

THE PHYSICAL REVIEW

A JOURNAL OF EXPERIMENTAL AND
THEORETICAL PHYSICS

CONDUCTED BY
THE
AMERICAN PHYSICAL SOCIETY

BOARD OF EDITORS

Managing Editor JOHN T. TATE, University of Minnesota, Minneapolis
I. S. BOWEN, R. S. MULLIKEN, H. D. SMYTH, E. U. CONDON, C. J. DAVISSON,
F. K. RICHTMYER, K. F. HERZFELD, A. W. HULL, F. W. LOOMIS

VOLUME 36, SECOND SERIES
JULY-DECEMBER, 1930

THE PHYSICAL REVIEW
MINNEAPOLIS, MINN.



CONTENTS

JULY 1, 1930

A Note on the Spectra of Doubly and Trebly Ionized Lead	STANLEY SMITH	1
Spark Spectrum of Cobalt (Co II)	J. H. FINDLAY	5
Spectra of Gases Lighted with Strong Electrical Discharges	E. O. HULBURT	13
Computation of the Effective Cross Section for the Recombination of Electrons with Hydrogen Ions	E. C. G. STUECKELBERG AND PHILIP M. MORSE	16
Recombination of Ions in Argon, Nitrogen and Hydrogen	OVERTON LUHR	24
Mobilities of Ions in Dry and Moist Air	JOHN ZELENY	35
Excitation Processes in the Hollow Cathode Discharge	RALPH A. SAWYER	44
Analytic Atomic Wave Functions	CLARENCE ZENER	51
Atomic Shielding Constants	J. C. SLATER	57
A Search for the Source of Dielectric Polarization	RALPH D. BENNETT	65
Infrared Filters of Controllable Transmission	A. H. PFUND	71
Velocity of Ultrasonic Waves in Water Vapor	GEORGE E. THOMPSON	77
Unreliability of Photographic Emulsions on Glass for Recording Distances and a Method of Minimizing this Defect	D. COOKSEY AND C. D. COOKSEY	80
Precision Measurements of the Glancing-Angle of Reflection from Calcite for Silver ($K\alpha_1$) X-Rays by the "Method of Displacement"	C. D. COOKSEY AND D. COOKSEY	85
Spherically Symmetrical Field in the Unified Theory	N. ROSEN AND M. S. VALLARTA	110
Gibbs-Dalton Law of Partial Pressures	LOUIS J. GILLESPIE	121
A Rational Basis for the Thermodynamic Treatment of Real Gases and Mixtures of Real Gases	JAMES A. BEATTIE	132
Letters to the Editor		146
Breadth of Compton Modified Line, <i>J. W. M. DuMond</i> —146; Raman Effect in Trimethylethylene, <i>Dorothy Franklin and E. R. Laird</i> —147; Photoionization of Salt Vapors, <i>A. Terenin</i> —147; Raman Effect in Solutions of Sodium Nitrate of Varying Concentration, <i>Vera Sterling and E. R. Laird</i> —148; Calculation of Energy Values, <i>Carl Eckart</i> —149; Some Peculiarities of the Spectrum of the Tungsten Mercury Arc, <i>W. E. Forsythe and M. A. Easley</i> —150; Experimental Evidence for the Existence of Quadrupole Radiation, <i>Rudolf Frerichs and J. S. Campbell</i> —151; Mobility of Na^+ Ions in H_2 , <i>Leonard B. Loeb</i> —152; Interaction between Excited and Unexcited Hydrogen Atoms at large Distances, <i>E. C. Kemble and F. F. Rieke</i> —153.		
Book Reviews		155

JULY 15, 1930

Incomplete Paschen-Back Effect	J. B. GREEN	157
Fine Structure of the K-Radiation of the Lighter Elements	LAWRENCE Y. FAUST	161
Spark Spectra of Silver and Palladium (Ag II and Pd II)—An Extension	H. A. BLAIR	173
Resonance (B-A) Band System of the Hydrogen Molecule	HUGH H. HYMAN	187
Luminescence of Zinc Sulphide Under the Action of Alpha, Beta and Gamma Rays	GEORGE S. GESSNER	207
A Second Ionization Potential in Potassium Vapor	A. L. HUGHES AND C. M. VAN ATTA	214
Absorption and Collision Broadening of the Mercury Resonance Line	M. W. ZEMANSKY	219
Effect of Small Angle Scattering on the Electron Absorption Coefficient	METTA CLARE GREEN	239
Rate at Which Ions Lose Energy in Elastic Collisions	AUSTIN M. CRAVATH	248
Method of Enhancing the Sensitiveness of Alkali Metal Photoelectric Cells	A. R. OLPIN	251
Infrared Absorption of Some Organic Liquids Under High Resolution. Part II	R. BOWLING BARNES	296
Effect of High Pressure on the Near Infrared Absorption Spectrum of Certain Liquids	J. R. COLLINS	305
Adsorption of Methyl Alcohol Films on Rock Salt	SHIRLEIGH SILVERMAN	311
Principal Magnetic Susceptibilities of Bismuth Single Crystals	ALFRED B. FOCKE	319
Discontinuous Changes in Length Accompanying the Barkhausen Effect in Nickel	C. W. HEAPS AND A. B. BRYAN	326
Isotopes of Nitrogen, Mass 15, and Oxygen, Mass 18 and 17 and their Abundances	S. MEIRING NAUDÉ	333
Margules Method of Measuring Viscosities Modified to Give Absolute Values	HOWARD R. LILLIE	347
An Erratum		363

Letters to the Editor	364
Interpretation of the Visible Halogen Bands, <i>Robert S. Mulliken</i> —364; Double Crystal Analysis of Scattered X-rays, <i>Newell S. Gingrich</i> —364; A Remark on the Paper of R. C. Tolman: "Mechanical Treatment of the Temperature Distribution in the Case of Radiation," <i>Wilhelm Anderson</i> —365; A Remark on the Foregoing Letter of W. Anderson— <i>R. C. Tolman</i> —365; Raman Spectra of Geometric Isomers, <i>C. F. Ffolliott</i> —367; Method Offered as a Means of Computing Planck's Constant Without Involving the Charge on the Electron, <i>Allen Lucy</i> —367; Gas Discharge Wave-length List in Extreme Ultraviolet, <i>Janet M. MacInnes and Joseph C. Boyce</i> —368.	
Book Reviews	369

PROCEEDINGS OF THE AMERICAN PHYSICAL SOCIETY

Ithaca Meeting, June 19-21, 1930; Minutes and Abstracts 1-33; Author Index	372
--	-----

AUGUST 1, 1930

Fine Structure of He as a Test of the Spin Interactions of Two Electrons	G. BREIT	383
Singlet System of Oxygen Arc Spectrum and the Origin of the Green Auroral Line	RUDOLF FRERICHs	398
Band Spectra Intensities for Symmetrical Diatomic Molecules	ELMER HUTCHISSON	410
Vibrational Quantum Analysis of the Potassium Infrared Absorption Bands	W. O. CRANE AND ANDREW CHRISTY	421
Rotational Motion of Molecules in Crystals	LINUS PAULING	430
Deflection of Electrons by a Magnetic Field on the Wave Mechanics	LEIGH PAGE	444
Absorption of X-Rays by Lithium	K. C. MAZUMDER	457
Wave-Length Measurements of Gamma-Rays from Radium and its Products	LUVILLE T. STEADMAN	460
Ionization of Carbon Dioxide by Electron Impact	H. D. SMYTH AND E. C. G. STUECKELBERG	472
Ionization of Nitrous Oxide and Nitrogen Dioxide by Electron Impact	E. C. G. STUECKELBERG AND H. D. SMYTH	478
Effect of Intense Electric Fields on the Photoelectric Properties of Metals	ERNEST O. LAWRENCE AND LEON B. LINFORD	482
Magnetic Isotropy of Copper Crystals	CAROL G. MONTGOMERY	498
Tension Coefficient of Resistance of Metals	HARRY ROLNICK	506
Vibrations of a Non-Planar Membrane	GEORGE R. STIBITZ	513
Capillary Retention of Liquids in Assemblages of Homogeneous Spheres	W. O. SMITH, PAUL D. FOOTE AND P. F. BUSANG	524
A Representation of the Dynamic Properties of Molecules by Mechanical Models	C. F. KETTERING, L. W. SHUTTS AND D. H. ANDREWS	531
Relation Between the Raman Spectra and the Structure of Organic Molecules	DONALD H. ANDREWS	544
Elastic Character of the Homopolar Chemical Bond	ROBERT C. YATES	555
Study of the Small Vibrations of Six Particles in a System Analogous to the Benzene Ring	ROBERT C. YATES	563
Coupled Vibrations with Applications to the Specific Heat and Infrared Spectra of Crystals	ARTHUR B. LEWIS	568
Studies in Contact Rectification. II. The Cupric Sulfide-Magnesium Junction	MILTON BERGSTEIN, J. F. RINKE AND C. M. GUTHEIL	587
Letters to the Editor		600
The Presence of Neutral Oxygen in the Gaseous Nebulae, <i>I. S. Bowen</i> —600; Photoelectric Outgassing, <i>Ralph P. Winch</i> —601; Effect of the Earth's Electric and Magnetic Fields on Ions in the Atmosphere, <i>Leigh Page</i> —601; Note on Wave-lengths in the Vacuum Copper Arc, <i>A. G. Shenstone</i> —602; The Electrolytic Dissociation of Nitric Acid as Revealed by its Infrared Absorption Spectrum, <i>E. L. Kinsey and J. W. Ellis</i> —603; The Optical Excitation Function of Helium, <i>Walter C. Michels</i> —604; Metastable Atoms and Electrons Produced by Resonance Radiation in Neon, <i>Irving Langmuir and Clifton G. Found</i> —604; On the Magnetic Deflection of Cosmic Rays, <i>Bruno Rossi</i> —606.		
Book Reviews		607

AUGUST 15, 1930

Report on Notation for Spectra of Diatomic Molecules	ROBERT S. MULLIKEN	611
Application of the Fermi-Thomas Statistical Model to the Calculation of Potential Distribution in Positive Ions	EDWARD B. BAKER	630
Fine Structure in the X-Ray Absorption Spectra of the K Series of the Elements Calcium to Gallium	BEN KIEVIT AND GEORGE A. LINDSAY	648
False Lines in X-Ray Grating Spectra	J. M. CORK	665
Arc Spectrum of Palladium	A. G. SHENSTONE	669
Intensity Measurements in the Spectrum of Nickel and Cobalt	L. S. ORNSTEIN AND T. BOUMA	679

Effect of the Motion of the Nucleus on the Spectra of Li I and Li II - - - - -	D. S. HUGHES AND CARL ECKART	694
Electronic States in the Visible Halogen Bands - - - - -	ROBERT S. MULLIKEN	699
Interpretation of Pressure and High Velocity Vapor Jets at Cathodes of Vacuum Arcs - - - - -	KARL T. COMPTON	706
Secondary Emission from Metals by Impact of Metastable Atoms and Positive Ions - - - - -	W. UYTERHOEVEN AND M. C. HARRINGTON	709
Extinction of Short A.C. Arcs between Brass Electrodes - T. E. BROWNE, JR. AND F. C. TODD		726
Restriking of Short A.C. Arcs - - - - -	F. C. TODD AND T. E. BROWNE, JR.	732
Photoelectric Behavior of Solid and Liquid Mercury - - - - -	DUANE ROLLER	738
Thermodynamic Treatment of Chemical Equilibria in Systems Composed of Real Gases. I. An Approximate Equation for the Mass Action Function Applied to the Existing Data on the Haber Equilibrium - - - - -	LOUIS J. GILLISPIE AND JAMES A. BEATTIE	743
Dielectric Constant of Carbon Dioxide as a Function of Temperature and Density - - - - -	FREDERICK G. KEYES AND JOHN G. KIRKWOOD	754
Some Applications of the Theory of Plastic Deformations of Ductile Metals - - - - -	A. NADAI	762
Attempt to Detect Collisions of Photons - - - - -	A. L. HUGHES AND G. E. M. JAUNCEY	773
Letters to the Editor - - - - -		778
Band Intensities, <i>Joseph Kaplan</i> —778; X-Ray Scattering Coefficient as a Function of Wave-length and Atomic Number, <i>Errol N. Coade</i> —778; Fluorescent Dry Plates for Photographic Photometry, <i>George R. Harrison and Philip A. Leighton</i> —779.		
Book Reviews - - - - -		781

PROCEEDINGS OF THE AMERICAN PHYSICAL SOCIETY

Eugene Meeting, June 19–21, 1930; Minutes and Abstracts 1–25; Author Index - - - - -	783
--	-----

SEPTEMBER 1, 1930

Double Crystal Study of Scattered X-Rays - - - - -	J. A. BEARDEN	791
Energy of $K\alpha_1$ of Copper as a Function of Applied Voltage with the Double Crystal Spectrometer - - - - -	JESSE W. M. DUMOND ARCHER HOYT	799
Projective Relativity - - - - -	OSWALD VEBLEN AND BANESH HOFFMAN	810
On the Theory of the Brownian Motion - - - - -	G. E. UHLENBECK AND L. S. ORNSTEIN	823
Appearance of Forbidden Lines in Spectra - - - - -	L. D. HUFF AND W. V. HOUSTON	842
Hyperfine Structures of Some Cd Lines and the Hypothesis of Nuclear Spin- C. L. ALBRIGHT		847
New Lines in the Arc and Spark Spectrum of He - - - - -	P. GERALD KRUGER	855
Structure of Emission Lines- - - - -	FRANK HOYT	860
Note on Frequency Shifts in Dispersing Media - - - - -	G. BREIT AND E. O. SALANT	871
Theory and Calculation of Screening Constants - - - - -	CARL ECKART	878
Reflection of Cd and Zn Atoms from NaCl Crystals - - - - -	HAROLD A. ZAHL	893
Determination of e/m for an Electron by Direct Measurement of the Velocity of Cathode Rays - - - - -	CHARLOTTE T. PERRY AND E. L. CHAFFEE	904
New Experimental Determination of Effective Cross-Sections for the Quenching of Hg Resonance Radiation - - - - -	M. W. ZEMANSKY	919
Some Measurements of the Longitudinal Elastic Frequencies of Cylinders Using a Magnetostriction Oscillator - - - - -	DAVID S. MUZZEY, JR.	935
Electrical Resistance of Ni and Permalloy Wires as Affected by Longitudinal Magnetization and Tension - - - - -	L. W. MCKEEHAN	948
On the Magnetic Properties of Metals - - - - -	FRANCIS BITTER	978
Scattering of Fast Electrons by Metals. I. The Sensitivity of the Geiger Point Discharge Counter - - - - -	CARL T. CHASE	984
High Potential X-Ray Tube - - - - -	C. C. LAURITSEN AND B. CASSEN	988
Linear Correction for Cathode Ray Oscillograph - - - - -	FREDERICK BEDELL AND JACKSON KUHN	993
Propagation of Luminosity in Discharge Tubes - - - - -	J. W. BEAMS	997
Simple Accurate Method for Measuring the Diamagnetic Susceptibility of Dissolved Substances - - - - -	SIMON FREED AND CHARLES KASPER	1002
Ultrasonic Velocity and Absorption in Oxygen- - - - -	W. H. PIELEMEIER	1005
Thermodynamic Treatment of Chemical Equilibria in Systems Composed of Real Gases. II. A Relation for the Heat of Reaction Applied to the Ammonia Synthesis Reaction. The Energy and Entropy Constants for Ammonia- - - - -	LOUIS J. GILLESPIE AND JAMES A. BEATTIE	1008
Letters to the Editor - - - - -		1014
Wave Mechanics of Deflected Electrons, <i>Carl Eckart</i> —1014; Magnetostriction in Nickel, <i>L. W. McKeehan</i> —1014; Wind Mixing and Diffusion in the Upper Atmosphere, <i>S. Chapman</i> —1014; Evidence for the Richtmyer Double Jump Hypothesis of X-Ray Satellites, <i>Jesse W. M. DuMond</i> —1015; Hyperfine Structure of X-Ray Lines, <i>F. K. Richtmyer, S. W. Barnes and K. V. Manning</i> —1017; The Angular Momentum of the Li ⁺ Nucleus, <i>L. P. Granath</i> —1018; Evidence for Be Isotope of Mass 8 in the BeH Band Spectrum, <i>William W. Watson</i> —1019; The Penetration of Radiation, <i>Elliot Q. Adams</i> —1020; New Bands in the Absorption Spectrum of Mercury, <i>J. G. Winans</i> —1021.		
Errata - - - - -		1022

SEPTEMBER 15, 1930

Canal Ray and Electron Excitation of the Band Spectrum of Nitrogen - - - - -	H. D. SMYTH AND E. G. F. ARNOTT	1023
Angle and Energy Distribution of Electrons Scattered by Helium, Argon and Hydrogen - - - - -	J. HOWARD McMILLEN	1034
Intensity of X-Ray Satellites - - - - -	F. K. RICHTMYER AND L. S. TAYLOR	1044
Analysis of Scattered X-Rays With the Double Crystal Spectrometer - NEWELL S. GINGRICH		1050
Scattering of Fast Electrons by Metals. II. Polarization by Double Scattering at Right Angles - - - - -	CARL T. CHASE	1060
Experimental Determination of the Change in Temperature Accompanying Change in Magnetization of Iron - - - - -	WALTER B. ELLWOOD	1066
New Method of Measuring the Variation of Specific Heats (c_p) of Gases with Pressure - - - - -	E. J. WORKMAN	1083
Note on the Pressure Variation of Specific Heats of Gases Derived from Compressibility Data - - - - -	L. G. HOXTON	1091
Letters to the Editor - - - - -		1096
Relative Efficiency of the Hg-arc Lines in exciting the Raman Spectrum of Benzol, <i>Sister Magna Werth</i> —1096; Orbital Valency, <i>James H. Bartlett, Jr.</i> —1096; Probable Number of Isotopes of Eight Metals as determined by a New Method, <i>Fred Allison and Edgar J. Murphy</i> —1097; Formation of Striae in a Kundt's Tube, <i>Rolla V. Cook</i> —1098; Intensity Changes of Cameron Bands in the Electrodeless Discharge, <i>Harold P. Knauss and Jack C. Cotton</i> —1099; On the Direction of Emission of Photoelectrons from Potassium Vapor by Ultraviolet Light, <i>Ernest O. Lawrence and Milton A. Chaffee</i> —1099; Electrostatic Surface Fields near Thoriated Tungsten Filaments by a Photoelectric Method, <i>Leon B. Linford</i> —1100.		

OCTOBER 1, 1930

Use of the Refraction of X-Rays for the Determination of the Specific charge of the Electron - - - - -	H. E. STAUSS	1101
X-Ray Scattering Coefficient as a Function of Wave-Length and Atomic Number - - - - -	ERROL N. COADE	1109
Atomic Scattering Powers of Nickel, Copper and Iron for Various Wave-Lengths - - - - -	RALPH W. G. WYCKOFF	1116
Theory of Complex Spectra - - - - -	E. U. CONDON	1121
Zeeman Effect in the ZnH and CdH Bands - - - - -	WILLIAM W. WATSON	1134
Principle of Identity and the Exclusion of Quantum States - - - - -	GILBERT N. LEWIS	1144
On the Wentzel-Brillouin-Kramers Approximate Solution of the Wave Equation - - - - -	L. A. YOUNG AND G. E. UHLENBECK	1154
On the Origin of the Bands in the Spectrum of Mercury Vapor - - - - -	S. MROZOWSKI	1168
Abnormal Shot Effect of Ions of Tungstous and Tungstic Oxide - - - - -	JOHN S. DONAL, JR.	1172
Distinction between Contact-Potential Effects and True Reflection Coefficients for Low-Velocity Electrons - - - - -	H. E. FARNSWORTH AND V. H. GOERKE	1190
Current, Pressure, and Frequency Relationships for the Initiation and Maintenance of the Electrodeless Glow Discharge - - - - -	MILTON L. BRAUN	1195
Absorption of Slow Hydrogen Positive Rays in Hydrogen - - - - -	ROBERT E. HOLZER	1204
Velocity Distribution of Secondary Electrons from Molybdenum - - - - -	THEODORE SOLLER	1212
Heat of Formation of Molecular Oxygen - - - - -	L. COVELL COPELAND	1221
Dielectric Constant of Helium - - - - -	J. V. ATANASOFF	1232
Potential and Potential Energy of Space Lattices - - - - -	C. N. WALL	1243
Origin of the Variations in the Sun's Rotational Velocity - - - - -	ROSS GUNN	1251
Triboluminescence - - - - -	R. E. NYSWANDER AND BYRON E. COHN	1257
Letters to the Editor - - - - -		1261
High Voltage Tubes, <i>M. A. Tuve, L. R. Hafstad and O. Dahl</i> —1261; Use of the Pierce Acoustic Interferometer for the Determination of Absorption in Gases for High Frequency Sound Waves, <i>Elias Klein and W. D. Hersberger</i> —1262; The Magnetic Moment of the Li Nucleus, <i>G. Breit and F. W. Doermann</i> —1262; Wind Mixing and Diffusion in the Upper Atmosphere, <i>E. O. Hulburt</i> —1264.		
Book Reviews - - - - -		1265

OCTOBER 15, 1930

Position and Structure of the Modified Line of the Spectrum of Scattered X-Rays - - - - -	F. L. NUTTING	1267
An Experimental Study of the Relative Intensities of X-Ray Lines in the Tantalum L-Spectrum - - - - -	VICTOR HICKS	1273
A Study of the Velocities of H^+ Ions Formed in Hydrogen by Dissociation Following Electron Impact - - - - -	W. WALLACE LOZIER	1285
Ionization of Helium, Neon, and Argon by Electron Impact - - - - -	PHILIP T. SMITH	1293

Ionization Potentials and Probabilities for the Formation of Multiply Charged Ions in Helium, Neon and Argon - - - - -	WALKER BLEAKNEY	1303
Thermionic Emission of Oxide Coated Cathodes Containing a Ni-Ba Alloy Core - - - - -	N. C. BEESE	1309
Shot Effect of the Emission from Oxide Cathodes - - - - -	H. N. KOZANOWSKI AND N. H. WILLIAMS	1314
A Photographic Method of Determining Atomic Structure Factors - - - - -	DAROL K. FROMAN	1330
A Note on the Extrapolation of Atomic Structure Factor Curves - - - - -	DAROL K. FROMAN	1339
Range of the α Particles from Thorium - - - - -	G. H. HENDERSON AND J. L. NICKERSON	1344
Possibilities of the Oscillating Arc in Spectrochemical Analysis - - - - -	E. Z. STOWELL AND W. S. HUXFORD	1348
Electro-Optical Modification of Light Waves - - - - -	L. H. STAUFFER	1352
Optical Excitation Function of Helium - - - - -	WALTER C. MICHELIS	1362
Organic Reactions in Gaseous Electrical Discharge I. Normal Paraffin Hydrocarbons - - - - -	ERNEST G. LINDER	1375
Polarized Fluorescence of Solutions of Rhodamine-B and Uranine - - - - -	ERNEST MERRITT AND DONALD R. MOREY	1386
Mobility of Aged Ions in Air - - - - -	OVERTON LUHR AND NORRIS E. BRADBURY	1394
On the Entropy of Hydrogen - - - - -	D. MAC GILLAVRY	1398
A New Relativity Theory of the Unified Physical Field - - - - -	WILLIAM BAND	1405
Letters to the Editor - - - - -		1413
Effect of Electric Field upon X-Ray Diffraction Pattern of a Liquid, G. W. Stewart—1413; Interpretation of the Spectra of CaF and SrF, A. Harvey and F. A. Jenkins—1413; Structure of K-radiation from C, B, and Be, Martin Soderman—1414; High Efficiencies of Emission from Oxide-Coated Filaments, B. J. Thompson—1415; Negative Ions in Hydrogen and Water Vapor, W. W. Lozier—1417; Wave Mechanics of Deflected Electrons, Leigh Page—1418.		
Book Reviews - - - - -		1419

NOVEMBER 1, 1930

Improved Technique for the Raman Effect - - - - -	R. W. WOOD	1421
Raman Spectra of Benzene and Diphenyl - - - - -	R. W. WOOD	1431
Heats of Condensation of Electrons on Several Metals in Several Ionized Gases - - - - -	C. C. VAN VOORHIS AND K. T. COMPTON	1435
Correlation of Atomic J Values and Molecular Quantum Numbers, with Applications to Halogen, Alkaline Earth Hydride, and Alkali Molecules - - - - -	ROBERT S. MULLIKEN	1440
A New Band in the Absorption Spectrum of Methane Gas - - - - -	DAVID M. DENNISON AND S. B. INGRAM	1451
Transverse Zeeman Effect of the Green Auroral Line; an Experimental Proof of the Existence of Quadrupole Radiation - - - - -	RUDOLF FRERICHS AND J. S. CAMPBELL	1460
Spectral Distribution of Energy Radiated from a New Type of Tungsten Mercury Arc - - - - -	B. T. BARNES	1468
General Electric Type S-1 Lamp as a Spectroscopic Source - - - - -	DONALD DOOLEY	1476
Behavior of a Mercury Vapor Arc with a Jet of Liquid Mercury as Cathode - - - - -	AUSTIN M. CRAVATH	1480
Diffraction of a Circularly Symmetrical Electromagnetic Wave by a Co-axial Circular Disc of Infinite Conductivity - - - - -	JOHN BARDEEN	1482
A Low Grid-Current Vacuum Tube - - - - -	G. F. METCALF AND B. J. THOMPSON	1489
Cataphoresis in Rotating Electric Fields - - - - -	E. M. PUGH AND C. A. SWARTZ	1495
Hall Effect and the Magnetic Properties of Some Ferromagnetic Materials - - - - -	EMERSON M. PUGH	1503
Letters to the Editor - - - - -		1512
The Molecular Field and Atomic Order in Ferromagnetic Crystals and in Hydrogenized Iron, L. W. McKeehan—1512; The Wave Mechanics of Deflected Electrons, Carl Eckart—1514; The Non-Statistical Solution of Einstein's Law of Gravitation in a Spatially Symmetrical Field, Hsin P. Soh—1515.		
Book Reviews - - - - -		1516

NOVEMBER 15, 1930

Scattering of Hard γ -Rays - - - - -	C. Y. CHAO	1519
Fine Structure of Certain X-Ray Emission Lines - - - - -	JOSEPH VALASEK	1523
Correction and Extension of the Series of the Silver Arc Spectrum, Ag I - - - - -	H. A. BLAIR	1531
I. Effect of Gases on the Optically Excited Cadmium I Spectrum - - - - -	PAUL BENDER	1535
II. Optical Excitation of Cadmium Hydride and Zinc Hydride Bands - - - - -	PAUL BENDER	1543
Isotope Effect on Band Spectrum Intensities - - - - -	J. L. DUNHAM	1553
Ultraviolet Light Theory of Aurorae and Magnetic Storms. (Continued) - - - - -	E. O. HULBURT	1560
Dielectric Constant of Ammonia as a Function of Temperature and Density - - - - -	FREDERICK G. KEYES AND JOHN G. KIRKWOOD	1570

Note on the Production of Extremely High Voltages - - - - -	M. A. TUVE	1576
A Two Dimensional Boundary Value Problem for the Transmission of Alternating Currents Through a Semi-Infinite Heterogeneous Conducting Medium - - - - -	HERBERT P. EVANS	1579
Letters to the Editor - - - - -		1589
Polarization of Mercury Lines in Stepwise Radiation, <i>Allan C. G. Mitchell</i> —1589; On the Attempt to Detect Collisions of Photons, <i>S. Vavilov</i> —1590; A Note on Zeeman Patterns, <i>Henry Norris Russell</i> —1590; Raman Effect of HBr and HI, <i>E. O. Salant and A. Sandow</i> —1591; Absorption and Collision Broadening of Resonance Radiation, <i>M. W. Zemansky</i> —1591; On the Incomplete Polarization of the Mercury Resonance Radiation, <i>S. Mrozowski</i> —1591; On the Entropy of Hydrogen, <i>W. F. Giaque and H. L. Johnston</i> —1592.		
Book Reviews- - - - -		1594

DECEMBER 1, 1930

On the Question of the Constancy of the Cosmic Radiation and the Relation of these Rays to Meteorology - - - - -	ROBERT A. MILLIKAN	1595
On the Electrical Resistance of Contacts between Solid Conductors - - - - -	J. FRENKEL	1604
X-Ray Absorption in Gases - - - - -	W. W. COLVERT	1619
Diffraction of X-Rays in Liquids: Effect of Temperature - - - - -	E. W. SKINNER	1625
On the Fluorescence of Quartz Under the Influence of Cathode Rays of Low Voltage - - - - -	HEINRICH PETERS	1631
Pressure and High Velocity Vapour Jets at Cathodes of a Mercury Vacuum Arc - - - - -	E. KOBEL	1636
Photoelectric Emission from Thin Films of Caesium - - - - -	L. R. KOLLER	1639
Magnetic Susceptibility of Gases II. Temperature Dependence - - - - -	FRANCIS BITTER	1648
Magnetic Properties of Certain Pt-Co and Pd-Co Alloys - - - - -	F. WOODBRIDGE CONSTANT	1654
Magnetic Isotropy of a Paramagnetic Alum - - - - -	C. G. MONTGOMERY	1661
A Method for Growing Large Crystals of the Alkali Halides - - - - -	JOHN STRONG	1663
Letters to the Editor - - - - -		1667
Use of the Pierce Acoustic Interferometer, <i>W. H. Pielemeier</i> —1667; Wave Mechanics of Deflected Electrons, <i>E. H. Kennard</i> —1667; Simple Isotopic Constitution of Caesium, <i>K. T. Bainbridge</i> —1668; Problems in Acoustic Interferometry with Gases, <i>J. C. Hubbard</i> —1668; Magnetostriction and Magnetic Hysteresis, <i>L. W. McKeehan</i> —1670; Note on the Source of Dielectric Polarization, <i>Ralph D. Bennett</i> —1670; A Diophantine Equation Connected with the Hydrogen Spectrum, <i>T. H. Gronwall</i> —1671.		
Book Reviews- - - - -		1673

DECEMBER 15, 1930

Polarization of the Continuous X-Rays from Single Electron Impacts - - - - -	BALEBAIL DASANNACHARYA	1675
Spectrum of the Radiation from a High Potential X-Ray Tube - - - - -	C. C. LAURITSEN	1680
Multiple Scattering in the Compton Effect - - - - -	JESSE W. M. DUMOND	1685
Design and Technique of Operation of a Double Crystal Spectrometer - - - - -	JESSE W. M. DUMOND AND ARCHER HOYT	1702
Value of e/m by Deflection Experiments - - - - -	G. E. UHLENBECK AND L. A. YOUNG	1721
Relativistic Wave Mechanics of Electrons Deflected by a Magnetic Field - - - - -	MILTON S. PLESSET	1728
Hyperfine Structure of S and P Terms of Two Electron Atoms with Special Reference to Li^+ - - - - -	G. BREIT AND F. W. DOERMANN	1732
Thermoanalysis of Metal Single Crystals and a New Thermoelectric Effect of Bismuth Crystals Grown in Magnetic Fields - - - - -	ALEXANDER GOETZ AND MAURICE F. HASLER	1752
Second Virial Coefficient for Gases: a Critical Comparison between Theoretical and Experimental Results - - - - -	HENRY MARGENAU	1782
Temperature Equilibrium in a Static Gravitational Field - - - - -	RICHARD C. TOLMAN AND PAUL EHRENFEST	1791
Letters to the Editor - - - - -		1799
The Inner Potential of a Copper Crystal, <i>H. E. Farnsworth</i> —1799; Differences in the Absorption Spectrum of Benzene in the Liquid and Vapor State, <i>E. D. McAlister and H. J. Unger</i> —1799; Relative Intensities in Hyperfine Structure Multiplets, <i>H. E. White</i> —1800. The Vibrational and Rotational Analysis of the S ₂ Bands, <i>S. M. Naude and Andrew Christy</i> —1801.		
Erratum - - - - -		1802
Index to Volume 36 - - - - -		1803

THE PHYSICAL REVIEW

A NOTE ON THE SPECTRA OF DOUBLY AND TREBLY IONIZED LEAD

BY STANLEY SMITH
UNIVERSITY OF ALBERTA
(Received May 27, 1930)

ABSTRACT

In the spectrum of Pb III three new singlet terms *viz.* $6s7s^1S_0$, $6s7p^1P_1$ and $6s7d^1D_2$ have been found to give rise to seventeen new lines which are here reported.

Certain discrepancies between the classification of terms by A. S. Rao and A. L. Narayan and the writer are discussed.

In the spectrum of Pb IV the previously published classifications of lines by J. A. Carroll, A. S. Rao and A. L. Narayan are discussed, and certain anomalies are pointed out. Two schemes different in some respects from those already put forward are suggested.

SPECTRUM OF Pb III

THE spectrum of Pb III has been discussed in several papers^{1,2,3} published during the past two years. The investigation of this spectrum has been continued by the writer and has led to the identification of three more singlet terms, which have been classified as $6s7s^1S_0$, $6s7p^1P_1$ and $6s7d^1D_2$. In the meanwhile a further paper by A. S. Rao and A. L. Narayan⁴ has appeared in which there is agreement with the writer with regard to the $6s7p^1P_1$ term but disagreement as to the identity of the term classified by the writer as $6s7s^1S_0$. As there are also further discrepancies between the results it was thought that it would be of interest to discuss these and to bring the information with regard to this spectrum up to date by adding a list of the new combinations which have been classified.

The data used in this investigation are the vacuum spark measurements of Mack,⁵ of R. J. Lang (unpublished) and of the writer.⁶ Spectrograms of the Schüler lamp discharge in the region from 1900Å to 7000Å obtained by the writer have also been found to be useful in this work. The writer is also

¹ K. R. Rao, A. L. Narayan and A. S. Rao. Indian Journ. Phys. 2, 467 (1928).

² S. Smith, Proc. Nat. Acad. Sci. 14, 878 (1928).

³ S. Smith, Phys. Rev. 34, 393 (1929).

⁴ A. S. Rao and A. L. Narayan, Zeits. f. Physik 59, 687 (1930).

⁵ J. E. Mack, Phys. Rev. 34, 17 (1929).

⁶ S. Smith, Trans. Roy. Soc. Canada 22, 331 (1928).

indebted to Dr. Lang for a plate of this spectrum taken on his vacuum spectrograph in the region 1300A to 2200A.

The two main points of disagreement between the classification of Rao and Narayan and that of the writer are in connection with the $6s7d^3D_{1,2,3}$ and $6s6d^1D_2$ terms. With regard to the $6s7d^3D_{1,2,3}$ terms Rao's choice does not lead to any observed lines in the predicted positions for the $6s6p^3P_{0,1,2} - 6s7d^3D_{1,2,3}$ combinations, whereas the terms selected by the writer do give fairly close agreement between predicted and observed lines for these combinations. Moreover the observed lines $\lambda\lambda 4094, 4128$, which apparently arise from combinations between $6s7d^3D_{1,2}$ and the newly found term $6s7p^1P_1$, may be considered as further evidence in support of the validity of the writer's choice of the $6s7d^3D_{1,2,3}$ terms. Turning now to the term $\nu = 104998$, classified by Rao as $6s6d^1D_2$ and by the writer as $6s7s^1S_0$, it will be noted that Rao gives $\lambda\lambda 4272, 4496$ as the combinations between this term and $6s7p^1P_1$ and $6s7p^3P_2$ respectively. If this classification is correct then the inner quantum number of the term in question clearly cannot be 0. However it is found that the wave-number difference between $\lambda\lambda 4272, 4496$ is 1163.6 whereas the value of $6s7p^3P_2 - 6s7p^1P_1$, deduced from the appropriate combinations using measurements in a region where the wave-lengths are known to a fairly high degree of accuracy, is 1158.4. This is so large a discrepancy that it throws doubt on the above mentioned classification of $\lambda\lambda 4272, 4496$. It is possible that $\lambda 4496$ is a $6s6d^3D$ combination as this line differs in wave-number from the line $\lambda 4400$, which also appears to be a line of doubly ionized lead, by 481.6. This is the value of the $6s6d^3D_{1,2}$ separation. The $6s6d^1D_2$ term has been previously given by the writer and $\lambda 3951$ appears to be the combination between this term and the newly found $6s7p^1P_1$ term and not an FG combination as classified by Rao. The lines $\lambda\lambda 2948, 3451$, given by Rao as $6s7p^3P_{1,2} - 6p7p^3P_2$ appear with considerable intensity on the Schüller lamp plates and are therefore to be attributed to Pb II.

The lines involving the new terms are given in Table I.

TABLE I. *New classified lines of Pb III.*

λ , A. air	Int.	ν	Classification	Term	Value
5780.0	3	17296	$6s7s^1S_0 - 6s7p^3P_1$		
*5191.9	3	19255	$6s6d^3D_2 - 6s7p^1P_1$		
*5064.4	1	19740	$6s6d^3D_1 - 6s7p^1P_1$		
4855.14	2	20591.0	$6p6p^3P_1 - 6s7p^3P_2$		
*4827.02	3	20710.9	$6s7p^1P_1 - 6s8s^3S_1$		
4596.53	1	21749.5	$6s6p^3P_1 - 6s7p^1P_1$	$6s7s^1S_0$	104998
4499.51	6	22218.4	$6s7p^1P_1 - 6s7d^1D_2$	$6s7p^1P_1$	81600
4272.63	5	23398.2	$6s7s^1S_0 - 6s7p^1P_1$	$6s7d^1D_2$	59382
4128.21	2	24216.8	$6s7p^1P_1 - 6s7d^3D_1$		
4094.68	3	24415.1	$6s7p^1P_0 - 6s7d^3D_2$		
3951.94	7	25296.9	$6s6d^1D_2 - 6s7p^1P_1$		
*3689.32	5	27097.6	$6s7s^3S_1 - 6s7p^1P_1$		
3530.35	1	28317.7	$6s7p^3P_1 - 6s7d^1D_2$		
λ , A. vac.					
1711.23	4	58437	$6s6p^1P_1 - 6s7s^1S_0$		
1118.67	4	89392	$6s6p^3P_1 - 6s7s^1S_0$		
1070.83	0	93385	$6s6p^3P_0 - 6s7s^1S_0$ (?)		
961.01	1	104057	$6s6p^1P_1 - 6s7d^1D_2$		

* Given by Rao and Narayan.

SPECTRUM OF Pb IV

The first investigation of this spectrum was made by Carroll,⁷ who gave the $6s^2S_1-6p^2P_{1,2}$ doublet, two of the $6d^2D_{2,3}-5f^2F_{3,4}$ triplet, and two choices for the $6p^2P_{1,2}-6d^2D_{2,3}$ triplet, the first of which included the line $\lambda 1069$, which has since been shown to be a Pb III line. An extension of this spectrum based on Carroll's identifications has recently been published by Rao and Narayan,⁸ but their classification does not appear to be a very probable one. The lines $\lambda\lambda 3909, 3279, 3089$, selected in Rao's scheme have been found to belong to Pb III. $\lambda\lambda 1726, 1796$ chosen by Carroll and by Rao as two of the $6d^2D_{2,3}-5f^2F_{3,4}$ triplet are found as very strong lines on the Schüller lamp spectrogram and therefore, in all probability, are to be attributed to Pb II. The writer has attempted to make a more probable selection, and a tentative scheme based on Carroll's second choice for the diffuse triplet is presented in Table II.

TABLE II. *Classified lines of Pb IV.*

λ I.A.	Int.	ν	$\Delta\nu$	Classification
*1028.61	15	97218	21063	$6s^2S_1-6p^2P_2$
*1313.12	15	76155		$6s^2S_1-6p^2P_1$
*922.53	4	108398	21057	$6p^2P_1-6d^2D_2$
*1116.10	5	89598		$6p^2P_2-6d^2D_3$
*1144.94	5	87341	2257	$6p^2P_2-6d^2D_2$
3002.78	2	33292.8	2258.4	$6d^2D_2-7p^2P_2$
3221.30	6	31034.4		$6d^2D_3-7p^2P_2$
3962.45	6	25229.8	8063.0	$6d^2D_2-7p^2P_1$
3052.66	7	32748.8	8063.1	$7s^2S_1-7p^2P_2$
4049.79	4	24685.7		$7s^2S_1-7p^2P_1$
2508.98	2	39844.8	8063.5	$7p^2P_1-7d^2D_2$
3087.10	4	32383.5		$7p^2P_2-7d^2D_3$
3145.60	2	31781.3	602.2	$7p^2P_2-7d^2D_2$

* Selected by Carroll.

An alternative classification of the triplets involving $6d^2D_{2,3}$ terms in which these terms are inverted, as in the case of the doublet D terms of Pb II,⁹ is given in Table III. In these tables the wave-lengths are expressed in I.A._{air} above 2000Å and in I.A._{vac} below 2000Å. Mack's measures are used for the $6P-6D$ triplet in Table III.

⁷ J. A. Carroll, Trans. Roy. Soc. A225, 357 (1925).

⁸ A. S. Rao and A. L. Narayan, Zeits. f. Physik 61, 149 (1930).

⁹ H. Gieseler, Zeits. f. Physik 42, 265 (1927).

TABLE III. *Alternative classification of lines of Pb IV.*

λ , Å.	Int.	ν	$\Delta\nu$	Classification
*890.78	5	112261		$6p\ ^2P_1 - 6d\ ^2D_2$
1096.47	2	91202	21059	$6p\ ^2P_2 - 6d\ ^2D_2$
*1116.09	7	89598	-1604	$6p\ ^2P_2 - 6d\ ^2D_3$
2864.54	7	34899.4		$6d\ ^2D_3 - 7p\ ^2P_2$
3002.78	2	33292.8	-1606.6	$6d\ ^2D_2 - 7p\ ^2P_2$
3962.45	6	25229.8	8063.0	$6d\ ^2D_2 - 7p\ ^2P_1$

* Selected by Carroll in his first choice of the diffuse triplet.

The fundamental triplet has not been found in either scheme and the $7p\ ^2P_{1,2}$ separation is larger than might be expected.

In conclusion I wish gratefully to acknowledge a grant from the National Research Council of Canada, which has been of assistance in this work.

THE SPARK SPECTRUM OF COBALT, Co II

By J. H. FINDLAY

PALMER PHYSICAL LABORATORY, PRINCETON UNIVERSITY

(Received May 19, 1930)

ABSTRACT

A further examination of the Co II spectrum, based on the previous work of Meggers, has been made. A magnetic analysis shows that Meggers' classification of the terms now called $d^7p\ ^5F^\circ$, $^5D^\circ$ should be interchanged, except for the term $^5F_5^\circ$. Since Meggers' results were obtained from intensity rules, the author's $^5F\ ^5F^\circ$ and $^5F\ ^5D^\circ$ multiplets show irregular intensities. The strongest lines in these multiplets are, respectively, $^5F_n\ ^5F_{n-1}^\circ$ and $^5F_n\ ^5D_n^\circ$. The magnetic analysis also shows that Meggers' terms 3D should be $d^7s\ ^5P$ and that his 3P , $^3D^1$, and 3F should be partly $d^7p\ ^5P^\circ$ and $^5D^\circ$. In addition, the terms $d^7s\ ^3F$, $d^7p\ ^3D^\circ$, $^3F^\circ$, $^3G^\circ$, $^5S^\circ$, $^5P^\circ$, $^5D^\circ$, and the lowest terms $d^8\ ^3F$ have been found. The location of the second member of the $d^7s\ ^5F\ ^3F$ series gives an I. P. of 16.9 volts from d^7s to d^7 and 17.3 volts from d^8 to d^7 , in practically exact agreement with the predictions of Dr. H. N. Russell.

INTRODUCTORY REVIEW

A PREVIOUS analysis of the first spark spectrum of cobalt was made by Meggers.¹ The purpose of the author's work was to extend Meggers' analysis with the aid of the Zeeman effect. The magnetic analysis afforded a change in the interpretation of several of Meggers' levels, and several new levels were found by the usual method of wave-number differences.

EXPERIMENTAL PROCEDURE

The author was fortunate in having the use of unpublished measurements and intensity estimates in the region from $\lambda 5000$ to $\lambda 2000$ made by Dr. Meggers of the Bureau of Standards. Further measurements were also made by the author of sharp lines in the range from $\lambda 2000$ to $\lambda 1940$ and of diffuse lines from $\lambda 3000$ to $\lambda 2550$, the standards being the copper arc and spark lines calculated by Shenstone.² Meggers' measurements were corrected to agree with these standards.

A Hilger E1 quartz spectrograph was used with Cramer Contrast and Hilger Schumann plates in taking photographs for wave-length determinations, sheets of very pure cobalt serving as electrodes.

Zeeman effect photographs were taken from $\lambda 3700$ to $\lambda 2190$ with the same instrument and an electromagnet, giving a field of about 35,500 gauss with pole pieces 1 cm in diameter and an air gap of about 3 mm. A button of cobalt about 1 mm thick clamped against one of the pole pieces of the magnet served as the anode, and a copper rod with a small tip on the end bent at right angles to the rest of the rod was used as the cathode of an arc, carrying a current of about 1 ampere at 250 volts, in taking most of the

¹ W. F. Meggers, Journ. Wash. Ac. Sci. **18**, 325 (1928).

² A. G. Shenstone, Phys. Rev. **28**, 449 (1926); **29**, 380 (1927).

TABLE I. Term table for Co II.

Config- uration	Designation		Level	g		Intervals (Higher J 's first)
	Author's	Meg- gers		Obs.	Landé	
$3d^8$	a^3F_4		0.0*			
$3d^8$	a^3F_3		950.3*			
$3d^8$	a^3F_2		1597.2*			
$3d^7(^4F)4s$	$4s^5F_5$	$5F_5'$	3350.5 *	1.39	1.40	
"	$4s^5F_4$	$5F_4'$	4028.9 *	1.36	1.35	
"	$4s^5F_3$	$5F_3'$	4560.8 *	1.25	1.25	
"	$4s^5F_2$	$5F_2'$	4950.0 *	1.00	1.00	
"	$4s^5F_1$	$5F_1'$	5204.5 *	.00	.00	
"	$4s^3F_4$		9812.7*	1.28	1.25	
"	$4s^3F_3$		10708.1*	1.10	1.08	
"	$4s^3F_2$		11321.5*	0.60	0.67	
$3d^7(^4P)4s$	$4s^5P_3$	$3D_3$	17771.5 *	1.70	1.67	
"	$4s^5P_2$	$3D_2$	18031.5 *	1.86	1.83	
"	$4s^5P_1$	$3D_1$	18338.5 *	2.48	2.50	
$3d^7(^4F)4p$	$4p^5F_5^{\circ}$	$5F_5$	45197.8*	1.40	1.40	
"	$4p^5F_4^{\circ}$	$5D_4'$	45378.8*	1.38	1.35	
"	$4p^5F_3^{\circ}$	$5D_3'$	45972.1*	1.26	1.25	
"	$4p^5D_4^{\circ}$	$5F_4$	46320.8 *	1.48	1.50	
"	$4p^5F_2^{\circ}$	$5D_2'$	46452.6*	1.02	1.00	a^3F 950.3, 646.9
"	$4p^5F_1^{\circ}$	$5D_1'$	46786.3*	.00	.00	$4s^5F$ 678.4, 531.9, 389.2, 254.5
"	$4p^5D_3^{\circ}$	$5F_3$	47039.0 *	1.51	1.50	$4s^3F$ 895.4, 613.4
"	$4p^5G_1^{\circ}$	$5G_1'$	47078.2 *	1.33	1.33	$4s^5P$ 260, 307
"	$4p^5G_2^{\circ}$	$5G_2'$	47345.7 *	1.27	1.27	$4p^5F^{\circ}$ 181.0, 593.3, 480.5, 333.7
"	$4p^5D_2^{\circ}$	$5F_2$	47537.1 *	1.52	1.50	$4p^5D^{\circ}$ 718.2, 498.1, 311.4, 146.6
"	$4p^5G_4^{\circ}$	$5G_4'$	47807.2 *	1.15	1.15	$4p^5G^{\circ}$ 267.5, 461.5, 343.5, 237.4
"	$4p^5D_1^{\circ}$	$5F_1$	47848.5 *	1.53	1.50	$4p^5G^{\circ}$ 792.3, 687.3
"	$4p^5D_0^{\circ}$		47995.1 *	0/0	0/0	$4p^5F^{\circ}$ 684.1, 532.2
"	$4p^5G_3^{\circ}$	$5G_3'$	48150.7 *	0.92	0.92	$4p^5D^{\circ}$ 717.4, 454.9
"	$4p^5G_2^{\circ}$	$5G_2'$	48388.1 *	0.33	0.33	$4p^5D^{\circ}$ -147.3, 19.3, 88.4, 109.4
"	$4p^5G_1^{\circ}$		48555.9*	1.20	1.20	$4p^5P^{\circ}$ 22.8, 298.1
"	$4p^5G_4^{\circ}$		49348.2*	1.09	1.05	$5s^5F$ 572.5, 580.5, 428.6, 280.2
"	$4p^5F_4^{\circ}$		49697.5 *	1.20	1.25	$5s^3F$ 864.6, 593.9
"	$4p^5G_3^{\circ}$		50035.9*	0.80	0.75	
"	$4p^5F_3^{\circ}$		50381.6 *	1.08	1.08	
"	$4p^5F_2^{\circ}$		50913.8 *	0.65	0.67	
"	$4p^5D_3^{\circ}$		51512.2*	1.32	1.33	
"	$4p^5D_2^{\circ}$		52229.6*	1.16	1.17	
"	$4p^5D_1^{\circ}$		52684.5*	0.45	0.50	
$3d^7(^4P)4p$	$4p^5S_3^{\circ}$		56010.6	1.99	2.00	
"	$4p^5D_3^{\circ}$	$3D_3'$	61240.8 *	1.51	1.50	
"	$4p^5D_2^{\circ}$	$3D_2'$	61260.1 *	1.51	1.50	
"	$4p^5D_1^{\circ}$		61348.5 *(?)	—	1.50	
"	$4p^5D_0^{\circ}$		61388.1 *	1.50	1.50	
"	$4p^5D_3^{\circ}$		61457.9 *	0/0	0/0	
"	$4p^5P_3^{\circ}$	$3P_2$	63344.1*	1.67	1.67	
"	$4p^5P_2^{\circ}$	$3F_2$	63366.9*	1.86	1.83	
"	$4p^5P_1^{\circ}$		63615.7	1.33	1.50	
"	$4p^5P_0^{\circ}$	$3P_1$	63665.0*	2.62	2.50	
$3d^7(^4F)5s$	$5s^5F_5$		84012.3 *			
"	$5s^5F_4$		84584.8 *			
"	$5s^5F_3$		85165.3 *			
"	$5s^5F_2$		85479.2*			
"	$5s^5F_1$		85593.9 *			
"	$5s^5F_0$		85874.1 *			
"	$5s^3F_3$		86343.8*			
"	$5s^3F_2$		86937.7*			

Zeeman effect photographs, the exposures of which were from 5 to 15 minutes. A blast of nitrogen blowing over the arc kept the cobalt from burning away too rapidly and, hence, made the arc run more steadily. Under these conditions, most of the lines appearing on the Zeeman effect plates were cobalt spark lines. However, in the region from $\lambda 3700$ to $\lambda 3000$ a spark discharge had to be used as a light source to bring out the spark lines. A few copper lines appeared on the plates. Of these $\lambda 3273.97$ ($^3S_{\frac{1}{2}} - ^2P_{\frac{1}{2}}$), $\lambda 2441.63$ ($^3S_{\frac{1}{2}} - ^4P_{\frac{1}{2}}$), and $\lambda 2181.71$ ($^2S_{\frac{1}{2}} - ^2P_{\frac{1}{2}}$) were used to determine the field. A quartz double image prism separated the parallel and perpendicular components of the patterns.

TERM DESIGNATION

The Hund theory predicts that the low terms should be 3F from the structure $3d^8$, and $^3\&^5F$, $^3\&^5P$, etc. from the structure $3d^74s$. The middle terms should be the $^3\&^5S^0$, P^0 , D^0 , F^0 , G^0 , etc. from $3d^74p$. Many of these terms have been discovered and are given in Table I together with the $^3\&^5F$ from $3d^75s$. The notation used is that recommended by H. N. Russell, A. G. Shenstone, and L. A. Turner.³

TABLE II. Resolved Zeeman patterns of Co II.

λ	$X - Y$	Z.E. Pattern	Remarks
3370.94	$4s^5P_1 - 4p^5D_0^0$	O(0.00) 2.40 C(0.00) 2.50	Good measurements not expected in this range.
2524.98	$4s^5F_2 - 4p^5F_2^0$	O(0.00) 0.68 C(0.00) 0.67	
2423.61	$4s^5F_1 - 4p^5F_2^0$	O(0.00, 1.10) 0.00, 1.10, 2.20 C(0.00, 1.00) 0.00, 1.00, 2.00	Discrepancy here unexplained.
2417.66	$4s^5F_4 - 4p^5F_4^0$	O(0.00) 1.39 C(0.00) 1.35	
2414.06	$4s^5F_3 - 4p^5F_3^0$	O(0.00) 1.26 C(0.00) 1.25	
2408.76	$4s^5F_2 - 4p^5F_2^0$	O(0.00) 1.01 C(0.00) 1.00	
2404.17	$4s^5F_1 - 4p^5F_1^0$	O(0.00) 0.00 C(0.00) 0.00	
2389.54	$4s^5F_2 - 4p^5F_1^0$	O(0.00, 0.92) 0.00, 0.92, 2.00 C(0.00, 1.00) 0.00, 1.00, 2.00	Discrepancy also unexplained.
2388.90	$4s^5F_5 - 4p^5F_5^0$	O(0.00) 1.39 C(0.00) 1.40	
2361.52	$4s^5F_1 - 4p^5D_2^0$	O(0.00, 1.50) 0.00, 1.50, 3.00 C(0.00, 1.50) 0.00, 1.50, 3.00	
2344.26	$4s^5F_1 - 4p^5D_1^0$	O(1.52), 0.00, 1.53 C(1.50), 0.00, 1.50	
2336.23	$4s^5F_1 - 4p^5D_0^0$	O(0.00) 0.00 C(0.00) 0.00	
2318.41	$4s^5P_1 - 4p^5D_0^0$	O(0.00) 2.48 C(0.00) 2.50	
2220.11	$4s^5P_1 - 4p^5P_2^0$	O(0.00, 0.88) 0.92, 1.86, faint. C(0.00, 0.67) 1.17, 1.83, 2.50	
2207.90	$4s^5P_1 - 4p^5P_2^0$	O(0.00, 1.18) 0.00, 1.33, faint. C(0.00, 1.00) 0.50, 1.50, 2.50	Unsymmetrical in π and σ . 0.50 components in σ unresolved.

³ H. N. Russell, A. G. Shenstone, L. A. Turner, Phys. Rev. **33**, 900 (1929).

ZEEMAN EFFECT

Several resolved patterns were obtained on the Zeeman effect photographs. Table II gives both the observed and calculated arrangement of these patterns. However, most of the lines appeared as simple triplets due to the low resolving power of the instrument. Nevertheless, a formula described by Shenstone and Blair⁴ allowed the calculation of g -values from the unresolved patterns. The g 's calculated from all the resolved and unresolved patterns are consistent with the assumption that all the terms have Landé g -values.

The magnetic analysis readily indicated that Meggers' classification of the 5F and $^5D'$ terms should be interchanged except for 5F_5 , his 3D terms should be $4s^5P$, and his 3P , $^3D'$, and 3F should be partly $d^7p^5P^0$ and $^5D^0$.

Since Meggers' results were based on intensity rules, the author's $4s^5F_4p^5F^0$ and $4s^5F_4p^5D^0$ multiplets show the irregular intensities indicated in Table III. In the case of spectra in which the Russell-Saunders coupling is broken down, there are usually irregular intensities, the g -values depart from Landé values, and the interval rule is not obeyed. In this spectrum, however, the interval rule is obeyed fairly well, and the terms have Landé g -values, yet two of the three principal multiplets show very anomalous intensities.

TABLE III. Intensities in the principal multiplets.

	$4s^5F_5$	5F_4	5F_3	5F_2	5F_1
$4p^2^5D_4^0$	25	80	10		
$^5D_3^0$		40	60	15	
$^5D_2^0$			30	30	10
$^5D_1^0$				30	25
$^5D_0^0$					20
$^5F_5^0$	100	10			
$^5F_4^0$	100	40	10		
$^5F_3^0$		80	40	10	
$^5F_2^0$			50	25	10
$^5F_1^0$				40	20
$^5G_5^0$	100				
$^5G_4^0$	8	75			
$^5G_3^0$	2	15	50		
$^5G_2^0$		3	20	40	
			4	15	30

IONIZATION POTENTIALS

The limits of the $4s^5F$, 3F series were determined by the application of a Rydberg formula to the two members of these series. However, on account of the inaccuracy of a Rydberg formula, this calculation did not, as is to be expected, give any indication of the four separate limits approached by the eight series.

The limit of the $4s^5F_5$ series gives an ionization potential of 16.9 volts from $3d^74s$ to $3d^7$, and 17.3 volts from $3d^8$ to $3d^7$. Using H. N. Russell's⁵

⁴ A. G. Shenstone and H. A. Blair, Phil. Mag. 8, 765 (1929).

⁵ H. N. Russell, Astrophys. J. 66, 223 (1927).

TABLE IV. *Classified lines of Co II.*

$\lambda(\text{Air})$	Int.	Auth.	$\nu(\text{Vac.})$	Combination
3621.22	100	M	27607.2	$4s^5P_3 - 4p^5F_4^\circ$
3578.03	30	M	27940.5	$4s^5P_2 - 4p^5F_3^\circ$
3555.93	10	M	28114.0	$4s^5P_1 - 4p^5F_2^\circ$
3545.03	25	M	28200.5	$4s^5P_3 - 4p^5F_4^\circ$
3517.48	10	M	28421.3	$4s^5P_2 - 4p^5F_3^\circ$
3514.21	5	M	28447.8	$4s^5P_1 - 4p^5F_2^\circ$
3501.73	200	M	28549.2	$4s^5P_3 - 4p^5D_1^\circ$
3446.40	100	M	29007.5	$4s^5P_2 - 4p^5D_3^\circ$
3423.85	75	M	29198.6	$4s^5P_1 - 4p^5D_2^\circ$
3415.78	75	M	29267.5	$4s^5P_3 - 4p^5D_3^\circ$
3388.18	50	M	29505.8	$4s^5P_2 - 4p^5D_2^\circ$
3387.72	60	M	29509.9	$4s^5P_1 - 4p^5D_1^\circ$
3370.94	50	M	29656.8	$4s^5P_3 - 4p^5D_3^\circ$
3358.59	10	M	29765.9	$4s^5P_3 - 4p^5D_2^\circ$
3352.80	30	M	29817.3	$4s^5P_2 - 4p^5D_1^\circ$
2943.16	30u	M	33967.2	$4p^3D_3^\circ - 5s^3F_4$
2930.45	10u	M	34114.5	$4p^3D_2^\circ - 5s^3F_3$
2883.43	1	F	34670.7	$4s^3F_3 - 4p^5F_4^\circ$
2880.32	3u	F	34708.2	$4p^3D_2^\circ - 5s^3F_2$
2870.03	3u	F	34832.7	$4p^3D_3^\circ - 5s^3F_3$
2848.36	5u	F	35097.6	$4p^3F_3^\circ - 5s^3F_4$
2845.64	2	F	35131.0	$4s^3F_2 - 4p^5F_2^\circ$
2834.92	2	M	35264.0	$4s^3F_3 - 4p^5F_3^\circ$
2825.22	8	M	35385.1	$4s^3F_4 - 4p^5F_3^\circ$
2821.63	5u	F	35430.1	$4p^3F_2^\circ - 5s^3F_3$
2818.86	1	M	35464.9	$4s^3F_2 - 4p^5F_1^\circ$
2810.85	5	M	35566.0	$4s^3F_4 - 4p^5F_4^\circ$
2807.17	2	M	35612.6	$4s^3F_3 - 4p^5D_1^\circ$
2798.92	2	F	35717.5	$4s^3F_2 - 4p^5D_3^\circ$
2796.86	2	F	35744.8	$4s^3F_3 - 4p^5F_2^\circ$
2793.93	20u	F	35781.3	$4p^3F_4^\circ - 5s^3F_4$
2779.82	20u	F	35962.9	$4p^3F_3^\circ - 5s^3F_3$
2775.11	20u	F	36024.0	$4p^3F_2^\circ - 5s^3F_2$
2766.85	30u	F	36131.6	$4p^3G_4^\circ - 5s^3F_4$
2764.75	1	F	36159.1	$4s^3F_4 - 4p^5F_3^\circ$
2753.38	10u	F	36308.2	$4p^3G_3^\circ - 5s^3F_3$
2738.32	1	F	36508.1	$4s^3F_4 - 4p^5D_1^\circ$
2736.91	2	M	36526.8	$4s^3F_2 - 4p^5D_1^\circ$
2734.68	10u	F	36556.6	$4p^3F_3^\circ - 5s^3F_2$
2727.91	20u	F	36647.3	$4p^3F_4^\circ - 5s^3F_3$
2714.40	15	M	36829.7	$\{4s^3F_2 - 4p^5G_3^\circ$ $\{4s^3F_3 - 4p^5D_2^\circ$
2709.12	10u	F	36901.4	$4p^3G_3^\circ - 5s^3F_2$
2707.55	30u	F	36922.8	$4p^3G_5^\circ - 5s^3F_4$
2706.72	50u	F	36934.2	$4p^3G_6^\circ - 5s^3F_5$
2702.19	20u	F	36996.0	$4p^3G_4^\circ - 5s^3F_3$
2697.02	3	M	37067.0	$4s^3F_2 - 4p^5G_2^\circ$
2694.65	25	M	37099.6	$4s^3F_3 - 4p^5G_4^\circ$
2686.97	1u	F	37205.6	$4p^3G_2^\circ - 5s^3F_2$
2684.50	50u	F	37239.8	$4p^3G_5^\circ - 5s^3F_4$
2676.03	20u	F	37357.7	$4p^3G_4^\circ - 5s^3F_3$
2669.89	10u	F	37443.6	$4p^3G_3^\circ - 5s^3F_2$
2666.82	5u	F	37486.7	$4p^3G_2^\circ - 5s^3F_1$
2663.52	60	M	37533.2	$4s^3F_4 - 4p^5G_5^\circ$
2662.64	2u	F	37545.6	$4p^3D_3^\circ - 5s^3F_4$
2653.68	15	M	37672.3	$4s^5P_1 - 4p^5S_2^\circ$
2653.16	1	F	37679.6	$4s^3F_3 - 4p^5G_2^\circ$
2652.36	5u	F	37691.1	$4p^3D_4^\circ - 5s^3F_5$
2639.26	2u	F	37878.1	$4p^3D_1^\circ - 5s^3F_1$
2632.22	30	M	37979.4	$4s^5P_2 - 4p^5S_2^\circ$
2629.01	0u	F	38023.7	$4p^3D_1^\circ - 5s^3F_1$
2626.89	10u	F	38056.4	$4p^3D_2^\circ - 5s^3F_2$
2622.06	5u	F	38126.5	$4p^3D_3^\circ - 5s^3F_3$

TABLE IV. *Continued.*

$\lambda(\text{Air})$	Int.	Auth.	$\nu(\text{Vac.})$	Combination
2614.37	20	M	38238.7	$4s^5P_3 - 4p^5S_2^\circ$
2612.63	10u	F	38264.1	$4p^5D_4 - 5s^5F_4$
2592.90	2u	F	38555.3	$4p^5D_2^\circ - 5s^5F_2$
2582.37	4u	F	38612.5	$4p^5F_5^\circ - 5s^5F_4$
2580.93	5u	F	38634.0	$4p^5F_4^\circ - 5s^5F_5$
2587.23	60	M	38639.8	$4s^5F_3 - 4p^5G_4^\circ$
2582.27	50	M	38714.0	$4s^5F_2 - 4p^5G_3^\circ$
2580.35	100	M	38742.8	$4s^5F_4 - 4p^5G_5^\circ$
2575.61	5u	F	38814.1	$4p^5F_5^\circ - 5s^5F_5$
2564.04	75	M	38989.3	$4s^5F_3 - 4p^5F_4^\circ$
2559.41	40	M	39059.8	$4s^5F_2 - 4p^5F_3^\circ$
2554.09	2u	F	39141.1	$4p^5F_2^\circ - 5s^5F_2$
2550.69	5u	F	39193.3	$4p^5F_1^\circ - 5s^5F_2$
2549.90	5u	F	39205.4	$4p^5F_4^\circ - 5s^5F_4$
2541.95	50	M	39328.1	$4s^5F_3 - 4p^5G_3^\circ$
2528.61	50	M	39535.5	$4s^5F_4 - 4p^5G_4^\circ$
2524.98	80	M	39592.4	$4s^5F_2 - 4p^5F_2^\circ$
2519.82	60	M	39673.4	$4s^5F_3 - 4p^5F_2^\circ$
2506.47	70	M	39884.7	$4s^5F_4 - 4p^5F_4^\circ$
2487.43	4	M	40190.0	$4s^5F_2 - 4p^5D_3^\circ$
2486.45	35	M	40205.8	$4s^5F_3 - 4p^5F_2^\circ$
2485.36	10	M	40223.5	$4s^5F_4 - 4p^5G_2^\circ$
2464.20	35	M	40568.8	$4s^5F_4 - 4p^5F_3^\circ$
2450.01	35	M	40803.8	$4s^5F_3 - 4p^5D_3^\circ$
2449.15	10	M	40818.1	$4s^5F_3 - 4p^5F_4^\circ$
2443.77	40	M	40908.0	$4s^5F_2 - 4p^5D_2^\circ$
2436.98	10	M	41021.9	$4s^5F_2 - 4p^5F_3^\circ$
2428.29	10	M	41168.7	$4s^5F_4 - 4p^5F_5^\circ$
2423.61	10	M	41248.2	$4s^5F_1 - 4p^5F_2^\circ$
2417.66	40	M	41349.7	$4s^5F_4 - 4p^5F_4^\circ$
2416.90	30	M	41362.7	$4s^5F_2 - 4p^5D_1^\circ$
2414.06	40	M	41411.4	$4s^5F_3 - 4p^5F_3^\circ$
2408.76	25	M	41502.5	$4s^5F_2 - 4p^5F_2^\circ$
2407.67	20	M	41521.3	$4s^5F_3 - 4p^5D_2^\circ$
2404.17	20	M	41581.7	$4s^5F_1 - 4p^5F_2^\circ$
2397.38	60	M	41699.5	$4s^5F_4 - 4p^5D_3^\circ$
2393.91	10	M	41759.9	$4s^5F_3 - 4p^5D_4^\circ$
2389.54	40	M	41836.3	$4s^5F_2 - 4p^5F_4^\circ$
2388.90	100	M	41847.5	$4s^5F_5 - 4p^5F_5^\circ$
2386.37	50	M	41891.9	$4s^5F_3 - 4p^5F_2^\circ$
2383.45	80	M	41943.2	$4s^5F_4 - 4p^5F_3^\circ$
2378.62	100	M	42028.3	$4s^5F_5 - 4p^5F_4^\circ$
2375.19	15	M	42089.0	$4s^5F_2 - 4p^5D_3^\circ$
2363.79	80	M	42292.0	$4s^5F_4 - 4p^5D_4^\circ$
2361.53	10	M*	42332.5	$4s^5F_1 - 4p^5D_2^\circ$
2353.43	60	M*	42478.0	$4s^5F_3 - 4p^5D_3^\circ$
2347.41	30	M*	42587.1	$4s^5F_2 - 4p^5D_2^\circ$
2344.26	25	M*	42644.0	$4s^5F_1 - 4p^5D_1^\circ$
2336.24	20	M*	42790.6	$4s^5F_1 - 4p^5D_0^\circ$
2330.37	30	M*	42898.5	$4s^5F_2 - 4p^5D_1^\circ$
2329.12	10	M*	42921.4	$4s^5P_1 - 4p^5D_2^\circ$
2326.49	25	M*	42970.0	$4s^5F_5 - 4p^5D_4^\circ$
2326.13	20	M*	42976.5	$4s^5F_3 - 4p^5D_2^\circ$
2324.32	40	M*	43010.2	$\{4s^5F_4 - 4p^5D_3^\circ$ $4s^5P_1 - 4p^5D_1^\circ$
2318.43	8	M*	43119.4	$4s^5P_1 - 4p^5D_1^\circ$
2314.99	30	M*	43183.5	$4s^5F_1 - 4p^5G_2^\circ$
2314.05	40	M*	43200.9	$4s^5F_2 - 4p^5G_3^\circ$
2313.60	8	M*	43209.4	$4s^5P_2 - 4p^5D_3^\circ$
2312.55	10	M*	43228.9	$4s^5P_2 - 4p^5D_2^\circ$
2311.62	50	M*	43246.5	$4s^5F_3 - 4p^5G_4^\circ$
2307.86	75	M*	43316.9	$\{4s^5P_2 - 4p^5D_1^\circ$ $4s^5F_4 - 4p^5G_5^\circ$

TABLE IV. Continued.

$\lambda(\text{Air})$	Int.	Auth.	$\nu(\text{Vac.})$	Combination
2301.42	15	M*	43438.1	$4s^5F_2-4p^5G_2^\circ$
2299.77	25	M*	43469.1	$4s^5P_3-4py^5D_3^\circ$
2298.74	10	M*	43488.6	$4s^5P_3-4py^5D_3^\circ$
2293.41	30	M*	43589.8	$4s^5F_3-4p^5G_3^\circ$
2292.00	40	M*	43616.6	$4s^5P_3-4py^5D_4^\circ$
2286.17	150	M*	43727.7	$4s^5F_5-4p^5G_5^\circ$
2283.54	20	M*	43778.2	$4s^5F_4-4p^5G_4^\circ$
2280.98	4	M*	43827.3	$4s^5F_3-4p^5G_2^\circ$
2272.28	20	M*	43995.1	$4s^5F_5-4p^5G_5^\circ$
2265.76	6	M*	44121.6	$4s^5F_4-4p^5G_4^\circ$
2248.68	8	M*	44456.7	$4s^5F_5-4p^5G_4^\circ$
2245.13	100	M*	44527.0	$4s^5F_4-4p^5G_5^\circ$
2232.08	50	M*	44787.4	$4s^5F_3-4p^5G_4^\circ$
2220.14	15	M*	45028.3	$4s^5P_1-4p^5P_2^\circ$
2217.30	4	M*	45085.7	$4s^5F_2-4p^5G_3^\circ$
2214.80	20	M*	45136.6	$4s^5F_3-4p^5F_4^\circ$
2211.44	30	M*	45205.3	$4s^5F_5-4p^5G_5^\circ$
2207.93	50	M*	45277.1	$4s^5P_1-4p^5P_2^\circ$
2206.21	75	M*	45312.4	$4s^5P_2-4p^5P_3^\circ$
2205.88	10	M*	45319.2	$4s^5F_4-4p^5G_4^\circ$
2205.53	20	M*	45326.4	$4s^5P_1-4p^5P_2^\circ$
2205.09	20	M*	45335.4	$4s^5P_2-4p^5P_3^\circ$
2203.44	5	M*	45369.4	$a^3F_3-4p^5D_4^\circ$
2202.96	100	M*	45379.3	$a^3F_4-4p^5F_4^\circ$
2200.42	25	M*	45431.5	$4s^5F_2-4p^5F_3^\circ$
2198.30	20	M*	45475.3	$4s^5F_3-4p^5G_3^\circ$
2193.61	100	M*	45572.7	$4s^5P_3-4p^5P_3^\circ$
2192.51	50	M*	45595.5	$4s^5P_3-4p^5P_3^\circ$
2190.69	75	M*	45633.5	$4s^5P_2-4p^5P_1^\circ$
2189.00	25	M*	45668.7	$4s^5F_4-4p^5F_4^\circ$
2187.05	25	M*	45709.4	$4s^5F_1-4p^5F_2^\circ$
2181.73	10	F	45820.8	$4s^5F_3-4p^5F_3^\circ$
2180.61	20	M*	45844.2	$4s^5P_3-4p^5P_2^\circ$
2174.94	2	M*	45963.9	$4s^5F_2-4p^5F_2^\circ$
2174.54	50	F	45972.3	$a^3F_4-4p^5F_3^\circ$
2173.33	60	M*	45997.9	$4s^5F_5-4p^5G_4^\circ$
2172.90	7	M*	46007.0	$4s^5F_4-4p^5G_3^\circ$
2158.16	2	M*	46321.2	$a^3F_4-4p^5D_4^\circ$
2156.95	40	M*	46347.1	$4s^5F_5-4p^5F_4^\circ$
2156.69	10	M*	46352.7	$4s^5F_4-4p^5F_3^\circ$
2147.38	2	M*	46553.6	$4s^5F_3-4p^5F_2^\circ$
2146.99	10	M*	46562.1	$a^3F_2-4p^5G_3^\circ$
2136.50	4	M*	46790.7	$4s^5F_2-4p^5D_3^\circ$
2133.47	10	M*	46857.2	$a^3F_3-4p^5G_4^\circ$
2129.17	1	M*	46951.8	$4s^5F_3-4p^5D_3^\circ$
2125.87	3	M*	47024.6	$4s^5F_1-4p^5D_2^\circ$
2117.95	8	M*	47200.4	$a^3F_3-4p^5G_3^\circ$
2114.40	2	M*	47279.7	$4s^5F_2-4p^5D_2^\circ$
2111.46	50	M*	47345.5	$a^3F_4-4p^5G_5^\circ$
2105.49	2	M*	47479.8	$4s^5F_1-4p^5D_1^\circ$
2105.34	3	M*	47483.1	$4s^5F_4-4p^5D_3^\circ$
2097.12	5	M*	47669.3	$4s^5F_3-4p^5D_2^\circ$
2094.24	1	M*	47734.8	$4s^5F_2-4p^5D_1^\circ$
2091.09	6	M*	47806.7	$a^3F_4-4p^5G_4^\circ$
2065.55	50	M*	48397.7	$a^3F_3-4p^5G_4^\circ$
2063.80	35	M*	48438.8	$a^3F_2-4p^5G_3^\circ$
2058.84	30	M*	48555.5	$a^3F_4-4p^5G_5^\circ$
2050.75	10	F	48746.8	$a^3F_3-4p^5F_4^\circ$
2049.19	2	M*	48784.1	$a^3F_2-4p^5F_3^\circ$

TABLE IV. *Continued.*

$\lambda(\text{Air})$	Int.	Auth.	$\nu(\text{Vac.})$	Combination
2036.61	3	M*	49085.4	$a^3F_3-4p^3G_3^\circ$
2027.08	20	M*	49316.1	$a^3F_3-4p^3F_2^\circ$
2025.80	10	M*	49347.2	$a^3F_4-4p^3G_4^\circ$
2022.35	20	M*	49431.4	$a^3F_3-4p^3F_3^\circ$
2011.52	5	F	49697.8	$a^3F_4-4p^3F_4^\circ$
2000.80	10	F	49963.7	$a^3F_3-4p^3F_2^\circ$
1997.93	3	F	50035.5	$a^3F_4-4p^3G_3^\circ$
1984.21	1	F	50381.5	$a^3F_4-4p^3F_3^\circ$
1974.38	1	F	50632.2	$a^3F_2-4p^3D_2^\circ$
1956.78	30	F	51087.6	$a^3F_2-4p^3D_1^\circ$
1949.46	20	F	51279.5	$a^3F_3-4p^3D_2^\circ$
1940.64	50	F	51512.3	$a^3F_4-4p^3D_3^\circ$

M—Meggers

M*—Meggers corrected

F—Author

equation to correct the calculation such that it may more nearly conform to results obtained from a Ritz formula, these ionization potentials become, respectively, 16.7 and 17.1 volts, which are in practically exact agreement with H. N. Russell's⁶ predictions.

Table IV gives all the identified lines of the spectrum.

In conclusion, I wish to thank Professor A. G. Shenstone for valuable aid and suggestions and Dr. W. F. Meggers for the use of his measurements and intensity estimates.

⁶ H. N. Russell, *Astrophys. J.* **66**, 1 (1927).

THE SPECTRA OF GASES LIGHTED WITH STRONG ELECTRICAL DISCHARGES*

BY E. O. HULBURT

NAVAL RESEARCH LABORATORY

(Received May 20, 1930)

ABSTRACT

Spectra of condensed discharges through hydrogen at pressures up to several cm of mercury showed, as usual, the Balmer lines merging into the continuous spectrum. With increasing strength of the discharge the Balmer lines widened, the higher members of the series disappeared and the continuous spectrum became more intense, until with 1 microfarad at 15 kilovolts there were no Balmer lines left at all, only the continuous spectrum and some absorption lines due to aluminum from the electrodes, etc. Helium, oxygen and nitrogen exhibited similar changes, i.e., with increasing intensity of the discharge in helium the lines gave way to a continuous spectrum, and in oxygen and nitrogen the molecular bands gave way to spark lines and these in turn to a continuous spectrum. The continuous spectra from all the gases were alike. The intensity distribution across the continuous spectrum was rather even and hardly that of a black body. In the strong discharges the external characteristics of the atoms were pretty well effaced and the conditions perhaps approached those in the interior of a star.

IT IS known that the spectrum of a gas varies with the pressure of the gas and with the type of electrical excitation, for example, the Balmer lines of hydrogen broaden with increasing pressure and intensity of the discharge. The experiments described in this paper were undertaken to find out what the spectrum of the gas is like when very strong discharges are used.

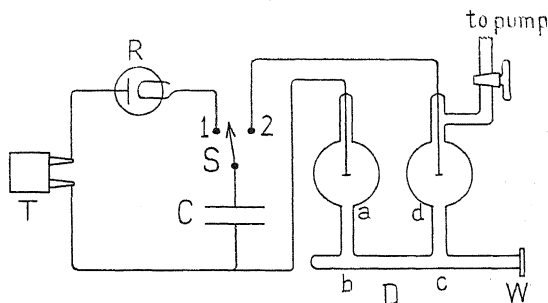


Fig. 1. Apparatus for sending strong discharges through the tube *D*.

A discharge tube *D*, Fig. 1, was arranged to be excited either directly by a 15000 volt, 25 cycle transformer *T*, or by a 0.002 microfarad condenser in series with a quenched gap to insure abrupt discharges, or by a 1 microfarad condenser. Fig. 1 gives a diagram of the apparatus for the last case.

* Published with the permission of the Navy Department.

With the switch *S* in position 1 the transformer *T* charged the condenser *C* through the rectifier *R*. When the switch was thrown quickly to position 2 by means of a spring the condenser discharged through the tube *D*. The arrangement was essentially that used by Anderson in his experiments with exploded wires.¹ The discharge tube was of glass with aluminum electrodes, the bulbs around the electrodes being about 5 cm in diameter. Sections *ab* and *cd* were 6 cm in length and *bc* was 7 cm in length and of internal diameter less than 1 cm. The light coming end-on through the quartz window *W* was photographed with a small quartz spectrograph. The discharge of the 1 microfarad condenser through the tube produced a blinding flash of light

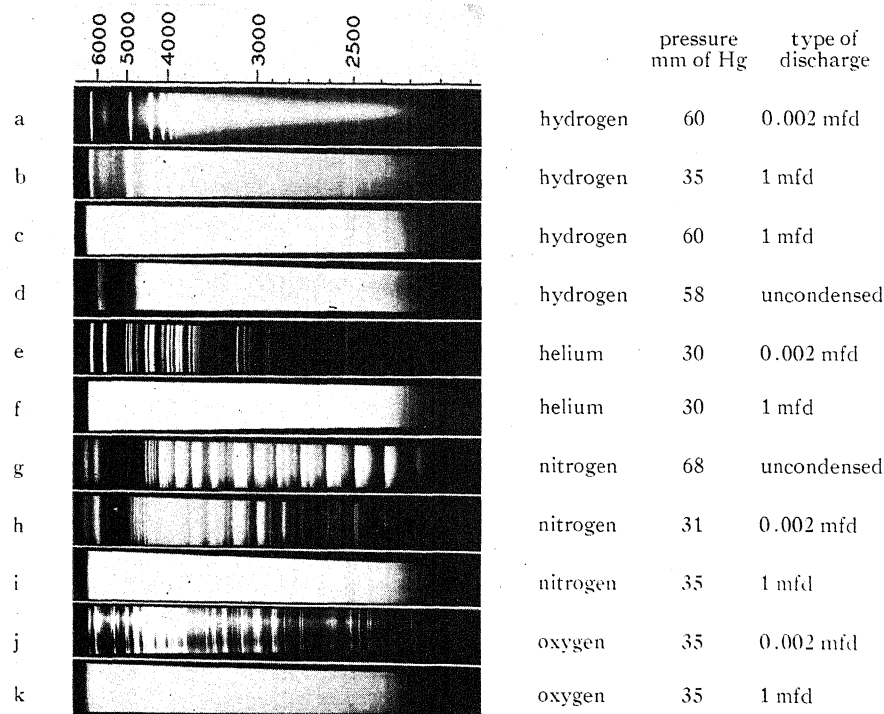


Fig. 2. Spectra of gases under various types of discharge.

and a fairly loud crack of sound, not so loud perhaps as the noise of an exploded wire. Usually a single discharge was sufficient to record the spectrum down to $\lambda 2000\text{\AA}$ in the ultra-violet. The pressure pulse in the tube sometimes blew off the quartz window, which was sealed on with wax. After a considerable number of discharges there were many fine superficial cracks on the interior surface of the portion *abcd* of the tube. None of the tubes, however, were broken by the violence of the discharge.

Some of the spectra of hydrogen, helium, nitrogen and oxygen are given in Fig. 2. Using the 0.002 microfarad condenser discharge the Balmer lines

¹ Anderson, *Astrophys. J.* **51**, 37 (1920); Smith *Astrophys. J.* **61**, 186 (1925); Anderson and Smith, *Astrophys. J.* **64**, 295 (1926).

of hydrogen widened with increasing pressure, as in strip *a* Fig. 2, the members of the series below H_γ disappeared and the continuous spectrum increased in intensity. With the 1 microfarad condenser and a discharge tube of 8 mm internal diameter between *b* and *c*, Fig. 1, there were only four Balmer lines left, these being much widened, and the continuous spectrum was intense, as in strip *b*. With the 1 microfarad condenser and a discharge tube of 4 mm internal diameter between *b* and *c*, Fig. 1, there were no Balmer lines left at all, only the continuous spectrum, as in strip *c*. The continuous spectrum was crossed by a few absorption and emission lines. Most of these were aluminum lines, but not all of them were identified. The spectra with the 1 microfarad condenser discharges were much the same for gas pressures from 20 to 60 mm of mercury, as might be expected on the idea that under such violent excitation the momentary pressure in the path of the discharge was very high and not dependent to a great extent on the pressure of the cold gas. Pressures greater than about 80 mm of mercury could not be used, for at greater pressures the discharge would not pass through the tube with the potentials available. It is interesting to compare strip *c* with strip *d* which is the spectrum of an uncondensed discharge through hydrogen at a pressure of 58 mm of mercury. This appears, except for its weakness at wave-lengths greater than 5000Å, much like strip *c*. The conditions of excitation of the gas for the two spectra were as different as could well be imagined, the one being a brilliant flash and the other a gentle blue glow, and yet the continuous spectra are somewhat similar.

Helium, nitrogen and oxygen, strips *e* to *k*, Fig. 2, exhibited changes similar to those of hydrogen, i.e. with increasing intensity of the discharge in helium the lines gave way to a continuous spectrum, and in oxygen and nitrogen the molecular bands gave way to spark lines and these in turn to a continuous spectrum. The continuous spectra from all the gases with the 1 microfarad condenser discharge were closely alike. A comparison with the lines of a mercury spectrum whose intensities were known² showed that the distribution of intensity across the continuous spectra was constant within two, and probably one, orders of magnitude from $\lambda 6000$ to 2000\AA . Thus, within the fairly large error of measurement, the intensity distribution did not seem to be that of a black body.

The general result of the experiments appeared to be that under the strong discharges the external characteristics, such as energy levels, etc., of the atoms of the gases were pretty well effaced. The atoms could no longer radiate their usual line or band spectrum but only a continuous spectrum. We may imagine that the conditions approached those in the interior of a star. It seems difficult at the present time to form a satisfactory quantitative theory of the continuous spectrum. In trampling on the atom we have at the same time trampled on theories of atomic behavior. It is hoped to extend the investigation using greater dispersion.

² Hulburt, Phys. Rev. **32**, 593 (1928).

COMPUTATION OF THE EFFECTIVE CROSS SECTION FOR THE RECOMBINATION OF ELECTRONS WITH HYDROGEN IONS

BY E. C. G. STUECKELBERG AND PHILIP M. MORSE
PALMER PHYSICAL LABORATORY, PRINCETON UNIVERSITY

(Received May 16, 1930)

ABSTRACT

The quantum-mechanical computation of the cross-section for combination of electrons with a positive point charge has been carried out in polar coordinates. This gives the fraction of the recombination to a final state of total quantum number n arising from recombination to the substates of different l values, making possible a comparison of the results with the experimental recombination intensities for alkali vapors to which the theory applies approximately.

AN ELECTRON passing by a hydrogen ion with a velocity equivalent to V volts can undergo a spontaneous transition to one of the states of a hydrogen atom. The probability with which such a process can occur has been treated by Kramers¹ and by Eddington² by the methods of the old quantum theory and the correspondence principle. Oppenheimer³ gives in his treatment of the motion of electrons in a Coulomb field the corresponding wave-mechanical expressions. The following paper gives certain additional calculations and numerical expressions for the probability of capture of electrons.

We recall the definition of the effective cross section of recombination: The decrease of the number N_+ ions per cm^3 is expressed by

$$\frac{dN_+}{dt} = -\alpha(v) \cdot N_+ \cdot N_- = -q(v) \cdot N_+ \cdot N_-' \quad (1)$$

N_- is the number of electrons per cm^3 having a velocity v relative to the ions. $N_-' = v \cdot N_-$ is the intensity of a stream of N_-' electrons per cm^2 per sec. $\alpha(v)$ is called the coefficient of recombination and $q(v)$ the effective cross section of recombination.

To find the probability of a transition of such an electron to one of the discrete states with negative energy one computes first the matrix element of the electric moment associated with the transition under consideration. As wave function in the initial state we require a solution $\psi_k(r, \cos \theta, \phi)$ of the wave equation in the force field of an ion of charge $Z \cdot e$, which becomes a plane wave at infinite distance, representing a stream along the x axis of N_-' electrons per cm^2 per sec.:

$$\lim_{r \rightarrow \infty} \psi_k = C \cdot \left\{ e^{i(Z/k a_0)x} + \frac{f(\cos \theta)}{r} \cdot e^{i(Z/k a_0)r} \right\} \quad (2)$$

¹ Kramers, Phil. Mag. 46, 836 (1923).

² Eddington, Internal Constitution of Stars, Cambridge (1926).

³ Oppenheimer, Zeits. f. Physik 55, 725 (1929).

and

$$\lim C \cdot \frac{h}{2\pi mc} \cdot \text{imag} (\bar{\psi}_k \text{grad } \psi_k) = N_-'$$

$$k^2 = \frac{R_V Z^2}{V} \quad (3)$$

V is the energy of the electrons and R_V is the ionization energy of a hydrogen atom in volts. a_0 is the radius of the first Bohr orbit in hydrogen. In the final state we take the known solution of the wave equation in polar coordinates $\psi_{n,l,m}(r, \cos \theta, \phi)$. Then we compute the matrix elements in the complex rectangular coordinates

$$\left. \begin{aligned} x &= r \cos \theta; & X^2(k, nlm) \\ u &= r \sin \theta \cdot e^{i\phi}; & U^2(k, nlm) \\ v &= r \sin \theta \cdot e^{-i\phi}; & V^2(k, nlm) \end{aligned} \right\} = \int \frac{x}{u} \bar{\psi}_k \psi_{nlm} d\tau_x \int \frac{x}{v} \bar{\psi}_k \psi_{nlm} d\tau \quad (4)$$

$$d\tau = \rho^2 \sin \theta d\rho d\theta d\phi$$

The relation between the matrix element $X(k, nlm)$ and the number of transitions per sec $q_x(k, nlm)$ N_-' giving light of frequency ν_n polarized in the x direction is

$$q_x(k, nlm) \cdot N_-' = \frac{64\pi^4}{3} \cdot \left(\frac{\nu_n}{c}\right)^3 \frac{\{\epsilon \cdot X(k, nlm)\}^2}{h} \quad (5)$$

Similar expressions hold for u and v . The total cross section for any given state n, l is

$$\begin{aligned} q(k, nl) &= q_x(k, nl0) + q_u(k, nl-1) + q_v(k, nl+1) \\ &= q_x + 2q_u. \end{aligned}$$

Oppenheimer⁴ computed by this method the $q(k, 10)$ and showed that it is asymptotically, for small velocities of the electron, proportional to Z^2/V . In a later paper he treated the problem for the excited states in parabolical coordinates⁵ using a wave function by Gordon⁵ and Temple,⁶ which satisfies Eq. (2). This method gives the expression of the total cross section summed over all l 's with the same n . The writers made use of the wave function used by Mott⁷ for the scattering of α -particles by nuclei in order to obtain the individual $q(nl)$'s. Mott's formula is in this notation:

$$\psi_k = i \cdot \left(\frac{N_-' \cdot h}{2\pi Z \epsilon^2}\right)^{1/2} \cdot \frac{k^{1/2} \cdot e^{(k\pi/2) + ik \log \rho}}{\sinh \pi k} \quad (6)$$

$$\sum_{\lambda=0}^{\infty} \frac{i^\lambda \cdot (\lambda + \frac{i}{2}) \cdot P_\lambda(\cos \theta)}{\Gamma(\lambda + 1 + ik)} \cdot \rho^\lambda \cdot \oint e^{\rho z} \cdot \left(z - \frac{i}{2}\right)^{\lambda-ik} \cdot \left(z + \frac{i}{2}\right)^{\lambda+ik} \cdot dz$$

⁴ Oppenheimer, Phys. Rev. **31**, 349 (1928).

⁵ Gordon, Zeits. f. Physik **48**, 180 (1928).

⁶ Temple, Proc. Roy. Soc. **121A**, 673 (1928).

⁷ Mott, Proc. Roy. Soc. **118A**, 542 (1928).

$\rho = (2Z/ka_0) \cdot r$ and the integral is to be taken along a single contour around $z = \pm i/2$. The asymptotic expansion for $r = \infty$ satisfies Eq. (2), having however in the first exponent an additional slowly varying logarithmic term (see Oppenheimer⁴ and Mott⁷). The evaluation of the integrals in Eq. (4) is done following a method given by Fues⁸ and used for similar problems by Oppenheimer.⁹ At one step one is left with an integral

$$J(k) = \oint \frac{\left(z - \frac{i}{2}\right)^{\lambda - ik} \left(z + \frac{i}{2}\right)^{\lambda + ik}}{\left(-z + \frac{k}{2n}\right)^{l + \lambda + s + 4}} dz$$

to be taken around $z = k/2n$. Its evaluation leads to the formulas 7a and 7b. for $q_z(nl)$ and $q_u(nl)$. 7c and 7d are the formulas taken from Oppenheimer's paper.³

Abbreviating: R for the Rydberg constant in frequency units

$$Q(\lambda, \alpha) = \sum_{p=0}^{p=\alpha} \binom{\lambda - ik}{p} \binom{\lambda + ik}{\alpha - p} \left(\frac{n + ik}{-n + ik}\right)^{(\alpha/2) - p},$$

$$S(k, l) = \frac{k^{2l+6}}{k^2(k^2 - 1^2)(k^2 - 2^2) \dots (k^2 - (l-1)^2)},$$

$$T(k) = \frac{e^{\pi k - 4k \tan^{-1}(n/k)}}{\sinh \pi k},$$

$$D = \frac{32 \cdot \pi^5 \cdot a_0^5 R^2}{3 \cdot Z^2 c^2}$$

$$F(\alpha \beta \gamma) = 1 + \frac{\alpha \cdot \beta}{1 \cdot \gamma} \cdot z + \frac{\alpha(\alpha + 1) \cdot \beta(\beta + 1)}{1 \cdot 2 \cdot \gamma(\gamma + 1)} z^2 + \dots$$

$$q_z(n, l) = D \cdot \frac{\nu_n}{c} \cdot \frac{(n - l - 1)!}{(2l + 1) \cdot (n + l)! n^{2l+4}} \cdot S(k, l) \cdot T(k)$$

$$\cdot \left\{ \sum_{s=0}^{s=n-l-1} \left(\frac{2}{n}\right)^s \cdot \left(\frac{R \cdot Z^2}{\nu_n}\right)^{s/2} \cdot \frac{(2l + 2 + s)!}{s!} \binom{n + l}{n - l - 1 - s} \right. \\ \cdot \left[\frac{4l}{k^2} \frac{RZ^2}{\nu_n} \cdot Q(l - 1, 2l + 2 + s) - \frac{(2l + s + 3)(2l + s + 4)(l + 1)}{(l + ik)(l + 1 + ik)} \right. \\ \left. \left. \cdot Q(l + 1, 2l + 4 + s) \right] \right\}^2 \quad (7a)$$

⁸ Fues, Ann. d. Physik **81**, 422 (1926).

⁹ Oppenheimer, Zeits. f. Physik **41**, 268 (1927).

$$q_u(n, l) = q_v(n, l) = D \cdot \frac{\nu_n}{c} \cdot \frac{(l+1)!(n-l-1)!}{(l-1)!(2l+1) \cdot (n+l)!n^{2l+4}} S(k, l) \cdot T(k) \cdot$$

$$\left\{ \sum_{s=0}^{s=n-l-1} \left(\frac{2}{n} \right)^s \left(\frac{R \cdot Z^2}{\nu_n} \right)^{s/2} \cdot \frac{(2l+2+s)!}{s!} \binom{n+l}{n-l-1-s} \right\} \quad (7b)$$

$$\left[\frac{4}{k^2} \cdot \frac{RZ^2}{\nu_n} O(l-1, 2l+2+s) + \frac{(2l+s+3)(2l+s+4)}{(l+ik)(l+1+ik)} \cdot Q(l+1, 2l+4+s) \right]$$

$$q_z(n) = \sum_{l=0}^{l=n-1} q_x(n, l) = 64D \cdot \frac{\nu_n}{c} \cdot \frac{k^6}{(n^2 + k^2)^2} \cdot T(k)$$

$$\sum_{s=0}^{s=n-1} \left| (n-s-1) \cdot F\left(-ik, 2+s-n, 1, \frac{-4ink}{(n+ik)^2}\right) \right. \quad (7c)$$

$$\left. - \left(n-s-1 - \frac{2ink}{n+ik} \right) F\left(-ik, 1+s-n, 1, \frac{-4ink}{(n+ik)^2}\right) \right|^2$$

$$q_u(n) = q_v(n) = \sum_{n=0}^{n=l-1} q_u(nl) = 64D \cdot \frac{\nu_n}{c} \cdot \frac{(4n)^2 k^{10}}{(n^2 + k^2)^4} \cdot T(k). \quad (7d)$$

$$\sum_{s=0}^{s=n-2} (s+1)(n-s-1) \left| F\left(1-ik, 2+s-n, 2, \frac{-4ink}{(n+ik)^2}\right) \right|^2.$$

For electrons whose kinetic energy is small compared with the term value of the final state, we substitute $w=z/k$ in the integral $J(k)$ and obtain

$$J(k) = k^{\lambda-l-s-3} \oint \frac{w^{2\lambda} \cdot e^{-1/w} \cdot dw}{\left(-w + \frac{1}{2n}\right)^{l+\lambda+s+4}}.$$

This integral is to be taken around the point $w=1/2n$ and is independent of k . Instead of formulas 7a and 7b we obtain 8a and 8b. 8c and 8d are the corresponding asymptotic expressions for $k=\infty$ of Eq. (7c) and (7d). For all states we obtain $q=A \cdot 10^{-20} \cdot Z^2/V$ for small V . Since in experiments on recombination the electron velocities are usually small, these formulas are sufficient in most cases.

Abbreviating

$$K(t, \lambda) = \sum_{\alpha=0}^{\alpha=t} \binom{t}{\alpha} \binom{2\lambda}{\alpha} \frac{\alpha!}{(2n)^\alpha} \cdot \sum_{\beta=0}^{\beta=t-\alpha-1} \binom{t-\alpha}{\beta} \binom{t-\alpha-1}{\beta} \frac{\beta!}{(-2n)^\beta}$$

$$E = \frac{4^7 \cdot \pi^5}{3c^3} \cdot a_0^5 R^3 R_v = 1.24 \times 10^{-19} \text{ cm}^2 \text{ volt}$$

$$M(t, \lambda) = \sum_{\alpha=0}^{\alpha=t} \binom{t}{\alpha} \frac{(-4n)^\alpha}{(\alpha + \lambda)!}$$

we obtain

$$q_x(nl) \sim \frac{E \cdot Z^2}{V} \cdot \frac{(n-l-1)! 16^l \cdot n^{2l+2}}{(2l+1) \cdot (n+l)! e^{4n}} \quad (8a)$$

$$\left\{ \sum_{s=0}^{s=n-l-1} \frac{(4n)^s}{s!} \binom{n+l}{n-l-s-1} [l \cdot R(2l+s+2, l-1) + (l+1) \cdot R(2l+s+4, l+1)] \right\}^2$$

$$q_u(nl) = q_v(nl) \sim \frac{EZ^2}{V} \cdot \frac{l(l+1) \cdot (n-l-1)! 16^l \cdot n^{2l+2}}{(2l+1) \cdot (n+l)! e^{4n}} \cdot \left\{ \sum_{s=0}^{s=n-l-1} \frac{(4n)^s}{s!} \binom{n+l}{n-l-s-1} [K(2l+s+2, l-1) - K(2l+s+4, l+1)] \right\}^2 \quad (8b)$$

$$q_x(n) = \sum_{l=0}^{l=n-1} q_x(n, l) \sim \frac{EZ^2}{V} \cdot \frac{1}{4n^2 \cdot e^{4n}} \cdot \sum_{s=0}^{s=n-1} \{ (n-s-1) \cdot M(n-s-2, 0) + (n+s+1) \cdot M(n-s-1, 0) \}^2 \quad (8c)$$

$$q_u(n) = q_v(n) = \sum_{l=0}^{l=n-1} q_u(n, l) \sim \frac{E \cdot Z^2}{V} \cdot \frac{4}{e^{4n}} \cdot \sum_{s=0}^{s=n-2} (s+1) \cdot (n-s-1) \cdot M(n-s-2, 1)^2. \quad (8d)$$

Empirical formulas are generally written in a form

$$q(n, l) = \text{const} \times \frac{1}{V \cdot \nu_{nl}^s}, \quad (9)$$

where ν_{nl} is the frequency of the emitted light, given for hydrogen by

$$\nu_{nl} = \nu_n = RZ^2 \left(\frac{1}{n^2} + \frac{1}{k^2} \right). \quad (10)$$

$s=2$ for the $2P$ band of Cs I (see report on recombination by Mohler¹⁰). Evaluating Eq. (8) for some of the lower states and abbreviating the algebraic expressions of k in frequencies according to Eq. (10) one obtains formulas 11, where

$$B = \frac{2 \cdot 4^6 \cdot \pi^5}{3} \cdot \frac{a_0 \cdot R^5 \cdot R_p \cdot Z^6}{c^3}.$$

¹⁰ Mohler, Phys. Rev. Supplement 1, 216 (1929).

$$\begin{cases}
 1s: q = q_x(10) = B \cdot T(k) \cdot \frac{1}{V \cdot \nu_1^2} \\
 2s: q = q_x(20) = \frac{B \cdot T(k)}{8} \cdot \frac{\nu_1}{V \cdot \nu_2^3} \\
 3s: q = q_x(30) = \frac{B \cdot T(k)}{27} \cdot \frac{\nu_1 \cdot \nu_2^2}{V \cdot \nu_3^5}; i = \left(\frac{27}{7}\right)^{1/2} \sim 2 \\
 2p: q = q_x(21) + 2q_u(21) = B \cdot T(k) \cdot \frac{RZ^2 \left(\frac{1}{36} \frac{\nu_j}{\nu_2} + \frac{1}{8} \right)}{\nu_2^3}; \\
 \quad j = \frac{2}{3}
 \end{cases} \quad (11)$$

This shows that the empirical way of writing the formulas involves frequency terms without physical meaning. The general form of the expressions (11) however is similar to Eq. (9), as T varies only slowly with k . None of these functions shows any maximum point corresponding to the results of Davis and Barnes experiment,¹¹ nor do any of the curves for higher states.

From formulas 8a and 8b the constants $A(nl)$ were computed for some of the lower states. The complexity of the sums increases greatly with larger n 's. Fig. 1 compares the exact and the asymptotic expressions for the 1s

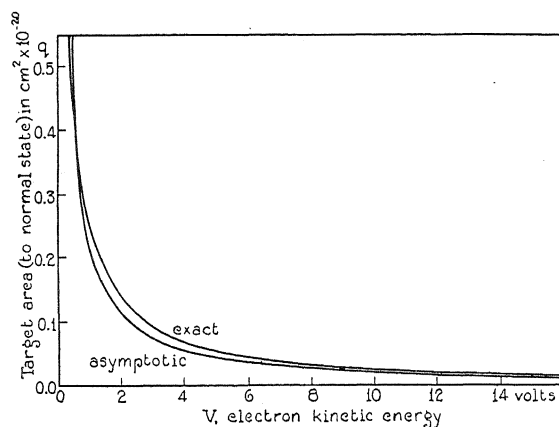


Fig. 1. Exact and asymptotic values of q for recombination to the 1s state.

state. Table I and Fig. 2 give the values of $A(n)$ for 1s, 2s, 2p, 3s, \dots , to 5s. The values of $\Sigma_l A(nl)$ is given in the last column of Table I and plotted as black dots in Fig. 2. The $\Sigma_l A(nl)$ have been computed by summing over the $A(nl)$ from Eq. (8a) and (8b), and to check it, also directly by Eq. (8c) and (8d). (Oppenheimer's formulas.)

¹¹ Davis and Barnes, Phys. Rev. **34**, 152 (1929); Barnes, Phys. Rev. **34**, 1224 (1929); **35**, 718 (1930).

TABLE I. Values for $A(nl)$ and $A(n) = \sum_{l=0}^{n-1} A(nl)$ in formula $q(nl) = A(nl) \cdot 10^{-20} \cdot Z^2/V \text{ cm}^2$.

terms	<i>s</i>	<i>p</i>	<i>d</i>	<i>f</i>	
<i>n</i>	$A(n0)$	$A(n1)$	$A(n2)$	$A(n3)$	$A(n)$
1	.227				.227
2	.0335	.109			.143
3	.0114	.0403	.0520		.104
4	.0053	.0190	.0318	.0254	.0814
5	.0030				

For a comparison of the absolute magnitude of the q 's with the experimental values obtained from recombination spectra, we compare in Table II the values as given by Mohler¹⁰ for the $1S$, $2P$ and $3D$ states of caesium for $V=0.2$ volts with the states $2s$, $2p$, $3d$ of hydrogen. There is little justification for picking these hydrogen states as comparison, except that their

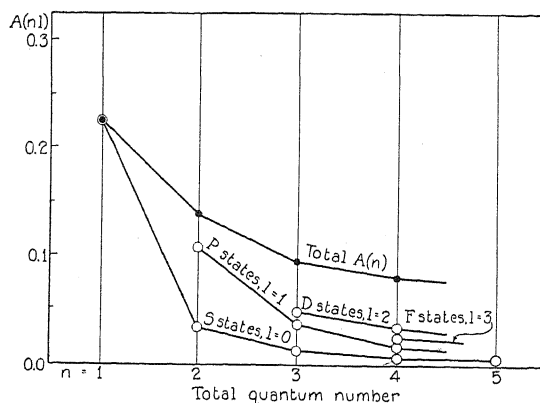


Fig. 2. Values of A in the formula $q = A \times 10^{-20} Z^2/V$ for recombination to various states.

effective quantum numbers most nearly correspond. For the P and D state we have a satisfactory agreement. The discrepancy of the $1S$ value is to be expected, since it is a highly penetrating orbit, and therefore would differ from a hydrogen-like behavior in a much greater degree than the P and D states. A similar disagreement is pointed out by Mohler¹⁰ in comparing the continuous absorption of these states with the theoretical computations for

TABLE II. Comparison of values of q for $V=0.2$ volts between caesium (experimental data) and hydrogen (theoretical data).

Cs		H	
term	q	term	q
1S	$0.015 \times 10^{-21} \text{ cm}^2$	2s	$1.7 \times 10^{-21} \text{ cm}^2$
2P	$6.0 \times 10^{-21} \text{ cm}^2$	2p	$5.5 \times 10^{-21} \text{ cm}^2$
3D	$6.0 \times 10^{-21} \text{ cm}^2$	3d	$2.6 \times 10^{-21} \text{ cm}^2$

the same hydrogen states by Oppenheimer.⁹ If one takes the states $6s$, $6p$ and $5d$ of hydrogen, whose *true* quantum numbers are the same as for the series electron of Cs in the considered states, the correspondence is improved with respect to the S -state (it being wrong by a factor 10 instead of 100) but the agreement for the P - and D -states is worse by a factor of about 10. This comparison is not given in Table II, because these higher terms have not been computed but only roughly extrapolated

It can not be expected to have any better agreement than this, since the wave function of the series electron in Cs is considerably different from that of any state in hydrogen. It is interesting to see that the best agreement for the P and D states is obtained by comparison with hydrogen states of the same effective quantum number.

Attempts to find an expression for the total target area

$$q = \frac{\sum_{n,l} A(nl) \times 10^{-20} \times Z^2}{V}$$

have not been successful.

The experiments by Davis and Barnes¹¹ can not be explained through spontaneous recombination of the electrons and α -particles and must therefore be due to some other mechanism.

THE RECOMBINATION OF IONS IN ARGON,
NITROGEN AND HYDROGEN

BY OVERTON LUHR

PHYSICAL LABORATORY, UNIVERSITY OF CALIFORNIA

(Received May 27, 1930)

ABSTRACT

Since free electrons are known to exist in ionized A, N₂ and H₂ these gases are employed in an effort to measure directly the coefficient of recombination for positive ions and electrons. At the same time the coefficient is determined for positive and negative ions in H₂ which would be expected theoretically to differ from other gases. The method is one using x-rays as the ionizing agent and has already been described by L. C. Marshall and the writer. Previous indirect methods and theory indicate that α , the coefficient of recombination for ions and electrons is of the order of 10^{-10} compared to 10^{-6} for positive and negative ions. In the present work results similar to those in air are obtained in the pure gases, and only a slight change in α is observed when sufficient O₂ is added to cause immediate attachment of the free electrons. Further direct tests in pure A, N₂ and H₂ indicate that negative ions are present in large quantities at all times, although a constant number of free electrons is also present. Hence it is probable that recombination was taking place between positive and negative ions rather than positive ions and electrons. It is assumed that as a result of the action of the ionizing agent negative ions are formed by attachment to excited metastable molecules in the case of A and N₂ and by attachment to atoms or triatomic molecules in the case of H₂.

In accordance with the criterion established in a previous paper for air, "absolute values" of α are set as follows:

Gas	Coefficient of Recombination
Air	$1.4 \pm 0.1 \times 10^{-6}$
O ₂	$1.5 \pm 0.1 \times 10^{-6}$
A	$1.2 \pm 0.1 \times 10^{-6}$
N ₂	$1.2 \pm 0.1 \times 10^{-6}$
H ₂	$0.32 \pm 0.05 \times 10^{-6}$

The results in H₂ show a constant value of $0.32 \pm 0.05 \times 10^{-6}$ which is much lower than in the other gases contrary to the prediction of the J. J. Thomson theory of recombination. However, the theory is deficient in certain respects which may explain this discrepancy.

INTRODUCTION

THE present work on the recombination of ions produced by x-rays is a continuation of previous investigations by L. C. Marshall¹ and the writer.² This second part was undertaken in an effort to measure directly the coefficient of recombination of positive ions and electrons, and at the same time to determine the coefficient of recombination in H₂ which would be expected to differ from other gases. Gases were used in which free electrons

¹ L. C. Marshall, Phys. Rev. 34, 618 (1929).

² O. Luhr, Phys. Rev. 35, 1394 (1930).

are known to exist for considerable periods of time. Thus in A, N₂ and H₂ free electrons will not attach to the normal molecules, but may attach to excited molecules or to molecules of impurity which may be present.

Theoretically it is to be expected that recombination between electrons and positive ions would proceed very slowly compared to that between negative and positive ions.³ This has in general been born out by numerous indirect spectroscopic methods of measurement⁴ and in one case by the direct measurements of Atkinson⁵ whose results, however, were inconclusive. Kenty,⁶ using spectroscopic methods and the Langmuir probe estimated the coefficient in very pure A to be of the order of 10^{-10} compared to 10^{-6} for positive and negative ions. Marshall,¹ with practically the same apparatus as that used by the writer believed he had found evidence of a low coefficient of recombination in pure A since the value was only about half that obtained when one cm partial pressure of O₂ had been added to the pure gas. The one cm of O₂ was sufficient to cause immediate attachment of all the free electrons present. Marshall used a metal ionization chamber where it is impossible to obtain the best conditions of purity, and he believed that the recombination in pure A was taking place principally between positive ions and negative ions formed by attachment of electrons to molecules of impurity.

In the present work it was found that Marshall's results were partially in error due to an unshielded lead (from the commutator to the ionization chamber) which caused a small statically induced charge to remain on the lower plate of the ionization chamber. No such effect was to be expected since the lead and lower plate were grounded through a half megohm resistance. However, because of the very high potentials in the room from the x-ray equipment, there was actually sufficient field to draw out most of the free electrons in 0.15 seconds, though there was no appreciable effect on the ions. Marshall attributed this loss of electrons to diffusion, but very little loss was observed in the present work even after a second, when the lead was shielded by enclosing it in a grounded metal tube. Also, the coefficient of recombination remained approximately the same when sufficient partial pressure of O₂ was added to any of the gases to obtain immediate attachment of the free electrons. This might indicate that the coefficient of recombination for positive ions and free electrons is nearly the same as for positive and negative ions, but it is believed that actually a considerable number of free electrons were attaching, possibly to impurities, but more likely to metastable excited molecules produced by the ionizing agent.

METHOD OF MEASUREMENT AND PRELIMINARY EXPERIMENTS

The apparatus has already been described by Marshall¹ and the writer,² and was used in exactly the same form in the present work. It consists of a rotating shutter and commutator mechanism which furnishes a means of

³ L. B. Loeb, *Trans. Am. Electrochem. Soc.* LV, 131 (1929).

⁴ R. Seeliger, *Phys. Zeits.* 30, 329 (1929).

⁵ R. d'E. Atkinson, *Zeits. f. Physik* 51, 188 (1928).

⁶ C. Kenty, *Phys. Rev.* 32, 624 (1929).

ionizing the gas in the ionization chamber by a flash of x-rays, then measuring the charge remaining at any time afterward by a suitable adjustment of the commutator and brushes. A sufficiently high field is applied to the lower plate of the ionization chamber through the commutator to produce a saturation current, thus sweeping all the ions of one sign to the upper plate almost instantly at any desired time. A neutralizing current is forced through a high resistance carbon line leak by means of a potentiometer, thus keeping the upper plate and electrometer system always at zero potential during the flash time and time of recombination.

The method of calculation is also the same as before, all values of α , the coefficient of recombination—obtained from the equation $\alpha = 1/t(1/n - 1/n_0)$ —being determined as a function of τ the age of the ions rather than t the total time of recombination.² In some cases this produced rather irregular results due to the very small differences in the potentiometer readings when the time of recombination was of the order of a few thousandths or a hundredth of a second. Thus very small errors in taking the potentiometer readings, due principally to fluctuations in intensity of the x-rays caused large errors in the values of α , and the plotted points do not always lie as close to a smooth curve as would be desired. However, since this method of calculation gives the only true picture of what is happening at any particular time, it was thought best to use it throughout.

Two small though important changes were made in the method of measurement. Instead of making use of the total volume of the ionization chamber ($10 \times 20 \times 7.5$ cm), the defining slit at the front of the chamber was narrowed down so that a beam of x-rays about 2.5 cm instead of 7.5 cm high passed between the plates. The volume of ionization was thus kept about 2.5 cm from each plate so that the possibility of diffusion of electrons to the plates with a resulting spuriously high coefficient of recombination would be at a minimum. On a kinetic theory basis it may be estimated that an electron would, on the average, diffuse a distance of two or three cm in as little as one-tenth of a second. However, this is extremely unlikely in the present case since the space charge produced by the positive ions remaining in the volume of ionization would prevent the electrons from diffusing to any great extent. Nevertheless, it was actually found in tests on A that the coefficient of recombination dropped off about fifteen percent as the distance of the x-ray beam from the plates was increased to a maximum.

The other change in the method of measurement consisted in having the sector opening the same for every run regardless of the commutator speed. This was necessary to produce sufficient ionization for convenient measurement. The sector opening was only 18° for A due to the intense ionization and 90° for air, N_2 and H_2 . Thus effectively older ions and more random distribution occurred at faster commutator speeds. Hence, α dropped more rapidly with time though the initial and final values remained the same as before, as shown by a comparison of the results in air obtained with the two methods. The situation was further aggravated by the high intensities of x-radiation which were necessary to produce sufficient ionization in H_2 and

N₂. As a result it is more difficult to set an "absolute value" for the coefficient of recombination as was done for air,² since the point at the end of the sharp drop due to nonrandom distribution is not clearly defined.

As in the previous work on air and O₂, all values of α are corrected for diffusion by assuming a swelling of the volume of ionization given by,

$$V = V_0 + 2A(\overline{\Delta x})_\tau$$

where V_0 is the initial volume, A is the area of the upper plate of the ionization chamber and $(\overline{\Delta x})_\tau$ is the average distance an ion will diffuse in time τ given by $(\overline{\Delta x})_\tau = (4D\tau/\pi)^{1/2}$ from the Brownian movement equation.⁷ D is the coefficient of diffusion given by $D = 0.0236k$ where k is the mobility of the ions. For air, A and N₂ the average mobility is about 2 cm per second per volt per cm, or D is 0.047. The mobility in H₂ is of the order of 6 cm per second giving D as 0.142. Owing to the use of a relatively small volume of ionization (though it was still 448 cm³ or seven times as large as that used by Marshall) the diffusion corrections were of the order of twenty percent at the longest time intervals but this correction gave results apparently consistent with the previous ones in air using larger volumes.

One extraneous effect observed in pure A, N₂ and H₂ is worthy of note. While Marshall was continually losing free electrons until there were very few left after 0.15 seconds, in the present work the negative readings were in general about three percent higher than the positive. This effect was evidently due to the presence of free electrons since the positive and negative readings became equal if sufficient O₂ was added to produce attachment. It was apparently not caused by a residual field as in Marshall's case since it was purely a percentage effect not varying with time. This possibility was further investigated by allowing x-rays to pass into the chamber with no field present to sweep out the ions. No appreciable charge was built up on the upper plate as long as the shielded lead was employed, but if the unshielded one used by Marshall was inserted a large positive charge accumulated indicating the loss of electrons to the lower plate. It was thought that possibly scattered radiation from the x-ray beam was in some way producing an excess of negative charges by photoelectric action on the metal surfaces, but photographs of the beam emerging from the ionization chamber showed it to be very sharply defined with no indication of any scattered radiation. The explanation may lie either in the presence of contact potentials or in a slight distortion of the field producing weak curved lines of force outside the volume of ionization which would sweep electrons of high mobility but not negative ions to the upper plate. The effect was not considered to be serious, however, since the positive readings were always used in calculating the coefficient of recombination. The negative readings would in general have given slightly higher values of α indicating a very small loss of electrons by diffusion from between the plates.

In regard to the purity of the gases, extreme care was taken so that the possibility of attachment of free electrons to molecules of impurity was

⁷ L. B. Loeb and L. C. Marshall, *Jour. Frank. Inst.* **207**, 371 (1929).

reduced to a minimum. The ionization chamber was thoroughly cleaned with cleaning solution to remove any organic materials. The A, N₂ and H₂ were first passed over copper heated to 400°C to remove the oxygen. They were then subjected to the same treatment as the air by passage through glass wool, sodium calcium hydrate, CaCl₂, P₂O₅ and two liquid air traps. The A, which was the purest obtainable in large quantities contained considerable N₂ as indicated by the presence of N₂ bands in the spectrum. Otherwise the gases were spectroscopically pure showing no evidence of organic compounds or oxygen when the discharge was observed with a large direct vision spectroscope.

Direct tests for the presence of free electrons. In view of the unexpectedly high values of α obtained in pure A, N₂ and H₂ it was thought desirable to test further for the presence of free electrons. In order to accomplish this a second brush was added to the commutator system so that an alternating potential could be applied to the lower plate of the ionization chamber. Thus by keeping the volume of ionization close to the lower plate and varying the driving and retarding potentials, the apparatus could be used to measure mobilities by the simple Rutherford alternating current method.⁸ Although the measurements were somewhat complicated by the presence of positive ions, the results in every case indicated two facts: (1) Only a part of the negative carriers were free electrons (probably twenty to forty percent) when the age of the ions was about 0.01 seconds, the newest that could be studied; (2) The total number of electrons remained approximately the same as the ions aged to 0.5 seconds or more, although a considerable portion of the negative carriers had disappeared by recombination. Thus negative ions and free electrons were probably both present in large quantities during the period of recombination, but there was no gradual attachment of free electrons taking place as would be expected if impurities were present. This can only lead to the conclusion that most of the attachment occurred within a few thousandths of a second after the formation of the ions, which would result if the effect were due to metastable excited molecules produced by the ionizing agent. This question will be considered further in the discussion of the results.

EXPERIMENTAL RESULTS

Values of the coefficient of recombination obtained in pure argon are shown in Fig. 1. The different curves correspond to commutator speeds varying from 16 to 1/2 revolutions per second. The initial concentration of the ions varied from about 2.5×10^6 ions per cm³ at 16 revolutions per second to 1.1×10^7 ions per cm³ at 1/2 revolution per second. The initial value of α at a time of 0.002 seconds is about 1.6×10^{-6} , and the value then drops off in a manner similar to that in air to about 0.55×10^{-6} at 0.75 seconds. A similar series of runs was next taken with the addition of 2 cm partial pressure of O₂ added to the A. This was sufficient to cause almost instant attachment of the

⁸ J. J. Thomson, *Conduction of Electricity Through Gases*, p. 102, III Edition, Cambridge 1928.

free electrons as indicated by the equality of the positive and negative readings. The results, however, (which are not shown in the diagrams)

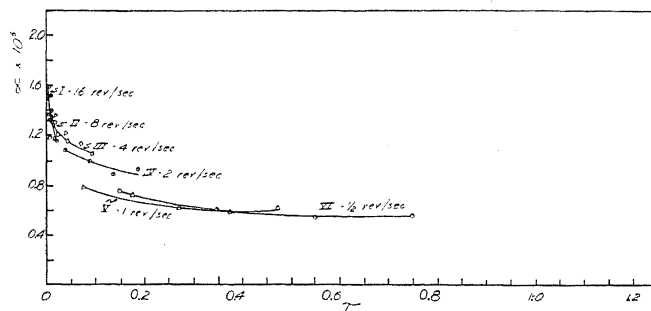


Fig. 1. Coefficient of recombination for pure argon.

were exactly the same as for pure A within the limits of experimental error except at the very shortest time interval (0.002 seconds) where $\alpha = 1.7 \times 10^{-6}$

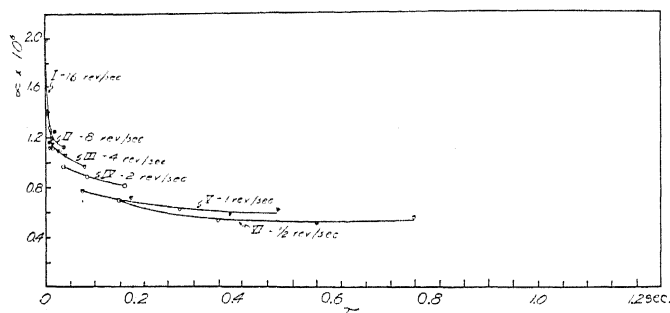


Fig. 2. Coefficient of recombination for argon with 15 cm partial pressure of O_2 .

instead of 1.6×10^{-6} . With the possibility that insufficient O_2 had been added, another series of runs was taken with 15 cm partial pressure of O_2 correspond-

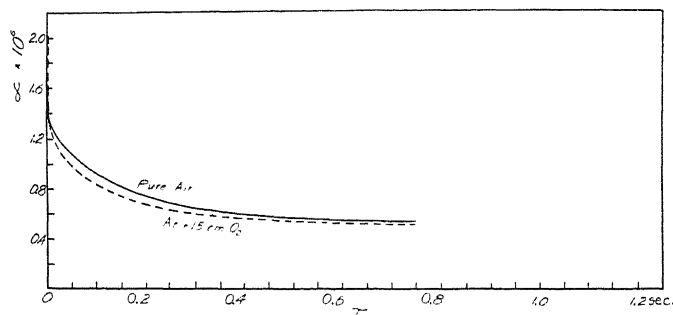


Fig. 3. Comparison of results in pure argon and argon with 15 cm partial pressure of O_2 .

ing to the N_2-O_2 mixture in air. The results shown in Fig. 2 were again almost the same as in pure A except at the very shortest time when $\alpha = 2.0$

$\times 10^{-6}$. A comparison of the results obtained with pure A and A+15 cm O_2 are shown in Fig. 3. Average values of α for any particular age τ are plotted against τ . The A+ O_2 curve starts higher, crosses the pure A curve at about 0.005 seconds and continues on slightly lower for the remainder of the time.

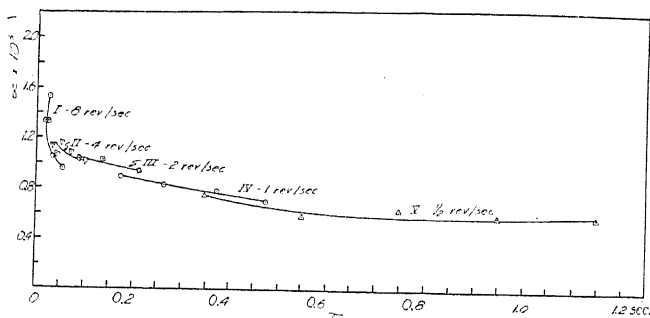


Fig. 4. Coefficient of recombination for pure nitrogen.

Fig. 4 shows the results for pure N_2 which are not far different from the corresponding values for A. It was impossible to obtain accurate results at the fastest commutator speed (16 revolutions per second) owing to the lack of sufficient concentration of ions. Even at 8 revolutions per second (time of

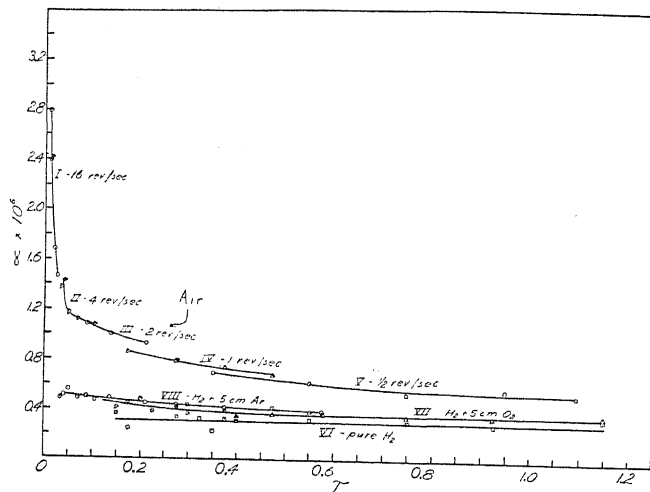


Fig. 5. Results for air and hydrogen.

exposure to x-rays 0.0156 seconds) the concentration was only 0.91×10^6 ions per cm^3 which gave rather inaccurate values of α .

Fig. 5 gives the results for air and H_2 . Curves I to V were taken in air for varying commutator speeds under the conditions corresponding to those for A and N_2 ; i.e. with constant sector opening of 90° and as high initial concentration as possible. The initial concentration varied from 0.79×10^6 ions per cm^3 at 16 revolutions per second to 4.8×10^6 at $1/2$ revolution per

second. The value of α varies from 2.8×10^{-6} at $\tau = 0.008$ seconds to 0.55×10^{-6} at $\tau = 1.15$ seconds.

Curve VI, Fig. 5 gives the results for pure H_2 , showing a constant value of 0.32×10^{-6} for α between 0.15 and 1.15 seconds. Owing to the extreme difficulty of obtaining sufficient concentration of ions, no runs at commutator speeds faster than one revolution per second could be taken. Even at one revolution per second (time of exposure to x-rays 0.25 seconds) only 0.46×10^6 ions per cm^3 were obtained. At $1/2$ revolution per second the initial concentration was 0.90×10^6 ions per cm^3 . Argon in varying quantities was then added to the H_2 to obtain greater concentration of ions, but made no appreciable difference in the value of α up to 5 cm partial pressure. The results for 5 cm partial pressure of A with H_2 are shown in Curve VIII, Fig. 5. The values of α are only slightly higher than for pure H_2 , starting at about 0.50×10^{-6} at $\tau = 0.03$ seconds (commutator speed 4 revolutions per

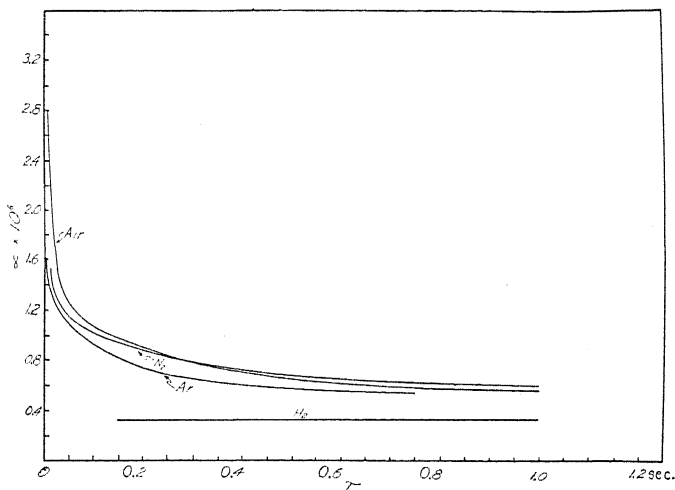


Fig. 6. Comparison of results for pure gases.

second) and dropping to 0.40×10^{-6} at $\tau = 0.6$ seconds. Runs at commutator speeds of 1 and $1/2$ revolutions per second were next taken with 5 cm partial pressure of O_2 added to pure H_2 to obtain attachment of the free electrons. The results (Curve VII, Fig. 5) again show only a small change from those in pure H_2 , α dropping from 0.45×10^{-6} at 0.15 seconds to 0.35×10^{-6} at 1.15 seconds. A final series of runs was taken with 5 cm partial pressure of A and 5 cm of O_2 added to pure H_2 but gave results identical with those for 5 cm partial pressure of A (Curve VIII).

A comparison of the results for air, pure A, pure N_2 and pure H_2 are given in Fig. 6. As in Fig. 3 average values of α are plotted against τ the age of the ions. Except at the shorter time intervals the results show a marked similarity for air, N_2 and A despite the fact that free electrons in large quantities were undoubtedly present in the N_2 and A. The values of α for H_2 are strikingly lower than those for the other three gases.

DISCUSSION OF RESULTS

From the results in the preceding section four facts stand out clearly:

(1) The coefficient of recombination for pure A and N_2 where free electrons should be present is only slightly lower than for air except at very short time intervals (probably 0.05 seconds or less) when random distribution of the ions has not been attained.

(2) The coefficient of recombination in pure H_2 is much lower than in the other three gases having approximately a constant value of 0.32×10^{-6} .

(3) The addition of sufficient O_2 to cause instant attachment of free electrons in A, N_2 and H_2 increases the value of α at the very shortest time intervals.

(4) In A and N_2 the addition of O_2 apparently results in a slight lowering of the values of α after random distribution has been attained.

Regardless of the question of recombination between positive ions and free electrons, one definite conclusion may be drawn from these facts. When free electrons are present, the value of α is lower at the very short time intervals indicating that random distribution is attained more rapidly. This is of course to be expected since electrons would diffuse evenly throughout the volume much more quickly than negative ions and the so-called initial recombination would not occur to as great an extent.

Interpretation of results in A and N_2 . In regard to the question of recombination between positive ions and electrons the results are inconclusive. If theory and previous spectroscopic results are to be relied on, α should be so small (of the order of 10^{-10}) that no recombination could be observed in the present work where the concentration of ions is of the order of 10^6 per cm^3 . Either, then, the spectroscopic results (obtained at low pressures and generally in the presence of rather high fields) are not applicable here, or else recombination was occurring in the present case only between positive and negative ions. If α for positive ions and electrons is very low, and attachment were taking place gradually, the curves would be expected to start at a low value of α for short times, then increase as time goes on until all the free electrons had attached. However, no such low value of α at short time intervals was observed, the values actually increasing rapidly down to 0.002 seconds. Finally, then, one of two conclusions may be drawn: either recombination between positive ions and free electrons is as rapid as that between positive and negative ions, or else a large portion of the free electrons had attached in less than 0.001 seconds. The second view is strongly supported by the evidence obtained in the tests for the presence of free electrons which have already been described.

In view of the precautions taken to obtain pure gases, and the results of the tests for free electrons which indicated that a definite number of electrons were present at all times, it does not seem likely that many electrons had attached to molecules of impurity in 10^{-3} seconds. Nevertheless, such a conclusion might conceivably be in error. As already mentioned there is however another mechanism by means of which attachment might have

taken place in A and N_2 . The intense hard x-rays and fast β -particles produced by them undoubtedly excite a large number of molecules. If these excited molecules remain in metastable states for a considerable period of time (as in the case of active N_2) impacts between the excited molecules and free electrons could give a means of dissipating the electron energy and allow attachment to form negative ions. An effect of this kind has been observed by da Silva⁹ who found some attachment in N_2 and H_2 which had been ionized by α particles. A similar process might occur in A which also has metastable states. On the other hand Loeb¹⁰ and Cravath¹¹ observed no attachment in these gases where the electrons had been produced by ultra-violet light and hot filaments.

Interpretation of results in H_2 . Hydrogen presents a different problem from A and N_2 since metastable excited states do not exist. However, attachment may still take place to atoms or triatomic molecules as indicated by the results of da Silva. Observations in H_2 by Langevin,¹² Townsend¹³ and McClung¹⁴ indicated that the coefficient of recombination was slightly lower than in air (1.4×10^{-6} compared to 1.6×10^{-6}) while in the present work α was found to be 0.32×10^{-6} for H_2 compared to 1.4×10^{-6} for air. The present results may be assumed more reliable owing to the improvements in technique now possible. On the other hand, J. J. Thomson's theory of recombination as modified by Loeb and Marshall⁷ gives much higher values of α for H_2 than for air, even assuming the molecular weight of the ions to be 32 (since the negative ion is ordinarily a molecule of impurity such as O_2). In this case it turns out that α is 2.34×10^{-6} compared to 1.62×10^{-6} for air. If the molecular weight is taken as 2.016, α is 9.50×10^{-6} . Since in pure H_2 , α is observed experimentally to be much lower than in air, this might be taken as an indication of the presence of a preponderance of free electrons which would recombine slowly. However, the addition of sufficient O_2 to produce attachment of the electrons should then bring the value of α up at least as high as for air, probably higher. As shown in Fig. 5 very little change was observed. The theory, however, is based on the assumption that if both ions suffer a single impact when they are within a defined distance d of each other they will lose all the excess kinetic energy gained as a result of their mutual attractions since the last impact. This single impact is assumed a sufficient condition for recombination. Since the mass of the ions is probably large compared to that of the molecules, a single impact may not suffice to remove the excess energy and the ions may drift apart without recombining. In other words, several impacts are probably required to reduce the excess energy, which fact cannot be taken into consideration by the theory as it stands. In this way α could be less for H_2 than for air in agreement with the experimental results.

⁹ M. A. da Silva, *Ann. de Physique* **12**, 100 (1929).

¹⁰ L. B. Loeb, *Kinetic Theory of Gases*, p. 507, New York, 1927.

¹¹ A. M. Cravath, *Phys. Rev.* **33**, 605 (1929).

¹² P. Langevin, *Ann. de Chim. et de Phys.* **28**, 433 (1903).

¹³ J. S. Townsend, *Phil. Trans. Roy. Soc. A***193**, 157 (1900).

¹⁴ R. McClung, *Phil. Mag.* **3**, 383 (1902).

Thus, in view of the experimental facts it is probable that the recombination observed in this work was taking place between positive and negative ions rather than positive ions and free electrons. The negative ions may have been formed by attachment of electrons to impurities but the evidence points strongly to the supposition that the attachment was to metastable excited molecules in the case of A and N_2 , and to atoms or triatomic molecules in the case of H_2 .

Values of the recombination coefficient in various gases. As indicated earlier it is more difficult to set an "absolute value" of α in this work than in the previous work on air owing to unfavorable experimental conditions. However, if the value of α for air is taken as $1.4 \pm 0.1 \times 10^{-6}$ at the point where the sharp drop due to non-random distribution ends, and the more gradual drop due to aging begins, comparison of the curves in Fig. 6 indicates a value of $1.2 \pm 0.1 \times 10^{-6}$ for A and N_2 . The value for H_2 may be more definitely set as $0.32 \pm 0.05 \times 10^{-6}$ since in this case there is no appreciable change with time.

A list of values for the coefficient of recombination determined by the above criterion for all the gases studied may then be given as follows:

<i>Gas</i>	<i>Coefficient of Recombination</i>
Air	$1.4 \pm 0.1 \times 10^{-6}$
O_2	$1.5 \pm 0.1 \times 10^{-6}$
N_2	$1.2 \pm 0.1 \times 10^{-6}$
A	$1.2 \pm 0.1 \times 10^{-6}$
H_2	$0.32 \pm 0.05 \times 10^{-6}$

In conclusion the writer wishes to express his sincere thanks to Mr. N. E. Bradbury for assisting in taking the readings and to Professor Loeb for his inspiring guidance throughout the course of these experiments.

THE MOBILITIES OF IONS IN DRY AND MOIST AIR

BY JOHN ZELENY

SLOANE PHYSICS LABORATORY, YALE UNIVERSITY

(Received May 26, 1930)

ABSTRACT

With the method recently described the distribution of mobilities of aged ions in dry air has been determined and the values for moist air remeasured because of a neglected correction in the previous results. In air dried by passage through metal tubes and filters immersed in liquid air the negative ions were found to consist of two main groups of which the less numerous group comprises about one third of the total number of ions and has a peak mobility only about 60 percent of that of the main group. The number of ions in the lesser group was relatively smaller in air dried by calcium chloride alone and their presence in still smaller numbers in air having a water content of 2 mg per liter accounts for the dissymmetry in the distribution curves of negative ions in moist air reported in the previous paper. The distribution curves for positive ions in dry air also show some indications of two groups of ions only here the ions of the less numerous group, which does not appear in moist air, have a peak mobility about 40 percent higher than those of the main group. The absolute values of the peak mobilities found for the main group of negative ions in the driest air used for a pressure of 76 cm and a temperature of 20°C was 2.45 cm/sec. This diminished to 2.37 cm/sec for air dried by calcium chloride, and to 2.08 cm/sec for air containing 2 mg of water per liter. Under the same conditions the mobilities of the positive ions increased in succession from 1.05 cm/sec to 1.10 cm/sec to 1.36 cm/sec. These large opposite changes produced by a small fraction of one percent of water molecules can only be explained on the supposition that aged ions in air consist of molecular clusters whose structure is affected by the presence of water molecules. The second group of negative ions cannot consist of ions having multiple electronic charges, because the mobility of these ions is smaller than that of the main ion group. It cannot arise from the presence of impurities condensable at liquid air temperatures. Since electrons do not readily become attached to nitrogen molecules, the central molecule of each of these ions is probably an oxygen molecule and the two cluster groups may arise either from a difference caused by a different point of attachment of the electron to the central molecule or from the nature of the molecule that first becomes attached to this central molecule in the process of cluster formation.

IN a recent paper¹ I reported some results on the mobilities of well-aged ions in moist air which showed that the ions of each sign are not all alike. No distinct groups were resolved but the mobilities in each case were found to be spread continuously over a range of values. Within this range, the positive ions as regards numbers present were distributed quite symmetrically about a most numerous kind, while the negative ions had mobility values extending much farther in the direction of lower mobilities than in the direction of higher mobilities.

¹ J. Zeleny, *Phys. Rev.* **34**, 310 (1929).

The method employed in the mobility measurements has some distinct advantages over other methods which have been used, and the work with it has now been extended to dry air.

The new results disclose for negative ions in very dry air a second group of ions comprising about one-third of the total number and having a mobility only about six-tenths of that of the ions in the main group. Indications of this new group in smaller numbers are well marked in air dried by passage through calcium chloride alone, and the presence of these ions in still smaller numbers also accounts for the lack of symmetry mentioned above in the distribution curves for negative ions in moist air.

Some indication too was found that among positive ions in very dry air a second group of higher mobility than that of the main group is also present.

The peak mobility of the main group of positive ions was found to decrease quite markedly when the air was dried, while that of the main group of negative ions increases with removal of moisture.

The method used consists in blowing a nonturbulent stream of air between two concentric cylinders, admitting ionized air into this stream through small openings in the outer cylinder, and measuring the distance the ions are carried down stream while they are crossing the space between the two cylinders under the action of an applied field.

The average velocity of the main air stream with which the velocity of the ions was compared was maintained throughout these measurements at approximately 8 cm/sec. This low velocity is well within the limits of nonturbulent motion in the apparatus used. The potentials used on the outer cylinder were such as allowed the ions in crossing to be carried down stream only far enough to permit an accurate determination of the distance, in order to keep the correction for ion diffusion as small as possible.

Reference should be made to the previous paper¹ for details regarding the apparatus and for the procedure used in reducing the observations, as well as for references to the work of other observers.

A few modifications were made in the apparatus. The connecting tubes were all made of metal or glass. The openings in the outer cylinder through which the ionized air is admitted into the main gas stream were enlarged and now consist of 20 slots along a circumference, each slot being 1 mm wide and 9 mm long. The total area of these openings is now such that with a stream of ionized air delivering 9.8 cc per sec. as was used throughout these measurements the correction which has to be applied to mobility determinations to allow for the penetration of this ion stream into the main air current is on the average less than one-half of one percent.

The movement of the inner cylinder with its insulated ion collector ring is now effected by a threaded micrometer head working on a rod extending from the system to be moved to the outside of the apparatus. This improvement makes possible more rapid and more accurate settings of the ion collector ring.

The radioactive material used for producing ions in the auxiliary chamber during these measurements consisted of a deposit of polonium on a nickel

strip which was wound around the outside of the outer cylinder a short distance up stream from the openings through which the ions entered the main gas stream. The polonium coating was sealed gas tight by a covering of thin condenser paper.

The age of the ions as they entered the main gas stream was on the average about 3 sec. although some of the ions were only about 1 sec. old.

The air for the main gas stream was supplied by the pressure system of the laboratory. To dry the air, it was passed in succession through a large filter, through a 16 cm wide bottle containing granulated calcium chloride, through a second filter, through a long copper coil of small diameter immersed in liquid air, and finally through a second copper coil immersed in a water bath maintained at room temperature. The air for the auxiliary ion bearing stream was passed through a similar, separate drying system. In some of the last measurements, additional filters immersed in liquid air were added to the drying system. These contained first a section filled with coarse metal filings to ensure a closer contact between the cold surfaces and the air, and then closely packed glass wool to remove any crystals of ice which might be blown along by the stream and later be changed to vapor.²

Measurements of the mobilities of both positive and negative ions were made not only in air dried as has just been described, but also in air dried much less thoroughly by calcium chloride alone, and in undried air of low but determined humidity. These last measurements are included because the absolute values given in my last paper for the mobilities in moist air are somewhat low owing to the fact that the air pressure at the gauge used for measuring the stream velocity was unwittingly allowed to exceed the limit within which no correction for this pressure had to be made. A mercury manometer, previously removed to avoid the presence of mercury vapor, was now kept at this gauge and the gauge was recalibrated for the same gas pressures as were used in the measurements.

AIR DRIED BY AID OF LIQUID AIR

Curve *A* of Fig. 1 gives an example of the way in which negative ions were found distributed along the inner cylinder, when the air used was dried as described above by passage through calcium chloride and through a long helical tube immersed in liquid air. The abscissas give the down stream distances from the place of entry of the ions into the air stream and the ordinates give the corresponding ion numbers. The difference of potential between the two cylinders was 12 volts. The curve of distribution is a compound one, and by drawing the two branches *c* and *d*, the sum of whose ordinates for any abscissa is equal to the corresponding ordinate of the experimental curve, the compound curve may be resolved into two simple curves having peaks at *a* and *b*. The observed distribution thus shows the presence of two distinct groups of ions, of which those of higher mobility are about twice as numerous as those of lower mobility. Some of the other

² H. A. Erikson, Phys. Rev. 34, 642 (1929).

similar observations show a small number of ions carried even farther down stream than is here apparent, indicating ions of still lower mobility. The mobility corresponding to the peak of the less numerous group of ions was found to be on the average 1.45 cm/sec. which is about six-tenths of the value for the main group.

Curve *B* of Fig. 1 is an example of corresponding results obtained for positive ions. The difference of potential between the cylinders was 15 volts. The main air stream and the ion bearing stream as well were passed in this case through calcium chloride and tubes immersed in liquid air and subsequently through a cylindrical metal box, also immersed in liquid air, which contained a layer of fine metal turnings and closely packed glass wool.

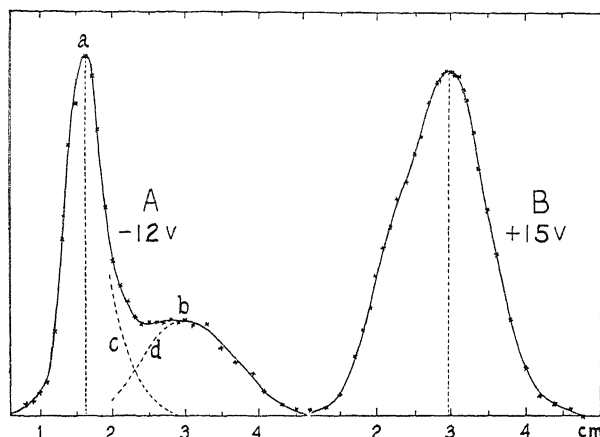


Fig. 1. Distribution of ions in dry air. Ordinates represent number of ions corresponding to down stream distances given as abscissas. Curve *A* is for negative ions in air dried by passage through tubes immersed in liquid air. Curve *B* is for positive ions where a filter immersed in liquid air was added to the drying system.

Curve *B* shows an entirely different distribution of ions than that found for negative ions. The dotted ordinate drawn through the peak of the curve shows that now the number of ions on the upstream side of the peak is greater than on the downstream side. There is a bulge in the curve near the abscissa distance 2.2 cm which appears also in all of the other similar observations, indicating the possible presence of an unresolved group of ions having a peak mobility of about 1.5 cm/sec., the mobility of the ions at the main distribution peak being here only 1.06 cm/sec.

A summary of the mobilities found for the peak of the distribution curves of the main group of ions in air dried by use of liquid air is given in Table I. The uncorrected potential of the outer cylinder relative to the inner one is indicated in each case. These results, as well as all others to be given, have been reduced to a temperature of 20°C and a pressure of 76 cm of mercury.

The unusually large difference between the positive and negative mobilities is to be noted. This difference is much larger than can be accounted for according to prevailing theories by a difference of mass alone. Linear dimen-

TABLE I. *Peak mobilities of predominant group of ions in very dry air.*

(a) Air dried by CaCl ₂ and tubes in liquid air.			
+12 volts	1.10 cm/sec.	-12 volts	2.40 cm/sec.
+15 "	1.06 "	-15 "	2.38 "
+20 "	1.07 "	-10 "	2.41 "
Positive ions	1.08 cm/sec.	Negative ions	2.40 cm/sec.
(b) Air dried by CaCl ₂ and tubes and filters in liquid air.			
+15 volts	1.04 cm/sec.	-15 volts	2.45 cm/sec.
+15 "	1.05 "	-15 "	2.44 "
+15 "	1.06 "		
+15 "	1.04 "	Negative ions	2.45 cm/sec.
Positive ions	1.05 cm/sec.		

sions of the ions must be invoked as a prominent factor in determining such variation in mobility.

The presence of the extra filters immersed in liquid air appears to have resulted in a more complete drying of the air, since the positive ion mobilities in (b) the lower portion of the table are on the average a little smaller than in (a) the upper portion, and those of the negative ions are a little larger. The amount of water remaining in the air after the above treatment must be very small. The computed amount at -194°C given in the International Critical Tables is 1.6×10^{-23} mg per liter; naturally such a low value cannot be approximated in the apparatus used.

The total spread of ions when they arrive at the inner cylinder as shown by the curves of Fig. 1 does not represent altogether ions of different mobilities. A part of the spread arises from diffusion and mutual repulsion of the ions during their passage between the two cylinders. A method of correcting for these effects is fully described in my previous paper,¹ and when applied to the results for positive ions shows that ions are present ranging in mobility from 0.83 cm/sec. to 1.58 cm/sec., the two possible groups present being treated as one. Owing to the partial overlapping of the two groups of negative ions, the spread of mobilities in the main group having the faster ions can only be obtained for the upstream side of the peak. The fastest ions here were found to have a mobility 11 percent greater than the peak mobility. In the group of lower mobility the estimated spread on either side of the peak mobility is between two and three times the above value.

The high value of the peak mobility of negative ions here given is in agreement with that obtained by Schilling³ likewise in very dry air but for ions of lesser age. The mobility of the positive ions here found for very dry air is lower than values hitherto reported. It must be remembered that this value corresponds to the peak of a distribution curve which shows strong indications of a less numerous group of higher mobility. Schilling makes note of the fact that the curves he obtained with positive ions, using the alter-

³ H. Schilling, *Ann. d. Physik* **83**, 23 (1927).

nating field method, were of a form to be expected from a mixture of different ions.

AIR DRIED BY GRANULATED CALCIUM CHLORIDE

A number of measurements were made with air dried by passage through granulated anhydrous calcium chloride only, this being known as a rather poor drying agent and leaving in air water to an amount of about 0.2 mg per liter.⁴

Examples of the ion distribution curves obtained under these conditions are given in Fig. 2, where curve *A* represents negative ions and curve *B* positive ions, the voltage used being 15 volts in each case.

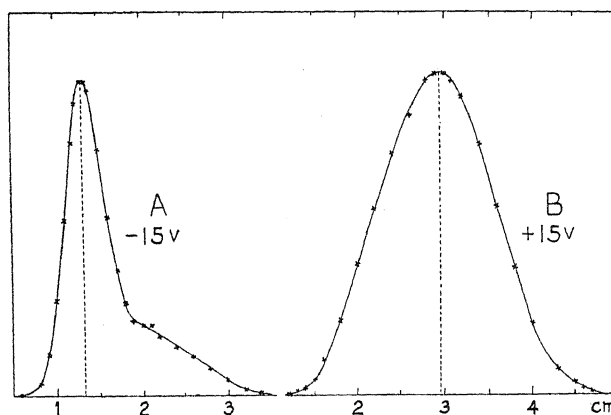


Fig. 2. Distribution of ions in air dried by calcium chloride. Curve *A*=negative ions. Curve *B*=positive ions.

The curve for the negative ions, in addition to the main group represented by the high peak, also shows the existence of ions of a smaller mobility but these are less numerous than was found to be the case (curve *A*, Fig. 1) with air more completely freed of water molecules.

The curve for the positive ions does not show the bulge seen on curve *B* of Fig. 1, although the dotted ordinate drawn through the middle of the peak helps to show the presence here also of a larger number of ions of mobility greater than the most numerous kind than there are of ions with a smaller mobility.

TABLE II. *Peak mobilities of ions in air dried by calcium chloride alone.*

+15 volts	1.10 cm/sec.	-12 volts	2.38 cm/sec.
+12 "	1.12 "	-20 "	2.33 "
+15 "	1.08 "	-10 "	2.35 "
+15 "	1.09 "	-15 "	2.41 "
+15 "	1.09 "		
+15 "	1.13 "	Negative ions	2.37 cm/sec.
Positive ions	1.10 cm/sec.		

⁴ A. T. McPherson, Jour. Am. Chem. Soc. 39, 1317 (1917).

Table II gives a summary of the results for the peak mobilities of ions in air of this degree of dryness.

The values for the positive ions are here a little larger and those for the negative ions somewhat smaller than those given in Table I.

The positive ion group was found to extend between the same limits as given above for positive ions in air dried by aid of liquid air. The main negative ion group extends from a peak mobility of 2.37 cm/sec. up to 2.54 cm/sec. The presence of a group or groups of negative ions of lower mobility here also prevents the getting of an estimate of the value of the lower limit of the mobilities in this main group.

AIR WITH AVERAGE WATER CONTENT OF 2 MG/LITER

Fig. 3 gives examples of the distributions found for ions in filtered air drawn directly from the pressure system of the laboratory, and containing on the average 2 mg of water per liter. The air for the auxiliary stream in

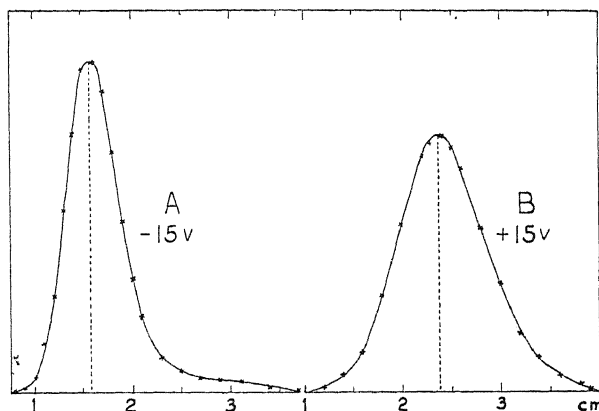


Fig. 3. Distribution of ions in air having a water content of 2 mg per liter. Curve *A* = negative ions. Curve *B* = positive ions.

which the ions were produced was supplied by a gasometer containing water and carried on the average 13.6 mg of water per liter. As this air did not mix with the main air stream, it is probable that the mobilities obtained are the same as would have been obtained had the ion bearing stream contained the same amount of water as was present in the main stream.

The positive ion distribution curve *B* shows the ions to be almost equally distributed on the two sides of the peak value. The negative ion curve *A* is again far from symmetrical but the group of ions of lower mobility, clearly indicated in Figs. 1 and 2, here shows only as an extended foot of the curve for the main ion group. It appears therefore that this low mobility group of ions forms a smaller and smaller portion of the whole number as the amount of water present in the air is increased. Its presence accounts for the lack of symmetry, reported in the previous paper, in the distribution curves for negative ions in moist air. The positive ions are spread over a somewhat smaller range of values here than is the case in dry air.

A summary of the results for moist air is given in Table III.

TABLE III. *Peak mobilities in moist air.*

Potential	Water content	Mobility	Potential	Water content	Mobility
+15 volts	1.90 mg/l	1.36 cm/sec.	-12 volts	1.45 mg/l	2.08 cm/sec.
+ 8 "	1.90 "	1.40 "	-15 "	1.98 "	2.05 "
+20 "	1.90 "	1.35 "	-12 "	1.98 "	2.07 "
+15 "	1.98 "	1.34 "	-12 "	1.74 "	2.12 "
+12 "	1.98 "	1.35 "			
+15 "	1.33 "	1.37 "		Negative ions	2.08 cm/sec.
+15 "	2.89 "	1.38 "			
Positive ions		1.36 cm/sec.			

The water content of the air used in the main gas stream is given in milligrams per liter in the second and fifth columns. The water molecules in the stream formed only about one quarter of one percent of the total number and yet their effect on the mobilities of the ions is seen, by comparison with the values of Table I, to be quite marked, the positive ion mobilities being increased by about 30 percent and the negative ions decreased by about 18 percent relative to those obtained in the driest air used. It is not possible to account for these large opposite effects on the two ions by an increase in the resistance to their motion due to the presence of the water molecules. It is necessary therefore to postulate that aged ions consist of molecular clusters and that the water molecules produce a change in their structure, such that the size of the positive ion cluster is diminished and that of the negative ion increased.

The increase in the mobility of positive ions produced by the presence of water molecules as given above confirms my earlier results and is in agreement with the results of Blanc⁵ and Laporte⁶ for ions of lesser age. Several other observers have obtained an opposite effect of moisture upon the mobility of positive ions, but it must be noted that in general the ions used have been much less aged than was the case in the experiments being reported. Valta⁷ using very young positive ions found their mobilities to decrease both with age and with water content of the air and has obtained in very dry air values as high as 6.8 cm/sec. Nolan and Nevin⁸ found remarkable fluctuations in the values of the mobilities of ions of both signs as the water content of the air was increased. It is difficult to reconcile all of these different experimental results on the effect of moisture on ionic mobilities in air.

The results given above clearly show the presence of two groups of aged negative ions in very dry air. The group of lower mobility has about one-half as many ions as the one of higher mobility. The relative number of these slower ions is considerably smaller in air dried by calcium chloride alone, and is still less in air having a water content of 2 mg per liter.

⁵ A. Blanc, Jour. de Physique 7, 825 (1908).

⁶ M. Laporte, Ann. de Physique 8, 466 (1927).

⁷ Z. F. Valta, Journal of Geophysics and Meteorology (Russian) 6, 197 (1929).

⁸ J. J. Nolan and T. E. Nevin, Proc. Roy. Soc. A127, 155 (1930).

It is of theoretical interest that among aged ions it is possible under any circumstances for two distinct groups of small ions to coexist. It is improbable that the new group consists of ions with multiple charges which tend to become reduced to unit charges in the presence of water molecules, since all of the evidence points either to an increase of mobility with increase of charge or to an independence of mobility of the ionic charge. The presence of some unusual impurity might be thought to give rise to the new ion group. If such an impurity consisted of vapors coming from the compression pump or elsewhere, we should expect its effect to be least pronounced or absent when the air was passed through tubes immersed in liquid air where such vapors would be condensed, whereas the opposite was found to be the case.

It is probable therefore that the two negative ion groups under discussion consist of clusters of molecules the center of each of which is a molecule of one of the chief constituents of the atmosphere, to which an electron has become attached. Since electrons do not attach themselves readily to nitrogen molecules the central molecules are probably oxygen molecules. The evidence available is not sufficient to account satisfactorily for the two negative ion groups, but we may suppose that the difference in cluster size arises either from a difference in place of attachment of the electron to the molecule or from a difference in the kind of molecules that by chance first become joined to the central charged molecules during the formation of the clusters.

I am indebted to Mr. R. S. Baldwin and to Mr. C. D. Bock for aid with the measurements.

EXCITATION PROCESSES IN THE HOLLOW CATHODE DISCHARGE

BY RALPH A. SAWYER

UNIVERSITY OF MICHIGAN, ANN ARBOR

(Received May 19, 1930)

ABSTRACT

The low potential gradients in the negative glow in a hollow cathode discharge in a rare gas make it a favorable source for the excitation of metallic spark spectra. The metal studied forms the cathode, and is brought into the discharge by cathode sputtering or evaporation. The excitation is limited by collisions of the second kind between gas and metal atoms and ions. The spectroscopic data of all the available cases have been examined to see what determines the processes occurring. In general only those processes occur in which the metal can be excited to some term in the spark spectrum with gain or loss of only a small amount of kinetic energy to balance the reaction equation. High melting point metals or those which sputter poorly cathodically enter the discharge in helium in the normal state or in a low metastable state of the atom. With low boiling points metals appreciable numbers of metal ions enter the reactions. In intermediate cases or in argon or neon, it is not always possible to predict if metal ions will enter the reaction or not. The conditions which determine the results are discussed.

THE excitation of metallic spectra by the discharge in a hollow cathode tube in a rare gas atmosphere has been discussed by Paschen,¹ Frerichs² and Takahashi.³ While there is general agreement that the excitation is mainly limited by collisions of the second kind between rare gas atoms or ions and metallic atoms or ions there has not been agreement as to the exact nature of the collisions. Paschen and Frerichs have attributed the fundamental process to collisions between metallic ions and excited metastable rare gas atoms. Takahashi on the other hand considers only normal or metastable metallic atoms which receive energy from metastable atoms or ions of the rare gases. On the basis of somewhat more experimental material than was available at the time the discussions mentioned above were written, it is now possible as will be shown in this paper to explain the processes involved somewhat more fully and to show that under suitable conditions any of the excitations proposed by the author's mentioned may occur.

The conditions on the hollow cathode are rather different from those in other discharges. With such a cathode, often though not necessarily inside a cylindrical anode, and an applied D.C. potential of 300 or 400 volts, at a suitable pressure which depends on the cathode dimensions, the discharge is almost wholly inside the cathode. The discharge then consists of a negative dark space close to the inner wall of the cathode and a very bright negative

¹ Paschen, Sitzungsber. d. Preuss. Akad. d. Wiss. p. 207 (1927).

² Frerichs, Ann. d. Physik 85, 362 (1928).

³ Takahashi, Ann. d. Physik 3, 49 (1928).

glow filling the cathode. The positive column practically disappears. This discharge was first used as a spectroscopic source by Paschen.⁴ It was explained by Günther-Schulze⁵ who showed that when the pressure was decreased in such a tube until the mean free path of electrons leaving the inner wall of the cathode was sufficient to bring them into the positive space charge of the opposite side of the inner wall they would there reduce this charge causing an increased current and a lower cathode fall of potential inside and so setting up a condition permitting a very much greater current density from the inner wall of the cathode than from the outer. The discharge then takes place chiefly inside the cathode. The pressure at which this effect will occur depends on the diameter of the cathode and the nature of the gas. It is a pressure such that the normal cathode dark space is about equal to the inner radius of the hollow cathode. The discharge however is formed inside the cathode with an abnormal dark space thickness much less than normal. This space inside the negative glow of the hollow cathode is nearly field free and ions may exist there in considerable concentrations and radiate freely even from states of high quantum number. The negative glow in the hollow cathode is very brilliant and this light source is one of the best for exciting the first spark spectra of the metals.

The metallic atoms which enter the discharge are removed from the cathode wall by ionic bombardment and evaporation. In the analogous case of cathode sputtering Von Hippel⁶ found with argon at 0.1 mm pressure in spectrograms of the light just at the cathode surfaces that the only spectral lines of the cathode material which appeared were the resonance lines of the atom. From this he concluded that the material is given off in an atomic state and arrives in the negative glow by a diffusion process. His theory is that intense local heating of the cathode by ion bombardment causes minute hot spots from which the cathode metal is evaporated. If the resonance lines of the cathode metal appear near the cathode, the cathode metal must enter the discharge as excited atoms as well as normal atoms. Ions knocked off the cathode could not normally penetrate the high cathode fall of potential in the hollow cathode (100–300 volts according to measurements of Schüler).⁷ We may expect in general in the negative glow of the hollow cathode reactions with metallic atoms both neutral and excited (in metastable states) although, as will be pointed out later, under certain conditions significant numbers of metal ions may enter the reactions. These metallic particles entering the negative glow suffer collisions with rare gas particles, or with electrons whose velocity is limited by collisions with rare gas atoms. The spectrum of the negative glow shows the spectrum of the ionized exciting gas very strongly. In fact with a grating not particularly good below $\lambda 300$ Sawyer and Lang⁸ observed in the discharge in helium as many as four

⁴ Paschen, *Ann. d. Physik* **50**, 901 (1916).

⁵ Günther-Schulze, *Zeits. f. Physik* **19**, 313 (1923).

⁶ v. Hippel, *Ann. d. Physik* **80**, 672 (1926) and **81**, 1043 (1926).

⁷ Schüler, *Phys. Zeits.* **22**, 264 (1921).

⁸ Sawyer and Lang, *Phys. Rev.* **34**, 712 (1928).

members of He II series 1^2S-m^2P beginning at $\lambda 304$ and Paschen⁹ under suitable pressure and current conditions has observed in the hollow cathode in helium Stark effect in the higher members of the helium series due to the electric fields of the great concentration of helium ions. It is then to be expected that excited atoms in the metastable state and ions in the normal state will be the predominating energy states in which the rare gas will be found and that the transfer of these energies to the metallic atoms will fix the limiting conditions of excitation for the spectrum of the metal.

To check these considerations there are available data for the hollow cathode excitation of aluminum, copper, magnesium and zinc in helium, argon and neon; cadmium in helium and argon; and gallium, mercury and thallium in helium.¹⁰ Not all of these data are well adapted for the study of the question in hand. In some cases the investigation did not cover a sufficiently wide spectral region to permit a certain determination of the kind of excitation attained in the discharge. In others the limit attained is low and so the terms too few and too far apart to fix the limit sharply. For the sake of completeness it has, however, all been assembled.

TABLE I. *Important energy levels of metallic spectra.*¹¹

Normal State of Atom				Metastable State of Atom			Normal State of Ion		
Config.				Config.			Config.		
Al	(s^2p)	$^2P_{1/2}$	42280	—	—	—	(s^2)	$1S_0$	151860
Ga	(s^2p)	$^2P_{3/2}$	48379	(s^2p)	$^2P_{1/2}$	47552	(s^2)	$1S_0$	165458
Tl	(s^2p)	$^2P_{3/2}$	49263	(s^2p)	$^2P_{1/2}$	41470	(s^2)	$1S_0$	164600
Mg	(s^2)	$1S_0$	61663	(sp)	3P_0	39813	(s)	$^2S_{1/2}$	121265
Cu	($d^{10}s$)	$^2S_{1/2}$	62306	(d^9s^2)	$^2D_{3/2}$	51105	(d^{10})	$1S_0$	163634
Zn	($d^{10}s$)	$1S_0$	75759	($d^{10}sp$)	3P_0	43450	($d^{10}s$)	$^2S_{1/2}$	144890
Cd	($d^{10}s^2$)	$1S_0$	72535	($d^{10}sp$)	3P_0	42420	($d^{10}s$)	$^2S_{1/2}$	136377
Hg	($d^{10}s^2$)	$1S_0$	84182	($d^{10}sp$)	3P_0	46536	($d^{10}s$)	$^2S_{1/2}$	151280

For each of the metals mentioned above Table I gives the electron configuration of the normal state of the ion and of the first state and of the lowest metastable state of the atom. In aluminum this metastable state is the lowest $^2P_{1/2}$ of the normal configuration and is too near $^2P_{3/2}$ to be differentiated in the data at hand. Table I also gives for each configuration the energy of removing the outermost electron from this configuration—that is to excite the metal to the lowest or normal state of its next ion. For con-

⁹ Paschen, Sitzungs. d. Preus. Akad. d. Wiss., p. 135 (1926).

¹⁰ Al in He, Sawyer and Paschen, Ann. d. Physik. **84**, 1 (1927).

Hg in He, Paschen, Sitzungs. d. Preus. Akad. d. Wiss., p. 3 (1928). and Naudé, Ann. d. Physik **3**, 1 (1929).

Cd and Zn in He, Takahashi, Ann. d. Physik **3**, 27 (1929).

Tl in He, Smith, Phys. Rev. **35**, 235 (1930).

Ga in He, Sawyer and Lang, Phys. Rev. **34**, 712 (1928).

All others, Frerichs, Ann. d. Physik **85**, 362 (1928).

¹¹ The data in table II are taken from Paschen-Götze "Seriengesetze der Linienspektren" or from the references in footnote 10.

venience in spectroscopic discussion this value is given in ν -units. It may of course be converted to equivalent volts by multiplying by 1.2345×10^{-4} . For the three rare gases the atomic energies available are, also in ν -units

	Energy of ionization	Energy of metastable state
Helium	198308	159830 (2^3S) or 166251 (2^1S)
Neon	173930	134819
Argon	127104	94546

From the energy available from the rare gas atoms together with the data of Table II there may be calculated the highest spectroscopic state of the metal ion which should be excited by any of the probable collisions of the second kind with a rare gas. Thus for example $\text{Zn}'(d^{10}s p^3 P_0) + \text{He}'(2^3S) \rightarrow \text{Zn}^+(?) + \text{He}(1^1S) + e$ we have:

energy to ionize metastable zinc	43450
energy to doubly ionize first zinc ion	144890
	<hr/>
	188340
energy of He (2^3S)	159830
	<hr/>
	28510

Thus, this reaction fails by 28510 ν -units to achieve second ionization, or a Zn II term of absolute value (measured from ionization) 28510 would just be excited. The results of such computations are listed in Table II, where in the column heads M stands for the metal concerned and G for the gas. Reactions with $\text{He}'(2^1S)$ are not listed. The results of a reaction with $\text{He}'(2^1S)$ may be obtained by subtracting 6421 from the term obtained by a reaction with $\text{He}'(2^3S)$.

TABLE II. *Excitation of metallic spectra in hollow cathode discharge in gases.*

	Calculated		Excitation			-Observed	
	$M+G'$	$M+G^+$	$M'+G'$	$M'+G^+$	M^++G'	Maximum	Limit
Al+He	40310	<i>1832</i>	—	—	-7970		1116
+Ne	65321	26210	—	—	<i>17041</i>		16943
+A	105594	73036	—	—	<i>57314</i>		56512
Ca+He	54007	<i>15529</i>	53180	<i>14702</i>	5628		12397
Tl+He	54033	<i>15555</i>	46240	7762	4770		12484
Mg+He	23098	-15380	<i>1248</i>	-37230	-38565		5419
+Ne	48109	<i>8928</i>	26259	-12922	-13534	8-10000	5419
+A	88382	55824	66532	33974	26719		17844?
Cu+He	66110	27632	54909	<i>16431</i>	3804	27-30000	16703
+A	131394	98836	120193	87635	<i>69088</i>		68837
Zn+He	60819	<i>22341</i>	28510	-9968	-14940	22-28000	-11400
+A	126103	93545	93794	61236	50344		27800?
Gd+He	49080	<i>10602</i>	18967	-19510	-23453	11-13000	-26800
+A	114364	81806	84251	51693	41831		46531
Hg+He	75632	<i>37154</i>	37986	-492	-8550	39-42000	-8019

The processes in italics are those which account for observed features of the spectra.

The experimental results of interest in this discussion are tabulated in the two right hand columns of Table II. In each case where it is certainly determined there is given the limit, that is, the highest spectral term of the metal ion excited in the rare gas atmosphere. There is also given any observed maximum of excitation—any terms which appear to be excited more strongly than immediately lower terms—indicating resonance phenomena in the exciting process.

A comparison of the calculated and observed excitation in Table II shows that many of the observed features of the spectra may be explained on the basis of various of the exciting processes. The cases will be discussed in order of their simplicity.

Aluminum, gallium and thallium are all high boiling point metals. Aluminum sputters cathodically less than any other metal tried. Consequently the concentration of these metals in the hollow cathode discharge in helium is very low; they react only as normal atoms or possibly in the case of gallium and thallium as atoms in the very low metastable $^2P_{1/2}$ state. The limit is clearly set in the case of excitation in helium by $M+G^+$ or $M'+G^+$. There are no resonance maxima in these cases because, although the process $M+G'$ must contribute to the excitation, the limit of this excitation falls where the spectral terms are not numerous enough nor close enough together to make such a maximum apparent.

In the case of aluminum in argon and neon a new effect enters. The limit here is obviously set by M^++G' . That is, metal ions are entering this discharge although the concentration of metal in these cases is still so small that metal ions are not to an appreciable extent current carriers, as does occur in cases to be mentioned later. The greater number of metal ions is here due probably to the heavier bombardment of the cathode by the heavier gas particles. A similar effect appears in the vacuum spark where increased voltage on the spark giving heavier bombardment of the electrodes brings higher ionized atoms into the spark.

The limit of excitation for magnesium in helium and neon appears to be set respectively by the reactions $M'+G'$ and $M+G^+$, although these cases have perhaps not been investigated over a sufficiently wide spectral range for absolute certainty as to the limit.² In the neon the excitation goes somewhat (1/3 volt) above $M+G^+$ and a maximum corresponding to resonance with this process in the series 3^2D-m^2F is clearly seen. The energy for overshooting of the limit, $M+G^+$, probably comes from kinetic energy of the atoms. The process, M^++G' , which sets the limit for Al+Ne probably does not occur here. It would call for excitation 13235 cm^{-1} beyond double ionization and as negative terms in Mg II are not possible and as there are no terms in Mg III as low as this, this process would involve freeing an electron with this surplus energy—a process which seems improbable. It will be seen that for magnesium and argon the limits of the five different processes are well separated and all positive. However, this case is not so favorable for observation as it seems for most of the limits are too low in the Mg II spectrum to allow maxima of excitation to be observed. It will

be noted from Table II that Frerichs observed excitation 10256 cm^{-1} above the highest limit. It is not clear how this can occur. A similar anomaly occurs with zinc in argon but in no other observed cases. It may be that here the reaction is with some high excited state of the metal atom but what state could occur with sufficient probability is not obvious.

Copper should offer an excellent opportunity to study excitation conditions in the rare gases since all the processes give rise to positive terms in Cu II. The copper spectrum is, however, unfortunately not completely analyzed and the combinations of the highest known terms lie largely in the extreme ultra violet. The highest term found by Kruger in helium, however, seems clearly to arise from $M' + G^+$. The process $M + G^+$ is responsible for a maximum of intensity found by Kruger for terms from $27\text{--}30000\text{ cm}^{-1}$. Frerichs' work in neon did not lead to determination of any limit, but in argon the limit is set by $M^+ + G'$ again, as with aluminum in neon and argon.¹²

Zinc, cadmium and mercury represent a different type of excitation condition. These metals have low boiling points and relatively high vapor pressure at the cathode temperature in the hollow cathode discharge. The ions of these metals enter the discharge in such concentrations as to carry a considerable part of the current. In fact in mercury the discharge may be operated without any rare gas using a carbon cathode and allowing the heat of the discharge to vaporize the mercury. Under such conditions we may expect that in all cases where the process $M^+ + G'$ gives rise to actual terms that this reaction will set the limit to the excitation. This is indeed the case as will be seen by reference to Table II. In all these metals negative terms in the spectrum of the ion are possible and have been found so that the excitation has been traced to the highest limit permissible in helium. In zinc and cadmium the limit given in Table II is in fact exceeded by $3000\text{ }\nu$ -units. This is possibly due to reaction with the higher metastable helium term (2^1S) which as pointed out previously would give excitation 6000 cm^{-1} higher than 2^3S which is given in the table. In the spectra of all these three metals some unclassified lines remain and more negative terms may be found to reach the limit $M^+ + \text{He}'$ (2^1S). In helium with each of these metals there is also found maxima of excitation explainable as resulting from $M + G^+$ which appears in these cases to be more probable than $M' + G'$ no doubt because M' is so high in these metals that it is less likely to be excited strongly than in the case of copper or magnesium. The metals have not been studied in neon with the exception of zinc where, however, the spectral range covered by Frerichs was not sufficient to permit conclusions to be drawn. In argon, however, the limit is clearly set by $M^+ + G'$ with cadmium while with zinc, as mentioned above, even this limit which is the highest set by the simpler reactions, is exceeded by 25000 cm^{-1} . This, as in the case of $\text{Mg} + \text{A}$, does not appear susceptible to obvious explanation.

¹² Frerichs terms have been corrected to the true lowest term in Cu II not known at the time of his work.

In conclusion it may be said that the excitation of metallic spectra in the hollow cathode discharge in rare gases does not give results which are entirely predictable. In general with metals which do not sputter too freely nor have too high vapor pressures at the cathode temperatures, as Mg and Al, the reaction $M+G^+$ together with $M'+G'$ and $M'+G'$, if M' is low, will occur, and the highest of these will set the limit to the excitation if this does not call for non-existent negative terms. With such metals in neon or argon M^++G' will in general occur due to the greater kinetic energy with which they bombard the cathode. With metals of high vapor pressure, as zinc, cadmium or mercury, M^++G' will always set the limit if the terms called for are possible—i.e. not impossible negative terms.

While the limit of excitation will be set by whichever of the possible processes, as described above, possesses the greatest energy which the metal atom or ion can absorb, the processes leading to lower excitations will manifest themselves by maxima of excitation of the terms with which they are nearly in resonance, providing these excitation levels fall where the M^+ terms are close enough together for such maxima to be distinguishable.

For metals intermediate between the types above discussed it does not appear on the basis of present information possible to predict the excitation conditions. Whether or not metal ions will play a conspicuous part in the excitation will apparently depend too much on current density, cathode temperature and gas pressure in particular cases. Altering any of these may influence widely the character of the discharge. It would seem that by placing the metal in a carbon cathode whose temperature could be controlled by the discharge current density or by external heating, it should be possible to pass at will, by varying the vapor pressure of the metal and the gas pressure from the case of low vapor pressure with $M+G^+$ as limit to that of high vapor pressure with M^++G' as limit. A complete theory of the discharge under all conditions and for all gases and metals is not yet possible.

ANALYTIC ATOMIC WAVE FUNCTIONS

BY CLARENCE ZENER
MANCHESTER, ENGLAND

(Received May 26, 1930)

ABSTRACT

The wave functions for the atoms Be, B, C, N, O, F, Ne, are written as simple analytic expressions with several parameters. The best values of these parameters are then determined by the variation method. In the final wave functions the effective quantum number is very nearly two, the radial node is so small as to have little effect upon the charge distribution, the coefficient in the exponential is related to an empirical "mean effective charge."

INTRODUCTION AND RESULTS

SEVERAL methods may be used to obtain approximate solutions of the wave equation for a many electron atom. Any one method cannot claim superiority in every respect. One naturally wants that type of solution which can be used to the best advantage. If he wants information derivable from a graphical $\psi\bar{\psi}$ distribution, then the Hartree¹ functions will be the best. In fact, the graphical method of integration, modified in the manner suggested by Slater² and Fock³ to include resonance, will give the best approximation in which the total ψ is built from functions of only one electron, and in which magnetic forces are neglected.

If all questions could be answered by graphical functions without an undue amount of labor, we would not be justified in finding a less correct analytical ψ . But the integrals representing the mutual potential energy of two atoms are of a type which can be readily evaluated only when the wave functions are given by analytic expressions. Moreover, these integrals become increasingly laborious as the complexity of the atomic functions increases. Hence it is desirable to know the best possible functions which can be represented by simple analytic expressions.

Such atomic functions may be obtained starting from the hydrogenic solutions, exact when the interaction between the electrons is neglected, then partially taking care of this interaction by putting parameters into the function wherever flexibility may be obtained without increased complexity. This method has been used to obtain an approximate eigenfunction for Li by Guillemin and Zener.⁴ In this paper the same method is applied to the normal states of the remaining elements in the first row of the periodic table.

¹ D. R. Hartree, Proc. Camb. Phil. Soc. **24**, 89-132 and 426-437 (1928).

² J. C. Slater, Phys. Rev. **35**, 210 (1930).

³ V. Fock, Zeits. f. Physik **61**, 126, (1930).

⁴ V. Guillemin Jr. and C. Zener, Zeits. f. Physik **61**, 199, (1930).

Slater⁵ has shown how to write the wave function of a many electron system without the use of the group theory. Since the normal states here considered are states of highest multiplicity, the complete ψ may be written

$$\psi = \frac{1}{n!^{1/2}} \sum_P (-1)^{\sigma_P} P u(1/x_1) u(1/x_2) u(s/x_3) \cdots \\ \delta(-\frac{1}{2}/m_{s_1}) \delta(\frac{1}{2}/m_{s_2}) \delta(-\frac{1}{2}/m_{s_3}) \cdots$$

n is the number of electrons; P is an operator which permutes the electron numbers; σ_P is the order of the permutation P ; $u(r/x_i)$ is a space coordinate function of the i^{th} electron in the r^{th} quantum state; $\delta(m_s/m_{s_i})$ is the spin function of the i^{th} electron in a state with spin component m_s . The summation is over all permutations.

We shall denote the states (100), (200), (21-1), (210), (211) by 1, s , a , b , c respectively. The normalised u 's which have been generalised from their hydrogenic form are

$$\begin{aligned} u(1/x) &= g_1 e^{-\gamma r} \\ u(s/x) &= g_2 r^{n^*-1} (1 - \alpha r^{-1}) e^{-\delta r} \\ u(b/x) &= g_3 \cos \theta r^{n^*-1} e^{-\delta r} \\ \left(\frac{a}{c} / x \right) &= g_4 \sin \theta e^{\pm i\phi} r^{n^*-1} e^{-\delta r} \end{aligned}$$

where r is written in units of a_H . In every atom the four parameters n^* , α , γ , δ are to be determined by finding that set which makes

$$J = \frac{\sum_{m_{s_i}} \int \psi H \bar{\psi} d\tau}{\sum_{m_{s_i}} \int \psi \bar{\psi} d\tau} \quad (1)$$

a minimum. H is the Hamiltonian operator without magnetic interactions. It is found that γ changes little from its value

$$\gamma = (N - 5/16)$$

in helium-like ions⁶ (N equals atomic number). In Ne, where interpenetration is the largest, the change is from 9.69 to 9.64. This variation in γ does not affect the minimal value of δ in the significant figures used. It is of interest to note that the resonance of the two $2s$ electrons counterbalances their interpenetration to give a net negative shielding of the K shell.

The minimal values of the remaining parameters are in Table I.

The small effect of α upon the charge distribution is shown in Fig. 1 for Be. Here the quantity

⁵ J. C. Slater, Phys. Rev. **34**, 1293 (1929).

⁶ J. Frenkel, Einführung in die Wellenmechanik, p. 291, Berlin, J. Springer, 1929.

$$D(x_1) = r_1^2 \sum_{m_{s_i}} \int \bar{\psi} \bar{\psi} dx_2 dx_3 dx_4 \sin \theta_1 d\theta_1 d\phi_1$$

in Be is plotted with $\alpha=0$, and its value for $\alpha=0.15$ is indicated by crosses.

TABLE I.

	Li^z	Be	B	C	N	O	F	Ne
$n^*(\pm .04)$	2.0	2.0	—	—	—	—	—	—
$\alpha(\pm .02)$.18†	.15	.10	.07	.05	—	—	—
$\delta(\pm .01)$.63	.96	1.26	1.59	1.92	2.24	2.56	2.88

z Taken from Guillemin and Zener, reference 4.

† ± 0.01

n^* has been varied only in Li and Be. Since in both atoms it has its hydrogenic value, it is to be expected to retain this value in the remaining atoms.

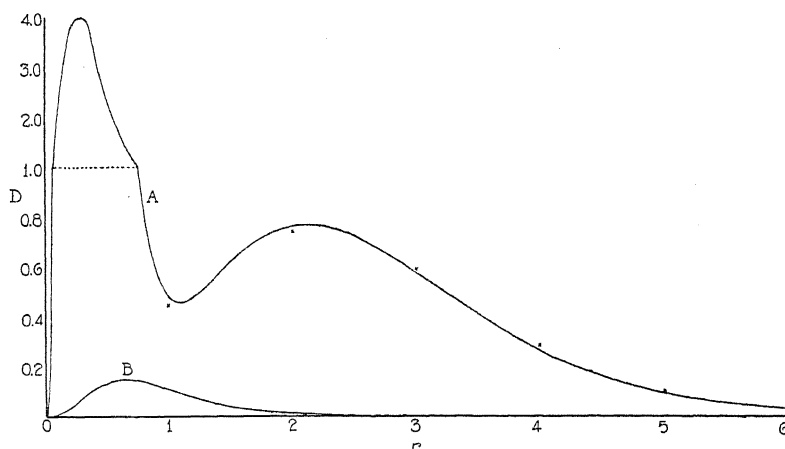


Fig 1.

A is electron density $\times r^2$ with $\alpha=0$, crosses indicate values when $\alpha=0.15$.

B is negative of resonance charge density $\times r^2$

In the elements Be to Ne δ is 0.05–0.06 less than the “mean effective charge” defined by

$$\bar{z} = n^*(\sum \epsilon_i / n)^{1/2}$$

in which $n^*=2$, n is the number of electrons in the L shell, and the ϵ_i are the successive ionization potentials of the L shell expressed in E_H units. It is of interest to have a table of \bar{z} for all the ions, as this relation will probably hold for the stripped atoms as well as for the neutral atoms. These are given in Table II. The \bar{z} 's of F and Ne are extrapolated, as well as of the negative ions.

When more than one electron is in the L shell, \bar{z} is seen to increase in steps of unity as the nuclear charge is increased. The addition of each electron after the first $2p$ electron reduces \bar{z} by 0.35.

TABLE II. \bar{z} of atoms and ions in first row. Numbers in parenthesis are ionization potentials.**

No. of electrons in L shell	1	2	3	4	5	6	7	8
Li	1.260 (.3970)	1.02						
Be	2.316 (1.341)	2.02 (.702)						
B	3.342 (2.793)	3.02 (1.79)	2.63 (.612)	2.28				
C	4.358 (4.747)	4.02 (3.36)	3.63 (1.795)	3.28 (.829)	2.93			
N	5.366 (7.198)	5.02 (5.40)*	4.63 (3.49)	4.28 (2.18)	3.93 (1.97)	3.58		
O	6.372 (10.15)	6.02 (7.97)*	5.63 (5.69)	5.28 (4.05)	4.93 (2.59)	4.58 (1.001)	4.23	
F	7.376	7.02	6.63	6.28	5.93	5.58	5.23	4.88
Ne	8.376	8.02	7.63	7.28	6.93	6.58	6.23	5.88

* Extrapolated potentials

** R. A. Millikan and I. S. Bowen, Proc. Nat. Acad. **13**, 531, (1927)INTEGRATION OF J

Upon the introduction of

$$H = \sum h_i(x_i) + \sum 2/r_{ij}$$

$$h_i = -\Delta_i + 2N/r_i \quad (2)$$

into (1) we see that J can be reduced to a function of the integrals

$$g = \int_0^\infty u(1/x)u(s/x)dx$$

$$h_n^m = \int u(m/x)hu(n/x)dx \quad (3)$$

$$K_{nq}^{mp} = \int u(m/x_1)u(n/x_1)\frac{2}{r_{12}}u(p/x_2)u(q/x_2).$$

To facilitate this reduction we define

$$U(P) = PU(1) = Pu(1/x_1)u(1/x_2)u(s/x_3) \dots$$

$$\Delta(P) = P\Delta(1) = P\delta(-\frac{1}{2}/m_{s_1})\delta(\frac{1}{2}/m_{s_2})\delta(-\frac{1}{2}/m_{s_3}) \dots$$

$$D(P', P'') = \sum_{m_{s_i}} \Delta(P')\Delta(P'').$$

The numerator of (1) becomes

$$\frac{1}{n!} \sum_{m_{s_i}} \int \left\{ \sum_{P'} (-1)^{\sigma_{P'}} P' U(1) \Delta(1) \right\} \cdot H \cdot \left\{ \sum_{P''} (-1)^{\sigma_{P''}} P'' U(1) \Delta(1) \right\} d\tau$$

$$= \frac{1}{n!} \sum_{P'} P' \sum_{m_{s_i}} \int U(1) \Delta(1) H \sum_P (-1)^{\sigma_P} P U(1) \Delta(1) d\tau$$

where $P' \cdot P = P''$, and hence $(-1)^{\sigma_{P'} + \sigma_{P''}} = (-1)^{\sigma_P}$.

Since the integrals and summation are independent of P' , and since there are in all $n!$ permutations, the numerator reduces to

$$\int U(1) H \sum_P (-1)^{\sigma_P} D(1, P) P U(1) d\tau. \quad (4)$$

Similarly the denominator becomes

$$\int U(1) \sum_P (-1)^{\sigma_P} D(1, P) P U(1) d\tau.$$

Observing that $D(1, P)$ vanishes whenever two electrons with opposite spin are permuted, and that $u(1/x)$ is orthogonal to $u(a/x)$, $u(b/x)$ and $u(c/x)$, the denominators for Be and the succeeding atoms reduce to

$$\int U(1) [1 - (13)] [1 - (24)] U(1) d\tau$$

$$= \left(\int u(1/x_1) u(s/x_3) [1 - (13)] u(1/x_1) u(s/x_3) dx_1 dx_3 \right)^2 \quad (5)$$

$$= (1 - g^2)^2.$$

Here the operator interchanging electrons i and j has been denoted by (ij) .

Putting (2) into (4) and using (5) gives the J 's for the various atoms in terms of the integrals (3).

$$J_{Be} = 2(h_1^1 + h_s^s - 2gh_s^1)/(1 - g^2) + [K_{11}^{11} + K_{ss}^{ss} + 2(2 - g^2)K_{1s}^{1s} \\ + (-2 + 6g^2)K_{ss}^{11} - 4g(K_{1s}^{11} + K_{ss}^{1s})]/(1 - g^2)^2$$

$$J_B = J_{Be} + h_a^a + [2K_{1a}^{1a} + 2K_{sa}^{sa} - K_{aa}^{11} - K_{aa}^{ss} + 2gK_{aa}^{1s} - 4gK_{sa}^{1a}]/(1 - g^2)$$

$$J_c^3P = 2J_B - J_{Be} + K_{ab}^{ab} - K_{bb}^{aa}$$

$$J_N^4S = 3J_B - 2J_{Be} + 2K_{ab}^{ab} - 2K_{bb}^{aa} + K_{aa}^{aa} - K_{cc}^{aa}$$

$$J_0^3P = 4J_B - 3J_{Be} + 3K_{ab}^{ab} - 2K_{bb}^{aa} + 3K_{aa}^{aa} - K_{cc}^{aa}$$

$$J_F^2P = 5J_B - 4J_{Be} + 4K_{ab}^{ab} - 2K_{bb}^{aa} + 6K_{aa}^{aa} - 2K_{cc}^{aa}$$

$$J_{Ne}^1S = 6J_B - 5J_{Be} + 8K_{ab}^{ab} - 4K_{bb}^{aa} + 6K_{aa}^{aa} - 2K_{cc}^{aa} + K_{bb}^{bb}$$

These expressions are the same as those given by Peierls⁷ except that he has assumed $g=0$ and the equivalence of such integrals as K_{ab}^{ab} and K_{aa}^{aa} .

COMPARISON OF ENERGY VALUES

A comparison of the observed energy required to strip the L shell in Be, B, C with the calculated energy of the L shell gives a measure of the approp-

⁷ R. Peierls. Zeits. f. Physik 55, 738 (1929).

riateness of our functions in representing the actual eigenfunctions. This is given in Table III.

TABLE III. *Energy of L shell in volts.*

	Li*	Be	B	C
obs.	5.37	27.64	70.3	145.2
calc.	5.32	25.86	68.1	142.7
error	.05	1.8	2.2	2.5

* Taken from Guillemin and Zener, reference 4.

The calculated energy of the L shell is to be defined as the minimum of J minus the calculated energy of the unperturbed K shell⁸

$$E_K = -2(N - 5/16)^2. \quad (6)$$

The calculated energies of the remaining L shells are 258.3, 417.8, 633.5, 919.0 volts for N, O, F, Ne, respectively. A comparison with extrapolated values of the empirical energies gives decidedly worse agreement.

It was found that in a series of ions, such as Be, B⁺, C⁺⁺, the discrepancy remains nearly constant between the empirical energies and those calculated from simple analytic functions. The helium series is of particular interest, where the energy⁶ is given by the function

$$\psi = g_h e^{-(N-5/16)(r_1+r_2)}.$$

TABLE IV. *Energy of helium-like ions (volts.)*

	He	Li	Be
obs	78.59	197.05 ^a	369.58 ^a
Calc.	77.05	195.44	367.94
Error	1.54	1.61	1.64

The multiplet separations have been calculated by the method given by Slater.⁵ They are from 1.5 to 2 times too large.

SUMMARY

Approximate solutions for the normal states of the elements in the first row have been calculated. The parameters in these solutions were either found to have nearly fixed values ($n^*=2$, $\gamma=N-5/16$, $\alpha \approx 0$), or values nearly equal to empirical quantities ($\delta = \bar{z}$). It is to be expected that these parameters will behave similarly in the ions of these atoms. By means of a table which is given for the \bar{z} of the various ions, one may thus write an approximate solution for all the ions, positive and negative, of the atoms in the first row. α will, however, become of increasing importance as the positive charge of the ions increases.

The writer wishes to express his gratitude to Professors Slater and Hartree for illuminating discussions. He also wishes to thank Harvard University for a Sheldon Fellowship which has enabled him to complete this work.

⁸ J. Frenkel, reference 6.

^a B. Elden and A. Ericson, *Nature* **124**, 688 (1929).

ATOMIC SHIELDING CONSTANTS

By J. C. SLATER

JEFFERSON PHYSICAL LABORATORY, HARVARD UNIVERSITY

(Received May 26, 1930)

ABSTRACT

In analogy with the method of Zener for the atoms from Li to F, simple rules are set up giving approximate analytic atomic wave functions for all the atoms, in any stage of ionization. These are applied to x-ray levels, sizes of atoms and ions, diamagnetic susceptibility, etc. In connection with ferromagnetism it is shown that if this really depends on the existence of incomplete shells within the atoms, rather far apart in the crystal, then the metals most likely to show it would be Fe, Co, Ni, and alloys of Mn and Cu (Heusler alloys).

IT IS often extremely useful to have simple approximations to the wave functions and energy levels of atoms and ions. Zener¹ has derived such functions for the atoms up to F, fixing the values of his parameters by variation methods. In the present paper, the functions are tentatively extended to the other atoms. The shielding constants and other parameters are not fixed by variation methods, but adjusted merely to get agreement with empirical values of stripped atom and x-ray energy levels, sizes, etc., so that the values do not have the certainty of Zener's calculations. It is to be hoped that eventually a variation calculation can be made here too; but we may anticipate that the figures given in this paper will be substantially verified, and in the meantime, an approximate set of functions is much better than none. The principal set of shielding constants which now exists is that of Pauling,² and it is believed that the present set is simpler, more general, and more accurate. The density functions derived from the present shielding constants agree fairly well with those found by Hartree's method, in cases where that has been carried out.

THE WAVE FUNCTIONS

The nodes in the wave function are found by Zener to be unimportant, and a glance at Hartree's distribution, say for Rb^+ , shows that they come much nearer the nucleus than for hydrogen wave functions, and are therefore less important. Consequently we neglect them entirely, taking as the radial part of the wave function of one electron simply

$$r^{n^*-1}e^{-(Z-s)/n^*r},$$

the asymptotic form at large distances for a hydrogen-like wave function of quantum number n^* in the field of a nuclear charge $(Z-s)$. Here Z is sup-

¹ C. Zener, *Phys. Rev.* **36**, 51 (1930); Guillemin and Zener, *Zeits. f. Physik* **61**, 199 (1930).

² Linus Pauling, *Proc. Roy. Soc. A* **114**, 181 (1927).

posed to be the actual charge on the nucleus, and s is a screening constant. We assign values of n^* , the effective quantum number, and $Z-s$, by simple rules, to the electrons in each shell in each atom or ion, and so have a complete set of one-electron wave functions. The method of combining such one-electron wave functions into functions for the whole atom has been described elsewhere.³

The values of n^* and $(Z-s)$ are given by the following rules:

(1) n^* is assigned by the following table, in terms of the real principal quantum number n :

$$\begin{aligned} \text{for } n &= 1, 2, 3, 4, 5, 6 \\ n^* &= 1, 2, 3, 3.7, 4.0, 4.2 \end{aligned}$$

(2) For determining $Z-s$, the electrons are divided into the following groups, each having a different shielding constant: $1s$; $2s, p$; $3s, p$; $3d$; $4s, p$; $4d$; $4f$; $5s, p$; $5d$; etc. That is, the s and p of a given n are grouped together (as Zener has done), but the d and f are separated. The shells are considered to be arranged from inside out in the order named.

(3) The shielding constant s is formed, for any group of electrons, from the following contributions:

(a) Nothing from any shell outside the one considered.

(b) An amount 0.35 from each other electron in the group considered (except in the $1s$ group, where 0.30 is used instead).

(c) If the shell considered is an s, p shell, an amount 0.85 from each electron with total quantum number less by one, and an amount 1.00 from each electron still further in; but if the shell is a d or f , an amount 1.00 from every electron inside it.

As a first example, we take C, $Z=6$. Here we have two $1s$ electrons, four $2s, p$ electrons. For effective nuclear charge, $Z-s$, we have

$$\begin{aligned} 1s: 6 - 0.30 &= 5.70 && \text{(Zener has 5.6875)} \\ 2s, p: 6 - 3(0.35) - 2(0.85) &= 3.25 && \text{(Zener has } 1.59 \times 2 = 3.18) \end{aligned}$$

As a second example, we take Fe, $Z=26$. There are two $(1s)$'s, eight $(2s, p)$, eight $(3s, p)$, six $(4d)$, two $(4s)$. The effective nuclear charges are

$$\begin{aligned} 1s: 26 - 0.30 &= 25.70 \\ 2s, p: 26 - 7(0.35) - 2(0.85) &= 21.85 \\ 3s, p: 26 - 7(0.35) - 8(0.85) - 2(1.00) &= 14.75 \\ 3d: 26 - 5(0.35) - 18(1.00) &= 6.25 \\ 4s: 26 - 1(0.35) - 14(0.85) - 10(1.00) &= 3.75. \end{aligned}$$

Finally we take Fe, lacking a K electron, so that there is only one $(1s)$, but otherwise it is as before. Then

$$\begin{aligned} 1s: 26.00 \\ 2s, p: 26 - 7(0.35) - 1(0.85) &= 22.70 \\ 3s, p: 26 - 7(0.35) - 8(0.85) - 1(1.00) &= 15.75 \\ 3d: 26 - 5(0.35) - 17(1.00) &= 7.25 \\ 4s: 26 - 1(0.35) - 14(0.85) - 9(1.00) &= 4.75. \end{aligned}$$

³ J. C. Slater, Phys. Rev. **34**, 1293 (1929).

THE ENERGY VALUES

The total energy of an atom or ion—the negative of the energy required to remove all electrons from the nucleus to an infinite distance—is found by Zener to be accurately given by the sum of the quantities— $((Z-s)/n^*)^2$ for all electrons of the atom (This is the significance of his connection of the shielding constant with the empirical “mean effective charge”). This is very reasonable. If we take as an atomic wave function a product of one-electron wave functions of our type, for each electron, then allow the energy operator to act on it, the result will consist of several parts, as one can readily verify: (1) the sum of $-((Z-s)/n^*)^2$ for each electron, times the function, coming from the second derivative in the Laplacian operator; (2) terms in $1/r$, and higher powers, times the function, coming from the Laplacian; (3) terms in $1/r$, times the function, coming from the potential energy. For the correct wave function, (2) and (3) will cancel each other, leaving just terms (1), a constant times the function, so that Schrödinger’s equation will be satisfied. It seems very reasonable that, in a wave function which is a good approximation, this will be nearly the case too. But this leaves as the energy just the sum which we have mentioned. We therefore take that as giving the energy of an atom or ion, saving ourselves by this simple rule from the necessity of computing the energy by the usual method of integrating H . This of course gives the energy in terms of the Rydberg energy.

As a first example, we take the energy required to remove all the L electrons from C . We have

$$\text{normal atom: } -2(5.70)^2 - 4(3.25/2)^2 = -64.98 - 10.56 = -75.54$$

$$\text{atom with } L \text{ electrons stripped off: } -2(5.70)^2 = -64.98$$

$$\begin{aligned} \text{Difference} &= \text{energy of removal} = 10.56 = 10.56 \times 13.56 \text{ volts} \\ &= 143.2 \text{ volts (correct, 145.2; Zener has 142.7)} \end{aligned}$$

As a second example, we take the energy required to remove any electron from the Fe atom, We have

$$\begin{aligned} \text{normal atom: } &-2(25.70)^2 - 8(21.85/2)^2 - 8(14.75/3)^2 - 6(6.25/3)^2 - 2(3.75/3.7)^2 \\ &= -2497.2 \end{aligned}$$

$$\begin{aligned} \text{atom lacking one } 1s \text{ electron: } &-1(26.00)^2 - 8(22.70/2)^2 - 8(15.75/3)^2 \\ &- 6(7.25/3)^2 - 2(4.75/3.7)^2 = -1964.6. \quad \text{Difference} = 532.6; \text{ observed} \\ &K \text{ absorption limit} = 524.0 \end{aligned}$$

$$\begin{aligned} \text{atom lacking one } 2s, p \text{ electron: } &-2(25.70)^2 - 7(22.20/2)^2 - 8(15.60/3)^2 \\ &- 6(7.25/3)^2 - 2(4.75/3.7)^2 = -2437.7. \quad \text{Difference} = 59.4; \text{ observed } L \text{ ab-} \\ &\text{ sorption limits, } L_{11} = 61.9, L_{21} = 53.4, L_{22} = 52.4 \end{aligned}$$

$$\begin{aligned} \text{atom lacking one } 3s, p \text{ electron: } &-2491.1; \text{ difference} = 6.1; \text{ observed } M_{11} \\ &= 7.07; M_{21}, M_{22} = 4.2 \end{aligned}$$

$$\begin{aligned} \text{atom lacking one } 3d \text{ electron: } &2496.4; \text{ difference} = 0.8; \text{ observed energy of} \\ &\text{ removal of } 3d \text{ electron from } Fe \text{ atom, by Moseley law in optical spectra,} \\ &0.8 \end{aligned}$$

$$\begin{aligned} \text{atom lacking one } 4s \text{ electron: } &2496.3; \text{ difference} = 0.9; \text{ observed energy of} \\ &\text{ removal of } 4s \text{ electron} = 0.58 \end{aligned}$$

It is interesting to notice in this example how the so-called "outer shielding" of the x-ray terms comes about, by the decrease of the shielding constants of the outer electrons when an inner electron is removed. It is also interesting to see how this rearrangement of shielding constants brings it about that the 3*d* electrons, although much further in than the 4*s*, still require about the same energy for their removal.

As a final example, we take the ionization potential of the alkalis:

normal Li: energy of *K* shell $-(1.30/2)^2$ = energy of *K* shell -0.423

ionized Li: energy of *K* shell; difference = 0.423; observed ionization potential = 0.397.

We observe that we can get these ionization potentials directly, without considering the inner shells. Thus we have for the ionization potentials:

$$\text{Na } (2.20/3)^2 = 0.537, \text{ observed} = 0.378$$

$$\text{K } (2.20/3.7)^2 = 0.354, \text{ observed} = 0.319$$

$$\text{Rb } (2.20/4.0)^2 = 0.302, \text{ observed} = 0.307$$

$$\text{Cs } (2.20/4.2)^2 = 0.274, \text{ observed} = 0.287$$

The examples which we have worked out are a fair sample of the energies obtained in general from the scheme; one sees that they are qualitatively accurate, though by no means to be trusted in detail. The principal criterion used in setting up the rules for the shielding constants has been to make the energy check fairly well with experiment.

SIZES OF ATOMS AND IONS

The maximum of the radial charge density for one of our shells comes, as we immediately find by differentiation, at $(n^*)^2/(Z-s)$. Thus our shielding constants permit us to compute the sizes of atoms and ions. For example, the radius, as defined in this way, of the outer, 4*s* shell of Fe is $(3.7)^2/3.75 = 3.65 = 1.95$ Angstroms. The radii of the outer shells, defined in this way, can be brought into interesting connection with the internuclear distances in valence compounds and in metals, in which the substances exist in the atomic state. For binding, we should expect that the electrons forming the bond would wish to have the maximum possible overlapping, which would come if the internuclear distance were the sum of the radii so defined, so that the maxima of density lay together. As a matter of fact, this is closely the case, when the valence electrons are *p* electrons; but when both valences are *s* electrons, the distances are smaller, about 2/3 of this. In any case, the correlation is quite good, and should be useful in predicting approximate internuclear distances where they are not known. We give, in Table I, the atomic radii so derived, and in Table II a number of internuclear distances, as observed in band spectra and crystals, together with the sum of the theoretical radii for comparison, and the ratio of the two. These ratios are, as we stated, about 1 when one or both valences are *p* electrons, but about 2/3 when both are *s* electrons. In a few cases, such as the hydrogen halides, where one might suppose the substances to be ionic rather than valence

compounds, the excellent agreement with our rule gives us confidence that the valence bond essentially describes the situation.

TABLE I. *Atomic radii (Angstroms).*

(These radii are the radii of the values for maximum radial density in the charge distributions of the outer shells of the neutral atoms, computed from the effective quantum numbers and effective nuclear charges by the formula $(n^*)^2/(Z-s)$.)

H	0.53	Na	2.17	K	3.32	Rb	3.86	Cs	4.25
Li	1.63	Mg	1.68	Ca	2.56	Sr	3.00	Ba	3.30
Be	1.09	Al	1.37	Sc	2.43	Y	2.84	La	3.12
B	.82	Si	1.15	Ti	2.32	Zr	2.71	—	—
C	.65	P	1.00	V	2.22	Nb	2.60	Ta	2.86
N	.55	S	.88	Cr	2.12	Mo	2.48	W	2.73
O	.47	Cl	.78	Mn	2.02		2.36		2.60
F	.41			Fe	1.95	Ru	2.28	Os	2.51
				Co	1.87	Rh	2.18	Ir	2.40
				Ni	1.80	Pd	2.10	Pt	2.31
				Cu	1.73	Ag	2.02	Au	2.22
				Zn	1.67	Cd	1.95	Hg	2.15
				Ga	1.46	In	1.71	Tl	1.88
				Ge	1.29	Sn	1.51	Pb	1.66
				As	1.16	Sb	1.35	Bi	1.48
				Se	1.05	Te	1.22		
				Br	.96	I	1.12		

TABLE II. *Internuclear distances in valence compounds (Angstroms).*

(Observed internuclear distances, observed from band spectra or crystal structure. Band spectrum data are taken from Report of National Research Council on Molecular Spectra in Gases, pp. 222-232, except for the following: BO, Jenkins, Proc. Nat. Acad. Sci. 13, 496, (1927); NO, Guillery, Zeits. f. Physik 42, 121 (1927), recalculated by Birge; OH, Report as above, but corrected by Birge; H₂O, Debye, Polare Molekeln, Hirzel, 1929, p. 85; HI, Czerny, Zeits. f. Physik 44, 236 (1927), calculated by Birge; H₂, Birge, Proc. Nat. Acad. Sci. 14, 12 (1928); Na₂, Loomis, Phys. Rev. 32, 223 (1928); MgH, Watson and Rudnick, Phys. Rev. 29, 413 (1927). Data on crystal structure are from Landolt-Börnstein, Tables, 5th Ed., Ergänzungsband.

The columns are as follows: (1) substances; (2) observed internuclear distances; (3) sum of atomic radii for outer shell, as given in Table I; (4) ratio of observed distance to sum of radii; (5) sum of atomic radii for inner incomplected shell, in substances which might be ferromagnetic; (6) ratio of observed distance to sum of radii of inner shells. Substances are divided into four classes: (a), molecules with one or both valences p electrons; (b) molecules with both valences s electrons; (c) crystals with one or both valences p electrons; (d) crystals with both valences s electrons.)

Part (a): Molecules with one or both valences p electrons.

(1) Substance	(2) Distance observed	(3) Sum of radii	(4) Ratio obs/calc
BO	1.21	1.29	0.94
CH	1.13	1.18	.96
CN	1.17	1.20	.98
CO	1.15	1.12	1.02
NO	1.15	1.02	1.12
N ₂	1.21	1.10	1.10
O ₂	1.20	.94	1.28
OH	.98	1.00	.98
H ₂ O	1.07	1.00	1.07
AlH	1.66	1.90	.87
AlO	1.62	1.84	.88
SiN	1.56	1.70	.92
I ₂	2.66	2.24	1.19
HF	.92	.94	.98
HCl	1.28	1.31	.98
HBr	1.42	1.49	.95
HI	1.62	1.65	.98

Part (b): Molecules with both valences *s* electrons.

(1) Substance	(2) Distance observed	(3) Sum of radii	(4) Ratio obs/calc
H ₂	.76	1.06	.71
Na ₂	3.08	4.34	.71
CuH	1.47	2.26	.65
AgH	1.63	2.55	.64
AuH	1.54	2.75	.56
MgH	1.74	2.21	.79
CaH	2.01	3.09	.65
ZnH	1.61	2.20	.73
CdH	1.78	2.48	.72
HgH	1.76	2.68	.66

Part (c): Crystals with one or both valences *p* electrons.

(1) Substance	(2) Distance observed	(3) Sum of radii	(4) Ratio obs/calc
C (diamond)	1.54	1.30	1.18
(graphite)	1.43	1.30	1.10
(ethane C—C)	1.55	1.30	1.19
C—N (KCN)	1.15	1.20	.96
Al	2.86	2.74	1.04
Si	2.35	2.30	1.02
Ge	2.44	2.58	.95
As	2.51	2.32	1.08
Se	2.35	2.10	1.12
In	3.24	3.42	.95
Sn (diamond lattice)	2.80	3.02	.93
Sn (white)	3.02	3.02	1.00
Sb	2.87	2.70	1.06
Te	2.87	2.44	1.18
Tl	3.36	3.76	.89
Pb	3.48	3.32	1.05
Bi	3.10	2.96	1.04

Part (d): Crystals with both valences *s* electrons.

(1) Substance	(2) Distance observed	(3) Sum of radii	(4) Ratio obs/calc	(5) Sum of radii inner shell	(6) Ratio obs/calc inner shell
Li	3.03	3.26	.93		
Be	2.23	2.18	1.02		
Na	3.72	4.34	.86		
Mg	3.22	3.36	.96		
K	4.50	6.64	.68		
Ca	4.97	5.12	.78		
Ti	2.93	4.64	.63	2.62	1.12
V	2.63	4.44	.59	2.22	1.18
Cr	2.51	4.24	.59	1.93	1.30
Mn	2.52	4.04	.62	1.71	1.47
Fe	2.50	3.90	.64	1.53	1.63
Co	2.51	3.74	.67	1.38	1.82
Ni	2.50	3.60	.69	1.27	1.97
Cu	2.54	3.46	.73		
Zn	2.67	3.34	.80		
Zr	3.18	5.43	.59	4.00	.79
Mo	2.72	4.96	.55	2.94	.92
Ru	2.64	4.56	.58	2.33	1.13
Rh	2.70	4.36	.62	2.11	1.28
Pd	2.73	4.20	.65	1.93	1.41

Part (d): Crystals with both valences s electrons—*Continued*.

(1) Substance	(2) Distance observed	(3) Sum of radii	(4) Ratio obs/calc	(5) Sum of radii inner shell	(6) Ratio obs/calc inner shell
Ag	2.88	4.04	.71		
Cd	2.96	3.90	.76		
Ta	2.83	5.72	.50	3.95	.72
W	2.73	5.66	.48	3.44	.79
Os	2.71	5.02	.54	2.72	1.02
Ir	2.70	4.80	.56	2.47	1.09
Pt	2.77	4.62	.60	2.25	1.23
Au	2.87	4.44	.65		

In studying valence, we are interested in the size of the outer shell, but for ferromagnetism the essential, as the writer has shown in an earlier paper,⁴ is the existence of an inner shell in process of formation, small enough so that the distance of separation is relatively great compared with the size of the shell. To see what metals should show ferromagnetism, if this idea is correct, we also give in Table II the radii for the d shells in process of formation in the transition groups, and the ratio of internuclear distance to twice this radius. This ratio is greater for Fe, Co, and Ni than for any other element, so that these would be most likely to be ferromagnetic. We might suppose that as two such shells were moved apart, the interaction was nonferromagnetic (the terms of lowest multiplicity lying lowest) out to about 1.55 times the sum of the radii; there the interaction would change sign, passing through a critical region (suggesting the fact that Mn sometimes shows magnetic properties, usually not). The first element beyond the critical region, Fe, would show the greatest ferromagnetism. As the internuclear distance still further increased, the exponential dropping off of the wave function would make the interaction less, resulting in weaker effects in Co and Ni. These conclusions are made much more reasonable by considering the Heusler alloys. Here Cu takes the place of Mn in an alloy with Al or other substance, and the alloy is almost as ferromagnetic as Fe. Now if Cu can replace Mn, it is presumably in a form with two $4s$ electrons, nine $3d$'s so that it has an open shell of d electrons, which is even smaller than for Ni (radius = $1.17/2A$). This very small radius, added to the large radius of Mn, gives a sum of $1.44A$, and a ratio intermediate between Fe and Co, suggesting a strong ferromagnetism, although Mn by itself is too big, Cu too small (and in ordinary Cu undoubtedly the $3d$ shell is closed anyway) to show ferromagnetic properties.

In ionic compounds, the atoms exist as ions, which have closed shells; and the interionic forces are repulsions (except for the electrostatic attractions), and account for the hardness and impenetrability of the structures. These repulsions become large, as has often been shown, as soon as the outer shells begin to overlap, and the internuclear distances in ionic crystals should be the sums of radii representing, not the radius of maximum density in the shell, but a considerably larger radius at which the charge just begins to become

⁴ J. C. Slater, Phys. Rev. 35, 509 (1930).

appreciable. It appears that the appropriate radius is roughly one at which the radial density becomes 10 percent of its maximum value. By solving the problem numerically, we find that for the density function we have used, this radius is a numerical factor times the radius of maximum density, this factor being 3.38 for $n^*=1$, 2.49 for $n^*=2$, 2.25 for $n^*=3$, 2.01 for $n^*=3.7$, 1.96 for $n^*=4.0$. Thus, finding the radius of maximum density, now for the ion rather than for the atom, and using these factors to get radii of 10 percent density, we get the ionic radii given in Table III. They should be compared with the ionic radii of Wasastjerna, which are to be added to give grating spaces, and which are also tabulated. It is seen that the agreement in general is decidedly good. This renders it highly probable that the atoms really exist in these compounds as ions, as has been supposed. Computed values are included for the inert gases, and these should be the radii of these gases, as derived in the kinetic theory. The latter of course vary over a considerable range, but our values seem to lie well within this range in each case. For example, for He, Jeans in his "Dynamical Theory of Gases" gives values from 0.99A to 1.10A, as determined by various methods; our value is 1.05A.

TABLE III. *Ionic radii (Angstroms).*

(Observed radii as given by Wasastjerna; see for instance W. L. Bragg, *Phil. Mag.* 2, 258 (1926); the sum of these radii gives the interionic distance in ionic crystals. Calculated values are for radius where density is 10% of its maximum value. This equals constant times $(n^*)^2/(Z-s)$, where the constant equals 3.38 for $n^*=1$, 2.49 for $n^*=2$, 2.25 for $n^*=3$, 2.01 for $n^*=3.7$, 1.96 for $n^*=4.0$)

Ion	Observed	Calculated	Ion	Observed	Calculated
H ⁻		2.57	Se ⁻		2.34
He		1.05	Br ⁻	1.92	2.02
Li ⁺	0.76	.67	Kr		1.77
Be ⁺⁺	(.3)	.49	Rb ⁺	1.50	1.58
			Sr ⁺⁺	1.20	1.43
O ⁼	1.32	1.37	Te ⁼		2.66
F ⁻	1.33	1.09	I ⁻	2.19	2.30
Ne		.91	Xe		2.02
Na ⁺	1.01	.77	Cs ⁺	1.75	1.80
Mg ⁺⁺	.75	.67	Ba ⁺⁺	1.40	1.62
Al ⁺⁺⁺	(.55)	.60			
Si ⁴⁺	(.3)	.54			
S ⁼	1.69	2.16			
Cl ⁻	1.72	1.79			
A		1.52			
K ⁺	1.30	1.33			
Ca ⁺⁺	1.02	1.17			

We can get a valuable check on the size of atoms by using the diamagnetic susceptibility, which is proportional to the mean value of Σr^2 . From our wave functions, by integration we find this quantity for one of the electrons to be $(n^*)^2 (n^*+1/2) (n^*+1)/(Z-s)^2$. For the inert gases, we have the following values:

	computed	observed
He	2.07	2.34
Ne	7.08	8.31
A	23.37	22.6

A SEARCH FOR THE SOURCE OF DIELECTRIC POLARIZATION

BY RALPH D. BENNETT

RYERSON PHYSICAL LABORATORY, UNIVERSITY OF CHICAGO

(Received May 23, 1930)

ABSTRACT

A brief discussion is given of the work of Hengstenberg on the same subject. A theory of the distortion of a polar cubic lattice by electric stress is derived with the method suggested by Richardson for calculating electric stress on the ions, and the frequency of residual rays for determining the restraining forces. The effect of the distortion on intensity of x-ray reflection is then calculated in the usual manner. Measurements of change in intensity of reflected x-rays were made with a precision of about 0.1 percent in the 4th and 5th orders for NaCl and the 5th order for KCl using gradients up to 700 kv/cm. It is concluded that the effect is probably not as large as predicted by Hengstenberg, i.e., the polarization is probably not due to motion of the ions as units. The precision of the experiments was not high enough to determine whether the theory derived here is correct.

IF A polar crystal is subjected to electric stress the positive and negative ions might be expected to be displaced in opposite directions. The distorted lattice would then reflect x-rays less intensely than before distortion. J. Hengstenberg¹ has derived a theory of this effect based on the assumption that the total polarization is due to the displacement of the ions as units. This assumption seems hardly justified since the polarization effects exhibited by nonpolar substances are of the same order of magnitude as those of polar substances. However Hengstenberg has tested his theory for KCl and found the experimental results in agreement.

A calculation of the electrostatic force due to an external field on an ion in a crystal of this type can be made following the method suggested by Richardson.² By considering the forces due to the condenser charge, the polarization charge, and the doublets in the neighborhood of the ion, the following equation is obtained:

$$f_e = \frac{K + 2}{3K} Ee \text{ dynes} \quad (1)$$

where K is the dielectric constant, E the field in e.s.u. per cm, and e is the electronic charge in e. s. u.

The binding forces on the atoms in a crystal can be calculated if we assume their resonance frequency to be that of the residual rays. The differential equation is:

$$m\ddot{x} + qx = 0$$

where m is the mass of the atom and q the restoring force per unit displacement.

¹ J. Hengstenberg, *Zeits. f. Phys.* **58**, 345 (1929).

² O. W. Richardson, *Electron Theory of Matter* p. 71 *et seq.*

A solution of the equation is:

$$x = A \cos (pt + \theta)$$

where

$$p = (q/m)^{1/2} = 2\pi\nu = 2\pi c/\lambda$$

λ being the resonance wave-length and c the velocity of light.

Then

$$q = 4\pi^2 c^2 m / \lambda^2 \text{ dynes/cm}$$

or for a displacement of δ cm

$$f_\delta = 4\pi^2 c^2 m \delta / \lambda^2. \quad (2)$$

If the binding forces for $\lambda = \infty$ are not substantially different from those for the wave-lengths of the residual rays then $f_\delta = f_e$ or combining Eqs. (1) and (2)

$$\frac{K+2}{3K} Ee = 4\pi^2 c^2 m \delta / \lambda^2$$

whence

$$\delta = \frac{\lambda^2}{4\pi^2 c^2 m} \frac{K+2}{3K} eE \quad (3)$$

If the lattice is distorted by moving alternate atoms in opposite directions in a cubic crystal, the intensity of the x-rays reflected may be shown to be:³

$$I_\delta = I_0 \cos^2 2\pi n \delta / D$$

where I_δ = intensity from distorted lattice

I_0 = intensity from undistorted lattice

n = order of reflection

δ = distance through which each atom is moved

D = distance between adjacent atomic layers.

The fractional change in intensity due to distortion is then:

$$\frac{\Delta I}{I} = \frac{I_0 - I_\delta}{I_0} = 1 - \cos^2 2\pi n \delta / D = \sin^2 2\pi n \delta / D$$

and for small values of δ

$$\frac{\Delta I}{I} = (2\pi n \delta / D)^2. \quad (4)$$

Combining Eqs. (3) and (4)

$$\frac{\Delta I}{I} = \left[\frac{(K+2)\lambda^2 n e}{6\pi K m c^2 D} \right]^2 E^2.$$

³ cf. A. H. Compton, X-rays and Electrons Chap. V.

With the values $e = 4.77 \times 10^{-10}$, $c = 3 \times 10^{10}$ and for NaCl

$$K = 6.12$$

$$\lambda = 52 \times 10^{-4} \text{ cm}$$

$$D = 2.81 \times 10^{-8} \text{ cm}$$

$$m = 23.00 + 35.46/2 \times 6.06 \times 10^{23} = 4.84 \times 10^{-23} \text{ grams}$$

and for KCl

$$K = 5.03$$

$$\lambda = 63.4 \times 10^{-4} \text{ cm}$$

$$D = 3.14 \times 10^{-8} \text{ cm}$$

$$m = 39.10 + 35.46/2 \times 6.06 \times 10^{23} = 6.18 \times 10^{-23} \text{ grams.}$$

For the 4th order NaCl $\Delta I/I = 0.89 \times 10^{-11} E^2$.

For the 5th order NaCl $\Delta I/I = 1.40 \times 10^{-11} E^2$.

For the 5th order KCl $\Delta I/I = 1.68 \times 10^{-11} E^2$.

These values are plotted in the dotted curves of figs. 3, 4 and 5. The corresponding values obtained from Hengstenberg's equations are represented by the dashed lines. The difference between these predictions would seem to be due to Hengstenberg's neglect of possible distortion of the ion under the influence of the applied electric field.

EXPERIMENTAL ARRANGEMENT

The source of x-rays was a water-cooled Coolidge molybdenum target tube immersed in oil and operated at from 30 to 45 ma. and 40 to 50 peak k. v. by a full wave rectifier. The crystals under test were mounted on the table of a spectrometer which also carried an arm for supporting the ionization chamber. The ionization currents were measured by means of a screen grid amplifier described in detail elsewhere,⁴ the variations in the plate current being measured by a galvanometer. A record of the galvanometer deflection was traced photographically on bromide paper, which was drawn at a constant rate by a synchronous-motor-driven reduction gear.

The crystals were mounted in a manner essentially the same as that used by Hengstenberg. This consisted of splitting the crystal as thin as conveniently possible, then mounting by means of sealing wax over a hole of about 7 mm diameter in a glass plate. After mounting, the crystal can be reduced to the desired thickness by washing with water. The thickness of the crystals used ranged from about 0.25 to 0.40 mm, a rough measurement being made by means of a dial test indicator before use, and more exactly by micrometer calipers after puncture. A circular piece of very thin aluminum foil was cemented with shellac to each side of the crystal for applying the electric stress.

The source of voltage for the crystals consisted of a kenotron rectifier set with a condenser, and could supply up to 21 k.v. direct current. This source was connected to the back foil of the crystal through a resistance of several megohms, the foil on the reflecting side being grounded. The high

⁴ R. D. Bennett, An Amplifier for Measuring Small Currents Rev. of Sci. Inst. in press.

voltage was switched on and off by means of a kenotron which when the filament was lighted served to ground the back surface of the crystal. The kenotron filament was switched by the same mechanism that moved the photographic paper, and an auxiliary light traced a record on the paper whenever the kenotron filament was lighted. The amplifier for the ionization

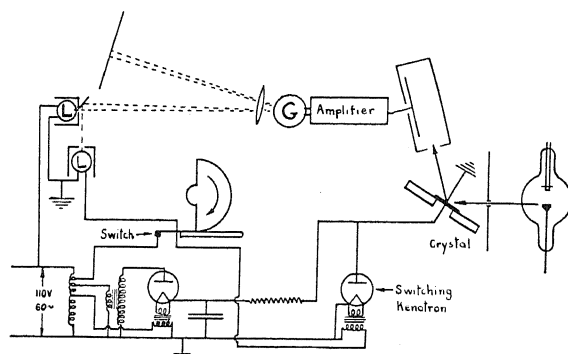


Fig. 1. Diagram of apparatus.

current was so sensitive to high frequency surges that this method of switching was necessary. For the same reason sources of sparking in the x-ray supply circuit had to be removed. Voltage on the crystal was measured by means of a spark gap. Fig. 1 is a diagram of the circuits.

The amplifier arrangement reads the ionization current directly, and the electrostatic capacity of the collector is so small that the ionization from the

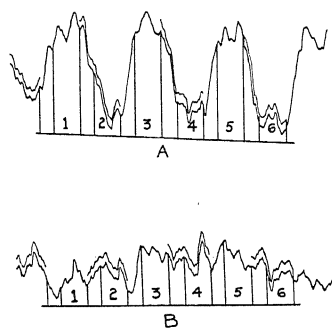


Fig. 2.

individual photoelectrons produces variations in the plate current. This makes the galvanometer trace a wavy line, the fluctuations being of the order of 1 percent in the arrangement used. Hence it was necessary, in order to measure to higher precision than 1 percent to take an average over a number of intervals. The method of analysis of the records is best shown by Fig. 2. The trace *A* is a calibration curve obtained by alternately inserting and removing a screen which absorbs a_0 percent of the x-ray beam. The sum of the areas 1, 3, 5 etc. is measured by means of a planimeter and an average area

s_0 found. From this is subtracted the average of the even areas s_e . Then $s_0 - s_e/a_0 = s_1$ gives the average area difference equivalent to 1 percent change in intensity. The curve B which is made with the field alternately on and off is then analysed in the same manner giving an average difference, say s_2 . Then the ratio s_2/s_1 gives the fraction of 1 percent change due to the field. The precision of the result will be proportional to the square root of the num-

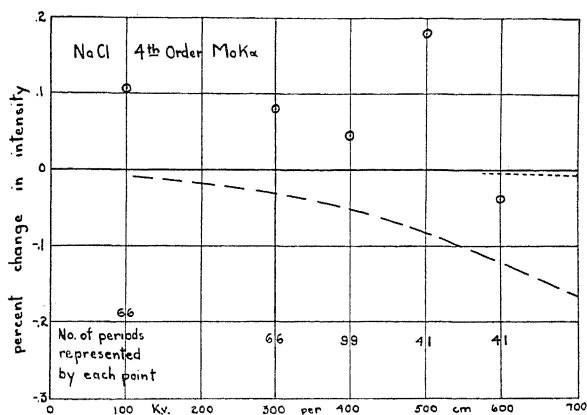


Fig. 3.

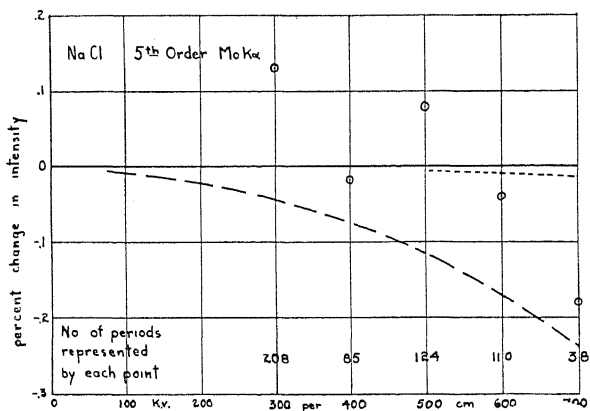


Fig. 4.

ber of periods averaged. Each period was 44.4 seconds, and approximately the first third of each interval was omitted to allow for adjustment of the recording system to a new value of ionization current.

Observations were made in the 4th and 5th order for rock salt and the 5th order for sylvine, the gradients ranging up to 700 k.v./cm. The tests under different gradients were grouped together in 100 k.v./cm. ranges, and the results are plotted in Figs. 3, 4 and 5.

The sensitivity of the apparatus was such that $1/30$ of one percent in the 5th order could just be detected if the deflection were steady. However to reduce the fluctuations to this level it would be necessary to increase the

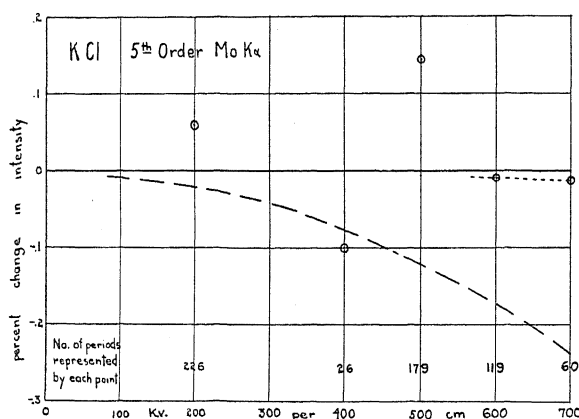


Fig. 5.

ionization current by a factor of $[1/(1/30)]^2 = 900$ which would hardly be possible. Increasing the electrostatic capacity of the recording system would be of no avail because there were irregular line voltage variations of about 1 percent.

CONCLUSIONS

The experimental results are not precise enough to tell definitely whether Hengstenberg's theory, the theory outlined above, or neither describes the effect. The 700 k.v./cm point on the 5th order NaCl curve falls very nearly at the value predicted by Hengstenberg's theory. It is doubtful whether this is more than a coincidence since it depends on a small number of observations. No other crystal stood this high field though many attempts were made to find one. The writer believes that from consideration of all the data, the effect is probably not as large as predicted by the Hengstenberg theory.

The KCl crystals used were very kindly furnished by Dr. E. F. Barker of the University of Michigan. I am also indebted to Professor A. H. Compton for advice and interest in this problem. The work was supported by the Utilities Research Commission as a part of their program of investigation of the properties of solid dielectrics at Ryerson Laboratory of the University of Chicago.

INFRARED FILTERS OF CONTROLLABLE TRANSMISSION

BY A. H. PFUND

ROWLAND HALL, JOHNS HOPKINS UNIVERSITY

(Received May 26, 1930)

ABSTRACT

When using an echelette grating for work in the infrared it is necessary to eliminate overlapping, higher orders. Since no adequate series of true filters covering the entire infrared is known, a new type of filter has been developed. Essentially, this type of filter consists of a powder spread uniformly over a surface of polished speculum. Short wave-length radiations are reflected diffusely while long wave-length radiations are largely transmitted since the Rayleigh scattering for long waves is feeble. The region of transition from opacity to transparency is controlled by choosing powders of proper particle-size and by depositing these in layers of appropriate thickness.

Specific examples, involving the use of particles whose mean diameter covers the range: 0.22μ to 2.5μ , are presented to show how filters for almost any portion of the spectral range: 2μ to 7.5μ may be largely freed from the effects of superposed, higher orders. Filters for greater wave-lengths may be produced by much the same methods.

FOR the attainment of large dispersion and high resolving-power in the infrared, the diffraction grating, in particular, the echelette grating is coming into wide use. It suffers, however, from one drawback, i.e. superposed orders. If for example, an echelette grating be adjusted for work in the first order near 3μ , there is superposed on this a large amount of second order 1.5μ energy, third order 1μ energy, etc. Due to the fact that the usual Nernst lamp has its energy maximum near 1.6μ , the energy of the contaminating radiations exceeds greatly the energy at 3μ . It is proposed to discuss in the following a new type of filter which, though by no means perfect, does minimize the effect of contaminating radiations.

The term filter is here employed in the broad sense of being a device which either isolates narrow spectral regions or which experiences a change from opacity to transparency within a relatively small wave-length interval. To be specific, a satisfactory filter for an echelette grating, operating between the limits 3μ to 3.5μ , would be one which is quite opaque for all radiations shorter than 1.75μ and quite transparent for radiations greater than 3μ . To realize so great a change in transparency within so narrow a spectral range is difficult.

Methods now in use for filtering out the undesirable radiations are here enumerated: I. Infrared monochromator.¹ II. Residual rays.² III. Reflection from rough surfaces.³ IV. True absorption filters.⁴ Without going

¹ Sleator, *Astro. Phys. J.* **48**, 127 (1918).

² Rubens and Aschkinass, *Ver. deutsch phys. Ges.* **17**, 42 (1898).

³ Gorton, *Phys. Rev.* **7**, 66 (1916).

⁴ Coblenz, *Supplementary Investigations of Infrared Spectra 5-7*, Carnegie Inst. of Washington (1908).

A very comprehensive list of references, dealing with the infrared, is to be found in "Le Spectre Infrarouge" by Jean Lecomte, Les Presses Universitaires de France (1928).

into a detailed discussion of the various devices it may be stated that most of them are limited in the range of spectrum which can be covered; again, some lack flexibility, i.e. if true filters or crystals (employed for residual rays) fail to show high transmission or reflection, respectively, in the region to be studied, there is nothing to be done about it. As for reflection from rough surfaces it may be said that the wave-length interval separating regions of low and high reflection is entirely too great to be considered seriously for the present purpose.

The new filters about to be described are a by-product of some work that is being carried out on the measurement of particle-size of finely divided powders by studying their transmission in the infrared. Rayleigh's inverse fourth power law of scattering is strictly applicable only if the particle-size be small in comparison with the wave-lengths employed. If, however, the particle-size be large in comparison with the wave-length, the particles assume the role of small mirrors which reflect vigorously. Consequently, if transparent particles of a uniform and suitable size be produced it will be found that they reflect the regions of short wave-lengths strongly and scatter those of great wave-length feebly. Used in transmitted light a film of such small particles will be virtually opaque to the short wave-lengths and highly transparent to the longer. Body-color, involving true absorption, plays no necessary part in the functioning of these filters.

The pulverized materials used in the construction of such filters must fulfill certain necessary conditions: 1. The material must be highly transparent in the spectral region to be studied. 2. A large range of particle-sizes must be available, and the particles in any individual class must be essentially constant in size. 3. The substratum on which the pulverized film is deposited must be transparent. 4. The films must be of uniform thickness.

Concerning condition (1) it may be said that short of 20μ , oxides, sulphides and halides have been found most transparent. Thusfar the most satisfactory films have been formed by the process of "fuming" as, for example, by allowing the oxide fumes from burning magnesium ribbon to collect on a plate. Condition (2) is not as yet realized. It is to be pointed out, however, that methods for accomplishing this purpose are known. The well-known process of "air-flotation" and subsequent settling has been used. Again, the method of successive centrifugings has been employed for bringing about uniformity of particle-size. The nature of the substratum (condition 3) depends largely upon the spectral region to be studied. Microscope cover glass 0.2 mm thick will serve up to 4μ while a thin plate of rock-salt will be useful at least up to 18μ . In order to eliminate completely the element of transparency of the substratum the procedure of coating a polished speculum plate with the pulverized film has been adopted—particularly for the region of long waves. Such a mirror will reflect all wave-lengths while the film will reflect the short waves diffusely but will transmit the long ones regularly. Attention is to be drawn to the fact that, while the widest possible spectral range may be covered by using a speculum or some other reflecting surface, the performance of such a "reflection" filter is less satisfactory than that of

a transmission filter. The reason is that the diffusely reflected light of shorter λ is in part added to the regularly reflected light in the case of the reflection filter, but not so in the transmission filter.

A few examples of the performance of these filters are here presented. Measurements were carried out by means of a rock-salt spectrometer and thermopile. Since it is difficult to control the film thickness accurately, it is necessary to resort to the use of a spectrometer in order to decide when a film of the proper characteristics has been deposited. In Fig. 1 are presented "transmission" curves (*A* and *B*) for zinc-oxide which was fumed on microscope cover glass. The fumes were supplied by an arc burning between zinc

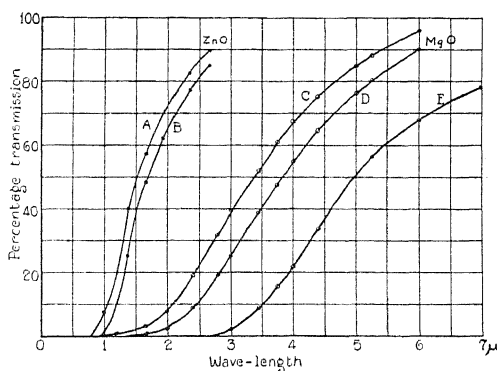


Fig. 1. Transmission curves for films of ZnO and MgO.

terminals. For the thicker film a deep, ruby-red image of an incandescent lamp filament was visible in transmitted light. A similar series for MgO, fumed on speculum is shown in curves *C*, *D* and *E* which apply to films of increasing thickness. In order to obtain the "incident energy" the oxide film was wiped off the speculum mirror.

It is known that zinc oxide particles are smaller than those of magnesium oxide. This is borne out by the curves which show that the transition region for ZnO lies at the shorter wave-lengths. While it is possible to shift this transition region somewhat in the direction of increasing wave-lengths by increasing the film-thickness, a limit is set to this mode of procedure as is evident from the decreasing slope of curve *E*, Fig. 1, in the region of high transparency. It is thus shown that, to produce filters for increasing wave-lengths, particles of increasing size must be used.

Even though a filter, as judged by its transmission curve, may appear to be entirely satisfactory, it is not necessarily so. The total energy associated with any wave-length is given by the product of the following quantities: 1. energy emitted by source. 2. transmission of total air-path. 3. reflection factor for the echelette grating, and 4. transmission factor for filter. This is illustrated in the following curves for films of increasing thickness. In Fig. 2 are plotted the true transmission coefficients of MgO plus cover glass while in Fig. 3 the actual energies are plotted for the same filters. The Nernst

lamp was operated at such a temperature as to place the wave-length of maximum emission at 1.9μ , no correction for irrationality of dispersion having been applied. It is this powerful maximum which must be rendered innocuous if regions of greater wave-length are to be studied. It is usually possible to realize any desired freedom from contamination from shorter wave-lengths; but this is accomplished at the expense of transmission. For the time being two arbitrary criteria for acceptable filters have been laid down, i.e. (1) the transmission, in the region under consideration, λ , must be at least 50%, (2) the energy at $\lambda/2$ ought not to exceed 5–10% of the energy at λ . Applying these criteria to specific filters it is evident that filter III, (Figs. 2 and 3) is

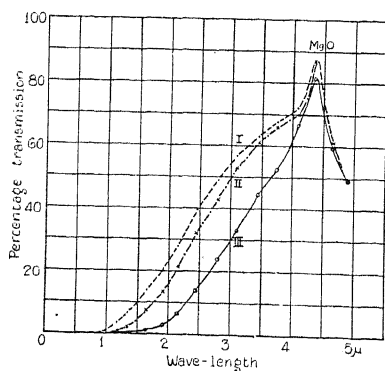


Fig. 2. Transmission curves for various thicknesses of MgO on glass of 0.2 mm thickness. Transmission of glass included in curves.

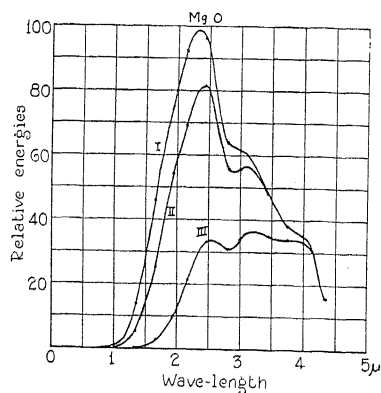


Fig. 3. Relative energies from Nernst lamp transmitted by same films shown in Fig. 2.

most satisfactory in the 3.75μ region. If a wedge-shaped film of oxide be deposited on an over-size speculum mirror, it is easy to pick out the position of the film having the best thickness. If, on the other hand, the film be deposited on microscope cover-glass the latter may be rotated about a vertical axis, thus changing the effective thickness of film, or again, a wedge-shaped film may be deposited.

While the deposition of fumed films is comparatively simple, it becomes difficult to make the thickness uniform whenever the pulverized material is furnished as a dry powder. It is proposed to form films of these materials by the well-known method of "air-flotation." For the time being, films were prepared by dispersing these pigments in water. A small amount of pigment and water were placed on a flat plate of glass and the mixture was ground to a paste of uniform consistency by means of a glass "muller." The latter was then used for applying the paste to the speculum surface. Unfortunately, films produced in this manner are non-uniform in thickness and, as a result the transition range is broadened out. While a graded series of NaCl powders would have been desirable it was found necessary to use such coarser particles as were available, despite the fact that they were known to have bands of

absorption in the region of longer waves. The series of filters shown in Fig. 4 were obtained through the use of the following powders whose respective average diameter of particle⁵ is given in Table I.

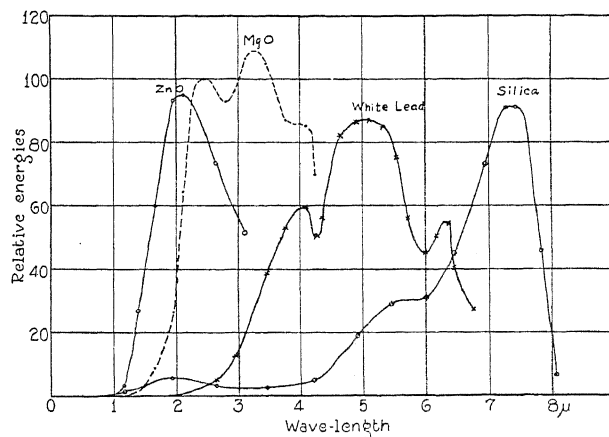


Fig. 4. Relative energies from Nernst lamp transmitted by various filters.

TABLE I.

Powder	Average particle diameter	Mode of application
I. Zinc oxide	0.22 μ	Fumed
II. Magnesium Oxide	0.35	"
III. Basic carbonate of white lead	0.50	Water Paste
IV. Silica	2.5	"

These curves for relative energies are so plotted that the maxima have approximately the same heights. Inspection shows that a very fair degree of separation between short and long waves has been effected and that, each filter may be used to advantage in the region of maximum energy. In fact it is evident that, following this general mode of procedure, a filter for almost any desired spectral region may be produced.

The sharp drop of the curve for Silica (SiO_2) near 8 μ is due to the true absorption of this material; the same may be said for the sharp drop at 7 μ for basic carbonate white lead. In this connection it may be stated that the writer has on record a large number of "transmission" curves for films of powdered sulphates and carbonates spread on polished speculum. These curves reveal a great deal more complexity than do the curves obtained by reflection from polished crystals. The results will be published at a later date.

In carrying out precise measurements with an echelette grating, together with these new filters, it is essential that the slight effect of superposed orders, higher than the first, be taken into account. To accomplish this, it is neces-

⁵ The measurements of particle-size were kindly carried out by Mr. G. S. Haslam of the Research Laboratory of the New Jersey Zinc Co.

sary to procure a series of filters whose characteristics are exactly the reverse of those already described. To be specific, if the 4μ region be studied, it is necessary to procure a filter which is entirely opaque at 4μ and highly transparent at 2μ and at all shorter wave-lengths. Fortunately, this problem is relatively simple. As is well known, layers of water, glass, quartz, fluorite, etc., when given the proper thickness, can be made to fulfill the conditions imposed on this type of filter. In this connection it is to be stated that, if nonaqueous filters be desired in the region of the near infrared, corex glass and a urea-formaldehyde condensation product known as Pollapos, are very effective. Corex glass of 3.2 mm thickness is opaque at 3μ while Pollapos of 4.5 mm thickness transmits virtually nothing at 1.6μ . It is hardly necessary to add that the effectiveness of a powder-filter can be increased by choosing a light source such that the emission of shorter wave-lengths is suppressed while that of the longer ones is enhanced as, for example, in case of the Welsbach mantle.

This report is incomplete since specific direction for powder filters covering the entire range of the infrared are not available. It is felt, however, that having described the general mode of procedure, the individual investigator will be guided in the production of filters required for his special needs.

VELOCITY OF ULTRASONIC WAVES IN WATER VAPOR

BY GEORGE E. THOMPSON
IOWA STATE COLLEGE, AMES, IOWA

(Received May 22, 1930)

ABSTRACT

The velocity of sound waves having a frequency of 108,600 cycles per second, has been measured in water vapor by a method similar to that used by Pierce for other gases. At a temperature of 27° C. the velocity is 432 meters per second.

SOME results by Pierce¹ for the velocity of ultrasonic waves in air showed much less than the expected variation of velocity with change of humidity. This situation suggested the desirability of making similar measurements in pure water vapor, so the present work was undertaken. More recently Reid² found the effect due to humidity which was expected on the basis of theory. It still seemed worth while, however, to continue the work with water vapor along the line originally planned.

DESCRIPTION OF APPARATUS

The sound chamber consisted of a cylindrical brass tube of 9.5 cm inside diameter and 25 cm in length. A plane reflector about 9 cm in diameter was moved back and forth by the calibrated screw *S*. (See Fig. 1) In order to

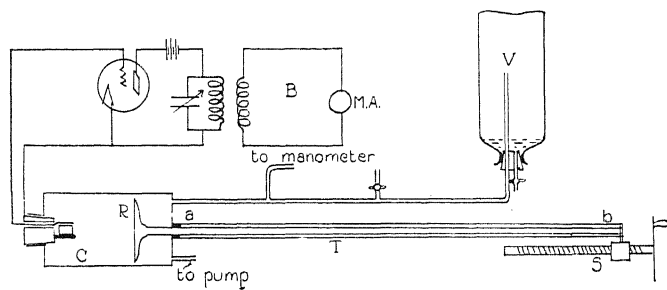


Fig. 1. Diagram of apparatus.

get an air tight joint at *a*, the rod carrying the reflector was enclosed in a rubber tube which was fastened to the sound chamber at *a* and to the rod at *b*. This arrangement permitted the reflector to be moved back and forth easily, the rubber being stretched or contracted to accommodate the motion of the rod. The rod was about 150 cm long. A spiral spring was placed around the rod and inside the rubber tube to keep the tube from gripping the rod when the pressure was reduced inside the chamber.

¹ G. W. Pierce, Proc. Am. Acad. of Arts and Sciences 60, No. 5 (1925).

² C. D. Reid, Phys. Rev. 35, 814 (1930).

The quartz crystal was mounted between electrodes on the end of a brass plug which was carefully ground to fit a tapered opening at the end of the chamber. The wire leading to the upper electrode of this crystal holder was insulated by filling the hole through which it passed with sealing wax. The lower electrode was not insulated from the plug so that connection to it was made by soldering a wire to the outside end of the plug.

The vapor was generated in a glass bottle *V* and pumped slowly through the chamber *C* during the course of the experiment. It was necessary to keep the pumps working continuously because the apparatus was not quite vacuum tight, the leak with the pump idle amounting to about one half centimeter of mercury pressure per hour.

The electrical circuit is fully shown in the figure and needs no detailed description. Instead of making observations on a d.c. meter placed in the plate circuit of the oscillator tube, a Weston, model 412, high frequency milliammeter (2 m.a. range) was placed in a resonant circuit which was coupled loosely with the oscillator. This circuit had a resistance of over 700 ohms and consequently tuned very broadly.

The temperature of the vapor was measured with a copper-constantan thermocouple placed in front of the crystal but above the direct path of the sound waves.

METHOD OF THE EXPERIMENT

Absolute measurement of velocity was not attempted. The velocity of the waves in air was assumed to be known and the velocity in the vapor determined by comparing the wave-length in vapor with the wave-length in air. In water vapor the crystal oscillations were somewhat irregular so that high precision of measurement could not be attained easily. Also the milliammeter fluctuations caused by the motion of the reflector were very slight due to the low density of the vapor. This difficulty was partly overcome by using a microscope to observe the movement of the pointer of the meter. In making measurements, the reflector was placed about 2.5 cm from the crystal face and at a position of minimum deflection, and the position read on the screw. Another position 20 half wave-lengths farther from the crystal was found and another reading taken. The settings were always made with the screw turning in the same direction.

SOURCE OF ERROR

It was considered likely that the greatest source of error would be the lack of purity of the vapor caused by air leakage. Consequently, extremely accurate measurement of temperature, pressure, frequency, and wave-length were not attempted.

In order that the wave-length be proportional to velocity the frequency of the crystal must not change when the nature of the surrounding gas is changed. A second oscillator was heterodyned with the crystal oscillator to give a beat note of about 200 cycles per second. Since no very appreciable change of pitch was produced by changing from air to water vapor, the frequency control was deemed satisfactory.

The screw was calibrated by comparison with a Gaertner comparator and found to be of sufficiently uniform pitch, the maximum variation from the average being about 0.009 mm. The average pitch was 2.509 mm.

RESULTS

The wave-length in air at 22°C was found to be 3.176 mm. Considering the velocity to be 345 meters per second, the frequency figures out to be about 108,600 cycles per second.

In Table I are values for the wave-length in water vapor. These are given in terms of the pitch of the screw and changed to mm after averaging.

TABLE I. *Wave-lengths in water vapor.* (Average, $1.586 \times 2.509 = 3.979$ mm, Vapor pressure, 1.4 cm of mercury, Temperature, 27°C).

1.581	1.585	1.566	1.597
1.610	1.605	1.591	1.600
1.593	1.567	1.588	1.588
1.576	1.572	1.597	1.572
1.575	1.576	1.604	1.572
1.588	1.596	1.578	

With the data of Table I, we get for the velocity of sound in water vapor at 27°C.

$$V = (3.979/3.176) \times 345 = 432 \text{ meters per second.}$$

Masson gives 401 meters per second as the velocity in water vapor at 0°C. Although no factor for temperature correction is available it seems that Masson's value is considerably below the value given above. Failure to provide air-free vapor for the determination would account for the low value. Since the effect of air in the vapor is to decrease the velocity, the largest value one can obtain for the velocity would presumably be most reliable.

With the value for the ratio of specific heats and density of water vapor given by Neyreneuf³ we get a theoretical value for the velocity of sound in water vapor at 27°C which is $V = 348(1.321/0.6143 \times 1.402)^{1/2} = 431$ meters per second. Neyreneuf's data were given for saturated vapor, whereas, the vapor pressure used in the present experiments was only slightly more than half that of saturated vapor. On the whole, the agreement is quite satisfactory, considering the errors involved in the measurement of the various quantities.

³ Neyreneuf, *Annals de chimie et de Physique* 9, 535, (1886).

UNRELIABILITY OF PHOTOGRAPHIC EMULSIONS ON GLASS
FOR RECORDING DISTANCES AND A METHOD
OF MINIMIZING THIS DEFECTBy D. COOKSEY AND C. D. COOKSEY
SLOANE PHYSICS LABORATORY, YALE UNIVERSITY

(Received May 19, 1930)

ABSTRACT

Superficial motions of double coated emulsions were investigated by Schlesinger's ink dot method. Also the positions of developed images with respect to corresponding latent images were studied for singly coated plates. Apparently *there are stresses in undeveloped gelatin emulsions that can be relieved* before plates are used for photographic purposes by soaking them in water followed by dehydration in alcohol, *thus greatly enhancing their reliability for recording distances*. This process we have termed *normalizing*. The maximum observed change in a distance between images, in their latent and developed states on a singly coated plate was 9μ without normalizing and 2.2μ with normalizing. The average change was likewise reduced to about one quarter. The advantage of normalizing is emphasized by the results reported in another paper.

MUCH effort has been expended in determining what reliance may be placed on photographic emulsions when used for recording the relative positions of star images and spectral lines. Many things affect the answer to this question. A very complete account of this subject, with bibliography, has been given by F. E. Ross.¹ Some years ago Professor Frank Schlesinger,² and recently E. Bäcklin,³ reached the conclusion that the position of a latent image is not appreciably altered in the processes of development. Schlesinger used a method of investigation in which artificial star images were produced on a photographic plate by spattering it with water-proof india ink. This plate was subjected to the ordinary developing, fixing and washing processes, except that the developing agent was omitted from the developer. The coordinates of a large number of ink dots were accurately determined before and after development. He reached the conclusion that any error due to distortion of the gelatin was negligible in comparison with the errors of measurement, and has since informed us that a subsequent unpublished investigation has led to the same conclusion.

During our work on the development of the "method of displacement" for measuring x-ray glancing-angles, we built and tested a specially designed spectrometer.⁴ The mechanical errors in this instrument and also the errors of manipulation were so small that they were negligible compared to the errors of measurement of distances between spectral images on photographic

¹ F. E. Ross, "The Physics of the Developed Photographic Image." Van Nostrand (1924).

² F. Schlesinger, Publications of the Allegheny Observatory, Vol. I, No. I.

³ E. Bäcklin, Inaugural Dissertation, Upsala (1928).

⁴ C. D. Cooksey and D. Cooksey, following paper. This issue.

plates. As this method is based partly on the assumption that the emulsion surfaces are plane and parallel, we decided to obtain plates more suitable for this purpose than those sold commercially. Through the kindness of Dr. C. E. K. Mees, the Research Laboratories of the Eastman Kodak Co. furnished us with "parallel plate" glass coated with a double thickness of x-ray emulsion. Several spectrograms of the $K\alpha_1$ line of silver were taken on these plates. Corresponding distances between images, which should have been constant to less than one micron, were found to differ between plates by as much as ten microns, a difference altogether too large to be accounted for by instrumental errors or those of measurement. In consequence, we were forced to suspect the constancy with which the position of a latent image is retained by its developed image, at least in the case of these double coated plates.

To investigate this, we adopted a modification of Professor Schlesinger's method. Plates were cut in strips 25 cm long and 3.4 cm wide (the size used for spectrograms) and spattered with water-proof india ink along their longer center-lines. The distances between ink dots were measured on a carefully calibrated Gaertner measuring engine, which is fully discussed in another paper.⁴ The errors of the screw, bearings and divided head were eliminated by always using exactly the same portion of the screw for the remeasurement of a given distance. The screw coördinate of each edge of each selected ink dot was determined three times. From the mean of these three determinations the distance between dot centers was obtained. The plates were measured before and after they were subjected to various soakings, dryings and development. The so-called developer used contained sodium sulphite, sodium carbonate and potassium bromide in the usual proportions, but no developing agent. The fixing bath contained sodium thiosulphate, sodium sulphite and acetic acid, but no alum or other hardener.

Preliminary investigations showed, as others had previously found, that the reliability of the gelatin was very dependent on the method of drying after development and washing. The essential factor in drying is that it shall take place uniformly. This condition is approached when the water is displaced from the gelatin by immersing the plate in strong ethyl alcohol; but as the alcohol will displace more water than is normally contained in the gelatin, the plate, if exposed to dry air, will become cloudy as the alcohol evaporates. This may be completely overcome by evaporating the alcohol in a humid atmosphere such as that in a box lined with wet blotting paper. As this part of the work was done in the summer, when the humidity is high, it was unnecessary to take this precaution. Furthermore we were led to believe that there were superficial longitudinal stresses in this gelatin, introduced while the emulsion was cooling during the process of manufacture. In order to relieve these stresses, plates were soaked in water for thirty minutes, dried in alcohol for twenty minutes and finally left to attain equilibrium in a humid atmosphere. This process, as applied to fresh plates, we have termed *normalizing*.

The accuracy of the measurements can be estimated from the following

data. The average variation of one setting from the mean of three settings on a given dot edge, obtained from 282 settings on 39 ink dots, was 0.19μ before, and 0.14μ after development, with a maximum variation from the mean of 0.7μ and 0.6μ respectively. The difference in accuracy is due to the difference in illumination before and after the silver salts had been removed. Eighteen distances on a developed plate, varying from 0.01 to 60 mm in length, were remeasured according to the above procedure on three different days during the course of a week. The average of the differences of these three determinations from their means was 0.09μ with a maximum variation of 0.3μ . Table I gives changes observed in distances between ink dots on a series of seven plates, measured before and after the plates were subjected to the treatments specified.

TABLE I. Comparison of changes in distance between ink dots on double coated plates resulting from various treatments.

measurement	Treatment before remeasurement ¹	No. of distances	Maximum change, μ	Average change, μ
None	developed and dried without alcohol	3	3.7	2.5
None	any wetting process and dried with alcohol	3	4.1	1.8
Wetted and dried with alcohol	wetted and dried with alcohol again	45	0.8	0.32
None	normalized	22	4.9	1.35
Normalized	developed and dried with alcohol	36	0.8	0.3

(By "developed" is meant 5 minutes and 20 minutes respectively in the developer and fixing bath described above, and 30 minutes in running water.)

These results seem to indicate that normalizing relieved stresses, thereby reducing the average relative displacements on development to about one-fifth. They lead to no conclusions as to the motions that may occur at the glass-gelatin surface or in intermediate layers. In connection with these results, Dr. Mees pointed out that certain precautions used in the manufacture of commercial plates were omitted by the Research Laboratory in preparing these double coated plates for our use.

In order to determine the reliability of the position of a developed image with respect to that of its latent image, the work was continued as follows. We constructed a template, about 78 mm long and 17 mm thick, of steel with ends lapped plane and parallel. Two parallel slits at a fixed distance apart were formed by bolting similarly prepared blocks to the ends of the template, the width of opening of the slits being adjusted to less than 0.02 mm by shims. By allowing x-rays to pass through the slits onto a photographic plate clamped to the template, very sharp-edged lines were obtained. Thirteen strips 3.4 cm wide were cut parallel to the 5 inch side of four 5×7 Eastman Universal plates taken from the same box. The emulsion of these plates is about 0.025 mm thick. The template, or rather the slits which terminated it, was photographed with x-rays approximately centered on ten of these strips. All thirteen strips were then normalized and the template rephoto-

graphed on nine of the strips, including, of course, some of those already bearing latent images. The strips were finally all developed in "Eastman X-ray Developer," fixed and washed. After washing they were soaked in strong alcohol for about 10 minutes and then dried in a humid atmosphere. The results of the measurements on the developed images are given in Table II.

TABLE II. *Comparison of reliability of normalized and unnormalized singly coated plates.*

	Unnormalized	Normalized
Number of distances measured	10	9
Maximum difference in lengths measured	9.0 μ	2.2 μ
Average difference from the mean	2.8 μ	0.7 μ
Probable error of one determination	$\pm 2.2\mu$	$\pm 0.5\mu$

As all these plates were handled in the same manner and subject to the same uncertainties of measurement, it is obvious that the *reliability of a photographic plate as a recorder of definite distances is greatly enhanced by the normalizing process*. However, by taking proper precautions during the process of manufacture, it might be possible to avoid the introduction of these stresses here relieved by normalizing. The fact that local stresses, due to non-homogeneity or other causes, may exist in gelatin, and do cause shifts of images by as much as 2μ is thoroughly treated by Ross. However, he states that 2μ is the maximum shift to be expected. We wish to call particular attention to the fact that we have found occasional motions as large as 9μ which occurred due to the relief of stresses existing in singly-coated commercial plates, and that if such stresses are not relieved before such a plate is used, it will not be reliable for positional recording. It would therefore seem to us advisable to subject plates to a normalizing process when they are intended for use in recording unique occurrences, such as eclipses, if intervals between images are of prime importance. Even when images may be recorded on many plates, given that the resulting definition permits of measurement to less than 2μ , normalizing will increase the self-consistency of measurements between plates in proportion to the accuracy of the individual measurements, as long as other causes of variation do not enter, such as pressure shifts of spectral lines, etc. This statement is, we hope, clearly verified by Table XI of another paper.⁴ It might not be amiss here to emphasize a point clearly demonstrated by Ross (page 197)¹ but contrary to what has been commonly assumed as an excuse for variations of measurements; viz., the non-uniformity of image contours. Our experience, in common with Ross's, is that well filled, sharply outlined images are just as liable to a shift as their "moth-eaten" relatives.

The particular object of this investigation was to determine a reliable method of handling spectrograms of sensibly the same dimensions as used by us in determining glancing-angles. During the course of the work we made certain observations which we did not feel called upon to verify because the normalizing process and subsequent drying with alcohol proved satisfactory for our purpose. However, we shall suggest conclusions which may be drawn

from them in the hope that they may be of interest. The edge-effects referred to by Ross and others have been reproduced by us, both with ink dots and developed images. The motions referred to in our tables are not due to edge effects, but frequently occur in the central region of the strips within a length of two or three millimeters. We found that we could control at will the direction of motion of an image by removing a strip of gelatin parallel to the image and at a distance of one centimeter or less from it. The evidence thus obtained, although not conclusive, indicated a compound effect made up of two independent causes; one, the diffusion of silver grains away from the drying edge* ("hydration gradient," cf. Ross), and the other, a contraction of the gelatin causing a bodily shift of the matrix toward the dried edge. It is believed that the former of these causes might readily change the scale of a photograph, in the region drying last, when alcohol is not used for dehydration.

We have been informed that gelatin, with or without the silver halides, normally contains about 15% water. One attempt was made to do away with the necessity of evaporating in a humid atmosphere by using about 75% alcohol. The resulting plate was free from clouding, but large stresses persisted in the gelatin. We therefore were content with the successful technique which employed the use of ethyl alcohol, at least 90% pure, and evaporation in a humid atmosphere. As the surface tension of alcohol is low, dirt specks adhere to the gelatin. Consequently all dust particles should be removed before the plate is placed in the alcohol, which in turn must be dust free. Although the plates used were soaked face up, we would suggest immersing them horizontally face down. If a plate is immersed standing in an approximately vertical plane, the gelatin will dry with ridges across its surface as though the displaced water had flowed down in tiny rivulets. The alcohol was evaporated with the plates in a plane making 45° with the horizontal, gelatin side up, and resting diagonally on one corner. However, we found no evidence to show that the drying position made any difference on alcohol soaked plates.

In conclusion we wish to express our indebtedness to Professor Frank Schlesinger and to the late Professor B. B. Boltwood for helpful suggestions in connection with this investigation. We are also indebted to Professors McKeehan and Uhler for advice in connection with the presentation of this work.

* Dr. Mees informed us that silver grains would diffuse into the region more highly saturated with water.

PRECISION MEASUREMENTS OF THE GLANCING-ANGLE OF REFLECTION FROM CALCITE FOR SILVER ($K\alpha_1$) X-RAYS BY THE "METHOD OF DISPLACEMENT."¹

BY C. D. COOKSEY AND D. COOKSEY
SLOANE PHYSICS LABORATORY, YALE UNIVERSITY

ABSTRACT

Part I. Method of displacement.—This method permits the determination of glancing-angles in terms of *linear measurements only*. It consists in letting a properly limited beam of x-rays, after reflection, fall on a photographic plate placed successively in two parallel positions which differ in distance from the crystal by a known amount. The theory of the method and its practical application to the present case are briefly discussed with references to Uhler's paper.

Part II. Apparatus and Adjustments.—A new high precision spectrometer, including a specially designed bearing on which the crystal rotates and a unique form of plate holder using air pressure to ensure the flatness of the photographic plate, is fully described. A *special* form of hot filament *cathode* which gives an approximately *linear source* of x-rays has been originated. Precision methods for adjusting and testing the reliability of the instrument are discussed at length. It is believed that the instrument is free from any defects that might cause a constant error of as much as 0.04" in the glancing-angle.

Part III. Experimental procedure.—The cleavage planes of a nearly perfect specimen of Iceland spar were used as grating. The bearing of its perfection on the widths of the spectral images is discussed. *The coefficient of expansion of calcite* normal to the cleavage planes was computed from the most reliable data obtainable. A mean value which is sufficiently precise, over a sixteen degree range, to reduce values of glancing-angles to 18°C within 0.008" is $1.02_3(10)^{-5}$ per °C. Attention is called to the fact that the commonly used value $1.04(10)^{-5}$ is not a sufficient approximation.

Distances between spectral images on each negative were measured on a Gaertner measuring engine, the errors of which were carefully investigated. The "displacements" of the photographic plate were equal to fixed intervals marked on a measuring bar and calibrated against the screw of the same measuring engine. The accuracy of these measurements and the effect of their errors on the glancing-angle are discussed.

The experimental procedure and precautions used in taking and measuring spectrograms are fully described. A complete protocol of observations is given for one plate. Evidence for the accuracy of the measurements is presented and discussed.

Part IV. Results.—The weighted mean value of the glancing-angle for the $K\alpha_1$ -line of silver from the cleavage planes of calcite at 18°C is $5^\circ 17' 13.81'' \pm 0.06''$ giving a wave-length, if $\log 2d_{18} = 0.7823350$, of 0.558238Å. This result is compared with those of other observers. It differs from Kellström's value quoted by the Int. Crit. Tables by more than ten times the combined probable errors. The only probable source of an adequate constant error in either result seems to lie in the crystal. Compton's measurements of the density of calcite are invoked to prove that different specimens of Iceland spar do differ enough in density to account for more than the discrepancy, if changes in density and grating space are interdependent.

¹ The final numerical results published in this paper have already been given by us in a letter to the Phys. Rev. [2] 35, 564 (1930) and Nature 125, 461 (1930).

PART I. THEORY OF THE METHOD OF DISPLACEMENT

VERY precise methods have been developed for measuring the glancing-angles at which characteristic x-rays are reflected by a crystal. In most cases where the highest precision has been attained, the results are based on measurements with a divided circle. In 1917 H. S. Uhler,² of this laboratory, suggested the so-called "Method of Displacement," by which glancing-angles are computed from linear measurements only. The method was given a preliminary trial, at the time, by Uhler and one of us³ and gave results of greater accuracy than any hitherto reported. The present work was undertaken for the purpose of developing this method to the high degree of precision of which it seemed capable. Unforeseen difficulties delayed the work until divided circle methods had been developed to give a precision that we could not expect to surpass. However, glancing-angles are of such importance that, it seemed to us, their values should be checked by an independent method of equal reliability, and therefore the work was continued.

The method is a photographic one and "consists in taking one exposure when the plate is at a certain distance from the crystal and then a second exposure when it is at a different distance from the reflector. The displacement of the spectral image, corresponding to some one wave-length, is a function of the distance through which the plate has been *translated* parallel to the collimation line. The form of the function and the details of the calculation of the glancing-angle depend respectively upon the value of the constant angle between the normal to the plate and the collimation line, and upon whether the measurements are absolute or are based upon adjacent images pertaining to known wave-lengths. The interval of translation may be determined with ease and great accuracy, whereas only an approximate value of the distance between the plate and the axis of rotation is required in any case."² It involves the fundamental assumption that the plate, in each of its chosen positions, intersects a region of the reflected beam in which the intensity is symmetrically distributed about a line which makes an angle with the axis of the incident beam equal to twice the glancing-angle. Such a region can be obtained approximately, in the case of a *perfectly selective* reflector, if the incident beam completely fills, and is limited by, two narrow slits whose long axes are parallel to the axis of rotation of the reflector; provided that the aperture of the beam in the plane of the long axes of the slits is sufficiently limited. The region then lies between the Bragg foci of the two slits. The condition that the reflector be *perfectly selective* is not fulfilled by real crystals, but it will be shown later that the crystal used in the present work reflected a beam of the required symmetry.

The function by which the glancing-angle can be computed from the measured data is easily derived from the geometry of Fig. 1. This figure is drawn in a plane which is perpendicular to the mutually parallel long axes of slits S_1 and S_2 , axis of rotation and reflecting planes of the crystal. For simplicity the axis of rotation is assumed to intersect the line of centers of

² H. S. Uhler, Phys. Rev. [2] 11, 1 (1918).

³ H. S. Uhler and C. D. Cooksey, Phys. Rev. [2] 10, 645 (1917).

the slits and to lie in the mean reflecting plane of the crystal, but the final result is independent of these assumptions. O is the point of intersection of the axis of rotation with the axis of the incident beam XX' . ORR' and OLL' represent reflected rays on either side of the direct beam and inclined to it at twice the Bragg angle of reflection, θ . LR and $L'R'$ are the parallel traces of the photographic plate in its two positions and intersecting the reflected rays at the points L, R and L', R' between the Bragg foci of the slits. The central ray, XX' , intersects the plate at the points C and C' and makes the angle ω with the normal to the plate, OPP' . The dotted lines LL'' and RR'' are drawn parallel to XX' .

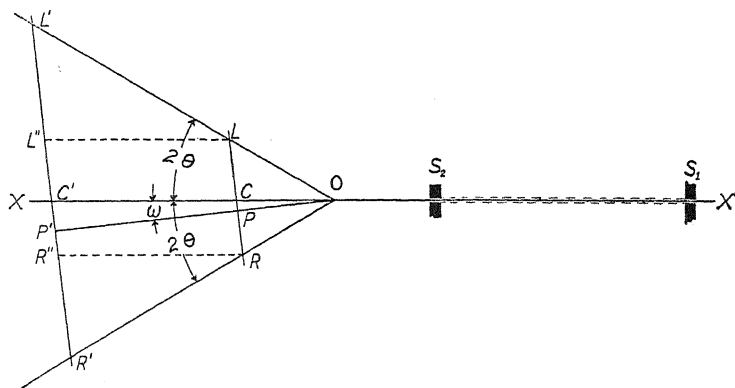


Fig. 1. Geometry of the "Method of Displacement."

If $x \equiv R'R''$, $y \equiv L'L''$, and $D \equiv CC'$, the angles θ and ω are given by

$$\tan 2\theta = \frac{2xy}{D(x+y)} \left[1 - \frac{D^2(y-x)^2}{4x^2y^2} \right]^{1/2} \quad (1)$$

$$\sin \omega = \frac{D(y-x)}{2xy} \quad (2)$$

If the plate is translated in the direction XX' , the quantities x and y are respectively equal to the distances between corresponding spectral images on each side of the image of the direct beam, and D is the distance the plate has been displaced. But if the direction of translation is inclined to XX' , the images of the undeviated beam taken in the two positions of the plate will not be superposed, and their separation must be measured and used in computing x and y from the separation of the spectral images. It is not difficult, in practice, to make this inclination so small that D may be taken as the distance the plate has been displaced in its line of motion without sensible error, but a corrected value of D can always be computed from this distance and the separation of the central images.

The quantity within the brackets in Eq. (1) is $\cos^2 \omega$, and therefore this term has very little effect on the value of θ , if ω is small. For small values of ω , the effect of this factor will be a maximum for glancing angles in the

neighborhood of $22^\circ 5'$. Even if ω is as great as $3.5'$, the omission of $\cos^2 \omega$ only causes an error of $0.03''$ at such glancing-angles, and at 5° , the region under investigation, the error is only $0.01''$. When $\cos \omega$ and the central image displacement can both be neglected, the glancing-angle may be computed with sufficient accuracy from

$$\tan 2\theta = \frac{L'R' - LR}{2D}. \quad (3)$$

Thus the result depends on the measurement of intervals— LR and $L'R'$ —each of which separates spectral images taken with the plate in a single position. This is an advantage if the spectral images corresponding to different positions of the plate have not the same width, and it is desired to use parallel hairs in the eye-piece of the measuring microscope.

A very full discussion of the geometry of image formation as applied to plane space-gratings, treated as perfectly selective reflectors, is to be found in Uhler's paper.² We therefore omit a detailed consideration of the effects of extreme rays and of inaccuracies in adjustment, and will merely cite these effects and the precautions taken to eliminate them in a later part of this paper.

PART II. APPARATUS AND ADJUSTMENTS

The work was begun on an apparatus, designed by one of us,⁴ but the results obtained lacked the accuracy of which the method was capable. Investigation showed the following defects: the apparatus as a whole was not sufficiently rigid; the plate-holder did not make the photographic plate flat and could not be displaced without fortuitous rotations; various parts of the apparatus were subject to distortion by small changes of temperature; and the axis about which the crystal rotated was indefinite. It was decided to build a new spectrometer which would be subject in use to no distortions causing a motion of one part relative to another of as much as 0.25μ . We are deeply indebted to Mr. Paul M. Mueller, then in charge of the Gauge Department of the Pratt and Whitney Machine Tool Co. of Hartford, Conn., for the design of a new spectrometer and plate-holder, which were built by that company under his constant supervision. The bearing for rotating the crystal was designed by him, and the unique form of plate-holder finally adopted was his original idea. We are also grateful to the Pratt and Whitney Co. for their very careful construction of the instrument.

Fig. 2 shows a view of the essential parts of the apparatus as set up for taking spectrograms. It is a tracing made from a photograph, and the wooden measuring stick, one-half meter long and divided in centimeters, fastened to base A, shows the scale in one direction. The radius of the divided circle table L is 13 cm, and the webbing of the castings varies in thickness from 1 to 1.5 cm. The whole assemblage weighs about 200 kg and rests on a stone-topped brick pier.

The primary base A is a standard Pratt and Whitney measuring engine bed, made of cast iron and aged by exposure to the weather for several years,

⁴ C. D. Cooksey, *Phys. Rev.* [2] **16**, 305 (1920).

after having been machined. The maximum vertical depth of the casting is 25 cm. The upper surface is 146 cm long and consists of two parallel ways or rails separated by a *T*-slot. The farther way is flat; the nearer is, in cross-section, an inverted 90° "V", truncated. After strains had been relieved by aging, the ways were scraped straight to conform to a "master." This base is supported on three leveling screws, furnished with lock nuts, one of which is near the forward end and directly under the center line between the ways. The bracket *M* which carries the forward slit S_1 fits the track and, when in use, is locked directly over this foot.

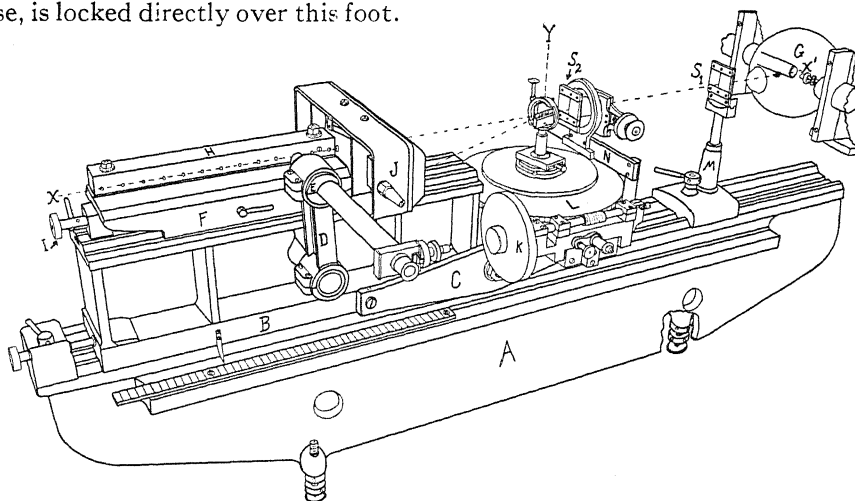


Fig. 2. Spectrometer assemblage.

The secondary base *B* is an iron casting in the form of an "I" beam, reinforced with heavy vertical cross webs. It is 56 cm long, 11.5 cm wide at top and bottom, and 16.5 cm high. The bottom surface was machined and scraped to fit the rails of base *A* accurately, so that *B* may be considered an integral part of *A* when locked in place. Thus, any bending stress due to a load on *B* will be resisted by a section of cast iron 41.5 cm deep. The position of *B* relative to *A* may be adjusted and fixed by means of the screw and clamp shown at the left of *B*. The upper surface of *B* consists of a track, a vertical cross-section of which is shown in Fig. 3.* The straightness and rigid-

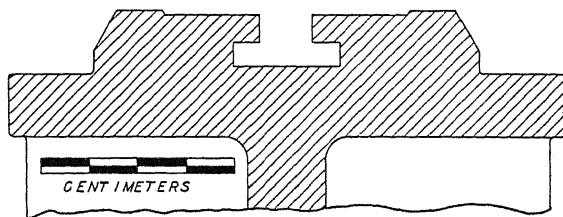


Fig. 3. Cross-section of ways on base *B*.

* Ways of this type were chosen because they have a vertical axis of symmetry and therefore permit the reversal of the "master" during the process of scraping the ways straight.

ity of these ways are essential to the success of the displacement method, as it is along them that the plate-holder carriage is moved. The scraping of the bearing surfaces of this track was done with extreme care. When assembled the track on *B* is very nearly parallel to that on *A*.

The plate-holder carriage *F* (the forward end of which is also shown in Fig. 4) rests on the track on *B*. It has bearing surfaces 15.5 cm long which were scraped to fit this track with great accuracy. It is provided with a slow motion adjusting screw *I*, and may be locked in position by a clamp operated by a level seen just to the right of the letter *F*. A portion of its upper surface was scraped flat and in the assemblage is parallel to the upper surfaces of the track on *B*, and serves as a seat for the measuring bar *H*. The forward end of the carriage is a vertical "goose-neck" having a horizontal hardened steel plate bolted to it. This plate has a "V" groove milled across its upper surface and serves as a support for the plate-holder *J*. The carriage with the bar and plate-holder weighs 15.1 kg.

H is a standard 12 in. Pratt and Whitney steel measuring bar, adapted for our use. The lower and back surfaces are scraped flat. In the front surface are thirteen hardened steel plugs with their outer ends ground and polished so that their surfaces lie all in one plane, parallel to the opposite surface of the bar. The plugs are numbered from left to right, beginning with zero and each has a very fine line, ruled with a diamond. The lines are accurately parallel and are approximately perpendicular to the lower surface of the bar. The distances between successive rulings are very accurately 1 "U. S. inch" each. The bar is held in place on the carriage by a tapered dowel pin which fits in a reamed hole at the left end of the bar. Two horizontal set screws (one of which is shown at *V* in Fig. 4) near the right hand end of the bar bear against a stud in the carriage which passes through an oversized hole in the bar. This permits the adjustment of the plane of the ruled plug surfaces parallel to the line of motion of the carriage.

The axis marked *XX'* in Figs. 1, 2, and 4 is defined as a line parallel to the line of motion of *F* and intersecting *Y*, the axis of rotation of the crystal, at the fixed elevation of the center of the slit *S*₂.

The microscope bracket *D* clamps to a short hollow cylinder which is bolted to a scraped surface on the central web of base *B*. The microscope is clamped in an eccentric collar *E* in the upper end of the bracket, and can be adjusted to any desired position. It is of 75-power and has a micrometer eye-piece. The movable reference lines ("crosshairs") are two fine diamond rulings on a glass plate and intersect at an angle of one radian. When the microscope is in proper adjustment the bisector of this angle is parallel to the vertical fiducial lines on the plugs of the measuring bar. An axial illuminator can be mounted on the forward end of the objective housing.

The bearing mechanism for rotating the crystal, and the slit *S*₂, are supported on a base which somewhat resembles a sled, the two runners of which embrace the lower edges of the base *B*. The nearer of these runners is shown in Fig. 2 and is labeled *C*. This base can rotate about an accurately fitting horizontal trunion bolt which passes transversely through the runners and *B*.

The lock nut and washers of the nearer end of this trunion are partly visible behind the wheel *K*. The base is adjusted and locked in position by means of two set screws in the left hand end of each runner; they bear against studs screwed into *B* through oversized holes in the runners. This mounting is thus a sort of cantilever and permits a necessary adjustment of the axis of rotation of the crystal with respect to the rest of the instrument.

Two vertical posts, one of which is shown, bolt to the forward end of the sled and have bolted to their upper ends a steel cross piece *N*, which in turn carries the adjustable mounting for the slit *S*₂. In the center of the sled is a scraped seat, with a large hole bored through it, to which is bolted the bearing for rotating the crystal.

The parts *B*, *C*, *D*, *F*, *J*, and *M* are made of cast iron. After being machined, but before the final finishing was done, they were artificially aged. The aging process was apparently effective, for none of the parts has shown any noticeable warping during several years.

A section of the plate-holder *J* in a plane parallel to that of *XY* is shown at (a) in Fig. 4 in position on the carriage *F*, and in perspective with the cover partly removed at (b). The holder is supported and positioned by two cone-pointed bolts, one of which is shown at *T*, and the round-ended screw *U*. The cone points fit in the slot milled across the steel plate which is bolted to *F*, and the screw *U* bears against a plane surface milled on *F*. The cone of one of the bolts is not coaxial with the bolt, thus permitting a small rotation of the plate-holder about a vertical axis. Adjustment about the line of the slot is made with the screw *U*. The center of gravity of the plate-holder is far enough forward of the screws *T* to keep the holder in position when the carriage is moved. The plate-holder is so compact that the distance from the center of the plate to the surface of the track below is only about 5.5 cm.

The plate-holder is of special design to ensure the flatness of the sensitized surface of the photographic plate. This surface is forced against two parallel flat surfaces on the cover, just to the left of *OO*, by thin walled rubber tubes *RR'* inflated with air at about two atmospheres pressure. The two surfaces *OO* are an integral part of a sufficiently large body of cast iron to prevent bending under this stress.

The cover of the plate-holder is one casting in the form of two *V*-sections joined together at both ends; these are reenforced by seven cross webs on each side, which terminate in bosses through which the fourteen screws *QQ* hold the cover to the back. Each of the *V*-sections is of the nature of a cantilever, such that the pressure on the surfaces *OO* causes a tension in the screws *QQ* and a pressure across the surfaces of contact between the cover and back of the plate-holder at *PP*. The back of the plate-holder offers about five centimeters depth of cast iron to resist both these stresses. The opposing surfaces of the cover and back, as well as the surfaces *OO*, were scraped plane to a high degree of precision. It had been the original intention of the designer to finish these surfaces by lapping, but it was feared that the slight peening action of the abrasive would only warp them. The edges of the sur-

faces were left sharp so that in working the two parts of the holder into contact dust particles would be removed.

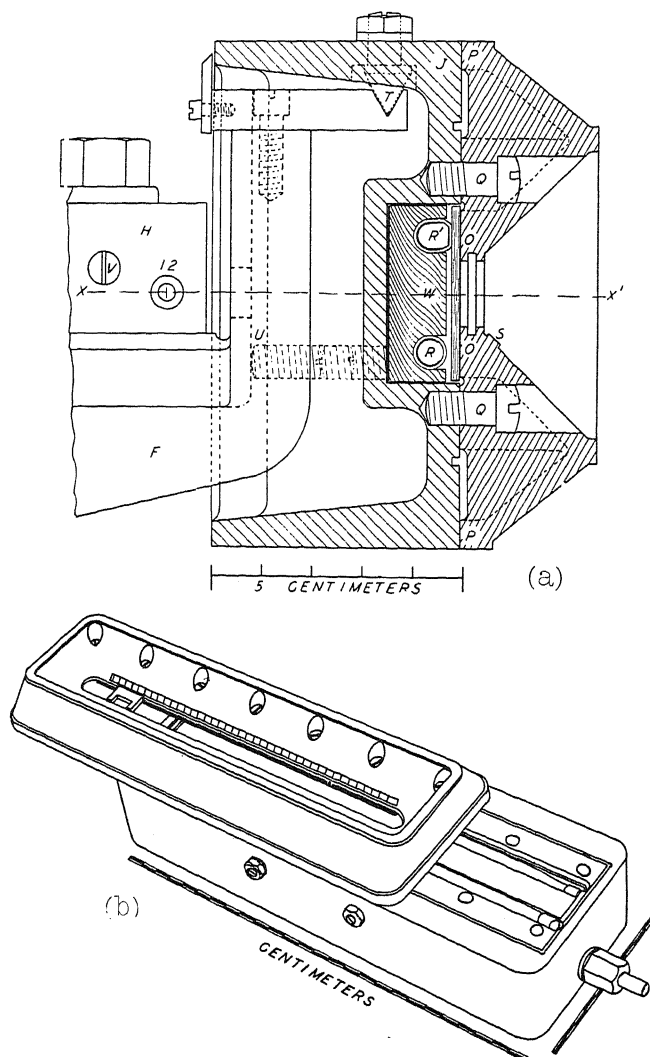


Fig. 4. Cross-section and perspective of plate-holder.

A strip of black paper, fitted into slots in the V-sections, covers the opening between the sections and serves as a light seal. A centimeter scale, ruled on the surface *S* along one side of the opening, facilitates the positioning of a lead screen when it is desired to shield a portion of the plate from x-rays. The photographic plates were cut in strips 25 cm long and 3.4 cm wide, dimensions such that the extreme edges of the strips extended slightly beyond the boundaries of the surfaces *OO*. This was to prevent irregularities in the edges of the gelatin from interfering with the proper seating of the plate.

The mahogany strip *W*, backed by a piece of velvet, and having two longitudinal grooves 6 mm wide milled in its front, affords support for the rubber tubes and distributes the pressure in them uniformly to the back of the plate-holder. The portions of the rubber tubes which press against the photographic plate are thinner than the remainder. We are indebted to Mr. G. W. Patterson of the Seamless Rubber Co. of this city for these tubes. Air is admitted to the tubes through a nozzle shown just below the letter *J*, Fig. 2. The tube *R'* is shown inflated in the section. When the tubes are deflated. There is ample clearance between the plate and the surfaces *OO* to prevent scratching of the gelatin while the cover is being worked into place. The plate-holder assemblage weighs 5.6 kg.

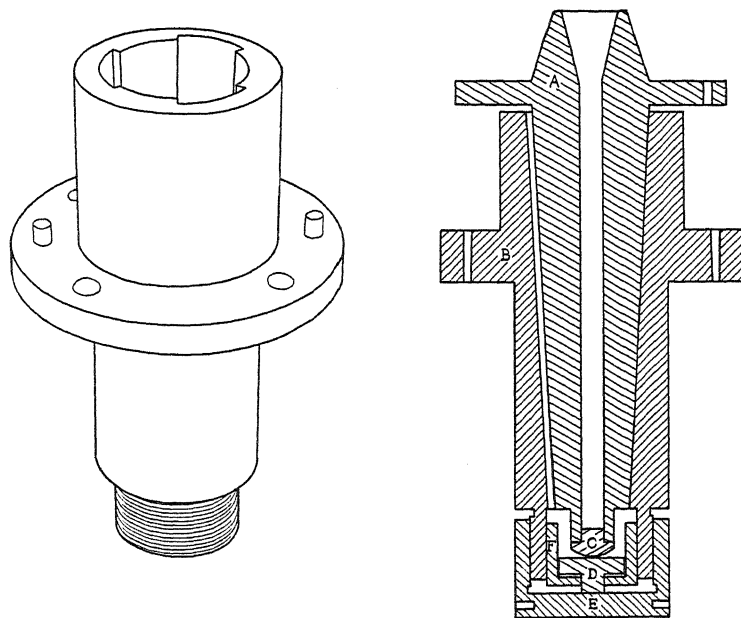


Fig. 5. Cone bearing.

The cone bearing for rotating the crystal is shown in Fig. 5. The flange on the seasoned cast iron sleeve *B* was scraped to fit its supporting seat on base *C*, Fig. 2, and the sleeve passes through the hole in this seat. The steel spindle *A* is a right circular cone supported by a hardened steel foot *C*; the lower surface of *C* is spherical and rests on the upper plane surface of *D*, also of hardened steel. The lower part of *D* is a stud which fits tightly in the sleeve *F*, and the latter has a sliding fit in *B* and a long enough bearing to keep *D* from rocking. The stud rests on the screw cap *E*, which is threaded to *B* with a fine thread and serves to adjust the bearing. By using a long tommy in the holes provided in *E*, the spindle and all its superstructure can easily be raised by as little as 2.5μ at a time. As the tangent of the semi-apical angle of the cone is slightly less than 0.06, an accurate means is at hand for adjusting the oil film separating the surfaces of *A* and *B* to the minimum thickness required for

lubrication. If this adjustment was correctly made at one angular position of the cone, it was found to be correct for all others, showing that the cone and its bearing fitted accurately. This corroborated what had already been inferred from the usual test with prussian blue. When the spindle was properly adjusted, a diminution in the thickness of the oil film of 0.3μ would cause the oil to cease acting as a lubricant. Therefore the cone may be considered to rotate in B about a practically *fixed* axis.

An essential feature of the design of the sleeve B is that portions of its bearing surfaces are relieved to insure the proper distribution of the oil and to prevent particles of foreign matter from getting between the bearing surfaces. This is done by removing one half the bearing area of B by three grooves, similar to rifling, but running parallel to the elements of the cone. The edges of these grooves were left sharp. This bearing was originally set up four years ago with "3 in 1" oil for lubricant, and the above tests and adjustment made. Since that time, no oil has been added, nor has any adjustment been found necessary by later tests. The oil shows no sign of having evaporated, or of becoming sticky after lying idle for six months at a stretch. It is doubtful if expensive watch oil would have been more satisfactory. If such a bearing was being built for continuous use, it would be well to replace the steel bearing surface of D by one of agate.

The spindle A is bolted to the divided circle table L , Fig. 2, and can be rotated by a tangent screw, the divided head of which appears at K in the figure. Screwed to the upper surface of this table and coaxial with it, is a circular brass plate with three radial slots 120° apart which serve to position the crystal holder or an auxiliary slit.

The bilateral slits, S_1 and S_2 , have gold jaws 2.4 mm thick, 2.5 mm wide, and 1 cm high, inserted in brass plates which slide in dovetails on the slit frames. The opposing surfaces of the jaws were carefully scraped flat. The slit widths can be varied by means of cams acting above their centers; but during the taking of spectrograms one jaw of each slit is held in place by two dowel pins, and the other jaw is clamped tight against platinum shims placed between the opposing surfaces above and below the limited portion of the slit used. The slit S_2 is at a fixed height above the supporting bar N , but S_1 can be raised or lowered. Both slits can be rotated about horizontal axes through their centers and about vertical axes, and can be translated at right angles to the plane XY .

The crystal holder assemblage is shown mounted on the table L . Its base is a brass disk with three cone feet which fit the slots provided for it. On this base is mounted a rectangular plate with lateral adjustment. The plate supports, in a vertical sleeve with locking set screw, a sliding post which carries at its upper end the outer of a pair of coaxial cylinders. The inner cylinder can be rotated with respect to the outer by a tangent screw. The crystal is fixed by soft wax with its working face against the surface of a slotted brass plate, which bolts inside the inner cylinder in such a manner that the axis of the latter lies approximately in the face of the crystal. Thus, the lateral and rotational adjustments of the crystal are independent. The

crystal holder can be replaced by an auxiliary slit (not shown) later referred to as S_3 . The latter is so adjusted that, when in place, its long axis coincides with the axis of rotation Y , and the plane through its upper corners contains the axis XX' .

The x-ray tube is mounted on a bakelite stand in a rectangular box of 5 mm lead sheet. The box is supported on two pieces of channel steel 31 cm deep which rest on the same pier as the spectrometer. The tube used in these experiments was entirely constructed in this laboratory and was of Coolidge type with 15 cm bulb. The target was a button of silver welded, to insure good thermal contact, to a water-cooled copper anode. The x-rays were taken at an angle of about 3.5° to the plane of the target. The cathode, heated by current from a storage battery, was designed to bring the cathode rays to an approximately line focus on the target. With this in view, the filament was wound in a spiral groove on a tapered mandrel, just as for a fine focus Coolidge filament; but, instead of being annealed between spherical surfaces, it was placed between cylindrical surfaces of 19 mm radius during annealing. This gave a focal spot on the target which was longer in one direction than in a direction at right angles; but, due to the magnetic field of the heating current, its long axis was inclined at an angle (roughly 45°) to the axis of the cylindrical filament. This is a drawback if it is desired to change the strength of the filament current after the tube has once been aligned with respect to the spectrometer. We hope to overcome this difficulty by the use of a non-inductive filament. Such a filament should have a greater thermionic emission at its center, owing to the elimination of the center lead, and should give an excellent focal spot distribution. We have succeeded in winding such a double filament, but have not had an opportunity to mount and try it.

The cooling water was circulated by a pump through a Ford automobile radiator and its temperature measured just before and just after passing through the anode. By regulating the speed of a fan blowing on the radiator, the temperature, and therefore the length of the anode could be held constant, thus keeping the focal spot on the line through the narrow slits used.

The source of potential for the tube was a 10 K.V.A. transformer connected to the 220 volt, 60 cycle, city supply. It was controlled by a variable inductive reactance in the primary and had a mechanical rectifier in the secondary, utilizing about one half of each side of the wave.

For precision measurements with the above described apparatus, it is essential that the plate-holder, when the carriage F is moved along its ways, should have rectilinear motion only; and that there should be no appreciable motion of the microscope relative to the crystal. It is also important to have the planes of the opposing faces of the slit jaws parallel to the plane XY , and the reflecting planes of the crystal approximately parallel to the axis of rotation. These adjustments were made with the aid of several steel mirrors of different thickness, each having two opposite reflecting surfaces accurately plane and parallel; and an auto-collimating device for detecting and measuring any rotation of the mirrors. The auto-collimator consisted of a 43 cm focal length objective with illuminated cross-hairs in its focal plane. The

90° cross-hairs, together with their reflected image, were viewed with a 20-power micrometer microscope. The sensitivity of this arrangement was 7, micrometer divisions per second of rotation of the mirror, and one-third of this rotation could be detected. For detecting small motions of one part of the spectrometer relative to another, two steel balls were fastened to one part, a third ball to another, and on a glass or hardened steel plate resting on these three balls was mounted a mirror facing the auto-collimator. When the balls bore on hardened surfaces, scrupulously clean, a relative motion of 0.01μ could be detected by this device.

Making use of this tilting mirror, it was found that the largest relative motion between the spectrometer microscope and the axis Y , due to moving the carriage F with the plate-holder along the ways, was the entirely negligible amount of 0.06μ . The carriage, when displaced the full length of the ways, rotated about horizontal and vertical axes perpendicular to its line of motion by the insignificant amounts of one and two seconds respectively, as measured with the auto-collimator. A sensitive spirit level showed no greater rotation about its line of motion.

These tests having been made, the sled C was adjusted, with the aid of the auto-collimator and mirrors until the Y -axis was perpendicular to XX' . A micrometer microscope, giving 45° deviation, was then clamped to the carriage F and adjusted until the axis of its objective coincided with the line XX' , thus supplying a means for bringing the centers of the slits S_1 and S_2 into this line.

The measuring bar was adjusted by a dial indicator until the scraped surface on the side opposite the plugs was parallel to XX' to within 3 seconds of arc. Since the surfaces of the plugs had all been ground and polished into one plane parallel to this scraped surface, this adjustment brought their surfaces parallel to XX' , and insured all of the diamond scratches being in focus without parallax as they came opposite the microscope, once this was focused on one of them.

By means of a mirror wrung to the vertical scraped surface of H , another on the divided circle table with its surfaces parallel to the axis Y , and mirrors clamped between the jaws of the slits S_1 and S_2 , the auto-collimator could be set with its axis normal to the plane XY , and the slits adjusted until the surfaces of their mirrors were parallel to this plane. The slit surfaces were thus adjusted parallel to Y within 30" and to XX' within 15". In a similar manner the plate-holder was adjusted so that the plane of the photographic plate would be approximately perpendicular to the axis XX' . The crystal, which had a cleavage face giving fair optical reflection, was similarly adjusted so that this face was parallel to the axis Y and as nearly as possible in this axis, the latter adjustment being made with a high power microscope. The various mirrors were brought opposite the auto-collimator by sliding the carriage B , and slit bracket M along the tracks on A . Wherever possible, the foregoing tests were checked with a spirit level sensitive to 5 seconds of arc per mm displacement of the bubble and, in some cases, with one of five times this sensitivity.

The greatest care was used to test the flatness of the opposing surfaces of the two parts of the plate-holder, not only when the plate-holder was disassembled and free from stress, but also when it was assembled and the air pressure applied.

The front portion, mounted on the carriage *F* in such a manner that it could be moved parallel to the surfaces *OO*, was examined with an interferometer using parallel and approximately monochromatic green light. The high portions of the scraping marks on these surfaces were so nearly continuous, and so well polished from working the two parts of the plate-holder together during assemblage, that the fringes were entirely unambiguous and could be counted. After allowing for the slight departure of the motion of *F* from a straight line, the surfaces *OO* were found to be flat to one fringe.*

The back of the plate-holder was similarly mounted on the carriage *F*, but the scraping marks were not close enough together to give useful fringes. However, with mirrors wrung to its surfaces in various places, it was tested both with the interferometer and the auto-collimator, and no evidence of an appreciable deviation from flatness was observed. This, together with the usual test for the fit of two scraped surfaces, convinced us that these surfaces were flat enough when separate and not under stress. Incidentally, the rectilinear motion of the carriage *F* was checked when these observations were made.

The plate-holder was then assembled with a photographic plate of "parallel plate" glass 1.5 mm thick in place. Tilting mirrors with short lever arms showed that contact between the surfaces *OO* and the gelatin surface was approximately complete at a pressure of 25 lb in⁻², because an increase to 30 did not diminish the separation of these surfaces by as much as 0.1 μ . A pressure of 12 was required to expand the rubber tubes. The photographic plate was then replaced by a strip of "parallel plate" glass of the same thickness, without gelatin, and this was examined with the interferometer, the air pressures varying from 20 to 30. The fringe system showed very little change after a pressure of 25 was reached, showing approximately complete contact at this pressure. Though the surface of "parallel plate" glass is not optically perfect, the interferometer could be set so that there were not more than one or two fringes in a distance of 3 cm at any part of the strip. The number of fringes per cm was determined for every centimeter of the useful length of the plate, as the plate holder moved parallel to the plane *OO* in front of the interferometer. This procedure was repeated with several other strips of "parallel plate." The data thus obtained gave no indication of a curvature of the surfaces *OO* which could cause a constant error in measurements of glancing-angles of as much as 0.04". The gelatin surface of ordinary commercial photographic plates, when examined with the interferometer, showed very rapidly changing local curvatures many times greater than any constant curvature that could be introduced by the plate-holder. It is in-

* The perfection of the spectrometer and plate holder is largely due to the painstaking care with which the scraped surfaces were fitted by Mr. Moody of the Pratt and Whitney Company.

teresting to note, in this connection, that when a strip of gelatin was removed from the plate, the fringe system associated with the remaining gelatin was usually continuous with that associated with the glass. This showed that the upper surface of the gelatin conformed pretty generally to the irregularities of the glass surface on which it was coated.

The spectrometer, having been adjusted and tested in the manner described, was next aligned with the source of x-rays. In order to obtain maximum intensity through two very narrow slits, it is necessary that the line of centers of the slits should pass through the center of the most intense region of the focal spot on the target. As the authors have previously shown,⁵ the focal spot is striated when the hot cathode is a spiral filament, being approximately a projection of the turns of the filament on the target. By taking x-ray photographs through S_1 when S_3 was in place and again through horizontal slits substituted for S_1 and S_2 , it was possible to adjust the tube and spectrometer so that the latter was approximately level, and the center line of S_1 and S_2 passed through the center of the most intense region of the focal spot. That this line coincided with the axis XX' , as previously defined, was also checked photographically with the aid of S_3 .

PART III. EXPERIMENTAL PROCEDURE

The crystal used was a calcite rhomb $12 \times 10 \times 7$ mm cleaved from a block of Iceland spar obtained from the "Marsh Collection," Yale University. This specimen is denoted by Ca 1. The largest cleavage face was used for reflection, and, as far as could be found by examinations with reflected light and with a microscope, the portion on which the x-rays fell was a plane. After mounting in the crystal holder with soft wax, this face was adjusted parallel to, and into coincidence with, the axis of rotation within $25''$ and 10μ respectively. A tilt of $25''$ would cause an error in the glancing angle under consideration of $0.0004''$.

Due to refraction, no crystal is a perfectly selective reflector, and therefore a monochromatic beam, upon reflection, will diverge beyond the limits of the rectangular region discussed by Uhler.² A sufficient measure of this divergence was obtained, without using a double crystal method, by comparing the angular width of the incident beam, as calculated from the slit widths, with the angle through which the crystal could be turned while still reflecting some energy of the wave-length under consideration. The limits of this angle were determined by finding the angular settings at which the crystal ceased to give an image on the photographic plate, during an exposure time a little too short to permit the formation of a perceptible image due to white radiation. This angle was approximately $46.8''$, with an extreme variation of less than 10 percent. As the beam was limited by the slits to an angular width of $26''$, the divergence due to the crystal was $20.8''$.

Table I gives a comparison between line widths calculated from the above angle and average line widths measured on the spectrograms, at three different distances from the crystal denoted by the plug numbers on the mea-

⁵ C. D. Cooksey and D. Cooksey, *Science* **58**, 382 (1926).

suring bar. The plate intersected the reflected beam near the Bragg focus of S_2 and S_1 in the first and third positions respectively and about half way between these foci in the second position. Considering the difficulty of de-

TABLE I. *Line widths at various positions of plate.*

Plug No.	0	6	11
Calculated	0.0249 mm	0.0400 mm	0.0535 mm
Measured	0.0276 "	0.0395 "	0.0519 "

termining line widths, the above figures are in fair agreement and give a reasonable indication of the perfection of the crystal. In practice it was found that a properly filled out image was obtained when the crystal was rotated through an angle of $18''$ symmetrically about the best setting; no additional width accrued due to energy from the wave-length under investigation through using a larger angle.

Uhler² has pointed out that oblique rays in a plane parallel to the axis of rotation of the crystal broaden the image asymmetrically. During the taking of spectrograms, the incident beam was limited by the following conditions: the widths of the two slits S_1 and S_2 were fixed by strips of platinum foil 0.02 mm thick, their lengths were limited to 3.2 and 2.5 mm respectively, and their distances from the crystal were 35.5 and 4.5 cm respectively. Limited thus, the maximum effect of oblique rays on the glancing-angle is the negligible amount of $0.02''$ for an eleven inch displacement.

In order to reduce the values of the glancing-angle obtained from the spectrograms to their values at a standard temperature, it is necessary to know the coefficient of expansion of calcite along the normal to its cleavage planes; i.e., the coefficient a_{18} in the formula $\sin\theta_{18} = \sin\theta_t [1 + a_{18}(t - 18)]$. W. Stenström⁶ gives the generally quoted approximate value of $1.04(10)^{-5}$ per degree centigrade, which is not precise enough to be used to correct data of the accuracy attained today. In obtaining this value, he assumed an angle of 45° between the optic axis and the normal to a cleavage plane, and $2.62(10)^{-5}$ and $-0.54(10)^{-5}$ per degree centigrade respectively for the coefficients parallel and perpendicular to the optic axis. We have recalculated the coefficient using the following constants: the axial angle of the crystal is $101^\circ 55.0' \pm 0.2'$ at 22°C as given by H. N. Beets;⁷ the mean coefficients of expansion parallel and perpendicular to the optic axis are $(\alpha_{\parallel} + 2\beta_{\parallel}t)$ and $(\alpha_{\perp} + 2\beta_{\perp}t)$ respectively where:

$$\begin{aligned}\alpha_{\parallel} &= +2.513\ 53\ (10)^{-5} & \beta_{\parallel} &= +0.001\ 18\ (10)^{-5} \\ \alpha_{\perp} &= -0.557\ 82\ (10)^{-5} & \beta_{\perp} &= +0.000\ 138\ (10)^{-5}\end{aligned}$$

in degrees centigrade as given by Benoît.⁸ The value of the coefficient a_{18} corresponding to these constants is:

⁶ W. Stenström, Dissertation, Lund (1919) p. 38.

⁷ H. N. Beets, Phys. Rev. [2] 25, 621 (1925).

⁸ R. Benoît, Travaux et Memoires du Bureau International des Poids et Mesures 6, 190 (1888).

$$a_{18} = 1.02_8(10)^{-5},^1$$

which, if used over a sixteen degree interval, will give the correction of the glancing-angle for the $K\alpha_1$ line of silver to 18°C within 0.008".

Table II gives $\log_{10}[1 + a_{18}(t - 18)]$ for the interval 10°C to 26°C.

TABLE II. *Temperature correction for calcite.*

$t^\circ\text{C}$	$\log [1 + a_{18}(t - 18)]$	$t^\circ\text{C}$	$\log [1 + a_{18}(t - 18)]$
10	0.999 964 46	18	0.000 000 00
11	968 90	19	004 44
12	973 34	20	008 88
13	977 79	21	013 32
14	982 23	22	017 76
15	986 67	23	022 21
16	991 12	24	026 65
17	995 56	25	031 09
18	0.000 000 00	26	035 53

A Gaertner measuring engine was used to measure the spectrograms and the distances between the fiducial lines on the measuring bar. The pitch of the screw is approximately 0.5 mm, and the least count of the divided head is 1μ . The errors of the screw were investigated by measuring, on successive parts of the screw, two overlapping 9 mm distances between fine lines on a glass plate manufactured by the Zeiss Company. As both these distances were within less than two divisions of a whole number of turns at all stations, errors of one turn did not enter. The settings were determined with parallel hairs in the eye piece of a three hundred power microscope. The algebraic sums of the residuals from the mean of the 9 mm lengths for successive intervals were plotted against the corresponding 9 mm stations on the screw. The errors so determined all lay within 0.1μ of a smooth curve. The errors in one turn were found at four stations, equally distributed along the screw, by measuring a 0.1 mm interval on the glass plate for successive fifths of the head. These errors are nearly sinusoidal and therefore are eliminated in the mean of three measurements started from three stations on the head, each of which is separated from the others by one third of a turn. As only relative linear measurements are involved in the displacement method, an absolute calibration of the screw was not made, although its units are termed millimeters throughout this paper.

For comparing the measuring bar with the screw the spectrometer microscope was used. The reliability of setting on the lines was found from the maximum variation between settings occurring in each of 143 groups, each group consisting of two to four settings on a line. The maximum variation of setting in one group was 0.9μ , and the average about 0.25μ . Table III gives the frequency of occurrence of the variations of different amount, from 0.1μ to the maximum, for all the groups.

TABLE III. *Frequency of occurrence of large and small variations in setting.*

Frequency of occurrence of a certain variation	25	28	35	23	14	6	8	1	1	2	0
Amount of variation in a group μ	.0	.1	.2	.3	.4	.5	.6	.7	.8	.9	1.0

The maximum amount that any setting differed from the mean in any of the 143 groups was 0.5μ . Thus it appears that, when the plate-holder is displaced by a certain interval on the bar, the chance will be very small that the actual displacement will differ from the measured value of the interval by as much as 1μ , in spite of the fact that the end positions of the interval are determined only once. Such an error in the displacement would cause an error of $0.07''$ in the glancing-angle under consideration.

The following procedure was adopted for obtaining spectrograms. 8×10 plates were cut in strips of the correct size and "*normalized*,"* the edge strips being discarded; after drying, the edges of the gelatin were carefully bevelled by cutting with a sharp knife blade, inclined at a slight angle with the plane of the plate, to remove irregular frills. A plate having been placed in the plate-holder, and the rubber tubes inflated, the holder was mounted on its carriage, with a lead screen so placed as to shield the plate from the lower half of the direct beam. Then the carriage was moved to that one of the desired positions which was most remote from the crystal and adjusted until, when locked, the setting of the microscope cross-hairs on the corresponding fiducial line of the bar appeared exact. After the lapse of at least twelve hours, the setting of the microscope was again scrutinized, but in no case was it necessary to readjust it.

With thermal equilibrium thus assured, the spectrogram was taken. First, with the divided circle set so that the crystal holder did not intercept the incident beam, a short exposure was made to record the upper half of the central image. Then the spectral line was taken on both sides of the direct beam, equal exposures being given for each of five angular positions of the crystal symmetrically spaced about the best setting on each side and covering a range of $18''$; this was repeated for each desired position of the plate-holder. The tangent screw was disengaged from the circle table before making an exposure to avoid unnecessary stress on the cone bearing, and the microscope setting was checked before and after the set of exposures for each spectral image. During each exposure, the temperature of the crystal was recorded from the reading on a calibrated mercury thermometer having five divisions per degree centigrade; this thermometer was so held by a clamp that its bulb was three centimeters from the crystal. After the last spectral image exposure the plate-holder was moved (when necessary) to that station which had been nearest the crystal, and a short exposure was made for the central image with the lead screen moved, and the crystal turned so as not to interfere with the direct beam. The plate-holder was then given a small transverse displacement, and the central image again taken for convenience in measuring the separation of the portions of the central images taken with the holder in its two extreme positions.

During exposures, the current through the x-ray tube was approximately 4 m.a.; and the filament current was regulated so as to maintain a brush

* By *normalizing* we mean soaking the unexposed plate in water for thirty minutes, then in strong ethyl alcohol for twenty minutes and finally leaving it to attain equilibrium in a humid atmosphere. The reasons for subjecting the plates to this process are fully discussed in another paper.¹⁴

discharge, with only occasional sparking, between the blunt points of a six inch spark gap in parallel with the tube. No attempt was made to get a more exact measure of the potential, but these operating conditions assured spectral images of ample density with exposures of moderate duration.

Table IV gives the detailed data recorded during the taking of a typical spectrogram, plate AG2, and Fig. 6 is a drawing to scale of this spectrogram.

TABLE IV. *Typical exposure record.*

Plate AG2. Line Ag $K\alpha_1$. Crystal Ca 1. S_1 —axis 35.5 cm. Plate—axis 32.7, 4.8, and 20 cm. S_1 and S_2 —0.02 mm. Spark gap 6 in. Tube current 4 m.a. Rheostat button 3. Filament current 3.7 amps. Set up 5 P.M. May 3, 1928. Exposures started May 4, 9:15 A.M., finished 11:45 A.M.

Exp. No.	Micr. set on plug	Crystal setting		Temperature		Air pressure plate-holder lb./sq. in.	Exp. time min.
		Deg.	Div.	Crystal °C	Anode °C		
1	11	out*					2
		343.0	6.0	24.7	28.0	27.2	6
		"	7.0	24.7	27.2		6
2	11	"	8.0	24.7	29.0		6
		"	9.0	24.9	28.2		6
		"	10.0	24.9	28.0	27.2	6
		152.0	439.0	25.0	28.0	27.1	6
		"	440.0	25.1	28.0		6
3	11	"	441.0	25.1	28.0		6
		"	442.0	25.2	28.1		6
		"	443.0	25.2	28.1	27.0	6
		152.0	439.0	25.3	27.8	27.0	3
		"	440.0	25.2	27.4		3
4	0	"	441.0	25.3	27.7		3
		"	442.0	25.3	28.0		3
		"	443.0	25.3	28.1	26.9	3
		343.0	6.0	25.3	28.1	26.9	3
		"	7.0	25.4	28.0		3
5	0	"	8.0	25.4	28.1		3
		"	9.0	25.4	28.2		3
		"	10.0	25.4	28.3	26.9	3
		343.0	6.0	25.5	28.2	26.9	5
		"	7.0	25.5	27.9		5
6	6	"	8.0	25.5	28.2		5
		"	9.0	25.5	28.3		5
		"	10.0	25.6	28.5	26.9	5
		152.0	439.0	25.6	28.6	26.9	5
		"	440.0	25.6	28.5		5
7	6	"	441.0	25.6	28.7		5
		"	442.0	25.6	28.7		5
		"	443.0	25.7	28.8	26.6	5
8	0	out*					1
9	0	out* (plate-holder displaced sideways 2 mm)					1

Remarks: Developed 4 min at 77°F, fixed 20 min, washed 30 min, rinsed in distilled water 10 min, and soaked in alcohol 20 min at 77°F, then dried in a humid atmosphere.

* Turned to give direct transmission.

After the plates were thoroughly dry, rulings were scribed at intervals on the gelatin surface (the dotted lines in Fig. 6) along a line through the centers of, and normal to, the spectral images, and all measurements were made along this line except those of the central image separation. If the spectral images were not filled out and black, they were discarded. Table

TABLE V. Plate AG2. Engine settings in millimeters.

Top Up				Top Down		
A	162.2487 92 78	162.0819 .0793 .0809	161.9182 89 67	23.7314 .7270 .7290	23.5627 20 26	23.4006 .3982 .4004
Mean	162.2486 (20.2°C)	162.0807 (20.0°C)	161.9179 (20.0°C)	23.7291 (20.0°C)	23.5624 (20.4°C)	23.3997 (20.2°C)
B	138.5332 14 33	138.3640 50 48	138.1996 .2004 .2000	47.4476 78 93	47.2782 95 89	47.1170 57 63
Mean	138.5326 (20.1°C)	138.3646 (20.0°C)	138.2000 (20.0°C)	47.4482 (20.0°C)	47.2789 (20.2°C)	47.1163 (20.2°C)
C	110.0780 64 77	109.9086 .9104 .9104	109.7470 84 76	75.9033 40 28	75.7361 61 41	75.5720 13 16
Mean	110.0774	109.9098 (20.1°C)	109.7477 (19.8°C)	75.9034 (20.1°C)	75.7354 (20.4°C)	75.5716 (20.3°C)
D	92.1552 69 55	91.9880 74 78	91.8245 40 51	93.8269 78 70	93.6567 84 79	93.4956 52 56
Mean	92.1559 (19.9°C)	91.9877	91.8245 (19.8°C)	93.8272 (20.0°C)	93.6577 (20.4°C)	93.4955
E	63.7039 60 59	63.5360 59 60	63.3716 20 29	122.2768 68 88	122.1082 77 81	121.9471 79 80
Mean	63.7053 (19.8°C)	63.5360 (20.2°C)	63.3722 (19.6°C)	122.2775 (20.2°C)	122.1080 (20.4°C)	121.9477 (20.4°C)
F	39.9994 90 70	39.8311 18 03	39.6623 37 48	145.9828 10 12	145.8144 66 31	145.6543 .6498 .6523
Mean	39.9985 (19.6°C)	39.8311 (20.2°C)	39.6636 (19.6°C)	145.9817 (20.4°C)	145.8147 (20.4°C)	145.6521 (20.4°C)
L	102.8114	102.6425	102.4800	83.1689 .1710	83.0037	82.8415
Mean	102.8114	102.6425	102.4800	83.1699	83.0037	82.8415
N	101.1121	100.9447	100.7813	84.8668 86	84.7000	84.5386
Mean	101.1121	100.9447	100.7813	84.8677	84.7000	84.5386
L	108.1553	107.9860	107.8243	82.8453	82.6748	82.5122
M	106.4640	106.2956	106.1320	84.5346	84.3655	84.2016

V gives the details of the measurements of the spectrogram illustrated. Before the value of the glancing-angle can be computed, the measured distances must be increased by the following quantities: $a \equiv$ screw correction; $b \equiv$ correction for difference between temperatures of plate when taken and

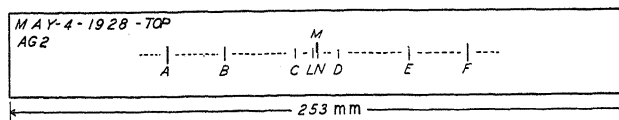


Fig. 6. Facsimile of spectrogram AG2.

when measured; $c \equiv$ lateral shift of plate-holder during displacement as indicated by central image separation. These corrections together with the corrected values of the distances between spectral images and their corresponding displacements are given in Table VI. The values of the angle

TABLE VI. Plate AG2. Corrections to measurements.

Distance Fig. 6		$a \times$ (10) ⁴ mm	Mean Temp. Diff. $\delta^\circ\text{C}$	$b \times$ (10) ⁴ mm	$c \times$ (10) ⁴ mm	Image separation corrected	Displacement mm
A-C	Up	+6.8	5.05	-9.7	-73	52.16406	279.44590 ± 0.00042
	Down	+0.7					
D-F	Up	+1.3	5.05	-9.7	+73	52.16378	
	Down	+4.7					
B-C	Up	+4.0	5.35	-5.6	-40	28.45062	152.42506 ± 0.00020
	Down	+1.6					
D-E	Up	+0.3	5.35	-5.6	+40	28.45471	
	Down	+1.0					

Differential thermal coefficient glass plate-screw $3.7 (10)^{-6}$ per $^\circ\text{C}$.

ω between the normal to the plate and the line XX' , computed by Eq. (2) from the data corresponding to the two different displacements, differ in magnitude and sign; but the more precise optical tests had shown very conclusively that the maximum rotation of the plate-holder, for any displacement along the tracks, was less than $2''$. Such differences are, therefore, probably due to residual fortuitous variations in position of a developed image with respect to its corresponding latent image,¹⁴ and the fact that commercial plates cannot be forced flat.

Table VII is given as an illustration of the accuracy with which the spectrograms could be measured. As shown in Table V, the distances be

⁹ A. Leide, Dissertation, Lund (1925).

¹⁰ A. P. Weber, Zeits. f. wiss. Photo. **23**, 149 (1925).

¹¹ K. Lang, Ann. d. Physik [4] **75**, 489 (1924).

¹² G. Kellström, Zeits. f. Physik **41**, 516 (1927).

tween pairs of lines were measured first with the plate in one position on the engine, and again when it was reversed ("top up", "top down"). The numbers tabulated are the differences between the means of these measurements in each position. The first three plates had lines corresponding to

TABLE VII. *Difference between measurements direct and reversed.*

Spectro-gram	Differences		Spectro-gram	Differences	
	11 in. displ.	6 in. displ.		11 in. displ.	6 in. displ.
AG1	0.25 μ	0.29 μ	AG3	0.56 μ	0.04 μ
AG2	0.20 μ	0.44 μ	AG4	0.81 μ	

both 11 and 6 in. displacements, but the fourth had only the former. The measurements on plate AG4 were repeated. If the new measurements are averaged with the first set, the corresponding difference is 0.72 instead of 0.81 μ . If it is assumed that the measurements can be in error by as much as 0.81 μ in the case of the 11 in. displacement, the resulting glancing-angle would be in error by 0.29". The maximum effect on this angle due to the uncertainty of setting on the bar is 0.07". Therefore it seems evident that there is a negligible chance that values of the glancing-angle obtained from different 11 in. displacements can fluctuate, due to errors of measurement, by as much as 0.36", assuming of course good lines on the spectrograms. Re-measurements made after a lapse of three months on another plate, AG5, by an independent observer gave glancing-angle values differing for the 5 and 6 in. displacements by 0.13" and 0.00" respectively.

TABLE VIII. *Effect of method of measurement. Plate No. AG9, 4 in. displacement, taken at 22.1° C. glancing-angle at 18° C.*

Measured at ° C.	Uncorrected for temp. of meas.		Corrected for temp. of meas.		Description of method of measurement
20.5	5° 17'	14.54"	5° 17'	14.42"	Deep focus objective; 57° cross-hairs; 18 X.
21.2	5° 17'	14.41"	5° 17'	14.34"	Same objective; parallel hairs separated to straddle width of remote lines; 18 X.
19.7	5° 17'	14.65"	5° 17'	14.48"	Shallow focus; parallel hairs same; 20 X.
Remote 17.0 Near 19.0	5° 17'	14.95"	5° 17'	14.43"	Same objective, but parallel hairs suitably adjusted to measure separation of remote and near lines independently; 20 X.

Spectral images taken with the plate in a remote position are broader than those taken with it near the crystal; therefore, if parallel hairs of fixed separation are used in the measuring microscope, their adjustment will not

be suitable for both types of images. Plate AG9 was measured under varying conditions of magnification, type of eye-piece and temperature, and Table VIII gives the glancing-angles thus obtained. It will be observed that the second column shows excellent agreement for different methods of measurement, especially when it is borne in mind that for such a short displacement a variation in the image separation of 0.2μ would change the glancing-angle by $0.20''$, and that the near and remote lines were of different width.

PART IV. RESULTS

The final results are given in Table IX. They were obtained from eight spectrograms, six of which were taken with the plate-holder in three, the remainder in only two, positions, but that nearest the crystal was the same for all. All the plates had been cut from the central portions of large plates; AG1 to AG4 from one Eastman "40," AG5 to AG7 from another, and AG9

TABLE IX. *Final data and results. Line; Ag ($K\alpha_1$). Crystal; Calcite (Ca 1).*

Spectro-gram	Displ't inches	Taken at ° C	Glancing-angle at 18° C	Mean values, probable errors of mean and of one determination respectively
AG1	11	25.2	5° 17' 13.68"	
" 2	11	25.1	14.00	$\theta = 5^\circ 17' 13.79''$
" 3	11	25.0	13.53	$R = \pm 0.075$
" 4	11	25.2	13.95	$r = \pm 0.15$
" 1	6	25.4	13.35	
" 2	6	25.4	13.78	
" 3	6	25.3	13.92	
" 5	6	21.4	13.03	$\theta = 5^\circ 17' 13.82''$
" 6	6	21.8	13.93	$R = \pm 0.092$
" 7	6	21.7	14.13	$r = \pm 0.29$
" 5	5	21.4	14.15	
" 6	5	21.7	13.43	
" 7	5	21.9	14.10	
" 9	4	22.1	14.42	

from an Eastman "Universal." If the values of the glancing-angle corresponding to eleven inch displacements are given twice the weight of the others, the following values are obtained:

$$\theta = 5^\circ 17' 13.81'' (\pm 0.06'') \text{ at } 18^\circ \text{C.}^1$$

$$\lambda = 0.5582384^1 (\log 2d_{18} = 0.7823350)$$

$$\pm 0.000002.$$

For comparison, the most reliable published results that we have seen are given with ours in Table X. In cases where the probable errors were not published we have calculated them from the data given. Omitting Kellström's second order value and weighting the others according to their probable errors,

$$\theta = 5^\circ 17' 14.66'' (\pm 0.036'') \text{ at } 18^\circ \text{C.}$$

TABLE X. *Comparison with results of others.*

Orders used	Glancing-angle	Probable error of		Av. deviation from mean	Source
		Mean	One det'n		
1	5° 17' 13.05"	0.4"	0.8"	1.0"	A. Leide ⁹
1 & 2	7.8	0.7	2.0	2.2	A. P. Weber ¹⁰
1	13.1	0.6	1.5	1.8	K. Lang ¹¹
1	15.2	0.045	0.12	0.13	G. Kellström ¹²
2	(10 37 9.8)	0.36	0.72	0.8	
				11 in. displ't	
				0.2	
1	13.81	0.06	0.13	Other displ't	Present work
				0.34	

DISCUSSION

Of the values given in the table, Kellström's first order determination has the smallest probable error and is the one quoted in the International Critical Tables. The value he gives for the wave-length determined from second order reflection would predict a first order glancing-angle ($5^\circ 17' 14.58'' \pm 0.18''$) approximately midway between his measured first order and ours and with four times his first order probable error. The fact that our value of the glancing-angle differs from his two values, and the latter differ among themselves, by about three times the sum of the respective probable errors would lead one to suspect that any one or all of the values may be affected by a constant error. From the point of view of agreement, the two sensibly identical values of Leide and Lang, large though their probable errors may be, favor our value rather than those of Kellström. The "Method of Displacement" may be subject to an error sufficient to account for our disagreement with Kellström's accepted value if the underlying assumption regarding the symmetry of the reflected beam is not fulfilled. However, the mean value of the glancing-angle computed from the eleven inch displacements only, where the plate was near a Bragg focus in both its positions, is sensibly the same as that from other displacements, where the plate intersected an intermediate portion of the beam in one position (Table IX). This fact confirms our belief that the reflected beam possessed the required symmetry, in spite of the fact that the crystal was not a perfectly selective reflector. The exhaustive tests to which the apparatus was subjected failed to show any defect which could cause an appreciable constant error. The only remaining source of such an error seems to be the crystal. The discrepancy between the results would be accounted for by a difference in grating space of seven parts in a hundred thousand between the crystals used. We have made use of only one specimen of Iceland spar while Kellström has used two (Pk 1 and Pk 2), although most of his data were obtained from Pk 1. He states that both crystals gave the same result within his limits of error. However, in the one case in which he used Pk 2 for a second order determination of the wave-length considered here his result is identical with that of our eleven inch displacements. We have been unable

to find any statement by Leide or Lang giving information concerning the particular specimens of calcite used by them. DeFoe and Compton¹³ have measured the density of specimens of calcite, obtained from various sources, within a probable error of $(10)^{-4}$ gm cm⁻³. They give values for two specimens from Iceland which differ by thirteen times this amount, indicating a real difference in density, even though they allow only half weight to the value for one of these specimens in computing the mean density of all the specimens. If all variations in density are reflected in differences of grating space, a difference in density of $6 \times (10)^{-4}$ gm cm⁻³ (less than half that found by DeFoe and Compton) between Kellström's crystal and ours would be sufficient to account for the difference in the values of the glancing-angle under consideration. The discrepancy might therefore be explained in this way, though it is doubtful that the observed differences in density are really due to variations in grating space.

TABLE XI. *Average variations in measured values of glancing-angle due to various causes.*

Displacements	11 in.	6 in.	5 in.	4 in.
<i>Average variations due to:</i>				
Variations in setting on bar	0.034"	0.06"	0.07"	0.10"
Unflatness of gelatin	0.17	0.31	0.37	0.50
Motions of images after exposure				
if plates are:				
normalized	0.25	0.46	0.56	0.69
not normalized	1.00	1.84	2.24	2.76
<i>Sum of average variations:</i>				
If plates are:				
normalized	0.45	0.83	1.00	1.29
not normalized	1.20	2.21	2.68	3.36
<i>Observed average variations</i>	0.20	0.33	0.30	—
<i>Observed maximum variations</i>	0.47	1.10	0.72	—

It is of interest to consider the effect on the final result of various causes of uncertainty in the directly measured quantities. The average difference between successive settings on the bar was 0.25μ , therefore any displacement of the plate-holder is subject to an average uncertainty of 0.5μ from this cause. Irregularities in the surface of the gelatin would cause the effective displacement to differ from the actual. An interferometer investigation of the gelatin surface of the developed spectrograms, when held in the plate-holder, showed that these irregularities could cause an average error in the displacement of 2.5μ . Our work on the unreliability of position of photographic images¹⁴ showed that the average error in the measured value of a fixed distance, as recorded on photographic plates, was 0.7μ when the plates had been normalized and 2.8μ when they had not. These errors, of course, include both the error of setting and that due to motion of the image. Though the images of the template slits¹⁴ could be set on more accurately than

¹³ O. K. DeFoe and A. H. Compton, Phys. Rev. [2] 25, 618 (1925).

¹⁴ D. Cooksey and C. D. Cooksey, Phys. Rev. preceding article.

spectral images, we shall assume that these figures include the average variations that might be expected in the remeasurement of a spectrogram. The effect of the average variation due to each of these causes on glancing-angle values, calculated for various displacements, is shown in Table XI.

These statistics not only emphasize the advisability of normalizing photographic plates before using them as accurate recorders of distances, but suggest that, even for small glancing-angles, the accuracy of the displacement method would be improved by the use of emulsions coated on good *plate* glass. With the accuracy of setting on spectral images limited as it is, there would seem to be no necessity for resorting to more accurate methods of measuring the displacement. Even though the apparatus is massive and so has a large thermal capacity, there is little doubt that better precautions for maintaining it at a constant temperature would have a beneficial effect. However, the manipulation in the present work was carried out with special reference to making the effects of temperature changes fortuitous.

In conclusion we wish to express our great appreciation of the encouraging and helpful interest shown, during the whole progress of this work, by Professor Uhler and Professor Emeritus Hastings of this department. We are also grateful to Dr. Albert W. Hull of the Research Staff of the General Electric Company for advice in connection with x-ray tubes and filaments, and to Professors McKeehan and Uhler for helpful suggestions in connection with the presentation of this investigation. In directing the construction and exhaustion of x-ray tubes, we have been greatly aided by experience gained in our long association with Mr. Alfred Greiner, formerly connected with this laboratory.

THE SPHERICALLY SYMMETRICAL FIELD IN THE UNIFIED THEORY

BY N. ROSEN AND M. S. VALLARTA

MASSACHUSETTS INSTITUTE OF TECHNOLOGY, CAMBRIDGE, MASSACHUSETTS

(Received May 15, 1930)

ABSTRACT

In this paper a systematic investigation of the spherically symmetrical static field in Einstein's unified theory of the electromagnetic and gravitational fields is given. The investigation is carried through in two cases: with and without time symmetry. By a time symmetrical field we understand one whose Riemann interval is not altered by changing $+dt$ into $-dt$.

To begin with we develop a generalization of the formulas for parallel displacement and covariant affine differentiation in Einstein's geometry which enables us to introduce orthogonal transformations of the local coordinates, so as to bring them formally into agreement with the Gaussian coordinates. We then solve the Einstein field equations $F^{\mu\alpha}=0$ and $G^{\mu\alpha}=0$, first without the assumption of time symmetry. We determine the values and the physical significance of the constants of integration by considering the case of a very weak field, and obtain asymptotically the classical Coulomb field (e/r^2) and the classical Newtonian potential ($-m/r$). Positive and negative electricity appear in the unified theory as given empirical facts, just as in the classical theory. In the present theory, however, the Newtonian field and the Coulomb field can be separated only asymptotically. In the immediate vicinity of a charged mass particle they are inextricably bound together.

Our solution gives a quadruple ("Vierbein")

$$\begin{aligned} {}_1h^1 &= 1 + e^2/r^4, & {}_2h^2 &= 1, & {}_3h^3 &= 1, \\ {}_4h^4 &= -(ie/r^2)(1 + e^2/r^4)^{1/2}, & {}_4h^4 &= 1 + m \int_r^\infty r^{-2}(1 + e^2/r^4)^{-3/2} dr. \end{aligned}$$

All the other components vanish. By a transformation of variables this is shown to reduce to the quadruple recently calculated by Einstein and Mayer.

The field equations are then solved with the assumption of time symmetry. The electrostatic field vanishes, but the component g_{44} of the metric form has approximately the Schwarzschild value, while the others have the Euclidean values. Because of the absence of a law of motion, no observable predictions having to do with the path of an exploring particle can be made. It is shown, however, that in the unified field the theory gives in the first approximation the same red shift as the 1916 theory. If it is assumed that the orbit of a planet is a Riemannian geodesic, as in the 116 theory, then the advance of the perihelion of Mercury comes out approximately 7" per century, that is, about the same as in the 1905 theory.

I. INTRODUCTION

A NUMBER of papers have recently appeared bearing on Einstein's attempt to construct a unified theory of the electromagnetic and the gravitational fields. The geometrical foundations of the new theory were laid down by Einstein in 1928,¹ without knowledge of the previous work of

¹ A. Einstein, Sitz. d. preuss. Akad. d. Wiss., 1928, p. 217; also Math. Ann. 102, 685, (1930), hereafter referred to as "E.1." The reader is referred to this paper for explanation of the symbols and operations used in the present article.

Cartan and others on the same subject.² In a paper following immediately thereafter Einstein³ suggested a unified field theory of the electromagnetic and gravitational fields in which the former was defined, in terms of the fundamental tensor h_s^λ of a torsion geometry with distant parallelism, through an electromagnetic potential $\phi_\lambda = \Lambda_{\lambda\sigma}^\sigma$, where $2\Lambda_{\lambda\mu}^\sigma = h_s^\sigma(h_{\lambda,\mu}^s - h_{\mu,\lambda}^s)$, and the latter through the usual gravitational potentials $g_{\mu\nu}$ defined in terms of the fundamental quantities h_λ^s by the relation $g_{\lambda\mu} = h_\lambda^s h_{s\mu}$. He further suggested a set of field equations for the determination of the tensor h_s^λ , obtained from the variational equation

$$\delta \int h g^{\mu\nu} \Lambda_{\mu\beta}^\alpha \Lambda_{\nu\alpha}^\beta d\tau = 0. \quad (1)$$

The spherically symmetrical statical field in the unified theory was then investigated by Wiener and Vallarta.⁴ In accordance with Einstein's definitions of the electric and gravitational fields, one had to expect that in the time symmetrical case one should obtain the Schwarzschild solution for the gravitational field of an uncharged mass particle, the Nordström-Jeffery solution⁵ for the charged mass particle and, asymptotically the classical potential $\pm e/r$ for the electrostatic field. Instead they found that in this case, adopting Einstein's definition of the electromagnetic potential, the electrostatic field vanishes and, further, the gravitational field obtained by solving the field equations (1) also vanishes. One of the present authors⁶ then pointed out that the vanishing of the electrostatic field is a consequence of the definition of the potential and has nothing to do with the particular choice of the field equations.

In 1929 Einstein modified his field equations several times. His first paper of that year⁷ contains a second set of field equations which leads, as shown by Salkover⁶, to the Schwarzschild solution for the gravitational field in the first approximation. In his second paper of that year Einstein⁸ gave a third set of field equations based on a new Hamiltonian. Wiener, in an unpublished paper, was then able to show that this new Hamiltonian is, except for nonsignificant terms, precisely the Hamiltonian of the gravitational theory of 1916, and therefore leads to the gravitational field described by the Schwarzschild solution. Wiener also showed that Levi-Civita's⁹ definition

² For a historical outline of the development of the Einstein geometry see a paper by E. Cartan, *Math. Ann.* **102**, 698, (1930).

³ A. Einstein, *Sitz. d. preuss. Akad. d. Wiss.* 1928, p. 224.

⁴ N. Wiener and M. S. Vallarta, *Proc. Nat. Acad.* **15**, 353, (1929), more specially *Proc. Nat. Acad.* **15**, 802 (1929).

⁵ See for example Eddington's "Mathematical Theory of Relativity," p. 82 and p. 185, Cambridge, 1923.

⁶ M. S. Vallarta, *Proc. Nat. Acad.* **15**, 784, (1929). The gravitational field obtained in this paper is vitiated by an error in transcribing the values of the electromagnetic potential from a previous paper by Wiener and Vallarta (footnote 4). The error was pointed out and corrected by M. Salkover, *Phys. Rev.* **35**, 209 and 214, (1930); acknowledgment by M. S. Vallarta, *Phys. Rev.* **35**, 435, (1930).

⁷ A. Einstein, *Sitz. d. preuss. Akad. d. Wiss.* 1929, p. 2.

⁸ A. Einstein, *Sitz. d. preuss. Akad. d. Wiss.* p. 156, 1929.

⁹ T. Levi-Civita, *Sitz. d. preuss. Akad. d. Wiss.* p. 137, 1929.

of the electric vector leads to a vanishing spherically symmetrical, time symmetrical electrostatic field.

The development of the theory entered a new phase with Einstein's 1930 papers. Giving up the previous attempt to describe the electromagnetic field in terms of a potential ϕ_μ and also, as it appears, the description of the gravitational field in terms of the potentials $g_{\mu\nu}$, except in the case of a weak field, he suggested a fourth set of field equations to determine the fundamental tensor h_s^{λ} .¹⁰ The present paper is concerned with the solution of these field equations in the spherically symmetrical case, with and without time symmetry. It will be shown that the former case leads to a vanishing electrostatic field, while the latter gives, asymptotically, the classical Coulomb field. We believe this is the first instance where the asymmetry of past and future has played a fundamental role in a *field* theory. Positive and negative electricity appear in the unified theory as *given* empirical facts, just as in classical theory. Both cases, with and without time symmetry, give asymptotically the classical Newtonian potential. By making a suitable transformation of variables we show that the quadruple ("Vierbein") obtained without the assumption of time symmetry is identical with that found by Einstein and Mayer¹¹ by a different method.

Comparison with experimental evidence having to do with the motion of an exploring particle is impossible at the present stage, because the law of motion has not yet been discovered, but it may be conjectured on the basis of our present results that the path of an uncharged exploring particle in the pure gravitational field is not a geodesic with respect to the Riemannian ds^2 as in the 1916 theory. However, the unified theory leads to predict a shift of spectral lines towards the red which in the first approximation agrees with that of the 1916 theory.

II. MATHEMATICAL INTRODUCTION

In problems involving spherical symmetry it is usually found that a considerable simplification is achieved if spherical space coordinates r , ϕ , θ are used to locate a point in the field. In the Einstein geometry as formulated by him this immediately leads to a difficulty, because he does not allow orthogonal transformations of the local quadruples ("Vierbeine") so that locally and at each point the local coordinates may formally be made to agree with the Gaussian coordinates. If local orthogonal transformations are made use of certain formal generalizations are necessary which we now proceed to establish.

Let $g_{\alpha\beta}$ and γ_{ab} be the fundamental metric tensors in the Gaussian and in the local (Euclidean or pseudo-Euclidean) system, respectively. We place following De Donder¹² and Wiener and Vallarta⁴ and using the customary tensor notation:

¹⁰ A. Einstein, Sitz. d. preuss. Akad. d. Wiss. 1930, p. 3; also E.1.

¹¹ A. Einstein and W. Mayer, Sitz. d. preuss. Akad. d. Wiss., p. 110, 1930; hereafter referred to as "E-M".

¹² T. De Donder, Comptes rendus, 1928, p. 817.

$$g_{\mu\nu} = \gamma^{ab} h_{a\mu} h_{b\nu} = h_{\mu}^b h_{b\nu} \quad (2)$$

$$g^{\mu\nu} = \gamma_{ab} h^{a\mu} h^{b\nu} = h_{\mu}^a h^{b\nu}. \quad (2a)$$

In these expressions Latin indices refer to the local system, Greek indices to the Gaussian system. The quantities $h_{a\mu}$ have thus tensorial character both in the local and in the Gaussian systems, but in raising or lowering local (Latin) indices, the local tensor γ_{ab} is used, whereas in the case of Gaussian (Greek) indices, the tensor $g_{\mu\nu}$ is used. In Einstein's papers where local Cartesian coordinates are used the distinction between co- and contravariant local indices does not occur. The transformation formulas from the local to the Gaussian system now become

$$A^\nu = h_s^\nu A^s = h^{s\nu} A_s, \quad A_\nu = h_\nu^s A_s = h_{s\nu} A^s \quad (3)$$

$$A^s = h_\mu^s A^\mu = h^{s\mu} A_\mu, \quad A_s = h_{s\mu} A^\mu = h_s^\mu A_\mu \quad (4)$$

and we have, as usual,

$$h_{s\mu} h^{s\nu} = h_\mu^s h_s^\nu = \delta_\mu^\nu, \quad h_s^\mu h_\mu^t = h_{s\mu} h^{t\mu} = \delta_s^t$$

where δ_ν^μ is the Kronecker symbol. Hence

$$A^2 = A_s A^s = (h_{s\mu} A^\mu)(h_\nu^s A^\nu) = \gamma_{st} h_\mu^t h_\nu^s A^\mu A^\nu = g_{\mu\nu} A^\mu A^\nu = A_\mu A^\mu$$

and the transformation formulas (3), (4), are shown to be compatible with the definition (2). Similar transformation formulas can be given for tensors of higher rank. Thus whether one works with local coordinates (Levi-Civita) or Gaussian coordinates (Einstein) is largely a matter of choice and convenience.

We now derive the generalized law of parallel displacement which formally allows local orthogonal transformations.¹³ The change δ of the local components of a vector (or tensor) for an infinitesimal displacement is, in accordance with the postulate of distant parallelism,

$$\delta A_s = \delta(h_{s\alpha} A^\alpha) = \delta(h_s^\alpha A_\alpha) = 0 \quad (5)$$

which gives

$$h_{s\alpha} \delta A^\alpha + h_{s,\beta}^\alpha A^\alpha \delta x^\beta = 0$$

$$h_s^\alpha \delta A_\alpha + h_{s,\beta}^\alpha A_\alpha \delta x^\beta = 0$$

where the dot indicates covariant differentiation referred to the local coordinates, i.e. to the form $\gamma_{ab} dx^a dx^b$. From this we obtain

$$\delta A^\alpha = -A^\sigma \Gamma_{\sigma\beta}^\alpha \delta x^\beta \quad (6)$$

$$\delta A_\alpha = A_\sigma \Gamma_{\alpha\beta}^\sigma \delta x^\beta \quad (6a)$$

where

$$\Gamma_{\sigma\beta}^\alpha = h^{s\alpha} h_{s\sigma,\beta} = -h_{s\sigma} h^{s\alpha}_{,\beta} \quad (7)$$

and

$$h_{s\sigma,\beta} = h_{s\sigma,\beta} - \{s\beta, t\} h_{t\sigma} - \{\sigma\beta, \alpha\} h_{s\alpha}. \quad (7a)$$

¹³ N. Rosen, "The Use of Polar Coordinates in Einstein's Geometry." S. M. Thesis, Mass. Institute of Technology; June, 1930.

As already mentioned above, the Christoffel symbols are defined through the tensor γ_{ab} by the usual formula

$$\{st, u\} = \gamma^{ub} [st, b] = \frac{1}{2} \gamma^{ub} \left(\frac{\partial \gamma_{sb}}{\partial x^t} + \frac{\partial \gamma_{tb}}{\partial x^s} - \frac{\partial \gamma_{st}}{\partial x^b} \right).$$

It is clear that a local orthogonal transformation can always be made whereby $\gamma_{ab} = \delta_{ab}$. Then obviously all the Christoffel symbols vanish and $h_{s\sigma, \beta} = h_{s\sigma, \beta}$ further $\Gamma_{\mu\nu}^\sigma = h^{s\sigma} h_{s\mu, \nu}$, in accordance with Einstein's definition (E.1, p.688, Eq. (12)). $\Gamma_{\mu\nu}^\sigma$ is in general different from $\Gamma_{\nu\mu}^\sigma$ and it can be readily shown that if $\Gamma_{\mu\nu}^\sigma = \Gamma_{\nu\mu}^\sigma$ then the space whose metric is defined by the $g_{\mu\nu}$ is Euclidean.

The law of covariant affine differentiation will now be derived. Since the local components A_s of a vector are covariant relatively to a transformation of the local coordinates, $A_{s, \alpha}$ is a tensor. Therefore $(h_s^\sigma A_\sigma)_{, \alpha}$ and

$$h_s^\sigma{}_{, \alpha} A_\sigma + A_{\sigma, \alpha} h_s^\sigma$$

or

$$A_{\tau, \alpha} + A_\sigma h_s^\sigma{}_{, \alpha} h_\tau^s = A_{\tau, \alpha} - A_\sigma h_{s\tau, \beta} h^{s\sigma} = A_{\tau, \alpha} - A_\sigma \Gamma_{\tau\beta}^\sigma \quad (8)$$

are tensors. This tensor we shall call the covariant affine derivative of A_τ with respect to x^α and denote it by $A_{\tau; \alpha}$. Analogously for a contravariant vector

$$A_{; \tau}^\sigma = A_{, \tau}^\sigma + A^\alpha \Gamma_{\alpha\tau}^\sigma, \quad (9)$$

which can readily be generalized to a tensor of any rank. From this we may also obtain the divergence $A^\sigma{}_{; \sigma}$ which is merely the contracted affine derivative.

If we take a scalar invariant Ψ and differentiate it covariantly twice we obtain

$$\begin{aligned} \psi_{; \alpha} &= \psi_{, \alpha} = \psi_{, \alpha} \\ \psi_{; \alpha; \beta} &= \psi_{; \alpha, \beta} - \psi_{; \sigma} \Gamma_{\alpha\beta}^\sigma = \psi_{, \alpha, \beta} - \{\alpha\beta, \sigma\} \psi_{; \sigma} - \psi_{; \beta} \Gamma_{\alpha\sigma}^\sigma \end{aligned}$$

hence interchanging α and β

$$\psi_{; \beta; \alpha} = \psi_{, \beta, \alpha} - \{\beta\alpha, \sigma\} \psi_{; \sigma} - \psi_{; \sigma} \Gamma_{\beta\alpha}^\sigma$$

and subtracting

$$\psi_{; \alpha; \beta} - \psi_{; \beta; \alpha} = \psi_{; \sigma} (\Gamma_{\alpha\beta}^\sigma - \Gamma_{\beta\alpha}^\sigma).$$

Therefore $\Gamma_{\alpha\beta}^\sigma - \Gamma_{\beta\alpha}^\sigma$ is a tensor of the third rank, once contravariant and twice covariant. We denote it by $\Lambda_{\alpha\beta}^\sigma$. By (7) and (7a) we have

$$\Lambda_{\alpha\beta}^\sigma = h^{s\sigma} (\{s\alpha, t\} h_{t\beta} - \{s\beta, t\} h_{t\alpha} + h_{s\alpha, \beta} - h_{s\beta, \alpha}) \quad (10)$$

Einstein originally assumed that the contracted tensor $\Lambda_{\alpha\sigma}^\sigma$ plays the role of the electromagnetic potential, but has now given up this assumption (E.1, p. 691). The tensor $\Lambda_{\nu\sigma}^\mu$, however, plays a fundamental role in the unified theory.

III. THE FIELD EQUATIONS AND THEIR SOLUTION

Einstein sets for his field equations (E.I p. 693):

$$F^{\mu\alpha} = 0, \quad G^{\mu\alpha} = 0$$

where $F^{\mu\alpha} = \Lambda^{\nu\mu\alpha}_{;\nu}$ and $G^{\mu\alpha} = \Lambda^{\alpha\mu\nu}_{;\nu} - \Lambda^{\sigma\mu\tau}\Lambda_{\sigma\tau}^{\alpha}$. For the purposes of this paper it is more convenient to write them $F_{\mu\alpha} = 0$ and $G_{\alpha\mu} = 0$. We now solve these equations under the assumption that time is not symmetrical. Wiener and Vallarta⁴ have suggested that for this case the covariant quadruple has the form*

$$\begin{aligned} {}^1h_1 &= U, & {}^1h_4 &= M, & {}^2h_2 &= 1 \\ {}^3h_3 &= 1, & {}^4h_1 &= N, & {}^4h_4 &= W \end{aligned} \quad (11)$$

where U, M, N, W are functions of r only. Transformed to Cartesian coordinates the contravariant quadruple h_s^λ becomes, as they have shown

$$\begin{aligned} h_s^\gamma &= x_s x_\gamma E(r) + \delta_{s\gamma}(s, \gamma = 1, 2, 3), \quad {}^4h^\gamma = G(r)x_\gamma \\ h_s^4 &= H(r)x_s, \quad {}^4h^4 = F(r) \end{aligned} \quad (12)$$

where $r = x_\gamma x_\gamma (\gamma = 1, 2, 3)$. This quadruple satisfies the Einstein-Mayer conditions (E-M, p. 112, Eq. (15); p. 113, Eq. (22). Since we include improper rotations their $C(r) = 0$. By a transformation of variable $x_4' = x_4 + \Psi(r)$, with Ψ arbitrary, we can always make h_s^4 vanish. Hence we may place without loss of generality $H = 0$, or $N = 0$.

The components of the tensor γ_{ab} are:

$$\gamma_{11} = 1, \quad \gamma_{22} = r^2 \sin^2 \theta, \quad \gamma_{33} = r^2, \quad \gamma_{44} = 1, \quad \gamma_{ab} = 0 \quad (a \neq b) \quad (13)$$

therefore the components of the tensor $g_{\mu\nu}$ are, from (2),

$$g_{11} = U^2, \quad g_{14} = g_{41} = UM, \quad g_{22} = r^2 \sin^2 \theta, \quad g_{33} = r^2, \quad g_{44} = M^2 + W^2 \quad (14)$$

and all the others vanish. Since g_{14} is not zero a change of sign of the variable t changes the sign of the term involving g_{14} in the metric fundamental form. If the variable t is to have its usual relativistic significance, time, then this can only mean that the asymmetry of past and future plays a role in the unified theory. As a matter of fact we shall see later that the condition for the existence of the electrostatic field of a particle is that there be non-symmetrical terms in time in the Riemann interval.

The tensor $\Lambda_{\nu\sigma}^\mu$ has the following non-vanishing components:

$$\begin{aligned} \Lambda_{14}^1 &= -\Lambda_{41}^1 = (MW' - M'W)/UW, & \Lambda_{13}^3 &= -\Lambda_{31}^3 = (U - 1)/r \\ \Lambda_{12}^2 &= -\Lambda_{21}^2 = (U - 1)/r, & \Lambda_{34}^3 &= -\Lambda_{43}^3 = -M/r \\ \Lambda_{24}^2 &= -\Lambda_{42}^2 = -M/r, & \Lambda_{14}^4 &= -\Lambda_{41}^4 = -W'/W \end{aligned} \quad (15)$$

where the prime indicates differentiation with respect to r .¹⁴ From these we find, after some calculation, the field equations:

* To avoid confusion we write in this and similar cases the local indices to the left of the symbols ${}^a h_\lambda$, and the Gaussian indices to the right.

$$F_{14} = -F_{41} = (1/U^2W^2)(MUWW'' - M''UW^2 - MUW'^2 - MU'WW' + M'UWW' + M'U'W^2) + 2(M - M'r)/r^2 = 0. \quad (16)$$

All the other components of the tensor $F_{\mu\nu}$ vanish identically. From the second field equation $G_{\alpha}{}^{\mu} = 0$ we find:

$$G_1^1 = 2(1 - U)/Ur^2 + (1/U^3W^4)(MM''UW^2 - M^2UWW'' + MUW'^2 + M^2U'WW' - MM'U'W^2 - M'^2UW^2) = 0. \quad (17)$$

$$G_1^4 = (1/U^2W^4)(MUWW'' - MU'WW' - MUW'^2 - M'UWW') = 0 \quad (18)$$

$$G_2^2 = (1/r^2U^3W^3)(2M^2U^2W - 2M^2UW - M^2U'Wr - 2M^2U^3W + 4U^2W^3 - 2UW^3 - U'W^3r - 2U^3W^3 + MM'UWr - M^2UW'r) = 0 \quad (19)$$

$$G_3^3 = G_2^2 = 0 \quad (19a)$$

$$G_4^1 = -[(M^2 + W^2)/U^4W^3](MUWW'' - M''UW - MU'W'^2 - MU'WW' + M'UWW' + M'U'W^2) + (2/Ur)[(M'W - MW')/UW - M/r] - (M^2 + W^2)(M'W - MW')W'/U^3W^4 - M(MW' - M'W)^2/U^3W^4 = 0 \quad (20)$$

$$G_4^4 = (1/U^3W^4r)(M^2UWW''r + UW^3W''r - M^2UW'^2r - M^2U'WW'r - 2UW^2W'^2r - U'W^3W'r + 2U^2W'W^3 - MM'UWW'r) = 0 \quad (21)$$

and all the other components of this tensor vanish identically.

From (16) we obtain

$$\frac{d}{dr}\left(\frac{M'W - MW'}{UW} + \frac{2M}{r}\right) = 0, \quad \phi_4 = \Lambda_{4\sigma}{}^{\sigma} = \text{const.} = c_1 \quad (22)$$

verifying the Einstein-Mayer relation $\phi_i = \text{const.}$ (E.-M., p. 115, Eq. (34)).

Since at infinity space is Euclidean we have the boundary conditions: for $r \rightarrow \infty$, $M \rightarrow 0$, $M' \rightarrow 0$, $U \rightarrow 1$, $W \rightarrow 1$. Hence $c_1 = 0$ and

$$W'/W = M'/M + 2U/r. \quad (23)$$

From (18) we have

$$W'/MUW = c_2 \quad (24)$$

and substituting in (21) we obtain

$$MW'r - 2MUW - M'Wr = 0 \quad (25)$$

verifying (23). $G_{\alpha}{}^{\mu} = 0$ is therefore compatible with $F^{\mu\alpha} = 0$ provided that c_1 vanishes, independently of the boundary conditions.

Substituting (23) in (17), or in (20), gives

$$W^2 = M^2/(U - 1) \quad (26)$$

whose logarithmic derivative is $2W'/W = 2M'/M - U'/(U - 1)$. Substituting W'/W from (23) we have $dU/(U - 1) = -4dr/r$ whose integral is

$$U = 1/(1 + c_2^2/r^4) \quad (27)$$

¹⁴ From these we readily find $\phi_1 = \Lambda_{1\sigma}{}^{\sigma} = 2(U - 1)/r - W'/W$, $\phi_2 = 0$, $\phi_3 = 0$, $\phi_4 = (M'W - MW')/UW + 2M/r$ as in a previous paper by Wiener and Vallarta. Here $\Lambda_{\nu\sigma}{}^{\mu} = \Gamma_{\nu\sigma}{}^{\mu} - \Gamma_{\sigma\nu}{}^{\mu}$, whereas in the previous paper $2\Lambda_{\nu\sigma}{}^{\mu} = \Gamma_{\nu\sigma}{}^{\mu} - \Gamma_{\sigma\nu}{}^{\mu}$.

where c_3^2 is an integration constant. We then have from (24), (26), (27) and the boundary conditions

$$1/W = 1 + c_4 \int_r^\infty r^{-2} (1 + c_3^2/r^4)^{-3/2} dr \quad (28)$$

where $c_4 = -ic_2c_3$. From (24) or (26)

$$1/M = (1/ic_3) \left(1 + c_4 \int_r^\infty r^{-2} (1 + c_3^2/r^4)^{-3/2} dr \right) r^2 (1 + c_3^2/r^4)^{1/2} \quad (29)$$

and we finally obtain the quadruple

$$\begin{aligned} {}_1h^1 &= 1/U = 1 + c_3^2/r^4, \quad {}_2h^2 = 1, \quad {}_3h^3 = 1 \\ {}_4h^1 &= -M/UW = -(ic_3/r^2)(1 + c_3^2/r^4)^{1/2}, \\ {}_4h^4 &= 1/W = 1 + c_4 \int_r^\infty r^{-2} (1 + c_3^2/r^4)^{-3/2} dr. \end{aligned}$$

All the other components vanish.

IV. CASE OF A WEAK FIELD AND DETERMINATION OF THE INTEGRATION CONSTANTS

For large values of r the quadruple $h_s{}^\lambda$ becomes

$${}_1h^1 = 1, \quad {}_2h^2 = 1, \quad {}_3h^3 = 1, \quad {}_4h^1 = -ic_3/r^2, \quad {}_4h^4 = 1 + c_4/r. \quad (30)$$

Einstein has suggested (E.I, p. 695) that in the first approximation the gravitational field is represented by $g_{\alpha\lambda}^* = h_{\alpha\lambda}^* + h_{\lambda\alpha}^*$, where $h_{\alpha\lambda}^*$ is an infinitesimal of the first order defined by $h_{\alpha\lambda}^* = \delta_{\alpha\lambda} h_{\alpha\lambda}^*$, $h_{s\alpha}^* = \delta_{s\alpha} - h_s^\alpha$. To the same approximation the electromagnetic field is defined by $a_{\alpha\mu}^* = h_{\alpha\mu}^* - h_{\mu\alpha}^*$. In the case we are considering all the components of $a_{\alpha\mu}^*$ vanish except the components a_{41}^* , a_{14}^* which give $a_{14}^* = -a_{41}^* = -ic_3/r^2$. If we now interpret this as the ordinary electromagnetic tensor then $a_{14}^* = -iE_r$. Asymptotically this should coincide with the Coulomb field for which $E_r = e/r^2$, hence the constant c_3 is to be interpreted as the electric charge. We note that this constant may be taken either positive or negative. Therefore positive and negative electricity must be taken in this theory as an empirical fact, just as in classical theory.

If we keep terms of the order $1/r$ only, all the components of the tensor $g_{\mu\nu}^*$ vanish except g_{44}^* which becomes $g_{44}^* = -2c_4/r$. To this order of approximation we may identify $g_{44}^*/2$ with the Newtonian potential as in the gravitational theory of 1916.¹⁵ Then the integration constant c_4 is to be interpreted as the gravitational mass.

Expanding in a power series we obtain, from (27), (28), (29):

$$\begin{aligned} U &= 1 - e^2/r^4 + \dots \\ 1/W &= 1 + m/r + (3/10)me^2/r^5 + \dots \\ M &= (e/r^2)(1 - m/r + m^2/r^2 + \dots). \end{aligned} \quad (31)$$

¹⁵ A. Einstein "Die Grundlagentheorie der allgemeinen Relativitätstheorie," p. 57, Leipzig, Barth, 1916.

From these expressions it is immediately seen that the electric and gravitational fields of a charged mass particle cannot be separated except when the distance r becomes sufficiently large. In the immediate neighborhood of the particle one cannot speak separately about a Coulomb field and a Newtonian field, as in classical theory, because they are inextricably bound together. This may be of importance in problems having to do with the stability of the nucleus and the constitution of the electron, but the time does not seem to have yet arrived when such problems can be treated quantitatively on the basis of the present theory, for reasons to be briefly discussed below.

V. COMPARISON WITH THE RESULTS OF EINSTEIN AND MAYER

With the interpretation of the integration constants obtained in the preceding section our quadruple becomes

$${}_1h^1 = 1 + e^2/r^4, \quad {}_2h^2 = 1, \quad {}_3h^3 = 1$$

$${}_4h^1 = - (ie/r^2)(1 + e^2/r^4)^{1/2}, \quad {}_4h^4 = 1 + m \int_r^\infty r^{-2}(1 + e^2/r^4)^{-3/2} dr.$$

To show the identity between our results and those of Einstein and Mayer we first make the transformation $x_4 = ix'_4$, both in the local and the Gaussian variables. The only component affected is ${}_4h^1$ which becomes

$${}_4h^1 = (e/r^2)(1 + e^2/r^4)^{1/2}.$$

We next revert to Cartesian coordinates, obtaining the quadruple (12) with

$$E = - (U - 1)/Ur^2, \quad F = 1/W, \quad G = - M/rUW$$

Lastly we make the transformation of the Gaussian space coordinates

$$x'^\alpha = e^{\int (u-1) d\tau/r} x^\alpha = (1 + e^2/r^4)^{1/4} x^\alpha \quad (\alpha = 1, 2, 3)$$

Remembering that h_s^γ transforms as a contravariant vector with respect to a change of Gaussian variables, i.e. according to the usual formula

$$(h_s^\gamma)' = h_s^\sigma \frac{\partial x'^\gamma}{\partial x^\sigma}$$

we obtain the quadruple

$$({}_1h^1)' = ({}_2h^2)' = ({}_3h^3)' = (1 - e^2/r'^4)^{-1/2}$$

$$({}_1h^4)' = ex'/r'^3(1 - e^2/r'^4)^{1/4}, \quad ({}_2h^4)' = ey'/r'^3(1 - e^2/r'^4)^{1/4},$$

$$({}_3h^4)' = ez'/r'^3(1 - e^2/r'^4)^{1/4}, \quad ({}_4h^4)' = 1 + m \int_{r'}^\infty r'^{-2}(1 + e^2/r'^4)^{1/4} dr'.$$

where $r'^2 = x'^2 + y'^2 + z'^2$. All the other components vanish. This is precisely the solution obtained by Einstein and Mayer by a different method.

VI. THE TIME SYMMETRICAL FIELD

By a time symmetrical field we understand one whose Riemann interval is not altered by changing $+dt$ into $-dt$. The condition for time symmetry is therefore that all the components of the tensor $g_{\mu\nu}$ shall vanish whenever either $\mu=4$ or $\nu=4$ except when $\mu=\nu=4$. This requires that $M=0$.

We solve the field equations $F^{\mu\alpha}=0$, $G_{\alpha}{}^{\mu}=0$ under this assumption. Without going into the detail of the calculations, which have already been reported at length in the preceding pages, we note the results: All the components of the tensor $F^{\mu\nu}$ vanish identically. The components of $G_{\alpha}{}^{\mu}$ which do not vanish identically are G_1^1 , G_2^2 , G_3^3 , G_4^4 . From these we get the equations:

$$G_1^1 = -2(U-1)/Ur^2 = 0$$

$$G_2^2 = G_3^3 = -[2(U-1)^2 + U'r/U](1/U^2r^2) = 0$$

$$G_4^4 = (1/U^3W^3r)(UWW''r - U'WW'r - 2UW'^2r + 2U^2WW') = 0.$$

The first equation admits evidently the only solution $U=1$, which is also a solution of the second. From the third we obtain $W'' - 2W'^2/W + 2W'/r = 0$ from which $W'r^2/W^2 = \text{const} = c_1$ and $1/W = c_1/r + c_2$. Using the boundary condition $1/W=1$ for $r \rightarrow \infty$ gives $c_2=1$; hence $W=1/(c_1/r+1) = 1 - c_1/r$ approximately. As before c_1 may be interpreted as the gravitational mass by noting that in a weak field g_{44}^* is twice the Newtonian potential. The quadruple is in this case:

$${}_1h^1 = U^{-1} = 1, \quad {}_2h^2 = 1, \quad {}_3h^3 = 1, \quad {}_4h^4 = W^{-1} = (m/r + 1).$$

All the other components vanish.

It is seen that in this case we obtain asymptotically the Newtonian potential just as in the previous case without time symmetry, but now there is no asymptotic electric field since all the components of $a_{\mu\nu}^*$ vanish. Thus the existence of an electrostatic field in the unified theory depends on the asymmetry of past and future ($-dt$ and $+dt$). We believe that this is the first instance that this asymmetry has been found to have any physical significance in connection with a field theory. The existence of the gravitational field, on the other hand, is apparently not connected with this asymmetry. We may perhaps have found here the fundamental difference, superficial similarity notwithstanding, between the gravitational and the electric field of a charged mass particle.

VII. CONCLUDING REMARKS

In the absence of a law of motion, not yet discovered, the path of an exploring particle in the unified field cannot be calculated. If it were assumed, for instance, that the orbit of a mass particle in a pure gravitational field is a geodesic with respect to the Riemannian ds^2 , as in the 1916 theory, then a simple calculation shows that in the case of Mercury the advance of the perihelion would be $7''$ per century, approximately. For the same reason the path of a light ray in the solar field cannot be predicted. If it were assumed that the path is a geodesic of zero length with respect to the Riemannian

nian interval, as in the 1916 theory, then the present experimental evidence would likewise furnish proof against rather than for the unified theory.

The shift of spectral lines towards the red, on the other hand, does not depend on the law of motion of an exploring particle, but only on the component g_{44} of the Riemann metric. One sees immediately from (14) and (31) that the red shift obtained on the basis of the present theory is the same to a first approximation as that predicted on the basis of the 1916 theory. To higher orders of approximation the present theory would lead to expect an effect depending also on the electric charge, but it seems difficult to devise an experiment to test this conclusion. In addition to the first order effect just discussed, the only evidence in favor of the unified theory seems to be that asymptotically it yields the classical Coulomb field and the classical Newtonian potential.

The two burning questions connected with the unified theory are, first, the discovery of the law of motion and, second, the discovery of a connecting link with quantum theory. The solution of these problems will inevitably lead to crucial experimental tests of its physical significance. While still far from the goal of investigations which we have pursued for some time, a few remarks may properly find expression at this time.

Because of the non-linear character of the field equations it is to be expected, just as in the case of the 1916 theory of gravitation, that these equations and the law of motion are not independent. If this conjecture is correct, then a systematic investigation by the method of Lanczos must lead either to the law of motion or to the proof that there is none. It should be emphasized that the choice of a law of motion is a considerably more difficult matter in the present theory than in the 1916 theory, because in the latter case the Riemannian geodesic is the natural generalization of the Euclidean straight line, so that even without a systematic investigation one would expect on the basis of the Principle of Equivalence that the path of the exploring particle is a geodesic. Such is not the case in the unified theory because there are too many intrinsically defined lines in the Einstein geometry, not merely the Riemannian geodesics, which asymptotically reduce to Euclidean straight lines. Hence the difficulty of finding the law of motion without a systematic investigation.

Until recently there seemed to be little doubt that the connecting link between the unified theory and quantum theory would be found through some generalization of the Dirac equations, as suggested by Wigner, Wiener and Vallarta, Tamm, Fock, Weyl and others. None of these attempts has proved satisfactory and some of them have been shown to be definitely erroneous. An entirely new method of attack, however, has been opened by the quantum electrodynamics of Heisenberg, Pauli, Jordan, and Fermi, but even then no great progress seems possible before this theory has been divested of its extreme formalism. A further discussion of these questions would evidently be very much out of place here, but we hope to return to them in the not too distant future.

THE GIBBS-DALTON LAW OF PARTIAL PRESSURES

BY LOUIS J. GILLESPIE

RESEARCH LABORATORY OF PHYSICAL CHEMISTRY, MASSACHUSETTS
INSTITUTE OF TECHNOLOGY*

(Received May 20, 1930)

ABSTRACT

Various formulations of Dalton's law are investigated thermodynamically. The Gibbs formulation is shown equivalent to the statement: The concentration of a gas is the same at equilibrium on either side of a membrane permeable to it alone. The ordinary form of Dalton's law has only a limited equivalence with the Gibbs form. The Lewis and Randall rule of fugacity is shown in many ways analogous to the Gibbs-Dalton law. Application to experimental data shows that the Gibbs-Dalton law, like the Lewis and Randall rule, though possible for gases which do not follow Boyle's law, is only an approximation. In the cases examined, the errors are opposite in sign to those of the Lewis and Randall rule. An outline is given for the application of the Gibbs-Dalton law to the study of equilibrium in gases, and the useful field of application is indicated.

1. THERMODYNAMIC THEORY

GIBBS formulated Dalton's law as follows:¹ "The pressure in a mixture of different gases is equal to the sum of the pressures of the different gases as existing each by itself at the same temperature and with the same value of its potential." He states "It is in this sense that we should understand the law of Dalton, that every gas is as a vacuum to every other gas." A study of Dalton's paper² shows that the spirit of Dalton's principle is very closely represented in the Gibbs formulation, which will hereinafter be called the Gibbs-Dalton law.

The Gibbs-Dalton law is in sharp contrast to the formulations now commonly given, which either omit entirely the essential idea of equilibrium,³ implied in the phrase "at the same temperature and with the same value of its potential," or state⁴ laws of vapor pressure of liquids in contact with inert gases, which laws assume zero the effects of varying pressure and composition, equations for which were given by Poynting and Raoult.

Gibbs disentangled the essential principle from these latter effects and generalized it, ignoring the unimportant distinction between vapor and gas.

* Contribution No. 242.

¹ Gibbs, *Scientific Papers*. I. Thermodynamics, p. 155. Longmans, Green and Co., New York, 1906 and 1928.

² Dalton, *Nicholson's Journ. Science* 5, 241 (1801).

³ Thus the equivalent of proposition (2) below is given by the *Encyclopedia Britannica*, Ed. 14, 6, 995; 13, 389 (1929), by Schaefer, *Einführung in die theoretische Physik*, II, 92, Berlin and Leipzig, 1929, and in a large number of texts on physical chemistry. No text has been found which shows an influence of Gibbs' formulation.

⁴ As in elementary texts on physics, following Ganot, *Traité de Physique*, Ganot, Paris, 1872.

He derived as a consequence of his formulation a series of propositions and pointed out that they, as well as the original formulation, are consistent and possible for gases obeying when pure any equations of state whatever. These propositions are involved in one extraordinarily condensed statement (page 157, just below equation 283). They may be stated as follows.⁵ 1. The concentration⁶ of any gas in a mixture is the same at equilibrium on either side of a membrane permeable to it alone. 2. The pressure of a gaseous mixture is equal to the sum of the individual gases as existing each by itself with the same temperature and volume as the mixture. (This is the common form of Dalton's law.) 3. Each of the quantities: the total energy, heat content, entropy, and $p-T$ and $v-T$ thermodynamic potentials (or free energies) equals the sum of the respective values for the individual gases as existing each by itself with the temperature and volume of the mixture. To these may be added another consequence,⁴ 4: The heat capacity at constant volume of a mixture of gases equals the sum of the heat capacities of the individual gases as existing each by itself at the temperature and volume of the mixture.

For let U be the energy and C the constant-volume heat capacity of the mixture, and U_{iv} and C_{iv} be the energy and heat capacity of any gas (i) of the mixture but in the pure state at the temperature T and the volume V of the mixture.⁷ Then Gibbs shows that $U = \sum_i U_{iv}$, from which $(\partial u / \partial T)_v = \sum_i (\partial u_{iv} / \partial T)_v$. Since $(\partial u / \partial T)_v = C$ we have therefore that $C = \sum_i C_{iv}$.

Gibbs states only one proposition in the nature of a converse, namely: 5. If the total $v-T$ thermodynamic potential (or Helmholtz free energy) of the mixture is equal to the sum of the values of this function for the several component gases existing each by itself in the same quantity as in the gas mixture and with its temperature and volume, then the Gibbs-Dalton law and all its consequences must hold. Two other converse propositions (6 and 7) may be added.

6. If the concentration of each gas in a mixture is the same at equilibrium on either side of a membrane permeable to it alone, the Gibbs-Dalton law and its consequences must hold. Let n_1 be the number of moles (or grams) of gas 1 in the mixture, of which the volume is V , and the pressure p , and let n_{1e} , V_{1e} , and p_{1e} be the corresponding quantities for the pure gas 1 in such a state as to be in equilibrium with the mixture with respect to transfer of gas 1. p_{1e} will be hereafter called the equilibrium pressure, and n_{1e}/V_{1e} the equilibrium concentration. Then by hypothesis,

$$n_1/V = n_{1e}/V_{1e}. \quad (1)$$

Gibbs' equation 98 is

$$dp = (S/V)dT + (n_1/V)d\mu_1 + (n_2/V)d\mu_2 + \text{etc.} \quad (2)$$

⁵ With less elegance, and with some redundancy.

⁶ As in moles per liter, or grams per cc. Dalton uses "density, considered abstractly," and Gibbs, "separate density," or simply "density," for what is now called concentration.

⁷ Naturally also, the same mass of pure gas is considered as is present in the mixture. This is understood to be the case in any of the comparisons, as otherwise no comparison is possible.

By substitution,

$$dp = (S/V)dT + (n_{1e}/V_{1e})d\mu_1 + (n_{2e}/V_{2e})d\mu_2 + \text{etc.} \quad (3)$$

Applying equation 98 in succession to the pure gases 1, 2, etc., we have

$$n_{1e}/V_{1e} = (\partial p_{1e}/\partial \mu_1)_T, \quad n_{2e}/V_{2e} = (\partial p_{2e}/\partial \mu_2)_T, \text{ etc.} \quad (4)$$

By substitution we have at constant temperature

$$dp = (\partial p_{1e}/\partial \mu_1)_T d\mu_1 + (\partial p_{2e}/\partial \mu_2)_T d\mu_2 + \text{etc.} \quad (5)$$

Since each pure gas remains in equilibrium with the mixture, μ and $d\mu$ for any gas is the same in the mixture as for the pure gas. Therefore the last equation may be immediately integrated at constant temperature to

$$p = p_{1e} + p_{2e} + p_{3e} + \text{etc.} + f(T), \quad (6)$$

since each term like $(\partial p_{1e}/\partial \mu_1)_T d\mu_1$ is at constant temperature of the form $(dz/dx)dx$, the variables having been separated. But $f(T)$ must be zero, in order that the expression shall reduce to the identity $p = p_{1e}$ for the special case in which the mixture is replaced with pure gas 1. Evidently the following law is in all ways equivalent to the Gibbs-Dalton law; (1): The concentration of each gas in a mixture is the same at equilibrium on either side of a membrane permeable to it alone.⁸

It should be noted that proposition 2, which is the form of Dalton's law commonly taught in texts on physical chemistry, is a consequence of the Gibbs form, but is less inclusive, as it asserts nothing about equilibrium. We may now show, however, that: (7). If we assume that the Gibbs form is true in the limiting case of infinitely large volumes, then proposition 3 asserted for all pressures, requires the validity of the Gibbs form at all pressures. Let the pure gases be kept throughout the variations at the volume and temperature and in the quantities present in the mixture, and consider variations of V and of n_1, n_2 , etc. Let the pressure and potential of the pure gas 1 at the temperature and volume of the mixture be represented by p_{1v} and μ_{1v} and likewise for other species. Then proposition 2 may be written

$$p = \Sigma(p_{1v} + p_{2v} + \text{etc.}) \quad (7)$$

Then

$$(\partial p/\partial n_1)_{T,v,n} = (\partial/\partial n_1)_{T,v,n} \Sigma(p_{1v}) = (\partial p_{1v}/\partial n_1)_{T,v}. \quad (8)$$

But⁹

$$(\partial \mu_1/\partial V)_{T,n} = -(\partial p/\partial n_1)_{T,v,n} \text{ and } (\partial \mu_{1v}/\partial V)_{T,n_1} = -(\partial p_{1v}/\partial n_1)_{T,v} \quad (9)$$

⁸ The same is true of the proposition: (1a) There is equilibrium when the concentration of a gas is the same on either side of the semipermeable membrane, (the temperature being uniform). This is because Gibbs proves (reference 1, page 67) that equality of potentials and temperature is necessary and sufficient for equilibrium. But even without this, physical reasoning shows that there is no point in observing the logical distinction between (1) and (1a).

⁹ These equations result from cross differentiation of Gibbs' Eq. (88).

and therefore

$$(\partial\mu_1/\partial V)_{Tn} = (\partial\mu_{1e}/\partial V)_{Tn_1}. \quad (10)$$

Hence, since equilibrium is supposed at zero pressure when in equal volumes the numbers of moles of kind 1 are equal in the pure gas and in the mixture, these volumes may be equally reduced as much as we please without changing the numbers of moles; the potentials will change by the same amounts for the pure gas and the mixture, so that their differences will remain zero, and the system will remain in equilibrium. Hence $p_1 = p_{1e}$, and similarly $p_2 = p_{2e}$, etc., and therefore

$$p = \Sigma(p_{1e} + p_{2e} + \text{etc.}) \quad (11)$$

But we believe that the Gibbs-Dalton law holds at zero pressure. When therefore we are interested solely in testing hypothesis or law by means of data, and not at all in developing or presenting a logical system, we may regard the simple additivity of pressures, as expressed in the common form of Dalton's law (proposition 2) as equivalent to the Gibbs formulation.

The theoretical treatment is incomplete if we omit to consider the form in which Dalton's law has frequently been used by specialists interpreting data. This is; (8) the equilibrium pressure of any gas in a mixture equals the total pressure of the mixture times its mole fraction in the mixture, or

$$p_{ie} = p(n_i/\Sigma_i n_i) = px_i, \quad (12)$$

where n_i is necessarily in moles rather than grams, and x_i is the mole fraction. When we come to examine the applicability of the Gibbs-Dalton law we should compare any success obtained with that obtained by the use of this form, which will be called Dalton's law in the ideal gas form.

Lurie and Gillespie¹⁰ pointed out that this form of Dalton's law contains the laws of Boyle and Avogadro. As their proof was incomplete in form, a complete proof is herewith given. Granted that $p_{ie} = px_i$ for every gas in a gas mixture. Then obviously $p = \Sigma_i px_i = \Sigma_i p_{ie}$, from which, according to the proof given by Gibbs, the concentration of any gas in the mixture, as n_i/V , equals the concentration of the pure gas when under its equilibrium pressure, as n_{ie}/V_{ie} . We have then

$$p_{1e} = px_1 = pn_1/\Sigma_i n_i \quad (13)$$

and

$$V_{1e}/n_{1e} = V/n_1 \quad (14)$$

From which,

$$p_{1e}V_{1e}/n_{1e} = pV/\Sigma_i n_i \quad (15)$$

Similarly

$$p_{2e}V_{2e}/n_{2e} = pV/\Sigma_i n_i \quad (16)$$

¹⁰ Lurie and Gillespie, Journ. Amer. Chem. Soc. 49, 1146 (1927).

Hence

$$p_{1e}V_{1e}/n_{1e} = p_{2e}V_{2e}/n_{2e}. \quad (17)$$

These equations must hold for equilibrium variations of the variables. Among the variables T , p , μ_1 , μ_2 , \dots , etc., only one relation (the fundamental equation) exists. Hence a variation in μ_1 is possible at constant μ_2 , μ_3 , etc., and T . Therefore at constant temperature a variation of p_{1e} is possible at constant p_{2e} , and constancy of p_{2e} requires at constant temperature a constant concentration n_{2e}/V_{2e} . Hence $p_{1e}V_{1e}/n_{1e}$ is a constant during variations of p_{1e} and if n_{1e} is arbitrarily held constant, pV is constant. This is Boyle's law. Furthermore, the constant $p_{1e}V_{1e}/n_{1e}$ is evidently independent in magnitude of the character of gas 1, and would be the same for some other gas. Hence this equation includes Avogadro's law, that n is the same for any gas when p and V are the same. If, also, these relations hold at any constant temperature, the expansions of the different gases must be alike. Hence this form of Dalton's law contains all of the laws of ideal gases except those relating to the energy (such as $(\partial u/\partial V)_T = 0$, or that pV is proportional to *thermodynamic* temperature), and, in the lack of a conventional name, may well be called Dalton's law in the ideal gas form.

The rule of Amagat,¹¹ that the volume of a gaseous mixture equals the sum of the volumes of the individual gases as existing each by itself at the temperature and (total) pressure of the mixture, is not here regarded as a form of Dalton's law.¹² It is analogous to the law of additive pressures (proposition 2) in many ways. Thus the fugacity rule of Lewis and Randall¹³ bears to this rule a relation similar to that existing between the Gibbs-Dalton law and the additivity of pressures. This fugacity rule, when the variable is changed from fugacity to chemical potential, states that the difference between the chemical potential of a gas in equilibrium with a mixture and the potential it would have at the temperature and pressure of the mixture is the same as for a system of ideal gases, i.e., $RT \ln x$. According to the Gibbs-Dalton law the difference between the potential of a gas in equilibrium with a mixture and the potential it would have at the temperature and volume of the mixture is the same as for a system of ideal gases, i.e., zero. As stated by Lewis and Randall, their rule implies the additivity (at constant temperature and pressure) of volume and heat content. As shown by the author,¹⁴ the additivity of volumes is enough, together with suitable assumptions relating to the gases at zero pressure (which may be, for example, that the rule is exact at zero pressure) to establish the rule. Furthermore, the rule makes the partial molal volume \bar{V}_1 of a gas in a mixture equal to the molal volume V_{1p} of the pure gas at the temperature and

¹¹ Amagat, Ann. chim. phys. [5] 19, 384 (1880); Compt. rend. 127, 88 (1898).

¹² Fortunately very few authors have called it Dalton's law. Curiously, this form was actually stated by Dalton, whereas the common form was not stated by him, though it was used. The two forms are naturally equivalent when ideal gases are under consideration, as was the case in all of Dalton's considerations.

¹³ Lewis and Randall, Thermodynamics, McGraw-Hill Book Co. Inc., New York, 1923.

¹⁴ Gillespie, Journ. Amer. Chem. Soc. 47, 305 (1925).

pressure of the mixture; that is, $\bar{V}_1 - V_{1p}$ and its temperature and pressure derivatives become zero. Examination now of equations 6a, 7, 10, and 14 of a previous paper¹⁵ will show that this leads to the following consequences. The difference between any one of the functions: the total energy, heat content, entropy, and $p-T$ and $v-T$ thermodynamic potentials for the mixture, as against the sum of the corresponding values of any function for the individual gases taken at the temperature and pressure of the mixture, must have at all pressures the same value as at zero pressure. This difference is zero for the energy and heat content, but is expressed in terms involving $\log x$ in the case of the entropy and the two thermodynamic potentials, whereas according to the Gibbs-Dalton law the corresponding differences (taken at the temperature and volume of the mixture) are all zero. Finally, the rule makes the heat capacities at constant pressure additive, since these are the temperature derivatives at constant pressure of the additive heat contents.

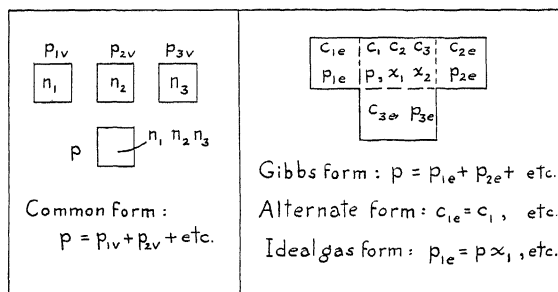


Fig. 1. Illustrating various forms of Dalton's law.

In Fig. 1 some of the principal relations among the forms of Dalton's law are shown and the use of symbols illustrated.

2. COMPARISON OF THE GIBBS-DALTON LAW WITH DATA

Figure 2 (L-G) Data of Lurie and Gillespie. These data are the values of p and x_1 for mixtures of ammonia (subscript 1) and nitrogen (subscript 2) at 45° observed for corresponding values of p_{1e} , which is the vapor pressure of barium chloride octammine corrected for the total pressure. In the former comparison, the quantities calculated and observed were the equilibrium pressure p_{1e} . A more direct comparison is here given between the calculated and observed values of x_1 . In the present calculations from the Gibbs-Dalton law the Beattie-Bridgeman equations of state¹⁶ for both gases were used. Fig. 2 shows the observed minus the calculated mole percent ammonia in percent deviation of the observed value. The percentage deviations are shown for the Gibbs-Dalton law (circles, solid line) and for Dalton's law in the ideal gas form (squares, broken line).

¹⁵ Gillespie, Phys. Rev. **34**, 1605 (1929).

¹⁶ Beattie and Bridgeman, Proc. Amer. Acad. Arts and Sci. **63**, 229 (1928).

Figures 2 and 3. Data of Larson and Black.¹⁷ These are the values of p and x_1 for mixtures of ammonia (subscript 1) and hydrogen-nitrogen (subscript 2) in a constant mole ratio of 3:1, observed for corresponding

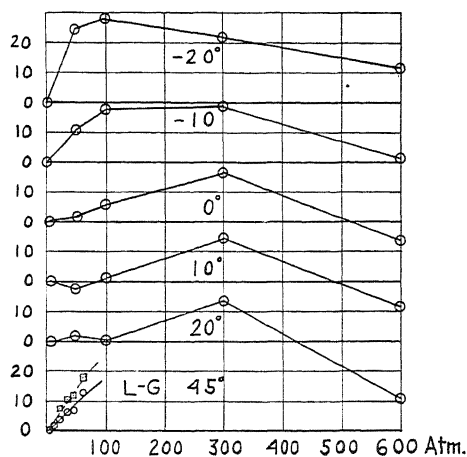


Fig. 2. Errors of the Gibbs-Dalton law.

values of p_{1e} , the vapor pressure of liquid ammonia corrected for the lowering due to dissolved gas and the raising due to the increased total pressure. The temperatures are from -20° to 20°C . The thermodynamic calculations

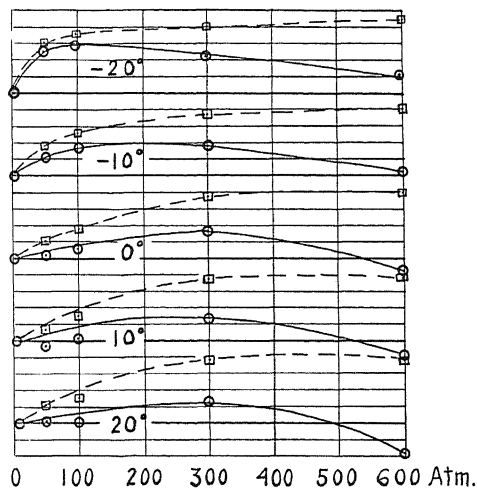


Fig. 3. Errors of the Gibbs-Dalton law.

were performed by Cupples¹⁸ for the purpose of determining the existence of a true "solvent action." Previous authors had ascribed deviations from

¹⁷ Larson and Black, *Journ. Amer. Chem. Soc.* **47**, 1015 (1925).

Dalton's law in the ideal gas form to the existence of a solvent action. The solvent action, as defined by him, is zero when the concentration of gas is the same at equilibrium on either side of an appropriate membrane. From the theoretical part above, it is evident that such calculations afford a direct test of the Gibbs-Dalton law. These calculations extend to 600 atmospheres, at which point the vapor pressure has been corrected to double its original value for the increase in total pressure. In applying this correction, the equation of state of ammonia has to be extrapolated well into the region of supersaturation and it is difficult or impossible at present to determine just how much reliance may be put on the calculations at the higher pressures. Consequently, more emphasis will here be put on the trends at the lower pressures. Figure 2 shows the percentage deviation, observed minus calculated mole percent ammonia, the percentage being based on the observed. As in the previous figure the deviation must be zero when the total pressure is equal to the normal vapor pressure, the mole fraction of ammonia then being unity. In Fig. 2 the points are connected by straight lines in order not to prejudice the smoothing. In Fig. 3 smoothed curves are drawn (solid lines near the circles) for the Gibbs-Dalton law, and also for the ideal gas form (broken lines and squares). The lines of zero deviation are heavy, and the scale divisions of ordinates are 10 percent in all cases.

Examination of the figures shows that the Gibbs-Dalton law fails to fit the data, especially at the lower pressures, where the calculations are most certain. It is true that in Fig. 2 at 10 and 20° the deviations are substantially zero for 50 and 100 atmospheres, and if only these two isotherms were given, one might conclude that the deviations appear to be zero, perhaps even above 300 atmospheres. This would involve the ignoring of the 300 atmosphere points. Taking the picture as a whole there appears to be no doubt that it is rather the 50 and 100 atmosphere points which are in error, and that the family of curves should be drawn with maxima, which move towards higher pressure at higher temperature. The deviations of the Gibbs-Dalton law are in all cases smaller than those of the ideal gas form, but the difference is not in most cases impressive. There is a hint that the contrary may be the case at sufficiently high pressures.

The existence of maxima in the curves seems consistent with the findings of Masson and Dolley¹⁹ in the cases of mixtures of ethylene with oxygen; here the deviations from the law of additive pressures also increase at first with pressure and pass through a maximum, in some cases changing sign at the highest pressures. In general it appears that the maximum occurs at lower pressures, the less perfect the gas mixture.

The foregoing conclusions, as respects the data of Larson and Black, are not the same as those drawn by Cupples. The principal reason for this appears to be that his plot, based on different variables, does not show the zero deviations which must occur at all temperatures in the limiting case in which the gas phase is pure ammonia.

¹⁸ Cupples, *Journ. Amer. Chem. Soc.* **51**, 1026 (1929).

¹⁹ Masson and Dolley, *Proc. Roy. Soc. London* **103A**, 524 (1923).

3. APPLICATION

By virtue of certain assumptions as to the properties of gaseous mixtures and pure gases at infinitely low pressures, which may for present purposes be freely expressed as follows: the behavior of real gases approaches that of ideal gases at zero pressure,—it is possible to correlate equilibrium data in a purely thermodynamic manner with pressure data for the pure gases in question and for mixtures of them, together with specific heats also, if temperature correlation is included. To avoid the necessity of data on gas mixtures, some assumption may be made regarding the pressures or volumes of gaseous mixtures, compared with those of their constituent pure gases. Only three such assumptions are to be found as the basis of methods which have received any degree of attention.²⁰ They are (1) the additivity of pressures or the Gibbs-Dalton law, (2) the additivity of volumes or the Lewis and Randall rule of fugacity, and (3) the additivity of equation of state constants, usually described in publications from this laboratory as linear combination of constants.²¹

Examination of the pressure data of mixtures, as well as application to equilibria, has shown that the third method is in general more accurate than the other two methods.²² Nevertheless the former two may be of service in special instances, due to the fact that in certain types of calculation they will require much less computation than the third method.

For calculations of the effect of pressure upon equilibrium constants the Lewis and Randall rule is especially adapted. It fits the Haber equilibrium data up to about 100 atmospheres.²³ A mass action equation may readily be derived from the Gibbs-Dalton law and the individual equations of state, but it has the disadvantage that the expression for the effect of pressure on the equilibrium constant involves terms in mole fractions, which would greatly complicate the calculation. Neither method can be trusted to give accurately the effect of varying mole fraction on the equilibrium constant.

For the calculation of the concentrations of a gaseous mixture which is in equilibrium with a liquid or other phase, or even for the calculation of the mole fractions of such a mixture, the Gibbs-Dalton law is especially adapted. It has an important advantage over the Lewis and Randall rule, that the

²⁰ We omit here the usual Dalton law in the ideal gas form, as its use is inconsistent with any equation of state but that of Boyle.

²¹ *I. e.*, linear in all the constants which are of the first power in the volume and in the square root of the cohesive pressure A constant, which root is of the first power.

²² Evidence in support of it may be marshalled from the following papers. Lurie and Gillespie reference 10; Keyes and Burks, *Journ. Amer. Chem. Soc.* **50**, 1100 (1928); Beattie, *Journ. Amer. Chem. Soc.* **51**, 19 (1929); Gillespie, *Phys. Rev.* **34**, 352 (1929); Beattie and Ikeshara, "An Equation of State for Gas Mixtures. II. A Study of the Methods of Combination of the Constants of the Beattie-Bridgeman Equation of State." (to be published soon); and Gillespie and Beattie, "Correlation of the Haber Equilibrium Data with Compressibilities and Specific Heats of the Pure Gases by Means of a Rational Mass Action Equation" (to be published soon).

²³ Gillespie, *Journ. Amer. Chem. Soc.* **48**, 28 (1926).

equations of state do not need such severe extrapolation into the region of supersaturation. Thus for the data of Lurie and Gillespie at a total pressure of 60 atmospheres, the equation of state needs extrapolation from 7.1 to 60 atmospheres in the one case and from 7.1 to but about 7.4 atmospheres in the other.

An outline of the calculations from the Gibbs-Dalton law follows.

Let $p_1 = f_1(T, n_1/V)$, $p_2 = f_2(T, n_2/V)$, etc., be the equations of state of the several gases. Then $p = f_1(T, n_1/V) + f_2(T, n_2/V) + \text{etc.}$, where p and V are the pressure and volume of the mixture and n_1, n_2 , etc., are the numbers of moles in the mixture.

Solution for the equilibrium pressure, p_{1e} , of a gas (1) in the mixture from known values of p and the mole fractions x_1, x_2 , etc., proceeds by putting $\sum_i n_i = 1$ and finding by trial a value of V which will satisfy

$$p = f_1(T, x_1/V) + f_2(T, x_2/V) + \text{etc.} \quad (18)$$

When the computed pressure finally checks the observed pressure, the final values of $f_1(T, x_1/V)$, $f_2(T, x_2/V)$, etc., are the calculated equilibrium pressures. Any equilibrium pressure is the pressure of the pure gas that would be in equilibrium with the mixture; and, when a liquid is in equilibrium with the mixture, the equilibrium pressure is equal to the vapor pressure of the liquid, corrected by means of Poynting's equation for the increased total pressure, and by means of Raoult's law for the solubility of the inert gases in the liquid.²⁴

Solution for the mole fractions from known equilibrium pressures and the known pressure of the mixture proceeds as follows. Calculate n_1/V from the equilibrium pressure p_{1e} of gas 1 by means of the equation of state:

$$p_{1e} = f_1(T, n_1/V) \quad (19)$$

by successive approximations. If the mixture is binary, $p_{2e} = p - p_{1e}$, and n_2/V may be similarly calculated from the equation of state of gas 2. If the mixture is binary with respect to a gas (1) like ammonia and a mixture (2) of gases in constant mole ratio, such as a 3:1 hydrogen-nitrogen mixture, treat this constant mixture (which will not change greatly through differential solubility) as a pure gas whose constants are obtained by "linear combination of constants,"^{21,22} unless the equation for the mixture has already been determined. If the mixture is ternary or more complicated, another equilibrium pressure must obviously be known for each added constituent. When in any case the values of n_1/V , n_2/V , etc. have been calculated, any mole fraction is immediately found from the relation

$$x_i = \frac{n_i/V}{\sum_i (n_i/V)} \quad (20)$$

In order to avoid some of the successive approximations, the volume equation of Beattie²⁵ may be used. The calculations may also be done

²⁴ This latter correction was found small by Larson and Black (17).

²⁵ $(V/n_i) = f_i(T, p)$, Beattie, Proc. Nat. Acad. Sci. 16, 14 (1930).

throughout by means of graphs. It is of course unnecessary to introduce fugacities²⁶ unless some of the experimental information is found expressed in terms of them.

4. THE SIGN OF THE ERRORS IN THE APPLICATION

At low pressures the partial volume \bar{V}_1 of a gas in a mixture is found in general to be greater than the molal volume V_{1p} of the pure gas at the pressure and temperature of the mixture.²⁷ From an equation previously given²³

$$RT \ln f_1 = \int_0^p (\bar{V}_1 - RT/p) dp + RT \ln p x_1 \quad (21)$$

the signs of the errors to be expected of the Lewis and Randall rule at low pressures can readily be determined. For according to the rule, $\bar{V}_1 = V_{1p}$, hence in applying the rule a value of the integral is virtually used which is too small algebraically. Hence the mole fraction x_1 calculated by the rule from a known fugacity f_1 (determined from the vapor pressure, of which it is an increasing function) will come out too large.

In the case of the Gibbs-Dalton law, no special study has been made of the analogous quantity $(\partial p / \partial n_1)$. It is worthy of notice, however, that the mole fractions calculated from the vapor pressures are too low at the lower pressures in the cases examined above. Thus, at least in these cases, the true value evidently lies between those given by the two approximate methods.

²⁶ If this is desired, the paper of Cupples may be consulted. (18).

²⁷ Gillespie, *Phys. Rev.* 34, 352 (1929).

A RATIONAL BASIS FOR THE THERMODYNAMIC TREATMENT OF REAL GASES AND MIXTURES OF REAL GASES

BY JAMES A. BEATTIE

RESEARCH LABORATORY OF PHYSICAL CHEMISTRY, MASSACHUSETTS

INSTITUTE OF TECHNOLOGY.*

(Received May 19, 1930)

ABSTRACT

From the general laws of thermodynamics and two isothermal assumptions, one of which states that at constant temperature the energy of a pure gas approaches a function of the temperature in the following manner:

$$U_1 = f_1(T) + \zeta_1 p$$

and the other that at constant temperature and composition the ratio of the equilibrium pressure of a gas in a mixture to the product of the mole fraction of the gas in the mixture multiplied by the total pressure of the mixture approaches unity in the following manner:

$$\frac{p_{ei}}{p x_i} = 1 + \xi_i p$$

where ζ_i and ξ_i are bounded parameters, it has been shown that the following relations hold for real gases or mixtures of real gases at infinitely low pressures:

(a). The ratio of the equilibrium pressure of a gas to the product of its mole fraction in the mixture multiplied by the total pressure of the mixture is unity.

(b). The ratio of the equilibrium concentration of a gas to its concentration in the mixture is unity.

(c). The ratio of the sum of the equilibrium pressures (or equilibrium concentrations) of the component gases to the total pressure (or concentration) of the gas mixture is unity.

(d). The entropy, energy, heat content, thermodynamic potentials and heat capacities at constant volume and at constant pressure of a mixture of gases are equal respectively to the sums of the entropies, energies, heat contents, thermodynamic potentials and heat capacities of the component gases existing each by itself with the same value of its volume, temperature and chemical potential as in the mixture. The above statement holds when the component gases exist each by itself with the same value of its volume and temperature as in the gas mixture and with the ratio of its concentration to its concentration in the gas mixture equal to unity.

(e). The energy, heat content and heat capacities of pure gases and of gas mixtures of constant composition are functions of the temperature.

(f). The difference between the heat capacity at constant pressure and that at constant volume of a pure gas or of a gas mixture is equal to the product of the total number of moles present multiplied by the gas constant R .

(g). The pressure-volume product for a pure gas or for a gas mixture is equal to the product of the total number of moles present multiplied by RT where R is a universal constant and T the Kelvin temperature.

* Communication No. 240.

1. INTRODUCTION

IN ORDER to give a general thermodynamic treatment for mixtures of real gases comparable to that given by Gibbs¹ for mixtures of ideal gases it is necessary to make several assumptions. Gillespie² has shown that a general relation for the isothermal variation of the mass action function K_p (which represents chemical equilibria in gaseous systems) can be derived from general thermodynamic considerations together with the one assumption: At very low pressures the "equilibrium pressure" of each gas in a mixture is equal to the product of the mole fraction of that gas in the mixture multiplied by the total pressure of the mixture. It has also been shown³ that relations for the variation of the thermodynamic properties of gas mixtures with temperature and pressure (or volume) can be derived from the above assumption and one other: At very low pressures the energy of a mixture of gases is equal to the sum of the energies of the component gases existing each by itself at the temperature and in the total volume of the mixture. Besides these two assumptions for gas mixtures, there was used the assumption that at very low pressures the pressure of a pure gas is equal to nRT/V .

De Donder⁴ has given relations for some of the thermodynamic properties of gas mixtures on the assumption that, as the pressure on the mixture is decreased at constant temperature, certain properties of the gas mixture approach those of mixtures of ideal gases. Keyes⁵ has given an equation for the mass action function K_p by use of the kinetic considerations from which the Keyes⁶ equation of state was derived.

It is to be noted that the assumptions which it has been found necessary to make relate to the thermodynamic properties of gaseous systems under low pressures. In the following treatment it is shown that all of the necessary relations for the treatment of real gases and mixtures of real gases can be derived from two assumptions, each of which are for isothermal conditions.

We shall consider two pressure regions:

(1) *Low pressures*, at which for all practical purposes terms of the order of p^2 can be neglected in comparison with unity, or with terms of the order of p .

(2) *Very low pressures*, at which for all practical purposes terms of the order of p can be neglected in comparison with unity. An asterisk placed after a thermodynamic quantity is used to denote the values which the quantity in question assumes in the region of very low pressures.

From an experimental standpoint one atmosphere may be considered a "low pressure" for the permanent gases at room temperature; and one centimeter of mercury, a "very low pressure."

¹ Gibbs, *The Scientific Papers of J. Willard Gibbs*, Longmans, Green and Co., New York, 1906; Vol. I, p. 150.

² Gillespie, *Jour. Amer. Chem. Soc.* **47**, 305 (1925); *ibid.* **48**, 28 (1926).

³ Beattie, *Phys. Rev.* **31**, 680 (1928); *ibid.* **32**, 691, 699 (1928).

⁴ De Donder, *Compt. rend. Acad. Sci. Paris* **180**, 1922 (1925). "L'Affinité," Gauthier-Villars, Paris, 1927.

⁵ Keyes, *Jour. Amer. Chem. Soc.* **49**, 1393 (1927).

⁶ Keyes, *Amer. Soc. Refrig. Eng. Jour.* **1**, 9 (1914); *Proc. Nat. Acad. Sci.* **3**, 323 (1917).

Throughout the present treatment we shall use the greek letters α , β , ζ , η , κ and ξ to denote bounded parameters; that is, parameters whose numerical magnitudes do not exceed an assignable upper limit. When occurring with the subscript 1, they refer to pure gases without reference to any gas mixture, and vary with the temperature; when used without subscripts or with the subscript i they refer to a mixture of gases and vary with the temperature and the composition of the mixture.

2. THE SYSTEM UNDER CONSIDERATION

Let p , V , T be the total pressure, total volume, Kelvin temperature and U , S , H , F_{VT} , F_{pT} , C_V , C_p be the total energy, entropy, heat content, thermodynamic potentials and heat capacities of a mixture of real gases consisting of n_1 , n_2 , \dots moles of the Gases 1, 2, \dots whose chemical potentials in the mixture are μ_1 , μ_2 , \dots . Let $C = \Sigma n_i/V$ be the concentration of the mixture; $C_i = n_i/V$ be the concentration of Gas i in the mixture; and $x_i = n_i/\Sigma n_i$ be the mole fraction of Gas i in the mixture.

Let p_{ei} , U_{ei} , S_{ei} , H_{ei} , $F_{VT_{ei}}$, $F_{pT_{ei}}$, $C_{V_{ei}}$, $C_{p_{ei}}$ be the pressure, energy, entropy, heat content, thermodynamic potentials, and heat capacities respectively of n_{ei} moles of the pure Gas i ($i=1, 2, \dots$) existing by itself in the total volume V , at the temperature T and with the chemical potential μ_i ; the quantities V , T and μ_i having identically the same values that apply to the gas mixture. Let $C_{ei} = n_{ei}/V$ be the concentration of the pure Gas i .

It is evident that the pure Gas i is in equilibrium with the gas mixture with respect to the isothermal transfer of Gas i from the vessel containing the pure gas to that containing the mixture or from the mixture to the pure gas, the chemical potential of the pure Gas i being kept equal to that of Gas i in the mixture throughout the process; that is, each gas would be in equilibrium with the gas mixture through a semipermeable membrane which permits only that gas to pass through. Hence the quantities with the subscript e will be called the "equilibrium" quantities.

Thermodynamic quantities with the subscript 1 refer to pure gases which are considered without relation to any gas mixture.

3. THE ASSUMPTIONS

Assumption 1: At all temperatures⁷ the energy of a real gas differs from a function of the temperature by a quantity which, at constant temperature, approaches zero with the pressure, p in the manner that $\zeta_1 p$ approaches zero with the pressure where ζ_1 and its derivative are bounded.

Assumption 2: At all temperatures⁷ the ratio of the equilibrium pressure of each gas in a mixture to the product of the mole fraction of that gas in the mixture multiplied by the total pressure p of the mixture differs from unity by a quantity which, at constant temperature and composition, approaches zero with the total pressure in the manner that $\xi_i p$ approaches zero with the total pressure, where ξ_i and its derivatives are bounded.

⁷ This means, of course, for the temperature range for which the resulting thermodynamic relations are to be used. The region in the immediate neighborhood of 0°K is to be excluded.

Thus for all temperatures we may write for low pressures:

$$U_1 = f_1(T) + \zeta_1 p \quad (1)$$

$$\frac{p_{ei}}{p x_i} = 1 + \xi_i p \quad (i = 1, 2, \dots). \quad (2)$$

In Eq. (1) U_1 is the energy of n_1 moles of any pure Gas 1, T the Kelvin temperature and p the pressure of the gas; the function $f_1(T)$ is a characteristic function of the temperature for each gas, and the parameter ζ_1 varies with the temperature. In Eq. (2) p_{ei} is the equilibrium pressure of Gas i , x_i its mole fraction in the mixture and p the total pressure of the mixture; the parameter ξ_i varies with the temperature and composition of the mixture.

At very low pressures (1) and (2) become:

$$U_1^* = f_1(T) \quad (3)$$

$$\left(\frac{p_{ei}}{p x_i}\right)^* = 1 \quad (i = 1, 2, \dots). \quad (4)$$

Thus:

At very low pressures the energy of a pure gas is a function of the temperature alone.

At very low pressures the ratio of the equilibrium pressure of a gas to the product of the mole fraction of the gas in the mixture multiplied by the total pressure of the mixture is unity.

4. THE EQUILIBRIUM CONCENTRATION

For the gas mixture we may write the fundamental equation:

$$V dp = S dT + n_1 d\mu_1 + n_2 d\mu_2 + \dots \quad (5)$$

and for each pure gas there is a relation of the type:

$$V dp_{ei} = S_{ei} dT + n_{ei} d\mu_i \quad (i = 1, 2, \dots) \quad (6)$$

where V , dT , $d\mu_1$, $d\mu_2$, \dots have identically the same values in (5) and (6). From (5) we see that:

$$\left(\frac{dp}{d\mu_i}\right)_{T, \mu} = \frac{n_i}{V}; \quad \left(\frac{dp}{dT}\right)_\mu = \frac{S}{V} \quad (i = 1, 2, \dots) \quad (7)$$

and from (6):

$$\left(\frac{dp_{ei}}{d\mu_i}\right)_T = \frac{n_{ei}}{V}; \quad \left(\frac{dp_{ei}}{dT}\right)_{\mu_i} = \frac{S_{ei}}{V} \quad (i = 1, 2, \dots) \quad (8)$$

The subscript μ to a partial derivative indicates that during the differentiation all of the μ 's are held constant, unless the differentiation is with respect to one of the μ 's in which case all of the other μ 's are held constant.

Eq. (2) can be written:

$$p_{ei} = p x_i (1 + \xi_i p) \quad (i = 1, 2, \dots) \quad (9)$$

Adding the equilibrium pressures for all of the gases in the mixture and placing $\sum x_i = 1$, we obtain:

$$\sum p_{ei} = p(1 + \xi p) \quad (10)$$

where ξ has been written for $\sum x_i \xi_i$. Differentiation of (10) successively with respect to μ_1, μ_2, \dots gives the relations:

$$\left(\frac{dp_{ei}}{d\mu_i} \right)_T = \left(\frac{dp}{d\mu_i} \right)_{T,\mu} (1 + 2\xi p) + p^2 \left(\frac{d\xi}{d\mu_i} \right)_{T,\mu} \quad (i = 1, 2, \dots) \quad (11)$$

Since:

$$\left(\frac{d\xi}{d\mu_i} \right)_{T,\mu} = \left(\frac{dp}{d\mu_i} \right)_{T,\mu} \left(\frac{d\xi}{dp} \right)_{T,\mu_2,\mu_3,\dots} \quad (i = 1, 2, \dots) \quad (12)$$

Eq. (11) may be written:

$$\left(\frac{dp_{ei}}{d\mu_i} \right)_T = \left(\frac{dp}{d\mu_i} \right)_{T,\mu} \left[1 + 2\xi p + p^2 \left(\frac{d\xi}{dp} \right)_{T,\mu_2,\mu_3,\dots} \right] \quad (i = 1, 2, \dots) \quad (13)$$

By Assumption 2 the partial derivative in the last term of (13) is bounded, and hence this term is of higher order than $2\xi p$. Replacing the partial derivatives of (13) by use of the relations (7) and (8) we obtain for low pressures the equations:

$$\frac{n_{ei}}{V} = \frac{n_i}{V} (1 + 2\xi p) \quad (i = 1, 2, \dots) \quad (14)$$

In terms of concentrations (14) becomes:

$$\frac{C_{ei}}{C_i} = 1 + 2\xi p \quad (i = 1, 2, \dots) \quad (15)$$

and at very low pressures:

$$\left(\frac{C_{ei}}{C_i} \right)^* = 1 \quad (i = 1, 2, \dots) \quad (16)$$

At very low pressures the ratio of the equilibrium concentration of a gas to its concentration in the gas mixture is unity.

Eq. (16) may be written in a form corresponding more closely to (4):

$$\left(\frac{C_{ei}}{C x_i} \right)^* = 1 \quad (i = 1, 2, \dots) \quad (17)$$

5. THE LAWS OF BOYLE AND AVOGADRO

Lurie and Gillespie⁸ have shown that if Eq. (4) holds at all pressures, then the gases obey the laws of Boyle and of Avogadro. Similar results may be obtained for real gases at very low pressures from the Assumption 2. When the relation (9) for each gas is divided by the corresponding relation (14), we obtain:

$$\frac{p_{ei}V}{n_{ei}} \frac{1}{1 + \xi_i p} = \frac{pV}{\Sigma n_i} \frac{1}{1 + 2\xi p} \quad (i = 1, 2, \dots) \quad (18)$$

Consider that n_{e1}, n_{e2}, \dots moles of the pure gases 1, 2, \dots and Σn_i moles of the gas mixture are placed in separate compartments each of volume V and at temperature T , and that the chemical potential of each of the pure gases has the same value during all variations as that which it has in the gas mixture. Let T, μ_1, μ_2, \dots be taken as the independent variables as in Eqs. (5) and (6). In the following discussion all variations are made at constant temperature. With μ_1 held constant both for the pure gas and the gas mixture we can vary μ_2, μ_3, \dots thus causing the pressures and concentrations of the Gases 2, 3, \dots and of the gas mixture to vary. From (6) we see that the first term of (18) for Gas 1 cannot vary except through the factor $(1 + \xi_1 p)$, but the effect of this variation can be made as small as desired by carrying out the whole process at sufficiently low pressures. At very low pressures the first term of (18) for Gas 1 may be considered constant during the given variations and hence each of the other terms must have remained constant during the variations. But Gas 2 or any other of the gases could just as well have been chosen as the one whose chemical potential was held constant. Hence for all isothermal variations of the chemical potentials at very low pressures:

$$\left(\frac{p_1 V_1}{n_1}\right)^* = \left(\frac{p_2 V_2}{n_2}\right)^* = \dots = \left(\frac{pV}{\Sigma n_i}\right)^* = \text{constant} = F(T). \quad (19)$$

The terms of (19) are each individually constant at constant temperature for gases or gas mixtures each confined in a cylinder. Hence the quantities $p_1^*, (V_1/n_1)^*, p_2^*, (V_2/n_2)^*, \dots$ which refer to the Gases 1, 2, \dots are no longer necessarily equilibrium values. The temperature function $F(T)$ is the same for all of the gases. For very low pressures we may write:

$$\frac{(pV)^*}{n_1} = F(T) \quad (20)$$

for any pure real gas; and:

$$\frac{(pV)^*}{\Sigma n_i} = F(T) \quad (21)$$

⁸ Lurie and Gillespie, Jour. Amer. Chem. Soc. **49**, 1146 (1927), See also Gillespie, Phys. Rev., **36**, 121 (1930).

for any mixture of real gases. Hence:

At very low pressures the laws of Boyle and Avogadro hold for all real gases and mixtures of real gases.

At very low pressures the ratio of the pressure to the concentration is the same function of the temperature for all real gases and mixtures of real gases.

Now

$$\left(\frac{dU}{dV}\right)_T = T\left(\frac{dp}{dT}\right)_V - p \quad (22)$$

and from this relation together with (1) and (20) it is evident that at low pressures:

$$\frac{pV}{n_1} = F(T) + \beta_1 p \quad (23)$$

or to the same degree of approximation:

$$\frac{pV}{n_1} = F(T) \left(1 + \frac{n_1 \beta_1}{V}\right) \quad (24)$$

where the subscript 1 refers to any pure gas and the parameter β_1 varies with the temperature. Moreover for gas mixtures at low pressures we can evidently write:

$$\frac{pV}{\sum n_i} = F(T) + \beta p \quad (25)$$

or to the same degree of approximation:

$$\frac{pV}{\sum n_i} = F(T) \left(1 + \frac{\sum (n_i) \beta}{V}\right) \quad (26)$$

where the parameter β varies with the temperature and composition of the mixture.

6. ADDITIVITY OF CERTAIN THERMODYNAMIC FUNCTIONS

Gibbs⁹ has shown that if the pressure of a mixture of gases is equal to the sum of the equilibrium pressures of the component gases then certain thermodynamic quantities are "additive." We can derive similar relations for real gases at very low pressures from the Assumption 2.

Differentiating (10) with respect to the temperature at constant μ_1, μ_2, \dots we obtain:

$$\sum \left(\frac{dp_{ei}}{dT}\right)_{\mu_i} = \left(\frac{dp}{dT}\right)_{\mu} (1 + 2\xi p) + p^2 \left(\frac{d\xi}{dT}\right)_{\mu} \quad (27)$$

⁹ Gibbs, Scientific Papers; Vol. I, p. 157.

which may be written:

$$\Sigma V \left(\frac{dp_{ei}}{dT} \right)_{\mu_i} = V \left(\frac{dp}{dT} \right)_{\mu} \left[1 + 2\xi p + p^2 \left(\frac{d\xi}{dp} \right)_{\mu} \right]. \quad (28)$$

The last term is of higher order than $2\xi p$ and may be neglected. Substitution from (7) and (8) into (28), gives for low pressures the result:

$$\Sigma S_{ei} = S(1 + 2\xi p). \quad (29)$$

The energy of the mixture is given by the relation:

$$U = TS - pV + \mu_1 n_1 + \mu_2 n_2 + \dots \quad (30)$$

and for each pure gas there is a relation of the type:

$$U_{ei} = TS_{ei} - p_{ei}V + \mu_i n_{ei} \quad (i = 1, 2, \dots) \quad (31)$$

Adding the Eqs. (31) for all of the gases composing the mixture and making use of the relations (10), (14) and (29), we obtain:

$$\Sigma U_{ei} = TS(1 + 2\xi p) - pV(1 + \xi p) + \Sigma(\mu_i n_i)(1 + 2\xi p) \quad (32)$$

Hence at low pressures:

$$\Sigma U_{ei} = U(1 + 2\xi p) + pV\xi p. \quad (33)$$

From the definitions:

$$H = U + pV \quad (34)$$

$$F_{VT} = U - TS \quad (35)$$

$$F_{pT} = U - TS + pV \quad (36)$$

and the relations already given, we find that at low pressures:

$$\Sigma H_{ei} = H(1 + 2\xi p) \quad (37)$$

$$\Sigma F_{VT_{ei}} = F_{VT}(1 + 2\xi p) + pV\xi p \quad (38)$$

$$\Sigma F_{pT_{ei}} = F_{pT}(1 + 2\xi p). \quad (39)$$

From (25) we note that at low pressures the quantity pV is bounded. By use of the relations already given and the first and second law equation, it can readily be shown that as the pressure on a gaseous system is isothermally reduced, the energy and heat content are bounded, and that the entropy and thermodynamic potentials approach plus or minus infinity in the same manner as $\pm \ln p$. But:

$$\lim_{p \rightarrow 0} p \ln p = 0$$

and hence at very low pressures:

$$\Sigma S_{ei}^* = S^* \quad (40)$$

$$\Sigma U_{ei}^* = U^* \quad (41)$$

$$\Sigma H_{ei}^* = H^* \quad (42)$$

$$\Sigma F_{VT\ ei}^* = F_{VT}^* \quad (43)$$

$$\Sigma F_{pT\ ei}^* = F_{pT}^* \quad (44)$$

At very low pressures the entropy, energy, heat content, and thermodynamic potentials of a mixture of real gases are equal respectively to the sum of the entropies, energies, heat contents, and thermodynamic potentials of the component gases existing each by itself with the same value of its volume, temperature and chemical potential as in the gas mixture.

Further, it is evident from (16) that the above statement applies when the component gases are each taken with the same value of its volume and temperature as in the gas mixture and with the ratio of its concentration to its concentration in the gas mixture equal to unity.

From (10) and (15) it is evident that at very low pressures:

$$\left(\frac{\Sigma p_{ei}}{p} \right)^* = 1 \quad (45)$$

$$\left(\frac{\Sigma C_{ei}}{C} \right)^* = 1 \quad (46)$$

At very low pressures the ratio of the sum of the equilibrium pressures (or equilibrium concentrations) of the gases composing a mixture to the pressure (or concentration) of the gas mixture is unity.

7. THE ENERGY

From Eqs. (1) and (33), we find that at low pressures the energy of a gas mixture can be written:

$$U = \Sigma f_i(T) + \zeta p \quad (47)$$

where the parameter ζ varies with the temperature and composition of the mixture. Hence:

$$U^* = \Sigma f_i(T). \quad (48)$$

At very low pressures the energy of a mixture of real gases is a function of the temperature and composition.

By use of (24) and (26) we can write (1) and (47) to the same degree of approximation in the more convenient forms:

$$U_1 = f_1(T) + \frac{\zeta_1'}{V} \quad (49)$$

$$U = \Sigma f_i(T) + \frac{\zeta'}{V} \quad (50)$$

where ζ_1' and ζ' have somewhat different numerical values from ζ_1 and ζ .

8. THE PRESSURE-VOLUME-TEMPERATURE RELATION

The following treatment is an adaptation of a method which Poincaré¹⁰ used for the case that the relations (3) and (20) hold for all pressures, and which is similar to a method that Phillips¹¹ applied for the case that the isometrics of a gas are strictly linear. We shall use the relations (49) and (24) which apply to real gases at low pressures, and (50) and (26) which apply to mixtures of real gases at low pressures.

Substitution of (49) into the first and second law equation:

$$dS = \frac{dU}{T} + \frac{p}{T}dV \quad (51)$$

gives:

$$dS = \left[\frac{1}{T} \frac{df_1}{dT} + \frac{1}{TV} \frac{d\zeta_1'}{dT} \right] dT + \left[\frac{p}{T} - \frac{\zeta_1'}{TV^2} \right] dV. \quad (52)$$

Since dS is a complete differential:

$$\frac{\partial}{\partial V} \left[\frac{1}{T} \frac{df_1}{dT} + \frac{1}{TV} \frac{d\zeta_1'}{dT} \right] = \frac{\partial}{\partial T} \left[\frac{p}{T} - \frac{\zeta_1'}{TV^2} \right]. \quad (53)$$

The quantities f_1 and ζ_1' do not vary with the volume, hence:

$$\frac{\partial}{\partial T} \left(\frac{p}{T} \right) + \frac{\zeta_1'}{T^2 V^2} = 0 \quad (54)$$

Integration of (54) at constant volume gives:

$$\frac{p}{T} + \frac{1}{V^2} \int \frac{\zeta_1'}{T^2} dT = \Phi \left(\frac{V}{n_1} \right). \quad (55)$$

For all values of the temperature other than zero, Eq. (55) may be written:

$$p = T \Phi \left(\frac{V}{n_1} \right) + \frac{n_1^2 \kappa_1}{V^2}$$

where κ_1 is bounded. From Eq. (24):

$$p = \frac{n_1}{V} F(T) + \frac{n_1^2 \beta_1}{V^2} F(T) \quad (56)$$

whence:

$$\frac{V}{n_1} \Phi \left(\frac{V}{n_1} \right) = \frac{1}{T} F(T) + [\beta_1 F(T) - \kappa_1] \frac{n_1}{VT}. \quad (57)$$

¹⁰ Poincaré, *Thermodynamique*, Gauthier-Villars, Paris, 2nd ed.; p. 160.

¹¹ Phillips, *Jour. of Math. and Physics* **1**, No. 1 (1921).

At very low pressures (57) becomes:

$$\frac{V^*}{n_1} \Phi \left(\frac{V}{n_1} \right)^* = \frac{1}{T} F(T) = \text{constant} = R \quad (58)$$

since a function of the volume can equal a function of the temperature only if each is constant. Hence:

$$F(T) = RT. \quad (59)$$

We would have obtained the same relation by use of Eqs. (50) and (26), and R would have the same value.

Thus Eqs. (23) and (24) for pure gases become:

$$pV = n_1 RT + n_1 \beta_1 p \quad (60)$$

$$pV = n_1 RT \left(1 + \frac{n_1 \beta_1}{V} \right) \quad (61)$$

and (25) and (26) for gas mixtures:

$$pV = \Sigma(n_i)RT + \Sigma(n_i)\beta p \quad (62)$$

$$pV = \Sigma(n_i)RT \left(1 + \frac{\Sigma(n_i)\beta}{V} \right). \quad (63)$$

Hence for real gases at very low pressures:

$$(pV)^* = n_1 RT \quad (64)$$

and for gas mixtures:

$$(pV)^* = \Sigma(n_i)RT. \quad (65)$$

At very low pressures the pressure-volume product for a real gas or for a mixture of real gases is equal to the product of the total number of moles present multiplied by RT where R is a universal constant and T the Kelvin temperature.

9. THE HEAT CONTENT

From the relations (1), (34) and (60) we can write for a pure gas at low pressures:

$$H_1 = f_1(T) + n_1 RT + \eta_1 p \quad (66)$$

where η_1 and its temperature derivative are bounded. Moreover from (47), (34) and (62), there results for a gas mixture at low pressures the relation:

$$H = \Sigma f_i(T) + \Sigma(n_i)RT + \eta p. \quad (67)$$

In (66) and (67), $f_1(T)$ (or $f_i(T)$) is the same function of the temperature as that which occurs in (1). At very low pressures (66) and (67) become:

$$H_1^* = f_1(T) + n_1 RT \quad (68)$$

$$H^* = \Sigma f_i(T) + \Sigma(n_i)RT. \quad (69)$$

10. THE HEAT CAPACITIES AT CONSTANT VOLUME AND AT CONSTANT PRESSURE.

Differentiation of (49) and (50), and of (66) and (67) according to the relations:

$$C_V = \left(\frac{dU}{dT} \right)_{V,n} \quad (70)$$

$$C_p = \left(\frac{dH}{dT} \right)_{p,n} \quad (71)$$

respectively, where the n denotes differentiation at constant composition, gives:

$$C_{V_1} = \frac{df_1(T)}{dT} + \frac{1}{V} \frac{d\zeta_1'}{dT} \quad (72)$$

$$C_V = \Sigma \left(\frac{df_i(T)}{dT} \right) + \frac{1}{V} \frac{d\zeta'}{dT} \quad (73)$$

$$C_{p_1} = \frac{df_1(T)}{dT} + n_1 R + \frac{d\eta_1}{dT} p \quad (74)$$

$$C_p = \Sigma \left(\frac{df_i(T)}{dT} \right) + \Sigma(n_i) R + \frac{d\eta}{dT} p \quad (75)$$

in which C_{V_1} and C_{p_1} refer to pure gases, and C_V and C_p to gas mixtures. Moreover it is evident that at low pressures:

$$C_{p_1} - C_{V_1} = n_1 R + \alpha_1 p \quad (76)$$

$$C_p - C_V = \Sigma(n_i) R + \alpha p \quad (77)$$

where α_1 and α are bounded. At very low pressures the relations (72) to (77) become:

$$C_{V_1}^* = \frac{df_1(T)}{dT}; \quad C_{p_1}^* = \frac{df_1(T)}{dT} + n_1 R \quad (78)$$

$$C_V^* = \Sigma \frac{df_i(T)}{dT}; \quad C_p^* = \Sigma \left(\frac{df_i(T)}{dT} \right) + \Sigma(n_i) R \quad (79)$$

$$C_{p_1}^* - C_{V_1}^* = n_1 R \quad (80)$$

$$C_p^* - C_V^* = \Sigma(n_i) R. \quad (81)$$

At very low pressures the heat capacities at constant volume and at constant pressure of a real gas are functions of the temperature, and those of mixtures of real gases are functions of the temperature and composition.

At very low pressures the difference between the heat capacity at constant pressure and at constant volume for a real gas or for a mixture of real gases is

equal to the product of the total number of moles present multiplied by the universal gas constant R .

From (78) and (79) it is evident that at very low pressures:

$$C_V^* = \Sigma C_{V_i}^* \quad (82)$$

$$C_p^* = \Sigma C_{p_i}^* \quad (83)$$

11. SUMMARY OF THE RELATIONS FOR VERY LOW PRESSURES

It has been shown that the two assumptions for low pressures:

$$U_1 = f_1(T) + \zeta_1 p \quad (1)$$

$$\frac{p_{ei}}{p x_i} = 1 + \xi_i p \quad (2)$$

together with the general laws of thermodynamics are the necessary and sufficient conditions for the following relations to hold at very low pressures:

Relations for real gases

$$(pV)^* = n_1 RT \quad (64)$$

$$U_1^* = f_1(T) \quad (3)$$

$$H_1^* = f_1(T) + n_1 RT \quad (68)$$

$$C_{V_1}^* = \frac{df_1(T)}{dT} \quad (78)$$

$$C_{p_1}^* - C_{V_1}^* = n_1 R \quad (80)$$

Relations for mixtures of real gases

$$(pV)^* = \Sigma (n_i) RT \quad (65)$$

$$U^* = \Sigma f_i(T) \quad (48)$$

$$H^* = \Sigma f_i(T) + \Sigma (n_i) RT \quad (69)$$

$$C_V^* = \Sigma \frac{df_i(T)}{dT} \quad (79)$$

$$C_p^* - C_V^* = \Sigma (n_i) R \quad (81)$$

Equilibrium relationships

$$\left(\frac{p_{ei}}{p x_i} \right)^* = 1 \quad (4)$$

$$\left(\frac{C_{ei}}{C_i} \right)^* = 1 \quad (16)$$

$$\left(\frac{C_{ei}}{C x_i} \right)^* = 1 \quad (17)$$

Additive relationships¹²

$$\left(\frac{\Sigma p_{ei}}{p} \right)^* = 1 \quad (45)$$

$$\left(\frac{\Sigma C_{ei}}{C} \right)^* = 1 \quad (46)$$

$$S^* = \Sigma S_{ei}^* \quad (40)$$

$$U^* = \Sigma U_i^* \quad (41)$$

$$H^* = \Sigma H_i^* \quad (42)$$

$$F_{VT}^* = \Sigma F_{VT_{ei}}^* \quad (43)$$

$$F_{pT}^* = \Sigma F_{pT_{ei}}^* \quad (44)$$

$$C_V^* = \Sigma C_{V_i}^* \quad (82)$$

$$C_p^* = \Sigma C_{p_i}^* \quad (83)$$

¹² When a thermodynamic quantity is bounded as the pressure approaches zero, it is not necessary to include the subscript e since in the region of very low pressures the value of the quantity does not change appreciably with pressure.

It is evident from the derivations given that each of the above relations holds at infinitely low pressures. Hence in each of these relations we may consider that the asterisk denotes "the limit of the quantity (to which the asterisk is attached) as the pressure on the system approaches zero at constant temperature, and subject to certain restrictions on the concentrations of the components." When no chemical reaction between the components of the system is contemplated, the restriction is simply that the composition of the system does not vary; when chemical reaction occurs the restriction is that the system be always maintained in equilibrium, and in this case a variation in composition will occur as the limit is approached. Thus for example, we may write:

$$\lim_{p \rightarrow 0} pV = n_1 RT$$

$$\lim_{p \rightarrow 0} U_1 = f_1(T)$$

$$\lim_{p \rightarrow 0} (C_{p1} - C_{v1}) = n_1 R$$

$$\lim_{p \rightarrow 0} \frac{p_{ei}}{p x_i} = 1$$

$$\lim_{p \rightarrow 0} S = \sum \lim_{p \rightarrow 0} S_{ei}$$

LETTERS TO THE EDITOR

Prompt publication of brief reports of important discoveries in physics may be secured by addressing them to this department. Closing dates for this department are, for the first issue of the month, the twenty-eighth of the preceding month; for the second issue, the thirteenth of the month. The Board of Editors does not hold itself responsible for the opinions expressed by the correspondents.

Breadth of Compton Modified Line

Professors Ross and Clark of Stanford, using the ingenious balanced filter method of Ross, have investigated the shifted line in the Compton effect for antimony, $K\alpha_1$ and $K\alpha_2$, lines scattered from beryllium. In this method the scattering angle is varied so as to vary the shift of the modified line. The scattered radiation is observed with an ionization chamber after passage through a silver filter and then a palladium filter balanced against the silver filter. The difference between the transmissions plotted as a function of the scattering angles exhibits peaks or fluctuations in the curve at the scattering angles of 55° and 75° corresponding to the points at which the shifted lines from $K\alpha_1$, $K\alpha_2$, respectively cross the silver edge of the spectral region defined by the balance filter method.

In view of the fact that the author has published experimental results¹ in which the breadth of the Compton line from molybdenum, $K\alpha_1$, $K\alpha_2$ scattered at nearly 180° from beryllium is too great to permit resolving the α_1 , α_2 peaks, it seems worth while pointing out that these two results are not necessarily discordant. The author's experimental results were accompanied with his theory of the breadth and structure of the Compton line according to which a prominent part of Compton line structure, due to scattering by the free or conduction electrons in metallic scatterers, has a breadth which can best be correlated with the velocities of these electrons required by the Fermi statistics and which furnishes confirmatory evidence of the correctness of the Fermi distribution of velocities for conduction electrons in contradistinction to the older Boltzmann statistics.

According to the author's theory, the breadth of the Compton line, however, depends not only on the velocity distribution

of conduction electrons, but also on the primary wave-length used and on the angle of scattering. In fact, for any given velocity β of randomly moving conduction electrons, the author's theory asserts that the contribution to the Compton line is a small rectangular element having a spectral breadth given by (formula (1), page 647)

$$\Delta\lambda = 4\beta\lambda^*.$$

In this formula, which gives the breadth of the Compton line as a function of scattering angle, the symbol λ^* stands for a wave-length which is defined thus:

$$2\lambda^* = (\lambda_c^2 + \lambda_1^2 - 2\lambda_c\lambda_1 \cos \theta)^{\frac{1}{2}}$$

λ^* is most easily visualized by a diagram. Construct a triangle, one angle of which equals the scattering angle, and having the two adjacent sides to this angle proportional respectively to the primary wave-length λ_1 , and the shifted wave-length λ_c , of the simple Compton theory, for initially stationary electrons. Then the third side of this triangle is proportional to $2\lambda^*$.

On the basis of this formula, the author has computed for the case of Ross' experiment

$$\theta = 75^\circ, \quad \lambda_1 = 469 \text{ X.U.}, \quad \lambda_c = 485 \text{ X.U.}, \quad \lambda^* = 292 \text{ X.U.}$$

$$\theta = 55^\circ, \quad \lambda_1 = 474 \text{ X.U.}, \quad \lambda_c = 485 \text{ X.U.}, \quad \lambda^* = 222 \text{ X.U.}$$

If one assumes in beryllium one conduction electron per atom, this would give a Compton line breadth for Ross' cases of 6.5 and 5X-units, respectively. This refers to the breadth of the line at the base of the part contributed by conduction electrons, which according to the author's calculation seems to come a little below half maximum value. Assuming

¹ J. W. DuMond, Phys. Rev., 33, 643-658 (1929).

two conduction electrons per atom, the corresponding breadths for Ross' cases are 8.4 X.U. and 6.36 X.U. respectively. It seems, therefore, safe to conclude that Ross' resolution of the doublet in the shifted radiation is for the conditions of his experiment not necessarily inconsistent with either the author's theory of Compton shifted line structure or with his published experimental observations.

At the present writing the author, in collaboration with Mr. H. A. Kirkpatrick, has just succeeded in obtaining photographic spectrograms of the Compton shifted line, using Mo $K\alpha_1$, α_2 scattered at 90° from graphite with a maximum inhomogeneity of scattering angle of less than one degree. The unmodified doublet is completely resolved on the negative and the Compton line appears

very broad and diffuse. This work is being done with the fifty-crystal spectrograph described in Review of Scientific Instruments, Vol. 1, No. 2, February 1930.

The author believes that this new instrument at last affords the possibility of investigating the whole question of Compton modified radiation under adequately pure conditions of scattering angle and spectral resolution. We feel that we can now announce with complete assurance that the Compton shifted line is more diffuse than the lines of the primary radiation.

J. W. M. DuMOND

California Institute of Technology,
Pasadena, California,
June 20, 1930.

The Raman Effect in Trimethylethylene

In some experiments made a year ago on the Raman effect in trimethylethylene several diffuse modified lines were found. The stronger correspond to infrared wave-lengths $3.44 \pm 0.05\mu$ and $8.4 \pm 0.2\mu$. Several fainter lines were found between these two. An anti-Stokes line corresponding to 8.4μ was also faintly seen excited by the mercury line 4358A. It seems probable that all these lines can be matched by absorption lines belonging to the group CH although no absorption line was found recorded as long as 8.4μ .

Accidental contamination with rubber added a continuous scattering, with a marked denser band beginning near the position of the strongest line, *ca* 4600A. A continuous

spectrum was obtained in about the same position when a little rubber was dissolved in carbon tetrachloride, making it probable that the effect was due to the rubber and not to a change in viscosity of less than one percent. In this case a suggestion of a second very broad band with maximum about 5500A was also found. If these bands were due to Raman scattering it would be necessary to think of the exciting mercury lines as 4046A and 3650A. The light appeared to be partially polarized.

DOROTHY FRANKLIN
E. R. LAIRD

Mount Holyoke College,
June 14, 1930.

Photoionization of Salt Vapors

The chief interest presented by the photoionization of the vapors of various compounds is that it may afford additional information regarding the structure of molecules. As far as I am aware no such work with the vapors of simple inorganic salts has as yet been done.

In an investigation undertaken by me on these lines with the vapors of halides of various metals, a marked photoionization of these vapors was observed. The illumination was produced by intense ultraviolet light of wave-lengths longer than 1850A. The photoeffect from the electrodes and the walls was negligibly small as compared with the photocurrent from the vapor, in some cases the latter was a hundred times as great as the

photocurrent which could be produced by direct illumination of the electrodes.

On raising the temperature of the salt thermal ionization currents could be observed without illumination, an effect which has been previously extensively studied by G. C. Schmidt and his co-workers (Ann. d. Physik **82**, 664 (1927) **2**, 313 (1929)). The photoionization begins generally at much lower temperatures than the temperatures at which the thermo-current is noticeable.

The salts studied first were TII, TlBr, TlCl. It has been previously shown in this laboratory (Butkow and Terenin, Zeits. f. Physik **49**, 865 (1928), Butkow, *ibid.* **58**, 232 (1929)) that the excitation energy of the first

electronic level of these molecules coincides very closely with the corresponding value for the Tl atom; the figures (in volts) are as follows: 3.4 for TII, 3.6 for TIBr and 3.8 for TICI as against 3.3 for Tl. It seems therefore that the Tl atom has to some extent an individual existence in the molecule and can be excited by light absorption independently of the other component, a view consistent with the fact that these molecules are "atomic" ones.

There arose naturally the question, whether the value of the ionization energy of the molecule would coincide with the ionization potential of Tl. The experiment showed, in fact, the existence of a strong photoionization of these vapors, the active wave-lengths lying on the short wave-length side of certain limits, which are 2140Å for TII and 2070Å for TIBr. Expressed in volts this gives for the assumed ionization potentials of TII and TIBr, 5.8 and 6.0 respectively, whereas the ionization potential of Tl is 6.1 V.

The agreement is sufficiently good to support the view that at these wave-lengths the ionization of the TIX molecules sets in, as the result of the liberation of an electron from the Tl atom. An explanation of the photocurrent by the dissociation of the TIX molecules into ions Tl^+ and X^- , improbable in itself, would give other threshold values than is the case here. It must be noticed that the range of ionizing radiation overlaps to some extent the range of wave-lengths producing the dissociation of the TIX molecules with subsequent emission of certain Tl lines, which has been thoroughly studied before (Terenin, *Zeits. f. Physik* **44**, 713 (1927); Butkow and Terenin, loc. cit.). The wave-length thresholds of these two processes are, however, quite different.

From the known equation: $D_m + I_a = I_m + D_{m+}$, where I_a , I_m are the ionization energies of the Tl atom and the TIX molecule respectively, D_m , D_{m+} —the dissociation energies of the neutral and the ionized molecule,

the value of D_{m+} can be computed to be 2.8V for TII⁺ and 3.3V for TIBr⁺. As the dissociation energies D_m of the neutral molecules are 2.5 and 3.2V respectively, it may be concluded that the molecular ions TIX^+ are more stable than the corresponding neutral molecules; this fact, interesting in itself, is consistent with other known data.

For TICI the threshold was found to be 1860Å, but this value is not quite certain owing to a dubious origin of the salt used in the experiment.

A marked decrease of the photosensitivity in the sequence TII, TIBr, TICI was noticed.

On raising the applied voltage from 50 to 600 V, the appearance of Tl arc lines could be observed in TII, but only during the illumination of the vapor. This can be explained as an excitation of the Tl atoms always present in the vapor, by the photoelectrons liberated from the molecules and accelerated by the field applied. There is, besides, the possibility of various dissociation and excitation processes induced in TII by these electrons.

Other volatile halides, e.g. AgI, PbI₂, PbCl₂, BiI₃, were also investigated, but they gave much smaller photoionization currents, than the Tl halides. In HgI₂ and CdI₂ no measurable effect could be observed.

The possibility of a photoionization seems to be dependent chiefly on the magnitude of the ionization potential of the metallic atom in the molecule, which must fall within the range of the ultraviolet frequencies used. The photoionization is more pronounced in the iodides and decreases in magnitude in the chlorides.

The magnetic mass analysis of the ions produced under various circumstances will facilitate, I hope, to a great extent the interpretation of the underlying processes.

A. TERENIN

Optical Institute,
Leningrad, Russia,
May 24, 1930.

The Raman Effect in Solutions of Sodium Nitrate of Varying Concentration

Experiments suggested by those of Rao on HNO₃ (*Nature*, **124**, 762 (1929)) have been made on the Raman spectrum of NaNO₃ at concentrations of 5, 10, and 30 percent and saturated. Exposures were made varying approximately inversely with the concentration from 39 hours down. The source of light

was a glass mercury arc, and the spectrograph a Hilger D78. The Raman line with frequency difference $1049 \pm 6 \text{ cm}^{-1}$ was found excited by the mercury lines 4358, 4077, and 4046, approximately equally strongly in the different cases, and no new lines were found either in the more dilute or in the saturated solution.

This remained true when the time of exposure for the saturated solution was increased to 15 hours. This line agrees with that found by Carrelli, Pringsheim and Rosen, (*Zeits. f. Physik* 51, 511 (1928)) and is attributed to the NO_3 ion, since they found it in solutions of different salts containing this ion. The present experiment confirms this and shows no indication of NaNO_3 molecules, although from conductivity measurements the partial dissociation theory would have said that nearly two-thirds of the salt was nondissociated in the saturated solution.

The water band was also found excited by the mercury lines 4358, 4077, 4046, and 3650. The water was redistilled. The ordinary

laboratory distilled water spectrum showed many lines, a number appearing like absorption lines although a photograph of the absorption in the region showed nothing. These lines could not be attributed to Raman scattering. The redistilled water spectrum showed only the water band in the region of wave-lengths shorter than 5460A except once a faint suggestion of an absorption line at 4859A, several lines still appeared at wave-lengths greater than 5790A.

VERA STERLING
E. R. LAIRD

Mount Holyoke College,
June 14, 1930.

The Calculation of Energy Values

A number of modifications of the Ritz method of calculating characteristic numbers have recently been applied to the quantum dynamical problem. I have tried another of these methods, which seems to possess several advantages.

The characteristic functions of an atomic system of N electrons whose coordinates are $(r_1, r_2 \dots)$ are approximated by polynomials of the requisite symmetry,¹ whose separate terms are of the type

$$u(\alpha, r_1) v(\beta, r_2) \dots$$

Taking a hint from the empirical formulae for energy levels, I assume that each of these functions, say v , is a characteristic function of a one-electron system whose nuclear charge

The rule has several advantages: (1) the approximate wave function involves at most N parameters. Others have often used more without obtaining results that are much more accurate than those given by the present choice. (2) It leads to a definite result for the approximate wave function, no matter what the atomic system under consideration may be. (3) Many of the integrals whose numerical values are needed have a simple form. (4) The same functions $u, v \dots$, recur in many different problems, so that when the numerical work required for one has been finished, much of the work for several others is also completed. This will be particularly true in the later parts of the periodic system.

The method has already been applied to

TABLE I

Z	Level	$T/(Z-1)^2$			$\alpha(1s)$	$\beta(2p)$
		Present method	Perturb. theory	Observ.		
2	He I, 2^1P	0.245	-0.039	0.2475	2.003	0.965
2	He I, 2^3P	0.262	+0.097	0.2657	1.99	1.09
3	Li I, 2^1P	0.245	0.173	0.250	3.007	1.94
3	Li I, 2^3P	0.261	0.224	0.263	2.98	2.16

is, say, β . These various "effective" charges α, β, \dots , are then determined so that the variation integral is a minimum, subject to the condition that the wave function is of the form just described. The justification for this choice of wave function is purely empirical at present, but it is believed that some theoretical justification for it may be found.

the particular case of the normal states of atoms of two electrons,² the result being

¹ This has also been suggested by V. Guillemin and C. Zener, *Zeits. f. Physik* 61, 199 (1930).

² J. Frenkel, *Einführung in die Wellenmechanik*, p. 291 ff. Berlin, J. Springer (1930).

that their term values are $2(Z-5/16)^2$, Z being the true nuclear charge. I have extended the calculations to the $2P$ and $3D$ states with the following results.

In Table I, T is the term value in units of $Rh\text{ cm}^{-1}$; the third column contains the result of a calculation based on the foregoing rule;

which is believed to have been sufficiently accurate. Although there are systematic deviations of the calculated from the observed values of $T/(Z-2)^2$, it is interesting to note that both sequences show a flat maximum near Be II. The calculated values of the screening constants $Z-\beta$ are not strictly

TABLE II. 3^3D-3^1D

	Present method	Perturb. method	Observation
He I	5.14×10^{-5}	$198. \times 10^{-5}$	3.68×10^{-5}
Li II	3.80×10^{-5}	$30. \times 10^{-5}$	2.68×10^{-5}

the fourth, the first-order result of perturbation theory; the fifth, the observed value. The quantities α and β are the effective nuclear charges for the $1s$ and $2p$ electrons, respectively. In the case of the $3D$ states, the screening constant $z-\beta$ proves to be so nearly unity that the Balmer formula may be used to calculate the absolute magnitude of the

comparable with those deduced from the observed doublet separation, but both sequences decrease monotonically.

Theory indicates that the method should be applicable to the 2^3S state of atoms with two electrons, but requires a slight modification for the 2^1S . A rough calculation verifies this. As soon as the calculations for these

TABLE III. $2P$ levels.

	$T/(Z-2)^2$		$Z-\alpha^*$	$Z-\beta$ (calc.)	$Z-\beta$ (observ.)
	Present Method	Observation			
Li I	0.255	0.2605	0.31	1.98	2.019
Be II	0.258	0.2620	0.32	1.95	1.937
B III	0.258	0.2609	0.32	1.93	1.884
C IV	0.257	0.2595	0.32 _s	1.91	1.858
N V	0.257		0.33	1.89	1.838
O VI	0.256		0.33	1.88	1.816

* Cf. Guillemin and Zener, reference 1.

term value. The difference 3^3D-3^1D may be calculated, however, and is compared with the results of perturbation theory and observation in Table II.

Having performed the calculations required for the foregoing cases, it was less than two hours' work to compute the following data for the sequence of three-electron systems. A graphical method of interpolation was used,

states have been made, it will be possible to calculate the normal states of the Li I sequence with very little additional labor. A more detailed account of this investigation will be published later.

CARL ECKART

Ryerson Physical Laboratory,
June 12, 1930.

Some Peculiarities of the Spectrum of the Tungsten Mercury Arc

In the course of an investigation of sources of ultraviolet radiation, it was found that the new General Electric Sunlamp in a quartz bulb gives a very intense continuous spectrum in the region from 4000Å to 2100Å. The source of the ultraviolet radiation is a 300 watt alternating current mercury arc between

hot tungsten electrodes with the bulb containing about 100 mm pressure of argon. With a Hilger E2 quartz spectrograph, an exposure of 10 to 15 seconds is sufficient to give an intense continuous background. The intensity of the continuous spectrum relative to the line spectrum can be increased by

burning the lamp at a higher voltage or by increasing the pressure of the mercury vapor in the lamp by external heating.

When the temperature of the mercury is increased, the mercury vapor absorption bands appear. The band at 2540A, first described by R. W. Wood (*Astrophys. J.*, vol. 26), is approximately 0.1A wide at a mercury temperature of 220°C (corresponding to a vapor pressure of 32 mm), and spreads toward longer wave-lengths until it reaches about 2576A at 407°C and 2652A at 426°C, (corresponding to a vapor pressure of 2316 mm). Wood found that this band did not extend beyond the resonance line on the short wave side. Our work with this arc, however, shows the resonance line disappearing at approximately 350°C and two narrow absorption bands appearing at approximately 2534A and 2532A. With further increase in the temperature of the mercury these bands merge with the 2540 band until at 426°C there is continuous absorption between 2530A and 2652A, with evidence of further absorption beyond 2652A.

The five fluted bands around 2345A appear between 320°C and 340°C and broaden as the temperature is increased until they extend over a range of about 16A at 420°C. The broadest of the bands is about 3A wide. The increased pressure also affects certain lines

in the region between 3500A and 2100A, some of the lines disappearing entirely at the higher temperatures.

Mercury in a separate quartz absorption cell shows a somewhat different absorption spectrum. The band at 2540A spreads toward the long wave-lengths as the vapor pressure increases until at a temperature of 456°C there is strong absorption of the radiation to 2652A and partial absorption to 2850A, and at 492°C (corresponding to a vapor pressure of 5420 mm) there is strong absorption to 2753A. The band does not extend beyond the resonance line on the short wave side. The fluted bands at 2345A appear at about 340°C and spread to either side until at 460°C the line at 2345A disappears and at 517° (corresponding to a vapor pressure of 7430 mm) the absorption between 2301A and 2350A appears to be continuous.

Further investigation of the absorption bands of both the excited and the unexcited mercury vapor is being made.

W. E. FORSYTHE

M. A. EASLEY

Lamp Development Laboratory,
Incandescent Lamp Department,
General Electric Company,
Cleveland, Ohio,
June 10, 1930.

Experimental Evidence for the Existence of Quadrupole Radiation

Rubinowicz (*Zeits. f. Physik* 53, 267 (1929)) has shown that spectral lines which violate the transition rule for l or j cannot be explained as dipole radiation, but must be attributed to multipole radiation.

Besides the nebular lines identified by Bowen, the best known line of this type is the green auroral line 5577A. According to McLennan the auroral line is the forbidden combination between the low metastable O I terms 1S_0 and 1D_2 . (The values of these terms have been accurately determined as $^1S_0=76037$ and $^1D_2=93962$ by one of the authors (F.) and will appear shortly in the *Phys. Rev.*)

Assuming that the auroral line is quadrupole radiation, Rubinowicz (*Zeits. f. Physik* 61, 338 (1930)) pointed out that not only those Zeeman components may be observed which correspond to the usual transition $\Delta m = \pm 1, 0$, but also components which correspond to the transitions $\Delta m = \pm 2$. The

latter have zero intensity when viewed longitudinally and were therefore not observed by McLennan and Sommer. According to Rubinowicz all of the above transitions show the same intensity when viewed perpendicularly to the field, with the exception of $\Delta m = 0$, which can only be observed at oblique angles with the field. Measurements of the transversal Zeeman effect thus make possible an experimental test for the existence of quadrupole radiation.

We have photographed the transversal Zeeman effect of the auroral line. The magnetic field was produced by a large solenoid previously constructed and calibrated by one of us (C.) for a precision determination of e/m by the Zeeman effect. With this solenoid it is possible to maintain a field of 7000 gauss continuously. The auroral line was produced by a d.c. discharge of 0.6 amperes through a mixture of argon and oxygen in a tube 30 mm in diameter. The tube

was silvered over the central portion to increase the intensity by multiple reflection. The light leaving the tube transversally through a slit in the silvering was reflected out of the solenoid by a 45° prism. The Zeeman pattern was photographed with a Fabry-Perot interferometer crossed with a prism spectrograph. By placing a thin calcite plate with proper orientation behind the spectrograph slit, each spectral line appeared separated into its π and σ components.

At a field of 2580 gauss and an interferometer separation of 0.6159 cm, the auroral line was resolved into four components. The displacement of the inner components was $0.92\Delta\nu_{\text{norm}}$, that of the outer components was $1.96\Delta\nu_{\text{norm}}$. The theoretical factors are

1 and 2, respectively. As was predicted the undisplaced line did not appear. We found that the outer components were polarized perpendicular to the field, and that the components displaced by $\Delta\nu_{\text{norm}}$, which in the normal effect are polarized perpendicular to the field, are in this case polarized parallel. This is in complete agreement with the theory of Rubinowicz.

We intend to investigate the Zeeman effect of other forbidden lines.

RUDOLF FRERICHS

J. S. CAMPBELL

Norman Bridge Laboratory of Physics,
California Institute of Technology,
Pasadena, California,
June 9, 1930.

Mobility of Na^+ Ions in H_2

The results of studies of mobilities of ions in mixtures showing the great importance of traces of impurities on mobilities,¹ the studies of Erikson² on the change of mobilities of positive ions with age at atmospheric pressures including the effects of impurities, and the prominence recently given the change of charge of initially ionized atoms and molecules in gases reported by Kallman and Rosen,³ indicating as previously emphasized the total ignorance as to the nature of the ionized carrier,^{4,1} led to the present investigations the first results of which it is desired to report at this time.

It seemed essential by as nearly an absolute a method as possible to measure the mobilities of a type of initially ionized carrier which would only reluctantly alter its charge in gases of reasonable purity over very short time intervals. To this end it was attempted to measure the mobilities of positive Na^+ ions from a Kunsman⁵ source, using a high frequency square wave form oscillator in fairly pure gases at low pressures. From the nature of the Kunsman sources the gas chosen was hydrogen purified by a process previously used by the writer.* A Kunsman source of positive ions with a square wave form oscillator, using the original Rutherford A.C. method with positive ions instead of negative ions, should: (1) give absolute values of the mobilities with no disturbing effects of gauzes as encountered in other A.C. methods,⁶ and with ions definitely emerging from one plane of the parallel plate electrode system; (2) give ions which retain

their positive charge in H_2 because of their low ionization potential; and (3) be capable of extension to very short time intervals. The chamber used was a brass one of a type previously described⁷ with electrodes altered to suit the Kunsman source. The source was a coating of Na catalyst, kindly sent the writer by Dr. Kunsman, on a thin Pt foil, spot welded onto a small oven of Ni containing a Pt spiral heating element insulated from it by "Insolute" cement. In practice it was heated to about 700°C and gave a copious supply of $+$ ions. It was mounted in the center of the upper plate of a parallel plate condenser in the gas, the lower plate going to ground through an electrometer system. The plate distance was 1.2 cm. By means of an oscillator first designed by J. L. Bowman,⁸ built here by Mr. J. E. McVay and adapted by the writer, good square wave form alternating potentials of from 10 to 150 volts with frequencies varying from 500 to 25,000 cycles per second have been achieved. It is probable that the upper frequency limit can be considerably extended. The first results covered a range of pressures from 0.5 to 7 cm of Hg and appeared of sufficient importance to report at this time, as the work will be interrupted for the period of a month or two by external demands on the writer.

Mobilities in H_2 were observed, beginning

* The H_2 was passed over hot Cu, NaOH, CaCl_2 , two meter long tubes of P_2O_5 and a special double liquid air trap immersed in liquid air.

at between 8 and 10 cm/sec. per volt/cm for $+$ ions at the lower frequencies, (500 cycles to 2000). Above frequencies of 2000 cycles the values of the mobilities increased, reaching a maximum of about 21 cm/sec. per volt/cm above 5000 cycles and remaining there up to 25,000 cycles. Between the lower and higher frequency values the curves indicated by their slopes the probable existence of two carriers present in varying proportions, which made the accurate assignment of mobilities uncertain. This uncertainty will have to remain until the new and somewhat difficult techniques involved shall have been perfected. Hence the results can be considered only as preliminary. The reduced mobility depends primarily on frequency and does not appear to depend on pressure. The correction of the results for temperature was not attempted, first, because the temperature correction for mobility is very uncertain⁹ and, secondly, it was not desired to encumber this already complex apparatus at this stage with the necessary added refinements. Since this work was done at constant density the temperature effects will not be great.

The results indicate that Na^+ ions in H_2 within 2×10^{-5} seconds (reciprocal of twice the frequency) after liberation have a little more than double the value of the mobility of the normal ions. These are probably the Na^+ atoms moving in the gas and impeded by their electrostatic attractions only. In 10^{-3} seconds these ions have in part either exchanged charges with other molecules or attached to molecules of H_2 , H_2O vapor (present in traces), or some other molecules to form molecular ions. Their mobility is of the order to be expected of the normal positive ions in H_2 as measured by an absolute method.⁶ The process (judging from the nature of the

curves) appears to be a process similar to that observed by Erikson² in his ageing experiments, that is a process which takes place in a single step. The present results differ from Erikson's in the much greater change in mobility occurring, an action which could be ascribed to the use of initial relatively stable Na^+ ions.

Note: Temperature measurements made since this letter indicate average temperatures of less than 130°C in the gas space between the plates. This lowers the average density by a factor of about 0.7 between the plates and indicates that all mobility values reported may be too high in absolute magnitude by a factor less than 1.43. It does not alter the relative changes with frequency.

LEONARD B. LOEB

Physical Laboratory,
University of California,
Berkeley, California,
June 4, 1930.

¹ L. B. Loeb, Phys. Rev. **32**, 81 (1928) and **35**, 192 (1930).

² H. A. Erikson, Phys. Rev. **33**, 403 and **34**, 635 (1929).

³ Kallman and Rosen, Zeits. f. Physik. **58**, 52 (1929) and **61**, 61 (1930).

⁴ Loeb and Marshall, Jour. Franklin Inst. **208**, 386 (1929).

⁵ C. H. Kunsman, Phys. Rev. **25**, 892 (1925).

⁶ L. B. Loeb, Jour. Franklin Inst. **196**, 537 and 771 (1923).

⁷ Loeb and Cravath, Jour. Opt. Soc. Am. **16**, 191 (1928).

⁸ J. L. Bowman, Phys. Rev. **24**, 31 (1924).

⁹ L. B. Loeb, Internat. Crit. Tables, **VI**, 114 (1929).

The Interaction Between Excited and Unexcited Hydrogen Atoms at Large Distances

Eisenschitz and London¹ have recently pointed out that when two similar atoms in different quantum states interact with one another a first order calculation of their mutual energy yields an inverse R^3 term corresponding to a dipole interaction. This term is the controlling one for large values of the internuclear distance R and may yield an energetic order for the different molecular terms at large distances quite different from that which occurs at short distances. As an example they cite the two quantum II

states of the hydrogen molecule whose potential energy curves were computed in first order approximation by Kemble and Zener.² For small internuclear distances the energetic order of the states is $H_{12}^{12} > H_{10}^{10} > H_0^0 > H_{11}^{11}$ as shown by Kemble and Zener, while for large distances the predominance of the $1/R^3$ term leads to the energetic order

¹ Eisenschitz and London, Zeits. f. Physik **60**, 491 (1930).

² Kemble and Zener, Phys. Rev. **33**, 512, (1929).

$H_{12}^{12} \leq H_9^9 > H_{10}^{10} \leq H_{11}^{11}$. The state $U_9(^1\Pi_+)$ in the notation of Eisenschitz and London) whose potential energy curve shows a marked minimum in the region of small values of R has a positive energy of interaction for large values of R corresponding to a repulsive force between the atoms. Similarly the state $U_{10}(^1\Pi_-)$ which shows marked repulsion at short distances, yields a weak attraction at very large distances.

the exact first order computations of Kemble and Zener to the internuclear distances $R=5, 6, 7, 10$. The results are shown in the accompanying table and figure.

The curves show that the crossing-point of the "potential" energy curves for the states 9 and 10 occurs farther out than supposed by Eisenschitz and London. Also the maximum in the potential energy of the state 9 and the minimum for the state 10 are less

TABLE I

R	H_9^9	H_{10}^{10}	H_{11}^{11}	H_{12}^{12}
	(volts above E_0)			
5	-0.21	0.27	-0.44	0.43
6	-0.038	0.057	-0.181	0.162
7	0.016	0.008	-0.081	0.068
10	0.014	-0.014	-0.016	0.016

As the computations of Kemble and Zener were not extended to internuclear distances larger than $R=4$ (here the unit of distance is the radius of the innermost Bohr orbit for the H atom) Eisenschitz and London made a necessarily crude interpolation between the asymptotic $1/R^3$ formula and the curves

pronounced than their interpolation would indicate, being almost imperceptible when plotted on the scale of the original graph of Kemble and Zener.

In the course of the computation here reported we have found the following misprints in the paper of Kemble and Zener.

Errata to paper by Kemble and Zener, Phys. Rev. 33, 512 (1929).

p. 525, Eq. (28): the second term in square brackets should be multiplied by $1/4$ to read

$$\frac{1}{4} \left(1 + R + \frac{R^2}{3} \right) \left(1 + \frac{R}{2} + \frac{R^2}{12} \right)$$

p. 526, Eq. (29): the sign of the third term in the right hand member should be positive.

p. 530, Eq. (35): should read

$$K_2^{(2)} = \frac{R^4}{3840} \int_1^\infty (\lambda^2 - 1)(\lambda^2 + 1/7) \left\{ (3\lambda + R)e^{-3\lambda R/2} - \left(\frac{3\lambda^2 - 1}{2} \right) e^{-\lambda R/2} [S'Ei\{- (\lambda + 1)R\} - SEi\{ -(\lambda - 1)R\} - S \ln \left(\frac{\lambda + 1}{\lambda - 1} \right)] - 3S\lambda e^{-\lambda R/2} \right\} d\lambda.$$

E. C. KEMBLE

F. F. RIEKE

Jefferson Physical Laboratory,
Harvard University,
June 11, 1930.

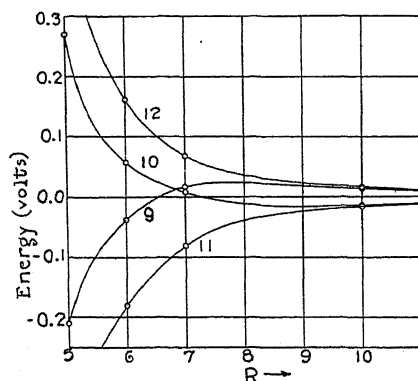


Fig. 1.

given by Kemble and Zener for short distances. This interpolation enabled them to estimate the positions and values of the minimum point in the H_{10}^{10} curve and the maximum in the H_9^9 curve. At London's suggestion, however, the writers have now extended

BOOK REVIEWS

Physique Moderne. GAETANO CASTELFRANCHI, (Translation from the Italian by M. A. Quemper de Lanascot), 2+660 pp., 147 figures, Albert Blanchard, Paris, 1930, Price 70 francs.

This is a summary of modern physics, written for the educated layman and for the scientist whose work lies outside the field of physics, rather than for the physicist or for the student of physics. For the most part, the mathematics is subordinated to such a degree that a person who has, or who once had, a slight acquaintance with the calculus, will be able to follow the treatment. The book differs somewhat in subject matter from volumes in English which have a similar purpose. An introductory chapter deals with history and with the most elementary facts in regard to atoms and molecules. There is a chapter on the classical theory of light and one which reviews the kinetic theory of gases from an elementary standpoint. Chapters IV and V on the Brownian movement and fluctuation phenomena are entertaining and give considerable insight into the physics underlying the statistical equations which govern these subjects. There are conventional chapters on special relativity and on electrons and positive rays. Then we have a discussion of x-rays, the determination of atomic numbers with their aid, and the structure of crystals. A chapter on radioactivity introduces the nuclear atom, which is first discussed from the standpoint of Rutherford's early scattering experiments. The concept of quanta is introduced via the black-body-radiation route. Bohr's theory of hydrogen is treated much as it is in any elementary English book on atomic structure. Chapter XIV develops the elements of generalized dynamics and applies them to the Zeeman and Stark effects. In the same chapter, we find a very brief account of line and band spectra and of Pauli's principle. Then we encounter specific heats, photoelectric effects (including a brief section on the experiments of Auger), the Compton effect, and other experiments on the structure of radiation. The treatment of magnetism is quite pleasing.

As the author says, his discussion of wave mechanics follows closely that of Darrow, published in the "Bell System Technical Journal" for 1927. The author's decision to do this is commendable, for the reviewer knows of no clearer treatment than that in Darrow's article. The principal application of wave mechanics given in this chapter is that of electron diffraction. The discussion of experiments on this subject is well written. The book ends with a chapter on the new statistics.

No doubt this book will be well received by persons who speak the Romance languages. Its subject matter is already well covered in English by a variety of entertaining and well written books, such as those of Darrow, Andrade, and Haas. The treatment is superficial and the book is not to be recommended as mental food for the serious student of physics. However, this criticism must not be interpreted severely, for the reviewer believes that the volume is well suited to the class of readers for whom it was obviously intended.

ARTHUR E. RUARK

Essai sur les Principes de la Thermodynamique. I.-N. LONGINESCU, with a preface by A. Boutaric, 80 pp., 13×20 cm. Société d'Éditions Scientifiques, Paris, 1929.

In this essay an attempt is made to embrace under the same broad point of view the First and Second Laws of Thermodynamics and the Principle of Least Action. This is done by a quasi-logical deduction from certain general philosophical considerations, among which the notion of causality is important. I do not suppose, however, that even the author would claim that this deduction has any binding logical force, or that more has been achieved than to show in a suggestive way that the notions of thermodynamics fit consistently into a broader sort of physical outlook. The work as a whole may be described as a pleasantly sophisticated essay, which the physicist already familiar with thermodynamics may read with a certain satisfaction, but which is not intended for the beginner or for the physicist who is seriously interested in resolving the logical difficulties in thermodynamics emphasized by recent developments.

P. W. BRIDGMAN

Radio Technic. VI. Die elektrischen Wellen. F. KIEBITZ. Pp. 125, 28 figs. Walter de Gruyter and Co., Berlin. Price RM 1.50.

This is a thin book of pocket size, the sixth of a series dealing with radio practice each by a different author and appearing under the general classification of "Sammlung Götschen." The booklet under review is concerned with an elementary exposition of the nature, propagation and reflection of electromagnetic waves and their radiation and reception by practical antennas and antenna systems.

The treatment is brief and in general takes the form of stating the equations of interest and considering their numerical application to commonly encountered oscillation circuits and radio antennas. The author usually gives the range through which a quantity under consideration may be expected to vary in practice. Although elementary, the treatment is sound and accurate, qualities not found in a great deal of the literature on radio recently appearing.

H. E. HARTIG

Die Grundgedanken der neueren Quantentheorie. O. HALPERN AND H. THIRRING. Pp. 241. J. Springer, Berlin, 1929.

This article is a separate issue from volume 8 of the annual "Ergebnisse der Exakten Naturwissenschaften." There are four chapters: Relativity and electron spin, One body problems, Many body problems, and Interpretation of the theory. The first chapter includes an account of the Dirac electron theory. The second treats a wide variety of problems, oscillator, rotator, hydrogen atom, radioactivity, dispersion and Compton effect, in a concise and simple manner. The third discusses symmetry of the eigenfunctions and simple applications to the helium atom, to band spectra, and gives an account of the new statistics. The last chapter gives an unusually clear account of the statistical interpretation and the uncertainty relation.

E. U. CONDON.

The Conduction of Electricity through Gases. K. G. EMELÉUS. Pp. X+94, 37 figures. E. P. Dutton and Co. Inc., New York City. Price \$1.10.

This book is one of a series of small monographs on physical subjects, edited by B. L. Worsnop. The author confines himself to a treatment of electrical discharges at low gas pressures. He condenses into a few small pages a great deal of information regarding the complex phenomena involved, and points out and briefly discusses some of the outstanding problems of the subject. A chapter is devoted to exploring electrodes.

JOHN ZELENY

THE PHYSICAL REVIEW

THE INCOMPLETE PASCHEN-BACK EFFECT

By J. B. GREEN

MENDENHALL LABORATORY OF PHYSICS, OHIO STATE UNIVERSITY

(Received May 23, 1930)

ABSTRACT

Darwin's calculations for the Zeeman effect have been applied to the most noted examples of discrepancy between the older quantum theory and experiment, those of the Cu $^2P^2D$ multiplet, and the Mg and Be $^3P^2S$ multiplets. The positions and intensities of the lines calculated are in very good agreement with the experiment. The distorted Zeeman patterns of $^3P^2D$ of Mg and $^2P^2D$ of Na are attributed to the action of the magnetic field on 3P and 2P separations.

HEISENBERG and Jordan,¹ and Darwin² have applied the new quantum mechanics to the calculation of the standard Zeeman effect at all field-strengths. This had previously been done only for weak and strong fields, but not for intermediate field-strengths. Kronig³ and Fowler⁴ have also given rules for intensities. Mensing⁵ has applied these results to the case of the $^2P^2D$ multiplet of sodium, and to the $^3P^2D$ multiplet of Mg, and has shown that the observed intensities are in excellent agreement with the theory.

In both of these cases, however, the D separation is practically zero, and we therefore have the case of a very strong field for the D separation while it is a very weak field for the P separation. In this paper the author has sought for some intermediate cases in which the field-strength gives separations of the same order of magnitude as the Zeeman separation.

I. THE SPECTRUM OF COPPER

The most conspicuous example of this sort is given by the excellent work of Back⁶ on the $^2P^2D$ multiplet of copper, $\lambda\lambda 5220, 5218, 5153$. In this case, the 2D separation is 6.90 cm^{-1} while the Zeeman separation is 1.76 cm^{-1} . From Darwin's work we get the formula for the positions of the levels in the magnetic field, W

¹ Heisenberg and Jordan, *Zeits. f. Physik* 37, 263 (1926).

² Darwin, *Proc. Roy. Soc. A*115, 1 (1927); see also K. Darwin, *Proc. Roy. Soc. A*118, 264 (1928).

³ Kronig, *Zeits. f. Physik* 31, 885 (1925).

⁴ Fowler, *Phil. Mag.* 1, 1079 (1925).

⁵ Mensing, *Zeits. f. Physik* 39, 24 (1926).

⁶ Back, *Ann. d. Physik* 70, 333 (1923).

$$\begin{aligned}
& - a_{m_l-1, m_s+1} \beta (l - m_l + 1) (s + m_s + 1) \\
& \quad + a_{m_l, m_s} [W - \beta \cdot 2m_s m_l - \omega(m_l + 2m_s)] \\
& \quad - a_{m_l+1, m_s-1} \beta (l + m_l + 1) (s - m_s + 1) = 0.
\end{aligned}$$

The a 's are numerical coefficients related to the intensities. We write down this equation for every permitted value of m_s and m_l and group the equations thus found into sets in which $m_s + m_l = m$, is the same. The determinant of each group thus found gives us the values of W for that particular value of m . For the intensity formulae, the reader is referred to Darwin's work.

In the case of the Cu multiplet, the value of $\beta = 6.90/5 = 1.38 \text{ cm}^{-1}$ for the 2D levels, and $248.3/3 = 82.77 \text{ cm}^{-1}$ for the P levels, while $\omega = 1.76 \text{ cm}^{-1}$. The results are given in Table I.

TABLE I

Position of undisturbed line	Observed position in magnetic field	Calculated new theory (1)	Calculated old theory (2)	Obs. Int.	Calc. Int. (1)	Cal. Int. (2)
5218.200	18.764	8.835	8.863	1	1	1
	.735	.770	.800	6	3	3
	.704	.715	.737	7	5	5
	.670	.673	.673	8	8	8
	.279	.276	.295	7	7	7
	.205	.205	.232	10	10	10
	.137	.137	.168	10	9.5	10
	.085	.090	.105	7	6	7
	17.729	7.727	.727	8	8	8
	.644	.647	.663	7	4.5	5
	.560	.573	.600	1	2	3
		.508	.537	0	.5	1
	20.857	20.864	20.837	2	1	3
	.600	.615	.585	5	4	4
5220.080	.433	.474	.459	8	4	10
	.282	.354	.332	4	1	3
	.148	.235	.206	1	1	1
	19.959	19.985	19.954	1	2	1
	.845	.846	.828	4	3	3
	.727	.726	.701	10	10	10
	.608	.604	.575	5	4	4
	.367	.356	.323	3	3	3
	53.652	3.652*	3.660	7	7.5	7.5
	—	.599	.598	0	2.5	2.5
5153.26	.292	.291	.291	10	10	10
	.228	.229	.229	10	10	10
	52.909	2.921	2.922	4	2.5	2.5
	2.850	.850	2.862	9	7.5	7.5

(The multiplet $^2P^2D$ of Cu, $H = 37,000 \text{ g}$)

* See text.

A study of the table shows that the newer theory gives much better agreement with experiment than the older theory for 5218 and 5220 except in one component 5220.433. All the other exceptions are very faint lines, which are too difficult to measure with any degree of accuracy. The distortion of intensities is also in the direction indicated by the newer theory.

5153 according to the new theory should be shifted 0.029Å to the red. This amount has been subtracted from all the calculated wave-lengths to show the distortion of the pattern, in almost complete agreement with the experiment.

II. THE SPECTRUM OF BERYLLIUM

Beryllium furnishes a very good example for the theory, since the 3P separation is very small, much smaller, in fact, in comparison with the field-strengths available, than the 2D separations of copper. We are, however, faced with a difficulty, in that the theory has been worked out for the "standard" Zeeman effect. This means that the coupling between the l and s vectors must be such that the ordinary Landé g and γ rules are obeyed. In the case of Be, we should expect the ratio $\Delta\nu_{21}/\Delta\nu_{10}=2:1$ whereas Back⁶ has found 3.58:1. The total separation is 3.02 cm^{-1} and if we take β for the P_{21} separa-

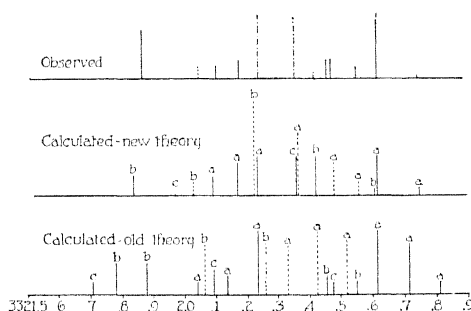


Fig. 1. The Zeeman effect of the Be $^3P^3S$ triplet. Lengths of lines indicate intensities. Dotted lines indicate parallel polarization, full lines perpendicular polarization, dot-and-dash lines double polarization. a indicates components of 3322.423. b indicates components of 3322.162. c indicates components of 3322.090.

tion, we get 0.59 cm^{-1} while for the P_{10} separation it is 0.33 cm^{-1} . Goudsmit⁷ has shown, however, that the γ -sum is independent of the l - s coupling and hence β has been chosen as $3.02/6 = 0.503 \text{ cm}^{-1}$.

The results are shown graphically in Fig. 1 for the $^3P^3S$ triplet at $\lambda 3322$. While they are not so satisfying as the results for Cu, they are still seen to be very good indeed. Two discrepancies in polarization are apparent, and the author has no explanation for these. The presence of a σ -component of 3322.455 is not accounted for by the theory. Back⁶ has attempted to account for the double polarization of the component of 3322.358 by saying that a σ -component of the line b has "crossed" a π component of the line a . The new theory shows no need for such an explanation, the double polarization being predicted.

III. THE SPECTRUM OF MAGNESIUM

The $^3P^3S$ triplet of magnesium, $\lambda\lambda 5183, 5172, 5167$ has been chosen as an example. Here, the 3P separation yields $\beta = 10.09 \text{ cm}^{-1}$, and from Back's

⁷ The Structure of Line Spectra, McGraw-Hill Company, 1930.

observations $\omega = 1.88 \text{ cm}^{-1}$. The results are indicated in Table II. The intensities are relative only within one line and not from line to line. The calculated shifts of the lines are in general in the correct direction, while the intensities are in excellent agreement with experiment.

TABLE II.

	Observed	Calculated (1)	Calculated (2)	Obs Int.	Calc Int. (1)	Calc Int. (2)
5183.558	84.545	84.548	84.540	1	1	2
	.309	.300	.295	8	3.5	8
	.055	.049	.049	10	8	10
	83.821	83.808	83.803	7	7	8
	.576	.566	.558	10	10	10
	.326	.317	.312	9	7.5	8
	.076	.067	.067	10	7.5	10
	82.834	82.826	82.821	8	4	8
	.589	.584	.576	3	1.5	2
5172.680	73.691	73.681	73.658	4	3	5
	.418	.408	.413	5	4	5
	72.932	72.919	72.924	8	8	8
	.441	.430	.435	8	7.5	8
	71.954	71.941	71.946	5	4	5
	.737	.724	.701	6	5	5
5167.342	68.299	68.245	68.318	3	2.5	2
	67.326	67.269	67.342	4	4	4
	66.342	66.293	66.366	1	1.5	2

Back⁸ has also measured the Zeeman effects of the $^3P^3D$ multiplet in magnesium, in which the 3D separation has disappeared. Here, too, the patterns are distorted, and not so simple as one is at first led to believe. The photographs in Back-Landé, "Zeemaneffekt und Multiplettstruktur" show this effect very clearly, and it is to be attributed to the fact that the magnetic field is beginning to affect the 3P separations as it does in the above example. In the $^2P^2D$ multiplet of sodium a similar effect is also taking place, and the pictures show a markedly distorted Zeeman pattern.

⁸ Back, Zeits. f. Physik 33, 379 (1925).

FINE STRUCTURE OF THE *K*-RADIATION OF THE LIGHTER ELEMENTS

BY LAWRENCE Y. FAUST

RANDAL MORGAN LABORATORY OF PHYSICS, UNIVERSITY OF PENNSYLVANIA

(Received May 19, 1930)

ABSTRACT

A vacuum spectrograph of simple construction is described in which it is possible to maintain bombarding currents of 150 milliamperes. With a line grating on glass (1179 lines per mm) photographs, some measurable in the second and third orders have been obtained of the soft x-radiation from beryllium, boron, oxygen and carbon, also from tungsten and certain heavier elements. Under analysis with a thermoelectric densitometer the *K* lines of the lighter elements, excepting oxygen, were found to be complex. The *K*-radiation of boron compounds contained 13 components, that of "pure" boron four, that of carbon nine whereas the beryllium radiation was still more complex. The relative intensities of these components was shown to depend on the energy used in stimulating them. The representative wave-length selected for the *K α* line was for oxygen 23.7A, for boron 69.3A, for carbon 45.3 while for beryllium the radiation embraced more than 15A with maxima at 107.2, 113.2 and 118.7A. The complex structure is thought to be partly a true fine structure and partly a system of satellites due to interaction with associated dissimilar atoms. A possible hypothesis is suggested in explanation of these results.

INTRODUCTION

THE possibility of diffracting soft x-rays from line gratings at small glancing angles was first pointed out by Professor A. H. Compton,¹ in 1923. Since that time important advances have been made, especially by Thibaud,² in the technique of this method, resulting in a number of valuable contributions to our knowledge of the frequencies and inter-relations of spectral lines in the soft x-ray region. Thibaud³ has measured the *K* lines of carbon, oxygen, nitrogen and boron and the *L*, *M*, and *N* radiations of several elements of high atomic number. Other investigators including Hunt,⁴ Osgood,⁵ Weatherby⁶ and Howe⁷ have concentrated on the measurement of the *K* line of carbon in view of its possible value as a calibrating or reference line. Söderman⁸ has made careful measurements of the *K* lines of the elements between magnesium and beryllium with the exception of neon. In addition to these wave-length measurements Bazzoni^{9,10} Faust and

¹ A. H. Compton, *Phil. Mag.* **45**, 1121 (1923).

² Thibaud, *Journ. de Phys. et le Rad.* **1**, 13 (1927).

³ Thibaud, *Comptes Rendus*, Jan., 1926. Thibaud, *Phys. Zeits.* **28**, 241 (1928).

⁴ Hunt, *Phys. Rev.* **30**, 227 (1927).

⁵ Osgood, *Phys. Rev.* **30**, 567 (1927).

⁶ Weatherby, *Phys. Rev.* **32**, 707 (1928).

⁷ Howe, *Proc. Nat. Acad. Sci. Mar.*, 1928.

⁸ Söderman, *Zeits. f. Physik* **52**, 795 (1929).

⁹ Bazzoni, Faust and Weatherby, *Nature*, May 11 (1929) p. 717.

¹⁰ Bazzoni, Faust and Weatherby, *Abstract, Am. Phys. Soc., Washington Meeting, Apr., 1929, Phys. Rev.* **33**, 1101 (1929).

Weatherby have studied the fine structure of the *K* lines of carbon and boron by densitometric methods.

It is evident that the line grating offers amongst other advantages the best means for investigating the *K*-radiation and associated *K*-absorption edges of the light elements. There is some reason to suspect that with the light elements the proximity of the *K* level to the exterior of the atom may cause a deviation from the simplicity of structure characteristic of *K* lines of the heavier elements. However, the researches listed above were for the most part carried out with too low resolving powers to bring out any fine structure in the *K* lines if such structure existed. The single exception to this statement is in the work of Bazzoni, Faust and Weatherby who densitometered the lines obtained in the first, second and third orders from a grating of 1179 lines per mm. These workers reported that the *K* line of carbon contains four components lying between 44.2, 44.9, 45.4 and 46.2A and that the *K* line of boron is of still more complex construction.

The investigation reported on in the present paper was undertaken to check in greater detail the measurements reported by these last mentioned authors and to extend such measurements to other elements of low atomic number.

THE APPARATUS

The apparatus consisted of a special vacuum spectrograph constructed of brass pipe in a design similar to that of Weatherby.¹¹ This apparatus differed from Weatherby's in several particulars. In the first place it was of larger diameter permitting the use of a photographic plate 5" long at a distance of 40 cm from the grating. In the second place the anode-cathode structure was altered to make closer adjustment of clearances possible and to obtain a higher electron current. Both anticathode and filament were mounted on standards attached to a single plate which was wax-sealed to the spectrograph. A spiral filament was centered in an adjustable steel focusing ring coaxial with the anticathode. This ring, which formed one of the filament leads, was earthed and was separately water-cooled by a jacket surrounding the anticathode and insulated therefrom by a Pyrex tube. The other filament lead and the anticathode itself were also each water-cooled and were suitably isolated electrically by Pyrex insulation. The maximum clearance between the cathode and anticathode structure did not exceed 1/8 inch. This design incorporates the advantages of Dershem's¹² tube but is much simpler.

In order to prevent the fogging of the photographic plate as much as possible, carbon paper was introduced into the path of the direct and reflected beams. Considerable scattering resulted from the use of carbon paper, and later aluminum foil was substituted. This substitution resulted in producing clearcut, sharply measurable images of the direct and reflected beams.

¹¹ Weatherby, reference 6.

¹² Dershem, Journ. Optical Society of America 18, 127 (1929).

Eastman x-ray plates were used in all the work with exposures varying from 15 minutes to six hours, three hours being the average.

The current to the anticathode was usually approximately 60 m.a. The driving potential was obtained from d.c. generators in series. A vacuum as low as 10^{-4} mm could be obtained in the spectrograph during operation by the action of a set of diffusion pumps.

The width of the two slits used in collimating the x-ray beam was 0.1 mm or less. The width of the grating used was 2 mm.

At this point attention may be called to the fact that Thibaud² has investigated the collimating properties of a grating at grazing angles. He obtains a formula for the variation of diffraction angle with the grazing angle.

$$\frac{di}{d\theta} = \frac{\theta/2}{(2n\lambda/d + (\theta/2)^2)^{1/2}}.$$

Thus when $\theta = 0$ the diffracted beam is parallel. The maximum variation of θ in this work due to the width of the grating and the width of the slits was $\Delta\theta = 5'$. Whence for a grating of 1179 lines per mm with an angle 3° at 50A, $di/d\theta = 0.2$. Thus corresponding to $5'$ for $\Delta\theta$ we have $1'$ change in i which corresponds at 50A to about 0.08A or about the experimental limit of accuracy. In general the values of θ and $\Delta\theta$ were about half the above values whence the error would be roughly 0.02A which is well within experimental error. It is therefore apparent that in the apparatus as used in this work errors due to lack of perfect collimation of the beams were negligible.

MEASUREMENTS

The determination of the wave-length of a line is dependent (Fig. 1) on the measurement of the angles α and θ and the grating constant d used in the formula:

$$n\lambda = 2d \sin(\alpha/2) \sin(\alpha + \theta)/2.$$

The constant d , obtained by the usual procedure employing the 5461 line of the Hg arc was found to be 8481.8A corresponding to a ruling of 1179 lines per mm. The grating used was furnished by Professor R. W. Wood, to whom we hereby acknowledge indebtedness. $\tan \theta$ can be obtained by

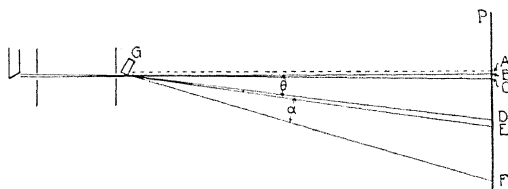


Fig. 1. Diagram of apparatus.

dividing the distance between the direct beam (BC , Fig. 1.) of x-rays passing by the grating and the beam (DE) reflected from the surface of the grating by the perpendicular distance (GA) from the effective center of the grating to the photographic plate.

The measurement of the distance GA was made on a comparator by comparison with a standard meter. The accuracy of this measurement was within 0.05 mm in 40 cm. Since care was taken to insure that the entire face of the grating was in the path of the incident beam, this measurement should correspond to the equivalent distance between grating and plate.

The distance BC to DE was found from a direct measurement on a Hilger traveling micrometer microscope of the extreme edges of the direct and reflected beams corresponding to the distance BE . This distance divided by the distance, GA , of the plate from the grating was taken as the corrected value for $\tan \theta$. An examination of Fig. 1 shows the justification of this procedure. BC is the direct beam image as found on the plate. In the absence of the grating this beam would extend from C to A . Thus AB is the position of the direct beam cut off by the grating and is therefore the effective direct beam. Then $BD + AB/2 + DE/2$ represents the real distance between the reflected beam and effective direct beam. The distance AB is measured by DE since the width of DE is due to the divergence of the direct beam. Whence $BD + AB/2 + DE/2 = BE$.

Having determined θ we find α by measuring $\alpha + \theta$. $\tan(\alpha + \theta)$ is equal to $BF + AB/2$ divided by the plate distance GA . In order to get $BF + AB/2$ it is necessary to add to BE which has been found already, the distance $EF + DE/2$.

Since the measurement of fine structure requires wave-length determinations for each component in the image F , the measurement of $EF + DE/2$ was carried out directly on the vacuum thermocouple densitometer. The width of the entrance slit in the diaphragm over the plate under investigation was 0.05 mm and this was therefore made the distance between successive plate settings in the line density measurements of the plates. To the moving part of the densitometer was attached a bar with fiducial mark which could be followed with the micrometer microscope and thus used to measure the distance that the plate moved.

In making a measurement the reflected line was placed in front of the densitometer slit. The plate was moved until the peak of the reflected line was found and the corresponding position of the fiducial mark was read on the micrometer. The plate was moved on its carriage until the diffracted line to be measured was near the slit. Readings on the galvanometer were taken every 0.05 mm from this point across the width of the diffracted line. Whenever the readings indicated a peak in the line, the position of the fiducial mark was read with the micrometer. The wave-length of each of these peaks was determined thus independently of the others in every case.

Curves produced by plotting the galvanometer deflections against wave-length proved to be reproducible in independent runs, thus suggesting the absence of any serious errors in this part of the work.

With the procedure described, measurements have been completed for the K lines of carbon, boron, oxygen and beryllium. These have been obtained in some cases in three orders. The combined effect of intensity of the line image and variation in dispersion for the different orders determined in

each case which order would give the best resolution of the fine structure under densitometer analysis.

CARBON

The lines of carbon were present on every plate although no carbon was placed on the anticathode. The source of this carbon is probably the grease vapor present at all times in the apparatus. In the 40 plates taken in this particular phase of the study (serial numbers 79 to 119) about 20 carbon lines were studied under the densitometer, the others being either too weak or too strong to give good resolution of the fine structure. Under visual observation most of the carbon lines appeared as continuous broad bands with maximum intensity on the short wave side. However, in several instances where small grazing angles were used, the first order carbon line appeared as a doublet, the shorter wave component being considerably the stronger.

A plot of the densitometer results obtained from a typical carbon line is shown in Fig. 2. Here the peaks indicate diminished transmission through the plates, i.e., the intensity maxima of x-radiation. It is apparent that here

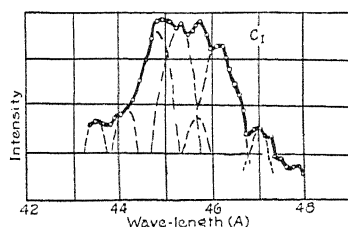


Fig. 2. Plot of densitometer results obtained from a typical carbon line.

we have a complex curve made up of several components. An attempt has been made to analyze this net curve into its constituents, a possible combination being shown in Fig. 2. An examination of this curve shows a rapid rise in intensity from the short-wave side to the first peak at 44.70 Å. A number of peaks follows with a gradual decrease in intensity to 46.20 where the curve again breaks in a sharp descent followed by a number of less prominent maxima. The small change of slope in the curve at 44.2 Å is a real effect and can be observed on all the curves of the carbon line. This demonstrates that the densitometer yields results sufficiently reproducible to attach a meaning even to a change of slope in the curve. The resolved lines shown in the figure are of course arbitrary to some degree. The position and magnitude of these components as shown do not represent the only way in which this curve could be built up. But little weight can be placed on the relative intensities of the minor components since that depends to a large degree on the method of choosing them.

The intensity of the line was found to depend on applied voltage. Although in general in soft x-ray spectroscopy the line intensity increases with

¹³ Dershem, Phys. Rev. 34, 1015 (1929).

the voltage and with increasing plate current, we find in the case of carbon that there is a decrease in line intensity with increase of these factors. This is in accord with the observations of Dershem¹³ who explained the effect as due to the burning off of the carbon from the anticathode by the greater energy used. Thus only faint carbon lines appeared at 2700 volts.

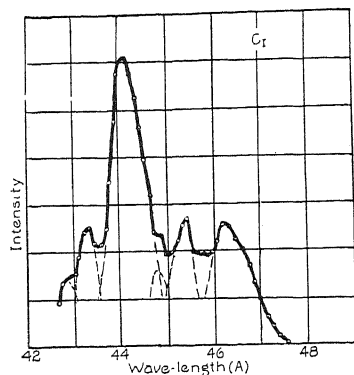


Fig. 3. Densitometer curve of the first order carbon line on a plate taken at 2300 volts.

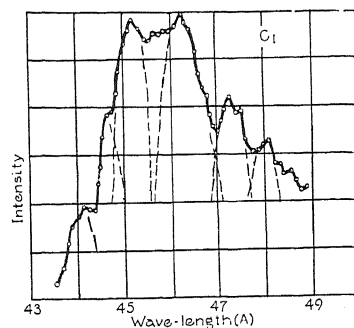


Fig. 4. Densitometer curve of the first order carbon line on a plate taken at 1500 volts.

It was found that the relative intensities of the components of the lines are dependent on the driving potential, the shorter wave components increasing in intensity relative to the long wave components at higher voltages. This interesting relation was specifically investigated by taking two series of plates under similar conditions excepting that the driving voltage for the one series was 1500 to 1600 volts and for the other series 2300 to 2800 volts.

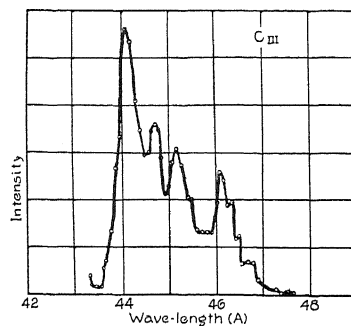


Fig. 5. Densitometer curve of a third order carbon line on a plate taken at 2500 volts.

Curves in Figs. 3 and 4 illustrate the different intensity distributions obtained in these tests. Fig. 3 is the densitometer curve of the first order carbon line on a plate taken at 2300 volts. This line under visual observation appeared as a doublet. A clearly defined peak is seen here at 43.3 Å. The curve then rises to a sharp maximum at 44.1 Å and shows two more distinct

peaks at 45.40Å. Comparison with Fig. 2 shows that the small change of slope in that curve has now risen to the chief peak, the longer wave peaks being of less intensity. This is the case for all curves of lines taken at voltages of 2300 volts or more and therefore shows a shift of the maximum to the short wave side with increasing voltage.

Fig. 4 is a first order carbon line taken at 1500 volts. The principal peak is now at 45.3Å with a second peak at 46.25. The short wave maxima have become reduced in intensity to mere kinks in the curve.

Fig. 5 is a densitometer curve of a third order carbon line showing unusually good resolution of the four principal maxima of the curve. This plate was taken at 2500 volts.

TABLE I

Plate No.	Order	Voltage	Wave-lengths of components of carbon.							
94	I	2300	42.70	43.23	44.10	44.70	45.4	46.25		
94	III	2300	42.90	43.24	44.00	44.65	45.25	46.00		
95	II	2300	42.60	43.06		44.48	45.28	46.20		
112	I	1900		43.45	44.05	44.62	45.35	46.20	46.55	
112	II						45.31		46.80	
97	I	1900				44.68	45.41	46.25		47.20
113	II	1900			44.25	44.70	45.26	46.20	46.57	47.00
114	I	1800			44.27	44.75	45.28	46.20		47.18
114	II	1800			44.30	44.70	45.25			47.79
116	I	1500			44.17	44.60	45.41	46.25		47.35
115	I	1700				44.61	45.34	46.23		47.12
115	II	1700	42.55	42.96	43.95	44.68	45.33	46.03		47.80
93	I	2300	42.50	43.40	44.12	44.70	45.30			
96	I	1900				44.33				
79	III	2500		43.30	44.01	44.71	45.11	46.11	46.45	46.90
87	I	1600	42.70	43.20	44.10	44.75	45.40	46.32	46.60	47.00
Ave. values			42.66	43.23	44.05	44.66	45.33	46.20	46.60	47.21
										47.70

Taking all of the curves together there appears to be sufficient reason for concluding that the carbon K line contains 9 components centered about 42.7, 43.2, 44.0, 44.7, 45.3, 46.2, 46.6, 47.2, and 47.7Å. We may also conclude that the relative prominence of these components and therefore the apparent position in the frequency scale of the unresolved line depends on the driving voltage, the maximum being 45.3Å at 1500 volts and at near 44.0Å at 2500 volts.

There is some uncertainty in the assignment of the title " $K\alpha$ " to any particular component because of this shift in the maximum from 44.0 to 45.3Å. Whatever the reason for the shift may be, it seems probable that the rate of decrease in intensity with decreasing voltage will be greater for the minor components than for the principal K line. Now since the 45.3Å component was the maximum at 1500 volts, the lowest voltage at which lines could be obtained, it is perhaps justifiable to assign to the $K\alpha$ line of carbon the wave-length 45.33Å.

No explanation can be offered at this time as to the significance of the fine structure here shown. Dr. C. B. Bazzoni has suggested that there is a possibility that the energy due to the excitation potentials of the other elements in combination with carbon interacts with the K -radiation of carbon to produce the satellite lines. The elements here in combination with the carbon are supposedly hydrogen and oxygen. It can be shown that the fre-

quency differences between the principal line and the various satellites are at least in qualitative agreement with this idea. There is also an agreement between the number of satellites observed and the number predicted from this consideration.

BORON

Boron lines were secured on 25 plates using boric acid, borax or boron on the anticathode. Fifteen of these lines were suitable for use in the densitometer. Second order boron overlapped the third order carbon line so that only the first order of boron could be measured.

The anticathodes of the boron compounds were prepared by fusing the compound on the anticathode. The line of pure boron was obtained by placing amorphous metallic boron obtained from Kahlbaum in a net-work of slots on the face of the anticathode.

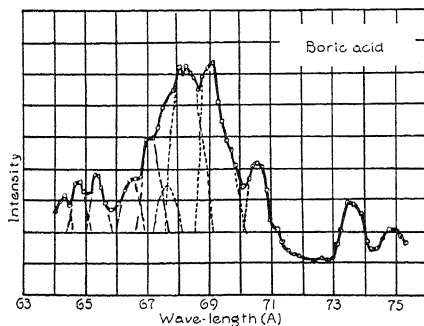


Fig. 6. Densitometer curve of a boron line taken with fused boric acid.

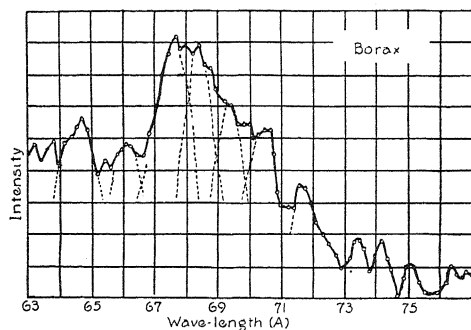


Fig. 7. Densitometer curve of a boron line taken with fused borax.

Under visual observation the $K\alpha$ line of boron appears as a continuous band broader than that of carbon. In several cases with small glancing angles the line appears to be just resolved into a doublet. The maximum of the line in general is on the short wave side. Two attendant lines on each side of the boron line are also visible to the eye in the spectra of boric acid and of borax. These attendant lines are absent in the spectrum of pure boron. This point was investigated carefully and plates from pure boron were obtained with lines even denser than the lines of the compounds with however no trace of satellites.

For given conditions of exposure the more intense lines of boron were obtained at higher voltages. Most of the lines of boron were obtained at 2300 volts more.

Fig. 6 shows a densitometer curve of a boron line taken with fused boric acid. This curve was resolved into components in a manner similar to that described for carbon. Fig. 7 is the plot of a line taken with fused borax on the anticathode. The conditions under which these plates were taken and the values of the resolved components are given in Table II

TABLE II.

Plate No.	Material	Voltage	Plate Distance	Wave-lengths of components of boron													
				66.43	67.37	68.28	69.30	70.30	71.63	72.67	73.26	73.90	75.00	76.60			
81	Borax	2500	30cm	64.85	67.30	68.12	69.15	70.22	71.20	72.67	73.26	73.90	75.00	76.60			
83	"	2300	30	64.50	67.30	68.30	69.33	70.00	71.26	72.24	73.10	73.75	74.90	77.00			
102	"	1870	30	64.81	67.40	68.30	69.35	70.00	71.25	72.00				77.10			
102(2)	"	1870	30		67.70	68.40	69.38	70.20	71.20					76.46			
88	"	1850	30	64.72	67.87	68.40	69.33	70.40	71.24	72.05	73.28	74.08	75.0	77.00			
68	Boric acid	2500		64.85	67.52	68.10	69.30	70.40	71.25	72.00	73.28	74.13	75.0				
71	"	2500		64.75	67.40	68.11	69.07	70.51	71.20								
72	"	2500		64.40	67.40	68.14	69.10	70.20	71.50	72.17	73.36	74.38		76.45			
96	"	1900	30	64.40	67.70	68.14	69.40	70.20	71.50	72.17	73.36	74.38					
97	"	1900	30	65.30	67.87	68.49	69.00										
73	Boron	2500	40		67.80	68.49	69.16	70.74									
74	"	2500	30		67.40	68.16	69.41	70.42									
94	"	2300	30		67.70	68.34	69.42	70.41									
95	"	2300	30		67.70	68.34	69.42	70.41									
114	"	1800	40		67.76	68.38	69.45	70.30									
Averages				64.68	65.45	66.55	67.61	68.38	69.33	70.36	71.32	72.03	73.20	74.00	74.95	76.75	

No marked difference is observed between the fine structure of the borax lines and the boric acid lines. The densitometer curves of pure boron are shown in Figs. 8 and 9. It is seen that but four components remain in the lines in this case. It would appear, therefore, that the presence of the attendant lines may be due to the association of the boron with other elements.

The curve of Fig. 8 is for a line taken at 2300 volts while Fig. 9 shows a curve of a line taken at 1800 volts. As in the case of carbon, a definite shift of the maximum to the short wave side occurs with increasing voltage. Reasoning in a manner similar to that used in selecting the wave-length of the $K\alpha$ line of carbon it would appear justifiable to assign a wave-length 69.33A to the $K\alpha$ line of boron.

The results in Table II seem to show that there are 13 components in the lines obtained from the boron compounds located at 64.68, 65.45, 66.55, 67.61, 68.38, 69.33, 70.36, 71.32, 72.03, 73.20, 74.00, 74.95, and 76.75A and that the spectrum of the K -radiation of the boron used contains four components at 67.61, 68.38, 69.33 and 70.36A. All of these figures are uncertain in the second decimal place.

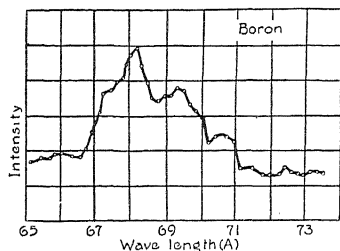


Fig. 8. Densitometer curve of pure boron line taken at 2300 volts.

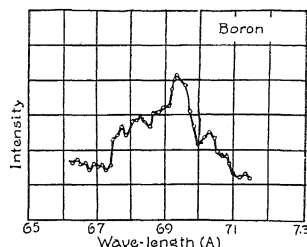


Fig. 9. Densitometer curve of pure boron line taken at 1800 volts.

It should be noticed that although the amorphous boron was "metallic" undoubtedly it contained appreciable percentages of oxide, hydride and probably nitride.

The explanation of the fine structure through the hypothesis of the development of addition and subtraction quanta through the interaction of the boron radiation with excited or neutral atoms associated in the molecular lattice is more difficult than for carbon. If we accept these results as showing that the K -radiation of boron is composed of four components, then to predict the fine structure of the compounds of boron on the above hypothesis, it is necessary to calculate these addition and subtraction quanta for each of the four compounds. Boron is associated with oxygen in fused boric acid and with sodium and oxygen in fused borax.

These calculations being carried out the number of satellites predicted is found to be substantially the same as the number observed. Also in many cases a close concordance between predicted and observed wave-length is found. However, due to the fact that the lines predicted due to sodium are in all cases coincident within 0.1A with oxygen lines or original component lines no definite conclusions can be formulated at this time.

There can be no doubt that these attendant lines are associated with the $K\alpha$ of boron. They do not seem to be due to any other element. In no case was it found possible to secure the attendant lines in the absence of the boron line. It is of some significance that in every case where the attendant lines appeared the oxygen line was present also.

OXYGEN

The $K\alpha$ line of oxygen appears on all plates of the boron compounds and on many others. Although several densitometer curves were taken of this

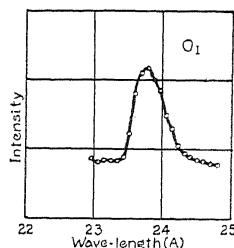


Fig. 10. Densitometer curve of a typical oxygen line.

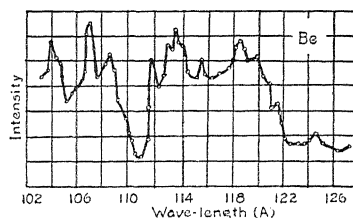


Fig. 11. Densitometer curve of the lines of beryllium.

line, only a single component appeared. Fig. 10 shows a curve of a typical oxygen line. The wave-length assigned to $K\alpha$ oxygen is $23.77 \pm 0.06\text{Å}$.

BERYLLIUM

A target of pure beryllium obtained from the Beryllium Company of America was used in the measurements of this element. Only faint traces of the presence of a line with three components could be obtained at 1800 volts using currents as large as 150 milliamperes for six hours. At 2700 volts beryllium lines of more intensity could be obtained using 40 milliamperes for two and a half hours. The line appears as a broad band with two distinct maxima. On the short wave side of this band a distinct line appears of the same intensity as the band.

Fig. 11 shows a densitometric curve of the lines of beryllium. Only four plates have been taken of this element of which three are suitable for use in the densitometer. It is not believed to be justifiable, therefore, to deduce values for the fine structure of the lines, but only for the three principal peaks. These maxima occur at $107.2 \pm 0.4\text{Å}$, $113.2 \pm 0.3\text{Å}$ and $118.7 \pm 0.2\text{Å}$. The great breadth, approximately 15Å , of this line is peculiar to this element and should be remarked.

DISCUSSION

It will be observed that the value we obtain for oxygen ($23.77 \pm 0.06\text{Å}$) is in good agreement with the value found by Söderman ($23.77 \pm 0.08\text{Å}$). Our value for beryllium ($113.2 \pm 0.3\text{Å}$) also checks with Söderman's value (113.4 ± 0.3) measured to the easily distinguishable maximum of this line.

The method of measurement used in our work in which a single component is selected from a group would seem to explain the divergence of our values for carbon and boron from those obtained by other investigators. Thus a visual measurement to the middle of the carbon line yields a value of 44.65A, in good agreement with the value of Söderman (44.70) and of Howe (44.62). The value (45.33) however, which we have finally selected based on a study of the components agrees very closely with the determination of Weatherby (45.4A). Similarly in the case of boron, a visual measurement to the middle of the line gives 67.8, in good agreement with Söderman's value ($67.80 \pm 0.2A$) and with that of Thibaud (68.0A) while the value here selected for the principal maximum is considerably higher, namely 69.33A.

The great breadth of the carbon, boron and beryllium lines must be accepted as a real effect, for the $K\alpha$ line of oxygen at 23.77A and the N doublets of tungsten at about 56A and 60A are fine lines.

In conclusion the author wishes to thank Dr. B. B. Weatherby who aided him in beginning this work. And especially does the author wish to express his thanks to Dr. C. B. Bazzoni under whom this work was carried out and whose many helpful suggestions and keen interest are largely responsible for the success of these measurements.

THE SPARK SPECTRA OF SILVER AND PALLADIUM
(Ag II AND Pd II)—AN EXTENSION

BY H. A. BLAIR

PALMER PHYSICAL LABORATORY, PRINCETON, N. J.

(Received June 9, 1930)

ABSTRACT

An attempt was made to excite the $4f$ electron spectrum of Ag II in the Schüller tube with helium. Failure is discussed assuming the excitation process Ag normal atom + He⁺. Some little extension was made to the lower spectrum. The Schüller tube was also used to extend the $4d^36s$ and $5d$ configurations of Pd II. About forty terms were added. A complete list of lines arising from high levels is given.

AG II

AN ATTEMPT was made, using the Schüller tube, to excite the spectrum connected with the $4f$ electron in Ag II. By Hund theory this should consist of the set of terms 3 and 1P , D , F , G , H in combination with the terms associated with the $5d$ electron. From analogy with other spectra the lines should lie in the lower half of the visible spectrum. Some fifty lines were measured in this region which could be allotted to the Ag II spectrum with reasonable certainty, but comparatively few were strong. About one quarter of these correspond to lines given in Kayser's Handbuch without displacement of wave-length. This lack of displacement further identifies these lines as being due to transitions from the $4f$ state for the following reason:—As is well known the lines due to transitions from high levels, which are diffuse when excited in the electric spark, are sharp when excited in the Schüller tube and besides have greater wave numbers by about two units. This means that the levels from which they arise are displaced by that amount toward their series limits. Since, however, the $4f$ levels will likely have a displacement similar to that known in the $5d$ it is to be expected that the lines due to transitions between them will not be displaced.

Among the lines observed some of the $5d$ differences were found, but it was not possible to identify any of the $4f$ terms with certainty on account of the fewness of the combinations. It appears that the Schüller tube is not well adapted to the excitation of this spectrum. This will be considered later in connection with the results in Pd II as well.

The spectral region from 2000 to 3000 Å which contains the lines of existing classifications of the silver spark, the most recent of which is due to Shenstone,¹ was also measured from Schüller tube plates. Shenstone's classification included all the predicted terms arising from the structures d^35s , $6s$, and $5d$, but the terms $5d^3P_0$ and $5d^1S_0$ were doubtful. The present measures gave about twenty new lines, some of which permitted these terms to be determined more reasonably, although the 1S_0 is much higher than expected

¹ Shenstone, Phys. Rev. 31, 317 (1928).

TABLE I. *Ag II terms.*

$d^9 5d^3 P_0$	89366.9	$d^9 5d^1 S_0$	95287.5
----------------	---------	----------------	---------

These new terms are given in Table I. To correspond with the other terms as previously given by Shenstone about 2 cm^{-1} should be subtracted.

In Table II are given the new lines as well as the few old ones whose allocations have been changed. In each case the wave number and wavelength are from Schüller tube measurements. From each of these also should 2 cm^{-1} be subtracted that they may fit Shenstone's terms. In the case of the old lines the authors and intensities are given.

TABLE II. *Ag II lines.*

Wave-length	Author	<i>I</i>	<i>I</i>	Wave number	Designation
3329.71	F	$3u$	10	30023.9	$5p^1 D_2^0 - 6s^3 D_2$
3146.10	B		8	31776.2	$5p^1 F_3^0 - 6s^3 D_2$
2801.93	B		4	35679.2	$5p^1 P_1^0 - 5d^3 S_1$
2752.19	B		4	36324.0	$5p^1 D_2^0 - 5d^3 D_3$
2743.78	B		15	36435.3	$5p^3 D_1^0 - 5d^3 P_1$
2728.73	B		3	36636.3	$5p^1 D_2^0 - 5d^3 D_2$
2656.59	E	$10u$	10	37631.0	$5p^1 F_3^0 - 5d^3 P_2$
2617.01	B		12	38200.1	$5p^3 D_1^0 - 5d^3 P_0$
2587.24	B		3	38639.7	$5p^1 P_1^0 - 5d^3 P_0$
2435.07	B		2	39434.8	$5p^3 P_0^0 - 5d^3 S_1$
2506.91	B		1	39877.8	$5p^3 F_3^0 - 5d^3 P_2$
2454.20	B		4	40734.2	$5p^3 P_2^0 - 6s^3 D_2$
2411.59	B		20	41453.8	$5p^3 D_1^0 - 5d^1 D_2$
2317.26	B		1	43141.1	$5p^3 P_1^0 - 5d^3 P_2$
2265.85	B		3	44120.5	$5p^3 D_1^0 - 5d^1 S_0$
2243.44	S	$9U$	40	44560.6	$5p^1 P_1^0 - 5d^1 S_0$
2240.47	B		3	44619.6	$5p^3 F_3^0 - 5d^3 D_1$
2226.02	S	$10U$	15	44909.2	$5p^3 P_1^0 - 5d^3 P_0$
2210.32	B		4	45228.2	$5p^3 P_2^0 - 6s^1 D_2$
2120.81	B		2	47136.9	$5p^3 P_1^0 - 5d^1 P_1$

S—Shenstone

F—Frings.

E—Exner & Haschek.

B—Author.

Some of the previously classified lines were greatly enhanced with the Schüller tube. These are $\lambda 3372$ from 1 to 50, $\lambda 3269$, 1 to 40, $\lambda 3223$, 3 to 40, $\lambda 3184$, $1u$ to 50, $\lambda 3129$, $1u$ to 20. No reason can be given for these marked changes of intensity. The remainder of the lines in the group to which they belong, the $6s$, although in most cases stronger, were not greatly different.

Pd II

The spectrum arising from the electron configurations $4d^9$, $4d^8 5s$ and $5p$ of Pd II has been very completely analyzed by Shenstone.² He was also able to classify a considerable number of the diffuse lines giving several of the $4d^8 6s$ and $5d$ terms. The present work is an extension of the analysis of the lines arising from the latter configurations.

Method of excitation. As with the silver, the Schüller tube was used for the excitation of the spectrum. The cathode used in each case was cylindrical, open at both ends, and measured 0.5 inches in diameter, and 1.5 inches in

² Shenstone, Phys. Rev. **32**, 1 (1928).

length. Helium was used to carry the current. It was purified by continuous circulation through a Misch metal discharge, and through chabazite cooled with liquid air. All gaseous impurities but hydrogen were soon removed by this method. A current of about 200 m.a. was used, the line voltage being 750 d.c. The gas pressure was kept between 3 and 4 mm, a much lower pressure, i.e., about 2 mm being found, as usual, to give the spark spectrum weakly compared with the arc. The photographs were made with the Hilger E1 quartz spectrograph. The extent of excitation is discussed later.

The data. In Table III is given a list of all the lines obtained, both classified and unclassified. The unassigned lines were included since the accuracy of measurement is probably sufficient to render a repetition of the

TABLE III. *Pd II* lines.

Wave-length	Author	I_1	I_2	Wave number	Designation
3382.57	S	1	10	29554.8	$ap^2F_{3/2}^0 - 6s^4F_{3/2}$
3377.35	B		2	29600.5	
3371.69	B		3	29650.2	
3365.99	B		2	29700.4	
3355.93	B		5	29789.5	
3352.19	B		3	29822.7	
3348.46	B		1	29855.9	$ap^2D_{3/2}^0 - ed^4F_{2/2}$
3348.11	B		1	29859.0	
3315.64	B		1	30151.4	
3282.96	B		1	30451.6	$kp^2H_{3/2}^0 - ed^2F_{3/2}$
3280.65	B		4	30473.0	
3278.05	B		3	30497.2	$cp^2F_{3/2}^0 - ed^4D_{3/2}$
3276.24	B		1	30514.0	
3274.96	B		3	30525.9	
3261.72	B	2u	2	30649.9	
3241.79	B		3	30838.3	
3237.44	B		1	30879.7	$ep^2P_{3/2}^0 - 6s^4P_{3/2}$
3221.12	B		1	31036.2	
3220.46	B		2	31042.5	$ep^2P_{1/2}^0 - 6s^2P_{3/2}$
3212.70	B		1	31117.5	
3210.48	B		6	31139.0	$ep^2D_{3/2}^0 - ed3s_{3/2}$
3206.88	B		3	31174.0	$ep^2S_{3/2}^0 - 6s^2P_{1/2}$
3206.39	B		1	31178.7	$cp^2F_{3/2}^0 - ed^4F_{4/2}$
3201.04	B		3	31230.9	
3189.34	B		4	31345.4	
3184.59	B		5	31392.1	$ap^4P_{1/2}^0 - 6s^4F_{2/2}$
3154.62	B		1	31690.4	
3153.16	S	10ua	10	31705.1	$ep^2P_{1/2}^0 - 6s^2P_{1/2}$
3149.83	B		1	31738.6	
3147.39	B		1	31763.2	
3146.51	B		1	31772.1	
3144.16	B		4	31795.8	
3138.33	B		3	31854.9	
3137.33	B		8	31865.0	$bp^4S_{1/2}^0 - 6s^4P_{1/2}$
3136.67	B		5	31871.7	
3135.41	S		3	31884.5	$bp^4D_{3/2}^0 - ed3s_{3/2}$
3123.61	B		3	32005.0	
3122.98	B		3	32011.4	
3117.70	B		1	32065.7	
3105.17	S	8uA	15	32195.1	$ap^4F_{2/2}^0 - 6s^4F_{3/2}$
3098.68	B		1	32262.4	$ep^2S_{1/2}^0 - edS_{1/2}$
3098.69	B		1	32263.3	
3091.28	B		1	32339.7	
3087.34	B		1	32381.0	

TABLE III (continued)

Wave-length	Author	I_1	I_2	Wave number	Designation
3086.26	S	3u	4d	32392.3	$\left\{ \begin{array}{l} ap^2F_{2\frac{3}{2}}^0 - 6s^2F_{3\frac{3}{2}} \\ ap^2F_{2\frac{3}{2}}^0 - 6s^4F_{2\frac{3}{2}} \end{array} \right.$
3083.18	B		1	32424.6	
3081.60	B		4	32441.3	
3079.97	B		2	32458.4	
3078.44	B		2	32474.6	
3077.01	B		6	32489.7	$bp^4D_{2\frac{3}{2}}^0 - ed3_{2\frac{3}{2}}$
3072.11	B		1	32541.5	
3068.88	E	3uA	8	32575.7	$ap^2D_{2\frac{3}{2}}^0 - 6s^4F_{3\frac{3}{2}}$
3055.07	S	10uA	35	32723.0	$kp^2G_{4\frac{3}{2}}^0 - 6s^2G_{4\frac{3}{2}}$
3053.87	B		4	32735.8	$kp^2G_{4\frac{3}{2}}^0 - 6s^2G_{3\frac{3}{2}}$
3040.16	B		2	32883.5	$cp^2D_{2\frac{3}{2}}^0 - ed3_{2\frac{3}{2}}$
3026.09	S	10uA	25	33036.3	$kp^2G_{3\frac{3}{2}}^0 - 6s^2G_{3\frac{3}{2}}$
3024.81	B		1	33050.3	$ap^2D_{1\frac{3}{2}}^0 - 6s^4F_{2\frac{3}{2}}$
3024.27	B		2	33056.2	
3020.86	B		1	33093.5	$bp^4D_{1\frac{3}{2}}^0 - ed4_{\frac{3}{2}}$
3018.95	B		3	33114.5	$bp^4S_{1\frac{3}{2}}^0 - 6s^2D_{2\frac{3}{2}}$
3014.72	S	5ua	4	33160.9	$bp^4P_{2\frac{3}{2}}^0 - 6s^2F_{2\frac{3}{2}}$
3013.59	S	5ua	4	33173.4	$bp^4P_{1\frac{3}{2}}^0 - 6s^2F_{2\frac{3}{2}}$
2997.49	B		8	33351.5	$kp^2F_{3\frac{3}{2}}^0 - 6s^2D_{2\frac{3}{2}}$
2989.61	B		1	33439.5	
2955.28	S	2uA	5	33827.9	$ap^2G_{3\frac{3}{2}}^0 - 6s^2F_{3\frac{3}{2}}$
2951.66	B		2	33869.4	$cp^2D_{1\frac{3}{2}}^0 - ed4_{\frac{3}{2}}$
2946.44	S	2uA	3	33929.4	$ep^2P_{1\frac{3}{2}}^0 - 6s^2P_{\frac{3}{2}}$
2944.53	B		1	33951.4	
2939.45	S	3uA	4	34010.1	$ep^2S_{\frac{3}{2}}^0 - 6s^2P_{\frac{3}{2}}$
2934.84	E	20uA	15	34063.5	$ap^4F_{3\frac{3}{2}}^0 - 6s^4F_{3\frac{3}{2}}$
2925.28	E	10uA	15	34174.8	$ap^2F_{2\frac{3}{2}}^0 - 6s^2F_{2\frac{3}{2}}$
2920.36	E	5uA	5	34232.3	$ap^2D_{1\frac{3}{2}}^0 - 6s^4F_{1\frac{3}{2}}$
2911.03	E	1uA	6	34344.1	$ep^2D_{2\frac{3}{2}}^0 - 6s^2P_{1\frac{3}{2}}$
2910.69	B		2	34346.1	
2900.25	E	2u	4	34469.7	
2889.97	E	2u	4	34592.3	$ep^2P_{1\frac{3}{2}}^0 - 6s^2P_{1\frac{3}{2}}$
2880.32	E	3uA	4	34708.2	$ep^2D_{1\frac{3}{2}}^0 - 6s^2P_{\frac{3}{2}}$
2877.88	E	100uA	20	34737.6	$ap^4F_{4\frac{3}{2}}^0 - 6s^4F_{4\frac{3}{2}}$
2871.20	E	100uA	25d	34818.5	$\left\{ \begin{array}{l} ap^2F_{3\frac{3}{2}}^0 - 6s^2F_{3\frac{3}{2}} \\ ap^2F_{3\frac{3}{2}}^0 - 6s^4F_{2\frac{3}{2}} \end{array} \right.$
2870.16	E	1uA	4	34831.0	$ap^2D_{1\frac{3}{2}}^0 - 6s^2F_{2\frac{3}{2}}$
2854.03	B		1	35027.9	
2853.51	S	10uA	10d	35034.3	$\left\{ \begin{array}{l} ap^4F_{2\frac{3}{2}}^0 - 6s^2F_{3\frac{3}{2}} \\ ap^4F_{2\frac{3}{2}}^0 - 6s^4F_{2\frac{3}{2}} \end{array} \right.$
2850.73	E	5uA	6	35068.4	$ap^2F_{2\frac{3}{2}}^0 - ed^4D_{2\frac{3}{2}}$
2837.48	E	20uA	25	35232.2	$cp^2F_{3\frac{3}{2}}^0 - ed3_{2\frac{3}{2}}$
2837.12	S	5uA	40	35336.7	$ap^2F_{3\frac{3}{2}}^0 - ed^4F_{3\frac{3}{2}}$
2826.33	E	3uA	4	35371.2	$ep^2D_{1\frac{3}{2}}^0 - 6s^2P_{1\frac{3}{2}}$
2822.94	E	10uA	8d	35413.6	$\left\{ \begin{array}{l} ap^2D_{2\frac{3}{2}}^0 - 6s^2F_{3\frac{3}{2}} \\ ap^2D_{2\frac{3}{2}}^0 - 6s^4F_{2\frac{3}{2}} \end{array} \right.$
2821.68	E	30uA	15	35429.4	$ap^4F_{4\frac{3}{2}}^0 - 6s^4F_{3\frac{3}{2}}$
2815.31	B		1	35509.6	
2808.75	B		1	35592.6	$\left\{ \begin{array}{l} bp^4D_{2\frac{3}{2}}^0 - ed9_{2\frac{3}{2}} \\ ep^2D_{2\frac{3}{2}}^0 - 6s^2D_{2\frac{3}{2}} \end{array} \right.$
2808.30	E	5uA	10	35598.3	$kp^2F_{2\frac{3}{2}}^0 - 6s^2G_{3\frac{3}{2}}$
2807.34	E	5uA	25	35610.4	$ap^2G_{3\frac{3}{2}}^0 - 6s^2F_{2\frac{3}{2}}$
2805.31	B		3	35636.2	
2800.74	B		10	35694.4	$bp^4D_{2\frac{3}{2}}^0 - 6s^4P_{1\frac{3}{2}}$
2800.44	E	5uA	20	35698.2	$ap^4G_{3\frac{3}{2}}^0 - 6s^4F_{3\frac{3}{2}}$
2792.68	B		1	35797.4	$ap^4F_{1\frac{3}{2}}^0 - 6s^4F_{3\frac{3}{2}}$
2791.62	B		2	35811.0	$bp^4D_{1\frac{3}{2}}^0 - 6s^4P_{1\frac{3}{2}}$
2791.32	B		1	35814.8	$cp^2P_{\frac{3}{2}}^0 - ed4_{\frac{3}{2}}$
2791.11	B		4	35817.5	
2787.73	E	100uA	50	35860.9	$ap^2G_{4\frac{3}{2}}^0 - 6s^2F_{3\frac{3}{2}}$
2781.48	B		5	35941.5	$ep^2D_{2\frac{3}{2}}^0 - 6s^2P_{1\frac{3}{2}}$

TABLE III (continued)

Wave-length	Author	I_1	I_2	Wave number	Designation
2781.32	B		1	35943.6	
2776.63	E	150uA	50	36004.3	$ap^4G_{3/2}^0 - 6s^4F_{4/2}$
2770.00	B		1	36090.5	
2765.83	B		4	36144.9	
2762.95	B		3	36182.5	
2751.55	B		3	36332.4	$bp^4D_{3/2}^0 - 6s^2D_{1/2}$
2751.06	E	4uA	8	36338.9	$bp^4D_{3/2}^0 - 6s^2D_{3/2}$
2750.51	S	1uA	4	36346.2	
2745.48	B		1	36412.7	
2732.36	B		3	36587.6	$cp^2D_{1/2}^0 - 6s^4P_{1/2}$
2732.07	B		5	36591.5	$cp^2D_{3/2}^0 - ed9_{2/2}$
2731.61	B		7	36597.6	$ap^2D_{3/2}^0 - 6s^4F_{1/2}$
2731.36	B		4	36600.9	$ap^2F_{3/2}^0 - 6s^2F_{2/2}$
2726.78	E	5uA	20	36662.4	$kp^2F_{3/2}^0 - 6s^2G_{4/2}$
2709.82	B		5	36891.9	$ep^2P_{1/2}^0 - fd\ 14$
2707.29	S	1u		36926.4	
2703.21	E	5uA	4	36982.0	$ap^4F_{1/2}^0 - 6s^4F_{1/2}$
2696.18	E	5u	6d	37078.5	$ap^4G_{3/2}^0 - 6s^2F_{3/2}$ $ap^4G_{3/2}^0 - 6s^4F_{2/2}$ $kp^2H_{3/2}^0 - 6s^2G_{4/2}$
2693.72	E	10uA	35	37112.4	$bp^4D_{3/2}^0 - 6s^2P_{1/2}$
2680.67	S	1u	3	37293.0	
2678.95	E	5uA	12	37317.0	$ap^4G_{4/2}^0 - 6s^4F_{4/2}$
2677.48	B		5	37337.4	$cp^2D_{3/2}^0 - 6s^2D_{3/2}$
2676.86	E	5uA	10	37346.1	$ap^4D_{3/2}^0 - 6s^4F_{2/2}$
2660.19	E	1u	5	37580.1	$ap^4F_{1/2}^0 - 6s^2F_{2/2}$
2653.57	B		2	37673.9	
2651.09	E	5uA	5	37709.1	$ap^4F_{2/2}^0 - ed^4D_{3/2}$
2650.38	B		5	37719.3	$cp^2P_{1/2}^0 - ed8_{1/2}$
2644.07	B		3	37809.2	$kp^2F_{2/2}^0 - fd14$
2641.67	B		8	37843.6	
2636.37	B		1	37919.6	$ap^2G_{4/2}^0 - ed^4D_{3/2}$ $ap^2F_{3/2}^0 - ed^4G_{4/2}$
2636.17	B		1	37922.5	
2633.41	B		1	37962.3	$cp^2P_{1/2}^0 - 6s^4P_{3/2}$ $ap^2F_{3/2}^0 - ed^4F_{3/2}$ $ap^4F_{2/2}^0 - ed^4F_{3/2}$
2632.33	E	2u	2	37977.8	$bp^4S_{1/2}^0 - fd13_{2/2}$
2630.78	B		3	38000.9	
2630.16	E	20uA	25	38009.2	$ap^4G_{4/2}^0 - 6s^4F_{2/2}$
2628.85	E	5uA	5	38028.1	$ap^4D_{1/2}^0 - 6s^4F_{3/2}$
2625.08	M	2uA	30	38082.7	$ap^2F_{2/2}^0 - ed^4G_{3/2}$
2624.63	E	2uA	3	38089.3	$ap^2D_{3/2}^0 - ed^4D_{3/2}$
2620.38	E	2uA	4	38151.0	$ap^4D_{3/2}^0 - 6s^4F_{1/2}$
2618.86	M	4uA	12	38173.2	$bp^4P_{2/2}^0 - ed3_{2/2}$
2618.01	S	2uA	4	38185.6	$bp^4P_{1/2}^0 - ed3_{2/2}$ $cp^2D_{1/2}^0 - 6s^2P_{1/2}$
2615.12	S	1u	25	38227.8	
2612.89	B		4	38260.4	$ap^4G_{2/2}^0 - 6s^4F_{1/2}$
2606.20	E	2uA	6	38358.6	$ap^2D_{2/2}^0 - ed^4F_{3/2}$
2600.79	B		1	38438.3	$cp^2P_{1/2}^0 - 6s^2D_{3/2}$
2597.52	B		1	38486.7	$ap^2F_{2/2}^0 - ed^2F_{3/2}$
2594.41	B		1	38532.9	$cp^2P_{1/2}^0 - 6s^4P_{1/2}$
2594.17	E	10uA	10d	38536.4	$ap^4G_{3/2}^0 - 6s^2F_{3/2}$ $ap^4G_{3/2}^0 - 6s^4F_{2/2}$ $cp^2F_{2/2}^0 - ed8_{1/2}$
2592.09	M	1u	2	38567.4	$bp^4D_{1/2}^0 - ed4_{1/2}$
2588.58	B		1	38619.6	
2587.15	E	3uA	50	38641.0	$kp^2G_{4/2}^0 - gd^2F_{3/2}$
2586.52	B		2	38650.4	$bp^4S_{1/2}^0 - fd14$
2583.02	B		6	38702.8	$kp^2G_{3/2}^0 - gd^2D_{2/2}$
2582.20	B		1	38715.1	
2580.23	B		1	38744.6	
2572.65	E	1uA	2	38858.8	$ap^4G_{2/2}^0 - 6s^2F_{3/2}$
2568.85	B		1	38916.2	$kp^2H_{4/2}^0 - 6s^2G_{4/2}$

TABLE III (continued)

Wave-length	Author	I_1	I_2	Wave number	Designation
2568.02	E	4u	10	38928.8	$kp^2H_{4\frac{1}{2}}^0 - 6s^2G_{3\frac{1}{2}}$
2567.20	B		3	38941.3	$cp^2F_{3\frac{1}{2}}^0 - ed8_{2\frac{1}{2}}$
2565.92	B		1	38960.7	$ap^4F_{3\frac{1}{2}}^0 - ed^4D_{3\frac{1}{2}}$
2565.72	B		1	38963.7	
2564.51	E	3uA	40	38982.1	$kp^2G_{3\frac{1}{2}}^0 - gd^2F_{2\frac{1}{2}}$
2563.33	S	2uA	2	39000.0	
2561.67	B		4	39025.3	
2561.43	B		2	39029.0	
2553.74	E	1	20	39146.4	
2552.26	B		2	39169.2	$cp^2P_{\frac{1}{2}} - 6s^2D_{1\frac{1}{2}}$
2551.54	B		4	39180.3	
2543.35	B		3	39306.4	$cp^2P_{\frac{1}{2}}^0 - 6s^4P_{\frac{1}{2}}$
2541.99	E	10uA	30	39327.4	$kp^2G_{4\frac{1}{2}}^0 - gd^2G_{4\frac{1}{2}}$
2539.30	E	50uA	10	39369.1	$ap^4D_{3\frac{1}{2}}^0 - 6s^4F_{4\frac{1}{2}}$
2535.94	E	1	10	39421.3	
2534.11	E	5uA	35	39449.7	
2533.94	B		10	39452.4	
2532.21	E	1u	15	39479.3	
2526.76	B		4	39564.5	
2525.19	E	4u	10	39589.1	
2521.30	E	2u	5	39650.2	$bp^4D_{3\frac{1}{2}}^0 - 6s^2G_{4\frac{1}{2}}$
2520.59	E	1	1	39661.3	$bp^4D_{3\frac{1}{2}}^0 - 6s^2G_{3\frac{1}{2}}$
2518.13	E	7uA	40	39700.0	$kp^2G_{3\frac{1}{2}}^0 - gd^2G_{3\frac{1}{2}}$
2515.33	E	5uA	20	39744.2	$bp^4P_{2\frac{1}{2}}^0 - 6s^4P_{2\frac{1}{2}}$
2513.11	B		1	39779.4	$ep^2P_{1\frac{1}{2}}^0 - fd14$
2511.22	B		2	39809.3	$ap^4D_{1\frac{1}{2}}^0 - 6s^2F_{2\frac{1}{2}}$
2508.92	E	10uA	8	39845.7	$ap^4F_{3\frac{1}{2}}^0 - ed^4F_{3\frac{1}{2}}$
2508.06	E	3uA	15	39859.5	$ep^2S_{\frac{1}{2}}^0 - fd14$
2500.11	S	1u	12	39986.2	
2499.11	E	5uA	6	40002.1	$ap^4F_{3\frac{1}{2}}^0 - ed^4G_{4\frac{1}{2}}$
2498.22	E	5uA	15	40016.4	$cp^2F_{2\frac{1}{2}}^0 - 6s^2D_{1\frac{1}{2}}$
2491.02	B		1	40132.1	$cp^2P_{\frac{1}{2}}^0 - 6s^2P_{1\frac{1}{2}}$
2488.62	B		1	40170.8	
2487.78	B		8	40184.4	$ap^4D_{2\frac{1}{2}}^0 - 6s^4F_{2\frac{1}{2}}$
2484.01	E	1	2	40245.3	
2482.60	E	1	1	40268.2	$bp^4D_{2\frac{1}{2}}^0 - 6s^2G_{3\frac{1}{2}}$
2481.75	E	2u	12	40281.9	
2479.03	E	20uA	12	40326.2	$ap^4F_{4\frac{1}{2}}^0 - ed^4D_{3\frac{1}{2}}$
2478.84	B		4	40329.2	$\left\{ \begin{array}{l} ap^2G_{3\frac{1}{2}}^0 - ed2_{2\frac{1}{2}} \\ ap^2D_{1\frac{1}{2}}^0 - ed4_{\frac{1}{2}} \end{array} \right.$
2478.57	B		2	40333.6	
2477.46	E	2uA	6	40351.7	$ap^2D_{1\frac{1}{2}}^0 - ed^4F_{1\frac{1}{2}}?$
2476.57	B		20	40366.2	
2476.11	B		1	40373.8	
2475.89	B		2	40377.3	
2473.52	B		5	40416.0	
2472.96	B		1	40425.2	
2471.45	B		1	40449.8	
2469.77	B		6	40477.3	$ep^2D_{2\frac{1}{2}}^0 - fd13_{2\frac{1}{2}}$
2469.06	B		2	40489.0	
2468.68	B		1	40495.2	$ap^4G_{3\frac{1}{2}}^0 - ed^4D_{3\frac{1}{2}}$
2467.92	E	1	2	40507.7	$ap^2F_{3\frac{1}{2}}^0 - ed^4G_{3\frac{1}{2}}$
2465.42	B		2	40548.8	
2463.97	E	1uA	4	40572.6	
2462.60	B		1	40595.2	
2461.89	B		4	40606.9	
2459.72	E	3u	7	40642.8	
2457.02	B		3	40687.4	
2456.31	B		2	40699.2	
2453.49	E	2u	6	40745.9	$ap^4F_{4\frac{1}{2}}^0 - ed^4H_{5\frac{1}{2}}$
2452.76	B		4	40758.1	$ap^2F_{2\frac{1}{2}}^0 - 6s^4P_{2\frac{1}{2}}$
2452.39	E	3u	20	40764.2	

TABLE III (continued)

Wave-length	Author	I_1	I_2	Wave number	Designation
2451.04	B		8	40786.2	
2450.95	E	10uA	8	40788.2	
2449.92	S	2u	4	40805.3	
2444.20	E	20uA	12	40900.7	$ap^2F_{3/2}^0 - ed^4F_{3/2}$
2443.88	B		1	40906.0	
2443.45	E	5uA	5	40913.3	$ap^2F_{3/2}^0 - ed^2F_{3/2}$
2442.01	B		2	40937.4	
2441.81	B		1	40940.8	
2440.01	B		6	40969.9	
2437.81	E	10uA	10	41007.9	$ap^4F_{4/2}^0 - ed^4F_{4/2}$
2436.39	E	20uA	25	41031.8	$ap^4F_{4/2}^0 - ed^4G_{3/2}$
2432.72	B		1	41093.8	$bp^4D_{3/2}^0 - fd12_{3/2}$
2431.46	B		25	41115.0	$ap^4F_{3/2}^0 - ed^4F_{3/2}$
2426.71	B		3	41195.6	
2426.08	E	8uA	30	41206.2	
2425.74	B		6	41212.0	$ap^4F_{4/2}^0 - ed^4F_{3/2}$
2425.02	B		3	41224.2	$bp^4D_{3/2}^0 - fd13_{3/2}$
2422.62	E	4uA	12	41265.0	$kp^2F_{3/2}^0 - gd^2D_{3/2}$
2422.37	B		8	41269.3	$ap^2D_{3/2}^0 - 1_{3/2}$
2421.95	E	2uA	4	41276.4	$ap^4G_{3/2}^0 - ed^4F_{4/2}$
2420.22	B		1	41306.0	$bp^4D_{3/2}^0 - fd10_{1/2}$
2419.41	E	2uA	4	41319.9	$ap^2F_{3/2}^0 - ed2_{3/2}$
2418.56	B		3	41334.4	
2418.33	B		3	41337.2	$bp^4P_{3/2}^0 - 6s^4P_{1/2}$
2417.09	B		3	41359.5	
2416.57	E	6uA	20	41368.3	$\left\{ \begin{array}{l} ap^4D_{3/2}^0 - 6s^4F_{1/2} \\ ap^4F_{4/2}^0 - ed^4G_{4/2} \end{array} \right.$
2416.32	B		2	41372.7	
2415.21	E	1uA	22	41391.6	
2414.95	B		2	41396.1	$ap^2F_{3/2}^0 - ed7_{3/2}$
2413.91	B		8	41414.0	$ap^2D_{1/2}^0 - 6s^4P_{3/2}$
2413.20	B		1	41426.1	
2411.67	E	5uA	15	41452.5	$ap^2G_{3/2}^0 - ed6_{3/2}$
2410.55	B		15	41471.6	
2408.47	B		1	41507.5	$ap^2D_{3/2}^0 - ed^2F_{3/2}$
2406.34	B		60	41544.2	$kp^2F_{3/2}^0 - gd^2F_{3/2}$
2405.99	E	1	2	41550.3	$ap^2G_{4/2}^0 - ed^4G_{3/2}$
2401.38	E	30uA	40	41630.1	
2401.13	B		12	41634.4	
2400.97	E	5uA	12	41637.1	$ap^2G_{3/2}^0 - ed^2G_{4/2}$
2400.31	E	1	2	41648.5	
2399.38	B		4	41664.6	
2398.72	B		25	41676.2	
2397.49	B		1	41697.6	$cp^2D_{2/2}^0 - fd10_{1/2}$
2398.38	B		1	41699.4	$bp^4D_{2/2}^0 - fd12_{3/2}$
2396.40	B		4	41716.5	$ap^2G_{4/2}^0 - 1_{3/2}$
2396.11	B		7	41721.6	
2394.55	B		8	41748.8	
2391.35	E	1	8	41804.6	
2391.06	B		3	41809.6	$cp^2D_{2/2}^0 - fd11_{1/2}$
2390.71	E	2uA	15	41815.8	$bp^4D_{1/2}^0 - fd12_{3/2}$
2389.89	E	1	2	41830.5	$bp^4D_{2/2}^0 - fd13_{3/2}$
2387.55	B		5	41871.1	
2386.25	B		20	41894.0	$bp^4P_{1/2}^0 - ed8_{2/2}$
2385.01	E	3uA	8	41915.6	$ap^2D_{2/2}^0 - ed2_{3/2}$
2383.43	E	4uA	15	41943.6	$ap^4F_{3/2}^0 - ed^4F_{3/2}$
2383.25	B		2	41946.6	$bp^4D_{1/2}^0 - fd13_{3/2}$
2382.70	B		7	41956.4	$ap^2G_{4/2}^0 - ed^2F_{3/2}$
2382.46	E	30uA	35	41960.5	
2382.26	B		2	41964.1	
2382.10	B		1	41966.9	$ap^4D_{3/2}^0 - 6s^2F_{3/2}$
2381.78	B		2	41972.6	$bp^4P_{3/2}^0 - 6s^2D_{1/2}$

TABLE III (continued)

Wave-length	Author	I_1	I_2	Wave number	Designation
2379.51	B		15	42012.6	$ap^4G_{a\frac{1}{2}}^0 - ed^4H_{n\frac{1}{2}}$
2379.31	B		10	42016.2	
2378.55	E	$2uA$	30	42029.5	
2376.77	B		2	42061.1	$bp^4D_{\frac{1}{2}}^0 - fd11_{\frac{1}{2}}$
2374.97	B		3	42092.9	$cp^2D_{\frac{3}{2}}^0 - fd12_{\frac{3}{2}}$
2374.23	B		4	42106.1	$bp^4S_{\frac{1}{2}}^0 - gd^2D_{\frac{3}{2}}$
2373.97	E	1	$8d$	42110.6	$bp^4P_{\frac{1}{2}}^0 - 6s^4P_{\frac{1}{2}}$
2372.96	E	2	4	42128.6	
2369.07	B		4	42197.8	$cp^2D_{\frac{1}{2}}^0 - fd10_{\frac{1}{2}}$
2368.54	B		4	42207.2	$ap^2D_{\frac{1}{2}}^0 - ed3_{\frac{3}{2}}$
2367.59	B		4	42224.0	$ap^2F_{\frac{3}{2}}^0 - ed5_{\frac{3}{2}}$
2365.46	E	$0uA$	20	42262.2	$kp^2H_{\frac{1}{2}}^0 - gd^2G_{\frac{3}{2}}$
2364.75	E	$3uA$	7	42274.9	$ap^4G_{\frac{3}{2}}^0 - ed^4F_{\frac{3}{2}}$
2364.61	B		7	42277.3	
2364.07	B		7	42287.0	
2363.91	B		6	42289.9	
2363.41	E	$5uA$	18	42298.8	$ap^4G_{\frac{1}{2}}^0 - ed^4G_{\frac{3}{2}}$
2362.95	B		8	42307.0	
2362.83	B		1	42309.2	$cp^2D_{\frac{1}{2}}^0 - fd11_{\frac{1}{2}}$
2361.23	E	$1uA$	15	42337.9	$ap^4F_{\frac{3}{2}}^0 - ed^4F_{\frac{1}{2}}$
2360.97	B		30	42342.5	$kp^2F_{\frac{3}{2}}^0 - gd^2D_{\frac{3}{2}}$
2360.76	B		1	42346.2	
2359.14	E	$4uA$	75	42375.3	$ap^4G_{\frac{3}{2}}^0 - 5d^4H_{\frac{6}{2}}$
2358.95	B		3	42378.8	
2357.43	B		3	42406.1	
2355.57	E	$3uA$	20	42439.5	$ap^4F_{\frac{3}{2}}^0 - ed5_{\frac{3}{2}}$
2355.34	B		3	42443.7	$ap^2F_{\frac{3}{2}}^0 - ed6_{\frac{3}{2}}$
2350.72	E	$1uA$	10	42527.1	
2349.38	B		2	42551.3	
2349.02	E	$2uA$	8	42557.9	
2347.76	B		25	42580.6	$kp^2F_{\frac{3}{2}}^0 - gd^2F_{\frac{3}{2}}$
2347.38	B		1	42587.5	
2347.17	E	$8uA$	10	42591.4	$ap^4F_{\frac{3}{2}}^0 - ed^4G_{\frac{3}{2}}$
2345.52	B		8	42621.4	$kp^2F_{\frac{3}{2}}^0 - gd^2F_{\frac{3}{2}}$
2344.77	B		1	42635.0	$ap^4G_{\frac{3}{2}}^0 - ed^4G_{\frac{3}{2}}$
2342.50	B		1	42676.3	
2341.93	E	1	6	42686.8	
2340.26	B		3	42717.2	$ap^2D_{\frac{3}{2}}^0 - ed^4F_{\frac{1}{2}}$
2339.95	E	1	15	42722.9	$cp^2D_{\frac{1}{2}}^0 - fd13_{\frac{3}{2}}$
2339.65	B		1	42728.3	
2338.10	E	$1u$	2	42756.7	$ap^4F_{\frac{3}{2}}^0 - 1_{\frac{3}{2}}$
2335.57	B		5	42802.9	
2335.43	B		3	42805.5	
2334.04	E	$1uA$	2	42831.0	$ap^2G_{\frac{3}{2}}^0 - ed7_{\frac{3}{2}}$
2333.32	B		3	42844.2	
2332.81	B		2	42853.6	
2332.47	E	$4uA$	8	42859.8	$ap^4D_{\frac{3}{2}}^0 - ed^4D_{\frac{3}{2}}$
2331.94	B		1	42869.5	
2329.96	E	$3uA$	5	42906.0	$ap^4G_{\frac{3}{2}}^0 - ed^4D_{\frac{3}{2}}$
2329.76	B		1	42909.7	$cp^2P_{\frac{1}{2}}^0 - fd11_{\frac{1}{2}}$
2328.56	E	$3uA$	4	42931.8	$ap^4G_{\frac{3}{2}}^0 - 1_{\frac{3}{2}}$
2327.35	M	$3uA$	8	42954.1	
2326.11	E	1	7	42977.0	$bp^4P_{\frac{3}{2}}^0 - 6s^2P_{\frac{1}{2}}$
2325.12	E	$3uA$	$3d$	42995.3	$cp^2F_{\frac{3}{2}}^0 - 6s^2G_{\frac{3}{2}}$
2324.07	E	$3uA$	8	43014.7	
2323.34	E	$2uA$	12	43028.2	$ap^2F_{\frac{3}{2}}^0 - 6s^2D_{\frac{1}{2}}$
2322.79	B		3	43038.4	$ap^2D_{\frac{3}{2}}^0 - ed6_{\frac{3}{2}}$
2320.56	B		$5d$	43079.7	$ap^4F_{\frac{1}{2}}^0 - ed4_{\frac{3}{2}}$
2319.40	E	$4uA$	10	43101.4	$ap^4F_{\frac{1}{2}}^0 - ed^4F_{\frac{1}{2}}$
2318.12	B		1	43125.1	$bp^4D_{\frac{1}{2}}^0 - fd14$
2317.96	E	$2uA$	5	43128.1	$ap^4D_{\frac{3}{2}}^0 - ed^4F_{\frac{3}{2}}$
2317.23	B		1	43141.7	

TABLE III (continued)

Wave-length	Author	I_1	I_2	Wave number	Designation
2315.65	B		5	43171.2	$ap^4G_{2\frac{1}{2}}^0 - ed^2F_{3\frac{1}{2}}$
2314.73	B		1	43188.2	
2314.47	E	1	4	43193.2	$cp^2P_{1\frac{1}{2}}^0 - fd12_{2\frac{1}{2}}$
2313.80	B		4	43205.7	
2312.29	B		6	43233.9	$ep^2P_{1\frac{1}{2}}^0 - gd^2D_{2\frac{1}{2}}$
2310.57	B		10	43266.0	$\left\{ \begin{array}{l} ap^2G_{4\frac{1}{2}}^0 - ed5_{3\frac{1}{2}} \\ kp^2F_{3\frac{1}{2}}^0 - gd^2G_{4\frac{1}{2}} \\ ap^4G_{4\frac{1}{2}}^0 - ed^4H_{5\frac{1}{2}} \end{array} \right.$
2307.40	E	20uA	25	43325.4	
2306.99	B		2	43333.2	
2306.71	B		2	43338.4	
2305.70	E	1	10	43357.3	
2304.89	S	1u	3	43372.7	$cp^2D_{1\frac{1}{2}}^0 - fd14$
2304.35	B		7	43382.8	
2303.47	B		1	43399.3	$ap^4F_{2\frac{1}{2}}^0 - 6s^4P_{2\frac{1}{2}}$
2303.28	B		1	43402.9	$ap^4F_{2\frac{1}{2}}^0 - ed2_{2\frac{1}{2}}$
2302.14	B		3	43424.4	
2295.71	B		4	43546.1	
2295.51	E	3uA	12	43549.9	$ap^2D_{1\frac{1}{2}}^0 - ed8_{2\frac{1}{2}}$
2294.02	B		4	43578.1	$ap^4G_{2\frac{1}{2}}^0 - ed2_{2\frac{1}{2}}$
2293.52	E	5uA	10	43587.7	$ap^4G_{4\frac{1}{2}}^0 - ed^4F_{4\frac{1}{2}}$
2292.97	B		2	43598.1	
2290.72	B		1	43640.8	$ap^2F_{2\frac{1}{2}}^0 - 6s^2D_{2\frac{1}{2}}$
2287.55	B		10	43701.3	
2286.78	B		8	43716.1	$kp^2H_{5\frac{1}{2}}^0 - gd^2G_{4\frac{1}{2}}$
2283.40	E	3uA	3	43780.9	
2283.09	B		3	43786.8	
2282.87	E	3u	5	43790.9	$ap^4G_{4\frac{1}{2}}^0 - ed^4F_{3\frac{1}{2}}$
2282.40	E	2	12	43800.9	$ap^2D_{2\frac{1}{2}}^0 - 6s^4P_{2\frac{1}{2}}$
2281.37	E		4d	43819.7	$\left\{ \begin{array}{l} ap^2D_{1\frac{1}{2}}^0 - 6s^4P_{\frac{1}{2}} \\ ap^2F_{2\frac{1}{2}}^0 - ed7_{2\frac{1}{2}} \end{array} \right.$
2280.43	B		25	43837.8	
2277.33	E	4ua	3	43897.4	
2275.92	E	5ua	10	43924.7	
2274.70	E	2ua	3	43948.3	$ap^4G_{4\frac{1}{2}}^0 - ed^4G_{4\frac{1}{2}}$
2272.13	B		1	43998.0	
2270.11	E	6uA	40	44037.1	$ap^4F_{2\frac{1}{2}}^0 - ed7_{2\frac{1}{2}}$
2269.11	B		1	44046.5	
2268.42	B		1	44069.9	
2266.43	B		2	44108.6	$ap^4D_{1\frac{1}{2}}^0 - ed^4F_{2\frac{1}{2}}$
2265.69	B		4	44123.0	$ap^4F_{4\frac{1}{2}}^0 - 1_{3\frac{1}{2}}$
2264.68	B		3	44142.6	$cp^2P_{\frac{1}{2}}^0 - fd10_{1\frac{1}{2}}$
2263.63	B		2	44163.2	$ap^4F_{1\frac{1}{2}}^0 - 6s^4P_{2\frac{1}{2}}$
2262.30	B		15	44189.0	
2261.72	E	2uA	20	44200.4	
2261.29	B		20	44208.8	
2260.45	E	6uA	18	44225.2	$ap^4G_{3\frac{1}{2}}^0 - ed^4G_{3\frac{1}{2}}$
2259.32	S	1u	5	44247.2	$ap^4D_{1\frac{1}{2}}^0 - ed4_{\frac{1}{2}}$
2259.03	S	1u	3	44253.1	$cp^2P_{\frac{1}{2}}^0 - fd11_{1\frac{1}{2}}$
2257.06	B		1	44291.7	$ep^2D_{1\frac{1}{2}}^0 - gd^2F_{2\frac{1}{2}}$
2254.30	B		20	44345.8	
2253.74	B		2	44357.0	
2252.98	B		1	44371.8	
2252.60	S	2u	5	44379.3	$ap^4G_{2\frac{1}{2}}^0 - ed^4F_{1\frac{1}{2}}$
2247.40	S	3	3	44482.0	$ap^4G_{2\frac{1}{2}}^0 - ed5_{3\frac{1}{2}}$
2245.11	S	1u	3	44527.3	$ap^4D_{1\frac{1}{2}}^0 - ed2_{2\frac{1}{2}}$
2243.47	B		4	44559.8	
2243.29	B		1	44563.5	
2243.17	S	0u	2	44565.8	
2242.54	B		7	44578.3	
2242.34	B		1	44582.3	$ep^2D_{2\frac{1}{2}}^0 - gd^2D_{2\frac{1}{2}}$
2241.51	B		4	44598.9	$ap^2D_{2\frac{1}{2}}^0 - ed8_{1\frac{1}{2}}$
2240.57	S	1u	2	44617.7	$ap^4G_{3\frac{1}{2}}^0 - ed^4F_{2\frac{1}{2}}$

TABLE III (continued)

Wave-length	Author	I_1	I_2	Wave number	Designation
2237.42	B		1	44680.5	$ap^4D_{3\frac{1}{2}}^0 - 6s^2F_{2\frac{1}{2}}$
2235.05	B		3	44727.7	
2234.25	B		15	44743.8	
2232.63	B		4	44776.2	
2231.36	B		10	44801.8	$ap^4F_{1\frac{1}{2}}^0 - ed7_{2\frac{1}{2}}$
2230.75	B		2	44814.0	
2230.43	B		4	44820.5	$\left\{ \begin{array}{l} ap^4D_{1\frac{1}{2}}^0 - ed^23_{2\frac{1}{2}} \\ ep^2D_{2\frac{1}{2}}^0 - gd^2F_{3\frac{1}{2}} \\ kp^2H_{4\frac{1}{2}}^0 - gd^2F_{3\frac{1}{2}} \end{array} \right.$
2229.76	B		4	44833.9	
2229.55	B		1	44838.1	
2228.68	B		1	44855.5	
2228.40	B		5	44861.2	$ep^2D_{2\frac{1}{2}}^0 - gd^2F_{2\frac{1}{2}}$
2224.91	B		1	44931.5	
2224.14	B		2	44947.1	
2223.63	S	25ua	25	44957.5	$ap^4D_{3\frac{1}{2}}^0 - ed^4D_{3\frac{1}{2}}$
2223.57	B		2	44958.6	
2222.20	S	25ua	25	44986.3	
2220.40	B		1	45022.9	
2220.20	S	0	5	45026.9	
2216.49	B		4	45102.2	$cp^2F_{2\frac{1}{2}}^0 - fd11_{1\frac{1}{2}}$
2212.50	B		1	45183.7	
2210.57	S	0u	2	45223.1	
2206.32	B		4	45310.1	
2205.95	B		1	45317.8	$cp^2P_{\frac{3}{2}}^0 - fd14$
2205.41	S	0u	25	45328.9	$bp^4D_{3\frac{1}{2}}^0 - gd^2D_{2\frac{1}{2}}$
2204.80	B		2	45341.4	
2204.55	S	0u	4	45346.5	
2201.97	B		1	45399.6	
2200.09	B		2	45438.4	
2196.16	S	1u	20	45519.7	$kp^2H_{4\frac{1}{2}}^0 - gd^2G_{4\frac{1}{2}}$
2193.88	S	0u	15	45567.0	$bp^4D_{3\frac{1}{2}}^0 - gd^2F_{3\frac{1}{2}}$
2193.47	S	3u	4	45575.5	
2192.69	B		7	45591.8	$kp^2F_{2\frac{1}{2}}^0 - gd^2G_{3\frac{1}{2}}$
2192.11	B		1	45603.8	
2191.92	B		3	45607.8	$bp^4D_{3\frac{1}{2}}^0 - gd^2F_{2\frac{1}{2}}$
2190.55	B		4	45636.3	
2190.45	S	10ua	7	45638.7	$ap^4D_{3\frac{1}{2}}^0 - ed^4F_{4\frac{1}{2}}$
2184.34	S	0u	2	45766.1	
2181.54	B		1	45824.7	
2180.72	S	0u	2d	45841.9	$ap^4D_{3\frac{1}{2}}^0 - ed^4F_{3\frac{1}{2}}$
2178.30	B		5	45892.9	$ap^4F_{4\frac{1}{2}}^0 - ed6_{3\frac{1}{2}}$
2172.92	B		3	46006.7	
2171.38	S	3u	1	46039.2	$ap^4D_{2\frac{1}{2}}^0 - 1_{3\frac{1}{2}}$
2166.36	B		3	46145.9	
2166.04	B		1	46152.6	$ap^4D_{1\frac{1}{2}}^0 - ed8_{1\frac{1}{2}}$
2164.41	B		3d	46187.4	
2163.18	B		2	46213.7	$bp^4D_{2\frac{1}{2}}^0 - gd^2F_{2\frac{1}{2}}$
2161.35	B		3	46252.9	$bp^4D_{3\frac{1}{2}}^0 - gd^2G_{4\frac{1}{2}}$
2158.74	S	0u	2d	46308.6	
2157.85	B		1	46327.6	$cp^2D_{2\frac{1}{2}}^0 - gd^2D_{2\frac{1}{2}}$
2155.91	B		2	46369.5	
2141.28	S	1u	1	46686.2	
2140.69	B		3	46699.1	
2124.33	S	1u	2	47058.8	$bp^4P_{\frac{1}{2}}^0 - fd11_{1\frac{1}{2}}$

E—Exner & Naschek

M—Meggers

S—Shenstone

B—Author

u—Diffuse

A—strong in arc

a—weak in arc.

Wave numbers measured, wave-lengths calculated.

 I_1 —Meggers' intensities except for Shenstone's lines. I_2 —Author's estimates from Schüler tube.

Author—Original observer.

work unnecessary. The standards used were the corrected Pd II sharp lines from Shenstone's classification. In general no greater variation than 0.5 cm^{-1} was necessary in satisfying the combination principle with new terms. All the normally diffuse lines were included, even when they had been previously given by Shenstone, since the accuracy of measurement is here much greater, since some of the classifications have been altered and since the usual displacement of the diffuse lines by $2\text{--}3 \text{ cm}^{-1}$ prevents a consistent scheme. The complete line list of Pd II is obtainable by adding that here given to that of Shenstone's sharp lines.

TABLE IV. *Origin of high terms of Pd II.*

Config.	Pd III Term	Added Electron	Theoretical	Terms	
				Empirical	
$4d^8$	3F	$6s$	$^4,^2F$	$6s^4,^2F$	
		$5d$	$^4,^2P, D, F, G, H$	$ed^4 D, F, G, H$	parts of
	3P	$6s$	$^4,^2P$	$6s^4,^2P$	parts doubtful.
		$5d$			None identified.
	1S	$6s$			None identified.
		$5d$			None identified.
	1D	$6s$	2D	$6s^2D$	
		$5d$	$^2S, P, D, F, G$	jd	Not nameable.
	1G	$6s$	2G	$6s^2G$	
		$5d$	$^2D, F, G, H, I$	$gd^2D, F, G.$	

In Table IV are given the electron configurations of the high terms, the predicted terms and those thought to have been found. The lettering corresponds to that in the list of high terms given in Table V. Where a term could not be reasonably placed in a group it was left unlettered.

The $6s$ group. It was found possible to complete the $6s$ group satisfactorily, except for the $^2P_{\frac{1}{2}}$ term, and possibly the $^4P_{\frac{1}{2}}$ term, the former being particularly doubtful, as it requires the crossing over of the components of the doublet.

The convergence of the terms is odd in part. The $^4F_{4\frac{1}{2}}$ $^4F_{3\frac{1}{2}}$ separation has decreased from 2013.3 to 692.2 in going from the $5s$ to the $6s$ group, and these terms appear to be approaching the same limit as would be expected with the inverted type of convergence pointed out by Shenstone,^{3,4} i.e., where equal J values do not cross. The $^4F_{2\frac{1}{2}}$ and $^2F_{3\frac{1}{2}}$ however, which are also expected to have the same limit have already crossed over each other, although just by one cm^{-1} . It would be interesting to find what would happen in the next series member as well as to investigate the "strong field" Zeeman pattern of the present one. The lines are too diffuse to do this with a source in air, but it might be accomplished at low pressure. The $^4F_{1\frac{1}{2}}$ and $^2F_{2\frac{1}{2}}$ have converged considerably, again as expected. The doubtful validity of two of the P terms renders a discussion of their convergence profitless. The 2D has converted from -1227.2 to -612.9 while the 2G which in the first member had an interval of only 108.2 has closed to 12.5. The indication is that each doublet is going to its own limit.

³ Shenstone, *Nature* **122**, 727 (1928).

⁴ Hund, *Zeits. f. Physik* **52**, 601 (1928).

TABLE V. *High terms of Pd II.*

No.	Term	Designation
*61	79535.0	$6s^4F_{4\frac{1}{2}}$ *
*62	80227.2	$6s^4F_{3\frac{1}{2}}$ *
*63	83065.0	$6s^2F_{3\frac{1}{2}}$ *
*64	83066.0	$6s^4F_{2\frac{1}{2}}$ *
*65	84249.0	$6s^4F_{1\frac{1}{2}}$ *
*66	84847.5	$6s^2F_{2\frac{1}{2}}$ *
*67	85123.5	$ed^4D_{3\frac{1}{2}}$ *
68	85543.5	$ed^4H_{5\frac{1}{2}}$ *
69	85740.9	$ed^4D_{2\frac{1}{2}}$ *
*70	85805.6	$ed^4F_{4\frac{1}{2}}$ *
71	85829.3	$ed^4G_{5\frac{1}{2}}$ *
72	85905.8	$ed^4H_{6\frac{1}{2}}$ *
*73	86009.3	$ed^4F_{3\frac{1}{2}}$ *
74	86166.0	$ed^4G_{4\frac{1}{2}}$ *
75	88754.7	$ed^4G_{3\frac{1}{2}}$ *
76	88920.4	$1s_{\frac{1}{2}}$ *
77	89147.2	$ed^4F_{2\frac{1}{2}}$ *
78	89160.0	$ed^2F_{3\frac{1}{2}}?$ *
79	89566.6	$ed\ 2_{2\frac{1}{2}}$ *
*80	89859.2	$ed\ 3_{2\frac{1}{2}}$ *
81	90345.9	$ed\ 4_{\frac{1}{2}}$ *
82	90368.7	$ed^4F_{1\frac{1}{2}}$ *
83	90470.5	$ed\ 5_{3\frac{1}{2}}$ *
84	90690.2	$ed\ 6_{3\frac{1}{2}}$ *
85	91430.6	$6s^4P_{2\frac{1}{2}}$ *
86	92068.7	$ed\ 7_{2\frac{1}{2}}$ *
87	92251.1	$ed\ 8_{1\frac{1}{2}}$ *
88	93063.6	$6s^4P_{1\frac{1}{2}}?$ *
89	93567.5	$ed\ 9_{2\frac{1}{2}}$ *
90	93700.7	$6s^2D_{1\frac{1}{2}}$ *
91	93837.4	$6s^4P_{\frac{1}{2}}$ *
92	93999.6	$6s^2P_{\frac{1}{2}}??$ *
93	94313.6	$6s^2D_{2\frac{1}{2}}$ *
94	94662.6	$6s^2P_{1\frac{1}{2}}$ *
*95	97625.0	$6s^2G_{4\frac{1}{2}}$ *
96	97637.5	$6s^2G_{3\frac{1}{2}}$ *
97	98674.0	$fd10_{1\frac{1}{2}}$ *
98	98785.1	$fd11_{1\frac{1}{2}}$ *
99	99068.6	$fd12_{1\frac{1}{2}}$ *
100	99199.3	$fd13_{2\frac{1}{2}}$ *
101	99849.0	$fd14$ *
102	103304.2	$gd^2D_{3\frac{1}{2}}$ *
103	103542.6	$gd^2F_{3\frac{1}{2}}$ *
104	103583.5	$gd^2F_{2\frac{1}{2}}$ *
105	104228.3	$gd^2G_{4\frac{1}{2}}$ *
106	104301.5	$gd^2G_{3\frac{1}{2}}$ *

* Previously given by Shenstone, reference 2.

Intervals

$6s^4F$	692.2	2838.8	1183.0
$6s^2F$	1782.5		
ed^4D	617.4	—	—
ed^4H	—362.5	—	—
ed^4F	203.7	3137.9	1221.5
ed^4G	336.7	2588.7	—
$6s^4P$	1633.0	773.8	
$6s^2D$	—612.9		
$6s^2G$	12.5		
gd^2F	40.9		
gd^2G	73.2		

The 5d group. The terms built on the $d^8\ ^3F$ of Pd III should be found in three groups with separations similar to those of the components of the 3F . This 3F of Pd III has not been found, but the $d^8s^2\ ^3F$ of Pd I which is known should have separations of about the same magnitudes. Its intervals are 3100 and 1500. The terms here designated "*ed*" which are considered to be those built on the 3F of Pd III are sharply divided into but two groups. The second group does in fact start at about 3,000 above the first but it shows no definite division within itself. This is to be expected, however, considering the narrowness of the interval.

The lower "*ed*" group which is quite distinct, which shows the proper quantum numbers to be based on the 3F_4 , and in which the naming of the terms was possible from intensities of combination is composed entirely of quartets of high inner quantum numbers. This apparent separation of the quartets and doublets seems to indicate the inverted type of convergence. In Ni I Russell⁵ found this situation with the quintets and triplets of the $d^8s\cdot 4p$ configuration, but it was not general throughout the spectrum.

The combinations made by the remainder of the "*ed*" group indicate a coupling in which the L vector is losing its identity. The "*fd*" group which is quite probably based on the 1D of the ion from its position, had to be left nameless also for this reason. The "*gd*" group gave much more complete combinations, and these terms could be assigned L values quite definitely. The "*gd*" 2H and 2I could not be found although the 2H at least should make sufficient combinations. It is noteworthy that the "*gd*" group lies at about 19,000 above the beginning of the "*ed*" just as does the $5s^2G$ above the $5s^4F$.

The unassigned lines. The type of coupling makes it difficult to find new terms by the method of differences as the expected differences frequently do not occur. The labor involved in a method of trial of lines is probably not warranted until more idea of the positions of the missing terms can be obtained. The several unassigned strong lines are quite likely due to missing terms of high L and J whose combinations will be very few.

Excitation limit with helium. The extent of excitation of these two spectra and the points of maximum excitation are in agreement with the discussion of these points by R. A. Sawyer.⁶ He has found that with metals of high melting point as cathodes where the presence of the atoms of the cathode substances in the discharge is due to sputtering rather than vaporization, that the principal processes of excitation start from the normal state of the atom. Thus the highest levels excited to any great extent will be those which lie at the energy of the helium ion, 24.48 volts, 198,290 cm^{-1} above the normal state of the metal atom. Further, there should be an intensity maximum at this energy as well as at 19.75 volts, the metastable potential of helium. Neither of the spectra here considered was measured in the region where the excitation maximum due to the metastable potential would occur, but they may be considered as regards the energy of the helium ion.

⁵ H. N. Russell, Phys. Rev. 34, 821 (1929).

⁶ Sawyer, Bulletin, Am. Phys. Soc. 5, No. 2, Abstract 22, April (1930).

In the case of silver the lowest term of the ion $d^{10} {}^1S_0$ is at $-39,163.9 \text{ cm}^{-1}$ from the $4d^9 5s {}^3D_3$ which has been used as the zero level. The ionization potential of Ag I is $59,370 \text{ cm}^{-1}$. Subtracting these energies from that of the helium ion leaves about $99,750 \text{ cm}^{-1}$ available for excitation, on the scale used. This is much too low for the $4f$ electron levels which from analogy with other spectra are to be expected to lie about $20,000 \text{ cm}^{-1}$ above the $5d$, i.e., at about $110,000$.

In the case of palladium the lowest term $4d^9 {}^2D$ is at $-25,081 \text{ cm}^{-1}$, while the ionization potential of Pd I is about $67,060$. About $106,150 \text{ cm}^{-1}$ is thus available for excitation, and there should be an intensity maximum of the lines arising from terms in this neighborhood. The " gd " doublet terms at $104,000$ do in fact give rise to the group of lines which, compared to the ordinary spark, is enhanced most in intensity and which is quite as strong as even the lowest of the high set of terms. Nothing can be said about the limit of excitation as no higher spectrum than the $5d$ was sought, and it is probably just within the available energy.

The author wishes to express his thanks to Professor A. G. Shenstone, under whose direction the work was done, and to the Carnegie Foundation through whose generosity the laboratory was enabled to procure a calculating machine which greatly facilitated the calculation of the wave-numbers from the measurements.

THE RESONANCE (*B-A*) BAND SYSTEM OF THE HYDROGEN MOLECULE

BY HUGH H. HYMAN
PHYSICAL LABORATORY, UNION COLLEGE
(Received June 3, 1930)

ABSTRACT

Part I. Experimental procedure. A three meter focal length vacuum spectrograph, designed by Professor J. J. Hopfield, has been constructed at the University of California and used to photograph the extreme ultraviolet hydrogen band spectra. A description of the type of mounting and method used to focus the instrument is given. The greater dispersion and resolving power has made possible the measuring of additional lines. New tables of frequencies are given.

Part II. Lines in sixty-eight bands have been given quantum assignments. On the basis of the old quantum theory the moment of inertia of the hydrogen in the normal (*A* level) state is found to be 0.4673×10^{-40} g cm² and the nuclear separation to be 0.7500×10^{-8} cm. In the first electronic excited state (*B* level) the moment of inertia is 1.4225×10^{-40} g cm² and the nuclear separation 1.308×10^{-8} cm. Comparison of the present results with those obtained by Richardson and Davidson in their study of bands found in the visible leaves no doubt but that the ultraviolet *B* state also is the lower state of the bands studied by them. This, then, verifies the assumption made by Birge and leads to the conclusion that the ionization potential of H₂ must be 15.34 volts to within a few hundredths of a volt.

Bands connected with vibrational levels *A*₀, *A*₁ and *A*₂ are not observed. In order to obtain the best possible value of *I*₀, data from all available sources were correlated and averaged. Birge and Jeppesen calculated accurate values of *B*₀ and *B*₁, for the normal level, from Rasetti's data on the Raman effect of gaseous hydrogen. Values for *B*₁ by the two methods agree to one part in seven thousand but their value for *B*₀ is 0.27 percent higher than the value given by the present method. This discrepancy points to an irregularity in the moment of inertia of hydrogen in the *v*=0 state of the normal electronic level, as has been pointed out by Birge and Jeppesen.

INTRODUCTION

INVESTIGATIONS of the fine structure of bands found in the extreme ultraviolet have been handicapped greatly by the low dispersion and resolving power of the instruments used in the photographic work. Professor J. J. Hopfield of the University of California has designed a vacuum spectrograph using a three inch grating, 15000 lines per inch, with a three meter focal length. It has been found that the instrument has a resolving power of 0.1Å and a dispersion of 2.76Å per millimeter in the second order. The spectrograph has been built in the shop of the Physics Laboratory of the University of California by Mr. W. R. Stamper and his assistants, following the plans furnished by Professor Hopfield.

The hydrogen bands of the extreme ultraviolet were photographed by the writer, this being the first vacuum work completed on the instrument.

Previous to the present work Dieke and Hopfield,^{1,2} by obtaining ab-

¹ Dieke and Hopfield, Zeits. f. Physik 40, 229 (1926).

² Dieke and Hopfield, Phys. Rev. 30, 400 (1927).

sorption and emission spectrograms, were able to give a complete analysis of the vibrational levels of the three known lower electronic states of the hydrogen molecule. These three states are known as the *A*, *B*, and *C* levels, the *A* level being the normal state of the molecule.

Schumann,³ Lyman,⁴ Witmer,^{5,6} Werner,⁷ Hori,⁸ and others had photographed and measured H_2 bands in the extreme ultraviolet. The bands photographed and measured by Werner constitute the *C-A* system, as given by Dieke and Hopfield. The Lyman-Witmer bands now are known to form the B_3-A_v transitions of the *B-A* system. These B_3-A_v bands are obtained when the discharge tube is filled with a mixture of argon and hydrogen. These same bands appear when only hydrogen is used in the tube, but generally are weaker, some of them being almost completely blended by more intense bands of the *B-A* system. Richardson, and his students,⁹ in a series of papers, have identified a great number of electronic levels of the hydrogen molecule. Birge¹⁰ assumed that the lower level of the Richardson "*A*" and "*B*" band systems¹¹ was identical with the *B* state of the bands in the ultraviolet. With a Ritz formula for the Richardson band system, Birge found the ionization potential of H_2 to be 15.34 volts. In the same paper a summary of the quantum levels and constants of the hydrogen molecule is given. Starting with the vibrational analysis as given by Dieke and Hopfield,^{1,2} Hori⁸ has obtained an analysis of the fine structure of the *C-A* bands. In the same paper he gave a preliminary analysis of the Lyman-Witmer progression (B_3-A_v), based on the assumed presence of *R*, *Q*, and *P* branches. For the latter work Hori used Witmer's measurements.

PART I. EXPERIMENTAL PROCEDURE

The instrument designed by Professor J. J. Hopfield and used for obtaining the spectrogram shown in Fig. 2 is so made that it is possible to obtain on the photographic plate any region of the spectrum. The plates are of such size that a span of 1200 Angstroms, in the first order can be photographed with one exposure. Arrangements have been made so that thirteen exposures may be taken on one plate. However, it has been found that limiting the number to five is more practical.

Type of mounting.

As the space to be evacuated needed to be kept a minimum, a modified form of the Eagle mounting¹² was used, instead of the Rowland type. The

³ W. Schumann, Werner Anzeiger 29, 230 (1892).

⁴ T. Lyman, Spectroscopy of Extreme Ultraviolet, (1914).

⁵ Witmer, Proc. Nat. Acad. Sci. 12, 238 (1926).

⁶ Witmer, Phys. Rev. 28, 1223 (1926).

⁷ Werner, Proc. Roy. Soc. 113A, 107 (1929).

⁸ T. Hori, Zeits. f. Physik 44, 11, 834 (1927).

⁹ Richardson and Davidson, Proc. Roy. Soc. 125A, 23 (1929), and article referred to in this paper.

¹⁰ R. T. Birge, Proc. Nat. Acad. Sci. 14, 12 (1928).

¹¹ Richardson and Davidson, Proc. Roy. Soc. 115A, 528 (1927).

¹² A. Eagle, Astrophys. J. 31, 120 (1910).

slit, the photographic plate, and the grating were all placed in a cast iron tube three meters long. Five sylphons served as a means for making the adjustments of the plate-holder and grating. These adjustments could be made after a vacuum had been obtained. A grating to be used in this manner must be capable of motion along the tube, and also of rotation about a vertical axis. Fig. 1A shows how this was accomplished. The grating is fastened to the carriage *C* which is mounted on the rails *R*. Rods *D* and *E* served to move the grating.

The position of the grating is shown by two dials placed at *A* and *B*. The plate-holder *F-G* is pivoted such that the line of rotation passes through the line of the slit and the radius of curvature of the holder is one-half the radius of curvature of the grating. The slit is at *S*.

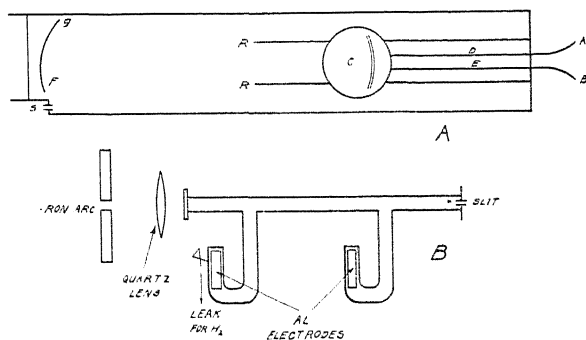


Fig. 1. Diagram of apparatus.

It is well known that in order to obtain the best definition with a concave grating the slit and the grating must be on a circle whose diameter is equal to the radius of curvature of the grating, and, in this case, all the spectral lines are focused on this same circle. The method of mounting fulfills these requirements. It can be seen that the exact position of four variables must be determined to obtain the focus.

Adjustment of the instrument.

The first work to be done was to focus the instrument for all regions of the spectrum. In the case of the Rowland mounting there is a standard method of procedure but in the mounting considered here the method is not so well established.

The first step in the adjustment was the leveling of the grating so that the images would all fall upon the horizontal opening over the plate. Once this position for the grating had been determined, this variable was eliminated.

The second step in the adjustment was to find the approximate settings of the plate, the grating, and the slit with respect to one another, for a definite region of the spectrum.

For convenience, a portion of the visible spectrum of the mercury arc was used. For approximate settings, the eye was used to examine the image

which was assumed to be formed on a photographic plate. When the adjustments were found sufficiently close to serve as a starting point, a photograph of the known lines of mercury was taken and examined for the purpose of determining the course of procedure. Upon examining these plates it was found that certain parts of the spectrum were in much better focus than others. This indicated that the angle of the plate-holder was not correct.

The question, then, was one of determining what changes were necessary in order to bring in focus all the spectrum that fell on this plate. This necessitated the determination of the angle of the plate, the angle of the grating and the distance of the grating from the slit.

To obtain these relations, the central part of the grating was covered. By covering the central part, each individual line appears as double, if not in focus.

With the central portion of the grating covered, photographs were taken and the doubling of the lines observed. At least three exposures were taken on one plate with the plate-holder fixed, the grating being moved along the tube.

One of these exposures was taken at what was considered the best focus for some part of the plate, and the other two on opposite sides of this point. On at least two of these exposures doubling occurred. By carefully measuring the distance between these doubled lines and then drawing graphs, the position of the grating for the focus of the line being considered was found. At least two lines on the plate, preferably at extreme ends, were used and from data obtained the position of the grating for the focus of a line that would fall on the slit was calculated. To determine the amount of rotation of the plate it was necessary to know, in addition to the above, the pitch of the screw that moved the grating and also the distance of the lines on the plate from the slit. It must be remembered that the focus moves in and out twice as fast as the grating moves.

If P_0 is the position of the grating for focus on the slit, P_a the position for the focus of the line being considered, k the pitch of the screw moving the grating, and d the distance of the line from the slit, then the grating must be moved approximately

$$\frac{2k(P_a - P_0)}{d} \times 57 \text{ degrees.}$$

By repeated trials the angle of the plate was determined as well as the position of the grating in the tube. Thus the four variables were determined that fixed the focus for the one region. This same process was repeated for each section of the spectrum. Allowance has been made for sufficient overlapping from one region to another.

After obtaining the focus from $\lambda 1000$ to $\lambda 6000$, photographs of the iron arc were taken ($\lambda 2300$ to $\lambda 6000$) and many of the lines identified and marked on the plates. These plates are on file for use as an easy method of identifying the exact region given by any one position.

Vacuum technique.

Perhaps one of the greatest difficulties to be overcome was the obtaining of a vacuum suitable for photographic work in the ultraviolet. The volume to be evacuated was approximately one hundred eighty liters. The surface of the iron pipe alone was over two and three-quarters square meters. The ends of the spectrograph were sealed with rubber gaskets and held firm by heavy bolts. The opening for inserting plates was sealed in the same manner. Five sylphons, three windows and two outlets also were potential sources of trouble. Several holes were found in the casting.

At first one mercury vapor pump backed by a large General Electric Company vacuum pump was used to evacuate the system. It was found that this was inadequate. A second mercury vapor pump was then inserted in parallel with the first.

The pressure inside the spectrograph under working conditions varied between 0.005 mm and 0.010 mm of mercury, as measured by a McLeod gauge.

Photographic work.

A π -shaped discharge tube, made of Pyrex with aluminum electrodes, was used. As the region photographed reached beyond the limit of transmission of quartz or fluorite, the discharge tube was fastened directly to the spectrograph. Current from a 11,500 volt transformer was used, and a water rheostat in series with the tube was so adjusted as to give a maximum of intensity without melting the tube. Approximately 0.5 of an ampere was run through the tube. Considerable difficulty was found in eliminating the continuous spectrum found when exposing the plate in the second order, but by grinding the inside of the tube until a rough surface was obtained, much of the continuous spectrum was found to disappear.

The hydrogen was generated electrolytically, passed through a drying tube of P_2O_5 , then through a capillary leak directly to the discharge tube. As the gas was being removed by a Cenco pump and also through the slit, it was necessary to have a continuous flow of hydrogen.

The evacuating pumps and the flow of hydrogen were started at least two hours before the photographic work, thus insuring a thorough flushing out of the discharge tube. Any trace of air was noticeable at once in the visible spectrum. The best plates obtained show no trace of known impurities. Schumann plates made by Hilger Company were used.

To make sure that no first order hydrogen lines were being photographed the discharge tube was run under the same conditions as were used for the good plates except that a quartz window was placed between the slit and the source of light.

In general, investigators in the extreme ultraviolet have been handicapped not only by low dispersion and low resolving power, but also by lack of suitable standards. As the measurements in this investigation were from plates showing the second order H_2 lines it was found possible to measure them using first order iron arc lines as standards.

TABLE I. *B-A Bands of hydrogen.* (*indicates known blend).

Band	I	R-branch		I	P-branch		Band	I	R-branch		I	P-branch	
		$m-\frac{1}{2}$	cm ⁻¹		$m-\frac{1}{2}$	cm ⁻¹			$m-\frac{1}{2}$	cm ⁻¹		$m-\frac{1}{2}$	cm ⁻¹
<i>B₀-A₃</i>	2	0	78,462				<i>B₁-A₇</i>	5B	0-1	67,268*	5	1	67,156*
	2	1	439	4	1	78,332*		2	2	221	4	2	038*
	1B	?	356*	1	2	160		4	3	133*	5	3	66,880*
	3	3	203*	5	3	77,937		00	4	011*	4	4	686*
	0	4	77,996*	4	4	654*		1	5	66,845	4	5	456*
	3	5	733*	4	5	317					00	6	196
<i>B₀-A₄</i>				2	6	76,943*	<i>B₁-A₈</i>	5	0-1	64,729*	3	1	64,619*
				4	7	496*		1	2	696	2	2	513
				2	8	020*		3	3	619*	1	3	362*
	3	0	74,992					0	4	526	000	4	204
	6	1	973	6R	1	74,856*		1	5	392*	4B	5	003*
	5	2	898	5	2	706	<i>B₁-A₉</i>	2	0	62,442			
<i>B₀-A₅</i>	5	3	767	6	3	501		1	1	434*	3	1	62,325*
	1B	4	579*	4B	4	243		5	2	421*	000	2	230
	4B	5	343*	8	5	73,937*		2	3	357*	1	3	115
	3	6	040*	1	6	562		3	4	298*	5	4	61,968*
				2	7	135*		4B	5	206	1	5	809
				000	8	72,674*		3	6	048*	3	6	612
<i>B₀-A₆</i>	1	0	71,749*				<i>B₂-A₂</i>	3	1	81,031	1	1	80,934*
	4	1	738*	5	1	71,621*		1	2	80,934*	0	2	754
	3	2	674*	4	2	481		1	3	768	00B	3	528
	4	3	560*	6	3	293					1	4	241*
	1	4	396	3	4	059		3B	5	267	3	5	79,982
	2	5	187	5	5	70,779*					3	7	010*
<i>B₀-A₇</i>				1	6	458*	<i>B₂-A₃</i>	4	1	77,562	3	1	77,456
	00B	7	70,631	2	7	098					1	2	299
	1	0	68,737					1	3	329*	5	3	087
	5B	1	729	4	1	68,614*					1	4	76,820*
	2	2	678*	1	2	486*					4	5	496*
	4	3	581*	4	3	315*	<i>B₂-A₄</i>	4B	0	74,343*			
<i>B₀-B₇</i>	0	4	441*	5	4	102*		6	1	327	4	1	74,221*
	1	5	258*	3	5	67,851*		1	2	252	4	2	078*
				000	6	564*		2	3	125	8	3	73,883
	3	0-1	65,953*	1	1	65,836*		8	4	73,937*	2	4	637*
	2	2	893*	00	2	721*		0	5	717*	4	5	344
	1	3	836*	2	3	567*		0B	6	411*	00	6	008
<i>B₀-A₈</i>	00	4	721	00	4	379*	<i>B₂-A₅</i>	000	0	71,337			
	2	5	567	1	5	156		3	1	319*	2	1	71,212*
	00	6	379	1	6	64,908*		000	2	257	1	2	081
	3	0-1	63,410*	0	1	63,303*		2	3	146	3	3	70,903*
	0	2	383	1	2	195*		0	4	70,994*	1	4	680*
	1	3	314	1B	3	057		5	5	779*	1	5	408*
<i>B₀-B₈</i>				1	4	62,862	<i>B₂-A₆</i>						
	4B	5	134*	00	5	717		1	1		0	1	68,441*
								1	2	68,492*	4	2	315
	000	1	61,126*	3	1	61,017*		1	3	401*	5	3	168*
	4	2	112*	2	2	60,919*		5	5	102*	0	5	67,721*
				3	3	814*		1	6	67,906*			
<i>B₁-A₃</i>	4B	0	79,772*				<i>B₂-A₇</i>						
	1	1	752*	2	1	79,642		1	2	68,492*	4	2	315
				2	2	476		1	3	401*	5	3	168*
	2	3	503*	4	3	251*		5	5	102*	0	5	67,721*
	0B	4	288	2	4	78,965		1	6	67,906*			
	3	5	010*	3	5	623	<i>B₂-A₈</i>	5	0-1	66,006*	3B	1	65,901
<i>B₁-A₄</i>	2	6	78,656*	00	6	228		1	2	65,967*	3	2	793*
				1B	7	77,776		2	3	893*	6	3	650*
	2	1	76,283	1B	1	76,171		3	4	793*	3	4	475
	1	2	204	2	2	020*		6	5	650*	4	5	270
	2	3	066	1	3	75,812					5	6	040*
				3	4	550	<i>B₂-A₉</i>	4B	0-1	63,718*	4	1	63,614*
<i>B₁-A₅</i>				0	5	237		1	2	693	2	2	518*
				2	6	74,873*		3	3	638	4	3	396
	0	0	73,050					000	4	556*	3	4	243*
	00	1	029					1	5	447	4	5	074*
	2	2	72,988	0	2	72,928*	<i>B₂-A₁₀</i>	3	0	61,689*			
	2	3	849*	1	3	615*		4	1	699	4	1	61,595
<i>B₁-A₆</i>	000	4	674*					3	2	689*	3	2	513
	3	5	458*	2	5	078*		3	3	654	3	3	411
	1	6	186*	1	6	71,749*		0	4	601	2	4	154*
	4	1	043	3	1	69,933		00	5	527	00	6	60,993*
	2	2	69,984	2	2	802					3	7	814*
	3	3	881*	3	3	626*	<i>B₃-A₃</i>	0	1		0	1	82,171*
<i>B₁-A₇</i>	2	4	730*	1	4	408		0	2	82,171*	000	3	81,767
	2	5	540*	4	5	151	<i>B₂-A₄</i>	00B	0	78,831			
	6	6	278	000	7	68,514		3	1	808	3	1	78,708*
								3	2	708*	1	2	551*
								3	3	568	4	3	332
								3	4	356*	3	4	062*

TABLE I. B-A. Bands of hydrogen (Continued).

Band	I	R-branch		I	P-branch	
		m- $\frac{1}{2}$	cm-1		m- $\frac{1}{2}$	cm-1
B ₁ -A ₅	1	5	075	3	5	77,733*
				2	7	76,931
	2	0	75,591	2	1	75,468
	0	1	569	1	2	323*
	1	2	492*	5	3	125*
B ₂ -A ₆	2	3	358	2	4	74,873*
				1B	5	579*
				4	6	221*
				0	7	73,821*
				3	1	72,458*
B ₃ -A ₇				2	3	146
				1	5	71,649*
				3	6	319*
	1	0	69,794	3	1	69,684*
	4	1	784	2	2	562*
B ₄ -A ₈	2	2	730*	4	3	399
	2	3	633	2	4	196*
	2	4	493	3	5	68,955
	00	5	312	2	6	678*
	00	6	092*			
B ₅ -A ₉	0B	0-1	67,248*	4	1	67,133
	000	2	205	4	2	038*
				5	3	66,880*
				4	4	686*
				1B	1	64,859
B ₆ -A ₁₀	3	1	64,961	2	2	782*
	2	2	932	3	3	638*
	2	3	871	0	4	486
	2	4	782*	3	5	307
	2	5	653*	000	6	106
B ₇ -A ₁₁	1	0	62,934	6	1	62,842
	5	1	942	5	2	758
	3	2	926	5	3	653*
	4	3	887	3	4	529
	0	4	826	3	5	387
B ₈ -A ₁₂	2	5	745	000	6	230
	5	6	653*	3	7	048*
				000	1	61,126*
				1	2	045
				4	3	60,965*
B ₉ -A ₁₃	2	3	197	2	4	871
	2	4	154	2	5	768
	4	5	112*			
				0	1	83,382*
				1	2	212
B ₁₀ -A ₁₄	1	2	382*	2	3	82,976*
	1	3	200*	000	4	679
	0	4	82,966	2	5	320*
B ₁₁ -A ₁₅	1B	0	80,045	3	1	79,921*
	2	1	017	1	2	752*
	3	2	79,921*	4	3	544*
	4B	3	772*	3	4	264*
	4	4	544	2	5	78,937*
B ₁₂ -A ₁₆	3	5	264*	1	6	551*
	0B	6	78,887	0B	7	127
B ₁₃ -A ₁₇	1	0	76,820*			
	2	1	781*			
B ₁₄ -A ₁₈	0	0	73,789	3	1	73,672
	4	1	770	2	2	538
	0	2	699	5	3	354
	2B	3	579	1	4	124
	0	4	411	2	5	72,849*
B ₁₅ -A ₁₉	3	5	185			
B ₁₆ -A ₂₀	0	0-1	70,994*	3	1	70,903*
	2	2		5	2	779*
	3	3		1	3	608
	1	4	680*	1	4	408
	1	5	458*	000	5	153
B ₁₇ -A ₂₁				3	6	69,881
				2	7	562*
B ₁₈ -A ₂₂						
B ₁₉ -A ₂₃						
B ₂₀ -A ₂₄						
B ₂₁ -A ₂₅						
B ₂₂ -A ₂₆						
B ₂₃ -A ₂₇						
B ₂₄ -A ₂₈						
B ₂₅ -A ₂₉						
B ₂₆ -A ₃₀						
B ₂₇ -A ₃₁						
B ₂₈ -A ₃₂						
B ₂₉ -A ₃₃						
B ₃₀ -A ₃₄						
B ₃₁ -A ₃₅						
B ₃₂ -A ₃₆						
B ₃₃ -A ₃₇						
B ₃₄ -A ₃₈						
B ₃₅ -A ₃₉						
B ₃₆ -A ₄₀						
B ₃₇ -A ₄₁						
B ₃₈ -A ₄₂						
B ₃₉ -A ₄₃						
B ₄₀ -A ₄₄						
B ₄₁ -A ₄₅						
B ₄₂ -A ₄₆						
B ₄₃ -A ₄₇						
B ₄₄ -A ₄₈						
B ₄₅ -A ₄₉						
B ₄₆ -A ₅₀						
B ₄₇ -A ₅₁						
B ₄₈ -A ₅₂						
B ₄₉ -A ₅₃						
B ₅₀ -A ₅₄						
B ₅₁ -A ₅₅						
B ₅₂ -A ₅₆						
B ₅₃ -A ₅₇						
B ₅₄ -A ₅₈						
B ₅₅ -A ₅₉						
B ₅₆ -A ₆₀						
B ₅₇ -A ₆₁						
B ₅₈ -A ₆₂						
B ₅₉ -A ₆₃						
B ₆₀ -A ₆₄						
B ₆₁ -A ₆₅						
B ₆₂ -A ₆₆						
B ₆₃ -A ₆₇						
B ₆₄ -A ₆₈						
B ₆₅ -A ₆₉						
B ₆₆ -A ₇₀						
B ₆₇ -A ₇₁						
B ₆₈ -A ₇₂						
B ₆						

An iron arc (see Fig. 1B) was used as the source of light for the comparison spectrum. The lens and the window shown were of quartz. The iron arc was run for five minutes before starting the hydrogen source and also for five minutes after stopping the discharge, thus enabling one to detect any shift in the lines while making the exposures.

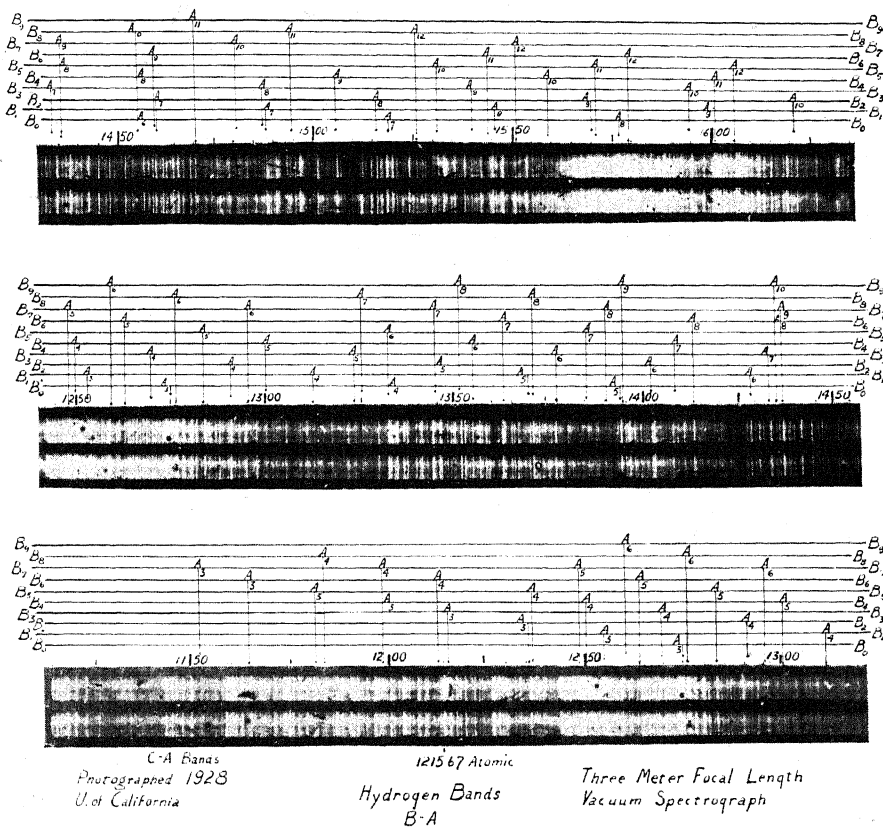


Fig. 2.

The shutter over the plate was so arranged that by turning a screw the iron lines did not cover all the plate that had been exposed to the hydrogen light. The iron lines may be seen in Fig. 2 and are easily distinguished from the hydrogen lines. On the same plate is found also an exposure showing only hydrogen lines.

Only plates that showed no displacement of the iron lines were used for measurement. It was found that the instrument was very sensitive to temperature changes. No special provisions had been made for maintaining a constant temperature, but care was taken in keeping the room as nearly as possible at one temperature while making the exposures.

Many iron lines suitable for standards were found between 2600A and

3300Å.¹³ For the H₂ lines below 1300Å, hydrogen lines were measured in the third order against iron lines as standards and these hydrogen lines were then used as standards in the second order. The iron lines used as standards were spaced approximately 100Å or less apart.

The measurements were made on a 200 millimeter comparator purchased by Professor R. T. Birge through the generosity of the Rumford Grant Committee of the American Academy of Arts and Sciences. It is believed that the measurements are in all cases accurate to approximately 0.05Å.

In general the lines listed were measured from two different plates.

Tables I and II give frequencies of the lines measured and intensities. Intensities are merely visual estimates. Table I also gives the quantum assignments as discussed in Part II.

TABLE II. *Frequencies of lines between $\lambda 1260\text{Å}$ and $\lambda 1640\text{Å}$ measured but not identified in this work.*

<i>I</i>	cm ⁻¹	<i>I</i>	cm ⁻¹	<i>I</i>	cm ⁻¹
1	79,990	000	72,752	2	65,765
3	78,766	0	629	2	743
1	666	1	431	2	627
1	527	000	419	000	593
1	512	000	396	3	226
3	495	000	272	3V	63,884
0	375	1B	051	000	843
000	260	000	71,635	2	806
1	248	0	534	2B	800
1B	182	00	436	0	795
1-	153	000	378	000	505
1	093	1	110	000	490
0	038	0	70,863	00	62,802
0	77,674	0	68,855	23	670
00	615	000B	68,756	2	408
0	356	000	523	1	313
1	188	00	326	2	270
00	149	00	67,398	1	126
00	73,741	000	185	1	120
1	664	1	66,993	1	61,795
00	418	1	413	2B	034
		1	355		
		1	65,985		

The focusing of the instrument was carried out in cooperation with Dr. C. A. Pulskamp, to whom the writer is indebted for his valuable aid in adjusting the instrument. The writer also wishes to express his thanks to Professor J. J. Hopfield, who suggested the problem and under whose direction the experimental work was started.

PART II. ROTATIONAL DATA

While the work on the fine structure of the hydrogen resonance bands was in progress Kemble and Guillemin¹⁴ published an article in which they concluded, on theoretical grounds, that the *B-A* system must consist of *R* and *P* branches only.

¹³ H. Kayser, and H. Konen, *Handbuch der Spectroscopie*, Vol. 7, (1924).

¹⁴ Kemble and Guillemin, *Proc. Nat. Acad. Sci.* **14**, 782 (1928).

Richardson and Davidson¹¹ have completed the fine structure analysis of certain bands found in the visible. It will be shown that there is a definite connection between this band system and the *B-A* system.

Schaafsma and Dieke¹⁵ have published rotational energy data, based on H_2 plates obtained by Dieke with Hopfield's 50 cm vacuum spectrograph at the University of California. The quantum assignments in the present paper were made entirely independent of their work. Data from their work have been used, with other data available, in calculating the moment of inertia of the molecule in the normal state.

Two brief accounts of the preliminary work on the *B-A* bands have been published in short articles to *Nature*.^{16,17}

The vibrational analysis as given by Dieke and Hopfield^{1,2} serves as a starting point for this work. All results are given in terms of the old quantum theory unless specified otherwise.

Verification of combination principle.

The lines of the three possible branches, *P*, *Q* and *R* of the usual quantum theory are defined as follows¹⁸

$$R_J = F'_{J+1} - F_J'' \quad (1)$$

$$Q_J = F_J' - F_J'' \quad (2)$$

$$P_J = F'_{J-1} - F_J'' \quad (3)$$

The *Q* branch is not observed in the *B-A* bands. Kemble and Guillemin¹³ have given as the theoretical reason for this that the *B-A* bands represent a transition from the $2^1\Sigma$ level to the $1^1\Sigma$ level.

From Eqs. (1) and (3) it follows¹⁹

$$R_J - P_J = F'_{J+1} - F'_{J-1} = 2\Delta F_J' \quad (4)$$

$$R_{J-1} - P_{J+1} = F'_{J+1} - F'_{J-1} = 2\Delta F_J'' \quad (5)$$

Eq. (4) shows that the values of $2\Delta F_J'$ may be obtained from any band if the *R* and *P* branches are known and the relative rotational quantum numbering of the lines has been found. The values of $2\Delta F_J'$ should be identical, within the limit of experimental error, for all bands of the *A* or n'' progression; that is, these values should be the same for all bands having the same upper level (*B*).

In the same manner, the values of $2\Delta F_J''$ should be the same for all bands having the same lower level. These facts are illustrated in Fig. 3.

¹⁵ Schaafsma and Dieke, *Zeits. f. Physik* **55**, 164 (1929).

¹⁶ Hyman and Birge, *Nature* **123**, 277 (1929).

¹⁷ Hyman and Jeppesen, *Nature* **125**, 462 (1930).

¹⁸ R. T. Birge, Chapter 4, p. 144 of Report of Committee on Radiation in Gases, Molecular Spectra in Gases, Bulletin No. 57 of the National Research Council, (1926). This bulletin is referred to hereafter as the "Report." In general the nomenclature in this paper is that used in the Report.

¹⁹ Report, p. 145.

The combination principle was first verified by choosing three bands such that two have the same B level and two the same A level, and finding differences between R and P lines such that equations (4) and (5) were satisfied.

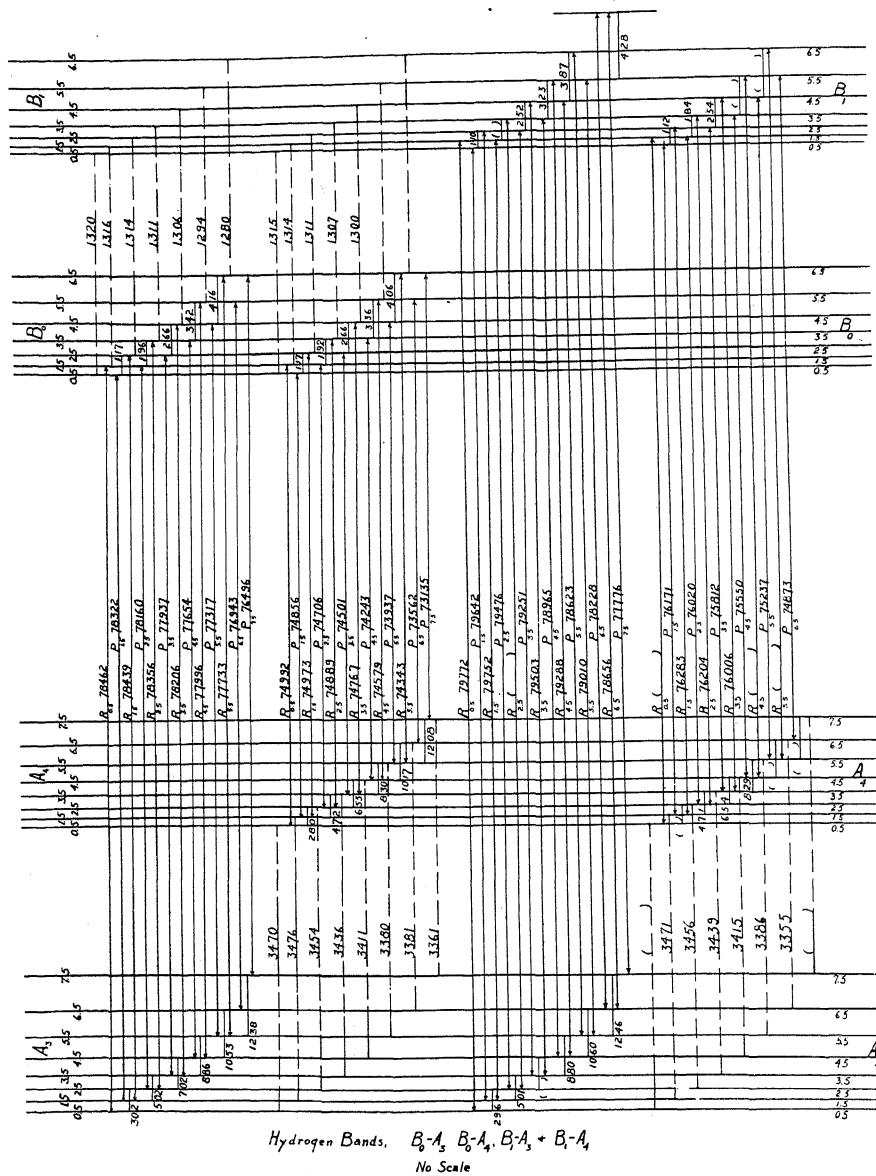


Fig. 3. Energy level diagram.

The vibrational analysis had been found by Dieke and Hopfield.² It was not necessary to know the true numbering of the lines in the bands. The method of obtaining this numbering will be explained later. The lines of the individual band were separated into R and P branches by the usual method of second differences.

After verifying the combination principle for these three bands, the work was extended to other bands. The results are collected in Tables I, III, and IV. Lines connected with sixty-eight bands were found. The results show alternating intensity of lines as is to be expected since the H_2 molecule is symmetrical.

 TABLE III. Average values of $2\Delta F'$.

k	1.5	2.5	3.5	4.5	5.5	6.5
B_0	116.4	192.9	266.3	338	411	475
B_1	111	184	254	324	390	434
B_2	104	176	242	314	375	403
B_3	100	169	234	296	350	419
B_4	97	165	225	279	318	331
B_5	93	155	215	274	324	
B_6	93	146	208	246	315	
B_7	86	138	187	254	287	
B_8	85	146	197	242	312	
B_9	86	115	202	223		

 TABLE IV. Average values of $2\Delta F''$.

k	1.5	2.5	3.5	4.5	5.5	6.5
A_3	295	502	702	881	1060	1249
A_4	285	475	652	830	1011	1217
A_5	268	445	617	780	923	
A_6	253	416	577	731	869	1033
A_7	230	386	533	679	802	896
A_8	214	364	493	607	755	
A_9	200	324	452	558	681	
A_{10}	175	289	400	500	581	694
A_{11}	169	260	341	426	501	558
A_{12}	148	271	335	414		

 TABLE IVa. Values of $2\Delta F''$ from Witmer and Hori.

k	1.5	2.5	3.5	4.5	5.5
$A_2(H)$		529			
$A_2(W)$	321	531			
$A_1(H)$		557	764	991	1231
$A_1(W)$	345	562			
$A_0(W)$	356	588			

To find m , the effective rotational quantum number, the $2\Delta F'$ values are plotted and extrapolated to $\Delta F=0$. m is now to be chosen so that ΔF equals zero when m equals zero and it is found that this condition is satisfied, at least to a close approximation, by assuming half integer values for m . Richardson and Davidson¹¹ referring to the lower level of bands analyzed by them, state " $m_0=0.50013$ and remains very close to $1/2$ throughout the vibrational levels." This level is now known to be identical with the B state as described in this paper.

Continuing the study of the B state later, it will be shown, by using the analytic method,²⁰ that the value of m is found to be a half-integer to

²⁰ Report, p. 173.

within 0.005, that is,²¹ α is zero or practically zero. At present we assume²² $m = k = J - 0.5$.

A second check on the assignment of the lines to the R and P branches was found by comparing the values²³ of $\omega_v(m)$ for the B level as obtained by

TABLE V. B -state. Average values of $\omega_v(m)$ (From both R and P lines). Values in parentheses are those obtained by Richardson and Davidson from bands in the visible.

m	0.5	1.5	2.5	3.5	4.5	5.5	6.5
$B_1 - B_0$	1318.5 (1318.345)	1315.8 (1316.41)	1312.4 (1312.55)	1307.0 (1306.94)	1300.6 (1299.68)	1289.8 (1290.99)	1279.9 (1280.94)
$B_2 - B_1$	1282.0 (1281.475)	1280.0 (1279.84)	1276.7 (1276.6)	1272.1 (1271.815)	1265.7 (1265.59)	1260.0 (1258.04)	1245 (1249.32)
$B_3 - B_2$	1244 (1246.71)	1244 (1245.25)	1240 (1242.38)	1238 (1238.12)	1234 (1232.61)	1223 (1225.89)	1217 (1218.02)
$B_4 - B_3$	1214 (1213.015)	1212 (1211.76)	1211 (1209.06)	1207 (1205.17)	1200 (1200.10)	1196 (1193.86)	1190 (1186.75)
$B_5 - B_4$	1179 (1179.95)	1180 (1178.77)	1176 (1176.33)	1174 (1172.74)	1167 (1168.03)	1164 (1162.25)	1160 (1155.5)
$B_6 - B_5$	1147 (1147.50)	1152 (1146.32)	1145 (1144.00)	1140 (1140.64)	1139 (1136.15)	1130.77 (1130.77)	1124.8 (1124.8)
$B_7 - B_6$	1115 (1115.5)	1112 (1114.32)	1112 (1112.04)	1105 (1108.7)	1102 (1104.3)		
$B_8 - B_7$	1086	1080	1079 (1081.29)	1078-	1068	1071	
$B_9 - B_8$	1052	1047	1038	1030	1028		

using the different A vibrational states as the base level. In a similar manner, but using different B vibrational states as base levels the values of $\omega_v(m)$ for the A level were found. Tables V and VI give the average values found. In making these averages the numbers obtained from the differ-

TABLE VI. A -state. Average values of $\omega_v(m)$.

m	0.5	1.5	2.5	3.5	4.5	5.5
$A_4 - A_3$	3470.0	3467.2	3454.7	3435.1	3413.5	3392
$A_5 - A_4$	3241.5	3236.0	3223.5	3207.3	3184.5	3153
$A_6 - A_5$	3012	3008.5	2995.8	2979.9	2956	2928
$A_7 - A_6$	2785.3	2774.9	2753.7	2746.1	2720	2692
$A_8 - A_7$	2543.7	2536.8	2524.5	2513	2513	2450
$A_9 - A_8$	2288	2288	2265	2241	2202	
$A_{10} - A_9$	2029	2018	2006	1984	1956	1918
$A_{11} - A_{10}$	1726	1720	1715	1689	1659	1627
$A_{12} - A_{11}$	1423	1414	1380	1358	1324	1303

ences of two frequencies neither of which was from blended lines were given weighted values. Fig. 3 also shows the values of $\omega_v(m)$. The numbers on this diagram are obtained by using P lines. Table V also gives (in parenthesis) the values as obtained by Richardson and Davidson¹¹ from their analysis of

²¹ Report, p. 137 gives $m = J - \epsilon^* = J - 0.5 - \alpha = k - \alpha$, where J is an integer and k a half-integer. This is in terms of the old quantum theory as used in this paper. In the new mechanics J is one unit less.

²² It is to be remembered that the value of $m - 1/2$ is the value of J for the new mechanics.

²³ Report, p. 113.

bands in the visible. The Richardson and Davidson measurements are from plates taken using a larger grating and the bands measured are in the visible. Their values of $\omega_v(m)$ are presumably the more trustworthy. It is to be remembered that an error of one-tenth Angstrom in the ultraviolet region considered here represents an error of between six and nine frequency units.

The values of $\Delta F'$ as obtained from the rotational energy function²⁴ also agree almost identically with those obtained by Richardson and Davidson from their data. They give a value of D_0 (their C) smaller than the theoretical value. The D_0 used in the present report is found theoretically and represents the best known method for obtaining this constant, while Richardson and Davidson have obtained the value empirically. More will be said about these constants later.

Birge¹⁰ in his summary of the quantum levels and resulting constants of the hydrogen molecule has taken the B state of the ultraviolet bands to be also the lower state of the Richardson "A" and "B" bands. This seemed justifiable at that time as the result of the close agreement of the vibrational data of Dieke and Hopfield² and of Richardson.¹¹

The far more accurate data of the present work confirms the assumption beyond all doubt, since the agreement of the spacings of all levels, both vibrational and rotational, is within the very small limits of experimental error. This verification of the assumption by Birge leads to the conclusion that the ionization potential of H_2 must be 15.34 volts to within a few hundredths of a volt, as given by Birge at that time.

Mention has been made of the rotational energy function

$$F = B_0 m^2 + D_0 m^4 + F_0 m^6 + \dots \quad (6)$$

It is from this equation that the actual spacings of the rotational energy levels are found. The value of B_0 is inversely proportional to the moment of inertia for no vibration and infinitely slow rotation.

Birge, in the Report,²⁵ gives three methods of handling the data obtained. Method one is purely empirical and is not to be considered here.

Method two is a rapid semigraphical method for evaluating B_0 .

From the rotational energy function, by assuming $m = k - \alpha$, one obtains, to a very close approximation when α is small.

$$\frac{\Delta F}{k} = 2B_0 - \frac{2B_0\alpha}{k} + 4D_0k^2 + 6F_0k^4. \quad (7)$$

In the present work α is zero, or at least very small. If we assume the value of F_0 to be small²⁶ we have

$$\frac{2\Delta F}{k} = 4B_0 + 8D_0k^2. \quad (8)$$

This equation represents a parabola with the vertex at $k = 0$.

²⁴ Report, p. 141.

²⁵ Report, pp. 169-173.

²⁶ Richardson and Davidson gave α equal to 0.0013, $F_0 = 1.3 \times 10^{-5}$.

The values of $2\Delta F/k$ for the B_0 state are

k	1.5	2.5	3.5	4.5
$\frac{2\Delta F}{k}$	77.60	77.16	76.09	75.11

These latter values were plotted against k and from this a fairly accurate value of $4B_0$ found directly.

D_0 is theoretically related to B_0 by the relation

$$D_0 = \frac{-4B_0^3}{\omega_0^2} \quad (9)$$

ω_0 is found by double extrapolation of the values of $\omega_v(m)$ to find the value of $\omega_0(0)$.

The final result of this extrapolation is that $\omega_0(0) = 1337.82 \text{ cm}^{-1}$.

Method three is strictly analytic and is the most accurate method of handling the data.

From the rotational energy function the following result is obtained, where $m = k - \alpha$

$$2\Delta F^* = 2\Delta F - 8D_0k^3 - 12F_0k^5 - 16H_0k^7 = (4B_0 + 8D_0)(k - \alpha) \quad (10)$$

if the values of F_0 and H_0 are zero.

The value of $2\Delta F^*$ may be called the reduced value of $2\Delta F$. The values of $2\Delta F$ are found directly. Values of F_0 and H_0 are assumed to be equal to zero. The value, $D_0 = -0.01647$, is found by using the approximate value of $B_0(19.46 \text{ cm}^{-1})$ found by method two in the theoretical Eq. (9).

In the equation $2\Delta F^* = 2\Delta F - 8D_0k^3$ the following values are found:

$2\Delta F$	k	$8 - D_0k^3$	$2\Delta F^*$
116.4	1.5	0.4447	116.845
192.9	2.5	2.059	194.959
266.3	3.5	5.649	271.949
338.0	4.5	12.007	350.009

The plot of $2\Delta F^*$ against k is a straight line, as predicted by the above theory.

The least squares solution of the equation

$$2\Delta F^* = (4B_0 + 8D_0)(k - \alpha) \quad (11)$$

accordingly gives the most probable values of B_0 and of α .

The solution gives

$$B_0 = 19.445 \text{ cm}^{-1}; \quad \alpha = -0.005 \text{ cm}^{-1}.$$

It is believed B_0 has a true probable error not exceeding one part in one thousand. The probable error in α is such that the true value may be zero.

Richardson and Davidson have found $B_0 = 19.455_5$.

The moment of inertia is found from the relation

$$I_0 = \frac{h}{8\pi^2 B_0 c} = \frac{27.66 \times 10^{-40}}{B_0} \text{ g cm}^2 \quad (12)$$

$$= (1.4225 \pm 0.003) \times 10^{-40} \text{ g cm}^2.$$

The error in B_0 is also to be found in the value of the moment of inertia. In addition there is a small probable error in the constant²⁷ 27.66×10^{-40} . The nuclear separation r_0 , in centimeters, is given by the relation

$$r_0 = (I_0/\mu)^{1/2} \quad \text{where}$$

$$\mu = 1.6490 \times 10^{-24} \frac{m_1 m_2}{m_1 + m_2} \quad \text{and}$$

m_1 and m_2 are the atomic weights of the two atoms.²⁸

The resulting value for the nuclear separation is

$$1.3084 \times 10^{-8} \text{ cm.}$$

The rotational energy function becomes

$$F = 19.445m^2 - 0.01647m^4 \quad (14)$$

$$m = \frac{1}{2}, 1\frac{1}{2}, 2\frac{1}{2} \text{ etc.}$$

The following is a comparison of the values of F obtained with those given by Richardson and Davidson:

Richardson and Davidson from bands in visible	$B-A$ bands found in ultraviolet
(cm ⁻¹)	(cm ⁻¹)
38.85	38.81
77.30	77.22
115.06	114.85
151.685	151.06
186.955	186.13

In the solution, Richardson and Davidson have used $D = -0.0152 \text{ cm}^{-1}$ instead of -0.01647 .

Constants for the normal level.

The evaluation of the moment of inertia of H₂, for the normal electronic level, has been carried out with the cooperation of Mr. C. Rulon Jeppesen, and the results have been reported briefly.¹⁷ In this case the values of $2\Delta F''$, as given in Table IV, begin at the vibrational level $v = 3$. For $v = 0, 1$, and 2 , the less accurate and extensive data of Hori,⁸ and Witmer,⁶ were used. These

²⁷ Birge, Phys. Rev. Supplement 1, 63 (1929) gives

$$h/8\pi^2 c = (27.65_{33} \pm 0.04) \times 10^{-40} \text{ g cm.} \quad (13)$$

²⁸ Constants used are those given by Birge, reference 27.

data are listed in Table IVa. In order to obtain the best possible value of I_0 , data from all available sources were correlated and averaged. These sources include Schaafsma and Dieke,¹⁵ in addition to those already quoted.

The various values of $2\Delta F/k$, resulting from the observations of the different observers, were plotted against k , on a large scale. In this case Eq. (7) becomes

$$\frac{2\Delta F_v}{k} = 4B_v + 8D_vk^2 + 12F_vk^4 \quad (15)$$

and the resulting curve, for each value of v , should be approximately a parabola with its vertex at $k=0$. Smooth curves were drawn through the plotted points, so as to satisfy, roughly, the form of Eq. (15). From these curves we obtain first approximate values of $4B_v$. These values were then plotted against v , and found to form a reasonably smooth curve. What appeared to be the best smooth curve was then drawn, and from—this, smoothed values of $4B_v$ were obtained. These smoothed values were now used to calculate theoretical values of D_v , using the theoretical relation²⁹

$$D_v = D_e - \beta(v + \frac{1}{2}) \quad (16)$$

where³⁰

$$\frac{\beta}{D_e} = -\frac{\omega_e}{24B_e} \left(\frac{\alpha}{B_e} \right)^2 - 5 \left(\frac{\alpha}{B_e} \right) + 8x_e. \quad (17)$$

The value of $\omega_e(4368.6 \text{ cm}^{-1})$ was obtained from a smooth curve, using data by Witmer.⁶ Still later work³¹ has led to 4371 cm^{-1} as the best value of ω_e , but the change is immaterial in connection with β . For B_e we used 60.16 cm^{-1} , as obtained by extrapolating our smooth B_v curve to $v = -\frac{1}{2}$. The slope of this curve, at $v = -\frac{1}{2}$, gives the value of α (2.68 cm^{-1}).

We could now calculate theoretical values of $8D_vk^2$, in Eq. (15). In order to calculate the final term in Eq. (15), we assumed³² that

$$F_v = F_e = \frac{D_e^2}{B_e} \left(2 - \frac{\alpha\omega_e}{6B_e^2} \right) \quad (18)$$

The true theoretical expression for F_v , as a function of v , has not yet been derived, but the last term in Eq. (15) is so small that any change of F_v with v is immaterial, for not too large values of k .

²⁹ In this case, the new mechanics relations have been used. In equations like (9), one should use D_e , B_e , and ω_e (values for $v = -1/2$) in place of D_0 , B_0 , and ω_0 , but numerically the change is insignificant.

³⁰ This theoretical expression for β/D_e is equivalent to that given by Pomeroy (Phys. Rev. 29, 59 (1927)), but is much simpler in actual use. It was suggested to us by Professor R. T. Birge.

³¹ R. T. Birge and C. R. Jeppesen, Nature 125, 463 (1930).

³² Compare "Report," p. 237, Eq. (198).

With these calculated values of D_v and F_v , we now obtained a value of $4B_v$ from selected points on the $2\Delta F_v/k:k$ curve, using Eq. (15). A weighted average of the resulting values of $4B_v$, for each value of v , was thus obtained. This process is equivalent to drawing a smooth curve through the plotted $2\Delta F_v/k$ points, having the theoretical *shape*, leaving only the constant term to be evaluated. Such curves, as actually drawn, were found to be quite as satisfactory as the original empirical curves. This is a most gratifying verification of theory, since the "distortion" of the H₂ molecule, with both rotation and vibration, is relatively large.

The new values of B_v were again plotted against v , and found to lie much more closely on a smooth curve than the original approximate values. The changes were, however, so small that it was deemed unnecessary to calculate *new* theoretical values of D_v (method of successive approximations). Since we had used the *finite* differences $2\Delta F_v$, the value of the constant term in Eq. (15) is, strictly, not $4B_v$, but³³ $4B_v + 8D_v$. The final smoothed values of B_v , obtained after this correction, are given in Table VII. They were then fitted, by least squares, to a third degree rational integral function, the result being

$$B_v = 60.587 - 2.7938(v + \frac{1}{2}) + 1.0500 \times 10^{-2}(v + \frac{1}{2})^2 - 24.058 \times 10^{-4}(v + \frac{1}{2})^3. \quad (19)$$

TABLE VII.

v''	$B_{v''}$ smoothed observed values	$B_{v''}$ calc. values
0	59.19	59.192
1	56.415	56.411
2	53.63	53.630
3	50.835	50.834
4	48.01	48.008
5	45.14	45.138
6	42.20	42.210
7	39.20	39.209
8	36.145	36.120
9	32.92	32.930
10	29.52	29.624
11	25.39	26.187
12	20.565	22.606

The calculated values, according to Eq. (19), are also given in Table VII. In this equation, the absolute term gives the value B_e for the hypothetical state of zero vibration ($v = -1/2$), according to the new mechanics. It corresponds to $I_e = 0.4565 \times 10^{-40}$ g cm² and $r_e = 0.7412 \times 10^{-8}$ cm. This is quite different³⁴ from Hori's value of $I_e = 0.467 \times 10^{-40}$. The value of B_0 .

³³ See Eq. (145), p. 174 of "Report."

³⁴ See reference 17 for a discussion of this point.

corresponding to $v=0$, is 59.192 cm^{-1} , giving $I_0=0.4675\times 10^{-40}$, $r_0=0.7500\times 10^{-8}$. These latter are the constants for the actual normal level of hydrogen.

As already noted, accurate data for $2\Delta F''$ values extend only from $v=3$ to 12, inclusive (Table IV). As can be seen from Table VII, Eq. (19) fits the data in a satisfactory manner only up to $v=9$. In fact, the B_v values for $v=10, 11, 12$, were not used in obtaining this equation, since they deviate sharply from any smooth curve. These higher values of v are close to dissociation, and the fact that the corresponding moments of inertia are appreciably larger than those given by the equation is not surprising.

The values of B_0, B_1 , and B_2 are not so trustworthy, but they do, perhaps accidentally, fit in very well with the values B_3 to B_9 . It would therefore appear that our final value of B_0 is reliable to about 0.2 percent. After this work was completed, Birge and Jeppesen³¹ calculated accurate values of B_0 and B_1 , from Rasetti's data³⁵ on the Raman effect in gaseous hydrogen. Their value of B_1 (56.4035 cm^{-1}) is in remarkable agreement with our value of 56.411 cm^{-1} , as given by Eq. (19), but their value of B_0 (59.354 cm^{-1}) is 0.27 percent greater than our value of 59.192 cm^{-1} . This discrepancy points to a real irregularity in the moment of inertia of hydrogen in the $v=0$ state, as discussed by Birge and Jeppesen. They discuss also an apparent irregularity in the frequency of vibration for this same level.

The final conclusion is then that Eq. (19), or Table VII, last column, gives reliable values of B_v'' from $v=1$ to 9 inclusive, but that the true value of B_0 is that given by Birge and Jeppesen, namely $B_0=59.354\text{ cm}^{-1}$, corresponding to $I_0=0.4660\times 10^{-40}\text{ g cm}^2$ and $r_0=0.7489\times 10^{-8}\text{ cm}^{-1}$. Because of the irregularity in the value of B_0 , it is impossible to give a reliable value of B_v , but it seems best, in calculating theoretical values of D_v and other derived constants, to use the value given by Eq. (19).

The experimental work and part of the theoretical work, of this investigation, were carried out at the University of California and the writer wishes to express his sincere thanks to Professor R. T. Birge of the University of California not only for the very obliging and valuable assistance that was given while the writer was at the University of California but also for the interest and advice he has given during the past year. He is also indebted to Mr. C. R. Jeppesen for his help in deriving the constants for the normal level.

³⁵ F. Rasetti, Phys. Rev. 34, 367 (1929).

THE LUMINESCENCE OF ZINC SULPHIDE UNDER THE ACTION OF ALPHA, BETA AND GAMMA-RAYS

BY GEORGE S. GESSNER

RANDAL MORGAN LABORATORY OF PHYSICS, UNIVERSITY OF PENNSYLVANIA

(Received May 21, 1930)

ABSTRACT

The luminescence of zinc sulphide under the action of α , β and γ -rays was studied with an especially designed brass capsule. The zinc sulphide was exposed to the α -rays or β and γ -rays, or α , β and γ -rays from radium or its products, while the luminescent material and the exciting agent were kept separate. In this way the effect of these rays upon the luminescent material was observed, separately and collectively. The experiment was made under practically constant temperature. The luminosity time curves for the three types of capsules were consistent in characteristics. It was found that for a time there was a definite increase in brightness; then the luminescence decreased under the constant action of the rays and rose again to a second maximum. This was followed by gradual decrease with time as long as observations were taken. The decay of luminescence of zinc sulphide, after the removal of the radio active source, showed that the decay curve is not of the type whose ordinate can be expressed by a single exponential term.

INTRODUCTION

THE action of α , β and γ -rays from radium or its products, upon luminous compounds has been studied by several experimenters¹ during the last two decades and theories have been formulated to explain their results.

Przibram² and his students found that the luminescence of some minerals increased under the action of β -rays and then gradually decayed after passing through a maximum. Smith³ found an increase in brightness at room temperature of chemically pure barium bromide.

Studies in luminosity of luminescent zinc sulphide under the action of α , β and γ -rays from radium or its products, up to this time, have been made using mixtures of the luminescent material and the radioactive exciting agent. One of the features of the present research was to keep the radioactive source separate from the luminescent material, thus avoiding the possible formation of complex products. Another feature was the use of a source of radiation which remained constant during the period of the experiment. Thus it was possible to observe the brightness as soon as the luminescent material was brought in contact with the radioactive source. This was not done in previous experiments on zinc sulphide because of the

¹ E. Rutherford, Proc. Roy. Soc. **83A**, 561 (1909-10), E. Marsden, Proc. Roy. Soc. **83A**, 548 (1909-10), Patterson, Walsh and Higgins, Proc. Phys. Soc. of London **4**, 215 (1917).

² K. Przibram and E. Kara-Michailova, Akad. Wiss. Wien, Ber **131**, 2A 285 (1923), **132**, 2A, 261 (1924).

³ L. E. Smith, Phys. Rev. **28**, 431 (1926).

time taken for the source of rays to become constant. It was also thought desirable to use a strong source of radiation, hoping thereby to hasten the decay.

Not only were the radioactive source and the luminescent material kept separate but the luminescent material was kept inclosed in a capsule so that it could be studied before bringing it in contact with the radioactive source or after its removal.

APPARATUS AND PROCEDURE

In order to keep the luminescent material separate from the radioactive source, brass capsules were prepared, as shown in Fig. 1, each consisting of five major parts. On a gold plate fitted snugly in a depression on the face of part (5) was placed a layer of radium sulphate in equilibrium

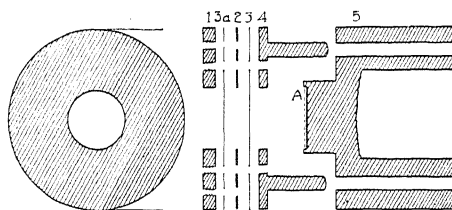


Fig. 1. Brass capsule.

with its decay products and covered with a coat of varnish. Such a plate furnishes a constant source of radiation permitting the α as well as the β and γ -rays to pass through. Part (4), serving to hold parts (1) and (5) together consists of a thin brass washer to which are fastened several legs fitting snugly into holes in part (5). Part (1) is a brass washer to which can be fastened part (2), an aluminum washer; a thin sheet of mica is

TABLE I.

Capsule	Radium content	Rays emitted
1	0.293 mg	α β γ
2	0.522	α β γ
3	0.910	α β γ
4	0.815	α β γ
A	2.40	α β γ
B	.16	β γ
C	2.8	α β γ
D	Pol.	

placed between the brass washer and the aluminum washer and parts (1) and (2) are fastened together by means of small screws. The luminescent material was placed in the opening in the aluminum washer (2) and the sample as well as the aluminum washer were covered with a piece of very thin mica (3). Against this mica disk part (4) was fastened by means of small screws. Thus the sample was separated from the radioactive source and also protected from contamination by radium and its products.

Three different kinds of capsules were prepared: (A) where the mica disk (3) was thin enough to allow α as well as β and γ -rays to pass through (in some cases the mica was replaced by aluminum foil); (B) where the mica (3) was thick enough to allow only the β and γ -rays to pass through; (C) where the layer of radium sulphate was replaced by a polonium plate, giving off chiefly α -rays. Thus it was possible to study the effect of α -rays or β and γ -rays or α , β and γ -rays upon the sample of zinc sulphide.

The luminosities of the different samples were measured by means of a Nutting polarization photometer. The arrangement of apparatus is shown in Fig. 2. The apparatus is so arranged that by changing the distance between the standard lamp and the ground glass screen, its illumination of the screen can be controlled. The standard lamp *S* is supplied by means of storage batteries and its voltage maintained constant by a potentiometer arrangement, and a ballast lamp to stabilize the current for small variations in the battery voltage. Light from the standard lamp is reflected by the rhomb *R*, thus passing through the polarizing Nicol *PN* and the photometer cube *C*. Light from the sample *B* is reflected by the prism *D* thus passing into the photometer cube *C*, and is again reflected as shown in Fig. 2.

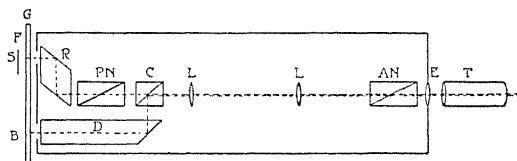


Fig. 2. Diagram of photometer.

In making an observation, the telescope is focused on the photometer cube and the field appears as two strips of reflected light from the sample *B* with the transmitted light from the standard lamp between them. By varying the intensity due to the standard lamp by means of the Nicol prism *AN*, the central strip is made alternately lighter and darker than the strips illuminated by the sample *B* until an intensity match is obtained. With the exception of the improvement in design of the capsule the apparatus is the same as that used by Smith³ in his study of barium bromide. The reference lamp *S* was a 110 volt incandescent carbon filament lamp operated at 60 volts. This lamp was compared with a lamp standardized by the Bureau of Standards. A green filter *F* was interposed to produce a better color match.

The brightness of the samples was readily calculated from the scale readings of the photometer and the constants of the apparatus. The photometer was graduated in logarithms of the ratio of the illuminating power of the standard lamp to that of the sample. If *K* is the transmission coefficient of the filter, *C*₁ the candle power of the standard lamp, *C*₂ the candle power of the sample, *d*₁ and *d*₂ their respective distances from the ground glass screen *G*,

$$\log_{10}(KC_1/d_1^2) - \log_{10}(C_2/d_2^2) = x \text{ (reading on photometer).}$$

If A is the area of the exposed luminous portion of the sample, the brightness B in apparent candle power per square cm is

$$B = (KC_1d_2^2)/(d_1^210^xA).$$

The sample of luminescent zinc sulphide approximately 0.020 cm in thickness was prepared and sufficient time allowed for the decay of the luminosity due to exposure to light in preparing. The sample was slipped on part (5) Fig. 1 and its luminosity read at intervals of a few minutes for the first hour, then at slightly longer intervals for the first day. All measurements were made at room temperature.

RESULTS

This study has shown that for crystalline zinc sulphide, there is first an initial growth to maximum value, then a decrease in luminosity followed by a second growth to a maximum, and then a very slow decay.

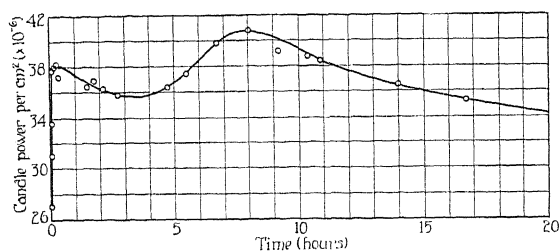


Fig. 3a. Luminosity curve, capsule (4), α , β , γ -rays. Zinc sulphide screen.

Figs. 3a and 3b show the variation of luminosity with time for two samples (4) and (A) (radium content given in Table I); from these curves will be seen that the maxima as well as the time required to reach these maxima are dependent upon the amount of radium present. Capsule (4) containing less radium than capsule (A) requires a longer time to reach the maximum values

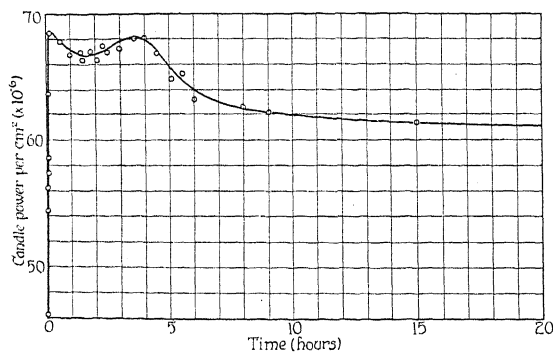


Fig. 3b. Luminosity curve, capsule (A), α , β , γ -rays. Zinc sulphide screen.

and these maxima are lower time to reach the maximum values and these maxima are lower than for capsule (A). Similar results were found for capsules (1), (2), and (3). Capsule (1) for example, containing 0.293 milli-

grams of radium, required about 5 hours to reach the first maximum and about 15 hours to reach the second maximum. The maximum brightness for capsule (1) was 1.65×10^{-6} candle power per square cm. In all the above cases the sample of zinc sulphide was bombarded by α , β , and γ -rays.

Fig. 4 is a luminosity time curve for capsule (C). In this case the luminescent material was bombarded by β and γ -rays only. This curve also shows

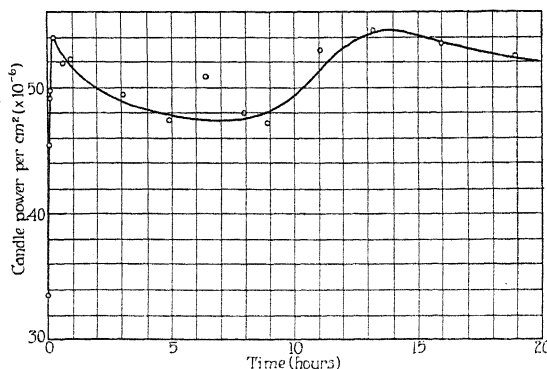


Fig. 4. Luminosity curve, capsule (C), β , γ -rays. Zinc sulphide screen.

the two maxima but the time required to reach the first maximum value was about 20 minutes and the second maximum about 13 hours.

Fig. 5 shows the curves of Fig. 3a, 3b and 4 plotted over a longer period of time. From this curve we can see that the rate of decay for capsule (A) after reaching its second maximum is greater than that of capsule (4). The

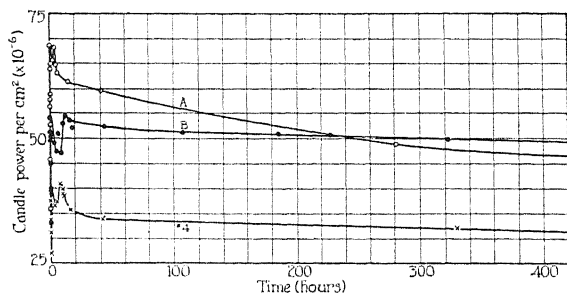


Fig. 5. Curves of Figs. 3a, 3b and 4 plotted over long periods of time.

decay of capsule (A) was not nearly so rapid as was expected from consideration of the amount of radium present in the two cases. It must also be noted that decay of luminescence for capsule (C) (which emits only β and γ -rays) after reaching the second maximum is much slower than for capsule (A).

The initial part of the luminosity time curve for capsule (D) is shown in Fig. 6. In this capsule the radium sulphate was replaced by a polonium plate so that the sample of zinc sulphide was bombarded chiefly by α -rays. Here also is seen the initial growth, decay and second maximum, followed by a gradual decay.

Fig. 7 shows the variation of luminosity with time for capsule (4) over a period of 400 days. Only one maximum is shown on this curve, this is due to the small time scale used in plottings. From this curve and similar curves

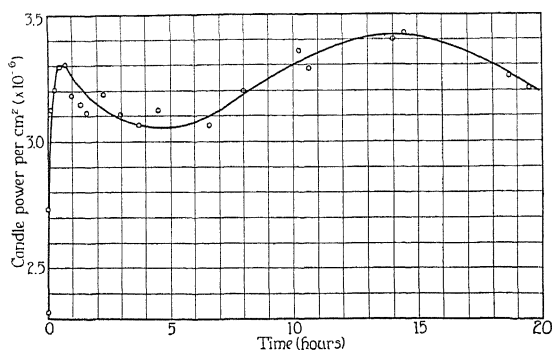


Fig. 6. Luminosity curve, capsule (D), Po α -rays. Zinc sulphide screen.

drawn over long periods, it was found that the decay of luminosity was not hastened as much as was expected by using a strong radium source.

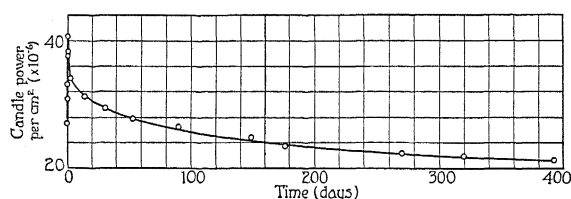


Fig. 7. Variation of luminosity with time for capsule (4) over a period of 400 days.

The theory of radioactive luminosity formulated by Walsh,⁴ in which the variation in brightness with time was expressed by the equation

$$\log \left[\frac{B}{(b + B)} \right] + a + kt = 0$$

where a , b , and k are constants, does not fit the observed decay curves of brightness found in this investigation.

Neither do the other theories mentioned by Walsh on radioactive luminescence explain the initial growth or the appearance of the second maximum, which was characteristic of all the curves plotted, whether the material was bombarded by α or β and γ , or α , β and γ -rays.

Since the luminescent material and the radioactive source were kept separate, it was possible to study the decay of the luminescent material after the radioactive source was removed. The screens containing the luminescent material were placed in contact with the exciting agent until the maximum brightness was reached and then the radioactive source was removed and the rate of decay of luminosity with time was studied. Fig. 8

⁴ J. W. T. Walsh, Proc. Phys. Soc. of London 39, 318 (1926-27).

shows the relation of brightness to time. The broken curve (with ordinates on the right) shows the relation between logarithms of intensity and time. From this curve it can readily be seen that the luminosity time curve, for a sample after the exciting agent was removed, is not of the type whose ordinate can be expressed by a single exponential term.

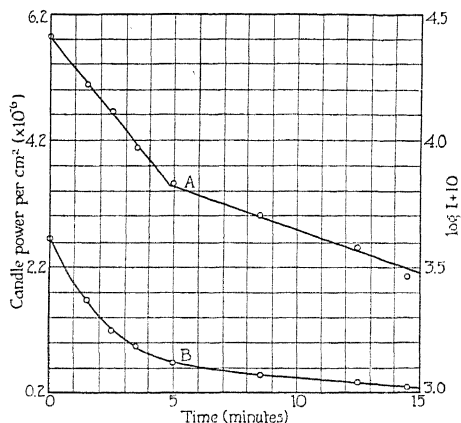


Fig. 8. Curve A = relation between logarithms of intensity and time.
Curve B = luminosity vs. time.

The fact that the decay of the zinc sulphide after removal of the exciting agent is not a single exponential may be an important factor in the formulation of a theory explaining the initial part of the brightness curves found in this investigation.

In conclusion the writer wishes to express his appreciation to Professor D. H. Kabakjian who suggested the problem, prepared the radium samples and under whose direction the work was carried out, and to Dr. E. E. Witmer for many helpful suggestions and discussions.

A SECOND IONIZATION POTENTIAL IN
POTASSIUM VAPOR

BY A. L. HUGHES AND C. M. VAN ATTA

WASHINGTON UNIVERSITY, SAINT LOUIS

(Received June 11, 1930)

ABSTRACT

The occurrence of a second peak in the photoionization curve of potassium vapor (Lawrence and Edlefsen) suggests that there might be a related peak (or discontinuity) in the curve for ionization by electron impact. The ionization in potassium vapor was investigated by Hertz' method of neutralization of space charge by positive ions. It was found that there was an abrupt increase in gradient of the ionization curve, indicating a second ionization potential at 0.97 ± 0.05 volt above the first one corresponding to the series limit. With mercury vapor, the apparatus indicated the presence of Lawrence's ultraionization potentials in mercury vapor, together with three new ones (10.40, 10.62, 10.88, 11.28, 11.40, 11.77, 12.16, 12.46).

INTRODUCTION

CERTAIN peculiarities in the photoionization curve of potassium in the vicinity of the series limit led to these experiments. Lawrence and Edlefsen¹ found that the photoionization of potassium is a maximum at the series limit (2856Å), diminishes to a minimum at 2700Å, and then rises to a second higher maximum at 2340Å. Mohler and Boeckner,² however, find that the ionization starts at the series limit and increases steadily. This curve resembles Lawrence's³ earlier results except for the fact that in the latter case the effect began at 2600Å. The peculiar form of the curve obtained by Lawrence and Edlefsen suggests that in ionization by electron impact something of a similar nature might be revealed. The only work which we can find on the ionization potential of potassium by electron impact is that done thirteen years ago by Tate and Foote,⁴ who identified roughly the ionization potential with the theoretical value corresponding to the series limit. They were interested only in establishing this approximate identity and made no attempt to study the shape of the ionization curve above the ionization potential. Another result which suggests that a careful study of the ionization curve for potassium might reveal peculiarities is Lawrence's discovery of the ultraionization potentials of mercury vapor (i.e., discontinuities in the ionization curve at 0.20, 0.89, 1.30 and 1.66 volts above the theoretical ionization potential corresponding to the series limit).

APPARATUS AND RESULTS

The method used for investigating the ionization potential was that originally used by Hertz. An oxide coated platinum filament, F , 11 mm long,

¹ E. O. Lawrence and N. E. Edlefsen, *Phys. Rev.* **34**, 1056 (1929).

² F. L. Mohler and C. Boeckner, *Bureau of Standards, Journal of Research* **3**, 303 (1929).

³ E. O. Lawrence, *Phil. Mag.* **50**, 345 (1925).

⁴ J. T. Tate and P. D. Foote, *Washington Acad. Sci. Jour.* **7**, 517 (1917).

was mounted in a rectangular box of monel metal, *B*, $25 \times 30 \times 15$ mm. A second oxide coated filament, *C*, was located just outside the box, opposite a small slit 0.6 mm in width. The slit was at right angles to the filament,

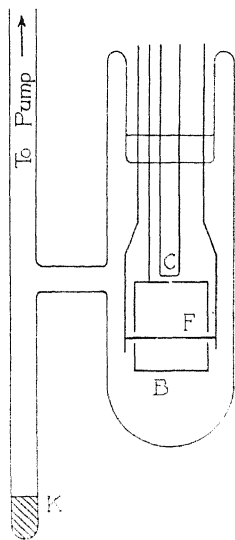


Fig. 1. Diagram of tube.

so that only those electrons coming from a nearly equipotential region of the filament, *C*, were allowed to enter the box. The potassium was dis-

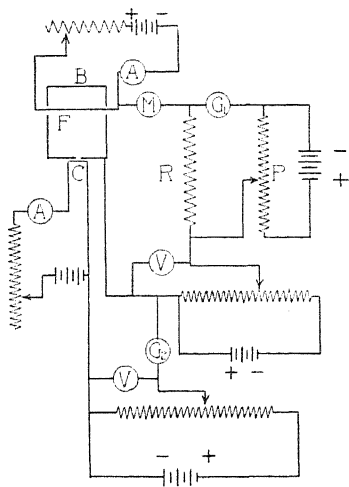


Fig. 2. Arrangement of balancing circuit.

tilled into a side tube, *D*. The whole of the apparatus, including part of the tube leading to the pump, was surrounded by a furnace, the temperature of which could be controlled.

To measure the change in the space charge limited current from F , caused by ionization inside the box, we used a balance arrangement, shown in Fig. 2. The thermionic current from the filament, F , passed through a resistance R . The voltage drop across R was balanced by an opposing potential from the potentiometer, P , through the galvanometer, G . Any change in the space charge limited current, far too small to be measured

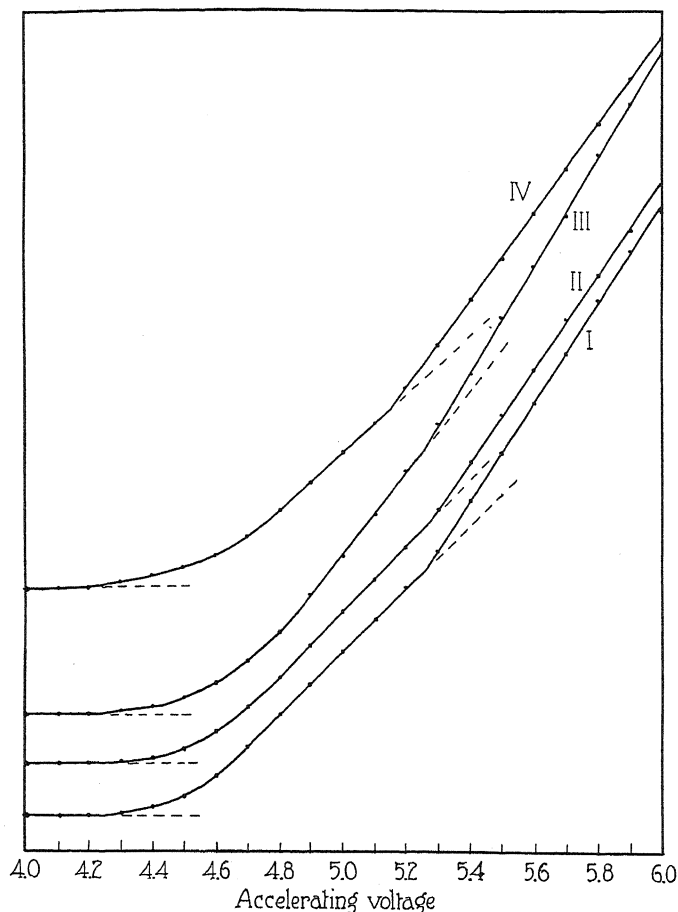


Fig. 3. Ionization curves for K vapor.

Curve:	I	II	III	IV
Temp.:	189	200	197	197°C

accurately on the micro-ammeter, M , could be easily read on the galvanometer. To secure steady conditions, batteries of large capacity were used.

In order that almost every electron from C entering the box should collide with a potassium atom, the apparatus was kept between 180°C and 205°C. This temperature range corresponds to a range of electronic mean free paths from 6 mm to 2 mm, and of vapor pressures from 0.0018 to 0.005 mm of mercury.

Under our final conditions, the space charge limited current from F was independent of the heating current for temperatures well below the rated limit of the filament. The presence of potassium in the apparatus increased the emission from filament C so much that sufficient electrons to cause measurable ionization were given off at a temperature below visible redness. Thus the velocity range of the emitted electrons due to temperature was small.

Some typical curves are shown in Fig. 3. Only relative values of the ionization potentials, of course, are given accurately by this method, since we had no easy way of correcting for the contact differences of potential involved. We have assumed that the initial rise in the curve corresponds to the ionization potential, which from spectroscopic data is 4.32 volts for potassium. All the curves show a second distinct discontinuity nearly one volt above the point at which ionization begins. The average of the separations between the first and second breaks for twenty-three curves is 0.97 ± 0.05 volts. It is interesting to note that just above the first break the curves merge into the horizontal axis asymptotically, making it difficult to determine the exact point at which ionization begins; whereas the second break is very sharp. The sharpness of the second break indicates that the velocity range of the ionizing electrons was small enough to show the true shape of the ionization curve. Thus we conclude that the rounding off of the first break is a true representation showing a slow increase in the ionization probability in the neighborhood of the ionization potential.⁵

As a check on the apparatus we also attempted to verify Lawrence's results on the ultraionization potentials of mercury vapor, before beginning the work on potassium vapor. We found that the discontinuities in mercury vapor were considerably more difficult to reproduce time after time than the single discontinuity in potassium. However, we obtained the following values for the ultraionization potentials of mercury, which are not wholly in agreement with those found by Lawrence.⁷

Lawrence's values	10.40	10.60		11.29		11.70	12.06
Our values	10.40	10.62	10.88	11.28	11.40	11.77	12.16 12.76

DISCUSSION

We may regard the discontinuity in the ionization curve at 0.97 volts above the first ionization potential as indicating the onset of an additional kind of ionization. This may be considered as a second ionization potential at $4.32 + 0.97 = 5.29$ volts. It is tempting to seek a correlation between the

⁵ Simultaneously with the measurement of the change in the space charge limited current by galvanometer G_1 , the total emission from filament C was measured on galvanometer G_2 . We found that the emission from C did not vary over 10 percent over the range of accelerating potentials used in producing the curves. Furthermore, the emission from C was a smooth, almost linear, function of the accelerating potential. Thus the discontinuity in the ionization curves above the ionization potential cannot be due to any abrupt change in the number of electrons entering the box.

⁷ E. O. Lawrence, Phys. Rev. 28, 947 (1926).

second ionization potential by electron impact and the short wave-length peak in Lawrence's work. We should expect to find the onset of a second type of photoionization at 2334Å, corresponding to 5.29 volts. However, in Lawrence's experiment, the second type of photoionization begins at 2700Å and rises to a maximum at 2340Å. Now the second break in our curves corresponds much more closely to the latter value, although we should have expected correlation with the former.

Until recently it was customary⁸ to associate the presence of the second ionization potential in photoionization in potassium with an effect on the molecule. Such evidence as we have as to the association in potassium vapor indicates that for every molecule, there are perhaps 5,000 atoms. Therefore, in order to account for the results, it has been suggested that, for light, the molecule has a much larger absorption coefficient than the atom. Since the change in slope at the second ionization potential in our ionization by electron impact curves is of the same order as the change in slope at the first, it would also mean a very large effective cross section for the molecule for electron impact as compared with the atom. Since this line of argument seems to lead to a conclusion which is difficult to believe, we are inclined to associate the second discontinuity with the onset of a second type of ionization in the atom, for which we have no theory.

A close correlation between the effects of light and electron impact is not to be expected. We know, for example, that in the excitation of an atom by light, the fit between the wave-length of the exciting light and the energy changes in the atom must be exact. However, in the case of electron impact, the colliding electron need have only *sufficient* energy. Similarly, in the field of ionization, we could hardly expect an exact parallelism between the effect of light and the effect of electron impact.

⁸ E. O. Lawrence, *Phil. Mag.* 50, 345 (1925), R. W. Ditchburn and F. L. Arnot, *Proc. Roy. Soc. A*123, 516 (1929).

ABSORPTION AND COLLISION BROADENING OF THE MERCURY RESONANCE LINE

BY M. W. ZEMANSKY*

PALMER PHYSICAL LABORATORY, PRINCETON, N. J.

(Received June 9, 1930)

ABSTRACT

Radiation emitted by a mercury resonance lamp. It is shown how an approximate expression for the frequency distribution of the radiation from a resonance lamp can be arrived at, and that it can be represented approximately by a Gauss error curve with a half-breadth depending upon the geometry of the lamp and upon the vapor density, and in general greater than that of the absorption line.

Absorption coefficient and ratio of emission to absorption line breadth. Assuming that all five components of the mercury resonance line are alike both in emission and in absorption, and that any one component of the emission and of the absorption line is a Gauss error curve of half-breadth $\Delta\nu_E$ and $\Delta\nu_D$ respectively ($\Delta\nu_D$ = Doppler breadth), the absorption of a slab of thickness l is calculated as a function of $\kappa(\nu_0)l$, where $\kappa(\nu_0)$ is the absorption coefficient for the center of any one of the components. From experimental values of the absorption, $\kappa(\nu_0)$ is found to be consistent with the theoretical value $1.41 \times 10^{-13}N$ (where N is the number of Hg atoms per cc) provided $\Delta\nu_E/\Delta\nu_D$ is taken to be 1.21 in these experiments, 1.46 in Orthmann's, 1.50 in Hughes and Thomas', 1.15 in Kunze's, and 1.15 in Kopfermann and Tietze's.

Lorentz collision broadening of the absorption line. A theoretical expression is obtained for the absorption coefficient when collision broadening is superimposed upon Doppler broadening, and is evaluated for different values of the frequency and of $\Delta\nu_C/\Delta\nu_D$ where $\Delta\nu_C$ is the Lorentz collision breadth and $\Delta\nu_D$ is the Doppler breadth. With $\kappa(\nu_0)l$ and $\Delta\nu_E/\Delta\nu_D$ equal to the values found for these experiments, the absorption is calculated as a function of $\Delta\nu_C/\Delta\nu_D$. From experimental values of the absorption of mercury vapor in the presence of H_2 , N_2 , A, CO, NH_3 , He, CH_4 , and C_3H_8 , $\Delta\nu_C$ is found as a function of the pressure of each gas. The curves of $\Delta\nu_C$ against pressure yield the effective broadening radius of each molecule, which is found to be directly proportional to the square root of the molecular diamagnetic susceptibility. On the basis of the Langevin theory this means that the effective broadening area of a molecule varies at the product of the number of outer electrons and the mean square radius of all the electronic orbits. The same result is obtained from the experiments of F üchtbauer, Joos and Dinkelacker.

ABSORPTION COEFFICIENT AND RATIO OF EMISSION TO ABSORPTION LINE BREADTH

THE transmission through mercury vapor of the radiation emitted by a mercury resonance lamp has been measured many times under apparently similar conditions, and yet the results have varied very markedly. The resulting values of absorption coefficient have differed from one another by as much as several hundred percent. In an investigation of the quenching of mercury resonance radiation by foreign gases which has been in progress for

* National Research Fellow.

the last two years it was found necessary to know the absorption coefficient of mercury vapor for mercury resonance radiation very accurately. Consequently, this quantity was studied rather carefully with a view to discover, if possible, the causes for the existing discrepancies. The present paper, it is hoped, will clear up those difficulties which have not already been solved by others, and will give a summary of all the work that has been done since 1925, as well as a new set of measurements of the absorption coefficient.

THE RADIATION EMITTED BY A MERCURY RESONANCE LAMP

It has been shown by Wood¹ that the mercury resonance line ($\lambda = 2537$) emitted by a mercury arc consists of five components of approximately equal intensity, and that all of these components are absorbed approximately equally by a column of mercury vapor. This has been substantiated by very careful measurements of the Zeeman effect of the mercury resonance line in a recent paper by Schein.² The intensity distribution of the radiation emitted by a mercury resonance lamp, however, is not known accurately as a function of the vapor density, the type of resonance lamp, dimensions, etc. It was assumed by Orthmann,³ Kunze,⁴ and Schein that the radiation emitted by a mercury resonance lamp was similar in intensity distribution to radiation whose half-breadth was equal to that of the absorption line but which had been absorbed slightly by passing through a thin layer of mercury vapor on its way out of the resonance lamp. This assumption was used by Orthmann and Kunze to calculate a correction factor which was applied to all the experimental values of the absorption. Schein, however, recognized that this assumption implies that the radiation emitted by a resonance lamp has a half-breadth slightly larger than that of the absorption line, and, by graphical means, estimated that, in his experiments, the ratio was 1.23.

The original supposition, namely, that the radiation emitted by a mercury resonance lamp is similar to that which results when a line of half-breadth equal to that of the absorption line passes through a thin absorbing layer, is only partly true, for when the vapor density in the resonance lamp approaches zero, the intensity should approach zero, whereas, according to the above assumption, it approaches a constant. A more satisfactory picture of the situation can be made on the basis of the following approximations:

1. The original stimulating radiation from the arc has a breadth that is so wide in comparison to the absorption line breadth of the vapor in the resonance lamp that it can be regarded as a continuous spectrum in the limited range of frequencies under consideration. Call this intensity A .
2. The radiation that is re-emitted in the body of the resonance lamp is a fraction ϵ of that amount of A which is absorbed in a column of average thickness l_1 . Call this radiation $A_1(\nu)$.

¹ R. W. Wood, *Phil. Mag.* **50**, 761 (1925).

² M. Schein, *Helv. Phys. Act.* Vol. II, Sup. I (1929).

³ W. Orthmann, *Ann. d. Physik* **78**, 601 (1925).

⁴ P. Kunze, *Ann. d. Physik* **85**, 1013 (1928).

3. The radiation that finally emerges from the resonance lamp is the radiation $A_1(\nu)$ after it has passed through a column of vapor of average thickness l_2 . Call this radiation $A_2(\nu)$.

The situation is represented graphically in Fig. 1.

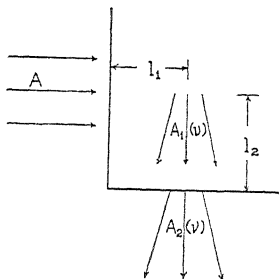


Fig. 1. Schematic representation of a resonance lamp.

Let us consider only one component of the mercury resonance line, inasmuch as all the components behave the same way. We have

$$A_1(\nu) = \epsilon A (1 - e^{-\kappa(\nu)l_1})$$

$$A_2(\nu) = A_1(\nu) e^{-\kappa(\nu)l_2}$$

where $\kappa(\nu)$ is the absorption coefficient of the vapor in the resonance lamp for the frequency range between ν and $\nu + d\nu$. Let us make the usual assumption:

$$\kappa(\nu) = \kappa(\nu_0) e^{-[2(\nu - \nu_0)/\Delta\nu_A]^2 \log_e 2}$$

where $\kappa(\nu_0)$ is the absorption coefficient for the center of the line of frequency ν_0 , and $\Delta\nu_A$ is the half-breadth of the absorption line. Calling $2(\nu - \nu_0)/\Delta\nu_A (\log_e 2)^{1/2} = \omega$, we have then

$$\kappa(\omega) = \kappa(0) e^{-\omega^2}.$$

Let us further assume that the geometry of the resonance lamp has been so arranged that l_1 is very nearly equal to l_2 . This is not essential, but it simplifies matters somewhat. Then, after substitution, we have

$$A_2(\omega) = \epsilon A (1 - e^{-xe - \omega^2}) e^{-xe - \omega^2} \quad (1)$$

where $x = \kappa(\nu_0)l_1 = \kappa(\nu_0)l_2$.

Plotting this expression for different values of x , it is found that it resembles a Gauss error curve fairly well with a half-breadth greater than that for the curve $e^{-\omega^2}$, that is, greater than the half-breadth of the absorption line. Calling this new half-breadth $\Delta\nu_E$, $\Delta\nu_E/\Delta\nu_A$ was found graphically to be 1.16 when $x = 0.25$ and 1.33 when $x = 0.50$. As the vapor density approaches zero, x approaches zero, and Eq. (1) approaches $x\epsilon A e^{-\omega^2}$, which is correct, because the intensity approaches zero, and the half-breadth approaches the absorption line breadth.

Burger and van Cittert⁵ considered the broadening of a spectral line by absorption and obtained an expression for the breadth as a function of x . Unfortunately, however, their results can not be applied to the case of a resonance lamp.

If there were some way of estimating x for a particular resonance lamp it might be worth while to use the expression given by Eq. (1) in what is to follow. Since, however, there is no way of knowing how accurately x can be estimated, it is better to replace Eq. (1) by a Gauss error curve of half-breadth $\Delta\nu_E$ where $\Delta\nu_E$ is to be determined by experiment.

Two types of resonance lamp have been used to obtain resonance radiation. In the first one, the resonance radiation is taken off the incident window at about 45° to the incident beam,⁶ and in the second, it emerges from a separate window at an angle of 90° to the incident beam.⁷ It is obvious that the second type can be designed to correspond to a much smaller value of x than the first. It is therefore to be expected that the experiments conducted with the 90° type will involve a smaller value of $\Delta\nu_E$ than those performed with one of the 45° type.

THE ABSORPTION OF RADIATION

When radiation of frequency between ν and $\nu + d\nu$ and intensity $K(\nu, 0)$ passes through an absorbing slab of thickness l with absorption coefficient $\kappa(\nu)$, then the transmitted radiation, $K(\nu, l)$ is given by⁸

$$K(\nu, l) = K(\nu, 0)e^{-\kappa(\nu)l}.$$

Let us suppose, as usual, that the emission and absorption lines are Gauss error curves with half-breadths $\Delta\nu_E$ and $\Delta\nu_A$ respectively. Then

$$K(\nu, 0) = K(\nu_0, 0)e^{-[2(\nu - \nu_0)/\Delta\nu_E]^2 \log_e 2}$$

$$\kappa(\nu) = \kappa(\nu_0)e^{-[2(\nu - \nu_0)/\Delta\nu_A]^2 \log_e 2}$$

and the absorption, A , is

$$A = 1 - \frac{\int_{-\infty}^{\infty} e^{-[\omega^2 + \kappa(\nu_0)l]e^{-(\Delta\nu_E/\Delta\nu_A)^2}} d\omega}{\int_{-\infty}^{\infty} e^{-\omega^2} d\omega}$$

where

$$\omega = \frac{2(\nu - \nu_0)}{\Delta\nu_E}(\log_e 2)^{1/2}.$$

For values of $\kappa(\nu_0)l \leq 1.5$, the series expansion of Eq. (2) is satisfactory for numerical computation

⁵ H. C. Burger and P. H. van Cittert, *Zeits. f. Physik* **51**, 638 (1928).

⁶ A. L. Hughes and A. R. Thomas, *Phys. Rev.* **30**, 466 (1927).

⁷ P. Kunze, reference 4.

⁸ A. v. Malinowski, *Ann. d. Physik* **44**, 935 (1914).

$$A = \kappa(\nu_0)l \cdot \frac{1}{\left(1 + \left(\frac{\Delta\nu_E}{\Delta\nu_A}\right)^2\right)^{1/2}} - \frac{[\kappa(\nu_0)l]^2}{2!} \cdot \frac{1}{\left(1 + 2\left(\frac{\Delta\nu_E}{\Delta\nu_A}\right)^2\right)^{1/2}} + \dots$$

$$\dots + (-1)^n \frac{[\kappa(\nu_0)l]^n}{n!} \cdot \frac{1}{\left(1 + n\left(\frac{\Delta\nu_E}{\Delta\nu_A}\right)^2\right)^{1/2}} + \dots$$

$$A = 1 - \frac{\int_{-\infty}^{+\infty} e^{-[\omega^2 + \kappa(\nu_0)l - (\Delta\nu_E/\Delta\nu_A)\omega]^2} d\omega}{\int_{-\infty}^{\infty} e^{-\omega^2} d\omega}.$$

TABLE I. Values of A .

$\frac{\Delta\nu_E}{\Delta\nu_A}$						
$\kappa(\nu_0)l$	0	.50	1.0	1.27	2.0	3.0
0.25	0.221	0.200	0.160	0.140	0.102	0.0723
.50	.393	.360	.291	.256	.188	.133
1.0	.632	.588	.486	.428	.316	.226
1.5	.777	.736	.619	.550	.400	.287
2.0	.865	.832	.711	.630	.472	.348
3.0	.950	.925	.820	.738	.564	.414
4.0	.982	.967	.878	.805	.622	.461
4.5	.989	.977	.897		.640	.480

For values of $\kappa(\nu_0)l > 1.5$ it was found more convenient to evaluate A graphically. The values of A for different values of $\kappa(\nu_0)l$ and $\Delta\nu_E/\Delta\nu_A$ are given in Table I, and are plotted in Fig. 2. Curves of A against $\kappa(\nu_0)l$ for various values of $\Delta\nu_E/\Delta\nu_A$ are shown in Fig. 3. DeGroot⁹ has given curves of the same character as those of Fig. 2, but in a form that is not very convenient for the purpose at hand.

When $\Delta\nu_E/\Delta\nu_A$ is known, a curve of A against $\kappa(\nu_0)l$ can be drawn, and from experimental values of A and l , $\kappa(\nu_0)$ can be obtained. Values of $\kappa(\nu_0)$ for mercury vapor at a density corresponding to 20° C obtained by different authors under different conditions are given in Table II.

It will be seen from Fig. 3 that, if a curve of A against $\kappa(\nu_0)l$ for $\Delta\nu_E/\Delta\nu_A = a$, where a is any number, be used in a situation which really requires the use of a curve for $\Delta\nu_E/\Delta\nu_A > a$, the resulting values of $\kappa(\nu_0)l$ will be too small. It is to be expected, therefore, that the smallest values of $\kappa(\nu_0)$ will correspond to the largest values of $\Delta\nu_E/\Delta\nu_A$. This is seen to be the case, for it was pointed out in the beginning that the 45° type of resonance lamp yields a broader line than the 90° type.

There is another important error that can result in a final value of $\kappa(\nu_0)$ that is too small, namely, the reception by the photoelectric cell of scattered

⁹ W. de Groot, *Physica* 9, 263 (1929).

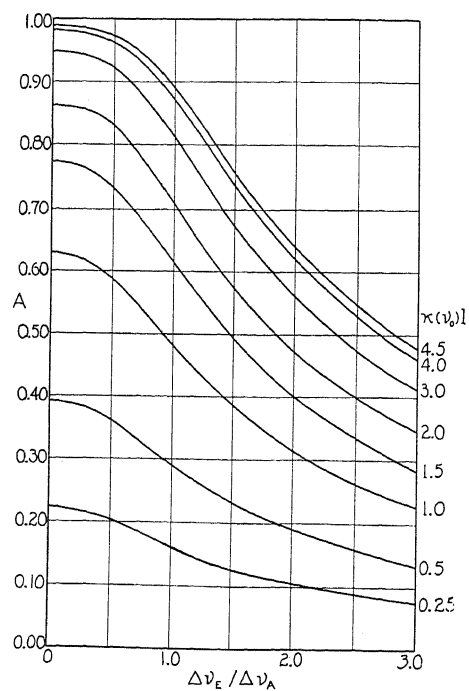


Fig. 2. Values of A for different values of $\kappa(\nu_0)l$ and $\Delta\nu_E/\Delta\nu_A$.

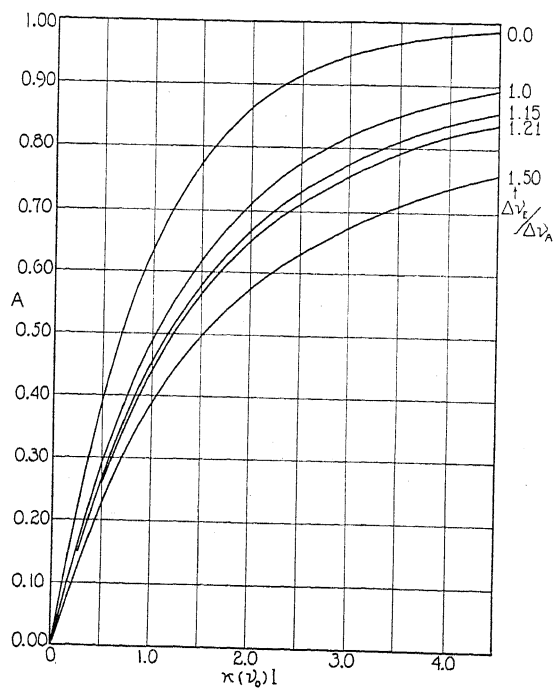


Fig. 3. Curves of A against $\kappa(\nu_0)l$ for various values of $\Delta\nu_E/\Delta\nu_A$.

TABLE II.

	Type of Resonance Lamp	Method of computing $\kappa(\nu_0)$ from A	at 20°C
Orthmann ³	45°	Used curve of A against $\kappa(\nu_0)l$ for $\Delta\nu_E/\Delta\nu_A=1$ and applied a correction factor to A to take into account absorption in the resonance lamp.	3.1
Hughes and Thomas ⁶	45°	Used exponential law of absorption which is equivalent to assuming $\Delta\nu_E/\Delta\nu_A=0$	1.24
Schein ²	90°	Used curve of A against $\kappa(\nu_0)l$ for $\Delta\nu_E/\Delta\nu_A=1.23$ but computed $\Delta\nu_E/\Delta\nu_A$ inaccurately.	3.77
Kunze ⁴	90°	Same as Orthmann	5.2
Kopfermann and Tietze ¹⁰	90°	Used formula due to Ladenburg for a situation in which the emitting and absorbing slabs are both infinitesimally thin.	5.2
Author	90°	Used curve of A against $\kappa(\nu_0)l$ for $\Delta\nu_E/\Delta\nu_A$ equal to that value which makes $\kappa(\nu_0)l$ vary linearly with Nl . This value was found to be 1.21.	5.61

radiation along with the transmitted radiation. If the photoelectric cell is placed close to the emerging window, and if the diaphragm which limits the incident beam is in front of the incident window, then a portion of the scattered radiation emitted by the *whole* emerging face is received by the photoelectric cell, resulting in a smaller value of A . It has been found by experiment that no scattered radiation reaches the photoelectric cell if the following conditions are adhered to:

1. The diaphragm limits the incident beam to a diameter of about 1 cm, and is placed over the *emerging* window.
2. The photoelectric cell is no nearer than 7 cm from the diaphragm.

It is believed that, in the experiments of Orthmann and in those of Hughes and Thomas, this was a possible source of error when the mercury vapor density was high enough to give rise to appreciable scattering. In all of the previous experiments, it is believed, an incorrect curve of A against $\kappa(\nu_0)l$ was used to compute the absorption coefficient.

APPARATUS

There is nothing essentially new in the apparatus used in these experiments, so that we shall limit ourselves to a very brief description.

Arc. Quartz mercury arc made by Cooper Hewitt, water-cooled and magnetically deflected.

Resonance lamp. 90° type with crystalline quartz windows cemented on with picein wax. Between it and the mercury diffusion pump there was a trap which was kept surrounded by ice. The drop of liquid mercury in a side tube was also kept in an ice bath. The exciting radiation from the arc illu-

¹⁰ H. Kopfermann and W. Tietze, *Zeits. f. Physik* 56, 604 (1929).

minated about 5 mm of the incident window and the resonance radiation was taken off an area of the emerging window about 5 mm in diameter.

Absorption cell. A disk of heavy Pyrex glass about 4.5 cm inside diameter, and 0.792 cm in length was cut as shown in Fig. 4. Two crystalline quartz windows were cut in the same way and cemented on with picein wax. This was then cemented to a Pyrex tube about 10 cm long and 2 cm in diameter in which was placed a drop of mercury. There was thus a large opening between the tube containing the drop of mercury and the absorption cell proper, which enabled equilibrium conditions to be obtained rapidly.

The absorption cell was connected to the pumps through a glass spiral about a foot in diameter, which had sufficient flexibility to allow the cell to be moved in and out of the path of the light beam. A diaphragm with an

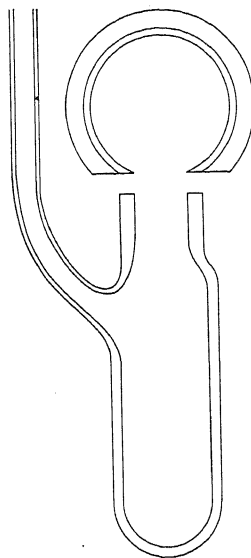


Fig. 4. Absorption cell.

aperture of about 1 cm remained fixed in space on the emerging side of the cell.

The photoelectric cell. The cell was made of fused quartz and had a platinum plate. It was first thoroughly cleaned and baked out, and then about 5 cm of H_2 was admitted. A discharge was passed through the H_2 by a small induction coil and then the H_2 was pumped out. This was repeated a few times until the platinum became slightly discolored. About 4 mm of H_2 was then introduced and the cell was sealed off. It was run on about 200 volts and a sensitive Compton electrometer was used to measure the current. The linearity of the cell at various voltages was tested with calibrated screens.

METHOD

With liquid air on the absorption cell the transmission of the quartz windows was measured and compared with the transmission of a piece of

cellophane which was mounted beside the cell and which came in front of the diaphragm when the cell was moved aside. The cellophane was used to cut down the intensity of the incident light by a known amount when it was measured. The mercury vapor in the absorption cell was maintained at constant density by a suitable substance contained in a Dewar flask which moved with the cell. Melting Benzol was used for the temperature 4.2°C and melting paraxylene for 12.1°C . Water was used for temperatures between 15 and 20°C . The absorption cell proper was always at room temperature which was held as near 20°C as possible. In calculating the number of mer-

TABLE III.

(1)	(2) Thickness l in cm	(3) Temp. $^\circ\text{C}$	(4) Nl $\times 10^{-13}$	(5) Absorption A	(6) $\Delta\nu_E$ — $\Delta\nu_A$	(7) $\kappa(\nu_0)l$ from Exp. plus Eq. (2)	(8) $\kappa(\nu_0)l$ Theor. Eq. (4)
Orthmann	0.85	2.7	0.706	0.346	1.46	0.82	0.995
		6.1	.970	.419		1.10	1.37
		11.5	1.60	.571		1.91	2.26
		12.0	1.68	.582		2.00	2.37
		15.5	2.28	.700		3.22	3.22
		18.0	2.85	.723		3.52	4.02
		19.3	3.18	.763		4.25	4.49
Hughes and Thomas	1.62	-13	.244	.202	1.50	.43	.344
		-8	.431	.309		.72	.608
		-3	.745	.440		1.23	1.05
		2	1.27	.554		1.83	1.78
		7	2.01	.660		2.79	2.84
		12	3.20	.755		4.32	4.51
Kunze	.301	0	.191	.161	1.15	.27	.269
		10	.494	.356		.72	.696
		15	.776	.489		1.12	1.09
		20	1.20	.620		1.70	1.69
Kopfermann and Tietze	.54	-11	.102	.115	1.15	.19	.144
		0	.343	.291		.55	.483
		10	.886	.539		1.31	1.25
		15	1.39	.661		1.95	1.96
		20	2.15	.741		2.60	3.03
Author	.792	0	.503	.370	1.21	.77	.71
		4.2	.752	.490		1.18	1.06
		12.1	1.58	.681		2.26	2.23
		15.4	2.11	.753		2.94	2.98
		20.0	3.15	.840		4.45	4.44

cury atoms per cc the vapor pressure was obtained from the International Critical Tables and the Knudsen correction was applied. In determining the transmission at a particular temperature, readings were taken through the cell and then through the cellophane at least six times.

Liquid air was put on the resonance lamp and the sensitivity of the photoelectric cell was increased by increasing the voltage. The absorption of the radiation emitted by the resonance lamp was then measured and found to be less than the radiation emitted by the lamp at 0°C . This was due to diffuse reflection in the resonance lamp of the edges of the broad 2537 line

from the arc. Other wave-lengths did not affect the photoelectric plate, for the reason that platinum treated with hydrogen has a long wave-length limit only a little above 2537. It was estimated that about 1 percent of the radiation from the resonance lamp at 0°C consisted of unabsorbable radiation. Every reading was therefore corrected to take account of this.

The results, along with those of others, are shown in Table III, and plotted in Fig. 5.

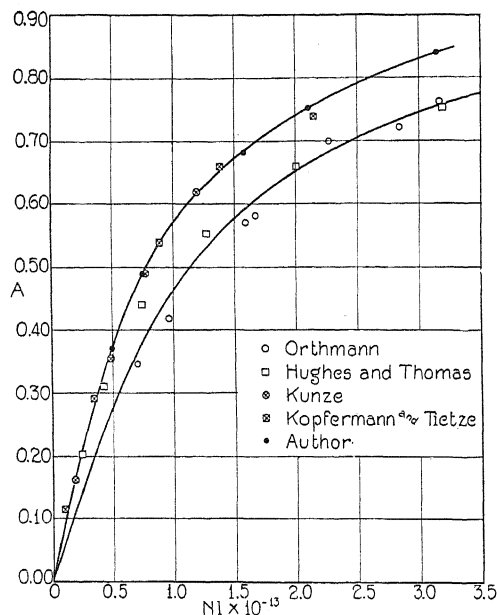


Fig. 5. A as a function of Nl .

It will be seen in Fig. 5 that all the measurements fall into two groups. those taken with the 90° type of resonance lamp, and those taken with the 45° type, the former yielding much larger values of the absorption. Both groups, however must correspond to the same values of $\kappa(\nu_0)l$. Inasmuch as it is impossible to calculate accurately $\Delta\nu_E/\Delta\nu_A$, the particular curve of A against $\kappa(\nu_0)l$ for each group is not immediately at hand. It must be chosen by appeal to theory as follows:

It is a well-known result that:¹¹

$$\int_0^\infty (\kappa\nu) d\nu = \frac{h\nu_0 N}{4\pi} B_{1 \rightarrow 2}$$

where N = no. of absorbing atoms per cc

ν_0 = frequency of center of line

$B_{1 \rightarrow 2}$ = Einstein coefficient defined in terms of light intensity, and where the integration is to be taken over all the fine structure components of the absorption line. Using the Einstein relations

¹¹ E. A. Milne, M.N. of R.A.S. **85**, 111 (1924).

$$\frac{A_{2 \rightarrow 1}}{B_{1 \rightarrow 2}} = \frac{2h\nu^3}{c^2} \cdot \frac{q_1}{q_2}$$

and $A_{2 \rightarrow 1} = 1/\tau$, we have

$$\int_0^\infty \kappa(\nu) d\nu = \frac{\lambda_0^2}{8\pi\tau} \cdot \frac{q_2}{q_1} \cdot N$$

and substituting $\lambda_0 = 2.537 \times 10^{-5}$ cm, $\tau = 10^{-7}$ sec.¹² and $q_2/q_1 = 3$, we get

$$\int_0^\infty \kappa(\nu) d\nu = 7.68 \times 10^{-4} N.$$

Since each component of the absorption line obeys

$$\kappa(\nu) = \kappa(\nu_0) e^{-[2(\nu - \nu_0)/\Delta\nu_A]^2 \log_e 2}$$

and since there are five components,

$$\begin{aligned} \int_0^\infty \kappa(\nu) d\nu &= 5 \left(\frac{\pi}{4 \log_e 2} \right)^{1/2} \kappa(\nu_0) \Delta\nu_A \\ &= 5 \times 1.07 \kappa(\nu_0) \Delta\nu_A \end{aligned}$$

whence finally

$$\kappa(\nu_0) l = \frac{1.44 \times 10^{-4}}{\Delta\nu_A} \cdot Nl. \quad (3)$$

In none of the experiments did the mercury vapor pressure ever become high enough to involve Lorentz collision broadening or Holtzmark coupling broadening of the absorption line. $\Delta\nu_A$ therefore, is the Doppler breadth $\Delta\nu_D$, and since the temperature of the absorption cell proper was always at 20°C, $\Delta\nu_D$ is constant. The Doppler breadth of a line is known to be $7.16 \times 10^{-7} \nu_0 (T/M)^{1/2}$ sec⁻¹ where T is the absolute temperature and M is the molecular weight. For mercury at 20°C, $\Delta\nu_D = 1.02 \times 10^9$ sec⁻¹, and consequently Eq. (3) becomes

$$\kappa(\nu_0) l = 1.41 \times 10^{-13} Nl. \quad (4)$$

In Fig. 6, Eq. (4) is shown as a heavy line. The individual points were obtained as follows:

A curve between $\kappa(\nu_0)l$ and A was sought which, in conjunction with the author's values of A , would give values of $\kappa(\nu_0)l$ that varied linearly with Nl . It was found that the curve corresponding to $\Delta\nu_E/\Delta\nu_A$ equal to 1.21 achieved this, and at the same time, agreed well with Eq. (4). Curves of $\kappa(\nu_0)l$ and A were then sought which, in conjunction with the other experimental values of A , would give values of $\kappa(\nu_0)l$ that agreed best with Eq. (4). In this way the curves corresponding to the values of $\Delta\nu_E/\Delta\nu_A$ given in Table III,

¹² R. Ladenburg, *Naturwiss.* **14**, 1208 (1926), H. W. Webb and H. A. Messenger, *Phys. Rev.* **33**, 319 (1929). For other references see M. W. Zemansky, *Phys. Rev.* **29**, 519 (1927).

column (6) were obtained, and the values of $\kappa(\nu_0)l$ in column (7) were obtained from these curves and experimental values of A . The values of $\kappa(\nu_0)l$ in column (8) were computed from Eq. (4). The agreement with theory is shown in Fig. 6.

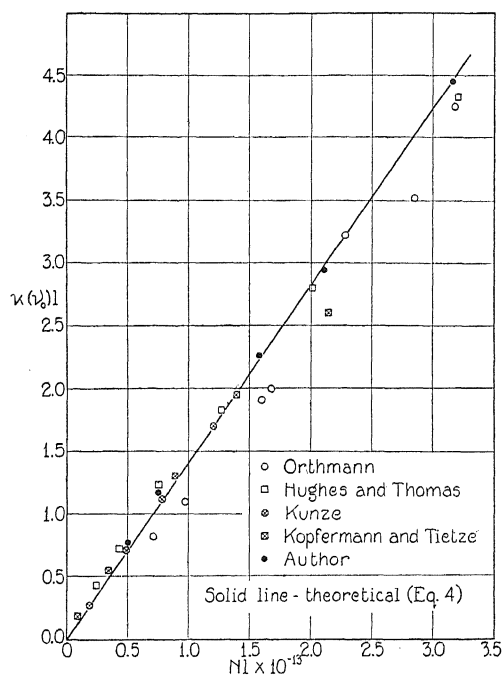


Fig. 6. $\kappa(\nu_0)l$ as a function of Nl .

LORENTZ COLLISION BROADENING

When an absorption line is broadened by Doppler broadening only, the absorption coefficient is given by

$$\kappa(\nu) = \kappa(\nu_0) e^{-[2(\nu - \nu_0)/\Delta\nu_D]^2 \log_e 2}$$

where $\Delta\nu_D$ = Doppler breadth. Under the influence of collision broadening, the absorption coefficient varies with the frequency according to a curve of the type

$$\frac{1}{1 + \left[\frac{2(\nu - \nu_0)}{\Delta\nu_C} \right]^2}$$

where $\Delta\nu_C$ = collision breadth = no. of impacts per sec./ π . With collision broadening superimposed on Doppler broadening

$$\kappa(\nu) = \frac{2\kappa(\nu_0)}{\pi\Delta\nu_C} \int_{-\infty}^{\infty} \frac{e^{-(2\delta/\Delta\nu_D)^2 \log_e 2}}{1 + \left[\frac{2}{\Delta\nu_C} (\nu - \nu_0 - \delta) \right]^2} d\delta$$

$$= \frac{2\kappa(\nu_0)}{\pi\Delta\nu_C} \int_{-\infty}^{\infty} \frac{e^{-[2/\Delta\nu_D(\nu-\nu_0-\delta)]^2 \log_e 2}}{1 + \left(\frac{2}{\Delta\nu_C}\delta\right)^2} d\delta$$

where $\kappa(\nu_0)$ = abs. coeff. of center of line when Doppler broadening only is effective, i.e., for zero pressure of foreign gas. Call

$$\frac{2(\nu - \nu_0)}{\Delta\nu_D} (\log_e 2)^{1/2} = q \quad \text{and} \quad \frac{\Delta\nu_C}{\Delta\nu_D} (\log_e 2)^{1/2} = p$$

and let

$$x = \frac{2\delta}{\Delta\nu_D} (\log_e 2)^{1/2}.$$

Then

$$\begin{aligned} \frac{\kappa(\nu)}{\kappa(\nu_0)} &= \frac{p}{\pi} \int_{-\infty}^{\infty} \frac{e^{-(q-x)^2}}{p^2 + x^2} dx \\ &= \frac{2p}{\pi} e^{-q^2} \int_0^{\infty} \frac{e^{-x^2} \cos 2iqx}{p^2 + x^2} dx. \end{aligned}$$

Now

$$\frac{1}{p^2 + x^2} = \int_0^{\infty} e^{-(p^2 + x^2)u} du$$

whence

$$\begin{aligned} \frac{\kappa(\nu)}{\kappa(\nu_0)} &= \frac{2p}{\pi} e^{-q^2} \int_0^{\infty} e^{-p^2 u} du \int_0^{\infty} e^{-(1+u)x^2} \cos 2iqx dx \\ &= \frac{2p}{\pi} e^{-q^2} \int_0^{\infty} e^{-p^2 u} du \frac{1}{2} \left(\frac{\pi}{1+u} \right)^{1/2} e^{q^2/(1+u)}. \end{aligned}$$

Let $1+u = t^2/p^2$, and we have, finally

$$\frac{\kappa(\nu)}{\kappa(\nu_0)} = \frac{2}{(\pi)^{1/2}} e^{p^2 - q^2} \int_p^{\infty} e^{-t^2 + (p^2 q^2 / t^2)} dt. \quad (5)$$

When there is no collision broadening, $p = 0$, and

$$\kappa(\nu) = \kappa(\nu_0) e^{-q^2} \frac{2}{(\pi)^{1/2}} \int_0^{\infty} e^{-t^2} dt = \kappa(\nu_0) e^{-q^2}.$$

At extremely high foreign gas pressures p is very large, and the original expression for $\kappa(\nu)/\kappa(\nu_0)$ can be shown to reduce to $1/(\pi)^{1/2} \cdot p/p^2 + q^2$. It can readily be verified that, for all values of p ,

$$\int_0^{\infty} \kappa(\nu) d\nu = \left(\frac{\pi}{4 \log_e 2} \right)^{1/2} \kappa(\nu_0) \Delta\nu_D$$

which is required by the constancy of the Einstein B coefficient.

In order to evaluate the integral in Eq. (5), we proceed as follows:¹³

Expanding $e^{p^2 q^2 / t^2}$ we have

$$\frac{\kappa(\nu)}{\kappa(\nu_0)} = \sum_{n=0}^{\infty} I_n(p) \frac{e^{-q^2} q^{2n}}{n!}$$

where

$$I_n(p) = \frac{2}{(\pi)^{1/2}} e^{p^2} p^{2n} \int_p^{\infty} e^{-t^2} \frac{dt}{t^{2n}}.$$

Integrating by parts (starting with (dt/t^{2n})) we obtain a convenient means for computing successively all the $I_n(p)$,

$$I_n(p) = \frac{p}{2n-1} \left(\frac{2}{\pi^{1/2}} - 2p I_{n-1}(p) \right)$$

and

$$I_0(p) = e^{p^2} \frac{2}{(\pi)^{1/2}} \int_p^{\infty} e^{-t^2} dt$$

which can be obtained from tables.

$\kappa(\nu)/\kappa(\nu_0)$ was evaluated for different values of p and q and the results are given in Table IV.

$$\frac{\kappa(\nu)}{\kappa(\nu_0)} = \frac{2}{\pi^{1/2}} e^{p^2 - q^2} \int_p^{\infty} e^{-t^2 + (p^2 q^2 / t^2)} dt$$

$$p = (\log_e 2)^{1/2} \frac{\Delta\nu_C}{\Delta\nu_D}, \quad q = (\log_e 2)^{1/2} \frac{2(\nu - \nu_0)}{\Delta\nu_D}$$

TABLE IV. Values of $\kappa(\nu)/\kappa(\nu_0)$.

$q \quad p$	0	0.5	1.0	1.5
0	1.0000	0.6157	0.4276	0.3216
0.2	.9608	.6015	.4215	.3186
.4	.8521	.5613	.4038	.3097
.6	.6977	.5011	.3766	.2958
.8	.5273	.4294	.3425	.2779
1.0	.3679	.3549	.3047	.2571
1.2	.2369	.2846	.2662	.2349
1.4	.1409	.2233	.2292	.2123
1.6	.0773	.1728	.1954	.1902
1.8	.0392	.1333	.1657	.1695
2.0	.0183	.1034	.1402	.1504

The absorption is given, as before, by

$$A = 1 - \frac{K(\nu_0, 0) \int_0^{\infty} e^{-[2(\nu - \nu_0) / \Delta\nu_E]^2 \log_e 2} \cdot e^{-\kappa(\nu) l} d\nu}{K(\nu_0, 0) \int_0^{\infty} e^{-[2(\nu - \nu_0) / \Delta\nu_E]^2 \log_e 2} d\nu}$$

¹³ I am indebted to Dr. T. H. Gronwall for the method of evaluating Eq. (5), and to Professor H. P. Robertson for valuable help throughout the calculation.

which becomes

$$A = 1 - \frac{\int_{-\infty}^{\infty} e^{-[(q/\Delta\nu_E/\Delta\nu_D)^2 + \kappa(\nu)/\kappa(\nu_0) \cdot \kappa(\nu_0)l]} dq}{\int_{-\infty}^{\infty} e^{-(q/\Delta\nu_E/\Delta\nu_D)^2} dq}$$

and which can be evaluated graphically for any situation in which $\kappa(\nu_0)l$ and $\Delta\nu_E/\Delta\nu_D$ are known. This was done for these experiments at 20 °C for which $\kappa(\nu_0)l = 4.44$ and $\Delta\nu_E/\Delta\nu_D = 1.21$, and for Orthmann's experiments at 15.5°C for which $\kappa(\nu_0)l = 3.22$ and $\Delta\nu_E/\Delta\nu_D = 1.46$. The results are given in Table V and Fig. 7.

$$A = 1 - \frac{\int_{-\infty}^{\infty} e^{-[(q/\Delta\nu_E/\Delta\nu_D)^2 + \kappa(\nu)/\kappa(\nu_0) \cdot \kappa(\nu_0)l]} dq}{\int_{-\infty}^{\infty} e^{-(q/\Delta\nu_E/\Delta\nu_D)^2} dq}$$

$$\frac{\kappa(\nu)}{\kappa(\nu_0)} = \frac{2}{\pi^{1/2}} e^{p^2 - q^2} \int_p^{\infty} e^{-t^2 + (p^2 q^2 / t^2)} dt.$$

TABLE V.

$\kappa(\nu_0)l$	$\frac{\Delta\nu_E}{\Delta\nu_D}$	p	$\frac{\Delta\nu_C}{\Delta\nu_D}$	A
4.44	1.21	0	0	0.840
		0.5	0.6	.833
		1.0	1.2	.775
		1.5	1.8	.707
3.22	1.46	0	0	.700
		.5	.6	.687
		1.0	1.2	.630
		1.5	1.8	.562

From the curves in Fig. 7 it is possible to obtain the collision breadth of the mercury absorption line merely by measuring the absorption. The advantage of this is that low enough foreign gas pressures may be used so that the five fine structure components of the mercury resonance line will not merge into one another, as was the case in the experiments of Füchtbauer Joos and Dinkelacker¹⁴ who broadened the line by foreign gases at pressures up to fifty atmospheres. There is one disadvantage, however, in that the asymmetry in the line broadening predicted by theory and observed by Minkowski¹⁵ in the case of sodium cannot be taken into account. It will be seen later how this affects the final results. Nevertheless it is believed that this method of measuring the magnitude of the collision breadth

¹⁴ C. Füchtbauer, G. Joos, and O. Dinkelacker, *Ann. d. Physik* **71**, 204 (1923).

¹⁵ R. Minkowski, *Zeits. f. Physik* **55**, 16 (1929).

of a line is superior to the photographic method, because it enables one to separate the collision breadth from the Doppler breadth easily. A spectrogram of an absorption line which has been broadened only slightly by a foreign gas could be used to obtain the collision breadth provided one plotted

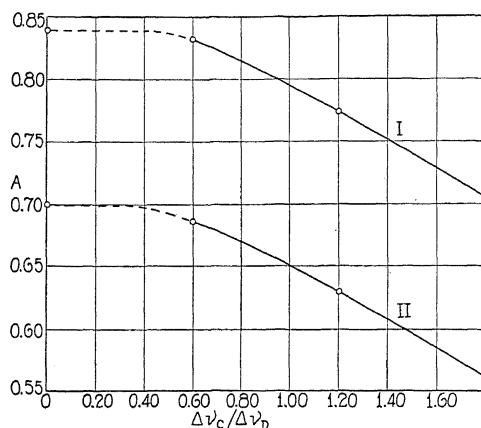


Fig. 7. A as a function of $\Delta\nu_E/\Delta\nu_D$. Curve I, $\kappa(\nu_0)l=4.44$, $\Delta\nu_E/\Delta\nu_D=1.21$. Curve II, $\kappa(\nu_0)l=3.22$, $\Delta\nu_E/\Delta\nu_D=1.46$.

measured values of $\kappa(\nu)/\kappa(\nu_0)$ against frequency, and compared these curves with those obtained from Eq. (5). A correction would have to be made, of course, for the frequency shift due to asymmetrical broadening. It is doubtful whether existing experimental data on absorption lines are sufficiently ac-

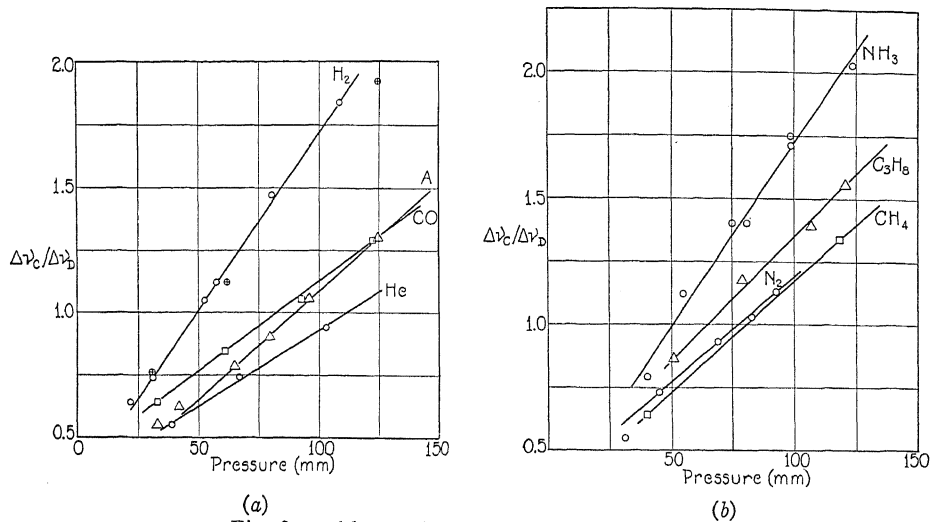


Fig. 8a and b. $\Delta\nu_C/\Delta\nu_D$ as a function of pressure.

curate for this purpose. The spectrograms of the 2537 absorption line obtained by Füchtbauer, Joos and Dinkelacker at very high foreign gas pressures yield values of the collision breadth that are somewhat in doubt be-

cause of the fact that the fine structure of the line has been completely wiped out. Nevertheless the values obtained by them are very interesting and will be referred to later.

TABLE VI.

Gas	Pressure in mm p'	Absorption A	$\frac{\Delta\nu_C}{\Delta\nu_D}$ from Fig. 7	Gas	Pressure in mm p'	Absorption A	$\frac{\Delta\nu_C}{\Delta\nu_D}$ from Fig. 7
H_2	0	0.840	0	CO	0	0.840	0
	22	.830	.64		33	.830	.64
	31	.821	.74		61	.812	.84
	53	.790	1.05		93	.790	1.05
	58	.783	1.12		123	.766	1.29
	81	.746	1.47	He	0	.840	0
	109	.702	1.84		39	.836	.55
H_2 (Orthmann)	0	.700	0		67	.821	.74
	31	.674	.76		103	.802	.94
	62	.638	1.12	NH_3	0	.840	0
	125	.548	1.92		40	.817	.79
N_2	0	.840	0		55	.783	1.12
	31	.836	.55		75	.754	1.40
	45	.822	.73		81	.754	1.40
	69	.802	.93		99	.717	1.71
	83	.792	1.03		99	.712	1.75
	93	.782	1.13		124	.680	2.03
A	0	.840	0	CH_4	0	.840	0
	33	.836	.55		40	.830	.64
	42	.831	.62		119	.760	1.34
	65	.817	.78	C_3H_8	0	.840	0
	80	.806	.90		51	.810	.86
	96	.790	1.05		79	.777	1.17
	125	.764	1.30		107	.755	1.39
					121	.736	1.55

A number of foreign gases were used to broaden the line, and the results are given in Table VI and in Fig. 8. It is seen in Fig. 8 that the collision breadth plotted against the pressure of the foreign gas does not yield a straight line passing through the origin, as it should according to the relation:

$$\Delta\nu_C = \frac{\text{no. of impacts per sec.}}{\pi}$$

It is believed that this is due to the failure to take into account the asymmetry in line broadening, but that the error will not be large if the linear portions of the curves are considered. The three points for H_2 shown in Fig. 8 obtained by Orthmann five years ago under entirely different conditions as to mercury vapor density, thickness of cell, type of resonance lamp, etc., agree well enough to constitute an excellent check on the method as a whole.

Calling Z the number of impacts per mercury atom per sec, we have from kinetic theory

$$Z = 2\sigma_E^2 \frac{9.71 \times 10^{18} p'}{T} \left(2\pi kT \left(\frac{1}{m} + \frac{1}{M} \right) \right)^{1/2}$$

where T is the absolute temperature, p' the pressure in mm, k Boltzmann's constant, m the mass of a mercury atom, M the mass of a foreign gas molecule, and σ_E the effective distance between centers.

Since $\Delta\nu_C = Z/\pi$,

$$\frac{Z}{p'} = \pi \Delta\nu_D \frac{\Delta\nu_C/\Delta\nu_D}{p'} = \pi \times 1.02 \times 10^9 \times \text{slope of line in Fig. 8} \quad (6)$$

and

$$\frac{Z}{\sigma_E^2 p'} = \frac{2 \times 9.71 \times 10^{18}}{T} \left(2\pi kT \left(\frac{1}{m} + \frac{1}{M} \right) \right)^{1/2} \quad (7)$$

from which σ_E^2 can be calculated.¹⁵ The values of Z/p' , $Z\sigma_E^2 p'$, and σ_E^2 obtained from these experiments along with those from the work of Fuchtbauer, Joos, and Dinkelacker are given in Table VII.

TABLE VII.

Gas	$\frac{Z}{p'} \times 10^{-7}$		$\frac{Z}{\sigma_E^2 p'} \times 10^{-22}$		$\sigma_E \times 10^8$		$(\sigma_E \times 1.80) - X_M \times 10^6 (-X_M)^{1/2} \times 10^3$	
	from Eq. (6)	from Eq. (7)	from Eq. (6)	from Eq. (7)				
Author								
He	1.94	1.29	15.0	3.88	2.08	1.87	1.37	
H ₂	4.48	1.83	24.5	4.95	3.15	3.94	1.99	
CO	2.32	.521	44.5	6.68	4.88	10.6	3.26	
N ₂	2.66	.521	51.0	7.15	5.35	11.8	3.44	
A	2.76	.448	61.5	7.85	6.05	18.0	4.24	
NH ₃	4.65	.653	71.2	8.45	6.65	19.0	4.36	
CH ₄	2.84	.671	42.3	6.51	4.71	12.2	3.50	
C ₃ H ₈	3.17	.431	73.5	8.58	6.78	40.5	6.37	
F. J. and D.								
H ₂	5.09	1.83	27.8	5.27	3.47	3.94	1.99	
N ₂	3.38	.521	64.8	8.05	6.25	11.8	3.44	
A	3.98	.448	88.9	9.44	7.64	18.0	4.24	
CO ₂	5.40	.431	125	11.2	9.40	18.7	4.32	
H ₂ O	4.37	.638	68.5	8.28	6.48	13.0	3.61	
O ₂	3.20	.491	65.1	8.07	6.27	para.		

DISCUSSION

It is seen from Table VII that all the values of σ_E^2 are larger than the normal ones, which vary from about 9 to 12×10^{-16} cm, in agreement with the ideas of Kallmann and London.¹⁷ The most striking result, however, is obtained if we adopt the point of view that, in the collision process, the mercury atom has a constant radius equal to the gas-kinetic radius (1.80×10^{-8} cm) and that each broadening gas has its own effective radius. The effective radius of each gas is then obtained by subtracting 1.80×10^{-8} from σ_E . Values of $\sigma_E - 1.80 \times 10^{-8}$ are given in Table VII along with values of

¹⁵ The values of σ_E^2 obtained from these experiments are to be regarded as lower limits because of the error in neglecting asymmetry. Relative values, however, are probably quite reliable.

¹⁷ Kallmann and London, Zeits. f. Phys. Chem. Abt. B, 2 (1929).

the molecular diamagnetic susceptibility, χ_M . All the values of χ_M are experimental ones¹⁸ except that for CO which was obtained by adding the susceptibilities of C and O. The justification for this is that it yields a result almost equal to that of N_2 which is known to be similar to CO in most of its properties.

In Fig. 9 the effective radius is plotted against the square root of the susceptibility, and very good straight lines are obtained for both Fuchtbauer's and these results. The agreement between the two lines is no less remarkable than the lines themselves, inasmuch as the two methods are so radically different. It is possible that the correct line lies between the two

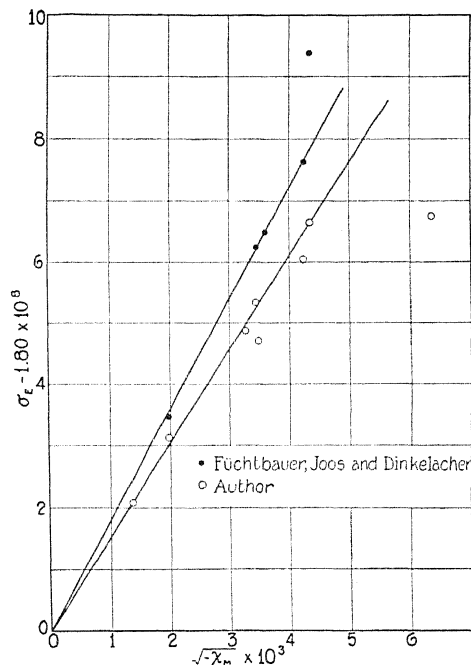


Fig. 9. σ_E as a function of $(-\chi_M)^{1/2}$.

because of the error that is peculiar to each method. The Langevin theory of diamagnetism allows us to give a meaning to this linear relation. According to the simple theory of diamagnetism for an atom, the atomic susceptibility is given by $-(e^2/6mc^2) n \bar{r}^2$ where n is the number of outer electrons of the atom, and \bar{r}^2 is the mean square radius of all the electronic orbits. Applying this relation to all the molecules in question, we get the result that the effective cross-section of a molecule for collision broadening is proportional to the number of outer electrons and to the mean square radius of the electronic orbits, a result that is quite interesting.

¹⁸ A. P. Wills and G. Hector, Phys. Rev. 23, 209 (1924), G. Hector, Phys. Rev. 24, 418 (1924), F. Bitter, Phys. Rev. 33, 389 (1929), Stoner "Magnetism and Atomic Structure."

According to this result, oxygen, although it is strongly paramagnetic, and cannot be plotted in Fig. 9, ought to behave like N_2 or CO, because O_2 has 16 electrons and a gas-kinetic radius of 1.47×10^{-8} cm, whereas N_2 and CO have each 14 electrons and radii equal to 1.58×10^{-8} cm and 1.60×10^{-8} cm respectively. The effective broadening radius of O_2 , according to Füchtbauer's results is 6.27×10^{-8} cm in good agreement with Füchtbauer's value for N_2 , 6.25×10^{-8} cm. The author did not use O_2 as a broadening agent for fear that at such high O_2 pressures, the inside walls of the absorption cell would become covered with HgO , which would lower their transmission and completely obscure any slight change in the absorption of the mercury vapor.

The only points that lie seriously off their respective straight lines in Fig. 9 are Füchtbauer's point for CO_2 and the author's for C_3H_8 . There is a possibility that the value for the diamagnetic susceptibility of CO_2 , -18.7×10^{-6} is too small. It was measured by Soné, whose value for N_2 is considerably smaller than the accepted value. It is not likely, however, that the value for the susceptibility of C_3H_8 , measured by Bitter, is too large, because it was based on Hector and Wills' values for N_2 and H_2 , and also because it fits in well with the higher hydrocarbons. Its departure from the line in Fig. 9 is much too great to be accounted for on the basis of experimental error. There is a possibility that, in the time that elapsed between its preparation and its use, it became contaminated. Unfortunately there was not sufficient time at the author's disposal to settle the question definitely. It would be very interesting to measure the effective broadening radius of all the gaseous hydrocarbons, as well as other organic gases, and it is quite likely that this will be done next year.

In conclusion, the author would like to express his indebtedness to Mr. L. J. Buttolph of the General Electric Vapor Lamp Co. for the loan of a mercury arc, and to Dr. J. R. Bates for his kindness in supplying methane and propane. It is a pleasure also to acknowledge my debt to the National Research Council for the opportunity of engaging in this research and to Professor K. T. Compton for the privilege of working in Palmer Physical Laboratory.

THE EFFECT OF SMALL ANGLE SCATTERING ON THE ELECTRON ABSORPTION COEFFICIENT

BY METTA CLARE GREEN

DEPARTMENT OF PHYSICS, UNIVERSITY OF CALIFORNIA

(Received June 7, 1930)

ABSTRACT

An indirect study of the scattering of electrons by gas molecules has been made by measuring electron absorption coefficients in an apparatus containing a Faraday cylinder of variable aperture. A straight path method was used in which electrons from an oxide-coated filament were given a desired velocity and made to traverse a 7.5 cm path to the collector. A retarding potential between the cylinder and its shield kept out all electrons which had suffered inelastic collisions as well as those which had been scattered outside of the collector opening. Measurements were made in argon, helium, hydrogen, and mercury vapor at accelerating potentials ranging from 11 to 196 volts. The radius of the cylinder aperture varied from one one-hundredth to one tenth of the path length. No consistent variation of the absorption coefficient with opening was found in any case. Theoretical calculations based on scattering laws obtained from inverse square or fifth power laws of force predicted relatively large variations. Calculations made assuming uniform scattering or the Sommerfeld law indicated small changes of the same order of magnitude as the deviations between individual values obtained in this experiment.

INVESTIGATIONS have recently been made by Dymond¹ and Watson,² Harnwell,³ and Arnot⁴ of the distribution of electrons scattered by gas molecules. The experimental curves showing the relation between the intensity of the scattered current per unit solid angle and the scattering angle all indicate relatively large scattering at small angles for both elastic and inelastic collisions. The initial steepness of the slopes of the curves increases with increasing initial electron velocity. Dymond and Watson's curve for elastic scattering of 210 volt electrons in helium gives very rough agreement with Born's⁵ theoretical curve calculated for slower electrons in hydrogen, but, as they point out, this fact is not very significant. Harnwell's original curves for elastic scattering in molecular and monatomic hydrogen compared total scattering between θ and $\theta + d\theta$ with scattering per unit solid angle given by the theoretical equation of Born. When corrected for this error,⁶ his experimental values of scattered intensity per unit solid angle are no longer in agreement with the theoretical values. Arnot found that the curve for elastic scattering of 82 volt electrons in mercury vapor had a steeper initial slope than that of Dymond and Watson's helium curve for electrons of the same

¹ E. G. Dymond, *Phys. Rev.* **29**, 433 (1927).

² E. G. Dymond and E. E. Watson, *Proc. Roy. Soc. Lon.* **122**, 571 (1929).

³ G. P. Harnwell, *Phys. Rev.* **33**, 559 (1929), **34**, 661 (1929).

⁴ F. L. Arnot, *Proc. Roy. Soc. A* **125**, 660 (1929).

⁵ M. Born, *Göttinger Nachrichten*, p. 146 (1926).

⁶ G. P. Harnwell, *Phys. Rev.* **35**, 285 (1930).

initial velocity. The experimental curves all indicate much less rapid change of scattered intensity with scattering angle at small angles than that given by the theoretical scattering law obtained from an inverse square law of force between the electron and the scattering particle.

Indirect evidence on the angular distribution of electrons scattered by molecules is given by measurements of electron absorption coefficients in gases and vapors. An electron beam is diminished in intensity by collision with molecules of a gas through which it passes, according to the equation, $I = I_0 e^{-\alpha p x}$, where I is the electron current reaching the end of the path, I_0 is the initial current, x , the path length, and α , the absorption coefficient.

Determinations of α all involve measuring the variation of the logarithm of the ratio of the final to the initial current with path length or gas pressure. The rate of variation of α with the diameter of the aperture of the Faraday cylinder used for collecting the final beam should depend on the angular distribution of the scattered electrons. Comparison of data so far collected with different experimental arrangements of apparatus indicates that α is practically constant for relatively large ranges of cylinder aperture. Brode⁷

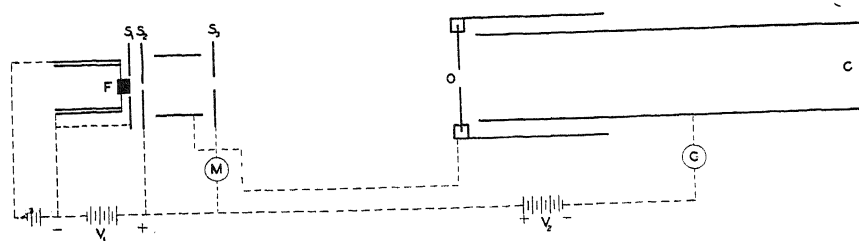


Fig. 1. Diagram of apparatus.

obtained very good agreement between values of α for cadmium vapor taken in very different types of apparatus. However, quantitative information cannot be obtained by direct comparison of other existing data.

Accordingly a direct experimental study of this question has been made in an apparatus in which a beam of electrons from a hot oxide-coated filament was given a definite velocity and then made to travel a straight path through gas at known pressure to a collector of variable opening.

The experimental arrangement is shown in Fig. 1. F is a small oxide-coated nickel cylinder which is welded to a tungsten wire and is a practically equipotential source of electrons.⁸ S_1 , S_2 and S_3 are circular holes of 5, 2, and 3 mm diameter respectively. C is a Faraday cylinder 9 cm long and 2 cm in diameter, whose shield has a magnetically-operated shutter-opening, O , similar to that of a camera. The diameter of O varied from 2.3 to 17 mm. The distance from S_2 to O is 7.7 cm. Accelerating and retarding potentials, V_1 and V_2 , were applied between the filament and second nickel plate and the Faraday cylinder and its shield, respectively. Galvanometers G and M measured the final electron current and the total emission through S_2 . The

⁷ R. B. Brode, Phys. Rev. 35, 504-508 (1930).

⁸ G. Hertz, and R. K. Kloppe, Zeits. f. Physik 31, 463 (1925).

metal parts were all made of nickel and the inside of the tube enclosing the whole apparatus was sputtered with nickel and grounded through M . The earth's magnetic field was neutralized by large Helmholtz coils.

Absorption coefficients were measured in argon, helium, molecular hydrogen and mercury vapor. Electron velocities corresponding to 13, 27.5, and 97 volts accelerating potential were used in argon, helium and hydrogen; in argon 47 and 196 volt electrons were also studied. 40 volt electrons were used in mercury.

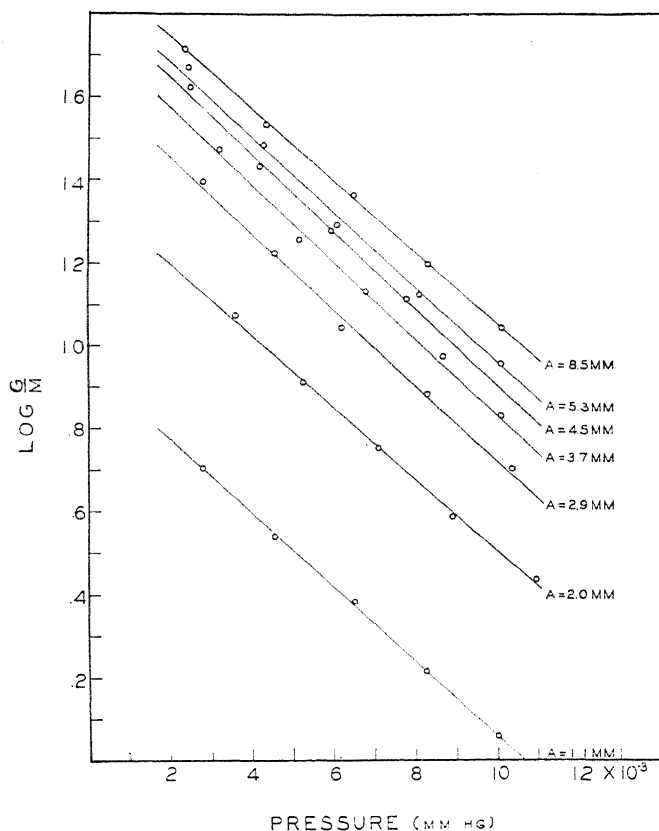


Fig. 2. Logarithm of ratio of current, G , at end of path to total current, M , as a function of pressure and aperture radius, A , for 97 volt electrons in argon.

The argon was purified in a calcium arc and the helium and hydrogen were passed through charcoal cooled in liquid air.

With constant accelerating potential, readings of G and M were made for from three to five different pressures for each cylinder aperture. From four to seven different apertures were used for each accelerating potential. The total electron current varied from 2 to 8×10^{-7} amperes, while the currents to the Faraday cylinder were from 2 to 100×10^{-9} amperes. Curves were obtained showing the variation of the final current with the total emission through S_2 for fixed values of pressure, aperture, and accelerating potential.

Readings were always taken in the region where the two currents were proportional to each other.

The true value of the electron velocity was determined by retarding potential curves. Each current, G , was taken as the difference between galvanometer scale deflections for a retarding potential about ten percent less than and one equal to the accelerating potential. The apparent size of the beam was determined by plotting values of G/M against aperture. The opening for which the G/M ratio fell to half its limiting value for wide openings was used to measure the beam radius. Under the conditions of this experiment this was approximately 3 mm.

TABLE I.

Aperture radius		Absorption coefficient, α				Mercury
		Argon				
(mm)	13v	27.5v	47.5v	96.5v	196v	37.5v.
1.1	64.8	43.2	34.4	30.4	18.3	94.5
2.0		43.5	37.5	30.1	20.2	84.5
2.9	70.9	43.9	35.8	30.6	19.9	82.4
3.7		43.2	35.2	31.0	19.8	84.5
4.5	68.6	43.5	35.8	31.4	22.0	89.0
5.3	67.4	42.9	33.8	30.7	21.7	
6.2						94.5
8.5	67.4	44.3	34.0	27.6	20.6	
Av. α	67.8	43.5	35.2	30.3	20.4	91.1

Aperture radius		Absorption coefficient, α				
		Helium		Hydrogen		
(mm)	13v	27.5v	97v	11.5v	27.5v	97v
1.1	14.9	10.8	3.21	27.0	15.1	11.2
2.9	15.2	10.8	3.54	27.0	16.5	10.5
3.7		9.6	4.05			
4.5	13.5	10.1	4.05	27.7	16.2	11.1
6.2			3.88	24.6	15.5	10.8
8.5	14.5	8.3	4.55	25.3	16.0	9.1
Av. α	14.5	9.9	4.12	26.3	15.9	10.5

The gas pressures varied from 2 to 12×10^{-3} mm for argon and helium, from 10 to 50×10^{-3} mm for hydrogen, and from 5 to 25×10^{-4} mm for mercury.

The value of the absorption coefficient was determined in each case by plotting the values of the logarithm of G/M (assumed to be proportional to $\log I/I_0$) against the gas pressure and dividing the slope of the straight line so obtained by the path length. The latter was not clearly defined in the apparatus, but it was assumed to be 7.5 cm. Correction was made for room temperature so that the values of α are in cm^2/cm^3 of gas at 1 mm pressure and 0°C . In Fig. 2 are shown the observed values of the $\log G/M$ plotted as a function of the pressure in argon at 97 volts: it appears that the relationship is linear.

Table I summarizes the experimental results for the variation of the electron absorption coefficients with aperture diameter. Figs. 3 and 4 represent these results graphically for some of the accelerating potentials in argon and hydrogen.

These values of α have a consistent tendency, except in the case of the low velocity measurements in hydrogen, to be higher than those recently obtained by Normand⁹ in this laboratory with a magnetic deflection method.

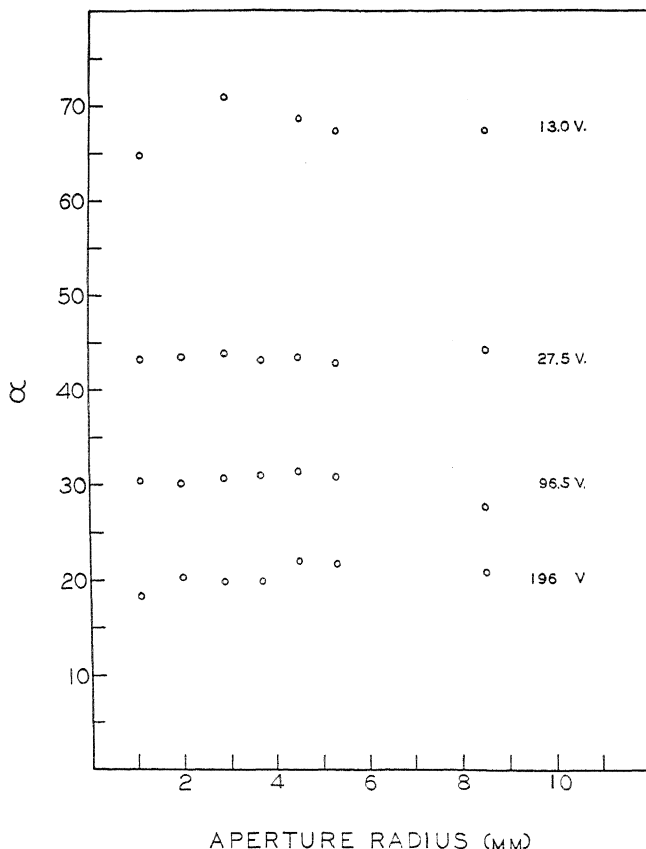


Fig. 3. Electron absorption coefficient α , as a function of aperture radius and accelerating potential in argon.

In helium this might be partly due to impurities, but it can hardly be ascribed to contamination in the case of argon, since most of the probable impurities would have lower values of α than argon. The difference has not been explained, but it is of interest to note that Jones¹⁰ got consistently higher values of α in mercury with a straight path method than with the magnetic deflection method.

As seen from the table of results, there is no consistent tendency for α to vary with aperture within the limits of error of these measurements.

⁹ C. E. Normand, Phys. Rev. **35**, 1217 (1930).

¹⁰ T. J. Jones, Phys. Rev. **32**, 459 (1928).

THEORETICAL DISCUSSION

Assuming an inverse square law of force between the electron and the scattering center one obtains with classical mechanics an expression for the

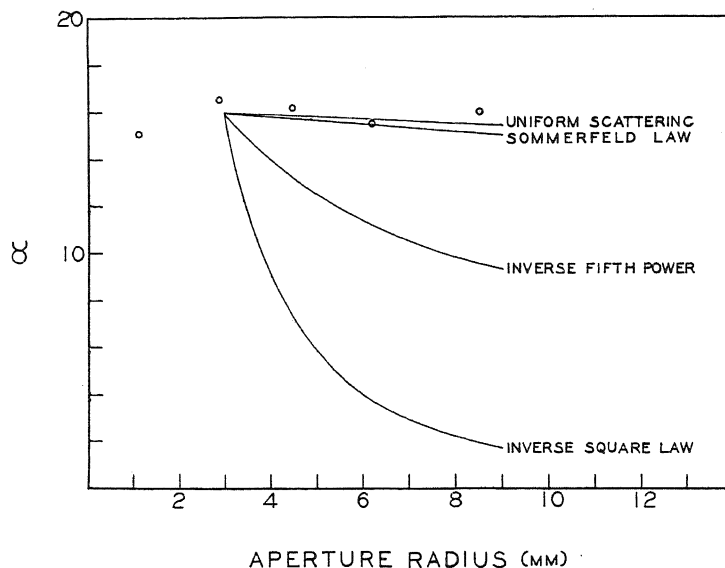


Fig. 4. Absorption coefficient for 27.5 volt electrons in hydrogen. Circles indicate observed values.

variation of intensity of elastically scattered electrons with scattering angle which is identical in form with that of Rutherford for the scattering of alpha-particles by heavy nuclei:

$$\frac{1}{n} \frac{dN}{dA} = \left(\frac{e^2 Z}{4Er} \right)^2 \frac{1}{\sin^4 \theta/2}$$

where θ is the angle between the original direction of the beam and the radius vector from the scattering center to the scattered particle, n is the intensity per unit area of the incident beam, dN/dA , the number of electrons which have been deflected through an angle θ and fall on unit area at a distance r from the scattering center, e , the electronic charge, E , the initial kinetic energy of the scattered particle, and Z , the atomic number of the scatterer.

Taking into consideration the polarization of the scattering particle by the passing electron Zwicky¹¹ obtained an inverse fifth power law of attraction which would give the scattering formula:

$$\frac{1}{n} \frac{dN}{dA} = \frac{K}{r^2} \frac{1}{(\cos^3 \theta/2 \sin^5 \theta/2)^{1/2}}$$

This is an approximate expression which is valid only for small angle scattering. K is a constant and the other symbols have the above meanings.

The scattering law derived by Sommerfeld¹² on the basis of the wave mechanics considers the interaction of the electron with the "electron cloud"

¹¹ F. Zwicky, Phys. Zeits. **24**, 171 (1923).

¹² A. Sommerfeld, Atombau und Spectrallinien, Wellenmechanischer Ergänzungsband, p. 231.

surrounding the nucleus of the scattering atom. The "electron cloud" is formed by the electrons outside the nucleus, all of which are assumed to be in the K -shell. The derivation neglects any disturbance of the electronic charge distribution of the atom by the field of the passing electron. The equation thus derived is:

$$\left| \frac{\psi_1}{\psi_0} \right|^2 = \left(\frac{e^2 Z}{4Er} \right)^2 \times \frac{1}{(\sin^2 \theta/2 + \alpha^2)^2}$$

In this formula, $|\psi_1/\psi_0|^2$ is the ratio of the intensity of the scattered to the initial beam per unit area and $\alpha = \lambda Z/2\pi a$ where λ is the wave-length of the electron in terms of Planck's constant, h , and its momentum, mv , and a is the radius of the first Bohr orbit of the atom. If α is very small, that is, for very fast electrons, this becomes the Rutherford formula. For slow electrons, of long wave-length, $\sin^2 \theta/2$ becomes negligible in comparison with α^2 and the formula becomes, merely:

$$\left| \frac{\psi_1}{\psi_0} \right|^2 = \left(\frac{e^2 Z}{4Er} \right)^2 \frac{1}{\alpha^4} = \left(\frac{h^2}{4\pi^2 m e^2 Z} \right)^2 \frac{1}{r^2}$$

This indicates uniform scattering in all directions. The above considerations would predict that the intensity of scattering per unit angle would show less variation with angle for slow electrons than that given by the Rutherford formula, but would approach it at higher velocities. That this has been found experimentally has been previously mentioned.

The scattering laws can be applied to determine the theoretical variation of the absorption coefficient with collector aperture by a double integration which takes into account all electrons scattered outside the aperture from every point in the path of the beam.

In the case of the scattering resulting from an inverse square law of force, if $\theta = \tan^{-1} a/(L-x)$ is the angle subtended by the aperture radius at the point of collision, the current scattered beyond the opening per unit intensity of the incident beam per scattering center is given by the expression:

$$\frac{dI}{I} = -K \int_{\tan^{-1} a/(L-x)}^{\pi} \frac{\sin \theta d\theta}{\sin^4 \theta/2} = -2K \left(\frac{(a^2 + (L-x)^2)^{1/2} + (L-x)^2}{a} \right)^2$$

a is the radius of the aperture, x , the distance from the beginning of the path to the point of collision, L , the path length, and $k = 2\pi(e^2 Z/4E)^2$. The same meanings will be attached to these symbols whenever they occur in the following discussion.

Multiplying by $N dx$ to get the effect of all the scattering particles, N being the number of molecules per cc, and integrating from $x=0$ to $x=L$, this equation becomes

$$\log \frac{I}{I_0} = -2KN \left(L + \frac{2}{3} \frac{L^3}{a^2} - \frac{2}{3} a^3 \pm \frac{2}{3} \frac{(a^2 + L^2)^{3/2}}{a^2} \right)$$

I_0 is the current when $x=0$. When a is very small in comparison with L , this may be simplified to:

$$\log \frac{I}{I_0} = -2KN \frac{4}{3} \frac{L^3}{a^2}$$

Since

$$\log \frac{I}{I_0} = -\alpha L p$$

$$\alpha = \frac{8KN}{3p} \frac{L^2}{a^2}.$$

That is, α should vary inversely as the square of the aperture radius. This theoretical variation of α is plotted for 27.5 volt electrons in hydrogen in the lower curve of Fig. 4. The constant K has been chosen arbitrarily to give the theoretical curve the experimental value at the point $a=3$ mm, this being the point at which the size of the collector opening equals that of the beam.

The above derivation, as well as those that follow, is approximate in that it considers only the scattering due to elastic collisions. At 27.5 volts in hydrogen, however, the fraction of inelastic scattering at small angles is small, as indicated by the work of Dymond and Watson and that of Harnwell on velocity and angular distribution of the two types of scattering. Further, this treatment neglects scattering due to collisions after the first and takes no account of space charge in the beam, nor of finite width of the beam. The effect of the size of the electron beam has been recently calculated by Beeck¹³ for the case of uniform scattering. Similar calculations for the scattering resulting from an inverse square law of force show that the effect of the size of the beam is to make the theoretical variation of α with aperture greater and thus to increase the discrepancy between the theoretical and the experimental curves.

The effect of aperture on α can be obtained for an inverse power law of force from the fact that $\tan \theta = CP/E$ where P is the potential energy of the electron at the point of nearest approach to the scattering particle and E is its initial kinetic energy. C is a factor of proportionality which depends on the power discussed. The above energy relation holds only for small angles of deflection. For an inverse n^{th} power law $\tan \theta = C'/(p^{n-1}V)$, V being the accelerating potential corresponding to the kinetic energy of the electron, and p , the distance of nearest approach. Noticing that all the electrons coming within a circle of radius, p , are scattered at angles greater than θ , one can write immediately for the total current of electrons scattered in all angles greater than θ from a volume of the beam dx cm long at a distance x from the beginning of the path,

$$-dI = I\pi p^2 N dx.$$

If for p^2 is substituted its value from the energy relation and for $\tan \theta$, its value, $a/(L-x)$, the expression becomes, on integration from $x=0$ to $x=L$

$$\log \frac{I}{I_0} = -\frac{K'}{a^{2/(n-1)}} L^{2/(n-1)+1}$$

$$\alpha = K'' \left(\frac{L}{a} \right)^{2/(n-1)}$$

Thus, for an inverse square law α varies inversely with a^2 as previously found. For the inverse fifth power law, $\alpha = k'''(L/a)^{3/2}$. A curve representing this

¹³ O. Beeck, Zeits. f. Physik 61, 251 (1930).

variation of α with a is plotted in Fig. 4. This curve was also arbitrarily made to have the experimental value $\alpha = 16$ for $a = 3$ mm.

Uniform scattering is obtained from the Sommerfeld formula by neglecting $\sin^2 \theta/2$ with respect to α^2 . The α in Sommerfeld's notation should not be confused with the α used as a symbol for the absorption coefficient. When the electron wave-length is long in comparison with the radius of the first Bohr orbit, the expression for the scattering at any distance x from the beginning of the path is:

$$\frac{dI}{I} = -\frac{2\pi}{\alpha^4} \left(\frac{e^2 Z}{4E} \right)^2 N dx \int_{\tan^{-1} a/(L-x)}^{\pi} \sin \theta d\theta = C \left[1 + \frac{L-x}{(a^2 + (L-x)^2)^{1/2}} \right].$$

From this, by integrating over the path one obtains:

$$\log \frac{I}{I_0} = -C(L-a + (a^2 + L^2)^{1/2})$$

or

$$\alpha = \frac{C}{Lp} (L-a + (a^2 + L^2)^{1/2}).$$

For small values of a compared to L

$$\alpha = C'(2 - (a/L)).$$

For molecular hydrogen the coefficient C' is arbitrarily chosen so that $C'(2-a/L)$ is equal to 16 for a 3 mm aperture. The resulting variation of α with aperture for uniform scattering is shown in Fig. 4.

For the numerical case chosen in Fig. 4 the value of Sommerfeld's α is about 0.7. In the above case $\sin^2 \theta/2$ is neglected in comparison with α^2 . When both terms are retained, the dependence of the absorption coefficient on aperture may be found by graphical integration. Fig. 4 shows the curve obtained from the Sommerfeld scattering law adjusted in the same manner as the other curves.

An examination of Fig. 4 shows that the dependence of α on aperture is greatest if an inverse square law of force is assumed and least in the case of uniform scattering as is to be expected. The variation of the experimental points is less than that predicted by the power laws and of the same order of magnitude as that given by the Sommerfeld or the uniform scattering law. The theoretical treatment given here deals only with absorption due to change in the direction of motion of the electron without change in energy. There is also some inelastic scattering which increases the absorption coefficient by an undetermined amount. If an arbitrary constant is added to the coefficients obtained from the scattering laws, any one of the curves can be made to lie within the limits of variation of the experimental points. To do this, however, assuming only scattering due to either an inverse square or fifth power law of force would assume that the scattering was largely inelastic, which is not the case, as we know from previous results. We may conclude, therefore, that the small angle scattering more nearly follows the Sommerfeld law than the inverse power laws, but may be a combination of uniform scattering with that due to some power law.

I am indebted to Professor R. B. Brode for proposing this study and for his continued assistance and interest throughout its progress.

THE RATE AT WHICH IONS LOSE ENERGY IN ELASTIC COLLISIONS

BY AUSTIN M. CRAVATH*

PALMER PHYSICAL LABORATORY, PRINCETON UNIVERSITY

(Received May 16, 1930)

ABSTRACT

The rate of energy loss of ions (including electrons) moving through a gas is rigorously calculated on the assumption that the ions and molecules are smooth elastic spheres with no attraction at a distance, having Maxwellian velocity distributions corresponding to the temperatures T_i and T_m respectively. The result is

$$f = \frac{8}{3} \frac{mM}{(m+M)^2} \left(1 - \frac{T_m}{T_i}\right)$$

where m and M are the masses of ion and molecule respectively, T_i and T_m are their temperatures, and f is the average energy loss per collision expressed as a fraction of the average ionic energy.

THERE are a number of problems in which ions (including electrons) move through a gas with an approximately Maxwellian velocity distribution corresponding to a temperature higher than that of the gas, and an expression for the rate at which the ions lose energy in elastic collisions is required. For instance, Compton¹ required it for his electron mobility equation. He deduced an approximate expression as follows. First he calculated the average energy loss for ions of given velocity striking molecules at rest at all angles from grazing to head on. He then corrected this for the motion of the molecules by finding how the energy loss for head on collisions was altered by a (one dimensional) molecular velocity distribution, and multiplying the expression for molecules at rest by this factor. The velocity distribution of the ions was not considered at all. Indeed there *is* no ion velocity distribution if one is merely interested in the average fraction of *its own* energy which an ion loses per collision. What was actually needed, however, was the average energy loss in all collisions expressed as a fraction, f , of the average energy (of all the ions in a given volume). The result obtained was

$$f = 2 \frac{m}{M} \left(1 - \frac{\Omega}{\omega}\right)$$

where m and M are the masses and ω and Ω the average energies of the ions and molecules respectively.

The present paper gives the rigorous calculation of the energy loss on the assumption that ions and molecules are smooth elastic spheres with no attraction at a distance, having Maxwellian velocity distributions.

* National Research Fellow.

¹ Compton, Phys. Rev. 22, 333 (1923).

The symbols which will be used are:

m = mass of ion.

M = " " molecule.

σ = sum of radii of ion and molecule.

T_i = absolute temperature of ions.

T_m = " " " molecules.

k = Boltzmann's constant.

n = number of ions per cm^3 .

N = " " molecules per cm^3 .

V = initial vector velocity of ion.

U = " " " " molecule.

$\mu = M/(m + M)$.

$W = (1 - \mu)V + \mu U$ = velocity of center of mass.

$R = V - W = \mu(V - U)$ = initial velocity of ion relative to center of mass.

D = unit vector giving direction of line of centers, from ion to molecule, at collision.

Q = total energy loss of all ions in 1 cm^3 in 1 sec.

$f = Q / \{(\text{no. collisions per } \text{cm}^3 \text{ per sec}) (\text{average ionic energy})\}$
= average fraction of average energy lost per collision.

To find the total energy loss, Q , we have simply to find the loss in each type of collision and then integrate over all the collisions in 1 cm^3 in 1 sec. A given type of collision is specified by given values of V , U , and D . In a collision, that component of R , the velocity of the ion relative to the center of mass, which is parallel to the line of centers, D , is reversed, and the perpendicular component is unaltered. Hence the final velocity of the ion is

$$V' = V - 2R \cdot DD$$

and the energy lost by the ion is

$$\frac{1}{2}mV^2 - \frac{1}{2}mV'^2 = \frac{1}{2}m\{4V \cdot DR \cdot D - 4(R \cdot D)^2\} = 2mR \cdot DW \cdot D$$

where W is the velocity of the center of mass.

The number of ions per cm^3 with velocity components between V_x and $V_x + dV_x$, V_y and $V_y + dV_y$, V_z and $V_z + dV_z$ is

$$dn = n(m/2\pi kT_i)^{3/2} e^{-mV^2/2kT_i} dV_x dV_y dV_z$$

where n is the number of ions per cm^3 and T_i is their temperature. Similarly, the number of molecules per cm^3 with given velocity is

$$dN = N(M/2\pi kT_m)^{3/2} e^{-MU^2/2kT_m} dU_x dU_y dU_z.$$

The number of collisions per cm^3 per sec. between ions and molecules of the above velocities in which the line of centers at impact lies within the solid angle $d\omega$ about the direction D is

$$dndN(V - U) \cdot D\sigma^2 d\omega = dndN(1/\mu) R \cdot D\sigma^2 d\omega$$

where σ is the sum of the radii of ion and molecule. The energy loss per cm^3 per sec. in these collisions of the given type is

$$(2mR \cdot DW \cdot D) \left\{ n(m/2\pi kT_i)^{3/2} e^{-mV^2/2kT_i} dV_x dV_y dV_z \right\} \\ \times \left\{ N(M/2\pi kT_m)^{3/2} e^{-MU^2/2kT_m} dU_x dU_y dU_z \right\} (\sigma^2/\mu) R \cdot D d\omega.$$

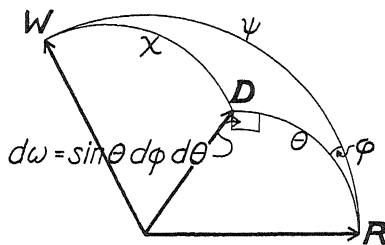


Fig. 1.

D may be expressed in polar coordinates ϕ and ϑ (Fig. 1) with the axis parallel to R and the plane $\phi=0$ containing W . Then

$$d\omega = \sin \theta d\phi d\theta$$

$$R \cdot D = R \cos \theta$$

$$W \cdot D = W \cos \chi = W(\cos \theta \cos \psi + \sin \theta \sin \psi \cos \phi)$$

and the total energy loss per cm^3 per sec. becomes

$$Q = \int_{-\infty}^{\infty} \int_{-\infty}^{\infty} \int_{-\infty}^{\infty} \int_{-\infty}^{\infty} \int_{-\infty}^{\infty} \int_{-\infty}^{\infty} \int_0^{2\pi} \int_0^{\pi/2} (2mnN\sigma^2/\mu) (m/2\pi kT_i)^{3/2} (M/2\pi kT_m)^{3/2} \\ e^{-mV^2/2kT_i - MU^2/2kT_m} R^2 W \cos^2 \theta \sin \theta \\ (\cos \theta \cos \psi + \sin \theta \sin \psi \cos \phi) d\theta d\phi dV_x dV_y dV_z dU_x dU_y dU_z$$

in which R , W , and ψ are all functions of $V_x \dots U_z$.

The integrations with respect to θ and ϕ may be performed immediately. For the remaining six integrations, V and U are replaced by R and W , expressed in polar coordinates. The result is

$$Q = 8(2\pi)^{1/2} n N \sigma^2 k^{3/2} \{mM(mT_m + MT_i)\}^{1/2} (m+M)^{-2} (T_i - T_m).$$

Finally, f , the average energy loss per collision expressed as a fraction of the average energy of the ions, is equal to Q divided by the number of collisions per cm^3 per sec. all divided by the average energy:

$$f = Q / \left\{ \left[n N \pi \sigma^2 \left(\frac{8kT_i}{\pi m} \right)^{1/2} \left(\frac{m}{M} \frac{T_m}{T_i} + 1 \right) \right] \left[\frac{3}{2} kT_i \right] \right\} \\ = \frac{8}{3} \frac{mM}{(m+M)^2} \left(1 - \frac{T_m}{T_i} \right).$$

METHOD OF ENHANCING THE SENSITIVENESS OF
ALKALI METAL PHOTOELECTRIC CELLS

BY A. R. OLPIN

BELL TELEPHONE LABORATORIES

(Received June 6, 1930)

ABSTRACT

A technique is described for sensitizing alkali metal photoelectric cells to light by introducing onto the metal surface small amounts of dielectrics, as oxygen, water vapor, sulphur vapor, sulphur dioxide, hydrogen sulphide, air, sodium bisulphite, carbon bisulphide, etc., or some organic compound as methyl alcohol, acetic acid, benzene, nitrobenzene, acetone, etc., or some organic dye as tropaeolin, rosaniline base, eosin, cyanine, kryptocyanine, dicyanine, neocyanine, etc. The marked increase in electron emission from the cathodes of cells so treated is due primarily to an increase in response to red and infrared light. Vacuum sodium cells have been produced, yielding photoelectric currents as high as 7 microamperes per lumen of white light of color temperature 2848°K and caesium cells yielding far greater currents.

The response of these cells is proportional to the intensity of the exciting light even for light of longer wave-lengths than that to which the cell responded before treatment.

Spectral response curves are similar for all cells using the same metal as cathode. These curves differ from the curves for the pure metal by the appearance of a new selective maximum at lower frequencies. This newly appearing maximum resembles the regular maximum for the untreated metal and is always separated from it by the frequency of a well-known line in the vibration-rotation spectrum of the dielectric molecules, usually the 1.5μ line so characteristic of oxygen-hydrogen, carbon-hydrogen or nitrogen-hydrogen linkages. The long wave limit shifts an amount agreeing with the separation of the maxima.

With a cell so designed that the cathode could be sensitized in a side chamber and then slipped into its proper place (thus keeping the anode free from light-sensitive materials), stopping potentials were obtained for electrons, liberated by monochromatic light, from a sodium cathode before and after treating it with sulphur vapor and air. For light of wave-lengths ranging from $\lambda 3500\text{\AA}$ to $\lambda 8000\text{\AA}$ falling on the treated cathode, the electron retarding potentials are found to vary linearly with the frequency of the exciting light, thus establishing the validity of Einstein's photoelectric equation for composite surfaces. From the slope of the straight line depicting this relationship, the value of Planck's constant h is found to be 6.541×10^{-27} , significant to three figures. An almost identical value is obtained for untreated sodium. The apparent stopping potentials, or voltages at which the photoelectric currents become zero are the same before and after the sulphur and air treatment. The voltage at which the current just saturates is always greater after treatment than before. This is a measure of the change in contact potential of the cathode due to the presence of the sulphur and air. Changes of approximately 0.8 volts are common.

The validity of Einstein's equation precludes the possibility of explaining the new maximum in the spectral response curve for a treated surface by a "Raman shift" of the incident light frequencies, even though the separation of these maxima is equal to certain well-known vibration-rotation frequencies of the dielectric molecules. It may be that the natural frequency of the alkali metal atom is diminished by the vibration frequency of the complex atom in which it is incorporated.

The Lindemann formula for the frequency of the selective photoelectric maximum [$2\pi\nu = (ne^2/mr^3)^{1/2}$], primitive though it seems in the light of modern theory, has always given values for the pure metals in close agreement with experimental determinations. The n term is determined by the valence of the substance, a choice of unity being used for the monovalent alkali metals corresponding to an electron revolving around a singly charged ion. A choice of 2, 3,—for divalent, trivalent,—substances corresponds to electrons revolving around doubly, triply—charged ions. Under certain conditions the alkali metals manifest different valencies, such for instance, as those exhibited in the oxide series Na_2O_2 , Na_2O , Na_3O , Na_4O . These compounds can be prepared in vacuum and are light-sensitive. Spectral response curves for such cells exhibit all the selective maxima called for by the Lindemann formula when the value of n is chosen to agree with the valence of the metal. Data are presented showing this condition to be general for the alkali metals, a maximum response to red or infrared light being dependent upon the formation of a subvalent compound, as a suboxide.

Attention is called to seemingly analogous phenomena in the fields of photoelectricity, photography, fluorescence and absorption.

THE work which culminated in the results to be reported in this paper was inspired by the simple inference that, since photoelectric emission from potassium is greatly increased by a non-conducting hydride film on the surface,^{1,2} some other dielectric film might be still more effective in the same sense. As will be seen the consequences were far-reaching. Not only have far more sensitive photoelectric cells been developed but their characteristics have been studied sufficiently to throw some light on the cause of the increase. Moreover, the results of the rather extensive research suggest plausible explanations of various phenomena in the fields of absorption, photoelectricity, fluorescence and photography.

A. APPARATUS FOR MEASURING PHOTOELECTRIC CURRENTS

The response of photoelectric cells to unresolved light was always measured on a high sensitivity Leeds and Northrup galvanometer, a system of external shunts being used to lower the sensitivity as the magnitude of the photoelectric currents increased. Currents as small as 10^{-10} amperes could be conveniently determined in this way with the instrument on which the largest currents obtainable were measured.

The photoelectron emissions for highly resolved light, represented by the ordinates of the spectral response curves which follow, were measured by a Compton quadrant electrometer using a resistance leak of the order of 10^4 megohms. By suitably adjusting the needle voltage, steady deflections were easily readable for currents as small as 10^{-14} amperes.

The source of light was usually a glowing tungsten filament of horizontal candle power about 70 and color temperature 2848°K . To resolve or disperse this light, a high precision Hilger monochromator was used. Proper corrections for the dispersion of the prism were made. All data plotted in the spectral response curves of this paper represent current per unit energy of the incident light, unless otherwise specified.

¹ Elster and Geitel, *Phys. Zeits.* **11**, 257 (1910).

² K. Moers, *Zeit. Anorg. Chem.* **113**, 179 (1920).

The ordinate values for any one figure are not directly comparable with those of any other.

B. SENSITIZATION OF CELLS WITH VAPORS FROM SULPHUR

1. *Potassium surfaces.* The first experiment with dielectric films on light sensitive cathodes was performed by admitting sulphur vapor to a potassium surface in vacuum. The technique involved in the manufacture of these cells is given here as typical of that for all the cells made and used throughout the series of tests herein reported, except where otherwise specified.

A glass bulb of the shape shown in Fig. 1. was connected to a vacuum pump by means of a distilling tube, in a side chamber of which was a slug of previously distilled potassium. In the center of the cells was a metallic

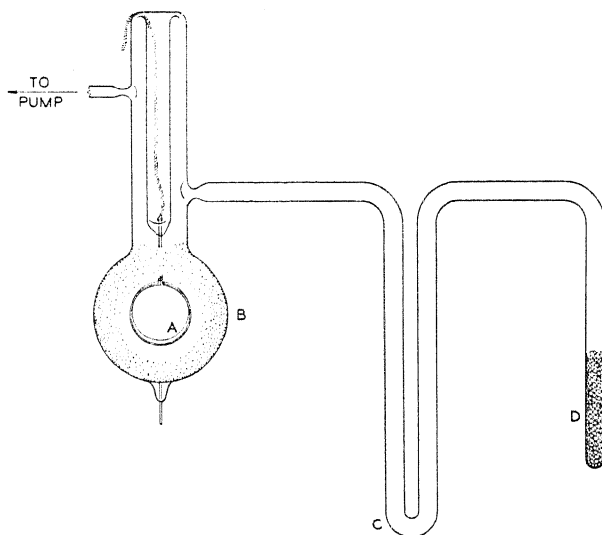


Fig. 1. Experimental type photoelectric cell. *A*-Ring-shaped anode. *B*-Bulb coated on inside with alkali metal to form cathode. *C*-Liquid air trap. *D*-Side arm containing dielectric.

ring *A* with a wire leading through the glass walls to form an anode. A lead-in wire came through the bottom of the cell to make contact with the potassium when it was deposited on the glass walls. A small glass tube *D* containing ordinary commercial flowers of sulphur was sealed onto the stem of the bulb. The U-shaped section *C* of this tube could be immersed in liquid air to trap the vapors coming from the sulphur.

After thorough evacuation of the system, the potassium in the distilling tube was melted and then distilled against the suction of the pump into the glass bulb and a coating made on the inner walls *B*. With a point flame a clear space about one inch in diameter for admitting the exciting light was made on the side of the bulb. As the light fell on the potassium surface, a galvanometer in series with the cell showed that a steady, though limited, emission of electrons was going on. The side tube containing sulphur was then heated and a very small amount sublimed onto the potassium coating.

The pump was left running during this treatment. The galvanometer registered an increased emission of electrons almost immediately and this continued until a certain critical amount of sulphur vapor had come in contact with the surface after which the number of electrons liberated by the light, began rapidly to decrease.

Table I gives a typical history of the treatment of a potassium surface with sulphur vapor, showing the relative current values for two different polarizing voltages at every stage in the process.

TABLE I.

Cathode History	P.E. Current at Cathode Voltages	
	-8	-50
Freshly distilled potassium	34.	38.
After admitting a trace of sulphur vapor	179.	217.
After admitting more sulphur vapor	905.	424.
Incident light diffused by ground glass	542.	542.
Slightly more sulphur admitted	840.	386.
Sulphur tube sealed off	846.	418.
Very low pressure of Argon	1360.	2280.
Argon pressure increased to 0.1 mm	1470.	4120.

It was noted that once the dielectric film began to build up, as shown by a change in the surface color, the current values were larger at low voltages than at high. This has been quite generally observed with this type cell, the voltage-current curves showing a maximum sometimes at cathode voltages as low as -5 volts. This maximum disappeared with the introduction of argon into the cell, and a general increase in measurable current even at low voltages was noted. A typical series of voltage current curves for a potassium surface treated with sulphur vapor is shown in Fig. 2. Another series for a rubidium cell similarly treated is reproduced in Fig. 3. The irregularities exhibited in these curves could be smoothed out by focusing the incident light on the side of the cell rather than the back, or by passing it through a diffusing glass. This suggested that they were due to the shape or design of the tube, an interesting observation which will be further discussed in a later section of this paper.

TABLE II.

Color of exciting light	EK filter used	KSH cell	KS cell	KH cell
White	None	374	374	374
Violet	#76	11	11	20
Blue	#78	93	101	132
Green	#60	59	85	44
Yellow	#16	120	72	9
Red	#29	58	11	1

It developed early in the work that the photoelectric emissions from potassium surfaces treated as described above were not only greater than those of potassium hydride cells for unresolved light, but the response to red light was decidedly larger. Even more striking results of this character were

obtained in some cases by flashing hydrogen on the surface treated with sulphur. Table II illustrates the relative sensitivities to colored light on a scale in which the emissions under the action of total light are made equal. The letters used to describe the cells refer to the elements known to be present at the cathode surface.

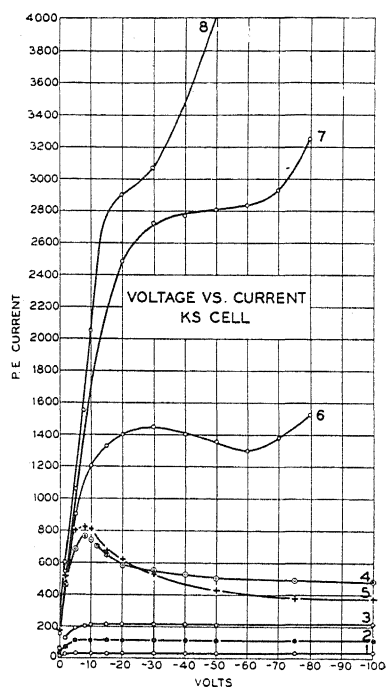


Fig. 2.

Fig. 2. Voltage-current curves for different stages in the manufacture of a potassium-sulphur vapor photoelectric cell. 1—For pure potassium cathode. 2—5—After successive treatments with sulphur vapor. 6—8—After successive admission of increasing pressures of argon.

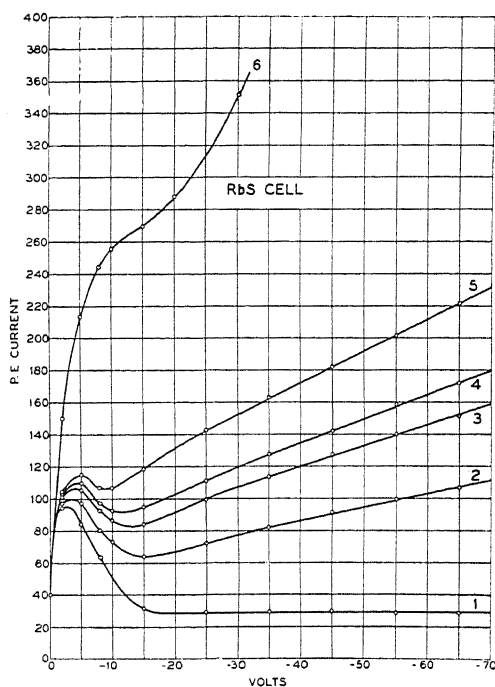


Fig. 3.

Fig. 3. Voltage-current curves for a rubidium-sulphur vapor photoelectric cell containing different pressures of argon. 1 Vacuum condition. 2—6 Argon pressure gradually increased.

The color temperature of the constant light source used in the preparation of this table was not known, but Fig. 4 shows the relative sensitivities of KH and KS cells to white light of color temperature 2848°K. The new cells were very stable and showed little change in emission upon aging, the tendency being rather frequently to increase slightly in sensitivity during the first few days after sealing off the pump. In Fig. 5 are plotted some curves showing relative sensitivities throughout the spectrum. These curves, taken with spectrally resolved light, are corrected so that the ordinates, representing current per unit of light energy incident on the surface, are equal at the selective maxima.

It will be noted that the large selective maximum for each of these curves lies in the blue-violet region of the spectrum but that the maximum for the potassium-sulphur cell is slightly displaced toward shorter wave-lengths. The long wave end of the curves for this cell can be represented as an amplified sensitivity curve for pure potassium plus an additional curve representing a new maximum symmetrically drawn about 6200Å. This maximum could be greatly enhanced by proper treatment and its importance should not be overlooked. It falls in that portion of the spectrum where the energy content of radiations from most illuminating systems is large, and its pres-

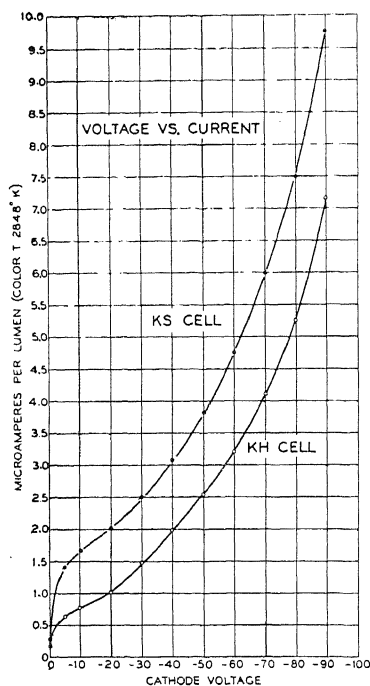


Fig. 4.

Fig. 4. Relative sensitivities of potassium-sulphur vapor and potassium-hydride photoelectric cells.

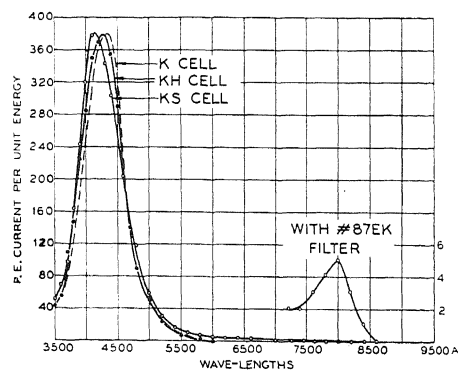


Fig. 5.

Fig. 5. Spectral response curves for potassium, potassium-hydride and potassium-sulphur vapor photoelectric cells.

ence figured strongly in increasing the response of a cell to white light. Further discussion of this part of the curve will be reserved for a subsequent section of this paper.

2. *Rubidium and caesium surfaces.* Encouraged by the increase in response to red light manifested by potassium cells treated with sulphur vapor, the same treatment was applied to rubidium and caesium. Since the selective maxima³ and the long wave limits⁴ for these two alkali metals are or-

³ F. Gross, *Zeits. f. Physik* 7, 316 (1921).

⁴ B. Gudden, "Lichtelektrische Erscheinungen" p. 40 Julius Springer, Berlin (1928).

dinarily found at greater wave-lengths than for potassium, it was thought that surfaces of these metals, treated as above, should yield electrons more freely than potassium when excited by red or infrared light. However, disappointment in this respect attended all early efforts, presumably because the low melting points and high vapor pressures of rubidium and caesium would not permit the formation of a definite surface structure. The results illustrated for a treated caesium film in Fig. 6, differ only from what would be expected with a pure caesium film by the presence of a maximum between 5000Å and 5500Å. This is the wave-length region at which caesium in bulk form has been observed to manifest a selective maximum.⁵

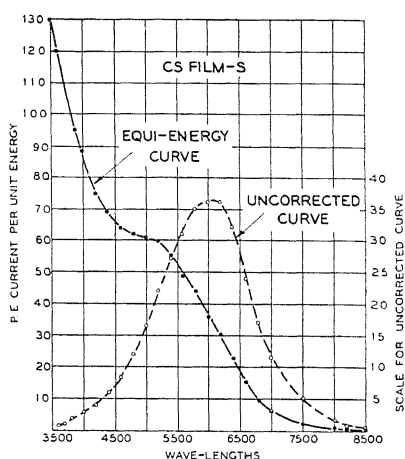


Fig. 6.

Fig. 6. Spectral distribution of sensitivity for a caesium film on magnesium plus sulphur vapor.

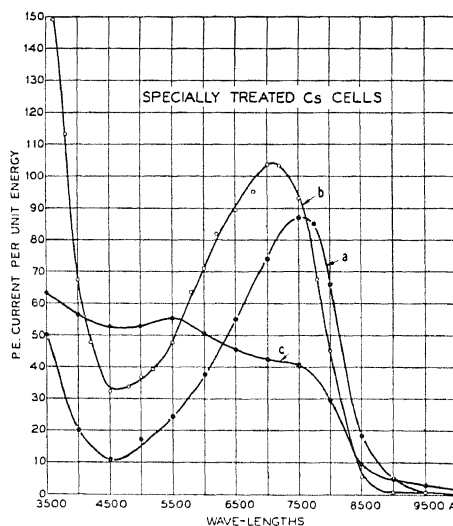


Fig. 7.

Fig. 7. Spectral distribution of sensitivity for a specially treated caesium photoelectric cell. Curves (a) and (b) were obtained from cells treated to give maximum response to red light. Curve (c) was obtained on a similar cell having less red sensitivity.

Early difficulties in treating caesium surfaces effectively with gases have in great measure been overcome by subsequent development of a technique for controlling the amounts of the various constituents which make up the cathode, so as to form the proper compounds. The rather remarkable results obtained with these cells supplement the data contained in this paper and will constitute the subject of a later publication. Suffice it to say that the photoelectric yield for properly treated caesium cathodes is almost entirely due to a marked response to deep red and infrared light, as shown in Fig. 7.

⁵ E. F. Seiler, *Astrophys. J.* 52, 3, 129 (1920).

3. *Sodium surfaces.* The difficulties which arose in connection with the manufacture of rubidium and caesium cells suggested the advisability of using sodium as the photosensitive material. It was found in fact that when sodium was treated similarly with sulphur vapor, photoelectric cells were evolved having much greater sensitivity than the potassium-sulphur cells previously described. Moreover, the cause of this was found to be increased response to light at the long wave end of the visible spectrum and in the infrared.

Fig. 8 shows a typical curve giving photoelectric current per unit of exciting light energy for such a cell throughout the spectrum. The maxi-

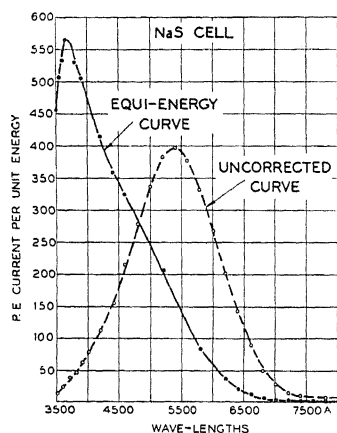


Fig. 8.

Fig. 8. Spectral response curve for a sodium-sulphur vapor cell. The broken curve is a plot of actual electrometer readings.

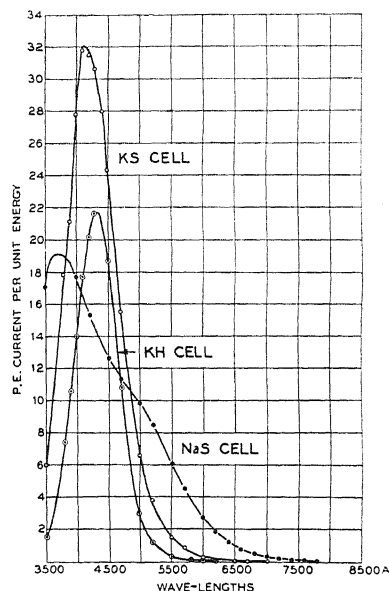


Fig. 9.

Fig. 9. Relative sensitivity of potassium hydride, potassium-sulphur vapor and sodium-sulphur cells throughout the spectrum.

mum at $\lambda 3600\text{Å}$ should probably appear at a slightly shorter wave-length as it is likely that some absorption of the incident light by the glass walls of the cell occurs below $\lambda 3800$ or 4000Å . However, the fact that Richardson and Compton⁶ found this maximum at $\lambda 3600\text{Å}$, and Pohl and Pringsheim⁷ at $\lambda 3400\text{Å}$ shows that the peak had not been shifted appreciably by the treatment with sulphur vapor. It was the appearance of a new maximum at approximately $\lambda 4800\text{Å}$ that was most significant. In Fig. 9 are found three curves comparing the spectral response of a sodium-sulphur cell with that of two types of potassium cell.

⁶ O. W. Richardson and K. T. Compton, *Phil. Mag.* 26, 549 (1913).

⁷ R. Pohl and P. Pringsheim, *Verh. d. D. Phys. Ges.* 14, 46 (1912).

By applying a point flame momentarily near the edge of the cell window and temporarily producing a vapor of the sodium and the gas occluded on it, a startling increase in sensitivity was brought about. The response of the surface to white light of color temperature 2848°K after this last treatment was about double that observed before. Moreover, the increase was again chiefly in the red and infrared regions, as shown in Fig. 10. The new spectral emissivity curve could be broken up into a regular curve for sodium greatly amplified plus a new curve with a pronounced maximum at approximately

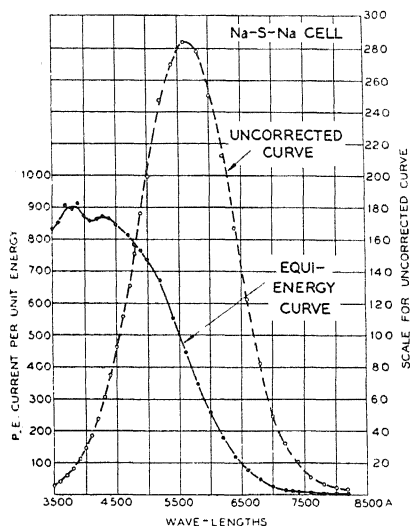


Fig. 10.

Fig. 10. Spectral response curve for sodium-sulphur vapor cell after deposition of a film of the mixture on the surface.

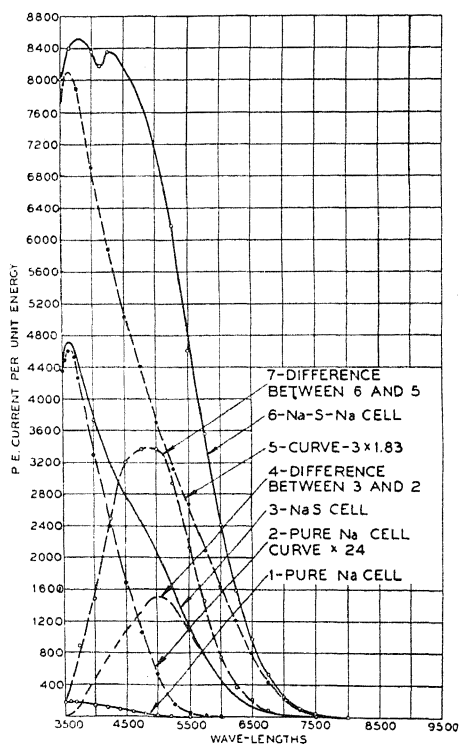


Fig. 11.

Fig. 11. Curves analyzing the increased sensitivity of sodium-sulphur vapor cells throughout the spectrum.

$\lambda 4800\text{Å}$. In Fig. 11 is found a record of the spectral distribution of emissions for each step in the sensitizing process.

At this stage in the development of these cells, air at atmospheric pressure was admitted onto the surface. Upon re-evacuation the cell showed absolutely no response to light of any color. By applying a point flame near the edge of the cell window momentarily and producing a vapor of sodium plus the adsorbed gases, a film deposited on the cathode surface which was strikingly sensitive to light. This experiment has been repeated with many

cells and the same effect always occurs. It appears that the effect is a broadening of the new selective maximum on the long wave side with a shift of the long wave limit to approximately 1μ , as shown in Fig. 12. Fig. 13 shows that

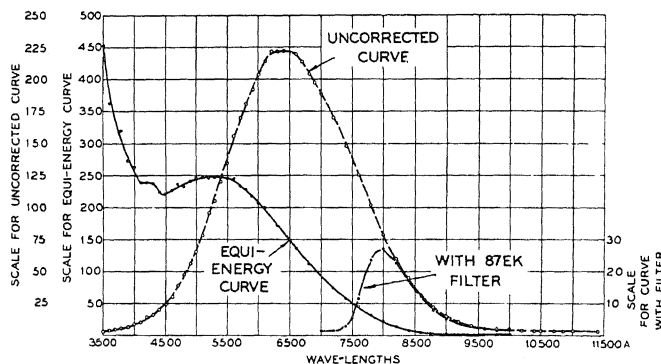


Fig. 12. Curves showing spectral distribution of sensitivity and long wave limits for sodium-sulphur-air cell. Actual electrometer readings are plotted in the broken curve, and current per unit energy in the so-called equi-energy curves.

pure Na surfaces can be sensitized to light of long wave-lengths by air and oxygen alone, but comparison with Figs. 12 and 14 indicates the advantage of the presence of sulphur vapor.

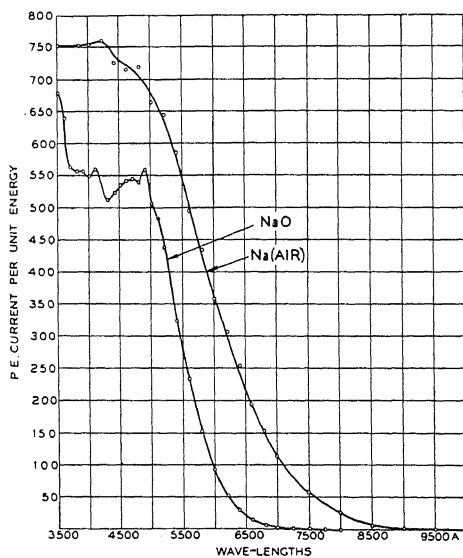


Fig. 13. Spectral response curves for sodium photoelectric cells treated with oxygen and air alone.

In Fig. 15 are given voltage-current curves for a typical potassium cell treated with sulphur vapor, a sodium cell similarly treated, another such

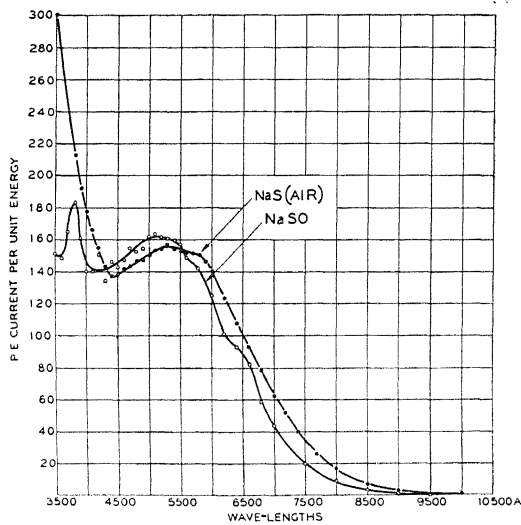


Fig. 14. Spectral distribution of sensitivity for sodium cells treated with sulphur and oxygen, and sulphur and air.

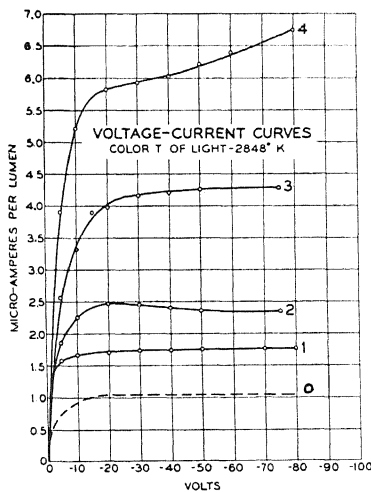


Fig. 15.

Fig. 15. Voltage-current curves for five different types of vacuum photoelectric cells when irradiated with light of color temperature 2848°K. 0—Potassium hydride cell. 1—Potassium-sulphur vapor cell. 2—Sodium-sulphur vapor cell. 3—Sodium-sulphur vapor cell with film on cathode. 4—Sodium-sulphur-air cell.

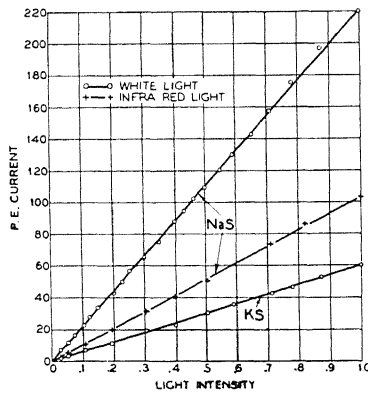


Fig. 16.

Fig. 16. Showing proportionality of response of sodium and potassium-sulphur vapor cells to white light and to infrared light.

sodium cell with a thin film deposited on top of the dielectric, and finally a sodium cell treated with both sulphur vapor and air as described above. None of these cells were gas filled so the ordinates represent true emissions from the surface. These emissions are in terms of microamperes per lumen, and the color temperature of the exciting light was 2848°K.

C. PROPORTIONALITY OF RESPONSE TO LIGHT

The relationship between the light intensity and photoelectric current was checked over an extensive range for both potassium and sodium surfaces sensitized by the methods described above. The results are depicted by the straight lines in Fig. 16. The variations in light intensity were effected by moving the lamp source along a photometer track. The measurements were made on a Compton electrometer, using the steady deflection method. The same linearity of response was noted when using a No. 87 EK filter (visually opaque) in the path of the light. This filter transmitted only light of greater wave-length than that to which the pure metals respond.

D. ATTEMPTS TO IDENTIFY THE ACTIVATING GAS IN THE VAPORS FROM SULPHUR

The words "sulphur vapor" have been used advisedly in the foregoing presentation, for it was early discovered that the actual sublimation of sulphur onto the surface was not essential. In fact, equally good cells were made with only the volatile gases liberated from sulphur on heating. These gases could be held in a liquid air trap between the sulphur and the cell, and then by lowering the liquid air flask properly, the amount of gas actually entering the coated cell could be accurately controlled.

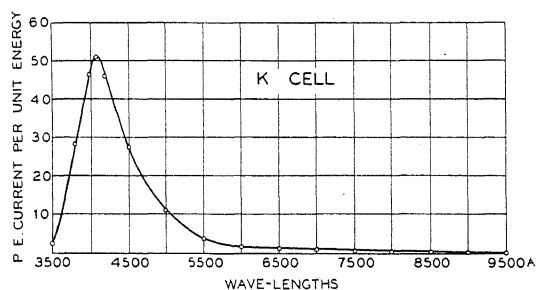


Fig. 17. Spectral response of a potassium photoelectric cell into which an unnoticeably small amount of vapor from sulphur had passed.

A surprising observation was that vapor in such small quantities as to be scarcely detectable with an ionization manometer gauge began to increase the sensitivity as soon as it entered the cell. In a way this was a fortunate discovery, for the amount of gas actually occluded or contained in commercial flowers of sulphur was decidedly small. Yet when a potassium cell with a side arm containing sulphur was sealed off the pump station, and a curve taken showing the spectral distribution of response to light (Fig. 17),

there was appreciable sensitivity out to 1μ . Evidently some gas had been liberated from the sulphur, but the amount was too small to be detected. This emphasizes the importance of taking added precautions against the presence of gas on surfaces to be used in determining the long wave limits of pure alkali metals, and suggests the likely cause for the wide discrepancies sometimes found in literature.

The question as to the nature of the activating gas contained in sulphur was a challenging one since that gas was present in such small quantities.

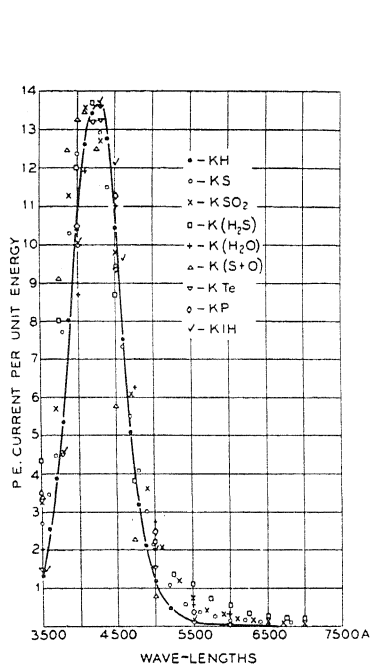


Fig. 18.

Fig. 18. Spectral response of potassium photoelectric cells, the cathodes of which were treated respectively with hydrogen, sulphur vapor, sulphur dioxide, hydrogen sulphide, water vapor, oxygen and sulphur vapor, tellurium vapor, phosphorous vapor and iodine vapor. The ordinates at the maximum are made equal.

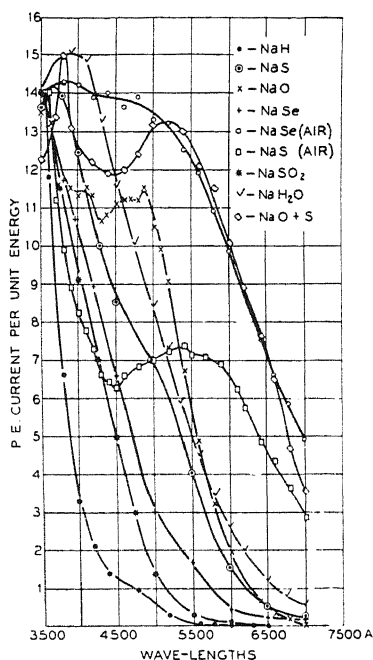


Fig. 19.

Fig. 19. Spectral distribution of sensitivity of sodium photoelectric cells treated with hydrogen, sulphur vapor, oxygen, selenium vapor, sulphur-dioxide, water vapor, oxygen and sulphur, and selenium and sulphur with air. These curves are corrected to correspond at approximately 3500 Å.

It certainly was not air, hydrogen, nitrogen or oxygen, for these gases could not be condensed at liquid air temperatures. It therefore seemed plausible to suppose that it was water vapor, hydrogen-sulphide or sulphur-dioxide; and direct tests were made to find how these gases act.

A large number of potassium and sodium cells were made, the coating of each being treated with one of the mentioned gases. All of the spectral response curves for potassium cells had selective maxima in the blue at

approximately the same wave-length, and the long wave limit did not vary appreciably from one cell to another. The gas producing results on potassium most nearly like those observed when using sulphur vapor was SO_2 , the only one to give the bright golden color and the one producing the most sensitive surfaces to unresolved light.

In Fig. 18 curves depicting the spectral distribution of electron emission are given for potassium cells sensitized with sulphur vapor, sulphur dioxide, hydrogen sulphide, water vapor, sulphur vapor plus oxygen, tellurium vapor, phosphorous vapor and iodine vapor. In all these cases it will be noticed that the selective maximum appeared at approximately the same wave-length, but generally was shifted to somewhat smaller values when sulphur

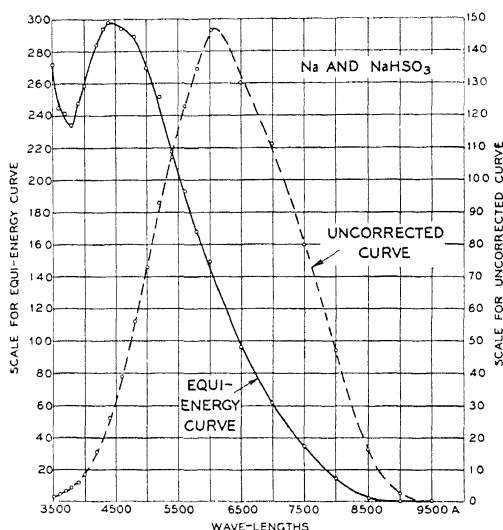


Fig. 20. Spectral response of sodium cell treated with sodium-bisulphite vapor.

was present in the activating gas. We thus find nothing to support Wiedmann's idea⁸ that the position of the maximum varies with the nature of the gas. It may be, however, that the relative *magnitudes* of the newly appearing maxima are influenced by the composition of the surface films.

With sodium the different gases produced markedly different curves (Fig. 19) and this gives us a better chance of identifying the vapor proceeding from the sulphur. In this case, it turned out that water vapor yielded the curve most resembling that due to the sulphur vapors, and incidentally colored the surface with a similar tint (dull grey); while sulphur dioxide alone provided a very different curve.

There seemed only one conclusion to draw from these tests. The activating vapor liberated from commercial flowers of sulphur must have been

⁸ G. Wiedmann, Verh. d. D. Phys. Ges. 16, 343 (1915).

a combination of water vapor and sulphur dioxide,⁹ and the dielectric films formed must have been sodium and potassium bisulphites. This conclusion seemed the more plausible when it was recalled that the sulphonc radical $\text{SO}_2 \cdot \text{OH}$ is an important radical in many organic dyes, and that investigators in the Eastman Research laboratory have succeeded in sensitizing photographic plates to light well into the infrared by the use of sodium bisulphite NaHSO_3 .¹⁰ A sodium cell was therefore made substituting sodium bisulphite for sulphur, and the spectral response of this cell (Fig. 20) was very similar to that obtained with sulphur and air. Moreover, the response was in almost identically the same spectral region to which the photographic plate treated with NaHSO_3 responded. The close correlation between these results in the fields of photoelectricity and photography suggests a common cause of the red sensitivity.

E. SENSITIZATION OF SODIUM AND POTASSIUM SURFACES BY ORGANIC DYES

There was no reason to suppose that sodium bisulphite is the only substance used in photography which could be applied in photoelectricity. Accordingly, other sensitizing dyes were introduced onto the light sensitive surfaces of alkali metals, and marked increases in photoelectric emission noted. In every case the amount of dye required was very small, as in plate sensitizing. The colors appearing on the cathode surfaces especially when thin films of sodium and potassium were added on top of the already treated surfaces were varied and beautiful.

Some of the side tubes containing the dyes had to be immersed in liquid air to prevent vaporization with possible decomposition under action of the pump. Others had to be warmed before they sublimed, and in such cases it is not only possible but likely that partial chemical decomposition occurred. In fact, Herndon and Reid's¹¹ study of the decomposition products of various alcohols, organic acids, acetates, benzenes, phenols, etc. upon heating to 400° suggests that the more complicated compounds break up into simple ones at considerably lower temperatures. Nevertheless, the well-known organic radicals which produce the absorption bands in the visible region, as the methyl group CH_3 , the nitroxyl group NO_2 , the amido group NH_2 , the bromine group, the methoxyl group CH_3O , the carboxyl group $\text{CO} \cdot \text{OH}$ and the sulphonc group SO_2OH , and many others probably are fairly stable.

The first dyes used contained the sulphonc radical and are not commonly used in photography. They were kept in a side tube beyond a liquid air trap, and heated after the alkali metal coating was made. When they were first heated, some gas passed through the liquid air trap into the cell and was

⁹ More recently Dr. G. T. Kohman of the Bell Telephone Laboratories has made a very ingenious analysis of the gases evolved from flowers of sulphur on heating and found water vapor and sulphur dioxide to be contained in greatest amounts, with also considerable hydrogen sulphide.

¹⁰ Capstaff and Bullock, *Brit. J. Phot.* **67**, 719 (1920).

¹¹ L. R. Herndon and E. E. Reid, *J.A.C.S.* **50**, 3066 (1928).

pumped out. This was probably nitrogen, hydrogen, or dry oxygen, or possibly some hydrocarbon compound, for it did not react with the alkali metal. The gas retained in the liquid air trap was very effective in sensitiz-

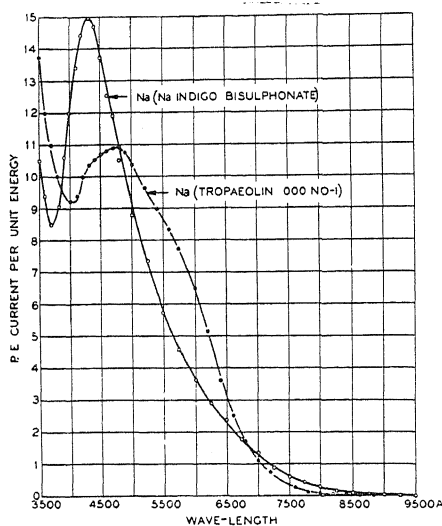


Fig. 21. (a) Spectral response curves for sodium photoelectric cells treated with the vapors of tropaeolin 000 No. 1 and sodium indigo disulphonate.

ing the metallic surface of the cell when allowed to enter in small quantities. A very thin film of the alkali metal deposited on the colored surface always enhanced the emission. In Fig. 21(a) are curves showing the response, in

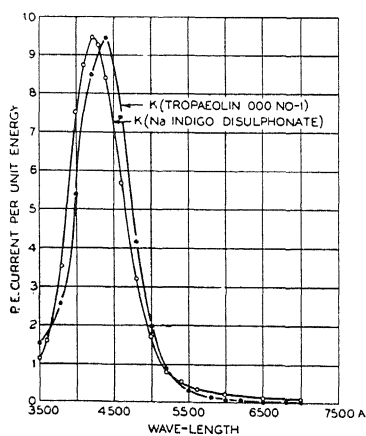


Fig. 21. (b) Spectral response curves for potassium photoelectric cells treated with the vapors of tropaeolin 000 No. 1 and sodium indigo disulphonate.

the visible and infrared, of sodium cells treated with the isomeric compounds tropaeolin 000 No. 1 [$\text{HO} \cdot \text{C}_{10}\text{H}_6 \cdot \text{N} : \text{N} \cdot \text{C}_6\text{H}_4 \cdot \text{SO}_3\text{Na}$] and sodium indigo disulphonate. Both compared favorably with the sodium-sulphur air cells

described in a previous section. Curves for the corresponding potassium coated cells, using these dyes, are given in Fig. 21(b).

To determine whether or not the sensitizing action was limited to compounds containing sulphur, a cell was made with rosaniline base $[\text{OH} \cdot \text{C}$

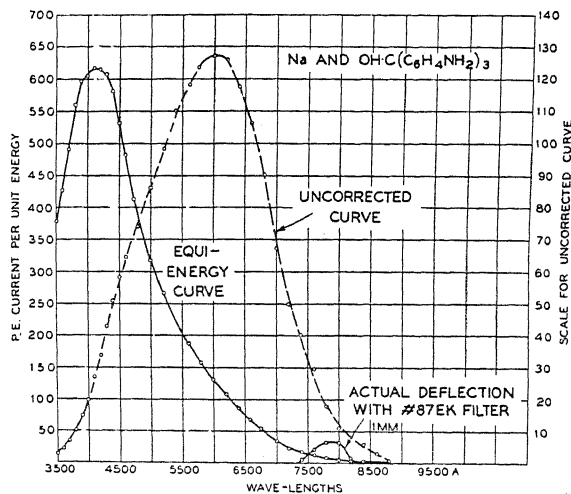


Fig. 22. Spectral response curve for a sodium cell treated with rosaniline base.

$(\text{C}_6\text{H}_4\text{NH}_2)_3]$ and a sodium coating. Although no sulphur was contained in this compound, the surface treated showed a good response to light throughout the visible and near infrared, as shown in Fig. 22.

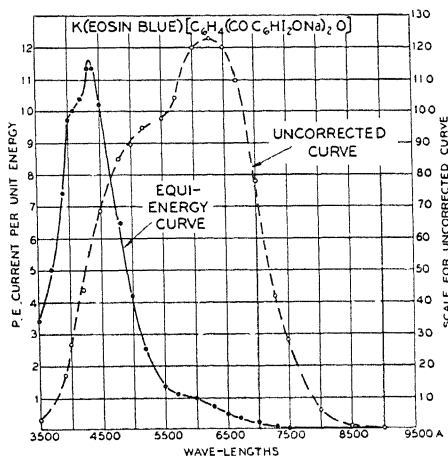


Fig. 23. Spectral response curve for a potassium photoelectric cell treated with eosin blue.

The remainder of the experiments to be reported in this section involve sensitizing dyes used in photography. Because of its historical importance, (it was first used to sensitize photographic plates to green and yellow light

in 1882) eosin [$C_6H_4(COC_6H_4ONa)_2O$] was tried first. Although it brought about a decided increase in sensitivity, it was not so satisfactory as many

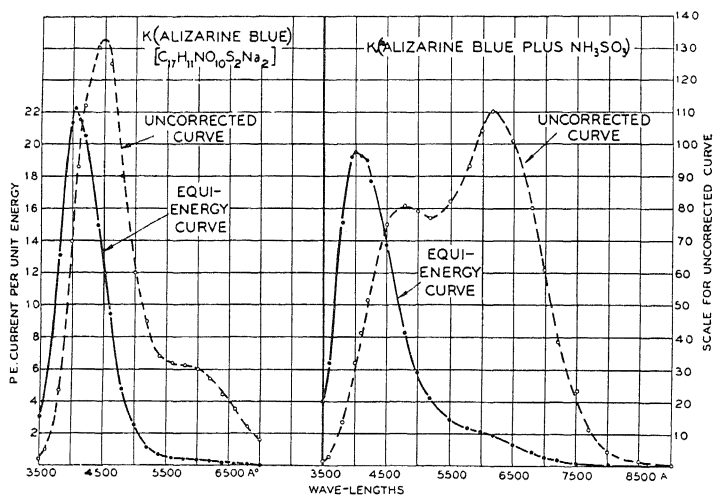


Fig. 24. (a) Spectral response curves for a potassium photoelectric cell treated with alizarine blue alone and one treated with alizarine blue plus ammonium sulphite.

others. In Fig. 23 is reproduced a spectral distribution curve for a potassium-eosin cell, showing the presence of the new maximum at longer wave-lengths very strikingly. The peculiar shape of the regular selective maximum will

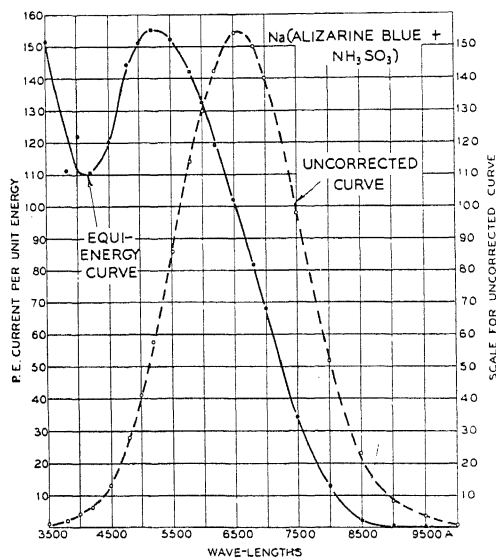


Fig. 24. (b) Spectral response curve for a sodium photoelectric cell treated with alizarine blue and ammonium sulphite.

be cited again in the discussion to follow. There appears to be a new peak at a slightly shorter wave-length.

Some have claimed astonishing results in sensitizing photographic plates to red by using alizarine blue [$C_{17}H_{11}NO_{10}S_2Na_2$];¹² and plates treated in addition with ammonia, have been reported sensitive out to about 1μ . In Fig. 24(a) is found a typical photoelectric emission curve for a potassium coating treated with alizarine blue and another curve for potassium treated also with the vapor from ammonium sulphite (NH_4SO_3). In Fig. 24(b) is a curve for sodium similarly treated. These curves show a response to light of all wave-lengths under 1μ , with the new maxima appearing at the same position as for the sulphur vapor cells. Here again is a close correlation between results obtained in the sensitizing of photoelectric cells and photographic plates.

Similar results attended the use of dicyanine, especially with addition of ammonium sulphite, and other dyes carrying the latter part of the same word

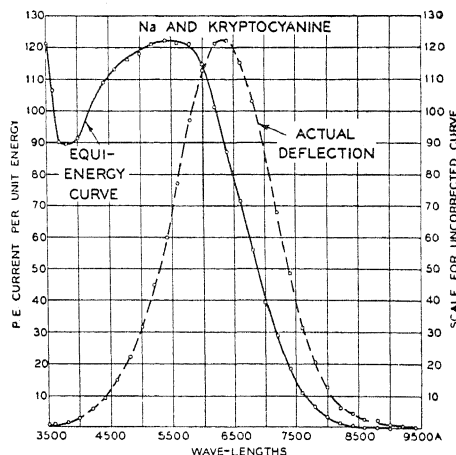


Fig. 25. Curve showing strikingly broad selective maximum in the spectral response curve for a sodium photoelectric cell treated with kryptocyanine.

in their trade names, as kryptocyanine and neocyanine. The spectral regions wherein these dyes are effective sensitizers of photographic plates is published in communication No. 255¹³ of the Eastman Research Laboratories where the latter two dyes were developed. Kryptocyanine should be better in the near infrared than dicyanine which in turn should be better than cyanine ($C_{29}H_{35}N_2I$). All of these indications were borne out on photoelectric cells, the dicyanine causing a greater electron emission from alkali metal surfaces than cyanine, and very small amounts of kryptocyanine producing one of the broadest selective bands so far observed in the spectral distribution curve for sodium cells. This last mentioned curve is found in Fig. 25.

F. SENSITIZATION BY COLORLESS DIELECTRICS

The position of the new maximum seems to be characteristic of the light sensitive metal and not the dielectric on its surface. It appeared likely,

¹² Scoble, Phot. J. **46**, 190 (1906).

¹³ M. L. Dundon, A. L. Schoerr, R. M. Briggs, J.O.S.A. and R.S.I. **12**, 397 (1926).

therefore, that any dielectric regardless of the peculiarities of its absorption spectrum, might bring out such a maximum. To test this, various colorless dielectrics and dielectrics practically transparent to visible light were substituted for the dyes. Most of these were liquids, but their vapors could easily be held in side tubes by means of liquid air. The technique employed in applying them was identical to that for the dyes.

Acetone ($\text{CH}_3 \cdot \text{CO} \cdot \text{CH}_3$), *acetic acid* ($\text{C}_2\text{H}_4\text{O}_2$), *carbon bisulphide* (CS_2), *methyl alcohol* (CH_3OH), *carbon tetrachloride* (CCl_4), *benzene* (C_6H_6), *chloroform* (CHCl_3), *phenyl mustard oil* ($\text{C}_6\text{H}_5\text{-N-C=S}$), *nitrobenzene* ($\text{C}_6\text{H}_5\text{NO}_2$), and *water-vapor* (H_2O) were used with more or less success. And surprising though it may seem, benzene and water vapor were the most effective, the red sensitivity of sodium surfaces properly treated with them being especially

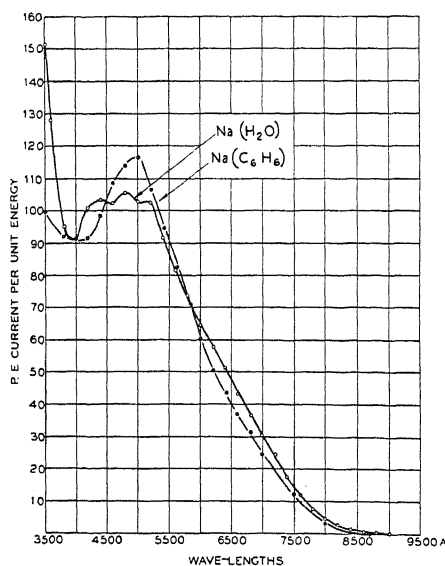


Fig. 26. Spectral response curves for sodium photoelectric cells treated with water vapor and with benzene.

marked, as shown in Fig. 26. There was absolutely no evidence of chemical action when benzene was admitted to the cell, even though a thin film of sodium was deposited on top of it. In fact, the surface of the completed photoelectric cell looked exactly like that of pure metallic sodium. This, of course, is not surprising since the alkali metals are preserved in benzene, but is cited here as evidence of the chemical purity of the sample used. In quite striking contrast to the behavior of benzene on sodium was that of water vapor, whose powerful affinity for the alkali metals makes it necessary to preserve them in benzene, oil, or sealed air-tight containers. Yet benzene and water vapor were alike in being able to increase photoelectron emissions from sodium and potassium surfaces.

In every case mentioned in the preceding paragraph, except that of CCl_4 , an appreciable amount of sensitivity to red was developed. Moreover, the

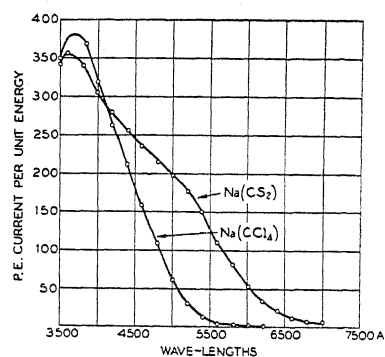


Fig. 27. Spectral response curves for sodium photoelectric cells treated with carbon bisulphide and with carbon tetrachloride.

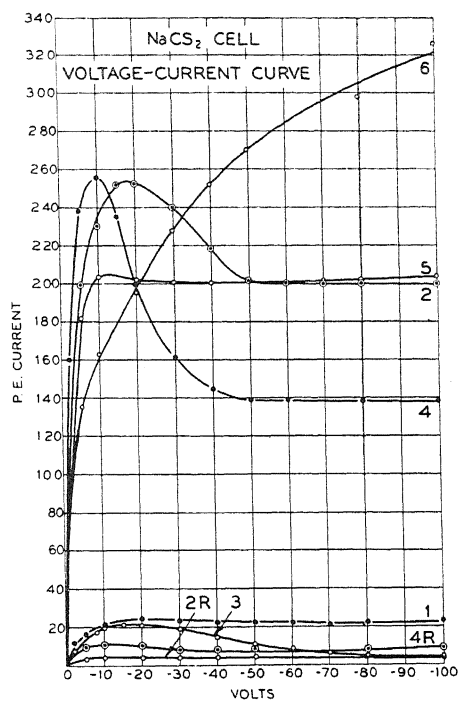


Fig. 28. Peculiarities noted in voltage-current curves for a sodium-carbon bisulphide photoelectric cell. 1—Supposedly pure sodium. 2—After first introduction of CS_2 on sodium surface. 2R—Same as 2 but for irradiation with red light only. 3—After additional CS_2 was introduced onto the surface. 4—After a film of sodium had been deposited from near the cell window. 4R—Same as 4 but for illumination with red light only. 5—Light focussed on cathode opposite cell window. 6—Light focussed on cathode adjacent cell window.

spectral distribution curves show evidence of a new maximum in the photoelectric emission curve near $\lambda 4800\text{\AA}$ for sodium and a much less pronounced peak at approximately $\lambda 6200\text{\AA}$ for potassium. When carbon tetrachloride was used no deflection of the galvanometer was observed when the exciting light was passed through a red filter, cutting out all wave-lengths under 6000\AA . In Fig. 27 are plotted wave-length vs. current curves for sodium surfaces sensitized with carbon tetrachloride and carbon bisulphide.

When working with carbon bisulphide (CS_2) and nitrobenzene ($\text{C}_6\text{H}_5\text{NO}_2$) the previously described peak in the voltage-current curve at low voltages was strikingly prominent. At one time during the treatment of sodium with CS_2 the current output with the cathode 15 volts negative was four to five times its value when this voltage was increased to 100 volts. A record of the change in shape of these curves as the sensitization process was carried out is included in Fig. 28. These will be discussed with those in Fig. 2 and 3 in the next section.

G. DISCUSSION OF RESULTS

A great mass of data has been presented. It now remains to be seen whether or not they can be correlated and interpreted. In all, over two hundred photoelectric cells involving the principles and technique herein discussed have been made, and most of them carefully studied. The collection of curves presented in the preceding sections of this paper may or may not in

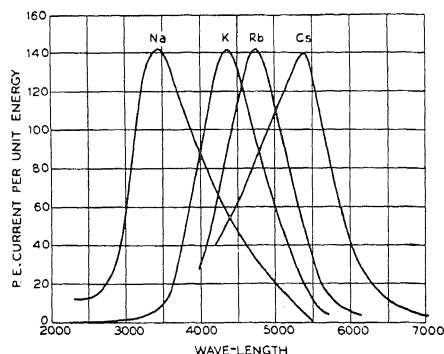


Fig. 29. Spectral response curves for the alkali metals. Curves for sodium and potassium reproduced from Pohl and Pringsheim⁷ and those for rubidium and caesium from Miss Seiler.⁵

every case refer to the best cell which could possibly be made with the stated materials; but they do display the properties of the cell when made according to the best technique at that time known.

A survey of the data presented in the form of spectral response curves revealed that the properties of the cells depended very much on the metal, very little on the dielectric. As pointed out previously (Fig. 11) each curve could be represented as the sum of the "regular" curve for the pure metal and a second curve with a maximum at longer waves. Only the *relative magnitudes* of the ordinates of these two curves seemed to be a function of the

dielectric. The so-called "regular" curves for the pure alkali metals are shown in Fig. 29. Each one will be seen to resemble a resonance curve, the area underneath being more or less symmetrically located on either side of the wave-length of light producing the greatest photoelectric current. These curves are not alone characteristic of the multiply distilled metals, but are also characteristic of these metals after a glow discharge has been passed through hydrogen at a pressure of a few millimeters on the surface. This fact caused Pohl and Pringsheim¹⁴ to refer to the metallic hydride surfaces as colloidal metal surfaces and attribute the increased response of such surfaces to light to the greater ease with which electrons might escape from tiny globules. This same fact caused Hallwachs and Wiedmann¹⁵ to claim that the photoelectric effect was a gas-metal phenomenon and that the maxima in the curves shown in Fig. 29 were dependent on the presence of hydrogen. At this stage in our discussion it is the *existence* of these maxima in the "regular" curves rather than the *cause* to which attention is called.

The "second" curve referred to above appeared as the "regular" curve shifted to longer wave-lengths. The amount of this shift was approximately the same for all cases excepting the ones in which sulphur or selenium plus oxygen or air and certain organic dyes, as kryptocyanine, were among the activating agents, in which cases it was somewhat greater, and the new maximum broader, as illustrated in Fig. 19. Slight variations in the separations of the two maxima, when several dielectrics were used, were dependent on the relative amounts of the different materials.

1. *Role of water vapor.* This analysis of the spectral response curves suggested that there is a single activating agent common to all the dielectrics introduced onto the alkali metal surfaces, with the possibility of one or more others in a few cases. Certainly it must be conceded that water vapor may have been present in every case. Every effort was made to eliminate it, the glass bulbs being carefully and thoroughly heated during the evacuating process. But, as mentioned earlier, the substances which were evaporated or sublimed onto the cathodes may have contained water. The glass tubes containing them could not be heated sufficiently to drive out all moisture before the alkali metal coatings were made. With liquids, it was necessary to immerse the side arm containing them in liquid air to keep them from evaporating and being pumped out. Moreover, the bulky, complex organic dye compounds usually occur in the form of very fine crystalline granules, undoubtedly containing water in small quantities. Some of the substances may have decomposed with formation of water vapor. There was no assurance that the samples of liquid dielectrics were absolutely water free, even though they were obtained from a reliable chemical house as certified chemically pure material. Take, for instance, benzene, a liquid easily obtained as "chemically pure" yet Manley¹⁶ reports experiments which seem to

¹⁴ R. Pohl and P. Pringsheim, *Verh. d. D. Phys. Ges.* **13**, 219 (1911); *Verh. d. D. Phys. Ges.* **15**, 173 (1913).

¹⁵ G. Wiedmann and W. Hallwachs, *Verh. d. D. Phys. Ges.* **16**, 107 (1914); G. Wiedmann, reference 8.

¹⁶ J. J. Manley, *Nature* **123**, 907 (1929).

indicate that benzene, when exposed to air, takes up moisture and holds it tenaciously. Certainly, the difficulties involved in handling liquids in an evacuated system make it impossible to eliminate water vapor altogether from the system.

Although the amount of water that could have been present with the dielectric was admittedly always small, it may not have been negligible. As a matter of fact, many of the experiments seemed to indicate that even *minute traces of moisture* were sufficient to sensitize alkali metal surfaces. One experiment consisted in sealing an empty glass tube on the side of a bulb and then during the pumping process immersing the tube in liquid air. After the bulb was coated, mere removal of the liquid air from the side tube permitted sufficient moisture to fall onto the metal coating to increase its response greatly. The characteristic of such a sensitized surface could be represented by the spectral response curve of Fig. 26. However, the total emission was not nearly so great as in the case of the cells containing sulphur vapor or organic dyes. It appeared, therefore, that the presence of water vapor in small quantities may have been advantageous, but was certainly not alone responsible for the whole of the observed increase in the photoelectric effect.

Perhaps the water vapor present with some such dielectric as sulphur was taken up as water of crystallization as alkali metal sulphides or sulphates were formed on the cathode surface. It is rather significant in this respect that the oxides, sulphides and sulphates of sodium and potassium quite generally hydrate if water is present, and the appearance of these hydrated crystalline forms resemble those of the photoelectric cell cathodes prepared as described earlier in this paper.¹⁷ This indicates that the surface films may have a definite configuration and the molecules a regular alignment, which really would be expected, for polar compounds in general are favorable to association, and this, as Gerlach¹⁸ commented, is a "preliminary stage of microcrystalline character." It is a well-known observation that while water of crystallization plays a definite role in the crystal structure, it reacts toward radiant energy as water vapor in its free liquid state.¹⁹

In connection with these remarks on water of crystallization, attention is called to the studies of Predwoditilew and Blinow²⁰ concerning the photoelectric emission of finely powdered crystalline sulphates. They announced a simple relation between the photoelectric current and the water of crystallization.

It occurred to us that the dielectric substance may form a surface film which reduces the work function; the molecules may well have been so aligned as to act as tiny grids setting up powerful fields which aided in pulling electrons from the alkali metals surface. This idea has been effectively

¹⁷ H. Bottger, Liebig's Ann. 223, 335 (1884).

¹⁸ W. Gerlach, "Matter, Electricity, Energy," p. 65-66.

¹⁹ W. W. Coblenz, Publication No. 35, p. 56 Carnegie Inst. of Washington, Bull. Bur. Stand. 7, 4, 619 (1911).

²⁰ A. Predwoditilew and W. Blinow, Zeits. f. Physik 42, 60 (1927).

used in interpreting long wave shifts, such as are caused by oxide coatings on filaments of thermionic tubes;²¹ but we do not see how it could explain the new selective maximum appearing simultaneously with the shift.

Richardson and Young²² had a theory that the two peaks in their spectral response curves for potassium treated with water vapor and flashed in hydrogen were due to the presence of multiple thresholds on a spotted cathode; but there is nothing in their discussion to explain why the selective maxima occur at the same wave-length for all dielectrics on a given metal; unless, of course, water vapor be the activating agent in them and act independently of and more effectively than any other substances with which it might be mixed.

2. *Lack of correlation between selective maxima and absorption bands in the visible.* We found no relation between the absorbing power of the various dielectrics for *visible* light and the sensitization which they brought about, although this conclusion might be modified if the actual absorption of the deposited films of these substances could be observed. As an example of this might be mentioned the case of water vapor with its weak absorption in the visible, producing better results than cyanine at the particular wave-lengths where this dye has powerful selective absorption (4500–6500A).²³

H. THEORETICAL CONSIDERATIONS

1. *Correlation of separation of maxima with infrared vibration-rotation spectra of the dielectrics.* The absorption of light by water vapor increases in the

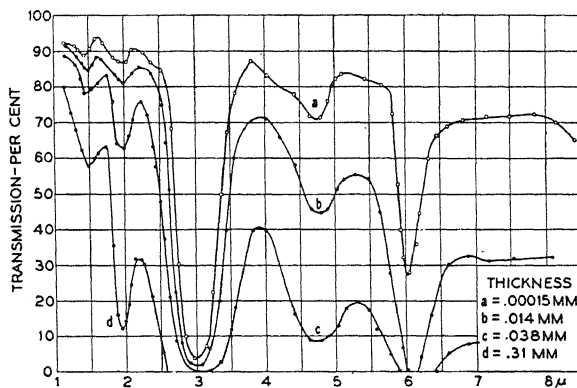


Fig. 30. Absorption spectra of thin films of water. Reproduced from Bull. Bur. Stand. 7, 4, 631.¹⁹

direction of increasing wave-length, and is very strong in the near infrared. It consists of a series of lines or narrow bands so related that if the frequencies of the powerful absorption bands near 6μ and 3μ be taken as fundamentals, other bands can be regarded as the first, second, and third harmonics of

²¹ J. A. Becker, Phys. Rev. 28, 341 (1926).

²² O. W. Richardson and A. F. A. Young, Roy. Soc. Proc. A107; 377 (1925).

²³ Bull. Bur. Standards No. 422 (1922).

these.²⁴ Also these frequencies seem to combine or add up to give other spectral lines. In general, frequencies corresponding to wave-lengths less than 1.5μ are not so strong (Fig. 30), but in the form of vapor or water of crystallization²⁵ the higher harmonics become sharper and more pronounced (Fig. 31), a line at 1.119μ being almost as strong as the 1.47μ line into which the 1.5μ band resolves itself. This absorption series, the "vibration-rotation

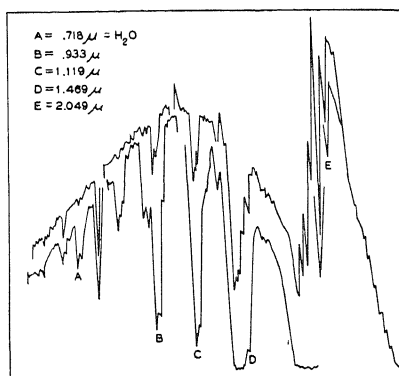


Fig. 31. Bolographic energy curves of the solar spectrum of a 60° glass prism, the upper one taken in February when the humidity was low and the lower one in September when the humidity was high. Curves reproduced after Coblentz from Fowle: *Smithsonian Misc. Coll.* Vol. 47, No. 1468, (1904).

spectrum," is due to interatomic vibrations within the molecule, or more specifically to vibrations set up between the hydrogen and oxygen atomic nuclei.

Now there seems to be considerable evidence that the increased photoelectric response is in some way, directly or indirectly, connected with this or a similar spectrum. For, in the first place, such absorption bands are quite characteristic of all compounds containing an oxygen-hydrogen carbon-hydrogen or nitrogen-hydrogen linkage, as shown in Table III.

TABLE III.

O-H Linkage ²⁶	C-H Linkage ²⁷	N-H Linkage ²⁷
3.06μ	3.28μ	2.90μ
1.469	1.68	1.50
1.119	1.145	1.03
.933	.874	.790
.718	.713	.648

There are other important bands of longer wave-length than 3μ , the ones near 6μ being particularly strong. However, (as pointed out by Ellis in discussing the bands listed here for the N-H linkage), the ones just tabulated

²⁴ H. A. Rowland, *Astrophys. J.* 6, (1897).

^{25,26} W. W. Coblentz, reference 19.

²⁷ J. W. Ellis, *Phys. Rev.* 33, 27 (1929), *Frank. Inst. J.* 208, 4, 507 (1929).

are of particular interest, for the positions of the bands are seemingly independent of the presence or nature of the solvent.

Since a band-system of the foregoing type is found in the spectra of so many different compounds involving hydrogen, it is reasonable to suppose that the vibrations to which such bands are due, occur in the molecules formed by the vapors which we brought into contact with alkali-metal surfaces.

Now we have observed a very interesting pair of numerical agreements, which are probably more than mere coincidences. On evaluating the shift in frequency δ of the long wave limit and the selective maximum, which occurs when an alkali metal is affected by one of the vapors in question, we found:

(a) In many cases this frequency-shift is equal to the frequency corresponding to the wave-length 1.5μ , which is that of a strong band in many molecules of the stated kind;

(b) In certain other cases, notably where sodium surfaces were involved, the frequency-shift is equal to the frequency corresponding to some wave-length near 1μ , where there are other bands.

A couple of other things suggest that the presence of hydrogen may be essential to these shifts: viz. Wiedmann's²⁸ data which suggested to him that not only the shifts but the actual maxima themselves are due to hydrogen; and the fact that CCl_4 contains no hydrogen, has no absorption-bands in the near infrared (Abney and Festing²⁹) and did not produce a frequency-shift, whereas CHCl_3 , with its hydrogen-content and its vibration-bands, did produce one.

We make, then, the tentative hypothesis that the frequency-shifts are due to the presence of molecules having natural vibration-frequencies equal to these shifts; and attempt to explain why such molecules should have that particular effect.

It may be that when an alkali-metal atom is incorporated into a molecule having an O-H bond (for example) the resulting complex molecule possesses a natural frequency equal to that of the alkali-metal, diminished by that appropriate to the O-H bond. It is well known that two electrical or two mechanical systems with natural frequencies of their own may be coupled into compound systems having a frequency which is the difference of theirs (cf. for instance Hartley and Peterson)³⁰. Something of the sort may occur here.

The newly-discovered phenomenon of the "Raman shift," however, offered a very tempting explanation.

2. *The Raman shift as an explanation of the frequency-shift of the spectral response curves.* In the language of the quantum-theory of light, a "Raman shift"³¹ occurs when a quantum or photon collides with a molecule, causes

²⁸ G. Wiedmann, reference 8.

²⁹ W. de W. Abney and E. R. Festing, Phil. Trans. **172**, III, 887 (1881).

³⁰ R. V. L. Hartley, Abs. 48, Bull. Am. Phys. Soc. **3**, 7 (1928); E. Peterson, Bell. Lab. Record **7**, 6, 231 (1928).

³¹ C. V. Raman, Ind. Journ. of Phys. **2**, 387 (1928); C. V. Raman and K. S. Krishnan, Roy. Soc. Lond. Proc. **A122**, A-789, 23 (1929).

the molecule to pass from its initial to another of its stationary states, receives the energy which the molecule gives up (or alternatively, gives up the energy which the molecules absorb) in making this transition, and flies off with energy correspondingly increased (or diminished). In the language of the wave-theory (Hartley³²) a Raman shift occurs when the frequency p of an incident wave-train of light is modulated by the frequency q of a natural vibration of the molecule on which the light falls, the shifted wave-trains being the "sidebands" of frequencies $p+q$, $p-q$, $2p-q$, etc.

Now suppose that some of the quanta striking the treated alkali-metal surface collide with molecules which are not in the normal, but in some excited state of vibration; and that in such a case, the molecule transfers to the quantum the amount of energy which it would release in the form of radiation, if it were spontaneously to relapse to a lower vibration-state; for instance, that it transfers the energy of one quantum of radiation of wave-length 1.5μ . Then the quanta which have made such collisions have their frequencies correspondingly augmented. If now they fall on the alkali metal and produce the photoeffect, it is the photoeffect proper to light of augmented frequency which they produce. The spectral-response curve would then be shifted because the frequency of the light itself is shifted before it reaches the photo-sensitive surface.

This idea was temporarily adopted as a working hypothesis; but a number of objections arose which are hard to surmount. In the first place, the sense of the shift is such that we must suppose the quanta to collide with molecules already excited. Now in a substance in thermal equilibrium, the proportion of molecules in any given state of excitation may be computed by Boltzmann's equation:

$$n = n_0 e^{(-\epsilon/kT)} \quad (1)$$

in which T stands for the temperature of the substance, k for the Boltzmann constant, n_0 for the number of molecules in the normal state or state of least energy, and ϵ for the energy of the given excited state referred to that of the normal state as zero. It seems unlikely that the proportion of excited molecules should be great enough to account for such results as those shown in Fig. 14 (for example) or in Fig. 32, where the "shifted" is as large as the regular maximum,—a result obtained when very thin films of potassium were flashed in hydrogen on oxidized copper plates. And it seemed doubly unlikely that the excited molecules should be numerous enough to explain the presence of such pronounced maxima at long wave-lengths as those shown in Fig. 7, where in the cases of curves (a) and (b) they are several times the magnitude of the regular maximum for caesium at $\lambda 5500\text{\AA}$.

One would expect encounters in which quanta give energy to normal molecules to be far more abundant than encounters in which quanta receive energy from excited molecules. In other words, if p stands for the frequency of the incident light and q for that of the vibrating molecule, the $p-q$ frequency should be more intense than the $p+q$ frequency and possibly present

³² R. V. L. Hartley, reference 30.

when the latter was not. There should then, be a new maximum, much stronger than the one which we have observed, located towards higher

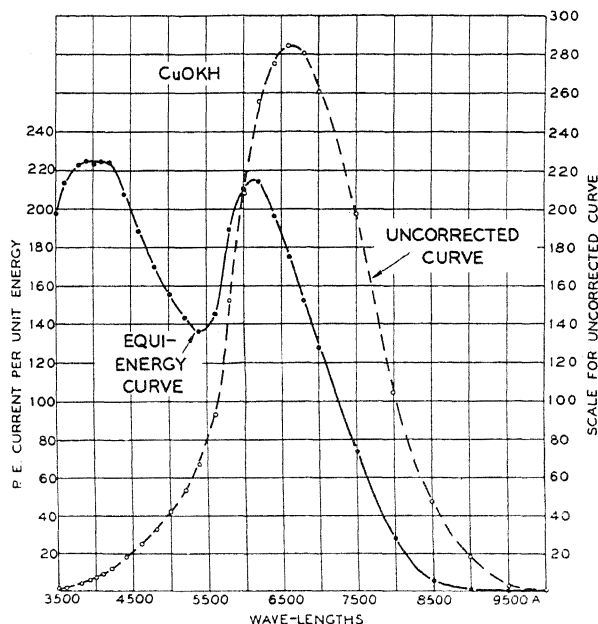


Fig. 32. Spectral response curve for a potassium film flashed in hydrogen on a copper-oxide plate

frequencies from the maximum characteristic of the pure metal. We were not fully equipped to investigate this region and so obtained no definite

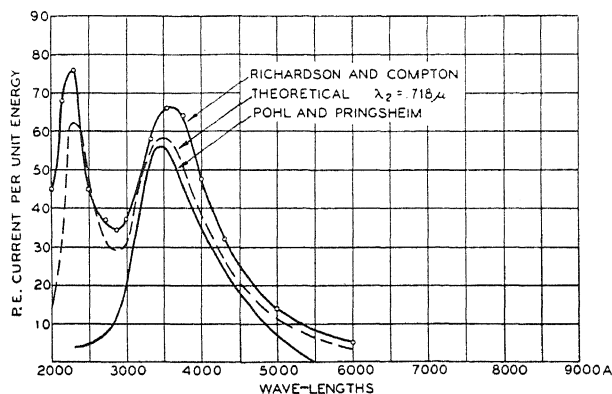


Fig. 33. Spectral response curves showing how Richardson's and Compton's observed double maxima for a sodium photoelectric cell appear as the regular selective maximum of Pohl and Pringsheim plus this maximum shifted to higher frequencies by an amount corresponding to the frequency of the $\lambda 0.718\mu$ water vapor absorption line.

information. However, the curves for caesium cells (Fig. 7) show evidence of a maximum at higher frequencies, and also the shift of the $\lambda 4360$ peak of

pure potassium to somewhat higher frequencies (Fig. 5) upon treatment with dielectrics might be explained by assuming the $p-q$ frequencies greater than the $p+q$ and taking q equal to the frequency of the intense 3μ water vapor band. Richardson and Compton have published a curve for sodium showing a peak at $\lambda 2270\text{\AA}$ in addition to the regular one at $\lambda 3600\text{\AA}$. Since the cell they used had electrodes sealed in with cement which would prevent thorough baking, water vapor was probably present. The ultraviolet peak could be explained as a $p-q$ frequency if we put q for the frequency of the 0.718μ line of the vibration-rotation spectrum of water vapor. In Fig. 33 is plotted a curve based on the assumption that this $p-q$ frequency produces

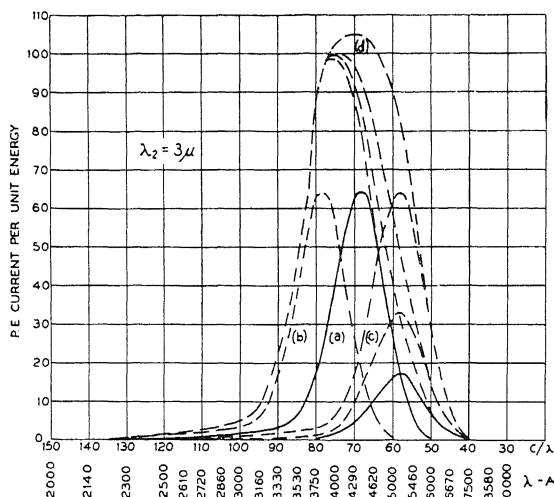


Fig. 34. Theoretical modifications of the spectral response curve for potassium photoelectric cells, assuming modulation of the incident light frequency p by the strong 3μ absorption band of water vapor. a) Curve for pure potassium (Pohl and Pringsheim). b) Curve (a) shifted to higher frequencies by an amount corresponding to $q=c/3\mu$ to show the effect of the $p-q$ side frequencies. c) Curve (a) shifted to lower frequencies by a similar amount to show the effect of the $p+q$ side frequencies. d) Composite curves assuming the presence of the incident light frequency p and the side frequencies $p \pm q$, illustrating the shift of the maximum to shorter wave-lengths with a decrease in the intensity of the $p+q$ sideband.

a maximum as strong as the unmodulated p frequency,—an assumption probably false. The shift of the long wave limit might also be taken to indicate the presence of a weak positive side frequency, also.

In Figs. 34 and 35 are plotted some theoretical curves for potassium cathodes, assuming the $p \pm q$ frequencies to be operative with varying intensities. In Fig. 36 is illustrated the close agreement between the theoretical and observed values. Similar curves for sodium may be shown.

We might avoid the need for postulating a transfer of energy to quanta from excited molecules by assuming that two quanta simultaneously strike a normal molecule and excite it, and a single quantum is then radiated having energy equal to the sum of their energies less that required to excite the mole-

cule. This seems a highly improbable event; but in any case the experiments which we are now about to describe exclude it, for if the theory were correct

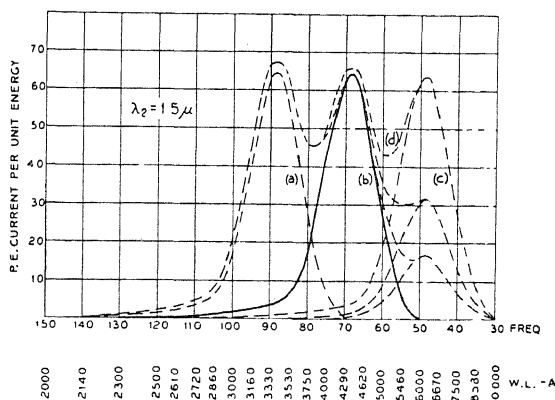


Fig. 35. Theoretical modifications of the spectral response curve for potassium photoelectric cells, assuming modulation of the incident light frequency p by the 1.5μ absorption band of water vapor. a) Curve for pure potassium (Pohl and Pringsheim). b) Curve (a) shifted to higher frequencies by an amount corresponding to $q=c/1.5\mu$ to show the effect of the $p-q$ side frequencies. c) Curve (a) shifted to lower frequencies by a similar amount to show the effect of the $p+q$ side frequencies. d) Composite curves assuming the presence of the incident light frequency p , and the side frequencies $p \pm q$, showing how the magnitude of selective maximum at $\lambda 6200\text{Å}$ might depend on the intensity of the $p+q$ sideband.

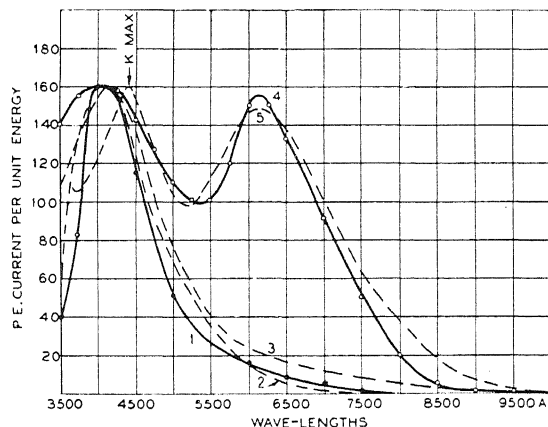


Fig. 36. 1—Experimental spectral response curve for a potassium cell after preliminary treatment with a dielectric. 2—Theoretical curve for a combination of light frequencies p and $p+q$, where $q=c/3\mu$ and the intensity of $p+q$ is considered one quarter that of the incident frequency p . 3—Theoretical curve for a combination of light frequencies p and $p+q$ where $q=c/1.5\mu$ and the intensity of $p+q$ is one-eighth that of p . 4—Experimental spectral response for a potassium film flashed in hydrogen on a copper-oxide plate. 5—Theoretical curve for a combination of light frequencies p and $p \pm q$ [$q=c/1.5\mu$] all of equal intensity.

the kinetic energy of the emerging electrons would be equal to $2h\nu$ minus the surface work function, instead of to $h\nu$ minus this function.

However, the gravest objection to the "Raman Shift" theory is that it requires that the electrons should receive the energy $h(\nu + \delta)$ rather than the energy $h\nu$ when the substance is illuminated by light of frequency ν ; so that the adverse voltage as read on the voltmeter which is required to stop the fastest electrons, the "apparent stopping potential," should be increased by the amount corresponding to $h\delta$ when the vapor is admitted to the metal. No such effect has ever been observed; but as the interpretation of the data requires an allowance for contact potential, this point must be left for discussion in the next section.

3. *Accurate determination of the stopping-potential vs. frequency curve and evaluation of h .* According to the well-known Einstein equation

$$Ve = \frac{1}{2}mv^2 = h(\nu - \nu_0) \quad (2)$$

the graph of stopping potential versus frequency should be a straight line of slope h . Our experiments have verified this prediction over a range of frequencies heretofore unemployed and extending into the infrared, have led to a very precise value of h , and have incidentally eliminated the idea mentioned above that a frequency $(2p - q)$ might result from the interaction of light with the molecules; for that idea would require a slope equal to $2h$.

A photoelectric cell was specially designed to avoid the deposition of photosensitive materials on the anode, for this is fatal to accurate determinations of stopping potentials as will be explained directly. As will be seen from Fig. 37, the cathode could be coated with freshly distilled sodium in one end of the tube and then transferred in vacuum to the other end where it became a central cathode surrounded by a cylindrical anode made of soot-coated nickel. Again at any time the cathode could be removed to its original position for further sensitization.

The potential drop across the electrodes of such a cell read on the voltmeter is of course not the true one; allowance must be made for contact difference of potential. The voltage at which the current just saturates would be that for the true potential drop equal to zero, if the anode completely encompassed the cathode. When there are small openings in the anode, such as a hole through which to introduce the exciting light, a slight positive potential is required to produce saturation of the photoelectric current. It is always possible, however, to find the effective or true zero voltage if the long wave limit is carefully determined, as will soon be shown. The true stopping-potential is then measured by the distance, along the axis of voltage, from that point to the point where the current just reaches zero. This last would not be true if the cylinder emitted electrons, for then there would be a "reverse" current when the field was so directed as to drive electrons from it to the central electrode, and the net current would vanish when this just balanced the direct current, not when the direct current itself vanished. But in our experiments the cylinder was not photosensitive at all, and there were never any reverse currents.

The photoelectric currents were measured by means of a Compton quadrant electrometer, using the constant deflection method. The cathode

was illuminated sometimes by the highly resolved light of a glowing tungsten filament, sometimes by means of the monochromatic lines of the quartz mercury arc. The arc lines used were isolated by passing the light through a Hilger quartz monochromator and using an Eastman filter which cut out all stray light of higher frequencies. The great amount of long wave-length

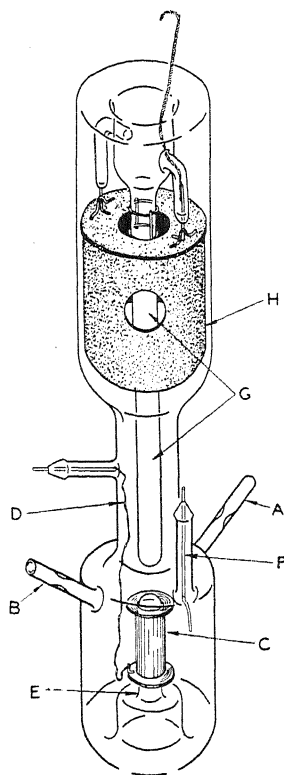


Fig. 37. Specially designed photoelectric cell for the study of stopping potentials. *A*—Tubular connection to evacuating system and entrance for sodium. *B*—Tube leading to side arm containing sulphur. *C*—Cathode of cell on which sodium is deposited. *D*—Phosphor bronze ribbon connecting cathode with external electrode. *E*—Glass stem supporting cathode while it is coated and sensitized and in which CO_2 snow was packed. *F*—Electrode forming electrical contact with coating of sodium used as temporary anode. *G*—Tube down which the sensitized cathode slides after it is sensitized and in which was kept a heating coil during the coating process. *H*—Insensitive anode to which the electrons were emitted after the tube was made.

energy radiated from a glowing tungsten filament made it easily possible to measure stopping potentials for light of wave-lengths up to 8000\AA with surfaces sensitized by means of dielectrics. This light was passed through a monochromator and a light filter cutting out higher frequencies, and the stopping potentials determined. Corrections for slit width were made before plotting the results. The stopping potentials were then redetermined using a

monochromator of different dispersion. The results obtained with the different instruments checked perfectly.

Both for pure sodium and sodium treated with sulphur vapor and air the curves obtained were straight lines of slope h , as shown in Fig. 38. The value of h obtained from the pure sodium cannot be considered so accurate as that obtained from the sensitized sodium surface because of the few points on the curve and the narrow spectral band to which they are confined. However, even the value $h = 6.6 \times 10^{-27}$ can be considered a fair check of this important constant.

The curve taken after sensitizing the sodium as described earlier in this paper was very carefully determined with wave-lengths of light varying from 3500\AA to 8000\AA , and, the value of h ($= 6.541 \times 10^{-27}$) can be considered

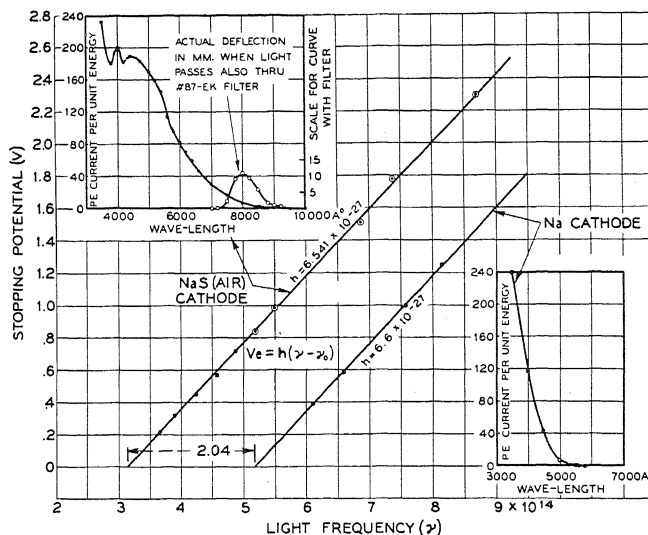


Fig. 38. Stopping potentials versus light frequencies for a sodium cathode before and after sensitizing it with sulphur and air treatments. The spectral response curves for both conditions are shown in the insets.

accurate to at least three significant figures. Perhaps this is the first time that stopping potentials for light of wave-lengths longer than $\lambda 5461\text{\AA}$ have been used in the determination of the value of h .

We never observed any line of slope $2h$. This excludes the idea of a transfer of energy to a normal molecule from two exciting quanta.

When we plot true stopping potentials (measured in the manner just described) against light frequency for pure sodium and treated sodium as is done in Fig. 38, we obtain two parallel lines displaced from one another by the frequency shift δ corresponding to 1.47μ which has already been emphasized. When we plot *apparent stopping potentials* as read by the voltmeter, the two lines fall on one another (Fig. 39). This signifies that the surface work-function of the treated surface has been diminished and the contact potential

increased by the amount corresponding in volts to δ . The electrons initially received the energy $h\nu$ from the quanta, but lose less of it in getting out through the surface, so that in effect their kinetic energy after escape is greater by $h\delta$ than it was with the pure sodium. By the Raman shift theory their kinetic energy would also have been greater by $h\delta$ after the treatment of the surface; but then the surface work function and the contact potential would have remained the same, and the apparent stopping potentials would have been shifted by δ .

To put the foregoing statements into algebraic form we may write the V of equation (2) as the sum of the P.D. registered by the voltmeter, say V_0 , and the contact potential difference K :

$$(V_0 + K)e = h(\nu - \nu_0) = \frac{1}{2}mv^2. \quad (3)$$

Now, it is generally agreed by all investigators that when the anode is preserved unchanged, and different surfaces are used as cathodes, the stopping potential for a given wave-length of light is the same for all. Therefore, if we use primes to denote the values of V_0 and K for treated as distinguished from untreated sodium, we have,

$$(V_0' + K') - (V_0 + K) = h/e(\nu_0 - \nu_0'). \quad (4)$$

If the light frequency remains unchanged, $V_0' - V_0 = 0$, and

$$K' - K = h/e(\nu_0 - \nu_0'). \quad (5)$$

If, however, the incident light frequency is modulated, and the surface work function remains unchanged, $V_0' - V_0$ would not be zero and Eq. (7) would not explain the facts. Here was a criterion for deciding whether or not the light was modulated.

The stopping potential curves shown in Fig. 39 all refer to the same cell, one of the type shown in Fig. 37. It will be seen that the apparent stopping potentials for a given wave-length of incident light are the same before introduction of the dielectric as after.³³ The increased velocity of emission of the electrons after treatment with sulphur and air was due to a reduction of the work-function of approximately 0.8 volt which was the contact difference of potential between pure sodium and the sodium treated with the dielectric. For this particular case, then, Einstein's equation might be extended to read:

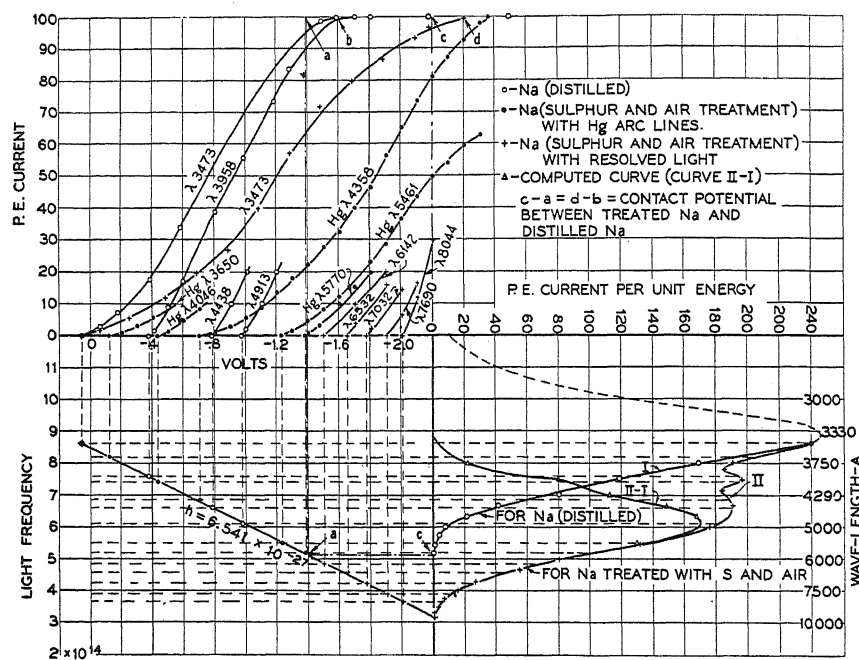
$$K' - K = \frac{h}{e}(\nu_0 - \nu_0') = \frac{h}{e} \frac{c}{1.47\mu}. \quad (6)$$

Here is ample evidence that the light frequencies incident on the surface are not modulated.

Referring again to Fig. 39 attention is called to the way in which all plots of the light frequency versus apparent stopping-potentials, (voltages

³³ Actually, the cathode voltage at which the current became zero was 0.5 volt more positive before admitting the dielectric than after, but this was due to the fact that the sulphur vapor and air which entered the cell had made the anode more electronegative as well as the cathode more electropositive.

at which no electrons reach the anode) fall on the same straight line which intersects the effective zero voltages at frequencies corresponding to the long wave limits of the respective cathodes. Failure of the voltage-current curves to break exactly at the effective zero is due to the fact that the anode did not enclose the cathode completely as explained above. A slight positive voltage had to be supplied to the anode before it gathered all of the emitted electrons. However, the separation of the voltages at which the currents saturate, designated by (b) and (d) and the separation of the effective zeros (a) and (c) are practically identical, and the relationship between the



that contact difference of potential was a property not alone of surfaces but of molecules and, as such, a measure of the relative number of available valence electrons under excitation of light, or the relative ease with which these loosely bound electrons can be liberated by light.

I. GENERALIZATION OF THE LINDEMANN FORMULA

In 1911 F. A. Lindemann³⁴ derived, from each of two very simple models, the following formula for a natural frequency ν which he proceeded to identify with the frequency of the selective photoelectric maximum:

$$2\pi\nu = (ne^2/mr^3)^{1/2} \quad (e, m \text{ charge and mass of electron}). \quad (7)$$

This is the frequency of an electron revolving in a circular orbit of radius r (or an elliptical orbit of major axis r) about a stationary charge of magnitude $+ne$. It is also the natural frequency of vibration of a system composed of two interpenetrating spheres of continuously-distributed positive and negative charge, having radii r , and total charges $\pm ne$ and $\pm e$ respectively.

Putting n equal to unity, and putting for r the radii of the atoms of the various alkali metals (obtained from their atomic volumes in the solid state) Lindemann obtained numerical values very close to the frequencies of the chief selective maxima of these metals as then known and subsequently checked (Pohl and Pringsheim, Braun,³⁵ Seiler,³⁶ and others). See Fig. 29. His values and the experimental ones, converted into wave-lengths, are shown in Table IV.

TABLE IV. *Specific wave-length of selective photoelectric effect.*

Metal	By Lindemann Formula	Observed
Cs	5500	5100
Rb	4900	4800
K	4380	4350
Na	3180	3400
Li	2360	2800

Subsequently Gross³⁷ showed that additional maxima observed by some workers for certain of the alkali metals fall at frequencies ν agreeing well with the formula

$$2\pi\nu = (ne^2/mr^3)^{1/2}$$

provided proper integer values be assigned to n .

Some of these agreements are so noteworthy, that it seems worth while to use the Lindemann model, primitive though it may appear in the light of recent theory. Now the choice of the value unity for n , which Lindemann

³⁴ F. A. Lindemann Verh. d. D. Phys. Ges. 13, 482 (1911). Verh. d. D. Phys. Ges. 13, 1107 (1911).

³⁵ Braun, "Die Photoelektrischen Wirkungen der Alkali Metalle in Homogenen Licht," Boun 1906.

³⁶ E. F. Seiler, reference 5.

³⁷ F. Gross, reference 3.

made, corresponds to an electron revolving around a singly-charged ion—the sort of ion one would expect from a monovalent substance, such as the alkali metals are. Such values as 2, 3, . . . for n would correspond to an electron revolving around a doubly-, triply-, . . . charged ion, such as a di-, tri- . . . valent substance would have. We might then say that in some atom-groups the alkali metals are divalent or trivalent, and that these are responsible for the maxima of higher frequencies which Gross considered.

Now in our experiments, we have checked several of the maxima to which the original Lindemann formula and the formula with Gross' modifications apply; and we have also observed maxima of lower frequency—those to which this paper is chiefly devoted—many of which are located at frequencies given by the Lindemann formula, provided that simple fractional values are assigned to the factor n .

Continuing with the model, we might say that such values of n are associated with atoms of valency $\frac{2}{3}$, $\frac{1}{2}$, and the like. To think of an electron revolving around an ion with net charge $+2e/3$ seems strange at first; but it is quite conceivable that the forces exerted on the electron by the other surrounding atoms might have the same net effect. We propose therefore to designate even the fractional values of n as "valencies".^{37a}

Our data, together with those of the observers already quoted, are listed in Tables V, VI and VII, being classified according to the metals involved. The second column of each table gives the various values assigned to n ; the third the corresponding wave-lengths, derived from the frequency computed by the generalized Lindemann formula; the fourth, the wave-lengths of the observed maxima; the fifth, the authorities. In the first column, we give the formulae for oxides in which the metal in question displays these valencies.

Now it is an important fact that most of these oxides are known to exist.³⁸

TABLE V. *Lindemann formula* $\nu_{\max} = (1/2\pi)(ne^2/mr^3)^{1/2}$.

Metal and its oxides	Valence of metal	λ_{\max} (Computed)	λ_{\max} (Observed)	Observer
Na	1.	3170	3400	Pohl and Pringsheim
Na ₄ O	0.5	4500	4700	Self (Figs. 14, 29, 42, 43.)
Na ₃ O	0.67	3900	4000	Self (Figs. 14, 42, 43.)
Na ₂ O	1.	3170	<3500	Self
Na ₂ O ₂	2.	2250	2270	Richardson and Compton ⁶
(Na ₂ O ₃)*	3.	1820		(On impure Na)

* Probably solid solutions or mixtures of R₂O₂ and R₂O₄.

Returning to the data reported in this paper, an attempt will now be made to interpret them in a way suggested by the Lindemann theory. Among

^{37a} Fractional valences are recognized by the chemists by such formulae as CdCl₂, 2.5 H₂O, CdSO₄, 2.66 H₂O (I.C.T. Vol. 1, p. 120).

³⁸ J. W. Mellor, "A Comprehensive Treatise on Inorganic and Theoretical Chemistry," Vol. 2, p. 485, Longmans, Green and Co. Ltd., London.

the oxides of sodium are listed Na_4O , Na_3O ,³⁹ Na_2O and Na_2O_2 , showing valencies for sodium ranging from 0.5 to 2. Since the likely presence of traces of water vapor in all the dielectrics introduced onto the alkali metals has been admitted and since atmospheric air was admitted in some cases,

TABLE VI. *Lindemann formula* $\nu_{\max} = (1/2\pi)(ne^2/mr^3)^{1/2}$.

Metal and its oxides	Valence of metal	λ_{\max} (Computed)	λ_{\max} (Observed)	Observer
K	1.	4380	4350	Pohl and Pringsheim
K_4O	0.5	6200	6200	Self (Fig. 34)
K_2O	1.	4380	4200	Self (Fig. 34)
K_2O_2	2.	3100	3130	Wiedmann
$(\text{K}_2\text{O}_3)^*$	3.	2520		
K_2O_4	4.	2240		
K_8O_5	1.25	3920	4000 to	Self (Fig. 34)
K_6O_4 †	1.33	3800	3500	
K_4O_3	1.5	3580		

* Probably solid solutions or mixtures of R_2O_2 and R_2O_4 .

† Probably aggregates or mixtures of R_2O and R_2O_2 .

it may well be that some oxide is formed on the cathode surface; and this may have been a suboxide. (The formation of the higher oxides should result in increasing the response to shorter wave-lengths.) As evidence that it actually was a suboxide, I cite experiments which showed that the cells

TABLE VII. *Lindemann formula* $\nu_{\max} = (1/2\pi)(ne^2/mr^3)^{1/2}$.

Metal and its oxides	Valence of metal	λ_{\max} (Computed)	λ_{\max} (Observed)	Observer
Cs	1.	5500	5100	Braun
Cs_7O	0.29	10200	5400	Miss Seiler
Cs_4O	0.5	7800	7700	Self (Fig. 8(a))
Cs_7O_2	0.57	7300	7200	Self (Fig. 8(b))
Cs_3O	0.67	6700		
Cs_2O	1.	5500	5500	Self (Fig. 8(c))
Cs_8O_5	1.25	4900		
Cs_6O_4	1.33	4750		
Cs_4O_3	1.5	4400		
Cs_2O_2	2.	3900	3900	Richardson and Compton ⁶
$(\text{Cs}_2\text{O}_3)^*$	3.	3160		
Cs_2O_4	4.	2760	2500	Richardson and Compton ⁶ (On impure Cs)

* Probably solid solutions or mixtures of R_2O_2 and R_2O_4 .

† Probably aggregates or mixtures of R_2O and R_2O_2 .

were red-sensitive only when very small amounts of the dielectrics were used. If a certain critical amount was exceeded the response to red decreased greatly, and soon entirely disappeared. If, however at this stage a point

³⁹ R. de Foicrand, *Compt. Rend.* 127, 364, 514 (1898).

near the cell window was heated, a vapor of sodium plus some of the dielectric was created in the cell. This lent itself to the formation of a subvalent compound on the surface and the characteristic response to light of long wavelengths was again in evidence. Moreover, the general appearance of the cathode of sodium cells so treated was exactly that of sodium suboxide, viz. a grey, porous surface crust.

Suboxides of potassium⁴⁰ and caesium⁴¹ are also known, but they are more difficult to prepare and apparently are only obtained by limiting the amount of oxygen first coming in contact with the metal. Really this is to be expected for it is impossible to prepare oxygen sufficiently dry that it will not react with either potassium or caesium, but sodium can be distilled in dry oxygen without reaction. In the case of caesium, the suboxides are only formed by limiting the amount of oxygen present and holding the temperature at a certain value. Naturally, then, it would be expected that sodium-suboxide photoelectric cells could be made with less difficulty than potassium or caesium suboxide cells. However, by flashing hydrogen on thin potassium films deposited on oxidized copper plates in vacuum, very much as Campbell⁴² has reported, a compound which apparently was potassium suboxide, was prepared. Also by proper control of the temperature, as caesium vapor came in contact with an oxidized silver plate in vacuum, caesium suboxide was formed. Each of these compounds produced a new and pronounced maximum in the spectral response curves, the former at 6200A and the latter at about 7700A. (See Figs. 32 and 7.)

There is no reason to assume, however, that such subvalent compounds are limited to the oxides. The main and limiting requirement for red sensitivity is undoubtedly the subvalent condition of the atoms in the molecules, and possibly these may be subhalides, subsulphides, or some other subvalent salts. However, not many such compounds are known; and water vapor was in all probability always present in the small amounts likely to form suboxides. The broadening of these maxima in cases when certain dyes or dielectrics were used (Figs. 12, 25) was probably due to intense absorption of these complex compounds on the long wave side of this maximum.

The work of Dima⁴³ on the oxides of manganese and various compounds of other metals suggests a similar theory; for using unresolved light, he found that the lower the valency of the metal in the compounds, the more photo-sensitive the compound. This may have been due to the shift of the maximum towards the red.

It is practically impossible to prepare a suboxide of a metal without at the same time forming some higher oxides as well. These should correspond to integer values of n in Lindemann's formula; and maxima explainable in this way have actually been observed. As in the case of the maximum for $n = 1$

⁴⁰ J. J. Berzelius, *Lehrbuch der Chemie*, Dresden 1, 749 (1825).

⁴¹ E. Reñgade, *Compt. Rend.* 148, 1199 (1909).

⁴² N. R. Campbell, *Phil. Mag.* 6, 633 (1928).

⁴³ Dima, *Compt. Rend.* 176, 1366 (1913); 177, 590 (1913).

shown by multiply distilled sodium, the additional maxima for treated sodium surfaces also generally fall at slightly greater wave-lengths than the computed values, (Table V). However, the second selective maximum observed in the ultraviolet by Richardson and Compton for sodium fits closely the maximum to be expected if $n=2$, the valence of Na in Na_2O_2 . The shift of the long wave limit to greater values suggests the presence of the suboxide ($n=0.5$) in small quantities. Since their experimental conditions precluded the possibility of thoroughly eliminating moisture from the glass walls, the likelihood of these compounds being present must be admitted.

The last three oxides listed in the potassium group (Table VI) may have been responsible for the apparent shift of the regular selective maximum for that metal to shorter wave-lengths as quite generally observed after treatment with the dielectrics, (Figs. 5, 23). Moreover, for $n=2$ (the valence of K in K_2O_2) Lindemann's formula gives a maximum at almost exactly the same wave-length as that attributed to oxygen on potassium by Wiedmann.

The difficulties in preparing pure, silvery caesium in bulk form may explain why most investigators seeking to establish the presence of a selective maximum at $\lambda 5500\text{\AA}$ ($n=1$ in the Lindemann formula) for caesium, found a greater peak in the ultraviolet. For, even after multiply distilling caesium in vacuum, it usually appears slightly golden in color as if containing some oxides. If the valence of Cs in these oxides is greater than unity ($n>1$) the selective maxima should fall in the ultraviolet, as observed. As a matter of fact, experiments show that by introducing caesium onto an oxidized plate under proper temperature conditions, the regular selective maximum ($n=1$) can be made to disappear almost entirely, as shown in Fig. 7, indicating that practically all free caesium had disappeared. At the same time the maxima due to the suboxides ($n<1$) and peroxides ($n>1$) become very pronounced.

In the foregoing computations the value of the atomic radius r was left unchanged as n was modified. The alkali metal atom in the molecule was considered as an isolated atom of normal dimensions but with a different force-constant.

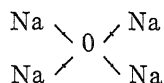
J. COMPARISON OF AFORE-MENTIONED HYPOTHESES

Two seemingly different and unrelated theories have been advanced to explain the displaced selective maximum. In the first one it was assumed that there is hydrogen present, a condition not unlikely since sodium and potassium absorb great quantities of this gas without any change in their metallic appearance, much as does palladium.⁴⁴ It is further assumed that addition of some such dielectric as oxygen or nitrogen results in the appearance of characteristic vibration-rotation frequencies which were apparently subtracted from the resonance frequency of the electron in the alkali metal atom. The other theory is based on the Lindemann equation, and accounts for the reduced resonance frequency as a consequence of a decreased binding

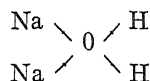
⁴⁴ P. Hautefeuille and L. Troost, *Ann. Chem. Phys.* (5), 2, 273 (1874), *Compt. Rend.* 78, 809 (1874).

force on the electron correlated with a change in the valence of the alkali metals in the molecules of the compound formed on the cathode, the atoms in a subvalent condition responding to light of longer wave-lengths.

Until more is known concerning valence and molecular structure, attempts to correlate the two theories would be outright conjecture. It may be that the reason the two theories appear to explain the same phenomena is that they are both built around similar structures. For example, the very unusual molecule Na_4O may be structurally written (for want of a better formula)



On the other hand, if hydrogen is assumed present with the alkali metals the introduction of oxygen (say) into a photoelectric cell and subsequent treatment, as described above, might result in the formation of molecules which may be written:



In this connection, it is significant that dry oxygen will not react with sodium. Now, the valence of the sodium atom in each of these compounds is identical, and yet the latter is shown to contain the atoms giving rise to the spectrum of water vapor. The valence of the sodium atoms being similarly reduced in each case, the resonance frequency of the valence electron would be correspondingly decreased and the response to long wave light increased.

Either theory may be made to account for the observation that for small ratios of oxygen atoms (say) to alkali metal atoms in a molecule, the response to red light becomes greater. This would be expected by the first theory, for when the atoms are attenuated, higher vibration-rotation frequencies become sharper, as pointed out previously for the case of water of crystallization.⁴⁵ It would also be expected by the second theory, for the valence of the metal and consequently the binding force on the electron would correspondingly be lessened.

K. IRREGULARITIES IN VOLTAGE-CURRENT CURVES EXPLAINED

The fact that higher voltages are required to bring about current-saturation when the surfaces are irradiated with light of large wave-lengths can be easily explained by a comparison of the contact potentials of the materials comprising the cathodes of red-sensitive cells. Experiment showed (Fig. 39) that the complex surface formed when the dielectrics were introduced onto an alkali metal cathode was electropositive with respect to the metal by as much as 0.8 volt, and since, within distances comparable to molecular diameters, both free atoms and these complex molecules were existing on the surface, electrons released from the molecules by long wave light would

⁴⁵ W. W. Coblenz, reference 19.

encounter strong opposing fields and their escape would be impeded. They would be pulled to the anode only when sufficient voltage was applied to offset these local surface fields. On the other hand, electrons released by light of shorter wave-lengths come primarily from the free atoms and since these are electronegative with respect to the molecules on the surface, the electrons encounter a helping rather than an impeding force. Consequently, the photoelectric current will saturate at lower voltages for blue light than for red light.

The phenomena, shown in Figs. 2, 3 and 28 and which might be called supersaturation, may be explained by the shape of the elements of the tube. To understand better why more electrons should reach the anode at low voltages than at high, the history of the cell will be reviewed. The first step after evacuation of the bulb was the coating of the entire inner walls with potassium or sodium. Next, by applying a fine point flame momentarily on the face of the bulb, the metal was caused to recede and form an opening through which light could enter the cell. But without thorough heating, the glass could not be made perfectly non-conducting; and on account of the

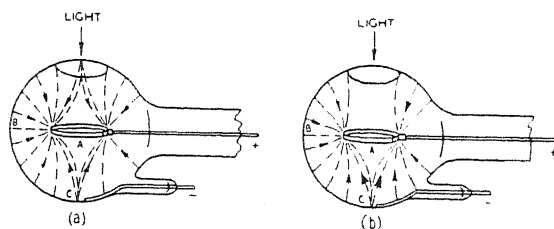


Fig. 40. Diagrams indicating the geometry of the electric fields within photoelectric cells having closed ring anodes (a) before treatment with dielectrics and (b) after such treatment.

low melting points of the alkali metals, prolonged heating of the "window" would have ruined the entire coating of the cell. Even if it were temporarily cleaned of all potassium, the high vapor pressure of the alkali metal produced by the heat of the flame would have deposited metal enough on the window to make it conducting afterward.

Now, the general shape of the electric field set up by an applied polarizing voltage within such a cell might be represented by the direction lines of diagram (a) Fig. 40. It is at once evident that the effect of increasing the polarizing voltage would be that of increasing the number of electrons reaching the anode up to complete saturation. This would result in a normal voltage-current relation. When, however, the conducting film on the glass window was destroyed by some active gas or dielectric, or by repeated heating afterward, the shape of the polarizing field changed to that illustrated by the directional lines of diagram (b). In effect the field between the window and the closed ring or anode was wiped out. From the point C the field spread radially toward the plane of ring A. For such a field there is a critical voltage at which the greatest number of emitted electrons arrive at a collector

located at some angle to the normal from an illuminated spot. These voltages have been computed for a similar case and published by Fry and Ives⁴⁶ and their computations experimentally verified by Ives, Olpin and Johnsrud⁴⁷ for central cathode photoelectric cells. The striking similarity of their curves and the voltage-current curves shown in Fig. 28, for illumination at back and side of cells treated with dielectrics, is illustrated in Fig. 41. It might also be that the greater energies of emission after treatment with the dielectric tended to augment this condition.

Apparently then, the closed ring used for the anode of these cells was responsible for these peculiarities in the voltage-current relation. Data

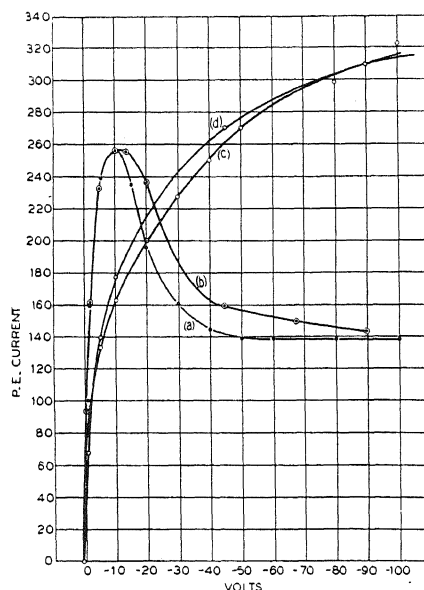


Fig. 41. Comparison of voltage-current curves obtained with photoelectric cells having closed ring electrodes as shown in Fig. 40(b) and voltage-current curves observed with anodes fixed at given angles to the normal to the cathode for cells having radial fields, as described by Ives, Olpin and Johnsrud.⁴⁷ a—Curve 4 of Fig. 28. Light incident at C (Fig. 40) b—Curve for a cell with a radial field when the collecting segment was located at 10° to the normal from the cathode. c—Curve 6 of Fig. 28. Light incident at B (Fig. 40). d—Curve for a cell with radial field when the collecting segment was located at 10° to the normal from the cathode.

obtained from cells having different shaped anodes, such as straight wires or grids, failed to show these peaks at low voltages. Finally a cell was made having a closed ring anode which could be rotated and set with its plane perpendicular to or parallel to the illuminated spot on the cell wall. Whenever, the plane of the ring was parallel to the back of the cell on which the light was falling, the peaks at low voltages appeared and whenever the ring was turned through 90° these maxima disappeared.

⁴⁶ T. C. Fry and H. E. Ives, *Phys. Rev.* **32**, 44 (1928).

⁴⁷ H. E. Ives, A. R. Olpin, A. L. Johnsrud, *Phys. Rev.* **32**, 57 (1928).

L. CONSIDERATIONS IN THE REALM OF PHOTOGRAPHY FLUORESCENCE AND LIGHT ABSORPTION

While there is not space for more extensive discussions, it seems important to call attention to apparently analogous phenomena in the fields of photography, light absorption and fluorescence. It certainly seems more than a coincidence that photographic plates and photoelectric cells can be sensitized to red and infrared light by such strikingly similar methods. The presence of traces of sulphur in the gelatines obtained from some sources has been given by investigators at the Eastman Research Laboratories⁴⁸ as an explanation for their high sensitivity to light. Certainly these experiments, together with those wherein photographic plates are sensitized to red and infrared light by means of organic dyes, suggest a close relationship between photographic and photoelectric phenomena.

Saha⁴⁹ and others have already advanced theories in which fluorescence with change of wave-length is attributed to modulation of the exciting light. In general, however, his conclusions have not been enthusiastically received, many unexplainable observations standing in the way of such a theory. Certainly, however, it should not be dismissed without further consideration. Such results as Wood and Kinsey⁵⁰ reported wherein the *D* lines of sodium were excited by radiation in the region of 5100–5250Å when the sodium vapor was mixed with low pressures of hydrogen, nitrogen or air, seem significant, indeed, since the wave-length region of the exciting radiation here coincides with that of the new photoelectric maximum in the spectral response curves for sodium cathodes treated with air, and the photoelectric threshold for pure sodium atoms coincides with the *D* lines.⁵¹

Many other closely analogous phenomena might be mentioned here; such, for instance, as the fact that the absorption lines of an absorbing medium are noticeably shifted to longer wave-lengths when the absorbing medium is dissolved in a dielectric.⁵² But these are beyond the scope of this paper.

ACKNOWLEDGMENT

To Mr. G. R. Stilwell for invaluable contributions to the technique and art involved in the manufacture of the cells described above, to Dr. Herbert E. Ives for careful consideration of problems encountered in this investigation and for helpful suggestions, and to Dr. K. K. Darrow and Dr. Homer H. Lowry for constructive study of this manuscript, the author expresses his heartiest appreciation.

⁴⁸ A. P. H. Trivelli, *Frank. Inst. J.* **205**, 111 (1928).

⁴⁹ M. N. Saha, D. S. Kothari, G. R. Toshniwal, *Nature* **122**, 398 (1928).

⁵⁰ R. W. Wood and E. L. Kinsey, *Phys. Rev.* **31**, 5, 793 (1928).

⁵¹ H.E. Ives and A. R. Olpin, *Phys. Rev.* **34**, 117 (1929).

⁵² Aschkinass and Schaeffer, *Ann. d. Physik* **5**, 489 (1901).

THE INFRARED ABSORPTION OF SOME ORGANIC LIQUIDS UNDER HIGH RESOLUTION

PART II

BY R. BOWLING BARNES

JOHN HOPKINS UNIVERSITY, BALTIMORE, MARYLAND

(Received June 9, 1930)

ABSTRACT

The study of the C-H vibrations bands, which occur in organic liquids between 3.0μ and 4.0μ , has been continued and extended. A more powerful spectrometer, with which wave-lengths can be determined as accurately as $\pm 0.001\mu$, has been developed for this work. Values are given here for water-vapor, benzene and toluene.

IN A recent paper,¹ we gave an account of an attempt to obtain very accurate values for the C-H absorption bands of various organic liquids. In this discussion we stated the wave-lengths of benzene and eight of its derivatives with an estimated accuracy of $\pm 0.003\mu$. This present paper is intended primarily to outline the developments in the construction of the spectrometer, and the improvements which have been made in the technique and methods. These advances enable us to state wave-lengths now as close as $\pm 0.001\mu$.

By using an echelette grating rather than a rock-salt prism, the resolving power may be increased by a factor of 10 or more. For instance, in this region of the spectrum, a 10 cm prism has a resolving power of only about 170. So, even by using four-prism dispersion, one still has a resolving power somewhat less than 1000, neglecting any loss due to the finite width of the slits. On the other hand, in the grating spectrometer described in our last paper, the theoretical resolving power was over 10,000. In this region, this puts the theoretical limit of resolution for the two types of spectrometers at 30 A'' and 3 A'' respectively, the approximation to these values being determined by the width of the slits and the perfection of the optical systems being used.

In striving to approach these theoretical limits of resolution one uses very narrow slits. When this is done however, another factor becomes of considerable importance in determining the actual limit. In a paper at the April meeting of the American Physical Society² we called attention to the effects of various aberrations in this respect.

If one is not fortunate enough to have properly parabolized mirrors, one must resort to the use of spherical mirrors "off the optic axis." As long as the numerical apertures are small, and the slits are comparatively wide, the effects of the aberrations introduced are negligible. But, if we use apertures as large

¹ R. Bowling Barnes, Phys. Rev. 35, 1524 (1930).

² R. Bowling Barnes and A. H. Pfund, Bulletin Amer. Phys. Soc. 5, 2 (1930).

as $f \cdot 4$ the effects of coma become very pronounced, and the image of the first slit is broad and is accompanied by a diffuse wing. This entire image cannot go through a narrow second slit, and consequently, if the eye is placed behind S_2 , or in the position of the thermocouple, it will receive light

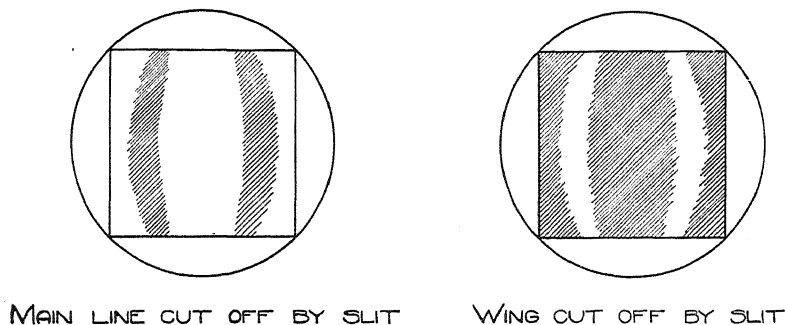


Fig. 1. Grating viewed through second slit of spectrometer when illuminated with monochromatic light. Spectral line is accompanied by a wing produced by the aberrations of the optical system.

from only a very small fraction of the grating, if the latter is illuminated with monochromatic light. Patterns such as those shown in Fig. 1 may be seen, the jaws of the slit having blocked off the light coming from some parts of the grating. However, if we use continuous radiation, such as that from a

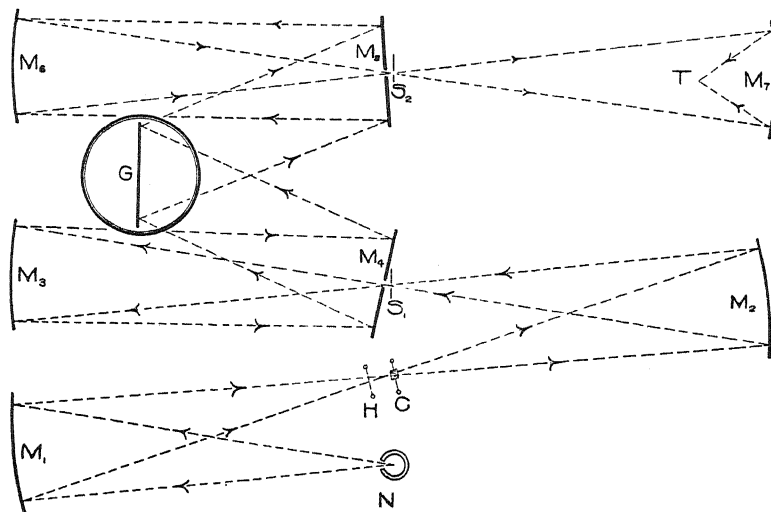


Fig. 2. Plan of spectrometer. Designed to minimize the effect of aberrations.

Nernst lamp, the spectrum falling upon S_2 will necessarily be very impure, and hence the resolving power will be correspondingly low. This diffuseness of the slit image is also a serious handicap in obtaining a very accurate calibration of the spectrometer.

The apparatus which we are using at present is a grating spectrometer, the plan of which is given in Fig. 2. It makes use of about 3.5 inches of a 3600 line per inch echelette grating, which gives it a theoretical resolving power of over 12,000. By a method analogous to that described by Pfund,³ we have been able to use $f \cdot 4$ spherical mirrors along the axis and so minimize all of these aberrations mentioned above. The radiation diverging from S_1 passes through a slot in M_4 , is collimated and returned along the axis by M_3 to the plane mirror M_4 which directs it to the grating. Similarly, the diffracted beam is reflected by M_5 to M_6 , the second spherical mirror, and this focusses upon S_2 which lies on the axis just behind M_6 , an image of S_1 that is sharp and free from aberrations. With this optical system, we have satisfied the condition that the thermocouple shall receive radiation which comes from the entire grating, when monochromatic light is used and the slits are very narrow.

CALIBRATION

A calibration more accurate than $\pm 5 \text{ A}''$, was obtained by observing the settings of the grating which would direct the various orders of the spectrum from a mercury lamp, on to the second slit. By interposing a plane mirror at 45° just behind S_2 , the transmitted light could be reflected into a microscope

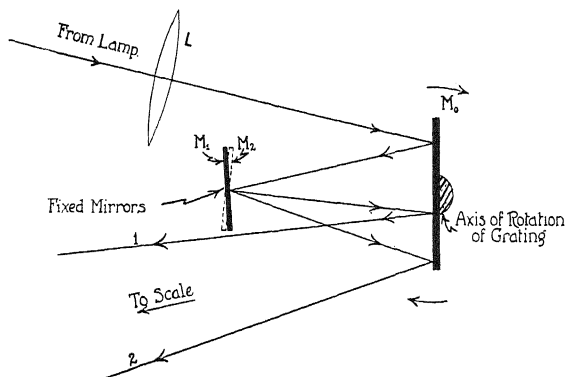


Fig. 3. Calibration mirror system.

which was a permanent part of the apparatus. This microscope was focussed upon S_2 , the crosshairs set upon the center of the slit, and then the latter was opened very wide. As the grating was rotated, the spectral lines passed in turn by the cross-hairs, and an observer could thus tell accurately when the grating was set so as to send known wave-lengths through S_2 . A second observer noted the grating positions by reading on a scale 3 m distant, the image of a lamp filament that had been twice reflected by a mirror which rotated rigidly with the grating. This was accomplished in the manner shown in Fig. 3. Light from an incandescent lamp after passing through a lens was reflected by M_0 to a fixed mirror M_1 , which returned it to M_0 . After a second

³ A. H. Pfund, J.O.S.A. 14, 377 (1927).

reflection by M_0 it was sent along path 1 to the scale upon which an image of the lamp filament was formed. This double reflection causes the beam of light to swing through an arc four (4) times that through which the grating is rotated. The linear displacement of the image of the filament thus becomes large. To avoid the necessity of having a very long scale, a second fixed mirror, M_2 , was mounted as is shown. The angle between M_1 and M_2 was adjusted so that as the grating and M_0 were rotated image 2 came onto the scale just as image 1 was going off the opposite end. If the grating must be rotated through a large angle, a third mirror M_3 could be mounted in a similar manner causing a third image to follow image 2. A linear motion of the filament image of 1 mm at 3 m scale distance, represents a rotation of the grating of about 17 sec. of arc. If the beam of light is allowed to be reflected by M_0 three times, a displacement of 1mm would represent a rotation of only 8.5 seconds. If necessary, more than three reflections can easily be used, and also the image of the filament can safely be read to 0.1 mm. This gives us a method of handling with ease rotations of the order of 1 second of arc. In all of this work the image was moved in steps of 1 mm, this indicating a change in the wave-length falling upon the thermocouple slightly less than 10 \AA '. The calibration was carefully checked from time to time, and was always known closer than $\pm 5 \text{\AA}'$.

PROCEDURE

At best, the point by point method which is usually employed in making infrared measurements is a rather long and tedious process. Every step taken to improve the instruments used, in regard to sensitivity and resolving power, requires that more readings per μ be taken. Obviously, with very high resolution the problem of making such measurements becomes painfully taxing. However, we have so improved our methods that at present we can measure the absorption at over 500 different grating settings within an hour, whereas last year 50 readings constituted a full hour's work. The most fundamental step in making this possible resulted from the recent work of Dr. Pfund on controllable filters for the infrared. Since a grating superposes orders, the effect of the second order of the 1.5μ region and the third order of the 1.0μ region must be eliminated, or to say the least, must be taken into account. For this purpose, one of the MgO filters described by Dr. Pfund⁴ is admirably suited. Also, a filter of a glass designed for use in solar observations was found, which was over 60 percent transparent at 3.5μ , and only 5 percent at 1.75μ and below. These filters, it is true, did not entirely eliminate the effect of the higher orders, but did succeed in reducing it sufficiently for our purposes. For instance, the one we used, though it had a transmission of only 5 percent at 1.75μ , due to the intense emission of the Nernst filament in that region transmitted enough higher order radiation to cause a contamination of the 3.5μ energy of 30 percent. It was shown separately, however, by using 100 percent 1.75μ energy, that in such small thicknesses the

⁴ A. H. Pfund, Phys. Rev. July 15, 1930.

absorption of these higher orders was negligible. So, by using either of these filters, the desired results were obtained.

Further, it was found that by proper shielding the zero drift of the galvanometer could be held to a very small amount and so, instead of reading the zero between each spectrometer setting as is customary, we used the method employed in instruments which record the galvanometer deflections automatically. The zero was read before and after each series of measurements, and the results corrected for the sloping base line caused by the zero drift. Some slight discrepancies in the relative intensities of the various bands may be introduced, because of the fact that we must assume that this zero drift was linear with time. Such errors however will be small, for evidence indicates that this drift is linear. One observer changed the spectrometer setting in intervals of 10 \AA , while the other read and recorded the respective galvanometer deflections. By plotting the results thus obtained we got directly a curve showing the energy transmitted (galvanometer deflections) for the various wave-lengths. The minima of these curves gave us the wave-lengths of the absorption bands.

It must be remembered that in using such a method the total energy transmitted at any wave-length is affected by many factors, namely: the emission of the source, the absorption of the atmosphere, the absorption of the empty cell, the absorption of the filter, and finally the absorption of the sample which is being studied. Separate experiments proved that the empty cell and the filter were not selective in their absorptions, but only reduced the values throughout the entire range by a constant factor. By making a series of measurements, with the absorption cell removed entirely, the combined results of the first two effects was obtained. In Fig. 4 (a) and (b) we have drawn two such curves. They are drawn from different base lines so they may be easily compared. Here we see some 65 or more weak bands, which are evidently due chiefly to the water vapor in the air. The trustworthiness and accuracy of the instrument and methods used, are shown by the manner in which the weak minima of these two curves check each other.

RESULTS

Last year⁵ readings were taken at intervals of 0.007μ on an instrument whose calibration was accurate to $\pm 0.0015\mu$ and the wave-lengths then stated were thought to be accurate to $\pm 0.003\mu$. This year readings were taken every 0.001μ , using an instrument calibrated to $\pm 0.0005\mu$, and therefore we believe that we can now state our wave-lengths to $\pm 0.001\mu$.

The absorption of benzene has been measured some 30 odd times this year, under many different conditions. We have used various cells, slit widths and thicknesses of solution. Fig. 4 (c) shows a sample curve for benzene, made with slits 0.1 mm wide (11 \AA 'slit width') and a thickness of 0.05 mm . In comparing this with a curve from last year, we find the same three strong bands located this year at 3.236μ , 3.257μ and 3.296μ . A careful study was made of the weaker indications of absorption lying on each side of the strong

⁵ R. Bowling Barnes, reference 1.

group of bands. It was noticed in the work last year, that while the 3 strong bands always checked in the different curves, these weaker ones rarely ever agreed exactly. By comparing the benzene curve with those for the atmosphere, we can see the reason for this. Since we have the absorption of water vapor superposed upon that of benzene, we must expect the locations of the benzene bands to be somewhat affected by the presence of the water bands. This effect will be rather slight in the case of very strong benzene bands.

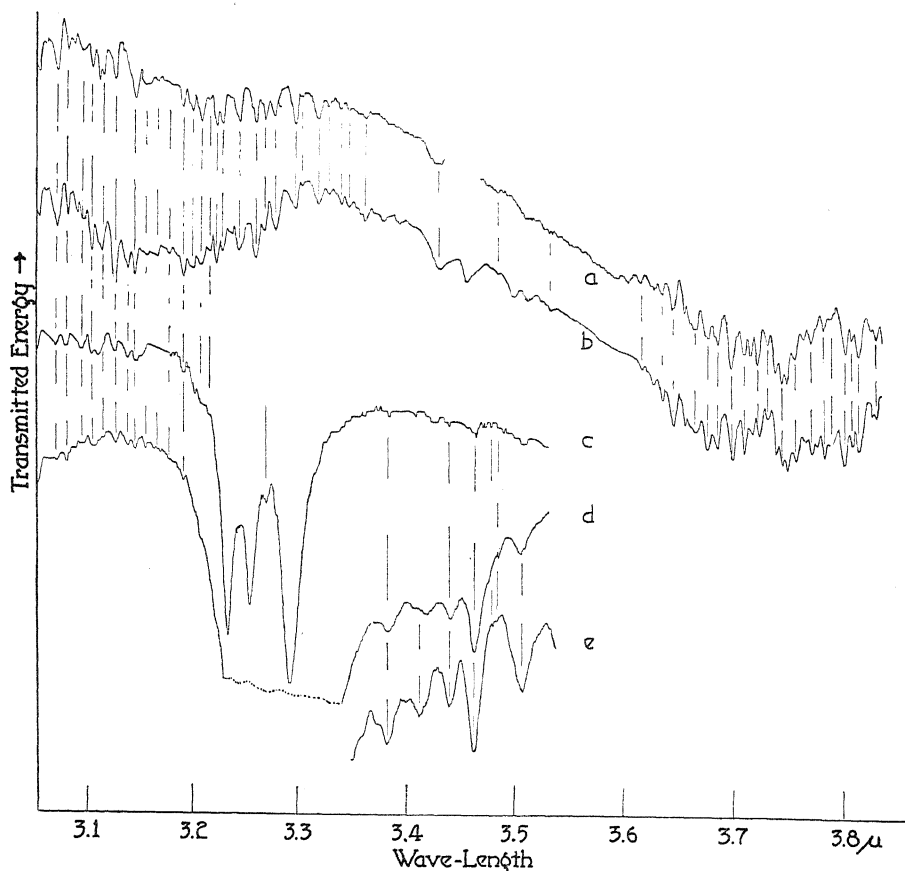


Fig. 4. Absorption curves. (a) and (b) atmospheric absorption. (c) benzene, $t=0.05$ mm. (d) benzene, $t=0.1$ mm. (e) benzene, $t=0.5$ mm.

However, in regions where the bands of the two compounds are of approximately the same intensity, a change in the partial pressure of the water vapor present in the room, may produce very noticeable changes in the absorption bands. In the previous work, since readings were taken only every 0.007μ , we always had the combined effect of benzene and water vapor, for neighboring bands could not be separated.

In order to identify further the weak benzene bands, we made measurements on benzene in 5 different thicknesses. Fig. 4 (c), (d) and (e) show a

comparison of 3 such curves, and it is easily seen that on the short wave-length side of the 3 strong bands, benzene has no absorption. However, toward longer wave-lengths several bands show decided changes as the thickness is increased. The bands which show these changes, do not correspond to any of the air bands, and thus we can say definitely just which of the weaker minima indicate benzene bands, and which, water vapor. With this process we finally arrived at the results given for benzene in Table I. Here we have also listed for reference the wave-lengths of the water-vapor bands.

Obviously, if we could eliminate this atmospheric absorption the results could be interpreted more easily and no doubt would be more exact. This could be done by taking one set of values through the compound and then a set through an empty cell, and subtracting the respective ordinates. This, however, would again require zero readings and would thus make the procedure very much longer and harder. The only course which offers a convenient solution to the problem seems to be to enclose the entire spectrometer in a vacuum, or to say the least, in an enclosure which has been carefully freed from water-vapor and CO_2 . The entire instrument from Nernst lamp to thermocouple must be in such an atmosphere. Czerny⁶ enclosed his spectrometer in a tin case, which contained trays of P_2O_5 and KOH . Plans are at hand for putting this instrument into just such an enclosure. Until this is accomplished however, we must continue to use our method of locating the atmospheric bands, and then picking them out of the other absorption curves.

TABLE I. *Wave-lengths of observed bands.*

Air	Air (con)	Air (con)	Air (con)	Air (con)	Benzene	Toluene
3.054 μ	3.193 μ	3.331 μ	3.633 μ	3.748 μ	3.236 μ	3.240 μ
3.073	3.202	3.342	3.642	3.754	3.257	3.263
3.083	3.210	3.348	3.654	3.762	3.296	3.301
3.093	3.217	3.364	3.659	3.768	3.383	3.386
3.098	3.224	3.379	3.664	3.781	3.412	3.426
3.106	3.230	3.397	3.675	3.787	3.440	3.489
3.115	3.241	3.430	3.685	3.801	3.463	
3.127	3.246	3.455	3.697	3.807	3.508	
3.139	3.267	3.485	3.709	3.813		
3.146	3.270	3.498	3.715	3.825		
3.153	3.281	3.512	3.721	3.830		
3.158	3.305	3.603	3.730			
3.178	3.312	3.614	3.736			
3.180	3.321	3.626	3.743			

In this manner, the bands of toluene were also located. Curve (d) of Fig. 5 shows this absorption clearly. The air bands are easily identified. The remaining bands, whose wave-lengths are given in Table I, agree nicely with those stated in the previous paper. Again we note only a slight shift toward longer wave-lengths in the locations of the three strong bands of the benzene C-H's. These shifts are 0.004 μ , 0.006 μ and 0.005 μ respectively. The minimum at 3.307 μ shows up in the other curves for toluene to be due to air. The general intensity distribution throughout this entire region is the same as that shown previously.

⁶ M. Czerny, *Zeits. f. Physik* **34**, 227 (1925).

Curve (b) of Fig. 5 shows an attempt to measure the absorption of cyclohexane at a thickness of 0.05 mm. As is shown in the curve the intensity of the absorption is extremely great. From 3.35μ to 3.46μ this thickness is opaque, the only energy transmitted being the 30 per cent contamination due to 1.75μ . The results were the same, using a film formed by putting one drop of the liquid between two cover glasses, which were then pressed together. Le Compte⁷ gives a curve for it, but does not mention the thickness. He

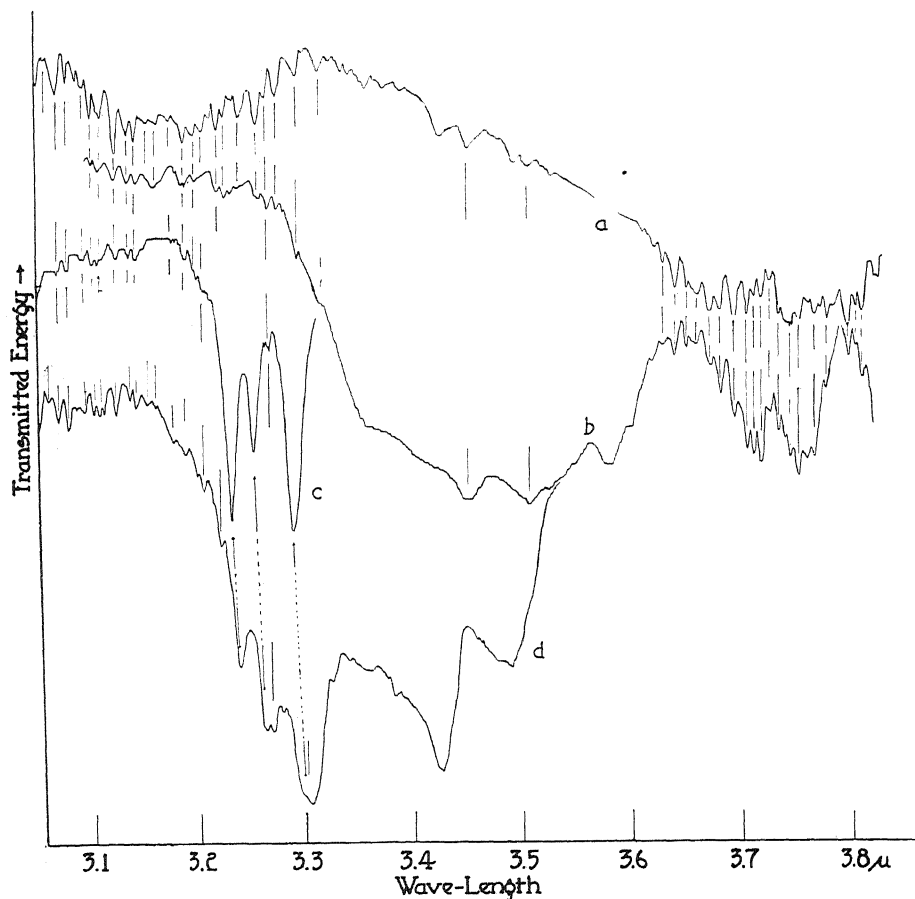


Fig. 5. Absorption curves. (a) atmospheric absorption. (b) cyclohexane, $t=0.05$ mm. (c) benzene, $t=0.05$ mm. (d) toluene, $t=0.05$ mm.

finds for it bands at 3.16μ , 3.26μ , 3.60μ and 3.90μ . We find the strong band somewhere between 3.35μ and 3.46μ . It is interesting to note that the three benzene bands are entirely absent. In this molecule no C atom has only one H atom attached as in benzene, but each has two. Apparently, the H-C-H vibrations are quite different from the C-H vibrations. Cyclohexene, also shows an extremely strong absorption in this region.

⁷ J. Le Compte, *Le Spectra Infrarouge.*, p. 218.

CONCLUSIONS

Specific heat calculations⁸ and Raman photographs⁹ each show definitely that the C-H linkage must vibrate with a frequency very close to 3.5μ . In most organic liquids then, we must expect to find very complex absorption bands in this region. Remembering that water also has a strong band close to 3.0μ , we see that almost every liquid will have pronounced absorption between 3.0μ and 4.0μ . The resulting fact, that so many liquids have complex bands around 3.5μ , makes this spectral interval a most interesting and fruitful source of information concerning the structure of the molecules. To obtain all of this information we must develop instruments of still higher sensitivity and resolving power. With the present spectrometers however, we can learn quite a bit.

In our first paper we showed several progressive shifts and changes in the bands, which were apparently connected with the symmetry and structure of the molecule. The curve on cyclohexane shows no trace of the three strong benzene bands. This is the first curve in which they have been entirely absent, and this is the first molecule we have examined which had no simple C-H bonds. Toluene and each of the other derivatives had some C-H linkages, in addition to their respective radicals. In these we found separate absorption due to the C-H, CH_3 , C_2H_5 and C_4H_9 groups. Here in cyclohexane the absence of bands for C-H gives us additional evidence, which seems to show a mutual effect between two neighboring C-H bonds. Every shift and intensity change tells something about the molecule, and it is hoped that a theoretical discussion of these will soon appear.

⁸ D. H. Andrews, *Chem. Reviews* 5, 4 (1928).

⁹ A. Dadiou and K. W. F. Kohlrausch, *Berichte der Deutschen Chemischen Gesellschaft* 2, 251 (1930).

THE EFFECT OF HIGH PRESSURE ON THE NEAR INFRARED ABSORPTION SPECTRUM OF CERTAIN LIQUIDS*

BY J. R. COLLINS

CORNELL UNIVERSITY

(Received June 5, 1930)

ABSTRACT

Certain absorption bands of liquid water, methyl alcohol, amyl alcohol, and toluene were studied when the liquids were subjected to high pressures. In the case of the first three liquids, pressures up to 5000 kg/cm² were used, and pressures up to 8000 kg/cm² were applied to the toluene. No change was found either in the spectral position or in the intensity of the bands studied. The results are of interest since a change in the polymerization of polar liquids is supposed to take place with increase of pressure. The absorption bands are characteristic of the molecules and hence a change in the position and intensity should accompany the change in polymerization. As no such change was observed, it is concluded that there is no change in polymerization in the pressure range studied. The pressure necessary to solidify toluene at 20°C. was found to lie between 8100 kg/cm² and 8300 kg/cm².

INTRODUCTION

THE anomalous properties of liquid water have been explained by the hypothesis that it is composed of two or more kinds of molecules. The simplest assumption is that water consists of the molecules (H₂O)₂ and (H₂O)₃ whose relative proportions depend on the physical conditions such as temperature, pressure, etc. Sutherland¹ has made calculations as to the relative amounts of the two constituents under various conditions of temperature. The author² has studied the near infrared absorption spectrum of liquid water from its freezing point to its boiling point and found changes which seem readily explained on Sutherland's assumptions. Redlich³ has used the author's results to calculate the relative amounts of the two kinds of molecules at various temperatures and finds fair agreement with similar calculations based on the change of magnetic susceptibility of liquid water as the temperature changes.

Sutherland explains the change in the viscosity of water with pressure by assuming that the degree of polymerization changes as the pressure changes. He estimates that a pressure of a few thousand atmospheres should convert all of the triple molecule into the simpler one. Hence, if one may interpret the change in the absorption spectrum as due to a change in the degree of polymerization, the absorption spectrum should show decided

* This investigation was supported by funds granted by the Heckscher Foundation for the Advancement of Research at Cornell University.

¹ Sutherland, Phil. Mag. 50, 460 (1900).

² Collins, Phys. Rev. 26, 771 (1925).

³ Redlich, Proc. Akad. Wissensch. Wien 53, 874 (1929).

changes as the pressure on the liquid is increased to several thousand atmospheres. Accordingly, the present experiments were undertaken to find if such changes do occur. Although the principal interest is in the case of water, the experiments were planned to include the study of toluene as a typical nonpolymerizing liquid and as many other liquids that do show polymerization as time would permit. The experiments were performed in the Jefferson Physical Laboratory at Harvard University, and the author is under deep obligation to Professor P. W. Bridgman who kindly designed the pressure chamber which provided plane parallel glass windows through which the radiation could be passed through the specimen.

APPARATUS AND EXPERIMENTAL PROCEDURE

The method of measurement was to pass a beam of radiation from an incandescent source through the chamber containing the liquid, to disperse the radiation by means of a spectrometer system and then to measure the intensity of the radiation at the exit slit of the spectrometer by means of a thermopile and galvanometer. On account of the impossibility of moving the absorption chamber, an indirect method of obtaining the fractional absorption of the liquid at the various pressures was used. Figure 1 illustrates

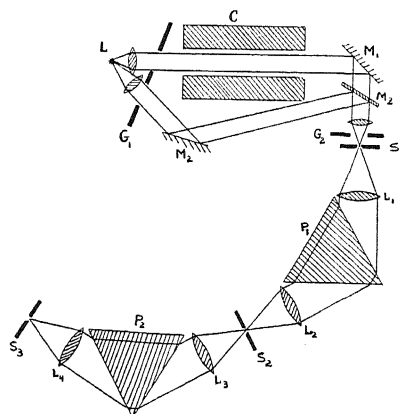


Fig. 1. Diagrammatic arrangement of apparatus.

diagrammatically the arrangement of apparatus. *L* is the filament of a street series incandescent lamp, from which two beams of parallel radiation are obtained. One of these beams passes through the absorption chamber *C* and is then focussed on the entrance slit of the spectrometer system. The other beam, after reflection from suitably placed mirrors, is also focussed on the slit of the spectrometer. By means of the shutter *G*₁ either of these beams may be blocked off and the intensity of the other measured by the thermopile. The beam which does not pass through the specimen serves as a standard of comparison, so that the absorption at any one pressure can be calculated if that at any other pressure is known. The absorption at atmospheric pressure was determined by a separate experiment.

The spectrometer used was a double Van Cittert spectrometer in which the slit S_2 is moved across the spectrum focussed in its plane. This movement allows any desired spectral position to be transmitted through the system. The double spectrometer is necessary to obtain the necessary purity of spectrum. The spectrometer was calibrated by means of emission lines from a mercury arc, and by means of the known positions of absorption bands of several liquids. Since the openings at the ends of the absorption chamber were only one quarter of an inch in diameter, the amount of radiation transmitted was very small. It was accordingly necessary to use a thermo-relay to magnify the galvanometer deflections. It was found that a magnification of fifty times was sufficient, and the Moll thermo-relay used was very steady at this magnification. On account of mechanical and electrical disturbances which were present in the daytime, all measurements were made at night.

Figure 2 shows the details of the mounting of the glass windows in the ends of the absorption cell. *A* is the window and was a cylinder of glass seven eighths of an inch in diameter and one and a quarter inches thick. A doubled piece of rubber tubing, *E*, was tightened around this window by

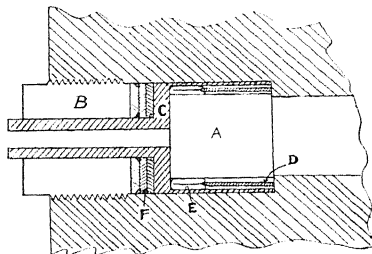


Fig. 2. Detail of mounting the windows in the pressure chamber.

means of the tube, *D*, and made a liquid tight seal between the window and holder *C*. This holder was forced in against the shoulder of the cell by means of the screw plug *B*. Packing at *F* was used to make the outside edge of the holder tight. When pressure was applied to the inside of the chamber, the window *A* was forced to a seat against the bottom of the holder. A thin washer of tin was placed between the window and bottom of the holder.

With plate glass as the material of the windows, pressures up to 10000 kg/cm² could be maintained for long periods of time. Unfortunately, however, plate glass has a strong absorption band in the spectral region being studied, and with the two windows only about one percent of the incident radiation was transmitted. Although several kinds of transparent glasses were tried, none were found which would allow pressures greater than about 5000 kg/cm² to be maintained for any length of time. Another arrangement which was used in the last part of the experiments was that described by Poulter,⁴ which allowed thin windows of plate glass to be used. These windows transmitted sufficient radiation to be measured. The holder, *C*, was

⁴ Poulter, Phys. Rev. 35, 297 (1930).

made solid and the inner end ground and polished to a plane surface. Then windows five sixteenths of an inch were cemented on to the end of the holder by a very thin layer of Canada balsam.

The original plan was to have the specimen placed in an absorption cell inside the pressure chamber so that the liquid transmitting the pressure would not contaminate the specimen. However, every liquid suitable for the transmission of pressure has strong absorption bands in the spectral region being studied, and so in the final arrangement the specimen filled the whole pressure chamber and as much of the pressure chamber above the absorption chamber as was possible without affecting the manganin coil whose resistance was measured as an indication of the pressure. Kerosene was used to transmit the pressure to the specimen liquid. A capillary tube connected the absorption chamber with the pressure producing apparatus and diffusion of the kerosene through this tube was apparently slow enough to prevent harmful contamination of the specimen. The test of this was to measure the absorption of the specimen after the pressure had been on for some time and then reduced to atmospheric pressure again. No change was noticed which could be ascribed to contamination of the specimen.

The procedure was as follows. The apparatus was assembled and a small pressure applied to find if the packing was liquid tight. Then by means of the shutters G_1 and G_2 the intensity of the two beams of radiation were obtained for various settings of the spectrometer system through the spectral region desired. Then the pressure was raised to about 1000 kg/cm² and the process repeated. Pressures higher than 5000 kg/cm² were not obtained under circumstances which permitted measurements of the absorption except in the case of toluene. This was possibly due to faulty assembly, although the same care was taken in all cases. This pressure is well in excess of that estimated by Sutherland for the complete conversion of the triple molecule of water into the simpler form.

A very interesting method of obtaining the pressure necessary for the solidification of toluene at 20° C. was to observe the interior of the pressure chamber by means of a reading telescope. When the pressure was slowly increased, fine needle like crystals would begin to form, and if the pressure was maintained, the whole of the liquid would become solid. On slowly reducing the pressure, the crystals would begin to melt. As the pressure was successively raised and lowered above and below the solidification point, the pressures at which the solidification and the melting took place came nearer to each other and after a great many trials, the final values obtained were: Freezing pressure 8300 kg/cm², melting pressure 8100 kg/cm².

RESULTS AND CONCLUSIONS

The results obtained for five absorption bands of water indicate that there is no change in the spectral position or intensity of the bands. The absorption bands of water which are studied are supposed to be the overtone bands of fundamental bands farther in the infrared. It was expected that these might show even greater changes than the fundamental bands would

show. Also they are not so intense as the fundamental bands so that reasonable thicknesses of the liquid could be used. When too thin layers are used, the thickness is increased at the higher pressures on account of the packing becoming compressed and thus allowing the windows to move outward. Only a few of the curves which were obtained are shown as they are all similar in that no change in spectral position is shown and only slight changes in intensity. These changes in intensity are ascribed to the increase in length mentioned above. Account was taken of the increase in density of the liquid as the pressure was increased.

A study of the absorption of toluene was made as an example of a non-polarizing liquid and thus, presumably, of a liquid whose molecules do not

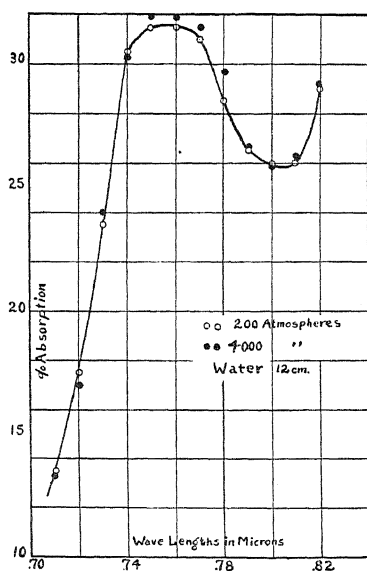


Fig. 3.

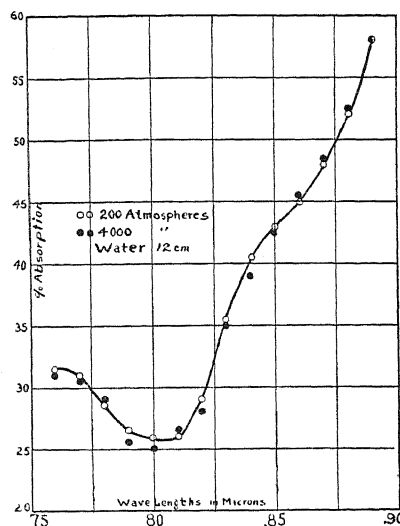


Fig. 4.

associate to produce complicated molecules. The two alcohols were studied as other examples of polymerized molecules.

Results are plotted for the lowest and highest pressures used as the results for the intermediate pressures lie intermediate between them. In the case of water several runs were taken at each absorption band and the results plotted are from one of the individual runs.

If we are to assume that changes in the absorption bands of a liquid should occur when the degree of polymerization changes, the results of these experiments indicate that no such change in polymerization occur in the pressure range used. It is difficult to imagine a process whereby an increase in pressure would cause a breaking up of the complicated molecules. Bridgman,⁵ in discussing the effect of pressure on the thermal expansion of water, concluded that his results do not indicate any breaking up of the complicated

Bridgman, Proc. Am. Acad. Arts, and Sci. 47, 544 (1912).

molecules. From other considerations, he concludes that the effect of pressure should be one of increasing the complexity of the molecules.

It is interesting in this connection to note that Stewart⁶ denies the existence of small molecular groups such as are postulated by Sutherland and others. His results on the x-ray diffraction halos produced by liquid water lead him to postulate the presence of very large groups of molecules with a regular arrangement, these groups having only a temporary existence to be succeeded by other similar groups. The results of the present experiments

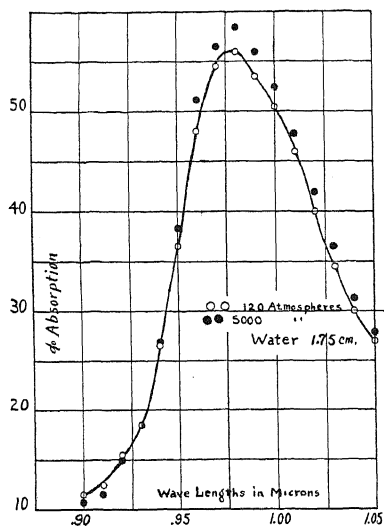


Fig. 5.

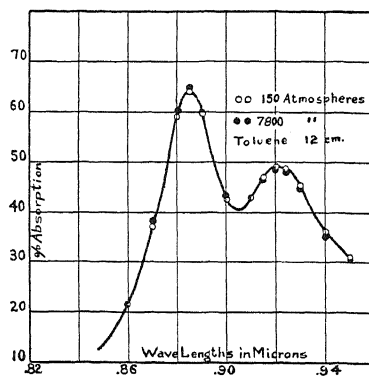


Fig. 6.

do not seem incompatible with this view of Stewart, as it seems likely that the absorption of the molecules within these groups would be different than that of the molecules not in the groups, and that there may be some effect of temperature on the number of molecules in the groups or on the time of existence of a given group.

The author wishes to make grateful acknowledgment of his indebtedness to Professor Bridgman for placing the pressure apparatus at his disposal. The author also feels under obligation to Mr. Mann, chief mechanic at Jefferson Laboratory, who helped by his skill and advice.

⁶ Stewart, Proc. Am. Phys. Soc. April, 1930.

ADSORPTION OF METHYL ALCOHOL FILMS ON ROCK-SALT

BY SHIRLEIGH SILVERMAN
JOHNS HOPKINS UNIVERSITY

(Received June 9, 1930)

ABSTRACT

The optical method of Rayleigh and Drude as recently modified by Frazer and Herzfeld has been applied to the study of methyl alcohol films on rock-salt. The isothermal adsorption has been studied at pressures ranging from 10^{-5} mm to 11 cm mercury. The results indicate that a unimolecular layer is formed at a pressure between 10^{-5} and 10^{-4} mm of mercury, with no further adsorption until the region of 2-3 cm, when a second layer begins to form, with completion at 9-10 cm. The thickness of these layers is calculated to be in the neighborhood of 4.5-5.0Å. The effect of thorough outgassing has been observed and the results have been interpreted to indicate that with decrease in temperature either an underlying unimolecular layer of water vapor is formed, or that there is a true increase in the natural ellipticity of the surface. In addition, it is possible to calculate the isothermal heat of adsorption from the experimental data.

INTRODUCTION

IF A beam of light be allowed to fall upon a plane surface of a transparent medium at the polarizing angle, the reflected beam is not found to be completely plane polarized, but is always elliptically polarized. Drude¹ has shown that the ellipticity of the reflected beam may be explained by assuming that there is not a perfectly sharp boundary between the two media, but that there is present a transition layer whose properties vary from the rare to the dense medium. This sheet whose index of refraction gradually changes from the value of 1 (assuming the 1st medium to be air or vacuum) to n , the refractive index of the 2nd substance, is known as the transition layer. Drude has worked out the equation which yields the relation between the observed ellipticity and the thickness of the transition layer; where we define as the ellipticity the ratio of the amplitudes of the minor and major axes of the ellipse of polarization.

The result is as follows:

$$\rho = \frac{\pi}{\lambda} \frac{(\epsilon_1 + \epsilon_2)^{1/2}}{\epsilon_1 - \epsilon_2} \int \frac{(\epsilon - \epsilon_1)(\epsilon - \epsilon_2)}{\epsilon} dz \quad (1)$$

where ρ is the ellipticity, ϵ_1 , ϵ and ϵ_2 are the dielectric constants of the first, the transition, and the second media respectively, λ the wave-length of the incident light, and z the position in the transition layer.

It is possible to determine a lower limit for the value of the thickness of the layer, L , which will not deviate very greatly from its true value. For a

¹ Drude, Theory of Optics, p. 287, Longmans (1901).

given value of ρ it is evident that L will attain its smallest value when ϵ is assumed to be a constant whose value is determined by making the factor $(\epsilon - \epsilon_1)(\epsilon - \epsilon_2)/\epsilon$ a maximum. This condition will be fulfilled when $\epsilon = (\epsilon_1 \epsilon_2)^{1/2}$. Setting the refractive index equal to the square root of the dielectric constant, the expression for the lower limit of L becomes:

$$\frac{L_{min}}{\lambda} = \frac{\rho}{\pi(1 + n^2)^{1/2}} \frac{n + 1}{n - 1} \quad (2)$$

where n is the refractive index of medium 2 with respect to medium 1.

Work by Langmuir, and later by Eucken, has formed the background for the theory that adsorption takes place in uniform monomolecular layers, and that each layer is completed before the formation of a subsequent one. Many other workers have substantiated this theory. However, many experimenters have worked with glass surfaces, with the resultant difficulty that it is very hard to describe the exact condition of the surface; to say nothing of the elaborate set-up required for the volumetric measurements on such large surfaces. Now, an adsorbed film fulfills the condition of Drude's transition layer. So, by taking a small cleavage surface of a crystal (two or three millimeters square was found to be quite large enough) which reflects nearly as well as plate glass, it is possible to calculate directly the thickness of the adsorbed layer by observing the changes in the ellipticity of the reflected light. The materials selected for this experiment were rock-salt for the transparent medium, because of the relative ease with which a perfectly clean surface may be prepared; and methyl alcohol for the vapor, because of the insolubility of rock-salt.

The equations of Drude require that the amplitude of the incident light in the plane of incidence be equal to the amplitude in the direction perpendicular to the plane of incidence. In early work on the measurement of thin films by Drude¹ and Rayleigh² the incident light is polarized at an angle of 45° at the plane of incidence. The ellipticity was measured by means of a Babinet compensator. Other investigators; Ives and Johnsrud³ and Ellerbroeck,⁴ have measured films; but in no case with an accuracy greater than several Angstrom units. The method has been considerably improved in this laboratory by Herzfeld and Frazer,⁵ and an accuracy of 3/10 to 4/10 Å has been attained. The essential improvements are: (1) the incident light is unpolarized, giving greater intensity while fulfilling the conditions set by the theory. (2) the ellipticity is measured photometrically with an accuracy unobtainable with a compensator. The present apparatus is very similar to that used by the above mentioned authors, with a few added refinements, particularly in the photometric arrangement.

The apparatus is shown diagrammatically in Fig. 1. The source of light was an Edison 500 C. P. Pointolite which gives a very intense beam that is

² Rayleigh, *Phil. Mag.* [6] 23, 431 (1903).

³ Ives and Johnsrud, *Journal of the Optical Soc.* 15, 374 (1927).

⁴ Ellerbroeck, *Arch. Neerland Sci.* 111, A10, 42-90 (1927).

⁵ Frazer, *Phys. Rev.* 33, 99 (1929).

quite uniform. After passing through a pin hole S_1 , the image of the hot tungsten plate was brought to a focus on a second pin hole S_2 and the beam made parallel by lens L_3 . A piece of clean plate glass M_1 was placed at a very slight angle to the beam, the transmitted light being allowed to fall upon the crystal and the reflected beam being used as the comparison beam in the photometer. The transmitted beam was reflected from the crystal R at the polarizing angle, passed through the analyzing nickel and brought to focus upon a piece of lightly ground glass G_1 . This serves to produce a very uniform field in the photometer. The beam is then made parallel by a lens L_5 , is passed by the edge of the mirror M_3 through the photometer P and the filter A , to the eye. The comparison beam was reflected successively from the mirrors M_1 and M_2 , brought to focus upon a bit of ground glass G_2 which formed a pin hole S_3 ; behind this was placed the photometric wedge W . The beam is again made parallel, and is reflected from the photometer mirror M_3 through the filter A to the eye.

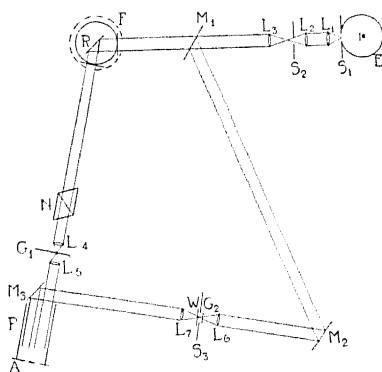


Fig. 1. Diagram of apparatus.

The photometer was of the Pfund split-field type, which consists of a mirror of a very sharp edge, set at an angle of 45° to the incident beams. One ray passes by the edge of the mirror and the other is reflected by it. The wedge was selected to give a linear transmission curve between ten percent and sixty percent; and was neutral as far as could be determined spectrophotometrically. In addition, screens were used which were calibrated against the wedge, and checked upon the same spectrophotometer. Inasmuch as the wave-length enters Drude's formula it is necessary to use a color filter. For this purpose, an aniline solution was found to be preferable to a monochromator since the intensity of the transmitted light is much greater. Such a solution was prepared by Professor Pfund, and the spectral centroid (5550A) calculated to an accuracy of about one percent.

The vacuum system itself merits a brief description. To prevent, as far as possible, contamination by stop-cock grease and occluded water vapor, a tube of activated coconut charcoal was placed between the crystal container and the rest of the system. The charcoal was previously outgassed by repeated heating to a dull red heat until no further gas was driven off. To make

certain that there was no backing-up on the far side of the charcoal plug, and auxiliary tube was connected to the container after the end of the main experiment. Pressure readings were found to be the same on both sides of the charcoal. The alcohol is kept in a trap and the vapor admitted as desired through a small stop-cock which was kept on the far side of the charcoal. The low pressures were read on a McLeod gauge. This was believed to be reliable as the pressure difference in the gauge at the highest pressures read was only 1.5 centimeters of mercury which is considerably below condensation pressure. As for occlusion of gases in the capillaries of the gauge, it was found that repeated pressure readings were quite consistent, so that it was not likely that our readings were affected. Higher pressures were read on the manometer.

EXPERIMENTAL PROCEDURE

The experimental procedure was as follows: a piece of rock-salt which was free of cloudiness was ground and polished along one edge at an angle of about 20° to the nearest cleavage plane. It was then cracked along the nearest cleavage direction and placed immediately in the container at the polarizing angle; and the apparatus was evacuated immediately. The polishing of the back plane at this angle of 20° removed entirely any reflection from the rear surface which would have vitiated our readings. The bottle containing the crystal was then heated and pumped out at a fairly good vacuum, 10^{-5} millimeters of mercury, for some hours. Methyl alcohol was admitted and the pressure noted; the nicol prism was set for minimum and maximum transmission, and the square root of the ratio of the readings gave the value of ρ . The temperature was measured and kept constant to within 5°C . The pressure was varied, and the readings taken again. This was repeated until the whole range between 10^{-5} mm and 11 cm had been covered. The temperature was then raised to the desired value, and the set of readings repeated. The alcohol was supplied by the Chemistry Department; no traces of water vapor or of any volatile organic substances were listed among the impurities.

Certain precautions were found to be quite necessary; (1) It is exceedingly important that no water vapor be present to be adsorbed on the surface; (2) No stop-cock grease or metal should be used in the set up as they might contaminate the surface; (3) The windows of the outfit must be free of double refraction; (4) The pressure in the gauge has to be corrected to give the pressure in the container as there is a temperature difference. As for the first precaution, it is impossible to state at present whether or not all traces of water vapor can be removed, even by continued heating at temperatures around 325°C . This will be discussed more fully at the end of the article. The second contamination was avoided more readily. The crystal was imbedded in a bead of molten silver chloride at the end of a glass rod, and the upper end of the rod was ground nicely to fit into a tube; no lubricant was used. This arrangement permitted very easy adjustment of the angle of reflection, and after the crystal was set at the polarizing angle, the tube was

sealed off. The windows were of Pyrex plate glass, which were very carefully annealed and tested between crossed nicols after being sealed to the container. To further test for double refraction a specimen was taken and its ellipticity determined in air and in the apparatus. The two values were identical. Knudsen's equation for the relative pressures on the two sides of a porous plug at absolute temperatures T_1 and T_2 respectively, is:

$$\frac{p_1}{p_2} = \frac{T_1^{1/2}}{T_2^{1/2}} \quad (3)$$

This equation fits our condition fairly closely for low pressures, and the correction was applied to all our low pressure readings; at high pressures the temperature correction is small enough to be neglected.

It was found possible to read the photometer to an accuracy of two percent. Accordingly, a group of eight or nine settings was taken for each reading, so that the probable error was quite close to one percent. Now,

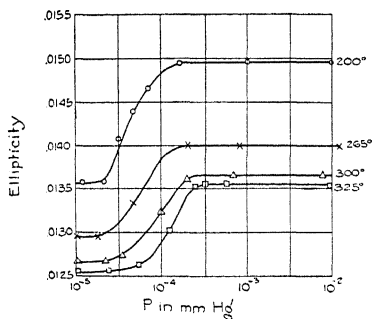


Fig. 2. Adsorption isotherms.

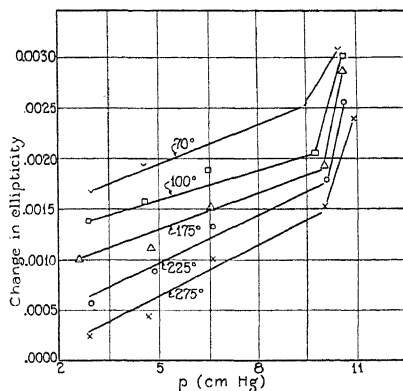


Fig. 3. Adsorption isotherms.

for $\lambda = 5550\text{\AA}$, a value of $p = 0.01$ means a layer about 45\AA thick. The values of p range from 0.0125 to 0.0170, so that the absolute error was about 0.5\AA . This is the same percentage error, but a slightly larger absolute error than is claimed by Frazer.⁵ In all cases the adsorption is found to be completely reversible, and an adsorbed layer can be removed at will, returning the surface to its original condition.

EXPERIMENTAL RESULTS

At 325°C and 10^{-5} mm pressure the ellipticity had a value of 0.01265. The value remained unchanged at twice this pressure and then increased to a value of 0.01365 at 2×10^{-4} mm from this pressure up to the neighborhood of 2 cm there was no further change in the ellipticity. From this point, the value increased linearly until 9.5–10 centimeters was reached, after which there was an abrupt increase in the ellipticity. The isothermal corresponding to 300°C showed a very similar curve, parallel and higher than the one at 325°C . At 10^{-5} mm the value was 0.0127, and above 10^{-4} mm the value was

0.0137. The same flat region extending to two or three centimeters was noticed, and the following portion proceeded as in the first case. The curves were repeated for intervals down to 75°C. In all cases the adsorption at lower pressures occurred roughly between 10^{-5} mm and 10^{-4} mm, and in all cases there was no further change until the neighborhood of two to three centimeters had been reached. Further, the ellipticity following two centimeters proceeded regularly until ten centimeters was reached. These curves are shown in Figs. 2 and 3.

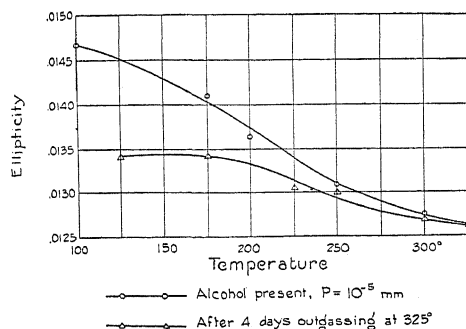


Fig. 4. Ellipticity as function of temperature. ($p=10^{-5}$ mm)

Lastly, the outfit was outgassed and the pressure was lowered to 10^{-5} mm, the temperature being 325°C. The pressure was kept constant and the temperature lowered progressively to 70°C, with readings being observed at intervals of about 50°C. The apparatus was then heated for three days at 325°C and 10^{-5} mm; it was then cooled over-night. Following, it was heated under the same conditions continuously throughout a period of four days. Readings were again taken at various temperatures as the cooling progressed. As will be seen from Fig. 4 at 325 degrees, the two curves coincide; their divergence is noticeable at 250°C, while at 100°C the increase in ellipticity for the clean surface in air is about 0.0008, and the corresponding increase for the surface in the presence of methyl alcohol is 0.00205.

INTERPRETATION AND DISCUSSION

The results of the preceeding section are summarized in the following table:

Temp.	$\Delta\rho_1$	$\Delta\rho_2$	L_1	L_2
325	0.0009		4.1A	
300	.00095		4.3	
275	.0011	.0011	4.9	4.9A
225		.0012		5.4
200	.0014		6.3	
175		.0009		4.1
100		.0008		3.6
75		.0008		3.6

Where $\Delta\rho_1$ is the change in ellipticity in the approximate interval of 10^{-5} to 10^{-4} mm and $\Delta\rho_2$ the change in ellipticity in the approximate interval of

2–10 cm; L_1 and L_2 are the respective thicknesses in Angstroms corresponding to $\Delta\rho_1$ and $\Delta\rho_2$. The average value of L_1 is 4.9A, and the average value of L_2 is 4.3A. These values agree fairly well with values calculated by means of the kinetic theory. Pictorially, this means that the first layer of methyl alcohol molecules first begins to be adsorbed on the surface at pressures slightly above 10^{-5} mm, and that the layer is complete at pressures slightly above 10^{-4} mm. The alcohol molecule is probably oriented with its long axis perpendicular to the surface, with the OH radical adjacent to the Na ions of the lattice. From the pressure of about 10^{-4} mm until the region of 2–3 centimeters there is no further adsorption. At this point the formation of a second layer commences, and becomes complete at around 9.5–10 cm. Whether or not the second layer is oriented cannot be said definitely, as the binding forces must be considerably weaker than in the case of the first layer.

While the interpretations of the isotherms are apparently clear, it is much more difficult to explain the changes with temperature. The curves of

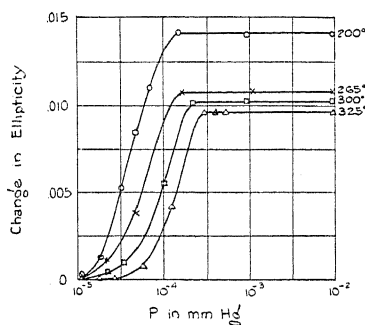


Fig. 5. Adsorption isotherms referred to a common origin.

Fig. 4 seem to show that the surface is clean at 325°C, so that the measured ellipticity must be natural to the clean surface. The increase in ρ with decrease in temperature may be explained in one of two ways. First, as the temperature is lowered, a single layer of water vapor might begin to form which is complete at temperatures around 100°C. This would mean, then, that at high temperatures there is adsorption only of methyl alcohol, but that at lower temperatures adsorption of both methyl alcohol and a layer of water vapor is observed. The second possibility is that there is no water vapor present and that the increase in ellipticity is indicative of an actual surface roughening with lowering of temperature. Very recently, Frazer⁶ has observed the same type of curve with an agreement which is very encouraging. He attributes the increase in ellipticity to an adsorption of air; however, this is rather unlikely. The only possible constituent of air that would be likely to adsorb so strongly would be water vapor. However, there is nothing conclusive to be drawn from the data thus far. Certain modifications in the crystal container will have to be introduced, as it does not now appear that outgassing by heat alone is sufficient to determine whether all traces of water vapor have been removed.

If the effect is actually due to temperature directly, then we can move the curves of Fig. 2 to a common origin at their lowest points as in Fig. 5. This will then give us a family of curves of true adsorption. Then it is possible to calculate the isothermal heat of adsorption by means of the Clausius-Clapeyron equation:

$$\frac{d(\log p)}{dT} = \frac{Q}{RT^2} \quad (4)$$

The approximate values obtained are: 7000 calories for the first layer and 2000 calories for the second layer, in the region of 250°C. However, theoretical considerations seem to be in favor of the first view as the theoretical value of Q is several times larger. If at 325°C the alcohol is adsorbed directly on the salt we could use as a rough approximation the following formula which is due to Nernst:

$$\log p = -\frac{Q}{4.51T} + 3 + 1.75 \log T \quad (5)$$

which, with a value of $p = 10^{-4}$ mm and $T = 600^\circ\text{K}$, yields a value of 40,000 calories per mol. On the other hand one can calculate the energy between an ion and a dipole of moment⁶ P , which is (PeN/r^2) ergs per mol. If we accept for r the value calculated from the hydration of the sodium ion, $r = 1.74\text{\AA}$, for P the value 1.7×10^{-18} ; one again finds for the value of Q about 40,000 calories per mol. On the other hand, we find for 200°C almost the same pressure, which would make Q about 21,000 calories; this decrease can best be accounted for as being due to an adsorption on a partly water covered surface. But the value of 7,000 calories as found experimentally is far too small to account for the vapor pressure as small as 10^{-4} mm at 300°C. One might state the argument in another form. One can expect that the equilibrium pressure of an adsorbed monomolecular layer and the vapor pressure of the substance in bulk to be similar, if the heat of adsorption and the heat of evaporation are similar. Water, with a heat of evaporation of about 9500 calories boils at 100°C; mercury with 13000 calories boils at 338°C. As the equilibrium pressure in the present case is 10^{-4} mm at 325°C, the heat of adsorption must be considerably higher than 13000 calories.⁸

The author wishes to take this opportunity to acknowledge many useful suggestions of Professor A. H. Pfund, concerning the optical set-up; and to express his sincere thanks to Professor Karl F. Herzfeld who has suggested this problem and whose assistance and supervision during its growth have been most helpful.

⁶ J. H. Frazer, *Phys. Rev.* **34**, 645 (1929).

⁷ K. Hojendahl, *Phys. Zeits.* **30**, 391 (1929).

⁸ K. F. Herzfeld, *Kinetische Theorie der Wärme*, p. 298 ff. Vol. 3, Müller-Pouillet, *Lehrbuch der Physik*.

THE PRINCIPAL MAGNETIC SUSCEPTIBILITIES
OF BISMUTH SINGLE CRYSTALS

BY ALFRED B. FOCKE

CALIFORNIA INSTITUTE OF TECHNOLOGY, PASADENA, CALIFORNIA

(Received June 9, 1930)

ABSTRACT

The Gouy method is used to determine the principal magnetic susceptibilities of bismuth single crystals grown by the method developed by Goetz. The specific susceptibility is shown to be a constant in all directions perpendicular to the principal crystallographic axis with a value of -1.487×10^{-6} . Parallel to the main axis the specific susceptibility is a minimum and has the value -1.046×10^{-6} . The mean is given then as -1.340×10^{-6} .

I. HISTORICAL

RECENT investigations by Goetz,¹ Goetz and Hasler,² and Goetz and Focke,³ concerning the effects of allowing one half of a single crystal of bismuth to crystallize in a strong magnetic field, have shown that different orientations are affected in different ways. The effects are a maximum if the principal axis is perpendicular to the field and a minimum if the axis is parallel to the field. This at once leads to the conclusion that if the susceptibility is a contributing factor in the effect, it must also have a maximum perpendicular to the main axis and minimum parallel to it. This supposition is sustained by the results obtained by Nusbaum.⁴ There is however an objection to accepting the absolute values of the results which he has reported since the value given by him as the maximum is still below that given in tables for the susceptibility of the heterogeneous crystal aggregate. Because of this, it was felt that a new determination of the principal susceptibilities of bismuth should be made.

II. PREPARATION OF CRYSTALS

The bismuth used in the crystals described in this paper was obtained from the Braun Corporation and subsequently vacuum distilled in an effort to purify it.

The single crystals were made by the method developed by Goetz.¹ Crystals are grown in this method, by moving a rod of the metal which is lying in a graphite trough through a furnace at such a speed that once a crystal begins to form, it can continue its growth throughout the entire rod, the orientation of the crystal being determined by inoculation. The orientations used were P_1 (principal axis perpendicular to the length of the rod) and P_3 (principal axis parallel to the length of the rod). The

¹ A. Goetz, Phys. Rev. 35, 193 (1930).

² A. Goetz and M. Hasler, to appear in Phys. Rev.

³ A. Goetz and A. Focke, to appear in Phys. Rev.

⁴ C. Nusbaum, Phys. Rev. 29, 905 (1927).

accuracy of the orientations could be checked after magnetic observations were taken by cleaving the crystal along the basal cleavage plane. In the case of the P_1 crystals, this plane was parallel to the rod making it possible to obtain a very accurate determination of the orientation. The crystals used were all correct to less than ten minutes of arc. The P_3 orientation could not be checked so accurately in this way since the cleavage plane is perpendicular to the rod but as no error could be noticed it was probably accurate to within two degrees.

The crystals were searched for strangers and twinning lamellae before and after the observations, by etching them in nitric acid. Only those crystals which were free from these imperfections were used as any such irregularities would have destroyed the accuracy of the results.

3. METHOD OF MEASUREMENTS

The Guoy method⁵ was chosen for making these measurements. The principal requirement of this method is that the sample must have a uniform cross section over the entire section in which the field gradient is appreciable. The condition of the extreme ends is not important as they are both located in uniform fields. Both of these facts were advantageous because long uniform single crystals were available and also the twinning lamellae at the ends of the crystals, which invariably are formed when bismuth is cleaved, would be in such a position as to have no effect upon the results.

The arrangement is shown in Fig. 1.

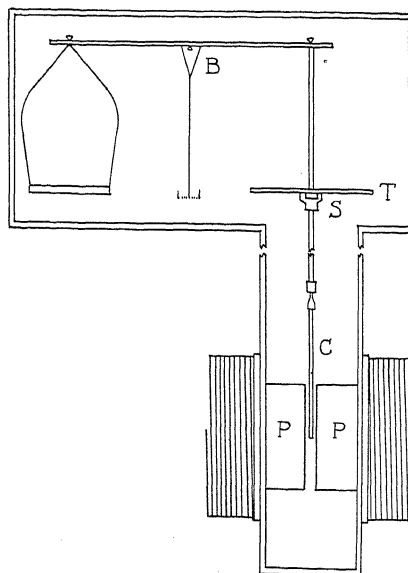


Fig. 1. Arrangement of apparatus.

An aluminum suspension S was designed to take the place of one of the regular pans of a sensitive analytical balance B . It was fitted with a divided

⁵ E. C. Stoner, *Magnetism and Atomic Structure*, p. 40, (1926).

torsion head T so that the sample could be rotated about the vertical axis. The lower end of the suspension was about eight centimeters above the pole pieces P of the magnet. This distance was great enough so that the suspension was totally unaffected by the magnetic field. The pole pieces were flat faced and ten centimeters in diameter, giving a very uniform field between them with comparatively little stray field. The crystals C were thirteen centimeters in length, thus placing the lower end on the axis of the pole pieces while the other end was in a field of negligible intensity.

The balance, suspension, crystal and the ends of the pole pieces were enclosed in a cabinet to prevent air currents from disturbing the apparatus.

The greatest error to be expected between any two determinations of the susceptibilities was about 2 percent. The greatest single source of error was in the determination of the area of the cross section of the crystals. Due to the peculiar shape caused by the method of growth, the only practicable way of measuring the cross sectional area was by computing it from the weight, length and density of the sample under consideration. The error thus introduced was about 1 percent. The field strength was measured with a Grassot fluxmeter introducing a possible error of 0.5 percent, and the force exerted upon the crystal by the field was accurate to within 0.3 percent. The greatest deviation actually observed was less than 1.5 percent.

4. THEORY OF THE METHOD

Let a crystal with principle susceptibilities k_1, k_2, k_3 be placed in a magnetic field as in Fig. 2.

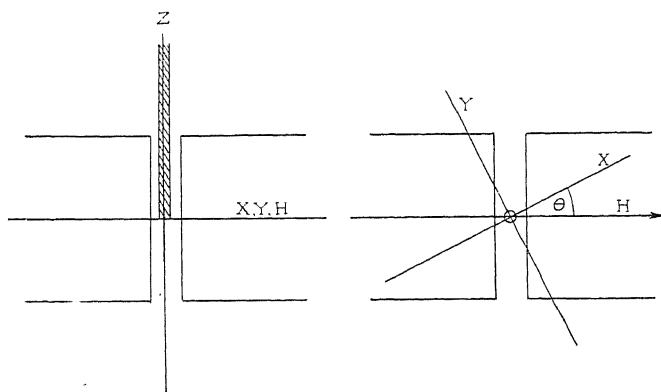


Fig. 2. Arrangement of crystal in magnetic field.

Take a set of axes parallel to the principal magnetic axes of the crystal with origin at its lower end.

Let z be parallel to the length of the crystal and let x make an angle θ with the magnetic lines of force. The boundary conditions will then be

$$H_x = H \cos \theta \quad H_y = H \sin \theta \quad H_z = 0$$

$$\frac{\partial H_x}{\partial x} = \frac{\partial H_x}{\partial y} = \frac{\partial H_y}{\partial x} = \frac{\partial H_y}{\partial y} = \frac{\partial H_z}{\partial x} = \frac{\partial H_z}{\partial y} = \frac{\partial H_z}{\partial z} = 0$$

if the diameter of the crystal is small in comparison to that of the pole-pieces.

The equation for the energy of a magnetic field in an anisotropic medium is given as

$$E = \frac{1}{8\pi}(\mu_x H_x^2 + \mu_y H_y^2 + \mu_z H_z^2)$$

where

$$\mu_x = 4\pi k_x, \mu_y = 4\pi k_y, \mu_z = 4\pi k_z$$

thus

$$E = \frac{1}{2}(k_x H_x^2 + k_y H_y^2 + k_z H_z^2).$$

The force in directions parallel to the axes is

$$F_x = \frac{\partial E}{\partial x} = \frac{k_x}{2} \frac{\partial H_x^2}{\partial x} + \frac{k_y}{2} \frac{\partial H_y^2}{\partial x} + \frac{k_z}{2} \frac{\partial H_z^2}{\partial x}$$

$$F_y = \frac{\partial E}{\partial y} = \frac{k_x}{2} \frac{\partial H_x^2}{\partial y} + \frac{k_y}{2} \frac{\partial H_y^2}{\partial y} + \frac{k_z}{2} \frac{\partial H_z^2}{\partial y}$$

$$F_z = \frac{\partial E}{\partial z} = \frac{k_x}{2} \frac{\partial H_x^2}{\partial z} + \frac{k_y}{2} \frac{\partial H_y^2}{\partial z} + \frac{k_z}{2} \frac{\partial H_z^2}{\partial z}$$

or

$$F_x = k_x H_x \frac{\partial H_x}{\partial x} + k_y H_y \frac{\partial H_y}{\partial x} + k_z H_z \frac{\partial H_z}{\partial x}$$

$$F_y = k_x H_x \frac{\partial H_x}{\partial y} + k_y H_y \frac{\partial H_y}{\partial y} + k_z H_z \frac{\partial H_z}{\partial y}$$

$$F_z = k_x H_x \frac{\partial H_x}{\partial z} + k_y H_y \frac{\partial H_y}{\partial z} + k_z H_z \frac{\partial H_z}{\partial z}$$

Substituting the boundary condition these equations reduce to:

$$F_x = 0$$

$$F_y = 0$$

$$F_z = k_x H_x \frac{\partial H_x}{\partial z} + k_y H_y \frac{\partial H_y}{\partial z}$$

$$F_z = k_x \cos^2 \theta H \frac{\partial H}{\partial z} + k_y \sin^2 \theta H \frac{\partial H}{\partial z}$$

$$F_z = [k_y + (k_x - k_y) \cos^2 \theta] H \frac{\partial H}{\partial z}$$

if $H=H$ when $z=0$ and $H=H_0$ when $z=z$ integrating over the volume we get

$$F = \int F_z dv = \int [k_y + (k_x - k_y) \cos^2 \theta] dx dy dz H \frac{dH}{dz}$$

or

$$k_y + (k_x - k_y) \cos^2 \theta = \frac{2}{(H^2 - H_0^2)} \frac{F}{A}.$$

If F is given in grams we have

$$k_y + (k_x - k_y) \cos^2 \theta = \frac{2gF}{A(H^2 - H_0^2)}.$$

In terms of the specific susceptibility x and if $H_0 \ll H$, we have

$$x_y + (x_x - x_y) \cos^2 \theta = \frac{2gF}{dAH^2}.$$

The similarity between this equation and that usually given for the Gouy method is seen at once by setting $x_x = x_y$ giving

$$x = \frac{2gF}{dAH^2}.$$

5. DISCUSSION OF RESULTS

Fig. 3 shows the result obtained when the principal axis of the crystal is parallel to the rod (P_3). In this case the axis is always perpendicular to the

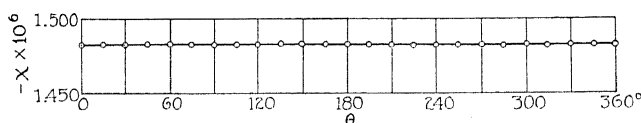


Fig. 3. Variation of specific susceptibility when major axis is parallel to length of the rod.

field and the distribution of the susceptibility in a plane perpendicular to the main axis is measured. It is seen at once that there is perfect circular symmetry about this axis.

Fig. 4 shows a compilation of five separate determinations of the variation of the susceptibility when the main axis is perpendicular to the rod, and a cosine square curve calculated from the average maximum and average minimum values of the susceptibility obtained in the cases of the five individual determinations. In the case of the maximum value the P_3 case is included. The agreement is evident showing that the variation definitely follows a cosine square law.

The principal susceptibilities of this bismuth may be given as $x_{min} = 1.046$ parallel to the main axis and $x_{max} = 1.487$ perpendicular to the main axis. The ratio of x_{max}/x_{min} is 1.425. This last point is particularly mentioned as it has been found that this ratio varies with varying amounts of impurities and an investigation of this effect is now in progress.

The susceptibility, calculated from these values, for a heterogeneous crystal aggregate is $-1.340, (2x_{max} + x_{min})/3$ agreeing very well with the values given in various tables.

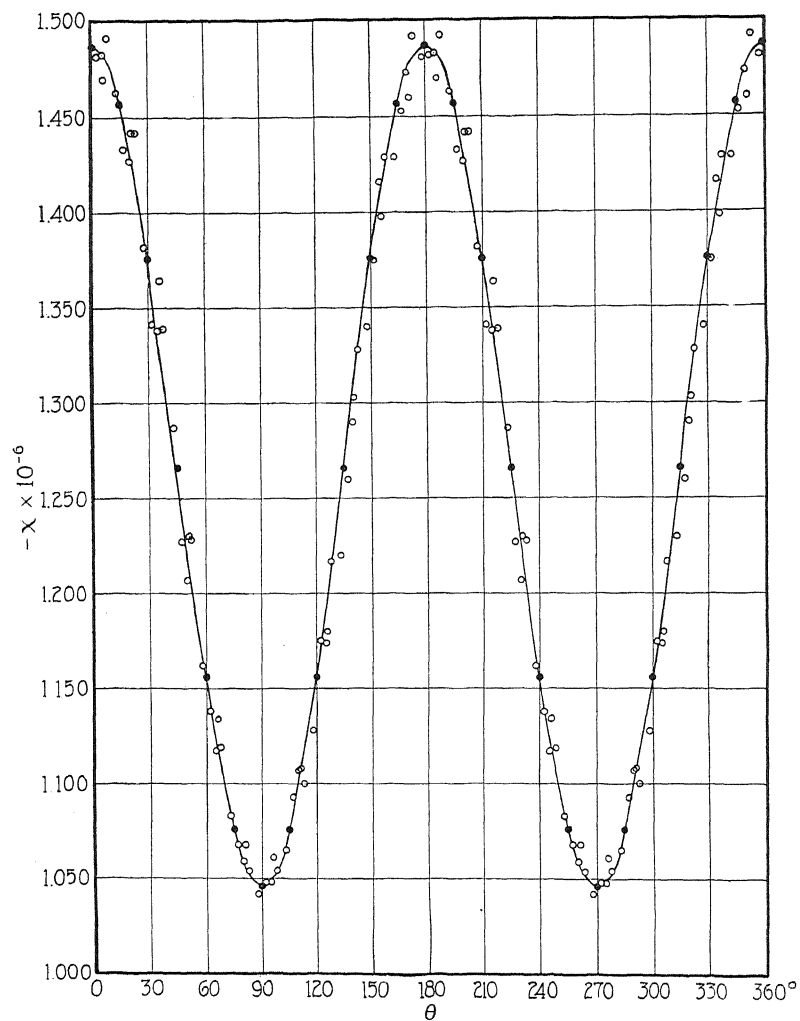


Fig. 4. Variation of specific susceptibility when major axis is perpendicular to length of the rod.

TABLE I. Data for figure 4.

Calculated Values		Crystal #120/11		Crystal #120/21	
θ	$-x \times 10^6$	θ	$-x \times 10^6$	θ	$-x \times 10^6$
0	1.487	13	1.463	2	1.482
15	1.457	28	1.392	17	1.433
30	1.376	43	1.287	32	1.341
45	1.266	58	1.162	47	1.227
60	1.156	73	1.083	62	1.138
75	1.076	88	1.042	77	1.068
90	1.046	103	1.065	92	1.048
105	1.076	118	1.128	107	1.093
120	1.156	133	1.220	122	1.175
135	1.266	148	1.340	136	1.260
150	1.376	163	1.429	152	1.375
165	1.457	178	1.481	167	1.453
180	1.487	193	1.463	182	1.482
195	1.457	208	1.392	197	1.433
210	1.376	223	1.287	212	1.341
225	1.266	238	1.162	227	1.227
240	1.156	253	1.083	242	1.138
255	1.076	268	1.042	257	1.068
270	1.046	283	1.065	272	1.048
285	1.076	298	1.128	287	1.093
300	1.156	313	1.220	302	1.175
315	1.266	328	1.340	317	1.260
330	1.376	343	1.429	332	1.375
345	1.457	358	1.481	347	1.453
360	1.487	13	1.463	2	1.482

TABLE I. (Continued).

Crystal #120/51		Crystal #120/61		Crystal #120/71	
θ	$-x \times 10^6$	θ	$-x \times 10^6$	θ	$-x \times 10^6$
8	1.492	5	1.483	6	1.470
23	1.442	20	1.427	21	1.442
38	1.339	35	1.338	36	1.364
53	1.228	50	1.207	51	1.230
68	1.119	65	1.117	66	1.134
83	1.054	80	1.059	81	1.068
98	1.054	95	1.048	96	1.061
113	1.100	110	1.107	111	1.108
128	1.217	125	1.174	126	1.180
143	1.328	140	1.290	141	1.303
158	1.429	155	1.416	156	1.398
173	1.492	170	1.473	171	1.460
188	1.492	185	1.483	186	1.470
203	1.442	200	1.427	201	1.442
218	1.339	215	1.338	216	1.364
233	1.228	230	1.207	231	1.230
248	1.119	245	1.117	246	1.134
263	1.054	260	1.059	261	1.068
278	1.054	275	1.048	276	1.061
293	1.100	290	1.107	291	1.108
308	1.217	305	1.174	306	1.180
323	1.328	320	1.290	321	1.303
338	1.429	335	1.416	336	1.398
353	1.492	350	1.473	351	1.460
8	1.492	5	1.483	6	1.470

DISCONTINUOUS CHANGES IN LENGTH ACCOMPANYING THE
BARKHAUSEN EFFECT IN NICKELBY C. W. HEAPS AND A. B. BRYAN
RICE INSTITUTE, HOUSTON, TEXAS

(Received May 15, 1930)

ABSTRACT

A heterodyne beat method is described by means of which displacements as small as 9×10^{-9} cm may be measured. When a nickel wire, 1.96 cm long and 0.01 cm in diameter, is subjected to a steadily changing magnetic field there is evidence of a sudden length change at the instant of a Barkhausen discontinuity of magnetization. For a nickel wire 2 cm long and 0.002 cm in diameter these sudden length changes were larger and could easily be measured. They were associated with every Barkhausen jump observed in the specimen. The largest one measured was 4.7×10^{-7} cm. Calculations based on the measurements of these magnetostrictive jumps give 3.7×10^{-7} cc. for the minimum value of the volume of the element which suffers the jumps. Reasons are advanced for believing that the sudden change in intensity of magnetization of this volume element cannot be less than 40 units nor more than 330. A qualitative theory of the phenomenon is given.

WHEN a ferromagnetic substance is magnetized by a field which changes continuously it is found that a part at least of the resulting change in intensity of magnetization takes place in sudden discontinuous jumps. This Barkhausen effect is usually observed by means of the induced voltages in a coil surrounding the specimen. Ferromagnetic substances also undergo a change of length when magnetized. There appears to be a very close relation between the magnetostrictive effect and the Barkhausen effect. One phenomenon has so far not been observed in a substance without the other, and both are affected by heat treatment and by mechanical strain.

It seemed probable therefore, that the discontinuities of magnetization should be accompanied by discontinuous changes in length of the specimen. This conclusion follows directly from one interpretation of McKeehan's¹ theory of atomic magnetostriction and is also in agreement with a theory of the Barkhausen effect which has been discussed by one of the authors.² In the experiments to be described a very sensitive and quick acting apparatus has been constructed and sudden changes in the length of a nickel wire have been observed to occur simultaneously with the Barkhausen discontinuities.

APPARATUS

The heterodyne beat method of measuring small capacity changes or small displacements is used. The apparatus, shown diagrammatically in Fig. 1, is a modification of that previously used by one of the authors.³ Oscillator A

¹ L. W. McKeehan, Jour. Frank. Inst. 202, 737 (1926).

² C. W. Heaps and J. Taylor, Phys. Rev. 34, 937 (1929).

³ A. B. Bryan, Phys. Rev. 34, 615 (1929).

is maintained at 1819 k.c. by a quartz crystal. Oscillator B , employing a shield grid tube, is the same as in the previous work except that different condensers are used. C_1 is a calibrated General Radio precision air condenser and is used for purposes of adjustment and calibration. C is a small condenser with two circular horizontal plates 2 cm in diameter. The top plate is supported by a 2 cm length of the nickel wire to be examined. It is steadied and vibrations are damped out by three short sections of rubber cut from ordinary rubber bands, arranged to press downward at three points on its upper surface. The lower plate is provided with a screw adjustment so that the spacing between the plates can be made very small. C is mounted near the center of the large solenoid S_1 , which is 15.7 cm long and has an inner diameter of 5.9 cm. The winding of S_1 and the leads to it are completely inclosed in a grounded copper shield. A field strength of 74.5 gauss per ampere is obtained.

Detector D includes a small loop antenna, a detector and a two stage amplifier. The radio frequency oscillations from A and B are picked up by D and the audible beat note between them is impressed on the telephone

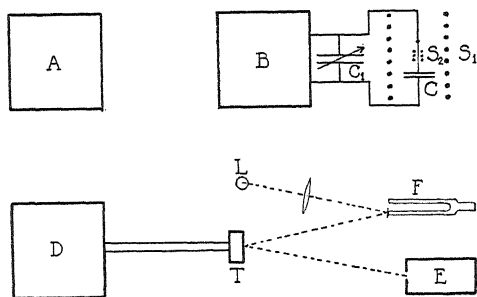


Fig. 1. Diagram of apparatus.

receiver T . A small mirror attached to T thus vibrates with the frequency of the beat note between A and B . A beam of light from lamp L , is reflected first from a mirror attached to one prong of a 300 cycle electrically driven tuning fork F . It is then reflected from the mirror attached to T and finally falls on a strip of motion picture film in camera E . The film moves downward while both mirrors are arranged to vibrate the beam of light in a horizontal plane. When the fork and heterodyne beat frequencies are about the same the combined motions of the two mirrors thus produce a sort of "photographic" beat as shown in Fig. 2. The frequency of this photographic beat is equal to the difference of the two component frequencies. When the field of S_1 produces magnetostriction in the nickel wire the capacity of C changes and there is a resulting change in the frequency of oscillator B , of the heterodyne note and of the photographic beat.

A time scale is obtained by focusing an image of the filament of an ordinary lamp on one edge of the film. The lamp carries 60 cycle alternating current and the filament vibrates with this frequency when a permanent magnet is brought near. This arrangement is not shown in Fig. 1.

The nickel wire passes through a small bakelite spool on which solenoid S_2 is wound. This solenoid is 0.65 cm in length and 1.58 cm in outside diameter and has 3960 turns. It is connected through a three stage amplifier to a second telephone receiver carrying a mirror. Light reflected from this mirror produces the third trace on the film, in this case a straight line which is broken when the sudden Barkhausen change in magnetization of the nickel wire induces a voltage in S_2 . None of this equipment except S_2 is shown in Fig. 1.

Suitable rheostats are used in series with S_1 to control the magnetizing current. A spiral of fine nickel wire is also connected in series with S_1 . This spiral may be heated by means of a nichrome heating coil which surrounds it, the resulting resistance change producing a slow continuous variation of current over a small range. The rheostats are so adjusted that this continuous change takes place over a range in which the Barkhausen discontinuities are largest.

THEORY OF THE MEASUREMENTS

Let the parallel plate condenser C have capacity C , area A , and plate distance d . Then $C = A/4\pi d$ and if d changes by a small amount δd we get $\delta d = -(A/4\pi C^2)\delta C$ where δC is the corresponding change in C .

Let n_0 be the frequency and C_0 the total capacity of oscillating circuit B . Then if we assume that n_0^2 is inversely proportional to C_0 it may easily be shown that a decrease δC_0 in C_0 will produce an increase δn in n_0 such that

$$\delta C_0 = C_0 \left[1 - \left(\frac{n_0}{n_0 + \delta n} \right)^2 \right] \quad (1)$$

or

$$\delta C_0 = 2C_0 \delta n / n_0 \quad (2)$$

for small changes. The only change in C_0 is that produced by the nickel wire in raising or lowering the upper plate of condenser C . Thus $\delta C_0 = \delta C$ and we get

$$\delta d = -AC_0 \delta n / (2\pi C^2 n_0). \quad (3)$$

In this equation δd is of course the desired change in length of the supporting nickel wire. All the quantities on the right may be easily determined. The area of A of the circular condenser plate as calculated directly from its measured diameter is 3.14 cm². The value of n_0 differs by a negligible amount from the known frequency of the quartz crystal used and may be taken as 1819 kilocycles. The other three quantities are found as follows:

- (1). *Determination of C_0 .*—A wavemeter is used to measure n_0 . Then a known large change in C_0 is produced by means of the calibrated variable condenser C_1 and the frequency $(n_0 + \delta n)$ is again measured. These readings and Eq. (1) give C_0 . The mean of several determinations is $C_0 = 597.4$ cm.
- (2). *Determination of C .* The reading of C_1 is noted when A and B are tuned to the same frequency. Then C is disconnected and B again tuned to the fre-

quency of A by adjusting C_1 . The increase of C_1 required for the retuning gives the value of C to be 41.2 cm.

(3). *Determination of δn .* Let n_A , n_B , and n_F be the frequencies of oscillator A , oscillator B , and the fork F , respectively. For simplicity assume $n_B > n_A$ and $(n_B - n_A) > n_F$. Then $(n_B - n_A)$ is the frequency of the heterodyne beat note between the two radio frequency oscillators and $(n_B - n_A - n_F)$ is the frequency of the photographic beat between this heterodyne note and the fork, as observed on the film. n_A and n_F remain constant. A decrease δd in the length of the nickel wire produces an increase δn in n_B and the frequency of the photographic beat increases to $(n_B - n_A - n_F + \delta n)$. Let $T = 1/(n_B - n_A - n_F)$ and $T' = 1/(n_B - n_A - n_F + \delta n)$ be the periods of the photographic beat before and after the change δd occurs, respectively. Then $\delta n = (T - T')/(TT')$. The periods T and T' are readily obtained from the film by means of the time scale. Obviously some care is necessary to determine whether an observed δn corresponds to an increase or a decrease in the length of the nickel wire.

To get an estimate of the smallest change in length which can be detected assume that $T = 1$ second and that a change in T of 10% can be observed. These conditions are obtained fairly easily. In this case $\delta n = 0.1$ cycle per sec. approximately, and from Eq. (3) $\delta d = 9.7 \times 10^{-9}$ cm. A higher sensitivity is obtained for larger values of T .

It should be mentioned that with this extremely high sensitivity there is always a gradual change in the beat frequency because of unavoidable temperature changes. Vibrations are perhaps an even more serious source of trouble. The condenser C was mounted on sponge rubber, a basement room was chosen for the experiment and records were taken at night; nevertheless seismic disturbances and a temperature drift were always in evidence. The sensitivity could no doubt be considerably increased by further efforts to eliminate these two disturbing factors.

RESULTS

The first specimen was a nickel wire 0.01 cm in diameter and 1.96 cm long. The photographic record showed several Barkhausen discontinuities. A curve was drawn with the period of the photographic beat plotted against time. Since the magnetizing current varied continuously with the time the curve indicated how the length of the wire varied as the field changed continuously. It was found that the smooth course of the curve showed breaks at two of the points where Barkhausen impulses occurred. However, since these breaks were only a little larger than the apparent discontinuities due to experimental error it was felt that the evidence was not entirely conclusive.

Accordingly a new nickel wire 0.002 cm in diameter and 1.98 cm long was prepared by immersing a larger wire for a short time in nitric acid. With a fine wire it was thought that the volume which gives the Barkhausen discontinuity by its magnetization change would be a larger percentage of the whole wire and would thus produce a proportionally larger effect on the gross magnetostriction of the specimen. The results seemed to justify

this idea. The magnetizing field was decreased from a large negative value to zero and then increased to a positive value of 18.6 gauss. A further slow increase to 26.1 gauss was then produced with the hot wire arrangement previously described and the photographic records were taken during this slow increase. There were usually one large Barkhausen impulse and two smaller ones in this region. Fig. 2 shows one of the three photographic records taken of the large impulse. The break at *A* shows the time of arrival of the impulse. The length *BC*, as measured on the time scale *F*, shows the period *T* of the photographic beat before the arrival of the impulse to be (70.2/60) sec. and the length *DE* shows the period *T'* after the impulse to be (10.5/60) sec. Hence $\delta n = (T - T')/(TT') = 4.85$, and from Eq. (3) the change δd in the length of the wire is found to be 4.7×10^{-7} cm. The change in this case was a contraction, showing that the intensity of magnetization had passed through its zero value and was increasing.

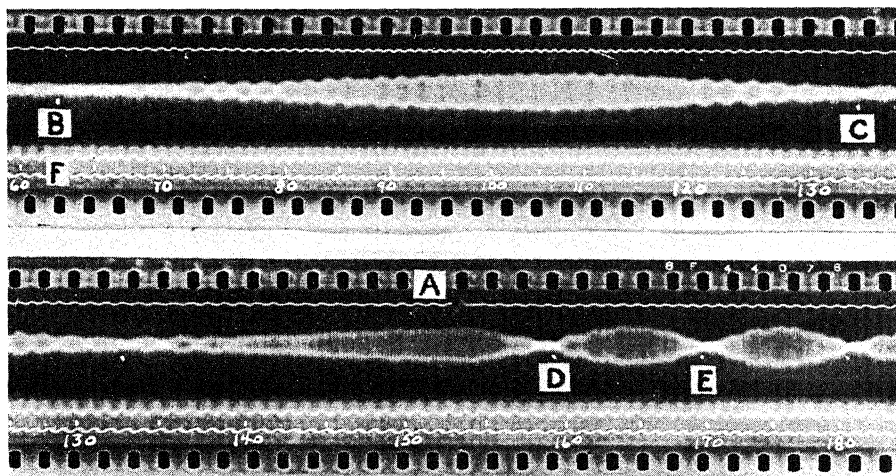


Fig. 2. Photographic record of frequency change. The lower record is a continuation of the upper with slight overlapping.

The two other records, taken in the same way, give values of 2.95×10^{-7} cm and 3.6×10^{-7} cm for this quantity. The three determinations thus give an average δd of 3.75×10^{-7} cm. The large impulse did not always occur at exactly the same magnetizing field value and it is probably not to be expected that the three determinations should be in exact agreement. Numerous additional visual observations with this same specimen showed that every Barkhausen impulse heard was invariably accompanied by a simultaneous sudden change in length of the wire.

DISCUSSION OF RESULTS

A qualitative theory of the Barkhausen effect to which the present experiments lend support has previously been proposed.² This theory ascribes the effect to the presence of stresses in the specimen. To be specific,

assume that there is one small volume element in the interior of the nickel specimen which is initially under tension. The two effects of tension on nickel are to produce a decrease in magnetic permeability and a relatively larger increase in the magnetostrictive contraction for a given intensity of magnetization.⁴ Consequently, when the specimen is magnetized the volume element under consideration will contract more than the surrounding material in spite of its abnormally low intensity of magnetization and the initial tension will increase until eventually there is some sort of slipping or rearrangement of the material and the tension is partially or completely released. This release causes a measurable change in length of the specimen only when the cross sectional area of the volume element is an appreciable part of that of the whole specimen. The sudden length change should thus be more prominent in fine wires, as has been observed in the present work. The release of tension also causes a sudden increase in the permeability and the intensity of magnetization of the volume element. Thus we get the Barkhausen effect. This increase in intensity of magnetization will in turn produce a secondary change in the field acting on all other parts of the specimen and in their intensities of magnetization and lengths, but this secondary effect is probably negligibly small.

The following calculation, based on the above conception of the Barkhausen effect, may be considered as a rough approximation. Assume that the volume element which has produced the experimentally observed effects has a length L parallel to the axis of the wire and a uniform cross sectional area a . Let δI be the sudden change in the intensity of magnetization I for the volume element and δL be the accompanying change in L which would result if the element were not restrained by the material around it. The actual length change, which may be identified with the observed δd , may reasonably be taken equal to $\delta L(a/a_0)$, where a_0 is the area of cross section of the whole wire. Ewing's⁵ I vs H curve and an unpublished $\delta L/L$ vs H curve obtained by the present writers together give $\delta L/(L\delta I) = 9.5 \times 10^{-9}$ for hard drawn nickel, the value being taken at a point on the hysteresis loop where $H = 20$ gauss and is increasing. The Barkhausen jumps for which δd was measured were near this point on the hysteresis loop. Then, assuming the magnetic similarity of the three samples of hard drawn nickel involved, the value $\delta L/L\delta I = 9.5 \times 10^{-9}$ may be taken as correct for the volume element considered. Replacing δL by $a_0\delta d/a$, and using the experimentally found values for δd and a_0 , we get $aL\delta I = 1.24 \times 10^{-4}$. Here aL is the volume V of the volume element. The exact value of V cannot be obtained because δI is unknown. However, the maximum value of δI may be taken to be 330, this being the approximate saturation value of I for nickel. The corresponding

⁴ McKeehan states, reference 1, that, "In the case of nickel the resultant orientation of atomic magnetic axes across the axis of tension, which reduces the ease of magnetization along the axis of tension, will increase the magnetostriction (contraction)." Bidwell's experiments, however, (Proc. Roy. Soc. A47, 469, 1890) do not seem to agree with this statement unless large magnetic fields and small tensions are used.

⁵ J. A. Ewing, "Magnetic Induction in Iron," p. 87.

minimum V is 3.76×10^{-7} cc, which is roughly one sixteenth of the total volume of the specimen.

Bozorth and Dillinger⁶ find that V varies over different parts of the hysteresis loop. Their value for the conditions of the present experiment is about 2×10^{-8} cc for annealed nickel, roughly a twentieth of the above found minimum value. However, they assume I to be a complete reversal from a saturation value in one direction to saturation in the other direction. With the same assumption in the present work the discrepancy between the two measurements is reduced to a factor of 10. This is not bad if we consider that the two determinations are widely different in character, that both are somewhat indirect, that the two specimens of nickel differ greatly in size and that one specimen is annealed and the other hard drawn. This last difference alone might account for the discrepancy since it is known that annealing reduces the Barkhausen effect.

The true δI is probably considerably less than the maximum of 330. An estimate may be made as follows. For a Barkhausen discontinuity to occur it is hard to see how the associated volume element could be greater than half the volume of the wire. Taking this value as a maximum for V the equation $V\delta I = 1.24 \times 10^{-4}$ gives $\delta I = 40$ as a minimum. The true δI is probably somewhere between the maximum of 330 and the minimum of 40, V having a corresponding intermediate value. The assumption of a complete reversal of the saturation value of I seems to be unwarranted. The length depends only on the magnitude of I and consequently it is difficult to see how a reversal, which involves no change in magnitude of I , could alone produce any permanent change in length, either the sudden δd of the present work or the gross magnetostriction as usually observed.

⁶ Bozorth and Dillinger, *Phys. Revs.* 35, 733 (1930).

THE ISOTOPES OF NITROGEN, MASS 15, AND
OXYGEN, MASS 18 AND 17, AND
THEIR ABUNDANCES

BY S. MEIRING NAUDÉ

RYERSON PHYSICAL LABORATORY, UNIVERSITY OF CHICAGO

(Received June 9, 1930)

ABSTRACT

I. The isotopes of nitrogen and oxygen.—The absorption spectrum of the NO γ bands, in particular that of the (0, 0) band at $\lambda 2269$, the (1, 0) band at $\lambda 2154$ and of the (2, 0) band at $\lambda 2052$ was studied in search of isotopes of nitrogen and in order to verify the recently discovered isotopes of oxygen of mass 18 and 17.

A hydrogen continuous source was constructed which could be operated by means of a 5 K.W. transformer which gave 0.5–0.75 amps. through the secondary. It was shown that the silvering of the capillary tube joining the electrodes acts as a catalyzing agent which accelerates the recombination of the hydrogen atoms to molecules thus increasing the intensity of the continuous spectrum. Owing to a chemical change in the fused quartz window on the hydrogen source which leaves the quartz coloured to a violet tint if light of shorter wave-length than $\lambda 1850$ falls on it, the intensity of the continuous spectrum below $\lambda 2300$ is reduced considerably. This was overcome by using a crystal quartz window which did not show this effect. The photographic plates were sensitized with vaseline.

A glass tube 92 cm long and 5 cm in diameter with quartz windows sealed onto either end was used as an absorption tube. NO was prepared by dropping a solution of NaNO_2 into FeSO_4 and H_2SO_4 .

Band heads were observed in all three bands investigated corresponding to the calculated heads for the four kinds of molecules $\text{N}^{14}\text{O}^{16}$, $\text{N}^{15}\text{O}^{16}$, $\text{N}^{14}\text{O}^{18}$ and $\text{N}^{14}\text{O}^{17}$, the maximum deviation of the observed wave-lengths from the calculated values being 0.035A. The results obtained therefore provide new evidence for the existence of a nitrogen isotope of mass 15 and verifies the existence of the oxygen isotopes of mass 18 and 17.

II. The relative abundance of O^{16} and O^{18} .—From the atmospheric bands of oxygen Babcock obtained the relative abundance of O^{16} and O^{18} to be 1250 with a probable error of 25 percent. $(\text{O}^{16})_2$ is symmetric whereas $\text{O}^{16}\text{O}^{18}$ is not. This may give different absorption coefficients for the two molecules. This difficulty disappears in NO. By comparing the pressures of NO in the absorption tube at which the (1, 0) P_1 $\text{N}^{14}\text{O}^{16}$ head could be made to have the same intensity as the P_1 $\text{N}^{14}\text{O}^{18}$ head the relative abundance of O^{16} and O^{18} was found to be 1075 ± 110 .

The relative abundance of N^{14} and N^{15} .—Because in the (1, 0) band the P_1 $\text{N}^{15}\text{O}^{16}$ head has the same intensity as the head Q_1 $\text{N}^{14}\text{O}^{18}$ head, the relative abundance of the N^{15} and O^{18} isotopes is inversely proportional to the relative intensity of the P_1 and Q_1 $\text{N}^{14}\text{O}^{16}$ heads. This relative intensity was found to be 0.65 ± 0.1 . The relative abundance of N^{14} and N^{15} is therefore 1075×0.65 or 700 ± 140 .

From the relative abundance of O^{16} and O^{18} , and O^{16} and O^{17} the mass of the O^{16} isotope was calculated to be 15.9980 ± 0.0002 if the atomic weight of the mixture of isotopes was taken to be 16.0000. Aston defines the mass of the O^{16} isotope as 16.000 and consequently his atomic weights are higher than the corresponding chemical atomic weights. The chemical atomic weights and Aston's should agree if we correct the O^{16} isotope to an atomic weight of 15.9980 ± 0.0002 , that is by 1.25 parts in 10000.

The mass of the N^{14} isotope was calculated to be 14.0069 ± 0.0012 which is in close agreement with Aston's corrected value of 14.0063 ± 0.0029 .

THE search for isotopes, especially among the lighter elements is important,¹ because, as is now generally believed,² any theory of nuclear structure will have to account for the existence or non-existence of all possible atomic species as well as for the regularities³ which exist among the different known isotopes. The occurrence of a certain isotope provides evidence that the corresponding configuration of electrons and protons in the nucleus must be stable. The discovery of the oxygen isotopes of mass 18⁴ and 17⁵ by Giauque and Johnston, and of the carbon isotope of mass 13 by King and Birge^{6,7} throws new light on the stability of atoms having the configurations corresponding to these atomic weights.

Recently the author⁸ reported that evidence had been found from the absorption spectrum of NO of the existence of the four kinds of molecules N¹⁴O¹⁶, N¹⁴O¹⁸, N¹⁴O¹⁷ and N¹⁵O¹⁶, thus not only verifying the existence of the oxygen isotopes of mass 18 and 17 but also proving the existence of an isotope of nitrogen of mass 15. In the meantime more evidence has been found for the existence of these isotopes. The relative abundance of the isotopic species of an element is considered to be a measure of the relative stability of the different atomic configurations constituting the isotopes. Therefore special care has also been taken to find as accurately as possible the relative abundance of the O¹⁸ and N¹⁵ isotopes with respect to O¹⁶ and N¹⁴ respectively.

Part I of this paper gives the evidence that has been found for the existence of the isotopes of nitrogen and oxygen, whereas Part II deals with the experiments carried out to find the relative abundance of the isotopes and the conclusions to which the obtained results lead.

PART I. THE ISOTOPES OF NITROGEN AND OXYGEN

Introduction. According to the theory of the isotope effect in band spectra^{9,10} a molecule containing a rarer isotope of one of the atoms con-

¹ W. F. Giauque, *Nature* **124**, 265 (1929). At the meeting of the "British Association for the Advancement of Science" held in South Africa in July, 1929, Sir E. Rutherford also pointed out that the determination of all the existing isotopes was one way of studying the structure of the nucleus.

² Cf. A. E. Ruark and H. C. Urey, "Atoms, Molecules and Quanta," McGraw-Hill Book Co., 1930, p. 39.

³ W. D. Harkins, *J. Am. Chem. Soc.* **39**, 856, 870 (1917), *Phil. Mag.* **42**, 305 (1926), *Chem. Reviews*, **5**, 371 (1928); Guido Beck, *Zeits. f. Physik* **47**, 407 (1928), **50**, 548 (1928), **61**, 615 (1930), H. A. Barton, *Phys. Rev.* **34**, 1228 (1929).

⁴ W. F. Giauque and H. L. Johnston, *Nature* **123**, 318 (1929); *J. Am. Chem. Soc.* **51**, 1436 (1929).

⁵ W. F. Giauque and H. L. Johnston, *Nature* **123**, 831 (1929); *J. Am. Chem. Soc.* **51**, 3528 (1929).

⁶ A. S. King and R. T. Birge, *Nature* **124**, 182 (1929); *Phys. Rev.* **34**, 376 (1929).

⁷ R. T. Birge, *Phys. Rev.* **34**, 379 (1929).

⁸ S. M. Naudé, *Phys. Rev.* **34**, 1498 (1929); **35**, 130 (1930).

⁹ R. S. Mulliken, *Phys. Rev.* **25**, 119 (1925).

¹⁰ In a Symposium of the Faraday Society held September 1929 on Molecular Spectra and Molecular Structure, Birge discusses methods by which the calculation of the rotational effect can be made more accurate. In this work the approximate formula given in Eq. (2) suffices as the analysis of the NO spectrum made use of here contains relatively large probable errors.

stituting the ordinary molecule, gives rise to a displaced band which corresponds exactly to that which originates from the ordinary molecules. The position of the displaced isotopic band can be calculated accurately by taking into account firstly, the displacement due to vibration:¹¹

$$\nu_2^v - \nu_1^v = (\rho - 1) [\omega_e'(v' + \frac{1}{2}) - \omega_e''(v'' + \frac{1}{2})] - (\rho^2 - 1) [\omega_e'x'(v' + \frac{1}{2})^2 - \omega_e''x''(v'' + \frac{1}{2})^2] \quad (1)$$

and secondly, the displacement due to rotation:

$$\nu_2^r - \nu_1^r = (\rho^2 - 1)\nu_1^r \quad (2)$$

where ν_1 refers to the ordinary molecule $N^{14}O^{16}$ and ν_2 to the isotopic molecule, e.g., $N^{15}O^{16}$, $\rho^2 = (\mu_1/\mu_2)$ where $\mu_1 = 1/M_1 + 1/M_2$ and $\mu_2 = 1/M_1 + 1/M_2'$, M_1 being the mass of the atom which is common to both molecules, and M_2' being the mass of the rarer of the isotopic species M_2 and M_2' , and where ω_e' , $\omega_e'x'$, ω_e'' , $\omega_e''x''$ are vibrational constants in the initial and final states respectively, and v' and v'' are the vibrational quantum numbers in these states.

The absorption spectrum is far superior to the emission spectrum for studying the isotope effect in a gas containing a rare isotope, for by increasing the length of the absorption tube and the pressure of the gas in the tube, the number of molecules in the path of the light can be increased practically indefinitely, and hence also the number of molecules containing a rare isotope. The lower the pressure, the sharper the absorption lines that are obtained. Therefore the absorption tube is chosen as long as possible and then the pressure of the absorbing gas is raised until the expected effect, if present, is observed.

The absorption spectrum of NO, especially the (0, 0) band at $\lambda 2269$, the (1, 0) band at $\lambda 2154$ and the (2, 0) band at $\lambda 2052A$, that belong to the γ system which is degraded towards the violet, offers a good opportunity for studying the isotope effect. This system of NO has been analyzed partly by Frl. M. Guillery¹² and partly by R. Schmid.¹³ Schmid worked on the (0, 0) and (1, 0) bands mentioned. The γ system of NO has a $^2\Pi$ lower level and a $^2\Sigma$ upper level. The separation of the $^2\Pi_{3/2}$ and $^2\Pi_{1/2}$ levels has been found to be 124.4 cm^{-1} . Because the $^2\Sigma$ level is single, every band will exist of a doublet, each having a Q and a P head.¹⁴ Of the (1, 0) band Schmid¹³ was able to measure only the Q_1 heads. The position of the P_1 heads could, however, be calculated with the help of the relation:

$$Q_1(J+1) - \Delta F'(J) = P_1(J) \quad (3)$$

¹¹ The notation used here is in accordance with the report of Prof. Mulliken to be published in the Phys. Rev. Cf. also R. S. Mulliken, Reviews of Modern Physics 2, 60 (1930).

¹² Frl. M. Guillery, Zeits. f. Physik 42, 121 (1927).

¹³ R. Schmid, Zeits. f. Physik 49, 428 (1928).

¹⁴ To avoid confusion the older notation for the heads according to Schmid is used here. The more recent nomenclature of these band heads is given by R. S. Mulliken, Phys. Rev. 32, 413 (1928).

given by him for the final state. This calculation gives 46391.3 cm^{-1} for the wave-number of the P_1 head which agrees with the measurements made in the course of the present work. The position of the P_1 and Q_1 heads of the (2, 0) band were calculated to be 48708.6 and 48736.1 cm^{-1} respectively. The vibrational constants ω_e , $\omega_e x$, used in computing the vibrational isotopic shift of the band heads, were calculated from the ω_0 and $\omega_0 x$ given by Birge:¹⁵ $\omega_e = \omega_0 + \omega_0 x$ and $\omega_e x = \omega_0 x$. The values thus found were $\omega_e' = 2365$, $\omega_e'' = 1902.19$, $\omega_e' x' = 13$, $\omega_e'' x'' = 13.88$. The calculated shifts with the corresponding wave-lengths are given in columns 4 and 5 of Table I.

The continuous source. As continuous light source a hydrogen lamp was constructed of Pyrex glass according to Bay and Steiner.¹⁶ The source could be operated with a 5 K.W. transformer giving from 0.5 to 0.75 ampere through the secondary. This gave a very intense continuous spectrum. The source was provided with a quartz window at either end. The second window allowed one to sight through the hydrogen source, thus greatly facilitating the lining up of the source, the absorption tube and the spectrograph, which is very important in the case of a long absorption tube, for in this way the maximum intensity can be obtained.

Some experiments were carried out to find out what function was fulfilled by the silvering of the capillary tube which joins the electrodes and in which the discharge takes place, as no conclusions were made in this respect by Gehrcke and Lau¹⁷ who first describe its use. It was found that, when the capillary tube was not silvered the discharge was distinctly red due to the H_α line becoming very prominent. On the other hand, when it was silvered the secondary and also the continuous spectrum of hydrogen which is emitted by the hydrogen molecule,¹⁸ became much stronger, H_α being reduced to about the same intensity as that of the secondary spectrum. The evidence thus points to the mechanism of the silvering being to catalyze the recombination of hydrogen atoms into which the molecules dissociate on giving out the continuous spectrum back to molecules, thus strengthening the secondary spectrum and hence also the continuous spectrum.

As is well known¹⁶ the observed intensity of the hydrogen continuous spectrum falls off rapidly below $\lambda 2400\text{A}$. Experiments were carried out to determine the cause of this phenomenon. It was noticed that a fused quartz window sealed onto the hydrogen tube gave a very strong fluorescence¹⁹ when the tube was in operation. After a window had been in use for about a week, it was replaced by a new one. It was then noticed that the used one had been discoloured to a violet tint, the pattern in it being the same as the one that was seen in fluorescence while the tube was in use. The hydrogen tube was now refilled and sealed off. Two absorption pictures were taken on the

¹⁵ R. T. Birge, "Molecular Spectra in Gases" p. 232.

¹⁶ Z. Bay and W. Steiner, *Zeits. f. Physik* **45**, 337 (1927); see also E. O. Lawrence and N. E. Edlefsen, *Rev. Scientific Instruments* **1**, 45 (1930).

¹⁷ E. Gehrcke and E. Lau, *Ann. d. Physik [IV]* **76**, 675 (1925).

¹⁸ J. G. Winans and E. C. Stueckelberg, *Proc. Nat. Acad. Sci.* **14**, 867 (1928).

¹⁹ H. W. Webb and Miss Helen Messenger, *Phys. Rev.* **34**, 1463 (1929).

same photographic plate, the first with the used quartz window and the second with an unused window in the light path. It was found that the used window absorbed very strongly in the region below $\lambda 2400\text{\AA}$. The used quartz window had to be ground down to about half the original thickness before the violet tint was removed. It is not known what the cause of this colouring is, but it seems likely that the SiO_2 constituting the quartz dissociates, giving free silicon. The wave-length causing this fluorescence must be shorter than $\lambda 1850$, the shortest wave-length transmitted by quartz, because the fused quartz windows used on the absorption tube showed no fluorescence and when the windows were removed after being in use for six months, no violet colouring could be observed. A crystal quartz window was ground and polished and used to replace the fused quartz window on the hydrogen source. The fluorescence in this window was distinctly less conspicuous and the intensity of the continuous spectrum obtained was much better. This window showed no violet colouring even after being in use for three months. It is therefore advisable to use crystal quartz instead of fused quartz windows on the hydrogen source for work in the far ultraviolet.

Procedure. A tube 92 cm long and 5 cm in diameter and with two quartz windows sealed onto either end served as absorption tube. The NO gas was prepared by dropping NaNO_2 into a solution of H_2SO_4 and FeSO_4 . The end of the dropping funnel was well below the surface of the liquid so that all the NO_2 formed could be reduced to NO by the FeSO_4 . The NO gas was left over the FeSO_4 for about a day so that the gas obtained was practically free from NO_2 . The NO gas was dried by passing it through a tube containing P_2O_5 . The pressure of the gas could be determined by means of a McLeod gauge.

An E1 Hilger spectrograph was used which had a dispersion varying from 1 mm = 1.9A at $\lambda 2269$ to 1.3A at $\lambda 2052$. The time of exposure varied from six to twelve hours. The best pictures were taken with 2 cm pressure of NO in the absorption tube. Speedway and Eastman 40 plates were used. The copper arc lines measured by Mitra²⁰ and corrected by Shenstone²¹ were used as comparison spectrum. In the region below $\lambda 2100$ the copper lines as given by Sommer²² are less accurately measured and consequently the measurements on the (2, 0) band are less accurate.

The insensitivity of the photographic plate in this region, $\lambda 2300$ to 2000\AA , was overcome by using a solution of five grams of vaseline²³ in half a liter of petroleum ether²⁴ as sensitizer according to Beach.²⁵ The solution was prepared and kept in a glass bottle. Before taking an exposure the photo-

²⁰ S. K. Mitra, *Ann. de Physique* 19, 315 (1923).

²¹ A. G. Shenstone, *Phys. Rev.* 28, 449 (1926).

²² L. A. Sommer, *Zeits. f. Physik* 39, 711 (1926).

²³ The vaseline used was the ordinary white product of Chesebrough Mfg. Co.

²⁴ The best results were obtained with petroleum ether made by the Mallinckrodt Chemical Works.

²⁵ A. C. G. Beach, *Nature* 123, 166 (1929); Cf. also H. R. Harrison *J. Opt. Soc. Am.* 11, 341 (1925).

graphic plate was dipped into the solution which had been previously poured into a flat dish. On taking it out an oscillatory movement was carried out in order to dry it in such a way that the film of vaseline formed on the surface of the plate after the petroleum ether had evaporated, should be as even as possible. An even film of vaseline was essential especially where a comparison was made between the intensity of two photographs on the same plate (as described in Part II), since the thickness of the film of vaseline determines the intensity obtained.

The plate was then inserted into the holder and the photograph taken in the ordinary way. Before the plate was developed, the vaseline was removed by rubbing its surface with cottonwool which had been soaked in acetone. The plate was then developed as usual.

Results. In all three bands bandheads are observed corresponding to the four types of molecules $N^{14}O^{16}$, $N^{15}O^{16}$, $N^{14}O^{18}$ and $N^{14}O^{17}$ except in the (0, 0) band where, owing to the smallness of shift and the proximity of the $N^{15}O^{16}$ head, the much weaker $N^{14}O^{17}$ head is not observed.

The results are tabulated in Table I being the average of the measurements on five different plates taken at different pressures.

TABLE I.

Band		Nomenclature wave-length and wave-number of $N^{14}O^{16}$ head	Type of molecule containing an isotope	Calculated shift $\nu_2 - \nu_1$ in cm^{-1}	Calculated wave-length in Å	Observed wave-length in Å
0,0	P_1	2269.40	$N^{14}O^{17}$	-2.595	2269.53 ₄	—
		44050.8 ₆₈	$N^{15}O^{16}$	-3.375	2269.57 ₄	2269.56
			$N^{14}O^{18}$	-4.952	2269.65 ₅	2269.69
1,0	Q_1	2153.63	$N^{14}O^{17}$	-35.193	2155.26 ₄	2155.23
		46418.5 ₇₇	$N^{15}O^{16}$	-45.729	2155.75 ₄	2155.73
			$N^{14}O^{18}$	-67.030	2156.74 ₅	2156.75
	P_1	2154.90	$N^{14}O^{17}$	-34.444	2156.49 ₃	2156.49
		46391.3	$N^{15}O^{16}$	-44.758	2156.95 ₇	2156.98
			$N^{14}O^{18}$	-65.615	2157.94 ₉	2157.98
2,0	Q_1	2051.01	$N^{14}O^{17}$	-66.401	2054.00 ₅	2054.02
		48736.1	$N^{15}O^{16}$	-86.282	2054.84 ₅	2054.82
			$N^{14}O^{18}$	-126.482	2056.54 ₆	2056.54
	P_1	2052.43	$N^{14}O^{17}$	-65.646	2055.13 ₅	2055.15
		48708.6	$N^{15}O^{16}$	-85.304	2055.96 ₅	2055.97
			$N^{14}O^{18}$	-125.055	2057.64 ₉	2057.66

In the preliminary publication⁸ mention was made of faint absorption bands appearing beyond the isotopic heads in the (1, 0) band, whose positions seemed to agree with the values calculated for a possible $N^{16}O^{16}$ head. This point has been the subject of further research. When the focus of the spectrograph was shifted so as to include the (2, 0) band, it was found that the β bands of NO^{26} which originate from the same $^2\Pi$ ground state as the γ bands, but have an upper $^2\Pi$ level different from the $^2\Sigma$ upper level of the

²⁶ F. A. Jenkins, H. A. Barton and R. S. Mulliken, Phys. Rev. 30, 150 (1927).

γ bands, also appear in absorption although very weakly. Now it happens that the heads of the *R* and *P* branches of the (1, 0) β band fall at $\lambda 2153.45$ and 2153.68\AA and thus on top of the (1, 0) γ band. Consequently these heads do not interfere with the isotopic bandheads. Because the β system is degraded towards the red, its rotational fine structure appears beyond the isotopic heads. The position of these rotational lines can be calculated from the relation

$$F = \text{const} + Aj + Bj^2 + Cj^3 + Dj^4$$

given by Jenkins, Barton and Mulliken.²⁶ All the observed absorption lines beyond the heads of the isotopic molecules could be accounted for in this way. The isotope N^{16} does therefore not exist (unless it is less abundant

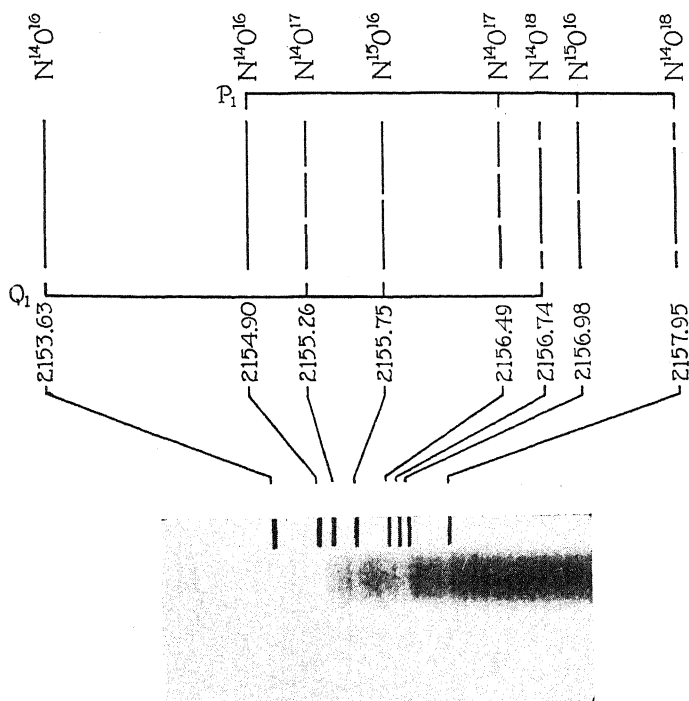


Fig. 1. The expected appearance of the band-heads of the (1, 0) band are sketched. The types of molecules giving these band-heads are given on the upper side of the figure and on the lower side the corresponding wave-lengths of the heads are given. The line on the lower side of the figure joins the Q_1 heads formed by the different types of molecules, whereas the upper line joins the corresponding P_1 heads.

Fig. 2. An enlargement of the observed appearance of the (1, 0) band. The positions of the band heads are indicated by lines which connect the heads to the corresponding heads in Fig. 1.

than O^{17}) especially since the (2, 0) band shows definitely no trace of the N^{16} isotope. The evidence the (1, 0) band gives for the other isotopes is, however, not effected by these faint absorption lines since the intensity of the isotopic heads is much greater than the rotational fine structure of the (1, 0) β band.

Because the P_1 and Q_1 heads of the (1, 0) band are separated by 27.3 cm^{-1} and the smallest displacement, namely that of the Q_1 head due to the $\text{N}^{14}\text{O}^{17}$ molecule is -35.193 cm^{-1} , one expects the six heads due to $\text{N}^{14}\text{O}^{17}$, $\text{N}^{15}\text{O}^{16}$ and $\text{N}^{14}\text{O}^{18}$ all to fall beyond the $\text{N}^{14}\text{O}^{16}$ P_1 head and to be observable as far as they do not overlap one another. In Fig. 1 a sketch is given of the expected appearance of the bandheads. In Fig. 2 a photograph (enlarged eight times) of the actual appearance of the (1, 0) band is reproduced. This photograph was taken with a pressure of 2 cm of NO in the 92 cm absorption tube, the time of exposure being ten hours.

Between the Q_1 $\text{N}^{14}\text{O}^{17}$ and $\text{N}^{15}\text{O}^{16}$ heads a faint absorption line is seen which could be shown to be due to the overlapping of three lines of the rotational structure belonging to the Q_1 $\text{N}^{15}\text{O}^{16}$, and $\text{N}^{14}\text{O}^{18}$ heads and the P_1 $\text{N}^{15}\text{O}^{16}$ head. The P_1 $\text{N}^{14}\text{O}^{17}$ head is not visible in this picture but in pictures taken at higher pressures one is able to observe and measure it accurately.

The separation of the P_1 and Q_1 heads in the (2, 0) band is 27.5 cm^{-1} . The displacement of the Q_1 $\text{N}^{14}\text{O}^{17}$ head is calculated to be 66.401 cm^{-1} and will therefore fall beyond the P_1 $\text{N}^{14}\text{O}^{16}$ head. All the isotopic heads are therefore expected to fall beyond the P_1 head. As can be seen from the calculated positions of these heads in column 5 of Table I, they are widely separated and can therefore be measured more accurately. The increased insensitivity of the photographic plate, however, makes a reproduction of the obtained pictures impossible.

The fine structure of the isotopic bands could also be measured when the overlapping was not too much. This corresponded very closely with the rotational fine structure of the main heads, so that it provides further decisive evidence that these heads must be due to the isotopic molecules.

To be absolutely sure that these bands might not perhaps be due to some other molecule, e.g. $(\text{NO})_2$, the absorption tube was replaced by a tube 1.2 cm in length and filled up to 75 cm pressure with NO. The light passing through this tube has to traverse about the same number of molecules of NO as in the case of the 92 cm tube with 1 cm pressure. If $(\text{NO})_2$ molecules were present their concentration should increase with the square of the pressure and the path being 75 times shorter, one would expect the effect due to these molecules to be 75 times as intense. The absorption of the isotope heads observed is quite similar to that obtained with the 92 cm tube, except that they are a little more diffuse, as one might expect owing to the high pressure. The measured shift agrees accurately with the above results.

This investigation therefore definitely proves the existence of an isotope of nitrogen of mass 15 and verifies the existence of the recently discovered isotopes of oxygen of mass 17 and 18.

PART II. THE ABUNDANCE OF O^{18} AND N^{15}

The relative abundance of O^{16} and O^{18} . The abundance of the oxygen isotope of mass 18 has been determined by Babcock²⁷ from the atmospheric

²⁷ H. D. Babcock, Proc. Nat. Acad. Sci. 15, 471 (1929); Phys. Rev. 34, 540 (1929).

bands of oxygen. Babcock took an absorption picture of the atmospheric bands using the sun as continuous light source and the oxygen in the atmosphere as his absorbing medium. In this way the heads of the displaced bands due to the $O^{16}O^{18}$ molecule could be photographed. On the same plate he took an absorption picture of the corresponding main bands due to $(O^{16})_2$ using a certain length of air path in the laboratory for the absorption. When the isotopic heads in the former appeared to him to be of the same intensity as the main heads in the latter picture, he concluded that the abundance of the molecules giving these bands should be inversely proportional to the number of oxygen molecules traversed in each case. The latter could be calculated from the known path lengths. In this way a relative abundance of one O^{18} isotope in every 1250 O^{16} was obtained as the weighted mean of 1175 and 1350.

The molecule $(O^{16})_2$ is symmetric whereas $O^{16}O^{18}$ is unsymmetric. These molecules may have different absorption coefficients which would affect the results obtained for the relative abundance. This difficulty disappears in the case of NO, for both $N^{14}O^{16}$ and $N^{14}O^{18}$ are unsymmetric. A redetermination of the abundance of O^{18} therefore seemed desirable.

The pressure of NO in the absorption tube could be varied thus giving different numbers of molecules in the light path, and could be measured accurately by means of a McLeod gauge. The pictures were taken on the same photographic plate, 5 mm apart, so that the condition of sensitizing and developing were exactly the same. The two pictures could be taken under the same experimental conditions and special care was taken to get the continuous background of the pictures of the same intensity.

The (1, 0) band is the best to apply this procedure to, because the intensity of the plate is still favourable and the displacement of the isotope heads is fairly large. The only displaced head to which the method can, however, be applied with certainty is the $N^{14}O^{18}$ head at $\lambda 2157.98$ corresponding to the P_1 head of $N^{14}O^{16}$ $\lambda 2154.90$. This head is displaced the farthest and consequently there is no overlapping of the fine structure of the less displaced isotopic heads. The fine structure of the (1, 0) β band mentioned above is so weak that it does not affect the accuracy with which the intensity of the displaced isotope head can be estimated.

The first pictures taken showed that the higher pressure caused the isotopic head to appear much broader than expected. Pressure broadening according to Lorentz²⁸ was at once suspected to be the cause. Two pictures were taken on the same plate, one with only 2.1 cm pressure of NO in the absorption tube, the other with the 2.1 cm of NO left unchanged but with 44 cm pressure of N_2 added, see Fig. 3. Since the N_2 has no absorption bands in this region it can only have the effect of pressure broadening according to Lorentz. A large number of investigators²⁹ have done work on the pressure

²⁸ H. A. Lorentz, Proc. Amsterdam 8, 501 (1906). For a discussion of this phenomenon according to the wave mechanics cf. J. Frenkel, Zeits. f. Physik 59, 198 (1930).

²⁹ Cf. W. Schütz, Zeits. f. Physik 45, 30 (1927) and the literature given there.

broadening in the case of atoms, and Teves³⁰ has extended this work to bands. The pressure in the absorption tube was therefore regulated as follows: If a pressure ratio of 1 to 1000, for instance, was desired, the tube was filled to 5 cm with NO and 65 cm of N₂ added. After an exposure with this pressure was finished, the pressure in the tube was changed to 0.005 cm of NO and 70 cm of N₂, and another picture taken on the same photographic plate. In both cases therefore the total pressure was the same, viz. 70 cms, and a large excess of N₂ was present. N₂ was chosen, chiefly because it has no absorption bands above $\lambda 1520\text{\AA}$ and also because it has about the same molecular radius as NO³¹, the latter factor influencing the broadening according to Lorentz and Frenkel. It was absolutely necessary to have N₂

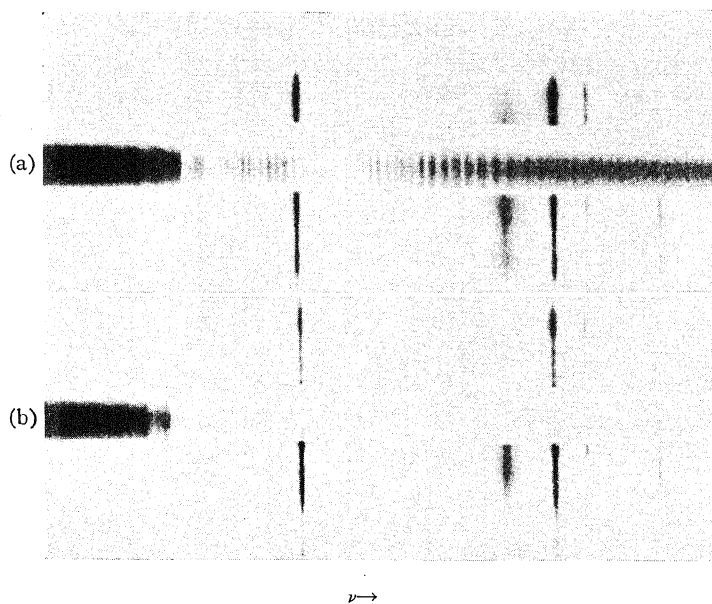


Fig. 3. (a) Absorption picture with 2.1 cm NO pressure. (b) Absorption picture with 2.1 cm NO+44 cm N₂ pressure. A comparison shows that in (b) every rotational line is broadened so much that the absorption becomes complete.

free from all traces of oxygen otherwise NO₂ would be formed in the absorption tube and this molecule gives a continuous absorption in the region in question. Pure N₂ was obtained by heating sodium azide in a flask from which all the air had been exhausted beforehand. The gas was then dried in a tube containing P₂O₅. Pictures were taken with pressure ratios varying between 1 in 1800 and 1 in 500. Definite differences in the intensity of the absorption of the main and isotopic heads were found for all ratios outside 1 in 990 and 1 in 1160. Within this region ten photographs were taken at different pressure ratios, but, as it is difficult to decide definitely about their intensities, an average is taken over all ten values giving as result a relative abundance

³⁰ M. C. Teves, *Zeits. f. Physik* **48**, 244 (1928).

³¹ P. M. Morse, *Phys. Rev.* **34**, 57 (1929).

of O^{18} of one in every 1076 O^{16} atoms. Taking the mean of the two extreme ratios where definite differences of the same amount could be observed in the intensities a ratio 1/1075 is found for the abundance. Although the first calculation gives a probable error of only three percent, the maximum error is given as ten percent, as systematic errors might occur in the method used. The abundance ratio of O^{16} to O^{18} is therefore given as 1075 ± 110 .

After obtaining the above result two comparison pictures were taken with helium instead of N_2 to make sure that no resonance effect between NO and N_2 was present. The pictures indicated that the given abundance ratio was correct.

The result differs by about 14 percent from that given by Babcock, but as Birge³² gives a probable error of 25 percent for Babcock's values this deviation does not seem too large. Further, Babcock compares the absorption of the oxygen in the laboratory and hence at atmospheric pressure with the oxygen in the atmosphere where the pressure varies exponentially to zero. Hence the pressure broadening which, as pointed out above, is very great, is much more effective in the first case where all the oxygen is at atmospheric pressure than in the second case where only the oxygen near the ground is at atmospheric pressure. This would give a result which would differ from the one obtained with the same pressure in both cases in the sense of the result found here.

Babcock finds the relative abundance of O^{18} and O^{17} to be eight to one. If a maximum error of ten percent is allowed for this value and the relative abundance of O^{16} and O^{18} is assumed to be 1075 ± 110 as found here, the relative abundance of O^{16} and O^{17} becomes 8600 ± 1750 .

The relative abundance of N^{14} and N^{15} . As stated above the overlapping of the fine structure due to the $N^{14}O^{18}$ molecule, made it impossible to determine the abundance of the $N^{15}O^{16}$ molecule in the same way. Here the circumstance that the $Q_1N^{14}O^{18}$ and $P_1N^{15}O^{16}$ heads lying close together are of the same intensity was made use of. At very low pressures practically no fine structure of the isotopic heads is present and therefore the conclusions following this observation are rigid. It was further noticed that the $P_1N^{15}O^{16}$ head was more intense than the $Q_1N^{15}O^{16}$ head. This resulted from the fact that the main $P_1N^{14}O^{16}$ head was less strongly absorbed than the corresponding Q_1 head. The ratio of the main P_1 and Q_1 heads could easily be determined by taking different pressures in the absorption tube and observing at which pressures the heads had the same intensity. The ratio of these pressures was found to be 0.65 ± 0.1 and this is evidently the intensity ratio of the main heads, the P_1 head being less intense. This result could also be verified by taking microphotometer curves of the heads with a Moll apparatus and averaging the area under each of the heads. This result agreed accurately with the above result. The fact that the $Q_1N^{14}O^{18}$ and $P_1N^{15}O^{16}$ heads are equally intense can therefore only be ascribed to the fact that the $N^{14}O^{18}$ must be less

³² R. T. Birge, Phys. Rev. Suppl. 1, 69 (1929).

abundant than the $N^{15}O^{16}$ in the same ratio as the Q_1 head is stronger than the P_1 head.

This result therefore gives us as relative abundance of $N^{14}O^{18}$ and $N^{15}O^{16}$ molecules the ratio 0.65 ± 0.1 and hence as the relative abundance of N^{14} and N^{15} the ratio 1075×0.65 or 700 ± 140 . In this case the maximum error is given as 20 percent, since the ratio 0.65 may be affected as much as ten percent by systematic errors.

Discussion. The existence of the O^{18} and O^{17} isotopes seems to be quite certain. This, however, affects Aston's³³ atomic weights determined by means of the mass spectrograph with respect to the chemical atomic weights.³⁴ Aston assumes the atomic weight of the O^{16} isotope to be 16.0000, whereas the chemical method defines the average atomic weight of the O^{16} , O^{17} and O^{18} isotopes as 16.0000. The actual atomic weight of the O^{16} isotope can now be calculated by making use of the relative abundance determined above. The atomic weight of the O^{16} isotope can be computed from the following relation:

$$1074 \times 8x + 8 \times 18 + 17 = (1075 \times 8 + 1)16.0000 \quad (4)$$

from which we get $x = 15.9980 \pm 0.0002$. We see therefore, that although the maximum error in the relative abundance of the oxygen isotopes is very large, the value of the atomic weight of the O^{16} is little affected. It is easily seen that it makes no difference in the result whether 18 or 17.991,³⁵ as recently found by Mecke and Wurm to be the atomic weight of O^{18} , is used. If the chemical atomic weight 16.0000 is our standard, Aston should use 15.9980 ± 0.0002 as the atomic weight of the O^{16} isotope, if he expects to obtain an agreement between his values and those obtained by chemical methods. This change in value of the O^{16} isotope used as standard by Aston corresponds to a change of 1.25 ± 0.13 in 10000. This does not mean that Aston's determinations of the atomic weights are less accurate than 1 in 10000 as given by himself, but just gives the amount by which all his values have to be corrected in order to allow a comparison with the values obtained by chemical methods.

We can now proceed to correct Aston's values by 1.25 ± 0.13 in 10000. In Table II the corrected values of Aston are compared with the chemical determinations. The elements chosen are those which have no isotopes as far as we know, or which have rare isotopes, as these are the only cases where a direct comparison is possible.

A comparison of columns 1 and 3 reveals a number of interesting points. In the case of hydrogen a correction of Aston's value makes the agreement worse, but the corrected value can be made to agree with the chemical value by assuming an error of 0.00011 which is well within the maximum error allowed for.

³³ F. W. Aston, Proc. Roy. Soc. 115A, 487 (1927).

³⁴ Cf. R. T. Birge, Phys. Rev. Supplement 1, 19 (1929).

³⁵ R. Mecke and K. Wurm, Zeits. f. Physik 61, 37 (1930).

TABLE II. *Atomic weights.*³⁶

Atom	Chemical method	Aston's mass spectrograph	Aston's values corrected by 1.25 in 10000
H	1.00777 ± 0.00002	1.00778 ± 0.00015	1.00766 ± 0.00016
He	4.0018 ± .0003	4.00216 ± .0004	4.00166 ± .00045
C	12.0025 ± .00019	12.0036 ± .0012	12.0021 ± .0014
N	14.0083 ± .0008	14.008 ± .0028	14.0063 ± .0030
O	16.0000 ± .0000	16.0000 ± .0000	15.9980 ± .0002
F	19.00	19.0000 ± .0019	18.9976 ± .0021
P	31.027	30.9825 ± .0046	30.9786 ± .0050
As	74.96	74.934 ± .010	74.925 ± .011
I	126.93	126.932 ± .025	126.916 ± .027

In the case of He the corrected value agrees to 1 in 30000 with the chemical value 4.0018. This correction therefore does away with a very bad discrepancy between Aston's values and the chemical values. Further, as pointed out by Birge³⁷ this value agrees accurately with Eddington's³⁸ calculated value for an ideal rigid nucleus. This agreement might be due to chance as the value still has a large maximum error and hence it cannot be assumed from this that the helium atom really has a rigid nucleus.

Birge and King have recently discovered an isotope of carbon of mass 13. One would therefore expect the chemical atomic weight to be higher than that found by Aston. The reverse is the case, however. If Aston's value is corrected one obtains a value of 12.0021 which is in close agreement with the chemical value 12.0025 and still allows for the presence of the isotope C¹³. From these values the calculated abundance of the C¹³ isotope is 1 in 2500 but this seems to contradict Birge's⁷ results according to which the C¹³ isotope should be more abundant relative to C¹² than the N¹⁵ relative to N¹⁴, but the given atomic weights still have a large probable error which may account for this discrepancy.

In the case of nitrogen the abundance of the N¹⁵ has been determined as 1 in 700 ± 140 N¹⁴ isotopes. From this we can determine what the expected atomic weight of the N¹⁴ isotope should be, for

$$700x + 15 = 701 \times 14.0083 \pm 0.0008 \quad (5)$$

or

$$x = 14.0069 \pm 0.0012.$$

This value agrees with Aston's corrected determination 14.0063 to within 1 in 20000.

For F, P and As the chemical values are given with less accuracy, but a comparison of Aston's corrected value of P with the chemical value leads

³⁶ Most of the values with their probable errors given in the first column are taken from the excellent discussion by R. T. Birge, *Phys. Rev. Supplement* **1**, 18 (1929). The values in column 2 with their maximum errors are obtained from Aston's paper, *Proc. Roy. Soc.* **115A**, 487 (1927). The chemical values for F, P, As and I are taken from the Second Report of the International Committee on Chemical Elements, *J. Am. Chem. Soc.* **47**, 597 (1925) and the German Committee, *Berichte* **62**, 1 (1929).

³⁷ R. T. Birge, *Phys. Rev.* **35**, 1015 (1930).

³⁸ A. S. Eddington, *Proc. Roy. Soc.* **A126**, 696 (1930).

one to suspect the presence of heavier isotopes of P in small quantities. Although less certain, the same seems to be indicated by the corresponding values for F and As.

Until 1928 the German Committee³⁹ gave the atomic weight of I as 126.92 and Birge⁴⁰ finds as weighted average of Clark's values 126.926. This indicates that the real chemical value for I may still be on the lower side of 126.932—the value that is now accepted—and such a value will be in better agreement with Aston's corrected value 126.916.

Although it is difficult to draw definite conclusions from the above, it is quite clear that the sooner an agreement is reached by chemists and physicists as to the value which should be used as standard of atomic weight, the less confusion will exist as to the most accurate atomic weights.

Mr. F. Bueso-Sanlehi started this work but had to leave before obtaining any definite results. I wish to thank Professor R. S. Mulliken who suggested the search for isotopes in these NO bands and also wish to thank him and Dr. A. Christy for their helpful suggestions and Professor H. B. Lemon for allowing me the use of the apparatus in his laboratory.

³⁹ Max Bodenstein, etc., *Berichte* 61B, 1–31 (1928).

⁴⁰ R. T. Birge, *Phys. Rev. Supplement* 1, 25 (1929).

THE MARGULES METHOD OF MEASURING VISCOSITIES
MODIFIED TO GIVE ABSOLUTE VALUES

BY HOWARD R. LILLIE

CORNING GLASS WORKS, CORNING, NEW YORK

(Received May 28, 1930)

ABSTRACT

Measurement of absolute viscosities. A method for determining absolute viscosities in a Margules rotating cylinder type viscometer, without the aid of calibrating liquids of known viscosities, is described. This method involves the determination of true viscosity by extrapolating apparent viscosities for several lengths of inside cylinder to that viscosity corresponding to infinite length. By this method the viscosity of the commercial castor oil used is found to be 9.99 poises at 20°C, and 4.61 poises at 30°C, as compared with 9.86 and 4.51 poises quoted in the Smithsonian Tables for pure oil at corresponding temperatures.

End corrections. The additional length to be applied to the measured length to correct for finite dimensions is computed for several inside cylinders or spindles. When the radius of the outer containing cylinder is 3.2 cm, and the ends of the spindle are 1.5 cm from the upper and lower boundaries of the liquid, the corrections for spindle radii of 0.556 cm and 0.477 cm are found to be 0.62 cm and 0.52 cm respectively as long as the length of the spindle is 5 cm or greater. Accordingly, the end correction is apparently proportional to the 1.18 power of spindle radius.

Constancy of calibrating factor. Comparisons are also made between relative viscosities measured by this method and those for the same liquids measured by capillary flow. Results indicate that within experimental error these relative values are the same by both methods, for viscosities between 5 and 3500 poises, showing that the calibrating factor of the concentric cylinder system is constant over this range of viscosities.

IN A previous paper,¹ the apparatus and method were described for measuring viscosities of molten glasses (10^2 to 10^7 poises) by the use of concentric cylinders. A simple way of determining the effect of the use of cylinders of finite length was also described. However, since this determination was made for only one viscosity—that of castor oil at room temperature—the question remained as to whether one can assume that the calibrating factor is entirely independent of viscosity when the ends of the cylinders are present. Measurements were accordingly undertaken with the object of comparing the relative viscosities of two liquids differing quite widely in this property, as found by the concentric cylinders and as given by the method of capillary flow, for which a constant calibrating factor is more generally accepted.

In a majority of cases, investigators of glass viscosities² have found, by more or less rigorous calibration with standard liquids, that the calibrating factor is apparently independent of viscosity. On the other hand, in an

¹ H. R. Lillie, *J. Am. Ceramic Soc.* **12**, 505-529 (1929).

² S. English, *J. Soc. Glass Tech.* **8**, 205 (1924). Stott, Irvine and Turner, *Proc. Roy. Soc. A* **108**, 154 (1925). Proctor and Douglas, *Proc. Phys. Soc. (London)* **41**, 500 (1929). M. Volarovich, *J. App. Phys. Moscow* **5**, 185 (1928).

investigation of the viscosities of soda-lime glasses over a large field of compositions, Washburn³ found that his factor existing between force per unit shear and viscosity apparently varied by a factor of about three over the range of viscosities dealt with. Comparisons made by others have shown that agreement between their results and those of Washburn can be reached only if his calibrating factor be changed to a constant or their own made variable.

Since in any rotation method the torque is simply proportional to the viscosity and to the velocity gradient at the very surface of the cylinder upon which the torque is exerted, a variation in the factor connecting torque and viscosity for a given total relative angular motion between the two cylinders, would indicate that the velocity gradient at the surface of the cylinder is not proportional to the total relative velocity alone. In other words, the velocity distribution would have to depend on viscosity. The result of this would be that if the temperature of a liquid, contained between a stationary cylinder and one rotating with a constant speed, be changed so as to alter its viscosity, some parts of the liquid would be thereby slowed down while others would rotate faster in order to change the velocity gradient to the cylinders' surfaces. This is only conceivable if centrifugal or other forces tending to disturb the regular motion of the liquid have more effect in the less viscous liquid. This may be true in the case of cylinders of finite length.

MEASUREMENT BY THE CONCENTRIC CYLINDER METHOD

Mathematical procedure.

As reported in the previous papers, viscosities have been measured without the aid of actual calibration with standard liquids, simply by determining the magnitude of the "end effect" at some arbitrary viscosity and assuming a constant calibrating factor for all viscosities. The end effect was determined by first finding the apparent viscosity of the liquid, using inside cylinders or spindles of various lengths, by using the formula

$$T = \frac{4\pi\eta\Omega R_1^2 R_2^2 l}{R_2^2 - R_1^2} \quad (1)$$

where T is the torque on the inner cylinder, η the viscosity, Ω the angular velocity of the outer cylinder, R_1 and l the radius and length of the inner cylinder and R_2 the radius of the outer rotating cylinder. These apparent viscosities were then plotted against reciprocals of spindle length and the "true" value of η corresponding to infinite length found by extrapolation. A correction to l was then found for each spindle. This correction is not the same for all lengths of spindles of the same diameter, supposedly because the amount of deformation of the flow surfaces around the body of the spindle depends on the length of the spindle itself.

Some minor changes have been made in the method of computation of apparent viscosity. We have the relations

³ Washburn, Libman and Shelton, Univ. of Illinois, Eng. Expt. Sta., Bull. No. 140 (1924).

$$T = K\theta = \frac{KZD}{2d}$$

and

$$\Omega = \frac{2\pi}{t},$$

where K is the constant of the suspension, determined as described in the previous paper, θ its angular displacement, D the deflection as read on a scale at a distance d from the mirror, Z the correction for straight scale and t the time for one revolution of the containing cylinder. Eq. (1) becomes

$$\frac{KZD}{2d} = \eta \frac{8\pi}{t} (\pi R_1^2 l) \frac{R_2^2}{R_2^2 - R_1^2},$$

or, for apparent viscosity,

$$\eta = \frac{ZDt}{d} \left[\frac{K}{16\pi V} \left(1 - \frac{R_1^2}{R_2^2} \right) \right] \quad (2)$$

where V is the total volume of the spindle. The quantity in the brackets is a constant for any one spindle since a constant value of $R_2 = 3.2$ cm was used during the whole investigation. All apparent viscosities were computed from this equation.

Fig. 1 represents diagrammatically the experimental viscometer used. A water bath is contained in a large cylindrical can placed on the rotating table V of the viscometer frame described previously. This can is surrounded by a galvanized water jacket J , the purpose of which is to maintain an external temperature below that of the bath. The outer cylinder of the measuring viscometer, C , containing the liquid under investigation, is supported at the center of the bath by a hollow pedestal of brass and is closed by a threaded top carrying a small upright tube which extends through the surface of the water bath and allows the inner cylinder or spindle E to hang into the liquid. This spindle is held by a brass connector D upon which is fastened the mirror M , all of which hangs from the calibrated steel wire suspension B . With the exception of spindle No. 53, described later, the two ends of the spindle were 1.50 cm distant from the surface of the oil and the bottom of the container.

The temperature is maintained constant by means of a vapor pressure regulator R constructed as shown. Methyl formate was found to be the most satisfactory liquid for actuating the mercury column. Various temperatures can be obtained by adjusting the pressure of air in the top part of the regulator. The contacts of the regulator are connected in series with a small flashlight dry cell and a telegraphic relay, both of which are fastened to the transite cover piece of the rotating can. This relay makes and breaks the circuit through the heater H consisting of three units of nichrome wire which can be connected in various ways depending on the temperature desired. The current for the heater is supplied through mercury cups at the extreme bottom of the viscometer frame. Circulation of the water bath is maintained

by a small toy electric motor directly connected to the shaft of the stirrer *A*. This stirrer is so built as to take water in from top and bottom and eject it tangentially at the center. Current for the motor is supplied by a large 4 volt storage battery, through brushes acting on rings around the outside of the jacket *J*. It was found necessary to house the motor completely to prevent disturbance of the spindle due to air currents from the armature. At times

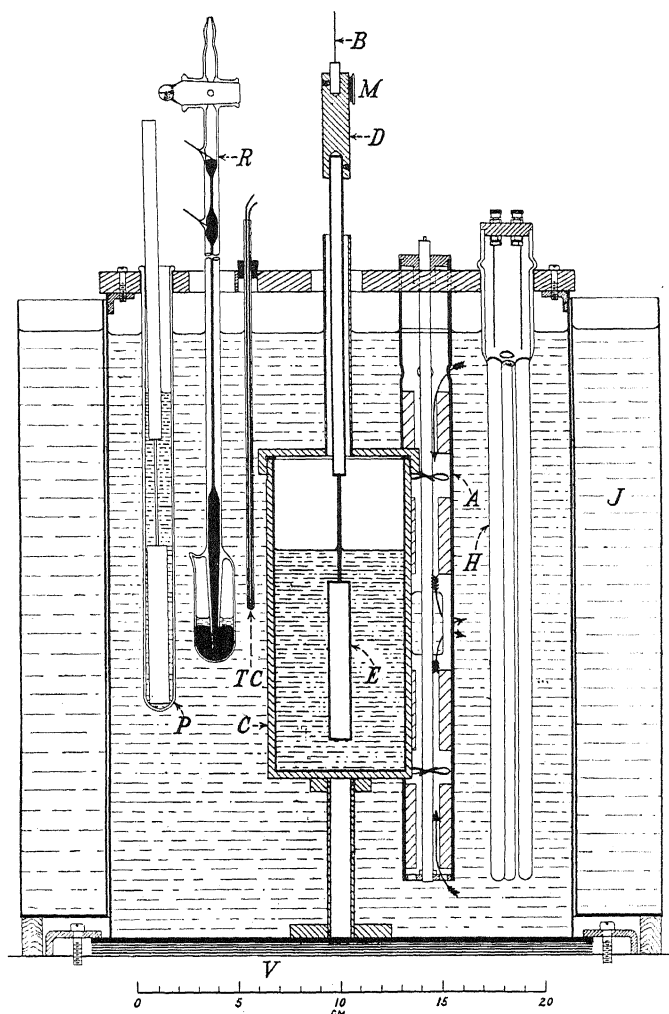


Fig. 1. Diagram of apparatus.

when various spindles were being used, one after another, a preheating tube *P* was installed containing some of the same oil as was being used in *C* so as to allow the next spindle to come to temperature before being placed in the central position. Temperatures were measured by means of three copper-constantan thermocouples placed as shown (*TC*) and connected in series through junctions kept at 0°C. A precision potentiometer accurate to less

than 1 microvolt was used for e.m.f. readings. These couples measured the average temperature of the bath to within 0.05°C and were sensitive to changes of less than 0.01°C . Their condition was checked periodically with a standard mercury thermometer to make sure that no short circuits were causing them to be far in error.

Temperature control.

Since all temperature readings made during actual viscosity measurements were for the water bath instead of for the liquid inside the viscometer proper, a few test runs were made to establish the relations between these temperatures. By placing a second set of couples in the center of the oil its temperature could be followed while the bath was cooling, heating, and just after it had come to equilibrium. In this way the following conditions were found:

Heater turned off: temperature lag 2.3°C , time lag 35 min.

Heater turned on: temperature lag 1.3°C , time lag 17 min.

(rate $0.08^{\circ}\text{C}/\text{min.}$)

Length of time after regulator began working, for oil to be

within 0.05°C of bath: 50 min.

within 0.01°C of bath: 70 min.

Accordingly, about two hours were always allowed, after the regulator began to function, before any viscosity readings were made. It was also observed that when the regulator had been in action for some time no periodic fluctuation of temperature in the oil could be detected.

Effective spindle length.

For determining "true" viscosities by extrapolating the apparent values for several spindles of equal radii but various lengths to the value corresponding to infinite length, five spindles of $3/8"$ diameter and five of $7/16"$ diameter were used. Their actual dimensions were:

No.	R_1	l	$1/l$	No.	R_1	l	$1/l$
101	0.4766 cm	10.14 cm	0.0986	106	0.5561 cm	10.22 cm	0.0979
102	.4771	7.61	.1314	107	.5562	7.60	.1315
103	.4769	5.08	.1969	108	.5564	5.12	.1953
104	.4768	3.80	.263	109	.5561	3.82	.262
105	.4770	2.53	.396	110	.5561	2.54	.394
Mean	0.4769			Mean	0.5562		

The observed apparent viscosities found by the use of these spindles (R_2 constant and equal to 3.2 cm) are shown in Table I. The ratios of viscosity at 23.40°C and 28.20°C to that at 19.97°C , as given by each spindle, are also shown. It is quite evident that over this small range of viscosities relative results are independent of the spindle used. A mean of these ratios for the two higher temperatures was accordingly taken, weighting each value according to spindle length, and all the viscosities recomputed back to the basis

TABLE I

Spindle No.	Observed Values						Mean μ	Values read from curve (Fig. 2)	
	19.97°C $\eta = 10.020$		23.40 $\eta = 7.633$		28.20 $\eta = 5.295$			App. η	l'
	App. η	l'	App. η	Ratio	App. η	Ratio			
101	10.53	0.51	8.03	0.762	5.61	0.533	0.55	10.53	0.51
102	10.67	.49	8.15	.763	5.62	.527	.52	10.70	.52
103	10.99	.49	8.41	.766	5.86	.534	.52	11.07	.52
104	11.29	.48	8.57	.760	5.92	.525	.47	11.33	.50
105	11.72	.43	9.10	.776	6.17	.526	.44	11.75	.43
106	10.63	.63	8.09	.761	5.63	.529	.62	10.63	.62
107	10.85	.63	8.28	.762	5.75	.529	.64	10.84	.62
108	11.27	.64	8.54	.757	5.90	.523	.61	11.24	.62
109	11.65	.62	8.83	.757	6.09	.522	.59	11.61	.60
110	12.19	.55	9.21	.756	6.43	.527	.54	12.16	.53
Mean ratios				.7618	.5284				

of 19.97°C. This process gave the points plotted in Fig. 2. Since for a given radius of spindle the relation between apparent viscosity and reciprocal of length appeared to be a linear one for values of l greater than 5 cm, this was assumed to be true and the apparent viscosities as given by the six longest spindles were used for determining the best pair of straight lines intersecting

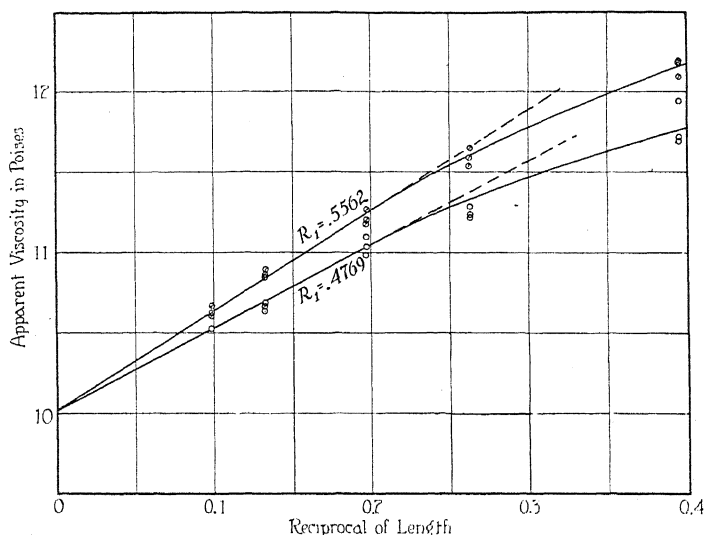


Fig. 2. Apparent viscosities of castor oil. Spindles 101-110 inclusive. Converted to 19.97°C

at $1/l=0$. In so doing it was discovered that the sum of the deviations become minimum for the two lines separately as well as collectively when the intercept was made at 10.020 poises. The average deviation in this case was about 0.3 percent, using only those spindles of length greater than 5 cm. The curved part of each line was drawn by estimate.

Using the extrapolated intercept as the true viscosity at 19.97°C and the mean ratios shown in Table I for computing the corresponding values at the

two higher temperatures, the following comparison is made with viscosities of pure castor oil as given by the Smithsonian Tables:

Temp.	Observed	Sm. T.
19.97°C	10.020 poises	9.92 poises
23.40	7.633	7.42
28.20	5.295	5.14
$\Delta \log \eta / \Delta 1/T$	297	302

Fig. 3 shows these two sets of data plotted as logarithms against the reciprocal of absolute temperature. This method of plotting was used in order to obtain a linear relation, thus facilitating interpolation. The figure includes also a similar curve for values proportional to viscosity as obtained later by capillary flow.

We now have sufficient means for computing some sort of correction to be applied to each spindle to account for the additional torque exerted by virtue of its finite length. Since others have assumed that this may be expressed in terms of an additional length of spindle which remains constant for a constant radius, it will be so computed in this case. If l' is this additional length, we have

$$l' = l \left(\frac{\text{app. } \eta}{\text{true } \eta} - 1 \right).$$

Values for this correction computed from observed apparent viscosities and for those read from the curves in Fig. 2 have been included in Table I. For lengths greater than 5 cm a constant correction is obtained for each radius as follows:

$$R_1 = 0.5562 \text{ cm, } l' = 0.620 \text{ cm}$$

$$R_1 = 0.4769 \text{ cm, } l' = 0.517 \text{ cm}$$

from which we have the relation:

$$l' \text{ proportional to } (R_1)^{1.18},$$

indicating that the end correction when stated in terms of additional spindle length varies approximately as the first power of radius.

Temperature runs.

In order to determine more accurately the temperature viscosity relations for the oil, a run was made with each of four spindles, in each case leaving the spindle undisturbed while the temperature was varied. For this purpose two spindles, No. 101 and No. 107, from the previous runs were used, together with two others of special sizes.

Spindle No. 53. In a previous trial of various spindles with specially shaped ends it was found that one with conical ends showed the least variation of torque with variation of the distance from the bottom of the oil to the end of the spindle. Many subsequent determinations of glass viscosities

were made using such a spindle, consisting of platinum-iridium and having the following dimensions:

$$R_1 = 0.477 \text{ cm}, \quad l = 3.82 \text{ cm}, \quad V = 3.010 \text{ cc},$$

where l is the length of the cylindrical portion. Each end of the large portion of the spindle terminated in a 90° cone, while the whole was supported by a stem of about 0.16 cm diameter. A duplicate of this spindle was made of iron and called No. 53. Its distance of 1.5 cm from the upper and lower boundaries of the oil was measured to its cylindrical portion instead of to its pointed ends.

Spindle No. 152. Another spindle used considerably in glass is the one of "sillimanite" described in the previous paper on glass viscosities. It is nearly the same as spindle No. 101 but is held by a porcelain stem of $1/4$ " double-bore thermocouple tubing. A similar one was made of brass of dimensions:

$$R_1 = 0.5151 \text{ cm}, \quad l = 10.18 \text{ cm}, \quad R' = 0.3174 \text{ cm}, \quad V = 8.960 \text{ cc},$$

where R' is the radius of the stem. This was called spindle No. 152.

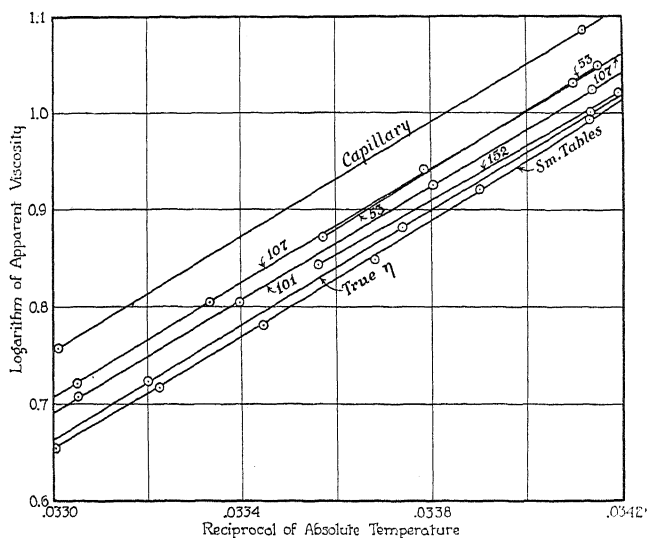


Fig. 3. Temperature runs in castor oil.

Table II gives the results for apparent viscosity of the castor oil obtained with these four spindles. The values for 20°C were interpolated on the curves in Fig. 3.

It is quite evident that the result obtained with spindle 152 at 19.47°C is in error since the slope of the curve for this spindle is less than for any of the others. Also, the similarity of No. 152 to No. 101 suggests an apparent viscosity at 20°C more nearly equal to 10.5. However, this trouble was not discovered until after the viscometer was dismantled and no redetermination was made.

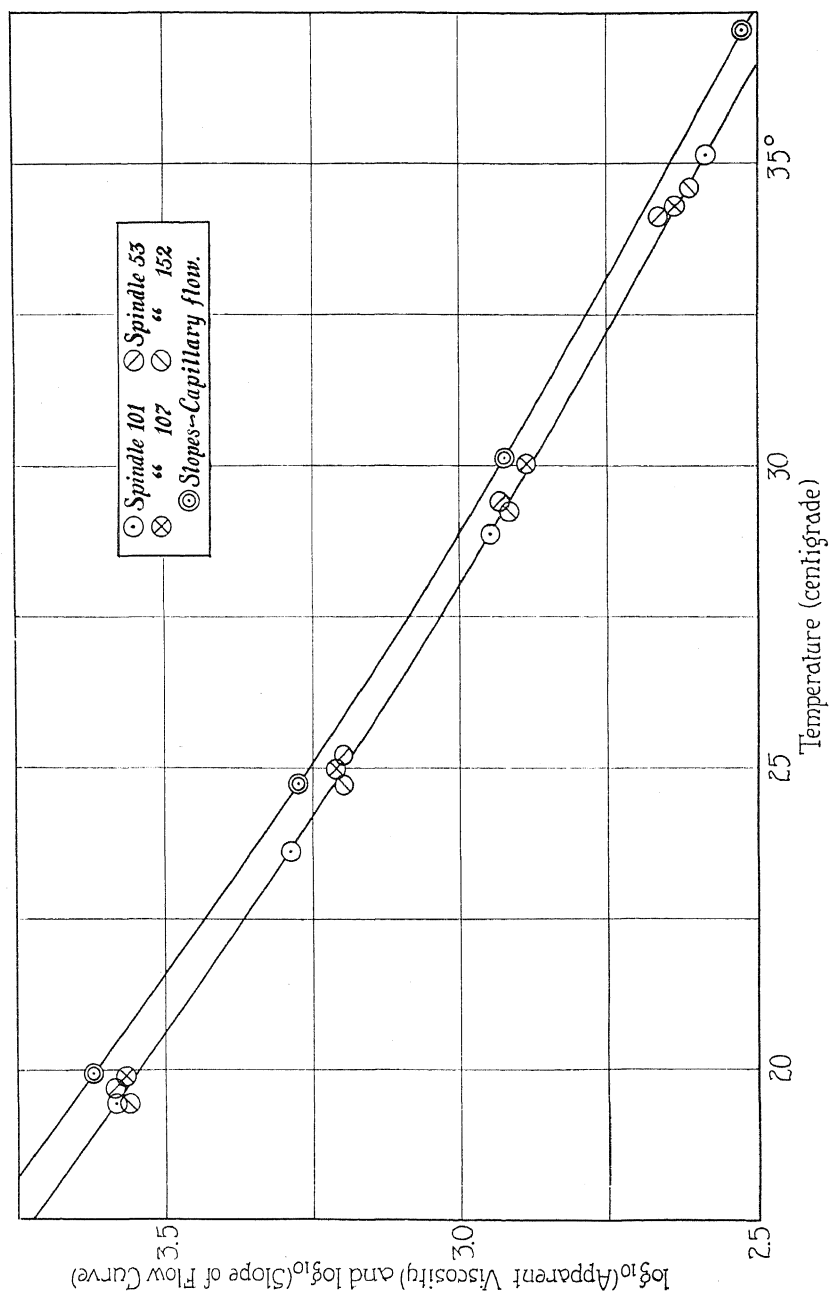


Fig. 4. Apparent viscosities of glucose solution.

TABLE II.

No. 101		No. 107		No. 53		No. 152	
Temp.	App. η	Temp.	App. η	Temp.	App. η	Temp.	App. η
19.94	10.57	20.00	10.99	19.84	11.20	19.47	10.52
20.00	10.50	20.30	10.74	20.00	11.04	20.00	10.10
22.83	8.44	23.00	8.77	24.87	7.45	24.97	6.97
26.46	6.38	26.99	6.36				
29.55	5.10	29.59	5.26				

Measurements in glucose solution.

For the purpose of measuring relatively high viscosities, a supply of heavy glucose solution was obtained from a candy making concern. At the time it was drawn from the large supply tank this solution was placed in several pint jars and kept tightly sealed until used for the various runs. It was found in preliminary tests that evaporation could be completely stopped and surface film thereby avoided by covering the surface of the glucose with a thin layer of oil. Observation also showed that the oil had no tendency to creep between the glucose and its container, while a sharp surface always showed between the two liquids. Accordingly, as soon as the glucose had been placed in the cylindrical container of the viscometer and the spindle had been put in place, a small quantity of oil was added. As a further test of constant concentration of the solution, the first temperature used in each viscosity run was repeated at the end of the run. Good checks were consistently obtained.

TABLE III.

No. 101		No. 107		No. 53		No. 152	
Temp.	App. η	Temp.	App. η	Temp.	App. η	Temp.	App. η
19.45°C	3836	19.90	3707	19.70	3842	19.45	3650
23.64	1940	25.00	1627	25.24	1576	24.74	1581
28.88	885	30.04	771	29.43	854	29.25	823
35.15	385	34.30	436	34.20	447	34.60	411

Table III gives the observed apparent viscosities of the glucose as found by the four spindles used in the similar runs in castor oil. Fig. 4 shows these results plotted in terms of their logarithms against temperature. The line drawn through the points is for spindle No. 101. The other three spindles would give three curves parallel to and near this line.

TABLE IV

Spindle No.	Apparent η for glucose				Oil at 20°C.	η glucose \div η oil at 20°			
	20°	25°	30°	35°		20°	25°	30°	35°
101	3506	1574	760	392	10.50	334.0	150.0	72.4	37.3
107	3608	1630	777	396	10.99	328.2	148.3	70.7	36.0
53	3658	1637	789	410	11.04	331.0	148.1	71.4	37.7
152	3342	1521	744	385	10.10	331.0	150.7	73.6	38.1
					Mean	331.1	149.3	72.0	37.3
						$\pm 0.5\%$	$\pm 0.7\%$	$\pm 1.4\%$	$\pm 1.7\%$

Table IV gives values read from this family of curves corresponding to the various temperatures stated. From these values have been computed the viscosities of the glucose solution relative to castor oil at 20°C, as determined with the same spindles (Table II).

MEASUREMENT BY CAPILLARY FLOW METHOD

The second part of the investigation consisted of measuring the relative viscosities of castor oil and glucose solution over the same range of temperatures by capillary flow. The same capillary viscometer was used for both liquids and the rates of flow so regulated as to make the maximum rates of shear as nearly as possible the same as those which prevailed in the cylinder method.

Apparatus.

The thermostat used was essentially the same as that described above for the rotating cylinder apparatus, with the exception of one slight change. A side tube was sealed into the regulator just above the top of the mercury column, this tube terminating in a large bulb immersed in the water bath. The purpose of this was to reduce further the effect of changing room temperature on the pressure over the column.

Fig. 5 is a sketch of the viscometer. Two similar reservoirs r_1 and r_2 are connected by the capillary C selected for roundness and uniformity of bore. The dimensions of the bore were found to be:

$$R = 0.1175 \text{ cm}; R^4 = 1.905 \times 10^{-4} \text{ cm}^4; L = 9.992 \text{ cm}$$

The ends of the capillary were ground and polished perpendicular to the axis. DeKhotinsky cement was used for fastening into the reservoirs, care being taken to have the two sides as symmetrical as possible. To avoid slipping when the higher temperatures and pressures were used, the bottom part of the viscometer was buried in plaster of Paris as shown. The reservoirs are fitted with screw tops A made of brass. The tubes t_1 and t_2 lead to a system of stopcocks which allow either tube to be connected to pressure or suction systems or to the volumetric manometer at will. This manometer is constructed as shown at the right of Fig. 5. The left-hand leg a is graduated in cm and has been calibrated for volume. The liquid used is diphenyl oxide, chosen for its low viscosity and low vapor pressure. By keeping the levels equal in tubes a and b by means of the counter columns of mercury in c and d , the volume of flow through the capillary C can be followed and measured. This flow is corrected for temperature differences between the bath and the room by the following:

$$F = V(T_1/T_2)$$

where F is the actual flow through C , V the volume registered in the manometer, T_1 and T_2 the absolute temperatures of bath and room respectively.

The pressure system contains a large carboy for holding the pressures constant during measurements.

Measurements for castor oil.

Technique: For creating such a small rate of flow as was desired, very small pressures were necessary. This meant that a difference in level in the two reservoirs would have an effect on the rate of flow. The following method was used for avoiding error from this source: Both reservoirs were first opened to

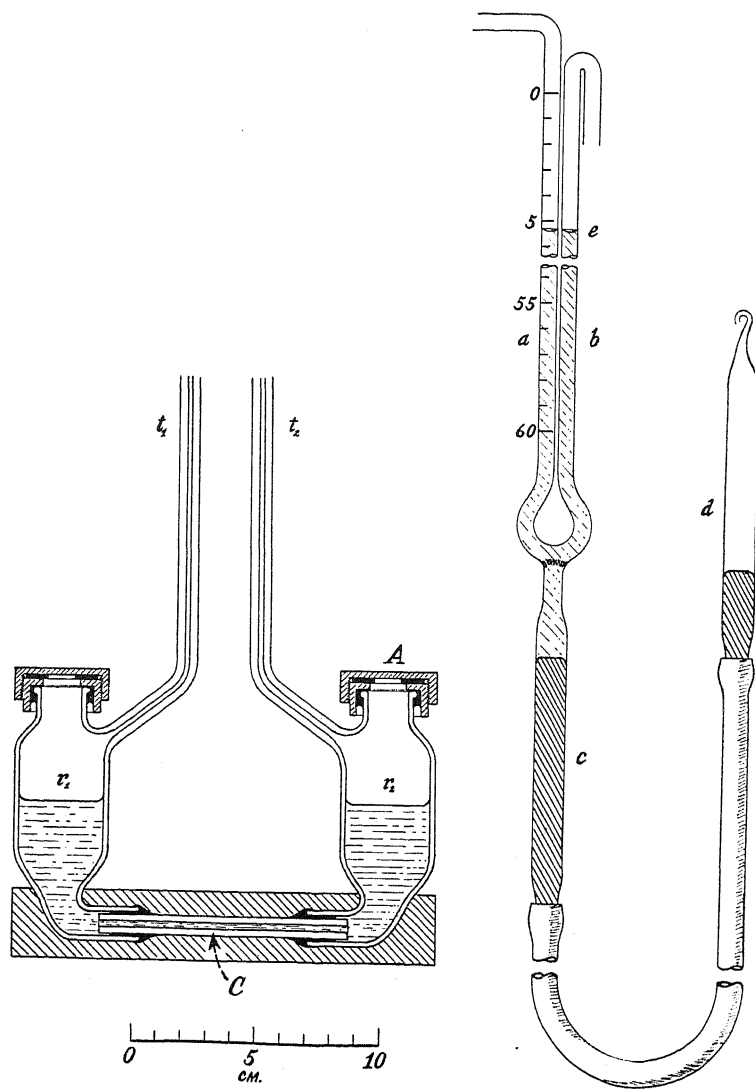


Fig. 5. Sketch of viscometer.

atmospheric pressure and the liquid allowed to come to rest. One tube, e.g. t_1 , was then connected to the volumetric manometer, the columns a and b being first adjusted to about the 30 cm mark. A slight suction was then caused in r_2 and the oil made to flow back until the columns a and b reached the 10 cm mark or thereabouts. At this time r_2 was connected to the pressure

system and, keeping atmospheric pressure in r_1 by lowering d to keep a and b on a level, time readings were made for each 2 cm drop in a by means of a split-time watch. These time readings were then plotted against the corresponding column positions, giving a slightly curved line whose slope at 30 cm was the rate of flow corresponding to zero hydrostatic pressure.

In the case of castor oil, pressures were measured by means of a Nujol manometer and later converted to the usual cm of mercury units.

Results: The actual numerical results will not be quoted here. Fig. 6 shows them graphically, the two kinds of points plotted representing the two

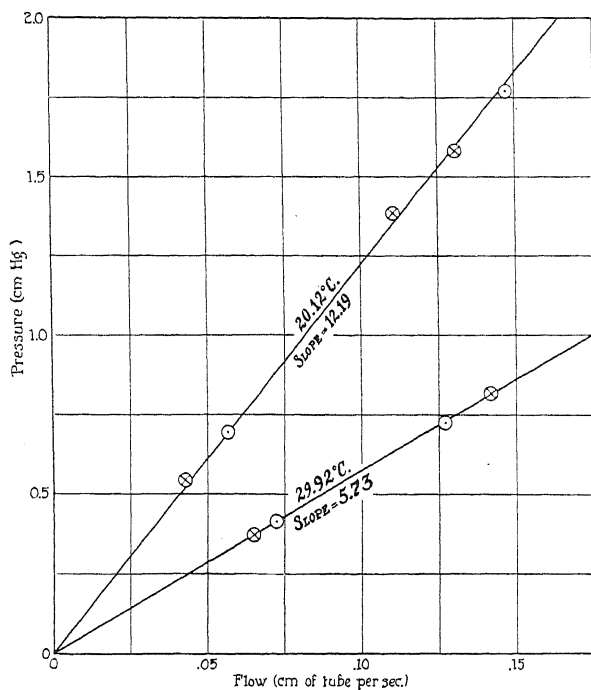


Fig. 6. Pressure-flow relations for new castor oil.

directions of flow through the capillary. It is evident that the system is quite nearly symmetrical and that the relation between rate of flow and pressure is a linear one. The slopes are:

29.92°C	5.73
20.12	12.19
20.00 (extrapolated)	12.31

These slopes, proportional to viscosity, have been plotted in Fig. 3. The value obtained in this case for $\Delta \log \eta / \Delta (1/T)$ is 297 as compared with 297 for the concentric cylinders and 302 for values from the Smithsonian Tables. This indicates that the oil itself differs slightly from that for which the viscosities in the Tables are quoted.

Measurements for glucose solution.

Technique. In order to have about the same rates of flow in the glucose solution as in the oil, very much higher pressures were used. This fact made the effect of difference of level between the two reservoirs negligible in comparison with the other forces acting. It was, therefore, unnecessary to carry out the procedures as outlined above, the flows being now measured simply by taking the total time for a certain flow—usually 10 cm in the volumetric manometer.

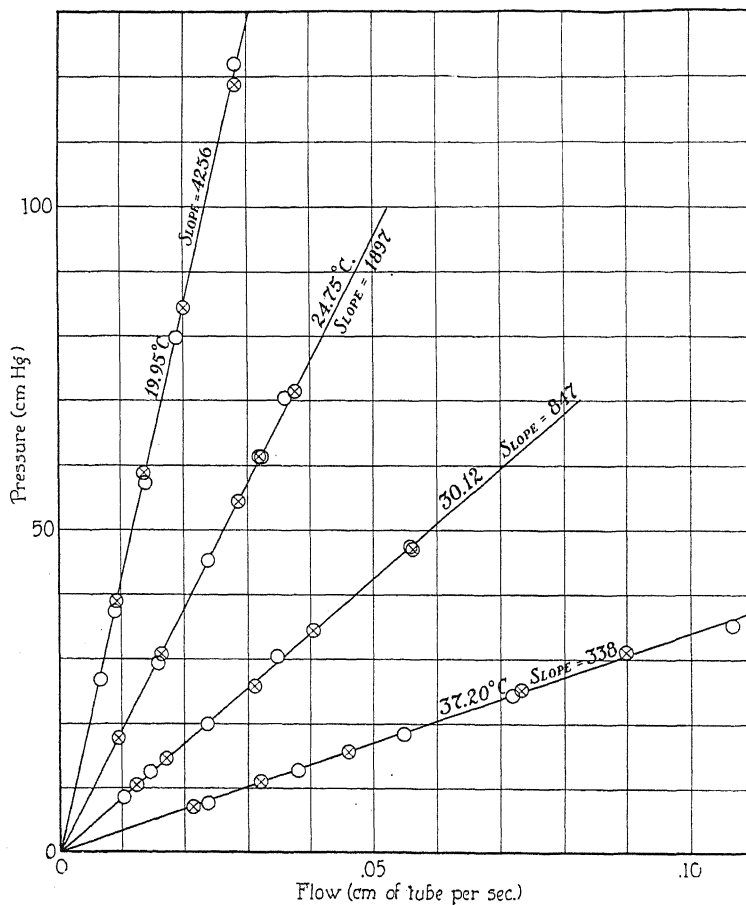


Fig. 7. Pressure-flow relations for glucose solution.

A covering of oil over the glucose was used as before and bubbles were eliminated by warming and slightly reducing the pressure for a very short time. In this case mercury was used in the pressure manometer. No suction was used over the glucose at any time during the measurements. It was found necessary to use a soft wax in the stopcocks of the pressure system. Pressure was obtained from a cylinder of nitrogen by the use of a reducing valve, a stopcock being closed between the pressure system and the reducing valve during the flow observations.

Results. Fig. 7 shows the pressure-flow relations for the glucose solution. As in the case of castor oil, it is evident that the two directions of flow agree and that the relations are represented by straight lines. It may be said in this connection that any small difference observed in apparent viscosity as the pressures were decreased seemed to be toward lower values instead of toward high ones as would be expected if plasticity were present in the glucose.

The slopes of the observed pressure-flow lines are:

37.20°C	338 ± 4	24.75°C	1897 ± 21
30.12	847 ± 11	19.95	4256 ± 53

These values, proportional to viscosity, are plotted logarithmically in Fig. 4. Values for the reference temperatures, interpolated by means of this graph, are shown in Table V, together with viscosities relative to castor oil at 20°C, as obtained by the two methods.

TABLE V.

Temp.	Interpolated slope	Oil at 20°C	η relative to castor oil at 20°		Deviation of cylinders from capillary
			capillary	cylinders	
20°C	4220 ± 53	12.31	342.5 ± 1.3%	331.1 ± 0.5%	-3.4% (±1.8%)
25	1824 ± 21		148.1 ± 1.1%	149.3 ± 0.7%	+0.8% (±1.8%)
30	865 ± 11		70.3 ± 1.3%	72.0 ± 1.4%	+2.4% (±2.7%)
35	446 ± 6		36.2 ± 1.3%	37.3 ± 1.7%	+3.1% (±3.0%)

The table also gives the deviations of values of relative viscosity as obtained by the cylinders from those by capillary flow. The figure in parentheses following each of these deviations is the sum of the estimated probable errors for the two methods taken to represent the probable error to which the final comparison is subject. The fact that this deviation is zero for about 2000 poises, while it must be zero also for the viscosity of the oil, indicates that errors in the measurements themselves, and in the various graphical interpolations made, are responsible for all the deviations. If this can be considered true it may be said that the calibrating factor of the concentric cylinders remains constant over the range of viscosities between 5 and 3500 poises. In any case the deviation from constancy is very small.

Rates of shear.

In the rotating cylinder system, the expression for rate of shear is:

$$s = \frac{2\Omega R_1^2 R_2^2}{r^2(R_2^2 - R_1^2)}.$$

This reaches a maximum when r is its minimum value R_1 , or maximum rate of shear

$$S = \frac{2\Omega R_2^2}{R_2^2 - R_1^2} = 2.06\Omega \text{ approximately.}$$

The values of Ω used were from 0.233 to 0.524 radians/sec. The maximum rates of shear, then, ranged from

$$S = 0.48 \text{ to } 1.08 \text{ cm/sec/cm.}$$

In the capillary flow system, rate of shear is expressed by

$$s = \frac{-4rQ}{\pi R^4}$$

which reaches a maximum numerical value at $r = R$, or

$$S = \frac{-4Q}{\pi R^3}.$$

In the experiments reported above, Q was expressed in terms of cm of tube in the volumetric manometer. To convert the values to cc/sec. we must multiply the numbers by the volume of tube per cm (0.1131). This gives values of Q from 0.0045 to 0.017 for oil and from 0.0011 to 0.0113 for the glucose. Using $R^3 = 1.62 \times 10^{-3}$ we have $S = 3.54$ to 13.4 for oil and 0.86 to 8.9 for glucose. Although these limits do not correspond exactly to those found for the cylinders, they are of the same order of magnitude and actually overlap to some extent.

Capillary end correction.

The equation for viscosity by the capillary flow method is, since the kinetic energy correction is negligible,

$$\eta = \frac{\pi P R^4}{8Q} \left(\frac{1}{L + \lambda} \right)$$

where P is pressure in dynes/cm², Q volume rate of flow and R and L the radius and length respectively of the capillary. λ represents a length that must be added to L to give the effective length of the constriction through which the liquid must flow.

The viscosity of the castor oil at 20°C, found by the concentric cylinders is 9.99 poises. The slope P/Q found as 12.31 by capillary flow is in terms of cm of mercury per unit velocity of the column in the volumetric manometer. It is equivalent to 1.445×10^6 in c.g.s. units. Then we have

$$\begin{aligned} L + \lambda &= \frac{\pi \times 1.905 \times 10^{-4} \times 1.445 \times 10^6}{8 \times 9.99} \\ &= 10.83 \end{aligned}$$

But since $L = 9.99$ cm,

$$\lambda = 0.84 \text{ cm or about } 3.5 \text{ diameters.}$$

The experience of others has shown that λ is usually of the order of a few diameters.

Acknowledgment.

In conclusion, the writer wishes to express his appreciation for the assistance rendered by Dr. G. S. Fulcher in the preparation of this paper.

ERRATUM

THE DISPERSION FORMULA AND RAMAN EFFECT FOR THE SYMMETRICAL TOP

BY MORRIS MUSKAT

(Phys. Rev. **35**, 1262, 1930)

Exponents of the form $(2\pi i/h) t(W_a - W_b)$ should be preceded by a minus sign so that $\nu_{jk} = (W_j - W_k)/h$ and $\eta = +8\pi^2 A\nu/h$.

In the bracket of (21) read $[1 + \dots]$ and in (25) $(j \mp 2m)$.

In $R(\nu + \nu_{j, j+1})$ the parenthesis should be $(j^4 + 3j^3 + 2j^2 + j^2 m^2 + 8jm^2 + 12m^2)$ so that the numerical factor in $I(\nu + \nu_{j, j+1})$ becomes $128/3$.

LETTERS TO THE EDITOR

Prompt publication of brief reports of important discoveries in physics may be secured by addressing them to this department. Closing dates for this department are, for the first issue of the month, the twenty-eighth of the preceding month; for the second issue, the thirteenth of the month. The Board of Editors does not hold itself responsible for the opinions expressed by the correspondents.

Interpretation of the Visible Halogen Bands

The familiar absorption band spectra of the halogen molecules in the visible (and partly in the near ultraviolet) are commonly attributed to a ${}^1\Sigma \leftarrow {}^1\Sigma$ electron transition. That the lower level is ${}^1\Sigma$ is practically certain from the fact that Cl_2 is diamagnetic and from other considerations, while the ${}^1\Sigma$ character of the upper state is then indicated by the structure of the bands (one P and one R branch). Now it is known that both states dissociate into normal 2P halogen atoms (the lower probably into ${}^2P_{1/2} + {}^2P_{1/2}$, the upper certainly into ${}^2P_{1/2} + {}^2P_{3/2}$). According to the rules of Wigner and Witmer, it can be shown that two normal halogen atoms can give three ${}^1\Sigma$ states, namely two ${}^1\Sigma_g^+$ states and one ${}^1\Sigma_u^-$ state. The normal molecular state can in all probability be identified with one of the two ${}^1\Sigma_g^+$ states. Now a ${}^1\Sigma_g^+$ state can combine spectroscopically with another ${}^1\Sigma$ state only if the latter is of the ${}^1\Sigma_u^+$ type. Since no such state can be derived from normal atoms, and since the upper level of the halogen bands certainly is derived from normal atoms, it is evident that the bands cannot be of the ${}^1\Sigma \leftarrow {}^1\Sigma$ type. (The same conclusion would be reached if we assume ${}^1\Sigma_u^-$ for the normal state; this assumption is however almost certainly not appropriate.)

The upper state must then be a state of some kind other than ${}^1\Sigma$, fulfilling the following conditions: (1) it must be derivable from normal atoms; (2) it must be capable of combining spectroscopically with the ${}^1\Sigma^+$ normal state, giving a P and an R branch. The only

state which fulfils these conditions is a ${}^3\Pi_{0u}$ state. We must, however, assume that only half of the rotational levels of the ${}^3\Pi_0$ state are active (in an ordinary ${}^3\Pi_0$ state, there are two closely adjacent rotational levels for each value of J). This at first seemingly arbitrary assumption is made plausible by a consideration of the fact that the dissociation energy of the electron level in question is of the same order of magnitude as the energy of coupling between the L and S vectors in the halogen atom. Under these circumstances the two sets of rotational levels of ${}^3\Pi_0$ may behave as if belonging to two separate electron levels, which we shall call 0^+ and 0^- . The halogen band can be interpreted by assuming that only combinations with the 0^+ level are observed. As for the 0^- level, it may be that it has a very small dissociation energy so that it gives only a continuous band spectrum, or it may be that its combinations with the normal state (Q branches only, they should be) are weak.

A consequence of the above interpretation is that the excited state of the halogen bands should be paramagnetic. This is in harmony with certain magnetic phenomena observed with these bands.

ROBERT S. MULLIKEN

University of Chicago,
Ryerson Physical Laboratory,
Fellow of the John Simon Guggenheim
Memorial Foundation, now in Leipzig.
June 14, 1930.

Double Crystal Analysis of Scattered X-rays

A series of double crystal experiments has been completed to determine accurately the magnitude of the Compton shift. In order to do this, the angle of scattering was made

as near to 180° as possible, so that variations in the scattering angle would result in small variations of the wave-length change. A metal x-ray tube of small diameter and with two

aluminum windows 0.05 mm thick was used. In a typical run, this tube carried 70 m.a. at 50 K.V., though occasionally higher currents were used. The x-rays passed through one aluminum window and were incident upon a large block of graphite placed four mm from that window. X-rays scattered from the graphite passed back through this window, and emerged from the other window on the opposite side of the tube, after which they were limited by two lead slits before striking the first crystal. This means that the x-rays were scattered at nearly 180° . The direct beam of x-rays emerging from the second window was carefully shielded, so that the only x-rays reaching the first crystal were those scattered by the graphite or by the thin windows. A test showed that no x-rays were scattered by the windows themselves.

The x-rays, after having been limited by the slits were reflected by two calcite crystals, set at the proper angle. Those x-rays, which were reflected from the second crystal, entered a carefully shielded ionization chamber, filled with methyl bromide. The amount of ionization produced at various angles of the second crystal was measured by means of an electrometer system having 6000 mm/volt sensitivity and about 35 cm capacity. The two crystals used were polished and gave a rocking curve in the parallel position, which was 20 seconds wide at half maximum.

Five different spectra were taken to determine the position of the $\text{MoK}\alpha_1$ modified line. The $\text{K}\alpha_1$ and $\text{K}\alpha_2$ lines of the modified beam were clearly separated. Fluorescent rays from Mo were used to determine the position of the unmodified $\text{K}\alpha_1$ line. The value of $d\lambda$ obtained was 0.04721Å with a probable error of $\pm 0.00003\text{Å}$, on the basis of D (calcite) = 3.02904.

The effective angle of scattering was calculated from the geometry of the slit-window system by dividing the target face into segments of area, the scattering block into small volumes and evaluating the angle between each area and each volume. The extreme values of the scattering angle ϕ were 153° and 175° . The value of $1-\cos \phi$ determined in the above manner was 1.9479. It is estimated that this value is accurate to ± 0.003 . From the equation $d\lambda = (h/mc)(1-\cos \phi)$, one calculates for h/mc the value $0.02424 \pm 0.00004\text{Å}$. This may be compared with 0.02417Å, the value for h/mc when the mass of the electron is deduced from spectroscopic determinations, and with 0.02428Å, the value for h/mc when the mass of the electron is deduced from deflection methods.

NEWELL S. GINGRICH

Ryerson Physical Laboratory,
The University of Chicago,
June 24, 1930.

A Remark on the Paper of R. C. Tolman: "Mechanical Treatment of Temperature Distribution in the Case of Radiation."

R. C. Tolman points out that heat, like every other form of energy, possesses weight, and that therefore gravitation must have an influence on the distribution of temperature throughout a system which has come to thermodynamic equilibrium. Tolman here observes: "The discovery of a dependence of equilibrium temperature on gravitational potential must be regarded as something essentially new in thermodynamics."¹

As against this I must remark that similar ideas have previously been expressed by my-

self.² In the publication referred to I gave some formulae, which differ from the corresponding ones given by Tolman only in some unessential details.

WILHELM ANDERSON

Tartu-Dorpat (Estonia).

¹ Richard C. Tolman, *Phys. Rev.* **35**, 904 (1930).

² Wilhelm Anderson, Über den Samazustand "ertser Art" und "zweiter Art," *Zeits. f. Physik* **58**, 440 (1929).

A Remark on the Foregoing Letter of W. Anderson

The Editor of the Physical Review has been good enough to send me a copy of the preceding letter before publication, and Dr. Anderson has also himself kindly sent me a reprint of the article to which he refers. In

this article Dr. Anderson has indeed expressed the opinion that the weight of energy should itself lead to a temperature gradient, and has thus given qualitative expression to an idea, which I believe to be essentially cor-

rect. Nevertheless, the quantitative implications of this idea can be ascertained with certainty only by a careful analysis in which the phenomena of gravitation are treated by the methods of general relativity. Such an analysis, however, is not presented by Dr. Anderson and I find myself unable to agree with the quantitative conclusions which he does obtain.

In considering the case of a system of gaseous molecules subjected to the action of gravity, Dr. Anderson does not make use of the idea that heat has weight, and comes to the conclusion that the temperature would fall to the absolute zero at levels too high for the molecules to obtain sufficient energy to reach. I should maintain on the other hand that in a treatment of thermodynamic equilibrium it was incorrect to consider the molecules separately from the radiation with which they are in equilibrium and that this radiation would have a finite temperature even at levels too high for the molecules to reach. Thus in the case of a spherical distribution of a perfect fluid, which could consist of molecules and radiation at lower levels and of pure radiation at higher levels, I should maintain that the temperature gradient would be given at all levels by my equation (54, loc. cit.)

$$\frac{d \log T_0}{dr} = -\frac{1}{2} \frac{d\nu}{dr} \quad (1)$$

and that there would be no discontinuity or drop to the absolute zero at levels too high for the molecules to reach.

In considering the case of pure radiation, Dr. Anderson does make use of the idea that energy has weight and proceeds in a manner in somewhat closer agreement with that which I should consider correct. Nevertheless, I believe that the non-relativistic treatment which he gives not only involves serious limitations but leads as well to a result which is essentially incorrect.

As to the limitations, it should be noted that this final result is expressed in terms of the quantities temperature T , height H , and gravitational acceleration g , which he does not interpret from the standpoint of the relativistic theory of gravitation. In place of his undefined quantity T he would presumably be willing to use the proper temperature T_0 which can be definitely defined as that measured by a local observer, but the

ideas of height H and gravitational acceleration g are necessarily restricted in their significance to fields weak enough so that the Newtonian treatment of gravitation becomes a correct approximation and this greatly limits the generality of his result.

Turning now to the correctness of the actual result which he does obtain for the temperature gradient in a field of radiation subjected to gravitational action, namely,

$$\frac{dT}{T} = -\frac{3}{4} \frac{g}{c^2} dH \quad (2)$$

we must compare this with the approximate result which can be obtained from my Eq. (1), when the gravitational field is weak enough so that the Newtonian treatment can be to some extent introduced as a first approximation. Under such circumstances we can then approximately identify the coordinate r with the height H and approximately replace the right hand side of the equation by $-g/c^2$, where g is the acceleration that would be experienced by a *slow moving* particle in the field in question. We thus obtain the different result

$$\frac{dT_0}{T_0} = -\frac{g}{c^2} dH \quad (3)$$

The incorrect factor $3/4$ appearing in Dr. Anderson's Eq. (2) is connected of course with the well-known fact, verified by the bending of light in the gravitational field of the sun, that the Newtonian approximations do not lead to correct results even in weak fields when particles are considered which are moving with velocities in the neighborhood of that of light.

At first sight it might appear as if the difference between the two formulae was an unessential detail, as suggested by Dr. Anderson. With this, however, I cannot agree since as shown in my article the formula (3) applies to matter in a weak gravitational field, and it would certainly be a thermodynamic catastrophe if a different formula (2) had to be applied to radiation, since this would force us to the conclusion that matter and the radiation in contact with it at a given level had to have *different* proper temperatures in order to be in equilibrium.

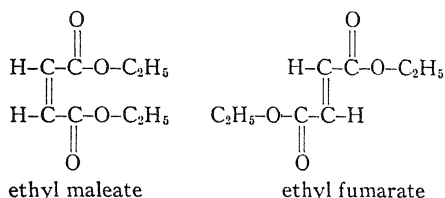
In conclusion, I am very grateful to Dr. Anderson for informing me of his earlier expression of the idea that the weight of energy should lead to a temperature gradient. Since I do not agree, however, with the con-

clusions as to temperature gradient drawn by Dr. Anderson and do not know of any other general and coherent treatment of the thermodynamic consequences of this idea, I hope Dr. Anderson will understand why

I still feel inclined to maintain that the discovery of the *correct* dependence of equilibrium temperature on gravitational potential must be regarded as something essentially new in thermodynamics.

Raman Spectra of Geometric Isomers

An investigation of the Raman spectra of the geometric isomers, ethyl fumarate and ethyl maleate, has disclosed a difference between them. In the spectrum of ethyl maleate we find a broad diffuse band at 4693A to 4699A. In the case of ethyl fumarate, the band is replaced by two distinct lines at 4692A and 4698A. The frequency difference between modified and unmodified lines for the first case is from 1636 cm^{-1} to 1683 cm^{-1} and for the second case, 1633 cm^{-1} and 1661 cm^{-1} . It has been suggested by others that a shift of about 1600 wave numbers is associated with the vibration frequency along a carbon oxygen double bond. In the accepted structural formulae of the two esters,



the only C=O double bonds are exterior to the chain. In the case of the maleate, the C=O double bonds are not symmetrically arranged with regard to either the double bond connecting the two chains, or the center of mass of the molecule. In the fumarate the C=O double bonds are symmetrically arranged with regard to this bond, which is also the center of mass of the system. In the spectrum of the maleate, the vibration along the two C=O double bonds may give rise to the broad band, while in the fumarate, they apparently give the separate lines.

The average value of the frequency shifts for the other lines common to both substances are,

$$\Delta\nu = 865, 1169, 1212, 1732, 3033, 3061\text{ cm}^{-1}.$$

The fumarate has in addition two very faint lines corresponding to a shift of 888 and 1361 cm^{-1} .

C. F. FOLLIOTT

Rensselaer Polytechnic Institute
Troy, New York
June 13, 1930.

A Method Offered as a Means of Computing Planck's Constant without Involving the Charge on the Electron

One notes that, numerically, the magnetic moment of an electron in ergs per gauss is equal to its charge in coulombs:

$$\begin{aligned} 3\frac{1}{2}he/4\pi mc &= e/c = 1.59 \cdot 10^{-20}; \text{ whence} \\ 3\frac{1}{2}h/4\pi &= m \quad \text{or} \\ h &= 4\pi/3\frac{1}{2}. \end{aligned}$$

Inserting the spectroscopic value of m , $0.9035 \cdot 10^{-27}$, one finds that $h = 6.555 \cdot 10^{-27}$ erg sec. To make the units cancel properly, one must give the spin vector the dimensions of seconds per centimeter squared, or time per unit area, dimensions which do not seem to have any obvious physical meaning. However, it passes the bounds of plausibility that the magnetic moment should be found numerically equal to the charge, or the angular momentum to the mass, without any physical basis. Two such coincidences to several significant figures in a range so enormous

would have a vanishingly small possibility of occurring, were there no physical basis for such concordance.

Unfortunately, the units are different even in ultimate rational units, for in this system charge, being a world-invariant, is expressed as a pure number; whereas magnetic moment is not.

One is reminded of the theory that mass is merely the effect of self-inductance or electrical inertia. Thus the mass of the electron might be due to the self-inductance of the current representing the spin, if a spinning electron may be said to constitute a current. Thus the equating of the angular momentum of the electron to its mass is qualitatively reasonable and could doubtless be made quantitatively exact by the use of an appropriate model.

It is to be noticed that $6.555 \cdot 10^{-27}$ erg

sec. as a value of h falls just within the limit of error which Birge allows. If M_h/m_e is taken as 1840 the agreement is better, h equalling $6.552 \cdot 10^{-27}$ erg sec.

As stated, the advantage of this method of calculating h is that it does not involve the charge on the electron, since the value of the mass of the electron may be found without reference to its charge as Houston has done by the relation between the Rydberg constants for hydrogen and ionized helium. Thus we may use this value of h for computing e . According to Birge's article in the first issue of the Physical Review Supplement, by the theory of ultimate rational units, the reciprocal of the fine structure constant equals 137.3, whence, using $6.555 \cdot 10^{-27}$ as the value of h , e is found to be $4.773 \cdot 10^{-10}$ e.s.u. The uncertainty in this value lies entirely in h , and therefore in the experimental value of the mass of the electron. This is about one-

twentieth of one percent, and since h occurs under a radical when one solves for e in the fine structure constant equation, the uncertainty in e is only $0.002 \cdot 10^{-10}$.

If the deflection mass instead of the spectroscopic mass of the electron is used, very disparate results are obtained for h and e .

The value of Avogadro's number obtained with the above value of e is identical with Birge's value of N .

It remains then to find some reason for the numerical equivalence of the magnetic moment and the charge of the electron, or of its angular momentum and mass, and the values of some of the more important physical constants may be established with less uncertainty than heretofore.

ALLEN LUCY

Stanford University,
May 15 to June 15, 1930.

Gas Discharge Wave-Length List in Extreme Ultraviolet

We have prepared a list, arranged in order of wave-length, of the published lines in the extreme ultraviolet ($\lambda 2500$ to $\lambda 100$) arising from discharges in gases. The elements included are hydrogen, helium, carbon, nitrogen, oxygen, neon, sodium, silicon, argon, and mercury. Thanks to support from the Carnegie Institution of Washington, it has been possible to publish a limited mimeographed edition of the list, copies of which have been sent

to a few spectroscopists to whom we thought it might be of particular use. We should be glad to give copies to any others who may write requesting them.

JANET M. MACINNES
JOSEPH C. BOYCE

Palmer Physical Laboratory,
Princeton University,
Princeton, N. J.
June 18, 1930.

BOOK REVIEWS

Einführung in die Wellenmechanik. L. DE BROGLIE. translated (from French to German) by R. Peierls. 219 pages. Akademische Verlagsgesellschaft, Leipzig, 1929. Price RM 13.80 bound.

The discoverer of the wave nature of the electron has written here a clear account of the development of wave mechanics starting with an account of classical mechanics and building on the analogy between the principle of least action and Fermat's principle in geometrical optics. The bulk of the book is occupied with a careful discussion of free motion of a particle and its relation to the wave packets from the standpoint of the uncertainty principle of Heisenberg and Bohr. In the last chapters elementary cases of quantization of energy levels in cases of periodic motion are discussed. There is no treatment of the radiation process nor of equivalence degeneracy in problems involving several equivalent particles nor of electron spin.

E. U. CONDON

Dielectric Phenomena in High Voltage Engineering. F. W. PEEK, JR. Pp. 410, figs. 267. McGraw-Hill Book Co., New York, 1929. Price \$5.00.

This is a third edition, the first having appeared in 1915. While the arrangement shows the effect of growth, involving some repetition, yet it has been thoroughly revised and brought up to date and constitutes an authoritative and exhaustive as well as very readable treatment of corona and spark-over phenomena. Mr. Peek is a leader in the field of high voltage engineering, and a large part of the material in the book is taken from his own experiments and those of his associates in the General Electric Company. Corona and spark-over in air, including lightning, are treated with great thoroughness, those in liquids and solids more briefly. The new material added to this third edition includes the results of recent studies of corona, extensive studies of the impulse breakdown of gases and insulation, cathode-ray studies of impulse breakdown in power transformers and other apparatus, and spark-over phenomena at very high voltages. Studies of artificial lightning with the author's five million volt impulse generator are of special interest.

The book contains mainly experimental data, with empirical laws and formulae, and relatively little mathematics.

ALBERT W. HULL

Elements of Electricity. ANTHONY ZELENY. Pp. xxiii+438, 267 figures, 12 appendices, McGraw-Hill Book Co., New York, 1930, Price \$3.00.

This excellent elementary text is the outgrowth of many years of teaching the subject of electricity to engineering, premedical and arts students in a first course of college physics. The subject is developed in a large number (30) of short chapters, at the end of each of which are a number of questions, problems and suggested experiments for lecture demonstration. The book is profusely illustrated by line drawings and half tones, including pictures of many of the pioneers in the subject. The appendices contain tables of numerical constants, definitions of electric and magnetic units, collections of laws, important dates, answers to problems, tables of squares, cubes and reciprocals, trigonometrical functions, and logarithms.

The text being designed for a first course, the subject is developed with the minimum of mathematical detail, no analysis more advanced than elementary algebra and trigonometry being used. The electron theory is introduced in the second article, and the subject is treated from this point of view throughout. After a brief discussion of electric charges and electric forces in the first chapter, the subject of magnetostatics is taken up, after which electrostatics is treated in more detail. The characteristics of the transformer and the subject of the generation and transmission of electric power are dealt with more extensively than in the usual elementary text, and chapters are devoted to discharge in gases at low pressure; measurement of

velocity, charge, and mass of electrons, protons and isotopes; production and detection of electromagnetic waves; electrical communication; and atmospheric electricity.

The outstanding feature of the book is the adoption by the author of modern points of view which have been all too slow in finding their way into elementary texts. Consequently the student does not have to "unlearn" much of what he reads before being able to advance further in the subject. This attitude is well exemplified by the author's sensible treatment of the ether. While not discarding the term itself, he points out the difficulties which have led to the abandonment of the old elastic solid medium, and makes clear that the subject can be treated without any reference to the ether, a form of treatment which he employs throughout. Again he emphasizes the importance of the elementary electric and magnetic fields associated with each electron and proton, as against the concept of the resultant field. Altogether too few writers seem to recognize the fact that "except in electrostatics and magnetostatics) it is these elementary fields which are fundamental and not the resultant field. Lack of recognition of this important fact can all too easily lead to grievous errors.

In his treatment of currents in metallic circuits the author takes the direction of flow of electrons as fundamental instead of that of the current. Whether this is pedagogically advantageous or not seems somewhat questionable to the reviewer, since it is likely to cause confusion in determining the direction of the magnetic field due to the current. In dealing with induced electromotive forces the author explains how the field of an accelerated electron urges neighboring free electrons in the opposite direction. This gives the student a picture of the mechanism of induction far superior to the usual treatment.

While certain minor details may be criticized, the book as a whole appeals very strongly to the reviewer as one which will give the elementary student an excellent foundation in the subject of electromagnetism. It is well printed, the type being of sufficient size to facilitate reading.

LEIGH PAGE

The Size of the Universe. LUDWIG SILBERSTEIN. Pp. viii+215, figs. 11. Oxford University Press, London 1930. \$3.50.

In this book Dr. Silberstein reexpresses and extends his previous treatment of the determination of the curvature radius of spacetime. The treatment presupposes the de Sitter line element for the universe in a static form, and makes no assumption as to a greater inherent probability of receding rather than approaching objects, in contradistinction to the treatment of Weyl and the corresponding non-static form for the de Sitter line element of Robertson. The estimates of radius are then based on correlations between the radial velocity and distance obtained from the consideration of five different groups of celestial objects. The groups used together with the varying values obtained for the radius were as follows:

- a. Eighteen globular clusters and the two Magellanic Clouds, 3.61×10^7 parsecs.
- b. Thirty-eight spiral nebulae, 7.32×10^8 parsecs.
- c. Twenty-nine cepheid variables, 1.46×10^6 parsecs.
- d. Thirty-five O-stars, 1.58×10^6 parsecs.
- e. Four hundred and fifty-nine stars from Young and Harper's list, 1.96×10^6 parsecs.

The most recent Mount Wilson results, of Hubble and Humason, showing a linear relation between apparent velocity of recession and distance of the extragalactic nebulae out to the enormous range of approximately 2.5×10^7 parsecs, were not available to Dr. Silberstein at the time of writing. In view of these facts, however, it would now appear to the present reviewer that cosmologies such as Silberstein's which do not expressly take account of the exclusively recessional motion of all the most distant objects would have to be superseded. In addition, it would seem that the use of stars within our own galactic system would have to be abandoned in favor of extragalactic objects for any form of cosmological determination.

Dr. Silberstein expresses throughout the book a most violent and unnecessary antipathy to the Einstein line element for the universe. This antipathy leads him to devote a whole chapter to a satiric and unjustified attack on the work of Hubble, for the sole apparent reason that Hubble has once made an estimate of the average density of matter in the universe which

could then be inserted in Einstein's formula for the radius of the universe. As a matter of fact, the work of Hubble and his collaborator Humason is by far the most important of all the observational contributions to the problems of cosmogony that have been made, and the estimate of mean density which he obtained is of great interest in interpreting the new non-static line element which now appears to be more satisfactory for cosmological speculations than either that of de Sitter or of Einstein.

The book exhibits a wealth of mathematical erudition and is written in a pungent and often illuminating style, although sometimes the style becomes perhaps too extravagant as for example in the following passage:

"If $a=r^*$, we have $\theta = \infty$, and, as we see directly from (108), each star will move uniformly on a straight line, utterly asocial, as it were, that, is, disregarding the presence of all other members of this galactic community. Thus, if their instantaneous velocities are haphazard in size and direction, the crowd will sooner or later be scattered to the four winds as in spite of all visual appearances; there is nothing to hold them together. And the more so, if the galaxy has swollen up beyond that critical radius of its mass total, the orbits then degenerating, by (109), into hyperbolic branches. Is in the wording of these results an illusion implied to communities of humans, a score or so of Nation-Galaxies, now stiffly coherent, now torn asunder, not only by foreign interference but as often by internal strife, with the greed and lust of power of the 'upper thousand' to urge the territorial expansion (growing a), and a huge majority of what some modern sociologists† refer to as the 'international mob,' but too eager to profit by every tumult, to tear down all social bonds, to set out on world-wide vagabondage, and mingling with deserters of other galaxies, sweep down every civilization, like the sand-laden winds of Sahara obliterate every hillock or oasis casually formed of stray particles through long years of slow and patient toil? I prefer to leave this question to my readers, the more so as I am the last man to desire to undermine their possibly strong confidence in a steady evolution and betterment of assemblages, both human and celestial, in an ever-mounting 'progress,' that is, as opposed to the hurricane-like 'cycloism' which is (not without weighty reasons) advocated by the aforesaid group of social philosophers. At any rate, some time spent now and then on such comparisons will not be entirely lost, provided that these are tempered by caution and self-criticism, and not poisoned by passion."

RICHARD C. TOLMAN

Grundzüge der theoretischen und angewandten Elektrochemie. GEORG GRUBE. Pp. xii+495, figs. 165. Published by Theodor Steinkopff, Dresden und Leipzig, 1930. Price bound, RM 30.

This treatise will be of treat interest to chemists and can be highly recommended to their attention. The author gives a clear and adequate account of theoretical electrochemistry in the first four chapters while he devotes the eight remaining chapters to numerous technical applications. The style is clear and the point of view is strictly up-to-date. It is a very satisfactory book.

F. H. MACDOUGALL

† Namely, the advocates of the theory of *social cycloism*. See a very interesting booklet on *Sozialphilosophie*, by Prof. L. Gumplowicz, Innsbruck, 1910.

PROCEEDINGS
OF THE
AMERICAN PHYSICAL SOCIETY

MINUTES OF THE ITHACA MEETING, JUNE 19-21, 1930

The 165th meeting of the American Physical Society was held in Ithaca, New York on Thursday, Friday and Saturday, June 19, 20 and 21.

The Council authorized a \$1.00 registration fee to be collected from the members attending this meeting.

The scientific sessions were all held in Rockefeller Hall. The presiding officers were Herbert E. Ives, John T. Tate, Dayton C. Miller, Ernest Merritt and Karl T. Compton.

On Wednesday, June 18, the Society was invited to be the guest of The Corning Glass Works for luncheon and an inspection trip through the Glass Works. There were 220 present at the luncheon at which we were honored by the presence of the Honorable A. B. Houghton.

On Thursday morning, June 19, from 10 a.m. to 1 p.m. the regular program for the reading of the thirty-three contributed papers was held. On Thursday afternoon a picnic was held at Buttermilk Falls and was attended by 247 persons.

On Friday morning, June 20, at 10 o'clock there were two invited papers on Astrophysics: S. A. Mitchell, Director, McCormick Observatory, University of Virginia, "Atomic Structure under Conditions of Temperature and Pressure Found at the Sun's Surface" and J. Q. Stewart, Princeton University Observatory, "The General Problems of Astrophysics with Special Reference to the Opacity of Gases." On Friday afternoon at 2 o'clock Sir William Bragg delivered an address on "Faraday's Diary." The attendance at this meeting was over 500. Among those attending this lecture were the delegates to the convention of Colloidal Chemists being held in Ithaca at the same time.

On Saturday morning, June 21, there were invited papers by F. Zwicky on "Secondary Structure of Crystals" and Arthur H. Compton on "X-ray Scattering and Atomic Structure."

In the afternoons of Thursday, Friday and Saturday informal conferences were held on the following topics: wave mechanics, dielectrics, biophysics, ionic and electronic emission, luminescence, astrophysics, electrons in metals, physical constants, molecular spectra, nuclei, quantum theory, x-rays and radio waves.

The delegates and their friends were housed in Risely Hall, one of the dormitories of the University. They all dined together in the beautiful dining room of this hall thus affording a most satisfactory opportunity to those attending the meeting to get together socially.

Meeting of the Council: At its meeting held on Friday morning, June 20, one person was elected to fellowship, one was transferred from membership to fellowship and nineteen were elected to membership. *Elected to Fellowship:* William Albert Noyes Jr. *Transferred from Membership to Fellowship:* J. J. Weigle. *Elected to Membership:* Warren F. Anderson, W. E. Bahls, Earle M. Bigsbee, Harry F. Blake, Charles P. Boner, Henry A. Boorse, Malcolm G. Colby, Ching Hsien Li, David Mann, F. L. Mears, Emerson M. Pugh, Leo J. Rysko, George H. Shortley Jr., Charles W. Sidney, Lewis K. Sillcox, Roger S. Strout, John H. Teeple, J. E. White, and Allan Williams.

The following resolution was passed by the Council and acclaimed by unanimous vote at the regular session of the Society on Saturday morning:

"That on behalf of the Council and of the membership of the American Physical Society we express to the local committee on arrangements, and to all those who assisted them, our great appreciation of the cordial hospitality and the splendid provisions they have made to make this first summer meeting of the Society so enjoyable and successful. We recall with pleasure that the Physical Review as well as the Society of Sigma Xi had their birth on this campus and we begin to appreciate this genius for giving new movements a vital beginning."

The regular program of the American Physical Society consisted of 33 papers. Numbers 15, 25, 28, 32, and 33 were read by title. The abstracts of these papers are given in the following pages. An **Author Index** will be found at the end.

W. L. SEVERINGHAUS, *Secretary*

ABSTRACTS

1. A new type of glow-discharge tube. HERBERT J. REICH, *University of Illinois*.—Several types of glow-discharge tubes are somewhat limited in their field of usefulness by the fact that the extinction potential is considerably lower than the ignition potential, making it difficult to control or stop the current after discharge commences. This difficulty may be overcome by incorporating an electron gun in the tube, and shooting a stream of electrons at high velocity between or through the glow electrodes. The discharge may thus be completely controlled at all times by a very small variation in the potential of the control electrode of the electron gun. A study of the characteristic curves of such a tube reveals a number of very interesting operating characteristics.

2. Preliminary measurements of the mean free path of potassium atoms in nitrogen. J. J. WEIGLE AND M. S. PLESSET, *University of Pittsburgh*.—The method of Taylor (*Zeits. f. Physik* 57, 242 (1929)) for the detection of beams of potassium atoms was used for a direct determination of their mean free path. A steel furnace with a single slit contained the potassium and was heated to about 150°C. At a distance of 10 cm a tungsten filament parallel to the slit, and surrounded by a slotted brass cylinder was used as a detector. The potassium atoms impinging on the hot filament are ionized and drawn to the cylinder by a suitable difference of potential. This positive ion current was measured as a function of the pressure of nitrogen filling the space between the filament and slit. Nitrogen pressures ranged from 10^{-2} to 10^{-6} cm of mercury. These ion currents are given by the equation $I = I_0 e^{-x/\lambda(p)}$ where I_0 is a constant, $\lambda(p)$ the mean free path at a given pressure p , and x the distance between the slit and filament. As λ is a known function of the average of the diameters of the potassium atom and nitrogen

molecule, this average was obtained from our measurements which gave values between 3×10^{-9} and 5×10^{-9} cm. These results are unexpectedly small. Experiments with a different apparatus are contemplated to disprove or confirm these preliminary results.

3. Organic reactions in gaseous electrical discharge. ERNEST G. LINDER, *Cornell University*.—A study of electrical discharge in a series of straight chain paraffin hydrocarbons indicates that the phenomenon is similar to that of electrolytic conduction in liquids, in so far as the amount of reaction (i.e., the amount of hydrogen liberated) appears to be proportional to the current, and independent of vapor pressure and voltage. There seems to be a simple relation between molecular size and the amount of hydrogen liberated.

4. On the recombination of electrons with caesium ions. E. H. KURTH, *California Institute of Technology*. (Introduced by F. Zwicky).—An apparatus was constructed in which electrons emitted from a caesium-on-tungsten oxide surface could be accelerated into an equipotential inclosure. A beam of caesium ions generated by a tungsten filament source and projected through the electron atmosphere in the box was collected on a plate. Electron currents up to 200 microamperes could be obtained with a few volts potential difference to the box. Positive currents were measured down to 10^{-9} amperes. When the electron velocities were varied over the range in which captures by caesium ions might be expected from the work of Davis and Barnes, no measurable decrease in the positive beam current was ever observed. The apparatus is being modified to permit tests for a considerably greater ratio of electron to positive currents.

5. Potential drop-current relations of a Geissler discharge from a hollow cathode. C. H. THOMAS, *Westinghouse Lamp Co., Bloomfield, N. J.*.—When a cold electrode, drilled to a depth $1/2$ inch with a drill 0.076 inch in diameter was used as a cathode in neon gas at pressures between 5 and 70 mm with electrode separation of 15 mm the cathode glow concentrated almost entirely in the hole. Under these conditions the potential drop-current curve for a thorium cathode shows a maximum in potential drop at a current of about 25 milliamperes. This potential drop decreases to a minimum at 50 milliamperes and subsequently attains a second maximum at 80–90 milliamperes. At a higher current a further decrease in potential drop resulted from thermionic emission. Similar curves for iron, misch meal and throrium-barium oxide cathodes in neon show a maximum at about 25 milliamperes but beyond that current their similarity to thorium curves disappears. Similar effects were observed in helium and argon. Potential drop-pressure curves for a cathode drilled with a 0.076 inch hole are given as well as the potential drop-size of hole curves which show that there is a minimum pressure for a given size hole in order that the cathode glow will concentrate in the hole. A hollow iron cathode in hydrogen at 23 mm pressure caused a decrease in the potential drop from 440 volts to 405 volts as the current was increased from 30 to 50 milliamperes.

6. The electrodeless discharge in mercury vapor. HERSCHEL SMITH, W. A. LYNCH AND NORMAN HILBERRY, *New York University, University Heights*.—The electrodeless discharge produced in Hg vapor inside the solenoid of a high frequency C. W. oscillator is studied in the pressure range between 0.004 mm and 0.8 mm of Hg. The characteristics of the two types of discharges reported by various authors (MacKinnon, Phil. Mag. Nov. 1929, Brasefield, Phys. Rev. May, 1930) are investigated in detail. Direct experimental evidence is given as to the electrostatic nature of the "glow" discharge and to the electromagnetic nature of the "arc" type discharge. Electromagnetic forces in themselves are found to be insufficient for the formation of the discharge but are sufficient for its maintenance. The "arc" type discharge is shown to be the more familiar ring discharge excited by damped oscillations. The currents in the oscillator coil necessary for the excitation of both types of discharge are examined as a function of the pressure at various frequencies. The curve for the glow discharge has a minimum within the given pressure range while that of the "arc" type discharge has both a minimum and a maximum. The form of these curves would seem to indicate the necessity for a complete revision of the present theories.

7. **Effect of collisions on potential distribution in positive ion sheaths.** H. P. ROBERTSON AND P. M. MORSE, *Princeton University*.—The potential distribution in a plane positive ion sheath is derived under the assumptions (1) an ion gives up a fraction θ of its kinetic energy at each collision, (2) the ions may be considered as following the lines of force and (3) the density of charge may be taken as i/v where v is the root mean square of the actual ionic velocities. The justification of assumption (2) is based on the considerations of v. Hippel, and that of (3) on the approximate agreement of dependence of potential on initial velocity for zero pressure with that obtained by previous workers (Schottky, Epstein, Fry, Langmuir). The rigorous solution of this problem gives the field strength and mean forward kinetic energy of the ions at any point in the sheath. The corresponding problem for cylindrical or spherical cathodes cannot be rigorously solved by the same methods, but can be treated by a method of approximations based on the rigorous solution for the plane case.

8. **The Hall effect in tellurium amalgams.** P. I. WOLD AND J. M. HYATT, *Union College*.—Certain aspects of the study of the Hall effect in crystalline materials suggested an attempt to make Te-Hg alloys. Amalgams were obtained of about 30% tellurium which were plastic when fresh but which became, in a few hours, quite hard and very friable. The plastic amalgam was placed in a mold as quickly as feasible and measurements on the Hall effect, the specific resistance and the longitudinal effect were started. The Hall effect commenced with very small values and built up steadily for two or three days. The Hall constants, after such time, were as high as 0.9, which is from 100 to 500 times the value when the amalgam was a half hour old. The authors are not aware of any previous case in which Hall effect has grown with time when temperature was constant and as a new phenomenon it seems to be of special interest. X-ray crystal photographs were taken of a sample of the amalgam as soon after making as possible and photographs taken within an hour show crystalline structure apparently as strongly as when two days old. The longitudinal effect started with very low values and increased steadily in about the same way as the Hall effect.

9. **Contact resistance and microphonic action.** FRANK GRAY, *Bell Telephone Laboratories, Inc.*—A mathematical theory is developed to explain the fact that conductivity of a contact between two carbon spheres changes with the force pressing the spheres together. It is assumed that the surface roughness of the carbon is equivalent to an assembly of minute spherical hills. On account of the elasticity of the material, both the macroscopic area of contact between the spheres and the microscopic areas of contact between the hills increase with contact force. The resulting relation between the contact resistance R and the contact force F is $R = A/F^{1/3} + B/F^{7/9}$ where A and B are constants. The last term of this equation, contributed by surface roughness, is almost the same as the corresponding term of the equation, $R = A/F^{1/3} + B/F^{6/9}$ which was developed by Professor P. O. Pedersen [Electrician, Feb. 4, 1916] on the assumption that carbon is covered with a thin, high resistance film. In other words, surface roughness behaves almost identically with a non-variable, high resistance film. Higher degrees of roughness increase the exponent of the last term. In the limit it becomes unity, and the roughness resistance then varies inversely as the contact force.

10. **Contact resistance and microphonic action.** F. S. GOUCHER, *Bell Telephone Laboratories, Inc.*—Previous work has shown that the conducting portions of contacts between single granules of microphone carbon are of the nature of carbon and that variations in contact area occur when the contact resistance is varied in a reversible resistance force cycle. An experimental study of the slopes of these reversible characteristics both for single contacts and aggregates shows them to be of the form $R = \text{const}(F)^{-n}$. The exponent n varies from cycle to cycle for equal force limits and the average value depends on the force limits. A maximum mean value independent of the force limits over a wide range, is obtained with the aggregates. This value is in agreement with the exponent in the second term of Gray's equation $R = (A/F^{1/3}) + (B/F^{7/9})$ [previous abstract] which indicates that an aggregate of contacts may, under certain conditions, behave as though it were a single contact between spheres having a rough surface. Values of n less than $1/3$ are obtained with both single contacts and aggregates. This is attributed to the effect of cohesive forces the existence of which was demonstrated by the sticking of contacts.

11. **Work functions and thermionic and constant "A" determined for thoriated tungsten.** W. B. NOTTINGHAM, *Bartol Research Foundation*.—The work function of a type T thoriated tungsten filament was determined with a 3.5 volt accelerating potential by measuring the thermionic current as a function of temperature over the range 1045°K to 1340°K. With the filament activated to give the maximum emission at 1100°K with a 20 volt accelerating potential, the effective work function ϕ' with 3.5 volts was found to be 2.59 volts. From measurements of the current-potential relationship at 1100°K, it was found that the 3.5 volt accelerating potential had reduced the work function by $\Delta\phi = 0.56$ volt. The work function at zero field is $\phi' + \Delta\phi = \phi_0 = 3.15$ volts. Using this value of ϕ_0 and the measured current, the thermionic constant is $A = 59.0$. Measurements made with a thorium covering *thicker* than that required to give the maximum emission as above, gave $\phi' = 2.8$ volts with 3.5 volts accelerating potential, $\Delta\phi = 0.3$ volt and therefore $\phi_0 = 3.1$ volts and $A = 56.0$. These data indicate that abnormally low values of A previously reported can be accounted for by the fact that the work functions were not measured at zero field. Langmuir found the contact potential between thoriated tungsten and clean tungsten to be 1.46 volts. Accordingly the work function of thoriated tungsten should be 4.53—1.46 = 3.07 volts which agrees with the above.

12. **The relation between the number of electrons ejected photoelectrically from the cathode and the time lag of the spark.** JOHN A. TIEDEMAN, *University of Virginia*. If the ions usually present in a spark gap in ordinary air are carefully removed by sweeping potentials an impulsive field of 75,000 volts/cm can be applied for at least 10^{-6} sec. without electrical breakdown. Strong ultraviolet irradiation of the cathode reduces the time lag to less than 10^{-8} sec. By means of biasing potentials and a steady source of ultraviolet light electrons could be liberated from the cathode only during the existence of a high electric field. The time lags were measured by the Lichtenberg figure method (Pedersen, *Ann. d. Physik* 71, 317 (1923)). By controlling the intensity of ultraviolet light on the cathode and the magnitude of the applied surge potential the time required for a known number of electrons to start the discharge in a field of known strength could be obtained. Between a Zn cathode and a steel anode spaced 2 mm electrons were ejected from the cathode at the rate of one in 3.3×10^{-9} sec. in an impulsive field with a maximum value of 75,000 volts/cm applied by a second spark, producing a time lag of 1.5×10^{-8} sec. while under the same conditions one electron per 9.5×10^{-9} sec. gave a time lag of 2.2×10^{-8} sec.

13. **Inhibition of photoelectric emission by near infrared light.** A. R. OLPIN, *Bell Telephone Laboratories, Inc.*—The response to potassium photoelectric cells to white light is greatly increased when small amounts of bromine or iodine vapor are distilled onto the cathode surface. Spectral distribution curves for cells so treated show a general increase in the response to light of all wave-lengths and a more marked increase to light at both ends of the visible spectrum. There is no measurable electron emission when the cells are irradiated with infrared light obtained by passing white light of color temperature 2848°K. through a #87 EK Wratten filter. If, however, the cathode already is emitting electrons under excitation with visible light when irradiation with infrared light occurs, a marked *decrease* in the photoelectric current is noted. Investigation shows that this decrease occurs only in the spectral regions where abnormally large increases are observed without the infrared light, and may amount to well over fifty percent for certain wave-lengths. Data showing some of the properties of this new effect, which has been observed for both potassium and sodium cells, are included. The phenomenon is closely analogous to the extinction of phosphorescence and destruction of the latent image on photographic plates by infrared radiations.

14. **On chain reactions caused by physical structure.** N. RASHEVSKY, *Westinghouse E. and M. Co., East Pittsburgh*.—In a previous paper (*Zeits. f. Physik* 59, 558 (1930)) it has been shown that when a substance is formed as a result of a reaction in a solution and is itself soluble in the surrounding liquid, this substance may exist as a separate phase, in shape of small drops, provided the size of the drops is above a certain critical value. Such drops cannot be formed spontaneously, but will continue to grow if brought from outside into the liquid. In the present paper, the case is considered, that the drop is constituted of several substances. Due to the interaction of the phenomena of diffusion and dissolution, the formation of the different sub-

stances will follow a definite order. Below a certain size, the drop cannot exist at all. Above it, it can be constituted only by one substance. With increasing size, the number of substances constituting the drop, increases. Applications to biological phenomena are discussed.

15. The corresponding state of maximum surface tension of saturated vapors. J. L. SHERESHEFSKY, *Mellon Institute of Industrial Research*. (Introduced by Paul D. Foote.)—The surface tension of a liquid is given by the expression (1) $\sigma = (rh/2)(\rho_1 - \rho_2)$, where h is the height of rise in a capillary of radius r , and ρ_1 and ρ_2 the densities of the liquid and vapor respectively. Writing the equation in the form $\sigma_r = rhe_1/2 - rhe_2/2$ and applying Antonow's rule, $rhe_1/2$ may be conceived as the true surface tension of the liquid, σ_r the relative surface tension, and (2) $\sigma_r = rhe_2/2$ where $rhe_2/2$ is defined as the surface tension of the vapor. Combining (1), (2), McLeods equation [$\sigma_r = c(\rho_1 - \rho_2)^{1/4}$] and Goldhammer's equation [$\rho_1 - \rho_2 = a(1 - T/T_c)^{1/3}$], an expression is obtained relating the surface tension of the vapor with the temperature, (3) $\sigma_v = K(1 - T/T_c)\rho_2$. It was found that σ_v goes through a maximum in the neighborhood of the critical temperature. Differentiating (3) the position of the maximum point is given by

$$(4) \quad \frac{d \log \rho_2}{dT} = \frac{0.4343}{T_c(1 - T_m/T_c)}.$$

By means of equation (4) the values of T_m/T_c for nineteen different substances were calculated and found to equal 0.91.

16. Fundamental correspondences between geometry and thermodynamics. JOHN Q. STEWART, *Princeton University*.—Continuing interpretation of thermodynamics as a physical symbolic logic (Phys. Rev. 34, 1289, (1929), etc.), the following equivalences exist between Euclidean plane geometry and the thermodynamics of reversible systems having two degrees of freedom. The vector corresponds to the working body; its magnitude, r , to volume, v ; x -component to internal energy, U ; y -component to entropy, S ; negative slope, $-m$, to temperature, T . Summing x and y components, respectively, when vectors are added, corresponds to conserving energy and entropy. The Pythagorean relation, $x = (r^2 - y^2)^{1/2}$, expresses the "equation of state" for the Euclidean plane. The corresponding special thermodynamic equation $U = (v^2 - S^2)^{1/2}$, implies reckoning U , v , s , in absolute units, for dimensional equivalence. In general, when U_2 replaces S_1 , and $-S_2$ replaces U_1 , while v remains unchanged, $-1/T_2$ replaces T_1 , and all relations of thermodynamics are preserved. This is on form of Lunn's important "principle of thermodynamic duality." (A. C. Lunn, Phys. Rev. 15, 269 (1920)). Evidently it corresponds to the geometrical symmetry accompanying rotation of axes through $\pi/2$. The general background of these studies is the philosophy of Leibniz. His logic possesses surprisingly close affiliations with thermodynamics.

17. Entropy, elastic strain and the second law of thermodynamics, the principles of least work and of maximum probability. W. S. KIMBALL, *Michigan State College, East Lansing, Michigan*.—By relying on the geometrical expression for weight, $W = N^N(r_1 r_2 \dots r_N)$, and taking strains to include unit extensions in velocity and momentum space as well as ordinary space, a relation is established between entropy and the total strain: $S = kY$, $Y = \log W$, where S is the entropy, k is Boltzmann's constant, Y the total strain and W the *a priori* probability. The Lagrange multiplier method is applied to statically indeterminate frames as well as gas theory, and shows in both cases that the principle of least work, or internal energy, is equivalent to the principle of maximum entropy, probability and strain. Furthermore the equilibrium equations which by the Lagrange method determine the equilibrium state are shown to represent balance between true stress and strain both in gas theory and in the statics of indeterminate frames, revealing the operation in these two domains of the same identical principles (not an analogy). The magnitude of the stress and strain acting in momentum space to maintain equilibrium are calculated for the case of perfect gas at temperature T , the stress being given by $(2\pi e)^{1/2} kT$, and the strain by $(2\pi e)^{1/2} / n$, and the modulus of elasticity is the familiar isothermal bulk modulus p . The outstanding experimental verification of the theory is the second law of thermodynamics. The automatic increases of entropy which it represents are explained as due to increased strain (in momentum space as well as ordinary space) under action of corresponding stresses, rather than as in statistics by the unsatisfactory ergodic hypothesis.

18. Energy changes related to the secondary structure of crystals. F. ZWICKY, *California Inst. of Technology*.—Theoretical considerations have led the author to the postulate of a secondary structure (Π) of large spacing, which is superposed on the primary structure (p) of crystals. According to the theory the Π -atoms are usually more densely packed than the p -atoms. It is $|E_{\pi}| > |E_p|$ where E_{π} and E_p are the respective atomic energies corresponding to the two structures. The p -atoms are therefore more easily removed from the crystal than the Π -atoms. Conditions may be reversed, however, by a plastic deformation inasmuch as this process diminishes $|E_{\pi}|$ into $|E_{\pi}'|$ but does not change E_p . These conclusions lead at once to an understanding of evaporation, etching and certain chemical reaction phenomena involving both perfect and plastically deformed crystals. As a practical criterion of the perfection or imperfection of a lattice the inequalities $|E_{\pi}'| \gtrless |E_p|$ may be used. More detailed considerations are of course required to distinguish crystals of the "metallic" type, which are both macroscopically and microscopically plastic from other types like NaCl which are macroscopically plastic but microscopically brittle. The theory further leads to the interesting conclusion that a voltaic potential difference should be found between Π -planes and p -planes a mounting in general to about 0.001–0.01 volts.

19. An x-ray study of the structure of electrets. MAURICE EWING, *University of Pittsburgh, Erie, Pa.*—Electrets were prepared by allowing a molten mixture of rosin, beeswax, and carnauba wax to solidify in a strong electric field, following Adams (Frank. Inst. J. **204**, 469). These were studied by means of a pinhole camera with filtered characteristic radiation from an x-ray tube having a molybdenum target. The patterns obtained all showed three well-defined rings, which indicated spacing of $3.69 \pm .02\text{\AA}$, $4.15 \pm .02\text{\AA}$, and $4.70 \pm .03\text{\AA}$. The 4.15\AA ring was about three times as intense as the others. When the specimen was set so that the angle between the direction of the x-ray beam and the direction in which the electric field had been applied was zero, each circle was of uniform intensity over its entire circumference; but when this angle was 90° , all circles showed a marked maximum of intensity in the regions in which they would intersect a line drawn through their common center parallel to the direction in which the field had been applied to the specimen.

20. Modified line in scattered x-rays. P. A. ROSS AND J. C. CLARK, *Stanford University*.—With balanced metal foils of silver and palladium in a manner previously described, (Proc. Nat. Acad. Sci. Vol. 9, July 1923; J. A. O. S. Vol. 16, June 1928) an attempt has been made to determine the width and structure of the modified $K\alpha_1$, $K\alpha_2$ lines of antimony scattered from beryllium metal. The differences in transmission between equivalent silver and palladium foils were plotted against scattering angle. With sufficiently narrow slits the differences showed clearly the passage, first of α_2 and then of α_1 past the silver K discontinuity with increasing scattering angle. With present intensity and resolution there is no indication of any step structure or any breadth of line inexplicable by lack of homogeneity of scattering angle in the scattering of antimony $K\alpha_1$, $K\alpha_2$ from beryllium at angles between 55 and 75 degrees.

21. Apparatus for measuring absorption coefficients of soft-x-rays in gases and the absorption in air of the $K\alpha$ line of carbon. ELMER DERSHEM AND MARCEL SCHEIN, *University of Chicago*.—The apparatus consists of an x-ray tube separated by a celluloid window about 2×10^{-4} mm thick from a spectrograph into which gases at various pressures may be introduced. Within the spectrograph beams of different wave-length are isolated by means of a ruled grating. The ratio of the intensity of a given spectral line when the spectrograph is filled with gas at a known pressure to the intensity of the line when the spectrograph is exhausted to a high vacuum is measured by a photographic method. Preliminary results for the mass absorption coefficient (μ/ρ) of air have been obtained for the $K\alpha$ line of carbon ($\lambda = 44.6\text{\AA}$). An average of 76 measures yielded the value $\mu/\rho = 5350 \pm 53$. This probable error of 1 percent compares very favorably with ionization chamber measurements of ordinary x-rays. Extrapolations of any of the various absorption formulae which are known to hold for ordinary x-rays yield values for the absorption coefficients of nitrogen and oxygen which are higher than the above but nevertheless of the same order of magnitude. The investigation is being continued with the use of pure gases and other wave-lengths.

22. Some measurements of currents through the walls of x-ray tubes. DONALD P. LEGALLEY, W. R. HAM, AND MARSH W. WHITE, *Pennsylvania State College*.—The walls of a Coolidge water cooled x-ray tube were coated with a thin layer of tin foil. The potential of this coating was varied from that of the anode, to that of the cathode in about 48 equal steps. With the walls, and the anode of the tube, at the same potential, surprisingly large currents were found to be flowing through the glass to the coating. These amounted to as much as 1 m.a., and 2 m.a. in most cases, but were found to be as large as 3 m.a. in some cases. As the potential of the walls was increased from the anode to the cathode, these currents were found to drop off rapidly, become negative, and fall to zero as soon as full retarding potential was reached. A wide range of tube voltages, and tube currents were used. Coating currents were plotted against retarding potentials, and reproducible curves secured, in which breaks occurred at certain retarding potentials time after time. It was found that the average values of these breaks corresponded to the values of the energy levels (in equivalent volts) of the material used in the anode of the tube.

23. Luminescence due to radioactivity. D. H. KABAKJIAN, *University of Pennsylvania*.—Results of several investigations on the nature and decay of luminescence due to radioactivity carried on under the direction of the author are reviewed. It is shown that the rise and decay of luminescence in various compounds, including phosphorescent zinc sulphide, cannot be explained on Rutherford's theory of "active centres." The observed facts can be explained qualitatively by assuming that the alpha, beta and gamma-rays produce excited molecules in the luminescent material. Return of these molecules to their initial state of more stable equilibrium results in emission of luminous energy. The rate at which this return takes place depends upon the thermal agitation of the molecules. The decay of luminescence is explained as due, not to the destruction of the hypothetical centres, but to the gradual increase of the absorption constant of the material for the light emitted, as evidenced by its discoloration. The disturbances produced by the exciting rays resulting in discoloration are more stable at ordinary room temperatures than those giving rise to luminescence but not necessarily so at higher temperatures. When a compound whose luminescence has decayed is brought to a temperature which removes discoloration it usually recovers its initial brightness.

24. The average life for ionized helium. LOUIS R. MAXWELL, *Bartol Research Foundation*.—The average life $T_{n,l}$ in energy states to ionized helium have been computed for levels up to $n=60$ by calculating all the transition probabilities from the level concerned. The transition probabilities can be obtained directly from known values of the (matrix amplitude)² as evaluated by the eigenfunctions for an electron in a Coulomb field. $T_{n,1}$ was found to increase proportional to n^3 starting with the extremely short time of 1.0×10^{-10} sec. for $n=2$. For other l values this relationship does not always hold but in general $T_{n,l}$ becomes greater for the higher states. T_n (an average mean life l not specified) has the calculated value of 1.3×10^{-10} sec. for $n=2$ which increases to 1.2×10^{-8} sec. for $n=6$. The method for measuring mean lives previously described by the writer (Phys. Rev. 33, 721, (1928)) has been applied to the 4686 series of He II. The displacements were found to become progressively greater in going from the lines 4686 (4→3) and 3203 (5→3) to 2733 (6→3) and to 2511 (7→3). Assuming that the excited helium ion is produced at a single collision then the lines exhibiting the greater shift must represent longer mean lives, which indicates that the average life becomes greater for the outer levels, in agreement with the theory. The above assumption has been substantiated for the line 4686 from intensity-current measurements.

25. The incomplete partial Paschen-Back effect in copper. J. B. GREEN, *Ohio State University*.—The study of the partial Paschen-Back effect in most elements has been limited to the cases in which the multiplet separation is very small compared with the normal Zeeman separation. Darwin has calculated the Zeeman effect for cases in which the magnetic separation varies from 0 to ∞ . His formulas have been applied to Back's measurements on the $^2P^2D$ multiplet of Cu, 5220, 5218, and 5153. These lines, while they show the ordinary characteristics for low fields, have distortions which are due to the small value of the 2D separation 6.90 cm^{-1} compared with the Zeeman splitting 1.74 cm^{-1} . The wave-lengths calculated on Darwin's theory are

in almost complete agreement with experiment. The calculated intensities cannot be compared since the observed intensities are only estimated, but they show qualitative agreement with experiment.

26. Interference measurements in the first spectra of krypton and xenon. C. J. HUMPHREYS, *Bureau of Standards*.—The wave-lengths of the stronger arc lines of krypton and xenon have been redetermined by the use of fixed etalons. The secondary standards of neon, photographed simultaneously with the spectrum under investigation, were used as a comparison. A sufficient number of krypton lines have been examined to permit fixing the relative values of the 1s terms and all the 2p and 3p terms. The accuracy of the term values is such that the average deviation of calculated combinations from the observed wave-numbers is one part in twenty million. The exact location of the combinations in the infrared region not photographically accessible can now be predicted with certainty. Such lines should prove useful wave-length standards for the infrared region. Further work is contemplated in the examination of the lines for hyperfine structure. It is apparent however from the extremely small variations of the term differences that the intensity of any satellites is too low to affect the wave-lengths. For the two strongest lines in the visible krypton spectrum, for which Perard at the International Bureau obtained wave-lengths 5570.2892 and 5870.9154A., we obtain 5570.2890 and 5870.9153A.

27. Spark spectrum of rhodium. A. G. SHENSTONE AND J. J. LIVINGOOD, *Princeton University*.—In the first spark spectrum of rhodium the following terms have been found: for the low structures, $4d^75s$, 5F , 3F , 5P , among the intermediate configurations $4d^75p$, 5F , 5D , 3G , 3F , 3D , 3G , 5D , 5P , 5S . A number of as yet unidentified levels have also been discovered in the low and middle group. The interval rule holds reasonably well for the low 5F and 3F , but not at all for the other multiplets. All are inverted, except the higher 5D from d^7p , which is reinverted, and 5F from the same structure which is partially reinverted. Preliminary investigation of the Zeeman effect indicates that the g-values do not coincide with the Landé predictions. Intensities in the multiplets show the same type of irregularity as occurs in the cobalt spark spectrum.

28. The structure of an emission line. FRANK C. HOYT, *University of Chicago*. The structure of an emission line within the frequency range of its natural width is calculated on the basis of Dirac's radiation theory as modified by Weyl. It is necessary to make use of a solution of the perturbation equations which is valid for a time long compared to the life-time of the excited state, which is in accord with the uncertainty principle. The result obtained is that the spectral distribution is that for a classical oscillator with damping constant $\frac{1}{2}A$, where A is the sum of the probabilities of spontaneous transition from the upper level to all states of lower energy.

29. Absorption and collision broadening of the mercury resonance line. M. W. ZEMANSKY, *National Research Fellow, Princeton University*.—With the assumptions that: (1) the half-breadth of the emission line $\Delta\nu_E$ from a resonance lamp is always greater than that of the absorption line, and depends on the vapor density, geometry, and the exciting line; (2) the half-breadth of the absorption line $\Delta\nu_D$ at low pressures and without any foreign gas is the Doppler breadth; (3) all five components of the $\lambda 2537$ line of mercury are alike both in emission and in absorption;—the absorption for thickness l is calculated as a function of $k(\nu_0)l$ and $\Delta\nu_E/\Delta\nu_D$, where $k(\nu_0)$ is the absorption coefficient for the center of any one of the components. From experimental values, $k(\nu_0)$ is found to be $1.41 \times 10^{-13} N$ where N is the number of atoms per cc. and $\Delta\nu_E/\Delta\nu_D$ is 1.21 in these experiments, 1.6 in Orthmann's, 1.50 in Hughes and Thomas', 1.15 in Kunze's and 1.15 in Kopfermann and Tietze's. The absorption coefficient in the presence of a foreign gas is calculated as a function of the frequency and of $\Delta\nu_C/\Delta\nu_D$ where $\Delta\nu_C$ is the Lorentz collision breadth, and the absorption is calculated as a function of $\Delta\nu_C/\Delta\nu_D$ for the values of $k(\nu_0)l$ and $\Delta\nu_E/\Delta\nu_D$ that hold in these experiments and in those of Orthmann. From experimental values of the absorption of mercury vapor in the presence of H_2 , N_2 , A , and CO , $\Delta\nu_C$ is found as a function of pressure for each gas. From these curves the effective cross-section is found.

30. Energy distribution in the ultraviolet spectrum of skylight. BRIAN O'BRIEN, *J. N. Adam Hospital, Perrysburg, N. Y.*—Energy distribution in the spectrum of sunlight scattered from the sky was measured by a method previously described (Phys. Rev. **33**, 640 (1929)) from $\lambda 4000\text{\AA}$ to $\lambda 2994\text{\AA}$ and compared to energy distribution in the direct solar beam. For very clear sky the ratio of intensity of sky, 90° from sun 60° from zenith, to intensity of sun is proportional to $1/\lambda^4$ over the above wave-length range. For sky uniformly cloudy showing faint blurr of sun, above ratio is nearly independent of λ , and energy distribution in direct solar beam agrees with that measured on very clear days for the same elevation of sun, even when absolute intensity in direct beam is reduced by clouds to $1/100$ that on a clear day. For hazy or slightly cloudy skys ratio of sky intensity to sun intensity increases with decrease in λ but less rapidly than $1/\lambda^4$, the scattering being made up of a molecular and a non-selective term. The values for the energy distribution in the spectrum of direct clear day sunlight $\lambda 3300\text{\AA}$ to $\lambda 2903\text{\AA}$ previously reported, (Phys. Rev. **33**, 1072 (1929)) (J.O.S.A. **20**, 150 (1930)), are thus applicable to sunlight through clouds or haze or scattered by clear or cloudy sky, providing the character of the scattering is taken into account. These results require that both non-selective and molecular scattering occur below the layer of atmospheric ozone, in agreement with accepted values for the height of this layer.

31. Behavior of positive ions in hydrogen. ALLAN C. G. MITCHELL, *Bartol Research Foundation*. In the present experiments, Li or Cs positive ions of various velocities are produced in a tube containing hydrogen molecules. The tube is immersed in liquid air, and the rate of decrease of pressure of hydrogen is measured as a function of the velocity of the positive ions. It is found that with no positive ions entering the tube there is a certain decrease in the pressure of the hydrogen due to its thermal dissociation on the hot filament and its subsequent condensation on the cold walls of the tube. With ions of energies from 15 to 320 volts flowing in the tube the rate of decrease of pressure is greater, showing a formation of some condensable product due to the action of the ions. The rate of pressure decrease with the voltage applied has been found to be proportional to the ion current flowing. The rate per unit current is proportional to the pressure; and the rate per unit current per unit pressure is practically independent of the voltage for Li or Cs ions of energies from 15 to 320 volts. The effect has been shown not to be due to secondary electrons. The number of hydrogen molecules disappearing per positive ion varies from 0.01 to 0.5. No critical voltage at which the effect starts has been found. A detailed account will appear shortly in the Journal of the Franklin Institute.

32. Chemical constitution and association. EUGENE C. BINGHAM AND HOLMES J. FURNWALT, *Lafayette College*. The authors have investigated the fluidities and densities and calculated the associations in several classes of homologous compounds, alcohols, acids, esters, ketones, mercaptans and hydrocarbons. In each case the association decreases as the hydrocarbon chain is increased, but a branched chain lowers the association, and the more, the closer the branch is attached to the middle of the molecule. The association is increased by certain associating groups such as hydroxyl, carboxyl etc. but these are least effective in bringing about association when they are placed at the center of the molecular chain. In the esters the association of different series e.g. the methyl esters, tends toward a definite value as the molecular weight is increased which is of course higher than the value toward which the ethyl esters approach. The association in excess of this minimum of any methyl ester has been found to be lowered quite precisely 46 percent by the addition of the methylene group necessary in going to the next higher member of the series. A recent note in Science indicated that for fifty-seven compounds the average deviation between the observed and calculated values is 0.9 percent.

33. The diffraction of hydrogen atoms. THOMAS H. JOHNSON, *Bartol Research Foundation*. The diffraction patterns which are formed when a very fine circular beam of hydrogen atoms is reflected from a cleaved 100 surface of a crystal of lithium fluoride have been photographed on a molybdenum oxide plate. Various arrangements of the crystal and plate were used. At normal incidence, with the plate perpendicular to the specularly reflected beam, the pattern consisted of two lines intersecting at right angles in the specular beam. These lines were parallel to the rows of similar ions on the surface of the crystal. The patterns for other

angles of incidence in both the 110 plane and the 100 plane have also been photographed and in each case the pattern is a set of conic sections which satisfy the two crossed grating formulae, $\cos\theta_0 - \cos\theta = n\lambda/d$; $\cos\phi_0 - \cos\phi = m\lambda/d$, where θ and ϕ are the angles between the beam and the two sets of lines of similar ions on the surface. The patterns observed correspond to $m=0$, $n=1$ and to $n=0$, $m=1$. The positions of maximum intensity correspond well with the calculated angles for the most probable wave-length in the Maxwellian distribution, if the wave-length is calculated from the velocity by the de Broglie formula, $\lambda = h/mv$.

AUTHOR INDEX

- Bingham, Eugene C. and Holmes J. Fornwalt—No. 32
- Clark, J. C.—see Ross
- Dershem, Elmer and Marcel Schein—No. 21
- Ewing, Maurice—No. 19
- Fornwalt, Holmes J.—see Bingham
- Goucher, F. S.—No. 10
- Gray, Frank—No. 9
- Green, J. B.—No. 25
- Ham, W. R.—see LeGalley
- Hilberry, Norman—see Smith
- Hoyt, Frank C.—No. 28
- Humphreys, C. J.—No. 26
- Hyatt, J. M.—see Wold
- Johnson, Thomas H.—No. 33
- Kabakjian, D. H.—No. 23
- Kimball, W. S.—No. 17
- Kurth, E. H.—No. 4
- LeGalley, Donald P., W. R. Ham and Marsh W. White—No. 22
- Linder, Ernest G.—No. 3
- Livingood, J. J.—see Shenstone
- Lynch, W. A.—see Smith
- Maxwell, Louis R.—No. 24
- Mitchell, Allan C. G.—No. 31
- Morse, P. M.—see Robertson
- Nottingham, W. B.—No. 11
- O'Brien, Brian—No. 30
- Olpin, A. R.—No. 13
- Plesset, M. S.—see Weigle
- Rashevsky, N.—No. 14
- Reich, Herbert J.—No. 1
- Robertson, H. P. and P. M. Morse—No. 7
- Ross, P. A. and J. C. Clark—No. 20
- Schein, Marcel—see Dershem
- Shenstone, A. G. and J. J. Livingood—No. 27
- Shereshefsky, J. L.—No. 15
- Smith, Herschel, W. A. Lynch and Norman Hilberry—No. 6
- Stewart, John Q.—No. 16
- Thomas, C. H.—No. 5
- Tiedeman, John A.—No. 12
- White, Marsh W.—see LeGalley
- Weigle, J. J. and M. S. Plesset—No. 2
- Wold, P. I. and J. M. Hyatt—No. 8
- Zemansky, M. W.—No. 29
- Zwicky, F.—No. 18

THE PHYSICAL REVIEW

THE FINE STRUCTURE OF He AS A TEST OF THE SPIN INTERACTIONS OF TWO ELECTRONS

BY G. BREIT

DEPARTMENT OF PHYSICS, NEW YORK UNIVERSITY

(Received June 16, 1930)

ABSTRACT

A tentative expression for the quantum Hamiltonian of two electrons has been set up in a previous paper. The equation is discussed again. It is shown that the last term in it is subject to doubt. The Hamiltonian is tested by applying it to the calculation of the fine structure of the $\text{He } 2^3P$ level. It is found that the above mentioned term in e^4 is in contradiction with experiment. Removing the term from the equation one is left essentially with Heisenberg's old Hamiltonian. The spin interaction in it is shown to agree well with experiment. The calculation has been applied also to Li^+ .

The essential improvements on previous work are: (1) an increase in the precision of the unperturbed eigenfunctions; (2) a determination from experimental data of a constant D which depends directly on spin—spin interactions (see Eq. (1) below) and which can be calculated with fair accuracy. Comparing the theoretical and empirical values of D a clearer test of the magnitude of spin—spin interactions can be obtained than by calculating the relative positions of the three components of the triplet. The reason for this is that the relative positions of the lines depend also on another constant C which is a difference of two approximately equal numbers and is more difficult to calculate accurately.

§I PURPOSE OF WORK AND RESULTS

THE motion of one electron in an external field is treated very satisfactorily by the Dirac equation. It is desirable to have a similar treatment of the two or many electron problem. A partial attempt in this direction has been made by the writer.¹ Considerations in configuration space and also the application of the Heisenberg-Pauli² wave field theory led to the Eq. (6) of the above paper. This equation appeared at the time as a likely one, but it was impossible to give a rigorous derivation. The writer has used the first form of the Heisenberg-Pauli theory. Because of the indefiniteness due to the infinite self interactions of point charges with themselves a certain amount of

¹ Breit, Phys. Rev. **34**, 553 (1929).

² W. Heisenberg and W. Pauli Jr., Zeits. f. Physik **56**, 1, 1929, Zeits. f. Physik **59**, 168 (1930).

arbitrariness was necessary in removing the infinite terms of the total energy. Also the interaction was derived only to the first approximation in e^2 . The same problem has been treated in more detail by Oppenheimer³ who showed that even to higher powers of e^2 the writer's Eq. (6) could be derived if certain infinite terms of the interaction energy are systematically neglected. However, Oppenheimer also shows that a strict application of the wave field theory leads to infinite relative displacements of the atomic energy levels. The failure of quantum mechanics to give a satisfactory account of the electromagnetic interaction of two particles appears to be connected with two difficult questions: (1) the size of the electron i.e. whether the electron can be located at a point and (2) the Dirac jumps to states of negative energy which make it impossible to have normal states for a finite number of particles. Neither of these questions can be answered at present and it seems that no satisfactory purely theoretical solution of the two electron problem can be obtained before this is done.

The derivation of (6) in configuration space was obtained by using Darwin's classical Hamiltonian function. The choice of quantum symbols has been made in such a way as to obtain equations of motion in agreement with the classical ones. This however was not sufficient to establish the validity of the equation. In fact a discussion in configuration space enables one to see a fault in the equation. In order to explain this unsatisfactory feature we explain first in somewhat more detail the satisfactory side of it. With (6) as it stands we have, omitting the external field, the following equations of motion:

$$(A) \quad \dot{x}_k^I = -c\alpha_k^I; \quad \dot{p}_k^I = -e_I e_{II} \frac{\partial}{\partial x_k^I} \left\{ r^{-1} - \frac{1}{2} [(\mathbf{a}^I \mathbf{a}^{II}) r^{-1} + r^{-3} (\mathbf{a}^I \mathbf{r})(\mathbf{a}^{II} \mathbf{r})] \right\}$$

The classical expressions obtained from Darwin's Hamiltonian are:

$$(B) \quad \dot{x}_k^I = v_k = \frac{p_k^I}{m_I} - \frac{p_k^I p_I^2}{2c^2 m_I^3} - \frac{e_I e_{II}}{2m_I m_{II} c^2} [p_k^{II} r^{-1} + r^{-3} (x_k^{II} - x_k^I)(p_{II} \mathbf{r})]$$

$$(C) \quad \dot{p}_k^I = -e_I e_{II} \frac{\partial}{\partial x_k^I} \{ r^{-1} - (1/2m_I m_{II} c^2) [r^{-1} (\mathbf{p}^I \mathbf{p}^{II}) + r^{-3} (\mathbf{p}^I \mathbf{r})(\mathbf{p}^{II} \mathbf{r})] \}.$$

The first equation (A) is an exact relation between the velocity and α_k . Equation (B) connects the velocities with the momenta. It was supposed that, in the sense of the correspondence principle, (B) is also true in the quantum theory. It then followed that (C) agrees with the second equation (A) to within terms in $(v/c)^2$. The p_k^I of Eq. (6) therefore replaces Darwin's \dot{p}_k^I because they have the same rate of change. The employment of equation (B) in the quantum theory is, of course, questionable. All that can be said is that the correct quantum equation should give (B) as an effective equation holding for wave packages. This has to be proved for whatever equation is finally devised.

³ J. R. Oppenheimer, Phys. Rev. 35, 461 (1930).

For the discussion of positive energy levels we can use the writer's Eq. (48) which is equivalent to (6). Here if terms in \hbar are dropped the Hamiltonian becomes exactly the classical one with the exception that the last term does not disappear. This shows that (B) and (C) are not satisfied consistently in Eq. (6) the error being of the order of e^4/mc^2r^2 . The writer is very grateful to Professors Pauli and Heisenberg for emphasizing the fact that this last term does not contain \hbar .

There is another unsatisfactory property of Eq. (6). Equation (B) gives p_k^I, p_k^{II} in terms of v_k^I, v_k^{II} . Thus

$$\mathbf{p}_I = m_I \mathbf{v}_I + m_I \mathbf{v}_I (v_I^2/2c^2) + (e_I e_{II}/2c^2) [r^{-1} \mathbf{v}_{II} + r^{-3} \mathbf{r} (\mathbf{v}_{II} \cdot \mathbf{r})]$$

This is a purely classical relation. In (6) \mathbf{p}_I is replaced by $(\hbar/2\pi i) \nabla_I$. For a single particle of charge e_I in an external field of vector potential \mathbf{A}_I we replace $m_I \mathbf{v}_I (1 - \beta_I^2)^{-1/2}$ by $(\hbar/2\pi i) \nabla_I - (e_I/c) \mathbf{A}_I$. In this case, to a sufficient approximation $\mathbf{A}_I = e_{II} \mathbf{v}_{II}/cr$. We should expect that a correct theory will replace $m_I \mathbf{v}_I (1 - \beta_I^2)^{-1/2} \cong m_I \mathbf{v}_I + m_I \mathbf{v}_I (v_I^2/2c^2)$ by $\mathbf{p}_I - (e_I e_{II} \mathbf{v}_{II}/c^2 r)$. We have identified however the quantum operator $(\hbar/2\pi i) \nabla_I$ with Darwin's \mathbf{p}_I . We see therefore that \mathbf{p}_I in (6) replaces the classical

$$\left[\frac{m_I \mathbf{v}_I}{(1 - \beta_I^2)^{1/2}} + \frac{e_I e_{II} \mathbf{v}_{II}}{c^2 r} \right] + \frac{e_I e_{II}}{2c^2} \left[-\frac{\mathbf{v}_{II}}{r} + \frac{\mathbf{r} (\mathbf{v}_{II} \cdot \mathbf{r})}{r^3} \right]$$

while it would be more satisfactory if it replaced only the first part of that expression. This means that if m_{II} becomes very large and the reaction on particle II negligible there is no exact agreement between (6) and Dirac's equation. It is thus seen that (6) is likely to be right only to the first order in e^2 . Also from the point of view of the wave field theory there is much less arbitrariness in the derivation of first order effects in e^2 .

With Eq. (6) it is possible to derive an equation involving two row, two column spin matrices and showing therefore the interaction of electrons as a function of their spins. This is Eq. (48). The interaction energy contains, in addition to the ordinary spin interactions, the extra term in e^4 . It is seen from the above considerations that the presence of this term is subject to doubt. In the writer's previous paper it has been supposed that the term might have a physical significance. Some rough estimates of the order of magnitude of its effect indicated that it might be reconcilable with experimental facts. It was felt however that a more accurate test is needed.

A possibility of testing the spin interaction in e^4 is offered by the fine structure of the He triplet spectrum and to some extent by that of Li^+ . It has been shown by Heisenberg⁴ that the inverted positions of the triplet components in these spectra can be explained by taking into account the interaction of electron spins with each other. The magnitude of the separations was also shown by him to be approximately in agreement with experiment. An attempt to refine Heisenberg's calculation has been made by Sugiura.⁵

⁴ Heisenberg, Zeits. f. Physik **39**, 499 (1926).

⁵ Sugiura, Zeits. f. Physik **44**, 190 (1927).

He considered in an approximate way the effect of polarization of the charge distribution formed by the inner electron due to the electric field of the outer one. A somewhat better agreement with the total separation in the yellow He has been obtained by using this correction. Gaunt⁶ has also attempted to improve on Heisenberg's calculation but has not reached a definite conclusion. The difficulty in the application of Gaunt's calculation lies in the insufficiently accurate unperturbed eigenfunctions used by him.

In the present paper the effect of all the spin interactions is calculated using unperturbed eigenfunctions determined by the variational equation derived in the writer's recent paper.⁷ These functions are also not exact but they are more accurate than those previously used. The result of the calculation is that satisfactory agreement with the experimentally observed fine structure is obtained if the extra terms in e^4 are neglected. The agreement with experiment is spoiled if the supposed additional effect of these terms is taken into account. This conclusion follows from the fine structure of He and to some extent also from the fine structure of Li^+ if the recent interpretation of the hyperfine structure of that spectrum is adopted.⁸ The conclusion is therefore that the terms in e^4 have no physical significance and that Eq. (6) is not correct to higher orders than e^2 . With terms of the first order in e^2 satisfactory agreement with experiment is obtained.

The present test is not able to distinguish between Gaunt's equation or Eq. (6) with the terms in e^4 omitted. Both of these agree with the observed fine structure. It is hard to believe however that the terms in $(1/2r)[(\mathbf{p}^I\mathbf{p}^{II}) + (\mathbf{p}^Ir)(\mathbf{p}^{II}r)/r^2]$ do not exist and are replaced by $(\mathbf{p}^I\mathbf{p}^{II})/r$. For this reason Gaunt's equation is also very likely to be incorrect. Further, Eq. (36) of the writer's previous paper is equivalent to Gaunt's and is seen also to contain terms in e^4 . These terms do not have any influence on the fine structure being of the form $(e^4/4mc^2r^2)(3 - 2(\sigma^I\sigma^{II}))$. They cannot have a physical significance since they do not vanish if $\hbar \rightarrow 0$.

The calculations which follow are rather laborious and it is advisable to explain at this point the comparison of the results with the experimental fine structure. The effect of spin interactions is taken into account by the ordinary method of perturbation calculations. Both in He and Li^+ this method should give, in the first order, results much more accurate than the experimental precision. This is seen directly from the fact that the separations in the fine structure are of the order of a few cm^{-1} while the total term value is of the order of $2 \times 10^4 \text{ cm}^{-1}$. In the perturbation calculation the effect of the spins is first of all neglected and the eigenfunctions used are determined. Their form is that of (21) in the writer's previous paper.⁷ Quite independently of the form of the function F it may be shown that the relative position of the three components of a triplet P term is given to the first order of the spin perturbations (and therefore very accurately in our case) by the following expression for the energy

⁶ Gaunt, Phil. Transactions of the Roy. Soc. A228, 151 (1929).

⁷ Breit, Phys. Rev. 35, 569 (1930).

⁸ Schüler and Brück, Zeits. f. Physik 58, 735 (1929).

$$E = E_0 + [-3(C + D), 2(D - C), 0] \quad (1)$$

for $j = 0, 1, 2$

where j is the inner quantum number, and C, D are certain integrals in terms of F . The term C is due to the interaction of the electric field with the electron spins. It is this term that gives rise to the ordinary multiplet structure and commonly goes under the name of the interaction of the spin with orbital angular momentum. By itself (i.e. neglecting D) it would give rise to the Landé interval rule. Although there are at present no accurate quantitative confirmations of the correctness of C , there appears to be no reason for doubting it particularly on account of the large number of cases which are in qualitative agreement and it is therefore supposed that the physical nature of C is correct. The integral D however involves the interactions of the two electronic spins with each other in the form of $f(r) (\sigma_1 \mathbf{r}) (\sigma_2 \mathbf{r})$.⁹ The questionable terms in e^4 give rise to a part of D which will be called D_1 , while the terms in e^2 give rise to another part D_0 .

$$D = D_0 + D_1 \text{ with terms in } e^4 \quad (2)$$

$$\text{or } D = D_0 \text{ without terms in } e^4$$

The experimentally known fine structure determines from (1) both $C+D$ and $C-D$, and therefore also C and D . These values will be called *empirical* values of C and D . The comparison with experiment is made by computing D according to the first and the second Eq. (2). It is found that the first equation is in disagreement with the empirical value of D while the second agrees well with it. This agreement does not appear to be accidental because D_0 consists mainly of terms of the same sign and also because the agreement holds in He and Li^+ .¹⁰

Since the physical nature of C appears to be sound this constant has been used as a check on the accuracy of the approximate form of F . It has proved difficult to obtain absolute agreement of the empirical and theoretical values of C . The difficulty lies in the laboriousness of the determination of eigenfunctions by the variational method and particularly in the fact that C is a difference of two numbers which are of approximately the same magnitude. These two approximately equal but opposite contributions to C are due to (1) the electric field of the nucleus acting on the spin of each electron and (2) the electric field of one electron acting on the spin of the other. The latter of these two effects turns out to be the larger one numerically. It depends essentially on the average value of $1/r^3$. From the agreement of the empirical and theoretical values of C it is possible to estimate the accuracy of the second part of C . The constant D_0 also depends essentially on $1/r^3$. The estimated accuracy of the second part of C gives one therefore a guide as to the accuracy of the computation for D_0 .

⁹ r is written here and later for the distance between the two electrons. The two electrons are referred to from now on as 1 and 2 rather than I and II.

¹⁰ The numerical calculations on Li^+ were made jointly with Mr. L. P. Granath of this

For He the result of the calculation is

$$(C, D_0, D_1) = (R_H \alpha^2 / 24) (-0.91, -0.62, +0.27) \quad (3)$$

where R_H is the Rydberg constant for hydrogen and α is the fine structure constant. In comparing this with empirical material we find somewhat different data. The results of Houston¹¹ and of Hansen¹² agree in giving $\Delta\nu_{02}/\Delta\nu_{12} = 14$ with $\Delta\nu_{02} = -3(C+D) = 1.068 \text{ cm}^{-1}$; $\Delta\nu_{12} = -2(C-D) = 0.077 \text{ cm}^{-1}$. The results of Wei¹³ are somewhat different giving $\Delta\nu_{02}/\Delta\nu_{12} = 10$ or 11. With the results of Hansen and Houston the empirical value of D is $(R_H \alpha^2 / 24) (-0.65) \text{ cm}^{-1}$ while using the results of Wei it is $(R_H \alpha^2 / 24) (-0.60) \text{ cm}^{-1}$. Either of these values is in good agreement with D_0 and is definitely in disagreement with $D_0 + D_1$. From the Hansen, Houston data we obtain as the empirical value of $C = -(R_H \alpha^2 / 24) 0.81$. This is not in very good agreement with the computed value listed in (3). However the agreement is as good as can be expected. This may be seen by considering the numerical part of the calculation for C . In the final step of the calculation we have $C = 1.302 R_H (\alpha^2 / 24) (1.020 - 1.719)$. The first of these numbers 1.020 is due to the action of the electric field of the nucleus and the second -1.719 is due to the field of the electrons. An error of 5% in the second number is likely to be accompanied by an approximately equal error in the opposite direction for the first number because the eigenfunction is normalized. An error of 10% in 1.719 is 0.17 and this constitutes an error of 24% in the result $-0.70 = 1.02 - 1.72$. It is therefore likely that the disagreement of 12% between the computed and the empirical value of C is an indication of an accuracy of about 2.5% in the computation of either the first or the second part of it. In other words the apparently low accuracy is due to the fact that C is the difference of two parts which are approximately equal in numerical magnitude. Using Wei's value for the separation ratio $C = -(R_H \alpha^2 / 24) (0.84)$. If this value is right the computation for C is correct to 8.3% and a likely accuracy of the calculation of each part is 1.7%. For Wei's value of the separation ratio the empirical values of both C and D come out lower than the calculated by consistent amounts. Using Houston and Hansen's observations the empirical D is higher than the calculated and the empirical C is lower. This is somewhat inconsistent because the error in the calculation is likely to be such as to overestimate the square of the eigenfunction for low r . It is likely however that neither the experiment nor the calculation is accurate enough to decide this point. It is only clear that the computed D_0 agrees well with either set of data and that the computed C , although different from the empirical, does not differ from it by more than can be explained by reasonable errors in the calculation. The presence of D_1 is definitely excluded since it would imply an inaccuracy of 43% in the calculation of D_0 . The value of the nuclear spin is immaterial for the present application.

laboratory and the writer is very grateful to him for his permission to quote here the results.

¹¹ Houston, Proc. Nat. Acad. 13, 91 (1927).

¹² Hansen, Nature 119, 237 (1927). Also see Grottrian Graphische Darstellung etc. vol. I, pp. 111-115, Springer, 1928.

¹³ Wei, Astrophys. J. 68, 194 (1928).

§II DETERMINATION OF APPROXIMATE UNPERTURBED FUNCTIONS

It has been shown by the writer⁷ that 3P states of a two electron configuration involving two electronic states with unequal azimuthal quantum numbers have the following complete set of normal orthogonal eigenfunctions

$$\begin{aligned} u_1 &= (3^{1/2}/4\pi)(F \sin \theta_1 e^{i\phi_1} - \tilde{F} \sin \theta_2 e^{i\phi_2}) \\ u_0 &= (6^{1/2}/4\pi)(F \cos \theta_1 - \tilde{F} \cos \theta_2) \\ u_{-1} &= (3^{1/2}/4\pi)(F \sin \theta_1 e^{-i\phi_1} - \tilde{F} \sin \theta_2 e^{-i\phi_2}) \end{aligned} \quad (4)$$

$$F = F(r_1, r_2; \theta), \tilde{F} = F(r_2, r_1; \theta)$$

where (r_1, θ_1, ϕ_1) , (r_2, θ_2, ϕ_2) are polar coordinates for each electron and $\cos \theta = \cos \theta_1 \cos \theta_2 + \sin \theta_1 \sin \theta_2 \cos(\phi_2 - \phi_1)$ so that θ is the angle between r_1, r_2 . This form is exact as long as the spin interactions are not brought in. If we had the exact form of F the whole problem could be solved quite accurately because as has been explained in §1 the first order of the perturbation calculation for the effect of spins should give a result of much higher accuracy than that of the experimental determinations. Unfortunately it is very difficult to determine F precisely and it is more practical to use good approximations for its form. Again, without approximations F is determined by the following conditions

$$\begin{aligned} \delta \int \left\{ \sum_{i=1,2} \left[\left(\frac{\partial F}{\partial r_i} \right)^2 - 2 \cos \theta \frac{\partial F}{\partial r_i} \frac{\partial \tilde{F}}{\partial r_i} + \left(\frac{\partial \tilde{F}}{\partial r_i} \right)^2 \right] + 2F^2/r_1^2 + 2\tilde{F}^2/r_2^2 \right. \\ \left. + 2 \sin \theta F \frac{\partial \tilde{F}}{r_1^2 \partial \theta} + 2 \sin \theta \tilde{F} \frac{\partial F}{r_2^2 \partial \theta} + \left(\frac{1}{r_1^2} + \frac{1}{r_2^2} \right) \left[\left(\frac{\partial F}{\partial \theta} \right)^2 - 2 \cos \theta \frac{\partial F}{\partial \theta} \frac{\partial \tilde{F}}{\partial \theta} + \left(\frac{\partial \tilde{F}}{\partial \theta} \right)^2 \right] \right. \\ \left. + (8\pi^2 m/h^2)(V - E)(F^2 - 2F\tilde{F} \cos \theta + \tilde{F}^2) \right\} dV = 0 \end{aligned}$$

$$dV = r_1^2 r_2^2 \sin \theta dr_1 dr_2 d\theta \quad (4)$$

with the normalization condition

$$\int (F^2 - 2F\tilde{F} \cos \theta + \tilde{F}^2) dV = 1. \quad (5)$$

The ranges of integration are here $0 < r_1 < \infty$, $0 < r_2 < \infty$, $0 < \theta < \pi$. In order to determine F precisely it would be sufficient to expand it in the form of a sum of a complete set of orthogonal functions with arbitrary coefficients and then to determine the coefficients by means of (4) and (5). Since the labor involved in this is very great and since the resultant series must subsequently be used in the perturbation calculation an approximate solution of the problem has been obtained by the current variety of the Ritz method. It has been supposed that to a sufficient approximation

$$F = r_1(1 + c \cos \theta) \exp[-ar_1/2 - br_2/2]. \quad (6)$$

This form is suggested by the usual screening considerations. The first electron (1) can be thought of approximately as moving in a screened field force subject to a potential $(Z-1)/e^2r$ while the second electron (2) is moving mainly in an unscreened field Ze^2/r . If this is supposed to be true then it is found that (1) is actually likely to be found outside of the region where there is a large probability of finding (2). Approximately therefore the radial part of (6) should give the solution. It is this kind of approximation that has been used by Gaunt with values of a, b derived directly by the screening considerations. This consideration is not exact and it can be improved by introducing the dependence on c and adjusting a, b, c so that (4), (5) are satisfied. The improvement to be expected from using (6) with adjustable constants amounts essentially to correcting the field of force acting on (1) for the incomplete screening of the nucleus by (2) and also to taking into account the fact that the two electrons cannot be considered as distributed on spherical shells and that the probability of a configuration r_1, r_2, θ depends on θ . We let

$$\begin{aligned} A_{r_i} &= \left(\frac{\partial F}{\partial r_i} \right)^2 - 2\mu \frac{\partial F}{\partial r_i} \frac{\partial \tilde{F}}{\partial r_i} + \left(\frac{\partial \tilde{F}}{\partial r_i} \right)^2; \mu = \cos \theta \\ A_\theta &= \left[\left(\frac{\partial F}{\partial \theta} \right)^2 - 2\mu \frac{\partial F}{\partial \theta} \frac{\partial \tilde{F}}{\partial \theta} + \left(\frac{\partial \tilde{F}}{\partial \theta} \right)^2 \right] (r_1^{-2} + r_2^{-2}). \\ B_\theta &= 2r_1^{-2}F^2 + 2r_2^{-2}\tilde{F}^2 + 2r_1^{-2} \sin \theta F \frac{\partial F}{\partial \theta} + 2r_2^{-2} \sin \theta \tilde{F} \frac{\partial \tilde{F}}{\partial \theta}. \end{aligned} \quad (7)$$

Substituting (6) and performing integrations involving only simple exponentials we find:

$$\begin{aligned} \int A_{r_i} dV &= (1 + c^2/3)(8a^{-3}b^{-3} + 24a^{-5}b^{-1}) + bc(16\beta^{-7} - 24a\beta^{-8}); \quad 2\beta = a + b \\ \int B_\theta dV &= 32a^{-3}b^{-3}(1 + c^2/3) - 32c\beta^{-6}; \quad \int A_\theta dV = (c^2/3)(192a^{-5}b^{-1} + 32a^{-3}b^{-3}) \\ \int (r_1^{-1} + r_2^{-1})(F^2 - 2\mu F\tilde{F} + \tilde{F}^2) dV &= (1 + c^2/3)(48a^{-4}b^{-3} + 96a^{-5}b^{-2}) - 64c\beta^{-7} \\ \int (F^2 - 2\mu F\tilde{F} + \tilde{F}^2) dV &= 192[(1 + c^2/3)a^{-5}b^{-3} - (c/2)\beta^{-8}]. \end{aligned} \quad (9)$$

The integrations involving r^{-1} are somewhat more complicated. Expanding r^{-1} in zonal harmonics and powers of r_1, r_2 , and then using¹⁴

$$\int_{-1}^{+1} \mu^n P_m(\mu) d\mu = \frac{2^{m+1}n!}{(n+m+1)!} \frac{\left(\frac{n}{2} + \frac{m}{2}\right)!}{\left(\frac{n}{2} - \frac{m}{2}\right)!} \quad (n \geq m) \quad (10)$$

¹⁴ Whittaker and Watson, *Modern Analysis*, p. 311.

we have

$$\begin{aligned} \int_{-1}^{+1} (1 + c\mu)^2 r^{-1} d\mu &= 2(1 + c^2/3)\rho_1^{-1} + (4c/3)\rho_2\rho_1^{-2} + (4c^2/15)\rho_2^2\rho_1^{-3} \\ \int_{-1}^{+1} \mu(1 + c\mu)^2 r^{-1} d\mu &= (4c/3)\rho_1^{-1} + (2/3 + 2c^2/5)\rho_2\rho_1^{-2} \\ &+ (8c/15)\rho_2^2\rho_1^{-3} + (4c^2/35)\rho_2^3\rho_1^{-4} \end{aligned} \quad (11)$$

with the convention

$$r_1, r_2 = \rho_1, \rho_2 \text{ if } r_1 < r_2; r_1, r_2 = \rho_2, \rho_1 \text{ if } r_1 > r_2$$

Using

$$\begin{aligned} \int \int_{r_1 > r_2} \exp(-ar_1 - br_2) dr_1 dr_2 &= a^{-1}(a+b)^{-1}, \\ \int \int_{r_1 < r_2} \exp(-ar_1 - br_2) dr_1 dr_2 &= b^{-1}(a+b)^{-1} \end{aligned} \quad (12)$$

we derive by successive differentiations with respect to a, b

$$\int_0^\infty \int_0^\infty r_1^2 r_2^2 \rho_1^{-1} \exp(-ar_1 - br_2) dr_1 dr_2 = 2[a^{-2}b^{-2}(a+b)^{-1} + a^{-1}b^{-1}(a+b)^{-3}] \quad (13)$$

Again using (12)

$$\int_0^\infty \int_0^\infty r_1^2 r_2^2 \rho_2 \rho_1^{-2} \exp(-ar_1 - br_2) dr_1 dr_2 = 6/[ab(a+b)^3].$$

Integrating (12) with respect to a and using

$$\int_0^\infty r^{-1} [\exp(-ar) - \exp(-(a+b)r)] dr = \log(1+b/a)$$

we get

$$\begin{aligned} \int_0^\infty \int_0^\infty r_1^2 r_2^2 \rho_2^2 \rho_1^{-3} \exp(-ar_1 - br_2) dr_1 dr_2 &= 24a^{-5} \log(1+a/b) \\ &+ 24b^{-5} \log(1+b/a) - 24(a^{-4} + b^{-4})(a+b)^{-1} - 12(a+b)^{-2}(a^{-3} + b^{-3}) \\ &- 8(a+b)^{-3}(a^{-2} + b^{-2}) - 6(a+b)^{-4}(a^{-1} + b^{-1}). \end{aligned} \quad (15)$$

Using (11), (13), (14), (15) one part of the integral involving r^{-1} is evaluated as

$$\begin{aligned} \int F^2 r^{-1} dV &= \frac{\partial^2}{\partial a^2} \int (1 + c\mu)^2 r^{-1} \exp(-ar_1 - br_2) dV = \frac{24}{ab(a+b)^2} \left[\frac{2a+b}{a^3b} + \right. \\ &\left. \frac{3a+b}{a(a+b)^3} \right] + c \left[\frac{16}{a^3b(a+b)^3} + \frac{48}{a^2b(a+b)^4} + \frac{96}{ab(a+b)^5} \right] + c^2 \left[192a^{-7} \log \right. \\ &\left. \frac{a+b}{b} - \frac{192}{a^6(a+b)} - \frac{96}{a^5(a+b)^2} + \frac{32}{5b^4a^2(a+b)} + \frac{32}{5b^4a(a+b)^2} \right] \end{aligned} \quad (16)$$

$$-\frac{56a^{-4} + (64/5)b^{-4}}{(a+b)^3} - \frac{24a^{-3} + (96/5)b^{-3}}{(a+b)^4} + \frac{48(a^{-2} - b^{-2})}{5(a+b)^5} + \frac{48(a^{-1} + b^{-1})}{(a+b)^5} \Big]$$

Another part of the integral in r^{-1} is given by the second line of (11). Using (12) we find

$$\begin{aligned} \frac{1}{2} \int_0^\infty \int_0^\infty r_1^3 r_2^3 \rho_2^3 \rho_1^{-4} \exp[-\beta(r_1 + r_2)] dr_1 dr_2 &= (720 \log 2 - 497.625) \beta^{-7} \\ \frac{1}{2} \int_0^\infty \int_0^\infty r_1^3 r_2^3 \rho_2^2 \rho_1^{-3} \exp[-\beta(r_1 + r_2)] dr_1 dr_2 &= (15/8) \beta^{-7} \\ \frac{1}{2} \int_0^\infty \int_0^\infty r_1^3 r_2^3 \rho_2 \rho_1^{-2} \exp[-\beta(r_1 + r_2)] dr_1 dr_2 &= (21/8) \beta^{-7} \\ \frac{1}{2} \int_0^\infty \int_0^\infty r_1^3 r_2^3 \rho_1^{-1} \exp[-\beta(r_1 + r_2)] dr_1 dr_2 &= (33/8) \beta^{-7}. \end{aligned} \quad (17)$$

Substituting these expressions (17) into the second line of (11) it is found that

$$\int \mu F \tilde{F} r^{-1} dV = \{3.5 + 13c + [2.1 + (8/35)(720 \log 2 - 497.625)]c^2\} \beta^{-7} \quad (18)$$

Combining (16) and (18) we also have $\int r^{-1}(F^2 - 2\mu F \tilde{F} + \tilde{F}^2) dV$. The variational Eq. (4) with the restricting condition (5) is now obtained by using (8), (9), (16), (18). On performing the substitutions it is convenient to use dimensionless variables x, y defined by

$$a = \alpha G, \quad b = \gamma G, \quad G = 8\pi^2 m Z e^2 / \hbar^2. \quad (19)$$

The constant G is related to the Rydberg constant by

$$4R_Z = GZ e^2. \quad (20)$$

The variational Eq. (4) becomes equivalent to the requirement that the fraction

$$\frac{E}{R_Z} = \frac{\alpha_0 + 2\alpha_1 c + \alpha_2 c^2}{\beta_0 + 2\beta_1 c + \beta_2 c^2} \quad (21)$$

should become a minimum. Here

$$\begin{aligned} \alpha_0 &= x^2 + y^2 - x - 2y + \frac{x}{Z} \left[\frac{x^2 y^2}{(x+y)^2} \left\{ \frac{2x+y}{x^2 y} + \frac{3x+y}{(x+y)^3} \right\} - \frac{56x^4 y^3}{3(x+y)^7} \right] \\ 2\alpha_1 &= x^5 y^3 \left\{ \frac{256y}{3(x+y)^7} - \frac{256xy}{(x+y)^8} - \frac{128}{3(x+y)^6} + \frac{512}{3(x+y)^7} \right. \\ &\quad \left. + \frac{2}{Z} \left[\frac{1}{3x^3 y(x+y)^3} + \frac{1}{x^2 y(x+y)^4} + \frac{2}{xy(x+y)^5} - \frac{104}{3(x+y)^7} \right] \right\} \\ \alpha_2 &= (5/3)y^2 + (5/9)x^2 - x/3 - 2y/3 + \frac{2}{Z} [x^5 y^3 (\zeta/180) - 6.48x^5 y^3 (x+y)^{-7}] \end{aligned} \quad (22)$$

$$\begin{aligned} \beta_0 &= 1, \quad 2\beta_1 = -128x^5y^3(x+y)^{-8}, \quad \beta_2 = 1/3 \\ \zeta &= 720x^{-7} \log(1+x/y) - 720x^{-6}(x+y)^{-1} - 360x^{-5}(x+y)^{-2} \\ &\quad + 24x^{-2}y^{-4}(x+y)^{-1} + 24x^{-1}y^{-4}(x+y)^{-2} - (210x^{-4} + 48y^{-4})(x+y)^{-3} \\ &\quad - (90x^{-3} + 72y^{-3})(x+y)^{-4} + 36(x^{-2} - y^{-2})(x+y)^{-5} + 180x^{-1}(x+y)^{-6} \\ &\quad + 180y^{-1}(x+y)^{-6}. \end{aligned} \quad (23)$$

The number 6.48 in the last term α_2 is the approximate value of $(32/15) [(21/8) + (2/7) (720 \log 2 - 497.625)]$. The result of minimizing (21) is¹⁵

$$x = 0.273, \quad y = 1.00 \quad c = -0.0089 \quad (25)$$

and the value of E/R_z corresponding to this is

$$E/R_z = -1.0654$$

while the experimental value is

$$(E/R_z)_{exp} = -1.0666.$$

Of the three constants entering the eigenfunction the constant x is the most important one for the following computations because it determines the mean radius of the outer electron and enters as a factor x^3 in most of the important terms of the formulas for fine structure separations. It should be observed here that the eigenfunction is sufficiently exact to determine the energy value to 0.1% which is a higher order of accuracy than that aimed at in the calculation of the fine structure.

§III SECULAR EQUATION FOR FINE STRUCTURE

Denoting, as is customary, the electronic spin functions by S_α, S_β with $S_\alpha = \begin{pmatrix} 1 \\ 0 \end{pmatrix}, S_\beta = \begin{pmatrix} 0 \\ 1 \end{pmatrix}$ we have a system of three normal orthogonal linearly independent functions

$$S_1 = S_\alpha^1 S_\alpha^2, \quad S_0 = 2^{-1/2}(S_\alpha^1 S_\beta^2 + S_\alpha^2 S_\beta^1), \quad S_{-1} = S_\beta^1 S_\beta^2 \quad (26)$$

the upper indices referring to the two electrons. These three functions when combined with the three coordinate functions (4) form a complete set of normal orthogonal functions of an unperturbed 3P state. The system may be arranged in a table as follows

m				
2	$u_1 S_1$			
1	$u_1 S_0$	$u_0 S_1$		
0	$u_1 S_{-1}$	$u_0 S_0$	$u_{-1} S_1$	
-1		$u_0 S_{-1}$	$u_{-1} S_0$	
-2			$u_{-1} S_{-1}$	

(27)

¹⁵ Dr. R. W. G. Wyckoff of the Rockefeller Institute has performed most of the numerical calculations on a calculating machine. The writer is very grateful to him for this assistance.

each row corresponding to a fixed magnetic quantum number m . The perturbation energy¹⁵ is

$$\Delta H = A\delta_1 + B\delta_2 + \mathcal{D}_0 + \mathcal{D}_1 \quad (28)$$

with

$$A = \frac{he^2}{8\pi m^2 c^2} \{ Zr_1^{-3} \mathbf{M}_1 + r^{-3} [(\mathbf{r}_1 - \mathbf{r}_2) \times (2\mathbf{p}_2 - \mathbf{p}_1)] \} \quad (28')$$

$$B = \frac{he^2}{8\pi m^2 c^2} \{ Zr_2^{-3} \mathbf{M}_2 + r^{-3} [(\mathbf{r}_2 - \mathbf{r}_1) \times (2\mathbf{p}_1 - \mathbf{p}_2)] \} \quad (28'')$$

$$\mathcal{D}_0 = R_0(r)(\delta_1 \mathbf{r})(\delta_2 \mathbf{r}), \quad R_0(r) = -(eh/4\pi mc)^2 3r^{-5} \quad (28''')$$

$$\mathcal{D}_1 = R_1(r)(\delta_1 \mathbf{r})(\delta_2 \mathbf{r}), \quad R_1(r) = (e^4/8mc^2)r^{-4} \quad (28''')$$

The \mathbf{M} are the orbital angular momentum operators $[\mathbf{r} \times \mathbf{p}]$. We have included here only those terms of the perturbation energy which have an influence on the fine structure and we have omitted therefore terms in $(\delta_1 \delta_2)$. The first three terms of (28) i.e. (28'), (28'') are of the second degree in the electronic charge e and the last is of the fourth degree. We have written this last term separately so as to be able to see the result with it and without it. Letting

$$C = A + B \quad (29)$$

we have

$$\begin{aligned} (A\delta_1 + B\delta_2)uS_1 &= C_z uS_1 + 2^{-1/2}(C_x + iC_y)uS_0 \\ (A\delta_1 + B\delta_2)uS_0 &= 2^{-1/2}(C_x - iC_y)uS_1 + 2^{-1/2}(C_x + iC_y)uS_{-1} \\ (A\delta_1 + B\delta_2)uS_{-1} &= 2^{-1/2}(C_x - iC_y)uS_0 - C_z uS_{-1} \end{aligned} \quad (30)$$

On the right side of these formulas all terms in the antisymmetric combinations $2^{-1/2}(S_\alpha^1 S_\beta^2 - S_\alpha^2 S_\beta^1)$ have been omitted since they do not belong to the triplet state. We are justified in doing this in the present calculation because the formulas (30) are to be used in the calculation of matrix elements for the secular equation and only matrix elements between eigenfunctions belonging to the unperturbed 3P state are of interest to us. Similarly we find¹⁷

$$\begin{aligned} (\delta_1 \mathbf{r})(\delta_2 \mathbf{r})S_1 &= z^2 S_1 + (2)^{1/2} z(x + iy)S_0 + (x + iy)^2 S_{-1} \\ (\delta_1 \mathbf{r})(\delta_2 \mathbf{r})S_0 &= (2)^{1/2} z(x - iy)S_1 + (x^2 + y^2 - z^2)S_0 - (2)^{1/2} z(x + iy)S_{-1} \\ (\delta_1 \mathbf{r})(\delta_2 \mathbf{r})S_{-1} &= (x - iy)^2 S_1 - (2)^{1/2} z(x - iy)S_0 + z^2 S_{-1} \end{aligned} \quad (31)$$

Formulas (30), (31) give the effect of all the operations due to the spins. Other angular momentum operations are involved in the operator C itself.

¹⁵ See (1). The σ 's are here Pauli's matrices with unchanged signs i.e. with signs opposite to those used in the above reference.

¹⁷ A systematic way of obtaining the matrices involved in (30) and (31) is to observe that $A\delta_1 + B\delta_2$ with symmetrical A, B is equivalent to an angular momentum matrix so far as operations on symmetric spin functions are concerned. From this point of view (30) is obvious and is easily generalized to any number of electrons. For (31) we can use (30) if it is remembered that $(\delta_1 \mathbf{r} + \delta_2 \mathbf{r})^2 = 2r^2 + 2(\delta_1 \mathbf{r})(\delta_2 \mathbf{r})$.

We see that

$$C = \frac{he^2}{8\pi m^2 c^2} \{ Z(r_1^{-3} \mathbf{M}_1 + r_2^{-3} \mathbf{M}_2) - 3^{-3} [(\mathbf{r}_1 - \mathbf{r}_2) \times (\mathbf{p}_1 - \mathbf{p}_2)] \}. \quad (30')$$

Applying C to the eigenfunctions u_1, u_0, u_{-1} it is found that

$$\begin{aligned} C_z(u_1, u_0, u_{-1}) &= C(u_1, u_0, u_{-1}) \\ (C_x + iC_y)(u_1, u_0, u_{-1}) &= C(0, -(2)^{1/2}u_1, (2)^{1/2}u_0) \\ (C_x - iC_y)(u_1, u_0, u_{-1}) &= C(-(2)^{1/2}u_0, (2)^{1/2}u_{-1}, 0) \end{aligned} \quad (32)$$

where

$$\begin{aligned} C = \left(\frac{eh}{4\pi mc} \right)^2 \left\{ Z \int \left[\frac{F^2}{r_1^3} + \frac{\tilde{F}^2}{r_2^3} - \left(\frac{1}{r_1^3} + \frac{1}{r_2^3} \right) F\tilde{F} \cos \theta + \frac{1}{2} \left(\frac{1}{r_1^3} \right. \right. \right. \\ \left. \left. - \frac{1}{r_1^3} \right) \left(\tilde{F} \frac{\partial F}{\partial \theta} - F \frac{\partial \tilde{F}}{\partial \theta} \right) \sin \theta \right] dV - 3 \int \frac{1}{r^3} \left[F^2 + \tilde{F}^2 - 2F\tilde{F} \cos \theta \right. \\ \left. + \frac{r_1}{r_2} \tilde{F}(F - \tilde{F} \cos \theta) + \frac{r_2}{r_1} F(\tilde{F} - F \cos \theta) + \frac{1}{2} \sin^2 \theta \left\{ r_2 \left(\tilde{F} \frac{\partial F}{\partial r_1} \right. \right. \right. \quad (33) \\ \left. \left. - F \frac{\partial \tilde{F}}{\partial r_1} \right) - r_1 \left(\tilde{F} \frac{\partial F}{\partial r_2} - F \frac{\partial \tilde{F}}{\partial r_2} \right) + \left(\frac{r_2}{r_1} - \frac{r_1}{r_2} \right) \left(\tilde{F} \frac{\partial F}{\partial \theta} - F \frac{\partial \tilde{F}}{\partial \theta} \right) \cot \theta \right. \\ \left. \left. - \left(\frac{r_2}{r_1} + \frac{r_1}{r_2} \right) F\tilde{F} \right\} \right] dV \right\}. \end{aligned}$$

It is also found that:

$$\begin{aligned} (2)^{1/2} z(x + iy) R(r)(u_1, u_0, u_{-1}) &= (0, Du_1, Du_0) \\ (2)^{1/2} z(x - iy) R(r)(u_1, u_0, u_{-1}) &= (Du_0, Du_{-1}, 0) \\ (x + iy)^2 R(r)(u_1, u_0, u_{-1}) &= (2Du_{-1}, 0, 0) \\ (x - iy)^2 R(r)(u_1, u_0, u_{-1}) &= (0, 0, 2Du_1) \\ (r^2 - 3z^2) R(r)(u_1, u_0, u_{-1}) &= (Du_1, -2Du_0, Du_{-1}) \\ z^2 R(r)(u_1, u_0, u_{-1}) &= (D'u_1, (D + D')u_0, D'u_{-1}) \end{aligned} \quad (34)$$

with

$$\begin{aligned} D &= \int \frac{1}{5} \{ 2(a\alpha + b\beta)^2 - (a\beta - \alpha b)^2 \} R(r) dV \\ D' &= \int \frac{1}{5} \{ (a\alpha + b\beta)^2 + 2(a\beta - \alpha b)^2 \} R(r) dV \end{aligned} \quad (35)$$

where

$$a = F - \tilde{F} \cos \theta, b = \tilde{F} \sin \theta, \alpha = r_1 - r_2 \cos \theta, \beta = r_2 \sin \theta. \quad (35')$$

In formulas (32), (34) we omit everywhere terms involving other functions than u_1, u_0, u_{-1} . The reason for this is the same as that for the omission of terms in $2^{-1/2} (S_\alpha^1 S_\beta^2 - S_\alpha^2 S_\beta^1)$ in (30), (31). These formulas (30), (31), (32), (34) can be used to form the secular determinant for the whole problem.

It is known that the matrix elements of ΔH between any two eigenfunctions belonging to different rows in (27) must vanish and that, therefore, the secular determinant can be broken up into five independent subdeterminants. With the aid of the results just described it is found that the subdeterminant $m=0$ is

$$\begin{vmatrix} -C - \lambda', & C + D, & 2D \\ C + D & -D - \lambda' & -C - D \\ 2D, & -C - D, & -C - \lambda' \end{vmatrix} = 0, \quad \lambda' = \lambda - D' \quad (36)$$

having roots $\lambda' = (-2C - 3D, 2D - C, C)$. The other subdeterminants are similarly found and give some of the same roots the first occurring on the whole 1, the second 3, and the third 5 times. The result is that the energy is to within a common additive constant

$$E = E_0 + [-3(C + D), 2(D - C), 0] \quad (1)^{18}$$

for $j=0, 1, 2$.

§IV COMPUTATION OF C AND D ¹⁹

Formula (6) is substituted into (33) and the integrations are performed. It is found that

$$\begin{aligned} \int (F^2 r_1^{-3} + \tilde{F}^2 r_2^{-3} - F\tilde{F} r_1^{-3} \cos \theta - F\tilde{F} r_2^{-3} \cos \theta) dV \\ = 8a^{-2}b^{-3}(1 + c^2/3) + 16c(a/2 + b/2)^{-5}. \end{aligned} \quad (37)$$

In the remainder of the calculation terms in c^2 are dropped, this being justified by the small numerical value of c .

$$\begin{aligned} \int r^{-3} \left\{ 2F^2 - 2F\tilde{F} \cos \theta + 2(r_1/r_2)(F\tilde{F} - \tilde{F}^2 \cos \theta) + (1/2) \sin^2 \theta \left[2r_2 \left(\tilde{F} \frac{\partial F}{\partial r_1} - F \frac{\partial \tilde{F}}{\partial r_1} \right) - 2(r_2/r_1)F\tilde{F} \right] \right\} dV \\ = 8 \left[\frac{1}{a^2 b (a+b)^2} + \frac{2b-a}{ab(a+b)^4} + \frac{20b}{(a+b)^6} \right] \\ + 16c \left[\frac{2b-a}{ab(a+b)^4} + \frac{2}{(a+b)^6} + 4.168 \frac{b-a}{(a+b)^6} \right]. \end{aligned} \quad (38)$$

Here $4.168 = (16/5) (120 \log 2 - 81.875)$. Substituting these expressions into (33), remembering the normalization condition (5) and (9), then substituting

¹⁸ The same result can be checked by using the theorem emphasized by Slater: the sum of the roots of a secular determinant is equal to the sum of the diagonal elements. The first row in (27) gives the last root ($j=2$), the second gives the sum of the last two, the third the sum of the three roots.

¹⁹ The writer is very grateful to Dr. F. W. Doermann for checking some of these formulas.

the dimensionless constants x, y by means of (19) and noting that $G^3\mu^2 = 4Z^3R_H\alpha^2$ we have

$$\left(1 - 128 \frac{x^5 y^3}{(x+y)^8} c\right) C = R_H Z^3 \alpha^2 x^3 \left\{ \frac{Z}{6} \left[1 - \frac{64 x^2 y^3}{(x+y)^5} c \right] - \frac{1}{2} \left[\frac{y^2}{(x+y)^2} + \frac{xy^2(2y-x)}{(x+y)^4} + 20 \frac{x^2 y^4}{(x+y)^6} \right] - c \left[\frac{xy^2(2y-x)}{(x+y)^4} + \frac{2x^2 y^3}{(x+y)^5} + 4.168 \frac{y-x}{(x+y)^6} \right] \right\}.$$

The first term involving Z is due to the action of the electric field of the nucleus and the remaining part of C is due to the interaction of the two electrons. It is seen that the two parts of C have opposite signs. For large Z the first part predominates and gives the usual effect for high atomic numbers. For small Z the second part may be numerically the larger one and C may be negative.

The part of D arising from \mathcal{D}_0 , given by (28''), is similarly found to be D_0 given by

$$\begin{aligned} \left(1 - 128 \frac{x^5 y^3}{(x+y)^8} c\right) D_0 = & - (R_H Z^3 \alpha^2 x^3 / 5) \left\{ \frac{y^2}{(x+y)^2} + \frac{xy^2(2y-x)}{(x+y)^4} \right. \\ & \left. + 2c \left[\frac{xy^2(2y-x)}{(x+y)^4} + \frac{xy^2}{(x+y)^3} - \frac{4x^2 y^3}{(x+y)^5} \right] \right\}. \end{aligned} \quad (40)$$

The part of D arising from \mathcal{D}_1 , given by (28'''), is, neglecting c altogether

$$\begin{aligned} D_1 = (R_H Z^2 \alpha^2 x^2 / 120) & \left[3 + \frac{256 x^3 y^3}{(x+y)^6} + 48 \frac{x^4 y^4 (x^2 + 3y^2)}{(x^2 - y^2)^5} \log \frac{x}{y} \right. \\ & \left. + 2x^2 y^2 \frac{x^4 - 11y^4 - 38x^2 y^2}{(x^2 - y^2)^4} + \frac{2x^2 y^2}{(x^2 - y^2)^2} + \frac{y^2 + 3x^2}{y^2 - x^2} \right] \end{aligned} \quad (41)$$

Substituting the numerical values of x, y, c of §2 the values of C, D_0, D_1 listed in §1 are obtained.

THE SINGLET SYSTEM OF THE OXYGEN ARC SPECTRUM
AND THE ORIGIN OF THE GREEN AURORAL
LINE

BY RUDOLF FRERICHS*

CALIFORNIA INSTITUTE OF TECHNOLOGY, PASADENA

(Received June 2, 1930)

ABSTRACT

The oxygen arc spectrum has been investigated under varied conditions in the extreme ultraviolet. A number of observed lines have been arranged in the singlet system of terms. The values of the low terms 1D_2 and 1S_0 have been fixed

AS J. C. McLennan has shown,¹ the green auroral line $\lambda=5577.35\text{\AA}$ gives the Zeeman pattern of a singlet line and is therefore probably the forbidden combination between the low metastable terms 1D_2 and 1S_0 of the oxygen atom. Although many attempts have been made to locate these terms, either by extrapolating the values of the corresponding terms of similar spectra or by connecting the structure of the oxygen band spectra with the dissociation energy, the exact position of these terms could not be fixed. The direct method of locating the terms by spectroscopic analysis was not used in former investigations.

The following paper gives an attempt to classify all the stronger ultraviolet singlet lines of the oxygen atom. The classification of singlet lines is usually more difficult than the classification of lines of higher multiplicity. Therefore, we have investigated the oxygen arc spectrum under different controlled conditions in order to obtain information regarding the excitation potential of the different lines. The results so obtained are given in part 2 after a short description of the experimental arrangement in part 1. Part 3 discusses the series analysis of the new lines.

APPARATUS AND PROCEDURE

Two different gratings were used. The first one, ruled by Anderson, (Focus = 1 m, area 5×8 cm, dispersion: first order 17A per mm) gives very good definition (see Table I) but unfortunately scatters the light so much that it could not be used for weak lines. The other one, ruled at the National Physical Laboratory, (Focus = 1 m, area 3.5×5 cm, dispersion 18A per mm) shows very bright and sharp lines down to 520A, the smallest wave-length here investigated, although it was not made with light rulings for the ultraviolet.

The spectrograph built for this investigation was very simply constructed. It consists of a brass tube which carries at one end the grating, at the other

* International Education Board Fellow.

¹ J. C. McLennan, J. H. McLeod, and McQuarrie, Proc. Roy. Soc. A114, 1 (1927). J. C. McLennan, J. H. McLeod and R. Ruedy, Phil. Mag. 6, 558 (1928); also L. A. Sommer, Zeits. f. Physik 51, 451 (1928).

end, the slit and holder for uncurved plates 1"×4" in size. The cover plates on the two ends of the spectrograph are sealed with rubber gaskets inserted in small circular grooves and are held in place with screws. These gaskets proved to be very satisfactory. Over one hundred exposures were made without the slightest trouble from leaks in the spectrograph.

Much care was taken in the arrangement of the pumping system and the light source. Small traces of oxygen in the spectrograph cause absorption of the light as well as serious fogging of the plates. In order to obtain as great a pressure difference as possible between the discharge tube and spectrograph we used two slits in series. The outer slit, narrow (0.01 mm) and short (2 mm) was sealed to the spectrograph so that the only communication between the discharge tube and the spectrograph was through this narrow aperture. A small distance behind this slit, there was a second slightly larger slit arranged at the end of a conical tube. One two-stage pump evacuated the space between these two slits, a second one the spectrograph directly, all connections were made with short and large tubes.

In order to make experiments on the excitation energy of the singlet lines the spectrograph was equipped with arrangements to work either with pure oxygen or with circulating mixtures of oxygen and rare gases. The oxygen was generated electrolytically. Small traces of hydrogen could be oxidized by a glowing platinum wire. The gas was dried with phosphorus pentoxide and then stored under low pressure in a bulb with a side tube immersed in liquid air. The flow of the oxygen in the discharge tube was regulated by a narrow capillary. A variable valve was not used but the amount of gas flowing in the tube was kept exactly constant by regulating the pressure in the storage bulb. The discharge tube was evacuated through two single stage pumps in series. For the experiments with pure oxygen, these four pumps were backed by an oil-pump. For the experiments with helium-oxygen and with neon-oxygen, the four pumps exhausted the gas from the spectrograph and discharge tube into a large bulb with a back pressure of about five millimeters. From this bulb the gas flowed back to the discharge tube through a heated quartz tube with copper oxide and a large charcoal trap in liquid air. The charcoal kept all impurities back and after a short time of circulation, the spectrum of the discharge tube was free from impurities. The charcoal also adsorbed the oxygen of the mixture and we had therefore to add continuously a small amount of oxygen to the rare gas after it had passed the charcoal. Argon is strongly adsorbed by charcoal. Therefore, the argon-oxygen mixture was circulated over calcium heated to about 300 degrees C in an iron tube and through a trap in liquid air, and new oxygen was added to replace that absorbed in the calcium tube.

The experiments were made with the positive column as well as with the hollow cathode in pure oxygen and in different mixtures. The discharge tube that was finally adopted had a diameter of about 15 mm and a length of 250 mm. Large electrodes of heavy aluminum allowed the use of currents of between 350 and 750 milliamperes. Direct current at 1300 volts was supplied by two small generators of 650 volts each, connected in series. Suit-

able ballast-resistance was used. The hollow cathode consisted either of a small aluminum tube 10 mm in diameter and 40 mm in length or of a hole of similar size in a solid piece of aluminum, which was cooled by water flowing through a copper-tubing surrounding the aluminum. The hollow cathodes carried currents of between 150 and 500 milliamperes.

TABLE I. Ultraviolet OI lines.

Intensity	Wave-length	Frequency obs.	Frequency calc.	Classification	
	1217.60	82128	82128	$2p^1S_0 - ({}^2P)3s^1P_1$	
	1152.06	86801	86801	$2p^1D_2 - ({}^2D)3s^1D_2$	
	999.47	100053	100053	$2p^1D_2 - ({}^2P)3s^1P_1$	
1	990.86	100922	100922	$2p^3P_0 - ({}^2D)3s^3D_1$	
3	990.27	100983	100983	$2p^3P_1 - ({}^2D)3s^3D_2$	
3	990.21	100989	100989	$2p^3P_1 - ({}^2D)3s^3D_1$	
4	988.84	101128	101128	$2p^3P_2 - ({}^2D)3s^3D_3$	
3	988.72	101141	101141	$3p^3P_2 - ({}^2D)3s^3D_2$	
1	988.66	101147	101147	$2p^3P_2 - ({}^2D)3s^3D_1$	II. Order
	935.15	106935	106934	$2p^1D_2 - ({}^2D)4s^1D_2$	
	922.02	108457	108457	$2p^1D_2 - ({}^2D)3d^1F_3$	
	882.88	113266	113265	$2p^1D_2 - ({}^2D)5s^1D_2$	
1	879.65	113681	113687	$2p^3P_0 - ({}^2P)3s^3P_1$	
			113744	$2p^3P_1 - ({}^2P)3s^3P_2$	
5	879.14	113747	113755	$2p^3P_1 - ({}^2P)3s^3P_1$	
			113761	$2p^3P_1 - ({}^2P)3s^3P_0$	
			113903	$2p^3P_2 - ({}^2P)3s^3P_2$	
4	877.97	113899	113914	$2p^3P_2 - ({}^2P)3s^3P_1$	
	861.63	116059	116058	$2p^1D_2 - ({}^2D)6s^1D_2$	I. Order
	850.74	117545	117544	$2p^1D_2 - ({}^2D)7s^1D_2$	
3	812.09	123139	123122	$2s^22p^4{}^3P_0 - 2s2p^5{}^3P_1$	II. Order
			123130	$2s^22p^4{}^3P_1 - 2s2p^5{}^3P_2$	
1	811.69	123200	123189	$2s^22p^4{}^3P_1 - 2s2p^5{}^3P_1$	
1	811.43	123239	123221	$2s^22p^4{}^3P_1 - 2s2p^5{}^3P_0$	
4	811.02	123301	123289	$2s^22p^4{}^3P_2 - 2s2p^5{}^3P_2$	
1	810.62	123362	123348	$2s^22p^4{}^3P_2 - 2s2p^5{}^3P_1$	
3	792.92	126346			II. Order
1	792.50	126274			
1	792.20	126231			
3	791.93	126183			
1	791.48	126116			
0	770.70	129752		{ 71	
1	770.28	129823			
2	769.39	129973		{ 150	
0	—	—			
1	756.7	132152		{ 158	
2	755.8	132310			I. Order
0	—	—			
1	749.3	133457	~133000	$2p^3P_{0,1,2} - ({}^2P)4s^3P_{0,1,2}?$	
1	748.4	133618			

In front of the slit, there was a small shutter which was closed before an exposure, while the discharge tubes were run at the heaviest possible currents until the last traces of visible bands and of the hydrogen lines disappeared. Table I gives the observed lines which we can attribute with safety to the spectrum of the oxygen atom. The exposures were made with times between 15 minutes and three hours. Most of the lines were measured in the second order against some lines of impurities: O II, NI, N II, CI, CII which have

been determined by Bowen and Ingram² with great accuracy, and which occurred weakly in our discharge. A few weaker lines have been measured only in the first order against O II, O I, Ne, He. As the intensities vary considerably with the source, intensity values are only relative and only given for lines which belong to one group.

THE EXCITATION POTENTIAL OF THE ULTRAVIOLET OXYGEN LINES

In order to obtain a classification of the oxygen lines, we investigated the spectrum under varied conditions. A few pictures were taken with the above mentioned positive column in the mixtures: He-O₂, Ne-O₂ and A-O₂. The pressure of the rare gas was not measured but was always adjusted to give the minimum potential drop across the tube. The amount of oxygen added continuously was so small that the stronger lines were just visible in a spectroscope of considerable dispersion. The excitation phenomena of mixtures of rare gases with other gases and vapors have been studied much and discussed in the last years. Although there are some discrepancies between the results of different observers, we can state with safety that the maximum amount of energy available in such a discharge is given by the ionization potential of the rare gas, when the amount of the other component of the mixture is small. These investigations differ only as to whether this amount is transferred to neutral atoms, to metastable atoms or to ions of the second component. In the case of discharges through mixtures of rare gases and molecular gases, the process is complicated by dissociation. By looking over various experiments carried on in this field, one gains the impression that the assumptions of different kinds of collisions are made *ad hoc* in order to obtain agreement with the observed facts.³ Therefore, because the prediction of the excitation limit of unclassified lines seemed to be rather uncertain, we have made no special assumptions as to the processes involved, but we have empirically calibrated our results by the well-known excitation energy of the already classified oxygen lines. Table II gives the results so obtained. The fifth column contains the excitation energy of the upper level of each line in frequency units, the second, third and fourth column the intensities in A-O₂, Ne-O₂ and He-O₂. Fig. 1 illustrates these results. The exposures are so chosen, that the resonance lines appear on all spectrograms with nearly the same intensity. In argon, only those lines whose upper level is not higher than about 100,000 frequency units above the ³P₂ level are excited with considerable intensity (>1). This photograph shows clearly that 1152 is the lowest excited line of the singlet system because the other lines are either very weak or absent in argon-oxygen. Neon has a very remarkable effect on the intensities. Table II shows that in neon, the line 935.15, whose upper level is about 122800 above the ³P term, is strongly

² I. S. Bowen and S. B. Ingram, Phys. Rev. **28**, 444 (1926).

³ For a discussion of the various kinds of collision which are necessary to explain the observed facts in mixtures of rare gases and molecular gases, see O. S. Duffendack and H. L. Smith, Phys. Rev. **34**, 68 (1929) and O. S. Duffendack and R. A. Wolfe, Phys. Rev. **34**, 409 (1929).

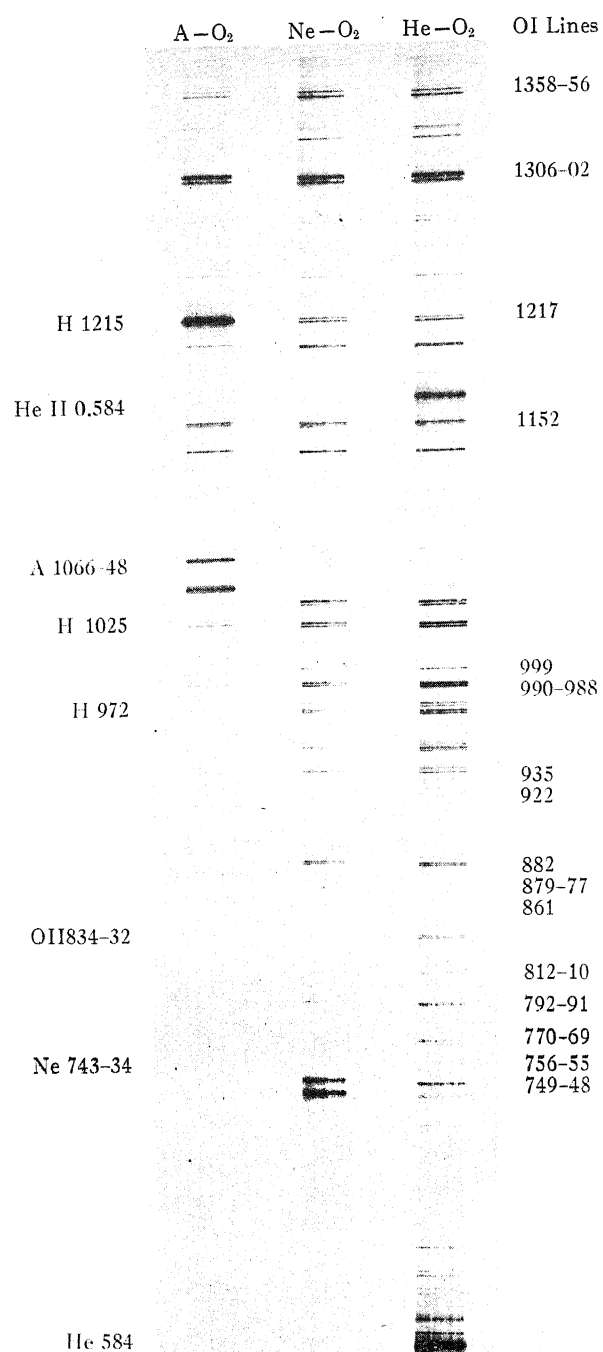


Fig. 1. The ultraviolet OI spectrum in A-O₂, Ne-O₂ and He-O₂.

excited. This phenomenon of increased intensities of certain lines in such discharges often has been mentioned.⁴ It occurs always when either the ionization energy or the energy of the metastable state of the rare gas is approximately equal to the excitation energy of the line of the other component.

TABLE II. *Intensities of the ultraviolet O I. Lines under different conditions.*

Wave-length	A-O ₂	Intensity Ne-O ₂	He-O ₂	Excitation energy frequency units
1358-56	4	6	6	73760
1306-02	10	10	10	76788
1217	—	3	3	115922
1152	3	4	5	102670
1041-39	1	4	5	95222
1028-25	1	4	5	97481
999	—	4	5	115922
990-988	1	5	8	101147
978-76	—	2	3	102406
973-71	—	2	3	102906
935	—	4	3	122803
922	—	—	1	124326
882	—	—	2	129134
879-77	—	4	4	113914
861	—	—	1	131927
850	—	—	0	133413
812-810	—	1	2	123348
792-791	—	2	3	126231
770-769	—	1	2	
756-55	—	0	1	
749-48	—	—	0	133618

These lines are strongly excited in helium-oxygen but on the other hand, some more lines can be observed in helium which are either weak or absent in neon.

A few words may be said about the excitation of the oxygen arc spectrum in other sources. The positive column in pure oxygen also shows these lines but the intensity at the same amount of current passing through the tube is much smaller than in the mixtures of rare gases and oxygen. In pure oxygen the lines show the usual decrease in intensity with increasing excitation.

The highest amount of excitation with direct current is obtained in the hollow cathode in pure oxygen. In the hollow cathode, all the lines of of O II which have been classified by Bowen⁵ are strongly developed. We also observed the hollow cathode discharge in mixtures of He-O and Ne-O. The spectra so obtained show generally the same lines as the spectra taken with the positive column. The intensity is much smaller and the spectra cannot be so brilliantly excited as in the positive column with great current density.

⁴ H. Beutler and B. Josephy, *Naturwiss.* **15**, 540 (1927); F. Paschen, *Berl. Ber.* p. 536. (1928); Y. Takahashi, *Ann. d. Physik* **3**, 25 (1929); R. A. Sawyer and R. J. Lang, *Phys. Rev.* **34**, 712 (1929).

⁵ I. S. Bowen, *Phys. Rev.* **29**, 38 (1927).

$3s^1D_2$. Our experiments on the excitation of the different lines (Table II) show that this last line has a lower excitation potential than the other two, in accordance with this classification.

We have now succeeded in finding five members of the series: $2p^1D_2 - ({}^2D)ns^1D_2$. According to Table III, their frequency differences are always between the corresponding frequency differences of the $({}^4S)ns^5S_2$ and $({}^4S)ns^3S$ terms. This demonstrates again how accurately the new terms can be obtained by the above mentioned displacement of the Runge-Paschen terms. We have used these five members to calculate the limit of this series in order to locate the important $2p^1D_2$ term.

These $({}^2D)ns^1D_2$ terms have for their limit the low metastable term 2D of the O II spectrum. This term has been located by Bowen⁸ not only by ultraviolet combinations with higher terms but also more accurately by the forbidden combinations with the lowest term: 4S , i.e. the nebular lines 3729.91 and 3727.12, according to his well-known theory. As Hund has shown in Table 34 of his book, the series of the 1D_2 terms have in this case the ${}^2D_{3/2}$ component of the doublet term for a limit. This term is inverted and according to Shenstone,⁹ there are some deviations known from Hund's rule in the case of inverted terms. But Shenstone states in his second paper that, in the case of the addition of an s -electron, this rule holds even for inverted terms. The possible error caused by a failure of Hund's rule would be in this case, ${}^2D_{3/2} - {}^2D_{1/2} = 20$ frequency units.

TABLE III. The OI series $2p^1D_2 - ({}^2D)ms^1D_2$.

$({}^4S)ns^3S_1$:	33043.3	13612.5	7425.6	4672.8	3210.2	2340.9
$\Delta({}^4S)ns^5S_1$:	19430.8	6186.9	2752.8	1462.6	869.3	
$2p^1D_2 - ({}^2D)ns^1D_2$ {	λ	1152.06	935.15	882.88	861.63	850.74
	ν	86801	106935	113266	116059	117545
	$\Delta\nu$	20134	6331	2793	1486	
$\Delta({}^4S)ns^5S_2$:	21710.5	6637.7	2902.9	1526.0	900.3	
$({}^4S)ns^5S_2$:	36069.0	14358.5	7720.8	4817.9	3291.9	2391.6

We have tried to get higher series members under conditions where the first four members are strong, but the fifth is always weak and it was not possible to obtain higher members. This is not astonishing when one considers how highly unstable such an atom is in a state 24,000 frequency units above the ordinary ionization limit. However, we can estimate the accuracy of this calculation in the following way. The value for the terms $({}^4S)ns^3S_1$ and $({}^4S)3s^5S_2$ which is obtained by applying the Rydberg formula to four series members departs only about 6 frequency units from the value which can be obtained by using eight or nine series members. Adding the fifth member reduces this error to 3 frequency units. We believe, therefore, that the error in the limit of our singlet series caused by this method of calculation is not greater than about 3 frequency units, because these terms are located

⁸ I. S. Bowen, reference 5.

⁹ A. G. Shenstone, Nature **121**, 619 (1928); Nature **122**, 727 (1928).

exactly between the corresponding $(^4S)ns^3S_1$ and $(^4S)ns^5S_2$ terms. The only important source of error will therefore be the comparatively small accuracy in the frequencies at these short wave-lengths.

By this determination the energy values of the terms involved in the emission of the green auroral line are fixed. As we have mentioned above, the classification of this line has been suggested some time ago by McLennan. In the meantime, many attempts have been made to locate these terms. Some predictions of their position have been made by assuming that the relative position of the metastable low terms 1S_0 and 1D_2 is the same for similar spectra. Sommer as well as Kaplan¹⁰ calculate from the known position of the 1S_0 , 1D_2 and 3P term in O III the distance $^1D_2 - ^3P$ to be about 15500 frequency units. This is apparently in very good agreement with the observed position although Sommer as well as Kaplan could not give any theoretical reason for their assumption. In a letter to Nature,¹¹ J. C. McLennan and M. F. Crawford find that the ratio $^1D_2 - ^3P : ^1S_0 - ^1D_2$ is constant and equal to 0.585 for selenium and tellurium and they assume that this ratio is the same for sulphur and oxygen. Thus, by using the value $^1S_0 - ^1D_2 = 17925$, they find $^1D_2 - ^3P = 10490$. But by comparing the relative positions of such terms in other columns of the periodic table: i.e., C I, Si I, Ge I, Sn I, Pb I or O II, S II, one finds that the ratio between the low terms in all the cases where they are known, is never constant and, therefore, it seems to be without any justification to predict unknown terms in this way.

Another method of prediction of the approximate position of this 1D_2 term is based on the calculation of the dissociation energy by means of the convergence point of the oxygen bands. Herzberg¹² has shown that the convergence limit of the Birge-Spencer bands does not correspond to a dissociation into two oxygen atoms in the normal 3P_2 state, but to a dissociation into one atom in the 3P_2 state and another atom in the 1D_2 state. By comparison of the so calculated dissociation energy $O_2 \rightarrow O_{1D_2} + O_{3P_2}$ with the chemically measured value $O_2 \rightarrow O_{3P_2} + O_{3P_2}$, one obtains the value $O_{1D_2} - O_{3P_2}$. In this way Mecke¹³ obtains $^1D_2 - ^3P_2 = 1.4$ volts, Henri¹⁴ $^1D_2 - ^1P_2 = 1.7$ volts the latter value being in better agreement with the observed value: 1.95 volts.

A few words may be said about some other combinations which can be calculated from the known position of the singlet terms. We have not found any intercombination between singlet and triplet terms. The theory of the intensity of intercombinations between singlet and triplet terms has been developed by Houston¹⁵ for atoms with two outer electrons. This theory predicts, in good agreement with the observations, that intercombinations are strong only when the interval between singlet and triplet terms is small compared with the intervals between the different components of the triplet

¹⁰ L. A. Sommer, *Zeits. f. Physik* **51**, 451 (1928); J. Kaplan, *Phys. Rev.* **33**, 638 (1929).

¹¹ J. C. McLennan and M. F. Crawford, *Nature* **124**, 874 (1929).

¹² G. Herzberg, *Zeits. f. Physik Chem.* **4**, 13, 233 (1929).

¹³ R. Mecke, *Naturwiss.* **17**, 996 (1929).

¹⁴ V. Henri, *Nature* **125**, 201 (1930).

¹⁵ W. V. Houston, *Phys. Rev.* **33**, 297 (1929).

TABLE IV. Term table of the OI spectrum.

$2s^2 2p^3$	$2p$	3P_2 : 109831 3P_1 : 109672 3P_0 : 109605	1D_2 : 93962	1S_0 : 76037	
		$2s^2 2p^3: ^4S$	$2s^2 2p^3: ^2D$	$2s^2 2p^3: ^2P$	$2s^2 p^4$
	$3s$	5S_2 : 36069.0 3S_1 : 33043.3	3D_3 : 8702.9 3D_2 : 8690.9 3D_1 : 8683.0 1D_2 : 7161.0	3P_2 : -4072.1 3P_1 : -4082.5 3P_0 : -4088.8 1P_1 : -6091	
	$3p$	5P_1 : 23211.9 5P_2 : 23209.2 5P_3 : 23205.8 3P_0 : 21207.7 3P_1 : 21207.7 3P_2 : 21207.2	3F_4 : -3876.1 3F_3 : -3883.0 3F_2 : -3888.7 $^3D_{1,2,3}$: -3456.4 3P_1 : -3459.8 1F_3 1D_2 1P_1	3D_3 : -17443.8 3D_2 : -17449.5 3D_1 : -17452.9 $^3P_{0,1,2}$ 3S_1 1D_2 1P_1 1S_0	
	$3d$	$^5D_{0,1,2,3,4}$: 12417.3 $^3D_{1,2,3}$: 12350.0	$^3G_{3,4,5}$ $^3F_{2,3,4}$ $^3D_{1,2,3}$ $^3P_{0,1,2}$ 3S_1 1G_4 1F_3 : -14495 1D_2 1P_1 1S_0	$^3F_{2,3,4}$ $^3D_{1,2,3}$ $^3P_{0,1,2}$ 1F 1D_2 1P_1	
	$4s$	5S_2 : 14358.5 3S_1 : 13612.5	$^3D_{1,2,3}$ 1D_2 : -12972	$^3P_{0,1,2}$ 1P_1	
	$4p$	5P_1 : 10742.5 5P_2 : 10743.7 5P_3 : 10734.3 $^3P_{0,1,2}$: 10157.5	$^3F_{2,3,4}$ 3D_3 : -15936.6 3D_2 : -15944.0 3D_1 : -15949.0 $^3P_{0,1,2}$ 1F 1D_2 1P_1	$^3D_{1,2,3}$ $^3P_{0,1,2}$ 3S_1 1D_2 1P_1 1S_0	
	$5s$	5S_2 : 7720.8 3S_1 : 7425.6	$^3D_{1,2,3}$ 1D_2 : -19303	$^3P_{0,1,2}$ 1P_1	
	$6s$	5S_2 : 4817.9 3S_1 : 4672.8	$^3D_{1,2,3}$ 1D_2 : -22096	$^3P_{0,1,2}$ 1P_1	
	$7s$	5S_2 : 3291.9 3S_1 : 3210.2	$^3D_{1,2,3}$ 1D_2 : -23582	$^3P_{0,1,2}$ 1P_1	
$2s^2 p^4$	$2p$				3P_2 : -13458.0 3P_1 : -13516.9 3P_0 : -13548.9

TABLE V. Transitions $2s2p^5 \rightarrow 2s2p^3np$ in the O I spectrum.

	3P_2 109831	$2s2p^4$ 3P_1 109672	3P_0 109605	3P_2 21207.2	$(^4S)2s2p^33p$ 3P_1 21207.7	3P_0 21207.7	$(^4S)2s2p^34p$ $^3P_{0,1,2}$ 10157.5	$(^4S)2s2p^35p$ $^3P_{0,1,2}$ 5968.6	$(^4S)2s2p^36p$ $^3P_{0,1,2}$ 3926.9
$^3P_2; \begin{cases} -13458.0 \\ -13516.9 \\ -13548.9 \end{cases}$ calc. $2s2p^33p_1; \begin{cases} -13458.0 \\ -13516.9 \\ -13548.9 \end{cases}$ 3P_0	123289 123348	123130 123189 123221	123122	34665.2 34724.1	34665.7 34724.6 34756.6	34724.6	23615.5 23674.4 23706.4	19426.6 19485.5 19517.5	17384.9 17443.8 17475.8
obs.	123301 811.02	123139 812.09	123139 812.09	34666.6 2883.78*	34666.6 2883.78*	34724.8 2878.95*	23615.5 4233.32	19426.6 5146.1**	17384.9 5750.42
	123362 810.62	123200 811.69	123139 812.09	34724.8 2878.95*	34724.8 2878.95*	34724.8 2878.95*	23674.4 4222.78	19485.5 5130.6**	17443.8 5731.0
		123239 811.43		34756.7 2876.30*	34756.7 2876.30*		23706.4 4217.09	19517.5 5122.1**	17475.81 5720.61

** Not observed.

* See: A. Fowler Proc. Roy. Soc. (A) 110, 476, (1926) unclassified OII lines.

term. Although this theory cannot be applied to the more complicated case of the oxygen atom, the very small intervals of the oxygen terms may be responsible for the missing intercombination lines. It is in agreement with Houston's theory that, in the case of selenium and tellurium, where the intervals are much larger, such intercombinations have been found by McLennan.

The green auroral line is according to its classification, the exact analogue of the nebular line 4363.21A. We should therefore expect to find also the other combinations ${}^3P_2-{}^1D_2$ and ${}^3P_1-{}^1D_2$ which correspond to the nebular lines 5006.84 and 4958.91A. According to Table IV, these lines are located at 6299 and 6363A with an error of approximately $\pm 5A$. These lines are neither found in the laboratory nor in the spectrum of the aurora or of the night sky.

Among the new triplet terms (Table IV), the term: $2s2p^5 {}^3P$ is especially interesting. By application of the irregular doublet law to the oxygen-like isoelectronic spectra, Mack and Sawyer¹⁶ have predicted its position as about 15000 frequency units above the ordinary ionization limit, the 4S term of the ion, in good agreement with the observed value. Under the unclassified lines in the near ultraviolet and in the visible, there are some triplets which give the intervals 58.9 and 32 frequency units. Table V shows that these triplets are combinations of this $2s2p^5 {}^3P$ term with the terms: $({}^4S)2s^2 2p^3 n p^3 P$. The combination $({}^4S)2s^2 2p^3 5p^3 P - 2s2p^5 {}^3P$ is not known, perhaps due to the small sensitivity of the photographic plates in this region. The term: $2s2p^5 {}^3P$ combines with a 3P term at 3926 and the application of the Rydberg formula shows that this term is the hitherto unknown term $({}^4S)2s^2 2p^3 6p^3 P$.

We are indebted to the Rockefeller Foundation for the grant of a fellowship, to Professor R. A. Millikan for extending the facilities of the Norman Bridge Laboratory and to Professor I. S. Bowen for helpful discussions and suggestions.

Note added with proof: Prof. Paschen writes me that he has recently observed the two lines ${}^3P_2-{}^1D_2$ and ${}^3P_1-{}^1D_2$ at 6300.06 and 6363.86A respectively in a discharge through pure oxygen. This proves that the above given calculation of the singlet terms is accurate within 0.5 frequency units. S. Goudsmit, Phys. Rev. **35**, 1325, (1930) finds by theoretical calculations the above mentioned value of McLennan in disagreement with our measurements. V. Kondratjew, Zeits. f. Phys. Chem. **B**, **7**, 70, (1930) obtains from the oxygen bandspectra the value 1.91 volts for the difference ${}^3P_2-{}^1D_2$ in very good agreement with the observed value 1.95 volts.

¹⁶ J. E. Mack and R. A. Sawyer, Phys. Rev. **35**, 299 (1930).

BAND SPECTRA INTENSITIES FOR SYMMETRICAL
DIATOMIC MOLECULESBY ELMER HUTCHISSON
BERLIN, GERMANY

(Received June 20, 1930)

ABSTRACT

The intensity of a spectral line may be calculated in the new quantum mechanics by evaluating the integral of the product of the electric moment and the wave functions of the initial and of the final states. The complete wave function may be written approximately as a product of a nuclear wave function and an electronic wave function. Furthermore, the electric moment can be approximately written as the sum of a function of the nuclear coordinates only and a function of the electronic coordinates only. For symmetrical diatomic molecules the term in the electric moment which is a function of the nuclear coordinates only is zero so that the intensity integral reduces to a double integral which may be written as a product of an electronic integral and a nuclear integral. The electronic integral is constant for all the lines corresponding to the same electronic transition and the integrand of the nuclear integral consists only of the product of the radial wave functions for the initial and the final states. The integration of the nuclear integral is carried out using harmonic oscillator wave functions whose origins are shifted due to the change of the nuclear separation during the electronic transition.

A comparison is made between the intensities calculated in the above manner and those obtained by experiment. In the case of Na_2 good quantitative agreement is obtained between the experimental and the calculated results. Accurate values of the moments of inertia in the initial and final states are not known for K_2 but it is possible to show that if a value of the change in the nuclear separations during the transition is assumed, agreement is possible for all of the lines corresponding to low quantum numbers. Good qualitative agreement is obtained for I_2 . Calculations are made for the absorption spectra and the $3'B-2'S$ emission band system of H_2 but the agreement in these cases is not as good as for Na_2 and K_2 .

I. INTRODUCTION

ON THE basis of the old quantum theory Condon¹ was able to show that in connection with a given electronic transition in a diatomic molecule certain transitions were more probable than others. His calculations were based upon Franck's² assumption that during an electronic transition nuclei which are originally in a non-vibrating state remain momentarily fixed because of their large masses compared with those of the electrons. Since the equilibrium distance between the nuclei is altered due to the motion of the electrons, the nuclei acquire a potential energy with respect to the new equilibrium points and begin to vibrate. The amplitude of the vibration acquired after the transition is approximately equal to the change in the equilibrium

¹ E. Condon, *Phys. Rev.* **28**, 1182 (1926).² J. Franck, *Trans. Faraday Society* (1925).

separations, therefore it is possible for the most probable nuclear transition to be calculated.

If the nuclei are vibrating in the initial state then almost any amplitude in the end state is possible. A calculation similar to that mentioned above can be employed except that instead of focusing our attention on the equilibrium position in the initial state, we focus our attention on the positions in which the nuclei spend most of the time. These positions will naturally be the turning points of the vibratory motion. With potential energy diagrams to determine the turning points of the vibration Condon was able to show that the positions of maximum intensities in the well-known double entry tables lie along a parabolic path and agree fairly well with experiment. As Condon's theory is essentially only one of transition probabilities the distribution in the initial state is not included.³

In a second paper Condon⁴ showed that the ideas expressed above on the basis of the old quantum theory could be carried over into the new quantum mechanics. In the new quantum mechanics the intensity of a spectral line may be calculated by evaluating the integral of the product of the electric moment and the wave functions of the initial and final states where the integration is carried out over all of the coordinates of the electrons and the nuclei. Thus a measure of the intensity is given by the expression (following Condon):

$$I = \int \int M(x, r) \psi_{e'n'}(x, r) \psi_{e''n''}(x, r) dx dr,$$

where M is the instantaneous electric moment, $\psi_{e'n'}$ and $\psi_{e''n''}$ are the wave functions of the initial and final states, x and r are total coordinates of the electron and of the nuclei respectively and e and n are electronic and vibrational quantum numbers. According to the work of Born and Oppenheimer⁵ the complete wave function ψ_{en} can be approximately expressed as a product of an electronic wave function $\Phi_e(x)$ and an oscillatory wave function $\Psi_{en}(r)$. The latter function corresponds to the motion of the nuclei moving under an effective force arising from the moving electrons and the repulsion of the nuclei. We may write our integral:

$$I = \int \int M(x, r) \Phi_{e'}(x) \Psi_{e'n'}(r) \Phi_{e''}(x) \Psi_{e''n''}(r) dx dr.$$

The electric moment is defined as the vector sum of the coordinates of the electrons times their charge and the coordinates of the nuclei times their charge. This may be approximately expressed in the following way:

$$M(x, r) = A(x) + B(r)$$

because during the transition of the electrons the nuclei remain practically fixed and the first term (representing the vector sum of the electronic charges

³ Cf. G. Herzberg, *Zeits. f. Physik* **49**, 761 (1928).

⁴ E. Condon, *Phys. Rev.* **32**, 858 (1928).

⁵ M. Born and Oppenheimer, *Ann. d. Physik* **84**, 457 (1927).

times x) will be a constant over the integration of the electron coordinates. The second term (representing the vector sum of the nuclear charge times r) will be a function of only the nuclear coordinates because the heavy nuclei cannot respond immediately to the changes in the electronic arrangement. We have therefore:

$$I = \int A(x) \Phi_{e'}(x) \Phi_{e''}(x) dx \int \Psi_{e'n'}(r) \Psi_{e''n''}(r) dr + \int \Phi_{e'}(x) \Phi_{e''}(x) dx \int B(r) \Psi_{e'n'}(r) \Psi_{e''n''}(r) dr.$$

The integrals involving the electron coordinates will be constant for a given electronic transition so that

$$I = C_1 \int \Psi_{e'n'}(r) \Psi_{e''n''}(r) dr + C_2 \int B(r) \Psi_{e'n'}(r) \Psi_{e''n''}(r) dr.$$

This integral cannot be evaluated in general because we do not know the ratio of the constants ($B(r)$ is probably a linear function). However if we restrict ourselves to symmetrical diatomic molecules the nuclear electric moment will always be zero so that the last term drops out and we have only

$$I = C_1 \int \Psi_{e'n'}(r) \Psi_{e''n''}(r) dr. \quad (1)$$

It is the purpose of this paper to evaluate this integral and to compare the results with experiment in several cases.

II. INTENSITIES FOR HARMONIC OSCILLATIONS

The approximate wave equation for the nuclear motions of the diatomic molecule may be written

$$\nabla^2 \Psi + \frac{8\pi^2\mu}{h^2} \left[W - \frac{Z^2 e^2}{r} + V_e(r) \right] \Psi = 0 \quad (2)$$

where Ze is the charge on one of the nuclei, μ is the equivalent mass ($= M_1 M_2 / M_1 + M_2$), r is the separation of the nuclei and $V_e(r)$ is the mean potential energy due to the electrons. The wave function may be separated into three functions in the usual manner by setting $\Psi = N\Phi(\phi) \cdot \Theta(\theta) \cdot R(r)/r$ where N is a normalizing factor. The equations in ϕ and θ will not have any effect⁶ on the calculated intensities of the spectral lines and we may therefore pass immediately to the equation in r

$$\frac{d^2 R}{dr^2} - \frac{m(m+1)}{r^2} R + \frac{8\pi^2\mu}{h^2} \left[W - \frac{Z^2 e^2}{r} + V_e(r) \right] R = 0 \quad (3)$$

⁶ A. Sommerfeld, *Ergänzungsband*, p. 69.

where m is the rotational quantum number. Making the substitution $\rho = r/r_0$ (r_0 = equilibrium separation of the nuclei) we obtain

$$R'' + \left[\frac{8\pi^2 J_0}{h^2} (W - f(\rho)) - \frac{m(m+1)}{\rho^2} \right] R = 0 \quad (4)$$

in which $J_0 = \mu r_0^2$ and $f(\rho)$ represents the effective potential energy.

In this paper we will restrict ourselves to linear oscillations and we may therefore put $f(\rho) = -D + [(2\pi\nu_0)^2 J_0/2] \xi^2$ where $\xi = \rho - 1$ and D is the dissociation energy and ν_0 is the frequency of vibration for very small amplitudes. Making use of this expression in Eq. (4) and expanding ρ in terms of ξ (or, one could set $m=0$) and finally making the substitution $\eta = 2\pi(\nu_0 J_0)^{1/2}/(h)^{1/2} \xi$, we obtain

$$R'' + \left[\frac{2}{h\nu_0} \left\{ W + D - m(m+1) \frac{h^2}{8\pi^2 J_0} \right\} - \eta^2 \right] R = 0 \quad (5)$$

which is the wave equation for the linear oscillator.⁷

The solution of this equation is well known and may be written

$$R_n = \frac{1}{N_n} e^{-\eta^2/2} H_n(\eta) \quad \text{and} \quad W + D - m(m+1) \frac{h^2}{8\pi^2 J_0} = \left[n + \frac{1}{2} \right] h\nu_0 \quad (6)$$

where n is the vibrational quantum number and $H_n(\eta)$ is a Hermitian polynomial.

We wish to evaluate the integral (1) which may now be written in terms of (ρ) and the radial wave function, in the following manner:

$$I = \text{const.} \int_0^\infty R_{e'n'}(\rho) R_{e''n''}(\rho) d\rho. \quad (7)$$

As far as the nuclei are concerned the effect of an electron transition is, that besides the change in the equilibrium positions of the nuclei there is also a change in the binding or potential energy such that the nuclei acquire a new vibration frequency after the transition. Therefore if we take $R_{e'n'} = (1/N_{n'}) e^{-\eta'^2/2} H_{n'}(\eta')$ as the nuclear part of the wave function for the upper state, we will have for the lower state $R_{e''n''} = (1/N_{n''}) \exp - [(\alpha\eta + \delta)^2/2] H_{n''}(\alpha\eta + \delta)$ where α and δ represent respectively measures of the change in frequency and the change in equilibrium position. From the definition of η we see that

$$\eta = [2\pi(\nu_0' J_0')^{1/2}/(h)^{1/2} r_0] r - 2\pi(\nu_0' J_0')^{1/2}/(h)^{1/2}$$

so that

$$\begin{aligned} \alpha\eta + \delta &= [(\alpha 2\pi(\nu_0' J_0')^{1/2}/(h)^{1/2} r_0')] [r + \delta r_0'/(h)^{1/2} 2\pi\alpha(\nu_0' J_0')^{1/2}] \\ &\quad - \alpha 2\pi(\nu_0' J_0')^{1/2}/(h)^{1/2} = [2\pi(\nu_0'' \mu)^{1/2}/(h)^{1/2}] r - 2\pi(\nu_0'' \mu)^{1/2} r_0''/(h)^{1/2}. \end{aligned}$$

Thus $\alpha = (\nu_0''/\nu_0')^{1/2}$ and

⁷ E. Fues, Ann. d. Physik **80**, 367 (1926).

$$\delta = (r_0' - r_0'') 2\pi(\nu_0''\mu)^{1/2}/(h)^{1/2} = 0.1221(r_0' - r_0'')(\nu_0''M)^{1/2}$$

where ν_0'' is expressed in cm^{-1} , M is the atomic weight ($\text{O} = 16$) of one of the atoms and $(r_0' - r_0'')$ is in Angstroms.

The integral (7) then becomes

$$I = \text{const} \int_{-\infty}^{+\infty} (N_{n'} N_{n''})^{-1} e^{-\eta^2/2} e^{-(\alpha\eta+\delta)^2/2} H_{n'}(\eta) H_{n''}(\alpha\eta + \delta) d\eta \quad (8)$$

where the limits are taken from $-\infty$ to $+\infty$ instead of from -1 to $+\infty$ since the addition of the region from -1 to $-\infty$ will not appreciably affect the value of the integral for small quantum numbers. The values of the normalizing factors are well known for the linear oscillator, being

$$N_{n'} = [2^{n'} n'! \pi^{1/2} h^{1/2} / 2\pi(\nu_0' \mu)^{1/2}]^{1/2} \quad N_{n''} = [2^{n''} n''! \pi^{1/2} h^{1/2} / 2\pi(\nu_0'' \mu)^{1/2}]^{1/2} \quad (9)$$

In order to carry through the integration of Eq. (8) the method used by Schrödinger⁸ in the Stark effect may be applied. The "erzeugende" function⁹ for the Hermitian polynomial is

$$\sum_{n'=0}^{n'=\infty} \frac{H_{n'}(\eta)}{n'!} s^{n'} = e^{-s^2+2s\eta}$$

and for the function of the lower state

$$\sum_{n''=0}^{n''=\infty} \frac{H_{n''}(\alpha\eta + \delta)}{n''!} t^{n''} = e^{-t^2+2t(\alpha\eta+\delta)}.$$

If these expressions are multiplied together and also multiplied by the exponentials in Eq. (8) we have after integration

$$\begin{aligned} \sum_{n'=0}^{n'=\infty} \sum_{n''=0}^{n''=\infty} \frac{s^{n'} t^{n''}}{n'! n''!} \int_{-\infty}^{+\infty} H_{n'}(\eta) H_{n''}(\alpha\eta + \delta) e^{-\eta^2/2} e^{-(\alpha\eta+\delta)^2/2} d\eta \\ = \int_{-\infty}^{+\infty} e^{-s^2+2s\eta-\eta^2/2} e^{-t^2+2t(\alpha\eta+\delta)-(\alpha\eta+\delta)^2/2} d\eta \\ = \left(\frac{2\pi}{\alpha^2 + 1} \right)^{1/2} e^{-\delta^2/2(\alpha^2+1)} e^{[(s^2-t^2)(1-\alpha^2)-2\alpha\delta s+2\delta t+4\alpha s t]/(1+\alpha^2)}. \end{aligned} \quad (10)$$

By expanding the last exponential factor in powers of s and t and then equating the like powers of s and t on both sides of the equation we obtain for the expression for the integral for each value of n' and n'' . Making use of Eqs. (9), Eq. (8) becomes

$$\begin{aligned} \int_{-\infty}^{+\infty} (N_{n'} N_{n''})^{-1} e^{-\eta^2/2} e^{-(\alpha\eta+\delta)^2/2} H_{n'}(\eta) H_{n''}(\alpha\eta + \delta) d\eta \\ = C_s \frac{(n'! n''!)^{1/2}}{2^{(n'+n'')/2}} \sum_{l=0}^{n' \text{ or } n''} \sum_{i=0}^{(n'-l)/2} \sum_{j=0}^{(n''-l)/2} a_{2l} b_{2i} c_{2j} d_{n'-2i-l} e_{n''-2j-l} \end{aligned} \quad (11)$$

⁸ E. Schrödinger, Ann. d. Physik **80**, 486 (1926).

⁹ Courant and Hilbert, Methoden der mathematischen Physik I (Berlin 1924) p. 76.

where

$$C_3 = \left(\frac{h}{2\pi^2 \mu \nu_0' \alpha (\alpha^2 + 1)} \right)^{1/2} e^{-\delta^2/2(\alpha^2+1)} \quad a_{2l} = \frac{1}{l!} \left(\frac{4\alpha}{1 + \alpha^2} \right)^l$$

$$b_{2i} = \frac{1}{i!} \left(\frac{1 - \alpha^2}{1 + \alpha^2} \right)^i \quad c_{2j} = \frac{1}{j!} \left(\frac{-(1 - \alpha^2)}{1 + \alpha^2} \right)^j$$

$$d_{n'-2i-l} = \frac{1}{(n' - 2i - l)!} \left(\frac{-2\alpha\delta}{1 + \alpha^2} \right)^{(n'-2i-l)}$$

$$e_{n''-2j-l} = \frac{1}{(n'' - 2j - l)!} \left(\frac{2\delta}{1 + \alpha^2} \right)^{(n''-2j-l)}$$

and where the upper limit of the first sum is the smaller of n' or n'' and the upper limits of the second and third sums are either the upper or lower figures depending upon whether $n-k$ is even or odd. In order to visualize these terms and to use them in the numerical calculations the smallest ones are given in Table I. The value of the integral for (n'', n') can be obtained from

TABLE I.

n'	n''	Value of the integral (11)
0	0	1
0	1	$(1/2^{1/2})e_1$
0	2	$(1/2^{1/2})[e_2 + c_2]$
1	1	$(1/2)[d_1e_1 + a_2]$
0	3	$(3^{1/2}/2)[e_3 + c_2e_1]$
1	2	$(1/2)[d_1e_2 + c_2d_1 + a_2e_1]$
0	4	$(3/2)^{1/2}[e_4 + c_2e_2 + c_4]$
1	3	$(3/8)^{1/2}[d_1e_3 + c_2d_{11} + a_2e_2 + a_2c_2]$
2	2	$(1/2)[d_2e_2 + c_2d_2 + b_2e_2 + b_2c_2 + a_2d_1e_1 + a_4]$
0	5	$(15^{1/2}/2)[e_5 + c_2c_3 + c_4e_1]$
1	4	$(3^{1/2}/2)[d_1e_4 + c_2d_{1e_2} + c_4d_1 + a_2e_3 + a_2c_2e_1]$
2	3	$(3/8)^{1/2}[d_2e_3 + c_2d_{2e_1} + b_2e_3 + b_2c_2e_1 + a_2d_1e_2 + a_2c_2d_1 + a_4e_1]$
1	5	$(15/8)^{1/2}[d_1e_5 + c_2d_{1e_3} + c_4d_1e_1 + a_2e_4 + a_2c_2e_2 + a_2c_4]$
2	4	$(3^{1/2}/2)[d_2e_4 + c_2d_{2e_2} + c_4d_2 + b_2e_4 + b_2c_2e_2 + b_2c_4 + a_2d_1e_3 + a_2c_2d_{1e_1} + a_4e_2 + a_4c_2]$
3	3	$(3/4)[d_3e_3 + c_2d_{3e_1} + b_2d_{1e_3} + b_2c_2d_{1e_1} + a_2d_{2e_2} + a_2c_2d_2 + a_2b_2e_2 + a_2b_2c_2 + a_4d_1e_1 + a_6]$
2	5	$(15/8)^{1/2}[d_2e_5 + c_2d_{2e_3} + c_4d_2e_1 + b_2e_5 + b_2c_2e_3 + b_2c_4e_1 + a_2d_1e_4 + a_2c_2d_{1e_2} + a_2c_4d_1 + a_4e_3 + a_4c_2e_1]$
3	4	$(3/8)^{1/2}[d_3e_4 + c_2d_{3e_2} + c_4d_3 + b_2d_{1e_4} + b_2c_2d_{1e_2} + b_2c_4d_1 + a_2d_{2e_3} + a_2c_2d_{2e_1} + a_2b_2e_3 + a_2b_2c_2e_1 + a_4d_{1e_2} + a_4c_2d_1 + a_6e_1]$
4	4	$(3/2)[d_4e_4 + c_2d_{4e_2} + b_2d_{2e_4} + b_2c_2d_{2e_2} + b_4e_4 + c_4d_4 + b_4c_4 + a_2d_{3e_3} + a_2b_2d_{1e_3} + a_2c_2d_{3e_1} + a_2c_2b_2d_{1e_1} + a_4d_{2e_2} + a_4c_2d_2 + a_4b_2e_2 + a_4b_2c_2 + a_6d_{1e_1} + a_8]$

$(n'n')$ by interchanging subscripts on "b" and "c" and on "d" and "e", i.e. $a_2b_2c_0d_1e_2$ becomes $a_2b_0c_2d_2e_1$. All coefficients with the subscript zero are equal to unity and are therefore omitted.

III. COMPARISON WITH EXPERIMENT

In the preceding section a formula is developed which allows the matrix elements of the electric moment to be calculated for vibration transitions in symmetrical diatomic molecules. The relative intensities of the bands in the electronic-vibration spectra of these molecules are calculated by squaring the integral (11) and multiplying by the fourth power of the frequency and by the

distribution factor of molecules in the initial state.⁹ It is somewhat difficult to know exactly what frequency to multiply by because the intensity obtained should apply to the sum of all the rotational transitions which have the same vibrational and electronic quantum numbers. If the rotational quantum number in Eq. (4) is set equal to zero then we should expect our calculated intensities to agree with those in the $Q(0)$ branch corresponding to the given electronic and vibrational transition. However, in any case, the changes in the frequencies associated with different vibrational transitions are very small since the change in vibrational energy is very small compared to the change in the electronic energy. Since the frequency factors do not appreciably affect the comparison of the calculated results with experiment, they have been omitted in the tables given below.

It is practically impossible at present to calculate accurately the expected intensity in emission spectra because the distribution factor for the initial state depends not only upon the temperature but also upon the method of excitation and upon whether or not the molecules have reached their initial excited levels by means of a transition from a higher level. It should be possible however, to calculate the relative intensities of those bands which originate from the same initial vibrational level and the emission diagrams should show agreement in the horizontal rows. In absorption spectra it is easily possible to calculate the expected absorption intensity for a given temperature because in this case the distribution factor is merely the appropriate Boltzmann factor. However, when we try to compare the calculated results with experiment we find that the exact temperature or pressure is seldom recorded in absorption spectrum intensity measurements. In the following calculated results no attempt has been made to include the temperature factor because of the uncertainty in the exact temperatures used in obtaining the experimental results. We have calculated the intensities for the first few vibrational levels only (because of the restriction to harmonic oscillations) so that in some cases the temperature distribution will not vary greatly from a uniform distribution and merely the squares of the integral (11) should be in approximate agreement with the experimental results, in other cases, only the agreement in the columns (for absorption) should be considered.

In making the theoretical intensity calculations the values of α and δ are first calculated. The value of α which is given by $(\nu_0''/\nu_0')^{1/2}$ is usually very well known since it comes from an analysis of the vibrational energy levels themselves. The value of α may therefore be determined to within three significant figures. The value of δ depends upon the values of the separations of the nuclei which in turn depend upon the values of the moments of inertia given by the analysis of the rotational spectrum. The values of the nuclear separations thus calculated are usually accurate only to within about 1 percent so that δ which depends upon the difference in the separations in the initial and final states ($\delta = 0.1221 (r_0' - r_0'') (\nu_0'' M)^{1/2}$) is, in general, susceptible to quite large errors. The next step in the calculations

⁹ Cf. A. Sommerfeld, *Ergänzungband*, p. 96.

is to evaluate the coefficients a, b, c, d , and e given after Eq. (11). The triple sum in Eq. (11) is then evaluated which in the highest state ($n'=4, n''=3$) considered, consists of 13 terms. In the diagrams given below the observed and calculated intensities are given in the usual double-entry form. In every case the observed intensities are placed on top and the corresponding calculated ones are given directly underneath them. Each element will be treated in a separate section.

a. Sodium.

The experimental and calculated data for the green absorption band of sodium (Na_2) are shown completely in Fig. 1. It may be seen that here the agreement is rather remarkable, perhaps much better than one would expect

$n' \backslash n''$	0	1	2	3	4
0	² 2.00	⁵ 4.52	⁵ 4.78	⁵ 5.32	⁴ 3.98
1	⁹ 5.82	⁶ 5.00	— 1.22	— 0.04	⁴ 1.32
2	⁸ 7.78	— 0.68	— 1.22	³ 3.26	— 1.70
3	⁶ 6.28	— 1.02	³ 3.26	² 0.40	— 2.38
4	⁵ 3.42	² 4.82	³ 0.60	— 1.53	

Fig. 1. Observed and calculated intensities in the green Na_2 absorption band. The observed values are placed on top.

with the available intensity measurements which are only estimates.¹⁰ The experimental intensities are taken from Fredrickson and Watson.¹¹ The values of the frequencies and of the nuclear separations are taken from Loomis and Wood¹² and give for α and δ the values 1.130 and 2.43 respectively. Fredrickson and Watson give the nonappearance of the bands (1-2), (2-1), (3-1), (2-2) and (1-3) as an especial characteristic of this system and the calculated intensities indicate very definitely the fact that these particular bands should be very faint. The calculated intensities in the positions (1-2) and (2-1) are quite sensitive to changes in the nuclear separations and indeed, when the writer first calculated these intensities, he used the value $r_0' - r_0'' = 0.40 \cdot 10^{-8}$ cm given by Fredrickson and Watson and found complete disagreement with experiment since the values in the positions (1-2) and (2-1) were approximately 12 on the same scale as used in Fig. 1. Later he found that Loomis

¹⁰ The Physical Review Referee has kindly pointed out that since at 1000°K the relative distribution in the initial states $n''=0,1,2,3,4$ is 1.00, 0.80, 0.64, 0.51, 0.41 respectively, the agreement in the top row of Fig. 1 can only be accidental and that the agreement in the columns only should be noticed.

¹¹ W. R. Fredrickson and W. W. Watson, Phys. Rev. **30**, 429 (1927).

¹² F. W. Loomis and R. W. Wood, Phys. Rev. **32**, 223 (1928).

and Wood had pointed out errors in Fredrickson and Watson's analysis and that they gave instead the value $r_0' - r_0'' = 0.33 \cdot 10^{-8}$ cm from which the values given were calculated.

b. Potassium.

Fredrickson and Watson¹¹ give an intensity diagram for the near red potassium absorption band which is very similar to the green band of sodium. However, as was the case with sodium, the nuclear separations which they give ($r_0' - r_0'' = 0.43 \cdot 10^{-8}$ cm) do not give calculated intensities which agree at all with experiment. It is interesting however, that because of the absence of the (1-2) and (2-1) bands and because of the likeness to Na_2 it is possible to estimate the change in the nuclear separation for K_2 . The value of δ which is obtained is almost the same as that for Na_2 and since $(\nu_0'' M)^{1/2}$ is practically identical in both cases the value of $r_0' - r_0''$ can be estimated to be close to the same value as for sodium ($0.33 \cdot 10^{-8}$ cm) although it may possibly be as low as $0.29 \cdot 10^{-8}$ cm. The agreement for only the first few terms when $0.33 \cdot 10^{-8}$ cm is used is shown in Fig. 2. The principle point in favor of the

$n' \backslash n''$	0	1	2
0	3 3.00	8 7.02	9 8.97
1	10 8.64	5 7.68	— 1.80
2	8 11.55	— 1.13	2 1.86

Fig. 2. Observed and calculated intensities in the near red K_2 absorption band. The observed values are placed on top.

argument for the change in separations chosen is that the *only* value, which gives a general agreement throughout all terms, is just the value which reduces the (2-1) and (1-2) terms to a very small value.

c. Iodine.

The iodine spectrum is characterized by the fact that intense bands correspond to changes of very large quantum numbers. Because of this fact it is obvious that we cannot expect to calculate the exact intensities by the integral (11) which is derived on the assumption of harmonic oscillations. We can however, draw important qualitative conclusions from this formula. If we restrict ourselves to the first column, that is, to all bands which result from a transition from the lowest initial vibrational state, we find that the most important term in the theoretical calculation is the d term which has the same index as the vibrational quantum number of the end state n' . The constants given by Mecke¹³ for iodine give $\alpha = 1.300$ and $\delta = 14.9$. Because of the large value of δ we find it is just the d coefficients which are extremely

¹³ Mecke, Handbuch der Physik XXI, p. 547.

large, in fact d_{14} is about 20,000 times d_0 . The values of the coefficients go up rather rapidly to a maximum at d_{14} and then slowly decrease. To calculate the intensities we must square these values of d and multiply by the square of the normalizing coefficient which tends to shift the maximum intensity in the direction of large quantum numbers. It requires therefore no stretch of the imagination to conclude that the first terms will be insignificant with respect to later ones and that observable terms will begin to appear at about $n'=14$ and extend out into the neighborhood of $n'=60$ or more. The appearance of lines in these positions is in agreement with the experimentally observed intensities.

Because of the effect of the Boltzmann distribution factor, there are very few molecules in the higher n'' states so that the absence of transitions starting from the higher n'' levels is explained even though their calculated transition probabilities are large.

d. Hydrogen.

In the absorption spectrum of hydrogen all the transitions have the same initial quantum level ($n''=0$) and we should therefore expect Eq. (11) to give a fairly accurate representation of their intensities. The intensity constants for the hydrogen absorption spectra are obtained from the molecular constants given by Richardson and Davidson¹⁴ and are $\alpha=1.786$ and $\delta=4.45$. The agreement of the calculated intensities with the absorption data given by Dieke and Hopfield¹⁵ is shown in Fig. 3. The agreement in this case is not

n'	0	1	2	3	4	5	6	7	8	9
I_0	2	6	8	5	4	8	3	6	4	6
I_c	1.0	7.2	22.5	38.5	39.0	20.7	4.2	0.02	1.2	0.19

Fig. 3. Observed (I_0) and calculated (I_c) intensities for the ultra-violet absorption spectrum of the hydrogen molecule. The initial vibrational state of all of these transitions is the same.

good although it will be seen that the theoretical calculations give about the right number of bands at least. No explanation of these discrepancies can be given but it must be realized that the intensities are in the extreme ultra-violet where it is very difficult to make accurate absorption estimates. Because of the similarity of the higher wave functions one would expect the intensities of the higher observed bands to become gradually smaller rather than to break off suddenly as is shown in the figure. It may be possible too that the fact that a harmonic oscillator was assumed will explain the discrepancies in the bands at the right of the figure.

Although as was stated earlier, we cannot expect very close agreement between emission spectra and the calculated intensities the emission spectra of the $3^1B \rightarrow 2^1S$ band system of hydrogen shows some interesting points. The notation and constants are taken from Richardson and Davidson¹⁴ and we find $\alpha=0.784$ and $\delta=-1.008$. The experimental values are taken from

¹⁴ A. W. Richardson and P. M. Davidson, Proc. Roy. Soc. A125. 35 (1929).

¹⁵ G. H. Dieke and J. J. Hopfield, Phys. Rev. 30, 400 (1927).

Kapucinsky and Eymers¹⁶ intensity measurements. These measurements are in the visible region and were carefully made by means of a registering microphotometer so that great faith may be had in the results. The experimental and calculated intensities are shown together in Fig. 4. It will be seen in this

$n \backslash n''$	0	1	2	3
0	286 286	95 223	29 41.8	9.1 1.4
1 2	375 137	35.4 42.6	159 257	56 26.9
2	75.2 73.5	395 72.4	5.4 6.6	61 194
3	(8) 32.6	102 88.4	142 10.9	29.3 24.6

Fig. 4. Observed and calculated intensities \bar{I} in the $3'B \rightarrow 2'S$ emission band system of hydrogen. The observed intensities are placed on top.

figure that good agreement is obtained except at the positions in which n changes by ± 1 units. At these positions the intensities are apparently reversed, that is, the one corresponding to a change in n of $+1$ agrees better in every case with the experimental intensity corresponding to a change of -1 in n and vice versa. No explanation of this fact can be given at the present time.

IV. CONCLUSION

On the basis of wave mechanics the intensity of a spectral line is measured by the integral of the product of the electric moment and the wave functions of the initial and of the final states. It is possible to carry this integration through approximately for vibration electronic transitions in symmetrical diatomic molecules. In this way a formula is developed for the intensity of any band in the electronic vibration spectra of these molecules. The intensities of certain spectral bands of Na_2 , K_2 , I_2 , and H_2 are calculated and in some cases rather good agreement with experiment is obtained. It should be noticed that although there are discrepancies in many of the results the general intensity values and the number of lines to be expected agree well with experiment in all cases in spite of the fact that the important constant (depending upon nuclear separations) varies from -1.01 in the $3'B - 2'S$ band of hydrogen to $+14.9$ in the absorption spectrum of iodine.

The writer wishes to express his sincere appreciation to Professor E Schrödinger for many helpful suggestions and for the privilege of using the facilities of the Institut für theoretische Physik at Berlin. The writer wishes also to thank the University of Pittsburgh for a grant which helped to make his stay in Europe possible.

¹⁶ W. Kapucinsky and J. G. Eymers, Proc. Roy. Soc. A122, 58 (1929).

VIBRATIONAL QUANTUM ANALYSIS OF THE POTASSIUM INFRARED ABSORPTION BANDS

BY W. O. CRANE AND ANDREW CHRISTY

RYERSON PHYSICAL LABORATORY, UNIVERSITY OF CHICAGO

(Received June 19, 1930)

ABSTRACT

The heads of the red system of the K_2 molecule have been remeasured, and twenty six new bands have been found. The vibrational constants derived from our measurements are: $\omega_e''=92.64\text{ cm}^{-1}$, $\omega_e''x''=0.354\text{ cm}^{-1}$, $\omega_e'=74.73\text{ cm}^{-1}$, and $\omega_e'x'=0.327\text{ cm}^{-1}$.

The bands of the infrared system of K_2 ($\lambda 7735$ to $\lambda 8850$) have been measured and a new vibrational analysis for this system is given, which removes the objections inherent in the analysis of Ritschl and Villars. The constants for this system, as found by us, are: $\omega_e''=92.64\text{ cm}^{-1}$, $\omega_e''x''=0.354\text{ cm}^{-1}$, $\omega_e'=69.09\text{ cm}^{-1}$, and $\omega_e'x'=0.153\text{ cm}^{-1}$. It is shown that the upper state of each of the two systems dissociates into a normal and a 2P excited atom. The energies of dissociation obtained for the upper levels of the two systems agree to within 0.02 volts, the average value being 2.41 volts. From this average value we obtain for the heat of dissociation of the lower level 0.81 volts, while from the formula $(\omega_e'')^2/4\omega_e'x''$, we obtain 0.75 volts.

THE absorption spectrum of the K_2 molecule thus far investigated contains three band systems: in the blue, $D\leftarrow A^1\Sigma$, ($\lambda 4243$ to $\lambda 4613$), in the red, $C^1\Pi\leftarrow A^1\Sigma$ ($\lambda 6280$ to $\lambda 6925$), and in the infrared, $B^1\Sigma\leftarrow A^1\Sigma$ ($\lambda 7735$ to $\lambda 8850$).

The vibrational analysis of the blue system has been given by Yamamoto^{1,2} The equation of the band heads in terms of half quantum numbers is:

$$\nu = 22970.0 + 61.28(v' + \frac{1}{2}) - 0.24(v' + \frac{1}{2})^2 - 92.54(v'' + \frac{1}{2}) + 0.353(v'' + \frac{1}{2})^2 \quad (1)$$

The red system, $C^1\Pi\leftarrow A^1\Sigma$, was analyzed by Fredrickson and Watson.³ The equation connecting the heads in terms of half quantum numbers is:

¹ H. Yamamoto, Nat. Research Council Japan 5, 146 (1929).

The equation actually given is:

$$\nu = 22954.6 + (61.13n' - 0.24n'^2) - (91.96n'' - 0.32n''^2)$$

The constants for the equation, according to Yamamoto, were obtained by the least square method. However, there must have been some error in the calculation of ω_0'' and $\omega_0'x''$. When the least square method is applied to all the intervals as actually obtained from the heads given in the paper the authors find: $\omega_0''=92.19\text{ cm}^{-1}$ and $\omega_0'x''=0.353\text{ cm}^{-1}$. These values are used in Eq. (1). These corrected values of the constants ω_0'' and $\omega_0'x''$ agree exactly with the constants as derived by the authors from the two other systems.

² See also W. Weizel and U. Kulp, Ann. d. Physik 4, 971 (1930). The analysis of the same system as given by these authors is based on seventeen heads measured by Walter and Barrat, Proc. Roy. Soc. A119, 257 (1928).

³ W. R. Fredrickson and W. W. Watson, Phys. Rev. 30, 429 (1927).

$$\nu = 15377.35 + 74.88(v' + \frac{1}{2}) - 0.30(v' + \frac{1}{2})^2 - 92.35(v'' + \frac{1}{2}) + 0.34(v'' + \frac{1}{2})^2 \quad (2)$$

The infrared system was first photographed by McLennan and Ainslee.⁴ They gave the measurements of nine heads extending from $\lambda 8212$ to $\lambda 8602$. It is mainly with the latter system that this paper deals.

The region of the spectrum from $\lambda 6200$ to $\lambda 8850$ was photographed in the first order of a Rowland concave grating giving a dispersion of 2.632 Å per mm. The vapor was contained in a glass tube 80 cm long heated electrically. The source of light was a 150 watt lamp. In the process of this investigation the heads of the bands of the red system were measured in an attempt to obtain a more accurate equation.

Shortly after this work had begun Ritschl and Villars⁵ published a short note on the vibrational analysis of the infrared system, $B^1\Sigma \leftarrow A^1\Sigma$, giving the following equation, as expressed in half quantum numbers:

$$\nu = 11584.9 + 71.43(v' + \frac{1}{2}) - 0.40(v' + \frac{1}{2})^2 - 91.40(v'' + \frac{1}{2}) + 0.30(v'' + \frac{1}{2})^2. \quad (3)$$

No data or measurements were given in that note and insofar as we know none were given subsequently. This equation has been tested by the authors and, as will be shown later, is probably incorrect.

RESULTS

Red system: In this system twenty six new heads were obtained bringing the total to seventy. These additional bands correspond to transitions involving higher quantum numbers than the bands measured by Fredrickson and Watson.³ With the new measurements the following equation was obtained:

$$\nu = 15377.73 + 74.73(v' + \frac{1}{2}) - 0.327(v' + \frac{1}{2})^2 - 92.64(v'' + \frac{1}{2}) + 0.354(v'' + \frac{1}{2})^2 \quad (4)$$

The new equation is believed to be more accurate since it includes heads of higher quantum numbers than Eq. (2). Table I gives the wave-length and wave-number values for this system. The average observed minus calculated difference is 0.39 cm^{-1} .

Far red system: The far red system contains many more observable heads than the one discussed above. Also, the bands are less clearly differentiated due to the great amount of overlapping throughout the entire system. This overlapping is also responsible for the presence of many faint markings on the plates whose appearance does not show whether they are heads or accidental condensations of lines. In all, two hundred apparent heads have been measured. It is doubtful, however, whether or not all of these are actually heads.

⁴ J. C. McLennan and D. S. Ainslee, Proc. Roy. Soc. A103, 304 (1923).

⁵ R. Ritschl and D. Villars, Naturwiss. 16, 219 (1928).

TABLE I. *Near red system.*

$v' - v''$	$\lambda_{(\text{air})}$ (\AA)	$\nu_{(\text{vac})}$ (cm^{-1})	O-C (cm^{-1})	$v' - v''$	$\lambda_{(\text{air})}$ (\AA)	$\nu_{(\text{vac})}$ (cm^{-1})	O-C (cm^{-1})
11-20	6922.19	14442.31	-0.96	3- 2	6489.03	15406.37	+0.64
10-19	6916.82	14453.53	-0.69	1- 0	6473.91	15442.35	-0.36
9-18	6911.37	14464.93	-0.30	2- 0	6443.15	15516.08	-0.05
8-17	6906.18	14475.80	-0.48	4- 1	6421.26	15568.96	-0.11
7-16	6900.86	14486.96	-0.44	3- 0	6413.03	15588.14	-0.75
6-15	6895.51	14498.21	-0.36	5- 1	6391.61	15641.01	+0.48
5-14	6890.49	14508.74	-1.05	4- 0	6383.67	15660.65	-0.36
4-13	6884.76	14520.82	-0.24	8- 3	6379.80	15670.15	+0.93
9-17	6873.70	14544.18	-0.95	7- 2	6371.53	15690.00	-0.25
8-16	6867.93	14556.40	-0.49	6- 1	6363.22	15710.98	-0.35
7-15	6862.24	14568.47	-0.24	10- 4	6360.99	15716.48	+0.04
6-14	6856.87	14579.89	-0.70	5- 0	6354.55	15732.41	-0.05
5-13	6850.94	14592.55	+0.03	13- 6	6351.42	15740.17	+0.59
4-12	6845.41	14604.40	-0.10	8- 2	6343.33	15760.23	+0.49
9-16	6835.88	14624.67	-1.06	16- 8	6343.33	15760.23	+0.57
8-15	6829.49	14638.33	+0.12	12- 5	6342.19	15763.08	+0.33
7-14	6823.96	14650.00	-0.74	7- 1	6334.63	15781.89	+0.41
6-13	6817.79	14663.47	+0.15	15- 7	6334.63	15781.89	-0.49
5-12	6812.00	14675.93	-0.03	11- 4	6333.90	15783.71	-0.26
4-11	6805.91	14689.06	+0.41	6- 0	6325.99	15803.44	+0.17
3-10	6800.33	14701.13	-0.26	10- 3	6325.03	15805.84	-0.41
5-11	6773.47	14759.42	-0.69	14- 6	6325.03	15805.84	+0.69
4-10	6767.00	14773.52	+0.01	9- 2	6315.90	15828.68	+0.09
3- 9	6760.79	14787.28	+0.32	13- 5	6315.90	15828.68	+0.71
2- 8	6754.68	14800.46	-0.01	8- 1	6307.05	15850.88	-0.09
1- 7	6748.22	14814.64	+0.61	12- 4	6307.05	15850.88	+0.03
4- 9	6728.08	14859.00	-0.07	7- 0	6298.11	15873.40	-0.01
3- 8	6721.19	14874.24	+1.01	11- 3	6298.11	15873.40	-0.39
2- 7	6715.08	14887.75	+0.30	10- 2	6288.51	15897.63	+0.86
1- 6	6708.78	14801.73	+0.02	13- 4	6280.79	15917.16	+0.08
0- 5	6702.38	14815.97	-0.07				
3- 7	6682.39	14860.59	+0.36				
2- 6	6675.79	14875.37	+0.24				
1- 5	6669.22	14890.11	+0.02				
0- 4	6662.51	15005.23	+0.09				
1- 4	6629.84	15079.15	-0.06				
0- 3	6622.81	15095.16	+0.21				
4- 6	6611.62	15120.74	+0.73				
3- 5	6605.11	15135.61	-0.68				
0- 2	6583.37	15185.60	+0.13				
4- 5	6573.06	15209.42	+1.01				
2- 3	6558.45	15243.31	+0.86				
0- 1	6544.13	15276.67	-0.03				
2- 2	6520.02	15333.19	+0.23				
1- 1	6512.58	15350.66	-0.11				
0- 0	6505.08	15368.35	-0.29				

The first step in the investigation was to test the formula of Ritschl and Villars. It was found that a large number of heads could be fitted into this formula if it were modified slightly. It was noticed further that on the basis of the above equation the distribution of the bands within the system was somewhat erratic. The main objections to this formula however were two: (1) the value of ω_e'' , (2) the heat of dissociation derived from their equation for the upper state.

It will be seen that ω_e'' of Eq. (3) differs somewhat from that of Eqs. (1) or (4). Ritschl and Villars did not state the number of heads from which Eq. (3) was derived, but it was thought that when a large number of heads

were included into this system the discrepancy would disappear. Indeed, we have found that the ω_e'' obtained by us, in testing Eq. (3), was 91.92, a difference of 0.72 cm^{-1} from the ω_e'' of Eq. (4), as compared with 1.24 cm^{-1} resulting from the equation as given by Ritschl and Villars. When, however, the value of 92.64 was inserted into Eq. (3) it was found that the deviations were far greater than the experimental accuracy warranted. The heads of the infrared system actually did not fit this modified equation. An attempt was then made to account for the discrepancy by the fact that the theoretical equations are derived for band origins, while in both systems band heads had been used. However with any reasonable assumption as to distance of heads to origins the correction introduced is about 1/100 of the above discrepancy.⁶

The second objection to Eq. (3) is the calculated heat of dissociation of the upper state. It has been assumed that the lowest state of K_2 , $A^1\Sigma$, dissociates into two normal potassium atoms, while the excited state, $C^1\Pi$, dissociates into a normal atom and an excited 2P atom as illustrated in Fig. 1. Birge⁷ using Eq. (2) calculated the heat of dissociation of the upper state as 0.57 volts. From this he derived the heat of dissociation for the lower state as 0.89 volts, by making use of the assumption noted above. Using the more accurate Eq. (4) we obtain for the upper state:

$$A^1\Pi: D' = \frac{(74.73)^2}{4 \times 0.327 \times 8106} = 0.527 \text{ volts} \quad (5)$$

and for the lower state:

$$A^1\Sigma: D'' = \frac{(92.64)^2}{4 \times 0.354 \times 8106} = 0.748 \text{ volts} \quad (6)$$

From Eq. (5) we obtain:

$$H_{\text{red}} = \frac{15377.73}{8106} + 0.527 = 2.424 \text{ volts} \quad (7)$$

where $H = \nu_e + D'$; ν_e being the electronic energy of the system involved and D' the heat of dissociation of the upper level of that system. D'' is not expected to be as accurate as D' since fewer levels are known for the lower state.

Reverting to Eq. (3) of Ritschl and Villars; the lower state of the infrared system is the same as that of the red system i.e., $A^1\Sigma$. Therefore we would expect the upper state to dissociate into one normal and one 2P excited atom, or into a normal atom and an atom with higher excitatoin potential than the atomic 2P state. Calculating D' from Eq. (3) we get:

$$D' = \frac{(71.40)^2}{4 \times 0.40 \times 8106} = 0.393 \text{ volts} \quad (8)$$

⁶ The values of ω_e'' as obtained independently from two different systems by Yamamoto and us agree to within 0.1 percent.

⁷ International Critical Tables, V, 410-418 (1929).

The total energy is:

$$H_{\text{infrared}} = \frac{11584.9}{8106} + 0.393 = 1.822 \text{ volts} \quad (9)$$

as compared with 2.424 volts.

H , as derived from Eq. (9) is too small, and since the first excited state of K is the 2P state, and there is no intermediate atomic state into which the molecule can dissociate the equation necessarily must be wrong. The difference, 0.608 volts, is almost twice as much as D' of Eq. (8) and although

TABLE II. *Far red system.*

$v'-v''$	$\lambda_{(\text{air})}$ (Å.)	$\nu_{(\text{vac})}$ (cm^{-1})	O-C (cm^{-1})	$v'-v''$	$\lambda_{(\text{air})}$ (Å.)	$\nu_{(\text{vac})}$ (cm^{-1})	O-C (cm^{-1})
0-4	8840.82	11308.06	+0.7	10-4	8342.49	11983.54	+1.9
4-7	8834.14	11316.60	-1.0	6-1	8339.84	11988.34	+1.2
3-6	8819.42	11335.54	+0.1	13-6	8331.28	12000.50	+0.2
2-5	8803.14	11355.84	+0.0	5-0	8321.93	12013.29	+1.5
0-3	8773.15	11395.28	-2.0	11-4	8298.35	12047.28	-0.0
4-6	8765.70	11404.97	+1.7	7-1	8294.79	12053.31	-0.8
3-5	8752.92	11421.62	-2.2	14-6	8286.48	12064.52	-0.6
2-4	8735.33	11444.61	-0.1	10-3	8280.21	12073.67	+1.3
6-7	8729.85	11451.81	+1.4	6-0	8275.42	12080.67	+1.6
1-3	8719.74	11465.13	-1.0	13-5	8270.51	12087.83	+0.1
0-2	8702.00	11488.46	+0.7	9-2	8206.70	12093.34	-2.4
4-5	8700.95	11489.85	-1.9	16-7	8259.44	12104.04	-2.1
1-2	8651.79	11555.20	+1.9	12-4	8255.02	12110.51	-2.7
5-5	8650.00	11557.52	-1.7	11-3	8237.91	12135.67	-1.4
0-1	8634.43	11578.41	-0.6	14-5	8226.85	12151.99	-1.5
4-4	8632.00	11581.60	+0.8	10-2	8220.09	12161.99	+0.1
8-7	8629.59	11584.82	+0.8	17-7	8214.24	12170.64	+0.6
3-3	8616.29	11602.74	-0.0	12-3	8192.50	12202.28	-0.2
2-2	8599.15	11625.66	-0.7	8-0	8186.45	12211.94	-0.8
6-5	8599.15	11625.66	-0.8	15-5	8181.49	12219.33	+1.3
1-1	8582.40	11647.80	0.0	11-2	8175.83	12227.80	+0.2
5-4	8582.40	11647.80	-0.5	18-7	8173.15	12231.83	-1.8
9-7	8580.66	11650.90	+0.6	21-9	8160.56	12250.70	+0.6
0-0	8566.30	11670.46	-0.1	20-8	8145.80	12272.90	-0.0
3-2	8549.89	11692.83	-0.4	19-7	8130.74	12295.64	-1.3
6-4	8533.51	11715.30	-0.3	15-4	8122.31	12308.39	+1.3
2-1	8532.50	11716.68	+0.4	11-1	8117.13	12316.26	-2.5
10-7	8532.50	11716.68	+0.3	17-6	8114.36	12320.45	-0.9
1-0	8515.75	11739.72	-0.0	14-3	8107.71	12331.55	-0.9
4-2	8499.51	11762.17	+1.1	16-4	8081.93	12369.90	-1.4
3-1	8483.08	11784.97	+0.5	23-9	8078.32	12375.41	+1.7
10-6	8468.23	11805.60	+1.5	12-1	8071.10	12384.00	-0.0
6-3	8468.23	11805.60	+0.2	19-6	8071.10	12384.00	-0.6
2-0	8468.23	11805.60	-2.6	22-8	8062.89	12399.09	+1.2
9-5	8453.60	11826.03	-0.4	11-0	8054.71	12412.69	+1.9
5-2	8450.75	11830.07	+1.4	20-6	8030.75	12448.77	+1.2
12-7	8438.04	11847.84	+0.3	13-1	8030.75	12448.77	-0.6
8-4	8438.04	11847.84	-1.4	19-5	8014.74	12473.59	+0.6
4-1	8434.47	11852.86	+0.6	21-6	7990.34	12512.48	+2.5
7-3	8419.99	11873.30	+1.0	14-1	7988.33	12514.77	+0.4
3-0	8418.25	11875.69	-0.7	24-8	7985.31	12519.57	-2.1
10-5	8405.84	11893.24	-0.7	17-3	7980.68	12526.84	+1.8
6-2	8403.55	11896.47	+0.6	27-10	7977.78	12531.36	-1.9
5-1	8387.83	11918.80	-1.1	13-0	7972.02	12540.43	+1.3
4-0	8370.62	11943.27	-0.9	23-7	7968.52	12545.97	-1.1
11-5	8359.85	11958.65	+0.4	16-2	7964.36	12552.50	+0.8
7-2	8358.61	11961.10	-1.8	26-9	7961.22	12557.44	-0.6

TABLE II. (Continued)

$v' - v''$	$\lambda_{(air)}$ (Å.)	$\nu_{(vac)}$ (cm ⁻¹)	O - C (cm ⁻¹)
19- 4	7956.88	12564.29	+2.1
22- 6	7952.69	12570.88	-1.8
15- 1	7946.90	12579.80	+1.1
25- 8	7943.48	12585.33	+2.2
18- 3	7942.32	12587.32	-1.3
21- 5	7934.69	12599.57	+1.0
14- 0	7931.11	12605.13	-1.0
24- 7	7929.25	12608.08	-0.6
27- 9	7922.18	12619.21	+0.3
20- 4	7918.90	12625.00	-0.1
23- 6	7911.95	12635.65	+1.0
16- 1	7907.23	12643.18	+0.3
29-10	7900.78	12653.50	-0.5
22- 5	7895.46	12662.00	+1.0
25- 7	7890.22	12670.40	+0.3
24- 6	7873.70	12697.00	+0.6
27- 8	7868.48	12705.45	+0.3
17- 1	7866.53	12708.60	+1.8
29- 9	7848.54	12737.70	-1.9
28- 8	7831.28	12765.80	+0.2
18- 1	7829.07	12769.40	0.0
31-10	7827.66	12771.70	-1.8
20- 2	7807.20	12805.30	-0.1
23- 4	7803.10	12812.20	+0.1
26- 6	7798.83	12818.90	-0.1
29- 8	7793.90	12827.02	+1.1
31- 9	7774.18	12859.60	+0.5
18- 0	7772.80	12816.60	-0.7
21- 2	7768.96	12868.96	-0.0
29- 7	7732.60	12911.60	-1.2
32- 9	7728.30	12918.80	+0.4

the equation from which the heats of dissociation are obtained may be first approximations, we would not expect that the deviations would be so large.

The equation of Ritschl and Villars was therefore abandoned and combinations between the heads were sought so that the ω_e'' derived from this system would be the same, within experimental error, as those obtained from the blue and the red systems. Such combinations were found, resulting in a new analysis in which 119 heads were included. The equation connecting these heads is:

$$\nu = 11683.58 + 69.09(v' + \frac{1}{2}) - 0.153(v' + \frac{1}{2})^2 - 92.64(v'' + \frac{1}{2}) + 0.354(v'' + \frac{1}{2})^2 \quad (10)$$

In this equation the origin and all the constants are different from those given by Ritschl and Villars. The average observed minus calculated value based on this equation is 0.93 cm.⁻¹. Table II gives the heads of the system and their assigned quantum numbers. The remaining 80 heads have been examined carefully and most of them are apparently accidental condensations of lines.

It is seen from Eq. (10) that the constants of the lower state are exactly the same as those of the red and blue systems.

HEATS OF DISSOCIATION

From the upper level of the red system we obtained $H_{\text{red}} = 2.424$ volts. Calculating D' from Eq. (10) we obtain:

$$B^1\Sigma: D' = \frac{(69.09)^2}{4 \times 0.153 \times 8106} = 0.962 \text{ volts} \quad (11)$$

and

$$H_{\text{infrared}} = \frac{11683.58}{8106} + 0.964 = 2.402 \text{ volts.} \quad (12)$$

The values of H as obtained from two different states agree within 1 percent.

From the blue system, we obtain:⁸

$$D' = \frac{(61.28)^2}{4 \times 0.24 \times 8106} = 0.483 \text{ volts} \quad (13)$$

and

$$H_{\text{blue}} = \frac{22970.0}{8106} + 0.483 = 3.311 \text{ volts.} \quad (14)$$

From the equation $H = \nu_{\text{e(mol)}} + D' = D'' + \nu_{\text{(atom)}}$ we obtain for the excitation potential of the atom $\nu_{\text{(atom)}}$:

$$\nu_{\text{(atom)}} = 3.31 - 0.81 = 2.50 \text{ volts} \quad (15)$$

as compared with

$$5^2S - 4^2S = 2.596 \text{ volts}$$

$$4^2D - 4^2S = 2.658 \text{ volts.}$$

The last two values are within the experimental error involved in Eq. (15). It is probable, however, that the upper state of the blue system is also $^1\Sigma$, which upon dissociating gives a normal atom and a 5^2S atom.⁹

Taking H'' as the mean of the two values in Eqs. (7) and (12) i.e. 2.41 volts we find that¹⁰

$$D'' = 0.81 \text{ volts}$$

On the other hand, from the constants of the lower state we obtain:

$$D'' = 0.75 \text{ volts}$$

a difference of only 0.06 volts between the two values.

⁸ These are essentially the same values as given by Yamamoto.

⁹ Professor Mulliken has pointed out that the lowest state of K_2 , (cf. the corresponding state of Na_2), since it is a singlet state, must be $A^1\Sigma_g^+$. The first excited state is $B^1\Sigma_u$, the second $C^1\Pi_u$ while the third is in all probability a $D^1\Sigma_u^+$. g (gerade) = even, u (ungerade) = odd, in the sense of these terms used by Hund.

¹⁰ We have taken $4^2S - 4^2P$ of the K atom to be 1.608 volts.

In Figure 1 the four $U(r)$ curves for the states A , B , C , and D , are drawn using the formula given by Morse.¹¹ r_0 values were obtained by means of the equation given in the same paper, i.e. $\omega_0 r_0^3 = 3000 \times 10^{-24}$.

The heat of dissociation for the normal state of K_2 was obtained by Carelli and Pringsheim¹² from two somewhat similar methods, the values given by them being 0.63 volts and 0.53 volts. Somewhat later Ditchburn¹³ calculated the heat of dissociation as 0.51 volts.

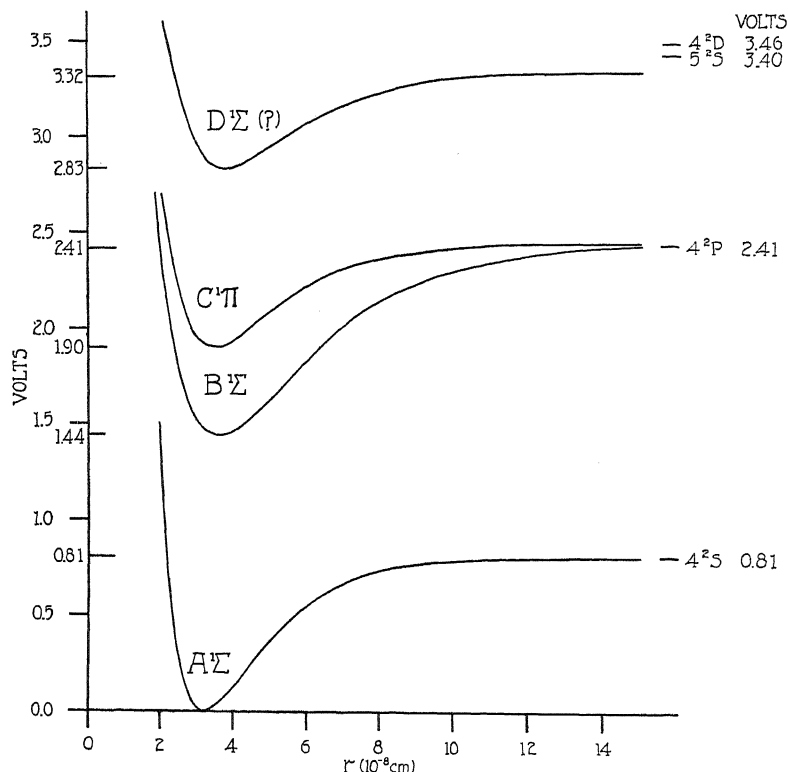


Fig. 1. $U(r)$ curves for the electronic states A , B , C and D .

In the experiment of Carelli and Pringsheim the vapor pressure of the molecules in thermodynamic equilibrium with the atoms was measured at several different temperatures. However the vapor pressure was not directly measured but was assumed to be proportional to the intensity of the band fluorescence produced when white light was passed through the vapor. The experimental errors involved in measuring the blackening of the plate etc. are rather large. Furthermore the heat of dissociation is obtained from the slope of the equation (first method, the second method is exactly analogous) $\log (IT) = f(1/T)$, where I is the intensity of the band fluorescence and T

¹¹ P. R. Morse, Phys. Rev. **34**, 61 (1929).

¹² A. Carelli and P. Pringsheim, Zeits. f. Physik **55**, 643 (1927).

¹³ R. W. Ditchburn, Proc. Roy. Soc. **A117**, 486 (1928).

the absolute temperature. It can be shown easily that this method would not give an accurate value of the heat of dissociation. A very slight change in the slope of the line drawn through their points would give a totally different value for the heat of dissociation. The value 0.75 volts is within their experimental error, and it is actually obtained from one of the four curves given in their paper.¹⁴

In Ditchburn's experiment white light was passed through a tube containing potassium vapor and the wave-length of the maximum in the region of continuous absorption was found. Ditchburn finds a maximum absorption at about 5820Å corresponding to 2.12 volts, and interprets this value as being the sum of the dissociation energy of the molecule in the lower state plus the energy required to excite the atom from the 4^2S to the 4^2P state. Since the latter energy is known accurately, he derives the dissociation energy of the molecule as $D'' = 0.5$ volts. The value obtained by him 2.12 volts, is to be compared with the mean value of H obtained from Eqs. (7) and (12), i.e. 2.41 volts. It should be noted that our value corresponds to a transition from the lowest vibrational state of A (refer to Fig. 1) to the threshold value of dissociation in the two upper states B and C , i.e. 2.41 volts corresponds to dissociation at $T = 0^\circ\text{K}$.

The position of the maximum in the continuum depends upon two factors, first, upon the number of molecules in the lower states from which by absorption of light a molecule dissociates, and second, upon the probability of such transitions. The first factor depends upon the temperature of the absorbing gas, while the second depends upon the shape of the $U(r)$ curves of the states involved, here A and C . It is seen from Fig. 1 that the maximum probability of transitions from A to the threshold value of C is from the vibrational level of A corresponding to an energy of 0.45 volts. However we would expect the number of molecules in this particular level to be less than that of lower vibrational states. Hence the maximum will occur for transitions arising from vibrational levels lower than 0.45 volts.¹⁵ Ditchburn's value indicates that the maximum corresponds to transitions from the vibrational level of 0.3 volts. He does not give the temperature at which this experiment was performed, however we can see from Fig. 1 that in general heats of dissociation obtained by measuring the wave-lengths of the region of maximum absorption from states A to C will be too low.

It is with pleasure that the authors acknowledge their indebtedness to Professor W. W. Watson for suggesting this problem and to Professor R. S. Mulliken for his valuable criticism and advice.

¹⁴ Carelli and Pringsheim, *Zeits. f. Physik* **44**, 645, dotted line of Fig. 2.

¹⁵ See discussion on transition probabilities by R. S. Mulliken, *Rev. Modern Physics* **2**, 78-83 (1930).

THE ROTATIONAL MOTION OF MOLECULES IN CRYSTALS

BY LINUS PAULING

GATES CHEMICAL LABORATORY, CALIFORNIA INSTITUTE OF TECHNOLOGY

(Received May 7, 1930)

ABSTRACT

It is shown by the discussion of the wave equation for a diatomic molecule in a crystal that the motion of the molecule in its dependence on the polar angles θ and ϕ may approach either one of two limiting cases, oscillation and rotation. If the intermolecular forces are large and the moment of inertia of the molecule is large (as in I_2 , for example), the eigenfunctions and energy levels approach those corresponding to oscillation about certain equilibrium orientations; if they are small (as in H_2), the eigenfunctions and energy levels may approximate those for the free molecule, even in the lowest quantum state.

It is found in this way that crystalline hydrogen at temperatures somewhat below the melting point is a nearly perfect solid solution of symmetric and antisymmetric molecules, the latter retaining the quantum weight 3 for the state with $j=1$ as well as the spin quantum weight 3. This leads to the expression

$$S = -n_A R \log n_A - (1 - n_A) R \log (1 - n_A) + n_A R \log 9 + S_{tr},$$

in which S_{tr} is the translational entropy, for the entropy of the solid at these temperatures. At lower temperatures (around 5°K) the solid solution becomes unstable relative to phases of definite composition, and the entropy falls to

$$S = n_A R \log 3 + S_{tr},$$

the entropy of mixing and of the quantum weight 3 for $j=1$ being lost at the same time. Only at temperatures of about 0.001°K will the spin quantum weight entropy be lost.

Gradual transitions covering a range of temperatures and often unaccompanied by a change in crystal structure, reported for CH_4 , HCl , the ammonium halides, and other substances, are interpreted as changes from the state in which most of the molecules are oscillating to that in which most of them are rotating. The significance of molecular rotation in the interpretation of other phenomena is also discussed.

I. INTRODUCTION

THE calculation of the difference in entropy of gaseous molecular hydrogen and crystalline hydrogen has recently been made by Giauque and Johnston.¹ At temperatures between the melting point (14°K) and about 10°K the heat capacity of the solid is well represented by a Debye function with $\beta\nu = 91^\circ$. Assuming the validity of extrapolation to 0°K by means of this function, it is found that the difference in entropy of the solid at 0°K and the gas at standard conditions is 29.7 ± 0.1 E. U. The molal entropy of the gas at standard conditions is given by the Sackur-Tetrode equation as 34.00 E. U., using the band spectrum value of the moment of inertia, and taking into account the symmetry number term ($-R \log 2$), the entropy of mixing of sym-

¹ W. F. Giauque and H. L. Johnston, J. A. C. S. 50, 3221 (1928).

metric and antisymmetric molecules, present in the ratio of $1:3(-1/4 R \log 1/4 - 3/4 R \log 3/4)$, and the nuclear spin quantum weight of the antisymmetric molecules ($3/4 R \log 3$). Thus the molal entropy of ordinary crystalline hydrogen (the metastable mixture of symmetric and antisymmetric molecules in the ratio of $1:3$) at temperatures somewhat below the melting point is found to be 4.3 ± 0.1 E. U. in addition to the translational entropy. In the attempt to account for this deviation from the value zero to be expected from the third law of thermodynamics, it was found necessary to carry through the quantum mechanical discussion of the motion of molecules in crystals.

Before proceeding with this task, it may be illuminating to mention the concept of the motion of a molecule in a crystal which we would form on the basis of classical mechanics. All but six of the degrees of freedom for the molecule can be assigned to represent relative motions of the atoms within the molecule, corresponding to internal oscillations. The six remaining degrees of freedom can be represented by the three coordinates x, y, z of the center of mass of the molecule referred to an arbitrarily chosen set of axes, and the Eulerian angles φ, θ, χ determining the orientation of the molecule with respect to the same axes. In case the forces between atoms in a molecule are much stronger than those between atoms in different molecules, a crystal of the substance may be considered as a first approximation to be a collection of rigid molecules held in a regular arrangement by the rather weak intermolecular forces. Each molecule will remain in the neighborhood of its equilibrium position, the coordinates x, y, z varying through only a small region of values about x_0, y_0, z_0 . Similarly, there will be one or more sets of values of φ, θ, χ for which the potential energy is a minimum, corresponding to equilibrium orientations of the molecule. There are two types of motion then possible for the molecule. If the potential energy for values of φ, θ, χ in the neighborhood of $\varphi_0, \theta_0, \chi_0$ is very small compared with that for other values, the difference being much larger than kT , the average molecule at the temperature T will carry out only small vibrations about its equilibrium orientation. This may be spoken of as oscillation about the equilibrium orientation. But if the potential energy undergoes a total variation smaller than kT , the kinetic energy of the average molecule will suffice to carry it into any orientation, so that the molecule will undergo non-uniform rotation, speeding up as it passes through the equilibrium orientations and slowing down as it goes over the potential maxima. A molecule with a given amount of energy and acted upon by a given potential would according to the classical theory assume a succession of orientations corresponding either to one or to the other of these possibilities, oscillation or rotation.

The introduction of the quantum mechanics does not require this picture to be changed essentially. The allowed states of the system can approximate either of two extremes, oscillation and rotation, or can lie between these extremes, approximating neither more closely than the other. For with the quantum mechanics, in contradistinction to the classical theory, the transition from one extreme to the other is unbroken.

II. THE DIATOMIC MOLECULE IN A CRYSTAL

In Fig. 1 there is shown the structure of the orthorhombic crystal iodine as determined with the use of x-rays.² The atoms are joined in pairs to form molecules by strong shared-electron-pair bonds, and the molecules are

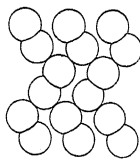


Fig. 1. The arrangement of atoms in one layer in a crystal of iodine. It is seen that the atoms are in groups of two (the molecules I_2) which are oriented by the intermolecular forces.

grouped together in such a way that the figure axis for each assumes a definite orientation. This is the equilibrium orientation, with the polar angle $\theta = 0$, say. The symmetry of the molecule requires that there also be another equilibrium orientation at $\theta = \pi$.

Let us consider a diatomic molecule in such a crystal. As a first approximation we may neglect the translational oscillations of the molecule under consideration and both the translational and rotational motion of the other molecules in the crystal. The wave equation then may be written

$$\nabla^2 \psi + \frac{8\pi^2 I}{h^2} (W - V) \psi = 0, \quad (1)$$

in which I is the moment of inertia of the molecule and $V = V(\theta, \varphi)$ is a potential function representing the averaged interaction of the molecule with surrounding molecules. The simplest form that can be given this function and have it represent a diatomic molecule with two equilibrium orientations is

$$V = V_0(1 - \cos 2\theta), \quad (2)$$

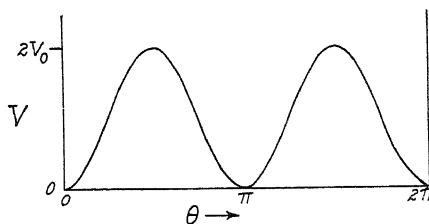


Fig. 2. The potential function $V = V_0(1 - \cos 2\theta)$.

in which V_0 is a constant. This potential function is shown in Fig. 2. The wave equation then becomes

$$\frac{1}{\sin^2 \theta} \frac{\partial^2 \psi}{\partial \phi^2} + \frac{1}{\sin \theta} \frac{\partial}{\partial \theta} \sin \theta \frac{\partial \psi}{\partial \theta} + \frac{8\pi^2 I}{h^2} (W - V_0 + V_0 \cos 2\theta) \psi = 0. \quad (3)$$

² P. M. Harris, E. Mack and F. C. Blake. *I. A. C. S.* **30**, 1583 (1928).

The characteristic value equation in θ obtained from this has not been solved except for limiting cases. The corresponding problem in a plane has, however, been fully treated. If the molecule were restricted to motion in a plane the wave equation would be

$$\frac{d^2\psi}{d\theta^2} + \frac{8\pi^2 I}{h^2} (W - V_0 + V_0 \cos 2\theta) \psi = 0 \quad (4)$$

or, writing

$$\alpha = \frac{2\pi^2 I}{h^2} (W - V_0)$$

$$q = \frac{\pi^2 I V_0}{2h^2},$$

$$\frac{d^2\psi}{d\theta^2} + (4\alpha + 16q \cos 2\theta) \psi = 0. \quad (5)$$

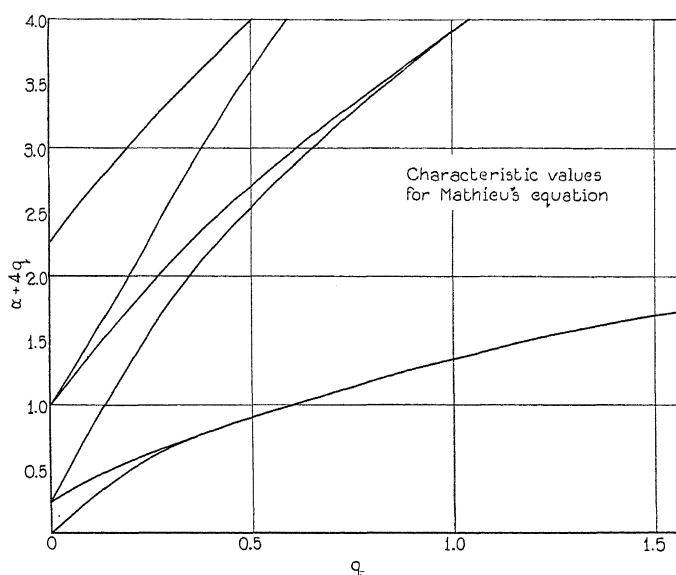


Fig. 3. The characteristic values for the six lowest Mathieu functions.

This equation is Mathieu's equation in the usual form.

The requirement that ψ be periodic in θ with the period 2π leads to the functions known as Mathieu functions.³ These are usually designated by the symbols ce_0 , se_1 , ce_1 , se_2 , ce_2 , etc. The functions and the corresponding characteristic values of α as functions of q have been evaluated by Goldstein.⁴ The energy values for the five lowest states are shown in Fig. 3. It is seen

³ E. Mathieu, *Liouville's Jour.* **13**, 137 (1868); Whittaker and Watson, "Modern Analysis," pp. 404-428. E. U. Condon, *Phys. Rev.* **31**, 891 (1928), pointed out that the Mathieu functions of even order are the eigenfunctions for the plane pendulum.

⁴ S. Goldstein, *Trans. Cambridge Phil. Soc.* **23**, 303 (1927).

that for $q=0$ Eq. (5) reduces to the equation for the plane rotator, with energy levels $W_m = (m^2 h^2 / 8\pi^2 I)$. For q large the eigenfunction ψ is appreciably different from zero only for values of θ close to 0 and π , and approximates a combination of Hermite orthogonal functions, the eigenfunctions for the harmonic oscillator. The energy levels for this case are $(n+1/2) h\nu_0$, in which $\nu_0 = h(2q)^{1/2} / \pi I$. Each energy level shows two-fold degeneracy, the corresponding eigenfunctions being approximately

$$\frac{1}{2^{1/2}} \{ \psi_n \theta / \theta_0 + \psi_n (\theta - \pi) / \theta_0 \} \quad \text{and} \quad \frac{1}{2^{1/2}} \{ \psi_n \theta / \theta_0 - \psi_n (\theta - \pi) / \theta_0 \},$$

in which $\psi_n(\theta/\theta_0)$ and $\psi_n((\theta-\pi)/\theta_0)$ represent Hermite orthogonal functions of the indicated arguments, and θ_0 is given by the equation $h\nu_0/2 = V_0\theta_0^2$.

This can be used as the basis of a perturbation treatment of the problem, using the method of variation of constants,⁵ as in the treatment of aperiodic phenomena.⁶ It is found that in case it were possible to carry out an experiment to determine whether the molecule were undergoing vibrations about $\theta=0$ or about $\theta=\pi$, with the use of a method of investigation involving an interaction unsymmetrical in the two atoms composing the molecule, the probability of observing the molecule in one orientation rather than the other would vary in a way corresponding to the molecule's changing end for end with a frequency given by the separation of adjacent energy levels (ce_0 and se_1 , ce_1 and se_2 , etc) divided by h . Reference to Fig. 3 shows that this frequency is very small for q large, justifying the interpretation of the corresponding states as oscillational states, the molecule oscillating about an equilibrium orientation and changing end for end only rarely. But for q small this frequency becomes large, approaching the principal frequency of motion of the molecule; then we say that the molecule is rotating, its rotation being made somewhat non-uniform through interactions with other molecules. The energy levels in this case approximate those for the free plane rotator, and their behavior for small values of q can be conveniently followed by perturbation methods using the rotator eigenfunctions as zeroth order eigenfunctions.

These considerations, involving a hypothetical investigation of the orientation of the molecule, are, while illuminating, not essential to the discussion of the type of motion of the molecule. We can define the motion of the molecule in a given state as oscillational in case the eigenfunction for that state can be closely approximated by a combination of Hermite functions and the energy of the state is given approximately by $(n+1/2) h\nu_0$. For rotational motion the eigenfunction and energy level should approximate those for a free rotator. This definition is equivalent to that given above: the study of Goldstein's Fourier series representation of the Mathieu functions shows that the transition of the eigenfunctions from approximation to Hermite

⁵ P. A. M. Dirac, Proc. Roy. Soc. A112, 661 (1926); J. C. Slater, Proc. Nat. Acad. 13, 7104 (1927); M. Born, Zeits. f. Physik 40, 172 (1926).

⁶ See the clear exposition given the process of radioactive decomposition by M. Born, Zeits. f. Physik 58, 306 (1929).

functions to approximation to sines and cosines takes place rather sharply at the value of q where the separation of adjacent energy levels becomes appreciable. A similar treatment can be applied to the spatial rotator with two potential minima. The discussion of the qualitative course of the energy levels and the nature of the eigenfunctions is similar to that given above, and a detailed treatment is not needed for our purposes.

III. ROUGH CRITERIA FOR OSCILLATION AND ROTATIONAL MOTION

Let us tentatively assume that the motion is oscillationa. Then we can approximate the lower part of $V(\theta) = V_0(1 - \cos 2\theta)$ by a parabola by expanding in powers of θ and $\theta - \pi$ obtaining $-2V_0\theta^2$ and $-2V_0(\theta - \pi)^2$ as the expansions in the neighborhood of $\theta = 0$ and $\theta = \pi$. These correspond to energy levels

$$W_n = (n + 1)h\nu_0, \quad n = 0, 1, 2, 3, \dots \quad (6)$$

for the two-dimensional harmonic oscillator, with

$$\nu_0 = \frac{1}{\pi} \left(\frac{V_0}{I} \right)^{1/2}. \quad (7)$$

In case that $W_n = (n + 1)h\nu_0$ is less than $2V_0$, the top of the potential hill separating the two-valleys, the molecule will change orientation only rarely. (The exceptional case with V_0 and n small for which there is a large probability of the molecule turning end for end even when its energy is not sufficient to carry it over the hill, is discussed later). But for W_n larger than $2V_0$ the motion will be rotational. Thus we obtain the following criteria:

$$\begin{aligned} n + 1 &< \frac{2\pi(IV_0)^{1/2}}{h}, & \text{oscillational motion,} \\ n + 1 &> \frac{2\pi(IV_0)^{1/2}}{h}, & \text{rotational motion.} \end{aligned} \quad (8)$$

The uncertain quantity of these expressions is V_0 . A rough value for it can be obtained from the observed heat capacity of the solid. If the molecules oscillate about equilibrium orientations the molal heat capacity would be given as a first approximation by the sum of a Debye function of parameter $\beta\nu$, corresponding to the translational oscillations, and twice an Einstein function of parameter $\beta\nu_0 = h\nu_0/k$, with ν_0 the characteristic frequency of Eq. (7). It is found that such a curve does not give a very close fit with observed heat capacities since the model is too greatly simplified; but the heat capacity curve does show that $\beta\nu$ and $\beta\nu_0$ are nearly the same for many substances and a rough value for them can be obtained by taking three times the temperature at which the heat capacity reaches 5 cal/mole degree; that is, half the high-temperature value for five degrees of freedom.⁷ Values of

⁷ This procedure is based on the fact that an Einstein function reaches half its maximum value at the temperature $0.33\beta\nu_0$.

TABLE I.

Molecule	$\beta\nu_0$	Θ	n_0+1	V_0	Heat of fusion and transition
				cal/mole	cal/mole
I ₂	75°	0.053°	350	25000	4000
N ₂	65°	2.33°	7.0	450	222
O ₂	70°	2.06°	8.5	600	306
CO	75°	2.65°	7.1	500	354
CH ₄	55°	8.5°	1.6	90	242
HCl	160°	14.9°	10.7	1700	760
HBr	125°	11.9°	10.5	1300	803
HI	105°	9.2°	11.4	1200	897
H ₂	<135°	82°	<0.4	<56	28

$\beta\nu_0$ for several substances⁸ are given in Table I, together with the characteristic temperature for rotational degeneracy, Θ , which is related to the moment of inertia I (obtained from band spectral data) by the equation

$$\Theta = \frac{h^2}{8\pi^2 I k} \quad (9)$$

The heat capacity of solid hydrogen provides no information regarding $\beta\nu_0$ for H₂. An upper limit for $\beta\nu_0$ can, however, be found in the following way. It is seen that for many substances the total heat change accompanying transitions and fusion is about equal to $V_0/2$ (compare columns 6 and 7 of Table I). Assuming this to hold for H₂, we find $V_0 = 56$ cal/mole, which, from the trend of the ratio $V_0/\Delta H$ with molecular weight, can be accepted as a maximum value. This corresponds to $\beta\nu_0 < 135^\circ$. The approximate constancy of $\beta\nu_0$ in the series I₂, O₂, N₂ suggests a value of this order of magnitude for H₂ also; it and derived quantities are included in Table I.

In terms of $\beta\nu_0$ and Θ the criteria 8 become

$$n + 1 < \beta\nu_0/4\Theta, \quad \text{oscillational motion,} \quad (10)$$

$$n + 1 > \beta\nu_0/4\Theta, \quad \text{rotational motion.}$$

The transition from oscillational to rotational motion should occur for $n = n_0$, with

$$n_0 + 1 = \frac{\beta\nu_0}{4\Theta} \quad (11)$$

Values of n_0+1 are given in Table I. There are also included data for unsymmetric molecules such as HCl. For these a reasonable potential function

⁸ Since these calculations were made some direct verification of them has been provided by the work of L. Vegard (Nature **125**, 14 (1930)) who has obtained spectra from solid nitrogen at very low temperatures involving an electronic transition, a change in oscillation within the molecule, and an additional energy change corresponding to frequencies of 40 cm⁻¹ and 69 cm⁻¹ which he interprets as oscillational jumps for the molecule in the lattice. One of these frequencies probably is the frequency of rotational vibration of the molecule. 40 cm⁻¹ and 69 cm⁻¹ correspond to $\beta\nu_0 = 57^\circ$ and 99° respectively, the first of which is in good agreement with the rough value 65° of Table I.

is $V = V_0(1 - \cos \theta)$, corresponding to an electric dipole in a uniform field. This leads to a transitional value n_0 given by

$$n_0 + 1 = \frac{\beta v_0}{\Theta}. \quad (12)$$

For CO it is doubtful as to whether 11 or 12 is more nearly applicable; the former has been used.

The value $n_0 + 1 < 0.4$ found for H_2 shows that *even in the lowest state* the molecules are rotating freely, the intermolecular forces producing only small perturbations from uniform rotation. Indeed, the estimated $\beta v_0 < 135^\circ$ corresponds to $V_0 < 28 k$, which is small compared with the energy difference $164 k$ of the rotational states $j=0$ and $j=1$, giving the frequency with which the molecule in either state reverses its orientation. The perturbation treatment shows that with this value of V_0 the eigenfunctions and energy levels in all states closely approximate those for the free spatial rotator.⁹

The other extreme is provided by I_2 , for which the transition from oscillation to rotation takes place at about $n = 300$. At the melting point the molecules are in states with $n = 10$ or 15 , so that there are no rotating molecules in this crystal. This agrees with the fact that equilibrium positions for the atoms have been found by x-ray methods.

The remaining substances form intermediate cases, the molecules in lower states oscillating and in higher states rotating. Whether the transition to rotational states takes place in the main before the crystal melts will be considered in Section V.

IV. CRYSTALLINE HYDROGEN AND ITS ENTROPY

In ordinary crystalline hydrogen there are three molecules with $j=1$ for every one with $j=0$. The eigenfunctions for these molecules approximate those for free molecules, namely

$$\begin{aligned} j = 0, \psi_0 &= 1/(4\pi)^{1/2}, \\ j = 1, \psi_1 &= (3/4\pi)^{1/2} \cos \theta, (3/4\pi)^{1/2} \sin \theta \cos \phi, (3/4\pi)^{1/2} \sin \theta \sin \phi, \end{aligned} \quad (13)$$

in terms of angles θ and ϕ relative to an arbitrary coordinate system. These rotating molecules interact with each other as though they were nearly spherically symmetrical.¹⁰ Hence we expect the crystal to have a close-packed structure—cubic close-packed, say, with molecules at 000 , $0\frac{1}{2}\frac{1}{2}$, $\frac{1}{2}0\frac{1}{2}$, $\frac{1}{2}\frac{1}{2}0$. This agrees with the known cubic symmetry of crystalline hydrogen.¹¹ The

⁹ It is worthy of especial mention that in the state with $j=0$ the molecules are to be considered as rotating when V_0 is sufficiently small (less than the separation of the levels $j=0$ and $j=1$) even though the energy of the state ($\sim V_0$) is not sufficient to carry the molecule over the potential maximum ($2V_0$). This is shown by the close approximation of the corresponding eigenfunction to the lowest tesseral harmonic and by the high frequency of end-for-end interchange given by the perturbation treatment, starting with oscillational eigenfunctions.

¹⁰ The forces holding the rotating molecules result from interpenetration of the molecules, as for the noble gases.

¹¹ The observed density 0.0808 at $11^\circ K$ corresponds to a unit with $a = 5.46 \text{ \AA}$, the distance between adjacent molecules being 3.86 \AA .

x-ray investigation of the crystals should not lead to the determination of atomic positions, but only of molecular positions.

In cubic close-packing each molecule is surrounded by twelve others, whose interaction with the central molecule can be represented by a potential function of cubic point-group symmetry in case that the twelve molecules are spherically symmetrical or oriented at random. The energy change produced by this potential function, f say, is

$$W^1 = \int \int \psi \bar{\psi} \sin \theta d\theta d\phi,$$

which is easily shown by the consideration of the symmetry of f to be the same for all four eigenfunctions. Thus a molecule of symmetrical hydrogen, with $j=0$, has in a crystal the same energy as a molecule of antisymmetrical hydrogen, with $j=1$. As a result the two forms of hydrogen should form a complete series of nearly perfect solid solutions, and, moreover, the energy content of the crystal, aside from rotational energy, should be independent of the composition. This has been verified by the measurements of Clusius and Hiller,¹² who found symmetrical hydrogen to have the same heat capacity and heat of fusion as the 1:3 mixture.

Additional experimental verification that molecules of hydrogen in condensed phases are in states approximating those for free molecules is provided by the Raman effect measurements of McLennan and McLeod.¹³ A comparison of the Raman frequencies found by them and the frequencies corresponding to the rotational transitions $j=0 \rightarrow j=2$ and $j=1 \rightarrow j=3$ (Table II) shows that the intermolecular interaction in liquid hydrogen produces only a very small change in these rotational energy levels.

TABLE II.

Transition	Raman effect	Band spectra
$j=0 \rightarrow j=2$	354 cm^{-1}	347 cm^{-1}
$j=1 \rightarrow j=3$	588	578
$0 \rightarrow 1$ in intramolecular oscillation	4149	4159

These considerations permit a calculation of the entropy of crystalline hydrogen at temperatures somewhat below the melting point. Ordinary crystalline hydrogen, consisting of the symmetrical and antisymmetrical forms in the ratio of 1:3, has an entropy of mixing of $-(1/4)R \log (1/4) - (3/4)R \log (3/4)$, for the solid solution can be considered ideal. The symmetrical molecules have a quantum weight 1 in the normal state, with $j=0$, and the antisymmetrical molecules a quantum weight 9, corresponding to the three rotational eigenfunctions for $j=1$, each of which is associated with any one of the three spin eigenfunctions. This gives a predicted total entropy of the solid at temperatures just below the melting point of

$$S_{H_2} = -\left(\frac{1}{4}\right)R \log \left(\frac{1}{4}\right) - \left(\frac{3}{4}\right)R \log \left(\frac{3}{4}\right) + \left(\frac{3}{4}\right)R \log 9 + S_{tr} = 4.39 \text{ E. U.} + S_{tr}, \quad (14a)$$

¹² K. Clusius and K. Hiller, *Zeit. f. phys. Chem.* **B4**, 158 (1929).

¹³ J. C. McLennan and J. H. McLeod, *Nature* **123**, 160 (1929).

in which S_{tr} is the translational entropy. This value is in excellent agreement with the experimental value $4.3 \pm 0.1 + S_{tr}$ of Giauque and Johnston.¹⁴ In general a mixture containing n_A mole-fraction of antisymmetric molecules would have

$$S = -n_A R \log n_A - (1 - n_A) R \log (1 - n_A) + n_A R \log 9 + S_{tr}. \quad (14b)$$

At very low temperatures a separation of the three rotational levels with $j=1$ will take place. This is a second-order effect, depending on the mutual orientation of two or more molecules. As an illustration, let us assume that we could obtain a crystal of pure antisymmetric hydrogen. At temperatures not too near 0°K the molecules would be in cubic close-packing, and an arbitrary molecule could be represented by any one of the three eigenfunctions with $j=1$. But there are possible states of the crystal somewhat more stable than those in which the three rotational eigenfunctions with $j=1$ are represented by random molecules. Thus if each molecule were in the state with $j=1$, $m=0$, corresponding to the eigenfunction $(3/4\pi)^{1/2} \cos \theta$, with θ referred to trigonal axes which for the various molecules are oriented as are the figure axes of CO₂ in crystals of this substance, then the energy of the crystal would be less than that of a crystal in which the three eigenfunctions with $j=1$ were represented at random. In crystalline CO₂ each molecule is surrounded by twelve others, of which the six in the equatorial plane point towards the central molecule, bringing six oxygen atoms to within 3.25 Å, while the other six molecules place oxygen atoms 4.12 Å away. As a result the stable orientation for the central molecule is along the trigonal axis. The distribution function $\psi^2 = 3/4\pi \cos^2 \theta$ for a hydrogen molecule with $j=1$ and $m=0$ shows a tendency for the molecule to line up parallel to the axis $\theta=0$, leading to the decreased energy of the CO₂-similar structure described above. Since this is a second-order effect the energy decrease will be considerably smaller than V_0 , of the order of magnitude of $V_0/5$. With V_0 equal to about 28 k at the most, the temperature at which this structure would become stable relative to the random one would be of the order of magnitude of 5°K.

With other simple ratios of symmetric to antisymmetric molecules other structures might become stable at very low temperatures. Since the energy change depends on the interaction of two antisymmetric molecules, which would drop off very rapidly as the molecules were separated, crystals containing only a small fraction of antisymmetric molecules would be unstable, breaking down into two phases, pure crystalline symmetric hydrogen and crystals with n_A (the mole-fraction of antisymmetric molecules) equal to 1, 1/2, or some other simple fraction. This process, involving diffusion of the molecules, might take some time, so that care would be necessary to insure equilibrium in the study of mixtures with n_A small.

The entropy change accompanying this transition is predicted to be

¹⁴ The possibility of the expression of the entropy of hydrogen as the sum of these terms was first noted by Giauque, who observed that it indicated the formation of nearly ideal solid solutions between symmetrical and antisymmetrical hydrogen and the retention of the quantum weight 9 for the latter.

$$S = -n_A R \log n_A - (1 - n_A) R \log (1 - n_A) + n_A R \log 3 \quad (15)$$

corresponding to the restriction of each antisymmetric molecule to one of the three rotational states with $j=1$, and to the removal of the entropy of mixing of the solid solution existing above the transition temperature.¹⁵ The entropy of the crystals then becomes

$$S = n_A R \log 3 + S_{tr}. \quad (16)$$

The discovery of a transition which we identify with this has been reported by Simon, Mendelssohn, and Ruhemann,¹⁶ who measured the heat capacity of hydrogen with $n_A=1/2$ down to 3°K. They found that the heat capacity, after following the Debye curve down to about 11°K, rose at lower temperatures, having the value 0.4 cal/deg., 25 times that of the Debye function, at 3°K. The observed entropy of transition down to 3°K, at which the transition is not completed, was found to be about 0.5 E.U. That predicted by Eq. (15) for the transition is 2.47 E.U.

In crystals for which n_0 is large, such as iodine, the lowest symmetric and the lowest antisymmetric state have practically the same energy and properties, and each corresponds to one eigenfunction only. As a result a mixture of symmetric and antisymmetric molecules at low temperatures will behave as a perfect solid solution, each molecule having just its spin quantum weight, and the entropy of the solid will be the translational entropy plus the same entropy of mixing and spin entropy as that of the gas. This has been verified for I_2 by Giauque.¹⁷ Only at extremely low temperatures will these entropy quantities be lost.

V. THE TRANSITION FROM OSCILLATIONAL TO ROTATIONAL MOTION

A consideration of the values of n_0 for CH_4 , N_2 , O_2 , and the hydrogen halides indicates that these molecules oscillate at low temperatures but go over mainly to rotational states before the melting point is reached. This process should be accompanied by thermal phenomena, as is shown by the following argument. With $n < n_0$ the eigenfunctions in θ and ϕ change only slightly as n is increased; the probability function $\psi\bar{\psi}$, with maxima in the neighborhood of the equilibrium values of θ and ϕ , falls off rapidly from these maxima, and increase in n causes only some spread, corresponding to larger amplitudes of oscillation. But a radical change takes place as n goes through the transition value. The eigenfunctions change completely in nature, becoming much more nearly constant, as may be verified by a study of the Fourier series coefficients given by Goldstein for the Mathieu functions. This change increases the repulsive forces between molecules, and tends to spread the crystal lattice

¹⁵ The entropy $n_A R \log 3$ arising from the three spin eigenfunctions for antisymmetrical molecules will be lost only at temperatures of the order of magnitude of 0.001°K, at which the very small nuclear interaction energy would become appreciable. It may be pointed out that the magnitude of the interaction energy with other molecules for the three states with $j=1$ as compared with the spin-rotation interaction energy is such as not to permit coupling of j and the spin moment to form a resultant.

¹⁶ F. Simon, K. Mendelssohn, and M. Ruhemann, *Naturwiss.* 18, 34 (1930).

¹⁷ Personal communication.

as soon as an appreciable number of molecules have begun to rotate. But spreading the lattice decreases the forces between molecules and decreases $\beta\nu_0$ and V_0 , so that more molecules can rotate. The effect builds up to give a transition, which often is not accompanied by an essential change in the structure of the crystal. The transition is usually not sharp, but covers a range of temperature of several degrees, and is foreshadowed on the low temperature side by an abnormal increase in heat capacity.

Such a transition is shown by methane.¹⁸ The heat capacity rises rapidly from 18°K to a very sharp maximum (over 48 cal/mole deg.) at 20.4°, and then drops sharply to 4.6 cal/mole deg. at 22.8°. The temperature of transition agrees with the low value (about 1) predicted for n_c . A methane crystal between 20° and 90.6°K (the melting point) would be described as consisting of rotating molecules in cubic close-packing;¹⁹ below 20° the tetrahedral molecules oscillate about equilibrium orientations. It would be very interesting to have Raman effect or infrared spectral data for solid methane; above 20° the lines should very closely approximate the rotation lines for the gaseous molecules, and below that temperature should show pronounced changes, the frequencies of the lines increasing and tending to become constant as the motion approaches harmonic oscillation.

The course of the heat capacity curves also indicates that the transitions shown by N₂ and O₂ at 35.4° and 43.76° respectively are accompanied by the setting in of rotation of the molecules. This is supported by the known crystallographic symmetry of the high temperature forms; nitrogen cubic (indicating cubic close-packing of N₂ molecules) and oxygen hexagonal (indicating hexagonal close-packing).

The gradual transitions shown²⁰ by HCl (at 98°K), HBr (at 89°, 113°, and 117°K), and HI (at 70° and 126°K) are to be given a similar interpretation.²¹ Each of the successive transitions in HBr and HI may be connected with incipient rotation about one crystal axis and the expansion of the crystal along that axis alone. In every case freely rotating molecules would assume a close-packed arrangement (cubic close-packing of molecules has been found with x-rays by Simon and Simson²² for the high temperature form of HCl); on cooling below the temperature at which oscillation sets in the molecules may merely orient themselves, giving a structure similar to that of CO₂, for example, or the orientation may be accompanied by a change of position of molecular centers. That this takes place for HCl is indicated by the low symmetry of the low-temperature form shown by Simon and Simson's powder photographs.

¹⁸ K. Clusius, *Zeits. f. phys. Chem.* **B3**, 41 (1929).

¹⁹ J. C. McLennan and W. G. Plummer, *Phil. Mag.* **7**, 761 (1929), have found that powder photographic data indicate cubic close-packing of the molecules.

²⁰ W. F. Giaque and R. Wiebe, *J. Am. Chem. Soc.* **50**, 101 (1928); **50**, 2193 (1928); **51**, 1441 (1929).

²¹ Giaque and Wiebe suggested essentially this explanation, writing "The results suggest the following possibility: the transition starts as a changing thermal equilibrium between energy states of the hydrogen iodide molecule, both in the same crystal lattice, but when a sufficient concentration of the higher energy state has been reached, the system becomes unstable and changes to a new crystalline form."

²² F. Simon and C. v. Simson, *Zeits. f. Physik* **21**, 168 (1924).

It is predicted that the dielectric constants of solid HCl, HBr, and HI at temperatures just below the melting points will be very high and dependent on the temperature, the values being given by Debye's theory of the orientation of electric dipole molecules; while the low-temperature forms will have low dielectric constants nearly independent of the temperature.

In general it is to be expected that rotational motion of molecules and complex ions of sufficiently low moment of inertia will set in below the melting point of the crystals. This condition of low moment of inertia is satisfied by complexes containing hydrogen atoms and one heavy atom. Thus the forces orienting the tetrahedral ammonium ion in an ammonium salt are much stronger than those acting on a methane molecule, so that the ion will oscillate until a much higher temperature than 20°K is reached; but this temperature of transition to rotational motion is still considerably below the melting point.

The transitions have been observed. Simon²³ and co-workers found from heat capacity measurements that ammonium chloride, bromide, and iodide show a gradual transition covering about a 10° range in the neighborhood 240°K, the nature of the phenomenon not depending essentially on the anion.²⁴ X-ray studies showed the crystal structure to be the same before and after the transition, which is accompanied by a small volume change, less than 1%. These investigators attribute the transition to the ammonium ion, but make no other suggestions as to its nature. The observed phenomena are just those expected to accompany the transition from oscillation to rotation of the ammonium ion, however. The increase in the transition temperature in the series NH₄I (-42.5°C), NH₄Br (-38.0°C), NH₄Cl (-30.4°C) further shows the expected effect of increasing interionic forces accompanying decreasing anion radius.²⁵

The rotation of the ammonium ion in salts at ordinary temperatures provides justification for the customary treatment of the ion as spherically symmetrical in the theoretical discussion of the structure of ionic crystals. Further, the rotation of molecules such as NH₃ and H₂O about symmetry axes accounts for the fact that these molecules occupy positions in crystals with symmetry elements not compatible with those of the non-rotating molecule. Thus in Ni(NH₃)₆Cl₂ the NH₃ molecules lie on four-fold axes, and in alum the H₂O molecules on three-fold axes. The rotation of the molecules,

²³ F. Simon, *Ann. d. Physik* **68**, 263 (1922); F. Simon and C. v. Simson, *Naturwiss.* **38**, 880 (1926); F. Simon, C. v. Simson, and M. Ruhemann, *Zeit. f. phys. Chem.* **129**, 339 (1927).

²⁴ A very small hump in the heat capacity curve at -30° was also found for ammonium fluoride; the interpretation of this is uncertain (the structure of this crystal is not the same as that of the other ammonium halides).

²⁵ Small maxima in the heat capacity curves of organic compounds are probably often due to the transition from oscillational to rotational motion of a part of the molecule. Thus the maxima shown by *o*-xylene, *m*-xylene, and hexamethylbenzene (reported by H. M. Huffman, G. S. Parks and A. C. Daniels, *J.A.C.S.*, **52**, 1547 (1930)) would be attributed to the rotation of the methyl groups, which have a low moment of inertia and can rotate about the single bond holding the group to the rest of the molecule. *p*-xylene shows no maximum, indicating that the orienting forces on the methyl group are larger, raising the transition temperature above the melting point.

however, gives them an effective infinite symmetry axis, which is compatible with these positions.

The possibility of rotation introduces considerable uncertainty in the conclusions reached by Hendricks²⁶ in regard to the nature of the aliphatic carbon chain. From the x-ray study of crystals of the mono-alkyl substituted ammonium halides he found that in a number of these crystals the alkyl ammonium ion lies on a four-fold axis of symmetry, a result which apparently excludes the usual staggered chain of carbon atoms, and which caused him to suggest that the chain really is straight. But the moment of inertia of a staggered chain about an axis along the chain would be very small, and we would expect rotation about this axis at ordinary temperatures, giving the chain an effective infinite symmetry axis, which is compatible with the x-ray data. Accordingly, Hendricks' investigation does not require that the staggered aliphatic chain be given up.²⁷

It has been found by Lyons and Rideal that solid unimolecular films on water of long chain hydrocarbons with polar ends exist in two possible forms, one with an area of 20.6\AA^2 per molecule, and the other, stable at higher temperatures, with an area of 26.2\AA^2 per molecule.²⁸ These authors suggest²⁹ that in the more compact form the staggered chains are interlocked, and fit together more closely than at higher temperatures when interlocking is not effective. This explanation is made somewhat more precise by the application of the considerations discussed in this paper. At low temperatures interlocking does take place, the molecules oscillating about certain equilibrium orientations. With increasing temperature rotation sets in, and the film expands; in this state the molecules would be well represented as circular cylinders with a radius equal to the maximum radius of the staggered chain. The phenomenon is exactly analogous to that giving rise to gradual transitions in crystals.

In molecules C_2X_6 , such as ethane, C_2H_6 , there exists the possibility of the two ends of the molecule rotating or oscillating relative to each other. In case that X is a large atom, as in C_2I_6 , the interaction of the two ends of the molecule will be large, and they will carry out small oscillations about the relative orientation in which the atom groups fit closely together, the six atoms X defining the corners of an octahedron. But in C_2H_6 the interaction of the two ends of the molecule will be small, and they will rotate freely about the single bond connecting the carbon atoms, with a frequency which is simply related to the rotational frequency of the entire molecule about its figure axis. The determination of the energy levels characteristic of this motion for molecules of this type, by means of Raman effect or infrared measurements, would permit the evaluation of the potential energy of the molecule as a function of the relative orientation of its ends.

I acknowledge with gratitude the inspiration and assistance received through conversations with Professor W. F. Giaque of the Chemistry Department of the University of California.

²⁶ S. B. Hendricks, *Zeits. f. Krist.* **67**, 465 (1928); **68**, 189 (1928); additional paper in press.

²⁷ Dr. Hendricks has informed me that he agrees with this conclusion.

²⁸ I am indebted to Professor J. W. Mc Bain for directing my attention to this work.

²⁹ C. G. Lyons and E. K. Rideal, *Nature* **125**, 455 (1930).

DEFLECTION OF ELECTRONS BY A MAGNETIC FIELD ON THE WAVE MECHANICS

BY LEIGH PAGE

SLOANE PHYSICAL LABORATORY, YALE UNIVERSITY

(Received June 26, 1930)

ABSTRACT

The wave equation for a stream of electrons passing through a uniform magnetic field is solved and the characteristic functions discussed. The motion at right angles to the field is found to be completely quantized.

The current density is investigated, and the mean square and mean fourth power radii of curvature found for each quantum state. The mean square radius of curvature is found to be the same for all quantum states of the same energy and identical with that predicted by the classical theory.

The mean radius of curvature is determined by interpolation and is found to be less than that predicted by the classical theory. Therefore values of e/μ calculated by means of the classical formula from measured values of the mean radius of curvature should be too large. The error is estimated and found to be of the same general magnitude as the discrepancy between the results of deflection experiments and those of spectroscopic measurements.

IN his review of the probable values of the general physical constants, Birge¹ gives for the best values of the ratio of charge to rest-mass of the electron:

$$\begin{aligned} e/\mu &= (1.769 \pm 0.002) (10)^7 \text{ abs e.m.u. from deflection experiments,} \\ &= (1.761 \pm 0.002) (10)^7 \text{ " " " from Zeeman effect,} \\ &= (1.761 \pm 0.001) (10)^7 \text{ " " " from H and He spectra.} \end{aligned}$$

The discrepancy between the value obtained from deflection experiments on the one hand and those obtained from spectroscopic evidence on the other is four times the probable error of the former, indicating that the difference is real and not merely the result of accidental errors. Now the value of e/μ obtained from deflection experiments is calculated on the classical electrodynamics, whereas the others are based on quantum theory. Therefore it is important to examine the Schrödinger theory of the motion of a stream of electrons in a uniform magnetic field in order to ascertain whether or not it introduces a correction into the classical formula for the radius of curvature r of the circular path of the electrons about the magnetic lines of force. This problem has been investigated by Alexandrow² on the basis of Dirac's theory. His second order wave Eq (10) differs from the Schrödinger equation which will be used in this paper only in the value of one of the constant coefficients—a difference which is quite negligible for the large energy values which are to be considered. Alexandrow obtains a solution of the wave equation which is everywhere finite and vanishes at infinity, and concludes that the motion is

¹ R. T. Birge, Phys. Rev. Sup. I, 47 (1929).

² W. Alexandrow, Zeits. f. Physik 56, 825 (1929).

not quantized, all values of the energy being allowed. His solution (11) however, contains the factor

$$e^{(k/2)\log(y+iz)} = r^{k/2} \left(\cos \frac{k}{2} \theta + i \sin \frac{k}{2} \theta \right)$$

in plane polar coordinates. Now, one of the requirements of the wave mechanics is that a solution, to be allowed, must be single valued. Therefore it would seem that $k/2$ in Alexandrow's solution must be an integer, and consequently the energy, which is a linear function of k , can assume only discrete values, indicating that the motion is quantized. In fact it will appear that Alexandrow's solution is just one of a multitude of characteristic functions corresponding to a stream of electrons of assigned energy.

SOLUTION OF THE WAVE EQUATION

The wave equation³ for electrons moving through a magnetic field is

$$-\frac{h^2}{8\pi^2\mu} \nabla \cdot \nabla \psi - \frac{eh}{2\pi\mu ic} \mathbf{a} \cdot \nabla \psi + \frac{e^2 a^2}{2\mu c^2} \psi + \frac{h}{2\pi i} \frac{\partial \psi}{\partial t} = 0, \quad (1)$$

where \mathbf{a} is the vector potential. If the field is uniform and in the X direction

$$\mathbf{a} = -j\frac{1}{2}Hx + k\frac{1}{2}Hy,$$

and if we introduce cylindrical coordinates r, θ, x the wave Eq. (1) becomes

$$\begin{aligned} -\frac{h^2}{8\pi^2\mu} \left\{ \frac{1}{r} \frac{\partial}{\partial r} \left(r \frac{\partial \psi}{\partial r} \right) + \frac{1}{r^2} \frac{\partial^2 \psi}{\partial \theta^2} + \frac{\partial^2 \psi}{\partial x^2} \right\} - \frac{ehH}{4\pi\mu ic} \frac{\partial \psi}{\partial \theta} \\ + \frac{e^2 H^2}{8\mu c^2} r^2 \psi + \frac{h}{2\pi i} \frac{\partial \psi}{\partial t} = 0. \end{aligned} \quad (2)$$

Putting

$$\psi \equiv X(x)R(r)e^{-im\theta}e^{-2\pi i(W/h)t},$$

where m must be an integer in order that the solution may be single valued, we are led to the two ordinary differential equations

$$\frac{d^2 X}{dx^2} + \frac{8\pi^2\mu}{h^2} W_x X = 0, \quad (3)$$

$$\frac{d^2 R}{dr^2} + \frac{1}{r} \frac{dR}{dr} + \left\{ \frac{8\pi^2\mu}{h^2} W_{r\theta} - \frac{2\pi eH}{hc} m - \frac{m^2}{r^2} - \frac{1}{4} \left(\frac{2\pi eH}{hc} \right)^2 r^2 \right\} R = 0, \quad (4)$$

W_x being the energy associated with the motion along the lines of force and $W_{r\theta}$ that with the motion in the plane at right angles to the magnetic field.

Equation (3) admits a continuous manifold of allowable solutions⁴ representing a uniform current parallel to the field. Our interest being confined to

³ Condon and Morse, *Quantum Mechanics*, p. 28.

⁴ Condon and Morse, p. 42.

the motion in the plane at right angles to the field, we may put $W_x = 0$, $W_r = W$ without limiting the generality of the solution. Our problem, then, is to find the allowed solutions of (4).

If we put

$$\rho^2 \equiv \frac{2\pi e H}{hc} r^2, \quad w \equiv \frac{4\pi \mu c}{he H} W,$$

(4) simplifies to

$$\frac{d^2 R}{d\rho^2} + \frac{1}{\rho} \frac{dR}{d\rho} + \left\{ w - m - \frac{m^2}{\rho^2} - \frac{1}{4} \rho^2 \right\} R = 0. \quad (5)$$

Making the substitution

$$R \equiv \rho^m e^{-\rho^2/4} V(\rho)$$

in (5), where we are supposing m to be positive, we get

$$\frac{d^2 V}{d\rho^2} + \left(\frac{2m+1}{\rho} - \rho \right) \frac{dV}{d\rho} + (w - 2m - 1)V = 0. \quad (6)$$

This equation can be simplified by changing the independent variable from ρ to x where $x \equiv \rho^2$. Then

$$4x \frac{d^2 V}{dx^2} + 2\{2(m+1) - x\} \frac{dV}{dx} + \{w - 2m - 1\} V = 0. \quad (7)$$

Assuming a series solution of the form

$$V = \sum_p A_p x^p$$

we find on substitution in (7)

$$4p(p+m)A_p = \{2p - w + 2m - 1\}A_{p-1}.$$

Therefore the two independent solutions of the differential equation are ascending series starting with x^0 and x^{-m} , that is, with ρ^0 and ρ^{-2m} . The second is inadmissible since it makes R infinite at the origin. Therefore we have to consider only the series which starts with a constant term. The successive coefficients are related by the equation

$$A_p = \frac{2p - w + 2m - 1}{4p(p+m)} A_{p-1}. \quad (8)$$

If the series fails to terminate, this relation may be written

$$A_p = \frac{1}{2p} A_{p-1}$$

for large values of p . Hence the function V approaches infinity for x infinite in the same way as

$$A_0 \left[\cdots \frac{\left(\frac{x}{2}\right)^p}{p!} + \frac{\left(\frac{x}{2}\right)^{p+1}}{p+1!} + \cdots \right] = A_0 e^{x^2/2},$$

making R become infinite of the order $e^{x^2/4}$. Consequently the only allowable solutions are those for which the series terminates. We see from (8), then, that

$$w = 2s + 1, \quad (9)$$

where s is a positive integer equal to or greater than m . The motion, therefore, is completely quantized, the energy values being

$$W = \left(s + \frac{1}{2}\right) \hbar \left(\frac{eH}{2\pi\mu c}\right), \quad s = 0, 1, 2, \dots \quad (10)$$

The last factor in (10) is just the frequency of revolution about the lines of force predicted by the classical theory.

Putting (9) into (8)

$$A_p = - \frac{(s-m) - (p-1)}{2p(p+m)} A_{p-1}. \quad (11)$$

It is more convenient to express the wave functions in terms of the quantum numbers s and k where $k \equiv s-m$, in place of s and m . The energy is a function of s alone, and for a given s , k may have any of the values $0, 1, 2, \dots, s$. For $k=0$ the polynomial V is a constant, for $k=1$ it consists of two terms, and so on. In terms of s and k (11) becomes

$$A_p = - \frac{k-p+1}{2p(s-k+p)} A_{p-1}$$

giving

$$V_{s,k} = \sum_{p=0}^k \frac{(-1)^p x^p}{2^p p! (k-p)! (s-k+p)!}, \quad k = 0, 1, 2, \dots, s, \quad (12)$$

and

$$R_{s,k} = A_{s,k} X^{(s-k)/2} e^{-x/4} V_{s,k}, \quad k = 0, 1, 2, \dots, s. \quad (13)$$

Alexandrow's solution of the wave equation is $R_{s,0} e^{-is\theta}$.

THE V POLYNOMIALS

Denote differentiation with respect to x by D . Then by differentiating (12) we find

$$V_{s,k} = -2DV_{s,k+1}. \quad (14)$$

Next we easily prove

$$V_{s,k} = \frac{1}{k! s!} x^{-(s-k)} e^{x/2} D^k [x^s e^{-x/2}], \quad (15)$$

which we can put in neater form if we write

$$X_s \equiv x^s e^{-x/2}.$$

Then (15) becomes

$$V_{s,k} = \frac{1}{k!s!} x^k X_s^{-1} D^k X_s. \quad (16)$$

From (14) and (15) we get the recursion formula

$$[2(s-k) - x]V_{s,k} = 2(k+1)V_{s,k+1} + xV_{s,k-1}. \quad (17)$$

The first four V polynomials are

$$V_{s,0} = \frac{1}{s!},$$

$$V_{s,1} = -\frac{1}{2s!} \{x - 2s\},$$

$$V_{s,2} = \frac{1}{2^2 2! s!} \{x^2 - 4sx + 4s(s-1)\},$$

$$V_{s,3} = -\frac{1}{2^3 3! s!} \{x^3 - 6sx^2 + 12s(s-1)x - 8s(s-1)(s-2)\}.$$

On account of (15) the zeros of $V_{s,k}$ between 0 and ∞ are the zeros of $D^k[x^s e^{-x/2}]$. The latter function vanishes at 0 and ∞ for all k 's less than s . Now $x^s e^{-x/2}$ has one turning point (maximum at $x=2s$). Consequently $D[x^s e^{-x/2}]$ has one zero between 0 and ∞ , and as it vanishes at both limits, it has two turning points. This requires $D^2[x^s e^{-x/2}]$ to have two zeros and three turning points and so on. Consequently $V_{s,k}$ has k zeros between 0 and ∞ for any k less than or equal to s . This means that all the roots of the equation $V_{s,k}=0$ are real and positive.

THE RADIAL FUNCTION

In terms of the quantum numbers s and m the differential Eq. (5) for R is

$$\frac{d^2 R}{d\rho^2} + \frac{1}{\rho} \frac{dR}{d\rho} + \left\{ 2s - m + 1 - \frac{m^2}{\rho^2} - \frac{1}{4} \rho^2 \right\} R = 0. \quad (18)$$

If we put $u \equiv \rho^{1/2} R$ this becomes

$$u'' + \left\{ 2s - m + 1 + \frac{1 - 4m^2}{4\rho^2} - \frac{1}{4} \rho^2 \right\} u = 0.$$

Denoting solutions for the same value of m but different values of s by u_{s_1} and u_{s_2} ,

$$2(s_2 - s_1) \int_0^\infty u_{s_1} u_{s_2} d\rho = 0 \quad (19)$$

showing that the u functions are orthogonal.

To normalize these functions we must determine the arbitrary coefficient $A_{s,k}$ in (13) so that

$$\int_0^\infty u_s^2 d\rho = \frac{1}{2} \int_0^\infty R_{s,k}^2 dx = 1, \quad (20)$$

where x , as before, stands for ρ^2 . Squaring (13) and using (15)

$$R_{s,k}^2 = A_{s,k}^2 x^{s-k} e^{-x/2} V_{s,k}^2 = \frac{A_{s,k}^2}{k!s!} V_{s,k} D^k [x^s e^{-x/2}].$$

Integrating by parts, with the aid of (14),

$$\int_0^\infty R_{s,k}^2 dx = \frac{A_{s,k}^2}{k!s!} \int_0^\infty V_{s,k} D^k [x^s e^{-x/2}] dx = \frac{2^{s-k+1}}{k!s!} A_{s,k}^2.$$

To satisfy (20) it is necessary that

$$A_{s,k} = \frac{1}{2^{(s-k)/2}} (k!s!)^{1/2} \quad (21)$$

and the normalized radial function is

$$\begin{aligned} R_{s,k} &= \frac{(k!s!)^{1/2}}{2^{(s-k)/2}} x^{s-k/2} e^{-x/4} V_{s,k} \\ &= \frac{1}{2^{(s-k)/2} (k!s!)^{1/2}} x^{-(s-k)/2} e^{x/4} D^k [x^s e^{-x/2}]. \end{aligned} \quad (22)$$

Also

$$R_{s,k}^2 = \frac{1}{2^{s-k}} V_{s,k} D^k [x^s e^{-x/2}]. \quad (23)$$

THE CURRENT

The quantity actually measured experimentally is the deflection of the current of cathode rays or electrons. The current density⁵ is given by

$$\begin{aligned} j &= \frac{eh}{4\pi\mu i} (\bar{\psi} \nabla \psi - \psi \nabla \bar{\psi}) - \frac{e^2}{\mu c} a \psi \bar{\psi} \\ &= -\frac{e^2 H}{2\mu c} \left\{ 1 + 2m \left(\frac{hc}{2\pi e H} \right) \frac{1}{r^2} \right\} R^2 r \theta_1 \end{aligned}$$

where θ_1 is a unit vector at right angles to r in the direction of increasing θ . It is clear from the form of this expression that the current lines are circles about the lines of force for all values of the quantum number m . The current between cylinders of radii r and $r+dr$ is

$$j_{s,k} dr = -\frac{eh}{8\pi\mu} \left\{ 1 + 2 \frac{s-k}{x} \right\} R_{s,k}^2 dx \quad (24)$$

⁵ Condon and Morse, p. 30.

in terms of the quantum numbers s, k and $x \equiv \rho^2$.

Since the constant factor appearing in (24) is of no significance for our purposes, let us consider the function

$$\begin{aligned} J_{s,k} &= \frac{1}{2} x^{1/2} \left\{ 1 + 2 \frac{s-k}{x} \right\} R_{s,k}^2 \\ &= \frac{1}{2^{s-k+1}} x^{1/2} \left\{ 1 + 2 \frac{s-k}{x} \right\} V_{s,k} D^k X_s \end{aligned} \quad (25)$$

and

$$\begin{aligned} J_{s,k} d(x)^{1/2} &= \frac{1}{4} \left\{ 1 + 2 \frac{s-k}{x} \right\} R_{s,k}^2 dx \\ &= \frac{1}{2^{s-k+2}} \left\{ 1 + 2 \frac{s-k}{x} \right\} V_{s,k} D^k X_s dx. \end{aligned} \quad (26)$$

First we will calculate the total current

$$I_{s,k} = \int_0^\infty J_{s,k} d(x)^{1/2} = \frac{1}{4} \int_0^\infty R_{s,k}^2 dx + \frac{s-k}{2^{s-k+1}} \int_0^\infty \frac{1}{x} V_{s,k} D^k X_s dx$$

corresponding to each normalized quantum state. The value of the first term on the right is $1/2$ from (20). To evaluate the second we note that if we integrate by parts with the aid of (14)

$$\int_0^\infty V_{s,k-p} D^k X_s dx = \frac{1}{2^{k-p} s!} |D^{p-1} X_s|_0^\infty = 0 \quad (27)$$

provided p is an integer greater than zero and less than k . Now, from the recursion formula (17),

$$V_{s,k} = \frac{s-k+1}{k} V_{s,k-1} - \frac{x}{2k} (V_{s,k-1} + V_{s,k-2}). \quad (28)$$

Consequently

$$\begin{aligned} \int_0^\infty \frac{1}{x} V_{s,k} D^k X_s dx &= \frac{s-k+1}{k} \int_0^\infty \frac{1}{x} V_{s,k-1} D^k X_s dx \\ &= \frac{s(s-1) \cdots (s-k+1)}{k! s!} \int_0^\infty \frac{1}{x} D^k X_s dx. \end{aligned} \quad (29)$$

But

$$\begin{aligned} \int_0^\infty \frac{1}{x} D^k X_s dx &= \int_0^\infty \frac{1}{x^2} D^{k-1} X_s dx = \cdots = k! \int_0^\infty x^{s-k-1} e^{-x/2} dx \\ &= k!(s-k-1)! 2^{s-k}, \end{aligned} \quad (30)$$

and

$$\int_0^\infty \frac{1}{x} V_{s,k} D^k X_s dx = \frac{2^{s-k}}{s-k} \quad (31)$$

Therefore the total current corresponding to each normalized quantum state is

$$I_{s,k} = \frac{1}{2} + \frac{1}{2} = 1 \quad (32)$$

independent of the quantum numbers s and k .

We are primarily interested in the radius of curvature r in the magnetic field of a current of electrons of kinetic energy W . From the defining equation for $x \equiv \rho^2$ and (10) we have

$$r^2 = \frac{2\mu c^2 W}{e^2 H^2} \frac{x}{2s+1} \quad (33)$$

which is to be compared with the formula

$$r^2 = \frac{2\mu c^2 W}{e^2 H^2} \quad (34)$$

of classical electrodynamics. In the experiments of Wolf,⁶ which Birge considers to be the most accurate for the determination of e/μ by the deflection method, s is of the order of magnitude of (10)⁸. Hence we are concerned only with states for which s is very large.

$$J_{s,0} \text{ AND } J_{s,1}.$$

Let us examine more closely the current densities $J_{s,0}$ and $J_{s,1}$ of the first two states of energy corresponding to the quantum number s . The first of these is

$$J_{s,0} = \frac{1}{2^{s+1} s!} \left(1 + 2 \frac{s}{x} \right) x^{s+1/2} e^{-x/2}. \quad (35)$$

Its only zeros are at $x=0$ and $x=\infty$. It has one maximum, at $x=2s$. The radius of curvature of the maximum current density, then, is given by

$$r_m^2 = \frac{2\mu c^2 W}{e^2 H^2} \frac{2s}{2s+1} \quad (36)$$

agreeing almost exactly for large s with the classical value (34). The maximum current density is

$$(J_{s,0})_{\max} = \frac{2^{1/2}}{s!} s^{s+1/2} e^{-s} \quad (37)$$

and in the neighborhood of the maximum we have approximately

$$\frac{J_{s,0}}{(J_{s,0})_{\max}} = e^{-(x-2s)^2/8s} \quad (38)$$

⁶ F. Wolf, Ann. d. Physik 83, 849 (1927).

for large s . Consequently the current density falls to $1/e^{\text{th}}$ of its maximum value at a point $\Delta x = 2(2s)^{1/2}$ to either side of the maximum. For $s = (10)^8$

$$\frac{\Delta x}{x_{\text{max}}} = \left(\frac{2}{s}\right)^{1/2} = 2^{1/2}(10)^{-4}$$

showing that the peak is extremely narrow.

The current density of the next state is

$$J_{s,1} = \frac{1}{2^{s+2}s!} \left\{ 1 + 2\frac{s-1}{x} \right\} (x-2s)^2 x^{s-1/2} e^{-x/2}. \quad (39)$$

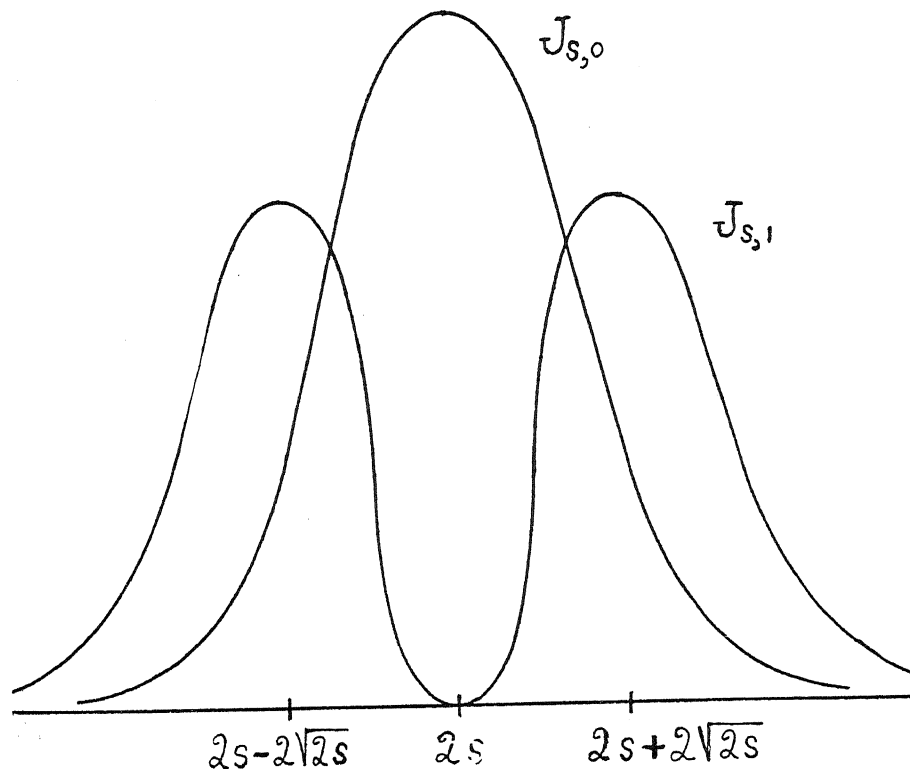


Fig. 1.

Zeros occur at $x=0$, $2s$, and ∞ . There are two maxima, at approximately $x = 2s \pm 2(2s)^{1/2} + 1$. The maximum current densities are approximately the same and equal to

$$(J_{s,1})_{\text{max}} = \frac{2^{3/2}}{s!} s^{s+1/2} e^{-(s+1)}. \quad (40)$$

The graphs of the two functions, $J_{s,0}$ and $J_{s,1}$ are sketched in Fig. 1 for large s , the origin being a great distance to the left of the center of the figure.

Evidently the zeros of $J_{s,k}$ between 0 and ∞ are identical with those of $V_{s,k}$. Thus $J_{s,k}$ has k zeros in this interval.

MEAN RADIUS OF CURVATURE

While the mean radius of curvature of each current cannot be evaluated easily on account of radicals appearing in the integrand, the mean square and the mean fourth power radius of curvature are readily obtained. From (26) and (32)

$$\begin{aligned}\overline{\rho^2} = \bar{x} &= \frac{1}{4} \int_0^\infty \{x + 2(s - k)\} R_{s,k}^2 dx \\ &= (s - k) + \frac{1}{2^{s-k+2}} \int_0^\infty x V_{s,k} D^k X_s dx,\end{aligned}\quad (41)$$

and

$$\begin{aligned}\overline{\rho^4} = \overline{x^2} &= \frac{1}{4} \int_0^\infty \{x^2 + 2(s - k)x\} R_{s,k}^2 dx \\ &= \frac{s - k}{2^{s-k+1}} \int_0^\infty x V_{s,k} D^k X_s + \frac{1}{2^{s-k+2}} \int_0^\infty x^2 V_{s,k} D^k X_s dx.\end{aligned}\quad (42)$$

To evaluate the integrals involved, we have, if we integrate by parts with the aid of (14),

$$\begin{aligned}\int_0^\infty x^p V_{s,k} D^k X_s dx &= \frac{1}{2^k} \int_0^\infty x^p V_{s,0} X_s dx - \frac{k p}{2^{k-1} 1!} \int_0^\infty x^{p-1} V_{s,1} X_s dx \\ &+ \frac{k(k-1)p(p-1)}{2^{k-2} 2!} \int_0^\infty x^{p-2} V_{s,2} X_s dx - \dots\end{aligned}\quad (43)$$

For positive integral values of p the series consists of a finite number of terms. Thus for $p=1$,

$$\begin{aligned}\int_0^\infty x V_{s,k} D^k X_s dx &= \frac{1}{2^k} \int_0^\infty \{x V_{s,0} - 2k V_{s,1}\} X_s dx \\ &= \frac{1}{2^k s!} \left[(k+1) \int_0^\infty x^{s+1} e^{-x/2} dx - 2ks \int_0^\infty x^s e^{-x/2} dx \right] \\ &= 2^{s-k+2} [(k+1)(s+1) - ks] = 2^{s-k+2} (s+k+1).\end{aligned}\quad (44)$$

Hence (41) becomes

$$\overline{\rho^2} = \bar{x} = (s - k) + (s + k + 1) = 2s + 1 \quad (45)$$

independent of the quantum number k . Putting this in (33) we find

$$r^2 = \frac{2\mu c^2 W}{e^2 H^2}, \quad (46)$$

which is identical with the classical formula (34). Hence we conclude that the mean square radius of curvature is the same for all quantum states of the same energy and identical with the square of the radius of curvature given by the classical theory.

Next we shall evaluate (42) for the mean fourth power radius of curvature. In this case we need in addition to (44) the integral (43) for $p=2$. The latter is

$$\begin{aligned} \int_0^\infty x^2 V_{s,k} D^k X_s dx &= \frac{1}{2^k} \int_0^\infty \{x^2 V_{s,0} - 4kx V_{s,1} + 4k(k-1) V_{s,2}\} X_s dx \\ &= \frac{1}{2^k s!} \left[\left(1 + \frac{3}{2}k + \frac{1}{2}k^2\right) \int_0^\infty x^{s+2} e^{-x/2} dx - 2ks(k+1) \int_0^\infty x^{s+1} e^{-x/2} dx \right. \\ &\quad \left. + 2ks(k-1)(s-1) \int_0^\infty x^s e^{-x/2} dx \right] \\ &= 2^{s-k+2} [(k+1)(k+2)(s+1)(s+2) - 2k(k+1)s(s+1) + (k-1)k(s-1)s]. \end{aligned} \quad (47)$$

Consequently (42) becomes

$$\begin{aligned} \overline{\rho^4} &= \overline{x^2} = 2(s-k)[(k+1)(s+1) - ks] \\ &\quad + [(k+1)(k+2)(s+1)(s+2) - 2k(k+1)s(s+1) + (k-1)k(s-1)s] \quad (48) \\ &= (2s+1)^2 + 2(2k+1)(2s+1) + 1. \end{aligned}$$

The mean fourth power of the radius of curvature, therefore, increases with increasing k and is greater than the square of the mean square radius of curvature for all quantum states of a given energy. If we average over all k 's from 0 to s we find

$$\overline{\rho^4} = \overline{\tilde{x}^2} = 8s^2 + 10s + 4. \quad (49)$$

DISCUSSION OF RESULTS

The usual experimental method of measuring the deflection of a stream of electrons by a magnetic field involves the determination of the mean radius of curvature rather than the mean square. On account of the slit or slits used to define the stream, we should expect the greatest number of electrons to be in the states for which k is small, for the increase of spread of J with increase in k would prevent electrons in the higher quantum states from passing through the slit system. In the absence of knowledge of the effect of slit width on the distribution of the electrons, no exact quantitative correction to the classical formula can be given. Certain qualitative conclusions may be drawn, however.

To obtain an estimate of the order of magnitude of the mean radius of curvature of the current for quantum number k we can make use of the known values of $\overline{\rho^0}$, $\overline{\rho^2}$ and $\overline{\rho^4}$. Putting $S \equiv 2s+1$, $K \equiv 2k+1$ we have from (32), (45) and (48)

$$\begin{aligned}\overline{\rho^0} &= 1, \\ \overline{\rho^2} &= S, \\ \overline{\rho^4} &= S^2 \left[1 + 2\frac{K}{S} + \frac{1}{S^2} \right].\end{aligned}$$

If the current distribution were perfectly sharp, we would have

$$\log \overline{\rho^n} = An. \quad (50)$$

If K is small compared to S , the values of $\overline{\rho^0}$, $\overline{\rho^2}$ and $\overline{\rho^4}$ show that the spread of the current is small. Hence we can determine the first order correction to (50) by writing

$$\log \overline{\rho^n} = An + Bn^2$$

and determining the constants A and B to fit the values found for the three means. This gives

$$\overline{\rho^n} = S^{n/2} \left[1 + 2\frac{K}{S} + \frac{1}{S^2} \right]^{n(n-2)/8} \quad (51)$$

Consequently interpolation gives for the mean radius of curvature

$$\begin{aligned}\bar{\rho} &= S^{1/2} \left[1 + 2\frac{K}{S} + \frac{1}{S^2} \right]^{-1/8} \\ &\div S^{1/2} \left[1 - \frac{1}{4} \frac{K}{S} \right].\end{aligned}$$

As this is less than $(2s+1)^{1/2}$ the square of the mean radius of curvature is less than the mean of the square. Hence, as e/μ varies inversely with r^2 , the calculation of e/μ by means of the classical formula will give too large a value of the specific charge of the electron. Therefore the error indicated by theory is of the right sign to explain the discrepancy between the results of deflection experiments and spectroscopic measurements.

To estimate the magnitude of the error we need the mean value of K for the electrons passing through the slit. The spread of the current is given by

$$\Delta\rho^2 = \int_0^\infty J(\rho - \bar{\rho})^2 d\rho = \overline{\rho^2} - \bar{\rho}^2 = \frac{1}{2}K.$$

The quantity $\Delta\rho$ measures the effective distance of the current either side of its mean position. It seems reasonable to infer that half the current passes through the slit when $\Delta\rho/\rho$ is equal to the ratio of the half width of the slit to the radius of curvature. Now the ratio of the half width of the slit to the radius of curvature in Wolf's experiments was 0.04 and s was approximately 1.7(10).⁸ So when

$$\frac{\Delta\rho}{\rho} = \frac{1}{2} \left(\frac{K}{S} \right)^{1/2} = 0.04 \quad \text{or} \quad \frac{K}{S} = 0.0032$$

half the current passes through the slit. Putting $S=3.4(10)^8$, $K=10.9(10)^5$ or $k=5.4(10)^5$. Consequently the ratio of the magnitude of each partial current to that of the next of lower index may be taken to be

$$\alpha = (\frac{1}{2})^{1/5.4(10)^5}.$$

The mean value of K , then, is

$$\bar{K} = \frac{1 + 3\alpha + 5\alpha^2 \cdots + (2s+1)\alpha^s}{1 + \alpha + \alpha^2 \cdots + \alpha^s} = 1 + \frac{2\alpha}{1-\alpha} \frac{1-\alpha^s}{1-\alpha^{s+1}} - \frac{2s\alpha^{s+1}}{1-\alpha^{s+1}}$$

$$\doteq \frac{2}{1-\alpha} = 1.56(10)^6.$$

The error in e/μ is that in $1/\bar{p}^2$, that is, $(1/2)\bar{K}/S$. Hence the order of magnitude of the error is

$$\frac{1}{2} \frac{\bar{K}}{S} = 0.0023.$$

As the actual discrepancy between the results of Wolf's deflection experiments and of spectroscopic observations is 0.0045 ± 0.0011 , we conclude that the error indicated by theory is of the correct order of magnitude as well as of the correct sign to account for the observed discrepancy. In view of the very rough calculation of the mean K , the numerical value obtained above cannot be considered as more than an estimate of the magnitude of the error. The agreement with the observed discrepancy is therefore as good as the method of calculation warrants.

The results of this investigation indicate that in measuring e/μ by the deflection method the classical formula is applicable only if (a) the ratio of slit width to radius of curvature is very small, or (b) the method is one in which the mean square of the radius of curvature is measured. In the latter case it makes no difference in what quantum states the electrons may be, for the mean square of the radius of curvature is the same for all states of the same energy and the value of e/μ is given correctly by the classical formula.

ABSORPTION OF X-RAYS BY LITHIUM

BY K. C. MAZUMDER

LONDON, ENGLAND

(Received May 26, 1930)

ABSTRACT

The mass scattering coefficient of lithium has been measured between the wave-lengths 0.587–0.100Å. The results for the long wave-lengths can be expressed by the equation $\mu/\rho = 0.94\lambda^3 + 0.162$. A very rapid bending of the curve towards the axis λ^3 is noticed below the wave-length 0.2Å.

LITHIUM is the lightest element studied in connection with x-ray absorption. Hewlett¹ worked with it twice but did not carry the investigation down to very short wave-lengths. More recently Mertz² attacked the problem afresh but he too, did not go beyond the wave-lengths used by Hewlett. The shortest wave-length used by Hewlett was 0.314 and that by Mertz 0.32Å. Both of these experimenters were engaged in measuring the scattered rays directly. In the present work, a wider range of wave-lengths, 0.587–0.100Å, was used in measuring in the straight-forward way the total absorption coefficient of lithium. The range of wave-lengths was sufficiently long to show that the absorption by even lithium did not follow the simple law $\mu/\rho = K\lambda^3 + \delta/\rho$ for short wave-lengths.

To prevent oxidation of lithium it had to be placed in an air-tight case the wall of which should not absorb any appreciable amount of rays. The scheme adopted in the present work made it unnecessary to measure by separate experiment the amount absorbed by the wall. A somewhat elliptical hole was cut into a steel rod of desired length. The diameter of the rod was equal to the inner diameter of the brass tube through which rays entered the spectrometer. The major axis of the hole was about two-thirds of the diameter of the rod and twice as much as the diameter of the piece of lithium. On either end of the rod was soldered a thick disk of steel with a hole at the center. One of the holes was sufficiently large to allow the lithium rod to be pushed into it. The other hole was so small as to be completely covered by the piece of lithium when it was in the path of the rays. One of the disks had a much larger diameter than the rod so that when the rest of the rod was pushed inside the brass tube the rays had no openings excepting the smaller hole at the center of the disks to enter the spectrometer. Thin pieces of mica were gummed on either end of the rod after the freshly cut lithium was placed inside. This arrangement was completely air-tight and lithium could be kept inside for weeks without any appreciable amount of oxidation taking place. By simply rotating the steel container through 180

¹ Hewlett, Phys. Rev. 17, 284 (1921); 20, 688 (1922).

² Mertz, Phys. Rev. 28, 891 (1926).

degrees it was possible to place the lithium in or out of the path of the rays. The same mica windows were in the path in both positions, so the correction for absorption by the walls of the container was not necessary.

The lithium used was obtained from Professor Lyman who procured it for his spectroscopic work. Professor Bridgman has samples of the same lithium analysed in connection with his high pressure work, only traces of aluminum were detected, the amount being 0.7 of 1 percent. The correction for aluminum was made by means of the equation $\mu/\rho = 15.5\lambda^3 + 0.147$, representing its coefficient of absorption. This equation was suggested by Professor Duane and the writer.³

The amount of the rays absorbed depending greatly upon the wavelengths it was necessary to use two pieces of lithium of lengths 5.3 cm and 2.9 cm, the former was used for the hard rays and the latter for the comparatively soft rays. The agreement between the results was very satisfactory.

In order to make measurements of the coefficient of absorption, the crystal and the ionization chamber were set in corresponding positions. The steel container with the lithium was placed in the brass tube. It was first kept in a position such that the lithium was out of the path of the rays. The ionization current was observed. The lithium was then placed in the path of rays by rotating the container through 180 degrees. The ionization current was again observed. Both of these readings were corrected for the natural leakage of the instrument and for stray radiations. From these two readings the corresponding mass absorption coefficient was calculated by means of the equation $\mu/\rho = (2.30/d.t) \log I_0/I$, d being the density and t , the length of the piece of lithium.

TABLE I.

λ in A	λ^3	μ/ρ	λ in A	λ^3	μ/ρ
0.587	0.202	0.330	0.368	0.0498	0.208
.535	.1529	.300	.315	.031	.192
.482	.112	.262	.2625	.018	.179
.429	.079	.237	.209	.009	.169
.368	.0498	.206	.185	.0063	.160
.473	.108	.263	.159	.004	.148
.421	.0745	.232	.144	.003	.134
			.102	.001	.114 (?)

The first five readings were taken with the shorter piece of lithium and the rest with the longer piece. The curve in Fig. 1 has been obtained by plotting the mass absorption coefficient against the tube of the corresponding wave-length. It is seen that the curve is not a straight line. It bends downwards in the region of short wave-lengths, the bending being noticeable in the neighbourhood of the wave-length $\lambda = 0.2A$. If the straight part of the curve is produced it cuts the axis at about 0.1625. This according to the theory is the mass scattering coefficient. The value obtained from J. J. Thomson's expression is 0.175, assuming that all the three electrons in the lithium atom scatter freely.

³ Duane and Mazumder, Proc. Nat. Acad. Sci. 8, 45 (1922).

The coefficient of λ^3 is found to be 0.94. The following equation represents approximately the mass coefficient of absorption for comparatively long wave-length

$$\begin{aligned}\mu/\rho &= 0.94\lambda^3 + 0.162 \\ &= 80.5 \times 10^{-3}(N^4/A)\lambda^3 + 0.162\end{aligned}$$

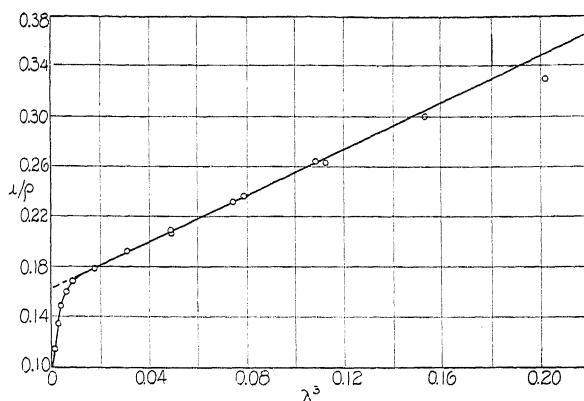


Fig. 1. Mass absorption coefficient plotted against cube of corresponding wave-length.

A and N are the atomic weight and atomic number of lithium respectively.

A slight bending is also noticed in the region of long wave-lengths.

In conclusion the writer wishes to thank Professor Duane for the kind interest he took in the work and for the facilities and suggestions he gave in conducting the experiment. This work was carried out in the Jefferson Physical Laboratory, Harvard University in 1923 but for various reasons it could not be published earlier.

WAVE-LENGTH MEASUREMENTS OF GAMMA-RAYS FROM RADIUM AND ITS PRODUCTS*

BY LUVILLE T. STEADMAN

SLOANE PHYSICAL LABORATORY, YALE UNIVERSITY

(Received June 16, 1930)

ABSTRACT

Wave-length measurements.—The wave-lengths of the gamma-rays in the spectrum of Ra, RaB, RaC, and RaD were determined by the method of crystal diffraction. The rays which experienced diffraction on transmission through a crystal of calcite were received in a Geiger counting chamber which was provided with a slit system that could be turned about a pivot situated at the chamber. By turning the crystal a little so that the diffracted rays were not able to enter the chamber, a method was developed for obtaining the background of the intensity curve and the intensities of the γ -rays, and for investigating the intensity of a possible continuous γ -ray spectrum. Practically all the wave-lengths found by other investigators were obtained and good agreement among all the results was noted. In addition, several other short wave-length γ -rays were found, of which the shortest was 0.42 X.U. Four of them were again determined from measurements made with a diamond which also revealed a γ -ray of wave-length 0.17 X.U.

Intensities of the rays.—In general the changes in intensity from one wave-length to another throughout the spectrum corresponded to those given by other workers, but the intensities of the rays were not found to vary as much.

Continuous spectrum.—A determination of the background of the intensity curve showed that no continuous γ -radiation of any appreciable intensity was present. A more precise measurement made at a wave-length of 53.9 X.U. indicated that a continuous spectrum of γ -rays if existing at all raises the background intensity to less than one tenth the height of the least prominent peaks here found. It has already been concluded from indirect reasoning that the continuous γ -ray spectrum is unimportant.

INTRODUCTION

THERE are several methods by which a rough estimate of the hardness of the gamma-radiation from radioactive elements has been obtained. The quantity which characterizes the hardness has been termed the effective wave-length, and its magnitude is closely associated with the wave-length of some line or lines of strong intensity in the source of the radiation. Kohlrausch,¹ Compton,² and Ahmad,³ have applied the x-ray absorption formula, $\mu = AZ + B\lambda^3 Z^4$, to their work on the absorption of γ -rays and have given λ_{eff} , for the hard γ -rays from RaC to be from 14 to 20 X.U. Similar results were obtained from measurements on the intensity of scattered rays by Owen-Fleming-Fage.⁴ The diffraction of γ -rays by a single atom depends

* Part of a dissertation presented for the degree of Doctor of Philosophy at Yale University.

¹ K. W. F. Kohlrausch, Wiener Ber. 126, IIa, 441, 683, 887 (1917).

² A. H. Compton, "X-Rays and Electrons," p. 390.

³ N. Ahmad, Proc. Roy. Soc. A109, 207 (1925).

upon the interference between the rays scattered by the electrons grouped close together in a heavy atom. Compton² has found $\lambda_{eff.} = 25$ X. U. by this method. He also obtained a value for $\lambda_{eff.} = 16$ X. U. by calculating the wave-length of the scattered rays from their absorption coefficient.

A quantitative investigation of the various wave-lengths in the γ -ray spectrum of a radioactive element was first made by Rutherford-Andrade.⁵ They used a crystal of rock salt to reflect the rays emitted by the disintegration products of radium contained in an emanation tube. The diffracted rays which emerged from the crystal at definite angles depending on their wave-lengths, were detected by their action on a photographic plate. However, the lines found by them belonged for the most part to the spectra of hard x-rays emitted by the atoms in the source after they had been excited by the nuclear γ -rays of high energy value.

The introduction of the counting method to the study of the high frequency γ -radiation from radium and its products by Kovarik⁶ enabled him to find many of the true nuclear γ -rays. The rays, after reflection by a calcite crystal were detected by means of a Geiger counter.

The problem was also taken up by several investigators^{7,8,9,10,11,12} who employed the β -ray spectrum method which makes use of the photoelectric effect of the γ -rays. Ellis-Skinner in particular give values for the wave-lengths of some twenty-two γ -rays of nuclear origin in RaB+RaC. In addition, relative intensities have been assigned to the lines. The theory in connection with this has been developed by Ellis-Wooster.¹³ They have taken into account the observed intensities of the β -ray groups as indicated by the photographic plate and also the probability of conversion of the γ -rays into β -rays. However, their method for obtaining the wave-lengths and the intensities of the γ -rays is not considered to be as direct and straightforward as that of crystal diffraction.

Recently, Frilley¹⁴ has made some experimental improvements in the method of Rutherford-Andrade and has been able to extend the measurements by means of photographic registration of the γ -rays. He has identified a large number of the wave-lengths obtained by the β -ray spectrum method. Great difficulty has always been experienced when trying to use the photographic plate to find rays of very short wave-length on account of the large quantity of primary radiation coming from the source. A general back-

⁴ E. A. Owen, N. Fleming, W. E. Fage, Proc. Phys. Soc. London **36**, 355 (1924).

⁵ E. Rutherford and E. N. daC. Andrade, Phil. Mag. [6] **27**, 854 (1914), [6] **28**, 263 (1914).

⁶ A. F. Kovarik, Phys. Rev. [2] **19**, 433 (1922).

⁷ E. Rutherford, H. Robinson and W. F. Rawlinson, Phil. Mag. [6] **28**, 281 (1914).

⁸ C. D. Ellis and H. W. B. Skinner, Proc. Roy. Soc. **A105**, 60 (1924).

⁹ C. D. Ellis and W. A. Wooster, Proc. Camb. Phil. Soc. **22**, 849 (1925).

¹⁰ O. Hahn and L. Meitner, Zeits. f. Physik **26**, 161 (1924).

¹¹ J. Thibaud, C. R. **179**, 1322 (1924), Journal de Physique [6] **6**, 82 (1925).

¹² L. F. Curtiss, Phys. Rev. [2] **27**, 257 (1926).

¹³ C. D. Ellis and W. A. Wooster, Proc. Camb. Phil. Soc. **22**, 595 (1925), Phil. Mag. [6] **50**, 521 (1925), Proc. Camb. Phil. Soc. **23**, 717 (1927).

¹⁴ M. Frilley, C. R. **186**, 137 (1928), Ann. de Physique [10] **11**, 483 (1929).

ground of stray and scattered radiation also makes it hard to distinguish very weak lines.

The general consensus of opinion thus far has been that there is no continuous spectrum for the γ -rays. This view has been arrived at on consideration of the results of several experiments including the counting by Kovarik¹⁵ of the number of γ -rays from RaB to RaC per atom disintegrating, the study of the intensities in the β -ray spectra by Gurney,¹⁶ the measurements by Ellis-Wooster¹³ on the heating effect of the γ -rays from RaB + RaC, and all the work mentioned above on the γ -ray wave-lengths and their intensities. It was concluded that the energy given off in the heating effect when the rays were absorbed in a suitable material could just about be accounted for by the total energy of all the monochromatic rays observed. There was no necessity for postulating a quantity of energy in the form of a continuous radiation. Because of the indirect method of measurement however it has usually been considered that there has been as yet no real proof either for or against the existence of a continuous spectrum.

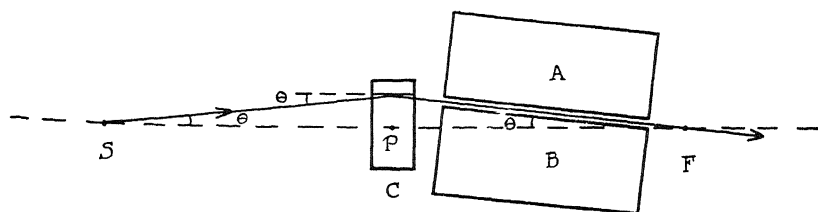


Fig. 1A. Crystal set.

In view of this fact and in particular because the lines determined by the β -ray spectrum method had not been completely checked by any crystal diffraction method, and in addition because some of the lines found by one observer had not been found by others, it was considered advisable to continue the investigation of these problems using the counting method. The experimental method used in the present measurements differed from that devised by Kovarik principally in the fact that diffraction of the rays was accomplished by transmission through a crystal instead of by reflection from the surface planes. The crystal was not rotated. Consequently there was one less experimental quantity to be determined and the range of the instrument in the direction of short wave-lengths was increased. The author was able to check nearly all the wave-lengths found before and to extend the measurements to several new γ -rays of very short wave-length. Additional direct evidence was obtained which supports the view of the non-existence of a continuous spectrum of any appreciable intensity. The intensity values found for the γ -rays are more or less in agreement with the results of other observers.

¹⁵ A. F. Kovarik, Phys. Rev. [2] **23**, 559 (1924).

¹⁶ R. W. Gurney, Proc. Roy. Soc. **A112**, 380 (1926).

EXPERIMENTAL METHOD

The diffraction of a single γ -ray is represented in Fig. 1A. S is a point source of the rays situated on the line SPF which may be considered as a line of reference. The crystal C is placed so that one set of its (1 0 0) planes is parallel to this line and perpendicular to the page. Then, a γ -ray of wave-length λ , coming from S and making an angle θ with the crystal planes, may undergo diffraction during transmission through the crystal, and if so the diffracted ray will pass over the point F . It can be shown from simple geometrical considerations that $FP = PS$ where P is a point at the center of the crystal. Such a ray must satisfy the Bragg formula for diffraction,

$$n\lambda = 2d \sin \theta$$

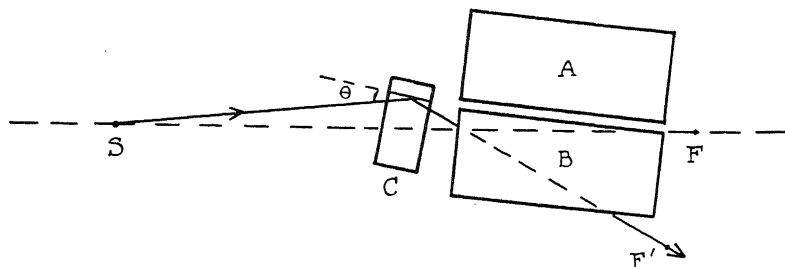


Fig. 1B. Crystal turned.

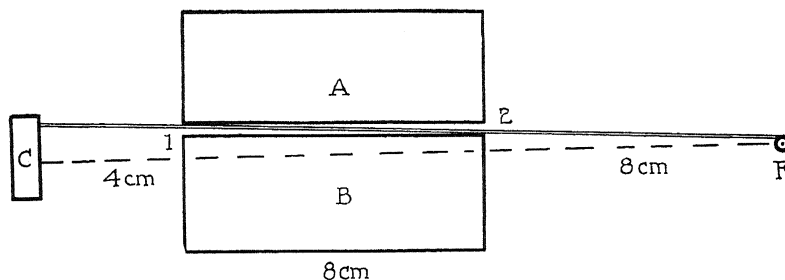


Fig. 1C. Diagram showing that the beam of monochromatic rays which passes into the counting chamber may have a width less than that of the slit.

where n is an integer, d the grating space, λ and θ the wave-length and angle of diffraction respectively. As the angles of diffraction concerned with here are all very small it is sufficient to use the formula $n\lambda = 2d\theta$. Furthermore, the cylindrical source that is used has a definite length and diameter and emits a great many rays in all directions; diffraction therefore will be possible for rays of all wave-lengths provided they are incident at the proper angle θ , and they will pass through the image of the source at F . The lead blocks A, B are shown in positions to form a deep slit or channel through which the rays may pass.

If a detector of γ -rays such as a Geiger counter is placed at F , the impulses which are counted will be due to several types of radiation. A considerable

number of γ -rays may pass right through the lead blocks A , B and come either from the source S or from sources of penetrating radiation in the neighborhood. The rays which pass through the deep slit may be diffracted γ -rays satisfying the above expression, rays which are scattered by the crystal and other parts of the apparatus, and also high speed electrons. At very small angles there will be, in addition, a considerable amount of direct radiation coming through the slit system from the source. If the axis of the slit passes through F and makes the angle θ with FPS the γ -rays diffracted at an angle θ are transmitted without absorption. The slit system is pivoted at F .

In Fig. 1B the crystal is shown turned through an angle of a few degrees about an axis perpendicular to the page. The conditions relating to the absorption and scattering by the crystal remain essentially the same for the two cases. Thus it is readily seen that by taking a γ -ray count for both positions of the crystal, one can obtain the background of the spectrum and the intensities of the γ -rays.

APPARATUS

The gamma-ray spectrometer was constructed as shown in Fig. 2. The base plate A , 24 in. by 8 in., was of cast iron and had strengthening ribs on the bottom. The lead blocks used to shield the source at S and to form

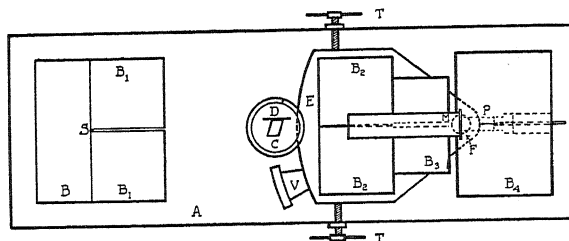


Fig. 2. Gamma-ray spectrometer.

the two slit systems were all 15 cm in height and about 8 cm thick, thickness being measured always in a direction along the axis of the instrument. The two blocks B_1 , B_1 placed about 3 mm apart were used to limit the angular width of the incident beam. The spectrometer rested on a stone pier.

The source of γ -radiation was a preparation of radium salt containing 5.002 mg of radium together with its disintegration products. The glass container was 7 mm long and about 1.5 mm inside diameter and, protected by its thin silver casing, was supported so that its long dimension was in the vertical direction. The experiments were concerned mainly with nuclear rays. Since therefore it was desirable to have as few hard x-rays as possible, no other absorbing material was placed between the source and the crystal.

The crystal holder of a Bragg x-ray spectrometer was used to support the crystal and to orientate it in its proper position. The calcite crystal was 7 mm thick, 10 mm wide, and 25 mm high. It was placed with one of its

faces in contact with the plate *D*. The vertical axis of the crystal holder together with the center of the source and the middle of the pivot determines the axis of the instrument. *D* was adjusted parallel to this by means of a straight edge. By turning the holder a little so that the horizontal peg in its edge was no longer in contact with the peg in the grooved disk beneath, the position illustrated in Fig. 1B was obtained. The distances between *S* and *C* and between *C* and *F* were each 20 cm.

A diamond crystal was also used to measure the shortest wave-lengths. Its dimensions were: height 9 mm, width 4 mm, and thickness 2.5 mm. The orientation of the (1 0 0) planes was determined by means of a goniometer. The grating space for the (1 0 0) planes in calcite is given as $3.0288 (10^{-8})$ cm. In the case of the diamond the 4th order reflection was the one used as the (1 0 0) planes give no 1st, 2nd, or 3rd order. For diamond $1/4$ of d_{100} is $0.885 (10^{-8})$ cm.

The steel plate *E* carrying the slit system could be turned in either direction about the 0.5 inch pivot by means of two small pitch screws. Its zero position with respect to the axis of the spectrometer was determined by the scale and vernier. The angular positions of the slit system, however,

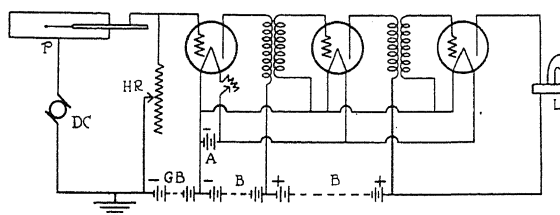


Fig. 3. Geiger counter and amplifier.

were measured by means of a lamp and transparent scale fastened to the wall at a distance of 286.48 cm from a lens and mirror *M*. The scale was accurately ruled in millimeters and one could estimate to 0.1 mm which corresponds to an angle of 3.600 sec. of arc. Since the angles to be measured were very small, the 0.2 mm distance corresponding to 7.200 sec of arc was taken as the unit of angular measurement. A lead plug 3 mm thick inside the slot cut through *B*₃ prevented high speed electrons from entering the counting chamber.

The counting chamber consisted of a brass cylinder 13 mm in diameter and 5 cm long with a 3 mm aluminum front, cast in the center of the lead block *B*₄ which was insulated from the base and to which the positive high potential connection was made. In especially damp weather dry dust free air was introduced into the chamber before counting. The potential necessary for operating the Geiger counter was supplied by a 3000 volt motor-generator set operating on 100 volts from a storage battery. The output was found to be very steady and constant to within 10 volts.

The electrical counting apparatus was essentially the same as that used by Kovarik.¹⁷ Similar arrangements have been used by others for counting

¹⁷ A. F. Kovarik, Phys. Rev. [2] 13, 273 (1919).

purposes. Fig. 3 is a schematic diagram of the electrical circuit. A loud speaker was used in the output circuit and the sharp clicks heard from it, one for each discharge in the chamber, were counted by a hand tally.

Platinum ball points about 0.003 inch in diameter were found to be very satisfactory. A point was made by melting one end of a half-inch piece of 0.001 inch hard drawn platinum wire in a very tiny gas-oxygen flame. As an indication of their practicability it may be said that throughout the experiments only about eight good points were used, and that with them somewhat more than two million γ -rays were counted.

PROCEDURE

The adjustment of the slit system was accomplished by placing one of the blocks B_2 on the carriage before the other and bringing its slit face into line with the axis of the spectrometer by means of a straight edge. The width of the slit formed by the two blocks was changed by moving the second block and inserting various thicknesses of paper between them, after which the paper was removed.

In general, the experimental procedure was to count the number of γ -ray impulses in a period of 20 minutes for each successive angular position of the slit, in order to obtain a curve of intensity plotted against angular measurement for the whole beam of diffracted rays. The slit system was always moved in the same direction in the course of a series of measurements. In each series a large portion of the spectrum was investigated.

In the preliminary work of measuring the wave-lengths the slit system was realigned several times and adjustments of the slit width and orientation of the crystal were made in order to obtain the best results. The positions D_1 and $-D_2$ of the peaks on either side of the zero were found for a number of wave-lengths. These positions were correlated in pairs and the mean zero of the spectrum determined from the average of $(D_1 - D_2)/2$ for all wave-lengths and used as a basis for further measurements.

The results showed that two diffracted rays could be completely resolved if their angular separation was about 20 sec of arc, corresponding to a difference in their wave-lengths of about 0.6 X.U. Calculation showed however, that for the smallest slit width, 0.126 mm, all the diffracted rays in a beam of at least 5 minutes angular width could pass through the slit and enter the counting chamber. Accordingly, the reasonable assumption was made that the slit must not be in perfect alignment with the image of the source, and in Fig. 1C is shown the manner in which a narrow beam of monochromatic rays from the crystal was assumed to pass through the slit.

Several experiments were performed later which confirmed this view. With the diamond crystal, no peaks could be found when the width of the slit was decreased from 0.126 to 0.063 mm, and also when the width at end 1 was increased to 0.126 again, the width at end 2 remaining 0.063 mm. But when the width at end 2 was made 0.126 and that at end 1 was changed to 0.063 the peaks reappeared. Furthermore, with the calcite crystal and a width of 0.19 mm, the peak at 35 X.U. was found again when the width

at end 1 was reduced to 0.126 mm, but the peak disappeared when end 2 of block *B* was moved the small distance 0.025 mm toward *A*. The position of *A* on the carriage was left unchanged throughout all the experiments. In order to calculate the resolving power, the position of the image of the source with respect to the pivot and the slit system must be known. Assuming their relative positions to be as shown in the figure, the two experiments indicated that two γ -rays could be resolved in the first case if their angular separation was about two minutes of arc and in the second case if the separation was less than one minute.

In the wave-length measurements it was found necessary to use three different slit widths, namely, 0.126, 0.19, and 0.38 mm. For angles of diffraction less than 40 units the first was used in order to have the rate of counting less than 55 per minute. The second was employed to decrease the slope of the background intensity curve for larger angles, and the third was found to be best for angles of diffraction greater than 195 units.

The portion of the background at large angles due to scattered rays was obtained from additional intensity measurements which were made with the slit closed. An intensity curve taken with the crystal removed did not show any peaks proving that they were due to diffracted rays only. A precise determination of the extent to which a possible continuous spectrum raises the background intensity was made by finding the intensities, for the two positions of the crystal, at a particular point on the curve where no peaks were to be expected either for first, second, or third order diffracted rays of any known wave-lengths.

The zero of the transparent scale was compared frequently with the zero of the steel scale and vernier. The deflections on the scale were noted at the beginning and at the end of each 20 minute period. In this way slight variations in the readings which occurred now and then due to the effect of temperature changes in the spectrometer were taken care of.

The operating potential on the Geiger counter was about 1800 volts, the exact value depending on the sensitive point in use. Its magnitude was always adjusted to the potential at which the impulses due to the γ -rays were slightly drawn out. The number of stray counts, or in other words, the number of impulses received when all sources of radiation were removed to a considerable distance, was about two or three per minute. A small test source placed in a definite position with respect to the counting chamber was used in standardizing the action of the points and in testing new ones. One person did the counting in all the experiments.

The expression for the probability of a number of counts n appearing in an interval of time for which x is the true average count was shown by Bateman¹⁸ to be,

$$P = \frac{x^n e^{-x}}{n!}.$$

¹⁸ H. Bateman, Phil. Mag. [6] 20, 704 (1910).

It has also been shown from this that the average deviation from the mean for a number of particles N counted in some interval of time t is $(nt)^{1/2}$, where n is the rate of emission. The probable deviation may therefore be taken as $0.67 (x)^{1/2}$.

Since in the counting experiments there was always the possibility of getting a large deviation at some time or another because of the random nature of the counts, it was the practice immediately to repeat a count

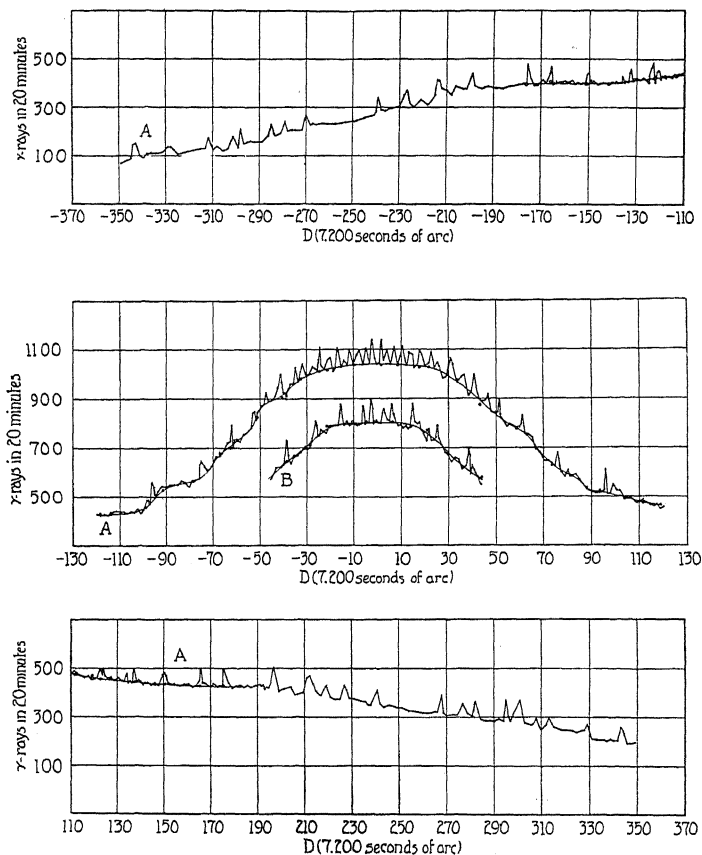


Fig. 4. Gamma-ray spectrum curves. Curve *A* is for the calcite, *B* for the diamond crystal.

which showed a large variation and average it with the other. If there was a true γ -ray intensity maximum or minimum for the position of the slit it was then confirmed, if not, the averaging process served to smooth out or reduce the magnitudes of the large deviations.

RESULTS AND DISCUSSION

The complete intensity curve is shown in Fig. 4 and is presented in three sections on account of its length. The experimental points have been joined by straight lines. Curve *B* was taken with the diamond crystal. The small

circles indicate the intensities obtained for the crystal turned and the base line of the spectrum has been drawn through them. The unit of the abscissa D is 7.200 sec. of arc and corresponds to a wave-length of 0.2115 X.U. for curve A and 0.0618 X.U. for curve B .

TABLE I.

D_1	$-D_2$	$(D_1 - D_2)/2$	λ X.U.	Intensity Rutherford- Andrade	Kovarik	Ellis- Skinner	Intensity, Thibaud	Frilley	Intensity Source of Rays
1260	1260	1260	266.5	262		264		265	RaD
1096	1098	1097	232.0	229		230.3		232	RaB
683	683	683	144.5					144	RaB
547	544	545.5	115.3	115					RaC
343	343	343.0	72.5	6	71	72.2			RaC
329	329	329.0	69.6	3				77 ² w.	RaB
312	313	312.5	66.1	4	66.1				Ra
308	308	308.0	65.2	2				65 w.	RaB
301	301	301.0	63.7	7					?
298	295	296.5	62.7	8		62.7	2		RaB
285	282	283.5	60.0	6		59.9	1		RaB
279	277	278.0	58.8	4	58.1				RaC
270	268	269.0	56.9	6					?
239	241	240.0	50.8	5		50.7	25		RaB
227	227	227.0	48.0	6	48.4				RaC
214	212	213.0	45.1	8		44.9	4		RaC
213	211	212.0	44.8	7		44.7	3		RaB
199.0	196.5	197.75	41.8	8		41.6	30	42.1 42	v.s. RaB
175.5	175.5	175.50	37.1	8	37.0	37.1	2		RaC
165.5	165.5	165.50	35.0	7		34.9	40	35.1 35	v.s. RaB
150.0	150.0	150.00	31.7	5		31.7	6		RaC
135.5	137.0	136.25	28.8	4		28.8	3	29.0	RaC
132.0	134.0	133.00	28.1	5	28.1				RaC
123.0	124.0	123.50	26.1	6		26.2	1	26.5 26	v.w. RaB
121.0	122.0	121.50	25.7	4		25.6	1		RaB
98.0	99.0	98.50	20.8	4					?
95.5	96.0	95.75	20.2	10		20.2	30	20.2 20	v.s. RaC
75.0	76.0	75.50	16.0	7				16.0 16	m. RaC
62.0	61.5	61.75	13.1	9		13.1	7	13.2	RaC
52.0	51.5	51.75	10.95	7		10.92	13	10.94	RaC
47.0	47.0	47.00	9.94	5		9.90	7	9.92	RaC
41.0	41.0	41.00	8.67	10		8.66	16		RaC
34.5	36.0	35.25	7.46	6					?
32.0	32.0	32.00	6.77	6		6.94	8	6.95	RaC
26.5	26.0	26.25	5.55	3		5.56	3	5.57	RaC
24.0	23.0	23.50	4.97	9					?
20.5	18.5	19.50	4.13	6					?
16.5	15.0	15.75	3.33	7					?
13.5	13.5	13.50	2.86	5					?
11.5	11.0	11.25	2.38	7					?
7.5	7.5	7.50	1.59	7					?
4.5	4.5	4.50	0.95	6					?
2.0	2.0	2.00	0.42	10					?
DIAMOND CRYSTAL									
38.5	38.5	38.50	2.38	10					?
26.0	25.5	25.75	1.59	8					?
15.5	15.0	15.25	0.94	9					?
6.0	6.5	6.25	0.39	7					?
2.5	3.0	2.75	0.17	9					?

The spectrum curve was obtained in five parts, a central portion extending to 45 units and two on either side with overlap. The parts were placed so as to give a continuous curve which was done by changing the ordinates by adding or subtracting a constant quantity. The actual intensity of the background was: 1040 γ -rays in 20 minutes at zero, 420 at 195, and 350 at 340. The intensity of the background for *B* was 1010 at zero, differing slightly from *A* because of a readjustment of the slit width. The large increase in intensity for angles less than 70 was due to γ -rays coming directly from the source. About 15 percent of the general background was made up of scattered rays. Because of the method of procedure in counting, previously described, it is estimated that the experimental error in the determination of the intensity of the background, and the intensities at most of the maximum and minimum points on the curve is about ± 15 γ -ray counts.

It is to be noted that the peaks on the curve are sharp and in general are defined by two or more points. No trouble was experienced in repeating the positions of the peaks and in fact many of the peaks were obtained several times. Taking the expected deviation to be $0.67 (x)^{1/2}$ it is seen that their heights above the background vary from 2 to 7 times the probable deviation depending on the intensity of the background.

The numerical results are given in the Table I. D_1 and $-D_2$ are the positions of corresponding peaks on both sides of the zero of the spectrum. The region of wave-lengths longer than 72.5 X.U. was not completely investigated so that no curves are shown. The values of the γ -ray wave-lengths and their intensities as found by other investigators are also included in the table for the purpose of comparison. The experimental error in the values of λ presented herewith is ± 0.1 X.U. except for wave-lengths longer than 41.8 where it is about ± 0.2 X.U. The four γ -rays of shortest wave-length were also obtained with the diamond crystal. The error in their wave-lengths is ± 0.03 X.U. Ellis-Skinner give an accuracy to their results of one part in 300. Frilley gives an experimental error of ± 0.5 X.U. Consequently there is good agreement among all the results. Many new rays were found and the diamond crystal made it possible to detect the extremely short wave-length of 0.17 X.U. Two additional determinations gave the same value.

The following γ -ray wave-lengths, reported by others for substances certainly present, were not found:

RaB $\lambda = 51.3$ X.U.	Thibaud, $\lambda = 51.5$	Frilley
RaB $\lambda = 47.5$		Ellis-Skinner
RaC $\lambda = 29.5$		Frilley
RaC $\lambda = 23.4$	Thibaud, $\lambda = 24$	Frilley

There is additional information in regard to a few of the wave-lengths, namely:

RaD $\lambda = 265$	Meitner, $\lambda = 264$	Curtiss
RaB $\lambda = 71$	Frilley, possibly 2nd order of $\lambda = 35$	
Ra $\lambda = 66$	Hahn-Meitner	

No particular effort was made to identify higher order diffracted rays and some of those presented in the table may be of that kind.

On account of the complex nature of the radioactive preparation used in the present experiments, it was impossible to tell the exact source of any of the rays. The assignments in the last column, some of which are doubtful, are also from other papers.

The relative intensities of the γ -rays are given in column 5. The height of a peak has been taken as the intensity and a number 10 means that 100 monochromatic rays in addition to the background were counted in 20 minutes. No correction has been made for the fact that three different sizes of slit were used. Some of the peaks were repeated using double the slit width but their heights were found to be increased only about 40 percent. It was therefore considered advisable not to assume any relation between the width of the slit and the intensity of the rays and so attempt to reduce them all to the same basis. On the whole the changes in intensity along the spectrum are in agreement with the results of other observers, but the intensities do not vary as much as in the results of Ellis-Skinner. Although the present method was quite straightforward it is not certain that this disagreement is particularly significant.

It may be seen from Fig. 4 that the base line passes through or a little above the bases of the peaks but not below them as would be the case if there was a continuous spectrum of any appreciable intensity. The more precise measurements made at a wave-length of 53.9 X.U. gave a γ -ray count of 6664 for the crystal set for diffraction through the slit and 6666 in the same length of time for the crystal turned. Since the probable variation in either of these numbers is about ± 0.8 percent, and the smallest peaks on that part of the curve are found to differ from the background by about 9 percent, it would seem that a continuous radiation if existing at all raises the background intensity to less than one-tenth the height of the least prominent peaks here found. Moreover these peaks belong to some of the weakest γ -rays.

It is to be noted that the very short wave-length γ -rays represent a large amount of energy as a wave-length of 1 X.U. corresponds to the energy of an electron after falling through a potential difference of some 12×10^6 volts. The relation between these γ -rays and other high frequency radiations may be inferred from a consideration of the work of Millikan-Cameron¹⁹ and many other investigators. No attempt has been made to correlate the new wave-lengths with the nuclear energy level theories put forward by Ellis²⁰ and others.

In conclusion the author wishes to express his appreciation to Professor A. F. Kovarik for suggesting and directing the work. He is also greatly indebted to Mr. Donald Cooksey for the loan of the diamond.

¹⁹ R. A. Millikan and G. H. Cameron, *Phys. Rev.* [2] **32**, 533 (1928).

²⁰ C. D. Ellis, *Proc. Camb. Phil. Soc.* **22**, 369 (1924).

THE IONIZATION OF CARBON DIOXIDE BY
ELECTRON IMPACTBY H. D. SMYTH AND E. C. G. STUECKELBERG
PALMER PHYSICAL LABORATORY, PRINCETON UNIVERSITY

(Received June 20, 1930)

ABSTRACT

A new mass spectrograph has been constructed entirely of glass except for the electrodes. Furthermore its design reduces thermal dissociation to a minimum. Using this apparatus the products of ionization in carbon dioxide have been studied. The primary ions are found to be CO_2^+ , CO^+ , O^+ and C^+ appearing at 14.4, 20.4, 19.6 and 28.3 volts respectively. There is also some O_2^+ produced as a secondary product with an ionization potential of 20.0 volts. Except for CO_2^+ minimum values for all the ionization potentials can be calculated and are found to agree within the limits of error with the observed values.

THE products of ionization in carbon dioxide as analyzed by a mass spectrograph have already been discussed in a brief note by the authors¹ and in a paper by Kallmann and Rosen.² The present paper constitutes a final report on the authors' work.

The method used was the familiar modification of Dempster's mass spectrograph first used by one of the authors³ in 1922 and since then employed by a number of different investigators. It will not be described in detail particularly as this entire field is to be discussed in a forthcoming article in *Reviews of Modern Physics*. There are, however, a number of minor improvements which should be mentioned.

In the first place the present apparatus is made entirely of glass. The "positive-ray box" which in previous experiments was a rectangular box of brass fitting between the poles of the magnet is now of one inch glass tubing bent in a semicircle and sputtered with platinum to prevent electrostatic charging. One end of this glass "positive-ray box" is sealed to the ionization tube and the other contains the Faraday box which receives the positive ions. This construction eliminates wax joints near the filament and metal parts that cannot be baked out. As a result of it and careful drying of the CO_2 , water vapor ions are negligible except at high pressures.

A second change of design is the use of an electron beam parallel to the magnetic field in order to minimize the bad effects of stray field. Such an arrangement has recently been used by Bleakney.⁴ A diagram of the central part of the present apparatus is given in Fig. 1.

¹ Smyth and Stueckelberg, *Helvetica Physica Acta* **2**, 303 (1929).

² Kallmann and Rosen, *Zeits. f. Physik* **58**, 52 (1929) and *Zeits. f. Physik* **61**, 61 (1930).

³ For references see Gurney and Morse, *Phys. Rev.* **33**, 789 (1929) or Kallmann and Rosen, reference 2.

⁴ Bleakney, *Phys. Rev.* **34**, 157 (1929), **35**, 139 (1930).

Finally and most important an attempt has been made to minimize dissociation by the filament. To do this the apparatus is so arranged that the gas first enters the ionization chamber from which it diffuses toward the pumps through the slits S_1 and S_2 and the circular opening O . Thus there is a continuous flow of gas from the ionization chamber through O past the filament. Unfortunately to get sufficient intensity of ionization the filament has to be very close to O so that there is still a certain amount of thermal dissociation. An attempt was made to get some quantitative estimate of this by thermocouple measurements of the temperature in the ionization chamber but the result was indeterminate. The positive-ray results themselves offer the most definite evidence of dissociation, as will appear below.

EXPERIMENTS AND RESULTS

Carbon dioxide was prepared by fractional distillation of commercial carbonic acid gas. After careful drying over phosphorous pentoxide it was

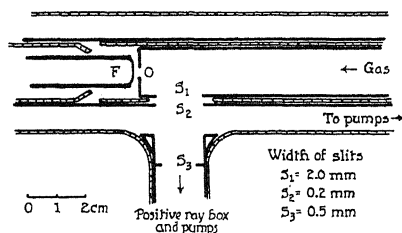


Fig. 1. Diagram of central part of apparatus.

admitted to the apparatus through traps cooled by CO₂ snow and showed no impurities in positive-ray analysis except a trace of water vapor.

First experiments confirmed what we had already found with the old apparatus and what has also been reported by Kallmann and Rosen, namely, that the ions produced are CO₂⁺, CO⁺, O⁺, C⁺, and O₂⁺. We then proceeded to study these ions in two ways, first by varying the pressure, second by observing critical potentials.

In the pressure runs the field V_1 accelerating the electrons was usually of the order of 40 volts. In both these runs and those on appearance potentials the space OS_1 is, of course, field free, the field V_3 between S_1 and S_2 is of the order of 8 volts and the field V_4 , between S_3 and S_4 , varies according to the mass of the ion according to the equation $(M/e)(V_3 + V_4) = K$ where M is the mass of the ion on the $H^+ = 1$ scale and K for this apparatus and the magnetic field used is about 2600. The pressure used for the most satisfactory of the appearance potential runs was of the order of 0.0008 mm so that the chances of collisions of the second kind or of other secondary effects were small. All the above conditions were varied at one time or another for purposes of control.

Pressure variation. In studying these effects due regard was paid to the recent remarks of Kallmann and Rosen concerning differential absorption

in the magnet space. One of us hopes to discuss this whole problem fully elsewhere, but we may say here that we observed the effect of varying the pressure in the magnet space on the intensities of CO_2^+ , CO^+ , O^+ , and C^+ . The effects were small in the range of pressures we were using and the relative intensities were not appreciably changed except in one case. The one ion which behaved differently from the others was C^+ which had an unusually long free path as might be expected from its low ionization potential.

In Fig. 2 the intensities of the different ions are plotted as functions of p_1 , the pressure in the ionization tube, for a typical set of observations. Two results are striking, the decrease of CO^+ and the increase of O_2^+ at higher

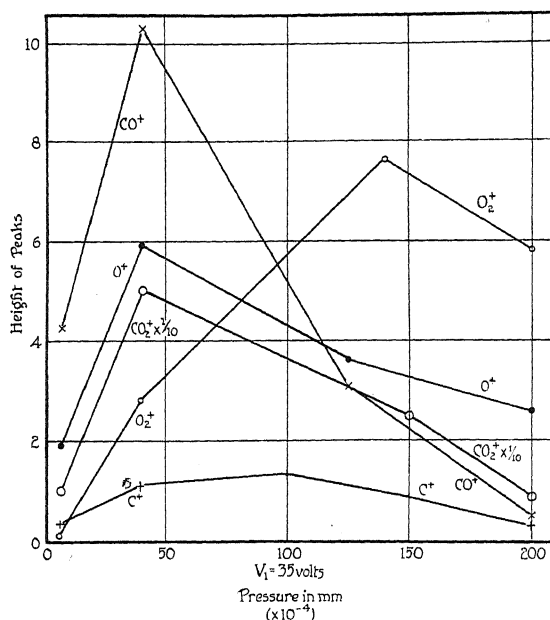


Fig. 2. Intensities of different ions plotted as functions of pressure in ionization tube for a typical set of observations.

pressures. The first is interpreted as the result of collisions of the second kind of the type $\text{CO}^+ + \text{CO}_2 \rightarrow \text{CO}_2^+ + \text{CO}$ which should be possible as the ionization potentials are only one or two tenths of a volt apart. At first sight this seems to contradict the statement above concerning the effect of pressure in the magnet chamber. But we may reconcile the results if we remember that the collision $\text{CO}_2^+ + \text{CO}_2 \rightarrow \text{CO}_2 + \text{CO}_2^+$ may also occur and would reduce the number of CO_2 ions getting through the magnet chamber but not the number of CO_2^+ ions produced in the ionization chamber. Thus collisions of the second kind in the magnet chamber may have little effect on the relative intensities of CO_2^+ and CO^+ but such collisions in the ionization chamber may greatly favor the CO_2^+ . Why the O^+ behaves like the CO_2^+ and CO^+ instead of like the C^+ is not certain. That the C^+ makes few collisions of the second kind is confirmed by its curve in Fig. 2. If that curve

is corrected for the effect of pressure in the magnet space it becomes of the same general type as the CO_2^+ etc. The O_2^+ curve remains as one of entirely different type, a type suggesting strongly a secondary effect. This is supported by the results of Kallmann and Rosen who observed only small traces of O_2^+ . Our final conclusion is therefore that all the ions are primary save O_2^+ .

Ionization potentials. In determining the ionization potential for different ions argon was used as a standard in the following way. Immediately before and immediately after several of the CO_2 runs argon was run into the apparatus and the electron accelerating voltage observed where A^+ ions were just noticeable. This voltage was the same within the limits of error before and after the CO_2 run and was taken as giving the proper correction to the observed value. That this procedure was justified is supported by the agreement between the ionization potential for CO_2^+ thus obtained and the value observed by Mackay.⁵ The ionization potentials for the other ions were then referred to that of CO_2 . A typical set of curves at an intermediate pressure is shown in Fig. 3. At lower pressures the O_2^+ usually can not be

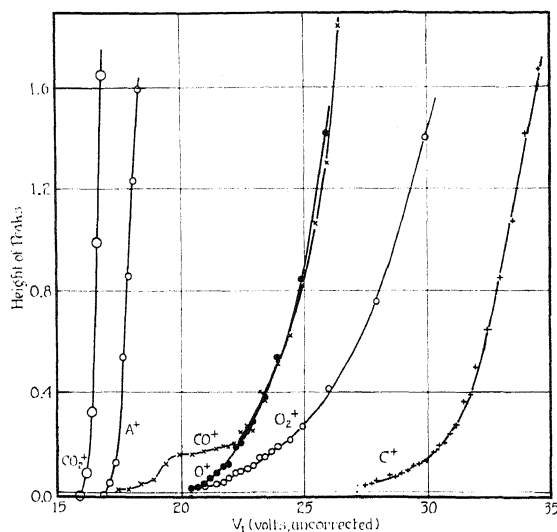


Fig. 3. Typical set of curves at intermediate pressure.

observed but the other curves cut the axis more sharply. The complete weighted results are tabulated below.

From both table and curves we see that CO^+ appears to have two critical potentials. From a comparison of these results with those of an earlier apparatus and from a study of the effect of pressure, filament temperature, etc., we have concluded that the lower potential is due to the presence of CO from thermal dissociation. Whether it may be a true critical potential for CO, to be identified perhaps with Mackay's higher ionization potential at

⁵ Mackay, Phys. Rev. 24, 319 (1924).

TABLE I. Observed critical potentials with weights.

Run	P	CO ₂ ⁺	A ⁺	CO ⁺		O ⁺	C ⁺	O ₂ ⁺
1	6 × 10 ⁻⁴	16.0(7)		20.0(6)	24(3)			
2	11.	15.5(5)		20.0(4)				
3	25.	15.5(6)	17.0(6)	19.0(4)	21.5(1)	21.0(4)		22.0(5)
4	100.	15.8(10)		19.0(4)		20.5(7)	28.0(2)	20.0(3)
5*	32.	16.0(10)	17.0(10)	18.0(5)	22.0(7)	21.0(5)	27.8(5)	21.6(5)
6	5.	16.3(8)	17.2(10)	17.0(5)	22.0(3)	22.0(5)	31.0(6)	
7	7.	16.0(9)		18.0(5)	20.8(6)	21.3(10)	31.0(6)	23.0(1)
8	6.	15.9(9)	17.5(10)	18.3(8)	22.7(10)	21.2(10)	30.5(5)	
9	7.	16.0(10)	17.5(10)	17.8(8)	22.0(10)	21.3(10)		
Weighted mean volts above CO ₂ ⁺			1.26	2.41	6.00	5.22	13.86	5.6
Value of ionizing potential with estimated error assuming I _{co₂} = 14.4.			15.66	16.8 ± 1.0	20.4 ± .7	19.6 ± .4	28.3 ± 1.5	20.0 ± 1.0

* Run shown in Fig. 3.

15.6 volts,⁵ or whether its position depends entirely on the amount of CO present we are not certain. We incline toward the latter view and would explain our previously reported value and that of Kallmann and Rosen in the same way. The higher break, on the other hand, we believe is a true ionization potential due to the direct production of CO⁺ from CO₂.

DISCUSSION

The results given above are particularly interesting because we can compare them with theoretical expectations. We know that carbon dioxide is a straight line molecule with the carbon atom in the middle. It is not surprising therefore that we can get CO₂⁺, CO⁺ and O⁺ all at comparatively low potentials but that to get C⁺ we must break away both oxygen atoms and ionize the remaining carbon so that we require considerably higher energy. Let us be more precise and calculate the minimum values where the different ions might appear. The calculations given in Table II are based on the following values.

Heats of Dissociation ⁶ Process		Volts	Ionizing Potentials ^{7,8,9,10}	
CO ₂ → CO + O		5.7	CO	14.2 ⁷
CO → C + O		10.	O	13.5 ⁸
O ₂ → O + O		5.6	C	11.2 ⁹
			O ₂	13.5 ¹⁰
			A	15.6 ⁹

⁶ Mecke, Zeits. f. Phys. Chem. B7, 108-129 (1930).⁷ Birge, International Critical Tables, Vol. 5.⁸ Frerichs, Phys. Rev. 34, 1239 (1929).⁹ Russell, Astrophys. J. 70, 16 (1929).¹⁰ Stueckelberg, Phys. Rev. 34, 65 (1929).

The probable errors given for the observed values are estimated and based on the assumption that 14.4 for CO₂⁺ is correct. The calculated probable error for $I_o - I_{CO_2^+}$ was only ± 0.074 volts but this is the best determined of the higher ionization potentials.

TABLE II.

Process	Calculated (volts)	Observed (volts)	
		K and R	This paper
CO ₂ →CO ₂ ⁺		14	14.4
CO ₂ →CO ⁺ +O	19.9	18	20.4±0.7
CO ₂ →CO+O ⁺	19.2	17	19.6±.4
CO ₂ →C ⁺ +O+O	26.9	29	28.3±1.5
CO ₂ →(CO ₂ ⁺ +CO ₂)→2CO+O ₂ ⁺	19.3		20.0±1.0

The good agreement between our results and the calculated ones is perhaps somewhat fortuitous considering the uncertainty of some of the heats of dissociation involved as well as the errors in our present experiments. It is difficult to make any comparison with the results of Kallmann and Rosen since they give neither experimental data nor estimated error. Their calculated values differ slightly from ours also, presumably due to use of different authorities for heats of dissociation but here again they do not give the data on which they base their estimates so detailed comparison is impossible.

The value calculated for the production of O₂⁺ postulates an intermediate process, the formation of an excited CO₂⁺ ion. If this is correct it means the CO₂⁺ ion has an energy level, perhaps a metastable one, at 5.6 volts above the normal. We are not yet in a position to judge of the reasonableness of this assumption.

Granting the minor uncertainties discussed in the above paragraphs and earlier it still seems clear that we have more complete knowledge of the effect of electron impact on CO₂ than on any other polyatomic molecule. Moreover it is very striking that the observed ionization potentials agree so closely with those calculated from energy considerations alone since such considerations give minimum values. Previous data, both ionization and thermochemical, on other polyatomic molecules are not so definite. Experiments are now being performed on N₂O and NO₂ molecules for which the heats of dissociation and ionizing potentials of the constituent parts are almost as well known as for CO₂.

THE IONIZATION OF NITROUS OXIDE AND NITROGEN DIOXIDE BY ELECTRON IMPACT

BY E. C. G. STUECKELBERG AND H. D. SMYTH
PALMER PHYSICAL LABORATORY, PRINCETON UNIVERSITY

(Received June 20, 1930)

ABSTRACT

The same apparatus used for the study of CO_2 has now been used to study the products of ionization in NO_2 and N_2O . Thermal dissociation is so serious in NO_2 that the results are somewhat unsatisfactory but NO_2^+ , N^+ and O_2^+ are found as primary ions and their appearance potentials determined approximately. In N_2O the results were more satisfactory and the appearance potentials 12.9, 16.3, 15.3, 21.4 were found for the primary ions N_2O^+ , O^+ , NO^+ , N^+ respectively. In both gases other primary ions were probably present but obscured by ions from products of thermal dissociation. As in CO_2 the observed potentials agreed within the limits of error with calculated values.

PURSUING the general scheme of investigating the simplest triatomic molecules the authors went on from the experiment on carbon dioxide reported in the preceding paper to study the products of ionization in nitrous oxide and nitrogen dioxide. These substances have almost the same advantages as CO_2 as far as our knowledge of their structure is concerned. Not only are the heats of dissociation of the gases themselves known but also the heats of dissociation and ionization potentials of their constituent parts, N_2 , O_2 , NO , N and O . Furthermore both N_2O and NO_2 are supposed to be triangular in structure furnishing an interesting contrast with CO_2 which is linear.

Experimentally, however, difficulties of two sorts arose. The first, which was foreseen, was the high degree of thermal dissociation which made any study of pressure variations futile and all results more difficult of interpretation. The second difficulty was a variable error in the voltage scale which made corrections uncertain and the determination of some of the ionization potentials less accurate than in CO_2 .

EXPERIMENTS AND RESULTS

The apparatus and procedure were the same as those described in the preceding case except that the electrode in front of the filament was changed from nickel to platinum and two fine wires welded across the hole O to make the field more uniform. (see Fig. 1 in previous paper).

The NO_2 was generated by heating $\text{Pb}(\text{NO}_3)_2$ and purified by fractional distillation. In the ionization chamber it was dissociated to such an extent that a typical mass spectrum showed NO^+ ions ten times more numerous than NO_2^+ and showed some N_2^+ and O_2^+ ions present. Therefore the possibility must be considered that the NO^+ , O^+ and N^+ ions observed came from ionization of NO , N_2 or O_2 rather than directly from NO_2 .

The N_2O was generated by heating NH_4NO_3 and was dried over P_2O_5 . The dissociation difficulty appeared here also but with certain differences. In this case the N_2O^+ was the strongest ion with O_2^+ and N_2^+ much stronger

and NO^+ relatively weaker than in the NO_2 mass spectrograms. But again care must be taken in interpreting results though in general they are better than in NO_2 .

Fortunately the resolution of the apparatus was excellent. Therefore it was possible to observe the appearance potentials of nearly all the stronger ions. The only exceptions were N_2^+ and O_2^+ in NO_2 where the great intensity of NO^+ obscured the appearance potentials of the neighboring ions.

Early in the experiments on NO_2 it was noticed that the appearance potential of NO^+ was not as far below that of argon as might be expected. Therefore it was decided to use the ionization potential of mercury as a second calibration point for correction of observed voltages. As may be seen in the tables below, this gave the surprising result that the observed appearance potential of the Hg^+ ion was only about 3.8 volts below that of the A^+ ion instead of the 5.2 which it should be. This is attributed to some variable charged layer or possibly some geometrical effect. Attempts were made to diagnose it more exactly by measuring the velocity and intensity characteristics of electrons reaching probes inserted just behind the hole O , or just above the slit S_1 (see Fig. 1 in previous paper) but the results were inconclusive. However plotting the observed values for A^+ , CO_2^+ and Hg^+ against their true values a correction curve can be drawn and observations of unknown ionization potentials corrected by it. Actually such an interpolation is required in only one case, N_2O^+ . Of the other three ions appearing below 14 volts, NO^+ and NO_2^+ both appear at approximately the same place as Hg^+ while the O_2^+ in the N_2O appears by interpolation at 13.5 which is in agreement with the accepted value of the oxygen ionization potential.

A typical ionization potential curve for N_2O is shown in Fig. 1 and the results of a number of runs on NO_2 and N_2O are tabulated below.

TABLE I.
A. NO_2

Run	P	Hg^+	Observed Ionization Potential				O^+	N^+
			NO_2^+	NO^+	A^+			
2	7×10^{-4}		15.0	14.5	18.2			
3	11		17.5	17.2	20.9			
4	10		17.0	16.5	18.9			
5	9	NO gas		17.5	20.0			
6	10		15.0	15.0	18.5	20.5		
7	10			14.5				
8	12		15.75	15.5	18.5	20.7		23.7

B. N_2O

Run	P	Hg^+	Observed Ionization Potentials (with weights)						O^+	N^+
			N_2O^+	NO^+	A^+	O_2^+	N_2^+			
1	25×10^{-4}		16.5(10)		19.0(10)					
2	18	13.8(10)	15.2(10)		17.3(10)					
3	7	13.6(10)	15.0(10)							
4	12	13.5(10)	15.0(10)		17.5(10)					
5	7		16.1(10)	18.3(10)			18.5(10)	19.7(2)	25.5(2)	
6*	12		16.5(10)	18.3(10)		17.0(10)	18.7(10)	19.5(2)	24.5(2)	
7	12		16.5(10)	17.8(2)	18.5(2)	17.0(10)	18.5(2)			

* Run shown in Fig. 1.

By using argon and mercury as reference points and using the correction curve discussed above we arrive at the following experimental values where

TABLE II

From	NO_2^+	N_2O^+	NO^+	O_2^+	N_2^+	O^+	N^+
NO_2	11.0?		10.5?			17.7?	20.8?
N_2O		12.9	15.3	13.5	15.5	16.3?	21.4

the question marks indicate that the accuracy is poor, perhaps 10% and we refrain deliberately from giving estimated errors for each separate potential. The ones not questioned are probably accurate to about half a volt.

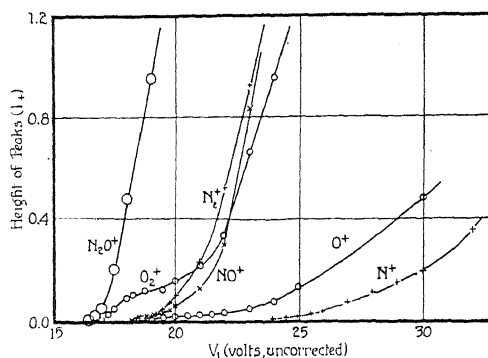


Fig. 1.

DISCUSSION

In comparing these experimental results with theoretical values we must remember that we can safely attribute an ionizing potential to NO_2 or N_2O

TABLE III.

Process	Heats of dissociation	Volts	Ionizing potentials	
	$\text{NO}_2 \rightarrow \text{N} + \text{O}_2$	4.3	N_2	16.5 ²
	$\text{NO}_2 \rightarrow \text{NO} + \text{O}$	3.3	N	14.5 ³
	$\text{N}_2\text{O} \rightarrow \text{N}_2 + \text{O}$	2.0	O_2	13.5 ⁴
	$\text{N}_2\text{O} \rightarrow \text{NO} + \text{N}$	4.6	O	13.5 ^{5,3}
	$\text{NO} \rightarrow \text{N} + \text{O}$	6.5	NO	9.4 ⁶
	$\text{N}_2 \rightarrow \text{N} + \text{N}$	9.1	A	15.6 ³
	$\text{O}_2 \rightarrow \text{O} + \text{O}$	5.6	Hg	10.4 ³

only of the observed value is lower than the theoretical value for production from N_2 , O_2 , or NO . Even the assurance of the chemists that no NO is to

¹ Mecke, Z. its. f. Phys. Chem. **B7**, 108-129 (1930).

² Estimated most probable value. Authorities differ.

³ Russell, Astrophys. J. **70**, 16 (1929).

⁴ Stueckelberg, Phys. Rev. **34**, 65 (1929).

⁵ Frerichs, Phys. Rev. **34**, 1239 (1929).

⁶ Birge, International Critical Tables, Vol. 5.

be expected in N_2O must be regarded with skepticism at first though it will be seen later to be verified. With the heats of dissociation given by Mecke¹ and the ionizing potentials from various sources given in Table II the minimum energy can be calculated for fifteen of the seventeen possible processes, which might be expected to occur in NO_2 or N_2O . The two ionization potentials that can not be predicted are, of course, simple ionization of N_2O and NO_2 without any dissociation. Without considering in detail the processes which might lead to each type of ion we may take one as typical. Consider NO^+ . In NO_2 it could be produced directly from NO_2 at 12.7 volts but actually it appears very strongly below this point so that presumably it comes from NO present as the result of dissociation and requiring only 9.5 volts for ionization. On the other hand in N_2O , NO^+ first appears at about 15.3 volts whereas it can first be produced directly from N_2O at 14.0. This suggests that it is actually being produced in this way and that there is no appreciable amount of NO itself present. This confirms the views of the chemists on the nature of dissociation in N_2O and allows us to throw out NO as a possible source of N^+ or O^+ in the experiments on N_2O . The results of arguments of this type are embodied in Table IV below.

TABLE IV.

Process	Theor.	Obs.	Remarks
$NO_2 \rightarrow NO_2^+$		11.0	
$\rightarrow NO^+ + O$	12.7		Obscured by $NO \rightarrow NO^+$
$\rightarrow NO + O^+$	16.8	17.7	Definitely occurs
$\rightarrow N + O_2^+$	17.8		O_2^+ present but I.P. obscured by NO^+
$\rightarrow N^+ + O_2$	18.8	20.8	Uncertain, perhaps due to NO
$N_2O \rightarrow N_2O^+$		12.9	
$\rightarrow N_2 + O^+$	15.5	16.3	Definitely occurs
$\rightarrow N_2^+ + O$	18.5		Obscured by $N_2 \rightarrow N_2^+$
$\rightarrow NO^+ + N$	14.0	15.3	Reasonably certain
$\rightarrow NO + N^+$	19.1	21.4	Reasonably certain

It seems that in every case where a definite conclusion can be drawn it is to the effect that the process to be expected does occur and at nearly the minimum possible energy. Perhaps the most interesting processes are $NO_2 \rightarrow N^+ + O_2$ and $N_2O \rightarrow N_2 + O^+$ which evidently do occur although the corresponding process $CO_2 \rightarrow C^+ + O_2$ does not occur. This is in perfect accord with our ideas as to the difference in structure of these molecules.

These results combined with those on CO_2 give a most satisfactory confirmation of predictions of ionization phenomena by the use of thermochemical data, a process that fell into disrepute after its early failure in the case of HCl . Unfortunately there are few other triatomic molecules for which we have sufficient data to make predictions. However the authors hope to continue the work as well as possible.

THE EFFECT OF INTENSE ELECTRIC FIELDS ON THE PHOTOELECTRIC PROPERTIES OF METALS

BY ERNEST O. LAWRENCE AND LEON B. LINFORD
UNIVERSITY OF CALIFORNIA

(Received June 20, 1930)

ABSTRACT

The photoelectric effect from thin films of potassium and oxygen on tungsten has been studied as a function of strong accelerating fields. Fields as high as 63,000 volts/cm were used which shifted photoelectric thresholds towards the red, the shifts being approximately proportional to the square root of the applied fields. An applied field of 36,000 volts/cm removed the threshold for a pure potassium layer on tungsten from 5620A to 5880A. A film of potassium on a very thick layer of oxygen on tungsten showed a threshold at 6800A which did not vary with applied accelerating fields. However the magnitude of the emission increased with the field suggesting that thick oxygen layers are rough and applied fields over most of such surfaces are much smaller than calculated from the geometry of the electrodes. A layer of potassium on a thin layer of oxygen on tungsten showed a threshold at 7350A for small applied fields which shifted to 7575A for a field of 18,600 volts/cm. A film of potassium on a thinner layer of oxygen—perhaps less than a monatomic layer—exhibited a threshold in small fields at 5830A which was shifted to 5960A by an applied field of 18,600 volts/cm. From the observations of the variations of the shifts with applied fields calculations of the surface fields were made after the manner of Becker and Mueller. It was found that outside the film of potassium on a thin layer of oxygen on tungsten the field followed closely the Schottky image law in the range 1.5×10^{-6} cm to 10^{-5} cm from the surface. The pure potassium film on tungsten exhibited surface fields which were closely image fields between 8×10^{-7} cm and 1.5×10^{-6} cm from the surface but which departed from the image law at greater distances. These observed departures were about equal to the image fields and were much smaller than the surface fields at like distances outside thoriated tungsten filaments as recorded by the thermionic measurements of several observers. The surface fields in excess of the image fields are ascribable to inhomogeneity of the surfaces, regions of different work functions having linear dimensions of the order of magnitude of 10^{-5} cm.

Shifts of photoelectric thresholds by strong accelerating fields are of particular theoretical interest for they involve changes of the work function of a surface without alterations of the other important characteristics of the metal. It is found that the form of the photoelectric sensitivity versus frequency curve remains unchanged over the range of observations and shifts along with the thresholds in intense fields. Thresholds are not sharp but approach the frequency axis tangentially. These observations are in excellent agreement with the theory of the photoelectric effect based on wave mechanics and the Fermi-Dirac distribution of the electrons in metals worked out by Wentzel and modified by Houston.

THE new quantum mechanics in the hands of Pauli, Sommerfeld, Wentzel, Fowler, Houston, Nordheim and others¹ has been highly successful in dealing with many general properties of metals, and has given a particularly satisfactory account of the emission of electrons from metal surfaces.

¹ An excellent résumé of the subject by L. Nordheim is to be found in *Phys. Zeits.* 30, 177 (1929).

The old concept of free electrons in metals has been revived, though to be sure the behavior of these electrons on the present theory differs radically from that of former views. For purposes of discussion of the experimental results herein described it is desirable to emphasize two characteristic features of the new theory.

The first has to do with the work function of a metal surface. The constant b in Richardson's thermionic equation and the photoelectric long wavelength limit have been regarded as measures of the minimum amount of energy given to an electron in the process of its ejection from a metal. On the older theory the free electrons possessed a Maxwellian distribution of velocities and were retained in the metal by a potential difference between outside and inside equal to the work function. The newer theory attributes a Fermi-Dirac distribution of velocities to the electrons and assigns a potential energy barrier at the surface which exceeds the maximum energy of the electrons at the absolute zero of temperature by the amount of the work function. The work function involves more than just the work required to eject an electron from inside to immediately outside a metal, for it includes as well the work required to remove it entirely away from the surface. Outside the metal an electron experiences a force of attraction to the metal produced by its image. In some cases inhomogeneous ion layers also produce electrostatic fields near metal surfaces which aid or oppose the removal of electrons.

It is obviously possible to introduce electric fields at metal surfaces which reduce the image and ion fields, and thereby cause reductions of the work function. Such reductions of the work function in strong fields have been observed by workers in the field of thermionics, and indeed variations of the thermionic emission with applied fields have been used to estimate surface electric fields.

The second feature of the new theory is that it yields a definite probability that an electron will pass into a region in which its classically computed potential energy is greater than its total energy before entering the region. The probability of finding an electron in such a region falls off exponentially with the distance into the region. This feature of the theory is one aspect of the wave nature of matter. It is possible to apply such a strong electric field at the surface of a metal that the potential within a few atom diameters of the surface becomes lower than the energy of some of the electrons within the metal. Any electron, which passes into this region of higher potential far enough to reach the point where the applied field has lowered the potential to that corresponding to the energy of the electron in the metal, will be accelerated away from the surface. This effect, which is analogous to the passage of light unaffected from one glass plate into another when the plates are close enough together, satisfactorily explains the observed emission of electrons in strong fields.

These effects of strong accelerating fields on the emission of electrons from metals, also should be clearly displayed by a dependence of photoelectric emission on such fields. The lowering of the work function by fields

should appear as a shift of the photoelectric threshold to the red, as has been pointed out by Becker and Mueller.² Similarly the ability of electrons to go through high potential barriers should be evidenced in a like manner. That effects of this sort exist, has been indicated by the observation of Ives³ who found difficulty in saturating photoelectric currents from thin alkali metal films, while currents from thicker ones were more easily saturated. Suhrmann⁴ also noted this lack of saturation, and its variation with the thickness of the film, and noted the further effect that the saturation becomes the more difficult the nearer the frequency of the incident light approaches the threshold value. The reports were only qualitative, and no mention was made of a possible shift in the threshold frequency being associated with the phenomena.⁵

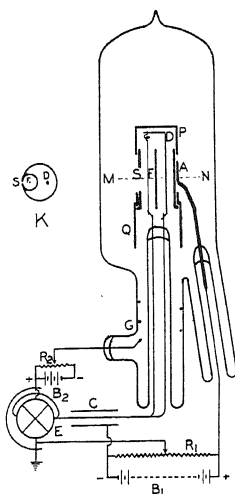


Fig. 1. Diagram of apparatus, showing a section through the photoelectric cell with a schematic diagram of the electrical connections. Also *K* a cross-section through the anode *A* on the line *MN*.

The present work was designed to investigate the matter in a quantitative manner with the primary view of verifying the predictions of the newer theories and also to use the experimental data to elicit information on the surface electrostatic forces near various metal surfaces.

APPARATUS AND EXPERIMENTAL METHODS

Figure 1 shows a section through the photoelectric cell and a schematic diagram of the electrical connections. *K* is a cross section through the anode *A* on the line *MN*. The anode was made from a solid block of nickel in the

² J. A. Becker and D. W. Mueller, *Phys. Rev.* **31**, 431 (1928).

³ H. E. Ives, *Astrophys. J.* **60**, 209 (1924).

⁴ R. Suhrmann, *Naturwissenschaften* **16**, 336 (1928).

⁵ Nottingham (abstract Feb. meeting Am. Phys. Soc.) has recently observed interesting shifts of photoelectric thresholds produced by very small applied fields.

form of two internally tangent cylinders. In their common wall was a 1 mm slit S , 1 cm long, to allow the light to fall on the tungsten filament F stretched along the axis of the inner cylinder. The filament was held in place by the nickel support D passing through the crescent shaped space between the two cylinders. The screw on cap P and the sliding sleeve Q were so arranged, that when in place they screened all parts of the cathode circuit, inside the tube, from light and external electrical effects. Both filament leads were carried out of the tube so that the filament could be glowed.

The tube was baked out under vacuum for 12 hours at a temperature of 500°C , the metal parts were heated with an induction furnace and the filament glowed at about 2200°C . The potassium was then distilled into the tube after repeated distillations, and the tube was sealed off when the pressure was less than 10^{-6} cm of Hg. To obtain a coating of oxygen on the filament, a little air was allowed into the tube, after baking out and before distilling the potassium, and then pumped out immediately.

Light from a 6 volt, 110 watt ribbon filament lamp, was dispersed by a Van Cittert type double monochromator, which gave light bands about 100 cm^{-1} units wide (corresponding to a width of 32 Å at 5600 Å) which were practically free from stray light. Any desired band of the visible spectrum could be selected by moving the middle slit. This made it unnecessary to change the adjustment of the last slit or of the photoelectric cell when measuring the current for various wave-lengths.

The photoelectric current was measured with a quadrant electrometer E using the accumulation of charge method. To prevent leakage of charge from the anode circuit to the electrometer circuit, a guard ring G consisting of several turns of tungsten wire was placed in the stem carrying the filament leads. Metal foil, used as a screen on the outside of the tube, was also connected to the guard ring circuit. A low voltage battery B_2 and potentiometer R_2 were used to balance out the effects of contact potentials.

The accelerating fields were produced by potentials from a 1500 volt bank of storage "B" batteries B_1 . These were connected across a resistance R_1 of about 5×10^5 ohms. Only a part of the battery potential was applied between the anode and the electrometer case. The remainder was used to produce a negative potential on the compensating condenser C . The ratio of the potentials on the anode and compensating condenser was so adjusted that the electrometer system was rendered immune to fluctuations in the voltage of the batteries.

The data are shown by plotting the sensitivity curves, that is the photoelectric current per unit light intensity against the frequency of the incident light in sec^{-1} units. The absolute values of the light intensity and of the photoelectric current were not determined. The maximum current was of the order of 10^{-14} amps.

The relative intensities of the light of the various wave-lengths were determined by a vacuum thermopile set in the place of the photoelectric cell.

The accelerating fields were calculated from the applied potentials and

the dimensions of the cylinder and filament. The inside diameter of the nickel cylinder was 0.228" or 0.579 cm. The field at the surface of the filament in the cell with a filament 0.9 mil (0.0023 cm) in diameter was $E=160$ V; and at the surface of the filament 3.0 mil (0.0076 cm) in diameter, $E=60.4$ V, where V is the applied voltage.

The small diameters of the filaments together with the fact that only about 0.7 cm of the filament was illuminated explain the small values of the photoelectric currents.

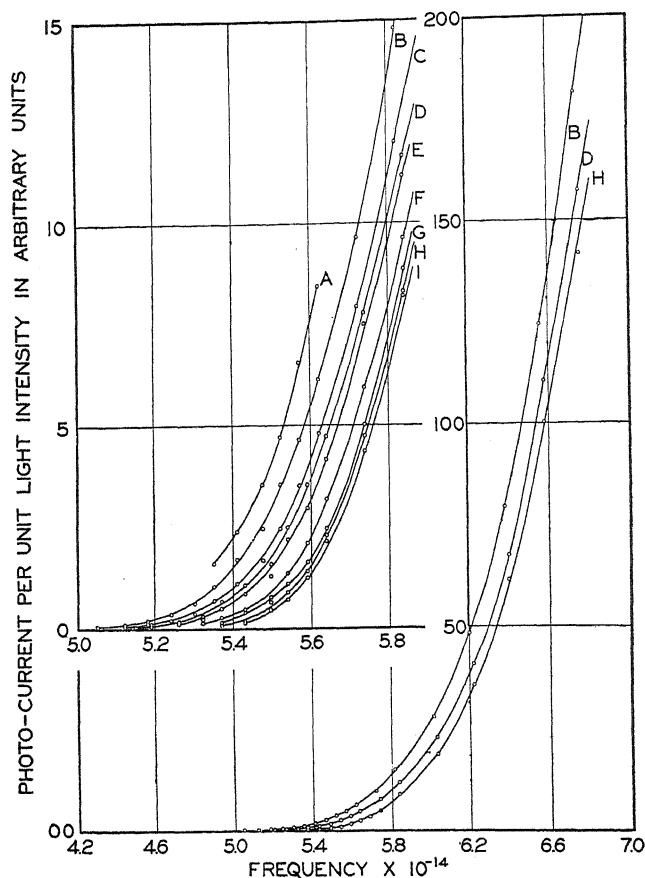


Fig. 2. The photoelectric current as a function of the frequency of the incident light for a potassium film on tungsten for various fields drawing electrons away from the surface. At right, complete curves for three values of the field. At left, similar curves for nine values of the field on an enlarged scale. The fields in volts per centimeter are for the curves A to I: A, 63, 100; B, 36,200; C, 22,100; D, 15,800; E, 9000; F, 3100; G, 1000 H, 260; and I, 0.

EXPERIMENTAL RESULTS

The photoelectric sensitivity curves for a film of potassium on the 0.9 mil tungsten filament, for different voltages are shown in Fig. 2. The three curves to the right are the sensitivity curves over the range of wave-lengths studied. The photoelectric threshold with an accelerating field of 260 volts/

cm, curve *H*, was 5620\AA ($5.35 \times 10^{14} \text{ sec}^{-1}$) and for fields of 36,200 volts/cm, curve *B*, the threshold was shifted to 5880\AA ($5.10 \times 10^{14} \text{ sec}^{-1}$).

At the left, the portions of the curves near the threshold are plotted on an enlarged scale. The scale of frequencies has been doubled and that of the current increased tenfold. The increased scale allows the current taken with

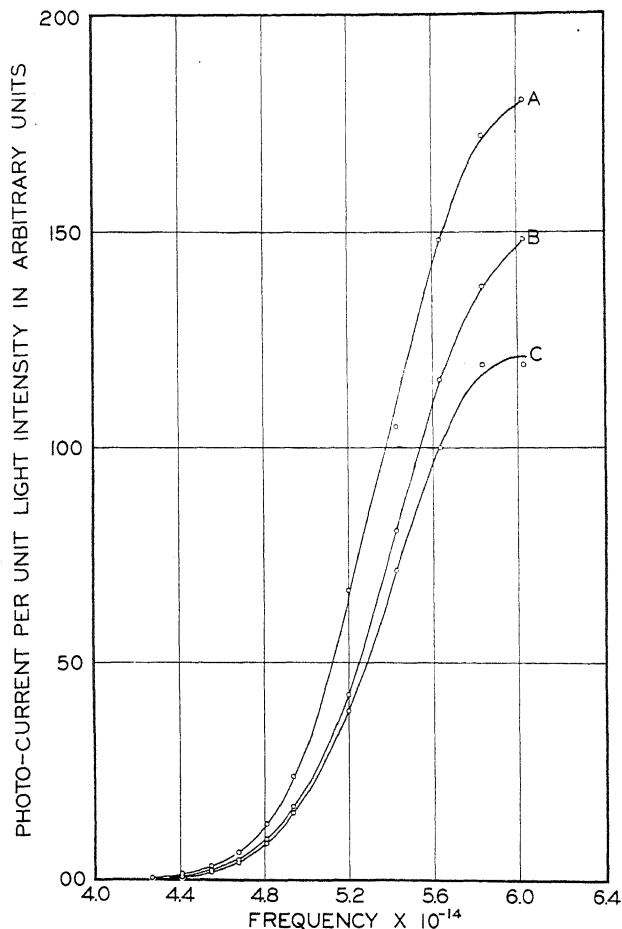


Fig. 3. The photoelectric current as a function of the frequency of the incident light for potassium on a thick layer of oxygen on tungsten. The fields in volts per centimeter for the curves *A* to *C*: *A*, 18,300; *B*, 4570; and *C*, 366.

the nine different accelerating fields to be plotted, while at the right only three representative ones have been selected. The fields for curves *A* to *I* in volts per centimeter are: *A*, 63,100; *B*, 36,200; *C*, 22,100; *D*, 15,800; *E*, 9000; *F*, 3100; *G*, 1000; *H*, 260; and *I*, 0. It was not possible to use higher electric fields, because of the setting in of field currents of the same order of magnitude as the photoelectric currents. *It is evident from the figure that the shift is not proportional to the strength of the field, but as will be shown later,*

is more nearly proportional to the square root of the field. Not only is the threshold shifted, but the entire sensitivity curve is displaced by the field. The curves do not meet the frequency axis at a finite angle, but approach tangentially, as near as can be experimentally determined. The recorded thresholds were arbitrarily chosen as the points where the currents became definitely measurable.

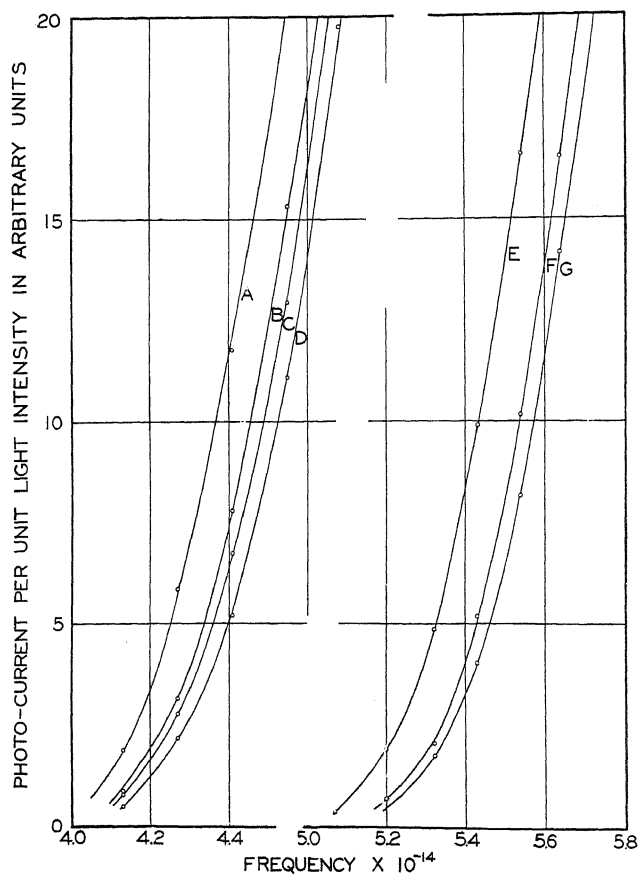


Fig. 4. The photoelectric current as a function of the frequency of the incident light. Curves A and D for the surface of figure 3 after being heated to 1100° C. The fields in volts per centimeter are: A, 18,600; B, 4650; C, 372; D, 0. Curves E to G show data obtained from the same surface after being heated to 1600° C. The fields are: E, 18,600; F, 372; and G, 0.

To test for the existence of contact potentials between the filament and anode, a photoelectric sensitivity curve was made with a retarding potential of 0.7 volts. The curve cut the frequency axis where the frequency was 1.3×10^{14} greater than for zero potential. This corresponds to a shift of 0.54 volts. Thus the contact difference in potential was less than 0.2 volt in a direction to produce an accelerating field.

A layer of oxygen was allowed on the 3.0 mil filament before the potassium was distilled into the tube. The results shown in Fig. 3 show that the thresh-

hold of this surface was not appreciably shifted by fields as large as 18,300 volts/cm. Near the maximum sensitivity, the emission with a field of 18,300 volts/cm was 1.5 times, and at 4570 volts/cm was 1.17 times the emission at 366 volts/cm (curves *A*, *B* and *C* respectively). The oxygen layer shifted the threshold from 5620Å for the pure potassium surface to 7100Å ($4.25 \times 10^{14} \text{ sec}^{-1}$). At the same time the nature of the surface was changed so that the threshold was little affected by the accelerating fields.

The filament was then heat treated at about 600° C for 5 minutes, allowed to cool and observations were made. It was then heat treated at successively higher temperatures up to about 1600° C. Curves *A* to *D*, Fig. 4, show the emission from the filament after being heated to 1100° C and then allowing the potassium to distil back onto the filament with the reduced oxide coating. Heat treating at this temperature produced the first observable difference from the unheated surface. Curves *E* to *G* show the results after the filament had been heated for a few minutes at 1600° C. These curves show only the region near the threshold on the enlarged scale used for the left half of Fig. 2. They are not continued to the frequency axis because when taking the data the region very close to the threshold was not measured in detail. However, single tests made near the threshold showed that for these surfaces these sensitivity curves are tangent to the zero axis.

Of interest is the fact that reducing the thickness of the oxygen film shifted the threshold still farther to the red, that is to 7500Å ($4.0 \times 10^{14} \text{ sec}^{-1}$), and then the further removal of the film shifted the threshold back to 5880Å ($5.1 \times 10^{14} \text{ sec}^{-1}$) or nearly back to the value found in the first cell.

The maximum photoelectric emission per unit light intensity of the surface with a thick oxygen layer and that of the same surface after being heated to 1100° C was about one-seventh that of the surface after most of the oxygen had been removed by heating to 1600° C. This latter surface had a photoelectric emissivity about equal to that of the pure potassium film on tungsten.

Throughout the investigation it was noted that after heating the filament, and thereby removing the potassium and some of the oxygen, from 24 to 48 hours elapsed before the characteristics of the surface became constant.

DISCUSSION OF RESULTS

Evaluation of surface fields from experimental data.

As previously stated, a considerable portion of the work function of metal surfaces can be accounted for by assuming that the field through which an electron leaves the surface is that due to its own image in the metal. This was considered by Lennard⁶ and Debye⁷ and discussed in detail by Schottky.⁸ If an electron is at a distance x from the surface, its image produces a field E_i of magnitude,

⁶ P. Lennard, Ann. d. Physik 8, 149 (1902).

⁷ P. Debye, Ann. d. Physik 33, 441 (1910).

⁸ W. Schottky, Phys. Zeits. 15, 872 (1914).

$$E_i = -\frac{e}{(2x)^2} = -\frac{e}{4x^2}. \quad (1)$$

The potential of the image field at the distance x from the surface, considering the zero potential to be at $x = \infty$ with no accelerating field, would be:

$$V_i = -\int_{\infty}^x E_i dx = -\int_{\infty}^x \frac{e dx}{4x^2} = -\frac{e}{4x}. \quad (2)$$

Now if an external accelerating field E_a be applied, its potential at a distance x from the surface would be:

$$V_a = -E_a x \quad (3)$$

and the potential resulting from the two fields, the sum:

$$V = -\frac{e}{4x} - E_a x. \quad (4)$$

To find the maximum potential, the derivative of Eq. (4) may be equated to zero which is the same as equating the resultant field to zero.

$$-\frac{dV}{dx} = E = -\frac{e}{4x^2} + E_a = 0. \quad (5)$$

Solving for the value of x at the maximum:

$$x_{\max} = \frac{1}{2} \left(\frac{e}{E_a} \right)^{1/2}. \quad (6)$$

Substituting this value in (4) gives the value of the maximum potential:

$$V_{\max} = -\frac{e}{4} 2 \left(\frac{E_a}{e} \right)^{1/2} - \frac{E_a}{2} \left(\frac{e}{E_a} \right)^{1/2} = -(eE_a)^{1/2}. \quad (7)$$

Since the potential of the free electron has been chosen as zero, $(eE_a)^{1/2}$ represents the reduction in the maximum of the potential energy curve due to the applied field E_a . If the image forces were the only ones acting on an electron leaving the surface, this reduction in potential would represent the reduction of the work function of the surface.

This simple explanation will not hold for all distances from the surface, since the integral in Eq. (2) becomes infinite for $x=0$, which would represent an infinite work function. However of course for distances of atomic magnitude from the metal, the image forces no longer are of this form. The precise manner in which the field departs from the ideal image law is of no consequence to the present discussion.

Regardless of the assumed law of force near the surface of the emitting metal, an increase in the strength of the accelerating field will reduce the work function of the surface. When an electron is leaving the surface of a metal under the combined action of the surface fields and an accelerating field, it is

retarded until it reaches a distance from the surface x_1 where the applied field equals the surface field. As soon as it passes that point it is free and is accelerated from the surface. If the accelerating field is increased by an amount ΔE_a in es units, the field which the electrons must overcome is reduced by an equal amount, and since the electrons must work against this field for a distance x_1 to escape, the decrease in energy necessary for unit charge to escape would be:

$$-\Delta\chi = x_1\Delta E_a. \quad (8)$$

Where $\Delta\chi$ is the change in the work function due to the change in the applied field ΔE_a . Dividing Eq. (8) by ΔE_a and considering the limit as ΔE_a approaches zero:

$$\frac{d\chi}{dE_a} = -x_1. \quad (9)$$

Thus observations on changes of the work function in strong fields yield directly the magnitudes of the electric fields near the surfaces. This method of evaluation of surface fields is due to Becker and Mueller.⁹

The above holds for any kind of electron emission, and the photoelectric threshold frequency gives a convenient measure of the work function as given by the Einstein relation:

$$h\nu_0 = e\chi. \quad (10)$$

Differentiating Eq. (10) and solving for $d\chi$ one obtains

$$d\chi = \frac{h d\nu_0}{e}. \quad (11)$$

Substituting the value of $d\chi$ from (11) into (9)

$$\frac{d\nu_0}{dE_a} = \frac{x_1 e}{h}. \quad (12)$$

Or expressing the field E_v in volts per centimeter:

$$\frac{d\nu_0}{dE_v} = -\frac{x_1 e}{300h} \text{ or } x_1 = -\frac{300h}{e} \frac{d\nu_0}{dE_v}. \quad (13)$$

Thus the distance from the surface x_1 where the applied field equals the surface field, is proportional to the slope of the ν_0 vs. E_v curve, evaluated at the particular value of the field in question.

This method of determination of the surface fields is independent of an exact measurement of the threshold, and depends only on the measurement of the displacements of the threshold. These displacements were measured a short distance away from the zero current axis, where the slopes of the curves were greater and the accuracy of the current measurements better.

⁹ See ref. 2.

This procedure was justified because the electric fields produced a parallel displacement of the curves. The shifts could thus be determined with considerable accuracy.

In Fig. 5 curve *A* shows the Schottky shift as calculated from Eq. (7) making allowance for the change in units. Curve *C* shows the shift of the threshold of the pure potassium surface from the data of Fig. 2. The sur-

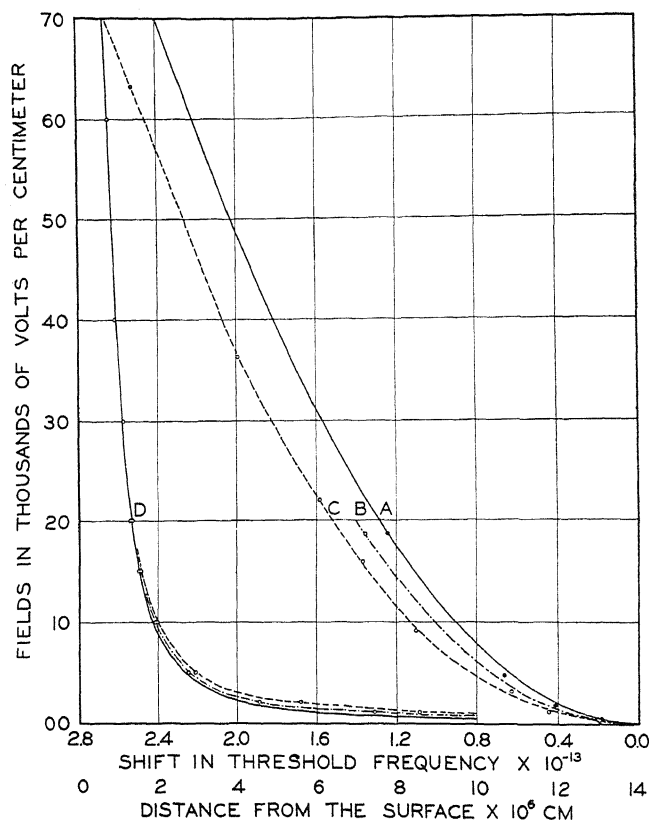


Fig. 5. Curves *A* to *C* show the shift of the threshold as a function of the field. Curve *A* the Schottky shift; *C*, the shift for the pure potassium surface; *B*, the shift for the surface heated to 1600° C, and the black dots the shifts for the surface heated to 1100° C. The curves *D* show the fields near the surface as a function of the distance from the surface. The type of line indicates the curve *A* to *C* from which it was deduced.

face with a thick oxygen layer showed negligible shift and was not plotted. The shifts measured from the curves *A* to *D* Fig. 4 were so nearly the Schottky values that the displacements are shown by the black dots only. This was the surface produced by heat treatment at 1100° C. Curve *B* shows the displacements measured from curves *E* to *G* Fig. 4, and shows the displacements of the threshold of the surface after being heated to 1600° C. From the three curves only two displacements could be measured, but

since both of these fell about midway between the theoretical curve and curve *C*, it was assumed that the complete curve was about as drawn.

The curves marked *D* show the fields calculated from the slope of the experimental curves *B* and *C* as compared with a calculated image field, drawn as a solid line. The single circles above fields of 20,000 volts/cm show the fields calculated from curve *C*. They show that the fields are very closely image fields between 7×10^{-7} and 1.2×10^{-8} cm from the surface. At greater distances, the fields of the two surfaces are greater than image fields. The field near the surface after it was heated to 1100°C is about the image field, and apparently the surface with a thick layer of oxygen under the potassium had only negligible fields which could be overcome by the applied fields.

It is of interest to note how closely the observed surface fields coincide with the image field within 1.2×10^{-6} cm of the surface. The deviation at greater distances is undoubtedly real though small. It is very small compared to the large deviations noted by Becker and Mueller,¹⁰ Reynolds¹¹ and others for thoriated tungsten surfaces.

The possible sources of fields greater than the Schottky fields at large distances from the surface have been discussed by many investigators.¹² The best explanation seems to be that the potassium film is not uniform over the surface, so that there are areas of different work functions. The areas of lower work function are electropositive with respect to those of higher work function. The electrostatic fields between these areas are in such a direction as to retard electrons leaving the surface through areas of lower work function. Near the threshold frequency, only the areas of lower work function are able to emit, and these electrons emerge with a retarding field equal to that of their image plus that due to the potential differences on the surfaces. The image field falls off as the square of the distance from the surface, while the fields due to these patches fall off much more slowly. Over the center of such a patch the field would be essentially constant to a distance comparable with about one-tenth of the diameter of the patch. Thus the extra field might be negligible compared to the image field near the surface and at greater distances become larger than the image field. It should be emphasized that to account for the deviation from Schottky fields at distances of 5×10^{-6} cm from these surfaces, it is necessary to postulate the existence of patches having a diameter about ten times this magnitude. Irregularities of atomic dimensions such as unequal distributions of ions over the surface as has been proposed by Suhrmann¹³ are not capable of accounting for the experimental facts.

Since the film of potassium on the layer of oxygen which removed the

¹⁰ See ref. 2.

¹¹ N. B. Reynolds, *Phys. Rev.* **35**, 158 (1930).

¹² O. W. Richardson and A. F. A. Young, *Proc. Roy. Soc. A* **107**, 377, (1925). See also work of Becker and Mueller, ref. 2, that of Reynolds, ref. 10, and of B. Gudden, *Naturwissenschaften* **16**, 547 (1928).

¹³ R. Suhrmann, *Naturwissenschaften* **16**, 616 (1928).

threshold farthest to the red exhibited very closely the Schottky field, it follows on this view that such films are homogeneous, and free from patches. In other words, the ions are distributed uniformly over the surface. Moreover it follows that the alkali film surfaces of the present experiments were much more homogeneous than the surfaces of thoriated tungsten studied by Becker and Mueller, Reynolds and others.

It is not evident why the surface with a thick oxygen layer should fail to show a reduction in the work function when the accelerating field is applied. There are two possible explanations. One is that the ions are about 300 atom diameters out from the surface of the tungsten, and the field between the positive potassium layer and the tungsten counteracts the image field in this region. At distances farther out, the image field is small and the counteraction of this by the applied field would not shift the threshold appreciably. The other postulates that the thick oxide layer is extremely rough, and the applied field can lower the work function of only the highest points, and since these constitute only a small part of the area, their emission would not appreciably affect the observed threshold. The principal part of the emission would occur from the hollows where the externally applied fields would be always greatly reduced. The small increase in the field would greatly assist the electrons emitted in the cavities to emerge without striking the walls of the cavity. This latter explanation seems to be more probable since this surface showed much poorer saturation than any of the others.

Comparison with theories of the photoelectric effect.

For the several surfaces and the many surfaces fields, i.e. the many thresholds studied in the present experiments the shape of the photoelectric sensitivity curves remained the same. Thus the form of the curve is practically independent of such superficial factors as the form of potential barriers at metal surfaces and therefore is of interest theoretically as well as experimentally.

From the standpoint of the wave mechanics, Wentzel¹⁴ has calculated the rate at which free electrons in a metal are excited to higher energy states which enable them to escape over the potential wall of a metal surface, when light falls on that surface. He finds that this rate Z for light of frequency ν having electric vectors proportional to E_x , E_y , E_z incident on a metal surface with the normal along the x direction is:

$$Z \sim \frac{1}{\nu^{7/2}} \xi^2 \left\{ E_x^2 + \frac{m}{2h\nu} \left[\frac{1}{2} \xi^2 E_x^2 + \eta^2 E_y^2 + \zeta^2 E_z^2 \right] \dots \right\} \quad (14)$$

where ξ , η , ζ are the velocity components of the electrons before the excitation by the light. He derived an expression for the total photoelectric emission from a surface by integrating the above expression over the distribution of energies of the electrons in the metal. In order to obtain approximate

¹⁴ G. Wentzel, in Sommerfeld's 60. Geburtstag Festschrift, Probleme der Modernen Physik, edited by P. Debye, p. 79. Leipzig, 1928.

expressions he assumed the distribution of energies to be the Fermi-Dirac distribution at the absolute zero of temperature—a distribution of the form:

$$n(\epsilon)d\epsilon = 4\pi \left(\frac{2m}{h^2} \right)^{3/2} \frac{(\epsilon)^{1/2} d\epsilon}{e^{(\epsilon-\bar{\epsilon})/kT} + 1} \quad (15)$$

where $n(\epsilon)d\epsilon$ is the number of electrons having energies between ϵ and $\epsilon+d\epsilon$. It is seen that at absolute zero the number increases as the square root of ϵ to a sharp upper limit for $\epsilon=\bar{\epsilon}$, the maximum energy of the Fermi distribution above which no electrons exist. The expression for the probability of excitation of an electron in the metal by impinging light indicates that the probability varies approximately as the square of the velocity of the electron and as the frequency of the light to the inverse 7/2 power. The Fermi distribution clearly led then to a formula for the total emission as a function of the frequency, having a sharp rise from a threshold value corresponding to the minimum energy necessary for an electron, having the maximum energy $\bar{\epsilon}$ of the Fermi distribution, to escape from the surface. The formula obtained in the case $\nu_0 < \nu < \nu_a$ is the following:

$$I \sim [\bar{\nu}^{5/2} - (\nu_a - \nu)^{5/2}] \nu^{-7/2} E_x^2 + \frac{1}{14} [\bar{\nu}^{7/2} - (\nu_a - \nu)^{7/2}] \nu^{-9/2} [3E_x^2 + 2E_z^2 + 2E_y^2] + \dots \quad (16)$$

Where $h\bar{\nu} = \epsilon$, the maximum energy of the Fermi distribution at 0°K, $h\nu_a = \epsilon_a$, the energy required by an electron at rest in the metal to escape over the potential barrier, and $\nu_0 = \nu_a - \bar{\nu}$ is the threshold frequency. For $\nu < \nu_0$ there is no emission, and for $\nu > \nu_a$, $I \sim \nu^{-7/2}$. The maximum of the photoelectric sensitivity curve is in the interval $\nu_0 < \nu < \nu_a$, and this comprises the frequencies used in the present research.

The above expression really gives the rate at which electrons in the metal acquire enough energy to emerge from the metal and of course is equal to the photoelectric emission provided that the excited electrons do not make an appreciable number of inelastic impacts before striking the surface of the metal normally. Houston¹⁵ has pointed out this tacit assumption of electron elastic impacts in Wentzel's derivation and believes a more nearly correct estimate of the photoemission would take account only of the electrons having great enough energies in their velocity components normal to the surface to escape. Integrating then the expression over the distribution of velocities normal to the surface in excess of a minimum value requisite to overcome the potential barrier, Houston has obtained the following expression:

$$I \sim \left(\frac{\bar{\epsilon}}{h\nu} \right)^{1/2} \left\{ \frac{E_x^2}{\nu} \left[1 + \frac{\bar{\epsilon}}{2h\nu} \right] + \frac{E_y^2 + E_z^2}{3\nu} \left[\frac{\nu - \nu_0}{\nu} \right] \right\} \left(\frac{\nu - \nu_0}{\nu} \right)^2 \quad (17)$$

where I is the photoelectric emission at 0°K, $\bar{\epsilon}$ corresponds to the maximum

¹⁵ We wish to thank Professor W. V. Houston for allowing us to read an unpublished manuscript dealing with this point.

energy of the electrons in the degenerate Fermi distribution and ν_0 is the threshold frequency.

Wentzel¹⁶ is in agreement with Houston on the necessity of taking account of the distribution in direction of the velocities of the electrons in the metal in computing the rate of emission and has modified his original expression (16) obtaining

$$I \sim 1/\nu^{7/2} \left\{ \frac{1}{3} \bar{\nu} [\bar{\nu}^{3/2} - (\nu_a - \nu)^{3/2}] - \frac{1}{5} [\bar{\nu}^{5/2} - (\nu_a - \nu)^{5/2}] \right\} E_x^2 \quad (18)$$

+ higher powers in $\bar{\nu}/\nu$ (for $T=0^\circ\text{K}$) which is essentially the same as Houston's formula in so far as the first term of the expansion in $\bar{\nu}/\nu$ is accurate.

It has been thought by some that photoelectric thresholds are sharp, and thus in accordance with Wentzel's formula¹⁶ and that lack of sharpness is ascribable to experimental errors, such as those introduced by scattered light. Others have observed photoelectric sensitivity curves approaching the frequency axis with zero slope, as is the case in the present experiments.¹⁷ A simple calculation shows that the rounding off introduced by the temperature effects accounts for about half of the observed lack of sharpness of the thresholds in the present experiments, if Wentzel's first method of calculation be assumed. *Houston's calculation (Eq. (17)) corrected for temperature effects is adequate to account for nearly the whole tailing off of the here recorded sensitivity curves.* In a later experiment it is hoped to verify the calculated magnitude of the temperature effect by studying the sensitivity as a function of the temperature.

Fowler¹⁸ has discussed the sharpness of photoelectric thresholds in a manner similar to Wentzel's original deduction, and therefore Houston's objections apply equally well to Fowler's conclusions that thresholds are sometimes sharp.

It has been mentioned that electrons can pass through regions of potential greater than that corresponding to their energy. The magnitude of the effect of applied fields at a metal surface is contained in the following formula:¹⁹

$$D(W) = \frac{4[W(W - \epsilon_a)]^{1/2}}{\epsilon_a} e^{-4\kappa(\epsilon_a - W)^{3/2}/3Ee}, \quad \kappa^2 = \frac{8\pi^2 m}{h^2} \quad (19)$$

where $D(W)$ is the probability that an electron with an energy W for the component of its velocity normal to the surface, will pass through a potential barrier whose maximum is ϵ_a volts greater than the zero of energy in the metal, when an accelerating field E is applied. For the maximum field, 63,000 volts/cm, used in the present experiments and assuming ϵ_a to be 7 volts, the probability $D(W)$ that an electron whose kinetic energy W is nor-

¹⁶ We wish to thank Professor Wentzel for this information sent to us in a private communication.

¹⁷ For discussion of this see B. Gudden, *Lichtelektrische Erscheinungen*, p. 37ff. Berlin, 1928.

¹⁸ R. H. Fowler, *Proc. Roy. Soc. A* **118**, 229 (1928).

¹⁹ See ref. 1.

mal to the surface is 0.1 volt less than ϵ_a , the amount required to go over the potential barrier, is less than 10^{-15} . It is evident therefore that this type of influence of the shape of the photosensitivity curve was inappreciable for the fields used in the present experiments. A more favorable case for the observation of this influence of strong fields on photoelectric emission would be that of a metal having a high work function like pure tungsten where much higher electric fields may be applied before the autoelectronic current becomes appreciable.

The changes of the whole photoelectric sensitivity curves produced by applied accelerating fields observed in the present experiments are of fundamental interest, for the effect of the applied fields is to alter the work function without affecting any other characteristics of a metal concerned in its photoelectric properties. Both Wentzel's and Houston's formulas agree in indicating that over the present range of observation the whole photoelectric sensitivity curve shifts by approximate parallel displacement along the frequency axis with the threshold. Alteration of the nature of the work function (the surface electrostatic fields) does not affect markedly the form of the sensitivity curve. *This prediction of the wave mechanical theory of the photoelectric effect is strikingly confirmed in the present experiments.*

THE MAGNETIC ISOTROPY OF COPPER CRYSTALS*

BY CAROL G. MONTGOMERY

SLOANE PHYSICS LABORATORY, YALE UNIVERSITY

(Received June 23, 1930)

ABSTRACT

The variation in the magnetic susceptibility with the direction of the applied field was investigated for large single crystals of copper. A modification of Curie's method of measurement was used. A Fourier analysis of the results indicates that there is no variation of susceptibility larger than 1%, a result consistent with the magnetic isotropy of cubic crystals predicted by the theory of W. Thomson.

I. INTRODUCTION

SINCE its conception in 1851, the description by means of the familiar ellipsoid of magnetization of the variation of the magnetic susceptibility of a non-ferromagnetic crystal with respect to the direction of the applied magnetic field has been accepted as correct until quite recently. It follows from this theory that for substances which form cubic crystals, there can be no dependence of the magnetic susceptibility upon direction of applied field so that the material must be magnetically isotropic.

In 1926, J. Forrest¹ performed some qualitative experiments on a number of cubic crystals and found that they were not isotropic, but that they showed variations in susceptibility as do single crystals of iron and nickel. McLennan and Cohen² investigated the magnetic susceptibility of large single crystals of a number of metals, and found that while bismuth seems to follow a law of variation with the direction of the magnetic field in accord with the accepted theory, antimony deviates noticeably from it. In addition, recent work³ on the Peltier and Thomson effects, which should obey the same symmetry relations as the magnetic susceptibility, seem also to show a deviation from the theory. Thus the accepted theory may have a more limited range of application than hitherto supposed, and it was deemed advisable to reinvestigate a cubic crystal, and to determine whether or not it is magnetically isotropic.

II. APPARATUS AND METHOD OF MEASUREMENT

In order to measure the susceptibilities of crystals it was decided to use a modification of Curie's method which has been developed to quite an extent by P. Weiss and his collaborators, a description of the final apparatus

* Part of a dissertation presented for the degree of Doctor of Philosophy at Yale University.

¹ J. Forrest, Trans. Roy. Soc. Edinburgh 54, 601-701 (1926).

² J. C. McLennan and E. Cohen, Trans. Roy. Soc. Canada [3] 23 III, 159-168 (1929).

³ H. D. Fagan and T. R. D. Collins, Phys. Rev. [2] 35, 421-427 (1930); P. W. Bridgman Proc. Amer. Acad. 63, 351-399 (1929).

being given by Foex and Forrer.⁴ The apparatus described below differs from theirs in several details.

A beam, 90 centimeters long, composed of three parallel lengths of quarter inch balsa wood, fastened at the ends and in the center at the corners of equilateral triangles, is suspended by five silk threads approximately 50 centimeters in length. These five suspensions are arranged so as to permit translation of the beam only in the direction of its length. They are hung at the top from a heavy iron frame in such a way that their lengths can be separately adjusted. The lower member of the beam is extended at one end and carries a small piece of aluminum with a vertical hole drilled in it about 2 centimeters deep. Into this hole fits the shaft of a crystal holder on which the crystal is placed. The crystal holder consists of a 7 centimeter length of #16 sterling silver wire on which fits a small cylindrical cap of amber, cut away at the top to fit the crystals, and graduated on the side every 10°. These graduations could be observed by means of a reading microscope and the azimuth of the holder thus read off. An electromagnet capable of producing fields up to about 5000 gauss was used. It was equipped with special pole pieces so as to obtain a field which has a high value of the product of the field by its derivative over a large area. Under the crystal holder, a small saddle, constructed out of copper wire and a small piece of paper, was fastened. This could hold either the crystals or the standard on the beam but was out of the field while measurements were being taken.

The other end of the balsa wood beam carried a celluloid cylinder 6 centimeters in diameter and 15 centimeters long, closed at one end, into which fits a piece of wood with a clearance all around of about 4 millimeters. This provides air damping which, combined with the electromagnetic damping of the sample in the field, is quite satisfactory.

At the center of the beam and perpendicular to it, is an aluminum arm extending some 10 centimeters out, to which is firmly waxed a phonograph needle pointing in the direction of the beam. This needle rests against and perpendicular to a microscope cover glass 1 centimeter in diameter. This is attached to the back of a galvanometer mirror suspended at both ends by a tightly stretched vertical quartz fiber of diameter about 50 microns. The plane of the cover glass makes an angle of 135° with the mirror. Light from an illuminated cross hair is reflected by the mirror and falls on a scale some two meters distant. Thus this arrangement acts as an optical lever and gives a total magnification of the motion of the beam of about 1000 times. The whole arrangement was placed in a wooden box having a large glass window on the side in order to stop air currents. The box was put on a stone pier in a sub-basement room to avoid mechanical vibrations.

When current is passed through the magnet coils, a force is exerted on the specimen and the beam will deflect until the force of gravity balances out the magnetic force. Suppose to do this the beam moves a distance x , and let l be the effective length of the suspensions, m the total mass of the suspended system, f the magnetic force, and g the acceleration of gravity.

⁴ G. Foex and R. Forrer, *Jour. de Physique* [6] 7, 180-187 (1926).

Then

$$x = fl/mg \quad \text{when } x \ll l.$$

Now if the crystal has a susceptibility* k in the direction of the field, we have

$$f = \int k H_y \frac{\partial H_y}{\partial x} dv$$

where the x -axis is in the direction of the beam, the y -axis in the direction of the field, and the integral is taken over the volume of the crystal. Now if the variation of f with respect to x is small, then

$$x = Ak$$

where A is a constant. Hence, if we have a substance with a known value of the susceptibility, we can measure the susceptibility of any other substance by determining the value of A .

In order to test the validity of the assumption that f does not vary appreciably with the position of the crystal, a series of values of x were measured for various values of the field strength. We see from the above equations that

$$x \sim H_y \frac{\partial H_y}{\partial x} \sim H^2$$

if the assumption is justified, and hence if we plot values of x as a function of H^2 we should get a straight line through the origin. With values of the field strength measured in arbitrary units by a ballistic method, we find that within the limits of accuracy of a reading, we do get such a straight line.

Measurements were made of the variation of susceptibility of single crystals of copper as a function of the azimuth of the field. Gold was used as the standard substance. We see that to compare susceptibilities of two substances by this method we must keep the mass of the beam constant. Hence the following procedure was followed in measurement. The gold standard was placed in the paper saddle, and a copper crystal in the crystal holder. Then a series of deflections of the spot of light was observed for 36 azimuths of the crystal. Then the crystal was removed and placed in the saddle, while the gold was placed in the holder. A series of deflections for four azimuths was then taken. Then both the crystal and the gold were placed in the saddle and the deflections due to the holder alone were observed for the same four azimuths.

The zero shift over the whole period of time required for one such set (about ten hours) was not more than 50 to 75 millimeters.

III. PREPARATION OF SPECIMENS AND DETERMINATION OF THEIR ORIENTATION

The copper crystals used in these experiments were obtained from the Hammond Metallurgical Laboratory, Yale University, through the courtesy

* This is not a true susceptibility, but the difference between the susceptibility of the crystal and the surrounding medium, in this case, air.

of Dr. C. H. Mathewson. They were prepared⁵ from the highest purity electrolytic copper by slowly lowering a graphite crucible containing the molten copper out of an induction furnace whose temperature at the center was maintained well above the melting point of copper. The rate of lowering was about 0.6 centimeter per hour. The single crystals so obtained were in the form of rough cylinders approximately a centimeter in diameter and 12 to 15 centimeters long. When these rods were etched in a 50 percent solution of nitric acid for a short time, and then washed, the surface of the rod would shine out brilliantly when held at certain positions with respect to parallel incident light. This is due to the fact that the etching process forms micro-

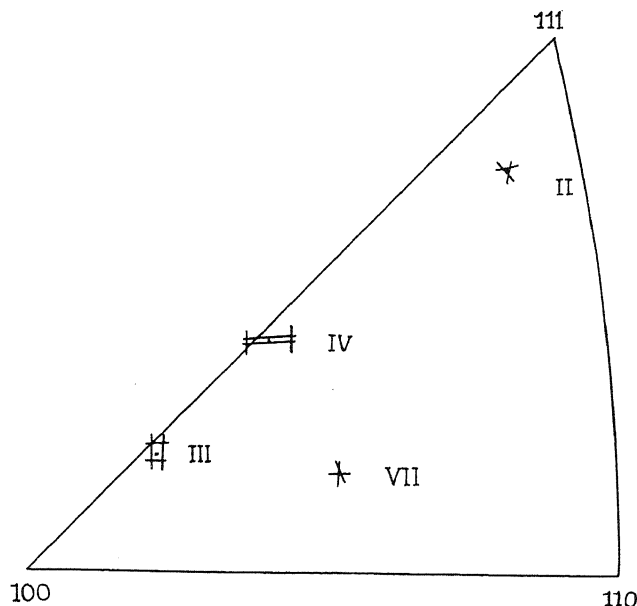


Fig. 1. Stereographic projection of the axes of the crystal rod.

scopic pits in the surface whose sides are definite crystal planes, and it is the light reflected from these pit-faces that gives rise to the selective reflection. It is evident that if the positions of these faces with respect to the rod as a whole could be determined, and the crystallographic form of these faces identified then the orientation of the crystal lattice with respect to the rod as a whole could be obtained. Bridgman⁶ has described one method of accomplishing this, but a more convenient, if not more accurate, arrangement was used here. The lenses were all removed from the telescope tube of a large polarizing spectrometer, and a plane piece of glass was fastened to the end of the telescope so that the normal to its plane was horizontal and made an angle of 45° with the axis of the telescope. The crystal rod was mounted horizontally and attached to a vertical circle carried by the

⁵ C. H. Mathewson and K. Van Horn, A. I. M. E. Tech. Pub. No. 301-E-109, Feb., 1930.

⁶ P. W. Bridgman, Proc. Amer. Acad. 60, 305-383 (1925).

collimator tube. The light of a small carbon arc with condensing lenses was thrown on the piece of glass on the telescope and reflected to the crystal. By changing the position of the crystal with respect to the light beam, it could be adjusted so that the light from a reflecting surface could be viewed through the telescope. The spherical coordinates of the normal to the pit-face could then be read off the horizontal and vertical circles. The points corresponding to these coordinates were then drawn on a 15 centimeter marble sphere, and the crystallographic planes corresponding to each reflection maximum could be identified. The position of the rod axis with respect to the crystal lattice was then determined by plotting the observed angles on a stereographic net.

Considerable difficulty was sometimes experienced in getting reflections which could be unambiguously identified. The etching process seems to be a difficult one to control satisfactorily, a condition due to the fact that the reaction is a complicated one and particularly dependent upon the amounts of the end-products present in the etching solution. Various concentrations of nitric acid were tried, and consistent results were obtained more often with a 50 percent by volume solution than with any other. Figure 1 shows the stereographic projection of the rod axes of the crystals used.

The specimens were prepared by cutting off a section from the long rod. In order to cut the single crystal rods without spoiling them by introducing too large strains, the following method was used. Two vises were set up and the jaws accurately aligned on the bench of a milling machine. The rod was well padded with paper and held firmly in one vise between two V-blocks. In the other vise was held a jig consisting of two guide slots attached to a piece of steel at right angles to its length. A hack saw blade, 0.025 inch (0.064 centimeter) thick, with all the set removed from the teeth, fitted into these two slots and could be moved only in the plane defined by them. From 30 to 40 minutes were taken to make a cut, and plenty of oil was used. When a section had been cut off, the burr was removed with a fine file and the surface removed in a 50 percent nitric acid solution until the characteristic shine was restored. Care had to be taken to keep the crystals away from moist air, as they tarnished quite rapidly.

The following table gives the dimensions of the crystals used.

Crystal	Diameter	Length	Mass
II	0.764 cm	0.991 cm	3.921 gram
III	0.767	0.968	3.849
IV	0.770	0.993	4.057
VII	0.772	0.942	3.927
Gold Standard	0.770	0.975	8.752

As a substance of standard susceptibility, a piece of gold was used. It was obtained from Baker and Co. who stated that the purity was over 99.99 percent. A piece was machined out whose size was close to that of the crystal specimens. The value of the susceptibility chosen was that obtained

by Owen,⁷ viz., -0.141×10^{-6} cgs. This same value was obtained by Seeman and Vogt,⁸ who have recently investigated copper-gold alloys.

No traces of ferromagnetic impurity could be detected in either the copper crystals or the gold standard.

IV. REDUCTION OF OBSERVATIONS AND RESULTS

In order to insure that the copper crystals used were sufficiently representative, average values of the susceptibility were obtained for each. Taking into account small corrections due to the magnetic effect of the crystal holder and of the air, we get the following values of the specific susceptibility of the different crystals:—

Crystal	$\chi_{\text{Cu}} \cdot 10^6$
II	-0.088
III	-0.075
IV	-0.086
VII	-0.091
Mean	-0.085

The spread of values here is just about that to be expected. Owen⁷ gives the value

$$\chi_{\text{Cu}} = -0.085 \cdot 10^{-6}.$$

In order to bring out any possible anisotropy in the susceptibility of copper it is sufficient to use relative values of the susceptibility only. The values of the deflections obtained with a crystal in the holder were therefore subjected to a Fourier analysis, obtaining the coefficients of the first four cosine and the first four sine terms.

We obtain the following results in millimeters.

$$\begin{aligned} x_{\text{Cu II}} = & 76.31 - 1.88 \cos \varphi - 0.68 \cos 2\varphi - 0.36 \cos 3\varphi \\ & + 0.30 \cos 4\varphi - 0.68 \sin \varphi - 0.44 \sin 2\varphi \\ & + 0.11 \sin 3\varphi - 0.61 \sin 4\varphi, \end{aligned}$$

$$\begin{aligned} x_{\text{Cu III}} = & 68.85 - 2.41 \cos \varphi - 0.36 \cos 2\varphi + 0.08 \cos 3\varphi \\ & - 0.05 \cos 4\varphi - 0.39 \sin \varphi - 0.16 \sin 2\varphi \\ & - 0.07 \sin 3\varphi - 0.05 \sin 4\varphi, \end{aligned}$$

$$\begin{aligned} x_{\text{Cu IV}} = & 75.88 - 0.95 \cos \varphi - 0.29 \cos 2\varphi + 0.16 \cos 3\varphi \\ & - 0.03 \cos 4\varphi - 0.45 \sin \varphi + 0.36 \sin 2\varphi \\ & + 0.15 \sin 3\varphi + 0.03 \sin 4\varphi, \end{aligned}$$

$$\begin{aligned} x_{\text{Cu VII}} = & 76.30 - 0.87 \cos \varphi - 0.26 \cos 2\varphi + 0.38 \cos 3\varphi \\ & + 0.02 \cos 4\varphi + 0.24 \sin \varphi + 0.41 \sin 2\varphi \\ & + 0.01 \sin 3\varphi + 0.00 \sin 4\varphi, \end{aligned}$$

$$\begin{aligned} x_{\text{Cu III}'} = & 68.92 + 1.02 \cos \varphi - 0.16 \cos 2\varphi - 0.08 \cos 3\varphi \\ & + 0.00 \cos 4\varphi - 1.96 \sin \varphi + 0.01 \sin 2\varphi \\ & + 0.02 \sin 3\varphi + 0.03 \sin 4\varphi, \end{aligned}$$

where φ is the azimuth as read. $x_{\text{Cu III}'}$ is a set of measurements made on crystal III in a different holder.

⁷ M. Owen, Ann. der Physik [4], 37, 657-699 (1912).

⁸ H. J. Seeman and E. Vogt, Ann. der Physik [5], 2, 976-990 (1929).

Figure 2 gives the observations for crystal III plotted as a function of the azimuth φ . The curve drawn is $A_0 + A_1 \cos \varphi + B_1 \sin \varphi$ as determined by the least squares analysis. Due to the fact that it was impossible to secure a holder which was perfectly straight and vertical, the crystal did not rotate exactly about its axis of figure. This gives rise to the large 360° period which the results show. That this is the case is supported by the fact that the 360° periods obtained by the least squares analysis are in close agreement in phase, with the exception of $x_{cu III}'$ which was made, as has been stated, with a different holder. An additional cause which contributes to this 360° period and may explain a shift in phase is the fact that the crystals were not exactly right circular cylinders. Thus we ascribe the whole of the 360° period to instrumental error. It is impossible to assign a crystallographic basis to the 360° period without attributing hemihedry to copper, for which there is, of course, no shadow of evidence.

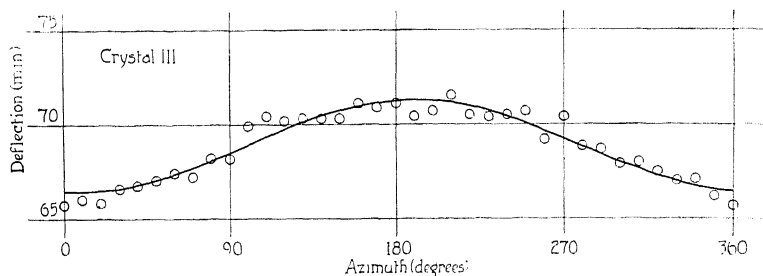


Fig. 2. Values of the deflection of the beam plotted against the azimuth of the crystal.

If there is any anisotropy, it must have four-fold symmetry about a $\langle 100 \rangle$ axis, three-fold symmetry about a $\langle 111 \rangle$ axis, and two-fold symmetry about a $\langle 110 \rangle$ axis. These are all the symmetry properties of a cubic crystal. Now, if without touching the apparatus we repeat a reading, on the average we will find that it cannot be reproduced closer than 0.5 millimeter. This is indicated on Fig. 2 where the diameter of the circles representing the observations gives what we may call the limits of "immediate reproducibility" of an observation. This represents a sort of minimum probable error. The actual probable error is much larger, as other factors such as the variation of temperature and humidity, which affect the length of the fibers, must be considered in assigning a proper value to the probable error. If we take this value of 0.5 millimeter as the minimum probable error, then we can compute from it the probable error in a coefficient of the Fourier series. For a series, representing 36 observations the probable error of a coefficient of a harmonic term is 0.236 times the probable error of a single observation, i.e., in the present case, 0.12 millimeter.

Now the axis of figure of crystal III lies near a $\langle 100 \rangle$ axis. Hence, if any anisotropy exists, we should expect a large term in 4φ . We see that the coefficient is actually less than half of the minimum probable error of that coefficient, i.e., it is sensibly zero. By the same reasoning the terms in 3φ are also sensibly zero. There is no physical justification for such terms.

In crystal II, whose axis of figure is close to a $\langle 111 \rangle$ axis, we should expect a large term in 3φ . Actually, the 4φ coefficient which has no significance for a three-fold axis, is larger than the 3φ coefficient, and the fact that both coefficients are larger than our minimum probable error should not therefore be taken as significant. We can therefore say that no three-fold symmetry can be detected with any degree of certainty. In a similar way the 3φ and 4φ coefficients of the more unsymmetrical cases of crystals IV and VII may be regarded as negligible.

It is to be noticed that in all cases the terms in 2φ have amplitudes larger than our assigned error. These can all safely be considered as due to the "spread" of the points. That is, we have chosen too small a value to represent our probable error. If we choose an error twice as great, viz., 1.0 millimeter, the probable errors in the 2φ terms become as large as the terms themselves.

We can therefore only ascribe any physical reality to the terms of period 360° , and these, it seems, are wholly due to instrumental defects. To assign a *limit of error* to this work it is only necessary to notice that the coefficients of terms of shorter periods than one revolution are all less than 1 percent of the whole effect, viz., less than about 0.7 millimeter. This represents, of course, not the probable error in a coefficient, but rather a limit of error; the actual probable error is less than this.

It is to be concluded from the experimental work described above that single crystals of copper show no variation of their diamagnetic susceptibility with the direction of the applied magnetic field greater than 1 percent.

The author wishes to express his sincerest appreciation to Dr. L. W. McKeehan for placing the facilities of the Sloane Physics Laboratory at his disposal, and for much helpful guidance and discussion during this work.

TENSION COEFFICIENT OF RESISTANCE OF METALS*

BY HARRY ROLNICK

SLOANE PHYSICS LABORATORY, YALE UNIVERSITY

(Received June 23, 1930)

ABSTRACT

A new method for measuring the change in resistance of a metal under tension has been developed and applied to fifteen metals. A direct current is sent through the wire under test while longitudinal vibrations set up in the wire cause the resistance and consequently the potential drop in the wire to fluctuate. These changes are amplified and measured. In this way it has been found that for bismuth, aluminium, manganin, and constantan the resistance decreases with tension while for all the other metals investigated the resistance increases with tension.

INTRODUCTION

THE change in electrical properties of metals under stress was first investigated by William Thomson, later Lord Kelvin, and described by him in a paper entitled "The Electrodynamical Qualities of Metals."¹ Due to the lack of sensitive apparatus, his experiments, which were conducted on copper and iron, gave untrustworthy results. Soon afterwards, H. Tomlinson,² at Lord Kelvin's suggestion, undertook to determine the exact change in resistance of wires caused by tension along their length. This remains the most extensive investigation on the subject. Other work has been done by W. E. Williams³ on bismuth; by Donaldson and Wilson⁴ on lead; and by N. F. Smith^{5,6} on iron, steel, copper, and brass. The most complete study in recent years has been made by P. W. Bridgman^{7,8,9} on many metals which he had at hand in the form of wires because of previous work on their pressure coefficients of resistance.

The method, a static one, used by all other investigators for studying these effects is to put a known load on the wires and then to measure the corresponding change in resistance. From this change is subtracted that produced by alteration in dimensions. The remainder is considered to be the change in resistance due to the stress.

The object of this research was the development of a dynamic method of

* Part of a dissertation presented for the Degree of Doctor of Philosophy in Yale University.

¹ W. Thomson, later Lord Kelvin. *Phil. Trans.* **146**, 649-672 (1856).

² H. Tomlinson, *Phil. Trans.* **174**, 1-172 (1883).

³ W. E. Williams, *Phil. Mag.* [6] **13**, 635-643 (1909).

⁴ J. A. Donaldson, and R. Wilson, *Proc. Roy. Soc. Edinb.* **27**, 16-20 (1907).

⁵ N. F. Smith, *Phys. Rev.* **28**, 107-121 (1909).

⁶ N. F. Smith, *Phys. Rev.* **28**, 429-437 (1909).

⁷ P. W. Bridgman, *Proc. Am. Acad.* **57**, 39-66 (1922).

⁸ P. W. Bridgman, *Proc. Am. Acad.* **59**, 117-137 (1923).

⁹ P. W. Bridgman, *Proc. Am. Acad.* **60**, 423-444 (1925).

measuring the tension coefficient of resistance and its application to metals whose coefficient is not easily obtained by static measurements. In the method finally adopted, the tension applied is alternating, in order to eliminate spurious effects due to thermoelectric forces and other effects of local or variable heating. A direct current is sent through the wire. As a result of the variations in resistance there are corresponding variations in the potential drop across the wire, and these are impressed on the grid of the first tube of calibrated amplifier, by means of which they are magnified and measured. From these data and the value of the direct current through the wire the change in resistivity due to tension is calculated.

APPARATUS AND PROCEDURE

The wire to be stretched, Fig. 1, is fastened at one end to a brass cylinder which is placed in a holder that can be moved by a screw in the direction of the wire axis to control the tension. The other end is wrapped around a hook. A glass rod, welded to the hook, connects it to the moving arm of a moving

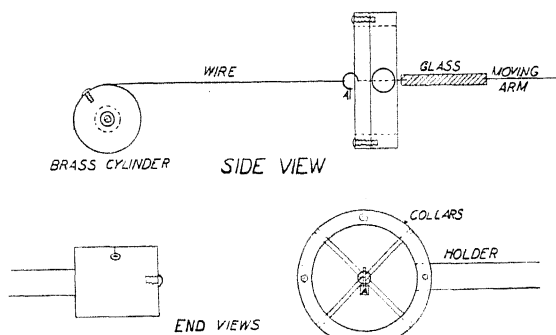


Fig. 1. Diagram of apparatus.

armature loud speaker unit. The hook is held in position by a cross-shaped piece of thin steel cut from an old telephone diaphragm. The ends of this cross are held fast between two brass collars. From them projects a rod which holds the collars securely. This arrangement keeps the motion of the hook axial.

The tension is applied by moving the brass cylinder back by means of the screw, thus stretching the wire. Care must be taken to avoid the production of standing transverse waves which will appear with amplitudes ranging from 1 mm to 5mm if the tension bears the appropriate relation to the length and density of the wire.

The glass rod is put in to insulate the wire from the loud speaker unit. Alternating current of 1025 cycles per second from a tube generator and amplifier is led into the loud speaker coil, and sets the wire into longitudinal vibration with a frequency equal to that of the alternating current. This frequency of current was chosen because it could be conveniently checked by a standard tuning fork making 1024 vibrations per second.

A battery, Fig. 2, sends a direct current through the wire. The change in resistance of the wire changes the potential drop across it, the alternating component is impressed on the grid of a vacuum tube of the amplifier. The choke coil, of 15 henrys inductance, makes the circuit impedance so high that the change in potential drop due to the current change is made negligible.

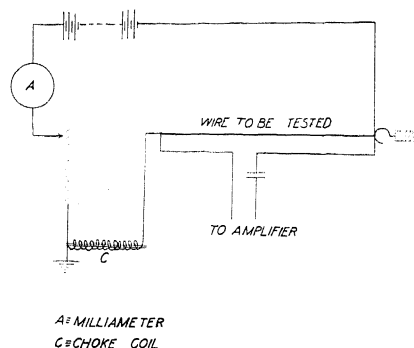


Fig. 2. Battery arrangement.

Fig. 3 is the wiring diagram of the six-tube resistance coupled amplifier. The amplifier is broken into two sets of three each, each part with its own batteries in a sheet tin box. Unless this is done the amplifier maintains continuous electrical oscillations. The connections to the first three tubes are arranged so that either one, two, or three may be used together with the last

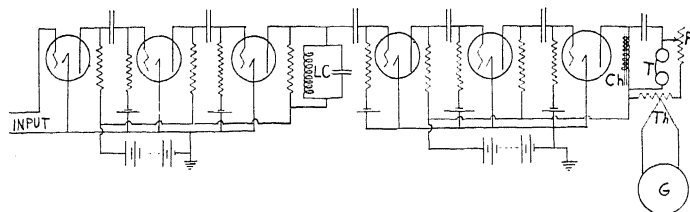


Fig. 3. Wiring diagram of the six tube resistance coupled amplifier.

three. It has been found difficult to get steady amplification without considerable noise with six tubes. Five tubes, with an amplification of about twenty-five thousand, gave very satisfactory performance and this number was used throughout the work. Between the third and fourth stages is fixed a circuit (LC) tuned to 1025 cycles. Its impedance to current of this frequency is five thousand ohms; to all other frequencies its impedance is considerably smaller. Thus it acts as a filter, being a low resistance shunt for all currents of frequencies other than 1025 cycles. Its use makes the amplifier very quiet. The negative side of the B battery and the metal shielding are grounded.

In the last stage is a power tube in the plate circuit of which is a hot-wire vacuum thermocouple (Western Electric No. 232) with an adjustable resist-

ance in series with it. The condenser (*C*) allows only alternating current to go through the thermocouple, which is used in connection with a galvanometer. The phones are used to detect any extraneous disturbance. The amplifier is first calibrated by sending a known e.m.f. into the input circuit and noting the deflections of the galvanometer in the output circuit.

The amplitude of vibration is measured with an optical lever. The back of a small light mirror about five millimeters in diameter is fastened to a tightly drawn fine wire, and the tip of the mirror rests against a small lip (*A* in Fig. 1) projecting from the hook to which the moving end of the vibrating wire is attached. Light from a slit is condensed on the mirror and focussed on a scale. As the lip moves back and forth the mirror is tipped about the wire holding it. The reflected image of the slit is drawn out into a band, whose width is proportional to the amplitude of vibration of the hook and the end of the wire.

One end of the specimen to be measured is fastened to the hook (Fig. 1) and the other end to the brass cylinder. A slight tension is put on the wire. The mirror is moved into such a position that an image of the slit is thrown on the scale. The oscillator is started and the wire forced into longitudinal vibrations, care being taken to avoid transverse vibrations. The amplifier is then switched on and the galvanometer reading noted. Then a small direct current is sent through the wire and the galvanometer reading again noted. This is repeated for different values of the direct current, which never exceeds a tenth of an ampere. The purpose of the several measurements is to decrease the effect of the errors from irregularities in the operation of the amplifier and those due to outside disturbances. Meanwhile the width of the band of light on the scale is observed from time to time. Galvanometer readings are taken only for equal amplitudes of vibration of the end of the wire, as shown by the width of the band of light. Some wires give considerable trouble in that the amplitude of vibration must be carefully adjusted to avoid breaking the wire in case transverse vibrations are set up.

After enough readings are taken the oscillator is stopped and the length of the wire and distance of the mirror axis from the wire are measured. The resistance of the wire is found with a wheatstone bridge.

MATERIALS TESTED AND THEIR METHOD OF PREPARATION

All the wires were either 0.004" or 0.005" in diameter, and all were obtained C.P. from Baker and Co., except molybdenum, tungsten, manganese, constantan, and nichrome. Molybdenum was from the Fansteel Products Co., tungsten from the Lamp Works of the General Electric Co. at Nela Park, manganin (84 Cu 4 Ni 12 Mn), constantan (60 Cu 40 Ni) and nichrome (85 Ni 15 Cr) from the Driver-Harris Co.

Annealing was effected by passing a current through the wire, except in the cases of aluminium and copper. Silver, gold, palladium, and platinum were annealed in air for an hour at a temperature about 300° below their melting points. Aluminium and copper were maintained for two hours at a temperature of 400°C in a steam bath. Molybdenum, tungsten, manganin,

and constantan were annealed in an atmosphere of hydrogen for one hour; manganin and constantan at 700°C, molybdenum at 2000°C, tungsten at 2500°C.

Bismuth, lead, tin and nichrome were not annealed; the first three are self-annealing and nichrome has such a high resistance that a large enough current could not be obtained with the power supply available.

Tin and bismuth were the most difficult to measure both on account of their softness and because the change in potential drop would not remain constant. In the results for these two wires abnormally large errors may be found.

MEASUREMENTS AND CALCULATIONS

Length of wire, distance of scale from mirror, width of light band, resistance of wire, direct current through wire, and galvanometer deflections are the only measured quantities. The first three give the fractional change in length of the wire; the last two enter in the calculations of the change of resistance. From the galvanometer deflection the potential difference impressed on the input of the amplifier is obtained and this equals the product of the direct current by the change in resistance. The fractional change in resistivity is calculated from the following relation:

$$\Delta R/R = (1 + 2w - K) \frac{\Delta l}{l} + \frac{\Delta \rho}{\rho}.$$

where w = Poisson's ratio, K = a constant and l = length of wire.

The factor $(1+2w)\Delta l/l$ is the change in resistance due to alteration of dimensions of the wire. In most cases the values of Poisson's ratio were taken from tables.¹⁰ For some metals this ratio was computed from the compressibility (k) and Young's Modulus (E) for the material. The formula used in $w = 0.5 - Ek/6$. Table I indicates how close the calculated values of

TABLE I.

Metal	$E \times 10^{-11}$	$k \times 10^{11}$	$Ek/6$	w (calculated)	w (observed)
Silver	7.90**	1.02	0.134	0.366	0.38*
Aluminium	7.05**	1.38	.162	.338	.34*
Gold	8.0**	.603	.0805	.42	.42*
Cadmium	5.0	2.27	.203	.297	.30*
Copper	12.3	.756	.155	.345	.35*
Iron	21.3	.606	.215	.285	.28*
Nickel	20.2	.542	.182	.318	.31*
Lead	1.62	2.38	.064	.436	.45*
Palladium	11.3	.536	.101	.40	.40*
Platinum	16.8	.372	.104	.396	.39*
Tin	5.43	2.02	0.183	.317	.33*

* E. Grüneisen, Ann. d. Physik [4] 25, 825-851 (1908).

** Kaye and Laby's Tables. E = Young's Modulus in c.g.s. units, k = compressibility in c.g.s. units, and w = Poisson's ratio.

the ratio are to observed values. All the values of the constants used were taken from the International Critical Tables unless otherwise noted. Young's

¹⁰ E. Grüneisen, Ann. d. Physik [4] 22, 801-851 (1907).

Moduli for molybdenum and nichrome were measured for this investigation with an apparatus constructed by Mr. L. R. Jackson of this laboratory.

The term $-K\Delta l/l$ is the change in resistance produced by a change in temperature of the wire as it is stretched and released. When a wire is suddenly stretched there will be a fall in temperature if the metal expands when heated and this temperature change is reversible.^{11,12} The change in temperature is given by the formula:

$$\Delta T = -TaP/C_p d$$

The fractional change in resistance due to this change in temperature is

$$\Delta R/R = -K\Delta l/l$$

$$K = abTE/C_p d$$

In these formulae T =absolute temperature; a =thermal coefficient of expansion; P =applied tension; C_p =specific heat; d =density; b =temperature coefficient of resistance; and E =Young's Modulus.

Table II contains the values of w and K used, together with the computed values of $\Delta R/R$, $\Delta\rho/\rho$, and $\Delta\rho/\rho$ divided by $\Delta l/l$.

TABLE II.

Metal	w	K	$\frac{\Delta l}{l} \times 10^4 (1+2w-K)$	$\frac{\Delta l}{l} \times 10^4$	$\frac{\Delta R}{R} \times 10^4$	$\frac{\Delta \rho}{\rho} \times 10^4$	$\frac{\Delta \rho}{\rho} \div \frac{\Delta l}{l}$
Silver	0.38	0.68	0.274	0.295	0.86	0.565	2.06
Aluminium	.34	.66	.80	.816	.274	-.542	-.68
Gold	.42	.563	.211	.27	.75	.48	2.27
Bismuth	.34	.40	.229	.294	-.50	-.794	-3.52
Copper	.35	.677	.629	.64	1.64	1.00	1.59
Molybdenum	.33	.402	.408	.514	.963	.449	1.10
Lead	.45	.424	.236	.349	.613	.264	1.12
Palladium	.40	.44	.327	.445	1.33	.885	2.70
Platinum	.39	.45	.395	.525	1.89	1.36	3.44
Tin	.33	.244	.216	.320	1.54	1.22	5.65
Tungsten	.32	.76	.827	.73	1.94	1.21	1.46
Zinc	.30	1.05	.172	.094	.638	.544	3.16
Manganin	.33	.00	.498	.83	.28	-.55	-1.10
Constantan	.33	.00	.517	.86	.735	-.125	-.246
Nichrome	.30	.02	.35	.55	.928	.378	1.08

The probable error in the resistance measurement, in the length of the wire, usually about sixty centimeters, in the distance of the mirror to the scale, and in the direct current is less than one-half of one percent in each case. The width of the light band, from one to four centimeters, was measured with a probable error of from one to three percent, being higher for smaller widths. The resultant error in the fractional change in length is about of the same magnitude. The probable error in measuring the alternating potential difference is dependent on the accuracy with which the amplifier has been calibrated and on the steadiness of the galvanometer deflections.

¹¹ W. V. Houston, Introduction to Mathematical Physics, p. 192.

¹² P. G. Nutting, Jour. Wash. Acad. of Sci. 19, 109-115 (1929).

The calibration is accurate to one percent, and the precision of the galvanometer reading is within two percent except in the measurements on bismuth and tin. For these metals, the galvanometer deflections were so unsteady as to cause a probable error of about ten percent in the potential difference measured.

Into the calculations there enter the thermal expansion coefficient, the temperature coefficient of resistance, the specific heat, Young's modulus and the density, all in correction terms, while Poisson's ratio enters directly. The uncertainty in the values of these constants varies considerably from metal to metal. The constants entering indirectly contribute about two percent to the uncertainty while Poisson's ratio can not be relied on within five percent. Thus the final results have errors of about seven percent due to constants used in calculating. Improved values of these constants will permit correspondingly greater accuracy in the final results. The measured quantities contribute about three percent more so that the possible error of the results is about ten percent. In the case of bismuth and tin the possible error is about 20 percent.

TABLE III. $\Delta\rho/\rho$ for a tension of 1 kg/cm^2 by different observers.

Metal	Bridgman	Tomlinson	Rolnick
Aluminium	$+1.8 \times 10^{-6}$	-0.63×10^{-6}	-0.96×10^{-6}
Silver	+3.4	+2.07	+2.51
Gold	+3.87		+2.86
Bismuth	-36.5		-32.2
Copper	+1.33	+.88	+1.32
Lead		+9.75	+7.0
Palladium	+1.66		+2.44
Platinum	+1.56	+2.25	+2.08
Tin		+5.89	+10.6
Zinc		+2.75	+3.26
Manganin	-.76		-.91

For bismuth, W. E. Williams gives $\Delta R/R = -53.5 \times 10^{-6}$ while the writer obtains $\Delta R/R = -28.1 \times 10^{-6}$.

In Table III is a comparison of my results with those of other investigators. These results have all been reduced to fractional changes of resistivity with a tension of 1 kg/cm^2 , using the values of Young's Modulus mentioned above. Considering the wide variation between the results of other workers, the present results tally fairly well with theirs.

The writer is deeply indebted to Professor L. W. McKeehan for his suggestion of the problem and for his advice and encouragement during its progress.

VIBRATIONS OF A NON-PLANAR MEMBRANE

BY GEORGE R. STIBITZ

CORNELL UNIVERSITY

(Received June 16, 1930)

ABSTRACT

Equations of motion are deduced for a non-planar membrane in small oscillation about any position of equilibrium. Cylindrical and conical membranes are discussed briefly as special cases; with certain types of boundary conditions there is no solution of the problem when stiffness is entirely omitted, and this is particularly true of the cone because of a characteristic singular point in the differential equations.

1. INTRODUCTION

NUMEROUS investigators have published studies of the vibrations of the plane membrane, including besides the usual circular drumhead the square, triangular and other shaped drumheads of uniform surface density and also the loaded drum, in which the density of the membrane is not uniform. Two articles in recent years have treated the statics of non-planar membranes, and to these the present writer is much indebted. They are the articles of Max Lagally¹ and of Frank Löbell.²

In this paper we will consider the problem of a membrane with very large elastic constants, whose middle surface is analytic and whose mass is uniformly distributed over that surface. We obtain the equations of motion for a general surface of this type as a system of three linear partial second-order differential equations. As a special case, we consider a type of symmetric vibration of a surface of revolution and finally the vibrations of a cone. In each case the vibrations are considered to take place about a strained equilibrium position of the membrane.

Let the middle surface of the membrane be described by a variable vector, r , drawn from any fixed point as origin. We can write r as a function of two parameters. Since the surface is analytic, it can be shown³ that the parameters, say u_1 and u_2 , can be so chosen that the lines described by the vector r when u_1 is constant and when u_2 is constant, respectively, are the orthogonal "lines of principal-curvature" of the surface.

Suppose that in such a surface tangential forces act. We define the stress component across any parametric curve u_1 (i.e. a curve along which u_2 is constant) as the vector force per unit length exerted by the "positive" part of the surface on the "negative" part across that curve. By "positive" part of the surface with respect to the curve $u_2 = K$, we mean that part defined by the inequality $u_2 > K$. The stress component across the u_1 curves we name σ_2 , and that across the u_2 curves, σ_1 .

¹ Max Lagally, *Zeits. f. Angewandte Math. u. Mech.* **4**, 377 (1924).

² Frank Löbell, *Zeits. f. Angewandte Math. u. Mech.* **7**, 463 (1927).

³ Blaschke, *Vorlesungen über Differentialgeometrie*, p. 62.

Let t_1, t_2 be the unit tangents along the u_1, u_2 curves respectively. If we assume the membrane to be perfectly pliable, then the stresses will lie entirely in the plane of t_1, t_2 . Their four scalar components in these directions we define by the vector equations,

$$\sigma_1 = \sigma_{11}t_1 + \sigma_{12}t_2, \quad \sigma_2 = \sigma_{21}t_1 + \sigma_{22}t_2. \quad 1.1$$

2. THE A, B AND C CONDITIONS OF THE MEMBRANE

For convenience in manipulation we define three states or conditions of the membrane. The first of these, state A , is the totally unstrained state. We will also refer to the middle surface of the membrane in this state as the surface A .

Next, let the membrane be stretched in any manner by forces exerted across its boundaries, and let it come to rest. Each element of the surface will then be in equilibrium under the stress forces acting tangentially across its own boundary. Call this state, B .

Finally, let the membrane undergo a small displacement from its equilibrium position B to a third position C . This last will not in general be an equilibrium position, the stress forces exerting a force P per unit area. The elastic constants for the displacement BC may be slightly different from those for AB ; call Young's modulus and Poisson's ratio for BC , E and κ respectively.

Let parametric lines u_1, u_2 as described in Sec. 1 be drawn on the surface B , these curves remaining fixed in space when the membrane moves to position C . Let v_1, v_2 be the parametric lines for the actual middle surface of the membrane, these lines moving with the membrane. We will so choose v_1, v_2 that when the membrane is in position B , v_1, v_2 coincide with u_1, u_2 .

Since we have assumed the elastic constants of the membrane to be large, the forces arising from displacements of the particles near a point p fixed in the middle surface can be assumed to be only those due to elastic strain of the element as long as the displacements lie in the tangent plane at p . Hence we can neglect the effect of rotation of the element when the axis of this rotation is perpendicular to the surface at p , for this type of displacement produces no strain in the element and the forces due to changes in the directions of the initial stresses will be negligible in comparison with forces due to the strains. On the other hand, displacements perpendicular to the surface do not produce strains in the element to the first order, and the only forces called into existence by such a displacement are those due to the changed directions of the initial stresses. Consequently we cannot neglect the component of rotation of the element which lies in the tangent plane.

3. THE ADDED STRESSES

Suppose q is a point on the middle surface near to p , both points moving with the membrane. Let q' and p' be the positions occupied by q and p when the membrane is in state B . Let t be the vector obtained by dividing the vector pq by the constant scalar $p'q'$ and then letting q approach p .

Then

$$t = \frac{\partial r}{\partial s}, \quad 3.1$$

where s represents arc length in the direction pq . In position C this tangent vector is different in magnitude and direction from the corresponding vector in position B ; let the difference vector be δt . Then evidently, if \bar{r} is the vector of the displacement BC , we have

$$\delta t = \frac{\partial \bar{r}}{\partial s}, \quad \delta t_1 = \frac{\partial \bar{r}}{\partial s_1}, \quad \delta t_2 = \frac{\partial \bar{r}}{\partial s_2}, \quad 3.2$$

in which the subscripts refer to cases in which pq lies along one of the coordinate lines.

Now in general the element about p undergoes a translation, a pure strain, and a rotation; let g denote the vector rotation and write with the usual notation for the components of strain:

$$\delta t_1 = g \times t_1 + \delta \epsilon_{11} t_1 + \delta \epsilon_{12} t_2, \quad 3.3$$

$$\delta t_2 = g \times t_2 + \delta \epsilon_{12} t_1 + \delta \epsilon_{22} t_2. \quad 3.4$$

Taking the scalar products $t_1 \cdot$, $t_2 \cdot$, with 3.3 and 3.4 and combining, we get, using 3.2,

$$\frac{\partial \bar{r}}{\partial s_1} \cdot t_1 = \delta \epsilon_{11}; \quad \frac{\partial \bar{r}}{\partial s_2} \cdot t_2 = \delta \epsilon_{22}; \quad 3.5$$

$$\frac{\partial \bar{r}}{\partial s_1} \cdot t_2 + \frac{\partial \bar{r}}{\partial s_2} \cdot t_1 = g \times t_1 \cdot t_2 + g \times t_2 \cdot t_1 + \delta \epsilon_{12} + \delta \epsilon_{21}. \quad 3.6$$

Noting that $g \times t_1 \cdot t_2 = -g \times t_2 \cdot t_1$ and $\delta \epsilon_{12} = \delta \epsilon_{21}$, we have

$$2\delta \epsilon_{12} = \frac{\partial \bar{r}}{\partial s_1} \cdot t_2 + \frac{\partial \bar{r}}{\partial s_2} \cdot t_1. \quad 3.7$$

Following the method of Lagally⁴ and Love⁵ except that we deal with two dimensions instead of three, we obtain the following formulas for the stresses in terms of the strains and the elastic constants:

$$\delta \sigma_{11} = 2\mu \delta \epsilon_{11} + \lambda(\delta \epsilon_{11} + \delta \epsilon_{22}), \quad 3.8$$

$$\delta \sigma_{12} = \delta \sigma_{21} = 2\mu \delta \epsilon_{12}, \quad 3.9$$

$$\delta \sigma_{22} = 2\mu \delta \epsilon_{22} + \lambda(\delta \epsilon_{11} + \delta \epsilon_{22}), \quad 3.10$$

where

$$\lambda = \frac{\kappa E \tau}{1 - \kappa^2}, \quad \mu = \frac{E \tau}{2(1 + \kappa)}. \quad 3.11$$

τ being the thickness of the membrane.

⁴ Lagally, Vektorrechnung, p. 260.

⁵ Love, Elasticity, p. 98-101.

4. FORCES ACTING ON THE MEMBRANE IN POSITION *C*.

It will be recalled that for the purpose of calculating the changes in stress due to rotation of the tangent plane we need consider only that component of the tangent variation which is normal to the surface; let this component of δt_1 and δt_2 be

$$\delta' t_1 = t_1 \left(\frac{\partial \bar{r}}{\partial s_1} \cdot t_3 \right), \quad \delta' t_2 = t_2 \left(\frac{\partial \bar{r}}{\partial s_2} \cdot t_3 \right). \quad 4.1, 4.2$$

Then the total vector stresses in position *C* are:

$$\text{across } v_2 \quad \bar{\sigma}_1 = (\sigma_{11} + \delta\sigma_{11})(t_1 + \delta' t_1) + (\sigma_{12} + \delta\sigma_{12})(t_2 + \delta' t_2), \quad 4.3$$

$$\text{across } v_1 \quad \bar{\sigma}_2 = (\sigma_{21} + \delta\sigma_{21})(t_1 + \delta' t_1) + (\sigma_{22} + \delta\sigma_{22})(t_2 + \delta' t_2), \quad 4.4$$

or, dropping second order terms, by 1.1,

$$\bar{\sigma}_1 = \sigma_1 + \sigma_{11}\delta' t_1 + t_1\delta\sigma_{11} + \sigma_{12}\delta' t_2 + t_2\delta\sigma_{12}, \quad 4.5$$

$$\bar{\sigma}_2 = \sigma_2 + \sigma_{21}\delta' t_1 + t_1\delta\sigma_{21} + \sigma_{22}\delta' t_2 + t_2\delta\sigma_{22}. \quad 4.6$$

The conditions for equilibrium between the stress forces and the surface forces can be obtained by direct consideration in the usual manner of an element bounded by parameter lines, or by the method of Löbell.² The conditions are given by the vector equation,

$$\left(G_1 - \frac{\partial}{\partial s_2} \right) \bar{\sigma}_2 + \left(G_2 - \frac{\partial}{\partial s_1} \right) \bar{\sigma}_1 + P = 0, \quad 5.1$$

where the G 's are the geodesic curvatures as defined below (6.2) and $-P$ is the external surface force per unit area.

Let

$$\delta\sigma_1 = \bar{\sigma}_1 - \sigma_1, \quad \delta\sigma_2 = \bar{\sigma}_2 - \sigma_2. \quad 5.2$$

Then, in position *C*,

$$-P = \left(G_1 - \frac{\partial}{\partial s_2} \right) (\sigma_2 + \delta\sigma_2) + \left(G_2 - \frac{\partial}{\partial s_1} \right) (\sigma_1 + \delta\sigma_1). \quad 5.3$$

But in position *B*, P is zero, i.e.

$$\left(G_1 - \frac{\partial}{\partial s_2} \right) \sigma_2 + \left(G_2 - \frac{\partial}{\partial s_1} \right) \sigma_1 = 0. \quad 5.4$$

Hence in position *C*

$$-P = \left(G_1 - \frac{\partial}{\partial s_2} \right) \delta\sigma_2 + \left(G_2 - \frac{\partial}{\partial s_1} \right) \delta\sigma_1. \quad 5.5$$

5. SCALAR COMPONENTS OF $\delta\sigma_i$ AND OF P

Assume as basic vectors the unit vectors t_1 and t_2 introduced in Sec. 1, and define $t_3 = t_1 \times t_2$. Define the components of \bar{r} , the vector of displacement BC , by

$$\bar{r} = r_1 t_1 + r_2 t_2 + r_3 t_3, \quad 6.1$$

and the normal and geodesic curvatures of the parametric lines by

$$\begin{aligned} N_1 &= -\frac{\partial t_1}{\partial s_1} \cdot t_3 = \frac{\partial t_3}{\partial s_1} \cdot t_1, & N_2 &= -\frac{\partial t_2}{\partial s_2} \cdot t_3 = \frac{\partial t_3}{\partial s_2} \cdot t_2, \\ G_1 &= \frac{\partial t_1}{\partial s_1} \cdot t_2 = -\frac{\partial t_2}{\partial s_1} \cdot t_1, & G_2 &= \frac{\partial t_2}{\partial s_2} \cdot t_1 = -\frac{\partial t_1}{\partial s_2} \cdot t_2. \end{aligned} \quad 6.2$$

The geodesic torsion, $(\delta t_1 / \delta s_2) \cdot t_3$, is zero for lines of principal curvature, as are also the scalar product of a unit vector and its derivative. Substituting from 6.1 and 6.2 in 4.1 and 4.2, we see that

$$\delta' t_1 = \left(\frac{\partial r_3}{\partial s_1} - r_1 N_1 \right) t_3, \quad \delta' t_2 = \left(\frac{\partial r_3}{\partial s_2} - r_2 N_2 \right) t_3. \quad 6.3$$

Similarly from 3.8–3.11, 3.5, 3.6, 6.1, 6.2, we have the result:

$$\delta\sigma_{11} = (2\mu + \lambda) \left(\frac{\partial r_1}{\partial s_1} - r_1 G_1 + r_3 N_1 \right) + \lambda \left(\frac{\partial r_2}{\partial s_2} - r_2 G_2 + r_3 N_2 \right), \quad 6.4$$

$$\delta\sigma_{22} = (2\mu + \lambda) \left(\frac{\partial r_2}{\partial s_2} - r_2 G_2 + r_3 N_2 \right) + \lambda \left(\frac{\partial r_1}{\partial s_1} - r_1 G_1 + r_3 N_1 \right), \quad 6.5$$

$$\delta\sigma_{12} = \mu \left(\frac{\partial r_1}{\partial s_2} + \frac{\partial r_2}{\partial s_1} + r_1 G_1 + r_2 G_2 \right). \quad 6.6$$

Comparing these results with 4.5, 4.6 and 5.2 we obtain finally:

$$\begin{aligned} \delta\sigma_1 &= \sigma_{11} \left(\frac{\partial r_3}{\partial s_1} - r_1 N_1 \right) t_3 + \left[(2\mu + \lambda) \left(\frac{\partial r_1}{\partial s_1} - r_1 G_1 + r_3 N_1 \right) \right. \\ &\quad \left. + \lambda \left(\frac{\partial r_2}{\partial s_2} - r_2 G_2 + r_3 N_2 \right) \right] t_1 + \sigma_{12} \left(\frac{\partial r_3}{\partial s_2} - r_2 N_2 \right) t_3 \\ &\quad + \mu \left(\frac{\partial r_1}{\partial s_2} + \frac{\partial r_2}{\partial s_1} + r_1 G_1 + r_2 G_2 \right) t_2. \end{aligned} \quad 6.7$$

Interchange of the subscripts 1 and 2 in 6.7 gives us the equation for $\delta\sigma_2$.

Substituting these results in the equation for P , (5.5), and carrying through the necessary algebra, we have P , the force per unit area due to the stresses, expressed in terms of components along the vectors t_i . Define the scalar components of P by

$$P = P_1 t_1 + P_2 t_2 + P_3 t_3. \quad 6.8$$

Resolving P into its components, we have ultimately:

$$\begin{aligned}
 P_1 = & -r_1 \left[2\mu G_1^2 + \lambda \frac{\partial G_2}{\partial s_1} + \sigma_{11} N_1^2 + 2\mu G_2^2 - \mu \frac{\partial G_1}{\partial s_2} \right] \\
 & - r_2 \left[(2\mu + \lambda) \frac{\partial G_1}{\partial s_1} + \sigma_{12} N_1 N_2 - \mu \frac{\partial G_2}{\partial s_2} \right] \\
 & + r_3 \left[(2\mu + \lambda) \frac{\partial N_1}{\partial s_1} + \lambda \frac{\partial N_2}{\partial s_1} + 2\mu G_2 (N_2 - N_1) \right] \\
 & - G_2 (2\mu + \lambda) \frac{\partial r_1}{\partial s_1} - \mu G_1 \frac{\partial r_1}{\partial s_2} - (4\mu + \lambda) \frac{\partial r_2}{\partial s_1} + 3\mu G_2 \frac{\partial r_2}{\partial s_2} \\
 & + [\lambda N_2 + (2\mu + \lambda) N_1] \frac{\partial r_3}{\partial s_1} + N_1 \sigma_{12} \frac{\partial r_3}{\partial s_2} + N_1 \sigma_{11} \frac{\partial r_3}{\partial s_1} \\
 & + (2\mu + \lambda) \frac{\partial^2 r_1}{\partial s_1^2} + \mu \frac{\partial^2 r_1}{\partial s_2^2} + \mu \frac{\partial^2 r_2}{\partial s_2 \partial s_1} + \lambda \frac{\partial^2 r_2}{\partial s_1 \partial s_2},
 \end{aligned} \tag{6.9}$$

from which P_2 is found by interchange of subscripts 1 and 2;

$$\begin{aligned}
 P_2 = & r_1 \left[N_1 G_1 \sigma_{12} + N_1 G_2 (\lambda + \sigma_{11}) + N_2 G_2 (2\mu + \lambda) - \sigma_{11} \frac{\partial N_1}{\partial s_1} - \sigma_{12} \frac{\partial N_1}{\partial s_2} \right. \\
 & \left. - N_1 \left(\frac{\partial \sigma_{11}}{\partial s_1} + \frac{\partial \sigma_{12}}{\partial s_2} \right) \right] + r_2 \left[N_2 G_2 \sigma_{12} + N_2 G_1 (\lambda + \sigma_{22}) + N_1 G_1 (2\mu + \lambda) \right. \\
 & \left. - \sigma_{22} \frac{\partial N_2}{\partial s_2} - \sigma_{12} \frac{\partial N_2}{\partial s_1} - N_2 \left(\frac{\partial \sigma_{22}}{\partial s_2} + \frac{\partial \sigma_{12}}{\partial s_1} \right) \right] - r_3 [(2\mu + \lambda) (N_1^2 + N_2^2) \\
 & + 2\lambda N_1 N_2] - \frac{\partial r_1}{\partial s_1} [N_1 (2\mu + \lambda + \sigma_{11}) + N_2 \lambda] - N_1 \sigma_{12} \frac{\partial r_1}{\partial s_2} \\
 & - N_2 \sigma_{12} \frac{\partial r_2}{\partial s_1} - \frac{\partial r_2}{\partial s_2} [N_1 \lambda + N_2 (2\mu + \lambda + \sigma_{22})] + \frac{\partial r_3}{\partial s_1} \left[\frac{\partial \sigma_{11}}{\partial s_1} + \frac{\partial \sigma_{12}}{\partial s_2} \right. \\
 & \left. - G_1 \sigma_{12} - G_2 \sigma_{11} \right] + \frac{\partial r_3}{\partial s_2} \left[\frac{\partial \sigma_{22}}{\partial s_2} + \frac{\partial \sigma_{12}}{\partial s_1} - G_2 \sigma_{12} - G_1 \sigma_{22} \right] \\
 & + \sigma_{11} \frac{\partial^2 r_3}{\partial s_1^2} + \sigma_{12} \left(\frac{\partial^2 r_3}{\partial s_1 \partial s_2} + \frac{\partial^2 r_3}{\partial s_2 \partial s_1} \right) + \sigma_{22} \frac{\partial^2 r_3}{\partial s_2^2}.
 \end{aligned}$$

6. EQUATIONS OF MOTION

The equations we have deduced are valid for any small displacement \bar{r} . If \bar{r} is a function of time, then P is also a function of time. We may suppose that at each instant each element of the membrane is vibrating under the influence of the tangential stress-forces P and the resistive forces due to the radiation of energy and to internal friction. Then the sum of the real forces acting on the element must be equal to the effective forces. Suppose

the resistive forces to be proportional to the velocity, $\dot{\bar{r}} = \delta \bar{r} / \delta t$. We can then write,

$$P - R\dot{\bar{r}} - m\ddot{\bar{r}} = 0, \quad R = \text{const.} > 0. \quad 7.1$$

The three scalar equations implied by 7.1 together with the value of P obtained from 6.9 and 6.10 furnish us with the required system of partial differential equations of motion of a general surface.

Let us seek normal vibrations of the form

$$\bar{r} = \rho e^{i p t}. \quad 7.2$$

Substituting in 7.1,

$$P^* - R i p \rho + m p^2 \rho = 0, \quad 7.3$$

where P^* is the function obtained by replacing each component of \bar{r} in P by the corresponding component of ρ . Equation 7.3 is then the equation for the amplitudes of the normal modes of vibration of the general surface.

7. APPLICATIONS TO SURFACES OF REVOLUTION

For the surface of revolution we choose as coordinates, (1) distance measured from the origin along a generator, $u_1 = s_1$, (2) the angle of revolution from a fixed plane, u_2 . If we consider only vibrations in which r_2 is zero, and in which r_1 and r_2 are functions of u_1 alone, then the amplitude equations become:

$$\begin{aligned} & -\rho_1 \left[\lambda \frac{\partial G_2}{\partial u_1} + \sigma_{11} N_1^2 + 2\mu G_2^2 + R i p - m p^2 \right] \\ & + \rho_3 \left[(2\mu + \lambda) \frac{\partial N_1}{\partial u_1} + \frac{\partial N_2}{\partial u_1} + 2\mu (N_2 - N_1) G_2 \right] \end{aligned} \quad 8.1$$

$$\begin{aligned} & - \frac{\partial \rho_1}{\partial u_1} G_2 (2\mu + \lambda) + \frac{\partial \rho_3}{\partial u_1} [\lambda N_2 + (2\mu + \lambda) N_1] + \sigma_{11} N_1 \frac{\partial \rho_3}{\partial u_1} + \frac{\partial^2 \rho_1}{\partial u_1^2} (2\mu + \lambda) = 0, \\ & \rho_1 \left[N_1 G_2 (\lambda + \sigma_{11}) + N_2 G_2 (2\mu + \lambda) - \frac{\partial N_1}{\partial u_1} \sigma_{11} - N_1 \frac{\partial \sigma_{11}}{\partial u_1} \right] \\ & - \rho_3 [(2\mu + \lambda) (N_1^2 + N_2^2) + 2\mu N_1 N_2 + R i p - m p^2] \\ & - \frac{\partial \rho_1}{\partial u_1} [N_1 (2\mu + \lambda + \sigma_{11}) + N_2 \lambda] + \frac{\partial \rho_3}{\partial u_1} \left[\frac{\partial \sigma_{11}}{\partial u_1} - G_2 \sigma_{11} \right] + \frac{\partial^2 \rho_3}{\partial u_1^2} \sigma_{11} = 0, \end{aligned} \quad 8.2$$

and the curvatures are,

$$N_1 = - \frac{y''}{(1 - y'^2)^{1/2}}, \quad N_2 = \frac{(1 - y'^2)^{1/2}}{y}; \quad G_1 = 0, \quad G_2 = - \frac{y'}{y}; \quad 8.3$$

where y is the ordinate of the generating curve, expressed as a function of u_1 , and the primes mean the ordinary derivative with respect to u_1 .

The equations for the cone are still simpler, for $y = u_1 \sin \alpha$, 2α being the

angle of the cone, and one easily sees that for equilibrium $\sigma_{11} = \text{const.}/u_1 = c/u_1$, so that the equations become, if $R=0$:

$$\frac{\partial^2 \rho_1}{\partial u_1^2} + \frac{1}{u_1} \frac{\partial \rho_1}{\partial u_1} + \frac{\kappa a}{u_1} \frac{\partial \rho_3}{\partial u_1} - \frac{a}{u_1^2} \rho_3 + \left(q^2 - \frac{1}{u_1^2} \right) \rho_1 = 0, \quad 8.4$$

$$\frac{c}{(2\mu + \lambda)u_1} \frac{\partial^2 \rho_3}{\partial u_1^2} - \frac{\kappa a}{u_1} \frac{\partial \rho_1}{\partial u_1} + \left(q^2 - \frac{a^2}{u_1^2} \right) \rho_3 - \frac{a}{u_1^2} \rho_1 = 0, \quad 8.5$$

where $a = \cot \alpha$, $q^2 = m p^2 / (2\mu + 2)$, m mass per unit area of the membrane. Let us introduce the new variable z for qu ; then, using primes here to denote differentiation with respect to z , we have,

$$\rho_1'' + \frac{1}{z} \rho_1' + \frac{\kappa a}{z} \rho_3' + \left(1 - \frac{1}{z^2} \right) \rho_1 - \frac{a}{z^2} \rho_3 = 0, \quad 8.4b$$

$$\rho_3'' - \frac{\lambda a}{eq} \rho_1' - \frac{2\mu + \lambda}{cq} \frac{a}{z} \rho_1 + \frac{2\mu + \lambda}{cq} \left(z - \frac{a^2}{z} \right) \rho_3 = 0. \quad 8.5b$$

If we suppose the initial stress to be different from zero everywhere in the range we are considering, then it is possible, by taking each of the first derivatives as a new dependent variable, to form a system of four simultaneous first-order differential equations, each of which has on the left side a different first derivative and on the right only an algebraic expression in the four unknowns; the right hand sides of these equations are all homogeneous and the coefficients of the unknowns are bounded and continuous for u greater than zero. Under these conditions it can be shown that four linearly independent continuous solutions exist throughout the range for which z is greater than zero. As is usual in vibration problems, there exists a discrete set of values of z , and so of p , for which the boundary conditions can be satisfied. In any given numerical case these can be found by numerical integration.

If, however, the initial stress is zero, i.e. $c=0$, then ρ_3'' disappears from 8.5b and it is not possible to throw the equations into the form specified above. If we then eliminate ρ_3 from 8.4b and 8.5b we obtain for ρ_1 a differential equation of the second order only, so that for ρ_1 we have only two index solutions and ρ_3 is given by 8.5b in terms of these. There are thus, in general, not enough independent solutions to satisfy the boundary conditions. Furthermore, the coefficients in the equation so obtained for ρ_1 , which is rather complicated and will not be written down here, has two pairs of singular points, one at $z^2 = a^2$, and the other at $z^2 = a^2(1 - \kappa^2)$. It is necessary to examine the solution for ρ_1 at these points by means of a series; we omit the rather tedious details and outline the result. In the region about $z=a$ we find that the indicial equation has the two roots 0 and 2. These differ by an integer, so that we can be certain of only one analytic solution through the point, but we find by actual calculation of the first three terms of the series that there are in fact two independent solutions, since if we use the zero root the second power of z has an arbitrary coefficient. Hence $z=a$ is

not an irregular singular point. Making the same kind of an examination of the point $z = a(1 - \kappa^2)^{\frac{1}{2}}$, however, we find the roots of the indicial equation to be 0 and 0. We can apply the usual method for finding the second solution⁶ and find for it

$$\bar{\rho}_1 = \rho_1 \int \frac{(z^2 - a^2)}{(z^2 - a^2 + a^2 \kappa^2)} \frac{dz}{z \rho_1^2}. \quad 8.6$$

This solution obviously has a pole of the first order at the point under consideration. Hence there is one and only one solution that is continuous throughout the range, $u_1 > 0$. Furthermore, although ρ_1 is continuous through the point $z = a$, yet ρ_3 is discontinuous there, for upon solving for ρ_3 in 8.5 we have

$$\rho_3 = a \frac{\rho_1 + \kappa z \rho_1'}{z^2 - a^2}, \quad 8.7$$

from which it is evident that ρ_3 has a pole of first order at this point.

Although it was thus impossible to obtain an actual solution from the equations for the case of a cone without initial stress, it seemed desirable to obtain a rough idea of what the vibrations may be like. Accordingly, the series for ρ_1 was evaluated near $z = a(1 - \kappa^2)^{\frac{1}{2}}$ for the case of a paper cone with a vertical angle of 120 degrees ($a = 0.58$) and the solution was then carried to $z = 7$ by numerical integration. The shape of the solution thus found suggests comparison with a sine curve. For very great distances out along the cone, 8.4b reduces to, $\rho_1'' + \rho_1 = 0$, so that ρ_1 approaches $\sin z$ while $\rho_3 \rightarrow 0$, which is simply the solution for a plane membrane of the same material. With this function as our norm, we find that the numerical solution, after vanishing at $z = 0.78$, showed a first node-to-loop distance of about 1.0 times the quarter wave-length for the plane longitudinal vibrations of the same frequency; the next succeeding node-to-loop distances were very roughly 1.2, 1.0 and 1.1 times the normal quarter-wave length. The second loop had an amplitude about two-thirds that of the first. Comparison might also be made with Bessel's function, for the equation differs markedly from

$$\rho_1'' + \frac{1}{z} \rho_1' + \rho_1 = 0$$

only within the first half wave or so and approximates to it very closely indeed beyond the first wave-length. The simplest solution of this equation $J_0(z)$ or Bessel's function of order zero, is very similar to the curve found here; the first two loops have an amplitude ratio of 3/4 as against 2/3 for the curve found for ρ_1 but this difference is in part due to their being displaced half a loop outward.

The singular point, $z = a(1 - \kappa^2 \alpha)^{\frac{1}{2}}$ occurs for ordinary materials where the distance from the axis along a line drawn perpendicular to the surface of the cone is about a seventh of a wave-length.

⁶ Ince, Ordinary Differential Equations, p. 22.

Because of the complexity of the equations of the cone it is difficult to examine the effect of reducing the basic stress. A case which is simple enough to handle mathematically, and which may suggest what happens to the vibrating cone under similar conditions, is the circular cylinder. For this membrane the equations are:

$$\rho_1'' + h\kappa\rho_3' + q^2\rho_1 = 0, \quad k\rho_3'' - h\kappa\rho_1' + (q^2 - h^2)\rho_3 = 0,$$

where k is the tension divided by $2\mu + \lambda$ and $1/h$ is the radius of the cylinder. Since all the coefficients are constants, we can assume a solution of the form,

$$\rho_1 = e^{nu_1}, \quad \rho_3 = \zeta e^{nu_1}.$$

We find that

$$\zeta = -\frac{n^2 + q^2}{h\kappa n}$$

and we obtain for n two pairs of solutions, of which one is independent of k to the first order whereas the other becomes infinite as k approaches zero: $n = q\{(q^2 - h^2)/[(1 - n^2)h^2 - q^2]\}^{1/2}$ or $\{(1 - \eta^2)h^2 - q^2\}/k^{1/2}$. As an illustration of the problem with boundary conditions, let the membrane be rigidly fixed at $u=0$ and $u=1$. We now find a variety of different modes of vibration, in fact, the spectrum of characteristic frequencies consists of three different ranges. There is an infinity of modes with frequencies such that $q^2 < h^2(1 - \kappa^2)$, which we may call the low-frequency range; and also an infinity of frequencies given by $q^2 > h^2$, called the high-frequency range; solutions corresponding to intermediate frequencies also exist, but whether they could be made to satisfy these boundary conditions was not definitely determined. The low-frequency modes with positive tension and the high-frequency modes with negative tension are found to be of the form, $n = \pm n_1 i$ or $\pm n_2$ and

$$\rho_1 = C \left[\sin(n_1 u_1 + \gamma) + \frac{n_1 \kappa^2 h^2}{n_2 (q^2 - h^2)} (e^{-n_2 u_1} \pm e^{-n_2 (1-u_1)}) \right],$$

$$\rho_3 = -\frac{n_1 \kappa h}{q^2 - h^2} C [\cos(n_1 u_1 + \gamma) - e^{-n_2 u_1} \pm e^{-n_2 (1-u_1)}].$$

As the basic stresses approach zero and $n_2 \rightarrow \infty$, we note that ρ_3 remains finite relative to ρ_1 ; the effect of the stress as seen in the exponential terms is merely to reduce ρ_3 rapidly to zero at the ends. That is, with vanishing stress the oscillations take on the form obtained from the differential equation for zero stress, while the boundary conditions for ρ_3 are satisfied by means of an added sharp kink at each end.

On the other hand, the high-frequency modes under tension, and the low-frequency modes under compression are of the form, with $n = \pm n_1 i$ or $\pm n_2$

$$\rho_1 = C_1 \sin(n_1 u_1 + \gamma_1) + C_2 \sin(n_2 u_1 + \gamma_2),$$

$$\rho_3 = b_1 C_1 \cos(n_1 u_1 + \gamma_1) + b_2 C_2 \cos(n_2 u_1 + \gamma_2).$$

The second pair of terms in this case represent a short-wave "crinkle" superposed upon the main wave-form represented by the first terms. In this case, as the basic stress vanishes, the wave-length of the crinkle approaches zero, but it appears that its amplitude does not vanish relative to the main wave.

The question obviously presents itself as to how the physical cylindrical membrane with fixed ends and without stress actually vibrates. We may suspect that the slight stiffness which such a membrane must actually possess takes the place of the small basic stress used above and that the modes actually found would have either a superposed crinkle throughout the length of the cylinder or a sharp kink at the ends, similar to what we have found by our analysis.

It seems possible that the difficulties which were encountered above in the case of the cone are in practice surmounted in a similar manner.

The writer wishes to acknowledge the assistance given by Professor E. H. Kennard during the preparation of this paper, especially in the latter part of the article, that dealing with the cylindrical membrane.

CAPILLARY RETENTION OF LIQUIDS IN ASSEMBLAGES OF HOMOGENEOUS SPHERES

BY W. O. SMITH, PAUL D. FOOTE AND P. F. BUSANG
GULF RESEARCH LABORATORY, PITTSBURGH, PA.

(Received June 16, 1930)

ABSTRACT

The pore space in an assemblage of uniform spheres was initially filled with liquid. After very slow drainage the amount of liquid retained by the spheres was experimentally measured. The liquid is retained in the form of rings at the contacts of adjacent spheres. The radii of curvature of the ring surfaces are computed in terms of surface tension, grain radius and pressure drop across the liquid-vapor interface, permitting calculation of the volume retained per sphere contact. The number of contacts per unit volume of spheres is obtained from porosity measurements using the theory developed earlier. Computed and observed data on total volume of retained liquid are in agreement.

IF THE pore spaces in an assemblage of spheres be completely filled by a liquid which is then allowed to drain, a portion of the liquid is retained. The retention occurs during the passage of the liquid-gas interface through the grain assemblage. It is current opinion, as expressed in the semi-technical literature, that such liquid remains in the form of a fairly uniform layer which envelops the separate grains. In order to account for the observed retention, the thickness of the layer would have to be several thousand molecular diameters. Molecular forces, however, decrease extremely rapidly with distance, and unless chemical reactions, such as those involving gel formation, take place, layers exceeding three molecular diameters are improbable. Much of the work on retention has been done with comparatively fine sands and the actual mechanism of the phenomenon has escaped notice. Under the microscope, however, one may readily observe that a small ring of liquid is retained at the point of contact of two spheres. This type of retention is easily demonstrated by dipping two small balls or shot in a liquid and observing the retained liquid when the spheres, in contact, are withdrawn. It also follows from thermodynamical considerations that the major retention occurs in this manner. Equilibrium requires a minimum of free energy, and when the spheres are sufficiently small that gravitational effects are negligible, a given amount of retained fluid must be so distributed that the surface energy is a minimum. This occurs when the liquid is collected about the points of contact of the spheres.

The ring volume can be calculated approximately. Consider a capillary ring of liquid as shown in Fig. 1 with the two principal radii of curvature y and R taken as positive numbers. Complete wetting or zero contact angle with the spheres is assumed. Let Δp be the difference in pressure just outside and inside the liquid surface, and let σ be the surface tension. Then

$$\Delta p = \sigma \left(\frac{1}{R} - \frac{1}{y} \right) \quad (1)$$

From geometry it follows, if r is the radius of the spheres, that

$$\frac{1}{R} = \frac{2(r-y)}{y^2} \quad (2)$$

and accordingly,

$$y = \frac{-3 + (9 + 8r\Delta p/\sigma)^{1/2}}{2\Delta p/\sigma} \quad (3)$$

Putting $y/r = k$ and $R/r = \alpha$, the volume v of the ring of liquid is readily found to be

$$v = 2\pi r^3 \frac{\alpha}{1+\alpha} f(k, \alpha) \quad (4)$$

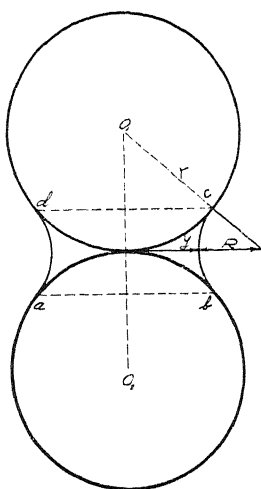


Fig. 1. Capillary ring of liquid between two spheres.

where

$$f(k, \alpha) = (k + \alpha)^2 - \alpha(k + \alpha) \left\{ 1 - \frac{1}{(1 + \alpha)^2} \right\}^{1/2} \\ - \alpha(k + \alpha)(1 + \alpha) \sin^{-1} \frac{1}{1 + \alpha} + \alpha^2 - \frac{\alpha}{1 + \alpha}.$$

This gives the volume of a single ring formed at a contact of two spheres in terms of parameters involving the quantity Δp which will be given consideration later.

In an earlier paper¹ the writers showed that in the natural piling of uniform spheres to a porosity P , the average number n of contacts per sphere is given by the approximate relation

¹ Smith, Foote and Busang, Phys. Rev. **34**, 1271-1274 (1929).

$$n = 6 \frac{1 + 1.828x}{1 + 0.414x} \quad (5)$$

where

$$x = (0.476 - P)/0.217$$

The number N of spheres per unit volume is

$$N = \frac{1 - P}{4\pi r^{3/3}} \quad (6)$$

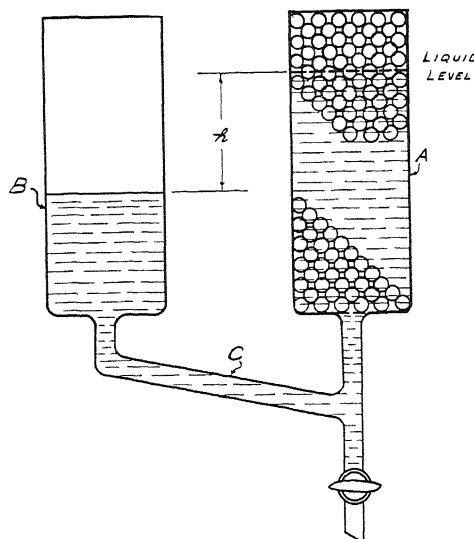


Fig. 2. Schematic diagram of drainage experiments in which the meniscus surface is above the free surface by the distance h equal to the capillary rise.

Since in the complete assemblage, two spheres determine a single contact, the number of contacts per unit volume is $Nn/2$ and the volume V of liquid retained per unit volume of packed space is

$$V = Nnv/2. \quad (7)$$

The value of Δp depends upon the manner in which drainage occurs. In general the flow of fluid through any single pore composed of three adjacent grains is along the axis normal to the plane of the grain centers, as is the case with a meniscus falling in a simple cylindrical tube. The interface always drops in a direction parallel to the axis of the tube provided that it is not too large. Let us consider a single contact and the pores on either side. As the complex meniscus of the whole sand body falls, the portion of it in this restricted region drops through the adjacent pore spaces wrapping itself around the contact point. As the interface falls further the liquid immediately under the contact point is constricted and finally breaks, leaving that around the contact in the form of a ring and separated from the main body

of liquid. The final curvatures of the ring are closely equal to those which it had just prior to breaking and these are determined by the pressure difference Δp prevailing at that instant, subject, of course, to the limitation that the spheres are not too large.

The simplest case is that in which Δp is the meniscus pressure drop prevailing at maximum capillary rise, a condition which can be produced by allowing the free liquid and meniscus to fall simultaneously and very slowly in a U-arrangement such as is shown in Fig. 2. *A* contains the grains and *B* provides the liquid receptacle and is connected to *A* by a small tube *C*. If now the liquid is allowed to drain from the system by bleeding it from the stop-cock, the meniscus will remain at a height *h* above the free liquid in *B* which will not differ greatly from normal capillary rise provided the drainage takes place sufficiently slowly. The pressure drop Δp across the meniscus formed by the liquid surface within the sphere assemblage is accordingly given by the capillary equation

$$\Delta p = \sigma \left(\frac{1}{r_1} + \frac{1}{r_2} \right) = \rho g h \quad (8)$$

where r_1 and r_2 are the principal radii of curvature of an element of the meniscus, ρ the density of the liquid, g the acceleration of gravity, and h the height of capillary rise for the particular element. In a paper on "Capillary Rise of Liquids in Homogeneous Sands," to appear later, the writers show that when h is large the average value of $\rho g h$ over the entire meniscus is given by the approximate relation:

$$\overline{\rho g h} = \frac{2\sigma}{r} \left(\frac{0.651 + 0.256x}{0.349 - 0.256x} \right) \quad (9)$$

From Eqs. (3), (8), and (9), we find

$$k = \frac{y}{r} = \frac{-3 + (9 + 8A)^{1/2}}{2A} \quad (10)$$

where

$$A = 2 \left(\frac{0.651 + 0.256x}{0.349 - 0.256x} \right)$$

and from Eqs. (2) and (10)

$$\alpha = k/(Ak + 1) \quad (11)$$

The Eqs. (10) and (11) determine α and k from which v can be calculated by substitution in Eq. (4).

It will be observed that retention of this type is independent of the density, surface tension and viscosity of the particular liquid used. No dependence on viscosity, of course, is to be expected because of the very slow rate of drainage. Also the retention per unit volume of packed space is inde-

pendent of the radius of the spheres used, being a function of the porosity alone as can be seen by substitution of Eqs. (4) and (6) in Eq. (7) from which we obtain

$$V = \frac{3}{4}n(1 - P)\frac{\alpha}{1 + \alpha}f(k, \alpha). \quad (12)$$

Fig. 3 shows the volume V of retained liquid per unit volume of packed space as a function of the porosity and is plotted from Eq. (12). A curve of this type is to be expected. While the number of contacts increases as we decrease the porosity, the height of capillary rise increases as do also the resulting ring curvatures. Hence the volume of a single ring must decrease with decreasing porosity, offsetting the increased number of contacts.

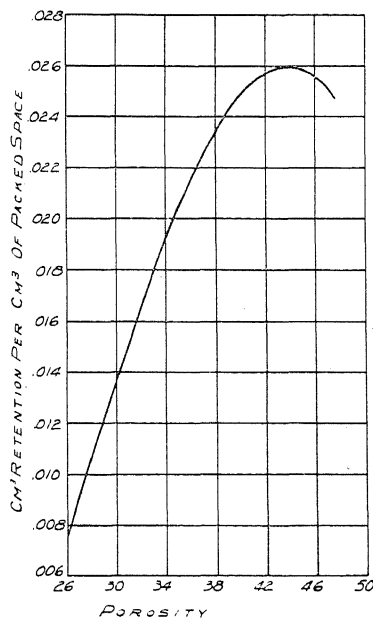


Fig. 3. Volume of retained liquid per unit volume of packed space as a function of porosity.

An experimental investigation was undertaken to test the validity of Eq. (12). The arrangement used is shown in Fig. 4. In principle it is a duplication of that shown in Fig. 2. A , C and D are spherical reservoirs each enclosing a volume of about two liters. A wire gauze was placed at the bottom of A in which the spherical grains were packed. C and D respectively served to fill and collect the liquid whose retention was to be investigated. B , a 3 cm cylindrical glass tube was used as a free liquid container during capillary drainage. a , b and c denote stop cocks for closing off the principal reservoirs. f and g are ground glass stoppers each provided with a small capillary to prevent excessive loss of liquid by evaporation, but permitting atmospheric pressure to prevail.

The procedure was to fill the flask *C* and weigh it. It was then placed in connection with the free liquid reservoir *B* by means of a large ground glass stopper *d*. With stop-cocks *a* and *c* open and *b* closed, the liquid was allowed to slowly fill *A* to the top of the grains. Valve *a* was then closed and the surplus liquid in *C* drained into the flask *D*, connected to the system *A* - *B* by a ground glass stopper *e*. The valve *b* was closed so that initially *B* was completely filled. Valve *b* was now opened a little and the liquid in the U-system *A* - *B* allowed to drop sufficiently slowly to keep capillary equili-

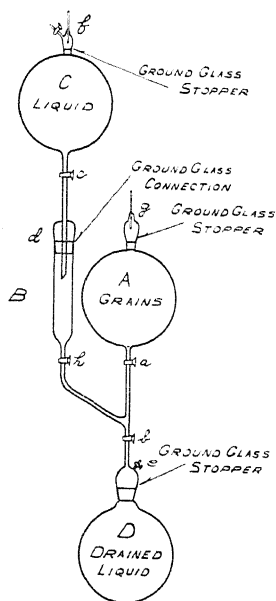


Fig. 4. Arrangement of apparatus in drainage experiments.

brum preserved. The surplus liquid was collected in *D* and weighed. That which remained in *A* was calculated from the difference in weights of liquid drained from *C* and into *D*.

With the smaller sizes the drainage time was necessarily longer, with a consequent increase in experimental losses. For this reason the retention of glass pearls and sands, was determined by taking small samples of about 100 grams each from the grain reservoir immediately after drainage. These were quickly weighed, dried in an oven at 80°C and reweighed, the difference being the weight of the retained liquid. Lead shot of radii 0.219 cm and 0.165 respectively as well as glass pearls of radii 0.0316 cm and standard Ottawa silica sand of radius 0.0443 cm were used in conjunction with a series of liquids of different surface tension and viscosity, the former varying between 25 and 72.8 dynes/cm and the latter from 0.009 to 1.38 poises. Kerosene was used in the cases of glass pearls and sands owing to the impracticability of the methods when volatile liquids such as CCl_4 are used. Its viscosity is such as to permit drainage in a reasonable time. Table I

summarizes the results. The observed retentions in cm^3 of liquid per cm^3 of packed volume are listed in column 5 of the table. Column 6 gives the corresponding quantities computed from Eq. (12). The agreement in general is good.

TABLE I. *Experimental data on retention.*

Grain Material	Grain Radius cm	Porosity	Liquid	Retention per cm^3		Density of Liquid	Surface Tension dynes/cm
				Obs.	Computed		
Lead Shot	0.219	0.404	CCl_4	0.0235	0.0250	1.587	24.9
			C_6H_6	.0261	.0250	.875	27.7
			$\text{C}_6\text{H}_5\text{CH}_3$.0258	.0250	.861	26.7
			Turbine Oil	.0201	.0250	.918	34.3
			Zephyr Oil	.0245	.0250	.846	30.9
			Cayuga Oil	.0222	.0250	.883	32.3
			$\text{C}_2\text{H}_5\text{OH}$.0246	.0250	.807	25.4
			Water	.0273	.0250	1.000	72.0
			Mean	.0243	.0250		
Lead Shot	0.165	0.396	CCl_4	.0264	.0279	1.587	25.0
			Zephyr Oil	.0285	.0279	.847	30.9
			Cayuga Oil	.0290	.0279	.847	32.3
			Pequod Oil	.0250	.0279	.893	33.7
			$\text{C}_2\text{H}_5\text{OH}$.0276	.0279	.807	25.6
			Water	.0283	.0279	1.000	72.8
			Mean	.0275	.0279		
Glass Pearls 20-24 mesh sand	0.0316	0.373	Kerosene	.0255	.0235	.811	28.6
	0.0443	0.359	Kerosene	.0292	.0222	.811	28.5

The results indicate that the wetting layer, a few molecules in thickness, is the only film present in assemblages of uniform spheres, and the volume of liquid so held is negligible in comparison with that found in the form of rings at the grain contacts. The quantities retained are obviously too large to be accounted for by the molecular forces involved in the formation of adsorbed films on a uniform surface. The shot and glass beads used had fairly uniform surfaces while the sand did not. Where rough surfaces are involved, small depressions filled with liquid can exist provided only that they are sufficiently deep to permit proper equilibrium curvatures. Such a type of surface film is permissible, and may account for the fact that the experimental values for sands are in excess of those calculated, although the lack of sphericity of the sand grains may be the controlling factor.

A REPRESENTATION OF THE DYNAMIC PROPERTIES
OF MOLECULES BY MECHANICAL MODELS

By C. F. KETTERING, L. W. SHUTTS AND D. H. ANDREWS

GENERAL MOTORS CORPORATION, RESEARCH LABORATORIES,¹ DETROIT, MICHIGAN.

(Received June 23, 1930)

ABSTRACT

Mechanical models have been constructed to represent the dynamical systems believed to exist in the molecule. Assuming that the intramolecular forces lie along lines associated with the chemical bonds and that for small vibrations they obey Hooke's law and have the mechanical character of spiral springs, it is possible to get a picture of the forces and masses which can be represented on a large scale by steel balls and spiral springs. Models have been constructed for some of the simpler non-polar molecules. They are found to have characteristic frequencies which correspond very closely to the frequencies observed in the Raman spectra, and it is possible by this means to identify the Raman lines with definite types of motion of particular atoms in the molecule. This substantiates the view that Raman lines correspond very closely to characteristic fundamental molecular frequencies.

INTRODUCTION

THIS paper describes an attempt to make some mechanical models of the dynamical systems of forces and masses which are found in real molecules. The possibility of doing this lies in the fact that according to optical and thermal data the smaller nonpolar molecules are dynamically rather simple.^{2,3} This simplicity is brought about in several ways. In the first place the only effective masses in the molecule are the nuclei of the atoms which may be regarded as point masses. The space relations of these masses to each other can be deduced to a large extent from the studies of the crystal lattice by means of x-rays. In the second place the forces in the molecule also appear to be simple in nature, lying for the most part along the lines which join the nuclei and which have been associated with the chemical bonds. In fact, the forces of the bonds are so much greater than any of the other forces acting on the atoms that they alone are of importance dynamically.

The problem is further simplified by the nature of the bond itself which behaves in a manner very analogous to a spiral spring. Thus for the small displacements with which we deal in studying the behavior of the molecule in the lowest vibrational levels we can see that the bond forces will obey

¹ The results reported here were arrived at largely as a development of the concepts of molecular structure originated by the senior author (C.F.K.). The success of the project is due chiefly to the cooperation of the many members of the laboratory staff who assisted in both the mechanical and physical part.

² J. W. Ellis, *Jour. Franklin Inst.* **208**, 517 (1929); E. O. Salant, *Proc. Nat. Acad. Sci.* **12**, 334, 370 (1926).

³ D. H. Andrews, *Proc. Roy. Acad. Amsterdam* **29**, 744 (1926); *Chem. Reviews* **5**, 533 (1928), *Phys. Rev.* **34**, 1626 (1929); **36**, 544 (1930).

Hooke's law with regard to the extension or compression of the bond. There is, however another feature of the mechanical nature of the bond which has been largely neglected heretofore. The organic chemist in trying to explain the behavior of ring compounds has suggested that the bonds from a carbon atom will normally bear certain spatial relations to each other. This normal position has been generally accepted as that in which the bonds make the tetrahedral angle with adjoining bonds. In a cyclic compound such as a ring composed of four carbon atoms, it has been assumed that a strain is introduced by the alteration of the angles between the bonds. The concept has thus arisen that, in addition to elasticity of stretching, the bond has also elasticity of bending. This idea has been substantiated by recent data from the Raman spectra which show the force necessary to bend a bond is about one fifth that necessary to stretch it.

Data from the Raman and infrared spectra, as well as from specific heats,³ have also indicated another regularity in the nature of the bond which simplifies considerably the construction of a mechanical model. It is found that the restoring force due to the stretching of a normal nonpolar bond is always about the same whether the bond be between two hydrogens, a hydrogen and a carbon, two carbons, a carbon and an oxygen, or any other similar position. It thus would appear to be possible to represent all the bonds in a mechanical model by means of the same kind of spiral spring. If the ratio of the stretching force constant to the bending force constant were chosen correctly it should be possible to make a model which would quite closely represent the actual molecule.

Until recently the data have been quite incomplete from which one could find the fundamental mechanical frequency in a molecule. Developments^{3,4,5} in the study of the Raman spectra, however, indicate that the frequencies found there do correspond rather closely to real mechanical frequencies in the molecule. It therefore seems probable that if a mechanical model of a molecule were correctly constructed the characteristic frequencies found in it should correspond term by term to the frequencies observed in the Raman spectra. We should be able to get from a Raman frequency to a model frequency and *vice-versa* by multiplying or dividing by the proper constant which depends on the ratio of the mass of the molecule to the mass of the model, and of the force of the chemical bond to the force of the spring which represents it.

THE CONSTRUCTION OF THE MODEL

The first problem in constructing the model was the determination of the ratio of the stretching to the bending force in the spring which was to be used to represent the chemical bond. In order to simplify the problem it was decided to omit the hydrogen atoms from the first series of models, thus representing only the atoms of atomic weight of twelve or greater. The hydrogens, being so light, have almost no appreciable energy at ordinary tempera-

³ A. Dadiou and K. W. F. Kohlrausch, *Berichte der Deutschen Chemischen Gesellschaft*, Jahrg. 63, 251 (1930).

⁵ A. S. Ganesan and S. Venkateswaran, *Indian Journal of Physics* 4, 195 (1929).

tures, and contribute very little to the dynamical character of the system. We were thus left with the problem of determining the nature of the bond between two atoms like carbon, oxygen, or chlorine.

We have a direct indication of the strength of the carbon-carbon bond in the Raman spectrum of ethane. There is one line at 990 wave numbers which with very little doubt corresponds to the frequency of vibration of the two carbon atoms. By means of the formula,

$$\nu = \frac{1}{2\pi} \left(\frac{k}{m} \right)^{1/2} \quad (1)$$

where ν is the frequency, m is the reduced mass of the system, and k is the force constant, we can calculate what the stretching force for the carbon-carbon bond will be. It turns out to be about 4×10^5 dynes per cm. Methyl alcohol which is dynamically similar to ethane gives a similar value for the force.

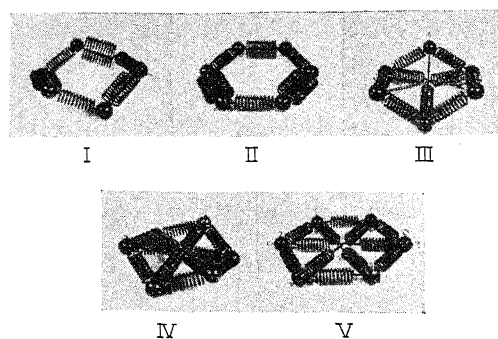


Fig. 1a.

The calculation of the bending force is quite a bit more uncertain as it is only involved when we have at least three atoms in the molecule. From the study of ethyl alcohol and benzene and its derivatives, the value of 0.66×10^5 dynes per cm has been calculated by defining the bending force as a force necessary to displace an atom in a direction perpendicular to the bond joining it to another atom which is held stationary. While this concept of the bending force may seem somewhat arbitrary, it would appear to be the best means of approach available at the time. A better knowledge of just what it is can probably be obtained as our knowledge of molecular dynamics increases.

From a consideration of these values, a helical spring to represent the bond was decided upon. It has the following characteristics:

Mean Diameter of Coil	13/16 in.
Diameter of wire	#11 (0.120)
No. of active turns	10
Free length	2-1/2 in.
Force per inch deflection	53 lbs.

The actual weight of the spring when completed was $1\frac{1}{2}$ ounces. Steel balls $1\frac{1}{8}$ in. diameter weighing 0.2 lbs. each were used to represent the carbon atoms. To obtain the desired value for the bending of the spring, the distance between the centers of the balls was set at $3\frac{3}{4}$ in. Some of the models constructed in these proportions are shown in Fig. 1a.

METHOD OF STUDY

In order to study the fundamental vibration frequencies of such models, it is necessary to activate them by means of vibrational impulses of various frequencies. This was successfully accomplished by using a rubber band to attach one of the balls to an oscillating arm having $\frac{1}{4}$ in. stroke. This arm was operated by a reciprocating yoke on an eccentric driven by a variable speed motor. The model was suspended on rubber bands in such a manner that the frequency of the natural period of the suspension was much lower than the lowest period in the model.

Since the vibrations of the models covered a range of frequencies from 200 to 3500 cycles per minute, it was necessary to use some special means of observation in order to determine the characteristic motion of the various vibration periods. This was accomplished by illuminating the model with a neon lamp of a specially constructed stroboscope giving a large field of illumination. The circuit breaker of the stroboscope was geared to the activating motor shaft so that the neon lamp flashed at a frequency 2% slower than the exciting frequency applied to the model. Thus when the model was vibrating, a slow motion image, 1/50th of the actual frequency, was obtained. Thus at a frequency of 3000 cycles per minute, the model would appear to move through one cycle per second making it very easy to study the characteristics of the motion.

The tuning was found to be very sharp. When the motor was running at a speed which did not correspond to a characteristic frequency, the model was absolutely quiet. When the motor speed came within about five percent of a characteristic frequency, however, the balls began to move over the paths characteristic of that frequency and with closer tuning would generally vibrate with an amplitude of the order of $1/2$ in. This, of course, depends on the type of motion and the point of activation to some extent. The tuning was sharp enough, though, so that the characteristic frequencies could be determined to within two or three percent, and it was easy to see just what type of motion corresponded to that frequency.

There was little complication because of harmonics. One or two of the lowest frequencies would sometimes appear when the speed of the motor was double their fundamental value, but could easily be recognized as harmonic because the balls were vibrating with twice the frequency which they should have had for that motor speed. The amplitude of these harmonics was always small. There seemed to be a little trouble from spurious vibrations, that is, vibrations occurring because the springs actually had mass. These are called spurious because they would not be found in the real molecule where the

only mass is in the nuclei. They were easily recognized by studying the motion of the springs under the neon light.

The method of study consisted in activating the model starting with a frequency of about 100 r.p.m. and raising the motor speed continuously to the maximum of 3600. As the characteristic frequencies were reached, they would be recognized by the appearance of motion of the balls under the neon light and the frequencies of revolution would be tabulated as read from a tachometer connected to the motor shaft. After going through the range of frequencies, a further study would be made by approaching each frequency carefully from above and below and observing as accurately as possible the motions of the balls at that frequency. The same model would be vibrated at several different positions by attaching the activating rubber band in various ways. It was found that while this sometimes altered the amplitude of the various frequencies, their values and number remained the same. In this way we have secured data on the characteristic frequencies of models of a number of the commoner organic compounds. A discussion is given in detail in the following paragraphs.

RESULTS

MODELS WITHOUT HYDROGEN REPRESENTED

Benzene. Benzene was chosen as one of the compounds for study because of the uncertainty regarding its structure. Five different models of benzene, illustrated in Fig. 1a, were constructed as follows:

I. The Kekulé formula. The six balls representing the carbon atoms are arranged in a hexagon, and joined with alternate single and double bonds so placed that the tetrahedral angle is formed between any two adjoining bonds. The double bonds are made by putting two of the standard springs in parallel. The result is a "puckered" hexagon.

II. The Kekulé formula, plane. This is similar to model I except that the bonds are so arranged that the balls form a hexagon in a plane.

III. Centric formula. In this model the six balls are joined by single bonds into a "puckered" hexagon. There are in addition three cross bonds joining carbon atoms opposite each other in the ring. Each of these cross bonds is formed of a standard spring with a sufficient extension of wire on one end to give it the necessary length. In model IIIa the three cross bonds can slide over each other freely. In model IIIb they are clamped together in the center.

IV. Centric formula. This is the same as the preceding model except that the cross bond is formed by two standard springs joined together in the center. In IVa the bonds slide freely at the center and in IVb they are clamped together.

V. Centric formula. This is similar to the preceding model except that the bonds are so arranged that the six balls lie in a plane.

In order to compare the frequencies found in these models with the Raman spectra, it is necessary to calculate a conversion factor for passing from r.p.m.

to wave numbers. This conversion factor C may be expressed in terms of the masses and elastic constants by means of the equation

$$C = \frac{\nu \text{ r.p.m.}}{\bar{\nu}} = 60c \left(\frac{k_s m_m}{k_m m_b} \right)^{1/2} \quad (2)$$

where $\bar{\nu}$ is the frequency in wave nos., ν r.p.m. is the frequency in r.p.m., k_m is the elastic constant for the bond in the real molecule, k_s is the elastic constant of the spiral spring, m_b is the effective mass of the ball, m_m the mass of the nucleus, and c the velocity of light.

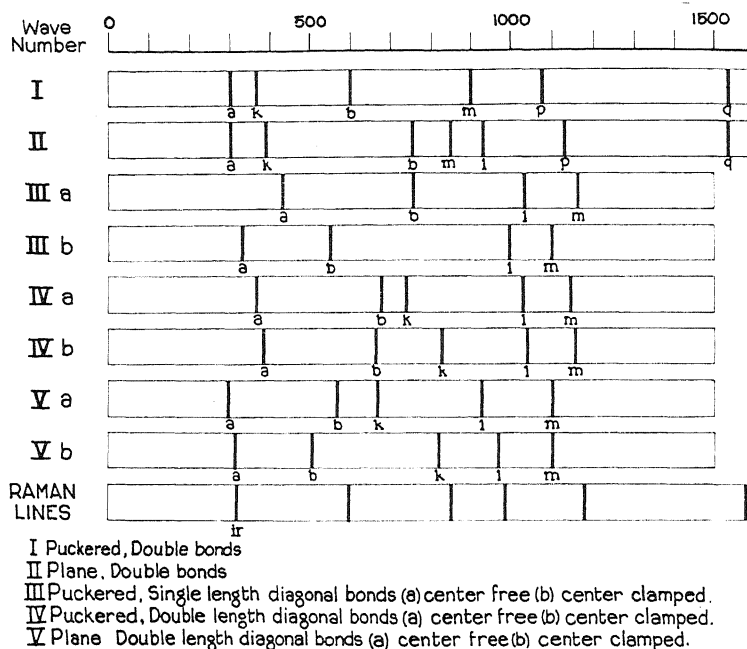


Fig. 1b. Models of benzene.

In the case of the fastest motion in benzene, the effective mass will be approximately that of a ball plus one and one-half springs. Of course this effective mass will be different for different types of vibration, but this seems to be sufficiently close approximation. Using the proper values, we find that C has a value of 3.1, which may be considered equal to three, within our limit of error.

The results of the study of these models are shown in Fig. 1b. The Raman spectrum for benzene is shown in the last line of the figure. The lines at 1500 cm^{-1} and at 3000 cm^{-1} (not shown) are almost surely due to the hydrogen which is not represented in this model. The four lines between 600 and 1200 cm^{-1} have been reported by almost everyone studying benzene and are known quite accurately. There seems to be also considerable evidence for a frequency in the neighborhood of 360 . A series of bands observed in the in-

frared^{6,7} indicate a fundamental frequency at 360 cm^{-1} and the specific heat⁸ of benzene also gives very strong evidence for a frequency in this neighborhood. These five frequencies then seem to be the characteristic frequencies due to the vibration of the carbon atoms in benzene.

As may be seen in Fig. 1b, the centric models are in fairly good agreement with the Raman spectrum. They show five fundamental frequencies of the type indicated in Fig. 2. These types of motion are also in agreement with those which had previously been assigned to benzene³ on the basis of its specific heat and Raman spectra. The degrees of freedom observed in the different types of motion add to give the correct number for the six carbon atoms, namely, twelve.*

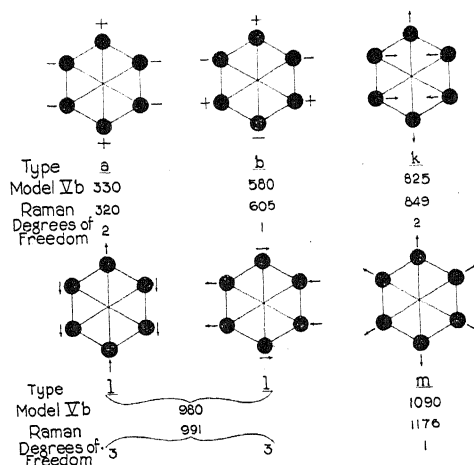


Fig. 2. Types of motion in benzene. + and - indicate motion out from and into plane of paper.

It is a little difficult to say just which model is in best agreement with the Raman spectrum. The evidence is perhaps a little in favor of *Vb*. This would be in accord with other observations which favor a plane hexagon for benzene. The double bond models, Kekulé formula, are distinctly different from the others in the higher frequencies. As may be seen in Table I, there is a frequency (*p*) which arises from a stretching of the single bonds. We would also expect a frequency (*q*) arising from a stretching of the double bonds. It was not possible with the present apparatus to excite this frequency because of the speed limitation of the motor, but calculation shows it would correspond to about 1540 cm^{-1} . As shown in the last column, there is fair agreement between these frequencies and the Raman frequencies at 1176 and 1592 cm^{-1} . It is true that we had assumed the latter to be close to a lateral motion of the

⁶ J. W. Ellis, Phys. Rev. **27**, 298 (1926).

⁷ L. Marton, Zeits. f. Phys. Chem. **117**, 97 (1925).

* The six carbon atoms with three degrees of freedom each give eighteen degrees of freedom in all. Subtracting six for the translation and rotation of the molecule as a whole, we should have twelve internal degrees of freedom.

TABLE I. *Models without hydrogen represented.* $\bar{\nu} = (r.p.m.)$.
Benzene

Model	I	II	IIIa	IIIb	IVa	IVb	Va	Vb	Raman ⁵
<i>a</i>	300	320	435	340	385	400	325	335	360*
<i>b</i>	615	770	755	—	650	665	580	585	605
<i>k</i>	390	400	—	550	735	850	680	815	849
<i>l</i>	950	940	1035	1000	1015	1015	945	955	991
<i>m</i>	—	865	1160	1150	1150	1150	1090	1080	1176
<i>p</i>	1080	1135	—	—	—	—	—	—	(1176)
<i>q</i>	(1540)	(1540)	—	—	—	—	—	—	(1592)

* Value from infrared spectra, see reference 6.

Toluene		
Type	Model	Raman ⁵
<i>t</i> ₁	205	215 cm ⁻¹
<i>t</i> ₂	235	
<i>a</i>	400	345
<i>b</i>	635	520*
<i>k</i> ₁	750	622
<i>k</i> ₂	835	730
<i>l</i> ₁	960	786
<i>l</i> ₂	990	1005
<i>m</i>	1150	1029
		1162

* Not observed by all investigators.

Models with chlorine 1.8ν = (r.p.m.).
Carbon tetrachloride Chloroform

Model	Raman ⁵	Model	Raman ⁵
220	216 cm ⁻¹	235	261 cm ⁻¹
305	313	360	367
—	459	—	669
—	762	—	762
1000	791	1195	1218
1540	1535	1750	1441

Models with hydrogen represented. $\bar{\nu} = (r.p.m.)$.
Ethane Ethylene Acetylene

Model	Raman ⁹		Model	Raman ⁸		Model	Raman ⁹	
C-C	1275	990 cm ⁻¹	C-C	1725	1623	C-C	2025	1960
H _t	{ 725	1460	H _t	{ 775	1342	H _t	750	
	{ 870			{ 825				
H _i	{ 2830	{ 2890	H _i	3000	{ 2880	H _i	{ 2960	
	{ 3000	{ 2950			{ 3019		{ 2980	
					{ 3240			
					{ 3272			

⁸ R. G. Dickinson, R. T. Dillon, and F. Rasetti, Phys. Rev. **34**, 582 (1929).⁹ M. Daure, Compt. Rend. **188**, 1452 (1929).

Methyl alcohol			Ethyl alcohol		
Model	Raman ⁵		Model	Raman ⁵	
C-O	1200	1031 cm ⁻¹	C-C-O $\begin{cases} x \\ y \\ z \end{cases}$	250	450 cm ⁻¹
H ₂	875	1257		1125	884
		1360		1350	1047
H ₂ $\begin{cases} \text{CH}_3 \\ \text{OH} \end{cases}$	2900	2834	H ₂	750	1461
	3000	2939			1165
					1276
			H ₂ $\begin{cases} \text{CH}_3 \\ \text{CH}_2 \\ \text{OH} \end{cases}$	2940	2872
				2960	2930
				3025	2973

hydrogens, but this is not absolutely certain. We may conclude that there is some evidence in favor of the double bonded structure, but until we are a little more certain of the correct way to represent the double bond, too much weight must not be placed on this evidence.

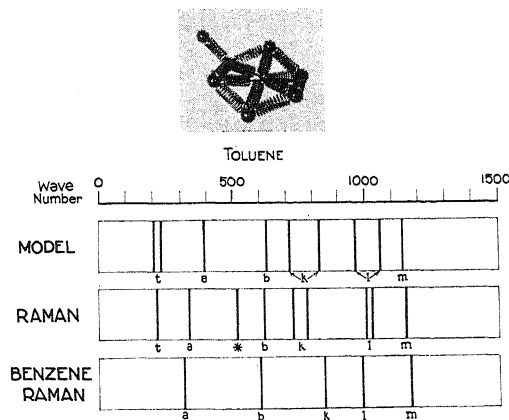


Fig. 3. Models of toluene.

Toluene. The model for toluene is the same as model IV_b of benzene, with a ball and spring added to represent the methyl group. This group is attached so that it lies in the plane of the ring. The results are shown in Fig. 3. The addition of the methyl group causes a splitting of two of the frequencies which involve several degrees of freedom into doublets. Apparently one of the lines represents a motion which has its principal axis through the pair of carbon atoms in the ring which are in line with the methyl group, and the other two correspond to types of motion with the principal axis passing through the other two carbon atoms in the ring. This splitting may be seen by comparing the Raman spectra of benzene and toluene, and the model duplicates it almost exactly. There are also two low frequencies which represent the motion of the methyl group like a tail wagging. This interpretation has been verified by the heat capacity³ which shows a large value at low temperatures which must be due to the presence of low frequencies.

Carbon tetrachloride. In order to investigate the effect of changing mass in the model, a representation of carbon tetrachloride has been constructed, the chlorine atoms being balls, the weight of which bears the proper ratio to the standard ball which represents the carbon atom. The results are shown in Fig. 4. If we use the same conversion factor of three, there is a discrepancy between the model frequencies and the Raman frequencies. This seems to be due to the fact that the force constant for the carbon-chlorine bond is somewhat smaller than for the carbon-carbon. An arbitrary conversion constant was therefore used which was somewhat smaller than the other one. There is no frequency in the model for the Raman line at 452 cm^{-1} . It seems quite possible that this is a first harmonic of the line at 216 cm^{-1} .

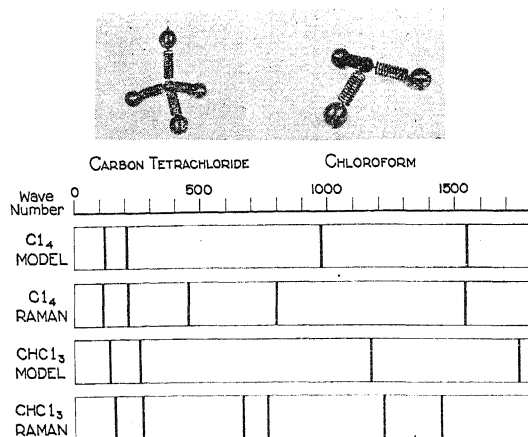


Fig. 4. Models of chlorine compounds.

Chloroform. This is just like the model for carbon tetrachloride except that the one chlorine atom has been omitted. If the value of the conversion constant suitable for the carbon-chlorine bond is used, the lines are in fair agreement with the Raman spectra.

MODELS WITH HYDROGEN REPRESENTED

In order to make a model in which the frequencies of the hydrogens could be represented and could be observable with the means at our disposal, it was necessary to change the scale of the model. For convenience we used, to represent the hydrogen, the ball which had previously represented the carbon, and carbon was now represented by a ball of twelve times the mass of the small ball. A spring of the same wire and same number of turns as before was used to represent the bond. Its length was, however, shortened by a third because in the molecule the distance separating C-H is 1 \AA , while that separating C-C is 1.5 \AA . With this means, models were constructed and vibrated and the results are as follows:

Ethane. In the model of ethane it was found that there was one frequency corresponding to the vibration of the two carbon atoms with respect to each

other, also vibration of the hydrogen atoms at approximately three times the frequency of the carbon atoms. Of course, a new conversion constant must be used now that the mass has been changed. It might be calculated from the one previously adopted, but the difficulty of correcting for the mass of the springs makes this almost impossible. Since we are primarily interested in the ratio of the frequencies, it seemed wiser to adopt an arbitrary constant, and as it happens that in this model r.p.m. corresponds almost exactly to wave numbers, we have taken the conversion constant to be unity for the sake of simplicity.

As may be seen in Fig. 5, the ratio of the carbon frequencies (C-C) to the longitudinal hydrogen frequencies (H_L) is approximately that found in the Raman spectra for longitudinal vibrations. The model, however, shows transverse frequencies for the hydrogen (H_T) around 800 cm^{-1} . The line in the

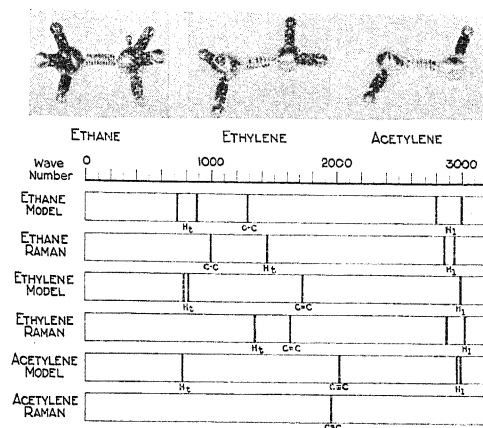


Fig. 5. Models with hydrogen represented.

Raman spectrum which has been identified with this vibration lies at 1420 cm^{-1} . The reason for this discrepancy between the model and the spectrum is hard to explain. Apparently the force constant for lateral displacement of the hydrogen is quite a bit larger than the corresponding force in the carbon-carbon bond. We can not hope, of course, for a perfect representation of the real molecule, and it seems that we must be content here with having the number of frequencies correspond while the numerical value of this type of frequency lies considerably lower in the model than it does in the spectrum.

Ethylene. By putting a double bond between the carbon atoms, we shift the carbon-carbon frequency to about 1700 cm^{-1} . This corresponds to the shift observed in the Raman spectrum. The frequencies of the hydrogen are but slightly affected as the spectrum also shows.

Acetylene. Putting a triple bond between the carbon shifts the frequency to a little over 2000 cm^{-1} . This corresponds to the spectrum observed.

Methyl alcohol. Dynamically, this is quite akin to ethane. We find about the same frequency for the vibration of the two heavy atoms and the frequen-

cies in the same region for the vibration of the hydrogens as shown in Fig. 6. Again transverse vibrations of the hydrogens lie considerably lower than the lines ascribed to them in the Raman spectra.

It is very interesting to see the distinction between the two lines around 3000 cm^{-1} . When the model is vibrated at 2900 cm^{-1} the three hydrogens of the methyl group move in toward and out from the carbon while the hydrogen attached to the oxygen stays quiet. At 3000 cm^{-1} the three methyl hydrogens become quiet and the hydroxyl hydrogen vibrates. Since the masses and forces are the same in each case, this difference in frequency must be due to the fact that we have three balls reacting against the central ball in the one case and only one in the other case. It would, therefore, look as if the lines in the Raman spectrum could be positively identified with specific atoms in the molecule.

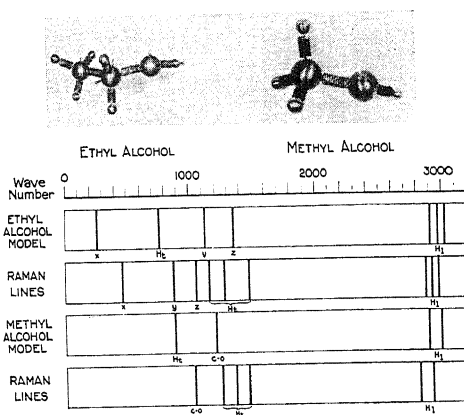


Fig. 6. Models with hydrogen represented.

Ethyl alcohol. This was constructed in the same way as the preceding models. We now have however, the possibility of three types of frequencies involving the large balls. The spectrum has the same general character as that of methyl alcohol. We now, however, find three lines around 3000 cm^{-1} . The lowest of these frequencies makes the three hydrogens in the methyl group vibrate while the others stand still. The next makes the two hydrogens in the CH_2 group vibrate, and the highest vibrates the hydrogen of the hydroxyl while the others remain quiet. We thus have a confirmation of the identification of these Raman lines with individual atoms. The transverse vibrations of the hydrogen again are lower than the lines identified with them in the Raman spectrum. The two upper vibrations (y , z) of the heavy atoms agree fairly well with the corresponding Raman lines. The lowest of the three (x) lies somewhat lower than the corresponding Raman line. This is probably due to the fact that in the model the mass is not distributed in space in the same way as in the molecule.

CONCLUSION

The general agreement which we have found between the characteristic frequencies of the models and the lines in the Raman spectra substantiates the character of the dynamical system in the molecule which we assumed in building the models. It seems reasonable to conclude that the molecular forces are directed along the lines associated with the chemical bonds and that mechanically, they are analogous to spiral springs. It appears also that the great majority of Raman lines have values of the frequency closely corresponding to fundamental mechanical frequencies in the molecule. Some of these frequencies are determined largely by the character of the whole molecule while others correspond to individual atoms or small groups of atoms. The mechanical model should prove very valuable in making these identifications and in ascertaining the structure of the molecule.

THE RELATION BETWEEN THE RAMAN SPECTRA AND
THE STRUCTURE OF ORGANIC MOLECULES

BY DONALD H. ANDREWS

CHEMISTRY LABORATORY, JOHNS HOPKINS UNIVERSITY

(Received June 23, 1930)

ABSTRACT

The following procedure is proposed for identifying the type of vibration in the molecule to which an observed frequency in a Raman spectrum corresponds. It is assumed that the only forces acting between the atoms in the molecule are those produced by the chemical bonds, and that there is a restoring force if the bond is stretched or if the angle which the bond makes with the other bonds on an atom is altered from the normal equilibrium value. It is also assumed that all non-polar chemical bonds have the same force constants in organic compounds. The different frequencies observed in the Raman spectra may then be considered as due solely to the variation in mass of the atoms concerned and to their space relation to each other, that is, whether they are in a straight chain, a branching chain, a ring, etc. It is possible to calculate in this way the number of Raman lines which should be observed for any compound, and the frequencies they should have. There is fair agreement with the observed spectra close enough so that the lines can be identified with different types of motion in the molecule.

INTRODUCTION

IN SPITE of the great deal of work which has been done on the Raman effect since its discovery two years ago we still lack a theory which is satisfactory for explaining at all completely the relation between the structure of organic molecules and the frequencies in the light which they scatter. The simplest explanation is that the shift in the frequency of the scattered light corresponds to a fundamental mechanical frequency in the vibrating molecule. This hypothesis has been supported by the extensive work of Dadiou and Kohlrausch¹ who have measured the Raman spectra for a large number of compounds, and have pointed out a great many significant relations between Raman lines and molecular structure in their own results and those of others working in this field. For example, certain special groups in a molecule such as hydrogen bound to carbon or two carbons bound by a double bond appear to have lines of definite frequency associated with them. Moreover, the calculation of the binding force between the atoms from the values of the Raman shifts lead to such uniform values among a wide variety of compounds that it seems reasonable to suppose that the frequencies of the Raman shift must correspond very closely to fundamental frequencies in the molecule.

Now, this hypothesis would also lead us to expect a close correspondence

¹ A. Dadiou and K. W. F. Kohlrausch: *Phys. Zeits.* **30**, 384 (1929); *Berichte d. deutschen chem. ges.* **63**, II, 251 (1930); *Wiener Berichte* IIa, **138**, 41, 336, 420, 607, 635, 799 (1929); **139**, 77 (1930).

between the frequencies of the Raman shifts and the frequencies in infrared absorption spectra. This has not been found to be true, particularly where the infrared absorption spectra can be interpreted with some degree of assurance, as in the simplest diatomic and triatomic molecules. However, Langer and Meggers² pointed out that in order to have such correspondence there must be a certain amount of freedom in the selection rules such as may not be found in triatomic or smaller molecules, but which may well be present in the case of molecules of more than six atoms, the class into which most organic compounds fall.

Granting that such a correspondence exists, the problem is still larger than merely finding relations between certain lines and certain characteristic groups in the molecule if we are to explain Raman spectra at all completely. Considering the mechanical nature of the vibrating system which we find in the molecule, it becomes evident that the majority of frequencies correspond to types of motion in which the whole molecule takes part rather than individual groups of two atoms. Now the problem of the dependence of frequencies on individual pairs of atoms as contrasted with the molecule as a whole is a moot question. Ellis³ and Marton⁴ have shown that certain band series in the infrared seem to be characteristic of pairs of molecules, and relatively independent of the structure of the molecule in which the pair is located. It appears, however, that this condition occurs only in special cases. For instance it may be due to the difference in mass of the vibrating particles. Thus in the case of hydrogen attached to carbon, we may expect the frequency ν , to be given rather closely by the equation for the harmonic oscillator

$$\nu = \frac{1}{2\pi} \left(\frac{k}{\mu} \right)^{1/2} \quad (1)$$

where k is the elastic constant of the C-H bond, and μ the reduced mass, determined by the equation

$$\frac{1}{\mu} = \frac{1}{m_1} + \frac{1}{m_2}$$

where m_1 is the mass of the hydrogen atom and m_2 the effective mass of the rest of the molecule. Since the ratio of m_2 to m_1 will nearly always be greater than twelve, it may be seen that the effect of the mass or structure of the rest of the molecule on the frequency will be small. Again this effect may be due to a pair of atoms being very tightly bound to each other and loosely bound to the rest of the molecule. An example of this is the $-\text{C}=\text{O}$ group which will be discussed later. On the other hand the majority of the frequencies will not depend on a pair of atoms, but on the nature of the molecule as a whole. This point is well brought out in Dennison's very complete analysis of the frequencies in me-

² Langer and Meggers, Bureau of Standards Journal of Research 4, 711 (1930).

³ J. W. Ellis, Phys. Rev. 27, 298 (1926).

⁴ L. Marton, Zeits. f. Phys. Chem. 117, 97 (1925).

thane.⁵ It is therefore, evident that if we are to explain the general nature of Raman spectra, we must formulate some ideas about the nature of the mechanical system in the molecule.

THE NATURE OF THE MECHANICAL SYSTEM IN THE MOLECULE

There appear to be a few simple postulates which give us a basis for a qualitative explanation of Raman spectra. They may be summarized as follows:

(1) The frequencies of the Raman shifts correspond to characteristic fundamental mechanical frequencies in the molecule.

(2) The masses in this vibrating mechanical system are the nuclei arranged in space as indicated by the x-ray studies of crystal structure and by the deductions from organic chemistry.

(3) The forces under which these masses vibrate may to a first approximation be considered as acting along the lines associated with the chemical valence bonds. They can be characterized by two elastic constants, one of which, the stretching constant, gives the restoring force when two atoms are pulled apart unit distance from their equilibrium position in the molecule. The other, the bending constant, gives the restoring force when the angle is altered between the bonds joining a central atom to two other atoms.

(4) The amplitude of vibration will be so small compared with the equilibrium distance between the atoms that the variation of the force with distance will obey Hooke's law.

(5) The elastic constants for any type of bond are independent of the structure of the molecule in which it occurs, if there are no neighboring dipoles.

The reasonableness of the first postulate, at least for the cases we are considering, seems to be granted by those who have carried on the work in this field up to the present time. The second is self-evident. The third will perhaps seem more reasonable to those who have studied molecules from the chemical point of view than to those who are more familiar with their physical aspects. Nearly every chemist feels that the structural formulas of organic chemistry have met with such broad success in correlating chemical facts that the implications behind them must be given great weight. These formulas are based primarily on the assumption of the constancy of valence, one for hydrogen, two for oxygen, three for nitrogen and four for carbon; and on the hypothesis that the structure of a group or radical may remain unchanged throughout a complicated series of chemical reactions involving other parts of the molecule. In explaining the infrared spectra of methane Dennison⁵ postulated forces acting between the hydrogens which were stronger than the forces joining the hydrogens to the carbon. It might be possible to reconcile the existence of such forces with the behaviour of atoms in organic molecules, but it is certainly much simpler to think of the invariance of structure during chemical transformations as due to forces which act in the place where we have pictured the bond.

⁵ D. M. Dennison, *Astrophys. J.* **62**, 84 (1925).

If, however, we are to confine the forces which determine the structure of the molecule to the lines associated with chemical bonds we must say something more about the nature of the force than merely calling it attraction or repulsion. For example, there is considerable evidence that a long chain of atoms has a certain tendency to stay straight, and that there is resistance to bending. This idea has been made use of in organic chemistry by postulating that the normal position for the four valences around the carbon atom is at the tetrahedral angle. It is found that when closed rings of less than five carbon atoms are made, where the angle between the valences is less than 109° , there is instability and a tendency for the ring to break. This was pointed out by Baeyer in his "strain theory" of the organic ring compounds. It has also been evident from the observations on the specific heats of organic compounds that there must be thermal vibrations which involve bending of the molecule. This has been pointed out by E. O. Salant⁶ and by the author⁷ who attempted a calculation of the force constants from specific heat data.⁸ Ellis has suggested that the 6.2μ band attributed to the C-H group is due to this type of vibration.⁹ In a diatomic molecule this characteristic of the forces would not of course come into play since the motion of the two atoms would have to be merely toward and away from each other in order to preserve the conservation of momentum. However, in a triatomic molecule we can expect a type of motion in which there is a variation of the angle between the lines joining the two outside atoms to the central atom, and in such a case it is possible to define the forces acting in terms of the increased separation of the atoms, stretching, and of the variation of the angle, bending.

The justification of the fourth postulate may be seen in a calculation of the energy of most of these compounds at room temperature. It is found that for nearly all types of motion the molecules are in the zero vibrational level. The transition which causes the Raman shift appears to be from the zero to the first vibrational state in nearly all cases. For vibrations of this amplitude we may expect the forces to obey Hooke's law, and we can therefore expect that the motion will be that of a harmonic oscillator. The frequency will be related to the force and mass by Eq. (1).

The fifth postulate states that the strength of the bond for small amplitudes of vibration depends only on the two atoms which it connects, and is relatively independent of the structure of the rest of the molecule. The strongest support for this lies in the constancy of the characteristic frequencies for such bonds as C-H, C=C, and C=O throughout extensive series of compounds. This has been clearly demonstrated in the results of a number of authors,¹ particularly Dadieu and Kohlrausch.¹ In fact it had been rec-

⁶ E. O. Salant, *Proc. Nat. Acad. Sci.* **12**, 334 (1926).

⁷ D. H. Andrews, *Proc. Roy. Acad. Amsterdam* **29**, 744 (1926). *Comm. Phys. Lab., Leiden*, Suppl. **56**, 16 (1926).

⁸ D. H. Andrews, *Chem. Reviews* **5**, 533 (1928). See also *Phys. Rev.* **34**, 1626 (1929), where a brief outline was given of the ideas presented in this present paper.

⁹ J. W. Ellis, *Jour. Franklin Inst.* **208**, 517 (1929).

ognized on the basis of infrared spectra and specific heat data that the non-polar bond joining together atoms of H, C, O or N has nearly always the same elastic constant. For the stretching¹¹ of the bond the value is generally about 4×10^5 dynes per cm. The latest values for the elastic constants of various bonds are tabulated by Dadiou and Kohlrausch¹ where it may be seen how remarkably uniform these values are.

MOLECULAR STRUCTURE AND RAMAN SPECTRA

These five postulates permit us to draw some conclusions as to what we will expect to find in the Raman spectra. In the first place, as has already been pointed out, the frequency of the hydrogen atoms will be relatively independent of the structure of the molecule, and will appear as the fastest of all the frequencies since hydrogen is so much lighter than any of the other elements. On the other hand in compounds of heavy atoms such as chlorine

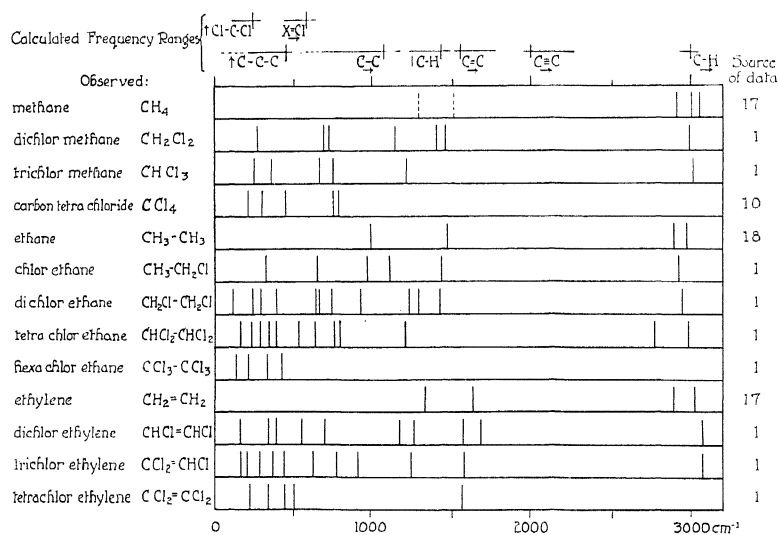


Fig. 1. Frequencies for three series of chlorine derivatives of methane, ethane and ethylene.

or bromine we will expect to find lines corresponding to much lower frequencies. Next with regard to the frequencies depending on the molecule as a whole we may say that the more complex the molecule, the lower the range of frequency, since a complex molecule will in general permit a kind of wave motion which will be of lower frequency than that for any pairs of atoms. By this effect frequencies may be secured which are as low as one tenth the value for a single pair of atoms, since the extension of the molecule into a chain may make possible very long wave length vibrations. On the other hand the frequency cannot be *increased* more than perhaps twenty percent

¹⁰ A. S. Ganesan and S. Venkateswaran, Indian Journal of Physics **4**, 195 (1929). A. Petrikaln and J. Hochberg, Zeits. f. Phys. Chem. **B3**, 217 (1929). P. Pringsheim and B. Rosen, Zeits. f. Physik **50**, 741 (1928).

¹¹ J. R. Bates and D. H. Andrews, Proc. Nat. Acad. Sci. (U. S. A.) **14**, 124 (1928).

by increasing complexity, since the number of forces acting on any one atom is limited to the number of valence bonds which it can possess. Thus, the only way of increasing the force acting on it is by introducing some strain, such as in ring formation and this effect is very small. With this in mind we may proceed to examine the frequencies which have been experimentally observed.

Lines associated with hydrogen. One of the earliest regularities to be pointed out in the Raman spectra was that of the lines in the neighborhood of 3000 cm^{-1} which appear to be due to the vibration of hydrogen attached to carbon. In Fig. 1 the frequencies have been plotted for three series of chlorine derivatives of methane, ethane and ethylene, respectively. It may be seen that in all compounds where hydrogen is present we have lines in the 3000 cm^{-1} region, but that when hydrogen is no longer present as in carbon tetrachloride, hexachlorethane, and tetrachlor ethylene there are no frequencies in this region.

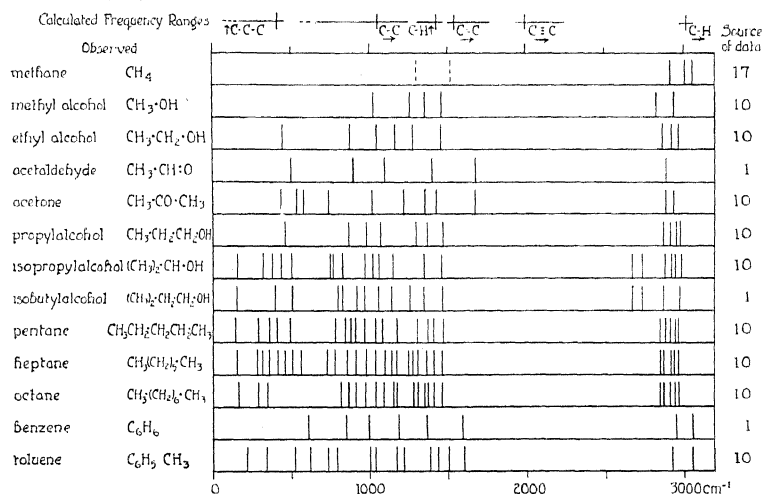


Fig. 2. Frequencies observed in a number of carbon compounds.

Further observation of these data, moreover, indicate that there is a region from about 1100 to 1600 cm^{-1} where this same regularity holds true. Now Dennison⁵ in his analysis of methane frequencies concluded that there would be two frequencies in this region, as shown by the dotted lines in Fig. 1, which correspond to motions of hydrogen of the type which we have called bending. It is a little surprising that no Raman frequencies were observed in the 1400 cm^{-1} region but this may be due to the difficulty of working with gases, or to the more rigid selection rules which we may expect to find in smaller molecules. Ellis⁹ also has suggested that the 6.2μ band in the infrared may be due to this type of motion. It therefore seems reasonable to say that we have in these two groups of frequencies, 3000 cm^{-1} and 1400 cm^{-1} , the frequencies of the two types of motion which we would expect the hydrogen atoms to have, namely stretching and bending. Granting

this, we may proceed to an explanation of the remaining lines outside these regions which may be due to the heavier atoms.

Carbon frequencies. Fig. 2 shows the frequencies observed in a number of carbon compounds. As is to be expected methane shows only frequencies in the region which we have associated with hydrogen. Passing to ethane, however, as is shown in Fig. 1, we have in addition to the lines around 1400 cm^{-1} and 3000 cm^{-1} a line at 1000 cm^{-1} and as has been concluded by others,¹ this appears to be the frequencies of two carbon atoms vibrating with respect to each other. The spectrum of methyl alcohol is very similar to this as we might expect since we have merely replaced a carbon by an oxygen atom.

If the frequencies in ethane at 1000 cm^{-1} are really due to the carbon-carbon vibration, we would expect it to shift when a single bond is replaced by a double bond. This is found to be true in the spectrum of ethylene in which the line at 1000 cm^{-1} disappears and the line at 1600 cm^{-1} appears.

There has always been considerable dispute among chemists as to whether a double bond is stronger or weaker than a single bond. This question has been ably discussed by Fajans¹² and the Raman frequencies substantiate

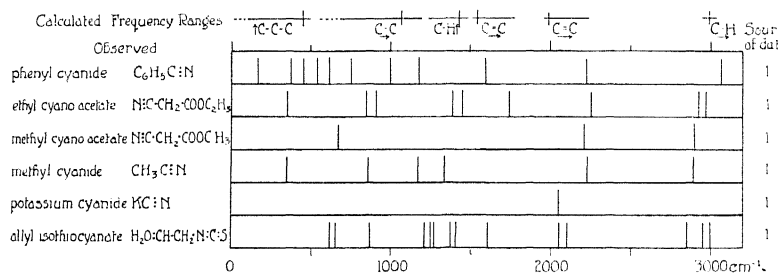


Fig. 3. Frequencies observed for a number of compounds containing triple bonds.

his conclusions. If we make use of Eq. 1 and calculate the elastic constant for these two frequencies, we find that the shift is that which would correspond approximately to the doubling of the elastic constant. This is an additional confirmation that we have identified the line correctly. Moreover if we examine compounds in which there are double bonds such as the $\text{C}=\text{O}$ bond in acetaldehyde and acetone we find frequencies in this region. Over twenty compounds have been examined by Dadieu and Kohlrausch¹ in which these frequencies due to the double bond appear. If we increase the strength of the binding still further by passing to the triple bond we find higher frequencies just as should be expected. Fig. 3 shows the frequencies observed for a number of compounds containing triple bonds.

This group of frequencies shows very well the way in which a frequency depending principally on the strength of one particular bond, in this case the triple bond, may also be influenced by the structure of the molecule.

¹² K. Fajans, Chem. Ber. 53, 643 (1920), 55, 2826 (1922).

If we regard these groups as of the type $X-C\equiv Y$ it may be seen that the frequency will depend on the linkage $X-C$ and on the mass of X as well as on $C\equiv Y$. Thus in acetylene, since the hydrogen, X , is light, the only effective force for this vibration is $C\equiv Y$, giving a frequency of about 1950 cm^{-1} . In compounds of the cyanide type, however, where X is a heavy atom the force $X-C$ also contributes to the vibration and we find the frequencies in the neighborhood of 2200 cm^{-1} . It is particularly interesting to note that in $KC\equiv N$ the frequency is again lower. It seems quite possible that this is due to the fact that the $K-C$ bond is presumably polar and much weaker than the $C-C$ bond.

Another interesting compound in this connection is allyl iso-thiocyanate where we have a carbon atom between two double bonds. Two double bonds so placed are as effective as a triple bond and we find a corresponding frequency.

Effect of increasing molecular complexities. Having identified the above lines which correspond to vibrations of pairs of atoms we may proceed to examine the frequencies which appear to be due to vibrations of the molecule as a whole. The simplest illustration of the effect of increasing the complexity may be seen by comparing methyl and ethyl alcohol. We may regard these as diatomic and triatomic molecules respectively since the hydrogens are so light that they do not affect appreciably the vibration of the heavy atoms. In methyl alcohol we have a single line at 1000 cm^{-1} due to the $C-O$ vibration, as would be expected for a diatomic molecule. In a triatomic molecule, however, we would expect three fundamental frequencies since the total number of degrees of freedom is nine and of these three will be translational, and three rotational for the molecule as a whole, leaving three for vibration. Now according to our postulates the effective forces joining the atoms will be the forces of the two chemical bonds, namely $C-C$ and $C-O$. For each of these bonds we will expect one restoring force if the bond is stretched and another restoring force if the angle between the two bonds is altered corresponding to a bending of the molecule. It is a little difficult to say off-hand what the relative values of these two forces will be but from the analogy of the stretching and bending frequencies for hydrogen attached to carbon, we may expect the bending force to be only about one-quarter as strong as the stretching force.

This particular case has been carefully investigated by Yates.¹³ He has assumed forces of this type and finds that there should result one comparatively low frequency corresponding to the bending of the molecule and two frequencies not far from that for the diatomic molecule. If we ascribe the three frequencies between 1200 and 1400 cm^{-1} in the ethyl alcohol spectrum to hydrogen, the three remaining lines are in good accord with Yates' calculation. The spectrum of acetaldehyde which may similarly be regarded as a triatomic molecule shows a close resemblance to that of ethyl alcohol as

¹³ Yates, The character of the elastic forces in the homopolar chemical bond. See succeeding article.

might be expected. If it is true that the line at 450 cm^{-1} corresponds to a bending of the molecule then the fact that this frequency becomes only slightly higher in passing from ethyl alcohol, $\text{C}-\text{C}-\text{O}$, to acetaldehyde, $\text{C}-\text{C}=\text{O}$ indicates that doubling the bond decreases the ease of bending only slightly. On the other hand the appearance of the line at 1600 cm^{-1} shows that the force involved in stretching has been greatly increased.

Passing to more complicated molecules, we now find low frequencies appearing presumably corresponding to the presence of wave motion involving more than three atoms. Moreover, the number of lines increases, and as we get to heptane we find a fairly even distribution of the lines from the hydrogen region down to the low frequencies. The experimental observation of these more complex compounds is somewhat difficult because of the tendency for fluorescence which gives a continuous background, masking many of the lines. A number of the lines are also of very low intensity so that the agreement between different observers for compounds of the complexity of heptane is rather poor. For that reason, it is dangerous to draw too definite conclusions. However, one or two points seem worth mentioning. Lewis¹⁴ in a study of the possible frequencies in compounds of this type points out that the frequencies should be fairly evenly distributed from the lowest, corresponding to the longest wave-length possible in the chain, up to the highest, corresponding to the vibration of a pair of atoms. Pentane and heptane have spectra in accord with this view. It also seems worth noticing that the number of lines below the hydrogen region, which we may take as ending at about 1100 cm^{-1} corresponds roughly to the number of degrees of freedom for internal vibration of the heavy atoms which would be calculated from the number of atoms present in the molecule. Thus for heptane we should have $(3 \times 7) - 6 = 15$. In the region below 1100 cm^{-1} where these frequencies should appear we find fifteen lines for heptane and twelve for pentane, but for octane there are only ten, so that the argument is hardly conclusive.

CONCLUSIONS

The way in which the above postulates accounts for the great majority of Raman lines may be seen from the following calculation. We take 5×10^5 and 0.6×10^5 dynes per cm for the stretching and bending constants respectively of the single non-polar bond. These are the best average values from the latest data and the actual values for the various bonds do not appear to deviate from these by more than ten per cent. We can then calculate the ranges in which frequencies should appear in the different compounds, from the atomic weights and number of bonds involved. The variation in frequencies between different compounds is thus considered to be due only to the variation in the masses of the atoms and in the number and position of the bonds. The stretching constant for a double bond is taken as twice that for a single bond, and for a triple bond, thrice.

¹⁴ A. B. Lewis, Coupled vibrations with applications to the specific heat and infrared spectra of crystals. P. 568, this issue.

The values of the frequency which would be expected for the vibration of pairs of atoms can be calculated quite simply with the help of Eq. (1). The results of these calculations have been summarized in Table I. The values for C-H, C-O, and C-N are in good agreement with the observed lines which have been attributed to these bonds.

The case of C_6H_5-Cl is not so clear. It has been difficult to say just which Raman line is due to the vibration of the Cl. However, a series has been observed in the infra-red by Ellis¹⁵ which appears to be due to this type of motion and its fundamental frequency agrees very well with that calculated here.

The C=C bond in ethylene has a frequency which is well accounted for if we take the elastic constant as twice that for the single bond. With the C=O bond, however, we find the frequency to be quite a bit higher. Here the carbon is also joined to two other carbon atoms and since these bonds probably make an angle of about 109° with the double bond we may say as

TABLE I.

Bond	Compound	μ	k	Frequency Calc.	Obs.
Stretching					
C-H	H_3C-CH_3	1.0	5×10^5 dynes/cm	2920 cm^{-1}	2950 ¹⁸
C-C	H_3C-CH_3	7.5	5	1070	990 ¹⁸
C-O	H_3C-OH	8.0	5	1030	1031 ¹⁰
C-Cl	C_6H_5-Cl	23.6	5	600	596 ¹⁵
C=C	$H_2C=CH_2$	7.0	10	1560	1600 ¹⁷
C=O	$(CH_3)_2-C=O$	8.0	15	1790	1704 ¹⁰
C \equiv C	$HC\equiv CH$	6.5	15	1990	1950 ¹⁸
C \equiv N	$C_6H_5-C\equiv N$	7.0	20	2210	2227 ¹
Bending					
H-C-H	CH_4	0.5	0.6	1430	1520 ⁵
C-C-O	CH_3-CH_2-OH		0.6	480	450 ¹⁰
Cl-C-Cl	CCl_4	17.5	0.6	240	216 ¹⁰

¹⁷ R. G. Dickinson, R. T. Dillon, and F. Rasetti, Phys. Rev. **34**, 582 (1929).

¹⁸ M. Daure, Compt. Rend. **188**, 1492 (1929).

a first approximation that the effective force acting on that side of the carbon atom will be about equal to a single bond. An approximate calculation then gives the frequency as 1790 cm^{-1} which accounts at least qualitatively for the increase in frequency over the value for ethylene.

In the same way we find that C \equiv C in acetylene has a frequency accounted for by thrice the value for the single bond while the $C_6H_5-C\equiv N$ frequency lies higher by about the amount we should expect from the addition of the extra bond to the carbon atom.

The calculation of the bending frequencies may be made most simply in the case of molecules like methane or carbontetrachloride. One of the types of motion with the slow frequency will be that where the central atom stands still and the outer atoms vibrate toward and away from each other in pairs without stretching the bonds. In other words, we have a pure type

¹⁵ Ellis, Phys. Rev. **28**, 25 (1926).

of bending motion. As a first approximation we can treat this by means of Eq. (1) since the motion of a pair of atoms will be the same as if they were directly joined by an elastic force. Giving the value of 0.6 dynes per cm to this effective force which we believe is brought about by the bending of the bonds, we find values as shown in the second part of Table I. The first agrees fairly well with the value ascribed by Dennison⁵ to this type of motion in methane. The second agrees with the slowest observed Raman frequency, and there is evidence that this frequency is the one associated with this type of motion in a study of molecular models to which reference will be made later.

The case of ethyl alcohol which is more complex has been treated by Yates.¹³ With these values in his equation we find 480 cm^{-1} for the frequency due to bending, in good agreement with the slowest observed Raman line.

The calculated frequencies are indicated in Fig. 1 by the vertical lines in the crosses at the top of the figure. The horizontal lines indicate roughly what we should expect from the modification of the frequency by additional bonds or chain formation. Thus, as we have seen in the case of $\text{C}=\text{O}$ the frequency is raised about five per cent by the addition of the two bonds on the left of the carbon. On the other hand by lengthening out the carbon chain as in pentane the original C-C frequency can in a sense be modified to perhaps a third of its value or less.

It may be seen that for the compounds, for which the Raman shift frequencies have been plotted in the figures, we find frequencies just in those ranges which we would expect according to the structure. This seems to be the best evidence we have that the postulates regarding the nature of the mechanical system in the molecule are reasonable and that the Raman frequency shifts do correspond to fundamental mechanical frequencies.

Considerable light has also been thrown on this problem by a study of mechanical models of molecules¹⁶ which was based on the ideas developed by C. F. Kettering on the nature of elasticity in molecules. The problem has also been discussed from several other points of view by Yates¹³ and Lewis¹⁴ to whose papers reference has already been made. The conclusions drawn from these different lines of approach to the problem seem to be in substantial agreement.

¹⁶ C. F. Kettering, L. W. Shutts and D. H. Andrews, p. 531, this issue.

THE ELASTIC CHARACTER OF THE HOMOPOLAR
CHEMICAL BOND

BY ROBERT C. YATES

MATHEMATICS DEPARTMENT, JOHNS HOPKINS UNIVERSITY

(Received June 23, 1930)

ABSTRACT

An attempt is made to obtain frequencies of internal vibrations of some organic molecules by the consideration of certain mechanical systems.

The system of three particles is studied assuming the forces of restitution elastic. Certain proportionality constants are determined, using a representative compound, which characterize the single valence bond. Calculated wave-numbers for CO_2 , CS_2 , CH_2Cl_2 , $\text{C}_2\text{H}_5\text{OH}$ are compared with observed data from Raman spectra.

I. INTRODUCTION

THERE has been a recent impulse on the part of the physical chemist to determine precisely the character of the chemical bond that retains the atoms in mutual attraction in molecular structures of organic compounds. An attempt in this direction has been made¹ under the assumption that the valence bond is of spring-like nature and the forces set up by a displacement are elastic. Mechanical models of representative molecules have been constructed accordingly and experiments run to observe the fundamental modes of vibration.² The correlation between such observed frequencies and those obtained from the Raman spectra was found to be surprisingly good. This prompted the desire to look more closely into several types of systems and to set up the dynamical equations of motion yielding frequencies that might be compared with experiment.

II. STATEMENT OF THE PROBLEM

We shall thus be concerned with the small vibrations of a system of particles about a position of stable equilibrium under certain definite assumptions, these assumptions to be supported by the closeness of agreement in the end.

The intramolecular forces that arise are set up by the mutual attraction and repulsion of the atoms, suggesting not only an elastic force between any two but also a force of restoration dependent on the angular divergence of neighboring bonds.

Definitely, it is assumed that the force tending to restore a particle after a displacement is the sum of two types of forces: the first acting along the

¹ D. H. Andrews, The Relation Between the Raman Spectra and the Molecular Structure of Organic Compounds, p. 544, this issue.

² F. Kettering, L. W. Shutts, D. H. Andrews, A Representation of the Dynamic Properties of Molecules by Mechanical Models, p. 531, this issue.

line of connection with another particle and proportional to the linear displacement (Hooke's law); the second acting at right angles to the first and proportional to the change in the angle between two adjoining bonds. This last may be restated as being proportional to the arc displacement.

We consider here only small displacements and higher order infinitesimals, in the presence of those of lower order, are neglected throughout. The motion of the particles is assumed to be in a given plane.

III. DETERMINATION OF THE FORCE CONSTANT k_1

Consider two particles of masses m_1 and m_2 constrained to linear motion. Assuming the force acting between them proportional to the displacement we find as is well known the frequency of vibration given by

$$\nu = (1/2\pi)(k_1/M)^{1/2} \quad (1)$$

where M denotes the relative mass $1/m_1 + 1/m_2$ and k_1 a factor of proportionality. If $m_1 = m_2 \equiv m$, we have

$$k_1 = 2\pi^2\nu^2m. \quad (2)$$

In order to evaluate k_1 we take the carbon-carbon combination of the diatomic molecule and assign the wave number of 1000 to motion along the line of connection.¹ This gives approximately $k_1 = 4 \times 10^5$ dynes per cm.

Before we may find a corresponding value for the remaining constant k_2 , that controls the restoring force arising from a change in the angle between neighboring bonds, we must look first at the system of three particles.

IV. THE SYSTEM OF THREE PARTICLES

Consider the system of three particles of masses m_1, m_2, m_3 , connected by two bonds as shown. We place the particles at the vertices of an isosceles triangle and select a reference frame with horizontal axis parallel to its base. These give the relations

$$\left. \begin{aligned} 2f/m_3 &= b/m_1 - c/m_2 \\ m_1d &= m_2a \end{aligned} \right\} \quad (3)$$

If the origin of coordinates be taken at the center of mass, we have

$$\left. \begin{aligned} f &= c - b \\ g &= a + d \end{aligned} \right\} \quad (4)$$

We introduce the notation:

$$\left. \begin{aligned} A &\equiv g/m_3 + a/m_1 \\ B &\equiv c/m_2 + f/m_3 = b/m_1 - f/m_3 \end{aligned} \right\} \quad (5)$$

so that $\tan \theta_2 = A/B$

Let the system be displaced to a position shown and let the components of displacement of the particles be $(1/m_i) \cdot (x_i, y_i)$.

The kinetic energy of the system is:

$$T = (\frac{1}{2}) [(\dot{x}_1^2 + \dot{y}_1^2)/m_1 + (\dot{x}_2^2 + \dot{y}_2^2)/m_2 + (\dot{x}_3^2 + \dot{y}_3^2)/m_3]. \quad (6)$$

The potential energy—dependent on the configuration—is composed of a potential V_1 due to linear displacement and V_2 due to rotation:

$$V_1 = (k_1/2)(\Delta d_1^2 + \Delta d_2^2) \quad (7)$$

$$V_2 = (k_2/2) \cdot \Delta S^2 = (k_2 d_1^2/2) \cdot \Delta \phi^2.$$

In order to find the explicit expressions for the quantities in (7) we obtain from the figure:

$$\left. \begin{aligned} d_1 \cdot \Delta d_1 &= -A(y_1/m_1 - y_3/m_3) + B(x_1/m_1 - x_3/m_3) \text{ etc.} \\ d_1^2 \cdot \Delta \phi &= d_1^2(\Delta \theta_1 - \Delta \theta_2) = A(x_1/m_1 - x_2/m_2) + B(y_1/m_1 + y_2/m_2 - 2y_3/m_3) \end{aligned} \right\} (8)$$

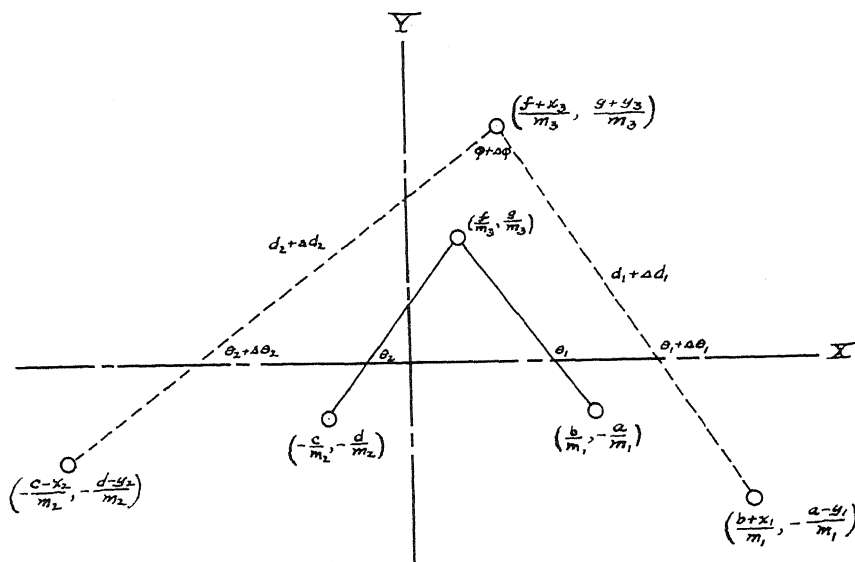


Fig. 1. System of three particles.

Since the resultant of the forces on the system is zero the center of mass will remain at rest in an inertial system. We may, therefore, write

$$\left. \begin{aligned} x_1 + x_2 + x_3 &= 0 \\ y_1 + y_2 + y_3 &= 0 \end{aligned} \right\} (9)$$

Furthermore the moment of the various forces about the origin is zero so that the angular momentum of the system about the origin is constant. Assuming that this angular momentum is zero, we have:

$$\begin{aligned} m_1 \begin{vmatrix} (b+x_1)/m_1 & -(a-y_1)/m_1 \\ \dot{x}_1/m_1 & \dot{y}_1/m_1 \end{vmatrix} + m_2 \begin{vmatrix} -(c-x_2)/m_2 & -(d-y_2)/m_2 \\ \dot{x}_2/m_2 & \dot{y}_2/m_2 \end{vmatrix} \\ + m_3 \begin{vmatrix} (f+x_3)/m_3 & (g+y_3)/m_3 \\ \dot{x}_3/m_3 & \dot{y}_3/m_3 \end{vmatrix} &= 0 \end{aligned} \quad (10)$$

which becomes on integrating:

$$By_2 = A(x_1 + x_2) + By_1. \quad (11)$$

The two energy functions may now be rewritten, because of the relations Eq. (9) and Eq. (11):

$$T = (\frac{1}{2}B^2) \{ [B^2/m_1 + A^2/m_2 + (A^2 + B^2)/m_3] \dot{x}_1^2 + (A^2 + B^2)(1/m_2 + 1/m_3) \dot{x}_2^2 + B^2(1/m_1 + 1/m_2 + 4/m_3) \dot{y}_1^2 + 2[A^2/m_2 + (A^2 + B^2)/m_3] \dot{x}_1 \dot{x}_2 + 2AB(1/m_2 + 2/m_3)(\dot{x}_1 + \dot{x}_2) \dot{y}_1 \} \quad (12)$$

$$V = (k_1/2d_1^2) \{ [(A^2 - B^2)/m_3 - B^2/m_1] x_1 + [(A^2 - B^2)/m_3] x_2 + AB(2/m_3 + 1/m_1) y_1 \}^2 + (k_1/2d_1^2) \{ [(A^2 + B^2)/m_3 + A^2/m_2] x_1 + (A^2 + B^2)(1/m_2 + 1/m_3) x_2 + AB(2/m_3 + 1/m_2) y_1 \}^2 + (k_2/2d_1^2) \{ AB(1/m_1 + 1/m_2 + 2/m_3) x_1 + (2AB/m_3) x_2 + B^2(1/m_1 + 1/m_2 + 4/m_3) y_1 \}^2. \quad (13)^*$$

These functions T and V must satisfy the Lagrangian equations of motion:

$$(d/dt)(\partial L/\partial \dot{x}_i) - (\partial L/\partial x_i) = 0 \quad (14)$$

where $L = T - V$. Inserting the expression L we have:

$$\begin{aligned} & [B^2/m_1 + A^2/m_2 + (A^2 + B^2)/m_3] \ddot{x}_1 + [A^2/m_2 + (A^2 + B^2)/m_3] \ddot{x}_2 + AB[2/m_3 + 1/m_2] \ddot{y}_1 = - (k_1/d_1^2) [(A^2 - B^2)/m_3 - B^2/m_1] \{ [(A^2 - B^2)/m_3 - B^2/m_1] x_1 + [(A^2 - B^2)/m_3] x_2 + AB[2/m_3 + 1/m_2] y_1 \} - (k_1/d_1^2) [(A^2 + B^2)/m_3 + A^2/m_2] \{ [(A^2 + B^2)/m_3 + A^2/m_2] x_1 + [A^2 + B^2][1/m_3 + 1/m_2] x_2 + AB[2/m_3 + 1/m_2] y_1 \} - (B^2 k_2/d_1^2) \cdot A \cdot [1/m_1 + 1/m_2 + 2/m_3] \{ A[1/m_1 + 1/m_2 + 2/m_3] x_1 + [2A/m_3] x_2 + B[1/m_1 + 1/m_2 + 4/m_3] y_1 \} \\ & [A^2/m_2 + (A^2 + B^2)/m_3] \ddot{x}_1 + (A^2 + B^2)[1/m_1 + 1/m_3] \ddot{x}_2 + AB[2/m_3 + 1/m_2] \ddot{y}_1 = - (k_1/d_1^2) [(A^2 - B^2)/m_3] \{ [(A^2 - B^2)/m_3 - B^2/m_1] x_1 + [(A^2 - B^2)/m_3] x_2 + AB[2/m_3 + 1/m_2] y_1 \} - (k_1/d_1^2) [A^2 + B^2][1/m_2 + 1/m_3] \{ [(A^2 + B^2)/m_3 + A^2/m_2] x_1 + (A^2 + B^2)[1/m_2 + 1/m_3] x_2 + AB[2/m_3 + 1/m_2] y_1 \} - (B^2 k_2/d_1^2)(2A/m_3) \{ A[1/m_1 + 1/m_2 + 2/m_3] x_1 + [2A/m_3] x_2 + B[1/m_1 + 1/m_2 + 4/m_3] y_1 \} \end{aligned} \quad (15)$$

$$\begin{aligned} & A[1/m_2 + 2/m_3] [\ddot{x}_1 + \ddot{x}_2] + B[1/m_1 + 1/m_2 + 4/m_3] \ddot{y}_1 = - (A k_1/d_1^2)(2/m_3 + 1/m_1) \{ [(A^2 - B^2)/m_3 - B^2/m_1] x_1 + [(A^2 - B^2)/m_3] x_2 + AB[2/m_3 + 1/m_2] y_1 \} - (A k_1/d_1^2)(2/m_3 + 1/m_2) \{ [(A^2 + B^2)/m_3 + A^2/m_2] x_1 + [A^2 + B^2][1/m_2 + 1/m_3] x_2 + AB[2/m_3 + 1/m_2] y_1 \} - (B^2 k_2/d_1^2)(1/m_1 + 1/m_2 + 4/m_3) \{ A[1/m_1 + 1/m_2 + 2/m_3] x_1 + [2A/m_3] x_2 + B[1/m_1 + 1/m_2 + 4/m_3] y_1 \}. \end{aligned} \quad (16)$$

These three Eqs. (15, 16, 17) define the motion of the system and are sufficient to determine the independent quantities x_1 , x_2 , y_1 .

* That the potential function as here written gives the correct forces is seen by calculating straight forwardly the forces acting on the separate particles. For example, the horizontal component of force acting on the first particle is $-(\delta V/\delta \cdot x_1/m_1)$.

On combining these we find:

$$\begin{aligned}
 & [B^2/m_1 + A^2/m_2 + 2B^2/m_3]\ddot{x}_1 + [(A^2 + B^2)/m_2 + 2B^2/m_3]\ddot{x}_2 + AB[1/m_2 - 1/m_1]\ddot{y}_1 \\
 & = (k_1/d_1^2) [(A^2 + B^2)/m_1 + 2B^2/m_3] \{ [(A^2 - B^2)/m_3 - B^2/m_1] x_1 \\
 & + [(A^2 - B^2)/m_3] x_2 + AB[2/m_3 + 1/m_1] y_1 \} - (k_1/d_1^2) [(A^2 + B^2)/m_2 \\
 & + 2B^2/m_3] \{ [A^2/m_2 + (A^2 + B^2)/m_3] x_1 + [A^2 + B^2][1/m_2 + 1/m_3] x_2 \\
 & + AB[2/m_3 + 1/m_2] y_1 \}
 \end{aligned} \quad (18)$$

which defines the particular type of motion that is unaffected by any bending of the bonds.

IV (B)

We now make the restriction that the two end particles be of the same mass, say $m_1 = m_2 \equiv m$. Eq. (18) becomes:

$$\begin{aligned}
 \ddot{x}_1 + \ddot{x}_2 & = - (k_1/d_1^2) [(A^2 + B^2)/m + 2B^2/m_3] (x_1 + x_2) \\
 & = - k_1(1/m + 2 \cos^2 \theta/m_3) (x_1 + x_2)
 \end{aligned} \quad (19)$$

where θ is a base angle (see table).

Thus the combined horizontal motion of the two end particles is simply harmonic. The third particle oscillates complementary to this.

Under this first restriction we solve Eqs. (15, 16, 17) explicitly for \ddot{x}_1 , \ddot{x}_2 , \ddot{y}_1 :

$$\begin{aligned}
 \ddot{x}_1 & = (k_1/d_1^2) \{ [(A^2 - B^2)/m_3 - B^2/m] x_1 + [(A^2 - B^2)/m_3] x_2 + AB[2/m_3 \\
 & + 1/m] y_1 \} - (2Ak_2/d_1^2) \{ A[1/m + 1/m_3] x_1 + [A/m_3] x_2 \\
 & + B[2/m_3 + 1/m] y_1 \} \\
 \ddot{x}_2 & = - (k_1/d_1^2) \{ [A^2/m + (A^2 + B^2)/m_3] x_1 + [A^2 + B^2][1/m + 1/m_3] x_2 \\
 & + AB[2/m_3 + 1/m] y_1 \} + (2Ak_2/d_1^2) \{ A[1/m + 1/m_3] x_1 + [A/m_3] x_2 \\
 & + B[2/m_3 + 1/m] y_1 \} \\
 \ddot{y}_1 & = - (Ak_1/d_1^2 B) \{ [(A^2 - B^2)/m_3 - B^2/m] x_1 + [(A^2 - B^2)/m_3] x_2 \\
 & + AB[2/m_3 + 1/m] y_1 \} - (2Bk_2/d_1^2) \{ A[1/m + 1/m_3] x_1 + [A/m_3] x_2 \\
 & + B[2/m_3 + 1/m] y_1 \}.
 \end{aligned} \quad (20)$$

If we are to find solutions of the type $x_i = C_i e^{\alpha t}$ for the differential equations (Eq. 20) we must require the vanishing of the determinant of coefficients:

$$\begin{vmatrix} \alpha^2 + a_{11} & a_{21} & a_{31} \\ a_{12} & \alpha^2 + a_{22} & a_{32} \\ a_{13} & a_{23} & \alpha^2 + a_{33} \end{vmatrix} = 0 \quad (21)$$

which is the characteristic equation—a cubic in α^2 —where the quantities a_{ij} are the constant coefficients that occur in the differential Eq. (20).

The determinant is readily reduced to:

$$\begin{vmatrix} \alpha^2 + b_{11} & 0 & 0 \\ a_{12} & \alpha^2 + b_{22} & a_{32} \\ a_{13} & b_{23} & \alpha^2 + a_{33} \end{vmatrix} = 0 \quad (22)$$

where

$$b_{11} = (k_1/d_1^2) [(A^2 + B^2)/m + 2B^2/m_3]$$

$$b_{22} = k_1 B^2/d_1^2 \cdot m + 2A^2 k_2/d_1^2 m$$

$$b_{23} = ABk_1/d_1^2 m - 2ABk_2/d_1^2 m$$

Solving Eq. (22) we get the two factors:

$$\alpha^2 + k_1(1/m + 2 \cos^2 \theta/m_3) = 0 \quad (23)$$

$$\alpha^4 + [(k_1 + 2k_2)/m + 2(k_1 \sin^2 \theta + 2k_2 \cos^2 \theta)/m_3] \alpha^2 + 2k_1 k_2 (2/m_3 + 1/m)/m = 0 \quad (24)$$

whose three roots $\alpha_1, \alpha_2, \alpha_3$, are pure imaginaries and we therefore write $\alpha_i^2 = -\mu_i^2$ from which we may obtain the normal fundamental frequencies of the system.

IV (c)

If all three particles were of the same mass, m , the foregoing expressions would simplify considerably. Under this restriction we rewrite Eq. (23):

$$\left. \begin{aligned} m\mu^2 - k_1(1 + 2 \cos^2 \theta) &= 0 \\ m^2\mu^4 - [(k_1 + 2k_2) + 2(k_1 \sin^2 \theta + 2k_2 \cos^2 \theta)]m\mu^2 + 6k_1 k_2 &= 0 \end{aligned} \right\} \quad (25)$$

The normal frequencies of this system are $\nu_i = (1/2\pi)\mu_i$ and the wave-numbers $\bar{\nu}$ are given by

$$\bar{\nu}_i = (\frac{1}{2})\nu_i \times 10^{-10} = \left(\frac{1}{6\pi}\right)\mu_i \times 10^{-10} \text{ cm}^{-1}. \quad (26)$$

V. DETERMINATION OF THE FORCE CONSTANT k_2

Referring to section III we proceed to calculate k_2 and for that purpose we select as most suitable a molecule of ethyl alcohol, the atoms arranged in groups as shown in the accompanying table.

We assume here that the bonds form the tetrahedral (approximately 109°) angle with each other in the position of rest. As an approximation, the atomic mass of the CH_2 group is taken as fourteen while the other two groups are assigned the average mass of sixteen. The mass of each group is supposed to be concentrated at the nucleus of each heavy atom. It is to be emphasized that there is no bond acting directly between the two end groups. We may thus apply Eqs. (25) of the preceding paragraph.

We find, on using the value of k_2 found in section III: $\bar{\nu}_1 = 1035$ as compared with the observed wave-number 1047.

TABLE I.

	Structure	Force Constants	Calculated			Observed		
			ν_1	ν_2	ν_3	ν_1	$\bar{\nu}_2$	ν_3
C_2H_5OH		$k_1=4$ $k_2=6$	1035	930	451	1047	884	450 ⁴
CO_2		$k_1=8$ $k_2=1.2$	1535	1320	703	3650	2350	683 ⁵
		$k_1=8$ $k_2=1.2$	1800	970	920			
		$k_1=32$ $k_2=4.8$	3600	1960	1820			
		$k_1=32$ $k_2=0.6$	3600	2817	978			
CS_2		$k_1=8$ $k_2=1.2$	1303	no value	no value	800	655	655 ⁴
		$k_1=4$ $k_2=6$	920	730	570			
CH_2Cl_2		$k_1=4$ $k_2=0.6$	917	1010	728	1151	715	283 ⁴
		$k_1=4$ $k_2=0.6$	1083	698	487			

⁴ A. S. Ganesan and S. Venkatesvaren, Indian Jour. Phys. 4, 195 (1929).⁵ R. H. Fowler, Statistical Mechanics, p. 64, Cambridge, 1929.

On using the other two fundamental wave-numbers 884 and 450 in the quadratic form (Eq. 23) we solve for k_2 , obtaining $k_2=0.6 \times 10^5$ dynes/cm as an average value. These values for the force constants had already been obtained in a very approximate manner from specific heats and Raman spectra.³

VI. SOME APPLICATIONS

We apply the results of the foregoing paragraphs to a few organic molecules, arranging the calculations in the accompanying table.

Carbon dioxide is definitely a double bonded structure and it was therefore supposed that the force constant k_1 would, in this case, be double its value for the single bond. It is found, however, that the values $k_1=32$; $k_2=0.6$ (or 1.2) dynes per cm gives results that best agree with experiment. The atomic arrangement is shown in table 2 under the heading "Structure," first with the bonds forming the tetrahedral angle and second with the atoms lying collinear. This last stable position seems to be most probable. The molecule of carbon disulphide gives best results if taken with the single bond. Dichlor methane not only seems to have a single bond structure but apparently has the straight line arrangement of its groups. Because of the agree-

³ D. H. Andrews Phys. Rev. 34, 1626 (1929).

ment between calculated and observed data in most of the cases considered it is fairly conclusive that the force constants as determined are quite valid. The percent of error is in itself not sufficient as an objection if it is considered that the frequencies might lie in the range of 100 to 10000 wave-numbers.

The writer is greatly indebted to Professor D. H. Andrews for suggesting the problem and to Professor F. D. Murnaghan for continued advice in the preparation of the paper.

STUDY OF THE SMALL VIBRATIONS OF SIX PARTICLES
IN A SYSTEM ANALOGOUS TO THE BENZENE
RING

BY ROBERT C. YATES

MATHEMATICS DEPARTMENT, JOHNS HOPKINS UNIVERSITY

(Received June 23, 1930)

ABSTRACT

The system of six particles is allowed to vibrate under certain restrictions, assuming an elastic nature for the restoring forces. Frequencies of vibration are obtained and compared with Raman data lending some support to the Claus construction of the benzene molecule.

INTRODUCTION

IN A previous paper¹ we have considered the small vibrations about a position of stable equilibrium of a system of three particles under the assumption that the forces set up by a displacement are elastic in character. It was definitely assumed that the restoring force was the sum of two types of forces; the first acting along the line of connection with another particle and proportional to the linear displacement; the second acting at right angles to the first and proportional to the change in the angle between two adjoining bonds. The results obtained for a few organic compounds pointed very strongly to the conclusion that two force constants $k_1 = 4 \times 10^5$ and $k_2 = 0.6 \times 10^5$ dynes per cm could be assigned as definite properties of the single valence bond which were independent of the particular molecule.

THEORY

In this paper we consider the system of six particles, (under the same assumptions as were taken for three particles), all of the same mass m lying in stable position at the vertices of a regular hexagon, whose side is of length a . Each particle has three connecting bonds as shown. If the angular momentum is zero and the center of gravity remains fixed, the system will have nine degrees of freedom. We, however, place certain restrictions on the motion of the system that will reduce considerably the order of the resulting characteristic determinant. The motion of the particles is assumed to be in a given plane and higher order infinitesimals, in the presence of those of lower order, are neglected throughout.

First we allow only motion along the 60 degree lines passing through the center of the hexagon. Let: (a) the displacement of the i^{th} particle from its position of rest be x_i ; (b) the change in the corresponding angles formed by the bonds be θ_i , and ϕ_i ; (c) the change in the length of the outside bonds be Δ_i . We have:

¹ R. C. Yates, The Elastic Character of the Homopolar Chemical Bond, p. 555, this issue.

$$\Delta_i = (x_i + x_{i+1})/2 \quad (i = 1, \dots, 6)$$

The energy functions are set up at once, following the procedure of the first paper:

$$\left. \begin{aligned} T &= (m/2) \cdot \sum_1^6 \dot{x}_i^2 \\ V &= (k_1/2) \cdot \sum_1^6 (\Delta_i^2 + x_i^2/2) + (a^2 k_2/2) \cdot \sum_1^6 (\theta_i^2 + 2\phi_i^2) \end{aligned} \right\} \quad (1)$$

If the center of mass is to remain fixed: $x_1 = x_4$, $x_2 = x_5$, $x_3 = x_6$, leaving three independent coordinates to fix the system.

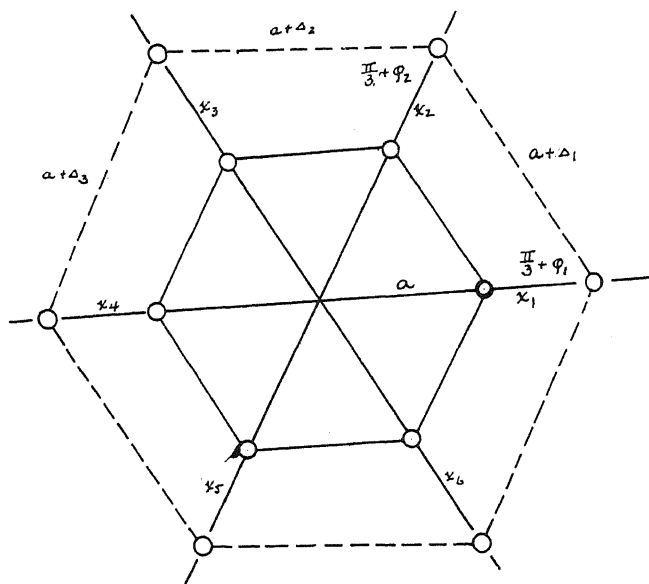


Fig. 1. Vibration along radial lines.

From the figure $\phi_1 = (3^{1/2}/a)x_2$, $\phi_2 = (3^{1/2}/a)x_3$, etc. and since $\theta_1 = \phi_1 - \phi_6$ etc., we may write Eqs. (1) in the final form:

$$\left. \begin{aligned} T &= m \cdot \sum_1^3 \dot{x}_i^2 \\ V &= (k_1/2) (2 \sum_1^3 x_i^2 + x_1 x_2 + x_1 x_3 + x_2 x_3) \\ &\quad + 6k_2 \left(2 \sum_1^3 x_i^2 - x_1 x_2 - x_1 x_3 - x_2 x_3 \right) \end{aligned} \right\} \quad (2)$$

The equations of motion are accordingly:

$$\left. \begin{aligned} 2m\ddot{x}_1 &= -(k_1/2)(4x_1 + x_2 + x_3) - 6k_2(4x_1 - x_2 - x_3) \\ 2m\ddot{x}_2 &= -(k_1/2)(x_1 + 4x_2 + x_3) - 6k_2(-x_1 + 4x_2 - x_3) \\ 2m\ddot{x}_3 &= -(k_1/2)(x_1 + x_2 + 4x_3) - 6k_2(-x_1 - x_2 + 4x_3) \end{aligned} \right\} \quad (3)$$

On combining the Eqs. (3), we find the set of normal coordinates

$$z_1 = x_1 + x_2 + x_3 \quad z_2 = x_1 - x_2 \quad z_3 = x_2 - x_3$$

with resulting frequencies:

$$\left. \begin{aligned} \nu_1 &= \left(\frac{1}{2\pi} \right) [(3k_1 + 12k_2)/m]^{1/2} \\ \nu_2 = \nu_3 &= \left(\frac{1}{4\pi} \right) [(3k_1 + 60k_2)/m]^{1/2} \end{aligned} \right\} \quad (4)$$

Secondly, we restrict the system to motion on a circle of arbitrary radius $(a+b)$. We select a polar system of reference with pole at the mass center and initial line passing through a vertex of the hexagon.

Let: (a) the angular displacement of the particles be θ_i ; (b) the change in the angles between adjoining bonds be $\alpha_i, \beta_i, \phi_i$, where $\phi_i = \alpha_i + \beta_i$; (c) the change in the bond length be Δ_i .

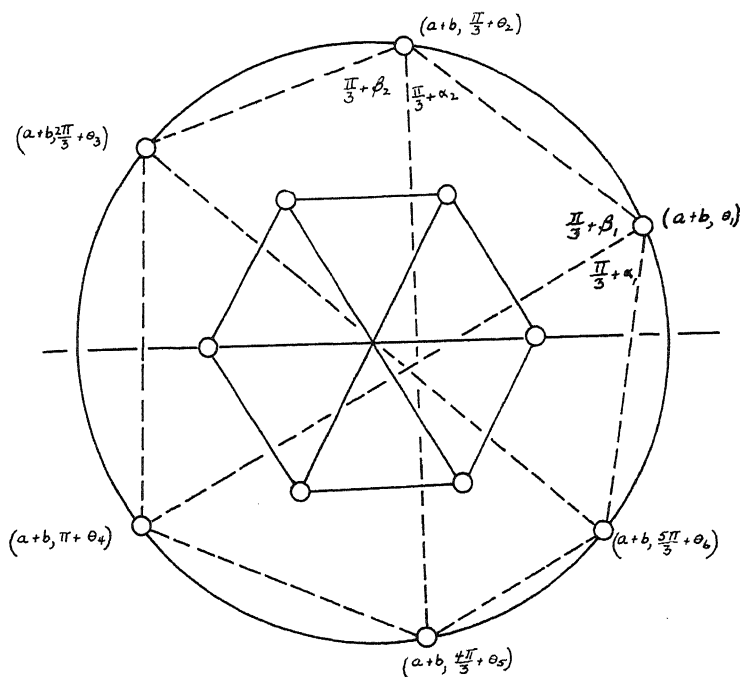


Fig. 2. Vibration on a circle.

The energy functions are:

$$\left. \begin{aligned} T &= (m/2)(a+b)^2 \sum_1^6 \dot{\theta}_i^2 \\ V &= (k_1/2) \left[\sum_1^6 \Delta_i^2 + 3b^2 \right] + (a^2 k_2/2) \sum_1^6 (\alpha_i^2 + \beta_i^2 + \phi_i^2) \end{aligned} \right\} \quad (5)$$

From an inspection of the figure we find

$$\left. \begin{aligned} \alpha_1 &= (2\theta_6 - \theta_1 - \theta_4)/2 & \beta_1 &= -(2\theta_2 - \theta_1 - \theta_4)/2 \\ \alpha_2 &= (2\theta_1 - \theta_2 - \theta_5)/2 & \beta_2 &= -(2\theta_3 - \theta_2 - \theta_5)/2 \end{aligned} \right\} \quad (6)$$

etc. which give expressions for ϕ :

$$\phi_i = \phi_{i-1} - \phi_{i+1}. \quad (7)$$

In order to fix the center of gravity at the pole we must have

$$\left. \begin{aligned} \theta_5 &= \theta_1 + \theta_2 - \theta_4 \\ \theta_6 &= -\theta_1 + \theta_3 + \theta_4 \end{aligned} \right\} \quad (8)$$

If we now put angular momentum about the center of mass equal to zero we obtain the further relation $\sum_1^6 \dot{\theta}_i = 0$. We thus eliminate θ_4 , θ_5 , and θ_6 by means of the equations:

$$\left. \begin{aligned} \theta_4 &= -\theta_1 - 2\theta_2 - 2\theta_3 \\ \theta_5 &= 2\theta_1 + 3\theta_2 + 2\theta_3 \\ \theta_6 &= -2\theta_1 - 2\theta_2 - \theta_3 \end{aligned} \right\} \quad (9)$$

We obtain now also from the figure

$$\left. \begin{aligned} \Delta_1 &= b + [a(3)^{1/2}/2](\theta_2 - \theta_1) & \Delta_4 &= b + [a(3)^{1/2}/2](3\theta_1 + 5\theta_2 + 4\theta_3) \\ \Delta_2 &= b + [a(3)^{1/2}/2](\theta_3 - \theta_2) & \Delta_5 &= b - [a(3)^{1/2}/2](4\theta_1 + 5\theta_2 + 3\theta_3) \\ \Delta_3 &= b - [a(3)^{1/2}/2](\theta_1 + 2\theta_2 + 3\theta_3) & \Delta_6 &= b + [a(3)^{1/2}/2](3\theta_1 + 2\theta_2 + \theta_3) \end{aligned} \right\} \quad (10)$$

With the foregoing expressions we may rewrite Eqs. (5) explicitly in terms of the three remaining independent coordinates θ :

$$\left. \begin{aligned} T &= m(a+b)^2[5\dot{\theta}_1^2 + 9\dot{\theta}_2^2 + 5\dot{\theta}_3^2 + 12\dot{\theta}_1\dot{\theta}_2 + 8\dot{\theta}_1\dot{\theta}_3 + 12\dot{\theta}_2\dot{\theta}_3] \\ V &= (k_1/2)[9b^2 + (3a^2/2)(36\theta_1^2 + 60\theta_2^2 + 36\theta_3^2 + 84\theta_1\theta_2 + 60\theta_1\theta_3 + 84\theta_2\theta_3)] \\ &\quad + a^2k_2[24\theta_1^2 + 60\theta_2^2 + 24\theta_3^2 + 66\theta_1\theta_2 + 30\theta_1\theta_3 + 66\theta_2\theta_3] \end{aligned} \right\} \quad (11)$$

The corresponding equations of motion are:

$$\left. \begin{aligned} m(a+b)^2(5\ddot{\theta}_1 + 6\ddot{\theta}_2 + 4\ddot{\theta}_3) &= -\frac{(9a^2k_1/2)(6\theta_1 + 7\theta_2 + 6\theta_3)}{3a^2k_2(8\theta_1 + 11\theta_2 + 5\theta_3)} \\ m(a+b)^2(2\ddot{\theta}_1 + 3\ddot{\theta}_2 + 2\ddot{\theta}_3) &= -\frac{(3a^2k_1/2)(7\theta_1 + 10\theta_2 + 7\theta_3)}{a^2k_2(11\theta_1 + 20\theta_2 + 11\theta_3)} \\ m(a+b)^2(4\ddot{\theta}_1 + 6\ddot{\theta}_2 + 5\ddot{\theta}_3) &= -\frac{(9a^2k_1/2)(5\theta_1 + 7\theta_2 + 6\theta_3)}{3a^2k_2(5\theta_1 + 11\theta_2 + 8\theta_3)} \end{aligned} \right\} \quad (12)$$

If here we make the change of variables: $z_1 = 2\theta_1 + 3\theta_2 + \theta_3$, $z_2 = \theta_1 + 3\theta_2 + 2\theta_3$, $z_3 = \theta_1 - \theta_3$, the last set of equations may be replaced by:

$$m(a+b)^2\ddot{z}_i = -9a^2(k_1/2 + k_2)z_i \quad (i = 1, 2, 3). \quad (13)$$

The characteristic of the differential Eqs. (12) is degenerate and for this particular type of motion there is but one frequency:

$$\nu = [3a/2\pi(a+b)][(k_1 + 2k_2)/2m]^{1/2}.$$

CONCLUSION

If the hydrogens in the benzene ring are grouped with the carbons and if we assume bonds passing through the center of the hexagon we may apply our results. Using the values for the elastic constants which were secured in the previous paper² the values for the three characteristic frequencies are found, as shown in Table I.

TABLE I.

Force constants	ν Calculated	ν Observed ⁴
$k_1 = 4 \times 10^5$	—	605
	—	849
$k_2 = 0.6 \times 10^5$	—	991
	1145	1176
	1305	
	1750	—

The frequencies in the Raman spectra, believed to be associated with the carbon atoms, are also given. Now it has already been deduced from a study of the relation between Raman spectra³ that the experimentally observed frequency of 1176 cm^{-1} should correspond to the type of motion where all the carbon atoms move in and out together along the lines through the center of the hexagon. The agreement between this value and the calculated one of 1145 cm^{-1} substantiates this view and indicates that the values chosen for the elastic constants are fairly correct. The other two calculated frequencies fail to agree with any of those experimentally observed. It appears probable that for these the restrictions imposed on the motion were so far removed from the actual state of the molecule that these types of motion do not exist in actuality.

The writer's appreciation is due Professor D. H. Andrews for many valuable suggestions and Professor F. D. Murnaghan for constructive advice in preparing this paper.

² R. C. Yates, reference 1.

³ C. F. Kettering, L. W. Shutts, and D. H. Andrews, *Phys. Rev.* **36**, 531 (1930). D. H. Andrews, *Phys. Rev.* **36**, 544 (1930).

⁴ A. S. Ganesan and S. Venkateswaran, *Indian Jour. Phys.* **4**, 195 (1929).

COUPLED VIBRATIONS WITH APPLICATIONS TO THE
SPECIFIC HEAT AND INFRARED SPECTRA OF
CRYSTALS

BY ARTHUR B. LEWIS

THE JOHNS HOPKINS UNIVERSITY

(Received June 23, 1930)

ABSTRACT

The free periods of certain coupled systems of linear oscillators are considered in this paper. The complete system discussed consists of p identical, coupled, groups; each group containing n identical linear oscillators. The equations of motion of such a system lead to a determinantal equation of the pn^{th} order, of which the well-known determinantal equations of the uniformly loaded string and the finite wave filter are special cases. The solution of this general determinantal equation has been reduced to the solution of certain trigonometric equations. A solution for the free periods of the system is obtained for the case in which the coupling between the groups is small compared to the internal forces of the groups. In case only one or two groups are present the resulting equations can be solved readily to any desired degree of approximation for any values of the forces whatever. Certain special cases are noted in which, for special values of the forces, exact solutions become possible.

Sample calculations have been carried out which illustrate the behavior of the pn free periods of a system of pn particles when various forces act between the particles of the system, and when the pn particles are rearranged in various ways. With the aid of the equations obtained above the specific heats of four of the normal alcohols have been computed at low temperatures and compared with the experimentally determined values. A reasonable agreement is obtained between the observed and computed values, but with the data at hand the agreement cannot be said to be conclusive.

1. INTRODUCTION

RECENT investigators in the infrared spectra of organic compounds^{1,2} have attained considerable success in organizing their data by assigning certain prominent bands which are common to all organic compounds to certain modes of vibration between the component parts of the molecules under investigation. It is generally agreed that the strong band at about 3.5μ in the spectra of organic compounds is to be identified with the vibration of the hydrogen atom against the carbon atom. Similarly the band at about 28μ is to be identified with the vibration of carbon against carbon. This assumption of the spring-like nature of these chemical bonds is supported by several lines of evidence. The assignment of a characteristic frequency to a given bond permits the calculation of the force constant of the bond. This in turn leads to the calculation of the heat of linkage.³ There is good agree-

¹ J. W. Ellis, Phys. Rev. **23**, 48 (1924); **27**, 298 (1926), **28**, 25 (1926).

² J. W. Sappenfield, Phys. Rev. **33**, 37 (1929).

³ Grundriss der Phys. Chem., A. Eucken, p. 459ff (1924) (References) J. W. Ellis, Phys. Rev. **33**, 27 (1929).

ment between the observed and computed values. Moreover these characteristic frequencies, when used in Einstein's formula,⁴ and Debye's formula,⁵ should give the specific heat curve of the compound at low temperatures. There seems to be reasonably good agreement between the computed curves and the observed values.⁶

It has therefore seemed worthwhile to consider a little more closely the free periods of vibration which one would expect from a mechanical model of one of these molecules, or from a group of molecules. To this end we shall consider the molecules under discussion as being represented by a series of massive particles attached at regular intervals to a massless elastic string. We shall first determine the free periods of a single group of massive particles, or of a single molecule, when various restrictions are placed on the ends of the molecule or group. We shall next consider the effect upon these periods of coupling two or more molecules or groups together, and shall thus determine the free periods of a system consisting of a number of identical molecules or groups coupled together. Such a system may be realized in the crystals of organic chain compounds. We shall finally be able to obtain the free periods of a single group of pn particles, and then to determine the effects produced on these frequencies by rearranging the pn component particles into various groupings (such as p groups of n particles each) keeping the total number of particles present always the same.

Mathematically we have here an extension of the problem of the vibration of a loaded string which has been treated by Lagrange,⁷ Lord Rayleigh,⁸ and others. The second order differential equations which arise from this problem are similar to those which arise in the solutions of the modes of vibration of other systems, particularly in the solution of wave filter problems. The analogous electrical case of the finite wave filter has been treated by Pupin,⁹ Campbell,¹⁰ Carson,¹¹ Wheeler and Murnaghan,¹² and others.

The method of solution consists, as usual, in setting up the differential equations of motion, which can be solved for periodic vibrations if a certain algebraic equation equals zero. This equation is known as the secular or characteristic equation. The roots of this equation give the frequencies of the free vibrations. In what follows we shall limit ourselves to motion in one dimension. In general, under these conditions, a system of N particles will possess N frequencies. If the system is free to move as a whole, or to rotate uniformly, the corresponding frequency is zero.

The system of particles which we shall discuss is obtained by arranging

⁴ A. Einstein, *Ann. d. Physik* **28**, 180 (1907).

⁵ P. Debye, *Ann. d. Physik* **39**, 789 (1912).

⁶ D. H. Andrews, *Proc. Roy. Acad. Amsterdam* **29**, 744 (1926); *Chemical Reviews* **5**, 533 (1928).

⁷ *Mecanique Analytique*, Lagrange, vol. 1, pp. 382-395 (1811).

⁸ *Theory of Sound*, Lord Rayleigh; vol. 1, p. 120 (1877).

⁹ M. Pupin, *Proc. A.I.E.E.* **16**, 93 (1899).

¹⁰ G. A. Campbell, *Bell System Tech. J.* p. 1, November 1922.

¹¹ *Electric Circuit Theory and Operational Calculus*, Carson, p. 132 ff. (1926).

¹² H. A. Wheeler and F. D. Murnaghan, *Phil. Mag.* **6**, 146 (1928).

pn equal particles into p groups of n particles each. We now introduce a small quantity, d , which we call the "coupling coefficient" and which measures the ratio of the force acting between the groups to the force inside of the group. An inspection of Fig. 1 will indicate that when $d=1$ the forces acting between the groups are the same as the forces acting within the groups, there is not longer any distinction between "groups," and we have the elementary case of the uniformly loaded string. The situation existing when $d=0$ must be examined with a little more care since d is defined as the ratio of two quantities. If d vanishes due to the fact that the internal forces present in each group are infinite we must say that we no longer have any vibrating group structure present. Our system will therefore vibrate as a uniformly loaded string of p particles, each of mass nm , the force constant of the string being that of the inter-group force. We have present the p frequencies characteristic of these p groups, while the other $p(n-1)$ internal frequencies

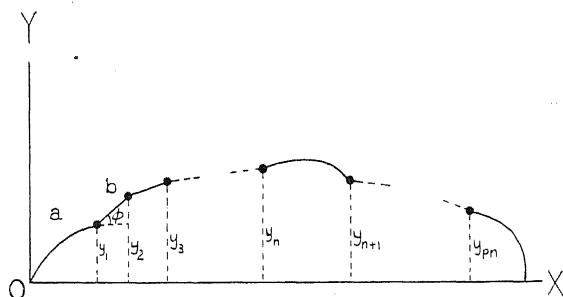


Fig. 1.

have been shifted to infinity. On the other hand if d vanishes due to the fact that the force between the groups has become infinitely small we must say that we have p groups present as before, but each infinitely removed from its neighbors and therefore entirely unaffected by them. We shall therefore expect the pn free periods of such a system to be the n free periods of a single group of n particles with free ends, each free period being repeated p times. These n frequencies characteristic of a single group of n particles with free ends will consist of one frequency, $\nu=0$, which corresponds to the vibration. When d has become small, but both forces remain finite, we can predict in a general way the behavior of the free periods. The p slowest vibrations will be slight modifications of the p vibrations which would be present if each group vibrated as a rigid whole, and on the other hand can be considered as corresponding to the p vibrations of frequency 0 for the p free molecules or groups. Similarly the $p(n-1)$ faster vibrations will be slight modifications of, and will therefore group themselves about, the $(n-1)$ internal vibrations which would be present if each group were entirely separated from its neighbors. While these, however, had been p -fold in the case of the independent molecules or groups, these p coinciding frequencies will be split up now into p separate components by the effect of the coupling.

II. STATEMENT OF THE MATHEMATICAL PROBLEM

Let us consider the motion of a massless, elastic string on which are fastened a number of massive particles of common mass " m ". Let these particles be arranged in identical and recurring groups of " n " particles, the common distance between particles of the same group being b . Let the distance between the n^{th} particle of any one group and the 1^{st} particle of the next group be a , there being p groups in all, see Fig. 1. Let the initial, uniform, tension in the string be T . Let us confine ourselves for the moment to small lateral displacements, all in the same plane, these displacements being so small that we may replace the sines of the angles by the angles themselves. This means that we can say, Fig. 1,

$$\sin \phi = \tan \phi = (y_r - y_{r-1})/a \text{ or } (y_r - y_{r-1})/b$$

We will so choose our axes that $y_0 = y_{pn+1} = 0$.

It is to be noted here that the introduction of the concept of an elastic spring under tension is a matter of convenience and not of necessity. In the same way we have restricted ourselves to small vertical displacements from convenience and not from necessity. We might have started equally well with a system of identical groups of particles in equilibrium under the influence of quasilastic restoring forces of any origin whatever. We have in this case to define a force constant which will be the restoring force per unit displacement acting on the r^{th} particle due to its displacement with respect to the $(r+1)^{\text{st}}$ or $(r-1)^{\text{st}}$ particle. This force constant we may call τ when the neighboring particle under consideration belongs to the same group as the r^{th} particle, and τ' when the neighboring particle under consideration does not belong to the same group as the r^{th} particle. The equations which will be obtained as Eqs. (1) will be found to follow immediately with the replacing of T/a and T/b by τ' and τ respectively. It will be noted in the following equations that the tension T always occurs in the expression T/a or T/b , which has the dimensions $F.L^{-1}$ as it should. It is apparent from what has been said that our coordinates y_r may be looked upon as generalized coordinates, the quantities which will occur in Eqs. (1) as $m\ddot{y}$ may be looked upon as generalized inertial forces, and the corresponding expressions such as $T/b(-y_{r-1} + 2y_r - y_{r+1})$ may be looked upon as generalized forces of restitution. The equations which will be obtained as Eqs. (1) are then equally capable of representing motions along the axis of X , perpendicular to the axis of X , rotations about this axis, or oscillations in properly coupled electrical circuits. The quantity defined as " d ", Eq. (3) will be given, in the light of the definitions of this paragraph as τ'/τ .

We can now write down the expressions for the kinetic and potential energy of the system,¹³ and set up the equations of motion by Lagrange's equations,

$$T - V = L$$

¹³ Partial Differential Equations of Mathematical Physics, Webster, p. 91, (1927).

The condition for a solution giving values for the C 's other than zero is that the determinant of the coefficients shall vanish. This gives a determinant of the pn^{th} order which we shall designate as F_p . It is to be understood by this notation that F_p represents the determinant of the pn^{th} order obtained from Eqs. (4) written for p identical groups of n particles each. We shall not be interested in this particular determinant when there are not exactly n particles in each group. The determinantal equation is

$$F_p = \begin{vmatrix} B-1 & 0 & 0 & 0 & 0 & 0 & 0 & 0 & 0 & \dots & \dots & 0 & 0 \\ -1 & A & -1 & 0 & 0 & 0 & 0 & 0 & 0 & \dots & \dots & 0 & 0 \\ 0 & -1 & A-1 & 0 & 0 & 0 & 0 & 0 & 0 & \dots & \dots & 0 & 0 \\ 0 & 0 & -1 & B-d & 0 & 0 & 0 & 0 & 0 & \dots & \dots & 0 & 0 \\ 0 & 0 & 0 & -d & B-1 & 0 & 0 & 0 & 0 & \dots & \dots & 0 & 0 \\ 0 & 0 & 0 & 0 & -1 & A-1 & 0 & 0 & 0 & \dots & \dots & 0 & 0 \\ 0 & 0 & 0 & 0 & 0 & -1 & A-1 & 0 & 0 & \dots & \dots & 0 & 0 \\ 0 & 0 & 0 & 0 & 0 & 0 & -1 & B-d & \dots & \dots & \dots & 0 & 0 \\ 0 & 0 & 0 & 0 & 0 & 0 & 0 & -d & B & \dots & \dots & 0 & 0 \\ \dots & \dots & \dots & \dots & \dots & \dots & \dots & \dots & \dots & \dots & \dots & \dots & \dots \\ 0 & 0 & \dots & \dots & \dots & \dots & \dots & \dots & \dots & \dots & \dots & \dots & \dots \\ 0 & 0 & \dots & \dots & \dots & \dots & \dots & \dots & \dots & \dots & \dots & \dots & \dots \\ 0 & 0 & \dots & \dots & \dots & \dots & \dots & \dots & \dots & \dots & \dots & \dots & \dots \\ 0 & 0 & \dots & \dots & \dots & \dots & \dots & \dots & \dots & \dots & \dots & \dots & \dots \\ 0 & 0 & \dots & \dots & \dots & \dots & \dots & \dots & \dots & \dots & \dots & \dots & \dots \\ 0 & 0 & \dots & \dots & \dots & \dots & \dots & \dots & \dots & \dots & \dots & \dots & \dots \\ 0 & 0 & \dots & \dots & \dots & \dots & \dots & \dots & \dots & \dots & \dots & \dots & \dots \end{vmatrix} = 0 \quad (5)$$

pn^{th}
order

For convenience the groups have been represented as having a limited number of terms, $n=4$.

This determinant is a function of the unknown $\lambda (=2\pi\nu^2$ where ν is the frequency) which is the variable entering through the quantities A and B . The solution of the problem will consist in finding those values of λ which will reduce the determinant to zero. A direct expansion of Eq. (5) will lead to an algebraic equation of the pn^{th} degree in λ . If it were possible to solve this algebraic equation, the resulting pn roots of λ would lead to the pn desired free periods of the system. This is the number of free periods which we expect from the number of degrees of freedom possessed by the system. Such a direct method of solution is not feasible in general. We must therefore look for transformations which will reduce Eq. (5) to a more tractable form. The general method of attack has been pointed out by Wheeler and Murnaghan.¹² The method consists essentially in reducing the expansion of Eq. (5) to a trigonometric equation in which the unknown, θ , is defined as a function of λ . The resulting trigonometric equation is well adapted to the processes of approximation.

An inspection of the determinant F_p will disclose that it is made up of certain simpler and recurring groups. As will be seen later the expansion of the complete determinant is obtained in terms of these sub-groups. We shall therefore define the following determinants:

$$D_n(d, d) = \begin{vmatrix} B & -1 & 0 & 0 & 0 \cdots & \cdots & 0 \\ -1 & A & -1 & 0 & 0 \cdots & \cdots & 0 \\ 0 & -1 & A & -1 & 0 \cdots & \cdots & 0 \\ \cdots & \cdots & \cdots & \cdots & \cdots & \cdots & \cdots \\ \cdots & \cdots & \cdots & \cdots & \cdots & \cdots & \cdots \\ 0 & 0 \cdots & \cdots & 0 & -1 & A & -1 & 0 \\ 0 & 0 \cdots & \cdots & 0 & 0 & -1 & A & -1 \\ 0 & 0 \cdots & \cdots & 0 & 0 & 0 & -1 & B \end{vmatrix} \quad (6)$$

n^{th}
order

$$D_n(1, d) = \begin{vmatrix} A & -1 & 0 & 0 \cdots & \cdots & 0 \\ -1 & A & -1 & 0 \cdots & \cdots & 0 \\ 0 & -1 & A & -1 \cdots & \cdots & 0 \\ \cdots & \cdots & \cdots & \cdots & \cdots & \cdots \\ \cdots & \cdots & \cdots & \cdots & \cdots & \cdots \\ 0 & 0 \cdots & \cdots & 0 & -1 & A & -1 & 0 \\ 0 & 0 \cdots & \cdots & 0 & 0 & -1 & A & -1 \\ 0 & 0 \cdots & \cdots & 0 & 0 & 0 & -1 & B \end{vmatrix} \quad (7)$$

n^{th} order.

$$D_n(1, 1) = \begin{vmatrix} A & -1 & 0 & 0 \cdots & \cdots & 0 \\ -1 & A & -1 & 0 \cdots & \cdots & 0 \\ 0 & -1 & A & -1 \cdots & \cdots & 0 \\ \cdots & \cdots & \cdots & \cdots & \cdots & \cdots \\ \cdots & \cdots & \cdots & \cdots & \cdots & \cdots \\ 0 & 0 \cdots & \cdots & 0 & -1 & A & -1 \\ 0 & 0 \cdots & \cdots & 0 & 0 & -1 & A \end{vmatrix} \quad (8)$$

n^{th} order

The determinant $D_n(1,1)$ is the determinant of the uniformly loaded string,¹³ and of the elementary wave filter.¹² The present notation has been adopted since the determinant $D_{pn}(1,1)$, see Eq. (8), can be obtained from the general determinant F_p , Eq. (5), by putting the quantity d everywhere equal to unity. The d 's then disappear from the determinant itself, and the quantity B becomes equal to the quantity A , see Eq. (3). Similarly the determinant $D_n(1,d)$ is obtained from the determinant $D_n(1,1)$ by replacing one of the A 's which constitute the terminal elements of the principal diagonal by the quantity B which is $A+d-1$. In the same way the determinant $D_n(d,d)$ is obtained from the elemental determinant $D_n(1,1)$ by replacing both of the A 's which constitute the terminal elements of the principal diagonal by the quantity B .

Let us now make the following definitions:*

* The author is indebted to Prof. F. D. Murnaghan for these substitutions.

$$H_p = F_p \mu^{-p} \quad (9)$$

$$\mu = + d(D_{n-1}^2(1, d) - D_n(d, d)D_{n-2}(1, 1))^{1/2} \quad (10)$$

$$\xi = \frac{D_n(d, d) - d^2 D_{n-2}(1, 1)}{\mu} \quad (11)$$

It can then be readily shown that the expansion of Eq. (5) is equivalent to

$$H_p = \xi H_{p-1} - H_{p-2}. \quad (12)$$

The condition that $F_1 = D_n(d, d)$ leads to the following definitions

$$H_0 = 1 \quad (13)$$

$$H_1 = \frac{D_n(d, d)}{\mu} \quad (14)$$

We see from an inspection of Eq. (12) and Eq. (11) that the general solution for H_p will depend upon the values assumed by the determinants which we have defined in Eqs. (6), (7) and (8). These determinants are special cases of the determinant F_p as should be evident from Eq. (5). Since a knowledge of these special cases is necessary for a complete solution, we shall digress here to consider the form assumed by F_p when we have only one group present, $p=1$.

III. SOLUTION OF CERTAIN LIMITING CASES

(A) The uniformly loaded string (Lagrange's problem).

The solution for the free periods of the uniformly loaded string, which is given by

$$D_n(1, 1) = 0$$

where

$$p = 1$$

$$d = 1 \text{ in Eq. (5)}$$

is so well known^{12,13} that we shall merely state the result here, since it will be used constantly in what follows. The determinant may be expanded yielding

$$D_n(1, 1) = A D_{n-1}(1, 1) - D_{n-2}(1, 1).$$

This gives

$$D_n(1, 1) = \frac{\sin(n+1)\theta}{\sin \theta} \quad (15)$$

if we make the substitution

$$A = (-mb\lambda)/T + 2 = 2 \cos \theta \quad (16)$$

The solution

$$D_n(1, 1) = 0$$

is given by

$$\theta = K\pi/(n+1), \quad K = 1, 2, \dots, n \quad (17)$$

The values of θ given by Eq. (17) together with Eq. (16) connecting $A(\lambda)$ and θ give us the free periods of the system. There are n possible frequencies, as is necessary for n particles.

(B) The single group of n particles with $d \neq 1$ at its terminal elements.

This case may be represented physically by a molecule, as of an organic chain compound, which is restrained at its ends by quasielastic restoring forces which differ from the restoring forces acting within the molecule itself.

Let us consider the case

$$F_1 = 0.$$

The solution in this case is exactly analogous to that of the finite wave filter,¹² and will be obtained in the same way. Let us generalize and assume that the coupling coefficient d is not the same at the two ends. The determinantal equation then becomes

$$D_n(d, d') = \begin{vmatrix} B & -1 & 0 & 0 \cdots & \cdots & 0 \\ -1 & A & -1 & 0 \cdots & \cdots & 0 \\ 0 & -1 & A & -1 \cdots & \cdots & 0 \\ \cdots & \cdots & \cdots & \cdots & \cdots & \cdots \\ \cdots & \cdots & \cdots & \cdots & \cdots & \cdots \\ 0 & 0 \cdots & \cdots & 0 & -1 & A & -1 \\ 0 & 0 \cdots & \cdots & 0 & 0 & -1 & B' \end{vmatrix} \quad n^{\text{th}} \text{ order.} \quad (18)$$

where

$$B = A + d - 1$$

$$B' = A + d' - 1$$

and all the other quantities have the same meanings as before. Direct expansion shows that

$$D_n(d, d') = D_n(1, 1) + (d + d' - 2)D_{n-1}(1, 1) + (d - 1)(d' - 1)D_{n-2}(1, 1).$$

With the aid of Eq. (15) this becomes, when $D_n(d, d') = 0$

$$D_n(d, d') = \frac{\sin(n+1)\theta + (d + d' - 2)\sin n\theta + (d - 1)(d' - 1)\sin(n-1)\theta}{\sin \theta} = 0 \quad (19)$$

It is apparent that Eq. (19) may be adjusted to any given values of the coupling coefficients d and d' . That is, we may now write the explicit expressions in terms of θ for $D_n(d, d)$, $D_n(1, d)$, $D_n(1, 0)$, and $D_n(0, 0)$ from Eq. (19). The solutions of the resulting trigonometric equations can be carried to as

high a degree of approximation as is necessary. Two cases, in which an exact solution becomes possible, are of interest.

The solution for a uniformly loaded string free at one end, $D_n(1,0)$, a case which was discussed but not carried to completion by Lagrange,⁷ is obtained by putting $d=1$ and $d'=0$ in Eq. (19). The equation for θ then readily reduces to

$$\frac{\cos(n + \frac{1}{2})\theta}{\cos n\theta \sin \theta/2} = 0$$

Whence

$$\theta = \frac{2k+1}{2n+1}\pi, \quad k = 0, 1, 2, \dots, n. \quad (20)$$

The solution corresponding to $k=0$ corresponds to a rotation and expansion of the entire system about its point of support, all the particles lying on a straight line. Besides, there are $(n-1)$ oscillatory motions.

The solution for a uniformly loaded string free at both ends, $D_n(0,0)$ is obtained by putting both d and d' equal to zero in Eq. (19). The trigonometric equation then becomes

$$\tan n\theta = 0$$

Whence

$$\theta = \frac{k}{n}\pi, \quad k = 0, 1, 2, \dots, (n-1). \quad (21)$$

The solution corresponding to $k=0$, which gives $\theta=0$ and consequently $\nu=0$, corresponds to a motion of the entire system as a rigid whole. If $k=n$, which gives $\theta=\pi$, we do not have a solution since in this case both numerator and denominator of Eq. (19) vanish and their ratio is not zero.

IV. SOLUTION OF THE GENERAL DETERMINANTAL EQUATION FOR p GROUPS, $H_p=0$

(A) Formal solution in terms of θ and Γ .

We can now proceed with the formal solution of the general determinant H_p .

$$H_p = \xi H_{p-1} - H_{p-2} \quad (12)$$

Eq. (12) is in the standard form¹² and if we make the substitution

$$\xi = 2 \cos \Gamma \quad (22)$$

the equation can be thrown into the form

$$H_p = \frac{\sin(p+1)\Gamma + d \sin(n-1)\theta/\sin \theta \times \sin p\Gamma}{\sin \Gamma} = 0. \quad (23)$$

The solution of our problem therefore consists in the solution of Eq. (23) together with our two equations of definition, Eqs. (16) and (22), which may be put in the form

$$\xi = \frac{2(1 - \cos \theta)(d - 1) \sin n\theta + 2d \sin \theta \cos n\theta}{d \sin \theta} = 2 \cos \Gamma \quad (24)$$

$$A = (-mb\lambda)/T + 2 = 2 \cos \theta \quad (16)$$

(B) Approximate solution of $H_p = 0$.

An exact solution of these equations is not, in general, possible. An approximate solution can be obtained, however, when the coupling coefficient d , is small. We have already found, Eq. (21), that when $d=0$ the values of θ are given by $(k/n)\pi$. Moreover, when $d=1$ the values of θ are given by $k\pi/(n+1)$, Eq. (17). We can therefore say, when d is small,

$$\theta_k = \frac{k\pi}{n} + \Delta\theta_k, \quad k = 0, 1, 2, \dots, (n-1) \quad (25)$$

where $\Delta\theta_k$ is a small quantity of order d or less. We shall now inquire as to the values assumed by the expression occurring in Eq. (23), $d \sin(n-1)\theta/\sin \theta$, when θ has the value given by Eq. (25). Direct substitution shows that

$$\frac{d \sin(n-1)\theta}{\sin \theta} \cong d(n-1).$$

If we will restrict ourselves to cases in which $d(n-1)$ is small in comparison with unity Eq. (23) becomes $\sin(p+1)\Gamma + (a \text{ small quantity of order } dn) \sin p\Gamma = 0$. An approximate solution for Γ will obviously lie near $(s\pi/p+1)$ and we therefore write for the solution of Γ

$$\Gamma_s = \frac{s\pi}{p+1} + \Delta\Gamma_s, \quad s = 1, 2, \dots, p \quad (26)$$

$\Delta\Gamma_s$ is a small quantity whose value is to be determined by successive approximations. In making this approximation we assume that $(p+1)\Delta\Gamma_s$ is so small that we can replace the sines of the angles by the angles themselves.

The substitution of Eqs. (25) and (26) in Eqs. (23) and (24) and the evaluation of $\Delta\Gamma_s$ and $\Delta\theta_k$ is tedious but straightforward, yielding finally for the pn desired values of θ ,

$$\left. \begin{aligned} \theta_{0s} &= 2 \left(\frac{d + d^2}{n} \right)^{1/2} \sin \frac{s\pi}{2(p+1)} \\ s &= 1, 2, \dots, p \\ (k &= 0) \\ \theta_{ks} &= \frac{k\pi}{n} + (-1)^k \frac{d}{n} \cot \frac{k\pi}{2n} \left[(-1)^k \left(1 + d - \frac{d}{2n} - \frac{d}{p+1} \right) \right. \\ &\quad \left. - \left(1 + d - \frac{d}{n} \right) \cos \frac{s\pi}{p+1} - (-1)^k \left(\frac{d}{2n} - \frac{d}{p+1} \right) \cos^2 \frac{s\pi}{p+1} \right] \\ s &= 1, 2, \dots, p \\ k &= 1, 2, \dots, (n-1). \end{aligned} \right\} \quad (27)$$

The frequencies of the free periods are obtained through the definition

$$A = (-mb\lambda)/T + 2 = 2 \cos \theta. \quad (16)$$

From this equation we readily obtain

$$\nu_{ks} = \frac{\lambda_{ks}}{2\pi} = \frac{1}{\pi} \sqrt{\frac{T}{mb}} \sin \frac{\theta_{ks}}{2}. \quad (28)$$

V. SOLUTION FOR TWO GROUPS COUPLED TOGETHER

The solution for the free periods of a system consisting of only two groups coupled together is of some interest, since the solutions can be obtained quite as directly as in the case of a single group, and can as readily be carried to any desired degree of accuracy. We shall therefore consider two cases in which there are only two groups present.

(A) Two groups coupled together and to fixed supports.

In this case in which we have two groups coupled together and to fixed supports we obtain from Eq. (5)

$$F_2 = D_n^2(d, d) - d^2 D_{n-1}^2(1, d). \quad (29)$$

The condition for a solution is, as usual,

$$F_2 = 0.$$

Using Eq. (19), ($d=d'$), and Eq. (15), this expression becomes

$$\left[\frac{\sin(n+1)\theta + 2(d-1)\sin n\theta + (d-1)^2 \sin(n-1)\theta}{\sin \theta} \right]^2 - d^2 \left[\frac{\sin n\theta + (d-1)\sin(n-1)\theta}{\sin \theta} \right]^2 = 0. \quad (30)$$

On transposing, extracting the square root, and using first the + and then the - sign, we obtain the two following equations

$$\frac{\sin(n+1)\theta + (d-2)\sin n\theta - (d-1)\sin(n-1)\theta}{\sin \theta} = 0 \quad (31)$$

$$\frac{\sin(n+1)\theta + (3d-2)\sin n\theta + (2d^2-3d+1)\sin(n-1)\theta}{\sin \theta} = 0 \quad (32)$$

The solution of these equations can be carried to as high a degree of approximation as is necessary, for any values of the coupling coefficient, d , whatever.

(B) Two groups coupled together, but with free ends.

We may also readily obtain the free periods of a system consisting of two groups of n particles each coupled together but with free ends. This means that $d=0$ at the 1st and 2 n th particles. The determinantal equation is

obtained from Eq. (5) written for only two groups when the terminal elements B of the principal diagonal are replaced by B' where

$$B' = A - 1.$$

Let us call this determinant F_2' . With the aid of these definitions we obtain by expansion as before, see Eqs. (6), (7) and (9),

$$F_2' = D_n^2(d, 0) + d^2 D_{n-1}^2(1, 0).$$

The condition for a solution is, as usual,

$$F_2' = 0.$$

With the aid of Eq. (19) this becomes

$$\frac{\sin(n+1)\theta + (d-2)\sin n\theta - (d-1)\sin(n-1)\theta}{\sin \theta} = \pm d \frac{\sin n\theta - \sin(n-1)\theta}{\sin \theta} \quad (33)$$

On expanding the multiple angles and collecting we have

$$\frac{2 \sin n\theta (\cos \theta - 1)}{\sin \theta} = 0 \quad (34)$$

and

$$\tan n\theta = \frac{d}{1-d} \cot \frac{\theta}{2}. \quad (35)$$

From Eq. (34) we have

$$\theta = \frac{k\pi}{n}, \quad k = 0, 1, 2, \dots, (n-1) \quad (36)$$

The n roots of Eq. (35) must be approximated.

It is interesting to note that if $d = \frac{1}{2}$, Eq. (35) also becomes capable of exact solution, the roots being given by

$$\theta = \frac{2k+1}{2n+1}\pi, \quad k = 0, 1, 2, \dots, (n-1)^\dagger \quad (37)$$

We obtain the free periods by means of our fundamental definition given in Eq. (16), $A(\lambda) = 2 \cos \theta$.

VI. DISCUSSION

A discussion of the results obtained here is most readily undertaken with the aid of a specific example. We have therefore represented in Fig. 2 the free periods which may be obtained from a group of 9 particles under the various arrangements discussed in this paper. For convenience the factor $(1/\pi)(T/m\bar{b})^{1/2}$ has been taken equal to unity. When we have the 9 particles

[†] Here again the value $k=n$, giving $\theta=\pi$, must be rejected due to the vanishing of the denominator in Eq. (33).

arranged in a uniform group and coupled to a supporting wall with a coupling coefficient $d=1$, we have the frequencies given by the well known formula. Eq. (17), as is shown in case (a). When the coupling coefficient between the group and the support is reduced to $d=0.1$, each of the previous frequencies is decreased, the slower ones more than the faster ones, as is illustrated in case (b). This slowing up of the frequencies with decreasing d is continued until, when $d=0$, the slowest frequency has become zero itself, see case (c). Now let the 9 particles be rearranged into 3 groups of 3 particles each, with a coupling coefficient $d=0.1$ between each group and between the end groups and the supporting walls. The 9 frequencies present rearrange themselves into three sharply defined groups of three frequencies each, see case (d). The number of groups of frequencies present is determined by the number of particles present in each group, that is by the internal structure of the

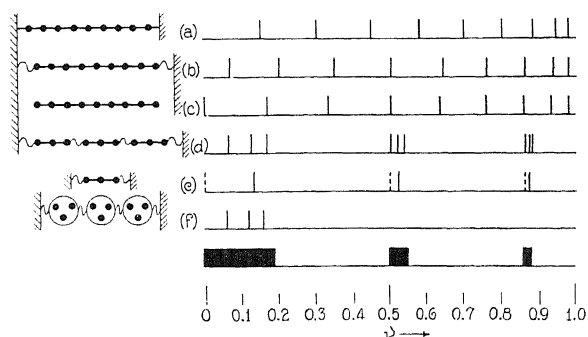


Fig. 2. The free periods obtained from various arrangements of a system consisting of 9 massive particles; $1/\pi \cdot T/m\bar{b}^{1/2}=1$

groups under consideration. On the other hand the number of separate frequencies present in each group of frequencies is determined by the total number of groups present in the system. In case (e) we have plotted the frequencies due to three particles arranged in a single group with coupling coefficient $d=0.1$. The dotted lines in case (e) represent the frequencies which would be present if $d=0$. Similarly in case (f) we have plotted the frequencies which would present if each group of case (d) vibrated as a rigid whole. We may speak of these frequencies as the "unmodified group vibrations" of such a system as that shown in case (d). Similarly the two higher frequencies of case (e) may be spoken of as the "unmodified internal vibrations." We may therefore say that the effect of rearranging a single group of pn particles into p groups of n particles each is to rearrange the pn free periods of the original group into n distinct groups of p frequencies each. Or, the effect of coupling together p originally independent groups of n particles each is to slightly modify the p slow group vibrations which would be present if each group vibrated as a rigid whole, and to split each of the $(n-1)$ internal vibrations into p separate components.

When the number of groups present has become infinite, as will be true for all practical purposes in any physical crystal, the number of frequencies

present in any one group becomes infinite and we have bands instead of groups, see case (g). The lower limit of each band is determined solely by the corresponding "unmodified" frequency of a single group with coupling coefficient $d=0$. See the dotted lines in case (e), Fig. 2. The upper limit, for any given band, is determined solely by the values of d and n , if $p=\infty$. The first and slowest band corresponds to the well-known Debye spectrum of group vibrations, but with a slightly modified upper limit.

Let us now inquire as to the distribution of the individual frequencies within these groups when p has become large but not infinite. To do this we form $(\partial\nu_{ks}/\partial s)$. From Eq. (28) we get

$$\frac{\partial\nu_{ks}}{\partial s} = \frac{1}{2\pi} \left(\frac{T}{mb} \right)^{1/2} \cos \frac{\theta_{ks}}{2} \frac{\partial\theta_{ks}}{\partial s}.$$

It is evident that the frequencies will be closest together, that is to say the density of lines in the elastic spectrum will be greatest, when $(\partial\nu_{ks}/\partial s)$ is a minimum. An investigation of the above expression with the aid of Eqs. (27) shows that, to a first approximation, the frequencies of the group, or Debye, vibrations crowd together or converge toward the high frequency limit of the group. The grouping of the frequencies is exactly analogous to that holding in cases (a), (b), and (c) of Fig. 2. In the case of the internal vibrations, to a first approximation, the frequencies converge toward both the high and low frequency limits of the group. The lines here have their minimum density at the center of the group.

It is not to be inferred from the preceding discussion of frequencies and bands that each of the frequencies predicted by Eqs. (27) can be expected to appear in the optical spectrum of the corresponding compound. The question of the optical activity of a given frequency is essentially a question concerning the electric moment of the molecule. It is hoped that an investigation of this question can be made at a later date.

VII. APPLICATION TO THE SPECIFIC HEATS OF ORGANIC COMPOUNDS

Although it is not the purpose of this paper to discuss in detail the applications of the equations just derived, an obvious example will be given. If we have, by any means, an approximate value for the forces of restitution acting upon an atom in a crystal of an organic chain compound, we have here the means for computing its free periods. By applying the proper Debye or Einstein functions we can then compute its specific heat as a function of temperature. The frequencies arising from the terms containing θ_{0s} , being molecular vibrations, will give rise to a Debye term. It is necessary then to know only the upper limit of the terms defined by θ_{0s} , that is θ_{0p} . When p becomes large this term becomes $\theta_{0p}=2(d+d^2/n)^{1/2}$. For the internal vibrations it will in general suffice to neglect the correction terms in Eqs. (27) and write $\theta_{ks}=k\pi/n$. In case the frequency band is unusually wide, as will be the case with the "internal" bands of hexyl alcohol, we may

use the average frequency of the band in the specific heat formula. Even in this case the correction is practically negligible.

For the force of restitution due to a displacement along the length of the molecular chain we will take 4×10^5 dynes/cm. This force will give a band in the neighborhood of 28μ for all our compounds. For the force of restitution due to a displacement perpendicular to the length of the chain we will take 0.12×10^5 dynes/cm. This value has been chosen more or less arbitrarily to fit the data. It is, however, of the same order of magnitude as the corresponding constants proposed by Andrews¹⁴ which range from 0.32 to 0.66×10^5 dynes/cm. It is to be noted that these constants are not forces of restitution due to a displacement along or perpendicular to the length of the valence bond itself, but are precisely as stated forces due to a displacement along or perpendicular to the length of the entire chain. The vibration of hydrogen against carbon has been neglected since others have shown that its effect is negligible.⁶

There seems to be no reliable method for computing the forces acting between the molecules in organic crystals. The Lindemann formula¹⁵ is strictly applicable to monatomic crystals, and Andrew's modification of it⁶ is of doubtful service here because of the high lack of symmetry of the chain molecules. The intermolecular forces have, therefore, been chosen arbitrarily. At low temperatures, 20°K , the internal vibrations have for the most part ceased to contribute to the specific heat. A Debye function has therefore been chosen to fit the data at this point. From the value of ν_0 so chosen it is possible to compute the corresponding force constant and the coupling coefficient d . This has been done.

The Debye function has been computed for three degrees of freedom, which assumes an isotropic crystal. The Einstein functions arising from the internal vibrations have been taken as having two degrees of freedom when the motion is perpendicular to the length of the chain, and one degree of freedom when along the length of the chain. The heat absorbed due to the expansion of the crystal has been computed according to Andrew's modification of Nernst's formula⁶

$$C_p - C_v = (C_v^2)_{\text{molecule}} \times \frac{T}{T_m} \times 0.0214$$

where $(C_v)_{\text{molecules}}$ is the specific heat at constant volume arising from the Debye terms alone, T is the temperature at which computations are being made and T_m is the melting point of the crystal under investigation.

Specific heat data are available for four of the normal alcohols. The computations have therefore been carried through for these substances. The frequencies found, neglecting the correction terms, as well as the total band width to be expected, expressed as percent of the corresponding uncorrected frequency, are summarized in Table I. In this table ν_0 represents the upper

¹⁴ J. R. Bates and D. H. Andrews, *Proc. Nat. Acad. Sci. (U.S.A.)*, **14**, No. 2, 124 (1928), D. H. Andrews, *Phys. Rev.* **34**, 1626 (1929).

¹⁵ F. A. Lindemann, *Phys. Zeits.* **11**, 609 (1910).

limit of the Debye terms, chosen arbitrarily to fit the data as stated above. The other frequencies, ν_1 , ν_2 , etc., represent the internal vibrations. The frequency bands, of width given by $\Delta\nu$, will always extend towards higher frequencies from the uncorrected frequency given in the table.

TABLE I.

	$10^{-11} \times$	ν_0	ν_1	ν_2	ν_3	ν_4	ν_5	ν_6
Methyl Alcohol	(Trans)	29	48					
	(Long)		277					
$\Delta\nu$ in %			0.6					
Ethyl Alcohol	(Trans)	25	35	60				
	(Long)		200	347				
$\Delta\nu$ in %			1.2	0.7				
Butyl Alcohol	(Trans)	48	22	41	57	67		
	(Long)		126	239	329	387		
$\Delta\nu$ in %			16	2.8	0.8	0.1		
Hexyl Alcohol	(Trans)	48	16	32	44	55	64	69
	(Long)		91	177	255	320	370	400
$\Delta\nu$ in %			36	6.4	2.3	1.0	0.4	0.1

Using these frequencies the calculations for ethyl alcohol give the following results, where $3D()$ represents a Debye function with 3 degrees of freedom, $1E()$ represents an Einstein function with 1 degree of freedom, etc.

TABLE II. *Ethyl alcohol*, $n=3$.

T°K	30	60	90	150
$3D(120/T)$	3.0	4.9	5.5	5.8
$1E(959/T)$	—	—	—	0.1
$1E(1660/T)$	—	—	—	—
$2E(166/T)$	0.5	2.2	3.0	3.6
$2E(288/T)$	—	0.8	1.8	2.9
C_v corr.	—	0.2	0.4	0.7
Total C_p , Cal/Mol	3.5	8.0	10.6	13.1

The computations for the other alcohols have been carried through and are plotted in Fig. 3, in which the solid lines represent the curves computed in the manner just indicated and the plotted points the observed values given by the authors indicated.

From the Debye functions chosen to fit the data at low temperatures we get values of ν_0 which give us values for the constant d for each substance in the manner indicated above. The results are as follows:

TABLE III.

Substance	No. groups	d
Methyl Alcohol	2	0.011
Ethyl Alcohol	3	0.012
Butyl Alcohol	5	0.070
Hexyl Alcohol	7	0.096

With the exception of ethyl alcohol the coupling coefficient varies approximately as the number of groups in the molecule. The low value of the coupling coefficient in the case of ethyl alcohol may have significance when considered in connection with the ease with which this substance forms glasses at low temperatures.

The agreement of the computed values with the observed values is as close as is to be expected, considering the very approximate nature of the calculations. There are, to be sure, no reasons for believing that these organic crystals are actually isotropic as has been assumed. Neither can we be particularly certain about the correction applied according to Nernst's formula for the conversion of C_v into C_p . The value of the constant 0.0214 was chosen originally to fit the data obtained in the case of certain metals and halogen salts,¹⁶ and we have no *a priori* reason for applying it directly

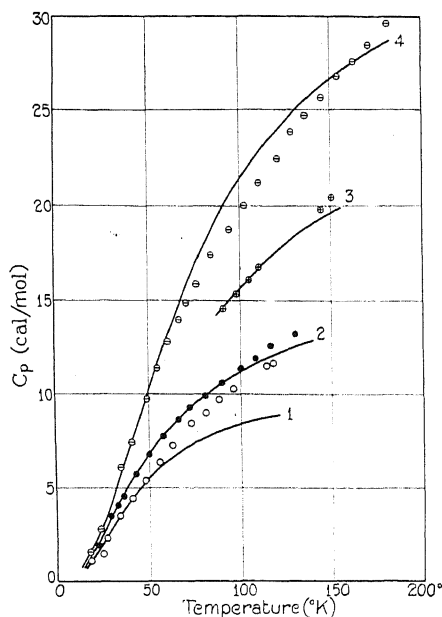


Fig. 3. C_p in cal/mol for the normal alcohols. (1) Methyl Alcohol K. K. Kelley, J. Amer. Chem. Soc. **51**, 180 (1929), (2) Ethyl Alcohol K. K. Kelley, J. Amer. Chem. Soc. **51**, 779 (1929), (3) Butyl Alcohol G. S. Parks, J. Amer. Chem. Soc. **47**, 338 (1925). (4) Hexyl Alcohol K. K. Kelley, J. Amer. Chem. Soc. **51**, 779 (1929).

to the case of organic crystals. Moreover these compounds have been treated as though each molecule was a uniformly loaded string which is actually not the case. The mass of the OH group is actually 17 as against 14 for the CH_2 group and 15 for the CH_3 group.

An additional remark should be made concerning the frequencies given in Table I. The values given under ν_0 , the upper limit of the Debye frequencies, have been chosen, as stated, to fit the data at 20°K and, so far as the comput-

¹⁶ W. Nernst and F. A. Lindemann, Zeit. f. Elektrochemie **17**, 818 (1911).

ations are concerned, may be looked upon as arbitrary constants. From these values of ν_0 values have been obtained for d which justify the original assumption that d is a small quantity. In the same way the absolute values of the frequencies of the internal vibrations are arbitrary, since the constant T/b was chosen more or less arbitrarily. These internal frequencies can therefore be considered significant only when taken in the ratio $\nu_1\nu_2\nu_3$ etc., or ν_1 (Methyl): ν_1 (Ethyl) etc. The results of applying Eqs. (27) to the computation of the specific heats of organic crystals are thus largely not characteristic of this paper. That is to say, for reasonable values of d , and within the limits of experimental error, Eqs. (27) indicate that the correction terms in the expressions for ν_{ks} are negligible, and the computation of the internal frequencies reverts to the well-known case of the uniformly loaded string with free ends.

No explanation is offered for the unusually high value of the specific heat of methyl alcohol as compared with the theoretical curve. On the other hand the manner in which the other experimental points have been reproduced by the theoretical curves is taken as evidence of the essential soundness of the underlying assumptions and calculations. If the data were available it would be highly desirable to carry through the corresponding calculations for the higher members of this or some similar series of compounds.

In conclusion the author wishes to acknowledge his indebtedness to Professor D. H. Andrews who originally suggested the problem and who has been most kind in discussing its details. The author is also indebted to Professor F. D. Murnaghan for valuable suggestions in connection with the mathematical treatment. Finally it is a pleasure to acknowledge the continual assistance of Professor K. F. Herzfeld under whose direction this paper was written.

STUDIES IN CONTACT RECTIFICATION. II. THE
CUPRIC SULFIDE-MAGNESIUM JUNCTION*BY MILTON BERGSTEIN, J. F. RINKE, AND C. M. GUTHEIL
RESEARCH LABORATORY, P. R. MALLORY AND CO., INC., INDIANAPOLIS, IND.

(Received June 19, 1930)

ABSTRACT

The commercial cupric sulfide magnesium junction consists of a disk of heat-treated, compressed cupric sulfide powder contacted under pressure with the suitably oxidized face of a magnesium disk. This rectifier is of the non-integral class and of the sulfide group. Oscillographic evidence indicates the formation of a film which possesses relatively high resistance to current flow from the magnesium to the cupric disk, slow partial destruction of the film on continued current flow in the opposite (low resistance) direction and "reformation" of the film within 0.004 sec when sufficient voltage is applied to send a current in the high resistance direction. Similar evidence indicates that there is no battery or thermoelectric effect within the junction of sufficient magnitude to account for rectification and that film "formation" and "destruction" are consequently electrothermic rather than electrolytic in origin. The phenomenon of "reverse rectification" is described. It is related to the a.c. voltage across the junction. Preliminary results for the relationship between efficiency and operating temperature of a bridge-type unit are in qualitative agreement with the theories which require film formation.

INTRODUCTION

A CONTACT rectifier is a device composed of dry dissimilar solids in good electrical contact through which current flows readily in one direction but not in the other. Contact detectors are of this class. They are merely small-current rectifiers. Rectifiers of the cupric sulfide-magnesium type and of the copper oxide-copper type are in commercial use for the rectification of large current at low voltages (usually below 120 volts). A cupric sulfide-magnesium rectifier unit of the bridge type may be made to output anywhere from 1 to 10 amperes d.c. using junctions of 0.515 sq. in. available area none of which are operated in parallel. The number of junctions used depends on the output voltage desired. The current density is higher in this type unit than in any other known commercial contact rectifier.

In a previous paper one of the authors¹ has divided rectifying junctions into general divisions according to mechanical structure and chemical constitution of the electro-negative member and has indicated what phenomena any accepted theory of contact rectification must at least qualitatively explain. Various fundamental mathematical theories² as well as

* Paper presented at the Washington meeting of the A. P. S., April 25, 1930.

¹ M. Bergstein, *Trans. Am. Electrochem. Soc.* **57**, Reprint 19 (1930)

² W. Schottky, *Zeits. f. Physik* **14**, 63 (1923), I. Stransky, *Zeits. Phys. Chem.* **113**, 131 (1925); R. Audubert and M. Quintin, *Compt. rend.* **188**, 52 (1929).

symbols of a more mechanical nature³ have been used to explain contact rectification. These latter depend on an analogy between contact rectifiers and electron tubes. The first theories proposed were based on a supposed thermoelectric or battery effect at the rectifying junction. These have been subjected to some criticism.⁴ Flowers⁵ favored a theory that a blocking film was alternately formed and destroyed on each half cycle and Goddard's⁶ experiments led him to the conclusion, in anticipation of the theories of Ruben and of Slepian,³ that film formation of some kind is a necessary corollary of contact rectification.

In work on the cupric sulfide-magnesium rectifier it became necessary to establish whether film formation within the junction between the members actually did take place, under what conditions, and in what time. The results of this investigation, and other previously unstudied phenomena of this rectifier junction also, are reported herein.

According to the classification already referred to,¹ the cupric sulfide-magnesium rectifier is of the non-integral class and the sulfide group.

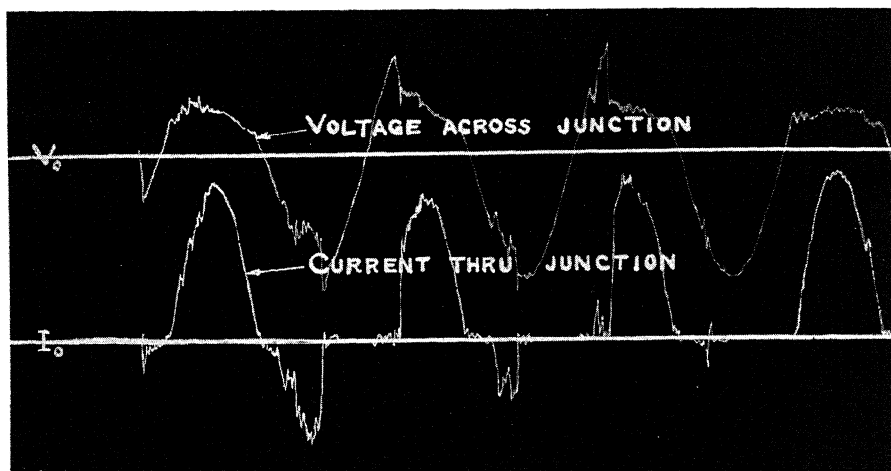


Fig. 1. Initiation of rectification.

EXPERIMENTAL

Nature of the rectifying junction. *Cupric sulfide disk.* The cupric sulfide disk (approximately 0.515 sq. in. in area) is prepared from compressed cupric sulfide powder which is subsequently heat treated to give a hard glassy mass and finally surface-ground to obtain a smooth finish.

³ S. Ruben, U. S. Pat. 1,751,361 (1930) (filed 1925), L. O. Grondahl, Science **64**, 306 (1926), J. Am. Inst. Elec. Eng. **46**, 215 (1927); J. Slepian, Trans. Am. Electrochem. Soc. **54**, 201 (1928).

⁴ F. Braun, Pogg. Ann. **153**, 566 (1874), Wied. Ann. **1**, 95 (1877); **4**, 476 (1878); G. W. Pierce, Phys. Rev. **29**, 478 (1909); Electrician **64**, 425 (1910).

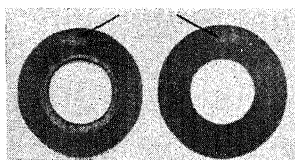
⁵ A. E. Flowers, Phys. Rev. **29**, 445 (1909).

⁶ R. H. Goddard, Phys. Rev. **34**, 423 (1912).

Particular care is taken in the heat treatment process to keep well below the dissociation temperature of cupric sulfide.

Magnesium disk. Pure magnesium strip of commerce is cleaned and mildly oxidized on the surface by one of a number of suitable processes either chemical or electrolytic. The nature of the oxidizing process is immaterial to this paper provided that a complete coat not so thick as to be too highly resistant be put on. The magnesium strip is subsequently cleaned on one face and punched into disks.

The junction. The oxidized surface of the magnesium disk is then contacted with one surface of the cupric sulfide disk and the two disks locked



CuS Mg
Fig. 2. Spots of adhesion.

together in a small vise under a pressure of several thousand pounds. The force required depends on the thickness of the oxide coat. When about 4 volts a.c. is applied to such a junction it attains rectifying properties in about the first four cycles as shown in the oscillogram of Fig. 1.

The direction of free passage of current is from cupric sulfide to magnesium. If the junction should now be removed from the vise, it is found

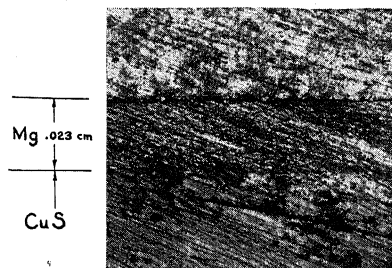


Fig. 3. Cross section of contact spot.

that the two disks are adherent and that the junction now has rectifying properties in spite of the removal of the pressure. If the two disks are pried apart, it is found that adhesion has occurred usually over a very small area. This is illustrated in Fig. 2 in which the points of adhesion on magnesium and cupric sulfide disks from the same junction are shown. If two such disks are again contacted with each other without the application of pressure, it is found that the junction is highly resistant and does not rectify. However, if pressure and voltage be applied as before, reformation takes place usually

at some others pot. In the adhesion between the two disks actual fusion takes place. As indicated in Fig. 3 the structures of both the magnesium and the cupric sulfide are considerably changed at the contact spot. We have shown that this spot is the only place where current flow actually takes place. The simple expedient employed was to cover all of the oxidized magnesium surface except one tiny spot with a coating of insulating varnish. A very small piece of lead was placed on the magnesium behind the clear

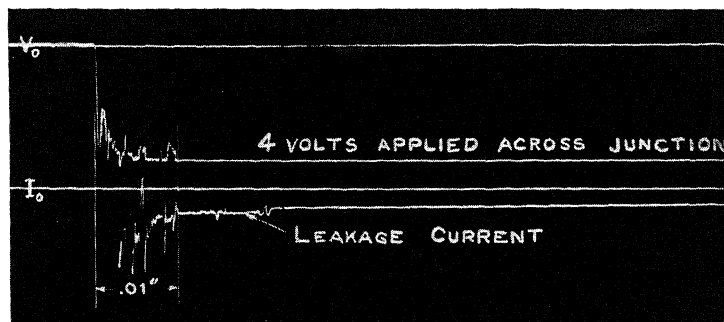


Fig. 4. d.c. formation of junction.

spot and the whole placed in a vise and assembled with a cupric sulfide disk as indicated above. The purpose of the lead was merely to deform the disk at the desired contact point and thus to effect contact with the cupric sulfide disk, which would have otherwise been separated from the magnesium disk by the thickness of the layer of varnish. It was found that a

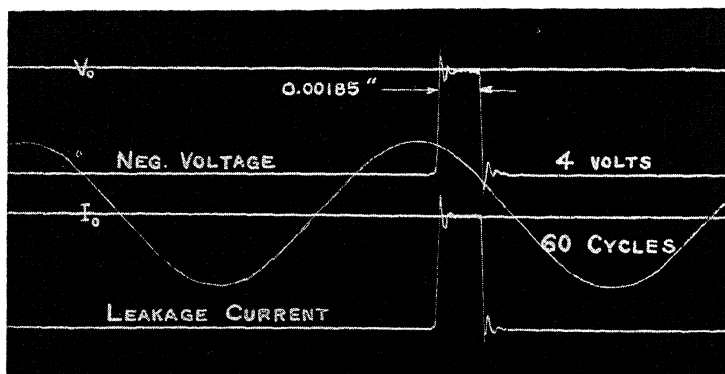


Fig. 5. Interruption in high resistance direction.

junction prepared in this way possessed substantially the same electrical characteristics as one prepared according to the standard practice thus establishing the fact that all the rectification and current flow takes place in the region of integral contact.

The film. Ruben³ has pointed out that the energy required for this "fusion" probably results from the I^2R loss in the oxide coating and that the

reaction results in the formation of a film to whose properties the behavior of the rectifier can be ascribed. Without examining any of the theoretical concepts involved we will here review the evidence we have accumulated indicating film formation.

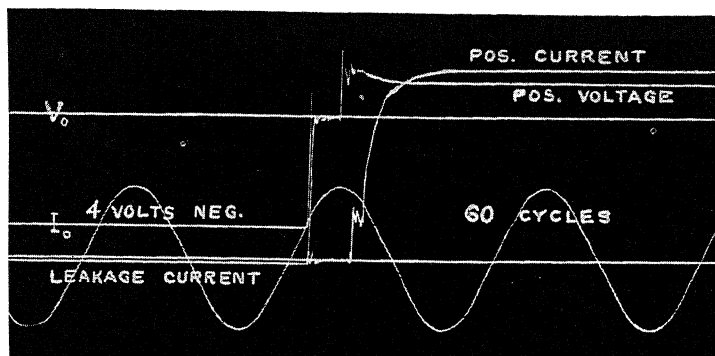


Fig. 6. Interruption in high resistance direction and reversal.

If, instead of applying a.c. to the unformed junction, approximately 4 volts d.c. is applied in the direction magnesium to cupric sulfide, the junction immediately becomes highly resistant in this direction and behaves as

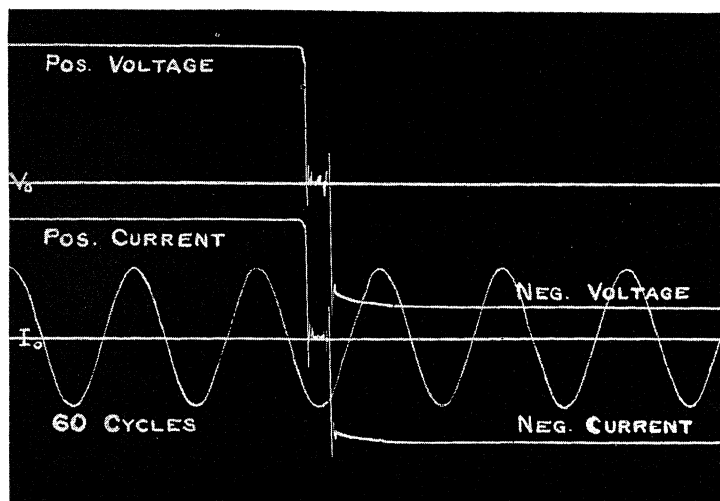


Fig. 7. Interruption in high resistance direction and reversal for cupric sulfide disk alone.

a normal rectifier when subsequently placed on a.c. The oscillogram of the development of this high resistance is shown in Fig. 4. Here we can observe that the resistance is initially extremely low but that in a period of approximately 0.02 sec. it increases to a value of the order of the final resistance in that direction.

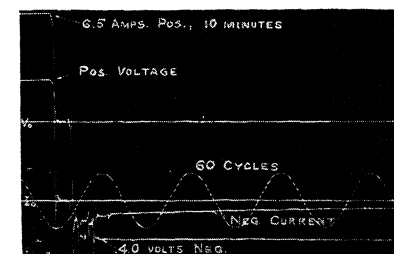
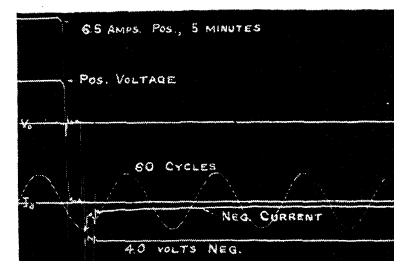
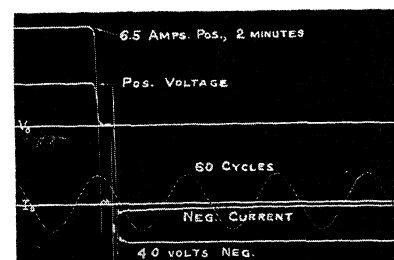
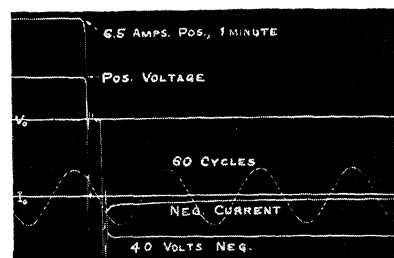
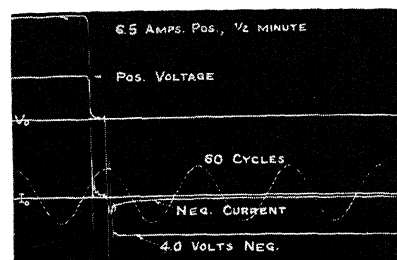
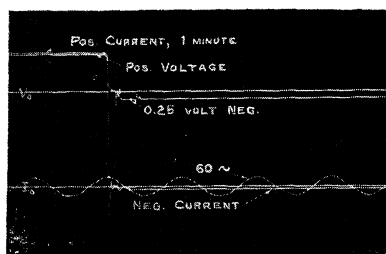
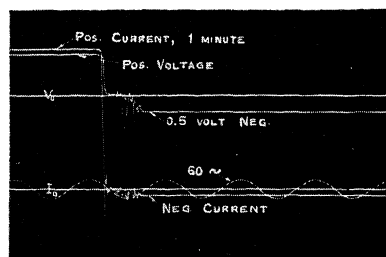
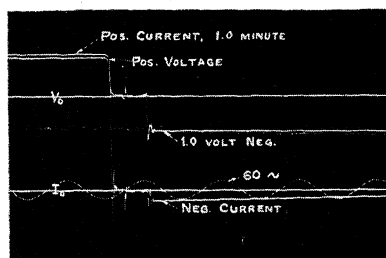
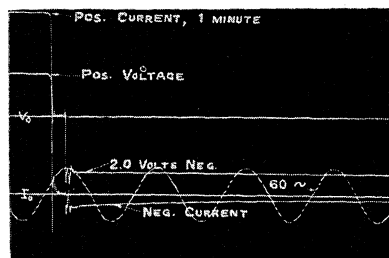
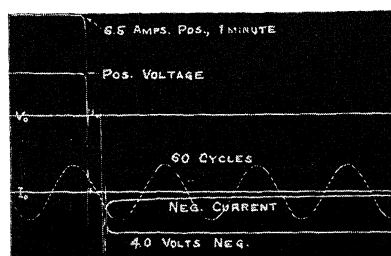


Fig. 8. Oscillograms of interruption and reversal after various periods of current flow in the low resistance direction.

Fig. 9. Oscillograms of interruption and reversal after identical periods of current flow in low resistance direction to varying direction.

This characteristic need not be ascribed to a film. It *must* be ascribed to the building up of a resistance and a film appears to be the only source of such resistance. In Fig. 5 we show an oscillogram of current flow in the high resistance direction momentarily interrupted. In this case there is no condition of building up of resistance. The current flow returns immediately to its former value on reclosing of the circuit indicating that whatever is responsible for the high resistance persists in its existence throughout the interval.

In Fig. 6 we show an oscillogram of current flow in the high resistance direction interrupted and reversed. The current does not rise to its maximum value at once on the reversal. About 0.005 sec. is required. However, as shown in Fig. 7, exactly the same phenomenon is observed for the cupric

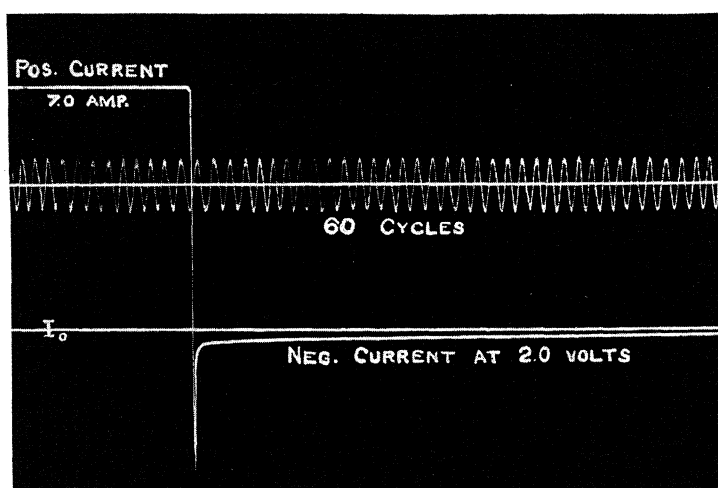


Fig. 10.⁷ Growth of resistance after reversal.

sulfide disk by itself between copper contacts. We would consequently be justified in saying that this oscillogram does not necessarily indicate destruction of the film lasting through that period of time. Indeed, the results obtained indicate that there is a gradual destruction of the film in a much longer time interval.

The method used in detecting this film destruction was: first, to form the junction by the regular method by applying an alternating current; second, to permit current to flow in the low resistance direction for varying periods of time; and third, to take an oscillogram at the moment of interruption and current reversal. In Fig. 8 is given a number of oscillograms taken after various periods of current flow in the low resistance direction. It is particularly notable as indicated by the increased time required to attain high resistance, that the apparent time of reformation of the film increases with the time that current has flown in the low resistance direction. Attention is pointed to the case of the unformed junction of Fig. 4 in which film for-

mation was even slower. In this case the complete interpretation of the succeeding figure in the next paragraph should be in point.

In Fig. 9 oscillograms are given for current reversals from low resistance to high resistance after identical periods of current flow but with varying voltage in the high resistance direction. The lower the voltage the longer is the time required for the high resistance to develop. This is exactly what would be expected if a definite amount of work be required to form a highly resistant intermediate layer. The oscillograms at 0.25 and 0.50 volts are, however, more difficult to explain. In these cases we do not have reformation of the film at all.

One possible interpretation of this phenomenon is that on current flow for any long time in the low resistance direction and destruction of the film small, complete, low resistance contacts are made between the cupric sulfide and the magnesium and that these contacts behave like fuses and can be "burned out" only at sufficiently high voltages. Only after "burning out" has occurred does film formation ensue. Indeed, all we may be observing in the apparent reformation of film may be "burning out" of the contacts. In Fig. 10 there is an oscillogram of a similar current reversal in which the recording film was revolved at lower speed. It can be seen that although the resistant film develops almost immediately it continues to "grow" through approximately 0.25 sec. Fig. 11 is a typical oscillogram indicating the opera-

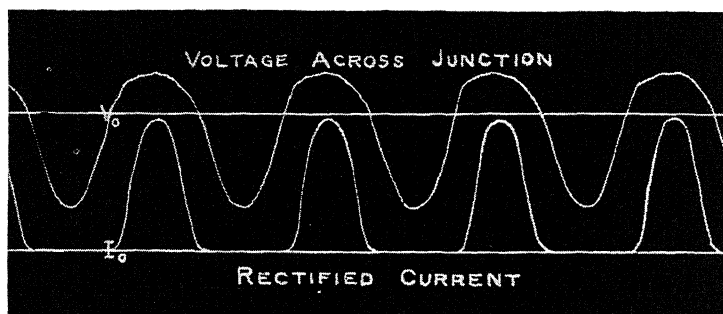


Fig. 11. Operation of a completely formed junction as a half-wave rectifier.

tion of a completely formed junction as a half-wave rectifier. In this illustration there is no sign of any destruction or reformation of a film in the time of a half-wave, but there is evidence that a certain critical voltage must be attained before current flow starts.

Battery and thermoelectric effects. The earliest explanations presented to explain contact rectification involved the propositions that rectification resulted because of a battery or thermoelectric effect within the junction. The first evidence contrary to this theory was presented by Braun,⁴ the discoverer of contact rectification. However, this theory is repeatedly reinvented for each new case of contact rectification and it is consequently necessary to examine the evidence in point that we have collected.

In Fig. 12 is illustrated in diagrammatic form the oscillograph circuit used for this study. V and A represent the voltage and amperage galvanometer vibrators in the oscillograph respectively. J represents the junction.

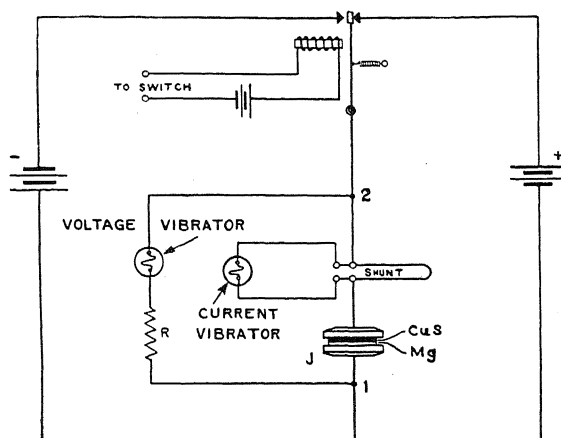


Fig. 12. Oscillograph circuit.

When current is flowing in the direction 1→2, the oscillograph can be adjusted so that the mirror displacements for V and A are in the same direction. If for any reason the circuit should be interrupted and there be a battery effect or thermoelectric effect opposed to the direction of the current, there should occur a reversal of the reading on A and a persistence of a deflection at V in the same direction as prior to the interruption. In other words, a reverse battery or thermoelectric effect will, on interruption of the

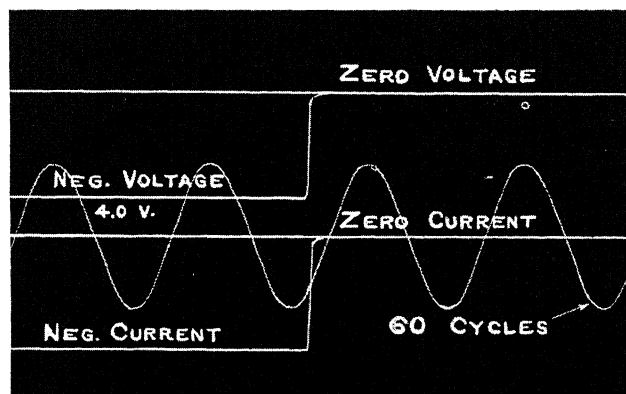


Fig. 13. Breaking circuit in high resistance direction.

circuit, give at least a momentary persistence of deflection of V . A failure to obtain this deflection, after interruption of the current in either direction, is indicated in Figs. 13 and 14. Particularly in the case of Fig. 13, where cur-

rent flow in the high resistance direction is interrupted, would this persistence of the voltage deflection be expected. The purpose of the oscillogram at *A* is merely to give an accurate indication of the time of interruption of

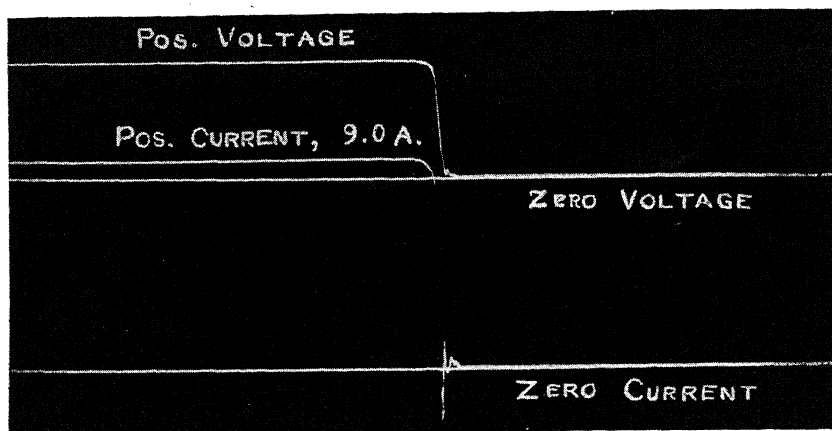


Fig. 14. Breaking circuit in low resistance direction.

the circuit. It is altogether possible that there may be a battery or thermoelectric effect of insufficient intensity to give an opposed deflection at *A*.

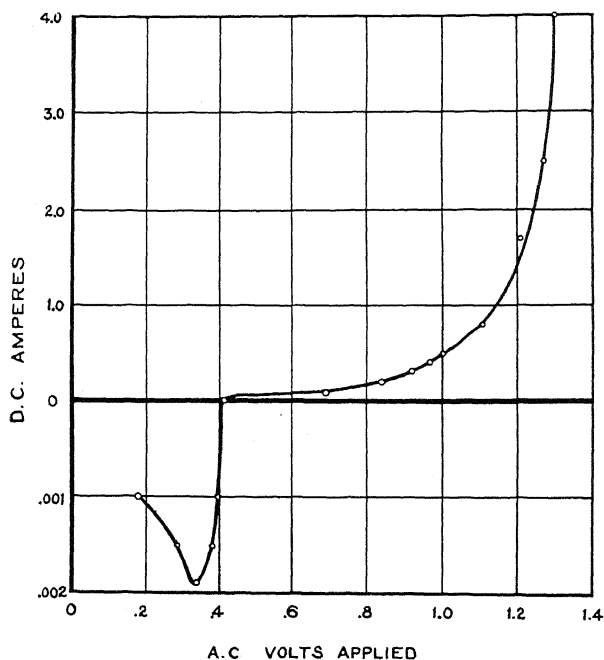


Fig. 15. Relation between d.c. amperes and impressed a.c. voltage.

The momentary opposed deflection on the current oscillograms of some figures at the moment of interruption is attributable to the inertial oscilla-

tion of the vibrator for it is similar in magnitude, direction, and period to the deflection on the voltmeter vibrator.

We may, therefore, conclude that there is no battery or thermoelectric effect in the cupric sulfide-magnesium junction of sufficient magnitude to account for its contact rectifying properties.

"Reverse rectification." The current efficiency of a rectifying junction has a theoretical maximum value for half-wave of 63.6 percent. It has been

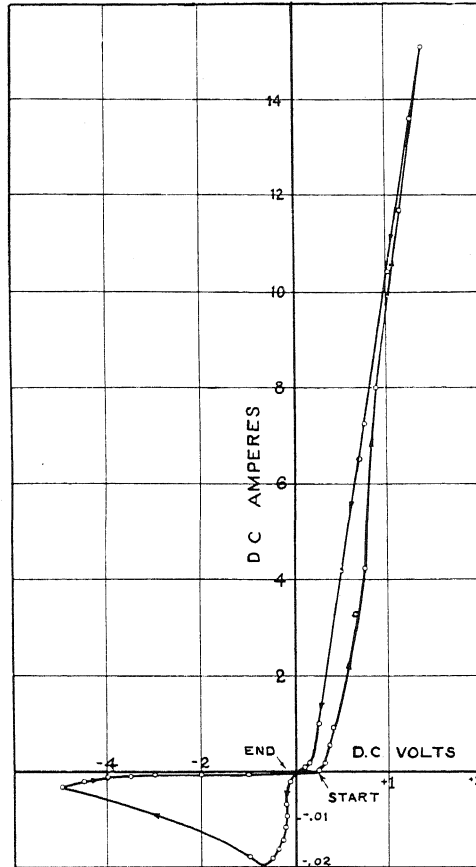


Fig. 16. Relation between d.c. amperes and impressed d.c. voltage.

known for some time that the current efficiency is a function of the applied a.c. voltage. For example, it is evident without any intimate knowledge of the properties of a rectifying junction that above some impressed voltage it will break down and cease to rectify. At that value it is obvious that the rectification efficiency is zero. It is not so well known that for some rectifiers the rectification efficiency decreases to zero at a small a.c. voltage. Goddard,⁶ among others has pointed out that the direction of rectified current is sometimes opposed to the direction predicted by experience for the junction studied. For example, if for the cupric sulfide-magnesium junction the

rectified current would flow in the direction magnesium to cupric sulfide, we would be observing the phenomenon of "reverse rectification." Tests that we have conducted indicate that the direction of rectification is related to the impressed voltage. The results are indicated in Fig. 15 in which we have illustrated a sharp reversal of current at approximately 0.4 volts a.c. A number of tests have indicated that the reversal always takes place in this region of voltage. It would be expected from this that the resistance of the junction would be lower at low negative voltages (i.e. from Mg to CuS) than at low positive voltages. This is verified by Fig. 16 in which the direction of taking current readings is indicated by arrows. In this figure also we may be impressed by the fact that there is an apparent destruction of a film which

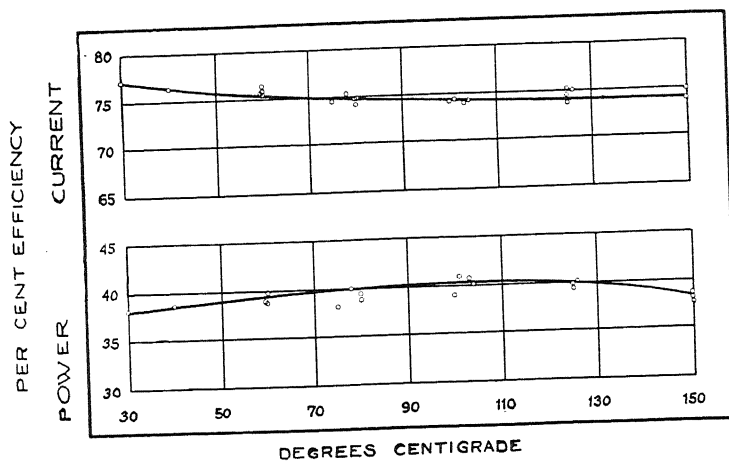


Fig. 17. Relation between efficiency of 4-junction bridge and temperature.

does not begin to reform until between -0.5 and -1.0 volts d.c. when reformation and negative increase of voltage are so rapid that no further readings are possible. This entire phenomenon is not made altogether clear in the light of the 0.25 and 0.50 volt oscillograms of Fig. 9 and the interpretation put on them. The conductive contacts, apparently, are of lower resistance than the film but we would expect them to carry current in both directions (if they do not "burn out") thus resulting in no rectification rather than in reverse rectification. The phenomenon will be subjected to further study.

Relationship between temperature and efficiency. The relationship between temperature and efficiency, for both power and current, is of great importance in the determination of the existence of a hypothetical film. Superficially, without too rigid analysis of the theories requiring the existence of a film in contact rectification, we may say that increase of temperature should be accompanied by lower current efficiency and, within limits, by higher power efficiency. A more detailed analysis of this aspect of the problem over a wide range of temperatures is reserved for a later paper. Fig. 17 indicates that this situation is true for a four junction bridge type rectifier.

The values graphed for power efficiency are arbitrary inasmuch as no correction has been applied for circuit conditions.

CONCLUSIONS

1. Oscillographic studies of the cupric sulfide-magnesium junction indicate film formation.
2. An explanation of the results obtained may be based on the hypothesis that "formation" of a film takes place on current flow in the high resistance direction and "destruction" on current flow in the low resistance direction for long intervals of times.
3. "Reverse rectification" is not easily explainable on any hypothesis so far presented. This problem is to be further studied.
4. The variation of efficiency of a bridge-type unit with temperature is in qualitative agreement with the requirements of theories that require film formation. This subject is to be discussed in greater detail in subsequent papers.
5. No battery or thermoelectric effect sufficient to account for the rectifying properties of the cupric sulfide-magnesium junction has been noted. It is consequently suggested that film formation and destruction are electrothermic rather than electrolytic in origin.

LETTERS TO THE EDITOR

Prompt publication of brief reports of important discoveries in physics may be secured by addressing them to this department. Closing dates for this department are, for the first issue of the month, the twenty-eighth of the preceding month; for the second issue, the thirteenth of the month. The Board of Editors does not hold itself responsible for the opinions expressed by the correspondents.

The Presence of Neutral Oxygen in the Gaseous Nebulae

The most stable configuration, s^2p^4 , of neutral oxygen gives rise to three terms, 3P , 1D and 1S . McLennan¹ has shown that the green auroral line corresponds to the $^1D-^1S$ transition. Recently Frerichs² by a very exhaustive analysis of the oxygen spectrum has been able to predict the positions of the $^3P_2-^1D$ and $^3P_1-^1D$ transitions at $6299 \pm 5\text{\AA}$ and $6363 \pm 5\text{\AA}$ respectively while a private communication to Dr. Frerichs from Professor Paschen states that he has found these lines in the laboratory at 6300.00\AA and 6363.86\AA .

Wright's³ list of nebular lines shows weak unidentified lines at 6302\AA and 6364\AA . In agreement with the corresponding transitions in O_{III} the $^3P_2-^1D$ line is two or three times as intense as the $^3P_1-^1D$ line. The general behavior of the lines in various nebulae is in agreement with this identification.

The question at once arises as to why the $^1D-^1S$ line alone occurs under auroral conditions while the $^3P-^1D$ lines alone appear in the nebulae. The theory of the transition probability⁴ due to quadrupole radiation (as these lines are "forbidden" by the ordinary selection rules no dipole radiation exists)⁵ shows that the mean life of the 1D state before transition to the 3P level is much longer, since it is an intercombination line, than that of the 1S state before transition to the 1D state. On the other hand the number of atoms reaching the 1S state is much less than that reaching the 1D state. This follows from the fact that nearly all of the atoms reaching the 1S state make the $^1D-^1S$ transition and thus arrive at the 1D state in addition to those that reach there directly. Since the 1D state has lower energy than the 1S state the number reaching it directly is also greater than that reaching the 1S directly.

Under nebular conditions the mean time between impacts with other atoms is large compared with even the longest of these mean lives and consequently the intensity of the lines is determined largely by the number of atoms reaching the respective upper states. Consequently we should expect the $^1D-^1S$ transition to be much weaker than the $^3P-^1D$ transition. This is verified by the observation that in O_{III} and N_{II} , which have the same set of low terms, the $^1D-^1S$ line is 1/20 to 1/50 as intense as the $^3P-^1D$ lines. A corresponding ratio in O_I would give the $^1D-^1S$ line at 5577\AA an intensity much below the limit that could have been observed, as the $^3P-^1D$ lines are fairly weak.

On the other hand under auroral condition the collisions between atoms are so frequent that the atom in the 1D is almost always taken out by a collision of the second kind before it can radiate the $^3P-^1D$ lines. The $^1D-^1S$ transition, however, has a high enough probability so that even under auroral conditions it can take place before a collision of the second kind removes the atom from the 1S state.

I. S. BOWEN

California Institute,
Pasadena,
July 19, 1930.

¹ McLennan, Proc. Roy. Soc. A120, 327 (1928).

² Frerichs, Phys. Rev. in press.

³ Wright, Studies of the Nebulae, Lick Observatory, p. 242.

⁴ Huff and Houstoun, Phys. Rev. in press.

⁵ Frerichs and Campbell, Phys. Rev. 36, 151 (1930).

Photoelectric Outgassing

While attempting to study the photoelectric emission from the two sides of an unbacked film of gold, 2×10^{-6} cm thick, it was found that the emission did not hold constant but increased with exposure to ultraviolet. With 360 hours of exposure of the film to ultraviolet the photo-current from the side where the light was incident increased 136 fold and at the same time the long wave limit shifted from 2000A to 2537A.

The emission from the unexposed face increased, in the first 50 hours, about one tenth as much as from the exposed face. It was found that the film was transmitting down to a wave-length of 2259A but only about 10 percent of the energy in the lines below 2537A was being transmitted. On exposure of the second face to the direct radiation of the arc its emission increased as in the case of the first face.

It was found that with the film charged positively, so that the electrons returned to the film after being ejected, the increase in emission was more rapid and the long wave limit shift was greater than when the film was charged negatively. In either case, when the film was exposed through a filter which absorbed all wave-lengths below 2800A but transmitted 55 percent of the total energy of the arc, there was no increase in emission.

A plate of solid gold was treated in like fashion and showed a similar increase in photo-current, which took place much more slowly, accompanied by a shift in long wave limit from about 2000A to 2482A.

At intervals during the exposure of the

specimen to ultraviolet fatigue curves, taken by leaving the specimen in a vacuum of 10^{-7} mm of Hg unexposed, showed during the first stages a rapid decrease in photo-current with time of standing, but, after 360 hours of exposure for the film and 160 hours for the solid gold, the photo-current from the former held constant for 3 hours, and from the latter $1\frac{1}{2}$ hours. This seemed to indicate that a fairly stable equilibrium had been reached, and the subsequent fatigue was consistent with the idea that it was due to return of gas to the surface.

The experiment was repeated, using a silver filament approximately 0.025 mm thick, and an increase in emission comparable to that for the gold film was obtained.

The probable explanation is that photoelectrons, both when ejected and returned to the surface by a reverse field, remove adsorbed gas from the surface.

Millikan¹ noted an increase in photoelectric emission on exposure of certain metals to ultraviolet, but did not note the corresponding change in long wave-length limit or that the photoelectrons themselves apparently play an important part in the outgassing.

Work is being carried forward testing this explanation and obtaining more data on photoelectric properties of thin films.

RALPH P. WINCH

Laboratory of Physics,
University of Wisconsin,
Madison, Wisconsin,
July 15, 1930.

Millikan, Phys. Rev. 29, 85 (1909).

Effect of the Earth's Electric and Magnetic Fields on Ions in the Atmosphere

In a recent letter¹ Hulburt has pointed out that the westward drift of ions in the upper atmosphere predicted in a previous paper of the writer² would be prevented by collisions of ions with neutral particles which partake of the earth's rotation. The predicted westward drift was obtained by neglecting the effect of collisions; it remains to consider the modifications of the theory necessitated by taking account of the effect of collisions of ions with neutral particles which rotate with the earth. A little consideration seems to show that the steady-state solution of the problem cannot be anything else than that

contained on page 830 of the paper² already referred to, where three regions were considered, (1) the interior of the earth, (2) the lower conducting atmosphere, (3) the upper atmosphere. The argument is as follows, references being to the May 1929 paper.²

1. Consider first an atmosphere containing no ions. This is the case treated on page 827. As there are no charges in the atmosphere, the potential outside the earth must be a solution of Laplace's equation relative to non-rotating observers, and the components of electric intensity relative to observers on the surface of the earth are given by (14).

It is evident that E_r' is upward (since M is negative) for $r > a$ at all latitudes and E_θ' is directed from the equator toward the poles.

2. Now suppose a few ions to be produced or injected into the earth's atmosphere. They tend to assume a westward drift, but, as Hulburt points out, collisions with neutral molecules interfere with this drift, causing a current in the direction of the electric field. The writer has already investigated the conductivities parallel and at right angles to the field in some detail.³ This current carries negative ions downward and toward the equator, and positive ions upward and toward the poles, and if the supply of ions is sufficient charges are produced just sufficient to annul the electric field relative to an observer at rest on the surface of the earth. No matter how long the mean free paths and how few the collisions this annulment of the electric field must take place after a sufficient lapse of time.

3. Finally, then, we must have the situation expressed by the equations on page 830, the radius b , however, being that of the outermost limit of the ionized atmosphere. On the surface of the earth we have the negative charge σ_{12} increasing from 0 at the poles to a maximum at the equator. The potential throughout the ionized atmosphere is given by V_2 . The atmosphere contains the volume charge ρ_2 which is positive over the poles and negative over the equator. The total charge in a spherical shell of radii r_1 and r_2 is zero, the volume charge being due merely to a separation of positive ions which have been urged poleward from negative ions which have been urged equatorward. The volume charge ρ_2 decreases in magnitude as the altitude increases, varying inversely with r^3 . Finally at the top of the ionized atmosphere is the surface charge σ_{23} , positive over the poles and zero at the equator. Outside the ionized atmosphere the potential is given by V_3 .

4. Now consider ions produced anywhere

in the ionized atmosphere ($r < b$). They suffer no drift at all due to the electric field, and rotate with the earth in so far as this effect is concerned. The gravitational drift is all that is left.

5. The case is different with ions reaching the earth from outside. So long as they are outside the ionized atmosphere they suffer the electrical drift (16) with a replaced by b . But when they begin to suffer collisions with air molecules the ions of opposite sign are separated just as in paragraph (2). The negative ones move downward annulling the surface charge σ_{23} , whereas the positive ones move upward and poleward. Effectively, then, the surface charge σ_{23} is raised and b is made larger.

6. Now suppose that ions disappear from the uppermost region of the atmosphere during the night. Then the upper limit of region (2) is depressed, that is, b becomes less. If after sunrise new ions are produced in the upper atmosphere outside the region (2) and in the region (3) which had lost its charge during the night, these new ions start drifting westward but collisions with neutral molecules cause the positives to move polewards and the negatives equatorwards as in paragraph (5). In this way the upper limit of region (2) is raised, b becoming greater.

7. It would seem, then, that ions produced in the portion of the atmosphere which is already ionized should experience no electrical drift relative to the rotating earth. Only those ions which come into the earth's atmosphere from outside or which are produced above the ionized region should suffer the westward drift, and this they should lose in time as a result of collisions.

LEIGH PAGE

Sloane Physics Laboratory,

Yale University,

July 14, 1930.

¹ Hulburt, Phys. Rev. 35, 1587 (1930).

² Phys. Rev. 33, 823 (1929).

³ Phys. Rev. 34, 763 (1929).

Note on Wave-Lengths in the Vacuum Copper Arc

Some months previous to publication, Dr. Kievin Burns sent me for criticism a typed copy of the paper "Wave-Lengths in the Spectra of the Vacuum Copper Arc" by Burns and Walters, publication of the Allegheny Observatory, Vol. VIII, No. 3. I did not fulfill my obligations as a critic

properly, for I failed to detect until recently, a rather important error which should have been obvious to me because of my previous work on the copper spark.

Burns and Walters wave-length determinations were made by the usual interferometer method which involves a preliminary wave-

length obtained from some other measurement. The preliminary wave-lengths used for Cu II lines were those given in the tables of spark spectra. Such a choice is perfectly right for low level spark lines, but unfortunately introduces an error of about 2.7 wave numbers into the results for all high level lines, since they appear with approximately that much greater wave number in arc exposures.

The authors of the paper intend to print a corrected list; but, in the meantime, it should be noted that the wave-numbers of all lines involving b^3D and b^1D of Cu II should be increased by approximately 2.7

cm^{-1} . These lines are useful as standards when they are produced in an arc, but not when the source is a spark. In the latter case they are diffuse and displaced to longer wave-length.

The great accuracy of the determination of the sharp lines of Cu II in the ultraviolet will be a boon to spectroscopists because those lines are by far the most useful as standards of measurement in the region $\lambda 2400$ – $\lambda 1940$.

A. G. SHENSTONE

Palmer Physical Laboratory,
Princeton University,
July 15, 1930.

The Electrolytic Dissociation of Nitric Acid as Revealed by its Infrared Absorption Spectrum

I. R. Rao has recently published an important paper in the Proceedings of the Royal Society (A127, 279, 1930) in which he describes a new method of estimating the percent dissociation of electrolytes. He has obtained relative values for the percent dissociation of nitric acid in solutions of varying concentration, which for the first time are independent of assumptions regarding the mobility of the ions. The method, which makes use of intensity studies of a Raman line scattered from water solutions of the acid and attributed to the NO_3 ion, was suggested by the earlier observations of Rao (Nature 124, 762, 1929), and independently by the observations of one of us (Phys. Rev. 35, 284, 1930), that large intensity shifts occurred in the Raman scattered lines as the acid was diluted, the presumption being that the lines which grew in intensity upon dilution arose from the NO_3 ion. Although most of this earlier work upon the Raman spectra was done by one of us in the months of April and May, 1929, publication was delayed until Rao's account of nearly identical results, in Nature, stimulated a short report in the February Physical Review. It was of course obvious that studies of the infrared absorption spectrum of the acid solutions should be made. These were begun and are still in progress. Since the work is being interrupted for a brief period, a short account of the results obtained so far seems advisable.

Records of the absorption of the acid solutions of varying concentration and of the fuming acid which contained about 5 percent water were taken on the self-recording quartz spectrograph described by one of us

elsewhere some years ago. The unexpected result obtained was that all the water solutions investigated, even the 70 percent commercial concentrated acid, in the region studied (2.4μ – 0.78μ), showed only bands which are unquestionably the water bands considerably sharpened and shifted slightly toward shorter wave-lengths, a circumstance which will be discussed in another place. It was only in the fuming acid that new strong maxima appeared which we attribute to the undissociated HNO_3 molecule. Absorption cells varying from less than 1 mm in length up to 10 cm have been employed. It is apparent that the concentration of the entity giving rise to these new maxima, which we believe to be the undissociated HNO_3 molecule, has been enormously reduced in as concentrated a solution as the 70 percent acid, reduced to a point where a column of the 70 percent acid 10 cm long showed no trace of the new maxima.

The bands in the fuming acid have been grouped into three sets, (1) a set of two due to water at 1.42μ and 0.96μ (2) a set of three which fit an anharmonic formula and extrapolate to a fundamental at 2.85μ of wave-lengths 1.47μ , 1.01μ , 0.78μ , and (3) a set of two at 2.12μ and 1.25μ which are interpreted as combinations between a fundamental observed in the Raman effect and bands of the anharmonic series. Others have appeared of whose nature it is yet too early to speak. Records of the acid vapor have been taken also as well as records of the 70 percent acid in which oxides of nitrogen have been dissolved. The vapor records exhibited, among other groups, a group forming an anharmonic

series which we believe to be the same as the series found in the liquid acid, but with every band characteristically shifted toward shorter wave-lengths. This matter is being investigated further. The records of the acid solutions of the nitrogen oxides show no trace of the fuming acid bands, a fact which indicates that these bands are not due to dissolved oxides of nitrogen. In regard to the anharmonic series found in the fuming acid, it is worth noting that the extrapolated fundamental at 2.85μ does not correspond to any fundamental yet observed by means of the

Raman effect. Rao reports a band at 3.01μ , but even this has repeatedly failed to appear on plates taken by one of us.

It is hoped that a fuller discussion can be given during the autumn months after experiments, which have been interrupted, are completed.

E. L. KINSEY
J. W. ELLIS

University of California at Los Angeles,
Los Angeles, California.

July 9, 1930.

The Optical Excitation Function of Helium

I have just completed a study of the optical excitation function of helium under conditions which permitted, simultaneously, a study of the electrical conditions in the discharge tube and a determination of the intensities. A new variation of the photographic method has been used for the measurement of the intensities, and the discharge tube has been designed with a view to the elimination of secondary electron emission and of ionization affects. Due to this design, and to a thorough cleaning of the electrodes, the dependence of intensity on either current or pressure is linear indicating that there is no ion current. In earlier work, this linearity has been expected but not obtained.

The results for the singlet system are largely in accord with those obtained by Elenbaas¹ and Hanle.² For the triplets, double maxima as reported by Elenbaas, have been found, although the location of these maxima differs somewhat from that previously found. This disagreement is particularly pronounced in

the case of the first maxima, which Elenbaas and Hanle both found in the region between 25 and 35 volts. With the present apparatus these maxima occur at approximately 28 volts and it has been possible to correct their position and shape in accordance with the experimentally determined velocity distribution curve of the electrons and the linear relation between current and intensity. This correction shows that the maxima are actually located at the excitation potentials and are of much greater height compared with the background than the experimental curves, without correction, would indicate.

A full report on the apparatus and results will be published in the near future.

WALTER C. MICHELS.

Norman Bridge Laboratory of Physics,
Calif. Institute of Technology,
Pasadena, California.

July 11, 1930.

¹ Elenbaas, *Zeits. f. Physik* 59, 289 (1930).

² Hanle, *Zeits. f. Physik* 56, 94 (1929).

Metastable Atoms and Electrons Produced by Resonance Radiation in Neon

In studies of arcs in pure neon at a few millimeters pressure, we have observed some phenomena which indicate that the resonance radiation from the arc can travel through the un-ionized neon beyond the end of the arc for distances of 20 to 30 centimeters, or more, and the absorption of this radiation produces, by excitation of the gas and by subsequent collisions of the second kind, metastable atoms at the rate of at least 10^{13} cm⁻³ sec⁻¹. In these experiments the neon arc carrying currents of approximately one ampere was passed through a long tube between a hot cathode at one end of the tube and an anode

placed near the center. One or more collecting electrodes were placed in the tube beyond the end of the arc, and, in some experiments, movable collectors were used whose distance from the end of the arc could be varied.

The metastable atoms thus produced beyond the end of the arc diffuse into contact with the walls or with metallic electrodes and liberate electrons from the glass or metal surfaces which have velocities of the order of 5 or 10 volts. The walls thus become positively charged and within the space there is a definite concentration of electrons. If a collector is maintained at, say, 70 volts

negative with respect to the anode, the electrons emitted by it serve as a measure of the concentration of the metastable atoms. The concentration of metastable atoms diffusing out of the arc should fall to $1/e^{\text{th}}$ of its value every time the distance is increased by an amount equal to 0.4 of the radius of the tube. Within a few centimeters of the end of the arc this theoretical decrement is actually observed, but at greater distances the concentration of metastable atoms decreases far more slowly.

The width of the line corresponding to the resonance radiation in the arc is far greater than that of the absorption line in the unexcited neon, which is determined mainly by the Doppler effect. Assuming this cause of broadening of the absorption line, it can be calculated that between parallel planes the energy absorbed per unit volume in the gas is inversely proportional to the distance from the source and thus, as the end of the arc is approximately a point source of this radiation, the rate of production of metastable atoms should vary approximately inversely as the cube of the distance from the end of the arc. The observed values are in accord with this theory.

The electrons in the tube generated at the walls by the metastable atoms give to the neon a conductivity whose value can be measured, and from the known mobility of the electrons in neon gas, the concentration of electrons can be calculated. For low voltages on the collectors, the currents are determined solely by this mobility of the electrons, and the volt ampere characteristics for small currents are thus linear on both sides of the zero point. For larger negative voltages, the current becomes limited by the number of electrons that can escape from the collector. For sufficient positive voltages, the currents increase more rapidly than corresponds to the linear relationships, this being due to ions produced within the tube by the acceleration of the electrons. The experiments prove that these ions are produced by the ionization of metastable atoms rather than normal atoms, for the rate of production of ions varies approximately with the square of the light intensity. These conclusions are confirmed by experiments with a shutter placed beyond the end of the arc, which can cut off the radiation without interfering with the diffusion of

atoms, ions, etc., past the shutter. It is thus proved that the production of metastable atoms is produced by light which travels only in straight lines. The fact that when the collector is positive the electron currents are also proportional to the light intensity proves that the electrons owe their origin not to photoelectric effect from the electrodes, but to the production of metastable atoms or excited atoms. Small disk-shaped collectors have also been used in which one side, which faces the source of resonance radiation, is covered with mica so that the exposed surface cannot receive radiation, and yet the electron current was nearly as great as if the mica were placed on the back side of the collector, proving that the electron currents are generated by metastable atoms which diffuse short distances to the electrode even when the resonance radiation does not reach the electrode itself.

Since the electrons emitted by the collectors possess considerable initial velocities, and since these electrons make elastic collisions with the neon atoms, it is impossible to obtain a saturation current from these electrodes at these gas pressures, for electrons which diffuse back to the electrodes have sufficient energy to be reabsorbed by it. A theoretical investigation shows that in this case the current i_x that flows between any two electrodes is given by the equation,

$$i_x = \frac{16\pi}{3} I_0 \lambda C(V/V_0) \frac{1}{\log(1 + V/V_0)}$$

where V is the potential difference between the electrodes, V_0 is the volt equivalent of the velocity with which the electrons are emitted from the cathode, I_0 is the theoretical saturation current density of the electrons emitted from the cathode, λ is the mean free path of electrons, and C is the electrostatic capacitance between the two electrodes (expressed in centimeters). Experiments show that this equation expresses well the volt ampere characteristics of neighboring electrodes in neon exposed to resonance radiation.

IRVING LANGMUIR
CLIFTON G. FOUNDT

Research Laboratory,
General Electric Company,
Schenectady, New York,
July 9, 1930.

On the Magnetic Deflection of Cosmic Rays

In a recent letter to this section, L. M. Mott-Smith¹ proposed an experiment for deflecting the cosmic rays in a magnetic field which made use of the magnetic induction in the inside of a magnetized iron bar.

This experiment has recently been performed by the writer, using identically the same arrangement and has been shortly described in "Rendicouti della R. Accademia Naxionale dei Lincei", Vol. XI, p. 478, March 1930.

Due to the exceedingly small frequency of coincidences, it was not possible during this first experiment to attain such an accuracy that the expected effect of electrons having a velocity of 10^9 volts lay outside of the average error. A new and more complete experimental set-up is at present under construction and will allow the application of the old method, as well as of a new method (for which Prof. Puccianti is to be thanked). The latter is based on the following principle. Above and below two oppositely magnetized iron bars, which lie close to each other in a horizontal plane, there are placed two counters with their axes parallel to the direction of magnetization. The electrons, passing through the upper counter will be either concentrated upon or deflected away from the lower counter, depending on the direction of magnetization.

Calculation has shown that, for a given size and separation of the counting-tubes, a much larger effect is to be expected from the latter method than from the former.

Moreover, for the explanation of such experiments, there are certain difficulties, which I (as well as L. M. Mott-Smith) did not consider at first. Namely, although the induction represents the average value of the microscopic magnetic field strength, it is probably not allowable *a priori* to assume that this average value is the true value which causes the electron deviation. An exact theoretical treatment of the problem has not been presented.

If the primary cosmic rays are an electron radiation, then (as has already been noted)² the earth's magnetic field must also be considered. The effect of the earth's field should be noticeable by an unsymmetric directional distribution of the intensity with respect to the perpendicular. Experiments are being prepared which will test such an effect.

Let us call V the velocity of the electrons in volts, R the earth's radius, M the magnetic moment of the earth, λ the magnetic latitude at the point of observation, θ the angle between the plane of the magnetic meridian and the direction of the path of the electrons (positive toward the east), a a constant, whose value is approximately 3×10^2 . Then the theory gives the following results. Electrons may impinge at a definite point of the earth's surface (when $V < aM/R^2$) only if the angle θ satisfies the following inequality:

$$\sin \theta > \frac{aM}{R^2 V} \cos \lambda - \left(\frac{aM}{R^2 V} \right)^{1/2} \frac{2}{\cos \lambda}$$

For example at a point where the magnetic latitude is $\lambda = 45^\circ$, if $(aM/R^2 V) = 16$ the above condition shows $\sin \theta > 0$. This means that the whole region west of the magnetic meridian is "in shadow". This case comes into consideration for electrons having a velocity of about 4.3×10^9 volt.

If $(aM/R^2 V) \cos \lambda - (aM/R^2 V)^{1/2} 2/\cos \lambda > 1$ the above inequality has no solution. This means that electrons can never impinge upon the point under consideration.

Here, however, diffusion and loss of velocity in the earth's atmosphere have not been taken into account.

BRUNO ROSSI

Physikalisch-Technische Reichsanstalt,
Charlottenburg, Berlin, Germany.

July 3, 1930.

¹ L. M. Mott-Smith, Phys. Rev. 35, 1125 (1930).

² Bothe u. Kolhörster, Das Wesen der Höhenstrahlung Zeits. f. Physik 56, 489 (1929).

BOOK REVIEWS

Structure of Line Spectra. PAULING AND GOUDSMIT. Pp. 263, figs. 68. McGraw-Hill Book Company, New York, 1930. Price \$3.50.

Goudsmit has often expressed the well-founded opinion that the phenomenally rapid rise of the Bohr theory was due more to the enthusiastic optimism of Sommerfeld than to the brilliancy of Bohr. The exposition of the Bohr-Hund theory that Pauling and he have given recently in their book, "Structure of Line Spectra," shows very markedly their conviction that optimism is also the proper treatment for a theory even when it is as fully developed as the Hund theory now is. I think most physicists will disagree with that idea. A severely critical attitude toward an established theory is much more apt to stimulate the increasingly difficult investigations which are necessary as the theory advances. The book under review will not accomplish that purpose for it leaves one with the impression that here is a practically closed chapter of physics. It seems regrettable that the authors have adopted such an attitude.

It is well known that the wave mechanics gives all the ordinary rules of spectra correctly, but it is also well known that most physicists would find it impossible to grasp the theory of spectra if it were presented solely as a problem in wave mechanics. The authors have wisely chosen to base their discussion on a vector model which can be easily visualized and which represents reasonably well the phenomena which can only be exactly described in terms of the quantum mechanics. Wherever necessary, the more correct methods and results of the mechanics are introduced, and references are made to the discussions of the same problems in Condon and Morse's "Quantum Mechanics."

The material is excellently arranged and is very lucidly explained. Goudsmit has always used the simplest methods to great advantage in his original papers, and the experimental spectroscopist will be grateful that that simplicity rules in this book. Particularly well-done is the discussion of hyperfine structure, which has recently assumed such importance. Goudsmit has been the leader in that part of the subject, and we can confidently expect him eventually to clear up the rather grave difficulties which, as he points out, still remain.

But, excellent as is this book, I cannot help regretting that the authors have not seen fit to make it a much more complete description of the theory and material of the subject. In many ways it falls behind Hund's "Linienpektren" published in 1927, particularly in the discussion of the relations between complicated spectra. Russell's papers on the energy of removal of electrons from various types of structure are very important for the understanding of spectra, but no discussion of such matters, nor of the limits of series in complicated cases, is given. The latter point should have been considered, if only because Hund's book contains erroneous conclusions.

It is worth drawing attention to the following statements which I believe are inaccurate or misleading. On page 71, Preston's rule for the Zeeman effect of series is stated without any qualification. That rule is true for the special case dealt with but is not generally true. On page 91, it is stated that all the symbols down to Z are needed to account for *observed* spectra. That is yet to be proved. On page 94, it is stated that triplet singlet combinations will "usually" appear not at all or with small intensities. The accuracy of that statement depends upon one's definition of "usually." Considering the authors of this book, the statement on page 98 is strange, "Thus $^3S-^3P$ consists of two lines $^3S_1-^3P_0$ and $^3S_1-^3P_2$." It is noted on page 139 that the intensity ratio for the combination $^2S-^2P$ is well verified by experiment on the sodium D -lines, but no mention is made that experiments on other similar pairs of lines disagree radically with the theory. On page 166 there are given rules governing the positions of terms within a configuration. Those rules are in reality fulfilled rather seldom except for the lightest atoms. One of the outstanding difficulties of interpretation is in direct violation i.e. the existence of inverted doublets in alkali spectra. This is not mentioned.

It is unfortunate that the authors did not choose to follow the recently accepted notation in which capital letters are used for the resultant quantum vectors of the atom.

Pauling and Goudsmit have written in this book an excellent account of the explanation of line spectra; but their optimistic attitude has prevented them from making it the complete account that many of us were expecting and that they are quite capable of giving.

A. G. SHENSTONE

The Analytical Expression of the Results of the Theory of Space Groups. RALPH W. G. WYCKOFF. 2nd edit. Pp. 239, figs. 222. Paper covers. Carnegie Institution of Washington 1930.

The first edition has long been out of print and in much demand, so that a simple reprinting would have met a very real need. The second edition, however, does far more than meet this need. The text has been completely rewritten in a more logical manner and, in most instances, with greater lucidity. The only additions here which are of doubtful value are the too greatly abbreviated discussions of the new space-group symbols of Hermann. Mere insertion of these symbols, and reference to the extensive original papers, would have been adequate. An important addition to the tables (132 pp.) of equivalent point coordinates and sub-groups for the 230 space-groups is the series of 200 well-planned and carefully drawn diagrams showing the *special* point-positions for all distinguishable cases. Drawings which show the distribution of symmetry-elements and *general* point-positions are available elsewhere, but these new diagrams with the information on sub-group symmetry contained in their captions, should be of great service in the solution of crystal structures by x-ray methods. The text diagrams are not quite as well drawn as those just mentioned. The original edition was remarkably free from errors. All the serious misprints known to the reviewer have been corrected in the new edition and in the parts newly set (the principal tables were copied photographically) only three trivial mistakes, easily corrected by the casual reader, have been noted in a rather careful survey. The author has always been a stickler for accuracy and has here upheld his principles to the letter.

L. W. MCKEEHAN

Das Ultrarote Spektrum. CL. SCHAEFER AND F. MATOSSÌ. Struktur der Materie X, Pp. 400, figs. 161, Julius Springer, Berlin, 1930. Price bound, R M 29.80.

Those interested in infrared spectroscopy have been very much pleased that during the past year and a half three excellent books have appeared on the subject. While each of the three has had its particular virtues, the volume by Schaefer and Matossi, the tenth of the Struktur der Materie monographs, is perhaps the most comprehensive and will be found to be the most generally useful.

The authors have devoted their first chapter to a careful description of the methods and instruments used in the measurement of infrared spectra. The second chapter deals with the source of infrared radiation, the hot body, and here the laws of black body radiation are given, as well as the measurements of actual hot bodies. The next chapter contains an account of the application of Maxwell theory and the manner in which the electrical and spectroscopic constants of a substance are related. The theory of the grating is also discussed.

The fourth chapter, of over a hundred and twenty pages, deals with the infrared spectra of gases and fluids. Following an exposition of the experimental methods, the authors develop the theory of the diatomic rotator-vibrator both by means of the classical and the wave theory and these results are carefully compared with the experimental data on HCl and other gases. The latter part of the chapter is devoted to a collection of the infrared data on polyatomic molecules together with many of the theories that have been proposed for their explanation. The fifth and last chapter deals with the infrared spectra of solid bodies. Beginning with the Born crystal lattice theory a fine account is given of all the more important experimental and theoretical material which forms the basis for our knowledge of this interesting subject.

It appears that this volume by Schaefer and Matossi may well be one of the important source books for the infrared for some years to come. It is an excellent compilation of all the available experimental material together with a sufficient account of the underlying theory to make the observational results intelligible. The treatment is very clear and the emphasis

which is placed on the theoretical interpretations tends to dispose of the difficulty that a survey of this character must always be somewhat uncritical in nature. The book may be enthusiastically recommended to those who are interested in the subject of the infrared.

D. M. DENNISON

Handbuch der Experimentalphysik. Herausgegeben von W. Wien und F. Harms unter Mitwirkung von H. Lenz. Band 24, 2. Teil. Röntgenspektroskopie. AXEL LINDH. Pp. viii + 436, figs. 197. Akademische Verlagsgesellschaft. Leipzig 1930. Price bound. R M 42.

When Siegbahn wrote his textbook on the spectroscopy of x-rays, he treated mainly the standard experimental methods and the general regularities in the spectra. The value of Lindh's book, aside from its bringing the bibliography up to 1929, lies chiefly in its shift of emphasis from these general regularities to the exceptions, such as the satellites of x-ray lines and the influence of chemical binding upon an atom's spectrum. The author's contributions in this last field prove him well fitted to discuss it.

After a general discussion of apparatus and gratings, the author considers the different series in detail and gives a general table of levels, revised to 1926. There is a short elementary chapter on the interpretation of the discrete x-ray spectrum. Intensity measurements, the continuous spectrum, and the auxiliary topics of the magnetic spectra of photoelectrons and photoelectric critical potentials, have their own chapters. The Compton effect is not mentioned.

A great part of the volume is given over to the compilation of data, which, when done critically or in connection with still mooted issues, is of course valuable in a handbook of experimental physics. But the inclusive reproduction of tables and figures from old work which can be seen now in some perspective, can hardly be justified. The devotion of a dozen pages to the square roots of all line frequencies (in addition to like data for absorption edges *and* term values), and the reprinting of four figures (122-125) of different ages giving $(\nu/R)^{1/2}$ as a function of Z , instead of one from the author's compiled table, are examples of such practise.

The interpretation of the lines would have been clearer if the author had given the modern spectroscopic L and J values of the levels, and shown in unified tables the two terms associated with each line, as well as the esoteric Greek notation.

J. MACK

Grundlagen der Hydromechanik. L. LICHTENSTEIN. Pp. 506, figs. 54. Julius Springer, Berlin, 1929. Price bound, R M 39.60.

This book by the well-known mathematician of the University of Leipzig constitutes volume 30 of the Springer collection *Die Grundlehren der mathematischen Wissenschaften in Einzeldarstellungen*. As might be expected it is very different from every other treatise on hydrodynamics, for the author, the fundamental problem of hydrodynamics is the integration of certain systems of partial differential equations with assigned boundary conditions and he calls to his aid all the resources of modern mathematics. This makes necessary a large amount of preliminary material; the first chapter is devoted to topology, the second gives a brief but interesting account of vector-analysis, the third treats potential theory, a subject to which the author has made valuable contributions, and so on. It is not until we reach page 290 that the equations of motion are derived. One of the most interesting and important chapters of the book is that devoted to the propagation of discontinuities, a difficult subject, the understanding of which is essential to any comprehension of wave motion. The last chapter is devoted to existence-theory questions.

The book could not profitably be recommended to a beginner, but to one who has studied Lamb and who wishes to understand more fully the mathematical foundations of the subject it should prove very valuable. For practical applications of the theory one must still turn to Lamb and to some such book as Tietjen's account of Prandtl's lectures on hydro- and aeromechanics. The printing has the high degree of excellence we have come to expect in the books of the Springer collection.

FRANCIS D. MURNAGHAN

Einführung in die Theoretische Physik. A. HAAS. Vol. I, Pp. X + 396 with 67 figures. Fifth and Sixth Editions. W. de Gruyter and Co., Berlin and Leipzig, 1930. Price bound R M 16.50.

In these last editions the subject matter of Professor Haas' excellent Introduction to Theoretical Physics has been completely worked over, and extensive revisions made both in arrangement and content. Whereas the third and fourth editions of the first volume, from which the English translation was prepared by Verschoyle, contained only two parts—Mechanics, and Theory of the Electromagnetic Field and of Light—, a third part on Thermodynamics has been added to the present editions with a consequent increase in length of some 90 pages.

The subject is developed in the author's customary clear and forceful style and the logical arrangement emphasizes the unity of the subject. Vector methods are used freely throughout the book, the theorems of vector analysis being developed as required. In spite of the fact that some writers in German are beginning to use at least parts of Gibbs' significant notation, the author adheres to the clumsy parentheses and brackets, grad's, div's and rot's. A comparison of any vector equation of a little complexity in the parenthesis-bracket notation (such as that on top of page 38) with the same equation in Gibbs' notation, would seem to be all that is necessary to convince anyone of the superiority of the latter.

Pedagogically the text may be criticized in that too frequently abstract theory is developed without any immediate application. Thus the deduction of Hamilton's canonical equation would appear more important to the student encountering them for the first time if the author had proceeded to the Hamilton-Jacobi equation and applied it to the solution of a few problems. Again Euler's equations for the rotation of a rigid body are developed without any considerable application being made.

As usual with Professor Haas' works, a high degree of scientific accuracy is maintained and misprints are nearly non-existent. These last editions will undoubtedly enjoy the high popularity of the earlier editions. The printing is excellent, but in this age of machinery it ought to be unnecessary for the reader to cut every page from preface to index.

LEIGH PAGE

Theoretische Physik. GUSTAV JÄGER. In five volumes. Vol. I Mechanik, Pp. 150; Vol. II Schall und Wärme, Pp. 133; Vol. III Elektrizität und Magnetismus, Pp. 151; Vol. IV Optik, Pp. 148, Vol. V Wärmestrahlung, Elektronik und Atomphysik, Pp. 130. W. de Gruyter and Co., Berlin and Leipzig, 1930.

These tiny volumes ($4\frac{1}{4}'' \times 6\frac{1}{4}''$) can be slipped in the pocket of the student who wishes to prepare for examination during his vacation. While elementary calculus is used freely, the mathematics is of the simplest. The first volume takes up the mechanics of particles including damped simple harmonic motion and Keplerian motion, mechanics of rigid bodies going as far as the symmetrical top under gravity, Lagrange's equations, the special relativity theory, the elements of the theory of elasticity, hydrodynamics of perfect fluids, Poiseuille's formula. The first quarter of Vol. II is devoted to the elements of acoustics, the remainder being concerned with conduction of heat, thermodynamics and kinetic theory of gases. Vol. III deals with electrostatics, magnetostatics, current electricity, electromagnetic induction, alternating currents, going as far as the development of Maxwell's equations. The volume on optics takes up the usual topics of geometrical and physical optics, and some electromagnetic theory of light, ending with a short section on x-rays. The last volume contains the theory of heat radiation, including the Stefan-Boltzmann law, Wien's displacement law and Planck's law, quantum theory of specific heats, the motion of electrons in electric and magnetic fields, metallic conduction, conduction in gases, deflection of alpha-rays, Bohr theory of the hydrogen atom, photo-electric effect, and Compton effect.

The books are clearly printed in type of normal size and strongly bound. The material is well chosen and the subject matter developed clearly and logically although in somewhat concise form. Each volume is provided with table of contents, index, and references for collateral reading.

LEIGH PAGE

THE PHYSICAL REVIEW

REPORT ON NOTATION FOR SPECTRA OF DIATOMIC MOLECULES

BY ROBERT S. MULLIKEN

RYERSON PHYSICAL LABORATORY, UNIVERSITY OF CHICAGO

(Received March 18, 1930)

I. INTRODUCTION

FOR some time there has been much confusion and little agreement between different investigators in the field of band spectra, in respect to the symbols used for quantum numbers, spectroscopic terms, spectrum lines, and molecular constants as obtained from spectrum analysis. In the hope of remedying this situation, a number of those interested in the subject discussed the matter at Washington in April, 1929, and reached a tentative agreement on certain main points. The writer then undertook to obtain further discussion by correspondence, and for this purpose sent out on August 10 a circular letter embodying the results of the above discussion, somewhat modified and amplified as a result of subsequent experience. Copies of this letter were sent to about eighty spectroscopists. Many replies were received, and the matter was also discussed at the Faraday Society symposium on band spectra at Bristol in September.¹ On the basis of the foregoing, and of the replies to a second circular letter, sent out November 1, and of considerable additional correspondence with various individuals, the following report was prepared in tentative form, and copies were sent out with a third circular letter on March 15, 1930. After some changes based on replies to this third letter, the report is now presented.

In this report, the expression "it is recommended" is used in some cases, "it is suggested" in others. The *recommendations* represent the opinion, either active or acquiescent, of nearly everyone whose opinion has become known to the writer. They deal for the most part with important points about which definite conclusions have been reached. The *suggestions* are of a more tentative character. They deal in part with less important points and with matters where the need of general agreement is less imperative than in the case of the

¹ "Molecular Spectra and Molecular Structure. A General Discussion held by the Faraday Society." Published in book form (Gurney and Jackson, 1930), also in Trans. Faraday Soc., pp. 611-950 (1929). In regard to nomenclature, cf. pp. 628-633 and pp. 768-772 and the Errata.

recommendations. In part they refer to topics which have not yet been sufficiently discussed to make definite recommendations.—In all the proposals given, the attempt has been made to take properly into account the varied needs of experimentalists and theorists.

The recommendations and suggestions given here have been made in such a way as to supplement and to be in harmony with those in the recent Report on Notation for Atomic Spectra.² In particular, the principle of using capital letters for quantum numbers representing angular momenta belonging to the molecule as a whole, and small letters for angular momenta of individual electrons, has been adopted. The recommendations apply for the most part only to diatomic molecules, but the manner of their extension to polyatomic molecules is in some cases obvious. Although a standard notation for polyatomic molecules would be very desirable, our knowledge of their spectra is as yet so undeveloped that it is perhaps best not to attempt this now. The only recommendation made here is that any notation chosen for polyatomic molecules be such as to harmonize with and supplement those used for atoms and diatomic molecules.

In addition to making recommendations and suggestions, opportunity has been taken to discuss a few matters of definition and nomenclature in regard to which misunderstandings have arisen or are likely to arise (Λ -type doubling, p -type multiplicity, band-origins, system-origins, "electronic," "vibrational," and "rotational" energy, etc.).

II. QUANTUM NUMBERS FOR MOLECULE AS A WHOLE

General. For the *vibrational quantum number*, v is recommended to replace the hitherto usual symbol n .³ The quantum number v has integral values (0, 1, 2, \dots), the vibrational energy being given by $E_v = (v + \frac{1}{2})h\nu_e + \dots$ (in regard to ω_e , cf. Section V).

For the resultant angular momentum of any molecule, and its projection on an external field, the quantum number *designations* J and M are respectively recommended ($M = J, J-1, \dots, -J$). These designations are identical with corresponding designations for atoms.⁴ The possible J values are 0, 1, 2, \dots for molecules with an even number of electrons, $\frac{1}{2}, 1\frac{1}{2}, \dots$ for those with an odd number. In certain coupling cases, J loses its meaning, and another quantum number K becomes prominent; in singlet states, J and K are identical, and may be used interchangeably: cf. p. 615 below.

Normal coupling: *Hund's cases a and b.* Before speaking in more detail about various quantum numbers associated with the angular momenta of

² H. N. Russell, A. G. Shenstone, and L. A. Turner, *Phys. Rev.* **33**, 900 (1929).

³ This change has been urged by a number of people, because of the increasing need of referring to v in the same paper, or even in the same sentence, in which n is used to designate the principal quantum number of an electron. The symbol v has already been used by J. H. Van Vleck (*Phys. Rev.* **33**, 477, 1929) and subsequently also by others.

⁴ The use of J both for resultant *atomic* and for resultant *molecular* angular momentum is likely to cause some confusion. If its use were less well established for molecules (in the form j), J ought perhaps to be replaced by some other symbol, such as P (Hund proposed the symbol p). If this were done, M for molecules should also be replaced by another symbol.

electrons and nuclei in various coupling cases, it is desirable to review briefly the underlying theory.⁵ We have always as angular momentum elements (1) the orbital angular momentum of the electrons, (2) their spin angular momentum, and (3) the angular momentum of the nuclear rotation. There are two coupling cases which may be regarded as normal,—cases *a* and *b* of Hund.

In both cases *a* and *b* we have for the resultant angular momentum of *spin* of the electrons a quantum number *S*, exactly as in an atom. Further, we have a quantum number [formerly called i_l , or σ_k or σ_l] for which the designation Λ is here recommended; $\Lambda h/2\pi$ represents (the numerical value of) the projection, on the electric axis of the molecule,⁶ of the resultant orbital angular momentum of the electron system. The resultant orbital momentum itself is not at all rigorously quantized in molecules; nevertheless in comparing a molecule with the atom which would be obtained if its nuclei could be united, a resultant orbital quantum number *L* may sometimes be assigned as in the case of the atom; then Λ is the projection of *L*.⁷ The possible values of Λ are 0, 1, 2,

In case *a* (possible only if $\Lambda > 0$) we have strong coupling of *S* to the electric axis, as a result of the magnetic field associated with Λ . Here the projection of *S* on the axis is a quantum number [formerly called i_s , or σ_s] for which the designation Σ is now recommended.^{7,8} Σ has values *S*, *S* − 1, . . . − *S*; it is considered to be a positive or negative quantity according as it is parallel or antiparallel to Λ . The numerical value of the algebraic sum of Λ and Σ is a quantum number [formerly called *i*, or σ] for which the symbol Ω is recommended. For given values of Λ and *S*, Ω has values $\Lambda + S$, $\Lambda + S - 1$, . . . $|\Lambda - S|$.⁹ $\Omega h/2\pi$ is the total angular momentum parallel to the electric axis. This may be considered as combining vectorially with the angular momentum of the nuclei (a vector perpendicular to the electric axis)¹⁰ to give the resultant angular momentum of the molecule (quantum number *J*, cf. Fig. 1). The possible values of *J* are Ω , $\Omega + 1$, $\Omega + 2$, The quantum num-

⁵ F. Hund, *Zeits. f. Physik*, **36**, 657 (1926). For further details, cf. R. S. Mulliken, *Reviews of Modern Physics* **2**, 60 (1930).

⁶ *I. e.*, on the line joining the nuclei.

⁷ More accurately, according to the new quantum mechanics, the resultant orbital angular momentum is $L^* h/2\pi$, where $L^* = [L(L+1)]^{1/2}$; then Λ is the projection of L^* (each in units $h/2\pi$). Similarly the angular momenta associated with *S*, *K*, *J*, J^a , *R*, *l*, are, in units $h/2\pi$, really S^* , K^* , etc., and Σ is really the projection of S^* , etc. [A recommendation of the symbols L^* , S^* , etc. is not intended here.]

⁸ Σ (Greek *S*) has been chosen,—after much discussion (the use of Greek *X* was at first proposed),—for the projection of *S*, in spite of the other common uses of this symbol, because its use here is analogous to that of Λ (Greek *L*) for the projection of *L*, and to the use of the symbols Σ , Π , Δ , . . . , (Greek *S*, *P*, *D*, . . . ,) for states with $\Lambda = 0, 1, 2, \dots$, as compared with *S*, *P*, *D*, for $L = 0, 1, 2, \dots$.

⁹ Usually, for a given Λ , a given value of Ω occurs only once, but if $S > \Lambda$, one or more values of Ω occur twice. For example, if we have $\Lambda = 1$, $S = 1\frac{1}{2}$, we have $\Omega = 2\frac{1}{2}, 1\frac{1}{2}, \frac{1}{2}, -\frac{1}{2}$ corresponding to $\Sigma = 1\frac{1}{2}, \frac{1}{2}, -\frac{1}{2}, -1\frac{1}{2}$.

¹⁰ The component of angular momentum perpendicular to the electric axis, which in the text is for brevity called "the nuclear angular momentum," is really *mainly* angular momentum of the nuclei, but *also* includes small contributions from orbital (and spin, in cases *a* and *c*) angular momenta of the electrons. Cf. R. S. Mulliken, reference 5.

bers associated with the molecule as a whole in case *a* are thus v ; L (sometimes, but never very rigorously quantized), Λ ; S , Σ ; Ω , J , M .

In case *b* we have Λ and S just as in case *a*, but S is not coupled to the electric axis, and there is no quantum number Σ . Case *b* exists whenever the magnetic field associated with Λ is too weak to couple S to the axis, a condition which is possible for any value of Λ , but which is automatically fulfilled when $\Lambda=0$. In case *b*, $\Lambda h/2\pi$ and the nuclear angular momentum¹⁰ combine to give a quantized resultant (cf. Fig. 1). For the corresponding

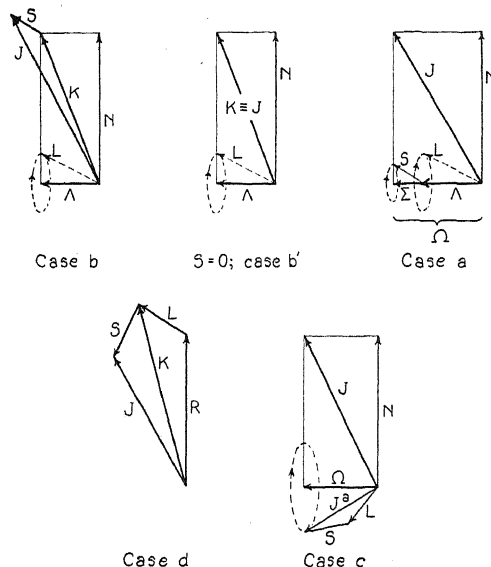


Fig. 1. Angular momentum vectors in Hund's cases *a*, *b*, *c*, *d*, expressed in units $h/2\pi$. In cases *a*, *b*, *c*, the angular momentum of the nuclear rotation¹⁰ is represented by N , which is *not* a quantum number; in case *d* it is represented by the quantum number R . In all the figures, the horizontal base line perpendicular to N represents the direction of the electric axis (line joining the two nuclei). In cases *a* and *b*, Λ is shown as the projection of L , which is represented as precessing around the direction of Λ , i.e. around the electric axis; L is given by a dotted line to indicate that it is not rigorously quantized. In case *a*, Σ is shown as the projection of S , which is represented as precessing around the electric axis.^{12a} In all cases, each pair of vectors which form a *resultant* must be thought of as precessing around the latter with a frequency which differs for each such pair. In each case, the only vector whose direction remains fixed is J . Precessing pairs are: Λ and N around J in the case $S=0$; Ω and N around J in cases *a* and *c*; Λ and N about K , and K and S about J , in case *b*; L and S about J^a in case *c*^{12a}; R and L about K , K and S about J , in case *d*. [The use of N in Fig. 1 is not intended as a notation suggestion to be followed. In Ref. 5 the writer has used O where N appears here, and has used N with a somewhat different meaning than here.]

quantum number [formerly called p_l or j_k] the designation K is now recommended.⁷ The possible values of K are Λ , $\Lambda+1$, $\Lambda+2$, \dots . There is usually a small magnetic field in the molecule parallel to K , so that K and S form a resultant J (cf. Fig. 1).^{7, 11} The quantity $J-K$ is often called ρ ; ρ is approxi-

¹¹ The combination of K and S to give J in a molecule is closely analogous to that of L and S to give J in an atom, and the designation K has been chosen with this in mind.

mately equal to the component of S parallel to J or K ; ρ has sometimes been thought of as a quantum number, but this is incorrect. The splitting of a rotational level with given K into two or more levels differing in J might be referred to as ρ -type multiplicity (the expression " ρ -type doubling" has been in common use for the case $S=\frac{1}{2}$). This is, however, not recommended. Such an expression as "case b spin multiplicity" would be better.

In the presence of a "weak" external field J gives M . If the field is strong enough, however, the coupling of K and S is broken down (molecular Paschen-Back effect) so that J loses its significance, while K and S separately give projections for which the designations M_K and M_S (magnetic quantum numbers) are recommended. (M_K has as possible values, $K, K-1, \dots, -K$; M_S has values $S, S-1, \dots, -S$). Here $M = M_K + M_S$.

Sometimes the coupling of K and S in case b is practically zero; this situation can conveniently be distinguished as case b' . In case b' , J is without significance. When $S=0$, cases a and b' become identical, as do K and J (cf. Fig. 1); here either K or J may be used to designate the resultant angular momentum; the designation K is the better in comparisons with case b' or b states with $S>0$, the designation J in comparisons with case a states.

Other coupling cases. In addition to cases a and b there are other less common cases which are nevertheless of sufficient importance to deserve consideration here. Hund's "case c " is an ideal limiting case in which L is assumed to be as rigorously quantized as in an atom, and, also, to be so strongly coupled to S as to give a quantized resultant as in an atom. *It is recommended that this resultant, which in an atom would be called J , be called J^a in the case of a molecule.*^{12, 12a} Λ and Σ here have no (quantum) meaning, but Ω is rigorously quantized, and is (the numerical value of) the projection of J^a on the electric axis. Ω has as possible values, J^a, J^a-1, \dots down to 0 or $\frac{1}{2}$ according as J^a is an integer or a half integer. Ω combines vectorially with the nuclear angular momentum to give J as in case a (cf. Fig. 1). In an external field J gives M .

In Hund's "case d ," examples of which are found in the higher electron levels of H_2 and He_2 , L is as rigorously quantized as in an atom,¹³ but is unusually little influenced by the electric axis, so that it does not give a projection Λ on the axis. S also exists as usual, but it does not give a projection Σ . In case d the angular momentum of the nuclei by themselves is quantized; for this the quantum number R [same as Hund's p_r] is recommended. ($R=0, 1, 2, \dots$). L is weakly coupled to R to give a resultant for which the designa-

¹² The superscript a serves to indicate the relation to the atomic J .

^{12a} There is also another, probably more important, form of case c in which L , J^a , and even S are not at all rigorously quantized, and in which Ω is the only rigorous electronic quantum number of the molecule. This case is found in loosely-bound molecular states formed by the union of two atoms one or both of which when alone has its own L and S strongly coupled to each other.

¹³ Actually in He_2 the relations are more complicated: we have essentially case b for the inner electron or electrons, but case d for the excited electron, whose l is coupled in accordance with case d to an R which is really the K of the He_2^+ ion.

tion K is recommended; K has the values $R+L$, $R+L-1$, \dots , $|R-L|$.¹⁴ K and S may now combine vectorially to give J , exactly as in case b (cf. Fig. 1.). In external fields we have, (1) in "weak" fields, a quantum number M as in previous cases; (2) in "strong" fields, M_K and M_S as in case b ; (3) in stronger fields, M_R , M_L , M_S . If, as is true in H_2 and He_2 , the coupling of K and S is very small, J is lacking in significance, just as in case b' . When $S=0$, we have $K \equiv J$. In such cases, we may speak of case d' . The quantity $K-R$ in case d' , like $J-K$ in case b (cf. above) is frequently called ρ ; ρ is here approximately equal to the component of L parallel to K or R ; it is not a quantum number.

As a variation on case d , we might have "case e ," in which L and S are coupled to give a J^a as in case c , while J^a and R give a resultant J .

III. TERM SYMBOLS

For coupling cases approximating Hund's a or b , or intermediate between them, the use of the symbols Σ , Π , Δ , Φ , Γ , H , \dots to indicate $\Lambda=0, 1, 2, 3, 4, 5, \dots$ is recommended. [Until recently the symbols S, P, D, \dots have been used for $\Lambda=0, 1, 2, \dots$ as well as for $L=0, 1, 2, \dots$.] In coupling cases resembling or tending toward case d , or also in theoretical discussions where a molecule is to be compared with the atom obtainable by uniting its nuclei, L values can be indicated by using the symbols S, P, D, \dots for $L=0, 1, 2, \dots$. To indicate both L and Λ , symbols such as $P\Sigma$, $D\Pi$, etc., may be used.

The multiplicity (equal to $2S+1$) should be indicated, as in the case of atoms, by a superscript at the left, as $^1\Sigma$, $^2\Pi$, etc. In coupling cases approximating case a , it is recommended that the value of $\Lambda+\Sigma$ be indicated by a subscript at the right.¹⁵ (For singlet states, however, no subscript is needed, since $\Sigma=0$ always, so that $\Lambda+\Sigma=\Lambda$; while for case b states no subscript is possible, since a quantum number Σ does not exist). Examples, $^1\Sigma$, $^1\Pi$, $^2\Sigma$, $^3\Delta_2$, $^4\Pi_{2\frac{1}{2}}$, $^4\Pi_{1\frac{1}{2}}$, $^4\Pi_3$, $^4\Pi_{-3}$.¹⁶

There are two kinds of Σ states, which differ in respect to the symmetry of their wave-functions with respect to a plane through the line joining the nuclei. In the one kind the *electronic factor* of the wave-function ψ (corresponding to the motion of the electrons with reference to the nuclei) is unchanged on reflection in such a plane, in the other kind it changes sign.

¹⁴ K in case d has a somewhat different physical meaning than K in case b , but is exactly like the latter in that it combines with S to give J . Further, there is a one to one correspondence between the K values in case d and those in case b , and K is quantized throughout the whole range of intermediate cases.

¹⁵ The recommendation that the value of $\Lambda+\Sigma$, rather than that of Ω , be used for the subscript in molecular multiplets is based on the fact that when $S>\Lambda$, $\Lambda+\Sigma$ takes on negative as well as positive values. In such cases [none of which, however, have yet been observed] it would not suffice to specify Ω , since $\Omega=|\Lambda+\Sigma|$. In $^4\Pi$ states, for example, we should have $\Omega=\frac{1}{2}$ for both $^4\Pi_3$ and $^4\Pi_{-3}$.⁹ In this connection it may be well to remind the reader that in molecular multiplets, in contrast to many cases of atomic multiplets with $L>0$, the full multiplicity is always developed whenever $\Lambda>0$. For example, the molecular level $^4\Pi$ is quadruple (cf. reference 9) while the atomic 4P is only triple.

¹⁶ For subscripts which are multiples of $\frac{1}{2}$, either of the two forms such as $\frac{3}{2}$ or $1\frac{1}{2}$ may be used, but the second form ($1\frac{1}{2}$) is preferable for typographical reasons (cf. reference 2, p. 900).

It is recommended that these be distinguished, when one wishes, by calling them respectively Σ^+ and Σ^- states.^{16a} [The designations Σ^+ and Σ^- respectively correspond to Σ and Σ' of Wigner and Witmer.^{17,18}]

In the case of homonuclear molecules (molecules composed of atoms whose nuclei are identical in charge and mass), any electron state may be either "odd" or "even."¹⁹ An electron state of a homonuclear molecule is said to be *odd* if the *electronic factor* of ψ changes sign on reflection in the midpoint of the line joining the nuclei, *even*, if it does not change sign.^{19,19a} It is recommended that the odd or even character of an electron state, *when known*, and *if desired*, be indicated by a subscript at the right of the electronic term symbol. The subscripts *g* (German *gerade*) for even terms and *u* (German *ungerade*) for odd terms are recommended.²⁰ Examples, $^1\Sigma_g$, or $^1\Sigma_g^+$, or $^1\Sigma_g^-$, $^2\Sigma_u$;

^{16a} Corresponding to the frequently used empirical designations such as Π_b and Π_a (cf. Section VI, Fig. 2, etc.), theoretical designations such as Π^+ (even terms^{19a} when K is even) and Π^- (odd terms when K is even) might be introduced, in analogy to Σ^+ and Σ^- .

¹⁷ E. Wigner and E. E. Witmer, *Zeits. f. Physik*, **51**, 859, 1928. In Σ^+ states the rotational levels with even values of K are "even" or "positive," those with odd K are "odd" or "negative," while in Σ^- states these relations are reversed.^{19a}

¹⁸ Wigner and Witmer's use of Σ where Σ^+ is proposed here is obviously undesirable, since the symbol Σ is needed to imply *merely* $\Delta = 0$ in cases where one cannot, or does not wish to, decide between Σ^+ and Σ^- , as well as in general discussions. Wigner and Witmer's use of Σ' where Σ^- is proposed here is undesirable because of the frequent use of the prime ('), in the analysis of spectra, to denote the upper of two energy levels.

¹⁹ The use of "odd" and "even" in this sense was introduced by Hund. Cf. the useful summary by W. Weizel, *Zeits. f. Physik*, **54**, 324-6 (1929).

^{19a} The words even and odd are applied by Kronig, in a sense different from that used by Hund,¹⁹ to the *complete* ψ function of any molecule, homonuclear or heteronuclear; a molecular term is odd or even in this sense according as its ψ function does or does not change sign on reflection in the origin of coordinates; this definition is the same as that which holds for odd and even atomic terms. Instead of "even" and "odd" Wigner uses "positive" and "negative" for atomic terms, and Wigner and Witmer (l.c., Ref. 17) for molecular terms.

In speaking of molecular terms, the designations "even" and "odd" (which may be abbreviated *g* and *u*, as in Fig. 2) may be preferred to "positive" and "negative" on two grounds: (1) they were introduced earlier (R. de L. Kronig, *Zeits. f. Physik*, **50**, 351, 1928), and (2) they refer to the same properties which in atoms are generally described by "even" and "odd." But "positive" and "negative" (which may be abbreviated $+$ and $-$) may be preferred on other grounds: (1) they avoid possible confusion with the earlier-introduced and equally well-founded use of "even" and "odd" in another sense for electronic terms;^{19a} (2) they avoid the confusing situation that molecular levels with even, or with odd, K values may be either "even" or "odd." In Fig. 2 and elsewhere in this report, "even" and "odd" are used, but the writer now intends personally to use "positive" and "negative."

²⁰ In the report on line spectra (reference 2), it was suggested that a superscript^o (degree mark) always be used for odd terms, and *no* superscript for even terms. It may be that this precedent should be followed, although "odd" and "even" do not have just the same meaning here as in atoms. But this would hardly be feasible anyway in molecular spectra, since in some cases we do not yet *know* whether a term is even or odd. Further, there are many purposes for which the odd or even character is a matter of indifference, and it is desirable in such cases to be able to drop the superscript, without thereby implying that the term is even. The choice of *g* and *u* in preference to the English *e* (even) and *o* (odd) is based mainly on the fact that *e* is often used as a subscript for other purposes, as in E_e and r_e , while *o* is easily confused with zero.

The choice of the subscript position is governed by the fact that *g* and *u* are sometimes

${}^2\Pi_{3g}$; ${}^3\Pi_u$. [The designations Σ_g^+ , Σ_u^+ , Σ_g^- , Σ_u^- , Π_u , Π_g , Δ_g , Δ_u , etc. as here proposed, respectively correspond to Σ_+ , Σ_- , Σ'_+ , Σ'_- , Π_+ , Π_- , Δ_+ , Δ_- , etc. of Wigner and Witmer.]

The term symbols just recommended are of course not sufficient to identify completely the electronic state of a molecule. This purpose can be accomplished by the use of an identifying symbol of an empirical character, as for example A , B , X , a , etc.; or by the use of a symbol describing the electron configuration (cf. section IV, below.) *It is recommended* that such symbols be placed before the symbol giving S , Λ and Σ , as in the following examples: $A {}^3\Pi_2$; $X {}^1\Sigma$; $1s\sigma^2 2p\sigma 2s\sigma {}^3\Sigma$ (if the meaning is clear from the context, this last may be abbreviated to $2s\sigma {}^3\Sigma$ or $2s {}^3\Sigma$). These and similar designations can be adapted to the individual case, and varied to suit the need of experimentalist and theorist.

If one desires to express the relation of a molecular electronic state to the states of its atomic dissociation products, it is suggested that designations such as the following be used: $X {}^1\Sigma({}^2S+{}^2P)$. Here 2S and 2P represent the states of the two atoms. If desired, the electron configurations of atoms and molecule can also be given.

Some writers have used a superscript number, appended to the electronic term symbol, to indicate v . Example, ${}^3\Sigma^2$, for $v=2$. It is suggested that this practice be avoided if possible, and that simpler, although longer, expressions such as "the level $v=2$ of ${}^3\Sigma$ " be used. In case, however, a necessity is felt for including v in the term symbol, it is suggested that this be given as a superscript *in parentheses to indicate* that it represents an element foreign to the rest of the symbol. Examples, ${}^3\Sigma^{(2)}$; ${}^3\Sigma_g^{-(2)}$.

If one needs to give the rotational quantum number (K or J) as well as v , it may be given in parentheses as in the following example: ${}^3\Sigma^{+(1)}(10)$, for $v=1$, $K=10$.

IV. QUANTUM NUMBERS FOR INDIVIDUAL ELECTRONS; ELECTRON CONFIGURATIONS

The designation Λ was recommended above as the quantum number for the component, parallel to the electric axis, of the resultant orbital angular momentum of the entire electron system. The *designation λ is now recommended* [to replace the former designation i_{lr} or σ_{lr} or σ_{k_r}] for the corresponding quantum number for an *individual electron*.²¹ It is recommended further

needed for *individual electrons* (cf. Section IV below), as in σ_g , σ_u , π_g , etc., where the superscript position would lead to awkwardness in the symbols for electron configurations. For example, $\sigma_g^2\sigma_u^2\pi_u^4$ is much less awkward than $\sigma^{g2}\sigma^{u2}\pi^{u4}$. It is also preferable in such symbols as ${}^2\Sigma_g^+$, ${}^2\Sigma_u^{+(1)}$, etc. In cases such as ${}^2\Pi_{3g}$ it is not so good, but also not very bad, and furthermore, one is usually not interested in the $\frac{1}{2}$ and the g at the same time, so that one will usually write just ${}^2\Pi_{\frac{1}{2}}$ or else ${}^2\Pi_g$, depending on the nature of the discussion.

²¹ The quantization leading to the assignment of λ values for individual electrons is rigorous only to the extent that the interactions of the electrons with one another can be replaced by an axially symmetrical electric field. Ordinarily, however, the assignment of individual λ values in molecules should be about as justifiable as the assignment of individual l values in atoms.

that electrons having $\lambda = 0, 1, 2, 3, 4, 5, \dots$ be respectively *designated* $\sigma, \pi, \delta, \phi, \gamma, \eta, \dots$ electrons. [These were formerly named s, p, d, \dots electrons by the present writer, although not with the same meaning as s, p, d, \dots in atoms.]

Under some circumstances quantum numbers n, l , and s can also be assigned to the individual electrons in a molecule, just as to those in an atom. In Hund's case d these quantum numbers have practically the same meaning as in an atom (examples, excited orbits of series electron in H_2, He_2).²² Ordinarily, however, n and l are not at all rigorous quantum numbers and have a definite meaning only in terms of some ideal limiting case, such as that of the atom which would be obtained ("united-atom") if one could unite the two nuclei of the molecule.^{22,23} To designate the values of l in a molecule the symbols s, p, d, \dots are recommended for $l = 0, 1, 2$, just as in the case of an atom. When n, l , and λ are all to be indicated for an electron, symbols such as $2p\sigma, 3s\sigma, 3p\pi, 4d\sigma, \dots$ are recommended; the number represents n . [In the notation formerly used by the present writer, the equivalents of these symbols are $2s^p, 3s^s, 3p^p, 4s^d, \dots$ respectively.]²⁴ When several electrons ($1, 2, 3, \dots$) are present, their several values of n, l, λ can be indicated, if desired, by numerical subscripts, as $l_1, l_2, \dots, \lambda_1, \lambda_2$, etc.

The quantum number λ represents the projection of l on the electric axis of the molecule.⁷ Ordinarily any λ is considered a positive quantity, but in a molecule with several electrons some of the λ 's must be considered as having a negative sign. Λ is then the algebraic sum of the individual λ 's. Those individual λ 's whose direction is opposite to Λ are regarded as having a negative sign.

Even when the assignment of an l value to an electron has little meaning there is still, in *symmetrical molecules*, a definite distinction between *odd* and *even* states of an electron. Thus one may speak of $\sigma_g, \sigma_u, \pi_u, \pi_g, \dots$ etc. electrons. Insofar as an l can be assigned, an even value of l always gives an even type of electron (σ_g, π_g etc.), and an odd value of l an odd type.—In a similar way, the even or odd character of the resultant electron state of a symmetrical molecule is determined, like that of an atom, by the (*arithmetic*) sum of the individual l values. If this sum is even, the term is even (Σ_g, Π_g, \dots etc.), and conversely.

Often one may wish to indicate not the "united-atom" values of l and n for an electron, but the values of l and n which the electron would have if the molecule were separated into its atoms. For this purpose, symbols such as $\sigma(1s), \sigma_g(2p), \pi(2p)$, etc., are suggested. Here the symbol σ or π gives the

²² For the series electron in H_2 and He_2 , most of the orbits are large compared with the distance between the nuclei, so that "united-atom" conditions are closely approximated.

²³ In terms of spherical coordinates (r, θ, φ) as in the ideal limiting case of the "united-atom," l is defined as $n_\theta + n_\varphi$, where n_θ and n_φ are quantum numbers associated with θ and φ . In terms of elliptical coordinates (ξ, η, φ), as in another ideal limiting case where the electrons move under the influence of two point charges (as in H_2^+), l is defined as $n_\eta + n_\theta$ ($\eta = \text{const.}$ is a hyperboloid of revolution).

²⁴ The symbols $2s^p$ etc. were introduced by the present writer (Phy. Rev. **32**, 186, 1928); $2p\sigma$, etc. by F. Hund. (Zeits. f. Physik, **51**, 759, 1928).

value of λ for the electron in the molecule, while the symbol in parentheses describes the state of the electron as it would exist in one of the atoms on dissociation of the molecule.

Electron configurations. A rather complete description of the state of a molecule is possible if the term symbol, which gives the quantum numbers associated with the molecule as a whole, is preceded by a set of symbols giving the electron configuration. Examples: $1s\sigma^2 2p\sigma^2 2s\sigma^2 2p\pi^3 {}^2\Pi$; or more briefly, $\sigma^2\sigma^2\sigma^2\pi^3 {}^2\Pi$; or, if the molecule is symmetrical, $\sigma_g^2\sigma_u^2\sigma_g^2\pi_u^3 {}^2\Pi_u$. The electron configuration designations used here are similar to those used in line spectra. Such a symbol as $1s\sigma^2$ really means $(1s\sigma)^2$, i.e., it indicates the presence of two $1s\sigma$ electrons; while σ^2 indicates any two σ electrons of identical type (equivalent σ electrons). The order in which successive symbols are written is that of decreasing firmness of binding.—Such a symbol as $\sigma^2\sigma^2\sigma^2\pi^3$ rather than $1s\sigma^2 2p\sigma^2 2s\sigma^2 2p\pi^3$ is often to be preferred, since the assignment of definite n and l values is usually rather lacking in meaning. The symbol $\sigma^2\sigma^2\sigma^2\pi^3$ signifies the existence of three different kinds of σ electrons without attempting to describe them in detail.

V. SYMBOLS FOR MOLECULAR CONSTANTS

The energy E of a diatomic molecule is commonly written as a sum of three parts (for exact definitions, cf. Section VI):

$$E = E_e + E_v + E_r \quad (1)$$

Here E_e is the "electronic energy," E_v is the "vibrational energy," and E_r is the "rotational energy."

For the energy of a molecule in a singlet state²⁵ we had according to the old quantum theory (using, however, the new symbols v and J in place of n and j)²⁶

$$E = E_e + hc[\omega_0 v - x\omega_0 v^2 + y\omega_0 v^3 + \dots] + hc[B_v(J^2 + \text{const.}) + D_v J^4 + F_v J^6 + H_v J^8 + \dots] \quad (2)$$

Here the first expression following E_e represented E_v , the second E_r . In Eq. (2), we had

$$B_v = B_0 - \alpha v + \gamma v^2 + \dots, \text{ where } B_0 = h/8\pi^2 c \mu r_0^2 = h/8\pi^2 c I_0. \quad (3)$$

Also,

$$D_v = D_0 + \beta v + \dots, \text{ where } D_0 = -4B_0^3/\omega_0^2. \quad (4)$$

In Eqs. (2)–(4), the subscript zero attached to a coefficient implied that this coefficient corresponded to $v=0$. At the same time, since the energy of vibra-

²⁵ The "const." in $(J^2 + \text{const.})$ depends on the electronic motions (cf. R. S. Mulliken, ref. 5, Eq. (29)). Small constants should also be added to the terms in J^4 , etc.; and other small terms should be added.

²⁶ The notation used for the coefficients in Eqs. (2)–(4) etc. is mainly that which is now most usual. Instead of ω_0 one often finds ν_0 or ω^0 ; instead of D_v , $-\beta$. The designation $y\omega_0$ in Eq. (2) and γ in Eq. (3) are not in common use, but have been introduced here to supply an existing lack. No recommendation of this use of y and γ is intended here.

tion was supposed to be zero when $v=0$, it implied a molecule with stationary nuclei in a state of *equilibrium*. Thus $c\omega_0$ was supposed to represent the frequency of vibration for $v=0$, and so the limiting frequency for infinitesimal amplitudes. Similarly B_0 referred to $v=0$, and so supposedly to a molecule in equilibrium; and the quantities r_0 and I_0 calculated by means of Eqs. (3) likewise were supposed to correspond to a molecule in equilibrium.

According to the new quantum theory, however, Eqs. (2)–(4) must be replaced by equations of the following form:^{26a}

$$E = E_e + hc\left\{\omega_0\left(v + \frac{1}{2}\right) - x\omega_0\left(v + \frac{1}{2}\right)^2 + y\omega_0\left(v + \frac{1}{2}\right)^3 + \dots\right\} \\ + hc\left\{B_v\left[\left(J + \frac{1}{2}\right)^2 + \text{const.}\right] + D_v\left(J + \frac{1}{2}\right)^4 + \dots\right\} \quad (2a)$$

$$B_v = B_0 - \alpha\left(v + \frac{1}{2}\right) + \gamma\left(v + \frac{1}{2}\right)^2 + \dots, \text{ where } B_0 = h/8\pi^2 c\mu r_0^2 = h/8\pi^2 cI_0 \quad (3a)$$

$$D_v = D_0 + \beta\left(v + \frac{1}{2}\right) + \dots, \text{ where } D_0 = -4B_0^3/\omega_0^2. \quad (4a)$$

If one assumes the validity of Eqs. (2a)–(4a) one gets somewhat *different numerical values* for E_e , ω_0 , x , B_0 , r_0 , I_0 , etc. than if one assumes Eqs. (2)–(4). In the literature most of the recorded values are based on Eqs. (2)–(4), although in some recent articles Eqs. (2a)–(4a) have been used as a basis of calculation. Thus the same symbols are now being used in different articles in two different ways, with resulting confusion on the part of the reader.

To remedy this situation a *revision of nomenclature is suggested*, at least for discussions dealing with the analysis of band spectra, such that Eqs. (2a)–(4a) are replaced by the following Eqs. (2c)–(4c).^{26, 26a, 27, 28} At the same time, equations of the form of Eqs. (2)–(4), except for the substitution of $(J + \frac{1}{2})^2$ for J^2 , may usefully be retained (Eqs. 2b–4b).²⁹ Eqs. (2b)–(4b) represent the more useful form for the empirical description of spectra, Eqs. (2c)–(4c) for the analysis of the isotope effect and for the theoretical application of band spectrum data as in the construction of $U(r)$ curves (cf. second paragraph following).

$$E = E_0 + hc\left[\omega_0 v - x\omega_0 v^2 + y\omega_0 v^3 + \dots\right] \\ + hc\left\{B_v\left[\left(J + \frac{1}{2}\right)^2 + \text{const.}\right] + D_v\left(J + \frac{1}{2}\right)^4 + \dots\right\} \quad (2b)$$

$$B_v = B_0 - \alpha v + \gamma v^2 + \dots \quad (3b)$$

$$D_v = D_0 + \beta v^2 + \dots \quad (4b)$$

$$E = E_e + hc\left\{\omega_e\left(v + \frac{1}{2}\right) - x_e\omega_e\left(v + \frac{1}{2}\right)^2 + y_e\omega_e\left(v + \frac{1}{2}\right)^3 + \dots\right\} \\ + hc\left\{B_v\left[\left(J + \frac{1}{2}\right)^2 + \text{const.}\right] + D_v\left(J + \frac{1}{2}\right)^4 + F_v\left(J + \frac{1}{2}\right)^6 + \dots\right\} \quad (2c)$$

^{26a} Although the form $(J + \frac{1}{2})^2$ is used here, it is immaterial to the present discussion whether this or the rival form $J(J+1)$ is used.

²⁷ The use of the symbol E for energy, as in E and E_0 , although it seems desirable, is not definitely included in the recommendations made here.

²⁸ The coefficients of Eqs. (2b)–(4b) are related to those of Eqs. (2c)–(4c) as follows: E_0 (Eq. 2b) = E_e (Eq. 2c) + $hc\left[\frac{1}{2}\omega_e - (1/4)x_e\omega_e + (1/8)y_e\omega_e + \dots\right]$; $\omega_0 = \omega_e\left[1 - x_e + (3/4)y_e + \dots\right]$; $x\omega_0 = \omega_e[x_e - (3/2)y_e + \dots]$; $y\omega_0 = \omega_e(y_e + \dots)$; etc.

²⁹ The quantities r_0 and I_0 calculated as in Eq. (3) are no longer of much interest, since they are not empirical coefficients, nor have they the theoretical importance of r_e and I_e .

$$B_v = B_e - \alpha_e(v + \frac{1}{2}) + \gamma_e(v + \frac{1}{2})^2 + \dots, \text{ where} \quad (3c)$$

$$B_e = h/8\pi^2 c \mu r_e^2 = h/8\pi^2 c I_e$$

$$D_v = D_e + \beta_e(v + \frac{1}{2}) + \dots, \text{ where } D_e = -4B_e^3/\omega_e^2. \quad (4c)$$

The coefficients ω_e , B_e , etc. and the quantities I_e and r_e (and E_e) refer to a molecule with stationary nuclei in equilibrium; such a molecule, however, in contrast to the state of affairs in the old quantum theory, would *not* at the same time have $v=0$. B_0 , D_0 , E_0 , etc., refer to a molecule with $v=0$.²⁹

For the *energy of dissociation* of a molecule, the symbol D has been widely adopted. To be accurate, one must distinguish D_e , the energy of dissociation for the imaginary case of a molecule with nuclei stationary at the distance r_e ; and D_0 or D , the energy of dissociation from the actual lowest energy level of the molecule ($v=0$). The values of D for various states of a molecule may be conveniently distinguished by putting identifying designations in parentheses, as $D(X)$ or $D(X^1\Sigma)$; $D(A^3\Pi)$; etc. In all cases the symbol D should stand for the energy of dissociation alone, and should not include, in the case of an excited electron state, the energy of excitation.

If the energy of a molecule in a definite electron state, with nuclei held stationary, is expressed as a function $U(r)$ of the distance between the nuclei, then $E_e \equiv U(r_e)$, while the dissociation energy $D_e \equiv U(\infty) - U(r_e)$. Also, $4\pi^2 \mu c^2 \omega_e^2 = (d^2 U/dr^2)_{r=r_e}$.

It may eventually be worth while to discard the heterogeneous and cumbersome set of symbols B_v , D_v , α , β , ω_e , $x_e \omega_e$, etc.²⁸ in favor of a simpler set. If, or when, this is done, the double use of D for heat of dissociation and for the coefficient of $(J+\frac{1}{2})^4$ might well be done away with. One might perhaps use d_v instead of D_v in the E_r expression (also, for consistency, f_v instead of F_v and possibly also b_v instead of B_v). This would, however, interfere with the possible future use of a , b , c , \dots in place of ω_e , $x_e \omega_e$, $y_e \omega_e \dots$ in Eq. (2c), or perhaps better in place of ω_0 , $x\omega_0$, $y\omega_0$, \dots in Eq. (2b); a , b , \dots have already often been used in this way.

VI. DESCRIPTION AND ANALYSIS OF SPECTRA

Term designations. In the analysis of spectra, one is usually concerned with the determination of energy values (E) or term-values (E/hc) through the use of the relation $\nu = (E' - E'')/hc$. The prime (') and double prime (') are used merely to indicate that $E' > E''$.²⁷ It is recommended that the *prime* and *double prime* be always used in a similar manner when one wishes to distinguish the *upper* and *lower* of two energy levels involved in the production of the lines of a band spectrum, and that this method be applied to all quantum numbers and coefficients pertaining to these energy levels. In discussing spectra, it is best to avoid where possible the expressions "initial" and "final" levels, since in terms of E' and E'' these have opposite meanings in absorption and emission spectra.

In the analysis of spectra, it is convenient to have a symbol to denote term-values. It is suggested that T be used for this purpose ($T \equiv E/hc$).³⁰ For

³⁰ The symbol F has sometimes been used for E/hc . (The present writer has in fact used this, and also F^{el} for E_e/hc , F^v for E_v/hc , and F^r for E_r/hc). But F has *usually* been used

the upper and lower levels involved in the production of a spectrum line, T' and T'' would be used.

In dealing with the analysis of a particular spectrum, the symbol T , followed by the rotational quantum number designation in parentheses, also the vibrational quantum number, if desired, as a superscript in parentheses, is suggested as a convenient symbol. Examples: $T(8)$, $T^{(2)}(8)$; also, $T_1(8\frac{1}{2})$, $T_{2a}(7\frac{1}{2})$, $T_a(9)$, etc., using numerical and literal subscripts in a manner to be discussed below in connection with the symbol F (cf. paragraphs following Eq. (7)).

For some purposes it is extremely convenient to have separate symbols for "electronic terms" (E_e/hc), "vibrational terms" (E_v/hc), and "rotational terms" (E_r/hc). It is suggested that the symbols G and F be used for vibrational and rotational terms respectively.³⁰ For electronic terms the symbol T_e is suggested. Thus we have, paralleling Eq. (1),

$$T = T_e + G + F. \quad (5)$$

Definitions of electronic, vibrational, and rotational energies and terms. It is important to define with some care the quantities F , G , and T_e , or the corresponding quantities E_r , E_v , and E_e . The following definitions appear to be unambiguous.

(1) The energy E_r is the difference between the energy of the actual molecule and that of an idealized molecule obtained by the following imaginary process: the rotation of the nuclei is gradually stopped without placing any new constraint on the vibration of the nuclei or on the electron motions, in such a way as might be realized by gradually (i.e. adiabatically) coupling an infinite moment of inertia to the axis of rotation of the molecule. In Eqs. (2c)–(4c), B_v and all the coefficients of powers of $(J+\frac{1}{2})^2$ then go to zero.

(2) The energy E_v is the difference between the energy of a molecule idealized just to the extent of making $E_r=0$ and the energy of a further idealized molecule obtained by the following imaginary process: the vibration of the nuclei is gradually stopped without placing any new constraint on the electron motions, in a way such as might be realized by leaving the charges of the nuclei unchanged but gradually increasing the masses until they are infinite. In Eqs. (2b)–(4b), ω_e and all the coefficients of powers of $(v+\frac{1}{2})$ then go to zero.

(3) The energy E_e is the total internal energy of a molecule in a definite electronic state with the nuclei stationary (this condition may be realized in imagination by making the masses infinite) at their equilibrium distance (r_e) apart. E_e consists of (a) kinetic energy of the electrons, plus (b) their potential energy with respect to the nuclei and to one another, plus (c) the mutual potential energy of repulsion of the two nuclei. As was mentioned above, $E_e \equiv U(r_e)$.

with the meaning E_r/hc , and this usage is therefore recommended here (cf. Eq. (5)). The use of T for E/hc (or for $-E/hc$, measured from an arbitrary zero of energy at ionization) has been frequent in the field of line spectra. The use of G for E_v/hc (cf. Eq. (5) and ref. 38) was suggested by Birge and recommended in the National Research Council Report on Molecular Spectra, but this recommendation has not been widely followed.

Rotational term differences. In the analysis of band spectra, it is customary to use such designations as $\Delta F(J)$, $\Delta_1 F(J)$, $\Delta_2 F(J)$ for the difference between two rotational terms differing only in the value of J . [Formerly Δf and ΔF were often used to distinguish these term intervals respectively for the upper and lower of the two electron levels involved, but it is recommended that this distinction be made only by the use of (') and (''), as in $\Delta F'$, $\Delta F''$].

It is recommended that in designating rotational term intervals, the forms which are defined in the following equations be used:^{31,32}

$$\Delta_1 F(J + \tfrac{1}{2}) = F(J + 1) - F(J) \quad (6)$$

$$\Delta_2 F(J) = F(J + 1) - F(J - 1). \quad (7)$$

Examples,

$$\Delta_1 F(3\frac{1}{2}) = F(4) - F(3); \quad \Delta_2 F(4) = F(5) - F(3).$$

In all states with $\Lambda > 0$ there are, for a given value of Σ and of J in case *a*, or of K and of J in case *b*, two rotational levels (cf. Fig. 2). (These are usually

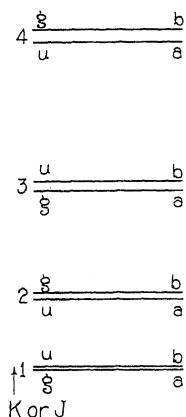


Fig. 2. Λ -type doublets for the case $S=0$, $\Lambda=1$. The order shown for the g and u levels represents only one of two possibilities; the case in which 1(g) lies above 1(u), 2(u) above 2(g), and so on, is the other (g and u respectively stand for even and odd^{19a}). There is also no fixed rule as to the relative position of a and b levels; nor is there any fixed rule for correlating the a , b , and the g , u descriptions (cf. references 35, 36, 19a).

very close together, but separate widely on approach to case *d*). This doubling may be called *Λ -type doubling* because it occurs if, and only if, $\Lambda > 0$. [It was formerly, but less correctly, called " σ -type doubling," where " σ " is a former designation for our present Ω .³³] It is suggested that, in each

³¹ $\Delta_1 F(J + \frac{1}{2})$ and $\Delta_2 F(J)$ may be read as "delta one $FJ + \frac{1}{2}$ " and "delta two FJ ."

³² $\Delta_1 F(J + \frac{1}{2})$ is commonly denoted by $\Delta_1 F(J)$, but the use of the symbol $\Delta_1 F(J + \frac{1}{2})$ as in Eq. (6) seems preferable. In practise, $\Delta_1 F(J + \frac{1}{2})$ is much less important than $\Delta_2 F(J)$, since $\Delta_1 F(J + \frac{1}{2})$ cannot be directly and exactly evaluated from the analysis of a spectrum; instead one usually obtains $F_a(J+1) - F_b(J)$, or $F_b(J+1) - F_a(J)$.

³³ The name " σ -type-doubling" was given by the writer before Hund's development of the theory of molecular electronic states, and was based on the idea that this type of doubling occurs whenever $\sigma > 0$ [in the present symbols, whenever $\Omega > 0$]. Later Hund showed that this doubling is to be expected, not whenever $\Omega > 0$ but whenever $\Lambda > 0$. Usually $\Lambda > 0$ and $\Omega > 0$

rotational doublet of this kind, the component levels be distinguished as a and b sublevels,³⁴ and that the term values be distinguished by corresponding subscripts, as, $T_a^{(v)}(J)$, $T_b^{(v)}(J)$, $F_a(J)$, $F_b(J)$.^{16a, 35, 36} For rotational term differences, we have then $\Delta_2 F_a(J)$, $\Delta_2 F_b(J)$, \dots etc.

In case b , it is necessary to provide a means of indicating both K and J . The writer^{35a} suggested the use of the symbols F_1 , F_2 ; $\Delta_1 F_1$, $\Delta_1 F_2$; $\Delta_2 F_1$, $\Delta_2 F_2$ for case b with $S = \frac{1}{2}$, where F_1 refers to the terms with $J-K = +\frac{1}{2}$ and F_2 to $J-K = -\frac{1}{2}$. For $S = 1$, the suggested symbols were F_1 , F_2 , F_3 , for $J-K = +1$, 0 , -1 respectively. These suggestions are now renewed,^{36b} with the added suggestion that this use of numerical subscripts be applied both to the rotational terms F and to the complete terms T ; when $\Lambda > 0$, a and b subscripts are needed in addition to the numerical subscripts. Examples, $T_1^{(v)}(J)$; $T_{2a}^{(v)}(J)$; $F_{2b}(J)$; $\Delta_2 F_1(J)$; $\Delta_2 F_{1a}(J)$; $\Delta_2 F_{2b}(J)$; $\Delta_2 F_{2a}(J)$, etc.; specifically, $\Delta_2 F_{1a}(5\frac{1}{2})$ would mean $F_{1a}(6\frac{1}{2}) - F_{1a}(4\frac{1}{2})$, with the K values 6 and 4. Sometimes when K is the important rotational quantum number, J is lacking in significance (case b' , cf. Section II above). In such a case, one naturally will use such forms as $\Delta_2 F(K)$, $\Delta_2 F_a(K)$. Also when $S = 0$, so that $J \equiv K$, one may use K instead of J as the argument of a ΔF expression.

Vibrational term differences. It is suggested that in designating vibrational term differences, the forms which are defined in the following equations be used.³⁷

$$\Delta G(v + \frac{1}{2}) = G(v + 1) - G(v) \quad (6)$$

$$\Delta^2 G(v) [\equiv \Delta G(v + \frac{1}{2}) - \Delta G(v - \frac{1}{2})] = G(v + 1) - 2G(v) + G(v - 1). \quad (7)$$

go hand in hand. A familiar exception is ${}^3\Pi_0(\Lambda = 1, \Omega = 0)$. Experimentally this shows Λ -type doubling as predicted by Hund.

³⁴ The use of the designations A and B was suggested by the present writer (Phys. Rev., 30, 791, 1928). Some people have followed this suggestion, others have substituted a and b . The difference is not essential, but a and b seem to be preferred by the majority. (These designations have nothing to do with Hund's cases a and b).

³⁵ The designations a and b are essentially temporary empirical labels, and have no definite relation to any designations of theoretical significance (but cf. ref. 36). For two formal schemes for choosing which levels to call a and which to call b , cf. (1) R. S. Mulliken, Phys. Rev. 28, 1205 (1926) and (2) R. S. Mulliken, Phys. Rev. 30, 791 (1927). Some writers follow the first scheme, more the second. Both schemes lead to the same use of the labels a and b in the case of Π states, but give opposite labellings in the cases of Σ and of Δ states.

³⁶ The division into a and b levels is related to the theoretical division (cf. Ref. 19a and Wigner and Witmer, l.c. Ref. 17) of all molecular terms into even or positive and odd or negative terms. In the case of Π states, if either of the methods of labelling mentioned in ref. 36 is followed, the result is usually that in the b set of sub-levels, the even-numbered levels are even and the odd-numbered are odd; in the a set of sub-levels, the relations are always the reverse of those in the b set. The nature of the correlation between a and b and even and odd levels is illustrated in Fig. 2. For the case of Σ levels, cf. reference 18. In the case of Δ , Φ , \dots levels, the relations are of the same type as in Π levels.

^{36a} Cf. R. S. Mulliken, Phys. Rev. 30, 788 (1927).

^{36b} A more logical method would be to use the values of $J-K$ as subscripts, as in $F_{+\frac{1}{2}}(J)$, $F_{-\frac{1}{2}}(J)$, $\Delta_2 F_{+\frac{1}{2}}(J)$, $Q_{-\frac{1}{2}-\frac{1}{2}}(J)$, instead of $F_1(J)$, $F_{2a}(J)$, $\Delta_2 F_1(J)$, $Q_{12}(J)$. But since the present notation is simple and reasonably satisfactory, it does not seem wise in this report definitely to suggest a change.

³⁷ $\Delta G(v + \frac{1}{2})$ and $\Delta^2 G(v)$ may be respectively read as "delta $Gv + \frac{1}{2}$ " and "delta second Gv ."

Examples, $\Delta G(3\frac{1}{2}) = G(4) - G(3)$; $\Delta^2 G(4) = \Delta G(4\frac{1}{2}) - \Delta G(3\frac{1}{2}) = G(5) - 2G(4) + G(3)$. It will be seen that the argument of ΔG is always a half-integer midway between the v values (always integers) of two energy levels, while the argument of $\Delta^2 G$ is always an integer. [$\Delta G(v + \frac{1}{2})$ as here used is synonymous with Birge's $\Delta G_{v+\frac{1}{2}}$ and with $\omega_{v+\frac{1}{2}}$ as introduced by Birge and Sponer.³⁸]

Band and system origins. In describing a band spectrum, it is convenient to consider the frequency of each line as a sum of three parts, just as it is convenient to consider the energy and the term-value each as a sum of three parts (cf. Eqs. (1), (5)). Thus for the wave number ν we may write³⁹

$$\nu = T' - T'' = (T_e' - T_e'') + (G' - G'') + (F' - F'') = \nu_e + \nu_v + \nu_r. \quad (8)$$

The concepts of the "origin" of a band and of a band system are frequently used in theoretical discussions. These can be unambiguously defined as follows.³⁹

System-origin: $\nu = \nu_e$

Band-origin: $\nu = \nu_e + \nu_v$.

These definitions do not in general correspond to wave-number positions which are of importance in the analysis of band spectra, except in the study of the isotope effect. Band and system origins are discussed here only in order to remove possible misconceptions as to their meaning.

In *simple types* of bands, an equation for the band lines can often be given in the form

$$\nu = \nu_0 + aM + bM^2 + \dots, \quad (9)$$

where M is a parameter which takes on positive and negative integral or half-integral values, related to values of K'' or J'' . The line given by $\nu = \nu_0$, and often other lines, are ordinarily missing. In the simplest cases, ν_0 is approximately the same as $\nu_e + \nu_v$, but the agreement is never exact if we use accurate expressions for E_e , E_v , and E_r ; and the difference between ν_0 and $\nu_e + \nu_v$ varies from one type of band to another. The term "band-origin" is often loosely applied to ν_0 , but it is evident that this usage is inaccurate and tends to produce confusion.

In a system of bands, the band origins can be expressed by the equation

$$\begin{aligned} \nu_e + \nu_v = \nu_e + \omega_e'(v' + \tfrac{1}{2}) - \omega_e''(v'' + \tfrac{1}{2}) \\ - x_e'\omega_e'(v' + \tfrac{1}{2})^2 + x_e''\omega_e''(v'' + \tfrac{1}{2})^2 + \dots \end{aligned} \quad (10)$$

The origin of the 0, 0 band (obtained by putting $v' = 0$, $v'' = 0$ in Eq. 10) obviously does not coincide with the origin of the band system ($\nu = \nu_e$). If

³⁸ For the original proposal to use ΔG , cf. the National Research Council Report on Molecular Spectra, p. 123, Eq. (76). (In Eq. (76) the old symbol n appears instead of v .) In regard to $\omega_{v+\frac{1}{2}}$ cf. R. T. Birge and H. Sponer, Phys. Rev. 28, 259, (1926).

³⁹ Where ν_v , ν_r are used here, other designations such as ν_n , ν_m are frequently used. No definite recommendation of ν_e , ν_v , and ν_r is intended here, although they are preferred by the present writer. It is pretty obvious, however, that ν_n and ν_m should be dropped, since their subscripts are the now discarded symbols n and m formerly used for the vibrational and rotational quantum numbers.

the old quantum theory formula for E_v (cf. Eq. (2)) were correct, the system-origin *would* coincide with the origin of the 0, 0 band. In existing tables of band spectrum data, based on the old quantum theory formulation, the origin, or even the ν_0 position, of the 0, 0 band is in fact commonly referred to as the system-origin.³⁹

Designations for band systems and bands. For designating a transition between two electronic states, it is suggested that the following forms be used: ${}^2\Pi \rightarrow {}^2\Sigma$ for emission bands (to be read " ${}^2\Pi$ to ${}^2\Sigma$ "); ${}^2\Pi \leftarrow {}^2\Sigma$ for absorption bands (this might be read " ${}^2\Pi$ from ${}^2\Sigma$ "); and simply ${}^2\Pi$, ${}^2\Sigma$ in general discussions. It is recommended that the equivalent form ${}^2\Sigma - {}^2\Pi$, which is analogous to atomic symbolism such as $1s - 2p$, be abandoned.⁴⁰ In the suggested symbols, the *first mentioned* (here ${}^2\Pi$) always refers to the state of higher energy.

In indicating the two vibrational levels concerned in the production of a particular band, one speaks of the (0, 3) band, the (5, 2) band, and so on, where the first number refers to v' , the second to v'' . Usually the parentheses can safely be dropped, so that one can write "the 0, 3 band," and so on.

Designations for band-lines. The lines of a band can always be divided into one or more series ("branches"). For all the lines in one branch, $J' - J''$ (also $K' - K''$ in case *b*) has a constant value. *It is recommended* that the symbols *O*, *P*, *Q*, *R*, *S* be used, in a way now to be described, to denote various types of branches. In case *a*, we define

$$\begin{aligned} O(J) &= T'(J-2) - T''(J) = \nu_e + \nu_v + F'(J-2) - F''(J) \\ P(J) &= T'(J-1) - T''(J) = \nu_e + \nu_v + F'(J-1) - F''(J) \\ Q(J) &= T'(J) - T''(J) = \nu_e + \nu_v + F'(J) - F''(J) \\ R(J) &= T'(J+1) - T''(J) = \nu_e + \nu_v + F'(J+1) - F''(J) \\ S(J) &= T'(J+2) - T''(J) = \nu_e + \nu_v + F'(J+2) - F''(J) \end{aligned}$$

In these symbols, the usual arbitrary convention has been adopted of *using the value of J''* , rather than that of J' or of $\frac{1}{2}(J' + J'')$, *as the argument*, but at the same time *substituting the symbol J for the symbol J''* for the sake of brevity. *It is recommended* that, to avoid confusion, the convention of using the value of J'' as argument be uniformly followed.

Branches $O(J)$ and $S(J)$ ordinarily exist only in Raman spectra, and there only in the form

$$\nu = \nu_{exc} \mp [O(J) \text{ or } S(J)].$$

Here ν_{exc} is the wave number of the exciting line; in $O(J)$ or $S(J)$, ν_e is zero in the cases usually investigated (vibration-rotation Raman bands), or ν_e and ν_v are both zero and at the same time we have only $S(J)$, not $O(J)$ (pure rotation Raman bands).

When, in case *b*, the fine structure corresponding to different values of $J - K$ is unresolved (case *b'*, cf. Section III), or narrow, one will naturally

⁴⁰ The form ${}^2\Sigma - {}^2\Pi$ is really sensible only in case each term is a member of a series converging to a known limit from which the term can be *measured downwards*. Except in H_2 and He_2 such series are not known for molecular terms, and the use of the corresponding notation has no point. Even in atomic spectra, its usefulness is limited to the simplest types of series spectra.

define and use $O(K), P(K), \dots$, in analogy to $O(J), P(J), \dots$, of case a . For example, in a ${}^2\Sigma, {}^2\Sigma$ transition, one has a branch $P(K)$ and a branch $R(K)$, each line of each branch being a usually narrow, often unresolved, doublet.⁴¹ Also when $S=0$, so that $J=K$, one may use K instead of J as argument.

In cases where both ΔK and ΔJ are important, it is necessary to designate both. For this purpose symbols such as $Q_{21}(J), R_{12}(J)$, etc. are suggested, in which J'' (written as J) is used as argument in the usual manner, and in which the numerical subscripts indicate values of $J-K$. It was suggested above that the rotational term designations F_1, F_2, F_3, \dots , be used in case b for $J=K+S, K+S-1, \dots, |K-S|$. Similarly,^{3, b} one may speak of branches $Q_{21}(J), R_{11}(J), Q_{22}(J), Q_{12}(J)$, etc., where the first numerical subscript refers to the upper energy level, the second to the lower. (Symbols such as $R_{11}(J)$ and $Q_{22}(J)$ can ordinarily be abbreviated to $R_1(J)$ and $Q_2(J)$.) For example, $Q_{21}(5\frac{1}{2})$ means $\nu_e + \nu_v + F_2'(5\frac{1}{2}) - F_1''(5\frac{1}{2})$, or, more briefly expressed, $T_2'(5\frac{1}{2}) - T_1''(5\frac{1}{2})$; here $K'=6, J'=5\frac{1}{2}, K''=5, J''=5\frac{1}{2}$, so that $K'-K''=+1$, while $J'-J''=0$. This notation is incomplete, however, until designations are added to indicate the a or b character of the rotational levels involved. When this is included, we have symbols such as $Q_{2a1a}(5\frac{1}{2}), Q_{2b1b}(5\frac{1}{2}), R_{1a1a}(J), R_{1b1a}(J), Q_{2b1b}(J)$, and $Q_{2a2a}(4\frac{1}{2})$ or more briefly $Q_2(4\frac{1}{2})$. If Λ' or Λ'' is zero, the a or b subscripts can be omitted.³⁶ The notation just suggested can be made more explicit by the addition of a superscript symbol to indicate $K'-K''$; examples, ${}^R Q_{2a1a}(5\frac{1}{2}), {}^R R_{1a1a}(J)$. The added superscript is, however, not necessary, since the value of $K'-K''$ is already implied in the remainder of the symbol. For a more detailed discussion of this notation, references 35 and 36 may be consulted.

In the analysis of band spectra, temporary designations for band lines are sometimes needed before the true J or K values involved are known. It is recommended that in such cases the lines and branches be designated and numbered in some way that will not be confused with approved theoretically significant designations. For example, one might use $X(m), Y(m), Z(m)$, etc.; or if ΔJ or ΔK is known, but the correct numbering is uncertain, $P(m), R(m)$, etc.; or $P_\alpha(m), P_\beta(m), R_\gamma(m), R_\delta(m)$, etc. The parameter m could be given values 1, 2, 3, \dots .

CONCLUSION

In Table I some of the most important changes recommended or suggested here are summarized.

TABLE I. Some new designations and some of their older equivalents.

New	Old	New	Old
v	n	λ	$i_{l\tau}, \sigma_{l\tau}, \sigma_{k\tau}$
J	j, m , etc.	$\sigma, \pi, \delta, \dots$	s, p, d, \dots
M	(magnetic quantum number)	$\{2p\sigma, 3s\sigma, 3p\pi, 3d\sigma, \text{etc.}\}$	$2s^p, 3s^s, 3p^p, 4s^d, \text{etc.}$
Λ	i_l, σ_k, σ_l	$T; T_e; G$	$E/hc; E_e/hc; E_v/hc$
Σ	i_s, σ_s, X	Λ -type doubling	σ -type doubling
Ω	i, σ	${}^2\Pi \rightarrow {}^2\Sigma$, or ${}^2\Pi, {}^2\Sigma$; etc.	${}^2\Sigma - {}^2\Pi$, etc.
K	p_l, j_k	Σ^+, Σ^-	Σ, Σ'
$\Sigma, \Pi, \Delta, \dots$	S, P, D, \dots	$\Sigma_u, \Sigma_u, \Pi_u, \Pi_g$, etc.	

⁴¹ Strictly, each line except the first is a triplet (cf. R. S. Mulliken, Phys. Rev. 30, 138, 1927).

Among those who have expressed approval of the recommendations and suggestions made in this report (except for possible minor reservations) are the following: H. S. Allen, G. M. Almy, E. Bengttson, R. T. Birge, A. Christy, E. U. Condon, F. H. Crawford, W. E. Curtis, D. M. Dennison, G. H. Dieke, R. Fortrat, A. Harvey, W. Heitler, G. Herzberg, E. L. Hill, E. Hulthén, F. Hund, F. A. Jenkins, W. Jevons, R. C. Johnson, J. Kaplan, E. C. Kemble, R. de L. Kronig, J. E. Lennard-Jones, F. London, F. W. Loomis, J. C. McLennan, R. Mecke, P. M. Morse, O. Oldenberg, R. W. B. Pearse, F. Rasetti, Lord Rayleigh, O. W. Richardson, B. Rosen, E. C. G. Stueckelberg, T. Takamine, H. C. Urey, J. H. Van Vleck, W. W. Watson, W. Weizel, E. Wigner, E. E. Witmer. The writer wishes to express his sincere thanks to these and others for their contributions in the way of criticisms, suggestions, and expressions of opinion. These form the basis of the present report. He is particularly indebted to Professors R. T. Birge and F. Hund for their very active cooperation and support.

THE APPLICATION OF THE FERMI-THOMAS STATISTICAL MODEL TO THE CALCULATION OF POTENTIAL DISTRIBUTION IN POSITIVE IONS

By EDWARD B. BAKER

DEPARTMENT OF PHYSICS, UNIVERSITY OF MICHIGAN

(Received June 26, 1930)

ABSTRACT

The statistical method of Fermi and Thomas of calculating atomic potential distributions has been extended to include positive ions. A table of potentials for any positive ion is given. The results have been applied to the calculation of (a) ionic radii, (b) successive ionization potentials, (c) deviations from the Mosely law in optical spectra.

I. THE THEORY

FERMI¹ and Thomas² have considered the electrons in a neutral atom as a completely degenerate electron gas under the influence of the Coulomb field of the nucleus. Assuming radial symmetry, and using Poisson's equation, the Fermi-Dirac statistics permitted a calculation of the distribution of potential for neutral atoms. The present work provides a generalization of the method to include all positive ions also.

Fermi and Thomas obtained the differential equation

$$\frac{1}{r} \frac{d}{dr} \left(\frac{1}{r} \frac{dv}{dr} \right) = -4\pi\rho = \frac{2^{13/2}\pi^2 m^{3/2} e^{5/2}}{3h^3} v^{3/2} \quad (1)$$

with the boundary conditions

$$v \sim Ze/r \text{ near } r = 0, \text{ or } \lim_{r \rightarrow 0} vr = Ze \quad (2.0)$$

$$v(\infty) = 0 \quad (2.1)$$

which determine the solution for the neutral atom uniquely. The additional condition

$$\int \rho d\tau = -Ze \quad (3)$$

is simultaneously satisfied.

Introducing dimensionless variables

$$\psi = v/\gamma; \quad \gamma = \frac{2^{13/3}\pi^{4/3}me^3Z^{4/3}}{3^{2/3}h^2} \quad (4)$$

¹ E. Fermi, Zeits. f. Physik **48**, 73 (1928).

² L. H. Thomas, Proc. Camb. Phil. Soc. **23**, 542 (1927).

and

$$x = r/\mu; \quad \mu = \frac{3^{2/3} \hbar^2}{2^{13/3} \pi^{4/3} m e^2 Z^{1/3}}$$

then Eq. (1) becomes

$$\frac{d^2\psi}{dx^2} + \frac{2}{x} \frac{d\psi}{dx} = \psi^{3/2} \quad (5)$$

Substituting $\phi = \psi x$, we have

$$\phi'' = \frac{\phi^{3/2}}{x^{1/2}} \quad (6)$$

and Eqs. (2) and (3) become

$$\phi(0) = 1 \quad (7)$$

$$\phi(\infty) = 0 \quad (7.1)$$

and

$$\int_0^\infty \phi^{3/2}(x)^{1/2} dx = 1. \quad (8)$$

For the positive ion having z electrons and the atomic number Z , which we shall call an ion of order σ ($\sigma = z/Z$), we have, in place of Eq. (3),

$$\int \rho d\tau = -ze \quad (9)$$

and, in place of Eq. (8),

$$\int_0^{x_m} \phi^{3/2} x^{1/2} dx = z/Z = \sigma. \quad (10)$$

Since Eq. (9) is not fulfilled by the former solution, it follows that the boundary condition, Eq. (2.1), must be modified, since Eq. (2.0) must remain the same. A suggestion of how this is to be done may be obtained by a comparison of Eq. (5) with the equations

$$\frac{d^2\psi}{dx^2} + \frac{2}{x} \frac{d\psi}{dx} = -\psi^n \quad (11)$$

which have been extensively studied by Emden³ in connection with the distribution of matter in polytropic gas spheres. Emden found that for certain values of n , and certain boundary conditions, there are solutions of Eqs. (11) describing gas spheres of *finite* radius. This suggests that Eq. (3) may also have such solutions if the boundary conditions are modified.

Fermi⁴ and Razetti⁵ have used the approximate potential

$$v = -\frac{e}{r} \left[1 + (Z-1)\phi\left(\frac{r}{\mu}\right) \right] \quad (12)$$

³ Emden, "Gaskugeln," Leipzig, 1907.

⁴ E. Fermi, Zeits. f. Physik 49, 550 (1928).

⁵ F. Razetti, Zeits. f. Physik 49, 546 (1928).

(where μ is evaluated for $Z-1$), for a singly ionized atom. This is obtained by considering the ion of nuclear charge Z as a neutral atom of nuclear charge $Z-1$ plus an extra proton in the nucleus. This approximation neglects the "packing effect" that the added proton will have upon the electron cloud. It is not possible to generalize this result for much higher ionizations, for then the neglect of the packing effect becomes serious. The present method is designed to remove this difficulty.⁶

We propose a model of the positive ion having a finite radius x_m , beyond which the charge density is zero. The solution ϕ_σ of Eq. (6), representing a positive ion of order σ , must obey the boundary condition

$$\phi_\sigma(x_m) = \phi_{\sigma m} = 1 - \sigma = 1 - z/Z \quad (13)$$

instead of Eq. (7.1). We find that ϕ_σ then fulfills the extra condition of Eq. (10). For the neutral atom $x_m = \infty$, Eq. (13) reduces to Eq. (7.1), and Eq. (10) reduces to Eq. (8), as required.

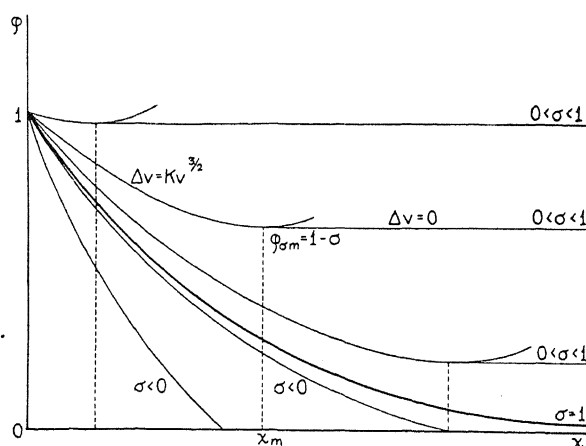


Fig. 1.

In Fig. 1 are displayed the possible forms the solution of Eq. (6) may take if the boundary condition of Eq. (7.0) is satisfied. The curve ϕ_1 is the only solution for which $\phi(\infty) = 0$, and is that already obtained for the neutral

⁶ The two dimensional analogue of Eq. (5) is

$$\frac{d^2\psi}{dx^2} + \frac{1}{x} \frac{d\psi}{dx} = \psi$$

the solution of which is any cylinder function $Z_0(ix)$. The only cylinder function which has the required logarithmic behavior for $x=0$, and which vanishes for $x=\infty$, is the Hankel function of the first kind $H_0^{(1)}(ix)$. As this function becomes asymptotically equal to $e^{-x}/x^{1/2}$, it can only represent a neutral two dimensional atom. The corresponding fact is true for Eq. (5); there is no solution of Eq. (5) which satisfies the conditions of Eqs. (2.0) and (2.1) other than the one obtained by Thomas and Fermi for neutral atoms. This can also be shown by a direct method of inequalities. This remarkable property of Eq. (5) made necessary the linking up of two solutions as described above.

atom by Fermi and Thomas. For this solution we have found the starting slope $\phi_1'(0) = -B_1 = -1.588558$.

Since the differential equation is of the second order, a particular value of the initial slope $-B_\sigma$ at $x=0$ uniquely determines a single solution passing

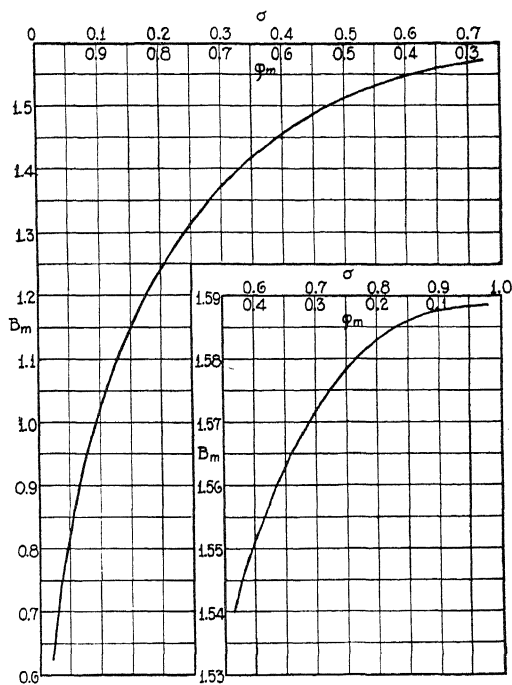


Fig. 2.

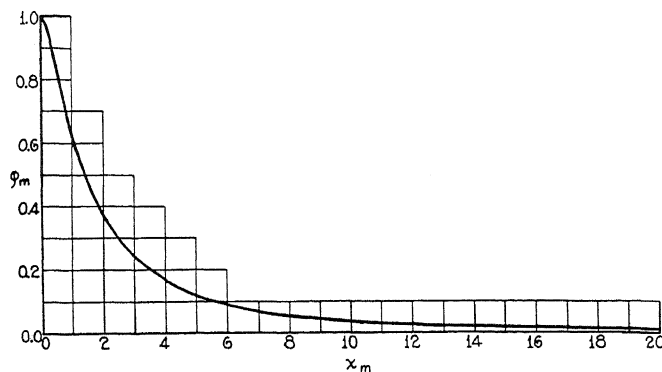


Fig. 3.

through $\phi=1$, $x=0$. All solutions with $0 > -B_\sigma > -\infty$ are single valued in ϕ , and no two cross each other.

All solutions with $0 > -B_\sigma > -B_1$ have each a single minimum, the coordinates of which $(\phi_{\sigma m}, x_m)$ are monotonous functions of B_σ (see Fig. 2), so that

the locus of minima (see Fig. 3) is monotonous in both x and ϕ . The ordinates at the minimum range from $\phi_{1m}=0$ to $\phi_{\sigma m}=1$, for values of B_σ from B_1 to B_0 respectively. These solutions describe any positive ion ($0 \leq \sigma \leq 1$) as far as the minimum, which is the boundary of the ion; beyond that point the Coulomb field requires a straight line parallel to $\phi=0$, and a distance $1-\sigma$ above it, corresponding to a solution of Laplace's equation, which joins at the minimum a solution ϕ_σ of Eq. (8). The value of σ which belongs to a solution ϕ_σ , having a starting slope $-B_\sigma$, is thus *determined* by numerical integration from $\phi=1$, $x=0$, $\phi'=-B_\sigma$ to the minimum, and by there *assigning* the value $1-\sigma$ to the ordinate $\phi_{\sigma m}$. The value of σ is known to characterize the straight line $1-\sigma=\phi$, which is the solution of Laplace's equation for the region outside of an ion of order σ . This condition expresses the fact that the potential of a positive ion must be

$$v \sim \frac{(Z-z)e}{r} = \frac{Ze}{r} (1-\sigma)$$

for large values of r .

All solutions of Eq. (8) with $-B_1 > -B_\sigma > -\infty$ lie below ϕ_1 and terminate abruptly at $\phi=0$, so that they do *not* represent negative ion distributions. Negative ions, as a matter of fact, will not find a place in any theory which assumes radial symmetry.

Since $x=0$, $\phi=1$ is a winding point with ϕ'' infinite, it is not possible to integrate from there using Taylor's series. Instead the expansions

$$\begin{aligned} \phi = 1 - Bx + \frac{4}{3}x^{3/2} - \frac{2}{5}Bx^{5/2} + \frac{1}{3}x^3 + \frac{3}{70}B^2x^{7/2} - \frac{2}{15}Bx^4 \\ + \frac{4}{63}\left(\frac{2}{3} + \frac{1}{16}B^3\right)x^{9/2} + \dots \end{aligned} \quad (14)$$

and

$$\begin{aligned} \phi' = -B + 2x^{1/2} - Bx^{3/2} + x^2 + \frac{3}{20}B^2x^{5/2} - \frac{8}{15}Bx^3 \\ + \frac{2}{7}\left(\frac{2}{3} + \frac{1}{16}B^3\right)x^{7/2} + \dots \end{aligned} \quad (15)$$

obtained by a method of successive approximations, are used, since they are rapidly convergent near $\phi=1$, $x=0$. Starting with an arbitrary value of B_σ , the integration is carried out to the minimum by an extension of the method given by Whittaker and Robinson⁷ for equations of the first order. The results must be given in a bivariate table, with values of ϕ for each value of x and B_σ or σ . This would be very extensive, were it not for the fact that, for each particular value of x , the values of both ϕ_σ and ϕ'_σ , from one curve to another, depend linearly upon B_σ . By means of the formulae:

$$\phi_\sigma = k(B_\sigma - B_p) + \phi_p \quad (16)$$

$$\phi'_\sigma = k'(B_\sigma - B_p) + \phi'_p \quad (17)$$

⁷ Whittaker and Robinson, "The Calculus of Observations."

and Table I, we may easily find the values of ϕ_σ and ϕ_σ' for each value of σ , at the values of x given in the table. For intermediate values linear interpolation is sufficiently accurate. The constants k and k' , being functions of x , are also tabulated, as well as the values B_p , ϕ_p and ϕ_p' of the reference solutions. The values of $B_{\sigma m}$ and $\phi_{\sigma m}$ are also listed; they are the initial slopes and minimal ordinates, respectively, of the solutions having their minima at the given value of x . Since $\phi_{\sigma m} = 1 - \sigma$, this part of the table is used to find the initial slope B_σ , needed in Eqs. (16) and (17), corresponding to the given order σ of the ion. This may also be done using Fig. 2. In Fig. 3 values of $\phi_{\sigma m}$ are plotted against x_m , and from this, since $\phi_{\sigma m} = 1 - \sigma$, we may find the radius x_m of an ion of order σ .

Values are listed from $x = 0.10$ to $X = 14.88$. For values of $x < 0.10$ the series in Eqs. (14) and (15) may be used.

II. IONIC RADII

Herzfeld⁸ has given a summary of some fourteen different methods of determining ionic radii, most of which are experimental, or semi-experimental. It may be seen from his collection of data, that the radius of any particular ion has a wide range of values, according to the method of determination. This uncertainty is not experimental, but lies in the variation of meaning of the radius with the method. It is consequently quite useless to

TABLE I.
 $B_p = 1.60$.

x	ϕ_p	$-(\partial\phi/\partial x)_p$	$-k$	$-k'$	B_m	ϕ_m
0.10	0.880448	1.0077	0.10126	1.0306	0.62221	0.97950
0.11	0.870539	0.9826	0.11159	1.0362	0.65170	0.97636
0.12	0.860832	0.9587	0.12197	1.0410	0.67901	0.97316
0.13	0.851358	0.9362	0.13240	1.0449	0.70399	0.96999
0.14	0.842103	0.9151	0.14287	1.0511	0.72935	0.96650
0.15	0.833053	0.8948	0.15342	1.0548	0.75166	0.96320
0.16	0.824201	0.8758	0.16401	1.0610	0.77453	0.95958
0.17	0.815535	0.8576	0.17464	1.0665	0.79592	0.95597
0.18	0.807046	0.8402	0.18418	1.0728	0.81678	0.95130
0.20	0.790574	0.80745	0.20576	1.0861	0.85655	0.94355
0.22	0.774731	0.7772	0.22761	1.0985	0.89248	0.93577
0.24	0.759471	0.7492	0.24971	1.1115	0.92596	0.92779
0.26	0.744751	0.72315	0.27208	1.1255	0.95746	0.91957
0.28	0.730535	0.69875	0.29473	1.1391	0.98658	0.91133
0.30	0.716792	0.67585	0.31765	1.1540	1.01434	0.90283
0.32	0.703492	0.6544	0.34089	1.1698	1.04059	0.89419
0.34	0.690609	0.63415	0.36447	1.1856	1.06513	0.88556
0.38	0.666003	0.5968	0.41251	1.2184	1.11013	0.86808
0.42	0.642812	0.5633	0.46193	1.2523	1.15018	0.85060
0.46	0.620895	0.5330	0.51275	1.2887	1.18639	0.83298
0.50	0.600134	0.50545	0.56505	1.3264	1.21892	0.81546
0.54	0.580427	0.4803	0.61888	1.3659	1.24839	0.79804
0.58	0.561684	0.4572	0.67434	1.4069	1.27500	0.78084
0.62	0.543825	0.4360	0.73146	1.4492	1.29916	0.76388
0.66	0.526781	0.41645	0.79031	1.4935	1.32216	0.74715
0.74	0.49490	0.3816	0.91345	1.5882	1.35972	0.71444
0.82	0.46561	0.35125	1.0443	1.6851	1.39155	0.68329
0.90	0.43858	0.3250	1.1833	1.7913	1.41856	0.65326
0.98	0.41352	0.30225	1.3310	1.9052	1.44136	0.62467

⁸ K. F. Herzfeld, *Jahrb. der Radioakt. und Elektronik* **19**, 259 (1922).

TABLE I. (continued)

x	ϕ_p	$-(\partial\phi/\partial x)_p$	$-k$	$-k'$	B_m	ϕ_m
1.06	0.39017	0.2819	1.4882	2.0239	1.46072	0.59744
1.14	0.36836	0.2639	1.6551	2.1502	1.47728	0.57148
1.22	0.34789	0.24825	1.8325	2.2866	1.49143	0.54684
1.30	0.32859	0.2341	2.0212	2.4293	1.50362	0.52339
1.38	0.31037	0.22175	2.2216	2.5827	1.51414	0.50112
1.46	0.29308	0.21075	2.4347	2.7470	1.52328	0.47987
1.54	0.27662	0.2006	2.6612	2.9547	1.53210	0.45732
<hr/>						
$B_p = 1.589$						
<hr/>						
1.649	0.28827	0.1546	2.9889	3.1213	1.53939	0.43653
1.822	0.26312	0.1361	3.5600	3.4885	1.55001	0.40192
2.014	0.23878	0.1186	4.2678	3.906	1.55863	0.36839
2.226	0.21538	0.1027	5.149	4.408	1.56569	0.33540
2.460	0.19305	0.08866	6.250	5.027	1.57136	0.30327
2.718	0.17180	0.07616	7.649	5.764	1.57579	0.27286
3.004	0.15167	0.06515	9.367	6.572	1.579133	0.24410
3.320	0.13266	0.05560	11.62	7.701	1.581780	0.21656
3.669	0.11472	0.04748	14.38	9.085	1.583774	0.18986
4.055	0.09776	0.04069	18.21	10.79	1.585230	0.16640
4.482	0.08165	0.03512	23.26	12.74	1.586243	0.14577
4.953	0.06619	0.03081	30.11	15.32	1.586989	0.12673
5.474	0.05105	0.02758	38.90	18.56	1.587515	0.10883
6.050	0.03587	0.02537	50.63	22.61	1.587878	0.09268
<hr/>						
$B_p = 1.5886$						
<hr/>						
6.686	0.04672	0.01340	66.60	28.12	1.5881234	0.07846
7.389	0.03817	0.01108	88.40	34.24	1.5882763	0.06679
8.166	0.03029	0.00932	118.2	42.37	1.5883801	0.05629
9.025	0.02286	0.00806	159.3	53.19	1.5884485	0.04699
9.974	0.01565	0.00723	216.3	66.97	1.5884921	0.03900
<hr/>						
$B_p = 1.58857$						
<hr/>						
11.02	0.01716	0.00434	296.0	85.30	1.5885191	0.03218
12.18	0.01252	0.00373	408.0	107.6	1.5885353	0.02666
13.46	0.00802	0.00335	563.0	136.7	1.5885454	0.02182
14.88	0.00341	0.00319	782.0	171.4	1.5885514	0.01798

expect quantitative agreement of the radii determined by this theory, which themselves have little real meaning, with his values. Never-the-less, they do correspond in order of magnitude, and show the same general variation with atomic number. The class of ions considered by Herzfeld is a restricted class, having values of z equal to $Z-q$, where q is the valence of the element Z . When their radii are plotted against Z , a Lothar Meyer curve is obtained. We have made a similar curve, Fig. 4, of the values found from Fig. 3, but only for elements having positive ions.

III. SUCCESSIVE IONIZATION POTENTIALS

Milne⁹ has applied the Fermi-Thomas theory of the neutral atom to the calculation of the total potential necessary to remove all of the electrons from

⁹ E. A. Milne, Proc. Camb. Phil. Soc. 23, 794 (1927).

a neutral atom. Since our theory also gives a description of positive ions, the natural extension of the work of Milne is the calculation of the *successive* ionization potentials of atoms, or the successive potentials necessary to remove the electrons from an atom one at a time, further "stripping" the atom at each step.

The method of calculation consists in finding the total potential $X = X(\sigma, Z)$, necessary to remove all of the electrons from each kind of a positive ion that an element of atomic number Z may have, including the neutral atom.

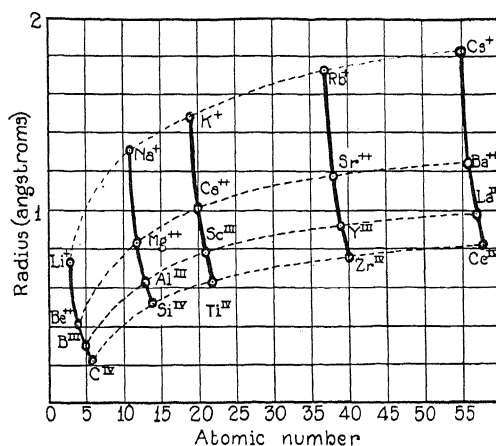


Fig. 4.

Successive differences of these quantities give the desired successive ionization potentials.

Milne considered the total electrostatic potential V to consist of two parts, Ze/r due to the nucleus, and $v(r)$ due to the charge cloud. At the nucleus $v(r)$ takes the constant value v_0 , the "back potential" of the charge cloud, and this he showed proportional to the starting slope of ϕ_1 , which is $-B_1$. There is a charge Ze at the nucleus, and at any other point a charge ρv . The total electrostatic potential is then

$$W = \Sigma \frac{1}{2} ev = \frac{1}{2} \int \rho v d\tau + \frac{1}{2} Ze v_0, \quad (18)$$

and the total energy is half of this.

The integral in the first term of Eq. (18) he showed to be proportional to B_1 , which becomes B_e for the ion. His result may be written:

$$X(1, Z) = -13.11 B_1 Z^{7/3} \text{ volts.} \quad (19)$$

He obtained his value of B_1 from Thomas' calculations of ϕ_1 near $x=0$, which, however, are slightly in error. Using our value of $B_1 = -1.588558$, we obtain

$$X(1, Z) = 20.824 Z^{7/3} \text{ volts} \quad (20)$$

which does not agree as well with experiment as Milne's

$$X(1, Z) = 17Z^{7/3} \text{ volts.} \quad (21)$$

This agreement must be regarded as accidental.

For the positive ion of order σ we obtain

$$X(\sigma, Z) = -13.11B_\sigma Z^{7/3} \text{ volts.} \quad (22)$$

If the approximation of Fermi and Razetti is generalized for ions of any order we obtain

$$X_F(\sigma, Z) = -13.11B_1 \frac{7}{13} \left(\frac{6}{7}\sigma + 1 \right) Z^{7/3} \text{ volts,} \quad (23)$$

since z must be used for the evaluation of v in the first term of Eq. (18). In successive differences only the term in Eq. (23) containing σ gives a contribution.

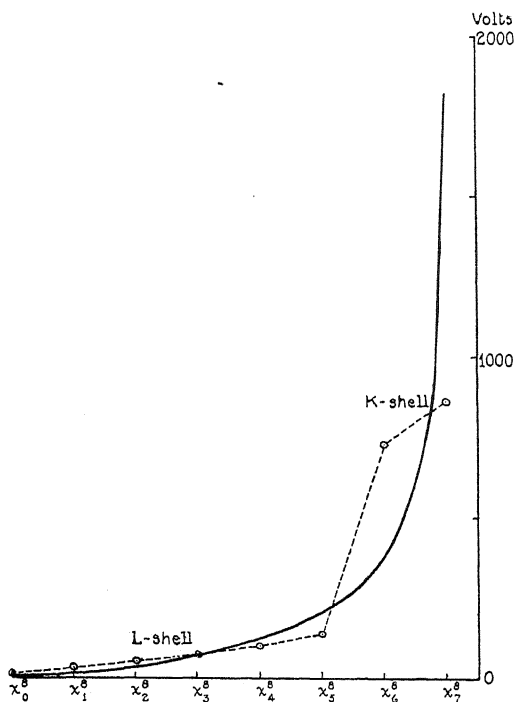


Fig. 5. Successive ionization potentials of oxygen. $Z=8$. Circles represent Hartree's Values.

In Figs. 5 and 6 we have plotted such differences of $X(\sigma, Z)$ for the elements oxygen and iron. The broken curves are the semi-experimental values of Hartree.¹⁰ As with most results of this statistical theory, a smooth curve

¹⁰ D. R. Hartree, Proc. Camb. Phil. Soc. 22, 473 (1924).

running through the jagged experimental one is obtained. Differences of X according to (23) give a curve of successive ionization potentials having a negative slope and going from the upper left hand corner to the lower right hand corner of the diagrams 5 and 6.

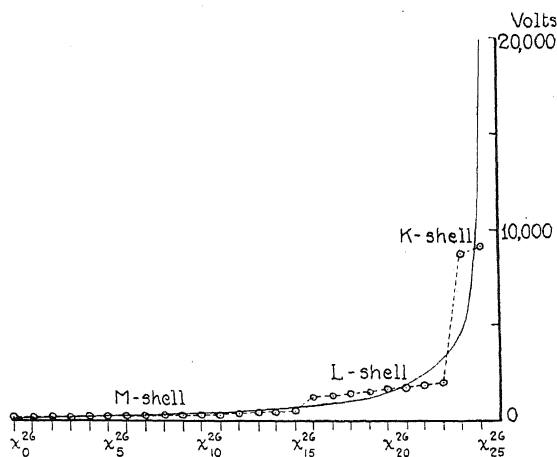


Fig. 6. Successive ionization potentials of iron. $Z=26$. Circles represent Hartree's values.

IV. APPLICATION TO THE BEHAVIOR OF OPTICAL TERM VALUES IN THE LIMIT OF VERY HIGH FREQUENCIES

Sommerfeld has shown that x-ray terms may be represented by the semi-empirical term formula

$$-\frac{T}{R} = [Z/n - a(Z, n) - b(n, l)]^2 + \alpha^2 \left[\frac{Z - d(n, l, j)}{n} \right]^4 \left(\frac{n}{j + \frac{1}{2}} - \frac{3}{4} \right) + \dots \quad (24)$$

Laporte¹¹ has shown that this same formula may be used to represent optical terms, though the number $a(Z, n)$, which represents the screening of the outer electrons, is zero for optical terms, and $b(n, l)$ is a function of Z , except for very high ionizations ($\partial < 1$). For low ionizations its dependence upon Z may be expressed as the series

$$b(n, l, Z) = A(n, l) + \frac{B(n, l)}{Z} + \frac{C(n, l)}{Z^2} + \dots \quad (25)$$

so that

$$\lim_{Z \rightarrow \infty} b(n, l, Z) = A(n, l). \quad (26)$$

It is possible to calculate the quantity $A(n, l)$, by means of the present theory, for hydrogenic ion series like Na I, Mg II, Al III, etc. It is also

¹¹ O. Laporte, "Sommerfeld Festschrift," Leipzig, 1928, p. 128.

possible to derive this from the experimental values of the line frequencies for such isoelectronic series. We shall be interested first in the latter problem.

Combining Eqs. (24) and (25) we have:

$$-\frac{T}{R} = \left\{ \frac{Z}{n} - \left[A(n, l) + \frac{B(n, l)}{Z} + \frac{C(n, l)}{Z^2} + \dots \right] \right\}^2 + \alpha^2 \left\{ \frac{Z - d(n, l, j)}{n} \right\}^4 \left(\frac{n}{j + \frac{1}{2}} - \frac{3}{4} \right) + \dots \quad (27)$$

Terms in α^2 and higher powers of α^2 represent the "relativity" correction, and if we subtract them from both sides of Eq. (27), we obtain the "reduced" term values t , thus

$$-\frac{t}{R} = -\frac{T}{R} - \alpha^2 \left\{ \frac{Z - d(n, l, j)}{n} \right\}^4 \left(\frac{n}{j + \frac{1}{2}} - \frac{3}{4} \right) + \dots = \left\{ \frac{Z}{n} - \left[A(n, l) + \frac{B(n, l)}{Z} + \frac{C(n, l)}{Z^2} + \dots \right] \right\}^2. \quad (28)$$

We wish now to be able to calculate $A(n, l)$ from observed values of t . This may be done in at least two ways.

The first is to take the square root of the absolute values of both sides of Eq. (28), obtaining:

$$\left(\frac{t}{R} \right)^{1/2} = \frac{Z}{n} - A(n, l) - \frac{B(n, l)}{Z} - \frac{C(n, l)}{Z^2} + \dots \quad (29)$$

which shows that the Moseley law holds for large values of Z . If we form the difference

$$\left(\frac{t(l_2)}{R} \right)^{1/2} - \left(\frac{t(l_1)}{R} \right)^{1/2} = [A(n, l_1) - A(n, l_2)] + \frac{1}{Z} [B(n, l_1) - B(n, l_2)] \quad (30)$$

and go to the limit for very large Z , we obtain the quantity

$$\lim_{Z \rightarrow \infty} \left\{ \left(\frac{t(l_2)}{R} \right)^{1/2} - \left(\frac{t(l_1)}{R} \right)^{1/2} \right\} = [A(n, l_1) - A(n, l_2)]. \quad (31)$$

This quantity may be directly calculated from the experimental term values of an isoelectronic sequence, it being the asymptotic value that the quantities in Eq. (30) seem to approach for the heavier elements in the sequence. Such quantities have been calculated by Wentzel¹² and Unsöld,¹³ on the basis of a model of the atomic core composed of concentric spherical surface charges. This quantity has the disadvantage that the absolute term values must be known in order to calculate it.

The second quantity which may be used as a medium of comparison of theory and experiment is the asymptotic value of the first differences, for

¹² G. Wentzel, *Ann. d. Physik* **76**, 803 (1925).

¹³ A. Unsöld, *Zeits. f. Physik* **33**, 843 (1925).

neighboring elements in the isoelectronic sequence, of the line frequencies themselves. We may form this quantity from Eq. (28). It is

$$\begin{aligned} & \lim_{Z \rightarrow \infty} \left\{ \frac{\nu(l_2, l_1, Z+1)}{R} - \frac{\nu(l_2, l_1, Z)}{R} \right\} \\ &= \lim_{Z \rightarrow \infty} \left\{ \left[\frac{t(n, l_2, Z+1)}{R} - \frac{t(n, l_1, Z+1)}{R} \right] - \left[\frac{t(n, l_2, Z)}{R} - \frac{t(n, l_1, Z)}{R} \right] \right\} \quad (32) \\ &= \frac{2}{n} [A(n, l_1) - A(n, l_2)], \end{aligned}$$

which is just $2/n$ times the quantity in Eq. (31).

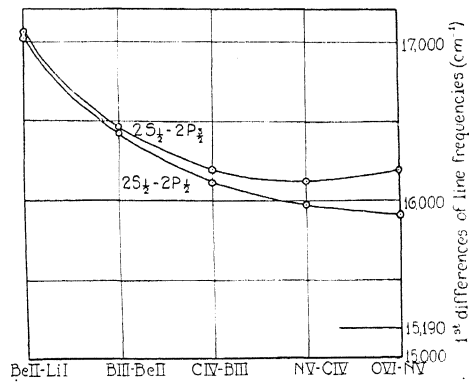


Fig. 7.

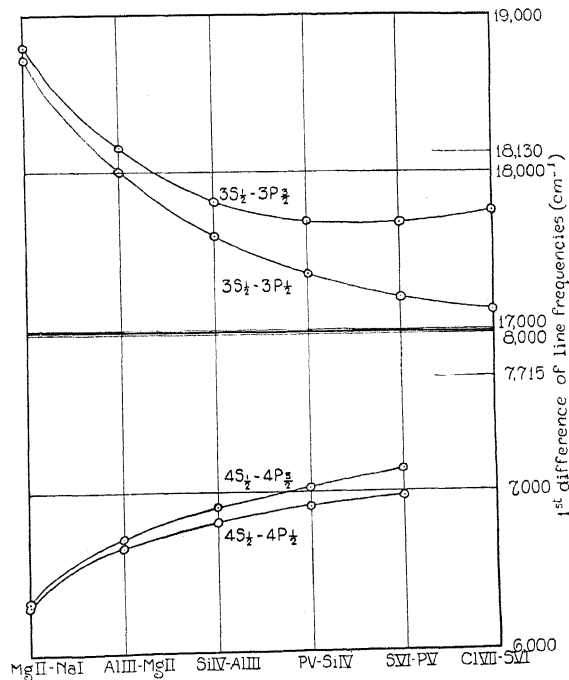


Fig. 8.

These two quantities, in Eqs. (31) and (32), have been calculated by means of this theory, and have been compared with the experimental values of Bowen and Millikan¹⁴ for the series Na I, Mg II, etc., and Li I, Be II, etc. in Figs. 7, 8, 9, and 10.

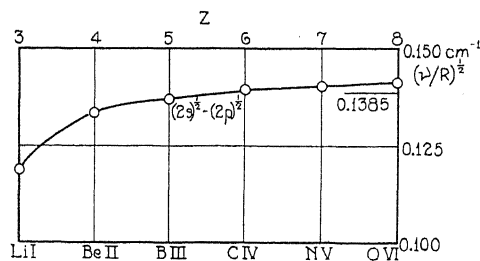


Fig. 9.

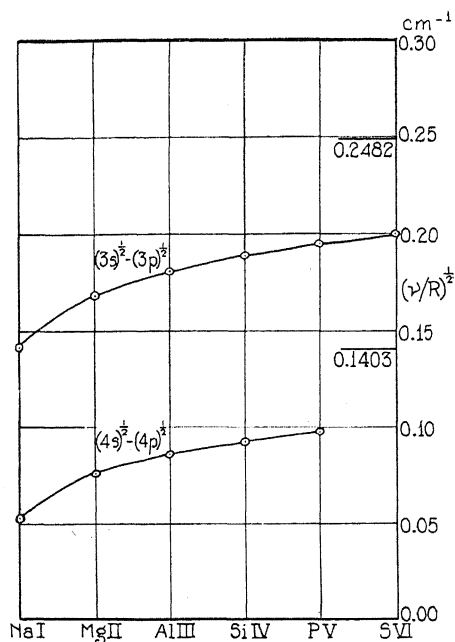


Fig. 10.

The use of the present theory to calculate these values involves the Schrödinger perturbation theory, since we are only interested in the energy values for large values of Z (σ nearly 0). We consider the core as a perturbation of an "hydrogenic" atom, writing the perturbation energy as

$$\epsilon = \frac{\int_0^\infty P(r) \psi^2 r^2 dr}{\int_0^\infty \psi^2 r^2 dr} \quad (33)$$

¹⁴ I. S. Bowen and R. A. Millikan, Phys. Rev. **25**, 299 (1925), **27**, 145 (1926).

where ψ is the wave function of the unperturbed hydrogenic atom, and $P(r)$ is the perturbation function of the core. We proceed to construct $P(r)$.

Consider an ion of nuclear charge Z , with z electrons in the core, and one valence electron in addition. The potential energy of the valence electron in the field of the nucleus plus core is

$$-\frac{Ze^2}{r}\phi_\sigma\left(\frac{r}{\mu}\right) \quad (34)$$

where ϕ_σ is the generalized Fermi function for an ion of order σ . The net charge of the ion is $(Z-z-1)$.

The potential energy of the valence electron in the field of the nucleus alone (of charge Ze) is

$$-\frac{Ze^2}{r}. \quad (35)$$

If we add and subtract Eq. (35) to Eq. (34), we still have the potential energy of the valence electron in the field of the nucleus plus core as

$$-\frac{Ze^2}{r} + \frac{Ze^2}{r}\left[1 - \phi_\sigma\left(\frac{r}{\mu}\right)\right] = -\frac{Ze^2}{r} + \Phi. \quad (36)$$

The quantity $\Phi = Ze^2/r[1 - \phi_\sigma]$ may be split into two parts Φ_1 and Φ_2 , such that

$$\Phi = \Phi_1 \text{ for } r \leq r_m$$

$$\Phi = \Phi_2 \text{ for } r \geq r_m,$$

where r_m is the radius of the core. If $r > r_m$, then

$$\phi_\sigma = \phi_{\sigma m} = 1 - \sigma = 1 - z/Z,$$

so that

$$\Phi_2 = \frac{Ze^2}{r}(1 - 1 + z/Z) = \frac{ze^2}{r}. \quad (37)$$

We may rewrite Eq. (36) in the form

$$-\frac{(Z-z)e^2}{r} + P(r) \quad (38)$$

where P is a function defined by

$$\begin{aligned} P &= \Phi_1 - Ze^2/r \text{ for } r < r_m \\ P &= 0 \quad \text{for } r > r_m. \end{aligned} \quad (39)$$

Now, if Z is very large, we may think of the valence electron as being primarily in the field of a point charge $(Z-z)e$, and then being perturbed by

another system, with the perturbation energy $P(r)$. So, without the perturbation we have an hydrogenic atom with nuclear charge $(Z-z)e$ (i.e. the quantity z is the first approximation to the screening number $b(n, l, Z)$).

If $Z \gg z$ (σ nearly 0), we may use the series approximation of ϕ_σ given in Eq. (14), since x_m is also nearly zero. By means of the analytical expressions of Eqs. (14) and (15) we are able to find an analytical expression for B_σ as a function of σ . To do this we notice that at the minimum

$$\phi' = 0 = -B + 2x_m^{1/2} - Bx_m^{3/2} + x_m^2 + \dots \quad (40)$$

Since both B and x_m are small, all terms after the first two are of lower order, so that, approximately,

$$B = 2x_m^{1/2}; \quad x_m^{1/2} = B/2; \quad x_m = B^2/4. \quad (41)$$

Then, substituting in Eq. (14), we have

$$\begin{aligned} \phi_m = 1 - \sigma &= 1 - B(B^2/4) + \frac{4}{3}(B/2)^3 - \frac{2}{5}(B/2)^5 + \dots \\ &= 1 - B^3/12 - B^5/80 + \dots \end{aligned} \quad (42)$$

or, to the same approximation as in Eq. (41),

$$B^3/12 = \sigma; \quad B = (12\sigma)^{1/3} \quad (43)$$

which is the required function. If we eliminate B from Eqs. (14) and (43), we obtain ϕ_σ in terms of x and σ explicitly. Thus

$$\phi_\sigma = 1 - (12\sigma)^{1/3}x + \frac{4}{3}x^{3/2} - \frac{2}{5}(12\sigma)^{1/3}x^{5/2} + \dots \quad (44)$$

and therefore

$$\begin{aligned} \Phi_1 &= \frac{Ze^2}{r} \left[(12\sigma)^{1/3}x - \frac{4}{3}x^{3/2} + \frac{2}{5}(12\sigma)^{1/3}x^{5/2} + \dots \right] \\ &= Ze^2 \left[\frac{(12\sigma)^{1/3}}{\mu} - \frac{4}{3} \frac{r^{1/2}}{\mu^{3/2}} + \frac{2}{5}(12\sigma)^{1/3} \frac{r^{3/2}}{\mu^{5/2}} + \dots \right]. \end{aligned} \quad (45)$$

Finally, we may write our perturbation function as

$$P(r) = Ze^2 \left[\frac{(12\sigma)^{1/3}}{\mu} - \frac{4}{3} \frac{r^{1/2}}{\mu^{3/2}} \right] - \frac{ze^2}{r}; \quad r \leq r_m \quad (46.0)$$

$$P(r) = 0; \quad r \geq r_m. \quad (46.1)$$

If we introduce the dimensionless variable

$$\rho = \frac{r}{r_0}; \quad r_0 = \frac{r(Z-z)}{na_0}, \quad (47)$$

where Ze = the real nuclear charge

$(Z-z)e$ = the nuclear charge of our hypothetical hydrogenic atom

a_0 = the normal radius of the hydrogen atom

n = the principal quantum number,

we have the perturbation function

$$Q(\rho) = P(r) = a + b\rho^{1/2} + c/\rho, \quad (48)$$

with

$$a = \frac{Ze^2(12\sigma)^{1/3}}{\mu} = \left(\frac{Ze^2}{a_0}\right) \frac{8Z^{1/3}}{3^{1/3}\pi^{2/3}} \quad (49.0)$$

$$b = -\frac{4Ze^2}{3\mu^{3/2}} \left(\frac{a_0 n}{2(Z-z)}\right)^{1/2} = -\left(\frac{Ze^2}{a_0}\right) \frac{32n^{1/2}}{9\pi(1-\sigma)^{1/2}} \quad (49.1)$$

$$c = -\frac{2ze^2(Z-z)}{a_0 n} = -2\left(\frac{Ze^2}{a_0}\right) \left(\frac{1-\sigma}{n}\right) \quad (49.2)$$

$$\rho_m = 2\frac{r_m}{r_0} = \frac{2r_m(Z-z)}{na_0} = (1-\sigma) \frac{\pi^{2/3} 3^{4/3} z^{2/3}}{4n} \quad (49.3)$$

and ϵ takes the form

$$\epsilon = \frac{\int_0^{\rho_m} Q(\rho) \psi^2(\rho) \rho^2 d\rho}{\int_0^\infty \psi^2(\rho) \rho^2 d\rho} \quad (50.0)$$

since $Q(\rho) = 0$ for $\rho \geq \rho_m$.

The limiting forms of Eqs. (49) for $\sigma = 0$ are

$$b]_{\sigma=0} = -\left(\frac{Ze^2}{a_0}\right) \frac{32n^{1/2}}{9\pi} \quad (50.1)$$

$$c]_{\sigma=0} = -\frac{2}{n} \left(\frac{Ze^2}{a_0}\right) \quad (50.2)$$

$$\rho_m]_{\sigma=0} = \frac{\pi^{2/3} 3^{4/3} z^{2/3}}{4n}. \quad (50.3)$$

We have passed to the limit several times during the process in order to simplify the calculations. The asymptotic form of the perturbation energy is

$$\epsilon_\infty = -L(n, l, z) \frac{Ze^2}{a_0} \quad (51)$$

If we were to extend the calculation for ϵ near the limit, we would find¹⁵

$$\epsilon = [-LZ + M + N/Z + \dots] \frac{e^2}{a_0}. \quad (52)$$

The energy of the unperturbed hydrogenic ion, of nuclear charge $(Z-z)e$, is

$$E = -\frac{e^2(Z-z)^2}{2a_0n} = -\frac{e^2}{2a_0n}(Z^2 - 2zZ + z^2) \quad (53)$$

and therefore the sum

$$E_p = E + \epsilon = -\frac{e^2}{2a_0n}[Z^2 - 2(Z - n^2L)Z + (z^2 - M) - N/Z + \dots] \quad (54)$$

is the energy of the perturbed ion. From this the reduced term value is seen to be

$$-\frac{t}{R} = \frac{1}{n^2}[Z^2 - 2(z - n^2L)Z + (z^2 - M) - N/Z + \dots] \quad (55)$$

In order to compare this with Eq. (28) we must place the square root of the right hand side under an indicated square. Thus

$$-\frac{t}{R} = \left\{ \frac{Z}{n} - \frac{1}{n}(z - n^2L) - \frac{M - 2zn^2L - n^4L^2}{2Zn} + \dots \right\}^2. \quad (56)$$

Comparing Eqs. (56) and (28) we may make the following identifications:

$$A(n, l) = \frac{1}{n}(z - n^2L) \quad (57.0)$$

$$B(n, l) = \frac{M - 2zn^2L - n^4L^2}{2n}, \text{ etc.} \quad (57.1)$$

From Eqs. (57.0) and (51) we may calculate quantities such as those of Eqs. (30) and (31).

The quantities of Eq. (30), which Wentzel introduced, must be calculated from "reduced" absolute term values. They are practically insensitive

¹⁵ Since the perturbation function has the form of Eq. (48), the perturbation integrals reduce to sums of integrals of the type

$$I(\mu, \nu) = \int_0^\nu x^{\mu-1} e^{-x} dx$$

which are known as "incomplete Γ -functions." They are special cases of the "confluent hypergeometric functions." Tables of these functions have been prepared by K. Pearson ("The Incomplete Γ -function"), but interpolation is very laborious. However, since we encounter only whole or half integral values of μ , it is much simpler to reduce the integrals to polynomials (integral values), or to polynomials plus Gauss error functions, by partial integration.

to relativity corrections, but the absolute term values are only known by somewhat approximate calculations from line frequencies. The unreduced values of Bowen and Millikan are plotted in Figs. 9 and 10.

The quantities calculated according to Eq. (31), though found directly from line frequencies, are very sensitive to relativity corrections, which are difficult to estimate accurately for s terms. Instead, in Figs. 7 and 8, the actual "unreduced" values are plotted for each of the doublet lines, to give an idea of the error involved in not reducing them. The lines on the right hand margin indicate the theoretical asymptotes.

In conclusion I wish to express my appreciation to Professor H. M. Randall, Director of the Physics department, for courtesies shown me during my graduate study at the University of Michigan. I am indebted to Professor O. Laporte for suggesting this problem to me, and for his constant advice. I also wish to thank Professors D. M. Dennison and E. A. Milne for valuable advice and criticism.

FINE STRUCTURE IN THE X-RAY ABSORPTION SPECTRA
OF THE *K* SERIES OF THE ELEMENTS CALCIUM
TO GALLIUM

BY BEN KIEVIT AND GEORGE A. LINDSAY

UNIVERSITY OF MICHIGAN

(Received July 10, 1930)

ABSTRACT

The *K* x-ray absorption spectra of the free elements Ca, Cr, Mn, Co, Ni, Cu and Zn have been photographed and for each of these elements an extended fine structure has been obtained. The fine structure, consisting of six or seven secondary edges, extends over an energy range of more than 200 volts. In every instance the element was used as the absorbing screen except Mn where it was present in the alloy manganin. No detectable difference was found in the absorption spectrum of copper between that obtained with a brass screen and that with the element alone. An attempt was made to show more definitely the relation of the $K\beta_2$ emission line to the principal *K* absorption limit for Fe, Co, Ni and Cu. Indications are that the main edge is produced by the ejection of a *K* electron to an optical level rather than to infinity. It is shown that the Kossel theory alone is quite inadequate to explain all the secondary edges. On the basis of multiple ionization the probable electron transitions have been determined and tabulated to account for the observed separations of the various secondary edges from the principal *K* edge. The methods employed herein to account for probable electron transitions, when applied to the transitions proposed by Ray, in his treatment of the fine structure in *K* and Ca, give very different energy values from those which he has computed.

INTRODUCTION

THE more or less complicated appearance of absorption spectra which is often found on the short wave-length side of the edge is known as absorption fine-structure. Stenstrom,¹ Fricke,² Hertz³ and Lindh⁴ were among those who made the earlier investigations. The latter made an extensive study of the *K* absorption spectra of the elements P(15) to Fe(26) and found as many as three white lines on the plates i.e., in addition to the ordinary absorption discontinuity there appeared lighter and darker regions on the short wave-length side. Coster and van der Tuuk⁵ found a very limited fine structure associated with the *K* edge of argon. An extended fine structure of the edge was found by Lindsay and Van Dyke⁶ in the *K* absorption of calcium, where the element was present in the crystals used as reflectors and served also in the capacity of absorbing material. Nuttall's⁷ investiga-

¹ W. Stenstrom, Diss. Lund, 1919.

² H. Fricke, Phys. Rev. **16**, 202 (1920).

³ G. Hertz, Zeits. f. Physik **3**, 19 (1920).

⁴ A. E. Lindh, Diss. Lund, 1923.

⁵ D. Coster, and J. H. van der Tuuk, Zeits. f. Physik **37**, 367 (1926).

⁶ G. A. Lindsay and G. Van Dyke, Phys. Rev. **27**, 508 (1926).

⁷ J. M. Nuttall, Phys. Rev. **31**, 742 (1928).

tion of the *K* edges of potassium and chlorine in compounds showed as many as five secondary edges. Voorhees and one of the authors⁸ have shown that the multiple structure for iron, both as a metal and in compounds, extends over a range considerably greater than that of any fine structure previously reported. They found that the outstanding features for the element alone were in the structure which was apparent in the main edge itself, the absence of the intense white-line absorption, the increase in extent or range of the secondary edges, and verified the fact that the free element has the principal absorption edge of longest wave-length⁹ which should therefore be more characteristic of the substance.

Since metallic iron afforded such an excellent fine-structure it was felt that other neighboring elements in the free state might also under suitable conditions, give an extended structure of the *K* absorption edge. Besides it was hoped that with information regarding the secondary edges of a considerable number of adjacent elements, it might be possible to arrive more readily at a satisfactory explanation for the observed phenomena. It was with such aims in view that the present work was undertaken. The general method employed was that of placing films of the absorbing metal in the path of the x-ray beam and obtaining photographic records of the absorption spectrum by reflection of the radiation from a sylvite or a calcite crystal.

APPARATUS AND EXPERIMENTAL PROCEDURE

A Siegbahn precision vacuum spectrograph was used for obtaining photographs of the absorption edges. For absorption spectra of all the elements investigated a natural potassium chloride crystal served as the reflector. The dispersion with this crystal varied from about 15 X.U. per mm for Ca to about 17 X.U. per mm in the case of zinc. Since the secondary edges become more crowded together with increasing atomic number it was necessary to increase the dispersion for Cu and Zn in order to obtain plates showing the fine structure which could be measured with a fair degree of accuracy. Accordingly, a calcite crystal was ground parallel to the (111) planes and mounted in the usual manner. This provided a dispersion of about 7 X.U. per mm.

Proper screens are one of the most essential requirements necessary to insure success in obtaining fine structure in the absorption edges. One must have uniformity as well as optimum thickness and both of these are troublesome factors in many cases. An excellent principal edge can be produced with screens which are either too thick or too thin to show the secondary edges. The surest method of determining the proper thickness is by trial.

Using such a trial method it was found that a nickel film about 0.007 mm thick gave excellent fine structure. This nickel had been prepared electrolytically and annealed in hydrogen. The copper, brass and zinc screens were prepared simply by carefully rolling out the metals to suitable thicknesses. It may be pointed out here that the results obtained for copper in

⁸ G. A. Lindsay and H. R. Voorhees, *Phil. Mag.* **6**, 910 (1928).

⁹ Kath. Chamberlain, *Nature* **114**, 500 (1924), *Phys. Rev.* **26**, 525 (1925).

brass showed no measurable deviations from that obtained when copper screens were used.

Considering the results obtained with brass screens for copper fine structure it was thought permissible to use an alloy of manganese as an absorber. Manganin, a copper-manganese alloy containing 15% manganese, was used since it could be easily rolled to the proper thickness and also because the manganese content is high in this alloy.

The preparation of cobalt screens presented no difficulties. The metal was deposited electrolytically on chromium plated electrodes from which it was then easily removed. The chromium screens required a different procedure. Due to its extreme hardness and brittleness rolling was out of the question. A layer of Cr about 0.003 mm thick was plated on a thin steel electrode. Then a thin coating of paraffin was applied over the Cr to strengthen the film, this added support being necessary during the following chemical process. HCl was used to etch away the iron from a small area leaving the Cr film which was supported by the remainder of the steel.

Calcium screens required extra precautions due to the rapid oxidation. Pure Ca was rolled out to the desired thickness and immediately given a thin coating of paraffin. In this manner Ca films could be used for a hundred or more hours.

Although no very definite results were obtained for gallium (31) and selenium (34), as far as fine structure is concerned, the preparation of these screens is described. Ga melts at 30.1°C . Like Hg in the liquid state its surface tension is great. Fortunately one is able to spread it out into a thin layer when applied on aluminum. If the Al is used in the form of thin foil there will be only a very slight amount of absorption due to this element since the wave-length of the *K* edge of Ga is below 1.2Å. Selenium screens were made by heating the element somewhat above its melting point and then when temperature conditions were just right it was possible to spread out the substance on thin pieces of paper. Here again the amount of absorption by the supporting material was negligible.

Measurements on all plates were made on a comparator having a least count of 0.005 mm. In making settings on the various edges the cross-hair of the instrument was brought across the blackening to such a position that it was possible just to see no falling off in the intensity on the long wave-length side of the cross-hair. Settings were also made on any good emission lines, if they were present on the plate, since they served as convenient reference lines to determine the wave-length of the principal edge and also permitted a check on the dispersion for the adjacent regions. The photometric curves incorporated in this paper were made on a Moll microphotometer. Duplicate runs over different portions of the plate gave curves which were essentially the same.

To aid in the interpretation of the fine structure data additional plates were made to show more definitely the location of the KB_2 line of an element with respect to the principal *K* absorption limit of the same substance. Copper, nickel, iron and cobalt were studied. The method employed was

to photograph on a plate the main K edge and any suitable reference line so that the distance between these two could be measured on the comparator. On another plate the emission spectrum of the element was obtained in which the $K\beta_2$ line was sufficiently prominent to be measured. The same reference line was photographed with the $K\beta_2$ line and therefore the distance between the lines could be determined. In each case of absorption the screens were of the free element, no attempt being made to obtain fine structure. For copper absorption the continuous spectrum came from a molybdenum target while in the other three cases a copper anode was employed. This procedure prevented the appearance of the $K\beta_2$ line in the absorption spectrum and therefore aided in making more reliable settings on the main edge. For the emission spectra targets of these various metals were used. At least two plates of each type for each element were obtained and measured.

In every case the value used in the computation of the wave-length of edge or line was the mean value of ten settings on the comparator. The general method used was that of reference measurements. Since the wave-length of the principal absorption edge depends upon the chemical combination of the absorber it was desirable to determine the wave-length of the absorption limits for each of the free elements studied. Having determined the wave-lengths of the main K edge for each element the wave-lengths of the secondary edges were computed by multiplying each linear separation, from the principal edge to the secondary edge, by the proper dispersion factor and subtracting each product from the known absorption limit. The reciprocal of the wave-length gives the frequency ν in cm^{-1} and division by the Rydberg constant 109737 gives ν/R for each edge. The separation $\Delta\nu/R$ of any secondary edge from the main edge may then be expressed in equivalent volts by multiplying the by the factor 13.56.

DATA AND RESULTS

I. Wave-Length determinations of principal K absorption limits.

In Table I have been recorded the mean values, expressed to the nearest 0.1 X.U., of the principal K absorption limits. The value of iron is included, this result having been taken from the work of Voorhees and one of the authors.⁸

TABLE I. Wave-lengths of the K absorption limits. λ in X.U.

Element	λ	Element	λ
20 Ca	3063.9	28 Ni	1484.6
24 Cr	2066.1	29 Cu	1377.8
25 Mn	1891.3	30 Zn	1280.8
26 Fe	1739.3*	31 Ga	1192.9
27 Co	1604.3	34 Se	977.8

* Lindsay and Voorhees.⁸

II. Absorption fine structure.

The general appearance of the plates showing absorption spectra in which the principal edges are accompanied by several secondary edges

may be seen in Fig. 1. The micro-photograms are reproduced in Fig. 2. The discontinuity designated by "K" marks the location of the main edge

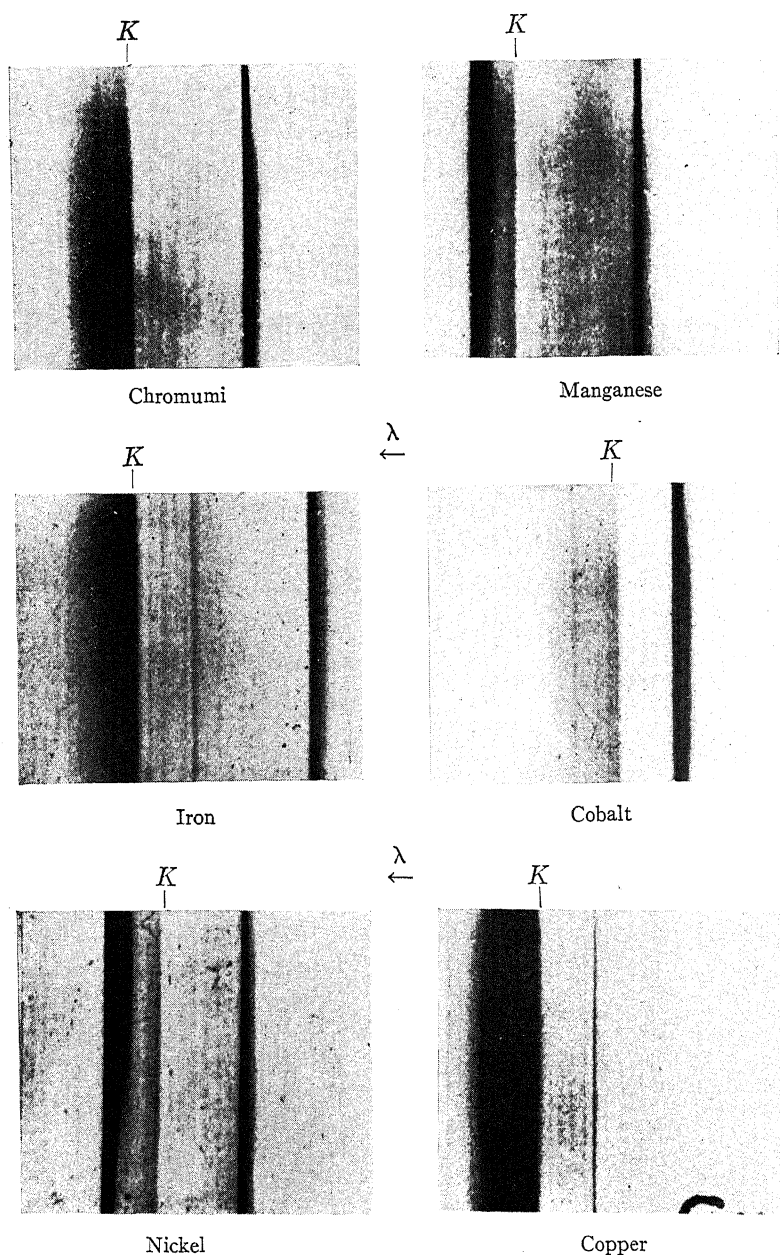


Fig. 1. Fine structure in the absorption spectra of the K series of several elements.

and it is in the lighter region to the short wave-length side of this edge that one observes the fine structure, whose general appearance is that of a series

of alternately light and dark regions. The "white lines" are not of the same width, nor of the same intensity, neither are they equally spaced on the plate but appear farther and farther apart as one proceeds to shorter wave-lengths. In the discussion below an attempt is made to trace the most

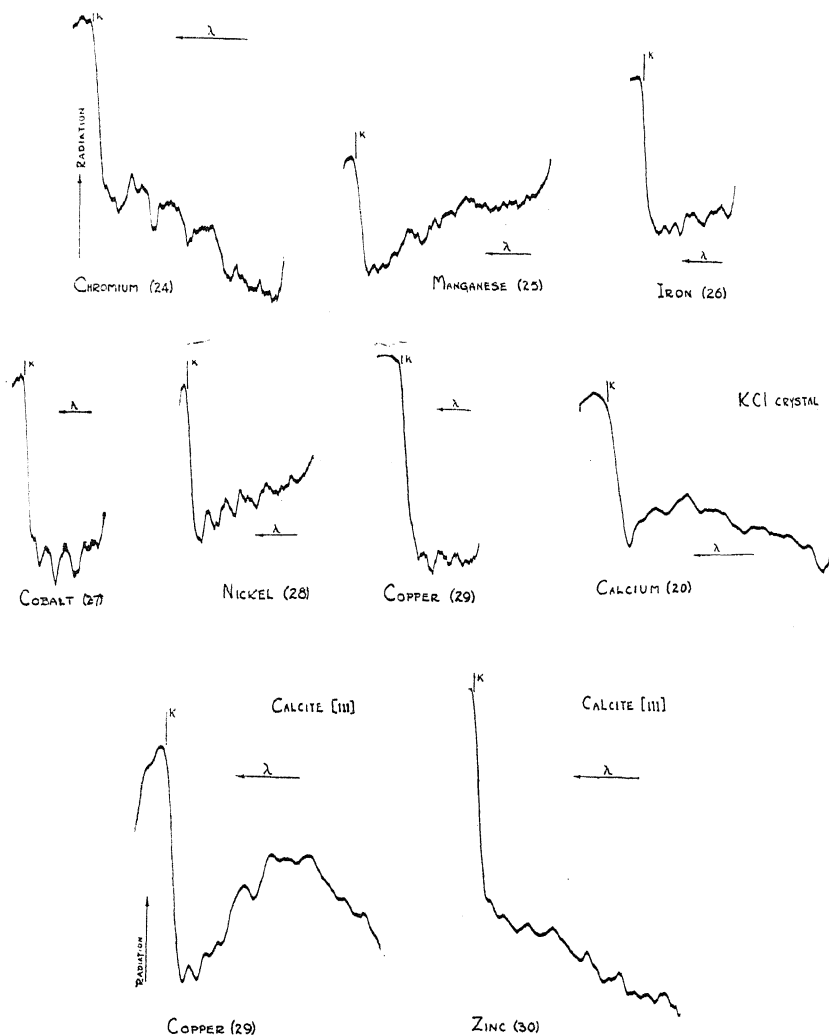


Fig. 2. Photometric records of *K* x-ray absorption spectra.

intense white line, or better, the adjacent secondary edge, through the various elements.

The results obtained from data on each element for which fine structure was observed and measured have been collected in Table II. In this table are given the mean values of the wave-lengths of the secondary edges, expressed to 0.1 X.U. together with the separations of these edges from the

TABLE II. Secondary absorption edges.

λ —Wave-length in X. U.					$\Delta(\nu/R)$ ΔV (volts)				Separation from Principal Edge				
λ $\left\{ \frac{\Delta(\nu/R)}{\Delta V} \right\}$	3063.9	3059.0	3048.5	3041.8	3034.7	3014.2	2987.3	2959.9					
Ca $\left\{ \frac{\Delta(\nu/R)}{\Delta V} \right\}$.48 6.5	1.50 20.2	2.16 29.3	2.87 38.9	4.90 66.4	6.93 94.0	10.45 142.					
Cr $\left\{ \frac{\Delta(\nu/R)}{\Delta V} \right\}$	2066.1	2060.5 1.19 16.2	2049.1 3.67 49.8	2040.0 5.66 76.7	2030.5 7.73 105.	2019.9 10.1 137.	2009.3 12.48 169.	1984.9 18.08 245.	1958.6 24.23 329.				
Mn $\left\{ \frac{\Delta(\nu/R)}{\Delta V} \right\}$	1891.3	1886.8 1.13 15.4	1880.6 2.73 37.1	1876.6 3.77 51.	1870.4 5.38 73.	1867.6 6.10 83.	1857.6 8.74 118.	1850.7 10.23 139.	1842.3 12.81 174.	1838.1 13.95 189.	1827.4 16.85 228.	1811.2 21.3 289.	1787.0 28.1 381.
Fe $\left\{ \frac{\Delta(\nu/R)}{\Delta V} \right\}$	1739.3	1737.1 .67 9.1	1731.4 2.39 32.4	1726.7 3.82 51.8	1721.1 5.54 75.	1715.2 7.36 100.	1706.9 9.90 134.	1701.3 11.7 159.	1690.9 14.9 202.	1683.4 17.4 236.	1663.0)* 24.0 325.		
Co $\left\{ \frac{\Delta(\nu/R)}{\Delta V} \right\}$	1604.3	1601.9 .86 11.6	1595.4 3.17 43.	1586.6 6.32 86.	1573.3 11.2 152.	1557.0 17.25 234.							
Ni $\left\{ \frac{\Delta(\nu/R)}{\Delta V} \right\}$	1484.6	1483.0 .69 9.3	1478.3 2.61 35.3	1471.0 5.65 77.	1458.2 11.14 151.	1449.4 14.97 203.	1442.7 17.86 242.	1431.3 22.95 311.	1413.0 31.2 423.				
Cu $\left\{ \frac{\Delta(\nu/R)}{\Delta V} \right\}$	1377.8	1375.8 .96 13.0	1374.2 1.74 23.6	1372.4 2.64 36.	1365.3 6.06 82.	1363.2 7.09 96.	1357.0 10.11 137.	1354.1 11.56 157.	1349.5 13.9 188.	1348.0 14.6 191.	1342.2 17.5 238.	1337.0 20.2 273.	1329.1 24.3 330.
Zn $\left\{ \frac{\Delta(\nu/R)}{\Delta V} \right\}$	1280.8	1278.7 1.15 15.6	1277.2 2.0 27.	1275.6 2.88 39.	1273.7 3.95 54.	1270.6 5.71 77.	1265.6 8.46 115.	1261.5 10.85 147.	1258.4 12.63 171.	1253.5 15.48 209.	1249.5 17.75 241.	1238.9 24.0 326.	

* Lindsay & Voorhees.⁸

principal edge. The separations are tabulated in ν/R units as well as in equivalent volts. The values for iron were taken from the results of Lindsay and Voorhees⁸ and were incorporated in order to have a complete sequence from Cr to Zn.

III. Relation between the $K\beta_2$ line and the principal K edge for the elements Fe, Co, Ni and Cu.

In the discussion of possible electron transitions corresponding to secondary edges it is evidently necessary to know as much as possible of the transition related to the principal edge. It has been rather assumed that the K electron goes to infinity. Now the $K\beta_2$ line represents a transition from the $N_{II,III}$ level to the K level, and if the K electron in absorption goes to infinity we should have for the elements here considered a difference between the K edge and the $K\beta_2$ line about equal to the first ionization potential.

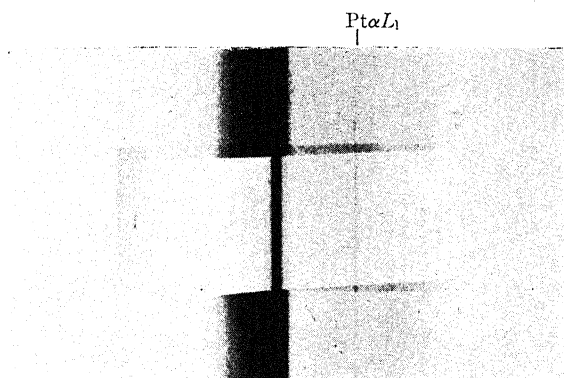


Fig. 3. K absorption and emission spectrum of copper.

Measurements from a number of plates of the relative positions of the K edge and the $K\beta_2$ line with respect to a chosen reference line show a separation smaller than that of the ionizing potential. The difference also varies with different elements. In fact, for nickel, what we have been accustomed to take as the position of the K edge is slightly longer in wave-length than the $K\beta_2$ line, while for Cu the two are sensibly the same. Fig. 3 shows the K absorption spectrum and the $K\beta_1$ and $K\beta_2$ emission lines for Cu photographed on the same plate. The reference lines is $PtL\alpha_1$.

THEORETICAL ASPECTS OF THE PROBLEM

Several hypotheses have been set forth to account for the observed structure of x-ray absorption edges. Since in this investigation free elements were used as absorbers there was no possibility of observing the white line absorption on the long wave-length side of the principal edge, similar to that found by Coster¹⁰ and by Lindh,¹¹ resulting from reduction of the com-

¹⁰ D. Coster, *Zeits. f. Physik* **25**, 83 (1924).

¹¹ A. E. Lindh, *Zeits. f. Physik* **31**, 210 (1925).

pounds in the screen by the x-ray beam thus producing some of the free element. It has been demonstrated that the free element has its principal absorption limit at a longer wave-length than any of the ionized forms.

According to Kossel's¹² viewpoint, published in 1920, the principal K absorption limit corresponds to the absorption of a quantum of energy sufficient to eject a K electron to the first permissible, unoccupied orbit. For the elements studied in this investigation this would mean a transition from the K level to the N_{II} level, or what is the same, from a $1s$ to a $4p$ state. That many atoms are excited to this state by the absorption of energy, is evidenced by the fact that the $K\beta_2$ line is emitted with considerable intensity by these elements. Thus one may conclude, as did Kossel, that the probability of a K electron stopping in the first unoccupied orbit is large. However, it is very likely that in many atoms the K electron would be ejected to the $5p$ or $6p$ level if the atom absorbed a quantum sufficient for such a jump. One would therefore expect absorption limits corresponding to these various transitions. The limiting position for these secondary edges would be that which corresponds to absorption of energy sufficient to remove a K electron completely from an atom. The energy required would be in excess of that for the principal edge by an amount corresponding approximately to the first ionization potential of an atom of atomic number one greater. The first ionization potentials for the elements under consideration are 6 to 9 volts. Edges within this small range are hardly to be detected although results indicate that the separation of the first secondary edge corresponds to the limiting value, that is, to the energy of ionization. Coster and Van der Tuuk in their study of the K edge of argon found a secondary edge at 1.7 volts from the main edge. They attributed this to the absorption of energy sufficient to eject a K electron to one of the optical levels of the atom.

There is rather convincing evidence that the main edge results from absorption of energy which will remove a K electron to an outer orbit rather than from that which would completely remove the K electron from the atom. As stated under Part III, the principal edge, at least for iron, cobalt, nickel and copper, has a separation from the $K\beta_2$ line which is never more than about half the ionizing potential. The $K\beta_2$ line is ascribed to the transition of an electron from the N_{II} level to the K level. To exactly what orbit the K electron goes in the absorption process is difficult to say, although the results would indicate an excitation to a higher optical level in the cases of cobalt, iron and copper than in nickel. Allowance for this condition was made in the determination to account for the secondary edges.

The extent of absorption fine structure such as that observed by Lindsay and VanDyke for calcium in calcium compounds, by Nuttall for potassium and for chlorine in compounds of those elements, by Lindsay and Voorhees for iron (free and in combinations), by Coster¹³ for copper and that by the authors has all been such that Kossel's theory, which he himself

¹² W. Kossel, *Zeits. f. Physik* 1, 119 (1920).

¹³ D. Coster, *Nature* 124, 652 (1929).

pointed out would explain only a small range of fine structure, would alone be quite inadequate to account for it. Secondary edges occur whose separations from the main edge are much greater than that which one could ascribe to an amount of energy of the order of the first ionization potentials. Thus one is led immediately to the supposition that a multiple ionization may result from the absorption of a single quantum of energy. It was this idea of multiple ionization that Wentzel¹⁴ proposed to account for the so-called "spark lines" or non-diagram lines which were found in x-ray emission spectra.

If Wentzel's hypothesis is a valid one to account for the emission of the "spark" lines then the atoms must absorb energy sufficient to excite them to the states which would give rise to such lines and one ought to be able to obtain absorption edges for the corresponding states. Lindsay and Voorhees, in their work on the K absorption in iron and iron compounds sought to locate an edge which would result when the incident quantum of energy ejected an L electron with a K electron. This edge would have a separation of about 750 volts from the principal edge. The indications of such an edge were too feeble to furnish any conclusive evidence for this double ionization. Likewise, no one has reported absorption edges to confirm a double ionization of the K state. However, this does not lead to the conclusion that simultaneous multiple ionization is improbable. Ionizations involving K and M or N electrons may occur and edges corresponding to these have been found by several investigators.

To calculate the energy difference in states represented by the separation of any secondary edge from the main edge one must know, or determine, or possibly assume, the electron transition which resulted from absorption of energy to produce the main edge. It was by means of measurements on the K edge and $K\beta_2$ line for several elements that one could say with some degree of assurance to which orbit the K electron went in the case of the main edge.

Consider first the zinc absorption spectrum. Zinc, atomic number 30, has the normal configuration of electrons $3d^{10} 4s^2$, and all the inner orbits are filled. To excite the atom to the K state means that a K electron must be ejected at least to an N_{II} level, i.e., to a $4p$ orbit. This will be designated by ($K \rightarrow N_{II}$). The ejected electron cannot stop in an inner orbit since there are no vacant ones in the neutral zinc atom. If this be the case then the wave-length for the main edge would correspond exactly to the wave-length of the $K\beta_2$ line. Although this was not verified for zinc in a manner similar to that for iron, nickel, cobalt and copper, there are other reasons to believe that one should attribute the main K edge to the transition $K \rightarrow N_{II}$ as recorded in Table III under zinc. In the first place it seems reasonable to assume that when one K electron is missing, then to an outer electron the nucleus and remaining K shell together, or the core of the atom, is very much like the central portion of the element with atomic number one

¹⁴ G. Wentzel, Ann. d. Physik 66, 437 (1921)

greater. Thus the nucleus and *K* shell of neutral zinc taken as a unit acts like a charge of 30-2 or 28 to an outer electron. This assumes that the *K* electrons have a complete screening effect. But with one *K* electron gone the effective charge would be 29. This is just the value of the charge of the

TABLE III. Probable multiple ionizations for secondary absorption edges.

Edge	Electron transitions	Separation from <i>K</i> edge in ν/R units	
	Calcium	Calculated	Observed
<i>K</i>	$(K \rightarrow M_{IV})$	0.00	0.00
1	$(K \rightarrow M_{IV}) + (N_I \rightarrow \infty)$	0.48	0.48
2	$(K \rightarrow M_{IV}) + (N_I \rightarrow \infty) + (N_I \rightarrow \infty)$	1.43	1.50
3	$(K \rightarrow M_{IV}) + (M_{III} \rightarrow \infty)$	2.70	2.87
4	$(K \rightarrow M_{IV}) + (M_I \rightarrow \infty)$	4.70	4.90
5	$(K \rightarrow M_{IV}) + (M_I \rightarrow N_{II}) + (M_{III} \rightarrow N_{IV})$	6.90	6.93
6	$(K \rightarrow M_{IV}) + (M_I \rightarrow \infty) + (M_I \rightarrow \infty)$	10.20	10.45
	Chromium		
<i>K</i>	$(K \rightarrow N_{II})$	0.00	0.00
1	$(K \rightarrow \infty) + (N_I \rightarrow O_{II})$	1.0	1.19
2	$(K \rightarrow N_{II}) + (M_{II} \rightarrow N_I)$	3.5	3.67
3	$(K \rightarrow \infty) + (M_{II} \rightarrow \infty) + (M_{IV} \rightarrow N_{II})$	5.3	5.66
4	$(K \rightarrow \infty) + (M_I \rightarrow \infty)$	7.55	7.73
5	$(K \rightarrow N_{II}) + (M_I \rightarrow M_{IV}) + (M_{II} \rightarrow N_I)$	10.1	10.1
6	$(K \rightarrow N_{II}) + (M_I \rightarrow N_{II}) + (M_I \rightarrow M_{IV})$	12.7	12.48
7	$(K \rightarrow N_{II}) + (M_I \rightarrow \infty) + (M_I \rightarrow \infty) + (M_{II} \rightarrow N_{IV})$	18.2	18.08
8	$(K \rightarrow \infty) + (M_I \rightarrow \infty) + (M_I \rightarrow \infty) + (M_{II} \rightarrow N_{IV}) + (M_{II} \rightarrow N_{IV})$	24.1	24.23
	Manganese		
<i>K</i>	$(K \rightarrow N_{II}) + (N_I \rightarrow M_{IV})$	0.00	0.00
1	$(K \rightarrow N_{II}) + (M_{IV} \rightarrow N_{II}) + (M_{IV} \rightarrow N_{II})$	1.2	1.13
2	$(K \rightarrow \infty) + (N_I \rightarrow \infty) + (M_{IV} \rightarrow N_{II})$	2.8	2.73
3	$(K \rightarrow \infty) + (N_I \rightarrow \infty) + (M_{IV} \rightarrow \infty)$	3.71	3.77
4	$(K \rightarrow \infty) + (M_{II} \rightarrow \infty)$	5.3	5.38
5	$(K \rightarrow \infty) + (M_{II} \rightarrow \infty) + (M_{IV} \rightarrow N_{II})$	5.9	6.10
6	$(K \rightarrow N_{II}) + (M_{II} \rightarrow \infty) + (M_{II} \rightarrow N_I)$	8.9	8.74
7	$(K \rightarrow \infty) + (M_{II} \rightarrow \infty) + (M_{II} \rightarrow N_{IV})$	10.1	10.23
8	$(K \rightarrow N_{II}) + (M_I \rightarrow \infty) + (M_{II} \rightarrow \infty)$	12.6	12.80
9	$(K \rightarrow N_{II}) + (M_{II} \rightarrow \infty) + (M_{II} \rightarrow \infty) + (M_{III} \rightarrow N_I)$	13.9	13.95
10	$(K \rightarrow \infty) + (M_I \rightarrow \infty) + (M_{II} \rightarrow N_I) + (M_{II} \rightarrow N_{IV})$	17.1	16.85
11	$(K \rightarrow N_{II}) + (M_I \rightarrow \infty) + (M_I \rightarrow \infty) + (M_{II} \rightarrow \infty)$	21.6	21.30
12	$(K \rightarrow \infty) + (M_I \rightarrow \infty) + (M_I \rightarrow \infty) + (M_{II} \rightarrow \infty) + (M_{II} \rightarrow N_I)$	27.9	28.10
	Iron		
<i>K</i>	$(K \rightarrow N_{II}) + (N_I \rightarrow M_{IV})$	0.00	0.00
1	$(K \rightarrow \infty) + (N_I \rightarrow N_{II})$	0.72	0.67
2	$(K \rightarrow \infty) + (N_I \rightarrow \infty) + (M_{IV} \rightarrow N_{II})$	2.4	2.39
3	$(K \rightarrow \infty) + (N_I \rightarrow \infty) + (M_{IV} \rightarrow \infty)$	3.73	3.82
4	$(K \rightarrow \infty) + (M_{II} \rightarrow \infty)$	5.8	5.54
5	$(K \rightarrow \infty) + (M_I \rightarrow M_{IV})$	7.4	7.36
7	$(K \rightarrow \infty) + (M_{II} \rightarrow N_I) + (M_{II} \rightarrow N_{IV})$	9.9	9.90
7	$(K \rightarrow N_{II}) + (M_I \rightarrow N_{II}) + (M_{II} \rightarrow M_{IV})$	11.9	11.70
8	$(K \rightarrow N_{II}) + (M_I \rightarrow M_{IV}) + (M_I \rightarrow N_{III})$	15.0	14.90
9	$(K \rightarrow \infty) + (M_I \rightarrow \infty) + (M_I \rightarrow N_{II}) + (M_{IV} \rightarrow N_{II})$	17.4	17.40
10	$(K \rightarrow \infty) + (M_I \rightarrow \infty) + (M_{II} \rightarrow N_I) + (M_{II} \rightarrow N_{IV}) + (M_{II} \rightarrow N_{IV})$	24.2	24.00
	Cobalt		
<i>K</i>	$(K \rightarrow \infty) + (N_I \rightarrow M_{IV})$	0.00	0.00
1	$(K \rightarrow \infty) + (N_I \rightarrow O_{II})$	0.86	0.86
2	$(K \rightarrow \infty) + (N_I \rightarrow \infty) + (M_{IV} \rightarrow O_{II})$	3.1	3.17
3	$(K \rightarrow \infty) + (M_{II} \rightarrow \infty)$	6.33	6.32
4	$(K \rightarrow \infty) + (M_{II} \rightarrow \infty) + (M_{II} \rightarrow M_{IV})$	11.23	11.14
5	$(K \rightarrow \infty) + (M_I \rightarrow \infty) + (M_I \rightarrow M_{IV})$	17.0	17.25

TABLE III. (Continued)

Edge	Electron transitions	Separation from K edge in ν/R units	
Nickel			
K	$(K \rightarrow M_{IV}) + (N_I \rightarrow M_{IV})$	0.00	0.00
1	$(K \rightarrow M_{IV}) + (N_I \rightarrow \infty)$	0.57	0.69
	$(K \rightarrow \infty)$	0.79	0.69
2	$(K \rightarrow \infty) + (N_I \rightarrow \infty) + (M_{IV} \rightarrow N_I)$	2.6	2.61
3	$(K \rightarrow M_{IV}) + (M_{II} \rightarrow N_{IV})$	5.7	5.65
4	$(K \rightarrow M_{IV}) + (M_{II} \rightarrow N_{IV}) + (M_{II} \rightarrow N_I)$	11.3	11.14
5	$(K \rightarrow M_{IV}) + (M_I \rightarrow N_{II}) + (M_{II} \rightarrow \infty)$	15.0	14.97
6	$(K \rightarrow M_{IV}) + (M_I \rightarrow N_{II}) + (M_I \rightarrow N_{III})$	18.0	17.86
7	$(K \rightarrow \infty) + (M_I \rightarrow \infty) + (M_I \rightarrow \infty) + (M_{IV} \rightarrow N_{II}^+)$	22.7	22.95
8	$(K \rightarrow \infty) + (M_I \rightarrow \infty) + (M_I \rightarrow \infty) + (M_{II} \rightarrow \infty)$	31.2	31.20
Copper			
K	$(K \rightarrow N_{II})$	0.00	0.00
1	$(K \rightarrow \infty) + (N_I \rightarrow N_{II})$.86	.96
2	$(K \rightarrow \infty) + (N_I \rightarrow \infty)$	1.72	1.74
3	$(K \rightarrow \infty) + (M_{IV} \rightarrow \infty)$	2.45	2.64
4	$(K \rightarrow N_{II}) + (M_{II} \rightarrow N_I)$	6.50	6.06
5	$(K \rightarrow N_{II}) + (M_{II} \rightarrow \infty)$	7.20	7.09
6	$(K \rightarrow N_{II}) + (M_I \rightarrow N_{II})$	10.10	10.11
7	$(K \rightarrow N_{II}) + (M_I \rightarrow N_{II}) + (M_{IV} \rightarrow \infty)$	11.7	11.56
8	$(K \rightarrow N_{II}) + (M_{II} \rightarrow \infty) + (M_{II} \rightarrow N_I)$	13.9	13.89
9	$(K \rightarrow N_{II}) + (M_{II} \rightarrow \infty) + (M_{II} \rightarrow N_{IV})$	14.5	14.60
10	$(K \rightarrow N_{II}) + (M_I \rightarrow \infty) + (M_{II} \rightarrow N_{IV})$	17.8	17.50
11	$(K \rightarrow N_{II}) + (M_I \rightarrow N_{II}) + (M_I \rightarrow N_{III})$	20.7	20.20
12	$(K \rightarrow N_{II}) + (M_I \rightarrow N_{II}) + (M_{II} \rightarrow N_{IV}) + (M_{II} \rightarrow N_I)$	24.3	24.30
Zinc			
K	$(K \rightarrow N_{II})$	0.00	0.00
1	$(K \rightarrow \infty) + (N_I \rightarrow N_{II})$	1.11	1.15
2	$(K \rightarrow \infty) + (N_I \rightarrow \infty)$	1.95	2.00
3	$(K \rightarrow \infty) + (M_{IV} \rightarrow \infty)$	2.88	2.88
4	$(K \rightarrow N_{II}) + (M_{IV} \rightarrow \infty) + (N_{IV} \rightarrow N_{II})$	3.95	3.95
5	$(K \rightarrow \infty) + (N_I \rightarrow \infty) + (M_{IV} \rightarrow \infty)$	5.75	5.71
6	$(K \rightarrow N_{II}) + (M_{II} \rightarrow \infty)$	8.24	8.46
7	$(K \rightarrow N_{II}) + (M_{II} \rightarrow \infty) + (M_{IV} \rightarrow \infty)$	11.0	10.85
8	$(K \rightarrow \infty) + (M_I \rightarrow \infty)$	12.88	12.63
9	$(K \rightarrow \infty) + (N_I \rightarrow \infty) + (M_I \rightarrow \infty)$	15.35	15.48
10	$(K \rightarrow N_{II}) + (M_{II} \rightarrow \infty) + (M_{II} \rightarrow \infty)$	17.3	17.75
11	$(K \rightarrow N_{II}) + (M_I \rightarrow \infty) + (M_I \rightarrow N_{II})$	24.14	24.00

core of neutral gallium. The electron configuration for gallium is $3d^{10}4s^24p$. Hence the K electron of zinc in being ejected by the absorption of energy sufficient to excite the K state would probably stop in the $4p$ orbit so as to give an outer configuration like gallium, and there would now be 29 electrons outside the K shell just as there are in neutral gallium.

Further evidence that this assumption is valid comes from the results expressed in Table III for the energy separations of the secondary edges in the zinc absorption spectrum. By taking the K electron to an N_{II} level for the main edge remarkably good agreement has been obtained between calculated and observed values for the energy separations of secondary edges from the K edge. The method employed in calculating these energy separations follows.

Column one in Table III lists the edges in order of decreasing wave-length beginning with the main edge (which has the longest wave-length) marked

"K". In the second column appear the probable electron transitions which involve absorptions of energy of sufficient amounts to account for the observed edges. Calculated and observed values (expressed in the customary ν/R units) of the energy differences which correspond to the separations of the main and secondary edges are given in the last two columns.

Confining attention to the tabulation on zinc, one notes that the K edge has been recorded as resulting from the transition $K \rightarrow N_{II}$ as mentioned above. The first secondary edge, might arise from the transitions:

$$(K \rightarrow \infty) + (N_I \rightarrow N_{II})$$

which may also be written as: $(K \rightarrow N_{II}) + (N_I \rightarrow \infty)$ although the former is easier to compute. The additional energy involved here, above that for $(K \rightarrow N_{II})$, may be determined since it amounts to:

$$(N_{II} \rightarrow \infty) + (N_I \rightarrow N_{II}).$$

Keeping in mind that the configuration after $(K \rightarrow N_{II})$ is $3d^{10}4s^24p$, it is evident that the term $(N_{II} \rightarrow \infty)$ requires energy measured by the first ionization potential for gallium which is 5.97 volts or 0.44 in ν/R units. One must then add to this the energy to excite a gallium ion from a $4s^2$ state to a $4s4p$ state. From Ga II, as given by Sawyer and Lang¹⁵, the separation of these states is about 0.67 in ν/R . Hence the total separation of the first secondary edge from the K edge is $0.44 + 0.67 = 1.11$ whereas the observed value is 1.15.

For edge #2 we have written:

$$(K \rightarrow \infty) + (N_I \rightarrow \infty)$$

and since we are interested in the separation from the K edge we may write:

$$(N_{II} \rightarrow \infty) + (N_I \rightarrow \infty).$$

The first term as before is the energy to ionize the gallium atom once leaving the configuration $4s^2$, and the second term is the energy to remove the second ion after the first one is gone or, in other words, the second ionization potential which one obtains from the Ga II spectrum. Its value is 20.45 volts or 1.51 in ν/R . Thus the energy difference is computed to be: $0.44 + 1.51 = 1.95$. This corresponds favorably with the observed value of 2.0.

The next edge involves changes in the atom whereby two electrons, a K electron and an M_{IV} electron, are ejected from the atom. The transitions are given by:

$$(K \rightarrow \infty) + (M_{IV} \rightarrow \infty)$$

Similar to the preceding case the first term requires 0.44 in ν/R units to ionize the atom once. With the values of the energy levels as given in the thesis of F.P. Mulder,¹⁶ the energy to remove an M_{IV} electron to an N_{II} level is found to be 1.6. But to remove the M_{IV} electron completely from

¹⁵ R. A. Sawyer and R. J. Lang, Phys. Rev. 34, 712 (1929).

¹⁶ F. P. Mulder, Diss. Groningen, 1927.

the atom will take more than that amount. In the computation for the first secondary edge it was seen that $(N_I \rightarrow N_{II})$ required 0.67 providing the K electron was ejected to infinity, while in #2 the energy was the second ionization potential if $(N_I \rightarrow \infty)$. Hence to take the M_{IV} electron out completely would require $1.51 - 0.67$ or 0.84 in addition to that necessary to eject it from an M_{IV} level to the N_{II} level. This gives as the total energy of separation of the third edge from the main edge:

$$0.44 + (1.6 + 0.84) = 2.88.$$

The observed value for this edge is also equal to 2.88.

Edge #4 may be accounted for by the transitions:

$$(K \rightarrow N_{II}) + (M_{IV} \rightarrow \infty) + (M_{IV} \rightarrow N_{II})$$

and for the separation value we need consider just the last two terms. With the K electron stopping in the N_{II} orbit the atom is much like neutral gallium. We need therefore 1.6 in ν/R to take an M_{IV} electron to the N_{II} orbit but this time only 0.44 more to remove it entirely from the atom since this amounts to the first ionization. Hence the term $(M_{IV} \rightarrow \infty)$ requires $1.6 + 0.44 = 2.04$. The next step necessitates the excitation of a second M_{IV} electron to the N_{II} level. Since one electron has already been taken from this group it should require more than 1.6 for the second M_{IV} electron. In order to estimate what increase ought to be made one needs to consider the value of the screening constant for the $M_{IV,v}$ levels, which Sommerfeld¹⁷ gives as 13.0. This means that the average screening effect for each electron is not more than about one half so that it seems reasonable to assume the value of the M_{IV} level to be increased by approximately one third the amount that the germanium M_{IV} level exceeds the gallium M_{IV} level. Thus the term $(M_{IV} \rightarrow N_{II})$ requires 1.9 and the total amount of energy that corresponds to the separation of edge #4 from the K edge is:

$$1.6 + 0.44 + 1.9 = 3.94.$$

Experimentally the separation was found to be 3.95.

The fifth secondary edge is associated with the following changes in electron configuration:

$$(K \rightarrow \infty) + (N_I \rightarrow \infty) + (M_{IV} \rightarrow \infty)$$

which may be written:

$$(K \rightarrow \infty) + (N_I \rightarrow \infty) + (N_I \rightarrow \infty) + (M_{IV} \rightarrow N_I)$$

since in both the resulting configuration is the same, and the latter form lends itself more readily to computation. Considering again only the energy corresponding to the separation of the secondary edge and the K edge we may write:

$$(N_{II} \rightarrow \infty) + (N_I \rightarrow \infty) + (N_I \rightarrow \infty) + (M_{IV} \rightarrow N_I)$$

¹⁷ A. Sommerfeld, "Atomic Structure and Spectral Lines," Methuen, London.

and recalling that the configuration after ($K \rightarrow N_{II}$) is $3d^{10}4s^2 4p$ we see that the first, second and third terms require energy equal to the first, second and third ionization potentials of gallium respectively. The last term amounts to the excitation of a Ga^{+++} ion from a $3d^{10}$ state to a $3d^9 4s$ state. From the Ga IV spectrum as reported by Mack, LaPorte and Lang,¹⁸ the separation of the terms $3d^{10}$ and $3d^9 4s$ is approximately 1.3. The four terms above give then:

$$0.44 + 1.51 + 2.5 + 1.3 = 5.75$$

compared with 5.71 which is the observed value for the separation in energy of the fifth secondary edge from the K edge.

In quite an analogous manner one can account for the other observed secondary edges. For each case one must choose those transitions such that the energy involved will correspond as nearly as possible to the observed values. This has been done for six more edges in zinc as well as for those found for the other elements studied. In most cases the agreement is good.

The question naturally arises as to the uniqueness of the transitions involved. Are there other possible combinations of transitions that will serve equally well to account for any given edge? In most instances the answer would probably be in the negative. One exception has been recorded in Table III for edge #1 in nickel. For the first few edges in each spectrum one must restrict the choice of electron transitions to those involving only the outer or valence electrons, since levels inside $M_{IV,V}$ are already too deep. In contrast with this one has difficulty (especially with the lighter elements studied) in finding transitions which involve enough energy to account for the shortest wave-length secondary edges. As mentioned above, changes calling for transitions from the L levels do not aid in this situation since one change such as ($L \rightarrow M$) would involve too much energy to account for any observed secondary edge.

The predominating factors which governed the choice of transitions to account for a given separation (other than that the total energy be correct) were:

- (1) the electron configuration corresponding to the K edge
- (2) minimum number of electron transitions.

The first of these had been discussed at length under the calculations of the various secondary edges. Some verification of the second is shown by the fact that the most prominent secondary edges seem to be associated with those changes in which the K electron and only one other (usually an M_I or an M_{II}) electron are excited. Thus two electron jumps seem more probable than those involving three or more, which is to be expected.

In connection with this characteristic feature concerning the excitation of M electrons with K electron it has been mentioned above that Coster has observed a fine structure in copper that is in good agreement with the results herein reported for that element. However, he obtained no secondary

¹⁸ J. E. Mack, Otto Laporte and R. J. Lang, Phys. Rev. 31, 748 (1928).

edges in zinc and attributed this negative result to the fact that in zinc (normal configuration $3d^{10}4s^2$) the $3d$ group of electrons is completely filled, so that it would be much more difficult to break into this configuration than it would be in the case of let us say—iron, nickel or even copper. A glance at Table III will indicate, however, that transitions of M electrons enter into practically every computation for zinc secondary edges.

When one compares the general method of computing the energy separations of the secondary edges from the K edge as outlined and applied in this investigation with the method used by Ray¹⁹ for potassium, calcium and chlorine, it is very evident that there will be wide deviations in the results. One or two specific calculations will be given to confirm this statement.

Ray has used the experimental data of Nuttall⁷ for potassium in various compounds, and also the data of Lindsay and Van Dyke⁶ for calcium in calcium compounds. The normal configuration of potassium is $2p^64s$. The K edge, according to Ray, is associated with the transition ($K \rightarrow \infty$). The first secondary edge is related to the change:

$$(K \rightarrow \infty) + (N_I \rightarrow \infty)$$

so that the separation of this edge from the main edge is due to the term ($N_I \rightarrow \infty$) which Ray gives as the first ionization potential of potassium or 4.1 volts. The observed value for the separation varies from 2.8 to 4.9 volts in different compounds. Several objections to this treatment may be noted.

In the first place, when the K electron is ejected either to an outer orbit or to infinity it seems more reasonable to assume that to an outer electron, such as an N_I electron, the core of the atom should be more like calcium than potassium. If the K electron remained in the outer portion of the atom then the transition ($N_I \rightarrow \infty$) ought to correspond to the first ionization potential of calcium (6.09 volts), instead of to that for potassium (4.3 volts). But with the assumption that the K electron is ejected to infinity one ought therefore to regard ($N_I \rightarrow \infty$) as requiring energy equal to the second ionization potential of calcium which is 11.8 volts rather than 4.1 volts. A further objection arises since the potassium is present as an ion and not as an atom in the free state. In the ionic state there might not even be an N electron which could be ejected. The calculations on subsequent edges for potassium are also open to quite similar objections.

Ray's treatment of the calcium edges seems equally unsatisfactory. The normal configuration is $2p^64s^2$ and for the K edge he has assigned the transition ($K \rightarrow \infty$). For the first edge he gives as the electron jumps:

$$(K \rightarrow \infty) + 2(N_I \rightarrow \infty)$$

so that the latter term involves the energy which corresponds to the separation of this edge from the main edge. This he gives as twice the first ioniza-

¹⁹ B. B. Ray, Zeits. f. Physik 55, 119 (1929).

tion potential for calcium (6.1 volts) or 12.2 volts, as compared with the observed value of 13.3 to 16.0 volts.

Neglecting the fact that the calcium is in a compound, the following interpretation of the transitions:

$$(K \rightarrow \infty) + 2(N_I \rightarrow \infty)$$

seems more preferable:

Since the K electron is completely ejected the atom is now much like ionized scandium (Sc^+). Removing one of the N_I electrons would require energy equal to the second ionization potential of scandium which is 12.8 volts. To remove the second N_I electron ought to take an amount of energy equal to the third ionization potential which is about 25 volts. Thus the total energy separation would be approximately 38 volts instead of 12.2 volts as given by Ray. The value for the next secondary edge in calcium is about 31 volts. Thus the transitions:

$$(K \rightarrow \infty) + 2(N_I \rightarrow \infty)$$

as chosen by Ray, which under our interpretation given above corresponds to an energy separation from the K edge of 38 volts, represent not only a great deal in excess of the 15 volts demanded for the first edge, but even too much to account for the separation of the second secondary edge from the main edge.

FALSE LINES IN X-RAY GRATING SPECTRA

By J. M. CORK

DEPARTMENT OF PHYSICS, UNIVERSITY OF MICHIGAN

(Received July 5, 1930)

ABSTRACT

Because of the arrangement of slits, x-ray source and diffraction grating generally employed in x-ray spectroscopy, certain false lines may be obtained on the photographic plate in addition to those due to defects in the grating. Spectrograms of such spurious lines having their origin in a non-uniform focal spot or reflection from slit faces, as well as those due to certain grating imperfections are shown. One type of companion line is present at wave-lengths about 13 percent greater than the parent line, whose origin is not explained.

THE existence and explanation of false lines in grating spectra in the optical region has been dealt with by many writers. Meggers and Kiess, Anderson and Runge¹ have treated the lines known as Rowland ghosts and Lyman ghosts in spectra obtained with several particular gratings. Since such false lines or 'ghosts' may occur in any spectral region and be of intensity comparable with that of fainter true lines, they may lead to confusion in interpretation of the spectra. In x-ray spectra, beside false lines of this type there may occur others due to the nature of the source. Fig. 1 shows spectrograms illustrating false lines of four different types. While with sufficient care most of these false lines may be avoided, the possibility of their existence makes them worthy of description.

The arrangement of x-ray source, slits and grating usually employed is shown in Fig. 2. Slit widths are generally less than 0.1 mm and the distance between slits *A* and *B* not less than 15 cm. The minimum width of spectral line to be expected for a given set of conditions may be readily computed by means of the diffraction formula $\lambda = d(\cos\theta - \cos\phi)$ where λ , d , θ and ϕ denote respectively wave-length, grating constant, grazing angle of incidence, and grazing angle of diffraction. For a slit width at *A* of 0.1 mm and distance between slits of 15 cm, assuming the grating very close to the second slit, a variation is obtained in the grazing angle θ at the grating of 2.27 minutes of arc which combined with an assumed width of 0.1 mm at *B* would give a maximum variation of 4.54 minutes of arc. It is perhaps remarkable that this apparently unfavorable slit arrangement when used with a grating having 30,000 lines per inch and an incident angle θ of 20 minutes of arc for the first order molybdenum *L* series lines as shown in *A* Fig. 1 should yield a variation in ϕ of only 40 seconds of arc. This divergence in the diffracted beam would cause an increment in width of line on a photographic plate at a distance of 50 cm of only 0.097 mm. For higher orders the width is cor-

¹ Meggers and Kiess, Anderson and Runge, Jour. Opt. Soc. and Rev. Sci. Ins. 6, 417 (1922).

respondingly reduced so that for the fourth order spectrum under the same conditions the maximum width increment is 0.0531 mm. Now while slits 0.1 mm wide when used with the 30,000 line grating as shown yield lines of satisfactory sharpness, with coarser gratings and larger values of the incident angle θ , much wider lines are produced. Thus for an incident angle of 40 minutes and a grating of 14,400 lines per inch a divergence in ϕ of 2.0 minutes of arc is obtained, giving a width increment of 0.29 mm for the first order L series lines of molybdenum.

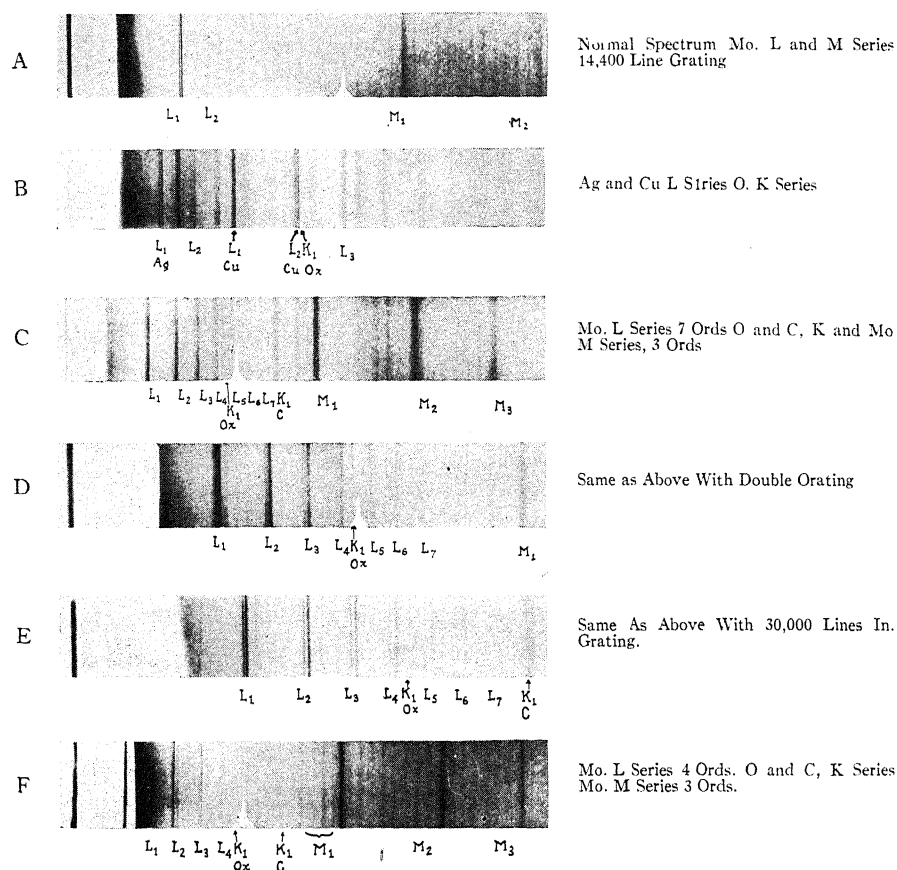


Fig. 1. Spectrogram showing false x-ray lines.

In this case the line very often appears to consist of a group of very fine lines. This fine structure may be due to either of two causes, namely (a) a multi-point focal spot on x-ray target, (b) reflection or scattering of ex-radiation from the faces of slit A. Spectrogram C in Fig. 1 illustrates this multiple structure. The $L\alpha_1$ line on the original photographic plate shows clearly as five fine lines. This is undoubtedly due to the existence of several radiating spots in the main focal spot. These fine spots originating perhaps by surface irregularities become heated to incandescence and are plainly

visible. A multiplicity of this sort might account for the fine structure reported for the $K\alpha$ line of carbon² as it would be in agreement with the statement that the relative intensity of the observed components varied with voltage. The second type of defect may be produced if the main part of the focal spot is not included between limiting lines drawn through slits *A* and *B* as shown in Fig. 2, but lies outside as at *C*. This may result in a line of the usual width with more intense blacking at either border, the type of line depending upon relative position of focal spot and slits as well as shape of slit faces. In spectrogram *D*, Fig. 1 each main line has a blacking of this type on the long wave length side disappearing at high orders. Similarly if the total focal spot is very small and located as at *m* in Fig. 2, then a strong-fine line with a faint companion on each side might be obtained. These defects may be largely reduced by using sharp slit faces arranged as shown in Fig. 2 with a narrow opening.

Another peculiar type of defect in spectra is shown in spectrogram *D*, Fig. 1. In this case each line is doubled and the distance between components

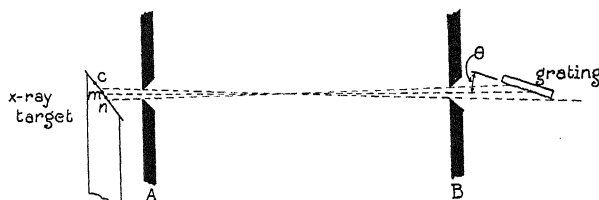


Fig. 2. Arrangement of target, slits and grating in x-ray spectrograph. (Relative slit width enlarged.)

is the same regardless of the distance between grating and photographic plate and varies only slightly with the spectral order. An examination of the grating showed that in the part of the surface being used there were two surface levels due perhaps to some abrupt change in condition during the ruling process, this being a portion of a test grating. Two such parallel gratings when used at grazing incidence would produce doubled lines having a minimum separation of $\sin\phi/\sin\theta$ times the difference in level. A proper selection of grating surface would of course avoid defects of this sort.

Rowland ghosts as observed in optical spectra would be difficult to observe in the x-ray region. They consist of spurious lines close to and on each side of the real line with apparent wave-lengths

$$\lambda_g = \lambda(1 \pm n/Nm)$$

where *n* and *m* denote the order of spurious line and order of real line respectively, and *N* stands for the number of lines ruled for one revolution of the ruling machine screw. These lines are due to the superposition of a coarser period upon the nominal period of the grating caused by imperfections connected with the pitch of the screw in the ruling machine. Such false lines may have intensities less than 1/1000 that of the parent line for gratings

² Bazzoni, Faust and Weatherby, *Nature* **123**, 717 (1929).

ruled on the excellent machines now existant. This low intensity, combined with the minute separation that would be obtained for say a 30,000 line per inch grating in high orders, make ghosts of this type of no moment in x-ray spectroscopy.

False lines of the Lyman type having wave-lengths such as $3/5$, $4/5$, $6/5$, $7/5$ etc. the wave-length of a real line but with intensities less than $1/1000$ that of the parent line might be observed in the x-ray region. These lines have been explained by Runge as due to the superposition of two periods on the grating, one large and one small but neither necessarily a simple multiple of the fundamental period, caused by some mechanical irregularity in the ruling machine. In spectrogram *F*, Fig. 1 the principal Mo *M* line whose wave-length is 64.52 Å is shown over-exposed in three orders. Situated almost symmetrically with each of these are two pairs of fainter lines. The inner pair is separated from the parent line by fractional wave-length differences of 0.067 less and 0.073 more than the central line. The wave-length (of that one) of the outer pair on the short wave-length side is 55.17 Å which agrees with a wave-length value already attributed to a molybdenum *M* line.³ The component on the long wave-length side may be a satellite of the type to be described in the following paragraph. Although the arrangement of these lines looks suspiciously like a parent line with satellites on either side, there is no definite assurance so far, that they are not all real lines.

It will be observed in Fig. 1 in every spectrogram that on the long wave length side of every strong line there appears a companion line of perhaps $1/10$ the intensity whose wave-length is approximately 1.133 times that of the strong line. The principal lines in most of these spectra are the Mo *L*, α_1 and β_1 lines. Wave-lengths greater than the α_1 and β_1 , by the factor 1.133 would come very close to the fainter Mo *L* series, 1 and η lines. However, the relative intensity of these lines is not similar to that found for the 1 and η lines in crystal spectrometry. Further, similar lines are found on the long wave-length side of the copper $L\alpha_1$ and oxygen $K\alpha$ lines in the same relative position as shown in spectrogram 3, Fig. 1. Accompanying lines of this sort were obtained in the same relative position, both with gratings ruled 14,400 lines per inch on the University of Michigan ruling machine and those with 30,000 lines per inch from Johns Hopkins University. At present a satisfactory explanation of these lines is not available.

³ Thibaud, Jour. Opt. Soc. & Rev. Sci. Inst. 17, 145.

THE ARC SPECTRUM OF PALLADIUM

BY A. G. SHENSTONE,

PALMER PHYSICAL LABORATORY, PRINCETON UNIVERSITY

(Received June 30, 1930)

ABSTRACT

A practically complete analysis of Pd I is given, based on previous analyses. The electron structures are d^{10} , d^9s , $6s$, $7s$, $8s$ (part of) d^8s^2 (incomplete) d^95p , d^8sp and d^96p (parts of), d^95d , d^96d (almost complete).

The presence of an unidentified level k_1 is discussed and it is shown that the only explanation within the Hund theory is that k_1 is a hyperfine structure component of $5d^3P_1$. Such an assignment presents very great difficulties.

THE ARC spectrum of palladium has played a considerable part in the development and correction of the Hund theory of atomic spectra. It was partially analyzed by Beals¹ and, later, more completely by McLennan and Smith² and by Bechert and Catalan.³ About the time when McLennan was engaged on the analysis, there appeared Hund's⁴ paper, on the correlation between components of terms and the components of the limit terms on which they are built. This circumstance was unfortunate because the accuracy of the theory was quite naturally accepted by McLennan and the naming of the levels of the spectrum was carried out to agree with that theory instead of with the usual criteria, intensities and Zeeman effects. A little later Hund's book⁵ was published; and, in it, McLennan's analysis of Pd I appeared as the most conclusive evidence for the theory of limits. That theory has since been proved to be correct in only a few trivial cases.⁶ The analysis of Pd I has been only partially corrected in a paper on Ag II by McLennan and McLay⁷ and by Shenstone.⁸ The present designation of terms was communicated to Gibbs and White and was used by them in their paper⁹ on Cd III.

The following analysis is based on the numerical analyses of McLennan and Smith, and Bechert and Catalan. A considerable number of new terms has been found, some of which can be identified as second series members of the d -electron series. The spectrum in the ultraviolet has been measured, and new lines have been found by long exposures throughout the whole visible and ultraviolet.

As much information as possible has been collected in the term table.

¹ Beals, Proc. Roy. Soc. 109A, 369 (1925).

² McLennan and Smith, Proc. Roy. Soc. 112A, 110 (1926).

³ Bechert and Catalan, Zeits. f. Physik 35, 449 (1926).

⁴ Hund, Zeits. f. Physik 34, 296 (1925).

⁵ Hund, Linien Spektren und Periodisches System.

⁶ Hund, Zeits. f. Physik 52, 601 (1929).

⁷ McLennan and McLay, Trans. Roy. Soc. Can. 22, 10 (1928).

⁸ Shenstone, Nature 121, 619 (1928).

⁹ Gibbs and White, Phys. Rev. 31, 776 (1928).

Electron configurations, the notation used by Bechert and Catalan, and by McLennan and Smith, the present notation, the level, the level connections, the g -values where known, the Landé g -values, and the Rydberg denominators are given in successive columns. The intervals and g -sums are tabulated separately at the end of the term table.

TABLE I. Term Table, Pd I.

Origin.	B. & C.	McL.	S.	Level	Obs. "g"	Landé "g"	Ryd. Den.
$4d^{10}$	1^1S_0	1^1S_0	a^1S_0	0.0			
$4d^9(^2D_{3/2})5s$	3^3D_3	1^3D_3	$5s^3D_3$	6564.0*	1.33	1.33	1.3446
"	3^3D_2	1^3D_2	$5s^3D_2$	7755.0*	1.17	1.17	1.3579
$4d^9(^2D_{1/2})5s$	3^3D_1	1^3D_1	$5s^3D_1$	10093.9*	.50	.50	1.3445
"	1^1D_2	1^1D_2	$5s^1D_2$	11721.7	1.00	1.00	1.3629
$4d^85s^2$	1^1G_4	b^3F_4	a^3F_4	25101.1*			1.2775
"	"	b^3F_3	a^3F_3	28213.5*			
"	"	"	a^3F_2	29711.0*			
$4d^9(^2D_{3/2})5p$	3^3P_2	1^3P_2	$5p^3P_2$	34068.8*	1.50	1.50	1.8185
"	3^3F_3	1^3F_3	$5p^3F_3$	35451.3*	1.08	1.08	1.8576
"	3^3F_4	1^3F_4	$5p^3F_4$	35927.8*	1.25	1.25	1.8717
"	3^3P_1	1^3P_1	$5p^3P_1$	36180.5*	1.42	1.50	1.8793
"	$3^3D_2'$	$1^3D_2'$	$5p^3D_2$	36975.8*	1.03	1.17	1.9038
"	$3^3D_3'$	1^3F_3	$5p^3D_3$	37393.5*	1.33	1.33	1.9171
$4d^85s^2$	"	"	a^3P_2	37952.0...			1.2935
$4d^9(^2D_{1/2})5p$	3^3P_0	1^3P_0	$5p^3P_0$	38088.0*			1.8318
"	3^3F_2	1^3F_2	$5p^3F_2$	38811.7*	.72	.67	1.8524
"	1^3F_3	$1^3D_3'$	$5p^1F_3$	39858.1*	1.08	1.00	1.8835
"	$3^3D_1'$	1^3P_1	$5p^3D_1$	40368.6*	.82	.50	1.8993
"	$1^3D_2'$	$1^3D_2'$	$5p^1D_2$	40771.3	1.14	1.00	1.9120
"	1^3P_1	$1^3D_1'$	$5p^1P_1$	40838.7	.76	1.00	1.9141
$4d^9(^2D_{3/2})6s$	a_3	2^3D_3	$6s^3D_3$	48804.2*			2.4394
"	b_2	2^1D_2	$6s^3D_2$	49019.5*			2.4537
$4d^85s5p?$	"	"	$z^3D^{70}?$	50910.4.	1.47?	1.50	
$4d^9(^2D_{1/2})6s$	d_1	2^3D_1	$6s^3D_1$	52336.3*			2.4389
"	"	"	1_3^0	52457.0	1.26?		
$4d^9(^2D_{1/2})6s$	e_2	2^3D_2	$6s^1D_2$	52487.7			2.4490
"	"	"	$z^3F_3^0?$	53761.6			
"	"	"	2_3^0	54335.9			
$4d^9(^2D_{3/2})5d$	f_1	a^3S_1	$5d^3S_1$	54574.1			2.9431
"	"	"	3_4^0	54600.2?			
"	"	"	4_3^0	54673.2	1.29?		
$4d^9(^2D_{3/2})5d$	3^3G_5	a^3G_5	$5d^3G_5$	54806.1*			2.9705
"	3^3G_4	a^3G_4	$5d^3G_4$	54811.3*			2.9711
"	h_2	a^3P_2	$5d^3P_2$	54820.6*			2.9722
"	i_1	a^3P_1	$5d^3P_1$	54822.7*			2.9724
"	k_1	"	k_1	54825.9*			
$4d^9(^2D_{3/2})5d$	l_3	a^3D_3	$5d^3D_3$	54947.7*			2.9875
"	m_2	a^1D_2	$5d^3D_2$	54998.5*			2.9937
"	n_3	a^1F_3	$5d^3F_3$	55012.2*			2.9954
"	o_4	a^3F_4	$5d^3F_4$	55025.2*			2.9970
"	p_0	a^1S_0	$5d^3P_0$	55373.0*			3.0279
"	"	"	6_2^0	55634.1*	.92?		
"	"	"	7_2^0	56335.9*			
"	"	"	8_4^0	56544.6*	1.06		
$4d^85s5p?$	"	"	$7^3D_3^0$	56910.9*	1.33	1.33	
"	"	"	9_2^0	57255.0*			
"	"	"	10_2^0	57565.2*			
"	"	"	11_2^0	57926.2*			
$4d^9(^2D_{3/2})7s$	"	a^3G_4	$7s^3D_3$	58064.1*			3.4581
"	"	"	12_2^0	58103.7*			
$4d^9(^2D_{3/2})7s$	q_2	3^1D_2	$7s^3D_2$	58138.3*			3.4721
$4d^9(^2D_{1/2})5d$	r_1	a^3P_1	$5d^1P_1$	58195.3*			2.9527

TABLE I. (Continued).

Origin.	B. & C.	McL.	S.	Level	Obs. "g"	Landé "g"	Ryd. Den.
$4d^8 5s 5p?$			$3^3 F_4^0$	58316.8	1.25	1.25	
$4d^9(^3D_{1\frac{1}{2}})5d$	3G_3	$a^3 G_3$	$5d^3 G_3$	58348.9 * . . .			2.9710
"	t_4		$5d^3 G_4$	58387.8 . . .			2.9757
"			13_s^0	58389.8 . . .			
"	u_1	$a^3 D_1$	$5d^3 D_1$	58408.1 . *			2.9781
"			14_2^0	58415.1 . .	.91?		
"	v_2	$a^3 D_2$	$5d^3 D_2$	58448.5 . .			2.9830
"	w_2	$a^3 F_2$	$5d^3 F_2$	58555.8 . *			2.9961
"	x_3	$a^3 F_3$	$5d^3 F_3$	58561.7 .			2.9968
"	y_0	$a^3 P_0$	$5d^3 S_0$	58681.3 .			3.0108
"			15_s^0	59143.1 .	1.04?		
"			16_1^0	59588.4 .			
"			17_2^0	59731.2 .			
$4d^9(^2D_{2\frac{1}{2}})6d$			$6d^3 S_1$	60225.8? .			3.9556
"			$6d^3 G_3?$	60315.5 *			3.9809
"			$6d^3 G_4$	60318.2 *			3.9817
"			$6d^3 P_2$	60322.0 . *			3.9829
"			$6d^3 P_1$	60323.4 . *			3.9832
"			$6d^3 D_3$	60370.4 . . *			3.9968
"			$6d^3 F_3$	60397.9 . . . *			4.0050
"			$6d^3 D_2$	60397.9 . . . *			4.0050
"			$6d^3 F_4$	60404.0 . . . *			4.0068
$4d^8 5s 5p?$			$3^3 F_3^0$	60722.6	1.20?	1.08	
"			18_1^0	60729.8			
$4d^9(^2D_1)7s$	z_1	$3^3 D_1$	$7s^3 D_1$	61602.8 * . . .			4.4581
"	a_2'	$3^3 D_2$	$7s^3 D_2$	61638.6 . . .			4.4649
$4d^9(^2D_{2\frac{1}{2}})8s$			$8s^3 D_3$	61736.2 . . .			4.4656
"			19_s^0	62316.3 . . .	1.08		
$4d^9(^2D_{2\frac{1}{2}})9s$			$9s^3 D_3$	63571.7? . . .			5.4715
$4d^9(^2D_{1\frac{1}{2}})6d$			$6d^3 G_3$	63853.0 * . . .			3.9806
"			$6d^3 G_4$	63872.7 . . .			3.9863
"			$6d^3 D_1$	63896.3 . *			3.9929
"			$6d^3 F_2$	63937.4 . *			4.0050
"			$6d^3 F_3$	63939.8 .			4.0059
$4d^9$			$4d^2 D_{2\frac{1}{2}}$	67236.0			
"			$4d^2 D_{1\frac{1}{2}}$	70775.0			
$4d^8 5s^2$			$5s^4 F_{4\frac{1}{2}}$	92307.0			
"			$5s^4 P_{2\frac{1}{2}}$	103507.5			

Column 1 Electron Configuration.
 " 2 Notation of Bechert and Catalan.
 " 3 Notation of McLennan and Smith.
 " 4 Notation of Shenstone.

Column 5 Numerical Value of Level.
 " 6 "g" Value, observed.
 " 7 "g" Value, Landé.
 " 8 Rydberg Denominator.

Term separations.

$d^9 5s$	3D	1191; 2339. 215; 3317.
$6s$		74; 3465.
$7s$		
$5p$	$^3P^0$	2112; 1908.
	D	-418; 3393.
	F	-477; 3360.
$5d$	3P	2; 550.
$6d$		1; ?
$5d$	D	51; 3410.
$6d$		17; 3498.
$5d$	F	-13; 3544.
$6d$		-6; 3540.
$5d$	G	5; 3538.
$6d$		3; 3535.
$d^8 s^2$	$a^3 F$	3112; 1497.

"g-sums"

Structure	J	Obs.	Landé.
$d^9 5s$	3	1.33	1.33
	2	2.17	2.17
	1	.50	.50
$d^9 5p$	4	1.25	1.25
	3	3.49	3.41
	2	4.39	4.34
	1	3.00	3.00

Certain levels given by other authors have not been included. They are given in Table II.

TABLE II. *Rejected terms.*

Author	Level	Explanation
McL. & S.	45489.3	Unidentified line
	56519.6	Unidentified line and spark line
	56695.	Unidentified line
	57650.	Unidentified line and spark line
	58028.	Unidentified line
	64701.	Insufficient evidence
B. and C.	49533.6	2 of 3 lines used elsewhere
	51285.0	2 or 3 lines are spark lines
	56168.4	2 or 3 lines used elsewhere

The 6 levels rejected from McLennan and Smith's list are all founded on lines observed by them in the underwater spark or in absorption in palladium vapor. These lines are all either spark lines or lines which have not been identified as palladium lines in any other source.

Of the 3 levels rejected from Bechert and Catalan's list, one is founded on spark lines, and the other two give only three combinations and of those, two in each case are lines otherwise used in the analysis. Those two levels are therefore possible but extremely improbable.

1. *Determination of the term types.* The information from which the term types may be determined consists of intensities of lines and Zeeman effects. For the low multiplets, the intensities¹⁰ give sufficient evidence that Bechert and Catalan's selection of terms was correct. The intensity diagram (Figure 1) demonstrates this result. Beals' Zeeman effect measurements must also be considered. These measurements are not altogether satisfactory since they are in some cases inconsistent. I have remeasured some of the ultra-

	$5s^3D_3$	3D_2	3D_1	1D_2
$5p^3P_2^0$	700R	75	20	50
3P_1		500r	75	50
3P_0			200	
3D_3	1000R	300		200
3D_2	50	500R	100	200
3D_1		100	400	200
3F_4	1000R			
3F_3	300r	600R		200
3F_2		20	400r	200
1P_1		10	200	250
1D_2	40	100	300	300
1F_3	50	200		500r

Fig. 1. Intensity diagram of low multiplets.

¹⁰ The intensities are Meggers' estimates and are somewhat different from those used in Table III of the paper, Phil. Mag. 8, 765 (1929).

violet lines, and from all the evidence available have calculated the probable values of the g -factors for a considerable number of terms. They are not to be considered as having an accuracy of better than about 3%. It is worth notice that the g -values would hardly permit of a choice between $5p^3D_1^0$ and $5p^1P_1^0$ although the evidence of the intensity diagram is reasonably certain.

The terms of prefix $5d$ are all from old levels. Intensities again suffice to determine the types unambiguously except perhaps for the two levels of $J=0$. The lower of the two levels has been chosen as 3P_0 because its combinations with triplet terms are considerably stronger than those of the higher level. In Ag II the equivalent levels in my analysis have both been found by Blair (to be published shortly) to be false and a new 3P_0 has been found which agrees in position and characteristics with the level chosen in Pd I. No very probable 1S_0 has been found in Ag II. The terms of prefix $6d$ were identified partly from intensities and partly from series extrapolation. In some cases they are doubtful levels and are followed by a question sign. In addition there are the terms of prefix $6s$, $7s$, $8s$, $9s$ which will be discussed below; and a large number of unidentified or doubtfully identified high odd levels. The designation of one level as k is carried over from Bechert and Catalan and the level is discussed below.

2. *Structures.* From the atomic number (46) of Pd it can be predicted that the spectrum should have low terms from the structures $4d^{10}$, $4d^95s$, $4d^85s^2$; and, from the general relations amongst similar structures in other spectra, their relative energies can be roughly predicted. Such a prediction is in agreement with the discovery of 1S_0 as the lowest term, 3D , 1D as the next and 3F as the next. The relatively high position of the 3F and, therefore, of all other terms based on $4d^85s$ makes the spectrum very much less complicated than Ni I in which $3d^94s$ and $3d^84s^2$ are of practically equal energy and importance. Except for a^3F and a^3P_2 no terms founded on $4d^85s$ can be definitely identified although a few high odd terms probably do belong to that structure.

3. *Limits.* All terms based on the ion $4d^9$ are prefixed by the symbols which indicate the quantum numbers of the one electron whose change of condition is responsible for the emission of spectral lines. Amongst the even terms it is possible to pick out directly three members of the series ns^3D^1D . A calculation of a Ritz formula then allows the prediction of the position of higher terms. The $8s^3D_3$ and the doubtful $9s^3D_3$ were found in this way. The series was then recalculated using the $6s$, $7s$, $8s$ terms. The limit of this series is $4d^9\ ^2D_{2\frac{1}{2}}$ of Pd II and the addition of 3529, known from Pd II, yields $4d^9\ ^2D_{1\frac{1}{2}}$. Those terms are given at the end of the table, together with $4d^85s\ ^4F_{4\frac{1}{2}}$ and $^4P_{2\frac{1}{2}}$ which were used to calculate the Rydberg denominators of a^3F_4 and a^3P_2 . The separation of the 2D limit is so great (3529) that even the $5p$ terms break up naturally into two groups corresponding to the components of 2D . This effect is very much more in evidence in the higher terms where we find the groups much closer together and separated by about 3500 wave numbers. In spite of such evidence of practically complete jj coupling, the intensities of the lines indicate at least as close an approach to

LS coupling as occurs amongst the lower levels. The $6d$ group of terms is new and almost complete. Its combinations with the $5p$ group give the diffuse lines in the visible and near ultraviolet previously unassigned. In particular, the two lines $\lambda 4020$ and $\lambda 4098$ which are given in the tables as reversed are in reality double lines and belong to this group. Part of one of these lines is unassigned though it would fit well as the prohibited combination $5p^3F_3^0 - 6d^3G_5$. There is therefore some doubt of the naming of 3G_5 .

The Rydberg denominator of every level whose limit is known is given in the term table. The values of these numbers for the $5d$ and $6d$ terms form confirmation of the accuracy of the calculation of the series limit.

The Ritz formula calculated from the terms $6s$, $7s$ and $8s^3D_3$ is

$$T = 67236 - T^1 = 67236.0 - \frac{R}{(n + 0.47681 - 2.037 \times 10^{-6}T^1)^2}$$

4. *High odd terms.* The wave-length list was extended as far into the ultraviolet as possible in the hope that the terms from the structure $4d^96p$ could be found and give some evidence concerning the still rather unsatisfactory theory of limits. A large number of levels was found in the proper energy range but in most cases there is insufficient evidence on which to classify them. There are undoubtedly numbers of odd levels of the structure $4d^85s5p$ in that same region and they naturally add to the difficulty. An attempt has been made to classify by means of Zeeman effects, but this also was not very successful. Some possible levels of the latter structure are indicated in the term table, the evidence being mainly Zeeman effect and intensity of combination with the term a^3F . A number of rather strong sharp lines in the region around λ 3000–3200 have been used to form these terms and there remain a few such lines unidentified.

5. *The level k_1 .* The designation k_1 for the level 54825.9 found by Bechert and Catalan has been retained as a distinguishing mark because of the very peculiar nature of that level. It is an even level of $J=1$ or 2 (but almost certainly 1) and it makes 5 exact combinations, all of which are diffuse.¹¹ It is distant from $5d^3P_1$ only 3.2 wave numbers and all of its combinations occur with those terms with which $5d^3P_1$ combines strongly. There are no other diffuse lines in Meggers' list except $\lambda 4631.37$, which is triply assigned.

There are three possible origins for the level k_1 : (1) A term of the system $4d^9nx$; (2) A term of the system $4d^85s\ nx$; (3) A hyperfine structure component of $5d^3P_1$. The first possibility may be eliminated by the observation that all terms of that structure which could have such an energy have been discovered. The second possibility reduces to a consideration of $4d^85s^2$ only, since all other even configurations yield terms much too high. The configuration d^8s^2 contains only one level of $J=1$. It is a 3P_1 level, but an examination of the analogous spectra Ni I, and Pt I and the spectrum Pd II demonstrates that k_1 is about 10,000 wave numbers too far above 3F_4 and 3P_2 . There is

¹¹ The line $\lambda 4816.27$ is of the same character as the other k_1 lines on Meggers' plates and has been so labelled in the wave-length list.

a remote possibility that the level is 1D_2 but it is at least 5000 wave numbers too high and it does not combine with either 1F_3 or 1D_2 . The third possibility, that k_1 is a hyperfine structure component of $5d^3P_1$, appears to be extremely improbable. There is certainly no expectation that a single level in a whole spectrum should show a structure of 3.2 units and that level one not involving an s -electron at all. If it is hyperfine structure, then the hyperfine structure is wider than the fine structure since $^3P_2-^3P_1$ is only 2.2 units.

I believe that the level k_1 is the only level yet found in any spectrum which cannot be logically explained on the Hund theory; but a single exception is sufficient to indicate that there is a factor which is yet to be considered. It would be of great interest to examine the Zeeman effect of a group of lines involving the levels $5d^3P_2$, 3P_1 and k_1 . The fields produced by an ordinary magnet are sufficient to produce the beginnings of a Paschen-Back effect of the three levels if they have the necessary structural affiliation.

I would like to point out in this connection that the type of analysis which has been carried out since the development of the Hund theory is unlikely to give anything but confirmation since the theory is assumed correct to start with. But that theory has been shown to be incorrect in one part, the prediction of limits, and it is possible that it is either incomplete or incorrect in other details. There is, of course, no doubt of the essential correctness of the theory.

The wave-length table (Table III) contains all the identified lines of Pd I and, in addition, the few remaining unidentified lines of any strength. The intensities are the estimates of Dr. Meggers except for a short range from $\lambda 3700$ to $\lambda 4500$ and a number of newly observed lines for which I have made estimates on about the same scale. As usual, Dr. Meggers has been extremely kind in placing at my disposal considerable unpublished data.

TABLE III

λ	I	A	ν	Combination	λ	I	A	ν	Combination
9234.02	1	M	10826.6	$a^3F_4-5p^3F_0^0$	7026.91	1	M	14227.1	$5p^1D_3^0-5d^3D_2$
8761.34	2	M	11410.7	$5p^3D_3^0-6s^3D_3$	7016.44	8	M	14248.3	$5p^3P_0^0-6s^3D_1$
8695.03	1	M	11497.7	$5p^1P_1^0-6s^3D_1$	6917.56	2	M	14452.0	$5p^3D_1^0-5d^3P_2$
8644.38	1	M	11565.0	$5p^1D_3^0-6s^3D_1$	16.56	9	M	14454.1	$5p^3D_1^0-5d^3P_1$
8399.06	2	M	11626.0	$5p^3D_3^0-6s^3D_2$	6914.98	2h	M	14457.4	$5p^3D_1^0-k_1$
8585.28	1	M	11644.6	$a^3F_3-5p^1F_3^0$	6892.52	0	M	14504.5	$a^3P_2-1^0$
8581.99	2	M	11649.1	$5p^1P_1^0-6s^1D_2$	78.35	2	M	14534.4	$5p^1P_1^0-5d^3P_0$
8532.67	2	M	11716.5	$5p^1D_3^0-6s^1D_2$	56.89	0	M	14579.9	
8451.93	0	M	11828.4	$5p^3D_3^0-6s^3D_3$	6833.42	8	M	14629.9	$5p^3D_1^0-5d^3D_2$
8353.54	2	M	11967.7	$5p^3D_3^0-6s^3D_1$	6784.52	10	M	14735.4	$5p^3P_2^0-6s^3D_3$
8300.81	5	M	12043.7	$5p^3D_3^0-6s^3D_2$	6774.54	12	M	14757.1	$a^3F_4-5p^1F_3^0$
8132.85	6	M	12292.4	$a^3F_4-5p^3D_3^0$	6739.16	0	M	14834.6	
7961.04	4	M	12557.7	$a^3F_3-5p^1D_3^0$	6712.10	0	M	14894.4	
7915.84	7	M	12629.4	$5p^1F_3^0-5d^1D_2$	6686.79	3	M	14950.7	$5p^3P_2^0-6s^3D_2$
7786.66	7	M	12839.0	$5p^3P_2^0-6s^3D_2$	85.71	2	M	14953.2	$5p^1F_3^0-5d^3G_4$
7763.99	12	M	12876.4	$5p^3F_3^0-6s^3D_3$	81.56	3	M	14962.4	$5p^1F_3^0-5d^3P_2$
7486.93	7	M	13352.9	$5p^3F_3^0-6s^3D_3$	62.86	4	M	15004.6	$5p^3D_1^0-5d^3P_0$
7391.91	8	M	13524.6	$5p^3F_3^0-6s^3D_1$	25.28	4	M	15089.5	$5p^1F_3^0-5d^3D_3$
68.14	15	M	13568.2	$5p^3F_3^0-6s^3D_2$	23.26	4	M	15094.1	$5p^3D_3^0-6s^1D_2$
7310.06	5	M	13676.0	$5p^3F_3^0-6s^1D_2$	6603.03	1	M	15140.4	$5p^1F_3^0-5d^3D_2$
7278.44	2	M	13735.4	$5p^1P_1^0-5d^3S_1$	6599.32	0	M	15148.9	
42.90	2	M	13802.8	$5p^1D_3^0-5d^3S_1$	97.08	1	M	15154.0	$5p^1F_3^0-5d^3F_2$
7228.99	1	M	13829.4	Pb?	6591.44	3	M	15167.0	$5p^1F_3^0-5d^3F_4$
7149.11	6	M	13983.9	$5p^1P_1^0-5d^3P_1$	6508.41	6	M	15360.5	$5p^3D_3^0-6s^3D_1$
*7147.45	1h	M	13987.2	$5p^1P_1^0-k_1$	6465.90	0	M	15461.5	
7115.84	3	M	14049.1	$5p^1D_3^0-5d^3P_2$	6464.68	0	M	15464.4	
7060.29	5	M	14159.8	$5p^1P_1^0-5d^3D_2$	6444.89	2	M	15511.9	$5p^3D_3^0-6s^1D_2$
52.04	2	M	14176.4	$5p^1D_3^0-5d^3D_3$	6342.46	1	M	15762.4	$5p^3F_3^0-5d^3S_1$
37.58	3	M	14205.5	$5p^3D_3^0-5d^3S_1$	6268.23	0	M	15949.1	Cu?

* Previously unpublished line observed by Dr. Meggers of the Bureau of Standards.

TABLE III (continued)

λ	I	A	ν	Combination	λ	I	A	ν	Combination
6244.78	1	M	16009.0	$5^sP_2^0-5^sD_2P_2$	4991.62	2	S	20028.0	$5^sD_2^0-6^sP_2D_2$
43.97	2	M	16011.0	$5^sP_2^0-5^sD_2P_1$	71.95	9	M	20107.3	$5^sP_2^0-5^sD_2P_1$
03.73	0	M	16114.9		62.05	0h	S	20151.4	$5^sP_2^0-12^sD_2$
03.13	0	M	16116.4		29.99	3	M	20278.4	
6195.61	2	M	16136.0	$5^sP_2^0-5^sD_2D_3$	24.20	2	M	20302.2	
88.02	6	M	16155.8	$5^sP_2^0-6^sD_2D_1$	4919.87	8	M	20320.1	$5^sP_2^0-5^sD_2D_1$
76.15	5	M	16186.8	$5^sP_2^0-5^sD_2D_2$	4875.43	20	M	20505.3	$5^sP_2^0-5^sD_2S_1$
70.94	5	M	16200.5	$5^sP_2^0-5^sD_2F_3$	36.44	4	M	20670.6	$5^sP_2^0-7^sD_2D_3$
36.99	1	M	16290.1		19.15	2	M	20744.8	$5^sP_2^0-7^sD_2D_2$
30.59	8	M	16307.2	$5^sP_2^0-6^sD_2D_2$	17.51	30	M	20751.8	$5^sP_2^0-5^sD_2P_2$
29.45	0	M	16310.2		17.02	9	M	20754.0	$5^sP_2^0-5^sD_2P_1$
01.65	0	M	16384.5	$5^sP_2^0-2^sD_2$	16.27	1h	M	20757.2	$5^sP_2^0-k_1$
6064.08	1	M	16486.0	$5^sP_2^0-5^sD_2S_1$	14.65	1	M	20764.2	$5^sP_2^0-7^sD_2D_1$
5995.94	0?	M	16673.3		06.37	1	M	20799.9	$5^sP_2^0-7^sD_2D_2$
78.96	0	M	16720.7	$5^sP_2^0-4^sD_2$	4799.02	1	M	20831.8	$5^sP_2^0-7^sD_2D_1$
74.03	0	M	16734.5	$5^sP_2^0-5^sD_2P_1$	90.85	2	M	20867.3	$5^sP_2^0-7^sD_2D_2$
5868.14	2	M	17036.4	$5^sP_2^0-6^sD_2D_2$	88.18	20	M	20879.0	$5^sP_2^0-5^sD_2D_2$
5782.14	3	M	17289.9	Cu	76.56	4	M	20929.7	$5^sP_2^0-5^sD_2D_2$
5778.85	1	M	17299.7	$5^sP_2^0-7^sD_2D_2$	73.37	0	S	20943.7	$5^sP_2^0-5^sD_2F_3$
59.92	4	M	17356.6	$5^sP_2^0-5^sD_2P_1$	71.37	0	M	20752.5	
39.68	7	M	17417.8	$5^sP_2^0-5^sD_2G_1$	93.52	0	S	20755.7	$5^sP_2^0-5^sD_2G_3$
37.65	4	M	17423.9	$5^sP_2^0-5^sD_2P_1$	61.88	3	M	20994.3	$5^sP_2^0-5^sD_2G_4$
36.52	12	M	17427.0	$5^sP_2^0-5^sD_2P_2$	24.01	6	M	21162.5	$5^sP_2^0-5^sD_2F_2$
30.52	0	M	17445.6						$5^sP_2^0-7^sD_2D_2$
5698.10	0	S	17544.9						$5^sP_2^0-5^sD_2F_1$
95.08	20	M	17554.1	$5^sP_2^0-5^sD_2D_3$	22.75	1	M	21168.2	$5^sP_2^0-7^sD_2D_1$
90.14	8	M	17569.4	$5^sP_2^0-5^sD_2D_1$	08.06	2	M	21234.3	$5^sP_2^0-7^sD_2D_2$
87.49	3	M	17577.6	$5^sP_2^0-5^sD_2G_3$	4700.12	1	M	21270.1	$5^sP_2^0-7^sD_2D_2$
80.80	2	M	17598.3	$5^sP_2^0-5^sD_2S_1$	4677.46	8	M	21373.2	$5^sP_2^0-5^sD_2G_3$
77.07	1	M	17609.9	$5^sP_2^0-5^sD_2D_2$	4664.54	0	M	21432.4	$5^sP_2^0-5^sD_2D_1$
74.25	3	M	17618.6	$5^sP_2^0-5^sD_2F_3$	32.63	3	M	21580.0	$5^sP_2^0-5^sD_2F_2$
70.90	0	S	17629.0	V?	31.37	2h	M	21585.9	$5^sP_2^0-5^sD_2F_1$
70.06	30	M	17631.6	$5^sP_2^0-5^sD_2F_4$	4589.99	4	M	21780.5	$5^sP_2^0-6^sD_2F_3(5^sD_2)$
68.42	3	M	17636.7	$5^sP_2^0-5^sD_2D_1$	59.83	1	M	21924.5	$5^sP_2^0-7^sD_2D_2$
55.42	10	M	17677.3	$5^sP_2^0-5^sD_2D_2$	52.91	4	M	21957.8	$5^sP_2^0-7^sD_2D_2$
42.71	8	M	17717.1	$5^sP_2^0-5^sD_2F_2$	41.13	10	M	22014.8	$5^sP_2^0-5^sD_2P_1$
21.33	3	M	17784.4	$5^sP_2^0-5^sD_2F_2$	23.33	1	M	22106.3	
19.46	12	M	17790.4	$5^sP_2^0-5^sD_2F_3$	16.20	10	M	22136.3	$5^sP_2^0-7^sD_2D_2$
08.02	7	M	17826.7	$5^sP_2^0-5^sD_2P_1$	4497.66	3	M	22227.6	$5^sP_2^0-5^sD_2D_1$
03.00	4	M	17842.6	$5^sP_2^0-5^sD_2S_0$	89.46	15	E	22268.2	$5^sP_2^0-5^sD_2D_1$
02.29	2	M	17844.9	$5^sP_2^0-5^sD_2P_2$	73.59	50	E	22347.2	$5^sP_2^0-5^sD_2P_0$
01.65	8	M	17846.9	$5^sP_2^0-5^sD_2P_1$	58.62	1h	K	22422.2	$5^sP_2^0-5^sD_2G_3$
5600.62	2h	M	17850.2	$5^sP_2^0-k_1$	43.04	5	E	22500.8	$5^sP_2^0-5^sD_2S_0$
5562.70	3	M	17971.9	$5^sP_2^0-5^sD_2D_3$	21.03	3	E	22612.8	$5^sP_2^0-7^sD_2D_2$
47.02	20	M	18022.7	$5^sP_2^0-5^sD_2D_2$	06.55	8	E	22687.1	$5^sP_2^0-7^sD_2D_2$
42.80	30	M	18036.4	$5^sP_2^0-5^sD_2F_3$	4388.62	5	E	22779.8	$5^sP_2^0-18^sD_2$
41.88	1	M	18039.4	$5^sP_2^0-5^sD_2D_1$	86.48	3	E	22790.9	$5^sP_2^0-7^sD_2D_2$
29.45	9	M	18080.0	$5^sP_2^0-5^sD_2D_2$	79.58	2	E	22826.8	$5^sP_2^0-7^sD_2D_2$
5496.85	6	M	18187.2	$5^sP_2^0-5^sD_2F_2$	60.23	8h	E	22928.1	$5^sP_2^0-6^sD_2P_2$
72.67	1	M	18267.5	$5^sP_2^0-6^sD_2D_1$	58.58	8	E	22936.8	$5^sP_2^0-5^sD_2G_1$
59.16	2	M	18312.8	$5^sP_2^0-5^sD_2S_0$	51.00	10h	E	22976.8	$5^sP_2^0-6^sD_2D_2$
35.16	7	M	18393.6	$5^sP_2^0-5^sD_2S_1$	4344.66	20h	E	23010.3	$5^sP_2^0-6^sD_2F_4$
27.69	4	M	18419.0	$5^sP_2^0-6^sD_2D_2$	28.04	2h	E	23098.7	$5^sP_2^0-6^sD_2F_2$
06.59	5	M	18490.9	$5^sP_2^0-5^sD_2G_3$	26.97	1h	S	23104.4	$5^sP_2^0-5^sD_2F_2$
5395.26	25	M	18529.6	$5^sP_2^0-5^sD_2G_4$	23.04	2h	E	23125.4	$5^sP_2^0-6^sD_2D_1$
94.76	6	M	18531.4		14.96	6h	E	23168.7	$5^sP_2^0-6^sD_2F_2$
85.44	2	M	18563.4		4281.89	3h	E	23347.6	$5^sP_2^0-6^sD_2P_2$
77.62	3	M	18590.4	$5^sP_2^0-5^sD_2D_2$	68.26	30hd	E	23422.2	$5^sP_2^0-6^sD_2F_2(5^sD_2)$
63.26	4	M	18640.2	$5^sP_2^0-5^sD_2P_2$	51.49	1	E	23514.6	$5^sP_2^0-7^sD_2D_1$
62.69	15	M	18642.2	$5^sP_2^0-5^sD_2P_1$	49.0	1h	E	23528.3	$5^sP_2^0-6^sD_2D_1$
61.72	2hv	M	18645.5	$5^sP_2^0-k_1$	41.7	1h	E	23568.8	$5^sP_2^0-6^sD_2F_2$
46.79	2	M	18697.6	$5^sP_2^0-5^sD_2F_2$	12.95	200	E	23729.7	$5^sP_2^0-5^sD_2F_3$
45.10	10	M	18703.5	$5^sP_2^0-5^sD_2F_3$	4169.86	20	E	23974.8	$5^sP_2^0-5^sD_2P_2$
12.57	12	M	18818.1	$5^sP_2^0-5^sD_2D_2$	66.31	10d	S	23995.3	$5^sP_2^0-7^sD_2D_2$
11.50	1	M	18821.9						$5^sP_2^0-6^sD_2G_3$
5295.61	50	M	18878.5	$5^sP_2^0-5^sD_2G_5$	62.84	3h	S	24015.3	$5^sP_2^0-6^sD_2G_4$
94.15	7	M	18883.5	$5^sP_2^0-5^sD_2G_4$	56.98	3	S	24049.2	$5^sP_2^0-6^sD_2F_3$
5256.17	10	M	19020.0	$5^sP_2^0-5^sD_2D_3$	52.12	3h	S	24077.3	$5^sP_2^0-6^sD_2P_2$
38.41	2	M	19084.5	$5^sP_2^0-5^sD_2F_3$	51.36	3h	S	24081.7	$5^sP_2^0-6^sD_2P_2$
34.85	20	M	19097.5	$5^sP_2^0-5^sD_2F_4$	40.83	5h	S	24142.9	$5^sP_2^0-6^sD_2D_2$
20.93	0	M	19151.6	Cu	28.37	3h	S	24215.8	$5^sP_2^0-6^sD_2D_2$
08.93	10	M	19192.5	$5^sP_2^0-5^sD_2P_0$	23.64	5	S	24243.6	$5^sP_2^0-1^sD_2$
5179.31	0	M	19302.7	$5^sP_2^0-9^sD_2$	4106.85	1h	S	24342.7	$5^sP_2^0-8^sD_2D_3$
63.83	40	M	19360.1	$5^sP_2^0-5^sD_2G_4$	4099.27	20h	S	24387.7	$5^sP_2^0-6^sD_2D_2$
61.36	5	M	19369.4	$5^sP_2^0-5^sD_2P_2$	98.87	10h	S	24390.1	$5^sP_2^0-6^sD_2G_1$
57.56	0	M	19383.6	$5^sP_2^0-5^sD_2P_1$	4090.05	2h	S	24442.7	$5^sP_2^0-6^sD_2D_3$
27.71	7	M	19496.5	$5^sP_2^0-5^sD_2D_3$	87.37	50	E	24458.7	$5^sP_2^0-5^sD_2P_0$
17.01	20	M	19537.3	$5^sP_2^0-5^sD_2G_3$	84.35	5h	S	24476.8	$5^sP_2^0-6^sD_2F_4$
14.38	8	M	19547.3	$5^sP_2^0-5^sD_2D_2$	82.72	1h	S	24486.6	$5^sP_2^0-5^sD_2F_2$
10.81	15	M	19560.9	$5^sP_2^0-5^sD_2F_3$	81.68	3h	S	24492.8	$5^sP_2^0-5^sD_2F_2$
07.43	1	M	19573.9	$5^sP_2^0-5^sD_2F_4$	20.66	5h	S	24864.5	
01.51	3	M	19596.4	$5^sP_2^0-5^sD_2D_1$	20.20	15h	S	24867.4	$5^sP_2^0-6^sD_2G_4$
5092.53	0	M	19631.1		11.74	0h	S	24919.8	$5^sP_2^0-6^sD_2D_2$
63.40	10	M	19744.1	$5^sP_2^0-5^sD_2F_2$	4007.5	3h	E	24946.2	$5^sP_2^0-6^sD_2F_3(5^sD_2)$
09.95	1	S	19954.7	$5^sP_2^0-6^sD_2P_2$	4004.93	1h	S	24962.2	$5^sP_2^0-1^sD_2$
04.99	0h	S	19974.5	$5^sP_2^0-11^sD_2$	3992.3	3h	E	25041.2	$5^sP_2^0-6^sD_2G_3$

TABLE III (continued)

λ	I	A	ν	Combination	λ	I	A	ν	Combination
3985.48	0h	S	25084.0	$5p^2F_2^0-6d^2D_1$	3075.17	10	M	32509.1	$a^2F_2-3^2F_2^0$
78.88	1h	S	25125.6	$5p^2F_2^0-6d^2F_2$	3066.09	3	M	32605.4	$a^2F_2-19_2^0$
58.64	200	E	25254.1	$5s^1D_2-5p^2D_2^0$	3055.30	100	M	32613.8	$5s^2D_2-5p^2D_1^0$
26.93	0	S	25458.0	$5p^2P_2^0-7s^1D_2$	3028.76	3	M	33007.2	
13.07	1	S	25548.2	$a^2F_2-3^2F_2^0$	3027.92	100	M	33016.4	$5s^2D_2-5p^1D_2^0$
3894.18	200	E	25672.1	$5s^1D_2-5p^2D_2^0$	3021.74	10	M	33083.9	$5s^2D_2-5p^1F_1^0$
73.57	1h	S	25808.7	$\{5p^2F_2^0-6d^2D_1$ $a^2F_4-2^2D_2^0$ $5p^2F_2^0-8s^2D_2$	3009.77	20	M	33215.5	$a^2F_4-3^2F_2^0$
				$5s^2D_2-5p^2P_2^0$	3002.66	50	M	33294.1	$5s^2D_2-5p^1F_2^0$
				$a^2F_2-4_2^0$	2936.77	2	S	34041.1	$a^2F_4-15_2^0$
3832.30	75	E	26086.6	$5s^2D_1-5p^2P_1^0$	2931.47	4	M	34102.6	$a^2F_4-19_2^0$
27.15	3	S	26121.9	$a^2F_2-2_2^0$	2922.50	40	M	34207.3	$5s^2D_2-5p^1D_2^0$
21.99	5h	S	26157.0	$5p^2P_2^0-6d^2S_1^2$	2875.75	2	M	34763.4	
18.89	1	S	26178.2	$5p^2F_2^0-9s^2D_2^2$	2806.45	1	M	35621.7	$a^2F_4-3^2F_2^0$
3807.87	5h	S	26254.0	$5p^2P_2^0-6d^2P_{2,1}$	2763.08	100R	M	36180.8	$a^1S_0-5p^2P_1^0$
3800.96	1	S	26301.7	$5p^2P_2^0-6d^2D_2$	2686.29	3	M	37215.0	$a^2F_4-19_2^0$
3799.16	75	E	26314.2	$5s^2D_2-5p^2P_2^0$	2605.08	4	M	38375.1	
78.28	1	S	26459.6	$a^2F_2-4_2^0$	2476.43	50R	M	40368.5	$a^1S_0-5p^2D_2^0$
54.85	1	S	26624.7	$a^2F_2-7_2^0$	2447.95	10R	M	40838.1	$a^1S_0-5p^1F_1^0$
18.91	100	E	26882.0	$5s^2D_1-5p^2D_2^0$	2360.51	5	M	42350.8	
3690.34	200	E	27090.1	$5s^1D_2-5p^2F_2^0$	2327.49	5	S	42951.5	$5s^1D_2-4_2^0$
54.41	2	E	27356.4	$a^2F_4-1_2^0$	2216.48	6	S	43155.5	$5s^2D_2-2^2D_2^0$
45.97	2	E	27419.8	$a^2F_2-6_2^0$	2276.54	2	M	43912.7	$5s^1D_2-6_2^0$
34.70	700R	E	27504.8	$5s^2D_2-5p^2P_2^0$	2254.28	15	M	44346.3	$5s^2D_2-2^2D_2^0$
13.39	0	S	27667.0	$5p^2P_2^0-8s^2D_2$	2240.76	4	M	44613.8	$5s^1D_2-7_2^0$
3609.56	600R	M	27696.3	$5s^2D_2-5p^2F_2^0$	2236.38	8	M	44701.2	$5s^2D_2-1_2^0$
3596.66	4	S	27795.7		2225.28	10	M	44924.1	
89.16	2	S	27853.7	$a^2F_2-10_2^0$	2195.49	6	M	45533.5	$5s^1D_2-9_2^0$
84.11	2	S	27893.0		2178.26	10	M	45893.7	$5s^2D_2-1_2^0$
81.06	1	S	27916.8		2174.67	4	M	45969.6	
77.56	1	S	27944.1	$5p^2F_2^0-6d^1G_1$	2172.92	10	M	46006.6	$5s^2D_2-2^2F_2^0$
71.16	200	M	27994.1	$5s^2D_1-5p^2P_1^0$	2151.00	5	S	46475.3	
66.63	5	M	28029.7		2142.11	10	S	46668.1	$5s^1D_2-13_2^0$
53.10	500R	M	28136.4	$5s^1D_2-5p^1F_2^0$	2130.69	3d	S	46918.2	$5s^2D_2-4_2^0$
43.25	1	S	28214.62	$a^2F_2-11_2^0$	2123.76	2	S	47071.4	
28.72	5	M	28330.8	$a^2F_2-8_2^0$	2118.09	6	S	47197.4	$5s^2D_2-2^2F_2^0$
21.14	2	S	28391.8	$a^2F_2-12_2^0$	2108.09	4	S	47421.1	$5s^1D_2-15_2^0$
16.95	500R	M	28425.6	$5s^2D_2-5p^2P_1^0$	2105.87	10	S	47471.3	$5s^2D_2-10_2^0$
3489.79	200R	M	28646.9	$5s^1D_2-5p^2D_1^0$	2092.61	7	S	47771.9	$5s^2D_2-2_2^0$
3488.15	1	M	28660.3	$a^2F_4-3^2F_2^0$	2089.97	2	S	47832.3	$5s^2D_1-11_2^0$
81.17	400R	M	28717.8	$5s^2D_1-5p^2F_2^0$	2088.47	8	S	47856.7	$5s^2D_1-16_2^0$
60.76	300R	M	28887.2	$5s^2D_2-5p^2F_2^0$	2087.93	10	S	47879.3	$5s^2D_2-6_2^0$
42.40	3	M	29041.2	$a^2F_2-9_2^0$	2082.24	10	S	48009.7	$\{5s^2D_1-12_2^0$ $5s^2D_2-17_2^0$ $5s^2D_2-3_2^0$
41.40	300	M	29049.6	$5s^1D_2-5p^1D_2^0$	2081.10	10	S	48036.2	
33.44	250	M	29117.0	$5s^1D_2-5p^1P_1^0$	2079.35	0	S	48076.5	
21.24	500	M	29220.8	$5s^2D_2-5p^2D_2^0$	2077.93	4	S	48109.4	$5s^2D_2-4_2^0$
19.66	6	M	29234.3	$a^2F_4-2_2^0$	2076.47	3	S	48143.2	
3406.04	3	M	29351.2	$a^2F_2-10_2^0$	2068.78	8	S	48322.2	$5s^2D_1-14_2^0$
3404.60	1000R	M	29363.6	$5s^2D_2-5p^2F_4^0$	2061.98	2	S	48481.5	
3396.79	4	M	29431.1	$a^2F_2-15_2^0$	2057.76	2	S	48580.9	$5s^2D_2-7_2^0$
89.05	3	M	29498.4	$a^2F_4-3_2^0$	2057.42	2	S	48588.9	
80.69	20	M	29571.3	$a^2F_4-4_2^0$	2042.98	3	S	48932.3	
73.02	300	M	29638.5	$5s^2D_2-5p^2D_2^0$	2040.19	0	S	48992.2	
46.12	0	K	29876.8	$a^2F_2-16_2^0$	2039.81	1	S	49008.3	$5s^1D_2-18_2^0$
21.00	5	M	30102.8	$a^2F_2-3^2F_2^0$	2019.75	4	S	49495.0	$5s^2D_1-16_2^0$
12.99	5	M	30175.6	$a^2F_2-13_2^0$	2019.53	4	S	49500.4	$5s^2D_2-9_2^0$
11.04	3	M	30193.3		2013.96	3	S	49637.4	$5s^2D_1-17_2^0$
10.14	2	K	30201.5	$a^2F_2-14_2^0$	2006.96	10	S	49810.5	$5s^2D_2-10_2^0$
3307.08	2	S	30229.5		λ (vac)				
3302.15	400	M	30274.6	$5s^2D_1-5p^2D_1^0$	2000.72	2	S	49982.0	$5s^2D_2-8_2^0$
3287.26	50	M	30411.7	$5s^2D_2-5^2D_2^0$	1993.18	3	S	50171.2	$5s^2D_2-11_2^0$
58.80	300	M	30677.3	$5s^2D_1-5p^1D_2^0$	1986.14	2	S	50348.7	$\{5s^2D_2-12_2^0$ $5s^2D_2-3^2D_2^0$ $5s^2D_2-3^2F_2^0$
3251.66	200	M	30744.7	$5s^2D_1-5p^1P_1^0$					
42.72	1000R	M	30829.4	$5s^2D_2-5p^2D_2^0$	1976.48	5	S	50594.9	$5s^1D_2-19_2^0$
32.33	5	S	30928.5	$a^2F_2-15_2^0$	1974.88	3	S	50635.9	$5s^2D_2-13_2^0$
18.98	20	M	31056.8	$5s^2D_2-5p^2F_2^0$	1973.94	3	S	50660.1	$5s^2D_2-14_2^0$
3179.41	8	S	31443.3	$a^2F_4-8_2^0$	1972.74	8	S	50690.8	$5s^2D_2-9_2^0$
3171.93	1	S	31517.5	$a^2F_2-17_2^0$	1968.33	5	S	50804.4	
3142.82	50	M	31809.4	$a^2F_4-3^2D_2^0$	1963.71	2	S	50924.0	
3114.05	200	M	32103.2	$5s^2D_2-5p^1D_2^0$	1945.98	2	S	51388.1	$5s^2D_2-15_2^0$
3109.19	5	M	32153.4	$a^2F_4-9_2^0$					

For convenience in visualizing the energy relations in the spectrum, a diagram of electron configurations is given in Fig. 2.

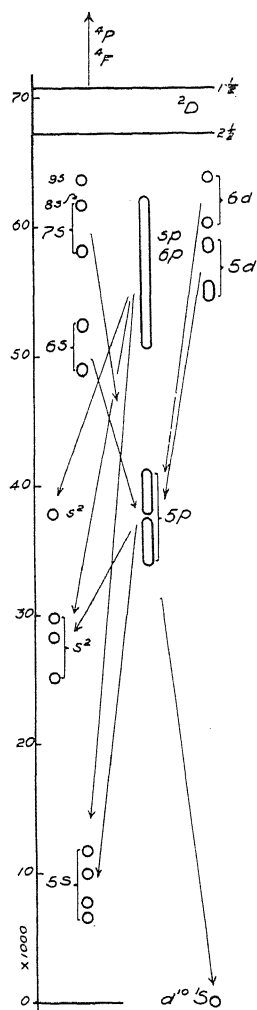


Fig. 2. Diagram of the energies of the electron configurations of Pd I. The last electron only is given except for structures based on 8 d electrons for which the characteristics of two electrons are given.

INTENSITY MEASUREMENTS IN THE SPECTRUM
OF NICKEL AND COBALT

BY L. S. ORNSTEIN AND T. BOUMA

PHYSICAL LABORATORY OF THE UNIVERSITY OF UTRECHT

(Received June 2, 1930)

ABSTRACT

Quantitative intensity measurements have been carried out in the Ni I and Ni II, and the Co I spectrum. The spectrographic outfit for the intensity measurements consisted of a stigmatic concave grating mounting used with step weakeners, and a Hilger E 1 used with the method of slit width variation. The *summation rules* have been tested both for *multiplets* and *supermultiplets*, also the intensity ratio for singlets and triplets, doublets and quartets. Serious divergencies have been found everywhere. In the Ni II spectrum an extension of the summation rules to supermultiplets gives better results in several cases. Intensity tables are given of the lines measured.

QUANTITATIVE intensity measurements have been carried out in the nickel I and II and the cobalt I spectrum. In the Ni I spectrum the analysis of Becher and Sommer¹ has been utilized; later on also the very extensive analysis by Russell, obtained through the courtesy of Professor Harrison.² For Ni II the analysis has been given by Shenstone;³ for Co I by Catalan and Bechert.⁴

In the Co II spectrum no intensity measurements have been carried out, the classified multiplets⁵ being situated in the far ultraviolet where intensity measurements meet with special difficulties.

Although the material used was the purest Ni and Co that could be obtained, the Ni contained some Fe, and the Co some Fe and Ni as impurities.

THE EXPERIMENTAL METHODS

In the first measurements for the Ni I spectrum an image of the light source through step-reducers was formed on the slit of a stigmatic concave grating-mounting; the line intensities was determined by the usual method.⁶ For the subsequent investigation a Hilger E 1 quartz-spectrograph was used. The density curves were obtained by the method of variable slit width.⁷

Frequently the photometer curves of two or more lines lying close together coalesced. In such cases it is necessary to change the photometer curve accurately point for point into the intensity curve of the complex of

¹ K. Bechert and L. A. Sommer, Ann. d. Physik 77, 351 (1925) and 77, 537 (1925).

² Afterwards published, Phys. Rev. 34, 821 (1929).

³ A. G. Shenstone, Phys. Rev. 30, 255 (1927).

⁴ Catalan and Bechert, Zeits. f. Physik 32, 336 (1925).

⁵ Meggers and Walters. Scientific Papers of the Bureau of Standards No. 551.

⁶ L. S. Ornstein, Intensity of Multiple Spectrallines, Proc. Phys. Soc. 37, 334 (1925).

⁷ L. S. Ornstein, Proc. Phys. Soc. 37, 337 (1925).

lines. The same thing is done for a neighbouring isolated line. It may be assumed that the shape of the intensity curve for all these lines is the same^s and that therefore the intensity curve of the complex can be analysed into a few separate curves of this shape.

THE FIRST MEASUREMENTS

The Ni I quintet $z^5G^0 - e^5F$ was photographed with the above mentioned concave grating in second order. The results will be found in Table I, and for 0.95 amp. also in an intensity scheme (Table II).

TABLE I. *Intensities of the lines of the $z^5G^0 - e^5F$ multiplet of Ni I.*

Line λ	Intensity		Line λ	Intensity	
	1.4 amp.	0.95 amp.		1.4 amp.	0.95 amp.
4900.97	1	~ 1	4714.416	100	100
4874.803	1.1	~ 1	4686.209	11	11
4814.59	0.95	~ 1	4648.656	40	44
4786.541	38	41	4604.990	27	25
4756.529	26	29	4600.364	10	9.5
4715.757	22	24.5	4592.532	17	16

TABLE II. *Intensity scheme for the $z^5G^0 - e^5F$ multiplet of Ni I.*

Statistical Weight	5	7	z^5G^0 9	11	13	Sum	Quotient
3	9.5					9.5	3.2
5	11	16				27	5.4
e^5F 7	~ 1	24.5	25			50.5	7.2
9		~ 1	29	44		74	8.2
11			~ 1	41	100	142	12.9
Sum	21.5	41.5	55	85	100		
Quotient	4.3	5.9	6.1	7.7	7.7		

According to the summation rule the quotients in Table II ought to be equal. The divergencies are serious, as will be seen. Self-reversal cannot be the cause of this divergency for it would diminish the contrasts, whereas the divergencies lie in the opposite direction.

Although in the case under consideration the summation rule does not determine the intensity of each line separately, it gives the ratio of the extreme diagonal terms; this ought to be 27:91 i.e. 29.7:100. As this is a sensitive test, the intensity ratio between these two lines has been measured several times. (Table III).

TABLE III.

Current	Int. proportion
2.4	10. 9:100
1.4	10. 15:100
1.4	9.9 :100
0.95	9.3 :100
0.95	9.6 :100

^s L. S. Ornstein and M. Minnaert, Zeits. f. Physik 43, 404 (1927).

As blending with impurity lines is out of question, the experimental ratio 9.6:100 differs from the theoretical 29.7:100.

In order to get more facts the measurements have been continued with the Hilger E 1 in the ultraviolet. Here fairly large regions could be photographed at once and with a sufficient dispersion.

The current used was the smallest possible (about 0.45 amp.) A preliminary examination with 0.80 and 0.45 amp. showed that difference between the intensities found for these currents is comparatively small.

A few intensity measurements have also been carried out in an arc with a pressure of 50 and 28 cm of air. These also did not show any appreciable difference for the intensity. Therefore the definitive measurements for Ni I and CO I have been carried out with a current of 0.45 amp. in air.

In the Ni II investigation a Leyden jar was charged by the secondary tension of an induction coil. The spark discharge of the jar took place via a self-induction between two small bars of nickel. Variations of the conditions of discharge could not be used here. Only, to get a current of small density, a Leyden jar of the smallest possible capacity was chosen.

THE DEFINITIVE MEASUREMENT

In each of the three spectra mentioned a region has been chosen in which a number of multiplets, suitable for intensity measurements was situated. The region was situated for Ni I between 2900 and 3800Å, for Ni II between 2450 and 3770Å for Co I between 2500 and 4500Å.

Besides the multiplets the intensities of all the lines appearing in the photographs have been measured. In the tables the intensities found by analysis of the photograms have been marked (1) when the analysis was certain, (2) when it was less certain and (3) when the analysis was very doubtful. Intensities marked (4) are inexact, owing to the slight density and the great influence of the irregularities which the photometer curve shows in the unexposed plate for that case. The tables are the least complete on the side of the largest wave-lengths where the dispersion was so small that several lines had to be omitted. The experimental facts have been used for testing: (1) the multiplet summation rules; (2) the supermultiplet summation rules; and (3) the intensity ratio for singlets and triplets, doublets and quartets. Generally the theoretical expectations are not fulfilled. For this reason we have limited our measurements to the spectral regions given below. Perhaps our material will be of some help in developing the intensity rules for the complicated spectra.

THE Ni I SPECTRUM

Besides the quintet $z^5G^0 - e^5F$ already mentioned 13 multiplets have been examined.

The intensities in horizontal and vertical direction have been formed and the quotients of intensity sums and statistical weights have been calculated in the same way as has been done for $z^5G^0 - e^5F$, the results are collected in Table IV.

TABLE IV. Intensity quotients in multiplets of Ni I.

No.	Multiplet Designation	Quotients									
1	$a^3D - y^3D^0$	35	28	17		36	29	16			
2	$a^3F - y^3D^0$	11.7	6.2	5.8		9.1	3.9	3.8			
3	$a^3D - y^3F^0$	34	18	7.4		25	25	23			
4	$a^3F - y^3F^0$	10	7.5	3.2		2.4	7.0	7.8			
5	$a^3F - z^3G^0$	3.2	6.5	4.2		2.6	8.5	6.1			
6	$a^3P - v^3D^0$	0.4	0.4	0.4		0.8	0.8	0.7			
7	$a^3D - z^3G^0$	4.5	1.7			6.2	2.3				
8	$a^3D - z^3F^0$	31	22	10		30	28	24			
9	$a^3D - z^3D^0$	23	[25]	18		[37]	29	10			
10	$a^3F - z^3D^0$	22	21.6	10.3		23.3	10.1	6.6			
11	$a^3F - z^3F^0$	21	12.1	5.9		12	17.6	6.7			
12	$a^3D - z^3P^0$	70	51	33		49	28	14			
13	$a^3F - z^3P^0$		4.3	2.4		3.1	1.4				
14	$z^5G^0 - e^5F$	3.2	5.4	7.2	8.2 12.9	4.3	5.9	6.1	7.7	7.7	

The quotients [25] and [37] have been deduced from sums containing a line, ordered doubly, so that they are too high by an unknown amount.

Only the multiplet 6 is in accordance with expectation (and multiplet 3 in one direction). In the case of all other multiplets the summation rules do not apply. In the case of the incomplete multiplets, e.g. $2^5G^0 - e^5G$ it also appears from the intensities of the lines present that the summation rule will not hold.

Supermultiplets. If singlet, triplet and singlet-triplet intercombinations are taken together, no satisfactory results are reached (Table V).

TABLE V. Supermultiplet sums and quotients of intensity.

Statistical weight	3	a^3D 5	7	a^1D 5	Sum	Quotient	
y^3D^0	3 5 7	61 47	43 55 48	40 71	39 20 43	143 162 162	48 32 23
y^1D^0	5	8.7	23		72	103.7	21
Sum		116.7	169	111	174		
Quotient		39	34	16	35		

In the same way the quotients in Table VI are found.

TABLE VI.

Combinations	Quotients							
$a^3D, a^1D - z^3D^0, z^1D^0$	24	[35]	28	22	[38]	32	11	42
$a^3D, a^1D - y^3F^0, y^1F^0$	34	25	7	15	25	25	28	25
$a^3D, a^1D - z^3F^0, z^1F^0$	36	33	10	33	30	39	31	46

Again, when either the multiplets or all the lines, coming from the same term, are taken together the summation rules do not apply, e.g. for y^5D^0 : (Table VII).

TABLE VII.

Statistical weight	5	a^3F 7	9	3	a^3D 5	7	a^1D 5	Sums	Quotient
γ^3D^0	35			61	43		39	178	59
5	5.2	26		47	55	40	20	193.2	39
7	5.2	1.3	34		48	71	43	202.5	29

Now we add up in Tables VIII and IX the spectral lines originating from the same level.

TABLE VIII.

	5	a^3F 7	9
z^1G^0		31	
z^3G^0	13	59.3	54.8
z^5G^0	1.6	11.8	22.2
z^1F^0	30	51	32
z^3F^0	60.4	123.3	60
z^5F^0	41.4	46.5	57.9
γ^1F^0	1.7	5.0	4.7
γ^3F^0	12	49.2	70
z^1D^0	1	54	
z^3D^0	116.3	71	59
z^5D^0		0.65	2.1
γ^1D^0	10.5	4.2	
γ^3D^0	45.4	27.3	34
z^1P^0	3.8		
z^3P^0	15.5	9.5	
Sum	352.6	543.8	396.7
Quotient	71	78	44

TABLE IX.

	3	a^3D 5	7
z^1G^0			42
z^3G^0		31	15.8
z^5G^0	1.7	20.7	23
z^1F^0		55	50
z^3F^0	91	139	168
z^5F^0	36	93.3	114.4
γ^1F^0			31
γ^3F^0	74	125	164
z^1D^0	2.4	13	2.8
z^3D^0	[110]	145	71.4
z^5D^0	0.8	3.7	[28]
γ^1D^0	8.7	23	
γ^3D^0	108	146	111
z^1P^0	17	40	
z^3P^0	146.6	140	100
Sum	596.1	974.7	918.4
Quotient	199	195	131

Here the divergencies are smaller than for the separate multiplets. Still it is not very likely that the few multiplets still wanting will be able to equalize the quotients.

According to Mack⁹ the multiplets arranged in Table X belong together. Equal quotients are not obtained in this way either. Especially the first column shows a great divergence.

Finally we shall consider the ratio between the sums of the intensities for the corresponding singlet-triplet multiplets. When intercombinations are absent a ratio of 1:3 can be expected.¹⁰ The values found for our case are shown in Table XI; the last column contains the ratios after dividing the intensities by the fourth power of the frequency. There is a fairly great difference between the experimental and the theoretical ratios. However, fairly strong intercombinations are present in all 5 cases.

Table XII contains the intensities for all the lines in the spectral region investigated; an (arbitrary) intensity of 100 has been awarded to the line 3524.543.

⁹ J. E. Mack, Phys. Rev. **34**, 17 (1929).

¹⁰ L. S. Ornstein and H. C. Burger, Zeits. f. Physik **40**, 403 (1926).

TABLE X.

Statistical weight	7	a^3D 5	3	a^1D 5	Sum	Quotient
z^3F^0 9	93				93	10
7	66	86		78	230	33
5	[9]	53	91	[27]	180	36
z^3D^0 7	66	64		65	195	28
5	5.4	80	41	50	176.4	35
3		1	69	3	73	24
z^3P^0 5	100	54	9.6	4	167.6	34
3		86	67	9.5	162.5	54
1			70		70	70
z^1F^0 7	50	55		124	229	33
z^1D^0 5	2.8	13	2.4	93	111.2	22
z^1P^0 3		40	17	106	163	54
Sum	392.2	532	367	559.5		
Quotient	56	106	122	112		

TABLE XI.

Combinations	Ratio	
$a^1D - y^1D^0$ and $a^3D - y^3D^0$	1:5.1	1:5.1
$a^1D - y^1F^0$ and $a^3D - y^3F^0$	1:4.8	1:4.5
$a^1D - z^1F^0$ and $a^3D - z^3F^0$	1:3.1	1:2.6
$a^1D - z^1D^0$ and $a^3D - z^3D^0$	1:3.5	1:3.2
$a^1D - z^1P^0$ and $a^3D - z^3P^0$	1:3.6	1:4.4

TABLE XII. Intensities of Ni I lines. Intensities marked (1) are certain, (2) less certain, (3) doubtful, (4) inexact because of small intensity and the influence of irregularities in the plate.

λ (Kayser) ¹	λ (I.A.)	Int.	λ (Kayser)	λ (I.A.)	Int.	λ (Kayser)	λ (I.A.)	Int.
2798.78	2798.651	23	3012.11	3012.007	72	3165.64	3165.513	0.8
2802.40	2802.28	3.1	3018.09	3017.96	0.3 (4)	3170.86	3170.73	0.3
2803.25	2803.15	1.4	3019.28	3019.150	42	3176.44	3176.30	0.4
2805.20	2805.081	4.7	3029.36	3029.30	0.6	3181.89	3181.75	3
2814.48	2814.37	0.5	3031.98	3031.869	28	3183.14	3183.05	0.8 (3)
2821.42	2821.296	31	3038.04	3037.940	55	3183.40	3183.26	1.9 (3)
2834.66	2834.550	4.2	3043.15	3043.012	26	3184.50	3184.372	11
2839.05	2838.97	1.3	3048.98		0.4	3191.97	3191.89	0.2
2849.93	2849.84	0.5	3050.92	3050.828	67	3195.67	3195.577	5.2
2865.61	2865.508	8.7	3054.42	3054.317	53	3197.22	3197.121	17
2868.85	2868.76	0.9	3057.76	3057.647	61	3199.44	3199.36	0.2
2905.85	2905.76	0.5	3064.75	3064.626	48	3200.50	3200.433	2.8
2907.58	2907.462	10.5	3066.59	3066.46	0.4	3202.21	3202.149	1.7
2914.12	2914.013	5.0	3080.91	3080.758	47	3207.05	3206.963	0.2
2916.95	2916.85	0.2 (4)	3097.27	3097.120	39	3210.00	3209.910	0.9
2917.60	2917.53	0.2 (4)	3099.25	3099.117	31	3213.53	3213.435	0.5
2931.03	2930.93	0.3 (4)	3101.67	3101.563	72 (1)	3214.17	3214.064	3.7
2932.74	2932.63	0.3 (4)	3101.99	3101.881	76 (1)	3216.93	3216.823	1.3
2944.06	2943.922	40	3103.60	3103.466	35	3217.93	3217.828	5.8
2958.39	2958.29	0.7	3107.83	3107.717	1.3	3219.92	3219.810	0.4
2969.30	2969.20	1.2	3114.26	3114.128	40	3221.41	3221.28	1.9 (1)
2973.84	2973.73	0.4	3116.84	3116.700	0.2 (4)	3221.81	3221.661	32
2981.80	2981.652	43	3129.42	3129.310	5.2	3223.66	3223.542	0.7
2983.56	2983.42	3.1	3132.68		0.3 (4)	3225.19	3225.030	39
2984.28	2984.129	34	3134.22	3134.106	74	3227.11	3226.992	8.4
	2991.103	1.7	3143.23	3143.117	0.4 (1)	3233.06	3232.945	46
2992.71	2992.597	42	3145.82	3145.707	9.5 (1)	3234.00	3233.88	0.7
2994.58	2994.458	42	3151.33	3151.29	0.15	3234.78	3234.658	31
3002.58	3002.492	71	3154.68	3154.58	0.5	3235.86	3235.764	1.0
3003.70	3003.628	55	3159.65	3159.524	0.7	3243.20	3243.064	50
3010.96		0.3	3164.30	3164.17	0.3	3245.47	3245.35	0.2

¹ H. Kayser. Handbuch der Spektroskopie.

TABLE XII (continued)

λ (Kayser)	λ (I.A.)	Int.	λ (Kayser)	λ (I.A.)	Int.	λ (Kayser)	λ (I.A.)	Int.
3248.56	3248.44	15	3443.14	3443.00	0.2 (4)	3670.60	3670.424	9.5
3249.55	3249.440	3.8	3444.36	3444.247	0.8	3674.30	3674.105	27
3250.90	3250.749	20	3446.40	3446.263	80	3688.59	3688.413	9.4
3264.56	3264.44	0.1 (4)	3453.02	3452.891	59	3694.07	3693.933	2.8
3268.21	3268.09	0.3	3458.60	3458.467	91	3697.05	3696.904	0.25
3269.08	3268.96	0.08 (4)	3461.80	3461.660	78	3713.84	3713.696	0.2 (4)
3271.25	3271.118	13	3464.25	3464.12	0.3 (4)	3715.65	3715.498	0.2 (4)
3273.62	3273.50	0.15 (2)	3467.61	3467.505	23	3722.64	3722.484	9.6
3276.66		0.15	3469.65	3469.484	30	3724.95	3724.815	0.25
3277.35	3277.23	0.15	3472.71	3472.545	64	3729.06	3728.919	0.2 (4)
3282.03	3281.876	0.5	3476.80	3476.66	0.4	3730.90	3730.745	0.5
3282.81	3282.701	9.3	3478.00	3477.876	0.2 (4)	3736.98	3736.811	20
3284.56	3284.432	0.4	3478.42	3478.302	0.4	3739.40	3739.229	5.2
3287.08	3286.953	9.0	3479.36	3479.263	0.5	3739.94	3739.787	1.5
3293.83	3293.674	0.4	3480.30	3480.170	0.4	3744.72	3744.560	0.5
3296.42	3296.264	0.15	3483.98	3483.776	66	3749.19	3749.042	2.1
3305.10	3304.951	0.7	3486.09	3485.892	14	3762.76	3762.62	0.3
3307.16	3307.014	0.2	3488.43	3488.293	0.4	3769.60		0.15 (4)
3309.56	3309.44	0.2	3493.11	3492.965	86	3772.67	3772.518	0.7
3310.35	3310.206	1.9	3496.47	3496.352	0.8	3775.75	3775.562	50
3312.49	3312.319	2.8	3501.02	3500.852	58	3778.20	3778.048	0.9
3313.15	3312.992	0.7	3502.73	3502.604	4.9	3783.72	3783.521	51
3315.82	3315.668	55	3507.85	3507.695	6.5	3792.48	3792.325	1.1
3320.42	3320.259	54	3510.52	3510.340	70	3793.79	3793.599	2.5
3322.50	3322.316	43	3512.08	3511.94	0.4	3807.35	3807.135	65
3326.80	3326.673	0.4	3514.10	3513.947	22	3811.46	3811.32	0.08 (4)
3327.52	3327.402	0.6	3515.21	3515.057	86	3831.89	3831.685	9.5
3328.85	3328.720	1.0	3516.33	3516.220	3.5	3833.00	3832.865	0.65
3332.31	3332.19	0.5	3518.80	3518.635	2.3	3844.40	3844.27	0.2 (3)
3335.72	3335.59	0.06	3519.97	3519.776	51	3844.71	3844.58	0.15 (3)
3337.15	3337.015	0.4	3523.23	3523.075	4.6 (2)	3858.51	3858.284	78
3338.90	3338.763	0.1 (2)	3523.61	3523.445	11 (2)	3863.21	3863.08	0.3
3339.20	3339.049	0.4 (2)	3524.68	3524.543	100	3889.84	3889.673	0.9
3359.30	3359.104	1.4	3526.67	3526.53	1.0	3909.10	3908.93	0.3
3361.75	3361.557	53	3528.13	3527.988	13	3912.47	3912.31	0.2 (2)
3362.97	3362.808	2.4	3529.02	3528.890	0.6 (1)	3913.14	3912.975	0.15 (2)
3363.76	3363.612	0.6	3529.76	3529.625	0.5 (1)	3942.00	3941.86	0.1
3364.75	3364.590	1.1	3530.73	3530.588	0.9	3944.29	3944.10	0.4
3365.92	3365.771	48 (1)	3537.35	3537.243	0.3 (4)	3954.70	3954.53	0.1
3366.32	3366.169	51 (1)	3537.72	3537.634	0.4 (2)	3962.25	3962.10	0.1
3366.95	3366.808	4.5 (1)	3542.14	3542.00	0.3 (4)	3970.65	3970.49	0.35
3368.05	3367.892	5.4	3545.30	3545.16	0.3 (4)	3972.32	3972.157	1.4
3369.71	3369.576	59	3548.32	3548.189	41	3973.71	3973.547	4
3372.19	3371.995	50	3551.71	3551.563	5.3	3974.82	3974.681	0.35
3374.42	3374.228	33 (1)	3553.64	3553.483	1.7	3984.29	3984.17	0.2
3374.82	3374.637	11 (1)	3560.05	3559.925	0.4	3994.15	3993.97	0.1
3375.70	3375.560	0.5	3561.90	3561.752	8.2	4006.30	4006.14	0.01
3376.46	3376.330	0.8	3566.51	3566.375	93	4010.14	4009.99	0.007 (4)
3380.71	3380.577	106 (3)	3572.02	3571.871	63	4017.67	4017.56	0.15
3381.01	3380.885	13 (3)	3576.08	3575.94	0.4	4019.20	4019.055	0.06
3387.54	3387.467	0.3	3577.36	3577.23	0.4	4025.60	4025.44	0.1
3391.20	3391.051	48	3588.07	3587.928	12	4057.45	4057.30	0.1
3393.10	3392.993	66	3597.86	3597.699	67	4064.55	4064.380	0.05
3396.31	3396.174	0.6	3599.66	3599.530	0.3	4069.39	4069.24	0.015 (4)
3397.37	3397.28	0.1	3602.41	3602.278	17	4073.08	4072.93	0.01 (4)
3401.31	3401.164	1.9	3607.00	3606.853	0.4	4075.00	4074.897	0.015 (4)
3403.58	3403.427	2.2	3609.48	3609.312	19	4086.30	4086.15	0.01 (4)
3409.74	3409.579	12	3610.61	3610.45	54	4098.30		0.01 (4)
3413.66	3413.478	55 (1)	3612.90	3612.732	50	4116.11	4115.980	0.04
3414.12	3413.943	34 (1)	3619.52	3619.391	124	4121.48		0.015 (4)
3414.91	3414.771	93 (1)	3624.89	3624.733	14	4123.94	4123.79	0.01 (4)
3420.88	3420.742	1.0	3630.01	3629.891	0.3	4138.67	4138.52	0.01 (4)
3421.49	3421.339	2.3	3635.10	3634.943	3.0	4150.53	4150.37	0.03
3422.47	3422.334	0.7	3641.75	3641.632	0.3	4164.80	4164.636	0.02
3423.00	3422.870	1.3	3642.52	3642.383	0.2 (4)	4167.07	4166.96	0.02
3423.87	3423.713	69	3662.10	3661.938	1.7	4184.65	4184.473	0.07
3433.74	3433.565	66	3664.27	3664.089	13	4195.72	4195.533	0.1
3435.63	3435.495	0.5	3666.16		0.2 (4)	4200.60	4200.466	0.15
3437.45	3437.283	53	3668.36	3668.200	0.4 (1)	4201.89	4201.728	0.15
3442.17	3442.017	0.9	3669.40	3669.233	6.6			
3442.67	3442.540	0.4						

THE NI SPARK SPECTRUM

Eight doublets and 4 quartets have been measured; the quotients of intensity sums and statistical weights are found in Table XIII.

TABLE XIII.

Multiplet Designation		Quotients							
1	$a^4D^1-d^4F^1$	—	1.2	1.0	1.3	—	1.7	1.4	1.65
2	$a^2P^1-b^2P$	5	4.95			5.8	4.55		
3	$a^2P^1-b^2D^1$	0.5	0.05			0.07	0.5		
4	$a^4G^1-d^4F^1$	1.6	2.0	2.35	2.9	1.9	1.7	2.0	1.8
5	$a^2G^1-d^2F^1$	1.6	2.1			1.7	1.3		
6	$a^4F-d^4F^1$	2.85	1.9	1.5	1.15	1.85	1.4	1.7	1.7
7	$a^2F-d^2F^1$	1.6	1.0			1.3	1.2		
8	$a^2D^1-d^2F^1$	0.87	0.85			1.3	1.1		
9	a^2G-b^2F	0.6	0.9			0.5	0.7		
10	$a^2D-a^2D^1$	2.8	1.1			2.6	1.3		
11	a^2D-a^2F	0.47	0.04			0.15	0.4		
12	$a^4P^1-a^4D^1$	3.2	2.15			5.0	3.25	0.85	—

For some of the multiplets the disagreement with the summation rule is not very great, for others, however, the divergencies are wide, e.g. in the case of Nos. 3 and 11, where the diagonal terms are by far the weakest.

Adding up the doublet and quartet systems and the intercombinations, we get the quotients of Table XIV.

TABLE XIV.

Combinations	Quotients											
$a^4D^1, a^4D^1-d^4F^1, d^2F$	—	1.5	1.65	1.3	0.9	0.85	—	1.7	1.4	1.65	1.7	2.0
$a^4G^1, a^2G^1-d^4F^1, d^2F^1$	1.6	2.0	2.35	2.9	1.6	2.1	1.9	1.7	2.0	1.8	1.7	1.3
$a^4F, a^2F-d^4F^1, d^2F^1$	2.85	1.9	1.7	1.16	1.6	1.15	1.85	1.4	1.7	1.8	1.3	1.5

If we add the multiplets which in the quartet systems start from a^4D^1 , we find the quotients shown in Table XV.

TABLE XV.

Statistical weight	a^4D^1				a^4F^1				a^4G^1				Sum	Quotient
	1	2	3	4	2	3	4	5	3	4	5	6		
d^4F^1														
2					3.7	2.0			3.2				8.9	4.5
3	3.4	0.3				2.3	3.5		2.5	3.5			15.5	5.2
4			4.0				3.3	2.6		3.3	6.1		19.3	4.8
5				6.6				5.8			3.8	10.7	26.9	5.4
Sum	—	3.4	4.3	6.6	3.7	4.3	6.8	8.4	5.7	6.8	9.9	10.7		
Quotient	—	1.7	1.4	1.7	1.9	1.4	1.7	1.7	1.9	1.7	2.0	1.8		

There is comparatively little difference between these quotients. If we add to them the small number of intercombinations that occur, we find $4.5|5.4|5.7|5.4|$.

In the same way we find:

TABLE XVI.

	a^2D^1			a^2F		a^2G^1		Sum	Quotient
	2	3		3	4	4	5		
d^2F^1									
3	2.6			3.8	0.9	4.8		12.1	4.03
4		3.4			4.0	1.9	6.6	15.9	3.98
Q	1.3	1.1	1.3	1.2	1.7	1.3			

These results are satisfactory if the occurring intercombinations are added, the quotients become 4.03 and 4.12.

In our material these two multiplets are the only ones which start from the same level. The quartet $a^4P^1 - a^4D^1$ has the same original level as number of intercombinations. But we cannot conclude from these measurements, as there are other lines in the part of the spectrum that has not been examined which start from the same level. However, it is remarkable that the intensity ratios of this quartet are largely corrected by the additions of the intercombinations.

TABLE XVII.

	a^4P^1			a^2F^1		a^2D			
	1	2	3	3	4	2	3	Sum	Quotient
1	2.7	0.5				0.5		3.7	3.7
2	2.3	2.0		0.4		1.0	0.4	6.1	3.6
a^4D^1 3		4.0		0.9	1.1	1.3	3.9	11.2	3.7
4			2.6		2.7		7.2	12.5	3.1

In combining lines with a common final level we again meet with the difficulty that our materials are not complete; various lines that ought to be included do not occur in the spectral region that has been examined. Still the influence of the additions of the other intensities can be seen from Table XVIII.

TABLE XVIII.

	a^2D			a^2P^1			a^4P^1		
	2	3		1	2		1	2	3
a^2F	0.3	1.25	b^2D^1	0.07	1.05	a^4D^1 5	6.5	2.6	
a^2D^1	5.2	3.8	b^2P	5.8	9.1	a^2D^1	1.7	2.7	
a^4D^1	2.8	11.5	b^4D^1	1.2		a^2F		1.2	
a^4F	0.5	0.3	b^4P	1.0	2.8	a^4F	0.3		
			a^2F		0.2				
Sum	8.8	16.85	b^2F		0.4	Sum 5	8.5	6.5	
Quotient	4.4	5.6				Quotient 5	4.3	2.2	
			Sum	8.07	13.55				
			Quotient	8.1	6.8				

We have considered also the intensity ratio for doublet-quartet systems.

TABLE XIX.

Combinations	Ratio
$a^2D - d^2F^1$ and $a^4D^1 - d^4F^1$	1:1.6
$a^2G^1 - d^2F^1$ and $a^4G^1 - d^4F^1$	1:2.4
$a^2F - d^2F^1$ and $a^4F - d^4F^1$	1:2.4

The last column is found after division by ν^4 . The ratio 1:2 is found only approximately; this cannot be attributed to the occurring intercombination lines (3, 2 and 0 respectively) as in the last case where they do not occur, the divergency is the same as in the other two.

In the following intensity table (Table XX) an intensity of 100 has been awarded to line 2437.884.

TABLE XX. *Intensities of the lines of Ni II.* Intensities marked (1) are certain, (2) less certain, (3) doubtful, (4) inexact because of small intensity and irregularities in the plates.

λ (Kayser)	λ (I.A.)	Int.	λ (Kayser)	λ (I.A.)	Int.	λ (Kayser)	λ (I.A.)	Int.
2416.21	2416.13	29	2834.66		0.7	3366.31		4.3 (1)
2419.40		0.8		2836.58	1.0	3366.92		1.7 (1)
2429.17		0.5 (4)	2842.55	2842.41	1.9	3369.71		20
2431.65	2431.57	1.2	2863.84	2863.69	5.2	3372.14		4.6
2433.64	2433.57	6.7	2864.4	2864.16	2.6	3374.13	3373.98	3.9 (3)
2437.98	2437.884	100	2865.63		0.6	3374.36		2.9 (3)
2441.77		1.0		2881.24	0.3	3374.77		1.6 (3)
2441.90		0.6		2882.54	0.8	3380.74		21.5 (2)
2451.05		0.8	2907.10		0.4	3381.04		6.5 (2)
2454.09		0.6	2913.71	2913.59	3.4	3391.20		11.4
2455.60	2455.51	1.8	2914.11		0.2 (3)	3393.16		23
	2459.32	0.3		2942.71	0.15 (4)	3396.25		0.5
2465.34		0.2	2944.03		4.8		3397.82	0.2 (4)
2472.27		1.0	2947.56	2947.45	1.7	3401.30		0.5
2473.28	2473.13	13.4	2969.32		0.6	3401.90	3401.76	0.5
2476.96		0.8	2981.81		5.7	3403.45		0.8
2484.41	2484.32	6.6	2984.30		2.8	3407.43	3407.30	2.7
2497.92	2497.80	1.0	2988.21	2988.05	1.2	3409.70		0.9
2503.47		0.8	2992.75		4.2	3413.61		5.0
2505.94	2505.84	7.3	2994.60		6.6	3414.05		2.5
2511.00	2510.87	98	3002.65		19	3414.91		34
2514.85	2514.75	3.4	3003.76		15	3421.47		0.6
	2520.33	0.15	3012.14		19	3423.88		14
	2525.42	4.0	3019.27		3.7	3433.70		17
2539.20	2539.09	2.6	3032.00		1.3	3437.42		14
2540.14		2.0		3032.44	0.3	3446.41		22.5
2546.01	2545.90	21	3038.09		13	3453.06		12.5
	2547.16	0.5 (4)	3045.16		1.2	3454.29	3454.16	1.3
	2549.56	1.8	3050.99		21	3458.62		28
	2551.04	1.1	3054.46		12	3461.84		23
	2555.13	3.5	3057.79		16	3465.77	3465.62	2.0
2557.98	2557.88	0.9	3064.12	3063.93	0.5	3467.63		1.1
	2560.30	3.2	3064.76		5.0	3469.61		2.0
	2565.36	0.6 (4)	3080.90		3.5	3471.50	3471.35	2.3
2566.12	2566.08	6.1	3087.20	3087.07	2.7	3472.71		13.4
2584.10	2584.01	3.2	3097.26		2.0	3483.95		7.2
	2587.25	0.4	3099.26		1.5	3486.05		0.6
2588.40	2588.31	0.4	3101.70		21 (3)	3493.13		25.5
	2592.54	0.07	3102.02		12 (3)	3501.04		5.6
2601.22	2601.126	3.8	3105.60		1.7	3502.74		0.3 (4)
	2605.45	2.5	3114.25		2.2	3507.84		0.5
2606.50	2606.40	4.8	3129.40		0.2	3510.52		15
2610.20	2610.08	10.7	3134.21		16	3511.8		0.3 (4)
2611.78	2611.66	1.6	3197.24		1.4	3514.13	3513.95	7.2
2615.29	2615.20	6.6	3214.21		1.2	3515.21		30
2623.25	2623.10	0.3 (4)	3216.95		1.0	3516.32		0.8
	2626.57	3.3	3217.95		2.0	3518.76		0.5
2630.40	2630.29	2.7	3221.43		1.0	3519.90		3.4
	2631.52	2.0	3221.80		2.2	3524.69		33
2632.98	2632.86	3.5	3225.18		3.0	3528.10		0.7
2647.15	2647.04	2.6	3227.14		1.0	3548.32		2.4
2648.85	2648.72	0.9	3233.05		9.8	3551.70		0.4 (4)
2655.6	2655.46	0.9 (2)	3234.76		2.5	3553.65		0.4 (4)
2656.05	2655.90	3.7 (1)	3243.20		6.0	3561.92		0.5
2659.8		2.5	3248.57		1.1	3566.55		23
2665.39	2665.25	2.0	3249.55		0.8	3572.06		7.5
2666.00	2665.86	0.8	3250.90		1.7	3576.91	3576.76	4.0
2670.45	2670.33	1.0	3271.26		0.8	3588.07		0.5
2679.35	2679.25	2.3	3275.03	3274.90	0.4	3597.86		7.7
2684.57	2684.41	5.8	3282.85		0.8	3602.44		0.9
2690.8	2690.62	1.9	3282.97		0.3 (3)	3609.49		1.5
2708.9	2708.78	3.3	3287.06		0.5	3610.68		8.1
2743.1	2743.01	4.0	3290.70	3290.54	0.3 (2)	3612.91		3.9
2746.85		1.4	3290.83	3290.69	0.5 (2)	3619.54		25
2759.15	2759.02	3.8	3305.10		0.3 (4)	3624.89		0.9
2760.82	2760.67	1.1	3312.46		1.0	3664.26		1.1
2768.9	2768.78	3.4	3313.12		0.6	3670.59		1.0
2775.45	2775.31	2.6	3315.80		7.0	3674.29		1.2
2794.93		0.7 (4)	3320.41		4.4	3688.57		0.5
2798.75		1.8	3322.46		3.1	3722.62		0.5
2802.4		0.2 (4)	3326.85		0.2 (4)	3736.96		0.8
2805.20		0.2 (4)	3350.56	3350.42	1.0	3739.38		0.4 (4)
2805.80	2805.67	3.6	3359.24		0.4	3769.62	3769.45	2.6
2808.47	2808.35	0.4	3361.73		5.0	3775.74		3.1
2821.45		2.3	3362.94		0.2 (4)	3783.67		3.6
	2825.23	1.1	3365.90		4.0 (1)	3807.29		5.1
						3858.50		9.7

THE CO I SPECTRUM

In Table XXI the computed quotients are given for all the multiplets measured. The indication of the multiplets is that of Catalan and Bechert. The quotients with question marks between brackets are too large, owing to lines which are ordered doubly in the multiplets to which they refer. In quartet No. 30 one of the lines in the multiplet itself has been ordered doubly; 4 quotients had therefore to be left out.

TABLE XXI

No.	Level	Quotients											
4	F^1-D^1	40	46					29	34				
5	F^1-D^2	108	56					73	42				
6	$F^1-\bar{F}^1$	35	34					26	41				
7	$F^1-\bar{F}^2$	75	67					102	47				
8	F^1-G^1	72	61					77	90				
9	F^1-G^2	98	47					95	85				
15	ϕ^2-d^3	6.1	6.5	7.5	8.0			10.3	8.3	15.5			
19	f^1-d^1	99	80	78	41			89	83	41	13		
20	f^1-d^2	16	16	15	10			10	12	11	6		
21	f^1-d^3	20	20	16	11			23	15	8	4.4		
22	f^2-d^1	35	76	71	52			29	54	51	38		
23	f^2-d^2	155	115	83	51			135	78	62	18		
24	f^2-d^3	4.4	4.8	7.4	7.6			5.7	5.9	6.4	2.4		
25	$f^1-\bar{f}^1$	89	72	[82]	30			75	70	60	[55]		
26	$f^1-\bar{f}^2$	59	30	22	17			38	36	29	17		
28	$f^2-\bar{f}^1$	[2.3]	2.4	3	7.7			1.0	[2.1]	3.5	8		
29	$f^2-\bar{f}^2$	132	118	[98]	49			157	[127]	79	49		
30	$f^2-\bar{f}^3$	11	—	11.5	—			21	—	12	—		
31	f^1-g^1	33	23	18	15			50	28	25	18		
32	f^1-g^2	38	30	10	7			25	30	29	14		
34	f^2-g^1	4.4	7.5	9.6	6.5			0.5	3.8	8.7	17.6		
35	f^2-g^2	142	89	61	26			88	97	93	80		
36	f^2-g^3	2.2	5.5	2.8	3.8			3.0	3.9	6.2	4.6		
81	$\phi^1-\phi^1$	1.6	2.6	2.6	3.3	4.4	1.1	2.2	2.2	3.0	3.4	5.3	
82	$\phi^1-\phi^1$	2.9	3.0	3.8	2.8	2.3	12	4.3	4.6	3.7	1.5	7.5	8.2

None of the 25 multiplets follows the summation rule. Neither are equal quotients obtained when doublet and quartet systems are taken together with their intercombinations. For a few of these systems the results are found in Table XXII.

TABLE XXII.

Terms	Quotients											
f^1, F^1 and g^2G^2	101	57	39	44	59	7	25	32	34	22	112	148
f^1, F^1 and g^1G^1	73	66	33	23	19	15	50	28	31	18	77	91
f^1, F^1 and $\bar{f}^2-\bar{F}^2$	78	73	65	33	53	46	38	38	34	17	150	83
f^1, F^1 and d^2-D^2	109	58	16	16	16	19	10	14	12	6	74	51

If we take together the lines which originate from the same level we find the quotients of Table XXIII.

TABLE XXIII.

Term	Quotient			
g^1	38	31	28	21
G^1	110	84		
g^2	181	133	120	33
G^2	138	84		

Although for the level mentioned here the system is complete, the results are not appreciably better than for the separate multiplets; sometimes (for G^1) even worse.

For the other terms the system is incomplete; of these only for d^3 a considerable improvement is found. Here we combine f^1-d^3 , f^2-d^3 , F^1-d^3 and p^2-d^3 and find the quotients 31, 32, 32 and 28. However, p^1-d^3 , p^2-d^3 and P^1-d^3 could not be taken into account as they did not occur in spectral region we investigated.

TABLE XXIV.

Final level	Quotients			
f^1	315	293	235	144
f^2	431	488	413	264
F^1	467	450		

Finally we can add all the lines with a common final level. In each of these 3 cases a few systems of lines are wanting (2, 2 and 3 respectively), but it is highly improbable that the quotients given, which have been derived from 16, 16 and 13 lines respectively, would be greatly influenced by these.

For the ratio of intensities of doublet and quartet systems the following values (after division by ν^4) are tabulated here:

TABLE XXV.

Multiplet	Ratio
F^1-D^1 and f^1-d^1	1:2
F^1-D^2 and f^1-d^2	1:0.22
$F^1-\bar{F}^1$ and $f^1-\bar{f}^1$	1:2.1
$F^1-\bar{F}^2$ and $f^1-\bar{f}^2$	1:0.4
F^1-G^1 and f^1-g^1	1:0.3
F^1-G^2 and f^1-g^2	1:0.22

In 4 of the 6 cases the doublet is even stronger than the quartet. This cannot be ascribed to the existing intercombinations as the divergencies in the case of the systems F^1-D^2 and F^1-G^1 , where the intercombinations are weak, is much the same as in that of F^1-F^2 and F^1-G^2 with their strong intercombinations. Whereas the division by ν^4 yields a fairly correct ratio in 2 cases, it increases the error in the other 4 cases.

All the intensity values found are shown in Table XXVI in which an intensity of 100 has been awarded to the line 3334.151.

TABLE XXVI. *Intensities of the lines of Co I.* Intensities marked (1) are certain, (2) less certain, (3) doubtful, (4) inexact because of small intensity and irregularities in the plates.

λ (Kayser)	λ (I.A.)	Int.	λ (Kayser)	λ (I.A.)	Int.	λ (Kayser)	λ (I.A.)	Int.
2441.15		9.4	2451.84		1.2	2464.30		2.8
2443.00		2.7	2453.50		2.0	2464.58		2.8 (2)
2443.63	2443.55	5.1	2456.31		12	2464.71		4.5 (2)
2443.89		2.2	2460.28		2.2	2467.80	2467.71	11
2446.60		0.9	2460.90	2460.81	11	2470.38		16
2449.24		1.4	2462.22		3.8	2473.02		10
2450.10		2.4	2463.85		6.0	2474.01	2473.92	8.7

TABLE XXVI (continued)

λ (Kayser)	λ (I.A.)	Int.	λ (Kayser)	λ (I.A.)	Int.	λ (Kayser)	λ (I.A.)	Int.
2476.73	2476.64	17	2650.04	2650.271	11	2929.62		5.1
2483.70		15	2650.40		11		2936.551	0.5 (1)
2485.44		0.9	2653.84		0.5 (4)		2942.630	0.5
2486.53		3.4	2661.80		1.0	2943.60		1.9
2488.55		3.0	2663.61		0.6	2955.50		1.6
2489.36		3.3	2669.65		1.0	2957.79		3.1 (2)
2494.05		5.2	2674.04		1.3	2969.70		0.7
2494.83		9.5	2676.06	2675.987	10	2975.56		0.6
2495.65	2495.56	13	2679.83		12	2977.56		0.5
2496.80		17	2680.20		2.6	2978.10		1.5
2500.60	2500.51	3.2	2685.44	2685.340	17	2982.37		1.0
2504.63		17	2694.50		2.1	2984.24		0.3 (4)
2505.2		1.4	2694.76		2.2	2987.28	2987.172	33
2506.55		7.7	2695.93	2695.853	20	2989.70	2989.599	36
2507.26		1.0	2705.50		1.5	2996.67		1.0
2511.12	2511.03	18	2705.94		3.7	2999.84		1.0 (2)
2513.01		9.3	2708.88		1.4	3000.66	3000.554	2.7
2513.20		6.4	2716.05		13	3005.86		3.2 (1)
2517.90	2517.81	23	2719.65		1.1	3006.10		0.8 (1)
2519.90		5.4	2722.20		1.4	3013.70	3013.598	24
2521.03		1.1	2728.86		1.0	3015.77		3.8
2521.49	2521.40	22	2731.20		5.7	3017.33		1.0 (3)
2525.09		6.5	2740.54		7.2	3017.66	3017.552	31
2528.67		11	2745.17		8.0	3019.23		0.7
2529.06	2528.97	23	2746.10		1.3	3022.47		3.2
2530.22	2530.13	21	2750.20		3.5	3023.66		0.5
2530.65		6.8	2752.21		1.7	3026.49		10.7
2531.45		4.0	2758.67		1.0	3028.31		0.6
2532.26		21	2761.49	2761.375	9.6	3031.43		2.4
2535.45		5.6	2763.19		1.0	3034.55	3034.426	15
2536.02	2535.93	21	2764.30	2764.193	12	3038.42	3038.304	2.1
2536.55		19	2766.31		1.0 (1)	3039.66		3.3
2538.45		2.7	2766.47	2766.37	4.2 (1)	3040.93		14
2542.05		5.2	2768.80		1.2	3042.60	3042.482	30
2544.34	2544.25	20	2772.80		1.6	3044.11	3044.007	50
2544.94		12	2775.06	2774.964	4.4	3045.13		0.7
2548.40		20	2775.29		0.7 (1)	3048.21		2.0 (2)
2549.37		14	2775.67		1.5	3049.00	3048.892	46
2553.09	2553.00	16	2778.92		8.7	3050.64		3.6 (2)
2553.44	2553.35	18	2786.00		2.2	3054.84	3054.724	4.4
2555.15	2555.06	17	2790.40		0.7	3060.17		7.9
2556.85		12	2791.13		1.7	3061.15		1.5 (1)
2559.48		4.6	2791.57		0.6	3061.94	3061.825	49
2561.37		2.0	2792.55		2.2	3062.33	3062.198	8.8 (1)
2562.22	2562.13	19	2796.33	2796.236	5.4	3064.49	3064.375	16
2564.14		8.3	2797.18		4.0	3070.94		1.3 (1)
2567.42	2567.33	20	2803.87	2803.775	11	3072.06	3071.954	9.4 (2)
2572.32		8.8	2804.25		1.0 (2)	3072.45	3072.346	56
2574.45	2574.36	18	2811.23		1.5	3073.64		3.3
2574.94		1.2	2811.64		2.6	3079.49	3079.390	4.9
2575.82		4.2	2815.06	2814.979	1.1	3082.73	3082.614	42
2578.99		2.5	2815.65	2815.557	16	3086.46		9.0 (2)
2580.43		20	2818.69	2818.596	2.2	3086.89	3086.778	71
2580.95		16	2820.11	2820.003	3.6	3087.86		2.1
2582.35		7.8	2821.86		1.6	3088.76	3088.676	0.9
2585.45	2585.36	11	2823.78		1.2	3089.68	3089.593	38
2587.30		9.0	2825.29		2.5	3090.36		3.0
2590.70		11	2826.91		1.9	3095.81		2.7
2591.78		12	2828.55		0.8	3096.50		2.9 (1)
2594.26	2594.176	6.6	2834.02	2833.928	1.9	3096.80		1.8 (1)
2595.31		1.9	2834.55	2834.425	1.7	3098.30	3098.195	35
	2596.000	0.6	2837.26		4.7	3099.76		2.1
2601.07	2600.991	4.9	2842.46		1.8	3102.49		4.0
2606.22		9.0	2850.15		4.3	3103.82		7.2 (1)
2610.86	2610.770	4.7	2851.05	2850.956	1.1	3104.12	3103.990	4.0 (1)
2613.60		1.4	2859.75	2859.660	2.4	3106.03	3105.920	1.4 (2)
2613.98		10	2861.48		0.5	3106.22	3106.136	1.5 (2)
2614.23	2614.132	5.4	2862.70	2862.610	7.0	3107.15		2.5
2614.45		0.9 (2)	2867.57		0.4	3107.65		1.3
2615.45		2.4	2872.60		3.7	3109.60		3.3
2616.34		4.1	2878.65		1.4	3110.12		3.0
2617.95		6.7	2879.71		3.1	3110.94	3110.817	3.3
2619.36		5.0	2882.34	2882.221	1.8	3111.45		1.4
2622.15	2622.064	14 (1)	2886.55	2886.448	20	3113.58		7.3
2622.35	2622.252	5.9 (1)	2892.37		1.8	3118.35	3118.240	4.8
2622.54	2622.434	11	2895.46		0.7 (3)	3118.76	3118.630	0.4 (1)
2623.54	2623.450	11	2895.57		1.6 (3)	3121.54	3121.414	30 (3)
2623.85		4.0	2899.91	2899.801	3.3	3121.69	3121.560	36 (3)
2627.13		3.5	2903.30		1.9	3126.85		3.4
2627.71	2627.641	23	2904.40		0.6	3127.35	3127.244	4.6
2630.05		2.3	2907.75		0.5	3129.10	3128.997	1.5
2640.33		1.5	2911.70	2911.560	0.7	3129.57		2.3
2642.97		2.1		2916.041	0.2 (4)	3132.33	3132.212	2.4
2644.89		4.9	2919.66		1.3	3136.81	3136.721	2.2
2646.51	2646.420	24	2927.78		5.0	3137.47	3137.325	49
2648.79	2648.648	51	2928.91	2928.819	4.4	3140.08	3139.943	42

TABLE XXVI (continued)

λ (Kayser)	λ (I.A.)	Int.	λ (Kayser)	λ (I.A.)	Int.	λ (Kayser)	λ (I.A.)	Int.
3140.83		1.4	3342.10		3.2	3495.83	3495.685	176
	3143.812	0.6	3342.88		11	3496.80	3496.682	38 (2)
3145.16		1.8	3344.36		1.0 (4)	3496.90		38 (2)
3147.19	3147.060	56	3347.10		7.1	3502.45	3502.281	89 (2)
3149.43	3149.304	28	3348.28		11	3502.80	3502.620	159 (2)
3150.82		5.3 (2)	3351.70		1.6	3503.85		2.4 (3)
3150.93		6.3 (2)	3354.51	3354.386	92	3504.89		2.4 (3)
3152.84		6.8	3355.27		2.3	3506.47	3506.315	138
3154.91		42	3356.59		3.8	3510.00	3509.844	122 (1)
3157.23		1.3	3356.97		1.3	3510.59	3510.419	92 (1)
3158.92	3158.769	48	3358.13		0.7 (4)	3512.80	3512.643	128
3159.80	3159.660	16	3359.42		5.6	3513.61	3513.483	89
3161.78		4.6	3361.72		6.0	3518.50	3518.353	215
3164.66		0.3	3362.93		6.7	3520.23	3520.087	78
3168.19		4.5	3363.41		3.1	3521.73	3521.572	186
3169.90		10	3363.89		2.2	3523.55	3523.438	155
3173.30		0.6	3364.38		3.0	3526.97	3526.856	99
3174.29		1.3	3365.13		1.2	3529.19	3529.037	83
3175.06		3.2	3367.25	3367.114	94	3529.92	3529.815	151
3177.40		7.0	3368.72		1.2	3533.51	3533.363	100
3179.98		0.5	3370.48	3370.330	15	3534.91		12
3180.42		1.7	3373.40		5.9	3543.43		27
3182.25		6.6	3374.42		4.4	3546.85		2.6
3186.05		0.8	3376.34		1.5	3548.60		5.8
3186.46	3186.346	6.4	3377.20		4.7	3550.78	3550.599	64
3188.50		8.8	3378.86		5.4	3552.90	3552.719	3.0 (2)
3189.87	3189.756	3.6	3381.65		2.2	3553.16		15 (1)
3191.44	3191.300	1.8	3383.07		16	3553.31		3.0 (3)
3193.30	3193.162	3.2	3384.09		2.2	3558.93	3558.780	15
3198.79	3198.664	2.3	3385.38	3385.227	81	3561.03	3560.896	103
3199.44	3199.325	1.4	3388.29	3388.175	95	3562.25		5.0
3200.15	3203.030	2.0	3390.54		2.5 (2)	3563.09		5.3
3210.35		3.4	3390.92		3.8 (2)	3565.09	3564.955	103
3210.96		1.6	3395.55	3395.378	135	3569.59	3569.382	185
3219.31	3219.155	12	3398.96		1.4	3575.13	3574.964	99 (2)
3224.80		2.0	3402.14		3.9	3575.53	3575.361	114 (2)
3227.15		1.8	3403.33		0.6 (4)	3578.21		4.5
3235.69		9.2	3405.27	3405.120	144	3579.04		4.5 (3)
3237.18	3237.028	24	3407.02		1.0 (4)	3579.15		3.6 (3)
3239.08		1.1 (4)	3409.29	3409.176	124	3582.02		1.7
3243.99		22	3412.50	3412.335	128	3584.94	3584.796	7.2 (3)
3250.17	3249.994	10	3412.79	3412.636	64 (1)	3585.33	3585.159	109
3254.37		20	3415.66	3415.527	3.0 (1)	3587.30	3587.188	223
3258.16		2.3	3417.32	3417.158	118	3595.03	3594.869	101
3260.99		13	3417.84		8.0 (3)	3596.67		2.4
3263.35		2.4	3417.93	3417.796	8.0 (3)	3602.22	3602.081	114
3264.96	3264.842	7.4	3420.64		1.9 (3)	3605.52	3605.367	74
3271.92		9.8	3420.95		4.7 (3)	3611.89		14
3276.60		2.8	3421.77		1.4	3615.54		4.3
3277.44		2.3 (2)	3423.03		3.1	3618.15	3618.006	2.5
3277.80		2.3 (2)	3424.67		11	3620.56		2.7
3278.96		5.1	3426.60		1.3	3624.54		2.6 (1)
3279.39		4.2	3428.34		5.2	3625.18	3624.955	11 (1)
3280.74		18	3428.89		1.8	3627.98	3627.807	90
3283.60		38	3431.76	3431.579	71	3631.59	3631.340	70
3287.34		7.7	3433.18	3433.043	170	3633.01		5.4
3292.24		1.3 (4)	3437.10		1.4	3634.86		7.0
3298.83		4.6	3437.83		5.8	3637.44		1.7
3304.03		0.8 (3)	3439.05		5.8	3636.84		4.7
3304.29		1.7 (1)	3443.06	3442.924	84 (1)	3639.60		17
3305.27		1.0 (4)	3443.79	3443.646	140 (1)	3641.94		7.0
3305.87		1.0 (4)	3449.26	3449.171	170 (3)	3643.35		14
3306.54		0.8 (4)	3449.54	3449.443	153 (3)	3645.34		3.6
3307.31		7.9	3452.44		3.8	3647.85	3647.663	37
3308.65		3.0	3453.66	3453.513	155	3649.49		7.8
3308.96		4.7	3455.33	3455.236	99	3651.41		2.3
3312.33		10	3457.05	3456.936	9.3	3652.70	3652.544	45
3312.99		1.6	3460.86	3460.732	2.4	3654.59		4.0
3314.21		9.9	3461.33		15	3657.10	3656.965	7.5
3315.20		1.1 (4)	3462.94	3462.807	144	3658.06		1.0 (4)
3318.55		1.8	3465.96	3465.796	87	3662.32		22
3319.31		2.2 (1)	3469.11		1.5	3670.20		1.0 (4)
3319.66		14 (1)	3471.53		4.7	3676.72		17
3320.00		4.9 (1)	3472.85		2.0	3683.22		41
3322.41		15	3474.17	3474.019	169	3684.65		5.2
3325.44		15	3476.50		2.1	3690.91		4.1
3327.14		14	3478.00		1.8	3693.63		15 (3)
3328.34		1.1	3478.60		8.7 (3)	3702.39		16
3329.16		0.8 (4)	3478.90		5.2 (3)	3704.22	3704.061	83
3329.63		4.3	3480.17		3.5	3707.62		3.9
3333.55	3333.390	13	3483.58	3483.415	99	3709.00		21
3334.31	3334.151	100	3485.51		21	3712.35		2.9
3337.34	3337.175	6.4	3487.84		4.8	3726.79		1.2
3338.68		0.6 (4)	3489.57	3489.406	166	3730.63		27
3339.97		9.0	3490.89	3490.741	20	3732.59		55
3341.52		5.0	3491.49	3491.324	76	3733.65		22

TABLE XXVI (continued)

λ (Kayser)	λ (I.A.)	Int.	λ (Kayser)	λ (I.A.)	Int.	λ (Kayser)	λ (I.A.)	Int.
3736.08		12	3972.69		3.5(2)	4270.60	4270.423	1.0
3740.34		2.1	3973.31	3973.148	13	4285.95	4285.787	2.8
3745.65	3745.501	107	3974.90	3974.732	17	4292.42		0.7
3750.07		14 (1)	3978.78	3978.656	11 (3)	4303.41	4303.236	1.3
3751.75		3.3	3978.99		7.1 (3)	4309.61	4309.418	0.4
3754.47		1.5	3979.67	3979.525	20 (1)	4331.43		1.2
3755.60		9.3	3987.25	3987.121	4.1	4339.81		2.8
3759.83		1.0 (3)	3990.45	3990.307	5.9	4371.31		1.4
3760.55		1.3 (3)	3991.68		7.7 (2)	4373.81		1.4 (1)
3774.75		2.9	3991.83	3991.693	7.0 (2)	4375.11	4374.940	1.4 (1)
3777.68		2.6	3994.70	3994.541	1.0 (3)	4391.70	4391.59	1.2 (1)
3783.87		0.6 (4)	3995.45	3995.312	244	4392.02		1.0 (1)
3808.25	3808.106	7.2	3998.09	3997.909	125	4402.86		1.0
3811.23	3811.070	1.9	3998.69	3998.554	1.0 (3)	4417.55	4417.425	1.5
3812.62		0.9	4003.85		0.5	4421.54	4421.359	1.3
3814.62		3.1	4011.10	4011.098	1.1	4431.79		0.8
3816.48		17 (2)	4014.09	4013.950	4.8	4445.88	4445.730	1.4
3816.61		13 (2)	4019.45	4019.300	2.7	4467.09	4466.888	4.7
3842.21	3842.056	137	4021.07	4020.904	38	4469.75	4469.569	10
3845.60	3845.474	235	4023.55		2.1	4471.76	4471.578	4.0
3850.27		1.2 (2)	4027.18	4027.044	11	4478.50	4478.345	1.6
3851.09	3850.949	7.7	4035.74		5.9	4484.11	4483.946	1.5 (2)
3852.00		2.4 (2)	4040.57		0.7 (3)	4494.94		0.6
3856.94		4.8	4040.95		0.5 (3)	4517.26	4517.121	2.8
3861.31	3861.168	80	4045.56	4045.397	51	4528.08	4527.936	0.8 (2)
3863.75		1.0	4049.43		0.6 (4)	4531.12	4530.985	48
3870.66		2.5	4053.10		1.3	4534.16	4533.998	6.1
3873.23	3873.117	188 (1)	4057.10		2.0 (1)	4543.98	4543.836	5.5
3874.09	3873.957	185 (1)	4057.36	4057.199	4.5 (1)	4549.83		11
3877.01	3876.840	37	4058.36	4058.188	9.6 (1)	4565.79		17
3882.06	3881.877	133	4058.76	4058.603	5.5 (1)	4570.21		1.4
3884.79	3884.609	11 (1)	4063.34	4063.19	2.0	4580.34	4580.133	2.6 (2)
3885.45	3885.281	5.0 (2)	4066.56	4066.378	36	4581.80	4581.618	25
3894.25	3894.086	285	4068.72	4068.553	9.4	4594.82		3.2
3895.15	3894.981	35 (1)	4076.30	4076.134	3.1	4597.09		3.0
3898.54	3898.499	1.6	4077.56		1.4	4623.20	4623.024	1.1
3904.23		1.9	4082.75	4082.606	2.0	4625.92		1.0
3906.46	3906.296	16	4086.49	4086.307	32	4629.52	4629.380	19
3910.13	3909.941	26	4092.56	4092.397	135	4637.56	4637.399	0.2
3917.80		8.6	4104.57	4104.430	0.8 (2)	4663.59	4663.411	11
3920.90		5.3	4104.91		1.8 (2)	4682.53	4682.363	6.6
3922.90	3922.764	8.1	4110.70	4110.544	77	4693.36	4693.193	2.8
3925.33		0.9	4118.96	4118.784	232	4698.56	4698.370	1.4
3929.43		1.1	4121.52	4121.329	306	4704.57		0.7
3934.07	3933.921	4.5		4130.538	0.4 (4)	4728.14	4727.924	2.2
3934.85		1.1	4132.30	4132.15	3.0	4735.04	4734.834	0.8
3936.13	3935.974	146	4150.62	4150.442	0.5 (4)	4737.95	4737.776	1.1
3939.00		0.8	4158.59		0.8	4749.89	4749.684	6.8
3941.06	3940.895	20	4162.38		1.3	4754.59	4754.372	1.3
3941.91	3941.735	39 (1)	4179.44		0.5	4756.93		0.8
3945.51	3945.323	27	4187.46	4187.248	1.5	4767.33		0.8 (2)
3946.75		1.0 (2)	4190.88	4190.709	15	4768.26	4768.096	1.2 (2)
3947.26	3947.132	1.3 (2)	4193.02		0.8 (4)	4771.27	4771.105	2.8
3952.46	3952.329	2.1 (3)	4198.56	4198.424	0.7 (4)	4776.49	4776.328	3.1
3953.10	3952.923	55	4234.17	4233.996	1.8	4780.14	4780.001	5.7
3956.42	3956.276	0.8	4242.07		1.0	4793.03	4792.867	8.5
3958.10	3957.935	26	4245.75		0.2 (4)	4813.67	4813.482	12
3961.15		3.3	4248.35		0.2 (4)	4840.42	4840.267	14
3969.28		11	4252.46	4252.303	6.9	4868.05	4867.680	18

THE EFFECT OF THE MOTION OF THE NUCLEUS ON THE SPECTRA OF Li I AND Li II

By D. S. HUGHES AND CARL ECKART

RYERSON PHYSICAL LABORATORY, UNIVERSITY OF CHICAGO

(Received July 7, 1930)

ABSTRACT

The wave equation for a system of N electrons (mass m) and one nucleus (mass M) is set up and solved approximately. If $W(m)$ are the energy levels for $M = \infty$, the energy levels for finite M are $(\mu W(m)/m) + \Delta W$, where $\mu = mM/(m+M)$ and ΔW is calculable.

In case $N=2$ or 3 , ΔW is zero except for P levels. For these it is given by Eq. (13), which is derived on the assumption that the wave function is a polynomial of hydrogen functions, each with its own effective nuclear charge. The values of the latter previously determined by one of the authors are used in comparing the calculation with Schüler's experimental data on Li II, $\lambda 5485$ and Li I, $\lambda 6708$. The agreement is satisfactory and eliminates one objection to Schüler's interpretation of $\lambda 5485$.

IT IS well known that the effect of the motion¹ of the nucleus on the spectra of hydrogen and ionized helium may be accounted for by replacing m , the mass of the electron, by $\mu = mM/(m+M)$, M being the mass of the nucleus. This simple procedure does not suffice for elements of more than one electron, and as an effect observed in the spectrum of lithium has been ascribed to this cause, a theoretical discussion of the expected effect seems in order. Some of the results obtained are applicable to the general case of N electrons, others only to Li I and Li II.

1. GENERAL

The kinetic energy operator for a system of N electrons and one nucleus is

$$T = -\frac{\hbar^2}{4\pi^2} \left\{ \frac{1}{2\mu} \sum_{k=1}^N \nabla_k^2 + \frac{1}{M} \sum_{(k,i)} \nabla_k \cdot \nabla_i + \frac{1}{2(M+Nm)} \nabla^2 \right\} \quad (1)$$

in which

$$\nabla_k = i \frac{\partial}{\partial x_k} + j \frac{\partial}{\partial y_k} + k \frac{\partial}{\partial z_k}$$

$$\nabla = i \frac{\partial}{\partial X} + j \frac{\partial}{\partial Y} + k \frac{\partial}{\partial Z}$$

where x_k, y_k, z_k are the rectangular coordinates of the k^{th} electron in a system whose origin is located at the moving nucleus, and (X, Y, Z) are the coordinates of the center of mass of the atom in another system of arbitrary fixed origin. The quantities m, M , and μ have the significance already defined.

¹ This term will be used to describe the translatory motion of the nucleus about the center of mass of the atom, as distinguished from the nuclear "spin".

The wave equation is thus

$$\{T + V(x) - W\}\psi = 0 \quad (2)$$

where V is the potential energy of the atom and is independent of the coordinates of the center of the mass. For simplicity, it may be assumed that the latter is at rest, so that ψ will also be independent of (X, Y, Z) .

If it be assumed that the characteristic values $W(m)$ and solutions $\psi(m)$ of Eq. (2) are known for $M = \infty$ (stationary nucleus), the effect of the finiteness of M may be approximately resolved into two parts:

- a. M is replaced by μ in $W(m)$ and $\psi(m)$.
- b. The energy level is displaced by an additional amount ΔW given by

$$\psi(m)\Delta W = H'\psi(m) = -\frac{h^2}{4\pi^2 M} \sum_{(k,j)} \nabla_k \cdot \nabla_j \psi. \quad (3)$$

The perturbed energy value is thus $W(\mu) + \Delta W$. The statement (b) assumes that there is no degeneracy other than that conditioned by the rotational symmetry of the problem (degeneracy in the magnetic quantum number).

These two effects may be treated independently; for the first,² it is necessary to investigate the dependence on μ of the characteristic values of the equation

$$-\frac{h^2}{8\pi^2 \mu} \sum_{1 \rightarrow N} \nabla_k^2 \psi + [V(x) - W(\mu)]\psi = 0. \quad (4)$$

Since $V = \sum (Ze^2/r_k) - \sum (e^2/r_{jk})$ is a homogeneous function of degree -1 in the 3 N variables³ the calculation may be made rigorously without knowing ψ : on introducing new variables $x_k' = \alpha x_k$, $y_k' = \alpha y_k$, $z_k' = \alpha z_k$, where $\alpha = \mu/m$, and noting that $V(x) = \alpha V(x')$, Eq. (4) becomes

$$-\frac{h^2}{8\pi^2 m} \sum_{1 \rightarrow N} \Delta_k'^2 \psi + [V(x') - W(\mu)/\alpha]\psi = 0.$$

Hence

$$W(\mu) = \alpha W(m). \quad (5)$$

Since α is less than 1, this causes a general contraction of the spectrum relative to that of an atom whose nucleus has infinite mass. This may be called the normal effect, since it is the only effect in the case of the simplest spectra.

The specific effect ΔW cannot be evaluated without some assumption regarding $\psi(m)$. It is simplest to assume it as a polynomial of hydrogen functions, each with a different nuclear charge determined by the variational method of calculating characteristic values.⁴ The coefficients of the poly-

² The calculation is merely an extension of that usually given for hydrogen.

³ This is true only if the electron spin energy is not included in V .

⁴ C. Eckart, Phys. Rev. **36**, 149 (1930). It is not known whether such a polynomial is really a good approximation to $\psi(m)$ or not, but it may be shown to yield approximately correct values for the energy. There is also some justification for its use in a perturbation calculation, but the magnitude of the error introduced is uncertain. Experience would seem to show that it is smaller than if the true nuclear charge was used in each hydrogen function; cf. W. Heisenberg, Zeits. f. Physik **39**, 511 (1926). Whatever may be the theoretical status of effective nuclear charges, it should be remarked that the values of Z_1 and Z_2 used in these calculations have not been determined *ad hoc* but are the results of independent calculations made without reference to the present problem.

nominal are determined so that $\psi(m)$ has the proper permutational symmetry. Calculations based on this assumption follow for the cases of two and three electron systems.

2. TWO ELECTRON SYSTEMS

The wave function may be approximated by

$$\psi = [u(1)v(2) \pm v(1)u(2)]/2^{1/2} \quad (6)$$

in which u is the characteristic function of the $1s$ state, v of the excited state (n, l), and the numerals designate the variables of the two electrons. The effective nuclear charge for the function u is to be taken approximately equal to Z , the true nuclear charge. If v represents a $2p$ state, its effective nuclear charge is approximately $Z_2 = Z - 1.0$. The precise theoretical⁴ values for Li II, 2^3P are $Z_1 = 2.98$, $Z_2 = 2.16$. The upper sign in Eq. (6) is for the singlet level, the lower for the triplet. The perturbation operator in this case is simply

$$H' = -h^2 \nabla_1 \cdot \nabla_2 / 4\pi^2 M$$

and

$$\Delta W = \iint \psi^* H' \psi d\tau_1 d\tau_2.$$

On integrating by parts with respect to the variables 2,

$$\Delta W = (h^2/4\pi^2 M) \iint (\nabla_1 \psi) (\nabla_2 \psi^*) d\tau_1 d\tau_2;$$

noting that

$$\int (\nabla u) u^* d\tau = \frac{1}{2} \int \nabla |u|^2 d\tau = 0,$$

and making use of Eq. (6), this reduces to

$$\Delta W = \pm (h^2/4\pi^2 M) \left| \int u^* \nabla v d\tau \right|^2. \quad (7)$$

This integral will be evaluated at the end of the next section.

3. THREE ELECTRON SYSTEMS

In this case, it may be well to take account of the permutation degeneracy directly: there are three independent characteristic solutions

$$\psi_1 = v(1)u(2)u(3), \quad \psi_2 = v(2)u(3)u(1), \quad \psi_3 = v(3)u(1)u(2) \quad (8)$$

and

$$H' = - (h^2/4\pi^2 M) (\nabla_1 \cdot \nabla_2 + \nabla_2 \cdot \nabla_3 + \nabla_3 \cdot \nabla_1). \quad (9)$$

The function u again represents the $1s$ state, this time with Z_1 approximately equal to $Z - 0.3$, while v , in the case of the configuration $(1s)^2 (2p)$, has the approximate nuclear charge $Z_2 = Z - 2.0$. In the case of Li I, 2^3P , the theo-

retical values are⁴ $Z_1=2.69$, $Z_2=1.02$. The Eq. (3) is to be replaced by the three equations

$$\begin{aligned} a\Delta W &= aA + bB + cB \\ b\Delta W &= aB + bA + cB \\ c\Delta W &= aB + bB + cA \end{aligned} \quad (10)$$

in which

$$\begin{aligned} A &= \iiint \psi_i^* H' \psi_i d\tau_1 d\tau_2 d\tau_3 \\ B &= \iiint \psi_i^* H' \psi_j d\tau_1 d\tau_2 d\tau_3. \end{aligned} \quad (11)$$

The quantities A and B are real and independent of i and j since the operator H' is symmetric in the three sets of coordinates. The determinant of Eqs. (10) has one single root $\Delta W = A + 2B$ and one double root $\Delta W = A - B$. The former belongs to a state which is excluded by the Pauli principle, the latter to the actual doublet state.

On substituting Eqs. (8) and (9) into (11), it is found that

$$A = 0, \quad B = - (h^2/4\pi^2 M) \left| \int u^* (\nabla v) d\tau \right|^2,$$

so that ΔW has the same functional form as in the case of a two electron system.

This integral is readily evaluated: as a generalization of a well-known equation, it is readily shown that

$$\begin{aligned} - (h^2/4\pi^2 m) \int u^* (\partial v / \partial x) d\tau &= (W_u - W_v) \int x u^* v d\tau \\ &= e^2 (Z_1 - Z_2) \int (x u^* v / r) d\tau, \end{aligned} \quad (12)$$

W_u and W_v being the Balmer term-values associated to u , Z_1 and v , Z_2 , respectively. By a slight generalization of the methods used to derive the selection principles for spectral lines⁵ it may be shown that both integrals on the right vanish unless the values of the azimuthal quantum numbers of u and v differ by exactly one unit. As u represents the $1s$ state, ΔW will therefore vanish unless v represents a p state, and the specific effect is shown only by P levels (in this approximation at least). The displacement of these is found to be

$$\Delta W = \pm \frac{128}{3} \frac{m}{M} R_\infty Z_1^5 Z_2^5 n^3 (n^2 - 1) \frac{(Z_1 n - Z_2)^{2n-4}}{(Z_1 n + Z_2)^{2n+4}}$$

⁵ A. Sommerfeld, *Wellenmechanischer Ergänzungsband*, p. 92. (Vieweg, Braunschweig, 1929).

in which R_∞ is the Rydberg constant, $2\pi^2me^4/h^2$, and n is the true principal quantum number. The increment of energy will be negative for the three electron system and the triplets of the two electron system, positive for the singlets.

4. COMPARISON WITH OBSERVED EFFECTS

H. Schüler⁶ has proposed an interpretation of the hyperfine structure of the Li II line 2^3P-1^3S , $\lambda 5485$, according to which the nucleus of Li (6) has no angular momentum while that of Li (7) has $1/2$ unit. On the basis of his analysis it is possible to calculate the displacement of the Li (6) lines from the position which the Li (7) lines would occupy if there were no nuclear spin. These displacements are given in the last column of Table I. The three values should be identical to at least two significant figures, so that the differences are to be ascribed to errors, either in measurement or interpretation, or in both.

TABLE I.

	Li (6)	Li (7)	$\Delta\lambda$
$^3P_0-^3S$	5484.10	5483.81	0.29A
$^3P_2-^3S$	5485.02	5484.69	0.32
$^3P_1-^3S$	5485.65	5485.31	0.34

Using the values of $Z_1=2.98$, $Z_2=2.16$ Eq. (13) yields 0.256 A for the displacement produced by the specific effect, while Eq. (5) yields 0.071 A for the normal effect. The resultant is 0.327 A, the Li (6) line being to the long wave-length side of Li (7). This value is in excellent agreement with those of Table I. This calculation therefore supports part of Schüler's interpretation of this line though the present considerations would not defend it against attacks from other directions.⁷

Schüler and Wurm⁸ have also found that the lines 2^2P-1^2S of Li I, $\lambda 6708$, are doubled, with a separation of 0.15A. This has been confirmed by one of us (H), the observed separation being between 0.155 and 0.160A. Assuming the nuclear spin to be $1/2$ for Li (7), the structure due to this cause should be only 0.03-0.04A wide. The effect has therefore been interpreted as being primarily due to the motion of the nucleus.

The calculated values, using $Z_1=2.69$ and $Z_2=1.02$ (cf. Section 4) are 0.087A for the normal effect and 0.036A for the specific, a total of 0.123A. The agreement is as good as might be expected, since the difference between observed and calculated is of the order of the unresolved spin structure.

We would like to conclude from these results that Schüler's interpretation of $\lambda 5485$ is correct, but, in view of the results Harvey and Jenkins⁷ have obtained from the band spectra of lithium, the question had best be left open.

⁶ H. Schüler, *Zeits. f. Physik* **58**, 741 (1929); and H. Brück, *ibid* **42**, 489 (1927).

⁷ A. Harvey and F. A. Jenkins, *Phys. Rev.* **35**, 789 (1930).

⁸ H. Schüler and E. Wurm, *Naturwiss.* **15**, 971 (1927).

ELECTRONIC STATES IN THE VISIBLE HALOGEN BANDS

BY ROBERT S. MULLIKEN*

RYERSON PHYSICAL LABORATORY, UNIVERSITY OF CHICAGO

(Received July 7, 1930)

ABSTRACT

It is shown on the basis of theoretical considerations that the well-known visible iodine absorption bands and the analogous bands of the other halogens almost certainly cannot correspond to a ${}^1\Sigma \leftarrow {}^1\Sigma$ transition as hitherto supposed. It is concluded that they belong to a ${}^3\Pi_{0u} \leftarrow {}^1\Sigma_g^+$ transition, with a case *c* ${}^3\Pi_0$ state whose Λ -type doubling is so wide that the state is split into two separate states which simulate a ${}^1\Sigma_u^+$ and a ${}^1\Sigma_u^-$ state. The observed bands involve however only the state which behaves like ${}^1\Sigma_u^+$, the ${}^1\Sigma_u^-$ -like state and the ${}^3\Pi_1$ and ${}^3\Pi_2$ states being unknown. The classification ${}^3\Pi_0$ really has little meaning, one needs for case *c* here a classification in which only Ω values and symmetry properties (+ or -, *g* or *u*) are significant. According to the above interpretation, the upper level of the halogen bands is paramagnetic, this is in harmony with certain magnetic phenomena observed with these bands. Electron configurations for the normal and excited states are suggested in the case of fluorine.

TWO identical atoms in the same 2P state¹ are capable, as one finds by applying the relations obtained by Wigner and Witmer,² of giving only the following set of molecular states: ${}^1\Delta_g$, ${}^3\Delta_u$, ${}^1\Pi_u$, ${}^1\Pi_g$, ${}^3\Pi_u$, ${}^3\Pi_g$, ${}^1\Sigma_g^+$, ${}^1\Sigma_g^-$, ${}^1\Sigma_u^+$, ${}^3\Sigma_u^+$, ${}^3\Sigma_u^-$, ${}^3\Sigma_g^-$. As we shall see, this is almost certainly⁵ in conflict with the current interpretation of the visible absorption bands of iodine and the analogous bands of the other halogens as ${}^1\Sigma$, ${}^1\Sigma$ transitions. The argument is as follows.

For convenience we shall speak in terms of the *chlorine* bands, since our knowledge is more well-rounded for these than for the bands of the other halogens. What is said is intended to apply to all the halogens, since there can scarcely be a doubt that the bands of the four molecules are all of the same type. In respect to some properties, the iodine bands are better known than the chlorine bands, but we shall feel free to apply this knowledge also to the latter. (1) That the *normal state* of Cl_2 is ${}^1\Sigma$ seems assured by the fact that chlorine gas is diamagnetic (Br_2 and I_2 are also known to be diamagnetic in the *liquid* state). This conclusion is strongly supported by a study of

* Fellow of the John Simon Guggenheim Memorial Foundation, now in Leipzig.

¹ For the prediction of the possible molecular states as given above, the division of the 2P normal state into ${}^2P_{3/2}$ and ${}^2P_{1/2}$ substates does not matter, by the "normal state" of the atom we mean either ${}^2P_{3/2}$ or ${}^2P_{1/2}$ or both.

² E. Wigner and E. E. Witmer, *Zeits. f. Physik* **51**, 883 (1928). The designations Σ^+ and Σ^- used here correspond to Wigner and Witmer's Σ and Σ^1 (also to their 0 and 0'). The subscripts *g* and *u* (gerade and ungerade) mean "even" and "odd". In the case of odd (even) states the electronic factor of the wave-function ψ does (does not) change sign on reflection in the midpoint of the line joining the nuclei. Σ_g , Π_u , Δ_g are respectively the same as Σ_+ , π_- , Δ_+ of Wigner and Witmer, while Σ_u , Π_u , Δ_u are the same as their Σ_- , Π_- , Δ_- .

possible electron configurations for the normal molecule.³ (2) That this $^1\Sigma$ state is either a $^1\Sigma_g^+$ or a $^1\Sigma_u^-$ state is shown by the fact that the rotational levels with odd values of K have the greater statistical weight.^{4,5} Either $^1\Sigma_g^+$ or $^1\Sigma_u^-$ is capable,—see above,—of being derived from two normal atoms.¹ Whether or not the normal states of the halogens *actually are* so derived is not essential to the present argument, but is nevertheless of interest. By extrapolation from the known vibrational levels of the normal state, as in the method of Birge and Sponer, one gets, for I_2 , Br_2 and Cl_2 , values of the energy of dissociation which agree well with the supposition that dissociation does give normal atoms.¹ Also, since all excited states of the atoms (including $F^+ + F^-$) lie high above the normal level, it is improbable that any of these could give normal atoms. (3) A consideration of possible electron configurations consistent with $^1\Sigma_g^+$ and $^1\Sigma_u^-$ shows that only $^1\Sigma_g^+$ is reasonable for the normal state of the halogens.⁶ But even if we should

³ A $^3\Pi_1$ state would also be diamagnetic, but such a state is very unlikely to be the normal state, since the correspondence $^3\Pi_2$ would probably also exist and be lower, assuming case *a* coupling, $^1\Sigma$ is also by far the most probable normal state on the basis of a study of electron configurations.

⁴ That the odd levels have the greater weight is shown in the case of Cl_2 by the band analysis of A. Elliot (Proc. Roy. Soc. 123A, 629, 1929). In the case of Br_2 an analysis of the bands is lacking, while in I_2 no alternations in intensity have been detected. If we represent the complete wave function ψ as a product of three factors, $\psi = \psi_{el}\psi_{rot}\psi_{nu-spin}$, then we know (a) ψ must on theoretical grounds (cf. R. S. Mulliken, Trans. Faraday Soc. No. 102, 25, Part II Nov. 1929) be antisymmetrical in the nuclei (An)⁵; (b) for the levels with greater statistical weight in any homonuclear molecule, $\psi_{nu-spin}$ is always symmetrical in the nuclei (Sy), for odd values of K in a Σ state, ψ_{rot} is always An . For the odd K values, therefore, in Cl_2 ψ_{rot} is An , $\psi_{nu-spin}$ is Sy , hence, since ψ itself must be An , ψ_{el} must be Sy . This is the case for either a Σ_g^+ or a Σ_u^- state. (The possibility of Σ^- states was overlooked in the writer's article just cited, and led to some erroneous conclusions in regard to O_2 , whose normal state is now known to be $^3\Sigma_g^-$.)

⁵ That the complete ψ must be An for a molecule whose nuclei contain each an odd number of (protons plus electrons), as theoretically predicted by Hund (cf. R. S. Mulliken, Ref. 4), is contradicted by the experimental results on N_2 , where ψ is Sy although the nucleus is composed of 21 particles (14 protons, 7 electrons). The most probable reformulation is that ψ has to be An if the nucleus of each atom contains an odd number at *protons* (and Sy if it contains an even number), regardless of the electrons. Since both the old and the new conditions for an An ψ are fulfilled for the Cl atom, it seems safe to take this for granted. If, however, the contrary should be true, the following results would hold: the normal Cl_2 molecule is $^1\Sigma_u^+$ or $^1\Sigma_g^-$ (both are improbable on the basis of a consideration of electron configurations), and dissociates giving at least one highly excited atom (this would hardly be possible to reconcile with data on the vibrational levels (cf. section (2) in the text above)), the excited molecule would then probably be $^1\Sigma_g^+$ or Σ_u^- , either of which is derivable from normal atoms¹, in agreement with section (5) in the text.

⁶ It is highly probable that the normal state of F_2 is a $^1\Sigma_g^+$ state with essentially the following electron configuration: $1s^2 2p^2 2s^2 3p^2 3d^2 2p\pi^4 3d\pi^4$. Possible $^1\Sigma_u^-$ states are derivable from $\dots 2p\pi^3 3d\pi^3 nx\sigma^2$ (n and x anything not already present) and $\dots 2p\pi^4 3d\pi^3 3p\pi$. The first of these (probably with $nx\sigma^2 = 4f\sigma^2$) might be derived from two normal atoms, but would surely be higher and be more unstable than the $^1\Sigma_g^+$ configuration mentioned above. The second ($\dots 3p\pi$) could probably be obtained only from one normal F atom and one excited atom with a $3p$ electron; the energy of excitation of the latter would be so great that it practically certainly could not give the normal state of F_2 . Analogous arguments apply to the other halogens.

assume ${}^1\Sigma_u^-$, we should still come to the conclusion that the halogen bands here under discussion cannot be a ${}^1\Sigma, {}^1\Sigma$ transition. (4) Assuming that the normal state is ${}^1\Sigma^g$ and that the coupling relations in both states correspond to Hund's cases *a* or *b*, the *excited state* can only be one of the following:⁷ ${}^1\Sigma_u^+$, or ${}^1\pi_u$, or ${}^3\Sigma_u^+$, or ${}^3\Pi_u$. (5) According to Franck's well-known interpretation of the convergence limits of the halogen bands, the excited state dissociates without question into two normal atoms,—more accurately, into one ${}^2P_{1/2}$ and ${}^2P_{1/2}$ atom. (6) Since a ${}^1\Sigma_u^+$ state cannot possibly be obtained from two normal atoms (cf first paragraph), the excited state cannot possibly be ${}^1\Sigma_u^+$, and the bands therefore cannot be of the ${}^1\Sigma, {}^1\Sigma$ type. The possibilities ${}^1\Pi_u$, ${}^3\pi_u$, and ${}^3\Sigma_u^+$ for the excited state remain, since all are consistent with dissociation into normal atoms.

None of the interpretations ${}^1\pi \leftarrow {}^1\Sigma$, ${}^3\pi \leftarrow {}^1\Sigma$, and ${}^3\Sigma \leftarrow {}^1\Sigma$ appear easy to reconcile with the observed structure of the bands, which (in Cl_2 and I_2 , F_2 and Br_2 not having been investigated as yet) consists definitely only of one *P* and one *R* branch, each composed of single lines arranged exactly as in the case of a ${}^1\Sigma, {}^1\Sigma$ transition. The absence of a *Q* branch probably rules out the possibility of a ${}^1\Pi$ upper level. ${}^3\Pi$ also seems unlikely unless its combinations with ${}^1\Sigma$ are restricted, say, to one component of the ${}^3\Pi_0$ level (see below). In favor of ${}^3\Sigma_u^+$ is the fact that in a ${}^3\Sigma \leftarrow {}^1\Sigma$ transition only a *P* and an *R* branch are expected. But one would expect these to consist of wide doublets as in the ${}^1\Sigma \leftarrow {}^3\Sigma$ atmospheric oxygen bands.⁸ That the observed lines are single seems hardly reconcilable with a ${}^3\Sigma, {}^1\Sigma$ combination. One might of course suppose that the ${}^3\Sigma$ rotational triplets are so narrow as to be unresolved, but, especially for the heavier halogens, this is wholly contrary to theory, as well as to experimental data on doublet separations in ${}^3\Sigma$ states. Another conceivable explanation would be that in the ${}^3\Sigma$ level the components with $J=K\pm 1$ are widely separated from those with $J=K$ and that, for unknown reasons, only combinations of the levels with $J=K$ with levels of the ${}^1\Sigma_g^+$ normal state are observed. This would give simple *P* and *R* branches in agreement with experiment, but it is very far-fetched.

An escape from these difficulties is to be found by noting a fact whose consequences have hitherto not been fully appreciated. In the excited states of the halogen molecules, the energies of dissociation *D* are very small ($D=0.55$ volts for I_2 , 0.39 volts for Br_2 , 0.23 for Cl_2 , and by extrapolation from the other halogens, about 0.1 volts for F_2); they are roughly about equal to the doublet separations between the ${}^2P_{1/2}$ and ${}^2P_{3/2}$ sublevels of the normal states of the halogen atoms (I, 0.94 volts, Br, 0.45 volts, Cl, 0.11 volts, F, 0.05 volts). From these figures we can conclude that, especially in the heavier halogens, the influence of the electric axis on the electron orbits

⁷ The following selection rules apply if both states correspond to coupling cases *a* or *b* or intermediate cases: $\Delta\Lambda=0, \pm 1$; Σ^+ terms combine with Σ^+ but never with Σ^- terms; in homonuclear molecules, even terms (*g*) combine only with odd terms (*u*). Quintet states are ruled out, for the excited state, by the fact that the latter dissociates into normal atoms (cf. list of possible states in first paragraph).

⁸ R. S. Mulliken, Phys. Rev. 32, 880 (1928).

is not large enough to break down, at any rate not at all completely, the coupling of each atomic L vector with its S vector. The quantum numbers $L_1, S_1, J_1, L_2, S_2, J_2$ of the two atoms still retain their significance to a considerable extent in the molecule. J_1 and J_2 give respectively quantum numbers Ω_1 and Ω_2 (or M_1 and M_2) which represent their projections on the electric axis. The only electronic quantum number which is significant for the molecule as a whole is Ω ($\Omega = |M_1 + M_2|$) Λ and S for the molecule as a whole are practically meaningless as quantum numbers; λ 's of individual electrons are even more completely lacking in significance; nevertheless Λ, S , and λ values can be formally assigned by imagining the nuclei pushed closer together. This coupling case can be classified as a form of Hund's case c ; in another form which has been more discussed, the molecule as a whole has an L and an S , which are strongly coupled to give a resultant J^a , which in turn gives a projection Ω .

For the *normal* states of the halogen molecules, where the D values are moderately large (assuming dissociation into two $^2P_{1/2}$ normal atoms, they are, $D = 1.53$ volts for I_2 , 1.96 volts for Br_2 , 2.54 for Cl_2 , and by extrapolation, about 3.1 volts for F_2), we may assume Hund's case a , or in I_2 perhaps a case intermediate between a and c .

In dealing with the present weak-binding form of case c , it seems best to designate different electronic states simply by numbers giving their Ω values (0, 1, 2, etc.), together with a superscript $+$ or $-$ when $\Omega = 0$ and a subscript g or u in the case of homonuclear molecules in order to designate certain symmetry properties of their ψ functions. Here g and u have the same meaning as in cases a and b . So do $+$ and $-$, but for convenience we may here define 0^+ and 0^- states as follows: in 0^+ states the even-numbered rotational levels ($J = 0, 2, \dots$) are even (in the sense of Kronig) or positive (in the sense of Wigner and Witmer), while the odd-numbered levels are odd or negative;⁹ in 0^- states the relations are reversed.¹⁰

As selection rules in case c here we have only the following: $\Delta\Omega = 0, \pm 1$; $\Delta J = 0, \pm 1$; $g \rightleftharpoons u$; even or positive combine only with odd or negative rotational levels. The intensity relations in the P, Q , and R branches should be governed, just as in case a , by the Hönl and London intensity formulas.¹¹ For example, transitions between a 0 and a 1 state should show a P , a strong Q , and an R branch. (The 1 state should have Ω -type doubling, vanishing with zero rotation, and similar to the Λ -type doubling for a $^1\Pi$ state in cases a and b ; and the P and R branches should make connection with one component of each Ω -type doublet, the Q branch with the other). Transitions

⁹ The words "even" [R. de L. Kronig, *Zeits. f. Physik* 50, 351 (1928)] and "positive" (Wigner and Witmer, ref. 2, 867, footnote) are here synonymous; likewise for "odd" and "negative".

¹⁰ For a discussion of the behavior of $^3\Pi_0$ states in the passage from case a to case c , cf. J. H. Van Vleck, *Phys. Rev.* 33, 501-2 (1929). Van Vleck points out that the a and b sets of sublevels of $^3\Pi_0$ behave like a $0^+, 0^-$ pair (similar to $^1\Sigma^+$ and $^1\Sigma^-$). In regard to notation use of $+$ and $-$ cf. ref. 2.

¹¹ H. Hönl and F. London, *Zeits. f. Physik* 33, 803 (1925) Cf. R. S. Mulliken, *Phys. Rev.* 29, 391, (1927) for discussion and applications.

between two 0 states should show only a *P* and an *R* branch, just as for $^1\Sigma$, $^1\Sigma$ transitions in case *a*. This latter fact, taken in connection with the selection rule even \rightleftharpoons odd for rotational terms, shows that only combinations between two 0^+ states, or between two 0^- states, but not those between a 0^+ and a 0^- state, are capable in case *c* of giving rise to spectrum lines.¹² In case, however, there should be a departure from the conditions of case *c* toward those of case *a*, *Q* branch combinations between a 0^+ and a 0^- state may also be expected (cf. next paragraph).

Let us now consider as a typical example, for a range of cases from *a* to *c*, a transition which in case *a* would be classified as $^3\Pi_0$, $^1\Sigma$. The $^3\Pi_0$ state has two rotational levels for each *J* value ($J=0, 1, 2, \dots$); these may be considered as derived from two electronic sublevels of $^3\Pi_0$, namely from a 0^+ and a 0^- sublevel.¹¹ In case *a*, we may probably expect a *P*, a *Q*, and an *R* branch in a $^3\Pi_0$, $^1\Sigma$ combination. For a $^1\Sigma^+$ type of $^1\Sigma$ state, the *P* and *R* branches come from the 0^+ levels of the $^3\Pi_0$, the *Q* branch from the 0^- levels. In the passage to case *c*, the *P* and *R* branches remain, but the *Q* branch 0^- , 0^+ combination should gradually fade out, while at the same time the 0^- levels may become widely separated¹¹ from the 0^+ levels.

In both limiting cases (*a* and *c*), and probably also in intermediate cases, the rotational energy for the $^3\Pi_0$ states is given by an expression of the form $E = \text{const.} + B_v J(J+1) + \dots$. The same expression for E' also holds for all electronic states in case *c*, as well as in case *a*.

We are now in a position to interpret the halogen bands from a more general viewpoint than that adopted at the beginning of this paper. Their observed structures show that they are a $0 \leftarrow 0$ transition; more specifically, since we have seen that the lower state is in all probability a $^1\Sigma_g^+$ and since they consist of *P* and *R* branches, we conclude that they are $0_u^+ \leftarrow 0_g^+$. As we have already seen, the 0_u^+ state cannot correspond to a $^1\Sigma_u^+$ state, since such a state is not derivable from normal atoms. In the list of states derivable from normal atoms (cf. first paragraph of paper), only one 0_u^+ state is to be found, namely the 0^+ component of the $^3\Pi_u$ state,¹³ and we therefore conclude that the upper level of the halogen bands is of this type. The absence of a *Q* branch corresponding to the 0^- component of $^3\Pi_u$ can be understood (cf. preceding paragraph) in view of the fact that we expect case *c* coupling here for the 0_u^+ state. It may even be that the 0_u^- state is much more unstable than the 0_u^+ , so that the corresponding band system $0_u^- \leftarrow 0_g^+$ (*Q* branches) may consist only of a continuous region: furthermore, it may be that this system is very weak.—It should be emphasized that the classification of the 0_u^+ level as belonging to $^3\Pi$ has only a formal meaning, since

¹² This is analogous to, but not (except in singlet states) identical with the rule that in combinations between Σ states only Σ^+ , Σ^+ and Σ^- , Σ^- are possible.

¹³ The other 0 states derivable from two equal 2P atoms are, 0^- from $^3\Pi_u$, 0^+ and 0^- from $^3\Pi_g$, two 0_g^+ states and one 0_u^- state corresponding to the three $^1\Sigma$ states (one of the 0_g^+ states is the normal $^1\Sigma_g^+$ state of the molecule), and two 0_u^- and one 0_u^+ state from the two $^3\Sigma_u^+$ states and the one $^3\Sigma_u^+$ state respectively. A $^3\Sigma^+$ state gives in case *c*, as is easily shown, one 0^- and one 1 state; a $^3\Sigma^-$ state, one 0^+ and one 1 state (cf. later paper).

quantum numbers Λ and S are not defined here in case c . Physically, this 0_u^+ level may have little resemblance to a ${}^3\Pi_0$ ordinary level of case a .

By application of the methods of Wigner and Witmer, it is possible to predict, for a loosely-bound case c molecule as here, the molecular states which can be derived from each of the individual combinations ${}^2P_{1\frac{1}{2}}+{}^2P_{1\frac{1}{2}}$, ${}^2P_{1\frac{1}{2}}+{}^2P_{\frac{1}{2}}$ and ${}^2P_{\frac{1}{2}}+{}^2P_{\frac{1}{2}}$.¹⁴ The results are, for the case of two equal atoms in the same 2P state: ${}^2P_{1\frac{1}{2}}+{}^2P_{1\frac{1}{2}}$ gives $3_u, 2_g, 2_u, 1_u, 1_g, 1_u, 0_g^+, 0_u^-, 0_g, 0_u^-$; ${}^2P_{1\frac{1}{2}}+{}^2P_{\frac{1}{2}}$ gives $2_g, 2_u, 1_g, 1_u, 1_g, 1_u, 0_g^+, 0_u^+, 0_g^-, 0_u^-$; and ${}^2P_{\frac{1}{2}}+{}^2P_{\frac{1}{2}}$ gives $1_u, 0_g^+, 0_u^-$.¹⁵ The fact that only ${}^2P_{1\frac{1}{2}}+{}^2P_{\frac{1}{2}}$ is capable of giving a 0^+ state is in satisfying agreement with the experimental fact that the upper level of the halogen bands, here classified as 0_u^+ , is actually derived from ${}^2P_{1\frac{1}{2}}+{}^2P_{\frac{1}{2}}$. The lower, 0_u^+ , level is probably derived from ${}^2P_{1\frac{1}{2}}+{}^2P_{1\frac{1}{2}}$, although ${}^2P_{1\frac{1}{2}}+{}^2P_{\frac{1}{2}}$ or ${}^2P_{\frac{1}{2}}+{}^2P_{\frac{1}{2}}$ is not theoretically impossible, and also experimentally not yet absolutely excluded.

Some additional items of evidence having a bearing on the above interpretation of the halogen bands will now be mentioned. (1) The fact that the I_2 bands show a Faraday effect¹⁶ may be cited as evidence in favor of a paramagnetic upper level. Now it can be shown that a case c molecular state with $\Omega=0$ and derived from a ${}^2P_{1\frac{1}{2}}$ plus a ${}^2P_{\frac{1}{2}}$ atom *should* be paramagnetic; and that in the passage to a case a ${}^3\Pi_0$ state, the paramagnetism must increase.¹⁷ Of course, as Kemble has pointed out,¹⁸ a magnetic moment might be developed by rotation, even in a ${}^1\Sigma$ state; and in a loosely bound molecular state such as we have here, a rather large moment might be developed in this way through uncoupling of the atomic J vectors from the electric axis. But it seems hardly likely that the small rotational energies involved in the case of the observed band lines are large enough to give rise to the magnetic effects observed. (2) The fact that the fluorescence of the I_2 bands is (in part) quenched by a magnetic field¹⁸ is further evidence in favor of a paramagnetic upper level. (3) If the bands are ${}^3\Pi_0 \leftarrow {}^1\Sigma$ one might expect their intensity to increase markedly in going from F_2 to I_2 , since the intensity of intersystem combinations is extremely weak for the lightest atoms like He,

¹⁴ The rules which govern this case, and some applications, will be discussed in a subsequent paper.

¹⁵ The group of states here predicted corresponds, as of course it must if correct, in a one to one manner to the set of states predicted by the Wigner and Witmer method for cases a and b , and given at the beginning of this paper. E.g., 3_u from ${}^2P_{\frac{1}{2}}+{}^2P_{\frac{3}{2}}$ corresponds to $\Omega=3$ of ${}^3\Delta_u$ at case a .

¹⁶ Cf. E. C. Kemble, Nat. Research Council Bulletin on Molecular Spectra, p. 347.

¹⁷ To get a state with $\Omega=0$ from ${}^2P_{\frac{1}{2}}+{}^2P_{1\frac{1}{2}}$, we must assume the J of the ${}^2P_{1\frac{1}{2}}$ atom oriented with a projection $M=\pm 1/2$ on the electric axis, the J of the ${}^2P_{\frac{1}{2}}$ atom with a projection $M=\mp 1/2$. Since Landé's g factor is $4/3$ for ${}^2P_{1\frac{1}{2}}$ and $2/3$ for ${}^2P_{\frac{1}{2}}$, the total magnetic moment parallel to the electric axis is $(4/3 \times 1/2 - 2/3 \times 1/2) = 1/3$ Bohr magneton. This holds for the limiting case of very loose coupling of the atoms. In a case a ${}^3\Pi_0$ state, we have a magnetic moment of ± 2 magnetons parallel to the electric axis due to the spin ($S=1, \Sigma=-1$) and of ∓ 1 magnetons due to $\Lambda=1$, making a net result of 1 magneton parallel to the electric axis. (The magnetic moment component perpendicular to the electric axis also in some cases contributes to the paramagnetism.)

¹⁸ W. S. Steubing, Ann. d. Physik 58, 55 (1919).

and increases with the intensity of the coupling of L and S vectors. The fact that the upper level is case c 0^+ rather than case a $^3\Pi_0$ should however probably diminish this effect since the molecular S loses its meaning in case c , but it might well still exist to a more or less marked extent, since it is likely that case a is more nearly approached in the lighter than in the heavier molecules. In the halogen bands in which we are interested, the spectrum consists of two parts, namely the bands proper (relatively weak), and the continuum (stronger). Since the continuum corresponds to transitions with r near r_e'' , and since we probably have case a for $r=r_e''$, the upper level should function here as a true $^3\Pi_0$ level, and the strong variation of intensity with molecular weight which is to be expected for intersystem combinations should make itself evident here. Experimentally the intensity of the bands proper increases rather rapidly in the order F_2 to I_2 , but this is at least partly explainable in terms of the $U'(r)$ and $U''(r)$ curves by means of the Franck idea as applied by Condon. So far as can be judged from available data,¹⁹ the absorption in the continuum is however also much stronger for iodine than for chlorine, and this effect cannot be attributed to the nature of the $U(r)$ curves. This relation is therefore in harmony with our expectation.

(4) If one assigns the electron configuration $1s\sigma^2 2p\sigma^2 3p\sigma^2 3p\pi^4 3d\sigma^2 3d\pi^4$ to the $^1\Sigma_g^+$ normal state of F_2 , and assumes that the excited state corresponds to $\dots 3d\pi^3 4f\sigma$ one removes the only known exception²⁰ to the writer's λ conservation rule (formerly called " $\sigma_{l,r}$ conservation rule") for molecule formation (Of course the configurations given here have a physical meaning only, for small values of the distance between the nuclei.) The writer is, however now inclined to believe that this rule has not much significance. For Cl_2 the corresponding configurations are $\dots 3s\sigma^2 4p\sigma^2 3p\pi^4 4d\sigma^2 4d\pi^4$ and $\dots 4d\pi^3 5f\sigma$ and so on.

¹⁹ Cf. International Critical Tables Vol. V, p. 269. The nature of the intensity relations can be judged by the following values of the absorption coefficient K in the equation $I = I_0 e^{-Kl}$ (l = length of absorbing path in cm, in gas or vapor). For the maximum of the continuous absorption, K has the following values: Cl_2 , $K \sim 2$ for $p = 760$ mm at $0^\circ C$; Br_2 , $K \sim 1.36$ for $p = 66$ mm at $16^\circ C$; I_2 , $K \sim 0.21$ for $p = 0.17$ mm (reduced to $0^\circ C$) and $K \sim 0.77$ for $p = 1.67$ mm (reduced to $0^\circ C$). If we assume the validity of Beer's law (but the data on I_2 show that it does not hold) we get for $p = 1.67$ mm at $0^\circ C$, $K \sim 0.013$ for Cl_2 , $K \sim 0.033$ for Br_2 , $K \sim 0.77$ for I_2 .

²⁰ R. S. Mulliken, Phys. Rev. **32**, 772 (1928).

AN INTERPRETATION OF PRESSURE AND HIGH VELOCITY VAPOR JETS AT CATHODES OF VACUUM ARCS

BY KARL T. COMPTON

MASSACHUSETTS INSTITUTE OF TECHNOLOGY

(Received July 1, 1930)

ABSTRACT

Tanberg's conclusion, that the evaporating vapor from the cathode of a copper vacuum arc escapes with a temperature of about $500,000^{\circ}\text{K}$, which is based upon measurements of the repulsive force against the cathode, is shown to be unnecessary. The observed pressures can reasonably be explained in terms of the "accommodation coefficient" of the incoming Cu ions. It is thus shown that the observed pressures are accounted for if the positive ions retain about 2 percent of their incident kinetic energy after neutralization at the cathode.

IN A recent article in this journal¹ Mr. R. Tanberg has described some very pretty experiments on arcs drawn from a copper cathode *in vacuo*, which prove that there is a pressure of approximately 0.015 gm per ampere against the cathode, and a pressure of similar order of magnitude against an insulated vane placed about 2 cm in front of the cathode. These pressures, which were corrected for several minor disturbing influences, indicate the existence of material ejected with high speed from the cathode, and the experiments showed that this material is uncharged. Since copper evaporated from the cathode during the experiments, Tanberg identified the jet of high speed material with this stream of evaporated copper. The measurements of the amount of evaporation and the magnitude of the pressure led him thus to the conclusion that this vapor jet has a velocity of the order of $16(10)^5$ cm/sec and hence that "the temperature existing at the cathode spot determined from the velocity of the cathode vapor is of the order of $500,000^{\circ}\text{K}$ " "far in excess of even the most extreme temperatures ever measured in connection with any physical phenomena of any duration!" In view of the importance of this conclusion, if true, in the interpretation of arc cathode phenomena, it is important critically to examine Mr. Tanberg's work and the possibility of some less startling interpretation of his experimental results.

There is one part of Mr. Tanberg's calculations which shows entire failure to comprehend the nature of the electrostatic forces exerted on a cathode by the intense field at its surface. These are attractive forces, tending to pull the cathode toward the discharge, and Mr. Tanberg adds an estimated force of this type to the observed repulsion, to obtain the "corrected" repulsive force due to the reaction of the escaping vapor stream. He fails to note, however, that this strong field at the cathode arises from the positive ion space charge near it, that the attraction is mutually between cathode and

¹ Tanberg, Phys. Rev. 35, 1080 (1929).

ions, and that when the ions strike the cathode, they deliver momentum to it at a rate which exactly counterbalances the electrostatic pull which they exerted on it before impact. That this follows from the elementary relation $\int F dt = \int m dv$ is obvious and has long been recognized in such problems.² Thus this electrostatic correction should not have been made. It happens, however, to be only a few percent of the observed force, so that correction of this error does not essentially alter the evidence for a high speed stream of neutral particles escaping from the arc cathode.

There is, however, a phenomenon occurring at cathodes which appears quite adequate to explain Mr. Tanberg's results without invoking any unusual temperature of cathode spot. It is the occurrence of an "accommodation coefficient" of positive ions, as recently reported to the American Physical Society by Dr. Van Voorhis and the writer.³ Positive ions, on striking the cathode, become neutralized but do not, on the average, give up enough of their kinetic energy to reach thermal equilibrium with the cathode. They rebound as neutral atoms from the cathode with some fraction β of their incident kinetic energy.

Although, as we have seen, the impact of a charged ion against the cathode contributes nothing to the pressure against it (on account of the counterbalancing pull during its attraction to the cathode), nevertheless if the neutralized ion leaves the cathode with any momentum there is imparted to the cathode an equal opposite momentum. The following calculations show that this type of momentum transfer seems easily adequate to account for the pressures observed by Mr. Tanberg.

Let f be the fraction of the total current which is carried by positive ions at the cathode, and let β be the fraction of the incident energy of the ion which is retained after neutralization. β is approximately equal to $1 - \alpha$, where α is the accommodation coefficient. The arc drop in a copper arc of high current density carried in copper vapor has been shown by Nottingham⁴ to be 20.5 volts. It appears certain that the fall space in such an arc is so thin that ions make few if any collisions while traversing it.

Taking data from one of Mr. Tanberg's typical experiments (test No. 353) we calculate the following data:

Positive ion current at cathode.....	11 <i>f</i> amps
Mass of Cu ions striking cathode per sec.....	0.00724 <i>f</i> gm
Number of Cu ions striking per sec.....	7.0(10) ¹⁸ <i>f</i>
Kinetic energy of an incident ion.....	3.26(10) ⁻¹¹ erg
Total kinetic energy of ions striking per sec.....	22.8(10) ⁸ <i>f</i> erg
Total kinetic energy of neutralized ions leaving per sec...	22.8(10) ⁸ <i>f</i> β erg
Total momentum of neutralized ions leaving per sec, which is equal to the pressure on the cathode.....	5.86 <i>f</i> (β) ^{1/2} gm
If neutralized ions escape in random directions, as is likely, the resultant pressure is.....	2.93 <i>f</i> (β) ^{1/2} gm

² Duffield, Burnham and Davis, Proc. Roy. Soc. 97, 326 (1920).

³ Van Voorhis and Compton, Phys. Rev. 35, 1438 (1930).

⁴ Nottingham, J. Frank. Inst. 207, 301 (1929).

We now equate this to the observed pressure (corrected for "electrodynamical" disturbances but not for electrostatic disturbances as explained above) and obtain

$$2.93f(\beta)^{1/2} = 193.2(10)^{-3}.$$

We must now decide what value to use for the fraction f of current carried by positive ions at the cathode. Knowledge of this quantity is still woefully uncertain, even in the case which has been most studied, the mercury arc,⁵ but all indications point to a value not far from $f=0.5$. Theoretically we would like perhaps to see a smaller value, but it seems impossible to find a much smaller value experimentally, unless we strain the interpretation of results. Furthermore, the present copper arc is probably of essentially the same type as the mercury arc.⁶ So we shall provisionally assume that $f=0.5$. Solving, then, for β we find

$$\beta = 0.0174; \quad \alpha = 0.9826.$$

Thus the pressures observed by Mr. Tanberg would be accounted for if less than 2% of the incident energy of the ions were retained after neutralization. If we had assumed a smaller value of f , β would have come out larger and α smaller. The accommodation coefficient of Cu ions has never been measured, but from analogy with other ions of about the same atomic weight we might easily expect Cu ions to possess an accommodation coefficient as small as 0.9. Hence these considerations appear to give ample leeway for a reasonable explanation of Mr. Tanberg's results.

A possible objection to this theory based on the fact that Cu ions should condense on the cathode on striking it is met by the fact that their energies correspond to temperatures far in excess of the boiling temperature of the metal.

In conclusion it may be pointed out that this criticism does not alter Mr. Tanberg's basic conclusion regarding a high speed neutral vapor stream. It merely suggests an electrical mechanism for the acquiring of these speeds instead of assuming a terrifically high temperature at the cathode.

An interesting test of this interpretation is now being made by repeating Mr. Tanberg's experiments with a non-volatizing cathode of tungsten in a rare argon atmosphere. Here there is no possibility of an evaporated vapor stream like that considered by Mr. Tanberg, but the pressure effect due to the accommodation coefficient of argon ions is calculable directly from the work of Van Voorhis and Compton, combined with collector measurements to give directly the actual positive ion current.

⁵ Compton and Van Voorhis, *Proc. Nat. Acad. Sc.* **13**, 336 (1927).

⁶ Compton, Paper read before A.I.E.E., Detroit, June 1927.

SECONDARY EMISSION FROM METALS BY IMPACT OF
METASTABLE ATOMS AND POSITIVE IONS

BY W. UYTERHOEVEN AND M. C. HARRINGTON

PALMER PHYSICAL LABORATORY, PRINCETON UNIVERSITY

(Received June 16, 1930)

ABSTRACT

Experiments on the secondary electron emission from nickel electrodes due to bombardment of positive ions and metastable atoms in a neon discharge under conditions simulating those at the cathode in a glow discharge are described. Measurements with a collector movable in a direction perpendicular to a fixed plane collector give approximate values of the proportion γ of the apparent positive ion current which is actually carried by secondary electrons. Values of 15-50 percent are found depending on the experimental conditions and degree of purity of gas. A perforated plate behind which is situated a Faraday box is used to separate the effects of the ions and metastable atoms. A preponderant part of the emission is ascribable to the metastable atoms, but values of the number α of free electrons per positive ion, are found to be 14 to 20 percent, varying approximately linearly for ions of velocities of 75 to 150 volts. The secondary electrons originate at the surface of the collector with about 12.5 volts maximum initial velocity.

IN ALL theories of the cathode fall in the glow discharge there has been assumed a source of electrons at the surface of the cathode or in the immediate neighborhood of it. Generally it is supposed that these electrons are liberated from the metal by the impact of positive ions. Although the existence of this phenomenon has been established by several experimenters, direct experimental evidence under conditions simulating those at the cathode is not very extensive. Most of the determinations of the secondary emission due to ion impact have been made with ions from a Kunsman source, and have proved that the effect was rather small.^{1,2} This is what one would expect if the secondary emission depended on the potential energy of the ion. A necessary condition for secondary emission would then be that the ionization potential of the gas atom $V_i \geq 2\phi$, where ϕ is Richardson's work function.³ In accordance with this view Penning^{4,5} found for Ne ions impinging on different metals, efficiencies which were appreciably larger than those which had been found for alkali ions, and a linear variation of the number α of secondaries per incoming ion with the energy of the latter. All observers point out that α depends markedly on the surface condition of the metal and, since practically all the measurements have been done in a rather high vacuum, it might well be that under the actual conditions

¹ Jackson, Phys. Rev. 30, 473 (1927).

² Oliphant, Proc. Camb. Phil. Soc. 24, 451 (1928).

³ Holst and Oosterhuis, Physica 4, 375 (1924).

⁴ Penning, Proc. Amsterdam Ac. 31, 14 (1927).

⁵ Penning, Physica 8, 13 (1928).

of the cathode fall α is very much larger. The present work^{6,7} is an attempt to determine α under conditions as similar as possible to those at the cathode of a glow discharge, where adsorbed atoms and ions may appreciably change the properties of the metal surface.

A few years ago one of the writers,⁸ using a plane Langmuir collector in the positive column of the glow discharge, obtained current-voltage characteristics differing from those obtained by Langmuir and Mott-Smith in the mercury arc.⁹ Comparison of the measured ion current density i_m to a negatively charged collector with the value i_c , calculated from the usual space charge equation, showed differences amounting to 40–50 percent of i_m , i_m being larger than i_c . The simplest interpretation of these results was the assumption of a secondary emission from the metal up to 40–50 percent of i_m . This, however, led to a value for α of the order of magnitude 1, and it was therefore suggested that possibly metastable atoms diffusing out of the discharge contributed to the electron emission when striking the metal plate.^{10,11} This estimate of i_c was based on the assumptions underlying the derivation of the space charge equation, the most important being in this case the absence of ionization in the sheath. This introduced some uncertainty in the interpretation referred to above. Therefore different methods were devised to determine the secondary electron part in the apparent positive ion current i_m to a negatively charged electrode.

APPARATUS

Since the electrodes are continuously bombarded by positive ions of high velocity, they sputter rapidly; accordingly a set of nickel electrodes (Fig. 1) was constructed which could easily be adjusted in the different tubes used in the experimental work. The discharge was of the hot cathode type to permit a wide variation of the current density. The cathode was an oxide coated nickel cylinder, (heated by a tungsten filament inside), the anode a large nickel plate or cylinder. The main collecting electrode P was a circular nickel disk (diameter 18.2 mm) with a coplanar concentric guard ring (outer diameter 29.2 mm). The latter was supported by the cylinder L , which shielded the space within it from the discharge; the cylinder L was in turn protected on its vertical side by a glass cylinder to avoid the collecting of too large positive ion currents and subsequent distortion of the potential distribution in the main discharge. The central plate P was supported by the cylinder M , which shielded the box B from uncharged particles diffusing through the slit S between the guard ring G and the plate P . The box B supported by the nickel rod R was cylindrical in shape, closed at the top and bottom. At the center of the upper cover was a circular hole (diameter 2 mm), which was immediately under a 0.74 mm hole at the center of the plate P .

⁶ Uyterhoeven and Harrington, *Science* **70**, 586 (1929).

⁷ Uyterhoeven and Harrington, *Phys. Rev.* **35**, 438 (1930).

⁸ Uyterhoeven, *Phys. Rev.* **31**, 913 (1928); *Proc. Nat. Acad. Sci.* **15**, 32 (1929).

⁹ I. Langmuir and Mott-Smith, *G. E. Rev.* **27**, 449 (1924).

¹⁰ Webb, *Phys. Rev.* **24**, 113 (1924).

¹¹ Oliphant, *Proc. Roy. Soc. A124*, 228 (1929).

The movable cylindrical collector C was also made of nickel. The collector used in the first type of tube (i.e. cylindrical tube, which we will designate by no. 1) was somewhat simpler in construction than that used in the later type of tube (no. 2) (See Fig. 1). Cylinder no. 1 (length 10.8 mm, diameter 7.3 mm) was divided into quarters by vertical nickel partitions. The lower end was covered with fine nickel gauze, the upper end closed by a piece of solid nickel, the inner side of which was cone-shaped to reduce electron reflection to a minimum. A glass cap fitting the cylinder left only the gauze-covered end exposed to the discharge. In the course of the work, this glass cap as well as the glass tubing protecting the leading-in wire for the cylinder became coated with sputtered metal. To eliminate as far as possible

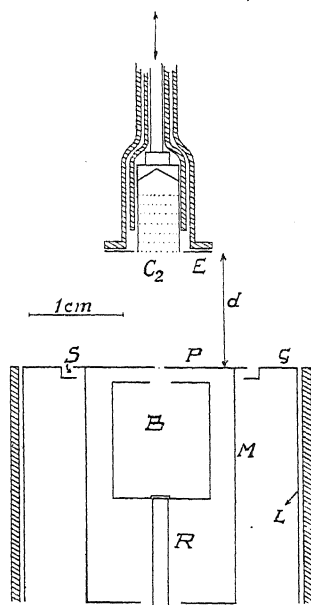


Fig. 1. Detail of collecting electrodes.

the resulting troubles the movable cylinder C_2 (diameter 4.8 mm) was fitted with a concentric guard ring E in the plane of the gauze-covered end (outer and inner diameter 11.0 and 5.4 mm respectively). Only the lower end of the guard-ring collected current, the back being protected by the glass cap enclosing the cylinder. The collector C was movable along its axis, i.e., perpendicular to the plane of the plate P , opposite to which it was placed.

The metal used in the construction of the electrodes was outgassed, before being used, by heating in vacuo to a red heat by high frequency induction currents.

Two types of tubes were used: first a cylindrical one (inner diameter 6 cm) with a bulbular enlargement at the cathode end and later a spherical one (diameter 15 cm). In the first the collectors were in the positive column and in the second in a uniform luminosity which filled the whole sphere.

During the measurements the neon gas was constantly circulating and passed through a misch-metal arc, while liquid air traps were used to avoid contamination of the neon by traces of mercury. The usual experimental technique in work of this kind was strictly followed (baking out of the tubes at high temperature while being evacuated, etc.).

EXPERIMENTAL METHODS AND RESULTS

Different methods can be applied for the measurement of the secondary emission. One, which was already referred to above, is to measure the apparent positive ion current to a negatively charged plane collector i_m , and simultaneously the thickness x of the dark space charge sheath. With the space charge equation the value of the positive ion current i_c corresponding to the potential difference between collector and space, and the thickness x may be calculated. If all the assumptions underlying the derivation of the space charge equation are satisfied, the difference $(i_m - i_c)$ gives a measure of the secondary electron emission. Due to a number of uncertain factors the values thus obtained in the earlier work were considered as provisional; the direct measurements here recorded check the order of magnitude of these earlier estimates.

First Method. Suppose the cylinder C is placed at a certain distance d from the plate and opposite to it. When C is made negative with respect to the surrounding gas, e.g., $V_c = -125v$, it will collect a certain positive ion current. The plate, originally floating, is now also made more and more negative with respect to the gas. If any secondary electrons are emitted from the plate, they will be accelerated by the electric field in the space charge layer and, after acquiring an energy corresponding to the potential of the plate with respect to the gas (potential drop in the sheath), increase the ionization in the space between the two collectors. So long as the plate is less negative than the cylinder, the electrons will not be able to run against the retarding potential in the sheath covering the cylinder. In this stage the ion current to the cylinder is slightly increasing (see Fig. 2, curve I , A to B), due to the additional ionization by the secondary electrons from the plate. When the plate potential V_P reaches V_C , there is a sudden decrease in the current i_c due to the incoming electrons, and this decrease is a measure of the secondary electrons leaving the plate P . The two principal factors to be considered in a quantitative analysis of these results, are the loss of energy of the electrons on their way from the plate to the cylinder and the decrease in intensity of the electron beam due to scattering.

Let us suppose for simplicity that the space potential in the discharge opposite to the plate is the same as the space potential in front of the cylinder. The difference in potential will actually be not more than a couple of volts, according to the theory of Tonks and Langmuir.¹² This simplification enables us to use the potentials of the cylinder and plate as measured with respect to the anode, since only the differences between V_C and V_P must be considered for the moment. If we use the extrapolated line AB (Fig. 2) as reference line,

¹² Tonks and Langmuir, Phys. Rev. **34**, 876 (1929).

the difference between its ordinate for a given value of $(V_P)_a$ and the corresponding ordinate of curve I gives the electron current collected at the cylinder. The curve I, read with respect to AB , is an integral curve, i.e., the difference for $(V_P)_a = -135v$, for instance, represents the number of electrons which on reaching the outer edge had an energy component normal to the bottom plane of the cylinder equal to or larger than $125v$. Since the potential of the plate is $(V_P)_a = -135v$, electrons are collected which have lost at most a forward component of momentum corresponding to an energy of 10 volts. Plotting the slope of the curve I, as read with respect to AB , we get a distribution curve (II, Fig. 2) of the electrons reaching the cylinder for the velocity component normal to the bottom plane of the cylinder.

Since the reception of electrons is confined to such a narrow region, say from $(V_P)_a = -112$ to about -160 in the case plotted (Fig. 2), we conclude that the electrons for this type of discharge arise at the plate P_c or very near

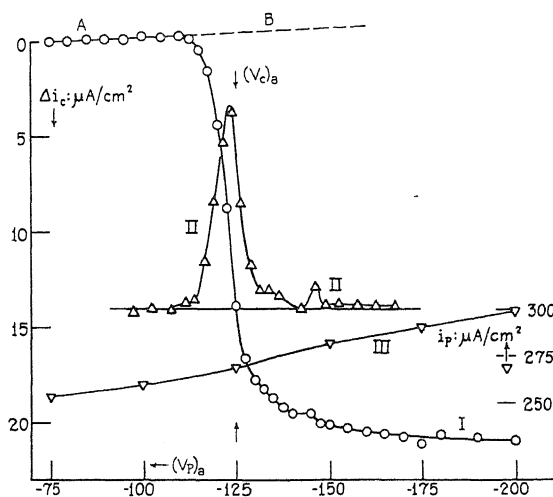


Fig. 2. Curve I.—Current to cylinder C as a function of the potential of the plate $(V_P)_a$ with respect to the anode. Cylinder potential $(V_C)_a = -125v$.

Curve II. Distribution curve for velocities of electrons (Component normal to plane of the end of C).

Curve III. Current to the plate i_P .

to it, for if appreciable numbers originated at other points of the sheath on P , the decrease in the curve would be much more gradual and extend farther to the right on the plot.

(Some objection may be raised against the use of the extrapolated line AB as zero line for the electron current reaching the cylinder. When the latter is absorbing part of the secondary electrons coming from the plate, $(V_P)_a$ more negative than $(V_C)_a$, the ionization produced by these in the space between plate and cylinder must be less than when the cylinder is reflecting the largest part $(V_P)_a$ less negative than $(V_C)_a$. When the pressure in the tube is made rather low ($p = 1 \times 10^{-2}$ mm or less) the slope of AB becomes

very small and the difference between the ordinate of AB and the curve rather large, so that this possible error must be small. In fact for pressures lower than 10^{-2} mm, the line AB is practically horizontal.)

Studying the velocity distribution curve II of Fig. 2 somewhat more closely, we notice first that the electrons start coming in when the retarding potential between cylinder and plate is about $-12.5v$. If the secondary emission is due to metastable neon atoms striking the plate, one must assume according to Oliphant¹¹ that the excess energy is transferred to the electron. Since the energy of a metastable neon atom ($2p^5.4s$) is about $16.5v$, taking for the work function of nickel $\phi_- = 4.4v$, we have for the maximum energy of the electron at the moment it leaves the plate $16.5 - 4.4 = 12.1$. If the secondary emission is due to positive ions, the maximum energy which the electron could carry away when leaving the plate would be $(V_i - 2\phi_-) = 21.5 - 8.8 = 12.7v$, where $V_i = 21.5v$ is the ionization potential for neon. Here $2\phi_-$ must be subtracted because the potential energy of the ion is used to liberate two electrons: one for neutralization of the ion and the secondary electron emitted from the plate. The value of the work function for nickel under the present conditions is not accurately known because the influence of adsorbed gas layers may change this appreciably. Van Voorhis¹³ found for molybdenum in a neon discharge $\phi_- = 3.68$, but the determination was made above the space potential so that the collector was receiving only electrons. In the present work it was found that the condition of the metal surface, when this is collecting electrons, may be somewhat different from that when bombarded with ions. The accuracy of this first method is not sufficient to decide between the two possible processes for the liberation of electrons mentioned above.

The form of the velocity distribution curve II (Fig. 2) does not change appreciably when the experimental conditions are varied. It seems to be practically independent of the plate voltage when this changes from $-75v$ to $-300v$. The maximum is rather sharp for low pressures and small distances of the cylinder from the plate. When the pressure is higher ($p = 5 \times 10^{-2}$ mm and more) or the distance d rather large the peak becomes less sharp; this is probably due to the impact suffered by the electrons on their path from plate to cylinder. At the same time the foot of the curve extends farther to the right, while a break appears in curve I (Fig. 2) at $(V_P)_a = (V_C)_a - 20$, (in the case of Fig. 2 at $(V_P)_a = -145v$). As may be seen from curve II of Fig. 2, which is a typical velocity distribution curve, there is no sharp maximum or minimum velocity as found by Oliphant¹¹ in his work on secondary emission by metastable He atoms. This may be partly due to a difference in the surface condition of the metal emitting the secondary electrons, but probably is mainly caused by scattering on their way from plate to cylinder. The maximum in the distribution curve corresponds always to a plate potential $(V_P)_a$ a couple of volts less negative than the potential of the cylinder. If the average velocity of the secondary electrons leaving the plate is a couple of volts, the velocity distribution curve will be of the form represented in Fig. 2.

¹³ Van Voorhis, recent unpublished work.

For a rational choice of the difference between the reference line AB and curve I of Fig. 2, representative of the secondary electron current collected by the cylinder, we must remember that, for a given value of the plate potential $(V_P)_a$, only those electrons reach the cylinder whose velocity normal to the space charge sheath corresponds to an energy equal to $(V_C)_a$. The loss of forward momentum of the part electrons coming from the plate is due to two effects: elastic scattering with change of direction of motion and inelastic impacts (excitation and ionization) with or without change in direction. The break in curve I (Fig. 2) referred to above may be due to excitation of neon, since the loss of energy corresponds roughly to 18 v.

To know the electron component of the plate current, i_p , we must extrapolate back the recorded electron currents, Δi_C . This requires a knowledge of the electron mean free path λ_- for the different velocities corresponding

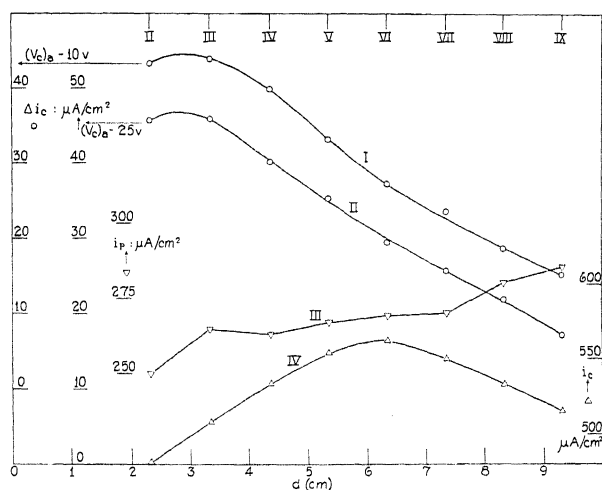


Fig. 3. Plate potential $(V_P)_a = -125$ v. $I = 450$ ma. $V = 59$ v. Pressure 8.8 to 9.2×10^{-3} Hg. Curve I: Δi_C for $(V_C)_a = 10$ v. vs. d . Curve II: Δi_C for $(V_C)_a = 25$ v. vs. d . Curve III: i_p in each case. Curve IV: i_C vs. d .

to $(V_P)_a$. As a first approximation we may take the gas-kinetic value for λ_- which for neon is 0.0737 cm at 1 mm pressure. Since the collecting cylinder C could be moved with respect to the plate, a direct determination of the electron mean free path would seem possible. The cylinder potential $(V_C)_a$ was given a definite value -125 and the variation of Δi_C with distance d studied, all other conditions being kept constant as well as possible. The two upper curves in Fig. 3 give Δi_C for $(V_P)_a = (V_C)_a - 10$ (curve I) and $(V_P)_a = (V_C)_a - 25$ (curve II), both plotted at the same scale but shifted the one with respect to the other to avoid confusion. The curves do not show an exponential decrease as would correspond to the simple formula $N_d = N_0 e^{-d/\lambda}$. The maximum in the Δi_C curve between positions II and III of the cylinder is due to the disturbing effect of the latter when it comes too near to the plate. As will be shown later, the secondary emission from the plate is due partly

to ion impact and partly to impact of metastable atoms. The latter are constantly diffusing from the center of the tube towards the wall and the presence of the cylinder in front of the plate probably disturbs the concentration gradients and decreases the number of metastable atoms striking the plate in unit time. To a certain extent this must also be true for the positive ion currents, but to a much smaller degree because of the correcting effect of space charges. The part of the curves to the right of position IV can be used for the calculation of the electronic mean free path. Table I gives the results of these computations. The first row gives the distance d of the

TABLE I.

Position	III	IV	V	VI	VII	VIII	IX
d	3.33	4.34	5.35	6.36	7.35	8.33	9.33
Δi_C	43.8	39.85	34.2	27.25	23.55	17.1	15.16
λ	10.6	6.5	5.7	6.8	4.3	4.7	
$p(10^{-3})$	8.8	8.7	8.9	9.2	9.2	9.2	9.5
λ_{pk}	8.9	9.0	8.8	8.6	8.6	8.6	8.3
i_p^-	63.7	64.4	62.6	57.2	55.6	45.2	46.8
i_p	259.5	257.	261.	263.5	269.	274.5	281.
γ	25	25	24	22	21	17	17

(V_c)_a = -125v. d in cm. λ in cm. Currents in $\mu A/cm^2$. p in mm of Hg.

cylinder from the plate, the second the electron currents at the cylinder (in $\mu A/cm^2$) for (V_P)_a = -135 v for different values of d . In the third are shown the values of the electron mean free path calculated from electron currents Δi_C for two adjacent positions. The fourth row gives the pressure in the tube for the different runs. (The small variation of the pressure shown in the table is due to the construction of the tube. The change in position of the cylinder influenced the rate of circulation of the gas in the tube and a readjustment of the pressure would have taken a rather long time. We thought it preferable to make all the runs in rapid succession to avoid a change in the discharge conditions, especially the purity of the gas.) The fifth line gives the gas-kinetic values for the electron mean free path corresponding to the pressures given in the fourth row. Most of our data have been taken with the cylinder in position IV, but much also in positions III and V. The sixth row of Table I gives the values of i_p^- calculated from those of Δi_C (second row) using the gas-kinetic mean free path for electrons (fifth row). The next row gives the total current to the plate i_p ($\mu A/cm^2$). On the last line are given the ratios of i_p^- to i_p (electron current to the total current) in percent of i_p called γ . In calculating values of i_p^- from the observed values of Δi_C , the gas kinetic values of λ were used in the exponential formula. Had the empirical values of row 3 been used, the values of i_p^- and hence of γ would have been still larger, except for positions III and IV in which there is the following geometrical complication. In the calculation of i_p^- from Δi_C the geometric arrangement of the apparatus must be taken into account. Part of the electrons colliding between plate and cylinder are scattered at small angles from their original direction and will still be collected. This effect will slow

down the decrease of the beam for positions of the cylinder near the plate. This may partly account for the large value of the electron mean free path obtained from the readings at positions III and IV.

The values for γ obtained from the different positions of the cylinder decrease when the distance d of cylinder to plate increases; this shows that the actual decrease of the electron current with distance is larger than would correspond to the exponential law $N = N_0 \exp(-x/\lambda)$ where λ is the gas kinetic value. Using the independent measurements obtained with the Faraday box (third method), it was found (under discharge conditions practically the same as in the case under consideration) that when the theoretical value for the electron mean free path is used in conjunction with the data obtained for Δi_C , at position IV, the value of i_{P^-} may be calculated quite accurately and consequently also that of γ . This would give in the present case a secondary emission of 24 percent. Even if we did not take into account the decrease of the secondary electron beam on its path from plate to cylinder, we would find, using the data of Table I, $\gamma = 17$ percent for position III and $\gamma = 16$ percent for position IV.

The values of γ obtained by the method outlined above vary within rather wide limits (15 to 50) according to the pressure and the degree of purity of the gas. In the runs which gave the data presented in Table I the neon contained slight traces of some impurity. The method under discussion does not permit a separation of the two effects which give rise to the secondary emission: impact of positive ions and impact of metastable atoms. The latter depending on the concentration of the metastable atoms in the discharge is likely to change considerably with the degree of purity of the gas. Table II gives some further illustrations. The values for γ at a given

TABLE II.

I	V	p	$(V_C)_a$	Δi_C	i_{P^-}	i_P	γ
433	68.7	8.5×10^{-3}	-75	35.5	56.8	215	26
433	67.8	8.6	-100	41.6	66.8	235.5	28
432	67.5	8.5	-125	44.8	71.6	258.8	28
432	69.	8.0	-150	43.7	67.9	271.5	25
430	70.	7.8	-175	45.2	69.4	274.5	25
430	70.	8.0	-200	45.7	70.9	287.	25
430	70.5	8.0	-225	48.7	75.6	302.5	25
500	43.2	1.9×10^{-2}	-100	46.3	103.5	268	38
500	43.	1.9	-150	46.9	104.8	279	38
500	42.5	1.9	-200	48.1	107.5	300	36
504	42.3	1.9	-250	48.9	109.3	321	34
507	42.4	1.9	-300	46.5	103.7	340	31

For first seven $d = 4.34$ cm, for last five $d = 3.33$ cm. I = total current through tube in m.a. V = drop across tube in volts. p = pressure in mm of Hg. Currents in cols. 5, 6, 7 in $\mu A/cm.^2$

pressure could be reproduced very well, but it was always found that higher pressures give larger values for γ (for a pressure variation from 5×10^{-2} mm to 8×10^{-3} mm). This variation of γ is principally due to the dependence of the concentration of metastable atoms on the pressure in the discharge tube.

We also tried to find the variation of γ with the plate potential $(V_P)_a$, the accelerating potential for the positive ions. As may be seen no appreciable variation was found. It is well known that the number α of electrons liberated per positive ion increases with the velocity of the ions. But in our case the emission i_P^- which gives γ is made up of two parts: electrons due to ions and electrons due to metastable atoms. Only the first part would vary with the plate potential and this part only contributes to α , so that the variation of i_P^- with $(V_P)_a$ is smaller according to the degree of preponderance of metastable atoms over ions as emitting agents.

We have for the present no definite interpretation for the decrease of γ with increasing $(V_P)_a$, which is especially marked in the lower set of Table II, where γ varies from 38 to 31 percent for $(V_P)_a$ varying from -100 to -300 v. One possibility is that the ions in falling through the sheath destroy a certain number of the metastables on their way to the plate; the larger $(V_P)_a$, the thicker the space charge sheath becomes, and, consequently, the loss of metastables due to positive ion impact also increases. Another effect of the ion impacts in the sheath could be the production of new metastable atoms by impact between fast ions and normal atoms, with a maximum for this process in the neighborhood of the normal cathode fall in neon which is around 100 v. Another possible, though improbable explanation is destruction of metastable atoms by absorbed light (red) or by impurities while traversing the sheath.

An interesting conclusion can be drawn from the data presented in Table II. In the noble gases the volt-ampere characteristic of a negatively charged plane collector (with guard ring) does not present a saturation character⁸ as in the case of mercury vapor.⁹ This may be attributed in part to the increase in ionizing power of the secondary electrons caused by the increase in the accelerating potential acting on them as the plate potential is made more and more negative. In the lower set of data in Table II this increased ionization is shown by the fact that i_P^- remains almost constant while i_P increases with the change in plate potential from -100 to -300 v. A more general case occurs in the upper set of data of Table II, where both i_P^- and i_P increase with increasing negative plate potential, indicating both increased ionization and increased secondary emission.

Second Method. The second method involves the use of the same electrodes as does the first method. In this the plate voltage $(V_P)_a$ is kept constant while the voltage of the movable cylinder $(V_C)_a$ is varied. The positive ion current collected by the cylinder therefore changes, decreasing with decreasing negative voltage, (right to left on Fig. 3). As the voltage of the cylinder becomes more positive and goes through the fixed voltage of the plate at point C, the cylinder current, i_C , shows an additional decrease (curve I, Fig. 4, B to C) due to the reception from the plate of secondary electrons which have previously been turned back. In the run to which Fig. 4 refers, the plate voltage $(V_P)_a$ was -100 v with respect to the anode, and the cylinder voltage $(V_C)_a$ was changed from -125 to -90 . The part AB of curve I, where no electrons are received, is extended in the dotted line BB' which indicates the value of the positive ion current collected by the cylinder.

(Since only the variations in the current are plotted, an arbitrary zero point is selected for convenience at *E*). The differences, *e*, between the measured current and the extrapolated positive ion current are plotted as a function of the cylinder voltage in curve II, which has the same general shape as curve I of Fig. 2. This curve is reversed right for left as compared with that of the first method since the potential changes are made in an opposite manner.

As in the first method it is seen that the electrons may have as much as 12.5 volts initial energy since they are received even when the cylinder is 12.5 volts more negative than the plate. The method of obtaining the reference line *ABB'* of curve I precludes the possibility of discerning a gradual rise in *FG* of curve II corresponding to that found in some cases in the curves of the first method, e.g., *AB* of curve I of Fig. 2. Otherwise, however, the remarks made in connection with the first method apply here. The value of

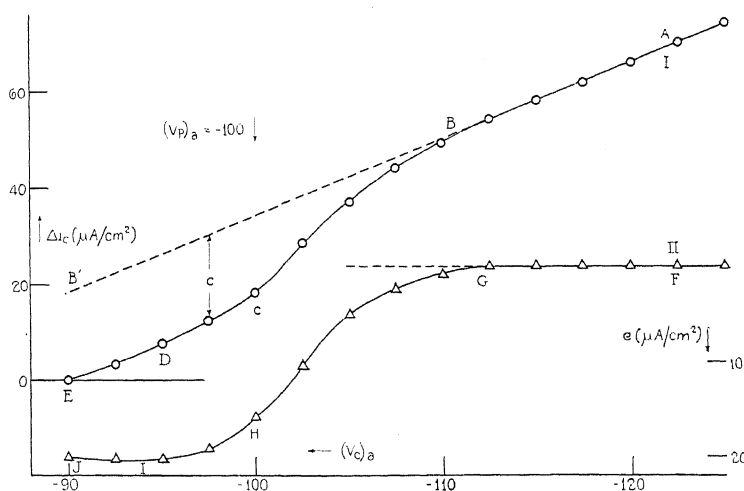


Fig. 4. Curve I. Change in i_c in $\mu A/cm^2$ vs. $(V_c)_a$. Curve II. Difference e vs. $(V_c)_a$.

the initial secondary electron current i_P^- may be calculated by using the gas-kinetic mean free path. In the case illustrated, γ was 33 percent of the measured plate current.

The results of this method corroborate those of the first method, but, since the first method permitted the use of a more sensitive galvanometer, most of the runs were made with the first method. Table III gives some illustrative material.

TABLE III.

p	λ_{gk}	$(V_P)_a$	i_P	Δi_C	i_P^-	γ
2.4×10^{-2}	3.3	-80	219	18	67	31
2.4	3.3	-100	232	20	76	33
2.8	2.8	-150	237	16	73	31
3.5	2.3	-80	204	9	64	31

p = pressure in mm of Hg. λ_{gk} = gas kinetic mean free path in cm. $(V_P)_a$ in volts. i_P , Δi_C , i_P^- in $\mu A/cm^2$. $\gamma = 100 i_P^- / i_P$.

Third Method. The first two methods are somewhat unsatisfactory, for in order to obtain quantitative data on the secondary emission some exponential decrease of the electron beam as it goes from the plate to the movable collector must be used. Since the appropriate value of the mean free path is not exactly known, there is some uncertainty in the results. Obviously, however, those methods give a lower limit to the secondary emission. The method now about to be described gives more definite information, which is free from the defect mentioned.

The movable cylinder *C* is not used and is drawn up out of the discharge. The plate (Fig. 1) has a hole at its center, behind which is the hole in the Faraday box *B*. The shield cylinder *M* attached to the plate *P* protects the box *B* from particles which may come through the annular slit *S* between the

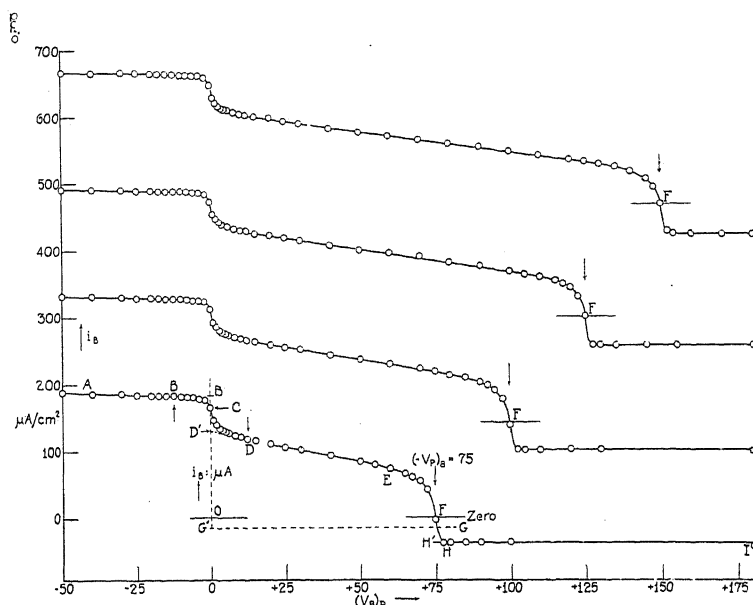


Fig. 5. Box current i_B vs. $(V_B)_P$ for plate potentials $(V_P)_a = -75, -100, -125$ and -150 .

plate and its guard-ring *G*. The reason for this will be discussed later. The plate *P* is given some definite potential $(V_P)_a$, measured with respect to the anode, and the box *B* is made positive or negative with respect to the plate. The total currents to the box and to the plate are measured. Suppose, for example, that the plate is made negative, say -75 volts, so that there is a positive ion current to it. Some of the ions accelerated in the sheath will go through the hole in the plate and into the box *B* beneath when the potential between the box and the plate $(V_B)_P$ permits them. Fig. 5 gives plots of the box currents i_B against the box potential measured with respect to the plate $(V_B)_P$, for plate potentials of $(V_P)_a = -75, -100, -125$, and -150 volts. The curves are plotted on the same scale, but the zero points indicated by the short horizontal lines at the points *O* and *F* are displaced to avoid superposition.

The behavior of the current is much more complicated than one would anticipate under the assumption that the secondary currents are due to positive ions alone. One would expect, for instance, that as the retarding voltage of the box increases, the box current would be constant up to the potential of the space from which the ions have come, at which it would fall sharply to zero and remain so for increasing retarding potentials. A comparison of the magnitude of this current per unit area of the hole with the measured current per unit area of the plate would then give the proportion of the plate current carried by the positive ions alone, assuming that secondary electrons ejected by the ions inside the box B would have a very small chance of escaping from it. The curves of Fig. 5 indicate that a more detailed study is necessary. The break in the current at point F occurs at a retarding box voltage $(V_B)_P$ equal to that of the negative plate voltage $(V_P)_a$, indicating that most of the ions come from a space whose potential is nearly that of the anode. The final value of the current received on B for higher retarding voltages is not zero but a constant negative quantity (points H to I of the plot, Fig. 5). Furthermore the curve $ABCD$ shows a diminution in the current when the box is brought from a negative potential with respect to the plate to a positive one. The magnitude of this diminution for any set of experimental conditions is independent of the potential of P .

In one set of electrodes the inner shield cylinder M (Fig. 1) was omitted, and in this case the action of metastable atoms could be particularly easily demonstrated. Assume that the ions which come through the hole in the plate P go directly into the box B whenever the potential is favorable, and that metastable atoms, on the other hand, are diffusing from the discharge in a random direction through the hole in the plate and the annular slit S . When the inner shield cylinder M was absent, the metastable atoms which came through the hole and the slit S struck the box B on its outer surface and also the under side of the plate and guard ring, and the inside of the outer shield cylinder L . When the potential of the box $(V_B)_P$ was made more and more positive with respect to the plate, any electrons liberated by the action of the metastable atoms on the inner side of the plate or outer shield cylinder L came to B . This current was considerably greater than the positive ion current coming through the hole to the box, since the measured current was negative. A reversed field gave a large current in the opposite direction. Furthermore, it was found that a field across the slit had no effect on these currents between the box B and the outer cylinder L , which again indicates that they are caused by the neutral metastable atoms. To test this the inner shield cylinder M was introduced and fastened to the under side of the plate P so that the space within was shielded from whatever particles might come through the slit S . This is the case for which the curves of Fig. 5 are plotted. Now the relatively large currents above mentioned are practically absent. The current now does not become negative until after the positive ions are repelled at the point F of the curve. The only opening through which the metastable atoms can come is the hole through which the positive ions also come. Part of the former having, as we assume, a random direction, go into

the opening in the box B where electrons ejected will have a very small chance of escaping. A certain proportion, p , of the metastable atoms hit either the outside of the box B , or the inner surfaces of the plate P or the cylinder M , from which the electrons liberated are drawn to the box B to be measured as an incoming negative current. An additional complicating effect caused by the ions repelled at the point F will be discussed later.

A similar argument explains the change in the current at the points BCD of the curve (Fig. 5) where $(V_B)_P$ passes through zero. When $(V_B)_P$ is negative, electrons liberated from the box by metastable atoms striking it on its outer surfaces are drawn from it to the surrounding shield cylinder M and plate P , since the latter are more positive. This appears in the galvanometer as an incoming positive current along with the true positive ion current i^+ . This current i_1^- is stopped when the potential difference $(V_B)_P$ is sufficiently positive to counteract the initial velocities of the electrons, say 12.5 volts, corresponding to the value found by methods one and two. The difference in ordinate CD' , therefore, gives a measure of i_1^- . On the other hand, when $(V_B)_P$ is positive, a secondary current i_2^- in the reverse direction flows, caused by the reception at B of electrons liberated on the inner sides of P and M by the action of the metastable atoms which strike them. The measured positive current i_B is then smaller than i^+ since the reception of electrons is equivalent in the galvanometer to a failure to receive positive ions. If, however, $(V_B)_P$ is decreased through zero, this current is stopped by 12.5 volts corresponding again to the initial energies of the electrons. The difference in ordinate CB' is therefore a measure of i_2^- .

Thus the electrodes shown in Fig. 1 enable us to estimate separately the magnitudes of the secondary emission due to metastable atoms and to positive ions. If we assume, as seems necessary, that the efficiency of production of electrons by metastable atoms is the same at all of the surfaces concerned, then the sum of i_1^- and i_2^- , or $B'D$ on the graph, represents the effect of the proportion p of the metastable atoms coming through the hole. Assuming, however, that each unit area of the plate P is struck by as many metastable atoms as come through the hole per unit area, a value of the secondary electron current liberated from the surface of P by the metastable atoms can be obtained as shown in the following paragraph. The remainder of the secondary emission from the plate is then ascribable to the effect of the ions, thus giving a measure for α , the percentage yield of free secondary electrons for positive ions.

The measured current to the plate i_P , must now be separated into its component parts, that due to the true positive ion current i^+ and that to the secondary emission i^- . Assume that the line ED extrapolated to D' gives the correct value for the positive ion current due to positive ions of the voltage of the plate with respect to the space outside. (The slope of ED is probably due to the distortion of the field at the hole as the potential of the box is changed.) The ordinate OD' , however, must be increased by the amount of the secondary current i_2^- flowing from M and P to B when $(V_B)_P$ is positive. ($B'C$ on the curve.) This lowers the zero line to G' where $OG' = B'C$, giving

i^+ as $D'G'$. The zero line through G' when extended to the right intersects the curve at G and does not coincide with HI , as might be expected from the explanation previously given. That, however, was obviously incomplete since it neglected the effect of the positive ions repelled from the box when $(V_B)_P$ was more positive than $(V_P)_A$ was negative. Presumably these either go back through the hole or strike the plate on its under side, where secondary electrons are liberated and drawn to the outside of the box, giving the current i_3^- (GH' on the curve). The ratio of this current to the positive ion current gives a value for α (Table IV, column 5) independent of the effect of the metastable atoms. This enables us to calculate the proportion, p , of the number of metastable atoms which do not enter the opening of the box B (equal to 74 percent with the electrodes used). This value is of the order of that to be expected from the geometry of the hole and box. $B'D$ of the graph is then divided by p to obtain the equivalent effect i_m^- of the total number of metastable atoms which come through the hole in the plate. (Table IV). The measured plate current i_P is diminished by i^+ to obtain i^- , the total secondary emission. γ is the ratio of 100 i^- to i_P . The part i_i^- , of the emission due to positive ions is the difference between i^- and i_m^- . A second value of α can then be calculated by dividing 100 i_i^- by i^+ . (Table IV, column 10).

TABLE IV.

$(V_P)_A$	i_P	i^+	i_3^-	α	i^-	γ	i_m^-	i_i^-	α
-75	240	146	21	14	94	39	74	20	14
-100	248	150	24	16	98	40	74	24	16
-125	253	153	26	17	100	40	74	26	17
-150	260	154	30	20	106	41	74	32	20

$p = 2.0 \times 10^{-2}$ mm of Hg. Currents are reduced to $\mu A/cm^2$.

Assuming that the decrease of α with decreasing ion velocity is linear, the value of α_0 for ions of zero velocity is about 7 percent as given by the runs of Table IV.

The values of α are somewhat uncertain since the results depend on a very small variation in the deflection of a sensitive galvanometer. The consistency of the data is indicated by a comparison of columns 5 and 10 of Table IV and by four other runs at $(V_P)_A = -125$ volts for instance, which gave respectively $\alpha = 18, 17, 18$ and 17 . The last of these was taken with about twice as much total current through the discharge, so that i^+ and i_i^- increased in about the same proportion. The values of γ obtained by this method check well with those obtained by methods one and two, where the three methods were used in immediate succession. For example at $p = 1.3 \times 10^{-2}$ mm of Hg, γ was found to be 30, 31 and 33 by methods one, two and three respectively. This degree of corroboration was obtained throughout, indicating that values of γ found by the first two methods were a few percent too small.

Some comparisons of this work with that of other observers can be made. A variety of gases and metals have been used. The experimental conditions

were not similar in many cases to those used here where the circumstances arising at the cathode in a glow discharge were counterfeited as nearly as possible. In Penning's experiments^{4,5} the positive ions from the main discharge tube traversed a canal in an electrode and entered a more highly evacuated vessel wherein the target was located. The value of α_0 (2 to 10) which he finds is approximately that given here, but the rate of increase of α with voltage is less than that which we find (about 0.02 or 0.03 per volt for iron in neon and less than 0.01 per volt for copper in neon as compared with 0.08 per volt for nickel in neon.*)

Found¹⁴ reports values of the secondary emission from tungsten electrodes in neon larger than those obtained here. His method is to compare the measured current at various electrode potentials with the area of the sheath calculated by the equation given by Langmuir and Mott-Smith.⁹ He assumes that the true positive ion current is proportional to the area of the sheath, while the secondary electron is constant. The larger emission which he finds may be a consequence of a greater purity of the neon since impurities destroy metastable atoms, to which he ascribes the preponderant part of the emission. His calculations, however, neglect several points: the effect of the second order plasma fields on the variation of the positive ion current with voltage, the additional ionization due to the increasing ionizing power of secondary electrons accelerated by increasing potentials, and the increase of α with voltage.

VELOCITIES OF ELECTRONS FROM THE DISCHARGE

The perforated plate and Faraday box system was used with the potential of the plate in the neighborhood of the space potential to determine electron velocities. In the case illustrated by Fig. 6, the plate was put at -25 v, and the current to the box measured as the potential of the box with respect to the plate was changed. The electrons which came through the hole were finally repelled by a retarding potential of -30 volts. The residual current for higher retarding potentials was not zero but positive indicating either that positive ions were coming through the hole in small numbers or that an electron current was released from the box. The latter in view of the phenomena described under method three is extremely probable. In any case, when the current as measured from the zero of the galvanometer is increased by the amount of the residual positive current, the $\log i_B$ vs. $(V_B)_P$ plot gives a straight line over a considerable portion whereas the corresponding plot of the apparent current is not straight over any part. This indicates that these electrons have a Maxwellian distribution of velocities of which the average, in

* During the writing of this article a paper on this subject by Oliphant appeared. Proc. Roy. Soc. A127, 373 (1930). He finds in experiments with an apparatus somewhat similar to that of Penning (for molybdenum and helium) a linear increase of α with the voltage of the impinging ions (about 25 for 200 v to about 120 for 1000 v, or 0.105 increase per volt); but he shows that below 200 v α is almost constant. A smaller α (not linear) is found for heat-treated targets. The velocity distribution curves are similar to those reported here (almost all velocities less than 20 volts), but only the runs taken with heat-treated targets show kinks (cf. Fig. 2).

¹⁴ Found, Phys. Rev. 34, 1625 (1929).

the case illustrated, corresponds to 7.3 volts. This was corroborated by measurements using the plate P as a plane collector, according to Langmuir's method,⁹ which gave in the present case 7.7 volts. This sort of agreement was obtained throughout. The space potential, about -20 or -25 volts with respect to anode, as indicated by Langmuir's method for a plane collector, was not exactly the same as that given under method three, namely, about that of the anode; but obviously the conditions are not comparable, for in one case the collector—a rather large one—was drawing a large negative current, while in the other a large positive one. The distribution of current going to the various electrodes is materially different in the two cases.

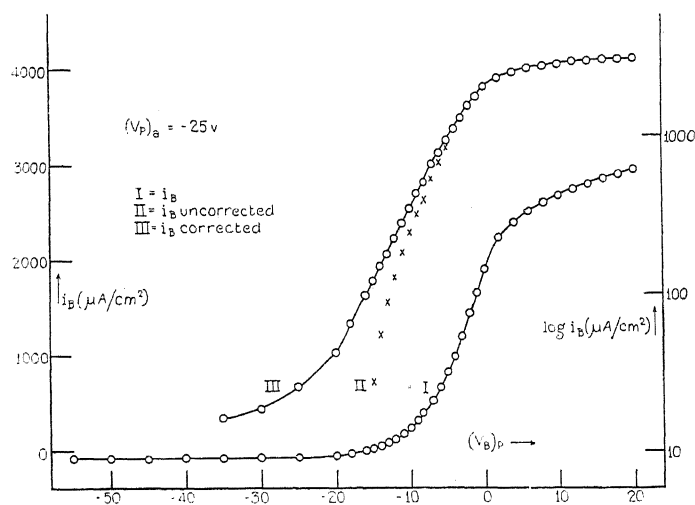


Fig. 6. Curve I. i_B vs. $(V_B)_P$ for $(V_P)_a = -25$ v. Curve II. Uncorrected $\log i_B$ vs. $(V_B)_P$. Curve III. Corrected $\log i_B$ vs. $(V_B)_P$.

In all runs taken for $(V_P)_a$ between 0 and -15 volts there was a break downward in the $\log i_B$ vs. $(V_B)_P$ curve at $(V_B)_a = -21$ or -22 volts which indicates a deficiency of electrons of a voltage corresponding to the ionization potential of neon.

There is some evidence for the reflection of electrons from the plate when it is receiving a large negative current, for the current per unit area of the hole received at the box when $(V_B)_P = 0$ is much more than the current per unit area to the whole plate, for example 4970 as compared with 3750 $\mu A/cm^2$, or 25 percent reflection. This varied under different experimental conditions and for different voltages of the plate from about 5 to about 50 percent. Unfortunately the data on this point are at present not sufficient to say anything further.

The junior author is extending this work to other gases and discharge conditions. In conclusion we wish to thank Professor K. T. Compton for his aid and advice during the course of the experiments and in the interpretation of the data.

EXTINCTION OF SHORT A. C. ARCS BETWEEN
BRASS ELECTRODES

BY T. E. BROWNE, JR., AND F. C. TODD

RESEARCH LABORATORY, WESTINGHOUSE E. AND M. COMPANY*

(Received June 26, 1930)

ABSTRACT

Results are given which show that the dielectric recovery after current zero, of short, stationary A.C. arcs between brass electrodes, is similar to that of cold-electrode arcs previously investigated and described. These results also show that the rate of recovery of dielectric strength of hot-electrode arcs after a current zero may be greatly increased by reducing, within limits, the electrode separation. A possible explanation on the basis of ionic diffusion to the electrode surfaces and the deionizing action of blasts of metal vapor from the boiling electrodes is mentioned.

THE recovery of dielectric strength by an A.C. arc, immediately after a current zero at which it is extinguished, has been studied by Slepian¹ with the result shown in Fig. 1. The short arcs studied were kept in rapid

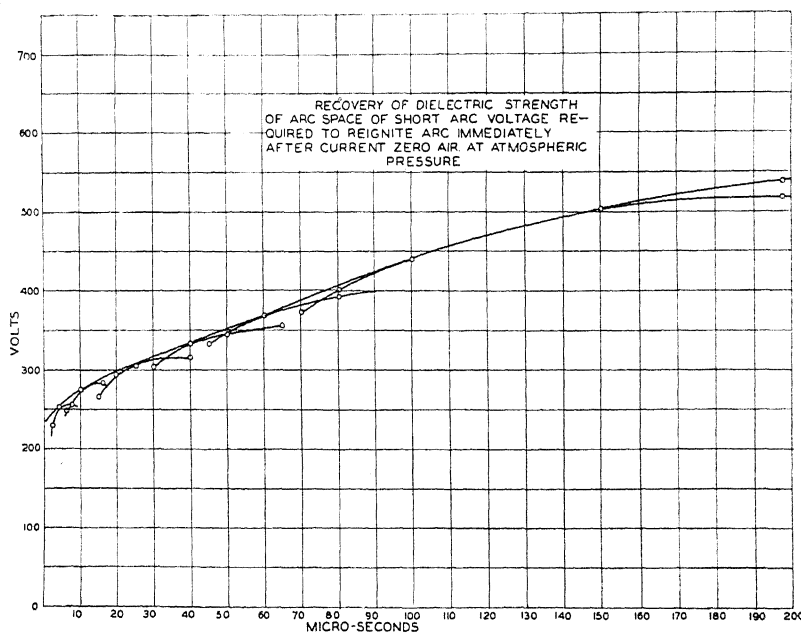


Fig. 1.

motion over copper surface terminals which are believed to have been cold. The ability to withstand about 230 volts was regained within less

* Scientific Paper No. 430.

¹ "Extinction of an A.C. Arc", J. Slepian, Trans. A.I.E.E. 47, 1398 (1928).

than a few micro-seconds after a current zero, and further dielectric strength was recovered thereafter at a much lower rate. The simple theory which Slepian gives identifies the quickly recovered dielectric strength with the minimum sparking potential or normal cathode drop in a glow in the gas next to the cathode. This should therefore be independent of current and of arc length. Slepian's theory also makes the slower further recovery of dielectric strength independent of current and arc length, but this part of his theory depends on the assumption that ions are lost from the arc space only by direct recombination. If other deionizing agents are not of negligible activity, such as for example, diffusion of ions into the electrodes, or diffusion into cooler surrounding gas with more rapid recombination there, then this slower later recovery should be influenced by arc length and current magnitude. The quickly recovered dielectric strength, however, should not be influenced by these other deionizing agents. Short stationary A. C. arcs in which the electrodes are hot might be expected to behave in a generally similar manner to the cold-electrode arcs which Slepian studied, provided that the boiling temperature of the electrode material is so low that appreciable thermionic emission is unlikely. Using stationary arcs with brass electrodes, the writers have conducted experiments which show that dielectric strength after current zero was recovered in the same manner as for the cold-electrode arcs of Slepian. The quickly recovered dielectric strength was independent of arc length, but the more slowly recovered dielectric strength varied with current and arc length, being greater for the smaller currents and shorter arc lengths.

APPARATUS AND METHOD

The circuit and the shape of the electrodes used in these tests are shown in Fig. 2. The source of power was a 100 KVA transformer bank with adjustable secondary voltage, whose primary was connected to a 2300-volt 60-cycle power line. The current was limited almost entirely by air-core reactors, having low power factor and comparatively low distributed capacitance. Following Slepian, the electrical transient of the circuit immediately after the extinction of the arc was controlled by shunting the arc electrodes with adjustable resistance made up of low-inductance wire-wound resistor tubes. To obtain the equivalent of exactly zero power factor in spite of resistance drops and arc voltage, a synchronous shorting switch was used to close the circuit at such a point on the voltage wave that the end of the first half-cycle of current occurred at the maximum of the sinusoidal generated voltage. An arc was formed almost immediately at the center of the electrodes by the burning of a fine (No. 40 B. & S.) copper fuse wire, and the ensuing number of half-cycles of arcing was counted by means of a direct-vision oscillograph. When the arc shunting resistance was high the arc would continue for many half-cycles; when the shunting resistance was low the arc would extinguish at the end of the first half-cycle. The resistance shunt was varied between trials until the value that would just cause the arc to go out at the end of the first half-cycle was determined within 5%. During a

short time after a current zero at which the arc is extinguished the voltage across the gap is approximately given by the formula:

$$e = E_m(1 - e^{-Rt/L}) \quad (1)$$

where E_m is the maximum of the generated voltage, R , the arc shunting resistance, and L , the inductance of the circuit. L was determined from the r.m.s. short-circuit current I by the relation:

$$E_m = 2^{1/2} \cdot 2\pi \cdot 60LI. \quad (2)$$

When the value of R is small, and the arc is extinguished at the first current zero, the impressed voltage given by (1) remains below the recovered dielectric strength of the arc space. When the value of R is large, and the

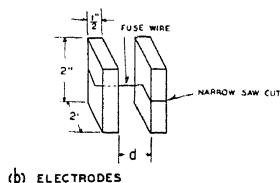
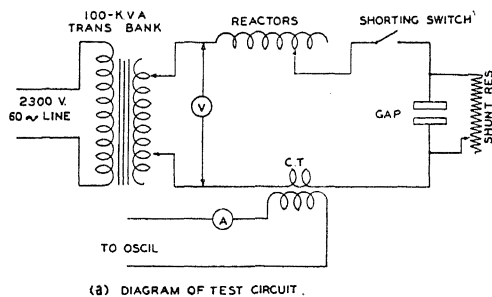


Fig. 2.

arc re-ignites, the curve of (1) will rise above the recovered dielectric strength of the arc space. For the critical value of R which just causes the arc to be extinguished at the first current zero, the curve of (1) must come up and just be tangent to the curve of the recovered dielectric strength of the arc space. By plotting a family of curves with different E_m 's, and corresponding critical R 's, the curve for the recovery of dielectric strength with time may be found by taking the envelope. No account is taken of distributed capacitance of the reactors and other parts of the circuit. Though these capacitances are comparatively small, they become appreciable when the critical value of resistance is high, and particularly when the shunt is removed altogether. The transient voltage will then generally rise in an oscillatory manner, reaching almost double the normal peak value. For this reason, tests in which nearly full voltage is recovered in less than ten micro-seconds are inaccurate and of value only for comparative purposes. Roughness of and

oxide formation on the electrodes after continued arcing may also cause considerable variation in results.

EXPERIMENTAL RESULTS

The curves of Fig. 3, which show results obtained for 1.6 and 3.2 millimeter arcs of 300 amperes, are similar in shape to curves obtained for cold-electrode arcs (Fig. 1). From these curves we see that the immediately

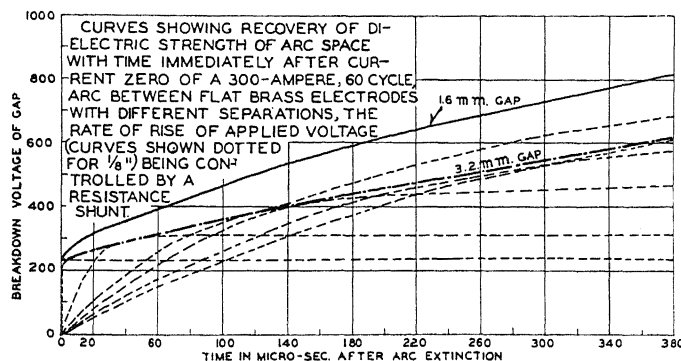


Fig. 3.

recovered ability to stand voltage is the same for the two arc lengths, but that after that the shorter arc recovers dielectric strength faster than the longer arc. Thus we are led to the interesting and at first sight paradoxical fact that a very short arc may be extinguished more easily than a longer arc.

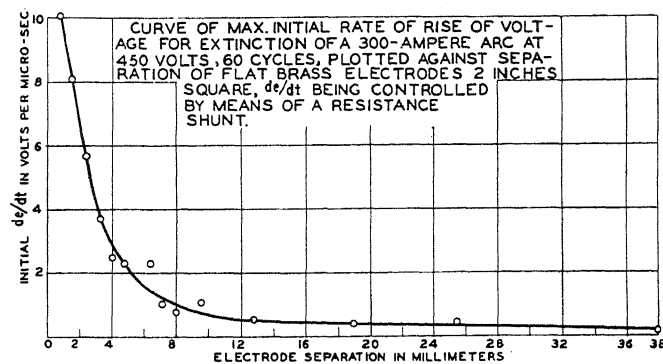


Fig. 4.

This influence of arc length on recovered dielectric strength was found to continue up to lengths of 5 cm and more, by tests on 300-ampere arcs in a 450-volt (r.m.s.) circuit. The critical shunting resistance for arc extinction was determined for different arc lengths, and the initial rate of rise of voltage for the transient corresponding to each critical resistance was computed. The results are shown plotted against arc length in Fig. 4. It is noticeable that the factor causing this variation with gap length is most effective as the electrode separation becomes less than one centimeter. As this factor is undoubtedly a

deionizing one, and is probably active during the arcing period as well as during the extinction transient, we might expect it to reveal itself in the magnitude of the arc voltage. Figure 5 shows the variation of arc voltage with gap length. The definite increase in slope for the smaller lengths affirms the presence, even while the arc current is flowing, of some deionizing action which is more effective for short arcs than for long.

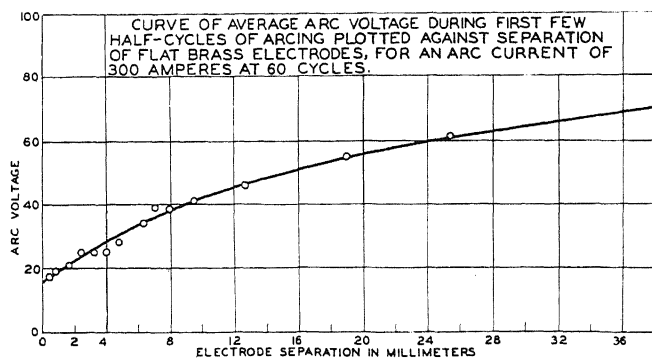


Fig. 5.

Figure 6 shows the results of tests at the same voltage and gap length but with currents ranging from 25 to 800 amperes. There is an undoubted decreasing tendency of these rather scattered values with increasing current.

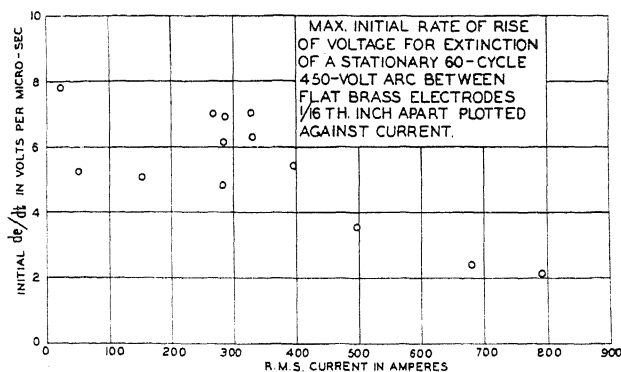


Fig. 6.

According to the approximate theory of Slepian for the dielectric recovery upon extinction of a short A. C. arc, all of the regained dielectric strength resides in a positive space sheath next to the cathode. Due to the high mobility of the electrons, this space charge sheath is formed with extreme rapidity upon application of voltage and is immediately able to withstand a minimum of two or three hundred volts, depending only on the electrode material and the gas medium. Further recovery of dielectric strength results from increase in thickness of this space charge sheath due both to growth of applied voltage and to the diminishing density of ionization next to the cathode.

In Slepian's theory the loss of ions was assumed to be due solely to direct recombination in the arc space. The results given here confirm the fundamental conception of the formation and growth of a cathode space charge sheath, but the large influence of electrode separation points to the presence of some deionizing agent other than direct recombination which becomes rapidly more effective as the arc length diminishes. Since diffusion of ions into the electrodes is a process fitting this description, approximate calculations were made to determine to what extent this can account for the observed results. So far, however, the simplified calculations, assuming all of the deionization to be due to diffusion alone, and neglecting such influences as the electric field, vapor emission from the electrodes, and diffusion to the surrounding air, seem to require a coefficient of diffusion far in excess of any reasonable value. This may indicate that diffusion to the electrodes is an unimportant factor, or it may simply mean that the present approximate method of calculation is unsound. It is also thought possible that other physical processes may enter considerably into the deionization of the arc space next to the cathode, such as for example, a blast of metal vapor from the violently boiling electrodes during the arcing period and perhaps for a very short time immediately thereafter, but this theory lacks verification as yet. Therefore, further work is being done in an effort to arrive at a more nearly satisfactory explanation of these results.

RESTRIKING OF SHORT A. C. ARCS

BY F. C. TODD AND T. E. BROWNE, JR.

RESEARCH LABORATORY, WESTINGHOUSE E. AND M. CO.*

(Received June 26, 1930)

ABSTRACT

The restriking after zero current of short stationary A.C. arcs with brass, copper, zinc, iron, tungsten and carbon electrodes, and of arcs moving rapidly over copper electrodes was investigated with a cathode-ray tube of the Braun type. The volt-ampere traces on the fluorescent screen showed clearly the voltage necessary to restrike the arc after current zero, and the effect of the electrode vapor on the magnitude and variation of the restriking voltage. The arcs with refractory electrodes, i.e. carbon and tungsten, showed traces differing from the arcs with the other metals in that no high voltage for restriking the arc appeared. This is believed to be due to the refractory electrodes being at a temperature high enough for thermionic emission. For the other electrode materials, re-ignition voltages of several hundred volts were observed, suggesting that re-ignition of the arc required breakdown of a gas layer by ionization by collision alone. The arcs which were rapidly moving over their electrodes usually restruck to a glow before breaking down to an arc. The magnitudes of the restriking voltage and the glow current depended upon the condition of the electrodes, magnitude of the driving magnetic field, and the transient characteristic of the circuit in which the arc was playing.

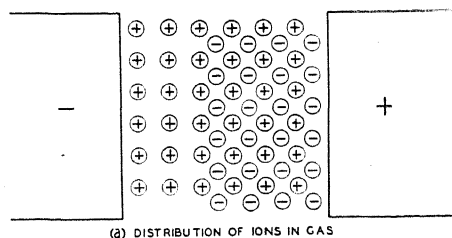
IT IS well known that although a carbon arc can be maintained in a low voltage A.C. circuit, in general, an A.C. arc with metallic electrodes cannot be maintained with less than a few hundred volts. This has been studied by means of volt-ampere traces on the fluorescent screen of a cathode-ray tube of the Braun type, developed by Zworykin for use in television. These investigations have brought out several interesting facts about the magnitude of the voltage required to restrike the arc, and the manner of breakdown.

Slepian¹ has attributed this peculiarity of arcs mentioned, to the formation immediately after current zero of a thin deionized layer of gas next to the cathode. With thermionic emission lacking, to re-ignite the arc this layer would need to be broken down by ionization by collision and would require several hundred volts. His theory is illustrated by Fig. 1 which is taken from the paper referred to above. Starting with a uniform distribution of ions when the current and voltage are zero, the increasing voltage will cause space charge sheaths to form next to the electrodes after the manner described by Langmuir in relation to probe electrodes in an ionized gas. Because the mobility of the electrons is much greater than that of the positive ions, most of the applied voltage will be across the space charge sheath at the cathode. The current densities in this sheath are very small and in order to

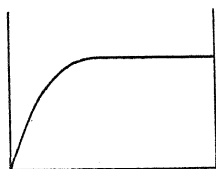
* Scientific Paper No. 431.

¹ "Extinction of an A.C. Arc," by J. Slepian, Journal of the A.I.E.E. October, 1928.

restrike the arc, the space charge sheath must be broken down. If there are no other ionizing agents, the breakdown must be by ionization by collision only, and is entirely similar to the breakdown of a short spark gap. It will, therefore, require a minimum of several hundred volts. If, however, there are other ionizing agents, breakdown will occur at a lower voltage.



(a) DISTRIBUTION OF IONS IN GAS



(b) POTENTIAL DISTRIBUTION IN GAS

Fig. 1.

It seems unlikely that the temperature of the electrodes can be raised much above the boiling point. Hence, for non-refractory metals, i.e. zinc brass, copper, and iron, thermionic emission is probably entirely negligible. Hence, for these metals, the space charge sheath must be broken down by ionization by collision only. But carbon and tungsten at their boiling points

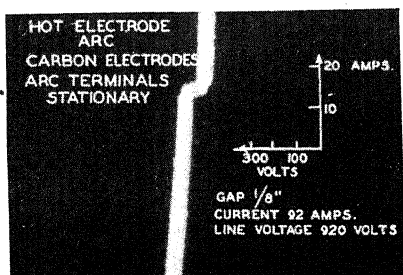


Fig. 2.

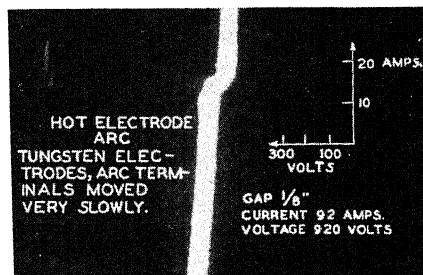


Fig. 3.

are at temperatures high enough for thermionic emission. Accordingly, for these electrode materials, we may expect breakdown of the sheath at low voltages. This occurs as is shown by the photographs of the dynamic volt-ampere characteristic on the fluorescent screen of the Braun tube. The photographs in Fig. 2 and 3 are for the carbon and tungsten arc respectively.

Fig. 4 shows the interpretation of Fig. 2 in the more familiar current and voltage against time relation. In Figs. 2 and 3 the current and voltage deflections are purposely not exactly in phase with the actual current and voltage and give the double line near current zero. The exposure for these photographs was 15 seconds, or included 900 retracings of the phenomenon.

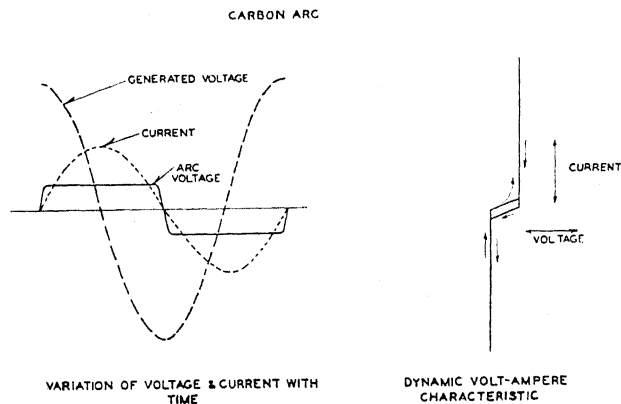


Fig. 4.

Returning now to the non-refractory metals, we shall expect to see much higher breakdown voltages, and since the space charge sheath is composed chiefly of the metal vapor, the breakdown voltages required for the various metals will in general be different. This is illustrated by Figs. 5, 6, 7, and 8 which give a portion of the dynamic volt-ampere characteristics near the reversal of current for zinc, copper, brass, and iron respectively. The current

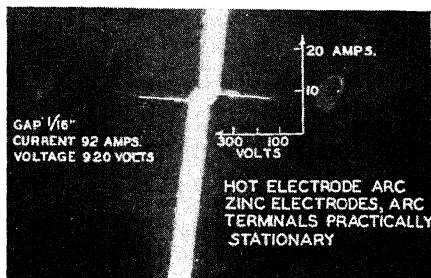


Fig. 5.

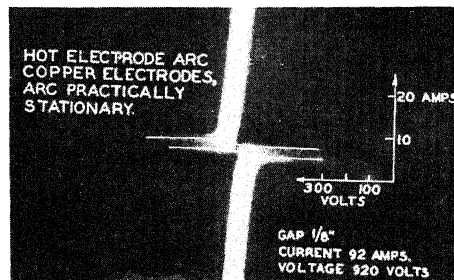


Fig. 6.

and voltage deflections are again not in phase with the actual current and voltage for Figs. 5 and 6, this displacement is to show the voltage before current zero as well as the restriking voltage. For the zinc arc, the restriking voltage is 280 volts and the voltage does not rise above arc voltage at the end of the half cycle. The stationary arc on copper has a peak restriking voltage of 360 volts, and the voltage before current zero rises to 280 volts.

The maximum restriking voltage for brass and iron were 255 and 290 volts respectively.

Fluctuations in the density of the breakdown voltage line indicates that reignition frequently occurred at low voltages in these stationary arcs. This requires some other ionizing agent than ionization by collision. What this

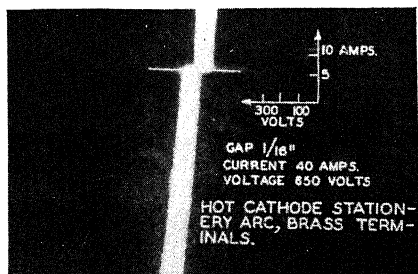


Fig. 7.

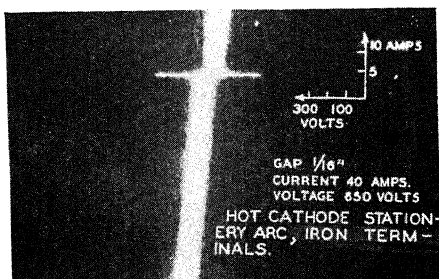


Fig. 8.

is is uncertain. Slepian suggests that the charging current to a particle or droplet making or breaking contacts with the cathode may cause a tiny spark which will make the space charge sheath collapse.

It is possible to cause an arc to move so rapidly over a clean smooth surface by means of a magnetic field that melting of the electrodes is prevented.

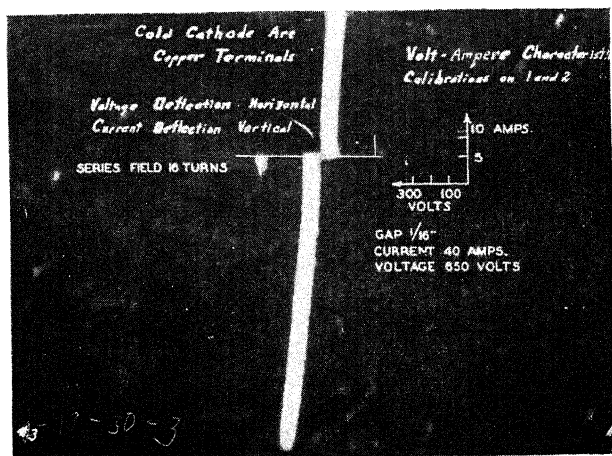


Fig. 9.

It is believed that the terminals of such an arc may be cold. The dynamic volt-ampere characteristic of such an arc is shown in Fig. 9. The maximum restriking voltage is 535 volts, the hesitation during the breakdown is at 325 volts. Fig. 10 is the interpretation of Fig. 9 in the more familiar relations, the scale is much expanded near the ends of the half-cycles for clearness. As

the impressed voltage increases by an oscillation at the natural period of the circuit, and as the density of ionization decreases due to recombination and discharging of ions into the electrodes, the thickness of the cathode space charge sheath increases. At peak value, the voltage across the sheath has exceeded the recovered dielectric strength, and the short gap breaks down by ionization by collision. The voltage drops from peak value to that of the

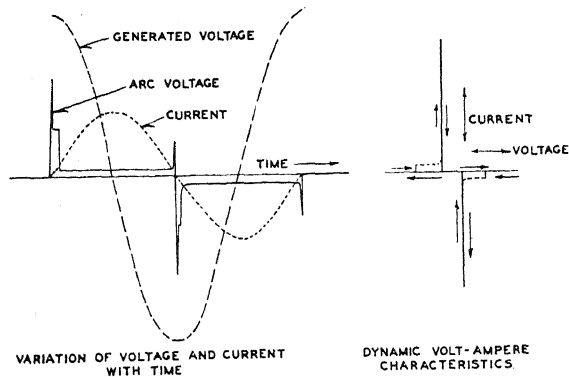


Fig. 10.

glow or occasionally even to arc voltage. The glow appears and remains a stable discharge until enough energy is put into the space adjacent to the cathode to give the conditions required by the cold electrode arc, then the transition from glow to arc abruptly occurs. The maximum glow current observed before transition to an arc was 4 amperes, and in this case meant that the glow was stable for longer than 10^{-4} seconds. The probability of a

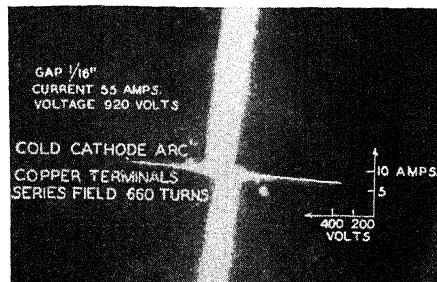


Fig. 11.

glow occurring seems to be less for the higher restriking voltage. It also appeared that the magnitude of the current to which the glow continued, and the probability of a glow occurring at all both increase as the electrode surfaces which had been initially cleaned with emery become oxidized. Slepian²

² "Theory of the Deion Circuit Breaker", J. Slepian Journal of the A.I.E.E., Feb., 1929.

had predicted that re-ignition of the cold electrode arc takes place first as a glow and his expectation is here confirmed.

Another dynamic volt-ampere characteristic similar to Fig. 9 is shown in Fig. 11, the only difference is that the driving magnetic field was 16 series turns for the former as compared to 660 series turns for the latter. The maximum restriking voltage in Fig. 11 is 1065 volts as compared to 535 volts for Fig. 9. In each case the glow occurs at 325 volts. This high restriking voltage can be obtained with the weaker field by shunting the arc with a resistance to slow down the rate of increase of voltage after current zero. This is due to the longer time the deionizing processes are active and the resulting thicker deionized layer requiring more voltage to breakdown.

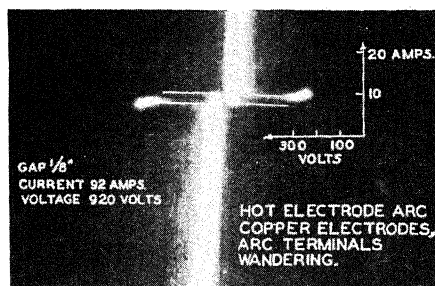


Fig. 12.

If an arc of approximately 90 amperes is drawn between plane electrodes with a fine fuse wire, generally the arc will not continue for several half-cycles where it was drawn but will wander about over the electrode surface. Judging by the trail, the arc does not move much while the current is flowing but restrikes after current zero to a position on one side of the position of the arc during the previous half-cycle. When moving in this manner tungsten and carbon arcs show a variable restriking voltage which may be quite comparable to that of non-refractory metals. The only metals among those tested which did not show this wandering behavior were zinc and to a certain extent brass. Copper arcs have a very peculiar volt-ampere characteristic while wandering as shown by Fig. 12. The hesitation at the peak of the restriking voltage varies from a minimum of about 250 volts to a maximum of about 325 volts.

THE PHOTOELECTRIC BEHAVIOR OF SOLID AND LIQUID MERCURY

BY DUANE ROLLER
UNIVERSITY OF OKLAHOMA

(Received June 26, 1930)

ABSTRACT

With monochromatic light, the photoelectric threshold wave-length for solid mercury, freshly distilled and frozen in vacuum, was $2750 \pm 25\text{\AA}$ for all temperatures between -190°C and the melting point. For room temperature it was $2735 \pm 10\text{\AA}$, confirming Kazda's value.

The photoelectric current excited by each of the lines 2537 \AA , 2653 \AA and 2700 \AA was independent of temperature between -190°C and *ca.* -125°C . Between *ca.* -125°C and -39°C there was a gradual small decrease in the current with increasing temperature, but this was not reproducible at definite temperatures and is attributed mostly to contamination and other secondary causes. With the possible exception of this decrease in current, there was no indication of an allotropic change in the mercury between -190°C and the melting point. The photoelectric current for the solid phase was always higher than that for the liquid at room temperature, possibly due to a change in the optical absorptivity of mercury with change in phase. Between -39°C and 0°C the emission curves show so much hysteresis that conclusions regarding this region are impossible.

THE photoelectric threshold for mercury at room temperature has been established at $\lambda_0 = 2735\text{\AA}$ by Kazda, Dunn and Hales.¹ Mercury at the melting point was investigated by Pohl and Gudden.² They were unable to detect any change in the threshold with melting but terminated their work with the conclusion that mercury is not a suitable metal for studying variations in the photoelectric effect at transition and melting points because of the difficulties inherent in such experiments at low temperatures. Recently, Margarete Grutzmann³ published a study of the photoelectric emission from mercury at low temperatures. No variation of the total emission with temperature was found and there was no change in the total emission at the melting point. Since monochromatic light was not used, it is impossible to interpret these results or to establish the behavior of the threshold.

The purposes of the present work with mercury were: (1) to find the effects of temperature and of changes in the state of aggregation on the photoelectric threshold and on the current excited by incident monochromatic light; (2) to check independently the value of the threshold at room temperature; (3) to seek evidence of a photoelectric nature regarding an allotropic change in mercury in the region between -190°C and the melting point. McKeehan and Cioffi⁴ determined the crystal structure of mercury

¹ C. B. Kazda, Phys. Rev. 26, 643 (1925); H. K. Dunn, Phys. Rev. 29, 693 (1927); W. B. Hales, Phys. Rev. 32, 950 (1928).

² Pohl and Gudden did not publish. This information was communicated to me by Dr. A. Goetz.

³ M. Grutzmann, Ann. d. Physik 1, 49 (1929). A comprehensive bibliography accompanies this paper.

⁴ McKeehan and Cioffi, Phys. Rev. 19, 444 (1922).

at -115°C and Alsen and Aminoff⁵ determined the structure at -78°C . The two results are very different and thus point to the existence of an allotropic modification of the mercury occurring somewhere between -115°C and -78°C .⁶ On the other hand, Lark-Horovitz⁷ has recently found that the crystal structure of mercury at the temperature of liquid air is identical with that at the temperature of a carbon dioxid-alcohol mixture.

The apparatus for the present work, Fig. 1, was made of Pyrex glass and had no cemented joints or stopcocks in the high-vacuum system. Light from a mercury arc, which had been carefully calibrated⁸ and which was operated with constant voltage, current and temperature, passed through a Hilger quartz monochromator and a quartz lens into the quartz window of the photoelectric cell, and then through a slit in the anode onto the bottom of the cell. The anode was a circular disk of tungsten 3 cm in diameter, welded with nickel to a heavy tungsten wire which lead out through a horizontal tube 12 cm long to a Dolazalek electrometer of sensitivity 1100 mm

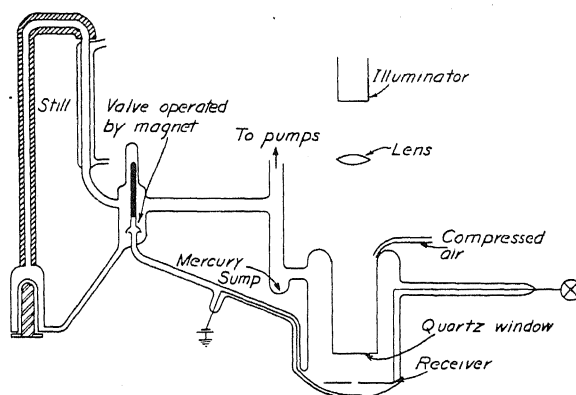


Fig. 1. Diagram of apparatus.

per volt at 1.5 m scale distance. The cell was shielded electrostatically by covering its outside walls with a paste made of powdered graphite, water, and a little water glass. When the cell was baked the graphite formed a hard conducting layer. Water glass, when used sparingly, apparently will not weaken Pyrex appreciably, for the cell was used for two months without breakage.

The mercury used as the cathode of the cell was cleaned and distilled by a special method⁹ and was then placed in the still, Fig. 1, where it was distilled repeatedly in high vacuum to remove occluded gases. Some of the mercury was then allowed to pass through a magnetically operated valve, Fig. 1, into the bottom of the cell, where it rested on the glass, but was in

⁵ Alsen and Aminoff, *Geol. Foren. i. Stockholm Forh.* 124 (1922).

⁶ Ewald and Hermann, *Zeits. f. Krist.* 65, parts 1-3, appendix (1927); *International Critical Tables*, 1, 340.

⁷ K. Lark-Horovitz, *Phys. Rev.* 33, 121 (1929).

⁸ C. B. Kazda, *Phys. Rev.* 26, 645 (1925).

⁹ D. Roller, *J. O. S. A.* 18, 537 (1929).

contact with a tungsten wire kept usually at a potential of 20 volts negative to ground.

The cooling of the mercury was accomplished variously with liquid air, liquid air and alcohol, solid carbon dioxide, and solid carbon dioxide and ether, contained in a specially designed Dewar flask which surrounded the cell up, to a point 7 cm above the surface of the mercury cathode. Temperatures were measured with a constantan-steel thermocouple, enclosed in a glass tube and immersed in the mercury. To retard the collection of moisture on the cold cell, a current of washed and dried air was played continuously on the window and walls. The points where the tungsten leads emerged from the cell were kept dry by means of small heating coils and drying materials. Surrounding the cell was a double-walled galvanized iron box, lined with asbestos, which helped to keep out moisture and which also served as an oven for baking the cell and as an additional electrostatic shield.

With the cell of Fig. 1 the threshold for mercury at room temperature was found to be at $2735 \pm 10A$, in agreement with the results of previous workers.¹⁰ This constitutes an independent check of the previous work, both because the mercury was here in contact with glass and tungsten, rather

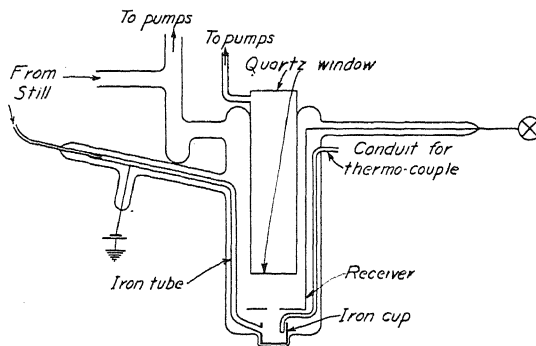


Fig. 2. Diagram of modified apparatus.

than iron, and because the cell involved relatively few metal parts and probably was more thoroughly outgassed than the cells previously used.

When it was attempted to use this cell for low temperature work several defects in its design became apparent and this led to the construction of a new cell, Fig. 2, which differed from the old one in the following respects. (a) A second quartz window was cemented to the cell at a point considerably above the region to be cooled, the space between the two windows being evacuated. This gave improved thermal insulation and also made it possible to dispense with the current of air on the cell. Compressed air usually contains oil which forms a film on the window; no simple way could be found for removing all the oil from the air. (b) The anode, including the lead through the glass wall of the cell, was cut out of a single sheet of tungsten. In the old cell, the anode consisted of a tungsten sheet welded to tungsten wire and it was the seat of thermoelectric forces which produced erratic effects during times that the temperature of the cell was changing. (c) An iron cup 2.5 cm in diameter served as a container for the mercury cathode, the size of this cup being such that light fell only on the central unstrained part of the frozen

¹⁰ Reference 1.

mercury. The mercury was admitted to the cup through an iron tube, so arranged that it did not need to pass through the glass wall of the cell. In the old cell the mercury ran in over the glass, resulting in the formation of electrostatic charges which would persist for as much as an hour. (d) The mercury pump attached to the cell was enlarged so that it could be immersed in liquid air, thus retarding the condensation of mercury vapor on the surface of the solid mercury cathode. Preliminary experiments had shown that without this protection enough mercury condensed on the surface of the empty iron cup, when the latter was cooled, to produce an appreciable photoelectric current. Experiments made very recently at the University of Oklahoma by Mr. Carl Woodward and the writer indicate that a thin film of frozen mercury deposited on iron has both a high photoelectric sensitivity and a threshold wave-length longer than 2735Å. In view of these results, it might be advisable to seal off the photoelectric cell from the pumps and mercury still before attempting to determine the threshold of solid mercury.

In order to determine the thresholds at various temperatures, measurements were made of the photoelectric current at a particular temperature as a function of wave-length. Thresholds were then determined in the usual way by plotting the current excited by unit intensity of the incident light as a function of wave-length.¹¹ In the region -190° to the melting point, the threshold was established at $2750 \pm 25\text{Å}$, independently of the temperature. Thus, within the experimental error, the threshold for solid mercury is the same as that for liquid mercury at room temperature. When the solid mercury was held at low temperatures for times exceeding about one hour, the threshold began to shift slowly to shorter wave-lengths. There was ample evidence that this shift was due to contamination.

Measurements were also made of the photoelectric current for a given line as a function of temperature. Results typical of sixty curves made for the lines 2537Å, 2653Å, and 2700 Å are shown in Fig. 3. The arrows indicate the direction of temperature variation. The time required to obtain data for a given curve varied between 30 minutes and 12 hours, depending upon the method of cooling and the number of observations made.

Fig. 3 shows that the sensitivity of the mercury to monochromatic light was practically independent of temperature in the region -190° to *ca.* -125° . Between the latter temperature and the melting point, -39°C , slight changes occur in the slopes of the sensitivity curves but these could not be reproduced at definite temperatures. They were found to be associated closely with changes in the level of the cooling agent surrounding the cell and with abrupt changes in the rate of warming and cooling. Experiments showed that contamination released from the walls of the cell lowered the sensitivity of the mercury. Abrupt changes in temperature had a marked effect on the appearance of the solid mercury surface, particularly when the mercury was near the melting point; thus it is very likely that such abrupt changes of temperature also affected the photoelectric efficiency of the mercury surface.

Nothing was observed in the region between -190° and -39°C that could be attributed to an allotropic change in the mercury. This excepts

¹¹ R. A. Millikan, *Phys. Rev.* 7, 380 (1916).

the slight decreases in sensitivity which always accompanied rises in temperature and which have been at least partly accounted for in other ways.

During melting and freezing the sensitivity of the mercury changed rapidly. In the region between -39° and 0° C the liquid mercury showed great susceptibility to some unknown contamination which lowered the sensitivity. The curves, Fig. 3, show so much hysteresis in this region that no conclusions can be made as to the effect of temperature on the liquid mercury. The contamination was of such a kind that it could be eliminated immediately from the mercury surface by heating the cell a few degrees above room temperature.

It is to be noted that the sensitivity of the solid mercury always was higher than that of the liquid at room temperature. Since the thresholds

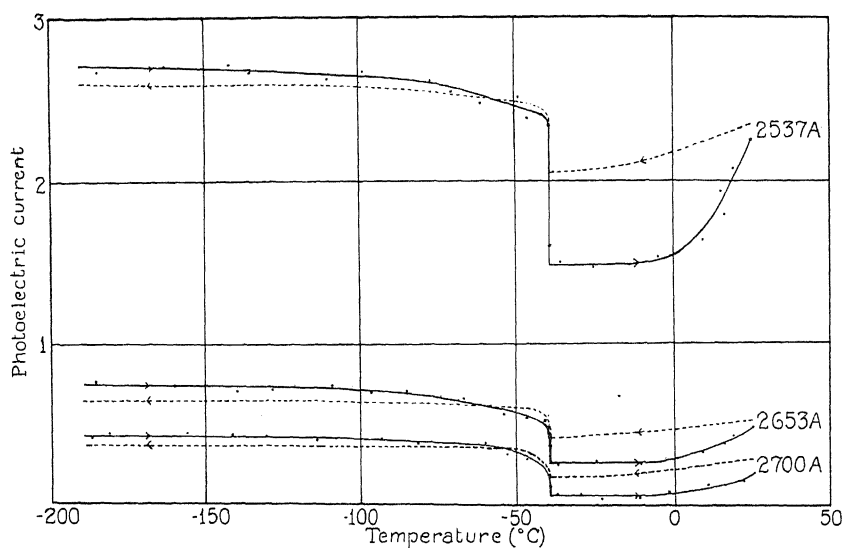


Fig. 3. Photoelectric current for lines 2537A, 2653A and 2700A as a function of temperature.

were found to be the same in the two cases, the higher sensitivity of the solid must be attributed to a change in the photoelectric efficiency of the mercury surface with change of state. This change in efficiency may be due to a change in the optical reflectivity of mercury with change of state. No exact information is at present available regarding the reflectivity of a very pure solid mercury surface formed in high vacuum although experiments are in progress. Haak and Sissingh¹² found no change in the optical constants of mercury either on freezing or in subsequent cooling down to -80° C, but the mercury surfaces used by them contained adsorbed layers of air.

This work was done in 1928 at the Norman Bridge Laboratory of Physics, California Institute.

It is a pleasure to acknowledge my indebtedness to Professor Millikan whose interest and guidance prompted the choice of subject and made the work possible.

¹² Haak and Sissingh, K. Akad. Amsterdam 21, 678 (1919).

THE THERMODYNAMIC TREATMENT OF CHEMICAL EQUILIBRIA IN SYSTEMS COMPOSED OF REAL GASES. I.
AN APPROXIMATE EQUATION FOR THE
MASS ACTION FUNCTION APPLIED
TO THE EXISTING DATA ON
THE HABER EQUILIBRIUM

BY LOUIS J. GILLESPIE AND JAMES A. BEATTIE

RESEARCH LABORATORY OF PHYSICAL CHEMISTRY, MASSACHUSETTS INSTITUTE OF TECHNOLOGY*

(Received June 30, 1930)

ABSTRACT

All of the equilibrium data on the ammonia synthesis reaction, which cover an extreme temperature range of from 325° to 952°C and an extreme pressure range (at some temperatures) of from 10 to 1000 atmospheres, are correlated with the compressibility and heat capacity data on the pure reacting gases by means of a rational and relatively simple equation for the mass action function K_p . In this equation the effect of temperature and of pressure on K_p are separated, the relation for the temperature effect being exact, but certain approximations being introduced for the sake of simplicity into the relation for the pressure effect.

All of the data on the ammonia synthesis equilibrium are represented within the experimental accuracy by the use of only two adjustable constants.

1. INTRODUCTION

THE use of high pressures in industrial chemical operations has disclosed numerous cases in which the deviations from the laws of ideal gases are of practical importance. We may mention the following two groups of phenomena:

1. When a vapor is condensed out of a gaseous mixture, more of the vapor has been found to remain uncondensed than would be expected from the laws of ideal gases. Typical cases¹ are the removal of ammonia from mixtures containing hydrogen and nitrogen, of carbon monoxide from water gas in the industrial preparation of hydrogen, and of nitrogen from nitrogen-hydrogen mixtures. The phenomenon has been studied by Pollitzer and Strebel,¹ Larson and Black,² Lurie and Gillespie,³ McHaffie,⁴ Eucken and Bresler,⁵ and Braune and Strassmann.⁶

2. In the fixation of nitrogen by the Haber process, the reaction for which is

* Contribution No. 245.

¹ Cited by Pollitzer and Strebel, *Zeits. f. phys. Chem.* **110**, 768 (1924).

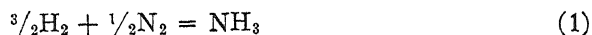
² Larson and Black, *J. Am. Chem. Soc.* **47**, 1015 (1925).

³ Lurie and Gillespie, *J. Am. Chem. Soc.* **49**, 1146 (1927).

⁴ McHaffie, *Phil. Mag.* (7) **1**, 561 (1926).

⁵ Eucken and Bresler, *Zeits. f. physik. Chem.* **134**, 230 (1928).

⁶ Braune and Strassmann, *Zeits. f. physik. Chem.* **143A**, 225 (1929).



there is a greater yield of ammonia as the pressure is increased than that calculated from the laws of ideal gases.^{7,8}

The deviations in these two classes of phenomena are due to the same cause, the failure of the ideal gas laws, and the explanation of one of these will furnish the basis for an understanding of the other. In the present paper we are interested in testing an improvement on the ideal-gas mass action law by the use of the existing data on the equilibrium of the chemical reaction given in Eq. (1).

Much of the interest in the mass action law has been confined to the case of solutions of electrolytes. In this laboratory, however, Keyes⁹ has for some years been collecting and correlating the compressibility data on gases in realization of their importance to chemistry in connection with the mass action law.

The thermodynamic connection between the mass action law and the pressure-volume-temperature relations for pure gases and gas mixtures has been given,¹⁰ the general relation being:

$$RT \ln (K_p/K_p^*) = - \sum \left\{ \nu_i \int_0^p [(dV/dn_i)_{T,p,n} - RT/p] dp \right\} \quad (2)$$

in which K_p is the "equilibrium constant" at the pressure p , and is defined by the relation:

$$\ln K_p = \sum (\nu_i \ln p x_i) \quad (3)$$

and K_p^* is the limiting value of K_p as the pressure on any mixture maintained in equilibrium is isothermally decreased to zero. The quantity ν_i is the coefficient of the substance i in the chemical equation for the given reaction and is negative if the substance disappears; x_i the mole fraction of substance i in the equilibrium mixture; and $(dV/dn_i)_{T,p,n}$ the partial molal volume of gas i in the mixture. A relation¹¹ for K_p in terms of the independent variables V and T is:

$$RT \ln (K_p/K_p^*) = \sum (\nu_i) RT \ln \frac{pV}{\sum (n_i) RT} - \sum \left\{ \nu_i \int_V^\infty [(dp/dn_i)_{V,T,n} - RT/V] dV \right\} \quad (4)$$

⁷ Larson and Dodge, *J. Am. Chem. Soc.* **45**, 2918 (1923).

⁸ Larson, *J. Am. Chem. Soc.* **46**, 367 (1924).

⁹ Keyes, *Am. Soc. Refrig. Eng. J.* **1**, 9 (1914); *Proc. Nat. Acad. Sci.* **3**, 323 (1917); Keyes and Felsing, *J. Am. Chem. Soc.* **41**, 589 (1919); *ibid.* **42**, 106 (1920); Smith and Taylor, *J. Am. Chem. Soc.* **45**, 2107 (1923); *ibid.* **48**, 3122 (1926); Beattie, *J. Am. Chem. Soc.* **46**, 342 (1924); Keyes and Burks, *J. Am. Chem. Soc.* **49**, 1403 (1927).

¹⁰ Gillespie, *J. Am. Chem. Soc.* **47**, 305 (1925), *ibid.* **48**, 28 (1926).

¹¹ Beattie, *Phys. Rev.* **31** 680 (1928), *ibid.* **3μ** 691 (1928). In Eq. 5 a new entropy constant has been used, as will be discussed in Part II.

wherein K_p^* is related to the temperature by the relation:

$$\ln K_p^* = \sum (\nu_i) (\ln T/T_0 - 1) - \frac{1}{RT} \sum \left\{ \nu_i \left[\int_{T_0}^T C_{V,i}^* dT - T \int_{T_0}^T \frac{C_{V,i}^*}{T} dT + u'_{0i} - Ts'_{0i} \right] \right\} \quad (5)$$

in which $C_{V,i}^*$ is the heat capacity at constant volume for gas i at zero pressure, and u'_{0i} and s'_{0i} are constants for gas i . These relations depend upon two assumptions¹² and the general laws of thermodynamics.

We may evaluate the partial derivatives of equations (2) or (4) graphically, by approximate methods, or from an equation of state of mixtures.

It has been shown¹⁰ that if the Lewis and Randall rule¹³ for calculating the fugacity of a gas in a mixture holds, then the partial derivative of Eq. (2) may be replaced by the molal volume of the pure gas at the temperature and pressure of the mixture, and Eq. (2) reduces to the simple, approximate relation:

$$RT \ln (K_p/K_p^*) = \sum \left\{ \nu_i \int_0^p [(RT/p) - (V_i/n_i)] dp \right\} \quad (6)$$

The differences between the molal volume and the partial molal volume have been studied for several mixtures.¹⁴ A further approximation of (6) is obtained by assuming the integrand constant during the integration and equal to its limiting value at zero pressure, which can be calculated from an equation of state for mixtures. The equation is^{10,15}

$$RT \ln (K_p/K_p^*) = - \sum \{ \nu_i (B_{0i} - A_{0i}/RT - c_i/T^3) \} p \quad (7)$$

where R is the ideal gas constant and B_{0i} , A_{0i} and c_i are equation of state constants for gas i .

Keyes¹⁶ has given an equation for the mass action function K_p for gases whose isometrics are linear by use of the kinetic considerations from which the Keyes equation of state was derived.⁹ Application of this equation to the Haber equilibrium data showed a tolerable agreement up to 600 atmospheres.

Gibson and Sosnick¹⁷ and Merz and Whittaker¹⁸ have calculated the fugacity of a gas in a mixture by graphic methods. In order to carry out the computation it is necessary to make some assumption regarding the expansion of gases on mixing at infinitely low pressures. They assumed this to be zero but this assumption is not supported¹⁴ by the experimental data.

Van der Waals hoped to determine an equation of state for gas mixtures from the equations of state of the gas constituents together with two

¹² Beattie, *Phys. Rev.* **36**, 132 (1930).

¹³ Lewis and Randall, *Thermodynamics and the Free Energy of Chemical Substances*. McGraw-Hill Book Co., New York, 1923, p. 226.

¹⁴ Gillespie, *Phys. Rev.* **34**, 352 (1929).

¹⁵ Gillespie, *Phys. Rev.* **34**, 1605 (1929).

¹⁶ Keyes, *J. Am. Chem. Soc.* **49**, 1393 (1927).

¹⁷ Gibson and Sosnick, *J. Am. Chem. Soc.* **49**, 2172 (1927).

¹⁸ Merz and Whittaker, *J. Am. Chem. Soc.* **50**, 1522 (1928).

adjustable constants, characteristic of every binary combination of constituents, the so-called interaction constants. Various methods for calculating these interaction constants from the values of the corresponding constants for the pure gases have been suggested. Keyes, working with an equation of state⁹ better adapted to representation of the compressibilities of the pure gases, found that a very simple method of calculating the interaction constants sufficed for the representation of the pressures of mixtures of methane and nitrogen measured by Keyes and Burks.¹⁹ Lurie and Gillespie³ were successful with the same method in accounting for their measurements of the effect of nitrogen on the vapor pressure of the system: barium chloride, barium chloride octamine. The necessary parameters for the gas mixture are calculated by a simple scheme, which may be designated as linear combination of constants:

$$k_x = k_1x_1 + k_2x_2 + \cdots = \Sigma(k_ix_i) \quad (8)$$

where k_x represents the parameter for the mixture and k_1, k_2, \cdots , represent the corresponding constants for the pure gases. All the constants for pure gases are dimensionally of the first power in the volume, except the cohesive pressure constant A , which is of the square of the volume. The linear combination rule is applied as above to the square root of the cohesive pressure constant, and directly to the others. A fuller discussion of the work of earlier investigators on the calculation of interaction constants is given elsewhere.²⁰ By means of this linear combination of constants we are able to calculate the values of the parameters for a mixture when the composition of the mixture and the constants of the pure gases are known, without the introduction of arbitrary constants.

In a series of investigations from this laboratory^{14,20,21} it has been found that when this scheme is applied in connection with the Beattie-Bridgeman equation of state²² the pressure-volume-temperature data on mixtures are represented very well, possibly within the experimental error. For chemical purposes it appears that a much smaller degree of success would suffice, as evidenced by the success obtained¹⁰ in representing the Haber equilibrium data to 100 atmospheres by the use of Eqs. (6) or (7).

Eq. (4) can be integrated¹¹ in terms of elementary functions by use of the Beattie-Bridgeman equation of state for mixtures. The equilibrium constant is expressed in terms of the temperature and the volume of the equilibrium mixture. This latter quantity must be computed from the equation of state, since the data are always given in terms of pressure and temperature, and hence an expression in terms of these latter variables is desirable. Eq. (2) gives such an expression, but the integration cannot be carried out in terms of elementary functions of the pressure and temperature from any of the usual equations of state.

¹⁹ Keyes and Burks, *J. Am. Chem. Soc.* **50**, 1100 (1928).

²⁰ Beattie and Ikehara, *Proc. Amer. Acad. Arts and Sci.* **64**, 127 (1930).

²¹ Beattie, *J. Am. Chem. Soc.* **51**, 19 (1929).

²² Beattie and Bridgeman, *Proc. Amer. Acad. Arts and Sci.* **63**, 229 (1928); *J. Am. Chem. Soc.* **50**, 3133 (1928); *Zeits. f. Physik*, **62**, 95 (1930).

II. A SIMPLE MASS ACTION EQUATION

A simple form of the mass action equation, explicit in the pressure, has been obtained¹⁵ by approximate integration of Eq. (2), and evidence given that this equation should furnish a very good approximation. The equation is

$$\ln K_p = \ln K_p^* - \left\{ \sum [\nu_i (B_{0i} - A_{0i}/RT - c_i/T^3)] + \sum [\nu_i (A^{1/2}_{0i} - \sum x_i A^{1/2}_{0i})^2/RT] \right\} p/RT \quad (9)$$

The same expression results if Eq. (2) is integrated by one form²³ of the Beattie-Bridgeman equation of state which expresses V as an explicit function of p and T , and if then terms containing powers of p higher than the first are dropped. Except for the terms involving the constant c , which does not occur in the Keyes equation of state, the above Eq. (9) is also equivalent to an approximate equation given by Keyes.¹⁶

For the quantity K_p^* which occurs in (9) we may use Eq. (5) which expresses K_p^* in terms of the energy and entropy constants and the heat capacities of the reacting gases. Or we may follow more closely the familiar treatment for ideal gases. One has every reason to expect that at very low pressure the van't Hoff isochor will hold. This we will write:

$$d \ln K_p^*/dT = \Delta H^*/RT^2. \quad (10)$$

Here ΔH^* is the heat absorbed in the reaction at zero pressure, and the derivative may be regarded as a total derivative. Kirchoff's law for the temperature coefficient of the heat of reaction is

$$d\Delta H^*/dT = \Delta C_p^* = \sum (\nu_i C_{p_i}^*). \quad (11)$$

In general C_p^* , the limiting value at zero pressure of the constant pressure specific heat, may be sufficiently well expressed as a function of the temperature by a series expansion:

$$C_{p_i}^* = R + A_i + B_i T + C_i T^2 \quad (12)$$

where R is the ideal gas constant and A_i , B_i , and C_i are constants for each gas.

Substituting (12) into (11) and integrating we obtain:

$$\Delta H^* = [\sum (\nu_i A_i) + \sum (\nu_i) R] T + \frac{1}{2} \sum (\nu_i B_i) T^2 + \frac{1}{3} \sum (\nu_i C_i) T^3 + I'. \quad (13)$$

Substitution of (13) into Eq. (10) and another integration give:

$$\ln K_p^* = \frac{\sum (\nu_i A_i) + \sum (\nu_i) R}{R} \ln T + \frac{\sum (\nu_i B_i)}{2R} T + \frac{\sum (\nu_i C_i)}{6R} T^2 - \frac{I'}{RT} + J' \quad (14)$$

Eq. (14) can be rearranged into the form

$$\log_{10} K_p^* - \frac{\sum (\nu_i A_i) + \sum (\nu_i) R}{R} \log_{10} T - \frac{M \sum (\nu_i B_i)}{2R} T - \frac{M \sum (\nu_i C_i)}{6R} T^2 = \frac{I}{T} + J \quad (15)$$

where M is the modulus of the common logarithms, 0.43429, \dots $I = -MI'/R$ and $J = MJ'$.

When an expansion similar to (12) (but omitting the constant R) is substituted into Eq. (5) for C_{V_i} , a relation similar to (15) results in which I

²³ Beattie, Proc. Nat. Acad. Sci. 16, 14 (1930).

and J are related to the energy and entropy constants of the reacting gases. These relations will be considered in a later paper.

III. TREATMENT OF THE DATA

Eqs. (9) and (15) are the basis for the present calculations. The former relation contains only the equation of state constants of the reacting gases, while the latter contains the heat capacity constants for the reacting gases and two arbitrary constants. Thus for the calculations of the effect of both pressure and temperature on the Haber equilibrium there are used only two adjustable constants, I and J , one of which might have been determined from a heat of reaction.

The data treated are those of Haber²⁴ which are at 30 atmospheres and extend from 561 to 952°C; and those of Larson and Dodge⁷ and of Larson⁸ (working at the Fixed Nitrogen Laboratory) which extend from 10 to 1000 atmospheres and from 325 to 500°C.

The equation of state constants for the various gases have been determined²⁵ from the available compressibility data, and are given in Table I.

TABLE I. *Values of the equation of state constants for the reacting gases. Units: normal atmospheres, liters per mole, degrees Kelvin ($T^{\circ}\text{K} = t^{\circ}\text{C} + 273.13$), $R = 0.08206$.*

Gas	A_0	B_0	c
Hydrogen	0.1975	0.02096	0.0504×10^4
Nitrogen	1.3445	0.05046	4.20×10^4
Argon	1.2907	0.03931	5.99×10^4
Ammonia	2.3930	0.03415	476.87×10^4

It will be noted that the constants for argon have been included. The reactant gas mixtures of hydrogen and nitrogen used by Haber, Larson and Dodge, and Larson contained 0.3 volume percent (which we shall assume to mean 0.3 mole percent) of argon. This argon must be taken into account in the calculation of the mole fractions of the gases composing the equilibrium mixtures from the stated analytical results, and must be included in the summation $\Sigma(x_i A_{0i}^{1/2})$ of Eq. (9); but does not enter elsewhere.

Larson and Dodge, and Larson calculated values of K_p from their analytical results by use of an approximate formula²⁶ that introduced errors which are now seen to be greater than those of experiment. Accordingly the values of K_p for these data were recalculated by use of the exact expression

$$K_p = \frac{\alpha/(1 + \alpha)^2}{[q - 3\alpha/2(1 + \alpha)]^{3/2} [r - \alpha/2(1 + \alpha)]^{1/2} p} \quad (16)$$

where α is the mole fraction of ammonia in the equilibrium mixture, q and r are the mole fractions of hydrogen and nitrogen in the reactant gas mixture,

²⁴ Haber, *Zeits. f. Elektrochemie* 21, 89 (1915).

²⁵ See reference (22) for the constants for H_2 , N_2 , and A. The values of the constants for NH_3 are given by Beattie and Lawrence, *J. Am. Chem. Soc.* 52, 6 (1930).

²⁶ Gillespie, *Jour. Math. and Phys.* 4, 84 (1925), especially p. 95.

being 0.762 and 0.235 respectively for these data. The values of K_p given by Haber were also checked by use of (16) and the given analytical data, the values of q and r being 0.752 and 0.245 for these data.

From the mole fraction of the gases in the equilibrium mixtures and the equation of state constants given in Table I, a value of K_p^* was calculated by use of Eq. (9) corresponding to each "measured" value of K_p (computed from Eq. (16)). At each temperature the values of K_p^* resulting from the treatment of the data at that temperature should be the same within the experimental error if Eq. (9) represents the pressure variation of K_p .

In order to correlate the values of K_p^* at different temperatures with the aid of Eq. (15) the specific heat constants A_i , B_i , and C_i were derived from the empirical equations of other observers, the reduction from 1 atmosphere to zero pressure being made by use of the relation

$$c_p = c_p^* + \left[\frac{2A_0}{RT^2} + \frac{12C}{T^4} \right] p \quad (17)$$

which gives sufficiently well the effect of pressure on specific heat.²⁷ These constants are given in Table II.

TABLE II. Values of the heat capacity constants of Eq. (12). Units: 15° calories per mole and per degree C; $R=1.986847$.

Gas	A	10°B	10°C	Ref.
Hydrogen	4.66	0.70	0.00	28
Nitrogen	4.82	0.33	0.05	29
Ammonia	6.04	0.71	5.10	30

The values of the left hand member of Eq. (15) were computed using the values of K_p^* obtained as described above and this quantity plotted against $1/T$. The values of the two adjustable constants I and J were determined from the best straight line drawn through the points, the deviations of the observed points from this line being shown in Fig. 1.

Knowing the two constants I and J we can compute K_p for any pressure and temperature by use of Eqs. (9) and (15). When the numerical values of all of the constants are included these equations become:

²⁷ Beattie, Phys. Rev. **34**, 1615 (1929).

²⁸ Partington and Shilling, "The Specific Heat of Gases", Van Nostrand, New York, 1924, p. 209.

²⁹ Partington and Shilling, *ibid.* p. 145. See also Shilling and Partington, Phil. Mag. (7) **6**, 920 (1928).

³⁰ Haber and Tamaru, Zeits. f. Elektrochemie **21**, 228 (1915). The values of C_p calculated by extrapolating the equation of Haber and Tamaru do not agree very well with the measurements of Osborne, Stimson, Sligh and Cragoe, Scientific Papers of Bureau of Standards **20**, 65 (1925). However the integral of $C_p^* dT$ from 0° to 150°C is in rather good agreement with the integrated value obtained from the results of the latter investigators, the difference being 3.7 calories per mole. The constants given are sufficiently accurate for our purposes.

$$\log_{10} K_p/K_p^* = \left[\frac{0.1191849}{T} + \frac{25122730}{T^4} + \frac{38.76816}{T^2} \Sigma(x_i A_{0i}^{1/2}) + \frac{64.49429}{T^2} (\Sigma x_i A_{0i}^{1/2})^2 \right] p \quad (18)$$

$$\log_{10} K_p^* = -2.691122 \log_{10} T - 5.519265 \times 10^{-5} T + 1.848863 \times 10^{-7} T^2 + \frac{2001.6}{T} + 2.6899 \quad (19)$$

where p is in atmospheres and T in degrees Kelvin; while x_i is the mole fraction of gas i in the equilibrium mixture and for A_{0i} is used the numerical value of A_0 for gas i given in Table I. In the summation $\Sigma(x_i A_{0i}^{1/2})$ the argon

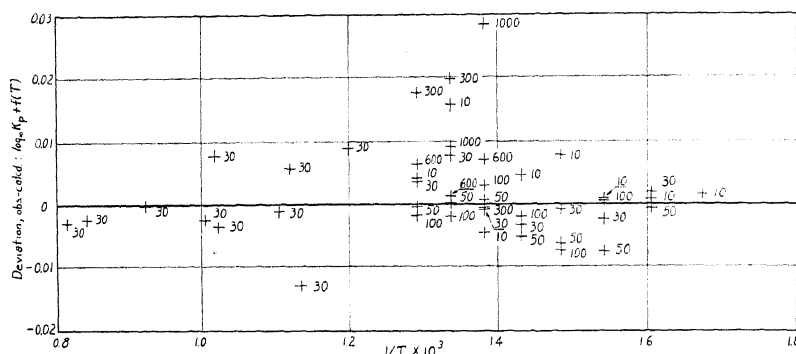


Fig. 1. Deviation of the observed value of $\log_{10} K_p + f(T)$, the left hand member of Eq. (15) from the best straight line through the points.

must be included. In evaluating this summation the experimental values were used for the x_i 's. This introduces a slight inconsistency since the values of x_i used in Eq. (18) should be those resulting from the solution of this equation. However the differences between the experimental and calculated values of x_i were sufficiently small so that the use of the latter values would in no case change the last figure given for α by more than one unit and this only at the highest pressures.

In Table III are given the values of the percentages of ammonia in the equilibrium mixture α computed from the "calculated" values of K_p resulting from Eqs. (18) and (19). There are also given the observed percentages, and in the last column the percentage deviation (percentage based on the observed mole percent of ammonia found in the equilibrium mixture). For the calculation of α from K_p , which is tedious to make directly, an approximate correction formula was derived by logarithmic differentiation of Eq. (16), which gives:

$$\Delta \alpha = \frac{2.3026 \Delta \log_{10} K_p}{\frac{1}{\alpha} - \frac{2}{1+\alpha} + \left[\frac{1}{1+\alpha} \right]^2 \left[\frac{2.25}{q - 3\alpha/2(1+\alpha)} + \frac{0.25}{r - \alpha/2(1+\alpha)} \right]} \quad (20)$$

TABLE III. Comparison of observed and calculated values of the mole percentages of ammonia in the equilibrium mixture.

The "calculated" values of the mole percentage of ammonia α give when substituted in Eq. (16) the values of K_p computed from Eqs. (18) and (19), and may be regarded as the best available values of α .

Temperature °C	Pressure atm.	Mole percent of ammonia in equilibrium mixture.		
		Observed	Calculated	100 $\frac{\text{obs.}-\text{calcd.}}{\text{obs.}}$
(a) Data of Fixed Nitrogen Laboratory: $q=0.762$, $r=0.235$.				
325	10	10.38	10.35	+0.29%
350	10	7.35	7.34	+0.14
	30	17.80	17.75	+0.28
	50	25.11	25.14	-0.12
375	10	5.25	5.24	+0.19
	30	13.35	13.41	-0.45
	50	19.44	19.66	-1.13
400	100	30.95	30.92	+0.10
	10	3.85	3.79	+1.56
	30	10.09	10.10	-0.10
425	50	15.11	15.27	-1.06
	100	24.91	25.16	-1.00
	10	2.80	2.77	+1.07
450	30	7.59	7.64	-0.66
	50	11.71	11.82	-0.94
	100	20.23	20.29	-0.30
475	10	2.04	2.06	-0.98
	30	5.80	5.81	-0.17
	50	9.17	9.16	+0.11
	100	16.35	16.27	+0.49
	300	35.5	35.5	± 0.00
	600	53.6	53.3	+0.56
500	1000	69.4	68.6	+1.15
	10	1.61	1.55	+3.73
	30	4.53	4.46	+1.55
	50	7.13	7.13	± 0.00
	100	12.98	13.02	-0.31
	300	31.0	30.3	+2.26
	600	47.5	47.4	+0.21
	1000	63.5	63.2	+0.47
561	10	1.20	1.19	+0.83
	30	3.48	3.45	+0.86
	50	5.58	5.58	± 0.00
	100	10.40	10.43	-0.29
	300	26.2	25.6	+2.29
	600	42.1	41.9	+0.48
(b) Data of Haber: $q=0.752$, $r=0.245$.				
561	30	1.97 _s	1.93 _g	+1.98
607	30	1.270	1.307	-2.91
620	30	1.192	1.177	+1.25
631	30	1.07 ₆	1.07 ₉	-0.28
704	30	0.627 ₆	0.632 ₆	-0.80
710	30	0.618 ₁	0.607 ₃	+1.75
722	30	0.557 ₆	0.560 ₃	-0.57
812	30	0.324 ₈	0.324 ₉	-0.03
914	30	0.192 ₁	0.193 ₂	-0.57
952	30	0.161 ₇	0.162 ₃	-0.68

by means of which the change in the mole fraction of ammonia in the equilibrium mixture $\Delta\alpha$ can be computed for a given change in $\log K_p$. Thus from each observed value of α and K_p , a value of α corresponding to the "calculated" K_p was obtained. This procedure was checked in several cases by calculation of K_p by substitution of the corrected values of α into Eq. (16).

In Fig. 2 is given a plot of the percentage deviation between the observed and calculated mole percentages of ammonia in the equilibrium mixture.

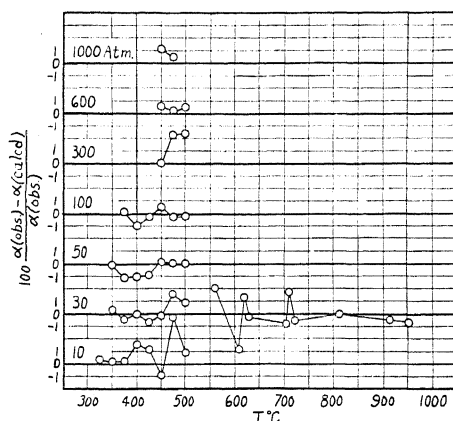


Fig. 2. Percentage deviation in the percentage α of ammonia in the equilibrium mixture. Each ordinate division represents 1%. A heavy base line representing zero deviation is used for each isobar.

IV. DISCUSSION OF THE RESULTS

The results of the calculations reported in Table III and exhibited in Figs. 1 and 2 may be briefly summarized as follows.

The average deviation in K_p for the results of the Fixed Nitrogen Laboratory is 1.18% and for those of Haber 1.09%, the average for all measurements being 1.16%. The distribution of positive and negative deviations is fairly good and it should be noted that with the exception of one point, the greatest errors do not occur at the extremes of pressure or temperature. This indicates that the equation is not failing progressively as the pressure or temperature is increased.

There is no indication of a discontinuity between the low pressure data of Larson and Dodge and the high pressure data of Larson. The discontinuity previously observed²⁶ in empirical smoothing was evidently produced by the use of inappropriate variables for the correlation. This is a case in which rational aid was clearly required for the discovery of appropriate variables.

The average difference between the observed and calculated mole percentages of ammonia in the equilibrium mixture, in percent of the observed mole percentage, is 0.73% for the Fixed Nitrogen Laboratory data, 1.08% for the Haber data, and 0.80% for both sets. We believe that this is well within the experimental accuracy of the measurements.

The calculated values of K_p and likewise of the percentage of ammonia α in the equilibrium mixture may be regarded as the best value deducible from the existing experimental observations. Our equation indicates that K_p and α depend on other variables than the temperature and pressure, for instance on the composition of the reactant gas mixture used in the production of ammonia (or on the equilibrium composition). Consequently Eq. (18) contains more information than can be presented in the form of a table such as Table III. This will be treated in a later paper.

V. CALCULATION OF THE COMPOSITION OF THE EQUILIBRIUM MIXTURE FROM THE INITIAL COMPOSITION

The calculation of the composition of the equilibrium mixture from the initial composition of the reacting mixture cannot be very conveniently made from Eq. (9), since the x_i 's in this relation are the equilibrium concentrations. However the last term of (9) is small¹⁰ in comparison with the other terms and may be neglected for a first approximation, giving Eq. (7) which does not contain any compositions. Thus in order to compute the composition of the equilibrium mixture at any pressure and temperature when the equation of state constants and the heat capacities of the reacting gases are given and the two constants I and J are known, we proceed as follows:

- (1) Compute a provisional value of K_p by use of Eqs. (7) and (15).
- (2) Calculate the corresponding provisional composition of the equilibrium mixture from the equation connecting K_p and these compositions. For the ammonia synthesis equilibrium this relation is Eq. (16).
- (3) Using these provisional equilibrium concentrations calculate a more exact value of K_p by use of Eq. (9), and correct the provisional equilibrium concentrations by use of an approximate correction formula similar to Eq. (20). In general even at the highest pressures no further approximation will be necessary. If required, however, these corrected equilibrium concentrations can be substituted again into Eq. (9) and a final value for K_p computed.

For the Haber equilibrium Eq. (7) becomes

$$\log_{10} K_p/K_p^* = \left[\frac{0.1191849}{T} + \frac{91.87212}{T^2} + \frac{25122730}{T^4} \right] p. \quad (21)$$

At 475°C and 1000 atmospheres Eq. (21) gives 0.01250 for K_p and the corresponding provisional value for α is 60.5%. From (18) and the provisional composition we find a value of 0.01483 for K_p , or 62.9% for α . One further approximation gives for the mol percent of ammonia at equilibrium, 63.2%, which is identical with the value given in Table III. For this calculation we have used $q = 0.762$ and $r = 0.235$ in Eqs. (18) and (20).

THE DIELECTRIC CONSTANT OF CARBON DIOXIDE AS
A FUNCTION OF TEMPERATURE AND DENSITY¹

BY FREDERICK G. KEYES AND JOHN G. KIRKWOOD**

RESEARCH LABORATORY OF PHYSICAL CHEMISTRY, MASSACHUSETTS INSTITUTE
OF TECHNOLOGY*

(Received June 12, 1930)

ABSTRACT

The dielectric constant of carbon dioxide has been measured over a wide range of temperature and density. It has been found that the Clausius-Mosotti function $(\epsilon-1)V/(\epsilon+2)$, although independent of temperature increases slowly with increasing density.

THE polarization of molecules by an homogeneous electric field has received adequate theoretical treatment. Both classical mechanics² and quantum mechanics³ lead to the following expression for the mean electric moment, m , of a molecule in weak fields at moderately high temperatures:

$$m = \left(\alpha + \frac{\mu^2}{3kT} \right) F$$

where F is the field strength, α the sum of the electronic and atomic polarizabilities, μ the permanent electric moment of the molecule, k Boltzmann's constant, and T the absolute temperature. The applicability of the above expression is further limited by the requirements that the frequency of the applied field be lower than any of the characteristic frequencies of the molecule, and that no transitions in internal atomic and electronic energy states occur with changing temperature.

The theory has been used with a large measure of success in the study of the molecular structure of gases of low density and of substances in dilute solution. In these cases the internal polarizing field may be calculated with very little ambiguity, and it is possible to obtain a relation between the dielectric constant of the substance and the constants α and μ of its constituent molecules.

The application of the theory to gases at high densities as well as to liquids and solids, has, however, been attended by great uncertainty because of the difficulty in calculating the average internal field effective in polar-

** National Research Fellow.

* Contribution No. 231.

¹ Preliminary work on air at low densities was carried out by Miss Charlotte T. Perry who constructed the first gas cell and measuring circuits.

² P. Debye, *Handbuch der Radiologie* 6, 600 (1925).

³ J. H. Van Vleck, *Phys. Rev.* 29, 727 (1927).

izing a molecule. The only guide in this matter has been the Clausius-Mosotti relation, which gives the molecular polarization as

$$\frac{\epsilon - 1}{\epsilon + 2}V = \frac{4\pi N}{3} \left(\alpha + \frac{\mu^2}{3kT} \right)$$

where N is the Loschmidt number, ϵ the dielectric constant, and V the molal volume. Several attempts have been made to verify the Clausius Mosotti law experimentally. Measurements of Tangl⁴ indicate that is valid up to a hundred atmospheres for air, nitrogen, and hydrogen at 20°C. It is to be noted, however, that the largest of his values of $\epsilon - 1$ are still so small that it is evident that the contribution of the polarization of the dielectric to the internal field is very small relative to the contribution of the external applied field. Measurements of Phillips⁵ on the refractive index of

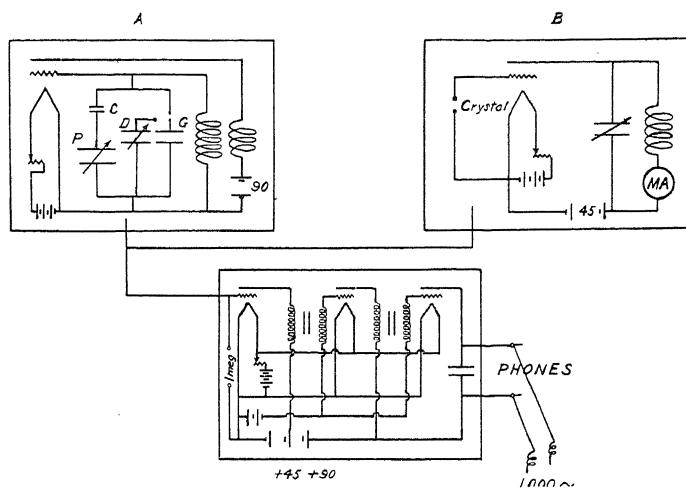


Fig. 1. Diagram of oscillator circuits.

carbon dioxide indicate that the corresponding Lorentz-Lorenz relation is valid even as far as the critical density for this substance. But the great experimental difficulties involved in the measurement of the refractive indices of compressed gases would make a verification of the values desirable.

In the present paper measurements of the dielectric constant of carbon dioxide over a wide range of temperature and density will be presented. We believe that they throw an important light on the limitations of the Clausius-Mosotti law, which the customary deduction, depending upon the cavity method for calculating the internal field, does more than suggest.

METHODS AND APPARATUS

Measurements of the dielectric constant were carried out by a resonance method which depended upon counting the beats between two heterodyne

⁴ K. Tangl, *Ann. d. Physik* **29**, 59 (1908).

⁵ P. Phillips, *Proc. Roy. Soc. A* **47**, 225 (1920).

oscillators. Since this method has been widely used in recent years, a detailed description will not be undertaken. The oscillator circuits (Fig. 1) were similar to those of Zahn.⁶ Oscillator *A* contained a condenser circuit consisting of the precision condenser *P*, the fixed mica condenser *C*, the gas condenser *G*, and the counterpoise condenser *D*. The precision condenser was a General Radio Variable Air Condenser, type 220, calibrated at the

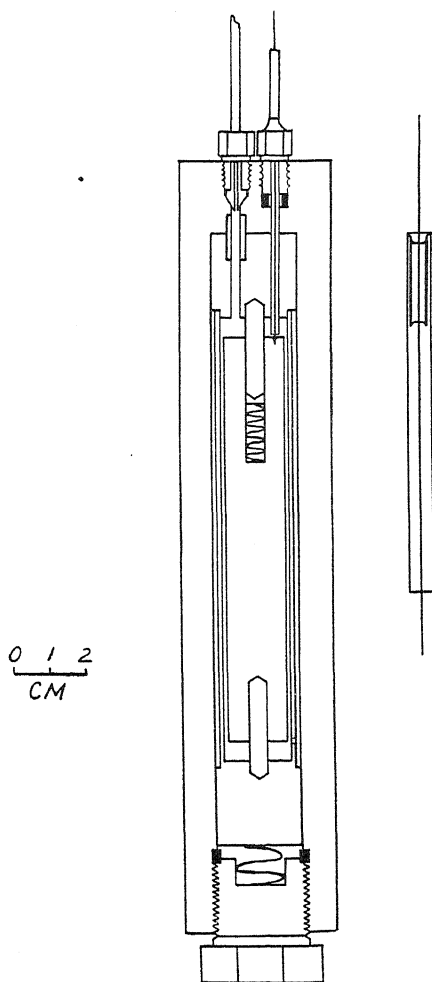


Fig. 2. Diagram of gas condenser.

Bureau of Standards. Sangamo fixed mica condensers of capacity appropriate to the magnitude of the dielectric constant to be measured occupied the position of *C*. All auxiliary capacities were calibrated in terms of the precision condenser at the working frequency. Oscillator *B* was maintained at a constant frequency of 1010 k.c. by means of a General Radio quartz crystal. The heterodyne note was amplified and then compared with the

⁶ C. T. Zahn, Phys. Rev. 23, 781 (1924).

1000 cycle note of a mechanical oscillator. The resulting beats were counted in telephone receivers.

The gas condenser, Fig. 2, was constructed of chrome vanadium steel. The high potential side consisted of a solid cylinder held in position by two quartz supports, conically ground at both ends and fitting accurately into the end members of the cell. The low potential side of the condenser consisted of a shell, one millimeter in thickness. The separation of the cylinder and shell was 0.3 mm. The length of the condenser was 16 cm. The entire cell was surrounded by a steel jacket which bore the stress of the pressure, reducing the elastic deformation of the condenser itself to a minimum. The correction for deformation due to compression of the walls never amounted to more than one percent of $\epsilon - 1$. The outer jacket was closed at the lower end and made pressure tight by means of an aluminum washer. The insulating joint, inset Fig. 2, which carried a lead from the oscillator to the inner cylinder of the condenser was constructed in the following manner. A two centimeter length of two millimeter steel tubing was welded into a seven centimeter length of three millimeter steel tubing. This was silver soldered into a fitting which was later made tight in the head of the gas cell by means of an aluminum washer. A section of lead glass capillary coated with a flux of the same coefficient of expansion as the steel was fused to the inner tube and around the platinum wire leading from the inner cylinder of the condenser. Below the seal, the lead was protected by a length of quartz capillary extending down to the point where it was made fast in the cylinder.

The free capacity of the gas cell was found to be $167.4\mu\mu f$. It was roughly calculated to be $165\mu\mu f$ from the dimensions of the cell.

The temperature of the gas cell was controlled in an oil bath of large heat capacity by means of a mercury regulator. Temperatures were measured with a platinum resistance thermometer.

The pressure line was constructed of Shelby steel tubing with double cone connections. Connection with the pressure gauge, of the floating piston type,⁷ was made through a mercury-in-steel U.

At the beginning of a series of measurements the oil bath was brought to the desired temperature and the variable condenser D was adjusted to the same capacity as the evacuated gas cell. They could be alternately inserted into the oscillator circuit by a switch of small capacity. Gas was then admitted from a steel reservoir in the pressure line, and the pressure brought approximately to the desired value by heating or cooling the reservoir. It was finally adjusted to the proper value by means of a mercury piston compressor. From the two readings of the precision condenser with G and D alternately in the circuit, the dielectric constant could be calculated. After completing a measurement, the pressure was increased by means of the mercury piston and measurements made at regular pressure intervals. The use of the counterpoise condenser D made it possible to compensate

⁷ F. G. Keyes and Brownlee, *Thermodynamic Properties of Ammonia*, Wiley and Sons 1916. F. G. Keyes and J. Dewey, *J.O.S.A.* 14, 491 (1927).

for drift in the oscillator between measurements. The dielectric constant was calculated by the following formula, evident from the condenser circuit:

$$\epsilon - 1 = \frac{C^2(P_2 - P_1)}{(P_1 + C)(P_2 + C)G_0}$$

Here P_1 and P_2 are the two readings of the precision condenser, C the capacity of the fixed condenser, and G_0 the free capacity of the gas condenser.

For each series of measurements, the function $(\epsilon - 1)/(\epsilon + 2)$ was plotted against the density. The point at which the extrapolated line intercepted the axis of $(\epsilon - 1)/(\epsilon + 2)$ was taken as the zero point to which all of the values of $\epsilon - 1$ were referred. The intercept was in every series of measurements small and sometimes negligible. It was evidently the result of an initial extraneous capacity change attending the introduction of the gas, caused by incomplete temperature equilibrium in the evacuated gas cell.

EXPERIMENTAL RESULTS

Measurements of the dielectric constant of carbon dioxide were made upon the gas at 35°, 70°, 100°; and upon the liquid at 0°. The results are listed in the following tables.

TABLE I. *Measurements on gaseous carbon dioxide at 100°.*

Pressure (atm.)	$\epsilon - 1$	Molal volume (cc)	Density (mols/liter)	$\frac{\epsilon - 1}{\epsilon + 2} V$
10	0.00753	2991	0.33	7.485
20	.01549	1461	.68	7.505
30	.02404	947	1.06	7.528
40	.03333	691	1.45	7.593
50	.04306	535	1.87	7.570
60	.05269	434	2.30	7.491
70	.06447	361	2.77	7.595
80	.07707	306	3.27	7.664
90	.09005	263	3.80	7.664
100	.1041	229	4.37	7.687
126	.1456	167	5.99	7.730
151	.1912	129	7.75	7.729

TABLE II. *Measurements on gaseous carbon dioxide at 70°.*

Pressure (atm.)	$\epsilon - 1$	Molal volume (cc)	Density (mols/liter)	$\frac{\epsilon - 1}{\epsilon + 2} V$
10	0.00831	2728	0.37	7.536
20	.01717	1321	.76	7.517
30	.02693	842	1.19	7.491
40	.03748	606	1.65	7.478
50	.04950	464	2.16	7.532
60	.06305	369	2.71	7.596
70	.07810	300	3.33	7.612
80	.09616	248	4.03	7.702
90	.1159	207	4.83	7.699
100	.1396	173	5.78	7.693
126	.2165	115	8.70	7.739
151	.3072	84.7	11.81	7.868

TABLE III. Measurements on gaseous carbon dioxide at 35°.

Pressure (atm.)	$\epsilon - 1$	Molal volume (cc)	Density (mols/liter)	$\frac{\epsilon - 1}{\epsilon + 2} V$
10	0.00971	2352	0.43	7.588
20	.02021	1135	.88	7.595
30	.03228	713	1.40	7.590
40	.04649	497	2.07	7.584
50	.06461	363	2.75	7.653
60	.08838	269	3.72	7.698
70	.1309	191	5.24	7.986
80	.3146	88.5	11.23	7.986
90	.4206	65.6	15.24	8.066
100	.4559	58.3	17.15	7.691

TABLE IV. Measurements on liquid carbon dioxide at 0°C.

Pressure (atm.)	$\epsilon - 1$	Molal volume (cc)	Density (mols/liter)	$\frac{\epsilon - 1}{\epsilon + 2} V$
50	0.6016	46.75	21.39	7.809
75	.6187	45.56	21.95	7.790
100	.6321	44.97	22.24	7.826
125	.6425	44.34	22.55	7.821
150	.6526	43.78	22.84	7.822
175	.6603	43.31	23.09	7.813
200	.6674	42.85	23.34	7.798

The molal volumes were obtained from Amagat's pressure volume temperature measurements, the best at present available for carbon dioxide. The Clausius-Mosotti function, $(\epsilon - 1)/(\epsilon + 2) V$, is expressed in cubic centimeters

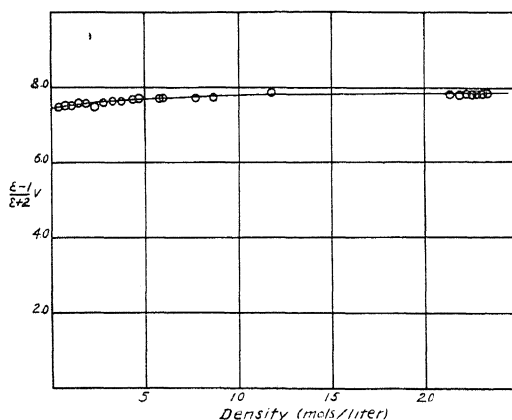


Fig. 3. The points above the density 20 are for the liquid at 0°; the others are for the gas at 100°.

per mol. At 35° above 60 atmospheres, the Clausius-Mosotti function, when plotted against the density, shows very great irregularity. We believe this to be due to error in Amagat's data, extremely probable in view of the very large value of $-(dV/dP)$ in this region. Except in this region, the

maximum error in measurements of Amagat which have been used is probably about 0.25%.

Extrapolation of $(\epsilon-1)V/(\epsilon+2)$ calculated from our measurements yields a value of about 7.4 cc in the low density region covered by other investigators. This is in satisfactory agreement with the value 7.3 cc calculated from the measurements of Zahn.⁸ We estimate the maximum random experimental error in $\epsilon-1$ to be $\pm 0.5\%$. With increasing density, it becomes progressively smaller. Absolute error originating in the calibration of the apparatus, we believe to be not more than one percent.

DISCUSSION

Within the limit of our experimental error, the Clausius-Mosotti function $(\epsilon-1)V/(\epsilon+2)$ is found to be independent of temperature. It is not, however, independent of density. To illustrate its behavior, $(\epsilon-1)V/(\epsilon+2)$, for the gas at 100°, as well as for the liquid at 0°, has been plotted against density in Fig. 3. The curve rises slowly with increasing density, but there is a gradual decrease in slope so that when the liquid densities are reached, it has become, within the limit of observation, parallel to the density axis. It is to be remembered however, that the deviation from the line

$$\frac{\epsilon-1}{\epsilon+2}V = \text{constant}$$

required by the Clausius-Mosotti law in its usual form, is small. Indeed the total increment in $(\epsilon-1)V/(\epsilon+2)$ in passing from the gas at the lowest density of the measurement to the liquid is only four percent.

A few brief speculations relative to the cause of the observed deviation from the Clausius-Mosotti law may be of value. The calculation of the average internal polarizing field F by the familiar cavity method yields

$$F = E + \frac{4\pi}{3}P \quad (1)$$

where E is the mean electric intensity in the dielectric and P the polarization per unit volume. The following formal generalization of the above expression has been suggested:

$$F = E + \nu P. \quad (1a)$$

Let us write

$$\nu = \frac{4\pi}{3} + \beta.$$

We also have at our disposal the familiar relations involving the displacement, D .

$$D = \epsilon E \quad (2)$$

$$D = E + 4\pi P \quad (3)$$

⁸ C. T. Zahn, Phys. Rev. 27, 455 (1926).

Moreover

$$P = \frac{N}{V} p_0 F$$

where N is the Loschmidt number, V the molal volume, and p_0 the molecular polarizability, $\alpha + \mu^2/3kT$. Elimination of D , E , and F from (1a), (2) and (3) gives

$$\frac{\epsilon - 1}{\epsilon + 2} V = \frac{4\pi N}{3} p_0 \frac{1}{1 - \beta N p_0 \rho} \quad (4)$$

where ρ is the density in mols per cubic centimeter. Eq. (4) may be made to conform to the curve of Fig. 3, if the polarizability p_0 is assumed to be a function of density of appropriate form. Change in the polarizability of a molecule with density could be attributed only to a change in the internal structure of the molecule or to molecular association. Such an hypothesis does not seem desirable without independent confirmatory evidence and in any case is of a purely qualitative nature. The fact that the carbon dioxide molecule gives no evidence of possessing a permanent electric moment is unfavorable to this type of explanation. Indeed, the polarizability, α , associated with the perturbation of the electronic orbits is not greatly affected even by interaction involving actual valence forces.

We are inclined to believe the cavity method of calculating the internal field is inexact and that the formal generalization (1a) is valid only if β is a function of density. If this view is accepted, we must conclude that the Clausius-Mosotti function, while furnishing a good approximation, is not an exact representation of the molecular polarization, $4\pi N p_0/3$, except in the limiting case of infinitely low density.

In conclusion, we wish to express our cordial appreciation to Professor H. B. Phillips for continued advice regarding the electrical circuits employed in these measurements.

SOME APPLICATIONS OF THE THEORY OF PLASTIC DEFORMATIONS OF DUCTILE METALS

BY A. NADAI

RESEARCH LABORATORIES, WESTINGHOUSE E. AND M. CO.*

(Received July 7, 1930)

ABSTRACT

A brief account will be given of the principal conditions which are available to express the equilibrium of stress in the plastic state of ductile metals. These conditions will be discussed for the case of rotationary symmetry in a plastic body. As an example several cases of plastic flow in a thick walled cylinder subjected to high internal pressure with and without longitudinal expansion will be treated. The distribution of stress during yielding is given for a long cylinder and for a flat ring, both subjected to radial pressure. How yielding and the plastic deformation spread through the walls of the cylinder has been shown.

1. GENERAL CONSIDERATIONS

CERTAIN ductile metals such as mild steel, if subjected to a state of homogeneous stress with increasing principal stresses show the remarkable behaviour of having a sharply defined limit of plasticity. It has been shown by numerous tests made within the last few years that for practical purposes, the reaching of the plastic state in a ductile polycrystalline metal such as steel, which has a well-defined limit of plasticity, under ordinary temperatures, depends on a stress-condition. This means that the plastic state is reached if a certain condition containing only the principal components of the stress tensor is fulfilled. Under a sharp limit of plasticity or a well-defined yield point it is understood, that permanent parts of the strain begin to develop only if the stresses satisfy the condition of plasticity mentioned before, and if the quantity expressed by the principal stresses on the left side of this condition is smaller than its limiting value a polycrystalline metal behaves like a perfectly elastic and isotropic material.

In this statement, the fact is included that in the first approximation it shall be permitted to assume that within certain amounts of plastic strain (of some few percent of the principal unit elongations) after the plastic limit has been reached, the three principal stresses do not change appreciably. In other words, it is permitted to assume that when plasticity is reached, the stresses remain constant and are independent of deformation as well as of the velocity of deformation.

A further consequence of these assumptions is that in general in a stressed body there will exist an elastic and a plastic region (or more plastic regions separated by elastic regions). In the plastic regions the deformations will have an elastic as well as a permanent part, while in the elastic region no permanent deformations exist.

* Scientific Paper No. 434.

By these restricting assumptions, the treatment of the problems of plastic flow is reduced from a question of dynamics to a question of pure statics. Hence, the six components of the stress tensor will have to be computed from the quasistatic equilibrium conditions, which will be identical with the equilibrium conditions of the stresses in an elastic material. They will also have to satisfy the conditions of plasticity and certain conditions expressing the manner in which stress and strain are connected during a steady, slow plastic flow.

It should be mentioned, that it is not difficult to work out the analysis of plastic flow under more general assumptions and to find solutions in certain simpler cases of plastic flow. It is thought to include in the assumptions such an experimentally known phenomenon as work hardening,¹ i.e. the fact that the stresses under which a metal is deformed plastically are dependent on the deformation and that the yield stresses gradually increase from zero with deformation. It is known that in soft annealed metals such as soft polycrystalline aluminum or copper, the plastic parts of the deformation are already developing under small stresses. In such metals a "yield point" cannot be observed if the annealed metal is stressed from the unstressed state. (But a yield point may appear and can be observed, if the metal was stretched to a certain amount, unloaded, and *again* stressed in the same sense). In this case, it is also not possible to distinguish a "plastic" portion within the stressed body from an "elastic" region, because the permanent part of the resulting strains increase gradually from zero and are hence encountered in all elements of the stressed piece of metal.

In this paper such cases will not be included, because the stress curves obtained by the simpler assumptions show already the characteristic facts related to the special cases of plastic flow treated here.

Regarding another effect, namely, the effect of the velocity of plastic deformation on the magnitude of the yield stresses producing this, it should be mentioned that tests made with single metal crystals as well as with polycrystalline ductile metals have shown that this effect is more pronounced at elevated temperatures (phenomenon of creep). For the plastic flow of steel at room temperatures, the effect can be considered as of a secondary order, if such phenomena as impact are excluded.

2. THE PLANE PROBLEM

If the stresses and strains depend only on two coordinates, for example, x, y , if rectangular or r, ϕ , if polar coordinates are chosen, we may distinguish two special cases in a similar manner as in the theory of elastic plane problems. We designate with s_x, s_y, s_z , the three components of normal stresses, with s_{xy} the only component of shearing stress, which is not vanishing, with $\epsilon_x, \epsilon_y, \epsilon_z$ the three components of strain and with ϵ_{xy} the unit shear component which is not vanishing.

¹ Some cases including the effect of work hardening were worked out in detail in A.S.M.E. Transactions, 1930.

3. THE PLANE STRAIN

In this case the unit extension $\epsilon_z = \text{constant}$, is a principal strain. Many examples of engineering practice are comprised under this heading. One case is especially simple, namely if $\epsilon_z = 0$. In this case the normal stress s_z is

$$s_z = \frac{1}{2}(s_x + s_y). \quad (1)$$

This follows from a rule of plastic flow.² If s_1, s_2 , and s_3 are the principal stresses and $\epsilon_1, \epsilon_2, \epsilon_3$ the principal strains during a steady slow plastic flow in which the directions of principal stresses do not change relatively to the stressed material, then

$$\frac{2s_2 - s_1 - s_3}{s_1 - s_3} = \frac{2\epsilon_2 - \epsilon_1 - \epsilon_3}{\epsilon_1 - \epsilon_3}. \quad (2)$$

Taking, for example, $\epsilon_3 = \epsilon_2 = 0$ and assuming that the volume during plastic flow is not changed:

$$\epsilon_1 + \epsilon_2 + \epsilon_3 = \epsilon_x + \epsilon_y + \epsilon_z = 0. \quad (3)$$

We see that

$$\epsilon_1 = -\epsilon_2 \text{ OR } \epsilon_x = -\epsilon_y$$

and with this (2) reduced to (1).

The following statements referring to plane strain with one vanishing principal strain $\epsilon_z = 0$ are limited to plastic regions where the permanent parts of the strains ϵ_x and ϵ_y are predominant, so that the elastic parts may be neglected. We may put then simply

$$s_z = \frac{1}{2}(s_x + s_y) \quad (4)$$

and we see that the principal stresses s_1 and s_2 are given by

$$\begin{aligned} s_1 &= \frac{s_x + s_y}{2} + s_m \\ s_2 &= \frac{s_x + s_y}{2} - s_m \end{aligned} \quad (5)$$

Where s_m designates the principal shearing stress

$$s_m^2 = \frac{(s_x + s_y)^2}{4} + s_{xy}^2. \quad (6)$$

In order to express the fact that we have an equilibrium of stresses in the plastic state, we have to introduce a *condition of plasticity*. Taking the general form of the second degree

$$(s_1 - s_2)^2 + (s_2 - s_3)^2 + (s_3 - s_1)^2 = 2s_0^2 = \text{const.}^3 \quad (7)$$

² See Der bildsame Zustand der Werkstoffe, J. Springer, Berlin, 1927 S. 51., or On the Mechanics of the Plastic State of Metals. A.S.M.E. Transactions, Applied Mechanics Division, 1930.

³ This condition of plasticity was proposed by R. v. Mises, by Huber, and H. Hencky and has been verified by the tests of W. Lode and Ros-Eichinger.

Where the constant s_0 designates the yield stress in pure tension, we see that this expression simplifies considerably and becomes

$$(s_1 - s_2)^2 = \frac{4s_0^2}{3} = \text{const.} \quad (8)$$

Writing the constant $s_0/3^{1/2} = k$ and using (5) and (6) this last equation can be expressed in terms of s_x , s_y , and s_{xy} as follows:

$$(s_x - s_y)^2 + 4s_{xy}^2 = 4k^2 = \text{const.} \quad (9)$$

This is the condition of plasticity for plane strain $\epsilon_z = 0$, which has to be combined now with the conditions of equilibrium.

$$\frac{\partial s_x}{\partial x} + \frac{\partial s_{xy}}{\partial y} = 0, \quad \frac{\partial s_y}{\partial y} + \frac{\partial s_{xy}}{\partial x} = 0. \quad (10)$$

A complete theory of integration of the three simultaneous equations for the three unknown functions s_x , s_y , and s_{xy} , has been worked out by H. Hencky⁴ and R. v. Mises.⁵ Solutions in polar coordinates including some properties of the so-called slip lines, which facilitate the discussion of the solutions have been investigated by the author.⁶

We may remark that the theory of plane plastic flow under the assumption $\epsilon_z = 0$ of a vanishing lateral extension ϵ_z is mathematically identical with the so-called theory of maximum constant shear. The only difference is, that the constant k in Eq. (9) has to be taken in the first theory $k = 2s_0/3^{1/2} = 0.577s_0$ and in the second $k = s_0/2 = 0.500s_0$.

If ϵ_z is not vanishing, but equals a constant, the theory is more complicated; one case is given below.

4. PLANE STRESS

In this case $s_z = 0$, the normal stress perpendicular to the xy plane vanishes. This case occurs in a thin sheet which is loaded in its plane, for example in a plate containing a circular hole and stretched in all directions by a uniform tensile stress. As in this case, the third principal stress $s_3 = 0$ vanishes, the condition of plasticity⁷ becomes in terms of principal stresses,

$$s_1^2 - s_1s_2 + s_2^2 = s_0^2 = \text{constant} \quad (11)$$

or in terms of the stress components s_x , s_y , and s_{xy} , in rectangular coordinates

$$s_x^2 - s_xs_y + s_y^2 + 3s_{xy}^2 = s_0^2 = \text{const.} \quad (12)$$

This equation again has to be combined with the two equilibrium conditions (10).

In rectangular coordinates s_1 and s_2 , equation (11) is that of an ellipse with the semi-axes $a = (2)^{1/2}s_0$ and $b = (2/3)^{1/2}s_0$. Hence in a thin plate stressed

⁴ H. Hencky, *Zeits. f. ang. Math. und Mechanik* 3, 241 (1923).

⁵ R. v. Mises, *Zeits. f. ang. Math. und Mechanik* 5, 147 (1925).

⁶ A. Nadai, *Zeits. f. Physik*, 106 (1924).

⁷ The author is much indebted to Mr. H. Friedman, who has carried out the computation.

in its plane, no normal stress component can ever become larger than $2s_0/3^{1/2}$, which is the maximum value of either s_1 or s_2 as coordinates of a point of the ellipse. This is $=1.155s_0$. There is therefore a distinct difference between the two states of plane stress $\epsilon_z=0$ and $s_z=0$, if plastic flow is considered. In the case $\epsilon_z=0$, the normal stresses may exceed the yield stress s_0 for pure tension considerably, and there are singularities of the stresses possible (for example, a "center of compression"). In the second case $s_z=0$, no stress component can become infinite, and singularities are not possible in this sense.

5. LONG CYLINDER YIELDING PLASTICALLY UNDER INTERNAL PRESSURE.

Let s_r and s_t be the radial and tangential normal stress components and s_z the axial normal stress. If the cylinder is not expanding or contracting in axial direction, the unit extension $\epsilon_z=0$ and the stress components s_r and s_t are given by the two equations

$$s_t - s_r = \pm \frac{2s_0}{3} \quad (13)$$

$$\frac{d(rs_r)}{dr} - s_t = 0. \quad (14)$$

The first is the condition of plasticity, the second the condition of equilibrium. A set of solutions satisfying these two equations and the two bound-

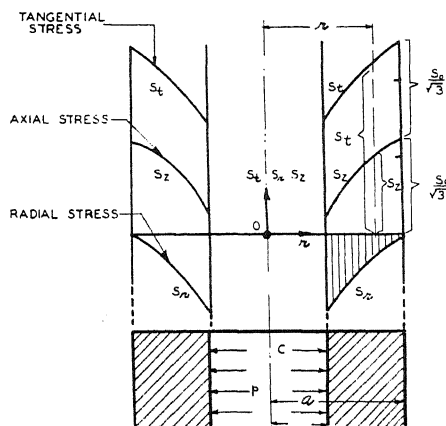


Fig. 1. Plastic flow in thick hollow cylinder stress distribution when axial elongation ϵ_z is equal to zero.

dary conditions, that at the inner surface for $r=a$ the radial stress must become equal to the pressure p and at the outer surface for $r=b$, s_r must vanish:

$$\begin{aligned} &\text{for } r = a, s_r = -p \\ &\text{and for } r = b, s_r = 0 \end{aligned}$$

is given by

$$\left. \begin{aligned} s_r &= -\frac{2s_0}{3^{1/2}} \ln \frac{b}{r} \\ s_t &= \frac{2s_0}{3^{1/2}} \left(1 - \ln \frac{b}{r} \right) \\ s_z &= \frac{2s_0}{3^{1/2}} \left(\frac{1}{2} - \ln \frac{b}{r} \right) \end{aligned} \right\} \quad (15)$$

This distribution of stress is shown in Fig. 1. The pressure p under which the cylinder will yield from the inner to the outer surface is found by the first formula of (15) by taking $r=a$:

$$p = \frac{2s_0}{3^{1/2}} \ln \frac{b}{a} \quad (16)$$

There s_0 designates the yield stress in pure tension.

6. YIELDING OF THIN PLATE WITH CIRCULAR HOLE OR OF FLAT RINGS RADIALY STRESSED

In this case $s_z=0$ and we have to combine Eq. (12) or if expressed in terms of the radial and tangential stress components s_r and s_t :

$$s_t^2 - s_t s_r + s_r^2 = s_0^2 = \text{constant} \quad (17)$$

with the equilibrium condition

$$r \cdot \frac{ds_r}{dr} = s_t - s_r. \quad (18)$$

Using here instead of s_t and s_r two new stress variables

$$\begin{aligned} s &= (s_t + s_r): 2 \\ s' &= (s_t - s_r): 2. \end{aligned} \quad (19)$$

We see that (17) takes the simpler form:

$$s^2 + 3s'^2 = s_0^2. \quad (20)$$

To satisfy this equation we put

$$s = s_0 \sin \theta, s' = \frac{s_0}{3^{1/2}} \cos \theta \quad (21)$$

and (18) takes the form

$$\frac{rd}{dr}(s - s') = 2s' \quad (22)$$

or

$$\frac{rd}{dr} \left(\sin \left(\theta - \frac{\pi}{6} \right) \right) = \cos \theta \quad (23)$$

whence by integration:

$$r^2 = c^2 e^{3^{1/2} \cdot \theta} \cos \theta \quad (24)$$

where c is a constant of integration. To determine its value, we have to express the radial and tangential stresses with the help of θ

$$\left. \begin{aligned} s_r &= \frac{2s_0}{3^{1/2}} \sin \left(\theta - \frac{\pi}{6} \right) \\ s_t &= \frac{2s_0}{3^{1/2}} \sin \left(\theta + \frac{\pi}{6} \right) \end{aligned} \right\} \quad (25)$$

If for $r=b$ the radial stress s_r shall vanish, we see that θ must be taken

$$\text{for } r=b, \theta = \theta_b = \frac{\pi}{6}.$$

If $\theta < \pi/6$, s_r will become negative, the radial stress will be a compression. On the contrary, if $\theta > \pi/6$, $s_r > 0$ and will be a tensile stress. Evidently the former case corresponds to the case of a ring with internal pressure and the latter case to a ring or plate with external tension. Now taking $\theta_b = \pi/6$ for $r=b$, the constant c in (24) is determined:

$$b^2 = c^2 \cdot \frac{3^{1/2}}{2} \cdot e^{\pi(3)^{1/2}/6} \quad (26)$$

We get finally from (24) and (26) the relation between the radius r and the parameter θ

$$r^2 = \frac{2b^2}{3^{1/2}} \cdot e^{3^{1/2}(\theta - \pi/6)} \cdot \cos \theta. \quad (27)$$

Thus the complete solution is obtained.

To get the pressure or tension p which must act on the circumference $r=a$ and produce yielding, the angle $\theta = \theta_a$ must be computed from the last equation by taking $r=a$ and thus p is given by

$$p = \frac{2s_0}{3^{1/2}} \sin \left(\frac{\pi}{6} - \theta_a \right). \quad (28)$$

To each value of θ_a corresponds a value of the ratio b/a and a radial and tangential stress s_r and s_t for $r=a$. This has been shown in Fig. 2, where the ratio of the two radii b/a and the two stress components at the circle $r=a$ are represented by curves. To find the pressure p for a given ring, we have to read the value of s_r for $r=a$ (that is of p) below the value of b/a . The stress distribution is also shown in Fig. 3, where the radial and the tangential stresses s_r and s_t are plotted as functions of the radial distance r of a point of the ring from its center.

Comparing the type of curves in Fig. 3 with the logarithmic curves for the distribution of stress obtained for the case of the yielding of a long cylinder under internal pressure p , (Fig. 1.) it can be seen that in the latter case with the increasing thickness of the hollow cylinder the pressure p is indefinitely increasing. In the case of a flat ring with free faces and stressed radially by

a pressure p acting on the inner circle, however, equilibrium is only possible, if the ratio of the outer to the inner radius is

$$1 < b/a < 2.963$$

For $b/a > 2.963$, no plastic equilibrium is possible in which the ring yields from its inner to its outer cylindrical surface.

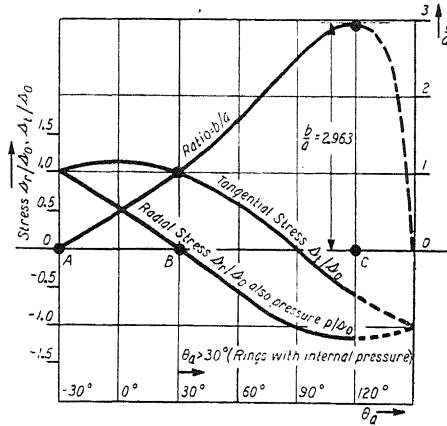


Fig. 2. Radial and tangential stress and ratio b/a plotted against parameter θ in circular plates with holes yielding under radial pressure.

7. PARTIAL YIELDING

Until now the only cases that have been treated were those in which the material in a hollow cylinder was yielding from the inner to the outer surface. If the pressure in a tube is gradually increasing from zero, the tube will be

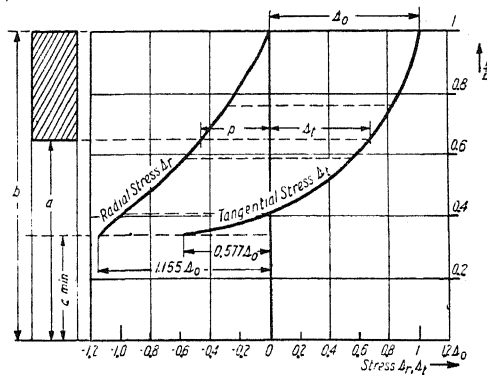


Fig. 3. Distribution of stress in circular plates with central hole, yielding under radial pressure p . a inner, b outer, radius to yield strain in tension.

stressed at first only elastically. Later, with the increasing pressure an annular region will become plastic, growing from the inner surface. For such values of the pressure, the tube must be divided in two portions $a < r < c$, and $c < r < b$, of which the former is stressed beyond the limit of plasticity and the latter only elastically. If, for example, the tube cannot expand in

the axial direction ($\epsilon_z=0$), first yield will occur at a pressure given by the well known formula

$$p_0 = \left(1 - \frac{a^2}{b^2}\right) \frac{p_0}{3^{1/2}} \quad (29)$$

derived from the stress conditions of an elastic tube. If $p > p_0$, the elastic stress distribution in the region $r > c$, will be obtained from the stresses for an elastic cylinder

$$\left. \begin{aligned} s_r' &= c_1 + \frac{c_2}{r^2} \\ s_t' &= c_1 - \frac{c_2}{r^2} \\ s_z' &= 2\nu c_1 \end{aligned} \right\} \quad (30)$$

where ν is Poisson's ratio and c_1 and c_2 are two constants, and the plastic stress distribution in the region $r < c$ will be given by

$$\left. \begin{aligned} s_r &= c_3 + \frac{2s_0}{3^{1/2}} \ln r \\ s_t &= c_3 + \frac{2s_0}{3^{1/2}} (\ln r + 1) \\ s_z &= c_3 + \frac{2s_0}{3^{1/2}} \left(\ln r + \frac{1}{2} \right) \end{aligned} \right\} \quad (31)$$

The three constants c_1 , c_2 , and c_3 can be determined from the conditions of continuity and the boundary conditions of the cylindrical surfaces $r=a$ and $r=b$. The result of the computation is

$$\text{Stresses in the elastic portion } c < r < b \quad \left\{ \begin{aligned} s_r' &= \frac{s_0}{3^{1/2}} \gamma^2 \left(\frac{1}{u^2} - 1 \right) \\ s_t' &= \frac{s_0}{3^{1/2}} \gamma^2 \left(\frac{1}{u^2} + 1 \right) \\ s_z' &= \frac{2s_0\nu}{3^{1/2}} \gamma^2 \end{aligned} \right. \quad (32)$$

$$\text{Stresses in the plastic portion } a < r < c \quad \left\{ \begin{aligned} s_r &= -p + \frac{2s_0}{3^{1/2}} \ln \frac{u}{\alpha} \\ s_t &= -p + \frac{2s_0}{3^{1/2}} \left(\ln \frac{u}{\alpha} + 1 \right) \\ s_z &= -p + \frac{2s_0}{3^{1/2}} \left(\ln \frac{\mu}{\alpha} + \frac{1}{2} \right) \end{aligned} \right. \quad (33)$$

where

$$\frac{r}{b} = u, \quad \frac{a}{b} = \alpha \quad \text{and} \quad \frac{c}{b} = \gamma. \quad (34)$$

The pressure required to produce yielding in the tube to the radius $r=c$ is found by

$$p = \frac{s_0}{3^{1/2}} \left(2 \ln \frac{\gamma}{\alpha} + 1 - \gamma^2 \right) \quad (35)$$

where s_0 is the yield stress in pure tension.

In Fig. 4 the pressures p required to produce progressive yielding through a hollow cylinder are shown for different ratios of $\alpha=a/b=0.1, 0.2 \dots$.⁷ The abscissae in this figure are $\gamma=c/b$, the ordinates the pressure p . For example, the curve belonging to $\alpha=0.8$ shows how the pressure p in a tube

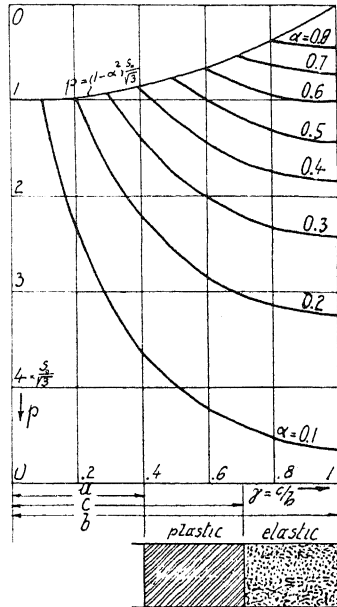


Fig. 4. Pressure p producing yielding plotted against ratio $\gamma=c/b$. c is radius of surface to which plastic region extends.

of the ratio a/b of the inner to the outer radius $=0.8$ would increase with the increasing radius c of the cylindrical surface, to which yielding has penetrated in the tube.

8. TUBE SUBJECTED TO INTERNAL PRESSURE AND AXIAL LOAD

The theory of the plastic flow of a thick walled cylinder which is exposed to a high internal pressure and which is permitted also to expand in the axial direction is considerably more complicated than the cases mentioned above with no axial expansion $\epsilon_z=0$. This case has been worked out elsewhere.⁸ We quote here the formulae. Let s and s' be

$$s = \frac{s_z + s_t}{2} - s_r, \quad s' = \frac{s_z - s_t}{2} \quad (36)$$

⁸ A.S.M.E. Trans., Applied Mechanics Division, 1930.

and u a variable parameter given by

$$u = \frac{1}{3^{1/2}} \left(1 + \frac{2\epsilon_a}{\epsilon_z} \right) \frac{a^2}{r^2} \quad (37)$$

where ϵ_a is the tangential unit elongation at the outer surface $r=a$ of the cylinder and ϵ_z the axial unit elongation, assumed to be uniform over the whole cross section of the tube, a is the outer radius, and b the inner radius of the tube.

Then the stress distribution is given by

axial stress:

$$s_z = s + s' + s_r \quad (38)$$

tangential stress:

$$s_t = s - s' + s_r \quad (39)$$

where

$$s = \frac{s_0}{2(3)^{1/2}} \cdot \frac{3^{1/2} + 3u}{(1 + u^2)^{1/2}} \quad s' = \frac{s_0}{2(3)^{1/2}} \cdot \frac{3^{1/2} - u}{(1 + u^2)^{1/2}} \quad (40)$$

and the radial stress is equal to

$$s_r = \frac{s_0}{3^{1/2}} \log_e \frac{u_a + (1 + u_a^2)^{1/2}}{u + (1 + u^2)^{1/2}} \quad (41)$$

The pressure p under which the whole tube will yield is

$$p = \frac{s_0}{3^{1/2}} \log_e \frac{u_b + (1 + u_b^2)^{1/2}}{u_a + (1 + u_a^2)^{1/2}} \quad (42)$$

with

$$u_a = \frac{1}{3^{1/2}} \left(1 + \frac{2\epsilon_a}{\epsilon_z} \right) \quad \text{and} \quad u_b = \frac{a^2}{b^2} u_a \quad (43)$$

A special case is that of a tube with no axial elongation $\epsilon_z=0$, where both constants u_a and u_b become infinite, but a careful consideration shows that the formulae (38–41) converge exactly to the simpler formulae already given by the Eqs. (15).

9. SUMMARY

The effect of the lateral (axial) extension E_z in the cases of plane plastic flow, which has not been considered until now, was investigated. The theory of plane plastic flow becomes more simple in two cases, namely (1) if the unit extension ϵ_z in the direction perpendicular to the plane xy vanishes: $\epsilon_z=0$ and (2) if the normal stress s_z on this plane is zero, that is, in the case of a thin sheet stressed in its plane. These cases were worked out for radial symmetry, containing the radial distribution of stress in a thick walled tube yielding under a high internal pressure, and assuming the tube restrained to expand in the axial direction and the radial distribution of stress in a flat circular ring yielding under radial pressure or tension.

Under the latter cases is included that of the plastic equilibrium of an infinite plate stretched uniformly in its plane and containing a circular hole. The case of partial yielding of a thick walled tube was shown and the pressures computed under which yielding penetrates to a given depth.

AN ATTEMPT TO DETECT COLLISIONS OF PHOTONS

BY A. L. HUGHES AND G. E. M. JAUNCEY

DEPARTMENT OF PHYSICS, WASHINGTON UNIVERSITY

(Received June 16, 1930)

ABSTRACT

Assuming that light is corpuscular and that collisions between light corpuscles (i.e. photons) can occur, it is shown that two photons of identical frequency ν , moving along paths which make an angle 2θ with each other, will on collision give rise to a photon of frequency $\nu(1 + \cos \theta)$ travelling forward along the line bisecting the angle. To test this, two beams of sunlight (one suitably deflected by a mirror), filtered through red glass, were passed through lenses 24 cm in diameter and of 33 cm focal length, so that the beams, whose axes made an angle of 120° with each other, intersected at a common focus. The point of intersection of the beams was examined through a green filter with the dark-adapted eye. No light was detected. Calculations show that if the photon has a cross section, its area must be less than 3×10^{-20} cm². From a result of Lord Rayleigh, some writers have suggested an area of the order of λ^2 for the photon. Our result shows the area to be of the order of $10^{-10}\lambda^2$.

1 INTRODUCTION

PHYSICISTS have become accustomed to the idea of the corpuscular nature of molecules, atoms, electrons, protons, alpha-particles and also, in some cases, of light. Collisions of molecules with molecules as in the kinetic theory of gases, of electrons with atoms as in critical potentials, of alpha-particles with the nuclei of atoms as in the Rutherford scattering experiments and of photons with electrons as in the Compton effect are familiar phenomena. It occurred to the writers that, if light has a corpuscular structure, collision phenomena should occur when two light beams cross each other—in other words, that two photons may collide and produce photons with energies different from the energies of the original photons.

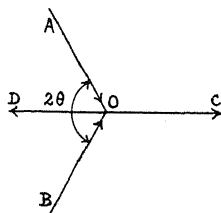


Fig. 1.

2. THEORY

Let two photons, each of energy $h\nu$, approach each other and collide as in Fig. 1, and let the angle between AO and BO , the paths of the two photons, be 2θ . The problem is to find the energy of the photon which after the collision proceeds along the bisector OC . If two photons arise out of the colli-

sion of two photons and if the principle of conservation of momentum may be applied to photons, the other resulting photon must travel along OD . Let the photon travelling along OC have the energy $h\nu_1$ and the photon along OD an energy $h\nu_2$. The conservation of energy gives

$$h\nu_1 + h\nu_2 = 2h\nu \quad (1)$$

and the conservation of momentum gives

$$h\nu_1/c - h\nu_2/c = 2(h\nu/c) \cos \theta \quad (2)$$

Whence

$$\nu_1 = \nu(1 + \cos \theta) \quad (3)$$

$$\nu_2 = \nu(1 - \cos \theta) \quad (4)$$

or, in terms of wave-length,

$$\lambda_1 = \lambda/(1 + \cos \theta) \quad (5)$$

$$\lambda_2 = \lambda/(1 - \cos \theta) \quad (6)$$

The theory thus leads to the expectation that, if two beams of monochromatic light cross each other, as in Fig. 1, light of a wave-length shorter than that of the two original beams will be observed in the direction OC . In particular, if $2\theta = 120^\circ$ and $\lambda = 6000\text{\AA}$, the wave-length observed in the direction OC will be 4000\AA . Accordingly an experiment was devised to test this prediction of the theory.

3. EXPERIMENTAL METHOD

A wide beam of sunlight entered a light-tight box AB through the lens C in Fig. 2 and was brought to a focus at O . A second beam after reflection

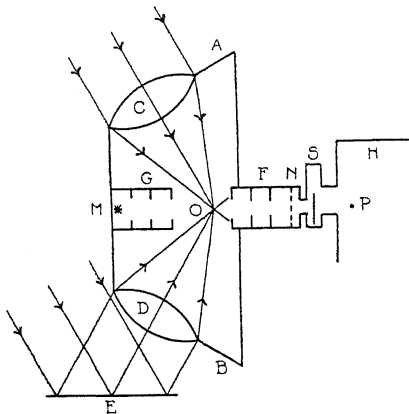


Fig. 2. Diagram of apparatus.

from the mirror E , which is rigidly attached to the box AB , passed through the lens D and was also brought to a focus at O . Thus two cones of light intersected at O . The diameter of each lens was 24 cm. For each lens, the focal length for the central and peripheral rays was 34.3 and 31.7 respectively. The area of cross section of the light passing through each lens was a minimum at 33 cm. The diameter of the

sun's image at this point was estimated to be 0.4 cm. This image occurred for each lens at O in Fig. 2. The head of the observer was enclosed in a light-tight helmet H , his eye being at P . The observer looked through the tube F and into the tube G . Both F and G contained diaphragms so as to prevent stray light from entering the eye. At the far end M of the tube G a small lamp was placed. The object of this lamp was to attract the attention of the eye to the direction PM . The line PM passed through O . The directions of the light rays passing through O were such that no direct rays from the lenses could enter the eye. The inside of the box AB was blackened so as to reduce scattering. Dustfree air was blown through the box AB in order to remove dust motes from the air at O and also to keep the inside of the box reasonably cool. The sunlight which entered the box through the lenses previously passed through plates of red glass. A quantitative curve for the transmission of this red glass was very kindly made for us by Professor H. M. Randall, of the University of Michigan, who found that the red glass transmitted wave-lengths between 5500 and 30,000Å. At N was placed a green filter, the transmission curve of which was supplied by the Eastman Kodak Company. The green filter transmitted light of wave-length shorter than 5200Å. At S was placed a shutter. The observer prepared his eye by sitting with his head in the helmet for 15 minutes. The lamp M was then switched on and the shutter S opened. The lamp was connected in series with a rheostat and increasing resistance was put into the circuit until the light of the lamp was just perceptible. After opening the lamp switch, the observer opened and closed the shutter S in order to determine whether or not green light was coming from O . The result was negative. The observer then rested his eye for a second 15 minutes when more observations were taken, a third set of observations were made at 45 minutes from the time when the helmet was first put on and a fourth set at 60 minutes. The eye is almost completely dark-adapted in 60 minutes, but nevertheless even after this time the result was negative.

As a check on the observations, a sliding shutter was made so that the proportion of sunlight entering the lenses could be suddenly changed from no light entering lens C and 100 percent of light entering lens D , to 50 percent entering each lens, and to no light entering lens D and 100 percent entering lens C . This shutter arrangement was outside the box AB and is not shown in Fig. 2. In whatever position the shutter was the same total amount of light passes through O . In the 50–50 percent position of the shutter the two light beams crossed at O and conditions were such as to allow collisions of photons, while in the 100–0 percent positions of the shutter the two light beams did not cross at O . While one person operated the shutter, another person who was the observer with his head in the helmet called whether or not he noticed a change in the light when a change was made in the position of the shutter. The usual observation was that there was complete darkness and no change. In those cases where the observer judged a change, there was no correlation between the observation and the position of the shutter, and the result was therefore negative. In order that the result might not depend

upon a particular observer, five different observers were used. All agreed in giving a negative result.

The apparatus was mounted so that the upper lens could be kept pointing toward the sun. The angle between the central rays passing through each lens was 120° . The peripheral rays of one lens made with the peripheral rays of the other lens angles varying from 80° to 160° . No lenses were used between the eye at *P* and *O* in Fig. 2, because of the well-known fact that the brightness of an object as seen by the eye cannot be increased by a lens system.

4. DISCUSSION OF RESULTS

The wave-lengths after collision at various angles, as calculated from Eq. (5), are shown in Table I.

TABLE I. *Change of wave-length on collision.*

Original wave-length	Wave-length after collision Collision angle		
	80°	120°	160°
5500A	3110A	3670A	4680A
6000	3400	4000	5110
7000	3970	4660	5960
8000	4530	5330	6810
9000	5100	6000	7670

It is seen that wave-lengths between 5500 and 9000A in the original beams produce wave-lengths after collision which can penetrate the green filter *N* in Fig. 2. Since the sensitivity of the eye rapidly decreases as the wave-length decreases below 4500A we shall consider only those wave-lengths between 4500 and 5000A which pass through the green filter. Let us assume that these are produced by the central rays passing through the lenses, then we are interested only in the wave-lengths 6750 to 7500A in the original beams. From data which were very kindly supplied to us by Dr. C. G. Abbot of the Smithsonian Institution, we estimate that the rate at which the energy of sunlight in a range 6750 to 7500A is incident on a surface perpendicular to the beam is about 0.12 cal/min. cm² at midday in the spring-time in St. Louis. The area of each lens is 453 cm² and the rate at which energy passes through each lens is therefore 54.4 cal/min. The coefficient of transmission for the red glass in the range 6750 to 7500A is 0.45 and the average wave-length is 7125A so that there are 3.7×10^{20} photons per minute passing through each lens. When the sliding shutter is used in the experiment in the 50-50 percent position, the number of photons in each beam passing through *O* in Fig. 2 is 1.85×10^{20} per minute. For simplicity we shall treat the beams which intersect at *O* as two square cylinders of side 4 mm, with 1.85×10^{20} photons passing through each cylinder per minute. Within a volume $(4 \times 4 \times 4)/\sin 120^\circ$ mm³ of one cylinder there will be at any instant of time 4.6×10^7 photons. Bombarding them from the second beam there will be 3.1×10^{18} photons/sec. If the effective collision area of each photon is *A* cm² the total area of the photons in the first beam presented to the photons in the second

beam is $4.6 \times 10^7 \times A$. The chance of a photon in the second beam colliding with any photon in the first beam is $4.6 \times 10^7 \times A / (0.4 \times 0.4) = 2.9 \times 10^8 \times A$. The total number of collisions per second will then be $9 \times 10^{21} \times A$. Ives¹ estimates that the pupil of the dark-adapted eye has a diameter of about 6 mm. The distance of the eye of the observer from O in Fig. 2 is 25 cm, so that the solid angle subtended by the pupil at O is 0.00044. Let us suppose that after collision the resulting photons are equally likely to travel in any direction. The number of photons entering the eye per second will then be $0.00044 \times 9 \times 10^{21} \times A / 4\pi = 3.3 \times 10^{22} \times A$.

There is some variation amongst different writers as to the energy of the smallest light stimulus which can be detected by the eye. Reeves² gives 19.5×10^{-10} erg/sec, Russell³ gives 7.7×10^{-10} erg/sec and Buisson⁴ 12.5×10^{-10} erg/sec. If we take the average of these values we shall at least have the correct order of magnitude. Assuming a wave-length of 5000A, we find that the minimal light stimulus is given by 336 photons entering the eye per second. Ives¹ gives the minimal light stimulus as 1000 photons per second. Using this value of Ives so as to be on the safe side, we obtain

$$3.3 \times 10^{22} \times A = 10^3$$

whence

$$A = 3 \times 10^{-20} \text{ cm.}^2$$

If the photons are thought of as having a circular cross section, this corresponds to a diameter of 2×10^{-10} cm. The result of our experiment is therefore that the collision area of a photon, if such a thing exists, is less than 3×10^{-20} cm².

Photons are supposed to obey the laws of the Bose-Einstein statistics and no two photons can occupy the same cell. A physical interpretation* of this may be that no two photons can be at the same place at the same time, and hence there can be no collisions of photons. Our result is compatible with this view. Lord Rayleigh⁵ has considered the case of a resonator being actuated by a plane wave and has calculated the area of the primary wave front which propagates the same energy as is dispersed by the resonator. This area is $\lambda^2 \pi$ where λ is the wave-length. This result has been said by some writers to indicate that the area of the cross section of a photon is of the order of λ^2 . According to this idea then we might have expected an area of cross section of 2.5×10^{-9} cm². Our experiment, however, gives an area less than 3×10^{-20} cm², which is of the order of 10^{-10} times the expected area.

We are indebted for information concerning the dark-adapted eye to Professor Allen of the University of Manitoba, to Dr. Jones of the Eastman Kodak Company, and to Dr. Priest of the Bureau of Standards. From this information, we have learned that the dark-adapted eye is the best instrument for making the observations in this experiment.

¹ H. E. Ives, *Astrophys. J.* 44, 124 (1916).

² P. Reeves, *Astrophys. J.* 46, 167 (1917).

³ H. N. Russell, *Astrophys. J.* 45, 60 (1917).

⁴ H. Buisson, *Astrophys. J.* 46, 296 (1917).

⁵ Lord Raleigh, *Phil. Mag.* 29, 209 (1915).

LETTERS TO THE EDITOR

Prompt publication of brief reports of important discoveries in physics may be secured by addressing them to this department. Closing dates for this department are, for the first issue of the month, the twenty-eighth of the preceding month; for the second issue, the thirteenth of the month. The Board of Editors does not hold itself responsible for the opinions expressed by the correspondents.

Band Intensities

The Franck principle concerning the most probable transitions between electronic states in molecules, has succeeded in explaining most of the cases of band intensities to which attention has been called. During the past two years I have observed several examples of band spectrum excitation which show extreme deviations from the above principle. Several such examples have already been pointed out by Birge in the National Research Council bulletin "Molecular Spectra in Gases." As far as I am aware however, very little attention has been paid to these exceptional cases, and it is my purpose here to point out one of the most interesting ones.

Lord Rayleigh studied the effect on the nitrogen afterglow of the admixture of inert gases with the glowing material and found that the intensity distribution among the first positive bands of nitrogen was considerably modified (especially so by helium). Now one can readily account for relative intensity changes between progressions in band systems, since these can be caused by variations in the relative number of molecules in the various initial vibrational states. The relative intensities of bands within a progression however, are definitely fixed by the Franck principle and can be determined from the

potential energy curves associated with the states involved in the emission of the bands. As far as I know, no discussion has as yet been given of relative intensity variations within progressions. It is just this type of intensity variation that is met in the experiments of Rayleigh and in some of my recent experiments. While no considerable discussion of this type of intensity change will be attempted at this time, it is worthwhile noting that should the cause of this intensity variation be a collision between a nitrogen molecule and a helium atom, then no energy transfer need take place during the process. If an energy transfer should take place between the two particles it would result in a change in the kinetic energies of the particles or in a redistribution of their excited states. Neither one of these would account for any variation of intensities within a progression. Since the purpose of this note has been simply to call attention to this type of intensity variation in band spectra further discussion will be left for a later communication.

JOSEPH KAPLAN

University of California at Los Angeles,
Los Angeles, California,
August 6, 1930.

X-Ray Scattering Coefficient as a Function of Wave-length and Atomic Number

Direct measurements of the mass scattering coefficient of x-rays have been made by Barkla and Dunlop, Hewlett, Mertz and others. In this experiment a modification of the ionization chamber used by Mertz was employed to measure simultaneously the radiation scattered at all azimuths. Improvements were made in the purity of the radiation employed and the measurements were extended to

longer wave-lengths and higher atomic numbers.

The source of x-rays was a water-cooled Coolidge tungsten-target tube. The current supplied to it was rectified by a full-wave kenetron rectifier operating on a balanced circuit. The tube was operated at from 35 to 50 peak K.V. with a current of 35 m.a.

Characteristic fluorescence radiation was

excited in radiators of Sn, Ag, Mo, and Se placed in the direct beam from the tube. The nature of the radiation was tested roughly by absorption measurements and found to be substantially pure.

This fluorescence radiation was collimated by a slit system into a beam one-half inch square in the path of which were placed hollow cylindrical scattering blocks of C, Al, Fe, Ag, Sn, and Au.

Scattered radiation from these blocks passed into a large ionization chamber the window of which was shaped like a segment of a sphere with the scattering block at its center. The chamber was of uniform depth and was filled with argon at atmospheric pressure.

A second ionization chamber, likewise filled with argon, was placed in the direct beam for absorption measurements. The electrodes of both chambers were connected to a Compton electrometer the sensitivity of which was about 10,000 mm scale divisions per volt at 2 meters. Lead screens were used to reduce the air scattering as much as possible.

The scattering blocks were mounted on supports of silk thread attached to wire

of such a thickness that one-half of the radiation used was absorbed by passing through them. For convenience the scattering of carbon, iron, silver, tin and gold was compared with aluminum and where it was not possible to obtain scattering blocks absorbing exactly half of the radiation, great care was taken to compare them with aluminum blocks of the same absorbing power.

The gold foil used was mounted on a celluloid base and was compared with an aluminum block also mounted on celluloid. In correcting for the scattering of the celluloid an amount was deducted equal to one-half the scattering from a celluloid block of the same dimensions.

For this and for all the other blocks corrections were made for air scattering and natural leak of the electrometer system. Due to the length of air path in front of the chamber and to the size of the chamber itself these were appreciable and their magnitude for longer wave-lengths and higher atomic numbers than those used made measurements by this method impracticable.

The results obtained are shown in Table I. The effective wave-length of the radiation

TABLE I. *Ratio of mass scattering coefficients of elements to aluminum for different wave-lengths.*

Scatterer	Radiator			
	Sn	Ag	Mo	Se
Au	5.49	6.75		
Sn	2.33	2.82	3.44	
Ag		2.65	3.51	
Fe	1.41	1.65	2.09	
C	1.07	0.95	0.87	0.79
Effective wave-length (calc.)	0.48 A	0.55	0.70	1.09

frames and were so placed in the path of the x-ray beam that radiation from every part of the first slit reached every part of the scattering block. Suitable filters were used to prevent fluorescence radiation excited in the scatterers from entering the ionization chamber.

The cylindrical scattering blocks were made

used was determined by averaging the wave-lengths of the $K\alpha$ and $K\beta$ lines weighted by their relative intensities.

ERROL N. COADE

Ryerson Physical Laboratory,
University of Chicago,
July 25, 1930.

Fluorescent Dry Plates for Photographic Photometry

We have recently shown (J.O.S.A. 20, 313, 1930) that problems of homochromatic photographic photometry can be greatly

simplified (especially in the Schumann region, where they had previously been impracticable) by coating ordinary dry plates with

fluorescent oils in the manner which Duclaux and Jeantet used to obtain increased sensitivity at short wave-lengths. We now find that a similar result can be obtained much more conveniently by using a dry transparent coating containing an aesculine solution as the fluorescing agent, while broadening of images and other difficulties can be minimized by making this coating an integral part of the plate. A Cramer Contrast Process Plate usually shows extreme variations of contrast between 3700 and 2300A; when such a plate was coated by pouring over it a mixture of two parts saturated solution of aesculine in water and one part 5% gelatine solution in water, which was allowed to dry for three days, it showed uniform contrast over the same range. A much more uniform coating can be obtained in this way than with the oils, and nothing need be removed prior to development, which should, however, be about twice as long as usual. The variation of sensitivity with wave-length is much less than with ordinary plates, and we believe that it can be made as negligible as the variation of contrast. The presence of the fluorescent layer appears to decrease greatly the amount of chemical fog produced, as was clearly shown by coating plates in certain regions only.

While the method can be applied in principle at all wave-lengths, its satisfactory extension to the region below 2000A depends on finding a carrier more transparent in that region than gelatin, while it could be used at wave-lengths greater than 3700A by coating a red sensitive plate with a substance fluorescing in that region. Preliminary experiments with a solution of chlorophyll have proven successful in giving uniform contrast up to where the green absorption band begins.

It should be emphasized that a decrease in sensitivity results at many wave-lengths when the fluorescent coating is used, as is indeed true of oil coatings also. This is usually an advantage in photometry, since the decrease is greatest at long wave-lengths where most other causes unite to give the greatest response. We expect to publish shortly a detailed account of our new methods of fluorescent photometry, which promise to greatly simplify not only homochromatic but heterochromatic photographic photometry as well.

GEORGE R. HARRISON
PHILIP A. LEIGHTON

Stanford University,
August 1, 1930.

BOOK REVIEWS

Einführung in die Theorie der Wärme, being volume V of *Einführung in die Theoretische Physik*. MAX PLANCK. 251 pages, 15×22.5 cm, S. Hirzel, Leipzig, 1930. Price 8 RM, bound, 10 RM.

This is the fifth and final volume of Planck's series on theoretical physics designed for reference by the student who wishes either to supplement a lecture course or even to work the subject up by himself. The first volume on general mechanics is already in its fourth edition. The second, third and fourth volumes deal respectively with the mechanics of deformable bodies, electricity and magnetism, and theoretical optics.

The book is divided into four parts: thermodynamics, heat conduction, thermal radiation, and atomistics and quantum theory. The first and third parts cover much the same ground as Planck's two books on general thermodynamics and thermal radiation, except that they are of necessity shorter and cannot go so much into the details of the applications. The second part, except for an interesting application of the second law to derive a necessary restriction which the equation of heat conduction must satisfy, is mostly occupied with the solution of the simpler problems of heat flow with different sorts of boundary conditions which were the conventional subject matter of books on the older mathematical physics, and is different in character from the rest of the book. The fourth part constitutes the most novel part, and is responsible for the somewhat unusual position of this volume on heat after the volumes on electrodynamics and theoretical optics. In this part the statistical method is introduced, the statistical significance of the thermodynamic concepts of temperature, entropy, and thermodynamic potential is developed, and applications made in deducing the equations of state of perfect gases and perfect solids and the value of the chemical constant. The close welding of the points of view of formal classical thermodynamics and statistical theory which is achieved in this book is very important for the student, and is something to which more attention might be paid in courses of instruction in this country.

The fundamental point of view of Planck in expounding the concepts at the basis of his statistical treatment may be described as "classical". It is a great merit of his clear exposition that the reader is driven to feel the inadequacy of many of these concepts in the light of the Heisenberg principle. Statistical mechanics cannot much longer avoid the task of making a clean-cut formulation of what is fundamentally observable and what is invention in its treatment of "microscopic states".

P. W. BRIDGMAN

Les Rayons X. J. THIBAUD. Pp. 218. Figs. 77. Librairie Armand Colin, Paris, 1930. Price 10 f. 50 (60 cents).

The excellence of the Collection Armand Colin and the favorable rate of exchange are two sound arguments for requiring of graduate students an early familiarity with French. Dr. Thibaud's book in this series gives a concise and lucid account of the important aspects of x-rays and their relation to allied physical problems. About one quarter of the text is usefully devoted to technique and applications; another short section deals with radiations in adjoining regions of the spectrum (gamma-rays and very soft x-rays) illustrating particularly the recent investigations of the author. Complicated mathematical discussions are avoided; formulas are in general quoted without derivation, but a bibliography shows where the information may be found if required. Unfortunately, the pocket size ($4\frac{1}{2}\times 7$ inches) of the volume makes some of the diagrams inconveniently small, and, as in many French texts, there is no adequate index. The book is to be recommended to those who desire a general survey of the subject before proceeding to the detailed study of some particular branch of x-rays.

THOMAS H. OSGOOD

X-Rays. B. L. WORSNOP. Pp. viii+101. Figs. 36. E. P. Dutton and Company Inc., New York, 1930. Price \$1.10.

This small volume is designed to provide for advanced students and for others whose main interest lies in some other field of physics a concise account of the subject of x-rays. The author gives a clear exposition of the phenomena of the production of x-rays, crystal reflection, scattering, emission and absorption and the photoelectric effect, with good descriptions of the fundamental methods of experiment. The last chapter deals with refraction and total reflection. Intermediate students studying x-rays for the first time in some detail will find in the easier portions of the book a useful summary of their subject.

The print and diagrams are excellent; there is an adequate list of standard reference books followed by a complete index.

THOMAS H. OSGOOD

Jahrbuch des Forschungs. Instituts der Allgemeinen Elektrizitäts-Gesellschaft, Erster Band, 1928-1929. Pp. 240. Julius Springer, Berlin, 1930.

This is a complete and uniform reprinting of thirty-five articles published by members of the staff of the Research Institute of the German General Electric Company during the years 1928 and 1929. The articles are arranged in groups according to subject matter (acoustics, electron physics, atomic physics, etc.) and each group is preceded by a brief statement concerning the material contained therein. In an introduction Dr. C. Ramsauer, the director, explains the aims and policies of the Laboratory and the purpose of the year book of which this is Volume I.

Among the papers of particular interest to physicists are those by Ramsauer and Kollath and by Bruche on the apparent cross-sectional areas of various atoms and molecules as determined by the Ramsauer method, and the numerous ones by Rupp on the diffraction of electrons.

The volume contains also a record of the public appearances of members of the staff together with a list of résumés and popular expositions published during the year but not reprinted in the present collection.

It is evident that every feature of this book has received most careful consideration, and that no expense has been spared to make it a model publication of its kind.

C. J. DAVISSON

PROCEEDINGS
OF THE
AMERICAN PHYSICAL SOCIETY

MINUTES OF THE EUGENE MEETING, JUNE 19-21, 1930

The 164th regular meeting of the American Physical society was held in Room 103, Deady Hall, University of Oregon, Eugene, Oregon, on Thursday afternoon, June 19, Friday June 20, and Saturday morning, June 21, in affiliation with Section B, Physics, of the Pacific Division of the American Association for the Advancement of Science.

The session on Thursday afternoon consisted of a joint symposium between the American Physical Society and the Astronomical Society of the Pacific and the general topic was the red shift in the spectra of distant light sources and its physical interpretation. There were three papers by invitation as follows:

1. **Apparent velocity shifts in the spectra of faint nebulae.**—MILTON L. HUMASON, *Mt. Wilson Observatory.*
2. **Distances of nebulae and their correlation with apparent velocities.**—EDWIN HUBBLE, *Mt. Wilson Observatory.*
3. **Significance of the velocity-distance relation from the standpoint of general relativity.**—RICHARD C. TOLMAN, *California Institute of Technology.*

On Friday morning preceding the presentation of papers the regular business session or meeting was opened for discussion of any business which might arise. On nomination Professor W. P. Boynton, Chairman of the Department of Physics, University of Oregon, presided at the meeting. It was moved, seconded and voted that the date of the 167th meeting of the American Physical Society which had been scheduled to be held at the University of California at Los Angeles on December 5 and 6, 1930, be changed as follows: The 167th meeting of the American Physical Society will be held at the University of California at Los Angeles on December 12 and 13, 1930, the meeting being a joint meeting between the American Physical Society and the Acoustical Society of America.

Following the morning session on Friday, there was a joint luncheon of the astronomers and the members of the American Physical Society at which 50 members were present.

Following the session on Saturday morning, June 21, the meeting adjourned, there having been 18 papers on the regular program and 7 papers on the supplementary program of which numbers 10, 16 and 25 were read by title. The abstracts of these papers are given on the following pages. An **Author Index** will be found at the end.

LEONARD B. LOEB, *Secretary for Pacific Coast.*

ABSTRACTS

1. The near infrared spectrum of Hg. H. J. UNGER, *University of Oregon*. (Introduced by E. D. McAlister.)—With a self-recording spectrometer the infrared spectrum of the Hg arc has been studied in the region 1 to 2μ . Several lines hitherto observed as single have been resolved into two or more lines. Of special interest are the groups of lines near 1.7μ and 1.2μ which contain the first and second members of the fundamental triplet series. The results obtained indicate that possibly the fundamental triplets are composed of six lines grouped as in the diffuse series.

2. Continuous spectrum in the region 500–1100. J. J. HOPFIELD. *University of California*.—An intense continuous spectrum has been observed in helium in the region 500–1100A. This is the only continuous spectrum known extending throughout the range 500–900A, and it therefore allows one to explore this interesting region for absorption spectra. I think the grating mounting used imposes the present ultraviolet limit of this spectrum. This spectrum is most intense when the helium bands are best developed, showing that they are closely related phenomena. To produce it the helium should be fairly pure, at a few millimeters pressure and a mild condensed discharge should be used. The spectrum contains the neon and helium lines which are useful as standards. It may also be satisfactorily observed in the second order. The spectrum resembles the continuous spectrum of hydrogen in the Schumann region. Its analogous explanation may be as follows. Two helium atoms each excited to the 2^3S state unite to form the molecule. The energy representing these changes is about 41.8 volts. If the electronic configuration of this molecule changes to that of the "normal," unstable state it immediately dissociates emitting 41.8 volts of energy. The continuous extension of this spectrum towards the red is due to the non-quantized kinetic energy subtracted from the above amount by the unbound atoms.

3. High resolution in the near infrared. E. D. McALISTER, *University of Oregon*.—With two 60° and one 30° prism (all of flint glass 4 inches high, 6 inches length of face) and a parabolic mirror 5.5 in. in diameter and 24 in. focal length in the Littrow form of mounting an effective slit width of $6A$ is obtained in the region 1 to 2μ . This type of mounting gives a dispersion equivalent to 5 sixty degree prisms. A special type of thermocouple is used for detection. The spectrograph is self-recording. With a galvanometer distance of 5 meters the zero drift in one hour's time is usually less than one millimeter. The construction of the thermocouple and housing are discussed and typical spectrograms are exhibited.

4. Some properties of the third positive carbon and associated bands. JOSEPH KAPLAN, *University of California at Los Angeles*.—The third positive group of CO, and the two systems usually associated with it, the $5B$ and $3A$, have been studied under a variety of excitation conditions in an attempt to excite progressions other than the $v'=0$ ones. Some interesting observations have been made. No progressions other than the $v'=0$ ones have been observed in spite of the fact that each of these groups has been intensely excited. This, together with other facts and observations can be interpreted as indicating that the levels involved in these three systems are triplet levels. A new system of bands similar in appearance to these bands has been observed. The 0-0 and 0-1 bands of the $5B$ group are exactly similar in appearance, but differ strikingly from the higher members of the group. The diffuse double-headed band observed outside the third head of the 0-0 $5B$ band and ascribed to CO_2 by Asundi is thought to be a real part of the CO band since a similar doublet is observed in the 0-1 band. A pair of complex but similar bands have been observed on the long wave-length side of the 0-0 $5B$ band and the 0-1 third positive band.

5. The classification of iron lines. HAROLD D. BABCOCK, *Mount Wilson Observatory*.—In an earlier discussion, (*Astrophys. J.* 67, 240, 1928), mean energy-levels were found for both upper and lower terms associated with each temperature class and pressure group. Repeating this work with more data, with weights proportional to the numbers of lines dependent on each term, and including King's study of dissymmetry in the high-current arc, (*Astrophys. J.*

62, 238, 1925), a broad parallelism is found between the three systems of classification. The terms of iron fall into three significant groups: 1, even terms of low level; 2, even terms of high level; 3, odd terms of medium level. The methods of classification may have a physical basis in the characteristics of these groups of terms. The energy level of a term, its odd or even character, and its part in the transition, i.e., whether it is the upper or the lower term involved, are factors which apparently determine the kind of lines associated with the term. This review of the data for iron may thus assist in the converse problem of finding the terms from observations of the position and peculiarities of a spectral line.

6. Reflection of x-rays from thin metallic films. JOS. E. HENDERSON AND E. B. JORDAN, *University of Washington*.—The critical angles of reflection for zirconium filtered molybdenum radiation have been investigated for sputtered gold and silver films of thicknesses ranging from very thin transparent films to thick opaque films. The gold films were backed with glass and the silver films with gold. Curves are plotted showing the critical angle as ordinate and thickness of the film as abscissa. For the gold on glass the curve rises, as the thickness increases, from the value for glass to a maximum value and then falls to a value which is independent of the thickness of the gold and therefore characteristic of gold. This value is approximately two-thirds of the maximum. As the above is a case for a material with critical angle larger than the backing material, silver on gold was investigated in order to obtain the opposite condition. The curve in this case again rises to a maximum greater than for gold alone for small thicknesses, falling to a value for large thicknesses which is less than the value for gold alone. A study of gold on silver is now in progress.

7. Experiments on the relative intensities of x-ray lines in the L -spectrum of tantalum. VICTOR HICKS, *University of California*.—The relative intensities of 17 lines in the L -spectrum of Ta have been investigated by the ionization spectrometer. The following precautions were taken: (1) the rays were taken at a glancing angle of 45° from a polished Ta surface, (2) a Ta filament was used, (3) the slits were enclosed in an arm of the tube, reducing the air path of the rays to 7 cm, (4) the coefficient of reflection of the crystal used was measured for the various wave-lengths by means of the double-spectrometer, (5) the absorption coefficients of the mica windows used were directly measured, (6) the rays were completely absorbed in methyl iodide vapor of known pressure, and (7) the slits were sufficiently wide to eliminate effects arising from the different natural widths of the lines. Measurements were taken at 30.6 K.V. and 20.7 K.V. and corrected to high voltage. The results for lines of small wave-length separation agree well with previous results of Allison and Armstrong and Jönsson on tungsten. For lines of larger wave-length separation ($L\alpha_1$, $L\beta_1$) the results of Jönsson are not confirmed, but the previous qualitative estimates of Allison and Armstrong are substantiated. The assumption that the ionization currents produced are proportional to the relative intensities is supported by recent work of A. H. Compton. If the ν^4 correction is made to the intensities at high voltage the sum rules are approximately valid except for lines having initial state L_1 . The intensity results are:

	l	α_2	α_1	η	β_4	β_1	β_3	β_2	β_7	$\beta_5 + \beta_{10}$
Rel. Int. at 30.6 K.V.	1.5	10.2	100	1.3	9.4	92.6	13.5	40.6	0.8	1.1
Rel. Int. at high V.	1.5	10.2	100	1.4	11.1	102.7	15.9	40.6	0.8	1.1

	β_8	γ_5	γ_1	γ_6	γ_2	γ_3	γ_4
Rel. Int. at 30.6 K.V.	0.8	1.24	29.1	0.6	4.98	7.08	2.20
Rel. Int. at high V.	0.8	1.38	32.3	0.7	5.88	8.37	2.60

8. Electronic emission from a metal target: bombarded with positive ions. C. L. UTTERBACK AND W. GEER, *University of Washington*.—Metal targets have been bombarded by positive ions whose energies varied from 200 to 750 volts, while the characteristics of the electron emission were studied. The secondary emission and positive ion currents were measured by galvanometers of sensitivities $8 \cdot 10^{-11}$ amperes and $6 \cdot 10^{-10}$ amperes, respectively. The secondary

emission has been found to depend upon the previous treatment of the target, especially in regard to the kind and amount of gas adsorbed and to the duration of the bombardment. These studies were made with positive ion currents as low as $3 \cdot 10^{-9}$ amperes, which is a smaller current than has been heretofore used in this connection.

9. The scattering of electrons in small angles by gas molecules and its effect on the electron absorption coefficient. METTA CLARE GREEN, *University of California*.—An indirect study of the scattering of electrons by gas molecules was made by measuring electron absorption coefficients in an apparatus containing a Faraday cylinder of variable aperture. A straight path method was used in which electrons from an oxide-coated filament were given a desired acceleration and made to traverse a 7.5 path to the collector. A retarding potential between the cylinder and its shield kept out all electrons which had suffered inelastic collisions as well as those which had been scattered outside of the collector opening. Measurements were made in argon, helium, hydrogen, and mercury vapor at accelerating potentials ranging from 11 to 196 volts. The radius of the cylinder aperture was varied from one hundredth to one tenth of the path length. No consistent variation of absorption coefficient with opening was found in any case. Theoretical calculations based on scattering laws obtained from inverse square or fifth power laws of force predicted relatively large variations. Calculations made assuming uniform scattering or the Sommerfeld law indicated small changes of the same order of magnitude as the observed experimental deviations.

10. The magnetic properties of dilute cobalt alloys. F. WOODBRIDGE CONSTANT, *California Institute of Technology*.—Continuing the investigation of the ferromagnetic properties of the cobalt atom when it is further and further isolated from other cobalt atoms by the presence of intervening non-ferromagnetic atoms, alloys of still higher platinum concentration than those previously reported on, (*Phys. Rev.* **34**, 1217, 1929), were tested magnetically. As found before, decreasing the cobalt content decreased the Curie point and magnetic hysteresis, the former, on the absolute scale, falling linearly. For comparison, similar alloys of palladium and cobalt were investigated, and found to behave similarly, thus confirming the view that the ferromagnetism of these alloys may be attributed to the cobalt atoms. The following table gives the Curie points in degrees Kelvin, and the maximum intensity of magnetization obtainable at the temperature of liquid air, (-194°C.):

		Curie Point	\dot{I}_{max}
10	% Co—90 % Pt	522°K	364
5	% Co—95 % Pt	322°K	254
3	% Co—97 % Pt	191°K	104
1.5	% Co—98.5% Pt	82°K	7
10	% Co—90 % Pd	508°K	223
5	% Co—95 % Pd	355°K	193

11. Discovery and rough measurement of a new electron inertia effect. S. J. BARNETT, *University of California at Los Angeles and California Institute of Technology*.—This effect, like its converse (Tolman and Stewart), was in the mind of Maxwell long ago (*Treatise* §574): An e.m.f. applied to a metallic conductor drives the free electrons and the remainder in opposite directions. A solenoid S is suspended vertical in a neutral region. If traversed by a current with its own natural frequency $\nu = \omega/2\pi$, the coil has a magnetic moment $\mu = M \sin \omega t$, and resonant vibration with amplitude A_M occurs. The rod holding the solenoid carries a magnet below, with horizontal moment m_0 , at the center of a small fixed Helmholtz coil H (constant Γ) with axis normal to m_0 . This coil, if traversed by a current $i = I \sin (\omega t + \epsilon)$, produces an amplitude A_I . When A_M is small theory gives

$$\left| 2 \frac{m}{e} \right| = \frac{A_M}{A_I} \cdot \frac{\Gamma m_0 I}{\omega M}$$

If S is surrounded by a longer solenoid S' (constant γ) properly connected in circuit (resistance R) with H , the sum of the torque on S due to electron inertia ($-2m/e \cdot \dot{\mu}$) and that on the mag-

net $(-\Gamma\gamma m_0 \cdot \dot{\mu})/R$, together with the amplitude, will vanish for one value R_0 of R . Then $-2m/e = (\Gamma\gamma m_0)/R_0$. For copper $2m/e$ has been determined both ways. The sign (from null method) proves e negative, and the magnitude is that expected within the limits of the experimental error (about 10%). The theory has been worked out completely. For large amplitudes the inertia torque contains a term involving the number of electrons per unit volume, whose determination refinements may perhaps make possible.

12. The recombination of ions in air and oxygen in relation to the nature of gaseous ions.

OVERTON LUHR, *University of California*.—The coefficient of recombination of ions in air and oxygen has been measured using an improved form of the method previously described by L. C. Marshall. The coefficient of recombination, α given by the law $dn/dt = -\alpha n^2$ is calculated from the integrated form $\alpha = 1/t(1/n - 1/n_0)$. It is found that α varies continuously with the age of the ions, dropping sharply within 0.05 seconds from 2.7×10^{-6} to 1.4×10^{-6} , then dropping more slowly to about 0.4×10^{-6} when the age of the ions is two seconds. Higher values of α are obtained when the initial concentration of the ions is smaller or when pure oxygen is used in place of air. In accord with Marshall and other observers, the sharp initial drop in α is assumed to be due to the initial non-random distribution of the ions. The later more gradual drop may be explained by assuming that the ions form heavy, slow moving clusters with molecules of impurity. The faster ions are constantly being removed at a high rate by recombination leaving the slow ions behind with a resulting increasingly low coefficient of recombination. The impurities may consist of nitric oxides, O_3 , or H_2O_2 formed by the ionizing agent. Taking the point at which the rapid decrease in α ends and the more gradual drop due to clustering begins, an "absolute value" of α for air is set at $1.4 \pm 0.1 \times 10^{-6}$.

13. Cataphoresis in rotating electric fields. E. M. PUGH AND C. A. SWARTZ, *California*

Institute of Technology.—A new method of making cataphoresis measurements on colloid particles has been developed and tested. The method makes use of a rotating electric field which causes the particles to move in circles. In this way, it is easily possible to test the effect of variable speed of the particle on the distribution of the diffuse electric double layer surrounding it. The results obtained indicate that this effect is negligible. Furthermore, it has been discovered that the mobility of the small particles (below 10^{-4} cm in diameter) fluctuates widely and this is made very evident to the eye by the fluctuations in the circular paths of the particles. The fluctuations are quite violent with particles as small as 10^{-6} cm diameter. Considerable study of these variations has been made as well as an attempt to explain them qualitatively.

14. Equations of state and thermodynamic functions for a substance with variable specific

heat. W. P. BOYNTON, *University of Oregon*.—General relations between the specific heat at constant volume (not assumed constant) and pressure, temperature and volume are deduced from the first and second laws of thermodynamics. Applying these to a generalized equation of the van der Waals type, expressions are derived for the specific heat at constant volume, energy and entropy. The Boynton and Bramley equation proposed in 1922 is shown to be a special case. Its difficulties and limitations are briefly discussed, and a modification having some advantages for very low temperatures is suggested.

15. A note on the quantization of the solar system. A. E. CASWELL, *University of Oregon*.—

A study of the relations between the mean distances of the planets from the sun, and of the satellites from their respective planets, the periodic times and the masses, seems to point to the operation of a number of causes, which results in a sort of quantization of distances, periods, and energies. Such a study gives some promise of revealing new principles that may aid in the solution of the problem of n bodies moving under the influence of an inverse square law.

16. Thermal expansion of M-M-M alloy. PETER HIDNERT AND W. T. SWEENEY, *U. S.*

Bureau of Standards.—In 1923 determinations were made at the Bureau of Standards, on the linear thermal expansion of a nickel alloy known as M-M-M alloy. This alloy was cast in a sand mold. The approximate composition was as follows: Nickel 61, copper 25, tin 9, iron

$3\frac{1}{2}$, manganese $\frac{3}{4}$, silicon $\frac{3}{4}$ percent. It is claimed that this alloy is acid resistant and resistant to the erosion of high temperature, high pressure steam. Manning, Maxwell and Moore, Inc., Bridgeport, Conn., prepared the alloy and furnished information about the treatment and the chemical composition. Data on tensile properties of M-M-M alloy are given in Circular of the Bureau of Standards No. 100 (2nd edition), p. 107. The following coefficients of linear expansion were obtained:

Temperature range	Average coefficient of expansion per degree centigrade
20 to 180°C	14.1×10^{-6}
180 to 350	15.6
350 to 485	18.5
20 to 350	14.8
350 to 500	18.7
20 to 485	15.9
20 to 500	16.0

After heating to 500° C. and cooling to room temperature, the cast alloy was found to be 0.02 percent shorter than the original length.

17. Polar properties of single crystals of ice. JOHN MEAD ADAMS, *University of California at Los Angeles*.—That the ice-crystal is unsymmetrical with respect to the basal (0001) plane has now been established by the observation that crystals twinned on this plane are separable into two kinds: (a) those which may develop pits at the ends of the *C* axis, and (b) those which may develop a cavity at the *middle* of the *C* axis. The phenomenon appears to suggest that the polar character of the crystal extends to the mechanism of thermal conduction in it.

18. Absorption coefficient of slow hydrogen positive rays in hydrogen. R. E. HOLZER, *University of California*.—With an ionization tube of the type employed by Smyth, Hogness and Lunn and others, and a magnetic field for resolution, the absorption coefficients of H^+ , H_2^+ , and H_3^+ in hydrogen were studied in the region between 50 and 300 volts. The gas pressures in the ionization and scattering chambers were controlled by steady flow through capillary tubes and were made nearly independent by the introduction of a high speed pump between the chambers. The variation of the intensity of a beam of ions of given mass and velocity was observed by means of a Compton electrometer as the pressure in the scattering chamber was changed. H_2^+ was absorbed more strongly than H_3^+ , and H^+ appreciably less than the other ions. All of the absorption coefficients rose with decreasing velocity.

19. The quenching of mercury resonance radiation by nitrogen and carbon monoxide. JOSEPH KAPLAN, *University of California at Los Angeles*.—All of the experiments on the quenching of mercury resonance radiation by foreign gases yield the result that CO is more effective than N_2 . The discovery by the writer of an intense single band in CO at 2575Å has suggested a more thorough comparison of the quenching powers of CO and N_2 than has heretofore been done. The new band appears under unusual discharge conditions and very closely resembles the fourth positive bands of CO. Therefore if it is interpreted as arising in a transition from some low lying level to the normal level of CO, the greater quenching power of CO over N_2 can be explained. N_2 possesses no electronic level around 5 volts and a calculation of the vibrational states of CO associated with the normal state shows that none of them agree as well with the energies of the 2^3P_1 and 2^3P_0 states of Hg as do the X_{18} and X_{19} states of N_2 . The latter fit almost perfectly and this close agreement suggests a discussion of the relative quenching power of N_2 and H_2 as well as a new explanation of Gaviola's photosensitized fluorescence of NH.

20. The recombination of ions in argon, nitrogen and hydrogen. OVERTON LUHR, *University of California*.—Since free electrons are known to exist in ionized A, N_2 and H_2 these gases are employed in an effort to measure directly the coefficient of recombination between

positive ions and electrons. Previous indirect methods and theory indicate that the coefficient of recombination, α is of the order of 10^{-10} for ions and electrons compared to 10^{-6} for positive and negative ions. In the present work results similar to those in air are obtained, only a slight change in α being observed when sufficient oxygen is added to cause instant attachment of the free electrons. Hence it is probable that recombination was taking place between positive and negative ions although free electrons were present initially in the pure gases. It is assumed that negative ions are formed by attachment to excited metastable molecules in the case of A and N_2 , and by attachment to atoms or triatomic molecules in the case of H_2 . In accordance with the criterion established in a previous paper for air, "absolute values" of α are set as follows: air, $1.4 \pm 0.1 \times 10^{-6}$; O_2 , $1.5 \pm 0.1 \times 10^{-6}$; A and N_2 , $1.2 \pm 0.1 \times 10^{-6}$; H_2 , $0.32 \pm 0.05 \times 10^{-6}$. The results in H_2 show a constant value of $0.32 \pm 0.05 \times 10^{-6}$ which is much lower than in the other gases contrary to the prediction of the J. J. Thomson theory of recombination. However, the theory is deficient in certain respects which may explain this discrepancy.

21. Further work on the rotation of soft iron and permalloy by magnetization and the gyromagnetic anomaly. S. J. BARNETT, *University of California at Los Angeles and California Institute of Technology*.—This is an extension of work reported in June 1927 and April 1928. By hundreds of days and hundreds of nights of labor, much interfered with by magnetic storms, great improvements have been effected in the methods and in the precision of the results. Nearly all of the observations have been made by one of the large deflection methods, perfected by (1) the use of improved commutators and brush systems, (2) the adoption of devices to eliminate rapidly systematic errors due to magnetostriction, and (3) the adoption of a more rigorous and systematic time schedule in the observation of deflections. The frequency range has been extended upward to about 21 cycles per second, and the range of magnetic field strengths has been extended downward to 2 and upward to 80 gauss (uncorrected for end effects). No differences in the gyromagnetic ratio have been revealed, except that (as formerly) the value found for permalloy slightly exceeds that found for iron. The new values are close to those previously published, m/e , the orthodox value for a spinning electron, being exceeded by several percent with great probability.

22. New oxygen spectra in the ultraviolet. J. J. HOPFIELD, *University of California*.—The resonance series of atomic oxygen has been extended to about twelve members and strong continuous spectrum was found to set in at the series limit and extend towards the ultraviolet. Many new lines, probably due chiefly to O_1 , have been found in oxygen and in oxygen-helium mixtures. A new progression of bands, forming a series of final vibration states, has been found in oxygen mixed with helium when a condensed discharge was employed. These seem to be fluorescent bands similar to those found in hydrogen by Lyman. The bands belong to an electronic system which has not been previously observed. The fine structure appearance seems to indicate that they are bands of normal O_2 . They resemble the Schumann bands in appearance, but they are degraded to the ultraviolet whereas the Schumann bands shade towards the red. The wave-lengths in vacuum are $\lambda 2031.5A$, (2077.3A), 2123.8A, 2170.7A and 2218.2A. The second band is masked by second order atomic lines. The first differences in cm^{-1} are (1085), (1053), 1018 and 987. The second differences are about $32 cm^{-1}$. $\lambda 2031A$ is probably the $v' = 0$ band but it is not certain that $v' = 0$ in this case.

23. New spectra in nitrogen. JOHN J. HOPFIELD, *University of California*.—With helium as a source of continuous light absorption band spectra of nitrogen have been found in the region $\lambda 600-1100A$. The bands in the region $750-1100A$ have not yet been measured. The only bands occurring below 750 are $\lambda 723.2$, 694.2, 681.7, 675.2 and 671.2A in absorption, and 715.2, 690.9, 680.1, and 674.3A is emission. They form approximate Rydberg series with the common limit of 18.6 volts, and represent the first case of a Rydberg series in molecules other than hydrogen and helium. These bands are provisionally ascribed to nitrogen and the limit (18.6) would represent ionization from an electronic state deeper than the normal one. In a nitrogen-helium mixture the resonance series of N_1 with $2p^4S(117345)$ as limit have been extended to ten members and a strong continuous spectrum has been found at the series limit. The

value of the 4S term remains unaltered by these new measurements. The series of lines ending on the metastable states $2p^2D$ and $2p^2P$ of nitrogen have been greatly extended but as yet not measured. In the helium-nitrogen mixture a new system of bands in emission has been observed. The bands shade towards the red and show alternating intensities of the lines. Approximate frequencies and provisional designations of the bands are: (0,0) $\lambda 1846.16A$, $\nu 54166$; (0,1) 52263, (0,2) 50390, (1,0) 56142, (1,1) 54235, (1,2) 52371, (1,3) 50532, (2,1) 56181, (2,2) 54311, (2,3) 52475, (2,4) 50677, (3,2) 56221, (3,4), 52584, (3,5) 50824.

24. On an electromagnetic theory of sight and color vision. S. R. COOK, *College of the Pacific*.—The paper reviews briefly the theories of color vision from that of Thomas Young to the latest photoelectric theory of Jenett Clark. It then makes the general hypothesis that the transmission of sight is a process equivalent to an alternating current of electricity set up in the rods and cones of the retina by the electromagnetic vibrations of light. The time of vibrations of this alternating current process is represented by the well-known formula $\nu = 1/2\pi[(1/CL) - (R^2/4L^2)]^{1/2}$. The receptors in the rods are tuned to all wave-lengths of light. The receptors in the cones are tuned to the special vibrations which they transmit, that is, some are tuned to red, others to green, and others to blue. Color blindness is the imperfect tuning of one or more special classes of receptors in the cones. Residual or after images may be the result of electrolytic action in the nuclear and ganglion cells, or it may be a physiological and psychological effect in the brain.

25. Mobility of Na^+ ions in H_2 . LEONARD B. LOEB, *University of California*.—A study of the mobility of Na^+ ions from a Kunsman catalyst source has been made in H_2 gas using a square wave from an oscillator with the original Rutherford A.C. method as adapted for use with a Kunsman source. The preliminary results cover measurements made from 0.6 to 7.0 cm Hg pressure, the chamber being of brass and filled with tank H_2 passed over hot copper and a purifying train of a standard sort used by the writer, including liquid air traps. Preliminary results were obtained for frequencies from 1000–50,000 half cycles. The reduced mobilities corrected for density but not for temperature (mobilities are little affected by temperature in moderate ranges) varied from 5 to 7 cm/sec per volt/cm at from 1000–5000 half cycles. Above this frequency they increased to a value of about 12 to 16 cm/sec per volt/cm at from 20,000 half cycles upward. The lower values were about those to be expected for normal positive ions in H_2 as affected by the uncertainty of gas temperature and density with the gradients produced by the source. The higher values probably correspond to the mobility of the Na^+ ions in H_2 , without any modification. The nature of the mobility curves obtained indicates that there are probably two carriers of different mobility existing simultaneously in the intermediate frequency range. This would point to a more or less abrupt transition from the one type of ion to the other.

AUTHOR INDEX

Adams, John Mead—No. 17

Babcock, Harold D.—No. 5

Barnett, S. J.—Nos. 11, 21

Boynton, W. P.—No. 14

Caswell, A. E.—No. 15

Constant, F. Woodbridge—No. 10

Cook, S. R.—No. 24

Geer, W.—see Utterback

Green, Metta Clare—No. 9

Henderson, Jos. E. and E. B. Jordan—No. 6

Hicks, Victor—No. 7

Hidnert, Peter and W. T. Sweeney—No. 16

Holzer, R. E.—No. 18

Hopfield, J. J.—Nos. 2, 22, 23

Jordon, E. B.—see Henderson

Kaplan, Joseph—Nos. 4, 19

Loeb, Leonard B.—No. 25

Luhr, Overton—Nos. 12, 20

McAlister, E. D.—No. 3

Pugh, E. M. and C. A. Swartz—No. 13

Swartz, C. A.—see Pugh

Sweeney, W. T.—see Hidnert

Unger, H. J.—No. 1

Utterback, C. L. and W. Geer—No. 8

THE PHYSICAL REVIEW

A DOUBLE CRYSTAL STUDY OF SCATTERED X-RAYS

BY J. A. BEARDEN

ROWLAND HALL, JOHNS HOPKINS UNIVERSITY

(Received July 14, 1930)

ABSTRACT

A study of the unmodified scattered x-rays has been made to detect possible fine structure lines as reported by previous experimenters. With copper and silver *K* series scattered by blocks of graphite and aluminum no trace of any fine structure lines was observed. The sensitivity of the apparatus was apparently many times that used by any previous experimenter. Experiments were also performed to measure the change in wave-length and the width of the modified line. It was found that the change in wave-length agreed within one percent with the change predicted by the quantum theory of x-rays scattered by free electrons. That is, with the equation $\delta\lambda = (h/mc)(1 - \cos \phi)$. The width of the modified line was found to be about twice as broad as it should have been from the divergence of the scattering angle.

SPECTROSCOPIC analyses of scattered x-rays have been made by numerous investigators¹ both by photographic and ionization methods. The results of these experiments have been in general to show the existence of two wave-lengths instead of the single exciting wave-length. The exciting wave-lengths have been found to appear (unmodified line) unchanged in wave-length and apparently unchanged in width. The modified wave-length (Compton effect) has in most experiments appeared broader than the unmodified line and its change in wave-length from the exciting wave-length seemed to be given by the quantum theory of scattering by free electrons.

With the introduction of the double crystal spectrometer² which secured high resolving power and great intensity it was possible to make a more detailed study of scattered x-rays than had been possible with the single crystal method. In a series of experiments by Davis³ and his collaborators using the double crystal method it was shown that both the modified and unmodified line was not a single line but a group of lines very close together. The relative intensity and position of the fine structure lines in the modified and the unmodified line were found to be similar. This result which indicated similar structure and width of the two lines was in definite disagreement

¹ A. H. Compton "X-rays and Electrons," p. 261, 270.

² Davis and Purks, Proc. Nat. Acad. 13, 419 (1927).

³ Mitchell and Davis, Phys. Rev. 31, 1119 (1928); Davis and Mitchell, 32, 331 (1928); D. P. Mitchell, 33, 871 (1929); Davis and Purks, 34, 1 (1929).

with earlier experiments using single crystals. However, few if any experiments had been performed in which such fine structure could have been detected. The wave-length of these fine structure lines was thought to be explicable on the quantum theory of x-rays scattered from bound electrons.

Since the announcement of this discovery several attempts have been made to find these fine structure lines with a single crystal by using very narrow slits and recording them on a photographic plate. In the first of these experiments by Ehrenberg⁴ a Seemann spectrograph with a calcite crystal was used. The scattering angle was 90° and the molybdenum $K\alpha$ x-rays were scattered from carbon. In the second experiments by Coster,⁵ a Siegbahn spectrograph was used. Carbon (graphite) was used as a scatterer and the molybdenum $K\alpha$ x-rays were used. Two scattering angles were used, one 25° to 50° , and the other a much larger angle which was not recorded. Since the separation of the fine structure lines from the parent line should be greater for the heavier elements Kast⁶ performed an experiment somewhat similar to Ehrenberg's but using aluminum as a scattering substance. In all these experiments no fine structure lines were observed. In these measurements the search has been to find the fine structure lines in the unmodified line because its width and position are independent of the scattering angle. Since a large fraction of the x-rays scattered by graphite or aluminum block may be due to the crystalline diffraction it is important to observe the modified line. In each of the above experiments the modified line was observed.

One of the greatest experimental difficulties in the study of scattered x-rays is the low intensity. Thus in the present experiment⁷ the arrangement of the apparatus was planned to secure the greatest intensity and at the same time to keep the stability of the apparatus such that all measurements could be reproduced from day to day.

The intensity of scattered x-rays⁸ is inversely proportional to the atomic number of the scatterer and inversely proportional to the cube of the wave length. Thus the use of carbon and other light elements have in most cases been used as the scattering material. The optimum wave-length is, however, not so easily determined. Previous experimenters have in general used either molybdenum or silver characteristic K x-rays. For the voltages usually employed the characteristic K -lines lie very close to the maximum intensity of the continuous radiation. This continuous radiation which is many times the intensity of the characteristic K -radiation is scattered from the scattering block and thence from the crystal into the ionization chamber. One has then the small effect of the characteristic K -lines superimposed upon a very intense background. In many experiments the intensity of the lines has been less than 10 or 15 percent of the total intensity recorded by the electrometer. However, if one uses long characteristic wave-lengths the scattering block

⁴ Ehrenberg, *Zeits. f. Physik* **53**, 234 (1929).

⁵ Coster, Nitta, and Thyssen, *Nature*, April 27 (1929).

⁶ Kast, *Zeits. f. Physik* **58**, 519 (1929).

⁷ Read at the Washington Meeting of the Am. Phys. Soc., April 1930.

⁸ Davis, *Phys. Rev.* **25**, 737 (1925).

can be made very thin and still absorb most of the characteristic x-rays and also scatter but very little of the intense short wave-lengths. The crystal angles are also much larger which reduces the general scattering in the direction of the ionization chamber. The writer has thus been able to make measurements using the copper $K\alpha_{1,2}$ lines in which the fine structure lines should be separated from the parent line many times as much as in experiments using shorter wave-lengths. Experiments have also been performed using the silver $K\alpha_{1,2}$ lines.

At first the scattering blocks were attached to the cathode inside the x-ray tube but it was found that the evaporation of the target condensed on the scattering block giving a detectable fluorescence radiation. By supporting the scatterer from the target as shown in Fig. 1 the condensation seemed to be much less. However, when the x-ray tube was greatly overloaded condensation of the target material could be observed on the scattering block. In order to avoid this difficulty the focal spot of the x-ray tube

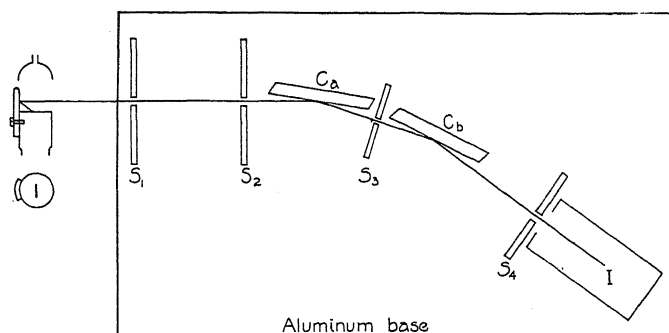


Fig. 1. Arrangement of apparatus as used in search of the fine structure in the unmodified line. In the experiment on the modified line the same arrangement was used except the scattering block was a cube supported by a small iron rod from the target.

was made large enough so that a minimum evaporation of the target occurred. The filament focusing cup used was very deep which gave a minimum number of "stray" electrons striking the scattering block. The shape and position of the focal spot were controlled as follows. A Helmholtz coil through which a 500 cycle current passed served to draw the circular focal spot out into a line focal spot. A second Helmholtz coil operated from a battery was used to locate the focal spot at any desired position on the face of the target. In the first experiments in which the fine structure was being sought in the unmodified line the focal spot line (10 mm \times 4 mm) was made parallel to the surface of the scattering block and placed about 4 or 5 mm from it. In this case the modified line was a broad band due to the large divergence in scattering angle. In the second experiment devised to measure the change in wave-length the focal spot line was made perpendicular to the face of the scattering block so the focal spot (10 mm \times 4 mm) appeared oblong when viewed from the scattering block. With this long focal spot the tube could

be operated at 75 m.a. and 50 k.v. but in order to make sure that no evaporation of the target occurred the current was never over 50 m.a. and voltage over 50 k.v. The x-ray tubes in all cases were kept connected to a mercury diffusion pump.

The spectrometer consisted of two separately mounted crystal tables which were rotated on accurately made centers by tangent screws. The ionization chamber (filled with argon for copper rays and methyl bromide for silver rays) was placed in a fixed position and the Compton electrometer mounted directly above it in order to reduce the electrical capacity to a minimum (15 cm). The sensitivity of the electrometer was about 20,000 divisions per volt. The two collimating lead slits (3 mm wide), the two crystal tables, and the ionization chamber system were mounted rigidly on an aluminum base so the whole outfit could be moved as a unit as shown in Fig. 1. The crystals used were split from a large very perfect calcite (Iceland spar) crystal. Three crystals were cut 2.5 cm \times 10 cm \times 1 cm and mounted in such a way that either surface could be used.

The position of the crystals and ionization chamber were determined by moving the aluminum base until the direct x-rays from the focal spot passed through the center of the slits S_1 and S_2 , Fig. 1. The crystal surfaces were placed parallel to and on the axis of rotation of the crystal tables. The crystal table C_a was then placed so the x-ray beam passed over the axis of the table and the crystal turned to reflect the $K\alpha_1$ line. Crystal C_b was then similarly adjusted to reflect the $K\alpha_1$ line which had previously been reflected from crystal C_a . Slits 4 mm wide were placed between the crystals and before the ionization chamber to reduce the amount of diffusely scattered rays entering the ionization chamber.

The aluminum base was then adjusted so that only the scattered rays from the scattering block could pass through the slits S_1 and S_2 . This was tested by placing a pin hole slit at the edge of slit S_1 on the side opposite the cathode and a photographic film over the slit S_2 . After a sufficient exposure to record an image of the target and scattering block a flash of light was passed through S_2 from the rear in order to record the exact position of the slit S_2 . The developed film then showed definitely whether or not direct rays were passing through the slits.

RESULTS

Copper $K\alpha_{1,2}$ scattered by graphite. The first experiment was performed with the first arrangement described above. That is, with the line of the focal spot parallel to the graphite and about 4 or 5 mm from it. The results are shown in the graph of Fig. 2. The approximate position of the two fine structure lines corresponding to those found by Davis are indicated by the solid vertical lines. The corresponding CK line would be at a scale reading of 3750 on the same graph. Measurements made in this region showed no line of measurable intensity. This graph is the average of several such curves. The intensity at the peak of the $K\alpha_1$ line was approximately 5/3 the intensity between the two lines.

Copper $K\alpha_{1,2}$ scattered by aluminum. Fig. 3 shows the results of the measurements on aluminum. The intensity of the $K\alpha_1$ peak in this case was about $3/2$ the intensity between the lines. Over the region where the fine structure lines should occur 10 sets of readings were taken. The average as shown in the graph shows no lines of intensity comparable to the α_1 and α_2 lines.

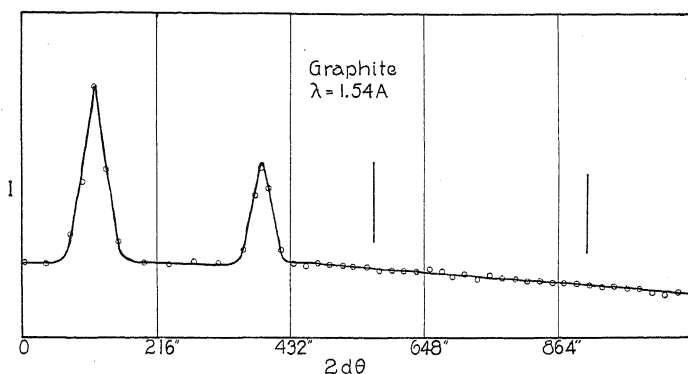


Fig. 2. The copper $K\alpha_{1,2}$ lines scattered by graphite. The two solid vertical lines are the positions corresponding to the fine structure lines as reported by Davis.

Silver $K\alpha_{1,2}$ scattered by carbon and aluminum. Figs. 4 and 5 show the results of experiments similar to those above using silver radiation instead of copper. The peak of the $K\alpha_1$ line with best conditions was about $5/3$ the intensity of the region between the lines. The solid lines indicate the positions where the fine structure should appear.

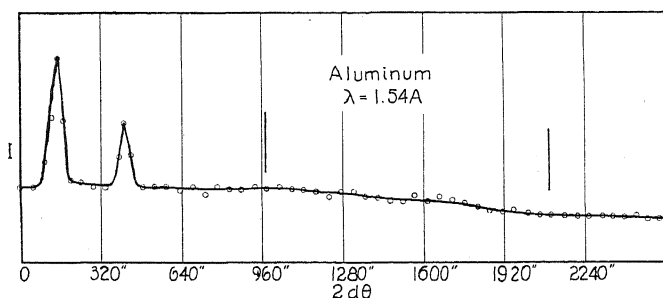


Fig. 3. Copper $K\alpha_{1,2}$ lines scattered by aluminum.

In experiments of this type it is essential that one make sure that the observed lines are not fluorescence lines due to a thin film of evaporated target material which condensed on the scattering block. The following facts appear to the writer to rule out such a possibility. First, in all cases the modified line was observed and qualitatively of the right relative intensity compared to the unmodified line as observed by other experimenters. Secondly, the ratio of intensity of the modified to unmodified line remained constant after many hours of operation of tube. This could not have been true if con-

stant evaporation of the target had been taking place and condensing on the scattering block. Third, a qualitative chemical analysis of the graphite

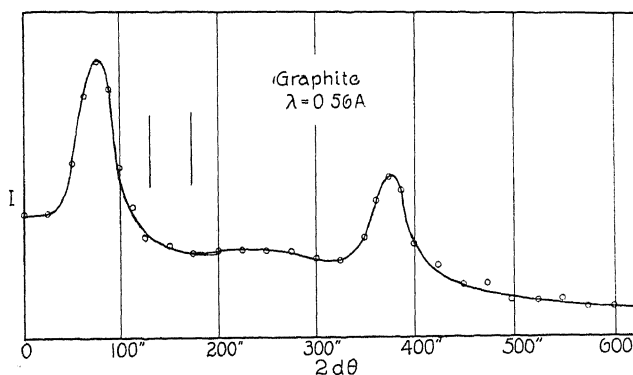


Fig. 4. Silver $K\alpha_{1,2}$ lines scattered by graphite.

and aluminum scattering blocks at the completion of the experiment showed no trace of copper or silver. The angle of scattering was in each case about 130° with a total divergence of 80° .

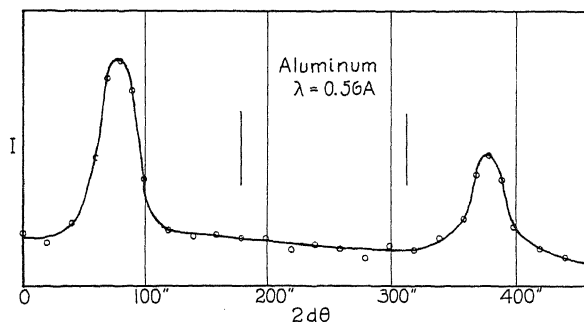


Fig. 5. Silver $K\alpha_{1,2}$ lines scattered by aluminum.

THE COMPTON EFFECT

Due to the difference in the experimental results obtained by various experimenter's³ it was thought worthwhile to make a series of measurements using the double x-ray spectrometer. Since the variation in the change of wave-length is a minimum at very large scattering angles one can use a rather wide divergence of scattering angle and still have sufficient narrowness of modified line to make accurate measurements. The wide divergence is necessary in order to have a measurable x-ray intensity in the scattered x-ray beam. In the present experiments an angle 154° to 176° was chosen in order that the two α lines should be completely separated. The graphite scattering block (1 cm^3) was supported by a small iron rod attached to the silver target of the x-ray tube. The distance from the front face of the scatterer to the center of the focal spot was 34 mm. The long focal spot ($10 \text{ mm} \times$

4 mm) in this case was made perpendicular to the face of the scattering block. Thus the focal spot when viewed from the scattering block appeared as an oblong focal spot 4 mm \times 2 mm. The position of the scattering block was carefully adjusted in the making of the x-ray tube so that a mean scattering angle of 165° was obtained. Pinhole photographs made after the adjustments of the slits S_1 and S_2 showed that the angle was very close to the desired angle. This procedure of definitely fixing the angle before any ionization measurements were made was adopted in order to reduce the "personal equation" to a minimum. The preliminary adjustment of the crystals C_a and C_b was accomplished by moving the aluminum base as was done above in the experiments on the unmodified line.

The x-ray intensity obtained in this arrangement was very much less than the previous experiments where a very large divergence of scattering angle was used. Thus the curve shown in Fig. 6 is the average of 9 curves taken over a period of 3 days. Every curve was very similar to the final

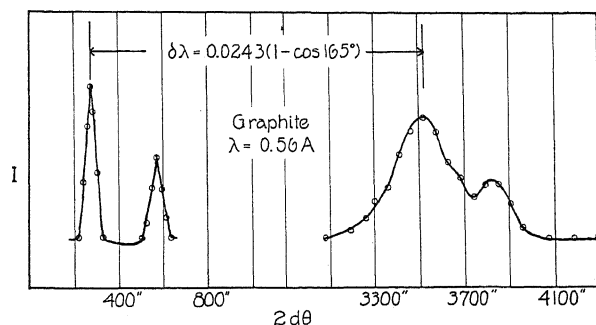


Fig. 6. Silver $K\alpha_{1,2}$ lines scattered by graphite. The unmodified α_1 and α_2 lines are shown.

average in its general shape and position of peaks. The change in wavelength on each curve agreed with the average very much closer than the scattering angle could be measured. Thus the limiting factor in comparing the change in wave-length with the theoretical value, was the determination of the scattering angle. As can be seen Fig. 6 the theoretical change in wave-length as predicted by the quantum theory of scattering by free electrons agrees very closely with the measured change. Considering the precautions taken in measuring the scattering angle it is believed that the agreement between theory and experiment is well within one percent. The modified α lines overlap some but the effect of this overlapping on the position of peaks must be very small.

In this type of experiment one can get more accurately the actual width of a line than by any previous method. It will be noticed in Fig. 6 that the two modified α lines are not completely separated. From the calculations of the divergence of the scattering angle the modified α lines are about 1.5 or 2 times as broad as they should be unless there is something in the scattering process which has not been taken into account in the theoretical cal-

culations. Evidence for a corresponding width has recently been obtained by Ross and Clark⁹ using an entirely different experimental arrangement. Several modifications of the quantum theory of x-ray scattering by free electrons have been made to take into account this increased width. However, more experimental evidence as to the exact width of the modified line is needed before detailed comparison can be made with the theories.

CONCLUSION AND DISCUSSION

Three conclusions may be drawn from the above experiments. First, no evidence of fine structure in scattered x-rays of short and long wavelengths has been obtained. Secondly, the change in wave-length seems to be accurately accounted for by the quantum theory of scattering by free electrons. Third, the width of the modified line is definitely greater than it should be due to the divergence in the scattering angle. These results are in general agreement with all the results obtained on scattered x-rays except those of Davis and his collaborators. Since their experiments are the only ones that have been published similar to the present experiments it should be of interest to compare the experimental arrangement of the two experiments for detecting the fine structure lines in the unmodified line.

The distance from the focal spot to the scattering block was about $1/2$ that used by Davis and Mitchell and about $1/4$ that used by Davis and Purks. The capacity of the electrometer and ionization chamber was about $1/4$ that by Mitchell. Therefore, the sensitivity of the writer's apparatus must have been at least 10 times as great as that used in their experiments. It should also be pointed out that the divergence of the scattering angle in the experiments of Davis and Purks on the modified line was so great (about 30°) that it would be impossible to observe any fine structure which was even partially obeying the usual quantum equation:

$$\lambda = 0.0243(1 - \cos \phi).$$

According to the usual interpretation of the quantum theory of x-ray scattering such fine structure lines certainly could not be present in the unmodified line and it is doubtful if they would occur in the modified line. It is also rather certain that such lines could not be classified as Raman lines for the scattering substances used. Theoretically, one should expect the Raman effect in the x-ray region to be a continuous spectrum instead of a line spectra, but calculations on the Raman intensity to be expected in the x-ray region show that it would be entirely too small to be measured by present methods. Thus if such lines exist the present experiments failed to detect them and existing theories do not seem adequate to explain them.

⁹ Paper given at Ithaca meeting of Am. Phys. Soc. June, 1930.

ENERGY OF $K\alpha_3$ OF COPPER AS A FUNCTION OF APPLIED VOLTAGE WITH THE DOUBLE CRYSTAL SPECTROMETER

BY JESSE W. M. DU MOND AND ARCHER HOYT
CALIFORNIA INSTITUTE OF TECHNOLOGY, PASADENA

(Received July 22, 1930)

ABSTRACT

With a double crystal spectrometer of special design here briefly described the following questions were investigated with a view to determining the origin of the satellite $K\alpha_3$ of copper.

(1) Dependence of intensity of satellite $K\alpha_3$ of copper on voltage with constant current.

(2) Dependence of intensity of parent line $K\alpha_1$ of copper on voltage with constant current.

(3) Ratio of intensities of satellite to parent.

(4) Dependence of satellite intensity on current at constant voltage.

The conclusions are (1) that the satellite is excited at a voltage differing from the excitation voltage of the parent line by too small an amount to be measured with certainty (less than 200 volts). (2) That the ratio of intensities of α_1 to α_3 as estimated from the *areas* of the spectral line structures is about 1:120. (3) That the intensity of the satellite $K\alpha_3$ of copper is strictly proportional to the current at constant voltage.

These facts seem to invalidate the Wentzel-Druyvesteyn "spark line" hypothesis as an explanation of $K\alpha_3$ of copper. Richtmyer's "double jump" hypothesis remains tenable.

In addition a doublet structure (separation of components about 2 X.U.) in $K\alpha_3$ of copper was observed (in accord with the doublet structure of this satellite in elements of lower atomic number).

INTRODUCTION

THE work described in this article was undertaken with the idea of testing whether the Wentzel-Druyvesteyn theory of x-ray satellites can explain the origin of the satellite $K\alpha_3$ of copper. Richtmyer¹ has recently proposed an alternative theory of the origin of satellites and the authors of this paper are indebted to his able discussion of the question for the stimulus to undertake this research.

According to the Wentzel-Druyvesteyn "spark line" theory the satellites are to be ascribed to electron transitions between multiply ionized states. The difference in frequency between the satellite and parent line is thus ascribed to a change in nuclear screening. This would require the atom emitting such a satellite to have lost at least two electrons from the high energy states (inner levels). As Richtmyer points out, this can occur either in two successive processes in which case the satellite should be extremely faint relative to the parent line and should vary in intensity as the square of the x-ray tube current or in a single process in which case the excitation potential of the satellite must be considerably higher than that of the parent line.

¹ Richtmyer, Journal Frank. Inst. 208, 325-361 (1929).

On Richtmyer's "double-jump" theory of satellites on the other hand the atom emitting the satellite is supposed to execute two electron transitions which simultaneously cooperate to produce one quantum of radiation. One of these transitions has as final level the level belonging to the series of the parent line. The other transition is one of relatively small energy between two outer atomic levels. Assuming that an atom is prepared for such a state of affairs by ionization of an outer and an inner level *in one process*, only very small differences need exist between the excitation potentials of satellites and their parent lines.

In view of these considerations, we have therefore in this research investigated the following questions.

- (1) Dependence of satellite intensity on voltage with constant current.
- (2) Dependence of parent line intensity on voltage with constant current.
- (3) Ratio of intensities of satellite to parent line.
- (4) Dependence of satellite intensity on current at constant voltage.

DESCRIPTION OF APPARATUS

The complete double crystal spectrometer outfit used in this work is of a new and original design and as a detailed description of it is to be given in a separate article soon to be published, it will only be briefly described here.

The ionization chamber is solidly fixed on top of the Hoffman vacuum binant electrometer with a very short wire connecting the collector to the suspension of the electrometer through a large diameter short evacuated sleeve. The capacity of the whole insulated system is about 12 e.s.u. The Hoffman vacuum electrometer affords high charge sensitivity and great stability. In order to reduce the fluctuations in ionization readings caused by radioactivity of the ion-chamber walls the chamber was built 25 cm in diameter. The chamber walls were grounded and the saturation potential was applied to an internal grid of fine nickel wires just large enough to enclose the x-ray beam and the collector. Particles emitted from the walls thus fall short of the grid and the ions they produce do not reach the collector.² The insulator used was quartz. The chamber was filled with about an atmosphere of methyl bromide and the internal grid was long enough so that 98% of the energy of the x-radiation as hard as molybdenum *K* series could be absorbed. The window consisted of a thin slab of very light wood known as Balsa wood treated with paraffin to make it gas tight. It had quite a large opening about 2.5×8 cm. The inner surface of the window was coated with an extremely thin sheet of aluminum beryllium alloy 0.0002" thick at the same potential as the grid. In this way, surface charges could not collect on the window and influence the collector. The entire system of ionization chamber and electrometer stood solidly fixed on a concrete slab. The ionization chamber and electrometer were standardized at frequent intervals with a radioactive source in a heavy lead case with a removable lead cover at a fixed distance of about a meter from the chamber. The radioactive source

² We have since learned from A. H. Compton that he has previously built ionization chambers of this type.

was equivalent to 0.0547 mg of radium. It was necessary to use such a weak source so as not to disturb other workers in the laboratory. From time to time, the source was checked against a radium standard. By these precautions, it was possible to insure that intensity readings taken with the ionization chamber on different days might be strictly comparable. With this apparatus it has been found possible to reproduce single readings to within about 3600 ions per second. Probably not all of this uncertainty is ascribable to the ion chamber and electrometer. This is equivalent to an uncertainty of 5.6×10^{-16} amperes. Currents of 6×10^{-14} amperes can therefore be measured with 1 percent accuracy in a single observation. The authors hope to improve these figures by certain projected refinements.

The calcite crystals are mounted on pivots 12.5 cm apart *and are rotated simultaneously* through equal and opposite angles with respect to the line of centers of the pivots by means of two lever arms 43.5 cm long actuated one by a right the other by a left hand screw thread on one and the same shaft. A second similar mechanism geared to the first through a 2:1 gear ratio serves to rotate the x-ray tube source around the pivot of the first crystal at twice the rate of angular speed of the crystal and also to rotate the entire system of x-ray tube and spectrometer around a fixed pivot under and in line with the pivot of the second crystal so that the outgoing beam from the second crystal always remains lined up with the window of the ionization chamber. The entire mechanism permits the exploration of a range of two degrees for the *grazing angles* of incidence with the crystals without resetting the crystals. The smallest divisions on the drum correspond to 10 seconds of arc for the grazing angle and tenths of these divisions are easily estimated. All backlash greater than 15 sec. of arc is eliminated with helical steel springs. The entire apparatus is surprisingly simple to construct involving scarcely any very precise machine work and is very convenient to operate. Great precautions were taken at the start to insure the proper orientation of the crystal faces. These faces were accurately set at a definite known angle with the line joining the centers of their pivots and accurately parallel to their axes of rotation and as nearly as possible coincident with their axes of rotation by means of a spectrometer fitted with a Gauss eyepiece. The above described design makes it possible to explore a large range of wavelengths by turning a single drum without having to re-set the crystals. The mutual rotations of the elements of the apparatus *insure that the same parts of the surfaces of the two crystals are reflecting the x-rays at all times.* This eliminates errors due to (1) Crystals having different reflecting power in different parts of their surface. (2) Reduction of intensity due to part of the beam not falling on the crystal. (3) Changes in intensity due to the beam passing through different parts of the x-ray tube window or the ionization chamber window.

The x-ray tube was an ordinary water-cooled Coolidge type fitted with a copper target to which we have added a side window of mica 12×3 mm and about 0.0008 inches thick. Charcoal and liquid air are used to maintain a very good vacuum. We are much indebted to Samuel K. Allison for

details of technique in making this window and also for his ingenious method of accurately controlling the filament heating current on the tube with a mercury column resistance. (Originally due to Paul Kirkpatrick).

A very convenient shielding box for enclosing the x-ray tube is made out of micarta tubing large enough in diameter to slip over the bulb and long enough completely to cover the tube. The micarta tube is wrapped outside with several layers of "lead rubber" such as is sold by medical supply houses for the protective aprons of röntgenologists. A shielding box so constructed of insulating materials can be made much smaller and lighter than the large metallic lead boxes ordinarily employed. This is essential for the spectrograph here described since the tube in its shielding box must rotate around the pivot of the first crystal when the wave-length settings are being made.

The high tension generator was manufactured by the Wappler Co. and consists of a high tension transformer, two valve tube rectifiers and a mica condenser in oil. It has proved very stable in operation. A rough estimate of the ripple has been made for the voltage of excitation of the K lines of copper by the use of a Western Electric Braun tube oscillograph. The ripple is not more than 10%. The authors do not believe that the conclusions drawn from the results here described would be greatly affected by the complete elimination of this ripple. The voltage output to the tube has been carefully calibrated at 5.6 m.a. load from 6 to 14 kilovolts by measuring the current through about 2.5 meg ohms consisting of a number of large standard resistances in series. This curve was extended upward by means of an Abraham & Villard electrostatic voltmeter and a point at about 50 k.v. was checked with a measurement of the short wave-length limit with a Seemann Spectrograph. The short wave-length limit was also observed for the crystal setting at which $K\alpha_3$ was found and the voltage calibration could thus be checked accurately at this important point.

The radiation passed through two openings—one near the tube and one near the ion chamber—whose height limited the angle of "cross fire" through the spectrometer to 2.4° or 1.2° deviation from a plane normal to the edge of the dihedral angle formed by the two crystal faces.

The two crystals used were cleaved from the same block the faces previously in contact being used. The crystal was of unknown origin. It was obtained from Wm. Gaertner. The dimensions of the faces are 4.6×7 cm. These crystals are not of as high precision as those reported by some investigators; however, they give a line breadth at half maximum for the molybdenum lines of 0.4 X.U. The copper lines have a breadth at half maximum of 0.60 X.U. with these crystals.

METHOD

A spectral curve was first run for the $K\alpha_1$ and α_2 of copper in order accurately to establish fixed points on the scale of angle settings. This curve is shown in Fig. 1. It will be noted that the background appears absolutely flat at the point marked $K\alpha_3$ where the satellite should occur. The intensity of

$K\alpha_3$ in the case of copper is so low, that it is quite imperceptible plotted to this scale. In order to bring out the line, it was found necessary to take every precaution to reduce the background of the ionization curves. This background is doubtless due to four causes:

1. The continuous or "white" x-radiation. This is probably very small with the double crystal spectrometer since this instrument selects an extremely narrow band of wave-lengths. It was reduced by diminishing the vertical divergence of the beams in the spectrometer.

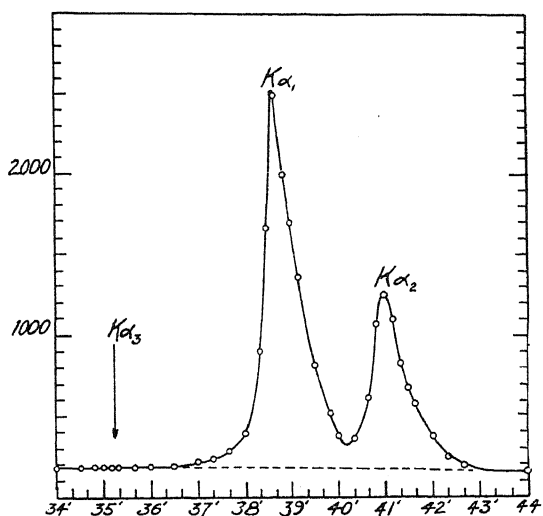


Fig. 1. $K\alpha_1$, α_2 of copper before taking precautions to reduce background in the neighborhood of α_3 . Note that α_3 is quite imperceptible. The abscissae represent the grazing angles between x-ray beam and calcite crystals.

2. The natural leak of the electrometer and ion chamber. This has been reduced to an extremely low value by the precautions mentioned in describing the apparatus.

3. Nonselective scattering (Compton modified) from the crystal faces and fluorescent radiation from the crystals.

4. Direct leakage of x-rays from the tube to the chamber without selective reflection from the crystals.

It was found that the last two causes of background could be greatly reduced in the case of copper radiation by using a thin sheet of nickel as a filter to cut down the bulk of hard white radiation from the tube without greatly reducing the line intensity. The filter was a sheet of nickel rolled down to about 0.0005" thick. Further reduction in the background was accomplished by great care in the arrangement of lead shields diaphragms etc. to preclude x-ray leakage and scattering to the highest possible degree and by reducing the vertical divergence of the x-ray beam through the spectrometer. We have succeeded in obtaining background ordinates of less than 1% of the maximum ordinate of $K\alpha_1$. See Fig. 2. This corresponds

to only about double the spontaneous ionization observed by Millikan for this vicinity.

The procedure was then to run a spectral curve of $K\alpha_3$ holding the primary voltage and the tube current very accurately constant. It was found necessary to run all such curves after midnight to have the necessary constancy of the power supply. The attention of one observer was almost completely occupied holding the milliamperes constant as observed with a telescope and cross hairs focussed on the needle and keeping the primary voltage constant throughout the run. Time of drift of the electrometer was observed between two fixed points on the scale with a stopwatch. In general, only one or two curves could be taken in a night.

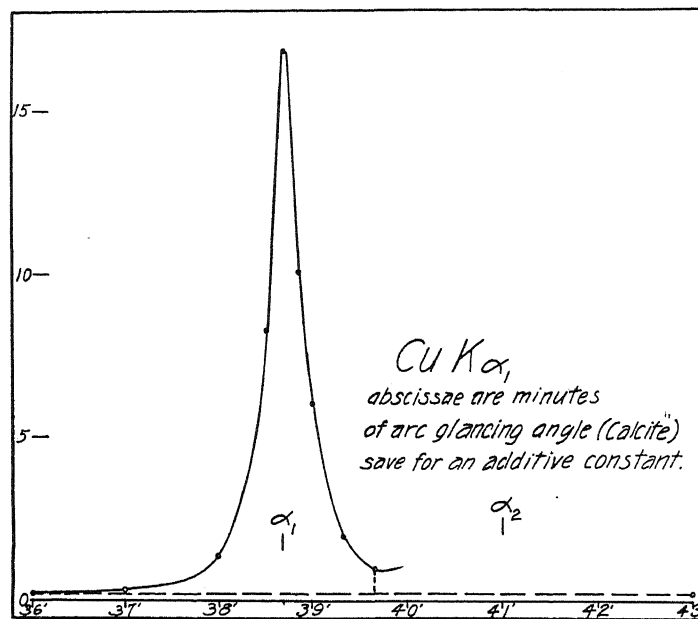


Fig. 2. Typical spectral curve of $K\alpha_1$ after taking full precautions to reduce background. From such curves as these the areas were taken for the purpose of determining α_1 intensities.

Although the background looks perfectly flat in the vicinity of $K\alpha_3$ in Fig. 1 when the sensitivity becomes sufficient to give good observations on $K\alpha_3$, the background is found to be increasing quite rapidly in this region. The "foot" of $K\alpha_1$ which is imperceptible relative to that line appears as a steep slope relative to the low intensity of $K\alpha_3$. Figs. 3 and 4 show the spectral curves taken on $K\alpha_3$ at various voltages all for the same current of 5.6 m.a. The enormous difference in intensity of the satellite and its parent will be appreciated when it is realized that the "saddle point" between α_1 and α_2 is about four times as high as the largest ordinates plotted in the curves of Fig. 3. The large background ordinates at 37' in the curves of Fig. 3 are only about 1/50th(!) of the maximum ordinate of α_1 .

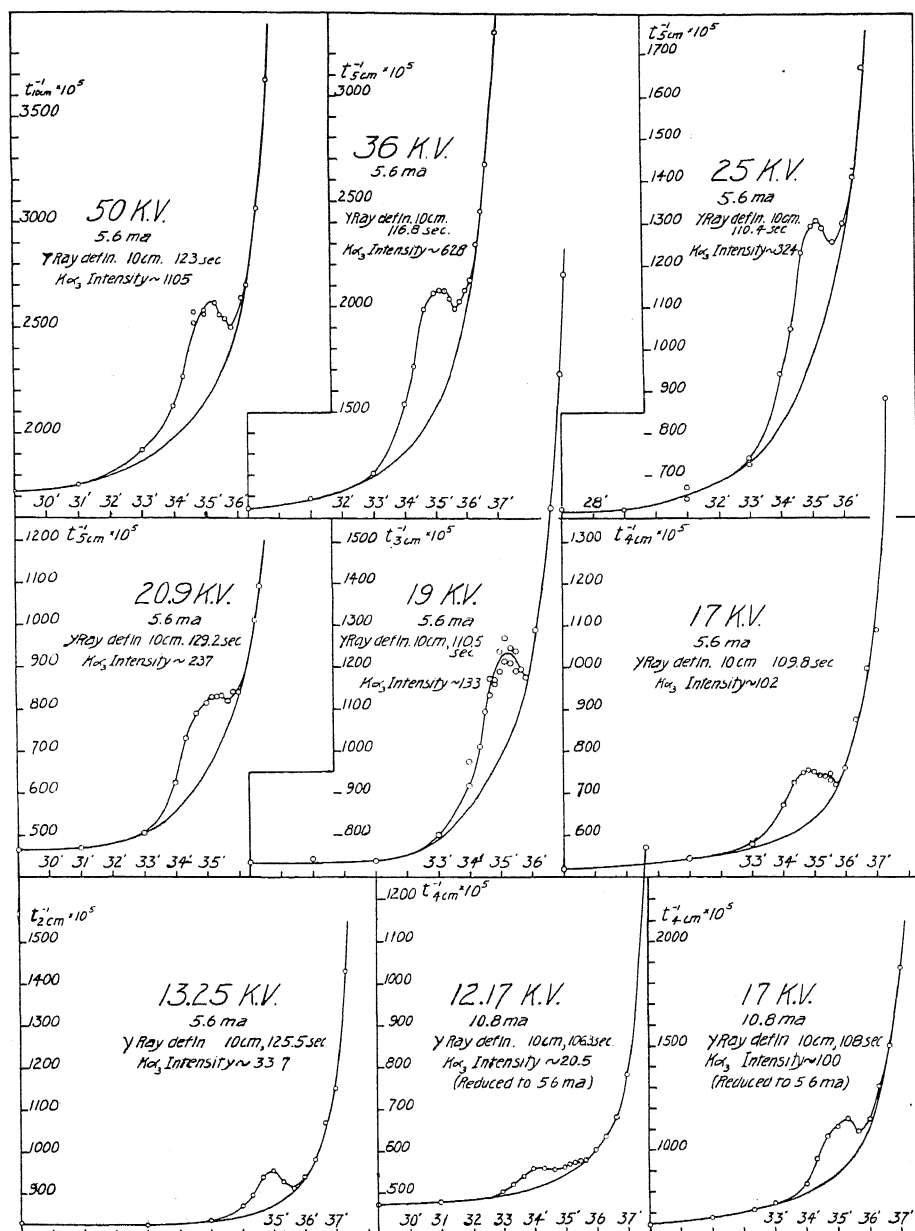


Fig. 3. Spectral curves of $K\alpha_3$. The area between the $K\alpha_3$ line and the interpolated background is taken as a measure of the intensity of the line. The sensitivity of the ion chamber and electrometer were calibrated in each case by taking the time for 10 cm deflection caused by γ rays from a radioactive source kept in a fixed position with respect to the apparatus. The calibrations are recorded on each curve shown. The ordinates of these curves are 10^5 times the reciprocals of the time in seconds required for a given number of cm deflection the number of cm being indicated as the subscript of the time. Note the partially resolved doublet structure which appears at the lower voltages.

The intensity of α_3 for the different voltages was obtained by interpolating the background curve under the region of α_3 as shown in the figure. This was done graphically with a spline. The areas of $K\alpha_3$ were then measured with a planimeter and checked by counting squares. These areas were then corrected according to the radioactive standardization of sensitivity for the time when the curve was taken. Not all the curves were observed for the same total deflection of the electrometer (in order to save time in the slow deflections) and this introduced another multiplying factor in the computation of the intensities from the measured areas. The different curves of α_3 are plotted to different ordinates scales introducing a third factor. The necessity of interpolating the background admittedly introduces an uncertainty in the measurements, but it is not possible to eliminate this.

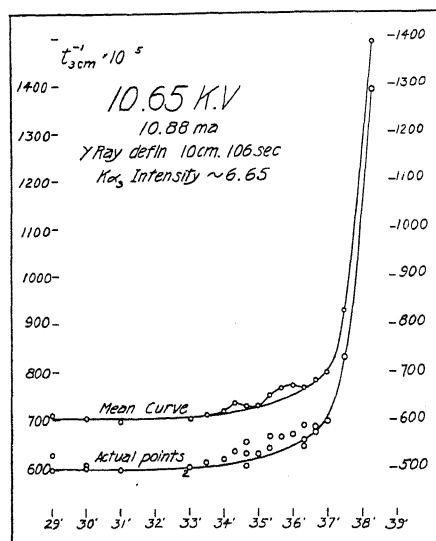


Fig. 4. Spectral curve of Cu $K\alpha_3$ at the lowest voltage where it was observed with certainty. Note the doublet structure. The actual observed points as well as the average curve are shown. The voltage here employed differs from the excitation voltage of the K series of copper by only 1.75 k.v.

From attempts to draw this interpolated background in different ways consistent with the background at considerable distance on either side of $K\alpha_3$ we have concluded that the uncertainty in area ascribable to this graphical interpolation is probably less than 5% of the total intensity in any case. Fig. 4 shows rather clearly a doublet structure in $K\alpha_3$ the separation of the components being about 2 X.U. Since it is the lowest intensity and voltage at which $K\alpha_3$ was observed with certainty, it is of especial interest. The voltage here differs from the excitation voltage of $K\alpha_1$ by only 1.75 k.v. Traces of the line were even thought to be detected at 9.75 k.v; but these results are rather uncertain.

A set of curves which it is not necessary to reproduce here was run for the line $K\alpha_1$ in the same way and for the same voltages and current as those shown in $K\alpha_3$.

RESULTS

Dependence of intensity on voltage. The intensities both of $K\alpha_3$ and $K\alpha_1$ are plotted (to different ordinate scales) as a function of the voltage squared in Fig. 5. It is seen that the intensities vary with voltage in almost identically the same manner. By projecting the nearly straight characteristic curves

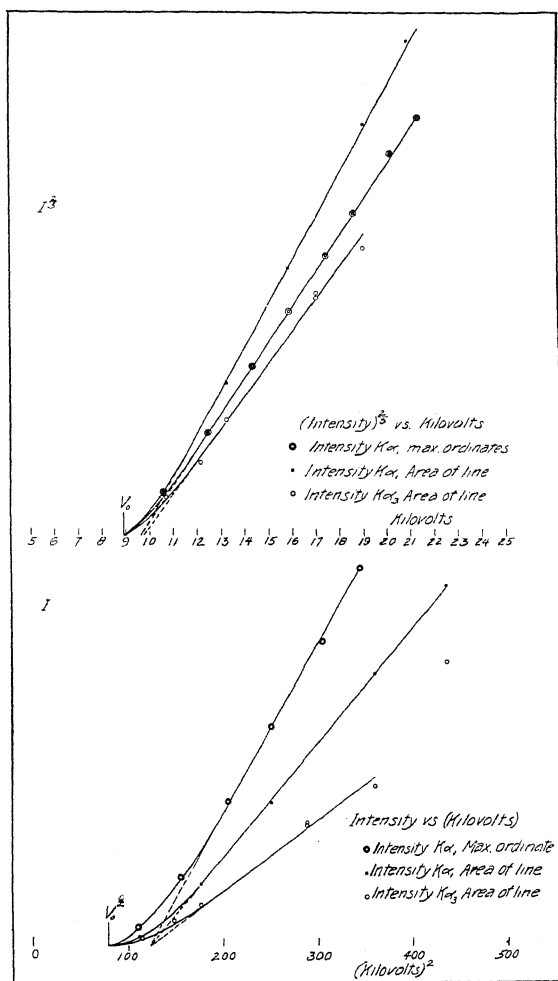


Fig. 5. Intensity of $K\alpha_1$ and $K\alpha_3$ as a function of voltage. These curves show how little difference (if any) exists between the excitation voltages of α_3 and α_1 . The upper curve ($I^{2/3}$ vs k.v.) is plotted for Webster and Clark's relation $I = \kappa(V - V_0)^{3/2}$ while the lower curve (I vs. (k.v.) 2) is plotted for Wooten's relation $I = C(V^2 - V_0^2)$.

until they intersect the axis of abscissae the difference in excitation potential between $K\alpha_3$ and $K\alpha_1$ is estimated to be less than 200 volts. These projected intersections are not the excitation voltages themselves, but from the work of Wooten³ it seems safe to assume that these intersections will serve to

³ Wooten, Phys. Rev. 13, 71 (1919).

indicate any difference that might exist in the excitation voltages of $K\alpha_3$ and $K\alpha_1$.

The upper curve in Fig. 5 represents $I^{2/3}$ vs. k.v. This method of plotting was adopted in order to rectify the curves in accordance with Webster and

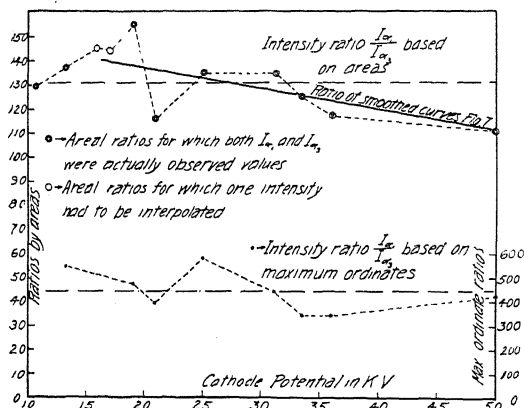


Fig. 6. Absolute ratio of $K\alpha_1$ to $K\alpha_3$ intensities from areas of spectral curves and also from maximum ordinates of each line at different voltages.

Clark's⁴ observed intensity relation $I = K(V - V_0)^{3/2}$. It has the advantage of giving a smaller fillet in the region near the critical excitation voltage. This

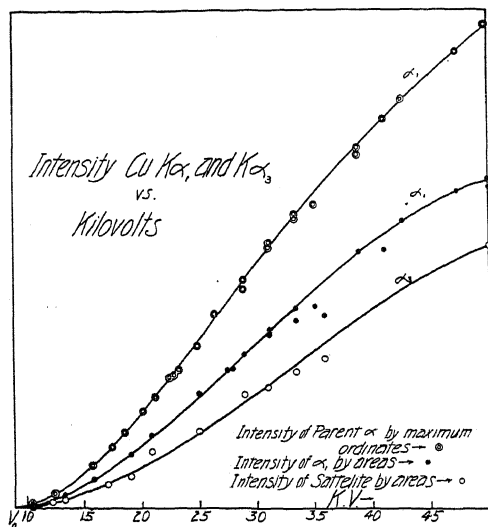


Fig. 7. Intensities of $K\alpha_3$ and $K\alpha_1$ for voltages up to five and one half times excitation voltage.

method of plotting also leads to the conclusion that $K\alpha_3$ differs in excitation voltage from $K\alpha_1$ if at all by less than 200 volts.

In Fig. 7 the intensities of $K\alpha_1$ by areas and ordinates and $K\alpha_3$ by areas

⁴ Webster and Clark. See Siegbahn's "Spectroscopy of X-rays," page 94.

are plotted up to 5.5 times excitation voltage. No very striking difference appears between α_1 and α_3 . On the whole the ratio $I\alpha_1/I\alpha_3$ seems to increase slightly with decreasing voltage, see Fig. 6, down to about 15 k.v. This suggests a slightly higher excitation voltage for $K\alpha_3$ than for $K\alpha_1$.

Below 15 k.v. however the ratio appears to decrease again. The difficulties of measuring $K\alpha_3$ in this region make this decrease uncertain.

$K\alpha_3$ is 6X.U. harder than $K\alpha_1$. This corresponds to about 35 volts. If Richtmyer's "double jump" hypothesis is correct, this extra energy might be assumed to be contributed by a peripheral electron dropping to say an M level of about 35 volts. It should then require at least 35 volts or perhaps slightly more to ionize such an M level preparatory to such a transition. Since the target of the x-ray tube is a solid body it seems probable that the M electron would have to be ejected beyond the densely packed levels of the conduction electrons satisfying the Fermi statistics.^{5,6} This would however require about 7 volts more. At the worst the Richtmyer "double jump" hypothesis could hardly require the $K\alpha_3$ line to be excited at voltages much more than 50 volts above the parent line, which is entirely consistent with the results reported in this paper.

The low intensity observed for $K\alpha_3$ of copper is also consistent with Richtmyer's hypothesis since the intensity of such a double transition depends on the "coupling" of the eigenfunctions for the four states involved which should be very much lower for copper than for the lighter elements in which $K\alpha_3$ appears more intensely.

2. *Ratio of intensities.* The ratio of intensities of $K\alpha_3$ to its parent $K\alpha_1$ based on areas is roughly constant for all voltages well above the excitation voltage and is found to be about 1:120. (See Fig. 6) The ratio of maximum ordinates of $K\alpha_1$ to $K\alpha_3$ is much larger than the ratio of areas because of the greater breadth of α_3 due to its doublet structure. This ratio is less accurately known but it is of the order of $I\alpha_1/I\alpha_3 = 440$.

3. *Dependence of $K\alpha_3$ on current.* This question was investigated by running two spectral curves of $K\alpha_3$ at the same voltage 17 k.v. one for 5.66 m.a. and one for 10.88 m.a. tube current. The conclusion from the measured areas is that the intensity of $K\alpha_3$ is accurately proportional to the first power of the current not to its square.

CONCLUSIONS

Although the difficulties and uncertainties of measurement of $K\alpha_3$ as a function of voltage caused by its extremely low intensity as compared to its parent line are admittedly considerable, it seems safe to conclude from this work that $K\alpha_3$ is excited at only very slightly higher voltages than $K\alpha_1$, the difference in excitation voltage being of the order of a few percent. It does not appear to us possible to explain the origin of $K\alpha_3$ of copper on the Wentzel-Druyvesteyn "spark line" theory. On the other hand, the results seem to be in accord with Richtmyer's "double jump" hypothesis.

⁵ A. Sommerfeld, *Zeits. f. Physik* **47**, 1-60 (1928).

⁶ Jesse W. M. DuMond, *Phys. Rev.* **33**, 643 (1929).

PROJECTIVE RELATIVITY

BY OSWALD VEBLEN AND BANESH HOFFMANN
DEPARTMENT OF MATHEMATICS, PRINCETON UNIVERSITY,

(Received June 16, 1930)

ABSTRACT

In this paper we show that the formalism of O. Klein's version of the five-dimensional relativity can be interpreted as a four-dimensional theory based on projective instead of affine geometry. The most natural field equations for the empty space-time case are a combination into a single invariant set of the gravitational and electromagnetic field equations of the classical relativity *without modification*. This seems to be the simplest possible solution of the unification problem.

When we drop a restriction on the fundamental projective tensor which was imposed in order to reduce our theory to that of Klein a new set of field equations is obtained which includes a wave equation of the type already studied by various authors. The use of projective tensors and projective geometry in relativity theory therefore seems to make it possible to bring wave mechanics into the relativity scheme.

1. INTRODUCTION

THE five-dimensional theory of relativity in the form in which it has been developed by O. Klein and others from the basic idea of Th. Kaluza,¹ need not be regarded as a five-dimensional theory. Its significance will be better understood if it is treated as a field theory of the four-dimensional space-time manifold of the ordinary relativity theory. But this field theory is stated in terms of what we call projective tensors to distinguish them from the classical or affine tensors. The projective tensors have sets of 5^k instead of 4^k components. Moreover they have in each coordinate system not one but an infinity of components dependent on a parameter x^0 . The components are functions of the form

$$T_{\sigma \dots \tau}^{\alpha \dots \beta} = e^{N x^0} f_{\sigma \dots \tau}^{\alpha \dots \beta}(x^1 x^2 x^3 x^4), \quad (1.1)$$

where $x^1 x^2 x^3 x^4$ are the coordinates, and N a constant which we call the index. We call the parameter x^0 the factor. The subscripts and superscripts $\alpha, \dots, \sigma, \dots, \tau$ take on the values² 0, 1, 2, 3, 4.

The projective tensors arise in the generalized projective geometry which may be briefly characterized as follows:

With any point $(x^1 x^2 x^3 x^4) = x$ of space-time there is associated an infinity of sets of differentials $(dx^1 dx^2 dx^3 dx^4) = dx$. These differentials are arbitrary numbers and may be regarded, in the usual manner of modern differential

¹ Th. Kaluza. Sitz. der Preuss. Akad. 966 (1921).

O. Klein. Zeits. f. Physik 37, 895 (1926); 46, 188 (1927).

A. Einstein. Sitz. der Preuss. Akad. 23; 26 (1927).

² We shall throughout this paper adhere to the convention that Greek suffixes shall take on values from 0 to 4 and Latin suffixes only the values 1 to 4.

geometry, as coordinates of another four-dimensional space, which we call a tangent space of the original underlying space. The point $dx=0$ is identified with the point x and will be called the point of contact. Thus to each point of space-time we have an associated tangent space. As usually studied in terms of the classical tensor analysis these tangent spaces are affine spaces. The theory of these tangent spaces together with the underlying space becomes a Riemannian geometry if a Euclidean metric is introduced in each tangent space by means of a quadratic differential form which we may write, remembering our convention regarding Latin indices, as

$$g_{ij}dx^i dx^j.$$

These tangent spaces can be converted into projective spaces by introducing points at infinity in the usual manner in each of them. The projective spaces can be studied analytically by means of homogeneous coordinates, $(X^0 X^1 X^2 X^3 X^4)$ and projective tensors. For the generalised projective geometry which thus arises the reader is referred to two papers by O. Veblen, "Generalised Projective Geometry," *Journal of the London Mathematical Society*, Vol. 4, p. 140 and "A Generalisation of the Quadratic Differential Form," *Quarterly Journal of Mathematics*, Oxford Series, Vol. I. p. 60; we shall refer to these papers as P. G. and Q. F. respectively. These papers contain references to the previous work on the generalised projective geometry by Weyl, Cartan, Thomas, Eisenhart and others.

The formalism of the generalised projective geometry includes a device which depends on the fact that there is a (1-1) correspondence between the points of the original four-dimensional space-time and a certain congruence of curves in a five-dimensional space. This congruence is such that in a particular coordinate system each curve is defined by the conditions

$$\begin{cases} x^i = \text{constant} \\ x^0 = \text{anything.} \end{cases}$$

Now the "sharpened cylinder-condition" which appears in Klein's, and independently in Einstein's, work on the Kaluza idea means that there is an invariant congruence of curves of exactly this sort in the five-dimensional space which they consider. Our point of view is that this five-dimensional space is without physical significance. It is merely a mathematical device to represent the points of space-time by the curves of an auxiliary 5-space.³ But in using this device we are dealing with the projective rather than the affine theory of space-time.

³ This point has been very clearly made by H. Mandel, *Zeits. f. Physik* **45**, 285 (1927), and *Phys. Zeits.* XXX (1929). This device is, at bottom, the same as that of using homogeneous coordinates in ordinary projective geometry. For this can be thought of as a representation of the points of a projective n -space by a congruence of lines in an affine $(n+1)$ -space. This is very clearly explained in a forthcoming paper, "The representation of projective spaces on affine spaces" by J. H. C. Whitehead, to be published in the *Proc. Lond. Math. Soc.*

2. ASSUMPTIONS AND DEFINITIONS

We shall now presuppose the generalized projective geometry as developed in P. G. and Q. F. In particular we assume that the homogeneous and non-homogeneous coordinates in tangent spaces are connected by the formulas

$$X^i = \frac{dx^i}{A} \text{ and } X^0 = \frac{1 - A_i dx^i}{A} \quad (2.1)$$

in which A is a projective scalar (which in Q. F. was taken to be of index 1) and

$$A_\alpha = \frac{\partial \log A}{\partial x^\alpha}. \quad (2.2)$$

Thus

$$A_\alpha X^\alpha = 0$$

is the equation of the hyperplane at infinity in each tangent plane. The inverse of (2.1) is

$$dx^i = \frac{X^i}{A_\alpha X^\alpha}.$$

In Q. F. we have the theory of a symmetric projective covariant tensor of the second degree, $G_{\alpha\beta}$, which may be thought of as determining a Cayley metric in each tangent space. The equation

$$G_{\alpha\beta} X^\alpha X^\beta = 0 \quad (2.3)$$

is unaltered by a change of coordinates and determines a unique quadric locus in each tangent space. The point of contact of the tangent space with the underlying space has homogeneous coordinates such that

$$X^i = 0.$$

The tangent lines to the quadric from this point meet it in points which all lie in a hyperplane

$$G_{\alpha 0} X^\alpha = 0. \quad (2.4)$$

The tangent lines generate a quadric cone with its vertex at the point $X^i = 0$. The equation of this cone is

$$\left(G_{\alpha\beta} - \frac{G_{\alpha 0} G_{\beta 0}}{G_{00}} \right) X^\alpha X^\beta = 0.$$

If we set

$$\frac{G_{\alpha\beta}}{G_{00}} - \frac{G_{\alpha 0} G_{\beta 0}}{G_{00} G_{00}} = g_{\alpha\beta}$$

we see that

$$g_{\alpha 0} = 0$$

and that this cone may be written

$$g_{ij}dx^i dx^j = 0$$

in nonhomogeneous coordinates. We shall identify the coefficients g_{ij} with the gravitational potentials of the ordinary relativity.

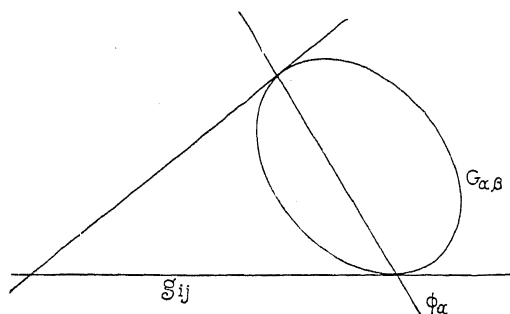


Fig. 1

Let

$$\frac{G_{\alpha 0}}{G_{00}} = \phi_\alpha.$$

Then ϕ_α is a projective vector of index zero such that

$$\phi_0 = 1.$$

We shall identify the components ϕ_i with the potentials of the electromagnetic field.

This treatment of the electromagnetic potentials as components of a projective vector is justified by the law of transformation. Under a pure transformation of coordinates

$$\begin{cases} \bar{x}^i = \bar{x}^i(x) \\ \bar{x}^0 = x^0 \end{cases}$$

the components ϕ_i transform like components of an affine vector,

$$\bar{\phi}_i = \phi_i \frac{\partial x^j}{\partial \bar{x}^i}, \quad \bar{\phi}_0 = \phi_0,$$

whereas under a change of factor

$$\begin{cases} \bar{x}^i = x^i, \\ \bar{x}^0 = x^0 + \log \rho(x^1, x^2, x^3, x^4), \end{cases}$$

we have

$$\bar{\phi}_i = \phi_i - \frac{\partial \log \rho}{\partial x^i}, \quad \bar{\phi}_0 = \phi_0.$$

Thus, under a change of factor ϕ_i changes by the addition of a gradient and so in any coordinate system is determined only to within an additive gradient,

which is the well-known property of the vector potential of the relativistic Maxwell field. We have also that the projective tensor

$$\phi_{\alpha\beta} = \frac{1}{2} \left(\frac{\partial \phi_\alpha}{\partial x^\beta} - \frac{\partial \phi_\beta}{\partial x^\alpha} \right)$$

is such that

$$\phi_{0\alpha} = -\phi_{\alpha 0} = 0$$

and thus ϕ_{ij} is affine and therefore uniquely determined in a given coordinate system.

The equation of the hyperplane (2.4) in non-homogeneous coordinates is

$$(\phi_i - A_i)dx^i + 1 = 0. \quad (2.6)$$

From the general theory G_{00} is a projective scalar of the same index as the projective tensor $G_{\alpha\beta}$. If we denote this index by $2N$,

$$\Phi = (G_{00})^{1/2}$$

is a projective scalar of index N and

$$\Phi_\alpha = \frac{1}{N} \frac{\partial \log \Phi}{\partial x^\alpha}$$

is a projective vector—a projective gradient—of index zero subject to the invariant condition

$$\Phi_0 = 1.$$

Then

$$\theta_\alpha = \phi_\alpha - \Phi_\alpha$$

is a projective vector such that

$$\theta_0 = 0$$

and hence such that θ_i are the components of an affine vector. The latter can be regarded as a normalized vector potential for the electromagnetic field.

It is possible to make the assumption

$$\Phi^{1/N} = A \quad (2.7)$$

which makes the relation between homogeneous and nonhomogeneous coordinates depend on the fundamental projective tensor $G_{\alpha\beta}$. This also reduces the equation of the hyperplane (2.4) in nonhomogeneous coordinates from (2.6) to the form

$$\theta_i dx^i + 1 = 0. \quad (2.8)$$

3. RESUMÉ OF FORMULAS

From the definitions in the last section we have

$$G_{\alpha\beta} = \Phi^2(g_{\alpha\beta} + \phi_\alpha \phi_\beta) = \Phi^2 \gamma_{\alpha\beta} \quad (3.1)$$

where $\gamma_{\alpha\beta}$ is a symmetric projective tensor of index zero, having $\gamma_{00} = 1$.

Let $\gamma^{\alpha\beta}$ be defined by the equation

$$\gamma^{\alpha\sigma}\gamma_{\beta\sigma} = \delta_{\beta}^{\alpha},$$

and g^{ij} by the equation

$$g^{ik}g_{jk} = \delta_j^i.$$

It is found that

$$\gamma^{ij} = g^{ij}$$

$$\gamma^{i0} = -g^{ij}\phi_j, \quad \gamma^{00} = 1 + g^{ij}\phi_i\phi_j.$$

Also that if γ is the determinant of the quantities $\gamma_{\alpha\beta}$ and g the determinant of g_{ij} , that

$$\gamma = g.$$

Whenever we have a projective tensor we shall raise and lower indices by means of the γ 's; but for an affine tensor we shall employ the g 's. We shall adhere to the further convention that whenever an index is raised it is the first index. For example consider the affine tensor

$$\phi_{ij} = \frac{1}{2} \left(\frac{\partial \phi_i}{\partial x^j} - \frac{\partial \phi_j}{\partial x^i} \right) = \frac{1}{2} \left(\frac{\partial \theta_i}{\partial x^j} - \frac{\partial \theta_j}{\partial x^i} \right)$$

defined in §2. We write

$$\phi_i^{\cdot} = g^{ik}\phi_{kj}. \quad (3.2)$$

Note that this fixes the sign of ϕ_i^{\cdot} .

There is a projective connection defined by the Christoffel formulas

$$\Gamma_{\beta\gamma}^{\alpha} = \frac{1}{2} \gamma^{\alpha\sigma} \left(\frac{\partial \gamma_{\gamma\sigma}}{\partial x^{\beta}} + \frac{\partial \gamma_{\sigma\beta}}{\partial x^{\gamma}} - \frac{\partial \gamma_{\beta\gamma}}{\partial x^{\sigma}} \right).$$

Its formal properties are the same as those of an affine connection in a space of 5 dimensions with a cylinder condition. Geometrically it defines an infinitesimal projective displacement from any tangent space to a "nearby" tangent space as explained in Q. F. §7. "Projective differentiation" is defined by the same formula as covariant differentiation and indicated by a semi-colon. Thus by the definition of Γ we have

$$\gamma_{\alpha\beta;\gamma} = \frac{\partial \gamma_{\alpha\beta}}{\partial x^{\gamma}} - \gamma_{\alpha\sigma}\Gamma_{\beta\gamma}^{\sigma} - \gamma_{\beta\sigma}\Gamma_{\alpha\gamma}^{\sigma} = 0.$$

From, $\Gamma_{\beta\gamma}^{\alpha}$ we can form the "projective curvature tensor"

$$B_{\beta\gamma\delta}^{\alpha} = \frac{\partial \Gamma_{\beta\gamma}^{\alpha}}{\partial x^{\delta}} - \frac{\partial \Gamma_{\beta\delta}^{\alpha}}{\partial x^{\gamma}} + \Gamma_{\beta\gamma}^{\epsilon}\Gamma_{\epsilon\delta}^{\alpha} - \Gamma_{\beta\delta}^{\epsilon}\Gamma_{\epsilon\gamma}^{\alpha},$$

the generalised Ricci tensor

$$B_{\beta\delta} = B_{\beta\alpha\delta}^{\alpha},$$

and the projective scalar

$$B = \gamma^{\beta\delta} B_{\beta\delta}.$$

We note that these quantities are of zero index; it follows that B is at the same time a projective scalar and an affine scalar.

For any projective tensor $T_{\alpha\beta}$ of zero index it follows from the laws of transformation that T^{ij} is an affine tensor; T_0^i is an affine vector; T_{00} is an affine scalar. Moreover these affine tensors completely determine the projective tensor when $T_{\alpha\beta}$ is symmetric.

Now let us denote the affine curvature tensor found from g_{ij} by R^i_{jkl} and let

$$R_{ij} = R^{\alpha}_{iaj} \quad \text{and} \quad R = g^{ij} R_{ij}.$$

Then we find⁴

$$\begin{aligned} B^{ij} &= R^{ij} + 2g^{st}\phi_s^i\phi_t^j \\ B_0^i &= \phi_{,s}^{is} = \frac{1}{g^{1/2}} \frac{\partial(\phi^{is}(g)^{1/2})}{\partial x^s} \\ B_{00} &= \phi_s^s\phi_s^t. \end{aligned}$$

Moreover we have

$$B = R - \phi_s^s\phi_s^t.$$

All this is derived more in detail in Q. F.

4. FIELD EQUATIONS, $\Phi = 1$

In the classical relativity the field equations are obtained by adding the Einstein tensor,

$$R^{ij} = \frac{1}{2}g^{ij}R,$$

representing the gravitational part, to the tensor,

$$S^{ij} = g^{st}\phi_s^i\phi_t^j + \frac{1}{4}g^{ij}\phi_s^s\phi_t^t$$

(as to the signs (see (3.2)) representing the electromagnetic part, and equating the sum to a stress-energy-momentum tensor T^{ij} ; thus

$$R^{ij} - \frac{1}{2}g^{ij}R + \alpha S^{ij} = \beta T^{ij},$$

where α and β are constants depending on the units used. There is also the set of Maxwell equations

$$\phi_{,s}^{is} = J^i$$

where J^i represents the current vector.

⁴ We shall denote covariant differentiation with respect to the g 's by a comma.

In generalizing this we first form a tensor,

$$\Gamma_{\alpha\beta} = B_{\alpha\beta} - \frac{1}{2}\gamma_{\alpha\beta}B,$$

analogous to the Einstein tensor. By appeal to the five-dimensional representation it is evident that this satisfies projective divergence conditions analogous to those satisfied by the Einstein tensor, i.e.

$$\Gamma_{\beta;\alpha}^{\alpha} = 0.$$

In this formula we must remember that the indices are raised and lowered by means of $\gamma^{\alpha\beta}$ and $\gamma_{\alpha\beta}$ and that the projective differentiation indicated by the semicolon is with respect to the projective connection $\Gamma_{\beta\gamma}^{\alpha}$.

As field equations in vacuo we propose

$$\boxed{\Gamma_{\alpha\beta} - \phi_{\alpha}\phi_{\beta}\Gamma = 0.} \quad (4.1)$$

These expand into the equivalent affine equations,

$$R^{ij} - \frac{1}{2}g^{ij}R + 2S^{ij} = 0. \quad (4.2)$$

$$\phi_{,s}^{is} = 0, \quad (4.3)$$

$$R = 0. \quad (4.4)$$

Equation (4.4) is not independent but is the result of contracting the first group with respect to g_{ij} . Hence our field equations are essentially (4.2) and (4.3) which are identical with those of the classical relativity. Hence the equations (4.1) afford a solution of the unification problem by combining the field equations for gravitation and electromagnetism into a single invariant set of equations. This is done without changing the physical significance of the quantities g_{ij} and ϕ_i in any way. But whereas the geometry underlying the pure gravitational theory is affine, that underlying the combination of gravitational and electromagnetic theory is projective.

5. VARIATIONAL DERIVATION OF THE FIELD EQUATIONS

The field equations (4.1) are necessary conditions that the quadruple integral

$$\int B(g)^{1/2} dx^1 dx^2 dx^3 dx^4$$

shall be stationary under variations of the functions $\gamma_{\alpha\beta}$. In calculating the variation we follow an elegant method due to Palatini.⁵ The functions $\delta\Gamma_{\beta\gamma}^{\alpha}$ are the differences of the components of two projective connections and are therefore components of a projective tensor. Taking the covariant derivative of this tensor we have

⁵ Attilio Palatini. Rend. del Circolo Matematico di Palermo XLIII, 205 (1919).

$$(\delta\Gamma_{\beta\gamma}^{\alpha})_{;\delta} = \frac{\partial(\delta\Gamma_{\beta\gamma}^{\alpha})}{\partial x^{\delta}} - (\delta\Gamma_{\beta\epsilon}^{\alpha})\Gamma_{\gamma\delta}^{\epsilon} - (\delta\Gamma_{\epsilon\gamma}^{\alpha})\Gamma_{\beta\delta}^{\epsilon} + (\delta\Gamma_{\beta\gamma}^{\epsilon})\Gamma_{\epsilon\delta}^{\alpha}.$$

We thus have

$$(\delta\Gamma_{\beta\gamma}^{\alpha})_{;\delta} - (\delta\Gamma_{\beta\delta}^{\alpha})_{;\gamma} = \delta B_{\beta\gamma\delta}^{\alpha},$$

and so, contracting with respect to α and γ

$$(\delta\Gamma_{\beta\alpha}^{\alpha})_{;\delta} - (\delta\Gamma_{\beta\delta}^{\alpha})_{;\alpha} = \delta B_{\beta\delta}.$$

Hence

$$\gamma^{\beta\delta}\delta B_{\beta\delta} = \{\gamma^{\beta\delta}(\delta\Gamma_{\beta\alpha}^{\alpha}) - \gamma^{\beta\alpha}(\delta\Gamma_{\beta\alpha}^{\delta})\}_{;\delta}.$$

So, remembering that $g=\gamma$, we have

$$\begin{aligned} & \int \gamma^{\beta\delta}(g)^{1/2}\delta B_{\beta\delta}dx^1dx^2dx^3dx^4 \\ &= \int \frac{\partial}{\partial x^{\delta}}[\gamma^{\beta\delta}(\delta\Gamma_{\beta\alpha}^{\alpha})(g)^{\frac{1}{2}} - \gamma^{\beta\alpha}(\delta\Gamma_{\beta\alpha}^{\delta})(g)^{\frac{1}{2}}]dx^1dx^2dx^3dx^4. \end{aligned}$$

Since the expression in the square brackets is independent of x^0 this integral is

$$= \int \frac{\partial}{\partial x^i}[\gamma^{\beta i}(\delta\Gamma_{\beta\alpha}^{\alpha})(g)^{\frac{1}{2}} - \gamma^{\beta\alpha}(\delta\Gamma_{\beta\alpha}^i)(g)^{\frac{1}{2}}]dx^1dx^2dx^3dx^4$$

= 0, by the generalized Green's theorem. We have, therefore,

$$\delta \int B(g)^{1/2}dx^1dx^2dx^3dx^4 = \int B_{\alpha\beta}\delta(\gamma^{\alpha\beta}(g)^{1/2})dx^1dx^2dx^3dx^4 = 0$$

Remembering that $\delta\gamma = -\gamma\gamma_{\alpha\beta}\delta\gamma^{\alpha\beta}$, this reduces to

$$\int \Gamma^{\alpha\beta}(g)^{1/2}\delta\gamma_{\alpha\beta}dx^1dx^2dx^3dx^4 = 0.$$

Since $\gamma_{00}=1$, $\delta\gamma_{00}=0$, but the remaining $\delta\gamma$'s are arbitrary. Hence we deduce that

$$\Gamma^{\alpha\beta} = \delta_0^{\alpha}\delta_0^{\beta}K$$

where K is some function of x^1, x^2, x^3, x^4 . Contracting by means of $\gamma_{\alpha\beta}$ we have at once

$$\Gamma = K.$$

Hence the condition for a stationary value of the integral becomes

$$\Gamma^{\alpha\beta} - \delta_0^{\alpha}\delta_0^{\beta}\Gamma = 0$$

or, in covariant form (4.1).

The equations $\Gamma_{\alpha\beta} - \phi_\alpha\phi_\beta\Gamma = 0$ may also be derived, without assuming that $\Phi = 1$, as the conditions that the integral

$$\int B(g)^{1/2} dx^1 dx^2 dx^3 dx^4$$

be stationary with respect to variation of the functions $G^{\alpha\beta}$. Since $B(g)^{1/2}$ is independent of Φ we have as before

$$0 = \delta \int B(g)^{1/2} dx^1 dx^2 dx^3 dx^4 = \int \Gamma_{\alpha\beta}(g)^{1/2} \delta \gamma^{\alpha\beta} dx^1 dx^2 dx^3 dx^4.$$

But

$$\gamma^{\alpha\beta} = \Phi^2 G^{\alpha\beta} = G_{00} G^{\alpha\beta}$$

and

$$\begin{aligned} \delta G_{00} &= \delta(G_{0\alpha} G_{0\beta} G^{\alpha\beta}) \\ &= G_{0\alpha} G_{0\beta} \delta G^{\alpha\beta} + 2G_{0\alpha} G^{\alpha\beta} \delta G_{0\beta} \\ &= G_{0\alpha} G_{0\beta} \delta G^{\alpha\beta} - 2G_{0\alpha} G_{0\beta} \delta G^{\alpha\beta} \\ &= -G_{0\alpha} G_{0\beta} \delta G^{\alpha\beta}. \end{aligned}$$

Hence

$$\delta \gamma^{\alpha\beta} = G^{\alpha\beta} \delta G_{00} + G_{00} \delta G^{\alpha\beta} = G_{00} \delta G^{\alpha\beta} - G_{0\alpha} G_{0\beta} \delta G^{\alpha\beta},$$

and so we must have

$$\int (\Gamma_{\alpha\beta} G_{00} - \gamma_{0\alpha} G_{0\beta} \Gamma)(g)^{1/2} \delta G^{\alpha\beta} dx^1 dx^2 dx^3 dx^4 = 0$$

giving, since we are assuming that $\Phi \neq 0$,

$$\Gamma_{\alpha\beta} - \phi_\alpha\phi_\beta\Gamma = 0.$$

6. FIELD EQUATIONS, ANY INDEX

It is natural to inquire next what sort of a theory arises from a study of a projective tensor $G_{\alpha\beta}$ of arbitrary index N . In case $N \neq 0$ there is a projective connection $\Pi_{\beta\gamma}^\alpha$ which satisfies the equations⁶ (Cf. Q.F. §5)

$$G_{\alpha\beta/\gamma} = \frac{\partial G_{\alpha\beta}}{\partial x^\gamma} - \Pi_{\alpha\gamma}^\epsilon G_{\epsilon\beta} - \Pi_{\beta\gamma}^\epsilon G_{\alpha\epsilon} = 0.$$

The components $\Pi_{\beta\gamma}^\alpha$ are Christoffel symbols of the second kind in terms of the $G_{\alpha\beta}$'s, but it is more convenient to express them in the form

$$\Pi_{\beta\gamma}^\alpha = \Gamma_{\beta\gamma}^\alpha + N(\delta_\beta^\alpha \Phi_\gamma + \delta_\gamma^\alpha \Phi_\beta - \gamma_{\beta\gamma} \Phi^\alpha),$$

where $\Gamma_{\beta\gamma}^\alpha$ is the projective connection employed in §3, and the indices of projective tensors are raised by means of the γ 's. Denoting the curvature tensor of the Π 's by $P_{\beta\gamma\delta}^\alpha$ and its contractions by $P_{\alpha\beta}$ and P we have (as in Q.F.)

⁶ We shall use the solidus "/" to denote projective derivation with respect to $\Pi_{\beta\gamma}^\alpha$.

$$P_{\alpha\sigma\beta}^{\sigma} = P_{\alpha\beta} = B_{\alpha\beta} + 3N(\Phi_{\alpha;\beta} - N\Phi_{\alpha}\Phi_{\beta} + N\Phi^{\sigma}\Phi_{\sigma}\gamma_{\alpha\beta}) + N\gamma_{\alpha\beta}\Phi^{\sigma}{}_{;\sigma}$$

and

$$P = B + 8N\Phi_{;\sigma}^{\sigma} + 12N^2\Phi^{\sigma}\Phi_{\sigma}.$$

The tensor analogous to the Einstein tensor is

$$\pi_{\alpha\beta} = P_{\alpha\beta} - \frac{1}{2}\gamma_{\alpha\beta}P.$$

The field equations analogous to those of §3 are

$$\pi_{\alpha\beta} - \phi_{\alpha}\phi_{\beta}\pi = 0.$$

These are expressible as the affine sets

$$\pi^{ij} = 0$$

$$P_0^i = 0$$

and

$$\pi_{00} - \pi = 0.$$

The last equation is an algebraic consequence⁷ of the set $\pi^{ij} = 0$.

Thus once more there are only fourteen algebraically independent equations involving the fifteen quantities $G_{\alpha\beta}$.

The affine form of these equations may be obtained by using (5.17) to (5.20) of Q.F.:

$$\pi^{ij} = \Gamma^{ij} - \frac{3N}{2}g^{ia}g^{jb}(\theta_{a,b} + \theta_{b,a}) - 3N^2\theta^i\theta^j$$

$$- 3N^2g^{ij}(1 + \theta^a\theta_a) + 3Ng^{ij}\theta^a{}_{,a} = 0,$$

$$P_0^i = B_0^i - 3N\phi_{;\sigma}^i\theta^{\sigma} + 3N^2\theta^i = 0,$$

and for completeness we give

$$\pi_{00} - \pi = R - 9N\theta^i{}_{,i} + 12N^2 + 15N^2\theta^i\theta_i = 0.$$

As already remarked, the last equation is a consequence of the first set. The significance of this equation comes out more clearly if we write it in terms of the projective scalar Φ . From (5.8) and (5.11) Q.F. we see that it is

$$R - 3N^2 + 9N\Phi^{\sigma}{}_{;\sigma} + 15N^2\Phi^{\sigma}\Phi_{\sigma} = 0.$$

On making the substitution

$$\Phi = \psi^{3/5}$$

⁷ This is a special case of a general theorem. If $A_{\alpha\beta}$ is any projective tensor

$$\begin{aligned} A &= \gamma_{\alpha\beta}A^{\alpha\beta} \\ &= (g_{\alpha\beta} + \phi_{\alpha}\phi_{\beta})A^{\alpha\beta} \\ &= g_{ij}A^{ij} + \delta_0^{\alpha}\delta_0^{\beta}A_{\alpha\beta} \\ &= g_{ij}A^{ij} + A_{00}. \end{aligned}$$

this becomes

$$\gamma_{\alpha\beta} \left(\frac{\partial^2 \psi}{\partial x^\alpha \partial x^\beta} - \Gamma_{\alpha\beta}^\sigma \frac{\partial \psi}{\partial x^\sigma} \right) + \frac{5}{27} (R - 3N^2) \psi = 0$$

or

$$\frac{1}{(g)^{1/2}} \frac{\partial}{\partial x^\alpha} \left((g)^{1/2} \gamma_{\alpha\beta} \frac{\partial \psi}{\partial x^\beta} \right) + \frac{5}{27} (R - 3N^2) \psi = 0.$$

This may be regarded as the relativistic wave equation studied by Klein, Gordon, Fock, and others.⁸

To be explicit, we may write it as

$$\begin{aligned} \frac{1}{(g)^{1/2}} \frac{\partial}{\partial x^i} \left(g^{ij} (g)^{1/2} \frac{\partial \psi}{\partial x^j} \right) - \frac{10N}{3} g^{ij} \phi_j \frac{\partial \psi}{\partial x^i} - \frac{5N}{3} \frac{1}{(g)^{1/2}} \psi \frac{\partial}{\partial x^i} (g^{ij} \phi_j (g)^{1/2}) \\ + \frac{25N^2}{9} g^{ij} \phi_i \phi_j \psi + \left(\frac{5}{27} R + \frac{20}{9} N^2 \right) \psi = 0. \end{aligned}$$

If we set

$$\begin{cases} N = \frac{3\pi mc}{(5)^{1/2} h} i \\ \phi_i = \frac{2}{(5)^{1/2}} \frac{e}{mc^2} V_i \end{cases}$$

we have

$$\begin{aligned} \frac{1}{(g)^{1/2}} \frac{\partial}{\partial x^i} \left(g^{ij} (g)^{1/2} \frac{\partial \psi}{\partial x^j} \right) - \frac{4\pi ie}{h} g^{ij} V_j \frac{\partial \psi}{\partial x^i} - \frac{2\pi ie}{h} \frac{1}{(g)^{1/2}} \psi \frac{\partial}{\partial x^i} (g^{ij} V_j (g)^{1/2}) \\ - \frac{4\pi^2 e^2}{h^2} g^{ij} V_i V_j \psi + \left(\frac{5}{27} R - \frac{4\pi^2 m^2 c^2}{h^2} \right) \psi = 0, \end{aligned}$$

and when g^{ij} have the values

$$\begin{pmatrix} 1 & 0 & 0 & 0 \\ 0 & 1 & 0 & 0 \\ 0 & 0 & 1 & 0 \\ 0 & 0 & 0 & -c^2 \end{pmatrix}$$

R vanishes and it becomes precisely the relativistic wave equation in a gravitation-free field.

The wave equation is invariant in form because the component T_{00} of any projective tensor $T_{\alpha\beta}$ is a projective scalar. This corresponds to the fact

⁸ See for example—O. Klein, *Zeits. f. Physik* **37**, 895 (1926), V. Fock, *Zeits. f. Physik* **39**, 226 (1926), W. Gordon, *Zeits. f. Physik* **40**, 117 (1926).

observed by several authors⁹ that we may alter the four-potential ϕ_i by a gradient provided we multiply the quantity Ψ by a suitable function. This is the effect of a change of factor. It is to be noted further that since θ_i is affine it is unaltered by a change of factor. The wave equation may thus be looked on as the normalizing condition satisfied by the affine four-potential θ_i .

We have been unable as yet to obtain satisfactory results from an attempt to interpret the terms involving θ_i in the other field equations as a quantum expression for the material tensor of the older theory.

The field equations,

$$\pi_{\alpha\beta} - \phi_\alpha\phi_\beta = 0$$

thus seem to bring the wave mechanics automatically into the relativity scheme of things. The difficulty is however that we do not know enough about the consistency of the equations. We have not succeeded in deriving them, or a satisfactory substitute, from a four-dimensional variational principle. The equations

$$\pi_{\alpha\beta} = 0$$

can, of course, be derived from a five-dimensional variational principle and as our equations are obtained from these by omitting

$$\pi_{00} = 0$$

they are presumably consistent when regarded as equations for determining $G_{\alpha\beta}$ as functions of x^0, \dots, x^4 . But are they consistent as equations for determining the G 's as functions of the form $\exp(Nx^0)f(x^1 x^2 x^3 x^4)$? We have set them down here because they seem to suggest an interesting possibility.

⁹ See F. London. *Zeits. f. Physik* **42**, 375 (1927), D. J. Struik and Norbert Wiener. *MIT Journal of Math. and Phys.* **7**, (1927-28), page I. Struik and Wiener show that the Klein theory, and hence of course the projective theory, can be regarded as the invariant theory of a linear partial differential equation of the second order. The latter theory is due to E. Cotton, *Ann. Ec. Norm. Sup.* (3) **17** (1900) pp. 211-244.

ON THE THEORY OF THE BROWNIAN MOTION

By G. E. UHLENBECK AND L. S. ORNSTEIN

UNIVERSITY OF MICHIGAN, ANN ARBOR AND PHYSISCH LABORATORIUM DER R. U. UTRECHT, HOLLAND

(Received July 7, 1930)

ABSTRACT

With a method first indicated by Ornstein the mean values of *all* the powers of the velocity u and the displacement s of a free particle in Brownian motion are calculated. It is shown that $u - u_0 \exp(-\beta t)$ and $s - u_0/\beta[1 - \exp(-\beta t)]$ where u_0 is the initial velocity and β the friction coefficient divided by the mass of the particle, follow the normal Gaussian distribution law. For s this gives the exact frequency distribution corresponding to the exact formula for \bar{s}^2 of Ornstein and Fürth. Discussion is given of the connection with the Fokker-Planck partial differential equation. By the same method exact expressions are obtained for the square of the deviation of a harmonically bound particle in Brownian motion as a function of the time and the initial deviation. Here the periodic, aperiodic and overdamped cases have to be treated separately. In the last case, when β is much larger than the frequency and for values of $t \gg \beta^{-1}$, the formula takes the form of that previously given by Smoluchowski.

I. GENERAL ASSUMPTIONS AND SUMMARY

IN THE theory of the Brownian motion the first concern has always been the calculation of the mean square value of the displacement of the particle, because this could be immediately observed. As is well known, this problem was first solved by Einstein¹ in the case of a *free* particle. He obtained the famous formula:

$$\bar{s}^2 = 2Dt = \frac{2kT}{f}t \quad (1)$$

where f is the friction coefficient, T the absolute temperature and t the time. The influence of the surrounding medium is characterized by f as well as by T . For this Einstein used the formula of Stokes, because almost always the particle is immersed in a liquid or gas at ordinary pressure. In that case the mean free path of the molecules is small compared with the particle, and we may consider the surrounding medium as continuous and may use the results hydrodynamics gives for the friction coefficient for bodies of simple form (sphere, ellipsoid etc.). This will depend on the viscosity coefficient of the medium and therefore be *independent* of the pressure.

But of course, when the surrounding medium is a rarefied gas (mean free path of the molecules great in comparison with the particle), the friction

¹ A. Einstein, Ann. d. Physik 17, 549 (1905). This and the further articles of Einstein have been collected in a book called: "Investigations on the theory of the Brownian Movement". Edited by R. Fürth, translated by A. D. Cowper. New York, Dutton. To this we shall always refer.

will change in character. Instead of a Stokes friction, we then get what we may call a Doppler friction and this can also be calculated for simple forms of the particle. It is based on the fact that a particle moving, say to the right, will be hit by more molecules from the right than from the left. This friction coefficient will be proportional to the pressure. To cover all cases, we will always leave the friction coefficient explicitly in the formulas.

The basis of formula (1), which since Einstein has been derived in various other ways,² has been almost always the equation of motion:

$$m \frac{du}{dt} = -fu + F(t) \quad (2)$$

where u is the velocity of the particle. Characteristically of this equation, the influence of the surrounding medium is split into two parts:

- (1) a systematic part $-fu$, which causes the friction
- (2) a fluctuating part $F(t)$. Concerning this we will naturally make the following assumptions:

A: The mean of $F(t)$, at given t , over an ensemble of particles (a large number of similar, but independent particles), which have started at $t=0$, with the same velocity u_0 , is zero. We will denote this by:

$$\overline{F(t)}^{u_0} = 0. \quad (3)$$

B: There will be correlation between the values of $F(t)$ at different times t_1 and t_2 only when $|t_1 - t_2|$ is very small. More explicitly we shall suppose that:

$$\overline{F(t_1)F(t_2)}^{u_0} = \phi_1(t_1 - t_2) \quad (4)$$

where $\phi_1(x)$ is a function with a very sharp maximum at $x=0$. More generally, when t_1, t_2, \dots, t_{n+1} are all lying very near each other, we assume:

$$\overline{F(t_1)F(t_2) \cdots F(t_{n+1})}^{u_0} = \phi_n(r, \theta_1, \theta_2, \dots, \theta_{n-1}) \quad (5)$$

where r is the distance perpendicular to the line $t_1=t_2=\dots=t_{n+1}$ in the $(n+1)$ dimensional $(t_1, t_2, \dots, t_{n+1})$ space, and $\theta_1, \theta_2, \dots, \theta_{n-1}$ are $(n-1)$ angles to determine the position of r in the subspace perpendicular to this line. The function ϕ_n has again a very sharp maximum for $r=0$. Further, when t_1, t_2, \dots, t_k are lying near each other, and also $t_{k+1}, t_{k+2}, \dots, t_l$ but far from the group t_1, t_2, \dots, t_k and so on, then:

$$\begin{aligned} \overline{F(t_1) \cdots F(t_k)F(t_{k+1}) \cdots F(t_l)F(t_{l+1}) \cdots F(t_m) \cdots}^{u_0} \\ = \overline{F(t_1) \cdots F(t_k)}^{u_0} \cdot \overline{F(t_{k+1}) \cdots F(t_l)}^{u_0} \cdot \overline{F(t_{l+1}) \cdots F(t_m)}^{u_0} \cdots \end{aligned} \quad (6)$$

The justification, or eventually the criticism, of these assumptions must come from a more precise, kinetic, theory. We will not go into that.

² Compare G. L. de Haas-Lorentz: Die Brownsche Bewegung (Braunschweig, Vieweg, 1913).

§3. In the later development, especially when given outside forces like gravitation were also considered, so that (2) had to be replaced by:

$$m \frac{du}{dt} = -fu + F(t) + K(x) \quad (2a)$$

the attention was fixed more on the determination of the frequency distribution of quantities like the displacement or the velocity. Given the value ϕ_0 of the quantity ϕ at $t=0$, we wish to find the probability $F(\phi_0, \phi, t)d\phi$ that after the time t the value lies between ϕ and $\phi+d\phi$. It is clear, that when we know $F(\phi_0, \phi, t)$ all mean values are determined. For instance:

$$\overline{\phi^k}^{\phi_0} = \int \phi^k F(\phi_0, \phi, t) d\phi.$$

The frequency distribution is the most general thing the theory can predict. In the case of a free particle, the function $F(x_0, x, t)$, which will now depend only on $x-x_0=s$, was already determined by Einstein. He found:

$$F(x_0, x, t) = \left(\frac{1}{4\pi Dt} \right)^{1/2} e^{-(x-x_0)^2/4Dt} \quad (7)$$

of which (1) is an immediate consequence. He derived this, by finding for F a partial differential equation, which in this case is the *diffusion equation*:

$$\frac{\partial z}{\partial t} = D \frac{\partial^2 z}{\partial s^2} \quad (8)$$

and of which $F(x_0, x, t)$ is then the so-called fundamental solution. This is that solution of (8) which for $t=0$ becomes $\delta(x-x_0)$, when $\delta(x)$ means the function, defined by the properties:

$$\delta(x) = 0 \quad \text{for } x \neq 0$$

$$\int_{-\infty}^{+\infty} \delta(x) dx = 1$$

This is clear from the definition of $F(x_0, x, t)$ because for $t=0$, there is certainty that $x=x_0$. Further there are boundary conditions, which express the behavior of the particle at the walls; in the case of a completely free particle they are simply $F=0$ for $x=\pm\infty$. The relation between the diffusion coefficient D and the friction coefficient f , Einstein then derived very simply, using the osmotic pressure idea.

This connection between the frequency distribution function and a partial differential equation of the parabolic type like (8), has later been generalized considerably by Smoluchowski, Fokker, Planck, Ornstein, Burger,

Fürth and others.³ The equation is generally called the Fokker-Planck equation. Especially for a particle under influence of outside forces, Smoluchowski showed that the generalization of (8) was:

$$\frac{\partial z}{\partial t} = - \frac{1}{f} \frac{\partial}{\partial x} (Kz) + D \frac{\partial^2 z}{\partial x^2} \quad (9)$$

For special forces (gravitation, elastic binding etc.) and by different boundary conditions, Smoluchowski, Fürth and others have determined the fundamental solution, and from this all sorts of mean values, which they have compared with experiments.

§4. With the results (1), (7), (8) and (9) of Einstein and Smoluchowski the problem seems completely solved. But there is one restriction, which was first stressed by Einstein. All these results hold only when t is large compared to m/f . The generalization of (1) for all times was given by Ornstein⁴ and Fürth⁵, independently of each other.

The result is:

$$\overline{s^2} = \frac{2mkT}{f^2} \left(\frac{f}{m} t - 1 + e^{-ft/m} \right) \quad (10)$$

For values of t large compared to m/f this becomes again Einstein's formula (1). For very short times on the other hand, we get:

$$\overline{s^2} = \frac{kT}{m} t^2 = \overline{u_0^2} t^2$$

as one would expect, because in the beginning the motion must be uniform.

The problem now arises to generalize the other results also. In part III we will do this for the frequency distribution $F(x_0, x, t)$. The result is rather complicated; for $t \gg m/f$ it goes over into (7), and (10) is an immediate consequence of it. The *method*, we used, was the momentum method. From the equation of motion (2), and using the assumptions (3) to (6), we could calculate the mean value of all the powers of

$$S = s - \frac{mu_0}{f} (1 - e^{-ft/m})$$

³ M. v. Smoluchowski, Phys. Zeits. **17**, 557 (1916). A. Fokker, Dissertation Leiden, 1913, p. 000. M. Planck, Berl. Ber. p. 324, 1927. L. S. Ornstein, Versl. Acad. Amst. **26**, 1005 (1917). H. C. Burger, Versl. Acad. Amst; **25**, 1482 (1917); L. S. Ornstein and H. C. Burger, Versl. Acad. Amst. **27**, 1146 (1919); **28**, 183 (1919). R. Fürth, Ann. d. Physik **53**, 177 (1917). R. Fürth gives a survey in Riemann-Weber, Die Partiellen Differential-gleichungen der Mathematischen Physik (Edited by R. v. Mises and Ph. Frank, Braunschweig Vieweg 1928) Vol. II, p. 177. Comp. also the article of F. Zernike, Handbuch der Physik, Vol. III, p. 456 (Berlin, Springer, 1928).

⁴ L. S. Ornstein, Versl. Acad. Amst. **26**, 1005 (1917) (=Proc. Acad. Amst. **21**, 96 (1919).

⁵ R. Fürth, Zeits. f. Physik **2**, 244 (1920).

and prove that S follows the normal Gaussian distribution law. We did not succeed in generalizing the diffusion Eq. (8), and determining the distribution function by this method.

As a preparation we derive in part II the frequency distribution function $G(u_0, u, t)$ for the velocity of a free particle in Brownian motion, first with the momentum method, and then also with the Fokker-Planck equation.

This extension to short times becomes especially interesting in the case of outside periodic forces. In part IV we shall treat the problem of the Brownian motion of an elastically bound particle. By using the same method as before, we could get exact expressions for the mean square of the displacement as a function of the initial deviation and of the time. The periodic, aperiodic and overdamped cases have to be treated separately. The way in which the equipartition value is reached for $t \rightarrow \infty$ is different in the three cases. In the last case, for very strong damping and $t \gg m/f$ the formula goes over into the result of Smoluchowski, which is a consequence of the frequency distribution function following from (9).

II. THE FREQUENCY DISTRIBUTION OF THE VELOCITY

§5. The problem is to determine the probability that a free particle in Brownian motion after the time t has a velocity which lies between u and $u+du$, when it started at $t=0$ with the velocity u_0 .

The first method to solve the problem is by calculating all the mean values $\overline{u^k}$ for given u_0 . As has first been shown by Ornstein⁶ for \bar{u} and $\overline{u^2}$, this is possible by integrating the equation of motion:

$$\frac{du}{dt} + \beta u = A(t)$$

when $\beta = f/m$ and $A = F/m$. Of course, the assumptions (3) to (6) hold for the fluctuating acceleration $A(t)$, as well as for the fluctuating force $F(t)$. Integrating we get:

$$u = u_0 e^{-\beta t} + e^{-\beta t} \int_0^t e^{\beta \xi} A(\xi) d\xi. \quad (11)$$

Taking the mean over an ensemble of particles, which have started at $t=0$ with the same velocity u_0 , and using (3) we get:

$$\bar{u}^{u_0} = u_0 e^{-\beta t}. \quad (12)$$

The mean velocity goes down exponentially due to the friction. Squaring (11) and taking the mean, gives:

$$\overline{u^2}^{u_0} = u_0^2 e^{-2\beta t} + e^{-2\beta t} \int_0^t \int_0^t e^{\beta(\xi+\eta)} \overline{A(\xi)A(\eta)} d\xi d\eta.$$

⁶ L. S. Ornstein, Proc. Acad. Amst. 21, 96 (1919).

By taking $\xi + \eta = v$, $\xi - \eta = w$ as new variables and by using (4), we can write for the integral:

$$\frac{1}{2} e^{-2\beta t} \int_0^{2t} e^{\beta v} dv \int_{-\infty}^{+\infty} \phi_1(w) dw = \frac{\tau_1}{2\beta} (1 - e^{-2\beta t})$$

because $\phi_1(w)$ is such a rapidly decreasing function, that we may integrate from $-\infty$ to $+\infty$. The value of the constant

$$\tau_1 = \int_{-\infty}^{+\infty} \phi_1(w) dw$$

we find with the help of the theorem of the equipartition of energy. For $t \rightarrow \infty$, we must have:

$$\lim_{t \rightarrow \infty} \overline{u^2}^{u_0} = \frac{\tau_1}{2\beta} = \frac{kT}{m}$$

so that:

$$\tau_1 = \frac{2\beta kT}{m} \quad (13)$$

Substituting, we get:

$$\overline{u^2}^{u_0} = \frac{kT}{m} + \left(u_0^2 - \frac{kT}{m} \right) e^{-2\beta t} \quad (14)$$

which shows, how the equipartition value is reached. So we can go on. Using the assumptions (3) to (6) for $A(t)$ and the fact that we must get the equipartition values for $t \rightarrow \infty$, we will prove in Note I, that for $u - u_0 \exp(-\beta t)$ the normal Gaussian distribution law holds. For the velocity itself we get, therefore, the distribution law:

$$G(u_0, u, t) = \left(\frac{m}{2\pi kT(1 - e^{-2\beta t})} \right)^{1/2} \exp \left\{ \frac{m}{2kT} \frac{(u - u_0 e^{-\beta t})^2}{1 - e^{-\beta t}} \right\} \quad (15)$$

which shows how the Maxwell distribution is reached, when at $t=0$ all the particles started with the same velocity u_0 .

§6. The second method for deriving (15) is, as we have already said, by constructing the Fokker-Planck partial differential equation for the problem, of which $G(u_0, u, t)$ is then the fundamental solution. We will first derive the equation in general and then later specialize to our case.⁷ Consider the distribution function $F(\phi_0, \phi, t)$. When t increases by Δt , ϕ will increase by a $\Delta\phi$, which will be different for every particle. Let the probability for an increase between the limits $\Delta\phi$ and $\Delta\phi + d(\Delta\phi)$ be $\psi(\Delta\phi, \phi, t) d(\Delta\phi)$. Writing $\phi' = \phi + \Delta\phi$ we have then:

$$F(\phi_0, \phi', t + \Delta t) = \int F(\phi_0, \phi' - \Delta\phi, t) \psi(\Delta\phi, \phi' - \Delta\phi, t) d(\Delta\phi) \quad (16)$$

⁷ Comp. F. Zernike, Handbuch der Physik, Vol. III, p. 457.

when we may suppose that the probability of an increase $\Delta\phi$ is *independent* of the fact that for $t=0$, $\phi=\phi_0$. We now develop the integrand after powers of $\Delta\phi$:

$$F(\phi_0, \phi' - \Delta\phi, t)\psi(\Delta\phi, \phi' - \Delta\phi, t) = F(\phi_0, \phi', t)\psi(\Delta\phi, \phi', t) \\ - \Delta\phi(F'\psi + F\psi') + \frac{\Delta\phi^2}{2}(F''\psi + 2F'\psi' + F\psi'') + \dots$$

The resulting integrals all have simple meanings, for instance:

$$\int \psi(\Delta\phi, \phi', t)d(\Delta\phi) = 1; \quad \int \Delta\phi\psi d(\Delta\phi) = \overline{\Delta\phi}; \quad \int \Delta\phi^2\psi'' d(\Delta\phi) = \frac{\partial^2}{\partial\phi'^2}\overline{\Delta\phi^2}$$

and so on. Developing the left hand side in powers of Δt , putting:

$$\lim_{\Delta t \rightarrow 0} \frac{\overline{\Delta\phi}}{\Delta t} = f_1(\phi', t); \quad \lim_{\Delta t \rightarrow 0} \frac{\overline{\Delta\phi^2}}{\Delta t} = f_2(\phi', t) \quad (17)$$

and supposing that:

$$\lim_{\Delta t \rightarrow 0} \frac{\overline{\Delta\phi^k}}{\Delta t} = 0 \quad \text{for } k > 2 \quad (18)$$

we get, when we write again ϕ for ϕ' :

$$\frac{\partial F}{\partial t} = \frac{1}{2}f_2\frac{\partial^2 F}{\partial\phi^2} + \left(\frac{\partial f_2}{\partial\phi} - f_1\right)\frac{\partial F}{\partial\phi} + \left(\frac{1}{2}\frac{\partial^2 f_2}{\partial\phi^2} - \frac{\partial f_1}{\partial\phi}\right)F. \quad (19)$$

We must of course in each special case determine the functions $f_1(\phi, t)$ and $f_2(\phi, t)$ and verify the supposition (18). We always can do that, when we know the equation of motion.

Let us return now to the velocity distribution. From the equation of motion we have:

$$u' - u = \Delta u = -\beta u\Delta t + \int_t^{t+\Delta t} A(\xi)d\xi$$

Using (3), we get therefore:

$$\overline{\Delta u} = -\beta u\Delta t = -\beta u'\Delta t$$

neglecting higher powers of Δt . From this:

$$\lim_{\Delta t \rightarrow 0} \frac{\overline{\Delta u}}{\Delta t} = f_1(u') = -\beta u'.$$

In the same way, we find using (4) as before:

$$\overline{\Delta u^2} = \tau_1\Delta t$$

so that:

$$f_2(u') = \tau_1 = \frac{2\beta kT}{m} = \text{const.}$$

All the higher powers of Δu become proportional to powers of Δt higher than the first, so that (18) is satisfied. We get therefore:⁸

$$\frac{\partial G}{\partial t} = \beta \frac{\partial}{\partial u} (uG) + \frac{\tau_1}{2} \frac{\partial^2 G}{\partial u^2} \quad (20)$$

The systematic way of finding the fundamental solution of this equation is by solving the equation:

$$\frac{\partial z}{\partial t} = \beta \frac{\partial}{\partial u} (uz) + \frac{\tau_1}{2} \frac{\partial^2 z}{\partial u^2}$$

when for $t=0$, $z=f(u)$. This is an ordinary boundary value problem, which can easily be solved by the method of particular solutions. By summing the infinite series which we get, one can write the solution:

$$z(u, t) = \int_{-\infty}^{+\infty} f(u_0) G(u_0, t) du_0$$

and G is then clearly the fundamental solution. For the details, see Note II. The result is again formula (15). One can derive the same result much more briefly when one is so clever as to substitute in (20):

$$G = (\phi)^{1/2} \exp \{ -(u - u_0 \chi) \phi \}$$

where ϕ and χ are functions of t only.⁹ This is suggested a little by the result one ought to expect. Substituting, one sees that (18) is fulfilled, when χ and ϕ are solutions of the ordinary differential equations:

$$\begin{aligned} \frac{d\chi}{dt} &= -\beta\chi \\ \frac{1}{\beta} \frac{d\phi}{dt} &= 2\phi - 4\phi^2. \end{aligned}$$

These can be immediately integrated, and the integration constants can be determined from the fact that for $t=0$ we must get $\delta(u - u_0)$ and for $t = \infty$ the Maxwell distribution law.

III. THE FREQUENCY DISTRIBUTION OF THE DISPLACEMENT

§7. The problem is to determine the probability that a free particle in Brownian motion which, at $t=0$ starts from $x=x_0$ with the velocity u_0 after the time t lies between x and $x+dx$. It is clear that this probability will depend only on $s=x-x_0$, and on t .

⁸ This equation has been derived already by Rayleigh (Phil. Mag. 32, 424 (1891) = Scient. Papers III, p. 473) and he gives also the fundamental solution (15). Later it has again been treated by v. Smoluchowski (Krakauer Ber. 1913, p. 418). Because Rayleigh's proof is a little artificial, and the treatment of v. Smoluchowski is not easily accessible, we thought it not superfluous to give the proof again.

⁹ Comp. Lord Rayleigh, reference 8.

We will use again the momentum method, and calculate all the mean values $\overline{s^{u_0}}$. This goes in an analogous way as with the velocity. By integrating (11) again we find:

$$x = x_0 + \frac{u_0}{\beta}(1 - e^{-\beta t}) + \int_0^t e^{-\beta \eta} d\eta \int_0^\eta e^{\beta \xi} A(\xi) d\xi \quad (21)$$

or integrating partially:

$$s = x - x_0 = \frac{u_0}{\beta}(1 - e^{-\beta t}) - \frac{1}{\beta} e^{-\beta t} \int_0^t e^{\beta \xi} A(\xi) d\xi + \frac{1}{\beta} \int_0^t A(\xi) d\xi.$$

Taking the mean, gives:

$$\overline{s^{u_0}} = \frac{u_0}{\beta}(1 - e^{-\beta t}) \quad (22)$$

which can be interpreted as the distance travelled in the time t with the mean velocity $\bar{u} = u_0 \exp(-\beta t)$. By squaring, averaging, and calculating the double integrals in the same way as before, we get:

$$\overline{s^2}^{u_0} = \frac{\tau_1}{\beta^2} t + \frac{u_0}{\beta^2} (1 - e^{-\beta t})^2 + \frac{\tau_1}{2\beta^3} (-3 + 4e^{-\beta t} - e^{-2\beta t}) \quad (23)$$

where the constant τ_1 is known from the corresponding calculation of $\overline{u^2}^{u_0}$. This result (23) was first derived by Ornstein; for very long times t it goes over in:

$$\overline{s^2}^{u_0} = \frac{\tau_1}{\beta^2} t = \frac{2kT}{m\beta} t$$

the result of Einstein. For very short times t on the other hand, we get:

$$\begin{aligned} \overline{s}^{u_0} &= u_0 t \\ \overline{s^2}^{u_0} &= u_0^2 t^2 \end{aligned}$$

The motion is then uniform with the velocity u_0 . Taking a second average over u_0 , remembering that $\overline{u^2}_0 = kT/m$, we get:

$$\begin{aligned} \overline{\overline{s}} &= 0 \\ \overline{\overline{s^2}} &= \frac{2kT}{m\beta^2} (\beta t - 1 + e^{-\beta t}) \end{aligned}$$

which is the result quoted above (formula 10). The calculation of the higher powers goes similarly. In the result we get constants $\tau_2, \tau_3 \dots$ which have been determined in part II in the corresponding calculation of $\overline{u^k}^{u_0}$ from the equipartition law. We can show in this way that for:

$$S = s - \frac{u_0}{\beta}(1 - e^{-\beta t})$$

again the normal Gaussian distribution law holds. For the details of the proof, see Note III. We get therefore:

$$F(x_0, x, t) = \left(\frac{m\beta^2}{2\pi kT(2\beta t - 3 + 4e^{-\beta t} - e^{-2\beta t})} \right)^{1/2} \exp \left[\frac{m\beta^2}{2kT} \frac{\{x - x_0 - u_0(1 - e^{-\beta t})/\beta\}^2}{2\beta t - 3 + 4e^{-\beta t} - e^{-2\beta t}} \right] \quad (24)$$

For large t this becomes of course the distribution law (7), already derived by Einstein. For $t \rightarrow 0$ it becomes $\delta(x - x_0)$ as it should.

§8. When we want to derive (24) in the same way as $G(u_0, u, t)$ from a partial differential equation we run into the following difficulty. According to the general Eq. (19), we have to calculate $\overline{\Delta x}$ and $\overline{\Delta x^2}$. Now it follows from the equation of motion, when the prime denotes the value of the quantities at the time $t + \Delta t$, that:

$$u' - u = -\beta(x' - x) + \int_t^{t+\Delta t} A(\xi) d\xi$$

so that:

$$-\beta(\overline{x' - x}) = -\beta\overline{\Delta x} = \overline{u'} - \overline{u} = u_0 e^{-\beta t} (e^{\beta \Delta t} - 1)$$

or:

$$\overline{\Delta x} = u_0 e^{-\beta t} \Delta t. \quad (25)$$

When one now calculates in the same way $\overline{\Delta x^2}$, then one finds that $\overline{\Delta x^2}$ becomes proportional to Δt^2 , so that the function f_2 in (19) would become zero, and the differential equation would become:

$$\frac{\partial F}{\partial t} = -u_0 e^{-\beta t} \frac{\partial F}{\partial x}$$

which does not become the diffusion equation for $t \gg \beta^{-1}$. On the other hand, when we suppose $t \gg \beta^{-1}$ and Δt so large that we may apply the formula of Einstein for $\overline{\Delta x^2}$, we have:

$$\begin{aligned} \overline{\Delta x} &= 0 \\ \overline{\Delta x^2} &= 2D\Delta t \end{aligned} \quad (26)$$

and this substituted in (19), gives immediately:

$$\frac{\partial F}{\partial t} = D \frac{\partial^2 F}{\partial x^2}$$

It seems impossible to derive from (19) the rigorous differential equation for $F(x_0, x, t)$, which for $t \gg \beta^{-1}$ would become the diffusion equation, and of which (24) would be the fundamental solution. The reason for this, it seems to us, is that in the derivation of (19) we suppose that the change Δx in the time Δt is independent of the fact that at the time $t=0$ the particle is at $x=x_0$ and has the velocity u_0 .

IV. THE BROWNIAN MOTION OF A HARMONICALLY BOUND PARTICLE

§9. We will first derive, following Ornstein¹⁰ the equation (9) first proposed by Smoluchowski from macroscopic considerations. We have to determine again $\overline{\Delta x}$ and $\overline{\Delta x^2}$. Now, when there are external forces the equation of motion is:

$$\frac{du}{dt} + \beta u = A(t) + \frac{1}{m}K(x).$$

Integrating as in §8, we get:

$$u' - u = -\beta(x' - x) + \int_t^{t+\Delta t} A(\xi)d\xi + \frac{1}{m}K\Delta t$$

from which follows, when we may neglect the influence of the initial velocity:

$$\overline{\beta\Delta x} = \frac{1}{m}K(x)\Delta t \quad (27)$$

so that:

$$f_1(x) = \frac{1}{\beta m}K(x) = \frac{1}{f}K(x).$$

When again Δt is not too small, we may put:

$$\overline{\Delta x^2} = \frac{2kT}{m\beta}\Delta t = 2D\Delta t \quad (28)$$

and substituting in the general equation (19), we get:

$$\frac{\partial F}{\partial t} = -\frac{1}{f}\frac{\partial}{\partial x}(KF) + D\frac{\partial^2 F}{\partial x^2}$$

which is (9).

Let us apply this to the case of a harmonically bound particle, for which:

$$\frac{1}{m}K(x) = -\omega^2 x$$

where ω is the frequency in 2π sec. We get then:

$$\frac{\partial F}{\partial t} = \frac{\omega^2}{\beta}\frac{\partial}{\partial x}(xF) + D\frac{\partial^2 F}{\partial x^2}.$$

This is completely similar to the equation (20) for $G(u_0, u, t)$. We find therefore for the fundamental solution

$$F(x_0, x, t) = \left(\frac{\omega^2}{2\pi\beta D(1 - e^{-(2\omega^2/\beta)t})} \right) \exp \left\{ -\frac{\omega^2}{2\beta D} \cdot \frac{(x - x_0 e^{-(\omega^2/\beta)t})}{1 - e^{-(2\omega^2/\beta)t}} \right\}$$

¹⁰ L. S. Ornstein, Proc. Acad. Amst. **21**, 96 (1919).

which gives:

$$\bar{x}^{x_0} = x_0 e^{-(\omega^2/\beta)t}$$

$$\overline{x^2}^{x_0} = \frac{kT}{m\omega^2} + \left(x_0^2 - \frac{kT}{m\omega^2} \right) e^{-(2\omega^2/\beta)t}.$$

This shows how the equipartition value is reached. For ω^2 very small we get approximately:

$$\bar{x}^{x_0} = x_0$$

$$\overline{x^2}^{x_0} = x_0^2 + \frac{2kT}{m\beta}t$$

which are the results for a free particle. We may not expect though, that the equations are generally valid. According to the derivation, there are clearly *two* limitations:

- a. Because we have used (27) and (28) which correspond to (26) in §8, we must expect (30) to hold only for times $t \gg \beta^{-1}$
- b. Because we have in (28) used the result for a *free* particle, we must expect (30) to hold only when β is large, the motion therefore being strongly overdamped. This is also the reason why apparently there is no distinction between the periodic, aperiodic and overdamped cases in the result for $\overline{x^2}^{x_0}$.

§10. To get exact results, we have to use the same method as before. We have first to integrate the equation of motion, and then take the average. The periodic, aperiodic and overdamped case must now be treated separately. We will indicate the calculations only for the periodic case.

The equation of motion is:

$$\frac{d^2x}{dt^2} + \beta \frac{dx}{dt} + \omega^2 x = A(t)$$

when at $t=0$, $x=x_0$ and $u=dx/dt=u_0$ we get from this:

$$u = -\frac{2\omega^2 x_0 + \beta u_0}{2\omega_1} e^{-\beta t/2} \sin \omega_1 t + u_0 e^{-(\beta/2)t} \cos \omega_1 t$$

$$+ \frac{1}{\omega_1} \int_0^t A(\xi) e^{-\beta(t-\xi)/2} \left\{ -\frac{\beta}{2} \sin \omega_1(t-\xi) + \omega_1 \cos \omega_1(t-\xi) \right\} d\xi$$

$$x = \frac{\beta x_0 + 2u_0}{2\omega_1} e^{-(\beta/2)t} \sin \omega_1 t + x_0 e^{-(\beta/2)t} \cos \omega_1 t + \frac{1}{\omega_1} \int_0^t A(\xi) e^{-\beta(t-\xi)/2} \sin \omega_1(t-\xi) d\xi$$

where:

$$\omega_1^2 = \omega^2 - \frac{\beta^2}{4}.$$

Supposing, in correspondence with (3):

$$\overline{A(\xi)}^{x_0 u_0} = 0$$

this gives immediately, for instance:

$$\bar{x}^{x_0 u_0} = \frac{\beta x_0 + 2u_0}{2\omega_1} e^{-(\beta/2)t} \sin \omega_1 t + x_0 e^{-(\beta/2)t} \cos \omega_1 t. \quad (31)$$

The mean value here has to be understood as follows. We have a canonical ensemble of harmonic oscillators, from which at $t=0$ we pick a sub-ensemble (A) of oscillators, which have a deviation and velocity x_0, u_0 , resp. and which we follow in their motion. At the time t we take an average over the x of the different members of this sub-ensemble (A), and the result is then given by (31). If we would follow a *sub-ensemble* (B), of which the members at $t=0$ had the deviation x_0 but arbitrary velocity, we would get at the time t a mean deviation, which will follow from (31) by taking the average over u_0 . Since in a canonical ensemble of oscillators the deviation is not correlated with the velocity, we may put:

$$\begin{aligned} \bar{u}_0^{x_0} &= 0 \\ \overline{u^2}^{x_0} &= \frac{kT}{m}. \end{aligned} \quad (32)$$

Using this, we get:

$$\bar{x}^{x_0} = x_0 e^{-(\beta/2)t} \left(\frac{\beta}{2\omega_1} \sin \omega_1 t + \cos \omega_1 t \right). \quad (33)$$

Let us now consider u^2 and x^2 . Using again the assumption analogous to (4):

$$\overline{A(t_1)A(t_2)}^{x_0 u_0} = \phi(t_1 - t_2)$$

where $\phi(x)$ is an even function with a sharp maximum at $x=0$, and calculating the double integrals exactly as before, we get:

$$\begin{aligned} \overline{x^2}^{x_0 u_0} &= \left(\frac{\beta x_0 + 2u_0}{2\omega_1} e^{-(\beta/2)t} \sin \omega_1 t + x_0 e^{-(\beta/2)t} \cos \omega_1 t \right)^2 + \frac{\tau_1}{2\omega_1^2 \beta} (1 - e^{-\beta t}) \\ &\quad - \frac{\tau_2}{8\omega_1^2 \omega_1^2} (\beta - \beta e^{-\beta t} \cos 2\omega_1 t + 2\omega_1 e^{-\beta t} \sin 2\omega_1 t) \end{aligned}$$

where we have put:

$$\begin{aligned} \tau_1 &= \int_{-\infty}^{+\infty} \phi(w) \cos \omega_1 w dw \\ \tau_2 &= \int_{-\infty}^{+\infty} \phi(w) dw. \end{aligned}$$

The condition, that for $t \rightarrow \infty$ we must get the equipartition value, gives us one relation between τ_1 and τ_2 . One would expect that from:

$$\lim_{t \rightarrow \infty} \overline{u^2}^{x_0 u_0} = \frac{kT}{m}$$

we would get a second relation, but the calculation of $\overline{u^2}^{x_0 u_0}$ shows that this is the same as the first. The fact that $\phi(w)$ has such a sharp maximum suggests, that in the integral for τ_1 we may replace $\cos \omega_1 w$ by unity, which would make $\tau_1 = \tau_2$. We can prove this more exactly by calculating $\overline{xu}^{x_0 u_0}$ ¹¹ and determining the limit for $t \rightarrow \infty$, which must be zero, because for $t \rightarrow \infty$ subensemble (A) must again become a canonical ensemble. We get in this way:

$$\tau_1 = \tau_2 = \frac{2\beta kT}{m}.$$

This solves the problem completely. Averaging again over u_0 , using (32) we get:

$$\overline{x^2}^{x_0} = \frac{kT}{m\omega^2} + \left(x_0^2 - \frac{kT}{m\omega^2} \right) e^{-\beta t} \left(\cos \omega_1 t + \frac{\beta}{2\omega_1} \sin \omega_1 t \right)^2 \quad (34)$$

which shows how the equipartition value is reached. So we can calculate all sorts of mean values. The further result is perhaps interesting, that:

$$\overline{xu}^{x_0} = \frac{1}{\omega_1 \omega^2} \left(\frac{kT}{m\omega^2} - x_0^2 \right) e^{-\beta t} \sin \omega_1 t \left(\cos \omega_1 t + \frac{\beta}{2\omega_1} \sin \omega_1 t \right)$$

which shows how the correlation between x and u , beginning with being zero, oscillates and goes to zero again for $t \rightarrow \infty$. Of course, averaging over x_0 , we get $\overline{xu} = 0$ as it must be.

§11. In the aperiodic case we get:

$$\overline{x^2}^{x_0} = x_0^2 \left(1 + \frac{\beta t}{2} \right) e^{-(\beta/2)t} \quad (33a)$$

$$\overline{x^2}^{x_0} = \frac{kT}{m\omega^2} + \left(x_0^2 - \frac{kT}{m\omega^2} \right) \left(1 + \frac{\beta t}{2} \right) e^{-\beta t}. \quad (34a)$$

The equipartition value is now reached monotonously. The calculation goes similarly, except that instead of the integral τ_1 , we have to introduce an integral:

$$\tau_1' = \int_{-\infty}^{+\infty} w^2 \phi(w) dw.$$

The calculation of $\overline{xu}^{x_0 u_0}$ proves then that this is zero, which could be expected.

In the overdamped case we get:

$$\overline{x}^{x_0} = x_0 e^{-(\beta/2)t} \left(\cosh \omega' t + \frac{\beta}{2\omega'} \sinh \omega' t \right) \quad (33b)$$

$$\overline{x^2}^{x_0} = \frac{kT}{m\omega^2} + \left(x_0^2 - \frac{kT}{m\omega^2} \right) e^{-\beta t} \left(\cosh \omega' t + \frac{\beta}{2\omega'} \sinh \omega' t \right)^2 \quad (34b)$$

¹¹ Here we use: $\int_{-\infty}^{+\infty} \phi(w) \sin \omega_1 w dw = 0$, which follows from the fact that $\phi(w)$ is an even function.

where:

$$\omega'^2 = \frac{\beta^2}{4} - \omega^2 = -\omega_1^2.$$

The equipartition value is again reached monotonously. It is easy to show further, that when $\beta \gg 2\omega$ and $t \gg \beta^{-1}$ these last equations go over into the results (30) of v. Smoluchowski, as we would expect according to the remarks at the end of §9.

§12. The problem of the rotatorial Brownian motion of a small mirror suspended on a fine wire, has been treated recently by S. Goudsmit and one of us,¹² by a method analogous to the well-known treatment of the shot effect by Schottky.¹³ If the displacement, registered during a time, long compared to the characteristic period of the mirror, is developed in a Fourier series, an expression was derived for the square of the amplitude of each Fourier component. It was found that this depended, besides on the temperature, on the pressure and molecular weight of the surrounding gas. This explains in principle, why the curves registered by Gerlach¹⁴ at different pressures, though all giving the same mean square deviation, are quite different in appearance. The calculations were made under the condition that the surrounding gas is much rarified, and though they can easily be generalized, the exact comparison with the experimental data of Gerlach is very difficult.

The results (33) and (34) (when we replace m by the moment of inertia) are in this respect much better. They could be tested easily, and they hold for all pressures of the surrounding gas. They show that, though the mean square deviation depends only on the temperature, the correlation between successive values of the deviation depends in a more interesting way on the surrounding medium. Its influence is expressed by the friction coefficient β .

NOTES

I. To prove that for $U = u - u_0 \exp(-\beta t)$ the normal Gaussian distribution law holds, we have to show that:

$$\begin{aligned} \overline{U^{2n+1}} &= 0 \\ \overline{U^{2n}} &= 1 \cdot 3 \cdot 5 \cdots (2n-1)(\overline{U^2}) \end{aligned} \quad (A)$$

We have from §5:

$$\begin{aligned} \bar{U} &= 0 \\ \overline{U^2} &= \frac{\tau_1}{2\beta}(1 - e^{-2\beta t}). \end{aligned}$$

From (11) we get further:

$$\overline{U^3} = e^{-3\beta t} \int_0^t \int_0^t \int_0^t e^{\beta(\xi_1 + \xi_2 + \xi_3)} \overline{A(\xi_1)A(\xi_2)A(\xi_3)} d\xi_1 d\xi_2 d\xi_3.$$

¹² G. E. Uhlenbeck and S. Goudsmit, Phys. Rev. **34**, 145 (1929).

¹³ W. Schottky, Ann. d. Physik **57**, 541 (1918).

¹⁴ W. Gerlach, Naturwiss. **15**, 15 (1927).

According to the assumptions made about $A(\xi)$ the integrand will be different from zero only in the neighborhood of the line $\xi_1 = \xi_2 = \xi_3$. Taking cylindrical coordinates with this line as z -axis, and using (5), we find:

$$\overline{U^3} = \frac{\tau_2}{\beta(3)^{1/2}} (1 - e^{-3\beta t})$$

where τ_2 denotes the constant:

$$\tau_2 = \int_0^\infty \int_0^{2\pi} \phi_2(r, \theta) r dr d\theta.$$

The value of τ_2 follows again from the equipartition law. For $t \rightarrow \infty$, $\overline{U^3}$ must go to zero, so that $\tau_2 = 0$.

Going to the fourth power we find:

$$\overline{U^4} = e^{-4\beta t} \int_0^t \int_0^t \int_0^t e^{\beta(\xi_1 + \xi_2 + \xi_3 + \xi_4)} \overline{A(\xi_1)A(\xi_2)A(\xi_3)A(\xi_4)} d\xi_1 d\xi_2 d\xi_3 d\xi_4.$$

When ξ_1 and ξ_2 are lying near each other and also ξ_3 and ξ_4 (but far from ξ_1, ξ_2), we will have according to (6):

$$\overline{A(\xi_1)A(\xi_2)A(\xi_3)A(\xi_4)} = \overline{A(\xi_1)A(\xi_2)} \cdot \overline{A(\xi_3)A(\xi_4)}$$

so that this integration region will contribute:

$$e^{-4\beta t} \frac{\tau_1^2}{4\beta^2} (e^{2\beta t} - 1)^2.$$

We will get this 3 times because we can divide $A(\xi_1) A(\xi_2) A(\xi_3) A(\xi_4)$ into two pairs in 3 ways. There remains the region in the neighborhood of the line $\xi_1 = \xi_2 = \xi_3 = \xi_4$. For this we get, introducing cylindrical coordinates and using (5):

$$\frac{\tau_3}{2\beta} e^{-4\beta t} (e^{4\beta t} - 1)$$

where:

$$\tau_3 = \int_0^\infty \int \int \phi_3(r, \theta, \theta_2) r dr dw$$

For $t \rightarrow \infty$ we get therefore:

$$\lim_{t \rightarrow \infty} \overline{U^4} = \frac{3\tau_1^2}{4\beta^2} + \frac{\tau_3}{2\beta}$$

but according to the Maxwell distribution law, we have:

$$\lim_{t \rightarrow \infty} \overline{U^4} = \lim_{t \rightarrow \infty} \overline{u^4} = 3 \left(\lim_{t \rightarrow \infty} \overline{u^2} \right)^2 = \frac{3\tau_1^2}{4\beta^2}$$

so that $\tau_3 = 0$ and we get:

$$\overline{U^4} = 3(\overline{U^2}).$$

To write down the general proof for (A) is tedious, because one has more and more integration regions to consider. However, since (A) holds for $t \rightarrow \infty$, one can convince oneself of the fact that only those regions where the ξ are lying in pairs near each other give a real contribution. All the other regions give contributions proportional to constants $\tau_k (k > 1)$ which by the equipartition law prove to be zero. This gives A_1 immediately and since the number of ways in which we can divide $2n$ objects into n pairs is $1.3.5 \cdots (2n-1)$ we get A_2 also.

II. When we substitute in (20):

$$x = \beta t$$

$$y = u \left(\frac{2\beta}{\tau_1} \right)^{1/2}$$

we get:

$$\frac{\partial z}{\partial x} = z + y \frac{\partial z}{\partial y} + \frac{\partial^2 z}{\partial y^2}$$

and we have to solve this when for $x=0$, $z=f(y)$ and for $y = \pm \infty$, $z=0$. By separating we find as a particular solution:

$$A_n e^{-nx} D_n(y) e^{-y^2/4}$$

where D_n denotes Weber's function of the n th order¹⁵

We have then to determine A_n :

$$f(y) = \sum_0^\infty A_n D_n(y) e^{-y^2/4}$$

which gives:

$$A_n = \frac{1}{n! (2\pi)^{1/2}} \int_{-\infty}^{+\infty} D_n(\eta) f(\eta) e^{-\eta^2/4} d\eta$$

and we get for the solution:

$$z(x, y) = \frac{1}{(2\pi)^{1/2}} \int_{-\infty}^{+\infty} d\eta f(\eta) e^{(\eta^2 - y^2)/4} \sum_0^\infty \frac{D_n(y) D_n(\eta)}{n!} e^{-nx} \quad (B)$$

We have now to sum the infinite series. As Professor H. A. Kramers showed to us, this can be done in the following way. Put, suppressing the arguments y and η :

$$M(x) = \sum_0^\infty \frac{D_n D_n}{n!} e^{-nx}$$

¹⁵ Comp. Whittaker-Watson, Modern Analysis, p. 347.

then:

$$-\frac{dM}{dx} = \sum_0^{\infty} \frac{D_{n+1}D_{n+1}}{n!} e^{-(n+1)x}.$$

Using the recurrence formula:

$$D_{n+1}(z) = zD_n(z) - nD_{n-1}(z)$$

we get:

$$-\frac{dM}{dx} = y\eta e^{-x}M - e^{-2x}\frac{dM}{dx} - \sum_0^{\infty} \frac{yD_{n+1}D_n + \eta D_n D_{n+1} - D_n D_n}{n!} e^{-(n+2)x}.$$

Calling the last sum N and using again the recurrence relation, we find:

$$N = (y^2 + \eta^2 - 1)e^{-2x}M - \sum_0^{\infty} \frac{yD_n D_{n+1} + \eta D_{n+1} D_n}{n!} e^{-(n+3)x}$$

Again using the recurrence relation, we find for the last sum

$$L = (2y\eta e^{-3x} - e^{-4x})M - e^{-2x}N.$$

Substituting back, we get for M the differential equation:

$$-(1 - e^{-2x})^2 \frac{dM}{dx} = M \{ y\eta e^{-x} - (y^2 + \eta^2 - 1)e^{-2x} + y\eta e^{-3x} - e^{-4x} \}$$

This we can immediately integrate, which gives:

$$M = \frac{C(y, \eta)}{(1 - e^{-2x})^{1/2}} \exp \left\{ -\frac{y^2 + \eta^2 - 2y\eta e^{-x}}{2(1 - e^{-2x})} \right\}.$$

The integration constant $C(y, \eta)$ can be determined from the fact that:

$$\lim_{x \rightarrow \infty} M = D_0(y)D_0(\eta) = C(y, \eta)e^{-(y^2 + \eta^2)/2}$$

which gives:

$$C(y, \eta) = e^{(y^2 + \eta^2)/4}.$$

Substituting in the solution (B) gives finally:

$$z(x, y) = \frac{1}{(2\pi)^{1/2}} \int_{-\infty}^{+\infty} d\eta f(\eta) \frac{1}{(1 - e^{-2x})^{1/2}} \exp \left\{ -\frac{(y - \eta e^{-x})^2}{2(1 - e^{-2x})} \right\}$$

which shows that the fundamental solution ($f(\eta)$ is then $\delta(y - y_0)$) is given by:

$$G(y_0, y, x) = \frac{1}{(2\pi(1 - e^{-2x}))^{1/2}} \exp \left\{ -\frac{(y - y_0 e^{-x})^2}{2(1 - e^{-2x})} \right\}.$$

Introducing again t and u , we get (15).

III. To prove that for $S = s - u_0/\beta(1 - e^{-\beta t})$ the Gaussian distribution law holds, we have to show again:

$$\overline{S^{2n+1}} = 0$$

$$\overline{S^{2n}} = 1 \cdot 3 \cdot 5 \cdots (2n-1)(\overline{S^2})^n \quad (C)$$

We have from §7:

$$\overline{S} = 0$$

$$\overline{S^2} = \frac{\tau_1}{2\beta^3}(2\beta t - 3 + 4e^{-\beta t} - e^{-2\beta t}).$$

The calculation of the 3-fold integrals in $\overline{S^3}$ is analogous to the calculation of $\overline{U^3}$ in Note I. We find that the result is proportional to τ_2 , and from Note I we know that $\tau_2 = 0$, so that:

$$\overline{S^3} = 0.$$

In the 4-fold integrals occurring in $\overline{S^4}$ we have to consider only the regions where $\xi_1, \xi_2, \xi_3, \xi_4$ are lying in pairs near each other, because the other regions will give results proportional to τ_3 which is zero, as is proved in Note I. The calculation gives:

$$\overline{S^4} = 3(\overline{S^2})^2$$

as could be expected. The factor 3 comes again from the fact that we can divide $\xi_1, \xi_2, \xi_3, \xi_4$ into two pairs in three ways. In the same way as in Note I then, one convinces oneself further of the truth of the general relations (C).

THE APPEARANCE OF "FORBIDDEN LINES" IN SPECTRA

BY L. D. HUFF AND W. V. HOUSTON

CALIFORNIA INSTITUTE OF TECHNOLOGY, PASADENA, CALIFORNIA

(Received July 23, 1930)

ABSTRACT

A rough calculation shows that the quadrupole term in the radiation of a forbidden line is usually larger than the dipole produced by an external electric field. This is not true, however, when there is an intermediate state, with which both initial and final states combine, and which lies close to one of them.

If the J selection rule is violated, and the Laporte rule is obeyed, the radiation cannot be due to the quadrupole term and must be ascribed to the octopole. Hg 2270 is such a line. An octopole transition will have a Zeeman effect distinctively different from that of a dipole or quadrupole.

THE ordinary spectroscopic selection rules are derived from a consideration of the "dipole radiation" only. This dipole radiation is essentially the first term in the series when the vector potential is developed in powers of the atomic radius divided by the wave-length of the emitted light. For most practical purposes, the first term of this series is amply sufficient to represent the experimental results; but in some cases where the first term is zero, it is necessary to consider the higher terms which give the quadrupole, octopole, etc.

Rubinowicz¹ has recently written a series of papers in which he has developed general methods for dealing with multipole radiation, and has applied them in some detail to quadrupole radiation. We wish to call attention in this note to a few additional properties of quadrupole radiation, and to point out the existence of lines which represent octopole radiation.

INTENSITY OF QUADRUPOLE RADIATION COMPARED WITH THAT DUE TO THE PERTURBATION OF THE ATOM BY AN ELECTRIC FIELD

The presence of an external field will always disturb an atom so that the dipole selection rules will no longer be strictly valid. Thus, it is sometimes thought that the appearance of a "forbidden line" is to be ascribed to an interatomic field sufficient to break down these rules. It is possible, however, to express the intensity of the quadrupole radiation, and of the radiation of the disturbed atom, in so nearly the same form that their relative probabilities can be inferred from a knowledge of the ordinary features of the spectrum. This comparison shows that in most cases, and particularly in the case of the auroral line, the fields necessary to produce the perturbation are much larger than are to be expected under the conditions of the experiments. With respect to the auroral line, Frerichs and Campbell² have already shown

¹ A. Rubinowicz, *Zeits. f. Physik* **53**, 267 (1929); **61**, 338 (1930).

² Frerichs and Campbell, *Phys. Rev.* **36**, 151 (1930).

its quadrupole nature from its Zeeman effect; but it is also of interest to see how the relative intensities of quadrupole and perturbed dipole may be correlated with other features of the spectrum.

Since the total intensity, in the presence of a vanishingly small magnetic field, is the same in all directions, we may take 4π times the intensity per unit solid angle in the z direction as the total intensity. For quadrupole radiation, we may write this as follows:

$$\begin{aligned} I_{kj} &= (16\pi^4 e^2 / c^5) \nu_{kj}^6 \left\{ \int \tilde{\psi}_k z (x + iy) \psi_j d\tau \right\}^2 \\ &= (16\pi^4 e^2 / c^5) \nu_{kj}^6 \left\{ \sum_l z_{kl} (x + iy)_{lj} \right\}^2 \end{aligned} \quad (1)$$

where

$$z_{kl} = \int \tilde{\psi}_k z \psi_l d\tau.$$

In this equation k and j represent the states between which the quadrupole transition takes place, ν_{kj} represents the frequency of the emitted light in sec^{-1} , while x , y , and z represent the coordinates of the electrons. A summation over all electrons is implied. The coordinates with the subscripts attached represent the components of the dipole moments connected with the indicated transition. Thus the quadrupole radiation may be expressed in terms of the dipole moments.³

The intensity of the quadrupole is thus expressed in terms of a sum of products of the dipole transitions to all the states l with which both k and j combine according to the dipole selection rules. In many cases the order of magnitude can be estimated by considering one term. However, an investigation of the convergence of the series would probably be rather difficult.

The intensity of a transition produced by a weak uniform electric field may be expressed in a similar way. Of course the interatomic fields which actually produce violations of the selection rules are not uniform fields, but the deviations from uniformity will produce an effect of higher order which we may neglect for a first approximation.

The solution of the Schroedinger equation with an electric field may be written in the first approximation

$$\psi_k' = \psi_k + F \sum_l A_{kl} \psi_l \quad (2)$$

where the ψ_l are the solutions with zero field and F is the field strength in electrostatic units per cm. The coefficients have the definition

$$A_{kl} = \frac{ez_{lk}}{h\nu_{lk}} \quad \text{and} \quad \tilde{A}_{kl} = \frac{ez_{kl}}{h\nu_{kl}}.$$

³ Bartlett, Phys. Rev. **34**, 1247 (1929).

The electric moments connected with a transition $k \rightarrow j$ are then

$$\begin{aligned}(x + iy)_{kj} &= F \left\{ \sum_l A_{jl}(x + iy)_{kl} + \sum_l \tilde{A}_{kl}(x + iy)_{lj} \right\} \\ &= F \sum_l \frac{e}{h\nu_{lj}\nu_{kl}} \{ (x + iy)_{kl} z_{lj} \nu_{kl} + z_{kl} (x + iy)_{lj} \nu_{lj} \}.\end{aligned}\quad (3)$$

With this expression, it is possible to write the intensity of the perturbed dipole transition.

$$I_{kj} = (2\pi^3 \nu_{kj}^4 F^2 / c^3) \left[\sum_l \frac{e}{h\nu_{lj}\nu_{kl}} \{ (x + iy)_{kl} z_{lj} \nu_{kl} + z_{kl} (x + iy)_{lj} \nu_{lj} \} \right]^2. \quad (4)$$

The summation is seen to contain the same quantities as are in Eq. (1) but with a slightly different dependence upon the frequencies. If we consider only one intermediate state, we can divide out the frequencies and determine the ratio of the radiation caused by an electric field to that normally due to the quadrupole term. For the auroral line if we consider only the 1P state next above the 1S and the 1D states, we get this ratio equal to $3 \cdot 10^{-16} V^2$ where V is the electric field in volts per cm. This indicates that, under ordinary conditions of excitation, the quadrupole term is much larger than the dipole. If, however, the intermediate state were closer to the two states involved in the transition or to one of them, so that the frequencies in Eq. (4) were smaller, the dipole would be relatively somewhat stronger. This is the case in the Stark effect in He where the intermediate level l is very close to the initial level k .⁴

Eq. (1) shows that a quadrupole transition between terms of different multiplicities will be weaker than the corresponding transition between terms of the same multiplicity in the same ratio as in dipole radiation, since one of the dipole moments must be that of an inter-combination. This explains why the auroral line is so much easier to produce in the laboratory than the corresponding intercombinations which appear in the nebulae.

SELECTION RULES FOR MULTIPOLE RADIATION

Rubinowicz has worked out the selection and intensity rules which are to be derived from Eq. (1). It is important, however, to notice the place which Laporte's rule holds. As this rule is now formulated, there are two kinds of terms which may be designated as odd and even terms. The rule states that for dipole radiation, odd terms combine only with even terms, and vice versa. In the quadrupole, however, odd terms may combine with odd terms, and even with even, since there are terms of the other kind with which each combine. But an odd term cannot combine with an even, since there can be no common state with which both can combine with a dipole moment. This can also be shown by the group theory of Neuman and Wigner.⁵ It is essential, then, for the existence of a quadrupole moment, that the Laporte rule be violated.

⁴ Jane Dewey, Phys. Rev. **28**, 1108 (1926).

⁵ Neumann and Wigner, Zeits. f. Physik **49**, 73 (1928).

The two selection rules which are rigorously valid for dipole radiation in any atom are Laporte's rule and the inner quantum number or the J rule. If the Laporte rule is obeyed, and the J rule is violated, neither the dipole nor the quadrupole moments can be different from zero. If such lines do appear, and $^1S_0 - ^3P_2$, $\lambda 2270$ in Hg is one of them, the radiation must be ascribed to an octopole moment.

We may make the following tabulation of the selection rules where the first column gives the first term in the series expansion which can be different from zero.

<i>Radiation</i>	<i>Laporte's Rule</i>	<i>J Rule</i>
Dipole	Obeyed	Obeyed
Quadrupole	Violated	Obeyed or Violated
Octopole	Obeyed	Violated

The 0-0 transition for J is always forbidden in the absence of an external field.

The intensity for an octopole transition can be represented in the same form as the quadrupole in Eq. (1), except that it is a function of a sum of products of three dipole moments involving two intermediate states. The intensity is correspondingly less than for a quadrupole.

THE ZEEMAN EFFECT OF OCTOPOLE RADIATION

The fact that the line Hg 2270 is much harder to produce than the auroral line lends some experimental support to the idea it is an octopole transition. It would be of some interest, however, to confirm the fact by an observation of the Zeeman effect. In an octopole line the magnetic quantum number can change by 0, ± 1 , ± 2 , ± 3 , but in the line Hg 2270 the change of ± 3 cannot appear since one state has an inner quantum number 2 and the other 0. Hence the pattern will be equivalent to a quadrupole except for the polarization. By the method of Rubinowicz it is possible to determine this polarization. It is not necessary to indicate the calculations since they follow Rubinowicz exactly; but the results are given in the table. This is distinctly different from the quadrupole polarization when viewed at right angles to the lines of force.

Polarization of the octopole Zeeman effect.

Octopole Moment	m jumps to	Polarization				
		$\alpha=0$	$\alpha=35^\circ$	$\alpha=45^\circ$	$\alpha=55^\circ$	$\alpha=90^\circ$
z^3	m	0	π	π	π	0
$z(x+iy)(x-iy)$	m	π	π	π	π	0
$z^2(x+iy)$	$m-1$	0	Elliptical	Elliptical	σ	Left Circular
$z^2(x-iy)$	$m+1$	0	"	"	σ	Right Circular
$(x+iy)^2(x-iy)$	$m-1$	σ	"	"	Elliptical	0
$(x+iy)(x-iy)^2$	$m+1$	σ	"	"	"	0
$z(x+iy)^2$	$m-2$	π	σ	"	"	0
$z(x-iy)^2$	$m+2$	π	σ	"	"	0
$(x+iy)^3$	$m-3$	σ	Elliptical	"	"	0
$(x-iy)^3$	$m+3$	σ	"	"	"	0

It is interesting to notice that the longitudinal effect has the same pattern in the octopole term as in the dipole and the quadrupole. Although in general an undisplaced component is permitted in the transverse effect, for the line Hg 2270 this will have zero intensity, so that the pattern will be the same as the quadrupole except for the reversed polarizations.

Note Added August 15: Dr. Bowen has called our attention to the fact that the line $\lambda 2270$ in Hg is probably due to the coupling of the nuclear spin with the electronic angular momentum. An estimate based on the relative separation of the multiplets and the hyperfine structure gives the right order of magnitude for the intensity. The statements made above with respect to J really refer strictly to the total angular momentum.

THE HYPERFINE STRUCTURES OF SOME CADMIUM LINES AND THE HYPOTHESIS OF NUCLEAR SPIN

By C. L. ALBRIGHT

DEPARTMENT OF PHYSICS, UNIVERSITY OF IOWA

(Received July 21, 1930)

ABSTRACT

Measurements have been made of the hyperfine structures of the cadmium lines $\lambda\lambda 5086, 4800, 4678, 3614, 3613, 3610, 3468, 3466, 3404$, and 6438 A.U. ($2^3P_{2,1,0} - 3^3S_1$, $2^3P_2 - 3^3D_{1,2,3}$, $2^3P_1 - 3^3D_{1,2,3}$, $2^3P_0 - 3^3D_1$, and $2^1P_1 - 3^1D_2$) using two quartz Lummer Gehrcke plates. The results are compared with those of MacNair and Schrammen, with fair agreement in general. $\lambda\lambda 3613$ and 3466 A.U. are single in agreement with Schrammen. Structure ascribed to $\lambda 3466$ A.U. by MacNair and to $\lambda 3613$ A.U. by Wali-Mohammad belongs to $\lambda\lambda 3468$ and 3614 A.U. respectively. An attempt is made to extend the application of the hypotheses of Schüler and Brück to the $^3P - ^3D$ lines. This succeeds fairly well save in the cases of $\lambda\lambda 3466$ and 6438 both of which are single whereas if the ideas of Schüler and Brück are accepted they apparently should show readily resolvable fine structure. It is also pointed out that the hypotheses of the above authors would require incomplete polarization of the $1^1S_0 - 2^3P_1$ resonance line in contrast to the observed value of 100%.

BY APPLYING Pauli's¹ idea of nuclear spin, Back and Goudsmit² have successfully explained the hyperfine structures in the bismuth arc spectrum. Schüler and Brück,³ in attempting to explain the hyperfine structures in the cadmium arc spectrum, have advanced the hypothesis that certain isotopes of cadmium have a nuclear moment of $1/2$ (measured in units of $\hbar/2\pi$), whereas other isotopes have a zero nuclear moment. They assume that in most lines the strong or main component is due to the isotopes with zero moment and attribute the remaining components to the isotopes having a nuclear moment $1/2$. These assumptions they showed were sufficient to explain the observed hyperfine structures of the cadmium lines starting on the 3S and ending on the 3P levels, provided the doubtful component at -0.060 cm^{-1} observed by Miss Schrammen⁴ in $\lambda\lambda 4800, 3133$, and 2775 A. U. is real. Schüler and Brück³ state that they observe a -0.060 cm^{-1} fine structure component in their work on the above cadmium lines. However, Janitzki⁵ using an echelon, and Fabry and Perot⁶ using their interferometer, did not observe the -0.060 cm^{-1} in $\lambda 4800$ A.U. Janitzki,⁷ Wali-Mohammad,⁸

¹ Pauli, *Naturwiss.* **12**, 741 (1924).

² Back and Goudsmit, *Zeits. f. Physik* **43**, 321 (1927); **47**, 174 (1928).

³ Schüler and Brück, *Zeits. f. Physik* **56**, 291 (1929); **58**, 735 (1929).

⁴ Schrammen, *Ann. d. Physik* **83**, 1161 (1927).

⁵ Janitzki, *Ann. d. Physik* **19**, 36 (1906).

⁶ Fabry and Perot, *Compte rendus* **126**, 407 (1898).

⁷ Janitzki, *Ann. d. Physik* **29**, 823 (1909).

⁸ Wali-Mohammad, *Ann. d. Physik* **39**, 225 (1912).

Takamine,⁹ MacNair,¹⁰ and the writer, using Lummer plates also have not observed it. Collins,¹¹ in this laboratory, using a Fabry and Perot etalon with separations 16, 10, 8, and 6 mm, has been able to find no evidence of this particular fine structure component.

Only three authors have investigated $\lambda 3133\text{A.U.}$ Miss Schrammen⁴ in her work on this line, questions the reality of the -0.060 cm^{-1} component, while MacNair¹⁰ and Wali-Mohammad⁸ fail to observe any fine structure having the value -0.060 cm^{-1} .

Miss Schrammen and Wali-Mohammad have investigated $\lambda 2775\text{A.U.}$ Here, again, Miss Schrammen is doubtful about the appearance of the fine structure component -0.060 cm^{-1} . Wali-Mohammad does not observe this particular satellite in $\lambda 2775\text{A.U.}$ The results of the above authors are stated in Table I.

TABLE I.*

$\lambda 5086$	$\lambda 5086$		$\lambda 4678$		
+76	-26	Janitzki ⁵	+30	-56	Janitzki ⁵
+76	-26	Wali-Mohammad ⁸	+31	-56	Wali-Mohammad ⁸
+77	-25	Takamine ⁹	+31	-57	Takamine ⁹
+77	-25	MacNair ¹⁰	+31	-56	MacNair ¹⁰
+76	-26	Schrammen ⁴	+30	-57	Schrammen
+85		Gehrcke and v. Baeyer ¹²	+35	-55	Gehrcke and v. Baeyer ¹²
+76	-24	Hamy ¹³	+32	-56	Luneland ¹⁴
+79		Luneland ¹⁴	+31	-56	Author
+76	-24	Fabry and Perot ⁶			
+79		Author			
$\lambda 4800$			$\lambda 3133$		
+58	-34	-81	+25	-12	-33
+58	-34	-81	+25	+6?	-11
+59	-33	-80	+33		-28
+58	-34	-81			
+62	+14?	-29			
+63		-38			
+61		-35			
+82		-82			
+62		-79			
		Author			
			$\lambda 2775$		
			+20	+5?	-8
					-24
					-27

* The wave-lengths are given in milli-Angstrom units with the zero or main line components omitted in each case.

Whether their hypotheses will apply with equal success to the explanation of the hyperfine structures of other cadmium lines Schüler and Brück do not say, though considerable data on lines other than the *S-P* triplets are available. The results of Miss Schrammen, of MacNair, and of the present author are presented in Table II. MacNair used two quartz Lummer plates of lengths 13 and 20 cm and thicknesses 4.40 and 6.55 mm respectively. Miss Schrammen had at her disposal one Lummer plate 14.5 cm long and 4.81 mm thick. As a source of light MacNair and Schrammen both used a water-cooled cadmium arc. The writer's observations were made with two Lummer plates of

⁹ Takamine, Proc. Tokyo Math-Phys. Soc. 8, 51 (1915).

¹⁰ MacNair, Phil. Mag. 2, 613 (1926).

¹¹ Collins, Results communicated verbally to the author.

¹² Gehrcke and v. Baeyer, Ann. d. Physik 20, 269 (1906).

¹³ Hamy, Comptes rendus 130, 489 (1900).

¹⁴ Luneland, Ann. d. Physik 34, 505 (1911).

¹⁵ Wali-Mohammad and Mathur, Phil. Mag. 4, 112 (1927).

lengths 20 and 13.5 cm and thickness 6.42 and 4.92 mm respectively, using as a source a long hydrogen discharge tube having a side tube containing a small amount of metallic cadmium. Heating this side tube distilled a small

TABLE II.*

$\lambda 5086$				$\lambda 3610$		
+77	-25		MacNair ¹⁰		-36	MacNair
+76	-26		Schrammen ⁴	+3?	-37	Schrammen
+79			Author		-37	Author
$\lambda 4800$				$\lambda 3468$		
+58	-34	-81	MacNair	+31	-15.5	MacNair ¹⁶
+62	+14?	-29	Schrammen	+31	-15	Schrammen
+62		-79	Author	+30	-17.9	Author
$\lambda 4678$				$\lambda 3466$		
+31	-56		MacNair	Single		MacNair ¹⁶
+30	-57		Schrammen	Single		Schrammen
+31	-57		Author	Single		Author
$\lambda 3614$				$\lambda 3404$		
+37.5	-23		MacNair	+17		MacNair
?	-22		Schrammen	+17		Schrammen
+39.9	-21		Author	+16		Author
$\lambda 3613$						
Not reported by MacNair						
Single			Schrammen			
Single			Author			

* The wave-lengths of the components are given in milli-Angstrom units with the zero or main line component omitted in each case.

amount of cadmium into the discharge resulting in an intense emission of the cadmium arc spectrum. The advantage of this source is that the vapor pressure of the cadmium may be kept so low that self reversal is entirely eliminated.

DISCUSSION

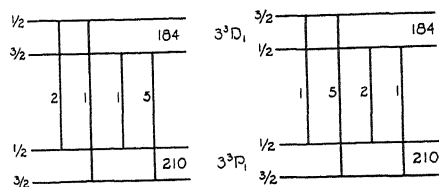
The results obtained on the lines $\lambda\lambda 5086$, 4800, 4678, and 3133 A.U. obtained by different observers appear to be in good agreement. Miss Schrammen alone has observed the -0.060 cm^{-1} component in $\lambda\lambda 4800$, 3133, and 3775 A.U. The writer was unable to observe $d\lambda = -0.025 \text{ A.U.}$ in $\lambda 5086 \text{ A.U.}$ and -0.030 A.U. in $\lambda 4800 \text{ A.U.}$ The source used by the writer apparently emits many satellites with an intensity relative to the main line much lower than that usually observed in a vacuum arc. This statement is based on a comparison of the reproductions of MacNair's spectrograms with the author's photographs, and on the fact that Lummer Gehrcke spectrograms made from a water-cooled mercury arc and from a mercury hydrogen discharge of the type here used for cadmium show that the satellites are far more intense relatively in the arc.

There is disagreement between MacNair and Wali-Mohammad as to the hyperfine structure of the cadmium triplet $\lambda\lambda 3614$, 3613, and 3610 A.U. By

¹⁶ The structure MacNair gives to 3466 is that for 3468.

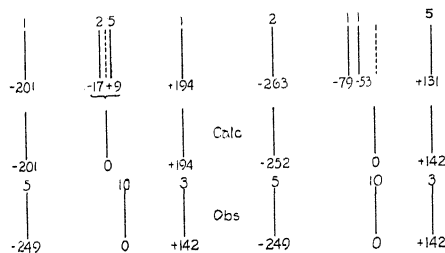
using an E-1 Hilger quartz spectrograph, the lines $\lambda\lambda 3614$ and 3613 A.U. can be resolved. It is found that $\lambda 3613$ is single.

MacNair¹⁰ and Schrammen⁴ disagree on the structures of the $\lambda\lambda 3468$ and 3466 A.U. lines. The results of the writer substantiate the conclusion drawn by Miss Schrammen that the hyperfine structure must be attributed to the $\lambda 3468$ A.U. line, while $\lambda 3466$ A.U. remains single.



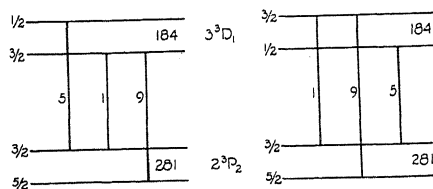
(a) Inverted D-Level

(b) Normal D-Level

Fig. 1. Energy level diagrams for $\lambda 3468$ A.U.

(a) Inverted D-Level

(b) Normal D-Level

Fig. 2. Structure of $\lambda 3468$ A.U.

(a) Inverted D-Level

(b) Normal D-Level

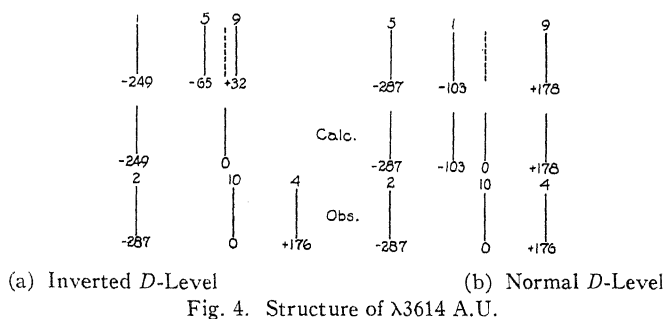
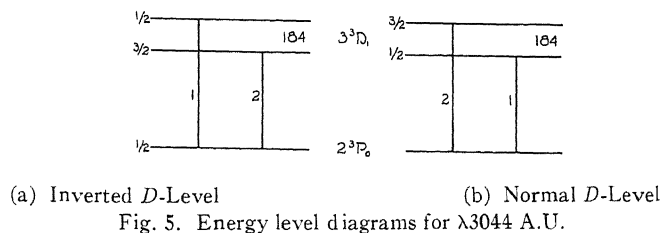
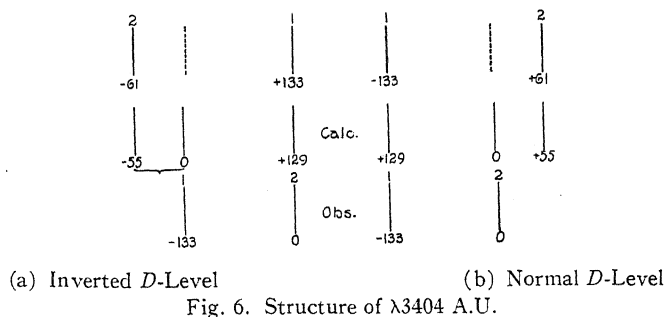
Fig. 3. Energy level diagrams for $\lambda 3614$ A.U.

If we accept the hypothesis of Schüller and Brück³ that the nuclear spin of certain cadmium isotopes is $1/2$, then each gross level, save those having the inner quantum number zero, will split into two, having fine quantum numbers $f = J \pm 1/2$. The levels 1^1S_0 and 2^3P_0 must therefore be assumed to be single, each having a fine quantum number $1/2$. That the levels are inverted has further been pointed out by Goudsmit.¹⁷

Since on the hypotheses of nuclear spin the 2^3P_0 level does not divide, any structure found in the lines ending on this level must be attributed to the upper levels involved. This fixes the doublet separations of 2^3S_1 , 3^3S_1 , and

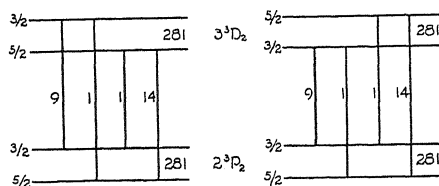
¹⁷ Goudsmit, Naturwiss. 41, 805 (1929).

4^3S_1 at 0.397, 0.369, and 0.354 cm^{-1} respectively. As 2^3S_1 is expected to be double any further frequency differences found in $\lambda\lambda 4800$ and 4678 A.U. must be due to the splitting of the 2^3P_1 and 2^3P_2 levels. To these levels Schöler and Brück³ assign separations of 0.210 and 0.300 cm^{-1} . Goudsmit¹⁷ however, has pointed out that 0.281 cm^{-1} is a more probable value for 2^3P_2 . With the structures of the $2^3P_{0,1,2}$ levels known, the lines $\lambda\lambda 3614$, 3613, 3610, 3468, 3466, and 3404 A.U. should give the separations of the $3^3D_{1,2,3}$ levels.

Fig. 4. Structure of $\lambda 3614$ A.U.Fig. 5. Energy level diagrams for $\lambda 3044$ A.U.Fig. 6. Structure of $\lambda 3404$ A.U.

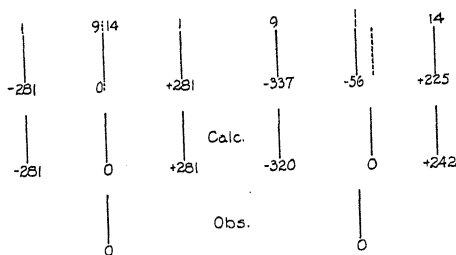
$\lambda 3404$ A.U. is found to be double with a separation of 0.133 cm^{-1} , which requires 3^3D_1 to have approximately this separation. As the line is double it follows that one of the observed components, the stronger of course, must be due to the fusion of the line due to the $i=0$ isotopes with one component of the pattern due to the $i=1/2$ isotopes. The $i=0$ line will, save for isotope shift, lie at the center of gravity of the $i=1/2$ pattern, and hence closest to the stronger component of that pattern, so that the long wave-length component observed in $\lambda 3404$ A.U. must be due to the $i=0$ isotope fusing with the stronger component of the $i=1/2$ isotope pattern. In order that the

stronger component of this pattern should have the longer wave-length, the $f=1/2$ fine structure level of 3^3D_1 must lie above the $f=3/2$ level. That is to say, 3^3D_1 unlike the 3^3P levels, is not inverted. Its separation must be somewhat greater than 0.133 cm^{-1} as this merely measures the separation of the weaker component of the $i=1/2$ isotope from the center of gravity of the stronger component due to this isotope and the line due to the $i=0$ isotope. Just how much greater the separation is we may see from the lines $\lambda\lambda 3468$ and 3614 A.U. The patterns of these lines have a spread of 0.394 cm^{-1} and 0.466 cm^{-1} respectively. Subtracting from these the separations of 0.281



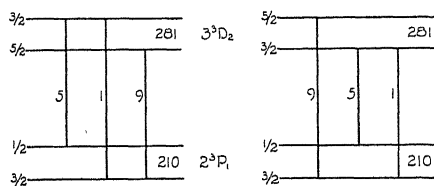
(a) Inverted D-Level (b) Normal D-Level

Fig. 7. Energy level diagrams for $\lambda 3613 \text{ A.U.}$



(a) Inverted D-Level (b) Normal D-Level

Fig. 8. Structure of $\lambda 3613 \text{ A.U.}$



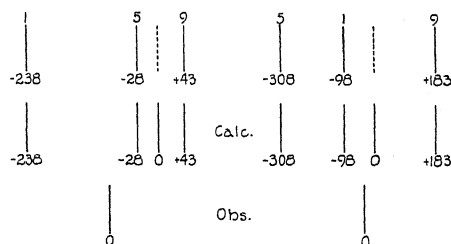
(a) Inverted D-Level (b) Normal D-Level

Fig. 9. Energy level diagrams for $\lambda 3466 \text{ A.U.}$

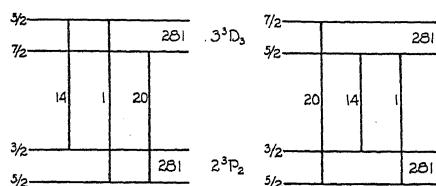
cm^{-1} and 0.210 cm^{-1} found in 2^3P_2 and 2^3P_1 we find 0.184 cm^{-1} and 0.185 cm^{-1} as the values of the separation of 3^3D_1 . The diagrams shown in Figs. 1 and 3 have been constructed using this separation, and the patterns shown in Figs. 2 and 4 are those to be expected if the line from the $i=0$ isotope lies at the center of gravity of the pattern due to the $i=1/2$ isotope. Components of the compound pattern which might be expected to fuse are bracketed. The agreement with the observed patterns drawn below is about as good as could be expected except that in $\lambda 3468 \text{ A.U.}$ the calculated intensity ratio

for the two clearly resolved satellites is $5/2$ whereas the observed intensities are in the opposite order, namely $2/4$.

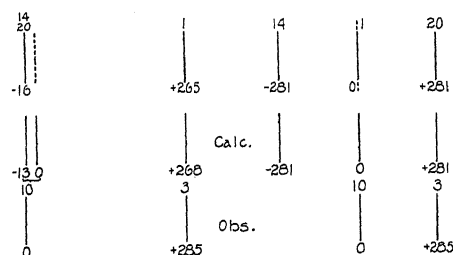
The energy level diagrams for $\lambda 3613$ A.U., using a normal and an inverted 3^3D_2 level, are shown in Fig. 7 while the structures which would be expected due to the $i=0$ and the $i=1/2$ isotopes are found in Fig. 8. If the 3^3D_2 level separation is 0.281 cm^{-1} then $3^3D_2-2^3P_2$ would have strong components close together so that they would coincide with the $i=0$ isotope. The two satellites



(a) Inverted D -Level (b) Normal D -Level
Fig. 10. Structure of $\lambda 3466$ A.U.



(a) Inverted D -Level (b) Normal D -Level
Fig. 11. Energy level diagrams for $\lambda 3610$ A.U.



(a) Inverted D -Level (b) Normal D -Level
Fig. 12. Structure of $\lambda 3610$ A.U.

$\pm 0.281 \text{ cm}^{-1}$ are probably too weak to be observed. The pattern to be expected if a normal 3^3D_2 level is used (see Fig. 8a) is three strong lines, two of which are due to the $i=1/2$ isotope and the other to the $i=0$ isotope.

From $\lambda 4800$ A.U. 2^3P_1 was found to have a separation of 0.210 cm^{-1} which if used in $\lambda 3466$ A.U. ($2^3P_1-3^3D_2$) results in a triplet structure, whereas the line is observed to be single. There is no possibility for the two strong, components having wave-lengths $d\lambda = +0.035$ and -0.053 A.U. to fuse with the $i=0$ isotope. If in Fig. 10b we use a normal 3^3D_2 separation in $\lambda 3466$ A.U. there should be predicted three clearly resolved components.

The line $\lambda 3610$ A.U. ($2^3P_2-3^3D_3$) is double whereas we would expect to find three components. However, two of these may be made to coincide if we give to 3^3D_3 the same separation (0.281 cm^{-1}) as 2^3P_2 . In Figs. 11 and 12 are shown the energy level diagrams, using inverted and normal 3^3D_3 levels, and the predicted and observed structure of $\lambda 3610$ A.U. The -0.013 cm^{-1} component shown in Fig. 12a lies very close to the $i=0$ isotope and as its intensity is large the fusing of this component with the $i=0$ isotope is entirely possible. The wave-length of the satellite would be about $+0.280 \text{ cm}^{-1}$, whereas the observed wave-length is $+0.285 \text{ cm}^{-1}$.

A difficulty arises in the calculation of the structure of $\lambda 6438$ A.U. ($2^1P_1-3^1D_2$), the cadmium red line. Wood¹⁸ has shown the presence of a fine structure component at $d\nu = +0.324 \text{ cm}^{-1}$ in $\lambda 2288$ A.U. ($1^1S_0-2^1P_1$). Since 1^1S_0 must be supposed to be single, the separation of 0.324 cm^{-1} must be placed in 2^1P_1 . If this value is used in $2^1P_1-3^1D_2$, there is no separation that can be given to 3^1D_2 to give the observed single structure of $\lambda 6438$ A.U.

The calculation of the polarization of resonance radiation for the $\lambda 3261$ A.U. line leads to values which are much lower than those which are actually observed.¹⁹

CONCLUSION

Since there is some doubt as to the reality of the -0.060 cm^{-1} component found in $\lambda\lambda 4800, 3133$, and 2775 A.U. by Miss Schrammen⁴ the hypotheses of Schüler and Brück can be said to apply only in part to lines beginning on the 3S and ending on the 3P levels.

The structures of the lines $\lambda\lambda 3468, 3614$, and 3404 A.U. show 3^3D_1 to be a normal level having a separation of 0.184 cm^{-1} . The lines $\lambda\lambda 3613$ and 3610 A.U. show that the 3^3D_2 and 3^3D_3 levels are inverted. The 3^3D_1 level was the only one found in this investigation to be normal.

The hypotheses of Schüler and Brück apply reasonably well to the $\lambda\lambda 3468, 3614, 3404$, and 3613 A.U. lines but fail to account for the structure of $\lambda 3466$ A.U. They predict structure for the $\lambda 6438$ A.U. cadmium red line whereas the single character of this line is definitely established. Finally, they predict a polarization of resonance radiation which disagrees materially with the observed value of 100%.

In conclusion the writer wishes to express his sincere thanks to the members of the Department of Physics for their interest. He particularly wishes to express his gratitude to Dr. A. Ellett who suggested the problem and whose interest and encouragement made the completion of this problem possible.

¹⁸ Wood, Phil. Mag. 2, 611 (1926).

¹⁹ Ellett, Phys. Rev. 35, 588 (1930).

NEW LINES IN THE ARC AND SPARK SPECTRUM OF HELIUM

BY P. GERALD KRUGER*

PHYSIKALISCH-TECHNISCHE REICHSANSTALT, BERLIN

(Received July 28, 1930)

ABSTRACT

Light source. The glow inside a Paschen hollow cathode was used as the light source. Carbon, tantalum, and tungsten were used as the cathode materials. Helium gas for these experiments was specially refined, so that only very slight traces of neon could be detected.

Apparatus. The spectra were photographed by two different gratings used alternately in a Sawyer vacuum spectrograph and in a grazing incidence vacuum spectrograph.

Results. The $1s^2S_{\frac{1}{2}}-np^2P_{\frac{1}{2}, \frac{3}{2}}$ series of He II was extended to nine members, and the wave-lengths of the intensity maxima were calculated, so that these wave-lengths can be used for standards in this region.

Lyman's line at 600.019A has been found to be a He band. The forbidden line $1s^2^1S_0-1s2s^1S_0$ is present. Another line, thought to be $1s2s^1S_0-2s^2^1S_0$, has been observed. The line 320.392A, first observed by Compton and Boyce, is surely a helium line, and very probably the transition $1s2p^3P_{012}^0-2p^3^3P_{012}$.

The 303 series is by far the strongest series in the helium spectrum when pure helium is used in the discharge lamp. When, however, slight impurities of oxygen or carbon are introduced, the 584 series of He I as well as the 600.019A band is greatly enhanced, and the 303 series is weakened.

The presence of the forbidden line $1s^2^1S_0-1s2s^1S_0$ is probably due to the fact that the levels concerned are metastable, and that the gas pressure in the discharge in the lamp was exceedingly low.

THE present investigation was carried out at the suggestion of Professor F. Paschen, and was an attempt to excite the $1s^2$ electrons of He I into the $2p^2$, $2s^2$, and corresponding states.

LIGHT SOURCE

The glow in the inside a Paschen hollow cathode was used as the light source. During the course of the experiments a carbon cathode 10 mm in diameter, a carbon cathode 22 mm in diameter, a tantalum cathode 10 mm in diameter, and a tungsten cathode 10 mm in diameter were used.

The helium gas used for these experiments was specially refined at the cold temperature laboratory of the Physikalisch-technische Reichsanstalt to remove traces of neon. This was done by liquifying the helium. One sample was collected during the liquification process, the other while the liquified helium was allowed to evaporate. Both samples were very pure, and only showed traces of the strongest neon lines when the discharge was maintained in the helium gas at high pressure. At low pressures, such as

* National Research Fellow.

were used when all exposures were taken, not even traces of the strong neon lines were visible.

APPARATUS

A vacuum one-meter spectrograph designed according to Sawyer¹ with a glass grating from Wood, ruled 30,000 lines per inch, was used to photograph the first thirteen exposures. The glass grating was then replaced by a spectrum metal grating from Hilger, ruled 15,000 per inch. Five more exposures were photographed with this set-up, repeating the most favorable conditions during the first thirteen.

In the meantime a grazing incidence spectrograph, built in the shops of the Physikalisch-technische Reichsanstalt largely according to the design of Siegbahn and described by Ericson and Adlen² was adjusted with the glass grating from Wood. This set-up gave a dispersion of about 3Å per mm at 300Å, and about 6Å per mm at 1000Å. Eight more exposures were made with this instrument, repeating the above experiments. The glass grating was then replaced by the metal grating, and seven more exposures taken in order to check completely all work. Thus a total of thirty-two photographs were taken under varying conditions of gas pressure, current density, cathode material, and type of apparatus and grating.

The essential difference between the grazing incidence spectrograph and the design of Siegbahn was that the slit, grating, and cassette were all mounted on a solid aluminum block which could be pulled out of the hull of the spectrograph without disturbing either the vacuum set-up or the adjustment in any way. This arrangement has several obvious advantages.

The reason for using the different cathodes mentioned above was to eliminate the possibility of attributing lines from the cathode substance to helium, and to find a cathode substance which sputtered as little as possible and which gave no lines in the vacuum region. Tungsten was found to be the most favorable.

Although various helium gas pressures and current densities were tried in the light source, it was found that the best conditions for exciting the helium spectrum were an exceedingly low gas pressure (i.e. a gas pressure so low, that it was just possible to maintain the glow discharge under a potential of 800 volts) and a current density of 150 to 200 m.a./cm².

RESULTS

Table I gives all of the observed members of the $1s^2S_{1/2} - np^2P_{3/2, 1/2}$ series of He II, and includes those members of the series which have previously been observed by Lyman³ and Compton and Boyce.⁴ Column one gives the estimated intensities of the lines; column three gives the calculated

¹ Sawyer, Jour. Opt. Soc. Am. 15, 305 (1927).

² Ericson and Adlen, Zeits. f. Physik 59, 656 (1930).

³ Th. Lyman, Astrophys. J. 60, (1924).

⁴ K. T. Compton and J. C. Boyce, Journ. Franklin Inst. 205, 497 (1928).

values which have been computed by using the formula given by F. Paschen⁵ and which applies the general and special relativity correction. These values are much more accurate than the observed values, and make the best avail-

TABLE I. Helium II lines.

Int.	$\lambda_{\text{vac. obs.}}$	$\lambda_{\text{vac. cal.}}$	$\nu \text{ cm}^{-1}$	Combination $1s-np$
50	303.782	303.7788	329,186.8	$1^2S_{1/2} - 2^2P_{3/2}^o$ $1\frac{1}{2}$
30	256.547	256.3145	390,145.6	$1^2S_{1/2} - 3^2P_{3/2}^o$ $1\frac{1}{2}$
20	243.222	243.0244	411,481.3	$1^2S_{1/2} - 4^2P_{3/2}^o$ $1\frac{1}{2}$
15	237.264	237.3297	421,354.7	$1^2S_{1/2} - 5^2P_{3/2}^o$ $1\frac{1}{2}$
10	234.340	234.3452	426,720.9	$1^2S_{1/2} - 6^2P_{3/2}^o$ $1\frac{1}{2}$
7	232.540	232.5821	429,955.5	$1^2S_{1/2} - 7^2P_{3/2}^o$ $1\frac{1}{2}$
4	231.472	231.4520	432,054.8	$1^2S_{1/2} - 8^2P_{3/2}^o$ $1\frac{1}{2}$
2	230.691	230.6836	433,494.1	$1^2S_{1/2} - 9^2P_{3/2}^o$ $1\frac{1}{2}$
1	230.208	230.1370	434,523.6	$1^2S_{1/2} - 10^2P_{3/2}^o$ $1\frac{1}{2}$
0		229.7343	435,285.4	$1^2S_{1/2} - 11^2P_{3/2}^o$ $1\frac{1}{2}$

able standards for this region. The observed values of this series given in column two have been computed from plates taken with the grazing incidence apparatus according to the following formula:

$$n\lambda = e(\sin \phi - \sin(\phi - x/R))$$

where ϕ is the angle between the incident ray and the normal, R is the diameter of the Rowland circle, and x is the distance from the direct image to the line. ϕ was empirically determined to be $81^\circ 34.225^{-1}$.

This computation, however, assumes that the plate, slit, and grating all lie accurately on the Rowland circle, and since this is probably not true, the deviations in column two may be explained in this way.

Column four gives the ν values in cm^{-1} for the wave-lengths in column three. Column five gives the spectroscopic transition.

Table II gives only those additional lines which have been photographed by both gratings used in both spectrographs, and which, therefore, may be attributed to the helium spectrum.

TABLE II. Helium I lines.

Int.	$\lambda_{\text{vac. obs.}}$	$\lambda_{\text{vac. cal.}}$	$\nu \text{ cm}^{-1}$	Combination
5	601.418	601.415	166,274.6	$1s^2 \ ^1S_0 - 1s2s \ ^1S_0$
2	357.507		279,714.8	$1s2s \ ^1S_0 - 2s^2 \ ^1S_0(?)$
8	320.392		312,117.6	$1s2p^3P_{012}^o - 2p^2P_{012}^o$

Line 600.019A has been commented upon by Lyman,³ Compton and Boyce,⁴ Paschen,⁵ and Sommer.⁶ During the course of the present investigation it has been photographed under all conditions, and always appears as a band having the sharp edge on the violet and shading toward the red. The band undoubtedly belongs to the helium spectrum, and may therefore be attributed to He₂.

⁵ F. Paschen, Sitzungsberichten der Preussischen Akademie der Wissenschaften 662, Berlin (1929).

⁶ Sommer, Proc. Nat. Acad. Sci. 13, 213 (1927).

Line 320.329A was first observed by Compton and Boyce,⁴ and is very likely the transition $2p^2\ ^3P_{012} - 1s2p\ ^3P_{012}^0$. This places the $2p^2\ ^3P_{012}$ term at -282894 cm^{-1} with respect to the He I limit. On the other hand, no trace of their line at 309.04A has been found on any of the plates taken during the present work. Other lines at 321.186A int. 2 and 322.517A int. 2, which would probably be $2p^2\ ^1S_0 - 1s2p\ ^1P_1^0$ and $2p^2\ ^1D_2 - 1s2p\ ^1P_1^0$ and which

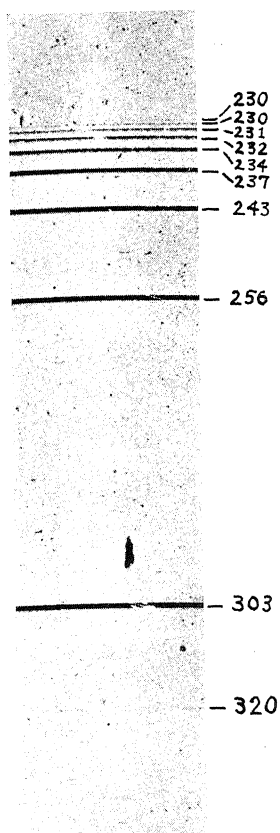


Fig. 1. np series of helium II.

would strengthen the classification of the line at 320.392A, have, however, only been photographed with the glass grating in the Sawyer spectrograph and are therefore not included in Table II.

Line 601.418A is without doubt the forbidden line $1s\ 2s^1S^0 - 1s^2\ ^1S_0$.

Line 357.507A may be $2s^2\ ^1S_0 - 1s\ 2s\ ^1S_0$, for it has the same characteristics as 601.418A, and never occurs when 601.418A is absent from the spectra. Moreover, G. W. Kellner⁷ has very kindly computed that the $2s^2\ ^1S_0$ should lie between $180,000\text{ cm}^{-1}$ and $200,000\text{ cm}^{-1}$ below the limit of He II. The

⁷ Privately communicated to the author, and for which due thanks are acknowledged.

above value would give $2s^2^1S_0$ a value of $-247,681$ which is about $191,000 \text{ cm}^{-1}$ below the limit of He II, thus fitting Kellner's calculation nicely.

A general survey of all plates taken shows the following results:

1. The 303 series is by far the strongest series in the helium spectrum, and appears most strongly when the pressure in the lamp is the smallest possible. In one hour, using the grazing incidence spectrograph, it was possible to photograph 8 members of the 303 series, and only four members of the 584 series which is the next strongest series in the helium spectrum. Increasing the time of exposure to six hours only added one member more to the 303 series. (See Fig. 1). It may also be remarked that under the same discharge conditions only four members of the 303 series could be photographed using the Sawyer spectrograph. This shows the enormous gain in light intensity which is obtained by the grazing incidence instrument when working in this region.

2. The 584 series as well as the band of He_2 , 600.019\AA , is greatly enhanced by the presence of small quantities of O_2 or C.

3. The $1s2s^1S_0 - 1s^2^1S_0$ never appears when the band 600.019\AA is missing, although the band has been present when 601.415\AA was not present.

4. Line 357\AA appears only when 601.415\AA is present.

The presence of the forbidden line $1s^2^1S_0 - 1s2s^1S_0$ is probably due to the fact that the discharge in the lamp was maintained in a very low pressure of helium. It is estimated that the pressure was 0.1 mm or less. Moreover, the levels concerned in this jump are highly metastable, which may account for the phenomena.

If the present interpretation is assumed to be correct, one would expect to find other radiation from transitions of the nature $2s^2 - 2s2p$ or $2s^22s - 3p$, etc. Although the plates were examined for such radiation, none were found.

The author wishes to take the opportunity to thank Professor F. Paschen for placing at his disposal the apparatus and shop at the Physikalisch-technische Reichsanstalt, and for the constant interest and kindly criticism which has been given him during the course of these investigations.

THE STRUCTURE OF EMISSION LINES

BY FRANK HOYT

RYERSON PHYSICAL LABORATORY, UNIVERSITY OF CHICAGO

(Received June 16, 1930)

ABSTRACT

A method for obtaining the intensity distribution in a spectral line is derived from Dirac's quantum theory of the radiation field. The calculations are carried out for the case of emission from a first excited state (resonance line) and show that the intensity of frequency ν is, in this case, proportional to $1/[4\pi^2(\nu_0 - \nu)^2 + (A/2)^2]$ where A is the rate at which atoms are leaving the upper state and ν_0 is the frequency of the transition. The half-width is therefore $1/2\pi$ times the Einstein probability coefficient for spontaneous transition to the lower state. The more general case where the lower state has a finite life time is not treated.

A general method for the treatment of radiation problems, which is essentially Weyl's modification of Dirac's method, is briefly described.

ANY theory of radiation predicts a finite width for emission lines, even under experimental conditions which eliminate Doppler effect and pressure broadening. Classically this "natural width" is attributed to the damping of the atomic oscillations which must accompany an emission of energy, and in the quantum theory a similar result is to be expected from the correspondence principle, the rate of damping being the total rate at which atoms are leaving the upper state. The calculations of the present paper confirm this expectation for the case of a resonance line,¹ and a formula is derived for the structure of the line. The method of treating the radiation field, which is that of Dirac as modified by Weyl,² is briefly described, and appears as a very natural extension of the usual procedure of wave mechanics.

THE RADIATION FIELD

If the configuration of a dynamical system can be described by any number of variables and the equations of motion written in the Hamiltonian form, the methods of wave mechanics are applicable. If the system is a radiation field the number of variables is infinite; nevertheless, if questions of mathematical rigor are disregarded, it seems possible to set up a wave equation and interpret its solutions in the usual way when these variables form a denumerable set, such as the development coefficients of the field vectors in a system of orthogonal functions.

Consider an electromagnetic field inside a cubical inclosure whose dimensions will eventually be allowed to become infinite. It can be completely specified by the values of a vector potential A at all points inside the in-

¹ Regarding the generalization to other cases see the note at the end of this paper.

² P. A. M. Dirac, Proc. Roy. Soc. A114, 243, 710 (1927); H. Weyl, Gruppentheorie und Quantenmechanik, Leipzig (1928) p. 89.

closure, provided A satisfies the relation $\nabla \cdot A = 0$. The fields are then $E = -(1/c) (\partial A / \partial t)$, $H = \nabla \times A$ and the total energy is

$$\mathcal{E} = \frac{1}{8\pi} \int \left[\frac{1}{c^2} \left(\frac{\partial A}{\partial t} \right)^2 + (\nabla \times A)^2 \right] dv. \quad (1)$$

The "equations of motion" are then the Maxwell field equations, but they may be replaced by the single equation

$$\nabla^2 A - \frac{1}{c^2} \frac{\partial^2 A}{\partial t^2} = 0,$$

which is completely equivalent to them. It is readily shown that this equation gives a set of ordinary equations for the development coefficients of A .² If a Fourier development is chosen the variables have a direct physical significance; we therefore write, for the field within a cube of length L ,

$$A = \sum_{\tau} a_{\tau} \exp 2\pi i k_{\tau} \cdot r, \quad a_{-\tau} = a_{\tau}^* \quad (3)$$

where $a_{\tau} = a_{\tau_1} + a_{\tau_2}$ is a complex vector, r a real vector from the center of the box, and k_{τ} is the vector with components τ_1/L , τ_2/L , τ_3/L . The integers τ_1 , τ_2 , τ_3 take on all positive and negative values. The condition $\nabla \cdot A = 0$ is fulfilled by taking a_{τ} perpendicular to k_{τ} , and a_{τ} is then specified by only two components.

Substituting Eq. (3) in Eq. (2), regarding the a_{τ} as functions of the time, gives the equations

$$\frac{d^2 a_{\tau}}{dt^2} + 4\pi^2 c^2 k_{\tau}^2 a_{\tau} = 0$$

which are the equations of motion for a system of independent linear oscillators with frequencies $\nu_{\tau}^2 = c^2 k_{\tau}^2$. On substitution of the solutions in Eq. (3) the field is represented as a linear superposition of plane-polarized, progressive waves, so that classically the a_{τ} are the amplitudes of such waves.

The Eqs. (3) may be put in canonical form with the Hamiltonian

$$H = \sum_{\tau} \frac{1}{2} |b_{\tau}|^2 + 2\pi^2 \nu_{\tau}^2 |a_{\tau}|^2$$

where $b_{\tau} = \dot{a}_{\tau}$ is the "momentum" conjugate to a_{τ} . It is easy to show, by substituting Eq. (3) in Eq. (1), that, independently of any boundary conditions,

$$\mathcal{E} = \frac{L^3}{4\pi c^2} \sum_{\tau} \frac{1}{2} |b_{\tau}|^2 + 2\pi^2 \nu_{\tau}^2 |a_{\tau}|^2$$

Therefore $H = (L^3/4\pi c^2) \mathcal{E}$, and the Hamiltonian is the energy of the inclosure, except for a constant factor.

For the purpose of quantization it is preferable to have real, scalar quantities for the variables instead of the complex vectors a_{τ} , and to have

the Hamiltonian equal to the energy. This is accomplished by using a slightly different representation of A . Let $I_r^{(\sigma)}$ ($\sigma=1, 2$) be two unit vectors chosen in some definite way in the plane perpendicular to k_r (plane of polarization), and $a_\rho^{(\sigma)}$ ($\rho=1, 2$) be the components of a_{r1} and a_{r2} in these directions. Then, on making use of the reality condition $a_{-r}=a_r^*$ Eq. (3) may be written

$$A = 2 \sum_r (\tau_1 \geq 0) a_{r1}^{(1)} I_r^{(1)} \cos 2\pi k_r \cdot r - a_{r2}^{(1)} I_r^{(1)} \sin 2\pi k_r \cdot r \\ + a_{r1}^{(2)} I_r^{(2)} \cos 2\pi k_r \cdot r - a_{r2}^{(2)} I_r^{(2)} \sin 2\pi k_r \cdot r$$

if one of the integers, τ_1 , is restricted to positive values. It is therefore seen that any real vector A satisfying the condition $\nabla \cdot A = 0$ can be written in the form

$$A = \sum_r (\tau_1 \geq 0) \sum_{\rho=1}^2 \sum_{\sigma=1}^2 q_{r\rho\sigma} A_{r\rho},$$

where $q_{r\rho\sigma}$ replaces $\pm 2a_{r\rho}^{(\sigma)}$ and the $A_{r\rho\sigma}$ are orthogonal vector functions into which, for convenience, a constant factor $2c(2\pi/L^3)^{1/2}$ has been introduced; explicitly they are

$$A_{r1\sigma} = 2c(2\pi/L^3)^{1/2} I_r^{(\sigma)} \cos 2\pi k_r \cdot r, \\ A_{r2\sigma} = 2c(2\pi/L^3)^{1/2} I_r^{(\sigma)} \sin 2\pi k_r \cdot r. \quad (5)$$

The constant factor has been so chosen that the energy is simply the Hamiltonian

$$\mathcal{E} = H_R = \sum_{\tau, \rho, \sigma} (\tau_1 \geq 0) [\frac{1}{2} p_{\tau\rho\sigma}^2 + 2\pi^2 \nu_\tau^2 q_{\tau\rho\sigma}^2],$$

where $p_{\tau\rho\sigma} = \dot{q}_{\tau\rho\sigma}$. The index τ determines the frequency and direction of a plane wave component, ρ distinguishes cosine from sine terms, and σ gives the direction of polarization.

For simplicity the vector potential may accordingly be written

$$A = \sum_\alpha q_\alpha A_\alpha \quad (6)$$

where α stands for τ, ρ, σ . The Hamiltonian for the radiation field is then

$$H_R = \sum_\alpha [\frac{1}{2} p_\alpha^2 + 2\pi^2 \nu_\alpha^2 q_\alpha^2] \quad (7)$$

where q_α and p_α are real.

WAVE MECHANICS OF AN ATOM IN A RADIATION FIELD

Suppose an atom, represented for simplicity as a single electron (mass μ , charge $-e$, momentum p) is placed at the center of the box. The classical Hamiltonian for the system "atom plus radiation field," neglecting spin and assuming $v^2/c^2 < 1$, can then be written

$$H = \frac{1}{2\mu} \left(\mathbf{p} + \frac{e}{c} \mathbf{A} \right)^2 + U + H_R$$

where U is the potential energy of the electron in the field of the nucleus and A and H_R are the functions of q_α , p_α given by Eqs. (6) and (7). The corresponding wave equation is $H\psi + (\hbar/2\pi i)\partial\psi/\partial t$ where H is the operator obtained by making the substitutions $\mathbf{p} = (\hbar/2\pi i)\nabla$, $p_\alpha = (\hbar/2\pi i)\partial/\partial q_\alpha$ and ψ is a function of the time t , the atomic coordinates \mathbf{r} , and the variables q_α which specify the field. This wave equation may be written

$$(H_0 + V)\psi(t, \mathbf{r}, q_\alpha) + \frac{\hbar}{2\pi i} \frac{\partial\psi}{\partial t} = 0$$

with $V = H_1 + H_2$, where

$$H_0 = -\frac{\hbar^2}{8\pi^2\mu}\nabla^2 + U + \sum_\alpha \left(-\frac{\hbar^2}{8\pi^2} \frac{\partial^2}{\partial q_\alpha^2} + 2\pi^2\nu_\alpha^2 q_\alpha^2 \right) \quad (8)$$

$$H_1 = \frac{e\hbar}{2\pi i\mu c} \sum_\alpha q_\alpha \mathbf{A}_\alpha \cdot \nabla \quad (9)$$

$$H_2 = \frac{e^2}{2\mu c^2} \sum_{\alpha, \beta} q_\alpha q_\beta \mathbf{A}_\alpha \cdot \mathbf{A}_\beta. \quad (10)$$

(The operators A and ∇ are commutative when $\nabla \cdot A = 0$.)

Such a wave equation differs from those usually encountered only in the fact that the number of variables is infinite. It may be treated by regarding V as a perturbation and using the method of variation of constants. This gives the solution in the form

$$\psi = \sum_a c_a(t) u_a(\xi) e^{-(2\pi i/\hbar) E_a t},$$

where $\xi = \mathbf{r}, q_1, q_2, \dots$, and the u_a are the normalized characteristic functions of the unperturbed problem. The c_a are determined by the differential equations

$$-\frac{\hbar}{2\pi i} \dot{c}_a = \sum_b V(ab) e^{-(2\pi i/\hbar) E_a t} c_b \quad (11)$$

where $V(ab)$ is the perturbation matrix

$$V(ab) = \int u_a^* V u_b d\xi.$$

In the case of the present wave equation the characteristic functions of the unperturbed system are

$$u_a = u_k(\mathbf{r}) \prod_\alpha u_{r_\alpha}(q_\alpha)$$

where $u_k(\mathbf{r})$ is the k -th characteristic function for the atom alone, and u_{r_α} is a Hermite orthogonal function, since the operator in H_0 that involves q_α is simply that for the energy of a linear oscillator (of unit mass). The corresponding characteristic value of the energy is

$$E_a = E_k + \sum_{\alpha} (r_{\alpha} + \frac{1}{2}) h\nu_{\alpha}.$$

A state of the unperturbed system is thus represented by a complex of quantum numbers $a \equiv (k; r_1, r_2, \dots)$ and the c_a may be given the customary probability interpretation (which is also a consequence of the general transformation theory). That is, $|c(t, k; r_1, r_2, \dots)|^2$ measures the probability of finding the atom to have the energy E_k and the α -th radiation component to have the energy $(r_{\alpha} + \frac{1}{2})h\nu_{\alpha}$, if the interaction between the atom and field is suddenly destroyed or becomes vanishingly small at time t . The energy of a field component in its lowest state $r_{\alpha}=0$ is still $(1/2)h\nu_{\alpha}$; this "zero-point energy" must be regarded as undetectable in the form of radiation.

PROPERTIES OF THE PERTURBATION MATRIX

The quantities $|V(ab)|^2$ eventually measure transition probabilities from state b to state a , and certain of their formal properties are of importance. Using Dirac's notation for a matrix element we may write $V(ab) = (k; r_1, \dots, |H_1| l; s_1, \dots) + (k; r_1, \dots, |H_2| l; s_1, \dots)$. A given element of $H_1 = (eh/2\pi i\mu c) \mathbf{A} \cdot \nabla$ is of the form

$$(k; r_1, \dots | H_1 | l; s_1, \dots) = \frac{eh}{2\pi i\mu c} \sum_{\alpha} \int u_k^* \mathbf{A}_{\alpha} \cdot \nabla u_l dv \\ \cdot \int \dots \int q_{\alpha} u_{r_1}^* \dots u_{s_1} \dots dq_1 \dots$$

Since $\int q_{\alpha} u_{r_{\alpha}}^* u_{s_{\alpha}} dq_{\alpha}$ is the (r_{α}, s_{α}) element of the coordinate matrix of a linear oscillator it is different from zero only when $s_{\alpha} = r_{\alpha} \pm 1$. Thus the only elements of H_1 different from zero are those corresponding to transitions in which the quantum number of only one radiation component changes by ± 1 , those of the others remaining constant. Inserting the well-known expressions for the coordinate matrices of the linear oscillator and the values of \mathbf{A}_{α} given in Eq. (5) the non-vanishing elements of H_1 may be written

$$(k; r_1, \dots, r_{\alpha} \dots | H_1 | l; r_1, \dots, r_{\alpha} - 1, \dots) = \left(\frac{hr_{\alpha}}{\pi\nu_{\alpha}} \right)^{1/2} \frac{e}{\mu} \mathbf{I}_{\alpha} \cdot \mathbf{P}_{\alpha}(kl) \cdot \frac{1}{L^3} \quad (12)$$

$$(k; r_1, \dots, r_{\alpha} \dots | H_1 | l; r_1, \dots, r_{\alpha} + 1, \dots) = \left(\frac{h(r_{\alpha} + 1)}{\pi\nu_{\alpha}} \right)^{1/2} \frac{e}{\mu} \mathbf{I}_{\alpha} \cdot \mathbf{P}_{\alpha}(kl) \cdot \frac{1}{L^3} \quad (13)$$

where

$$\mathbf{P}_{\tau\rho\alpha}(kl) = \frac{h}{2\pi i} \int \begin{matrix} \cos \\ \sin \end{matrix} \left\{ 2\pi \mathbf{k}_{\tau} \cdot \mathbf{r} u_k^* \nabla u_l dv \right. \quad \left. \begin{matrix} (\cos & \text{for } \rho = 1) \\ (\sin & \text{for } \rho = 2) \end{matrix} \right\} \quad (14)$$

Elements of the first kind correspond to transitions of the atom from state l to state k accompanied by emission of radiant energy, those of the second kind to the same atomic transition accompanied by absorption.

It will be seen at once that for radiation components of not too short wave-length $P_\alpha(kl)$ reduces to the (kl) element of the atomic momentum. This will be the case when the trigonometric factor may be replaced without appreciable error by its value at the nucleus. In general this means $\nu_\alpha = c|k_\alpha| < 10^{-8}$ cm, so that for visible light

$$\begin{aligned} P_{\tau 1\sigma}(kl) &= p(kl) = 2\pi i \mu \nu(kl) \mathbf{r}(kl) \\ P_{\tau 2\sigma}(kl) &= 0. \end{aligned} \quad (14a)$$

As will appear later the most important matrix elements for spontaneous emission are those of the form $\langle k; 0, \dots, r_\alpha=1, 0, \dots, |H_1|l; 0, \dots \rangle$, which may be abbreviated to $\langle k1_\alpha | H_1 | l0 \rangle$, if it is understood that all quantum numbers not specified are zero. Their squares

$$| \langle kl_\alpha | H_1 | l0 \rangle |^2 = \frac{\hbar}{\pi \nu_\alpha} \left(\frac{e}{\mu} \right)^2 | I_\alpha \cdot P_\alpha(kl) |^2 \cdot \frac{1}{L^3}$$

refer to transitions of the atom accompanied by "emission of one quantum" of a definite frequency, direction and state of polarization specified by α . In their dependence on frequency and direction as specified by τ they are continuously variable in the limit $L \doteq \infty$, and may be regarded as point functions defined at the points with rectangular coordinates $\tau_1/L, \tau_2/L, \tau_3/L$, in a three dimensional " k -space." The volume element $dk_1 dk_2 dk_3$ in this space is $1/L^3$. It is more convenient, however, to use a system of spherical coordinates, as in this case $\nu/c = |\mathbf{k}|$ represents distance from the origin. If $d\Omega$ is an infinitesimal solid angle in the direction of \mathbf{k} we may write for the volume element

$$dk_1 dk_2 dk_3 = (\nu^2/c^3) d\nu d\Omega.$$

Direction and frequency are now specified by continuous variables ν and $\Omega = (\theta, \phi)$ which replace the index τ so that

$$| \langle k, 1_{\nu\sigma} | H_1 | l0 \rangle |^2 = \frac{\hbar}{\pi \nu} \left(\frac{e}{\mu} \right)^2 | I_\sigma(\nu, \Omega) \cdot P_\sigma(kl; \nu, \Omega) |^2 \cdot \frac{\nu^2}{c^3} d\nu d\Omega. \quad (15)$$

It will be convenient to replace sums of such elements over τ by integrals over ν and Ω .

The matrix elements of $H_2 = (e^2/2\mu c^2) \mathbf{A} \cdot \mathbf{A}$, on the other hand, are of the form

$$\begin{aligned} \langle k; r_1, \dots | H_1 | l; s_1, \dots \rangle &= \frac{e^2}{2\mu c^2} \sum_{\alpha, \beta} \int \mathbf{A}_\alpha \cdot \mathbf{A}_\beta u_k^* u_l d\nu \\ &\cdot \int \dots \int q_\alpha q_\beta u_{r_1}^* \dots u_{s_1} \dots dq_1 \dots \end{aligned}$$

For optical frequencies they will vanish except when $k=l$, i.e. when the state of the atom does not change; at the same time *two* radiation components can change their quantum numbers, again by ± 1 . These elements are responsible for direct scattering of light (Dirac's true scattering) but are unimportant for spontaneous emission. Since they are of the second order in $(1/L^3)^{1/2}$ they are negligible when added to elements of H_1 .

SPONTANEOUS EMISSION OF A RESONANCE LINE

The usual method of solving the variation equations (11) is to substitute in the right hand members the values of the c_a at time $t=0$. Integration then gives an approximation which is valid for a short time—in general short compared to the life-time of an excited state. On re-substitution, higher approximations may be found. By proceeding in this way it is possible to obtain all of Dirac's results for emission, absorption, and dispersion. In fact, the present equations differ from those of Dirac only in that the c 's give the probability of finding a system in a given stationary state, while his give the probability of finding a given distribution of a number of systems among the various stationary states.

This method of solution is inadequate, however, if we wish to investigate the structure of a line within its natural width, as may be seen by appealing to the uncertainty principle. As applied to energy and time this states that any limitation Δt in the time of an energy measurement will introduce an unavoidable uncertainty in the energy of amount $\Delta E = h/\Delta t$. For a component of the radiation field $E \approx h\nu$, and hence

$$\Delta\nu \approx \frac{1}{\Delta t}.$$

It is well known that the natural width of an emission line is approximately $1/T$, where T is the life-time of the upper state. Hence a solution of Eqs. (11) which is valid only for $t \ll T$ cannot predict the result of a frequency measurement of accuracy greater than $\Delta\nu = 1/T$. Actually, as Pauli has shown,³ Dirac's results give only the total probability of finding a light quantum in a given range of stationary states extending over the natural width.

It is possible to obtain, however, a solution of the variation equations which is valid for any value of t *much greater* than the life-time. This will not be subject to the foregoing restrictions, and we shall see that it gives a reasonable formula for the shape of an emission line.

Written explicitly the Eqs. (11) are

$$-\frac{h}{2\pi i} \dot{c}(k; r_1, \dots) = \sum_{l, \alpha} (k; r_1, \dots | H_1 | l; r_1, \dots r_\alpha \pm 1, \dots) \\ e^{(2\pi i/h)(Ek - El + h\nu_\alpha)t} c(l; r_1, \dots r_\alpha \pm 1, \dots) \\ + \text{terms in } H_2$$

³ Probleme der Modernen Physik, Leipzig, 1928, p. 30.

where the \pm sign means inclusion of both terms in the sums. If we are interested only in the solutions for large values of the time it will be legitimate to retain on the right only those terms which are constant or vary slowly with the time, since the effect of those which vary rapidly and periodically will average out. The "resonance" or "secular" terms are those for which $E_k = E_l \pm h\nu_\alpha$ is zero or very small, so that they are just those which correspond to transitions in which the total energy is conserved.

To describe spontaneous emission we wish a solution for initial conditions such that at time $t=0$ it is certain that all atoms are in an excited state m , while all radiation components are unexcited. We therefore suppose only $c(m; 0, \dots)$, is initially different from zero. From the infinite set of equations it is then possible to discard any sub-set containing only c 's which are not coupled with $c(m; 0, \dots)$ since such a set will have only the trivial solution that all the c 's which it contains remain practically zero. Terms in H_2 may also be neglected compared to those in H_1 as they are of the second order in $(1/L^3)^{1/2}$. At the same time we may retain only the resonance terms. If this process of elimination is carried out consistently for the special case that m is the first excited state of the atom, so the only state of lower energy is the normal state $k=n$ the only equations which survive are the following:

$$-\frac{h}{2\pi i} \dot{c}(n1_\alpha) = H_1(\alpha 0) e^{-2\pi i(\nu_0 - \nu_\alpha)t} c(m0), \quad (16)$$

$$-\frac{h}{2\pi i} \dot{c}(m0) = H_1(0\alpha) e^{2\pi i(\nu_0 - \nu_\alpha)t} c(n1_\alpha). \quad (17)$$

where $(E_m - E_n)/h = \nu_0$ and $H_1(\alpha 0)$ is put for $\langle n1_\alpha | H_1 | m0 \rangle$.

A solution of these equations which is valid when only $c(m0)$ is initially different from zero may be obtained in the following manner: From Eqs. (16),

$$\dot{c}(n1_\alpha) = -\frac{2\pi i}{h} H_1(\alpha 0) \int_0^t e^{-2\pi i(\nu_0 - \nu_\alpha)s} c(m0) ds$$

and substituting these integrals in Eq. (17) gives the integral equation

$$\begin{aligned} \dot{c}(m0) = & -\left(\frac{2\pi}{h}\right)^2 \sum_\alpha |H_1(\alpha 0)|^2 e^{2\pi i(\nu_0 - \nu_\alpha)t} \\ & \cdot \int_0^t e^{-2\pi i(\nu_0 - \nu_\alpha)s} c(m0) ds \end{aligned} \quad (18)$$

for $c(m0)$ as a function of the time.

The sum with respect to α may be partly replaced by an integral, since, as already explained, $|H_1(\alpha 0)|^2$ is a continuously varying function of ν and Ω in the limit $L \rightarrow \infty$. From Eq. (15) it is seen to be of the form

$$|H_1(\alpha 0)|^2 = f_{\rho\sigma}(\nu, \Omega) \nu d\nu d\Omega, \quad (19)$$

where

$$f_{\rho\sigma}(\nu, \Omega) = \frac{h}{\pi c^3} \left(\frac{e}{\mu} \right)^2 |I(\Omega) \cdot P_{\rho}(nm; \nu, \Omega)|^2. \quad (20)$$

Eq. (18) then becomes

$$\dot{c}(m0) = - \left(\frac{2\pi}{h} \right)^2 \sum_{\rho, \sigma} \int_0^{2\pi} d\Omega \int \nu \left\{ f_{\rho\sigma} e^{2\pi i(\nu_0 - \nu)t} \int_0^t e^{-2\pi i(\nu_0 - \nu)s} c(m0) ds \right\} d\nu.$$

(The integration with respect to Ω is only over a hemisphere because of the restriction $\tau_1 \geq 0$.)

It will now be shown that Eq. (18) has a solution of the form $c(m0) = Ce^{-\kappa t}$, and κ will be determined. Substituting this expression in Eq. (18) gives

$$\kappa e^{-\kappa t} = - \left(\frac{2\pi}{h} \right)^2 \frac{1}{2\pi i} \sum_{\rho, \sigma} \int d\Omega \int f_{\rho\sigma} \frac{e^{2\pi i(\nu_0 - \nu)t} - e^{-\kappa t}}{\nu - \nu_0 + i \frac{\kappa}{2\pi}} \nu d\nu. \quad (21)$$

The integral with respect to ν may be written

$$\begin{aligned} I = & \int F(\nu) \frac{e^{2\pi i(\nu_0 - \nu)t}}{\nu - \nu_0 + i \frac{\kappa}{2\pi}} d\nu \\ & - e^{-\kappa t} \int F(\nu) \frac{\nu - \nu_0}{(\nu - \nu_0)^2 + \left(\frac{\kappa}{2\pi} \right)^2} d\nu \\ & + i \frac{\kappa}{2\pi} e^{-\kappa t} \int F(\nu) \frac{1}{(\nu - \nu_0)^2 + \left(\frac{\kappa}{2\pi} \right)^2} d\nu, \end{aligned}$$

where $F(\nu) = \nu f_{\rho\sigma}$. The three integrals may be evaluated without difficulty when it is assumed that κ is vanishingly small compared to ν_0 and that $F(\nu)$ vanishes for large values of ν in such a way that the integrals converge for high frequencies. The first assumption is certainly valid, since, as will be seen, 2κ is the transition probability; the second has not been rigorously proved, but has been assumed by Dirac in his calculations, and is plausible because $F(\nu)$ contains factors of the form $\int \cos 2\pi k \cdot r u_n^* \Delta u_m dv$ which vanish for high frequencies. The limits of integration may then be extended from 0 to ∞ , and $F(\nu)$ replaced by $F(\nu_0)$, since, because of the resonance when $\nu = \nu_0$ the contribution to the integral near the resonance point is the predominant part. The first integral may be extended to a closed path in the

complex plane and by Cauchy's theorem its value is $= 2\pi i F(\nu_0)e^{-\kappa t}$. The second vanishes because of the factor $\nu_0 - \nu$, while the last may be reduced to the form $\int_{-\infty}^{\infty} d\xi / (\xi^2 + a^2) = \pi/a$ and contributes $i\pi F(\nu_0)e^{-\kappa t}$. Hence

$$I = -\pi i \nu_0 f_{\rho\sigma}(\nu_0, \Omega) e^{-\kappa t},$$

and Eq. (18) is satisfied with

$$\kappa = \frac{1}{2} \left(\frac{2\pi}{h} \right)^2 \nu_0 \sum_{\rho\sigma} \int d\Omega f_{\rho\sigma}(\nu_0, \Omega). \quad (22)$$

The solution of the set of differential equations is completed by substituting $c(m0) = c^{(0)}(m0)e^{-\kappa t}$ in Eqs. (16) and integrating, which gives

$$c(n1_\alpha) = c^{(0)}(m0) \frac{2\pi i}{h} H_1(\alpha 0) \frac{e^{-\kappa t} e^{-2\pi i(\nu_0 - \nu_\alpha)t} - 1}{2\pi i(\nu_0 - \nu_\alpha) + \kappa} \quad (23)$$

$$c(m0) = c^{(0)}(m0) e^{-\kappa t}. \quad (24)$$

Turning to the physical interpretation of the results just obtained, it is seen from Eq. (24) that the number of atoms in the upper state m falls off exponentially with the time, since $|c(m0)|^2$ is the total probability of finding the atom in state m . This number is proportional to $e^{-2\kappa t}$, so that $\kappa = (1/2)A$, where A is the Einstein probability coefficient for spontaneous transition. (It will be shown presently that the value of A given by Eq. (22) coincides with that derived from the correspondence principle.) From Eq. (23), on squaring, we obtain the total probability of finding the α^{th} radiation component to have the energy $h\nu_\alpha$. For $t \gg 1/\kappa$ this is

$$|c(n1_\alpha)|^2 = |c^{(0)}(m0)|^2 \frac{\left| \frac{2\pi}{h} H_1(\alpha 0) \right|^2}{4\pi^2(\nu_0 - \nu_\alpha)^2 + \left(\frac{A}{2} \right)^2}$$

which gives the final energy distribution in the line. (For sufficiently large values of the time the atom and field can certainly be regarded as uncoupled.) On summing over all values of α it can be shown that the total energy is $|c^{(0)}(m0)|^2 h\nu_0$, as it must be. Since, for $\nu_\alpha \approx \nu_0$, $|H_1(\alpha 0)|^2$ can be regarded as independent of α , and since, in the limit $L \doteq \infty$, $|H_1(\alpha 0)|^2$ is proportional to $d\nu$, the intensity $I(\nu)$ per unit frequency interval is

$$I(\nu) = \text{const} \frac{1}{4\pi^2(\nu_0 - \nu)^2 + \left(\frac{A}{2} \right)^2}. \quad (25)$$

This is just the intensity distribution calculated from the Fourier analysis of a classical oscillator with damping constant $(1/2)A$. Since this damping of the amplitude of the virtual oscillator is just what is required to preserve the energy balance when the atoms leave the upper state, according to

Einstein's law, at rate A , it is seen that Eq. (25) gives the result to be expected from the correspondence principle.⁵ The half-width (width at half maximum is readily seen to be $(1/2\pi)A$, or $(1/2\pi)$ times the reciprocal of the lifetime of the upper state.

In conclusion it will be shown that the value of κ given by Eq. (22) is actually $\frac{1}{2}$ the usual expression for the probability coefficient:

$$A(mn) = \frac{(2\pi\nu_0)^4}{h\nu_0} \left(\frac{2e^2}{3c^3} \right) 2 |r(mn)|^2$$

derived from the correspondence principle on the assumption that only dipole radiation need be considered. Under these conditions (not too short wave-length) the factor $\sum_p |I_\sigma \cdot P_p(\nu_0, \Omega)|^2$ occurring in Eq. (22) becomes simply $4\pi^2\nu_0^2 |I_\sigma \cdot r(mn)|^2$ (Cf. Eq. (14a)). If the space degeneracy of the atom is not removed by an external field the \cos^2 in the scalar product may be averaged over all orientations of the atom, introducing a factor of $1/3$ and removing any dependence on the direction of polarization (σ) and Ω . With this simplification it is readily seen that κ is $1/2$ the value of $A(mn)$ given by Eq. (26). For short wave-lengths the factor $\cos 2\pi k \cdot r$ in P cannot be regarded as unity. It can be shown, however, that in this case κ is still one half the rate of emission of radiant energy calculated classically from the Schrödinger charge and current density associated with the transition, the trigonometric factor taking care of the retardation.

The method which has been used for emission lines is obviously capable of extension to the case of absorption under various conditions, and the results will be discussed in a future paper.

Note added in proof: Since the above article was sent to press a paper has been published by Weisskopf and Wigner* on the natural widths of emission lines.

Comparison with their results showed an error in the author's generalization of the above results to the case of lines other than a resonance line. A paragraph dealing with this generalization has therefore been deleted in the proof. Weisskopf and Wigner arrive at the important conclusion that the half-width in the general case is $1/2$ times the sum of the total probabilities of spontaneous transition from the upper and lower states. Their method is similar to that of the present paper and gives, of course, the same result for a resonance line. Equations equivalent to those on which they base their treatment of other cases can be derived from Eqs. (11) above.

⁵ Cf. W. Pauli, Handbuch der Physik, Vol. XXIII, p. 70.

* Zeits. f. Physik 63, 54 (1930).

NOTE ON FREQUENCY SHIFTS IN DISPERSING MEDIA

BY G. BREIT AND E. O. SALANT

DEPARTMENT OF PHYSICS, NEW YORK UNIVERSITY

(Received July 1, 1930)

ABSTRACT

The propagation of a light wave through a dispersing medium is discussed. The absorption frequencies of the medium are shown to be the absorption frequencies of the coupled system formed by molecules contained in a cavity elongated in the direction of the electric intensity of the incident wave. The cavity is supposed to contain a large number of molecules and yet to be small compared to the wave-length.

The absorption bands of the coupled system are discussed. For tenuous media the shift is small and of the order of the Lorentz-Lorenz shift. The modification introduced by the quantum theory consists in replacing the classical $e^2/8\pi^2 m\nu$ by $|x(I, II)|^2$ where $x(I, II)$ is the unperturbed matrix element of the polarization in the fixed direction X , the normal state is I , the excited state II . In this approximation the shift is obtained by replacing the classical e by Dennison's effective charge. For regular arrangements of molecules, no broadening due to coupling is expected.

For dense media there are additional effects even to the first order. These are: (1) the electrostatic interaction of a molecule with its neighbours due to its excitation, (2) the effect of the finite space extension of the $u_I^* u_{II}$ charge distribution. A comparison of the measured shifts in liquid HCl and HBr with the extrapolation of the Lorentz-Lorenz formula modified by $|x(I, II)|^2$ is made. The observed shift is much too large to be explained without taking into account effects (1), (2). Particle exchange has been neglected.

IT IS well known that the modern quantum theory explains satisfactorily the main features of the phenomena of dispersion. In the considerations published so far the main emphasis has been on the behavior of a single atom. The conclusion reached is that an atom scatters electromagnetic waves as though the incident wave induces a polarization given by the Kramers-Heisenberg formula. The coherent radiation is therefore reradiated by the atom very much as though it contained a number of classical harmonic oscillators with resonant frequencies equal respectively to all the possible atomic absorption frequencies. It is our purpose to consider here the effect of the interaction of neighbouring molecules and in particular to ascertain the difference between the absorption frequencies of the dispersing medium and the corresponding frequencies of free atoms.¹

Just as in the classical theory of dispersion we may define in the quantum theory local and average field intensities.¹ The local electric intensity d

¹ In the classical theory of dispersion there is a difference between these two. The effective dielectric constant ϵ is connected with the deformability α by $\epsilon - 1 = N\alpha/[4\pi + \alpha(\epsilon - 1)]$ where α depends on the geometrical arrangement of molecules and N is the number of molecules per unit volume. The atomic absorption frequencies correspond to $\alpha = \infty$ and the absorption frequencies of the medium correspond to $\epsilon = \infty$. The two occur in general for different frequencies. See H. A. Lorentz Theory of Electrons, Chapter IV, Wolf and Herzfeld Handbuch der Physik Geiger Scheel, Vol. XX, p. 511.

varies rapidly within a molecule and the average electric intensity E varies appreciably only in a region containing many molecules. The validity of Maxwell's equations for the local field quantities (d, h) implies by the classical reasoning of averaging also the validity of similar gross equations for the averaged field quantities (E, H). This part of the theory is entirely unchanged. For nonmagnetic media the modification introduced by the quantum theory comes in only at the point of establishing a relation between E and the average polarization P .

To find this relation we use again the well-known classical reasoning. A cavity containing a large number of molecules is formed. A molecule inside the cavity is acted on (1) by E , (2) by E' due to the other molecules in the cavity, (3) by the surface charges due to P giving a local intensity E'' . It is not quite right however at this point to adhere to the classical reasoning. The force E' is not the only effect of the neighbouring molecules. All the molecules in the cavity must be considered as forming one coupled system. The polarization of this under the influence of $E + E''$ may be worked out. For a cavity of a known shape E'' depends on P in a known way. In particular an elongated cavity parallel to P gives $E'' = 0$. The resonant frequencies of the coupled system formed by molecules inside an elongated cavity give therefore the absorption frequencies of the medium, for at these resonant frequencies P/E is infinite.

At this point we call attention to the fact that the coupled system formed by molecules inside a spherical cavity has a different set of absorption frequencies. They are exposed however also to a different field: $E + 4\pi P/3$. The spectrum of the spherical cavity does not correspond to $P/E = \infty$ but to $P/E = -3/4\pi$. We shall see presently that the results of considering these two shapes are consistent with each other, as one would expect.

We must also point out that a system of loosely coupled molecules in a cavity has a very large number of absorption frequencies lying close to an absorption frequency of a free molecule. They form a band having a certain width which as has been pointed out by Schütz-Mensing² is in some cases approximately equal to the Lorentz-Lorenz shift. The polarizability of a quantum system is given by

$$\alpha = \frac{2}{h} \sum_m \frac{\nu_{mn} |X(mn)|^2}{\nu_{mn}^2 - \nu^2} \quad (1)$$

where n is the normal level in which the system is supposed to be, m is any excited level, and $X(mn)$ is the matrix element of the polarization of the system in the direction of the incident electric intensity. Our problem consists in finding the maximum of (1) as a function of ν . The frequencies lie so close together that we cannot observe the individual maxima of (1). Also α does not actually become infinite at $\nu = \nu_{mn}$ on account of radiation damping. The maximum of (1) can be taken to lie at

$$\nu = \sum_m \nu_{mn} |X(mn)|^2 / \sum_m |X(mn)|^2 \quad (2)$$

² Schütz-Mensing, Zeits. f. Physik 61, 655 (1930) J. Frenkel, Idem. 59, 198 (1930).

the weighted mean of the individual absorption frequencies in the band. Most of the calculations necessary for the evaluation of (2) have already been carried out by Frenkel² in connection with the resonance broadening of spectral lines.

All the molecules in the cavity form a coupled system. For each individual molecule there is a normal state I and an excited state II. For the whole system we consider the non-degenerate state described by the zero approximation function

$$\psi_I = u_I(q_1) u_I(q_2) \cdots u_I(q_n). \quad (3)$$

Here the u 's are eigenfunctions of the individual molecules and the q_i are the coordinates describing their configuration. We also consider the degenerate excited state described in the zero approximation by a linear combination

$$\psi_{II} = \sum_i a_i u_I(q_1) \cdots u_{II}(q_i) \cdots u_I(q_n). \quad (4)$$

There are in general n functions ψ_{II} corresponding to n levels. The perturbation energy may be taken to be

$$H' = \sum_{i < k} H_{ik}(q_i, q_k). \quad (5)$$

The mutual coupling gives to the first order of the perturbation calculation a change in the energy of the state described by (3)

$$w_I = \sum_{i < k} H_{ik}(I I / I I) \quad (6)$$

where

$$H(ab/cd) = \int u_a^*(q) u_b^*(q') H(q, q') u_c(q) u_d(q') dq dq'.$$

The perturbations of (4) are given by the secular equation

$$w_{II} a_i = \left(\sum_k H_{ik}(II I / II I) + \sum_{k, l \neq i} H_{il}(I I / I I) \right) a_i + \sum_k H_{ik}(II I / I II) a_k. \quad (7)$$

Multiply (6) by a_i and subtract from (7) ... Then

$$(w_{II} - w_I) a_i = \sum_k [H_{ik}(II I / II I) - H_{ik}(I I / I I)] a_i + \sum_k H_{ik}(II I / I II) a_k \quad (8)$$

is the secular equation determining the shifts in the frequency $(w_{II} - w_I)/h$. This is very similar to Frenkel's (7a) although we do not confine ourselves to atoms describable by simple linear displacements as he does. In (8) we see first of all a frequency displacement given by the coefficient of a_i

$$\frac{1}{h} \sum_k [H_{ik}(II I / II I) - H_{ik}(I I / I I)]. \quad (9)$$

This is easily interpreted as the increase of electrostatic energy of the single molecule i due to its excitation $I \rightarrow II$ with all the other molecules. For molecules well inside the cavity (9) is independent of i . At the boundary it depends on i . The number of molecules inside is much larger than that at the boundary and to a first approximation we consider (9) as a constant. The non-diagonal terms in (8) are intimately connected with the Lorentz-Lorenz shift. Their character stands out best if the molecules are supposed to be small in comparison with their distance apart. The coefficient H_{ik} (II I/II) is then the mutual electrostatic energy of two dipoles of moment

$$|x(I, II)| \quad (10)$$

at a distance r_{ik} (the distance between molecules i and k). In the matrix element (10) x is the resultant polarization of an individual molecule in the fixed direction x . Under these conditions the problem is mathematically equivalent to that treated by Frenkel. Neglecting the effect (9) the energy shifts $w_{II} - w_I = \lambda$ satisfy

$$\lambda_r a_{ri} = \sum_k \alpha_{ik} a_{rk}, \quad \alpha_{ik} = r_{ik}^{-3} (1 - 3 \cos^2 \theta_{ik}) |x(I, II)|^2 \quad (11)$$

where θ_{ik} is the angle made by r_{ik} with the x axis. The total and individual polarizations are connected by

$$X_r(I, II) = \sum_i a_{ri} x(I, II). \quad (12)$$

It is a mathematical consequence of (11) and (12) that

$$\begin{aligned} \sum_r |X_r(I, II)|^2 &= n |x(I, II)|^2 \\ \sum_r |X_r(I, II)|^2 \lambda_r &= |x(I, II)|^2 \sum_{k,l} \alpha_{kl} \quad \bar{\lambda} = (1/n) \sum_{k,l} \alpha_{kl} \\ \sum_r |X_r(I, II)|^2 \lambda_r^2 &= |x(I, II)|^2 \sum_{k,i,l} \alpha_{ki} \alpha_{il} \quad \bar{\lambda}^2 = (1/n) \sum_{k,i,l} \alpha_{ki} \alpha_{il} \text{ etc.} \end{aligned} \quad (13)$$

It should be noted here that these formulas can be applied to the calculation of the weighted mean of any power of λ .

The results of (13) depend on the space distribution of molecules. A simple type of distribution is the cubical arrangement discussed by Lorentz. The number of molecules in the cavity being large $\sum_i \alpha_{il}$ is practically independent of i as long as the molecule is inside. The number of particles at the boundary being relatively small we have from (13)

$$\overline{\lambda^m} = \frac{1}{n} \cdot (n\bar{\lambda}) \cdot \bar{\lambda} \cdots \bar{\lambda} = \bar{\lambda}^m. \quad (14)$$

This is not an exact result but it is the more exact the larger the cavity and becomes therefore applicable in the case of very long wave-lengths. It means that in this limiting case the frequency is shifted without broadening. In

order that this be true it is essential to have a regular arrangement of molecules i.e. such an arrangement that $\Sigma_l \alpha_{kl}$ is independent of k . A statistical space distribution will of course give rise to broadening as has been found by Frenkel. For a longitudinal cavity $\Sigma_{k,l} \alpha_{kl}$ can be evaluated by surrounding the point k by a sphere S . Then $\Sigma_l \alpha_{kl}$ inside S vanishes for the cubical arrangement. In the region between S and the outside boundary of the cavity the summation is replaced by an integral which is identical with the integral of the classical dispersion theory. It is transformed into a surface integral representing the effect of classical surface charges due to polarization. The contribution of the boundary of the cavity is zero if it is sufficiently elongated. The contribution of the surface of S is

$$- (4\pi/3) |x(I, II)|^2 N$$

where N is the number of molecules per unit volume. Summing this over k is equivalent to multiplying by n . Substituting $\Sigma_{k,l} \alpha_{kl}$ in (13) it is found that

$$\lambda = - (4\pi/3) |x(I, II)|^2 N. \quad (15)$$

In the special case of an almost harmonic oscillator of charge e , mass m , frequency ν the frequency shift $\bar{\lambda}/h$ is on substitution of $|x(I, II)|^2 = e^2 h / 8\pi^2 m \nu$ for the fundamental, $\Delta\nu = -Ne^2/(6\pi m \nu)$ in agreement with the result of the classical dispersion theory.

Let now the cavity be spherical and the arrangement of molecules cubical as before. Then the surface integral over the sphere S is equal and opposite to the surface integral over the boundary of the cavity and $\bar{\lambda} = 0$. By (1) and the first equation (13)

$$\frac{P}{E + (4\pi/3)P} = \frac{N\alpha}{n} = \frac{2N\nu_{I\ II} |x(I, II)|^2}{h(\nu_{I\ II}^2 - \nu^2)} \quad (16)$$

the other states III, IV, . . . being neglected here. The external force acting on the spherical cavity is, as mentioned before, $E + (4\pi/3)P$. The absorption frequency always corresponds to $P/E = 0$ and the right side of (16) is therefore $3/4\pi$. This gives

$$\nu - \nu_{I\ II} = - \frac{8\pi N \nu_{I\ II} |x(I, II)|^2}{3h(\nu_{I\ II} + \nu)} \quad (15')$$

which agrees with (15) if $\nu - \nu_{I\ II}$ is small.

If the arrangement of molecules is not cubical $\Sigma_l \alpha_{k,l}$ over a sphere does not necessarily vanish. This changes the factor $4\pi/3$ in (15) into a where a depends on the geometry of the arrangement entirely as in the classical theory. Also if the distribution of molecules is sufficiently statistical $\Sigma_l \alpha_{kl}$ is not independent of k . Then (14) is not true. Still for a spherical cavity and a statistical distribution $\Sigma_{k,l} \alpha_{kl} = 0$ so that in this case (15) holds although the line is broadened as shown by Frenkel and Schütz.

For molecules which are not small in comparison with their average distance apart formula (8) may be used. Formulas (13) may not be used accurately. Approximately however they remain correct if α_{ik} is replaced by H_{ik} (II, I/I, II). In performing $\sum_l H_{kl}$ between S and the outside boundary of the cavity, H_{kl} may be taken to be α_{kl} quite accurately because S itself contains many molecules and r_{kl} is large. Over the inside of S however $\sum_s H_{kl} \neq 0$. We have then in general

$$\bar{\lambda} = \sum_k \{ H_{ik}(\text{II}, \text{I/II}, \text{I}) - H_{ik}(\text{I}, \text{I/I}, \text{I}) \} + \sum_k \overline{(S)H_{ik}(\text{II}, \text{I/I}, \text{II})} - (4\pi/3) |x(\text{I}, \text{II})|^2 \cdot N \quad (17)$$

the averaging being performed over the molecule i .

Measurements of shifts of the 0→1 vibrational frequency of HCl and HBr have been made by E. O. Salant and A. Sandow.³ The frequencies observed in the liquid state were different from those in the gaseous. The pure Lorentz-Lorenz shift given by (15) (15') can be calculated from a knowledge of the absorption coefficient. This is

$$J_{\text{I, II}} = 8\pi^3 N \nu |x(\text{I}, \text{II})|^2 / (3hc). \quad (18)$$

Expressing with Dennison⁴ $J_{\text{I, II}}$ in terms of the effective charge $e_{\text{I, II}}$ of the molecule i.e. defining $e_{\text{I, II}}$ by

$$|x(\text{I}, \text{II})|^2 = e_{\text{I, II}}^2 h / 8\pi^2 m \nu \quad (19)$$

the frequency shift

$$\Delta \nu_{\text{I, II}} = - N e_{\text{I, II}}^2 / 6\pi m \nu_{\text{I, II}} \quad (20)$$

where m is the reduced mass. For HCl Dennison's best value of $e_{\text{I, II}}$ is 0.949×10^{-10} e.s.u., ν_0 is 2886 cm^{-1} . Substitution into (9) gives $\Delta \nu_{\text{I, II}} = 2.99 \times 10^{-3} \text{ cm}^{-1}$ per atmosphere pressure at 0° C . Applying the formula to the liquid state we find that the observed shift of 105 cm^{-1} is roughly 48 times larger than that given by (20). (In the note by Salant and Sandow³ a factor $1/4\pi^2$ has been omitted in the expression $\Delta \nu$ which led to the impression that the difference between Dennison's effective charge and the electronic charge e accounted for the observed shift). It thus becomes apparent that there are other more serious reasons for the shift than the pure Lorentz-Lorenz effect (20). This is further supported by the fact that the harmonic of HCl shows a shift of the same order as the fundamental. Since by (15) and (18) the Lorentz-Lorenz shift is proportional to J/ν and since the absorption coefficient of the 0→2 transition (unpublished infrared measurements of West and Salant) is weaker than that of the 0→1 the Lorentz-Lorenz shift alone cannot account for the observed shift.⁵ The actual shift must therefore be connected with the other effects given by the first two terms of (17).

³ E. O. Salant and A. Sandow, Phys. Rev. **35**, 214 (1930).

⁴ D. M. Dennison, Phys. Rev. **31**, 503 (1928).

⁵ Dunham calculates from his own and Bourgin's data $J_{02}/J_{01} = 0.0161$. See J. L. Dunham, Phys. Rev. **34**, 438 (1929).

This conclusion has been reached above by considering the measurements. It can also be seen by taking into account the mutual distances of molecules in the liquid and their dimensions. It is clear that they are by no means far apart and that the space occupied by $u_I^* u_{II}$ is by no means negligible. The molecules are in fact so close together that we would not expect the first order result (17) to hold with any accuracy. All that can be claimed is that the three kinds of effects given in order in (17) as the pure electrostatic, the energy exchange, and the Lorentz-Lorenz effect will all contribute to the shift. In addition there may enter the effect of particle exchange which, for simplicity, has been neglected. The degeneracy connected with space quantization has not been considered explicitly. It is however easily removed by applying an auxiliary field parallel to E . Formulas (18), (19) have been used as though this were done.

THE THEORY AND CALCULATION OF SCREENING
CONSTANTS

BY CARL ECKART

RYERSON PHYSICAL LABORATORY, UNIVERSITY OF CHICAGO

(Received July 26, 1930)

ABSTRACT

It is shown that if H is the negative energy operator, and ϕ any function satisfying the boundary conditions of quantum dynamics and possessing the symmetry properties characteristic of a given spectral series, then $E = \int \phi^* H \phi d\tau$ is a lower limit to the term-value of the lowest level of that series. If the integral is evaluated for various ϕ 's, the largest value obtained will be the best approximation to this term value. The method is applied to various electronic configurations with satisfactory results. The degree to which ϕ approximates the wave function of the state is not determined, but it is shown to be likely that the approximation is not good at large distances from the nucleus.

THE empirical interpretation of x-ray spectra has long been based on the idea that each electron of an inner shell screens the outer electrons from the field of the nucleus. The outer electrons are supposed to move in an approximately central field, much as though the inner electrons were not present and the nucleus had an effective charge less than its true charge. Millikan and Bowen have also shown that this idea is applicable to many optical spectra.

Quantum dynamics has furnished a qualitative justification for this idea, but the effective nuclear charges have never been deduced from first principles in any systematic way. It is true that L. Pauling¹ has obtained numerical values for them which are in excellent agreement with observation, but his calculation begins with the wave equation of a single electron moving in the field of an artificial distribution of charges on spherical surfaces. This amounts to assuming the general form of the result, and neglecting some of the finer features of the problem. J. Frenkel² has used the method which forms the subject of the present paper. He calculates the screening constant for the normal state of helium-like atoms, but assumes it to be applicable to any state. It was found empirically (cf. Section 5) that the method fails miserably when applied to $(1s)(2s) 2^1S$, but, remarkably enough, gives very good results for $(1s)(2s) 2^3S$. This is shown to be a consequence of a definite limitation on the method, which is applicable only to the lowest state of any spectral series. (Section 1.).

The method is analogous to that first used by Ritz³ to calculate characteristic numbers. The Ritz method has already been used to solve problems

¹ L. Pauling *Zeits. f. Physik* **40**, 344 (1926).

² J. Frenkel, *Einführung in die Wellenmechanik*, p. 291. (Berlin, Julius Springer, 1929). Also Guillemin and Zener, *Zeits. f. Physik* **61**, 199 (1930).

³ W. Ritz, *Journ. f. reine u. angew. Math.* **135**, 1 (1909).

of quantum dynamics,⁴ but the investigators have not adhered very closely to the original procedure,⁵ and it appears that the deviations are largely responsible for the success of the calculation. They are all in the direction indicated by the empirical theory of screening. In this paper, a theoretical justification for them is given and the original Ritz procedure is abandoned⁶ entirely. This simplifies the calculations considerably without greatly reducing the accuracy of the result. If higher accuracy is required, however, the Ritz method may be superposed as was done by Kellner and Hylleraas.

It may be well to make a few general remarks about the various kinds of screening constants⁷ (or effective nuclear charges). These numbers are essentially parameters determining an average value of the electrostatic field in which an electron moves, and there will be as many different ones as there are different ways of averaging. The present paper will be primarily concerned with that effective charge which is to be used in the wave function. The approximate value of the main energy term is also obtained, from which that screening constant called σ_1 by Pauling could be calculated if it were desirable. This latter is responsible for the "screening doublets"; the "spin" screening constant is not calculated.

1. THE DIRECT METHOD OF CALCULATING CHARACTERISTIC NUMBERS

The fundamental equation of a characteristic value problem may be written

$$H\psi_n = W_n\psi_n, \quad (1)$$

which is normally a partial differential equation, H being an operator, W_n the characteristic number, and ψ_n a function of the coordinates. This equation is to be solved subject to certain boundary conditions, and possesses solutions satisfying these only for certain values of W_n , say

$$W_1 \geq W_2 \geq W_3 \geq \dots \quad (2)$$

(In quantum dynamics there is always a greatest W if this letter denotes the negative energy or term value.) For the following, it will be convenient to use the letters $\phi, \phi', \phi'' \dots$ to denote functions which satisfy the boundary conditions just mentioned, but are otherwise arbitrary. If the operator H is hermitian the characteristic solutions ψ_n of Eq. (1) may be normalized so that

$$\int \psi_n \psi_m^* d\tau = \delta_{nm} \quad (4)$$

⁴ G. W. Kellner, *Zeits. f. Physik* **44**, 91, 110, (1927), E. Hylleraas, *Zeits. f. Physik* **48**, 469 (1927).

⁵ Courant-Hilbert, *Mathem. Methoden der Physik* p. 157 (Berlin, J. Springer, 1924).

⁶ This has also been done by V. Guillemin, Jr. and C. Zener, *Zeits. f. Physik* **61**, 199 (1930); C. Zener *Phys. Rev.* **36**, 51 (1930).

⁷ For details, see L. Pauling and G. Goudsmit "Structure of Line Spectra," pp. 61, 180, 188 (McGraw-Hill, 1930).

and any of the functions ϕ may be expanded in a convergent series:

$$\phi = \sum a_n \psi_n, \text{ where } a_n = \int \phi \psi_n^* d\tau \quad (5)$$

If ϕ is itself normalized, i.e., if

$$\int |\phi|^2 d\tau = 1, \text{ or } \sum |a_n|^2 = 1 \quad (6)$$

then the integral

$$E = \int \phi^* H \phi d\tau \quad (7)$$

possesses certain important properties. For convenience, it will be called the variational integral and any normalized ϕ will be called a comparison function.

On substituting the expression (5) for ϕ into Eq. (7) and making use of Eqs. (1) and (4), it follows that

$$E = \sum |a_n|^2 W_n.$$

It is immediately seen that if all the a 's are zero except one ($\phi \equiv \psi_m$) then $E = W_m$; if ϕ differs only little from ψ_m , E will approximate W_m . To investigate this approximation, it is necessary to study the difference

$$W_m - E = \sum_n |a_n|^2 (W_m - W_n). \quad (8)$$

Because of the inequalities (2) the difference $W_1 - E$ must always be positive, since $W_1 - W_n \geq 0$, and W_1 is therefore the maximum value assumed by the variational integral for any comparison function whatever. If E has been evaluated for various comparison functions, then the largest of these values will be the best approximation to W_1 .

This reasoning applies only to the largest characteristic number, but if the first $m-1$ coefficients of the expansion (5) are all zero, it will apply equally to W_m . It is often possible to find comparison functions satisfying this condition, even though the functions ψ_n are not known exactly. A simple example is afforded by an atomic system with two electrons. If x_1, x_2 be their cartesian coordinates (the spin variables are entirely neglected) it is known that

$$\psi_1(x_1, x_2) = \psi_1(x_2, x_1)$$

and hence if

$$\phi(x_1, x_2) = -\phi(x_2, x_1)$$

it follows from Eq. (5) that $a_1 = 0$. Any antisymmetric comparison function will thus furnish a lower limit to the second characteristic number.

Similarly, if M be the operator associated to the angular momentum of the system and the comparison function be restricted by the equation

$$M^2\phi = L(L+1)\phi$$

where $L=0, 1, 2, \dots$, then the value of E obtained will be a lower limit to the lowest (largest W) S, P, D, \dots , term, respectively.

These results afford a basis for a direct method of calculating those characteristic values to which they apply. If comparison functions $\phi, \phi', \phi'' \dots$ are known, which result in values $E \leq E' \leq E'' \leq \dots$, it may be presumed that this sequence of numbers will converge toward the corresponding W_n . The proof of this convergence will usually be difficult, and no attempt will be made to construct one in this paper. Instead, a mode of reasoning will be adopted which is much simpler.

It depends on the fact that there exists one comparison function which has a certain theoretical justification:⁸ if the operator H be written $H' + H''$, it is known from perturbation theory that

$$\begin{aligned}\psi_n &= \phi_n + \dots \\ W_n &= W_n' + W_n'' + \dots\end{aligned}\tag{9}$$

where

$$H'\phi_n = W_n'\phi_n\tag{10}$$

and

$$W_n'' = \int \phi_n^* H'' \phi_n d\tau.\tag{11}$$

The function ϕ_n is the first term of an infinite series and is generally accepted as a "zeroth" approximation of ψ_n , while $W_n' + W_n''$ is the "first" approximation to W_n . For physical purposes, they may therefore be taken as standards by which other approximations are to be judged—if $|W_n - E| < |W_n - W_n' - W_n''|$ then E will be a good approximation according to this criterion. The direct method immediately enables us to find a good approximation whenever it is available and ϕ_n is known.

The operator H' and the function ϕ_n will usually depend on a numerical parameter Z (say the nuclear charge); if this parameter, whose true value is a part of the given data, be allowed to assume arbitrary values α in ϕ_n , then

$$E(Z, \alpha) = \int \phi_n^*(\alpha) H''(Z) \phi_n(\alpha) d\tau\tag{12}$$

will certainly be a lower limit to W_n . If $E(Z, \alpha)$ possesses a maximum for $\alpha = Z_e$ then it immediately follows that

$$W_n - E(Z, Z_e) \leq W_n - E(Z, Z) = W_n - W_n' - W_n''.$$

⁸ The mathematician might not agree to the soundness of the theory, but it has the general assent of physicists.

Hence $E(Z, Z_e)$ is a good approximation according to the criterion adopted above. This is the explanation of the recognised fact that the substitution of effective charges and quantum numbers in formulas deduced from perturbation theory usually improves their agreement with observational data. It goes farther, however, and indicates when the process will certainly be successful and when it is likely to fail; in the former case, the numerical value of the "effective" parameter is determinate. It should be noted that $E(Z, Z_e)$ depends on the true, as well as on the effective, value of the parameter. This affords a theoretical clue to the use of "inner" and "outer" effective charges.

In the previous paragraph, only one parameter has been treated, but there is no limit to the number which can be introduced into ϕ_n provided only that its symmetry properties be left undisturbed. Any degeneracy in the characteristic values of H' must be removed in determining ϕ_n by perturbation theory.

2. APPLICATION TO THE CONFIGURATION $(1s)^2$

The details of this method may most simply be illustrated by its application to the configuration $(1s)^2$ (normal state of helium), and this case will therefore be treated even though it has already been published by Frenkel.²

The operator H is

$$H = \nabla_1^2 + \nabla_2^2 + 2Z/r_1 + 2Z/r_2 - 2/r_{12} \quad (13)$$

where the indices denote the coordinates of the two electrons, which are measured in units of $a_H = 0.528\text{\AA}$. The constant W is the negative energy, measured in units of $Rh \text{ cm}^{-1} = 13.53\text{v.}$, and Z is the true nuclear charge in units of e . These units and designations will be used throughout the following. The operator H' is taken to be

$$H' = \nabla_1^2 + \nabla_2^2 + 2Z/r_1 + 2Z/r_2$$

whose characteristic function for the $(1s)^2$ configuration is

$$\begin{aligned} \phi(Z) &= u(Z, 1)u(Z, 2) \\ u(Z, k) &= (Z^3/\pi)^{1/2} \exp(-Zr_k) \end{aligned} \quad (14)$$

A comparison function may be obtained from this in various ways, the simplest being

$$\phi(\alpha) = u(\alpha, 1)u(\alpha, 2); \quad (15)$$

substituting this in the variational integral, one finds (cf. Section 7) that

$$E(Z, \alpha) = 2[2(Z - 5/16)\alpha - \alpha^2]. \quad (16)$$

This expression has a maximum for $\alpha = Z_e = Z - 5/16$ so that

$$E(Z, Z_e) = 2Z_e^2$$

is independent of Z in this case. The ionizing potential of the $(1s)^2$ state may be calculated from this by subtracting Z^2 , the energy of the hydrogen-like ion.

The values given by this formula are compared with those from other sources in Table I.

TABLE I. Ionizing potentials of $(1s)^2$.

Atom	$V = 2Z_c^2 - Z_2$	V (Calc. §6)	V (Observ.)
He I	1.70		1.81
Li II	5.45	5.50	5.564*
Be III	11.20	11.26	11.315*
B IV	18.95	19.00	
C V	28.70	28.75	

* B. Elden and A. Ericson, Nature **124**, 688 (1929).

A somewhat better approximation would be obtained by using

$$\phi(\alpha, \beta) = [u(\alpha, 1)u(\beta, 2) + u(\alpha, 2)u(\beta, 1)]/[2(1 + c^2)]^{1/2} \quad (17)$$

$$c = \int u(\alpha, 1)u(\beta, 1)d\tau_1 = 8\alpha^{3/2}\beta^{3/2}/(\alpha + \beta)^3$$

as comparison function. The variational integral is then

$$E(Z, \alpha, \beta) = 2Z\alpha + 2(Z - \sigma)\beta - (\alpha^2 + 2\alpha\beta c^2 + \beta^2)/(1 + c^2)$$

where

$$\begin{aligned} \sigma\beta &= \iint [\phi(\alpha, \beta)]^2/r_{12}d\tau_1d\tau_2 \\ &= \frac{\beta}{1 + c^2} \left[1 - \frac{2x + 1}{(x + 1)^3} + \frac{20x^3}{(x + 1)^5} \right], \quad x = \alpha/\beta. \end{aligned}$$

It is difficult to determine the maximum of this function analytically, but a numerical approximation method yields a value of 5.755 for $\alpha = 2.14$, $\beta = 1.19$ in the case of He I ($Z = 2$). This corresponds to 1.755 for the ionizing potential—a value as good as Kellner's fourth approximation.

The interest does not center on an accurate determination of this ionizing potential, however: in the case of He I, it has been calculated very accurately by Hylleraas (loc. cit.) and the others of this isoelectronic sequence may be calculated more accurately by the indirect method explained in Section 6. The comparison function of this configuration is of great interest, however, for it enters into many of the other configurations considered later. The relative simplicity of the function $\phi(\alpha)$, Eq (15), leads one to use it rather than the more elaborate one.

3. APPLICATION TO THE CONFIGURATIONS $(1s)(2p)$ AND $(1s)(3d)$

The wave equation for these configurations is that of Eq. (13); the comparison function is to be taken as

$$\phi(\alpha, \beta) = [u(\alpha, 1)v(\beta, 2) \pm u(\alpha, 2)v(\beta, 2)]/2^{1/2} \quad (18)$$

where u is the function defined by Eq. (14) and in the case of $(1s)(2p)$,

$$v(\beta, k) = Y_1 \cdot (\beta^3/6)^{1/2} (\beta r_k/2) \exp(-\beta r_k/2) \quad (19)$$

is the characteristic function of the $(2p)$ state of a hydrogen atom with nuclear charge β ; Y_1 is a normalized surface spherical harmonic of order 1. The upper sign is to be taken for the 1P , the lower for the 3P level. The value of the variational integral is found to be

$$E(Z, \alpha, \beta) = (2Z - \alpha)\alpha + [2(Z - \sigma) - \beta]\beta/4 \quad (21)$$

where

$$\sigma = I \pm J$$

and, with $x = \alpha/\beta$

$$I = (4/\beta) \iint \{ [u(\alpha, 1)v(\beta, 2)]^2 / r_{12} \} d\tau_1 d\tau_2 \quad (22)$$

$$= 1 - (6x + 1)/(2x + 1)^5$$

$$J = (4/\beta) \iint \{ u(\alpha, 1)v(\beta, 1)u(\alpha, 2)v(\beta, 2) / r_{12} \} d\tau_1 d\tau_2 \quad (23)$$

$$= (7/3)64x^3/(2x + 1)^7.$$

The function $E(Z, \alpha, \beta)$ has a maximum for the values of α and β which satisfy the equations $\partial E/\partial \alpha = 0$, $\partial E/\partial \beta = 0$, or

$$\alpha = Z - (d\sigma/dx)/4 \quad (24)$$

$$\beta = Z - \sigma - xd\sigma/dx.$$

These are readily solved by a semi-graphical method of approximation: σ and $d\sigma/dx$ are plotted from the values of I , J , and their derivatives given in Table II. As a rough approximation, $(1 - \sigma)$ and $d\sigma/dx$ may be neglected,

TABLE II. Values of I , J , and their derivatives.

x	I	dI/dx	J	dJ/dx
1.3	0.9854	0.0302	0.0418	-0.0654
1.4	0.9881	0.0234	0.0358	-0.0556
1.5	0.9902	0.0182	0.0308	-0.0468
1.6	0.9919	0.0146	0.0265	-0.0396
1.7	0.9932	0.0118	0.0230	-0.0334
1.8	0.9943	0.0094	0.0200	-0.0292
1.9	0.9951	0.0077	0.0175	-0.0236
2.0	0.9958	0.0066	0.0153	-0.0204
2.1	0.9964	0.0051	0.0135	-0.0184

whence $\alpha = Z$, $\beta = Z - 1$. The values of σ and $d\sigma/dx$ for these values are taken from the graphs and substituted in Eq. (24), giving a better approximation to α and β ; continuing the process, the roots are soon found with sufficient accuracy, and the maximum value of E is then calculable. The results of such calculations are summarized in Table III, V being the ionizing poten-

tial of the state in units of 13.53 v. The numbers in the last two columns are the roots of Eq. (24).

TABLE III. Ionizing potentials of (1s)(2p).

Level	$V/(Z-1)_2$		α	β
	Calc.	Obs.		
He I, 2^1P	0.245	0.2475	2.003	0.965
He I, 2^3P	0.262	0.2657	1.99	1.09
Li II, 2^1P	0.245	0.250	3.007	1.94
Li II, 2^3P	0.261	0.263	2.98	2.16

To treat the configuration (1s) (3d) only slight changes are necessary: the function u remains the same, while

$$v(\beta, k) = Y_2 \cdot (8\beta^3/1215)^{1/2} (\beta r_k/3)^2 \cdot \exp(-\beta r_k/3),$$

$$E(Z, \alpha, \beta) = (2Z - \alpha)\alpha + [2(Z - \sigma) - \beta]\beta/9,$$

$$\sigma = I' \pm J',$$

$$I' = (9/\beta) \iint \{ [u(\alpha, 1)v(\beta, 2)]^2 / r_{12} \} d\tau_1 d\tau_2 \quad (25)$$

$$= 1 - (12x + 1)/(3x + 1)^7,$$

$$J' = (9/\beta) \iint \{ u(\alpha, 1)v(\beta, 1)u(\alpha, 2)v(\beta, 2)/r_{12} \} d\tau_1 d\tau_2$$

$$= (4/5) \cdot 729x^3/(3x + 1)^9.$$

In this case, σ is so nearly unity that $\alpha = Z$ and $\beta = Z - 1$ is a sufficient approximation if only the center of gravity of the 1D and 3D terms is required. Their separation may be calculated from J' : it is

$$\Delta W = 4(Z - 1)J'/9 = (6)^4 Z^3 (Z - 1)^7 / [5(4Z - 1)^9].$$

The numerical values of this expression are compared with the observed values in Table IV.

TABLE IV. 3^3D-3^1D .

	Calc.	Obs.
He I	5.14×10^{-5}	3.68×10^{-5}
Li II	3.80×10^{-4}	2.68×10^{-4}

4. THE CONFIGURATION (1s)² (2p)

For this configuration, the energy operator is

$$H = \sum_{k=1}^3 (\nabla_k^2 + 2Z/r_k) - \sum_{(k,j)} (2/r_{kj}). \quad (26)$$

Since two electrons are in the $1s$ state, the two ways of introducing variable parameters discussed under Eqs. (15) and (17) are available; the former is much the simplest, so that it may be chosen:

$$\phi(\alpha, \beta) = u(\alpha, 1)[u(\alpha, 2)v(\beta, 3) - u(\alpha, 3)v(\beta, 2)]/2^{1/2}, \quad (27)$$

v having the significance of Eq. (19). The variational integral reduces to

$$E(Z, \alpha, \beta) = 2[2(Z - 5/16) - \alpha]\alpha + [2(Z - \sigma) - \beta]\beta/4 \quad (28)$$

with (cf. Eqs. (22) and (23))

$$\sigma = 2I - J.$$

The maximum value of this expression may be determined as already described. The results are shown in Table V, the ionizing potential of the state being obtained by subtracting $2(Z - 5/16)^2$ from the maximum value of E . There are systematic differences between the calculated and observed values of $V/(Z - 2)^2$ but both sequences show a flat maximum near Be II. This indicates that the method is capable of giving information even regarding the finer features of the dependence of W_n on Z . The systematic deviations could undoubtedly be diminished if the more complex function (17) were used for $(1s)^2$.

TABLE V. Ionizing potentials of $(1s)^2(2p)$.

Atom	$V/(Z-2)^2$		$Z-\alpha^\dagger$	$Z-\beta$	
	Calc.	Obs.*		(Calc.)	(Obs.)*
Li I	0.255	0.2605	0.31	1.98	2.019
Be II	0.258	0.2620	0.32	1.95	1.937
B III	0.258	0.2609	0.32	1.93	1.884
C IV	0.257	0.2595	0.32 ₅	1.91	1.858
N V	0.257		0.33	1.89	1.838
O VI	0.256		0.33	1.88	1.816

* Millikan and Bowen, Phys. Rev. 27, 144 (1926). The observed values of $Z-\beta$ are taken from the spin doublet separation, and are only qualitatively comparable with the calculated values.

† Cf. Guillemin and Zener, loc. cit.

5. THE CONFIGURATION $(1s)(2s)$

This electronic configuration gives rise to two levels, 2^3S , 2^1S , of which the former is the lowest, the latter is the second term of its series. The method may be expected to fail when applied to 2^1S , and does so.

The energy operator is that of Eq. (13), and the comparison function is

$$\phi = [u(\alpha, 1)v(\beta, 2) \pm u(\alpha, 2)v(\beta, 1)]/[2(1 \pm b^2)]^{1/2}, \quad (29)$$

u being given by Eq. (14) and

$$v(\beta, k) = (\beta^3/8\pi)^{1/2}(1 - \beta r_k/2) \exp(-\beta r_k/2), \quad (30)$$

$$b = \int u(\alpha, 1)v(\beta, 1)d\tau_1 = (2x)^{3/2}(x-1)/(x+\frac{1}{2})^4. \quad (31)$$

The variational integral reduces to

$$E(Z, \alpha, \beta) = \{ [2(Z - \sigma_1) - \alpha]\alpha + [2(Z - \sigma_2) - \beta]\beta/4 \} / (1 \pm b^2)$$

with

$$\sigma_1 = \pm (Z - \beta)b^2x/(1 - x)$$

$$\sigma_2 = A \pm [B - (Z - \alpha)b^2/(1 - x)]$$

$$A = \frac{4}{\beta} \iint \frac{[u(1)v(2)]^2}{r_{12}} d\tau_1 d\tau_2 = 1 - \frac{1}{4} \left\{ \frac{4x+1}{(x+\frac{1}{2})^3} - \frac{5x+1}{(x+\frac{1}{2})^4} + \frac{3}{8} \frac{6x+1}{(x+\frac{1}{2})^5} \right\}$$

$$B = \frac{4}{\beta} \iint \frac{u(1)v(1)u(2)v(2)}{r_{12}} d\tau_1 d\tau_2 = \frac{x^3}{2} \frac{20x^3 - 30x + 13}{(x+\frac{1}{2})^7} \quad (33)$$

The derivatives of the function E are too complex to be used in computation, and it is simpler to calculate E numerically for various values of α and x , the maximum value being determined by graphical interpolation. The numerical work was simplified considerably by first tabulating the values of A , B , and b^2 (Table VI); this was also a saving of time, since these functions also enter into the work on $(1s)^2(2s)$ and other more complex configurations.

TABLE VI.

x	b^2	A	B	C
1.0	0.0000	0.8396	0.0876	0.00000
1.1	0.0025	0.8504	0.1044	0.00216
1.2	0.0079	0.8604	0.1220	379
1.3	0.0143	0.8692	0.1400	497
1.4	0.0205	0.8772	0.1564	582
1.5	0.0263	0.8848	0.1716	641
1.6	0.0312	0.8916	0.1844	681
1.7	0.0352	0.8980	0.1952	706
1.8	0.0381	0.9036	0.2040	719
1.9	0.0404	0.9092	0.2112	724
2.0	0.0419	0.9140	0.2164	723
2.1	0.0429	0.9184	0.2204	716
2.2	0.0434	0.9228	0.2232	707
2.3	0.0435	0.9268	0.2248	694
2.4	0.0433	0.9304	0.2252	680
2.5	0.0428	0.9336	0.2252	

The values of the ionizing potential and effective charges as calculated for 2^3S are given in Table VII. The ionizing potential calculated for 2^1S

TABLE VII. Ionizing potentials of $(1s)(2s)2^3S$.

Atom	Calc.	Obs.	α	β
He I	0.334	0.350	2.01	1.53
Li II	1.21	1.22	3.03	2.56

was in each case somewhat greater than that for 2^3S —in direct contradiction to observation. It was attempted to improve matters by choosing $\beta = Z - 5/16$

which makes the ϕ of Eq. (29) orthogonal to the approximate wave function for 1^1S :

$$u(Z - 5/16, 1)u(Z - 5/16, 2).$$

This reduced the calculated ionizing potential too much. Perhaps a method of this sort might be worked out using the expression (17) for the wave function of 1^1S .

6. THE CONFIGURATION $(1s)^2(2s)$.

The operator H is that of Eq. (26) and the comparison function is

$$\phi = u(\alpha, 1)[u(\alpha, 2)v(\beta, 3) - u(\alpha, 3)v(\beta, 2)]/[2(1 - b^2)]^{1/2} \quad (34)$$

with v defined by Eq. (30) and b^2 as in Table VI. The variational integral reduces to

$$E(Z, \alpha, \beta) = \{ [(2 - b^2)(2Z - \alpha) - \tau]\alpha + [2(Z - \sigma) - \beta]\beta/4 \} / (1 - b^2) \quad (35)$$

where

$$\begin{aligned} \sigma &= 2A - B + 8C - (z - 1 - \alpha)b^2/(x - 1) \\ \tau &= 5/4 - 2(z - 1 - \beta)b^2x/(1 - x). \end{aligned} \quad (36)$$

A and B have the values given in Table VI and

$$\begin{aligned} C &= \frac{b^2(\alpha^2 - \beta^2/4)}{2\beta(\alpha - \beta)} - (b/\beta) \iint \{ [u(1)]^2 u(2)v(2)/r_{12} \} d\tau_1 d\tau_2 \\ &= (2x^3)^{1/2} b(3x^2 + 2x - \frac{1}{4}) / (3x + \frac{1}{2})^4 \end{aligned}$$

is also given in that table.

TABLE VIII. Ionizing potentials of $(1s)^2(2s)$.

Atom	V		$Z - \alpha$	$Z - \beta$
	Calc.	Obs.		
Li I	0.456	0.397	0.30	1.22
Be II	1.41	1.34	0.30	1.16
B III	2.85	2.79	0.28	1.07
C IV	4.80	4.745	0.29	1.04

The maximum value of this function was again determined by plotting it for various values of α and x . The resulting ionizing potentials are all too high, as is shown in Table V. This is because the value $2(Z - 5/16)^2$ is consistently less than the energy of $(1s)^2$; a better comparison with observation is obtained if the observed ionizing potential be subtracted from the maximum value of E . The result should be a lower limit to the true energy of $(1s)^2$. The third column of Table I contains the values of the ionizing potential of helium-like ions calculated in this way; the agreement with observation is good. The values for B IV and C V are as good as any available, and are presumably about 0.05-0.06 units lower than the true values.

7. FORMULAE USED IN EVALUATING THE FOREGOING INTEGRALS

The following is a brief summary of formulae, most of them well-known, which were used in evaluating the integrals of the foregoing sections. The functions u and v satisfy the equations

$$\Delta^2 u + 2\alpha u/r = \alpha^2 u/n^2$$

$$\Delta^2 v + 2\beta v/r = \beta^2 v/m^2$$

n and m being integers. Each has the form $X(r) Y_l(\theta, \phi)$, Y_l being a normalized surface spherical harmonic of order l (l is the azimuthal quantum number). The X 's are also supposed normalized. From these definitions, it follows that

$$\int u[\nabla^2 u + 2Zu/r]d\tau = (2Z - \alpha)\alpha/n^2$$

(u may of course be replaced by v if other appropriate changes are made);

$$\begin{aligned} & \int [u\nabla^2 v + v\nabla^2 u + 4Zu/r]d\tau \\ &= 2b\{[\alpha^2(Z - \beta)]/n^2 - [\beta(Z - \alpha)]/m^2\}/(\alpha - \beta), \\ b &= \iint uv d\tau, \end{aligned}$$

The quantity b will vanish unless the azimuthal quantum numbers of u and v are equal.

If f and g are any functions independent of ϕ and θ , it may be shown that

$$\begin{aligned} & \iint \{f(r_1)[Y_l(\theta_1, \phi_1)]^2 g(r_2)/r_{12}\} d\tau_1 d\tau_2 \\ &= \int_{r_1=0}^{\infty} f(r_1)r_1 \int_{r_2=0}^{r_1} g(r_2)r_2^2 dr_2 dr_1 \\ &+ \int_{r_1=0}^{\infty} f(r_1)r_1^2 \int_{r_2=r_1}^{\infty} g(r_2)r_2 dr_2 dr_1, \end{aligned} \tag{40}$$

and

$$\begin{aligned} & \iint \{f(r_1)Y_l(\theta_1, \phi_1)g(r_2)Y_l(\theta_2, \phi_2)/r_{12}\} d\tau_1 d\tau_2 \\ &= \left\{ \int_{r_1=0}^{\infty} f(r_1)r_1^{1-l} \int_{r_2=0}^{r_1} g(r_2)r_2^{l+2} dr_2 dr_1 \right. \\ &+ \left. \int_{r_1=0}^{\infty} f(r_1)r_1^{2+l} \int_{r_2=r_1}^{\infty} g(r_2)r_2^{1-l} dr_2 dr_1 \right\} / (2l + 1). \end{aligned}$$

In evaluating the integrals with respect to r_1 and r_2 the following formula is useful:

$$\int_r^\infty r^n e^{-\alpha r} dr = (n!/\alpha^{n+1}) \sum_{k=0}^n (\alpha r)^k / k!. \quad (42)$$

8. DISCUSSION OF THE RESULTS

The primary object of all calculations like the foregoing must be to determine the functions ψ_n approximately, or at least to approximate the electron density which is defined by

$$D(1) = 2 \int |\psi_n(1, 2)|^2 d\tau_2$$

in the case of two electrons. It may be hoped that an approximation will be obtained if a comparison function is substituted in this integral and its parameters are given the values determined as described.

While this paper was being written, two others dealing with the same subject were published by C. Zener⁹ and J. C. Slater.¹⁰ These authors use comparison functions ϕ which are much simpler than those used in the present calculations. This is presumably justified, for Zener has shown that the first term of the parenthesis $(1 - \beta r_k/2)$ in Eq. (30) has very little effect on D . If this is true only for that value of β which makes the variational integral a maximum, then it is significant in the matter discussed in the preceding

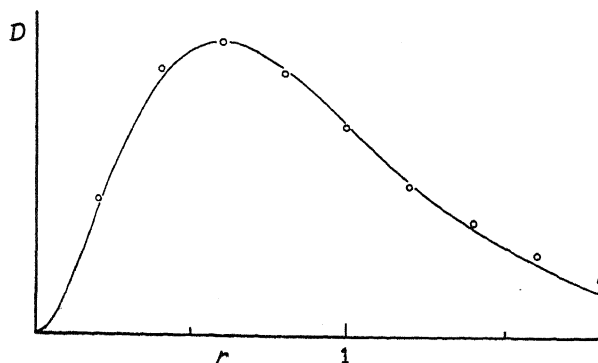


Fig. 1.

paragraph: it indicates that the same D is obtained for two comparison functions. But if the same is true for a wider range of β , then the observation merely means that this term may be neglected in evaluating D (or E), but does not give any information regarding the invariance of D —the difference between the two comparison functions is then trivially slight.

⁹ C. Zener, Phys. Rev. **36**, 51 (1930).

¹⁰ J. C. Slater, Phys. Rev. **36**, 57 (1930).

The functions $\phi(\alpha)$, Eq. (15), and $\phi(\alpha, \beta)$, Eq. (17), may be compared in this respect. At first glance, they are widely different, but a closer examination shows that if r_1 and r_2 are of the same order of magnitude and not too large, $\phi(\alpha, \beta) \sim \exp[-(\alpha + \beta)(r_1 + r_2)/2]$. In this region the two are not appreciably different, therefore, and the result of the comparison will be open to much the same doubt as Zener's. It is to be noted that the variational integral is a maximum for $2\alpha = 3.38$ if $\phi(\alpha)$ is used, and for $\alpha + \beta = 3.33$ if $\phi(\alpha, \beta)$. In Fig. 1, the curve represents the D obtained from $\phi(\alpha)$, the circles, the values of $1.56 D$ obtained from $\phi(\alpha, \beta)$. The relative values of D obtained from the two functions are thus nearly the same in the region $r < 1.5a_H$ but their absolute values differ by more than 50%. The reason for this becomes apparent on noting that $D[\phi(\alpha)]$ approaches zero like $\exp(-3.38r)$ for large values of r , while $D[\phi(\alpha, \beta)]$ approaches $\exp(-2.38r)$. The only rigorous conclusion is that the electron density calculated in this way may be quite inaccurate at infinity. It seems quite likely, however, that its behavior for small values of r is correctly given.

I wish to acknowledge my indebtedness to Mrs. Ardi's T. Monk, who performed many of the computations required for this work. Among other things not so easily enumerated, Tables II and VI are due to her.

Note added in proof: The following considerations afford a means of estimating the error introduced by the use of approximate wave functions. Let ψ_1 be the true wave function of the lowest state of a series and ϕ an approximation to ψ_1 ; both will be supposed real and normalized. The error introduced by using ϕ will generally be of the order of magnitude ϵ , where

$$\begin{aligned} \epsilon^2 &= \int (\psi_1 - \phi)^2 d\tau \\ &= 2 - 2a_1 \end{aligned} \quad \text{by Eq. (5)} \quad (43)$$

The expression for E (Eq. 7)) may be written

$$\begin{aligned} E &= a_1^2 W_1 + \sum_{n>1} a_n^2 W_n \\ &\leq a_1^2 W_1 + W_2 \sum_{n>1} a_n^2 && \text{by Eq. (2),} \\ &= a_1^2 W_1 + W_2 (1 - a_1^2) && \text{by Eq. (6);} \end{aligned}$$

hence

$$(W_1 - E)/(W_1 - W_2) \geq 1 - a_1^2 = 1 - (1 - \epsilon^2/2)^2.$$

If ϵ is not too great, this is equivalent to

$$\epsilon^2 \leq (W_1 - E)/(W_1 - W_2). \quad (44)$$

The values of W_1 and W_2 are known from experiment so that an upper limit for ϵ may be calculated, which probably does not differ greatly from the true value.

Eq. (44) indicates that $W_1 - E$ is proportional to the second power of ϵ —a result which was obvious anyway—and that the factor of proportionality is not W_1 but $(W_1 - W_2) < W_1$. These two facts explain the remarkably small

values of $W_1 - E$ obtained above. They also show why the calculations of Section 6 yielded better values for the ionizing potentials of $(1s)^2$ than did those of Section 2.

In calculating other quantities than the energy, the error will be of first order in ϵ , which may therefore be taken as the probable fractional error. This should be the case in calculating the density function D ; for $\phi(\alpha)$ Eq. (44) yields $\epsilon \leq 0.27$ for $\phi(\alpha, \beta)$, $\epsilon \leq 0.19$. The difference 50 percent in the values of D obtained from the two functions is thus no greater than might be expected.

In the case of Li II, 2^3P and Li I 2^2P , the values of ϵ for the functions given in Sections 3 and 4 are ≤ 0.12 and ≤ 0.19 respectively. These functions have been used elsewhere to calculate the relative displacements of Li (6) and Li (7) lines because of the motion of the nucleus.¹¹ The probable errors of these calculations can now be estimated:

Li II $\lambda 5485$	$\Delta\nu = 0.327 \pm 0.031 \text{ cm}^{-1}$
Li I $\lambda 6708$	$\Delta\nu = 0.123 \pm 0.007 \text{ cm}^{-1}$

The errors are small since only a part of the calculated value is affected by the error in the wave function.

¹¹ D. S. Hughes and C. Eckart, Phys. Rev. **36**, 694 (1930).

REFLECTION OF CADMIUM AND ZINC ATOMS FROM
SODIUM CHLORIDE CRYSTALS

BY HAROLD A. ZAHL

PHYSICAL LABORATORY, STATE UNIVERSITY OF IOWA

(Received July 16, 1930)

ABSTRACT

A beam of zinc atoms reflected from a sodium chloride crystal is in part specularly reflected. The specular beam was investigated: (1) by measuring the velocity distribution of the atoms composing the specular beam; and (2) by examining the specular beam after reflection from a second crystal. A difference in angle of 22.5° between the two crystals does not greatly reduce the intensity of the specular beam. It is concluded that if velocity selection or a space-grating type of reflection of zinc is present it is not very pronounced.

Double reflection experiments of cadmium from sodium chloride crystals have been repeated and apparently evidence for both space and surface-grating phenomena found in certain cases. It is suggested that individual differences in crystals may be an important factor in causing these differences.

INTRODUCTION

THE wave-particle dualism of an atom required by the new quantum mechanics has for some time been investigated by the reflection of atoms from a crystal or ruled grating.¹

In a paper by Ellett, Olson and Zahl² it was shown that a beam of uncharged cadmium atoms undergoes reflection from a sodium chloride crystal such that the specular beam consists of atoms possessing for the most part a velocity within a definite range. They suggest that the phenomenon may be due to a space-grating type of reflection. A formula of the type

$$\lambda = \frac{h}{mv} = 2d \left(1 - \frac{\phi}{\frac{1}{2}mv^2} - \cos^2 \theta \right)^{1/2}$$

may be made to fit their data if ϕ , the average potential energy of the cadmium atom within the crystal, is not taken as constant but as varying with the angle of incidence. As further evidence for a velocity selection the same writers show that a beam of cadmium atoms incident on a first crystal of sodium chloride is not specularly reflected from a second crystal unless the angle the incident beam makes with both crystals is the same or nearly the same.

The reflection experiments of Knauer and Stern³ who used helium and molecular hydrogen incident on sodium and potassium chloride crystals, indicate the presence of a surface diffraction phenomenon. Estermann and

¹ See J. B. Taylor, *Phys. Rev.* **35**, 375 (1930) for a more complete list of references.

² A. Ellett, H. Olson and H. Zahl, *Phys. Rev.* **34**, 493 (1929).

³ F. Knauer and O. Stern, *Zeits. f. Physik* **53**, 779 (1929).

Stern⁴ find that the reflection of helium and molecular hydrogen from crystals of lithium fluoride conclusively shows the cross-grating nature of the diffraction. Johnson⁵ has found that atomic hydrogen reflected from lithium fluoride produces a pattern which satisfies simple cross-grating formulae.

Ellett and Olson⁶ have shown that a beam of sodium atoms incident on sodium chloride gives no indication of specular reflection. Taylor¹ has worked with alkali metals other than sodium and finds no specular reflection of lithium, potassium or caesium from crystals of sodium chloride or lithium fluoride. There is also no evidence of specular reflection of cadmium or arsenic from crystals of orthoclase or fluorite.²

It is difficult, at this stage of the problem to conceive why some atoms and molecules should be reflected from crystal surfaces in accordance with surface-grating theory while a heavier atom such as cadmium should penetrate at least apparently through several reflecting layers of the crystal and be specularly reflected only if the atom's initial velocity corresponds to a certain wave-length. There is also the question why in certain cases no reflection occurs at all.⁷

It is not the purpose of this paper to attempt a solution of the problem. The apparent necessity for the consideration of two distinct phenomena adds considerable complexity to the general case of the reflection of atoms and molecules from crystals.

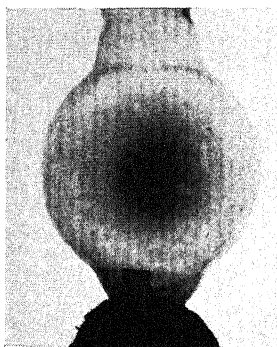


Fig. 1. Specular deposit obtained with zinc reflected from sodium chloride at an angle of 45° .

EXPERIMENTAL

I. Reflection of zinc from sodium chloride.⁸

A beam of zinc atoms issuing from a molybdenum boiler at 600°C is

⁴ I. Estermann and O. Stern, *Zeits. f. Physik* **61**, 95 (1930).

⁵ T. H. Johnson, *Phys. Rev.* **35**, 1432 (1930).

⁶ A. Ellett and H. Olson, *Phys. Rev.* **31**, 643 (1928).

⁷ Taylor suggests in the case of the alkali metals mentioned above that the presence of no reflection may in part be due to the ease of absorption of these metals on surfaces.

⁸ A preliminary report of part of the work on zinc herein described was read at the Christmas meeting of the American Physical Society at Des Moines.

in part specularly reflected when incident upon a freshly cleaved clean sodium chloride surface. This was determined by placing a crystal within a bulb which was surrounded by liquid-air, a defined beam of zinc atoms entering through a small opening and striking the crystal surface. Since all atoms after leaving the crystal must strike a liquid-air cooled surface every atom could be accounted for. Fig. 1 shows a specular spot thus obtained when the crystal surface was set at 45° relative to the direction of the incident beam. The specular spot is not sharply outlined and fades into a back-ground of diffusely scattered atoms which possess a maximum on the normal to the crystal surface. It will be remembered that random scattering results in a distribution according to the well-known cosine law.

II. Direct measurement of the velocity distribution of the atoms composing the specular beam.

The apparatus employed was essentially the same as that by which the velocity distribution of cadmium atoms after reflection was measured.²

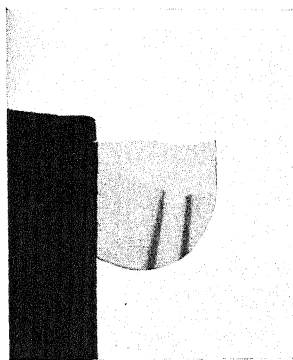


Fig. 2. A typical deposit obtained with specularly reflected zinc after passing through the velocity-analyzer.

Briefly, the atoms after reflection from a large area of the crystal surface were all condensed except a narrow beam which passed through a slit placed very close to the first disk of a rotating sectored-disk velocity-analyzer.⁹ The atoms which passed through the defining slit and were moving in a direction appropriate to the velocity of the analyzer passed through the sectored disks and were condensed on a liquid air cooled glass surface. Rotation of the analyzer first in one direction and then the other resulted in the formation of two deposits. Fig. 2 shows a photograph of a typical set of deposits obtained in this manner. Microphotometer curves of the deposits when translated into relative density gave the velocity distribution of the atoms contributing to the deposits. Such curves for zinc reflected from sodium chloride

⁹ J. A. Eldridge, Phys. Rev. 30, 931 (1927).

are shown in Fig. 3,¹⁰ together with the rate of rotation of the disks, the geometric outline and the velocity corresponding to the observed separation of the deposits. The best mean values for the velocities corresponding to different angles of incidence are given in Table I.

TABLE I. *Experimental values of the velocities of a specular beam of zinc atoms reflected from crystals of sodium chloride.*

θ	vel (m/sec)			Average
22.5°	763	736	761	753
45°	666	672	683	674
67.5°	712	689	695	699

It is a question as to how much weight may be assigned to these measured values of the velocities. The resolving power of the apparatus was considerably lower in the case of the high-speed zinc atoms than in that of the much slower cadmium atoms. A monochromatic (single velocity) beam would

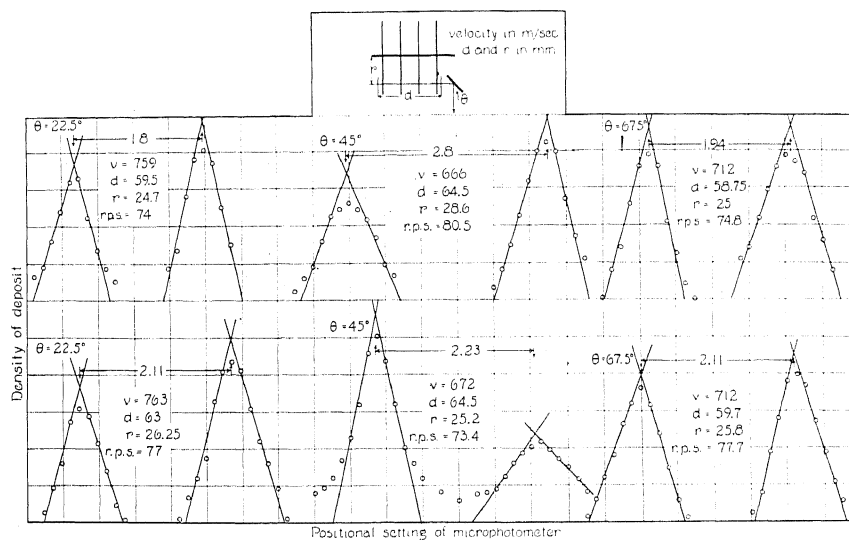


Fig. 3. Density curves obtained from deposits such as are shown in Fig. 2.

give a velocity distribution closely resembling the triangles of Fig. 3, but due to the low resolving power a beam of zinc atoms possessing a Maxwell distribution of velocities would also give an approximate triangle not very much wider at the base. The isosceles appearance of the velocity triangles is different from a curve produced by a Maxwell distribution of velocities, but

¹⁰ Approximate relative densities were obtained with a microphotometer-density curve experimentally calibrated for cadmium. This was deemed permissible since the density of the lines was not great enough to cause specular reflection of light. That is, the deposits could be considered as made up of an aggregate of individual scattering centers. In regions of such low density the calibration curve for cadmium plotted on semi-logarithmic paper is quite linear.

other than that the measurements offer no strong evidence for the presence of velocity selection.

III. Multiple reflection of zinc from sodium chloride.

If a space-grating type of reflection occurred resulting in the specular beam being made up of atoms possessing nearly equal velocities, then reflection from a second crystal should be total if the angles were the same and the specular reflection should drop off as the angle of the second crystal is changed. The rate at which the specular beam dropped off as a function of the change in angle would be a measure of the resolving power of the crystal for the atoms in question.

A description of the type of apparatus used may be found in an earlier reference to some similar experiments with cadmium.² Aside from some differences in the way the atom gun was mounted the methods were identical.

Runs were made, first with both crystals making an angle of 45° with respect to the incident beam, and second with the first crystal at 45° and the

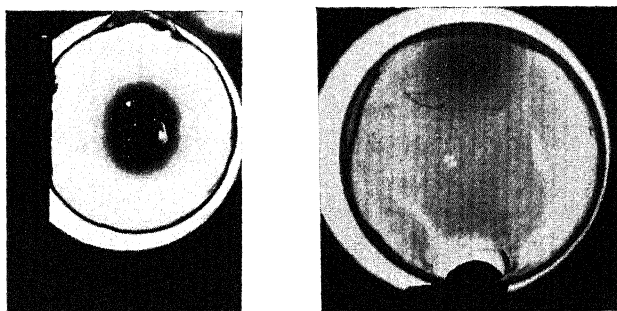


Fig. 4. (a) Specular deposit of zinc obtained after double reflection from sodium chloride, the incident beam making an angle of 45° with both crystals. (b) Same as (a) except the beam was incident on the second crystal at 22.5° .

second at 22.5° . The alignment of both crystals was taken care of optically by sending a beam of light over the path to be traversed by the atoms. Since the measurements of II indicate a maximum velocity difference when the crystals are set at 45° and 22.5° , it would be under these conditions that selective reflection should be in greatest evidence.

In Fig. 4(a) is shown a specular deposit condensed on the walls of the bulb surrounding the second crystal, both crystals set at 45° .¹¹ The deposit was several times dense enough to be opaque yet there was no trace of any diffuse back-ground. At a conservative estimate, at least 95 percent of the atoms incident on the second crystal were specularly reflected. The presence of almost total reflection differs considerably from all experiences with zinc

¹¹ Microphotometer curves of these specular deposits were not made because of their opacity to ordinary light. An attempt to obtain a density picture by means of x-rays greatly reduced by the characteristic absorption of the metal was not successful.

reflected from one crystal. Cosine scattered atoms become in evidence, in the case of single crystal reflection, soon after the appearance of a specular spot.

Fig. 4(b) is a photograph of a deposit made under identical conditions except that the second crystal was set to receive the beam from the first at an angle of 22.5° . The specular deposit is quite evident together with a faint diffuse back-ground which was entirely lacking in the runs made with equal angles. (Photographic comparison of course only serves as an approximation).

A comparison of (a) and (b) of Fig. 4 indicates that if one is to consider velocity selection as the explanation of these phenomena then the resolving power of sodium chloride for zinc must be extremely low. Following the x-ray analogy, the low resolving power shown by the reflection of zinc could be explained by assuming that the incident zinc atoms penetrate but very few of the reflecting planes of the crystal. If it be assumed that no selective reflection was present it will then be necessary to introduce some other explanation as to why the zinc atoms when both angles are equal, are almost totally reflected from the second crystal but not from the first.

In Fig. 4(b) a dense thread-like line can be seen to twist around the lower edge of the specular deposit. This curious structure appeared as though it was formed by a very dense "ray of zinc" which slowly moved through an irregular path and finally stopped after doubling back. The small circular spot which represents either the terminus or the start of the trace was many times heavier than either the thread-like deposit or the specular deposit. It has been observed but once. No explanation can be put forth at this time.

IV(a). Multiple reflection of cadmium atoms from sodium chloride.

It was considered desirable to repeat the experiments on double reflection of cadmium² since the experiments on zinc discussed in III gave no conclusive evidence of velocity selection.

In Fig. 5(a) is shown a typical specular deposit condensed on the walls of a liquid-air cooled bulb surrounding the second crystal, both crystals being set at 45° . Within one or two percent the entire incident beam was found to go into the specular deposit. The deposit was many times dense enough to be opaque.

In Fig. 5(b) is shown a photograph of a deposit produced under identical conditions except that the beam from the first crystal was incident on the second at an angle of 22.5° with the surface. A specular deposit is clearly in evidence but the boundary is not well defined and there is present considerable diffuse scattering having a maximum on the normal to the reflecting area of the crystal. The rim of the hemisphere due to the random scattered atoms is clearly discernible. Approximately 50-65 percent of the beam incident on the second crystal was specularly reflected, the remaining atoms contributing to the diffuse back-ground.

The absence of any random scattered atoms when the crystals are set at equal angles and the presence of such atoms when the angles are different

indicate that selective reflection is present though not in so marked a degree as found in cases previously reported.

A curious phenomenon was observed in the particular run illustrated by Fig. 5(b). Almost on the normal to the surface of the second crystal a quite noticeably dense rectangular deposit appeared. In Fig. 5(c) is shown this deposit, the specular deposit of Fig. 5(b) appearing at the edge of the photograph.

Because of the incident beam having the shape of a cone it is hard to conceive of any mechanism whereby a square deposit could be obtained by ordinary reflection or even evaporation from the crystal surface. However, since the crystal was fastened to the heating unit by means of fine copper

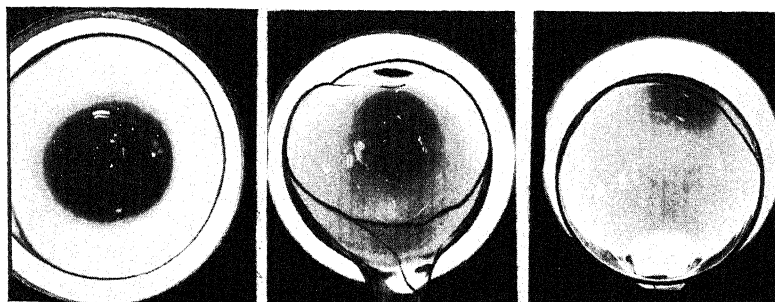


Fig. 5. (a) Specular deposit of cadmium obtained after double reflection from sodium chloride, the incident beam making an angle of 45° with both crystals. (b) Same as (a) except the beam was incident on the second crystal at 22.5° . (c) Curious rectangular deposit found almost on the normal to the crystal surface.

wires which passed over the unused region of the crystal some of the atoms (when the second crystal is set at 22.5° relative to 45° for the first) would strike the wires after reflection since the diffusely scattered atoms spread over a complete hemisphere. There is no reason to believe however, that these atoms which leave the crystal at grazing angles would be scattered in any way but at random. Even if these atoms were in some way directed towards and contributed to the rectangular deposit the few atoms intercepted would hardly account for the number found in this deposit.

This phenomenon has not been observed in any case other than when the first crystal was at 45° and the second at 22.5° , and in fact, it has been observed but twice under these conditions.

IV(b). Multiple reflection of cadmium atoms using the same set of crystals for different angles.

All atomic reflection experiments so far reported in this paper have been made with crystals freshly cleaved before each run. Immediately after cleavage they were mounted, placed into position for the experiment and the air pumped from the system. Out-gassing by heating was never commenced until shortly before the run. In a word, such a treatment and direct compari-

son afterwards assumes equal behavior of all sodium chloride crystals under like conditions.

The experiments described here differ from those of III and IV(a) in that the apparatus was so designed that the reflected beam from the second crystal could be studied as a function of the angle of incidence using the same set of crystals for the comparison.

The essential features of the apparatus are brought out in Fig. 6. A beam of cadmium atoms defined by a system of liquid-air cooled slits strikes the first crystal which is fixed at 45° . A portion of the specularly reflected beam is re-defined by a second opening and then passed to the second crystal which is mounted on a ground-glass joint so that the angular relation between the incident beam and the crystal surface can be varied. The second specularly reflected beam is thrown on to the liquid-air cooled surface of a

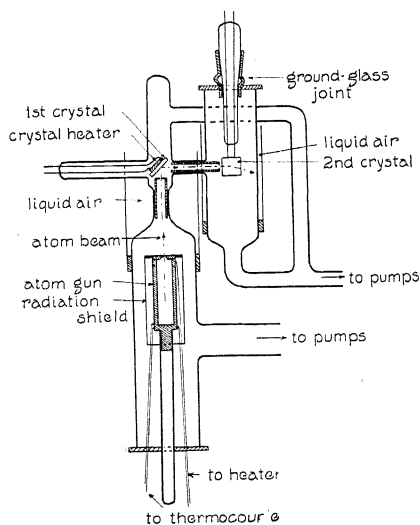


Fig. 6. Apparatus used for experiments described in IV (b).

glass cylinder. Two angles were studied during a run, the crystal being thrown over from one position to another at ten minute intervals to compensate for any change in the density of the atomic beam. A complete run took about three hours or one and one-half hours at each angle. At the end of a run the glass cylinder was cut up and the deposits studied with the help of a microphotometer.

Because of the lack of time only two runs have been made with the apparatus. In the last of the two runs it was found that even when the second crystal was at 18° relative to 45° no trace of selective reflection occurred. The greater number of atoms contributed to the specular deposit with but little indication of random scattering.

In Fig. 7 are shown the microphotometer curves across the central sections of the specular deposits when the first crystal was held at 45° and the

second alternately changed from 45° to 18° . The curves were not drawn to represent relative density because the central portions of the deposits so closely approached opaqueness that the cadmium microphotometer-density curve was not applicable. The relative slopes however, and the breadth of the deposit would not be greatly altered even if a translation were made. The

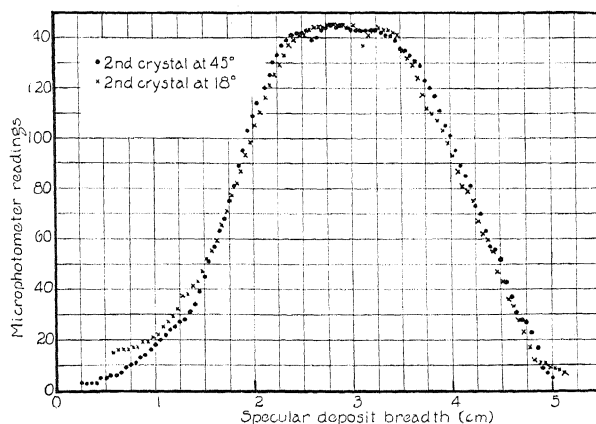


Fig. 7. Microphotometer curves across central sections of specular deposits shown in Fig. 8.

agreement of the two curves is within the limits of the microphotometer error.

In Fig. 8(a) and (b) the photographs of the two specular deposits are shown. These pictures were taken by means of reflected light unlike the transmitted light photographs of the other deposits shown earlier. In Fig.

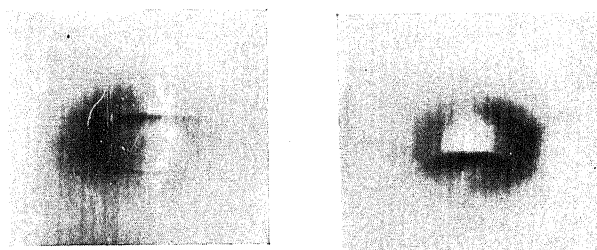


Fig. 8. Reflected light photographs of specular deposits obtained with apparatus shown in Fig. 6. (a) Both crystals set at 45° . (b) First crystal at 45° and the second at 18° .

8(a) is shown the result obtained when both crystals were set at 45° . Quite noticeably, two lines streak across the central part of the deposit. The microphotometer faintly records the broader line as a decrease in density. Fig. 8(b) represents the situation obtained when the second crystal was at 18° relative to 45° for the first. A curved broad line traces around the lower edge of the deposit. This line is also recorded as representing a decrease in

actual density. Other than this principal line three curved streamers can be distinguished leaving the central spot. It is difficult to say more than this. The pattern is very faint and if the missing part of a symmetrical pattern is present it does not appear on the photograph, neither does it show up on the original.

These deposits suggest what may be evidence of a surface-grating phenomenon.

DISCUSSION

The double reflection experiments with zinc described in III show no positive evidence for velocity selection as a function of the angle of incidence. Moreover, since the measured velocities of specularly reflected zinc fall closely in the region of the most probable velocity of zinc at that temperature they cannot be considered with the same degree of confidence as the similar cadmium measurements which gave values considerably off the most probable velocity.

It may perhaps be a coincidence, but if values for ϕ be calculated by substitution of the measured velocities of zinc into the equation mentioned earlier, then values are obtained which closely approximate those for cadmium at similar angles. The values obtained for both zinc and cadmium are contrasted in Table II. The agreement is quite close but whether this carries any significance is not known.

TABLE II. *Calculated values of ϕ for zinc and cadmium.*

θ	22.5°	45°	67.5°
$\phi_{\text{Zn}} 10^{13}$	4.4	12.1	22.2
$\phi_{\text{Cd}} 10^{13}$	4.84	13.2	19.6

The appearance of two distinct phenomena in the case of cadmium after multiple reflection from sodium chloride was rather surprising. It was believed that all runs were made under identical experimental conditions. The crystals, however, were not laboratory grown but were the natural mined product and although a critical selection was made of each crystal before it was used, it cannot be said the crystals were perfect. Unfortunately, each group of experiments described was made with crystals cleaved from different blocks. It is possible that individual differences in crystals of sodium chloride may in part be responsible for the differences in results as reported herein. It is of interest to note in this connection that Dempster¹² has found that in reflecting positive ions from surfaces of calcite great differences have appeared with two different crystals.

Whether or not reflection from two different crystals is necessary for producing patterns as shown in Fig. 8 is not known at present though such patterns have never been observed from single crystal reflection. It may be that reflection from the first crystal removed atoms of such velocities as would have made the pattern obscure had a single reflection alone been

¹² A. J. Dempster, Phys. Rev. 35, 1405 (1930).

recorded. The absence of any appreciable diffuse back-ground of random scattered atoms for either angle is an indication that the reflection was not devoid of some velocity selection. Experience from single crystal reflection invariably has shown that with a specular deposit equivalent in density to those of Fig. 8 there is always present a considerable diffuse back-ground. In fact, early experiments² show but 17 percent of the incident beam contributing to the specular deposit. There is reason to believe, however, that considerable variation from that specific percentage takes place depending on the crystal.

The incompleteness of the patterns of Fig. 8(a) and (b) makes it difficult to attempt to fit the data with cross-grating formulae. It is probable that a clearer pattern may result if the crystal be oriented so that rows of similar ions run parallel and perpendicular to the plane of the incident beam. The present experiment was with alternate positive and negative ions parallel and perpendicular to the plane of incidence.

CONCLUSIONS

No general conclusions can be drawn concerning the above experiments. More data are first necessary. The problem of the reflection of heavy atoms from crystals is far from a satisfactory solution. It appears that what was first thought to be a case of space-grating reflection with velocity selection depending on the wave-length of the atom now spreads into a problem of greater complexity.

The writer wishes to express his appreciation to Professor A. Ellett under whose direction this work was carried out and to the Research Department of the General Electric Company who so kindly furnished the molybdenum guns used in the experiments with zinc.

A DETERMINATION OF e/m FOR AN ELECTRON BY DIRECT MEASUREMENT OF THE VELOCITY OF CATHODE RAYS

BY CHARLOTTE T. PERRY* AND E. L. CHAFFEE

CRUFT LABORATORY, HARVARD UNIVERSITY

(Received July 12, 1930)

ABSTRACT

The velocity of cathode rays, driven by potentials of from 10,000 to 20,000 volts, is measured directly by timing the passage of the electrons between two localized transverse high-frequency electric fields 75 cm apart. Those electrons which pass undeflected travel the distance between the deflecting fields in an even multiple of half a cycle of the oscillating fields. The velocity thus obtained, combined with the expression for the energy imparted to an electron in falling through a measured difference of potential, gives the value of e/m_0 .

The mean value thus obtained is

$$e/m_0 = (1.761 \pm 0.001) \times 10^7 \text{ abs. em units}$$

This value is in agreement with the values obtained by spectroscopic methods and does not agree with the most accurate previous value obtained for free electrons. A possible explanation for the discordant value previously obtained for free electrons is given.

INTRODUCTION

THE ratio of the charge to the mass of an electron has been measured by many investigators using various methods, a description of which is given in several places, among which may be mentioned the paper, "The Probable Values of the General Physical Constants," by R. T. Birge in the first issue of the Physical Review Supplement. It seems unnecessary here to review the previous work but it might be helpful to point out that the various methods of measurement may for convenience be classed in two general groups. The *first* group includes those experiments made with free electrons, as cathode rays, photo-electrons or β -particles. The *second* group of experiments involves spectroscopic measurements and hence deals with electrons within atoms.

Most of the methods of the first group involve the deflection of rapidly moving electrons by transverse magnetic or electrostatic fields or both. The most accurate work of this type is that of F. Wolf¹ using a method first suggested by H. Busch.² Briefly, his experiment consisted in projecting into a longitudinal magnetic field a diverging cone of cathode rays and adjusting the strength of the field to bring the rays to a focus. Wolf's result, corrected by Birge for the difference between the international and absolute volt, is

* Holder of the Margaret E. Maltby Fellowship, awarded by the American Association of University Women, 1928-1929.

¹ F. Wolf, Ann. d. Physik 83, 849 (1927).

² H. Busch, Phys. Zeits. 23, 438 (1922).

$$e/m_0 = (1.7689 \pm 0.002) \times 10^7 \text{ abs. em units}$$

where m_0 is the mass of the electron at rest.

A few of the methods of the first group are somewhat more direct than those to which reference has just been made. These methods involve a direct determination of the velocity of the electrons combined with the equation giving the energy imparted to an electron when accelerated by a longitudinal electric field. The relativity mass of an electron is

$$m = \frac{m_0}{(1 - (v^2/c^2))^{1/2}} \quad (1)$$

where m_0 is the mass at rest, v is the velocity of the electron at which it possesses mass m , and c is the velocity of light. The energy given to an electron in falling through a difference of potential E is

$$\int_0^v v d(mv) = m_0 c^2 \left[\frac{1}{(1 - v^2/c^2)^{1/2}} - 1 \right] = eE. \quad (2)$$

Historically Wiechert³ in 1899 was the first to make a direct measurement of the velocity of cathode rays by timing their passage between two points by means of damped high-frequency electric oscillations.

In 1912 one of the authors⁴ reported at a meeting of the Physical Society some determinations of e/m_0 made by an improved direct method. This work was suspended, however, until better facilities were available.

The present work reported below was resumed about two years ago with further improvements in method and technique made possible by the development of vacuum-tube oscillators and the installation of the 100,000-volt storage battery in the Cruft Laboratory.

Kirchner⁵ last November reported some preliminary measurements using practically the same method as that described in this paper. His results, obtained for accelerating voltages not exceeding 2500, agree approximately with Wolf's value given above.

Some of the experiments of the second group made upon bound electrons involve the measurement of the Zeeman separation in a known magnetic field. The most accurate work of this kind is that of Babcock.⁶ With certain selected lines in the spectra of chromium, zinc, cadmium, and titanium he obtained a weighted mean value

$$e/m_0 = (1.7606 \pm 0.0012) \times 10^7 \text{ abs. em units}$$

Another method of obtaining the value of e/m_0 from spectroscopic measurements depends upon the Bohr-Sommerfeld theory for an atom consisting of a single electron moving around a positive nucleus. This method involves

³ E. Wiechert, Wied. Ann. 69, 739 (1899).

⁴ E. L. Chaffee, Phys. Rev. 34, 474 (1912).

⁵ F. Kirchner, Phys. Zeits. 30, 773 (1929).

⁶ H. D. Babcock, Astrophys. J. 58, 149 (1923); 69, 43 (1929).

the Rydberg constant for hydrogen and ionized helium. Houston⁷ using this method obtained a value which, corrected by Birge, is

$$e/m_0 = (1.7608 \pm 0.0008) \times 10^7 \text{ abs. em units.}$$

In view of the disagreement in the values of e/m_0 obtained by the experiments on free and on bound electrons, a disagreement greater than the probable errors of the experiments, Birge said "it seems to be necessary to assume two different values of e/m , one to be used in all cases involving atomic structure, and the other involving free electrons." The value of e/m_0 obtained in the present work using free electrons, i.e.,

$$e/m_0 = (1.761 \pm 0.001) \times 10^7 \text{ abs. em units,}$$

agrees well with the values obtained from spectroscopic data, and it is hoped will help to resolve the unpleasant suggestion made by Birge of the necessity of retaining two values for e/m_0 .

METHOD AND APPARATUS

The value of e/m_0 was obtained through a direct measurement of the velocity of free electrons, and the use of the energy equation for a moving charge. The method of velocity measurement was briefly as follows.

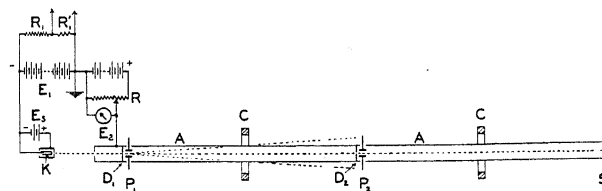


Fig. 1. Diagram of tube.

A highly evacuated cathode-ray tube was placed parallel to the earth's magnetic field, and a stream of electrons projected along its axis by means of a high potential. A diagram of the tube is shown in Fig. 1, in which K is the cathode, and the batteries supplying the driving potential are shown at E_1 and E_2 . The anode, shown at A , was a long hollow metal cylinder, within which the electrons travelled with constant velocity. Placed in their path were two high-frequency electrostatic fields, furnished by small parallel plates activated by a high-frequency oscillator. The pairs of plates, shown at P_1 and P_2 , were a known distance apart, and so connected that the two fields were 180° out of phase. A group of electrons passed P_1 undeflected each half cycle. If the time required for these electrons to travel the distance between P_1 and P_2 was a half cycle (or any multiple of a half cycle) of the oscillator, they were also undeflected by P_2 and so made a single central spot on the fluorescent screen S . But if their velocity was too great, they

⁷ W. V. Houston, Phys. Rev. 30, 608 (1927).

reached P_2 before the field there was zero, and were deflected. Alternate groups were deflected in opposite directions. Hence two spots appeared on the screen S . The same was true if the electron velocity was too small. For a fixed frequency of the oscillator, the potential on the tube was gradually increased until the two spots moved into one. If the voltage was increased still further two spots again appeared. The voltages causing similar patterns on both sides of the single spot were averaged to obtain the voltage corresponding to the correct velocity.

The cathode-ray tube was of Pyrex glass enclosing the metal parts, and was evacuated by a four-stage mercury diffusion pump, with an oil backing pump. The mercury pump was of steel, and was placed about two meters away from the tube to prevent its magnetic field from disturbing the electrons. The pump tube was 2.5 centimeters in diameter to allow rapid exhaustion, and near the cathode-ray tube it passed through a large trap cooled with liquid air.

The cathode of the tube, shown in cross-section in Fig. 2, was an indirectly-heated nickel thimble K , with the heating coil of tungsten wire located inside along the axis. A small spot of oxide on the end of the thimble gave

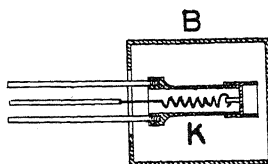


Fig. 2. Cross-section of cathode.

good emission when the nickel was only a dull red. A shallow open cylinder attached to and extending beyond the end of the thimble, caused the emitted electrons to take the form of a solid cone of rays. The negative terminal of the high-potential source was connected directly to the thimble.

A shielding cylinder of nickel, shown at B in Fig. 2, enclosed the cathode. This shield was pierced by a millimeter hole in front of the oxide coating, and was kept at a constant potential of about 20 volts positive with respect to the cathode by the battery E_s in Fig. 1. This small potential started the electrons away from the cathode, and those passing through the millimeter opening formed a narrow beam of rays falling upon the anode.

A water-cooled wax joint allowed the cathode to be removed for repairs without disturbing the shielding cylinder, whose millimeter opening was accurately aligned with two others in the anode.

The anode was a hollow aluminum cylinder 150 centimeters long, which was connected to the positive side of a 2,000-volt storage battery through a potential divider shown at R_2 in Fig. 1. The negative side of this battery was grounded, as was also the positive side of the high-potential battery E_1 connected to the cathode. The battery E_1 was a portion of the 100,000-volt storage battery in the Cruft laboratory, and could only be varied by steps

of 1,600 volts. The use of the second battery permitted continuous variation of the driving potential.

The deflecting plates at P_1 and P_2 , together with their neighboring diaphragms, were similar, and a cross section of the arrangement (labelled for P_1) is shown in Fig. 3. The deflecting plates were of aluminum, approximately 5 millimeters long and 3 millimeters wide, and were separated by

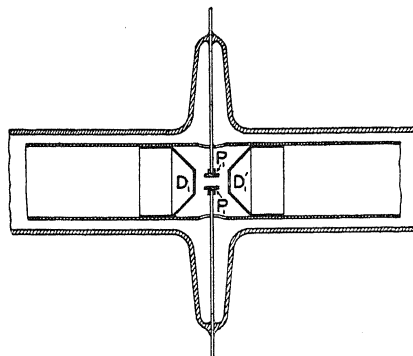


Fig. 3. Arrangement of deflecting plates and diaphragms.

about 3 millimeters. A diaphragm with a central millimeter hole, shown at D_1 in Figs. 1 and 3, was located above the plates P_1 to limit the electron stream to a narrow pencil of rays. A similar diaphragm D_2 was located above the plates P_2 to allow only the electrons that were undeflected by P_1 to pass through P_2 . Diaphragms with 3 millimeter holes were placed below the plates, to prevent reflection of electrons from the inside of the tube and to balance geometrically the diaphragms D_1 and D_2 . One of these is shown at D'_1 in Fig. 3.

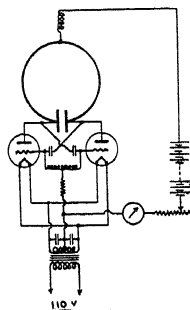


Fig. 4. Arrangement of connections.

A fluorescent screen S was placed at the lower end of the cylindrical anode, and a window was cut in the metal tube for observation of the fluorescent spot. The diaphragm D_2 was also covered with fluorescent material, and a similar window supplied. This was used to observe the amount of deflection caused by the plates P_1 and also for the adjustment of the focusing coils,

the use of which is discussed farther on. Both windows in the tube were covered with fine copper gauze.

The distance between P_1 and P_2 was taken as the distance between the centers of the two pairs of plates, and was found to be 75.133 centimeters. This distance was accurately determined by means of a cathetometer and comparison with a standard meter rod checked by the Bureau of Standards.

The oscillator consisted of two 75-watt vacuum tubes, type 846, connected in push-pull arrangement to reduce second harmonics. The connections are shown in Fig. 4. The plate potential was 2000 volts. Small variations of wave-length were produced by means of a tuning condenser connected across the inductance in the oscillatory circuit. Larger variations were made by changing the inductance. In this manner the wave-length was varied from 3 to 6 meters.

The short-wave oscillator was inductively coupled at the center to a pair of parallel wires. These parallel wires were about 5 centimeters apart, approximately one-half wave-length long, and bent into a V with rounded vertex so that the ends could connect with the pairs of plates P_1 and P_2 . The mid-points of the parallel wires were connected by a two-megohm resistance, the center of which was grounded to drain off any accumulated charge on the plates.

The success of this method of velocity measurement depends upon the accuracy to which the phase difference between the electric fields at P_1 and P_2 is 180° . Although theoretically the phase difference should be 180° if the node of the stationary wave system on the wires remains fixed, the system was constructed to be geometrically as symmetrical as possible to aid in securing this result. The position of the grounding resistance on the parallel wires could be varied considerably without any detectable effect upon the experimental results, showing that this resistance had no appreciable influence upon the phase difference at P_1 and P_2 . In the course of the experiment different degrees of coupling to the oscillator were used, the oscillator was tuned above and below resonance with the wire system, the time of flight of the electrons between P_1 and P_2 was in some cases a whole cycle and in others a half cycle of the oscillations and yet all results were in close agreement. This consistency seems to allay all doubt as to the correctness of the assumption of the 180° phase relation.

For any one reading, the frequency was kept constant as indicated by beats with a harmonic of an oscillating crystal. Since the harmonics used ranged from the 28th to the 49th, it was impractical to make direct use of the beats between the crystal and the short-wave oscillator. Hence an intermediate oscillator of wave-length about 28 meters was used to produce beats with both. During each reading the frequency was checked several times by listening to the two sets of beats. The harmonics used were the 4th to the 7th of the crystal, and the 4th to the 8th of the intermediate oscillator and were identified by means of a calibrated wavemeter loosely coupled to the intermediate-frequency oscillator.

The frequency of the crystal was measured with the aid of Professor G. W. Pierce, in terms of a 1000-cycle clock, driven by a magnetostriction rod. The frequency of the crystal was found to be

$$n = 1,680,890 \text{ cycles per second,}$$

correct to 1 part in 40,000.

Allowing liberally for slight variations from zero beats in the case of both oscillators, (200 cycles for the intermediate, and 1000 cycles for the power oscillator), the error in frequency was less than 1 part in 20,000.

The voltage between ground and cathode (E_1 in Fig. 1) was measured by means of two resistances R_1 and R'_1 and a potentiometer. R'_1 was an accurately-known resistance of 89.958 ohms, and the potential drop across it was measured with the potentiometer and a standard cell. For potentials less than 12,000 volts, R_1 was a manganin wire resistance of 895,130 ohms, while for higher potentials a similar resistance of 6,936,600 ohms was used.

The high resistances were measured on a Wheatstone bridge, carefully insulated for leakage. The other members of the bridge were composed of two resistances of 500,000 ohms, and two of 100,000 ohms, which were carefully measured by building up from a 10,000-ohm Leeds-Northrup sealed standard. A substitution method was used throughout this work. The Wheatstone bridge was balanced by the addition in one arm of a decade box with a maximum resistance of 99,999 ohms. Each coil of this box was measured in terms of a sealed standard of the same size, and here again the substitution method was employed. The resistance of 6,936,600 ohms was measured in sections of about 1,000,000 ohms each for greater accuracy.

The 10,000-ohm Leeds-Northrup standard was checked against two others of the same type, and all three agreed to better than 1 part in 10,000. The one with the most recent certificate from the Bureau of Standards was taken as correct.

The resistance of 895,130 ohms was tested for changes in its value due to the current carried, and corrections of 3 to 5 parts in 10,000 were made according to the load. The resistance of 6,936,600 ohms carried so little current that no correction was required.

The 89.958-ohm resistance was measured in terms of a 100-ohm sealed standard, which had recently been checked.

The potentiometer was a new one, and was checked for equality of intervals. The standard cell was checked against three others, one of them a new one, and all four agreed to better than 1 part in 10,000. The new cell was taken as correct.

The variable voltage applied to the anode was measured by a General Electric voltmeter, which had been calibrated by a potentiometer for division errors. Allowance was made for a slight irregularity at the beginning and end of the scale.

The adjustment of the voltage until the two electron spots just came together, and again, until they just separated, was the most uncertain part of the experiment. A single spot appeared throughout a voltage change of 400

or 600 volts, and separate settings on either side of this range could not be made with more accuracy than one division on the voltmeter, corresponding to 20 volts. Hence many pairs of settings were made for one determination, and the midpoints of these pairs averaged. All settings were made in the dark, and so should be truly independent, and for reasons of symmetry, the voltage was always changed in such a manner that the two spots were brought together for each setting.

The use of concentrating coils to focus the electron stream, which was mentioned above, was necessary and yet undesirable. They were coils of about 2,000 turns, 15 centimeters in diameter, encircling the tube, and giving magnetic fields symmetric with the axis of the tube. One was placed midway between the deflecting plates at P_1 and P_2 , and the other an equal distance below P_2 . These are shown at C in Fig. 1. Without the coils, the electron stream spread out, giving a spot about a centimeter in diameter on the screen just above P_2 . This was too large and also too faint for accurate work. Furthermore, the axis of the tube was not placed exactly parallel to the earth's field, and hence the electron spot was not central. The first concentrating coil focused the electrons in a small, intense spot, and brought them over to a central position. The second coil merely made the final adjustment more accurate by increasing the intensity and decreasing the size of the two spots on the final screen.

The use of the first coil was, however, undesirable, for it imparted a spiral motion to the electrons, thus increasing slightly the distance they travelled in the observed time. Also, if the strength of the magnetic field was such that the electron stream was accurately focused, the transverse electric field at P_1 had no effect on the position of the spot. In order to get a deflection, the coil had to be used off focus, and the amount of deflection depended on how much the focus was displaced. As the voltage range between each pair of settings depended upon the amount of deflection obtained, varying the current through the coils greatly varied the individual settings. However, readings were made under many different conditions of focusing, and the midpoints of the voltage pairs were in close agreement as shown by the following tables.

As to the increase in path due to the spiral motion of the electrons, the following estimate was made. By gradually increasing the current in the coil, the amount of rotation of the spot was found to be less than 180° . The distance from the center of the screen to that of the undeflected spot was about 1 centimeter, which would make the electron stream about 0.5 centimeter from the axis of the tube in the plane of the concentrating coil. With the magnetic field acting, however, the electron path would be concave toward the axis and so this distance would be decreased. From symmetry the maximum departure occurs in the plane of the coil. Assuming the path to be a helix on a cylinder of diameter 0.5 centimeter, the increase in path was found to be 1 part in 4500. This makes a decrease in e/m_0 of 1 part in 2,250, or 0.0008.

As the voltage on the tube was increased to 20,000, the undeflected spot became more central, and so this error should have been reduced. Therefore, a definite upward trend in e/m_0 with increasing voltages would have indicated an appreciable error due to this cause; however, no such trend was observed. Hence it seems reasonable to state that the error in e/m_0 from the use of the coils was not more than 0.0008.

RESULTS

Voltage measurements were made for six frequencies of the oscillator, and in order to average out unknown errors as much as possible, the settings for each frequency were made in groups over a period of several days. A sample group of such measurements is shown in Table I, where the actual voltmeter settings are given, with the midpoint of each pair, and the corresponding

TABLE I. *Sample group of settings.* 48th harmonic of the crystal beating with the fundamental of the oscillator. Frequency = 80,683,000 cycles/sec. Times of passage between plates = 1 cycle. Velocity = 0.60619×10^{10} cm/sec.

Voltmeter settings (factor = 20)	Midpoint	$E_1 + E_2$ Total voltage for midpoint	δ from the average voltage
63-79	71	10776	10
61-80	70.5	10766	0
62-79	70.5	10766	0
62-80	71	10776	10
63-77	70	10756	10
64-76	70	10756	10
65-76	70.5	10766	0
61-79	70	10756	10
62-79	70.5	10766	0
61-80	70.5	10766	0
62-79	70.5	10766	0
63-79	71	10776	10
		Av. 10766	Av. 5

voltage. The pairs of settings were influenced by the intensity of the spots, the power of the oscillator, and how close together the spots were brought, and so varied considerably. However, their midpoints were in good agreement, each group being very consistent within itself, and all the groups for any one frequency agreeing well with each other.

Tables II to VII give all the settings made at each frequency, arranged in groups as they were taken. For each group, the settings giving the same midpoint are combined, and the corresponding voltage listed. The average voltage for this frequency is also given, and the deviation of each setting from this average. The value of e/m_0 corresponding to the average voltage is computed from the energy equation

$$\frac{e}{m_0} = \frac{c^2}{E} \left[\frac{1}{(1 - v^2/c^2)^{1/2}} - 1 \right]$$

The average deviation and probable error of e/m_0 are calculated from the

voltage deviations. In these tables, all voltages have been changed to absolute volts by use of the conversion factor 1.00046 given by Birge.⁸

TABLE II. *Summary of observations with frequency of 80,683,000 cycles/sec. 48th harmonic of the crystal beating with the fundamental of the oscillator. Times of passage between plates = 1 cycle. Velocity = 0.60619×10^{10} cm/sec.*

No. of settings	Voltage $E_1 + E_2$	δ from the av. voltage
11	10759	4
6	10769	6
1	10749	14
1	10739	24
1	10729	34
10	10757	6
7	10767	4
1	10777	14
10	10760	3
4	10770	7
2	10790	27
8	10769	6
2	10759	4
Table I {	6	3
	3	13
	3	7
6	10764	1
6	10754	9
Total No. 88	Av. 10763	Av. 6.2
<hr/>		
Av. $e/m_0 = 1.7613 \times 10^7$ abs. em units.	Av. deviation = 0.0010	
Max. $e/m_0 = 1.7668 \times 10^7$	Prob. error = 0.0001	
Min. $e/m_0 = 1.7568 \times 10^7$		

TABLE III. *Summary of observations with frequency 82,364,000 cycles/sec. 49th harmonic of the crystal beating with the fundamental of the oscillator. Time of passage between plates = 1 cycle. Velocity = 0.61882×10^{10} cm/sec.*

No. of settings	Voltage $E_1 + E_2$	δ from the av. voltage
7	11235	3
4	11245	13
1	11215	17
1	11255	23
5	11236	4
4	11226	6
2	11246	14
7	11220	12
6	11230	2
Total No. 37	Av. 11232	Av. 7.9
<hr/>		
Av. $e/m_0 = 1.7612 \times 10^7$ abs. em units	Av. deviation = 0.0012	
Max. $e/m_0 = 1.7639 \times 10^7$	Prob. error = 0.0002	
Min. $e/m_0 = 1.7576 \times 10^7$		

⁸ R. T. Birge, Phys. Rev. Supp. 1, 1 (1929).

The error introduced by assuming that the midpoint of the two voltage settings agrees with the midpoint of the two corresponding velocities, is

TABLE IV. *Summary of observations with frequency 47,065,000 cycles/sec. 28th harmonic of the crystal beating with the fundamental of the oscillator. Time of passage between plates = $\frac{1}{2}$ cycle. Velocity = 0.70723×10^{10} cm/sec.*

No. of settings	Voltage $E_1 + E_2$	δ from the av. voltage
5	14853	28
1	14843	18
3	14824	1
2	14814	11
2	14804	21
1	14834	9
4	14817	8
3	14827	2
3	14837	12
8	14818	7
2	14828	3
2	14808	17
1	14798	27
Total No. 37	Av. 14825	Av. 11.6
Av. $e/m_0 = 1.7608 \times 10^7$ abs. em units		Av. deviation = 0.0014
Max. $e/m_0 = 1.7640 \times 10^7$		Prob. error = 0.0002
Min. $e/m_0 = 1.7575 \times 10^7$		

that of substituting a linear for a square root relation. For voltage settings differing by 400 volts, this error for a total potential of 10,000 volts amounts to 1 part in 10,000. For higher voltages it is less than this, becoming 1 part

TABLE V. *Summary of observations with frequency 50,427,000 cycles/sec. 30th harmonic of the crystal beating with the fundamental of the oscillator. Time of passage between plates = $\frac{1}{2}$ cycle. Velocity = 0.75774×10^{10} cm/sec.*

No. of settings	Voltage $E_1 + E_2$	δ from the av. voltage
6	17117	19
2	17127	9
1	17137	1
4	17157	21
4	17147	11
2	17167	31
6	17127	9
6	17137	1
Total No. 31	Av. 17136	Av. 12.4
Av. $e/m_0 = 1.7601 \times 10^7$ abs. em units		Av. deviation = 0.0013
Max. $e/m_0 = 1.7622 \times 10^7$		Prob. error = 0.0002
Min. $e/m_0 = 1.7569 \times 10^7$		

in 40,000 at 20,000 volts. This enters directly in e/m_0 , and is such as to increase the tabulated values, but is negligible in comparison with other errors.

TABLE VI. *Summary of observations with frequency of 52,948,000 cycles/sec. 63d harmonic of the crystal beating with the second harmonic of the oscillator. Time of passage between plates = $\frac{1}{2}$ cycle. Velocity = 0.79563×10^{10} cm/sec.*

No. of settings	Voltage $E_1 + E_2$	δ from the av. voltage
8	18993	0
5	19003	10
2	18983	10
9	18986	7
2	18996	3
1	18976	17
5	18996	3
3	19006	13
1	18986	7
Total No. 36	Av. 18993	Av. 6.0
Av. $e/m_0 = 1.7600 \times 10^7$ abs. em units		Av. deviation = 0.0006
Max. $e/m_0 = 1.7616 \times 10^7$		Prob. error = 0.0001
Min. $e/m_0 = 1.7588 \times 10^7$		

TABLE VII. *Summary of observations with frequency of 53,789,000 cycles/sec. 32d harmonic of the crystal beating with the fundamental of the oscillator. Time of passage between plates = $\frac{1}{2}$ cycle. Velocity = 0.80826×10^{10} cm/sec.*

No. of settings	Voltage $E_1 + E_2$	δ from the av. voltage
7	19622	4
5	19612	14
8	19625	1
5	19635	9
1	19615	11
6	19637	11
4	19627	1
2	19617	9
Total No. 38	Av. 19626	Av. 6.6
Av. $e/m_0 = 1.7610 \times 10^7$ abs. em units		Av. deviation = 0.0006
Max. $e/m_0 = 1.7622 \times 10^7$		Prob. error = 0.0001
Min. $e/m_0 = 1.7599 \times 10^7$		

TABLE VIII. *Summary of results.*

	Velocity ($\times 10^{10}$) cm/sec.	No. of settings (weighting factors)	Av. e/m_0 ($\times 10^{-7}$) abs. em units	δ from 1.7609	Av. δ of settings from 1.7609
Table II	0.60619	88	1.7613	0.0004	0.0011
Table III	0.61882	37	1.7612	0.0003	0.0012
Table IV	0.70723	37	1.7608	0.0001	0.0014
Table V	0.75774	31	1.7601	0.0008	0.0013
Table VI	0.79563	36	1.7600	0.0009	0.0010
Table VII	0.80826	38	1.7610	0.0001	0.0006

Weighted average $e/m_0 = 1.7609 \times 10^7$ abs. em units

Weighted average deviation of the six values of e/m_0 from 1.7609×10^7 0.0004

Probable error (obtained by weighting the deviations from 1.7609×10^7) 0.0002

Table VIII summarizes these results, giving the six average values of e/m_0 for the six frequencies used. The values of e/m_0 for each frequency are more consistent with each other than with those obtained for other frequencies, and for this reason the six average values of e/m_0 are treated as six single determinations, weighted proportionally to the number of settings from which they are derived. The weighted average e/m_0 so obtained is

$$e/m_0 = (1.7609 \pm 0.0002) \times 10^7 \text{ abs. em units,}$$

with an average deviation of 0.0004, and a probable error of 0.0002, both similarly computed.

In view of the foregoing errors the final value of e/m_0 from the present work is conservatively written

$$e/m_0 = (1.761 \pm 0.001) \times 10^7 \text{ abs. em units.}$$

This method is, however, capable of much more accuracy, and the work is being continued with some improvements in technique.

CONCLUSION

Because of the difference between the present value

$$e/m_0 = (1.761 \pm 0.001) \times 10^7$$

and that obtained by Wolf,

$$e/m_0 = (1.769 \pm 0.002) \times 10^7$$

it may be noted that in one particular the two experiments differed quite markedly, that is, in their sensitiveness to the presence of residual gas. The effect of gas in the path of electrons is to retard them by an amount dependent upon their speed. J. J. Thomson⁹ deduced the relation

$$v_0^4 - v_x^4 = ax$$

for the slowing down of electrons in metals. Here v_0 is the initial velocity, v_x the velocity after travelling a distance x in the substance, and a is a constant dependent upon the metal.

Widdington¹⁰ tested this formula for metals, and also for air, obtaining for the constant in the latter case

$$a = 2 \times 10^{40}$$

when $p=760$ millimeters. Assuming that a is directly proportional to the pressure of the gas, the equation becomes

$$v_0^4 - v_x^4 = \frac{2(10^{40})px}{760}$$

⁹ J. J. Thomson, *Conduction of Electricity through Gases*, 2nd. edition, p. 378.

¹⁰ R. Whiddington, *Proc. Roy. Soc. A86*, 360 (1912).

where p is the air pressure in millimeters of mercury. If the change in velocity is small,

$$v_0^4 - v_x^4 = 4v^3 dv$$

or

$$\frac{dv}{v} = \frac{2(10^{40})px}{4(760)v^4}.$$

Thus the percentage change in v is much less at higher speeds.

To compute a few cases actually involved, take first the present experiment. Here the distance x was 75 centimeters, and the voltage varied from 10,000 volts to 20,000 volts.

$$E = 10,000 \text{ volts} \quad v = 0.60 \times 10^{10} \text{ cm/sec} \quad \frac{dv}{v} = 0.39p.$$

$$E = 20,000 \text{ volts} \quad v = 0.80 \times 10^{10} \text{ cm/sec} \quad \frac{dv}{v} = 0.12p.$$

In Wolf's experiment, $x=30$ centimeters, and the voltage varied from 3,500 volts to 4,500 volts.

$$E = 3,500 \text{ volts} \quad v = 0.35 \times 10^{10} \text{ cm/sec} \quad \frac{dv}{v} = 1.31p$$

$$E = 4,500 \text{ volts} \quad v = 0.37 \times 10^{10} \text{ cm/sec} \quad \frac{dv}{v} = 1.05p$$

Thus the percentage change in electron velocity introduced by the same gas pressure is much less for the present work than for Wolf's experiment.

To consider the effect of such a change in velocity upon the calculated values of e/m_0 take first the present work. The energy equation gives

$$\frac{e}{m_0} = (\text{const}) \frac{v^2}{E}$$

approximately, and hence, if the measured velocity is too small for the applied potential, the calculated value of e/m_0 is too small. However, the change in velocity increases threefold as the voltage is reduced from 20,000 to 10,000 volts. Hence, if this error were appreciable, the calculated values of e/m_0 should show a definite trend with voltage. The absence of such a trend seems to show that this error was negligible in the present work.

In Wolf's experiment,

$$\frac{e}{m_0} = (\text{const}) \frac{E}{H^2}$$

approximately, and the energy equation is assumed as the relation between the velocity and potential. If the velocity is decreased due to the presence

of gas, the potential measured is larger than that actually corresponding to the average velocity, and so the calculated value of e/m_0 is too large. Moreover, no trend in his results can be expected, as the error does not change appreciably over the voltage range used. Wolf made no estimate of the gas pressure in his apparatus. If Whiddington's formula is assumed, a pressure of 0.004 mm would be sufficient to explain the discrepancy between his value of e/m_0 and the present one.

It is fully realized that in applying Whiddington's formula to the present case, a very great extrapolation is made. The value of a was obtained by measuring the distance required to halt an electron whose path was through air at atmospheric pressure. Yet here it is used to calculate a small percentage loss in the velocity of electrons passing through gases at extremely low pressures. Therefore, no great confidence can be placed in the resulting numerical values. In fact for electron velocities approximating those used in the present experiment Bohr¹¹ obtained from theoretical considerations a value of the constant a equal to about one-half that given by Whiddington.

¹¹ N. Bohr, *Phil. Mag.* **25**, 10 (1913).

NEW EXPERIMENTAL DETERMINATION OF EFFECTIVE
CROSS-SECTIONS FOR THE QUENCHING OF
MERCURY RESONANCE RADIATION

BY M. W. ZEMANSKY*

PALMER PHYSICAL LABORATORY, PRINCETON, N. J.

(Received July 14, 1930)

ABSTRACT

Theory of the quenching of resonance radiation. The problem of the quenching of resonance radiation by foreign gases is treated on the basis of Milne's theory of diffusion of radiation extended to take account of (1) a collimated incident beam, (2) a finite emission line, (3) a finite absorption line, (4) impacts of the second kind, and a curve is obtained from which one can find the number of impacts of the second kind corresponding to any experimentally observed value of the quenching. The effect of metastable atoms is discussed and a theory of their behavior outlined.

Measurement of the quenching of mercury resonance radiation. The scattered radiation emerging from an absorption cell containing mercury vapor in the presence of a foreign gas was measured as a function of the gas pressure with apparatus designed to agree closely with the requirements of the theory. From the theoretical curve the number of impacts of the second kind was obtained, and from this the effective cross-section for quenching was calculated for the following gases: O_2 , H_2 , CO , NH_3 , CO_2 , H_2O , N_2 , CH_4 , C_2H_6 , C_3H_8 , C_4H_{10} , He and A . The values of the effective cross-section for quenching are tabulated along with those for depolarization of resonance radiation and for collision broadening. The quenching cross-sections of CO , NH_3 , CO_2 , H_2O , N_2 , CH_4 , C_2H_6 and C_4H_{10} are shown to be connected with the difference between the energy of the transition $2^3P_1 \rightarrow 2^3P_0$ of Hg and the vibrational energy of the molecules, in qualitative agreement with the theory of Kallmann and London.

INTRODUCTION

THE quenching of mercury resonance radiation has been used by many investigators as a method of studying impacts of the second kind, and has provided rough estimates of the effective cross-sections for such impacts.¹ The most extensive investigation was carried out by Stuart² in 1925 who obtained quenching curves for mercury resonance radiation in the presence of H_2 , O_2 , CO , CO_2 , H_2O , Ne , A , and He , the order representing the relative quenching ability. In Stuart's paper, and in many later papers by others,³ attempts were made to calculate from these quenching curves the effective cross-sections associated with each gas. It is unnecessary at this point to go carefully into all the faults of these calculations, because they will become apparent in what is to follow. It is sufficient merely to mention that the

* National Research Fellows.

¹ P. Pringsheim, "Fluoreszenz und Phosphoreszenz" Vol. VI Struktur der Materie.

² H. A. Stuart, Zeits. f. Physik. **32**, 262 (1925).

³ M. W. Zemansky, Phys. Rev. **31**, 812 (1928); P. D. Foote, Phys. Rev. **30**, 288 (1927); E. Gaviola, Phys. Rev. **33**, 309 (1929); E. Gaviola, Phys. Rev. **34**, 1049 (1929).

results varied widely among themselves, to such an extent that it was apparent that what was needed was not more theories to explain Stuart's curves, but new experiments performed in such a manner that they would lend themselves to accurate calculation on the basis of the existing theory of the process, namely, Milne's theory of the diffusion of radiation.

It is the purpose of this paper to treat the problem on the basis of this theory taking into account (1) the geometrical character of the incident radiation, (2) the finite spectral width of the incident radiation, (3) the geometry of the slab of mercury vapor, (4) the finite width of the absorption line, (5) the accurate value of the absorption coefficient of mercury vapor for the 2537 line. In part II new experimental data are given on the quenching of mercury resonance radiation, obtained with apparatus designed to comply with the requirements of the theory, and finally, effective cross-sections are obtained for the following gases: H_2 , O_2 , CO , NH_3 , CO_2 , H_2O , N_2 , A , He , CH_4 , C_2H_6 , C_3H_8 , and C_4H_{10} .

THEORY OF THE QUENCHING PROCESS

Consider a mass of gas, enclosed between the planes $x=0$ and $x=l$, exposed to isotropic radiation at the face $x=0$ whose frequency lies between ν and $\nu+d\nu$ and which is capable of raising the atoms from the normal state 1 to the excited state 2. Suppose at any moment that there are n_1 normal atoms per cc capable of absorbing this radiation and n_2 excited atoms per cc capable of emitting this radiation. Then it was shown by Milne,⁴ on the basis of Einstein's radiation theory, and *without appeal to the analogy with molecular diffusion*, that n_2 at any point is given by:

$$\frac{\partial^2}{\partial x^2} \left(n_2 + \tau \frac{\partial n_2}{\partial t} \right) = 4\kappa^2 \tau \frac{\partial n_2}{\partial t} \quad (1)$$

where τ is the life-time of the excited atom in sec, and κ is the absorption coefficient of the gas in cm^{-1} for the radiation between ν and $\nu+d\nu$. This equation holds for all values of n_2 and n_1 provided $n_2 \ll n_1$, which is undoubtedly the case for light intensities employed in the laboratory. It is *not* restricted in the way that the molecular diffusion equation of kinetic theory is, namely, to short mean free paths. Furthermore, Milne showed that the forward flux of radiation at any point is given by

$$\pi I_+ = \frac{\pi\sigma}{n_1} \left[\left(n_2 + \tau \frac{\partial n_2}{\partial t} \right) - \frac{1}{2\kappa} \frac{\partial}{\partial x} \left(n_2 + \tau \frac{\partial n_2}{\partial t} \right) \right] \quad (2)$$

and the backward flux, by

$$\pi I_- = \frac{\pi\sigma}{n_1} \left[\left(n_2 + \tau \frac{\partial n_2}{\partial t} \right) + \frac{1}{2\kappa} \frac{\partial}{\partial x} \left(n_2 + \tau \frac{\partial n_2}{\partial t} \right) \right] \quad (3)$$

⁴ E. A. Milne, Journ. Lon. Math. Soc. 1, Part I (1926).

where

$$\sigma = \frac{q_1}{q_2} \cdot \frac{2h\nu^3}{c^2}$$

and q_1 and q_2 are the statistical weights of the normal and the excited states respectively. It must be remembered that n_1 , n_2 , κ , I_+ and I_- are all functions of the frequency.

The $\partial n_2/\partial t$ that appears in these expressions represents the resultant rate of formation of excited atoms under the influence of the absorption of radiation, spontaneous emission, and stimulated emission. In order to take into account impacts of the second kind, and also a superimposed collimated beam of light of the same frequency at the face $x=0$, we have to consider two further rates: (1) rate of decay of excited atoms due to impacts of the second kind equal to kn_2 , and (2) rate of formation of excited atoms due to absorption of the collimated beam incident on the face $x=0$, equal to $B_{1 \rightarrow 2}n_1(K'/4\pi)e^{-kx}$ where $B_{1 \rightarrow 2}$ is the Einstein coefficient defined in terms of light intensity and K' is the intensity of the collimated beam before it enters the slab of gas. In virtue of Einstein's relation

$$B_{1 \rightarrow 2} = \frac{q_2}{q_1} \cdot \frac{c^2}{2h\nu^3} \cdot \frac{1}{\tau} = \frac{1}{\sigma\tau}$$

rate (2) can be put in the form $(n_1K'/4\pi\sigma\tau) \cdot e^{-kx}$.

We have now to replace $\partial n_2/\partial t$ in Eqs. (1), (2), and (3) by

$$\frac{\partial M_2}{\partial t} + kn_2 - \frac{n_1K'}{4\pi\sigma\tau}e^{-kx}$$

and to put the new $\partial n_2/\partial t$ equal to zero, in order to represent the stationary state. Eq. (1) then becomes

$$\frac{\partial^2 n_2}{\partial x^2} = 4\kappa^2 \frac{\tau k}{1 + \tau k} n_2 - 3 \frac{\kappa^2 n_1 K' e^{-kx}}{4\pi\sigma(1 + \tau k)} \quad (4)$$

and Eqs. (2) and (3) become

$$\pi I_+ = \frac{\pi\sigma}{n_1}(1 + \tau k) \left(n_2 - \frac{1}{2\kappa} \frac{\partial n_2}{\partial x} \right) - \frac{3}{2} \frac{K'}{4} e^{-kx} \quad (5)$$

$$\pi I_- = \frac{\pi\sigma}{n_1}(1 + \tau k) \left(n_2 + \frac{1}{2\kappa} \frac{\partial n_2}{\partial x} \right) - \frac{1}{2} \frac{K'}{4} e^{-kx}. \quad (6)$$

If, now, we do away entirely with the isotropic radiation and keep only the collimated beam, we have the boundary conditions that

when $x=0$, $I_+ = 0$

and when $x=l$, $I_- = 0$.

Putting $\gamma = 2\kappa(\tau k/1 + \tau k)^{1/2}$, the solution of Eq. (4) is

$$n_2 = A \cosh \gamma x + B \sinh \gamma x - 3 \frac{n_1 K' e^{-kx}}{4\pi\sigma(1 - 3\tau k)}. \quad (7)$$

Introducing the auxiliary parameter $\beta = \sinh^{-1} \sqrt{\tau k}$ and noticing that $\sqrt{1+\tau k} = \cosh \beta$, $\sqrt{\tau k} = \sinh \beta$, Eqs. (5) and (6) become

$$\pi I_+ = \frac{\pi \sigma}{n_1} \cosh \beta [A \cosh (\gamma x - \beta) + B \sinh (\gamma x - \beta)] - \frac{3K'e^{-\kappa x}}{2(1-3\tau k)} \quad (8)$$

$$\pi I_- = \frac{\pi \sigma}{n_1} \cosh \beta [A \cosh (\gamma x + \beta) + B \sinh (\gamma x + \beta)] - \frac{K'e^{-\kappa x}}{2(1-3\tau k)}. \quad (9)$$

The boundary conditions require

$$A \cosh \beta - B \sinh \beta = \frac{3n_1K' \operatorname{sech} \beta}{2\pi\sigma(1-3\tau k)}$$

$$A \cosh (\gamma l + \beta) + B \sinh (\gamma l + \beta) = \frac{n_1K' \operatorname{sech} \beta}{2\pi\sigma(1-3\tau k)} e^{-\kappa l}$$

whence

$$A = \frac{3 \sinh (\gamma l + \beta) + e^{-\kappa l} \sinh \beta}{\sinh (\gamma l + 2\beta)} \cdot \frac{n_1K' \sinh \beta}{2\pi\sigma(1-3\tau k)}$$

$$B = \frac{-3 \cosh (\gamma l + \beta) + e^{-\kappa l} \cosh \beta}{\sinh (\gamma l + 2\beta)} \cdot \frac{n_1K' \operatorname{sech} \beta}{2\pi\sigma(1-3\tau k)}$$

and we have, from Eq. (8),

$$\pi I_+ = \frac{K'}{2(1-3\tau k)} \left\{ \frac{3 \sinh [\gamma(l-x) + 2\beta] + e^{-\kappa l} \sinh \gamma x}{\sinh (\gamma l + 2\beta)} - 3e^{-\kappa x} \right\}$$

The scattered radiation emerging from unit area of the face $x=l$, will then be equal to:

$$\pi I_{x=l}^+ = \frac{K'}{2(1-3\tau k)} \left\{ \frac{3 \sinh 2\beta + e^{-\kappa l} \sinh \gamma l}{\sinh (\gamma l + 2\beta)} - 3e^{-\kappa l} \right\}$$

and finally, putting in the value of β

$$\pi I_{x=l}^+ = \frac{K'}{2(1-3\tau k)} \left\{ \frac{6(\tau k(1+\tau k))^{1/2} + e^{-\kappa l} \sinh 2\kappa l \left(\frac{\tau k}{1+\tau k} \right)^{1/2}}{\sinh \left(2\kappa l \left(\frac{\tau k}{1+\tau k} \right)^{1/2} + 2 \sinh^{-1} (\tau k)^{1/2} \right)} - 3e^{-\kappa l} \right\} \quad (10)$$

$$= K'F(\kappa l, \tau k). \quad (11)$$

Two special cases are of interest, namely $\tau k=0$ and $\tau k=1/3$. When $\tau k=0$

$$F = \frac{1}{2} \left[\frac{3 - (3 + \kappa l)e^{-\kappa l}}{1 + \kappa l} \right]$$

and when $\tau k = 1/3$, going back to Eqs. (4), (5), and (6), we get

$$F = \frac{3}{4} \left[\frac{6\kappa l - 1 + e^{-2\kappa l}}{9e^{\kappa l} - e^{-\kappa l}} \right]$$

The function F was evaluated for a number of values of κl and of τk , and the results are given in Table I and in Fig. 1.

TABLE I. Values of

$$F(\kappa l, \tau k) = \frac{1}{2(1 - 3\tau k)} \left[\frac{6(\tau k(1 + \tau k))^{1/2} + e^{-\kappa l} \sinh 2\kappa l \left(\frac{\tau k}{1 + \tau k} \right)^{1/2}}{\sinh \left(2\kappa l \left(\frac{\tau k}{1 + \tau k} \right)^{1/2} + 2 \sinh^{-1} (\tau k)^{1/2} \right)} - 3e^{-\kappa l} \right]$$

$\kappa l \backslash \tau k$	0	0.05	0.10	0.20	0.333	0.50
0.5	.194	.175	.164	.143	.125	.107
1.0	.290	.260	.236	.198	.160	.128
1.5	.332	.282	.244	.195	.150	.118
2.0	.344	.273	.227	.168	.124	.092
2.5	.334				.0968	
3.0	.320	.219	.163	.106	.0704	.0488
3.5	.300				.0504	
4.0	.280	.158	.104	.0590	.0351	.0224
4.5	.260				.0241	
5.0	.243	.108	.0628	.0308	.0163	.00968

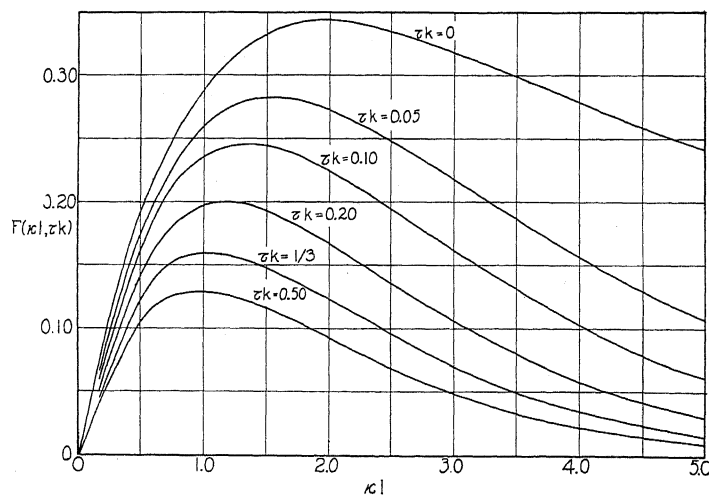


Fig. 1. The function F evaluated for a number of values of κl and of τk .

It will be remembered that this calculation was carried out for only an infinitesimal frequency band lying between ν and $\nu + d\nu$. Let us therefore write Eq. (11) as follows:

$$\pi I_+(\nu, l, \tau k) = K(\nu, 0) F(\kappa(\nu)l, \tau k).$$

We now assume that the emission line can be represented by a Gauss error curve of half-breadth $\Delta\nu_E$, and that the values of τk correspond to foreign gas pressures that are so small that no Lorentz collision broadening results. Then the absorption line can also be represented by a Gauss error curve whose half-breadth is the Doppler breadth, $\Delta\nu_D$. We have then

$$K(\nu, 0) = K(\nu_0, 0)e^{-[2(\nu-\nu_0)/\Delta\nu_E \cdot (\log_e 2)^{1/2}]^2}$$

$$\kappa(\nu) = \kappa(\nu_0)e^{-[2(\nu-\nu_0)/\Delta\nu_D \cdot (\log_e 2)^{1/2}]^2}$$

or, calling

$$\frac{2(\nu - \nu_0)}{\Delta\nu_D}(\log_e 2)^{1/2} = q$$

$$K(\nu, 0) = K(\nu_0, 0)e^{-(q\Delta\nu_D/\Delta\nu_E)^2}$$

$$\kappa(\nu) = \kappa(\nu_0)e^{-q^2}$$

The total scattered radiation emerging from unit area of the face $x=l$ is

$$S = \int_0^\infty \pi I_+(\nu, l, \tau k) d\nu$$

$$= \int_0^\infty K(\nu_0, 0)e^{-(q\Delta\nu_E/\Delta\nu_D)^2} F[\kappa(\nu_0)le^{-q^2}, \tau k] d\nu$$

where the integration is to be extended over all the fine structure components of both the emission and the absorption lines.

The total incident radiation per unit area is

$$K_0 = \int_0^\infty K(\nu_0, 0)e^{-(q\Delta\nu_D/\Delta\nu_E)^2} d\nu$$

and the "quenching" is

$$J = \frac{S/K_0 \text{ for } \tau k = \tau k}{S/K_0 \text{ for } \tau k = 0}$$

$$= \frac{\int_{-\infty}^\infty e^{-(q\Delta\nu_E/\Delta\nu_D)^2} F[\kappa(\nu_0)le^{-q^2}, \tau k] dq}{\int_{-\infty}^\infty e^{-(q\Delta\nu_E/\Delta\nu_D)^2} F[\kappa(\nu_0)le^{-q^2}, 0] dq} \quad (12)$$

J can be obtained by graphical integration with the aid of Fig. 1 as soon as $\kappa(\nu_0)l$ and $\Delta\nu_E/\Delta\nu_D$ are known. A complete discussion of these quantities for mercury vapor will be found in a recent paper by the author.⁵ In these experiments $\kappa(\nu_0)l$ was 4.44 and $\Delta\nu_E/\Delta\nu_D$ was 1.21. The results of the graphical integration are given in table II and Fig. 2. From Fig. 2 we can obtain τk for any experimentally determined value of J . It is seen that, when $J=0.50$, $\tau k=0.114$, a result very different from what would be obtained if

⁵ M. W. Zemansky, Phys. Rev. 36, 219 (1930).

the theorem of Stern and Volmer⁶ were used. According to this theorem, which was used by Stuart in interpreting his quenching curves, when $J=0.50$, $\tau k=1$.

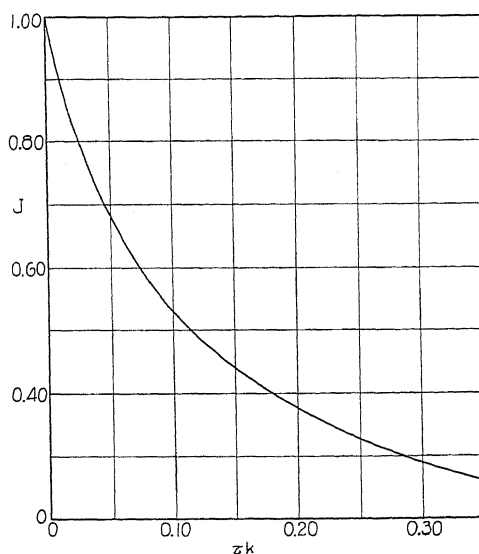


Fig. 2.

TABLE II.

$$J = \frac{\int_{-\infty}^{\infty} e^{-(q/\Delta\nu_E/\Delta\nu_D)^2} F(\kappa(\nu_0) l e^{-q^2}, \tau k) dq}{\int_{-\infty}^{\infty} e^{-(q/\Delta\nu_E/\Delta\nu_D)^2} F(\kappa(\nu_0) l e^{-q^2}, 0) dq}$$

τk	J
0.00	1.000
0.05	.683
.10	.528
.20	.374
.333	.268
.50	.199

APPARATUS AND METHOD

The essential difference between the method of Stuart and the one used here is that Stuart measured the resonance radiation that was re-emitted from the incident face of the resonance lamp that contained the foreign gas, whereas, in these experiments, the scattered radiation that passed *through* a slab of mercury vapor in the presence of a foreign gas was measured. Experimentally, Stuart's method is simpler, but it does not lend itself to accurate calculation. The apparatus used in these experiments was designed to comply with the calculation that has just been given. It is shown

⁶ O. Stern and M. Volmer, Phys. Zeits. 20, 183 (1919).

schematically in Fig. 3, and is exactly the same apparatus that was used to measure the absorption and collision broadening of the mercury resonance line. The arc, resonance lamp, and absorption cell are all described in the paper just referred to along with the manner in which the photoelectric

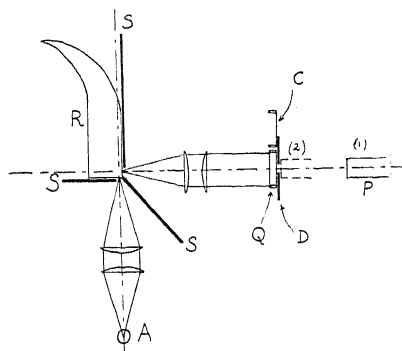


Fig. 3. Diagram of apparatus. *A*, arc. *S*, shield. *R*, resonance lamp. *Q*, absorption cell (can move to be replaced by *C*). *C*, cellophane (can move to be replaced by *Q*). *D*, diaphragm (stationary in space). *P*, photoelectric cell (can move from position (1) to position (2)).

cell was sensitized. The geometrical features of the photoelectric cell which are important in measuring the scattered radiation are shown in Fig. 4. The grid, a coarse mesh of fine platinum wire spot-welded to a circular frame of heavy platinum wire, was mounted against the window of the cell,

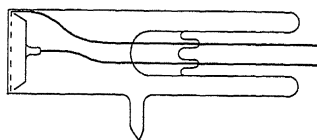


Fig. 4. Photoelectric cell.

and the plate, a cup-shaped piece of platinum, was placed as close as possible to the grid. The plate could receive, therefore, a large solid angle of radiation from a source immediately outside the window.

The radiation passing through the diaphragm *D* in Fig. 3 is composed of two parts: the unabsorbed portion of the incident collimated beam *K*,⁷ and the scattered resonance radiation *S*. When the photoelectric cell is in position (1), about 7 cm away from the diaphragm, it receives an entirely negligible fraction of *S*, and consequently, in this position *K*/*K*₀ can be measured in the manner described in the paper on absorption. With the photoelectric cell in position (2), close up against the diaphragm, both *K* and a constant fraction of *S* are received, say *K* + ϵS , and the measurement of (*K* + ϵS)/*K*₀ is made. Subtracting *K*/*K*₀ from (*K* + ϵS)/*K*₀, we get ϵS /*K*₀, and dividing by ϵS /*K*₀ when no foreign gas was present, *J* is obtained.

$$^7 K = \int_0^\infty K(\nu, l) d\nu, K_0 = \int_0^\infty K(\nu, 0) d\nu \text{ and } K' = K(\nu, 0).$$

The fraction ϵ depends upon the relative size of the diaphragm and photoelectric plate, the distance between them, and the law of distribution in angle of the emerging resonance radiation. It was judged to be in the neighborhood of 90%. No attempt was made to take into account the difference between the reflecting power of the quartz window of the photoelectric cell for the collimated radiation and that for the scattered radiation, because it is believed that the error was within experimental error. The mercury vapor in the resonance lamp was kept at a density corresponding to 0°C by suitable ice baths, and the drop of mercury in the stem of the absorption cell was kept at 20°C with an allowance of no more than $\pm 0.05^\circ\text{C}$. Under these conditions $\kappa(\nu_0)l$ and $\Delta\nu_E/\Delta\nu_D$ are known to be 4.44 and 1.21 respectively.

Every precaution possible was taken to insure purity and dryness of the gases that were studied. The pressures employed never reached a value sufficient to cause Lorentz collision broadening. It was not possible to test carefully the degree to which the absorption cell (which was 0.792 cm thick and 4.5 cm in diameter) approximated the infinite slab required by theory. No change, however, was observed in the value of J when the

TABLE III.

Gas	Pressure in mm: p	J	τk from Fig. 2	Gas	Pressure in mm: p	J	τk from Fig. 2
H ₂	0.010	0.90	0.011	NH ₃	0.15	0.78	0.029
	.021	.84	.019		.38	.60	.074
	.030	.74	.037		.49	.56	.087
	.043	.71	.044		.57	.49	.118
	.052	.68	.051		.75	.45	.142
	.065	.62	.067	CO ₂	.38	.72	.041
	.072	.59	.076		.63	.62	.067
	.090	.56	.087		1.02	.51	.111
	.100	.49	.119		2.73	.26	.351
	.107	.48	.124	H ₂ O	1.0	.63	.064
	.127	.43	.155		1.5	.54	.095
	.160	.37	.203		2.33	.41	.170
O ₂	.033	.83	.021	N ₂	1.35	.88	.014
	.043	.80	.026		2.62	.80	.026
	.056	.72	.041		2.95	.795	.027
	.078	.68	.051		4.04	.72	.041
	.078	.66	.056		5.00	.69	.048
	.082	.65	.058		5.70	.65	.058
	.112	.60	.073		7.50	.58	.078
	.120	.61	.070		8.00	.59	.076
	.120	.57	.083	C ₃ H ₈	.46	.80	.026
	.143	.54	.095		1.04	.61	.070
CO	.150	.51	.108		2.10	.43	.155
	.177	.46	.136				
	.139	.81	.024				
	.22	.70	.047				
	.26	.66	.056				
	.27	.66	.056				
	.36	.61	.070				
	.45	.54	.095				
	.54	.48	.127				
	.59	.47	.133				

diameter of the diaphragm D was varied from 0.5 cm to 1 cm, and when the diameter of the collimated incident beam was varied slightly. It is believed that a cell whose diameter is roughly five times its thickness is a good experimental approximation to an infinite slab.

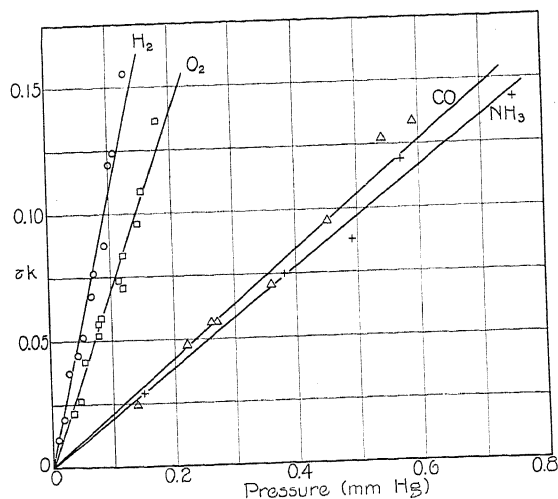


Fig. 5. τk plotted against pressure, p .

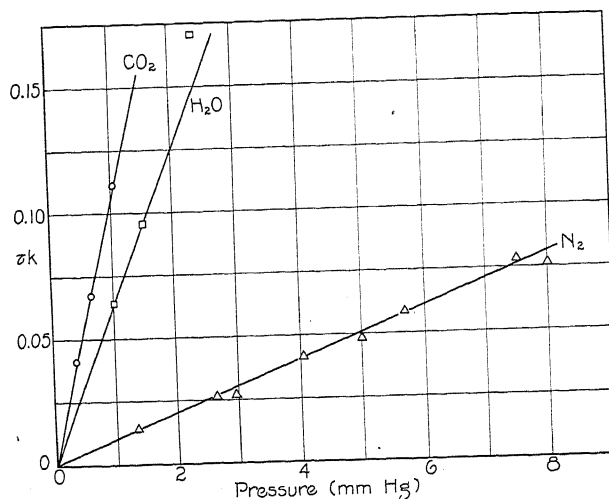


Fig. 6. τk plotted against pressure, p .

Values of J at various pressures for all the gases studied are given in Table III along with the values of τk obtained from Fig. 2, and τk is plotted against the pressure p in Figs. 5 and 6.

FINAL RESULTS

It is seen in Figs. 5 and 6 that the curves of τk against p are all straight lines. It will be remembered that k was defined as the number of impacts

of the second kind per second per excited atom. By an impact of the second kind, we mean here *any* process, other than spontaneous or stimulated emission, which transfers the excited mercury atom from the 2^3P_1 state to *any* other state, not necessarily to the normal state. For example, in the case of N_2 , k probably represents the number of times per sec that an excited 2^3P_1 mercury atom is lowered to the metastable 2^3P_0 level. The fact that the τk against p curve for N_2 is a straight line, indicates that the metastable atoms formed are destroyed by diffusion to the walls so rapidly that the number of upward transitions from 2^3P_0 to 2^3P_1 is negligible. If this were not so, the curve would not be a straight line. This point will be treated more fully later. If the effect of some gas is to perform both transitions, $2^3P_1 \rightarrow 2^3P_0$ and $2^3P_1 \rightarrow 1^1S_0$, then k is the sum of the rates at which each go on. Since, however, it is impossible to separate the two parts of k in this case, we shall have to be content to describe the effect of each gas as due to either one or the other of these transitions. It is not likely that a gas will perform both with equal probability. A mixture of two gases, however, should give a value of k equal to the sum of the separate values. This was tested by comparing the effect of air with the effect of N_2 and O_2 . For O_2 , $\tau k = 0.68p$; for N_2 , $\tau k = 0.01p$; and for air, $\tau k = 0.14p$, whence for $p = 1$, $1/5 \times 0.68 + 4/5 \times 0.01 = 0.144$ in good agreement.

From kinetic theory we have,

$$\tau k = 2\tau\sigma_E^2 p \frac{9.71 \times 10^{18}}{T} \left(2\pi k' T \left(\frac{1}{m} + \frac{1}{M} \right) \right)^{1/2} \quad (13)$$

where p is the pressure in mm, T is the absolute temperature, k' is Boltzmann's constant, m is the mass of a mercury atom, M is the mass of a foreign gas molecule, and σ_E is the distance between centers at impact. We shall call σ_E^2 the "effective cross-section for quenching."

Since τ is 10^{-7} secs and $T = 293^\circ K$

$$\frac{\tau k}{\sigma_E^2 p} = 3.32 \times 10^8 \left(\frac{1}{m} + \frac{1}{M} \right)^{1/2} \quad (14)$$

and from Figs. 5 and 6

$$\tau k/p = \text{slope of line in Fig. 5 or 6}$$

from which σ_E^2 can be calculated. The values of $\tau k/p$, $\tau k/\sigma_E^2 p$, σ_E^2 , σ_N^2 are given in the first four columns of Table IV. σ_N is the sum of the radius of a mercury atom (1.80×10^{-8} cm) and the gas-kinetic radius of a foreign gas molecule. The point of view adopted heretofore has been that there is associated with the excited Hg atom and with each foreign gas molecule a constant radius, and that the total number of collisions between them is given by substituting the sum of these radii for σ_E in Eq. (13). Then the number of impacts of the second kind is obtained by multiplying the right hand member of Eq. (13) by a probability. In all of the papers on this subject one will find estimates of the radius of an excited Hg atom and calculations of these probabilities. The point of view adopted here is

TABLE IV.

Gas	(1) $\tau k/p$ from Figs. 5 and 6	(2) $\tau k/\sigma_E^2 p \times 10^{-15}$ from Eq. (14)	(3) $\sigma_E^2 \times 10^{16}$ Quenching	(4) $\sigma_E^2 \times 10^{16}$ Normal	(5) $\sigma_E^2 \times 10^{16}$ depolarization	(6) $\sigma_E^2 \times 10^{16}$ collision broadening
O ₂	0.683	0.491	13.9	10.7	5.70	65.1
H ₂	1.10	1.83	6.01	8.89	3.55	24.5
CO	.212	.521	4.07	11.6		44.5
NH ₃	.192	.653	2.94	10.8		71.2
CO ₂	.107	.431	2.48	11.6	53.4	125.
H ₂ O	.0637	.638	1.00	10.0	51.4	68.5
N ₂	.0100	.521	.192	11.2	36.4	51.0
CH ₄	.004	.671	.0596	11.6		42.3
C ₂ H ₆	.021	.506	.415	16.4		
C ₃ H ₈	.070	.431	1.62			73.5
C ₄ H ₁₀	.158	.385	4.11			
He	0.00	1.29	0.00	7.83	10.7	15.0
A	0.00	.448	0.00	10.4	19.0	61.5
Hg		.258		13.0	15500	

more in line with the ideas of quantum mechanics in which one is inclined to ascribe a cross section to each *process* that can take place between two colliding molecules. Of course the two points of view amount to the same thing numerically, because the σ_E^2 in Eq. (13) is equal to

probability \times (excited Hg radius + foreign molecule radius)²

Using the values of probability and excited Hg atom radius obtained by Stuart,² and by Gaviola,³ and using the low pressure parts of the $\tau k - p$ curves given in the author's previous paper on this subject,³ the corresponding values of σ_E^2 were obtained and compared with those in Table IV. The comparison is shown in Table V.

TABLE V. Comparison of values of effective cross-section for quenching.

Gas	$\sigma_E^2 \times 10^{16}$ Stuart 1925	$\sigma_E^2 \times 10^{16}$ Gaviola 1929	$\sigma_E^2 \times 10^{16}$ Author 1928	$\sigma_E^2 \times 10^{16}$ These Experiments
O ₂	59		20	13.9
H ₂	27	20	8.8	6.01
CO	48	54	13	4.07
CO ₂	12		3.2	2.48
H ₂ O	3.9	3.8	1.2	1.00
N ₂	.63	2.0	.23	.192

The values given in Table IV for the hydrocarbons were obtained from measurements of the quenching by Bates⁸ who used the same method as that employed here. In order to avoid the tedious graphical integration that is necessary to obtain the correct $J - \tau k$ curve for Bates' apparatus, the following method was used: A $\tau k - p$ curve was obtained with *this* apparatus for propane and was compared with a $J - p$ curve for propane obtained with Bates' apparatus. From these two curves a $J - \tau k$ curve was drawn that could be used for all the other gases studied by Bates.

⁸ J. R. Bates, Journ. Amer. Chem. Soc. not yet published.

The quenching of argon and helium was tested and found to be negligible in the pressure range where there is no collision broadening. At higher pressures there would presumably be a decrease in resonance radiation, but the correct value of τk could not be inferred from the $J-\tau k$ curve of Fig. 2. It would not be worth while, moreover, to compute a set of $J-\tau k$ curves corresponding to various collision breadths, because at high pressures the rate at which metastable atoms are being raised from the 2^3P_0 to the 2^3P_1 state is no longer negligible. Approximate corrections for collision broadening were made by Bates in the case of methane at high pressures, and the effect of these upward transitions was shown very definitely.

THEORY OF THE EFFECT OF METASTABLE ATOMS

Suppose that the following processes are taking place: (1) transitions from 2^3P_1 to 2^3P_0 , (2) diffusion of metastables to the walls, (3) transitions from 2^3P_0 to 2^3P_1 , and that, at any moment there are n_1 2^3P_1 atoms, n_0 2^3P_0 atoms and n normal atoms. Let the rate at which (1) is going on be $k_1 n_1$, and the rate of (2) be $D(\partial^2 n_0 / \partial x^2)$, and the rate of (3) be $k_0 n_0$, where D is the diffusion coefficient of metastable atoms. Then, considering the equilibrium of the 2^3P_1 and the 2^3P_0 states separately, we obtain the two equations:

$$\frac{\partial^2}{\partial x^2} [n_1(1 + \tau k_1) - \tau k_0 n_0] = 4\kappa^2 \tau [k_1 n_1 - k_0 n_0] - \frac{3nK'}{4\pi\sigma} \kappa^2 e^{-\kappa x}$$

$$D \frac{\partial^2 n_0}{\partial x^2} = - [k_1 n_1 - k_0 n_0]$$

which must be solved simultaneously. They lead to the following equations:

$$\frac{\partial^2}{\partial x^2} [n_1(1 + \tau k_1) + n_0(4\kappa^2 \tau D - \tau k_0)] = - \frac{3nK'}{4\pi\sigma} \kappa^2 e^{-\kappa x} \quad (15)$$

$$\frac{\partial^2}{\partial x^2} (k_1 n_1 - k_0 n_0) = \frac{4\kappa^2 \tau k_1 + k_0/D}{1 + \tau k_1} (k_1 n_1 - k_0 n_0) - \frac{3nK'}{4\pi\sigma} \frac{k_1 \kappa^2}{1 + \tau k_1} e^{-\kappa x} \quad (16)$$

which can be solved very easily.

The forward and backward fluxes of radiation are:

$$\pi I_+ = \frac{\pi\sigma}{n} \left\{ [n_1(1 + \tau k_1) - \tau k_0 n_0] - \frac{1}{2\kappa} \frac{\partial}{\partial x} [n_1(1 + \tau k_1) - \tau k_0 n_0] - \frac{3}{2} \frac{K'}{4} e^{-\kappa x} \right\}$$

$$\pi I_- = \frac{\pi\sigma}{n} \left\{ [n_1(1 + \tau k_1) - \tau k_0 n_0] + \frac{1}{2\kappa} \frac{\partial}{\partial x} [n_1(1 + \tau k_1) - \tau k_0 n_0] - \frac{1}{2} \frac{K'}{4} e^{-\kappa x} \right\}$$

The four arbitrary constants in the solutions of Eqs. (15) and (16) are obtained from the boundary conditions that

$$\begin{aligned} & \text{when } x=0 \left\{ \begin{array}{l} I_+ = 0 \\ n_0 = 0 \end{array} \right. \\ & \text{and when } x=l \left\{ \begin{array}{l} I_- = 0 \\ n_0 = 0 \end{array} \right. \end{aligned}$$

and finally πI_+ at $x=l$ can be obtained.

In the final integration over the emission and absorption lines, account would have to be taken of collision broadening. It has not seemed worth while to carry this out in view of the fact that no experiments have been done that can be handled by these equations. It is the opinion of the author, however, that no really reliable information can be obtained about the formation of metastable atoms until some such procedure is adopted. The information yielded by measuring the absorption of a line originating from the metastable level is not very exact. Measurements of the life-time of metastable Hg atoms in the presence of foreign gases,⁹ however, can yield quite reliable values of k_0 and D but not of k_1 .

DISCUSSION

According to the ideas of Kallmann and London¹⁰ the effective cross-section for quenching should depend upon the nature of the two colliding molecules, the law of interaction between them, and the difference between the energy that one has to give and the energy that the other has to take. The law of interaction depends on whether the transition of the Hg atom is optically allowed or not. We should therefore expect those molecules which produce the transition $2^3P_1 \rightarrow 1^1S_0$ to behave differently from those which produce the transition $2^3P_1 \rightarrow 2^3P_0$. There is good evidence to show that O_2 and H_2 produce the first transition and that the other molecules produce the second.

It is generally conceded that excited Hg atoms dissociate H_2 molecules. Since the energy of an excited Hg atom is 4.86 volts and the dissociation energy of H_2 is 4.42 volts, the difference is 0.44 volts. To calculate the energy difference in the case of oxygen we have to consider two possibilities: (1) $Hg^* + O_2 \rightarrow Hg + O_2^*$, in which the oxygen molecule is raised to a vibrational level. According to Mitchell,¹¹ the oxygen molecule has a vibrational level exactly at 4.86 volts, making the energy difference zero. (2) $Hg^* + O_2 \rightarrow Hg + O$, which¹² required an amount of energy equal to the heat of dissociation of O_2 (5.5 volts) minus the heat of dissociation of Hg O. Estimating this last quantity from thermochemical data to be about 0.5 volt, we get for the desired energy difference, $5.5 - .5 - 4.86 = 0.14$ volts. It has not been decided which one of these processes is responsible for the quenching, but since both involve a smaller energy difference than in the case of H_2 the fact that σ_E^2 is larger for O_2 than for H_2 is at least accounted for.

The quenching cross-sections of the other molecules can be accounted for in terms of the difference between the energy that the Hg atom has to give up in the transition $2^3P_1 \rightarrow 2^3P_0$ (0.218 volts) and the vibrational energy that can be taken up by a colliding molecule. Since 0.218 volts corresponds to a wave-length equal to 5.66μ , it is necessary to find out from the infrared absorption spectrum of a gas the wave-length of that band which lies nearest

⁹ M. W. Zemansky, Phys. Rev. **34**, 213 (1929).

¹⁰ Kallmann and London, Zeits. f. Phys. Chem. B2, 207 (1929).

¹¹ A. C. G. Mitchell, Journ. Frank. Inst. **206**, 817 (1928).

¹² A. Leipunsky and A. Sagulin, Zeits. f. Phys. Chem. B1, 362 (1928).

5.66 μ . This information was obtained from Schaefer and Matossi's "Das Ultrarote Spektrum" for every molecule except C_3H_8 and N_2 . The energy of the first vibrational state of the N_2 molecule was obtained from the International Critical Tables. The results are shown in Table VI and in Fig. 7.

TABLE VI.

Gas	$\sigma E^2 \times 10^{16}$ for Quenching	Wave-length in μ of Band nearest 5.66 μ	Corresponding volts = $1.234/\lambda(\mu)$	Energy difference (volts)
CO	4.07	4.66	.265	+0.047
NH ₃	2.94	6.132	.202	-0.016
CO ₂	2.48	4.88	.253	+0.035
H ₂ O	1.00	6.267	.197	-0.021
N ₂	.192		.288	+0.070
CH ₄	.0596	7.67	.161	-0.057
C ₂ H ₆	.415	6.85	.180	-0.038
C ₄ H ₁₀	4.11	5.67	.218	0.00

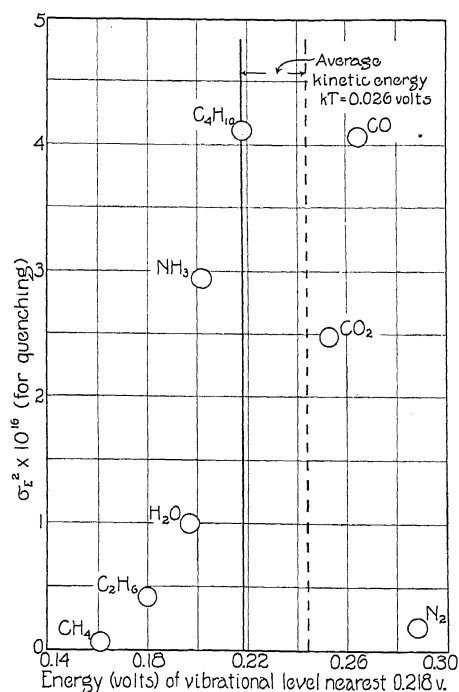


Fig. 7.

The interesting features of Fig. 7 are:

- (1) The points determine roughly a "resonance curve."
- (2) The points are *not* distributed symmetrically about the line drawn at 0.218 volts.
- (3) The point for CO is quite far away from any curve that the other points would suggest. This discrepancy is beyond the limits of experimental error.

(4) The points are approximately symmetrical about a line drawn midway between 0.218 volts and $0.218 + \text{average kinetic energy}$.

(5) There is no marked difference between the behavior of those molecules which have strong dipole moments, and those which have none. According to Kallmann and London's theory, the points should be symmetrical, and the magnitude of the cross-sections should be much larger than the normal cross-sections. One is not justified, however, in attempting to apply their theory completely to these results, because their calculation referred to a much simpler situation than the one involved here.

In columns (5) and (6) of Table IV the effective cross-sections for depolarization of resonance radiation and for collision broadening of the absorption line are given for convenience in comparison. Those for collision broadening were taken from the author's recent paper,⁵ and those for depolarization were calculated in the following way from data given by Keussler:¹³ The percentage polarization of resonance radiation was assumed to follow the law:

$$P = \frac{P_0}{1 + \tau Z}$$

when P = percent polarization with no foreign gas, and τZ = number of depolarizing collisions per life-time per excited atom. τZ is therefore $P_0/P - 1$, and from curves of P against the pressure τZ was calculated and plotted against the pressure. The slopes of the best straight lines that could be drawn were then used to furnish values of σ_E^2 in the manner already described. To obtain the value for pure mercury vapor, the slope as $p \rightarrow 0$ was used, in order to eliminate the effect that the imprisonment of resonance radiation has on the depolarization.

So far, it has not been possible to find a relation between the various kinds of cross-sections, although one would expect that some relation ought to exist. In a rough way, those gases which quench most depolarize least, a result that Keussler pointed out in comparing his results with those of Stuart.

In conclusion, the author would like to thank Mr. Buttolph of the General Electric Vapor Lamp Company for the loan of a mercury arc, and Dr. J. R. Bates for his kindness in supplying data on the hydrocarbons. It is a pleasure also to express my indebtedness to Professor H. P. Robertson for very valuable help in the calculation, to Professor K. T. Compton for the privilege of working at Palmer Physical Laboratory and to the National Research Council for the opportunity to do this research.

¹³ V. Keussler, *Ann. d. Physik* **82**, 793 (1927).

SOME MEASUREMENTS OF THE LONGITUDINAL ELASTIC FREQUENCIES OF CYLINDERS USING A MAGNETOSTRICTION OSCILLATOR

BY DAVID S. MUZZEY, JR.

CRUFT LABORATORY, HARVARD UNIVERSITY

(Received July 21, 1930)

ABSTRACT

Cylindrical rods cut from two samples of stainless steel are excited to longitudinal vibration in a magnetostriction oscillator and the resonant frequencies at which the rods control the oscillator are measured by beating with a crystal oscillator of known frequency. Many rods of each material are measured in order to test the theoretical relation given by Lord Rayleigh between the natural longitudinal frequency and the dimensions, in particular the effect of the diameter of the rod on its frequency.

Evidence is presented to show that, in general, the frequency measurements are good to 0.01 percent or better. The lengths of the rods are known to 0.02 percent or better and the diameters to from 0.05 percent to 0.5 percent according to the size of the rod.

A very brief theoretical discussion is given to show that if Rayleigh's frequency equation for the "free-free" longitudinal vibration is sound then the theory of G. W. Pierce for the magnetostriction oscillator leads to approximate frequency equation of the same form but with slightly different constants for the case where the cylinder is driven in a magnetostriction oscillator at resonance.

The relation between the measured frequencies and the dimensions is shown graphically for each of the two kinds of stainless steel. On the same graphs are plotted curves for the theoretical formula with constants chosen to give the best fit with the experimental points. Agreement of 0.2 percent or better is obtained for one of the samples and 0.1 percent or better for the other. It is pointed out that in all probability a large part of this deviation from the theoretical curves is due to the lack of uniformity of consistency in the alloys used.

THE magnetostriction oscillator, invented by Professor G. W. Pierce,¹ offers a means of maintaining and accurately measuring the frequencies of longitudinal elastic vibrations in bars and rods. The method is, of course, limited to the ferromagnetic metals and only such of those as show strong magnetostrictive properties, but the frequencies can be measured to one part in ten thousand so that it has been interesting to change the dimensions of a cylinder of stainless steel in small steps and determine its longitudinal frequencies after each cutting. By this process it has been possible to examine the nature of the dependency of frequency on the length and diameter of the cylinder over a certain range of dimensions. It turns out, as will be seen, that this relation between the frequencies and the dimensions is very nearly that predicted for the "free-free" vibrations of a cylinder by elastic theory.²

¹ G. W. Pierce, Proc. Am. Acad. Sci. 63, (1928).

² "Mathematical Theory of Elasticity" by A. E. H. Love. Cambridge University Press.

EXPERIMENTAL

The apparatus used consisted of a magnetostriction oscillator with one stage of amplification, a piezoelectric oscillator also with one stage of amplification, and an audiofrequency meter with telephones. These three pieces were connected together as shown in Fig. 1. The outputs of the two oscillators were joined and connected to the input of the frequency meter so that any audible beat frequencies could be measured.

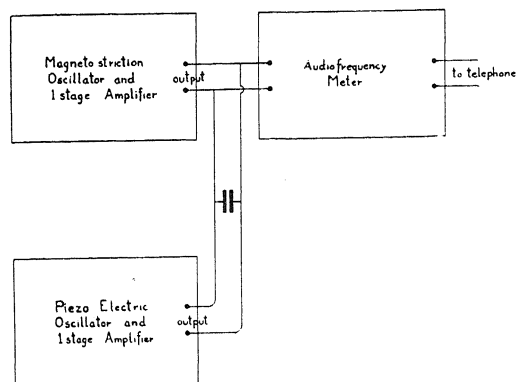


Fig. 1. Showing the arrangement of the apparatus.

The magnetostriction oscillator was of the type invented by Professor Pierce and described by him in the paper referred to in footnote¹ below. It was a commercial model manufactured by the General Radio Company, of Cambridge, Massachusetts. In Fig. 2 the wiring diagram for this oscillator and its accompanying single stage of amplification is reproduced

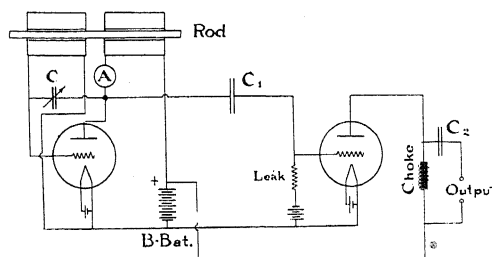


Fig. 2. The wiring diagram of the magnetostriction oscillator.

from Professor Pierce's paper. In as much as the oscillating circuit must be tuned to a natural period of the rod to start it vibrating, any one pair of coils (i.e. grid and plate coils) is useful only for frequencies falling within a certain range which is determined by the range of the variable condenser. For this research it was desirable that the oscillator be tuneable to any frequency between five thousand and one hundred thousand cycles without disturbing the rod in the coils. To effect this the grid and plate coils were

made up of four coils each as is shown by the wiring diagram in Fig. 3. The two four-point switches enable one to change the coil combination without disturbing the rod. The method of mounting the rod by balancing it on a narrow wooden support placed between the grid and plate coils is also shown in Fig. 3. The plate winding is about the rod on one side of its center and the grid winding on the other side.

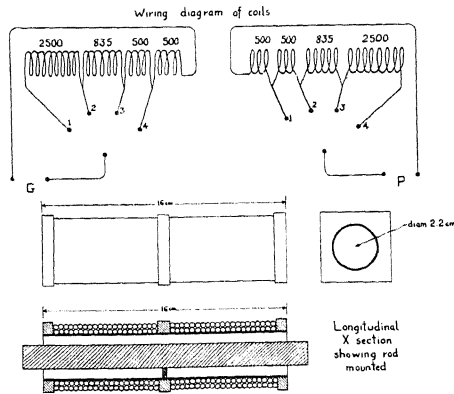


Fig. 3. The wiring diagram and mounting of the coils.

The circuit of the piezoelectric oscillator with its single stage of amplification is shown in Fig. 4. The quartz crystal was one of the Cruft Laboratory standards known as number 28. It maintained the frequency of the oscillator

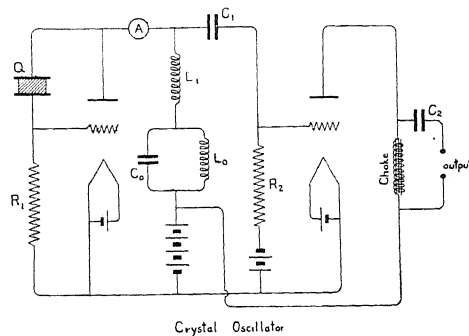


Fig. 4. The wiring diagram of the piezoelectric oscillator.

circuit at $28,067.5 \pm 0.2$ cycles. This frequency was determined at the start of the research by calibrating the piezoelectric oscillator in the manner described on pages 18–19 of Professor Pierce's paper "Magnetostriction Oscillators."¹ Since it was found that other factors prevented the measurement of the rod frequencies to better than one part in ten thousand this accuracy was considered sufficient in checking the crystal calibration at the close of the research. The crystal frequency was then found to be $28,069 \pm 2.0$ cycles. The apparatus was mounted in a "constant temperature"

room whose temperature did not change by more than two degrees centigrade throughout the year and in as much as the temperature coefficient of frequency for the crystal in the mounting used had been found to be about one cycle in one hundred thousand per degree centigrade at 20°C. it was not necessary to correct the crystal frequency for temperature to ensure accuracy to one part in ten thousand.

The audiofrequency meter was identical with the one described on page 22 of "Magnetostriction Oscillators."¹ The wiring diagram given there is reproduced in Fig. 5. The instrument has three ranges covering frequencies of from 500 to 5000 cycles and is equipped with a direct reading scale.

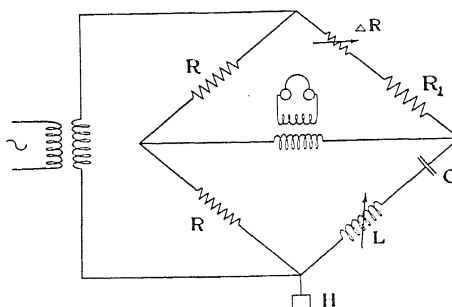


Fig. 5. The wiring diagram of the audiofrequency meter.

The rods measured were of commercial stainless steel. For the first three series of measurements all the rods were cut from a single cylinder which was 24.338 cm long by 1.8057 cm in diameter. For the first series this piece was shortened by steps which became smaller as the rod grew shorter. After each cutting the frequencies of all the modes of longitudinal vibration that could be excited were measured. For the second and third series two of the pieces left from the cuttings of the first series were reduced in diameter a little at a time, frequencies being measured for each diameter. The rods measured in the fourth and fifth series were all cut from a second piece of stainless steel obtained from another source. At the start it was machined to a length of 12.9837 cm and a diameter of 1.9050 cm. For the fourth series of measurements the diameter was cut down in small steps and for the fifth series the piece that remained was shortened in steps.

Stainless steel was chosen for these measurements simply because it is easily obtained and works well in the magnetostriction oscillator. Each of the samples was annealed and each rod was permanently magnetized before its frequencies were measured.

The machining of the rods was done as accurately as was possible in the shop of the Cruft Laboratory. The lengths of the rods were uniform over the end faces to within some two or three ten thousandths of an inch so that the lengths of rods that were longer than two inches were known to one part in ten thousand or better. All of the diameters were uniform to within one half of one thousandth of an inch and for most of the rods the uniformity was

considerably better than this. The possible error in the value taken as the diameter of any rod varied between one percent and one tenth of one percent according to the size of the rod. Since changes in diameter have a much smaller effect on the frequencies of longitudinal vibration than changes in the length this accuracy was sufficient for the purpose of this research.

The method of procedure was as follows: The rod whose frequency was to be measured was inserted in the coils and balanced on the narrow wooden support (see Fig. 3). After time had been allowed for the rod to come to the temperature of the surrounding air the magnetostriction oscillator was turned on and tuned by means of the condenser till the needle of the plate circuit direct current milliammeter "kicked," showing resonance of the oscillator with a mode of vibration of the rod. Then the crystal oscillator was turned on and the magnetostriction oscillator readjusted so that the milliammeter needle was at the peak of its "kick." Finally the frequencies of the audible beats between the two oscillators were measured with the audio frequency meter. A record was kept of the beat frequencies, the condenser setting, the positions of the switches on the grid and plate coils (see Fig. 3), the temperature of the air surrounding the rod, and the dimensions of the rod. In order to use these beat frequencies to determine the frequency of the rod one must know beforehand the approximate value of that frequency. This was obtained by using the simple formula given by elementary theory, namely

$$f = \frac{n}{2l} \left(\frac{E}{\rho} \right)^{1/2}$$

where

f = frequency, $n = 1, 2, 3$, etc. any + integer.
 l = length of the rod, E = Young's modulus
 ρ density of the rod.

The density of each of the samples was measured and the value of E given in Professor Pierce's paper¹ for stainless steel was used.

With the exception of the lengths of the four longest rods all the dimensions were measured with micrometer calipers. Enough readings were taken in each case to determine the uniformity of the dimension in question. The four lengths which were too long for the largest available micrometer were measured by using a cathetometer and an auxiliary cylinder marked with a fine scratch parallel to its plane ends.

Table I below is a sample of the data taken for the frequency measurements on a single rod. The abbreviations heading the columns of this table are to be interpreted as follows:

N refers to the mode of longitudinal vibration, $N = 1$ for the fundamental, $N = 2$ for the next to the gravest mode etc.

P and G refer to the positions of the switches of the plate and grid coil respectively i.e. the combination of coils being used in each case. Under *Cond.* are the condenser settings. Under *Temp.* are the temperatures of the air about the rod. The beat frequencies are tabulated under *Beats*. f heads the

column of computed rod frequencies and in the next column these frequencies are corrected to twenty degrees centigrade which was taken as the standard temperature. The pairs of numbers in the last column refer to the harmonics (produced in the vacuum tubes) of the rod and crystal frequencies that are causing the beat frequency measured.

TABLE I. *Sample of data: Frequency measurements on rod No. 6 of the first series, beating with crystal No. 28, $f=28,067.6$ March 13, 1929.*

N	P	G	Data		Beats	f	Results	C-R
			Cond.	Temp.			f at 20°	
1	2	2	28	23.5	1893	23,788	23,799	6-7
1	2	2	28	23.5	4275	23,793	23,804	1-1
1	2	2	28	23.5	2388	23,788	23,799	5-6
1	3	2	53	23.5	4280	23,788	23,799	1-1
1	3	2	53	23.5	2386	23,787	23,798	5-6
1	3	3	62	23.5	1898	23,787	23,798	6-7
1	3	3	62	23.5	4280	23,788	23,799	1-1
1	3	3	62	23.5	1420	23,786	23,797	17-20
2	3	3	23	23.5	1861	47,399	47,422	5-3
2	4	3	48	23.5	1898	47,412	47,434	5-3
2	4	4	94	23.5	1830	47,389	47,412	5-3
3	4	3	23	23.5	747	70,543	70,576	5-2
3	4	4	45	23.5	744	70,541	70,574	5-2

In the above table are the data from just one of the sets of measurements made on rod #6. Every rod was subjected to two or more independent sets of measurements with intervals ranging from several hours to several days between them. The temperature was often different at the times of these repetitions so that the agreement of the frequencies found for the standard temperature furnished a check on the value of the temperature coefficient of frequency used. (This coefficient was taken from Professor Pierce's paper "Magnetostriction Oscillators."¹) An examination of the complete data shows that in many of the measurements two or more beat frequencies were observed and recorded for the same mode of vibration of the rod and with the same coil combination and condenser setting. An example of this may be seen in the sample data above for the fundamental mode of rod #6. Separate computations of the rod frequency from these beat frequencies served as a check on the calibration and readability of the audiofrequency meter. Furthermore, in many cases, a vibration-mode of a rod could be excited with two or more different combinations of coils in the grid and plate circuits of the oscillator. This may also be noted in the sample above. The results of these measurements with different coils furnished a check on the assumption that the frequencies might be considered peculiar to the rods and the effects of the coils neglected.

With a very few exceptions, 19 in the 133 measurements made, all the frequencies obtained for any one mode of any one rod under these different conditions agreed to better than one part in ten thousand when reduced to the standard temperature. The second gravest mode of rod #6 was one of the exceptions to this as may be seen from the sample data above. This experimental fact is the foundation for the statement that the frequencies could be

measured to one part in ten thousand or better. In plotting the results the mean of the several frequencies found for each mode of vibration of each rod was taken as the frequency of that mode.

THEORETICAL

The equations for the elastic vibration of a "free-free" cylindrical rod have been solved approximately by Pochhammer³ and by Chree.⁴ The solution is approximate in that it does not satisfy the boundary condition that the tractions or tangential forces on the ends of the rod must be zero. As Love⁵ points out, the tractions on the ends introduced by this solution are small if the radius of the rod is small compared to its length. The frequencies of the rod are given by an equation in Bessel's functions and their derivatives but if one neglects the fourth and higher powers of na/l one may obtain the following expression for the frequency: (see Love, pages 289-290)

$$f = \frac{n}{2l} \left(\frac{E}{\rho} \left(1 - \frac{n^2 \pi^2 \sigma^2 a^2}{2l^2} \right) \right)^{1/2} \quad (1)$$

where f = frequency, $n = 1, 2, 3$, etc. i.e. a positive integer, l = length of rod, E = Young's modulus, ρ = density of rod, σ = Poisson's ratio, a = radius of rod.

Lord Rayleigh⁶ has obtained the same result much more simply by assuming the standing waves in the rod to be made up of plane waves normal to the longitudinal axis. Under this assumption all the boundary conditions can be fulfilled and the frequency is given by

$$f = \frac{n}{2l} \left(\frac{E}{\rho \left(1 + \frac{n^2 \pi^2 \sigma^2 a^2}{2l^2} \right)} \right)^{1/2} \quad (2)$$

where the letters have the same meanings as above. This equation becomes identical with (1) if $(na/l)^4$ is negligible with respect to 1.

Since the effects of "viscosity" in the rod have been neglected in what has been said above, the resonance frequencies for "forced-free" vibration will be given to the same degree of approximation by these same equations. However, in this research the rods were not "forced" in the usual sense of the word for the reaction of the vibrations of the cylinders on the oscillator was an important part of the operation of the apparatus and may not be neglected. Briefly, the changing magnetic induction in the rod due to the changing current in the coils forces vibration of the rod, which vibration, in turn, changes the magnetic flux in the rod and sets up E.M.F.'s in the coils. When the electric circuits are tuned to resonance with a mode of

³ L. Pochhammer, *J. für Math.*, Crelle, **881**, 324 (1876).

⁴ C. Chree, *Quart. Jour. of Math.* **21**, (1886).

⁵ "The Mathematical Theory of Elasticity," by A. E. H. Love, fourth ed., Camb. Univ. Press.

⁶ "Theory of Sound," by Lord Rayleigh, Vol. 1.

vibration of the rod there is a sudden change in the impedance of the coils due to the "motional" impedance of the rod. This sudden change in the impedance of the coils produces a change in the average plate current and therefore kicks the needle of the D.C. plate circuit milliammeter.

Now one can put into the equations of motion for the rod (assuming a plane wave after Rayleigh,—see Love⁵ page 428) terms to take care of the forcing of the rod by magnetostriction as well as the magnetostrictive reaction of the vibrations of the rod on the magnetic induction through the coils. (see Pierce's "Magnetostriction Oscillators"¹). If the amplitude of the alternating magnetic induction in the rod is small enough so that one may say that the longitudinal "pressure" on a small piece of the rod is proportional to the induction in that piece, i.e. $p = qB$, where q is a constant; and if the strains produced in the rod are small enough so that one may say that the magnetic induction caused by them (longitudinal strains) is proportional to them i.e. $B' = q'(\delta\xi/\delta x)$, where q' is a constant and ξ is the displacement in the x direction which is along the longitudinal axis of the rod, then the equation of motion is linear and the frequencies for resonance are given by

$$f = \frac{n}{2l} \left(\frac{E'}{\rho \left(1 + \frac{n^2 \pi^2 \sigma^2 a^2}{2l^2} \right)} \right)^{1/2} \quad (3)$$

which is the same as formula (2) except that E is replaced by E' where

$$E' = E + qq'.$$

Assuming that E' , ρ , and σ are the same for all the rods of the same material this formula gives a relation between the dimensions and frequencies of the rods that can be tested by the results of the measurements described above. Actually E and ρ may vary slightly from one rod to another because the materials used were commercial alloys and the original cylinders may have varied slightly in consistency. Furthermore the values of q and q' depend on the magnetic polarization of the rod,⁷ though less in the case of stainless steel than in that of some of the other magnetostrictive metals that might have been used for the research.⁸ This polarization was not the same for the different rods for they were all magnetized in the same field wherefore the shorter ones were left with less residual magnetism than the longer ones because of the demagnetizing effect of their ends.

It should also be pointed out that formula (3) applies only when the surfaces of the rods are entirely free from forces. Actually, in these experiments the rods were surrounded by the atmosphere and supported at their midpoints on a narrow piece of wood. To test the effect of the air about the rod the first four modes of rod #2 were measured both in the atmosphere and with rod and coils inside a large brass cylinder in which the pressure was reduced to five millimeters. The frequencies were found to

⁷ Honda, Shimizu, and Kusakabe, *Phil. Mag.* **4**, 459 (1902) and 537 (1902).

⁸ K. C. Black, *Proc. Am. Acad. Sci.* **63**, 49 (1928).

be the same to the limit of accuracy of the measurements i.e. one part in ten thousand. This, of course, does not show that under certain conditions of resonance of the rod's frequency with a natural period of the air column formed by the tubing on which the coils are wound the frequency of the rod will not be affected. In connection with the support, it was found that substituting two supports at the ends of the rod for the one at the center did change the frequencies of the lower modes of vibration by several hundredths of a percent while hanging the rod on a linen thread at its mid-point did not change the frequencies. Furthermore it was noticed that if a rod was slightly unbalanced so that one of its ends touched the wall of the surrounding tube the frequency was not measureably changed.

For convenience the frequency equation (3) above may be re-arranged to give

$$\frac{2fl}{n} = \left(\frac{K}{1 + C(n^2 a^2 / l^2)} \right)^{1/2} \quad (4)$$

where

$$K = \frac{E'}{\rho} \quad \text{and} \quad C = \frac{\pi^2 \sigma^2}{2}$$

and since the theory on which this frequency equation is based assumes plane standing waves in the rods one may call $2l/n$ the wave-length in the rod, whence

$$\frac{2fl}{n} = \text{wave velocity}$$

and

$$\frac{na}{2l} = \frac{\text{radius}}{\text{wave-length}}.$$

RESULTS

The results of these frequency measurements are shown graphically in Figs. 6 to 10. The ordinates in each case are the values of $2fl/n$ (the "wave velocity") while the abscissa are the common logarithms of $100 na/l$. (na/l is the ratio of diameter of the rod to "wave-length").

In Fig. 6 are plotted the results for the first series of measurements in which rod #1 (length 24.338 cm, diameter 1.8057 cm) was shortened in fourteen steps to a final length of 3.2299 cm. In this series eight modes of vibration could be measured for the longest rod, six for the second longest rod, four for each of the next two in order of length, three for each of the next three, and the fundamental mode only for the remaining shorter rods. The numbers beside the points refer to the rods. For instance, there are eight points numbered 1 which are the plottings of the eight modes of the longest rod of the series. The curve drawn out in the figure is the graph of

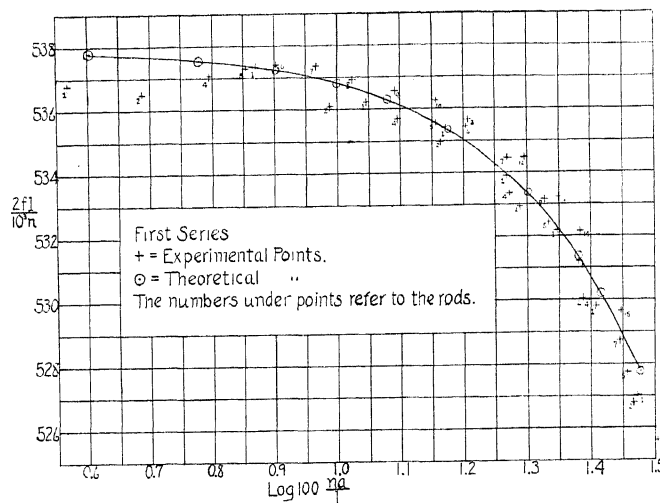


Fig. 6. Graph showing relation between the velocity of the standing wave components and the ratio of diameter to wave-length for the first series.

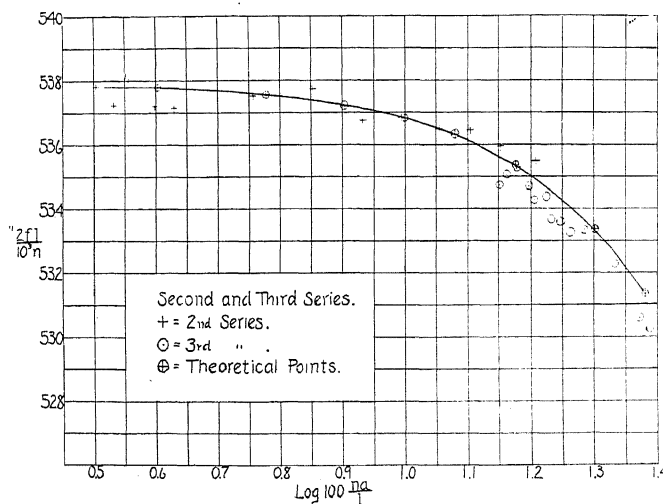


Fig. 7. Graph showing relation between the velocity of the standing wave components and the ratio of diameter to wave-length for the second and third series.

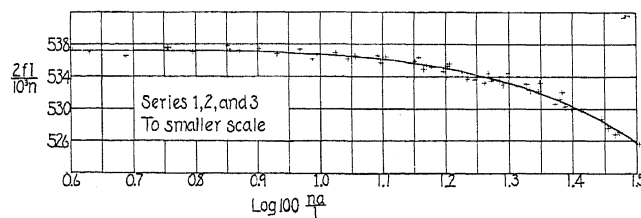


Fig. 8. Graph for the first second and third series to smaller scale to aid in fitting a curve to the points.

Eq. (4) with E'/ρ taken equal to 28.945×10^{10} and σ taken as 0.30. It will be noticed that the experimental values of $2fl/n$ fall within two tenths of a percent of the values given by this curve.

In Fig. 7 are plotted the results of the second and third series. The second series of measurements was made on a piece left from the cuttings

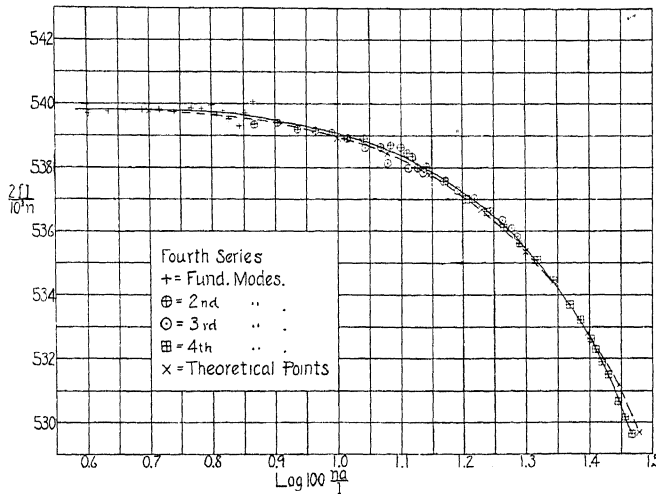


Fig. 9. Graph showing the relation between the velocity of the standing wave components and the ratio of diameter to wave-length for the fourth series.

of the first series (length 5.5946 cm) which was turned down till it became too small to control the oscillator. The third series was made by turning down a shorter piece (length 3.6995 cm) from the first series. The curve drawn is the graph of Eq. (4) using the same values for the constants as in Fig. 6.

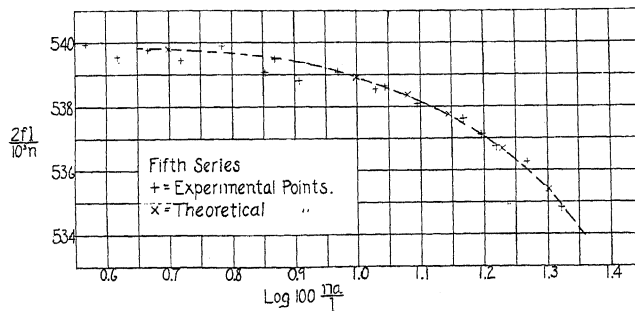


Fig. 10. Graph showing the relation between the velocity of the standing wave components and the ratio of diameter to wave-length for the fifth series.

The method of obtaining the constants for plotting this curve of Eq. (4) was to plot the points of the first three series all together and to a smaller scale so that the best fitting curve might be drawn through them. (See Fig. 8.) The coordinates of two points chosen at random from the opposite

ends of this curve were substituted into Eq. (4) to obtain the constants for plotting the theoretical curves shown in Figs. 6 and 7.

In Fig. 9 are plotted the results of the fourth series of measurement in which a new sample of stainless steel (length 12.9837 cm, diameter 1.9050 cm) was turned down in sixteen steps to a diameter of 0.9588 cm. For most of the rods of this series it was possible to measure the first four modes of vibration the exceptions being cases in which the frequency of the third mode was such that good audible beats with the crystal standard could not be obtained. In this case the plotted points indicate clearly the path of the experimental curve which was drawn in without replotting to a smaller scale. (The solid curve in Fig. 9.) By trial it was found that putting E'/ρ equal to 29.171×10^{11} and σ equal to 0.30 made the graph of Eq. (4) fit this experimental curve best. The two curves coincide except for the large values of na/l , where the theoretical curve is shown by the dashed line. It will be noted that for this series all the experimental points fall within one tenth of one percent of the theoretical curve.

In Fig. 10 are shown the results of the fifth series in which the last rod of the fourth series was shortened in six steps to a final length of 5.9375 cm. The curve shown in the figure is the graph of Eq. (4) with the same constants as were used for the theoretical curve on Fig. 9. Here again the experimental points have ordinates within one tenth of a percent of the ordinates of the theoretical curve.

The average density for the first sample of stainless steel (first three series) was 7.65 grams per cc hence the value of E' for this sample was 22.1×10^{11} dynes per cm^2 . The second sample (fourth and fifth series) had an average density of 7.69 grams per cc and hence an E' of 22.4×10^{11} dynes per cm^2 . These values for E' are about what one would expect for the Young's modulus of steel showing that the product of the magnetostrictive constants q and q' is small. ($E' = E + qq'$.)

SUMMARY AND DISCUSSION OF RESULTS

The lower modes of longitudinal vibration of magnetized cylinders of stainless steel have been measured with an accuracy of one part in ten thousand. These cylinders varied in length from twenty four centimeters down to slightly more than three centimeters and in diameter from nearly two centimeters to less than three tenths of a centimeter. The lengths were known to one or two parts in ten thousand and the diameters with varying accuracy, but none to better than one part in five thousand. (Some of the small diameters were not known to better than 0.5 percent.) The product of frequency by length was therefore known to some two or three parts in ten thousand. Nevertheless, the experimental values of $2fl/n$ when plotted against $\log 100 na/l$ varied as much as one or two parts in one thousand from the curve of the theoretical formula with values for the constants chosen to give the best fit.

This theoretical formula (Eq. (3) above) is based on Lord Rayleigh's theory⁶ for the longitudinal vibrations of a cylinder taking account of the radial motion and G. W. Pierce's theory¹ for the magnetostriction oscillator.

As has been pointed out, it assumes the simple form presented above only because of several assumptions beyond those ordinarily made in applying the elastic theory. It was assumed that the standing waves in the rods were plane and that the action and reaction between the alternating magnetic field and the vibrating rod were small enough in magnitude that the relations between them might be considered linear. Furthermore the cylinders were treated as though free of all body and surface forces and of uniform consistency throughout. The actual experimental conditions may have been sufficiently different from these ideal ones to account for the deviations of the experimental points from the theoretical curves. It is not possible to say which factor or factors caused these deviations and all that one is justified in concluding is that, for stainless steel cylinders of the dimensions used, the frequencies are given by equation (3) to within one or two tenths of one percent.

The fact that the first sample of stainless steel showed variations from the expected curve of as much as 0.2 percent while the second sample agreed with the theory to better than 0.1 percent may mean that the first sample was not as uniform in consistency as the second and that therefore a large part of the deviation is due to the fact that the samples were merely pieces of the commercial alloy. This supposition is born out by the further fact that density measurements made on two pieces cut from opposite ends of the first sample differed by almost one percent.

There is no reason why other magnetostrictive metals subjected to these same measurements should not yield as good agreement with the theory, provided they come as near to being uniform, homogeneous, isotropic substances and provided the rods of different sizes are so magnetized that the permanent magnetic polarizations in each will be nearly the same. This last precaution was not taken in this research because of the small effect of polarization on frequency for stainless steel reported by K. C. Black.⁸ As a matter of fact, when all the rods are magnetized in the same field as in these measurements the first order effect due to the different permanent polarizations will not change the form of the frequency Eq. (3) but only the apparent value of Poisson's ratio (σ). This is because the actual field in the rod may be expressed approximately as a function of the ratio of the diameter to the length.⁹

This research has also yielded values of the E' and the σ of Eq. (3) for the two samples of stainless steel. These constants are respectively Young's modulus and Poisson's ratio, each with an added term or terms arising from the fact that the rods are driven by magnetostriction and are magnetically polarized. It turns out however that these constants have values that are very close to those of Young's modulus and Poisson's ratio for steel (as far as we know) so that the added terms must be small.

The measurements described in this paper were carried out in the Cruft Laboratory at Harvard University under the direction of Professor G. W. Pierce.

⁹ J. C. Maxwell, *Electricity and Magnetism*, Vol. I.

ELECTRICAL RESISTANCE OF NICKEL AND PERMALLOY WIRES AS AFFECTED BY LONGITUDINAL MAGNETIZATION AND TENSION

By L. W. McKEEHAN

SLOANE PHYSICS LABORATORY, YALE UNIVERSITY

(Received July 14, 1930)

ABSTRACT

The changes in the electrical resistance of ferromagnetic metals in magnetic fields and under mechanical stresses are abnormal in comparison with such changes in non-ferromagnetic metals. Published results for nickel and nickel-rich alloys, reviewed in detail, show wider diversity than can be ascribed to accident. A full bibliography is included.

Simple cases of these magneto-resistance and elasto-resistance effects have been studied in permalloys containing from 45 to 90 percent nickel. The results of two series of experiments, in 1923 and 1929, are presented, and show that both effects have, in these ferromagnetic alloys, the same origin. This common origin can be considered as the orientation, by one means or the other, of atomic magnetic axes associated in each atom with mechanical asymmetry.

The connection between these resistance effects and magnetostriction is emphasized. Conclusions are drawn as to the kinds of re-orientation involved in magnetizing and as to the relative importance in the observable effects of intra-atomic and inter-atomic magnetic fields. Questions for further experiment are raised.

INTRODUCTION

THE changes in the electrical resistance of solid metallic conductors when subjected to the action of magnetic fields have attracted the attention of one hundred and twenty-eight investigators. The changes in resistance of such conductors when compressed or distorted have been measured or discussed by ninety-one. Thirteen names appear on both lists, so that no novelty can here be claimed for the idea that there is an intimate connection between the two effects. Recent improvements in magnetic materials have, however, made a study of this connection much easier and have suggested that in it may lie important clues for solving the problem of ferromagnetism. The new data collected in such a study, and reported below in some detail, make it interesting to review previous data of comparable character, the discrepancies in which have become more puzzling as the technique of measurement has improved.

Magneto-Resistance.

On the basis of their changes in electrical resistance when placed in a strong magnetic field, metals and alloys may be assigned to one or the other of two groups. Members of the first and more numerous group increase in resistance whatever may be the relative directions of the current, i and the applied magnetic field, H . Members of the second group increase in re-

sistance if i and H are parallel, decrease if i and H are perpendicular. One observer¹ has reported *decrease* in resistance for both parallelism and perpendicularity of i and H in copper-rich alloys with low temperature coefficients of resistance, e.g. constantan. If confirmed this necessitates a third group.

Members of the second group show relatively much larger changes of resistance than those of the first group for values of H of the order of 10^3 gauss, and relatively much smaller changes for values of H of the order of 10^5 gauss.² All members of the second group are ferromagnetic, and no ferromagnetics occur in the first group. The magneto-resistance effect in non-ferromagnetics is only measurable with accuracy in very intense magnetic fields at room temperature,² or in somewhat less intense fields at low temperatures.³ The change in resistance depends simply upon H , though the exact form of dependence is not yet agreed upon.⁴ In ferromagnetics, on the other hand, the effect attains its limit in fields of such moderate intensity that the whole course of the phenomenon has been accessible to investigation for a long time. The diversity of reported results is surprising and deserves more consideration than it has hitherto received.

Elasto-Resistance.

Ferromagnetic metals are also sharply distinguishable from non-ferromagnetics on the basis of the changes in resistance which they temporarily suffer during elastic deformation. Many experiments on these elasto-resistance effects are difficult to interpret because of poorly defined initial conditions or inhomogeneity of applied stresses. In general, however, the resistance in ferromagnetics is more sensitive to non-isotropic stresses⁵ and less simply related to the intensity of stress, than in non-ferromagnetics.

REVIEW OF PREVIOUS WORK

Among ferromagnetic metals and alloys, nickel and nickel-rich alloys are especially interesting in this connection because of the relative simplicity they offer. Nickel is the only ferromagnetic element that has no phase change below its melting point.⁶ This means, for one thing, that its physical condition is little liable to alteration by thermal treatment. Nickel is also superior to iron for studies on polycrystalline specimens because, as its magnetostriction⁷ suggested, and as has since been demonstrated,⁸ the magnitude of the longitudinal magneto-resistance effect— i and H parallel—is nearly the same for all directions in a monocrystalline specimen. This means that polycrystalline nickel, and nickel-rich alloys over the appropriate

¹ J. Obata, Bibliography Item 29.

² P. L. Kapitza, Proc. Roy. Soc. A123, 292-341, 342-372 (1929).

³ W. Meissner, H. Scheffers, Phys. Zeits. 30, 827-836 (1929).

⁴ W. Meissner, H. Scheffers, Naturwiss. 18, 110-113 (1930); P. L. Kapitza, Proc. Roy. Soc. A126, 683-695 (1930).

⁵ As will be shown below, permalloy of critical composition—with about 81 percent nickel—is exceptional in this respect.

⁶ S. B. Hendricks, M. E. Jefferson, J. F. Shultz, Zeits. f. Krist. 73, 376-380 (1930).

⁷ Y. Mashiyama, Sci. Rep. Tohoku Imp. Univ. [I] 17, 945-961 (1928).

⁸ S. Kaya, Bibliography Item 35.

range of composition in each system, should, except for such minor differences as may be due to preferred orientation of the crystallites, behave like monocrystalline metal. The corresponding expectancy does not exist in the case of polycrystalline iron, since the longitudinal effect in iron monocrystals⁹ differs widely in magnitude for crystallographically different directions. What has so far been reported regarding the magnetostriction of cobalt monocrystals,¹⁰ and the conditions for the stability of hexagonal cobalt,¹¹ make it likely that anisotropy will modify the magneto-resistance effect in polycrystalline cobalt even more than in polycrystalline iron.

For the reasons just presented it seems best to limit the review of previous work to that which deals with nickel and nickel-rich alloys at room temperature or lower. It will also be necessary to omit all results on the transverse magneto-resistance effect, since the transverse effect is peculiarly subject to errors caused by magnetization in undesired directions. In studies on the longitudinal effect errors due to failure of exact parallelism of i and H are serious only in the highest fields and the maximum increase in resistance, though reached in less than the greatest applied field, and followed by a steady decrease in resistance in greater fields, is only slightly less than for perfect alignment.¹² As regards elasto-resistance the review will consider only the effects of tension, since tensile stress is the only homogeneous non-isotropic stress that can easily be applied, and is therefore the type of stress selected in the experiments here to be reported. Even with these rather drastic limitations there remain about forty papers to be considered. The use of tables and graphs thus appears necessary.

TABLE I-A. Longitudinal magneto-resistance in nickel.¹³

	Specimen ¹⁴	Tension kg/mm ²	H_{\max} gauss	H for— gauss	$(\Delta R/R)_{\max}$ percent	Fig- ures
1	Prism $0.30 \times 1.32 \times 3.0$ cm ³	—	—	—	0.7	—
2A	Rod 0.7 cm diam. as cast	—	80	80	0.45	1
2B	0.105 cm diam. annealed	—	42	42	0.45	1, 3
2C	same	2.3	42	42	0.34	3
2D	same	6.9	42	42	0.29	3
3	0.033 cm diam.	—	—	—	— ¹⁵	—
4	Electrodeposited film	—	—	—	1.5	—
5A	ditto	—	1376	1376	2.023	—
5B	ditto	—	1211	1211	1.928	2
5C	ditto	—	1410	1410	1.643	2
5D	ditto	—	1361	1361	1.139	2
6A	0.01551 cm diam. unannealed	—	167	167	1.29	2

⁹ W. L. Webster, Proc. Roy. Soc. A113, 196–207 (1926).

¹⁰ Z. Nishiyama, Sci. Rep. Tohoku Imp. Univ. [I] 18, 341–357 (1929).

¹¹ H. Masumoto, Sci. Rep. Tohoku Imp. Univ. [I] 15, 449–477 (1926); A. B. Cardwell, Proc. Nat. Acad. Sci. 15, 544–551 (1929); *loc. cit.*⁶

¹² W. M. Jones, J. E. Malam, Bibliography Item 26.

¹³ Especially in the earlier work the nickel may have been far from pure.

¹⁴ The number designating a specimen refers to the item in the Bibliography wherein the data occur. A letter is added to distinguish the several specimens, or states of one specimen, covered by one numerical reference. Except as noted, specimens were drawn wires.

¹⁵ The specimen was coiled and placed in a uniform field so that the purely longitudinal effect was not measured. As far as the data go they are in qualitative agreement with those of Tomlinson.

TABLE I-A (continued)

	Specimen	Tension kg/mm ²	H_{\max} gauss	H for gauss	$-(\Delta R/R)_{\max}$ percent	Fig- ures
6B	0.02563 cm diam. annealed	—	130	130	2.04	2
7A	Diam. not given	—	4130	2280	1.23	—
7B	0.1 cm diam.	—	170.4	170.4	1.77	—
8A	0.102 cm diam. unannealed	—	738.7	738.7	1.500	—
8B	0.047 cm diam. annealed	—	602.5	602.5	1.331	—
8C	Strip 0.027×0.30 cm ²	—	671.0	671.0	1.431	—
8D	Strip 0.027×0.15 cm ²	—	700.6	700.6	1.296	—
9A	0.102 cm diam. unannealed	—	64	64	0.514	1
9B	0.047 cm diam. annealed	—	63.3	63.3	0.683	1
9C	Strip 0.027×0.30 cm ²	—	67.2	67.2	0.687	1
11	0.04 cm diam.	—	3300	3300	1.439	2
12A	0.0765 cm diam.	—	165	165	0.72	1
12B	ditto	—	450	450	1.29	2
12C	ditto	—	11000	790	1.70	—
12D	0.0200 cm diam.	—	18000	2000	1.56	—
13	Diam. not given	—	24000	1500	1.5	—
14A	0.012 cm diam.	—	420	420	0.97	2, 3
14B	same	4.4	420	420	1.09	—
14C	same	8.8	370	370	1.10	—
14D	same	26.6 ¹⁶	320	320	1.05	3
14E	same	44.2 ¹⁶	425	425	1.27	3
14F	same	62.0 ¹⁶	425	425	1.08	3
15	0.013 cm diam.	—	69.5	69.5	0.755	1
16A	0.035 cm diam. unannealed	—	785	785	1.90	2
16B	0.035 cm diam. annealed	—	785	785	1.42	2, 3
16C	0.021 cm diam. unannealed	—	560	560	2.14	2
16D	0.014 cm diam. unannealed	—	785	785	3.07	2
16E	0.014 cm diam. annealed	—	785	785	1.97	2
16K	0.035 cm diam. annealed	2.18	795	795	1.53	—
16L	same	5.44	795	795	1.66	—
16M	same	10.9	800	800	1.87	3
16N	same	21.8	800	800	2.36	3
16P	same	32.7 ¹⁷	800	800	2.25	3
17	Diam. not given	—	34	34	1.040	1
18A	Diam. not given	—	900	900	1.60	2
20	0.0035 cm diam. at -190°C	—	3000	3000	5.5	—
21A	0.050 cm diam.	—	2200	1250	2.35	2
21B	0.017 cm diam.	—	9300	4000	1.26	2
22A	0.00206 cm diam.	—	29000	2800	1.462	—
22B	0.00159 cm diam.	—	28500	2800	1.418	2
23	"Thin" strip 2.1 cm wide	—	57	57	0.64	1
24A	0.0425 cm diam. annealed	1.77	1000	1000	1.46	3
24B	same	8.8	1000	1000	1.86	—
24C	same	17.7	1000	1000	2.20	3
24D	same	26.2 ¹⁷	1000	1000	2.23	—
24E	same	31.9 ¹⁷	1000	1000	2.15	3
25	0.0015 cm diam.	—	2600	1000	1.30	2
26	0.00206 cm diam.	—	14500	3000	2.347	2
27	0.022 cm diam.	—	1900	1900	0.90	2
29A	Diam. not given	—	15400	3500	1.22	2
31A	0.15 cm diam.	—	1390	1390	1.77	2, 3
31B	same	12.9	1610	1610	2.46	3
31C	same	26.1 ¹⁷	>1700	1700	2.60	3
33	0.125 cm diam. annealed at 950°C	—	1100	450	1.48	2
35A	Polycrystalline prism 0.125×0.125×2 cm ³	—	1387	539	2.16	2
35B	<100> prism 0.125×0.125×2.6 cm ³	—	1415	943	1.97	2
35C	<110> prism 0.130×0.155×2.2 cm ³	—	1375	903	2.33	2
35D	<111> prism 0.090×0.113×1.3 cm ³	—	1368	520	2.41	2
37	0.0051 cm diam.	—	180	180	0.46	1
39	Diam. not given. 0.6 percent Mn	—	500	500	1.34	—
40	0.02 cm diam.	—	255	255	1.15	—

¹⁶ Probably above the elastic limit for annealed nickel. The smooth progression of the curves indicates therefore that the wire was not annealed.

¹⁷ Probably above the elastic limit for annealed nickel.

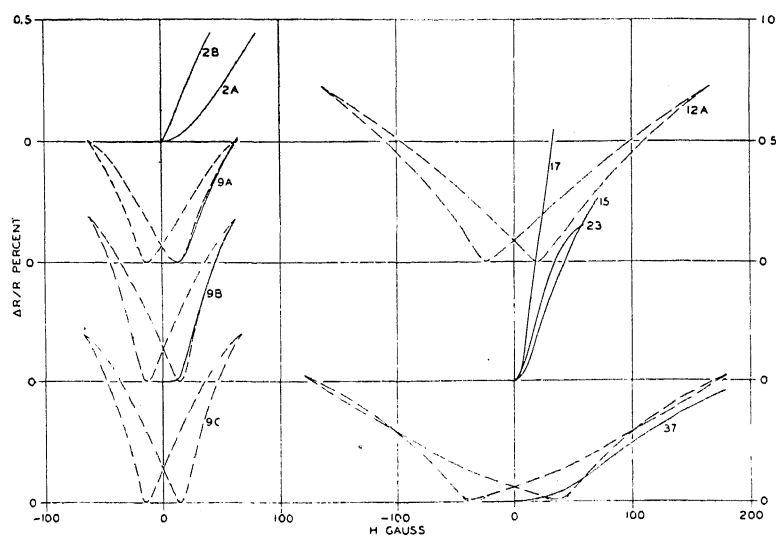


Fig. 1. Longitudinal magneto-resistance in nickel. Previously published results.

TABLE I-B. Longitudinal magneto-resistance in nickel alloys.

Specimen ¹⁴	Tension kg/mm ²	H_{max} gauss	H for gauss	$-(\Delta R/R)_{max}$ percent	Figure
16F Platinite [Ni 47 Fe 53?] 0.035 cm diam. unannealed	—	580	500	0.31	4
16G ditto annealed	—	740	405	0.028	—
16H Nickel-steel [Ni 27 Fe 73?] diam. not given	—	800	80	0.0045	—
16J Rheostene [Ni 26 Fe 74?] diam. not given	—	—	—	0.0018	—
16Q Platinite [Ni 47 Fe 53?] 0.035 cm diam. unannealed	18.5	630	300	0.16	4
16R same	22.9	770	300	0.13	—
18B Ni 24 Fe 76 Diam. not given	—	800	300	0.06	—
18C Ni 27.9 Fe 72.1 Diam. not given	—	800	300	0.0065	—
18D Ni 35.5 Fe 64.5 Diam. not given	—	800	300	0.08	—
18E Ni 40 Fe 60 Diam. not given	—	800	300	0.14	—
18F Ni 44 Fe 56 Diam. not given	—	800	300	0.155	4
18G Ni 48.7 Fe 51.3 Diam. not given	—	800	300	0.23	4
18H Ni 57 Fe 43 Diam. not given	—	800	350	0.46	4
18J Ni 70 Fe 30 Diam. not given	—	800	350	0.72	4
24F Monel, Ni 68 Cu 29.5 Fe 1.5 Mn 1 un- annealed. Diam. not given	3.95	250	100	0.164	4
24G same	13.8	250	150	0.226	—
24H same	23.7	250	175	0.246	4
24J same	33.6	250	200	0.250	—
24K Monel, Ni 68 Cu 29.5 Fe 1.5 Mn 1 an- nealed. Diam. not given	3.95	250	75	0.166	4
24L same	13.8	250	100	0.185	—
24M same	23.7	250	125	0.192	4
24N same	33.6	250	175	0.194	—
29B Ni 72.86 Fe 20.09 Mn 7.04. Diam not given	—	20000	—	-0.059 ¹⁸	—
29C Ni 56.31 Fe 25.43 Cr 15.57 Mn 3.19. Diam. not given	—	1300	600	0.035	—
29D Ni 58.30 Fe 22.28 Cr 15.21 Mn 2.60	—	1200	500	0.056	—

¹⁸ Probably in error, as this composition is ferromagnetic and should give a positive value for $\Delta R/R$.

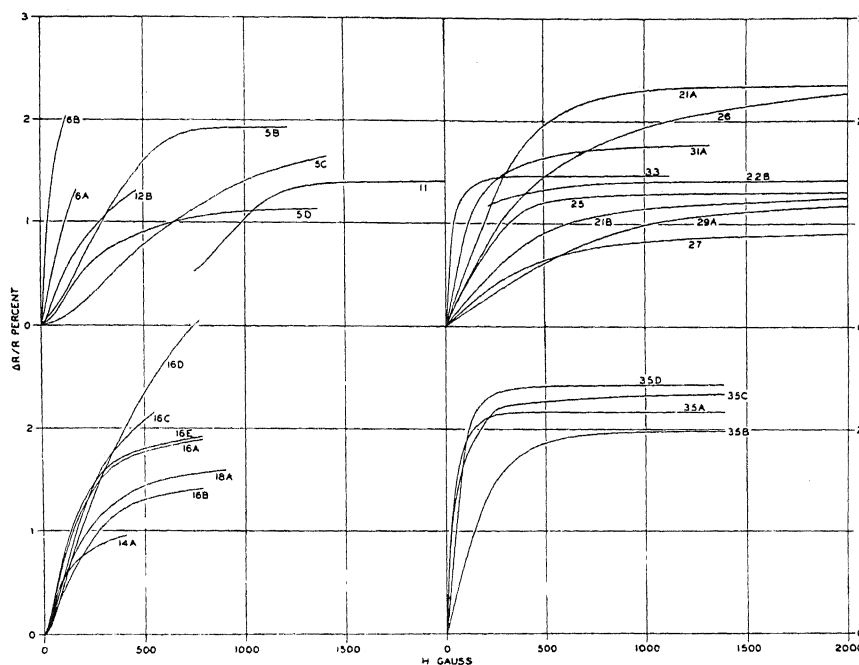


Fig. 2. Longitudinal magneto-resistance in nickel. Presiously published results.

TABLE II. *Elasto-resistance in nickel¹³ under tension.*

Specimen ¹⁴		T_{max} kg/mm ²	T for kg/mm ²	$-(-\Delta R/R)_{max}$ percent	Figure
2E	0.086 cm diam. annealed. Cyclic state	27.4	13	0.420	5
2F	same	30.8	13	0.415	—
2G	same	34.2	15	0.351	—
2H	same	37.7	15	0.321	—
2J	same	41.1	15.5	0.292	5
2K	0.078 cm diam. annealed. Cyclic state	37.6	16.5	0.500	5
2L	same after 25 kg/mm ² at 100°C	37.6	19.5	0.514	—
10A	0.0251 cm diam. unannealed	23	18	0.105 ¹⁹	5
10B	same. Later	24	14	0.074 ¹⁹	5
19A	0.024 cm diam. Loading	42	28	0.050	5
19B	same. Unloading	42	14	0.055	5
28A	0.0259 cm diam. Loading	15.5	11.0	1.68x ²⁰	6
28B	same. Unloading	15.5	9.5	1.76x ²⁰	6
28C	same. Loading	17.6	9.5	2.12x ²⁰	6
28D	same. Unloading	17.6	8.5	2.00x ²⁰	6
28E	same. Loading	18.0	9.5	1.76x ²⁰	6
28F	same. Unloading	18.0	8.5	1.28x ²⁰	6
30A	0.0129 cm diam. annealed. Loading at 0°C	19.0	17.1	0.157	5
30B	same. Unloading at 0°C	19.0	14.3	0.173	5
32	Cast rod 0.317 cm diam. annealed	19	19	0.48	—
34	Strip 0.012x1.25 cm ²	3.78	3.78	0.54	—
36	0.056 cm diam.	—	—	0.8	—
38	0.046 cm diam.	—	—	— ²¹	—

¹⁹ Referred to initial state with 10 kg/mm².²⁰ Referred to initial state with 3.8 kg/mm² and expressed in arbitrary units not convertible into percent by means of reported data.²¹ Reported data show a minimum in R but do not permit calculation of either T or $\Delta R/R$.

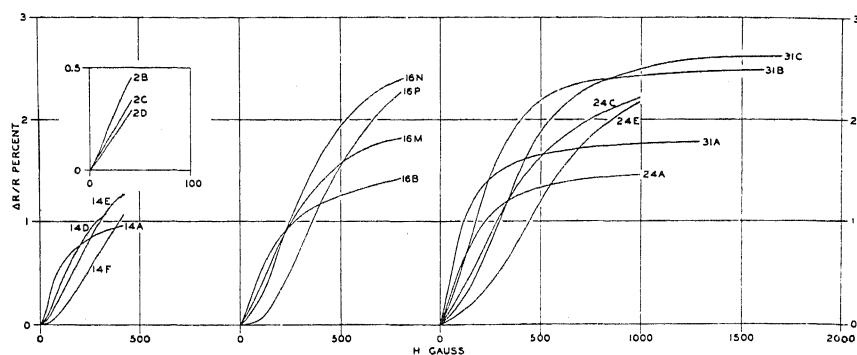


Fig. 3. Effect of tension on longitudinal magneto-resistance in nickel.
Previously published results.

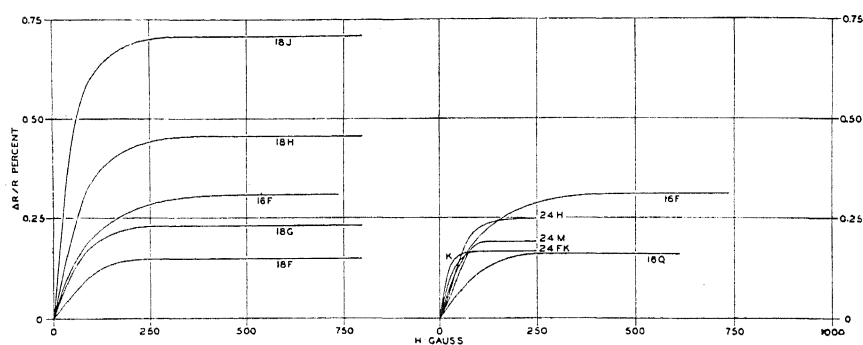


Fig. 4. Longitudinal magneto-resistance in nickel-iron alloys and effect
of tension thereon. Previously published results.

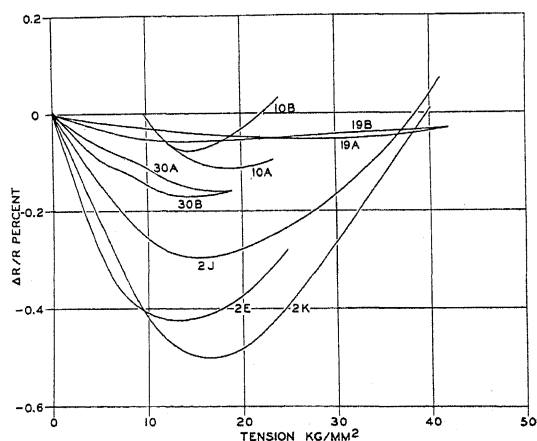


Fig. 5. Elasto-resistance in nickel for tension.
Previously published results.

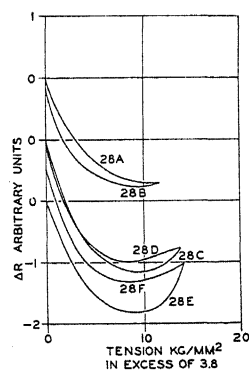


Fig. 6. Elasto-resistance in nickel
under tension, after Nobile.

Tables I and II summarize the magneto-resistance and elasto-resistance data so far published. Figures 1 to 6 present curves selected to show the wide range of the reported results for nickel and a few nickel alloys. Many of these curves have been plotted from tables and are here presented for the first time in graphical form.²² No effort has been made to distinguish those few sets of data in which correction has been made for the self-demagnetizing field. Except for short thick specimens of high magnetic permeability this correction would affect the appearance of the curves but little. Certain results of particular significance will be referred to in the discussion of the new material reported below.

Bibliography

1. Thomson, W.: Proc. Roy. Soc. 8, 546-550 (1857).
On the electro-dynamic qualities of metals:—Effects of magnetization on the electric conductivity of nickel and of iron.
Also in Phil. Mag. [4] 15, 469-472 (1858).
2. Tomlinson, H.: Phil. Trans. Roy. Soc. 1881 174, 1-172 (1883).
The influence of stress and strain on the action of physical forces.
3. Faé, G.: Atti Veneto [6] 5, 1405-1446 (1887).
Influenza del magnetismo sulla resistenza elettrica dei conduttori solidi.
4. Goldhammer, D. A.: Ann. d. Physik [3] 31, 360-370 (1887).
Ueber den Einfluss der Magnetisirung auf die electrische Leitungsfähigkeit der Metalle.
5. Goldhammer, D. A.: Ann. d. Physik [3] 36, 804-824 (1889).
Ueber den Einfluss der Magnetisirung auf die electrische Leitungsfähigkeit der Metalle. II.
6. Gol'gammer, D. A. [Goldhammer, D. A.]: Sobranie protokolov zasiedaniï sektsiï fiziko-matematicheskikh nauk obshchestva estestvoispytatelei pri imperatorskom kazanskom universitet. 8, 57-128 (1890).
Ob izmienenii elektroprovodnosti matallov pri namagnichenii [On the alteration of the electrical conductivity of metals by magnetization.]
7. Garbasso, A.: Atti Torino 26, 839-853 (1891).
Dell'influenza della magnetizzazione sulla resistenza elettrica del ferro e del nichel.
8. Cantone, M.: Rend. Lincei [5] 1 i, 424-431 (1892).
Sulla variazione di resistenza del ferro e del nichel nel campo magnetico.
Additional information regarding the same experiments in Rend. Lincei [5] 1 ii, 277-284 (1892).
Influenza del magnetismo trasversale sulle variazioni di resistenza del ferro e del nichel magnetizzati longitudinalmente.
9. Cantone, M.: Rend. Lincei [5] 1 ii, 119-126 (1892).
Contributo allo studio della variazioni di resistenza del nichel nel campo magnetico.
10. Cantone, M.: Rend. Lincei [5] 6 i, 175-182 (1897).
Sulle variazioni di resistenza prodotte dalla trazione nell'argentana e nel nichel crudo.
11. Bamberger, K.: Dissertation Rostock (1901) 31 pp.
Widerstandsmessungen im Magnetfelde.
12. Barlow, G.: Proc. Roy. Soc. 71, 30-42 (1902).
On the effects of magnetisation on the electric conductivity of iron and nickel.
13. Dongier, R.: Seances soc. franç. de phys. Résumés 61* (1902).
Variation de la résistance électrique du nickel dans le champs magnétique.
14. Williams, W. E.: Phil. Mag. [6] 4, 430-434 (1902).
On the magnetic change of length and electrical resistance in nickel.

²² Curve 2B has been drawn on the assumption that the value for $\Delta R/RH$ given by Tomlinson for annealed nickel in his Table XXIII is that for a specimen earlier described for which only relative values of $\Delta R/R$ are cited.

15. Knott, C. G.: *Trans. Roy. Soc. Edinburgh* **40**, 535-545 (1903).
Change of electrical resistance of nickel due to magnetization at different temperatures.
16. Williams, W. E.: *Phil. Mag.* [6] **6**, 693-697 (1903).
The influence of stress and of temperature on the magnetic change of resistance in iron, nickel, and nickel-steel.
17. Knott, C. G.: *Trans. Roy. Soc. Edinburgh* **41**, 39-52 (1904).
Magnetization and resistance of nickel wire at high temperature.
Also in *Festschrift Ludwig Boltzmann* 333-340 (1904).
18. Williams, W. E.: *Phil. Mag.* [6] **9**, 77-85 (1905).
On the magnetic change of resistance in iron, nickel, and nickel-steel at various temperatures.
19. Ercolini, G.: *Nuovo cimento* [5] **14**, 537-564 (1907).
Variazioni della resistenza elettrica del nichel assoggettato a deformazione.
20. du Bois, H. [E. J. G.]: *Handelingen van het XIIde nederlandsch natuur- en geneeskundig congres. Utrecht, 1909.* p. 128.
Over den invloed van temperatuur en magnetisatie op den gelijkstroomweerstand van nikkell.
21. Heaps, C. W.: *Phil. Mag.* [6] **22**, 900-906 (1911).
The effect of magnetic fields on metallic resistance.
22. Owen, E. A.: *Phil. Mag.* [6] **21**, 122-130 (1911).
The change of resistance of nickel and iron wires placed longitudinally in strong magnetic fields.
23. Knott, C. G.: *Proc. Roy. Soc. Edinburgh* **33**, 200-224 (1913).
Changes of electrical resistance accompanying longitudinal and transverse magnetizations in nickel.
24. Smith, A. W.: *Phys. Rev.* [2] **1**, 339-354 (1913).
The Hall effect and some allied effects.
25. Jenkins, W. A.: *Phil. Mag.* [6] **27**, 731-739 (1914).
On the effect of a magnetic field on electric resistance.
26. Jones, W. M., Malam, J. E.: *Phil. Mag.* [6] **27**, 649-659 (1914).
The electrical resistance of nickel in magnetic fields.
27. Heaps, C. W.: *Phys. Rev.* [2] **6**, 34-42 (1915).
The magnetostriction and resistance of iron and nickel.
28. Nobile, A.: *Rendi. Napoli* [3] **27**, 52-60 (1921).
La resistenza elettrica dei fili di nichel sottoposti a trazione.
29. Obata, J.: *Researches Electrotechnical Laboratory (Tokyo) No. 101* 427-446 (1921).
The effect of magnetic fields on electrical resistance of some alloys.
Also in *Nagaoka Anniversary Volume* 219-239 (1925).
30. Bridgman, P. W.: *Proc. Amer. Acad.* **57**, 39-66 (1922).
The effect of tension on the electrical resistance of certain abnormal metals.
31. Smith, A. W.: *Phys. Rev.* [2] **19**, 285-299 (1922).
The effect of tension on the change of thermoelectric forces by magnetization.
32. Bridgman, P. W.: *Proc. Amer. Acad.* **59**, 117-137 (1923).
The effect of tension on the thermal and electrical conductivity of metals.
33. McCorkle, P.: *Phys. Rev.* [2] **22**, 271-278 (1923).
Magnetostriction and magnetoelectric effects in iron, nickel and cobalt.
34. Bridgman, P. W.: *Proc. Amer. Acad.* **60**, 423-449 (1925).
The effect of tension on the transverse and longitudinal resistance of metals.
35. Kaya, S.: *Sci. Rep. Tohoku Imp. Univ.* [I] **17**, 1027-1037 (1928).
The magneto-resistance effect in single crystals of nickel.
36. Seth, J. B., Anand, C.: *Phys. Zeits.* **29**, 951-952 (1928); **30**, 32 (1929).
Veränderungen im Widerstand beim Spannen von Nickeldraht.
37. Vilbig, F.: *Archiv f. Elektrotechnik* **22**, 194-219 (1929).
Über Widerstandsänderung verschiedener Metalle in Magnetfeldern.

38. Bedi, R. S.: Phys. Zeits. **31**, 180-182 (1930).
Widerstandsveränderungen bei längsgespanntem Nickeldraht.
39. Gerlach, W.: Zeits. f. Physik **59**, 847-849 (1930).
Magnetische Widerstandsänderung und spontane Magnetisierung.
40. Stierstadt, O.: Phys. Zeits. **31**, 561-574 (1930). Die Änderungen der elektrischen Leitfähigkeit ferromagnetischer Stoffe in longitudinalen Magnetfeldern.

Comments on Bibliography.

Tomlinson's work on elasto-resistance (Item 2) is not strictly comparable with later work because he usually accommodated a wire to the maximum load he intended to apply, that is, he repeatedly loaded and unloaded the wire until its resistance changes became cyclic. A wire so treated does not, if the range of stress is more than a few kg/mm², retain its initial properties.

Goldhammer (Items 4, 5 and 6) was the first to observe that there was a remanent magneto-resistance, and introduced great improvements in the control of temperature and in the method of making measurements. He attempted to prove that

$$R = R_0 + AI^2$$

where R_0 is the resistance of an unmagnetized wire, I its magnetization, and A a constant. Even his own data show this relation to be inexact. His last and most important paper appeared only in Russian and is available to most physicists in a single inadequate abstract. I am indebted to Dr. D. E. Olshevsky for its translation. In his second paper he reports the interesting fact that the change in resistance for magnetization is greater after preliminary magnetization at right angles.

Cantone (Items 8, 9 and 10) was the first to obtain the now familiar "butterfly" loops in magneto-resistance. His elasto-resistance data did not disclose "lag" or "priming," but those of Ercolini (Item 19) show lag and Nobile (Item 28) found both effects in a single specimen for different ranges in tension.

The most interesting of the recent papers is that of Vilbig (Item 37). Though he seems not to be acquainted with the history of magneto-resistance he reports some curious variations in resistance for values of H in the neighborhood of the coercive force. There appear from his data to be two distinguishable states of nickel in this region, in one of which (*stabile Zustand*) the resistance variations are reversible, in the other of which (*labile Zustand*) they are irreversible.

The most recent work on elasto-resistance (Items 36 and 38) suffers from a really astonishing paucity of both data and historical background.

NEW DATA

First Series, 1920-1923.

Late in 1920 Dr. H. D. Arnold²³ was struck by the fact that usual methods of measuring the electrical resistance of wires gave erratic results in the case of an alloy containing 77 percent nickel, 23 percent iron. He traced

²³ Director of Research, Bell Telephone Laboratories (in 1920, Engineering Department, Western Electric Company).

this variability to the unsuspectedly large effects of moderate tension and of stray magnetic fields—especially the magnetic field of the earth—and showed that for this particular composition of what was later called permalloy, tension and magnetization were roughly equivalent in their effects upon resistance. He expressed this equivalence by the equation

$$\Delta R = f(H + kT)$$

where $f(x)$ is a function of x which has a maximum value within easily attainable limits of H and T , and k is a constant roughly equal to 0.0035 if H is in gauss and T in kg/mm^2 .

In 1922²⁴ I examined the data upon which this conclusion was based and decided that the equivalence of H and T was not so perfect as Arnold's equation suggests. For low values of H and T the best value of k is considerably greater than 0.0035, meaning that the ΔR —*vs.*— H curve rises more steeply from the origin than does the ΔR —*vs.*— T curve if they are so plotted as to agree best in their middle ranges.

During the summer of 1923 my assistant, Mr. P. P. Cioffi, who had also assisted in the experiments of 1920, measured for me the changes in resistance under tension, magnetization, and combinations of tension and magnetization, in the series of permalloys of special purity used by Dr. O. E. Buckley and myself in a study of changes in magnetization curves and hysteresis loops due to tension.²⁵ Other permalloys, of commercial purity, were also available and were measured at this time. The methods of supporting and stretching the wires, and of measuring changes in magnetizing field and magnetization have been fully described.²⁶ The additional apparatus needed for resistance measurements consisted of current connections at the ends of the wire under test, two fine wires welded to the specimen in the region of uniform magnetization to serve as potential taps, and a potentiometer for measuring the difference of potential between these taps under the various conditions. In these experiments there was no provision for protecting the specimen from heating by the magnetizing solenoid, so that H could not conveniently be made much more than 6 gauss.

The results of these tests confirmed the existence of a transition in properties at a composition in the neighborhood of 81 percent nickel. A brief note dealing with a single composition (78.5 percent nickel) was presented at a meeting of the Physical Society late in 1923.²⁷ One of the drawings then exhibited was published about three years later,²⁸ together with a statement regarding the signs of magneto-resistance and of elasto-resistance in tension on both sides of 81 percent nickel. The method of reducing the

²⁴ At the Bell Telephone Laboratories.

²⁵ O. E. Buckley, L. W. McKeehan, *Phys. Rev.* [2] **26**, 261–273 (1925). These same wires were also used in later work on magnetostriction: L. W. McKeehan and P. P. Cioffi, *Phys. Rev.* [2] **28**, 146–157 (1926).

²⁶ P. P. Cioffi, *J. Opt. Soc. and Rev. Sci. Inst.* **9**, 53–60 (1924).

²⁷ H. D. Arnold, L. W. McKeehan, *Phys. Rev.* [2] **23**, 114 (1924).

²⁸ L. W. McKeehan, *J. Franklin Inst.* **202**, 737–773 (1926); especially pp. 762–763.

observations at the time they were made—by slide-rule—obscured the fact that they are self-consistent to a high degree and, in the aggregate, present interesting information regarding magneto- and elasto-resistance in general. The whole set of data has recently been reduced by methods which preserve the precision really attained,²⁹ and a considerable number of representative curves are here presented for the first time.

Fig. 7 shows the effect of tension alone for a total of 27 annealed³⁰ specimens of (about) one millimeter wire in the range from 65 to 90 percent nickel. Lines which terminate at relatively small values of tension belong to specimens—all of the purer series—which suffered from crystalline brittleness.

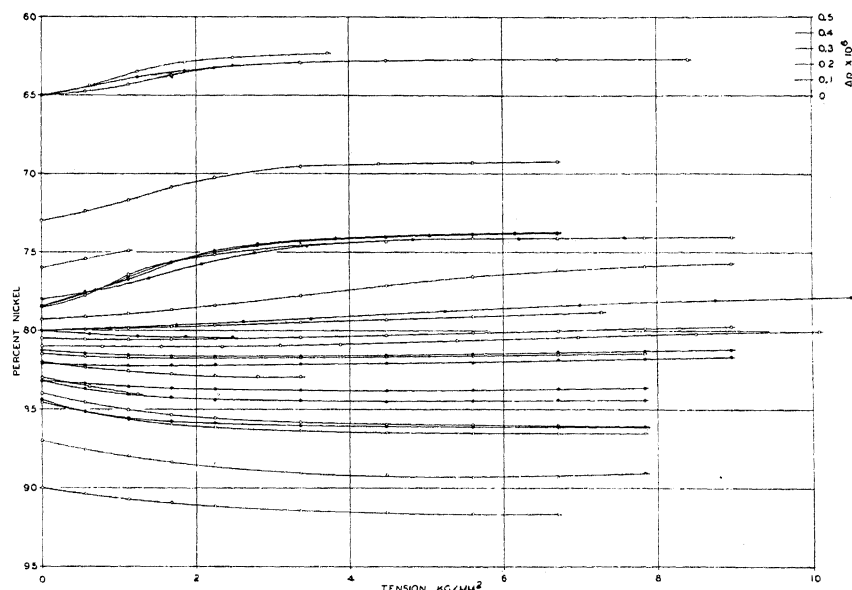


Fig. 7. Elasto-resistance in permalloy under tension—1923.

It will be noticed that these short curves are only a little steeper and straighter than those for neighboring alloys of more normal mechanical soundness.

Fig. 8 shows how the application of a magnetic field has different effects under different steady tensions, including zero tension in each case.

It will be noticed that I have departed from precedent in plotting the change in resistivity,³¹ $\Delta\rho$, rather than the proportional change in resistance, $\Delta R/R$. This departure seemed advisable because the resistance, R , for specimens of equal dimensions, and with it the resistivity, ρ , and the ratios $\Delta R/R$ and $\Delta\rho/\rho$ vary widely with nickel content—by a factor of 6 within

²⁹ I am indebted to my former colleagues at the Bell Telephone Laboratories for the loan of notebooks containing the original records of these experiments.

³⁰ Held at 960° C in vacuum for one hour and cooled to room temperature in about an hour.

³¹ The resistivity ρ has *not* been corrected for changes in dimensions of the specimens under tension. These changes were not measured and in comparison with such large changes as here occur the correction due to these elastic deformations is safely negligible.

the range covered—and because, for one and the same nickel content R , ρ , $\Delta R/R$ and $\Delta\rho/\rho$ are correspondingly sensitive to small differences in purity, in mechanical soundness and in thermal state or history. As the specimens were not all of the same diameter ΔR was an unsuitable index of the effect under investigation and $\Delta\rho$ was the only quantity fairly characteristic of nickel content alone. It can be argued that the effect of tension or of a magnetic field is to produce, increase or diminish an additive resistivity of the same kind as that due to alloying, *i.e.* independent of the change in resistivity due to change in temperature and, presumably, equally independent of additive resistivities due to structural imperfections and the

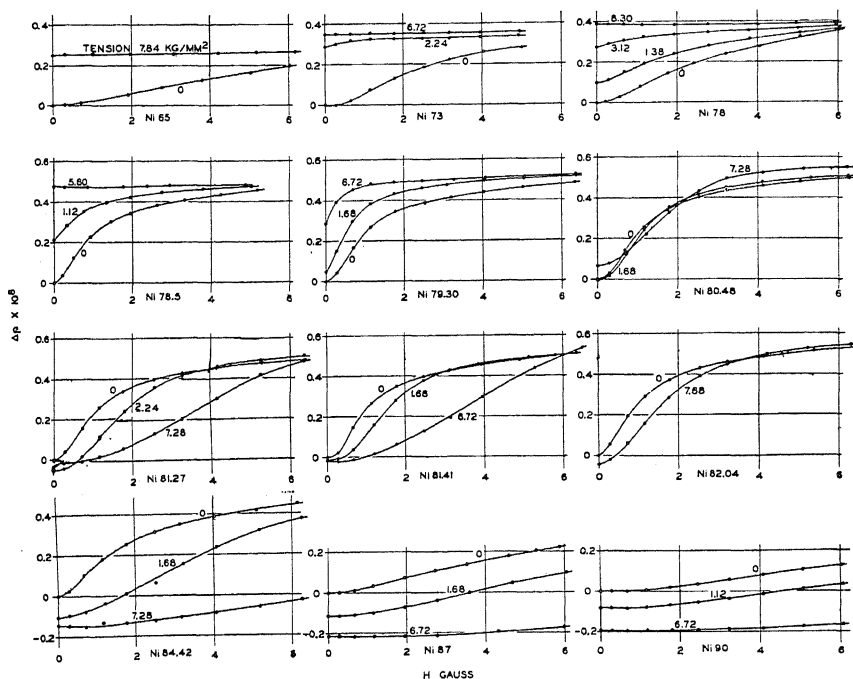


Fig. 8. Effect of tension on longitudinal magneto-resistance in permalloy—1923.

like. In case it is desired to convert any value of $\Delta\rho$ into the proportional change $\Delta\rho/\rho$ to be expected in pure, sound, metal the values of ρ given by Sizoo and Zwicker³² are probably the best available.

The purer series of alloys were made in such small lots that they could not easily be analysed, and for the same reason the probable error in their compositions is large. Some of the discrepancies in Fig. 7 are probably due to deviations of actual from intended nickel-iron ratio in members of this series, especially at about 80 percent nickel where a small change in composition changes the sign of elasto-resistance. Wherever, in Fig. 8, the

³² G. J. Sizoo and C. Zwicker, *Zeits. f. Metallkde.* **21**, 125–126 (1929). These authors are probably wrong in ascribing every peculiarity of the ρ -vs.-nickel content curve to the existence of a definite nickel-iron compound.

nickel content is given to hundredths of a percent this datum is the result of one or more analyses on wire drawn from the same casting. It cannot be expected, however, that the nickel content of any particular specimen is known with a smaller probable error than ± 0.2 percent.

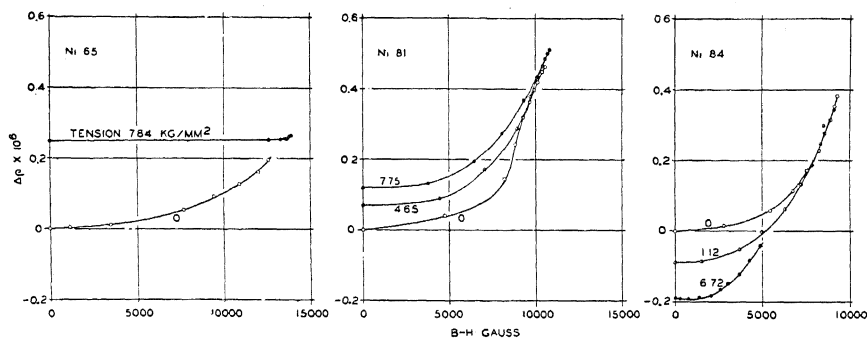


Fig. 9. Effect of tension on longitudinal magneto-resistance in permalloy, as a function of magnetization—1923.

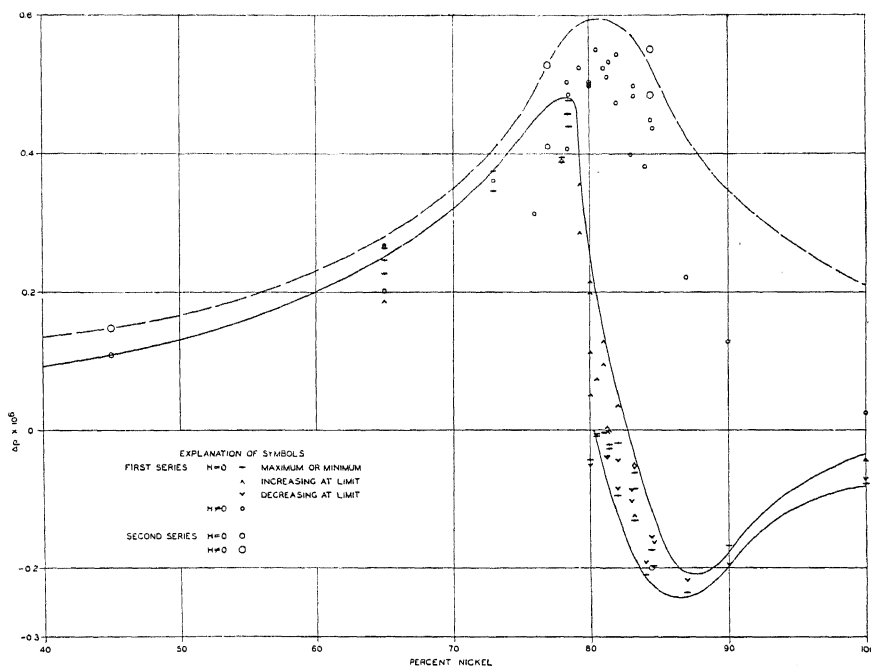


Fig. 10. Magneto-resistance and elasto-resistance in permalloy, as a function of nickel content.

The magnetization curves for the alloys particularly studied by Dr. Buckley and myself²⁵ were also obtained at about the same time as the resistivities and have been used to obtain—in Fig. 9—the relation between $\Delta\rho$ and $B-H$ in the cases of three compositions. These curves are not so simple as to suggest that much would be gained if it were possible to obtain like curves for all of the specimens. One objection to such an attempt is that

measurements at a single value of H can easily be repeated with accuracy by using high-capacity storage batteries and resistance boxes, whereas a value of $B-H$ is hard to duplicate.

Fig. 10 presents many of the results displayed in Figs. 7 and 8, and additional results of the same sort from experiments for which detailed curves are not here reproduced. It shows that for permalloys with less than about 79 percent nickel the effect of tension is of the same sign as that of magnetization, and that the greatest positive value of $\Delta\rho$ due to tension within the elastic limit in this range of composition may be nearly as great as that due to magnetization alone or to any combination of pull and magnetic field. Between 79 and 100 percent nickel tension within a safe limit is incompetent to increase the resistivity as much as magnetization can, so that the full line which runs close beneath the broken line for low nickel content here drops far beneath it. It is worthy of remark, however, that the course of the curves at the safe limit in tension makes it not unlikely that if the necessary tensile stress could be applied without damage to the specimen the final resistivity in tension might again be nearly as high as that produced by magnetization.

Beyond a somewhat ill-defined point which has been chosen in Fig. 10 at 80.5 percent nickel, the initial effect of tension is to diminish ρ so that ρ passes through a minimum within the safe range of loading. Close to or at the same critical composition the magneto-resistance effect passes through a well-marked maximum.

The data of 1923 do not permit any very definite statements regarding the effects of magnetization in permalloys with more than about 83 percent nickel, because H could not be pushed high enough to obtain the saturation value of $\Delta\rho$. The results of previous investigators on pure or nearly pure nickel have been used to establish the right-hand end of the broken line in Fig. 10 and the gap has been filled in on the supposition that the magneto-resistance effect at saturation is roughly symmetrical about the maximum near 81 percent nickel.

Series of 1929-1930.

An additional series of experiments was undertaken in this laboratory about a year ago with the idea of extending the range in H and to clear up a difficulty which can best be understood by reference to Fig. 8. While it is abundantly clear that the principal effect of increasing H from zero is to increase ρ , there are numerous $\Delta\rho$ -vs.- H curves which first pass through a shallow minimum.³³

Since the procedure in 1923 included a preliminary demagnetization³⁴ it seemed impossible to explain this minimum as due to the suppression of an initial magnetization in a direction opposite to that in which H was increased during the experiment itself. It appeared possible that the process

³³ The reality of these minima was not apparent until the data had been reanalysed as explained above.

³⁴ By decreasing to zero amplitude an alternating magnetic field in the presence of a constant field adjusted to compensate the vertical component of the earth's magnetic field.

of demagnetizing might have heated the specimen, the initial drop in ρ then being attributable to cooling. Both purposes required better control of the temperature of the specimen and advantage was accordingly taken of some improvements in technique devised for the even more exacting requirements met in studying magnetostriction.³⁵

The new magnetizing coil was wound on a double-walled glass jacket inside which were the specimen, potential leads and search coil. There was now—as there had not been in the magnetostriction studies—a source of heat inside the jacket, since a current had to be maintained in the specimen to permit the measurement of its resistance. It was therefore necessary to pass a heat-absorbent material through the jacket rather than to evacuate and silver it. In order to prevent the condensation of atmospheric water vapor on parts within the jacket, and to make it feasible to leave the lower end open so as to constrain the loaded end of the specimen to the least possible degree, the tap-water used as a coolant was circulated through the jacket at a temperature several degrees above that of the room. Most of the heat necessary to maintain this excess temperature was furnished by a manually controlled gas heater. Final adjustment, usually to 26°C, was effected by a 400-watt electric heater controlled by a mercury-under-hydrogen switch operated by a thermostat of the Stirlen type³⁶ between the electric heater and the jacket. With a convenient flow of water it was found by direct experiment that the temperature of a representative specimen did not vary by as much as 0.01°C during normal operation. For a magnetizing current corresponding to $H = 50$ the rise in temperature of the specimen produced a change in resistance negligible in comparison with those to be measured. The barometric height affects the equilibrium temperature of the cooling water, and other things, particularly the room temperature, make slight differences in the temperature of a specimen for the same water temperature. For these reasons sets of data taken at intervals of a day or more frequently yielded slightly different values of ρ for what were meant to be identical conditions. Such differences are believed, for reasons already mentioned, to have little or no effect upon the values of $\Delta\rho$, provided a standard magnetic and mechanical condition can be reestablished at intervals to furnish a bench-mark.

The three alloys chosen for study contained about 45, 77 and 85 percent nickel, and were furnished by the Bell Telephone Laboratories in the form of 40-mil (about one millimeter) wires. Analysis of one of these and analyses of materials of similar manufacture indicate the presence of impurities about as follows:

Co	0.2 percent	Si	0.01
Mn	0.2	C	0.01
Al	0.05	S	0.005
Cu	0.05	P	trace

³⁵ *loc. cit.*²⁵ second reference.

³⁶ A mercury column balanced by the vapor pressure of a suitable mixture of ethanol and ethyl ether in a bulb completely submerged in a small reservoir.

Suitable lengths of the hard-drawn wires were straightened and then were heated, while hanging vertically in hydrogen at atmospheric pressure, to about 1000° for one hour by passing an alternating electric current through them. Cooling was rapid. Care was taken to avoid bending or twisting the prepared specimens, even elastically, and the results obtained with good specimens did not depend upon the order in which experiments were performed.³⁷

Figs. 11 to 13 inclusive present resistivity changes as a function of H for loops repeatedly traversed between equal positive and negative values of $H(\pm 23.4 \text{ gauss})$, under various steady tensions well within the elastic limit. In 45- and 77-nickel permalloy the magneto-resistance effect is

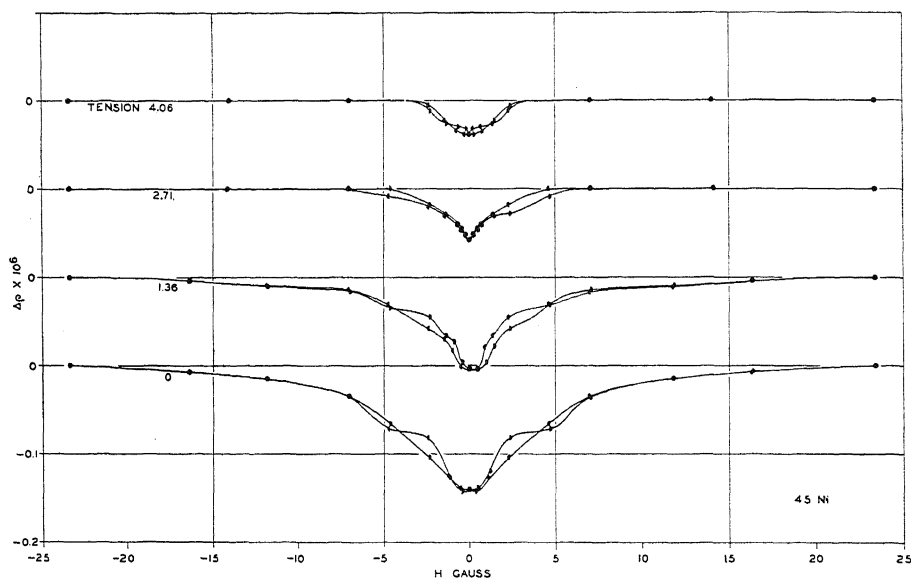


Fig. 11. Effect of tension on longitudinal magneto-resistance in permalloy with 45 percent nickel. Major loops.

thoroughly saturated at the peak value of H so that this condition of maximum resistivity was chosen as standard. With this convention $\Delta\rho$ is negative and passes through its maximum negative value near $H=0$. In 85 permalloy (84.41 by analysis) the effect is hardly saturated by $H=23.4$ even for zero tension. All values of $\Delta\rho$ were therefore obtained with respect to the highest value of ρ in the experiment under zero tension, and the difference in level with difference in tension in Fig. 13 is not as significant as in Figs. 11 and 12.

The method of taking observations, in which corresponding points for $+H$ on the descending branch and for $-H$ on the ascending branch are taken in quick succession, tends to make the errors symmetrical, since accidental causes more often than not produce like errors in consecutive

³⁷ The less consistent behavior of certain specimens is described later.

measurements of nearly equal values of ρ . This is very evident in Figs. 11 and 13. In Fig. 12, however, the curves are noticeably asymmetric. Still more asymmetric results were obtained in certain preliminary experiments on other specimens of 77 and 85 percent permalloy. The search for the cause of this asymmetry led to clearing up one of the questions at issue and must therefore be described in some detail.

In the preliminary experiments the $\Delta\rho$ -vs.- H curves were analogous rather to normal magnetization curves than to hysteresis loops. That is, H_{\max} was repeatedly increased, ρ being measured only for $+H_{\max}$ and $-H_{\max}$

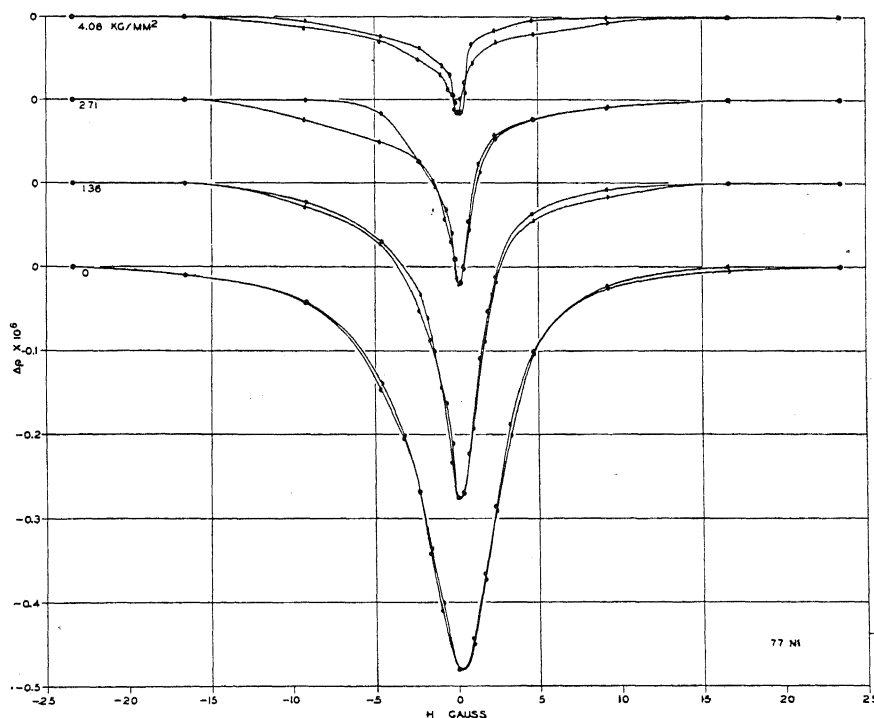


Fig. 12. Effect of tension on longitudinal magneto-resistance in permalloy with 77 percent nickel. Major loops.

at each step, so that the curve obtained was the locus of the tips of loops like those given in Figs. 11 to 13 for a particular value of H_{\max} . Fig. 14 gives part of the results obtained in this way for a particular specimen of 77 percent permalloy.³⁸ The curves are lettered to distinguish the order in which they were obtained, and black dots mark the starting points the centers of the ranges in H . The maximum applied field in these experiments—70 gauss—largely exceeds the limits of the figure. The value of ρ for great

³⁸ The points upon which these curves depend have been omitted from Fig. 14 in the interest of simplicity. There are for each curve more than 60 measured values of $\Delta\rho$ with the range shown.

applied fields is the bench-mark for $\Delta\rho$ in each case. It will be noticed that ρ reaches its limiting value within the limits of the figure on only two curves, *viz.* on the negative side of curve *D*, and on the positive side of curve *G*.

The very striking thing about Fig. 14 is that applying H in one direction from the starting point decreases ρ just as applying H in one direction in the experiments of 1923 (see Fig. 8) sometimes decreased ρ . But now that *both* signs of applied field are used the smooth course of the $\Delta\rho$ -*vs.*- H curves through their starting points makes it evident that the initial states are not of any particular significance in respect to magneto-resistance.

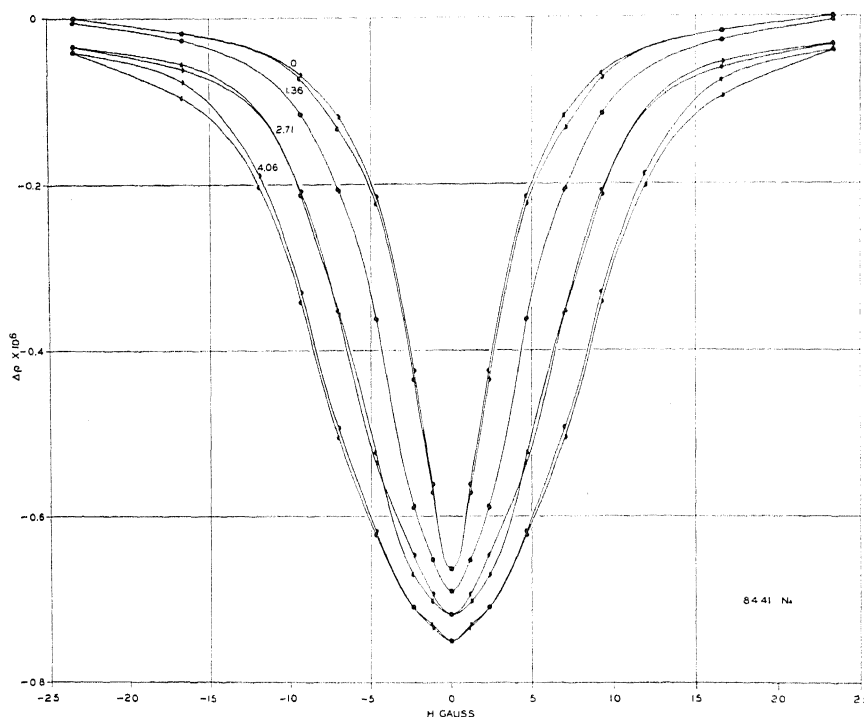


Fig. 13. Effect of tension on longitudinal magneto-resistance in permalloy with 85 percent nickel. Major loops.

An attempt had, of course, been made in every case to select a significant initial state, that of complete demagnetization in zero applied field. The process employed for this selection is one of those described in an earlier paper.³⁹ In it the specimen is carried repeatedly around a hysteresis loop of suitable range in H . It is then observed whether the changes in B corresponding to equal steps in H from the two tips of the loop are or are not equal. If they are equal the loop is symmetrical and its center is at $H=0$. If they are not equal the stray fields producing the asymmetry of the loop must be compensated before a demagnetizing process can be really effective.

³⁹ L. W. McKeehan, P. P. Cioffi, J. Opt. Soc. Amer. and Rev. Sci. Instr. **9**, 479-485 (1924).

In the experiments here under discussion the specimen to be tested had been used in the manner just described in adjusting the magnetic field applied to compensate that of the earth.⁴⁰ It had already been observed with some alarm that the compensating field so fixed varied much too widely. The obvious explanation was that the particular specimen in use did not follow symmetrical hysteresis loops in zero field. When the loops were forced to pass through four symmetrically disposed points—the tips and the two test

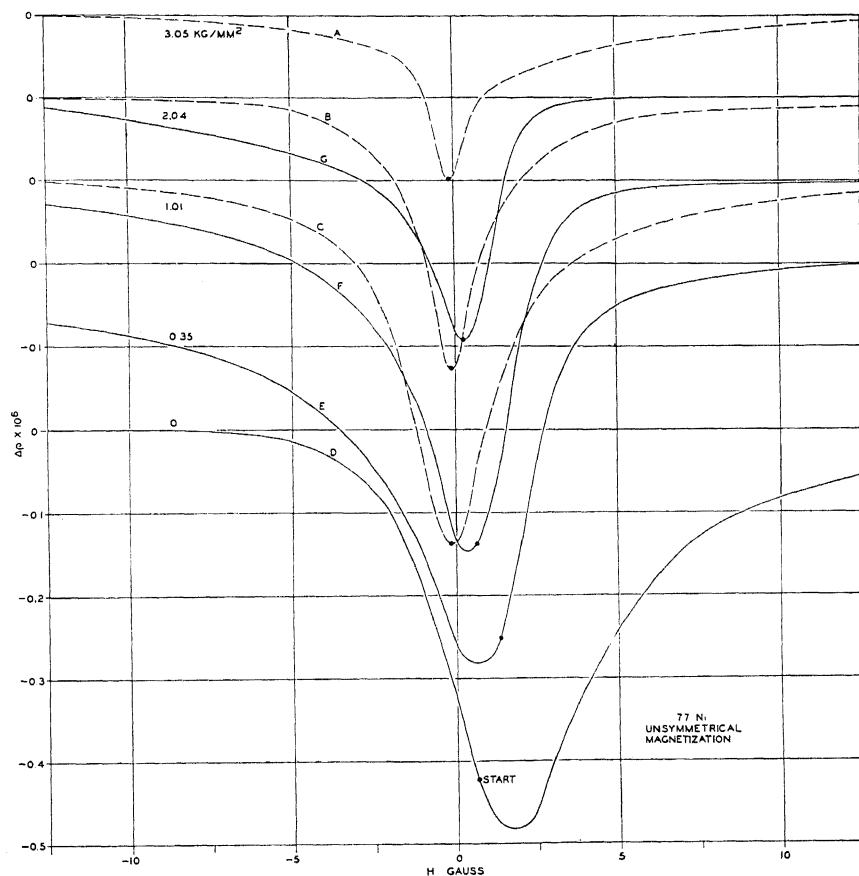


Fig. 14. Effect of tension on longitudinal magneto-resistance in permalloy with 77 percent nickel—unsymmetrical magnetization.

points—the middle did not therefore lie at $H=0$ and when “demagnetized” at this fictitious origin for H the specimen was left partly magnetized. As soon as this was realized a specimen known to give hysteresis loops symmetrical about $H=0$ was substituted for the suspect specimen and the true earth’s compensating field thus measured. The results of this auxiliary experiment have been used in fixing the abscissas of the starting points in Fig. 14.

⁴⁰ The magnetizing solenoid carries a separate winding for this purpose. *loc. cit.*²⁶

The question still remaining was why the specimen followed asymmetrical loops and how their asymmetry could change as profoundly as it evidently had between the experiments recorded in curves *C* and *D* of Fig. 14. Trial of several specimens prepared in the same way showed that asymmetry was more likely to appear in specimens which were slightly bent or otherwise visibly damaged than in those which passed every visual test. It has long been known⁴¹ that the passage of an electric current through an apparently well-annealed wire will develop in it a magnetic asymmetry that is relatively persistent but that can be altered by reversing the direction of the current, by mechanical twisting, by vibration and the like. The reason for this is

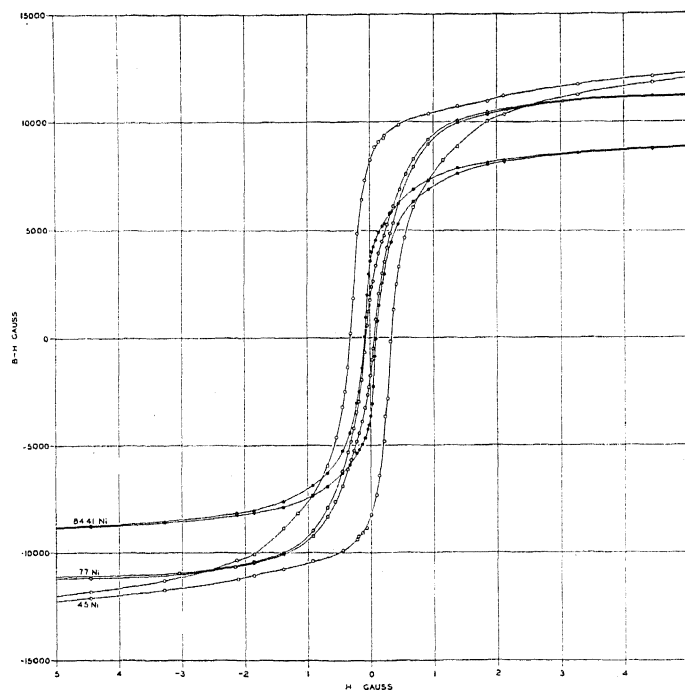


Fig. 15. Hysteresis loops for permalloy specimens of Figures 11, 12 and 13.

to be looked for in the mechanical history of the particular piece, especially in twisting and untwisting operations. In the wires here used, made in small lots and with much handling, it is not at all surprising that specimens from the same lot should show local differences in subliminal twist in the finally annealed condition. Neither is it surprising that this mere ghost of a dead twist might have been altered by accident in the interval between the taking of data for curves *C* and *D*.

The specimens used in getting Figs. 11 to 13 give symmetrical hysteresis loops, as is shown, for zero tension, in Fig. 15. This confirms the conclusion as to their relative excellence derived from the magneto-resistance tests

⁴¹ D. E. Hughes, Proc. Roy. Soc. 32, 25-29 (1881).

already described, in which the earth's compensating field was correctly adjusted. Besides the wide loops of Figs. 11 to 13, and some still wider, a great many narrower loops have been traced. A few of these are presented in Fig. 16.

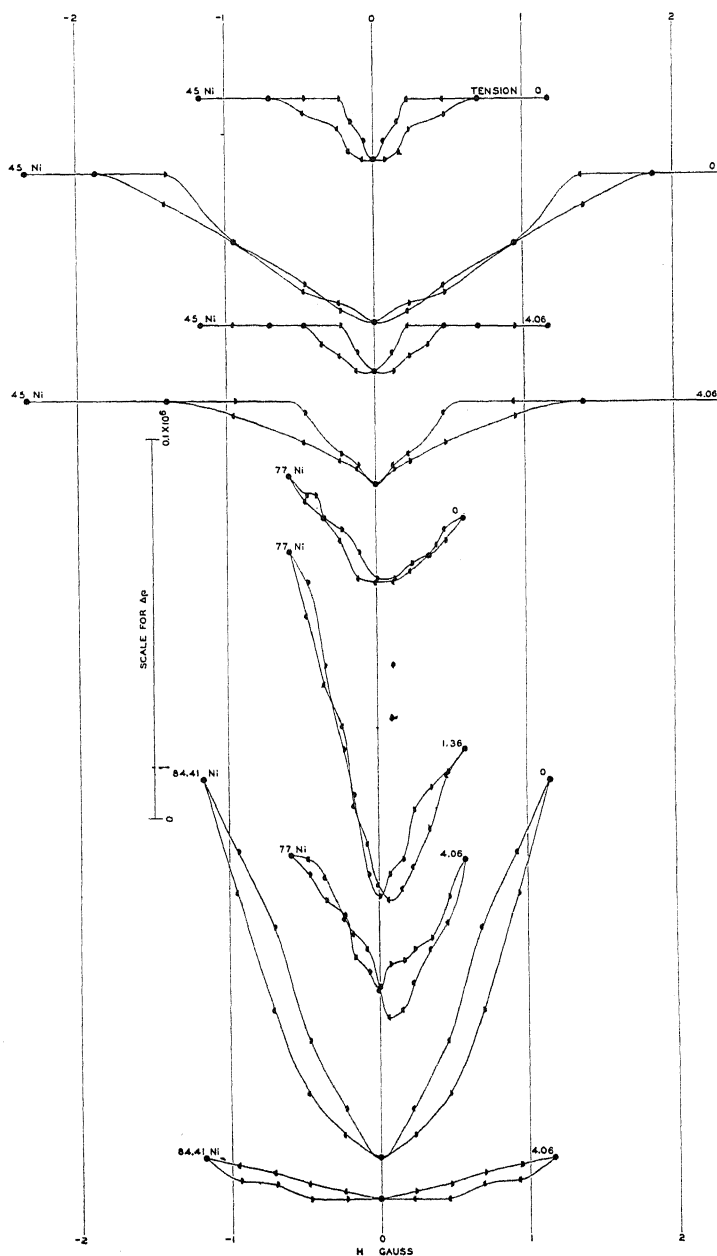


Fig. 16. Longitudinal magneto-resistance in permalloy specimens of Figures 11, 12 and 13. Minor loops.

In all the work so far described in this section the changes in magnetization, corresponding to each change in H were followed ballistically, so that $\Delta\rho$ has also been obtained as a function of the magnetization ($B-H$). Figs. 17 and 18 show some characteristic curves of this sort. As in the first series,

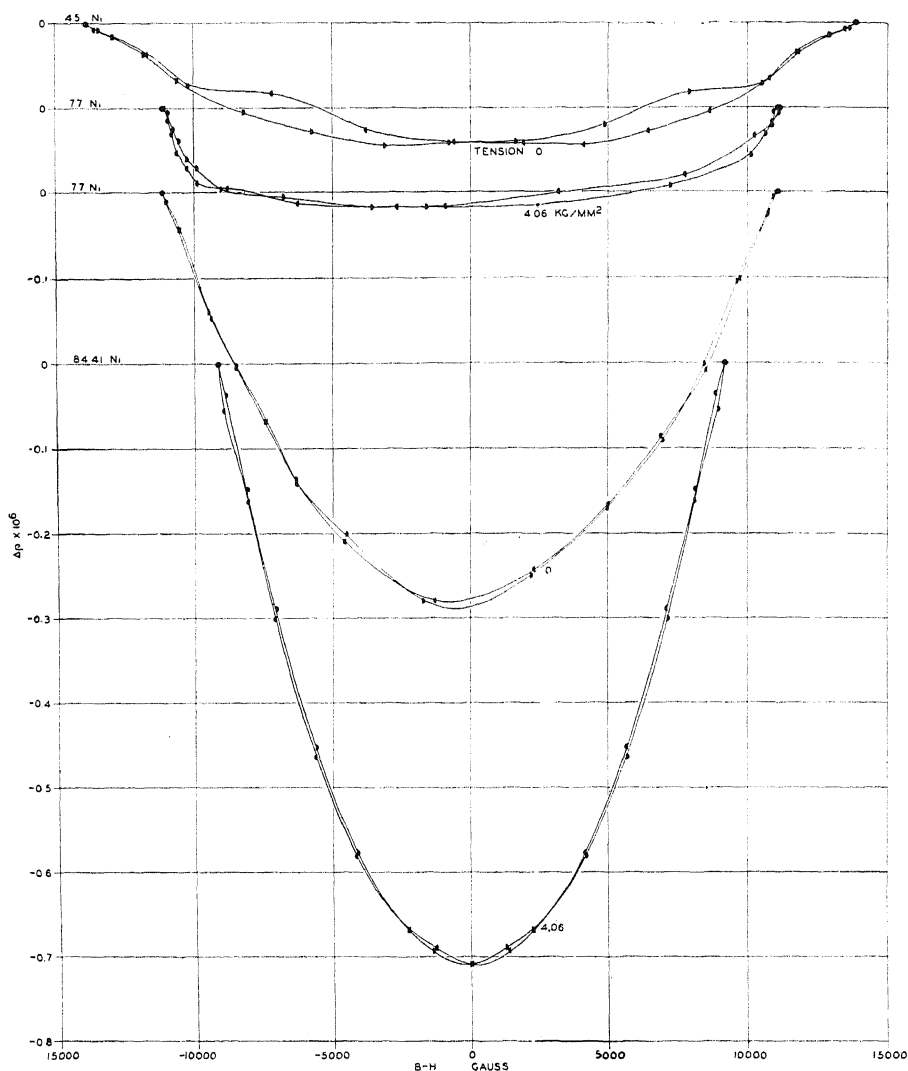


Fig. 17. Longitudinal magneto-resistance as a function of magnetization for permalloy specimens of Figures 11, 12 and 13. Major loops.

however, there is little or no advantage in thus presenting the results, and there is some loss in considering the relations between two dependent variables rather than between one dependent and one independent.

The bizarre appearance of Fig. 11 made it seem possible that the magnetization of the specimen had been notably discontinuous. The magnetic meas-

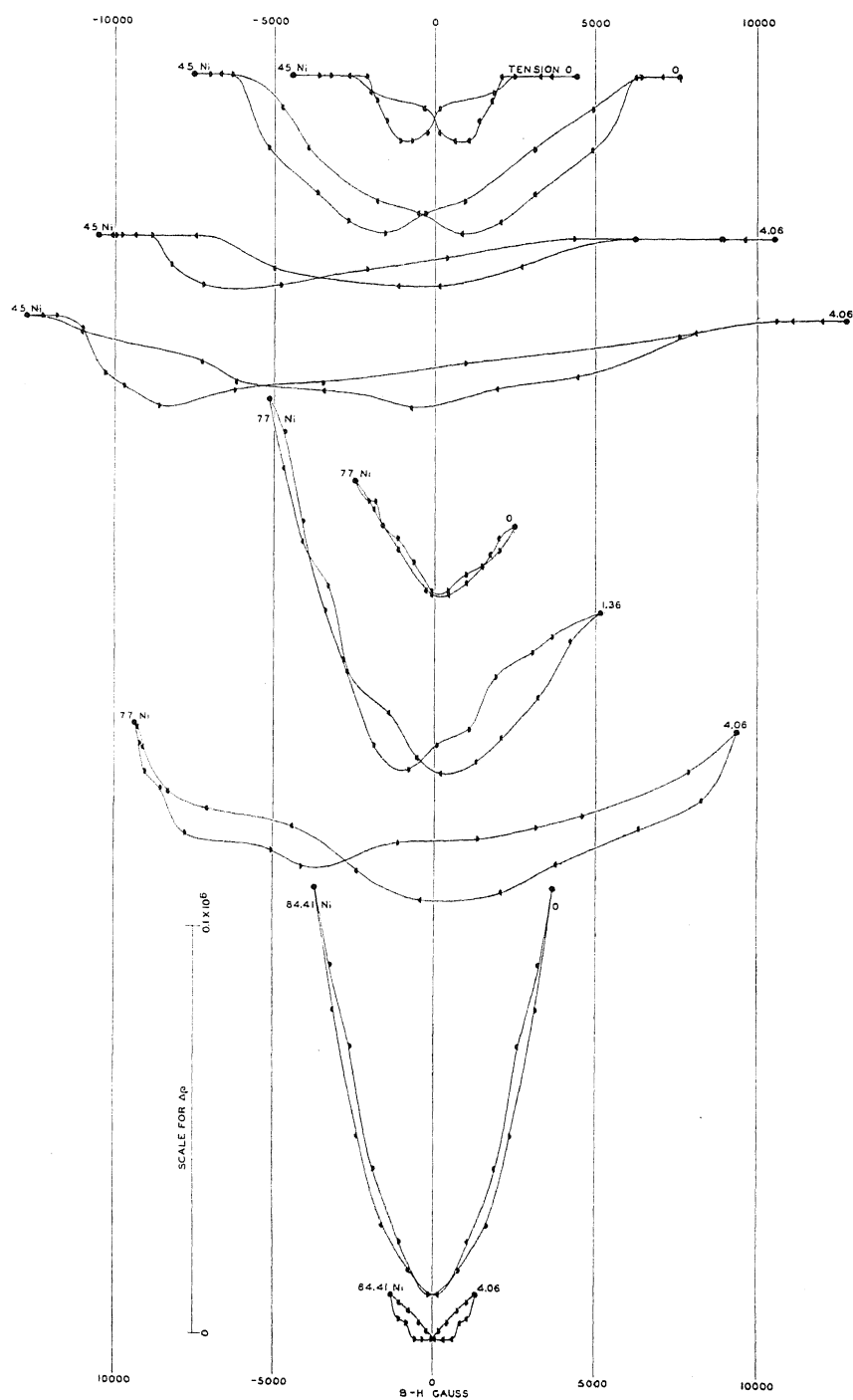


Fig. 18. Longitudinal magneto-resistance in permalloy specimens of Figures 11, 12 and 13, as a function of magnetization. Minor loops.

urements shown in Fig. 15 disposed of this idea and it seemed advisable to measure the variations in ρ during a loop traversed as smoothly and continuously as possible. Since the jerkiness of the previous traverses⁴² was largely due to the inclusion of ballistic measurements of magnetization changes this feature was dropped for the special experiment. A potential divider was so constructed of slide-wire resistances that the current through the magnetizing coil could be varied continuously in either direction between about +1 amp. and -1 amp. This current was measured by a microammeter across shunts of such low resistance that the transfer of the microammeter from one shunt to another in changing the range of this make-shift ammeter did not sensibly disturb the current being measured. The resistivity was now measured for consecutive points around a loop about as wide as those in Fig. 11 and under no tension. The results in ρ are plotted in Fig. 19 which shows a highly irregular loop with the three main crossings seen in Fig. 11 and a pair of more doubtful crossings on one side only. It must be concluded that the principal irregularities are not due to the step-by-step character of the earlier tests on this specimen.⁴³

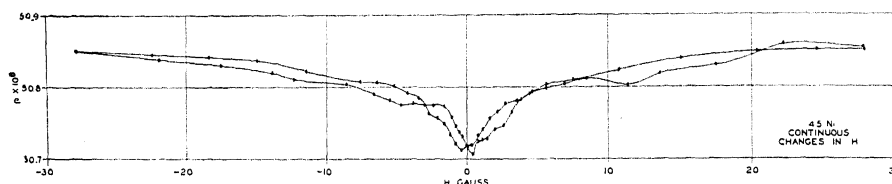


Fig. 19. Longitudinal magneto-resistance in permalloy with 45 percent nickel, for continuous variation of magnetizing current. Major loop.

Points have been placed on Fig. 10 to show that the new data support and extend the old. For 45 and 77 percent nickel the correspondence is good. For 85 percent nickel arbitrary correction terms (-0.112 and -0.079 in $\Delta\rho$) have been applied to lower the points plotted for this alloy until the points for tension alone agree with the earlier curve. Such a correction would be theoretically justified if the annealed specimen had its structure modified in the way that low tensions favor. It would probably be more logical, however, to suppose that all three alloys suffered in the same way but to a smaller extent. This would involve raising all the plotted points that have been derived from the second series of experiments by about 0.05 in $\Delta\rho$. The trend of the new points would still agree with that of the old, but the magneto-resistance limit would have to be raised higher than it has been drawn.

DISCUSSION OF RESULTS

In this discussion I propose to regard the specimens as assemblies of atoms, for the most part associated with the points of a space-lattice, and, as far as may be, to interpret the findings in terms of atomic properties and

⁴² *loc. cit.*,²⁶ control of magnetizing current by a battery of knife switches.

⁴³ There was an interval of seven months between the tests here compared.

inter-atomic relations. This mechanistic method has pictorial advantages and probably will serve to describe the phenomena as well or better than the more up-to-date statistical method.

The difference, emphasized in the introduction, between magneto-resistance in ferromagnetics and in other metals, suggests that the disturbance of electric conduction producible by magnetic fields has, in ferromagnetics, already proceeded far in zero *applied* field. Let us assume, therefore, that the most important part of each atomic domain in a ferromagnetic metal is occupied by a self-maintained magnetic field so intense that in comparison with it the most intense fields yet used in the study of magneto-resistance are nearly negligible.⁴⁴ Applied fields can therefore only affect conduction in ferromagnetics by aligning these atomic fields and by the relatively trivial changes in inter-atomic regions which must result from such alignment.

Kapitza² has supposed that conduction is affected almost as much by random local fields and by uniform fields of the same average scalar magnitude. The present suggestion is that this small difference in effect is the whole magneto-resistance effect in ferromagnetics.

The principal result of the experiments on permalloy is (*cf.* Fig. 10) that the maximum effect of tension in a particular class of alloys is nearly equivalent to the maximum effect of magnetization, and that both agents together are no more effective than magnetization alone. This means that the atomic fields we have postulated can be aligned by tension as well, or nearly as well, as by magnetization. If the alignment effected by tension is as nearly perfect as that effected by an applied magnetic field, the slightly smaller change in resistivity for tension is to be explained as due to the lower average magnitude of the interatomic field between oppositely directed atomic magnets. Otherwise we must neglect the effect of regions remote from any magnetic element, and explain the lower efficacy of tension by supposing, probably in accordance with fact, that the mechanical stress within the stretched specimen is not as homogeneous as the magnetic field due to current in an enclosing solenoid. It is obvious that mechanical stresses can only affect the orientation of atoms with less than spherical symmetry, and that the asymmetry must be spatially related to the magnetic axis in each atom.

This line of reasoning applies also to cases where the initial effect of tension and the effect of longitudinal magnetization are opposite in sign. Here we have only to assume that moderate tension renders the arrangement of atomic magnetic axes less nearly parallel and more nearly transverse to the direction of current.

The plausibility of these assumptions is much greater in view of the

⁴⁴ It may be noted that a magnetic dipole having the magnetic moment associated with each atom of nickel at saturation produced a field in excess of 3×10^5 gauss throughout less than one percent of the atomic volume, so that a magnetic element much less compact than a dipole is indicated. The intense magnetic fields here dealt with should not be confused with the "molecular field" of Weiss which controls the interaction of atoms and must be located principally in interatomic regions.

measurements on magnetostriction,³⁵ which show that tension decreases the magnetostrictive expansion in permalloys with less than about 81 percent nickel, and increases the magnetostrictive contraction in those with more than this nickel content. There is, to be sure, an element of extrapolation in establishing a quantitative relation between magnetostriction and elasto-resistance effects. The maximum magnetostrictive strain is much less than the strain necessary to saturate the elasto-resistance effect. (There is as yet no proof that the elastic and magnetic strains are exactly similar.) Secondary effects are therefore to be expected in tension rather than in magnetization. The change in sign of $\partial\rho/\partial T$, at an attainable value of T , in nickel and nickel-rich alloys is such a secondary effect that may well repay further study.

A striking feature of Fig. 10 is the maximum in $\Delta\rho$ for magnetization at about the critical composition dividing alloys which expand when magnetized from those which contract. Striking as this maximum is, it may be unimportant in the theory of these phenomena. The current maintained in the wires for resistance measurement produces a transverse magnetic field which, near the surface of the wire, is enough, by itself, to maintain approximate magnetic saturation in the more easily magnetizable permalloys. What is measured, then, is the whole change in resistance from a condition of transverse magnetization to one of longitudinal alignment. The fact that the peak value is about twice that for pure nickel (where the transverse magnetization is certainly slight) lends support to this hypothesis, since the transverse effect, when correctly measured in ferromagnetics is always of about the same magnitude as the longitudinal effect, and opposite in sign.⁴⁵

The irregularity of many curves and the confusion of points near 81 percent nickel in Fig. 10 are not regarded as being especially significant. It seems more reasonable to suppose that local variations in composition are chiefly responsible. If the resistivity varies from point to point the distribution of current over the cross-section also varies from point to point and the average resistivity as measured is not a simple space-average but a more sensitive function of the independent variables. The 45 percent alloy lies near a resistivity maximum and the critical region is one where resistivity changes rapidly with composition. Changes in flux distribution over the cross-section, involving changes in resistivity, provide a secondary source of non-uniformity of current.

More important than these casual irregularities is the definite evidence, most strikingly presented in Figs. 9 and 17, that $\Delta\rho$ is not, for these materials,

⁴⁵ Considerations of the same sort support the negative correction used in placing points on Fig. 10 for 84.41 Ni (Second Series). In annealing a vertically hung wire of this composition both the heating current and the weight of the specimen conspire to establish transverse settings of the atomic axes, and thus to decrease the subsequent decrease of ρ under tension, to increase the increase of ρ for magnetization. For the other alloys treated in the same way the heating current and the weight of the specimen act in opposite senses upon the arrangement of atomic axes. The wires of the first series were annealed horizontal in a tube furnace, so that no such correction was called for in plotting the results.

any simple function of the magnetization. This is no surprise, because it is implied by the fact, already noted, that magnetization of certain stretched alloys does not change their resistance. Such magnetization must be regarded as due to the reversal in direction of atomic magnets originally anti-parallel to the applied magnetic field. It will be natural, therefore, to expect that any changes in magnetization due to reversals will be without effect upon electric conduction.

In well-annealed strain-free metal changes in magnetization involve at each stage both reversals of atomic magnets and changes of another sort which may conveniently be pictured as rotations of the elementary magnets through less than 180° . It has been suggested in an earlier paper⁴⁶ that reversals involve no hysteresis, as they have no effect upon magnetostriction. The smooth curvatures of the hysteresis loops plotted in Fig. 15 are therefore taken to indicate that partial rotations occur at all stages. Consistent with these ideas is the smooth and nearly parabolic course of $\Delta\rho$ -vs.- $(B-H)$ curves under these conditions. As suitable stresses are applied, the separation of the two modes of magnetization becomes sharper, the reversals occurring within a narrower range of H and accounting for a larger fraction of the whole change in magnetization. The hysteresis loops become more nearly rectangular,⁴⁷ hysteresis losses and magnetostriction decrease, and as the new data show, the central portions of $\Delta\rho$ -vs.- $(B-H)$ curves become so flattened that they no longer suggest parabolas.⁴⁸

Minor hysteresis loops always have some area, and in accordance with the ideas just presented, must therefore involve both reversals and partial rotations. It is consistent with our picture of the phenomenon, therefore, that there are sensible changes in ρ in traversing loops wholly within the limits of the flat central portion of more extensive loops. Though the changes in magnetization might have been accounted for by reversals alone, all the experimental evidence is against this supposition.

There remains one paradoxical fact which gives further information about the mechanism of electric conduction. Though it is necessary to proceed well toward magnetic saturation before the magneto-resistance effect becomes important, the effect saturates sharply before magnetic saturation is attained. This must mean that the disorganization of electric conduction is sensibly complete before exact parallelism of magnetic axes obtains. One or both of the following conclusions are reasonable.

In the first place we may argue that this experimental fact proves that many paths of electric conduction are oblique to the wire axis. The average velocity of electrons is, of course, still along this axis, but small deviations of magnetization from exact parallelism with the axis become unimportant in fixing the mean resistivity.

⁴⁶ L. W. McKeehan, Phys. Rev. [2] 28, 158-166 (1926).

⁴⁷ *loc. cit.*²⁵ first reference.

⁴⁸ Actually the smoothest and most regular of these curves require $n > 2$ in any assumed relation of the form $\Delta\rho = (\Delta\rho)_0 + A |(B-H)^n|$.

In the second place we may argue that only when the adjacent atoms in a crystal are oriented in particular ways with respect to the line joining their centers, is conduction along that line unhindered, and that reversing either or both of these atoms leaves the favorable condition unaltered. If this be admitted it follows that as soon as the applied magnetic field reaches such a value that any favorable aspect of adjacent atoms is improbable, further increase of applied field, though it increases the probability of exact parallelism—magnetic saturation—can have no further effect upon conductivity.

A decision between these conclusions can be made by measuring the resistivity of monocrystalline specimens in directions inclined to the axis of magnetization.

The diversity of results presented in the review of previous work is now seen to be a natural consequence of the inter-play of magneto-resistance and elasto-resistance changes. Among the most puzzling of the early results were the cases reported by Williams⁴⁹ in which annealing diminished the saturation value of $\Delta R/R$ due to magnetization. We now explain this anomaly by the existence in his unannealed wires of a preferred orientation of atomic axes due to tension, and the return to a more nearly random distribution of magnetic axes in the process of annealing.

Part of the spread of values in the earlier literature must be due to abnormalities in resistivity. Low values of $\Delta R/R$ are particularly suspect, since the purest specimens would have the highest values of this quotient.

It will be noticed in Figs. 2, 3 and 4 that the magneto-resistance effect saturates sharply whatever its maximum magnitude, and that the initial slopes of the several curves vary widely. The latter fact points to the existence in the various specimens of widely different initial conditions. Even if the maximum resistance in each case had been chosen for reference the resulting curves could not be superposed. This suggests that in the state of maximum resistance different specimens have different distributions of internal stresses tending to disorganize the arrangement of atomic magnetic axes produced in magnetizing.

CONCLUSION

The principal features of magneto-resistance and elasto-resistance in nickel and permalloy for longitudinal magnetization and tension have been presented and discussed. Previous results and the results of new experiments can be adequately explained in terms of atomic orientation provided: (1) each atom has a fixed magnetic moment and a magnetic axis definitely related to its mechanical asymmetry; (2) magnetization is effected by two processes, conveniently termed reversals and partial rotations of atomic magnets, the relative importance and sequence of which depend principally upon mechanical stresses; (3) electrical conduction is affected primarily by the atomic magnetic fields within single atoms, secondarily by the mutual

⁴⁹ Bibliography Item 16.

aspect of adjacent atoms, and little or not at all by applied magnetic fields of the order of a few thousand gauss.

Matters requiring further study are: (1) the change in sign of $\partial\rho/\partial T$ as tension passes a critical value in nickel and nickel-rich alloys, (2) the early saturation of the magneto-resistance effect, and (3) the irregular progress of magneto-resistance changes in low applied fields.

It is a pleasure at this time to acknowledge the contributions of several persons not already mentioned in the text of this report or in previous papers. Chief among these is my present assistant, Mr. L. R. Jackson, whose ingenuity, skill and patience have been unfailing. I am indebted to Dr. R. M. Bozorth and others at the Bell Telephone Laboratories for numerous services in connection with the procurement of materials. Dr. O. E. Buckley of the same organization has helped me frequently by critical comment and discussion, especially regarding the theory of ferromagnetic phenomena.⁵⁰

⁵⁰ A brief note on this matter has been published: L. W. McKeehan, O. E. Buckley, *Phys. Rev.* [2] **33**, 636 (1929).

ON THE MAGNETIC PROPERTIES OF METALS

BY FRANCIS BITTER*

CALIFORNIA INSTITUTE OF TECHNOLOGY

(Received July 7, 1930)

ABSTRACT

It is shown that the susceptibility of copper and silver is structure sensitive. Annealing increases the diamagnetism and drawing decreases it. It is suggested that uncertainty concerning the state of a metal as well as uncertainty concerning its purity may account for the large spread of observed values of the susceptibility. It is shown that the Pauli paramagnetism of the free electrons and the diamagnetism of the ions taken together are not sufficient to explain the susceptibility of the alkali metals. It is suggested that partly bound electrons should be taken into consideration. Several effects are predicted by means of which the total susceptibility can be analyzed and its component parts measured separately.

OUR knowledge of the processes which contribute to the magnetic properties of metals has been considerably increased in recent years, but it has been impossible to submit any theories to an accurate experimental check because of the very large discrepancies between various observed values. The results for the susceptibilities of the alkali metals, for example, are contained in the following table.

TABLE I. *Specific susceptibility* $\times 10^6$.

	Honda ¹	Owen ²	Bernini ³	Sucksmith ⁴	McLennan ⁵	Lane ⁶
Li	—	3.1	.5	3.8	—	—
Na	.51	.50	.54	.59	.59	.65
K	.40	.63	.63	.51	.45	.54
Rb	—	.076	—	.07	.17	.21
Cs	—	-.10	—	-.05	.18	.22

The agreement is best for sodium, but even here the large value is 30% higher than the low one. Magnetic measurements on solids are so straightforward that it seems out of the question to attribute these discrepancies to experimental error, and it necessarily follows that different samples of these metals may have susceptibilities varying by amounts of the order of the susceptibility itself. In this connection, the question of impurities is an

* National Research Fellow.

¹ K. Honda, Ann. d. Physik [4] 32, 1027 (1910).

² M. Owen, Ann. d. Physik [4] 37, 657 (1912).

³ A. Bernini, N. cim. [5] 7, 441 (1904); Phys. Zeits. 6, 109 (1905). The value for Li is 3.8 and not 0.38 as given in the Landölt Bornstein tables.

⁴ W. Sucksmith, Phil. Mag. [7] 2, 21, (1926).

⁵ J. C. McLennan, R. Ruedy and E. Cohen, Proc. Roy. Soc. [A] 116, 468 (1927).

⁶ C. T. Lane, Phil. Mag. [7] 8, 354 (1929); Phys. Rev. [2] 35, 977 (1930).

important one. It has generally been assumed that only ferromagnetic impurities could account for errors of such size, and in most of the work, iron has been tested for chemically and magnetically, and corrections applied on the assumption that the iron was present in its magnetically most active form. But even with such corrections, the agreement is poor, and it becomes necessary to find another reason for the disagreement between observed values.

A hint as to what this uncertainty in magnetic measurements on metals is due to is given by the following considerations. We now know that conduction electrons do play a part in magnetic phenomena; and we know that, in general, properties due to conduction electrons, such as conductivity, change of resistance in a magnetic field, etc., are structure sensitive properties. Consequently, it seems reasonable to suppose that magnetic phenomena are also structure sensitive. In other words, we suppose that the susceptibility of a metal can be altered by mechanical working. In order to test this assumption, I undertook a few simple experiments with the help of Mr. J. Foladare. We used the Gouy method.⁷ The sample, in the form of a cylinder about 12 cm long and 1 or 2 mm in diameter, was suspended from one arm of a beam balance. The lower end of the sample was in a homogeneous magnetic field. The magnetic force in dynes is then given by

$$F = \frac{1}{2}KH^2A \quad (1)$$

where K is the volume susceptibility, H is the magnetic field strength, and A is the cross-sectional area of the sample. Copper and silver wires were used. The copper was slightly paramagnetic, probably due to impurities, but the silver was diamagnetic and probably quite pure. The procedure for copper was to take a long piece of wire and to cut it into lengths of about 15 cm. These were then stretched by various amounts, and their susceptibilities measured. As the diameters were equal before stretching, the diameters after stretching are a measure of the total distortion. Typical results are given in Table II.

TABLE II. *The effect of stretching on the magnetic susceptibility of a copper wire.*

Susceptibility in arbitrary units	Diameter of sample after stretching
3.2	1.67 mm
3.4	1.63 mm
4.1	1.57 mm
4.8	1.41 mm

This shows that stretching increases the susceptibility. The last sample above was then annealed by heating to red heat for about 15 minutes in a quartz furnace. During the heat treatment the sample was immersed in a CO₂ atmosphere to prevent oxidation. After the sample had cooled off, it was again measured, and its susceptibility was found to have changed

⁷ See for instance, E. C. Stoner, *Magnetism and Atomic Structure*, p. 40.

from 4.8 to 3.4. It was then stretched again, so that its diameter changed from 1.4 mm to 1.36 mm, and the susceptibility increased to 4.1. Silver gave similar results. For example, stretching a given sample so that its diameter changed from 1.66 mm to 1.56 mm changed its susceptibility from -4.2 to -3.3 .

Although the data obtained are very few, until further information is available, it seems reasonable to suppose that, just as hardening in general increases the resistance of a metal, it also increases the paramagnetic component or decreases the diamagnetic component of its susceptibility. The significance of this result will be further discussed below. At this point, I merely wish to point out that structural features must be taken into account in subsequent measurements; that other mechanical deformations may play an equally important though different role (twisting, stretching within the elastic limit, compression, etc); and that impurities may have a considerable influence on the above effects, especially if the rate of cooling is taken into account.⁸

Let us return now to a closer examination of the experimental facts and their significance. For simplicity, I shall deal with the alkali metals, though many of the considerations apply to other substances as well. We have, then, experimental values for the susceptibility within a certain range for each substance, and it is proposed to determine something about the mechanisms which must be assumed to explain the results. Theoretically we know that there exist two components at least of the susceptibility. One is the diamagnetism of the ions in the metal. This, if measured per unit volume, is designated by K_i . It is independent of the temperature except when the number of free electrons is not constant, and its absolute value can be estimated both theoretically and experimentally. It is structure insensitive. The other component is the paramagnetism of the free electrons due to their spins, and has been calculated by Pauli.⁹ It is also structure insensitive, and is given by one of the following formulae

$$K_p = \frac{1}{4\pi} \left(\frac{3}{\pi} \right)^{1/3} \frac{e^2}{mc^2} n^{1/3} \quad (2)$$

$$= \frac{1}{4\pi} \left(\frac{3}{\pi} \right)^{1/3} \frac{e^2}{mc^2} \alpha^3 n \quad (3)$$

$$= \frac{3}{10} \frac{n\mu^2}{\epsilon_0} \quad (4)$$

Here it is assumed that there is one free electron per atom. n is the number of atoms per cm^3 ; α is the lattice constant, such that for a simple cubic lattice $\alpha^3 n = 1$; μ is the magnetic moment of the electron; and ϵ_0 is the zero-point energy of the electrons. The first form of the formula is most useful for com-

⁸ W. G. Davies and E. S. Keeping, *Phil. Mag.* [7] 7, 152 (1929).

⁹ W. Pauli, *Zeits. f. Physik* 41, 100 (1927).

parison with experiment, and will be discussed more fully below. The second form shows that K_p is comparable with K_i ,

$$K_i = - \frac{1}{6} \frac{e^2}{mc^2} \Sigma r^2 n \quad (5)$$

where Σr^2 refers to the summation of the average value of r^2 over all the electrons in the ion. Thus for large ions with many electrons, it is to be expected that $|K_i| > |K_p|$, whereas for small ions like Li, as a more detailed consideration shows, $|K_i| < |K_p|$. The last form, Eq. (4), is perhaps most useful in anticipating what would happen in a metal in which some of the electrons are partly bound. Such a binding might be thought of as a dropping of electrons into potential energy holes, with a consequent decrease in ϵ_0 and an increase in K_p . In this sense formulae (2) and (3) may be thought of as lower limits which actual bodies approach when their electrons may be considered really free. Another way of interpreting the increase in susceptibility due to binding is to suppose that, as the electrons travel through the metal, they are occasionally caught by an atom, and add to the paramagnetism through their orbital motions. To these processes, one would still have to add any diamagnetism of the free electrons. A calculation of the quantity has been carried out¹⁰ in an approximate fashion, and it has the same form as Eq. (3), but the numerical factor must be open to considerable doubt because in the approximation used any one cell in the lattice was assumed identical with all the others, thus omitting fluctuations which most certainly occur, and which may be of considerable importance for diamagnetism. The diamagnetism of partly bound electrons, especially those which are concerned in holding the atoms of the metal together, must also be considerable, especially in substances like bismuth with an unusually large diamagnetism which is known to be structure sensitive. In the case of bismuth and allied metals, it is certainly related to the unusual crystal structure, but it is well to keep in mind the possibility that in other metals a similar process may also take place, though of course to a much lesser extent.

The first point to be checked concerns the absolute values of the susceptibilities. Table III shows the situation.

TABLE III. Comparison of theoretical and experimental values for the susceptibility of the alkali metals. Volume susceptibility $\times 10^6$.

	K_p	K_i	$K_p + K_i$	K experimental
Li	.79	-.31	.48	.27 to 2.04
Na	.66	-.45	.21	.49 to .63
K	.51	-.37	.15	.35 to .55
Rb	.49	-.56	-.07	.14 to .34
Cs	.45	-.64	-.20	-.19 to .41

The values for K_i are taken from Stoner¹¹ and are dependable as to order

¹⁰ F. Bitter, Proc. Nat. Acad. Sci. 16, 95 (1930).

¹¹ E. C. Stoner, Magnetism, p. 101 (1930).

of magnitude except for Li, where the true value may be much nearer zero. The outstanding feature of the table is that the observed values are more paramagnetic than the calculated ones. Especially for lithium this seems to be the case. I measured a sample of Li in the form of a wire made by sucking molten Li into a glass tube, pulling the sample out by one end after it had cooled, and finishing the magnetic measurements rapidly in air before appreciable oxidation had set in. The result was a specific susceptibility equal to 3.8×10^{-6} , in good agreement with the larger values in Table I. A spectral analysis of the sample, for which I am indebted to Professor Badger, revealed chiefly magnesium and other alkali metals as impurities, with no detectable traces of iron, and in view of Owen's work, it does not seem possible that this high value is due to iron. A further investigation to determine the origin of the large discrepancy between 3.8 and 0.5 should prove very interesting. The possibility that a radio-active impurity might produce such a high value, perhaps through nuclear excitation, was also investigated, but this was found to be very improbable, as the zero count of a Geiger counter was not observably changed by the presence of the lithium in direct contact with the counter chamber.¹² Whatever these high values are due to, there unquestionably is another phenomenon to be considered, and this most probably is related to the partly bound electrons. More experimental data are needed to help in satisfactorily interpreting the spread of the observed values.

Besides measurements on pure substances, measurements on alloys of the alkali metals in each other should prove especially interesting, as these substances, except lithium, are not supposed to be crystalline at ordinary temperatures. If further investigation shows that accurately repeatable measurements can be made on pure substances, it would even be possible to check the dependence on n in Eq. (2) by determining whether the deviation from linearity of the susceptibility of these alloys as a function of concentration of the components was representable by the $n^{1/3}$ dependence on the density given in Eq. (2).

A further consequence of the assumption that a part, at least, of the susceptibility of metals is due to free electrons, is that there must exist a small "magneto-electric" effect, analogous to a thermo-electric effect. If one end of a wire is in a magnetic field H , the other end in a field zero, the electrons at the two ends have different energies, the difference being of the order of magnitude $\frac{1}{2}K_e H^2 \text{ ergs/cm}^3$, where K_e is the volume susceptibility of the electron gas, and might be less than K_p above due to a possible diamagnetic effect.¹³ If we assume $K_e = 0.5 \times 10^{-6}$ and a very large $H = 50,000$ gauss, such as might be used for such an experiment, this would give 625 ergs per cm^3 . To calculate the energy per electron this quantity must be divided by n , which for silver, for instance, is 5.9×10^{22} , and we have about 1.1×10^{-23} ergs per electron. Translated into electron volts this gives 10^{-8}

¹² I am indebted to Dr. Van den Akker for performing this experiment for me.

¹³ In this connection I want to point out that such a "magneto-electric" effect is to be expected for ferro-magnetic substances as well as others, though its order of magnitude cannot, so far as I am aware, be calculated.

volts as the potential difference for the two ends of the conductor. To detect such an effect would probably be difficult, but certainly possible. A convenient form would be that of the thermocouple, but instead of keeping the two junctions at different temperatures, it would be necessary to keep them at the same temperature, but at different field strengths. In this way it would be possible to measure separately the susceptibility of the free electrons.

One more effect can be predicted; namely, a dependence of the susceptibility on the field strength in the neighborhood of Kapitza's critical field strength,¹⁴ called by him H_k . These are the field strengths at which the dependence of the change in resistance on magnetic field goes over from a quadratic to a linear function. Above this field strength the susceptibility should approach a more paramagnetic value and should become more structure insensitive, and the difference in the susceptibility of an annealed wire above and below H_k should be of the order of magnitude of the change produced by annealing a hard drawn wire. These conclusions are based on the following picture of the mechanism. Kapitza's work has shown that some property of the electrons exists which has not been taken into consideration in the theoretical analyses. It is a property which controls the behavior of the electrons in a magnetic field, and is very probably related to the residual resistance and supra-conductivity. It is structure sensitive. Such a property is contained in the "large orbits" of bismuth electrons. For simplicity let us refer to it merely as an orderliness in the motion of some of the electrons in a lattice. This order is responsible to some extent for conduction and diamagnetism. Either a magnetic field or mechanical distortion has the effect of destroying this order, and consequently of increasing the resistance and decreasing the diamagnetism. The picture accounts in a rough way for the facts, and predicts the above mentioned dependence on the field strength above H_k . This "orderliness" must of course not be interpreted too literally. It is really only another way of referring to Kapitza's inner "fields."

¹⁴ P. Kapitza, Proc. Roy. Soc. [A] **123**, 292 (1929).

THE SCATTERING OF FAST ELECTRONS BY METALS. I. THE SENSITIVITY OF THE GEIGER POINT- DISCHARGE COUNTER

BY CARL T. CHASE

NEW YORK UNIVERSITY, UNIVERSITY HEIGHTS, N. Y.

(Received July 5, 1930)

ABSTRACT

This paper presents new information on the sensitivity of the Geiger point-discharge counter. The type of counter used here, with a cylindrical chamber, the open end being covered with thin foil, is not sensitive to electrons of all velocities at the same time. The velocity sensitivity depends on the voltage applied to the counter, higher velocities being registered at higher voltages. This information may have an important bearing on past experiments looking for electron polarization.

INTRODUCTION

A NUMBER of experiments have been reported which were designed to search for evidences of polarization in a beam of electrons, from this and various other laboratories. They have been of many kinds, such as double scattering at right angles, transmission through crossed magnetic fields, double reflection at grazing incidence, etc., and have involved both fast and slow electrons.¹⁻⁸ All experiments with slow electrons have given negative results, while some of the experiments with fast electrons have shown evidences of polarization effects. As far as any theory is available, the prediction is that the spin vector of the electron may possibly show itself as the analog of a transverse vector in the electron waves, but only when the electrons have high velocities.^{9,10}

POINT-DISCHARGE COUNTERS

These counters have never been regarded as entirely satisfactory, and have given different results in the hands of different workers. Their chief recommendation lies in the fact that when they do count an electron, the time of arrival of the electron is known to within a moderate fraction of a second. This fact has seemed to imply that all the electrons arriving at the counter are registered, since the arrival of those which are counted is so de-

¹ Cox, McIlwraith, and Kurrelmeyer, *Proc. Nat. Acad. Sci.* **14**, 544 (1928).

² Chase, *Phys. Rev.* **34**, 1069 (1929).

³ Myers and Cox, *Phys. Rev.* **34**, 1067 (1929).

⁴ Davisson and Germer, *Phys. Rev.* **33**, 760 (1929).

⁵ Wolf, *Zeits. f. Physik* **52**, 314 (1928).

⁶ Joffé and Arsenièva, *Comptes rendus* **188**, 152 (1929).

⁷ Rupp, *Zeits. f. Physik* **53**, 548 (1929).

⁸ Rupp, *Zeits. f. Physik* **61**, 158 (1930).

⁹ Darwin, *Proc. Roy. Soc.* **A116**, 227 (1927).

¹⁰ Mott, *Proc. Roy. Soc.* **A124**, 425 (1929).

finitely marked. For most of the experiments in which these counters have been used the time of arrival is immaterial, and the only information desired is the number of particles which arrive at the counter under certain conditions in the apparatus through which the electrons have passed.

We consider counters made with a cylindrical chamber of ebonite or glass, the point being of fused platinum wire, as described in previous papers. When the number of particles counted is plotted against the voltage applied, different types of curves are obtained, depending on whether the open end of the chamber is uniformly covered with thin foil, or whether the window is a small hole in a larger metal plate.¹³⁻¹⁵ In the latter case the number of counts increases rapidly, after counting starts, as the voltage is increased, until a point is reached when the curve suddenly becomes nearly horizontal.¹⁴ When this saturation point is reached, a large increase in voltage produces small change in the number of counts, unless the voltage is made too high, when the curve starts upward again, and soon rises almost vertically. Operation is best just above the first bend of the curve, and this voltage is generally called the working voltage. After the second bend spontaneous discharges become numerous, and the point soon fails.

In contrast to this is the operation of counters in which the open end is covered with a uniform thin foil, or when the end is left completely open (with metallic walls in the latter case). The curve of number against voltage then climbs steadily, the number counted increasing uniformly to large numbers, merging finally and steadily with increased voltage to the state where spontaneous discharges predominate. It is hard to say where the best working voltage is in this case, since it is plain that many electrons are not being counted unless the voltage is so high that the counter can in no way be depended upon. Besides, if this curve continues upward indefinitely, how should we treat the first bend in the curve for the counters just mentioned, which was regarded as the point where electrons were quantitatively counted?

THE VELOCITY-SENSITIVITY OF POINT-DISCHARGE COUNTERS

The only information so far available as to how effective these counters are for counting electrons of different velocities is indirect. Kovarik and McKeehan have measured the velocity spectrum of beta-particles, using counters with sharp steel points.¹¹ Their results are in agreement with more recent photographic measurements of Curie and d'Espine.¹² More recently Riehl has made experiments with the same view in mind as has the present paper.¹⁴ He used counter windows of thick material, with a small hole in the center covered with thin foil, and obtained curves of number against voltage showing saturation, as explained above. He varies the pressure of gas in his counters, and plots curves of "starting potential" and "saturation poten-

¹¹ Kovarik and McKeehan, *Phys. Rev.* **8**, 574 (1916).

¹² Curie and d'Espine, *Comptes rendus* **181**, 31 (1925).

¹³ Bennett, *J.O.S.I.* **16**, 339 (1928).

¹⁴ Riehl, *Zeits. f. Physik* **46**, 478 (1928).

¹⁵ Chase, unpublished data.

tial" against gas pressure. These potentials in each case are less for smaller gas pressures. He then plots curves of number of particles counted, presumably for the so-called saturation, or working, potential. These again rise with increased pressure, until a saturation value is reached, and show that beta-particles whose speeds are less than 0.4 of the velocity of light are "quantitatively counted" in air at pressures as low as 7 mm of mercury, while for the faster particles from radium *E*, the curves do not reach saturation until the pressure is 1100 mm of mercury. The peak of the velocity spectrum of radium *E* occurs in the region of speeds of about 0.8 of the velocity of light. In the experiment with radium *E*, a magnetic field was applied through the apparatus to bend slow electrons out of the path. For fields strong enough to bend most of the electrons slower than those last mentioned out of the path, the curve has the same form as the curve for no field. Saturation occurs at the same pressure, and the curve can be obtained from the curve for no field by decreasing the ordinates in a constant ratio. This suggests that his counter was counting only electrons of one velocity range, probably the faster ones.

MEASUREMENT OF VELOCITY-SENSITIVITY

We have constructed a magnetic spectrograph for testing directly the velocity-sensitivity of these counters. Radium *E* was used as a source, and the electrons passed through the field in a good vacuum. Windows of aluminum, 0.02 mm thick, closed the vacuum cell at each side; air at atmospheric pressure was in the counter, which was of the type used previously in this laboratory, the open end being covered uniformly with thin aluminum leaf. It was found that the number of particles of different velocities which was counted depended on the voltage applied to the counter in a very definite way. At low voltages, just after the counter began to operate, many slow electrons were counted. At higher voltages, more fast electrons were counted, and what was surprising, fewer slow ones. At very high voltages, so high that the counter was beginning to misbehave, the same number of electrons was counted as at the moderate voltage, but the electrons counted were faster still. The fact that the same number of the higher velocity electrons was counted at the higher voltage as the number of moderately fast electrons had been at the lower voltage was due to the fact that there were no more fast electrons to count; otherwise the number counted would have continued to rise with increased voltage.

To make things doubly sure, the counter and source were rigidly mounted facing each other, with air between and ten cm apart. When set for low velocity electrons, as indicated by the magnetic deflection experiment, a piece of paper 0.28 mm thick held directly in front of the counter cut down the count by twelve percent, while with the voltage as high as the counter could stand the paper had no effect whatever on the number counted. We made sure that the counts at the high voltage were not spurious counts; they were actual electron counts. It is well known that the high speed electrons are far more penetrating than are the slower ones. It may be noted that besides

computing the velocities by measurement of the magnetic field strength, the spectrum was measured with a gold leaf electroscope, and found to be in agreement with the photographic work of Curie and d'Espine.¹²

RESULTS FOR POLARIZATION EXPERIMENTS

In this laboratory Cox, McIlwraith, and Kurrelmeyer¹ caused electrons from a milligram of radium to be doubly scattered at right angles, the targets being of gold, and the electrons being detected with Geiger counters. The three claim to have found a real effect of a new kind, in that more electrons were scattered in one of the transverse positions than in the other. The present writer then set up a new, though similar, apparatus, in which the scattering material was lead. This apparatus gave the same effect as had the earlier one. At this stage it was discovered that a large part of the counts was due to gamma-rays, and a new apparatus designed to eliminate this gave consistent, negative results.²

The criterion used in weighing these results was that of self-consistency. The later work of Chase was far more consistent than had been that of the earlier three, and this was taken as a measure of its correctness. From the results contained in this paper it appears that this later work did not include a count of the faster electrons. Thinner windows allowed more slow electrons to get through. The increased number of electrons in turn allowed the operation of the counter at lower voltages, making for more consistent results, but counting only the slower electrons. The number of slow electrons given off by a sample of radium is much greater than the number of fast ones, due to absorption in the source, unless this is spread out in a layer a few molecules thick, which was not true in our case. The foregoing shows the need for further work on these experiments, which we have undertaken.

Our electron currents are much too small to use electrometers, and gold leaf electroscopes hold great promise. A carefully made and shielded electroscope will detect the formation of a few ions per cc per second, and should have no difficulty in detecting as few as one electron per minute. In fact, during the preliminary experiments which led to this paper it was found that a rather poorly made electroscope was as sensitive as the Geiger counters which we have used, the natural rate of fall of the leaf being the same proportionate amount of what was to be measured as were the number of spurious discharges of the counter to the number of real counts.

We accordingly adopt the gold leaf electroscope and proceed to an experimental survey of the field of electron scattering, with an eye open for polarization effects. The next paper will concern double scattering at right angles, and will appear shortly.

HIGH POTENTIAL X-RAY TUBE

By C. C. LAURITSEN AND B. CASSEN
CALIFORNIA INSTITUTE OF TECHNOLOGY

(Received July 14, 1930)

ABSTRACT

An account is given of further development work on the high potential x-ray tube at the California Institute of Technology. Details of the construction of the tube and its housing are presented. The housing, which is a concrete structure erected on the floor of the high potential laboratory, makes it possible to operate and make observations at close range. The tube has been equipped with a hot cathode and a tungsten target, thus rendering it more suitable for spectrographic work. High speed cathode rays outside of the tube have been obtained by replacing the target by thin windows of mica or metal. Continuous operation is possible over a period of several hours at six hundred kilovolts and with a space current of three to four milliamperes. A comparison between different types of high potential x-ray tubes and of different methods of operation is contained in the discussion.

INTRODUCTION

A PRELIMINARY report describing an attempt to develop apparatus for generating x-rays of short wave-length was presented some time ago by Lauritsen and Bennett.¹ The investigation showed that it is possible to obtain satisfactory operation up to 750 kilovolts by means of apparatus constructed along the general lines described, i.e. apparatus which cannot be baked out, but in which the electrode distance is small and the glass is shielded against bombardment.

Since then the x-ray tube has been rebuilt in a more permanent form and further development work has been carried on. Satisfactory operation has been obtained at somewhat higher potentials, still using the same method of operation, i.e. making use of cold emission as the sole source of electrons and operating intermittently so that the maximum potential is applied only one second out of eight, the potential during the interval being about one half of the maximum potential. In addition, satisfactory continuous operation up to 600 kilovolts has been obtained when a hot cathode was used for furnishing the electrons.

THE TUBE

The x-ray tube was rebuilt primarily to allow operation and observation at close range. For this purpose a concrete housing was constructed, the general plan of which is shown in Fig. 1 whereas Fig. 2 is a cross-section through the tube and housing.

As may be seen, this housing is divided into two compartments by a concrete partition which is two feet thick. The glass section of the tube is

¹ C. C. Lauritsen and R. D. Bennett, *Phys. Rev.* **32**, 850 (1928).

mounted on top of the housing and the base, which consists of a steel tube one meter long, forty centimeters in diameter and of six millimeter wall thickness, protrudes down through the ceiling into one of the compartments.

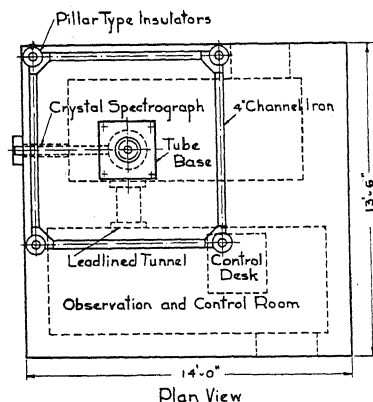


Fig. 1. General plan of apparatus.

This compartment also contains the liquid air trap and the vacuum pumps described in the previous paper.

The second compartment contains the control desk for operating the high potential transformers as well as the vacuum gauge and various meters for measuring current and potential, etc. A lead-lined opening in the concrete

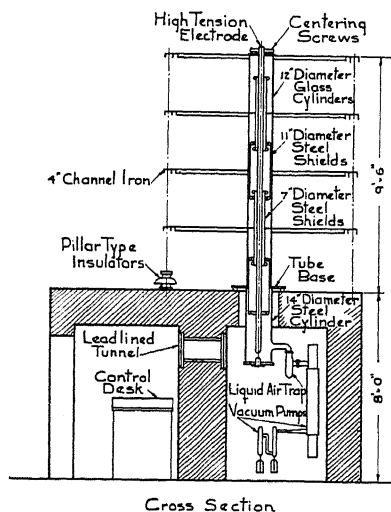


Fig. 2. Cross-section through tube and housing.

partition is provided for making absorption measurements and other observations on the radiation.

Sheets of galvanized iron are placed under all the walls, and the top of the housing is completely covered with sheets of the same material, carefully

soldered together and connected at all four corners to the bottom sheets by means of copper conductors. A heavy copper conductor makes connection to the station ground. The tube base is insulated from the housing and connected to ground through two milliammeters, one for reading alternating current and the other for reading the unidirectional current through the tube.

The upper section of the tube is as previously described with the exception that the four torus-shaped corona shields have been replaced by horizontal plates of galvanized iron sheets, eight feet square. These are supported on frames of four-inch channel iron carried on insulators of the pillar type. These plates produce a very uniform field along the glass and provide a considerable capacity across each section, thus effectively preventing punctures and flashovers due to surges.

HOT CATHODE

For many purposes it is desirable to have a well-defined focal spot rather than the somewhat erratic source inherent in cold emission. For this reason the upper electrode was constructed with a recess at its lower extremity into which a small spiral filament was placed. Fig. 3 shows in detail the construction and relative position of the electrodes. The filament is a small spiral

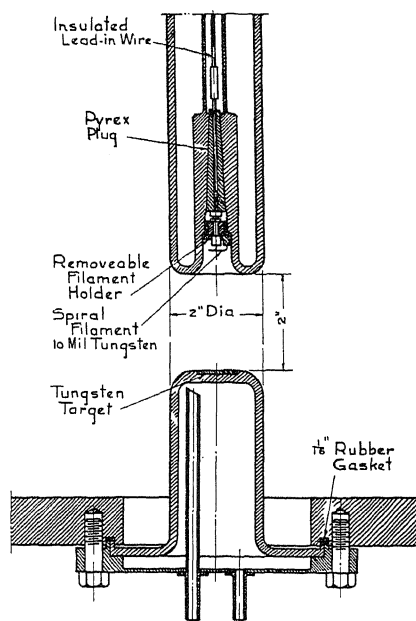


Fig. 3. Detail of construction and relative positions of electrodes.

of ten mil tungsten wire mounted in a removable holder to facilitate replacement. It is accessible through the opening in the bottom plate when the lower electrode is removed. One end of the filament is connected to an insulated central terminal of the filament holder. This terminal makes contact with an insulated lead-in wire sealed in through a tapered Pyrex plug. The other

end of the filament is connected through the holder to the electrode proper. The filament is heated by means of a six-volt storage battery placed on top of the tube structure. The heating current is controlled by means of a slide wire operated through long cords.

The target consists of a tungsten disk, two millimeters thick and two centimeters in diameter, embedded in the steel electrode. The distance between the electrodes is approximately five centimeters and both are water cooled by means of the cooling system previously described.

With this arrangement continuous operation is possible up to somewhat over 600 kilovolts with a unidirectional current of three to four milliamperes through the tube. The diameter of the focal spot is approximately five millimeters. The current is, of course, limited only by the heat dissipating ability of the target. Under these conditions the cold emission is usually negligible so that the radiation originates almost entirely in the focal spot and is confined to the concrete housing. This is very essential, both on account of the safety of the operators and of the shielding of the sensitive instruments required especially for absorption measurements.

CATHODE RAYS

In order to test the possibility of obtaining high speed electrons outside of the tube, the target was temporarily replaced by a thin window. A mica window was found to be satisfactory provided the current was limited to a very small value by keeping the filament at low temperature. Metal foils of two to three mil thickness permit the use of considerably larger currents. A very intense and concentrated beam was obtained and the usual phenomena such as glowing of crystals etc. could be observed.

DISCUSSION

The greatest difficulty in connection with the construction and operation of vacuum tubes for high potentials is caused by cold emission. This must therefore be minimized as far as possible or else rendered harmless. The first is best accomplished by thorough outgassing or, if this is not possible, by keeping the potential gradients between the different parts below a safe limit. The second is accomplished by shielding the glass against bombardment by stray electrons.

Two principal types of high potential tubes have been developed so far, each having its advantages and disadvantages and each being best suited for a particular purpose.

The most important feature of the first type is that the tube is constructed in sections in such a manner that only a fraction of the potential across the tube is applied between any two adjacent metal parts within the tube. The first tube of this type was developed by Coolidge² who described successful experiments with cathode rays up to 900 kilovolts. Excellent progress with tubes of this type has been made by Tuve, Hafstad and Dahl,³ who have

² W. D. Coolidge, *J. Frank. Inst.* **202**, 639 (1926).

³ Tuve, Hafstad and Dahl, *Phys. Rev.* **35**, 1407 (1930).

constructed tubes which they report are capable of withstanding as much as 1900 kilovolts.

These tubes were carefully cleaned and pumped to a high vacuum. This is essential with this type since the electrons must travel the full length of the tube in order to get from the filament to the target. This distance is necessarily great even if the tube is designed for use under oil. If the mean free path is insufficient the electrons will collide with the gas molecules and thus not reach the target with maximum velocity. Furthermore, unless the tube has been well outgassed, many of the electrons will undoubtedly strike the walls and shields on their way through the tube and thus liberate large quantities of gas. It is doubtful if a well-defined focal spot can be obtained with this construction.

The second type, which has been developed at the California Institute, is characterized by the fact that the full potential is applied directly between two electrodes which are comparatively close together. This increases the difficulties due to cold emission, but the vacuum requirements are not nearly as severe as in the case of the first type because the distance between the filament and the target is only a few centimeters instead of a meter or more.

This type is well suited for producing x-rays of great intensity, but is presumably not capable of development for as high potentials as are certain other types. It seems likely that a combination of the two types here described offers advantages over any of the tubes now in use.

Our experience so far with alternating current operation indicates that the method is practical for investigating the x-ray region up to at least 600 kilovolts and there is every reason for believing that it will be possible to extend this range considerably. The advantage of the method lies in the great intensity available with continuous operation. This is extremely important for many investigations.

There can be little doubt, however, that other methods of operation will prove more suitable for much higher potentials. This has been beautifully demonstrated by the recent work of Breit, Tuve and Dahl⁴ in their work with resonance coils. The instantaneous value of the energy may in this case be enormous although the average is quite small. This, of course, solves not only the problem of power source, but also the difficulty of dissipating the heat in the target.

In conclusion, we wish to express our thanks to Dr. R. A. Millikan for his interest in the work and the Carnegie Corporation of New York for financial support.

⁴ Breit, Tuve and Dahl, *Phys. Rev.* 35, 51 (1930).

LINEAR CORRECTION FOR CATHODE RAY OSCILLOGRAPH

BY FREDERICK BEDELL AND JACKSON KUHN

CORNELL UNIVERSITY, ITHACA

(Received July 7, 1930)

ABSTRACT

The deflection of the cathode beam in a cathode-ray oscillograph tube, while substantially proportional to the voltage applied to the deflecting plates within the tube, is not proportional for small voltages in tubes commonly used. This non-linearity is due to the heavy cloud of ions between the plates. In the practical use of such a tube error due to this non-linearity is avoided by applying a bias to the plates so as to work on the straight part of the curve.

IN A cathode-ray oscillograph the deflection of the cathode beam is proportional to the electromagnetic field through which it passes. While in an ideal case the deflection is likewise proportional to the electrostatic field through which the beam passes, there are certain disturbing elements in cathode-ray tubes, as usually constructed, which need to be taken into consideration, particularly when the deflection is small.

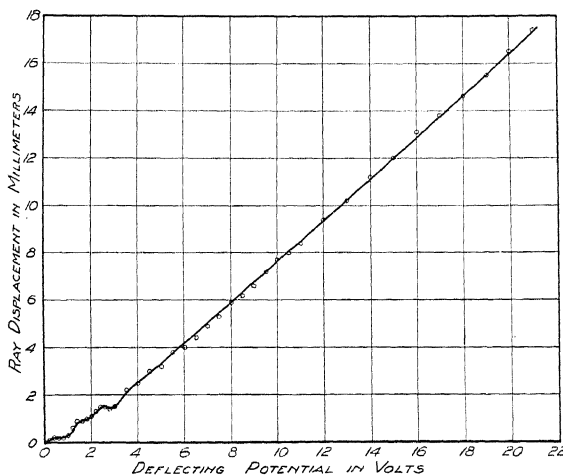


Fig. 1. Relation between deflection and applied e.m.f.

Fig. 1 shows the relation between the deflection and applied e. m. f. in a W. E. 224-B cathode-ray oscillograph tube, in which the electrostatic field is obtained by applying the e.m.f.s., which are to be measured or compared, to two pairs of deflecting plates, located inside the tube, between which the beam passes. It is seen that when the applied e.m.f. exceeds 3 volts, giving an observed deflection of 2.5 mm, or more, the curve is practically a straight line, while for smaller values the proportionality does not hold.

This is further shown in Fig. 2, obtained by applying a periodic e.m.f. to one pair of deflecting plates and a constant e.m.f., varied by steps of 10 volts, to the other. The second set of more or less parallel lines was obtained by

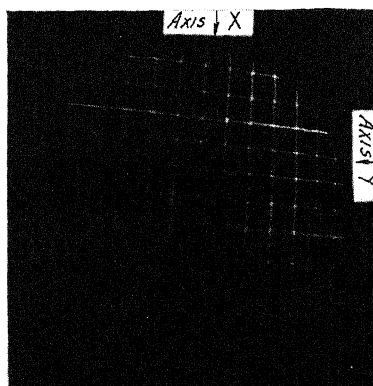


Fig. 2. Displacement of X and Y axes, vertically and horizontally, by 10-volt steps. Distance of camera from screen: 18 inches.

repeating, with the connections to the plates reversed. The vertical line marked " Y -axis" corresponds to zero e.m.f. on the X plate; the lines on the left and right corresponding to negative and positive e.m.f. s of 10, 20, 30

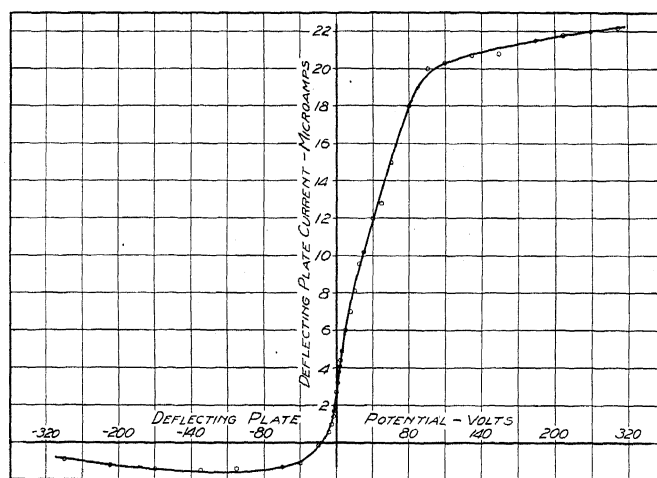


Fig. 3. Plate current for different plate voltages, using deflecting plate Y ; anode potential 400 volts.

volts, etc. Similarly the horizontal line marked " X -axis" corresponds to zero e.m.f. on the Y plate. Negative and positive refers to the potential of the free plate with respect to anode.

Under ideal conditions, we should have in Fig. 2 a system of square coordinates made by two systems of equidistant parallel lines. Departure from this condition is caused by the non-linear calibration, as shown in Fig. 1, and other causes which will not be analyzed here, as the curvature of the screen, location of the camera, etc.

The non-linearity of the relation between plate potential and the resulting beam deflection, as shown in Fig. 1, is due to the heavy cloud of ions between

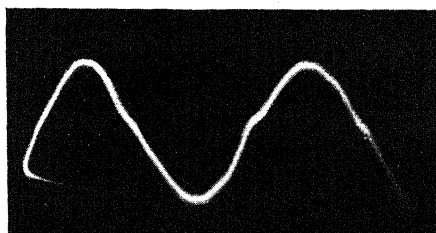


Fig. 4. Effect of non-linearity shown by bump in what should be smooth curve.

the deflecting plates. An idea of the number of ions can be obtained from the curve in Fig. 3, which shows the plate current corresponding to different plate voltages. The presence of these ions between the plates masks the effect of the applied potential, so that the potential gradient at the beam is not proportional to the applied potential. This masking effect is, of course, more marked at the lower potentials. At high potential this effect is negligible as the ions are swept away. The relation between deflection and deflecting potential is now linear within the limits of observation, although there are probably slight departures due to critical potentials.

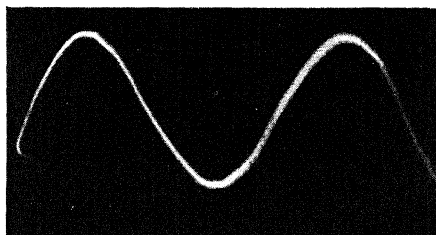


Fig. 5. True curve, without bump, obtained with stabilized oscilloscope with linear scale.

So far as the practical applications of the tube are concerned, the cure for the non-linearity of the calibration curve in Fig. 1 is obvious: to shift the zero by applying a plus or minus bias to the deflecting plates so as to work on the straight part of the curve. For the plate current to be a minimum the biasing potential should be negative, as shown in Fig. 3. A biasing potential of about 50 volts applied to both plates will displace the spot diagonally to the periphery of the screen, outside the area in which observations

are made. The spot may be restored to an artificial zero position near the center of the screen by a constant magnetic field, so that the curve as observed will never pass through the real zero, now displaced to the periphery of the screen, with its non-linear error. In other words, the observed deflections, both horizontal and vertical, will always be on the straight part of the calibration curve shown in Fig. 1.

As ordinarily used, without a corrective device, a cathode-ray oscillograph, when connected to a smooth nearly sinusoidal e.m.f., does not show a smooth curve but shows a curve with a little bump, as in Fig. 4. On the stabilized oscilloscope¹ used by the authors, equipped with linear correction as here described, the true curve without this bump is shown as in Fig. 5. The horizontal and vertical scales are both truly linear. The authors were assisted by G. B. Engelhardt in the experimental work. The investigation was carried on under a grant from the Hecksche Research Council.

¹ F. Bedell and J. G. Kuhn, *Rev. Sci. Insts.* 1, 227 (1930).

THE PROPAGATION OF LUMINOSITY
IN DISCHARGE TUBES

BY J. W. BEAMS

UNIVERSITY OF VIRGINIA

(Received July 18, 1930)

ABSTRACT

The velocity of propagation of luminosity in long discharge tubes, when a high potential was suddenly applied to one electrode, was studied by means of a mirror rotating between 2000 and 3000 revolutions per sec. Air and hydrogen at pressures from 0.04 to 0.5 mm of mercury were used in the tube. The luminosity always moved from the electrode to which the potential was suddenly applied toward the electrode maintained at ground potential. The velocity of the luminosity after progressing a few centimeters from the electrode to which the surge potential was applied, travelled with almost a constant speed, usually within the limits of 10^8 to 10^{10} cm/sec, depending upon the conditions of the experiment. A qualitative explanation of the results is offered based upon the formation of space charge.

IN THE case of long discharge tubes J. J. Thomson¹ was the first to observe that the luminosity did not start simultaneously throughout the length of the tube but traversed it from anode to cathode at a finite and measurable velocity. The potential across his tube was applied by attaching its electrodes directly to the terminals of an induction coil and the velocity of luminosity was measured by reflecting the light from two portions of the tube, several meters apart, by means of a rotating mirror, into the field of view of a measuring telescope. He experimented with a large variety of electrodes and came to the conclusion that the velocity was independent of the size, shape and material of the electrodes. For the velocity of the luminosity through a discharge in air at a pressure of 0.5 mm of mercury in a glass tube 5 mm in diameter, he found a velocity greater than half that of light. From this high value of the velocity he was able to conclude that the propagation of the luminosity was not due to the motion of the emitting atoms and molecules because of the absence of an observable Doppler effect in the spectrum lines. Several years later J. James² using the method of Abraham and Lemoine³ was unable to observe a velocity of propagation such as might be expected from the experiments of Thomson; while the writer⁴ using a somewhat similar method to study the order of appearance of spectrum lines in discharge tubes, obtained results in qualitative agreement with those of Thomson.

Whiddington⁵ Zeleny and others have observed moving pulses of luminosity in a discharge tube the electrodes of which were attached to the terminals of a storage battery. The current, at least in some cases, was intermittent and the velocity of the moving pulses was much smaller than

¹ Recent Researches, 115, 1893.

² J. James, *Ann. d. Physik* **15**, 954 (1904).

³ Abraham and Lemoine, *Ann. Chem. et Phys.* **20**, 264 (1900).

⁴ J. W. Beams, *Phys. Rev.* **28**, 475 (1926).

⁵ Whiddington, *Nature* **115**, 506 (1925).

to keep the electrodes Q and N at ground potential until the sudden impulsive potential was applied. R_1 also prevented the spark A from stopping before the discharge in the tube could start and thus avoided troublesome oscillations. The high capacity grounds G_1 , G_2 and G_3 , G_4 were independent and special precautions were taken to insure that the impulsive potential surge at A did not change the potential at G_3 and G_4 until the discharge of the tube was initiated. Impulsive surges were applied to the tube every second and the observations were obtained by waiting until the tube flashed at the proper time for its image to fall into the telescope T . The stellite mirror M was rotated between 2000 and 3000 revolutions per sec and the distance AM was one meter. The high rotational speed of the mirror was obtained by the method of Henriot and Huguenard⁶ modified to insure greater stability and flexibility.⁷ The tube was exhausted through a P_2O_5 trap by means of a "Hyvac" oil pump and the pressure was measured on a McLeod gauge.

The first tube 490 cm in length was constructed of glass tubing 5 mm in diameter with electrodes made of 50 mil tungsten wire sealed through the glass as shown in the drawing. In the initial experiments air was used at pressures from 0.04 to 0.5 mm of mercury and later hydrogen was used over the same range. For impressed potentials of between 20,000 volts and 40,000 volts the time between the appearance of the light at A and at B was much greater than the time between the appearance of the light at B and D . In almost every case the time between the appearance of the light at D and at E was too small to measure. This short time between the appearance of the light at D and E resulted from the fact that the width of A was always more than four times that of E . Therefore E was considerably over-volted and its time lag made very small.⁸

The phenomena usually observed can be described as follows: Soon after the appearance of the light at A an intense luminosity having the shape of a solid cylinder with a conical tip, progressed relatively slowly toward B . The base of the cylinder remained at Q and the moving tip was on the axis of the tube. At a distance (usually not greater than 40 cm in these experiments) the moving tip appeared to flatten into a plane and traversed the remaining length of the tube with a much higher speed. For example in the case of hydrogen at approximately 1.5 mm mercury pressure and a gap width of 8 mm at A , the light from A appeared 1.2×10^{-6} sec. before that from B , while D appeared in only 1.2×10^{-7} sec. after B . When the light at the point P midway between B and D was brought into the field of view of T , by means of an auxiliary mirror and lens not shown in the figure, it was found to appear at a time approximately half way between B and D . This showed that the velocity from B to D was roughly constant and equal to about 4×10^9 cm/sec. in this special case. On the other hand, since the

⁶ Henriot and Huguenard, *Comptes rendus* **180**, 1389 (1925); *Jour. d. Phys. et Rad.* **8**, 443 (1927).

⁷ Beams, *Rev. Sci. Inst.* (in press)

⁸ Beams, *Jour. Frank. Inst.* **206**, 809 (1928).

distance from *Q* to *B* was 50 cm the velocity of the luminosity between the two points could not have been greater than 3.8×10^7 cm/sec. or 1000 times less than the velocity from *B* to *D*. The time between the appearance of the luminosity at *A* and *B* was influenced by a number of factors. It was decreased with increasing potential and also with increasing conductivity of the tube. The charge on the walls the shape and material of the electrodes, together with the sputtering of the electrodes on the walls of the tube are probably very important factors.

After the luminosity finally attained the higher velocity, it apparently was not affected by the type of electrodes and did not depend critically on the pressure or voltage applied at *Q*. There was, however, some increase in velocity with voltage. Also when the pressure was adjusted so as to decrease the effective resistance of the tube the velocity was increased. At pressures from 0.2 mm to 0.4 mm of mercury, the light at *B* would usually first appear somewhat fainter than at *D* but become of equal intensity soon after *D* became luminous. Sometimes at the higher pressures (0.4 mm to 0.5 mm of mercury) a very intense luminous pulse not longer than 50 cm would traverse the tube from *Q* to *N* at a velocity of about 4.5×10^9 cm/sec., regardless of the polarity of the impressed surge (30,000 volts). As soon as the pulse of luminosity reached *N* the whole tube became luminous throughout. Many cases have also been observed where the luminous pulse traveled first from *Q* to *N* followed by the luminosity progressing from *N* to *Q*.

In order to study the effect of the walls on the high velocity luminous propagation, a long discharge tube, made of flexible thick rubber pressure tubing 5 mm inside diameter was substituted for the glass tube. The light was viewed through short sections of glass tubing connecting the rubber tubing at *A*, *P* and *D*. The electrodes were made of aluminum rods fastened into glass tubes by sealing wax. With this arrangement, although (in the case where the pressure and impressed voltage were the same) the velocity was actually measurably less than in the glass tube, the inductance and capacity of the tube as a whole were shown not to be important factors in determining the luminous velocity. By folding the tube its inductance as a whole could be almost eliminated and still the phenomenon was approximately the same as with it folded in such a way as to make its inductance a maximum. However, the inductance and capacity of the tube for electric impulses, which reach their maximum in a time much shorter than that required for the impulse to traverse the tube, may be an important factor, but the effect of this could not be thoroughly tested.

It is obvious as pointed out by Thomson that the high velocity of luminosity cannot be due to the movement of the emitting atoms and molecules because of the absence of a large Doppler effect. Nor can it result from charged atoms or molecules of any kind moving along the tube, for even the total impressed voltage is many times too small to give the ions a velocity comparable with that of the luminosity. Consider now a typical case of hydrogen at 0.2 mm pressure with a 30,000 volt positive surge impressed on the electrode *Q*. Light from *A* appeared about 7×10^{-7} sec. before it did

at *E* and at *B* approximately 10^{-7} sec. before it did at *D* and *E*. The velocity of the luminosity from *B* to *D* was therefore 4.9×10^9 cm sec. If the impressed voltage was distributed uniformly across the tube, the field would be 61.2 volts/cm. An electron would fall through roughly 24 volts between collisions and therefore could ionize the hydrogen gas throughout the length of the tube. It is not very probable, however, that many free electrons would be present in the tube at the time of the application of the potential and the fields would not be great enough to produce much ionization by positive or negative ions. The current would be small and *E* would remain non-luminous until space charges so arranged themselves as to allow considerable current to traverse the tube. This time required for the space charges to form throughout the tube works out to be too long and further the luminosity would be expected to appear gradually throughout the whole positive column rather than abruptly at the electrode *Q* and move toward *N*. It is possible that the luminosity did not strictly follow the current rush yet the experiments definitely showed, by the very small time between the appearance of the light at *D* and *E*, that the amount of current flowing out of the tube is very small until the luminosity completely traversed the tube. In the above discussion the assumption that the impressed voltage was uniformly distributed is of course not true for impressed surges having wave fronts which reach their peak value in a time less than the length of the tube divided by the velocity of the electromagnetic wave along the tube. This might double the field but only for a time small in comparison to the time required for the tube to start discharging. The comparatively long time between the appearance of the light at *A* and at *B* also makes it very unlikely that the velocity of luminosity observed can be identified with velocity of the potential wave along the tube.

However, when the process of formation and distribution of space charge in the tube is examined more carefully it may be possible to find a qualitative explanation of most of the results observed. The important factors in starting the ionization at *Q* seem to be the influence of the walls and the size and shape of the electrode to which the high potential is applied. In the neighborhood of the electrode, due to its shape and irregularities, the field is very high and intense ionization should take place. This ionization due to the large difference in the mobilities of positive ions, negative ions and of electrons respectively should result in the establishment of a space charge. This space charge, once formed near the high potential electrode *Q* must move down the tube regardless of the polarity of the applied potential because of the changes it produces in the field near its edges. The luminosity should then follow roughly the region of intense ionization.

The time between the appearance of the light at *A* and at *B* would then represent the period required to build up the space charges to a critical value around the high potential electrode *Q*, while the higher velocity of luminosity between *B* and *D* would represent the velocity with which the intense ionization moved.

A SIMPLE ACCURATE METHOD FOR MEASURING THE DIAMAGNETIC SUSCEPTIBILITY OF DISSOLVED SUBSTANCES

BY SIMON FREED AND CHARLES KASPER
UNIVERSITY OF CALIFORNIA, BERKELEY, CALIFORNIA

(Received July 15, 1930)

ABSTRACT

A quasi-null method has been developed for determining very accurately the diamagnetic susceptibility of dissolved substances. Two independent runs with 2.521 M. sodium iodide agreed easily within ± 0.06 percent. Its advantages over other methods are discussed. Several other kinds of investigations to which this method may be applied are pointed out.

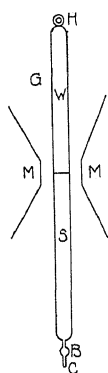
THE need of an accurate method for measuring the diamagnetic susceptibility of dissolved substances has long been recognized.

The present method is a simple modification of the standard method of Gouy. The modification resides in the elimination of the effect produced by almost all of the solvent, a procedure which can take advantage of the sensitivity of a micro-balance. Hitherto, the susceptibilities of the solutions were measured against air or vacuum and all the errors in the measurements had to be borne by the solute alone. The new method measures the susceptibility of the solute almost directly and it measures the solute against the solvent.

In this way, the actual pull suffered by the solution in the magnetic field is slight, it is less sensitive to the fluctuations in the current going through the coils (highly sensitive ammeters are unnecessary), the tube is not urged out of its position in the field by the dissymmetries which exist there, and indeed almost all the advantages of a null method are realized.

The method shall be illustrated with a run on a solution of sodium iodide, 2.521 M (vol.).

Fig. 1. *MM* are the pole pieces of an electromagnet. *G* is a glass tube with a glass partition *P* in the center of the pole gap and *G* extends on both sides to fields of negligible intensity. The upper part of the tube *W* contains the solvent, in this case water, and the lower half contains the solution, that of sodium iodide. By employing a little bulb *B* with constrictions on both sides and by having the end *C* drawn into a capillary, no trouble is experienced in keeping the air bubble (the space present above the solution when the tube is sealed off) from rising to the top of *S*. The tube *G* is suspended by braided silk thread at the hook *H* from the stirrup of a Sartorius micro-balance having a capacity of 20 gm and a sensitivity of ± 0.001 mg.



In this work a sensitivity of ± 0.01 mg was usually obtained. Finer reproducibility than this was reached in the measurements with the sodium iodide solution.

TABLE I. *Diamagnetic susceptibility of sodium iodide.*

Amperes	Pull in mg	Calibration in mg (against air)	$X_{gr.}^a$
35	1.238	11.31	0.3941
40	1.362	12.48	0.3937
45	1.466	13.43	0.3938
50	1.558	14.23	0.3943

(a) The results show an average deviation of 0.06 percent.

An independent determination gave a result equal to the one above within the limits stated. All of the pulls had a slight correction for the non-uniformity in the glass of the tube. The correction was found by measuring the change in weight when both the upper and lower parts of the tube were filled with water.

The same sample of water was employed for both the standard and the solutions. An absolute accuracy of ± 0.06 percent cannot be claimed for the determination. It is merely a measure of its reproducibility. If the calibration had been made with a solution of nickel chloride in the lower portion of the tube *G* instead of air, the reproducibility in the calibration would have been as good as that with sodium iodide. (The pull in the calibration against air was about ten times that with sodium iodide and a fluctuation in the current, for example, effects a proportionate change in the total pull. The absolute change then in the calibration is about ten times that in the run, and it is the absolute change which determines the accuracy of the susceptibility.) The use of nickel chloride would then have permitted an absolute determination of the diamagnetic susceptibility to within 0.2 percent¹ the accuracy with which the susceptibility of nickel chloride is known.

However, if the susceptibility of a diamagnetic salt is once accurately determined, the susceptibility of other diamagnetic salts can be determined relative to it with even greater precision, since the full advantages of a null method can be more nearly realized.

The sample of sodium iodide which we employed to test the reproducibility of the method was as pure as we could obtain. We did not analyze the salt, for it was not our purpose to find its absolute susceptibility. It still may be worth while to compare the result with the reliable determination of Ikenmeyer² who recently perfected a torsion method employing a non-homogeneous field.³ Ikenmeyer did not analyze his material for impurities.

¹ Brant, Phys. Rev. 17, 678 (1921).

² Ikenmeyer, Ann. d. Physik 5, 1, 169 (1929).

³ The torsion methods in the past have been subject to many inaccuracies, although their sensitivity leaves nothing to be desired. The difficulty seems to lie in placing the bob exactly in the same field gradient. And again, the inaccuracy incurred by the total solution is assumed by the solute alone.

He obtained -60.4×10^{-6} per mol, while our value is -59.1×10^{-5} . Under the circumstances the agreement is satisfactory. Several other determinations are recorded in the literature, but they differ from the above by about 15 percent.

The quasi-null method just described is applicable to many problems. It may be employed in order to determine accurately the susceptibility of paramagnetic substances in great dilution. It may also serve to measure accurately diamagnetic as well as paramagnetic substances in non-aqueous solvents, for the susceptibility of the solvent itself need not be known to the extreme precision which previous methods have required.

ULTRASONIC VELOCITY AND ABSORPTION IN OXYGEN

BY W. H. PIELEMEIER

DEPARTMENT OF PHYSICS, PENNSYLVANIA STATE COLLEGE

(Received July 22, 1930)

ABSTRACT

The velocity and absorption in oxygen at room temperature were measured at five ultrasonic frequencies located in the two octaves, 316 to 1264 kc/sec. The observed velocities reduced to 0°C do not differ more than 0.2% from Dulong's observed value of V_0 for audible sound (317.2 m/sec). The theoretical value ($V_0 = (\gamma p/d)^{1/2}$) is 314.76 m/sec. The observed absorption values vary with frequency as expected but the deviations from the theoretical values are greater than the velocity deviations.

IN MAKING the velocity and absorption determinations for air published in an earlier article¹ deviations from the theoretical values were found. These deviations are thought to be due to various causes. In order to gain more information on the subject it was decided to test oxygen and nitrogen separately.

APPARATUS

The sources of the high frequency sound were piezoelectric oscillators made of quartz. These square slabs of natural crystal were sputtered with platinum on their two large faces as stated in the earlier article.¹ The electric circuit was altered but slightly. The radiometer was fitted with a small 45 degree reflector so as to render the vertical sound beam horizontal so it could be directed against the pressure vane. The radiometer could be interchanged with the interferometer mirror without any further alteration of the apparatus. With the lowest frequency crystal it was necessary to put a tuned inductance and capacity in series with the load coil in order to suppress a neighboring frequency. The oxygen was dried by bubbling it through concentrated H_2SO_4 and by placing a dish of P_2O_5 or $CaCl_2$ in the gas chamber. For the later measurements a hair hygrometer was placed in the box.

RESULTS

Tables I and II present the results of individual runs although a number of runs were made at each frequency. The number of significant figures given in the tables is justified by the precision of the data and by the slopes of the absorption curves for individual cases but the variation in the successive values of V_0 at a given frequency is about 0.1 percent and the variation in the values of A_t is too great to be explained by the temperature changes between runs.

¹ The Pierce acoustic interferometer as an instrument for the determination of velocity and absorption. Phys. Rev. 34, 1184 (1929).

V_t , in Table I, represents the observed velocity at the temperature, t , given in the second column; V_0 represents the velocity reduced to 0°C ;

TABLE I. *Interferometer determinations.*

Frequency Kilocycles	t $^\circ\text{C}$	V_t m/sec	V_0 m/sec	k_t /cm	A_t cm	Humidity %	Date
1219.0	23.5	330.91	317.52	0.42	$3.1(10)^{-4}$	Approx. 20	Dec. 31, 1930
1166.0	20.8	329.18	317.32	0.44	3.5 "	18	May 15, 1930
655.5	21.3	329.58	317.43	0.21	5.3 "	Approx. 20	3-22-30
389.3	24.4	331.1	317.2	0.103	7.4 "	"	4-2-30
316.2	25.9	332.3	317.7	0.102	11.2 "	24	6-3-30

K_t represents the ordinary absorption constant defined by the equation $I = I_0 e^{-Kx}$; A_t is defined as $A_t = k_t \lambda^2$; similarly for Table II.

TABLE II. *Pressure vane determinations.*

Frequency Kilocycles	t $^\circ\text{C}$	k_t /cm	A_t cm	Date	Humidity %
1219	19.6	0.533	$3.85(10)^{-4}$	1-21-30	—
1166	26.5	0.583	4.68 "	5-10-30	26
655.5	21.0	0.219	5.51 "	3-18-30	—

Theoretical $V_0 = (\gamma p/d)^{1/2} = 314.76$ m/sec

Dulong's Observed $V_0 = 317.2$ m/sec (for audible sound)

$$\text{Theoretical } A_{20} = \frac{4\pi^2}{ap} \left[\frac{4}{3} - u' + \left(\frac{C_p}{C_v} - 1 \right) \frac{K}{C_p} \right] = 3.65(10)^{-4}$$

DISCUSSION OF RESULTS

On account of an originally greater variation in the values of V_0 the crystal frequencies were checked. Radio crystals with oven controlled frequency were used as standards for this purpose. Some of these were at hand in the college broadcasting station, where the checking was done, but frequencies from crystals in Philadelphia and other cities were used also. The lowest frequency (316.2 kc/sec) was not redetermined.

A slightly decreasing velocity with diminishing sound intensity was observed. In a few runs minor peaks, due to higher order reflections, were observed, which, when used to calculate V_0 , gave values near the theoretical value, 314.76 m/sec. Data of this type for another paper are being taken. Instead of substituting in the formula, $V = (\gamma p/d)^{1/2}$, directly, the ratio of the value of $(\gamma p/d)^{1/2}$ for O_2 and its value for air was multiplied by the theoretical value of V_0 for air. This method is not subject to uncertainty in the value of g and hence in p if the two densities were determined at the same place. For this calculation the *relative* density (1.1053) of oxygen and air was used; i.e. $V_0 = 331.60(\gamma')/\gamma(1.1053)^{1/2}$. Here γ' designates the ratio C_p/C_v for oxygen. Its value is given by Lummer and Pringsheim as 1.3977.

The close agreement of the velocity values in Table I with each other and with Dulong's value probably indicates that all were made at somewhat

the same sound intensity. This was roughly determined for crystal *A*, by using a vane suspended by a tungsten wire of known diameter. Near the crystal it was approximately 15 ergs/sec per cm².

This investigation shows the velocity and absorption deviations for oxygen to be similar to those for air. Many observers have published values for V_0 in air very near the theoretical value but for oxygen this is not the case.

Apparently the excess absorption band for O₂, as for air has its upper limit near 1200 kc/sec. The *radiometer* values of k and A are probably the more reliable because they are more directly related to the readings.

THE THERMODYNAMIC TREATMENT OF CHEMICAL
EQUILIBRIA IN SYSTEMS COMPOSED OF REAL GASES.II. A RELATION FOR THE HEAT OF REACTION
APPLIED TO THE AMMONIA SYNTHESIS
REACTION. THE ENERGY AND ENTROPY
CONSTANTS FOR AMMONIA.

BY LOUIS J. GILLESPIE AND JAMES A. BEATTIE

RESEARCH LABORATORY OF PHYSICAL CHEMISTRY, MASSACHUSETTS INSTITUTE
OF TECHNOLOGY*

(Received July 28, 1930)

ABSTRACT

From the two adjustable constants obtained by the authors' treatment of the data on the ammonia synthesis equilibrium, there are calculated the energy and entropy constants for gaseous ammonia referred to the energy and entropy of hydrogen and nitrogen as having the value zero at 0°C and 1 atmosphere. The energy constant for ammonia is $-10058.1 \pm 15^\circ$ -calories per mole and the entropy constant $-16.6491 \pm 15^\circ$ -calories per degree C per mole.

Values of the usual thermodynamic function at 0°C and 1 atmosphere are given in this system for hydrogen, nitrogen, and ammonia.

A rational and simple relation is given for the variation with both pressure and temperature of ΔH , the heat absorbed in a chemical reaction at constant pressure in systems composed of real gases. Values of this heat are computed for several pressures and temperatures for the ammonia synthesis reaction.

1. INTRODUCTION

IN THE first paper,¹ the authors applied a rational and relatively simple relation for the mass action function K_p to the existing data on the ammonia synthesis equilibrium, the equation for which is



In the method used, the effects of pressure and of temperature on K_p were separated; one expression, into which certain approximations had been introduced, giving the variation of K_p with pressure; and the other, which contained no approximations, giving the variation with temperature. We are concerned in the present paper with the latter effect.

The temperature variation of K_p^* (the limiting value of K_p as the pressure on a reacting mixture maintained in chemical equilibrium is isothermally reduced to zero) can be related² to certain energy and entropy constants for the reacting gases. The relation is:

* Contribution No. 246.

¹ Gillespie and Beattie, Phys. Rev. in press.² Beattie, Phys. Rev. **31**, 680 (1928).

$$\ln K_p^* = \sum(\nu_i) \left(\ln \frac{T}{T_0} - 1 \right) - \frac{1}{RT} \sum \left\{ \nu_i \left[\int_{T_0}^T C_{V,i}^* dT - T \int_{T_0}^T C_{V,i}^* \frac{dT}{T} + u_0'{}_i - T s_0'{}_i \right] \right\} \quad (2)$$

where ν_i is the number of moles of Substance i in the stoichiometric equation for the chemical reaction, being negative if the substance disappears in the reaction; $C_{V,i}^*$ the constant-volume heat capacity of Substance i at zero pressure; $u_0'{}_i$ and $s_0'{}_i$ the energy and entropy constants for Substance i at some standard temperature T_0 ; and R the ideal gas constant. The summation extends over all of the gases taking part in the chemical reaction.

The integration constants u_0' and s_0' can be related quite simply to expressions which occur in the theory of ideal gases. For the molal energy of an ideal gas:

$$u = \int_{T_0}^T C_V dT + u_0' \quad (3)$$

and for the molal entropy there are two expressions depending upon the choice of independent variables:

$$s = \int_{T_0}^T C_V dT/T + R \ln V/n + S_0 \quad (4)$$

or

$$s = \int_{T_0}^T C_V dT/T + R \ln T/T_0 - R \ln p + s_0'. \quad (5)$$

In the previous publication² the entropy constant used in the various equations for real gases was S_0 , that is the one referring to V and T as independent variables. If we choose 0°C and 1 atmosphere as the standard state, there is a numerical simplification in using the energy and entropy constants u_0' and s_0' as defined above: For ideal gases these integration constants are equal, and for real gases they are approximately equal, to the energy and entropy, respectively, of a mole of the gas in the standard state. The relation between the two integration constants is:

$$S_0 = s_0' - R \ln RT_0. \quad (6)$$

One way to interpret the integration constants u_0' and s_0' is as follows: The quantities u_0' and $s_0' - R \ln p$ are for real as well as ideal gases the molal energy and entropy, respectively, of the gas at T_0 and at an infinitely low pressure.

We can expand $C_{V,i}^*$ in a power series of the temperature

$$C_{V,i}^* = A_i + B_i T + C_i T^2 \quad (7)$$

where A_i , B_i , and C_i are constants for each gas. Substitution of (7) into (2) and carrying out the indicated integration gives:

$$\log K_p^* = \frac{\sum(\nu_i A_i) + \sum(\nu_i) R}{R} \log T + \frac{M \sum(\nu_i B_i)}{2R} T + \frac{M \sum(\nu_i C_i)}{6R} T^2 + \frac{I}{T} + J \quad (8)$$

where

$$I = \frac{M}{R} \left[\Sigma(\nu_i A_i) T_0 + \frac{\Sigma(\nu_i B_i)}{2} T_0^2 + \frac{\Sigma(\nu_i C_i)}{3} T_0^3 - \Sigma(\nu_i u_0' i) \right] \quad (9)$$

$$J = \frac{M}{R} \left[-\Sigma(\nu_i A_i) - \Sigma(\nu_i) R - \Sigma(\nu_i B_i) T_0 - \frac{\Sigma(\nu_i C_i)}{2} T_0^2 + \Sigma(\nu_i s_0' i) \right] \quad (10)$$

$$- \frac{\Sigma(\nu_i A_i) + \Sigma(\nu_i) R}{R} \log T_0.$$

The quantity $M = 0.43429 \dots$ is the modulus of the common logarithms, which are denoted by \log .

In the treatment of the data on the ammonia synthesis equilibrium, values of K_p^* were computed from each given value of K_p . From the values of A, B, and C given in Table I the next three terms of Eq. (8) were computed for each temperature, subtracted from $\log K_p^*$, and the difference plotted against $1/T$. The values of the two adjustable constants I and J were then determined from the best straight line through the points. The resulting numerical relation for $\log K_p^*$ is:

$$\log K_p^* = -2.691122 \log T - 5.519265 \times 10^{-5} T$$

$$+ 1.848863 \times 10^{-7} T^2 + \frac{2001.6}{T} + 2.6899. \quad (11)$$

TABLE I. Values of the specific heat constants of Eq. (7). Units: 15° calories per mole and per degree C; $R = 1.986847$.

Gas	A	$10^3 B$	$10^6 C$
Hydrogen	4.66	0.70	0.00
Nitrogen	4.82	0.33	0.05
Ammonia	6.04	0.71	5.10

2. THE ENERGY AND ENTROPY CONSTANTS

Substitution of the values of I and J from (11) into Eqs. (9) and (10), and using the values of the other constants from Table I gives:

$$\Sigma(\nu_i u_0' i) = -10059.2 \text{ } 15^\circ \text{ calories} \quad (12)$$

$$\Sigma(\nu_i s_0' i) = -16.6532 \text{ } 15^\circ \text{ calories per degree C} \quad (13)$$

A consistent system of energy and entropy values may be constructed³ by assigning arbitrary values (say zero) to the energy and the entropy of all elementary substances in some standard state, say 0°C and 1 atmosphere. This system of values can readily be interpreted in terms of any other system as for instance that used by Rodebush and Rodebush,⁴ who use 0°K for the standard temperature. It should be noted however that for a practical sys-

³ Beattie, Phys. Rev. **32**, 691 (1928).

⁴ Rodebush and Rodebush, Int. Critical Tables, McGraw-Hill Book Co., New York, 1929; Vol. V, p. 84.

tem there are many advantages in favor of the use of 0°C as the standard temperature. In the system of Lewis and Randall⁵ the standard state for a gas is defined in terms of unit fugacity. This makes, as they note, their standard state of a gas a hypothetical one which corresponds to no real state of the gas. In our system the standard state is the same for a gas as for a liquid or solid.

Since hydrogen and nitrogen are each gaseous in the standard state, we may compute their energy and entropy constants from the relations⁵

$$u_0' = \frac{U}{n} + \frac{nA_0}{V} \left[1 - \frac{na}{2V} \right] + \frac{3nRc}{VT_0^2} \left[1 + \frac{nB_0}{2V} - \frac{n^2B_0b}{3V^2} \right] \quad (14)$$

$$s_0' = \frac{S}{n} - R \ln \frac{V}{nRT_0} + \frac{nRB_0}{V} \left[1 - \frac{nb}{2V} \right] + \frac{2nRc}{VT_0^3} \left[1 + \frac{nB_0}{2V} - \frac{n^2B_0b}{3V^2} \right] \quad (15)$$

where A_0 , a , B_0 , b and c are constants in the Beattie-Bridgeman equation of state, and U/n and S/n are the molal energy and entropy of the gas at T_0 and the molal volume V/n . Placing $U=0$ and $S=0$ and using $T_0=273.13$

TABLE II. Values of the equation of state constants. Units: normal atmospheres, liters per mole, degrees Kelvin ($T^\circ K = t^\circ C + 273.13$); $R=0.08206$.

Gas	A_0	a	B_0	b	c	Normal volume
Hydrogen	0.1975	-0.00506	0.02096	-0.04359	0.0504×10^4	22.4252
Nitrogen	1.3445	0.02617	0.05046	-0.00691	4.20×10^4	22.4015
Ammonia	2.3930	0.17031	0.03415	0.19112	476.87×10^4	22.1022

and using the values of the normal volumes and of the constants listed in Table II gives for hydrogen and nitrogen the energy and entropy constants listed in Table III. Use of these values in Eqs. (12) and (13) leads to the energy and entropy constants for ammonia given in Table III.

TABLE III. Values of the energy and entropy constants for hydrogen, nitrogen and ammonia. Units: 15°-calories, degrees Centigrade, moles.

Gas	Energy Constant (u_0')	Entropy Constant (s_0')
Hydrogen	0.215	0.00079
Nitrogen	1.602	.00587
Ammonia	-10058.1	-16.6491

From the energy and entropy constants for hydrogen, nitrogen, and ammonia we have computed the molal energy and entropy of these three gases at 0°C and 1 atmosphere together with their molal heat content and thermodynamic potentials defined by the usual relations

⁵ Lewis and Randall, *Thermodynamics and the Free Energy of Chemical Substances*, McGraw-Hill Book Co., New York, 1923.

⁶ Beattie, *Phys. Rev.* **32**, 699 (1928). In Eq. (15) the new entropy constant has been used, which accounts for the RT_0 in the denominator of the term $R \ln(V/nRT_0)$.

$$H = U + pV \quad (16)$$

$$F_{VT} = U - TS \quad (17)$$

$$F_{pT} = H - TS. \quad (18)$$

These values are given in Table IV. They are given to more significant places than the data warrant, but these calculation figures were intentionally retained in order that relative values may be accurately computed.

TABLE IV. Values of several thermodynamic quantities for one mole of hydrogen, nitrogen and ammonia at 0°C and 1 atmosphere; and the increase Δ of these quantities when one mole of ammonia is formed from its elements all reactants and products being at 0° and 1 atmosphere. Units: 15°-calories, degrees Centigrade, moles.

	Hydrogen	Nitrogen	Ammonia	Δ
U	0	0	-10078.0	-10078
H	543.0	542.4	-9542.9	-10628
S	0	0	-16.7220	-16.722
F_{VT}	0	0	-5510.7	-5511
F_{pT}	543.0	542.4	-4975.6	-6061
pV	542.96	542.39	535.14	-550.50

3. THE HEAT OF REACTION

A general relation⁶ for the heat content of n moles of a pure gas in terms of the independent variables p and T is:

$$H = \int_0^p \left[V - T \left(\frac{dV}{dT} \right)_p \right] dp + nh' \quad (19)$$

where

$$h' = \int_{T_0}^T C_V^* dT + RT + u_0' \quad (20)$$

and V is the volume of n moles of the gas. When the integrand of (19) is evaluated by means of the form of the equation of state explicit in V , we obtain:

$$H = \left[B_0 - \frac{2A_0}{RT} - \frac{4c}{T^3} \right] np + nh' \quad (21)$$

where terms containing powers of p higher than the first have been omitted. This approximation corresponds to the approximation used in the equation for the effect of pressure on K_p (Eq. (9) of the first paper¹). It is believed that no better value for the heat of reaction would be obtained by retaining the terms in higher powers of p , since the values of the constants I and J were obtained from relations containing this simplification.

The heat absorbed at constant pressure by a chemical reaction is

$$\Delta H = \Sigma(\nu_i H_i) \quad (22)$$

whence

$$\Delta H = [\Sigma(\nu_i B_{0i}) - 2\Sigma(\nu_i A_{0i}/RT) - 4\Sigma(\nu_i c_i/T^3)]p + \Sigma(\nu_i h'_i) \quad (23)$$

where by use of Eqs. (7), (9) and (20) we find that

$$\Sigma(\nu_i h_i') = [\Sigma(\nu_i A_i) + \Sigma(\nu_i)R]T + \frac{\Sigma(\nu_i B_i)}{2}T^2 + \frac{\Sigma(\nu_i C_i)}{3}T^3 - \frac{R}{M}I \quad (24)$$

When the numerical values of the various constants are included, there results from (23) and (24) the relation

$$\Delta H = - \left[0.54526 + \frac{840.609}{T} + \frac{459.734 \times 10^6}{T^3} \right] p - 5.34685T \quad (25)$$

$$- 0.2525 \times 10^{-3}T^2 + 1.69167 \times 10^{-6}T^3 - 9157.09$$

in which ΔH is the heat absorbed in the formation of one mole of ammonia from its elements in 15°-calories, p is in atmospheres and T in degrees Kelvin. The reduction factor 24.212127 15°-calories per liter-atmosphere was used in the term evaluated from the equation of state constants. Values of ΔH computed from (25) for several pressures and temperatures are given in Table V.

TABLE V. Heat evolved ($-\Delta H$) in the formation of one mole of ammonia from its elements at several temperatures and pressures.

Temp. °C	0	300	500	600	700
Pressure, atm.	$-\Delta H$ in 15°-calories				
1	10630	11990	12660	12890	13040
100		12430	12920		13230
300		13320	13450		13610
600		14660	14240		14190
1000		16440	15290		14950
1 (Haber)	From 10950 to 11000			13000	

The values at 0° and 600°C and 1 atmosphere are given for comparison with the calorimetric measurements of Haber.⁷ No calorimetric determinations of the heat of formation of ammonia have been made at high pressures. It should be noted that our calculations indicate that at high pressures there is a considerable increase in the heat evolution—the effect being about 20 percent for 1000 atmospheres at 500°C.

At about 400 to 500 atmospheres, depending on the temperature, the temperature coefficient of the heat of reaction changes sign.

The agreement of our value at 1 atmosphere and 600° with the direct measurement of Haber is within 1 percent, and is satisfactory. The measurement of Haber at 1 atmosphere and 0° was carried out in a hot chamber within the calorimeter and is probably not so accurate as the measurements at higher temperatures.

⁷ Haber, Zeits. f. Elektrochemie 21, 191, 206 (1915).

LETTERS TO THE EDITOR

Prompt publication of brief reports of important discoveries in physics may be secured by addressing them to this department. Closing dates for this department are, for the first issue of the month, the twenty-eighth of the preceding month; for the second issue, the thirteenth of the month. The Board of Editors does not hold itself responsible for the opinions expressed by the correspondents.

Wave Mechanics of Deflected Electrons

Under a similar title,¹ Leigh Page discusses the wave mechanics of the deflection of cathode rays by homogeneous fields. The greater part of the discussion is entirely correct and is a valuable contribution to our knowledge of wave functions. It is therefore unpleasant to have to point out that the major conclusion is incorrect: wave mechanics and classical mechanics do agree in the formulae by which they relate \bar{p} , the mean radius of curvature of the cathode beam, to (e/m) and the field strength. This has been proven by Kennard² with complete rigor. Mr. Page reaches the opposite conclusion only be-

cause this calculation of \bar{p} is an interpolation between the values of $\bar{p}_0 \equiv 1$ and \bar{p}^2 , \bar{p}^4 which are calculated accurately. The difference between $(e/m)_{\text{defl}}$ and $(e/m)_{\text{cp}}$ can therefore not be explained as a difference between wave and classical mechanics.

CARL ECKART

University of Chicago,
Chicago, Illinois,
August 15, 1930.

¹ Leigh Page, Phys. Rev. **36**, 444 (1930).

² E. H. Kennard, Zeits. f. Physik **44**, 344 (1927).

Magnetostriction in Nickel

In a recent article in this journal¹ C. W. Heaps and A. B. Bryan quote a statement of mine² in regard to the effect of tension upon the magnetostrictive contraction observed in nickel, and point out that the results reported by S. Bidwell³ would, if correct, require my statement to be limited to relatively high

magnetic fields and low tensions. I wish to point out that more recent work, particularly that of S. R. Williams,⁴ indicates that no change in sign of the effect of tension on magnetostriction is to be expected in pure annealed nickel, properly demagnetized in zero applied field.

L. W. MCKEEHAN

Sloane Laboratory,
Yale University,
August 13, 1930.

¹ Heaps and Bryan, Phys. Rev. [2] **36**, 326-332 (1930).

² McKeehan, J. Franklin Inst. **202**, 761 (1926): "In the case of nickel . . . tension . . . will increase the magnetostriction (contraction)."

³ Bidwell, Proc. Roy. Soc. **47**, 469-480 (1890).

⁴ S. R. Williams, Phys. Rev. [2] **4**, 288 (1914); **10**, 129-139 (1917); School Science and Mathematics **22**, 859-871 (1922).

Wind Mixing and Diffusion in the Upper Atmosphere

My attention has lately been called to a letter by Dr. E. O. Hulburt, under the above title (in your issue of July 1, 1929, p. 161) which had escaped my notice. It seems desirable to state that the substance of what was published on this subject in my paper, to which he refers, was in writing before Dr.

Maris' work became known to me, either by the Abstract of 1927 December, or by his paper of 1928 December, which had been kindly sent to me in 1928 May. The absence of a reference to Dr. Maris was intended to indicate this independence implicitly; a mention of his work, coupled with an explicit

claim to independence, seemed to me a less courteous step. No question of priority of publication did or could arise, as this was assured to him by his abstract of 1927 December.

The height at which mixing ceases is important for the constitution of the upper atmosphere, but it remains speculative because the degree of mixing by winds at great heights is not known. For some years prior to 1920 the height was generally assumed to be about 10 km; E. A. Milne and I then broke away from that idea (Q. J. R. Meteor. Soc. 46, 357, 1920), but not to the extent that Dr. Maris and I have since thought necessary. In

1926 (Proc. R. Soc. A111, 4, lines 24-26) I mentioned the possibility that mixing extends up to auroral heights, though without giving my reasons. Early in 1927 Mr. T. W. Dickson and I made calculations as to the rate of diffusive stratification of the air at great heights, but in view of the abstract and paper by Dr. Maris we have not published them. Such calculations were made as early as 1914 by Gouy (Comptes rendus 158, 664).

S. CHAPMAN

Imperial College of
Science and Technology,
London,
July 28, 1930.

Evidence for the Richtmyer Double Jump Hypothesis of X-Ray Satellites

Richtmyer¹ has recently proposed the hypothesis that many of the x-ray satellite lines may be due to double transitions in which two electron transitions cooperate to emit one quantum. I should like to call attention to a number of known facts about x-ray satellites which are very satisfactorily explained on this hypothesis several of which facts have not yet been mentioned by Richtmyer.

The main facts known and published to date about x-ray satellites may be roughly summarized as follows:

1. Definition: An x-ray satellite is a line whose frequency is not directly derivable from the known system of x-ray absorption levels. (Lines which *can* be so derived are called "diagram" lines.)

2. Satellites are generally very close to some "parent" diagram line and on the short wave-length side.

3. The same satellite can be identified for different elements and the frequency difference $\Delta\nu$ between the satellite and the parent line follows a Moseley diagram when $(\Delta\nu/R)^{1/2}$ is plotted against atomic number Z .

4. Satellites are much less intense than the parent line. They appear abruptly in the series of increasing atomic numbers about at the point where a new electron shell two levels higher (at least) than the terminal level of the parent line starts to form. Thus K satellites appear about when the M level starts to form.

5. They are intense near this abrupt beginning point and fall off in intensity relative to the parent line as the atomic number increases.

6. Richtmyer believes he has observed

something like a continuous spectrum associated with the satellites of a given parent line.

As additional information to the above facts the author in collaboration with Mr. A. Hoyt has just finished an investigation with the double crystal spectrometer soon to be published in this Journal on the excitation potential of the satellite $K\alpha_3$ of copper. We find

7. That the satellite $\text{Cu } K\alpha_3$ is excited at not more (if at all) than 200 or 300 volts higher critical potential than the parent line (89 K.V.).

8. That the satellite intensity is rigorously proportional to the exciting cathode-ray current.

9. That the ratio of the intensities $K\alpha_3/K\alpha_1$ is about 1/120 based on the areas of the lines α_3 and α_1 (integrated over their breadth), but only about 1/440 based on the maximum ordinate values. In other words, α_3 is nearly 4 times as broad as α_1 .

10. $K\alpha_3$ of Cu is a doublet. This is in accord with recent observations of Richtmyer and with the doublet structure of $K\alpha_3$ for lighter elements.

Let us now consider how many of the above facts are explained and correlated by the Richtmyer double jump hypothesis. For definiteness and lucidity let us consider the line $K\alpha_3$ of copper as explained by the double transition $N \rightarrow M$ and $L \rightarrow K$. As Richtmyer has pointed out facts (1) to (3) inclusive are explained since the extra energy of the satellite as compared to its parent represented by

¹ Richtmyer, Jour. Frank. Inst. 208, 325-361 (1929).

the frequency difference $\Delta\nu$ is interpreted as the energy of the transition $N \rightarrow M$ which is of the right order of magnitude and would of course follow a Moseley diagram.

Fact (4) is explained because unless there were at least two levels above the terminal level of the parent line any double transition that might occur (e.g. $M \rightarrow L$; $L \rightarrow K$) would be equivalent to a diagram line ($M \rightarrow K$). The fact that the satellites do not appear at exactly the point in the atomic table where the third level higher up starts to form (sometimes one or two atomic numbers lower) is not to be taken as contrary evidence because it must be recollected that x-ray satellites always come from targets in the *solid* state and it is highly likely that the peripheral electrons of atoms in a crystal lattice behave differently from those of free atoms as in the vapor state.

Fact 6 needs no comment that Richtmyer has not already made.

Facts 7 and 8 seem to invalidate the Wentzel-Dryvesteyn spark line hypothesis which requires for say a K satellite that the atom be doubly ionized in deep levels. This would have to be done either (a) in a single collision in which case the excitation potentials of satellites would be much greater (about double) than the excitation potentials of the parent, or (b) in two successive collisions in which case the intensity of the satellite would vary as the square of the current. Facts 7 and 8 are in accord with the double jump hypothesis since only a few extra volts would be necessary to ionize the M level at the same time as the K level in the case of K satellites.

Facts 5 and 9 are in accord with information given the writer by J. R. Oppenheimer on the theory of the probability of double excitation and double emission. Quoting from a letter of Oppenheimer's to the writer he says,

"If there were no coupling between the M , N electrons on the one hand with the K , L electrons, then both the probability of a double excitation and that of a double emission would vanish; because of the coupling in each case the ratio of the probability of the double jump to that of the single jump involving only the more tightly bound electron has a finite value; the value of the ratio r is very nearly the same for the excitation and the emission so that $R \sim r^2$. Nor r is given by the overlapping, or quantitatively by the so-called scalar product of the wave functions

for an electron in the M and N shells, when the interaction of all electrons is considered, and this in turn is given, as one sees, by working out the perturbation of the electrons on each other, roughly by the square of the mean interaction of an L and an M electron divided by the square of the energy difference $M-N$. If one takes your value of 30 volts for the $M-N$ difference and your value for $R=1/240$, [assuming a doublet $K\alpha_3$ of two equal members] then one gets for the mean interaction energy about 8 volts, which is not at all unreasonable for an L and an M electron of copper. (The apparent neglect of the K and N shells comes from this, that the mean interaction of electrons in these states is negligibly smaller than the $L-M$ interaction.) I believe, therefore, that Richtmyer's interpretation is applicable to this satellite."

Dr. W. V. Houston has pointed out that the progressive decrease of intensity of a given satellite with increase of atomic number is beautifully explained by the above remark of Oppenheimer for since the ratio

$$R = r^2 = \left[\frac{(\text{mean interaction energy of } L \text{ and } M)^2}{(\text{energy difference } M-N)^2} \right]^2$$

the decrease of R with atomic number is seen to be due to the Moseley increase of the energy difference $M-N$ entering to the fourth power in the denominator of the above expression.

Finally the writer believes there may be some significance in the apparently greater breadth of the satellite $K\alpha_3$ of copper. As mentioned under (9), the ratio of $K\alpha_3/K\alpha_1$ for areas (1/120) disagrees with the same ratio for maximum ordinates (1/440) by a factor of almost 4. If the satellite were a poorly resolved doublet of two equally intense lines the disagreement would be by a factor of two only. If the lines were not equally intense the factor would be less than two. To explain a factor of more than two, it is necessary to suppose that each of the two members of $K\alpha_3$ are broader than the parent line $K\alpha_1$, indeed almost twice as broad. The writer wishes to suggest that this extra breadth may be precisely attributed to the almost continuous dense distribution of energy levels for the peripheral (N) electrons required in the solid target by the Fermi

statistics shown by A. Sommerfeld.² The energy of the $N \rightarrow M$ transition would be indefinite to just the extent defined by the energy breadth of the Fermi distribution of the conduction electrons in copper. The excess broadening of $K\alpha_3$ of copper over $K\alpha_1$ corresponds to an energy of about 12 volts a value which is in qualitative agreement with the probable energy value of the Fermi distribution as well as the experimental and theoretical uncertainties warrant.

The field of x-ray satellites may therefore prove to have an important bearing on the field of the electron theory of metals and metallic conductors making possible a study

of the behavior of peripheral electrons *in the solid state* which would be impossible with optical spectra.

It would seem that about all the known facts of x-ray satellites are explained qualitatively by Richtmyer's double-jump hypothesis and only await further experimental work for a quantitative verification.

JESSE W. M. DU MOND

California Institute of Technology,
Pasadena, California,
August 6, 1930.

² A. Sommerfeld, *Zeits. f. Physik* **47**, 1-60 (1928).

Hyperfine Structure of X-Ray Lines

In the June 15 (1930) issue of *The Physical Review* Professor G. Breit discusses the possible effect of nuclear spin on x-ray terms. By straightforward calculation from the Dirac equation for a Coulomb field of force, and by use of only minor approximations, he shows that K terms of the heavier elements should be split into two components with a frequency difference $\Delta\nu$ given by

$$\Delta\nu = \left(\frac{8\pi^2 mc^2}{h^2} \right)^3 \cdot Z^3 \cdot \left(k + \frac{1}{2} \right) \cdot \frac{1840\mu}{2k\mu_0(2\rho^2 - \rho)} \text{cm}^{-1}$$

where m , c , h , Z have their usual meanings; k and μ are respectively the angular momentum and magnetic moment of the nucleus; μ_0 is the Bohr magneton; and ρ is $(1 - \alpha^2)^{1/2}$, where $\alpha = (2\pi e^2 / ch)Z$. Taking $k = 9/2$ and assuming $1840\mu / 2k\mu_0 = 1$, Breit finds that the $WK\alpha_1$ line should contain two components separated by 7.3 volts—or by 1 part in 8092. In wave-length, this is a separation of $\Delta\lambda = 0.026$ X.U., taking $\lambda K\alpha_1$ of tungsten as 208.8 X.U.; in angle, it is a separation of 0.86 seconds of arc, for a calcite crystal, first order.

With the direct-reading two-crystal spectrometer developed in this laboratory (*Phys. Rev.* **35**, 1428, June 1, 1930) we have searched for this predicted fine structure of $WK\alpha_1$. We were unsuccessful in detecting any certain

evidence in first order, but on going to the higher resolution available in fifth order we find distinct evidence that there are two peaks separated, in that order, by some 5'' of arc—corresponding to a $\Delta\lambda$ in first order of about 0.03 X.U., substantially as predicted by Breit. A qualitative check was obtained by observations in fourth order. The long wavelength component appears to be the more intense by some 25 or 50 percent. However, the measurements as yet are not sufficiently precise to warrant reporting more than qualitative data as regards separation or relative intensity.

To check whether this separation might possibly be due to some peculiarity of the crystals used we very carefully repeated the observations on first order; and also measured the $MOK\beta$ doublet. Crystal imperfections, e.g., twinning, should cause the same apparent angular separation into components, regardless of wave-length. In these cases no separations as great as 1'' of arc could be found.

A detailed report will be made later after we have had opportunity to obtain more precise and complete data.

F. K. RICHTMYER
S. W. BARNES
K. V. MANNING

Physical Laboratory,
Cornell University,
Ithaca, N. Y.,
August 15, 1930.

The Angular Momentum of the Li_7 Nucleus

There are at present two discordant estimates of the angular momentum of the Li_7 nucleus. Harvey and Jenkins¹ arrive at the value $i=3/2$ using the alternating intensities of the Li bands. Schüler and Brück² use the hyperfine structure of the $1s2p^3P \rightarrow 1s2s^3S$ line of Li^+ as observed by Schüler and infer the angular momentum to be $1/2$. I have made additional observations on the same hyperfine structure pattern and my results support strongly the value of Jenkins, being definitely in disagreement with the value of Schüler and Brück.

The apparatus used for excitation of the Li^+ spectrum is practically identical with that developed by Schüler and the line was photographed in the second order of a 21 foot concave grating³ having a dispersion of 1.3A/mm in the second order. The Li used was obtained through the courtesy of the Maywood Chemical Co., Maywood, N. J. and is manufactured by them.

The pattern obtained is very similar to Schüler's with the following essential differences. (a) Component (12) is absent on all of my plates. This component was attributed by Schüler to a ghost and it does not fit any reasonable interpretation of the spectrum. (b) Component (1) appeared definitely both in strong and in weak fields and has, according to my estimates the same relative intensity with respect to components (3) and (2) under both sets of conditions. According to Schüler and Brück this component appears only in strong fields. It was discarded by them in the classification of the lines.

The presence of component (1) makes it impossible to adopt the value $1/2$. The closely spaced group (3), (2), (1) can be due only to a transition $^3P_0 \rightarrow ^3S_1$. The upper level being single the lower level 3S_1 must be triple, which is impossible for $i=1/2$. The possible values of i are therefore $i=1, 3/2, 2$. The position of the components (3), (2), (1) has been measured and is in essential agreement with Schüler's results. The "interval ratio" is according to Schüler's⁴ measurements $\Delta\lambda_{32}/\Delta\lambda_{21}=0.19/0.12=1.58$ and according to preliminary measurements I find the ratio to be $1.61(5) \pm 0.02(3)$. The error given in my ratio was derived from the mean deviation in the comparator readings. There is a possibility that the third figure may also be subject to a systematic error due to the proximity of

(1) to (2). There appears to be a discrepancy in Schüler's data; the ratio obtained from his wave-length differences being in disagreement with that obtained from his frequency differences. The theoretical value of this interval ratio is according to Goudsmit and Bacher⁵

$$(i+1)/i = 2, 5/3, 3/2$$

for $i = 1, 3/2, 2$.

Schüler's measurements thus agree about equally well with $i=3/2$ and $i=2$ and mine agree best with $i=3/2$. A calculation of the position of the lines for $i=3/2$ and of their relative intensities, using the approximations of Goudsmit and Bacher and of Hill⁶ shows that the remainder of the pattern is also in agreement with $i=3/2$.⁷ Components (13), (5) are presumably unresolved doublets and components (8), (4) are unresolved triplets. Two components of the $^3P_2 \rightarrow ^3S_1$ pattern would be too faint to observe. No definite conclusion as to i can be reached using this part of the pattern on account of its complexity. In the group (3), (2), (1) however the lines are single and definitely resolved. As has just been explained $i=1/2$ is excluded by the presence of component (1), $i=1$ is excluded by the separation ratio which according to my observations is also in better agreement with $i=3/2$ than with $i=2$.

L. P. GRANATH

Department of Physics,
New York University,
University Heights.

¹ Harvey and Jenkins, Phys. Rev. 35, 789 (1930).

² Schüler and Brück, Zeits. f. Physik 58, 735 (1929).

³ The Anderson grating used at present in this mounting is the property of Townsend Harris Hall, College of the City of New York.

⁴ Schüler, Zeits. f. Physik 42, 487 (1927).

⁵ Goudsmit and Bacher, Phys. Rev. 34, 1501 (1929).

⁶ Hill, Proc. Nat. Acad. 15, 779 (1929).

⁷ I have been informed of this by Professor G. Breit. I understand from him that Professor Goudsmit has calculated the same pattern with the same results. Through the courtesy of Professor Pauli we learned of a forthcoming paper in the Zeits. f. Physik by Mr. Guttinger of Zurich in which Schüler's pattern is brought into agreement with $i=3/2$.

Evidence for Be Isotope of Mass 8 in the BeH Band Spectrum

Consideration of the regularities¹ in a table of the α -particle plus proton and electron content of the known nuclei leads to the prediction that the mass 8 should be found as an isotope of Be. The fact that the mass spectrograph fails to reveal this isotope for Be would indicate that if present it must be very much less abundant than the 9. This is also indicated by the atomic weight of Be which is still given as greater than 9 (9.02 is the latest value). An isotope of Be of mass 10 is not to be expected because of the disturbance of the symmetry in the table of isotopes just mentioned.

Judging from its success in demonstrating the presence of the weak isotopes C¹³, N¹⁵, O¹⁷, and O¹⁸, the band spectrum method should detect this Be⁸ even though it may represent but a very small fraction of the total in ordinary Be. Band spectra due to the diatomic molecules BeF, BeO, and BeH only are known, and unfortunately these can only be obtained in emission from an arc, which is not the ideal source for isotope study. Of these three band systems, that due to BeH at $\lambda 4990$ is by far the easiest to obtain in intense exposure at high dispersion, and therefore, since its bands also have the open fine structure characteristic of the diatomic hydrides, it is the best for this investigation. The mass factor $\rho^2 - 1 = 0.0125$ for BeH is not as large as that for BeO, but nevertheless it is large enough so that the rotational isotope effect for lines not too near the origin of the band is greatly in excess of the smallest line separation detectable at this wave-length under ordinary conditions on high dispersions-plates.

I have made a comparison of the predicted positions of Be⁸H lines for the ($\frac{1}{2}$, $\frac{1}{2}$) band with those of some very weak lines found on a spectrogram of this band system used for a previous investigation,² with the result that there is good evidence for the existence of Be⁸. The following table gives the comparison of some of the calculated and observed displacements of these weak lines from the corresponding Be⁹H lines (in cm^{-1} units):

	Calc.	Obs.
P(11)	-2.32	-2.46
P(17)	-3.17	-3.12
P(18)	-3.28	-3.39
P(19)	-3.37	-3.37

	Calc.	Obs.
P(21)	-3.52	-3.73
R(9)	+2.73	+2.93
R(10)	+2.98	+2.74
R(11)	+3.24	+3.07
R(12)	+3.49	+3.28
R(16)	+4.43	+4.71

The line designations here are those of reference 2 reduced by $1\frac{1}{2}$ units to give the proper K'' values. This table is incomplete because of the fact that the majority of the weak Be⁸H lines lie so close to over-exposed main lines of this and the overlapping ($3/2$, $3/2$), ($5/2$, $5/2$), and ($7/2$, $7/2$) bands as to be obliterated by the solarization accompanying these stronger lines. Since this spectrogram was taken in the first order with a dispersion of but 2.76Å per mm, much of this obscuring could be eliminated by the higher dispersion and resolution of a third order spectrum. Work is now in progress with an improved light source to obtain an intense exposure of these bands at this higher dispersion.

In making the calculations of these isotope shifts it is highly important to take account of the higher powered terms in the rotational energy expression because of the large rotational distortion present in these bands.² Even the sixth powered term with a mass factor $\rho^6 - 1$ is appreciable for $K'' > 18$. Since the vibrational constants have not been directly measured,² there is a slight uncertainty in the exact value of the vibrational isotope shift for the ($\frac{1}{2}$, $\frac{1}{2}$) band, but this cannot introduce much of an error into the calculations. For the rotational B_0 constants are nearly the same in both the initial and final states, and it is therefore certain that the two vibrational frequencies differ but little. And since the vibrational isotope shift is proportional to the difference between the vibrational constants in the two states, it is certainly therefore quite small (the estimated constants² yield $+0.11 \text{ cm}^{-1}$).

WILLIAM W. WATSON

Sloane Physics Laboratory,
Yale University,
August 27, 1930.

¹ Cf., for example, G. Beck, *Zeits. f. Physik* 47, 407 (1928).

² W. W. Watson, *Phys. Rev.* 32, 600 (1928).

The Penetration of Radiation

In the therapeutic use of radiation, as in photochemistry, it is an axiom that only that radiation which is absorbed is effective, and that its immediate effect is located at the place where it is absorbed.

Both in heat therapy and in treatment with x-rays, it is frequently desired to produce effects at a definite depth in the tissues, and to do so with a minimum of unwanted effects at the surface (e.g., erythema), and elsewhere. The selection of the proper wave-length of radiation requires a knowledge of the coefficient of absorption of the radiation as a function of depth in the tissues. Since, however, it will frequently be necessary to act in the absence of such detailed information, it may be of interest to consider a simple special case, which may in many cases correspond rather closely to the actual conditions:

Assume that the place at which it is desired to produce the effect is far enough from the surface of emergence of the radiation,—or the coefficient of reflection low enough,—so that reflection at the surface may be neglected. Assume that the absorbing power of the tissue is uniform, and that scattering is either small enough, or great enough, so that the degree of scattering does not change with depth.

The intensity of radiation flux will then vary exponentially with depth, x :

$$J_x = J_0 e^{-kx}.$$

The rate of energy absorption at depth, x , will be given by

$$-J_x' = -dJ_x/dx = J_0 k e^{-kx}$$

New Bands in the Absorption Spectrum of Mercury

Two new continuous bands have been found in the absorption spectrum of mercury. Preliminary measurements give the wave-lengths at the maxima as 1807 and 1685. These bands correspond to known absorption bands of cadmium and zinc at wave-lengths 2212, 2114, and 2064, 2002 respectively.

The mercury bands were photographed with a small vacuum fluorite spectrograph with a hydrogen discharge tube as a light source. The absorption cell was made of fused quartz. It contained very thin windows which had been drawn in to a hemispherical shape to withstand atmospheric pressure. The short wave limit of transparency for this cell was 1550.

and the fraction relative to the initial flux J_0 ,

$$-J_x'/J_0 = k e^{-kx}.$$

The coefficient of absorption, k , will be a function of the wave-length of the radiation. To make the fraction absorbed at depth x a maximum.

$$\frac{d}{dk}(k e^{-kx}) = 0 = e^{-kx} - k x e^{-kx}$$

whence $kx = \infty$, or 1. The first value corresponds to a minimum (complete absorption before reaching depth, x), whence the desired solution $kx = 1$, indicates that the energy flux at depth, x , should be the e^{th} part of that at the surface ($1/e = 0.368$). A more penetrating radiation will be transmitted too far, and a less penetrating radiation absorbed too soon, to produce a maximum effect at depth, x .

It should be remarked, that this solution is the optimum only on the assumption that the total energy flux is to be kept as low as possible. If the limiting factor is the absorption at the surface, the ratio of the absorption at the surface to that at depth, x , will approach unity as k becomes vanishingly small. In this case, therefore, the radiation should be as penetrating as possible.

ELLIOT Q. ADAMS

Elliot Q. Adams,
Lamp Development Laboratory,
General Electric Company,
Nela Park, Cleveland, Ohio,
August 26, 1930.

With increasing pressure of mercury vapor in the absorption cell, the absorption line 1849 ($1S-2^1P$) broadens symmetrically until it reaches the band at 1807, after which it broadens only toward longer wave-lengths. This development with pressure of the $1S-2^1P$ line and its relation to the 1807 band of mercury is quite the same as the developments of the corresponding lines (2288, 2134) and bands (2212, 2064) in cadmium and zinc vapors respectively (Phil. Mag. 7, 555. 1929).

If the interpretation given to these absorption regions in cadmium and zinc vapors be applied to the present observations on mercury, the energy of dissociation of the unexcited mercury molecule is 0.20 volts.

This value is about one-fourth that obtained by Mrozowski from the convergence limit of a series of flutings and from the change in intensity of fluorescence with super-heating (*Zeits. f. Physik* 50, 657, 1928; 55, 338, 1929). Kuhn has shown (*Zeits. f. Physik* 63, 458, 1930) that Mrozowski's method for computing convergence limits could not be applied to molecules like Hg_2 . Rollefson (*Phys. Rev.* 35, 1177, 1930) has pointed out that the value of D computed from the decrease in intensity of fluorescence with super-heating may be in error because some of the absorption may arise from colliding Hg atoms and not from

Hg_2 molecules, and that the value of D so obtained was much greater than should be expected for molecules formed from closed shell atoms like Hg.

The interpretation given the absorption spectrum of Cd and applied here to Hg is not yet fully established. However, it gives at least a value of D of the right order of magnitude even though considerably higher than that obtained by Koernicke (*Zeits. f. Physik* 33, 219, 1925).

J. G. WINANS

University of Wisconsin,
August 22, 1930.

ERRATA

STUDIES IN CONTACT RECTIFICATION. II. THE CUPRIC SULPHIDE-MAGNESIUM JUNCTION.

BY MILTON BERGSTEIN, J. F. RINKE, AND C. M. GUTHEIL
(Phys. Rev. **36**, 587, 1930)

The figures above the captions on page 592 should be interchanged. The caption on Fig. 9 should read:

Fig. 9. Oscillograms of interruption and reversal after identical periods of current flow in low resistance direction to varying voltage.

THE PHYSICAL REVIEW

CANAL RAY* AND ELECTRON EXCITATION OF THE BAND SPECTRUM OF NITROGEN

BY H. D. SMYTH AND E. G. F. ARNOTT

PALMER PHYSICAL LABORATORY, PRINCETON UNIVERSITY

(Received July 28, 1930)

ABSTRACT

The idea is suggested that the excitation of band spectra by canal ray* impact on the one hand, and by electron impact on the other, may give quite different intensity distributions. The results of three groups of experiments on the band spectra of nitrogen are presented.

In the first, the relative intensities of the lines in the 3914 negative band were studied. There seemed to be a small weakening of the lower rotational lines in the canal-ray excitation compared to electron excitation.

In the second, the relative intensities of the second positive group and of the negative group were observed in a canal-ray beam. The intensities of the transitions from high initial vibrational states were abnormally great. The variations in comparison plates taken by us and by others with various sources were so great that no satisfactory standard of comparison could be chosen as representing excitation purely by electron impact.

This suggested the third phase of the work, a study of the excitation by a beam of 700 volt electrons. This gave a most unusual distribution of intensity with nearly all the energy in the $0 \rightarrow 0$ and $0 \rightarrow 1$ bands of the negative group and a similar concentration in the second positive group.

INTRODUCTION

THE theory of the relative intensities of the lines in a band and the bands in a system has been rather fully developed.¹ There is no need to reproduce it here in detail but we may recall one guiding principle, that due to Franck and Condon. According to this notion an electron striking a molecule can alter only the electronic configuration without having any direct effect on the vibration or rotation of the nuclei.

Initially, the authors were interested in a case where this principle certainly should not apply, namely, excitation by canal ray* impact. In such a case the impacting ion might be expected to transfer both angular and vibrational momentum to the molecule being excited and consequently to produce a different distribution of intensity from that observed with pure

* The term "canal ray" is used throughout this paper to include both the positive ions and high speed neutralized molecules that emerge behind the perforated cathode of a discharge. It seems better to restrict the term positive ray to ionized molecules.

¹ See Mulliken, *Revs. of Modern Phys.* **2**, 79 (1930) and references cited there.

electron excitation. It might be expected, therefore, that, in a given band, the higher rotational members of all branches would be relatively stronger than when excitation was by electron impact and, similarly, that, in a given system, the bands corresponding to higher initial vibrational states should be relatively stronger than when excitation was by electron impact. A search for such effects was undertaken.

The bands of nitrogen were chosen for examination because more is known about them than about the bands of any other gas of equal experimental convenience. There have, of course, been many studies of the excitation of spectra by canal rays and in particular the bands of nitrogen have been studied. But the point of view was so different from our present one that no very satisfactory evidence on intensity distribution is available. Detailed discussion of previous work will be more intelligible later on in connection with our own results.

But the earlier work did suggest what we found to be the case, namely that the intensities are not strikingly different from those usually published and ascribed to pure electron excitation. It became necessary therefore to examine these "electron excitation experiments," considering carefully the evidence on relative intensities and their variation with varying conditions of source. For example, Birge gives a set of intensity estimates on the second positive nitrogen bands. He says² this illustrates "the most common type of intensity distribution." Yet in a footnote he says "the relative intensity of the bands in this system is very sensitive to changes in self-induction, capacity and other experimental conditions. Hence it is very difficult to give a normal intensity distribution." Yet he does treat this particular distribution as the "normal" intensity distribution and proceeds on this basis. For the sake of convenience we will also speak of this particular distribution as "normal." Birge has apparently studied deviations from this "normal" intensity considerably but his only reference³ is to a fifteen line abstract and we can find no complete account of his investigations. Fortunately, other authors are not so hesitant about publishing their results and theories, imperfect though they be. Herzberg^{4,5} in a series of papers has given an excellent account of the variations of intensity distribution in the nitrogen bands under different conditions of excitation and the factors to be considered in accounting for the observations theoretically. However, in all his experiments he used an electrodeless discharge so that it is difficult to say exactly what the conditions of excitation were. Apparently the only experiments where the excitation was certainly by single electron impact were those whose object was to determine the critical potentials of various band systems.⁶ Consequently the electron speeds used were low.

Both in Birge's "normal" case and in those reported by Herzberg the intensity distribution is of the type predicted by theory. That is, if the

² Birge, *Molecular Spectra in Gases*, Bull. Nat. Res. Council, 57, 135 (1926).

³ Birge, *Phys. Rev.* 25, 240, 1925.

⁴ Herzberg, *Ann. d. Physik*, 86, 189 (1928).

⁵ Herzberg, *Zeits. f. Physik* 49, 761 (1928).

⁶ See references 16, 17, 18.

system is arranged in a square array with the bands of the same initial vibration state all in the same row and the bands of the same final state all in the same column (See Tables I to IV), the most intense bands lie on a parabola whose vertex is toward the $0 \rightarrow 0$ band and whose shape depends on the nuclear binding in the initial and final electronic states. The distributions differ only in rate of falling off of intensity with increasing distance from the vertex of the parabola. This is just the kind of effect we may expect from canal-ray excitation. It is clear, therefore, that control experiments with electrons must be made before any conclusions can be drawn from those on canal rays. Furthermore experiments with electrons are of importance for direct comparison with theory. This, then, became the secondary object of our work.

Though our experiments have suffered many interruptions and are by no means complete, we believe them of sufficient importance to report. We feel this the more strongly because we are convinced that progress in this field has been retarded by the substitution of abstracts, footnotes and "private communication" for frank and full publication.

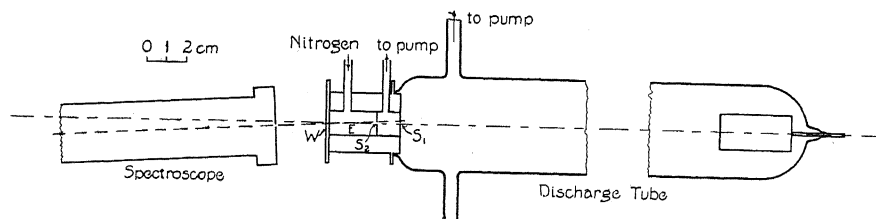


Fig. 1. Schematic diagram of canal ray apparatus.

CANAL RAY EXCITATION

First experiments

At the Chicago meeting of the Physical Society last November we reported⁷ the results of shooting canal rays from a mixture of nitrogen and mercury into an atmosphere of nitrogen. The apparatus, Fig. 1 and Fig. 2 (a), consisted of a cylindrical discharge tube into the end of which a brass water-cooled cathode was sealed with wax. The slits S_1 and S_2 behind each other in the cathode defined a canal-ray beam which shot into the space E in front of the quartz window, W . Nitrogen generated from ammonia and bromine and stored over P_2O_5 flowed continually into the chamber E and out through the slits and the evacuation tube between the slits. The discharge contained mercury at approximately room temperature and a certain amount of nitrogen that diffused through the slits. The discharge was run with a 15,000 volt transformer and with a kenotron in circuit for rectification. Pressure and voltage conditions were varied until a fairly intense canal ray beam appeared; the pressure of nitrogen finally used was of the order of 0.04 mm in the space E . In these early experiments there was sometimes a certain amount of secondary discharge within the cathode. In taking photographs the spectroscope was set at a slight angle to the beam as shown in Fig. 1. This angle had to be very small to get good intensity yet large enough so

⁷ Smyth and Arnott, Phys. Rev. 35, 126, 1930.

that no light came through the slits S_1 and S_2 into the spectroscope. The difficulty of this adjustment and the occasional secondary discharge made these preliminary results less reliable than later ones since the spectrum photographed may not have been entirely due to canal-ray excitation.

Photographs were made first with a constant deviation small glass Hilger instrument and then with a small one-meter concave grating. The plates made with the prism spectroscope covered the region from about 4900 to 3900A.U. with sufficient intensity and resolving power for the study of the bands of the second positive and the negative groups which lie in this region. The lines in the bands were not resolved but in the stronger bands the positive (R) and negative (P) branches were separated. In the grating spectra, in the second order, all the lines of the R and some of those in the P branch were resolved. In both cases very long exposures of the order of 30 to 80 hours were required to bring out any considerable intensity. Ilford Panchromatic plates were used with the prism spectrograph and Eastman Panchromatic films with the grating.

The first photographs taken with the prism instrument showed both negative and second positive bands present with the 4278 and 3914 negative bands predominating. The relative intensity of the bands seemed approximately "normal" but there appeared to be an abnormal separation of the positive and negative branches. These facts suggested that the vibrational intensity might be the same as in electron excitation but that the lower rotational states were abnormally weak.

Attention was therefore concentrated on getting grating photographs and then making exact measurements on the relative intensities of the lines in the bands 3914 and 4278. Photographs were also made with an electrodeless discharge and compared with the canal-ray plate both visually and with a densitometer; the results of Fassbender⁸ and of Ornstein and van Wijk⁹ were also compared. The experimental result seems to be a small but definite weakening of the lower rotational transitions in the canal-ray plate. This was the stage of the work reported at Chicago. Since that time we have been more meticulous about our conditions of excitation and avoidance of light from the main tube, as we will describe presently. Unfortunately this made it impossible to get photographs with the grating even with exposures of as much as 72 hours and therefore no further quantitative evidence is available on the relative intensities of the lines in a single band.

Searching the older work, we find the published reproductions of Fulcher^{10,12} and of Rau^{11,12} have sufficient resolution to show the fine structure of the 4278 band. Fulcher's is the clearer picture and looks very much like ours, but the problem needs more accurate experimental work before any certain conclusion can be drawn.

⁸ Fassbender, *Zeits. f. Physik* **30**, 73 (1924).

⁹ Ornstein and van Wijk, *Zeits. f. Physik* **49**, 315 (1928).

¹⁰ G. S. Fulcher, *Astrophys. J.* **35**, 101 (1912).

¹¹ H. Rau, *Ann. d. Physik* **73**, 266 (1924).

¹² Wien-Harms, *Handbuch der Exp. Phys.* XIV, p. 687, and p. 690.

Later experiments

A number of changes were now made in the apparatus. A General Electric high potential set made up of transformer, kenotrons, condensers and resistances and supposed to give a constant potential was substituted for the transformer. This meant that the canal rays would now be of nearly uniform energy instead of having energies ranging from zero to the maximum voltage of the secondary of the transformer. The other principal change was in the mounting of the discharge tube which was tilted until at an angle of about thirty degrees from horizontal. This made it possible to head the spectroscope directly at the canal ray beam without its receiving any light through the slits S_1 and S_2 from the discharge tube. To prevent reflected light from getting into the spectroscope the inside of the cathode was painted black. There were some further minor modifications in the cathode which need not be described. The new set-up is shown in Fig. 2 (b).

This new outfit ran very much more smoothly than the old as long as no more than a few milliamperes were drawn from the high potential set.

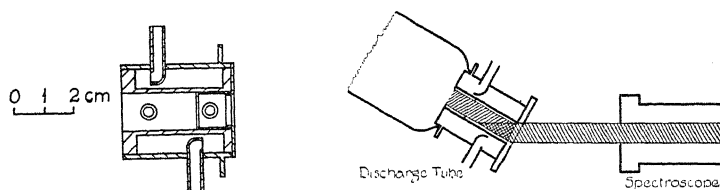


Fig. 2. (a) Details of water-cooled cathode. (b) Second arrangement of tube and spectroscope.

At such currents and with a voltage of 5000 it was possible to get a clearly defined beam which seemed just about as bright as the one we had been using. Nevertheless we were unable to get more than a few mercury lines on any spectra taken with the grating.

Returning to the small glass instrument several satisfactory spectra were obtained. They were very similar to those obtained before showing the same wide separation of positive and negative branches in the 4278 band, but showing a slightly higher intensity in the higher vibrational bands. It was obviously desirable to cover a greater range of the spectrum than was possible with this instrument so a Type E315 Quartz Hilger spectroscope was tried. The first photograph was a little overexposed but the second was very satisfactory. It was an exposure of fifty hours during which the tube ran perfectly steadily at a voltage of 5500 to 6000 with a pressure of 0.04 mm of nitrogen in the cathode and a sharply defined bluish canal-ray beam reaching without scattering to the quartz window.

This plate covered the spectrum range from $\lambda = 5790$ to $\lambda = 2100$, but above 4708 there was very little on it and the dispersion was small. Measurements and densitometer records were made of this entire plate. Besides the negative and second positive groups of bands it showed many mercury lines and many nitrogen spark lines. As impurities there were the resonance lines of Al and Cu and a few other Al lines. These might all be expected since the

main part of the cathode was brass but with an aluminum disk over the front of it to reduce sputtering. Unexpected and unaccounted for were a

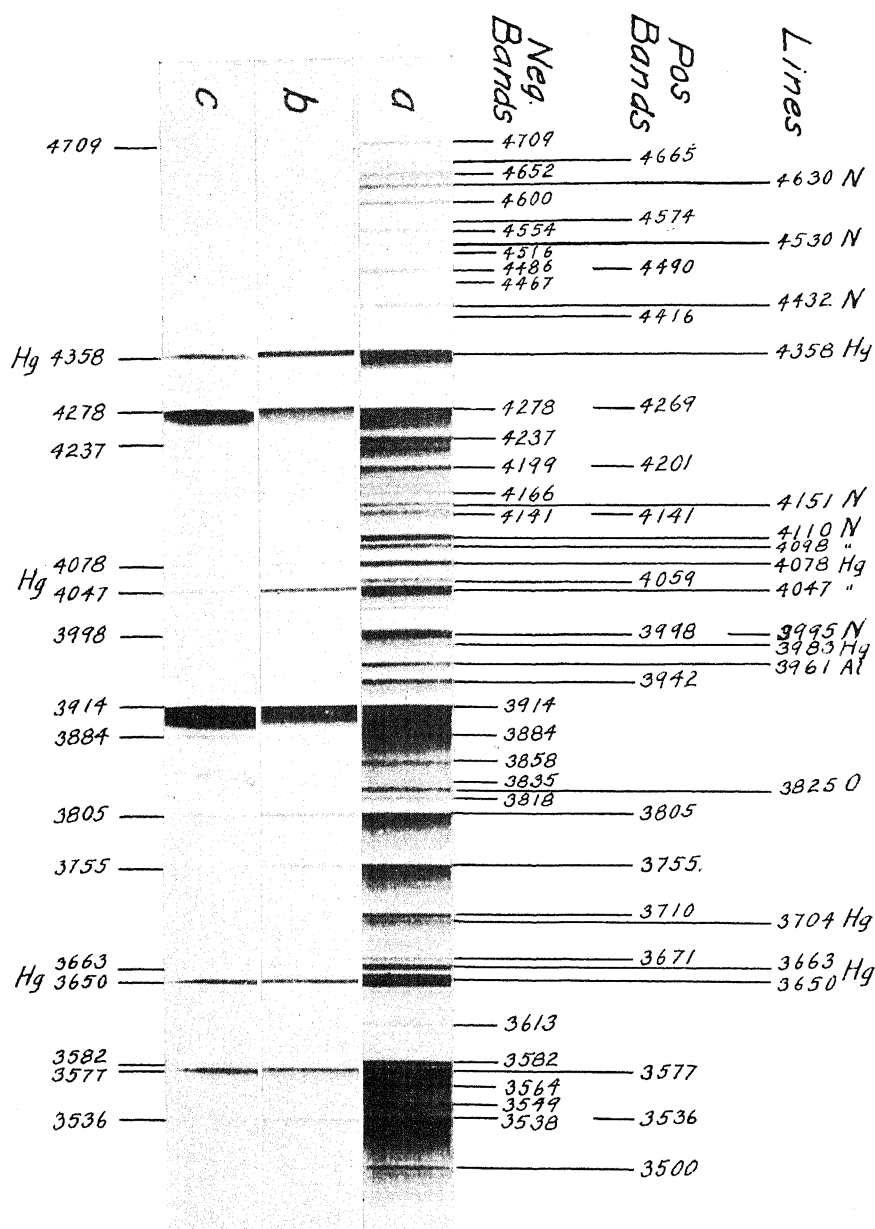


Fig. 3. Spectrograms taken with E315 quartz Hilger spectroscope. (a) Canal ray beam (5500 volts). (b) Discharge used as source of canal rays. (c) Electron beam (700 volts).

number of oxygen lines chiefly below 3000Å.U. Finally there were a few faint bands in the neighborhood of 2500 which may have been the fourth positive group of nitrogen.

In Fig. 3 (a) a section of this plate is reproduced. The print is a little over exposed to show some of the fainter bands, in particular the one at 3613. From a study of this plate and the densitometer records of it, it was possible to estimate the intensity of most of the bands of both the second positive and the negative groups. In some cases the resolution was so poor that an estimate was dubious or impossible. This is indicated in the tables below which give the results of visual and densitometer estimates of the relative blackening of the photographic plate.

TABLE I. *Densities of second positive group. Canal-ray excitation plates.*

$v' \backslash v''$	0	1	2	3	4	5	6	7	8	9
0	3371 18	3577 11	3805 12	4059 8	4344 *	4666 4				
1	3159 15	3339 3	3536 6*	3755 12	3998 10*	4269 *	4574 00			
2	2977 12	3136 14	3309 6*	3506 4	3710 10	3942 9	4201 *	4490 4*		
3	2820 2*	2962 12	3116 10	3284 6	3469 1	3671 7	3894 *	4141 *	4416 1	
4		2814 4	2953 12	3104 7	3268 6	3446 0	3642 4	3857 *	4094 *	4356 *

* Wholly or partially obscured by another line or band.

Considering first the second positive group one could hardly ask for a more perfect parabolic intensity distribution. In general it agrees very well with the intensities given by Birge. One curious point is the extreme weakness of the 4574 band. This is confirmed by the other plates taken with this type of excitation in contrast to the comparison plates but we have no explanation for it. Looking for the effect we expected, an enhancement of the bands coming from the higher initial states of vibration, we find nothing very striking but a distinct tendency for the intensities in the 4th and 5th rows to be relatively stronger than in the figures published by Birge. They are also stronger than in our own comparison plates which will be discussed more fully below.

Turning to the negative bands, perhaps the most striking result is the presence of the "tail bands" first reported by Herzberg.⁴ The strongest of these at 3613 is on the reproduction Fig. 3 (a) where it is hoped that the shading off to the red may be seen. It is very clear in the original. The band 4→0 at 2885A.U. is also identifiable on our plate, observed for the first time so far as we know. The absence of the higher sequences is presumably due to the low sensitivity of the plate in the region where they lie but had they been present they would not have been resolved.

The general run of intensities is very similar indeed to that given by

Herzberg,⁵ for the case of strong excitation. Possibly in our case there is a slightly greater intensity in the lower rows of the table corresponding to higher initial vibrational states but certainly this is not sufficiently marked to be a proof of the effect we are seeking.

TABLE II. *Densities of negative group. Canal-ray excitation plates.*

$v' \backslash v''$	0	1	2	3	4	5	6	7	8	9
0	3914 20	4278 15	4709 7							
1	3582 15	3884 12	4237 12	4652 7						
2	3308 7*	3564 12	3858 9	4199 10	4600 9					
3	3078 17	3299 8	3549 12	3835 6	4166 7	4554 6*				
4	(2885) (1)	3076 1*	3293 8	3538 10*	3818 8	4141 7*	4516 4			
5					3533 5*	(3807) *		4486 6*		
6									4467 5	
7										4459 *
8										
9										
10							2987 0	3174 0	3381 2	3613 7
11									3223 1	

* Partially or entirely obscured by other lines or bands. The band 14-10 at 3217 was also noted with intensity 0.

Nor does study of our own comparison plates strengthen our case. These were made with one spectroscope or the other with the following sources (a) a capillary Geissler tube discharge (b) the first transformer discharge used as a source of canal rays (c) an electrodeless discharge (d) the end of the positive column toward the cathode in the high voltage discharge finally

used as canal-ray source. Of these comparisons the first three all gave about the same results, the second positive group, as in Birge's "normal" distribution, was somewhat weaker in the lower rows than in Table I, while the negative bands were also perhaps a little weaker in the high initial vibration bands. In the case of the (d) comparison, the intensities were entirely different. They are given in Table III and can be seen in Fig. 3 (b).

TABLE III. *Density distribution in high voltage discharge plit's.*
Negative Bands Second Positive Bands

$v' \backslash v''$	0	1	2	3
0	15	12	8	
1	6	6	7	
2				1

$v' \backslash v''$	0	1	2	3	4
0	15	14	10	2	
1	10	4	10	10	
2		4*		2	3

* Partially obscured by neighboring line.

Obviously this distribution has a relatively higher concentration in the lower vibrational bands than the canal-ray excitations given in Table I and II, or than in other comparison plates. It agrees quite well with Herzberg's "weak" excitation as far as the negative bands are concerned. He gives no intensities for the positive bands so comparison is not possible.

Originally we intended to study positive ion excitation and compare it with electron excitation. By this time we were pretty well convinced that we had no pure electron excitation spectra for comparison. Therefore we proceeded to get some.

ELECTRON EXCITATION

In making comparison plates with electron impact we wished to change conditions as little as possible and therefore used a tube, Fig. 4, very similar to that used for positive ions. However in order to reduce the length of exposure necessary, a filament source of electrons was used. As shown in

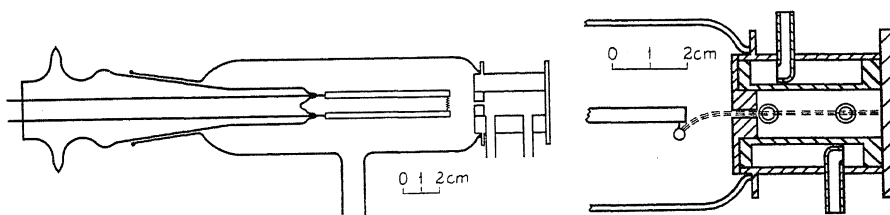


Fig. 4. (a) Schematic diagram of electron beam apparatus. (b) Details of filament, electron beam and water-cooled anode.

the figure the filament was mounted below the hole in the anode so that none of its light got into the excitation chamber. A small electromagnet was then used to bend some of the electrons into the path shown in Fig. 4. With a voltage of 700, a current to the anode of 70 milliamperes, a pressure of 0.06 mm in the excitation space and of 0.006 mm in the discharge tube a sharp luminous beam was obtained. Part of a spectrogram taken of this beam with the type E315 Quartz Hilger is given in Fig. 3(c). This was an exposure of

two hours with an Eastman Speedway plate. The estimated densities of the negative and positive bands are given below in Table IV.

TABLE IV. *Density distribution with excitation by a Beam of 700 volt electrons.*
Negative Bands Second Positive Bands

$v' \backslash v''$	0	1	2	3
0	40	25	5	—
1	8	8	7	1
2				

$v' \backslash v''$	0	1	2	3	4
0	12	14	8	1	
1	10	1	8	7	*
2	1	1	—	—	1

Clearly we have here an extreme concentration of intensity in the low initial vibration states.

GENERAL DISCUSSION

Before making any attempt to interpret the results presented above they will be compared with previous work. First, as to the positive ray results, the photograph published by Stark and Hermann¹³ shows the nitrogen canal-ray spectrum between 5500 and 3550A.U. Both the negative and positive bands are present and though the reproduction is not good enough to pick out many of the bands, there is at least no conspicuous departure from the intensity distributions of Tables I and II. A study of Fig. 4, in Fulcher's paper¹⁰ gives a similar result. Again the reproduction given by Wilsar¹⁴ shows the intensities of the first two sequences of the negative bands with intensities approximately like those of Table II. Doubtless a study of the original plates of these experimenters would yield really satisfactory intensity estimates. Dr. C. J. Brasefield has kindly turned over to us some early plates which he took in his work on canal rays in hydrogen¹⁵ at a time when he was being troubled with nitrogen as an impurity. One of these plates shows eight members of the 4708 and four of the 4278 sequence of the negative bands. Their intensity is approximately as given in Table II and not at all like Table III or IV. Thus what evidence there is agrees with ours.

The question may be raised whether the excitation in all these experiments is actually by canal-ray impact. There are two other possibilities. The excitation of the N_2^+ ions might occur in the discharge before their passage through the cathode. This seems unlikely in view of the distance between the slit S_1 (Fig. 1) and the place where the spectrum is observed, the observations of Wien on the decay of the N_2^+ bands, and the pressure in the observation chamber. Or the excitation might be by secondary electrons. Considering the sharpness of the beam and the fact that it was observed nearly a centimeter beyond the last slit, this seems unlikely also.

Granted that the excitation is by canal-ray impact is the radiation observed from the canal ray or the molecule that is struck? If we are interested only in the conversion of kinetic energy of translation into energy of vibration or rotation this is not a fundamental question since it is immaterial which molecule is stationary. However, this question raises the point which was the

¹³ Stark and Hermann, *Phys. Zeits.* **7**, 92 (1906).

¹⁴ Wilsar, *Ann. d. Physik* **39**, 1251 (1912).

¹⁵ Brasefield, *Phys. Rev.* **31**, 215 (1928).

chief concern of the previous papers we have been discussing, the Doppler effect. They all agree that there is no Doppler effect in the positive bands when they are observed in the canal-ray spectrum but there is not complete agreement on the negative bands. The consensus of opinion appears to be that it is either absent or very small.^{11,12} In our experiments there was no sign of doubling in the bands, and as it was extremely unlikely that the shifted bands should be present without any trace of the unshifted we concluded that the Doppler effect was small or absent. But for some of the lines in the better resolved part of the spectrum there appeared to be both a shifted and an unshifted line of about the expected separation.

The conclusion is then that the intensities given in Tables I and II are confirmed by the older work and actually represent the excitation of band spectra by rapidly moving molecules of nitrogen or mercury. These molecules may or may not be charged.

Returning to the electron excitation, previous work needs to be considered. The remarkable fact is that there seems to be so little. Several authors have studied the excitation potentials of the various band systems of nitrogen^{16,17,18} but of these apparently only Kneser worked with electron speeds as high as 100 volts, and made some slight study of the variation in the intensity of the different bands. His results, for both electrons of 100 volts and electrons of about 30 volts, are not very complete but as far as they go, show an intermediate intensity distribution between those of Tables I and II and those of Table III but nearer Table III. As far as one can judge from reproductions published in some of the other papers mentioned, Kneser's work is typical of the results with electron impact below 100 volts. Apparently no one has worked before with electron impact at higher voltages. Our photographs with 700 volts are a start and it is in this direction that we expect to continue our work next year.

FINAL SUMMARY AND CONCLUSION

Reviewing the whole situation we see that the parabolic intensity distribution is maintained under all types of excitation. It is presumably characteristic of the transition probabilities and therefore may be expected to be independent of excitation conditions. But the distribution along the parabola varies greatly. At one extreme with canal-ray excitation we have the intensity spread well out along the parabola toward higher quantum numbers. At the other extreme with high voltage electron excitation we have the intensity very much concentrated at the head of the parabola. This much is in accord with our original notion that the canal-ray impact may convey vibrational momentum and the electron impact may not. Intermediate types of distribution are obtained from impact of low velocity electrons and from various types of discharge. Surprisingly the electrodeless discharge supposed to be purely electronic in its excitation, gives the distribution most nearly like the canal-ray excitation. This is probably due to secondary effects which raise large numbers of the molecules into high vibration states.

¹⁶ Turner and Samson, *Phys. Rev.* **34**, 747 (1929).

¹⁷ Spöner, *Zeits. f. Physik* **34**, 622 (1925).

¹⁸ Kneser, *Ann. d. Physik* **79**, 597 (1926) and others.

ANGLE AND ENERGY DISTRIBUTION OF ELECTRONS
SCATTERED BY HELIUM, ARGON AND HYDROGEN

BY J. HOWARD McMILLEN

WASHINGTON UNIVERSITY, ST. LOUIS, MISSOURI

(Received July 30, 1930)

ABSTRACT

The distribution of electrons rebounding at definite angles from gaseous molecules was investigated. An electrostatic re-focussing arrangement was used to analyse the energies of the electrons. In helium, it was possible to identify the following energy losses at several angles, 21.12, 22.97, and 23.62 volts for a primary electron beam of 50 volts, but not the 19.77 and 20.55 volt losses.

The number of electrons, rebounding without loss of energy, was measured for different angles of rebound (7° to 60°) from argon, helium, and molecular hydrogen molecules, and for various energies (50 to 150 volts). A scattering curve was also obtained in helium for 100 volt electrons that had lost 21.12 volts energy. In almost all cases, the number scattered decreased rapidly as the angle increased. The higher the energy of the electrons, the more rapidly did the number fall off with increasing angle. The steepness of the curves increases as we go from argon to helium to hydrogen for the slower electrons. For the faster electrons their curves are practically superposable.

The results were compared with those of other observers and with the theoretical predictions of Mott, Mitchell and Sommerfeld.

INTRODUCTION

AN INVESTIGATION of single scattering of electrons by gaseous molecules has become a subject of particular interest, in that it enables one to appraise certain theoretical predictions of the new quantum mechanics and to verify the choice of external atomic fields used in the application of the general scattering theory.

The general theory of scattering was first investigated, from the point of view of wave mechanics, by Born.¹ Sommerfeld² and Mitchell,³ using Born's general theory, have calculated the angular distribution of elastically scattered electrons in argon. Mott⁴ has done the same for helium and Born⁵ for atomic hydrogen. Few experimental measurements, however, have been made on the scattering of electrons by gaseous molecules. Dymond and Watson⁶ have measured the distribution of inelastically and elastically scattered electrons in helium, using 210 volt electrons. Their results agreed well with the calculations of Mott. Harnwell,⁷ with 120 and 180 volt electrons, has measured the scattering in atomic and molecular hydrogen. Arnot⁸

¹ M. Born, *Zeits. f. Physik* **38**, 803 (1926).

² *Atombau und Spektrallinien Wellenmechanischer Ergänzungsband*, p. 226.

³ A. C. G. Mitchell, *Nat. Acad. Sci. Proc.* **15**, 520 (1929).

⁴ N. F. Mott, *Proc. Cam. Phil. Soc.*, **25**, 304 (1929).

⁵ M. Born, *Göttingen, Nachr.* p. 146 (1929).

⁶ Dymond and Watson, *Proc. Roy. Soc.* **125A**, 660 (1929).

⁷ G. P. Harnwell, *Phys. Rev.* **34**, 661 (1929).

⁸ F. L. Arnot, *Proc. Roy. Soc.* **125A**, 660 (1929).

obtained scattering curves for 80 volt electrons in mercury vapor. Little work has been done, however, using a large range of velocities in conjunction with several scattering gases.

It was the purpose of this investigation to measure and compare the angular distribution of electrons elastically scattered by the three gases, helium, argon and molecular hydrogen, when colliding electrons of several energies are used. The energies used were 50, 75, 100 and 150 volts. The angles investigated ranged from 7° to 60° . The distribution of inelastically scattered electrons in helium was likewise determined for 100 volt electrons. This investigation also includes a measurement of the energy losses in helium at various angles.

DESCRIPTION OF APPARATUS

The apparatus used in this investigation may be briefly described as consisting of an electron projector *A*, a collision chamber *B* and an analysing chamber *C*. A diagram is given in Fig. 1. Electrons leaving the projector *A* were scattered by the gas molecules in chamber *B*. After single collisions in *B* the electrons passed through the slit s_4 into the analyser *C*. The two cylindrical plates, *M* and *N* in *C*, when set at the correct potentials, deflected the electrons into the Faraday cylinder *F*.

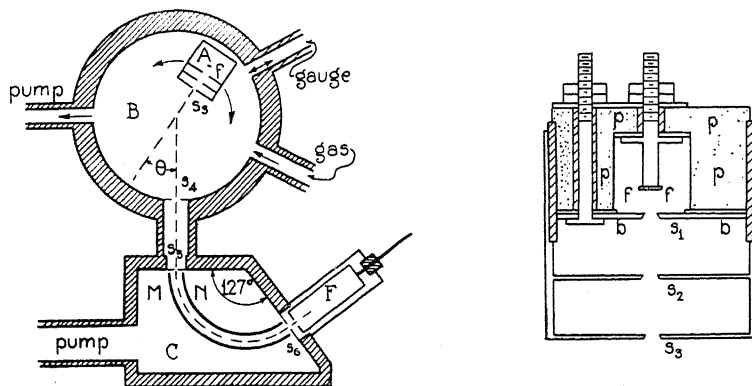


Fig. 1. Diagram of apparatus.

The projector, as shown in Fig. 1, consisted of an oxide coated filament *f*, a grid *b* with slit s_1 , a final grid with the two slits, s_2 and s_3 , and a back plate *p*. All parts were made of brass, with the exception of the plate *p*, which was constructed of aluminum alloy. A glass cylinder and mica sheets were used as insulators. The potential on the final double slits, s_2 and s_3 , determined the energy of the electrons projected through the slit. The potentials on *b* and *p* were fixed so as to give the maximum emission from the projector, or gun, as it is sometimes called. The slits of the gun play an important part, since they are the chief source of slow electrons. Their lips were sharply bevelled and sooted to eliminate slit-scattering. The dimensions of the slits were $s_1 = 1 \text{ mm} \times 15 \text{ mm}$, $s_2 = 0.8 \text{ mm} \times 14 \text{ mm}$, $s_3 = 0.4 \text{ mm} \times 14 \text{ mm}$.

The projector could be rotated about the axis of the cylindrical chamber *B*. In *B* the electrons collided with the gaseous molecules and were reflected

at various angles. Only those electrons which were reflected at an angle θ entered the analysing chamber. This angle was determined by the gun-setting. The gun was fastened to a brass tube which fitted into a ground glass joint. The ground glass joint was waxed into the back end of the brass chamber *B*. On to the front end was fastened a thick glass plate. A copper screen placed on the inside surface of the glass plate insured the equipotentiality of chamber *B*.

The analysing chamber was connected to the collision chamber *B* by a short brass tube. The two chambers were separated by two slits; s_4 , 2mm \times 14mm and s_5 , 0.3mm \times 10mm. The angle subtended at s_5 by s_4 measured one and a half degrees. The cylindrical plates *M* and *N* were bolted to the wall of the chamber and insulated from it by sheets of mica. The radii of curvature of the plates were 50 mm and 60 mm respectively. The plates formed an arc which subtended an angle of $127^\circ 17'$. It has been shown, and predicted by theory, that the potential difference between the plates necessary to deflect electrons from s_5 to s_6 is proportional to the energy of the electrons. The particular chamber and the properties of the electrostatic analysing method have been described by Hughes and Rojansky⁹ and Hughes and McMillen.¹⁰ The Faraday cylinder was connected to a Compton electrometer.

The gas to be investigated flowed into chamber *B* through a small capillary and was pumped out by a mercury diffusion pump. This arrangement maintained a steady pressure and a fresh supply of pure gas in the collision chamber *B*. The pressure was read on a McLeod gauge. To secure high pumping speeds, a glass tube of large diameter connected the analysing chamber with a Gaede two stage steel diffusion pump. The gases used in this experiment were helium, hydrogen and argon. Helium was purified by slow passage over charcoal at liquid air temperature. The hydrogen was obtained by heating a palladium tube. A discharge in the presence of calcium vapor was employed to purify the argon. To freeze out the mercury liquid air traps were inserted. The following pressures in mm of Hg were used with the following gases: helium, 0.008 mm; hydrogen, 0.006 mm; argon, 0.004 mm.

ENERGY LOSSES IN HELIUM

To measure the energy losses, the projector was set at some fixed angle and the electron current to the Faraday cylinder noted for each set of potentials on the deflecting plates. The energy of the deflected electron is readily obtained from the potential on the deflecting plates when the ratio of the energy of the deflected electron to the deflecting potential is known. This ratio was established when no gas was in the apparatus. One can then obtain a set of curves plotting the number of electrons against their energy. Unfortunately, because of excess scattering of the slits and other unaccounted for defects in the apparatus, the original curves had to be modified by subtracting from them spurious peaks and background scattering which were also present in the absence of any gas.

⁹ Hughes and Rojansky, Phys. Rev. 34, 284 (1929).

¹⁰ Hughes and McMillen, Phys. Rev. 34, 291 (1929).

In Fig. 2 can be seen an energy loss curve for helium. This curve was taken with electrons of 50 volts energy and indicates the energy losses for those deflected at 10° . The abscissa measures the energy of the electrons after collision, while the ordinate measures the number of electrons having that particular energy. The energy loss is also indicated in the diagram. The main peak at 50 volts, comprised of electrons making elastic impacts, is many times higher than the remaining peaks and extends off the figure. A group of peaks is seen near 30 volts energy region, indicating losses of the order of 20 volts. In this group there are three distinguishable peaks. The obvious lack of symmetry of the main energy-loss peak suggests a smaller peak, or peaks, overlapped by the main peak. One notes, too, on the low

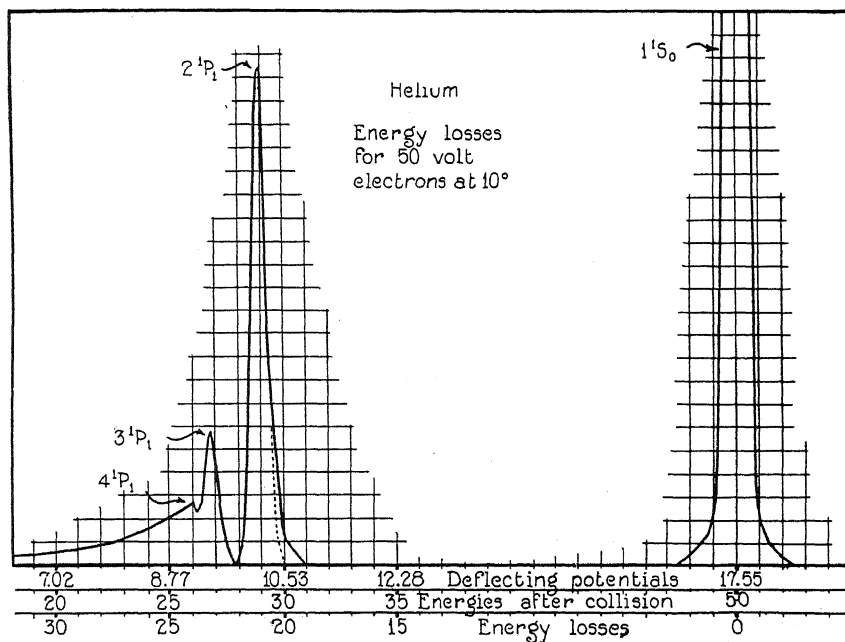


Fig. 2. Energy losses in helium for 50 volt electrons simultaneously deflected at 10° .

energy side of the last peak, that there is a gradual shading off in intensity. Fig. 3 shows the main energy-loss peak and the composite subsidiary peak for 100 volt electrons. For the case of electrons of 100 volts energy the lesser peaks have become indistinguishable because of the poor resolving power at higher voltages. These curves are similar to those obtained by Dymond,¹¹ who used the magnetic deflection method.

In identifying these energy-loss peaks great care was taken in measuring the magnitude of the energy loss of the main energy-loss peak, and the remaining peaks were then referred to it. The procedure was carried out in the following way: the main beam of electrons was directed into the gas at a definite energy, as read on the accelerating voltmeter. With the deflecting potential set at the value to give the main energy-loss peak, the energy of the

¹¹ E. G. Dymond, *Phys. Rev.*, **29**, 433 (1927).

original beam was lowered until the main beam reached an energy value such as to be directed into the Faraday cylinder. The reading of the voltmeter under those conditions subtracted from the original setting read directly the energy loss in volts. This method of measurement demanded only two readings and both readings were taken on the same voltmeter, thus giving greater accuracy. Also the difference read in this manner was three times the corresponding unconverted reading on the deflecting potential voltmeters.

A set of 15 readings over a range of 50 to 150 volts gave for the main energy-loss peak an average energy loss value of 21.50 with the probable

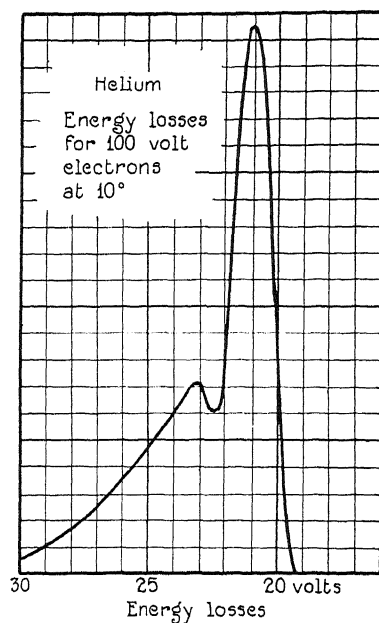


Fig. 3. Energy losses in helium for 100 volt electrons simultaneously deflected at 10° .

error of 0.15 volts. One has from spectroscopic data the following possible energy losses: 19.77, 20.55, 21.12, 22.98, 23.63, etc., corresponding to the transitions $1^1S_0-2^3S_1$, $1^1S_0-2^1S_0$, $1^1S_0-2^1P_1$, $1^1S_0-3^1P_1$ and $1^1S_0-4^1P_1$ respectively. The above measured-loss 21.5 lies closer to the spectroscopic value 21.12 than to any of the others, which indicates that the main energy loss peak corresponds to the 21.12 loss or to the first transition in the principal series, $1^1S_0-2^1P_1$. This choice is further supported by a series of measurements taken on the other two peaks. These measurements were taken directly from the energy-loss curves and measured as separations of the two small peaks from the main energy-loss peak. These measured separations of the two small peaks from the main energy-loss peaks showed that in matching experimental separations of energy losses with the various combinations of possible separations taken from spectroscopic data a good match was obtained by assigning to the main energy-loss peak the transition

$1^1S_0-2^1P_1$, as was done above, and to the next two peaks the transitions $1^1S_0-3^1P_1$ and $1^1S_0-4^1P_1$ respectively. The averaged separation between the first main peak and the next was 2.13, while the spectroscopic difference between 2^1P_1 and 3^1P_1 is 1.85. The averaged experimental separation between the two lesser peaks is 0.82, and the spectroscopic difference between 3^1P_1 and 4^1P_1 is 0.65. This is fairly good agreement, in view of the uncertainty of measurement for the low intensity peaks. Dymond, in his paper on electron scattering, attributed the main energy-loss peak to the 20.55 loss, which, in view of the above results, seems to be untenable. Further support for the identification of this main energy-loss peak as the 21.12 loss peak is obtained from probability considerations. Attributing the main energy-loss peak to the transition associated with the 21.12 loss indicates, in view of the prominence of this peak, that this loss is by far the most probable in the 50 volt energy range. This is in accord with the work of Glockler,¹² who measured double impact losses in helium by the partial current method. Glockler's most prominent double impact peak, 40.86, was assigned to the transitions 21.12 and 19.77, the 21.12 loss occurring when the colliding electron had 40.86 volts energy. Dymond,¹³ also using the double impact method, found that the most probable loss in this energy range was 20.9 ± 0.2 , which, in view of the present work, should be assigned to the 21.12 loss. However, Dymond assigned this energy difference to the 20.55 transition.

The indication of one or more peaks on the high energy side of the $1^1S_0-2^1P_0$ peak is in such a position as to be due to either a 19.77 loss, a 20.55 loss, or both. The gradual tapering off in intensity evident after peak C can be explained, as was done by Dymond and Watson, as the composite of the peaks of decreasing intensity corresponding to the remaining lines in the principal series. It is interesting to note that no peak appears corresponding to the energy lost in ionization, i.e. at 24.5 volts. In the first place, the efficiency of ionization is low for 50 volt electrons and, in the second place, there are now two electrons after collision, and conceivably, they may share the excess energy in all possible combinations.

The energy-loss values showed no variation when measurements were made for various angles. The angles used ranged from 0° to 20° . It was also observed that there were no variations in the energy-loss values outside of the experimental errors of the apparatus when colliding electrons of energies ranging from 40 to 150 volts were used.

ANGULAR DISTRIBUTION OF REBOUNDED ELECTRONS

The angular distribution curves for electrons making elastic impact were determined for the two monatomic gases, helium and argon, and the diatomic gas hydrogen. The energies of the colliding electrons ranged from 50 volts to 150 volts, while the angles investigated extended from 7° to 60° . An inelastic scattering curve was also obtained for helium with electrons of

¹² G. Glockler, *Phys. Rev.* **27**, 423 (1926).

¹³ E. G. Dymond, *Proc. Roy. Soc.* **107A**, 291 (1925).

100 volts. These curves have been plotted so as to indicate the proportionate number of electrons scattered per unit solid angle at the angle indicated. The abscissa is calibrated in degrees, while the ordinate is graduated in

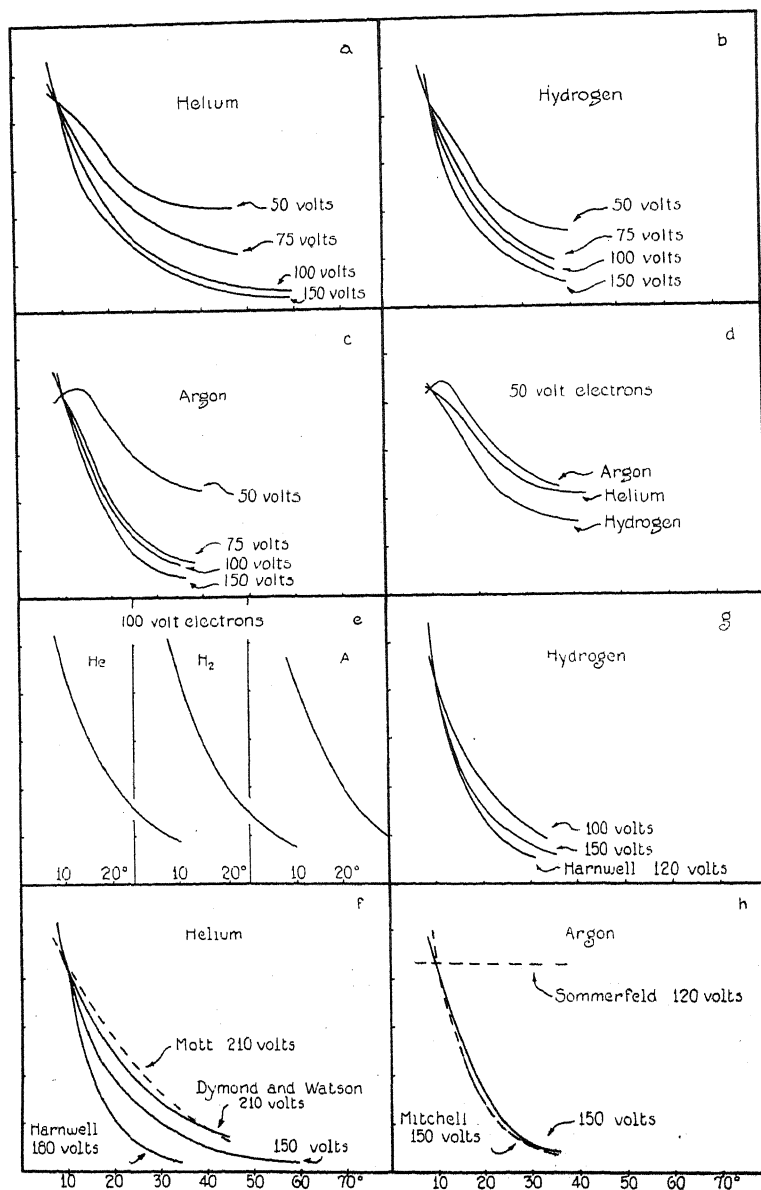


Fig. 4. Distribution per unit solid angle of elastically scattered electrons.

arbitrary numbers. All curves given in the accompanying figures were so arranged as to coincide at 10° . This was a necessary procedure because of the difficulty one encounters in attempting to measure the absolute value of the intensity of the scattered electrons.

A scattering curve was obtained by setting the potentials on the deflecting plates in the analyser to correspond to one of the peaks of the energy-loss curve and by measuring the electron current to the Faraday cylinder for various settings of the projector. The total number scattered upon a collision with an energy-transfer or upon elastic collision at any angle is proportional to the area under the corresponding peak of the energy-loss curve taken at that angle. A separate investigation showed that the area under the peak was proportional to its height, which justifies the procedure of taking the height of the peak as a measure of the number scattered at that angle. There were always present in the scattering curves some spurious electrons. In order to correct for these, their magnitude was determined by a separate set of readings with no gas in the apparatus and subtracted from the original curve. The magnitude of this spurious curve was much greater, however, than its effective magnitude when the gas was present. This was due to the fact that the electrons causing the spurious peaks were partially absorbed or scattered by the gas molecules as they pass from the gun slit to the analysing chamber slit. Hence the spurious curve obtained with no gas in the apparatus was reduced before being subtracted from the original curve. A further correction had to be applied to the original scattering curve in order to correct for the variation of scattering volume with changes in the angle of the projector. It is apparent that the collision volume, the volume common to the emission wedge from the projector and the reception wedge of the slit s_3 , varies as $1/\sin\theta$. To reduce, then, one's readings to the same volume of collision, one multiplies the results by the $\sin\theta$.

The angle θ was measured accurately by a protractor and pointer arranged outside the apparatus. Because of the fact that the gun emitted a wedge-shaped beam of electrons, some electrons were measured after having been deflected at an angle other than that of θ . This discrepancy in the value of θ became appreciable only for small values of θ . The co-latitude angle measured in the plane perpendicular to the paper in Fig. 1 remains the same for all settings of the projector. Its magnitude is approximately equal to the length of the slit-entrance of the Faraday cylinder divided by the path from the gun to the Faraday cylinder. It is about 2° .

The elastic scattering curves, i.e., curves indicating the angular distribution of electrons rebounding from elastic collisions, can be advantageously studied, by comparing curves for one gas with electrons of various energies and then by comparing the curves for the various gases with colliding electrons of the same energy. The three sets of curves taken with the three gases, helium, argon and hydrogen, are shown in the accompanying figure; helium, Fig. 4(a); hydrogen, Fig. 4(b); argon, Fig. 4(c). An inspection of these curves shows the following characteristics:

(a) First, one observes that the curves for electrons of lower energy are much less steep than those of higher energy. That is to say, the higher the energy of the electrons, the less the deviation from the undeflected path. This is true for all three of the gases used.

(b) It can also be seen that the change in slope of these curves is more

evident in the comparison of the 100 volt and 50 volt curves than in the comparison of the 100 volt and 150 volt curves. Thus, the change in slope with energy of the colliding electron is more marked at low velocities.

(c) One further notes a change in shape of the low energy curves. These curves flatten out at small angles, indicating a smooth hump in this small angle region. The higher energy curves, on the other hand, rise steeply with no suggestion of becoming horizontal. The argon curve for 50 volts, Fig. 4(b), has a definite hump at 12° .

(d) In Fig. 4(d) are superimposed the 50 volt curves of the three gases, helium, hydrogen and argon. The curves are very different, argon showing a much greater degree of scattering than helium and helium a greater degree than hydrogen.

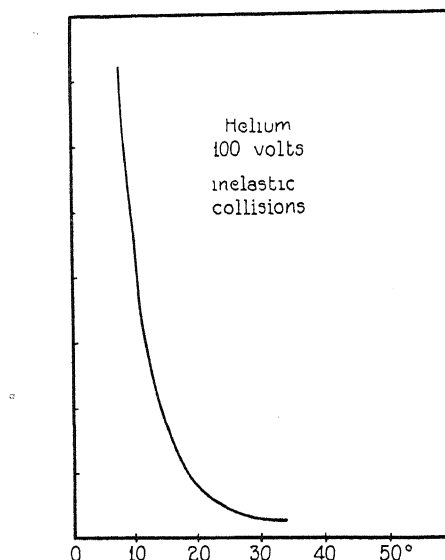


Fig. 5. Distribution per unit solid angle of electrons scattered from helium molecules with a loss of energy corresponding to the transition $1^1S_0-2^1P_1$.

(e) For electrons of greater energy, energies of 100 or 150 volts, the curves for the three gases do not differ much. An inspection of Fig. 4(e) shows that there is very little difference between the three curves when the 100 volt electrons were used. The change in slope, then, for various gases is only evident with electrons of low energy.

It was also possible to obtain an angular distribution curve for electrons having lost energy upon collision. In Fig. 5 is shown the distribution for electrons having lost energies corresponding to the $1^1S_0-2^1P_1$ transition in helium. The curve drops off rapidly, showing that electrons losing energy are only slightly deflected by the collision. Dymond and Watson's inelastic curve is in agreement with the one obtained in this investigation.

DISCUSSION OF SCATTERING MEASUREMENTS

Although these scattering curves allow certain definite observations to be made concerning the behavior of scattered electrons when the scattering

gas is varied and when the energy of the colliding electrons is varied, no simple collision process, such as that used most successfully by Rutherford in his theory of α -ray scattering, based on classical methods, is forthcoming. A collision theory based upon the new mechanics, however, has been developed by Born. All collision theories make this one observation; namely, the decrease in the degree of scattering for electrons of higher energy, an observation in accord with the results obtained in this investigation.

For helium Mott has applied this general theory to elastic collisions, assuming an atomic force field given by Hartree's selfconsistent fields. The result, however, applies to relatively fast electrons and has only been worked out for 210 volt electrons. An experimental curve for scattering in helium has been obtained by Dymond and Watson for 210 volt electrons which agrees well with Mott's theoretical curve, but which is less steep than our 150 volt curve, as can be seen in Fig. 4(f). This difference between the results of Dymond and Watson for 210 volt electrons and our results for 150 volt electrons is of too great a magnitude and in the wrong direction to be explained as a difference caused by the use of two different electron velocities. Harnwell, in a qualitative investigation of helium, observed very little difference in the degree of scattering by helium and by hydrogen (an observation verified in this investigation for high velocity electrons). If this is so, Harnwell's hydrogen curve may be used as an estimate of his helium scattering curve. Investigation of Fig. 4(f) shows that this curve is much steeper than either Dymond and Watson's or the author's. These three measurements of elastic scattering in helium, although at variance with each other, are all much closer to the prediction of Mott, based on the new mechanics, than to the results obtained when one assumes the Coulomb field.

In Fig. 4(g) can be seen Harnwell's 120 volt hydrogen curve and the 100 and 150 volt hydrogen curve as obtained in this investigation. (Harnwell's curve has been replotted from the original data to indicate the number scattered per unit solid angle at the angle θ . The original data was given as the number scattered in the total solid angle subtended between θ and $\theta + \Delta\theta$). Harnwell's curve is much steeper than either our 100 or 150 volt curve. It is difficult to explain this discrepancy. No theoretical results have been given for molecular hydrogen.

Both Mitchell and Sommerfeld have calculated the degree of scattering for argon. Sommerfeld has applied Born's general collision theory and obtained an atomic force field by assuming that all the electrons were situated in the K shell. For 120 volt electrons Sommerfeld finds practically no change in the number of electrons scattered as the angle is increased from 0° to 90° . This does not agree with the results obtained above. Mitchell has adopted an atomic field force given by Fermi and calculated the degree of scattering in argon for electrons of various velocities. Fig. 4(h) shows good agreement for the 150 volt electrons. The figure also gives Sommerfeld's results approximately. Mitchell's curves for the lower velocities did not agree well with our experimental values. (Dr. Mitchell very kindly contributed the data, as yet unpublished, used in drawing the above curve.)

In conclusion I wish to thank Professor A. L. Hughes, under whose direction this work was carried out.

THE INTENSITY OF X-RAY SATELLITES*

By F. K. RICHTMYER** AND L. S. TAYLOR

CORNELL UNIVERSITY AND BUREAU OF STANDARDS

(Received July 14, 1930)

ABSTRACT

By means of the two-crystal ionization spectrometer measurements have been made of the wavelengths and intensities relative to $K\alpha_1$ of the satellites $K\alpha_{3,4}$ of Cu (29). $K\alpha_{3,4}$ has characteristics of a doublet and is separated, photographically, for elements below Sc(21) but is unresolved for elements of higher atomic number. The greater resolving power of the two-crystal spectrometer shows that this "doublet" contains, probably, more than the two components $K\alpha_3$ and $K\alpha_4$, the wavelengths of which latter were found, respectively, to be 1531.15 and 1530.15 X.U. The intensity of either of these components, at 40 K.V., is of the order of 0.25 percent of the intensity of $K\alpha_1$. A similar study of the $K\alpha_{3,4}$ doublet of Ni (28) suggests that this doublet may contain four components.

IT IS generally agreed that x-ray satellites have their origin in "doubly ionized atoms" for which reason these lines are sometimes called "spark lines." A knowledge of the intensities of the satellites relative to each other and to the intensities of the respective parent lines should therefore provide a basis for estimating the relative probabilities of single and double ionization in the target of the x-ray tube. Such information would materially assist in clarifying the present theories regarding the origin of these lines.

Up to the present only the roughest estimates of the intensities of satellites have been made. Practically all studies of satellites have been made by the photographic method. To bring out the satellites on a photographic plate requires that the parent lines should, usually, be very much over-exposed, so that direct comparison of intensities is difficult. Further, many of the satellites lie "in the shadow" of the parent line, the shape of which, were there no satellites, must be estimated (guessed!) in order to make even a semiquantitative determination of relative intensity.

According to such estimates as are available the relative intensities of satellites vary from a small fraction of one percent to several percent of the intensities of the respective parent lines. The several satellites of a given line vary among themselves. For example, the $K\alpha$ doublet has several satellites of which the doublet $K\alpha_{3,4}$ is much more intense than $K\alpha_{5,6}$. $K\alpha_4$ is more intense, perhaps by a factor of two, than $K\alpha_3$, for elements in the neighborhood of $Z=20$. But for Si(14) and below, $K\alpha_3$ is the more intense. The $L\alpha$ doublet, likewise, has several satellites², $L\alpha^i$, $L\alpha^{ii}$, $L\alpha^{iii}$. . . $L\alpha^{vi}$ in order of

* For preliminary report see Science 70, 616 (Dec. 20, 1929).

** The senior author wishes to express his thanks to the Heckscher Research Council of Cornell University for a grant in aid of this research.

¹ For a discussion of x-ray satellites and their origin see M. J. Druyvesteyn, Dissertation, Groningen, 1928. F. K. Richtmyer, Franklin Inst. Journal 208, 337ff (1929).

² For terminology see F. K. Richtmyer, Jour. Franklin Inst., reference 1.

decreasing wave-length. Of these $L\alpha^{ii}$ and $L\alpha^{iii}$ are the most intense. $L\alpha^n$ and $L\alpha^{vi}$ are very faint.

The relative intensities vary, for any given satellite, with atomic number. The $K\alpha_{3,4}$ doublet is relatively strong for $Z=20$; it is very faint for $Z=30$ and practically disappears for $Z=33$. $K\alpha_{5,6}$ is easily observed from Na(11) to Si(14) but disappears above S(16).

It is also probable, since the excitation voltages of satellites are somewhat higher than those of the parent lines, that the law of increase of intensity with voltage differs from the corresponding law for the parent line, and hence, at least for voltages not too far above the excitation voltage, that the intensity of a satellite relative to parent line depends, for a given element, on the voltage.

The present investigation was undertaken to obtain information which might serve as a starting point for a systematic study of this general problem. The $K\alpha_{3,4}$ doublet of Cu(29), a (photographically unresolved) satellite of the $K\alpha_{1,2}$ doublet, was chosen as most suitable for an initial study. An x-ray tube with a copper target can be built to stand, with water cooling, an input of at least 2500 watts. And Davis and Slack have developed a window thin enough to transmit to the outside of the x-ray tube, a substantial proportion of $CuK\alpha$ radiation so that it may be studied by an ionization spectrometer. The two-crystal x-ray spectrometer developed by Bergen Davis³ and his collaborators is particularly suited for this purpose, partly because of its high resolving power and partly because of the intense beam of monochromatic radiation which it delivers.

With the two-crystal spectrometer and water-cooled, copper-target tube with thin window, observations were made of the apparent energy distribution through the line $CuK\alpha_1$ and to a considerable distance toward shorter wave-lengths. The method of making observations requires no special comment, save only that every effort was made to maintain conditions constant during a run, by manually controlling voltage and tube current. The x-ray tube was run at approximately 40 kv and 50 ma.

The results are best shown by Fig. 1 which is the average of several runs. The abscissae represent Bragg reflection angles in seconds (starting from an arbitrary zero). The ordinate scale *A* gives the intensity distribution through the line $K\alpha_1$. The measurements below 300" are plotted to ordinate scale *B*. A distinct "hump" is observed to extend from about 60" to 200". The observed points above and below this "hump" define a smooth line, *abc*. If the ordinates of this line be subtracted from the observations and these differences plotted on the abscissae scale there results the line *pqr*, which is the $K\alpha_{3,4}$ satellite of Cu(29). Photographic determination (by Siegbahn) of $K\alpha_{3,4}$ places the doublet (unresolved on the photographic plate) at 150" as shown at "C" on the abscissae scale.

³ A substantial proportion of the work herein described was done in the Physical Laboratory at Columbia University with the double x-ray spectrometer, x-ray plant and accessory equipment previously assembled by Professor Bergen Davis. To him and his colleagues, particularly Mr. Beller, the authors wish to express sincere thanks not only for the use of the apparatus, including the specially constructed x-ray tube, but for many other courtesies and suggestions during the progress of the work.

It is obvious that $K\alpha_{3,4}$ as here observed by the ionization spectrometer is at least a doublet, as Siegbahn found it to be by the photographic method for elements of atomic number below Sc(21). For, not only does the line have the appearance of a close doublet in spite of some scattering of the points, but, as shown on Fig. 1, the width at half-maximum of $K\alpha_1$ is 28 seconds of arc, while the corresponding width of $K\alpha_{3,4}$ is 83". This suggests that $K\alpha_{3,4}$ may contain several components. The resolution is not sufficient to warrant an attempt accurately to determine these components. If, however, starting from the long-wave-length side, a line $rq'p'$, Fig. 1, be constructed with the same width at half-maximum as $K\alpha_1$, the long-wave-length component of $K\alpha_{3,4}$ can be approximately located. This long-wave-length component,

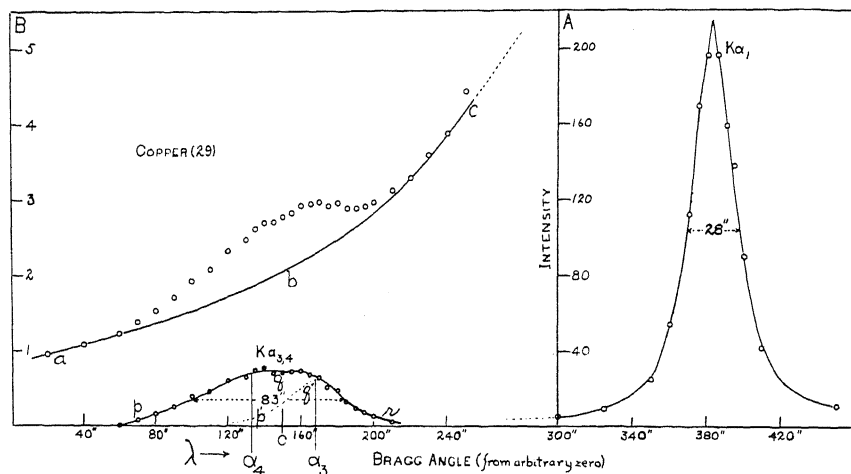


Fig. 1. Energy distribution through $K\alpha_1$ of Cu(29) including its satellites $K\alpha_{3,4}$. The abscissa scale represents Bragg reflection angles, in seconds, from an arbitrary zero. (The actual Bragg angle for Cu $K\alpha_1$ (calcite) is about $14^\circ 42'$). Ordinate scale A gives the distribution through $K\alpha_1$. Ordinate scale B applies to the short wave-length "foot" of $K\alpha_1$ as shown by the line abc . The satellite doublet, $K\alpha_{3,4}$, shown by the line pqr , is the difference between the smooth line abc and the corresponding observed points. Two of the components of $K\alpha_{3,4}$ are estimated to be at " α_3 " and " α_4 ", respectively. The photographic method locates the doublet at "C".

i.e. $K\alpha_3$, is thus located at " α_3 " on the graph. Taking the maximum ordinate of the remainder as the next component, we locate $K\alpha_4$ at " α_4 " on the graph. We are then able to compute the wave-lengths of $K\alpha_3$ and $K\alpha_4$ as follows:

	$K\alpha_3$	$K\alpha_4$
$\Delta\theta$ from $K\alpha_1$	217"	252"
λ from $K\alpha_1$	6.15 X. U.	7.15 X. U.
λ ($\lambda K\alpha_1 = 1537.30$ X. U.)	1531.15"	1530.15"
$\Delta\nu/R$ from $K\alpha_2$	3.85	4.23
$(\Delta\nu/R)^{1/2}$ from $K\alpha_2$	1.96	2.06

Siegbahn gives 1530.7XU. as the wave-length of the (photographically unresolved) doublet $K\alpha_{3,4}$ of Cu (29). The mean of the wave-lengths given above is 1530.65XU.

One of us⁴ has shown that a simple relation exists between the frequency ν of a satellite and that of the corresponding parent line; namely, $(\Delta\nu/R)^{1/2}$ is a linear function of atomic number, where R is the Rydberg constant and $\Delta\nu$ is the difference in frequency between the satellite and the parent line. For the $K\alpha_{3,4}$ satellites it was found that this linear relation held if $\Delta\nu$ was taken as the difference in frequency between $K\alpha_3$ or $K\alpha_4$ and the parent line $K\alpha_2$ (instead of $K\alpha_1$). The graph of this relation is shown in Fig. 2. The data for

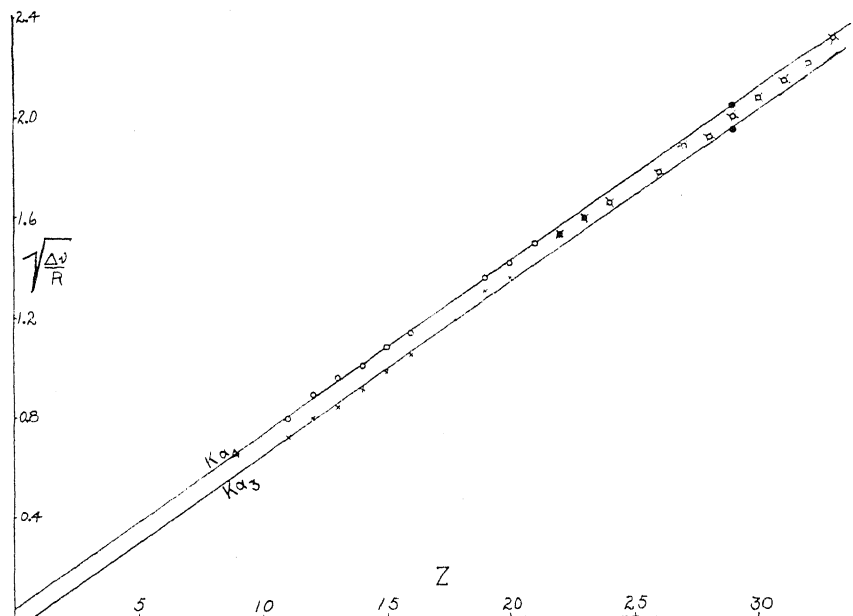


Fig. 2. The square root of the difference in frequency between a satellite and its parent line is a linear function of atomic number. Upper line: Square root of difference in frequency between $K\alpha_1$ and $K\alpha_2$; lower line, same for $K\alpha_3$. Source of data: Na(11) to Ni(28) from Siegbahn; Cu(29) to As(33) from F. K. R. at Cornell University). The solid circles are the present measurements for Cu(29) by the two-crystal ionization spectrometer.

the elements Na(11) to Ni(28) are taken from Siegbahn. Below Ca(20) the two components are resolved and are shown, respectively, by circles (for $K\alpha_4$) and crosses (for $K\alpha_3$). From Sc(21) to Ni(28) the "circle-cross" represents the unresolved doublet. The last five points (circle-cross), namely Cu(29) to As(33) are from unpublished data taken by one of us (F.K.R. at Cornell University). It is seen that these unresolved points fall between the two parallel lines defined by the elements, below Ca(20), for which the doublet is resolved.

⁴ F. K. Richtmyer, Phil. Mag. **6**, 64 (July, 1928); Franklin Inst., Jour. **208**, 325 (Sept., 1929). Also F. K. Richtmyer and R. D. Richtmyer, Phys. Rev. **34**, 574 (1929)

The two solid circles at Cu(29) represent the doublet as resolved by the two-crystal spectrometer (See above data table). The closeness with which these two points fall on the respective lines seems to justify the conclusion that the difference in $(\Delta\nu/R)^{1/2}$ is constant and independent of atomic number, which empirical fact forms a basis for the term "doublet" as applied to $K\alpha_{3,4}$.

Referring now to Fig. 1 the maximum ordinate of $K\alpha_{3,4}$ is about 0.72; that of $K\alpha_1$ is about 215. The intensity of the components of $K\alpha_{3,4}$ is not greater than $0.72/215 = 0.0034$ of that of $K\alpha_1$, and in reality is somewhat less, since the line pqr has a higher maximum than any of its components. In round numbers, therefore, we may say that $K\alpha_1$ is some 400 times as intense as the $K\alpha_{3,4}$ satellites for the element Cu(29) at 40 kv.

A similar study was made of the $K\alpha_{3,4}$ of Ni(28). The results of two runs at two different voltages are shown at A and B of Fig. 3. The satellites are

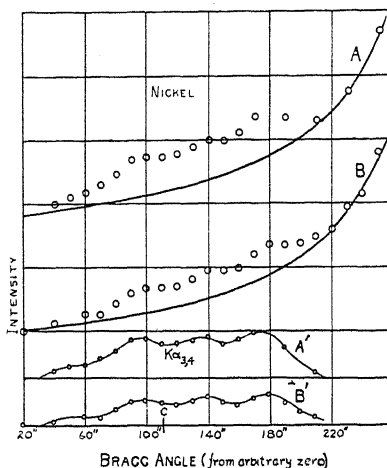


Fig. 3. The $K\alpha_{3,4}$ satellites of Ni(28). A and B represent observed energy distribution along the foot of $K\alpha_1$ of Ni, for two different tube voltages; A' and B', the corresponding energy distribution through the satellites. The photographic method places the (unresolved) satellite at "C".

are shown at A' and B'. Photographic measurement places the doublet at "C." Further measurements are necessary to determine whether $K\alpha_{3,4}$ for Ni actually has three (or perhaps four) components as these data seem to indicate. Unpublished data⁵ at Cornell University show that $K\alpha_3$ splits up into two components for elements below S(16).

No determination of the intensity of $K\alpha_{3,4}$ for Ni(28) relative to $K\alpha_{1,2}$ has been made since, as may be observed from Fig. 3, the absence of observations on the short-wave-length side makes it impossible to locate the base line accurately. However, the order of magnitude of relative intensity is the same as for Cu(29).

Since $K\alpha_1$ and $K\alpha_2$ originate from the same initial ionized state, namely single K-ionization, we may, by analogy, assume that the components of

⁵ By O. Rex Ford.

$K\alpha_{3,4}$ originate in the same double ionized state which we may for the present call a KX -ionization, "X" standing for a missing electron the identity of which is as yet undetermined. Let P_K and P_{KX} be the relative probabilities of these single and double ionizations, respectively, under any given set of conditions—tube current, voltage, etc. Then, these data on relative intensities of one of the components of $K\alpha_{3,4}$ to $K\alpha_1$ make possible the estimate that (for Cu(29) at about 40 kv).

$$P_{KX}/P_K \geq 1/400.$$

This estimate, of course, is very rough and gives only the order of magnitude of the ratio, as may be seen from the following: A K -ionized atom may return to the normal state by various routes. As a first step, it may emit any one of the diagram lines of the K series; or, as a result of autophotoelectric absorption, it may emit a photoelectron. We may expect, likewise, that a KX -ionized atom might return to the normal state in various ways other than by the emission of $K\alpha_{3,4}$. Indeed, there is some evidence⁶ to indicate that, associated with some, at least, of the satellites, there is a continuous spectrum which may account for a considerable proportion of the doubly ionized atoms. The asymmetry of the satellite curves in Figs. 1 and 3—i.e., these curves are less steep on the short wavelength side—is suggestive of a continuous spectrum similar to that found with $L\alpha$ satellites in Fig. 1 of the article just cited⁶.

It is hoped later to make a more extensive report on relative intensities of satellites on the basis of work now in progress at Cornell University.

⁶ F. K. Richtmyer and R. D. Richtmyer, Phys. Rev., reference 4.

AN ANALYSIS OF SCATTERED X-RAYS WITH THE DOUBLE CRYSTAL SPECTROMETER

BY NEWELL S. GINGRICH

RYERSON PHYSICAL LABORATORY, UNIVERSITY OF CHICAGO

(Received August 7, 1930)

ABSTRACT

X-rays from a molybdenum target were scattered by graphite at approximately 109° and 161° . The scattered rays were analyzed with a double crystal spectrometer. When scattering at 109° was used, no indication of the fine structure lines, reported by Davis and his collaborators, could be found. When scattering at 161° was used, the modified $K\alpha_1$ and $K\alpha_2$ lines were definitely separated. The value of $\delta\lambda$ was $0.04721 \pm 0.00003\text{\AA}$, the value of $(1 - \cos\phi)$ was 1.9479 and the calculated value of h/mc was $0.02424 \pm 0.00004\text{\AA}$.

INTRODUCTION

WHEN monochromatic x-rays are scattered by matter, both their intensity and their wave-length are changed. A theory explaining their change in wave-length was suggested by A. H. Compton,¹ in 1922. This theory assumed that x-rays were scattered by free electrons and gave the equation,

$$\delta\lambda = (h/mc)(1 - \cos\phi) \quad (1)$$

for their change in wave-length. In the above equation, $\delta\lambda$ represents the change in wave-length; h , Planck's constant; m , the mass of an electron; c , the velocity of light; and, ϕ the angle of scattering. The change in wave-length has been measured by many investigators,² and their results have for the most part agreed very well with the theory. In 1924, A. H. Compton³ proposed a theory for the scattering of x-rays by bound electrons. The energy equation for this type of scattering is

$$h\nu = h\nu' + h\nu_s + mc^2[(1 - \beta^2)^{-1/2} - 1] + \frac{1}{2}MV^2 \quad (2)$$

where h is Planck's constant, ν the frequency of the incident x-rays, ν' the frequency of the scattered x-rays, ν_s the characteristic frequency of the s^{th} level in the atom, $mc^2[(1 - \beta^2)^{-1/2} - 1]$ the kinetic energy of the recoil electron, and $\frac{1}{2}MV^2$ the kinetic energy given to the atom of mass M . The kinetic energy given to the atom is negligible, so that only the first three terms on the right hand side of Eq. (2) need be considered. If the recoil electron has zero velocity, we have a special case in the predictions of the theory. The equation for this case is.

$$h\nu = h\nu' + h\nu_s. \quad (3)$$

¹ A. H. Compton, X-rays and Electrons, p. 260.

² A. H. Compton, X-Rays and Electrons, p. 270.

³ A. H. Compton, X-Rays and Electrons, p. 285.

When converted into wave-lengths, the equation becomes,

$$\delta\lambda = \frac{\lambda^2}{\lambda_s - \lambda} \quad (4)$$

where $\delta\lambda$ is the change in wave-length of the incident radiation, λ_s the characteristic wave-length of the s^{th} level, and λ the wave-length of the incident radiation. This is the x-ray analogue to the Raman effect with light.

Davis and Mitchell,⁴ Mitchell,⁵ and Davis and Purks⁶ have reported a fine structure, predicted by this special case of scattering by bound electrons, with various materials used for scattering. They have also reported the existence of spectral lines whose wave-lengths are given by the equation

$$\delta\lambda = \frac{h}{mc}(1 - \cos \phi) + \frac{\lambda^2}{\lambda_s - \lambda} \quad (5)$$

except that the constant h/mc should be about 9 percent less than the theoretical value 0.0243A. DuMond⁷ has observed small humps on the modified line scattered from Be, but was unable to interpret them in the above fashion. Coster,⁸ Ehrenberg,⁹ and Kast¹⁰ were unable to detect any fine structure with scatterers of graphite and aluminum.

All the investigators who observed the fine structure lines used the double crystal spectrometer, while those who did not observe them, used a single crystal spectrograph. With this in mind, the writer has reexamined the spectrum of scattered x-rays using a double crystal spectrometer. Two separate experiments have been performed.

METHOD I

X-rays were scattered from a block of graphite in air at about 109° with a divergence of angle of $\pm 9^\circ$. The scattered radiation was limited by two lead slits before striking the first crystal of a double crystal spectrometer. The radiation reflected from the first crystal according to Bragg's law, was again reflected by the second crystal. The reflection from the second crystal entered an ionization chamber after passing through three lead slits. The ionization produced in the methyl bromide in the chamber was measured by a Compton electrometer. A diagram of the apparatus is shown in Fig. 1.

APPARATUS I

An oil immersed, full wave rectifier unit supplied voltages up to 60 peak kv and currents up to 110 ma. The unit was housed in a tank $14'' \times 25'' \times 34''$, and all parts at high voltage were immersed in oil except the insulated lead to the x-ray tubes.

⁴ D. P. Mitchell, Phys. Rev. **33**, 871 (1929).

⁵ B. Davis and D. P. Mitchell, Phys. Rev. **32**, 331 (1928).

⁶ B. Davis and H. Purks, Phys. Rev. **34**, 1 (1929).

⁷ J. W. M. DuMond, Phys. Rev. **33**, 643 (1929).

⁸ Coster, Nature **123**, 642 (1929).

⁹ Ehrenberg, Zeits. f. Physik. **53**, 234 (1929).

¹⁰ Kast, Zeits. f. Physik **58**, 519 (1929).

Two metal x-ray tubes of small diameter were used. The distance from the center of the targets to the windows was $7/8$ inch, and the aluminum windows were usually as thick as 0.05 mm. The size of the focal spots was adjusted by means of movable focal cups and in this experiment was the same as the size of the Mo buttons on the targets. Though the use of such large focal spots increased the divergence of the angle of scattering to some extent, it increased the possible input of the tube greatly. These tubes were connected in parallel, and a current of 50 ma was carried by each one. The potential usually used was 45 peak kv.

The double crystal spectrometer used was one made by the Société Genevoise. The first crystal table was graduated in one minute intervals, and its position could be estimated to a quarter of a minute. The second crystal table and ionization chamber circle were graduated in minutes, but by means of ocular micrometers, their positions could be read to one second of arc.

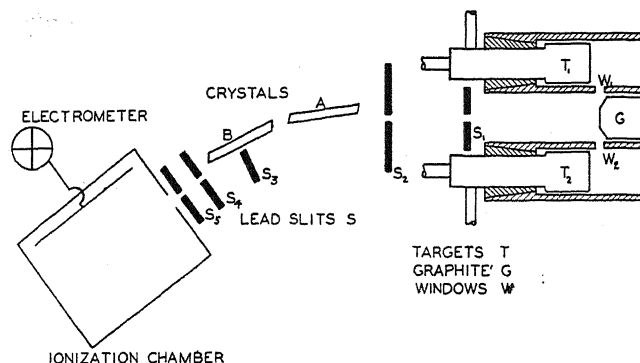


Fig. 1.

Crystals of calcite with their cleavage surfaces polished were used to reflect the x-rays. With the notation adopted by Allison and Williams,¹¹ the half width W at half maximum obtained with these crystals in the $(1, -1)$ position, was ten seconds of arc. With the crystals in the $(1, 1)$ position, the value of W for $\text{Mo } K\alpha_1$ was 20 seconds. Though this resolution is not as good as that obtained by those¹² who have used cleavage faces of calcite, it is sufficient for the purposes of these experiments.

The ionization chamber was of brass, 10 cm long, and was filled with methyl bromide. There was a short lead to a Compton electrometer, which was equipped with a needle only 6 mm long. The capacity of the system was thus very small.

METHOD OF MEASUREMENT I

(a) *The measurement of $\delta\lambda$.* The spectrometer was lined up by using direct radiation. There was sufficient intensity to observe the $\text{Mo } K\alpha_1$ and $K\alpha_2$ lines reflected from the second crystal, with a strip of fluorescent screen when

¹¹ S. K. Allison and J. H. Williams, *Phys. Rev.* **35**, 149 (1930).

¹² B. Davis and H. Purks, *Phys. Rev.* **34**, 181 (1929).

the room was partly darkened. Scattered rays were then sent through the same slit system, and the readings of the ionization current were taken as the second crystal was turned through intervals of 7.5 seconds of arc. A plate of Mo was occasionally used in place of the graphite as a check on the alignment of the system. The angular distance between the undisplaced $K\alpha_1$ line and any other line was measured from the plot of intensity vs. crystal angle. The value of $\delta\lambda$ was then calculated from the equation for the dispersion of the double crystal spectrometer,

$$\frac{\delta\theta_B}{\delta\lambda} = \frac{n_A}{2D \cos \theta_A} + \frac{n_B}{2D \cos \theta_B} \quad (6)$$

where the subscript A refers to the first crystal, the subscript B refers to the second crystal, and D is the grating space of calcite.

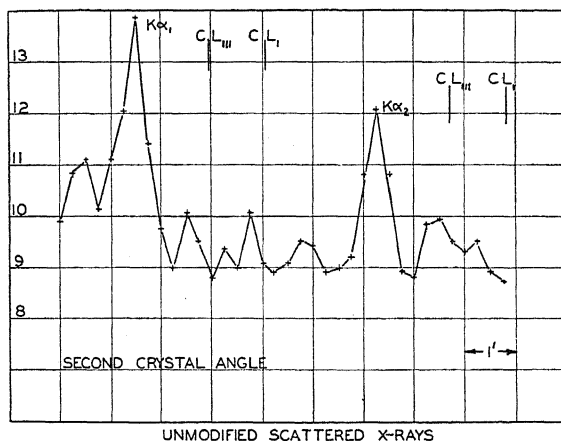


Fig. 2.

(b) *The measurement of ϕ .* In this experiment the measurement of the effective angle of scattering ϕ was not done with great care. However, it is sufficiently accurate to show a qualitative agreement between Compton's theory and this experiment. The extreme values of ϕ were got by geometrical considerations of the target-window-slit system, and the value of ϕ given is the arithmetic mean of the two extremes.

RESULT I

The results of this experiment are shown graphically in Figs. 2 and 3. Fig. 2 shows the undisplaced $K\alpha_1$ and $K\alpha_2$ lines as obtained from x-rays scattered at 109° . They appeared consistently at the same position, whether scattered radiation from graphite or fluorescent radiation from Mo was used. The space between these lines shows fluctuations, but no fluctuation greater than the experimental error encountered in working with as feeble radiation as was used here.

Fig. 3 shows the graph of Fig. 2 plotted on a smaller scale together with a continuation of the spectrum out as far as the modified line.

Readings were taken at smaller intervals than shown, but, since they agreed substantially with those plotted, are not included in the graph. Fig. 2 is the average of six typical curves, and the part of Fig. 3 not shown in Fig. 2 is the average of five curves.

DISCUSSION AND CONCLUSION I

The fine structure lines from a carbon scattering block, as reported by Davis and his collaborators, were found at the positions indicated by the lines CL_{111} and CL_1 in Fig. 2. It will be seen that the present experiments give no indication of lines in these positions.

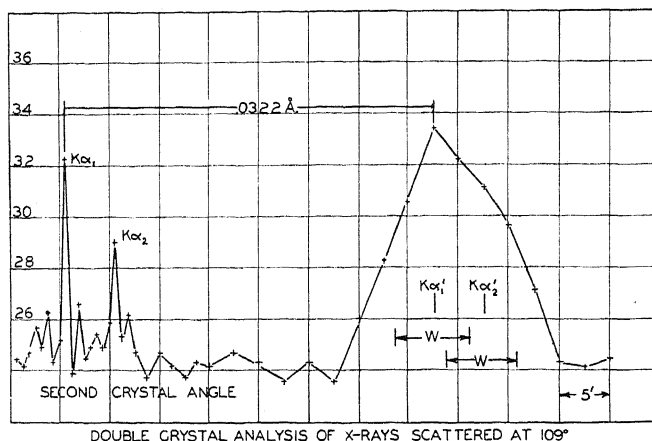


Fig. 3

Carrelli¹³ has made a calculation to learn upon what factors the intensity of these fine structure lines depends. If the photon incident upon the atom lifts a K electron to a $1s$ level, the intensity I of the shifted line should be proportional to the following expression:

$$I \sim Z^{-3} \frac{\left[1 + \frac{E_e}{E_u}\right]^4}{\left[1 + \frac{E_e}{4E_u}\right]^4}.$$

If the incident photon lifts a K electron to the $2p$ level, the intensity I of the shifted line should then be proportional to:

$$I \sim Z^{-3} \frac{E_e \left[1 + \frac{E_e}{4E_u}\right]^4}{E_u \left[1 + \frac{4E_e}{E_u}\right]^6}.$$

¹³ A. Carrelli, Zeits. f. Physik 61, 632 (1930).

Somewhat similar expressions are given for the case of an L electron being lifted to a $1s$ or a $2p$ level. These latter two expressions show that the intensity of a line caused by the removal of an L electron, is less than that for the removal of a K electron. In order to obtain greater intensity of the lines, the following three conditions must be fulfilled:

(a) Use substances presenting semi-optical lines. (b) Use substances of low atomic number. (c) Use exciting wave-lengths, directions of observation, and substances for which the ratio E_e/E_u is very high. Here E_e is the kinetic energy of the electron emitted for the Compton effect in one particular direction, and E_u is the energy of the level from which the electron is lifted. These are fulfilled reasonably well in this experiment, so that nearly the optimum intensity could be expected.

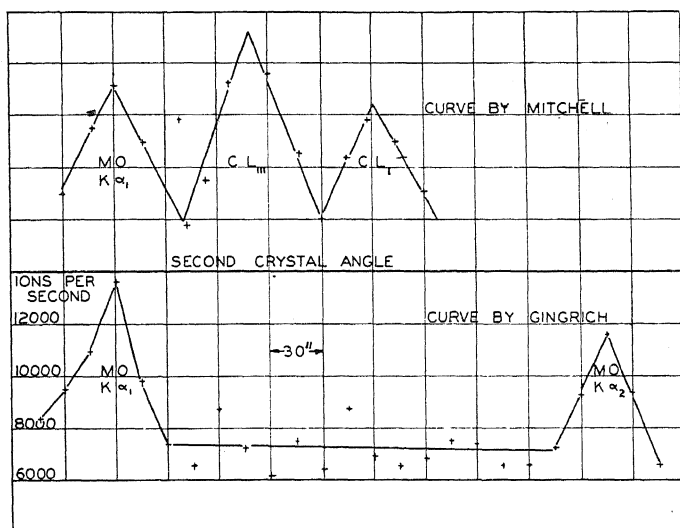


Fig. 4.

In Fig. 4 is reproduced a curve published by Mitchell⁴ reporting fine structure lines in x-rays scattered from carbon. It will be noted that the modified lines are of the same order of intensity as the unmodified lines. This is true also for the curves published by Davis and Mitchell⁵ and Davis and rks.⁶ Fig. 3, on the other hand, shows no indication of fine structure lines between $\text{MoK}\alpha_1$ and $\text{K}\alpha_2$ of greater intensity than 15 or 20 percent of the undisplaced α_1 line. The fluctuations between the bases of α_1 and α_2 could hardly be interpreted as fine structure lines since they do not have the width characteristic of a true line resolved by the spectrometer. The separate spectra taken had larger fluctuations than the average of all six spectra, but no consistently high readings were obtained at points between the α_1 and α_2 lines. Since the ionization produced by one alpha-particle during the time of taking an observation is comparable with the ionization measured, it is evident that the chance fluctuations observed could easily be produced by a slight radioactivity of the chamber.

Bearden¹⁴ reported the completion of a similar experiment, shortly after these results were obtained. His conclusions are essentially the same as the writer's,¹⁵ except that in his experiment, the intensity of the fine structure lines could be no more than 10 percent of the undisplaced α_1 line. Bearden used a scattering block inside the tube, and since a slight deposit of the target metal on the scattering block would produce relatively strong fluorescent rays, his method has been criticized by those who report evidence of fine structure. However, Bearden's chemical analysis of the scattering block may invalidate this criticism. This objection does not hold in the present experiment.

From this experiment, the conclusion is drawn that no fine structure of intensity greater than 15 or 20 per cent of the unmodified radiation is present in radiation scattered at 109° by graphite.

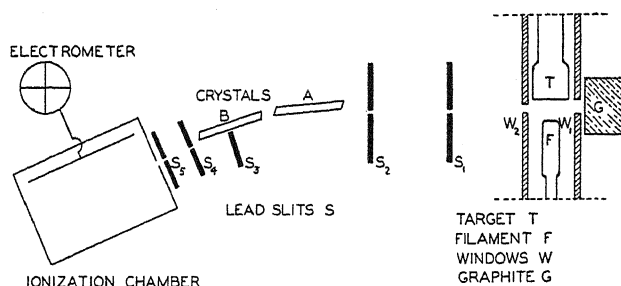


Fig. 5.

METHOD II

X-rays were scattered at 161° from a block of graphite in air. The smallest angle of scattering possible was 153° and the largest angle of scattering possible was 175° . Except for the fact that the x-rays were scattered at a different angle, the method in this experiment was essentially the same as that in the first experiment. A diagram of the apparatus is shown in Fig. 5.

APPARATUS II

The same source of high voltage was used in this experiment as was described under Apparatus I.

One metal x-ray tube of small diameter was used. The distance from the center of the target to the windows was $7/8$ inch. This tube had two windows instead of one as in the first apparatus. The second window was diametrically opposite the first window. The size of the focal spot was adjusted with a movable focal cup. With a voltage of 50 peak kv across the tube, a current of 100 ma. was used through the tube. Occasionally only 60 ma. were used.

The same double crystal spectrometer, crystals, and detecting devices were used as are described in Apparatus I.

¹⁴ J. A. Bearden, *Phys. Rev.* **35**, 1427 (1930).

¹⁵ N. S. Gingrich, *Phys. Rev.* **35**, 1444 (1930).

METHOD OF MEASUREMENT II

Measurement of ϕ . In order to measure accurately the effective angle of scattering, the following procedure was followed. Pinhole pictures of the focal spot were taken, and the variation of intensity of the x-rays from various

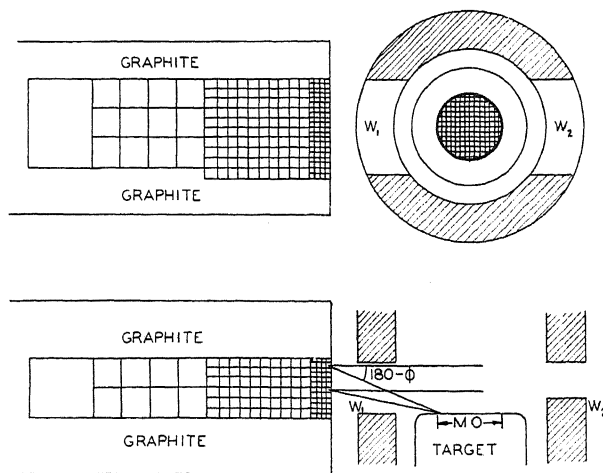


Fig. 6.

portions of the target was measured. The Mo target was then marked off with millimeter squares, as indicated in Fig. 6, and a weighting factor was associated with each square in accordance with the relative intensity of x-

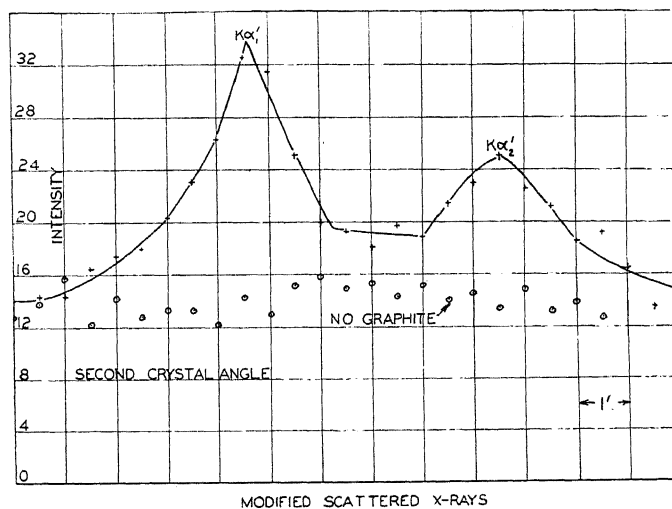


Fig. 7.

rays from this square. The scattering block was then divided into small segments of volume as shown.

The angle of scattering caused by the x-rays from each element of target area to each element of scattering volume was calculated geometrically. The

cosine of each angle thus obtained was multiplied by the number representing the relative intensity of the x-ray from the area used, was multiplied by the relative volume of the element of scatterer considered, and then by a factor correcting for the absorption of the x-rays in the graphite. These values of the weighted cosines were then averaged. The grand average of the weighted cosines as thus calculated was 0.9479 , with an estimated probable error of ± 0.003 .

RESULTS II

Fig. 7 shows the average of five curves taken of the modified beam. The α_1 and α_2 modified lines are definitely separated.

Fig. 8 shows the complete spectrum of scattered x-rays.

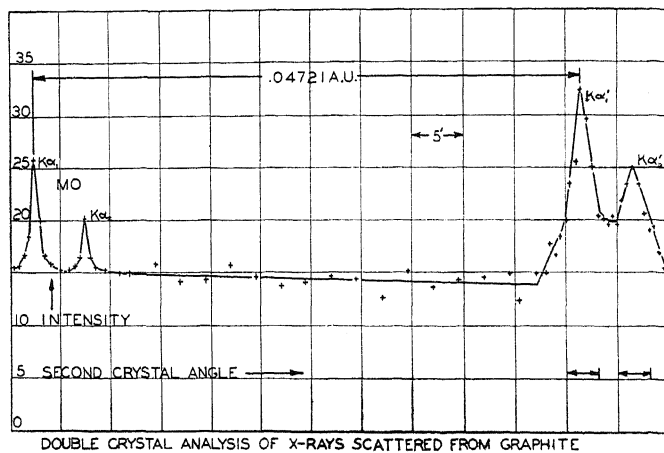


Fig. 8.

The value of $\delta\lambda$ obtained from five separate determinations, as calculated from Eq. (6), using $D = 3.02904\text{\AA}$, was $0.04721 \pm .00003\text{\AA}$ when the probable error is calculated in the usual manner. Using for the cosine of the angle of scattering the average value 0.9479 ± 0.003 , we obtain from Eq. (1),

$$\frac{h}{mc} = 0.02424 \pm .00004.$$

DISCUSSION AND CONCLUSION II

Kallmann and Mark¹⁶ obtained fairly accurate measurements of the change in wave-length of scattered x-rays with the single crystal photographic method. From scattering at 72° , the value of $\delta\lambda$ was 0.0170\AA , and by substitution in equation (1), one finds that $h/mc = 0.0246\text{\AA}$. From scattering at 90° , the value of $\delta\lambda$ was 0.0241\AA and that of h/mc was 0.0241\AA .

H. M. Sharp¹⁷ has measured $\delta\lambda$ using the single crystal, and, combining this value with his value of $(1 - \cos \phi)$, obtains the experimental value

¹⁶ H. Kallman and H. Mark, *Naturwiss.* 13, 297 (1925).

¹⁷ H. M. Sharp, *Phys. Rev.* 26, 691 (1925).

$$\frac{h}{mc} = 0.02432 \pm .00009A.$$

The value of the ratio h/mc as calculated from the accepted values of the constants differs according as the deflection or the spectroscopic value of e/m is used. In the former case, Birge¹⁸ finds

$$\frac{h}{mc} = 0.02428A$$

and in the latter case

$$\frac{h}{mc} = 0.02417A.$$

The value found from the present experiment lies between these extremes. There is thus no indication of a departure of the experiments from the predictions of Compton's theory of scattering.

These experiments were carried out under the supervision of Professor A. H. Compton and the writer is indebted to him for his encouragement and helpful suggestions. The writer also wishes to express his appreciation of the many very helpful practical suggestions given by Dr. R. D. Bennett.

¹⁸ R. T. Birge, Phys. Rev. Supplement 1, 1 (1929).

THE SCATTERING OF FAST ELECTRONS BY METALS. II. POLARIZATION BY DOUBLE SCATTERING AT RIGHT ANGLES

BY CARL T. CHASE

NEW YORK UNIVERSITY, UNIVERSITY HEIGHTS, N. Y.

(Received July 28, 1930)

ABSTRACT

The first paper of this series discussed methods of counting fast electrons, a consideration of which has shown the need for further experiments looking for polarization of fast electrons. The present paper concerns a search for polarization by double scattering at right angles, using radium E as a source, and a sensitive gold leaf electroscope to detect the arrival of the scattered electrons, the slower electrons being eliminated from the experiment. A peculiar type of polarization appears, which can be described as follows, using the notation of previous papers. At moderate electron speeds the number counted in the configuration called 0° is greater than the number counted at 180° . This effect does not appear for very slow electrons. As the speed of the electrons approaches that of light, the above type of polarization persists, and another type appears, superposed upon the first; the number counted at 270° becomes greater than the number counted at 90° . Previous experiments of a similar nature, in which one or the other of the above effects appears, are discussed.

THE reasons for performing this work are inherent in the results, and will accordingly not be discussed at this point. We proceed immediately to a description of the experiment, which will be followed by a comparison with other similar experiments.

A sectional diagram of the apparatus used is shown. In this diagram, lead shielding is depicted by double cross-hatching, the brass apparatus itself being shown in section by single cross-hatching. The two lead targets, as well as the radium source, are completely inked in. The sketch is drawn to scale. The radium source consists of a number of old radium emanation tubes containing radium D, E, etc., cut in half and bound in a bundle, open ends toward the upper target. The source is firmly attached to the shaft carrying the upper target, which can be rotated by the handle shown at the top, the shaft passing through the cover in a ground joint. By this means the configuration of the electron path is altered. The apparatus is kept evacuated by means of the tube shown at the right. The window at the immediate left of the lower target is of aluminum, 0.03 mm thick, while the window in the wall of the electroscope is of aluminum, 0.04 mm thick.

The case of the electroscope is made of lead, as shown, the only openings being two circular windows for observing and illumination, covered with glass; the window covered with aluminum for the entrance of the electrons; and the small opening at the left through which a glass tube projects. A wire through this glass tube serves to charge the leaf system. The case contains a drying agent. This type of electroscope has proved most satisfactory.

The lead case protects the leaf to a large extent from the soft radiations always present, from the laboratory walls, air, etc. By having the leaf system completely enclosed in the case, any ionization present in the air from whatever cause is not able to affect the rate of fall of the leaf, this making for consistent operation at all times. A further benefit is that the sulphur plug, on which the leaf system is mounted, does not become contaminated, as would be the case if it projected into the air of the room. The electroscope is sensitive to vibration, and its rate of fall for a given amount of entering radiation changes to some extent with the temperature of the room in which it is used, but with ordinary laboratory precautions it has proved to be the most sensitive and reliable instrument for detecting small amounts of ionizing radiation which the writer has ever used. The rate of fall of the leaf is observed by means of a microscope with a magnifying power of about twenty-five dia-

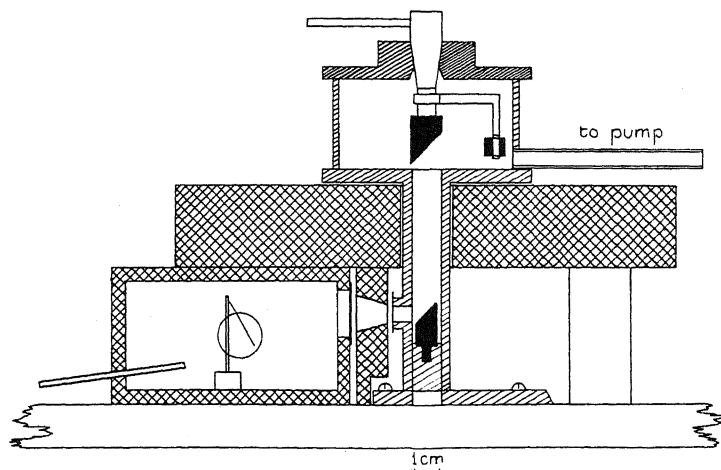


Fig. 1. Diagram of apparatus.

eters, provided with a scale in the eyepiece. This electroscope is far more sensitive than the point-discharge counters which we have used, to say nothing of its infinitely greater reliability and ease of use. The one disadvantage, that it is very sensitive to gamma-rays, can be eliminated by proper shielding. We may mention here that readings should not be taken immediately after charging the leaf, for if any spark passes in the charging process, ions are formed which are a few moments in disappearing.

If very fast electrons are desired, one thinks immediately of using radium C as a source. Radium E emits very fast electrons, but the peak of intensity in the velocity spectrum of radium C occurs in a region of higher velocity than is the case for radium E. By using plenty of radium E, however, and screening out the slower rays, it is possible to obtain a sufficient number of electrons with high enough speeds. Radium C emits powerful gamma-rays, while radium E emits gamma-rays of very feeble intensity and penetrating power. We have accordingly decided to continue to use radium E as a source, cutting out the slower electrons by means of absorbing screens

placed in front of the electroscope. We are concerned here with electrons having speeds from about 0.7 to 0.95 of the velocity of light.

The configuration shown in the diagram is called 0° . The configurations 90° , 180° , and 270° are obtained by rotating the plug, upper target, etc., clockwise as seen from above.

Counts are taken in several ways. First, counts are taken continuously around the circle, taking the time required for the leaf to drift over a given part of its scale at the settings 0° , 90° , etc., continuing round and round as long as possible. Then counts are taken alternately at two of the positions,

TABLE I. Numbers refer to relative counts, and are not corrected for the "zero rate of fall" of the electroscope. This is done on the curve. The experimental error is one percent, obtained from the accuracy obtainable in taking individual readings, and from a consideration of the final data.

At 0°	At 90°	At 180°	At 270°	Weight
1.000	0.972	1.009	1.024	1
1.000	0.975	1.075	1.075	1
1.000	0.997	0.986	1.005	1
1.000	0.990	0.986	1.015	1
1.000	0.988	1.000	1.008	1
1.000	0.994	0.976	1.010	1
1.000	1.034	1.041	1.044	1
1.000	—	0.950	—	4
—	1.000	—	1.030	3
—	1.000	—	1.040	3
—	—	1.000	1.020	2
1.000	—	0.933	—	1
—	1.000	—	1.030	2
—	—	1.000	0.969	2
1.000	—	—	1.003	1
1.000	—	1.037	—	2
—	1.000	0.933	—	2
Means (Weighted)				
1.000	0.993	0.985	1.021	

counting repeatedly at first one, then the other of the two, to get a determination of the ratio of the numbers of electrons counted in these two configurations. The process is then repeated for another pair, etc. The results are shown in tabular form. The weight attributed to each run is determined by the relative number of counts made in each position. The weighted average of all the runs is plotted.

We discuss first the asymmetry as between the configurations 90° and 270° . This asymmetry has not been predicted in any theory. It has been observed first by Cox, McIlwraith, and Kurrelmeyer,¹ in experiments using point-discharge counters, being observed in two separate pieces of apparatus of different size. It also appeared in a third apparatus of the same nature made by the writer,² but not in later experiments³ which seemed at the time to be the most consistent and conclusive of the entire series; these experiments have been rediscussed in a previous paper³ to which the reader is re-

¹ Cox, McIlwraith, and Kurrelmeyer, Proc. Nat. Acad. Sci. 14, 544 (1928).

² Chase, Phys. Rev. 34, 1069 (1929).

³ Chase, Phys. Rev. 36, 984 (1930).

ferred. The argument was that the point-discharge counters have been found by experiments with a magnetic beta-ray spectrograph to register only the slower electrons unless the potential applied to the counter is raised to such a high value as to render the life of the point, the time during which it gives reliable results, very short. In the three cases mentioned above in which this effect appeared, the apparatus was so constructed that the electrons had to pass through about 0.2 mm of mica and aluminum, which cut out the slower rays. The small number of electrons left forced the use of high voltages on the counters, in order to obtain any electron counts at all. These high voltages in turn made the counters more unreliable than ever, but also made them sensitive to the very fast electrons. Gamma-ray counts were predominant in the total count, but in the positions 90° and 270° should have been of equal intensity.

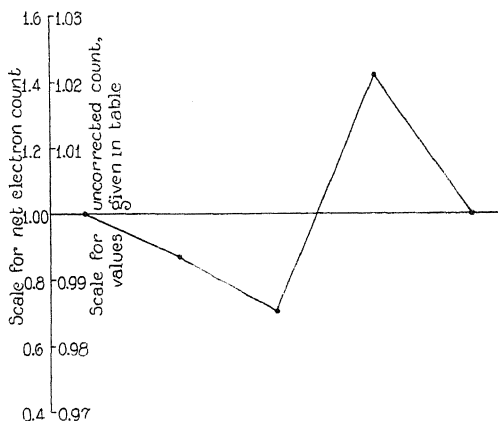


Fig. 2.

The experiment of Chase which gave a negative result eliminated the gamma-ray counts, and by decreasing the window thickness to 0.04 mm increased the number of electrons which arrived at the counter, these added electrons being the slower ones which had previously been excluded. With more electrons to count, the counters could be operated at lower voltages, sufficiently low for the points to give consistent results for a whole day. We have shown³ that these consistent results did not include the faster electrons, and any polarization effect is predicted for fast electrons. At the time the consistency of the results were convincing, and it was thought that electrons having speeds of say 0.5 of the velocity of light were to be considered as fast. We now see that for the purpose of discussing the effect with which we are concerned, these speeds are to be regarded as slow, and speeds of at least 0.7 of the velocity of light are necessary.

The following can be said of the present experiments; the asymmetry between the counts at 90° and 270° is always observed, which was in no sense true before. Not only every single run, but even all the readings in every run, with few exceptions, show the effect. As an interesting sort of check, the apparatus which had previously given a negative result² was set

up again; with counters used as they had been before, at lower voltages, the results were negative as before, but with high voltages on the counter, high enough to ruin the point within an hour or two, the effect was very likely to appear. Making no changes except in the voltage on the counter, the effect could be accentuated or suppressed.

It will also be noted that in the average more electrons are counted at 0° than at 180° , though this effect is not so consistently observed as that between the other two positions. The position of the point at 180° on the curve must therefore be regarded as the least reliable of the set.

Mott has predicted⁴ on the basis of the Dirac electron theory that this experiment should show a polarization effect in that an asymmetry should be observable between the two positions 0° and 180° . This effect is supposed to be more definite for fast electrons and heavy scattering materials. He predicts equal counts for the positions 90° and 270° . A previous experiment of the writer² showed an effect of this nature, more electrons being counted in the 0° position than in the opposite position by 4 percent. Nothing was claimed for this result, because the targets were so close together that it seemed plausible that the electrons would find it easier to get through the apparatus in the 0° position. The targets are now farther apart, since fewer electrons per second are permissible with the increased sensitivity of the electroscope, and beam divergence is much less than before. The previous objection is, therefore, no longer valid. That the effect is not due to the penetration of gamma-rays is shown by the fact that the presence or absence of the lead shield between apparatus and electroscope had little if any effect. A piece of paper held in the path of the rays, in front of the electroscope, cut down this asymmetry to a very small figure.

A similar experiment has been performed by Rupp,⁵ but slower electrons from a filament were used, and instead of scattering the electrons at right angles, the rays were reflected at grazing incidence. He observes an asymmetry of 12 percent with more electrons counted at 0° than at 180° , for filament electrons accelerated through 80 kilovolts. The asymmetry is less for 40 kilovolt electrons, and disappears for 10 kilovolt electrons. The above applies to gold targets; he does not observe the effect for slow electrons with gold targets, nor for fast electrons with beryllium targets. Neither does he observe the asymmetry between 90° and 270° , which is in accordance with our contention concerning the electron speeds necessary to observe this effect.

It has not been shown that Mott's prediction applies directly to reflection at grazing incidence. Further, one might say that electrons would find a freer path through Rupp's apparatus in the 0° position, especially the fast ones. His results, however, appear to be beyond argument of this sort, since his effect is not observed for light targets, all else remaining the same.

We may say in general that there are several unsatisfactory things about this experiment. For instance, electrons hitting the lead targets produce

⁴ Mott, Roy. Soc. Proc. **A124**, 425 (1929).

⁵ Rupp, Zeits. f. Physik **61**, 158 (1930).

secondary gamma-radiation, that from the lower target being able to affect the electroscope. Also, secondary gamma-radiation from the upper target may eject electrons from the lower target which will be counted. Besides, we do not know how the electrons which are finally counted are related to those originally falling on the upper target. They may be the same ones, either with the original velocity, or, which is more probably the case in view of experiments with absorbing screens of paper before the electroscope, with diminished velocities. Lead screens cannot be used to test this point, since electrons produce secondary gamma-rays when they fall on lead. For this reason we used paper screens. The counted electrons may also be secondary, tertiary, etc. electrons produced by the primaries. These points will have to be tested in auxiliary experiments.

The next paper will deal with scattering at right angles, but the electrons will be those which have been scattered by transmission through thin foils, in contrast to the present case in which diffusely reflected electrons were used. We shall return later to the present experiment using reflected electrons, in order to get a more exact measurement of the effect. It seems better to postpone this until we have found in how many ways the effect can be obtained.

AN EXPERIMENTAL DETERMINATION OF THE CHANGE IN
TEMPERATURE ACCOMPANYING CHANGE IN
MAGNETIZATION OF IRON¹

BY WALTER B. ELLWOOD

DEPARTMENT OF PHYSICS, COLUMBIA UNIVERSITY

(Received July 21, 1930)

ABSTRACT

Apparatus.—An apparatus is described which permits the measurement of the change in temperature of a ferromagnetic material consequent upon a change in its magnetization. The test specimen, of peculiar form and construction, is placed in a specially designed calorimeter. Around this is wound a solenoid which furnished the magnetizing field. Changes in temperature are measured by means of 102 thermocouples connected in series to a sensitive galvanometer. Methods are described for minimizing thermal and thermoelectric disturbances. The sensitivity of the system is such that a temperature change of 2.26×10^{-6} °C can be detected. This corresponds to a thermal energy change of 87 ergs per cm³ for steel.

Results.—Results are reported on for two specimens of carbon steel containing 1.08 percent and 1.35 percent carbon respectively. Detailed data are presented showing the relationship between temperature change and magnetizing field as the material is carried through various symmetric and asymmetric cycles of magnetization.

The following is typical of a symmetric cycle which starts with the steel in a saturated condition. As the magnetizing field is diminished from +290 to +20 gauss the temperature of the steel rises gradually; this is followed by a very marked cooling between +20 and -8 gauss; if the magnetizing field is further diminished from -8 gauss through the coercive force (-9.6 gauss) to -90 gauss a sudden rise in temperature indicates the release in this region of the major portion of the hysteretic energy; between -90 and -290 gauss the steel cools gradually.

Temperature changes for smaller cycles of magnetization are qualitatively the same as for the large cycle, except that the second cooling may be absent. Similar sharply defined regions of heating and cooling are characteristic of the different asymmetric cycles investigated.

It appears that the total amount of hysteretic heat developed depends upon the rate of performance of the cycle, at least for those cycles which nearly saturate the steel. A rapid traversal yields a greater total heat than a slow traversal.

A—OBJECT

THE object of this research is to measure the spontaneous change in temperature of a specimen of iron which occurs when the magnetic state of the iron is altered in any way. As was pointed out by Larmor,² calorimetric data of this sort are essential to the formulation of a theory of the energy in a magnetized medium. The experimental results here reported are intended as a contribution to such a theory.

What follows will be better understood if it is stated at once that the experiment here contemplated necessitates the measurement of a change in

¹ The author's preliminary report of this work appeared in *NATURE* 123, 797 (1929).

² Larmor, *Proc. Roy. Soc.* 71, 239 (1903).

temperature of the order of one hundred thousandth of a degree Centigrade in a space surrounded by a magnetizing current dissipating as much as four kilowatts of power.

B—APPARATUS

(a) **Material.** The magnetic material used in this research is a carbon steel commercially known as "drill rod."

The sample of drill rod which yielded the observations reported in *Nature*¹ contained 1.35% carbon. Fig. 1 is a microphotograph of this material; it shows tiny globules of cementite (Fe_3C) in a matrix of *almost* divorced pearlite.³

The material used in the present series of experiments contains 1.08% carbon. A microphotograph of a sample of this steel (Fig. 2) shows it to be an annealed mechanical mixture of cementite in a ferrite matrix. The coarse globules of cementite are characteristic of *completely* divorced pearlite.

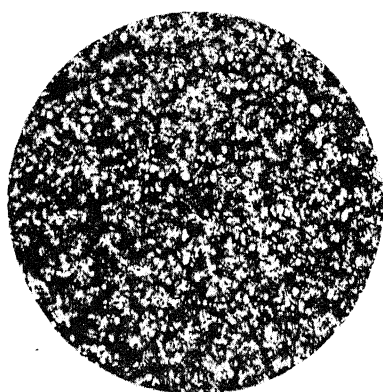


Fig. 1. Microphotograph of 1.35% carbon steel (500x).

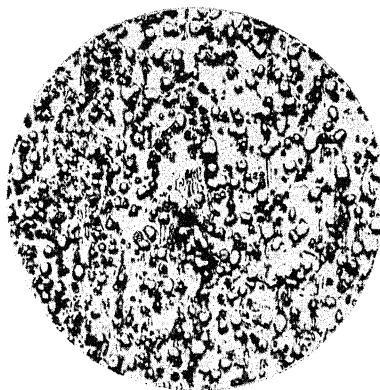


Fig. 2. Microphotograph of 1.08% carbon steel (500x).

(b) **The test specimen.** The test specimen consists of 104 bars of the 1.08% carbon steel 1 mm in diameter (drill rod size #57), selected for magnetic uniformity. These bars are mounted on the surfaces of seven concentric coaxial cylinders, the lengths of the bars in the several cylinders being so adjusted as to give the aggregate the form of an ellipsoid of revolution of major axis 60 cm and minor axis 3.4 cm. The frame for holding the bars consists of six hard rubber disks held together with brass rods.

Between the iron bars are mounted an equal number of copper bars of the same diameter and length. The function of these copper bars is described below.

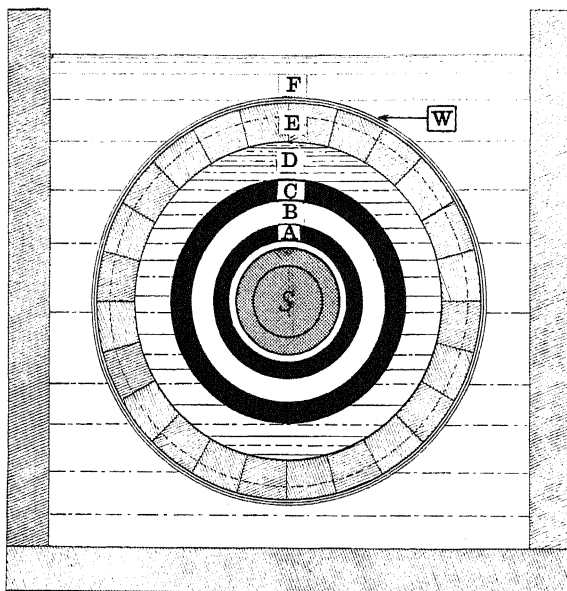
(c) **The calorimeter.** Fig. 3 shows a cross-section of the calorimeter in which the experiment was performed. The specimen *S* is imbedded in rice flour,⁴ and placed in an evacuated glass tube 5 cm in diameter about 1

³ Pearlite is a mechanical mixture of iron and iron carbide containing about 0.9% carbon.

⁴ International Critical Tables—Thermal Conductivities of Powders. Vol. II, p. 315. (The thermal insulation of rice flour plus a vacuum is here shown to be superior to the thermal insulation of a vacuum alone).

meter long, the inner surface of which is silvered and electrically grounded. The glass tube is surrounded by a hard rubber tube, *A*, an air space, *B*, and a second hard rubber tube, *C*. The wall thickness of the hard rubber tubes is approximately 1 cm. *E*, is a redwood cylinder, 1.8 cm thick, upon which the magnetizing solenoid, *W* is wound.

A centrifugal pump, delivering 1.5 liters per second, maintains a continuous circulation of water through the space *D* and an auxiliary tank not shown in the figure. The temperature of this water is controlled by means of a mercury-in-glass thermostat⁵ operating a 1000 watt incandescent light



SECTION OF CALORIMETER-SOLENOID.

Fig. 3.

bulb, both located in the tank. Water from the city mains at a temperature below 15°C is added continuously to the circulating water to compensate for evaporation and leakage, and for the heat from all other sources except the lamp. The fluctuations in temperature of the water in the space *D* under operating conditions have a maximum amplitude of 0.01°C with a period of 5 seconds.

A continuous flow of water, *F*, from the city mains surrounds the solenoid. This flow effectively removes most of the power dissipated in the coil, which may be as much as 4 kilowatts.

The calorimeter just described entirely eliminates thermal disturbances as a source of error in the measurements.

(d) **The solenoid.** The solenoid consists of two layers of #16 B and S gauge enamelled, double cotton covered copper wire. The insulation was

⁵ Eight-inch metastatic thermoregulator made by the American Instrument Company.

saturated with asphaltum paint as the coil was wound. The winding is 114 cm long and 19 cm in diameter. It is tapered at an angle of $1^{\circ} 16'$ for a distance of 27 cm at each end in order to secure greater uniformity of field.⁶ The magnetic field does not vary more than 1% over the space occupied by the specimen.

(e). **The thermocouple system.** Temperature changes of the 104 iron bars constituting the test specimen are measured by means of 102 thermo-

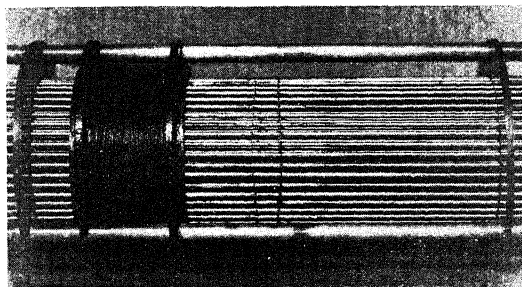


Fig. 4. Photograph of the assembly of rods and thermocouples.

couples in series. These thermocouples are constructed by connecting adjacent iron and copper bars alternately with short lengths of #40 copper and #34 constantan wire. These bits of wire are soldered to the bars with ordinary soft solder. The temperature of the copper bars, being comparatively unaffected by the magnetic field, thus affords a reference point from which to measure a change in temperature of the iron bars.

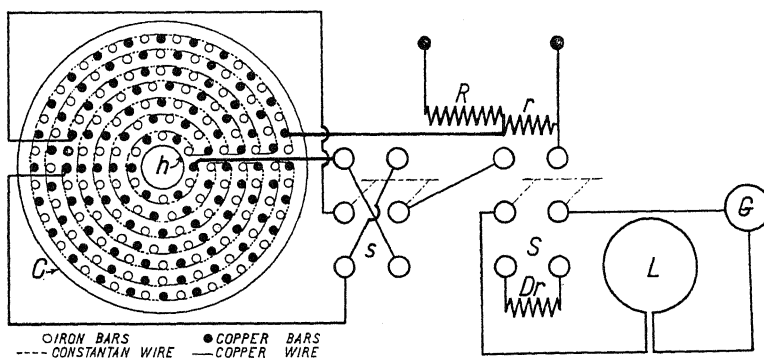


Fig. 5. Thermocouple circuits.

Fig. 4 shows the assembly of copper and iron rods in which the thermocouples may be seen to the right of the coil. This coil, which is displaced to the left in the photograph, is used in the magnetic measurements to be described later.

Fig. 5 is a diagram of the thermocouple and galvanometer circuits. The thermocouples are connected in series so as to form two groups of 51 couples

⁶ L. Houllévigie, J. de Phys. [3] 7, 466-468 (1898).

each, which groups may, in turn, be connected either in series aiding or in opposition by means of switch *s*. Switch *S* connects the galvanometer to the thermocouples or to an equal non-inductive resistance *Dr* which serves as a dummy. Resistances *R* (400000 ohms) and *r* (0.400 ohms) constitute the calibrating potentiometer. The resistances *r*, *R*, *Dr*, and the switches *s* and *S*⁷ are placed in a wooden box covered with heavy felt. The switches are operated at a distance by piano wires passing through holes in the sides of the box. In series with the galvanometer, *G*, is a single turn of wire, *L*, 10 cm in diameter, so placed as to compensate entirely the inductive effect of the lead wires.

The galvanometer is a Leeds and Northrup d'Arsonval type HS 2285x with a critical damping resistance of 12 ohms, a period of 10 seconds and a sensitivity of 103 mm per microvolt at a scale distance of 6 meters. It is mounted in a box filled with cotton batting on a specially constructed suspension which reduces the effects of vibration to a satisfactory minimum. The metal platform of the suspension is grounded.

Since thermal disturbances are completely eliminated as a source of error, the accuracy of the thermal measurements is limited solely by the magnitude of the variation of the parasitic electromotive forces in the galvanometer circuit. With the precautions mentioned above the maximum variation in the parasitic electromotive forces over a period of 3 hours is 0.1 microvolt. This appears in the form of a slow drift in the galvanometer zero, amounting in all to 10 mm under operating conditions. Since the time required to complete a single observation is not more than 5 minutes the error due to this source is negligible. Accordingly the accuracy of the method is equal to its sensitivity, and permits the detection of a change in temperature of the iron of 2.26×10^{-6} degrees Centigrade.

C—METHOD OF MEASUREMENT

(a) **Magnetic.** The specification of the magnetic state of the iron involves the determination of the relation between the magnetic field intensity, *H*, and the intensity of magnetization, *J*. Because of the ellipsoidal form of the specimen the magnetic field intensity in the iron bars is the same as that in the interspace between them. This quantity is measured directly by means of a ballistic galvanometer and a small calibrated solenoid (*h*, Fig. 5) of 1041 turns placed axially at the center of the ellipsoid. The intensity of magnetization can then be calculated if the total magnetic flux through the ellipsoid is known. This quantity is likewise measured ballistically, with the aid of a 48 turn coil (*C*, Fig. 5) of known area wound around the ellipsoid at its center. The change in intensity of magnetization in the iron can now be obtained as follows:

Let

ΔH = change in the magnetic field intensity as measured above,

ΔF = change in the total flux through the coil *C*,

⁷ Walter P. White, Journ. Amer. Chem. Soc. 33, 1856 (1914), also Journ. Amer. Chem. Soc. 33, 2296 (1914).

ΔB = change in the magnetic flux density *in* the iron,

A = total cross sectional area of coil C ,

a = cross sectional area of the 104 iron bars.

$$A' = A - a$$

Then

$$\begin{aligned}\Delta F &= \Delta B a + \Delta H A' \\ &= \Delta(H + 4\pi J)a + \Delta H(A - a) \\ &= \Delta H A + 4\pi a \Delta J;\end{aligned}$$

Hence

$$\Delta J = (\Delta F - \Delta H A) / 4\pi a$$

The independent variable in the magnetic measurements is actually the magnetizing current, I . A specially constructed rheostat permits the variation of this current in steps of any desired magnitude by opening or closing knife switches. The values of J and H corresponding to specified values of the magnetizing current are now determined as follows: (1) The iron is first placed in a suitable cyclic state by repeated reversals of the magnetizing current. (2) The subsequent magnetic state of the iron is then varied in steps in any desired manner. (3) Corresponding $J-H$ curves are constructed by summing the successive increments in these quantities, obtained in the manner described above.

All the magnetic paths whose thermal relations are here investigated start at some point on a hysteresis loop. It is, therefore, important to determine these loops as precisely as possible. Errors intrinsic to the step by step summation method can be detected by reducing the number of steps to one. This gives an overall check on the end points. The absolute values of J are calculated from its maximum value. The latter is assumed to be $\frac{1}{2}$ the observed change in J in passing in a single step from one tip of the hysteresis loop to the other. The absolute values of H are calculated from its value when $J=0$, i.e. from the coercive force. When $J=0$, H is simply the magnetic field intensity of the solenoid alone. The corresponding solenoid current is obtained graphically by plotting J against the current. The value of H when $J=0$ is then calculated from the current and the constant of the solenoid.

(b) **Thermal.** As stated above, the object of this research is to measure the changes in temperature of the iron which accompany changes in H and J , produced and evaluated in the manner just described. It is assumed that this temperature change occurs simultaneously with the change in magnetization. Immediately thereafter the induced change in temperature decays logarithmically⁸ due to radiation and to conduction through the rice flour and across the thermocouple wires. The experimental procedure for obtaining the initial value of this quantity is as follows:

1. The thermocouple galvanometer is switched from the dummy resistance to the thermocouples and the deflection noted. This deflection of

⁸ The average thermal time constant is 32 seconds.

about 10 mm is due to the constant parasitic e.m.f.'s in the switches and the thermocouple leads. It is taken as the zero in reckoning subsequent deflections. The small value and the constancy of this quantity indicate establishment of thermal equilibrium in the calorimeter.

2. The galvanometer is switched back to the dummy resistance.
3. At time $t=0$ the desired change in magnetizing current is effected.
4. Immediately thereafter the galvanometer is switched from the dummy resistance to the thermocouples.
5. At $t=10$ seconds the galvanometer deflection is noted. It is again noted at $t=20$ seconds.

6. These galvanometer deflections are directly proportional to the corresponding thermal *emf*'s. ($1\text{ mm}=0.01\text{ microvolt}=2.26\times 10^{-6}^{\circ}\text{C.}$) The *emf* corresponding to the temperature at time $t=0$ is obtained by extrapolation.

7. At the end of 5 minutes thermal equilibrium is reestablished and the operations 1 to 6 are repeated for a new change in magnetizing current. The magnetic path under investigation is thus traversed in successive steps of appropriate magnitude.

8. Curves showing the relation between temperature and magnetic field intensity for the complete magnetic process are constructed by summing the increments in temperature obtained in this manner. It is to be noted that a cooling of the iron is indicated by a galvanometer deflection in the opposite direction to that which indicates heating.

D. EXPERIMENTAL RESULTS

(a). **Thermal relations.** The observed magneto-thermal relations are exhibited graphically in Figs. 6 to 12. As has been stated, the iron is placed in a cyclic state by a dozen reversals prior to each experiment, and is left in the condition of maximum magnetization for the cycle. In the figures the entire hysteresis loop of the cycle is shown by a curve in part solid and in part dotted. The solid curve shows the magnetic path actually traversed in the experiment. The direction of traversal is indicated by arrows and the starting point by a dot. The solid curve upon which the observations are plotted gives the relation between the total temperature change and the magnetic field intensity, as the path is traversed. This curve is constructed in the manner described in paragraph 8 of the preceding section. The temperature change indicated by an ordinate of this curve is the total change in temperature which would have resulted if no heat had been lost in the process of measurement. The temperature corresponding to the zero ordinate is 18°C and is the same for all curves.⁹

⁹ The cooling observed at the upper end of the thermal curve of Fig. 6 was not revealed by the preliminary experiments reported in *Nature*, owing to outstanding parasitics and low sensitivity. Since these experiments were performed, the short period parasitics have been practically eliminated, and the galvanometer sensitivity has been doubled. A reexamination of this specimen, which contained 1.35% carbon, showed a cooling at the upper end of the thermal curve of approximately the same amount as that observed in the neighborhood of $H=0$, i.e., the curve is qualitatively the same as Fig. 6, the cooling effects being smaller.

Fig. 12 gives a plot of the data obtained for the so called "virgin curve" of magnetization. The iron was demagnetized by means of a 60 cycle alternating magnetic field of diminishing amplitude and also by the method of repeated reversals with identical results.

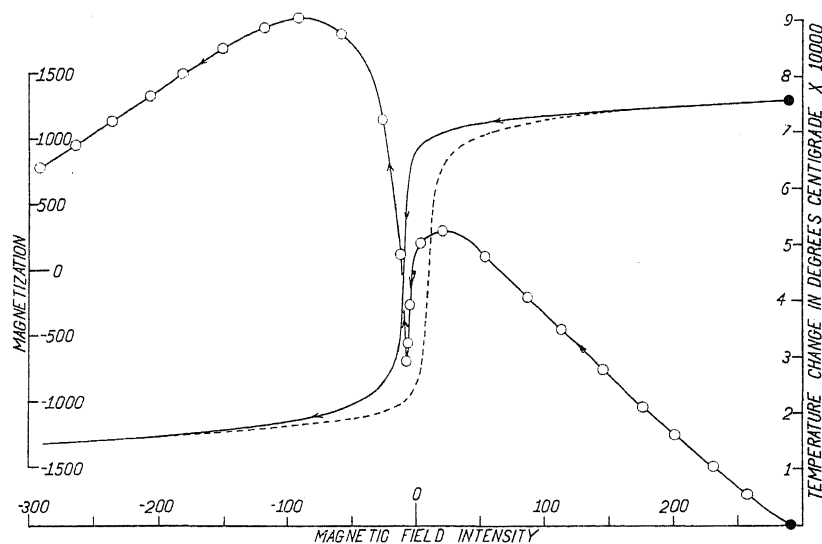


Fig. 6. The magneto-thermal relations associated with the largest hysteresis loop.

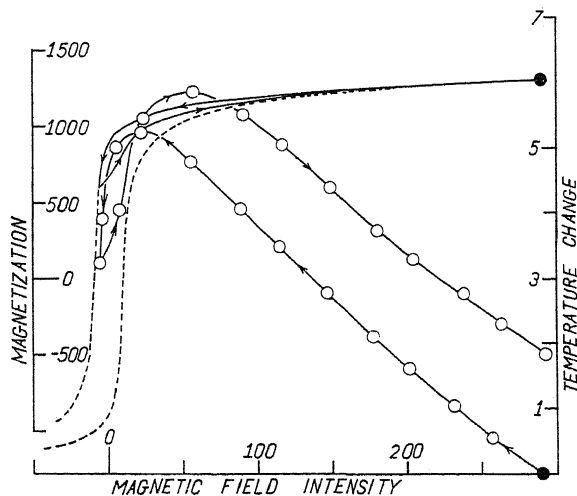


Fig. 7. The magneto-thermal relations associated with an asymmetric loop formed between $H = 290$ gauss, and zero impressed field.

Table I contains the experimental data for the curves of Fig. 6, and illustrates the way in which the curves are constructed. In this table the observed change in temperature is given in millimeters deflection of the

galvanometer. The calibration constant of the galvanometer thermocouple system is 2.26×10^{-6} degrees C per mm deflection.

TABLE I. Data for curve of Figure 6.

Step	Field Current (Amps.)	ΔH	ΔI	Observed ΔT in mm	H gauss	J	Total Change Temp. (mm)
Start	35.1				284	1316	0.0
1	32.0	-27.3	-14.1	19.5	257	1302	19.5
2	28.8	-26.3	-15.0	21.3	231	1287	40.8
3	25.3	-29.8	-18.1	24.2	201	1269	65.0
4	22.5	-23.9	-16.3	21.3	177	1252	86.3
5	18.9	-31.1	-23.4	28.8	146	1229	115.1
6	15.0	-32.3	-29.1	30.5	114	1200	145.6
7	11.8	-26.4	-19.3	24.5	87.7	1181	170.1
8	7.94	-33.3	-46.8	31.0	54.4	1134	201.1
9	4.01	-32.8	-79.4	19.3	21.6	1054	220.4
10	1.91	-17.0	-100.9	-9.8	4.6	953	210.6
11	0.50	-9.2	-206.0	-47.0	-4.6	747	163.6
12	0.00	-2.0	-150.4	-29.0	-6.6	597	134.6
13	-0.50	-1.2	-234.0	-15.0	-7.8	363	119.6
14	-1.90	-3.8	-790.0	82.5	-11.6	-427	202.1
15	-4.01	-13.3	-406.0	103.3	-24.9	-833	305.4
16	-7.97	-31.4	-216.7	65.5	-56.3	-1050	370.9
17	-11.95	-33.3	-88.0	11.8	-89.6	-1138	382.7
18	-15.1	-26.6	-42.7	-7.5	-116.0	-1181	375.2
19	-18.9	-32.8	-39.1	-16.0	-149	-1220	359.2
20	-22.7	-31.8	-29.4	-19.5	-180	-1249	339.7
21	-25.6	-24.4	-19.2	-16.8	-205	-1268	322.9
22	-28.7	-30.8	-15.2	-19.3	-235	-1283	303.6
23	-32.2	-27.4	-17.2	-18.0	-263	-1300	285.6
24	-35.3	-28.4	-15.1	-17.2	-291	-1316	268.4
					± 9.6	0	

Tables II to VI contain the data from which were plotted the curves of Figs. 5 to 11 respectively.

TABLE II. Data for curves of Figure 7.

Step	Field Current I (Amps.)	ΔH	ΔJ	Observed ΔT in mm	H	J	Total change in T (mm)
Steps 1 to 12 are the same as in Table I.							
13	1.9	13.2	219	35	6.6	766	169.6
14	4.0	15.4	196	60	22.0	962	230
15	7.9	33.4	130	18	55.4	1092	248
16	11.9	33.4	62	-15	88.8	1154	233
17	15.1	26.2	34	-20	115.0	1188	213
18	18.9	32.5	34	-28	147.5	1222	185
19	22.7	31.7	26	-28	179.2	1248	157
20	25.5	24.2	18	-19	203.4	1266	138
21	29.1	32.3	18	-23	235.7	1284	115
22	32.3	27.5	16	-20	263.2	1302	95
23	35.3	29.3	14	-20	292.5	1316	75

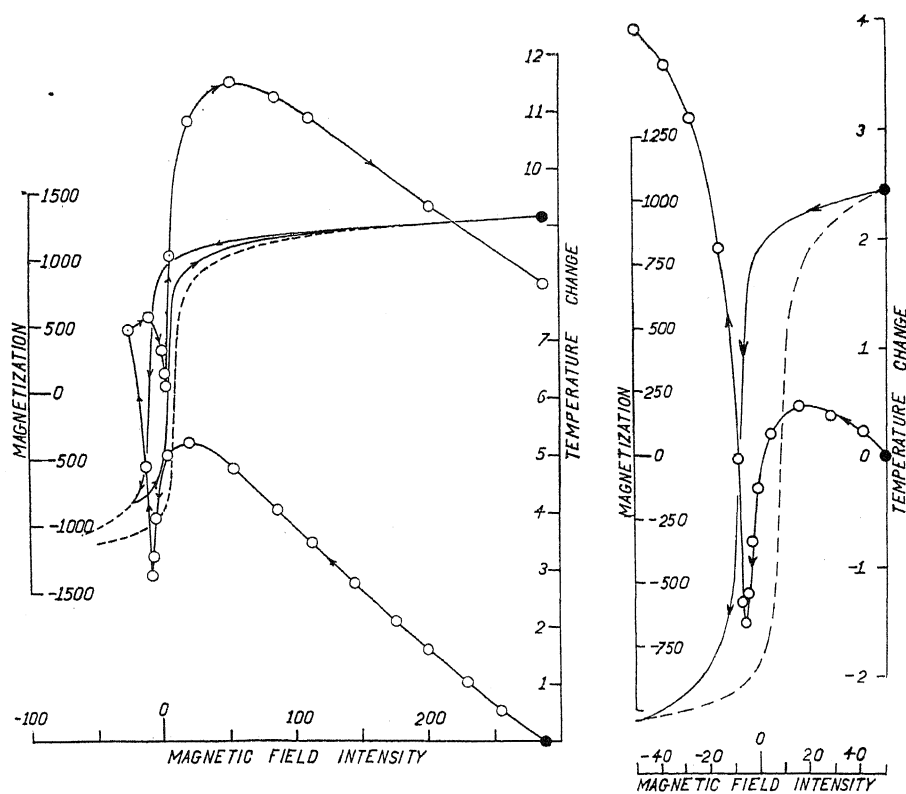


Fig. 8. The magneto-thermal relations associated with an asymmetric hysteresis loop formed between $H = -25$ and $H = 290$ gauss.

Fig. 9. The magneto-thermal relations associated with the medium sized hysteresis loop.

TABLE III. Data for curves of Figure 8.

Step	Field Current I (Amps.)	ΔH	ΔJ	Observed ΔT in mm	H	J	Total change in T (mm)
Steps 1 to 15 are the same as in Table I.							
16	-1.9	15.8	88.1	10	-9.2	-737	315
17	-0.5	9.4	182	-25.5	0.2	-555	290
18	-0.0	1.8	137	-17.5	2.1	-418	272
19	0.5	1.1	223	-9.5	3.2	-195	263
20	1.9	3.6	794	98.5	6.8	599	361
21	4.0	13.8	336	99.5	20.6	935	461
22	8.0	32.5	149	30.0	53.1	1084	491
23	12.0	33.7	65	-11.5	86.5	1149	479
24	15.1	26.2	35	-16.0	112.9	1184	463
25	25.9	90.7	81	-65.5	203.7	1265	398
26	36.1	89.5	51	-59.5	293.2	1316	338

TABLE IV. Data for curves of Figure 9.

Step	Field Current (Amps.)	ΔH	ΔJ	Observed ΔT in mm	H	J	Total change in T
Start	7.21				49	1044	0.0
1	5.87	-11.2	-23.3	10.0	39.7	1021	10.0
2	4.56	-10.9	-28.0	6.0	26.8	993	16.0
3	3.08	-12.5	-46.9	3.5	14.3	946	19.5
4	1.62	-11.0	-85.4	-11.0	3.3	860	8.5
5	0.83	-5.1	-116.2	-21.5	-1.8	744	-13.0
6	0.39	-2.2	-96.8	-21.0	-4.0	648	-34.0
7	0.00	-1.5	-129.7	-20.5	-5.5	518	-54.5
8	-0.39	-1.1	-184.0	-11.5	-6.6	334	-66.0
9	-0.83	-0.9	-262.0	8.0	-7.7	72	-58.0
10	-1.62	-2.2	-445.0	56.5	-9.9	-373	-1.5
11	-3.08	-7.8	-394.0	83.0	-17.7	-767	81.5
12	-4.58	-11.5	-158.0	51.0	-28.8	-925	139.5
13	-5.90	-10.4	-73.4	21.0	-39.2	-998	153.5
14	-7.25	-11.0	-45.9	14.0	-50.2	-1044	167.5
					± 8.1	0	

TABLE V. Data for curves of Figure 10.

Step	Field Current (Amps.)	ΔH	ΔJ	Observed ΔT in mm.	H	J	Total change in T
Start	3.80				21.1	857	0.0
1	3.50	-2.5	-9.4	2.0	18.5	847	2.0
2	3.05	-3.6	-15.9	3.0	14.9	831	5.0
3	2.78	-2.2	-10.9	1.0	12.7	820	6.0
4	2.42	-2.8	-16.5	1.0	9.9	804	7.0
5	2.02	-3.0	-21.7	0.0	6.9	782	7.0
6	1.63	-2.9	-29.4	-3.0	4.0	753	4.0
7	1.23	-2.7	-39.3	-5.0	1.3	714	-1.0
8	0.83	-2.4	-57.6	-9.0	-1.1	656	-10.0
9	0.39	-2.4	-95.0	-17.0	-3.5	561	-27.0
10	0.10	-1.3	-90.6	-14.0	-4.8	470	-41.0
11	0.00	-0.4	-34.1	-3.5	-5.2	436	-44.5
12	-0.10	-0.3	-36.6	-3.5	-5.5	399	-48.0
13	-0.39	-0.8	-144.1	-5.0	-6.3	255	-53.0
14	-0.83	-0.8	-260.0	+10.0	-7.1	-4	-43.0
15	-1.24	-1.0	-235.5	22.5	-8.1	-240	-20.5
16	-1.63	-1.3	-194.1	29.0	-9.4	-434	8.5
17	-2.03	-1.9	-142.7	30.0	-11.3	-577	38.5
18	-2.42	-2.2	-96.4	26.5	-13.5	-673	65.0
19	-2.81	-2.3	-63.9	18.0	-15.7	-737	83.0
20	-3.07	-1.8	-38.4	14.0	-17.6	-775	97.0
21	-3.51	-3.3	-52.0	17.0	-20.9	-827	114.0
22	-3.81	-2.2	-29.3	9.5	-23.1	-857	123.5

TABLE VI. Data for curves of Figure 11.

Step	Field Current (Amps.)	ΔH	ΔJ	Observed ΔT in mm.	H	J	Total change in T
Steps	1 to 11 are the same as in Table V						
12	0.40	-2.8	-25.4	1	-1.8	461	-43.5
13	0.84	-3.1	-26.2	3.5	1.3	487	-40.0
14	1.64	-5.5	-87.6	14.0	6.8	575	-26.0
15	2.80	-7.8	-139.5	32.5	14.6	715	6.5
16	3.82	-7.7	-83.3	23.0	22.3	798	29.5

The three magnetic cycles which were investigated are shown together in Fig. 13. The results obtained are indicated roughly by the broken lines

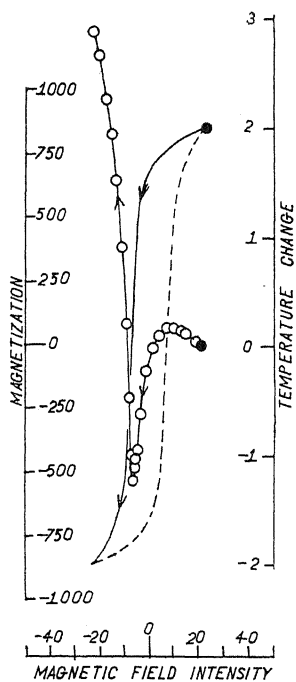


Fig. 10. The magneto-thermal relations associated with the smallest hysteresis loop studied.

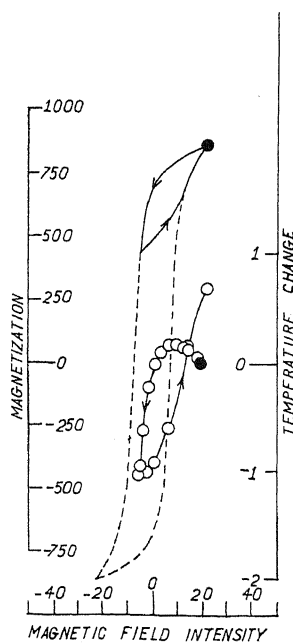


Fig. 11. The magneto-thermal relations associated with an asymmetric loop formed between $H = 22$ gauss, and zero impressed field.

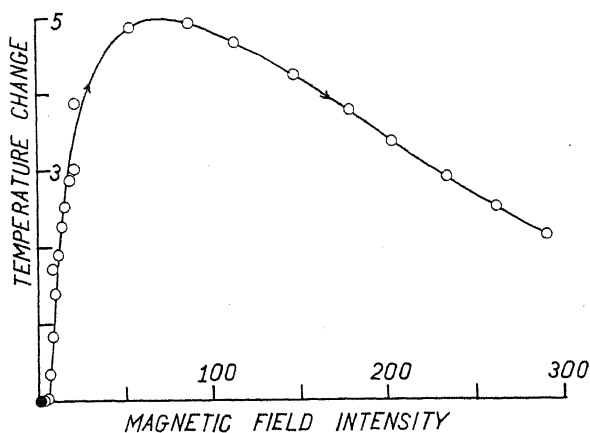


Fig. 12. The magneto-thermal phenomena of the "virgin curve."

L and L' . The intersection of these lines with the loops correspond to the successive maxima and minima of the *temperature-magnetic field intensity*

curves. If one is traversing *any* magnetic path in the direction of decreasing magnetic field intensity, and if one views the line L in the direction indicated by the arrow, then cooling is observed along those portions of the path which lie to the right of the line and heating along those portions which lie to the left. In traversing *any* magnetic path in the direction of increasing magnetic field intensity, the line L' is to be used in exactly the same way.

(c). **Energy.** In order to convert temperature changes as indicated by galvanometer deflections into heat developed in ergs it is necessary to know the following quantities:

1. The galvanometer calibration constant,
2. The thermoelectric power of the copper constantan couple,
3. The specific heat and the density of the iron,
4. The effect of the solder and the thermocouples upon the thermal capacity of the iron.

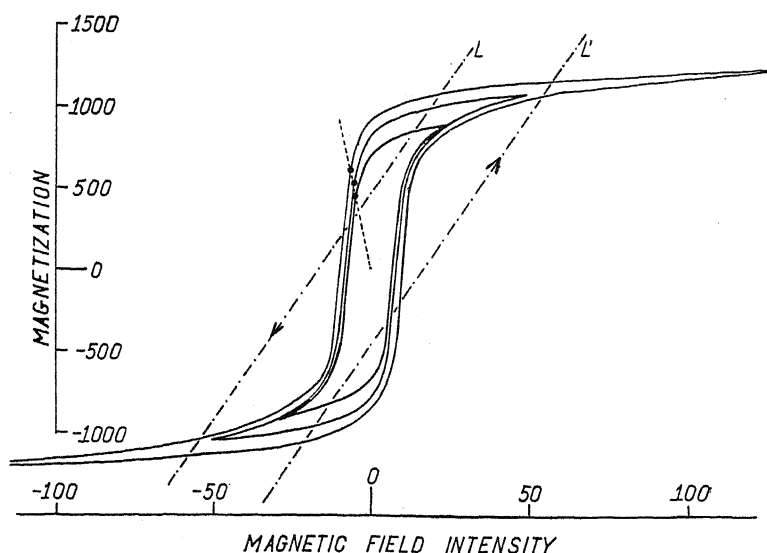


Fig. 13. Summary of observations on hysteresis heats.

The galvanometer calibration constant was obtained by means of the potentiometer heretofore described. It is 103 mm per microvolt.

The thermoelectric power of a couple composed of the wires used in this experiment was carefully measured. For a single couple it is 41.75 microvolts per degree C.

The value which is here adopted for the specific heat of the steel used in this research is 0.116 gm calories per °C.¹⁰ This quantity was not measured. The measured density of the steel used is 7.75 g/cc.

¹⁰ The International Critical Tables page 118, Vol. V, give the specific heat of steel in terms of the temperature and the carbon content. Between 0 and 100° C the specific heat in joules per gram is $0.4661 + 0.0184 \times (\% \text{ carbon})$. Taking 4.18 joules per calorie the specific heat for 1.08% carbon steel is 0.116 which is the value used here. Other authorities give values ranging from 0.098 to 0.118 but are not explicit as to the kind of steel described.

The thermal capacity of the solder and thermocouple wires is assumed to be that of a sheath of solder 0.005 cm thick surrounding each bar. This introduces an additive correction of 3% to the calculated energies. The temperatures given in the Tables I to VII have not been corrected for the effect of the solder.

The results of the energy calculations are presented in the following table.

The iron, being initially in a cyclic state, is carried through a half cycle of magnetization by diminishing H in successive steps of varying magnitude. Column 2 of Table VIII gives the number of such steps and therefore an indication of the manner of performance of the half cycle. Column 3 con-

TABLE VIII.

Cycle	No. steps per half cycle	Heat developed per half cycle (ergs)	
		from thermal obs.	from hysteresis loop
Largest	1	28 800	29 000
	2	27 750	
	4	27 150	
	14	23 300	
	24	23 400	
Medium	1	15 300	17 000
	14	14 600	
Small	1	9 950	11 500
	22	10 800	

tains the observed total heats developed, corrected for the effect of the solder. Column 4 gives the half area of the three hysteresis loops expressed in ergs.

Too much significance should not be attached to a comparison of the energy values given in columns 3 and 4. The combined cumulative error inherent in both the magnetic and thermal measurements must be expected to appear in such a comparison. However, the interesting result here definitely exhibited, is the fact that the heat developed in the large cycle of magnetization depends upon the manner in which the cycle is performed.

It appears that in a cycle of magnetization which saturates, or nearly saturates, the iron the heat developed during a slow traversal of the cycle is appreciably less than that given by the area of the hysteresis loop, though the latter also represents magnetic data taken during a slow traversal.

If one views the possibility of the storage of energy in the iron in the form of magnetostrictive strain as well as in the form of heat, then one is lead to the conclusion that a slow cycle of magnetization which leaves the iron in the same magnetic state should, for the case under review, leave the iron with a permanent or semi-permanent elongation. This effect should be absent if the cycle be traversed rapidly. This phenomena has been observed elsewhere¹¹ and is now the subject of further investigation in this laboratory.

¹¹ S. R. Williams, Phys. Rev. 34, 258 (1912), also see Ewing, 1st. Ed. p. 74 also p. 327.

E. SOURCES OF ERROR AND PRECISION OF MEASUREMENT

(a). **Magnetic measurements.** The uncertainty in the absolute value of H varies for the different magnetic paths but in no case amounts to more than 3%. As regards J , the larger paths could be repeated to 1% while for the smaller paths the uncertainty may be as large as 5%. In general the reproducibility of the magnetic data indicates a precision of 5% or better in the determination of ΔH and ΔJ .

The uniformity of the magnetic field throughout the test specimen is examined as follows:—The inner group of 51 thermocouples is connected in series opposing the outer group of 51 thermocouples, and the magnetization is reversed from maximum to maximum producing a deflection of 7 mm. If the 102 thermocouples had been connected in series aiding, the heat developed by the process would have produced a galvanometer deflection of 330 mm. The observed deflection of 7 mm indicates that the magnetic field is uniform to 2% over the cross-section of the ellipsoid.

A further check on the magnetic behavior of the aggregate of bars is obtained as follows:—Consider a typical H - J hysteresis loop. If now a line be drawn through the origin and through the point on the loop corresponding to the zero value of magnetizing current in the solenoid, (e. g. the dotted line in Fig. 13), then the tangent of the angle between this line and the J axis is the so called "demagnetizing factor" of the specimen. This follows immediately on setting $H_0 = 0$ in the expression

$$H = H_0 - NJ,$$

in which, H_0 = the field of the magnetizing current, and N = demagnetization factor or form factor. Values of N for the ellipsoid determined in this manner from the three hysteresis loops agree to 5% and exhibit no systematic variation.

(b). **Thermal measurements.** Since the thermal measurements may be repeated to the limit of accuracy stated above, any sources of error appearing therein must be systematic. Sources of systematic error considered are the following:

1. The radiation correction,
2. Eddy currents,
3. Time lag in magnetization,
4. Effect of magnetic field on the thermoelectric power.

1. *Radiation correction.* The logarithmic decay of the thermocouple *emf* is slightly different for each observation. This is due to a change in temperature of the rice flour environment of the iron bars, and a change in temperature of the copper bars, resulting from preceding operations. As has been stated, the extrapolation to zero time is performed for every observation. The validity of the method of extrapolation is established over the experimental range of the temperature changes both for heating and cooling in the following manner:

An *emf* equal and opposite to the sum of the extrapolated *emf* and the steady switch parasitic *emf* is inserted in the thermocouple circuit by means of the potentiometer R, r , of Fig. 5. The desired temperature change is then effected and the galvanometer is immediately connected to the thermocouple potentiometer circuit. The correctness of the extrapolated thermal *emf* is indicated by an initial zero galvanometer deflection.

2. *Eddy currents.* An estimate of the eddy current loss in the cylindrical bars may be obtained from the following formula,¹²

$$Q = (\Delta B)^2 \times \frac{\lambda R^2}{8t},$$

in which Q = heat per unit volume in ergs, R = radius of a single bar, λ = electrical conductivity of the material, t = time required to establish the change ΔB , and $\Delta B = \Delta H + 4\pi\Delta J$.

In the derivation of this formula it is assumed that ΔB varies linearly with ΔH and that ΔH varies linearly with the time. An oscillogram of the increasing current in the solenoid indicates that t is of the order of 0.01 second, assuming that H and J follow in time the impressed magnetizing field. It follows that the heat due to eddy currents in the iron is a negligible factor in this experiment. The same applies to the heat due to eddy currents in the copper bars except on those portions of the hysteresis loop over which the change in J is smaller than the corresponding change in H . There calculation shows that the eddy current heat in the copper may be of the same order of magnitude as that in the iron, though not of the same order as the cooling actually observed. The following experiment proves that there is no measurable difference between the eddy current heat developed in the copper and the iron in this portion of the loop. A reduction of the field from +290 to +150 gauss causes a heating of the iron, while an increase of the field from +150 to +290 gauss produces an equal cooling. Thus, if this loop be traversed very rapidly there is no net change in temperature of the iron. The fact that one side of this loop is thermally equal and opposite in sign from the other side shows that in this region the effects of eddy currents are quite inappreciable.

3. *Time lag in magnetization.* It will be observed on reference to Fig. 5 that the flux from 59 iron bars links the thermocouple circuit. Accordingly any time lag in magnetization would induce uncompensated electromotive forces in this circuit after the galvanometer is connected therein. The absence of any such effect is established by connecting the 48 turn coil to a highly sensitive ballistic galvanometer immediately after the reversal of the maximum magnetizing field. No deflection is observed.

4. *Effect of magnetic field on thermoelectric power.* The thermoelectric power of a couple composed of the wires used in this experiment was found to be unaffected by a strong magnetic field.

¹² U. Adelsberger, Ann. d. Physik [4] 83, 199 (1927).

¹³ U. Adelsberger, Ann. d. Physik [4] 83, 184 (1927).

F. REMARKS

The problem of the present paper has recently been attacked by Adelsberger,¹³ F. W. Constant,¹⁴ and Honda, Okubo, and Hirone.¹⁵ The several experimental methods devised by these investigators were not so elaborate as the present method. None of them report any of the cooling effects characteristic of the curves submitted above. Adelsberger worked with tungsten steel and a special Krupp steel and Constant with K. S. magnet steel. Since it is not definitely known that the cooling takes place in any other material than carbon steel of the sort used in this experiment, Honda's results for carbon steel are the only ones which offer any definite basis for comparison. The sensitivity of Honda's apparatus, as given by Table II of this paper, was 14.5 mm per 100,000 ergs of heat developed, which is to be compared with 1150 mm per 100,000 ergs for the present method. This, together with the method of observation adopted by Honda and his collaborators, may account for their failure to observe the cooling effects. However, since Honda's steel contained only 0.2% carbon, and since the cooling effects noted in our 1.08% carbon steel differ markedly in magnitude from those in our 1.35% carbon steel, the evidence is not conclusive that the cooling effects are a general property of steels. Further experiments bearing on this point are now in progress.

In conclusion I wish to acknowledge my indebtedness to those without whose cooperation this work could not have been accomplished; in particular to Dr. William Campbell who made the microphotographic analysis and to Dr. Harold Fales who made the chemical analysis of the steels; to Dr. Walter P. White for advice on the thermocouple assembly and manipulation; and to Dr. S. L. Quimby who suggested the problem and followed its progress with helpful counsel and encouragement.

¹⁴ F. W. Constant, *Phys. Rev.* **32**, 486 (1928).

¹⁵ Honda, Okubo, and Hirone, *Sci. Rep. of the Tohoku Imp. Univ.* [I] **18**, 409 (1929).

A NEW METHOD OF MEASURING THE VARIATION OF THE SPECIFIC HEATS (c_p) OF GASES WITH PRESSURE

By E. J. WORKMAN

UNIVERSITY OF VIRGINIA

(Received August 7, 1930)

ABSTRACT

A method is described whereby the ratio of c_p at a high pressure to c_p for the same gas at a pressure of one atmosphere taken as a standard is determined. The continuous flow principle is used in such a way that the necessity for measuring gas flow and heat input is avoided. A stream of gas at high pressure is brought to a temperature t_1 and passed through a heat interchanger acquiring there a temperature t_2 , after which it is throttled to atmospheric pressure, brought to a temperature t_3 and returned to the heat interchanger, where its temperature again becomes t_2 . The ratio of c_p at a high pressure to that at atmospheric pressure is equal then to $(t_3 - t_2)/(t_2 - t_1)$ plus certain small corrections. Measurements on commercial oxygen taken at a mean temperature of 26° C and pressures ranging from 15 to 100 atmospheres indicate a pressure coefficient of this ratio of 0.00165 ± 0.00005 per atmosphere.

IN CONSIDERATION of the need for further data on the specific heats of gases the present work was undertaken with the object of developing a method of determining the variation of c_p with pressure for a number of gases over a large range of pressure and temperature. Air^{1,2} and ammonia³ are the only gases on which direct measurements on c_p have been made over a considerable range of pressure. Indirect determinations follow from data on the Joule-Thomson effect. Here we note the work of Burnett⁴ on CO₂ and Roebuck⁵ on air. Recently Beattie⁶ and Bridgeman⁷ using the Beattie-Bridgeman equation of state have calculated c_p as a function of pressure and temperature for air and ammonia.*

The method of measurement to be described in this paper is of value because of its simplicity and the fact that the usual calorimetric errors are easily detected and in most cases eliminated. It possesses the advantage of avoiding the measurement of quantities of matter and of energy. On the other hand relative values only are determined.

A schematic arrangement of the apparatus is shown in Fig. 1. B and B' are constant temperature baths and I is a heat interchanger. The gas at high

¹ Lussana, Nuov. Cim. 1894 to 1908.

² Holborn and Jacob, Berl. Ber. 1, 213 (1914); also Zeit. Inst. 31, 116 (1911).

³ Osborne, Stimson, Sligh and Cragoe, Sci. Papers Bureau of Standards 20, 65 (1924).

⁴ Burnett, Phys. Rev. 22, 590 (1923).

⁵ Roebuck, Proc. Amer. Acad. Arts and Sciences 60, 537 (1925).

⁶ Beattie, Phys. Rev. 34, 1615, (1929).

⁷ Bridgeman, Phys. Rev. 34, 527, (1929).

* For a review of the earlier work on this subject, see Partington and Shilling, "Specific Heats of Gases," London, 1924.

pressure passes through the tube *a* in the bath *B* where it comes to a fixed temperature. It then passes through the interchanger where its temperatures on entering and leaving are measured. After leaving the interchanger the pressure is reduced almost to one atmosphere by the reduction valve *V*. It now passes through a second constant temperature bath *B'*, back through the interchanger, and escapes. The temperatures at entrance and exit are measured as before.

The interchanger is so constructed that the two gas streams, after passing through a region where their entrance temperature are measured, are brought into such intimate thermal contact that they leave the interchanger at approximately the same temperature.

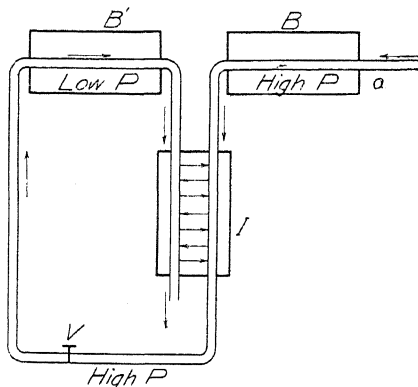


Fig. 1. Schematic arrangement of apparatus.

If there is no net passage of heat from the interchanger to the surroundings, then the amount of heat gained by one stream is equal to that lost by the other. Further, since these streams are equal, it follows that the ratio of the two specific heats are inversely as the temperature changes in their respective lines; i.e. $(c_p)/(c_p)_0 = (t_3 - t_2)/(t_2 - t_1)$ †. Methods of applying small corrections to values thus obtained will be discussed later.

During the course of this work three different types of interchangers were constructed and used. The third and best will be described in detail. Fig. 2 shows a sectional drawing of the third interchanger. For convenience it is made schematic to the extent that only one gas line (low pressure) is shown entering and leaving. Except for a smaller diameter and a greater wall thickness the construction of the high pressure line where it enters and leaves is the same. In general the heavy lines represent polished copper and the light lines German silver, thinly copper-plated. The low pressure gas enters at *a* from the bath, its line of flow being protected by the heavy copper shield *S*₁ which is thermally coupled to the bath and the tube *a* within the bath.

† Recently attention has been directed to the work of Callendar (Roy. Soc. Phil. Trans. 212, 1 (1912) and of Romberg Amer. Acad. Proc. 57, 377-387 (1912) where the variation with temperature of the specific heat of water was determined by a similar method of flow calorimetry.

At *b* the gas is stirred by a small tuft of steel wool and passes along the thermometer tube *c* where it is further stirred in its path by small fins soldered to *c* (not shown).

At *d* the gas passes out through a copper tube which bends back sharply (not shown in drawing) and passes to *e* along the length of the shield *S*₂, to which it is soldered for thermal contact. The section *gg'* is interposed between the thermometer cell and the point *g* beyond which interchange begins, in order to minimize errors arising from heat conduction. Both this section and the corresponding section *uu'* of the high pressure line pass parallel to each other in a dead air space bounded by the tube *f*.

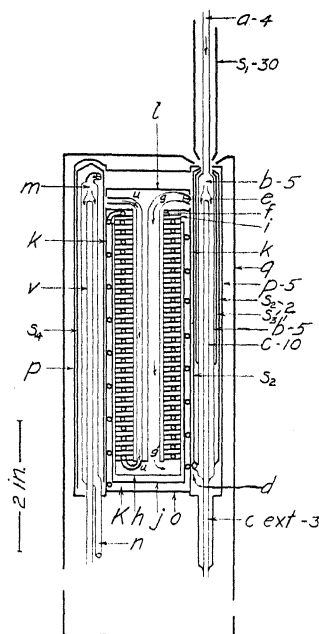


Fig. 2. Sectional drawing of interchanger. Copper in heavy lines, German silver in light lines. Letters refer to text; numbers indicate thickness of the walls in thousandths of an inch.

About the tube *f* are two thin copper ribbons wound helically and spaced as shown. To these are tin soldered the high pressure line shown by the small circles. Fitting snugly over this helical ribbon is a cylinder *h* closed at lower end. The two gas streams are therefore constrained to spiral around an axis (twenty-four times) in passing from *g'* to *i*, both being closely coupled thermally.

The cylinder *h* above referred to has a double wall, the outside of which *j* is of copper with an intervening dead air space. The high pressure line is wound on the outside of the cup as shown, soldered in place, and closed over with a thin copper cylinder *k* which makes a tight enclosure and extends across the upper end to provide the shield *l*. The two gas streams flow around seven or eight times before reaching the end chamber *K*. From *k* the low pressure gas enters a copper tube, which is soldered, as in the case of the inlet

tube, to a shield S_4 and leads to the tube m which is exactly similar in size and arrangement to the inlet tube b . The gas leaves by way of the tube n (shown in part) and passes out into the room.

After the interchange of heat and before the exit temperatures are measured, both exit streams are put in good and approximately equal thermal contact with the end plate o as a means of making a base for the external shield p which surrounds the interchanger and provides it with an equal temperature boundary. A heavy copper cylinder q provided with a heating coil acts as a heater guard and is kept at the same temperature as the surface of the interchanger. This is accomplished by adjusting the heater current to maintain a zero reading on a five-junction copper-constantan thermocouple connected differentially between the constant temperature boundary (near its base) and the inside of the heater guard.

The thermal capacity of the interchanger, including the four thermometer tubes is equivalent to approximately 18 grams of water and requires on the average about 35 minutes to attain a steady state with a flow of 50 cc/sec. at atmospheric pressure.

The two baths are exactly similar, each consisting of an outer bath which contained an electric heating coil and thermostat as well as a large coil through which the gas flows, and an inner bath without heating or cooling coils which served to smooth out temperature fluctuations due to the heater current in the outer bath which surrounds it. The bath liquid was kerosene. The similarity of the baths and their thermostat mountings made it possible quickly to reverse the order of the bath temperatures.

All temperature measurements were made with copper-constantan, thermocouples, used differentially. The tubes c and v (Fig. 2) were provided for the insertion of a five-junction thermocouple to read the temperature change in the low pressure line. A similar arrangement was used for the high pressure line. In addition, for the purpose of checking, a two-junction couple was provided for the two inlet temperatures and a similar one for the two outlet temperatures. Only the copper lead wires were permitted outside the heater guard. Potential differences were measured with a White single potentiometer using the usual auxiliary equipment.

The similarity of the thermoelectric properties of the thermocouples was established by standardization and the formula of Adams⁸ was used in obtaining the temperature intervals from the bridge readings in microvolts.

Pressure readings were taken on a spring gauge, devised by combining an optical indicating arrangement (telescope, mirror and scale) with a high class Bourdon spring of the type used in hydraulic gauges. This arrangement gave approximately 530 scale divisions for a pressure of 100 kg/cm². The gauge was calibrated against a Pratt and Whitney dead-weight gauge.

Commercial oxygen gas (water free) with a flow of approximately 50 cc/sec. was used. Two cylinders connected in parallel provided a reservoir sufficiently large to permit the taking of temperature and pressure readings continuously, thus eliminating the necessity of pressure control on the high

⁸ Adams, J. Wash. Acad. 3, 469 (1913).

pressure side. The flow of gas was controlled from the low pressure side by adjusting an ordinary pressure reduction valve in such a way as to maintain a constant pressure (11 pounds/sq. in.) on a glass capillary leak.

The bath temperatures were controlled by mercury-in-glass thermostats so as to maintain one gas inlet stream at approximately 33.2°C and the other at approximately 18.8°C.

In making a run the baths were brought to steady state of temperature regulation and the gas started through the interchanger. The heater guard temperature was then adjusted until it was the same as the surface of the interchanger. After the steady state had been reached a zero reading on the heater guard thermocouple was maintained for about 15 minutes before taking calorimetric measurements. In regulating the guard temperature the observer also gave attention to the room temperature. It was thought desirable that the room temperature should be kept fairly constant with respect to the outside temperature of the interchanger, which differed from the arithmetic mean of the bath temperatures depending upon the pressure of the high pressure gas and the order of the bath temperatures. This was accomplished by keeping the room temperature such that the heater guard temperature could be regulated by limiting its power input to the small range 0 to 0.35 watt. After the heater guard thermocouple had indicated zero for 15 to 20 minutes, readings were taken on the pressure gauge and the four thermocouples. From two to four sets of readings were taken in a given pressure range. The bath thermostats were then interchanged thus reversing the order of the bath temperatures and another group of readings taken at a somewhat lower pressure.

Let the subscript 1 be applied to the state of the high pressure gas upon entering the interchanger and the subscript 2, to that upon leaving. Similarly let the subscripts 3 and 4 apply to the low pressure line entering and leaving respectively. Further, let i stand for the function $u + pv$. Now if q is the heat from various outside sources gained per gram for both streams, we have

$$q = i_2 - i_1 + i_4 - i_3. \quad (1)$$

Now it is reasonable to assume that the variation of these functions is linear over the small range of temperature and pressure in each gas line. We then get

$$q = c_p [T_2 - T_1 + \mu(p_1 - p_2)] + (c_p)_0 [T_4 - T_3 + \mu_0(p_3 - p_4)] \quad (2)$$

where the subscript 0 applies to conditions at atmospheric pressure and μ is the Joule-Thomson coefficient. It finally follows that

$$\frac{c_p}{(c_p)_0} = - \frac{T_4 - T_3 + \mu_0(p_3 - p_4)}{T_2 - T_1 + \mu(p_1 - p_2)} + \frac{q}{(c_p)_0 [T_2 - T_1 + \mu(p_1 - p_2)]} \quad (3)$$

Since we measure $(T_4 - T_3)/(T_1 - T_2)$ we write Eq. (3) in the form:

$$\frac{T_4 - T_3}{T_1 - T_2} = \frac{c_p}{(c_p)_0} + \phi(\mu, q) \quad (4)$$

where $\phi(\mu, q)$ is a correction term. The sign of this term is changed, but not its value if we interchange the bath temperatures; so that these corrections can be eliminated. The whole problem thus centers on the accurate measurement of the various temperatures. With an ideal interchanger in which pressure drops and thermal leakages are negligible we see from what has been said before that the last term in Eq. (4) would vanish.

The mean values of the ratio on the left of Eq. (4) for each group of readings were calculated and they are shown plotted against the corresponding mean pressures in Fig. 3. Curve 1 represents values obtained when the high pressure bath was maintained at 33.2°C and the low pressure bath at 18.8°C; while curve 2 gives the values obtained with the reverse order of bath temperatures. The fact that curves 1 and 2 do not coincide and pass through

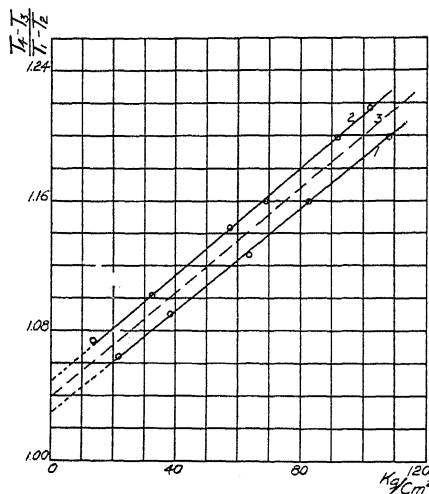


Fig. 3.

the point $p = 1$ atmosphere and $(t_4 - t_3)/(t_1 - t_2) = 1$ gives evidence that we are not dealing with the ideal calorimeter just referred to.

In order that the difficulties might have further study a set of observations was taken with both baths set at 26°C and a flow of 50 cc/sec. A cooling effect in each gas stream as it passes through the interchanger was observed. The magnitude of the effect for three different pressure regions is shown in Table I.

If corrections of the type given in the last column of Table I were to be applied along the length of the two curves the general effect would be to change the shape of each slightly and bring them somewhat closer together. Since the proposed corrections would not affect in any sense the mean curve 3 of 1 and 2 they are not applied. These corrections include the Joule-Thomson effect, velocity cooling and possible index errors; and we conclude that the mean curve is independent of the Joule-Thomson effect and heat leakage q .

A part of the separation between curves 1 and 2 might be attributed to

temperature effects upon the specific heat c_p of oxygen. Since there is considerable evidence to show that c_p at atmospheric pressure changes very slightly with temperature in the region in which we are interested, we shall consider it as constant. On the other hand, c_p at pressures of 60 and 100 kg/cm² decreases quite considerably with temperature increase between 0 and 50°C. Data of this type on oxygen are lacking but if we adopt values calculated by Beattie⁶ or by Bridgeman⁷ for air and make corrections to curves 1 and 2, assuming air and O₂ to be alike in these respects, we find that the correction is more than sufficient to bring them together at 100 kg/cm² pressure. If, on the other hand, we use observed values quoted by Beattie,

TABLE I

High pressure kg/cm ²	High Pressure line cooling °C	Low Pressure line cooling °C	Calculated correction factor for corresponding points on 1 and 2, Fig. 3.	
13	0.023	0.020	Curve 1	1.008
			Curve 2	0.992
64	0.008	0.008	Curve 1	1.002
			Curve 2	0.998
83	0.015	0.012	Curve 1	1.003
			Curve 2	0.997

the corrections so obtained are not sufficient to reduce the divergence between 1 and 2 at 100 kg/cm² by more than 50 percent. If we make similar corrections at lower pressures, 0 to 20 kg/cm², it is seen that the effect almost vanishes. It should be observed, however, that the corrections listed in Table I for this region are almost sufficient to bring the two curves together.

It is apparent therefore, that uncorrected curves obtained in the manner that 1 and 2 were obtained will never coincide for the large temperature intervals here used and may have slopes such that the divergence between them will increase slightly with increases in pressure. It is equally apparent however, that we are justified in drawing a mean curve 3.

The residual errors giving the effect of moving the mean curve 3 upward by approximately 4 percent must be due to difficulties in measuring temperature changes in one of the thermometer tubes. The difficulty doubtless lies in the fact that heat is conducted along the high pressure entrance thermometer tube. An examination of the entrance thermometers in the interchanger gives evidence of the possibility of some interchange of heat between the two gas streams before the temperatures are determined. The effect of this is to induce a temperature gradient in the thermometer cells and therefore an uncertainty in meaning of the temperature readings. The results indicate that this effect is larger in the case of the high pressure line as might be expected from the construction. It also appears in this connection that errors of this type depend only on the general temperature distribution in the apparatus to a high degree of approximation. The slopes of the curves in Fig. 3, therefore, are not affected appreciably. It is of especial interest to note that

with the first (and very faulty) apparatus curves were obtained intersecting the horizontal axis at about 30 kg/cm² having, however, approximately the same slope as the mean curve here given.

The apparatus was designed to work in the region from 20 to 200 atmospheres and therefore too much confidence should not be placed in measurements taken at pressures lower than 20 atmospheres.

The mean value of the slope between 30 and 100 kg/cm² is 0.00160 per unit of pressure here used, or 0.00165 per atmosphere. The value obtained from the first apparatus mentioned above is 0.00176 per atmosphere and that from a second apparatus is 0.00171 per atmosphere. The two earlier sets of apparatus, moreover, embodied a radically different method of measuring temperatures, namely that the thermometer tubes and their respective shields for measuring t_1 and t_2 were located in the baths B and B' (Fig. 1).

Although the present work has been done on oxygen, it is not without interest to compare results with those already obtained for air. The experimental work of Roebuck gives 0.00140 per atmosphere, while the calculations of Beattie from the Beattie-Bridgeman equation of state yield, 0.00166 per atmosphere. The experiments of Holborn and Jacob while performed at 59°C (where the value 0.00119 emerges) may be reduced to the temperatures of these experiments by using the calculations of Beattie, resulting in the value 0.00162 per atmosphere.

The agreement in the values for $(d/dp) [c_p/(c_p)_0]$ as obtained by the use of three calorimeters is considered sufficient evidence for establishing the validity of the method for precise work. This point could be made more impressive if space could be taken to describe in detail the great differences in type and quality of the three sets of apparatus. The arrangement of the apparatus last used possesses many defects, many of which can be almost completely eliminated by more careful design and construction. Perhaps the most important feature of the method over and above its simplicity is the fact that the sources of error speak their presence in the nature of the results which it yields.

Plans to investigate gases other than oxygen and to extend the readings over a range of temperature were brought to a halt by the development of a leak in the interchanger. This, together with the fact that designs for an improved apparatus were in mind, made it seem wiser to publish the results already obtained and defer the general survey until the new designs could be realized.

In conclusion the author wishes to express thanks to Professor L. G. Hoxton who proposed the method for his interest during the progress of the work.

NOTE ON THE PRESSURE VARIATION OF SPECIFIC
HEATS OF GASES DERIVED FROM COMPRESS-
IBILITY DATA

BY L. G. HOXTON

UNIVERSITY OF VIRGINIA

(Received August 7, 1930)

ABSTRACT

Values of the rate of variation of c_p with pressure at constant temperature as calculated from p - v - T data and as determined by direct experiment are compared for oxygen and air over a pressure range of 20 to 100 atmospheres and at 26° C. The calculated values, while of the same order of magnitude as the experimental, are shown to be very sensitive to small variations in the coefficients of the "equation of state" employed; also to modifications in the method of approximation used in handling such equations. The conclusion is reached that this rate probably diminishes slowly with rising pressure for oxygen in the field considered and that its calculated values cannot at present approach in accuracy what may reasonably be expected from direct calorimetric experiments.

THE computation of thermodynamic properties of gases from p - v - T data has recently been brought forward by Beattie and Bridgeman who have developed an "equation of state"¹ and have applied it with surprising success to the evaluation of the Joule-Thomson effect and the heat capacity at constant pressure (c_p) for air.^{2,3,4} Also a new method for the experimental determination of the relative values of c_p at different pressures and the same temperature is reported elsewhere in this issue by E. J. Workman. It would seem of interest, therefore, to compare the result there given for oxygen with calculated values and, if possible, to draw conclusions as to the applicability of computations of this nature.

Since the thermodynamic relation essential in this connection, namely

$$\left(\frac{\partial c_p}{\partial p}\right)_T = -T \left(\frac{\partial^2 v}{\partial T^2}\right)_p \quad (1)$$

involves, in effect, the curvature of a graph adjusted to experimentally determined points, often far apart, one is led to expect that a large variety of values for the curvature are possible depending upon the form of the equation employed and upon the number of points; further, that any equation of state which is adjusted to fit over a wide range of data, which is its usual purpose, may not be so suitable as an interpolation formula utilizing

¹ J. A. Beattie and O. C. Bridgeman, Jour. Am. Chem. Soc. 50, 3133 (1928); also Zeits. f. Physik 62, 95 (1930).

² O. C. Bridgeman, Phys. Rev. 34, 527 (1929).

³ J. A. Beattie, Phys. Rev. 34, 1615 (1929).

⁴ J. A. Beattie, Phys. Rev. 35, 643 (1930).

closer points merely. An ideal case, in fact, would be the one where the points are so closely distributed that interpolation by successive differences alone might be used.

In what follows calculated values of the same quantity for oxygen will be compared among themselves and with experiment, with a view to getting some idea of the magnitude of the divergencies resulting from different methods of treatment. Air, to a lesser extent, will be included also. This quantity, δ , say, will be the change in c_p per atmosphere relative to its value at one atmosphere, the temperature being constant and taken as 26°C. That is

$$\delta = \frac{1}{(c_p)_0} \left(\frac{\partial c_p}{\partial p} \right)_T \text{ parts per atmosphere} \quad (2)$$

where the subscript 0 refers to a pressure of one atmosphere and T is taken as 299°K. The pressures considered cover a range from 20 to 100 atmospheres.

The result found by Workman for this quantity was

$$\delta = 0.00165 \text{ parts per atmosphere} \quad (3)$$

which exhibited no variations greater than the errors of experiment over the entire range of pressures.

Beattie,³ in computing the heat capacity per mol for air at constant pressure gives the approximation

$$C_p = C_p^* + \left(\frac{2A_0}{RT^2} + \frac{12c}{T} \right) p. \quad (4)$$

The factor in parentheses is equal to the left hand member of Eq. (1) since C_p^* is constant. If we employ the values of the constants for oxygen given by Beattie and Bridgeman,¹ namely, $R=0.08206$, $A_0=1.0763$ and $c=12 \times 10^4$ and, in addition, the value 6.98 cal. per mol per degree⁵ at 26°C, we obtain

$$\delta = 0.00166 \quad (5)$$

The compressibility data of Holborn and Otto⁶ offer another means of approach. They are to be found summarized in the form

$$pv = A + Bp + Cp^2$$

where the values of A , B , and C , which are functions of the temperatures only, are each given for 0°C, 50°C, and 100°C respectively. The pressure range goes up from 1 to 80 meters of mercury so that the data are excellent for comparison here. A three-constant formula for interpolation over temperature at constant pressure is required. Fortunately, rather than use a power series of the form

$$pv = d + et + ft^2$$

⁵ International Critical Tables, V. 82.

⁶ L. Holborn and J. Otto, *Zeits. f. Physik* 33, 1 (1925).

a. three-constant formula may be derived from the equation of van der Waals

$$\left(p + \frac{a}{v^2}\right)(v - b) = RT$$

which, after terms in the second and higher orders of the small constants a and b are neglected, takes the form

$$pv = bp + RT - \frac{ap}{RT} = g + ht + \frac{k}{273 + t},$$

say, for constant pressure. Any required coefficient in the second formula may be determined from the values of pv at the three given temperatures. The last coefficient only is needed, for

$$T\left(\frac{\partial^2 v}{\partial T^2}\right)_p \quad \text{may be taken as} \quad \frac{2k}{p(t + 273)^2}.$$

This procedure, when followed out gives

$$\delta = 0.00191 - 2.35 \times 10^{-6}p. \quad (6)$$

Likewise, the result from the power series formula is

$$\delta = 0.00165 - 2.13 \times 10^{-6}p. \quad (7)$$

which, though less valuable, is not without an interest for comparison.

In an earlier paper by the same authors,⁷ of which the one just cited seems to be a revision, the quantities A and B are given values identical with those of the later paper, while C is given values one tenth as great at 50°C and 100°C and a value about 0.13 as great at 0°C. The constant term, 0.00191 in Eq. (6) or 0.00165 in Eq. (7) is unaffected but the linear term is greatly affected in proportion to its magnitude. Thus, if the values given in the earlier paper are used as they stand, the term is reduced to a little over one third value, while if, on the other hand, a correcting factor of ten is applied to the earlier paper (making thus eight of the nine values in the two papers agree) the linear term is more than tripled. (It seems possible that the earlier paper contains a misprint).

TABLE I. Values of $(1/(c_p)_0)(\partial c_p/\partial p)_T$ at 26° for oxygen.

p , atm.	Eq. (3)	Eq. (5)	Eq. (6)	Eq. (7)
20	0.00165	0.00166	0.00186	0.00161
60	.00165	.00166	.00177	.00152
100	.00165	.00166	.00168	.00144

For convenience of comparison, the values of δ as given in Eqs. (3), (5), (6), and (7) are collected in Table I and set down for the mean and extreme pressures under consideration.

⁷ L. Holborn and J. Otto, Zeits. f. Physik 10, 367 (1922).

It appears, first, that the computed and experimental values are of the same order of magnitude; secondly, that the computed values vary among themselves in a way that indicates great sensitiveness to the particular method of treating the data and, by inference, to small variations in the data themselves. In the third place it is quite probable that δ decreases slowly with rising pressure in this part of the field; for, this is indicated by the method of interpolation just employed. Also it is indicated qualitatively by the application of Eq. (1) to an equation of state such as that of van der Waals. On the other hand the absence of variation in the computed column headed "Eq. (5)" is subject to some doubt. For, in a reference, which includes Eq. (4), from which this column is deduced, the author states: "These relations represent the data* surprisingly well; so well, in fact, that some compensation must have taken place between the various approximations made." It follows, fourthly, that the agreement of the values in this column with the experimental values is probably accidental. A final conclusion may be drawn that, if we set down, say, one percent as a reasonable limit to the accuracy now promised by direct experiment such as those of the relative type already referred to it is useless at present to expect calculations from p - v - T data to approach this. One might look forward, in fact, to putting into practice a reversed type of computation applying thermodynamic data in correcting or filling out data on compressibility.

The last conclusion is further borne out by available experimental data and calculations for air. Thus Roebuck⁸ gives a table of values for c_p over a field of temperatures and pressures far exceeding that considered here. From his tables one may obtain a mean value

$$\delta_a = 0.00140 \quad (8)$$

where δ_a applies to air instead of oxygen.

From Beattie's computed tables,³ or Eq. (4), one obtains

$$\delta_a = 0.00165. \quad (9)$$

The constants given for air in the paper just referred to are, however, not all just the same as those given in an earlier paper¹ and repeated in a later paper.¹ This different set, when applied in Eq. (4), gives

$$\delta_a = 0.00146. \quad (10)$$

Bridgeman,² on the other hand, using the same equation and the same constants as Beattie but employing a different mathematical treatment, publishes a similar table from which is derived

$$\delta_a = 0.00176. \quad (11)$$

The divergence here is sufficient to bring out the point in question. It is of interest to note, in passing, the way in which the two terms in the parenthesis of Eq. (4) contribute to the values given in Eqs. (9) and (10).

* For air.

⁸ J. R. Roebuck, Proc. Am. Ac. Arts Sci. 60, 537 (1925).

If we consider, as is natural, that the term $2A_0/RT^2$ is representative of molecular attractions, then 62% of the first value and 85% of the second come out as contributions from molecular attractions. This is a further forcible illustration of the sensitiveness of the computed values of thermodynamic quantities to small variations in the value of the coefficients in equations of state arising from small changes in the data themselves or in the processes of adjusting the equations to them.

It should not be overlooked that the calculated values of Beattie and Bridgeman and the experimental values of Roebuck show in the actual magnitude of c_p an agreement much better than might be implied in the foregoing. It is in the differences between values of c_p rather than in the whole quantities themselves that the proportionate irregularities show up the more plainly. Here, indeed, appears again one of the reasons for conducting direct calorimetric experiments.

LETTERS TO THE EDITOR

Prompt publication of brief reports of important discoveries in physics may be secured by addressing them to this department. Closing dates for this department are, for the first issue of the month, the twenty-eighth of the preceding month; for the second issue, the thirteenth of the month. The Board of Editors does not hold itself responsible for the opinions expressed by the correspondents.

Relative Efficiency of the Hg-Arc Lines in Exciting the Raman Spectrum of Benzol

The Raman spectrum of benzol was studied by Wood's method, modified to give better results and greater convenience and economy of operation. The Raman tube used was about 30 cm long and 3 cm in diameter, silvered and painted with black Duco on the outside, except for the flat end and a strip about 2 cm wide and 15 cm long, on the side of the tube through which the light of a Cooper-Hewitt 220-volt quartz Hg-arc was permitted to enter. The tube was surrounded by two concentric glass jackets. The innermost one, for solutions of color filters, was omitted when no filters were employed. The outermost tube formed the cooling system. Through it, tap water (whose temperature is very constant in this laboratory) was circulated during exposures. It was found that by omitting the screens and lens usually employed in Wood's method and bringing the flat end of the Raman tube close to the spectrograph slit much better spectra were obtained. The problem of aligning the tube was greatly simplified, and all stray light from the room could be screened off completely by wrapping several layers of black cloth around the end of the Raman tube and slit end of the spectrograph.

The color filters which gave the best results were: 1. Ammoniacal copper sulphate, which transmitted the 4358 and 4047 groups strongly and eliminated the effect of the 3650 group and the 4916, 5461, and 3341 lines; 2. Alcohol

solution of quinine sulphate with "Blue Manhattan Lamp Coloring" painted on the outside walls of both filter and water jackets transmitted only the 4358 group. By spreading a thin layer of vaseline over the Duco the chemical action of the color filters on the paint was effectively prevented.

The Raman patterns for the different exciting lines were charted and found to be complete and identical for the 3650 group and 4047 and 4358 lines, while those for the weaker Hg-arc lines 4108, 4347, 4339 were very incomplete, only the strongest Raman frequency (992) appearing in each case. Many Raman lines coincide with arc lines or other Raman lines. This makes the determination of the efficiency of the exciting lines difficult. Results obtained thus far do not confirm the Fourth Power (Rayleigh) Law in the spectral region 3341-4358. Ornstein and Rekveld report this law to hold for carbon tetrachloride in the region 4047-5461. The higher frequencies appear somewhat more efficient in the excitation of the Raman lines. Equal intensities of incident frequencies are practically equally efficient. The intensities of the lines were measured and calculated by a microphotometer using a carbon ribbon lamp as standard and check well with those of other investigators.

SISTER MAGNA WERTH

University of Minnesota,
September 5, 1930.

Orbital Valency

It has been suggested by Heitler¹ that, in the formation of molecules, the orbital angular momenta may play a rôle analogous to that of the spin angular momenta, in that

there is a tendency toward compensation. Just what the precise relationships are, and what special rules hold (as to the order of the molecular terms) for this so-called orbital valency, if it has a meaning, have not been made clear.

¹ W. Heitler, Naturwiss. 17, 546 (1929).

To investigate the situation, I have studied the problem of the interaction of two identical atoms, each with one p valence electron. These give rise to the following² molecular states: $^1\Delta_g$, $^3\Delta_u$, $^1\Pi_g$, $^1\Pi_u$, $^3\Pi_g$, $^3\Pi_u$, $^1\Sigma_g^-$, $^3\Sigma_g^-$, $^1\Sigma_g^+$, $^1\Sigma_u^+$, $^3\Sigma_u^+$, $^3\Sigma_u^+$. These are thus twelve states, and *a priori* it is not evident in what order their energies occur, and which of them correspond to repulsive states. It seems that one must ascertain this by a calculation similar to that of Kemble and Zener³ for the two-quantum excited states of H_2 . This has been done in the present work.

In order to avoid analytical difficulties (and at the same time to follow the work of Zener)⁴ an atomic wave-function with the radial part $R(r) = \text{const. } re^{-kr}$ has been adopted. Since we are not primarily interested in the absolute values of the energies, but only in their relative positions, it would seem that this assumption is sufficient. A complete treatment would also include other wave-functions but the work has been quite complicated in the above case, which is probably the simplest of all.

When, now, the potential energy for a given value of kR (where R is internuclear distance)

is calculated, it is found to be proportional to k , so that the relative positions of the states are not influenced by a change in k . This is true for any function of the form $R(r) = \text{const. } r^n e^{-kr}$.

The complete potential energy curves have not as yet been obtained, but for the special value $kR = 6$, it is found that the lowest state is a $^1\Sigma_g^+$. The other $^1\Sigma_g^+$, together with $^1\Delta_g$ and $^3\Sigma_g^-$, are repulsive, while all the remaining states, including $^3\Delta_u$ and the Π states, seem to be attractive. Whether any of the states cross each other or not is not as yet known.

A full account of the work, together with various numerical tables will be published as soon as time permits.

JAMES H. BARTLETT, JR.
Parker Travelling Fellow

Jefferson Physical Laboratory,
Harvard University,
August 30, 1930.

² See R. S. Mulliken, Phys. Rev. **36**, 611 and 699 (1930).

³ E. C. Kemble and C. Zener, Phys. Rev. **33**, 512 (1929).

⁴ C. Zener, Phys. Rev. **36**, 51 (1930).

The Probable Number of Isotopes of Eight Metals as Determined by a New Method

In our study of some twenty-five metallic elements in inorganic compounds (Phys. Rev. **35**, 124, 1930; a detailed report of our results is in Press in the *Journal of the American Chemical Society*) we have found that the number of minima of light, or so-called differential time lags, characteristic of each compound is in general the same as the number of known isotopes of the metal. This is true whether the metal be in the chloride, sulphate, nitrate or hydroxide form, a rather extensive series of each having been studied. The same has been found true more recently for several other inorganic salts which we have had the opportunity to study. The method therefore appears to afford a new means of determining the number of isotopes of the metallic elements. It is really to be expected, in the light of our previous experimental results, that each isotope would produce a separate minimum of light corresponding to its mass, for we have found that the positions of the minima of the inorganic compounds are some inverse function of the chemical equivalent of the metallic element of the compound. The scale readings of the

minima of the isotopes of a given element, however, appear in general to vary directly with the masses of the individual isotopes, a conclusion which is based upon the order in which the minima characteristic of the given element make their first appearance as the concentration, beginning with extreme dilution, is gradually increased.

It occurred to us to find the number of characteristic minima of some elements of which no isotopes have been reported. We have therefore recently made a study of the elements listed below, finding for each the number of minima indicated.

Gold,	2 minima.
Palladium,	3 "
Platinum,	2 "
Rhodium,	1 "
Ruthenium,	2 "
Tantalum,	3 "
Thallium,	2 "
Thorium,	3 "

If, as seems very probable, our method detects the presence of the isotopes of the metals of inorganic compounds, our results are to be interpreted as showing that the above named

metals have the number of isotopes represented by the number of minima recorded. These elements, for the most part, were studied in the chloride, sulphate and nitrate compounds and the number of the minima for each element was the same in each of the three compounds. Since the relationship connecting scale reading, or time lag, with atomic mass is not known with sufficient accuracy to yield values of atomic masses closer than some two or more units in the case of

the foregoing metals, we are unable at present to determine the exact masses of these isotopes. This we believe may be possible, however, with further studies, along with a quantitative estimate of the abundance of the different isotopes.

FRED ALLISON
EDGAR J. MURPHY

Department of Physics,
Alabama Polytechnic Institute,
August 30, 1930.

The Formation of Striae in a Kundt's Tube

Some experimental work has been carried on by the author from time to time on the formation of striae in a Kundt's tube. An article was written for *Nature* 118, 157 (1926) also for *Science* and *School Science and Mathematics* the same year setting forth a method of producing these striae by means of a sounding organ pipe.

Since the summer of 1924 observations seemed to show a rotation of the dust particles on each side of the striae and in July 1929 the author succeeded in showing conclusively that such rotation does take place.

A glass tube about 150 cm long and about 2 cm inside diameter had some burned cork scrapings scattered along its inside and a sheet tin piston connected to one prong of an electrically driven tuning fork was used to excite the air vibrations in the tube. The piston was inserted a short distance into the end of the tube and the other end of the tube was closed with a tight fitting cork. When the fork was made to vibrate complete disks of cork dust were produced across the tube at the antinodes and close observation showed that at each disk two distinct orbits of rotating particles were present, one on each side of a single striation, one clockwise, and on the opposite side a counterclockwise rotation. The rotations take place so that the particles leave the top of the striation and enter at the bottom of the same striation. Midway between two adjacent striae little striae lower than the others tend to form but are soon destroyed by the rotations mentioned above, the dust particles forming these lower striae being pulled away in opposite directions and forced into the two adjacent striae at the bottoms of the same. Thus the dust particles are pulled away from a line approximately midway between adjacent striae in opposite directions and forced into the major striae at their

bottoms. When the agitation of the dust particles is violent the striae at the antinodes, especially those extending completely across the tube as disks, do not remain always in one position but very often they merge into each other. When the agitation is less violent as in the case where the striae do not extend completely across the diameter of the tube from top to bottom, there seems to be two orbits of rotation on each side of a striation, one above the other, rotating in opposite directions so that the direction of rotation is from near the middle of the striation, one orbit entering the top of the striation, and the other orbit entering the bottom of the striation, somewhat as two meshed cogwheels directly above the other, would rotate.

While there seems to be experimental evidence in the scientific literature for the support of the explanation of the formation of striae in a Kundt's tube as given by Koenig, *Wied. Ann.* t XLII, pp. 353, 549, 1891, the author is inclined to believe that the formation of these striae may be satisfactorily explained in a manner similar to the explanation for the formation of ripple-mark in sand as given by Darwin, *Proc. Royal Soc.* Vol. 36, p. 18, Oct. 18, 1883.

In the summer of 1927 the author was able to maintain two paper segments, cut in a shape similar to a dust striation, upright in the tube and when pith dust was also present a violent somewhat elliptically shaped rotation about an inch long along its major axis parallel to the axis of the tube, was produced. Also a single segment of paper similar to a dust striation has been maintained upright in the tube for a short time by means of the air vibrations.

In the summer of 1927 striae were obtained by the author by allowing puffs of air produced by interrupting a continuous air stream

from a small glass nozzle by a rotating siren disk and then allowing these puffs to enter a glass tube, one end of which was corked and in which pith dust was distributed along the bottom. These striae were formed when the air jet was interrupted too slowly to produce an audible tone.

The author is continuing his investigation of these striae photographically and is making

an effort to determine the effects produced by forming them in various gases and in tubes of various diameters and lengths, and when produced by sources of various frequencies.

ROLLA V. COOK

Bethany College and Indiana University,
Bloomington, Indiana,
August 12, 1930.

Intensity Changes of Cameron Bands in the Electrodeless Discharge

The band spectra of carbon monoxide obtained in the electrodeless ring discharge have been photographed by the writers under various conditions in order to determine to what extent this source permits controlled excitation, or modification of relative intensities of different band systems. Pronounced intensity changes have been observed, and of these the variations of the Cameron bands are most striking.

The Cameron bands (Phil. Mag. 1, 405, 1926) were discovered in a discharge tube containing neon and a little CO. They involve transitions from the $^3\Pi$ state which is somewhat metastable, to the $^1\Sigma$ or normal electronic state of the molecule, and are not easy to obtain in emission, although Hopfield and Birge (Phys. Rev. 29, 922, 1927) without giving details, report finding them in both emission and absorption. Since the initial state has a long life, the bands would be expected to appear only at relatively low pressures, because of the longer interval between impacts. This led Herzberg (Zeits. f. Physik 52, 815, 1928) to look for them in his careful study of the CO spectra obtained in the electrodeless ring discharge maintained by a damped wave oscillator. Although he kept the gas at quite low pressures, the Cameron bands were not present on his plates.

The oscillator used in the present work is tube driven, with a frequency of about five millions cycles, and a power input variable from about five to one hundred watts. With

low power input, the Cameron bands were entirely missing; with increased power they began to appear, and with the highest input they were well developed, with about the same intensity on a microphotometer record as the bands of the fourth positive group lying near them. The exposure in the last case was for 20 minutes, and the pressure was 0.09 mm. Herzberg's excitation apparently is comparable to that of our oscillator with low power input.

Another effect of the high power input was to produce a rise in pressure, in contrast to the decrease or "clean up" obtained with low power. The increase was as much as five fold, far more than could be explained by the rise in temperature. Since there is considerable carbon deposited in the vessel, a release of adsorbed gas from this finely divided carbon, caused by the rise in temperature, must probably be held responsible for the pressure increase.

A quartz spectrograph of low dispersion has been used in searching for intensity changes; since it was proved that the relative intensities of bands can be varied in the electrodeless discharge, it is planned to continue this work with higher dispersion.

HAROLD P. KNAUSS
JACK C. COTTON

Mendenhall Laboratory of Physics
Ohio State University,
August 29, 1930.

On the Direction of Emission of Photoelectrons from Potassium Vapor by Ultraviolet Light

The wave mechanics (A. Sommerfeld, Atombau und Spektrallinien, Wellenmechanisches Ergänzungsband, p. 213) predicts that the most probable direction of ejection of photoelectrons by polarized light is in the plane of the light beam and the electric vector, the lateral distribution varying as the square

of the cosine of the azimuth angle. This has been most satisfactorily shown to be true for light of x-ray frequencies by the well-known experimental work of several investigators.

We have been concerned with examining the same phenomenon in the optical region. Ultraviolet light of wave-length in the region

of 2400Å from a monochromator was polarized by a pile of quartz plates and passed through a jet of potassium vapor. A cylindrical grid provided a field-free space in the region of the illuminated vapor so that electrons passed out of the grid in the original directions of ejection by the light. A slit and faraday cylinder arrangement served for the measurement of the number of photoelectrons ejected in various directions relative to the electric vector of the exciting light. Though the energies of ejection were less than one volt-electron, the experiments have clearly shown that the optimum direction is that of the electric vector. Approximately twice as many

electrons were observed to be ejected in the direction of the electric vector as at right angles thereto. It seems probable that the electrons observed as ejected at right angles to the electric vector were scattered by the vapor. Correcting for this scattering the observed variation with angle of ejection follows the cosine squared law deduced by Sommerfeld on the basis of the wave mechanics.

ERNEST O. LAWRENCE
MILTON A. CHAFFEE

Department of Physics,
University of California, Berkeley,
September 8, 1930.

Electrostatic Surface Fields near Thoriated Tungsten Filaments by a Photoelectric Method

The electrostatic fields acting on electrons emitted from a thoriated tungsten filament¹ were studied by the photo-electric method described in a paper by E. O. Lawrence and the writer.² The cell was essentially the same as that used in the previous work. In the absence of potassium, a calcium deposit in a side tube immersed in liquid air was used as a getter.

The applied accelerating fields varied from 360 volts/cm, with a corresponding threshold at 4900Å (6.1×10^{14} sec⁻¹), to 48,200 volts/cm, with a corresponding threshold at 5500Å (5.5×10^{14} sec⁻¹). The apparent reduction in the work function by the increased field was 0.25 volt. This reduction is much larger than was produced by corresponding fields on potassium films, or the reduction which would occur if the Schottky (image force) law held. In the latter case the reduction would be 0.08 volts.

When the fields are calculated, as in the previous work, they are found to approximate the Schottky fields at distances less than 1.5×10^{-5} cm. At 10^{-5} cm from the surface there is a field of about 6000 volts/cm, and at 8×10^{-5} cm from the surface, a field of about 1000 volts/cm. The image fields at these distances are 350 volts/cm and 6 volts/cm respectively. The observed fields are very nearly the same as those Becker and Mueller³ calculated for 70% thoriated tungsten from thermionic data. The agreement between the

two independent methods of determining the fields is striking, and shows that sufficiently large fields are present near thoriated filaments to cause the noted deviations from Schottky's thermionic emission equation.

The hypothesis that the thorium ions exist on the surface in patches⁴ which are electropositive with respect to the tungsten, appears best to explain the fields. Electrons emitted through these patches would not only be retarded by the image field, but also by the field between the patches and the ions. A uniform charge distribution on the surface could not cause the observed fields.

The writer intends to continue the studies under different methods of activation before making a detailed report of the work.

LEON B. LINFORD

University of California,
Berkeley, California,
September 9, 1930.

¹ A 4.4 mil thoriated tungsten filament (T122×10) kindly furnished by the Bell Telephone Laboratories, New York.

² Lawrence and Linford, Phys. Rev. 36, 482 (1930).

³ Becker and Mueller, Phys. Rev. 31, 431 (1928).

⁴ Reference 12 of the paper by Lawrence and Linford lists several articles on the theory of patches.

THE PHYSICAL REVIEW

THE USE OF THE REFRACTION OF X-RAYS FOR THE DETERMINATION OF THE SPECIFIC CHARGE OF THE ELECTRON

BY H. E. STAUSS*

RYERSON PHYSICAL LABORATORY, THE UNIVERSITY OF CHICAGO

(Received July 14, 1930)

ABSTRACT

The discrepancies in the determination of the value of the fundamental constant e/m by the two different methods developed so far make desirable the development of new methods for its evaluation. The index of refraction of x-rays offers one method. According to the theories developed so far, in the case of a dispersive medium with no critical frequencies near the frequency of the incident radiation, the value of e/m may be expressed in terms of well-known constants, the wave-length of the incident radiation, and δ (one minus the index of refraction).

Index of refraction of quartz for $\text{MoK}\alpha_1$ and $\text{K}\beta$ radiation. A new method of using the prism with x-rays has been developed and used to determine δ . For crystalline quartz of density 2.6480 gm/cm^3 , δ was determined for the $\text{K}\alpha_1$ radiation of molybdenum as $1.804 \pm 0.001 \times 10^{-6}$ and for the $\text{K}\beta$ as $1.436 \pm 0.001 \times 10^{-6}$.

The calculation of e/m is complicated by the discrepancies that have arisen in the absolute determinations of x-ray wave-lengths. Using the absolute wave-lengths as determined from the results of Bäcklin, Bearden, and Cork, the values of e/m all lie between the values given by the spectroscopic and deflection methods, and they have nearly as great a range as the difference between the two older values. For this reason no definite conclusion can be made as to the most probable value of e/m .

INTRODUCTION

THE index of refraction of x-rays has, in addition to its intrinsic interest, an interest on account of the discrepancies in the evaluation of some of the fundamental constants existing at the present time. So far a number of different dispersion theories have been developed for the x-ray region, but they all agree in the limiting case when the frequency of the radiation is greatly different from the natural frequencies of the medium, when they all lead to

$$\delta = 1 - \mu = \frac{ne^2}{2\pi m\nu^2} \quad (1)$$

where μ is the index of refraction, n is the number of electrons per cm^3 in the refracting medium, e is the electronic charge, m the electronic mass, and ν the

* National Research Fellow.

frequency of the radiation. If this formula is assumed correct, one of the constants can be evaluated in terms of the others and δ . Ordinarily it would not seem feasible to determine any of the constants in terms of δ ; but in view of the great discrepancy in the value of e/m as determined by the two methods developed so far,¹ there is need of additional methods of determining e/m . An attempt to evaluate this fundamental constant from the refraction of x-rays thus seemed desirable.²

In Eq. (1) n may be replaced by Ndz/M , where N is Avagadro's number, d the density of the medium, z the "molecular number", and M the molecular weight; and ν may be replaced by c/λ , where c is the velocity of light and λ the wave-length of the radiation. Ne/c in turn is Faraday's constant in e.m.u. With these values, Eq. (1) may be solved for e/m as

$$\frac{e}{m} = \frac{2\pi M\delta}{Fd\lambda^2} \text{ in e.m.u.} \quad (2)$$

Of the quantities on the right, all except λ and δ are known or can be determined with high precision. The value of λ is in doubt on account of the discordant results obtained in its absolute determination by the several observers. Whenever λ can be assumed to be known, δ is the limiting factor in the evaluation of e/m . It will be noticed that Eq. (2) is independent of e , the value of which is also in doubt.

For the determination of δ it was decided to use the deviation produced by a prism and to develop the method suggested in an earlier paper.³ There it was shown that the maximum deviation of a beam of x-rays can be obtained either with the beam striking the first face of the prism at nearly the critical angle of reflection, the method used by Larson, Siegbahn, and Waller,⁴ or with the beam striking the second face internally at nearly zero glancing angle of incidence and leaving at nearly the critical angle of reflection. In the second method the refracted beam is less divergent than the incident beam, and all wave-lengths suffer maximum deviation simultaneously. There is the disadvantage that an angular rotation must be used that must be measured with high precision.

THEORY OF EXPERIMENT

The experimental procedure adopted can be explained by reference to Figs. 1 and 2. Radiation from the slit S fell upon the prism P , which had its refracting edge A over the center of rotation of a spectrometer. Slightly to the front and to the side of the prism was a lead block B which acted with the prism as a sort of Seemann slit. The primary beam was defined by A and B . Refraction occurred in the neighborhood of A . After the primary and re-

¹ R. T. Birge: Phys. Rev. Supplement 1, 43 (1929).

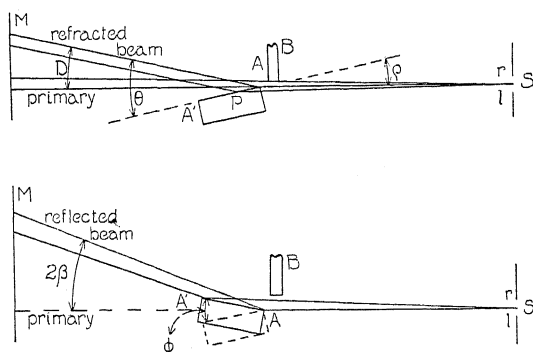
² It is a great pleasure to acknowledge that Professor A. H. Compton suggested the desirability of such a determination of e/m .

³ H. E. Stauss, J. O. S. A. 19, 167 (1929).

⁴ A. Larson, M. Siegbahn, and T. Waller, Phys. Rev. 25, 245 (1925).

fracted beams were registered on the photographic plate M , the prism was rotated through a small angle ϕ to the position of Fig. 2, and the beam was totally reflected from the face AA' at the angle β .

The value of δ is most readily calculated from $\mu = 1 - \delta = \cos \rho$, where ρ is the internal glancing angle with the face AA' and θ is the external angle. Assuming a single ray to be striking at A and assuming the ray to suffer no



Figs. 1 and 2. Diagrammatic sketch of experimental arrangement.

deviation at the first face, ρ and θ can be determined from ϕ , β , and D , where D is the angle of deviation.

$$\begin{aligned}\phi &= \theta + \beta & \text{or} & & \theta &= \phi - \beta \\ \theta &= D + \rho & \text{or} & & \rho &= \theta - D.\end{aligned}$$

Substituting these values in the expression for μ , and solving for δ

$$\delta = D(D + 2\rho)/2. \quad (3)$$

The values of D and ρ need a slight correction ($1/3''$) on account of the deviation in passing through the first face; but this can easily be calculated.

In practice the rays from the slit S are divergent. The simplest experimental procedure is to make all measurements from the edges produced by the radiation from the edge r (of the slit S) that passed A . The errors introduced by measuring edges will be discussed later. In the case of the refracted beam, the ray defined by A and r lies within the beam. Theoretically refraction occurs all along AA' . Practically absorption limits the effective length of the refracting face. For the experiments reported here, the intensity of the refracted radiation that emerged 1 mm from A was only 9 percent of that which emerged at A . The change in ρ produced by the penetration produces a negligible effect upon θ ; so the refracted radiation from r may be considered a band of parallel radiation, of width about 0.002 mm. A correction of this amount can be made to the position of the refracted beam. It is evident that the width of the refracted beam is determined almost solely by the slit S .

In practice it was found advisable to use two different widths of the slit S for the refracted beam and for the primary and reflected rays. The former

varied from 0.1 to 0.3 mm in different trials; the latter was always 0.012 mm. The changes in width could be made accurately with a micrometer screw that formed part of the slit. On account of the changes in width, the position in the refracted beam corresponding to r had to be calculated in order to obtain D_r . This can be done from the relation $\cos \theta = \mu \cos \rho$ or $\theta^2 = \delta + \rho^2$, since $D = \theta - \rho$. In practice the refracted beam was not as sharp as was to be expected; so to diminish the chances of error, both edges of the refracted beams were measured and averaged. In the case where two strong beams of different wave-length overlap, as is the case for the two $K\alpha$ lines, another correction is necessary, which can be shown to be approximately

$$\Delta D = \theta \Delta \lambda / \lambda.$$

The position of D_r is then obtained from the average position by the formula

$$D = D'_{Av} - \frac{\Delta \theta'_i - \Delta \theta'_r}{2} + \theta \frac{\Delta \lambda}{2\lambda} \quad (4)$$

where the primes apply to the greater slit-width, and $\Delta \theta'_i$ and $\Delta \theta'_r$ are the corrections to be made in θ (and hence in D) on account of the changes of ρ produced by changing the slit-width. No correction was made for the γ line overlapping the β line because of the great difference in intensity. The corrections were always less than 1 percent.

The accuracy of the experiment depends to a very great extent upon the second or refracting face of the prism. It should be good up to the very edge A because half of the radiation is transmitted within 0.28 mm of A . The prism used in this experiment was a piece of crystalline quartz which had been cut from a larger pitch-polished surface. It was good to a quarter of a fringe and showed no peculiarities at the edges. Nevertheless, the refracted beam was more diffuse than was to be expected, and there was a band of radiation lying between the primary and refracted beams whose presence had not been foreseen. If in the preparation of the plate, even a slight bending occurred very near the edge A , it might affect the results by changing the inclination of parts of the refracting face. Moreover, a polished surface is never a geometrical plane, and the exact character of the surface is problematical. The observed abnormalities may in some way be due to surface effects. For this work it has been assumed, though it is difficult to prove, that the cause of the diffuseness does not displace the centers of the refracted beams.

Another factor affecting the accuracy of the experiment is the location of the edges of the beams. All the beams have penumbras within which the intensity falls from the maximum to zero. The calculations made above have all assumed that measurements can be made to the edge of zero intensity. This obviously is incorrect. On the other hand, the grains in an x-ray plate have considerable size, and the blackening may even run past the zero edge. A priori it is difficult to predict the positions that will be measured. It is possible to design more involved arrangements that permit

the centers of lines to be measured, and the results obtained by the present method seem to justify further work with such an arrangement.

EXPERIMENTAL ARRANGEMENT AND PROCEDURE

All the experimental work was done in a basement room. The plate-holder and the slit *S*, Fig. 1, were two meters apart, with a Geneva optical spectrometer midway between them. The telescope and collimator of the instrument were removed; and a special turntable was made that rotated with the scale of the instrument, so that its motion could be measured. The table was provided with perpendicular slides for centering the refracting edge of the prism. The slit, taken from a Geneva double x-ray spectrometer, was aligned by taking advantage of the striations present in a beam of x-rays from a narrow slit, the analogues of the spiral formed by a pinhole. An optical prism with its base 90° to the refracting edges was mounted on the table, and the slit adjusted until one of the striations and an edge of the prism were parallel. Other objects mounted on the table thereafter could be aligned by reference to the striations. That the method was satisfactory is shown by the fact that no systematic deviations were ever observed in reflection or refraction which could be attributed to inclination of the slit to the prism edge or reflector.

The plate-holder was made approximately perpendicular to the x-ray beam in both the vertical and horizontal directions. As the apparatus was used, the deviation from normal was too small to produce appreciable differences in the results. To obtain the distance from the refracting edge to the photographic plate, a piece of glass was substituted for the latter, a steel rod pressed against it, and the distance from the end of the rod to the refracting edge of the prism measured with a travelling microscope. The length of the bar was obtained by comparison with a standard meter. It is believed that this distance was determined with an error of less than 0.1 mm or 0.01 percent.

The prism, for most of the trials, had its refracting edge formed by the polished surface and a narrow bevel at 45° to it. The theory of the prism shows that the value of the prism angle is of minor importance in producing the deviation and this angle was assumed to be $135^\circ \pm 15^\circ$. To test the validity of this procedure the bevel was removed and a face was cloth-polished at 90° to the refracting surface. Later the prism was beveled again because, in the polishing, the tool had overlapped and injured the edge slightly. This was shown by the diffuseness produced at the edge of the reflected beam.

The $K\alpha_1$ and $K\beta$ radiations of molybdenum were used for the measurements. A water-cooled, self-rectified tube was run at 42 K.V. maximum and 20 ma. The times of exposure were adjusted to avoid over-exposure of the different lines. Eastman x-ray plates were used and the measurements made with a Gaertner comparator reading to 0.001 mm.

The experimental procedure finally adopted was as follows. The prism was set in position for refraction, the slit *S* opened to the desired width, and an exposure made for 1 to 2 hours, with the position of the direct beam cov-

ered with a lead sheet. The slit was then narrowed to 0.012 mm, the lead removed, and the primary beam registered for about four minutes. This position was read on the scale of the spectrometer, thirty settings of the cross-hair in the micrometer eye-piece of one of the reading microscopes being made on the edge of one mark on the scale. The prism was then rotated until the face AA' (Fig. 2) could reflect, a matter of 7', and an exposure made for about ten minutes, the lead sheet again blocking out the primary beam. This position was read thirty times on the same edge of the same mark on the scale. Thus the measurement of the angular displacement was thrown entirely upon the micrometer screw of the reading microscope. The screw was calibrated at three greatly different positions on the spectrometer scale. The order of the procedure was changed in as many ways as possible in the different trials in order to eliminate any systematic error due to the order. Measurements of the photographic plates were made to both the right and the left to avoid errors in estimating the edge in coming to it from within or without the beam. Nine positions were measured on each plate, and five measurements, to both right and left, made at each position.

RESULTS

After the experimental method had been developed to a satisfactory state, eleven trials were made. In one of the trials the plate became fogged and difficult to measure. It is listed in Table I, but is not used in the final average. On another plate, where the value of ρ was 17'', the $K\beta$ line was not sufficiently strong to be measured accurately under the same conditions as the $K\alpha$ line. The first two trials were made on the original prism; the next four on the right-angled prism; and the rest on the final bevelled prism (all being the same block of quartz). The probable error of a single determination of δ , as deduced from the deviations of the various readings and the arbitrarily assigned errors was much less than the differences between the various trials. In the experiment every factor that seemed to have any influence on the

TABLE I. *Values of δ .*

Trial	ϕ	$S(mm)$	ρ	$\delta K\alpha_1 \times 10^6$	$\delta K\beta \times 10^6$
1	6'10"	0.322	48"	1.818	1.447
2	4'56"	0.322	59"	1.819	1.447
3*	6' 9"	0.322	28"	1.756	1.457
4	5'40"	0.322	51"	1.821	1.450
5	4'44"	0.222	17"	1.791	
6	6'11"	0.222	1'40"	1.794	1.424
7	7'37"	0.322	42"	1.783	1.425
8	7'10"	0.222	2'41"	1.795	1.421
9	7' 7"	0.322	2'22"	1.805	1.448
10	7' 6"	0.222	2'20"	1.793	1.428
11	6'56"	0.122	2'14"	1.819	1.431
Average (omitting 3)				1.804 $\pm .001$	1.436 $\pm .00085$

* Plate fogged.

result was varied, except the slit-width for the reflected and primary beams. The values of δ show no systematic variation with any of the quantities. The variations seem to be due to the measurements of the plates. If it can be assumed that the variations in δ are purely accidental in origin, the probable error of the average may be calculated. The results of the trials are shown in Table I, together with the variables entering into the experiment. The character of the refraction spectrum is shown in Fig. 3.

At the time this investigation was begun, there seemed to be one absolute determination of x-ray wave-lengths of outstanding accuracy, and the evaluation of e/m seemed to be very feasible. Since that time a new set of experi-

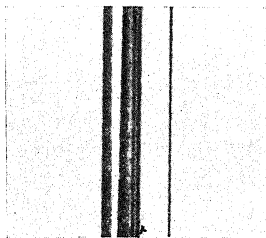


Fig. 3. A refraction spectrum of the molybdenum radiation formed by quartz. From right to left are the reflected beam, the $K\alpha$ line, and the $K\beta$ line. At the left is the primary beam. Between it and the $K\beta$ line can be seen the radiation refracted at small angles.

ments has been performed with is not in agreement with the others and the question of the accuracy of the grating measurements of x-rays has been raised. The question of the value of x-ray wavelengths is now about as uncertain as the problem of the value of e/m . Consequently the value of e/m has been calculated for the values of λ as determined by crystal measurements and by Bäcklin,⁵ Bearden,⁶ and Cork,⁷ without passing any judgment upon the relative accuracies of the determinations. The absolute values for the molybdenum radiation were calculated from the proportion

$$\frac{\lambda_1 \text{ (corrected)}}{\lambda_1 \text{ (crystal)}} = \frac{\lambda_2 \text{ (grating)}}{\lambda_2 \text{ (crystal)}}$$

where λ_2 is the wave-length used in the absolute determinations, and the values of λ (crystal) have been corrected for refraction. If it is assumed that the differences between the observers are due to the experimental arrangements and the gratings, for the present purpose it is sufficient to use only one wave-length of each observer to calculate the molybdenum lines. The results are shown in Table II. The lines used as standards were chosen because they were single.

To obtain the values of e/m , the most probable values of the constants as given by Birge¹ were used. The density of the quartz was determined as

⁵ E. Bäcklin, Dissertation, Upsala (1928).

⁶ J. A. Bearden, Proc. Nat. Acad. Sci. 15, 528 (1929)

⁷ J. M. Cork, Phys. Rev. 35, 1456 (1930).

TABLE II. *Absolute values of λ as determined by different observers.*

Observer	λ used	$\lambda\alpha_1(AU)$	$\lambda\beta(AU)$
Crystal Method		0.7078	0.6314
Bäcklin	Mo $L\beta$.7087	.6322
Bearden	Cu $K\beta$.7095	.6329
Cork	Mo $L\beta$.7100	.6333

2.6480 ± 0.0003 gm/cm³; the molecular weight was taken as $60.06 \pm .03$. The results are listed in Table III. The probable errors are calculated from those

TABLE III. *The values of e/m .*

Observer or method	$e/m \times 10^{-7}$ determined from $K\alpha_1$	$e/m \times 10^{-7}$ determined from $K\beta$
Crystal	1.773	1.773
Deflection	$1.769 \pm .002$	
Bäcklin	$1.768 \pm .007$	$1.769 \pm .007$
Bearden	$1.764 \pm .001$	$1.765 \pm .001$
Cork	$1.762 \pm .0013$	$1.763 \pm .001$
Spectroscopic	$1.761 \pm .001$	

given by Bäcklin and Bearden without evaluation, and from an arbitrary error of 0.01 percent assigned to Cork's results. This is not meant to imply any judgment as to the relative accuracy of the experiments.

It is clear that the determination of e/m from the refraction of x-rays must wait upon the solution of the absolute values of x-ray wave-lengths. The range of values of e/m , as determined from the values of the different investigators, is nearly as great as the original differences in e/m . If the average of all the experimenters is taken, the resulting value⁸, 1.765×10^7 , lies midway between the two older values. The two later experiments lead to a value closer to the spectroscopic value, but this does not warrant a definite conclusion, since one of them gives a result nearly midway between the older values. Whenever the absolute values of x-ray wave-lengths are known accurately, the method of this paper offers a way of evaluating e/m that is independent of the older methods and of the same order of accuracy.

I wish to thank the physics department of the University of Chicago for the apparatus placed at my disposal, and Professor A. H. Compton for his interest in all stages of the work.

⁸ If the dispersion formula had been used in the form

$$\delta = \sum_i \frac{n_i e^2}{2\pi m(\nu^2 - \nu_i)^2}$$

where ν_i is a critical absorption frequency of the dispersive medium, the values of δ and e/m would be increased by unity in the last significant place.

X-RAY SCATTERING COEFFICIENT AS A FUNCTION
OF WAVE-LENGTH AND ATOMIC NUMBER

BY ERROL N. COADE

RYERSON PHYSICAL LABORATORY, UNIVERSITY OF CHICAGO

ABSTRACT

The mass scattering coefficients for Au, Sn, Ag, Fe, and C were compared with those of Al for wave-lengths between $\lambda=0.48\text{\AA}$ and $\lambda=1.09\text{\AA}$ by collecting the scattered radiation in an ionization chamber surrounding the scatterer on one side. The primary beam consisted of characteristic fluorescence radiation excited in radiators of Sn, Ag, Mo, and Se by a water-cooled tungsten tube. The ratios obtained are shown in the table.

With Hewlett's measurement of the absolute value of the mass scattering coefficient of carbon these ratios can be transformed into absolute scattering coefficients.

INTRODUCTION

WHEN x-rays pass through an absorbing screen part of the energy of the beam is spent in ejecting photoelectrons and part is scattered. If μ is the total absorption we may write

$$\mu = \tau + \sigma$$

where τ is the true absorption due to the ejection of electrons, and σ the absorption due to scattering. The fraction of the energy scattered per gram of the scattering substance is σ/ρ , the mass scattering coefficient. The experiment to be described was undertaken to measure σ/ρ directly, and to aid in determining the value of the true absorption from the known values of the total absorption. Another purpose was to find reliable values of σ/ρ to check current theories of the scattering by complex atoms.

Direct measurements of the mass scattering coefficient of x-rays have been made by Barkla and Dunlop, Hewlett, Mertz and others. Barkla and Dunlop¹ observed the scattering at 90° of filtered white radiation from an x-ray tube striking scatterers of different materials. It may be pointed out that these experimenters did not measure the true scattering coefficient because all their measurements were made at right angles to the primary beam. This would be adequate if the angular distribution of scattering were the same for all elements; but such is not the case. We know that as heavier atoms are used the angular distribution changes, with an increasing preponderance of scattering taking place in the forward direction. This scattering in excess of that called for on Thomson's theory was at that time considered to be extra-radiation, not connected with the scattering process, and was purposely excluded from measurement. In their experiments the purity of the primary radiation left much to be desired, since it consisted of direct radiation from an x-ray tube filtered through absorbing screens. This was

¹ Barkla and Dunlop, *Phil. Mag.* 31, 222 (1916).

used because with fluorescence radiation the intensity of the scattered beam was so small that it could not be measured accurately. Barkla and Sale² repeated the experiment with modifications.

For the same reason Hewlett³ used direct radiation for his primary beam. This radiation was, however, from a molybdenum target, and was filtered through a zirconium screen, thus giving a large proportion of homogeneous rays. By moving his ionization chamber to measure the intensity of scattering at all azimuths he was able to integrate the intensity distribution and get the true scattering coefficient. His method, however, required so many observations that its application over a wide range of elements and wavelengths would be very tedious.

It was undoubtedly for this reason that Mertz⁴ adopted a large ionization chamber surrounding the scattering block, which would receive the scattering for all azimuths. His measurements, however, were confined to elements of low atomic numbers with Na the highest. He likewise used white radiation from an x-ray tube filtered through Al and Cu. The effective wavelength was varied by changing the tube potential. Mertz used solid scattering blocks and had troublesome corrections to make for the absorption of the blocks. His ionization chamber was filled with air and he had difficulty in obtaining sufficient intensity to extend his measurements to higher atomic numbers and longer wavelengths.

APPARATUS

In the present investigation a modification of the chamber used by Mertz was employed to measure simultaneously the radiation scattered at all azimuths. Improvement was made in the quality of the x-ray beam by using fluorescence radiation excited in blocks of Se, Mo, Ag, and Sn by direct radiation from an x-ray tube. The scattering blocks were of Al, C, Fe, Ag and Sn. Suitable filters placed in the primary or secondary beam prevented fluorescence rays excited in the scatterer from entering the ionization chamber.

The source of x-rays was a water-cooled Siemens tube of the Coolidge type with a tungsten target surrounded by a copper screen. Current was supplied to the tube from a transformer, whose secondary current was rectified by a full-wave kenotron rectifier, using a balanced circuit. The tube potential was from 35 to 50 peak k.v. with a current of 35 ma.

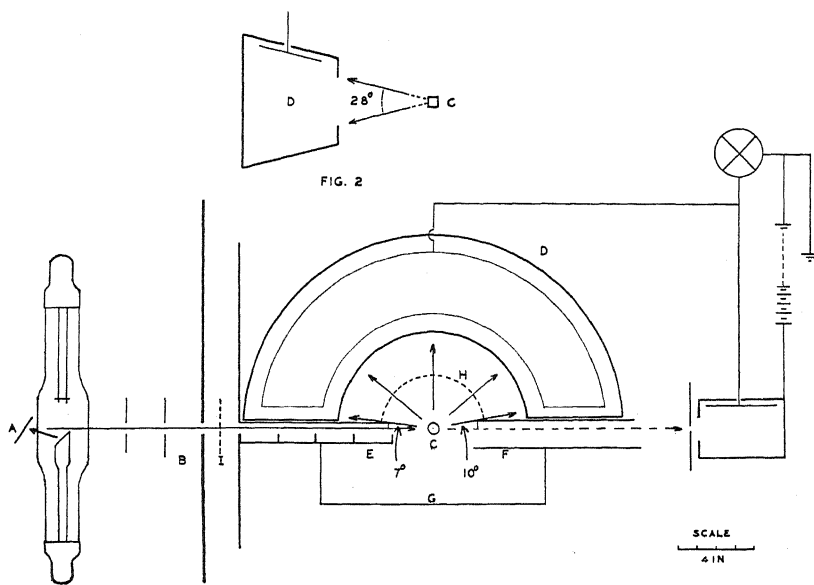
The experimental arrangement is shown in Fig. 1. The radiators, *A*, were placed three cm from the x-ray tube and directly in front of a system of collimating screens, *B*, with openings one-half inch square. The beam of fluorescence radiation, which we will call the primary beam, passed through these openings and struck the scattering blocks at *C*. Since no direct radiation from the tube was allowed to reach the scatterer the beam consisted almost entirely of fluorescence *K*-rays.

² Barkla and Sale, *Phil. Mag.* 45, 743 (1923).

³ Hewlett, *Phys. Rev.* 20, 688 (1922).

⁴ Mertz, *Phys. Rev.* 28, 891 (1926).

The ionization chamber, *D*, shown also in Fig. 2, was so shaped that it would receive the x-rays scattered between two planes meeting along the path of the primary beam at an angle of 28° . The chamber was of the same depth throughout, so that the path of all the scattered x-rays through it would be the same. The extreme rays entering the chamber from the center of the block made angles of 10° and 173° respectively, with the forward direction of the primary beam.



Figs. 1, 2.

The window of the ionization chamber was covered by celluloid. A protecting ledge about the window prevented x-rays from striking the walls or the electrode, which consisted of an aluminum plate, the same shape as the top of the chamber, and mounted in the upper portion of the chamber. The entire outside of the chamber and all the electrometer connections were covered with $1/32''$ lead. Lead screens, *E* and *F*, were used to reduce the effect of air scattering from the path of the primary beam. A lead screen *G*, enclosing the scattering block and the window of the ionization chamber was found useful in excluding stray radiation. Absorbing screens were placed at *H* and *I* when required. The chamber was filled with argon at atmospheric pressure and was connected to a Compton electrometer, the sensitivity of which was about 10,000 mm per volt.

The scattering blocks were then mounted on supports of silk thread attached to wire frames and were so placed in the path of the x-ray beam that radiation from every part of the first slit reached every part of the scattering block.

FILTERS

Radiation of wave-length other than that desired was prevented from

entering the ionization chamber by filters of aluminum, silver, or tin placed in the primary or secondary beam or both. In addition, the potential of the tube was altered from 35 peak k.v. for Mo and Se to 50 peak k.v. for Ag and Sn. For scattering blocks of carbon and aluminum the *K*-radiation is so soft that it is absorbed by the air before reaching the ionization chamber. Consequently no filter was required. For the iron scatterer a filter of aluminum 0.2 mm in thickness was used to remove 99 percent of the *K*-radiation. When the scatterer was silver no filter was required for Mo radiation, but for Ag radiation filters of silver, each absorbing 50 percent of the *K*-rays, were placed in both the primary and secondary beams. The same filters were used for the scattering of Ag radiation by tin. When tin was used to scatter Sn rays a filter of tin was placed in the primary beam to absorb 50 percent of the characteristic radiation. This presumably absorbed more of the short wave-lengths present and prevented the excitation of fluorescence Sn rays. When Se rays were scattered by tin no filter was used, since the potential, 35 peak k.v., was too low to excite the fluorescence radiation. When gold was used to scatter Ag or Sn rays, an aluminum filter 1.2 mm thick was placed in the secondary beam to absorb the *L*-radiation.

The gold foil used was mounted on a celluloid base and was compared with an aluminum scattering block, likewise mounted on celluloid. In correcting for the scattering of the celluloid an amount was deducted equal to one-half of the scattering from a celluloid block of the same dimensions. For this and for all the other scattering blocks corrections were made for air scattering and for the natural leak of the electrometer system. Due to the length of air path in front of the chamber and to the size of the chamber itself, these corrections were appreciable, and their magnitude for longer wave-lengths and higher atomic numbers than those used made measurements by this method impracticable.

MEASUREMENT

The measurement of the mass scattering coefficient was made as follows: Let I_0 be the intensity when no scatterer is in the path of the primary beam, I_1 be the intensity when an aluminum block is in the path of the beam, I_2 be the intensity when an iron (or other) block is in the path, m_1 be the mass of the aluminum scatterer and m_2 be the mass of the iron (or other) scatterer. Then the ratio of the mass scattering coefficients of the two materials is

$$\frac{(\sigma/\rho)_{Fe}}{(\sigma/\rho)_{Al}} = \frac{m_1}{m_2} \times \frac{I_2 - I_0}{I_1 - I_0}.$$

The resulting ratios are shown in Table I and are plotted in Fig. 3. Data obtained by Barkla and Dunlop¹ are included for comparison.

The purity of the primary radiation was tested roughly by absorption methods and the beam was found to be approximately monochromatic. No attempt, however, was made to measure the wave-lengths accurately, because it was felt that better results could be obtained from published

TABLE I. *Ratio of mass scattering coefficients of elements to that of aluminum for different wave-lengths*

Scatterer	Radiator			
	Sn	Ag	Mo	Se
Au	5.49	6.75		
Sn	2.33	2.82	3.44	
Ag		2.65	3.51	
Fe	1.41	1.65	2.09	
C	1.07	0.95	0.87	0.79
Effective Wave-length (calc.)	0.48A	0.55	0.70	1.09

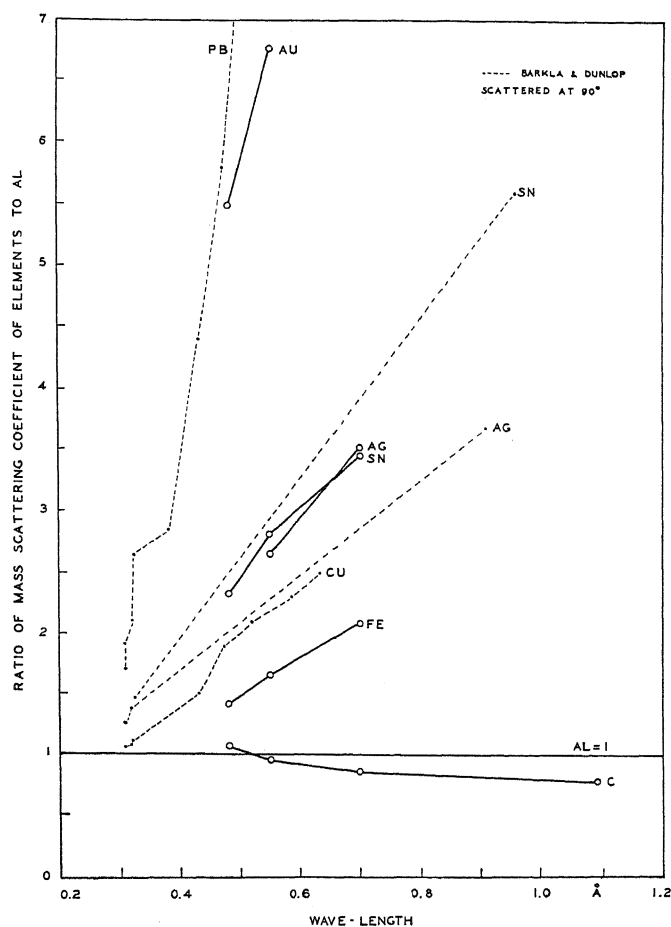


Fig. 3.

values for x-ray spectrum lines. Accordingly the wave-lengths of the K_{α} and K_{β} lines of each element were weighted according to the relative

intensities of each line,⁵ and the average obtained. The weights are contained in the following table:

TABLE II.

Atomic No.	Element	Intensity ratio
34	Se	6.0
42	Mo	5.5
47	Ag	4.7
50	Sn	4.7

ABSOLUTE MASS SCATTERING COEFFICIENTS

The absolute values of the mass scattering coefficient can be deduced from Hewlett's measurements on carbon. He found³ that $\sigma/\rho = 0.200$ for $\lambda = 0.7\text{\AA}$. The corresponding value of μ/ρ for the same wave-length was found also by Hewlett⁶ to be $\mu/\rho = 0.532$. Substituting in

$$\frac{\tau}{\rho} = \frac{\mu}{\rho} - \frac{\sigma}{\rho}$$

one obtains $\tau/\rho = 0.332$

But τ is known to be very nearly proportional to λ^3 i.e.

$$\frac{\tau}{\rho} = K\lambda^3.$$

Therefore, for $\lambda = 0.7\text{\AA}$, $K = 0.968$ whence $\tau/\rho = 0.968\lambda^3$

From the equation

$$\frac{\sigma}{\rho} = \frac{\mu}{\rho} - \frac{\tau}{\rho}$$

We obtain the value of σ/ρ for carbon for the other wave-lengths as given in the following table:

TABLE III. *Mass scattering coefficients for carbon.*

Element	λ	σ/ρ (calculated)
Sn	0.48A	0.183
Ag	0.55	0.186
Mo	0.70	0.200
Se	1.09	0.330

With these values for carbon in Table I the absolute values of the mass scattering coefficients for the other elements were calculated and are shown in Fig. 4. Data obtained by Mertz for carbon are shown by the broken line for comparison.

⁵ Siegbahn, Spectroscopy of X-rays, p. 96. These data are for the ratio of lines excited by cathode rays. That the ratio is the same for fluorescent lines has been shown in the case of Ag K-rays by A. H. Compton, Proc. Nat. Acad. Sci. 14, 549 (1928).

⁶ Hewlett, Phys. Rev. 17, 284 (1921).

The writer is indebted to Professor A. H. Compton for suggesting this experiment and for invaluable advice during the course of the investigation.

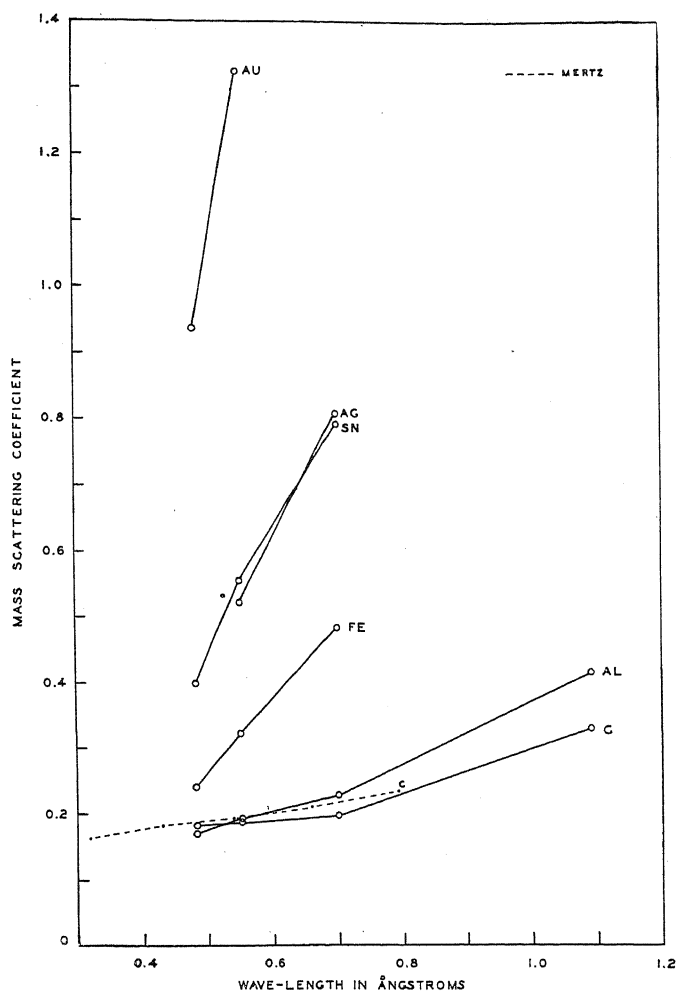


Fig. 4.

THE ATOMIC SCATTERING POWERS OF NICKEL,
COPPER AND IRON FOR VARIOUS WAVE-
LENGTHS

BY RALPH W. G. WYCKOFF

ROCKEFELLER INSTITUTE FOR MEDICAL RESEARCH, NEW YORK CITY

(Received June 26, 1930)

ABSTRACT

Atomic scattering powers are measured for the atoms in metallic nickel, copper and iron when they are reflecting the $K\alpha$ lines of molybdenum, copper, nickel and iron. These data show that the scattering power of an atom passes through a minimum at its K absorption limit and attains a maximum at, or near, its "resonance" wave-length. The atomic F -curves of the nickel atom in metallic nickel and in NiO are practically identical.

THE data of this paper consist in measurements of the scattering powers of the metals nickel, copper and iron for the $K\alpha$ lines of molybdenum, copper, nickel and iron. Previous work from this laboratory with metallic copper and iron¹ showed that the reflecting powers of an atom might be considerably different for different wave-lengths. Studies² of NiO have indicated that the scattering power of nickel decreases as the wave-length used approaches its K critical absorption limit from the high frequency side and that it rises again after the limit is passed. The following results³ suggest that this variation is generally to be expected.

F -curves for metallic nickel have been measured using the $K\alpha$ lines of molybdenum, copper, nickel and iron. The previous data from metallic copper and iron have also been extended through observations with copper, nickel and iron rays. The experimental procedures and the calculations leading to absolute F -values are the same⁴ as those which have already been described. The $K\alpha$ lines of molybdenum were obtained by filtering the beam from a General Electric diffraction x-ray tube through a ZrO_2 filter; all other radiations were the unfiltered output of Siemens-Phoenix tubes equipped with appropriate targets. Calculation showed, however, that none of the measured $K\alpha$ reflections was, under the conditions of the experiment, contaminated by other wave-lengths.

The specimens studied were chemically pure, powdered metals which were passed through a fine meshed sieve and formed into suitable cakes by pressure applied in an ordinary vise. The surfaces of the preparations made in this way were filed and brushed before use in order to remove any super-

¹ A. H. Armstrong, Phys. Rev. **34**, 931 (1929).

² R. W. G. Wyckoff, Phys. Rev. **35**, 583 (1930).

³ cf. R. W. G. Wyckoff, Phys. Rev. **35**, 215 (1930).

⁴ A. H. Compton, X-rays and Electrons (New York, 1926), Chap. V; R. W. G. Wyckoff and A. H. Armstrong, Zeits. f. Krist. **72**, 319 (1929).

ficial layer which might show a preferred orientation. Two samples each of nickel and copper, one of domestic and the other of foreign manufacture, gave concordant results. The iron used was an imported preparation of pure electrolytic metal.

The relative intensities of the various measured reflections are listed in Tables I and II together with the intensities of (220) of NaCl which has served

TABLE I. *Relative intensities of the measured powder reflections from metallic nickel.*

Plane	Mo $K-\alpha$	Relative Intensities for		Fe $K-\alpha$
		Cu $K-\alpha$	Ni $K-\alpha$	
111	374.6	431.2	412.4	226.5
200	181.6	192.1	185.7	[100]
220	[100]	[100]	[100]	—
113	102.9	107.4	—	—
222	34.1	32.0	—	—
400	—	—	—	—
133	30.6	—	—	—
240	28.6	—	—	—
224	18.3	—	—	—
333}	18.5	—	—	—
115}				
220 of NaCl	571.7	107.7	93.3	49.1

TABLE II.

Radiation	Reflection	Intensity of reflection (220, NaCl=100)	F for 110, Fe
Cu $K-\alpha$	110, Fe	51.9	11.48
Ni $K-\alpha$	110, Fe	37.5	9.77
Fe $K-\alpha$	110, Fe	609.2	13.45
Cu $K-\alpha$	220, Cu	94.2	—
Ni $K-\alpha$	220, Cu	88.4	—
Ni $K-\alpha$	200, Cu	167.7	—
Fe $K-\alpha$	200, Cu	153.7	—
Fe $K-\alpha$	111, Cu	330.1	—

as standard. Since the absolute reflecting power of no crystal is known for any of the wave-lengths used except Mo $K\alpha$, it has, as before, been assumed that $F(220, \text{NaCl})$ is independent of wave-length and equal⁵ to 15.62. Though this assumption is almost certainly not strictly accurate, it probably does not depart far from the truth. When absolute F 's shall have been determined for these longer wave-lengths, it will be easy to shift the present results to conform with them.

The F -values calculated from the intensity data of Tables I and II are dependent upon the absorption coefficients that are used. Experimental values exist for most of these coefficients. Except for metallic copper when absorbing Cu $K\alpha$ and metallic iron when absorbing Ni $K\alpha$ radiations, they are in satisfactory agreement with the values calculated by Jönsson's general formula.⁶ Even in the most unfavorable case, the choice of extreme values of absorption coefficients makes a difference of only 0.4 of an absolute F -unit.

⁵ R. W. James and E. M. Firth, Proc. Roy. Soc. 117A, 62 (1927).

⁶ E. Jönsson, Uppsala Univers. Årsskrift (1928).

For the sake of uniformity and completeness, calculated μ/ρ 's as shown in Table III, have been employed throughout.

The resultant reflection F 's are recorded in Tables II, IV and V and in Figure 1. Several comparisons are possible between these data and the

TABLE III. Absorption coefficients used in calculating F -values.

Absorber	Density	Mo $K-\alpha$	Absorbed Wave-length		Fe $K-\alpha$
			Cu $K-\alpha$	Ni $K-\alpha$	
Nickel	8.90	423	432	549	825
Copper	8.95	—	468	586	886
Iron	7.92	—	2556	3124	570
NaCl	2.16	18.0 ₁	161. ₂	196. ₂	306. ₈

TABLE IV. Absolute F -values of the nickel atom in metallic nickel.

Plane	$\sin \theta/\lambda$	Mo $K-\alpha$ (0.710 Å)	Radiation		Fe $K-\alpha$ (1.932 Å)
			Cu $K-\alpha$ (1.537 Å)	Ni $K-\alpha$ (1.655 Å)	
111	0.246	18.06	14.94	15.92	16.05
200	.284	16.89	13.70	14.71	14.69
220	.402	12.91	10.57	11.29	—
113	.471	11.10	8.73	—	—
222	.492	11.64	8.32	—	—
400	—	—	—	—	—
133	.619	8.37	—	—	—
240	.635	8.36	—	—	—
224	.696	7.48	—	—	—
333}	.738	7.01	—	—	—
115}					

TABLE V. Absolute F -values of the copper atom in metallic copper.

Plane	$\sin \theta/\lambda$	Cu $K-\alpha$ (1.537 Å)	Radiation		Fe $K-\alpha$ (1.932 Å)
			Ni $K-\alpha$ (1.655 Å)		
111	0.241	16.60	—		14.59
200	.278	14.90	14.57		13.72
220	.392	11.53	11.18		—
113	.461	9.56	—		—
222	.481	9.10*	—		—

* The relative intensities of the reflections in this column (compared with 220) are those found by A. H. Armstrong (reference 1).

results of previous measurements. The $F(220, \text{Cu})$ for Cu $K\alpha$ is in fairly good agreement with existing information, but $F(110, \text{Fe})$ for the same radiation falls considerably below the published⁷ value. Additional observations with iron powder from the source which supplied the earlier experiments make it seem probable that there was some preferential orientation in the previous powder cake. Of interest is the comparison that can be made between the F -curves of metallic nickel and of the nickel ion⁸ in NiO. This comparison

⁷ A. H. Armstrong, reference 1.

⁸ R. W. G. Wyckoff, Phys. Rev. **35**, 583 (1930).

is shown graphically in Figure 2 for Mo $K\alpha$, Cu $K\alpha$ and Ni $K\alpha$ rays. The agreement is especially close for the Mo $K\alpha$ and Cu $K\alpha$ curves.

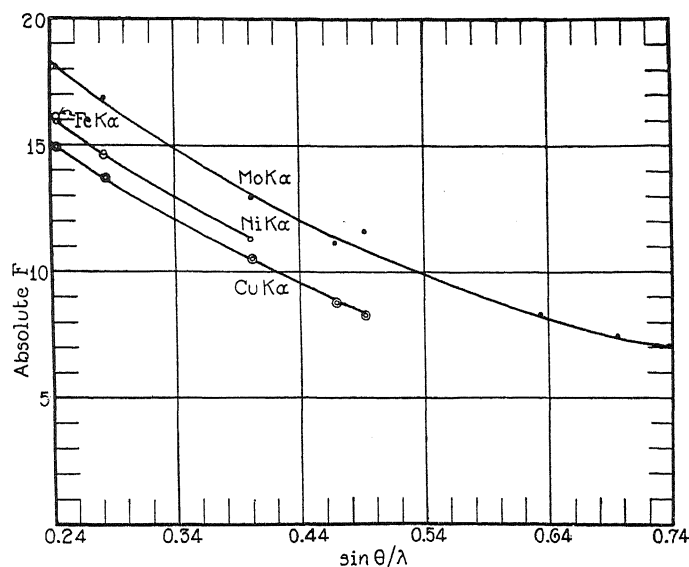


Fig. 1. The experimentally determined F -curves of metallic nickel for Mo $K\alpha$, Ni $K\alpha$ and Cu $K\alpha$ radiations. The two observed points for Fe $K\alpha$ rays are shown as large open circles.

Points on the F -curve for nickel with molybdenum radiation could be measured for reflections more complicated than (333; 115). Such reflections would be hard to determine with accuracy, however, because they are insignificant compared with the background of secondary nickel radiation

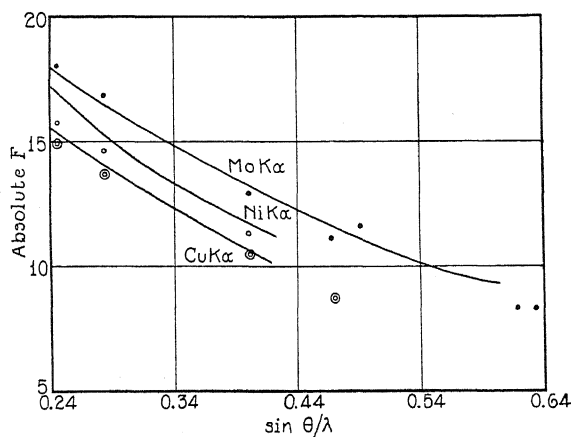


Fig. 2. The F -curves for the nickel atoms in NiO crystals are shown as full lines. Observed points for nickel atoms in metallic nickel appear as black circles (for Mo $K\alpha$), open circles (for Ni $K\alpha$) and ringed circles (for Cu $K\alpha$).

excited by the Mo $K\alpha$ lines. The first, (111), reflection of nickel occurs at so great an angle ($\sin \theta/\lambda = 0.246$) that much of the complete F -curve of metallic

nickel is of necessity extrapolated. This fact seems to prevent any important physical significance being attached to the electron-distribution curves that are calculated by Fourier analysis from the extrapolated forms of this F -curve.

The F -values of this paper show clearly the way in which the reflecting power of an atom varies with the wave-length of the x-rays scattered. The phenomena are illustrated by the (200) reflections of nickel as plotted in Figure 3. All of the other data of the present paper as well as those from NiO

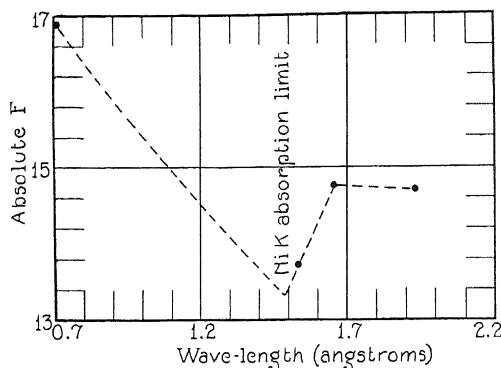


Fig. 3. The dotted curve indicates the variation of the scattering power of nickel with wave-length. The full circles are the measured values of the (200) reflection of metallic nickel.

agree with this figure in showing that the scattering power of an atom is at a minimum close to its K critical absorption limit, that it attains a maximum at, or near, its "resonance" wave-length, but that the reflecting power falls off only slowly on the long wave-length side of this frequency. The photographs made by Mark and Szilard⁹ of RbBr using strontium and bromine radiations are obviously an expression of the same variation.

It is hoped through additional experiments to put these scattering powers for long wave-lengths upon an accurate absolute scale.

⁹ H. Mark and L. Szilard, *Zeits. f. Physik* 33, 688 (1925).

THE THEORY OF COMPLEX SPECTRA

BY E. U. CONDON

PALMER PHYSICAL LABORATORY, PRINCETON UNIVERSITY

(Received August 27, 1930)

ABSTRACT

Extending the paper of Slater (Phys. Rev. **34**, 1293, 1929) on complex spectra, it is pointed out that assignment of definite electron configurations to spectral terms is an approximate procedure and only has meaning when the multiplet systems of the several configurations are widely separated. The effect of including spin terms is sketched. Non-diagonal matrix elements for the N -electron problem are reduced to corresponding elements for the 2-electron problem, as Slater did for the diagonal elements. Two-electron jumps occur because of the fact that spectral terms may not be precisely labelled by means of electron configurations.

IN A paper of this same name, Slater¹ has given a direct treatment of the application of the first order perturbation theory to the central field approximation to the atom model. He neglects spin forces in the Hamiltonian and so his results correspond to pure Russell-Saunders coupling of the angular momentum vectors, all intervals inside of the multiplets being zero. The electrostatic interaction gives the classification into multiplet levels and the calculations provide definite predictions concerning the intervals between the several multiplets which belong to the same electron configuration.

These intervals are found to be expressible in terms of certain double integrals over the radial factors of the eigen-functions of an electron moving in the central field which is made the starting-point of the perturbation calculation. For a configuration which gives n multiplets, there are thus $(n-1)$ intervals. Slater's first-order calculation expresses these $(n-1)$ intervals in terms of a fewer number (say, m) of integrals, usually, so even if one regards all of the integrals as independently adjustable, the theory predicts certain relations between the intervals. One may choose values for the m integrals as if they were independent so as to get the best fit possible in order to obtain a kind of test of Slater's results. Such a test of the results can be made comparatively simply without going into the more difficult question of determination of the best central field and the radial eigen-functions associated with it. If a good representation of the data is obtained on treating the m integrals as independent, the question still remains whether the m values assigned are compatible with the central field eigen-functions in view of the fact that they are not really independent. However, if a good representation cannot be obtained even by treating the integrals as independent, it certainly will not be improved when allowance is made for the fact that they are not independent.

¹ Slater, Phys. Rev. **34**, 1293 (1929).

With such considerations in mind an attempt was made to apply Slater's results to a larger number of cases than he has treated in the examples at the end of his paper. It quickly became apparent that the intervals between the multiplets usually disagree badly with the first-order calculations. It is therefore necessary for an adequate theory of complex spectra to extend the calculations to a higher degree of approximation. Some results in that direction are the subject of this paper.

1. Definitions and Notation. The starting point, as with Slater, is a model of the atom in which N electrons each move, without influencing each other, in the same central field which has the potential energy, $-U(r)$. Only eigen-functions that are anti-symmetric in all pairs of electrons are used and so an eigen-function is specified by giving a *complete set* of $4N$ quantum numbers. A complete set consists of N *individual sets* which are called (n, l, m, k) these being the (n, l, m_l, m_s) of Slater. Each electron has four coordinates (x, y, z, s) . The first three give its position and the fourth the z -component of spin angular momentum. For short the Greek letters, $\alpha, \beta, \gamma, \delta \dots$ are written for separate individual sets. Also the capitals $A, B, C, D \dots$ are written as abbreviations for different complete sets.

By Pauli's exclusion principle all individual sets in a complete set must be different, and two complete sets are not considered as different if they differ merely in regard to the order of listing of the same N individual sets. Nevertheless for definiteness a definite order of writing the individual sets in a complete set is adopted and adhered to during the calculations.

Since anti-symmetric eigen-functions are used there is no one-to-one correspondence between individual electrons and individual sets of quantum numbers. This means that an expression commonly used in spectroscopy such as "the excited electron is in a $4f$ state" refers to the presence of a $4f$ individual set in the complete set of quantum numbers. The electron configuration of a given complete set means the list of n, l values of the individual sets. Thus there are generally a number of different complete sets belonging to each configuration. Since the energy of a particle in a central field depends only on n and l , all of the complete sets belonging to a certain configuration have the same energy in the zeroth approximation from which the start is made.

For the one-electron eigen-function having the individual set α , written as a function of the first electron's coordinates, the notation $u_\alpha(1)$ is used, replacing Slater's $u(n_1/x_1)$. ψ is defined as

$$\psi = u_\alpha(1) \cdot u_\beta(2) \cdot u_\gamma(3) \cdots u_\xi(N)$$

so that the normalized eigen-function for the complete set A is

$$\Psi_A = (N!)^{-1/2} \sum_P (-1)^p P\psi$$

in which P stands for a permutation of the indices $1, 2, 3 \cdots N$ in ψ relative to the $\alpha, \beta, \gamma \cdots \xi$. The summation extends over all $N!$ such permutations and p has the parity of P .

For the matrix component of any quantity as H which connects the states having the complete sets A and B , the Dirac notation $(A | H | B)$ is used, so that

$$(A | H | B) = \int \bar{\Psi}_A H \Psi_B$$

where \int means integration over the $3N$ position coordinates and summation over the N spin coordinates.

2. Formulation of the energy level problem. The starting point is an exact solution of the quantum mechanical problem for a fictitious atom whose Hamiltonian is E where

$$E = \sum_1 \left[\frac{1}{2\mu} (p_{x1}^2 + p_{y1}^2 + p_{z1}^2) - U(r_1) \right] \quad (2.1)$$

where \sum_1 means that the same functional form is to be written down successively as depending on the coordinates of all N electrons and the results added together.

A form of the Hamiltonian for real atoms that is much nearer to the truth is

$$H = \sum_1 \left[\frac{1}{2\mu} (p_{x1}^2 + p_{y1}^2 + p_{z1}^2) - \frac{ze^2}{r_1} + V(r_1) M_1 \cdot s_1 \right] + \frac{e^2}{2} \sum_{1,2} \frac{1}{r_{12}} \quad (2.2)$$

In this the terms $V(r_1) M_1 \cdot s_1$ represent the energy of interaction of each electron's spin with its own orbital angular momentum. $V(r_1)$ is to be chosen in some way along lines of the semi-empirical discussions of the "screening for the spin doublets" of other workers. The question will not be discussed further in this paper. $M \cdot s$ is the scalar product of orbital and spin angular momentum for an electron. $\sum_{1,2}$ means a summation over all pairs of electrons, the two indices varying independently so that each pair is counted twice. Since the operators for E and H do not commute with each other, the matrix for H will not be diagonal in terms of the representation that is based on the eigen-functions of E . The problem of finding the energy levels for H is that of finding a transformation to the diagonal form for the matrix for H .

How the function $U(r)$ is to be chosen will not be discussed here. An approximate theoretical treatment, such as that of Thomas and Fermi, or a semi-empirical method of the sort studied especially by Hartree may be used. Slater studied the Hamiltonian (2.2) with omission of the spin term. Houston,² Bartlett,³ and Gaunt,⁴ have considered special cases of (2.1) counting the spin term and Goudsmit⁵ has recently extended their results by a clever device.

² Houston, Phys. Rev. **33**, 297 (1929).

³ Bartlett, Phys. Rev. **35**, 229 (1930).

⁴ Gaunt, Proc. Roy. Soc. **A122**, 513 (1929).

⁵ Goudsmit, Phys. Rev. **35**, 1325 (1930).

When the spin term is omitted the Hamiltonian H commutes with both the sum of the z -components of orbital angular momentum, and the sum of the z -components of spin angular momentum. Therefore H has no matrix components connecting states of E for which either of these sums is different. In terms of the quantum numbers introduced in §1 the quantities are Σm and Σk , the sums being over all the individual sets belonging to a complete set. Slater makes very good use of these results to calculate the energies of all the multiplets arising from a configuration (except for those configurations in which more than one multiplet of the same kind appears) without having to calculate any non-diagonal matrix components.

If the spin term is not omitted one still has the result that H commutes with the total sum of the z -components of both orbital and spin angular momentum although it no longer commutes with each sum separately. Therefore, even with spin counted there will be no matrix components of H connecting states for which the values of $\Sigma(m+k)$ differ.

There is another important property of the Hamiltonian which arises from its isotropy with regard to different orientations of the coordinate axes. The isotropy means that there is still a degeneracy, that of space quantization, associated with the Hamiltonian, so that the degeneracy of E is not completely removed by the inclusion of the spin and electrostatic repulsion terms which are the essence of the transformation from E a diagonal matrix to H a diagonal matrix. With each eigen-value of H can be associated a maximum value of $\Sigma(m+k)$ which is represented among the eigen-functions belonging to that eigen-value. This number is the quantum number J of that energy level. The isotropy then brings with it the result that there are other eigen-functions for which $\Sigma(m+k)$ has the values $J-1, J-2 \dots, -J$ all of which have the same eigen-value. The proof of this is best obtained by appeal to group theory.

If one uses the perturbation theory to find approximately the transformation from E diagonal to H diagonal, by treating $(H-E)$ as a perturbation, the success of the calculation in the first-order requires that the eigen-values of H which "grow out of" a particular eigen-value of E remain close together compared with the distance of the particular eigen-values of E from its nearest neighbor in the spectrum of E . This is a well known property of the perturbation theory and shows itself in many particular instances. Perhaps the Paschen-Back effect in the anomalous Zeeman effect is the best known of these. In it the effect of a uniform magnetic field on an atomic energy level is required. The first-order calculation is correct only if the spread of the energy levels growing out of the unperturbed level is small compared to the distance from the unperturbed level to its nearest neighbor in the unperturbed scheme. If this condition is not fulfilled then the second order perturbation becomes important. An important second-order correction implies that an important alteration of the eigen-function has taken place so that, when it is expanded in terms of the eigen-functions of E , it begins to have an important component of the eigen-function of the neigh-

boring level of E in addition to the eigen-function of the level from which it grew.

Therefore as the second-order correction becomes more important the quantum numbers which were appropriate to labelling the different eigenvalues of E become less and less appropriate for the labelling of the eigenvalues of H . They cease to be "good quantum numbers" to use a curiously apt expression introduced by Mulliken⁶ in a discussion of the correlation of atomic energy levels with those of diatomic molecules.

3. Validity of configuration assignments. All discussions of complex spectra have hitherto been based on the idea that an electron configuration could be assigned uniquely to each energy level. That this procedure is only of approximate validity is seen at once from the foregoing discussion. The

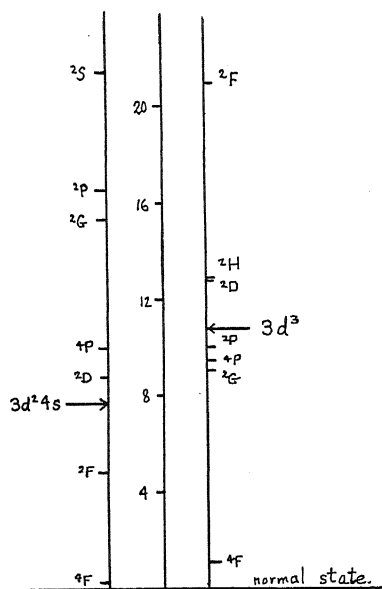


Fig. 1. The two lowest configurations in $Ti II$. Theory predicts another $2D$ for $(3d)^3$ which has not been found; the arrow shows the center of gravity of the known terms, which is therefore not the exact center of gravity of the whole configuration. The center scale is in thousands of cm^{-1} .

criterion can be so formulated: *The assignment of a definite electron configuration to a group of multiplets is only exact insofar as the spread of the levels belonging to one configuration is small compared to the distance (on the energy level diagram) of the spread of levels belonging to the neighboring configurations.*

It is evident that this criterion for the case of the electron configuration quantum numbers is of the same form as the well known criterion for deciding between "weak" and "strong" magnetic fields in the Paschen-Back effect.

The importance of raising this point lies in the fact that complex spectra have already been analyzed in which the criterion for definite assignments

⁶ Mulliken, *Reviews of Mod. Phys.* **2**, 60 (1930).

of electron configurations is not fulfilled. A noteworthy instance⁷ is that of Ti II as analyzed by Russell.⁸

In Fig. 1 are plotted the levels corresponding to the two lowest configurations in Ti II as assigned by Russell. The arrows in each column give the centers of gravity of all the terms in the column, weights being assigned according to their values of $(2J+1)$.

It is evident that here, if anywhere, one may expect an appreciable effect of what may be suitably called interaction of neighboring electron configurations. Except for the overlapping of $d^3\ ^2H$ and $\ ^2D$ and of $d^3\ ^2P$ and $\ ^4P$ the distance between multiplets is large compared to intervals inside the multiplets, so that the criterion for Russell-Saunders coupling is fulfilled. The $\ ^2H$ and $\ ^2D$ can show no interaction, though, since they have no common value of J , whereas it is expected that the nearness of $\ ^2P$ to $\ ^4P$ will disturb the intervals. This is in fact the case, the ratio of the observed intervals being 3.82 against a theoretical (Landé) value of 1.67.

Perhaps the best way to present the situation is by reference to Slater's diagrams (loc. cit. p. 1301) of the energy matrix. Referring to his Fig. 2, one may suppose that the upper double-shaded square is the matrix for the different complete sets belonging to $(3d)^24s$ and the next double-shaded square is the similar matrix for complete sets belonging to $(3d)^3$. Slater says that the terms in the singly-shaded rectangles (these are the matrix components connecting the complete sets in $(3d)^24s$ with those in $(3d)^3$) are negligible. This is often the case but the point that is made here is that they are not negligible in a case where the distance between the centers of gravity of the terms coming from the same configuration is small or comparable with the spread of the multiplets arising from the two configurations separately. In case the configurations overlap, as they do in the special instance of Ti II one needs to consider the larger square which includes the two doubly-shaded squares and the two singly-shaded rectangles that border them.

If one next makes use of the exact theorem that there are no matrix components connecting complete sets for which $\Sigma(m+k)$ differs the large square is considerably simplified. It can be rearranged so that complete sets belonging to either configuration but having the same $\Sigma(m+k)$ are in adjacent rows and columns and then the large square corresponding to the two configurations taken together will break up into a series of smaller squares. If one wishes further to neglect the spin terms, as Slater does, then these smaller squares may be broken up into still smaller ones since then both Σm and Σk separately have to be equal in the quantum numbers labelling rows and columns.

The actual procedure in applying the diagonal sum method will be illustrated in terms of d^2s and d^3 although the numerical application of the formulas to $(3d)^24s$ and $(3d)^3$ in Ti II will be reserved to a later paper. One has first to set up the scheme of complete sets of quantum numbers for each config-

⁷ I am indebted to my friend, Prof. J. E. Mack, for directing my attention to this case.

⁸ Russell, *Astrophys. J.* **66**, 283 (1927).

uration, just as Slater does. For example, Table I gives the quantum numbers for the (*dds*) configuration.

TABLE I. Sets of quantum numbers for (*dds*) configuration.

$\Sigma k =$	3/2 (+++)	1/2 (+-+)	(++-)
$\Sigma m = 4$		(220)	
3	(210)	(210) (120)	(210)
2	(200)	(200) (020) (110)	(200)
1	(2-10) (100)	(2-10) (-120) (010) (100)	(2-10) (100)
0	(2-20) (1-10)	(2-20) (-220) (1-10) (-110) (000)	(2-20) (1-10)

In this table are listed the *m* values that may be associated with the sets of spin (*k*) values that head the columns. The corresponding table for *d*³ is Table II.

TABLE II. Sets of quantum numbers for (*ddd*) configuration.

$\Sigma k =$	3/2 (+++)	1/2 (++-)
$\Sigma m = 6$		(212)
5		(211) (202)
4		(210) (201) (2-12) (102)
3	(210)	(21-1) (200) (2-11) (2-22) (101) (1-12)
2	(21-1)	(21-2) (20-1) (2-10) (2-21) (100) (1-11) (1-22) (0-12)
1	(21-2) (20-1)	(20-2) (2-1-1) (2-20) (10-1) (1-10) (1-21) (0-11) (0-22)
0	(20-2) (10-1)	

In these tables it is not necessary to list the quantum numbers for negative values of Σm and Σk as these do not give additional information.

The multiplet schemes corresponding to the two configurations are given superposed in the Table III, the first line in each cell being the contribution from *d*²*s* and the second that from *d*³.

TABLE III. Multiplets for *d*²*s* and *d*³.

$\Sigma k =$	3/2	1/2
$\Sigma m = 6$		
5		² H
4		² H ² G
3	⁴ F	² H ² G ² F ⁴ F
2	⁴ F	² H ² G ² F ² D ² D ⁴ F
1	⁴ F ⁴ P	² H ² G ² F ² D ² D ² P ⁴ F ⁴ P
0	⁴ F ⁴ P	² H ² G ² F ² D ² D ² P ² S ⁴ F ⁴ P

Now if the interaction between configurations can be neglected the diagonal sum method gives a value for the sum of the energies of all the multiplets

lying on each line separately in each cell. But if the interaction is important then the diagonal sums must be taken simply cell by cell, this gives only half as many equations and so the power of the diagonal sum method is greatly diminished (just as it is greatly diminished when spin is not neglected). Neglecting the interaction the diagonal sum method in this case is capable of giving the energy of each multiplet except that it can only give the arithmetic mean of the two 2D 's which arise from d^3 . Allowing for the interaction it gives much less: now the 2H and the 2S are the only ones given directly, also given are the arithmetic means of the two 4P 's the two 4F 's, the three 2D 's, the two 2P 's, the two 2F 's and the two 2G 's.

In order to get the actual separation of the terms of similar multiplet character whose sums only are given one needs to have the non-diagonal elements of the energy matrix.

With these at hand one can set up the secular determinants for each cell and get the roots of the secular equations. This looks formidable at first sight because the determinants are of the order equal to the number of multiplets in each cell. But the diagonal sum method can be used to depress the order of the secular equations so that one needs only to solve a quadratic where there are two multiplets of the same kind, a cubic if there are three, and so on.

Perhaps it is helpful here to point out how the diagonal sum method works when spin is not neglected. In that case one can not write an equation that the sum of the terms in each cell of the $\Sigma m, \Sigma k$ diagram is equal to the sum of the corresponding diagonal elements of the energy matrix. Also one needs a complete table covering the negative values of Σk as well as the positive. For simplicity the argument will be presented in terms of the sp configuration, which has already been fully treated by Houston.⁹ One has for $\Sigma m, \Sigma k$:

sp

$\Sigma k =$	1 (++)	0 (+-) (-+)	-1 (--)
$\Sigma m = 1$	(01)	(01) (01)	(01)
0	(00)	(00) (00)	(00)
-1	(0-1)	(0-1) (0-1)	(0-1)

Arranging by values of $\Sigma(m+k)$ one sees that the values of $\Sigma(m+k)$ and the number of complete sets by which each value is realized is

$\Sigma(m+k)$	Realizations	Terms represented
2	1	3P_2
1	3	3P_2 3P_1 1P_1
0	4	3P_2 3P_1 3P_0 1P_1
-1	3	3P_2 3P_1 1P_1
-2	1	3P_2

⁹ Houston, Phys. Rev. 33, 297 (1929).

The third column gives the energy levels whose sum is given by applying the diagonal sum method to all complete sets which have the same value of $\Sigma(m+k)$. Just as the diagonal sums, without spin, fails to give the separation between two multiplets of the same kind, so here with spin it fails to give the separation between two levels having the same J value. To get the separation one would need to solve a quadratic equation, which is what Houston did. And generally, the diagonal sums alone will give simply the arithmetic mean of all the terms in the configuration that have the same J value. To get them separately one has to use the non-diagonal elements and solve an algebraic equation whose degree is equal to the number of times the particular J value occurs. This statement is the starting point of Goudsmit's recent work on the transition from Russell-Saunders to jj -coupling.

Of course it is evident that if perturbations by an external magnetic field are included the method of diagonal sums gives the derivation of the g -sum rules that play such an important role in the theory of the anomalous Zeeman effect. But similarly if one wants to find the individual g 's for n terms of the same J value then an algebraic equation of the n^{th} degree has to be solved, and this is true whether the n terms come from the same configuration or not.

4. Non-diagonal matrix elements. The diagonal sum method works only with the diagonal matrix elements of the energy and is quite powerful. It gives the energies of each multiplet belonging to a configuration if the interaction between configurations is neglected and if all multiplets are of a different kind. To go beyond this and find the separations between two multiplets of the same kind, or to allow for interaction of configurations and for other questions it is necessary to know the non-diagonal elements.

Two types of symmetrical function of the electron coordinates are of especial importance. One is of the form $F = \Sigma_i f(1)$, that is, the sum of the same function of each one of the electron's coordinates occurring one at a time. The other is $G = \Sigma_{12} g(1,2)$, that is, the sum over all possible pairs of electrons, of a symmetrical function of the coordinates of both of them. Slater has carried out the calculation for the diagonal elements, the extension to the non-diagonal elements is very easy and almost exactly like Slater's work so only the results will be stated.

For a quantity of the type F , the matrix components, $(A | F | B)$, connecting states with the complete sets A and B are as follows:

- (a) They vanish if B differs from A in regard to more than one individual set.
- (b) If B differs from A solely in regard to one individual set then

$$(A | F | B) = \int_1 \bar{u}_\alpha(1) f(1) u_{\alpha'}(1)$$

where α and α' are the only individual sets of A and B respectively which are not equal.

- (c) The diagonal element $(A | F | A)$ is worked out by Slater. Its value is

$$(A | F | A) = \sum_{\alpha} \int_1 \bar{u}_{\alpha}(1) f(1) u_{\alpha}(1)$$

where the sum extends over all the individual sets in the complete set A .

An immediate corollary of the results (a) and (b) is that if $f(1)$ is a quantity which is a diagonal matrix in the one-electron problem, then F is a diagonal matrix in the N -electron problem. This is perhaps the simplest way of proving that the total z -component of spin and the total z -component of orbital angular momentum are diagonal matrices in the representation used for this approach to the theory of complex spectra.

Similarly the matrix components, $(A | G | B)$, for a quantity of the type G can be reduced as follows:

(d) They vanish if B differs from A in regard to more than two individual sets.

(e) If B differs from A only in that two of its individual sets which one may call α', β' differ from the individual sets of A , called α, β , then

$$(A | G | B) = \left[2 \int_{1,2} \bar{u}_{\alpha}(1) \bar{u}_{\beta}(2) g(1, 2) u_{\alpha'}(1) u_{\beta'}(2) - 2 \int_{1,2} \bar{u}_{\alpha}(1) \bar{u}_{\beta}(2) g(1, 2) u_{\beta'}(1) u_{\alpha'}(2) \right].$$

(f) If B differs from A only in that its individual set, α' , differs from the individual set, α , in A then

$$(A | G | B) = 2 \sum_{\beta} \left[\int_{1,2} \bar{u}_{\alpha}(1) \bar{u}_{\beta}(2) g(1, 2) u_{\alpha'}(1) u_{\beta}(2) - \int_{1,2} \bar{u}_{\alpha}(1) \bar{u}_{\beta}(2) g(1, 2) u_{\beta}(1) u_{\alpha'}(2) \right]$$

where \sum_{β} means a summation in which β runs over the $N-1$ individual sets that are common to A and B .

(g) The diagonal element $(A | G | A)$ is given by Slater. It is

$$(A | G | A) = \sum_{\alpha, \beta} \left[\int_{1,2} \bar{u}_{\alpha}(1) \bar{u}_{\beta}(2) g(1, 2) u_{\alpha}(1) u_{\beta}(2) - \int_{1,2} \bar{u}_{\alpha}(1) \bar{u}_{\beta}(2) g(1, 2) u_{\beta}(1) u_{\alpha}(2) \right]$$

the summation running over all pairs of individual sets.

These results show further simplifications for quantities that are independent of spin. For $u_{\alpha}(1)$ one has

$$u_{\alpha}(1) = v_{\alpha}(1) \delta(s_1, k_{\alpha})$$

where $v_{\alpha}(1)$ is a function of the position coordinates only. In the preceding formulas \int_1 means integration over the position coordinates and summa-

tion over the spin coordinate. If $f(1)$ or $g(1,2)$ do not depend on spin the summation over s can be carried out at once. The results are:

$$(b) \quad (A | F | B) = \delta(k_\alpha, k_{\alpha'}) \int_1 \bar{v}_\alpha(1) f(1) v_{\alpha'}(1)$$

$$(c) \quad (A | F | A) = \sum_\alpha \int_1 \bar{v}_\alpha(1) f(1) v_\alpha(1)$$

$$(e) \quad (A | G | B) = 2 \left[\delta(k_\alpha, k_{\alpha'}) \delta(k_\beta, k_{\beta'}) \int_{1,2} \bar{v}_\alpha(1) \bar{v}_\beta(2) g(1, 2) v_{\alpha'}(1) v_{\beta'}(2) - \delta(k_\alpha, k_{\beta'}) \delta(k_\beta, k_{\alpha'}) \int_{1,2} \bar{v}_\alpha(1) \bar{v}_\beta(2) g(1, 2) v_{\beta'}(1) v_{\alpha'}(2) \right]$$

$$(f) \quad (A | G | B) = 2 \delta(k_\alpha, k_{\alpha'}) \sum_\beta \left[\int_{1,2} \bar{v}_\alpha(1) \bar{v}_\beta(2) g(1, 2) v_{\alpha'}(1) v_\beta(2) - \int_{1,2} \bar{v}_\alpha(1) \bar{v}_\beta(2) g(1, 2) v_\beta(1) v_{\alpha'}(2) \right].$$

$$(g) \quad (A | G | A) = \sum_{\alpha, \beta} \left[\int_{1,2} \bar{v}_\alpha(1) \bar{v}_\beta(2) g(1, 2) v_\alpha(1) v_\beta(2) - \delta(k_\alpha, k_\beta) \int_{1,2} \bar{v}_\alpha(1) \bar{v}_\beta(2) g(1, 2) v_\beta(1) v_\alpha(2) \right].$$

A consequence of the limitation (d) is that there is no first-order interaction between two neighboring configurations that differ in regard to more than two electrons. This result is hardly likely to be of much importance for two configurations that differ in regard to as many as three electrons will, in general, lie in widely separated parts of the energy level diagram so the interaction would be negligible anyway.

This completes the reduction of the non-diagonal elements to integrations over the coordinates of only one or two electrons. If in particular $g(1,2)$ is of the form $1/r$ additional developments may be made in which $1/r_{12}$ is expanded in a series of spherical harmonics and so all the integrals can be expressed, as Slater does for the ones occurring in the diagonal elements, as a sum of certain integrals over the radial eigen-functions multiplied by coefficients that are certain integrals of spherical harmonics. The calculations involve some more general coefficients than Slater's a 's and b 's. Detailed developments of this part of the reduction will be reserved for a later paper.

5. Two-electron jumps. An immediate application of the results of the preceding section is to the question of "two-electron jumps." These are transitions between energy levels whose configurations differ in regard to two of the sets of nl values. Such transitions are usually weak compared to the more usual one-electron jumps. One may also have "zero-electron

jumps," that is, transitions between terms arising from the same configuration. This is the usual way of stating the case, in which one speaks as though each term is uniquely associated with a single configuration of the central field approximation.

The interaction between a light wave whose vector potential is given by $A(x, y, z)$ and an atom consisting of N electrons is measured by a term in the Hamiltonian of the form

$$\sum_1 A(x_1, y_1, z_1) \cdot p_1$$

where p_1 is the momentum of the first electron. This form embraces quadrupole and all multipole radiations. The dipole radiation which is the first approximation is obtained by replacing $A(x, y, z)$ by its value at the center of the atom and writing

$$A(0, 0, 0) \cdot \sum_1 p_1$$

which is valid if the wave-length is great compared to the size of the atom so that A does not vary much over the size of the atom. Now even the exact interaction is of the form of the sum of the same operator function of the coordinates of each electron summed over each of the electrons. Therefore one sees that its matrix components connecting complete sets which differ in regard to more than one individual set vanish.

In other words, if assignment of electron configurations to energy levels were an exact procedure there would be no two-electron jumps. Thus the existence of two electron jumps is an indication of a break-down of exact configuration assignments.

This point is similar to the one that the existence of inter-system combinations, i.e. transitions between states of different multiplicities, is an indication of the break down of exact assignment of L and S values of the terms, i.e. break-down in the Russell-Saunders coupling scheme.

There is an interesting question of language involved here. If the expression "electron jump" is to be translated into quantum mechanics as meaning a change in an (nl) individual set in going from an initial state to a final state, then, strictly, only one-electron jumps occur. But the exact eigen-function of each energy level has in its make-up components belonging to several different configurations of the central field model, whereas it has been the custom to assign to the energy level one configuration which is presumed to be the one that has the largest component in the expansion of the exact eigen-function. One-electron jumps are the only ones really occurring but since the exact eigen-function has other configurations in it than the principal one from which it derives its configuration name, there will appear to be two-electron jumps when the transitions are described solely by reference to the single configuration name that is assigned to each level by the customary procedure. It is the same with inter-system combinations: the selection rule $\Delta S=0$ is exact, but the actual energy levels have components in their eigen-functions corresponding to more than one value of S ; then when

one persists in labelling the terms simply with the value of S most strongly represented in the eigen-function he is confronted with apparent violations of this selection rule.

The break-down of exact configuration assignments also has important implications for the theory of relative intensity of spectral lines. Ornstein and Burger¹⁰ have already shown that when inter-system combinations have appreciable intensity that they must be appropriately reckoned in the application of the intensity sum rules. This point is brought out clearly also in recent work by Harrison.¹¹ That is, the sum rules have to be applied to all the lines arising from transitions between all the terms of the initial and final configurations. Evidently all this has to be extended one step further for cases in which the interaction between two configurations is important. For simplicity suppose the initial state levels can be all given a fairly exact configuration assignment but that for the final state there are two configurations in interaction. Then the sum rules for intensities will have to be extended to summations over all lines terminating on any of the levels belonging to both of the interacting configurations. Detailed consideration of the intensity relations will be postponed to a later paper.

This paper was written at Stanford University during the summer quarter. The writer takes pleasure in this opportunity to thank the Stanford physicists for their cordiality and especially Professor G. R. Harrison for stimulating discussions on spectroscopy. He is also indebted to Professor J. E. Mack for discussions last winter at the University of Minnesota.

¹⁰ Ornstein and Burger, *Zeits. f. Physik* 40, 403 (1926).

¹¹ Harrison, *J. Opt. Soc. Amer.* 19, 109 (1929).

THE ZEEMAN EFFECT IN THE ZnH AND CdH BANDS

BY WILLIAM W. WATSON

SLOANE PHYSICS LABORATORY, YALE UNIVERSITY

(Received August 15, 1930)

ABSTRACT

The Zeeman effect in the ${}^2\Pi \rightarrow {}^2\Sigma$ bands of ZnH at $\lambda 4326$ and CdH at $\lambda 4509$ which involve strictly case (a) ${}^2\Pi$ states and ${}^2\Sigma$ states with large ρ -type doubling is reported in detail. Field strengths up to 30,400 gauss were used, together with a large concave grating in a parallel light mounting which gives a dispersion in the third order of about 1.44Å per mm in this region.

Analysis of the ZnH and CdH bands.—Intensity relations among the 12 branches of each band are discussed. The ρ -type doubling in the ${}^2\Sigma$ states is found definitely to be proportional to $K + \frac{1}{2}$ rather than to K .

The Zeeman effect patterns.—The positions and widths of the blocks of components for all the lines are computed by means of the quantum mechanics formulas of E. L. Hill. Observed and computed patterns are shown to be in excellent agreement on a number of details unique to these bands. Diagrams and tables of data showing these details are given for $H = 16,400$ gauss for the lines of several branches.

INTRODUCTION

WITH the aid of the formulas recently developed by Hill¹ for the Zeeman effect in doublet molecular states, quantitative consideration of the rather complex Zeeman patterns in doublet bands is now possible. Agreements with the predictions of the theory have been obtained by Almy and Crawford² in the ${}^2\Pi \rightarrow {}^2\Sigma$ MgH bands, by the writer and W. Bender³ for the lower rotational states in the ${}^2\Pi \rightarrow {}^2\Sigma$ CaH bands, and by Almy⁴ for the ${}^2\Sigma \rightarrow \Pi^2$ OH bands. The present paper gives a comparison of the computed Zeeman pattern with some of the details of the effect of a magnetic field on the lines of the ${}^2\Pi \rightarrow {}^2\Sigma$ bands of ZnH at $\lambda 4326$ and of CdH at $\lambda 4509$ which differ from any patterns reported for these other bands.

A few measurements on the Zeeman effect in the $\lambda 4326$ ZnH band have previously been given by Hulthén⁵ and by the writer and B. Perkins.⁶ This earlier work was confined to observations only on the most obvious features of the action of the field, notably the doubling of the lines of low rotational quantum number in the Q_1 , R_1 , and ${}^PQ_{12}$ branches⁷ with component separation approaching at the origin $2\Delta\nu_n$, and ignored the obscurer details which

¹ E. L. Hill, Phys. Rev. **34**, 1507 (1929). Additional treatment by Hill of the effect in ${}^2\Sigma$ states when ρ -type doubling is not neglected is given by G. M. Almy, Phys. Rev. **35**, 1502 (1930).

² G. M. Almy and F. H. Crawford, Phys. Rev. **34**, 1517 (1929).

³ W. W. Watson and W. Bender, Phys. Rev. **35**, 1513 (1930).

⁴ G. M. Almy, Phys. Rev. **35**, 1495 (1930).

⁵ E. Hulthén, Thesis, Lund 1923.

⁶ W. W. Watson and B. Perkins, Jr., Phys. Rev. **30**, 592 (1927).

⁷ Hulthén designated these branches Q_2 , R_2 , and Q_1 respectively. The notation used throughout the present paper follows the latest recommendations.

now are of major interest for comparison with the theory. Particularly puzzling was the reported absence of any effect on the lines of the $^0P_{12}$ and P_1 branches. The incompleteness of these data was due in part to the lack of any guiding theory, and apparently in part also to insufficient exposure-time when obtaining the spectrograms. New high dispersion plates were obviously necessary, and it was decided to include the CdH bands in the investigation in order to note the effect of the very near approach to strictly case (a) conditions in the $^2\Pi$ state (strong orientation of the electronic spin in the direction of the electric axis in the molecule). There is also a considerable increase in the magnitude of the p -type doubling of the lower $^2\Sigma$ state in the CdH bands, the effect of which is discussed below.

It should perhaps be emphasized that these band spectra due to diatomic hydride molecules (and the He_2 bands) constitute, because of the wide spacing of the rotational lines in their fine structure, the best available material for the complete study of the effects of a magnetic field. Even in these bands there is usually a certain amount of overlapping of field patterns from lines of different branches.

EXPERIMENTAL PROCEDURE

As in the CaH investigation, the source was an intermittent d.c. arc operating in a modified Back chamber mounted between the pole faces of a large water-cooled Weiss electromagnet. The pole faces were 2 cm in diameter, spaced 6 mm apart, the maximum field strength in this gap being about 31,000 gauss. The moving electrode was a block of either Zn or Cd c.p. metal about 5 mm square and 3 to 4 mm thick riveted on to the flattened end of a length of 1/8 inch round brass rod. The fixed electrode was a thin strip of Cu, insulated from the pole face by a sheet of mica. A slow stream of hydrogen gas from a commercial cylinder was pumped at about 5 cm of Hg pressure through the arc chamber. The arc current was usually held at 2 amperes. Because of the relatively large size of the Zn or Cd electrode, about five hours of exposure could usually be obtained before renewal of the electrode became necessary.

The spectrograms were obtained in the third order of the large concave grating mounted in parallel light, the dispersion being from 1.43 to 1.46 Å per mm. Field strengths of 9,600, 16,400, and 30,400 gauss were used for both the ZnH and the CdH bands. The strength of the magnetic field was determined by measurements on the patterns of the Zn triplet $\lambda\lambda 4680, 4722, \text{ and } 4811$ as well as that of the $\lambda 4413$ Cd intercombination line ($3/2$ normal triplet). Exposure times of 9 and 10 hours sufficed for good registration of the ZnH bands on Eastman 40 plates at all field strengths, but the CdH band lines are more weakened when the field is thrown on, so that 18 hours of exposure were required with a field of 30,400 gauss to give their patterns with fair intensity. With the same setting without the magnetic field, good spectrograms of these bands could be obtained in 15 minutes. This no-field comparison and an iron arc spectrum were photographed on every plate in addition to the field exposure.

THE ANALYSIS OF THE ZNH AND CDH BANDS

These bands have been completely measured and analysed by Hulthén,^{5,8} the latest interpretation being by Mulliken⁹ to whose article reference should be made for an energy level diagram showing all the observed transitions. The 12 possible branches of ${}^2\Pi \rightarrow {}^2\Sigma$ bands arising from all the transitions obeying the selection rule $\Delta J = 0, \pm 1$ are present and with good intensity in both of these band systems. This is due to, or is to be correlated with, the fact that the upper ${}^2\Pi$ states are close to strict case (a), as judged by the large separation between the ${}^2\Pi_{3/2}$ and ${}^2\Pi_{1/2}$ levels (330 cm^{-1} for ZnH, 1001 cm^{-1} for CdH), and that the doublet separations in the lower ${}^2\Sigma$ levels are quite appreciable. The lines of the satellite branches are thus nicely separated from those of the main branches and are of comparable intensity, which are points of importance for our present work. As a matter of fact, since among the satellite lines and lines for which $\Delta K = 2$ the intensity rule $Q > R > P$ holds as for the main branches, the lines of low and intermediate J values in the ${}^PQ_{12}$ and ${}^RQ_{21}$ satellite branches are just about as intense as the accompanying main branch lines (P_1 and R_2 respectively) in the ZnH bands,¹⁰ and are even stronger than the main branch lines in the CdH bands.

In order to compute the Zeeman patterns, one must know the exact magnitude of the ρ -type doubling in the ${}^2\Sigma$ state. This doubling is measured directly by the separation of the satellite and main lines having the same K values. There is the possibility of obtaining four such $\Delta\nu$'s for each K in each band and the set of average values yields the constant a in the expression $\Delta\nu = a(K + \frac{1}{2})$ which has been shown¹¹ theoretically to be the correct formula. These data taken from the present measurements of the no-field comparison spectra, indicate definitely that the doubling is proportional to $K + \frac{1}{2}$ rather than to K , in agreement with the theory. The calculations give for the ρ -type doublet widths $0.223(K + \frac{1}{2})$ for ZnH and $0.592(K + \frac{1}{2})$ for CdH. Hulthén¹² gives $2.10(K + \frac{1}{2})$ for this same doubling in the corresponding lowest ${}^2\Sigma$ state with $v'' = 0$ for HgH. The course of this doubling in this sequence of similar molecules would seem to indicate the importance of the rotational distortion of the electronic motions as the principal cause.^{11,3}

THE ZEEMAN EFFECT IN THE ZNH BANDS

The action of the magnetic field on the upper ${}^2\Pi$ state may be computed with Hill's quantum mechanics formulas,¹ it being sufficiently accurate to use his Eq. (12) to give the magnetic sublevels:

⁸ E. Hulthén, *Zets. f. Physik* **32**, 32 (1925).

⁹ R. S. Mulliken, *Phys. Rev.* **32**, 388 (1928).

¹⁰ It has been previously stated (ref. 9) that the satellite and $\Delta K = 2$ branches are, on the whole, only about half as intense as the main branch lines. Visual estimates of relative intensities in the present measurements indicate that for both ZnH and CdH the main Q branch lines are more intense than the ${}^PQ_{12}$ and ${}^RQ_{21}$ line more nearly in the ratio 10:8 or 10:9.

¹¹ J. H. VanVleck, *Phys. Rev.* **33**, 467 (1929).

¹² E. Hulthén, *Zeits. f. Physik* **50**, 319 (1928).

$$W = B \left\{ (J + \frac{1}{2})^2 - \Lambda^2 + \beta(\Lambda^2 + \frac{1}{2}) \pm \frac{1}{2} [(2J + 1)^2(1 - \beta)^2 + \Lambda^2(\lambda + \beta)(\lambda - 4 + 5\beta)]^{1/2} \right\} \quad (1)$$

The upper sign is to be associated with the F_2 levels ($J=K-\frac{1}{2}$), and the lower sign with the F_1 levels ($J=K+\frac{1}{2}$). The quantity $\beta = (\Delta\nu_n/B)M/J(J+1)$, $\Lambda=1$ for a Π state, and for this (0,0) ZnH band $B=7.3 \text{ cm}^{-1}$ and $\lambda = +45 \text{ cm}^{-1}$. Calculation shows that the $2J+1$ sublevels formed from each original level of total angular momentum J are symmetrically placed about the no-field position.

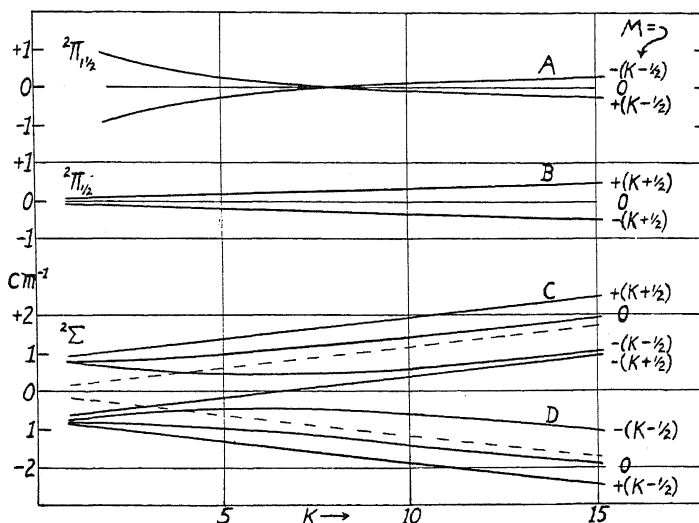


Fig. 1. Magnetic energy levels for the $^2\Pi$ and $^2\Sigma$ states of the ZnH $\lambda 4326$ band. Only the levels for the extreme values of M are shown; the other magnetic levels should be spaced quite uniformly between these extreme levels. Note that the displacements in the $^2\Pi$ states are symmetrical about the no-field position. The dashed lines for the $^2\Sigma$ state represent the no-field positions of the two members of the ρ -type doublet. The positions and widths of the branches may be computed from the displacements in this diagram, noting that $\Delta M=0$, and ± 1 only, and taking the proper ΔK for the branch in question.

The behavior of the $^2\Sigma$ state in the field is discussed by Almy.⁴ If $\Delta\nu_n$ for the field strength in question is considerably larger than the ρ -type doubling at the origin of the band, there should be a molecular Paschen-Back effect, with the spin oriented either parallel or anti-parallel to the field. But the internal field which tends to orient the spin is still present, and therefore each member of this twice normal doublet is split into $2J+1$ magnetic sublevels. As K increases the spread of these magnetic levels about the no-field position should be from about $+\Delta\nu_n$ to $-\Delta\nu_n$, representing the various space orientations of the spin in the field. The position of these sublevels is given quantitatively by Hill's formula:

$$W = \pm \frac{1}{2} \{ \nu_0^2 + 4M\nu_0\Delta\nu_n / (K + \frac{1}{2}) + 4\Delta\nu_n^2 \}^{1/2} \quad (2)$$

where ν_0 is the p -type doublet width for the K level being considered, the $+$ sign is for the F_1 levels ($J=K+\frac{1}{2}$), and the $-$ sign for the F_2 levels ($J=K-\frac{1}{2}$). For the two outermost levels $M=\pm(K+\frac{1}{2})$ of the $J=K+\frac{1}{2}$ states, the energies are given by

$$W = \nu_0/2 \pm \Delta\nu_n. \quad (3)$$

For the sake of brevity, some of the principal features of the calculated and observed Zeeman patterns for one field strength only, 16,400 gauss, will be given here. All of the conclusions are substantiated by the measurements at the lower and higher field strengths. Fig. 1 is a plot to scale showing the course of the magnetic levels for which $M=\pm J$ for the $^2\Pi$ and the $^2\Sigma$ states when $\Delta\nu_n=0.77$ cm $^{-1}$ (16,400 gauss). The levels for all of the intermediate values of M are spaced quite uniformly between these extreme levels. From this level diagram, paying due regard to the selection rule $\Delta M=0, \pm 1$ and

TABLE I. Comparison of calculated and observed patterns for $Q_1+Q_{R_{12}}$ branches. ZnH (0,0) band. $H=16,400$ gauss. These results are plotted in Fig. 2. All calculations and observations in cm $^{-1}$ with reference to the no-field position of Q_1 as origin. $+$ values are on the high frequency side, $-$ values on low frequency side. * indicates inaccurate because of an overlapping pattern.

K''	Q_1 block		$Q_{R_{12}}$		Cross-over components	
	Obs.	Calc.	Obs.	Calc.	Obs.	Calc.
0	-0.80	-0.77	+0.67	+0.77		
1	-0.76	-0.63	+0.79	+0.72 to +1.08		
2	-0.63	-0.55	+0.72 to +1.24	+0.70 to +1.32		
3	-0.60	-0.49	+0.55 to +1.60	+0.60 to +1.60		
4	-0.60	-0.15 to -0.63	+0.88 to +1.78	+0.82 to +1.85	+0.65	+0.62
5	-0.67 to -0.10	-0.60 to -0.00	+1.09* to +2.06	+0.88 to +2.10	+0.61	+0.60
6	-0.50 to +0.11	-0.58 to +0.10	+1.15 to +2.52	+0.95 to +2.35	+0.52	+0.55
7	-0.54 to *	-0.55 to +0.15	+0.95 to +2.80	+1.05 to +2.60		
8	-0.49 to +0.61	-0.52 to +0.50	+1.14 to *	+1.16 to +2.85		
9	-0.45 to +0.47	-0.50 to +0.48	+1.37 to +3.20	+1.30 to +3.15		
10	-0.46 to +0.50	-0.45 to +0.47	+1.70 to +3.38	+1.46 to +3.38		
11	-0.34 to +0.43	-0.40 to +0.42	+1.80 to +3.60	+1.60 to +3.62		

to the proper changes in K for the various transitions, the blocks of components in the Zeeman patterns may be drawn. Comparison with the similar energy level diagram given by Almy for OH (reference 4, Fig. 4) is of interest. The arrangement of the levels in the $^2\Sigma$ state is almost identical because of the approximate equality of the p -type doubling, but in the $^2\Pi$ state there is a marked difference, noteworthy being the crossing of the levels at $K=9$ in the $^2\Pi_{1/2}$ set and the very slow, gradual increase in the spread of the levels in the $^2\Pi_{3/2}$ set.

We at once have the explanation of Hulthén's findings that the lines in some of the branches become doublets in the field, with doublet interval approaching $2\Delta\nu_n$ at the origin. These branches all represent transitions from the $^2\Pi_{1/2}$ upper level, and it is seen that for low K values the magnetic levels are here closely spaced about the no-field position. The magnetic sublevels in the $^2\Sigma$ state tend to group themselves into two sets separated by an inter-

val of about $2\Delta\nu_n$, and hence the possible transitions from the ${}^2\Pi_{3/2}$ levels to the levels in these two sets will be observed as two blocks of unresolved lines with this separation. Some examples of these field doublets may be seen in Fig. 5.

The only field doublet with really sharp components observed on our plates is that for the $Q_1(\frac{1}{2})$ line. This happens to be the only transition from the anomalous lowest ${}^2\Pi_{3/2}$ level with $K=1$, $J=\frac{1}{2}$, which is magnetically insensitive,¹³ to the lowest ${}^2\Sigma$ level with $K=0$, $J=\frac{1}{2}$, which splits into a twice normal doublet. The observed doublet interval for this line is 1.47 cm^{-1} , as against $2\Delta\nu_n = 1.54\text{ cm}^{-1}$.

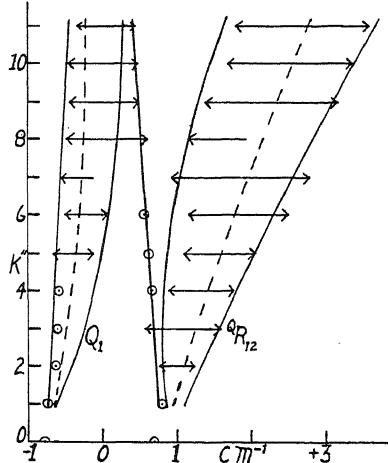


Fig. 2. Comparison of the computed and observed Zeeman patterns for the $Q_1 + {}^Q R_{12}$ lines of the ZnH band at 16,400 gauss. All displacements are reckoned with respect to the no-field Q_1 line positions. The dashed lines represent $M' = M'' = 0$, and divide equally the total number of components in each block. The crossing-over lines between the two blocks represent the two possible transitions to the $M = -(K + \frac{1}{2})$ level of the ${}^2\Sigma$ state in Fig. 1. Observed narrow components are represented by small circles, broader components by double-headed arrows.

Table I and Fig. 2 give a detailed comparison of the positions and widths of the blocks of Zeeman components, as obtained from Fig. 1, with the experimental values for the $Q_1 + {}^Q R_{12}$ lines. Such main lines and satellites must be considered together for each K'' , for these transitions become intermingled in the field. The agreement in general is seen to be good. An interesting detail is the detection of the component crossing over from its association with the broader ${}^Q R_{12}$ block to the narrower Q_1 block as K increases. This component arises from two transitions to the $M = -(K + \frac{1}{2})$ level which is to be noted in Fig. 1 crossing over between the two groups of magnetic levels in the ${}^2\Sigma$ state. The 30,400 gauss plate shows this narrow crossing-over component much more definitely both in these patterns as well as in those of other lines, particularly in the ${}^S R_{21}$ patterns. The low frequency edges of the narrower Q_1 portions of these patterns are stronger because of the greater

¹³ Cf. Hill, reference 1 page 1516.

crowding of the components on this side (the dashed lines in the diagrams of Zeeman patterns represent $M' = M'' = 0$, and divide equally the total number of components in the block in each case). The greater width of the blocks of components for the lines of the satellite branches, such as the positive or ${}^Q R_{12}$ blocks of Fig. 2, and the ${}^O P_{12}$ and ${}^S R_{21}$ branches, is caused by the reversal of the order of the magnetic levels in the transitions $A \rightarrow C$ or $B \rightarrow D$ in Fig. 1. Remembering that M can change by only 0 or ± 1 in the transition, it is seen

TABLE II. Zeeman patterns of the first ${}^O P_{12}$ lines. ZnH, (0,0) band. $H=16,400$ gauss. Displacements with respect to no-field position.

J''	Weak neg. component		Strong pos. component	
	Obs.	Calc.	Obs.	Calc.
$1\frac{1}{2}$			+0.50	+0.60
$2\frac{1}{2}$			+0.46	+0.51
$3\frac{1}{2}$	-1.30	-1.20	+0.06 to +0.65	-0.03 to +0.80
$4\frac{1}{2}$	-1.41	-1.40	-0.08 to +0.75	-0.21 to +0.83
$5\frac{1}{2}$	-1.60	-1.60	-0.14 to +0.76	-0.40 to +0.85
$6\frac{1}{2}$	-1.82	-1.82	-0.33 to +0.74	-0.50 to +0.90
$6\frac{1}{2}$	-1.97	-2.00		

that the energy shifts are greater for these transitions than for the transitions $A \rightarrow D$ and $B \rightarrow C$. This is not the case for the CdH band patterns (see below). Fig. 5 shows several of these ${}^Q I + {}^Q R_{12}$ patterns.

The ${}^O P_{12}$ and P_1 branches are now found to exhibit Zeeman patterns quite similar to all of the other branches. The ${}^O P_{12}$ branch proceeds to longer wave-lengths from the ${}^2\Pi_3$ origin in a region clear of all other branches. These lines have no satellites, and yet, in agreement with the theory, they

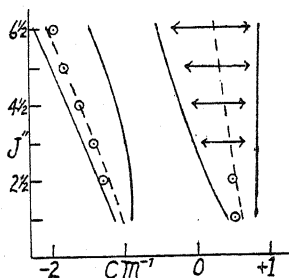


Fig. 3. Computed and observed patterns for the first lines in the ${}^O P_{12}$ branch of the ZnH band with $H=16,400$ gauss. The negative block is observed only as a weak, rather narrow line, the position of which in every case agrees well with the portion of the predicted block in which the components are more crowded together.

show two blocks of components coming from the transitions from the ${}^2\Pi_3$ magnetic levels to the two groups of magnetic levels in the ${}^2\Sigma$ state in Fig. 1. The comparison of the predicted and observed patterns for the first lines of the branch is shown in Fig. 3 and in Table II. In agreement with the theory, no crossing-over field component is found, since because of the selection rule for M and the fact that $\Delta K=2$ for these lines, transitions to the crossing-over magnetic level in the ${}^2\Sigma$ state cannot occur. The negative block is observed only as a weak narrow line whose position agrees well with that

of the center of the predicted components. Even though the positive block is considerably the broader, it is much stronger than the narrow negative block; about in the ratio 10:1 for $^0P_{12}(6\frac{1}{2})$. The same great intensity difference for the two blocks of a pattern is observed for the lines of the R_1 and $^S R_{21}$ branches, which also have no satellites in the no-field spectrum. This result is apparently contrary to the observations of Almy⁴ on corresponding lines in the OH bands, and must be related to the much closer approach of ZnH to case (a) in the $^2\Pi$ state. For in the CdH bands, for which the $^2\Pi$ state is even closer to case (a), and with a larger doubling in the $^2\Sigma$ state, there is no trace of these weaker blocks in the patterns of these three branches. These transitions in the absence of an external field would involve the ex-

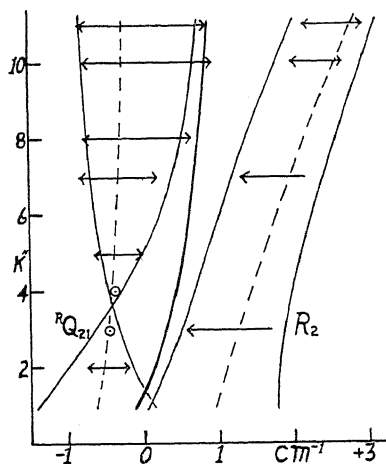


Fig. 4. Zeeman patterns of the $R_{Q_{21}} + R_2$ lines of the ZnH band for $H=16,400$ gauss. All displacements are with reference to the no-field $R_{Q_{21}}$ positions. Note particularly the observed constriction in the width of the $R_{Q_{21}}$ block of components at $K''=3$ and 4.

cluded jumps $\Delta J = \pm 2$, and hence with increasing interaction energy of the spin in the molecule (increasing importance of J), these intensity differences evidence the decreasing effectiveness of the field in breaking down this internal coupling.

Because of the relative peculiarities of the course of the magnetic energy levels in the $^2\Pi_{1/2}$ and $^2\Sigma$ states in Fig. 1 at the low K values, the computed pattern blocks for transitions such as $R_{Q_{21}}$ show a constriction at about $K''=3$ or 4. Fig. 4 illustrates this phenomenon for this particular branch. Experimentally it is found that the block of components is of about the same width for $R_{Q_{21}}(2\frac{1}{2})$ and $(5\frac{1}{2})$, and that both of these are distinctly broader than the $R_{Q_{21}}(3\frac{1}{2})$ and $(4\frac{1}{2})$ patterns. The latter are, as a matter of fact, no broader on the plate than the no-field comparison lines. Similar excellent agreement with the theory on this point is found in the $^S R_{21}$ patterns. The degree of fit between the predicted and observed patterns for the measurable $R_{Q_{21}}$ patterns can be judged from Fig. 4. It should be mentioned that measurement of the exact position of the edges of many of these broad patterns

is difficult, and that therefore exact coincidence with the predicted outlines of the patterns is not to be expected.

THE ZEEMAN EFFECT IN THE CdH BANDS

The magnetic energy levels for both of the CdH states involved in the $\lambda 4509$ band may be computed from Eqs. (1), (2), and (3), with $B = 6.0 \text{ cm}^{-1}$, $\lambda = +169 \text{ cm}^{-1}$, and the ρ -type doubling in the $^2\Sigma$ state as given above. The results plotted as in Fig. 1 are similar to those for ZnH, with the following main points of difference. In the $^2\Pi_{1/2}$ state the two extreme levels start at $K=2$ exactly as for ZnH, but rather than crossing each other at a low K value, they converge symmetrically and more gradually to about zero separation at $K=17$. The two extreme levels in the $^2\Pi_{3/2}$ state do not diverge so rapidly, the interval of each from the no-field position being but 0.13 cm^{-1} at $K=15$. And finally in the $^2\Sigma$ state the two groups of magnetic levels diverge of course more rapidly because of the larger ρ -type doubling, while

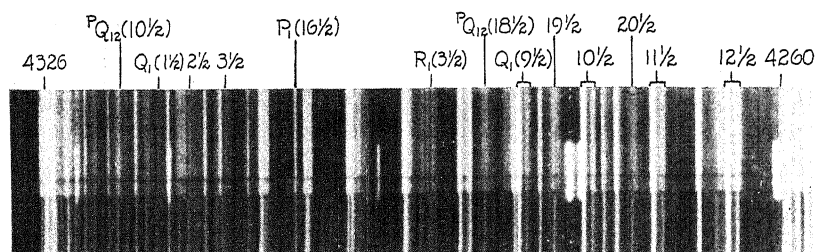


Fig. 5. Reproduction of the portion of the (0, 0) ZnH band between the $^2\Pi_{1/2}$ and $^2\Pi_{3/2}$ origins at $H=16,400$ gauss. The doublet structure of the first Q_1 and R_1 lines is evident. The high frequency weaker component of the patterns $Q_1(9\frac{1}{2})$ to $(12\frac{1}{2})$ is opposite the $^Q R_{12}$ satellite in each case. Notice the breadth of these satellite field blocks (also $^P Q_{12}(18\frac{1}{2})$, $(19\frac{1}{2})$, and $(20\frac{1}{2})$) as compared to that of the $P_1(16\frac{1}{2})$ line.

the two curving levels with $M = -(K - \frac{1}{2})$ swing around more sharply in the region of low K values and at $K=7$ are already spaced at a distance $\Delta\nu_n$ from the no-field positions.

The main differences between the Zeeman patterns of the CdH and ZnH lines due to these variations in the level scheme just mentioned are: first, that for CdH the two blocks of patterns arising from the transitions to the two sets of levels in the $^2\Sigma$ state diverge more rapidly from each other as K increases; second, that all of the blocks of components except those associated with the $^R Q_{21}$, $^Q P_{21}$, and $^S R_{21}$ transitions are for $K > 5$ about $2\Delta\nu_n$ in width, while the patterns of the lines of these three branches approach this width gradually as K approaches the value 17; third, the vanishingly weak intensity of some of the blocks of components already discussed in the ZnH section of this paper.

Comparison of the computed and observed patterns for one set of transitions, $R_2 + ^R Q_{21}$, will suffice. This comparison is made in Table III and in Fig. 6 for the first seven lines in these branches. The calculated and observed widths and positions agree about as well as could be expected. Particularly

satisfying is the observation of the constriction in the width of the ${}^RQ_{21}$ block at $K''=3$. The ${}^RQ_{21}$ patterns are stronger than the corresponding R_2 patterns, even more so than the ratio of the intensities of the no-field comparison lines. This is due perhaps entirely to the fact that the ${}^RQ_{21}$ blocks are narrower. Also the low frequency edges of the ${}^RQ_{21}$ patterns and the high

TABLE III. *CdH* (0,0) band. Zeeman patterns of $R_2+{}^RQ_{21}$ lines. $H=16,400$ gauss. Refer to Fig. 6. All displacements are with respect to R_2 no-field position. * indicates presence of overlapping pattern.

K''	R_2 block		${}^RQ_{21}$ block	
	Obs.	Calc.	Obs.	Calc.
1	-2.04*to +1.52*	-2.10 to +1.50	same. see note below	
2	-0.88 to +1.23	-0.75 to +1.30	-2.00*to -1.31*	-2.05 to -1.35
3	-0.87 to +1.06	-0.80 to +1.15	-2.33 to -1.97	-2.36 to -1.80
4	-0.60 to +1.00	-0.82 to +1.05	-2.25*to -2.92*	-2.28 to -3.05
5	-0.70 to +0.91	-0.82 to +0.95	-2.68*to -3.58*	-2.80 to -3.75
6	-0.74 to +0.80	-0.81 to +0.92	-3.52 to -4.30	-3.30 to -4.37
7	-0.84 to +0.84	-0.80 to +0.90	-3.87 to -4.85	-3.87 to -5.00

Note: The measurements affected by overlapping patterns are made by noting the patterns of the lines of the same branch immediately preceding and following the line causing the fusion, and so determining the excess attributable to the R_2 or ${}^RQ_{21}$ line. These estimates are of course somewhat inaccurate.

frequency edges of the R_2 patterns are the stronger as they should be because of the slightly greater concentration of components on these sides of the blocks respectively. The ${}^RQ_{21}(12\frac{1}{2})$ pattern is of uniform intensity over all, however, for the $M'=M''=0$ line dividing equally the total number of components becomes centered for the higher K levels.

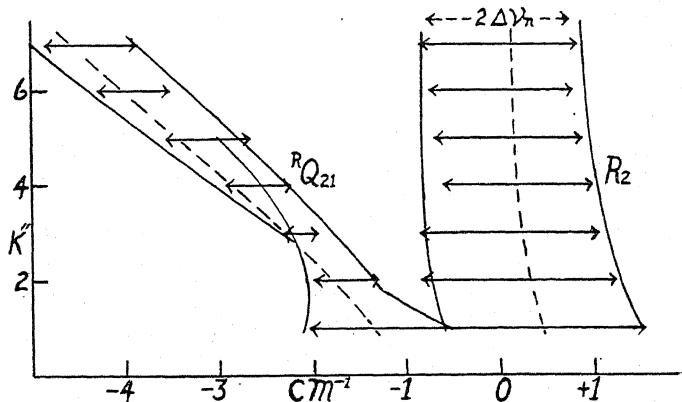


Fig. 6. Comparison of computed and observed Zeeman patterns for the $R_2+{}^RQ_{21}$ lines of the *CdH* (0,0) band at $H=16,400$ gauss. Note the rapid assumption of the width $2\Delta\nu_n$ for the R_2 block of components as K increases, the narrowing of the ${}^RQ_{21}$ block at $K''=3$, and the rapid separation of the two blocks with K due to the larger ρ -type doubling.

Many more similar comparisons of these magnetic field effects in these two band systems with the predicted appearance of the patterns from Hill's quantum mechanics formulas might be presented. Enough of the details unique to these bands have been given, however, to demonstrate the good agreement between the theory and the observations.

THE PRINCIPLE OF IDENTITY AND THE
EXCLUSION OF QUANTUM STATES

BY GILBERT N. LEWIS

DEPARTMENT OF CHEMISTRY, UNIVERSITY OF CALIFORNIA

(Received August 11, 1930)

ABSTRACT

In classical physics it was assumed that a system of two bodies, both having the same mechanical and electrical properties, would show the same behavior regardless of their complete identity. This assumption, that gave rise to the paradoxes of Gibbs and of Einstein which are here discussed, must be abandoned in atomic physics. We must distinguish sharply between identical particles and those that are only quasi-identical, in the sense that they are the same in mass, charge and the potential fields to which they give rise. All of the results which have hitherto been obtained in quantum mechanics are valid even if we assume that two particles such as two electrons or two helium nuclei are only quasi-identical. The postulate of complete identity is a new mathematical condition which, operating simultaneously with the wave equation and its boundary conditions, restricts the number of possible solutions of the equation and thus gives rise mathematically to a number of exclusion laws such as those which have been empirically obtained.

The assumption of identity is equivalent to the mathematical assumption that the ordinary configuration space is degenerate, in the sense that one portion is a mere reflection of another. By this method it is shown that if the wave function is a scalar, the laws of exclusion are obtained without ambiguity. Thus a perfectly symmetrical diatomic gas in its simplest electronic state can have only even rotational levels. It is pointed out that the experimental results with $O_2(O_{16}O_{16})$ and He_2 show that these atoms exist in a single *nuclear* state. It is predicted that with heavier atoms both even and odd states will be found owing to the existence of isobars. The monatomic gas is then discussed and it is shown that, if the Schrödinger function is a scalar, only the Bose-Einstein statistics are possible.

The phenomenon of spin introduces a vector character into the wave function. If we assume that the spin factor changes sign upon reflection when the number of units of spin is odd but not when the number of units of spin is even, we have all the cases of exclusion now known, including the case of the nitrogen molecule. As an example of the method, the problem of the helium atom is discussed.

THERE is at present a great interest in the various rules for the exclusion of certain quantum states, of which rules Pauli's was the prototype; and many speculations are rife concerning those quantum states which are supposed to issue from the mathematics of quantum mechanics, but of which it is said that they "do not exist in nature." I have therefore decided to present, before all their applications have been worked out, certain ideas through which I wish to show that all such exclusion rules become direct mathematical consequences of quantum mechanics when full consideration is given to the identity of certain elementary particles.

In the last century there was no convincing evidence that any two atoms of a given species could be assumed to be exactly alike, but we are now convinced, although the number of atomic species has been largely increased

by the discovery of isotopes, that the individuals within any one species are in all respects identical. This identity has been tacitly recognized without a complete realization of the remarkable consequences to which it leads. For the first intimation of these consequences we must go back to a notable discussion by Willard Gibbs.

THE PARADOXES OF GIBBS AND OF EINSTEIN

In "The Equilibrium of Heterogeneous Substances," Gibbs, obtaining an expression for the increase of entropy when two gases are mixed, commented as follows: "It is noticeable that the value of this expression does not depend upon the kinds of gas which are concerned, . . . except that the gases which are mixed must be of different kinds. If we should bring into contact two masses of the same kind of gas, they would also mix, but there would be no increase of entropy." He goes on to say, "Now we may without violence to the general laws of gases which are embodied in our equations suppose other gases to exist than such as actually do exist, and there does not appear to be any limit to the resemblance which there might be between two such kinds of gas. But the increase of entropy due to the mixing of given volumes of the gases at a given temperature and pressure would be independent of the degree of similarity or dissimilarity between them. We might also imagine the case of two gases which should be absolutely identical in all the properties (sensible and molecular) which come into play while they exist as gases either pure or mixed with each other, but which should differ in respect to the attractions between their atoms and the atoms of some other substances, and therefore in their tendency to combine with such substances. In the mixture of such gases by diffusion an increase of entropy would take place, although the process of mixture, dynamically considered, might be absolutely identical in its minutest details (even with respect to the precise path of each atom) with processes which might take place without any increase of entropy."

As the increase of entropy remains constant when the two gases that are mixed continuously approach complete identity, then by the doctrine of limits, the same increase must be found in the limiting case of identity; but since there is no change of entropy on mixing two identical gases, we are here confronted with a real paradox. In other words, some one link in the chain of reasoning must be fallacious. Despite the penetrating genius of Gibbs, it would have been too much to expect of him in his time to resolve this paradox, but since the advent of quantum theory it is easy to see where the difficulty lies. The false step was made in assuming that two species could approach identity by a continuous path. We are now aware that even atoms of the same species can not be regarded as identical if they are in different quantum states, since these quantum states constitute a discrete series.

While the formal paradox is thus resolved, we are left with a feeling that the phenomenon discussed by Gibbs is still antagonistic to some underlying physical principle; for quantum states, while always distinguishable from

one another, may lie very close together. We have long been taught that the behavior of a physical system is completely determined by such quantities as mass and potential, and we therefore feel that systems which are almost exactly alike with respect to such quantities must behave nearly the same. These ideas brought over from the older physics we must now abandon.

The paradox of Gibbs is important not only as the first intimation of a new kind of principle operating in physical science, but also because when it is stated in modern terms it suggests a general rule that is immediately applicable to problems of atomic and molecular structure. The entropy of a system under given conditions is a measure of the number of its quantum states that are compatible with these conditions. When we find, other things being equal, that the entropy of a system is greater when it is composed of two kinds of particles than when it is composed of one kind, this means that the number of quantum states is reduced in the case of identical particles. This rule holds, for reasons that we shall see presently, not only for the great aggregates of particles with which thermodynamics deals, but also for the simplest atomic systems.

Let us next turn to a problem presented by Einstein, who, in his work on the monatomic gas, discovered the remarkable deviation from the laws of the perfect gas which must result when the same individual quantum numbers may be assigned to two or more particles. I quote from the closing paragraph of his paper.¹ "Finally I may call attention to a paradox, the solution of which I have sought without success. There is no difficulty in treating, by the method here given, the case of the mixing of two different gases. In this case each molecular species has its separate "cells." Thence follows the additivity of the entropies of the components of the mixture, and each component behaves, with respect to molecular energy, pressure, and statistical distribution, as if it alone were present. Therefore a mixture with the molecular numbers n_1 , n_2 , where the molecules of the first and second species differ indefinitely little from each other, (especially with respect to the molecular masses m_1 , m_2) exhibits, at a given temperature, a different pressure and distribution from a single gas with $n_1 + n_2$ molecules of practically the same mass, and at the same volume. This, however, appears as good as impossible."

Here is a paradox only if we take over from classical physics the idea that the behavior of a system is determined by such quantities as mass and potential alone. This, however, is the very idea that we have now agreed to abandon. The equations of Einstein, like the equations of Gibbs, must be accepted. It must be admitted that the equation of state for a mixture of isotopes is unlike that for either pure isotope, although at present this seems beyond the limits of experimental proof. This is true not only of two nearly identical substances, but as Dr. Mayer and I have shown,² it is also true for molecules of the same substances if they are in different quantum states. Thus a gas composed of normal and one composed of metastable

¹ Einstein, Berlin Ber. 267 (1924).

² Lewis and Mayer, Proc. Nat. Acad. 15, 208 (1929).

mercury atoms may exhibit the same pressure under like conditions, but a mixture of the two must have a different pressure.

IDENTICAL AND QUASI-IDENTICAL SYSTEMS

An electron in a sodium atom is distinguishable from an electron in a chlorine atom, but if we imagine the two interchanged, the resulting system differs from the original in no way whatsoever. In the same sense, two helium atoms may be regarded as intrinsically identical, but not always two lithium atoms, for one may have the mass 6, and the other the mass 7. We may even have two isotopes of nearly, or exactly, the same mass. Such "isobars" are found in the radioactive series where two atoms have the same atomic number and, except for their small differences in energy, the same atomic weight, and yet differ in origin and in later radioactive behavior. Two such particles may be regarded as composed of the same number of protons and electrons in a different arrangement, or, as we now say, they represent the same system in two different quantum states. We might even find two atoms with precisely the same mass (analogous to optical isomers) or, in other words, the lowest energy level of the nucleus may be degenerate. Nevertheless, two such atoms, or two such states of an atom, must not be regarded as identical, though they may be so regarded for most purposes.

When two non-identical particles have the same, or nearly the same, values for those quantities which enter into the quantitative statement of a certain problem, they may then be called quasi-identical. Whether those values could be precisely the same for non-identical particles is doubtful. Suppose, for example, that in a certain problem we are concerned with the mass and charge of two particles, and with the potential field to which each gives rise. In the case of two isobars of identical mass and charge, the potential field would presumably be different at very small distances from the atomic center. If we held those prejudices which made the equations of Gibbs and of Einstein seem paradoxical, we should expect to detect such lack of complete identity only by measurements of extreme refinement, calculated to show the minute differences to which we have referred. On the other hand, by using the principle which I am here developing, the roughest sort of observation, such as the mere inspection of a spectrogram, may suffice to decide as to the identity of the particles.

THE QUANTUM STATES OF A DIATOMIC MOLECULE

When the electronic states are not such as to produce complications, the rotation and vibration states of a diatomic molecule have been treated with complete satisfaction by the methods of Schrödinger as applied to a two-body problem. Let us consider two quasi-identical atoms, A_1 and A_2 , with the same mass, m , and a potential field for each atom which depends only upon the distance from the other. The Schrödinger equation then reads

$$\frac{\partial^2 \psi}{\partial x_1^2} + \frac{\partial^2 \psi}{\partial y_1^2} + \frac{\partial^2 \psi}{\partial z_1^2} + \frac{\partial^2 \psi}{\partial x_2^2} + \frac{\partial^2 \psi}{\partial y_2^2} + \frac{\partial^2 \psi}{\partial z_2^2} + \frac{8\pi^2 m}{h^2} (E - V) \psi = 0 \quad (1)$$

where the coordinates x_1, y_1, z_1 , and x_2, y_2, z_2 are associated, respectively, with the first particle and with the second, and ψ is a (real or complex) scalar function of the coordinates.

Such an equation, even when the potential V is given as an explicit function of the coordinates, does not suffice to determine ψ , but only restricts the range of its possible values. This range is further restricted if we impose such further specifications as are known as boundary conditions. In the present case we employ the condition that ψ shall remain finite and continuous. The continuous range of the solutions of Eq. (1) is then reduced (when $E < 0$) to a discontinuum of discrete proper-functions. Any additional condition which operates simultaneously with Eq. (1) and its boundary conditions will in general further diminish the range of the solutions. This lies at the very root of mathematical reasoning. In the present case, where the solutions are already reduced to a discrete series, the assumption of identity will in general eliminate some of these solutions.

We need not go through the familiar process of integrating Eq. (1), but merely recall that the coordinates are first transformed to coordinates of the center of gravity and the relative coordinates x, y, z , where $x = x_1 - x_2$, etc. The equation may then be split into two equations, of which the second involves only x, y and z . Again, transforming to ordinary polar coordinates, r, ϕ and θ , the equation is further separated and integrated. The whole proper-function ψ now appears as the product of several partial functions of which those that depend upon ϕ alone and upon θ alone are

$$\Phi = e^{im\phi}, \quad (2)$$

$$\Theta = \frac{(2j)! \sin^m \theta}{2!(j-m)!} \left(\cos^{j-m} \theta - \frac{(j-m)(j-m-1)}{2(2j-1)} \cos^{j-m-2} \theta + \dots \right). \quad (3)$$

where j and m are integers.

We must now find the consequences of imposing the *additional* mathematical condition that the two particles are not merely quasi-identical, but are identical. This can affect the result not by any modification of the solutions previously obtained but only by an elimination of some of them. In proceeding to the mathematical calculation a serious difficulty appears at the outset because in setting up Eq. (1) we associated one particle with the coordinates x_1, y_1, z_1 , and the other with the coordinates x_2, y_2, z_2 . As the two particles are indistinguishable this is no longer possible. It might be possible to devise a new mathematical method in which the identity of the particles is recognized from the beginning, but until such a method has been invented we must start as before with the fiction of quasi-identical particles and later make a correction for the consequences of this fiction. This must be done by recognizing that the six dimensional space $x_1 \dots z_2$, is a degenerate or "mirror" space, in the sense that the conditions in one-half of the space must be an exact reflection of those in the other half. Thus, any condition prevailing in the point $x_1=a, y_1=b, z_1=c$ and $x_2=d, y_2=e, z_2=f$ must be exactly reflected at the point $x_1=d, y_1=e, z_1=f$ and $x_2=a, y_2=b$ and $z_2=c$.

This may be illustrated in the simple two-dimensional space represented in Fig. 1. In this space of the coordinates x_1 and x_2 the diagonal dotted line acts as the mirror and all conditions on one side of this line are automatically reproduced by reflection on the other side. Thus the point P'' is the reflection of the point P' . A scalar function of position must be the same even to sign at the two points. On the other hand, this need not be true of a vector function of position. Suppose that we are considering a planar vector or 2-vector (which in this two dimensional space acts as a pseudo-scalar) of which the magnitude is represented by the area of a circle and its direction by an arrow, as in the figure. It is evident that the vector is reflected as a vector of the same magnitude but of opposite direction.³

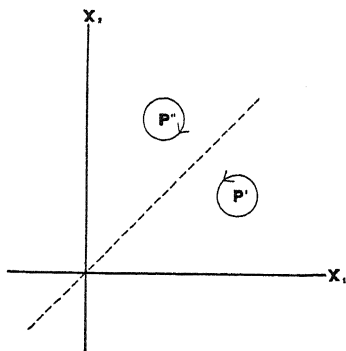


Fig. 1.

Returning to the diatomic molecule we see that the principle of identity requires that the scalar function ψ , must be the same, even to sign, at two mutually reflecting points. If ψ is broken into several factors, then, because of the variety and the arbitrariness of the ways in which a quantity may be factored, our rule of invariance to reflection need not apply to the individual factors, but only to their product.

When as before we transform to new coordinates all the degeneracy of the space remains in the space of the relative coordinates. $x = x_1 - x_2$ can not be distinguished from $-x = x_2 - x_1$, so that every point has its reflection at a diametrically opposite point. When, therefore, we finally change to polar coordinates, the value of ψ at a given point (ϕ, θ) must be the same as at the reflected point $(\phi' = \pi + \phi, \theta' = \pi - \theta)$. If now we examine Eq. (2) and (3) we see that Φ changes sign, if ϕ is replaced by $\pi + \phi$, whenever m is odd, and Θ changes sign, if θ is replaced by $\pi - \theta$ whenever $j - m$ is odd. Therefore, in order that ψ have the same sign at reflected points it is necessary that $j - m$ be even when m is even and that $j - m$ be odd when m is odd; thus, j must always be even. In other words, of all proper-functions which are

³ While the pseudo-scalar in two dimensional space (which may be regarded as the vector product or outer product of two linear or 1-vectors) changes sign on reflection, in four dimensional space the pseudo-scalar does not change sign on reflection. In six dimensional space the pseudo-scalar again changes sign.

solutions of the former set of mathematical conditions only those with even values of j are solutions of the new set of mathematical conditions.

These deductions are completely corroborated by experiment. Not only from spectroscopic observations but also from the entropy determination of Giauque and Johnston,⁴ we know that the molecule $O_{16}O_{16}$ has only half as many quantum states as a molecule of unlike particles. On the other hand $O_{16}O_{17}$ and $O_{16}O_{18}$, discovered by Giauque and Johnston, show all the states corresponding to the solution of the quasi-identical problem. Moreover, such particles as O_2 and He_2 , with identical particles, have in their simplest electronic states only the *even* rotational states. This agreement of our deductions with experiment is to be regarded not as a corroboration of our mathematical method, which, I believe, requires no such corroboration, but rather as a justification of the application of the *scalar* equation, Eq. (1), to the simple problem of two bodies.

The experimental results go farther and give us an insight into the nucleus itself, for if the atoms O_{16} and He existed to an appreciable degree in more than one nuclear quantum state, the lines now missing in the molecular spectra would have been found, and their intensities would inform us concerning the relative amounts of the different isobars. Such isobars were not perhaps to be expected in these simple nuclei, but in elements of higher atomic weight, where many isotopes have been discovered, we may expect to find lines in the spectra of the diatomic molecules which give definite evidence of the existence of isobars.

It can not be too strongly emphasized that the conclusions hitherto obtained are in no way dependent upon the particular choice of the Schrödinger equation. They will be entirely similar if we use the relativistic form of that equation, or indeed, any equation whatsoever that defines a *scalar* function of position and that determines proper-functions, with the aid of its boundary conditions.

THE MONATOMIC GAS

Let us consider next the simplest of all 2-body problems: namely, that of two quasi-identical particles in a box free from potential fields except at, or very near, the boundaries. The new boundary condition is that ψ shall be zero outside the box. If we assume an equation such as Eq. (1) in which V is omitted, it is easily separated by writing $\psi = \psi_1\psi_2$. We thus obtain two sets of partial proper-functions so that, if ψ_{1m} represents the first particle in the m 'th quantum state, and ψ_{2n} represents the second in the n 'th state, the product of the two is a proper-function for the whole system.

On account of the quasi-identical nature of the two particles $\psi_{1m}\psi_{2n}$ is associated with the same energy as $\psi_{2m}\psi_{1n}$ and therefore any linear aggregate of these two is also a solution of the equation. It is customary to take as the two orthogonal solutions

$$\psi^+ = \psi_{1m}\psi_{2n} + \psi_{2m}\psi_{1n}; \quad \psi^- = \psi_{1m}\psi_{2n} - \psi_{2m}\psi_{1n}. \quad (4)$$

⁴ Giauque and Johnston, J. Am. Chem. Soc. 51, 3300 (1929).

Let us now once more replace the condition of quasi-identity by the condition of identity. There are no longer two degenerate states, $\psi_{1m}\psi_{2n}$ and $\psi_{2m}\psi_{1n}$; the single state is completely specified by stating that one particle is in state m and the other in state n . To proceed more formally, we know again that the space $x_1 \cdots x_2$ is a degenerate or "mirror" space in which every point P' has its reflected point P'' . Owing to the identity of the particles $\psi_{1m}\psi_{2n}$ at P' is the same as $\psi_{2m}\psi_{1n}$ at P'' , and $\psi_{2m}\psi_{1n}$ at P' is the same as $\psi_{1m}\psi_{2n}$ at P'' . Of the two functions ψ^+ and ψ^- of Eq. (4), the former remains unchanged during reflection, the latter changes sign and must therefore be excluded if the whole wave function is a scalar.

This reduction of the two sets of proper-functions to the single function ψ^+ corresponds to the smaller entropy of a system of identical particles discussed by Gibbs, and constitutes the difference between the Bose-Einstein statistics and the statistics of Boltzmann.

If, however, we are dealing with a system in which ψ is not a scalar but changes sign on reflection (as in the case exemplified in connection with Figure 1) then of the functions ψ^+ and ψ^- the former would have been excluded and only the latter allowed. It is to be noted that, because of its form, ψ^- always disappears when both particles are in the same quantum state; that is, when $m=n$. We therefore have a system following the Fermi statistics.

It is easy to generalize to a large number, N , of identical particles. Here the configuration space becomes highly degenerate and may be divided into $N!$ equal pyramidal regions such that if conditions are given throughout one of these regions they are obtained by reflection in all the other regions. Instead of the pair of mutually reflecting points in the previous case we now have $N!$ mutually reflecting points. Furthermore, in the system of N particles the $N!$ degenerate states of the quasi-identical particles are reduced to a single state in the case of identity.

Any one of the quasi-identical states may be obtained from any other by a series of single reflections, each of which may be interpreted as the interchange of a single pair of particles. They may be divided into two groups according as they may be obtained from a chosen state by an even or odd number of reflections. The sum of one group added to the sum of the other group gives the single function that we have called ψ^+ , and the sum of one group subtracted from the sum of the other gives ψ^- .

If the whole wave function is a scalar, ψ^+ is the only function allowed and the number of quantum states corresponds to the Bose-Einstein statistics. If, however, the whole wave function changes sign with each single reflection, ψ^- is the only function allowed. The terms in ψ^- vanish pair by pair whenever two of the particles are in the same state and we thus have the Fermi statistics. In neither case do we have any of the so called "mixed types" of proper-functions.

THE PROBLEM OF SPIN

The principle of identity tells us without ambiguity how many of the various sets of quantum states obtained in the case of quasi-identity are ex-

cluded in the case of identity. If the nature of the wave function is known it tells further just which sets of quantum states are excluded. Thus if the wave function is a scalar we have seen how simply we are led to the exact exclusion laws.

Further than this our principle can not go alone, but it will enable us to codify in a simple manner certain laws derived from experiment. The discovery of a fourth quantum number, the quantum number of spin, is incompatible with any equation of the type of Schrödinger's. It introduces a new and, in spite of the brilliant work of Dirac, a still mysterious element into quantum mechanics.

We shall assume (1) that in the absence of spin any system may be adequately interpreted by means of a scalar equation of the type of Schrödinger's. The principle of identity then states that the whole wave function remains unchanged upon reflection. Thus, for example, any particles, neutral or charged, that are not associated with spin obey the Bose-Einstein statistics.

We shall further assume (2) that every system may be described by means of a *scalar* wave function Ψ which, at least in certain limiting cases, may be regarded as the product of a function ψ , which satisfies an equation of the Schrödinger type, and a quantity σ , which may be called the factor of spin, and may be regarded as the product of the spin factors of the individual particles.

Our final assumption (3), which now generalizes assumption (1), is that for particles with an even number of units of spin σ is unchanged by reflection, but that for particles having an odd number of units of spin any product of the individual spin factors changes sign with each single reflection (interchange of two identical particles). As far as I have at present been able to see, these simple assumptions cover all known cases of the exclusion of quantum states, including the case of the nitrogen molecule. In thinking over the consequences of these assumptions, I have had the benefit of many discussions with Professor G. E. Gibson, to whom I wish to express my gratitude.

I shall give only one example of the application of these rules to atomic problems. If, in considering the helium atom, we should make the provisional assumption that the two electrons are only quasi-identical, we would obtain all of the results obtained by Heisenberg in his treatment of the problem, but when we introduce the further condition of identity one set of quantum states is excluded. Let us see what these quantum states are.

With Eq. (1), the center of gravity of the atom being taken as the origin and the possibility of motion of the nucleus being neglected, we may neglect that part of V which depends upon the interaction of the two electrons, since we are now concerned not with the energies of the quantum state, but only with their number and characterization. The equation can then be separated into two similar "hydrogen-like" parts and each leads to its own set of proper-functions so that any one from one set multiplied by any one from the other gives a solution of Eq. 1. Proceeding as in a previous case, we obtain the double set of functions given in Eq. 4, ψ^+ and ψ^- .

Since, however, each electron has one unit of spin the whole wave function of the system is not ψ but $\Psi = \psi\sigma$, where σ is the product of the two individual spin factors, either of which may have one of the two values α or β . Thus, treating σ in the ordinary way as a proper-function, it has four possible values which may be written as (a) $\alpha_1\alpha_2$; (b) $\beta_1\beta_2$; (c) $\sigma^+ = \alpha_1\beta_2 + \alpha_2\beta_1$; (d) $\sigma^- = \alpha_1\beta_2 - \alpha_2\beta_1$.

So far we have been assuming provisionally that the two electrons are only quasi-identical. We now introduce the condition of identity and employ the rule that each product of the individual spin factors changes sign upon reflection, so that when we pass from a point P' to its reflected point P'' , $\alpha_1\alpha_2$ goes into $-\alpha_2\alpha_1$, $\beta_1\beta_2$ into $-\beta_2\beta_1$, $\alpha_1\beta_2$ into $-\alpha_2\beta_1$ and $\alpha_2\beta_1$ into $-\alpha_1\beta_2$. Of the four values of σ given above the only one that does not change sign upon reflection is σ^- .

Now the whole wave function Ψ , must not change sign; therefore, σ^- can be combined only with ψ^+ and the other three values of σ can be combined only with ψ^- . We thence obtain, by methods too familiar to repeat, the quantum states of the helium atom which are experimentally found; and our rule of exclusion covers in this, as it will in other cases, the Pauli principle.

ON THE WENTZEL-BRILLOUIN-KRAMERS APPROXIMATE SOLUTION OF THE WAVE EQUATION

BY L. A. YOUNG AND G. E. UHLENBECK

DEPARTMENT OF PHYSICS, UNIVERSITY OF MICHIGAN

(Received August 25, 1930)

ABSTRACT

A discussion of the Wentzel-Brillouin-Kramers method of obtaining an approximate solution of the wave equation is given from the point of view that it forms a link between the quantum theory of Bohr and the new quantum mechanics. This becomes clear when one compares the probability distributions (see Figs. 2 and 3) and calculates the mean values \bar{r}^k (see Table I). It is shown that for high quantum numbers these become the classical values. The method leads also, as shown by Zwaan, to quantization by the classical phase integrals with the use of half-integer quantum numbers. In the last section the method is applied to the charged shell atom model. It is shown that the condition of smooth joining of the wave function is practically equivalent to half-integer quantization of the sum of the inner and outer phase integrals. Of course there is no longer a sharp distinction between penetrating and non-penetrating orbits. The Landé formula for the doublet separations is derived. The value of $\psi^2(0)$, which occurs in the calculation of the hyperfine separations in 2S states, is also given.

I. GENERAL CHARACTER OF WENTZEL-BRILLOUIN-KRAMERS APPROXIMATE SOLUTION

THE method proposed by Wentzel and Brillouin and later developed by Kramers and Zwaan¹ for obtaining an approximate solution of the one-dimensional wave equation²

$$\psi''(x) + Q^2(x)\psi = 0 \quad (1)$$

where $Q^2(x) = (8\pi^2m/h^2)(E - V(x))$ in which E is the total energy and $V(x)$ the potential energy of the system consists, as is well known, in substituting into Eq. (1) an expression of the form

$$\psi = \exp \left\{ \frac{2\pi i}{h} \left(S_0 + \frac{h}{2\pi} S_1 + \frac{h^2}{4\pi^2} S_2 + \cdots \right) \right\}$$

where S_0, S_1, S_2, \cdots are functions of x to be determined. One finds easily by successively equating the coefficients of equal powers of $h/2\pi$ to zero that

$$S_0 = \pm \int^x Q dx$$

¹ G. Wentzel, *Zeits. f. Physik* **38**, 518 (1926); L. Brillouin, *C. R. Juli*, 1926; H. A. Kramers, *Zeits. f. Physik* **39**, 828 (1926); H. A. Kramers and G. P. Ittmann, *Zeits. f. Physik* **58**, 217 (1929); A. Zwaan, *Utrecht Dissertation*, 1929.

² It should be noticed that $Q(x)$ is proportional to the linear momentum $p(x)$ and therefore to the velocity $v(x)$.

$$S_1 = + \frac{i}{2} \log Q$$

$$\vdots \quad \quad \quad \vdots$$

$$\vdots \quad \quad \quad \vdots$$

One obtains therefore as a first approximation to a solution of Eq. (1)

$$\psi_{\text{appr}} = Q^{-1/2} \left\{ c_1 \exp \left(\frac{2\pi i}{h} \int^x Q dx \right) + c_2 \exp \left(- \frac{2\pi i}{h} \int^x Q dx \right) \right\}$$

The integration constants c_1 and c_2 must now be so chosen that in regions where a motion was possible classically ($Q^2(x) > 0$) ψ has an oscillatory character while in regions where $Q^2(x) < 0$ we have solutions behaving as a linear combination of increasing and decreasing exponentials.

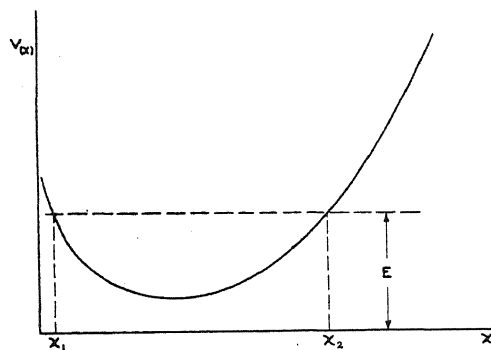


Fig. 1.

If, for example, we are considering a potential function of the type sketched in Fig. 1 the approximate solution will have the forms

$$\begin{aligned} \psi_{\text{appr}} &= A Q^{-1/2} \cos \left\{ \int_{x_1}^x Q dx + \delta \right\} & x_1 < x < x_2 \\ &= B Q^{-1/2} \exp \left\{ \int_x^x Q dx \right\} & x < x_1 \\ &= C Q^{-1/2} \exp \left\{ \int_{x_2}^x Q dx \right\} & x > x_2. \end{aligned} \quad (2)$$

These solutions have been so chosen that they become zero for $x = \pm \infty$ as they must if they are to correspond to an eigenfunction of the discrete spectrum of the wave equation.

When the expressions (2) are approximations to one and the same exact solution it is clear that there must be relations connecting the constants of amplitude and phase A , B , C , and δ . These relations are given by Kramers and Zwaan. They say that an increasing exponential solution like $\psi_{\text{appr}} = Q^{-1/2} \exp \left\{ \int^x Q dx \right\}$ is "connected" with an oscillatory solution $\psi_{\text{appr}} = Q^{-1/2}$

$\cos\{\int^x Q dx - \pi/4\}$ while a decreasing exponential solution $\frac{1}{2}Q^{-1/2}\exp\{-\int^x Q dx\}$ must connect with an oscillatory function $Q^{-1/2}\cos\{\int^x Q dx + \pi/4\}$. These formulas completely determine δ but the constants A , B , and C are determined only within a common multiplicative constant which may be fixed by normalization.

The value of this approximate solution is two-fold; first, of course, it can lead to valuable results in cases where the exact solution is unknown or difficult to handle; in the second place it has the advantage that it is a link between the classical quantum theory of Bohr and the exact quantum mechanics. One may say that it shows how from the viewpoint of the latter, at least in the case of one-dimensional problems, the classical physicist ought to have treated his problems to obtain the best results. We will illustrate this in general:

a. by showing that the approximate solution leads to a determination of the energies by quantization of the classical action integrals with the sole difference that half-integer quantum numbers must be used instead of whole numbers.

b. by considering the probability distribution $P_{\text{appr}} = \text{const} \psi^2_{\text{appr}}$ and comparing it with the classical probability which is inversely proportional to the velocity, that is $P_{\text{class}} = \text{const}/v = \text{const}/Q$ as well as with the exact probability functions $P_{\text{exact}} = \text{const} \psi \bar{\psi}$.

In sections II and III for the case of hydrogenic atoms and the charged shell atom model we will show in more detail how the Wentzel-Brillouin-Kramers approximate solution fills the gap between the older and newer theories.

2. If we consider a potential function of the type sketched (Fig. 1) corresponding to an allowed energy E such that the classical motion was periodic and bounded by the points x_1 and x_2 we may apply the connection formulas at these points obtaining as our approximate solution for this region either

$$Q^{-1/2} \cos \left\{ \int_x^x Q dx - \pi/4 \right\}$$

or

$$Q^{-1/2} \cos \left\{ \int_x^{x_2} Q dx - \pi/4 \right\}$$

We shall require that these two expressions join smoothly at every point x of the interval x_1 to x_2 (or, in other words the two must be identical). Since the solutions are determined only within an arbitrary multiplicative constant we must have $\psi_1'/\psi_1 = \psi_2'/\psi_2$ where ψ_1 and ψ_2 denote the two alternative cosine-like solutions for this region. This condition requires that

$$\tan \left\{ \int_{x_1}^x Q dx - \pi/4 \right\} = - \tan \left\{ \int_x^{x_2} Q dx - \pi/4 \right\} \quad (3)$$

This has the solution $\int_{x_1}^x Q dx = -\int_x^{x_2} Q dx + (n_x + \frac{1}{2})\pi$ from which we see

$$\int_{x_1}^{x_2} Q dx = (n_x + \frac{1}{2})\pi \quad (4)$$

This relation determines the allowed energies and from our previous remark concerning the relationship between $Q(x)$ and the linear momentum $p(x)$ we see that this is equivalent to quantization by the action integrals of the Bohr theory with the single difference that half-integers now appear instead of the integers of the older theory.

$$I = \oint p dq = (n + \frac{1}{2})h \text{ instead of } I = nh.$$

This was first made clear by Kramers and later expressed in practically the above form by Zwaan in his Utrecht dissertation. It is felt that this affords a justification for the half-integer quantization which was found empirically to be so successful in certain problems, particularly in the interpretation of the vibrational spectra of diatomic molecules.

3. In discussing the character of the approximate solution we shall speak of the derived probability functions rather than the solutions themselves. As unnormalized probability functions we have

$$\begin{aligned} P &= \frac{1}{4} Q^{-1} \exp \left\{ -2 \int_{x_1}^x Q dx \right\} & x < x_1 \\ &= Q^{-1} \cos^2 \left\{ \int_{x_1}^x Q dx - \pi/4 \right\} & x_1 < x < x_2 \\ &= \frac{1}{4} Q^{-1} \exp \left\{ -2 \int_x^{x_2} Q dx \right\} & x > x_2. \end{aligned} \quad (5)$$

First of all we notice that in the region $x_1 < x < x_2$ the probability is a positive oscillatory function with an amplitude equal to Q^{-1} —exactly the classical probability function. The close relation of this probability to the corresponding classical quantity is brought out if we write

$$P = Q^{-1} \cos^2 \left\{ \int_{x_1}^x Q dx - \pi/4 \right\}$$

in the equivalent form

$$P = \frac{1}{2} Q^{-1} - \frac{1}{2} Q^{-1} \sin \left\{ 2 \int_{x_1}^x Q dx \right\}. \quad (6)$$

The first term in this expression is just the classical probability. In calculating mean values the second term will contribute little due to its alternating sign and we will obtain to a first approximation the classical result with half-integer quantum numbers.³ In the limit of large quantum numbers the ratio of the contribution of the second term to that of the first will vanish.

³ It is now clear that the classical analogue of the matrix element X_{nm} connected with the transition between two states characterized by, say, the energies E_n and E_m is given by

The probability functions in the tail regions ($x < x_1$, $x > x_2$) had no meaning in the Bohr theory and it may be shown that their contribution may be considered as a small correction to the results obtained from the region in which a motion was classically possible. In the exact wave mechanical theory, however, the tail regions are not so sharply marked off from the interval⁴ x_1 to x_2 and it may be shown that the results obtained by using the approximate solution lie between those of the classical theory and those of the Schrödinger theory.

Summarizing we see that the approximate probability function $P_{\text{appr}} = c\psi_{\text{appr}}^2$ has in common with the exact probability $P_{\text{exact}} = c\psi_{\text{exact}}^2$ an oscillatory character in the region $x_1 < x < x_2$ and the existence of exponentially decreasing tails. With the classical probability function it has in common that at x_1 and x_2 it becomes infinite⁵ and that the amplitude of the oscillatory part is equal to the classical probability function. See Figs. 2 and 3.

II. APPLICATION TO HYDROGENIC ATOMS

4. The three dimensional motion of a charged particle (electron) in a central Coulomb field is described by a wave equation of the form

$$\Delta_3\psi + \frac{8\pi^2m}{h^2}\left(E - \frac{Ze}{r}\right)\psi = 0$$

where Δ_3 is the Laplace operator for three dimensions. Introduction of spherical polar coordinates allows the separation of this partial differential equation and the solution may be written $\psi = R(r)y_l(\theta, \phi)$ and y_l is a spherical harmonic of the l^{th} order. By the substitution $w = rR$ the radial equation is reduced to the form

$$w'' + Q^2(r)w = 0$$

where

$$Q^2(r) = \frac{2Z}{r} - \epsilon - \frac{l(l+1)}{r^2}.$$

In this expression Z/r is the potential energy of an electron at a distance r from a Z -fold charged positive nucleus, ϵ is the total energy of the electron, and l has the physical meaning of total angular momentum.⁶

$$X_{nm} = \int \frac{X}{(Q_n Q_m)^{1/2}} dx \sqrt{\left[\int \frac{dx}{Q_n} \int \frac{dx}{Q_m} \right]^{1/2}}.$$

⁴ From Eq. (1) we see that at the points x_1 and x_2 $\psi''(x) = 0$ so that these points are the outer inflection points of the exact solution.

⁵ ψ_{appr}^2 is, however, still integrable.

⁶ All quantities are measured in the rational units first proposed by Hartree (D. R. Hartree, Proc. Camb. Phil. Soc. **24**, 89, 1928). In this system of units energy is measured in multiples of the negative energy of the hydrogen atom in its lowest stationary state; distances in terms of a unit equal to the radius of the first Bohr orbit of hydrogen; and time in units $1/4\pi cR$ where c is the velocity of propagation of light in vacuum and R is the Rydberg constant in sec^{-1} .

The above equation is of the form considered in the preceding section and the approximate solution considered there will be applied to the determination of the properties of hydrogenic atoms. Naturally, we ask first as to whether or not the correct energies are obtained when half-integer quantization is employed. We must evaluate the integral

$$\int_{r_1}^{r_2} \left[\frac{2Z}{r} - \epsilon - \frac{l(l+1)}{r^2} \right]^{\frac{1}{2}} dr$$

and equate it to $(n_r + \frac{1}{2})\pi$. The above integral was well known in the older theory giving

$$\pi(Z/\epsilon^{1/2} - [l(l+1)]^{1/2}) = (n_r + 1/2)\pi$$

or

$$\epsilon = \frac{Z^2}{(n_r + \frac{1}{2} + [l(l+1)]^{1/2})^2}.$$

It is apparent that we do not obtain the familiar Balmer formula except in the limit of large l values. If, however we replace $l(l+1)$ by $(l + \frac{1}{2})^2$ the correct result is obtained.

We shall now investigate the properties of the approximate eigenfunctions more closely. In the region $r < r_1$ we may choose either the positive or the negative exponential. This corresponds to our freedom of choice of either of the two roots of the indicial equation of the exact solution. We consider only the root which gives a solution vanishing at the origin and which behaves for very small values of r like r^{l+1} . The approximate solution based upon the negative exponential behaves for r very small like $r^{[l(l+1)]^{1/2} + \frac{1}{2}}$. Again the replacement of $l(l+1)$ by $(l + \frac{1}{2})^2$ leads to an agreement between the approximate and exact solutions. This is considered to be a sufficient argument for the consistent use of half-integers not only for the radial quantum number but for the azimuthal quantum number as well. Hereafter we shall consider $Q^2(r) = 2Z/r - \epsilon - (l + \frac{1}{2})^2/r^2$ instead of the expression previously used.

5. From the wave mechanics it has become clear that most if not all observable properties of an atomic system can be expressed in terms of mean values of certain functions of the coordinates of the system. In the case of hydrogenic atoms for example the mean values $\overline{r^k}$ where k is a positive or negative integer, are very important. If P represents the probability function as a function of r we may write

$$\overline{r^k} = \frac{\int r^k P dr}{\int P dr}.$$

This expression may be used for the calculation of mean values classically if $P = P_{\text{class}}$ and the range of integration is over that region of the variable

where $Q^2(r) > 0$; wave mechanically if $P = P_{\text{exact}}$ and the range of integration is extended from 0 to ∞ ; and by the Wentzel-Brillouin-Kramers approximation method if the approximate probability functions (5) are used and the integration taken over the entire range of the variable. For the latter case we may write

$$\overline{r^k} = \frac{\int_0^{r_1} P_{\text{app}}^{(1)} r^k dr + \int_{r_1}^{r_2} P_{\text{app}}^{(2)} r^k dr + \int_{r_2}^{\infty} P_{\text{app}}^{(3)} r^k dr}{\int_0^{r_1} P_{\text{app}}^{(1)} dr + \int_{r_1}^{r_2} P_{\text{app}}^{(2)} dr + \int_{r_2}^{\infty} P_{\text{app}}^{(3)} dr} = \frac{I_k^{(1)} + I_k^{(2)} + I_k^{(3)}}{I_0^{(1)} + I_0^{(2)} + I_0^{(3)}}.$$

By referring to Eqs. (6) we see that

$$I_k^{(2)} = \int_{r_1}^{r_2} P_{\text{app}}^{(2)} r^k dr = \int_{r_1}^{r_2} \left(\frac{1}{2} P_{\text{class}} - \frac{1}{2} Q^{-1} \sin \left\{ 2 \int_{r_1}^r Q dr \right\} \right) r^k dr = C_k - U_k$$

If we now consider

$$(\overline{r^k})_{\text{class}} = C_k / C_0$$

we obtain

$$\overline{r^k} \cong \overline{r^k}_{\text{class}} \left(1 + \frac{I_k^{(1)} - U_k + I_k^{(3)}}{C_k} - \frac{I_0^{(1)} - U_0 + I_0^{(3)}}{C_0} \right). \quad (7)$$

The above integrals were evaluated after making certain simplifying assumptions. It can be shown that for high total quantum numbers the correction terms vanish. In general, using (7) we get results lying between the classical values with half integer quantum numbers and the exact values. As an example we have tabulated $\overline{r^2}$.

TABLE I. *Hydrogenic atoms.*

	Class	Class (half-integers)	W.B.K.	Exact
$n=1, l=0$	1.0	2.1	2.5	3.0
$n=2, l=0$	34.0	38.5	40.8	42.0
$n=2, l=1$	16.0	26.5	28.6	30.0

In Figs. 2 and 3 the radial probability functions for the 3s and 3d states of hydrogen respectively have been plotted as a function of r . These examples illustrate the relation of the Wentzel-Brillouin-Kramers approximation to the results obtained by the exact wave mechanics.

6. In treating the frequency splitting in hyperfine structure due to the interaction of the extra-nuclear electrons with the nuclear magnetic moment it becomes necessary to calculate the magnetic field at the nucleus due to the orbital motion of the electron. This may be shown, in a classical way, to be proportional to $\overline{r^{-3}}$ and it would seem probable that the wave mechanical treatment should follow the classical treatment closely. However from the

fact that the exact solution of the Schrödinger equation behaves in the neighborhood of the origin like r^{l+1} and the probability distribution like $r^{2(l+1)}$ it is clear that $\overline{r^{-3}}$ diverges for s -states ($l=0$). This difficulty is only cleared

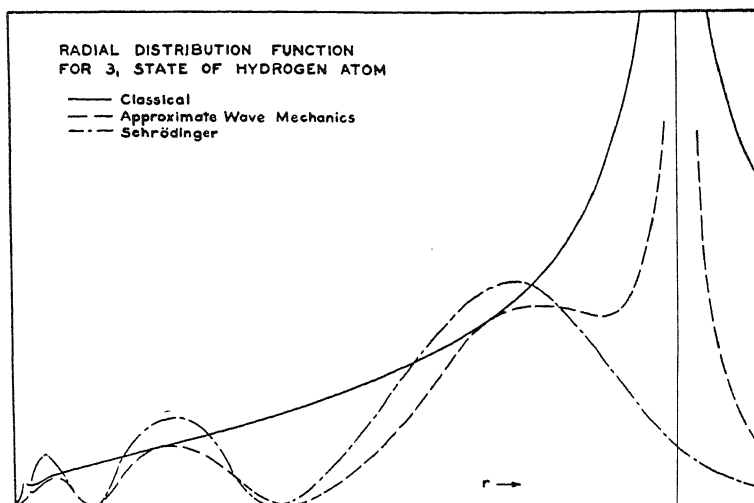


Fig. 2.

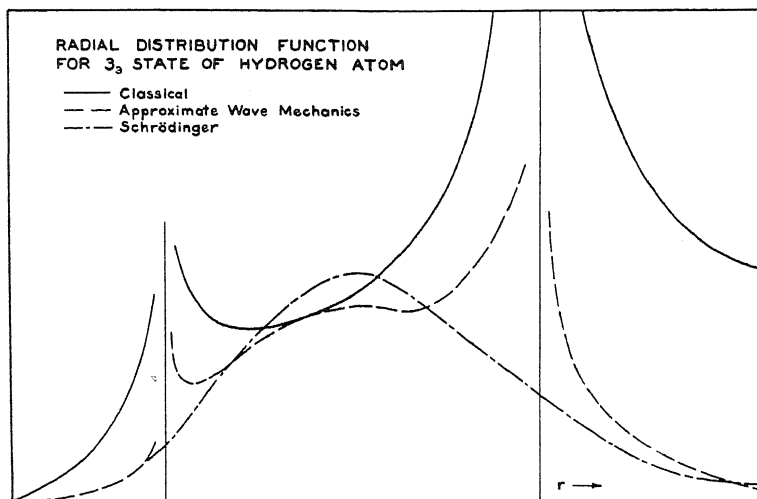


Fig. 3.

up when we treat the problem by means of the Dirac theory of the spin electron. Fermi and Hartree⁷ have shown that for s -states we have only to replace $l \times \overline{r^{-3}}$ by $\frac{1}{2}R^2(0)$ where $R(0)$ is the value of the normalized radial eigenfunction at the origin, to obtain the correct results. Thus for $l \neq 0$ we have $\overline{r^{-3}}$:

⁷ E. Fermi, *Zeits. f. Physik* 60, 320 (1930); D. R. Hartree, *Proc. Camb. Phil. Soc.* 25, 225 (1929).

Classical	Classical (half integers)	W. B. K.	Exact
$\frac{Z^3}{n^3(l+1)^3}$	$\frac{Z^3}{n^3(l+\frac{1}{2})^3}$	$\frac{Z^3}{n^3(l+\frac{1}{2})^3}(1 + \text{corr.})$	$\frac{Z^3}{n^3l(l+\frac{1}{2})(l+1)}$

While for $l=0$ we have:

$\frac{1}{k}r^{-3}$		$\frac{1}{2}R^2(0)$	
Classical	Classical (half integers)	W. B. K.	Exact
$\frac{Z^3}{n^3}$	$\frac{4Z^3}{n^3}$	const. $\frac{Z^3}{n^3}(1 + \text{corr.})$	$\frac{2Z^3}{n^3}$

For the case of $\frac{1}{2}R^2(0)$ by the Wentzel-Brillouin-Kramers approximation we are particularly interested to find out whether or not we obtain good agreement with the exact value since analogous methods when applied to the observed hyperfine structure of the alkali atoms can give valuable information concerning the structure of these nuclei.

For this case we may write

$$\frac{1}{2}R^2(0) = \frac{1}{2} \frac{\lim_{r=0} \frac{1}{4r^2Q} \exp \left\{ -2 \int_{r_1}^r Q dr \right\}}{I_0^{(1)} + C_0 - U_0 + I_0^{(3)}}.$$

Calculation of the numerator and using the values of the normalization integrals given in the appendix we find

$$\frac{1}{2}R^2(0) \cong \frac{\exp 2}{\pi} \cdot \frac{Z^3}{n^3} \left(1 - \frac{1}{24n^2} \right) \left(1 - \frac{I_0^{(1)} - U_0 + I_0^{(3)}}{C_0} \right). \quad (8)$$

A numerical calculation for the states having $n=1, 2, \infty$ was made and the coefficients of Z^3/n^3 were found to be 2.60, 2.40, and 2.35. These are to be compared with the exact coefficient which is just 2.

III. APPLICATION TO THE CHARGED SHELL ATOM MODEL

7. The difficulties encountered in representing the properties of an alkali atom in the quantum mechanics are much the same as in the older theories. The calculation of the interaction between all the electrons of the atom seems to be a problem of the future. At present the only possibility seems to be to represent by some simple model as many of the properties of the atom as possible. The simplest mode of procedure is to assume that the core electrons act as a spherically symmetrical charge distribution about the nucleus and that the optical electron moves in the field of the nucleus and this charge distribution. Some progress has been made in the determination of the appropriate charge distribution by various investigators. The unfortunate thing about their results, however, is that the mathematical methods to which they lead are of a purely numerical or graphical type. Clearly one must idealize the problem if one is to obtain results of any generality. The simplest idealization that one can make is to consider the core electrons con-

centrated in one or more spherical surface distributions of charge about the nucleus. If we adopt this charged shell model our mode of procedure is quite clear.

Consider an atom with a Z -fold charged nucleus surrounded by a spherically charged shell at a distance r_0 from the nucleus. Suppose the total charge in this shell to be $Z - z$ electrons. We will then have to deal with two functions Q^2 instead of one; namely

$$Q_i^2(r) = \frac{2Z}{r} - \frac{2(Z - z)}{r_0} - \epsilon - \frac{(l + \frac{1}{2})^2}{r^2}$$

$$Q_0^2(r) = \frac{2Z}{r} - \epsilon - \frac{(l + \frac{1}{2})^2}{r^2}.$$

We shall seek solutions of the two differential equations

$$w_i'' + Q_i^2(r)w_i = 0 \quad r < r_0$$

$$w_0'' + Q_0^2(r)w_0 = 0 \quad r > r_0$$

which join smoothly at $r = r_0$ (a smooth join means $w_i'/w_i = w_0'/w_0$ at $r = r_0$). Freedom of choice of r_0 still remains and we shall suppose that it has been chosen to lie within the region where a motion was possible classically.

The first question we must consider is concerning half-integer quantization. To answer this consider the two approximate solutions

$$w_i = Q_i^{-1/2} \cos \left\{ \int_{r_1}^r Q_i dr - \pi/4 \right\}$$

$$w_0 = Q_0^{-1/2} \cos \left\{ \int_r^{r_2} Q_0 dr - \pi/4 \right\}$$

The smooth joining condition given above leads to

$$- \tan \left\{ \int_{r_1}^{r_0} Q_i dr - \pi/4 \right\} - \frac{1}{2} Q_i^{-2}(r_0) Q_i'(r_0)$$

$$= \tan \left\{ \int_{r_1}^{r_2} Q_0 dr - \pi/4 \right\} - \frac{1}{2} Q_0^{-2}(r_0) Q_0'(r_0)$$

(note that $Q_i(r_0) = Q_0(r_0)$) which by the introduction of the notation

$$\int_{r_1}^{r_0} Q_i dr - \pi/4 = \alpha$$

$$\int_{r_0}^{r_2} Q_0 dr - \pi/4 = \beta$$

$$\frac{1}{2} Q_0^{-2}(r_0) \{ Q_0'(r_0) - Q_i'(r_0) \} = \eta$$

may be written

$$\tan \alpha + \tan \beta = \eta.$$

If $Q_0'(r_0) - Q_i'(r_0)$ were equal to zero (the inequality existing corresponds to the fact that the electric force has a discontinuity at r_0) we would have $\eta = 0$ whence

$$\tan \alpha + \tan \beta = 0$$

$$\alpha + \beta = \eta_r \pi$$

or

$$\int_{r_1}^{r_0} Q_i dr + \int_{r_0}^{r_2} Q_0 dr = (\eta_r + \frac{1}{2})\pi.$$

That is to the order of accuracy with which we may replace η by zero half-integer quantization is retained. The method used here should be compared with the corresponding procedure used in the treatment of hydrogenic atoms.

When η may not be considered zero it is necessary to consider

$$\tan \alpha + \tan \beta = \eta.$$

In case η is small we may write

$$\int_{r_1}^{r_0} Q_i dr + \int_{r_0}^{r_2} Q_0 dr = (\eta_r + \frac{1}{2})\pi + \tan^{-1} \eta.$$

The evaluation of this expression gives the possible energies for the charged shell model as a function of the quantum numbers and of r_0 —that is a Rydberg formula which is the analogue of the Balmer formula for the terms of hydrogen-like atoms.

It is perhaps worth while to remark that the deviation from half-integer quantization found here is a defect of the charged shell model and that if we replaced it by a model using the charge distributions of Hartree or Fermi⁸ we would again have half-integer quantization.

8. We can now use the approximate wave functions to calculate the quantities $\overline{r^k}$ for alkali-like atoms. All correction integrals will be neglected (in other words, the calculation is purely classical) since the value of r_0 is so uncertain, that greater accuracy is unwarranted. We have, then, to consider the integrals

$$\int_{r_1}^{r_0} r^k Q_i^{-1} dr \quad \text{and} \quad \int_{r_0}^{r_2} r^k Q_0^{-1} dr$$

These may be replaced approximately by

$$\int_{r_1}^{r_1'} r^k Q_i^{-1} dr \quad \text{and} \quad \int_{r_2}^{r_2'} r^k Q_0^{-1} dr$$

where r_2' and r_1' are the inner and outer roots of Q_0^2 and Q_i^2 respectively.

⁸ D. R. Hartree, Proc. Camb. Phil. Soc. 24, 89 (1928); E. Fermi, Zeits. f. Phys. 48, 73 (1928).

Using the notation introduced in section II. for hydrogenic atoms we may write immediately:

$$\overline{r^k} = \frac{E^{-1/2}C_k^{(i)} + \epsilon^{-1/2}C_k^0}{E^{-1/2}C_0^{(i)} + \epsilon^{-1/2}C_0^{(0)}} \quad (9)$$

where we have put

$$E = \epsilon + \frac{2(Z - z)}{r_0}.$$

Application of this formula for $\overline{r^{-3}}$ gives

$$\overline{r^{-3}} = \frac{Zz^2}{n_{\text{eff}}^3(l + \frac{1}{2})^3} \quad (10)$$

where $\epsilon = Z^2/n_{\text{eff}}^2$ and we neglect $\epsilon^{-1/2}C_3^{(0)}$ against $E^{-1/2}C_3^{(i)}$ and $E^{-1/2}C_0^{(i)}$ against $\epsilon^{-1/2}C_0^{(0)}$. This gives the well-known Landé formula⁹ for the doublet separations in optical spectra.

Following Schrödinger¹⁰ we could choose r_0 as the perihelion distance of the parabolic orbits of hydrogenic atoms $r_0 = (l + \frac{1}{2})^2/2z$. It is felt, however that this choice of r_0 has lost some of its physical meaning since the development of wave mechanics.

A procedure analogous to that used for hydrogenic atoms for the determination of $\frac{1}{2}R^2(0)$ gives

$$\frac{1}{2}R^2(0) \cong 2.35 \cdot \frac{Zz^2}{n_{\text{eff}}^3} \left(1 - \frac{2z}{3Z} + \dots \right).$$

Replacement of " $2Z^3/n^3$ " by the above expression in the formula for the frequency separation in hyperfine structure of the 2S states of alkali atoms¹¹ gives for the product of the Landé g -value of the nucleus and the mechanical moment of nucleus and electron

$$\begin{aligned} g(i)(i + \tfrac{1}{2}) &= 2.51 \text{ for Na} \\ &= 1.76 \text{ for Rb} \\ &= 3.67 \text{ for Cs} \\ &= 5.33 \text{ for Tl.} \end{aligned}$$

Fermi, using his statistical atom model and numerical calculation of the eigenfunctions, has given the values 4.11 and 1.89 for Na and Cs respectively.

⁹ The analogous approximation can always be made when k is negative. For example, we obtain

$$\overline{r^{-4}} = \frac{\frac{3}{2}Z^2 - \frac{1}{2}(l + \frac{1}{2})^2E}{(l + \frac{1}{2})^5z\epsilon^{-3/2}} \cong \frac{3}{2} \frac{Z^2z^2}{n_{\text{eff}}^3(l + \frac{1}{2})^5}$$

Of course this like (10) will hold only for $l > 0$ since for $l = 0$, $\overline{r^{-3}}$ and $\overline{r^{-4}}$ diverge. For positive values of k similar approximations may be made giving, for example

$$\overline{r^2} = \frac{1}{2} \frac{n_{\text{eff}}^2}{z^2} \left\{ 5n_{\text{eff}}^2 - 3 \left(l + \frac{1}{2} \right)^2 \right\}.$$

¹⁰ E. Schrodinger, Zeits. f. Physik 4, 347 (1921).

¹¹ S. Goudsmit and L. A. Young, Nature 125, 461 (1930).

It is unfortunate that it is difficult to give a criterion for the accuracy of these results. One can hardly expect them to be correct except as to order of magnitude.

APPENDIX

MEAN VALUE INTEGRALS

In calculating the mean values \bar{r}^k for hydrogenic atoms the following integrals were encountered:

$$I_k^{(1)} = \frac{1}{4} \int_0^{r_1} r^k Q^{-1} \exp \left\{ -2 \int_r^{r_1} Q dr \right\} dr$$

$$C_k = \frac{1}{2} \int_{r_1}^{r_2} r^k Q^{-1} dr$$

$$U_k = \frac{1}{2} \int_r^{r_2} r^k Q^{-1} \sin \left\{ 2 \int_{r_1}^r Q dr \right\} dr$$

$$I_k^{(3)} = \frac{1}{4} \int_{r_2}^{\infty} r^k Q^{-1} \exp \left\{ -2 \int_{r_2}^r Q dr \right\} dr.$$

The integral C_k was evaluated exactly, but it was necessary to introduce simplifying assumptions in evaluating the correction integrals $I_k^{(1)}$, U_k , and $I_k^{(3)}$. It was found that

$$\begin{aligned} C_k &= \frac{1}{2} \pi \epsilon^{-1/2} P^{(k+1)/2} P_{-(k+2)} \left(\frac{1}{2} S P^{-1/2} \right) & k < -1 \\ &= \frac{1}{2} \pi \epsilon^{-1/2} P^{(k+1)/2} P_{k+1} \left(\frac{1}{2} S P^{-1/2} \right) & k \geq -1 \end{aligned}$$

where P is the product of the roots of Q^2 , r_1 and r_2 , and $P_m(x)$ is the m -th Legendre polynomial of the argument x . No general formula was found for the integral $U_{(k)}$ but after simplifying approximations had been made it was possible to evaluate the integrals for special values of k with the results:

$$U_2 \cong \frac{(-1)^{n_r}}{16} \pi \epsilon^{-1/2} \left[3D^2 S \frac{J_1(\xi)}{\xi} + S^3 J_0(\xi) \right]$$

$$U_{-2} \cong (-1)^{n_r} \pi \epsilon^{-1/2} S^{-1} \left[J_0(\xi) + \left(\frac{D}{S} \right)^2 \frac{J_1(\xi)}{\xi} + 3 \left(\frac{D}{S} \right)^4 \frac{J_2(\xi)}{\xi^2} + \dots \right].$$

The values of U_k for other values of k were obtained by use of the recurrence relation

$$U_{k-1} = \frac{2}{k+1} \frac{dU_k}{dS}.$$

In these relations $S = r_1 + r_2$, $D = r_2 - r_1$, $\xi = (n_r + \frac{1}{2})\pi$, and $J_n(\xi)$ is the n -th Bessel function of the argument ξ . The integrals $I_k^{(1)}$ were found to be given approximately by:

$$I_k^{(1)} \cong \frac{(l + \frac{1}{2})^{2k+2} \exp \{ l + \frac{1}{2} \}}{2^{k+1} (2l + k + 5)}.$$

Finally, for the integrals $I_k^{(3)}$ we find

$$I_2^{(3)} = \frac{1}{8} r_2^3 \epsilon^{-1/2} \exp\left(\frac{\beta}{2}\right) \left[\left(1 + \frac{1}{2\beta}\right) K_0\left(\frac{\beta}{2}\right) + \left(1 + \frac{3}{2\beta} + \frac{2}{\beta^2}\right) K_1\left(\frac{\beta}{2}\right) \right]$$

$$I_1^{(3)} = \frac{1}{8} r_2^2 \epsilon^{-1/2} \exp\left(\frac{\beta}{2}\right) \left[K_0\left(\frac{\beta}{2}\right) + \frac{\beta+1}{\beta} K_1\left(\frac{\beta}{2}\right) \right]$$

$$I_0^{(3)} = \frac{1}{8} r_2 \epsilon^{-1/2} \exp\left(\frac{\beta}{2}\right) \left[K_0\left(\frac{\beta}{2}\right) + K_1\left(\frac{\beta}{2}\right) \right]$$

$$I_{-1}^{(3)} = \frac{1}{4} \epsilon^{-1/2} \exp\left(\frac{\beta}{2}\right) K_0\left(\frac{\beta}{2}\right)$$

$$I_{-2}^{(2)} = \frac{1}{4} \beta r_2^{-1} \epsilon^{-1/2} \exp\left(\frac{\beta}{2}\right) \left[K_1\left(\frac{\beta}{2}\right) - K_0\left(\frac{\beta}{2}\right) \right]$$

$$I_{-3}^{(3)} = \frac{1}{6} \beta r_2^{-2} \epsilon^{-1/2} \exp\left(\frac{\beta}{2}\right) \left[\beta K_0\left(\frac{\beta}{2}\right) - (\beta-1) K_1\left(\frac{\beta}{2}\right) \right]$$

where $\beta = 2\epsilon^{-1/2} r_2$ and $K_\nu(x)$ is the Bessel function of the third kind of order ν .

ON THE ORIGIN OF THE BANDS IN THE SPECTRUM OF MERCURY VAPOR

(REMARKS ON A PAPER BY R. ROLLEFSON)

BY S. MROZOWSKI

PHYSICAL LABORATORY, SOCIETY OF SCIENCES AND LETTERS, WARSAW

(Received July 28, 1930)

ABSTRACT

Arguments of Rollefson, admitting the existence of molecules of small energy of binding in mercury vapor, are criticized. It is shown that the experimental facts lead to the following conclusions: (1) That absorption is due to the molecules which exist before irradiation of the vapor; (2) probably all absorption bands have the same origin; (3) the bands are due to molecules with great energy of binding (17 kcal/mol); and (4) the emission bands lying in the region of the absorption bands are emitted by the molecule in returning to its normal electronic level.

A new observation is made of shaded absorption bands at 2267 and 2247A.

IN A very interesting paper¹ Rollefson tries to reconcile the contradictory results given by Franck and Grotrian² and Koernicke³ and those which the author has obtained.⁴ Rollefson concludes that different bands in mercury vapor spectrum have different origin, particularly the band 2540A may be accounted for the presence of Hg_2 molecules having small energy of binding (1.4 kcal/mol). The existence of such molecules seems very probable from the theoretical standpoint. Leaving aside the theoretical discussions the author will try in this paper to consider critically the arguments of Rollefson only from the point of view of experimental facts. In this connection the author would like to point out a series of very simple experimental facts, which were generally not taken into account in building the hypotheses relating to the origin of the band spectrum of mercury vapor.

We have to remark that the contradiction pointed out by Rollefson does not exist, for the author has shown in a former paper,⁵ that Koernicke, (and probably also Franck and Grotrian, whose preliminary measurements were improved by Koernicke) applied an erroneous formula and therefore the results cannot be convincing. Up to the time of a precise repetition of the measurements of Koernicke, there is no need to search for new points of view which would reconcile the results of Koernicke and those of the author.

To recall the complicated structure of the absorption bands of mercury vapor the graph of this band spectrum is given in Fig. 1.

The band series a^5 and e were found by Rayleigh, b and c is the fine struc-

¹ Rollefson, Phys. Rev. 35, 1177 (1930).

² Franck and Grotrian, Zeits. f. techn. Physik 3, 194 (1922).

³ Koernicke, Zeits. f. Physik 33, 219 (1925).

⁴ Mrozowski, Zeits. f. Physik 55, 338 (1929).

⁵ The fact that these bands can be due to Hg_2O molecules (Walter and Barrat, Proc. Roy. Soc. A122, 201, 1929) does not influence the consideration in this paper.

ture of the 2540A band discovered by Wood and Voss,⁶ *d* the bands observed long ago by Wood, finally the two shaded bands *f* and *g* were found by the author on the photographs of absorption bands. The absorption tube in these experiments had a length of 40 cm. A hydrogen quartz lamp wholly immersed in water, with electrodes also cooled by running water, was used

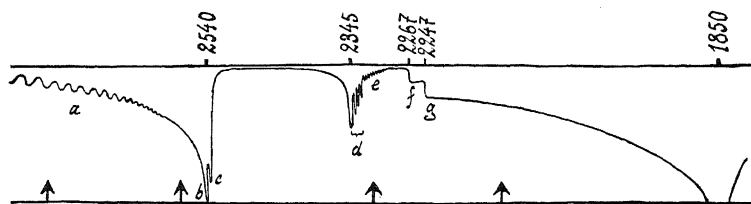


Fig. 1.

as the source of the continuous spectrum. (At 3000 volts a current of 2 amp. could be maintained, but in the experiments 0.5 amp. was mainly used.) The shaded bands *f* and *g* are represented in Fig. 2 where we have

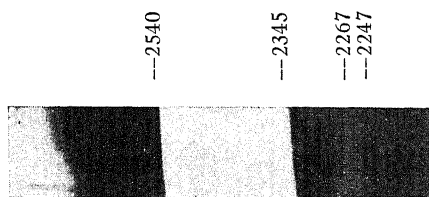


Fig. 2.

a photograph taken by a small Liess spectrograph type A.

Different hypotheses were made about the origin of the mercury absorption bands. One of these was, that the molecules which are responsible for the absorption are formed from excited and unexcited atoms during the irradiation. But the fact that the spectral lines of other elements separated by the monochromatic illuminator are absorbed (and excite the band emission) is in contradiction with the former hypothesis. In general the experiments show conclusively, that: (1.) The absorption is due to the molecules which exist before the irradiation of the vapor, because the form of the absorption bands does not depend in wide limits upon the intensity of the light transmitted through the vapor (variations of time of exposure from $\frac{1}{2}$ min. to 24 hours were used by the author). Nor do these bands depend upon the distillation of vapor (Niewodniczański).⁷

The theory of quasimolecules of Born and Franck and the theory of Oldenberg (interaction of radiation and impact) which is identical with it can only explain the widening of the atomic absorption lines which appears in dense vapor, but they cannot explain the complicated structure of the band

⁶ Wood and Voss, Proc. Roy. Soc. A119, 698 (1928).

⁷ Niewodniczański, Compt. Rend. Soc. Pol. de Physique 3, 31 (1927).

absorption spectrum of mercury vapor. There remain two possibilities: molecules with small or great energy of binding. In the first place it is to be proved, that: (2.) Probably all the absorption bands of mercury vapor have the same origin. This can be seen on the basis of the former measurements of dependence of the band absorption coefficient upon the temperature of saturated mercury vapor, made for wave-lengths 2749, 2573 and 2144A⁴ and also recent measurements made with a quite different method for wave-lengths 2749, 2573, and 2313A⁸ by the author. All these experiments show a good proportionality between the dependences of the absorption coefficients for four different wave-lengths lying in different absorption regions (corresponding spots are marked by arrows in Fig. 1). These measurements show further that: (3.) The bands are due to atoms or molecules with great energy of binding (17 kcal/mol). The heat of evaporation found from the change of the absorption coefficients is, on the average, 12 kcal/mol; we can say that the absorption is due to atoms (the heat of evaporation $\lambda_1 = 14.5$ kcal/mol; the difference could be explained by experimental errors) or molecules with energy of binding approximately of 17kcal/mol ($= 2\lambda_1 - 12\text{kcal/mol}$) The suggestion of Rollefson, that in the case of absorption of the line 2573A two different phenomena overlap: the absorption of molecules of small energy of binding and of quasimolecules (relatively the interaction of radiation and impact) does not evidently suffice to explain the experimentally shown proportionality of absorption coefficient for the wave-length 2573A to the concentration of atoms (approximately), for the phenomena mentioned are proportional to the square of density of vapor (heat of evaporation of $2\lambda_1$ also), which is too far outside the limits of the experimental errors of the methods applied.

Considering the emission bands of mercury vapor, we can refer to the graph shown in a recent paper of the author⁹ (Fig. 4 of the paper; the only uncertainty relating to the emission in the 2000–1850A interval in fluorescence was explained recently by Eliashewich and Teremin¹⁰ in agreement with the predictions of the author). Contrary to the suggestion of Rollefson, we have to assume, that (4.) The emission bands lying in the regions of the absorption bands (therefore excluding only the continuous band 4850A) are emitted by the molecules returning to their normal electronic level. That is shown by the proportionality of the intensity of fluorescence to the intensity of the exciting light (Wood and Voss⁶) and the fact, that for monochromatic excitation even of very weak intensity (time of exposure on a small spectrograph 100 hours) there appears the anti-Stokes part of the fluorescence band. For example, the band of Steubing (2350-2000A, the author has previously shown that they belong to the pure vapor of mercury⁴) is emitted by the transition to the normal electronic level and shows a series of separated oscillation bands. Therefore we can affirm that the molecules in the normal and in the excited states alike ought to have a relatively great energy of

⁸ Mrozowski, *Wszechswiat* 3, 101 (1930).

⁹ Mrozowski, *Zeits. f. Physik* 62, 314 (1930).

¹⁰ Eliashewich and Terenin, *Nature* 125, 856 (1930).

dissociation. That is in agreement with conclusion 3, for from the modern point of view about the structure of the atomic spectra we have to omit the first case of point 3. Moreover we can remark, that by assuming with Rollefson that the band 2540A is due to molecules of small energy of binding, it should be difficult to explain the structure of that band observed in emission by Takeo Hori.¹¹

Although the correlation of molecular and atomic electron levels given previously by the author⁴ may be considered only as provisional, it seems to us however, that the result given by the experiments, namely that there are molecules of mercury vapor with great energy of dissociation, is a very important one. We have to bear in mind that in the first place there is a contradiction with the results of measurements of the mercury vapor density on the one hand and with the theoretical view on the possibility of formation of such molecules from atoms with closed electronic shells on the other hand. The explanation of these contradictions can be expected from new precise measurements.

¹¹ Takeo Hori, *Zeits. f. Physik* **61**, 481 (1930).

ABNORMAL SHOT EFFECT OF IONS OF TUNGSTOUS
AND TUNGSTIC OXIDE

BY JOHN S. DONAL JR.

UNIVERSITY OF MICHIGAN

(Received August 18, 1930)

ABSTRACT

Part I. The formation of positive ions of tungstous and tungstic oxide. It was found that when oxygen attacks a hot tungsten filament, positive ions are formed, and a mass spectrograph test has shown these ions to be a mixture of tungstous and tungstic oxide. The positive ion current is proportional to the pressure of the gas, as is the rate of formation of the oxide. The evaporation of an oxide layer following the pumping away of the oxygen, yields an ion current which falls away exponentially with the time. The ratio of the number of charged particles of the oxide, to the number of uncharged particles, is approximately one in twenty thousand, and this ratio does not vary greatly with the temperature of the tungsten filament.

Abnormal shot effect of the currents of positive ions. When the positive ions are drawn to a collecting electrode, in series with which there is a tuned shot circuit, an abnormal shot voltage is developed. The hypothesis is advanced that this shot voltage arises from fluctuations in the inter-electrode capacitance of the tube, caused by variations in the thickness of the electron sheath surrounding the anode as the sheath is penetrated by the positive ions. On this basis, an expression for the resulting mean square shot voltage is presented. This expression was found to be correct as regards the variation of the shot voltage with the ion current, and it has yielded reasonable values for the change in the inter-electrode capacitance.

Part II. Abnormal shot effect due to the trapping of the positive ions. When positive ions of tungstous and tungstic oxide were trapped in the minimum of potential surrounding a hot cathode, an abnormal shot voltage resulted. This abnormality was found to vary inversely with the square of the resonance frequency of the tuned shot circuit, analogously with the "flicker-effect." An expression for the mean square shot voltage has been developed, which permits the calculation of the average plate current increase due to the trapping of a single ion. The simultaneous measurement of the shot voltage and the total plate current increase has permitted the determination of the number of electrons released by each positive ion, and also the average time of trapping of the ions. From a knowledge of the trapping time, values of the electron space charge density in the minimum of potential were computed. These values were in agreement with those computed from a knowledge of the filament temperature, and the space current, and the two methods of arriving at the space charge density yielded magnitudes which varied in the same manner with the electron current through the tube.

INTRODUCTION

IT IS well known, particularly from the work of Kingdon and Charlton,¹ that positive ions produced at the surface of a hot filament may become trapped in the minimum of potential adjacent to the cathode surface, and will in that case cause a partial break-up of the space charge and a release of electrons to the anode. It was felt that the fluctuations of the plate current

¹ K. H. Kingdon and E. E. Charlton, Phys. Rev. 33, 1011 (1929).

due to this trapping process would develop an abnormal mean square shot voltage across a tuned shot circuit, and that from measurements of this voltage much information concerning the process could be obtained.

It was proposed to make use of the fact that caesium vapor becomes ionized upon contact with a hot tungsten filament, but in the course of some other work it was found that positive ions are produced when oxygen attacks a hot tungsten surface, and this source of ions was used in the experiments. Part I will be devoted to a brief discussion of this phenomenon, and of the experimental conditions governing the formation of the ions.

Before undertaking the work to be described, measurements were made of the charge carried by electrons in temperature limited currents from the filaments of several commercial vacuum tubes. These determinations were carried out with the idea of placing the apparatus in correct operating condition, use being made of the known charge carried by the electron.

As a preliminary piece of work, a determination was made of the charge of electrons produced by the ionization of argon gas. In the course of this work, large abnormalities were found to be present, as long as the electron currents were space charge limited. A detailed study of these effects was made, but space will not permit further discussion here. It will suffice to say that, when the abnormalities were eliminated, the electrons produced by the gas ionization were found to carry the accepted value of electronic charge, within the probable error of the experimental work.

The shot effect apparatus used in these determinations was of essentially the same design as that employed by Williams and Vincent,² in previous researches on the measurement of the charge of the electron. The experimental tubes were assembled by the writer, and varied considerably in design. The vacuum system employed was capable of maintaining a pressure of 10^{-7} mm of mercury, and was equipped with the means of introducing and mixing various gases.

PART I. THE FORMATION OF POSITIVE IONS WHEN A HOT TUNGSTEN FILAMENT IS ATTACKED BY OXYGEN GAS

It is well known, from the work of Langmuir and others, that hot tungsten is attacked by oxygen gas, with the formation of tungstic oxide. The rate of attack is proportional to the oxygen pressure, if the filament is maintained at a constant temperature. When the metallic surface is above about 1250°K , the oxide is thrown off, but when the surface temperature is below this value, the oxide forms a thick layer and the filament is very perceptibly darkened. If the coating is permitted to form on the metal, the rate of attack by the gas is decreased.

In the course of some experiments on the abnormal shot effect of currents of positive ions from pure tungsten filaments, the ions were accelerated through gases. It was found that when oxygen was admitted to the system, the positive ion current was greatly increased, and that the increase was directly due to the oxygen itself. It was immediately surmised that the ions

² N. H. Williams and H. B. Vincent, *Phys. Rev.* **28**, 1253 (1926).

were those of tungstic oxide, with the possibility of tungstous oxide being present also. Langmuir,³ in one of his earlier papers, has shown that the attack of a tungsten surface by oxygen must take place in two steps, and he has suggested that the first may well be the formation of tungstous oxide on the metallic surface, oxygen further uniting with this compound to form the common trioxide.

As would be expected, the number of positive ions formed is very much a function of the gas pressure, the filament temperature, and the area of the tungsten surface. An idea of the magnitude of the positive ion current may be had from the fact that with a tungsten surface 1 cm² in area, held at a temperature of 2300°K, one may expect the saturation value of the positive

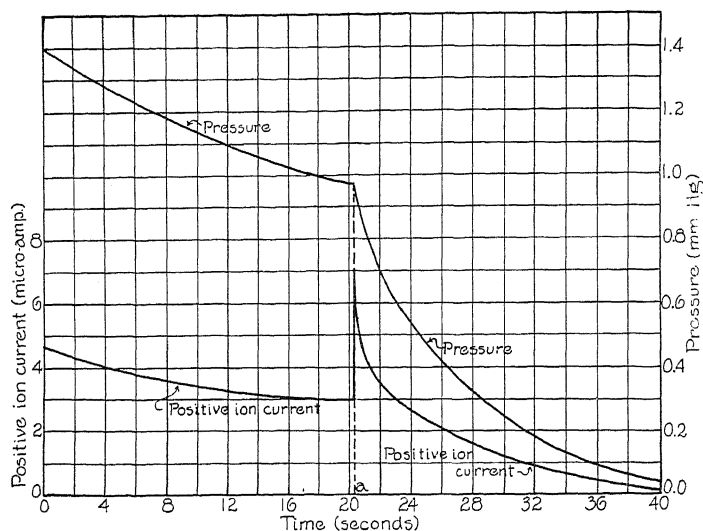


Fig. 1. Behavior of positive ion current and gas pressure, before and after evaporation of oxide layer.

ion current to be of the order of 5×10^{-5} amperes, with an oxygen pressure of 1 mm of mercury. This current is quite naturally difficult to maintain, since the gas is removed exceedingly rapidly by the filament, which is in turn eaten away. These facts have made the determination of the exact experimental relationships difficult and in some cases impossible.

As the result of experiments made with over one hundred tubes, it has been found that the rate of formation of the positive particles is directly proportional to the amount of oxygen entering into chemical combination with the tungsten to form the oxide, and it was upon this fact that the assumption as to the nature of the ions was based.

The behavior of the positive ion current and the gas pressure, with the time, is illustrated in Fig. 1. To the left of the point (a) on the time axis the filament temperature was so low that the oxide remained on the metallic surface. The positive ion current and the rate of decrease of gas pressure

³ I. Langmuir, Proc. Am. Chem. Soc. 37, 1139 (1915).

were therefore low. At the arbitrary point (*a*) in time the filament temperature was increased sufficiently to break away the oxide layer and to prevent its re-formation. It will be noted that the positive ion current increased sharply and then fell away rapidly, as did the gas pressure, since the rate of clean-up by the fresh metallic surface was very much greater and the temperature had been increased. It will be seen from the figure that the ion current was proportional to the gas pressure, at the points beyond (*a*) in time. The rate of formation of tungstic oxide is already known to be proportional to the gas pressure, and we thus see the direct relationship between the rates of formation of the ions and of the oxide. Subsequent determinations of the variation of the ion current with the oxygen pressure have shown the direct

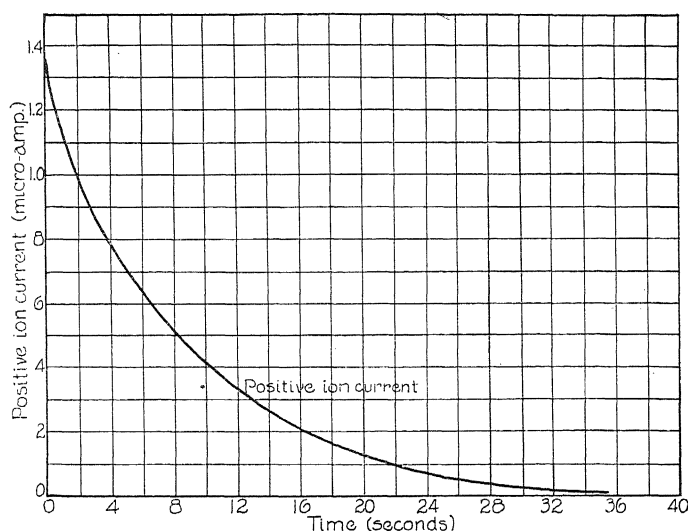


Fig. 2. Positive ion current obtained during the evaporation of an oxide coating from a tungsten filament.

proportionality to hold rigidly when the other experimental conditions are maintained constant.

It was naturally supposed that the ionization process takes place either at the moment of formation of the oxide or at the instant when the particle leaves the metallic surface, and that once the oxide is formed the oxygen gas is no longer essential. In order to test this assumption, an oxide layer was formed on a relatively cool filament, the remaining gas then pumped away and the tube walls well out-gassed. Following this treatment the filament temperature was increased sharply to a value slightly above that which would just permit the adherence of the coating. The variation of the ion current with time was then determined and the result is illustrated in Fig. 2.

From the shape of the curve of Fig. 2, it is apparent that the number of charged particles leaving the filament was proportional to the amount of oxygen resident there. No appreciable gas was given off during this breakdown process.

At the writer's request, L. P. Smith and L. Barnes, of Cornell University, lately have been so kind as to make a mass spectrograph determination of the nature of the positive ions under discussion. Their results are illustrated in Fig. 3.

It will be noted from the figure that both the singly charged dioxide and trioxide ions were present, in the approximate ratio of one to three, respectively. The presence of the dioxide ions is particularly interesting, in the light of Langmuir's conclusions as to the nature of the two-step process involved in the oxide formation.

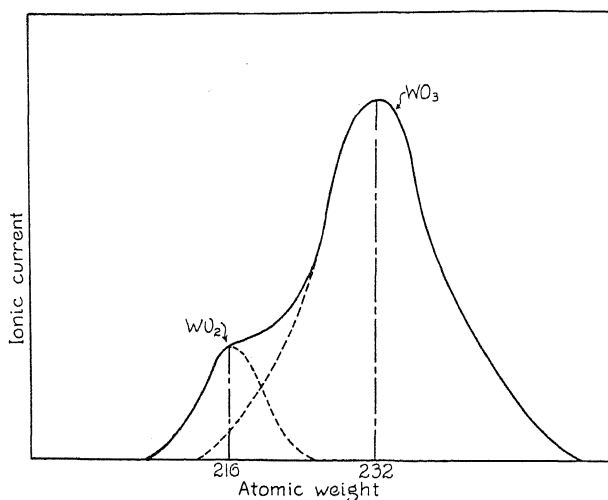


Fig. 3. Mass-spectrograph determination of the nature of the ions formed when oxygen attacks a hot tungsten filament.

THE RELATIVE NUMBER OF OXIDE PARTICLES WHICH LEAVE THE SURFACE CARRYING A CHARGE

Experiments were undertaken to determine what proportion of the particles of the oxide actually becomes charged, and how this proportion varies with the temperature of the metallic filament. In order to accomplish this, a tungsten filament was heated in an atmosphere of oxygen of a known initial pressure and volume. The total number of removed molecules of oxygen was computed from the change in pressure during the period of operation of the filament, and from this was determined the number of molecules of either WO_2 or WO_3 formed. During the heating of the filament the saturation value of the positive ion current to the cathode was measured, and the graphical integration of this curve yielded the number of ionized molecules of oxide.

The results of several representative determinations are presented in Table I. Since WO_2 is unstable chemically, the values have been computed on the basis of WO_3 alone. It is of course possible that all of the WO_2 leaving the filament was charged, and in fact it may have left the filament only by virtue of its charge.

The runs of Table I were made at different filament temperatures. The results, as regards the variation of the numbers of charged particles with the temperature, are particularly interesting. One would perhaps expect the oxide molecules to become charged more readily at the higher temperatures. This is obviously not the case, the trend being decidedly in the opposite direction toward the end of the table. It must be pointed out, however, that the smaller relative numbers of charged particles at the higher temperatures may be spurious. With the exceedingly hot filaments used in the latter runs of the table, the electron emission was high, from actual measurements, and there was a dense electron space charge surrounding the filament, which may well have brought about the removal of many of the oxide ions by recombination.

TABLE I. *Values of the ratio of the number of uncharged particles of WO_3 , to the number of charged particles.*

Run	Approximate filament temperature	M/M_+
4,5	Below oxide evaporation point	14840
6	" " " "	15580
2	Just above oxide evaporation point	14940
13	" " " "	14920
14	" " " "	13800
10	Bright yellow heat	17560
15	" " " "	17220
16	" " " "	16080
17	" " " "	15960
19	White heat	20600
20	" " " "	19940
22	" " " "	20560
23	" " " "	22600
1	Just below burn-out temperature	40400
8	" " " "	38560
9	" " " "	69200

We may conclude that, in spite of the great variation in gas pressure, filament surface condition and surface temperature from run to run, the ratio of the number of charged particles to the number of uncharged particles was of the order of one to twenty thousand and that, as regards temperature in particular, no marked variation was found.

It may be of interest to know that in experiments in which the temperature was increased uniformly until the filament burned out, the positive ion current almost invariably decreased slightly at the temperatures just below the fusion point of the tungsten. From the other results, this indicates a decrease in the rate of formation of the oxide at the highest temperatures, a result which has been predicted by Langmuir.⁴

ABNORMAL SHOT EFFECT CAUSED BY THE POSITIVE IONS OF WO_2 AND WO_3

A brief discussion of a series of determinations of the shot voltage developed by the currents of positive ions will now be presented. A tuned shot circuit was placed in the lead to the collecting electrode, and it was found that when the positive ion current traversed this circuit the resulting mean square

⁴ I. Langmuir, Proc. Am. Chem. Soc. 37, 1139 (1915).

shot voltage was abnormal by a factor as great as one thousand, depending upon the experimental conditions.

It was apparent that the magnitude of the shot voltage was very greatly dependent upon the emission of electrons from the hot anode, entirely aside from the rate of attack by oxygen. In short, not only the positive ions were necessary to develop the abnormal shot voltage, but an electron space charge was necessary as well. This fact is clearly illustrated in the plots of Fig. 4, which are representative of many such runs.

Fig. 4 illustrates the variation of the positive ion current, the abnormal mean square shot voltage and the electron emission (determined subsequently with duplicated experimental conditions as to pressure and tempera-

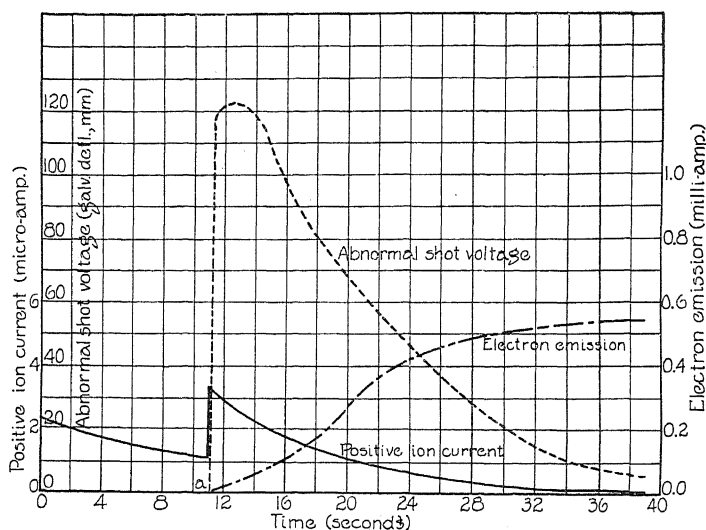


Fig. 4. Behavior of abnormal shot voltage and electron emission, following evaporation of oxide layer.

ture) as functions of the time. Again at the arbitrary time (*a*) the filament was heated sufficiently to break away the oxide layer. It will be noted that before the oxide was evaporated there was a current of positive ions, as in Fig. 1, but there was no electron emission nor was there any abnormal shot voltage. With the ion currents used, the normal shot voltage was so small as to be unmeasurable. As soon as the oxide layer was removed, however, a shot voltage, abnormal by a factor of approximately 1000, appeared, whereas the positive ion current increased by only a factor of two. It is to be particularly noted that the electron emission began to build up as soon as the layer was evaporated, increasing rapidly as the oxygen was removed from the tube. A large number of determinations were made in order to check this point, and in all cases it was found that the positive ion current alone was a necessary but not sufficient condition for the abnormal shot voltage fluctuations, the electron space charge being essential also.

In order to explain the observed mean square shot voltage, several hypotheses were considered. It will be remembered that the field used in these experiments was a retarding one for electrons, which therefore could only leave the hot anode by virtue of their emission velocities. This resulted in an equilibrium being established between the electrons leaving the filament and those returning, the only electrons present in the tube being those in the dense sheath close to the anode surface. The only direct current traversing the shot circuit was the positive ion current, and this had been found insufficient to yield the abnormality without the presence of the electron space charge.

Of the hypotheses advanced to explain the abnormality, all but one were found to be untenable, due to the peculiar experimental conditions. The theory adopted was that the abnormality arose from fluctuations in the inter-electrode capacitance of the tube itself, caused by variations in the size of the electron space charge sheath about the hot anode as the sheath was penetrated by the massive positive particles of oxide.

On the basis of the above assumption, the writer has developed an expression for the mean square shot voltage to be found across a tuned shot circuit, in terms of the number of positive particles formed per second and the average change in the inter-electrode capacitance due to the passage of a single ion. For this expression we have:

$$\bar{E}^2 = \frac{2NK^2V^2\overline{\Delta C}^2L^2A_0^2A}{R^2C^2}. \quad (1)$$

Here, N is the number of positive ions formed per second, K a constant depending upon the time constant of the circuit, V the negative plate potential in volts, $\overline{\Delta C}$ the average change in the inter-electrode capacitance due to the passage of a single ion, L , R , C are the constants of the tuned shot circuit, A_0 the voltage amplification of the amplifier at resonance frequency and A is the area under the amplifier resonance curve, as plotted against the frequency.

By comparing the \bar{E}^2 of Eq. (1) with the normal shot effect \bar{E}^2 , as developed in a tube known to yield the accepted value of the electronic charge it was found possible to measure $\overline{\Delta C}$ without a knowledge of the circuit constants or the characteristics of the amplifier.

Under the experimental conditions, Eq. (1) could only be subjected to direct test as regards the variation of \bar{E}^2 with N . The form of this variation was determined, and the result was entirely in accordance with the equation. Also, from measurements of \bar{E}^2 , values of $\overline{\Delta C}$ were computed, and these were found to be of the order of 10^{-4} times the actual electrode capacitance of the tube. Since, if Eq. (1) were based upon wrong assumptions, we might just as readily obtain values for $\overline{\Delta C}$ greater than the electrode capacitance itself, the computed results are thought to lend considerable support to the assumption as to the nature of the abnormality.

PART II. ABNORMAL SHOT EFFECT DUE TO THE TRAPPING OF POSITIVE IONS IN THE MINIMUM OF POTENTIAL

Introductory. This portion of the investigation was undertaken in order to test the writer's prediction that if positive ions were to become trapped in the minimum of potential surrounding a hot cathode, an abnormal shot effect would result. One would expect the ion, when trapped, to alter the potential distribution in the space charge region, and to cause an increase in the current to the plate, which increase should persist for the duration of the stay of the ion in the region surrounding the cathode. This change in the current would not be constant, of course, but would itself fluctuate as the ion oscillated about its mean position. The phenomenon would be fundamentally different in its effect upon the shot circuit, however, from the simple passage of an ion across the tube. In the latter case the duration of the event would certainly be less than the period of the tuned shot circuit used in these experiments (10^{-5} seconds). If the ion were to become trapped, however, and if neither the loss of ions by escape from the ends of the electrodes nor the loss by recombination with electrons were excessive, the duration of the event might be expected to be greater than the period of the tuned shot circuit. As has been pointed out by W. Schottky,⁵ the theoretical attack for these two cases is fundamentally different.

It was further hoped that the method of attack evolved by Schottky could be made applicable to the abnormal shot effect resulting from the trapping of the ions, and that, on this basis, a simple experimental procedure could be developed for determining the average effect of the positive ions under different conditions.

Finally, the writer wished to find a means of checking both the applicability of the Schottky theory and the quantitative experimental results to be obtained.

Preliminary experiments. In the course of the work with argon, mentioned in the Introduction, it had been found that the positive ions formed by the ionization of the gas yielded a very abnormal mean square shot voltage. This was due to the release of groups of electrons from the space charge region, as a result of the low mobility of the ions in comparison with the electron mobility. This phenomenon did not lend itself to quantitative measurements, however, since the ions were dependent upon the field for their formation, the ionization causing great instability in the tube plate characteristic and erratic readings as a consequence. Furthermore, there was no dependable method of measuring the actual number of ions formed per second.

When use was made of the ions formed by contact with oxygen with the hot tungsten filament, however, the phenomenon was fully under control. The number of ions formed was not a function of the field, but, the filament temperature being constant, was governed entirely by the oxygen pressure. This yielded separate control of the number of ions and of the space charge

⁵ W. Schottky, Phys. Rev. 28, 74 (1926).

density, and the number of ions formed per second could be measured at once by simply reversing the potential of the collecting electrode.

With the use of oxygen, and when the electron currents were space charge limited, it was found that the mean square shot voltage was abnormal by a factor of from 100 to 1000, depending upon the density of the space charge. The abnormality disappeared as soon as the electron currents were temperature limited. It remained to be determined whether or not the large shot voltage was due to the trapping of the ions, giving a result of the same nature as the "flicker effect."

Schottky⁶ has shown that, if the abnormal shot effect is caused by a primary event whose duration is greater than the period of the tuned shot circuit used, we would expect the shot voltage to vary inversely as the square of the resonance frequency of the tuned circuit. The particular case for which Schottky's theory was developed was the shot effect found experimentally by J. B. Johnson,⁷ and explained on the basis of fluctuations in emission caused by the temporary residence of foreign molecules on the emitting surface. This phenomenon followed the inverse square variation with the frequency of the tuned shot circuit.

Determinations were made of the trend with frequency of the abnormality in argon, and of the abnormality resulting from the positive ions of tungstous and tungstic oxide. In the former case, no definite frequency variation was found in the region from 100 to 250 kilocycles. In the latter case, however, the shot voltage was found to exhibit, within a few percent, the inverse square frequency variation. This at once classified the abnormality in oxygen as a phenomenon of the nature of the "flicker effect," with a primary event lasting longer than the period of the tuned shot circuit, and indicated that the cause of the abnormality was undoubtedly the trapping of the positive ions in the region of the minimum of potential, rather than the simple passage of an ion through the space charge region.

Theory. If we let γ be the average plate current increase due to the trapping of a single positive ion, we find that it is possible to obtain an expression for γ in terms of quantities easily measured experimentally. It may be pointed out that for the moment we are not interested in the factors limiting the duration of this average current increase, but only in the fact that, as was determined by the experimental frequency trend, the duration of the increase is substantially greater than the period of the tuned shot circuit.

The shot circuit consists of a tuned impedance in the plate lead of a two electrode tube and, in addition to the steady average value of the plate current, we have flowing through it a fluctuation current (due to electrons released from the space charge region) which may be written in terms of its Fourier components as follows:

$$j = \sum_{k=1}^{\infty} A_k \cos \omega_k t + \sum_{k=1}^{\infty} B_k \sin \omega_k t = \sum_{k=1}^{\infty} C_k \sin (\omega_k t + \Phi_k) \quad (2)$$

⁶ W. Schottky, Phys. Rev. 23, 74 (1926).

⁷ J. B. Johnson, Phys. Rev. 26, (July, 1925).

where A_k , B_k , and C_k are partial current amplitudes and ω_k is $2\pi x$ the frequency of the k th component.

Of course:

$$\left. \begin{aligned} \overline{A_k^2} + \overline{B_k^2} &= C_k^2 \\ \overline{A_k^2} &= \overline{B_k^2} \end{aligned} \right\} \quad (3)$$

and:

Schottky⁸ has evaluated these coefficients in his treatment of the "flicker effect," with the only difference that the fluctuations in the electron current originated at the cathode surface, rather than at the potential minimum, as in our case. Schottky obtained the result:

$$\overline{A_k^2} = \overline{B_k^2} = \frac{2}{T} \cdot \frac{\beta^2 \gamma^2 \alpha}{\alpha^2 + \omega_k^2} = \frac{2}{T} \cdot \frac{n \gamma^2}{\alpha^2 + \omega_k^2} \quad (4)$$

(since $\overline{\beta^2} = N_0$ from probability considerations, and $N_0 \alpha = n$.)

In this expression T is a time of observation, α the reciprocal of the time of trapping of an ion, N_0 the average number of ions in the space charge region at any instant, β the momentary deviation from this average, n the number of ions formed per second and ω_k is $2\pi x$ the frequency of the k th component of the fluctuation current.

We therefore have:

$$\overline{C_k^2} = \frac{4}{T} \cdot \frac{n \gamma^2}{\alpha^2 + \omega_k^2} \quad (5)$$

If a fluctuation current j is passed through a tuned shot circuit, and the resulting voltage fluctuations across the terminals of the tuned shot circuit are amplified, Williams and Vincent⁹ have shown that the mean square shot voltage is given by:

$$\overline{E^2} = \sum_k \overline{E_k^2} = \frac{L^2 A_0^2}{2R^2 C^2} \sum_{k=1}^{\infty} C_k^2 \Phi(x) \quad (6)$$

where A_0 is the voltage amplification of the amplifier at resonance frequency and $\Phi(x)$ is the curve obtained by plotting the relative power output at different frequencies against $x = \omega_k / \omega_0$.

If $dx = 2\pi / \omega_0 T$ be substituted in (6), together with C_k^2 from Eq. (5), we obtain:

$$\overline{E^2} = \frac{1}{\pi} \cdot \frac{L^2 A_0^2}{R^2 C^2 \omega_0} \int_0^{\infty} \frac{n \gamma^2}{x^2 + \alpha^2 / \omega_0^2} \Phi(x) dx. \quad (7)$$

The integrand of Eq. (7) may be considerably simplified if $\alpha \ll \omega_0$. In the experimental case, α will be found to be of the order of 10^4 and ω_0 was approximately 10^6 . Therefore α^2 / ω_0^2 was approximately 10^{-4} and could be neglected in comparison with x^2 , which was very nearly unity.

Eq. (7) then becomes:

⁸ References 5 and 6.

⁹ N. H. Williams and H. B. Vincent, Phys. Rev. **28**, 1253 (1926).

$$\overline{E^2} = \frac{n\gamma^2 L^2 A_0^2}{R^2 C^2 \omega_0} \int_0^\infty \frac{\Phi(x)}{x^2} dx. \quad (8)$$

A further simplification may also be carried out. If we write $1/z$ for x in the integrand of (8), we obtain:

$$\overline{E^2} = \frac{n\gamma^2 L^2 A_0^2}{R^2 C^2 \omega_0} \int_0^\infty \Phi\left(\frac{1}{z}\right) dz. \quad (9)$$

But it may be shown that if the amplifier resonance curve is sharp and symmetrical, as is true in the experimental case, we may write:

$$z = 1/z$$

with an error of only about 0.1%.

Thus:

$$\Phi\left(\frac{1}{z}\right) \cong \Phi(z)$$

and (9) becomes:

$$\overline{E^2} = \frac{n\gamma^2 L^2 A_0^2}{R^2 C^2 \omega_0} \int_0^\infty \Phi(x) dx \quad (10)$$

This equation may be written in terms of the frequency, since $x = \omega/\omega_0$ and $\nu = \omega/2\pi$. We thus obtain:

$$\overline{E^2} = \frac{2n\gamma^2 L^2 A_0^2}{R^2 C^2 \omega_0^2} \int_0^\infty \Psi(\nu) d\nu. \quad (11)$$

But $\int_0^\infty \Psi(\nu) d\nu$ is the area under the curve obtained by plotting the relative amplifier out-put voltage, for constant input, against the frequency, and may be called A .

Thus:

$$\overline{E^2} = \frac{2n\gamma^2 L^2 A_0^2 A}{R^2 C^2 \omega_0^2}. \quad (12)$$

Circuit constants and the necessity of plotting the resonance curve may be eliminated by comparing this $\overline{E^2}$ with the normal shot effect $\overline{E^2}$ obtained from a comparison tube known to yield the accepted value of electronic charge, and in which the electron current has been adjusted to give the same $\overline{E^2}$ as the abnormal effect.

Thus:

$$\frac{2n\gamma^2 L^2 A_0^2 A}{R^2 C^2 \omega_0^2} = \frac{2i_0 \epsilon L^2 A_0^2 A^{10}}{R^2 C^2}. \quad (13)$$

In the second member of this equation, ϵ is the electronic charge and i_0 the electron current necessary to yield the desired value of $\overline{E^2}$.

Simplifying, we obtain:

¹⁰ N. H. Williams and H. B. Vincent, Phys. Rev. 28, 1253 (1926).

$$\gamma = \omega_0 \left(\frac{i_0 \epsilon}{n} \right)^{1/2} \quad (14)$$

which is the expression for the average plate current increase due to the trapping of a single positive ion. From a consideration of the right hand side of the equation, it will be seen that we now have a means of determining experimentally the size of the primary event of the phenomenon in question.

In the course of the experimental work it was found, as would be expected, that during the attack of the filament by oxygen the shape of the plate current characteristic of the tube was altered. The break-up of the space charge by the positive ions resulted in an increase in current in the range of plate potentials wherein the current was limited by space charge. The effect of this may be seen in Fig. 5. The method of taking this plate current characteristic will be discussed in a subsequent paragraph.

If we let Δi_p be the increase in plate current, at any one plate potential, due to the action of all of the ions, and let τ be the average time of life of an ion in the minimum of potential, we see that $\gamma\tau$ is the average charge released by one ion, and $n\gamma\tau$ is the charge released per second, which is precisely the total change in the current.

Therefore:

$$\Delta i_p = n\gamma\tau. \quad (15)$$

It may now be seen that, if n is known from the saturation value of the positive ion current with reversed field, Δi_p known by direct measurement, and γ computed from the shot effect determinations, substituted in Eq. (14), we have a means of computing τ , the average time of life of the ions in the minimum of potential.

In addition, it is of interest to determine a value of the number of electrons released by each positive ion. This may be had by dividing Δi_p by the saturation positive ion current under reversed fields.

It seemed possible that, from the value of τ , the magnitude of the space charge density in the minimum of potential might be computed and checked against magnitudes computed from a knowledge of the filament temperature and the space current. It was thought that this might offer a means of verifying our theory, in particular the applicability of the "flicker-effect" Fourier coefficients to this experimental case.

The writer is not aware of any exact formula connecting τ and the electron space charge density, but Kingdon and Charlton¹¹ have given the approximate relation:

$$\rho = \frac{\left(\frac{2\pi m}{KT_f} \right)^{1/2}}{4\pi b^2\tau} \quad (16)$$

where m is the electron mass, T_f the filament temperature, and b is a parameter having the value 3.25×10^{-7} for a temperature of 1700°K .

¹¹ K. H. Kingdon and E. E. Charlton, Phys. Rev. 33, 1012 (1929).

It is obvious that, in making use of this equation, we are assuming that the life of the positive ions is limited solely by recombination with electrons. The other principal factor which might limit the time of existence of the ions in the minimum of potential is escape from the ends of the electrodes. In order to test for this effect, a special tube was constructed, having shields over the ends of the plates which could be so charged as to repel the ions back into the region about the filament. It was found that the effect of loss by escape was not appreciable with the low gas pressures at which the latter work was carried out. The region of pressure in which it was necessary to work will be discussed in a following paragraph.

The method of computing the space charge density in the minimum of potential, from a knowledge of the filament temperature and the space current, is too well known to require description. We need only refer the reader to the papers of Langmuir¹² and Kingdon and Charlton.¹³

In the present work, we could not hope to check very closely the values computed by the last mentioned method, since Eq. (16) is not exact. However, since the rate of recombination must certainly vary directly with the space charge density, the variation:

$$\rho \sim \frac{1}{\tau} \quad (17)$$

may be expected to be true. In short, if our theory is correct, we would expect the values of ρ computed from the experimental results to behave, with some variable such as the space current, in the same manner as the values of ρ computed from purely theoretical considerations. If our theory were incorrect, this would certainly be most unlikely. This, then, yielded a means of testing the ideas outlined in this section.

Experimental Procedure. In the final experimental runs, made to test the foregoing theory, the oxygen pressure was maintained constant by pumping air through a slow-leak stop-cock and past the hot filament. Control experiments showed that the nitrogen and water vapor from the air were entirely inert and acted in no way to invalidate the work.

Determinations of the variation of the positive ion current with the oxygen pressure demonstrated a direct proportionality, from the lowest measureable pressures until the chemical action was so rapid as materially to decrease the surface of the filament during a run. At the higher gas pressures the number of positive ions formed per second was computed from direct measurement of the positive ion current under reversed field. At the low oxygen pressures, where the ion current was unmeasurable with a microammeter, readings of the current were taken at the higher pressures and the values extrapolated.

Before admitting oxygen to the tube, the vacuum plate current characteristic was taken. (See Fig. 5.) The utmost care was necessary in the determination of this curve, as the amount of oxygen given out by the

¹² I. Langmuir, Phys. Rev. 21, 419 (1926).

¹³ K. H. Kingdon and E. E. Charlton, Phys. Rev. 33, 1011 (1929).

walls and electrodes, even after considerable baking and out-gassing, was sufficient to raise the characteristic curve in the region of space charge limited currents. This led to erroneous values of Δi_p .

Δi_p would be expected to vary linearly with the gas pressure, from Eq. (5), and a number of experiments were carried out to determine the range of gas pressures in which this was true. It was found that, with the tubes used, the linear variation held only up to pressures of the order of 10^{-4} mm of mercury. At higher gas pressures, Δi_p exhibited a saturation, no doubt partially due to the increased effect of the escape of the ions from the ends

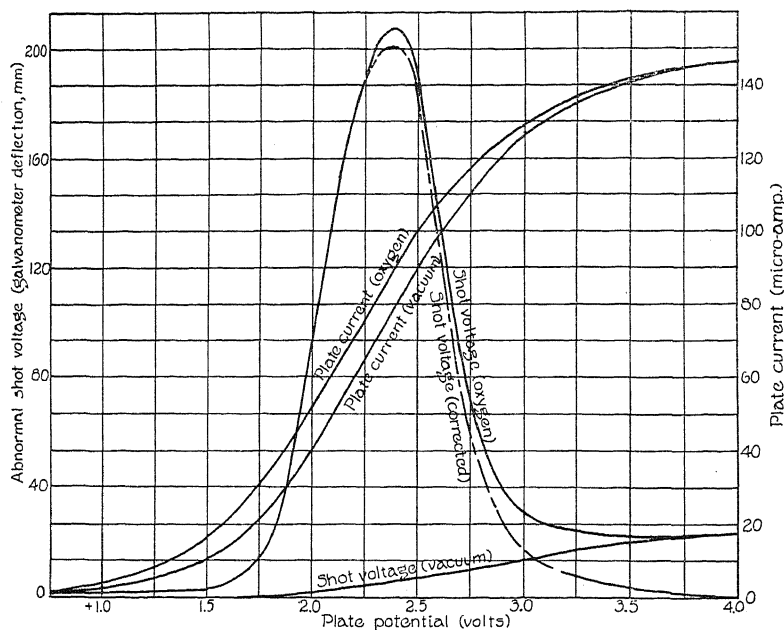


Fig. 5. Plate currents and mean square shot voltages as functions of the plate potential, in a vacuum and in oxygen.

of the electrodes. At the same pressure, ρ_m also began to fall away rapidly from the values computed by Langmuir's equations. For these reasons the pressures used in the final experiments were of the order of 10^{-4} mm of mercury or less.

Following the taking of the plate characteristic curve in a vacuum, the oxygen pressure was adjusted to the desired value and a determination of n made. The plate current characteristic of the tube was re-taken, together with the corresponding values of the abnormal mean square shot voltage. These latter were determined by means of the standard shot circuit and an amplifier which had been calibrated in terms of electron currents in a tube known to yield the accepted value of the electronic charge.

The values of γ , τ and ρ_m were computed from equations (14), (15) and (16), respectively. ρ_m was also computed from the equations of Lang-

muir and Kingdon and Charlton, and these latter space charge densities were compared with those obtained from the experimental results.

Results. Only one typical experimental run will be presented here. Fig. 5 illustrates the variation of the plate current in a vacuum and in oxygen, with the positive plate potential, and also the variation of the mean square shot voltage in both cases, with the same independent variable. The actual computations of γ , τ and ρ_m were carried out from the dotted curve.

TABLE II. Values of η , γ , τ and ρ_m , computed from the experimental results illustrated in Fig. 5.

E_p (volts)	η	γ (amperes)	τ (sec.)	ρ_m (experimental)	ρ_m (theoretical)
1.50	1.24×10^3	0.925×10^{-10}	2.13×10^{-4}	0.55×10^9	0.42×10^9
1.55	1.36	1.18	1.850	.637	
1.60	1.46	1.44	1.610	.728	
1.65	1.58	1.85	1.360	.861	
1.70	1.68	2.09	1.270	.920	
1.75	1.80	2.72	1.050	1.118	.790
1.80	1.94	3.27	.94	1.241	
1.85	2.06	3.94	.83	1.410	
1.90	2.22	4.92	.72	1.635	
2.00	2.38	6.98	.57	2.041	1.390
2.05	2.52	7.85	.52	2.230	
2.10	2.60	8.71	.45	2.630	
2.15	2.44	9.22	.41	2.820	
2.20	2.40	9.61	.38	3.080	
2.25	2.20	10.08	.35	3.360	2.130
2.30	2.14	10.32	.33	3.550	
2.35	2.10	10.52	.32	3.690	
2.40	2.06	10.31	.31	3.750	
2.45	2.00	10.08	.308	3.800	
2.50	1.80	10.00	.284	4.110	2.960
2.55	1.70	9.24	.293	3.990	
2.60	1.60	8.38	.303	3.860	
2.65	1.40	7.65	.291	4.02	
2.70	1.10	6.54	.267	4.38	
2.75	.90	5.65	.254	4.60	3.740
2.80	.80	4.95	.257	4.55	
2.85	.60	4.50	.212	5.50	
2.90	.50	3.96	.200	5.84	
2.95	.44	3.42	.205	5.70	
3.00	.40	2.92	.218	5.36	4.470
3.05	.34	2.83	.191	6.12	
3.10	.20	2.63	.121	9.65	
3.15	.16	2.42	.104	—	
3.20	.10	2.31	.069	—	
3.25	.04	2.06	.031	—	—

This last was obtained by first adjusting the vacuum shot voltage curve for the fact that the actual plate currents were higher in the second case, and then subtracting the result from the shot voltage curve obtained in oxygen.

The oxygen pressure chosen for this particular determination was 3.75×10^{-5} mm of mercury, which was well within the range of the linear variation of Δi_p with the gas pressure.

In Table II we have listed, for different plate potentials, the computed values of η (the average number of electrons released by each positive ion), γ , τ , and the experimentally determined values of ρ_m , which are the mag-

nitudes of the electron space charge density in the potential minimum, computed from the experimental results. In the last column are listed the values of ρ_m computed from the equations of Langmuir and Kingdon and Charlton. It will be noted that both η and γ reach a maximum, but not at the same plate potential, since η is proportional to the product of τ and γ . The values of τ are seen to decrease throughout the table, since the space charge (and hence also the amount of recombination with electrons) is decreasing. It will be noted that the values of τ are substantially greater than the period of the tuned shot circuit, which was in this case approximately 4×10^{-6} seconds.

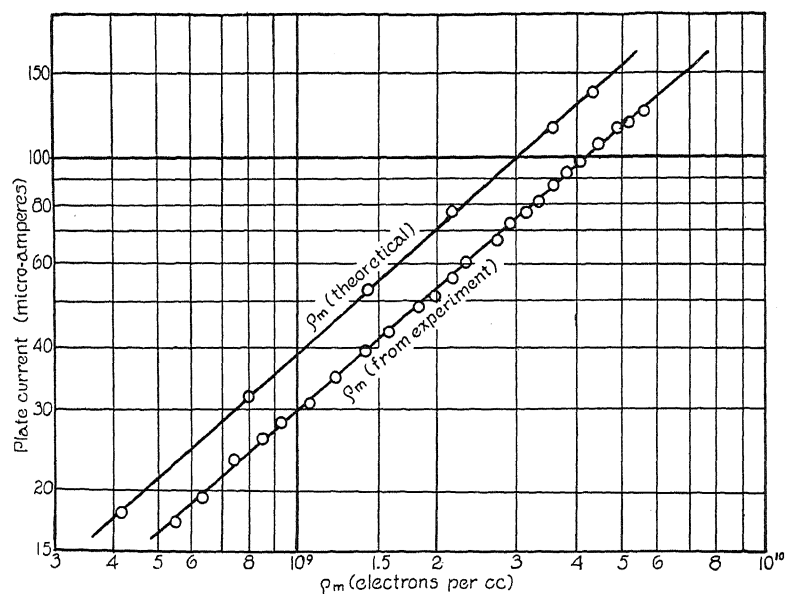


Fig. 6. Logarithmic plots of ρ_m , computed by the two different methods, against the logarithm of the space current.

In Fig. 6 we have the two different sets of values of ρ_m plotted against the space current, to logarithmic scales. As indicated in the last two columns of Table II, the values of ρ_m computed from the experimental results, agree with the values computed from purely theoretical considerations, within the probable error of the experiments and of Eq. (16). Fig. 6 shows that the two values of ρ_m varied in almost an identical manner with the space current, in spite of the fact that the experimentally determined magnitudes continue across the maxima of both the shot voltage and of Δi_p . (Fig. 5)

SUMMARY AND CONCLUSIONS

In the first part of this report, the formation of charged particles of tungstous and tungstic oxide was described. As far as the writer is aware, this has not been reported in the literature, and it is thought that the

results will be of interest to those working with the general problem of emission from various types of filaments.

In Part I we briefly described the abnormal shot effect resulting when the positive ions formed at the surface of the filament were accelerated through the dense electron space charge region surrounding the hot tungsten surface. This abnormality is interesting in that the fluctuations were not those of the direct current traversing the tuned shot circuit, since the large shot voltage was absolutely dependent upon the presence of the electron space charge. On the hypothesis that the primary event in the process is the fluctuation in the inter-electrode capacitance of the tube itself, due to variations in the thickness of the dense electron sheath, we were able to develop an expression for the mean square shot voltage in terms of the change in capacitance. Computations of ΔC from the experimental results yielded values which were entirely consistent with the actual electrode capacitance of the tube.

In Part II a study was made of the abnormal shot effect resulting from the trapping of the positive ions in the potential minimum surrounding the hot cathode. Tests of the frequency trend demonstrated that the phenomenon was of the nature of the "flicker-effect," the primary event persisting for a time longer than the period of the tuned shot circuit. From a consideration of the effect of the fluctuations upon the tuned circuit, an expression was developed for the experimental determination of the average increase in plate current caused by the trapping of a single ion. In addition, a means was found for determining the average time of life of an ion in the potential minimum, and the average number of electrons released by each ion.

As a means of checking the applicability of the theory, the values of the electron space charge density in the potential minimum were computed, and compared with the values obtained from a knowledge of the filament temperature and the space currents. The two sets of magnitudes of ρ_m were in agreement within the probable error of the experimental results and the equations used, and they were found to vary in exactly the same manner with the space current itself, throughout the range of plate potentials in which the currents were space charge limited. It is considered that these results lend strong support to the theory outlined in Part II.

As regards the technical aspects of the problem, it is obvious that the abnormal shot effects dealt with, and those mentioned in the introduction, are contributory factors to the noise in commercial vacuum tubes. The technique of abnormal shot effect should prove to be a powerful tool for the investigation of tube noise, and for the determination of the means of its elimination.

In conclusion, the writer wishes to express his indebtedness to Professor N. H. Williams, of this Department, under whose direction the work was carried out.

DISTINCTION BETWEEN CONTACT-POTENTIAL EFFECTS AND
TRUE REFLECTION COEFFICIENTS FOR
LOW-VELOCITY ELECTRONS

BY H. E. FARNSWORTH AND V. H. GOERKE

BROWN UNIVERSITY, PROVIDENCE, R. I.

(Received August 28, 1930)

ABSTRACT

A method is described for determining the apparent electron reflection coefficient in two ways in the same apparatus such that a distinction may be made between a contact potential and a true reflection coefficient for very low-velocity electrons. The results indicate that for a copper target which has been heated at red heat for some time in a high vacuum, the true electron reflection coefficient approaches a zero value as the primary voltage approaches zero, and that the apparent increase in the reflection coefficient below about one volt, is due to a change in the contact potential between the target and the surrounding electrodes. The value of this change for the specimen tested is approximately 1.2 volts.

IN MAKING observations on total secondary electron emission from a metal target, it is found that after the target has been heated at red heat the *apparent* reflection coefficient* passes through a minimum at a bombarding potential of about one volt, and then rapidly increases as the voltage is further decreased.¹ In the past this has been attributed to a contact potential between the degassed target and the surrounding metal electrodes. Thus, if the target assumes a negative potential of one volt, say, with respect to its surroundings as a result of heat-treatment, then all primary electrons having an energy less than one equivalent volt are turned back from the target, and consequently the *apparent* reflection coefficient is increased. There is, however, the possibility that the effect in question is at least partly due to an appreciable *true* reflection coefficient for the degassed target at the voltage in question. From theoretical investigations by Nordheim,² in terms of the new quantum mechanics, it appeared that a large reflection coefficient may exist for very low-speed electrons, although a small but appreciable value was later predicted when taking into account the effect of an image force.

Former experiments have not permitted a distinction between an effect of contact potential and a *true* reflection coefficient. Most experimenters in this field have not concerned themselves with the voltage region as low

* The term "reflection coefficient" is used here in place of "coefficient of secondary emission" as in former papers by Farnsworth since all of the electrons leaving the target for the voltages in question are presumably reflected primary electrons. The word "*apparent*" is used to indicate that the reflection coefficient as observed by the method in question may not be the true one.

¹ H. E. Farnsworth, Phys. Rev. 20, 358 (1922).

² L. Nordheim, Zeits. f. Physik 46, 833 (1928); Proc. Roy. Soc. A121, 626 (1928).

as one volt because of the difficulty of obtaining a narrow beam of electrons of measurable intensity under these conditions. It, therefore, seemed desirable to attempt an experimental determination of the true nature of the above mentioned increase in the *apparent* reflection coefficient with decreasing voltage. Not only is this important from the theoretical aspect but the result enters into the determination of the experimental voltage of electron diffraction beams from single crystals, and hence into the evaluation of the inner potential of the crystal and consequently of the refractive index as previously emphasized by Farnsworth.³ If the phenomenon is partly or wholly one of contact potential, then a correction must be applied to the impressed primary voltage, or the potential of the crystal must be changed by an amount equal to this correction. If the phenomenon involves only an actual reflection coefficient then no such correction should be made. Hence the accuracy of the experimental voltages is limited by the uncertainty of this correction.

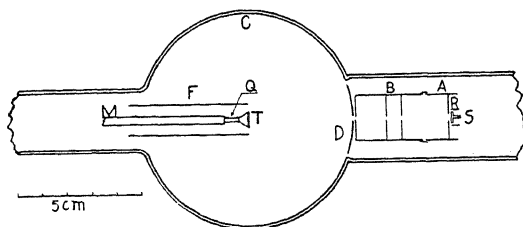


Fig. 1. Diagram of experimental tube.

APPARATUS AND METHOD

The essential parts of the apparatus are shown diagrammatically in Fig 1. The electron gun *SRAB* is similar to that previously described.⁴ The molybdenum diaphragm *D* forms a part of the sphere *C*. The inner surface of the Pyrex sphere *C* is made conducting by evaporation from a molybdenum filament and contact is made by a tungsten wire, not shown, which is sealed through the sphere. The copper target *T* is supported by a quartz strip *Q* which is attached to a molybdenum frame *M*. The target and its support may be moved horizontally by means of a magnetic control into the side tube where the target may be heated at red-heat by high-frequency induction. The copper Faraday cylinder *F* may also be moved horizontally into the same side tube where it may be heated separately at red-heat by high-frequency induction. The target is a disk cut from the same piece of copper as the Faraday cylinder.

All of the glass parts are Pyrex with no ground joints or wax seals. The tube was kept attached through a liquid air trap to the vacuum system which consisted of two mercury diffusion pumps in series backed by an oil pump. The preliminary baking and vacuum conditions were similar to those in the previous experiments on secondary electron emission by Farnsworth.⁴ No

³ H. E. Farnsworth, Phys. Rev. 34, 679 (1929).

⁴ H. E. Farnsworth, J.O.S.A. & R.S.I. 15, 290 (1927).

observable increase of pressure on a McLeod gauge occurred during 24 hours while the pumps were not running. Further, the secondary electron characteristics of the copper target remained constant for more than 24 hours after heating at red-heat, thus indicating a negligible effect due to the residual gas.

The method of distinguishing between contact potential and a *true* reflection coefficient consists in observing the *apparent* reflection over the region of low voltages by the following two methods. (1) With the target *T* in the forward position, i.e. at the center of the sphere *C*, the secondary current from the target is the sum of the currents to *C* and *D*, while the total or primary current is that to all of the electrodes *T*, *C*, *D*, and *F*. Under these conditions only a very small current reaches the cylinder *F* by reflection from the sphere. The *apparent* reflection coefficient or ratio of secondary to primary current is thus obtained at small voltage intervals over the range in question. (2) With the target *T* removed to the back end of the cylinder *F*, the combination forms a Faraday absorbing cylinder. The total or primary current is the current to this Faraday cylinder. The current to the target *T* when in its forward position is obtained as in method (1). The difference between the total current and the current to the target is the secondary or reflected current, and the ratio of this to the total current is then the *apparent* reflection coefficient given by this method. It is seen that this *apparent* reflection coefficient will equal the *true* reflection coefficient if *T* and *F* are at the same potential.

The total current as obtained by this method should check with that given by method (1) if all of the metal electrodes *T*, *C*, *D*, and *F* are at the same potential. It will also check even if *T* is at a slightly different potential. In this case the electrons are all deflected to the inner surface of the cylinder instead of some striking the target. If, however, the cylinder *F* is one volt negative, say, with respect to *C* and *D* then no electrons having energies less than one equivalent volt will enter the cylinder so that the total current as obtained by method (2) will be zero while method (1) will indicate a total current greater than zero. Since the current to the target *T* in its forward position is the same in the two methods, it follows that the *apparent* reflection coefficients given by the two methods will not be the same. If, on the other hand, the *true* reflection coefficient of the target after red-heat treatment increases as the primary voltage is decreased below about one volt, and if no appreciable potential difference has been introduced by this heating, then the *apparent* reflection coefficients determined by methods (1) and (2) will be the same and equal to the *true* reflection coefficient for any given primary voltage.* A determination of the *apparent* reflection coefficient by these two methods for various primary voltages both before and after heating the target *T* and cylinder *F* at red-heat should then distinguish between a change

* This presupposes that all the electrodes *T*, *C*, *D*, and *F* were at the same potential before separately heating the target at red-heat. This was approximately the case since methods (1) and (2) gave the same result after baking the whole apparatus but previous to separately heating any of the electrodes.

due to an alteration in the contact potential and one due to an altered *true* reflection coefficient. This method depends for its success upon the elimination of a contact potential between the target *T* and cylinder *F*. For this reason these two electrodes were cut from the same piece of copper sheet and given heat treatments as nearly alike as possible.

The electron currents were measured by a sensitive galvanometer.

RESULTS

After baking the whole tube but before heating either the target or cylinder at red-heat, measurements by methods (1) and (2) gave the same result. The reflection coefficient decreased with decreasing primary voltage, and appeared to approach a zero value for zero primary voltage. After heating

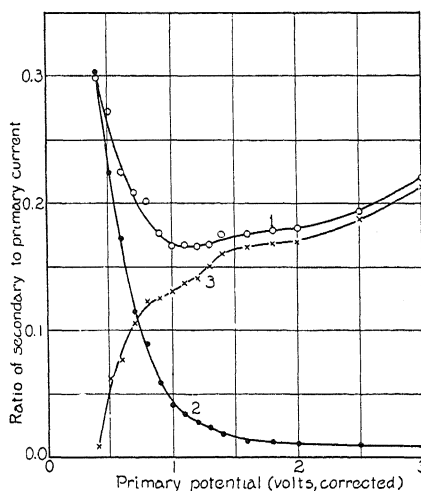


Fig. 2. Reflection coefficients by the two methods.

the target *T* alone at red-heat for several minutes, the formerly-observed increase in the *apparent* reflection coefficient, for primary voltages below about one volt, made its appearance. Both methods (1) and (2) gave the same result. This is shown in Fig 2 curve I for primary energies below 3 equivalent volts. After heating the cylinder *F* at red-heat, the results obtained by the two methods were not the same. With the target withdrawn to the back of the cylinder some of the low-velocity electrons were turned back from the cylinder and struck the sphere *C* and diaphragm *D*, thus resulting in an apparent reflection coefficient from the open end of the cylinder. The possibilities of the cylinder not being completely absorbing or of the spreading of the primary beam are eliminated by the results obtained previous to the heating of the cylinder for the primary velocities in question. Curve 2, Fig. 2 shows the *apparent* reflection coefficient from the open cylinder. Curve 3 shows the reflection coefficient from the target obtained by method (2). This was taken after the previous heat-treatment of the target and cylinder

were as nearly the same as possible. It is to be observed that this curve approaches a zero value as the primary voltage is decreased. The fact that it appears to cross the zero axis at a fraction of a volt probably has no significance. The voltages plotted represent the mean values which have been corrected for the velocity of electron emission from the filament, and for contact potential between the filament and other metal electrodes. Since the distribution of energies of the primary electrons covers at least one equivalent volt, the average value has little significance when only a few tenths of a volt are involved. Other curves corresponding to those shown in Fig. 2 were obtained when it was known that the conditions of the target and cylinder were not identical. In these cases the curves corresponding to curve 3 occupy positions between curves 1 and 2 of Fig. 2, as is to be expected. In all, the target and cylinder were each heated at red-heat temperatures such that excessive evaporation of copper occurred for periods totalling something over an hour. This heating removed sufficient gas to assure that the conditions of the target and cylinder were very nearly the same.

The results of this investigation indicate that for a copper target which has been heated at red-heat for some time in a high vacuum, *the electron reflection coefficient approaches a zero value as the primary voltage approaches zero* and that the *apparent* increase in the reflection coefficient below about one volt, which is observed only after red-heat treatment of the target, is due to a *change in the contact potential* between the target and the surrounding electrodes. The value of this change, which depends on the previous heat-treatment, is approximately 1.2 volts for the copper specimen tested.

CURRENT, PRESSURE, AND FREQUENCY RELATIONSHIPS FOR THE INITIATION AND MAINTENANCE OF THE ELECTRODELESS GLOW DISCHARGE

BY MILTON L. BRAUN

UNIVERSITY OF NORTH CAROLINA

(Received July 3, 1930)

ABSTRACT

Critical current and critical pressure values for the initiation of a discharge and their relation to the excitation frequency have been investigated by means of the electrodeless glow discharge for hydrogen, oxygen, carbon dioxide, and nitrogen. A departure from the usual definition of the critical point has been made in choosing as the criterion for its location the approximate center of the bend on the graph showing the relation between the current necessary to start the discharge and the pressure. By this method it was found: (1) that the critical current varies as the square of the wave-length; (2) that the critical pressure varies as the square of the wave-length; and (3) that the ratio of the critical current to the critical pressure is constant for a given gas. The current necessary to maintain the glow was also investigated, and formulas obtained expressing relationships between maintaining current, initiating current, wave-length, and pressure.

INTRODUCTION

RELATIONSHIPS between the minimum potential necessary to initiate a luminous discharge of electricity and the pressure of the gas through which the discharge takes place have long been investigated for several types of discharge. The pioneer work of Paschen¹ with spark discharge between parallel plate electrodes resulted in the generalization known as Paschen's law; namely, that for all values of pressure down to a limiting critical value, the minimum potential necessary to create a discharge is proportional to the product of the distance between the electrodes and the pressure of the gas. More recent investigations have shown that there exists a certain pressure for which the potential required to initiate the discharge is a minimum. This condition is referred to as the critical point.

The existence of critical points may be inferred from the works of several experimenters who had objectives other than the determination of critical values. Among such studies may be mentioned that of Frey,² who used a high potential battery discharge between ordinary electrodes in various mixtures of hydrogen and nitrogen; that of Kirchner,³ who used continuous-wave, high-frequency discharge in hydrogen, oxygen, neon, and air, with various distances between electrodes; and that of Huxley,⁴ who used an undamped electrodeless discharge in the study of corona effects for helium and neon.

¹ F. Paschen, *Ann. d. Physik* 37, 69-96 (1889).

² B. Frey, *Ann. d. Physik* 85, 381-424 (1928).

³ F. Kirchner, *Ann. d. Physik* 77, 287-301 (1925).

⁴ L. G. H. Huxley, *Phil. Mag.* 5, 721-737 (1928).

Comparing the internal and the external electrode methods, with various distances between the electrodes, and using undamped oscillatory discharges in air, Gutton and his fellow workers^{5,6} observed critical points for a number of excitation frequencies corresponding to certain wave-lengths between 12,000 m and 27 m (2.5×10^4 and 1.1×10^7 sec⁻¹), reporting in addition the existence of a critical point for a 6,000 km wave-length (a 50 cycle oscillation). However, they found no critical point for a 24.9 m wave-length (1.2×10^7 sec⁻¹) though extending the observation down to pressures as low as 0.005 mm. There seems to be no simple relationship between their critical points, except that in the case of internal electrodes both coordinates of the critical point gradually increase with an increase in the frequency of oscillation. C. and H. Gutton⁷ found that with hydrogen instead of with air the existence of critical points was restricted to a decidedly narrower frequency range, those corresponding to 110 m and 20.5 m wave-lengths being respectively above and below the critical range.

Critical points for 320, 160, and 80 m wave-lengths were found by Hayman⁸ while using external electrodes with helium excited by continuous-wave radiation, but none was observed by him for a 40 m wave-length. Townsend and Nethercot,⁹ however, also working with a 40 m undamped excitation but with nitrogen instead of with helium, not only encountered a critical point but were able also to determine that the potential coordinate was about one third less for external than for internal electrodes, other factors, including the critical pressure (0.04 mm), being equal. The comprehensive work of Heidemann¹⁰ with hydrogen showed that with a 450 m wave-length the critical potential was nearly twice as great with external than with internal electrodes, but that the corresponding critical pressure was about one third less. It was also shown by Heidemann that an increase in the frequency resulted in a decrease in the critical potential, while the change in the critical pressure was irregular, the trend being toward an increase.

That the damped wave electrodeless ring discharge also gives rise to critical points was shown by J. J. Thomson,¹¹ by Bergen Davis,¹² and by Mierdel.¹³ The data given in their papers, however, are insufficient to warrant any comparative conclusions. Thomson states¹⁴ that an increase in frequency results in an increase in the critical pressure. Although only two frequencies were used by Davis, his work showed that with the higher frequency both the critical potential and the critical pressure were increased. A continuous-wave electrodeless glow discharge in a cylindrical tube was

⁵ C. Gutton, S. K. Mitra, and v. Ylostal', *Compt. Rend.* **176**, 1871-1874 (1923).

⁶ C. Gutton, *Compt. Rend.* **178**, 467-470 (1924).

⁷ C. and H. Gutton, *Compt. Rend.* **186**, 303-305 (1928).

⁸ R. L. Hayman, *Phil. Mag.* **7**, 586-596 (1929).

⁹ J. S. Townsend and W. Nethercot, *Phil. Mag.* **7**, 600-616 (1929).

¹⁰ E. Heidemann, *Ann. d. Physik* **85**, 649-686 (1928).

¹¹ J. J. Thomson, *Phil. Mag.* **4**, 1128-1160 (1927).

¹² B. Davis, *Phys. Rev.* **17**, 501-505 (1903); *Phys. Rev.* **20**, 129-150 (1905).

¹³ G. Mierdel, *Ann. d. Physik* **85**, 612-640 (1928).

¹⁴ J. J. Thomson, reference 11, p. 1144.

recently used in a study of critical points for neon, helium, and oxygen by Gordon and Dushman.¹⁵ Although they employed only three wave-lengths their results taken as a whole, showed that, an increase in frequency reduced the values of the critical point, with the exception, in the case of oxygen, of the pressure component.

It should be noted that the critical point has usually been given in terms of pressure and of the potential difference between electrodes, either internal or external. In the case of the electrodeless discharge investigators either have employed some artificial method of obtaining a value of the potential, or have discarded its use, choosing in its place the value of the current in the circuit of the exciting coil. The latter method is employed on the reasonable assumption that the strength of the field set up is proportional to the current that sets it up, at least for constant frequencies. While admitting the desirability of having direct potential measurements it must be recognized that the reliability of measurement of the mean square current by hot wire instruments gives this method an advantage over methods which purport to indicate the potential difference between selected points or along chosen paths within the field, and which associate the discharge itself with these more or less arbitrarily chosen potentials.

In the present work the critical point was determined for several gases in terms of the pressure and of the mean square value of the current in a coplanar excitation coil, the electrodeless glow discharge taking place in a spherical bulb placed at the center of the coil. The minimum current to maintain the glow at given pressures was also investigated.

APPARATUS AND PROCEDURE

The apparatus used in this experiment consisted of (1) a gas control system, and (2) an electric circuit producing continuous-wave, high-frequency radiation. Low pressures were obtained by means of a vacuum pump, and evaluated by means of a McLeod gauge. The entire gas system (Fig. 1), including the discharge bulb of 6.5 cm radius with gas inlet at the bottom, was an integral one constructed of Pyrex glass. The inner surface of the bulb was partially freed from moisture and occluded gases by the application of heat, and while the bulb was still warm the desired gas, from steel tank storage, was slowly passed through the system under slight pressure. Then in order to impregnate the walls of the bulb with the gas under consideration the confined gas was subjected to a pressure of about two atmospheres. Within an hour the pressure was slowly released to the desired value by opening the upper stop-cock, with the pump running. During the taking of data for a given charge of gas the pump was in continuous operation, the stages of pressure being controlled by the stop-cock on the pump side of the gauge, the gas, of course, passing only in the direction of lower pressure, out of the bulb into the pump. It was found that the stop-cock constrictions retarded the complete equilization of pressure in the system for an appre-

¹⁵ N. T. Gordon and S. Dushman, *Phys. Rev.* **33**, 632 (1929), abstract.

cial time, and this was taken into consideration before the pressure was determined.

The field which excited the glow discharge was generated by a tuned-plate tuned-grid system (Fig. 2). Oscillations were set up by a UV-205-A transmitting Radiotron, the plate of which was fed by a 1000 volt generator, filament current being supplied by a center-tapped transformer. Current in

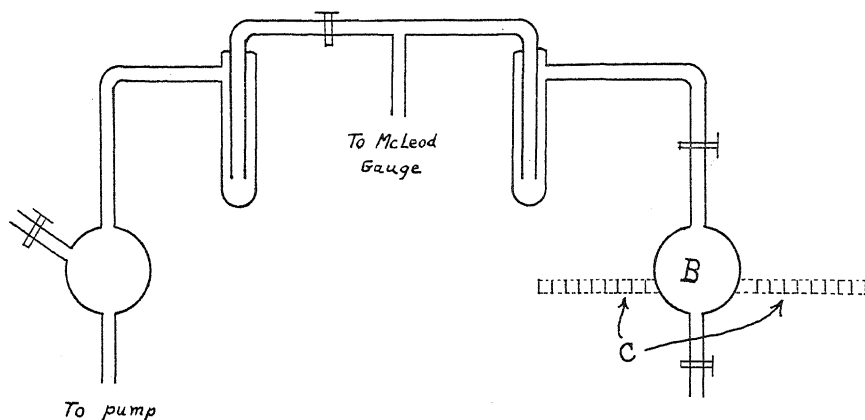


Fig. 1. Gas control system, showing radiating coil *C*, and discharge bulb, *B*.

the co-planar radiating coil was controlled not directly but by means of a suitable rheostat in the primary circuit of the filament transformer. Precaution was taken to keep the range of the filament current well within the linear section of the potential-current characteristic of the tube. The mean square value of the high frequency current was obtained by a hot wire ammeter having scale range from 0.2 to 2.0 amperes in .04 ampere divisions. The frequency

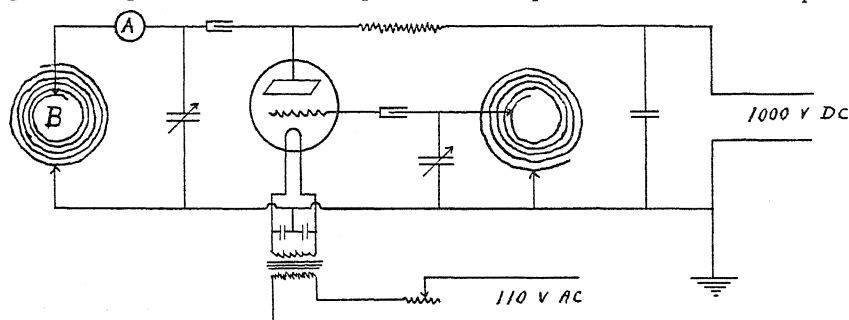


Fig. 2. Tuned-plate, tuned-grid, oscillatory circuit. Electrodeless glow discharge bulb placed at *B*.

of oscillation was controlled by manipulation of the condensers, while wave-length values were obtained directly from a precision wavemeter.

The initiating current was ascertained by adjusting the condensers for the predetermined wave-length, and, as the filament current was gradually increased, by noting its corresponding value in the radiating circuit at the moment when the visual discharge flashed on. The minimum maintaining

current was similarly obtained by noting, as the coil current was gradually diminished, its value just when the luminosity collapsed. Observations were taken within pressure limits of 2 to .002 mm of mercury in varying intervals which had their smallest values in the vicinity of the critical point. At each pressure, observations were made for wave-lengths between 90 and 160 m (or between 3.34×10^6 and $1.88 \times 10^6 \text{ sec}^{-1}$) in five-meter steps. In order to assure simultaneous values in the variables, the pressure was read both before and after the several current observations were made. The pressure was then reduced, and another set of observations taken at each of the desired wave-

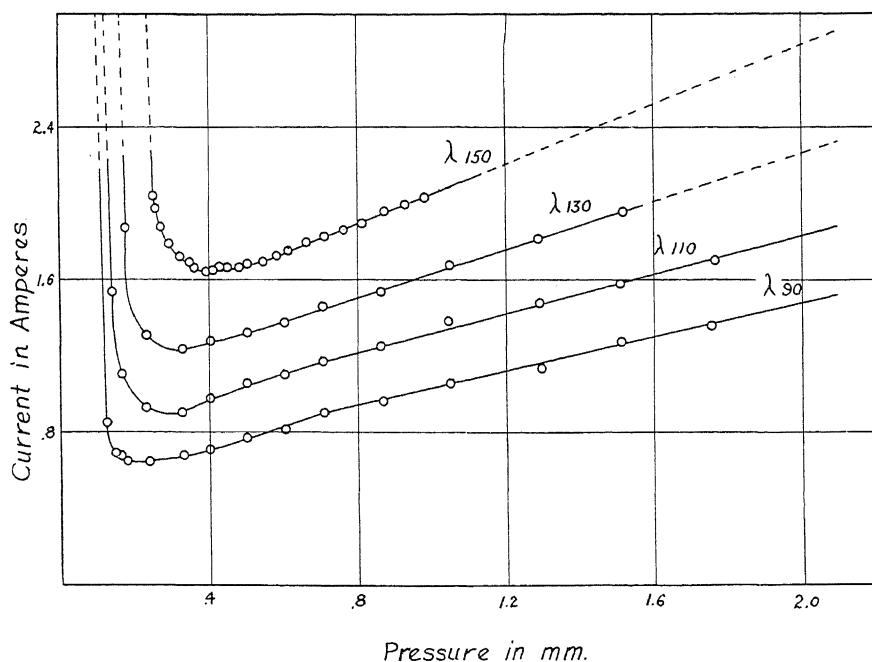


Fig. 3. Current to initiate the electrodeless glow discharge in nitrogen as a function of pressure.

lengths. Reliable results were obtained only after a time interval of 15 to 20 seconds from a previous discharge, it being found that an appreciable time was required for recombination in the gas to take place.

MINIMUM CURRENT TO INITIATE THE GLOW

On plotting for a given wave-length the value of the initiating current as a function of pressure, it was found that for pressures greater than the critical, but not excessively greater, the current necessary to initiate the glow discharge is approximately a linear function of the pressure. This relationship is probably not a true linear one, for the curve tends to bend downward after a pressure several times the critical pressure is passed. Typical of the results obtained are the curves for nitrogen shown in Fig. 3. It will be seen that as the knee of the curve is approached from higher pressures, the regularity of the slope breaks down and passes into a rapidly changing one which seems

to rise asymptotically with the axis of ordinates. This indicates either that as the pressure is indefinitely decreased the initiating current is indefinitely increased, or that there is a pressure lower than which a discharge cannot be obtained. The knee of a representative curve is shown in detail in Fig. 4, which indicates values for oxygen on a 120 m excitation. For each gas and frequency investigated the curvature of the knee appears to be circular, and it is noted that the radius of curvature becomes smaller as the wave-length is decreased.

DETERMINATION OF THE CRITICAL POINT FROM THE DATA

Because of the rather large radius of curvature at the knee of the initiating current graph it was found impossible accurately to locate the critical point

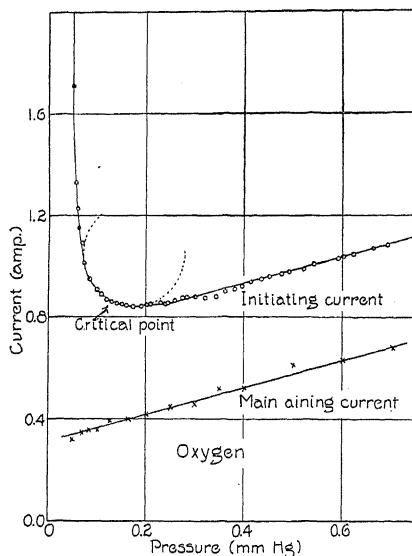


Fig. 4. Initiating current and maintaining current in oxygen as functions of pressure. Wave-length 120 meters.

by strict adherence to definition. This difficulty was also recognized by J. J. Thomson.^{14,16} Critical points as arrived at by Davis¹² were determined by the intersection of lines tangent to either end of the knee, or by the intercept of the projected linear section of the curve on the axis of ordinates. In deciding upon the critical point the present work used for its criterion the central or bisecting point of the knee, thereby permitting its locus to remain on the curve.

The justification of this criterion for the location of the critical point lay in the simple relationships between the variables to which it led. In addition

¹⁶ J. J. Thomson, "Conduction of Electricity Through Gases," Cambridge, 1st ed (1903), p. 362; 2nd ed (1906), p. 446.

to the difficulty of exact location, decided irregularities arose both between the points themselves and their relation to the frequency when a literal specification of minimum current and its corresponding pressure was followed. Values of the critical point as derived by this center-of-the-bend method are shown in Table I, where I_c is the critical current in amperes, P_c the critical pressure in millimeters of mercury, and λ the excitation wave-length in meters.

TABLE I. *Critical points for the initiation of the electrodeless glow discharge. Critical current, I_c , is measured in amperes; critical pressure, P_c , in mm of mercury; and excitation wave-length, λ , in meters.*

λ	Hydrogen		Oxygen		Carbon Dioxide		Nitrogen	
	I_c	P_c	I_c	P_c	I_c	P_c	I_c	P_c
90	0.44	0.110	0.50	0.070	0.63	0.132	0.68	0.155
95	.48	.120	.56	.086	.68	.140	.72	.168
100	.54	.135	.60	.094	.72	.150	.78	.180
105	.58	.150	.66	.100	.79	.165	.86	.200
110	.64	.160	.72	.105	.87	.185	.94	.215
115	.68	.170	.80	.120	.94	.200	1.03	.230
120	.74	.185	.86	.131	1.02	.215	1.09	.250
125	.80	.200	.92	.140	1.09	.230	1.16	.265
130	.86	.215	.99	.145	1.15	.240	1.24	.280
135	.94	.235	1.08	.164	1.24	.260	1.33	.300
140	1.02	.255	1.15	.174	1.33	.278	1.42	.321
145	1.10	.275	1.25	.185	1.39	.290	1.47	.335
150	1.18	.295	1.34	.200	1.46	.305	1.62	.370
155	1.26	.315	1.40	.210	1.54	.320	1.68	.380
160	1.34	.340	1.48	.222	—	—	1.76	.400

CRITICAL POINT RELATIONSHIPS

The coordinates of the critical point being designated as the critical current and the critical pressure, it was found that for a given gas the critical current and the excitation wave-length may be expressed in terms of each other by the relationship,

$$I_c = a\lambda^2 + b, \quad (1)$$

where a and b are constants which have been evaluated for each gas, where I_c is the critical current in the oscillatory circuit measured in amperes, and where λ is the excitation wave-length in meters.

The relationship between the critical current and the wave-length does not in any way predict what the relationship between the critical pressure and the wave-length shall be. It was found, however, that for a given gas the critical pressure, too, is dependent upon the square of the wave-length in accord with the relationship,

$$P_c = c\lambda^2 + d, \quad (2)$$

where c and d are constants, P_c the critical pressure in millimeters of mercury, and λ the wave-length in meters. That the critical pressure increases with the square of the wave-length, or decreases with an increase of frequency, stands in contrast to the conclusions of Davis¹² and of Thomson¹⁴ who found that for the electrodeless ring discharge an increase of frequency gave rise to an increase in the critical pressure.

Upon combining equations (1) and (2) it is seen that

$$I_c = kP_c + h, \quad (3)$$

where k and h are new constants. A graph of the critical points themselves not only gave a linear relationship, but also showed upon extrapolation that the straight line passed through the origin of the co-ordinate system. In other words it seems that within experimental limits the ratio I_c/P_c is the derived slope, k , itself. That the constant h does not come out to be zero is probably due to experimental error, and it is therefore concluded that

$$I_c/P_c = k \quad (4)$$

where k is equivalent to the ratio a/c from equations (1) and (2). Table II gives values obtained for the constants, while Fig. 5 shows the relationships between the three variables for one of the gases studied.

TABLE II. Evaluated constants for equations (1)—(4).

	Hydrogen	Oxygen	Carbon-Dioxide	Nitrogen
$a \times 10^5$	5.18	5.72	6.00	6.39
b	0.012	0.037	0.145	0.166
$c \times 10^5$	1.30	0.84	1.25	1.44
d	0.002	0.008	0.031	0.040
h	0.006	-0.016	-0.005	-0.011
$k = a/c$	3.98	6.82	4.80	4.43
$k = I_c/P_c$	3.99	6.67	4.77	4.39

MINIMUM CURRENT TO MAINTAIN THE GLOW

The minimum current necessary to maintain the glow for a given gas and frequency was found to be in direct proportion to the pressure. This relation showed no deviation at low pressures but continued linearly through the critical point to the low pressure limit of the apparatus. In order to obtain values of the minimum maintaining current for pressures lower than those for which the glow could be initiated, the discharge was effected at a higher pressure, and the pressure then reduced to the desired value while the discharge was in operation. The current was then gradually reduced until the glow became extinguished.

The minimum maintaining current was found to be a direct function not only of the pressure but also of the wave-length. The following empirical expressions give values for the minimum current, I_m amperes, required to maintain the glow, in terms of pressure and of wave-length:

$$\left. \begin{aligned} \text{Hydrogen } I_m &= (0.0044 + 0.0023P)\lambda - 0.20 \\ \text{Oxygen } I_m &= (0.0054 + 0.0044P)\lambda - 0.34 \\ \text{Nitrogen } I_m &= (0.0057 + 0.0038P)\lambda - 0.40 + 0.16P \end{aligned} \right\} \quad (5)$$

The maintaining current for the carbon dioxide glow was not investigated.

Perhaps of more importance than the relations determining the maintaining current are the connecting relations between the maintaining and the initiating currents. In presenting these relationships it is noted first that, for a given wave-length, and for pressures which lie within the restricted linear

section of the initiating current curve, there is a constant difference between the maintaining current and the initiating current. This difference may be expressed as

$$I_m = I_i - w \quad (6)$$

where I_m and I_i are the minimum maintaining and initiating currents respectively, and where w is the difference between them. The value of w was found to depend upon the nature of the gas, and the wave-length. The smallest observed value of w occurred with hydrogen at the shortest wave-length, while the greatest difference between the currents was found in the case of nitrogen at its longest wave-length. A representative relationship

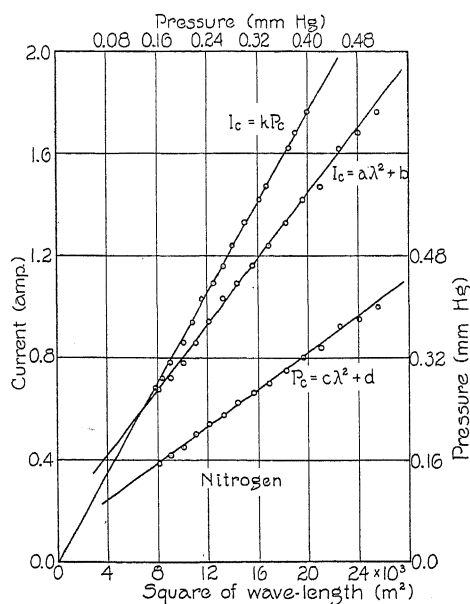


Fig. 5. Typical relation between critical current, critical pressure, and wave-length.

between maintaining and initiating currents is shown in Fig. 4. Including wave-length as one of the variables, the relationship between the two currents for the three gases investigated was found to be as follows:

$$\left. \begin{aligned} \text{Hydrogen } I_m &= I_i - 0.0044\lambda + 0.20 \\ \text{Oxygen } I_m &= I_i - 0.0062\lambda + 0.26 \\ \text{Nitrogen } I_m &= I_i - 0.0064\lambda + 0.19 \end{aligned} \right\} \quad (7)$$

The permissible values of I_i , of course, are those for which the linear relationship between I_i and P is best satisfied.

It is beyond the scope of this article to propose a theoretical explanation of the observed phenomena or of the relationships deduced therefrom. In conclusion the writer expresses his sincere thanks to Dr. Otto Stuhlman Jr. for suggestions given.

THE ABSORPTION OF SLOW HYDROGEN
POSITIVE RAYS IN HYDROGEN

BY ROBERT E. HOLZER

UNIVERSITY OF CALIFORNIA, BERKELEY

(Received August 26, 1930)

ABSTRACT

An experimental method for studying the absorption of slow hydrogen positive rays in hydrogen is described. The absorption coefficients of H^+ , H_2^+ and H_3^+ in hydrogen were measured in the region between 60 and 850 volts. The absorption coefficient of H_3^+ was found to be smaller than that of H_2^+ and very much nearer the absorption coefficient of H^+ in magnitude. The absorption coefficient of H_2^+ decreased from a value of $40 \text{ cm}^2/\text{cm}^3$ at 60 volts velocity to $20 \text{ cm}^2/\text{cm}^3$ at 850 volts and that of H_3^+ decreased from $17 \text{ cm}^2/\text{cm}^3$ at 60 volts to $12 \text{ cm}^2/\text{cm}^3$ at 500 volts. The absorption coefficient of H^+ remained nearly constant at $8 \text{ cm}^2/\text{cm}^3$, about one-half the kinetic theory value. No minimum of absorption was observed for any of the ions in the region investigated. Qualitative experiments upon the nature of the absorbing process indicate that the absorption of H_2^+ is probably due to neutralization while scattering is probably the most important factor in the absorption of H^+ and H_3^+ ions.

INTRODUCTION

THE first quantitative measurements on the absorption of very slow protons in hydrogen were made by Aich¹ in 1922. Using a Lenard type of apparatus he found that the collision radius of an H_2 molecule and a 25 volt proton was approximately the same as the kinetic theory value of the radius of the H_2 molecule. In 1925, Dempster,² using the type of apparatus which he had previously described, studied the absorption of 900 volt protons in hydrogen. Since the beam of protons was absorbed in a magnetic field, a proton which was neutral over part of its path would have the apparent radius of its path increased while one which lost velocity would have its apparent path radius decreased. Dempster observed no neutralization or loss of velocity equivalent to a change of 2 volts in the 900 volt accelerating potential as the pressure in the absorbing chamber was increased from 0.00017 to 0.008 mm of mercury. Dempster therefore concluded that at 900 volts the proton moved through several hydrogen molecules without apparent neutralization or loss of velocity, that between 900 and 25 volts there was a critical potential at which the proton lost its ability to penetrate the hydrogen molecule and that between 900 and 13,000 volts³ there was another critical potential at which the proton acquired the ability to ionize the hydrogen molecule. He notes that "Electrons acquire the velocity of protons used in this experiment by falling through 0.5 volt and it is significant

¹ W. Aich, *Zeits. f. Physik* 9, 372 (1922).

² A. J. Dempster, *Proc. Nat. Acad. Sci.* 11, 552 (1925).

³ E. R  chardt, *Ann. der Physik* 73, 228 (1924).

that electrons of this speed pass through many molecules without absorption."

While the work of G. P. Thomson⁴ on protons of between 5,000 and 25,000 volts velocity does not lead to a direct measurement of the effective size of the hydrogen molecule, his conclusions are worthy of note. Measuring the scattering of a beam of protons in hydrogen by observing blackening of a photographic plate beyond the edge of the image of the geometrical beam, he found: (1) appreciable small angle scattering in the velocity range studied, (2) a rapid decrease of scattering between 5,000 and 25,000 volts, (3) single scattering below 0.01 mm, (4) proportionality between scattering and pressure between 0.001 mm and 0.012 mm and (5) an inverse cube law of force at scattering centers.

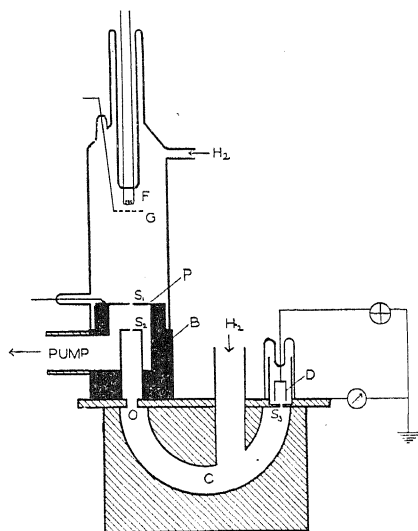


Fig. 1. Diagram of apparatus.

The present experiment was undertaken to measure quantitatively the absorption of protons in hydrogen in the region between the measurements of Aich and Dempster and to compare the absorption of protons with the previously unmeasured absorption of H_2^+ and H_3^+ in hydrogen.

APPARATUS

The apparatus employed in the experiment consisted essentially in an ionization tube of the type used by Smyth,⁵ Hogness and Lunn⁶ and others for producing the hydrogen ions under controlled conditions and a Dempster⁷ mass spectrograph for analyzing the rays. A simple diagram of the apparatus is shown in Fig. 1.

⁴ G. P. Thomson, *Phil. Mag.* **1**, 961 (1926).

⁵ H. D. Smyth, *Phys. Rev.* **25**, 452 (1925).

⁶ T. R. Hogness and E. G. Lunn, *Proc. Nat. Acad. Sci.* **10**, 398 (1924).

⁷ A. J. Dempster, *Phys. Rev.* **11**, 316 (1918).

Electrons from the incandescent filament, F , were accelerated toward the grid, G , by a potential difference of 60 volts. The primary ions were produced by electron impact in the space between G and the plate P . The spacing of F and G was 0.5 cm and of G and P , 10 cm. A drift field of 4 volts carried a small fraction of the ions formed between G and P through slit S_1 , into the highly evacuated space between S_1 and S_2 where the major part of the accelerating potential was applied. The plate P was insulated from the adjacent metal parts B by a mica disk and picene wax. All metal parts in the ionization tube at ground potential (B) were completely covered by mica and wax.

S_1 and S_2 , defining the beam of ions, were each 0.1 mm wide and 3 mm long. Their separation was 1 cm. The path of the beam between S_1 and O was shielded by a soft iron block, B , to which the ionization tube was waxed. The block, in turn, was soldered to the brass absorption and analyzing chamber placed between the pole faces of a large electromagnet so that the field was perpendicular to the plane of the diagram. When an ion passed S_2 it entered the absorption chamber and when it emerged from O it was deflected in a semicircular path the radius of which was determined by the mass and velocity of the ion and the strength of the magnetic field. If the magnetic field was so adjusted that the radius of the path was 4.75 cm the ion reached the slit S_3 , 1.5 mm wide and 3 mm long, at the entrance to the collecting chamber. The total path length between S_2 and S_3 was 20.0 cm. A Faraday cylinder 0.5 cm in diameter and 1 cm deep was used to collect the ions. It was connected to a Compton electrometer and was insulated from the apparatus by 3 cm of Pyrex glass.

The pressure control was effected by steady flow through capillary leaks from reservoirs to the ionization and absorption chambers, respectively. The gas flowed from the chambers through S_1 and S_2 into the space evacuated by a Gaede three stage mercury vapor pump. Liquid air traps were included in all the vacuum lines and gas feeds to the apparatus. The pressures in the ionization and absorption chambers were practically independent. With a pressure of 0.0120 mm in the ionization, the "back pressure" built up in the absorption chamber was 0.0003 mm. A change of 0.006 mm in the absorption chamber produced a change of less than 1.5 percent (minimum detectable on the McLeod gauge) in the ionization chamber. The pressure in the ionization chamber was approximately 0.01 mm and that in the absorption chamber, between 0.007 and 0.001 mm.

The gas was electrolytic (tank) hydrogen which was passed over hot copper turnings at 300°C, stored over P_2O_5 and finally passed through two liquid air traps after leaving the capillary while the pressure was less than 0.015 mm.

The magnetic field, calibrated by a test coil and Grassot fluxmeter, was found to be roughly proportional to the current flowing in the coil of the magnet when care was taken to reverse the magnet current before measurement.

The apparatus described produced a heterogeneous beam of hydrogen ions,

all of which had fallen through the same accelerating potential (i.e. within 4 volts). As the magnetic field was increased the rate of deflection of the electrometer reached several maxima corresponding to the various products of ionization. A typical graph of the results is shown in Fig. 2. All of these products of ionization have been observed previously.

MEASUREMENTS

The absorption of the various ions was measured in terms of the absorption coefficient which appears in the well known absorption formula $I = I_0 e^{-\alpha x p}$, in which I_0 is the initial intensity of a beam of particles, I , the intensity of the beam after traversing a gas layer x cm thick at a pressure of

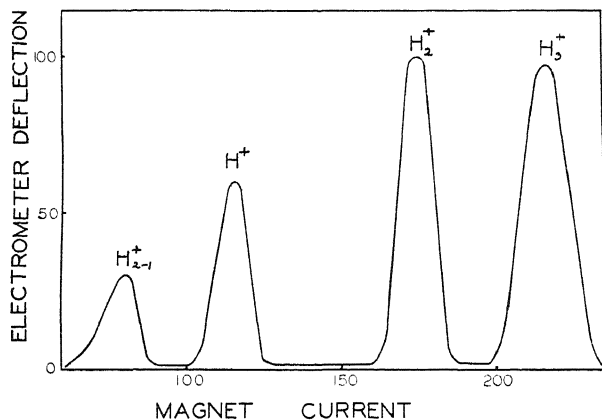


Fig. 2. Analysis of the products of ionization.

p mm, and α is the absorption coefficient, the effective absorbing cross-section of all of the molecules in 1 cubic centimeter of gas at 1 mm pressure. The equations

$$I_1 = I_0 e^{-\alpha x p_1} \quad (1)$$

$$I_2 = I_0 e^{-\alpha x p_2} \quad (2)$$

indicate the respective intensities of a beam originally of intensity I_0 after passing through a layer of gas, x cm thick, first at pressure p_1 and later at pressure p_2 . Dividing (1) by (2) and taking the natural logarithm of both sides of the resulting equation,

$$\ln I_1/I_2 = \alpha x(p_2 - p_1).$$

Solving for α ,

$$\alpha = \frac{1}{x(p_2 - p_1)} \ln \frac{I_1}{I_2}.$$

This equation is valid as long as I_0 remains unchanged and at once suggests a method of determining the absorption coefficient without measuring the absolute value of I_0 .

In the experiment, I_0 was the intensity of a beam of ions of given mass and velocity that would have reached the Faraday cylinder had the absorption chamber been kept at high vacuum. I_0 was directly proportional to the intensity of the beam which entered S_2 and was roughly proportional to the current which reached the plate containing S_2 . Since I_0 was a rather critical function of the filament current, the ionization tube pressure, and the applied potentials, keeping it constant was perhaps the greatest experimental difficulty encountered. A milliammeter measuring the differential current to P was used as an indicator of tube conditions while a galvanometer connected between the main metal portion of the apparatus and ground was used to determine the constancy of I_0 .

The procedure in determining a value of α for a given ion at a particular velocity was briefly as follows. The tube was allowed to reach a steady state. The magnetic field was so adjusted that the maximum of one of the "peaks" (see Fig. 2) was observed. The rate of deflection of the electrometer (I_1) was recorded while the gas in the absorbing chamber was maintained at a given value p_1 (measured by a McLeod gauge). In practice the value of I_1 was taken as the average of three or four trials. The pressure was quickly raised by compressing the gas in the reservoir behind the leak to the absorbing chamber. Within a minute and half equilibrium was reached at the new pressure, p_2 , which was 2 or 3×10^{-3} mm higher than p_1 , and I_2 was measured. The pressure was then lowered to p_3 , nearly the same as p_1 , and the process was repeated. The set of measurements usually required from 7 to 10 minutes. The data thus obtained were sufficient to determine two values of α which served as an additional check on the constancy of conditions. In those cases where the values of α differed by more than 25 percent and the galvanometer showed signs of fluctuation, the measurements were discarded. If, however, the galvanometer deflection steadily increased or decreased, an average of the values of α was taken as a fair approximation to the true absorption coefficient.

It was necessary to be certain that the accelerating potential did not vary, for a change sufficient to shift a peak one quarter of its width was in most cases sufficient to render the coefficient meaningless.

The formula $I = I_0 e^{-\alpha x p}$ holds when α is independent of the pressure or when $\log I \propto p$. Independent measurements were made to check this point. The relation was found to hold in the region studied, i.e., between 0.001 and 0.007 mm. This result is in accord with the results of G. P. Thomson for faster positive rays cited above. A further piece of evidence on this point is that α seemed to be essentially the same no matter what absolute values of p_1 and p_2 were used.

To obtain some idea of the processes involved in absorption of the ions a series of intensity measurements was made with a number of settings of the magnetic field for each of several pressures. The results of the measurements are shown graphically in Fig. 4. The meaning of the curves is briefly discussed in the following section.

DISCUSSION OF RESULTS

The absorption of the various hydrogen ions in hydrogen is of interest since H^+ resembles the electron more than any other positive ion, H_2^+ is similar to H_2 in structure and H_3^+ has a mass comparable to that of H_2 but is unlike it in structure.

The absorption coefficients of H^+ , H_2^+ , and H_3^+ in hydrogen were observed in a region between 60 and 850 volts. The actual velocity ranges studied were 1.1 to 4.1×10^7 cm/sec for H^+ , 0.76 to 2.9×10^7 cm/sec for H_2^+ , and 0.62 to 1.79×10^7 cm/sec (corresponding to the range from 60 to 500 volts) for H_3^+ . The results are shown graphically in Fig. 3.

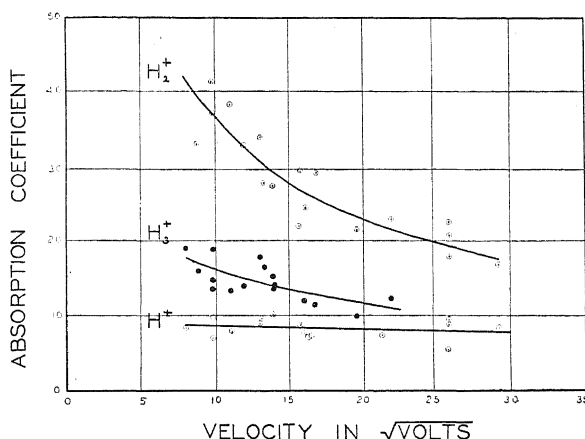


Fig. 3. Absorption coefficients.

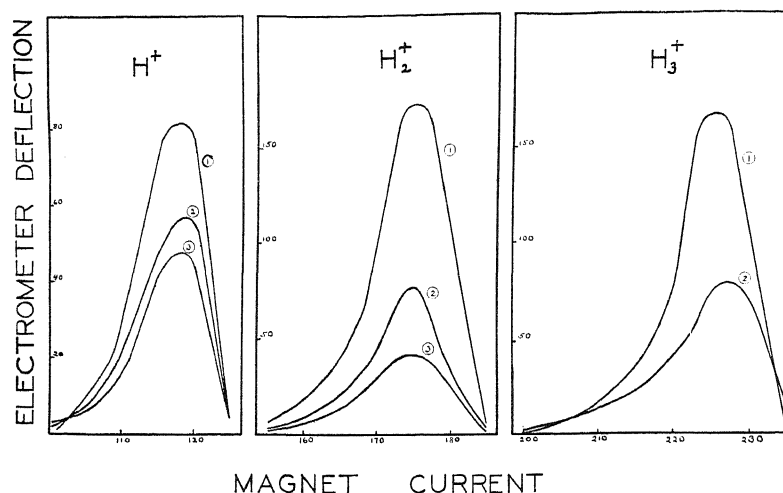
H_2^+ has markedly the largest coefficient varying from $40 \text{ cm}^2/\text{cm}^3$ at 60 volts to $20 \text{ cm}^2/\text{cm}^3$ at 850 volts. Assuming the radius of the ion given by Birge⁸ and the kinetic theory value of the radius of the molecule, α would be $64 \text{ cm}^2/\text{cm}^3$. This value of α is definitely of the same order of magnitude as the experimental value of α at 60 volts. The absorption coefficient for H_3^+ is smaller and varies less, decreasing from $17 \text{ cm}^2/\text{cm}^3$ at 60 volts to $12 \text{ cm}^2/\text{cm}^3$ at 500 volts. The absorption coefficient for H^+ is nearly constant at $8 \text{ cm}^2/\text{cm}^3$, roughly half the kinetic theory value assuming H^+ of negligible dimensions.

In surveying the results, it is at once apparent that the kinetic theory "size" is not as important a factor in determining the absorption coefficient as the possibility of an energy transfer from the ion to the molecule. One would scarcely anticipate a lower value of α for H_3^+ in H_2 than H_2^+ in H_2 yet the value is not only smaller but far nearer H^+ than H_2^+ at the lower velocities. This result may be due to the fact that energy of ionization of an H_2 molecule is equivalent to the energy of neutralization of an H_2^+ ion and that a capture of an electron by an H_2^+ ion in H_2 is very probable. Since the

⁸ R. T. Birge, Proc. Nat. Acad. Sci. 14, 12 (1928).

same is probably not true of H_3^+ , it is less likely to be eliminated by neutralization.

An examination of Fig. 4, showing the intensity and width of the H_2^+ peak at various pressures indicates that there is no spreading due to small angle scattering and no shift of the peak with increasing pressure. The process of absorption of the H_2^+ ion eliminates it completely from the beam. Since the free path is relatively long at the pressures used neutralization of the



Curve	H^+ $p \times 10^3$	H_2^+ $p \times 10^3$	H_3^+ $p \times 10^3$
1	0.0	1.8	0.0
2	2.1	2.9	2.3
3	4.3	3.5	

Fig. 4. Relative absorption of the products of ionization.

ion would definitely eliminate it from the beam. Neutralization and some large angle scattering are evidently the most important factors in the absorption of H_2^+ in H_2 .

The H_3^+ peak broadens with increasing pressure and diminishes in area. Since neutralization is not very probable the chief factor in the absorption of H_3^+ is presumably scattering. Some dissociation may occur although this point cannot readily be checked with the present type of apparatus.

The principal process in the absorption of H^+ is apparently scattering since in Fig. 4 the width at half-maximum does not decrease as the pressure increases and the bases of the peaks show a tendency to spread. Neutralization is not very probable since the energy of ionization of H_2 does not correspond to the energy of neutralization of H^+ .

J. S. Thompson⁹ has shown that α is a function of the geometry of the

⁹ J. S. Thompson, Phys. Rev. 35, 1196 (1930).

apparatus when small angle scattering is important. Since the results in Fig. 4 indicate very little small angle scattering, it is assumed that α is not markedly a function of the apparatus for any of the ions, less so for H_2^+ than either of the others.

The experimental value of α for H^+ at 60 volts is about one-half of Aich's value at 25 volts. These results are not discordant since one expects scattering to increase with decreasing velocities, very markedly in the region below which a minimum of absorption can be expected. However, the value of α does not show any sign of approaching zero at 900 volts as agreement with Dempster's results would require. Since Dempster gave no indication that the pressure in the ionization chamber was independent of the pressure in the absorption chamber, an increase in the intensity of the initial beam of hydrogen ions due to increased pressure in the ionization chamber may have masked the absorption effect.

The results of this experiment give no indication of a minimum of absorption of protons at 900 volts where the *Handbuch der Physik*¹⁰ has interpreted Dempster's results as showing a Ramsauer effect. G. P. Thomson's¹¹ investigations of the scattering of protons in argon and helium indicate that the shape of the absorption curve for protons is similar to the shape of the absorption curve for electrons in these gases in the same velocity ranges. If this conclusion may be carried over to the case of the absorption of protons in hydrogen, a minimum of absorption is to be expected at 1800 volts instead of 900 volts, since Normand¹² has found a minimum of absorption for electrons in hydrogen at 1 volt. It is hoped that measurements of the absorption of 1800-volt protons in hydrogen can be made with the present apparatus in the very near future.

It is a pleasure to acknowledge my indebtedness to Professor R. B. Brode for suggesting this problem and for offering valuable advice and assistance throughout the course of the experiment.

¹⁰ *Handbuch der Physik*, Bd. 24, S. 100.

¹¹ G. P. Thomson, *Phil. Mag.* 2, 1076 (1926).

¹² C. E. Normand, *Phys. Rev.* 35, 1217 (1930).

THE VELOCITY DISTRIBUTION OF SECONDARY ELECTRONS FROM MOLYBDENUM

BY THEODORE SOLLER

DEPARTMENT OF PHYSICS, AMHERST COLLEGE

(Received August 25, 1930)

ABSTRACT

The velocity distribution curves of secondary electrons from a molybdenum target for primary electron velocities from 7.5 to 100 volts are obtained by an improved apparatus, using the magnetic deflection method. Distribution curves quite similar to those observed by others for different metals are obtained, showing a broad low-velocity maximum of secondary electrons and a sharp "reflected" peak whose measured velocity in all cases turned out to be approximately 2 volts less than the corresponding accelerating voltage. It is shown that this should be so, from a consideration of contact potentials.

The effect of gas content of the surface on the velocity distribution was investigated. Heating at a temperature of approximately 850°C for 20 hours produced only slight changes in the curves. A prolonged heating of 41 hours at approximately 1250°C caused a marked decrease in the low-velocity maximum and an increase in the height of the "reflected" peaks. Both changes are ascribed to the removal of gas from the surface.

The curve giving the height of the "reflected" peaks as a function of the velocity of the primary electrons has several maxima. There is a fair correlation between the voltages to which these maxima correspond and the "critical potentials" of Mo observed by Petry.

INTRODUCTION

SEVERAL investigators¹⁻⁹ have been interested in the distribution in velocity of the secondary electrons which are emitted from metals when bombarded by a stream of electrons. The velocity distribution of these electrons has been most commonly obtained by subjecting the electrons in question to a uniform and known magnetic field of variable strength, and either measuring the number of electrons which reached a fixed collector as the field was varied, or else by receiving the electron spectrum on a photographic plate upon application of a constant magnetic field.

It seemed worth while to do further work along this line for the following reasons: (a) practically no attention has been paid to the effect of gas on the surface of the target upon the velocity distribution curves; (b) no work

¹ J. A. Becker, Phys. Rev. 23, 664 (1924); 24, 478 (1924).

² E. L. Rose, Phys. Rev. 25, 883A (1925).

³ A. Becker, Ann. d. Physik 78, 228 (1925).

⁴ C. F. Sharman, Proc. Camb. Phil. Soc. 23, 523 (1927); 23, 922 (1927).

⁵ D. Brown and R. Whiddington, Nature 119, 427 (1927).

⁶ J. B. Brinsmade, Phys. Rev. 30, 494 (1927).

⁷ E. Rudberg, Proc. Roy. Soc. A127, 111 (1930).

⁸ D. A. Wells, Phil. Mag. 5, 367 (1928).

⁹ H. E. Farnsworth, Phys. Rev. 25, 41 (1925); 31, 405 (1928).

of this nature has been reported on Mo, which lends itself readily to the process of outgassing because of its high melting point; (c) better vacuum conditions were desirable; and (d) the methods previously employed seemed to have one serious disadvantage in that no means of measuring the intensity of the incident beam of primary electrons was available. Consequently the curves obtained have been but apparent velocity distribution curves since nothing was known about the constancy of the primary electron beam impinging upon the target. The present experimental arrangement eliminates this difficulty.

APPARATUS

Fig. 1 gives a schematic diagram of the apparatus and electrical connections. The metal parts of the apparatus were constructed entirely of molybdenum, with the exception of F_1 (Pt foil coated with oxides) and F_2 (tungsten). Electrons were accelerated between F_1 and E and then proceeded

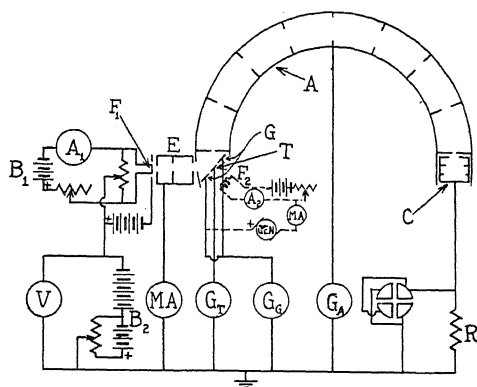


Fig. 1. Diagram of apparatus and electrical circuit.

to the target T , which consisted of two parts electrically insulated from one another, but in the same plane. Secondary electrons proceeding from the target in the direction of the first slit in the slit system A (called the analyzer) traveled in a circular path due to a uniform magnetic field produced by a pair of large Helmholtz coils and the earth's field. Those whose radius of curvature was 7 cm reached a collector C placed immediately behind the last slit. By varying the field, electrons of various velocities could be measured by the electrometer connected to C . Since the primary beam of electrons was also in this same magnetic field, their path would also be curved. Taking this into account, the angle between the direction of the incident electrons and that of the secondary electrons measured was in the neighborhood of $70\text{--}75^\circ$. The target was so constructed that only electrons from the central portion could reach the collector C . The target could be outgassed by electron bombardment from the filament F_2 behind it, without much danger of having the front surface contaminated by evaporated tungsten. Electron currents to G , T , and A were measured by galvanometers, as shown in the figure.

The metal parts of the tube were baked in a high vacuum before assembly, and great care was taken not to introduce contamination during assembly. The entire apparatus in its Pyrex tube was then attached to the pumping system and baked out at a temperature of 475°C for 30 hours. The pumps were kept running during the whole course of the experiment, pressures being read by a McLeod gauge sensitive to 10^{-6} mm Hg.

METHOD OF CALCULATION

The velocity distribution was obtained by plotting the ratio of the current to the collector C to the current to the target T for various values of the magnetic field. As is well known, the deflections of the galvanometers G_G , G_T , and G_A do not measure the number of electrons striking the guard-target, target, and analyzer respectively, but rather the difference between this and the number that leave. The whole enclosure A , G , T may however be considered as being approximately a "black body" for electrons incident upon the target. Consequently, if we designate the currents as measured by the various galvanometers simply by the letters referring to those parts, then $(A+T+G)$ may be taken as a measure of the total primary current striking T and G . The number of electrons "sticking" to the whole target is measured by $(T+G)$. Hence the ratio $(T+G)/(T+G+A) = F$ gives the fraction of the total current striking T and G which is measured by the galvanometers G_T and G_G . In order to get the true electron current to the *effective* portion of the target, the current as measured by G_T , being T , must be multiplied by $1/F$. Hence the total effective primary current is

$$I_{\text{target}} = T \frac{T + G + A}{T + G}.$$

Furthermore, the ratio $I_{\text{electrometer}}/I_{\text{target}}$ for various values of the field, H , will not give the correct velocity distribution, because the effective width of the slit system varies directly with the velocity of the electrons whose velocity is to be measured. Hence, in plotting the curves, this ratio was reduced to the same effective slit width by dividing in each case by the value of the magnetic field. For convenience, this magnetic field was measured in tenths of gauss, and the ordinates of all curves are the ratio $I_{\text{electrom}}/I_{\text{target}}$ divided by the value of the magnetic field.

METHOD AND RESULTS

The velocity distribution curves shown in Fig. 2 were obtained after baking out the apparatus but without any special outgassing of the target. These curves are quite similar to those reported by Brinsmade⁶ for Al. The essential features of these curves are a broad low-velocity group of electrons and a sharply defined high-velocity group. The value of the velocity of this group as calculated from the radius of curvature and the field strength in all cases turns out to be somewhat less than the accelerating potential as measured by the voltmeter V . That this should be so is evident

from the following considerations: The limiting case of a thermion from the filament is one which has just enough energy to escape from the filament. This may be designated as Φ_F , the work-function of the filament. This electron is then acted on by the field due to the applied e.m.f. V , by the contact e.m.f. $V_{C,TF}$ between the target and filament, and also by the field due to Φ_T , the work-function of the target, before it gets into the target. Therefore its kinetic energy in the target would be $e(V - V_{C,TF} + \Phi_T) = e(V - \Phi_T + \Phi_F + \Phi_T)$ since $V_{C,TF} = \Phi_T - \Phi_F$, and consequently the kinetic energy in the target is $e(V + \Phi_F)$. The secondary electrons measured would not have a kinetic energy equal to this, however, since they would lose kinetic energy equal to $e\Phi_T$ in emerging from the target, neglecting any loss of energy while in the metal. Hence the kinetic energy measured would be given by $e(V + \Phi_F - \Phi_T) = e(V - \{\Phi_T - \Phi_F\}) = e(V - V_{C,TF})$ and one would not expect

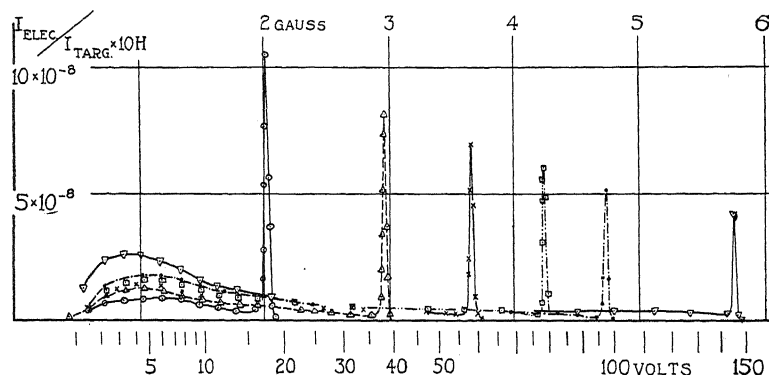


Fig. 2. Curves showing the velocity distribution of secondary electrons from a Mo target after baking out apparatus at 475°C for 30 hours.

the equivalent velocity (in volts) of the swiftest secondary electrons to coincide with V , the applied voltage, but to differ from this by an amount $\Phi_T - \Phi_F$ or $V_{C,TF}$. The above assumes no contact potential between the target and the analyzer. If there be a contact potential between T and A , $V_{C,AT} = \Phi_A - \Phi_T$ then the kinetic energy of the electrons after entering the analyzer slit would be $e(V - V_{C,TF} - V_{C,AT})$ or $e(V + \Phi_F - \Phi_A) = e(V - \{\Phi_A - \Phi_F\}) = e(V - V_{C,AF})$. This contact potential $V_{C,AF}$ between the analyzer and filament is independent of changes in Φ_T due to the outgassing or other causes. In the present work, the accelerating voltage was very nearly 2 volts higher than the measured velocity of the electrons comprising the high-velocity peak. This would indicate that Φ_A is greater than Φ_F by 2 volts, which is a reasonable order of magnitude, and in the right sense. It would be reasonable to suppose, then, that the electrons which make up this peak are those which correspond in energy to the primary electrons.

The low-velocity group of electrons would include, as Sharman⁴ suggests, electrons released by any characteristic corpuscular radiation excited in the atoms of the target by the primary beam, and also products of collision between primary electrons and free electrons in the target, as well as with

gas on the surface. It will be noticed that the magnitude of the low-velocity group increases with increasing velocity of the primary electrons, and there also appears to be a shift in the maximum toward higher velocities at the same time. These observations agree with those of Brinsmade.⁶ At the higher primary velocities there is a small region on the low-velocity side of the full-velocity peak in which very few electrons are found. This has also been observed by Sharman,⁴ Brown and Whiddington,⁵ and Brinsmade,⁶ working with other metals. Recently E. Rudberg,⁷ using an apparatus of very much

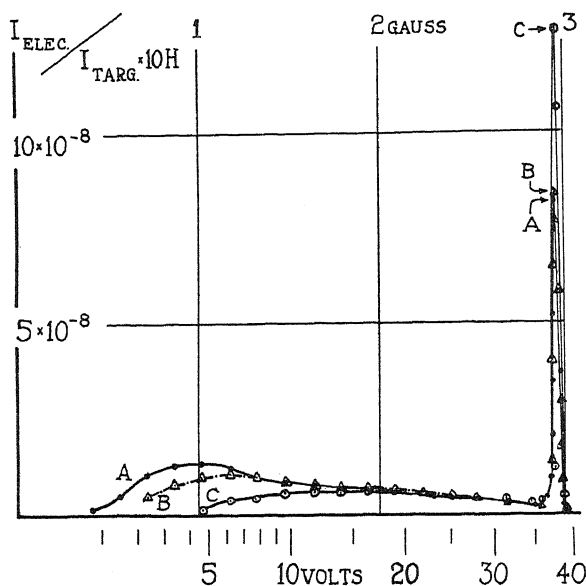


Fig. 3. Curves showing the effect of heat treatment on the velocity distribution of secondary electrons, for a primary accelerating voltage of 40 volts. *A*, after baking out at 475°C for 30 hours. *B*, after electron bombardment (850°) for 20 hours. *C*, after additional bombardment (1250°) for 41 hours.

higher resolving power and primary electrons of upwards of 200 volts, has shown that in this region there appear one or more maxima, indicating a certain kind of critical potentials for the substances studied.

The above runs were repeated after the target was outgassed for a period of 20 hours at a dull red heat. The differences between the curves thus obtained and the previous ones are not very great, the full-velocity maxima being practically the same in height, and the low-velocity group having its maximum slightly shifted toward higher velocities. The curve for 40 volts primary velocity is representative of what took place and is shown in curve *B* of Fig. 3, curve *A* being the original curve for this voltage. It is quite possible that heating at this low temperature does not cause a great change in the gas content of the surface itself, over what is produced by the original baking.

The target was then heated for a period of 41 hours at a much higher temperature, estimated at 1250°C, and during the last five hours of this the

temperature was raised still higher. During this last period the pressure in the system was too low to be readable on the McLeod gauge, even while the target was being bombarded. This condition was taken as an indication that this prolonged heat-treatment had removed practically all of the gas adsorbed on the surface of the target as well as a great share of the occluded gas. A series of curves was now taken as quickly as possible covering the range up to 100 volts at 5-volt intervals, in order to get more complete information as to the velocity distribution as a function of the primary velocity.

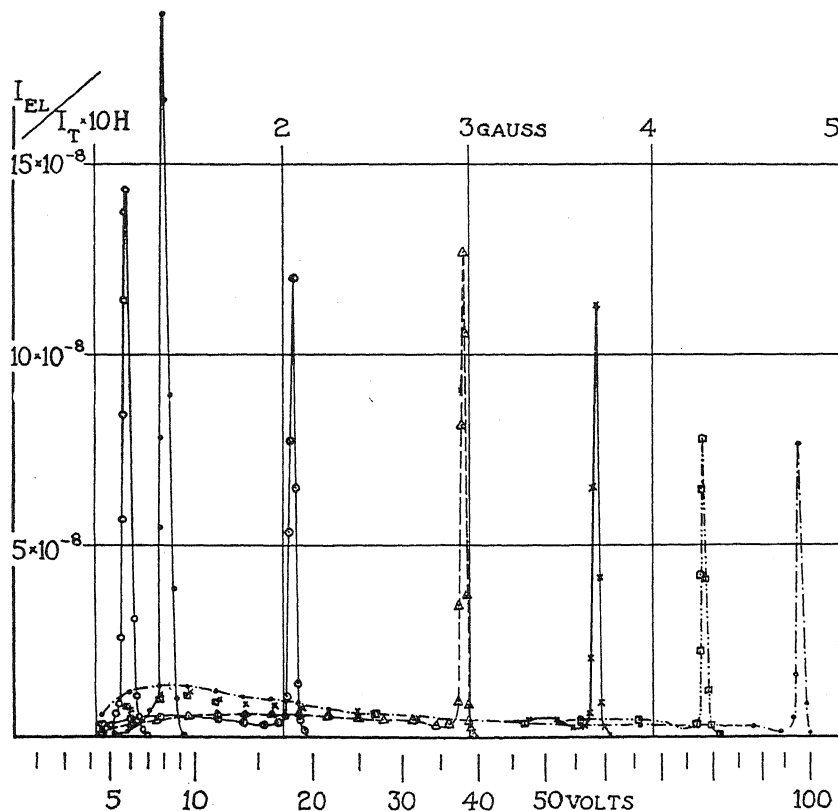


Fig. 4. Curves showing the velocity distribution of secondary electrons from Mo target after 61 hours heating at temperatures between 850° and 1250°C. The curves are for primary accelerating voltages of 7.5, 10, 20, 40, 60, 80 and 100 volts.

In the light of recent studies by Davisson and Germer¹⁰ these curves cannot be interpreted as representing a gas-free surface condition, but the amount of gas accumulated on the surface when these measurements were taken must have been relatively small.

The changes introduced by this heat-treatment were identical for all velocities of primary electrons, and consequently it will suffice to give the results for the 40-volt curve. This is curve C of Fig. 3. It will be observed

¹⁰ L. H. Germer, Bell Syst. Tech. Journ. 8, 591 (1929).

that the full-velocity peak is considerably higher, and that the low-velocity peak has practically disappeared. Fig. 4 shows the curves for accelerating voltages of 7.5, 10, 20, 40, 60, 80, and 100 volts, after this last outgassing. The last five of these curves correspond in voltage to the first five in Fig. 2, and show clearly the changes both in the full-velocity peaks and in the low-velocity maxima. It will also be noted that for accelerating potentials under 15 volts practically all of the secondary electrons have the full velocity of the primary electrons. This would indicate either a pure reflection up to this point, or else perfectly elastic collisions. The separation into two groups begins to appear around 15 volts, and above this the separation is quite marked. This behaviour has also been noticed by Farnsworth⁹ and Brinsmade⁶ working with other metals.

The decrease in the low-velocity group upon heat-treatment can be explained if we suppose that the electrons comprising this group are the result of collisions between primary electrons and gas atoms. This group would then decrease as the number of gas atoms on the surface was reduced. The results of Brinsmade⁶ also fit in with this hypothesis, since he obtained a maximum at almost exactly the same voltage from an Al target which had not been outgassed except by baking. If this maximum were due to a characteristic of the metal itself, one would not expect it to come at the same voltage for Al and Mo. The appearance of a slight low-velocity maximum for primary velocities above 40 volts may reasonably be due to collisions between primary electrons and atoms in the target, such that the resulting secondary electrons get through the surface of the target only after the energy of the primary electrons has reached a definite lower limit. This effect might reasonably be masked by the "gas" effect before thorough outgassing. The increase in the high-velocity or reflected group is also ascribed to the removal of gas from the surface, and parallels the experience of Davisson and Germer¹⁰ who found that the reflected beams of electrons were much more pronounced when the target was relatively free of gas than when it was covered with many layers of gas atoms.

A rough idea of the relation between height of the full-velocity peak and the velocity of the electrons can be obtained by drawing a curve through the tips of the peaks of Fig. 4. In order to get better information regarding this point, the target was outgassed for 5.5 hours at a bright yellow heat, and immediately thereafter the readings were taken which are collected in the curves of Fig. 5. Curve 1 shows the first run, which extended to 40 volts, after which fluctuations in the battery voltage caused trouble. Curve 2 was obtained several hours after this, and extends to 100 volts. A third curve after still further outgassing failed to materialize because the last heating had evaporated enough tungsten to destroy the insulation between the target and its guard, making similar measurements impossible. The two curves of Fig. 5 agree pretty well in form, considering the difficulty encountered in trying to set exactly on the peak for each voltage.

One might expect that wave-interference maxima due to the microcrystalline structure of the target would show up under the conditions re-

presented in Fig. 5. Although some of the maxima can be accounted for in this way with reasonable assumptions, there are evidently more variables involved than were under control; consequently the details of computation are here omitted. Another interpretation of these maxima is that they may represent certain "critical potentials" of Mo. In comparing the positions of

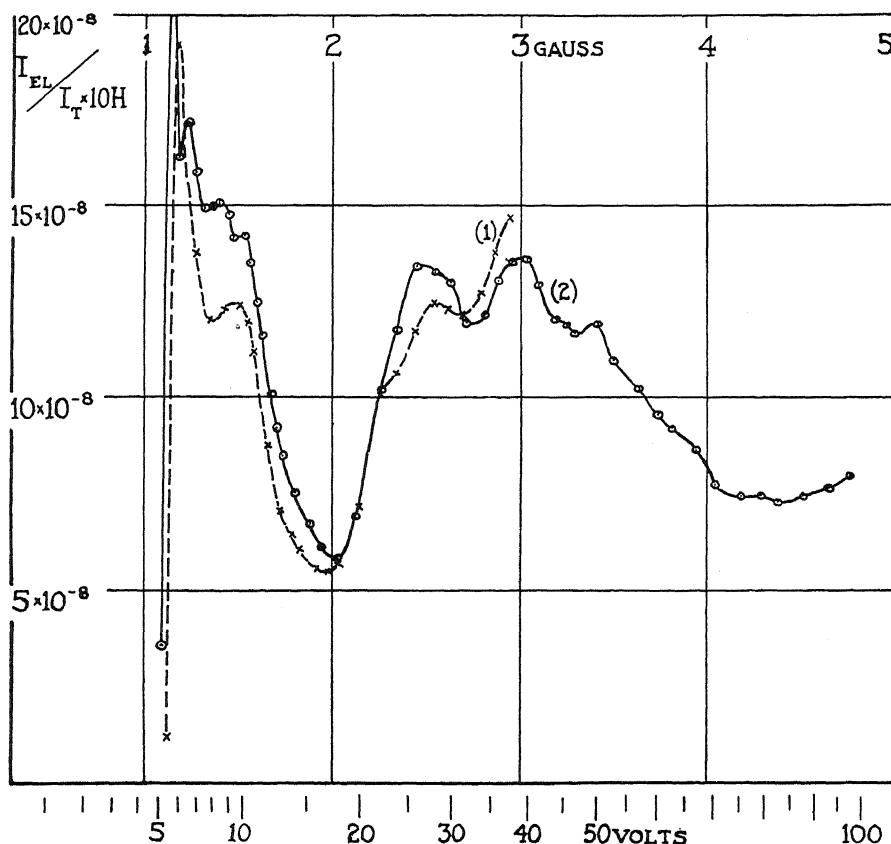


Fig. 5. Curves showing the heights of the full velocity peaks as a function of their velocity after thorough outgassing. Curve 1, first run. Curve 2, second run.

the maxima in Fig. 5 with the "critical potentials" which Petry¹¹ obtained in studying the ratio of total secondary to total primary electron currents for a Mo target, it is found that there is a very fair correlation between the two. Although the velocities at which the maxima occur do not coincide in the two cases, the velocities of the electrons in the target in both cases turn out to be very nearly the same, when proper corrections are applied to take care of the difference in work-function of the two sources, voltage drop along the filament, and initial velocity of emission of electrons.

¹¹ R. L. Petry, Phys. Rev. 26, 346 (1925).

¹² J. M. Hyatt and H. A. Smith, Phys. Rev. 32, 929 (1928).

J. M. Hyatt and H. A. Smith¹² working with a different type of apparatus, also find slight breaks in their curves for Mo, to which they attach no significance because they were not reproducible.

Further work needs to be done in order to prove or disprove this interpretation of the peaks. It does not seem probable that they can be due to eccentricities in the apparatus, since the irregularities appear only after considerable outgassing (Fig. 4) and not for the initial state (Fig. 2). The work is being continued at the University of Wisconsin, where the present work was done.

In conclusion, the writer wishes to express his thanks to Dr. C. E. Mendenhall for suggesting the problem and for his generous assistance throughout the work.

THE HEAT OF FORMATION OF MOLECULAR OXYGEN

By L. COVELL COPELAND¹

JEFFERSON PHYSICAL LABORATORY, HARVARD UNIVERSITY

(Received August 25, 1930)

ABSTRACT

An apparatus has been constructed and described for the production of atomic oxygen and the direct determination of the heat of formation of molecular oxygen. A series of determinations have been conducted in the pressure range of 0.1 to 0.55 mm of mercury. The heat of formation of molecular oxygen was determined by these experiments as 131,000 ($\pm 6,000$) calories or 5.7 (± 0.3) volts per gram molecular weight. Several of the properties of atomic oxygen have been investigated including the possibility of long-lived metastable states.

INTRODUCTION

THE dissociation energy of molecular oxygen has been determined by several indirect methods, the probable values ranging from 110,000 calories or 4.8 volts to 162,000 calories or 7.05 volts. In this work a direct calorimetric determination has been made. In preliminary reports by Bichowsky and the author² the presence of atomic oxygen in the gas issuing from a discharge tube was first demonstrated and a few of its properties determined. The method employed for the determination of the heat of association of atomic oxygen is the same as that used by Bichowsky and the author in their determination of the heat of formation of molecular hydrogen.³

Electrolytic oxygen was admitted to the electrodeless discharge bulb *D*, Fig. 1, at a determined rate of flow by the capillary *A*. The gas partially dissociated by the discharge from the high frequency current in *H*, passes through a set of orifices *B* and is associated on the palladium black surface of the calorimeter *E*. The temperature rise of the calorimeter above the temperature of the constant temperature bath *I* gives the energy of association of the partially dissociated gas. The percent of atomic oxygen in the gas is determined from the formula $2\alpha/(1+\alpha) = 3.41(1 - P_N/P_D)$ where α is the percent dissociation, P_N is the pressure of the gas on the high pressure side of the orifices *B* under steady state conditions of no dissociation, before the discharge is turned on, P_D is the pressure of the gas at the same point under the steady state conditions involving dissociation when the discharge is going. As the development of this formula from Knudsen's formula for the rate of flow of gas through a small orifice is given completely in a former paper³ it will not be repeated here.

¹ National Research Fellow in Chemistry.

² Bichowsky and Copeland, *Nature* **120**, 729 (1927); *Phys. Rev.* **31**, 1113(A) (1928).

³ Bichowsky and Copeland, *J.A.C.S.* **50**, 1315 (1928).

APPARATUS

The source of oxygen was a water-cooled electrolytic generator with nickel electrodes and CO_2 -free potassium hydroxide solution as electrolyte. The rate of flow of gas into the apparatus was determined by capillary *A*. As the rate of flow of gas through a capillary is dependent on the pressure on the high pressure side, a manometer *M* was attached to the generator line which actuated a relay to control the D. C. current to the generator and thereby maintained the source of oxygen at constant pressure. Capillary *A* was also immersed in the constant temperature bath *I* (for simplification the sketch does not illustrate this). The rate of flow of oxygen into the

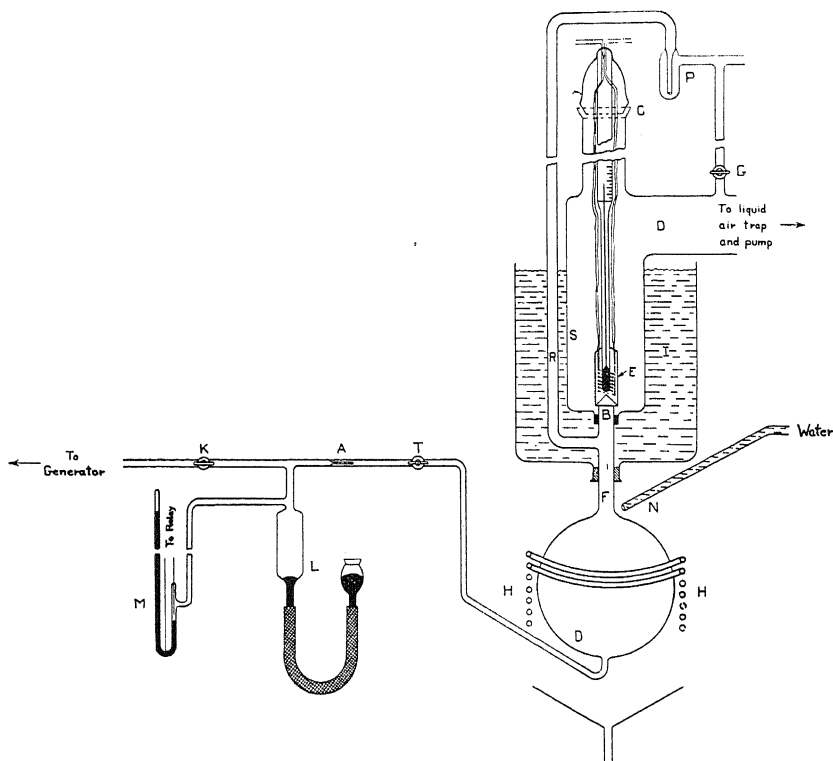


Fig. 1. Diagrammatic sketch of apparatus.

apparatus was measured by means of the pipette and leveling bulb *L*. The volume of the pipette between the two scratches on the capillary tubes on either end was accurately known. In determining the rate of flow, stop-cock *K* was closed and the time required to fill the pipette with mercury from the leveling bulb was taken on a stop watch, care being taken to maintain constant pressure as indicated by manometer and relay.

The discharge bulb *D* was made from a 500 cc round bottom flask. During an entire experiment this bulb was covered with running water from tap *N* discharging into the funnel placed beneath the bulb. The induction coil *H* was constructed of seven turns of 1/8 inch copper tubing

through which water was circulated to keep it cool. The current was supplied from an induction furnace circuit which consisted of 3kva 1-100 transformer, two 0.035 microfarad oil condensers and a quenched spark gap. The dissociated gas left the discharge bulb through the tube *F* which was a 1 cm piece of tubing about 13 cm long and terminated in the set of orifices *B*.

The use of Knudsen's formula for the flow of gas through orifices is applicable only if the area of the orifice is small in comparison to the mean free path of the gas, and the thickness of the plate in which the orifice is made must also be small in comparison to the diameter of the hole. Thus at 0.1 of a mm pressure the diameter of these orifices and the thickness of the wall in which they were made had to be of the order of magnitude of 0.1 mm.

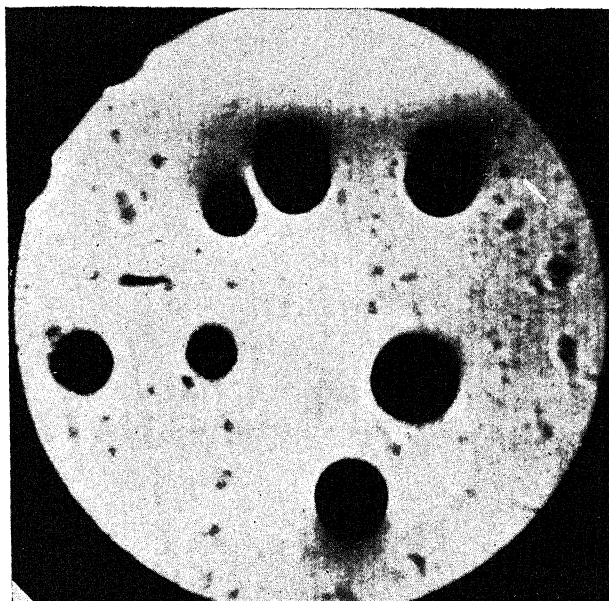


Fig. 2. Microphotograph of a portion of one set of orifices.
Largest holes 0.2 mm in diameter.

Sets of orifices containing 15 to 40 such holes were obtained in the following manner. The end of a piece of Pyrex tubing was blown out to give a large fragile bubble of glass about 0.1 mm in thickness. A small section of this thin glass was placed on a carbon plate and the end of a piece of 1 cm cross-section Pyrex tubing was heated to flowing temperature and then pressed against the thin glass thus sealing it to the end. A piece of 1/32 inch tungsten wire was mounted in the chuck of a jeweler's lathe and a fine centered point produced by burning it with an oxygen flame while the lathe was rotating. This fine drill was then heated red hot with an air flame and the thin wall lightly brought to the hot point. After considerable practice several very satisfactory sets of orifices were obtained. A microphotograph of a portion of one of these sets is shown in Fig. 2 in which the largest hole is about 0.2 mm in

diameter. These orifices were sealed to tube *F* and fastened into the bottom of the calorimeter jacket *S* with sealing wax, to facilitate centering and replacement.

The pressure at *B* was measured on a large thermostated McLeod gauge which was connected to the apparatus through *R*, a tube of 1 cm diameter. This gauge was read with a cathetometer. A liquid air trap *P* was inserted in the McLeod gauge line in order to keep mercury out of the apparatus because it destroyed the atomic gas and poisoned the catalytic surface of the calorimeter.

Stop-cock *G* was closed during the run but opened as a bypass to protect the fragile orifices when it was desired to change the pressure in the apparatus by more than a few cms. This bypass was also of assistance when evacuating the entire apparatus before starting a run.

The calorimeter *E* was constructed of a cylinder of platinum foil 1.5 cm in diameter and 4.5 cm long. This cylinder was closed at the bottom end by a platinum foil cone and sealed to the bulb of a Beckmann thermometer with Wood's metal. A coil of enameled nichrome wire with enameled copper potential and current leads was sealed in the Wood's metal. This coil was for the calibration of the calorimeter. On the conical surface of the calorimeter was deposited electrolytically an even layer of palladium black. The Beckmann thermometer and calorimeter were sealed into the upper section of a ground joint *C* with sealing wax. Tube *D* served to conduct the gas to the conventional liquid air trap, mercury pump, fore pump, and low pressure McLeod gauge. The thermostat *I* consisted of an inverted bottle from which the bottom had been removed. It was fastened to *F* with a rubber stopper and supported separately. In addition to what is shown in Fig. 1, the thermostat contained a toluene thermoregulator, stirrer, lamp, Beckmann thermometer, cooling coil, and capillary *A*. The temperature of the water in the thermostat could be maintained constant to within 0.01°C.

SOME QUALITATIVE PROPERTIES OF ATOMIC OXYGEN

The first experiments² made on the study of atomic oxygen made use of a discharge tube containing aluminum electrodes for dissociating the gas. The electrodeless discharge produced a much larger percentage of atomic gas due to the absence of any metal that could produce a "clean up" effect. This fact is in accord with the observations of Kurt and Phipps.⁴ Also in agreement with these authors it was found that water vapor was necessary for the establishment of dissociation. This fact was demonstrated very convincingly in the following manner. A 500 cc long-neck distilling flask was evacuated and then filled with moist oxygen gas to a pressure of about 0.2 mm and sealed off from the apparatus. When this bulb was held in the induction coil of the oscillating circuit a greenish blue discharge with a red center appeared that showed in the hand spectroscope, the line spectra of O I and the first three members of the Balmer series against a dark back-

⁴ Kurt and Phipps, Phys. Rev. 34, 1357 (1929).

ground. If the neck of the bulb was now placed in liquid air the entire character of the discharge slowly changed, the lines fading out and a banded background developing till finally $H\alpha$ the last to disappear, left nothing but a banded spectra. When the liquid air was removed, the reverse phenomena took place till at the end of a few minutes nothing but line spectra again remained. There were also a few specks of foreign material on the sides of the bulb that were incandescent when the line spectra were present and invisible when the band spectra were predominant. If the neck of the bulb was first cooled in liquid air and then placed in the exciting field, the first flash showed red and then immediately changed to the blue banded spectra. The interpretation is that the removal of water vapor by freezing it out with liquid air either prevented the dissociation of the O_2 molecule or, in analogy to Wood's⁵ explanation of the role of water vapor in the production of atomic hydrogen, the removal of water vapor exposed the dry glass walls which were sufficiently catalytic for the recombination of oxygen atoms to cause their complete removal. In either case excited atoms were not present in the dry bulb in sufficient number to produce detectable line spectra or cause the foreign particles to glow by the heat of recombination of oxygen. The energy of the discharge was then taken up in the excitation of the molecules as shown by the ensuing band spectra. As another illustration of the necessity of water vapor it should be mentioned that when liquid air was applied to the inlet line of the apparatus between *A* and *D* during the discharge there was a gradual decrease in pressure and a steady drop in the temperature of the calorimeter indicating a decreased percentage of dissociation. Both of these readings returned to their former value when the liquid air was removed.

Although these experiments do not show any optimum pressure for dissociation as mentioned by Kurt and Phipps,⁴ it should be noted that any dependence of dissociation at the orifices on pressure is probably completely masked by the changes in the surface conditions of exit tube *F* which was frequently changed throughout the course of these experiments and by changes in the rate of flow of gas through the apparatus.

Mercury vapor is very readily oxidized to the yellow form of mercuric oxide by atomic oxygen. Unless liquid air is maintained on the traps on all lines leading to a source of mercury vapor the cooler portions of the apparatus soon become coated with a yellow sheen due to this oxide.

Traces of nitrogen give the familiar greenish afterglow due to the metastable molecules. At the same time some compound is formed, possibly an oxide of nitrogen which will travel through the liquid air traps and react with mercury leaving a dirty black deposit⁶ that destroys the use of McLeod gauges. For the above reasons tank oxygen could not be used in these experiments.

⁵ Wood, Proc. Roy. Soc. 102, 1 (1922).

⁶ This black deposit may be removed without disassembling the apparatus even if it can not be heated, by filling the contaminated section with a few tenths of a millimeter of hydrogen and passing a discharge through that portion with an induction coil such as is used in testing for leaks.

Atomic oxygen like atomic hydrogen will cause small specks of substances, catalytic for the recombination, to glow white-hot in the dissipation of the energy of this reaction. A rough qualitative study of five metals was made to find a suitable catalyst for the surface of the calorimeter. Wires of these metals about 0.002 inches in diameter and 1 inch long were mounted on magnetic probes in another apparatus so they could be moved towards or away from the discharge bulb in vacuum. It was found that palladium, platinum and nickel were readily heated to glowing by the atomic oxygen but that copper and tungsten* were not visibly affected. Palladium was apparently the most active and both palladium and platinum wires could be melted by bringing them too close to the discharge or increasing the flow of gas suddenly. Although it was necessary to bring the wires to within 10 cm of the discharge bulb to start them glowing, after they were hot they could be removed as far away as 35 cm from the discharge bulb in the direction the gas was flowing where they would still glow visibly and apparently indefinitely. This initial lag which was always present if the wire for any reason became cooled is believed to be due to a surface layer of gas or water vapor which prevented the reaction taking place except at high concentrations of atomic gas. Once the reaction was started the temperature of the wire kept its surface free until it was allowed to cool again. Platinum was first chosen at the most practical catalyst for recombination but subsequent experiments showed it was not sufficiently effective. Every collision of an oxygen atom did not mean capture for recombination. (See blank experiments) Palladium black however both because of its greater area and its greater activity was found to be sufficiently effective.

EXPERIMENTS ON HEAT OF FORMATION

At the beginning of all experiments the capillary *A* was closed off by the stop-cock *T* and the bypass *G* was opened. The apparatus was then evacuated until the McLeod gauge showed a "flat gauge," approximately 10^{-6} mm. Stop-cock *T* was then opened and the bypass *G* closed. The following readings were taken periodically; the pressure on both sides of the orifices, temperature of the bath, the temperature of the calorimeter and the laboratory air temperature. Occasional checks on the rate of flow were made. When steady-state conditions were obtained, which generally required one to two hours, readings of all temperatures and pressures were taken every 10 minutes for a period from half an hour to an hour. If these readings showed no appreciable drift the discharge was turned on and the process of obtaining steady state readings repeated. After the discharge was turned off a new steady state set of readings was obtained and at the same time the calibration of the calorimeter was made by passing sufficient current from a 12 volt storage battery through a variable resistance and ammeter and the heating coil of the calorimeter to maintain the temperature of the Beckmann thermometer at the same point as it was during the discharge. These ammeter

* In atomic hydrogen tungsten wires glow and platinum wires do not glow except with a large excess of oxygen. (See Wood, ref. 5).

readings and the reading of the potential drop across the heating coil gave an amount of energy per minute which was equal to that received by the calorimeter per minute during the discharge. The following computations are for Experiment 1.

Rate of flow of oxygen corrected to normal temperature and pressure 0.66014 cc/min.

Average pressure at *B* during last half hour of steady state of discharge 0.3544 mm.

Average pressure at *B* during last half hour of steady state of no discharge 0.3099 mm.

$$2\alpha/(1 + \alpha) = 3.41(0.3544 - 0.3099)/0.3544 = 0.4282$$

$$= 27.24 \text{ percent of dissociated O}_2$$

$$0.660 \text{ cc/mm} \times 0.2724 = 0.180 \text{ cc dissociated O}_2/\text{min.}$$

0.123 amps at 0.60 volts required to maintain the calorimeter at the temperature obtained during discharge.

$$0.123 \text{ amps} \times 0.60 \text{ volts} \times 60 = 4.428 \text{ joules/min}$$

$$= 1.058 \text{ calories/min}$$

$$22,412 \text{ cc/gr mol. wt} \times 1.058 \text{ calories/mm} \div 0.180 \text{ cc/min}$$

$$= 131,645 \text{ calories/gr molecular wt.}$$

Table I gives the recorded data and results of fifteen experiments and one blank experiment, which will be explained later, arranged in the chronological order in which they were performed. Column 2 gives cc/min which is the rate of flow of oxygen corrected to normal temperature and pressure. Column 3 (P_D) gives the average pressure of the steady state during discharge

TABLE I.

Experiment number	cc/min	P_D mm of Hg	P_N mm of Hg	Percent Dissociation	cal/min	ΔH cal/mol
1	0.660	0.3544	0.3099	27.24	1.058	131,645
2	0.660	0.3522	0.3109	24.94	0.964	131,267
3	0.660	0.3085	0.3087	0.00	0.000	
4	0.667	0.2036	0.1789	26.15	1.222	156,985
	0.667	0.2032	0.1789	25.67	1.200	156,987
5	0.667	0.2012	0.1792	22.92	1.048	153,611
6	0.378	0.1088	0.0998	16.46	0.454	163,244
7	0.373	0.1089	0.0995	17.35	0.474	164,201
8	0.815	0.2455	0.2189	22.70	1.272	154,045
9	0.111	0.3766	0.3245	30.86	0.203	132,886
	0.111	0.3757	0.3245	30.27	0.188	125,489
10	0.168	0.5555	0.4813	29.51	0.288	130,381
11	0.064	0.2152	0.1905	24.38	0.121	172,360
12	1.129	0.5533	0.4867	25.84	0.176	135,023
13	1.129	0.5560	0.4846	28.03	0.177	125,239
14	0.947	0.4657	0.4150	22.76	0.130	135,197
15	0.947	0.4661	0.4163	22.06	0.127	134,633
16	0.361	0.1784	0.1626	17.87	0.456	159,382

and Column 4(P_N) the average pressure of the steady state after discharge. Column 5 gives the percent dissociation calculated from the pressure differences. Column 6 cal/min gives the energy in calories per minute required in the calibration of the calorimeter to bring it to the same tem-

perature as it was during the steady state of discharge. Lastly are listed the computed values of the heat of formation in calories per gram molecular weight. In Experiments 4 and 9 two separate steady states were obtained with the discharge on, involving different temperatures of the calorimeter. For this reason two separate computations were made on these experiments.

Blank experiments. In experiment 3 a strip of platinum foil coated with palladium black was inserted in tube *F*. The purpose of this foil was to associate all the atomic oxygen before it reached the orifices and calorimeter. The results of this experiment showed that there was no observable difference of pressure between the steady state of discharge and the steady state of no discharge and that there was no observable heat effect in the cal-

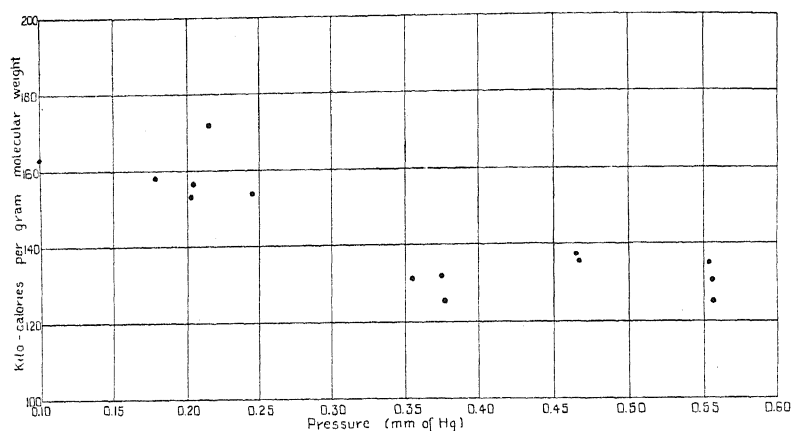


Fig. 3. ΔH -pressure plot of Table I.

orimeter. These results show that the observed pressure change in the other experiments was due to atomic oxygen which was completely associated by the palladium black surface to molecular oxygen and that there was no thermal leakage from the electrodeless discharge or exciting circuit to the calorimeter. These results were not obtained with a clean platinum surface in place of the palladium black. In the first experiments on this problem a shiny platinum surface was left on the calorimeter. Very inconsistent values were obtained for the heat of formation ranging from 50,000 to 150,000 calories. A similar blank with shiny platinum showed that only about 30% of the atoms were being associated. In all subsequent experiments the palladium black surface has been used. Whenever the calorimeter was removed a new surface of palladium black was deposited. This precaution was followed because one experiment not reported here, conducted after the apparatus had been standing for some time without liquid air on the traps, gave a value of 100,000 calories. Subsequent examination of the calorimeter surface showed an iridescently colored surface and minute drops of mercury visible with the aid of the microscope.

As a check on the possibility that the field of coil *H* might cause a temperature rise in the calorimeter not noticed in the blank experiment the oscillating current was allowed to pass through the coil when the pressure was too low to excite a discharge, 10^{-4} mm and also when the pressure was so high that only a faint glow was visible, 10 mm. In both cases there was no discernable temperature rise in the calorimeter. There was no appreciable stray discharge to the calorimeter. To demonstrate this fact an auxiliary electrode was sealed into a side arm on *F* and grounded through a galvanometer. No current passed through the galvanometer during the discharge.

In all these experiments the pressure of the low pressure side of the small holes was about 1/80th of that on the high pressure side.

DISCUSSION

It should be noted that all values obtained from experiments where the pressure was below 0.3 of a mm are higher and not as consistent as the values obtained from those experiments conducted at higher pressures. Fig. 3 is a plot of all values of Table I in kilocalories as abscissas against pressure

TABLE II.

Author	Source	Value cal/gr mol.wt.
Warburg ⁸	Photochemical formation of O ₃	138,000
Born and Gerloch ⁹	" " "	162,000
Eucken ¹⁰	Heat of formation of CO	253,000-423,000
Wulf ^{11,12}	Ionization potentials	56,000-138,000
Hogness and Lunn ¹³	Ionization potentials of O ₂	150,000
Birge and Sponer ¹⁴	Absorption bands of O ₂	162,000
Birge ^{15,16,17,18}	" " "	138,000
Herzberg ¹⁹	" " "	149,500
Kassel ^{20,21}	Decomposition of O ₃	110,000
Mecke ^{22,23,24}	Predissociation in NO ₂ bands	128,000
Henri ²⁵	Predissociation in SO ₂ bands	126,400
Kaplan ²⁶	Birge's paper	131,000
Kondratjew ²⁷	Predissociation in NO ₂ bands	118,000
Rodebush and Troxel ²⁸	Direct calorimeter measurement	131,000
Baxter ²⁹	Predissociation bands of NO ₂	115,000
Average value of nine high pressure runs of this paper		131,300

⁷ Copeland, J.A.C.S. 52, 2580 (1930).

⁸ Warburg, Zeits. f. Electrochemie 26, 58 (1920).

⁹ Born and Gerloch, Zeits. f. Physik 5, 433 (1921).

¹⁰ Eucken, Ann. d. Chemie 440, 111 (1924).

¹¹ Wulf, J.A.C.S. 47, 1944 (1925).

¹² Wulf, Proc. Nat. Acad. Sci. 14, 615 (1928).

¹³ Hogness and Lunn, Phys. Rev. 27, 733 (1926).

¹⁴ Birge and Sponer, Phys. Rev. 28, 259 (1926).

¹⁵ Birge, Phys. Rev. 27, 641 (1926).

¹⁶ Birge, Nature 122, 842 (1928).

¹⁷ Birge, Phys. Rev. 34, 1062 (1929).

¹⁸ Birge, Trans. Faraday Soc. (1929).

¹⁹ Herzberg, Zeits. f. Phys. Chemie 4B, 223 (1929).

²⁰ Kassel, Phys. Rev. 34, 817 (1929).

²¹ Kassel, Zeits. f. Phys. Chemie 2B, 264 (1929).

²² Mecke, Naturwissenschaften 51, 996 (1929).

in millimeters of mercury as ordinates. In a former note⁷ the value obtained at low pressures was presented. Since that time the last eleven experiments given here have been made. Since the high pressure values are consistent among themselves within the experimental limits of accuracy over a range of pressure from 0.35 mm of mercury to 0.56 mm of mercury, the average of these results is taken as the correct value. It is quite possible that the high values at low pressures are due to excess energy from metastable oxygen atoms which would have a longer life at lower pressures due to the fewer number of collisions. It was on this assumption that the high pressure measurements were made. Further confirmation of this point was sought by making a few runs with the discharge bulb moved 42 cm away from the calorimeter. Under these conditions it would be expected that there will be a decrease in the percentage of the atoms in the metastable state, by the time they reached the calorimeter. Also there will be a decrease in the total number of atoms. Unfortunately experiments made with longer paths have not proved to be sufficiently reliable to draw any conclusions.

Table II gives the reported values of the heat of formation of molecular oxygen and the experimental source from which the computation was made.

All values of experiments made at pressures above 0.3 mm of mercury agree within 6,000 calories of their average which is therefore taken as the experimental error.

It is of considerable interest that the preliminary report of Rodebush and Troxel is also from a direct calorimetric determination which differs but slightly from the method reported here. The agreement of our results is of more significance because of the differences in the method which include a fundamentally different application of Knudsen's formula for the measurement of the percent of dissociation. This result agrees also with that of Kaplan's and within the experimental limits with those of Mecke and Henri.

For a discussion of the theoretical assumptions involved in this method the reader is referred to the paper of Bichowsky and Copeland.³ In addition to what is stated there concerning the validity of the use of Knudsen's formula it should be mentioned that in this work it was found that the ratio of the rate of flow of oxygen to the pressure was a constant for each set of orifices over the range of pressures used.

The author wishes to acknowledge his indebtedness to Dr. F. R. Bichowsky who first suggested this problem and the method used. He also wishes to acknowledge the valuable assistance received from Mr. Foster Rieke including the final perfection of the method of making the sets of orifices. He

²³ Mecke, *Nature* **125**, 526 (1930).

²⁴ Mecke, *Zeits. f. Phys. Chemie* **7B**, 108 (1930).

²⁵ Henri, *Nature* **125**, 275 (1930).

²⁶ Kaplan, *Phys. Rev.* **35**, 436 (1930).

²⁷ Kondratjew, *Zeits. f. Phys. Chemie* **7B**, 70 (1930).

²⁸ Rodebush and Troxel, *J.A.C.S.* **52**, 3467 (1930).

²⁹ Baxter, *J.A.C.S.* **52**, 3468 (1930).

is indebted to Professor L. C. Graton for the microphotographs. In conclusion he also wishes to thank Professor E. C. Kemble and the other members of the Physics Department of Harvard University for their valuable assistance in the direction of the activities of his fellowship.

THE DIELECTRIC CONSTANT OF HELIUM

BY J. V. ATANASOFF

DEPARTMENT OF PHYSICS, UNIVERSITY OF WISCONSIN

(Received August 11, 1930)

ABSTRACT

The most successful study of unperturbed helium in its normal state has been made by Hylleraas, using the Ritz method. The Schrödinger partial differential equation is reduced to an equivalent problem in the calculus of variations and this problem is then solved by a so-called direct method.

In the present paper an extension is developed to the Ritz method, forming a theory which is applicable to perturbation problems. This theory is applied to a study of the normal helium atom under the influence of an electric field. As in the usual perturbation theory, the characteristic energy parameter E and the characteristic function ψ are assumed developable in power series in the field strength F , but now the coefficients in these expansions are given in terms of problems in the calculus of variations. The work of Hylleraas furnishes a knowledge of the terms in both expansions independent of the field strength. Then the minimization of a single integral furnishes values of ψ_1 and E_2 , the subscript of each denoting the power of F for which it forms the coefficient. Values of these coefficients are calculated to three approximations by the direct method. From E_2 we may calculate the dielectric constant in the usual way giving

$$\epsilon = 1.0000665,$$

a value 5 percent below the accepted value of $\epsilon = 1.000070$. One should note that it is a characteristic of the Ritz method that further approximations can only increase the value of ϵ , bringing it into better agreement with the experimental value.

THE value of the dielectric constant of an atom depends on the manner in which the normal energy levels are affected by a perturbing electric field. Unperturbed helium in the normal state has been most successfully studied, with the so-called Ritz method, by Kellner¹ and later by Hylleraas in two papers which we shall refer to as Hyl. I² and Hyl. II.³ The work of Hylleraas in his second paper possesses the great advantages of simplicity and of rapidity of convergence. These advantages seem to be founded in his exclusive use of distances rather than angles as variables. In the present paper we shall employ his results for that description of unperturbed normal helium which forms the starting point for our perturbation calculation.

A. THE RITZ METHOD AND PERTURBATION THEORY

§1. *The Ritz method and the characteristic value problem.* The ordinary way to solve a problem in the calculus of variations is to set up the corresponding Euler differential equations and find the solution which fits the boundary conditions. Under certain restrictions it is possible to reverse this procedure; i.e.,

¹ G. W. Kellner, *Zeits. f. Physik* **44**, 91, (1927).

² E. A. Hylleraas, *Zeits f. Physik* **48**, 469, (1928).

³ E. A. Hylleraas, *Zeits. f. Physik* **54**, (5, 6) 347 (1929).

given a differential equation, it is possible to find the corresponding problem in the calculus of variations. If then this variation problem can be solved by one of the so-called direct methods, which do not make use of Euler equations, we have a possible method for the solution of the differential equation.

The direct method of Ritz⁴ consists in starting with an independent and complete (but not necessarily orthogonal) system of given functions

$$\phi_1, \phi_2, \phi_3, \phi_4 \dots$$

each exactly satisfying the boundary conditions in the domain being studied. In the integral

$$I = \int F\left(x, y, \dots, \psi, \dots, \frac{\partial \psi}{\partial x}, \frac{\partial \psi}{\partial y}, \dots\right) dx dy \dots$$

to be minimized, one substitutes $\psi_n = \sum_1^n a_i \phi_i$, the a 's being undetermined coefficients. The resulting integral, which we may call I_n , becomes a function of the a 's and its minimization becomes an ordinary minimum problem. The a 's are then determined by the relations $\partial I_n / \partial a_i = 0, i = 1, 2, \dots, n$. Then n is increased, and under ordinary conditions the sequence ψ_n approaches the solution ψ to the problem, while the corresponding sequence I_n approaches the minimum value of the given integral. One may, on physical grounds, be able to choose the initial terms of the functional sequence ϕ_i so they are near the real solution, thus securing rapid convergence.

Now the self-adjoint equation⁵

$$L[\phi] = (a\phi_x)_x + (b\phi_x)_y + (b\phi_y)_x + (c\phi_y)_y + d_x\phi + e_y\phi - f\phi = 0, \quad (1)$$

in which ϕ, a, b, \dots, f are functions of x, y , is the most general homogeneous linear second order partial differential equation which is the Euler equation for a problem in the calculus of variations. In fact, if we consider solutions which are single valued, continuous and which vanish at the boundary Γ of a closed region G , then (1) is the Euler equation for a problem

$$\iint_G Q[\phi, \psi] dx dy = \min. \quad (2)$$

in which

$$Q[\phi\psi] = a\phi_x\psi_x + b\phi_x\psi_y + d\phi_y\psi_x + c\phi_y\psi_y + b\phi_x\psi + d\psi_x\phi + e\phi_y\psi + e\psi_y\phi + f\phi\psi.$$

Under the above conditions the extended Green formula becomes

$$\begin{aligned} \iint_G Q[\phi, \psi] &= - \iint_G \phi L[\psi] dx dy, \\ &= - \iint_G \psi L[\phi] dx dy; \end{aligned} \quad (3)$$

⁴ W. Ritz, J. reine angew. Math. 135, 1-61. Collected works, pp. 192-250. Paris, 1911.

⁵ The discussion of this paragraph is restricted for simplicity to the case of two independent variables. This restriction is not essential and the generalization is immediate.

for the usual integrations over Γ vanish.

The above statements assume that (2) actually possesses an extreme other than the trivial value zero. However, the homogeneous unconstrained problem does not possess such a minimum. Consider, however, the constrained problem

$$\int_G Q[\phi, \phi] d\tau = \min., \quad (4)$$

subject to the condition

$$\int_G \rho \phi^2 d\tau = 1, \quad (5)$$

where $d\tau$ is an element of coordinate space and ρ is a given function of the coordinates. By the ordinary methods of the calculus of variations the Euler equation in this case is

$$L[\phi] + e\rho\phi = 0. \quad (6)$$

When the integral (4) is minimized subject to (5), ϕ satisfies (6). Then by (3), (6) and (5) in turn,

$$\int Q[\phi, \phi] d\tau = - \int \phi L[\phi] = e \int \rho \phi^2 d\tau = e, \quad (7)$$

so that the extreme values of the integral are the characteristic values of (6).⁶

§2. *Extension to include perturbation effects.* Next we extend the above methods to enable us to investigate the effect upon the characteristic value e and the characteristic function ϕ of a small parameter f in L . Suppose

$$\begin{aligned} L[\phi] &= L_0[\phi] + fL_1[\phi] \\ \phi &= \phi_0 + f\phi_1 + f^2\phi_2 + \cdots \\ e &= e_0 + fe_1 + f^2e_2 + \cdots \end{aligned} \quad (8)$$

Then

$$O[\phi, \phi] = Q_0[\phi, \phi] + fQ_1[\phi, \phi].$$

Substitute (8) in (4) and (5) and collect powers of f . The zeroth order term furnishes⁷

$$- \int \phi_0 L_0[\phi_0] d\tau = \int Q_0[\phi_0, \phi_0] d\tau = \min. = e_0, \quad (9)$$

subject to

$$\int \rho \phi_0^2 d\tau = 1; \quad (10)$$

⁶ For the material of this section, see Courant und Hilbert, *Methoden der mathematischen Physik*, Berlin, 1924.

⁷ The minimum problem changes to a maximum problem because of the negative sign in Green's formula.

while from (6), ϕ_0 satisfies the Euler equation

$$L_0[\phi_0] + e_0\rho\phi_0 = 0. \quad (11)$$

The first order term furnishes

$$- \int (\phi_1 L_0[\phi_0] + \phi_0 L_0[\phi_1] + \phi_0 L_1[\phi_0]) d\tau = \min = e_1, \quad (9')$$

subject to

$$2 \int \rho \phi_0 \phi_1 d\tau = 0. \quad (10')$$

Equation (9') reduces by (3), (11), and (10') to

$$- \int \phi_0 L_1[\phi_0] d\tau = \int Q_1[\phi_0 \phi_0] d\tau = e_1; \quad (12')$$

for since ϕ_0 is fixed by (9), there is no variation.

The quadratic terms in the parameter f furnish

$$\begin{aligned} - \int (\phi_2 L_0[\phi_0] + \phi_1 L_0[\phi_1] + \phi_0 L_0[\phi_2] + \phi_1 L_1[\phi_0] + \phi_0 L_1[\phi_1]) d\tau \\ = \min = e_2, \end{aligned} \quad (9'')$$

subject to

$$\int \rho(\phi_1^2 + 2\phi_0\phi_2) d\tau = 0; \quad (10'')$$

and 9'' becomes by (3), (11), and (10''),

$$\begin{aligned} - \int (e_0\rho\phi_1^2 + \phi_1 L_0[\phi_1] + 2\phi_1 L_1[\phi_0]) d\tau, \\ = \int (Q_0[\phi_1\phi_1] + 2Q_1[\phi_1\phi_0] - e_0\rho\phi_1^2) d\tau = \min = e_2. \end{aligned} \quad (12'')$$

Hence we see that by solving (9) subject to the constraint (10) and then (12'') subject to (10'), one obtains e_0 , ϕ_0 , e_2 and ϕ_1 , while e_1 is directly obtained from the integral (12').

B. PRELIMINARIES TO CALCULATION

Units and the Schrödinger equation. If one uses a unit of length $a_H/2Z = \hbar^2/8\pi^2 mZe'^2$, a unit of energy $Z^2 R\hbar$ and a unit of charge e' , the field θ will, following its customary definition, be measured in terms of the unit $16\pi^4 m^2 Z^3 e'^5/\hbar^4$. Then the wave equation for a helium atom in an electric field is

$$(\Delta_1 + \Delta_2)\psi + \left(\frac{\lambda}{4} + \frac{1}{r_1} + \frac{1}{r_2} - \frac{1}{2r_{12}} + \frac{\theta}{4}(z_1 + z_2) \right) \psi = 0$$

Here λ is the energy parameter; $r_1, r_2, r_{12}, z_1, z_2$ are distances of the electrons from the nucleus, distance between the electrons, and z coordinates of the electron measured parallel to the field. For further simplicity we make the substitutions $\lambda/4=e$ and $\theta/4=f$ which reduce the Schrödinger equation to

$$(\Delta_1 + \Delta_2)\psi + (e + 1/r_1 + 1/r_2 - 1/2r_{12} + f(z_1 + z_2))\psi = 0$$

Let E be the energy of an atom when placed in an electric field F . Then the expansion

$$E = E_0 + E_1F + E_2F^2 + E_3F^3 + \dots$$

is useful in the discussion of the dielectric properties of the atom. This equation may be thought of as being written in ordinary units, while in the special units here employed,

$$e = e_0 + e_1f + e_2f^2 + \dots$$

If the units of this equation are to be consistent we must have e_2 measured in a unit $h^6/512\pi^6m^3z^4e'^6$ times as large as the unit of E_2 .

The dielectric constant. If ϵ is the dielectric constant and N is the number of molecules per unit volume at the temperature and pressure at which ϵ is measured, it is true that

$$\epsilon - 1 = -8\pi NE_2,$$

or

$$\epsilon - 1 = - \frac{e_2 h^6 N}{64\pi^5 z^4 e'^6 m^3}$$

in the units here employed. An experimental value⁹ for $\epsilon - 1$ is 0.000070 and this requires e_2 to be -88 (at 0°C and 760 mm of Hg).

Coordinates to be used. Hylleraas (II) has shown the great advantage of using the distances which occur in the potential terms as coordinates. For unperturbed helium he used as coordinates the distances r_1, r_2, r_{12} , the three angles which might be added to these distances to make a complete set of coordinates being ignorable. In our case we may use as coordinates $r_1, r_2, r_{12}, z_1, z_2$, the one other azimuthal coordinate being ignorable because of the symmetry of the problem.

Six dimensional Laplace operator in coordinates $r_1, r_2, r_{12}, z_1, z_2$. Suppose $\psi = \psi(r_1, r_2, r_{12}, z_1, z_2)$, in which

$$\begin{aligned} r_1^2 &= x_1^2 + y_1^2 + z_1^2, & r_2^2 &= x_2^2 + y_2^2 + z_2^2, \\ r_{12}^2 &= (x_1 - x_2)^2 + (y_1 - y_2)^2 + (z_1 - z_2)^2, \\ z_1 &= z_1, & z_2 &= z_2. \end{aligned}$$

Then $(\Delta_1 + \Delta_2)\psi =$

$$\frac{\partial^2 \psi}{\partial r_1^2} + \frac{2}{r_1} \frac{\partial \psi}{\partial r_1} + \frac{\partial^2 \psi}{\partial r_2^2} + \frac{2}{r_2} \frac{\partial \psi}{\partial r_2} + 2 \frac{\partial^2 \psi}{\partial r_{12}^2} + \frac{4}{r_{12}} \frac{\partial \psi}{\partial r_{12}}$$

⁸ J. H. Van Vleck, Proc. Nat. Acad. 12, 663 (1926).

⁹ Herzfeld and Wolf, Ann. d. Physik 76, 71 and 567, find $\epsilon - 1 = 0.0000693$ from extrapolation of optical data. Direct measurement usually gives results somewhat higher. C. P. Hochheim, Verh. D. Phys. Ges. 10, 446 (1908): $\epsilon - 1 = 0.000074$.

$$\begin{aligned}
& + \frac{r_1^2 - r_2^2 + r_{12}^2}{r_1 r_{12}} \frac{\partial^2 \psi}{\partial r_1 \partial r_{12}} + \frac{r_2^2 - r_1^2 + r_{12}^2}{r_2 r_{12}} \frac{\partial^2 \psi}{\partial r_2 \partial r_{12}} + \frac{2z_1}{r_1} \frac{\partial^2 \psi}{\partial r_1 \partial z_1} \\
& + \frac{2(z_1 - z_2)}{r_{12}} \frac{\partial^2 \psi}{\partial r_{12} \partial z_1} + \frac{2z_2}{r_2} \frac{\partial^2 \psi}{\partial r_2 \partial z_2} + \frac{2(z_2 - z_1)}{r_{12}} \frac{\partial^2 \psi}{\partial r_{12} \partial z_2} \\
& + \frac{\partial^2 \psi}{\partial z_1^2} + \frac{\partial^2 \psi}{\partial z_2^2}.
\end{aligned}$$

Jacobian. The differential expression just written is not self-adjoint. We can make it so by multiplication by the Jacobian of the transformation from rectangular coordinates to the coordinates $r_1, r_2, r_{12}, z_1, z_2, \chi$ in which χ is some angle that has been added to make the coordinate system complete. If one computes this Jacobian and then eliminates the ignorable coordinate χ by integration over it, the result is, aside from trivial constant factors,

$$\rho = \frac{r_{12} r_1 r_2}{q^{1/2}},$$

in which

$$\begin{aligned}
-q = & 4r_1^2 z_2^2 + (4r_{12}^2 - 4r_1^2 - 4r_2^2) z_1 z_2 + 4r_2^2 z_1^2 \\
& + r_{12}^4 - 2r_{12}^2 r_1^2 + r_1^4 - 2r_{12}^2 r_2^2 - 2r_1^2 r_2^2 + r_2^4.
\end{aligned}$$

To simplify connection with Hylleraas II on which we shall depend for the unperturbed characteristic functions, we make the further change of the variable

$$\begin{aligned}
s &= r_1 + r_2, \\
t &= -r_1 + r_2, \\
u &= r_{12}.
\end{aligned}$$

The Jacobian of this last transformation is a constant so that the Jacobian weight factor of the combined transformation is essentially

$$\sigma = \frac{(s^2 - t^2)u}{q^{1/2}},$$

in which

$$\begin{aligned}
-q = & (s - t)^2 z_2^2 + (4u^2 - 2s^2 - 2t^2) z_1 z_2 + (s + t)^2 z_1^2 \\
& + u^4 - u^2(s^2 + t^2) + s^2 t^2.
\end{aligned}$$

We omit the differential expressions for $(\Delta_1 + \Delta_2)\psi$ in the coordinates s, t, u, z_1, z_2 , but give rather the formulation of the problem in the calculus of variations

$$\begin{aligned}
Q_0[\psi, \psi] &= P[\psi, \psi] - \sigma \left(\frac{2}{s - t} + \frac{2}{s + t} - \frac{1}{2u} \right) \psi^2, \\
Q_1[\phi, \psi] &= -\sigma(z_1 + z_2)\phi\psi,
\end{aligned}$$

in which

$$\begin{aligned}
 P[\psi, \psi] &= 2\sigma\psi_s^2 + 2\sigma\psi_t^2 + 2\sigma\psi_u^2 \\
 &+ 4\sigma \left\{ \frac{s(u^2 - t^2)}{u(s^2 - t^2)} \psi_s + \frac{t(s^2 - u^2)}{u(s^2 - t^2)} \psi_t \right\} \psi_u \\
 &+ 4\sigma \frac{z_1}{s-t} (\psi_s - \psi_t) \psi_{z_1} + 2\sigma \frac{z_1 - z_2}{u} \psi_u \psi_{z_1} \\
 &+ 4\sigma \frac{z_2}{s+t} (\psi_s + \psi_t) \psi_{z_2} + 2\sigma \frac{z_2 - z_1}{u} \psi_u \psi_{z_2} + \sigma\psi_{z_1}^2 + \sigma\psi_{z_2}^2.
 \end{aligned}$$

Limits of integration. If $d\tau$ is an element of coordinate space, i.e., if $d\tau = ds dt du dz_1 dz_2$, then

$$\int d\tau = \int_0^\infty ds \int_0^s du \int_0^u dt \int_{-(s-t)/2}^{(s-t)/2} dz_1 \int_A^B dz_2,$$

where A and B are roots of $q=0$. These limits only cover part of space in which $r_2 > r_1$. Now in the normal state the wave function is symmetrical in the two electrons and so the limits just written produce one-half of the total integral. This factor of one-half is, however, easily compensated for by using the same limits in the normalization.

The integrals involved. The fact that the limits A and B are zeros of q or infinities of σ is of importance in performing the integrations over the z coordinates. A and B are clearly branch points of the integrand. In general, they will be the only singular points in the finite z_2 plane. So one easily finds by integration in the complex plane

$$\begin{aligned}
 \int_{-(s-t)/2}^{(s-t)/2} \int_A^B \sigma z_1^2 dz_1 dz_2 &= \frac{\pi}{12} u(s-t)^3 (s+t) \\
 \int_{-(s-t)/2}^{(s-t)/2} \sigma z_1 z_2 dz_1 dz_2 &= \frac{\pi}{12} u(s^2 - t^2)(s^2 + t^2 - 2u^2) \\
 \int_{-(s-t)/2}^{(s-t)/2} \int_A^B \sigma z_2^2 dz_1 dz_2 &= \frac{\pi}{12} u(s+t)^3 (s-t) \\
 \int_{-(s-t)/2}^{(s+t)/2} \int_A^B \sigma dz_1 dz_2 &= \pi u(s^2 - t^2).
 \end{aligned}$$

The last result should be the weight factor when there are no z coordinates. Hylleraas II gives the weight factor

$$\frac{u(s^2 - t^2)}{8}$$

for this case, showing that his normalization differs from ours by a factor 8π .

The other integrals that we shall need to evaluate are all of the form

$$\int_0^\infty ds \int_0^s du \int_0^u dt e^{-as} s^p t^q u^r = \frac{1}{a^{p+q+r+3}} \frac{(p+q+r+2)!}{(q+1)(r+q+2)}.$$

C. ACTUAL CALCULATION OF DIELECTRIC CONSTANT

We are now prepared to carry out the actual minimization of

$$I = \int \{Q_0[\psi_1, \psi_1] + 2Q_1[\psi_1, \psi_0] - e_0 \sigma \psi_1^2\} d\tau = \min = e_2, \quad (1)$$

when ψ_0 is given, subject to

$$\int \sigma \psi_0 \psi_1 d\tau = 0. \quad (2)$$

The function ψ_1 must, of course, satisfy all the conditions imposed on any solution of the Schrödinger equation. But, in addition, it must be symmetrical in the coordinates of the two electrons for it forms part of the wave function for a par-helium state. This requires, since $s=r_1+r_2$ and $t=-r_1+r_2$ that $\psi_1(s, t, u, z_1, z_2) = \psi_1(s, -t, u, z_2, z_1)$. The actual choosing of the functional form will depend on physical knowledge and experience with previous trials. For the form of Q_0 and Q_1 , see page 1237.

First approximation. It is easily shown when this same method is applied to hydrogen that a very simple wave function of the form

$$\psi_1 = \alpha_1 e^{-r/2z}$$

gives results for $-e_2$ that are only 11% low. By ideas which will be given later we easily generalize this to apply to helium thus obtaining¹⁰

$$\psi_1 = \alpha_1 e^{-c_1 s/2} (z_1 + z_2). \quad (3)$$

If one substitutes this in the expression (1) to be minimized and uses as ψ_0

$$\begin{aligned} \psi_0 &= e^{-c_1 s/2} (1 + c_2 u + c_3 t^2), \\ c_1 &= 0.908, \\ c_2 &= 0.0726, \\ c_3 &= 0.0083; \end{aligned} \quad (4)$$

(one of the results of Hylleraas II which gives the normal energy level to within 1/30%) one obtains on integration

$$I = \frac{\pi}{6c_1^6} \{391.1\alpha_1^2 - 5787\alpha_1\} = \min.$$

Now α_1 for a minimum is 7.40, so that

¹⁰ Professor Van Vleck has suggested that the most general form of ψ_1 is $\psi_1 = z_1 f(s, t, u) + z_2 f(s, -t, u)$. It is easily seen that this form satisfies the non-homogeneous wave equation for the perturbing function.

$$I = \frac{\pi}{c_1^6}(-3,568).$$

But ψ_0 is not normalized. We divide I by the normalization factor¹¹

$$\frac{\pi}{c_1^6}65.587,$$

and then find

$$-e_2 = 54.4$$

a value 37 percent low as compared with the accepted value $-e_2 = 88$ (page 1236).

Second approximation. We know that for normal hydrogen in our coordinates

$$\begin{aligned}\psi_0 &= \frac{1}{2}e^{-r/2}, \\ \psi_1 &= \frac{1}{4}z(r-4)e^{-r/2},\end{aligned}$$

and consequently to a second approximation

$$\psi = \psi_0 + f\psi_1 = e^{-r/2} \left\{ \frac{1}{2} + f \frac{z}{4}(r-4) \right\}.$$

If one neglects interactions between the electrons in a helium atom, the Schrödinger equation becomes separable and the true wave function for the perturbed problems becomes

$$\psi = e^{-r_1/2-r_2/2} \left\{ \frac{1}{2} + f \frac{z_1}{4}(r_1+4) \right\} \left\{ \frac{1}{2} + f \frac{z_2}{4}(r_2+4) \right\}.$$

Thus

$$\psi_1 = e^{-s/2} \left\{ z_1 \left(\frac{r_1}{8} + \frac{1}{2} \right) + z_2 \left(\frac{r_2}{8} + \frac{1}{2} \right) \right\},$$

for ψ_1 is the coefficient of f in the power development of ψ . It is natural to generalize this into¹¹

$$\psi_1 = e^{-c_1 s/2} \{ z_1(\alpha_1 + \alpha_2 s - \alpha_3 t) + z_2(\alpha_1 + \alpha_2 s + \alpha_3 t) \} \quad (5)$$

in which α_1, α_2 , and α_3 are unknown constants. We choose for c_1 the value that Hylleraas used in formula (4) (i.e., $c_1 = 0.908$). One notices that this function remains unchanged by interchanging the electrons, and that it is orthogonal to the ψ_0 given in (4), i.e.,

$$\int \sigma \psi_0 \psi_1 d\tau = 0.$$

We substitute this expression (5) in the integral (1) to be minimized using (4) as ψ_0 , and obtain after carrying out the integrations

¹¹ The normalization factors are most easily obtained by multiplication of Hylleraas' factors by 8π due to difference in normalization and division by c_1^6 to take care of his change in scale.

$$I = \frac{\pi}{c_1^6} (65.2\alpha_1^2 + 485.8 \times 2\alpha_1\alpha_2 + 4770 \times \alpha_2^2 + 38 \times 2\alpha_1\alpha_3 \\ + 303 \times 2\alpha_1\alpha_3 + 979 \times \alpha_3^2 \\ - 479 \times 2\alpha_1 - 4447 \times 2\alpha_2 - 1287 \times 2\alpha_3) = \min.$$

To find the minimum, we solve the linear equations

$$\frac{\partial I}{\partial \alpha_1} = 0$$

$$\frac{\partial I}{\partial \alpha_2} = 0$$

$$\frac{\partial I}{\partial \alpha_3} = 0$$

and obtain

$$\alpha_1 = 1.87, \quad \alpha_2 = 0.673, \quad \alpha_3 = 1.03.$$

On substitution of these values in the quadratic expression we find

$$I = 5091 \frac{\pi}{c_1^6}.$$

So $-e_2 = \frac{5091(\pi/c_1^6)}{65.59(\pi/c_1^6)} = 78$. This is 11 percent below the experimental value of $-e_2 = 88$.

Third approximation. We now extend the function ψ_1 by the addition of a term in u ; $\alpha_1, \alpha_2, \alpha_3, \alpha_4$ being new unknown constants

$$\psi_1 = e^{-c_1 s/2} \{ (\alpha_1 + \alpha_2 s - \alpha_3 t + \alpha_4 u) z_1 \\ + (\alpha_1 + \alpha_2 s + \alpha_3 t + \alpha_4 u) z_2 \}.$$

It now seems worth while to employ for ψ_0 the final and best result Hylleraas obtained in his second paper. This is

$$\psi_0 = e^{-c_1 s/2} (1 + c_2 u + c_3 t^2 + c_4 s + c_5 s^2 + c_6 u^2), \\ c_1 = 0.9100, \\ c_2 = 0.0885, \\ c_3 = 0.0080, \\ c_4 = -0.0252, \\ c_5 = 0.0021, \\ c_6 = -0.0020. \quad (7)$$

This wave function is sufficiently accurate to give the normal energy level of helium to within 0.01 percent of its experimental value.

On substitution of these expressions and integrating, the following quadratic expression is obtained

$$I = \frac{\pi}{c_1^6} [65.14\alpha_1^2 + 483.39 \times 2\alpha_1\alpha_2 + 4716.1\alpha_2^2 \\ + 37.59 \times 2\alpha_1\alpha_3 + 292.7 \times 2\alpha_2\alpha_3 + 974.3\alpha_3^2 + 269.58 \times 2\alpha_1\alpha_4 \\ + 2598.3 \times 2\alpha_2\alpha_4 + 499.3 \times 2\alpha_3\alpha_4 + 1922.5\alpha_4^2 \\ - 465.46 \times 2\alpha_1 - 4336.4 \times 2\alpha_2 - 1240.6\alpha_3 \\ - 2960.1 \times 2\alpha_4] = \min.$$

Minimizing as before yields

$$\alpha_1 = 0.825, \alpha_2 = 0.456, \alpha_3 = 0.815, \alpha_4 = 0.596$$

$$I = \frac{\pi}{c_1^6} (-5124).$$

The normalization factor is now

$$\frac{\pi}{c_1^6} 61.496.$$

This yields $-e_2 = 83.4$ which is less than 5 percent below the experimental value of $-e_2 = 88$.

It remains the author's pleasant duty to express his appreciation to Professor J. H. Van Vleck, to Professor G. Wentzel, and to Professor Warren Weaver for much helpful advice given throughout the preparation of this paper.

Note added in proof. The quantity e_2 is given by equation C(1) as the minimum value of an integral with respect to the variations of an unknown (and thus determined) function ψ_1 , the function ψ_0 being assumed known. Prof. J. H. Van Vleck has kindly suggested that one should emphasize the following consequence of this: That first order errors in ψ_1 will only produce second order errors in e_2 but that on the contrary first order errors in ψ_0 will likely produce first order errors in e_2 . This shows mathematically the importance of an accurate knowledge of the unperturbed state in the calculation of the dielectric constant.

THE POTENTIAL AND POTENTIAL ENERGY OF SPACE LATTICES

By C. N. WALL

NORTH CENTRAL COLLEGE, NAPERVILLE, ILLINOIS

(Received July 24, 1930)

ABSTRACT

The electrostatic potential of a general space lattice is developed. The space lattice is characterized by a base cell containing a finite set of positive point charges arbitrary in strength and position, and a negative space charge of arbitrary density, subject to the condition that the total charge in the cell is zero.

Next the expression for the lattice energy is obtained in the form of a triply infinite series. It is shown that the coefficients in this series representing the distribution of the negative space charge can be identified with the structure factors of the lattice or crystal provided we replace the negative space charge by a corresponding electron distribution.

An application of this theory is made to the three halides NaCl, NaF, and LiF. The lattice energy of each crystal is calculated for different grating spaces. In all three cases it is shown that the lattice energy has a minimum in the neighborhood of the accepted grating space for the crystal under consideration. The agreement is better for NaCl than for NaF or LiF.

THE ELECTROSTATIC POTENTIAL

THE electrostatic potential of an infinite space lattice with an arbitrary distribution of point charges in the base cell can be determined by a method due to Ewald.¹ This method consists in considering a continuous periodic distribution of charges the density of which can be represented by a triple Fourier series without a constant term.² The potential of such a system can be represented by a similar Fourier series whose coefficients can be determined by the use of Poisson's equation. Finally one arrives at the required result by taking the limiting case in which the continuous space charge shrinks into a discrete set of point charges. If, in this process, we allow the positive space charge to shrink into point charges but keep the negative charge as a continuous distribution of electricity, we obtain a space lattice with cells consisting of a set of positive point charges (nuclei) surrounded by an atmosphere of negative electricity which may be identified with the electron distribution under certain conditions. It is the potential and potential energy of such a space lattice which we wish to determine.

Let us consider the base cell of our lattice to be defined by the three vectors a^1, a^2, a^3 . Our lattice can be built up by a simple translation of this base cell in three space directions defined by a^1, a^2, a^3 . The lattice shall be referred to the rectangular axes x_1, x_2, x_3 whose origin shall be at a vertex

¹ P. P. Ewald, *Ann. d. Physik* **64**, 253 (1921).

M. Born, *Problems of Atomic Dynamics*, 158-162 (1926).

² The lack of a constant term in the series means that the total charge in any cell of the lattice is zero.

of the base cell. The rectangular components of the three base vectors shall be designated by a_i^m ; $m, i=1, 2, 3$. a_i^m is the x_i th component of the a^m th vector. The volume of the base cell shall be $\Delta = |a_i^m|$. We introduce the three vectors of the reciprocal lattice b^1, b^2, b^3 with their components b_j^n defined by the equations

$$\sum_{i=1}^3 a_i^m b_i^n = \begin{cases} 0 & \text{if } n \neq m \\ 1 & \text{if } n = m \end{cases}; \quad m, n = 1, 2, 3.$$

Let there be p positive point charges in the base cell, the k th charge having a strength e_k and coordinates x_i^k . The negative space charge shall have a density distribution of $\rho(x_1, x_2, x_3)$ in the base cell. We impose the condition that

$$\sum_{k=1}^p e_k + \iiint \rho dx_1 dx_2 dx_3 = 0$$

where the integral is taken throughout the entire base cell. This condition is equivalent to the statement that the total charge in the base cell, and therefore in any cell, is zero.

With this brief description of the lattice under consideration, we write down at once the potential of this lattice as given by Ewald's method.

$$V = \frac{1}{\pi\Delta} \sum'_{l_1, l_2, l_3 = -\infty}^{\infty} \left\{ \frac{A_{l_1 l_2 l_3} + B_{l_1 l_2 l_3}}{\sum_{j=1}^3 \left(\sum_{n=1}^3 l_n b_j^n \right)^2} \right\} \exp \left(i2\pi \sum_{j,n=1}^3 l_n b_j^n x_j \right) \quad (1)$$

where the coefficients $A_{l_1 l_2 l_3}$ and $B_{l_1 l_2 l_3}$ are given by the equations

$$\left\{ \begin{aligned} A_{l_1 l_2 l_3} &= \sum_{k=1}^p e_k \exp \left(-i2\pi \sum_{j,n=1}^3 l_n b_j^n x_j^k \right) \\ B_{l_1 l_2 l_3} &= \iiint \rho(\xi_1, \xi_2, \xi_3) \exp \left(-i2\pi \sum_{j,n=1}^3 l_n b_j^n \xi_j \right) d\xi_1 d\xi_2 d\xi_3 \end{aligned} \right\} \quad (2)$$

the integration to be taken throughout the base cell. The coefficients $A_{l_1 l_2 l_3}$ are functions of the positions and the strengths of the positive point charges, and the coefficients $B_{l_1 l_2 l_3}$ are functions of the distribution of the negative space charge. The total potential V is obviously the sum of the separate potentials of the positive and the negative charges, but the above series written with all of the $B_{l_1 l_2 l_3}$ coefficients omitted does not represent the potential of the positive charges alone. Rather it gives the potential of the positive charges imbedded in a negative space charge of uniform density such that the total charge in any cell is zero. It is seen by Eqs. (2) that for $\rho = \text{constant}$, $B_{l_1 l_2 l_3} = 0$ except for $l_1 = l_2 = l_3 = 0$, and this term is omitted in the series in Eq. (1) as indicated by the prime on the summation sign.

THE POTENTIAL ENERGY

Having calculated the potential of the space lattice under consideration we turn to the problem of determining the potential energy of the lattice,

or rather the potential energy of a single cell of the lattice. For this calculation we make use of Green's theorem which may be written in the form

$$\begin{aligned} & \iiint V \nabla^2 V dx_1 dx_2 dx_3 \\ & + \iiint [(\partial V / \partial x_1)^2 + (\partial V / \partial x_2)^2 + (\partial V / \partial x_3)^2] dx_1 dx_2 dx_3 \\ & + \sum \iint V (\partial V / \partial n) dS = 0 \end{aligned}$$

where the symbols have their customary significance.

The potential energy of the base cell will be given by the expression

$$(1/8\pi) \iiint [(\partial V / \partial x_1)^2 + (\partial V / \partial x_2)^2 + (\partial V / \partial x_3)^2] dx_1 dx_2 dx_3$$

where the integration is taken throughout the base cell. However this expression will give an infinite energy because of the presence of positive point charges in the cell of infinite self-energy. We can overcome this difficulty by deleting each of the positive charges with a small sphere of radius δ and subtracting off the self-energy of these positive charges. The resultant potential energy of the cell which we shall designate by Φ will then be given by the equation

$$\begin{aligned} \Phi = \lim_{\delta \rightarrow 0} \left\{ (1/8\pi) \iiint [(\partial V / \partial x_1)^2 + (\partial V / \partial x_2)^2 \right. \\ \left. + (\partial V / \partial x_3)^2] dx_1 dx_2 dx_3 - \sum_{k=1}^p (e_k)^2 / 2\delta \right\} \quad (3) \end{aligned}$$

where the integration now extends through-out the base cell excluding the p small spheres of radii δ .

By the use of Green's theorem Φ can be written in the form

$$\begin{aligned} \Phi = \lim_{\delta \rightarrow 0} \left\{ - (1/8\pi) \iiint V \nabla^2 V dx_1 dx_2 dx_3 \right. \\ \left. - (1/8\pi) \sum \iint V (\partial V / \partial n) dS - \sum_{k=1}^p (e_k)^2 / 2\delta \right\}. \quad (4) \end{aligned}$$

Now $\nabla^2 V = -4\pi\rho$ and $\iint V (\partial V / \partial n) dS$ vanishes over the external surface of the cell because of the periodicity of V and $\partial V / \partial n$.³ Thus the surface integral of $V \partial V / \partial n$ reduces to that over the small spheres alone. Eq. (4) may now be written

³ If some of the point charges lie on the bounding surface of the cell, they may be deleted by small hemispherical indentations precisely as is done in the theory of elliptic functions.

$$\Phi = \lim_{\delta \rightarrow 0} \left\{ (1/2) \iiint \rho V dx_1 dx_2 dx_3 - (1/8\pi) \sum_{k=1}^p \iint V (\partial V / \partial n) dS - \sum_{k=1}^p (e_k)^2 / 2\delta \right\}. \quad (5)$$

But $\lim_{\delta \rightarrow 0} (1/2) \iiint \rho V dx_1 dx_2 dx_3$ is equal to $(1/2) \iiint \rho V dx_1 dx_2 dx_3$, the integral being taken through-out the entire base cell, since the integral of ρV through-out any of the small spheres goes to zero as δ goes to zero. Also it is not difficult to show that

$$\lim_{\delta \rightarrow 0} \left\{ - (1/8\pi) \sum_{k=1}^p \iint V (\partial V / \partial n) dS - \sum_{k=1}^p (e_k)^2 / 2\delta \right\} = \left(\frac{1}{2} \right) \sum_{k=1}^p e_k V_k'$$

where V_k' is the potential at the point charge e_k with that charge removed. Making these substitutions in Eq. (5) we obtain

$$\Phi = \left(\frac{1}{2} \right) \iiint \rho V dx_1 dx_2 dx_3 + \left(\frac{1}{2} \right) \sum_{k=1}^p e_k V_k'. \quad (6)$$

Substituting in Eq. (6) the value of V as given in Eq. (1) we get

$$\Phi = (1/2\pi\Delta) \sum_{l_1, l_2, l_3=-\infty}^{\infty} \frac{(A_{l_1 l_2 l_3} + B_{l_1 l_2 l_3}) B_{-l_1 - l_2 - l_3}}{\sum_{j=1}^3 \left(\sum_{n=1}^3 l_n b_j^n \right)^2} + \left(\frac{1}{2} \right) \sum_{k=1}^p e_k V_k'. \quad (7)$$

Let us consider the quantity $(1/2) \sum_{k=1}^p e_k V_k'$ appearing in Eq. (7). V_k' is the potential at the k th positive charge with that charge removed. It is made up of two parts, that due to all the other positive charges, and that due to the negative space charge. Calling the former V_{k+}' and the latter V_{k-}' we see by the use of Eq. (1) that

$$\begin{aligned} \left(\frac{1}{2} \right) \sum_{k=1}^p e_k V_k' &= \left(\frac{1}{2} \right) \sum_{k=1}^p e_k (V_{k+}' + V_{k-}') \\ &= \left(\frac{1}{2} \right) \sum_{k=1}^p e_k V_{k+}' + (1/2\pi\Delta) \sum_{l_1, l_2, l_3=-\infty}^{\infty} \frac{B_{l_1 l_2 l_3} A_{-l_1 - l_2 - l_3}}{\sum_{j=1}^3 \left(\sum_{n=1}^3 l_n b_j^n \right)^2}. \end{aligned} \quad (8)$$

Substituting in Eq. (7) the results expressed in Eq. (8) and collecting terms we obtain Φ in its final form

$$\Phi = (1/2\pi\Delta) \sum_{l_1, l_2, l_3=-\infty}^{\infty} \frac{B_{l_1 l_2 l_3} B_{-l_1 - l_2 - l_3} + 2A_{l_1 l_2 l_3} B_{-l_1 - l_2 - l_3}}{\sum_{j=1}^3 \left(\sum_{n=1}^3 l_n b_j^n \right)^2} + \left(\frac{1}{2} \right) \sum_{k=1}^p e_k V_{k+}'. \quad (9)$$

Eq. (9) gives in compact form the potential energy of the base cell of the lattice under consideration. Given the quantities a_j^n , e_k , x_i^k , and the func-

tion $\rho(x_1, x_2, x_3)$, the value of Φ may be calculated by Eq. (9). A method devised by Ewald enables us to calculate the quantity $(1/2) \sum_{k=1}^p e_k V_k' +$ without too much difficulty.⁴

An examination of Eq. (9) shows that the potential energy of the cell consists of three parts. The first part is the energy of the negative space charge and involves the coefficients $B_{l_1 l_2 l_3}$, $B_{-l_1 -l_2 -l_3}$. The second part is the mutual energy of the negative space charge and the positive point charges. It involves the coefficients $A_{l_1 l_2 l_3}$, $B_{-l_1 -l_2 -l_3}$. The third part as given by $(1/2) \sum_{k=1}^p e_k V_k' +$ is the energy of the positive point charges. The first and third parts are essentially positive while the second part is negative.

The expression for Φ as given in Eq. (9) has some advantages over the expressions usually given for the potential energy of a lattice cell. It is usually assumed that the ions making up an ionic crystal can be treated as point charges. No attempt is made to take into account the actual distribution of electrons around the nuclei. As a result it is necessary, for the sake of achieving equilibrium, to introduce an additive term in the energy expression representing the effect of certain repulsive forces existing between the ions. In the expression here developed we have taken into consideration the distribution of the electrons in the crystal in so far as it is possible to replace a negative space charge by a corresponding electron atmosphere. This obviates the necessity of introducing extra terms representing repulsion since the sheath of electrons around each nuclei will automatically bring into play repulsive forces of considerable magnitude when the ions are close together.

Furthermore the coefficients $B_{l_1 l_2 l_3}$ which play an important part in this theory can, with only a few minor assumptions, be identified with the structure factors of the crystal in question.⁵ The structure factors for some crystals have been determined experimentally. For these crystals Φ may be calculated not only for the accepted crystal parameters but also for arbitrary parameters. This enables us to determine parameter values which give minimum values of Φ and therefore states of stable equilibrium. In the following section we give the results of some determinations of Φ for the halides NaCl, NaF, and LiF.

APPLICATIONS

The halides NaCl, NaF, and LiF are simple cubic crystals. The expression for Φ as given in Eq. (9) becomes considerably simpler for this type of a crystal. We carry through the computation of Φ for NaCl as illustrating the general method. In order to use the experimentally determined values of the structure factors it is necessary to take the origin at the heaviest ion in the crystal.⁶ This is at the Cl ion for NaCl.

There are two kinds of ions in the NaCl crystal so that

⁴ e. g. M. Born, 159-162.

⁵ A. H. Compton, X-Rays and Electrons, Chap. 5 (1926).

⁶ R. J. Havighurst, Phys. Rev. 29, 4 (1927).

$$e_1 = e_3 = e_5 = e_7 = 17e, \quad \text{and} \quad e_2 = e_4 = e_6 = e_8 = 11e$$

where e is numerically equal to the charge on the electron. Since NaCl is a cubic crystal we have

$$a_i^n = \begin{cases} 0 & \text{if } n \neq j \\ a & \text{if } n = j \end{cases}, \quad \text{and} \quad b_i^n = \begin{cases} 0 & \text{if } n \neq j \\ b & \text{if } n = j \end{cases}.$$

Evidently $a=1/b$ and $\Delta=a^3$. There are eight ions in each cell so that k runs from 1 to 8. The coordinates of the nuclei of these ions are

$$x_1^1 = x_2^1 = x_3^1 = x_2^2 = x_3^2 = x_2^3 = x_1^4 = x_3^4 = x_1^5 = x_1^6 = x_2^6 = x_3^7 = 0,$$

and

$$x_1^2 = x_1^3 = x_3^3 = x_2^4 = x_2^5 = x_3^5 = x_3^6 = x_1^7 = x_2^7 = x_1^8 = x_2^8 = x_3^8 = a/2.$$

We consider $\rho(\xi_1, \xi_2, \xi_3)$ as an even function of its arguments so that

$$\begin{aligned} B_{l_1 l_2 l_3} &= \iiint \rho \exp [-i2\pi b(l_1 \xi_1 + l_2 \xi_2 + l_3 \xi_3)] d\xi_1 d\xi_2 d\xi_3 \\ &= \iiint \rho \cos [2\pi b(l_1 \xi_1 + l_2 \xi_2 + l_3 \xi_3)] d\xi_1 d\xi_2 d\xi_3 = B_{\pm l_1 \pm l_2 \pm l_3}. \end{aligned}$$

So far we have considered ρ to be the negative space charge density in the crystal. We assume that it may be set equal to $-e\sigma$ where σ is the electron density in the crystal. But

$$\iiint \sigma \cos [2\pi b(l_1 \xi_1 + l_2 \xi_2 + l_3 \xi_3)] d\xi_1 d\xi_2 d\xi_3 = 4F_{l_1 l_2 l_3},$$

where $F_{l_1 l_2 l_3}$ is the l_1, l_2, l_3 structure factor for the NaCl molecule in the crystal.⁷ The factor 4 enters because there are four molecules in each cell of the crystal. Thus we have

$$B_{\pm l_1 \pm l_2 \pm l_3} = -4eF_{l_1 l_2 l_3}.$$

The expression for Φ with the above modifications now takes the form

$$\Phi = \left(\frac{1}{2}\right) \sum_{k=1}^8 e_k V'_k + (1/2\pi a) \sum'_{l_1, l_2, l_3=0} \delta_{l_1 l_2 l_3} \left(\frac{-8e\alpha_{l_1 l_2 l_3} F_{l_1 l_2 l_3} + 16e^2 (F_{l_1 l_2 l_3})^2}{l_1^2 + l_2^2 + l_3^2} \right) \quad (10)$$

where

$$\delta_{l_1 l_2 l_3} = \begin{cases} 8 & \text{if none of the subscripts are zero,} \\ 4 & \text{if only one of the subscripts is zero,} \\ 2 & \text{if only two of the subscripts are zero} \end{cases},$$

and where

$$\alpha_{l_1 l_2 l_3} = \begin{cases} 112e & \text{for the subscripts all even} \\ 24e & \text{for the subscripts all odd} \\ 0 & \text{otherwise} \end{cases}.$$

⁷ A. H. Compton, p. 160.

We are now in a position to calculate Φ for NaCl by the use of Eq. (10). The calculation of the term $(1/2) \sum_{k=1}^8 e_k V_{k+1}$ is a rather long and laborious process. The standard method due to Ewald⁸ is used for this calculation and need not be repeated here. The result for NaCl is $355e^2/a$. This amounts to less than three percent of the total value of Φ and thus contributes little to the energy of the cell.

The values of the structure factors for NaCl, and also for NaF and LiF, have been taken from a table of structure factors given by R. J. Havighurst.⁶ These values as given by Havighurst include the Debye temperature factor. Using forty of these values and substituting in Eq. 10 we obtain for Φ of NaCl the value

$$\Phi(\text{NaCl}) \equiv -13590 e^2/a_0$$

where $a_0 = 5.628 \times 10^{-8}$ cm. This value of Φ cannot be compared with Born's value of the potential energy of a NaCl cell since this value includes the energy of the ions and takes into account the electron distribution in the crystal.

It is possible to compute $\Phi(\text{NaCl})$ for various arbitrary values of the grating space since the structure factors for various values of a can be determined. The same can be done for NaF and LiF. The results are shown in tabulated form. a_0 represents the accepted grating space for the crystals under consideration and has the values $a_0(\text{NaCl}) = 5.628 \times 10^{-8}$ cm., $a_0(\text{NaF}) = 4.620 \times 10^{-8}$ cm, and $a_0(\text{LiF}) = 4.014 \times 10^{-8}$ cm. Values of $w = (a_0/e^2) \Phi$ are shown for the grating spaces $0.75a_0$, a_0 , $1.25a_0$, $1.50a_0$, and $2.00a_0$.

TABLE I

	$0.75a_0$	a_0	$1.25a_0$	$1.50a_0$	$2.00a_0$
$w(\text{NaCl})$	-11860	-13590	-12850	—	—
$w(\text{NaF})$	-4350	-5360	-5470	-4850	—
$w(\text{LiF})^9$	-1710	-1950	—	-1980	-1800

An examination of Table I yields the interesting fact that a minimum value of w , and therefore of Φ , occurs for each of the three crystals in the neighborhood of the accepted grating space for that crystal. For NaCl a minimum occurs in the interval defined by $0.75a_0 < a < 1.25a_0$. It is quite likely that $w = -13590$ at $a = a_0$ is an actual minimum for NaCl, as it should be from theoretical considerations.

For NaF a minimum value of w lies in the interval $0.75a_0 < a < 1.50a_0$ but it appears to be closer to $a = 1.25a_0$ than to $a = a_0$. For LiF a minimum lies in the interval $0.75a_0 < a < 2a_0$ but it appears to be closer to $1.5a_0$ than to a_0 . The reason for this shifting of the minimum value of w toward values of a greater than a_0 in the case of NaF and LiF is not clear. It may be that

⁸ M. Born, 158-162 (1926).

⁹ The term $(1/2) \sum_{k=1}^8 e_k V_{k+1}$ has been omitted for LiF.

w has not been determined accurately enough to make the difference between the values of w at a_0 and at $1.25a_0$ or $1.5a_0$ significant. Or it may be that we are not justified in assuming that a negative space charge can be replaced by an electron distribution in the case of NaF and LiF, since the total number of electrons per cell diminishes rapidly as we go from NaCl to LiF. NaCl has 112 electrons per cell, NaF has 80, and LiF has only 48.

Although we have determined approximately the position of a single minimum value of Φ for each of the three crystals, there remains the question as to whether or not this is the only minimum value of Φ . From the form of Eq. 10 and from the general relation between the structure factors and the grating space we hazard the guess that it is, although this conjecture has not been proved.

By the general method outlined in this paper one ought to be able to determine other crystal parameters besides grating spaces. Also it may be possible to relate Φ , the lattice energy which is not a directly measurable quantity, to other quantities which are measurable by some kind of a cyclical process as has been done by Born and others.

ORIGIN OF THE VARIATIONS IN THE SUN'S ROTATIONAL VELOCITY

BY ROSS GUNN

NAVAL RESEARCH LABORATORY, WASHINGTON, D. C.

(Received August 23, 1930)

ABSTRACT

The observed variations of the sun's rotation with solar activity are shown to be accounted for by changes of the electric and magnetic fields in the solar atmosphere. It is assumed that the sun's electric field arises from an electron or negative ion current flowing away from the sun's surface. The ionized atmosphere offers electrical resistance to the current and calculations show that the heat generated in the solar atmosphere is an appreciable fraction of the total radiated light energy. The electric field is thus correlated with the solar constant and since the solar constant is known to vary with the sunspot cycle, the atmospheric electric field, and hence the rotational period, must go through similar variations in magnitude. The subatomic processes which might give rise to the solar current are mentioned.

SIMULTANEOUS spectroscopic determinations of the sun's rotational velocity made at different observatories agree exceptionally well in magnitude but observations over long periods of time show that the velocities are not constant. The observed variations cannot be attributed to errors of observation or to a real change in the rotation of the entire solar mass. Newall¹ and Halm² have studied the observational data and definitely conclude that at times of maximum sun spot activity the sun revolves with an apparent speed that is greater by a few percent than the average; while at minimum activity, it rotates slower than the average. In addition to this type of variation there are observed temporary and local fluctuations which may amount to as much as ten percent of total superimposed velocity. These variations of velocity have been attributed to many causes, but no generally acceptable explanation has been given.

In an earlier paper³ it was shown that the anomalies of the sun's rotation arose from the combined electric and magnetic forces acting on the ions of the solar atmosphere and that the only fundamental solar rotational period which can be observed directly, is the period of rotation of the sun's magnetic pole. With a knowledge of this fundamental period the surface velocity of the sun proper is readily calculated for any given point. To this velocity must be added the atmospheric drift which arises from the sun's magnetic and electric fields and may amount to as much as one quarter of the surface velocity. The magnitude of this superposed atmospheric velocity u is given by

$$u = \frac{E \times B}{B^2} = \frac{E}{B} \sin \beta \quad (1)$$

¹ Newall, Monthly Notices, R.A.S. 82, 101 (1921).

² Halm, Monthly Notices, R.A.S. 82, 479 (1922).

where E and B are the electric and magnetic fields respectively, and β is the angle between E and B . We have seen that this additional velocity has the correct value and distribution to account for the anomalous rotation if the sun carries a negative charge sufficiently great to produce a radial electric field of 0.013 volts/cm at a level in the reversing layer where the magnetic field is 25 gauss.

At any given latitude and level the angle β between E and B may be considered constant and it is clear from Eq. (1) that fluctuations in the velocity of the solar atmosphere are to be expected if the ratio of E to B changes for any reason whatsoever. Observations show that the atmospheric drift at any given level and latitude may increase by as much as ten percent from a time of minimum to maximum solar activity. We may attribute this increase in the atmospheric drift velocity to: (a) an increase in E ; (b) a decrease of B ; and (c) a readjustment of both E and B .

The magnetic field B at any given level in the solar atmosphere is determined primarily by the magnetic permeability of adjacent layers, and we have seen³ that due to the diamagnetic action of the atmospheric ions the effective magnetic permeability is much less than unity. The intensity of magnetization I for the region is readily calculated and it is found³ that

$$I = - \frac{NkT}{B(1 + (R/\lambda)^2)} \quad (2)$$

where N is the number of ions per cm³, k the Boltzman constant, T the absolute temperature, λ the ion mean free path, and B the magnetic induction. The radius R of the circle generated by the ion as it spirals about the impressed magnetic field is given by

$$R = mV/Be = (2mkT)^{1/2}/Be \quad (3)$$

where m is the mass of the ion, V its velocity and e the ionic charge in e.m.u. Making use of the usual relations it is found that the magnetic permeability μ of the solar atmosphere at any level in terms of the observed magnetic field B is given by

$$\mu = \left[1 + \frac{4\pi NkT}{B^2(1 + (R/\lambda)^2)} \right]^{-1} = \left[1 + \frac{4\pi NkT}{B^2 + 2mkT/e^2\lambda^2} \right]^{-1} \quad (4)$$

In the reversing layer observation requires a permeability much less than unity and a long ion free path. Hence it follows from Eq. (4) that $4\pi NkT/B^2$ must have a value of the order of unity. This is the approximation which has been used heretofore to determine the pressure distribution in the solar atmosphere and it was found³ that this approximation led to a mean atomic weight for the ions constituting the solar atmosphere of 3.3, a value in fair accord with the more recent unpublished determination of Professor Menzel.⁴ The important thing to note in present discussion is that

³ Gunn, Phys. Rev. 35, 635 (1930); 33, 614 (1929); 32, 133 (1928); 34, 335 (1929).

⁴ H. N. Russell, Astro. Jour. 70, 1 (1929).

the magnetic permeability of the solar atmosphere decreases with increasing values of (N) the specific ionization.

It seems well established that the value of the solar constant⁵ increases by three percent from sunspot minima to maxima and that the radiation in the ultraviolet may increase by as much as thirty percent. This increase in radiation increases the specific ionization and decreases the permeability which in turn reduces the magnetic field at a given level. This reduction of the magnetic field increases the velocity of the atmospheric drift and at sun spot maxima we find, in accord with observation, that the solar rotational velocity is a maximum. It seems unlikely that this effect alone will account for the entire observed changes even though it is of the correct sign. We shall see that variations of the electric field appear to be of more importance in causing the observed changes in the rotational velocity.

In an earlier paper on the anomalous solar rotation³ it was shown that the observed atmospheric motions demanded the existence of an electric field in the reversing layer which is directed radially inward and which has an equatorial value of 0.013 volts/cm at a representative level in the reversing layer. No attempt was made to account for the presence of this field, although the calculations showed that the potential difference between the sun and free space amounted to at least 10^6 volts and the phenomena giving rise to the electric field must therefore be quite energetic. The required electric field may arise from some unknown cause but at the present time it seems correct to assume that the presence of the electric field is evidence of a current of electrons or negative ions which flow constantly outward from the sun to free space. In order to calculate the total electric current discharged by the solar atmosphere on our assumption it is necessary to note that diamagnetism confines the entire solar magnetic field to the solar atmosphere, and ions which eventually leave the sun, no matter where they leave the surface, must drift across the magnetic field and not along it. We have seen³ that the electrical conductivity of long free path ions moving across a magnetic field was very much smaller than the conductivity for ions moving in zero field or moving parallel to the magnetic field. In the present case we will not be greatly in error by taking the mean conductivity nearly equal to the conductivity of a typical level in the reversing layer near the equator. In this region the ions necessarily move across the magnetic field, and the usual expression for the electrical conductivity is reduced by a large factor dependent upon the ratio of the mean free path to the radius R of the ion path. If we take ion pressures in the reversing layer which are consistent with earlier work it seems likely that the electrons within the layer contribute but slightly to the electrical conductivity³ and that the current is carried almost entirely by ions. The electrical conductivity (σ) of highly ionized stellar matter has been worked out by Chapman⁶ who gives a mean value for the conductivity in the reversing layer of 1.7×10^{-11} e.m.u. This value is probably too large at the specific level in which we are interested, for here the magnetic field appreciably

⁵ Report Astro. Observ. Smithsonian for 1923, p. 109.

⁶ Chapman, Monthly Notices R.A.S. 89, 54 (1928).

affects the conductivity of the ions as well as the electrons. We can do no better at the present time than adopt the foregoing value although it may be considerably in error. The mean current density i of negative charge flowing away from the sun is simply $i = \sigma E$ where $\sigma = 1.7 \times 10^{-11}$ e.m.u. and E is 1.3×10^6 e.m.u. Thus the current density in this region is roughly 2×10^{-5} e.m.u. per cm^2 and if we assume this special region to be representative of the whole surface, the total solar current amounts to 1.3×10^{18} e.m.u.

The potential difference between free space and the base of the reversing layer has been calculated³ and found to approximate 1.5×10^{14} e.m.u. Moreover an extrapolation has been made extending down to the solar surface proper and the potential difference between the surface and free space was found to be 6.6×10^{15} e.m.u. This value may be taken as an upper limit and is based on the rather doubtful assumption that the drift velocities of the deep atmospheric layers are identical with the drift velocities in the reversing layer.

The solar atmosphere offers electrical resistance to the outward flow of current and the heat generated in the reversing layer by this process is radiated away into free space. The total electrical power dissipated in the form of heat in the solar atmosphere is simply the product of the total current and the potential difference. Thus the total electrical power dissipated in the reversing layer is 2×10^{32} ergs/sec and the total electrical power dissipated in all the surface layers cannot exceed 8×10^{33} ergs/sec. Since the total solar radiation is 3.8×10^{33} ergs/sec, we are driven to conclude that electrical heating effects in the solar atmosphere regulate to a certain degree the amount of light energy radiated into free space. The calculations which have been made are not sufficiently precise to warrant the conclusion that electrical heating effects are the only effects of major importance but they do indicate clearly that electrical phenomena may control to a marked degree the amount of energy transferred from the sun's interior to the solar atmosphere.

The introduction of an electrical mechanism to account for the transfer of energy from the interior of a star to its surface and hence, by radiation, to free space would profoundly modify many present astrophysical conceptions. It seems likely that the electrical effects will account for certain puzzling discrepancies which are now found in a comparison of the physical properties of different stars. A discussion of these astrophysical consequences must be postponed.

As a direct result of our conclusions in regard to the electrical energy dissipated in the solar atmosphere, we see that a direct relation exists between the amount of light energy radiated by the sun and the electric field produced in the reversing layer. Thus if the solar atmospheric current is increased by some subatomic or other process the radial electric field will increase, as will the total radiation. Observation shows⁵ that at sun spot maxima the solar constant increases by a few percent, which indicates that the solar electrical field must have increased. The resulting increase in the electric field increases the superposed drift velocity of the solar atmosphere and this in turn increases the apparent observed rotational velocity. The above theoretical

discussion suggests that the electric field and hence the superposed drift velocity is approximately a linear function of the solar radiation, if we consider small variations. This is in complete accord with observation and is reliable evidence for the physical reality of the theory.

We have no direct clue to the phenomena which take place inside the sun and give rise to the outward negative atmospheric current. It is certain that similar phenomena give rise to the observed atmospheric current of the earth and because the potential differences encountered are so great it seems likely that the current systems arise from some subatomic transformation. G. C. Simpson⁷ has suggested that electricity might be generated spontaneously within the earth while Swann⁸ has considered the effects arising from the death of positive electricity. Swann did not discuss the important question of the origin of the energy for such a transformation. Unless the law of conservation of energy is entirely ignored, the death of electricity must be accompanied by the absorption of energy during its transformation, for death of the charge is electrically equivalent to its transfer to infinity. This requires energy and unless this energy is supplied by subatomic processes it seems clear that death cannot take place. W. Anderson⁹ has avoided the above difficulties and he accounts for the earth's electric field by a single postulate. Anderson notes that the solar radiation must arise in some manner from the annihilation of matter and instead of assuming that the proton and electron vanish simultaneously with resultant radiation, or that the charge alone vanishes, he assumes that the proton's mass and charge both vanish while the associated electron wanders off into free space giving rise to certain solar and terrestrial phenomena. By this postulate Anderson was able to calculate the total solar current from the total solar radiation since one electron must appear for every proton annihilated and he found the total current to be 4×10^{16} e.m.u. Comparison of this value with 130×10^{16} e.m.u. computed above suggests that Anderson's postulate may yield the correct results, for the numerical value of the conductivity which has been chosen here, is probably too great. This postulate also connects directly the solar radiation with the solar electric current and therefore changes in the total radiation should be accompanied by rotational changes.

In his discussion of the source of solar energy Jeans¹⁰ suggests that the energy arises from purely radioactive transformations of a material having a higher atomic weight than uranium. If this is the case it is not unlikely that the transformation results in a residue of electrons and perhaps several electrons may be released by the conversion to radiation of the mass of a single equivalent proton. By incorporating such hypothesis in the author's theory, the above numerical values can be brought into accord with solar radiation data. So far as can be determined at the present time, the author's postulate, or that of Anderson, cannot be shown to be inconsistent with any

⁷ G. C. Simpson, *Monthly Weather Review* **44**, 121 (1916).

⁸ Swann, *Jour. Franklin Inst.* **201**, 143 (1926).

⁹ W. Anderson, *Zeits. f. Physik*, **42**, 475 (1927).

¹⁰ Jeans, *Astronomy and Cosmogony*.

known fact. These postulates do, of course, readily account for the earth's observed electric field as well as that of the sun.

The anomalies of the solar rotation and its fluctuations, in the light of this and previous work, must be attributed primarily to the solar magnetic field and some special mechanism which gives rise to moderately large electric fields in the solar atmosphere. The electric fields are not so large that they could be detected by their Stark effect, and it is important to investigate carefully the less direct proofs of their existence. The theory is noncommittal in regard to the origin of the electric fields but the rough agreement between the present calculations and the values given by very simple and not unreasonable postulates are suggestive of some mechanism whereby subatomic transformations result necessarily in the release of negative electricity.

TRIBOTHERMOLUMINESCENCE

BY R. E. NYSWANDER AND BYRON E. COHN

DEPARTMENT OF PHYSICS, UNIVERSITY OF DENVER

(Received August 22, 1930)

ABSTRACT

Glass, certain crystals and frits are rendered thermoluminescent by the process of grinding, emitting light of very low intensity. The phenomenon is observed not only in samples of low purity but also in compounds prepared from chemically pure grade materials. Quantitative measurements of light intensity were made by means of a polarization photometer. The particles tested were graded in size by means of a set of screens ranging from 20 to 200 mesh. The results show that the quantity of emitted light depends upon the nature of the substance and the size of the particles, and diminishes slowly with the time after grinding. Common glass tubing crushed to various grain sizes emitted the maximum amount of light when the linear dimensions of the average mesh size fell between 0.015 cm and 0.025 cm respectively.

CERTAIN substances, when powdered, store up energy which is released by heat in the form of light of very low intensity. As in other types of thermoluminescence, the temperature of emission is below that of incandescence. Wiedemann¹ applied the term triboluminescence to the light given off when certain materials are rubbed or scratched and Levison² designated as tribophosphorescence the luminescence of more prolonged duration excited by rubbing. The term tribothermoluminescence has been given to the phenomenon under consideration which involves the process of grinding followed by the application of heat.

Tribothermoluminescence has been observed in crystals, glasses and frits. In all cases the material tested was first heated in an electric furnace to destroy any trace of thermoluminescence which might have been present, and then ground in a mortar and screened to the desired size. Tribothermoluminescence was observed in clear, colorless crystalline fluorite, and also in lithium borate which forms a white vitreous opaque mass (frit) when fused, as well as all samples of clear colorless glass tested with the exception of a specimen of chemically pure boric anhydride.

The energy of triboluminescence has been discussed by Imhof,³ Trautz⁴ and Schmidt.⁵ One of these suggested explanations involves the recombination of electrons displaced by the process of rubbing, in the other the energy is the result of small electric sparks induced by differences of potential, the electrical doublet theory. In the case of tribothermoluminescence the latter

¹ E. Wiedemann, *Wied. Ann.* **34**, 446 (1888); *Nature* **27**, 181 (1889).

² W. Levison, *Science* **19**, 826 (1904).

³ A. Imhof, *Phys. Zeits.* **18**, 78 (1917) and **20**, 131 (1919).

⁴ M. Trautz, *Ion* **2**, 77.

⁵ H. Schmidt, *Phys. Zeits.* **19**, 399 (1918).

theory does not seem directly applicable after the following test. The particles immediately after grinding were immersed in an electrolyte of dilute nitric acid which would allow the recombination of all electric charges which might result from the process of grinding. The glass was then washed with distilled water filtered and dried in the dark. After this treatment to remove all electric charges, the glass showed the usual thermoluminescence.

Ultraviolet light is very active in exciting the energy of the thermoluminescence in glass.⁶ If ultraviolet light is emitted in the process of grinding, this might be the source of energy of the thermoluminescence of the glass particles. Accordingly, three similar samples of glass were tested in the following manner. The first was ground in a mortar in the usual way, i.e. in the presence of air. The second sample was ground under water then washed in distilled water and dried. The third sample was ground in a dark solution washed and dried as before. The presence of the water and the opaque solution would re-

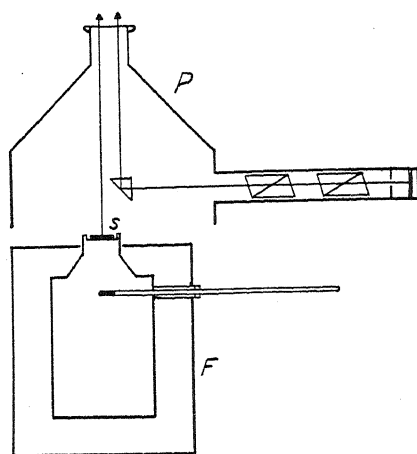


Fig. 1. Diagram of apparatus showing arrangement of polarization photometer and furnace.

duce through absorption the light radiated to the adjacent particles by the process of grinding. When these samples were tested for thermoluminescence the first emitted a much larger quantity of light than the second, and the second emitted more than the third, which gave out scarcely more than the threshold value.

All light measurements were made by means of a polarization photometer.⁷ The usual form was modified to allow a larger angular contrast background, as shown in Fig. 1, in which *P* is the photometer, *F* the furnace and *S* the substance to be tested. The samples were heated in small brass cups with cavities 0.8 cm diameter and 0.4 cm deep, which were placed on top of the large brass post of the electric furnace. By means of a thermometer in the furnace it was possible to hold the temperature of the sample constant for any period. Light measurements were made at time intervals from the

⁶ Nyswander and Cohn, *J.O.S.A.* 20, 131 (1930).

⁷ Nyswander and Lind, *J.O.S.A.*, and *R.S.I.* 13, 651 (1926).

beginning to the end of the period of luminescence. These light intensities were plotted as ordinates with the corresponding time intervals measured from the beginning of luminescence as abscissas. The total quantity of light emitted by the sample is proportional to the area under the curve. These areas were measured by means of a planimeter. All light measurements are expressed in terms of relative values.

The quantity of light emitted by the material was found to be dependent upon (1) the nature of the substance, (2) the size of the particles, (3) the time elapsed after the process of grinding. The effect of the nature of the material is brought out by the following measurements of the light given out by fused sodium borate glass as compared with zinc borate glass (45.5 percent zinc

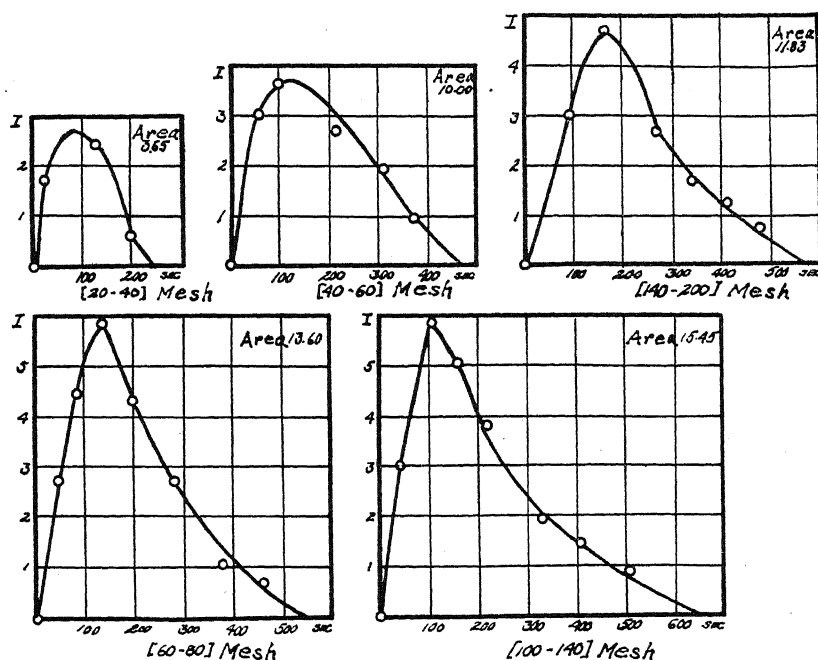


Fig. 2. Total quantities of light emitted by glass for various screen sizes.

oxide to 54.5 percent boric acid). The total quantities of emitted light in the two cases are 16.5 and 1.72 respectively. The two sets of measurements were made under similar conditions. The particles were sieved between 180 and 200 mesh screens, and the temperature of the furnace was 330°C. The results also show that chemically pure grade materials sometimes exhibit tribothermoluminescence.

To determine the effect of grain size on the quantity of light emitted, the particles were separated into groups by means of a series of screens. To obtain the size of the screen openings, eight measurements were made on different parts of each screen by use of a comparator, and the mean value used. Ordinary soft glass tubing was heated to remove all traces of luminescence

and then ground in a porcelain mortar and sieved. The graded sizes were heated in the furnace held at 360°C and a series of intensity-time curves were obtained and plotted as shown in Fig. 2. The areas of these curves were then used as ordinates with the mean of the two corresponding mesh openings as abscissas and plotted as shown in Fig. 3. Curve *A* represents the total light energy for the graded sizes two days after powdering, while *B* was determined 24 days after grinding. The difference between these two curves clearly

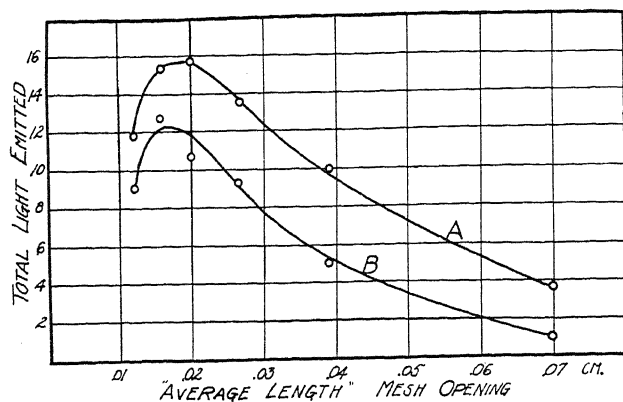


Fig. 3. Variation of emitted light as dependent upon grain size.

shows the decay of luminescence with time. The smaller the size of the particles the greater the amount of energy stored, however, the smaller the size of the particles the less the quantity of light which reaches the surface through a given thickness of the powdered material. These two factors would seem to determine the position of maximum light emission of the curves *A* and *B*. Tribothermoluminescence has been observed in glass of sizes less than 100 mesh one year after it had been powdered.

LETTERS TO THE EDITOR

Prompt publication of brief reports of important discoveries in physics may be secured by addressing them to this department. Closing dates for this department are, for the first issue of the month, the twenty-eighth of the preceding month; for the second issue, the thirteenth of the month. The Board of Editors does not hold itself responsible for the opinions expressed by the correspondents.

High-Voltage Tubes

As a more detailed paper will perhaps not be justified for some time, it may be of interest to report that we have obtained measurements which satisfactorily verify the production of high-speed electrons and of very penetrating x-rays, in the region above 1,000 kilovolts, using the high-voltage Tesla coils and cascade tubes previously described,¹ and that the H_p -values of the highest-speed electrons roughly correspond in voltage equivalents (according to the standard β -ray tables) to the peak voltages of the Tesla coil as measured by the capacity-potentiometer. These measurements have been carried out at voltages considerably below the maximum voltages which we have previously applied to tubes, to reduce the insulation difficulties which are experienced when working near the limit which the apparatus will attain.

A 12-section tube placed inside of a 6-inch diameter Tesla coil having taps on the winding connected to the separate electrodes of the tube has been used, the grounded end of the tube projecting through the oil-tank between the poles of an electromagnet. A slit-system defines a beam of electrons which strikes at will a fluorescent screen or a photographic plate enclosed in 3, 6, and 10 sheets of 0.01 mm aluminum-foil. The distribution of the magnetic field is carefully determined by the triangular search-coil method described in Thomson's "Positive Rays". Unfortunately only very rough spark gap voltage-measurements were obtained during these tests, but the indicated voltages for a series of four plates, for example, were about 900 kilovolts for the first two and 1,000 to 1,300 kilovolts for the last two, the highest H_p -values for which electrons were definitely detected on the plates corresponding to 850, 980, 1,110, and 1,130 kilovolts respectively. The in-

tensity of the electron-stream at the plate is rather low, approximately 500 primary sparks being required for a satisfactory exposure-density through 0.10 mm of aluminum at the maximum H_p -value. A 2-mil tungsten-filament constituted the electron-source at the high-voltage end of the tube; with the filament cold the tube was perfectly dark and no electrons could be detected.

A Geiger-Müller tube-counter mounted in a 6-inch lead-shield at a distance of 55 cm to one side of the copper slit-system in the tube showed no evidence of radiation through 1 inch of lead when the tube was operated as above described. Due to the very short on-time of the high-voltage pulses (resonant frequency about 30,000 cycles) and the very small part of the emission from the filament which would thus be effective, only a very small intensity of radiation could be expected, and consequently a "flashing" tube was resorted to in order to have a more copious emission available at the peak of the voltage-wave. The first observation showing penetrating radiation was made in January, using a similar "flashing" tube. The tube and the Tesla coil were placed end to end in the tank, thus applying the high voltage directly to the end electrodes only, causing it to flash; all other electrodes were electrically floating (no potentiometer was used, but external shields surrounded each tube-section as previously described).¹ This tube was operated at a voltage of 1,100 to 1,300 kilovolts, the H_p of the electrons being continuously observed on the fluorescent screen. As the voltage required to cause the tube to flash slowly increased, and the intensity of the flashing was somewhat irregular, absorption measurements were necessarily rough, but

¹ Phys. Rev. 35, 51, 66, and 1406 (1930).

during counting periods of about ten minutes, running the Tesla coil at 65 sparks per minute, approximately six extra counts per minute were produced through a 1-inch lead absorption-screen, two extra counts per minute through 2 inches of lead, and 28 extra counts per minute through 5/8 inch of lead. The absorption coefficients obtained from the above data are thus of the expected magnitude. The sensitivity of the Geiger counter, which has a residual of about 20 counts per minute, is such that 0.105 mg of radium at a distance of 75 cm produces 26 extra counts per minute through two inches of lead (89 extra counts per minute through 1 inch of lead). The average intensity of the radiation from the tube (at only 66 sparks per minute) is thus very low, but the estimated instantaneous radium equivalent is considerable, and this can be increased by the use of a tube adapted for the production of radiation, the above data being obtained with

the tube arranged for the $H\beta$ -measurements.

The production of "artificial β - and γ -rays" in the region above 1,000 kilovolts has thus been demonstrated. Work is now in progress on the acceleration of protons to radioactive speeds.

M. A. TUVE
L. R. HAFSTAD
O. DAHL

Department of Terrestrial Magnetism,
Carnegie Institution of Washington,
September 11, 1930.

Note added September 12, 1930.

By an amusing coincidence the August 29 issue of *Die Naturwissenschaften* arrived just after the writing of the above note, and it contains a letter by A. Brasch and F. Lange describing the spectacular performance of their high-voltage tube at 2.4 million volts. They are to be congratulated without reserve on the success of their work.

M. A. T., L. R. H., O. D.

Use of the Pierce Acoustic Interferometer for the Determination of Absorption in Gases for High Frequency Sound Waves

In recent articles in this journal, W. H. Pielemeier (Phys. Rev. **34**, 1184, 1929; Phys. Rev. **36**, 1005, 1930) reports determinations of the absorption coefficient in gases for high frequency sound. He employs both the Pierce acoustic interferometer and a torsion vane method. The observations by the first method reveal that as the sound path in the gas is increased the changes in plate current through the tube diminish, and from this rate of diminution Pielemeier attempts to calculate the absorption coefficient. We do not believe this procedure to be entirely justified. The variations in plate current are a function not only of the absorption in the gas but of the circuit constants as well. For we are here dealing with decrements in coupled circuits. The network may be con-

sidered as made up of a crystal circuit with a decrement which depends upon the reflector position in the gas; also this crystal is coupled to a plate circuit with its own decrement. Hence, uncorrected observations on changes in plate current through the tube give no information concerning the absolute absorption in the gas. Experiment has shown us that these changes in current depend both on the reactance and the decrement of plate circuit.

ELIAS KLEIN
W. D. HERSHBERGER

Naval Research
Laboratory,
Bellevue, D. C.
September 15, 1930.

The Magnetic Moment of the Li_7 Nucleus

Using the experimental data on the hyperfine structure of the alkalis, Fermi¹ and Hargreaves have computed approximate values of the magnetic moments of their nuclei. Goudsmit and Young² have estimated the magnetic moment of the Li_7 nucleus on the simplifying assumption that the coupling to the nucleus takes place entirely through the 1s electron. The apparent inconsistency of their results may be due in

part to the experimental difficulty of separating the structure of the $^3S_1-P_1$ and $^3S_1-P_2$ groups. In part it is probably due to their using $(1/2)(h/2\pi)$ for the nuclear

¹ E. Fermi, *Zeits. f. Physik* **60**, 320 (1930).
J. Hargreaves, *Roy. Soc. Proc.* **124**, 568 (1929); **127**, 141 and 407, (1930).

² S. Goudsmit and L. A. Young, *Nature* **125**, 461 (1930).

spin, their main object being to show that the magnetic moment is of the order of magnitude of the theoretical magnetic moment of the proton.

It has since been shown by Granath³ that the main reason for using $i=1/2$ for the nuclear spin is absent. The frequency separations between components agree best with $i=3/2$ which is also in agreement with the band spectrum results of Harvey and Jenkins.⁴ Goudsmit, Güttinger⁵ and ourselves have known for some time that this value of i is fairly consistent with the experimental pattern. The nuclear g factor is on this hypothesis in the neighborhood of 2.3, this value being obtainable directly from Schüler's frequency table and the formula used by Goudsmit and Young.

We have undertaken to make a more accurate calculation for the g factor. Our special reason for doing so is that the electronic configuration of the 3S_1 level is especially simple and appears to be favorable for accurate results. We have also been intrigued by the possibility that the g factor might be 2 exactly which would speak in favor of regarding the magnetic moment of Li , as due to three protons acting independently. It is our purpose to report here briefly on the results of our calculations.

The work of Casimir and of Fermi shows in the case of one electron that it is essential to consider the problem from the point of view of Dirac's electron equation. A non-relativistic equation cannot be expected to give even approximately correct results for S electrons because in the immediate vicinity of the nucleus the electron velocity cannot possibly be regarded as small. There exists at present no satisfactory relativistic treatment of two particles. Nevertheless, for the present purpose, it is possible to form a reasonable extension of the one-electron treatment. In a discussion of light atoms it is possible to treat the one-electron problem also by means of an equation of the Pauli-Darwin type, i.e. employing two rather than four components for ψ . Darwin⁶ has shown how such an equation can be derived from the original four-component Dirac form. The interaction energy with the nuclear magnetic moment μ is then to a sufficient approximation

$$H' = (e/mc) [1 + (E - mc^2) + eA_0/2mc^2] (\mathbf{M}\mathbf{u}) r^{-3}$$

$$\begin{aligned} & + (hec/2\pi) [2mc^2 + eA_0]^{-1} \{ -r^{-3}(\mathbf{u}\mathbf{d}) \\ & + 3(\mathbf{r}\mathbf{d})(\mathbf{r}\mathbf{u}) \} \\ & + (hec/2\pi) [2mc^2 + eA_0]^{-2} (e\mathcal{E}) \{ r^{-2}(\mathbf{u}\mathbf{d}) \\ & - r^{-4}(\mathbf{r}\mathbf{d})(\mathbf{r}\mathbf{u}) \} \end{aligned} \quad (1)$$

The charge of the electron is taken to be $-e$, E is the total energy, m and c are respectively the mass and the velocity of light, A_0 is the electrostatic potential due to the nucleus, \mathcal{E} is the electric intensity due to the nucleus, r is the displacement vector from the nucleus to the electron, \mathbf{M} is the angular momentum vector operator, and σ is Pauli's spin vector. In the first term the square bracket can be omitted for anything but s terms. For s terms it enforces the convergence of the otherwise divergent integrals for r^{-3} . The second term is the closest analogy of the dipole interaction of the nuclear and electronic magnetic moments. On account of the square bracket its effect disappears for s terms. The third term, involving the electric intensity \mathcal{E} is negligible except for s terms. If the square bracket in the second term were absent the result would be indeterminate. In fact it may be shown that if μ were the limit of a space distribution of magnetization the result of the second term would be $(-1/2)$ of the correct total result.

For two electrons we postulate the interaction energy to be the sum of two terms of the type of (1) one term in each electron. The first order perturbations for the energy of a 3S term come out without further approximations to be given by

$$\begin{aligned} w &= w_1(1, -(1/i), -(i+1)/i) \\ w_1 &= (16\pi/3)\mu\mu_0\int\psi^2(0, q)dq \end{aligned} \quad (2)$$

where μ_0 is the Bohr magneton and $\psi(q_1, q_2)$ is the nonrelativistic Schroedinger wave equation. The letter q_1 stands collectively for the Cartesian coordinates of electron 1, and simi-

³ L. P. Granath, Phys. Rev. **36**, 1018, (1930).

⁴ A. Harvey and F. A. Jenkins, Phys. Rev. **58**, 789, (1930).

⁵ We should like to express at this point our appreciation to Professor Goudsmit and to Professor Pauli. It is through the courtesy of the latter that we have received proofs of a paper by Güttinger which is in press in the Zeitschrift für Physik and which shows in detail how $i=3/2$ accounts for Schüler's pattern.

⁶ C. G. Darwin, Proc. Roy. Soc. **118**, 654, (1928).

larly q_2 for those of 2. The splitting is proportional to the probability of finding an electron in a unit volume at the nucleus. By means of (2) one can calculate a correction factor to be used in the formulas of Goudsmit and Bacher.⁷ This factor is

$$f = 2 \int \psi^2(0, q) dq / \int \psi_1 S^2(q) dq.$$

In order to obtain f and hence μ it is necessary to find a solution of the two-electron non-relativistic wave equation. In the absence of an analytic solution we have tried a number of wave functions adjusted for the minimum energy by the variational method. Among these the function

$$(r_1 - c) \exp [-(a/2)r_1 - (b/2)r_2] \\ - (r_2 - c) \exp [-(a/2)r_2 - (b/2)r_1]$$

appears to be best suited for the purpose. It gives when minimized for a, b, c an Eigenwert which is in excellent agreement with experiment. In terms of the ionization potential of Li^{++} the Eigenwert obtained is -1.1354 which may be compared with the spectroscopic value -1.1358 . The best values of a, b, c are 0.38, 1.00, 3.18. The correction factor f is for these values of $a, b, c, f = 1.063$. Using this factor and making the slight correction in the frequency of Schüler's component,³ mentioned by Granath,³ the g factor becomes 2.13 for $i = 3/2$. This is closer to 2 than the uncorrected value 2.3. The remaining difference of 6% appears to be too large to be accounted for by experimental error. The accuracy of the theoretical calculation may, of course, be questioned. An estimate of it may be made by the method recently published by Eckart.⁸ Such an estimate would

lead one to suppose that the result is accurate only to about 7%. In this special case, however, our experience with other trial functions as well as a more detailed consideration of the possible errors indicate that Eckart's accuracy criterion is likely to be too conservative. *The present evidence is, therefore, that if the nuclear spin is 3/2, Schüler's observed frequency separation between components (1) and (3) speaks in favor of a nuclear magnetic moment greater than that of three protons by about 6%.*

It should be noted that we base ourselves entirely on Schüler's observed frequency separation between components (1) and (3) because the other components of the pattern are not sufficiently resolved to make definite conclusions possible. It is also not out of place to emphasize here that in our calculation the magnetic field due to the electrons has been supposed to have no effect on the nuclear magnetic moment. An estimate shows this field to be about 4.5×10^6 gauss. An exact experimental test of the interval ratio given by (2) may show to what extent the nuclear magnetic moment is affected by this magnetic field.

G. BREIT

F. W. DOERMANN

Department of Physics,
New York University,
September 15, 1930.

⁷ S. Goudsmit and R. F. Bacher, *Phys. Rev.* **34**, 1501 (1929).

⁸ Carl Eckart, *Phys. Rev.* **36**, 878 (1930). Note also Eckart's function for ³S closely resembling ours.

Wind Mixing and Diffusion in the Upper Atmosphere

I am glad to see that Professor Chapman (*Phys. Rev.* **36**, 1014, 1930) agrees with me in thinking that there is no question of Dr. Maris' priority in the development of the subject of wind mixing and diffusion in the upper atmosphere. At the same time Professor Chapman claims that his work was independent of that of Dr. Maris. The internal evidence in his paper (*Proc. Roy. Soc. A*, **122**, 369, 1929) does not support this claim. To give one example; on page 375 he wrote, "It is here assumed that the mixing ceases at 110 km," with no indication of any calculation which would justify such an exact assumption. Maris had already written (*Nature*,

December 1927) "This 'diffusion' level for hydrogen would move from infinity down to 142 km in one day, at the end of five days it would be at a height of 127 km and in 50 days it would be at 113 km. The corresponding levels for helium would be at 137, 120 and 106 km, respectively." And in *Terr. Mag.* **33**, 233 (1928) after five printed pages of calculation and close physical reasoning Maris gave (Table 3) the diffusion levels of six atmospheric gases for summer, winter, day and night which "averaged about 110 km."

E. O. HULBURT

Naval Research Laboratory,
September 19, 1930.

BOOK REVIEW

Enführung in die Mechanik und Akustik. Dr. R. W. Pohl, Professor of Physics in the University of Göttingen. Pp. 240, figs. 440. Julius Springer, Berlin, 1930. Price R.M. 15.80.

This book is the first part of Professor Pohl's lectures concerning experimental physics. Other parts are to appear within a few years. This first part is not a complete text of mechanics and acoustics, but rather an exposition of the fundamental experiments in this subject. Mathematical demonstrations are generally omitted. The book contains numerous lecture experiments that are quite new to the reviewer. In its 244 pages there are 440 figures illustrating the experiments performed. In many of these shadow pictures are used instead of photographs of the apparatus. These seem to be a successful feature of the book. The author has prepared a work that will prove interesting and stimulating to students and teachers of physics and to others interested in the subject.

G. W. STEWART

Differential Equations, F. R. MOULTON

There is a large class of people, and among them most physicists, who have occasion to solve differential equations, who like to think with care, and who feel more or less ashamed of themselves when they proceed to do all sorts of curious things with series in seeking solutions of the equations in the doubtfully happy belief that somewhere or other there are some mathematicians or theorems so "pure" that they may shoulder all the iniquities of the mathematically wicked and somehow or other show that they are justified. Yet, when these lost souls turn to the realms of pure analysis for guidance, they are apt to be appalled by the necessity of wading through an infinite complexity of unappealing arguments and symbols—of η 's which are smaller than ϵ 's and can never be smaller than ξ 's, and so forth. To all such as these, Professor Moulton's book should be of the greatest value, representing as it does, the viewpoint of one interested fundamentally in the logical foundations of the subject, and at the same time, in its practical applications in astronomy, ballistics, etc.

The book is concerned almost entirely with "ordinary" differential equations, a couple of pages on "partial" differential equations being introduced merely to show the general relation of the considerations there involved to those of ordinary differential equations. Professor Moulton commences by emphasizing the fact that any problem having as its outcome the solution of a set of differential equations may be considered, logically, in four parts—formulation of the problem in terms of the properties of the functions involved—proof of the existence of a solution of the problem—determination of the properties of the solution—development of practical means of obtaining the solution. Then follows a discussion of the reduction of differential equations to "Normal Form." The second chapter is devoted to the formal construction of solutions in terms of power series in the independent variable, and to the subject of convergence of the solution. Chapter III deals with the construction of solutions in the form of power series in a parameter, again with a careful discussion of the question of convergence. Chapter IV treats the subject of solution by the method of variation of parameters. The general procedures in all of these cases are amply illustrated by practical examples; and, in the form of an appendix will be found a very useful collection of such theorems in analysis as are used in the logical development of the text. The appendix should be of particular value to the physicist whose acquaintance with these theorems dates back to a not too complete comprehension of their content gained in his student days, and who would otherwise lose much time in digging them out of the standard treatises on analysis. After devoting Chapter V to Integrals of Differential Equations and Chapter VI to Analytic Implicit Functions, the author proceeds in Chapters VII to X, to take up the solution of special problems which, while of fundamental practical interest in themselves, are chosen primarily to illustrate different methods of setting about the solutions of problems, having in mind the conditions and requirements of the special problem in hand. In the chapter on the "Sine Amplitude Function" in particular, the author emphasizes

how it is possible to obtain much information regarding the nature of a function defined by a differential equation without recourse to an actual solution of the equation itself.

Chapters XI and XII contain an admirable account of the method of solution by "Successive Integrations" and one acquires a certain aesthetic satisfaction from the author's emphasis on the fact that the process is not fundamentally an approximation, but is, in the limit, logically exact in the same sense that other limiting processes in analysis such as the expression of functions in series, may be regarded as logically exact. In Chapter XII the application of the method is set out in detail, even to the extent of suggestions in the matter of actual numerical procedure.

After devoting Chapter XIII to the Cauchy-Lipschitz method of solution the author proceeds, in Chapters XIV to XVII to discuss in detail the subject of linear differentials of various types, with applications. The last chapter is devoted to "Differential Equations with Infinitely Many Variables."

The work throughout is written in an exceptionally clear vein. Even in the parts of a more purely mathematical nature, conglomerations of symbols are minimized in favor of the spirit of the processes discussed, so that the reader is brought to a sympathetic interest in the significance and reality of content of the steps taken in place of being left, as is so often the case, with profound respect for the complexities of the subject coupled with a sense of relief that he does not have to do that kind of thing himself.

The addition of Historical Notes at the end of each chapter serves further to humanize the subject, and, by a curious freak of the mind, tends to render more clear the purport of many things by sheer realization of the fact that these matters were not always clear to the pioneers of the science itself.

W. F. G. SWANN

THE PHYSICAL REVIEW

THE POSITION AND STRUCTURE OF THE MODIFIED LINE OF THE SPECTRUM OF SCATTERED X-RAYS

By F. L. NUTTING

RYERSON PHYSICAL LABORATORY, UNIVERSITY OF CHICAGO

(Received August 22, 1930)

ABSTRACT

Measurements have been made by both photographic and single-crystal ionization methods of the shift in wave-length of scattered x-rays at angle of about 170° . The photographic method was that introduced by Sharp, but the $K\beta$ line of molybdenum was used. Two exposures of several hundred hours each were obtained. Analyses of the microphotographic records gave, from the shift of the center of gravity of the lines, $h/mc = 0.02305A$, and from the shift of the peaks, $h/mc = 0.2374A$. From the difference between different exposures, it is suspected that some hidden source of error is present, perhaps due to the effect of the $K\gamma$ line. Some 600 ionization curves give as an average $h/cm = 0.0240 \pm 0.00024A$. These results, compared with those of other experimenters, fail to indicate any definite departure from the theoretical value of $h/mc = 0.2422A$. This does not support the findings of Davis and Purks, who report a value of $0.022A$. The form of the spectral lines observed seems inconsistent with a fine structure of the modified line such as reported by Davis and Purks. The modified line is however found to have a considerable natural breadth.

THE well-known expression given by A. H. Compton for the change of wave-length of x-rays scattered at any angle,

$$\delta\lambda = \frac{h}{mc}(1 - \cos \phi), \quad (1)$$

has been tested by many experimenters.² Though the results of most of these investigations have been in close agreement with the theoretical formula, recent studies by Davis and Purks and by Davis and Mitchell have appeared to show a wave-length change considerably smaller than the predicted value. It has therefore seemed worth while to try some new experiments of a precision type to measure the wave-length change. Both photographic and ionization methods were employed.

¹ A. H. Compton, *Phys. Rev.* **21**, 207 and 483 (1923).

² E.g. A. H. Compton, *Phys. Rev.* **22**, 409 (1923); P. A. Ross, *Proc. Nat'l Acad.* **10**, 304 (1924); H. M. Sharp, *Phys. Rev.* **26**, 691 (1925); Kallmann and Mark, *Naturwissenschaften* **14**, 3 (1925); Davis and Mitchell, *Phys. Rev.* **32**, 331 (1928); J. W. M. DuMond, *Phys. Rev.* **33**, 643 (1929); Davis and Purks, *Phys. Rev.* **34**, 1 (1929).

PHOTOGRAPHIC METHOD

The photographic method employed was in principle the same as that used by Sharp.² The apparatus consists of an x-ray tube with narrow glass walls and a thin glass window w (Fig. 1). The rays are scattered from a paraffin radiator R through an angle ϕ of almost 180° , and are reflected from a polished calcite crystal, through a 0.1 mm. slit S . The spectrum is recorded on a photographic plate P . This construction gives only small variations in the angle of scattering for rays coming from different parts of the scattering block.

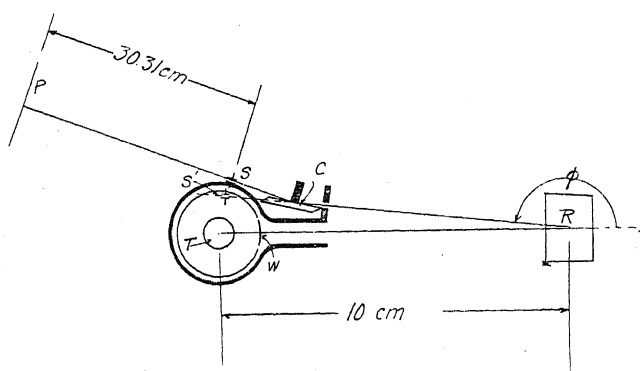
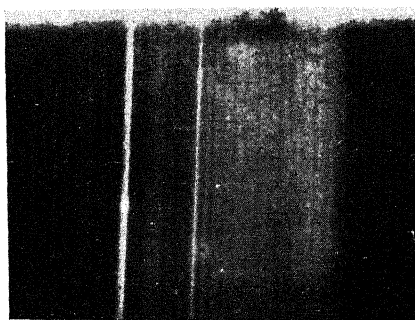


Fig. 1. Arrangement of apparatus.

In Sharp's experiments it was not possible to resolve the α doublet of the molybdenum rays which were used, and still retain sufficient intensity, and this incomplete resolution made necessary complicated corrections. In the present experiments, therefore, the measurements were made on the $K\beta$ line of molybdenum, which is a doublet so narrow that it may be treated as a single line.

Fig. 2 Photograph of Mo K spectrum.

Two good exposures of several hundred hours were made, with the tube operating on a diffusion pump, at about 38 m.a. and 40 peak kv. To obtain standard reference lines, a molybdenum plate was placed in front of the paraffin radiator, and in some 50 hours a fluorescence spectrum of suitable

intensity was recorded without changing the position of the photographic film. Figure 2 shows one of the photographs thus obtained. The α_1 , α_2 , β and γ lines of the fluorescent spectrum are clearly visible, as well as the short wave-length continuous spectrum, the modified β line, and (faintly) the modified α line.

A microphotometric record of this film (the average of 11 curves on different parts of the spectral lines), taken with a Moll microphotometer, is shown in Fig. 3.

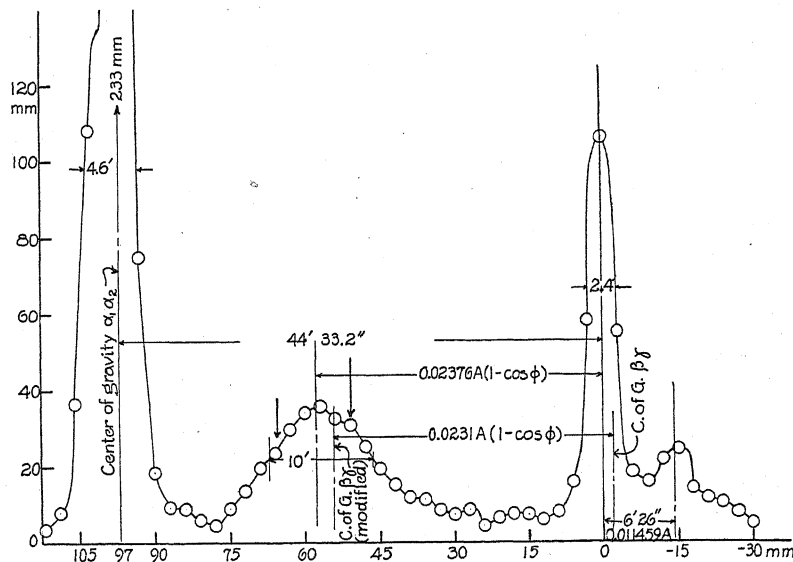


Fig. 3. Microphotometric analysis of Fig. 2. Mo K radiation; scatterers Mo plate and paraffin; $\phi = 169^\circ$. Mean microphotometric curve.

Making use of Allison and Armstrong's values for the wave-lengths of the molybdenum K lines, the mean of several measurements on the *center of gravity* of the modified $\beta\gamma$ line (cf. Fig. 3) give,

$$\delta\lambda = \lambda_{\beta\gamma\text{mod}} - \lambda_{\beta\gamma} = 0.045686A.$$

The mean value of $1 - \cos \phi$ was found to be 1.9816, whence by Eq. (1),

$$h/mc = 0.02305A.$$

A similar measurement on the *peaks* of the β line and the β modified line, after correcting for the effect of the unresolved γ modified line in the manner described by Sharp,² gives

$$h/mc = 0.02374A.$$

For each individual film the consistency of the measurements was such as to indicate an error of about 1 percent. The results of the two films differed however by about 2.5 percent. This discrepancy suggests that there may be a hidden source of error, perhaps in the effect of the γ line on the position

of the modified peak which, would vary with the conditions of exposure and development. The measurement on the center of gravity depends upon the selection of a base line, and is thus less reliable than the measurement of the peak. It is doubtful therefore whether the observed difference between these results and the value $h/m = 0.02422A$, calculated³ from the accepted values of the constants, is of real significance.

IONIZATION METHOD

The values of h/mc obtained from these photographs depart from the accepted value of this quantity in the same direction though not as far as do the values obtained by Davis and his collaborators using the double crystal spectrometer. It was thought worth while therefore to repeat the measurement by an ionization method which should be free from the errors suspected in the photographic work.

In this method two Pyrex x-ray tubes with molybdenum targets were placed side by side, and a Soller⁴ slit was used to increase the intensity of the modified radiation to be measured. Because of the low intensities of scattered radiation, an accurate determination of the position of the modified β line could not be made. The α doublet was therefore used, assuming in all calculations that $I_{\alpha_1} = 21\alpha_2$, so that the common center of gravity would be $1/3$ of their separation distance from α_1 .

The experimental arrangement is shown in Fig. 4. To prevent melting

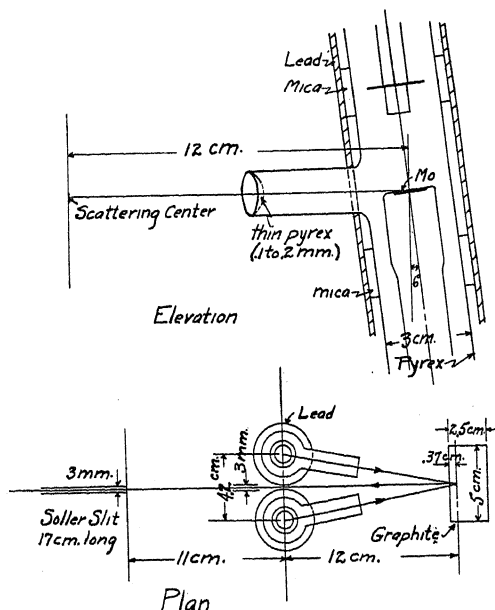


Fig. 4. Experimental arrangement for the ionization method.

³ This is the average of the values 0.02417 and 0.02428 calculated by Birge (Rev. of Mod. Phys. 1, 64, 1929) from the spectroscopic and the deflection values of e/m respectively.

⁴ W. Soller, Phys. Rev. 23, 292 (1924).

of the waxed ground joint near the cathode of the x-ray tube, it was necessary to maintain a jet of compressed air on each tube. The tubes were operated continuously at 50 kv peak and about 30 m.a. each. The ionization chamber was sulphur insulated and filled with argon. A block of graphite was used as the scattering material. The angle measurements were made from a slow motion screw attached to a Bragg spectrometer. Calibration by a mirror, lamp and scale, showed the readings to be reliable to within 3 seconds over the range of angles used.

Some six hundred runs were made over both the modified and the unmodified lines, and the difference between the positions of their peaks noted. This gave

$$\delta\theta = 27' 11.6'',$$

whence, using $D_{\text{calcite}} = 3.029\text{\AA}$,

$$\delta\lambda = 0.04757\text{\AA}.$$

The mean scattering angle was $168^\circ 39'$, whence

$$(1 - \cos \phi) = 1.9804,$$

and by Eq. (1),

$$h/mc = 0.0240 \pm 0.00024\text{\AA},$$

This result differs from the theoretical value of 0.02422\AA by less than the probable experimental error.

TABLE I. *Comparison of results.*

Author	Method	h/mc	Probable error per cent	Deviation from theory percent
Theory	Accepted values of constants	0.02422	0.3	—
Kallmann and Mark	Mo K , photographic	0.0242	1.	0
Sharp	Mo K , photographic	0.02432	0.4	0.4
Davis and Purks	Mo K ionization double crystal	0.0221	—	—9.
Dumond ⁵	Mo K Photographic	0.0234	—	—3.
Nutting ⁶	Mo K , (Photographic (peak)	0.02374	1(?)	—2.
Nutting	Mo K ionization, single crystal	0.0240	1	—0.9
Gingrich ⁷	Mo K ionization Double crystal	0.02424	0.2	0.1

⁵ This is the writer's estimate from the data published by DuMond.

⁶ The measurement on the center of gravity is not included for reasons given above.

⁷ N. S. Gingrich, *Phys. Rev.* **36**, 364 (1930).

This result was published after the work here described was completed.

It will be seen that most of the experiments lie somewhat below the value required by theory. However, the deviation is smallest for the experiments that seem to be most reliable, and it thus appears doubtful whether the difference is a real one. At least it can be said that the large deviation of the measurement of Davis and Purks is not confirmed by the other measurements.

STRUCTURE OF LINES

In the photographic method, there was a maximum spread of the modified line of 2.86 percent due to scattering angle variation. As is shown in Fig. 3, the modified line is not symmetrical, the long wave-length side being steeper. If we assume the same three principal components of the β modified line (neglecting γ of $1/7.7$ the intensity) as those given by Davis and Purks² for the α_1 line, they would have produced a high peak at the position indicated in Figure 3 by the long arrow and a much weaker one further out (shorter arrow). There is a mere suggestion only of such components in the curve. There seems to be no way in which sharply defined components such as those reported by Davis and Purks could form a curve like the one found in these experiments.

An examination of Figure 2 shows that the resolving power of the spectrograph was sufficient to separate the lines of the α doublet of molybdenum, which are 0.0043Å apart. The range of wave-lengths of the modified line due to the variation of 2.86 percent in $(1 - \cos \phi)$ is 0.0007Å, which is small in comparison with the apparent width of about 0.004Å of the β line. This means that the variation in scattering angle results in no appreciable widening of the lines. The apparent broadening of the modified line as compared with the fluorescent lines must therefore mean a variation in wave-length of the rays scattered at a definite angle, in accord with the conclusion of previous observers.

AN EXPERIMENTAL STUDY OF THE RELATIVE INTENSITIES OF X-RAY LINES IN THE TANTALUM L -SPECTRUM

BY VICTOR HICKS

UNIVERSITY OF CALIFORNIA, BERKELEY

(Received September 10, 1930)

ABSTRACT

The relative intensities of 17 lines in the L spectrum of tantalum have been investigated by the ionization spectrometer. The following precautions were taken: (1) the rays were taken at a glancing angle of 45° from a polished tantalum surface; (2) a tantalum filament was used; (3) the slits were enclosed in an arm of the tube reducing the air path of the rays to 7.35 cm; (4) the coefficient of reflection of the crystal used was measured for the various wave-lengths by means of the double-spectrometer; (5) the absorption coefficients of the mica windows used were directly measured; (6) the rays were completely absorbed in methyl iodide vapor of known pressure; and (7) the slits were sufficiently wide to eliminate effects arising from the different natural widths of the lines. Measurements were taken at 30.6 kv and 20.7 kv and corrected to high voltage. The results for lines of small wave-length separation agree well with previous measurements of Allison and Armstrong and Jönsson on tungsten. For lines of larger wave-length separation ($L\alpha_1$, $L\beta_1$) the results of Jönsson are not confirmed, but the previous qualitative estimates of Allison and Armstrong are substantiated. The assumption that the ionization currents produced are proportional to the relative intensities is supported by recent work of A. H. Compton. If the ν^4 correction is made to the intensities at high voltage, the sum rules are approximately valid except for lines having initial state L_I . The intensity results are:

	l	α_2	α_1	η	β_4	β_1	β_3	β_2	β_7
Rel. Int. at 30.6 kv	1.5	10	100	1.3	9.3	93	13	40	0.8
Rel. Int. at high V.	1.5	10	100	1.4	11.	103	16	40	0.8
	$\beta_5 + \beta_{10}$	β_9	γ_5	γ_1	γ_6	γ_2	γ_3	γ_4	
Rel. Int. at 30.6 kv	1.1	0.8	1.2	29	0.6	5.0	7.2	2.2	
Rel. Int. at high V.			1.4	32	0.7	5.9	8.5	2.6	

INTRODUCTION

THE relative intensities of the lines in the tantalum L spectrum have been investigated with an ionization spectrometer, the method used being similar to that previously employed by Duane and Patterson,¹ Allison and Armstrong,² and Allison.³ Considerable work has previously been done on the relative intensities in the tungsten L spectrum (atomic number 74). Duane and Patterson investigated the relative intensities of lines in the α , β , and γ groups, the members of which do not differ greatly in wave-length. They did not attempt to compare intensities of lines in different groups. Allison and Armstrong repeated and extended this work, and in addition made some qualitative estimates of the relative intensities of the more intense

¹ Duane and Patterson, Proc. Nat. Acad. Sci. 6, 518 (1920) 8, 85 (1922).

² Allison and Armstrong Phys. Rev. 26, 714 (1925).

³ S. K. Allison, Phys. Rev. 30, 245 (1927), 32, 1 (1928).

lines in the various groups, thus linking them together. Jönsson⁴ investigated the relative intensities in the L series of tungsten, using a Geiger counter, and gave results for all the lines in the L spectrum. Within the α , β , and γ groups, where wave-length differences are small, the results of Allison and Armstrong and Jönsson were in fair agreement, but for lines of wider wave-length separation (i.e. those separated by the $L_{II}L_{III}$ frequency difference) there were large discrepancies. For instance, Allison and Armstrong reported that $L\beta_1(M_{IV}L_{II})$ was slightly more intense than $L\alpha_1(M_V L_{III})$ whereas Jönsson found the intensity ratio of α_1/β_1 to be 100/51.8. He ascribed this lack of agreement to the fact that there was more absorption in the target in the experiments of Allison and Armstrong than in his; this explanation seemed quite reasonable, because they had obtained evidence of the L critical absorption discontinuities of the target in their general radiation spectrum.

The present experiments on tantalum (atomic number 73) were undertaken in order to add to our knowledge of the L -series intensities in general, and to investigate the cause of the discrepancies mentioned above in particular. They show that Jönsson's explanation of the differences cannot be correct.

APPARATUS

(1) *Power supply.* The high voltage direct current generating apparatus was that used by S. K. Allison for his measurements on the L -series of uranium.³ The potential difference applied to the x-ray tube was measured with an electrostatic voltmeter, consisting of a dumbbell hung on a bifilar suspension between two parallel plates, the whole being enclosed in a grounded metal case. A lens system formed an image of an incandescent lamp filament on a ground glass scale at a distance of 3.8 meters from a mirror mounted on the vertical axis of the dumbbell. The voltmeter was calibrated in the following manner: the crystal table angle corresponding to the K absorption limit of molybdenum was first carefully determined by observing the reflected intensities while moving the crystal through small angular steps with a thin molybdenum sheet in the path of the beam. The crystal was then set at the proper position to reflect the wave-length corresponding to this absorption limit, and the sheet of molybdenum removed. The limiting voltage to excite this wave-length was then determined by lowering the voltage in steps until no reflected intensities were observed. Three other points were taken on the calibration curve by the use of thin sheets of silver, tin, and cadmium.

The experiments were performed largely at 30.6 kv, although some measurements were taken at 20.7 kv. With two condensers in series in the high potential circuits, each of 0.050 mf capacity, the calculated fluctuation in the high voltage at 30.6 kv was 0.4 percent when a tube current of 3 ma was used. It was found convenient to operate the tube with the cathode grounded through the milliammeter.

(2) *X-ray tube.* The x-ray tube, the glass parts of which were constructed of Pyrex, is shown in Fig. 1. The most important features of this tube were:

⁴ A. Jönsson *Zeits. f. Physik* 36, 426 (1926).

(1) The slits were built into the tube as an integral part, thus cutting down the path of the rays in air; (2) the orientation of the cathode stream with respect to the axis of the tube could be changed while the tube was evacuated, thus permitting the focal spot to be brought opposite the slits. The slits were of iron, mounted on a tube of iron enclosed in a glass arm of the x-ray tube. The width of the slits was 0.18 mm, the height 1.6 cm, and the distance between the slits was 40.0 cm. This limited the horizontal angular width of the beam to approximately 3 minutes of arc. The x-ray beam left the tube through a mica window in a brass cap on the arm carrying the slits. As the slit system was fixed with reference to the anode, it was necessary to adjust

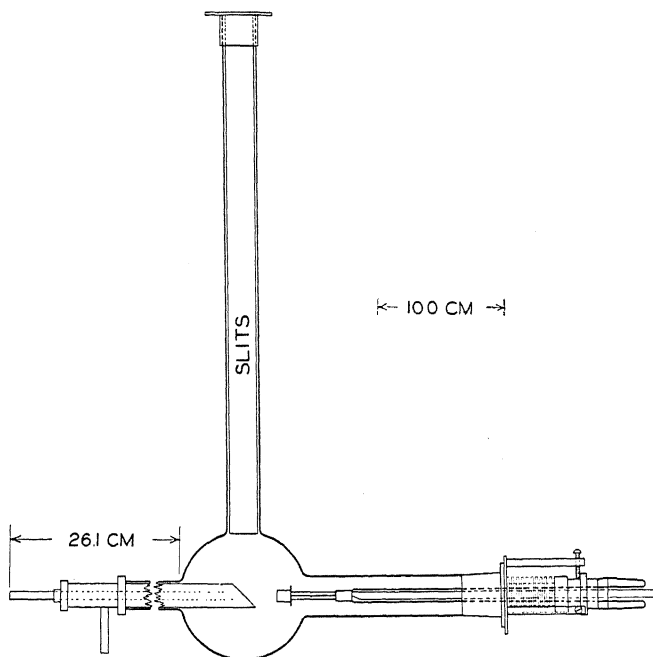


Fig. 1. Diagram of x-ray tube.

the position of the focal spot on the anode. This was accomplished by having a section of the arm of the tube carrying the cathode made of flexible silphon copper tubing. The orientation of the cathode beam with respect to the axis of the tube could then be changed by set screws, two of which are indicated in Fig. 1.

The anode was made of copper. A piece of sheet tantalum and a spool of tantalum wire 0.025 cm in diameter for filaments were given us by the Fansteel Products Co. The tantalum was 99% pure. The tantalum was spot-welded to a piece of nickel, and then the nickel soldered to the anode. With the tantalum spot-welded in about twenty points, no local heating was experienced at the low tube currents used, and the target was not pitted at the close of the experiments.

The anode was cooled by pumping kerosene through it. This prevented any electrical conduction to ground which might have taken place if water were used for cooling.

The x-ray tube was exhausted continuously while being operated. The tube and the glass part of the vacuum system were mounted on a stand which permitted translation, rotation, and leveling of the tube.

(3) *Spectrometer.* The spectrometer was of the Bragg type. Angular settings of the crystal were read with microscopes on an accurately divided circle 25.4 cm in diameter; settings could be made to 15 seconds of arc with ease, more precise settings were not necessary in this work. The axis of the spectrometer was 48 cm from the focal spot of the x-ray tube.

(4) *Ionization chamber.* The ionization chamber was of the type described by Williams and Allison.⁵ It was made of a Pyrex glass tube 4.7 cm in internal diameter and 33 cm long. To one end were attached the tubing and valves for introducing the gas and a ground glass joint for an iron guard ring. An amber plug supporting a nickel rod fitted tightly into the guard ring. The nickel rod was connected to the electrometer by very carefully shielded wires. Just inside the inner wall a cylinder of nickel gauze was placed as the charged electrode. The length of the gauze was 28 cm, and the nickel rod was 1.4 cm from the nearest point of the gauze. The end of the chamber towards the crystal was closed with a brass cap having a slit 0.3 cm wide by 2.9 cm high, over which a piece of mica was sealed with deKhotinsky cement. The effective angular width of this slit at the axis of the spectrometer was about 4°, so that it was not necessary to move the ionization chamber frequently when taking readings. A potential of 170 volts supplied to the nickel gauze by means of a dry battery was sufficient to insure saturation currents through the gas in the chamber, since frequent trials during the measurements showed that the rate of deflection of the electrometer was proportional to the electron current in the x-ray tube. Methyl iodide was used as the absorbing gas. A clear colorless liquid was obtained by stirring the methyl iodide with granulated zinc to remove any traces of free iodine. The liquid was then filtered into a small bulb, frozen by immersion in liquid air and the bulb sealed to the ionization chamber through a stopcock. The ionization chamber was then evacuated, keeping the methyl iodide immersed in liquid air, and the methyl iodide vapor introduced into the chamber through phosphorus pentoxide by allowing the liquid to warm up to room temperature gradually. Air was finally introduced over phosphorus pentoxide to bring the vapor in the chamber to atmospheric pressure.

(5) *Electrometer.* The electrometer was a Compton type used heterostatically. The currents were measured by observing the time rate of charging of the insulated pair of quadrants. A sensitivity of about 1800 scale divisions per volt with a mirror to scale distance of 1.75 meters was sufficient for the majority of the measurements.

⁵ Williams and Allison, J. Opt. Soc. Am. and Rev. Sci. Inst. 18, 473 (1929).

METHOD OF MEASURING INTENSITIES

A fundamental assumption in this method of measuring relative intensities is that the observed ionization currents are proportional to the intensities of the x-ray beams entering the ionization chamber, even when these beams differ in wave-length. This assumption will be discussed later. At present the method of obtaining what may with strict accuracy be called the relative ionization currents from the observed electrometer readings will be described. These were taken as proportional to the height of the tip of the peak representing the line above the base-line of scattered and general radiation. This method is justified if the following conditions hold true: (1) the curve representing each line must be symmetrical about the center of the line; (2) the resolution must be great enough so that the radiation due to a line is negligible at a distance from the center of the line equal to twice the wave-length separation from the nearest line; (3) the resolution must not be so great that the natural breadths of the lines play any part in the curve representing the line. Allison⁶ has found that in the iridium L spectrum the line $L\beta_2$ has an angular width at half-maximum corresponding to a range of reflection of about 45 seconds of arc from a single crystal of calcite in the first order. The angular width of the beam was 3 minutes of arc, and all the lines measured had the same full width at half-maximum, namely $2'30''$, so it is seen that assumption (3) was fulfilled. The angular width of the beam was not so great, however, as to violate the second assumption. For instance, the base-line for $L\alpha_1$, according to this method, is taken at an angle corresponding to $\lambda_{\alpha_2} + \Delta\lambda$, where $\Delta\lambda$ is the wave-length separation of α_1 and α_2 . By the symmetry of the lines, the radiation at this point is the fraction of α_2 appearing under α_1 plus baseline currents. The intensity at this point, however, was found to be very little different from that of the base-line farther away in agreement with condition (2).

CORRECTIONS TO BE APPLIED TO OBSERVED READINGS

Corrections to be applied to observed values arise from the following: (1) absorption of the rays in the target of the tube, (2) absorption in the mica windows in the tube and ionization chamber, (3) absorption by the air traversed by the beam, (4) incomplete reflection by the calcite crystal, (5) partial absorption in the ionization chamber. In computing the corrections for these factors ((4) excepted) the mass absorption coefficients of the materials were assumed to vary with the cube of the wave-length throughout the tantalum L spectrum. If μ is the absorption coefficient of the material for the line $L\alpha_1$, μ' that for another line, and t the thickness of the material, the correction to be applied to the intensity of the line relative to that of α_1 is

$$e^{-(\mu-\mu')t}$$

(1) The radiation used in the experiments was taken at an angle of 45° from the target face so that the thickness of the target traversed was the same for the impinging electrons and the emerging x-rays. No evidence of the L_{II} or L_{III} absorption discontinuities in the general radiation spectrum

⁶ S. K. Allison, Phys. Rev. 34, 176 (1929).

was found, as in the previous work of Allison and Armstrong on tungsten. The extent of the correction to be applied for this effect is probably less than 5 percent and is rather uncertain,⁷ so that no such correction has been applied here.

Further, since a tantalum filament was used throughout the experimental work, no foreign substance could have been deposited on the face of the target. This eliminates a doubtful correction which may enter when the target and filament are not of the same substance.

(2) The absorption coefficients of the mica used for windows were found by direct measurement to be 138 for Ta $L\alpha_1$, 93.5 for Ta $L\beta_1$ and 60.4 for Ta $L\gamma_1$. These values are approximately proportional to the cube of the wave-length, as expected. The total thickness of mica in the path of the beam was 0.0053 cm.

(3) Due to the fact that the slit system was a part of the x-ray tube, and therefore evacuated, the distance travelled by the x-rays in air was only 7.35 cm. From the values of μ/ρ for air listed in the International Critical Tables⁸ a mean value of 8.65 was computed for the mass absorption coefficient of air for the wave-length corresponding to $L\alpha_1$ of tantalum. The values of μ/ρ for the other lines in the spectrum were obtained from this value by assuming a variation proportional to λ^3 .

(4) The final measurements of the relative intensities of the lines $L\alpha_1$, $L\beta_1$ and $L\gamma_1$ which were used to link together the intensities in the α , β , γ groups were made with a crystal whose reflection coefficients for these wave-lengths were directly measured by the method of Davis and Terrill.⁹ The double spectrometer constructed in this laboratory and described by Williams and Allison⁵ was used, with a tungsten target tube. The voltage used was sufficiently low to prevent second order reflections at the angles concerned. The reflection coefficients per degree for the $L\alpha_1$, $L\beta_1$ and $L\gamma_1$ lines of tungsten were found to be 0.00208, 0.00222, and 0.00232 respectively. The corresponding wave-lengths in X.U. are 1473.5, 1279.2, 1095.5. The correction to be applied to the tantalum spectrum was computed from these values.

⁷ The measurements of Backhurst (Phil. Mag. 7, 353 (1929)) on the absorption coefficients of platinum and gold through the region of their L absorption discontinuities has made it possible to calculate these corrections to the platinum L spectrum, assuming that the penetration of the electrons in the target is roughly given by the Thompson-Whiddington law. The critical L series ionization potentials of platinum average about 13kv. Using values of the constant in the Thompson-Whiddington law from the paper of Terrill (Phys. Rev. 22, 101 (1923)) it is found that 34 kv electrons incident will penetrate 1.1×10^{-4} cm before their velocity is reduced to 13 kv. The depth of penetration of a large majority of the electrons is considerably less than this, due to the curving paths, and furthermore the classical theory predicts that they are most efficient in ionizing when their energy is twice that of the level to be ionized, that is, 26 kv electrons are most efficient in excitation of the platinum atom to the L state. If then we assume that the effective absorbing layer is half that above, and use Backhurst's absorption coefficients, we find that the largest correction to be applied in the L spectrum is a 5 percent reduction in $L\beta_1$ with respect to $L\alpha_1$.

⁸ International Critical Tables vol. VI, p. 16.

⁹ Davis and Terrill, Phil. Mag. 44, 463 (1923).

(5) The International Critical Tables⁸ list four mass absorption coefficients for methyl iodide corresponding to wave-lengths in the tantalum L spectrum. From these, a mean of 251 was computed for this coefficient for $Ta L\alpha_1$. The vapor pressure of the methyl iodide in the ionization chamber was 24 cm, the temperature, 20°C. This corresponds to a density of 2.17×10^{-3} gm/cm.³ Neglecting the absorption of the air introduced into the chamber, these data indicate that 99.9 percent of the line of shortest wave-length, γ_4 , was absorbed in the chamber. It is thus evident that no correction need be applied for the relative absorption in the ionization chamber.

RESULTS

The principal results of the investigation are shown in Table I, which gives the results of measurements taken at 30.7 kv. In column 6 of this table a factor is given by which the intensities at high voltage can be calculated. The intensities calculated by this factor would not take account of absorption in the target which might become more pronounced at high voltage. In making this calculation it was assumed that the variation of intensity with voltage of a line can be represented by

$$I_v = C(V - V_0)^{1.8}. \quad (2)$$

The exponent 1.8 was chosen, not from any independent determination of the variation of the intensity of lines in the tantalum L spectrum with voltage, but from the previous values of Jönsson⁴ who found 1.7 for tungsten, and Allison³ who found 1.8 for uranium. The voltage corrections to be applied to the tantalum L spectrum at 30.6 kv are small and the difference between the corrections computed with exponents 1.8 or 1.7 would be negligible.

TABLE I. *Relative intensities of lines in the tantalum L spectrum from ionization measurements at 30.6 kv.*

Line	Wave-length X.U.	Obs. Rel. intensity	Corr. factor for absorption	Rel. Int. 30.6 kv.	Factor to give rel. int. at high voltage	Rel. int. at high voltage.
l	1724	1.0	1.43	1.5	1.00	1.5
α_2	1530	10	1.02	10	1.00	10
α_1	1519	100	1.00	100	1.00	100
η	1466	1.4	.91	1.3	1.11	1.4
β_4	1343	12	.77	9.3	1.18	11
β_1	1324	122	.76	93	1.11	103
β_3	1304	18	.74	13	1.18	16
β_2	1282	56	.72	40	1.00	40
β_7	1260	1.1	.71	0.8	1.00	0.8
$\beta_5 + \beta_{10}$	1251	1.6	.70	1.1		(1.1)
β_9	1243	1.2	.69	0.8		(0.8)
γ_5	1170	1.9	.64	1.2	1.11	1.4
γ_1	1136	47	.62	29	1.11	32
γ_6	1110	1.1	.60	0.6	1.11	0.7
γ_2	1103	8.3	.60	5.0	1.18	5.9
γ_3	1097	12	.60	7.2	1.18	8.5
γ_4	1062	3.8	.58	2.2	1.18	2.6

The observed relative intensity of $\alpha_1:\beta_1:\gamma_1$, listed as 100:122:47 in column 3 of Table I has already been corrected for the measured coefficient of reflection of the calcite crystal used. The values observed without this correction were 100:128:52. Each value given in column 3 of Table I is the result of at least four independent measurements, which were averaged.

In the β group of lines, β_1 and β_6 could not be separated in the first order because of the wide slits used. Previous measurements with tungsten^{2,4} indicate that β_6 is about 2 percent as strong as β_1 ; thus a large error in the measurement of β_1 could not be made by the inclusion of β_6 under part of the curve. β_3 and the non-diagram line β_{10} have the same wave-lengths in tantalum; the sum of their intensities is given in the table, but not corrected to high voltage. No attempt was made to separate the very weak line β_8 from β_2 .

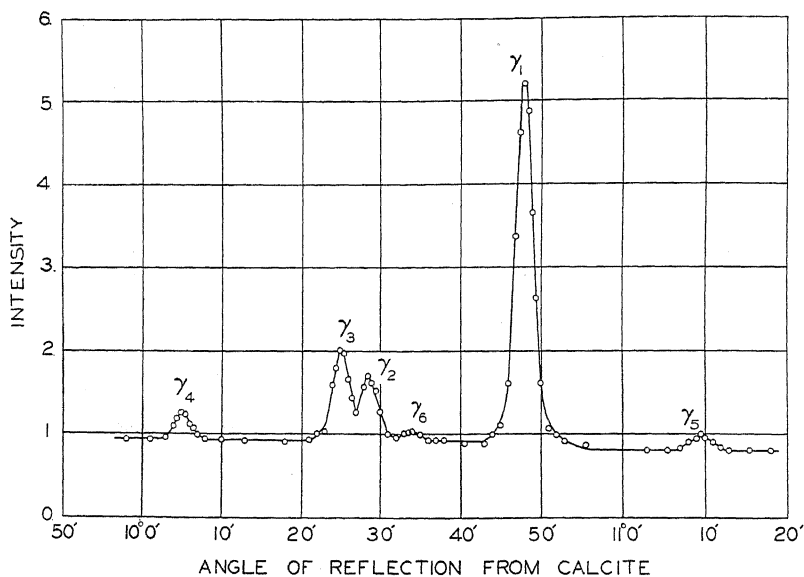


Fig. 2. Tantalum L spectrum, γ group.

In the γ group intensity measurements were made on all the lines listed by Lindh¹⁰ for tantalum. A typical ionization spectrum of the $L\gamma$ group is shown as Fig. 2.

DISCUSSION OF THE EXPERIMENTAL METHOD

Mention has previously been made in this paper of the grouping of the L -series lines (except the weak lines l and η) in three regions of small wavelength range compared to that of the spectrum as a whole. This fact makes it convenient to divide the problem of determining the relative intensities of the lines into two problems: (1) finding the relative intensities of the lines in a single group; (2) comparing the intensities of lines in different groups. The first of these problems seems to be comparatively simple. All investiga-

¹⁰ A. E. Lindh—Handb. der Experimentalphysik XXIV 2 Teil, p. 154 (1930).

tors have found the relative intensities of α_1/α_2 to be 100/10 or 100/11. Table II shows the results of three different investigations in the β and γ groups of the adjacent elements, tantalum and tungsten. The results of Allison and Armstrong quoted in Table II are the results originally in their paper multiplied by the appropriate high voltage factor to bring them to the same basis as the others.

TABLE II. *Relative intensities of lines in groups of small wave-length separation.*

Line	<i>L</i> β group.			Line	<i>L</i> γ group		
	Ta (73) Hicks	W (74) Allison and Armstrong	W (74) Jönsson		Ta (73) Hicks	W (74) Allison and Armstrong	W (74) Jönsson
β_1	(100)	(100)	(100)	γ_1	(100)	(100)	(100)
β_2	39	43	39	γ_2	18	15	16
β_3	16	16	16	γ_3	27	24	22
β_4	11	8.2	10	γ_4	8.1	7.5	6.5
β_5		.41	.39	γ_5	4.4	3.0	4.5
β_6		1.8	1.9	γ_6	2.2	2.3	3.3

In the measurement of the relative intensities of the lines $\alpha_1:\beta_1:\gamma_1$, representative of the α , β , and γ groups respectively, much larger differences between the measurements of Jönsson and the ionization chamber measurements are found. This is illustrated in Table III. It is evident that when larger wave-length separations are involved, much lower intensities for the

TABLE III.

Line	Ta (73) Hicks	W (74) Allison and Armstrong	W (74) Jönsson
α_1	(100)		(100)
β_1	103	"slightly more intense than α_1 "	51.8
γ_1	32	"more than $\frac{1}{2}$ as intense as β_2 "	9.1

shorter wave-length lines were obtained with the Geiger counter (Jönsson) than with the methyl iodide ionization chamber. The differences cannot be due to a sudden change in relative intensities between the elements tantalum and tungsten. In preliminary trials in these experiments a tungsten target was used and it was found that β_1 was somewhat more intense than α_1 , as previously reported by Allison and Armstrong, although quantitative measurements were not carried out on tungsten in the present research. In a later paper Jönsson has himself pointed out¹¹ that in the sensitive region near the point in the counter only a small fraction of the radiation is absorbed, and from the known absorption coefficients this fraction must vary with the wave-length of the line. Although Jönsson corrected his observations in the *L* series of the elements of atomic numbers 42-47 for this partial absorption, he did not apply this correction to his results on tungsten and platinum.

¹¹ Jönsson, *Zeits f. Physik* **46**, 383 (1928).

If this correction is applied to his results as given in column 4 Table III, values somewhat nearer those in column 2 are obtained. The remaining discrepancy may be due to the photo-electron range which in air is great enough to allow the ejected electrons to escape from the sensitive region near the point without producing their full quota of ions.

In the present research an experiment was performed to demonstrate the effect of this partial absorption in the detecting device. The methyl iodide vapor was pumped out of the ionization chamber and dry air admitted to a pressure of 15 cm. In a chamber 28 cm long this gives the same mass of air in the path of the x-ray beam as in Jönsson's experiments where a chamber 5.5 cm long was used at atmospheric pressure. Ionization measurements of $\alpha_1:\beta_1:\gamma_1$ were carried out in this air-filled chamber, and all corrections for absorption outside the chamber were made. The resulting "intensities" at high voltage were 100:43:5.7, which is of the order of Jönsson's results as quoted in column 4 of Table III. It must therefore be concluded that Jönsson's results in tungsten and platinum for lines of different groups are seriously in error due to neglect of this partial absorption factor.

Another difference between Jönsson's method of measuring and the one reported here is that his measurements were taken at 20 kv and extrapolated to high voltage, whereas the present measurements were taken at 30.6 kv and extrapolated. In order to find out if part of the differences between these results and his were due to this cause, a number of observations were made on the relative intensities of $\alpha_1:\beta_1:\gamma_1$ at 20.7 kv. These are listed in Table IV.

TABLE IV. *The ratios $\alpha_1:\beta_1:\gamma_1$ from measurements at 20.7 kv.*

Line	Observed rel. int.	Corr. factor for absorp.	Rel. Int. 20.7 kv.	Voltage Corr.	Rel. Int. high voltage
α_1	(100)	1.00	(100)	1.00	(100)
β_1	112	.76	85	1.24	105
γ_1	46	.62	28	1.24	35

The "observed relative intensities" given in column 2 of this table have already been corrected for the variation of the coefficient of reflection of the crystal with wave-length. From a comparison of Table IV and Table I it is apparent that measurements taken at 20.7 kv give approximately the same values as those taken at 30.6 kv when extrapolated to high voltage.

The method of measuring relative intensities used here has received considerable support from recent work by A. H. Compton.¹² Compton has shown that unless the saturation currents obtained in his ionization chamber (corrected for the fraction of the beam absorbed in the chamber, and the fraction of the fluorescent radiation produced in the chamber which escaped to the walls without production of photo-electrons in the gas) were proportional to intensities, the efficiency of production of fluorescent radiation for a given atom would be found to vary with the wave-length of the primary radiation. Compton states that his experiments support the conclusion that the ioniza-

¹² A. H. Compton, Phil. Mag. 8, 961 (1929).

tion by β -rays per unit energy is independent of their energy. Such conclusions had already been reached by Kulenkampff,¹³ Kircher and Schmitz¹⁴ and Crowther and Bond,¹⁵ but the experimental arrangement used by Compton was more like that used in these experiments in that he used an ordinary methyl bromide filled chamber rather than air. In the present experiments, the tantalum radiations entering the ionization chamber were never sufficiently hard to excite the K series of the iodine; only the relatively soft L series of wave-length around 2.8A could be emitted. From the dimensions of the chamber it may be calculated that only a negligible fraction of this iodine fluorescent radiation could reach the walls without expending itself in the production of photo-electrons. Furthermore, the range of the photo-electrons ejected by the tantalum L series wave-lengths from the iodine atoms was not over 2.5 mm as can be calculated from the Thompson-Widdington law. Therefore no photo-electrons could have reached the walls of the chamber without producing their full quota of ions.

DISCUSSION OF RESULTS

If it is conceded that the ionization method, as employed here and by Allison and Armstrong in tungsten, and Allison in thorium and uranium gives the correct relative intensities of the lines, the present results give the problem of the intensities of x-ray lines in the L -series an entirely new aspect. It is necessary to assume that the agreement between the measurements of Jönsson on tungsten (74) and those of Allison on thorium (90) and uranium (92) was fortuitous, and that the relative intensities in the L series undergo a large change in the region between atomic numbers 73 and 92. This is illustrated in Table V.

TABLE V. *Relative intensities at high voltage in the tantalum and uranium L-series*

	l	α_2	α_1	η	β_6	β_2	β_4	β_5	β_1	β_3	γ_5	γ_1	γ_2	γ_3	γ_6	γ_4
Ta(73) (Hicks)	1.5	10	100	1.4		40	11	<1.1	103	16	1.4	32	5.9	8.5	0.7	2.6
U(92) Allison	2.4	11	100	1.0	1.6	28	4.1	6.4	49	4.2	0	12	1.5	1.4	2.2	0

The development of the new quantum mechanics has made it increasingly evident that there is a factor in the expression for the intensities of spectral lines which is the fourth power of their frequency.¹⁶ This ν^4 correction is to be applied to widely separated multiplets in optical spectra, and the intensities so corrected should be governed by the sum rules or their extension in case the Boltzmann factors are not appreciably different for the initial levels of the transition. In the L -series, instead of the Boltzmann factor, we have an ionization function, which gives the relative number of atoms in the target ionized in the L_I , L_{II} , L_{III} levels by the impinging electrons.

¹³ H. Kulenkampff, Ann. d. Physik **79**, 97 (1926).

¹⁴ Kircher and Schmitz, Zeits. f. Physik **36**, 484 (1926).

¹⁵ Crowther and Bond, Phil. Mag. **6**, 401 (1928).

¹⁶ For instance Pauling and Goudsmit: The Structure of Line Spectra, McGraw Hill (1930) pp. 128-143.

Allison¹⁷ has pointed out that if the classical ionization function is taken, the relative intensity at high voltage of two lines having different initial states is very nearly equal to the ratio of the product of the transition probability by the statistical weight of the initial state. Since the transition probabilities involve ν^3 this suggests a ν^3 correction for lines involving different L sub-levels. Table VI gives the observed and corrected intensities and comparison with sum rule values.

TABLE VI.

Lines		Experimental relative intensities.	Corrected for ν^4 .	Corrected for ν^3 (for lines of different initial states)	Sum rules
$\alpha_1:\alpha_2:\beta_1$	$\left\{\begin{array}{l}\text{Ta}(73) \\ \text{U} (92)\end{array}\right.$	$\begin{array}{l}100:10:103 \\ 100:11:49\end{array}$	$\begin{array}{l}100:10:59 \\ 100:11:19\end{array}$	$\begin{array}{l}100:10:68\} \\ 100:11:24\}$	100:11:56
$l:\eta$	$\left\{\begin{array}{l}\text{Ta}(73) \\ \text{U} (92)\end{array}\right.$	$\begin{array}{l}100:93 \\ 100:46\end{array}$	$\begin{array}{l}100:49 \\ 100:15\end{array}$	$\begin{array}{l}100:57\} \\ 100:20\}$	100:50
$\beta_3:\beta_4$	$\left\{\begin{array}{l}\text{Ta}(73) \\ \text{U} (92)\end{array}\right.$	$\begin{array}{l}100:69 \\ 100:98\end{array}$	$\begin{array}{l}100:78 \\ 100:120\end{array}$	$\begin{array}{l}\} \\ \end{array}$	100:50
$\beta_2:\gamma_1$	$\left\{\begin{array}{l}\text{Ta}(73) \\ \text{U} (92)\end{array}\right.$	$\begin{array}{l}100:80 \\ 100:43\end{array}$	$\begin{array}{l}100:49 \\ 100:19\end{array}$	$\begin{array}{l}100:56\} \\ 100:23\}$	100:50
$\gamma_3:\gamma_2$	$\left\{\begin{array}{l}\text{Ta}(73) \\ \text{U} (92)\end{array}\right.$	$\begin{array}{l}100:69 \\ 100:107\end{array}$	$\begin{array}{l}100:71 \\ 100:112\end{array}$	$\begin{array}{l}\} \\ \end{array}$	100:50

From Table VI it is seen that a ν^4 correction brings the relative intensities of lines in tantalum multiplets containing the large $L_{II}L_{III}$ separation surprisingly near the sum rule values. In uranium, on the other hand, the experimental results, uncorrected for frequency, are near the sum rule values, and if frequency corrections are made, wide departures from the rules are found.

In x-ray spectra, in contrast to optical spectra, there always exists the possibility of an internal radiationless transition, or Auger effect. If the probability of such an event taking place varies with the atomic number of the element, and is different for different L -series lines, an explanation of Table VI could perhaps be presented on this basis. So very little is known about the Auger effect for L -series lines, however, that at present, speculation seems futile.

It is indeed a pleasure to thank Professor S. K. Allison for the suggestion of this problem and for valuable assistance during the investigation.

¹⁷ S. K. Allison, Phys. Rev. 32, 1 (1928).

A STUDY OF THE VELOCITIES OF H^+ IONS FORMED IN HYDROGEN BY DISSOCIATION FOLLOWING ELECTRON IMPACT

BY W. WALLACE LOZIER

PHYSICAL LABORATORY, UNIVERSITY OF MINNESOTA

(Received September 11, 1930)

ABSTRACT

An apparatus is described which is suitable for a study of the velocity distribution of ions formed by single electron impact. Electrons, confined to a narrow beam by a magnetic field, pass along the axis of two coaxial cylinders, ionize the gas, and are collected by a trap. The thick, inner cylinder, which is slotted, serves to allow only ions moving perpendicularly to the electron beam to pass to the outer collecting cylinder. A retarding voltage is applied between the cylinders. A study of the positive ion current collected as a function of the retarding voltage permits a determination of the velocity distribution of the ions. The above method is employed in a study of hydrogen.

Velocity distribution of H^+ ions formed by electron impact in H_2 . Theory shows that when the H_2 molecule is ionized by electron impact, it may prove unstable and dissociate into $H^+ + H$ (or H') or into $H^+ + H^+$ if two electrons have been removed. The H^+ ions thus formed possess kinetic energy. The H^+ ions coming from dissociation into $H^+ + H$ should occur at minimum electron velocities of about 27 to 40 volts, possessing roughly 5 to 11 volts velocity; while the H^+ ions resulting from removal of two electrons occur at minimum electron velocities of 46 to 56 volts, possessing 7.5 to 12.5 volts velocity. In agreement with the predictions of the theory it was found that the velocities of those ions resulting from dissociation into $H^+ + H$ and $H^+ + H^+$ together with the minimum velocities necessary to produce them satisfy linear relationships.

INTRODUCTION

AS PREDICTED by Condon¹ and first experimentally verified by Bleakney and Tate² and Bleakney³ the ions formed by electron impact in hydrogen will, in general, if molecular dissociation follows the ionization process, acquire kinetic energies corresponding to several electron-volts. The repulsive forces which are operative in the dissociation process and to which the ions owe their resultant kinetic energies are due, in case both electrons are removed from the H_2 molecule, to the ordinary classical repulsion of two protons. In the case of the removal of but one electron from the molecule, however, the repulsive forces between the proton and the neutral (or possibly excited) H atom are non-classical and find their interpretation in terms of the quantum mechanics.⁴ For this reason a more precise experimental study of the energy distribution among the ions so formed than was

¹ E. U. Condon, Phys. Rev. 35, 658 (1930) (Abstract).

² W. Bleakney and J. T. Tate, Phys. Rev. 35, 658 (1930). (Abstract).

³ W. Bleakney, Phys. Rev. 35, 1180 (1930).

⁴ Burrau, Kgl. Danske Vid. Selskab. Math-fys. Med. 7, 14 (1927). P. M. Morse and E. C. G. Stueckelberg, Phys. Rev. 33, 932 (1929).

possible with the experimental arrangement of Bleakney and Tate was deemed advisable and was undertaken at their suggestion.

PREDICTIONS OF THE THEORY

The theoretical potential energy curves for the hydrogen molecule given by Bleakney from sources quoted in his article³ are reproduced in Fig. 1. The ordinates of these curves represent the potential energies, in volts,

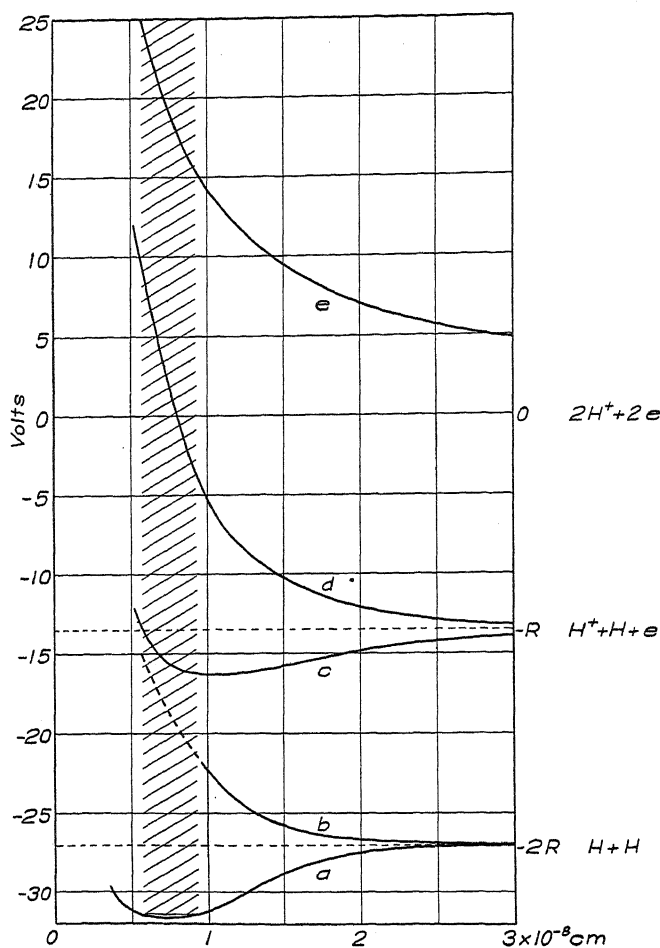


Fig. 1. Potential energy curves for the H_2 molecule.

of the various modes of bringing together the constituents of the hydrogen molecule as a function of the nuclear separation in Angstrom units. The zero of energy is taken with all of the constituents an infinite distance apart.

Curves *a* and *b* represent the two modes of bringing together two normal H atoms to form an H_2 molecule. The state *b* is unstable, while the state *a* represents the stable H_2 molecule. Curves *c* and *d* represent the two modes of bringing together a proton and a normal H atom to form the H_2^+ molecular ion. Curve *e* represents the one mode of bringing together two protons

to form an unstable H_2^{++} ion. The shaded area on the diagram represents approximately the range of separation of the two H atoms in the lowest vibration state of the H_2 molecule. It must be pointed out that this region is not entirely definite. The relative probability of finding the normal molecule with a given separation is greatest for the position of minimum potential energy and diminishes for separations greater or less than this. There is, however, some slight probability of finding the molecule with separations lying outside the shaded area.

The Franck-Condon principle states that transitions caused by electron impact, from the normal state to the states represented by the upper curves will be undergone without appreciable change in the nuclear separation. The molecule can be raised to the various states by an impacting electron possessing sufficient energy. Transitions to the state *b* would result in the dissociation of two normal atoms having from 3 to 6 volts kinetic energy. These have no significance for the present experiment, for the products would be uncharged. Transitions to state *c* would result in two possibilities. If the molecule be raised to any potential below -13.5 volts there would be formed stable H_2^+ . However, for transitions to slightly higher potentials dissociation could result, giving H^+ and H possessing small amounts of kinetic energy. Only slight evidence for this transition was observed in the present experiment, however it has been observed by Bleakney³ and has been suspected by others.⁵ At minimum electron velocities of 27 to 40 volts, transitions to state *d* should be effected, resulting in dissociation into H^+ and H, each having velocities of 5 to 11 volts. With minimum electron velocities of 46 to 56 volts transitions to *e* should be possible, resulting in two H^+ ions having from 7.5 to 12.5 volts velocity. These are the transitions with which these experiments are concerned. The values given assume the transitions to take place within the shaded area. Since there is some probability of finding the molecule with separations beyond this region we would not expect the velocity distribution of the ions to terminate abruptly at the given values, but quite rapidly decrease beyond these.

In addition to these potential energy curves, there are a number of similar ones, not shown, corresponding to the removal of one electron from the H_2 molecule followed by dissociation into H^+ and H in its various excited states. In these experiments there was observed no evidence of transitions leading to dissociation into $H^+ + H'$. This leads one to suspect a relatively low probability for these processes.

Relations between energy of ions and energy of impacting electron. The electron velocity necessary to produce a given velocity ion from one of the states may well be called the ionization potential for the formation of an ion of that velocity from the specified state. If the initial energy of the molecule be E_1 , that after dissociation E_2 , the ionization potential V_i , and the kinetic energy of the ions V_F , then for the states *d* and *e*, or any similar ones,

⁵ H. D. Smyth, Proc. Roy. Soc. A105, 116 (1924) and Phys. Rev. 25, 452 (1925). T. R. Hogness and E. G. Lunn, Proc. Nat. Acad. Sci. 10, 398 (1924) and Phys. Rev. 26, 44 (1925).

$$V_i = (E_2 - E_1) + 2V_F. \quad (1)$$

This assumes; the dissociating entities possess equal kinetic energies, and no radiation takes place during the process of dissociation. For transitions to the state d this becomes

$$V_F = \frac{1}{2}V_i - \frac{1}{2}(31.4 - 13.5) \text{ (volts)} \quad (2)$$

While for transitions to the state e

$$V_F = \frac{1}{2}V_i - \frac{1}{2}(31.4 - 0). \quad (3)$$

These are the equations of straight lines with the slope one-half. Regardless of the shape of the potential energy curve for either of these states, the velocities of the ions and their ionization potentials must satisfy the relations above. The shape of the potential energy curves would, however, have an effect upon the form and range of the velocity distribution curve of the ions.

THE APPARATUS

The apparatus, shown in Fig. 2, was constructed of copper and was sealed in a Pyrex glass tube, which was then evacuated and baked out

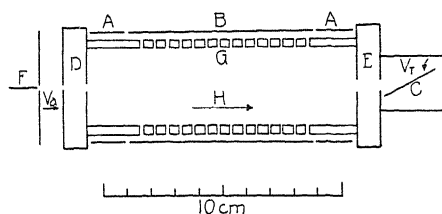


Fig. 2. Diagram of the apparatus.

several hours at 400° C. The source of electrons was a fine, sharply-pointed tungsten wire filament. An accelerating potential V_a was applied between the mid-point of the filament and the diaphragms D . The electrons passed through the holes in D and then through those in the diaphragms E and were finally collected at C . V_T was a potential of 175 volts holding the electrons to the plate C . A magnetic field H in the direction of the electron beam prevented any lateral spread. The electrons in traversing their path ionized the gas and ions were liberated, presumably in all directions. G was a circular cylinder with its axis along the electron beam. In it were cut a number of slots running around the circular boundary of the cylinder. These served to define the directions of the positive ions issuing from the electron beam and let pass only those ions having velocities very nearly perpendicular to the axis of the cylinder. These slots were of dimensions, 0.5 mm wide and 3 mm thick, requiring that the ions have 98 percent of their velocity or 96 percent of their volt-velocity perpendicular to the electron beam in order to pass through the slots. Parts A were cylindrical guard rings to B . Between A and G could be applied on the ions a retarding potential V_R . A Compton

electrometer with suitable carbon ink shunts was connected between *A* and *B* to measure currents to *B*.

The flow method was used to obtain a supply of hydrogen, which was admitted through a palladium tube surrounded by an electrical heating coil. The pressure used was estimated to be of the order of 2.0×10^{-4} mm Hg.

It was necessary to use electron currents of from 5 to 8 microamperes to obtain measureable positive ion currents.

For all of the data shown there was an initial velocity correction of 1.5 volts to be applied to the potential V_a . This was determined by noting the ionization potential of mercury vapor, which was not completely eliminated from the tube but was reduced to a very low pressure by liquid oxygen.

For such light ions as those of hydrogen the effect of the magnetic field upon the ions is not negligible. The effect was calculated. If ions be formed at the center of the cylinder with volt velocity V_F and pass out perpendicularly to the axis of the cylinder and are just able to reach *B*, in the presence of a retarding potential V_R and the magnetic field H , then

$$V_F = V_R + 300b^2eH^2/8mc^2 \text{ (volts)} \quad (4)$$

where b is the radius of the collector *B* in cm, e/m is the specific charge for the ion in e.s.u./gr., and H is the magnetic field in gauss. For H^+ ions, using the constants of the apparatus, this becomes

$$V_F = V_R + 0.63 \times 10^{-4}H^2 \text{ (volts)}. \quad (5)$$

For 100 and 150 gauss this correction becomes 0.63 and 1.42 volts, respectively.

VELOCITY DISTRIBUTION OF THE IONS

The relative abundance of the positive ions at the various values of V_R was found by measuring the change in the electrometer current on varying V_R by a small amount ΔV , one-half of this on each side of the voltage V_R . Graphically, it was found that $\Delta V = 0.5$ volts was a small enough differentiating potential to give within the experimental error the form of the derivative curve of the total positive ion current-retarding potential curve for ions having velocities greater than 1.5 volts. The results are shown in Fig. 3. The magnetic field used was 100 gauss except in the 200 and 250 volt curves, for which it was 150 gauss. These curves were all taken at the same pressure and as shown have been reduced to equivalent electron current.

Curves of the ions without appreciable kinetic energy are not shown because the presence of mercury ions invalidated the results. It should be remarked, that, because of the magnetic field, theoretically there should be collected no H_2^+ ions having velocities of formation less than 0.3 volts. Actually a high peak is observed, coming in at about 15.5 volts electron velocity, with a velocity distribution maximum at about 1.0 volts. This is a much larger velocity than their expected temperature velocity at 25°C . It is to be remarked that the low velocity ions might be bent into small circles by the magnetic field, thereby creating an appreciable positive ion space charge which would impart to the ions some kinetic energy. Or, there

might exist an appreciable contact potential between the collecting cylinder and the defining cylinder *G*. Nevertheless, the corrections given by Eq. (5) were those applied.

For electron velocities up to 45 volts the maximum *D* of the velocity distribution curve shifts toward higher velocities as would be expected, for the electrons are acquiring sufficient velocities to produce the higher velocity ions. From 45 to 55 volts it remains approximately unchanged. Beginning

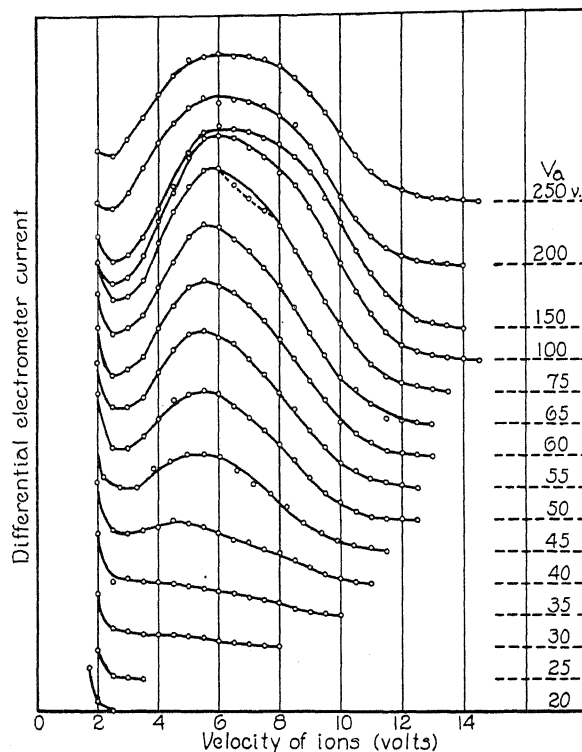


Fig. 3. Velocity distribution of the positive ions. An initial velocity correction of 1.5 volts should be applied to the values of V_a . The velocities of the ions have not been corrected for the effect of the magnetic field.

at about 60 volts the higher velocity ions increase noticeably in numbers, while the increase below the maximum is comparatively smaller. This is attributed to the yield of ions from the state *e*.

IONIZATION POTENTIALS

Ionization potentials for those ions resulting from transitions to state *d* were determined by setting a certain retarding potential V_R and varying the potential V_a until positive ion current began to reach *B*.

Ionization potentials for those ions formed by transitions to state *e* required a little different procedure. Theoretically those ions having velocities between 7.5 and 11.0 volts could also be obtained by transitions to state *d*.

Therefore for this range the ionization potentials must be detected as upward breaks in the positive ion current vs. electron velocity curves for the various values of V_R . These results are shown in Fig. 4. In these curves the

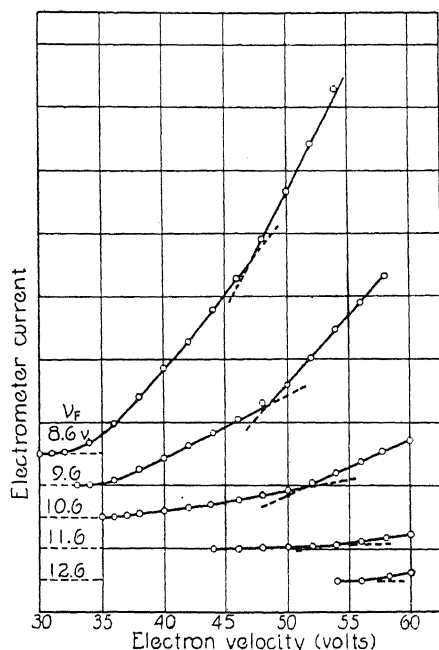


Fig. 4. Curves showing positive ion current reaching collecting cylinder against a definite retarding voltage, as a function of the electron velocity. The accelerating potential should be increased by 1.5 volts.

values of V_R have been corrected for the effect of the magnetic field. The electron velocities should however be increased by 1.5 volts, the initial velocity correction. The ionization potentials were determined and the results were plotted in Figs. 5 and 6. In Fig. 5 the straight line gives the theoretically predicted values for the state d , and Fig. 6 those for the state e .

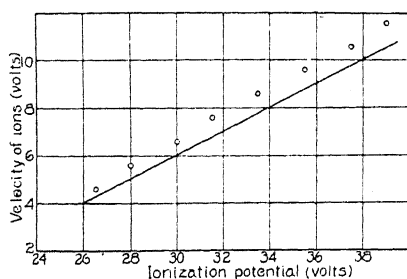


Fig. 5.

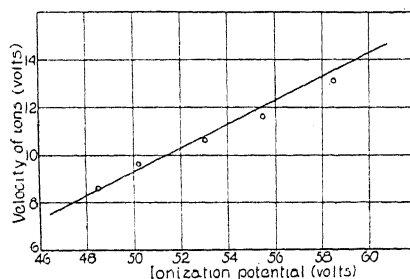


Fig. 6.

Relations between the velocities of the ions and their ionization potentials for transitions to states d (Fig. 5) and e (Fig. 6). The straight lines represent the theoretical relations and the circles represent the experimental values.

The circles give the experimental points. In these figures the above-mentioned corrections have been made.

Of the possible disturbing effects mentioned above, space charge would account for the direction of the discrepancy in Fig. 5. The effect of contact potential might cause a deviation in either direction. However, applying such a correction, the points in Fig. 6 would then lie below the straight line. But it is to be noticed that in Fig. 4 the breaks were taken at the intersections of the extrapolated straight lines, while it may be that they should have been taken at lower electron velocities, corresponding to the point where the smooth curve began to break away from the first straight line. In the last two curves of Fig. 4 the currents were quite small and the intersection with the zero axis is rather indefinite. This is to point out that the discrepancies are by no means serious.

CONCLUSIONS

The results of the present work constitute a striking confirmation of the essential correctness of the quantum mechanical theory of the hydrogen molecule. They provide a new method of attack on the general problem of molecular mechanics which will supplement the information gathered from the studies of band spectra by revealing the energy content of the unstable configurations of the molecule.

The experiments are now being extended to other gases. In conclusion, the writer wishes to express his gratitude to Professor John T. Tate and Dr. Walker Bleakney for their suggestion of the problem and for many practical aids throughout the investigation.

THE IONIZATION OF HELIUM, NEON,
AND ARGON BY ELECTRON IMPACT

BY PHILIP T. SMITH

PHYSICAL LABORATORY, UNIVERSITY OF MINNESOTA

(Received September 11, 1930)

ABSTRACT

Quantitative measurements have been made of the total number of positive charges produced per electron per cm path at a definite pressure, in helium, neon, and argon, as a function of the energy of the impacting electrons out to 4500 volts. In helium the maximum efficiency 1.256 occurs at 110 volts, in neon 3.008 at 170 volts, and in argon 13.01 at 88 volts.

An empirical relation has been found which expresses the efficiency of ionization of helium within the experimental error for energies greater than 60 volts.

The data obtained differ considerably from that found by previous investigations, but because of the more precise length of path from which the positive ions were measured and the more accurate knowledge of the energy of the electrons as well as the elimination of secondary electrons, it is believed that the results presented here are the most accurate thus far obtained.

SEVERAL investigations have been made of the efficiency of ionization by electron impact in various gases.¹⁻⁹ Five different methods have been used, with results which are not in satisfactory agreement. The most extensive investigations were those of Hughes and Klein³ and Compton and Van Voorhis.^{1,2} After applying certain necessary corrections to the data of Hughes and Klein, Compton and Van Voorhis² were able to make these data qualitatively substantiate their own. Jones⁴ and Bleakney⁵ using a method suggested by Professor Tate measured the efficiency of ionization in Hg vapor with results which agreed only qualitatively with those of Compton and Van Voorhis.

Hummel⁶ who studied Ne, A, and K by a method similar to that of Jones also agreed only qualitatively with Compton and Van Voorhis for Ne and A. The complicated effects present in the method used by Jesse⁷ make it impossible to compare his results with those of the others. Finally the results of von Hippel⁸ and Funk⁹ cannot be reconciled at all with the results of the other observers.

Because of these discrepancies in the measured values of the efficiency of

¹ Compton and Van Voorhis, *Phys. Rev.* **26**, 436 (1925).

² Compton and Van Voorhis, *Phys. Rev.* **27**, 724 (1926).

³ Hughes and Klein, *Phys. Rev.* **23**, 450 (1924).

⁴ T. Jones, *Phys. Rev.* **29**, 822 (1927).

⁵ W. Bleakney, *Phys. Rev.* **34**, 157 (1929); **35**, 139 (1930).

⁶ A. D. Hummel, Thesis, University of Illinois (1928).

⁷ Jesse, *Phys. Rev.* **26**, 208 (1925).

⁸ von Hippel, *Ann. d. Physik* **87**, 1035 (1928).

⁹ Funk, *Ann. d. Physik* **4**, 149 (1930).

ionization it was thought desirable to redetermine them by a method as free as possible from those sources of error which are inherent in most of the methods previously used and also to extend the work to higher voltages.

In this paper are presented the results obtained by using a method similar to that employed by Jones,⁴ Bleakney⁵ and Hummel.⁶

APPARATUS AND PROCEDURE

The apparatus, Fig. 1, was made of copper with Pyrex insulation. It was baked out at a bright red heat before, and at about 400°C for two days after, it was placed in the tube. A Pyrex tube with no wax joints was used. It was surrounded by a solenoid to develop the magnetic field H which facilitated the separation of the positive ions from the electrons and also served to define the electron beam. The electron source was the filament F made of fine tungsten wire bent in the form of a hairpin about 1 mm wide. The holes

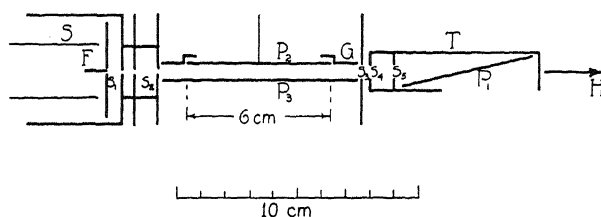


Fig. 1. Diagram of apparatus.

S_1 and S_2 were about 1.5 mm in diameter. This arrangement eliminated the presence of secondary electrons from the metal parts, since the magnetic field and not the slits defined the electron beam. Thus none of the electrons could collide with any metal until they reached the collecting plate P_1 which was connected to the grounded box T through a galvanometer G_1 (sensitivity 1500 megohms) and a set of B batteries (400 volts). S_3 was 5.5 mm in diameter while S_4 and S_5 were 5 mm in diameter.

The plate P_1 was covered with soot and, as stated above, maintained 400 volts positive with respect to T . Thus any electron which left P_1 would be in a field whose direction was nearly perpendicular to the axis of the tube and would have to go through a retarding potential of 400 volts before it could leave T . That P_1 collected all of the electrons is indicated by Fig. 2 in which the electron current to P_1 , for various values of V_a , as a function of the potential of P_1 is shown.

The plate S_1 , shield S , and the filament F (heated by the current from an insulated battery) were at the same potential $-V_a$ with respect to S_2 which was grounded.

The plate P_2 , 6.05 cm \times 2 cm was connected to the guard-ring G through the galvanometer G_2 (sensitivity 45,000 megohms) which measured the positive ions produced by the electrons in the 6.05 cm path directly below P_2 . The positive ions were drawn out of the electron beam by an electric field between P_2 and P_3 which were 6 mm apart and maintained at 4 volts difference of potential. G and P_3 were connected together by a high resistance,

the midpoint of which was grounded, so that the speed of the electrons would not be appreciably altered after they left the last slit S_2 until they passed through S_4 which was at the same potential as S_2 .

Compton and Langmuir¹⁰ have pointed out that probability of ionization by an electron in terms of the total number of collisions made per unit path by the electron is not easy to measure nor to define accurately, and consequently it is better "to deal directly with the more accurately determined quantity, the number of new electrons produced by ionization per unit path at a specified gas pressure by an electron of given energy. This may be called

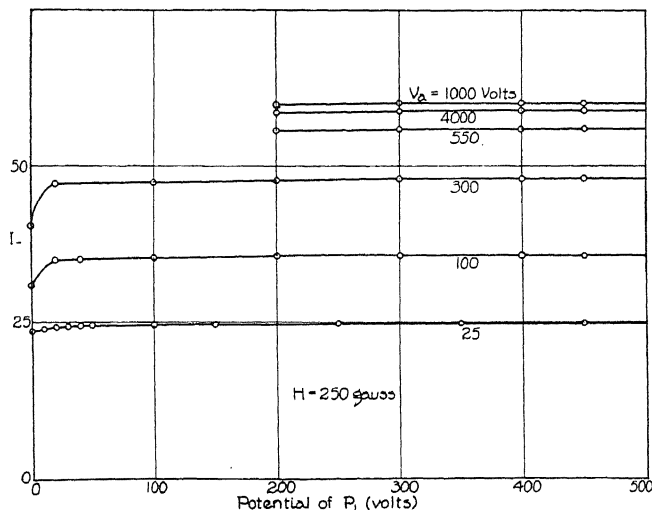


Fig. 2. Characteristics of electron trap.

the probability of ionization per unit path at unit pressure." In the present paper this quantity will be called the "efficiency of ionization," with the further specification that the temperature be 0°C .

The efficiency of ionization, ϵ , as defined above is given by the relation

$$\epsilon = (I_+/I_-) [(T_1 T_2)^{1/2} / 273 l p]$$

where I_+ is the positive ion current collected by the plate P_2 and measured by the galvanometer G_2 , I_- the electron current collected by P_1 and measured by the galvanometer G_1 , T_1 and T_2 the respective absolute temperature of the McLeod gauge and apparatus, l the length of the plate P_2 , and p the pressure of the gas in mm of Hg. T_1 was measured by a thermometer and T_2 by a thermocouple connected to the center of P_2 and at one edge, P_2 serving as one junction.

For He and Ne pressures from 1.0 to 1.6×10^{-3} mm of Hg were used. In argon the final results were obtained by using a pressure of 0.277×10^{-3} . At these pressures the ratio of the maximum positive ion current to plate P_2 to the electron current to P_1 was always less than 0.02, consequently the electron current could at the most not be more than 2 percent too high,

¹⁰ Compton and Langmuir, *Rev. of Mod. Phys.* **2**, 129 (1930).

even though the new electrons from the positive ions were measured. At these pressures the chance of an electron colliding more than once before it reaches the electron trap T is small enough to be neglected.

The electron current¹¹ collected by P_1 , which came from the ions formed within T , was smaller than the accuracy with which the total electron current could be measured.

Fig. 3 is a typical saturation curve for the positive ion current to P_2 . The positive ion current to P_2 is shown as a function of the difference of potential in volts between P_2 and P_3 , with the magnetic field H equal to 250 gauss, the field used throughout this investigation. Similar curves up to $V_a = 4500$

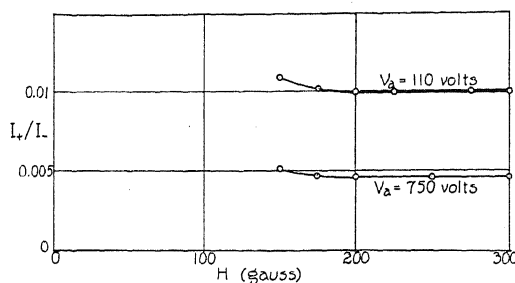


Fig. 3. Typical saturation curve for positive ions.

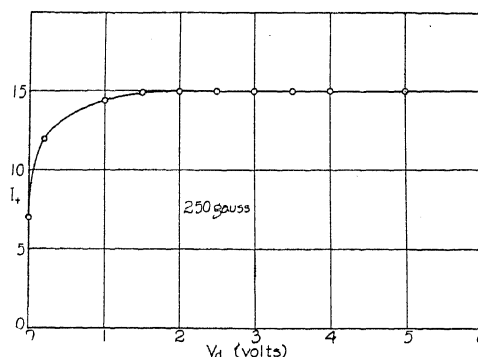


Fig. 4. The ratio of the positive ion current to the electron current as a function of the magnetic field.

volts were obtained. That none of the positive ions measured came from T was concluded, since no positive ions were collected when V_a was less than the ionization potential of the gas in the tube, with P_1 at a high potential.¹²

¹¹ The total current to T and P_1 , was not measured by a single galvanometer, since such an arrangement would have required a well insulated set of "B" batteries which were not available. The electrical circuit was, however, arranged so that the current to either could be measured at any time without altering any of the conditions existing in the tube.

¹² The question as to whether any photo ionization might be present which would alter the values of ϵ was experimentally tested. P_2 was removed and replaced by a narrow plate to collect the ions formed by direct impact. On each side of this plate was a wider plate connected to an electrometer. The results showed that if any photo ionization did occur it was too small to effect the efficiency measurements.

Fig. 4 indicates that the ratio of the positive ion current to the electron current was independent of the magnetic field, near the value used when readings were taken. The higher ratio obtained with lower magnetic fields is explained by the spreading of the electron beam, since a negative current was collected on *T* with the lower fields. This current was just great enough to account for the increase in the ratio. With higher fields no electron current was collected by either *S*₃ or *T*.

The gases used were commercially pure. The helium and neon were further purified by connecting to the tube a charcoal trap immersed in liquid oxygen. The purity of the helium is indicated by the curve for helium in Fig. 7, that is, any appreciable amount of foreign gas would have resulted in ionization below the ionization potential of helium. Helium has the highest ionization potential and the lowest efficiency of any of the gases. Dr. Bleakney made an analysis with a mass spectrograph of the neon used and found a trace of helium present (not more than one percent). Helium is the only gas with an ionization potential higher than that of neon and consequently the curve in Fig. 8 would not show the presence of a small amount of helium. However the presence of one percent of He in Ne would not affect the results by more than 2/3 percent, since the efficiency is not very different for the two gases. Charcoal absorbs a little more neon than helium but the results are probably not off by more than one percent due to the presence of the helium. Bleakney found no impurities at all in the argon for which CO₂ snow in acetone was used in place of the liquid oxygen.

The pumps were sealed off from the tube by a mercury trap. (The mercury vapor was frozen out by a trap immersed in liquid oxygen.) The gas to be studied was allowed to leak into the tube through a small capillary until the desired pressure was obtained, after which the flow was cut off. No ionization could be detected before the gas was admitted, although an electron current four or five times that used in taking the readings was employed. The tube was allowed to stand for about two hours after the gas had been admitted, to be sure that a pressure equilibrium had been established between the charcoal and the gas. It was found that the variations in the pressure were less than one percent over a period of 12 hours. After a complete set of observations had been taken, readings were repeated at intervals over the entire range of accelerating potentials used. Any observation could be checked to within one percent. Curves obtained on different days checked very closely except at the highest potentials where variations of several percent occurred.

In the calibration of the McLeod gauge, etc., an attempt was made to reduce all constant errors to a minimum.

RESULT

Fig. 5 shows the results obtained for He, Ne, and A up to 1500 volts, (readings were taken up to 4500 volts). The efficiency of ionization as defined above is shown as a function of the accelerating potential of the electrons.

The break in the curve for argon at about 57 volts was at first hard to

account for, since the energy necessary to form A^{++} as a primary product is 43.51 volts.¹³ The results of Bleakney¹⁴ however indicate that this would be expected, due to the peculiar form of the efficiency of ionization curve for A^{++} .

Professor Tate has derived the empirical relation

$$\epsilon = 3.383(V_0/V_a)^{1/2} [1 - e^{-54V_0/V_a}]^{1/2} [1 - e^{-(V_a - V_0)/2.28V_0}]$$

which expresses the efficiency of ionization of helium within the experimental error for $V_a > 60$ volts out to 4500 volts. Below 60 volts this formula yields values of ϵ which are higher than the observed values, since the observed values approach a linear function of V_a near the ionization potential while the above formula does not.

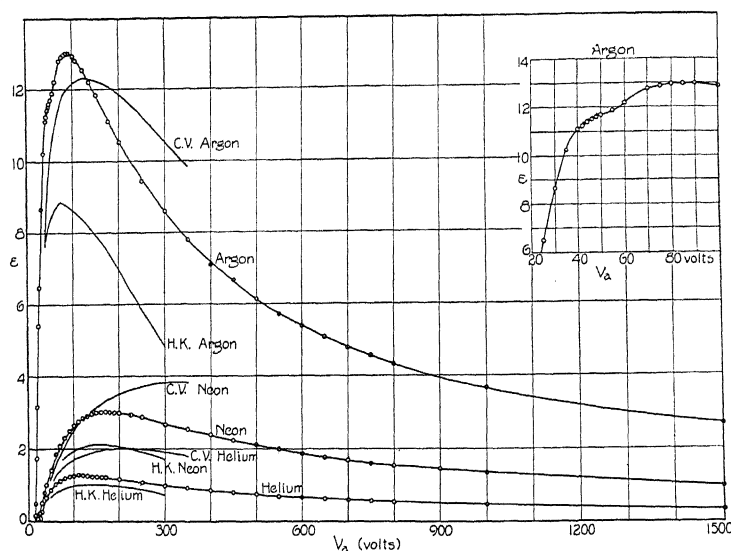


Fig. 5. The efficiency of ionization of He, Ne, and A as a function of the energy of the impacting electrons in volts, reduced to 1 mm pressure at 0°C.

It would seem that the above expression is more than a mere empirical formula, since there are in it only two constants which determine the shape of the curve, the constant 3.383 being only a scale factor.

These results were obtained with electron currents of from 1 to 3×10^{-7} amperes for $V_a < 2000$ volts, beyond which the currents used were from 8 to 10×10^{-7} amperes. For $V_a > 100$ volts the efficiency of ionization was independent of the electron current over the range 5×10^{-8} to 10^{-6} amperes, but for $V_a < 100$ volts it was found that the form of the curves began to change appreciably with electron currents greater than about 5×10^{-7} amperes. This could be accounted for by the increasing space charge at higher current densities which would decrease with increasing V_a , causing

¹³ K. T. Compton, J. C. Boyce, and H. N. Russell, Phys. Rev. 32, 179 (1928).

¹⁴ W. Bleakney, see the following paper in this issue.

the voltage correction also to decrease with increasing V_a . In the results given here, the current density was always low enough so that this effect was not appreciable.

The temperature of the tube, about 87°C , was the same as the temperature of the solenoid and consequently the whole apparatus inside the tube came to the same temperature.

The same data are given in Fig. 6, but in order to show the results out

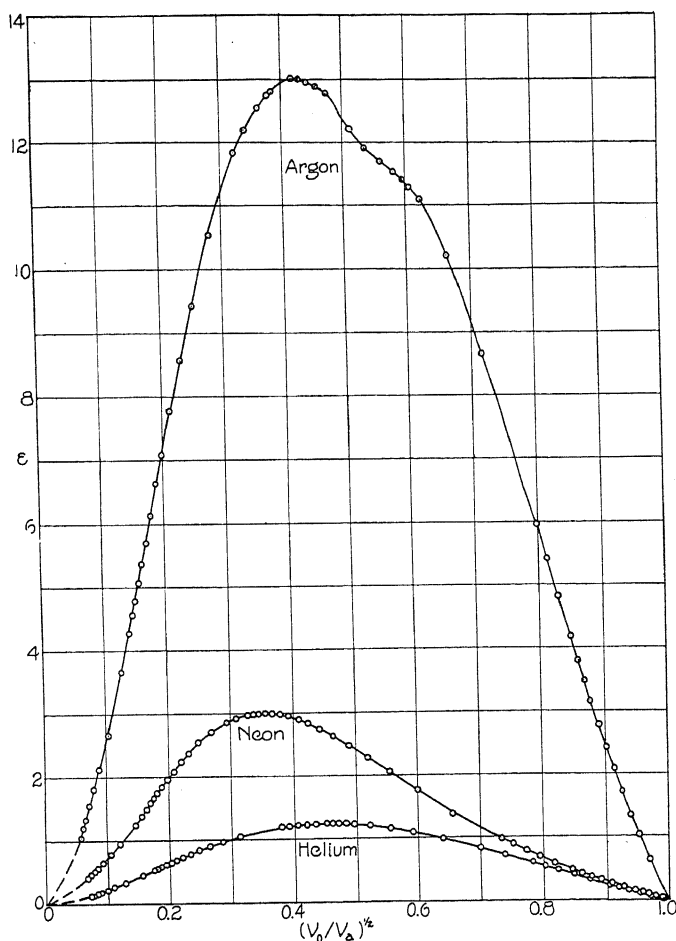


Fig. 6. The efficiency of ionization of He, Ne, and A as a function of $(V_0/V_a)^{1/2}$, reduced to 1 mm pressure at 0°C .

to 4500 volts the efficiency is shown as a function of $(V_0/V_a)^{1/2}$ when V_0 is the ionization potential of the gas and V_a the accelerating potential of the electrons.

The results are also given in the following table. The efficiency of ionization as defined, represents the average total number of positive charges per electron per cm path at 1 mm pressure and 0°C . The values of V_a have been corrected for contact e.m.f.'s initial velocity, etc., in the following manner.

To obtain a correct voltage scale the curves in Fig. 7 were drawn.¹⁵ The extrapolated straight lines were assumed to be the correct curves, the curved part being due to the velocity distribution of the electrons. All of the

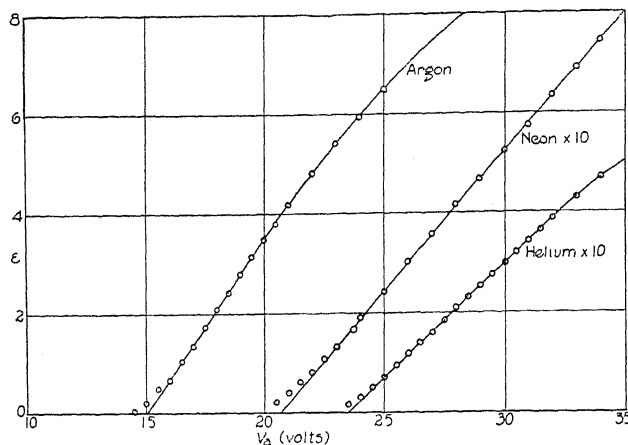


Fig. 7. The efficiency of ionization as a function of the energy of the impacting electrons, near the ionizing potential. The ionization potential of helium was assumed to be 24.48 volts, that of neon 21.47 volts, and that of argon 15.69 volts.¹⁵

curves do not show the same correction since the apparatus was changed several times and new filaments inserted.

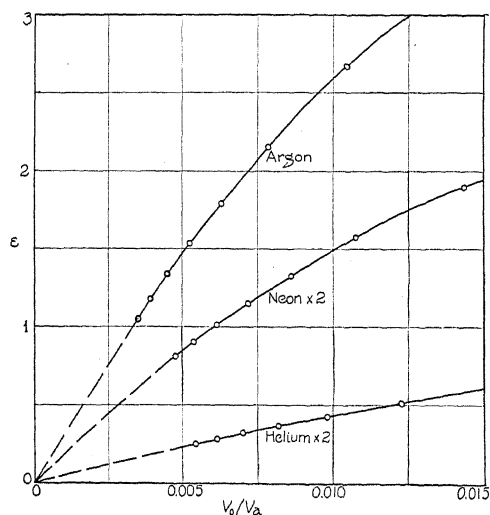


Fig. 8. The efficiency of ionization as a function of (V_0/V_a) for large values of V_a .

The curves in Fig. 7 also indicate that the efficiency of ionization is a linear function of the energy of the impacting electrons near the ionization potentials of the gases studied, whereas at higher velocities, Fig. 8, the

¹⁵ The values of ionization potentials were obtained from the Int. Crit. Tables, Vol. VI, p. 70.

efficiency apparently becomes inversely proportional to the energy. This was found to be approximately true with beta-particles in an article by W. Wilson.¹⁶ J. J. Thomson¹⁷ theoretically arrived at a formula which represents the efficiency of ionization as being inversely proportional to the energy of an impacting electron with energy much greater than the minimum ionizing energy. The formula does not, however, at all represent the observed data at lower energies and yields values much too low at higher energies. Bohr¹⁸ was able however partly to account for this discrepancy by considering the ionization due to the secondary electrons emitted in the process of forming the ions. In the present investigation this factor

TABLE I. *Efficiencies of ionization expressed as numbers of positive charges per electron per cm path per mm pressure at 0°C for various electron velocities.*

V_a	He	Ne	A	V_a	He	Ne	A
16.0			0.22	70	1.110	2.110	12.75
16.5			0.58	75			12.87
17.0			0.93	80	1.178	2.340	12.95
17.5			1.29	85			12.98
18.0			1.65	90	1.220	2.520	13.00
18.5			2.00	100	1.245	2.660	12.90
19.0			2.35	105	1.251		12.80
19.5			2.70	110	1.256	2.770	12.75
20.0			3.07	115	1.255		
20.5			3.40	120	1.250	2.860	12.53
21.0			3.75	130	1.247	2.930	
22.0		0.032	4.65	135			12.20
22.5		0.057		140	1.241	2.964	
23.0		0.087	5.12	150	1.228	2.987	11.83
23.5		0.118		160	1.216	3.000	
24.0		0.142	5.62	170	1.200	3.008	
25.0	0.022	0.198	6.16	175			11.10
25.5	0.045			180		3.005	
26.0	0.069	0.253		190		2.998	
26.5	0.092			200	1.149	2.988	10.53
27.0	0.114	0.307		225		2.935	
27.5	0.138			250	1.060	2.867	9.43
28.0	0.161	0.365		300	0.971	2.710	8.58
28.5	0.184			350	0.902	2.541	7.78
29.0	0.207	0.420		400	0.836	2.367	7.08
29.5	0.229			450	0.778	2.199	6.64
30.0	0.251	0.476	8.43	500	0.728	2.081	6.13
32.0	0.340	0.588		550	0.685	1.950	5.73
34.0	0.431	0.699		600	0.643	1.840	5.37
35.0			10.08	650	0.612	1.740	5.07
36.0	0.515	0.803		700	0.584	1.664	4.78
38.0	0.583	0.903		750	0.558	1.580	4.55
40.0	0.633	1.000	10.93	800	0.530	1.517	4.32
42.0			11.18	900		1.390	
44.0			11.39	1000	0.448	1.290	3.66
45.0	0.760			1500	0.328	0.950	2.67
46.0			11.52	2000	0.260	0.788	2.15
48.0			11.61	2500	0.215	0.663	1.79
50.0	0.860	1.470	11.68	3000	0.183	0.575	1.53
55.0	0.940		11.87	3500	0.162	0.510	1.34
60.0	1.025	1.830	12.15	4000	0.142	0.455	1.18
				4500	0.127	0.407	1.05

¹⁶ W. Wilson, Proc. Roy. Soc. **85**, 240 (1911).

¹⁷ J. J. Thomson, Phil. Mag. **23**, 449 (1912).

¹⁸ N. Bohr, Phil. Mag. **30**, 581 (1915).

however would be negligible, since the number of secondary electrons would be of the same order of magnitude as the positive ion current. A beam of electrons of this magnitude could not produce an appreciable number of ions, no matter what their energy might be.

The writer hopes in the near future to study the efficiency at higher energies since the present apparatus was not suitable for potentials greater than 4500 volts.

DISCUSSION

A comparison of the results of the present investigation for Ne, He, and A is shown in Fig. 5. The results of the other observers have been reduced to the same temperature and pressure conditions. The corrections which Compton and Van Voorhis² applied to Hughes' and Klein's data have not been made, although the temperature of their tube was assumed to be 60° C.²

Because of the definite length of path from which the positive ions were measured, and the more accurate knowledge of the energy of the impacting electrons as well as the elimination of secondary electrons, it is believed that the results presented here are more accurate than those of the previous investigations.

Although Hummel used the same method, the distorted fields in the ionizing chamber and the presence of secondary electrons from the slits which defined his electron beam, makes a comparison with his data difficult.

It is a pleasure for the writer to express here his gratitude to Professor John T. Tate, who suggested the method used and under whose guidance this work was carried out. Thanks are also due to Dr. Walker Bleakney for his constant interest and many suggestions.

IONIZATION POTENTIALS AND PROBABILITIES FOR
THE FORMATION OF MULTIPLY CHARGED IONS
IN HELIUM, NEON AND ARGON.

BY WALKER BLEAKNEY

PHYSICAL LABORATORY, UNIVERSITY OF MINNESOTA

(Received September 11, 1930)

ABSTRACT

The multiply charged ions in helium, neon and argon have been studied with a mass spectrograph previously described. In helium the He^+ ion showed up strongly but only faint evidence for the formation of He^{++} was found and no quantitative data for its relative intensity could be obtained. Neon yielded the three ions Ne^+ , Ne^{2+} and Ne^{3+} as the result of single electron impacts occurring respectively at minimum electron energies of 21.5, 63, and 125 volts. Curves which illustrate the efficiency for the formation of these ions expressed in number of ions per electron per cm per mm pressure at 0°C as a function of the electron velocity exhibit maxima for Ne^+ and Ne^{2+} of 2.75 and 0.16 at 150 and 250 volts respectively. In argon the five ions A^+ , A^{2+} , A^{3+} , A^{4+} and A^{5+} were observed. The ionization potentials for the first four were found to be respectively, 15.7, 44, 88 and 258 volts for single impact. The efficiency curves show maxima of 11.4, 1.1 and 0.04 at 50, 115 and 250 volts for A^+ , A^{2+} and A^{3+} respectively. In the curves for Ne^{3+} and A^{4+} are found several upward breaks beyond their ionization potentials which indicate other higher critical potentials for their formation.

INTRODUCTION

A METHOD of studying the multiply charged ions produced by electron impact in gases at low pressures has recently been described¹ and some results in mercury vapor and hydrogen have been reported. It is the purpose of the present paper to describe the results of a similar study of the ionization products in the rare gases—helium, neon and argon. Barton² has previously studied argon with a mass spectrograph. Certain improvements in the present method over those formerly employed have yielded new data, particularly in the experiments on neon and argon.

APPARATUS AND PROCEDURE

The apparatus employed in this investigation was essentially the same as that used in the study of ions in mercury vapor and hydrogen.¹ The reader is therefore referred to this earlier work for a detailed description of the method. The gases were admitted to the apparatus through a fine capillary at one end of the tube and the pressure could be varied by opening or closing with a mercury cut-off constrictions of different sizes in the pumping line leading from the other end of the tube. The pressures found suitable varied from 5 to 50×10^{-5} mm Hg. Helium from a steel drum was purified by passing it over charcoal immersed in liquid oxygen. The neon and argon were admit-

¹ W. Bleakney, Phys. Rev. 34, 157 (1929); 35, 139 (1930); 35, 1180 (1930).

² H. A. Barton, Phys. Rev. 25, 469 (1925).

ted to the apparatus directly from the Pyrex containers supplied by the Air Reduction Company without further purification. A preliminary study of the ions showed the helium and argon to be quite pure while the neon contained a slight amount (less than one percent) of helium. There was always present in the tube, however, even before any gas was admitted through the capillary, traces of some impurities which were identified as hydrogen, water vapor, and carbon monoxide. The number of ions due to these impurities was very small compared to those of the gas under investigation necessitating a correction usually of about one percent in the cases of argon and neon. It was only in the determination of ionization potentials, where it was necessary to measure very small currents, that the impurities caused any trouble, and here their effect was minimized by proper adjustment of pressure and current density. In all the results presented in this paper the data have been corrected as far as possible for the effect of impurities.

RESULTS

Helium. The singly charged He^+ ion formed, of course, a very strong peak in the analyzer. Unfortunately for this work the H_2^+ ion has the same e/m as He^{2+} and since there was always, as mentioned above, a trace of hydrogen present in the tube it was impossible to get any quantitative measure of the number of He^{2+} ions produced. However, the evidence at electron velocities of several hundred volts pointed toward the existence of He^{2+} but certainly less than one percent of all the helium ions formed were doubly charged.

Neon. The three ions Ne^+ , Ne^{2+} , and Ne^{3+} were found in neon and their ionization potentials were determined from the data shown in Fig. 1. Here the maximum heights of the peaks in the e/m analysis curves are plotted as functions of the electron velocity expressed in volts. With carbon dioxide snow on the trap a sufficient amount of mercury vapor remained in the tube to calibrate the voltage scale by means of the Hg^+ ion whose ionization potential was assumed to be 10.4 volts. Thus all of the ionization potentials could be measured without altering any of the conditions in the tube. The critical potentials obtained for ionization at single impact together with the estimated limits of experimental error are given in the second column of Table I. The agreement with the values calculated from spectroscopic data demonstrates the reliability of the method. The experimental error increases with increasing charge on the ion because of decreasing intensity and lack of complete resolution

TABLE I. *Ionization potentials in neon for single electron impact.*

Ion	Experimental	Spectroscopic
Hg^+	10.4 volts	10.39 ³ volts
Ne^+	21.5 \pm 0.1	21.47 ³
Ne^{2+}	63.0 \pm 0.5	62.4 ⁴
Ne^{3+}	125.0 \pm 1.0	

³ International Critical Tables VI, p. 71.

⁴ H. N. Russell, K. T. Compton and J. C. Boyce, Proc. Nat. Acad. Sci. **14**, 280 (1928).

The curves for Ne^{2+} and Ne^{3+} shown in Fig. 1 have a peculiar shape, unlike the others, suggesting more than one process for the formation of these ions. Particularly in the case of Ne^{3+} the curve shows two definite upward breaks, the first occurring in the neighborhood of 143 and the second at about 157 volts. These are perhaps to be correlated with the energies necessary to remove different electrons from the neon atom. For instance it may require 125 volts to remove three $2p$ electrons, 143 volts to remove two $2p$ and one $2s$ at a single blow and 157 volts to remove one $2p$ and two $2s$ electrons in one group, all three processes resulting in Ne^{3+} ions.

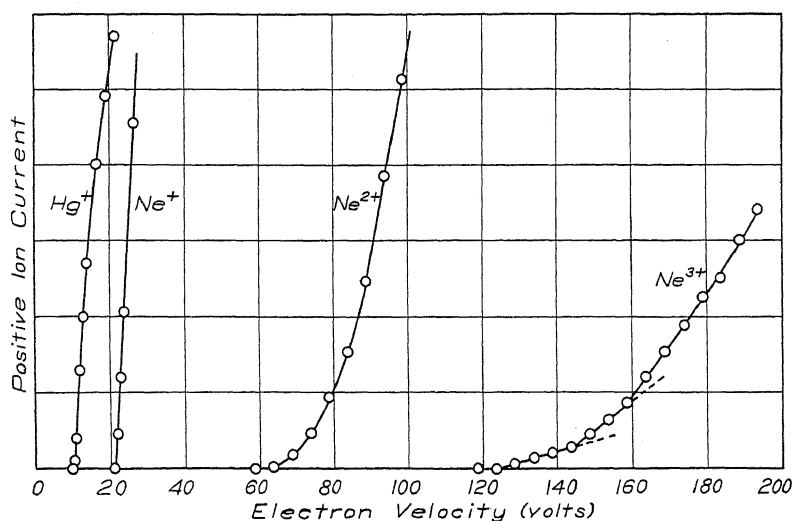


Fig. 1 Curves showing the ionization potentials in neon. The ordinate scale is an arbitrary one and differs for each curve.

The areas under the peaks in a set of runs carried out at various electron velocities were measured to determine the fractions of the total current carried by the several types of ions. The results are shown in Fig. 2 where the ordinates represent the percent of the total positive ion current to be assigned to the Ne^+ , Ne^{2+} and Ne^{3+} ions. It will be noticed from the figure that beyond 200 volts approximately 88 percent of the current is made up of singly charged ions while doubly charged ions account for about 11 percent.

The data of Fig. 2 combined with the measurements of the total ionization given by Smith⁵ enable one to calculate the probability of ionization for each type of ion. The result is obtained by multiplying the ordinate of Fig. 2 by the total ionization for that particular value of the electron velocity as given by Smith and dividing by the number of charges on the ion. Figure 3 shows the results of this calculation where the ordinates represent the probabilities of ionization expressed in numbers of ions per incident electron per cm path per mm pressure at 0°C as a function of the electron velocity. The curves for Ne^+ and Ne^{2+} exhibit broad maxima of 2.75 and 0.16 at 150

⁵ P. T. Smith, see the preceding paper of this issue.

and 250 volts respectively while that for Ne^{3+} shows no maximum in the range studied.

Argon. A study of the mass spectrum of argon revealed the five ions A^+ , A^{2+} , A^{3+} , A^{4+} and A^{5+} each one formed, it is believed as the result of a

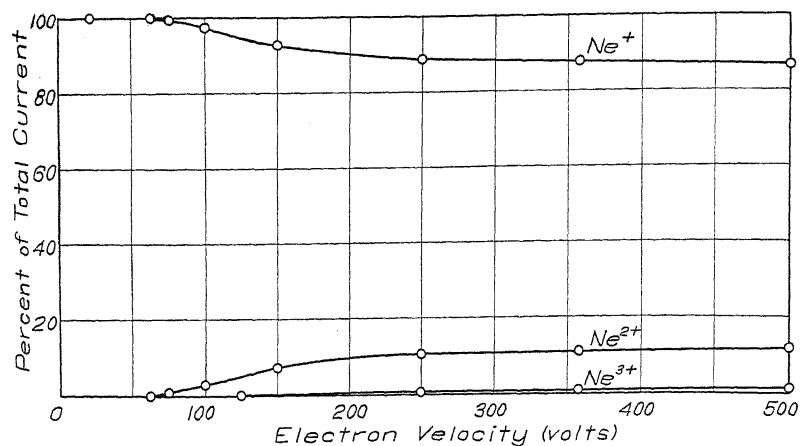


Fig. 2. Percent of total positive ion current ascribed to the different ions.

single electron impact. The intensity of A^{5+} was so small that no attempt was made to measure the number quantitatively. It can only be said that its formation certainly occurs at electron velocities below 500 volts. The ioniza-

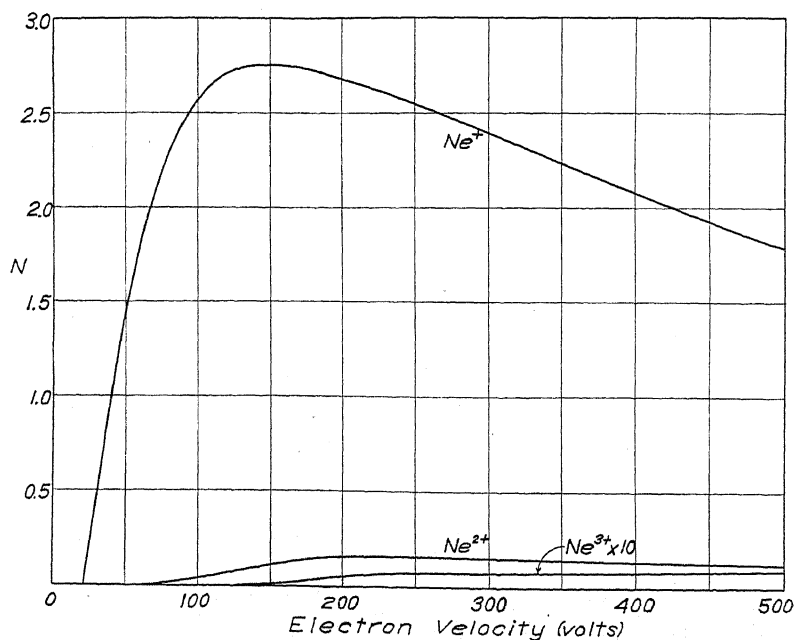


Fig. 3. Actual number of ions, N , formed per electron per cm per mm pressure at 0°C .

tion potentials for the first four ions were determined from the data shown in Fig. 4 and the values are given in Table II. It will be seen that the agreement with the spectroscopic values are quite satisfactory. The value 44.0 for A^{2+}

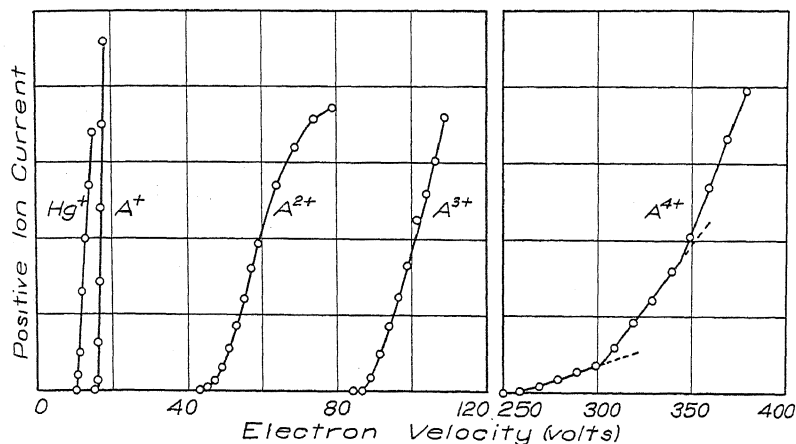


Fig. 4. Curves showing the ionization potentials in argon. The ordinate scale is an arbitrary one and differs for each curve.

checks quite well that found by Barton² which becomes 45.8 when his voltage scale is corrected to make A^+ appear at 15.7 volts.

TABLE II. Ionization potentials in argon for single electron impact.

Ion	Experimental	Spectroscopic
Hg^+	10.4 volts	10.39 ³
A^+	15.7 ± 0.1	15.69 ³
A^{2+}	44.0 ± 0.5	43.51 ⁶
A^{3+}	88 ± 1	
A^{4+}	258 ± 3	
A^{5+}	Less than 500	

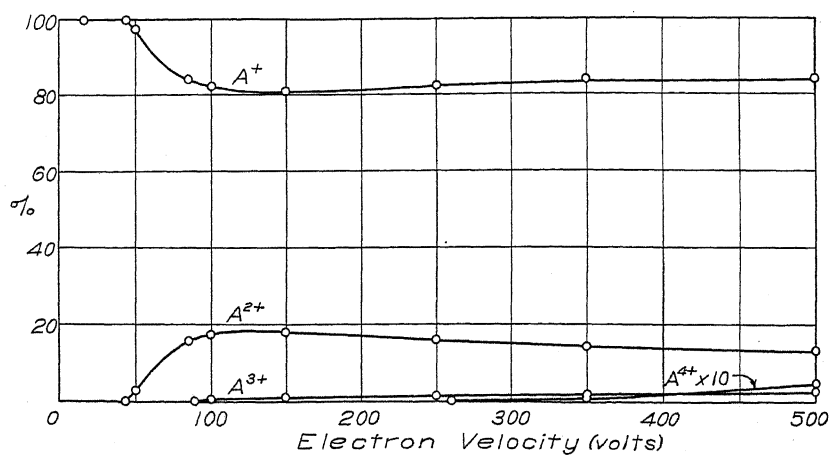


Fig. 5. Percent of total positive ion current ascribed to the different ions.

⁶ K. T. Compton, J. C. Boyce and H. N. Russell, Phys. Rev. 32, 179 (1928).

Like neon, the curves for the multiply charged ions in argon show peculiar shapes indicating more than one process of formation, and especially is this true of the fourth ion where upward breaks occur in the neighborhood of 300 and 340 volts. In all of the runs made these breaks consistently appeared but the values of the abscissas where they began did not check very well because of the difficulty encountered in holding the magnetic field perfectly constant. Hence the values given may be in error by several volts. It is hoped that these phenomena may be more carefully investigated in future work.

The fractions of the total positive ion current carried by the several ions are illustrated in Fig. 5. It appears that at least 80 percent of the current may always be ascribed, under the conditions of this experiment, to the singly charged ion in the range studied. Using again the data of Smith⁵ the probabilities of producing the first four ions as a function of the electron velocity have

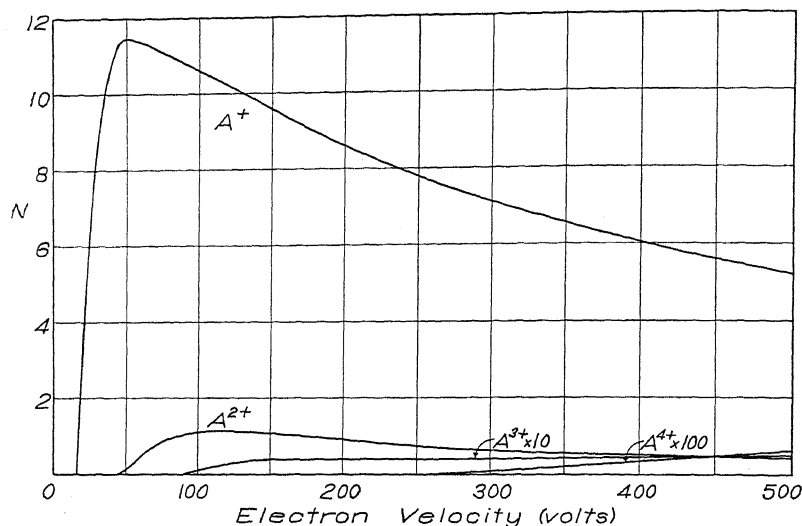


Fig. 6. Actual number of ions, N , formed per electron per cm per mm pressure at 0°C .

been calculated and are given by the curves of Fig. 6. The A^+ ion rises very sharply to a maximum value of 11.4 at 50 volts while the A^{2+} ion reaches a value of 1.1 at 115 volts. The number of A^{3+} ions shown only a very broad maximum of 0.04 beyond 150 volts and the A^{4+} curve continues to rise as far as 500 volts. The position for the maximum in the A^+ curve coincides very well with that observed by Barton² but none of the upward breaks observed by him beyond this point were found, probably because the present work was carried out at much lower pressures.

It is believed that work of this nature is of sufficient interest and importance to merit further investigation along the same line. It is planned, therefore, to extend the experiments during the next year to other gases and vapors in an attempt to gain further information on the mechanism of ionization by electron impact.

The author is ever grateful to Professor John T. Tate for his keen interest and helpful guidance during the course of this work.

THERMIONIC EMISSION OF OXIDE COATED CATHODES
CONTAINING A Ni-Ba ALLOY CORE

BY N. C. BEESE

WESTINGHOUSE LAMP CO., BLOOMFIELD, N. J.

(Received September 8, 1930)

ABSTRACT

An appreciable increase in thermionic emission from oxide coated filaments has been obtained by introducing a small percentage of metallic barium (approximately 0.15 percent) into the nickel core material. Comparisons made on the electron emission of this alloy with pure nickel and also with the nickel alloy after the barium had been extracted always showed the influence of barium in the base metal.

INTRODUCTION

SEVERAL theories have been advanced to account for the activity of an oxide-coated cathode. One explanation requires metallic barium* on the surface of the oxide coating.^{1,2,3,4} More recent investigations^{5,6} indicate the influence of the core material. The following explanation of enhanced emission from oxide-coated cathodes has been given by Reimann and Murgoci.⁵ The thermionic activation is accompanied by coating the surface of the core metal by a monatomic layer of barium or a double atomic layer of barium and oxygen. In either case the core metal acquires a high electron emissivity, and the electrons pass from the metallic core to the oxide coating thermionically. The electrons are then carried to the exterior surface of the coating by circulating barium atoms. The thermionic emission of the cathode as a whole is limited either by the coating or by the core,—whichever of the two systems has the lesser thermionic emissivity.

Lowry⁶ has indicated the importance of the core metal in oxide-coated filaments. He finds that Konel metal filaments give usable thermionic currents at much lower temperatures than similarly coated platinum filaments. The large thermionic currents at comparatively low temperatures in the case of coated Konel filaments suggested the assumption that thermionic currents originated at the layer of barium atoms occluded on the core. The electrons emitted from this surface diffuse through the interstices in the oxide coating into the vacuous space.

Since metallic barium seems to be the active agent in releasing an abundance of electrons from an oxide-coated cathode, a small continuous supply of

* Barium is used to represent all of the alkaline earth metals.

¹ Koller, *Phys. Rev.* **25**, 671 (1925).

² Espe, *Wiss. Veroff. aus dem Siemens Konzern* **5**, 29 and 46 (1927).

³ Rothe, *Zeits. f. Physik* **36**, 737 (1926).

⁴ Becker, *Phys. Rev.* **34**, 1323 (1929).

⁵ Reimann and Murgoci, *Phil. Mag.* [VII] **9**, 440 (1930).

⁶ Lowry, *Phys. Rev.* **35**, 1367 (1930).

barium atoms from the core material added to that from the decomposed BaO coating should produce and maintain a somewhat larger source of electrons than if the coating alone furnished the source. If an enhanced emission is due to the core surface being partially covered with adsorbed barium atoms, an internal source of metallic barium should be very desirable in furnishing a uniform layer of adsorbed atoms. This resembles the process of emission from thoriated tungsten filaments. If the large emission from oxide-coated filaments is due to barium atoms adsorbed on the exterior oxide surface, the barium from the core would augment the supply furnished by the BaO. Besides increasing the activity of the filament, the migration of the metallic barium atoms from the volume of the core should maintain an increased emission for a considerable period of time. Whether the barium atoms remain at the core-coating interface or are carried to the surface of the oxide cannot be determined by the experiments to be described. However their contribution to the total emissivity of the filament is quite noticeable.

METHOD AND RESULT

An alloy containing approximately 0.15 percent metallic barium in an essentially nickel base was obtained from the A. C. Spark Plug Company of Flint, Michigan. This alloy was formed into a ribbon 0.025 inch \times 0.002 inch. In the comparison with pure nickel filaments, a piece of pure nickel wire was drawn and rolled to the same dimensions. The filaments were coated by spraying them with a mixture of equal weights of BaCO₃ and SrCO₃ in an amyl acetate suspension, or they were coated by passing them through a water-suspension of the carbonates followed by baking in an atmosphere of CO₂. The filaments were mounted in structures similar to the UX-281 Radiotrons.

The tubes were exhausted with a two-stage mercury condensation pump backed by a Cenco oil pump. A liquid-air trap was placed between tubes and pumps. Pressures of about 10^{-5} mm of mercury as measured on a McLeod gauge were obtained before the "getter" was flashed and the tubes sealed off.

Four sets of tubes of three each were made as follows:—(1) and (2) Alloy filaments and pure nickel filaments respectively having a heavy coating weight of carbonate mixture; (3) and (4) alloy filaments and pure nickel filaments respectively having a light coating weight of carbonate mixture. The heavy coating of carbonates was applied by the "spray" method and had 8.0 mg of carbonate mixture per cm² of surface. The light coatings were applied by the "drag" method and had 2.3 mg of carbonates per cm² of surface.

Fig. 1 indicates the relative emission currents obtained by averaging the values from the first two types of filaments. The thermionic emissions in milliamperes per square centimeter of filament surface are plotted as ordinates and times are plotted as abscissae. Both types of filaments were operated with an energy input of 4 watts per cm² of radiating surface. This value was chosen as it is the operating condition of filaments in most commercial tubes. During life the tubes had 220 volts A.C. applied between filaments

and plates while for test purposes the measurements were made with 150 volts D.C. applied to the plates. The thermionic emissions from the pure nickel filaments were nearly constant throughout the 500 hours life test. The alloy filaments had initial emissions about equal to the emission from

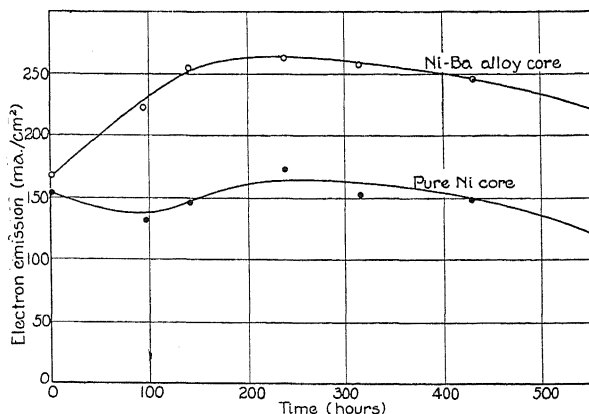


Fig. 1. Comparison of electron emission from pure Ni and alloy cores coated with a heavy coating weight of oxides.

the pure nickel filaments. This initial emission in both cases is attributed to the oxide coating and the activity of the pure nickel filament throughout its life is due to the oxide or the products of decomposition of the oxide. During operation the alloy filaments gave a constantly increasing emission for the first 150 hours, attaining a value about 70 percent larger than that of the pure nickel filaments. The larger emission was then maintained throughout the remainder of the life test. This increased emission is attributed to the fact that barium was slowly diffusing out of the volume of the core material and becoming adsorbed metallic barium at the core-coating interface or on the oxide surface. The emission from the pure nickel filaments was satisfactory for radio-tube purposes, and is the activity generally found in UX-281 type tubes.

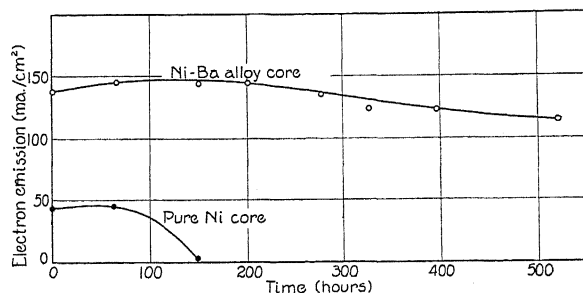


Fig. 2. Comparison of electron emission from pure Ni and alloy cores coated with a light coating weight of oxides.

In Fig. 2 is depicted the relative values of emission from filaments coated with a light coating weight of oxides. The activity of the pure nickel

filaments was low initially and had a life of only 150 hours, while the activity of the alloy filaments was comparable to that of the pure nickel filaments coated with the heavy coating weight of oxides. In this comparison the barium from the core accounts for nearly all the useful thermionic emission. It has been the writer's experience that a low initial emission and a relatively short useful life is generally associated with very light coating weights of carbonates.

Having thus accounted for the appreciable differences in thermionic activity of the two kinds of coated filaments, operated for at least 500 hours with a filament energy consumption of about 4 watts per cm^2 , a further test was applied. A piece of the barium-nickel alloy filament was heated in a well exhausted vacuum tube to approximately 1300°C until the barium had been diffused to the surface of the filament and evaporated. Initially the current drawn from the filament was of the order of 25 m.a. while after this

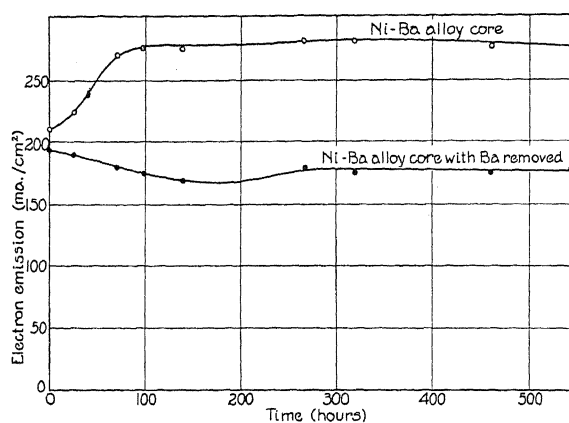


Fig. 3. Comparison of the activity of an alloy core filament with one having its barium content removed.

vacuum treatment currents of only a few microamperes could be obtained. This filament, supposedly free from barium content, was coated with a coating weight of 3.5 mg of carbonates per cm^2 , together with an alloy filament that had not received the preliminary vacuum treatment. Measurements taken at intervals during the life test of these two tubes revealed that the treated filament corresponded to the pure nickel type having a constant activity, while the untreated wire gave the characteristic alloy filament type of life history. These data are recorded graphically in Fig. 3 and show the great similarity to the curves of Fig. 1.

The data recorded in the three graphs were taken under the conditions that 4 watts of energy were being radiated per cm^2 of filament area, and do not show the actual differences in activity because of space charge limitation with 150 volts plate potential. A lower filament temperature, such as that produced by a radiation of 2 watts per cm^2 , would give a better indication of the relative differences in emissivity and would produce much larger ratios,

but the chosen value of 4 watts per cm^2 is representative of the normal operation of most commercial tubes.

Fig. 4 shows the relation between filament temperatures in watts per cm^2 and electron emission in m.a. per cm^2 . Curves *A* and *B* are taken from part of the data of Fig. 1 at the time $t = 240$ hours, while curves *C* and *D* are taken

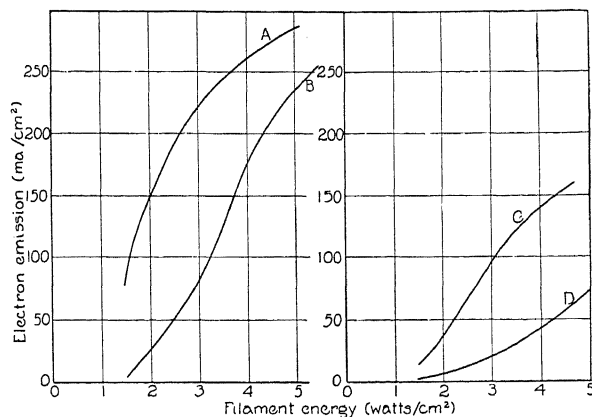


Fig. 4. Curves *A* and *B* are associated with data in Fig. 1 at $T = 240$ hours; Curves *C* and *D* are initial values associated with data of Fig. 2 at $T = 0$ hours.

from part of the data of Fig. 2 at the time $t = 0$ hours. The curves represent the averages of the various groups of tubes of 3 each. The slopes of the curves, especially at the higher plate currents, indicate the effect of space charge.

CONCLUSION

The operating life history of the filaments recorded in the three graphs shows the increased activity obtained from oxide-coated cathodes that have a slight amount of metallic barium contained in the nickel core. This is especially true in the filaments covered with a light coating weight of oxide. The core material, in this case at least, has an important influence on the amount of emission.

SHOT EFFECT OF THE EMISSION FROM OXIDE CATHODES

BY H. N. KOZANOWSKI AND N. H. WILLIAMS

UNIVERSITY OF MICHIGAN

(Received August 23, 1930)

ABSTRACT

Experimental procedure in the study of fluctuations in the space current of a thermionic emitter is outlined. A new method of measuring *shot-circuit impedance* is introduced. Conditions under which the observed fluctuations may be applied to determine the electronic charge are pointed out. A method is described whereby the frequency of oscillating circuits used in this investigation may be determined and controlled. An investigation has been made of the fluctuations associated with the emission from barium-strontium oxide cathodes, particularly in the space charge region. The presence of positive ions in the emission from oxide coatings has been experimentally verified. These positive ions moving in an electron space charge cause abnormally high shot-fluctuations in an aperiodic circuit at high amplifier frequencies. The characteristic fluctuations associated with the emission from oxide cathodes have been reproduced in a vacuum tube of special design in which positive ions from an independent Kunsman potassium ion emitter interact with electron space charge about a metal emitter. This is taken as evidence that the same process goes on in the emission from barium-strontium oxide cathodes. Some results obtained in a study of the shot effect of films evaporating from a tungsten wire are included.

THE shot effect has been successfully used in the determination of electronic and ionic charge by an entirely independent method. The emitters used for electronic currents in these determinations have been pure metals such as tungsten or thoriated tungsten. Williams and Huxford,¹ in the determination of the positive ion charge, used a Kunsman potassium ion emitter. This work was done at shot-amplifier frequencies in the region of 100,000 cycles per second. It was found that even at these frequencies, abnormal fluctuation voltages occur in the case of certain oxide electron emitters. It was to discover the underlying mechanism of these fluctuations that this investigation was carried out. A brief description of the apparatus and experimental procedure follows.

THE SHOT CIRCUIT AND AMPLIFIER

An experimental arrangement for studying the shot effect of thermionic currents is shown in Fig. 1. The vacuum tube *S*, consisting of a collector plate and an emitter is mounted in a shielding compartment. The emitter is heated by a storage battery located outside this compartment. The accelerating potential is applied to the collector plate through a wire-wound resistor *R*. It can be seen from the diagram of Fig. 1 that the positive end of the high potential battery is grounded to the shield. The negative terminal

¹ N. H. Williams and W. S. Huxford, Phys. Rev. 33, 773 (1929).

is connected to the filament leads, which are carefully insulated from direct current grounds, but are kept at ground potential for high frequency currents by the use of a one microfarad condenser having very low leakage current.

If the emitter is heated by means of the storage battery, and a positive potential is applied to the collector plate through the resistor R , electrons will flow from the emitter to the collector. The value of the electron space current is given by the direct current milliammeter A . If the electron stream were perfectly continuous, only a direct difference of potential would exist between A and B equal to $I_0 R$. But since the arrival of electrons at the plate is a discontinuous process, voltage fluctuations will occur across the resistance AB . These fluctuations will be called the "shot voltage" between A and B . The space current and the space charge conditions in the tube can be controlled by variation of the emitter heating current and the accelerating potential across the tube.

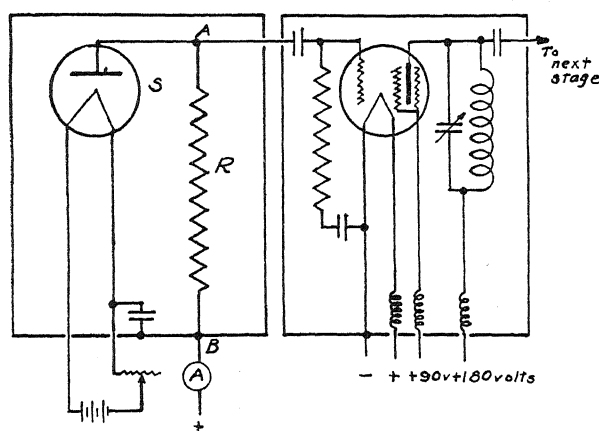


Fig. 1. Aperiodic shot effect.

The shot voltage developed across AB is impressed on the grid-filament circuit of a tuned-plate five-stage amplifier employing screen-grid tubes. Thus a narrow band of frequencies from the total "shot voltage" is selected and amplified. Coupled loosely to the tuned-plate circuit of the last amplifier tube is a coil of a few turns of wire. Voltages induced in this coil by alternating currents in the plate circuit cause current to flow through a 990 ohm vacuum thermal junction connected across it. The magnitude of the thermoelectromotive force is directly proportional to the heating of the junction and hence to the square of the current in the circuit or to the square of the voltage across it. In this manner a direct current galvanometer across the thermoelement is used to detect high frequency voltages.

It is evident that an amplifier correctly designed, and operated under suitable conditions will show a linear relation between the input and output voltages. Since both the input voltage and output current, which is proportional to the output voltage, are measured by the thermo-junctions in cir-

cuits to be described later, the fidelity of the amplifier may be determined by a plot of input against output galvanometer deflections. This must give a straight line relation for all normal voltages applied to the amplifier.

GENERAL EXPERIMENTAL PROCEDURE

In an experimental determination of the value of the electronic charge, the following method is employed:

The amplifier and shot-tube emitters are heated for about thirty minutes before actual observations begin. In this way the amplifier reaches a stable condition which can be maintained indefinitely. The plate circuit of the shot tube is then closed, giving a definite space current through the tube which is measured by ammeter *A* of Fig. 1. The shot voltage across the resistance *AB* is applied to the grid-filament circuit of the screen-grid amplifier, giving a deflection on the output galvanometer, *G*₀, which is proportional to the mean square voltage across *AB*. The shot circuit is then disconnected and a sine voltage is applied to the amplifier at its resonant frequency. This sine voltage is then varied until the deflection obtained with a definite space current in the shot circuit is reproduced. The magnitude of this sine voltage is the quantity *V* of the equation

$$\epsilon = V^2/2A i_0 Z^2$$

as derived by Williams and Vincent.² Thus a measurable sine voltage at the resonant frequency of the amplifier is substituted for the actual voltage existing across *AB* due to the shot effect. Under ordinary conditions, this voltage is of the order of 25 micro-volts. Its value is obtained from the inductive drop along an inductance potentiometer.

In order to obtain the value of the charge of the electron from the equation of the shot effect, the quantities *A* and *Z* must be determined. *A* is the amplifier resonance area and is a constant for any series of measurements. The impedance *Z* of the shot circuit, measured between *A* and *B*, is a function of the space charge in the shot tube. The method of determining *Z* is discussed in the following section. Substitution of the quantities, *i*₀, *V*², *A*, *Z*² in the shot equation gives the charge of the electron. The space current and the accelerating voltage in the shot tube are varied, and conditions under which the true value of the electronic charge is given by the shot effect equation can be studied. Obviously, this method of investigation will show any abnormalities in the shot-effect characteristics of a given vacuum tube.

When thermionic currents of 300 microamperes or less are used in the shot tube, the deflection of the amplifier output galvanometer is small. Then the duplication of this deflection using only the inductance potentiometer results in large inaccuracies, since the *I* of *IωLd* is small. In order to minimize this error, the current is attenuated to a small fraction of its original value and this fraction is passed through the inductance potentiometer. The complete circuit used for the duplication of output galvanometer deflections due to the shot effect of the thermionic current in the tube *S* is shown in

² N. H. Williams and H. B. Vincent, Phys. Rev. **28**, 1250 (1926).

Fig. 2. With the use of the attenuator, high frequency voltages of the order of 10 microvolts can be measured with a probable error of one percent.

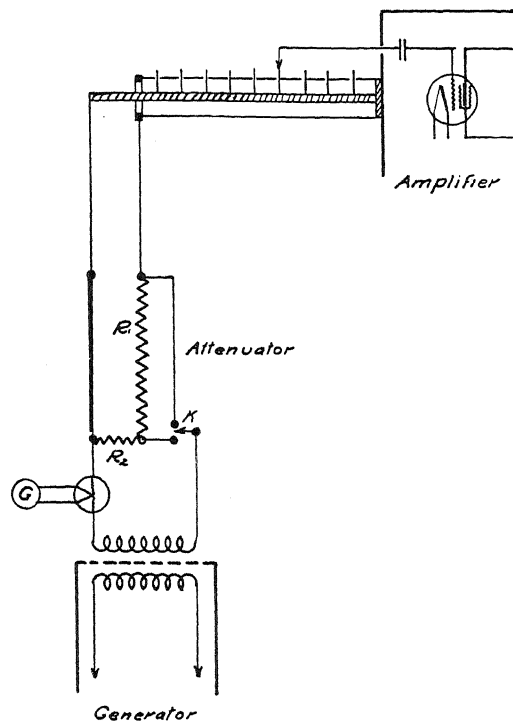


Fig. 2. Inductance potentiometer and attenuator.

MEASUREMENT OF IMPEDANCE OF THE SHOT CIRCUIT

The impedance of the shot circuit involved in the equation

$$\epsilon = V^2/2A i_0 Z^2$$

is that between the points A and B (Fig. 3) across which the voltage due to the fluctuations from the long time mean value of the space current is developed.

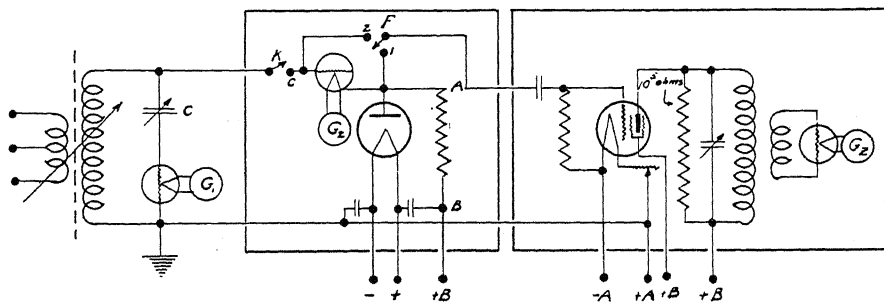


Fig. 3. Measurement of shot circuit impedance.

A process of measuring the impedance which is more direct than that of Williams and Huxford³ and experimentally very simple has been developed. It was found that a coil and thermojunction system G_2 , Fig. 3, coupled to the tuned plate circuit of the *first* screen-grid amplifier tube gives practically a linear response to the square of the high frequency voltage applied to the grid-filament circuit of the amplifier, if the tuned plate circuit is shunted by a resistance of the order of 100,000 ohms. In this way, the impedance of the plate circuit to the high frequency current, and the voltage amplification are lowered. We see that as the external impedance is made lower, say by shunting the tuned circuit with a high resistance, the voltage across it due to a given voltage applied to the grid filament circuit will decrease. The response of the first amplifier tube to various voltage inputs to the grid filament circuit is shown in curves I and II of Fig. 4.

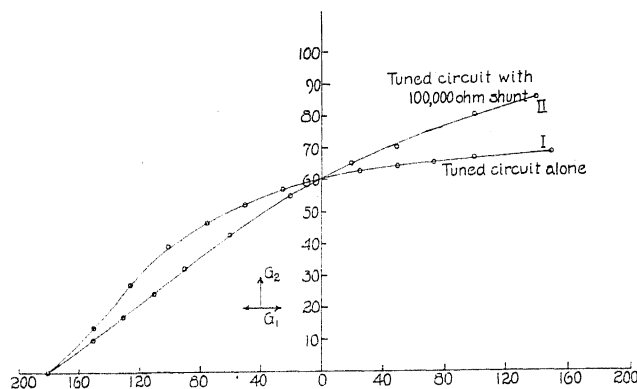


Fig. 4. Response of first amplifier tube as a high frequency voltmeter.

If any voltage at the resonant frequency of the amplifier is applied to the circuit at CB , Fig. 3, a current I_2 will flow through it. Also a deflection proportional to the square of the voltage between A and B will be observed on the galvanometer of G_2 . The thermojunction measuring the current I_2 into the shot circuit is then shorted by key F , thus eliminating the voltage drop along it. The deflection previously obtained on the galvanometer of the system coupled to the plate circuit of the first amplifier tube is now duplicated by varying the current through the standard condenser, C . As the amplifier tube responds to the mean square voltage between A and B regardless of phase, it is evident that the voltage giving the same output deflection without the thermojunction G_2 in the circuit is now exactly the same as previously existed between A and B . The impedance of the circuit is then given directly by E'/I_2 where E' is the voltage applied directly between A and B for the observed deflection on G_2 , and I_2 is the current read by the thermojunction system G_2 . We have then, for the impedance of the shot circuit between the points A and B ,

$$Z = I_1'/I_2 C \omega.$$

³ N. H. Williams and W. S. Huxford, Phys. Rev. 33, 773-778, (1929).

Typical impedance characteristics of vacuum tubes, investigated under conditions of constant current at various voltages between the anode and cathode are shown in Fig. 5.

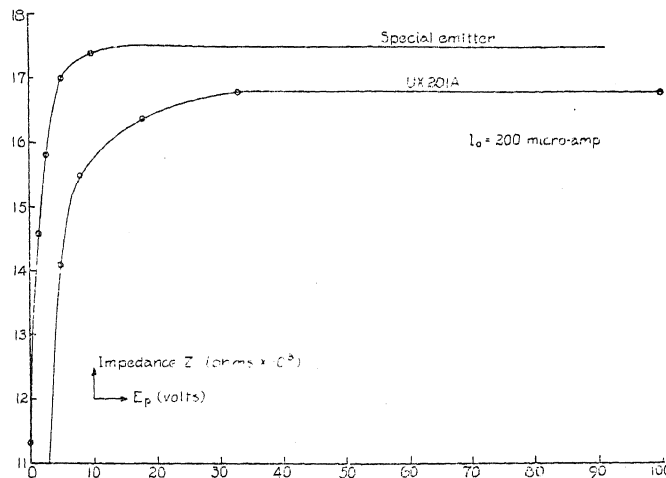


Fig. 5. Typical impedance characteristics of vacuum tubes.

FREQUENCY DETERMINATION AND CONTROL

We see that

$$\epsilon = V^2 / 2A i_0 Z^2$$

the shot effect equation, can be written in the form

$$\epsilon = \frac{I^2 \omega^4 L^2 C^2}{2A i_0 I_1^2 / I_2^2}.$$

This follows from the fact that v , the high frequency voltage applied to the input circuit of the amplifier at its resonant frequency to give the same output deflections as the shot effect associated with a definite space current, is obtained from the inductance potentiometer and is given by

$$V = I \omega L.$$

Also the impedance Z is given by E/I_2 or as outlined in a previous section,

$$Z = I_1 / I_2 C \omega.$$

It is evident that oscillator frequency, entering the expression in the fourth power must be accurately determined and completely controlled.

Methods have been used whereby the frequency of the generator can be determined and held constant to one part in 100,000. A self-maintained tuning fork whose frequency may be varied from 800 to 1000 cycles per second is used as a primary standard of audio frequency. This is calibrated by a synchronous-motor clock which operates continuously when the fork is in operation. The audio frequency is introduced in the input circuit of a distor-

tion amplifier. By the use of several stages of amplification, harmonics of the audio frequency as high as 150 times the fundamental can be obtained. These are easily identified by a precision wave-meter and tuned circuits together with a heterodyne oscillator. By adjusting the frequency of the fork so as to obtain a zero beat of a harmonic with the fundamental frequency of a crystal-controlled or Hartley oscillator, the latter can be easily calibrated to an accuracy well within the needs of the procedure.

A crystal-controlled oscillator having a frequency of 117,034 cycles per second was calibrated by the procedure outlined and used as a high frequency standard. This was coupled to the Hartley oscillator used for the calibrating shot voltage and impedance measurements by means of pick-up coils and the amplified beat note was kept at one or two cycles per second. An audio frequency amplifier and dynamic loud speaker allowed the coupling between the crystal and the Hartley oscillator to be made so loose that there was no possibility of reaction of the circuits. The standard oscillator and audio amplifier were operated during actual observations so that any change in the frequency of the Hartley oscillator due to change of plate and filament voltage could immediately be noted and corrected.

In the determination of the resonance curve of the high frequency shot amplifier, the ratio of the amplification of a given voltage input at various frequencies to that at resonant frequency is measured. A convenient method of obtaining known frequencies in the pass band of the amplifier is that of selecting frequencies of the distortion amplifier in a suitable range. The Hartley oscillator is then adjusted to zero beat with these frequencies, whose separation is given immediately by the fundamental frequency of the tuning fork. Thus the resonance curve can be determined without the use of a wave-meter and with much greater precision and speed.

MEASUREMENT OF THE ELECTRONIC CHARGE FROM THE THERMIONIC EMISSION OF A METAL

Measurement of the shot effect of thermionic currents from a pure metal offers few complications and yields, under proper conditions, the accepted value of the electronic charge. The shot tubes used consist of a cylindrical collector plate of nickel, and a co-axial tungsten or thoriated tungsten emitter. The pressure in selected tubes is probably of the order of 10^{-6} mm of mercury. These tubes have been well outgassed and flashed with a getter. No evidence of ionization of the residual gas with the voltages employed has been found.

The shot effect associated with various anode currents from 100 to 6000 microamperes was studied. In all cases investigated, it may be said that the apparent charge of the electron, as given by the equation $\epsilon = V^2/2Ai_0Z^2$, agrees within the limits of experimental error with the values obtained by previous investigators, if the electron current leaving the cathode is temperature limited. That is, conditions in the experimental tube are such that all of the electrons leaving the emitter with a random distribution in time arrive at the collector in the same manner. Experimentally this condition can be

realized if the accelerating voltage across the tube is high and the space current is low. When an increase of the accelerating voltage causes no further increase in the space current, the electron stream is purely temperature-limited. Substitution of observed quantities under these conditions in the shot effect equation will give the accepted value of the electronic charge.

The space current for any given emitter temperature will be a function of the accelerating voltage up to the saturation region. When voltages higher than the saturation voltage are applied, little or no increase in the space current is observed. Thus a possible method of studying the shot effect associated with thermionic emission is that of holding the emitter at a constant temperature, and varying the voltage across the tube.

It is essential to distinguish very carefully between the value of " ϵ " obtained by the substitution of measured quantities in the equation of Williams and Vincent when the fundamental assumptions of Schottky's small-shot theory are fulfilled and values obtained when they obviously are not. Thus *only* at high accelerating potentials and low space currents, giving no first order space charge interaction of electrons, are we justified in using the equation as a measure of the electronic charge. At low voltages and high space-currents the equation merely gives values which are proportional to the voltage fluctuations occurring in the shot tube and circuit.

When the voltage between the emitter and the collector is low, the current is no longer temperature-limited and the space-charge density near the emitter may become very large. An electron emitted from the cathode is acted upon by a repulsive force due to the electrons in the space charge sheath. The redistribution in time due to such interaction is to make the fluctuations smaller than those existing with the same current at higher voltages. This we call space-charge depression. Under these conditions the deflections of the output galvanometer may become very small. An extensive investigation of space-charge depression of shot fluctuations is now in progress in this laboratory. Another effect, the fluctuation of the space charge itself, has been studied in the case of the electron emission from barium-strontium oxide coated cathodes. The shot effect of this emission has been investigated and the cause of certain abnormal defects has been determined.

SHOT EFFECT OF THE EMISSION FROM BARIUM-STRONTIUM OXIDE CATHODES

During the summer of 1928, Williams and Huxford investigated the shot effect of electron currents from barium-strontium oxide emitters. The tube used contained a cylindrical quartz sleeve wound with platinum wire and then coated with a layer of barium-strontium carbonate mixture. The sleeve was surrounded by a co-axial cylinder as anode. Current passed through the platinum wire heats the emitter. The tube used had a geometry identical with the Kunsman emitter of positive ions described by Huxford.⁴ It was hoped that the results obtained with the Kunsman emitter of positive ions

⁴ W. S. Huxford, Dissertation, University of Michigan, 1928.

and an emitter of electrons such as barium-strontium oxide would allow calculation of the influence of the mass of the carrier on the space charge.

This tube was sealed onto a high vacuum system and baked and outgassed with the induction furnace until the vacuum could be maintained at 10^{-6} mm of mercury. With the vacuum system in operation the shot effect characteristics of the two were studied. The ordinary shot effect curves for an electron emitter were expected. Actually it was found that the shot effect behaved very abnormally under certain conditions of space charge. The shot-effect characteristics are graphically shown in Fig. 6. Four complete shot-characteristic curves were taken with this tube. The tube was on the pumps continually and the emitter was being heated except for a very short time between curves II and III when the system was brought to atmospheric

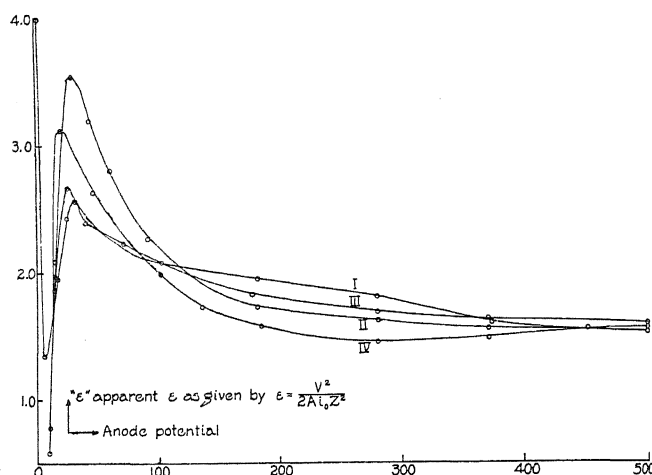


Fig. 6. Shot effect of electrons from barium oxide. $I_0 = 200$ microamps.

pressure for adjustment. We notice the characteristic space-charge depression at very low accelerating voltages on the tube. As the voltage on the tube is increased, v^2 increases very rapidly, reaches a maximum, and falls rapidly with a further increase of accelerating potential. From then on, with further increase of accelerating potential the behavior is similar to that in a metallic emitter. At high accelerating voltages, the value of v^2 is such as to give values of the electronic charge which agree with the accepted value within the limits of experimental error. Thus, since there is no possibility of gas ionization, and the abnormally high fluctuations disappear with high accelerating potentials, when space charge is obliterated, it appears that there exists an agency which operates on the space charge in such a manner that large, mean-square fluctuations are produced. It should be noted that there is a very good correlation between the length of time that the emitter has been heated, or activated, and the magnitude of the space-charge peak. In the following sections the cause of these fluctuations will be discussed and experimentally verified by an independent method.

In order to obtain more data on the shot effect with oxide coated emitters, commercial tubes of the UY-227 type were studied. These are the familiar indirectly heated barium-strontium oxide cathode type, designed for alternating current operation. During the process of activation the barium and strontium carbonates break down into the oxides, with the evolution of carbon dioxide. Thus the gas content of a tube of the 227 type is higher in general than that of a tube employing a pure metal emitter. In every case, the shot-fluctuation voltages at high accelerating potentials are from three to four times normal value. The deflection of the high frequency amplifier output galvanometer, which is proportional to v^2 , is not steady but may fluctuate from its mean position by as much as 25 percent. This is a good indication of the presence of gas in the tube.

If an evacuating system is sealed on to any of the commercial tubes studied, and the tube is well outgassed and held on the vacuum system at a pressure of 10^{-6} mm of mercury, a curve of " ϵ " against the accelerating voltage using a constant space current is found which has all of the essential characteristics of the oxide emitter described by Williams and Huxford. Thus we can conclude that even a small amount of gas in a shot tube will introduce fluctuations over and above the normal fluctuations in purely thermionic emission. This action of the gas is probably due to the positive ions and electrons obtained by ionization. In order to correlate the effects in the space charge region, all tubes subsequently studied were investigated under a high vacuum.

ACTIVATION OF THE EMITTER AND SHOT EFFECT IN THE SPACE CHARGE REGION

Commercial tubes whose emitters were unactivated were fitted with a five-millimeter-diameter evacuating tube and were sealed on to the evacuating system to obtain a high pumping speed. The pressure was brought down to 10^{-5} mm of mercury and the tube was then baked for 2 or 3 hours with an electric furnace at a temperature of 350–400°C, with the emitter operated at half-voltage. Large quantities of gas were evolved in the process. Toward the end of the treatment, the emitter was operated at normal temperature. The metal parts of the tube were then outgassed with an induction furnace. The emission from the cathode was measured by applying a low voltage between the cathode and the collector plate. By overheating the emitter for a short time and then bringing it back to its normal operating temperature, it was found that the emission materially improves. An application of the induction furnace in the early stages of activation causes the emission to decrease temporarily.

A detailed study shows that a very good correlation exists between the shot effect associated with the emission from an oxide cathode and the degree of activation of the cathode. The shot effect characteristics were determined under conditions of constant anode current for various anode voltages at successive stages in the activation of the emitter. They are represented in the curves of Fig. 7. In the case of curve I, we see the begin-

ning of a small peak in the space charge region. The high values of v^2 at higher voltages are obviously due to gas ionization as is shown by the sharp upward trend beyond 120 volts. A comparison of the curves shows that the magnitude of the peak in the space-charge region increases with the length of time the emitter has been heated. Curve III shows complete stability even at high voltages. A study of the activation curves of the emitter shows an increase in the reverse current as the emitter becomes more activated. This indicates that positive ion emission increases. These results show that the

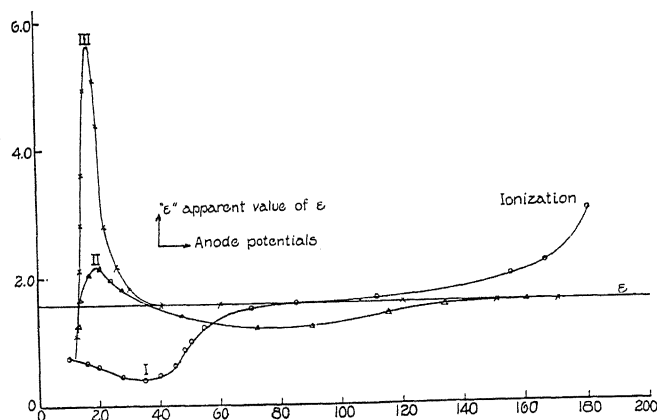


Fig. 7. Shot effect of electrons from barium oxide. $I_0 = 200$ microamps.

fundamental cause of the abnormal fluctuations in the space charge region is the activity of positive ions emitted from the oxide cathode into the space charge region.

A study of the activation of oxide emitters shows that the electron emission increases with the length of time the cathode has been heated. If the cathode is overheated, the electron emission rapidly improves to a maximum value and then slowly decreases. An oxide emitter may be completely activated merely by a prolonged heat treatment, gas-ion bombardment not being at all necessary to the process. At the time of the decrease of electron emission, measurable amounts of reverse current may be detected between the emitter and the plate if a negative potential is applied to the latter. By a high overheat it is possible to get 10 microamperes or more of reverse current. A more critical investigation shows that the reverse current does not consist entirely of positive ions in all cases. For one commercial tube, only 10 percent of the total reverse current was found to consist of positive ions. The remainder is due to photo-emission of electrons from the plate and grid elements by the radiation from the cathode. This has been verified by illuminating the elements with light from an external source, keeping the barium-strontium emitter cold. The magnitude of the current thus obtained is of the same order as with the cathode hot. If the plate and grid are negative with respect to the oxide emitter and they are photo-active, we are unable to

distinguish between positive ions going to them from the oxide and photoelectrons going in the opposite direction. The photoactivity of the grid and plate is very probably due to the evaporation of barium or barium oxide from the cathode and a recondensation on these elements so as to give a surface with a low photoelectric work function.

The problem of identifying positive ions in the emission from barium-strontium cathodes was solved by the use of the familiar magnetron method of Hull.⁵ He has shown that in the case of co-axial cylindrical emitter and collector and a uniform magnetic field applied along the axis of the system, the magnetic field required to prevent electrons or ions emitted by the inner cylinder from reaching the outer collector is given by

$$H = \left(\frac{8m}{e} \right)^{1/2} \frac{V^{1/2}}{R}$$

where m is the mass of the electron or ion, e is the charge of the electron or ion, V is the accelerating potential between the cylinders and R is the radius of the outer collecting cylinder. This assumes that the ratio of the radius of the inner cylinder to that of the outer cylinder is small. We see immediately that for a given voltage, the magnetic field required to prevent a barium or strontium ion from reaching the plate will be about 500 times that required for an electron. For

$$\frac{H_p}{H_e} = \left(\frac{m_p}{m_e} \right)^{1/2}.$$

A special tube containing a unipotential oxide-coated emitter and a nearly co-axial collecting cylinder of molybdenum was constructed. The radius of the collector was large compared to that of the emitter. The plate was therefore located so far from the emitter that recondensation and consequent photo-activity was very small. A solenoid consisting of several thousand turns of copper wire, layer wound, was so constructed that the special tube could be placed in the core with the collector and emitter axes parallel to the magnetic field produced by passing a direct current through the solenoid. Thus the above equation for the motion of the electrons or positive ions under the influence of the electric and magnetic field applies in all detail.

A potential of 22 volts positive with respect to the emitter was applied to the collector. A reflecting galvanometer of sensitivity 10^{-8} amperes was used to measure the space current. When the magnetic field was applied, the current dropped to 20 percent of its original value. It did not drop to a smaller value probably due to a lack of complete symmetry in the arrangement of the emitter and collector. This is the behavior to be expected with electrons. More elaborate experiments might serve to detect the presence of negative oxygen ions in the emission. The potentials were then reversed and the emitter heated until the same space current was again obtained. Application

⁵ A. W. Hull, Phys. Rev. 18, 31 (1921).

of a magnetic field now caused less than 0.5 percent decrease in the space current. This can be taken as conclusive evidence that heavy ions are emitted from oxide emitters. Evidence from photoelectric long wave limits points to these ions being barium or strontium. Absolute determination of the magnetic field would allow the mass of the ions to be determined. However, a mass spectograph analysis would perhaps be easier to carry out and would yield information about the relative proportions of the various ions present.

A report by Glass⁶ on the variation in emission of oxide filaments assumes that all of the reverse current is composed of positive ions. Obviously he has neglected the possibility of photo-emission from the grid and plate. This in commercial tubes is of the same order as the emission of positive thermions.

SHOT EFFECT AT CONSTANT EMITTER TEMPERATURE

In order to obtain the preceding shot-effect curves with constant space current for a range of accelerating voltages it is necessary to vary the temperature of the emitter over a rather wide range. This raises a question as to whether the abnormal fluctuations may not be due to a property of the emitting surface at a certain temperature. To test this point, characteristics of the shot effect were obtained under conditions of constant emitter temperature. The power input to the cathode was held constant at a convenient value, and the fluctuations as observed by the output galvanometer of the high frequency amplifier were studied as a function of the space current as the accelerating potential was varied. The space-current characteristic and the fluctuations observed are plotted against accelerating voltage in Fig. 8. We notice first the typical lack of saturation of the oxide emitter. Here again we have the familiar space-charge depression of fluctuations at very low voltages, then a space-charge peak at higher accelerating field, and finally a portion where the fluctuations are directly proportional to the space current. This is shown by the space current and fluctuation curves becoming parallel. Absolute values of Z and V^2 under these conditions will yield the true value of the electronic charge. Thus it is evident that the peak is not due to changes in the structure of the emitter with temperature, but is a function of space charge. A series of curves taken with various power inputs to the cathode shows that the peak moves toward higher voltages with increased emission.

At a critical value of space charge, a positive ion emitted from the cathode travels in the direction of the potential minimum. By virtue of its large mass and consequent low mobility, it can release a large number of electrons from space charge. Langmuir⁷ has shown that a single ion can release several hundred electrons from space charge. The random emission of positive ions from the cathode and their passage through the space charge region causes large fluctuations in the space charge, producing an abnormally high V^2 across the shot circuit. It is natural to suppose that the magnitude of

⁶ Myron S. Glass, *Phys. Rev.* **28**, 521 (1926).

⁷ Irving Langmuir, *Phys. Rev.* **33**, 954 (1929).

the peak will be a function of the amplifier frequency. Peaks have been found at audio frequencies with oxide coated commercial tubes in this laboratory by Mr. Thatcher. The frequency characteristics of the phenomenon are now

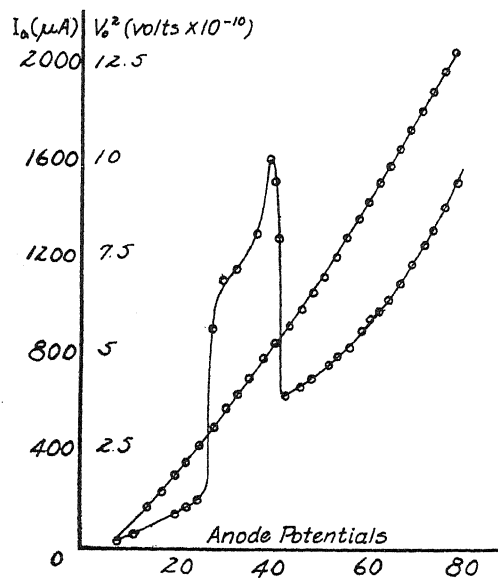


Fig. 8. Shot effect with barium oxide emitter at constant temperature. $I_f = 1.71$ amp., $E_f = 2.66$ volts.

under investigation. It is to be observed that when space charge is obliterated by the use of high accelerating potentials, the mechanism of the fluctuation

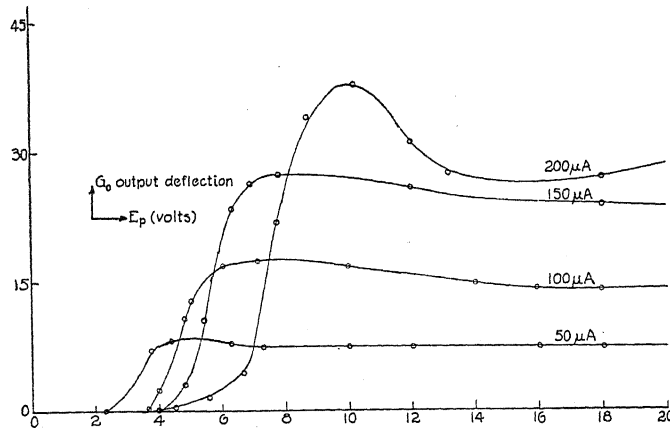


Fig. 9. Position of space charge shot effect peak for various I_0 values. Barium oxide emitter.

no longer exists. Positive ions emitted from the cathode are unable to travel in the tube because of the adverse field, and there are no space charge electrons to be released. Therefore, under these conditions, the true value of

the electronic charge is obtained. As the space current becomes smaller and smaller we would expect the magnitude of the space charge peak to decrease. A series of four curves given in Fig. 9 taken with four constant space currents at various accelerating voltages shows the dependence on current. The results are of the same nature as Johnson reports with the flicker effect at low frequencies. If the space current is low enough, normal fluctuations are obtained.

AN EXPERIMENTAL VERIFICATION OF THE SPACE CHARGE EFFECT

Since the abnormal behavior of the fluctuation voltage is due only to positive ions in the presence of an electron space charge, an attempt was made to reproduce artificially the conditions believed to exist with an oxide emitter. A vacuum tube containing two independent emitters mounted very close together and surrounded by a cylindrical collector plate was constructed. The first emitter is a pure tungsten wire which emits only

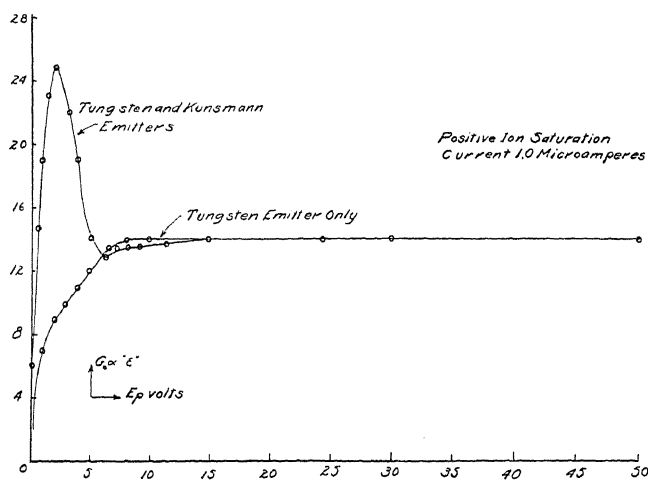


Fig. 10. Shot effect for special tube. $I_0 = 150$ microamps.

electrons when heated. The second is a Kunsman oxide emitter. This, at a temperature of about 900°C , gives off positive potassium ions and a small number of electrons. The ratio of the positive ion to the electron emission is about 1000 to 1 at 900°C . If the shot effect of each emitter is studied separately, the results obtained are normal. That is, at low voltages, the fluctuation voltage is very low due to the effect of space charge on the random distribution in time of the emitted ions or electrons. However, if the two emitters are operated simultaneously, positive ions emitted by the Kunsman emitter, will, at low voltages across the tube, travel into the electron space charge region. Space-charge density can be controlled by the temperature of the tungsten emitter, and by the voltage between the emitters and the anode. A typical curve for this tube operated under conditions simulating those believed to exist in an oxide-emitter tube is given in Fig. 10. A curve for the tungsten emitter alone is also included. The

space current in the tube using first only the tungsten emitter, and then the combination of tungsten and Kunsman emitters, was held constant at 150 microamperes. The general characteristics of the shot effect are those obtained with the oxide coated emitter. It is interesting to note that as soon as space charge is removed, the peak disappears.

Thus it has been shown that the abnormally high shot voltage observed in the space charge region when an oxide emitter is used can be duplicated by the interaction of positive ions from an independent emitter with an electronic space charge. The thermions from a Kunsman⁸ emitter have been identified by the mass spectograph as positive potassium ions. The abnormally high shot effect observed disappears when the source of positive ions has been cut off, and also disappears at high accelerating potentials. Therefore, we have conclusive evidence that the abnormal shot effect is due to positive ions moving through space charge.

SHOT EFFECT OF EVAPORATING SURFACE FILMS

During the study of the shot effect, a special tube containing a barium oxide and a tungsten emitter mounted close to one another was used. This tube was very highly evacuated and thoroughly outgassed, and then sealed off. The oxide emitter was thoroughly activated during the process of evacuation. No trace of residual gas was detected with the voltages applied to the tube. The tungsten emitter alone gave normal shot effect. If, however, the barium oxide emitter was operated for a short time with the tungsten cold, and then the tungsten emitter was suddenly brought to full brilliancy, the shot-output galvanometer gave a deflection of the order of 3000 mm. This decreased exponentially with the time to the normal value of 30 mm corresponding to the shot effect associated with the space current used. On the basis of Becker's⁹ work with oxide emitters, it is probable that some barium of the surface layer of the activated emitter evaporates from the oxide emitter and condenses on the tungsten emitter. On bringing this tungsten emitter to its operating temperatures suddenly, the barium evaporates in the form of barium ions which interact with the space charge in the usual manner. No such surge was noticed with a high accelerating voltage across the tube. The same phenomenon was noticed with the Kunsman tungsten emitter tube.

Absolutely no surge is noticed on bringing the tungsten emitter to full brilliancy after it has been thoroughly cleaned of this layer by operating at a high temperature for three or four minutes. The decay of the surge due to a layer formed by evaporation of either barium or barium oxide onto the tungsten emitter can be controlled by varying the operating temperature. It appears that the process of this film leaving the surface is quite the same as occurs in the deactivation of a thoriated tungsten emitter. No evidence of such a surge was found using a thoriated tungsten emitter brought suddenly to a temperature where the thorium leaves the tungsten and leaves it deactivated. This can probably be interpreted to mean that thorium leaves a thoriated tungsten emitter in a neutral state and not as an ion.

⁸ N. A. Barton, C. P. Harnwell, C. H. Kunsman, *Phys. Rev.* **27**, 739-746 (1926).

⁹ Joseph A. Becker, *Phys. Rev.* **34**, 1323 (1929).

A PHOTOGRAPHIC METHOD OF DETERMINING
ATOMIC STRUCTURE FACTORS

BY DAROL K. FROMAN

RYERSON PHYSICAL LABORATORY UNIVERSITY OF CHICAGO

(Received August 27, 1930)

ABSTRACT

The intensities of x-rays reflected from powdered crystals of magnesium oxide and potassium chloride were measured photographically. It was found that this method made possible the measurement of somewhat higher orders of reflection from powdered crystals than have been determined by the ionization method. The radial electron distribution for each of the atoms was determined and the results indicate that both compounds form polar crystals.

INTRODUCTION

ELECTRON distributions and atomic structure factors have been determined by many experimenters from measurements of the intensity of monochromatic x-rays reflected by the various atomic planes of a powdered crystal mass. It has been shown¹ that the electron distribution in a crystal can be represented by a Fourier series, each term of which depends on the intensity of the corresponding order of reflection. In order to evaluate as many terms of this series as possible, and thus to determine the electron distribution with precision, it is important to measure the higher orders of reflection. Since the intensities in the higher orders are often so small that ionization measurements are inaccurate, it was thought that the cumulative property of the photographic film might be used to obtain better measurements in this region.

APPARATUS AND EXPERIMENTAL PROCEDURE

A schematic arrangement of the apparatus is shown in Fig. 1. A cylindrical lead camera, *C*, was supported on an insulating stand about one inch from a Coolidge x-ray tube with an Mo target. The middle portion of the tube was covered with tin foil, which was connected to the camera to prevent sparks puncturing the glass. X-rays from the target fell on a calcite crystal, *K*₁, which was so oriented that the *K*_α line was reflected through the slits in the camera to the sample of powdered crystal, *S*. A photographic film, *F*₁, was bent to fit the inside of the camera, and a zirconium oxide filter placed just in front of it. The main x-ray beam, after transmission through the sample, was caught in a lead shield, *L*. Sometimes the crystal *K*₁ was removed and the direct rays allowed to fall on the sample, only the filter being used to limit the wave-lengths of the x-rays. In this case the intensity was increased greatly.

¹ A. H. Compton, "X-rays and Electrons," p. 164.

The samples were powdered crystal cylinders about 1 mm in diameter and 6 mm long. The powder was passed through a 200 mesh screen and was fine enough to eliminate primary extinction.² An emulsion of the powder in a little household cement and amyl acetate was made, and the cylinders were formed by extruding the mixture through a small circular aperture. These cylinders, although containing only about eight percent by weight of celluloid, were quite stable.

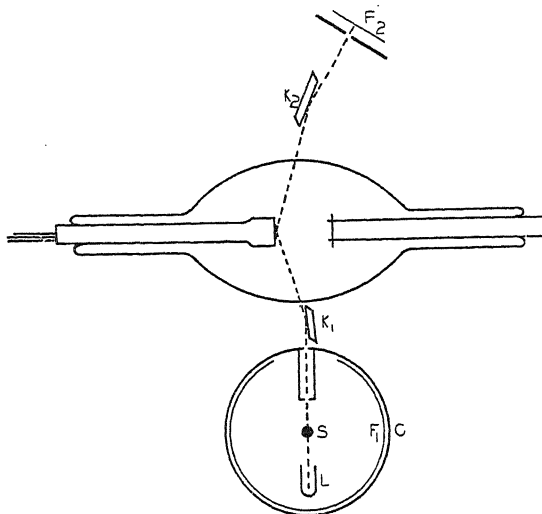


Fig. 1. Arrangement of apparatus.

During an exposure the K_{α} line from another crystal, K_2 , was allowed to fall on a second film, F_2 . A series of exposures with different exposure times was taken giving lines whose relative intensities were known, since it was assumed that the effect on the film was a function of the product of the intensity and the time of exposure. Both films were always cut from the same piece, developed together and given identical treatment. The films were examined with a Moll microphotometer and the galvanometer deflections measured for the various lines. The known intensities of the lines on film F_2 provided a calibration curve from which the relative intensity of any point on film F_1 could be determined. Fig. 2 shows a typical calibration curve obtained in this way. The ordinates are proportional to the exposure times and thus they represent relative intensities. A plot of intensity, determined in this way, against θ always showed that the powdered crystal lines were very nearly triangular and that their widths were constant. Thus the intensity of the peak was proportional to the integrated intensity, P_s , of the line and it was necessary to measure only this peak intensity. Fig. 3 shows a microphotometer trace of a typical film of the reflections from KCl. The line $D. B.$ is the zero position of the galvanometer. An absolute determination of the intensity of one line was made by a photographic comparison with

² R. J. Havighurst, Phys. Rev. **28**, 869 (1926).

the known reflections of NaCl. In this case the lines were of different widths and it was necessary to take the area under the intensity curve for the integrated intensity.

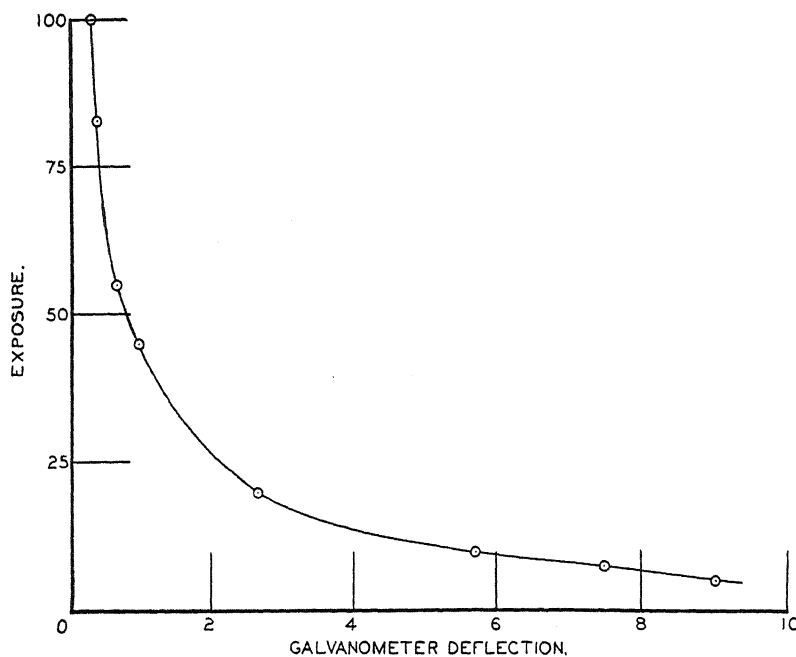


Fig. 2. Intensity calibration curve.

The structure factors were computed from the relation:³

$$F^2 = AP_s \sin^2 \theta \cos \theta / p(1 + \cos^2 2\theta) \quad (1)$$

in which P_s is the power in the reflected beam, θ the grazing angle of reflection and p the number of planes per unit cell contributing to reflection at angle θ . A represents a group of constants which were determined from the comparison with NaCl.

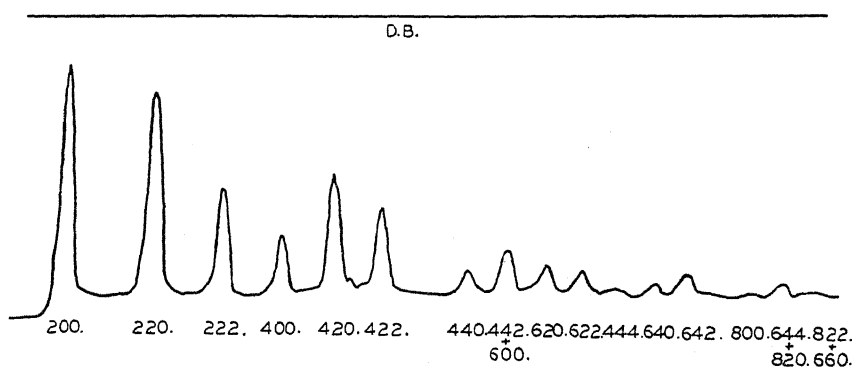


Fig. 3. Microphotometer trace of film.

³ A. H. Compton, "X rays and Electrons," p. 131.

RESULTS

Measured values of the relative intensities, P_s , and the corresponding structure factors, F , are given in Tables I and II for MgO and KCl re-

TABLE I. *Structure factors of MgO.*

Line	$\sin \theta$	P_s	F
111	0.1464	21.8	2.46
200	0.1691	353.0	13.25
220	0.2390	199.0	10.15
311	0.2804	22.1	2.85
222	0.2929	55.1	8.19
400	0.3380	21.2	6.41
331	0.3684	9.16	2.50
420	0.3780	46.8	5.83
422	0.4140	27.5	4.99
511+333	0.4392	4.25	1.81
440	0.4782	5.25	3.68
531	0.5000	1.40	0.997
442+600	0.5071	11.2	3.66
620	0.5344	5.66	3.07
533	0.5542	1.00	1.36
622	0.5606	4.80	3.03
444	0.5856	1.64	3.22
711+551	0.6036	0.8	0.949
640	0.6095	3.54	2.85
642	0.6324	6.17	2.77
731+553	0.6492	0.955	0.91
800	0.6762	0.658	2.71
733	0.6918	0.451	1.14
820+644	0.6970	3.68	2.31
822+660	0.7172	2.56	2.26
555	0.730	0.155	1.18
662	0.745	1.46	2.11
840	0.755	1.36	2.03
911+753	0.769	0.655	0.815
842	0.773	2.12	1.80
664	0.793	1.08	1.80
931	0.805	0.25	0.608
844	0.827	1.12	1.78
933+755+771	0.840	1.23	1.06
10,00+860	0.845	0.605	1.14
10,20+862	0.862	2.38	1.42
951	0.875	1.58	1.38
10,22+666	0.878	1.66	1.72
953	0.905	1.09	1.06
10,40+864	0.907	0.977	0.815
1042	0.924	0.769	0.835
11,11+775	0.936	0.396	0.570
880	0.956	0.250	0.815
882	0.962	0.818	1.00
11,31+955	0.966	0.256	0.313
1044	0.969	0.733	0.890

spectively. The probable errors in the intensities are about five percent in the highest values and about twelve percent in the smallest. Figs. 4 and 5 show the structure factors plotted against $\sin \theta$ for MgO and KCl respectively. No odd order reflections were obtained from the latter crystal. The intensities of several lines of high order of reflection which have not been measured by the ionization method have been determined. For example ionization measurements on MgO have not been carried past $(\sin \theta)/\lambda = 1$, whereas

TABLE II. Structure factors of KCl

Line	$\sin \theta$	P_s	F
200	0.1131	680.	12.08
220	0.1599	393.0	9.33
222	0.1959	127.0	8.04
400	0.2261	57.5	7.26
420	0.2529	144.0	6.50
422	0.2770	87.7	5.60
440	0.3199	19.3	4.36
600+442	0.3392	34.5	4.36
620	0.3575	19.8	3.56
622	0.3750	17.1	3.50
444	0.3918	5.07	3.48
640	0.4078	9.60	2.90
642	0.4231	14.5	2.66
820+644	0.4663	11.1	2.60
822+660	0.4798	3.8	1.82
662	0.4984	1.83	1.62
840	0.5051	2.57	1.95
842	0.5173	3.62	1.34
664	0.5307	4.26	2.10
844	0.5534	2.14	1.54
10,20+862	0.5769	2.05	0.90
10,22+666	0.5876	1.01	0.96

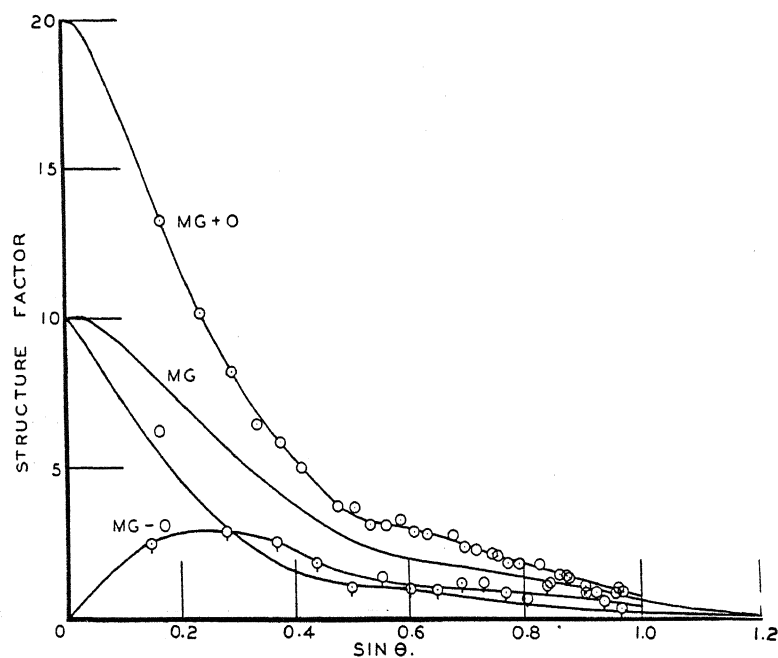


Fig. 4. Structure factors of MgO.

measurements were made with the photographic method as far out as $(\sin \theta)/\lambda = 1.35$.

The radial electron distribution for the different atoms,⁴

⁴ A. H. Compton, "X-rays and Electrons," p. 164.

$$U = (8\pi r/D^2) \sum_{n=1}^{\infty} nF_n \sin(2\pi nr/D) \quad (2)$$

where n is the order of reflection and F_n the corresponding structure factor, was determined by a mechanical synthesis. The synthesis was made with Michelson's⁵ harmonic analyser which is designed to analyse a curve into its first eighty Fourier components. To synthesize, it was necessary only to displace the ends of push rods distances proportional to the corresponding coefficients and, upon turning a crank, the result was traced out. Friction of

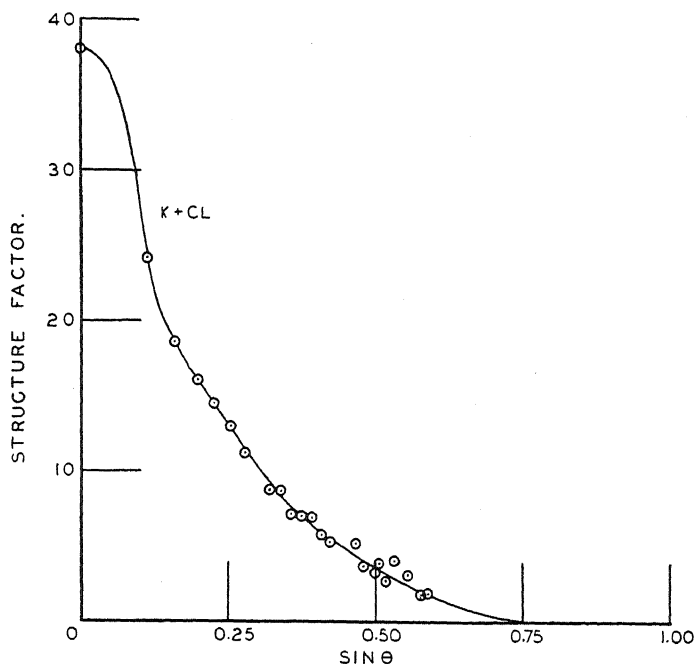


Fig. 5. Structure factors of KCl.

the pen point caused some error, so instead of a pen a slit was attached to the tracing arm which moved at right angles to its length. Back of this slit another stationary slit was placed at right angles to the first. Sensitized paper was used on the movable table and the curve traced by means of a beam of light passing through the crossed slits. Arbitrary grating spaces were chosen and the values of nF_n were set on the synthesizer. It will be seen from Eq. (2) that the result was a curve for U/r . A typical example of the analyzer trace is given in Fig. 6, which shows U/r for oxygen. The curve was obtained by multiplying the ordinates of this curve by their respective abscissas. Arbitrary grating spaces of 4.82 and 7.10 Å were chosen for MgO and KCl respectively. Somewhat different results for Mg and O might be expected in the U curves for different extrapolations of the odd order

⁵ A. A. Michelson and S. W. Stratton, *Amer. Journ. Sci.* 5, 1 (1898).

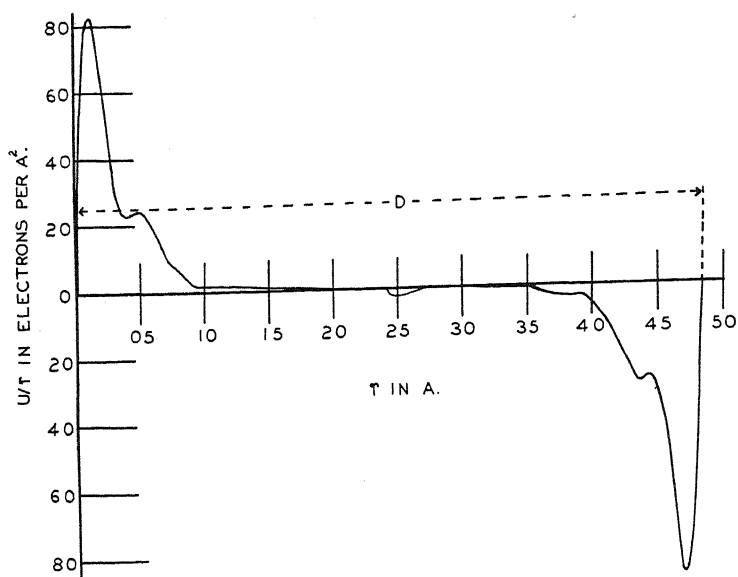


Fig. 6. Harmonic analyzer trace.

structure factor curve. Fig. 7, curve 1, shows the electron distribution of oxygen when the odd order structure factor curve is extrapolated to zero for

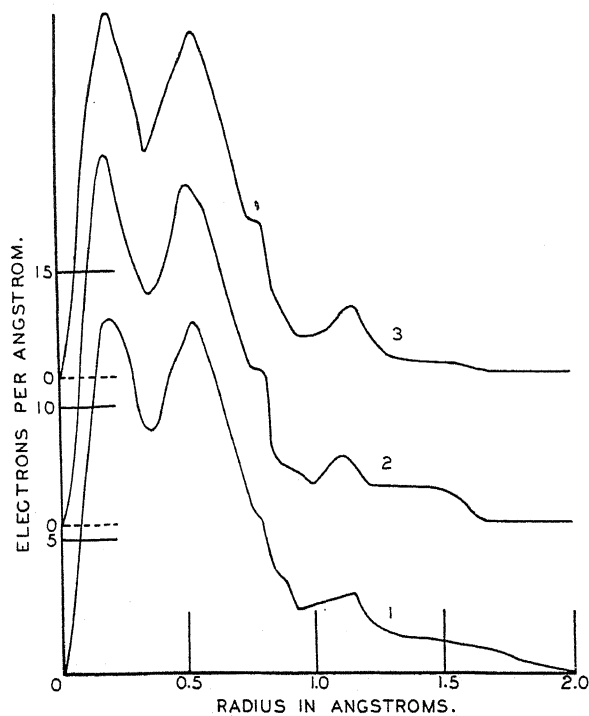


Fig. 7. Electron distribution of oxygen.

$\sin \theta = 0$. Curve 2 shows U for extrapolation to $F=2$ and curve 3 for extrapolation to $F=4$ at $\sin \theta = 0$. The three curves will be seen to be very similar. The area under such a curve represents the total number of electrons

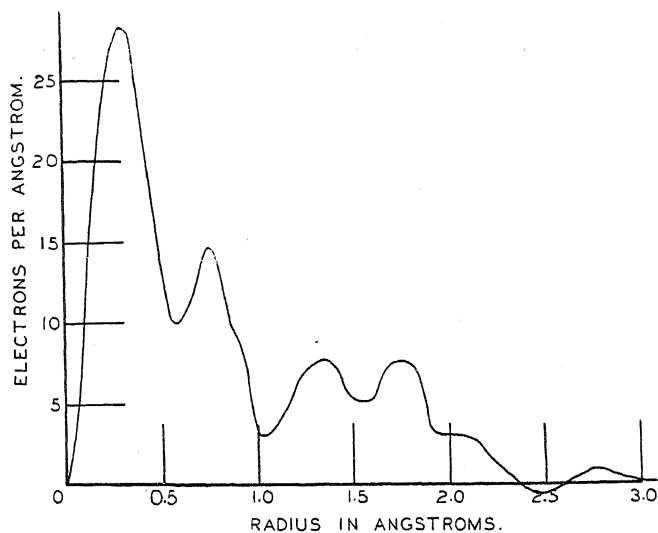


Fig. 8. Electron distribution of magnesium.

in the atom. The area under curve 1 is equivalent to 9.4 electrons and the areas under curves 2 and 3 are slightly greater than this, but the differences are not as great as 1 and 2 electrons respectively. Fig. 8 gives U for Mg for

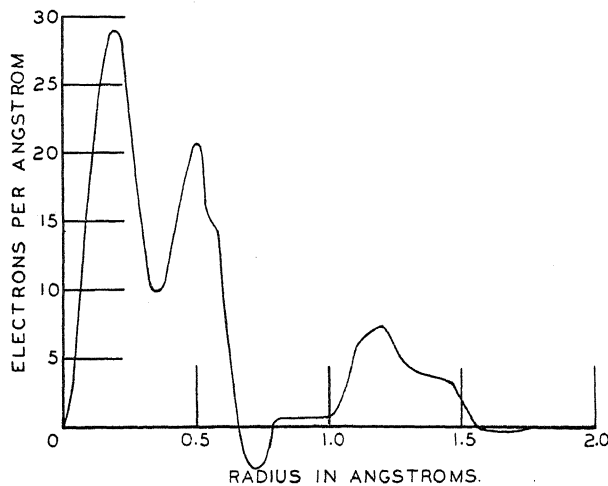


Fig. 9. Electron distribution for K and Cl.

extrapolation to zero, and Fig. 9 shows U for K and Cl, which, since the odd orders do not appear, cannot be distinguished by this method. Structure factors corresponding to reflections of different orders from the (111) planes were used throughout the analysis.

The total number of electrons per atom as determined from⁶

$$Z = -2 \sum_{n=1}^{\infty} (-1)^n F_n \quad (3)$$

was found to be 9.30 for oxygen, 10.32 for magnesium and 18.0 for both chlorine and potassium. This indicates polar crystals probably consisting of $\text{Mg}^{++}\text{O}^{--}$ and $\text{K}^{+}\text{Cl}^{-}$. The results for MgO are in fair agreement with those obtained by Wollan.⁷ The important differences are that the structure factor for the (111) plane was found to be somewhat less than for the (311) plane, Wollan finding them to be about equal; and that the structure factor curves are slightly higher than Wollan's for large values of $\sin \theta$. If the (111) factor is less than the (311) factor it is an indication that the odd order curve, (Fig. 4) should be extrapolated to zero. James and Brindley⁸ have measured the structure factors for KCl but it is a little difficult to compare their results with those reported here, since they do not give their original data and have applied some unknown corrections.

In conclusion the writer wishes to express his appreciation to Professor A. H. Compton, who suggested this problem, for his many very valuable suggestions during the course of the work.

⁶ A. H. Compton, "X-rays and Electrons," p. 165.

⁷ E. O. Wollan, *Phys. Rev.* **35**, 1019 (1930).

⁸ R. W. James and G. W. Brindley, *Proc. Roy. Soc.* **121**, 155 (1928).

A NOTE ON THE EXTRAPOLATION OF ATOMIC STRUCTURE FACTOR CURVES

BY DAROL K. FROMAN

RYERSON PHYSICAL LABORATORY, UNIVERSITY OF CHICAGO

(Received August 27 1930)

ABSTRACT

An approximate extrapolation formula for atomic structure factors of high order has been deduced from the form of the electron distributions indicated by the wave equation. The result is compared with the structure factors determined from Hartree's¹ electron distribution for Na^+ . The agreement is good enough to warrant the use of the formula in extrapolating experimentally determined structure factor curves. It is shown that an analogous treatment can be applied to the "S" curves obtained from the scattering of x-rays by gases.

EXTRAPOLATED STRUCTURE FACTORS

THE structure factors of the first few orders of reflection can be determined without great difficulty, and a rational method of extrapolation of the structure factor curve to high orders may be valuable.

The radial electron distribution $U(r)$, and the n th order structure factor, F_n , are related² by Eq. (1).

$$J(r) = (8\pi r/D^2) \sum_{n=1}^{\infty} nF_n \sin(2\pi nr/D) \quad (1)$$

where D is the first order grating space. Multiplying by $\sin(2\pi mr/D)dr$ and integrating from 0 to $D/2$

$$\begin{aligned} \int_0^{D/2} \frac{U(r)}{r} \sin \frac{2\pi mr}{D} dr &= \frac{8\pi}{D^2} \int_0^{D/2} \sum_{n=1}^{\infty} nF_n \sin \frac{2\pi mr}{D} \sin \frac{2\pi nr}{D} dr \\ &= \frac{8\pi}{D^2} \sum_{n=1}^{\infty} nF_n \int_0^{D/2} \sin \frac{2\pi nr}{D} \sin \frac{2\pi mr}{D} dr \\ &= 0 \text{ for } m \neq n \\ &= \frac{8\pi}{D^2} mF_m D/4 \text{ for } m = n. \end{aligned}$$

Putting $m = n$ and solving for F_n ,

$$F_n = (D/2\pi n) \int_0^{D/2} \frac{U(r)}{r} \sin \frac{2\pi nr}{D} dr. \quad (2)$$

The Schrödinger equation for the hydrogen-like atom

¹ D. R. Hartree, Proc. Camb. Phil. Soc. **24**, 189 (1928).

² A. H. Compton, "X-rays and Electron," p. 164.

$$\Delta^2 \Psi + (8\pi^2 m / h^2)(E + Ze^2/r)\Psi = 0 \quad (3)$$

has a solution separable in the polar coordinates, r , θ and ϕ ,

$$\Psi = R(r)P_l^m(\cos \theta)e^{im\phi} \quad (4)$$

where m is the magnetic quantum number, l the azimuthal quantum number minus 1 and P_l^m is the Legendre polynomial of degree l and order m .

$\Psi\Psi^*$ when suitably normalized, represents the density of electricity at the point (r, θ, ϕ) and averaging over the sphere of radius r ,

$\overline{\Psi\Psi^*} = a_{lm}R^2$ where a_{lm} is the average "square" of the angle functions.

Substituting the assumed solution (4) in equation (3) an equation in R and r is obtained which has as its solution³

$$R(r) = e^{-\rho/2} \rho^l \sum_{\nu=0}^{n_r} b_\nu \rho^\nu$$

where $\rho = 2r/r_0 = 2r/(-h^2/8mE)^{1/2}$, $n_r = n - (l+1)$, n being the total quantum number, and $b =$

$$\frac{(\nu + l + 1)(\nu + l) + 2(\nu + l + 1) - l(l + 1)}{\nu + l + 1 - n} b_{\nu+1}$$

But

$$\begin{aligned} U(r) &= 4\pi r^2 \overline{\Psi\Psi^*} \\ &= 4\pi r^2 a_{lm} e^{-\rho} \left[\sum_{\nu=0}^{n_r} b_\nu \rho^{\nu+l} \right]^2 \\ &= 4\pi r^2 a_{lm} e^{-\beta r} \left[\sum_{\nu=0}^{n_r} D_\nu r^{\nu+l} \right]^2 \end{aligned} \quad (5)$$

where $\beta = 2/r_0$ and $D_\nu = (2/r_0)^{\nu+l} b_\nu$

Since the number of nodes in $R(r)$ is not affected by screening, let us assume that the general shape of the electric density distribution curve for any one electron in an atom or ion is given by an equation similar to (5). However, since $R(r)$ will not be identical for electrons in corresponding orbits of different atoms, the recursion formula for the D 's will not be assumed to hold.

Then for any atom or ion with N electrons

$$U(r) = \sum_{i=1}^N \alpha_{l_i m_i i} r^2 e^{-\beta_i r} \left[\sum_{\nu=0}^{n_{r_i}} D_{\nu i} r^{\nu+2l_i} \right]^2$$

where

$$\alpha_{l_i m_i i} = 4\pi r^2 a_{l_i m_i i}$$

and substituting in equation (1),

$$F_n = \frac{D}{2\pi n} \sum_{i=1}^N \int_0^{D/2} \alpha_{l_i m_i i} r e^{-\beta_i r} \sum_{j=0}^{n_{r_i}} \sum_{k=0}^{n_{r_i}} D_{ji} D_{ki} r^{j+k+2l_i} \sin \frac{2\pi n r}{D} dr. \quad (6)$$

³ A. Sommerfeld, "Wellenmechanischer Ergänzungsband," p. 72.

Let γ_i be the total quantum number of the i th electron. Then $\gamma_i = \gamma_{ri} + l_i + 1$. The powers of r in the integrand run from 1 to $2(n_r + l_i) + 1$, i.e. from 1 to $\gamma_i - 1$ inclusive. Hence the integral is of the form:

$$I = \int_0^{D/2} \sum_{s=1}^{2\gamma_i-1} a_s r^s e^{-\beta_i r} \sin \frac{2\pi n r}{D} dr.$$

Each term of this integral can be integrated by parts successively, which reduces the power of r by 1 each step, and results in a series which, after substitution of limits, is of the form

$$\frac{\epsilon_1 n}{(\beta_i^2 + 4\pi^2 n^2/D^2)} + \frac{\epsilon_2 n}{(\beta_i^2 + 2\pi^2 n^2/D^2)^2} + \frac{\epsilon_3 n}{(\beta_i^2 + 4\pi^2 n^2/D^2)^3} + \dots$$

Summing over the s 's will change only the constants, ϵ .
Hence

$$I = \sum_{p=1}^{2\gamma_i} \frac{J_p n}{(\beta_i^2 + 4\pi^2 n^2/D^2)^p}$$

where the J 's are constants and equation (6) becomes

$$F_n = \sum_{i=1}^N \sum_{p=1}^{2\gamma_i} A_{pi} / [B_i + (n/D)^2] \quad (7)$$

where the A 's are constants and

$$B_i = 8\pi^2 m E_i / 4\pi^2 h^2.$$

In any practical case, $m = 9 \times 10^{-28}$ gm, $h = 6.5 \times 10^{-27}$ erg sec, $E \leq 10^{-10}$ ergs for most of the electrons in atoms for which structure factors are determined. Hence

$$B \leq 0.5 \times 10^{16} \text{ cm}^{-2} \leq 0.5A^{-2},$$

and B will be less than $(n/D)^2$ for $(n/D) > 0.7$ except, perhaps, the K electrons of heavy atoms and will usually be less than $(n/D)^2$ for $(n/D) > 0.2$.

Expanding F_n in powers of $B/(n/D)^2$ we have,

$$F_n = a_1 \left(\frac{n}{D} \right)^2 + a_2 \left(\frac{n}{D} \right)^4 + \dots \quad (8)$$

in which the a 's are undetermined constants. Since

$$n\lambda = 2D \sin \theta$$

$$\begin{aligned} F_n &= a_1/4 \left(\frac{\sin \theta}{\lambda} \right)^2 + a_2/16 \left(\frac{\sin \theta}{\lambda} \right)^4 + \dots \\ &= b_1 \left(\frac{\sin \theta}{\lambda} \right)^2 + b_2 \left(\frac{\sin \theta}{\lambda} \right)^4 + \dots \end{aligned} \quad (9)$$

If it is desired to extrapolate an experimental structure factor curve

account must be taken of the effect of temperature. It has been shown⁴ that the integrated intensity reflected at an angle θ is proportional to $e^{-B\sin^2\theta}$, where B is a function of the temperature and contains the factor $1/\lambda^2$.

Since $F_n^2 \sim P_s$, the structure factor at any temperature, T , is

$$F_{nT} = F_{n0}e^{-(B/2)\sin^2\theta}$$

and Eq. (9) becomes:

$$F_{nT} = e^{-(B/2)\sin^2\theta} \left[b_1 / \left(\frac{\sin \theta}{\lambda} \right)^2 + b_2 / \left(\frac{\sin \theta}{\lambda} \right)^4 + \dots \right]. \quad (10)$$

Waller⁵ finds a function for B which for Na at 290°K gives $B = 3.74/\lambda^2$.

Using this value of B the first two terms in Eq. (10) were fitted by least squares to the structure factors computed by Holbrook⁶ from Hartree's⁷

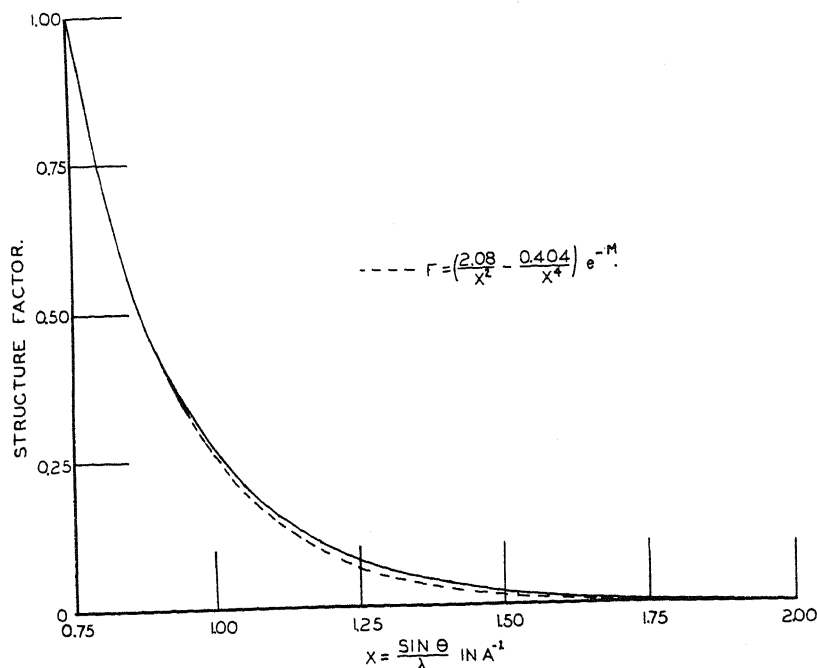


Fig 1. Extrapolated structure factors.

electron distribution for Na^+ . The constants b_1 and b_2 were determined to fit the computed structure factors over the range from $(\sin \theta)/\lambda = 0.75$ to $(\sin \theta)/\lambda = 0.95$, which is about the end of the measurable values. Using these values of b_1 and b_2 the curve was extrapolated to $(\sin \theta)/\lambda = 2.00$. Fig. 1 shows the computed and extrapolated structure factors. The maximum deviation of the extrapolated curve from the true structure factor is 0.015

⁴ P. Debye, Ann. d. Physik 43, 49 (1914).

⁵ I. Waller, Zeits. f. Physik 17, 398 (1923).

⁶ B. D. Holbrook, A paper not yet published.

⁷ D. R. Hartree, Proc. Camb. Phil. Soc. 24, 189 (1928).

electron and the fit is much better in most places. The entire structure factor for Na^+ is not shown since the vertical scale would need to be compressed ten fold to do so, and on such a scale the deviations of the extrapolation from the true values would not be noticeable.

APPLICATION TO SCATTERING FROM GASES

It might be noted here that an exactly analogous treatment can be applied to the electron distribution as determined from gas scattering. In this case⁸

$$U = Zr \sum_{n=1}^{\infty} A_n \sin \frac{2\pi nr}{2a} \quad (11)$$

where Z is the atomic number, a the radius of the atom, and A_n is a function of the intensity of x-rays scattered at angle ϕ . n is given by $n = (4a/\lambda) \sin(\phi/2)$. In Eq. (11), the A_n replaces the nF_n and the $2a$ replaces D in Eq. (1). Hence Eq. (8) can be replaced by

$$A_n = (n/D) [a_1/(n/D)^2 + a_2/(n/D)^4 + \dots] \quad (12)$$

$$\begin{aligned} &= \frac{4}{a} \frac{a_1}{\left(\frac{\sin \phi/2}{\lambda}\right)} + \left(\frac{4}{a}\right)^3 \frac{a_2}{\left(\frac{\sin \phi/2}{\lambda}\right)^3} + \dots \\ &= b_1/\left(\frac{\sin \phi/2}{\lambda}\right) + b_2/\left(\frac{\sin \phi/2}{\lambda}\right)^3 + \dots \end{aligned} \quad (13)$$

In conclusion the writer wishes to express his thanks to Professor A. H. Compton for suggesting this problem and indicating the general method of attack.

⁸ A. H. Compton, *Phys. Rev.* **35**, 933 (1930).

THE RANGE OF THE α PARTICLES FROM THORIUMBY G. H. HENDERSON AND J. L. NICKERSON
DALHOUSIE UNIVERSITY, HALIFAX, N. S.

(Received September 5, 1930)

ABSTRACT

The range of the α particles from thorium has been found from Wilson expansion chamber photographs to be 2.59 ± 0.05 cm. This agrees reasonably well with the Geiger-Nuttall relationship and greatly extends its applicability.

INTRODUCTION

THE ranges of the α -particles from most radioactive substances are known to a few tenths of one percent. The least accurately known is thorium, the longest lived of all the radioelements, for which only one determination worthy of consideration has been made. This was in 1911 by Geiger and Nuttall¹ and later corrected by Geiger² to the value 2.90 cm at 15°C and 760 mm. A more recent but tentative value of 2.75 cm was made by one of us³ but the uncertainty involved was felt to be too great. This uncertainty in the range of thorium is the more regrettable since these values differ markedly from that predicted by the Geiger-Nuttall relationship between range and transformation constant. In view of recent theories of nuclear structure and α -particle emission it is of great interest to determine if this discrepancy is real or only due to experimental error.

METHOD

The difficulty in determining the range for thorium lies in its weak activity, which precludes the use of the usual methods. The method adopted was that of photographing the tracks in a Wilson expansion chamber, modified to deal with this inactive source. The thorium source was made as extended in size as possible, covering most of the wall of the chamber, while automatic photographing had to be dispensed with to economize film and the photographs taken by the operator after the appearance of the tracks. The practicability of this method had already been proved in this laboratory for the α -particles from UI and UII, by Laurence,⁴ whose paper may be referred to for details.

The Wilson chamber was about 6 cm in diameter, actuated by a spring and cam mechanism and driven by a motor at the rate of 15 expansions per minute. On the appearance of an α -particle track an electrical contact made by the operator opened the camera shutter, shut off the motor and applied

¹ Geiger and Nuttall, *Phil. Mag.* **22**, 613 (1911).

² Geiger, *Zeits. f. Physik* **8**, 45 (1922).

³ Nickerson, *Trans. N. S. Inst. Sci.* **17**, 172 (1929).

⁴ Laurence, *Phil. Mag.* **5**, 1027 (1928).

a brake. Readings of temperature and pressure were then made. The camera had an f. 4.5 lens and used moving picture film. Light was supplied by a carbon arc.

Besides the tracks from thorium there were also longer tracks from isotopes which might strike the top or bottom of the chamber. It was necessary to photograph a large number of tracks so as to smooth out the probability variations in this background before the range of the α -particles from thorium itself could be clearly distinguished. The work was very tedious, for on the average about 200 expansions were necessary per track. Photographs of about 900 tracks were obtained, of which some 420 were judged sharp enough to be measured satisfactorily.

SOURCE

Two samples of thorium were used. One was a commercial sample of thorium nitrate, which contained a small amount of the isotope ionium, arising from the small percentage of uranium ordinarily mixed with thorium ores.

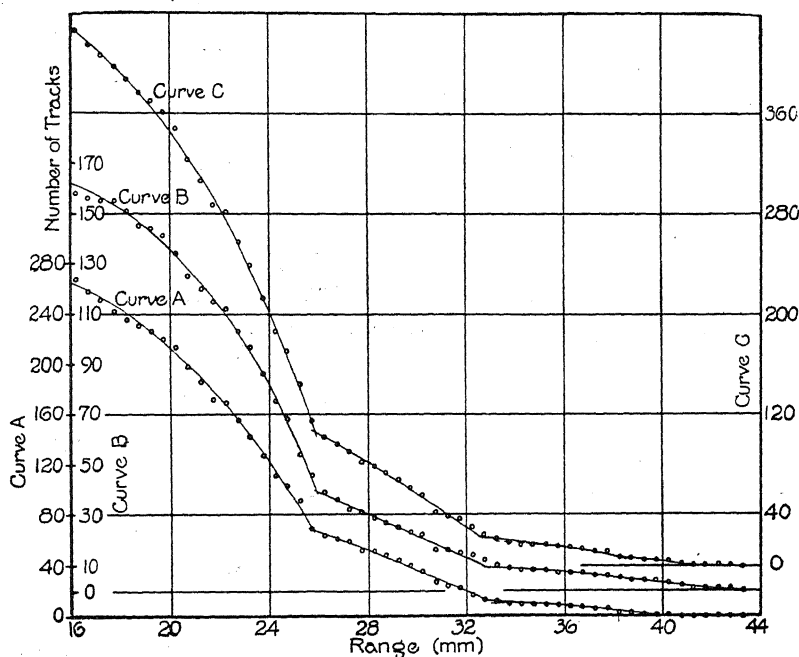


Fig. 1.

The other was a small sample of thorium hydroxide practically free of uranium, kindly furnished by Professor Soddy.

After much experimenting, the following method of preparing the sources was adopted. The sample was put into solution, some lead nitrate added and then the lead together with radioactive isotopes was precipitated by hydrogen sulphide. The thorium remained in solution and was then precipitated as hydroxide by ammonia, leaving ThX in solution. The hydroxide was dried, turned into the oxide by heating and then ground very fine in an agate mor-

tar. The thorium oxide dust was then brushed on to mica strips, which had been covered on one side by very soft wax. The finest of the dust adhered to the wax and with some practice it was found possible to obtain sources of the desired thickness, which appeared very uniform under low magnification. The thickness was determined by weighing and was generally made equivalent to about 1 mm of air. The mica strips were about 11×0.6 cm and covered most of the wall of the chamber, leaving a space to admit the light. To minimize the growth of later products, a source was not used for more than 30 hours after preparation but was replaced by a freshly made one.

RESULTS

The tracks were measured, corrected for pressure, temperature, water vapor, finite thickness of source and obliquity of tracks as described by Laurence.⁴

The results obtained are shown in Fig. 1. The abscissae represent the range in air at 15°C and 760 mm and the ordinates the number of tracks greater than the corresponding range. Curve *A* represents the results with uranium-free thorium, curve *B* those with commercial thorium, and curve *C* the combined results. The axis of abscissae of each succeeding curve has been raised for clearness.

It is satisfactory to find that the two different samples of thorium give clear-cut and almost identical ranges. From the combined results the range of thorium α -particles is taken to be

$$2.59 \pm 0.05 \text{ cm at } 15^\circ\text{C and } 760 \text{ mm pressure.}$$

THE GEIGER-NUTTALL RELATIONSHIP

This relationship is best illustrated by a diagram. In Fig. 2 $20 + \log \lambda$ (where λ is the transformation constant) is plotted against the log of the range at 15°C. Most of the values for the ranges are due to Geiger, the value of UI being that of Laurence⁴ and that for Th our present value. The error in each range, as assigned by the experimenters themselves, is indicated by the size of the dot or circle representing the α -particle concerned.

This diagram shows that both UI and Th fit the straight lines reasonably well. Even if UI and Th be left out it can be seen that no straight line can be drawn for any of the three radioactive families which will fit the results within the limits of experimental error. In fact a straight line can be drawn as shown passing through all points of the thorium family including thorium with an average deviation no greater than that shown by least squares⁵ for the five remaining members of that family. (In considering these deviations, of the order of less than 1 percent, it should be remembered that the range itself is defined in a somewhat arbitrary manner.)

Thus the conclusion may be drawn that Th and UI fit the Geiger-Nuttall relationship about as well as the other substances. It should be pointed out that this represents an enormous extension of the applicability of this relationship. In the case of thorium it involves a change of the transformation

⁵ Meyer u. Schweidler, Radioaktivität, 2nd ed. p. 50.

constant by a factor of 10^{10} , a change greater than the whole range of values covered by the remainder of the family.

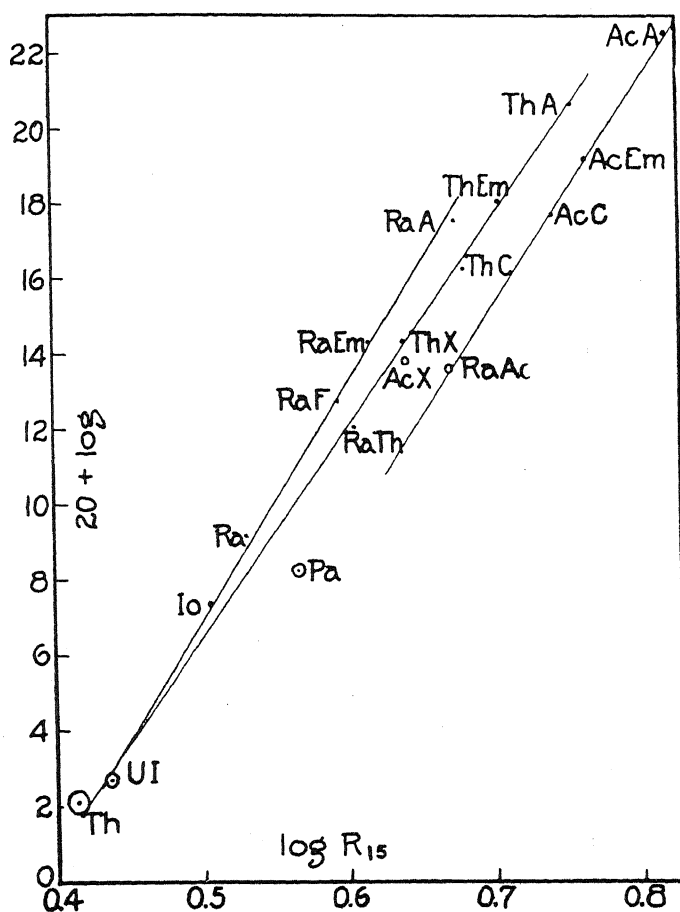


Fig. 2.

REMARKS

It will be noted that the number of thorium tracks does not become constant with decreasing range, owing to the geometrical conditions imposed by the boundaries of the chamber.

Traces of the ranges of other α -particles from isotopes are to be seen on the curves. That of ionium is fairly clear at about 3.26 cm (accepted range 3.194 cm). Further along are slight signs at 3.8 cm (protoactinium, 3.67 cm?) and at 4.1 cm (radiothorium 4.02 cm?). Tracks longer than about 4.3 cm could not be measured in the chamber and tracks as long as those of radiothorium would be very rare owing to the small permissible solid angle. The kink in the curve at about 3.0 cm would seem to be due to probability effects.

In conclusion we wish to thank Professor F. Soddy of Oxford for purifying and furnishing the sample of thorium.

POSSIBILITIES OF THE OSCILLATING ARC
IN SPECTROCHEMICAL ANALYSISBY E. Z. STOWELL AND W. S. HUXFORD
UNIVERSITY OF MICHIGAN, ANN ARBOR

(Received September 3, 1930)

ABSTRACT

It is shown experimentally that none of the alkali metals will allow radio-frequency oscillations to be generated across an arc in hydrogen, but that the alkaline earths will do so: a confirmation and extension of previous work. Spectra have been photographed of the two groups of elements when burned in the hydrogen arc, and the intensification and reduction of the lines of various elements is described. The effect of a minute quantity of Mg in large amounts of Rb and Na is described in detail, as well as the method by a quantitative estimate of the amount might be reached. No satisfactory explanation for the complicated phenomena of the oscillating arc has yet been found.

I. INTRODUCTION

A PREVIOUS paper¹ established as a fact of experience that an atmosphere of hydrogen is essential for the production of undamped high-frequency oscillations across an arc, and that in general these oscillations are then generated only if the cathode contains an element of even atomic number in its composition. Upon examining the spectra of these even elements while the arc is in the oscillating state, it is found that the even elements are intensified out of proportion to the odd. This suggests the use of an arc of this character in spectrochemical analysis.

The following work was done with a home-made arc, designed to permit rapid changes of electrodes. The arc operated on 220 volts dc, drawing 5 amps. on striking and 2.25 to 2.5 amp. while oscillating. Both electrodes were watercooled; the water did not reach the electrode tips, which could therefore be unscrewed from the arc without danger of water leakage. For the elements studied in these experiments it was necessary to use hollow copper cups as cathodes, in which was placed the element to be studied. The blank cups by themselves would not sustain a dc arc in hydrogen; this copper contained Ti and a small trace of Ca as impurities. Practically all spectra described below show these elements so that the effects cannot be ascribed to them. Commercial hydrogen was fed from a tank into the arc chamber and burned at the exhaust. The gas pressure inside the chamber was therefore fixed at one atmosphere. The arc flame was along the axis of the magnetic field. A radio-frequency circuit tuned to about 1000 meters wave-length was connected across the arc.

The spectrograph used was a double prism combination of glass built in the physics shops. The region photographed was 3500–5200Å, with Eastman

¹ Stowell and Redeker, Phys. Rev. **34**, 978 (1929).

Process plates. Exposures intended for comparison with one another, as, for example, an arc in the oscillating state as against the same arc in the non-oscillating state, were taken on the same plate and given identical exposures with the same arc current.

II. STUDY OF THE ALKALIS AND ALKALINE EARTHS AS CATHODES IN THE OSCILLATING ARC

The work cited in the previous paper¹ had indicated that the alkalis would not permit the generation of radio-frequency oscillations, while the alkaline earths would allow the oscillations to be generated. This has now been tested for the alkalis Li, Na, K, Rb and Cs, and for the group II elements Be, Mg, Ca, Sr and Ba; and is found to hold for these 10 elements.

This suggests the possibility of using the presence of current in the oscillating circuit as an indication of the presence of the elements of group II; this possibility is discussed in Section V.

III. SPECTRA OF ALKALI METALS IN HYDROGEN

Although none of the alkali metals allowed oscillations to be generated, the spectrum of the dc arc in hydrogen was photographed for comparison with the alkaline earths. The nature of the spectra are indicated in Table I.

TABLE I. *Nature of spectra obtained with dc arc in hydrogen.*

Element	Observed	Balmer lines
Li	Li I, Na I, K I, Rb I, Cs (trace) Cu, Ti	No
Na	Na I, K I, Rb I, Ca I, Ca II, Sr I, Sr II, Ba I, Ba II, Cu, Ti	No
K	K I, Rb I, Cs I (trace) continuous spectrum, no Cu or Ti.	No
Rb	Rb I, Na I, K I, Cs I, Ca I, Ca II, Sr I, Sr II, Mg I, Cu, Ti.	Yes
Cs	Cs I, Rb I, continuous spectrum, no Cu or Ti.	No

The elements used were of the ordinary grade obtainable in a chemical laboratory and no effort was made to purify them further as the effect of the impurities was of interest.

Only one of the spectra showed Balmer lines; that using a Rb cathode. This spectrum is also noteworthy in that it is the only one showing Mg as impurity. Ca, Sr and Ba had appeared above with the Na cathode in the Table, but the presence of these three elements appears to be insufficient to excite the Balmer lines; the appearance of the Balmer lines must therefore be connected with the presence of Mg. Owing to the fact that one of the Balmer lines, H_{β} let us say, may be of the order of 100 times the intensity of the sensitive Mg triplet at $\lambda 3838$, it is possible that the presence or absence of H_{β} might prove a method of detection of traces of Mg so minute that the sensitive lines of the element do not appear. If, for example, the intensities on the Rb plate were all reduced by a factor of 10, H_{β} would still be easily observable while $\lambda 3838$ would be wiped out.

The only other interesting feature of these plates is the large amount of continuous spectrum using K and Cs, and the simultaneous disappearance of Cu and Ti lines.

IV. SPECTRA OF BE, MG, CA, SR AND BA IN HYDROGEN

As all these elements allowed oscillations to be generated, a comparison was possible between their spectra in air, and in hydrogen with both the oscillating and the non-oscillating condition. The latter condition was obtained by opening the oscillating circuit.

The comparison is shown in Table II. One effect readily seen is the tendency of the arc in hydrogen, particularly when oscillating, to bring out impurities that were weak or absent in the arc in air. The Be used, for exam-

TABLE II. Comparison between arc spectra in air and in hydrogen (oscillating and non-oscillating) for the alkaline earth metals.

Cathode Element	Arc in Air	Non-oscillating Arc in Hydrogen	Oscillating Arc in Hydrogen			
			Elements intensified	Elements weakened	Elements not in non-osc. arc	New Elements
Be	CaI, CaII, SrI, BaII MnI	CaI, CaII, SrII, BaI BaII, MnI, Mo, V, Fe, Balmer Lines, and 2 bands of BeH ₂ (?)	CaI CaII MnI	Ba, Sr, Fe, Mo, V, Balmer lines		
	Cu, TiI, Be	Cu, TiI, TiII, Be	TiII	Cu, TiI		
Mg	CaI, CaII, SrI, SrII BaII, MnI	BaI, MgI, MgII and Balmer Lines	BaI MgI MgII	Balmer Lines	CaI CaII SrI SrII BaII MnI TiII	PbII
	Cu, TiI, MgI, MgII	Cu, TiI				
Ca	SrI, SrII, BaI, BaII	SrI, SrII, BaI, BaII, MgI, AlI and Balmer lines	SrI, SrII BaI, BaII MgI, AlI and Balmer Lines Ca			MnI
	Cu, TiI, CaI, CaII	CaI, CaII, Cu, TiI, TiII				
Sr	CaI, CaII, BaI, BaII MnI (trace)	CaI, BaI, BaII, MgII and Balmer Lines.	CaI, BaI, BaII, MgII and Balmer lines Cu, TiI, Sr		MnI CaII	MgI
	Cu, TiI, SrI, SrII	Cu, TiI, SrI, SrII			TiII	
Ba	CaI, CaII, SrI, SrII MnI (trace)	Balmer Lines	Balmer Lines BaII		CaI, CaII SrI, SrII MnI	
	Cu, BaI, BaII	Cu, BaI, BaII		Cu		

ple, did not show Mo and V impurity until burned in hydrogen. It happens that in this case the addition of the oscillating circuit did not bring out any new impurities. With the Mg cathode, the oscillating condition shows spectra of many more elements than in the non-oscillating condition, and even shows one element, Pb, which did not appear in the arc in air. With a Ca cathode, Mn is thus brought out, and with a Sr cathode, Mg.

All of these spectra contain Balmer lines under all conditions. The addition of the oscillating circuit weakens the Balmer lines from Be and Mg and strengthens those from Ca, Sr and Ba.

V. ATTEMPTED USE OF THE OSCILLATING ARC IN QUANTITATIVE ANALYSIS

Six samples of Na₂SO₄ (with Ca impurity) were prepared with the following amounts of MgSO₄ as a known impurity: No. 1, 0%; No. 2, 0.0001%; No. 3, 0.001%; No. 4, 0.01%; No. 5, 0.1%; No. 6, 1.0%. No oscillations

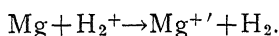
were obtained with No. 1; Nos. 2-6 inclusive gave oscillations, somewhat unsteady but easily readable on a radio-frequency ammeter with a 3 ampere maximum scale reading. It seems certain that the oscillations resulted from the presence of the Mg and not the Ca. The Mg triplet at $\lambda 3838$ did not appear until No. 6 was reached, so that in this case the presence of oscillations furnished a more sensitive criterion for the presence of Mg than the appearance of the sensitive lines of Mg. It is probable that smaller amounts of Mg than 0.0001% could be detected by replacing the radio-frequency ammeter by a thermogalvanometer or thermojunction.

The magnitude of the radio-frequency current in the above cases took approximately the theoretical value when oscillations occurred; i.e., the needle varied from zero to $(1/2^{1/2})$ dc amps. Hence no estimate could be made of the relative amounts of Mg from the current readings.

VI. DISCUSSION

It is of interest to compare these results with those of Crew.² In the case of a dc Mg arc in a hydrogen atmosphere he finds weakening of the copper and calcium impurity. In the non-oscillating condition, we find the Mg triplet at $\lambda 5183$, the Mg II doublet at $\lambda 3538$, and the doublet of Ca II at $\lambda 3933$ - 3969 , all completely suppressed; all reappeared with the closing of the oscillating circuit. The three green lines of copper were suppressed in both conditions, but the doublet at $\lambda 4023$ - 4063 occurred weakly in both. The vanishing of the CaII doublet is quite unusual, as it is well known for its persistence. $\lambda 4481$ of MgII was increased in intensity several fold by the addition of the oscillating circuit.

Other investigators of the excitation of the MgII spectrum in the presence of hydrogen³ were unable to excite either $\lambda 4481$ or $\lambda 3538$ - 3535 . This was in a low-voltage arc free from the effects of cumulative ionization which probably occurs in an arc at atmospheric pressure. Hence the mechanism of the excitation of this spectrum is not as simple as indicated by their equation



In all of the oscillating arcs, the Balmer series is obtained, indicating the presence of atomic hydrogen. So far it has not proven possible to write a general equation between the energy of the various states of the hydrogen atom and the cathode vapor, after the manner of Mohler⁴ and Kaplan,⁵ which would account for the lines observed, and at the same time explain the preference of the oscillations for even-numbered cathodes, and the absence of oscillations in all gases except hydrogen.

² Crew, *Phil. Mag.* **7**, 312 (1929).

³ Duffendack, Henshaw and Goyer, *Phys. Rev.* **34**, 1132 (1929).

⁴ Mohler, *Phys. Rev.* **29**, 419 (1927).

⁵ Kaplan, *Phys. Rev.* **31**, 997 (1928).

ELECTRO-OPTICAL MODIFICATION OF LIGHT WAVES

By L. H. STAUFFER

DEPARTMENT OF PHYSICS, UNIVERSITY OF CALIFORNIA

(Received August 30, 1930)

ABSTRACT

Broadening of the satellites of the Hg green line $\lambda 5461$ was observed when the light passed between the plates of a Kerr cell on which was impressed a varying E.M.F. having a frequency of $2 \times 10^7 \text{ sec}^{-1}$. The E.M.F. was obtained by superposing the output of a vacuum tube oscillator upon a steady potential of about 7000 volts. The maximum oscillator voltage was about 5000 volts. With this voltage the fine structure of the Hg green line became so diffuse that two satellites having a separation of 0.045 Å were scarcely resolved by the Lummer-plate. The broadening was observed to increase rapidly with the oscillator voltage. The observed effect is predicted by the classical electromagnetic theory and the quantum theories of dispersion of Kramers-Heisenberg, Schrödinger, and Dirac. The high frequency voltage effects a rapid variation of the refractive index of the nitrobenzene in the Kerr cell which in turn produces a corresponding variation in optical path, giving the source a virtual velocity, and thereby producing a Doppler effect. The magnitude of the observed broadening is in agreement with the predictions of theory.

INTRODUCTION

IT HAS been shown experimentally by E. Rupp¹ that monochromatic light suffers a slight change in wave-length when sent through an electro-optical shutter actuated by a high frequency oscillator. Rupp's shutter consisted of a Kerr condenser with nitrobenzene as a dielectric, placed between crossed Nicol prisms. When an E.M.F. is applied to the Kerr cell plates, the dielectric becomes doubly refracting and the second Nicol allows some of the light to pass through it. When an alternating E.M.F. is applied, the beam is interrupted with a frequency dependent on the frequency of the applied field. If the shutter opens and closes n times per second, theory predicts that the emergent beam should contain the original frequency and two "side frequencies" differing by $\pm n$ from the original frequency. These beat frequencies, of course, are due entirely to the rapid interruption of the beam and should be present even if the beam were interrupted by a mechanical shutter.

Shortly after Rupp's results were published, Wawilow² and others pointed out another phenomenon which must be considered when an electro-optical shutter is used. A variation in field strength produces a corresponding change in the refractive index of the liquid in the Kerr cell which, in turn, effects a change in optical path. This variation in optical path would give the source a virtual velocity and, in accordance with classical electromagnetic theory (Doppler's principle) a change in frequency would result.

¹ E. Rupp, *Zeits. f. Physik* **47**, 72 (1928).

² Wawilow, *Zeits. f. Physik* **48**, 600 (1929).

The experiment here reported was undertaken with the hope of testing the adequacy of the classical theory in explaining the above mentioned effect. Though to be sure, the quantum theories of dispersion of Kramers and Heisenberg³ Schrödinger,⁴ and Dirac⁵ are in agreement with the classical theory in this regard, there remains a reasonable suspicion that quantum phenomena might enter to modify the expected results. Indeed, such a possibility is suggested by a curious anomaly reported by A. Bramley.⁶ He photographed the arc spectrum of iron through a water Kerr cell on which was impressed the output of a high frequency oscillator. With relatively low voltages, he was able to detect shifts of certain lines toward the red end of the spectrum—shifts in magnitude very many fold greater than expected from theory.

GENERAL THEORY

Assuming the results of the classical electromagnetic theory, it is not difficult to deduce the frequency modification undergone by a train of light waves when it traverses a medium subjected to an electric field of varying intensity.

W. A. Michelson⁷ has generalized Doppler's principle to cover the case of a rapid variation of the refractive indices of the media traversed by a light ray. If ν is the observed frequency of the light then according to Michelson's formulation

$$\nu = \nu_0 \left[1 \pm \frac{1}{c} \sum_i \frac{d}{dt} (\mu_i l_i) \right] \quad (1)$$

where ν_0 is the frequency of the radiation as it leaves the source, c is the velocity of light in vacuum, l_i the distance traversed in a medium having an index of refraction μ_i and t the time. For the case of a single medium of fixed extent (1) reduces to

$$\nu = \nu_0 \left(1 \pm \frac{l}{c} \frac{d\mu}{dt} \right) = \nu_0 \pm \Delta\nu. \quad (2)$$

If a change in refractive index is effected by applying an electric field of strength E , P. Langevin⁸ has shown theoretically that

$$\frac{\mu_p - \mu_0}{\mu_s - \mu_0} = -2 \quad (3)$$

where μ_0 is the refractive index of the medium for zero field strength and μ_p and μ_s the indices for light polarized with its electric vector parallel and perpendicular respectively to the direction of the field. This relation has been

³ H. A. Kramers and W. Heisenberg, *Zeits. f. Physik* **31**, 681 (1925).

⁴ E. Schrödinger, *Ann. d. Physik* **81**, 108 (1926).

⁵ P. A. M. Dirac, *Proc. Roy. Soc. A* **114**, 710 (1927).

⁶ A. Bramley, *Jour. Franklin Inst.* p. 315, March 1929.

⁷ W. A. Michelson, *Astrophys. Jour.* **13**, 192 (1901).

⁸ P. Langevin, *Le Radium* **7**, 249 (1910).

experimentally verified by Pauthenier⁹ in his measurement of absolute retardation in the Kerr effect. It is also well established that the relative retardation in phase of the components of the ray vibrating parallel and perpendicular to the field is given by

$$\phi = 2\pi B l E^2 \quad (4)$$

in which B is the Kerr constant and ϕ is the retardation in radians. The difference in the optical paths of the two components is

$$\frac{\phi \lambda}{2\pi} = (\mu_p - \mu_s) l = B l E^2 \lambda \quad (5)$$

in which λ is the wave-length in vacuum. This gives the relation

$$B E^2 \lambda = \mu_p - \mu_s. \quad (6)$$

Expressions for μ_p and μ_s may now be obtained by combining (3) and (6), the result of which is

$$\mu_p = \mu_0 + 2 B E^2 \lambda / 3 \quad (7)$$

and

$$\mu_s = \mu_0 - B E^2 \lambda / 3. \quad (8)$$

The frequency change $\Delta\nu$ for light polarized with its electric vector parallel to the applied field may now be obtained by taking account of equations (2) and (7). This yields.

$$\Delta\nu = \frac{\nu_0 l}{c} \frac{d\mu_p}{dt} \quad (8a)$$

or

$$\Delta\nu = \frac{2 B \lambda_0 \nu_0}{3c} l \frac{dE^2}{dt} \quad (8b)$$

but since $\nu_0 \lambda_0 = c$

$$\Delta\nu = \frac{4}{3} B l E \frac{dE}{dt} \quad (8c)$$

APPARATUS AND PROCEDURE

The experimental arrangement (see Fig. 1) consists essentially of a Kerr cell, K , coupled to a vacuum tube oscillator, a mercury arc, M , as a light source, and a Lummer-Gehrcke plate, L , as a spectroscope. The mercury arc was water cooled to reduce Doppler broadening and was operated at the lowest current density which would maintain a steady arc. Light from the arc passes between the plates of the Kerr cell and is polarized with its electric vector parallel to the field by the Nicol prism, N_3 . A constant deviation prism D serves as a monochromator to separate the green line $\lambda 5461$. The interference pattern produced by the Lummer plate may be observed

⁹ M. Pauthenier, Comptes rendus 170, 803 (1920).

visually or photographed at E . The retardation can be measured at any time during the course of the experiment by observing the deflection of the galvanometer, G , which is actuated by current from the photoelectric cell P . A beam of light from the incandescent lamp, S , is sent through the cell in a direction crosswise to the plates and is polarized by the Nicol, N_1 in a plane making an angle of 45° with the vertical. When a difference of potential is applied to the plates the vertical component is retarded and the horizontal component advanced so that the light leaves the cell elliptically polarized and part of it can pass the second Nicol, N_2 , which is crossed with respect to N_1 . As will be shown later, the arrangement may be used to measure the field applied to the cell.

The design of the apparatus is governed largely by equation (8c) which gives the frequency change in terms of the Kerr constant of the liquid used in the cell, the length of the plates, the field strength and its time derivative.

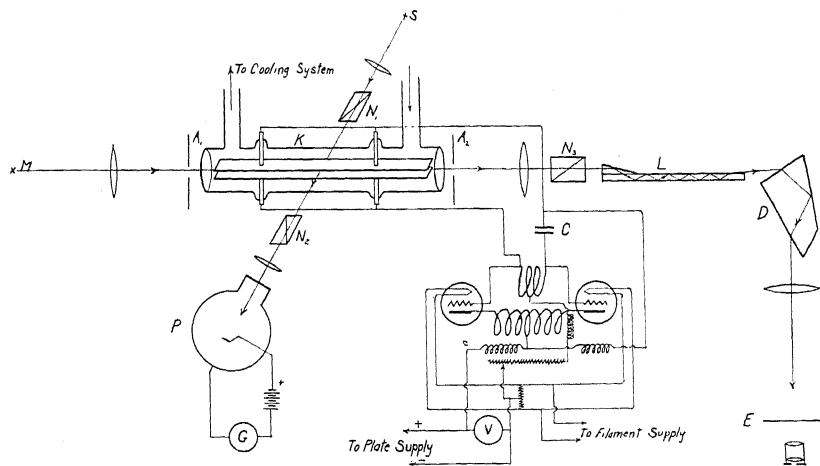


Fig. 1. Diagram of apparatus.

Nitrobenzene was chosen as the dielectric to be used in the cell for the reason that it has the largest Kerr constant of any known substance (3.5×10^{-5}). The quantity $E(dE/dt)$ may be made large by superimposing the oscillator output on a steady potential, in this case the plate potential of the oscillator.

The time rate of the field of course depends on the natural period of the oscillatory circuit, which is limited by the capacity of the Kerr cell. Since nitrobenzene has a specific inductive capacity in the neighborhood of 40, the capacity of even a small cell is comparatively high. The capacity was reduced as much as possible by making the plates narrow.

The Kerr cell used had nickel plates 10 cm by 2 mm with slightly rounded corners. The plate separation was 2 mm. Short tungsten leads of large diameter were used in order to reduce heating by the high frequency currents.

Considerable difficulty was at first encountered, due to the failure of the nitrobenzene to withstand the intense high frequency fields.

To reduce the conductivity to a minimum, the liquid was purified by treating with a weak base such as aluminum or calcium oxide to remove acids and then double distilling in vacuum during which process all water vapor was frozen out with liquid air. After such treatment, the liquid would

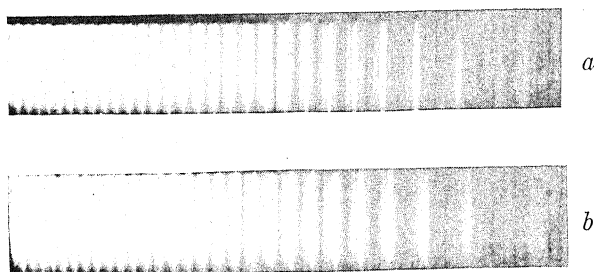


Fig. 2. Photographs of fine structure of Hg green line
(a) Unmodified spectrum. (b) Modified spectrum.

stand very high D. C. potentials, but heated badly, and broke down when subjected to high frequency fields. To keep the nitrobenzene cool, a water cooled circulatory system was devised, which consisted of a small four

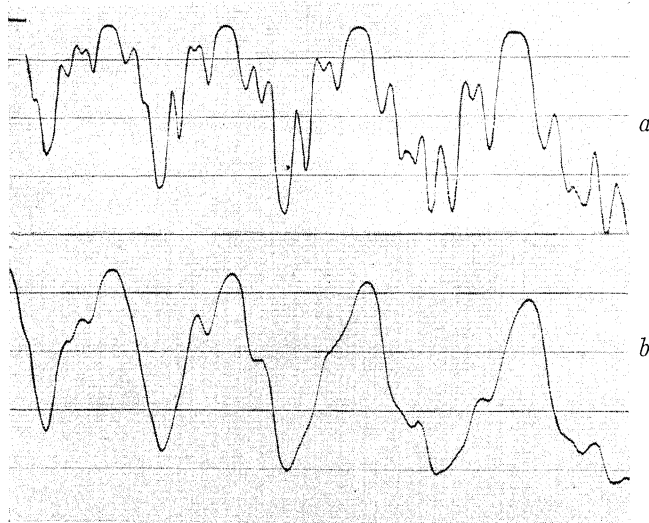


Fig. 3. Microphotometer curves. (a) Unmodified. (b) Modified.

bladed propeller rotating in a vertical chamber connected to the Kerr cell by tubes surrounded by water jackets. The whole was made of Pyrex glass to avoid contaminating the nitrobenzene. The liquid was found to withstand a much higher voltage when kept cool by this method.

A diagram of the push-pull oscillator used is shown in Fig. 1. Two 100 watt Radiotrons of the type UX-852 were employed with between 7000

and 8000 volts on the plates. The highest frequency that could be attained with the Kerr cell used was about $2 \times 10^7 \text{ sec.}^{-1}$. The plate voltage of the oscillator is applied to the cell by inserting a large condenser *C*, and connecting the isolated terminal of the cell through a choke to the positive side of the plate circuit.

Visual observations of the fine structure of the mercury green line revealed a slight broadening of the components when the oscillator was operating. The effect was repeatedly confirmed by photographing. Fig. 2a and b shows the interference pattern of the Lummer-Gerhcke plate without and with the oscillator in operation. Fig. 3 shows microphotometer curves of the unmodified and modified patterns.

The procedure followed in photographing was to take an exposure under no voltage conditions with the circulator operating and then directly underneath on the same plate an exposure with the oscillator in operation. The overloaded oscillator could only be operated over intervals of about 10 seconds without danger of overheating the tubes and Kerr cell. The second exposure was, therefore, broken up into a number of 10 second intervals.

DISCUSSION OF RESULTS

The appearance of the fine structure pattern of the Hg green line is shown in Fig. 2a. A large number of orders are present and as the photograph shows, the dispersion diminishes toward the lower orders. The main line and five satellites are clearly resolved on the original plates but the enlarged reproduction shows less detail. The designation and wave-length separations of the satellites are taken from a paper by McLennan¹⁰ reporting some work on the Hg green line in which he used a Lummer plate. In

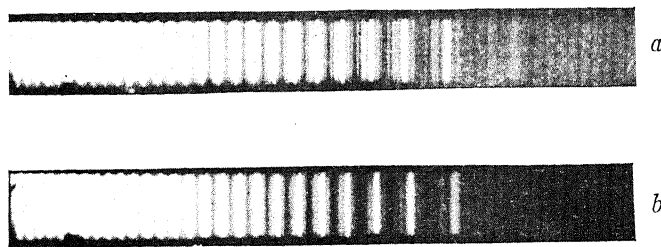


Fig. 4. Photographs of fine structure with reduced oscillator voltage.

all the photographs shown the negative satellites are on the right. The satellite -6 is separated from the main line by an interval of -0.237\AA and overlaps into the succeeding order where it is seen between the main line and the satellite $+3$. The wave-length separations from the main line of the satellites -6 , -5 , -4 , $+3$ and $+4$ are -0.237 , -0.102 , -0.0698 , $+0.852$ and $+0.128$ respectively.

The fine structure of the line as modified by a high frequency field of approximately 22,500 volts per centimeter superimposed on a steady field

¹⁰ J. C. McLennan, Proc. Roy. Soc. 102, 33 (1922).

of 36,000 volts per centimeter is shown by Fig. 2b. This gives a calculated broadening of over 0.01 Angstroms.

Microphotometer curves of the unmodified and modified lines are shown in Fig. 3a and b. The results obtained in a later trial with an oscillating field of 19,600 volts per centimeter and a steady field of 40,000 volts per centimeter are shown in Figs. 4 and 5.

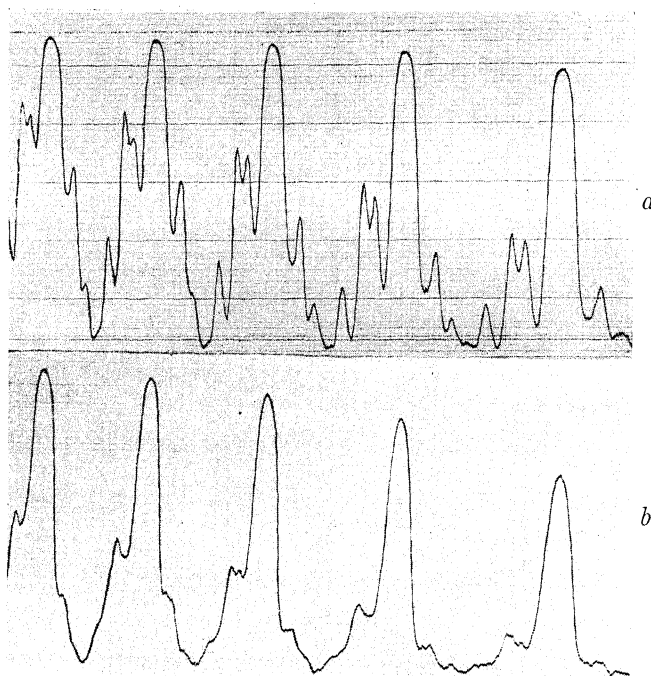


Fig. 5. Microphotometer curves. (a) Unmodified. (b) Modified.

In order to calculate the frequency change $\Delta\nu$ in terms of deflections of the galvanometer, G , and known constants of the apparatus it is necessary to modify equation (8b) by making the substitution

$$E = E_1 + E_0 \sin 2\pi nt$$

where E_1 is the steady field strength, E_0 the peak field strength of the oscillator, n the oscillator frequency and t the time. E_1 and E_0 are expressed in electrostatic volts per centimeter. Equation (8b) now becomes

$$\Delta\nu = \frac{2B\lambda_0\nu_0 l}{3c} \frac{d}{dt}(E_1 + E_0 \sin 2\pi nt)^2 \quad (9)$$

Taking the time average by integration over a quarter cycle gives

$$\frac{\overline{\Delta\nu}}{\nu_0} = \frac{8\lambda_0 B n l}{3c} (E_0^2 + 2E_1 E_0) \quad (10)$$

where $\overline{\Delta\nu}$ is the average value of the frequency change. Now if the intensity of the light reaching the photo-cell at any time t be represented by I we have in accordance with classical optics

$$I = I_0 \sin^2(\phi/2) \quad (11)$$

where I_0 is the intensity of light coming from the Nicol prism, N_1 , and ϕ is the retardation. By substituting the value of ϕ given by equation (4) into (11) the expression for the intensity becomes

$$I = I_0 \sin^2 \pi B w (E_1 + E_0 \sin 2\pi n t)^2 \quad (12)$$

in which w is the width of the plates. In this experiment it can be shown that the average value of the retardation is small since w is only 2 millimeters. It is, therefore, permissible within the limits of error of the experiment to replace the sine by the angle itself. This is done to facilitate the integration of equation (12) to get the time average of the intensity I . The result of the integration is

$$\bar{I} = I_0 \pi^2 B^2 w^2 (E_1^4 + 3E_0^2 E_1^2 + 3E_0^4/8) \quad (13)$$

Eliminating B between (10) and (13) the following expression is obtained

$$\frac{\overline{\Delta\nu}}{\nu_0} = \frac{8\lambda_0 n l I^{1/2} (E_0^2 + 2E_0 E_1)}{3\pi c w I_0^{1/2} (E_1^4 + 3E_1^2 E_0^2 + 3E_0^4/8)^{1/2}} \quad (14)$$

Since the galvanometer deflections are small and the photoelectric current is proportional to the intensity, the ratio of intensities may be replaced by the ratio of the corresponding deflections. It is also more convenient to deal with the ratio of E_0 to E_1 than to use the equation (14) as it stands. Designating the ratio E_0/E_1 by a , equation (14) becomes

$$\frac{\overline{\Delta\nu}}{\nu_0} = \frac{8\lambda_0 n l D^{1/2} a (a + 2)}{3\pi c w D_0^{1/2} (1 + 3a^2 + 3a^4/8)^{1/2}} \quad (15)$$

or in terms of λ_0 the average change in wave length $\overline{\Delta\lambda}$ is

$$\overline{\Delta\lambda} = \frac{8\lambda_0^2 n l D^{1/2} a (a + 2)}{3\pi c w D_0^{1/2} (1 + 3a^2 + 3a^4/8)^{1/2}} \quad (15a)$$

D_0 , the deflection corresponding to the intensity I_0 , may be obtained by uncrossing the Nicols by an angle θ and observing the deflection D_θ . D_0 is then given by the relation $D_\theta = D_0 \sin^2 \theta$.

The ratio, a may be obtained as follows. Let I_1 be the intensity of light reaching the photo-cell when a field E_1 is applied to the Kerr cell. Equation (13) then becomes

$$I_1 = I_0 \pi^2 B^2 w^2 E_1^4 \quad (16)$$

When the high frequency field is superimposed the intensity is given by equation (13). Dividing (16) by (13) and replacing the ratio of intensities by the ratio of the corresponding galvanometer deflections one gets

$$\frac{D_1}{D} = \frac{E_1^4}{E_1^4 + 3E_1^2E_0^2 + 3E_0^4/8} = \frac{1}{1 + 3a^2 + 3a^4/8} \quad (17)$$

The value of a may now be obtained with sufficient accuracy by plotting a curve of D_1/D for values of a ranging from 0 to 2. Knowing E_1 from the reading of the voltmeter, V , the value of E_0 is available when a is known. The reason for not measuring E_0 by means of a voltmeter will be evident to those familiar with the difficulties in making accurate measurements of large currents or voltages at high frequencies.

The ratio of the length to the width of the plates was corrected for edge effect by taking measurements with the photo-cell and crossed Nicol arrangement, lengthwise as well as crosswise of the plates with the field on. As equation (13) shows the intensity is proportional to the square of the effective path traversed in the field, it was thus found that the value of $1/w$ must be reduced by 8.5 percent.

At first thought it might seem easy to measure the change in wavelength by taking measurements on the microphotometer curves of the fine-

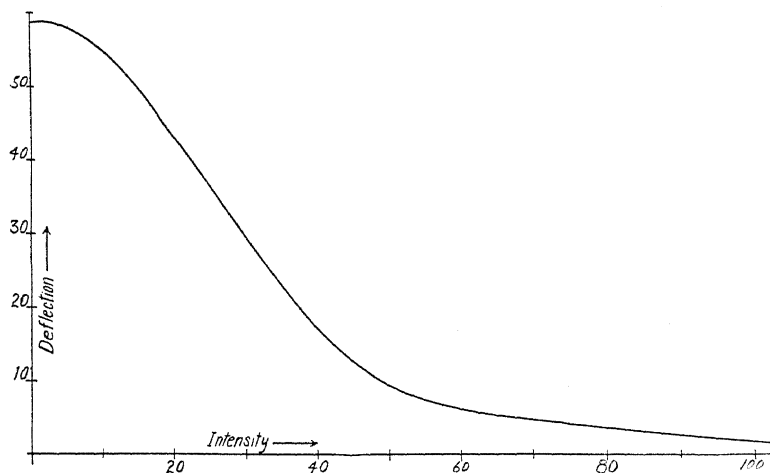


Fig. 6. Blackening curve for photographic plates.

structure patterns. The half-width of a satellite before the field was applied might be compared with the half-width of the modified satellite but this would probably not correspond to the average wave-length change given by equation (15a). It is also evident that the photographs of the modified and unmodified patterns are not comparable unless the exposures are the same since the width of the lines is influenced by the length of exposure. Since the ordinates of the microphotometer curves represent blackening and not intensity, it is necessary to know the blackening as a function of intensity for a given plate before two satellites can be compared. In view of these considerations one can only expect rough agreement between measured and calculated values of the wave-length change.

The procedure finally followed was to select a plate such as the one shown

in Fig. 4 where the modification is not so great as to obliterate the structure and to measure the change in half-width of the main line. To facilitate intensity measurements the unmodified fine structure was photographed, the Lummer plate removed and a slit and a Nicol prism placed in the path of the beam. A series of exposures was then taken on the same plate, the intensity of the beam being varied by rotating one of the Nicols a known amount before each exposure. The plate was then microphotometered and a curve of intensity against deflection was plotted. The curve is shown in Fig. 6. The deflections (plotted as ordinates) are measured from the line of absolute blackening on the microphotometer curves. Thus a large deflection means a low intensity. The intensity relations between the fine structure components were found to vary slightly from order to order of the interference pattern. It was found that over the range of the five highest orders in which intensity measurements were made that the intensity of the satellite +3 remained very nearly half that of the main line. In no order was the variation greater than six percent. The peak of the satellite +3 was therefore taken as the ordinate representing half-intensity for the main line in any given order. The dispersion was obtained by measuring the distance between the peaks of the satellites +3 and +4 which have a wave-length separation of 0.043A. The results obtained from the curves shown in figure 4 are presented in Table I.

TABLE I. *Results obtained from the curves of Fig. 4.*

Order	Dispersion mm/A	Broadening mm	Half-width Change/2 A
I	100	2.40	0.012
II	82.3	1.80	0.011
III	71.2	1.40	0.0098
IV	66.7	1.40	0.010
			0.0107 Mean

The average change in wave-length as given by equation (15a) is 0.0078A. The maximum change in wave-length may be secured by calculating the maximum value of dE^2/dt and introducing it in place of the average value as has been done. The calculation is straightforward but rather long. It yields a result which is 1.4 times as large as the average value, 0.0078. The factor 1.4 is not a constant but varies with a , the ratio of E_0 to E_1 . The maximum value of $\Delta\lambda$ is therefore about 0.011 Angstroms, slightly greater than the mean value given in the table.

Thus, within the experimental uncertainty (about 20 percent), the magnitude of the observed change in frequency is in agreement with the predictions of the classical theory and the several quantum theories of dispersion. No anomalous effects of the kind reported by Bramley were detected in the course of the experiment.

The author is indebted to Professor E. O. Lawrence, who suggested this experiment, for his constant assistance and many helpful suggestions.

THE OPTICAL EXCITATION FUNCTION OF HELIUM

BY WALTER C. MICHELS

NORMAN BRIDGE LABORATORY, CALIFORNIA INSTITUTE, PASADENA

(Received September 6, 1930)

ABSTRACT

With a discharge tube which has been considerably modified from the designs previously used, and with a technique specially developed to eliminate the effects of collisions of the second kind and ionization and recombination, the author has completed a study of the excitation function of helium for electrons with energies between the excitation potentials and one hundred volts. Two new features are introduced, namely, experimental conditions under which a linear dependence of intensity on either current or pressure is obtained, and an actual determination of the electron velocity distribution curve. The intensity curves, by themselves, agree fairly well with those obtained by earlier workers but, by the innovations mentioned above, it has been possible to correct these curves to obtain the true optical excitation function values. The corrected results show that each line has a maximum excitation probability either at or within a few tenths of a volt of the excitation potential, and that the probability drops off quite rapidly above this value, more rapidly for the triplet system than for the singlet.

INTRODUCTION

SINCE the publication of the original work of Hughes and Lowe¹ on the variation of the intensities of the lines of the helium spectrum with change of velocity of the exciting electrons, a large number of workers have made studies in this field. While the results of these investigations have been somewhat discordant, two papers, those of Hanle² and Elenbaas,³ give results which show at least qualitative agreement between themselves and with the publication mentioned above. A study of the intensity-voltage curves given by these authors seems to enable certain conclusions to be drawn:

- (1) All lines of the triplet system appear at their excitation potentials and show sharp maxima somewhere between these potentials and 35 volts.
- (2) All lines of the singlet system increase in intensity rather rapidly just above the excitation potential, and show moderately flat excitation curves, with maxima between 60 and 150 volts.

While these points have been fairly definitely established in earlier investigations, the author has felt that certain discrepancies in the published results demanded further investigation. Elenbaas, for example, finds double maxima for most of the lines while Hanle, Hughes and Lowe find but one maximum for each line. The positions of the maxima also vary quite widely among the different investigations.

Before entering into a discussion of the present work, it may be well to

¹ Hughes and Lowe, Proc. Roy. Soc. A104, 480 (1923).

² Hanle, Zeits. f. Physik 56, 94 (1929).

³ Elenbaas, Zeits. f. Physik 59, 289 (1930).

define just what interpretation shall be placed on the term "optical excitation function." In order that spurious results due to the apparatus may be eliminated, it would seem well to define this function as *the relative probability that light of a particular wave-length be emitted when an isolated atom experiences a collision (defined, for example, by kinetic theory considerations) with an electron moving with a specified velocity.* This definition imposes two definite restrictions on the experimental conditions:

(1) The requirement of isolation demands that the effects of collisions of the second kind, collisions with the walls, etc., be kept negligible, and that there shall be not more than a negligible amount of light emitted due to ionization and subsequent recombination.

(2) The exciting electron beam must be as nearly homogenous as possible, and the extent of departure from homogeneity must be determined.

The work now being reported was undertaken with these limitations definitely in mind and an attempt has been made to devise tests showing to what extent each requirement has been satisfied.

THE DISCHARGE TUBE

The final design of discharge tube used for the excitation of the spectrum is shown in Fig. 1. Electrons from the ten mil tungsten filament were accelerated through the first slit, 2 by 20 mm, which was about 2 mm distant from

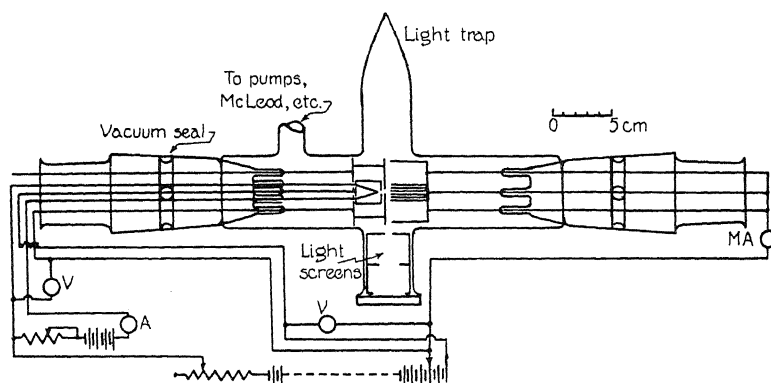


Fig. 1. Discharge tube with wiring diagram.

the filament. This slit was maintained at a potential difference of about sixteen volts above the second slit, about one mm away, and of the same size. Beyond this was a clear, field free space of 4 mm length, in which the emission was observed, and the plate, which was composed of a number of parallelo-piped boxes, 20 mm deep. All electrodes were of nickel. The various potentials were maintained by a bank of storage cells.

A remark in regard to the choice of the filament may be desirable. In the early part of the work tubes with oxide coated platinum emitters, usually of the unipotential type, were tried, in the hope of obtaining a very homogenous electron beam. Velocity distribution curves taken on these tubes showed,

invariably, a very large percentage of slow electrons, distributed between zero velocity and that applied to the slits. This difficulty was finally traced to secondary electrons, emitted from the slits, due to barium distilled onto their surfaces from the cathode. With its low work function, this material acted as a particularly efficient secondary emitter. The loss in homogeneity due to the voltage drop across the tungsten filament was much more than compensated for by the decrease in these secondaries.

In addition to the change to a tungsten filament, certain other precautions against secondary electrons were taken. The difference of potential, previously mentioned, between the two slits served to sweep back any secondaries formed at the edges of the second slit. The particular plate design used was also adopted for the elimination of this effect. With the large metal surface and the small opening obtained by this construction, the plate acted as a black cavity, not only for the electrons but also for ultraviolet light from the excited atoms. Reflected, secondary, and photo-electrons were therefore neither recorded in the current measurements nor allowed to enter the space in which light emission was observed.

The tungsten filament introduced a further difficulty in the large amount of continuous light which it furnished. This light gave a background on the plates which was comparable with the exposures produced by the lines themselves until the light trap and screens shown were introduced. The tube was painted, outside, with a dead black lacquer, with the exception of the plate glass window through which observations were taken.

Frequent filament replacements necessitated the ground glass joint construction shown in the figure. Stop-cock grease was used only on the outer portions of the joints, and the vacuum seals were pumped continuously except during the actual exposures, to keep vapor from reaching the electrodes. The construction prevented baking, however, and the following method was used for cleaning the electrodes. After the apparatus had been opened to air, a charcoal trap, in close proximity to the tube, was baked at 350–400°C for about twelve hours. Liquid air was then placed on this trap and the filament emission gradually built up until about four milliamperes flowed to the plate, with an accelerating potential of 300 volts. Under these conditions the electrodes, near the filament, were glowing at a dull red. During the clean-up action, if the filament current was held constant, the current to the plate increased for a few hours, then decreased slightly to a constant value. In general, the heating and bombardment were continued for ten to twelve hours, with the vacuum pumps running. The tube was then ready for operation. For subsequent exposures, if air had not been admitted, bombardments of three to four hours were found to be sufficient. This clean-up technique was found to be absolutely essential, as will be explained later.

The current vs. retarding potential curve shown in Fig. 2a was obtained with this tube after such treatment and with the pumps maintaining a vacuum of about 10^{-5} mm as measured by a McLeod gauge. The accelerating potential was 100 volts. The graphical differentiation of this curve gives the velocity distribution curve of Fig. 2b. By far the greater part of the elec-

tron beam is included within a five volt band, just accounted for by the filament potential drop. As the retarding potential was applied between the last slit and the plate, both of nickel, the 1.2 volt difference between the fastest electrons and the accelerating potential may be taken as the contact potential. This measurement checked, within the accuracy to which the voltage could be held constant during an exposure (about ± 0.3 volt), with the first appearance of the various lines at their excitation potentials. The "tailing off" of the distribution curve toward lower velocities may probably be attributed to a certain amount of electron reflection and secondary emission

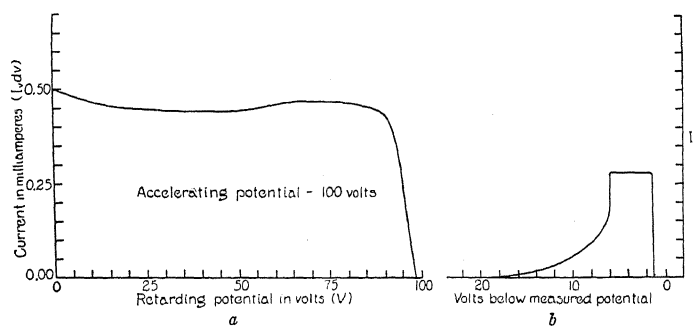


Fig. 2. Electron velocity distribution.

which was not eliminated. This region, however, accounts for only 30 percent of the total current, and this is much better than was obtained with any other type of tube construction which was tried.

The helium was purified as previously described⁴ and was passed through the charcoal trap before entering the tube. This helium was never left in the tube for more than three or four hours of operation, after which it was pumped out and the clean-up process was repeated, before fresh gas was inserted.

INTENSITY MEASUREMENTS

A photographic method was used for the measurement of the intensities, the optical set up being that shown in Fig. 3. A glass spectrograph, with an F 2.7 telescope lens was used for the photography. The extreme speed of this instrument made it possible to obtain exposures of satisfactory density with the discharge tube in 10 to 20 minutes, but made the obtaining of a continuous comparison spectrum a matter of some difficulty. In order to obtain a continuous spectrum of sufficiently low intensity, the scheme shown was resorted to. A ribbon filament tungsten lamp was mounted 70 cm from the optical axis. The light from a 3.25 mm section of the middle of the filament (which was 2 mm wide) was allowed to fall on the small right angled prism mounted on the axis. One face of this prism was ground to a focal length of 25 mm, so that a very much reduced image of the filament was formed on the optical axis. This image was used as a secondary source, and only the

⁴ Hodges and Michels, Phys. Rev. 32, 913 (1928).

light from it intercepted by the slit of the instrument was used for the calibration exposures. The Nicol prism, mounted directly in front of the slit, was arranged so that the two components of polarization could be measured separately and combined later to give the total intensity, thus eliminating errors due to the unequal treatment of the two components by the glass prism.

The 6 to 1 reduction obtained in the spectrograph made it impossible to use the "stepped reducer" method of plate calibration which had been utilized in previous work. It was necessary, therefore, to take a series of five or six calibration exposures. It seemed better, consequently, to eliminate the re-

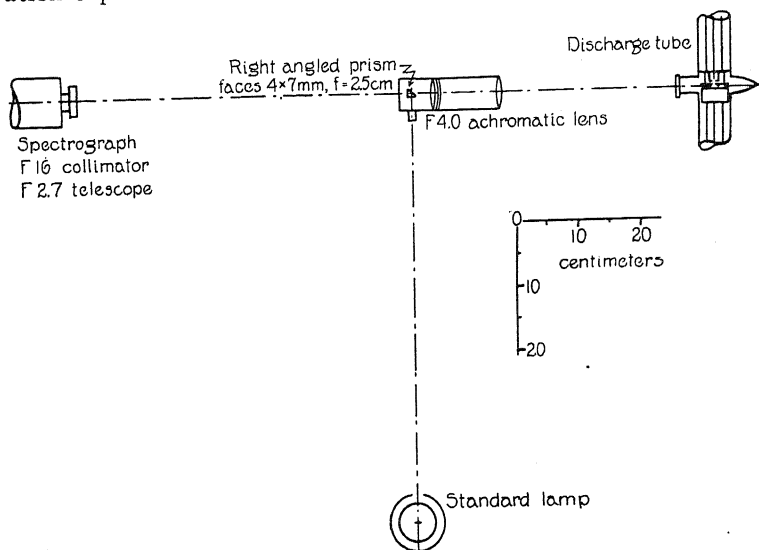


Fig. 3. Optical system.

ducers entirely, and to use a temperature variation of the standard lamp for the intensity steps. This was made particularly convenient by a new method of plotting the calibration curves.

In the older method, the density is plotted against the logarithm of the exposure, or, when the time is held constant, as it was in this work, against the logarithm of the intensity. This plot is widely used because it gives, over a large range of exposures, a straight line, in accordance with the Swartzchild formula. We now recall that tungsten, in the visible region, closely follows Wien's law:

$$I_{\lambda,T} = \epsilon c_1 \lambda^{-5} e^{-c_2/\lambda T}.$$

If, in this formula, we consider the emissivity, ϵ , to be a constant independent of temperature, as it is, very nearly, and vary the temperature, T , for a given wave-length, λ , we find that:

$$\log I_T = a - b/T,$$

where a and b are constants, so that, if the density be plotted against the reciprocal temperature, the straight line of the Swartzchild formula is re-

tained. A typical set of calibration curves for the Ilford panchromatic plates used in this investigation is given in Fig. 4. After the calibration curves had been obtained, the temperature of the tungsten lamp necessary to produce the same density as the helium exposure could be read from them, and the intensity corresponding to this temperature calculated from Wien's law. Correction was then made for the dispersion of the spectrograph to give the final intensities.

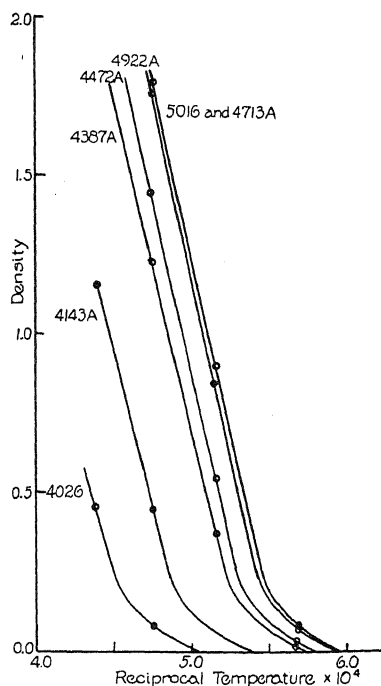


Fig. 4. Plate calibration curves.

The temperatures of the standard lamp were measured with a Leeds and Northrup optical pyrometer, the residual error of which was determined by a Bureau of Standards Calibration to be 2°C . The deviation measure of the temperature measurements was also about 2°C , so the temperature was accurate to about 3°C . Correction for the emissivity of tungsten was made according to the data of Forsythe and Worthing.⁵

It was possible to take fourteen exposures on a single plate. Of these, five, in general, were needed for continuous calibration exposures. The other nine were therefore used for helium spectra, taken under different excitation conditions. The plates were soaked in running water for five minutes, then developed according to the "brush method" recommended by Bloch.⁶ With this treatment, it was found that errors introduced due to difference of posi-

⁵ Forsythe and Worthing, *Astrophys. J.* **61**, 146 (1925).

⁶ Bloch, *Phot. J.* **61**, 425 (1921).

tion on the plate were negligible. The plates were microphotometered in an instrument built at the Institute.

INTENSITY VARIATIONS WITH CURRENT AND PRESSURE

In nearly all previous investigations, tests of the dependence of intensity on the current and pressure have been tried. In most of these tests, a linear relationship has been expected but not found. If we define the excitation function for an isolated atom as was done above, it is obvious that the experimental conditions should be such that the intensity of any line should be proportional to the number of impacts between electrons and the atom in unit time. This number, moreover, is proportional to the current. Also, if the pressure is sufficiently low so that the mean free path is large compared with the linear dimensions of the apparatus, the kinetic theory exponential expression for the number of impacts can be expanded to the first order, and a linear relationship is obtained between the number of impacts and the pressure. From these considerations we should expect, if we have isolated behavior, a linear relationship between either intensity and current or intensity and pressure for any line.

If the condition of isolation is not satisfied, there are several possibilities. In the first place, two atoms, both excited to metastable levels, may collide. In this case, the number of metastable atoms should vary linearly with the current or pressure, so that a quadratic variation of intensity would be expected. Another possibility is emission due to ionization and recombination. For this phenomena we again have the density of ions and the density of electrons each depending linearly on the current and pressure, so we should once more expect a quadratic law. In the general case, then, when some atoms act as isolated, while others are influenced by surrounding atoms, the law of variation between intensity and current or pressure will be a combination of the linear and quadratic variations. In the first work done with the present apparatus, such a law was found to hold, with the quadratic term accounting for about half of the intensity at 100 volts, with a current density of 0.0125 amperes per sq. cm, and a pressure of 0.10 mm of mercury. As the voltage decreased, the importance of the quadratic term also decreased, becoming negligible at about 50 volts.

The difficulty with the above interpretation lies in the fact that the experimentally determined coefficient of the quadratic term is much larger than would be expected. Since the mean distance from any point in the space being observed to the electrodes was of the order of two millimeters, thermal agitation would carry any ion or atom to the wall in $5(10)^{-6}$ seconds. For ions, any positive space charge built up would greatly reduce this time. If the ions are neutralized and the metastable atoms drop back to the ground state, as would be expected on collision with the metal electrodes, the chance for the occurrence of these secondary phenomena would be very small, especially since, with the highest current and pressure ever used, collisions between an electron and any given atom occur once in two or three tenths of a second, and the concentration of metastable atoms, ions and electrons could not attain any very high value.

These difficulties of interpretation were removed by the clean-up treatment outlined above. It was found, after this treatment, not only that a linear relationship was obtained, but also that the constant of proportionality was identical with the coefficient of the linear term previously found. A typical plot of the results finally obtained is shown in Fig. 5, for the line 4472 Å, taken at 100 volts. The spread of the observed points in this figure will also give an idea of the accuracy of measurement possible with the methods used. The variable chosen for the abscissa in this curve is the product of current and pressure. This, obviously, gives the same curve as either, plotted alone, would give, and at the same time saves space.

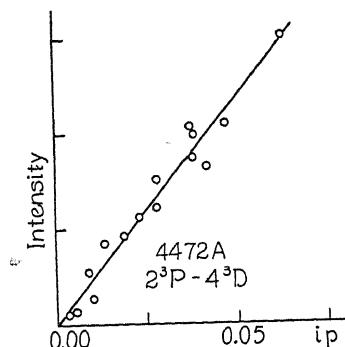


Fig. 5. Intensity variation with current and pressure.

The explanation, possibly, of the change in behavior after cleaning is that the electrodes, when coated with a layer of impurities (stop-cock grease or atmospheric molecules) act very inefficiently for the neutralization of the ions, and allow a large space charge to build up, thus increasing the relative importance of the recombination spectra. Data on the reflection of positive ions from dirty surfaces do not seem to be complete enough to give an answer on this point. Other evidence for the decrease of positive ions after the clean-up was given by the voltage-current curves, which showed no break in passing through the ionization potential.

The linear law finally obtained has been taken as proof that the atoms truly act in an isolated manner, and that contributions due to collisions of the second kind, recombination, etc., have been reduced to negligible proportions.

INTENSITY VARIATIONS WITH VOLTAGE

Figs. 6 and 7 give the intensity-voltage relationships found. These curves were obtained by a series of exposures at pressures between 0.04 and 0.08 mm and with currents of 0.300 to 0.600 ma. By means of the linear relationships established, all these exposures could be reduced to a common pressure and current before plotting. While the relative intensities between the lines are approximately correct, those of wave-length shorter than 4500 Å may be somewhat in error, due to absorption in the glass prism, through which the

line spectra and the continuous light did not have identical paths. This, of course, does not affect the shape of the curve for any individual line, but merely the relative heights.

In Fig. 6 the results for the singlet system are shown, plotted on a logarithmic scale for convenience. The weak lines of the singlet sharp series, while

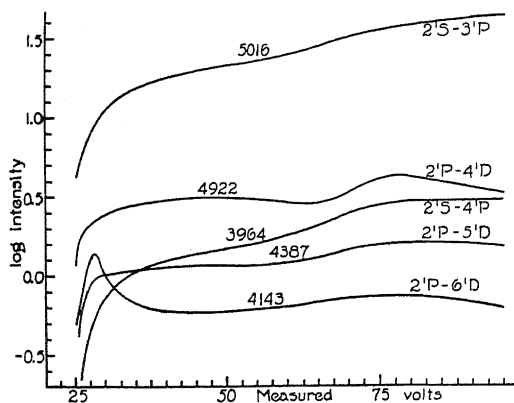


Fig. 6. Intensity-voltage relationships—singlet system.

they were resolved from nearby strong lines, were not far enough removed so that the microphotometer measurements could be relied upon, consequently no results are given for them. The first member of the diffuse series (6678 Å) has also been omitted due to the continuous background from the tungsten filament, which was very appreciable in this region. It will be noticed that

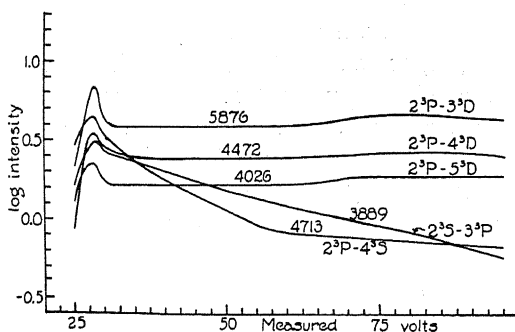


Fig. 7. Intensity-voltage relationships—triplet system.

the two lines observed in the principal series are apparently just approaching maxima at 90 to 100 volts, in quite good agreement with the results of Hanle and Elenbaas. In the diffuse series, 4922 shows two maxima, at 50 and 80 volts, as was found by Elenbaas. The other two lines observed show maxima at 80 volts, and 4143 has a sharp peak at 28 volts. This is the only singlet line showing this low voltage peak. A close examination of the curves will show that, in every case, a point of inflection occurs between 60 and 70 volts, indicating, apparently, some change in the excitation conditions in this region.

The behavior of the triplet system, as shown in Fig. 7, is somewhat different from that of the singlets. At least one member of each series has been observed in this case and all show sharp maxima at 28 volts. The behavior of the diffuse series is remarkably different from the other two, in that the intensity at voltages above the peak does not drop off rapidly. This series also shows maxima at about 80 volts as did the diffuse singlet series. All lines show the same inflection point between 60 and 70 volts as was shown by the singlets.

THE OPTICAL EXCITATION FUNCTION

In previous work, the plot of intensity vs. voltage given above has been taken as the curve of the optical excitation function, on the assumption of an absolutely monochromatic electron beam. With the experimentally determined distribution curve available, however, it is clear that, in the neighborhood of the excitation potential, part of the change in intensity, at least, is due to a change in the number of effective electrons, rather than to a variation in their velocity. The distribution curve shows that 96% of the electrons are included within a range of 10.8 volts. If the excitation potential of a given line, then, is 23 volts, it is clear that, taking into account the 1.2 volt contact potential, the effective current is increasing until a measured voltage of 35 volts has been reached. If the optical excitation function is defined for a monochromatic beam, which is not obtained experimentally, then the intensity will be given by:

$$I = C \int_0^{\infty} F(v) i(V_m, v) dv$$

where C is a constant, $F(v)$ is the optical excitation function for the voltage v , and $i(V_m, v)$ is the current distribution function (i.e. the height of the curve of Fig. 2b) for the same voltage, and for a given value of V_m as defined below. We know, however, that below the excitation potential V_0 the optical excitation function must have the value zero and that above a certain maximum voltage, V_m (1.2 volts below the measured potential), the current distribution function is zero. Making the corresponding change of limits and taking the constant into the function, we have:

$$I = \int_{V_0}^{V_m} F(v) i(V_m, v) dv.$$

Taking the derivative with respect to V_m .

$$\frac{dI}{dV_m} = F(V_m) i_m + \int_{V_0}^{V_m} F(v) \frac{di(V_m, v)}{dV_m} dv$$

where $F(V_m)$ is the value of the excitation function at the maximum voltage and i_m is the height of the flat portion of the distribution curve. Solving for $F(V_m)$ and choosing units so that i_m is unity:

$$F(V_m) = \frac{dI}{dV_m} - \int_{V_0}^{V_m} F(v) \frac{di(V_m, v)}{dV_m} dv.$$

Fortunately, when V_m is less than five volts above the excitation potential di/dV_m is zero throughout the range of integration, and the equation for $F(V_m)$ reduces to the first term. In this range, then, the optical excitation function may be directly determined from the slope of the intensity-voltage curve. This determination supplies a set of values of the function which may be combined with the values of di/dV_m read from Fig. 2a and graphically integrated to give the second term for the computation of the function at voltages not more than ten volts above the excitation potential. The new points thus obtained may be used in turn for calculating still higher voltages.

In Figs. 8 and 9 the results of these computations are shown. While the calculations could not be carried down to the excitation potential itself, due to the large error that would be introduced by a small error in the determina-

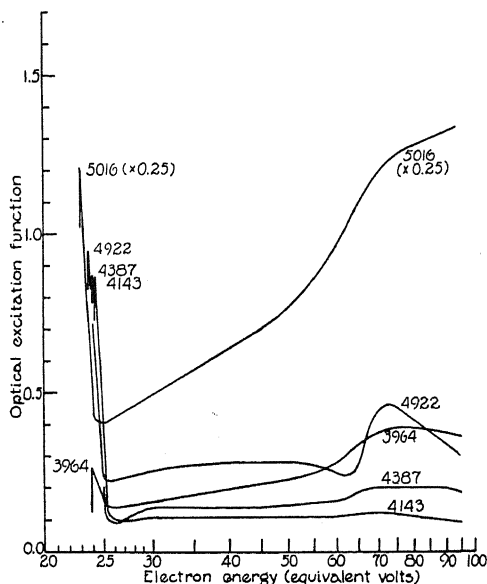


Fig. 8. Optical excitation function—singlet system.

tion of the velocity distribution, they have been carried to within half a volt of that potential. As the optical excitation function is still rising in value at that point, it has been assumed that the peak actually occurs at the excitation potential, and the curves have been extrapolated accordingly. In the figures, a logarithmic scale has been chosen for the voltages and parts of the curves approaching the peaks have been omitted in order to avoid congestion.

It will be noticed that the function, for all lines, exhibits a sharp peak at the excitation potential and a more or less constant value for all higher voltages. The width of the peak itself is, in general, about two volts. Whether

this width is real or is the result of experimental difficulties with voltage control, determination of velocity distribution, etc. cannot be decided with the present data.*

As would be expected from Figs. 6 and 7, the triplets are distinguished from the singlets by the fact that, in general, their ratio of peak height to background height is greater. The singlet principal series seem to be anoma-

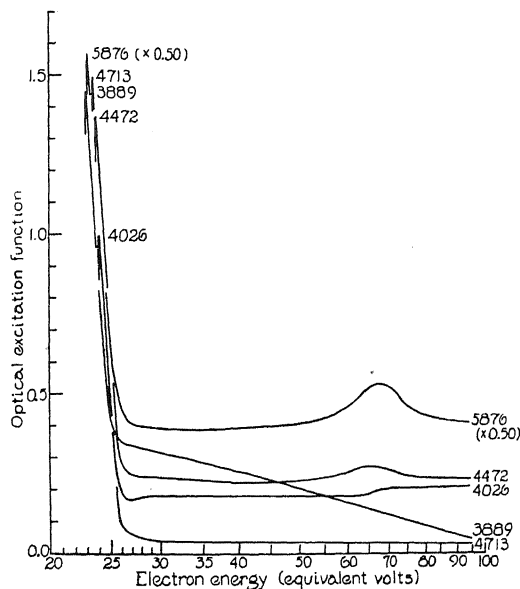


Fig. 9. Optical excitation function—triplet system.

lous in that its background value is of the same order of magnitude as the height of its maxima, and the two members observed show a much greater ratio of intensities than do the succeeding members of any other series. This may be connected with the fact that the normal state of the atom is a 1S level, with allowed transitions to the 1P levels.

CONCLUSIONS

We may summarize the new facts in regard to the optical excitation function of helium which have been brought forward in this investigation:

- (1) It is possible, by proper apparatus and technique, to obtain experimental conditions under which the atoms act in an isolated manner, with no appreciable effect of recombination. The test for this condition is a linear dependence of intensity on either current or pressure, within a limited range.
- (2) The optical excitation function has been shown to have a similar behavior for all lines, in that a sharp maxima is observed either at or very near to the excitation potential.

* It would seem probable that this peak may actually consist of a series of maxima, here unresolved, corresponding to the various excitation levels of the helium atom.

(3) Between 60 and 70 volts an irregularity occurs in the function, possibly due to some new mode of excitation entering in this region.

(4) The singlet and triplet systems are distinguished by the fact that, in the former, excitation is accomplished with fairly high probability by electrons with all energies above that just necessary for excitation, while, in the latter, those electrons with just sufficient energy to excite are much more efficient than those with greater energy.

In conclusion the author wishes to express his extreme gratitude to Drs. R. A. Millikan, I. S. Bowen, and W. V. Houston, whose constant interest has been of great aid in the completion of this investigation. He also wishes to thank Mr. A. B. Anderson for assistance in taking some of the data.

ORGANIC REACTIONS IN GASEOUS ELECTRICAL DISCHARGE I. NORMAL PARAFFIN HYDROCARBONS

BY ERNEST G. LINDER*

CORNELL UNIVERSITY

(Received September 4, 1930)

ABSTRACT

An apparatus is described for subjecting vapors to an electrical discharge. Vapor pressure and current are variable. Different fractions of the gaseous reaction products can be collected and their rates of accumulation measured. A study of *n*-decane vapor with this apparatus, with current values of from 0.5 to 2.5 m.a., voltage approximately 450 volts, and pressures from 0.2 to 4.5 mm of mercury, indicates that electric conduction in gases may follow an electrochemical equivalence law similar to Faraday's law of electrolytic conduction in liquids. Evidence has been obtained showing the amount of reaction to be proportional to the current, and independent of voltage and vapor pressure. Among the reaction products is a wax-like substance which deposits on the cathode only. The rate of production of gaseous reaction products has been measured for various values of discharge currents and vapor pressure. Curves and tables are given showing the relation between molecular size and rate of production of various fractions of the gaseous reaction products, for a series of seven normal paraffin hydrocarbons. A brief theoretical discussion is given.

INTRODUCTION

OF THE many investigations of electrical discharges in gases the greater part has been carried out with stable gases, whereas gases which undergo chemical changes in the discharge have been comparatively neglected. The work described below is the first set of a series of measurements which may eventually include all available hydrocarbons, and possibly also some oxygen-containing compounds, such as alcohols, ethers, ketones and esters. The purpose of the investigation is to try to shed some light on chemical action in electrical discharge, and to contribute something to the knowledge of the relation between molecular structure and chemical reactions, especially in regard to hydrocarbon chain structure.

APPARATUS AND PROCEDURE

The apparatus (Fig. 1) consists of a bulb *E* for containing the liquid hydrocarbon, the discharge chamber *D*, the trap *T*, the mercury vapor pump *P*, and the storage chamber *S*, from which tubes *G* and *F* lead to a McLeod gauge and oil pump respectively. The bulb *E* can be immersed in a constant-temperature bath and runs made at constant vapor pressure. The discharge chamber *D* consists of a two-liter Pyrex bulb; the purpose of the large volume being to minimize any possible influence of the walls on the chemical

* Detroit Edison Research Associate. The work described in this article is a part of an investigation of the fundamentals of organic dielectrics being carried on at Cornell University. It is supported by a fund provided by the Detroit Edison Company.

action. The two aluminum disk electrodes are about 2.5 cm in diameter and about 8.5 cm apart. They are mounted on heavy, glass-covered tungsten wires which in turn are sealed through ground glass stoppers, so that the electrodes may be removed from the bulb for cleaning. The trap *T* is of the ordinary type except that there is a ground joint near the top to facilitate cleaning, and the inside tube is cut shorter than usual and is flared at the end to prevent clogging by frozen hydrocarbons. The storage chamber *S* has a capacity of about 13 liters. The electrical energy for the discharge is supplied by a transformer in series with a single kenotron.

When the apparatus is in operation a continuous current of vapor flows from *E* to *T* where it condenses. The chamber *D* is therefore filled with hydrocarbon vapor whose pressure is determined by the temperature of *E*. In the few cases where runs were made at temperatures higher than that of

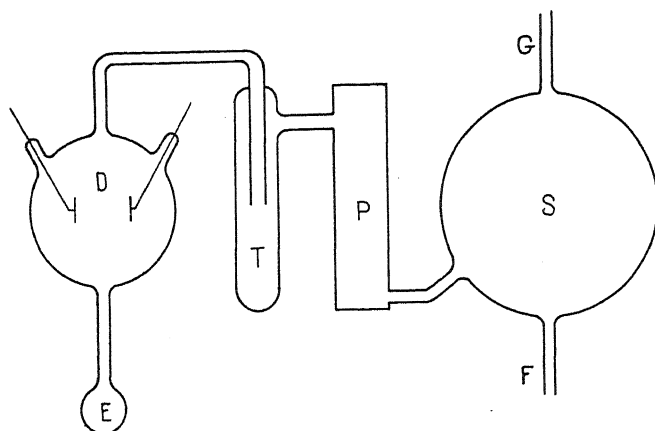


Fig. 1. Diagram of apparatus.

the room, *E* was removed, the hydrocarbon was placed in *D* itself, and *D* was entirely immersed in a constant-temperature bath. The runs were all made with such a high rate of vapor flow from *E* to *T* that all gaseous reaction products were swept out of *D* before there was any appreciable reverse reaction. This was shown by the fact that the results were independent of the vapor pressure, and consequently of the rate of flow. The discharge may therefore be considered as taking place through essentially pure hydrocarbon vapor.

Either liquid air, or a slush of carbon dioxide snow and ether was used as a refrigerant for the trap *T*, depending upon what fraction of the gaseous products it was desired to collect. With carbon dioxide cooling, *n*-hexane vapor was found to pass easily through the trap, while *n*-heptane was stopped. Since the vapor pressures of these two substances at -77°C are about 0.1 and 0.02 mm of mercury respectively, it can be concluded that substances of vapor pressures below 0.02 mm at the temperature of the trap will not pass, whereas those of vapor pressures above 0.10 mm will pass. This means, for example, that in the normal paraffin series, with liquid air cooling, only

H₂, CH₄ will pass, while with carbon dioxide cooling H₂, CH₄, C₂H₆, . . . , C₆H₁₄ will pass, and higher members of the series will be stopped.

Runs were made on seven normal paraffin hydrocarbons, n-pentane, n-hexane, n-heptane, n-octane, n-decane, dodecane, and n-tetradecane. All were obtained from the Eastman Kodak Company, and were of the highest degree of purity provided by them, except n-pentane which was the "practical grade." However it is believed that small amounts of impurities have no appreciable effect on the phenomena reported here, since in a series of about fifty runs, made on the same sample of n-decane, the results toward the end of the series were the same as at the beginning. A similar observation was made also with some of the other hydrocarbons, but the number of runs was not so great.

RESULTS

The discharge was run with currents from 0.5 to 2.5 m.a. for the n-decane measurements, and 1.0 m.a. for the other substances. The voltage could not be varied independently; it made wide fluctuations (sometimes as large as 25 percent) about 500 volts for all compounds. In appearance the discharge was essentially the same for all hydrocarbons investigated. There was only a very slight visible glow around the cathode, and frequently none at all. The glow was most apparent at the lower pressures, and hardly perceptible at all at pressures as great as 1.0 mm. The most conspicuous feature was the large number of sparks scintillating on the surface of the cathode. The sparks were small and bluish, and appeared in about equal numbers on the back and front of the disk. At the beginning of a run, when only a thin layer of wax had formed, they appeared evenly distributed, but later on, became more or less concentrated in small regions or spots. These spots finally became black as if the wax had been carbonized. Sparks also appeared on the surface of the anode, but they were much fewer in number and did not shift about, remaining fixed and glowing for minutes at a time. They were yellow or white rather than blue in color.

Previous work has shown that in general the effect of an electrical discharge in a hydrocarbon gas is to cause an apparently complicated chemical reaction resulting in solid, liquid and gaseous products. With the writer's apparatus the solid products were deposited mostly upon the cathode with slight traces of deposits on the glass walls, the gaseous products were pumped over into the storage chamber *S*, while the liquid products (if any) condensed in the trap. However, no evidence of liquid products was found, the same sample of n-decane having been run through the apparatus about fifty times without showing evidence of contamination or change of any sort.

The wax which formed on the cathode has not been analyzed by the writer, but analyses of similar, if not identical compounds by others¹ indicate

¹ S. C. Lind, *The Chemical Effects of Alpha Particles and Electrons*, The Chemical Catalog Co., 1928, Amer. Chem. Soc. Monograph No. 2, page 158. C. F. Hirshfeld, A. A. Meyer, L. H. Connell, *Study of the Mechanism of Cable Deterioration*, Detroit Edison Co., printed but not published by the Association of Edison Illuminating Companies, 1928, page 111.

that it is a complex hydrocarbon of high molecular weight. It is insoluble in all common organic solvents.

The gases produced by the discharge were pumped into the chamber *S*. Typical curves showing the pressure increase are given in Fig. 2, in which

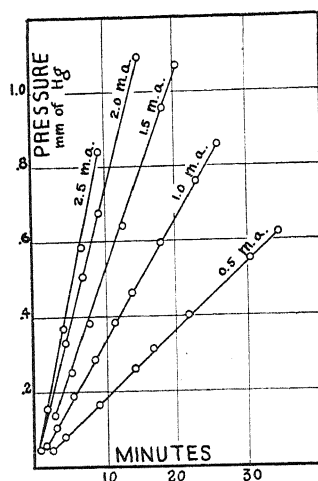


Fig. 2. Pressure-time curves for n-decane for various values of discharge current.

the time of duration of the discharge is plotted horizontally, and the pressure in *S*, vertically. Curves are given for five different values of discharge current from 0.5 to 2.5 ma., as indicated. The graphs are straight lines

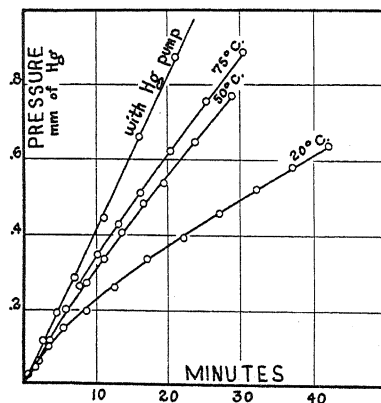


Fig. 3. Pressure-time curves showing effect of accumulation of reaction products on rate of reaction in n-tetradecane.

through the origin. Runs of a duration of 80 minutes showed no departure from this linear relationship. This is true in spite of the fact that at the beginning of the run the electrodes were clean whereas at the end the cathode

was coated with a heavy layer of wax. It seems that the wax deposit on the cathode has no effect on the production of gas.²

A linear relation between pressure and time is not found unless the gaseous products are removed from the reaction chamber sufficiently fast. If the mercury pump *P* is not in operation the products will be removed from *D* only by the pumping action of the vapor stream flowing from *E* to *T*. In most cases this will not effect a complete removal. Fig. 3 shows graphs for n-tetradecane. The three curved lines were obtained with the liquid hydrocarbon held at 20°, 50°, and 70°C, as shown. The straight line was obtained with the pump *P* in operation. It can be seen that the curved lines have at the origin the same slope as the straight line, but their slope decreases as the

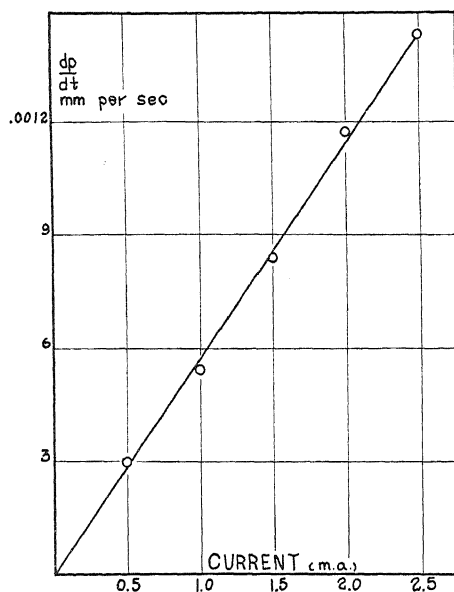


Fig. 4. Proportionality between discharge current and rate of reaction in n-decane.

discharge continues. This is probably due to the accumulation of reaction products in *D*, and consequent reverse reactions, or conduction of current by non-reacting ions. These hypotheses are supported by the fact that as the temperature of the liquid hydrocarbon is raised, and the rate of flow of vapor from *E* to *T* thereby increased, the pumping action of the vapor stream increases, the reaction products are more efficiently swept from *D*, and the curves approach closer to the straight line. A similar result was obtained with n-decane.

Plotting the slopes of the lines of Fig. 2 against discharge current, a straight line passing through the origin is obtained, as shown in Fig. 4.

² J. C. McLennan, M. W. Perrin, H. J. C. Ireton, Proc. Roy. Soc. 125, 246 (1929), bombarded with cathode-rays a similar wax formed from acetylene and found no evidence of gas evolution.

The numerical data are given in Table I. This indicates that under the conditions of this experiment, the relation between current and rate of reaction is of the type,

$$dp/dt = ki \quad (1)$$

where k is a constant depending only on the kind of hydrocarbon, and i is the current. In other words it seems that conduction in gases may follow an electro-chemical equivalence law similar to Faraday's law of electrolytic conduction in liquids. It appears quite certain however, that the mechanism in the case of gases must be very different from that of electrolysis.

TABLE I. Rate of production of gas in *n*-decane vapor for various values of discharge current.

Current (m.a.)	dp/dt (-77°C)
0.5	0.000300
1.0	.000546
1.5	.000842
2.0	.001180
2.5	.001441

The rate of reaction has been found to be independent of pressure and the voltage between the electrodes. There is some evidence that it is independent also of the distance between the electrodes. These points are discussed somewhat more in detail below.

(1) *Effect of pressure.* Table II gives dp/dt for different pressures, with carbon dioxide cooling on the trap. It will be seen that dp/dt is constant,

TABLE II. Rate of gas production and vapor pressure.

Hydrocarbon	$t^{\circ}\text{C}$	V.P. (mm Hg)	dp/dt (-77°C)
dodecane	0		0.000645
	22		640
n-decane	0	0.20	547
	22	1.25	555
	24	1.50	539
	40	4.50	533
n-octane	-15	.90	523
	0	2.95	511
n-heptane	-20	.63	800
	-17	.80	867
	0	11.45	816

within the experimental error, over a wide range of pressures, for a given compound. In the case of *n*-heptane the pressure change is over 1700 percent, whereas the corresponding change in dp/dt is only 2 percent. The vapor pressure data for dodecane were not available, but are probably similar to those of *n*-decane.

(2) *Effect of voltage.* Although it was not possible to determine the effect of different voltages by independently varying the potential difference between the electrodes, the automatic fluctuations in this quantity during the course of the runs served the purpose. These voltage changes were commonly as large as 25 percent yet no effect due to them was noticeable. The pressure-time curves were always straight lines as shown in Fig. 2. Hence it appears that if the current is held constant, the rate of reaction is unaffected by changes of potential difference between the electrodes.

(3) *Effect of electrode spacing and shape.* For the n-decane runs, two discharge bulbs were used, which were similar except that the distance between the electrodes was 5.5 cm in one and 8.5 cm in the other. The first gave as an average $dp/dt = 0.000546$, while the single run made with the latter gave $dp/dt = 0.000521$. Since the positive column was longer in the second case than in the first it can be concluded that in the case of n-decane any action which may occur in the positive column must be negligible in comparison with that occurring near the cathode.

As a further test of the locus of the reaction a point electrode about 1.0 mm in diameter and 1.0 cm long was substituted for the disk-shaped cathode. The electrode spacing was 8.5 cm. This gave $dp/dt = 0.000660$, an increase of about 27 percent over the rate obtained with the disk electrode. This indicates that the reaction goes to completion in the gas phase rather than on the electrode surface, but the difference is not sufficient to make the result conclusive.

Results similar to these have been obtained by a few other workers for other substances. Kirkby³ studied the synthesis of water in the glow discharge and obtained a linear relation between current and amount of water formed. He also observed that most of the action occurred in the neighborhood of the cathode and that this was independent of pressure. Günther-Schulze⁴ found the rate of reaction to be proportional to the current for the synthesis of water in the glow discharge for currents from 20 to 120 ma. The rate was independent of pressure. He found similar results for the synthesis of ammonia. A. Keith Brewer and J. W. Westhaver⁵ have made an extensive study of the synthesis of ammonia, and also nitrogen dioxide. They also find proportionality between current and rate, and independence of pressure. They show that most of the reaction occurs in the neighborhood of the cathode and that it apparently goes to completion in the gas phase rather than on the surfaces of the walls or cathode.

The rates of gas production for each of the seven normal paraffin hydrocarbons are given in table III, and shown graphically in Fig. 5. These rates are for a current of 1.0 m.a. The subscripts -77 and -182 indicate the use of carbon dioxide and liquid air, respectively, as the refrigerant on the trap.

³ P. J. Kirkby, *Phil. Mag.*, [6] 7, 223 (1904); 9, 175 (1905); 13, 289 (1907); *Proc. Roy. Soc. A* 85, 151 (1911).

⁴ A. Günther-Schulze, *Zeits. f. Physik* 21, 50 (1924).

⁵ A. Keith Brewer and J. W. Westhaver, *J. Phys. Chem.* 33, 883 (1929); 34, 159 (1930); 34, 554 (1930).

TABLE III. Rate of gas production for normal paraffins (discharge current = 1.0 m.a.)

Hydrocarbon	Formula	$\frac{dp}{dt}$ (-77°C)	$\frac{dp}{dt}$ (-182°C)
n-pentane	C_5H_{12}	—	0.000208
n-hexane	C_6H_{14}	0.000757	.000173
n-heptane	C_7H_{16}	.000828	.000167
n-octane	C_8H_{18}	.000510	.000163
n-decane	$\text{C}_{10}\text{H}_{22}$.000546	.000174
dodecane	$\text{C}_{12}\text{H}_{26}$.000642	.000291
n-tetradecane	$\text{C}_{14}\text{H}_{30}$.000702	.000346

The rates are expressed in mm of mercury per second increase in pressure in the storage chamber S.

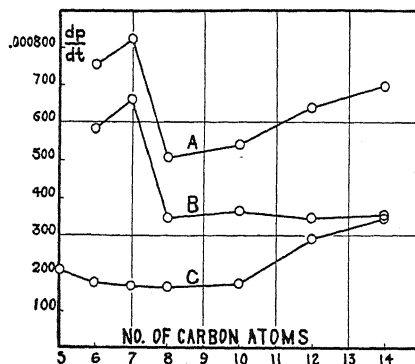


Fig. 5. Relation between molecular size and rate of reaction. Curves A and C represent data taken with carbon dioxide and liquid air respectively as refrigerants. Curve B was obtained by subtracting C from A.

In Fig. 5, curve A represents the rates of gas production with carbon dioxide cooling, curve C with liquid air cooling, while curve B was obtained by subtracting C from A. Although the writer has made no analyses of the gases collected, some idea of their composition may be obtained from these curves. Obviously they must be hydrocarbons or hydrogen. As was stated above, those having a vapor pressure greater than 0.1 mm at the temperature of the trap will pass through it, whereas those whose vapor pressure is less than 0.02 will be stopped. Hence the gases represented by curve C likely include hydrogen and methane, their vapor pressures being well above the limit. Ethylene, propylene and acetylene may also be present, for their vapor pressures, although not available for this temperature, may also be above the limit. Hirshfeld, Meyer, and Connell⁶ have analysed the gases given off when liquid normal paraffins are rayed with cathode-rays from a Coolidge cathode-ray tube and found them to be made up of from 72 to 91 percent of hydrogen, 1.8 to 3.0 percent of methane, and 6.3 to 26.4 percent of undetermined light hydrocarbons. Reference to Fig. 5 will show that in a

⁶ C. F. Hirshfeld, A. A. Meyer, L. H. Connell, *Study of the Mechanism of Cable Deterioration*, 1929. (See reference 1.)

gaseous electrical discharge a considerably smaller percent of hydrogen is obtained, curve *C* representing the maximum possible amount. On the other hand, the light hydrocarbons are present in larger amounts as shown by curve *B*. This may be due to the lower energy of the impacting electrons in the gaseous discharge. Or, it may be due to the longer period of bombardment in the cathode-ray experiments, in which the liquid hydrocarbons were exposed to the rays for periods of a few hours length. Polymerization and condensation may therefore have progressed further.

Heptane and hexane show a much greater production of light hydrocarbon gases than the others, as is shown by the hump in curve *B*. For these two substances the pressure-time curves (with carbon-dioxide as refrigerant) were not straight lines, as shown in Fig. 2, but broken lines each made up of two straight sections; the second section in each case was less steep than the first. This was due to the presence of hydrocarbon gases which condensed in the McLeod gauge, as soon as the difference in the mercury levels became equal to their vapor pressure at room temperature. The break for n-heptane occurred at a difference in mercury levels of about 120 mm, while that for n-hexane occurred at about 140 mm. No breaks in the pressure-time curves were found for any other substances.

DISCUSSION

Previous work^{1,5,7} indicates that chemical action in electrical discharge is initiated by positive ions. Once positive ions are formed the reaction appears to take place in one of two ways, (1) by a *chain mechanism* such as postulated by Bodenstein,⁸ in which "there is formed an unstable intermediate product, rich in energy, which on further reaction gives rise not only to the final product, but also to another intermediate product which regenerates the same process again and again," or (2) by a *clustering process*, such as has been assumed by Lind in connection with his work on α -ray bombardment, and according to which positive ions attract surrounding neutral molecules forming an ion cluster which reacts chemically upon neutralization.

It seems that a satisfactory theory of chemical action in electrical discharge should be in harmony with the above hypotheses, and in addition should explain the following experimental facts: (1) proportionality between current and rate of reaction; (2) independence of rate of reaction on pressure; (3) occurrence of the greater part of the reaction in the neighborhood of the cathode. (These facts are supported not only by the work reported in this article but also by that of Kirkby, Günther-Schulze, and Brewer and Westhaver, mentioned above.)

A simple mechanism which meets these requirements is the following: Consider the electrons leaving the cathode. These traverse the cathode potential drop and thereby acquire energy which is expended in collisions in

⁷ S. C. Lind, *Science* **67**, 565 (1928).

⁸ Max Bodenstein, *Chem. Reviews* **7**, 2, 215 (1930).

the dark space and negative glow. We assume that the positive ions formed by these collisions serve as the initiators of the chemical action, giving rise to either chain or cluster processes.

Proportionality between current and rate of reaction will follow from this hypothesis if there is a constant ratio between the current and the number of positive ions formed in the dark space and negative glow. The existence of such a ratio seems quite likely for the ranges of pressure and current under consideration. Such a constant ratio would exist (1) if there were a constant ratio between the current and the number of electrons leaving the cathode, or in other words, between the number of electrons leaving and the number of positive ions arriving; and (2) if there were a constant ratio between the number of electrons leaving the cathode and the number of positive ions formed in the dark space and negative glow. Both of these assumptions are in good agreement with the generally accepted ideas of the glow discharge, and it seems likely that they are valid.

Independence of the rate of reaction of pressure can be explained by the relation $pd = \text{const.}^9$, where p is the pressure and d is the width of the dark space. From this it is clear that any change in pressure is compensated for by such a change in d that the amount of gas subjected to bombardment by electrons from the cathode remains constant. In other words, as the pressure changes the mean free path of the electrons changes so that the same number of collisions is made as before. Changes in pressure may be regarded as only magnifying or reducing the dimensions of the active region surrounding the cathode, but not affecting the total number of positive ions formed therein.

This picture disregards the action in the positive column. Any reaction which may occur there is probably due to the formation and recombination of ions which never reach the electrodes and hence have no relation to the current. In the experiments discussed here this action has apparently been small in amount, and could probably be made as small as desired by making the positive column sufficiently short.

The occurrence of the greater part of the reaction in the neighborhood of the cathode is obviously accounted for by this mechanism. It would be expected that the negative glow would be the seat of most of the reaction because of the high energy of the electrons and the high density of positive ions in that region.

Among the experimental results, which are not yet well-established, are: First, the apparent independence of reaction rate on electrode spacing, found in the case of *n*-decane. On the basis of the suggested mechanism this means only that in this case the amount of reaction in the positive column is negligible. Second, the independence of the reaction rate on voltage. It seems likely that the voltage fluctuations were caused by inconstant conditions on the wax-covered cathode surface. The cathode potential drop depends only on the nature of the gas, hence it must have remained constant, and thereby yielded a constant reaction rate regardless of the voltage across the electrodes.

⁹ L. H. Dawson, *Phys. Rev.* 30, 119 (1927).

The results presented in this article are not such as to distinguish between a chain and cluster mechanism. However, a cluster mechanism is indicated by the formation of the wax, which is apparently a hydrocarbon of high molecular weight such as would be formed by polymerization or condensation. It seems likely that these heavy molecules form on the surface of the cathode rather than in the gas phase, since such large clusters would probably be unstable in the gaseous state,¹⁰ even though chemical forces were added to the ordinary forces of electrostatic induction between an ion and surrounding neutral molecules.

In conclusion the writer wishes to express his appreciation to those of the Departments of Physics and Chemistry of Cornell University who were helpful in this work, to Dr. H. A. Trebler for his interest in the problem and his valuable suggestions, and to Prof. Vladimir Karapetoff, who is in general charge of the above mentioned research program on insulation at Cornell University. He wishes especially to thank Mr. C. F. Hirshfeld, chief of research, and Mr. Alex Dow, president, both of the Detroit Edison Company, for the financial support which made the above described work possible, and for permission to publish the results.

¹⁰ J. J. Thomson, *Conduction of Electricity Through Gases*, 3rd Ed., p. 66.

THE POLARIZED FLUORESCENCE OF SOLUTIONS
OF RHODAMINE-B AND URANINE*BY ERNEST MERRITT AND DONALD R. MOREY
CORNELL UNIVERSITY

(Received August 30, 1930)

ABSTRACT

Measurements have been made of the extent of polarization in the fluorescence light from glycerine solutions of uranine and rhodamine-B. The results indicate that the fluorescence light is polarized to the same extent throughout any one fluorescence band; or, if there is a variation which these experiments have failed to detect, it cannot be much greater than one percent. These results thus confirm the observations of Wawilow and of Pringsheim and Wawilow. In the case of uranine the width of the fluorescence band is such that the frequency at the short-wave edge exceeds that at the long-wave side by more than twenty-five percent. The results therefore add support to the view that a fluorescence band is to be regarded as a unit. This view is still further strengthened by the fact that under some conditions of concentration there is evidence of the existence of two bands in the fluorescence spectrum of uranine, the polarization being constant throughout each band but different for the two bands.

If we adopt the usually accepted explanation of the cause of polarization in viscous solutions the results are best explained by the assumption that the duration of the fluorescence process is the same for all wave-lengths in a fluorescence band and that the duration is less for the small band of uranine than for the principal band. If this explanation is correct it may still be that the broad fluorescence band of uranine is really a group of overlapping lines; but if so the duration of the excited state is the same for all lines of the group. An alternative view, with which these results are altogether consistent, is that discussed by one of the writers in a previous paper, viz. that only a single electron transition is involved, and that the breadth and shape of the fluorescence band are determined by the disturbing effect of the solvent.

WHEN viscous solutions of the organic dyes are excited to fluorescence the emitted light is found to be partially polarized. The polarization is most marked when a solvent like glycerine is used, but it can be detected by sufficiently sensitive methods even in aqueous solutions. In its dependence upon the direction of observation and the direction of the electric vector of the exciting light this polarized fluorescence is qualitatively similar to the light scattered by small particles in the Tyndall effect.

All of the attempts that have been made to give a theoretical interpretation of the phenomena have involved two assumptions, namely: (1) that the active molecule is anisotropic, so that both the probability of excitation and the polarization of the emitted light are dependent on the orientation of the molecule; and (2) that the duration of the excited state is finite—or, in other words, that the act of emission requires an appreciable time. In solutions having small viscosity thermal agitation causes the orientation of the excited

* The investigation of which the work here described forms a part has been supported by a grant from the Hechscher Foundation for Research² at Cornell University.

molecule to change so rapidly that the fluorescence light may be regarded as coming from molecules having a nearly random orientation and the polarization is small. In viscous solutions emission occurs before the molecules have had time to change their orientation and the polarization may be quite marked. In general, therefore, strong polarization of the emitted light indicates either large viscosity or short duration of the excited state. While there are difficult points that are not yet cleared up and seemingly contradictory experimental results that are yet to be explained this interpretation of the observed effects is in the main satisfactory.

The study of polarized fluorescence thus offers a means of obtaining information on two important points connected with radiation, viz., the symmetry of the molecule as exhibited in the processes of absorption and emission, and the duration of these two processes. So little is known about what goes on in a molecule while it is absorbing or emitting radiation, and the means by which we may hope to add to our knowledge are so few, that the study of polarized fluorescence would seem to deserve even greater attention than it has received.

The experiments here described were undertaken in the hope of determining by means of polarization measurements whether or not the duration of the fluorescence process is the same for different parts of the fluorescence band. If it is the same we should expect the emitted light to be polarized to an equal extent for all wave-lengths in the fluorescence spectrum. The results of previous experiments bearing on this point are contradictory. Weigert¹ found the polarization greatest at the red end of the fluorescence spectrum. Wawilow and Lewschin,² working with filters to separate different spectral regions, found the polarization practically the same throughout the spectrum. This result was later confirmed by Wawilow³ for fluorescein and rhodamine by spectrophotometric measurements. With aesculin, both in sugar solutions and in solid gelatin, Pringsheim and Wawilow⁴ found the polarization greatest at the short wave side of the band and least at the long wave edge, the value at the center of the band being intermediate between the two. On the other hand aesculin in glycerin showed nearly equal polarization throughout.

If the percentage polarization really does give an indication of the duration of the fluorescence process it is a matter of importance to reach a decision among these conflicting results, for such a decision would help in forming an opinion as to the type of emission process that is involved. Are we, for example, to treat the fluorescence of solutions as involving essentially the same processes as the fluorescence of gases, the observed differences being simply the result of the disturbing effect of the solvent? In some cases, notably that of benzene, this procedure certainly seems to be justified. If it is generally applicable, the broad and seemingly continuous fluorescence band of a substance like uranine must be thought of as being really a group of overlapping narrow

¹ F. Weigert, *Phys. Zeits.* **23**, 232 (1922).

² S. J. Wawilow and W. L. Lewschin, *Zeits. f. Physik* **16**, 135 (1923).

³ S. J. Wawilow and W. L. Lewschin, *Zeits. f. Physik* **32**, 721 (1925).

⁴ P. Pringsheim and S. J. Wawilow, *Zeits. f. Physik* **37**, 705 (1926).

bands which we have not yet been able to resolve. In this case the different parts of the emission band are due to different electron transitions and it would seem not unreasonable to expect the duration of the excited state to be different at different points in the spectrum. On the other hand it may be that the complexity of the active molecule and the enormous forces exerted on it by the solvent make necessary some new method of treatment. It has in fact been found that the disturbing effect of the solvent is sufficient, even if only one electron transition is involved, to account not only for the width of the band in the case of fluorescein and rhodamine but also for certain peculiarities in the form of the absorption band and in the relation between fluorescence and absorption⁵ There remains also the possibility that chemical action brought about by the exciting light is an important factor, possibly an essential factor, in the fluorescence of liquids and solids. While knowledge of the matter in which the polarization depends upon the wave-length cannot be expected to settle the question as to what line of attack should be followed it should at least be helpful.

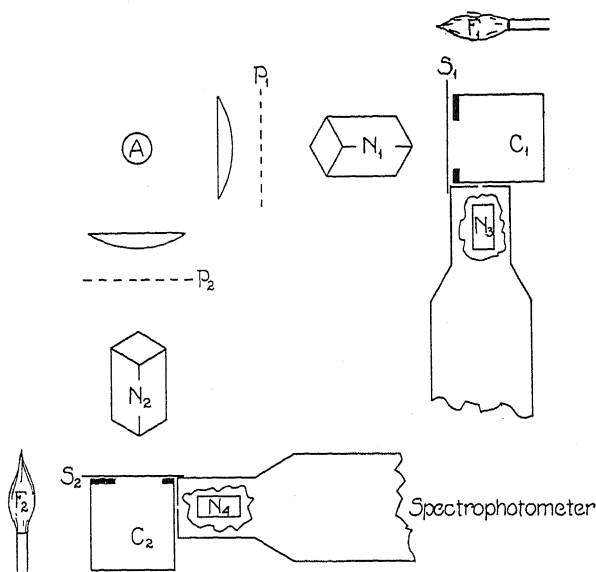


Fig. 1. Arrangement of apparatus.

EXPERIMENTAL

The arrangement of apparatus is shown in Fig. 1. The cells C_1 and C_2 containing identical solutions of uranine or rhodamine-B were placed before the two collimator slits of a large Lummer-Brodhun spectrophotometer. Fluorescence was excited in C_1 and C_2 by light from the mercury arc A , and the two fluorescence spectra were photographed at the same time and on the same plate. The blackening of the photographic plate was measured by a Moll

⁵ E. Merritt, Phys. Rev. 28, 684, (1926).

microphotometer, the two records being superposed, so that any differences could be readily detected. The two exciting beams could be polarized either in the horizontal or vertical plane by the nicols N_1 and N_2 . Screens of blue glass, S_1 and S_2 , cut out from the exciting beams nearly all light falling within the fluorescence band. There was enough transmission in the long wave region, however, and sufficient reflection from the cell walls, so that the strong lines 5461, 5770 and 5790 were frequently present in sufficient intensity to make a faint record on the photographic plate. In such cases they served as a check on the accuracy with which the two microphotometer records were superposed. To make certain that some check of this kind should be available sodium flames F_1 , F_2 were placed in front of each collim-

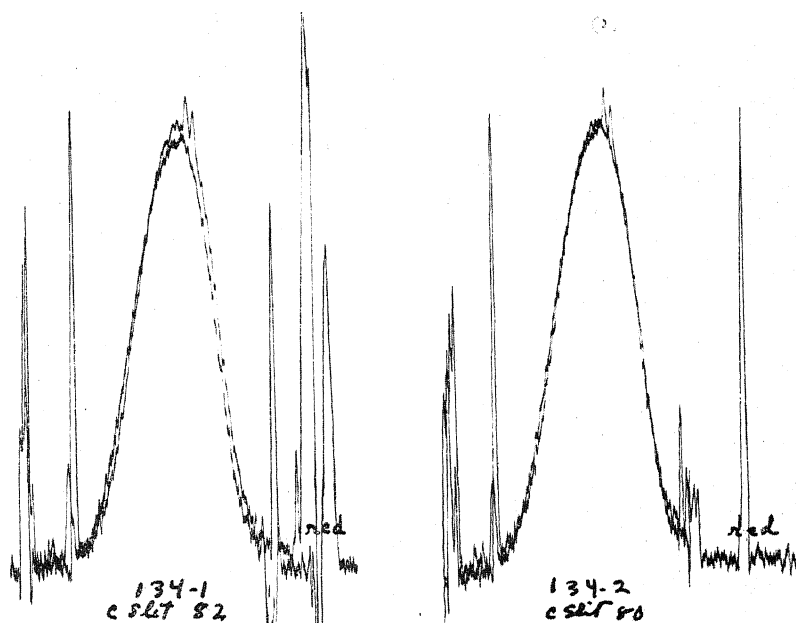


Fig. 2. Showing the effect of changing the opening of one spectrophotometer slit from 80 div. to 82 div., the other remaining unchanged.

ator, so as to have the sodium line show on the photographic plate. This wave-length is incapable of exciting fluorescence in the solutions tested. The screens S_1 and S_2 and the glass walls of the two cells proved to be so nearly free from strain that their depolarizing action was negligible. Analyzing nicols N_3 and N_4 , were carried in the collimator tubes as shown.

Ordinarily the nicols N_1 and N_2 were both set so that the electric vector of the exciting light was in the vertical plane and were then left in this position. This procedure was made necessary by the fact that any change in the setting of N_1 or N_2 altered the distribution of the exciting light over the surface of the corresponding cell C_1 or C_2 ; and since the fluorescence light suffered absorption by the solution a slight change in the path of the fluores-

cence light through the solution was likely to result in an apparent change in the distribution of energy throughout the fluorescence band.

The adjustment was first tested by photographing the two spectra when both analyzing nicols (N_3 and N_4) were set with their principal planes horizontal. In this case the microphotometer records should be identical. Small inequalities in the intensity of the two bands were corrected by inserting pieces of clear glass in the path of one of the exciting beams at P_1 or P_2 . The shapes of the bands were made similar by adjusting nicols N_1 and N_2 to make sure that the two beams of fluorescence light suffered equal absorption. The sensitiveness of the method varied from plate to plate, for the exactness with which the two curves could be made to coincide varied with the amount of grain structure fluctuations to be found on the microphotometer records. The time of exposure which made the density most sensitive to changes in intensity was determined roughly by trial. In Fig. 2, superposed microphotometer records are shown for a solution of rhodamine in glycerine, in one case when the two spectra were adjusted as nearly as possible to equal intensity and in the other when the width of one of the two slits was changed from 80 divisions to 82 divisions. From tests of this kind it seems safe to conclude that a change of 1 percent in the relative intensities of the two spectra could be detected with considerable certainty. There was no indication of errors due to variations in the emulsion from point to point; for after the two spectra were adjusted to equality exposures on different plates, or on different parts of the same plate, gave consistent results.

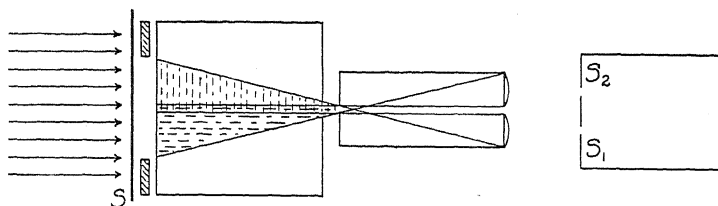


Fig. 3.

After the adjustment of the apparatus had been checked in this way one of the analyzing nicols was turned through 90° and the two bands were photographed again. By placing clear glass plates in the path of one of the exciting beams the intensities of the two bands were again made as nearly as possible equal. If the polarization of the fluorescence is the same for all wave-lengths it should be possible to bring the two microphotometer records into coincidence throughout the whole width of the fluorescence band.

To determine the actual magnitude of the polarization for the different solutions a Koenig-Martens spectrophotometer was used. Wawilow has described two methods by which the instrument may be utilized for such a determination,⁶ both of which involve the assumption that the polarization of the light entering one slit is the same as that entering the other. This

⁶ S. J. Wawilow, *Zeits. f. Physik*, 32, 721 (1925).

makes it advisable to observe the fluorescence in the direction of the incident light (Fig. 3) rather than at right angles (Fig. 4); for we find that the fluorescence light originating at a greater distance from the exciting source shows less polarization than that excited in those parts of the solution that are nearer the source. Two causes probably contribute to this result, namely: (1)

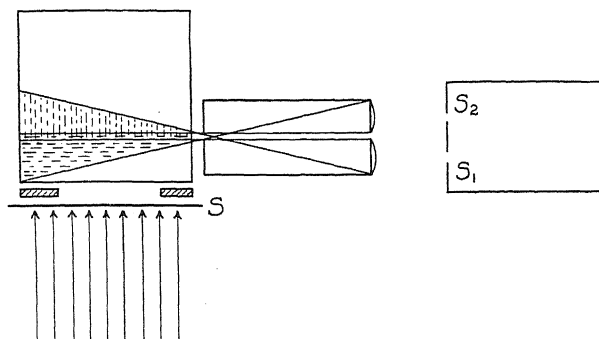


Fig. 4.

The longer wave-lengths in the exciting beam suffer greater absorption by the solution than do the shorter wave-lengths; so that the fluorescence from the front of the cell is excited by radiation whose average wave-length is longer than that of the exciting light which penetrates to the rear of the cell and excites fluorescence there. Since it has been shown experimentally that the percentage polarization becomes less as the wave-length of the exciting light is decreased,⁷ we should expect the polarization to be greatest where the exciting light enters the cell. (2) The fluorescence originating in the rear of the cell is partly excited by fluorescence light from the front of the cell, which is at most about 35 percent polarized. This weakly polarized exciting light results in fluorescence with much less polarization than that of the rays producing it

The results of measurements made with the cell arranged as in Fig. 3 are given in Table I. For each solution the instrument was set on the middle of

TABLE I. *Results of measurements with cell arranged as in Fig. 3.*

Uranine in glycerine		Method 1	Method 2	Average
gms/cc	gm mol/liter			
10^{-3}	.0027	21%	23%	22%
10^{-4}	.00027	36	38	37
10^{-5}	.000027	34	41	38
$10^{-3} + 10^{-2}$ Na_2CO_3		15	18	17
$10^{-4} + 10^{-3}$ Na_2CO_3		25	27	26
$10^{-5} + 10^{-4}$ Na_2CO_3		32	38	35

the fluorescence band and to gain intensity the slits were opened to 2 mm. No attempt was made to determine a possible variation of polarization

⁷ P. Fröhlich, *Zeits. f. Physik* 35, 193 (1926); W. L. Lewschin, *Zeits. f. Physik*, 26, 278 (1924)

throughout the band by the visual method. It will be noticed that the two methods give reasonably consistent results except for the most dilute solution. The differences probably result not so much from errors in setting as from a change in the distribution of the exciting light over the cell when the polarizing nicol is turned or removed.

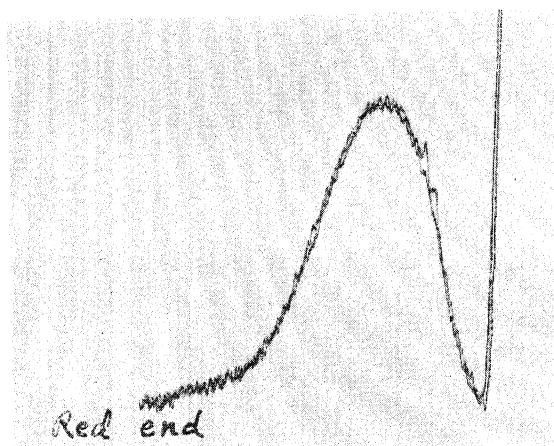


Fig. 5. Rhodamine-B in glycerine. Comparison of fluorescence produced by unpolarized exciting light with that excited by polarized light having the electric vector vertical. Observed from the side.

RESULTS

Three solutions of uranine in glycerine (concentrations 10^{-3} , 10^{-4} , and 10^{-5} gr/cc) and one of rhodamine-B in glycerine (concentration 10^{-4} gr/cc) were tested in this way. In some cases the comparison was between the

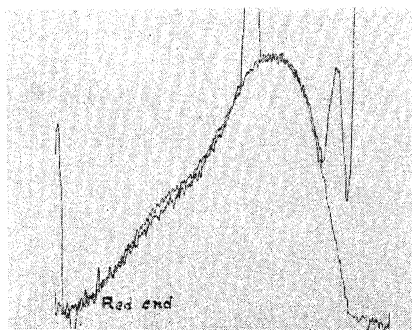


Fig. 6. Uranine in glycerine 10^{-5} gr/cc. Comparison of vertical and horizontal components of fluorescence produced by polarized exciting light.

fluorescence excited by unpolarized light and that observed when the excited light was polarized. In other cases the horizontally and vertically polarized components of the fluorescence light were compared.

For the rhodamine-B solution the fluorescence was found to be polarized to the same extent throughout the spectrum. The superposed microphotometer records for the polarized and unpolarized fluorescence are shown in Fig. 5.

In the case of uranine the microphotometer record sometimes showed a small band on the short wave-length side of the main band, probably corresponding to the similar small band found in the absorption spectrum. [See Fig. 6]. In the more concentrated solutions and in freshly prepared dilute solutions this small band did not appear. In neither band was there anything to indicate a variation of polarization with wave-length. The records indicate that the percentage polarization of the small band is distinctly greater than that of the principal band.

THE MOBILITY OF AGED IONS IN AIR

BY OVERTON LUHR AND NORRIS E. BRADBURY
PHYSICAL LABORATORY, UNIVERSITY OF CALIFORNIA

(Received September 2, 1930)

ABSTRACT

The mobility of air ions produced by x-rays has been measured by the simple Rutherford alternating current method. No change in mobility with age could be detected for ions aged as long as one second. The weighted average of the results gives 1.64 ± 0.05 and 2.25 ± 0.05 cm/sec per volt/cm for the mobilities of positive and negative ions respectively. No completely satisfactory explanation has been found for the continual decrease in the coefficient of recombination with age while the mobility remains unchanged. When moist air from the room was substituted for carefully dried air the mobility dropped to 1.4 and 1.8 cm/sec per volt/cm for positive and negative ions.

INTRODUCTION AND METHOD

IT HAS been recently shown in this laboratory¹ that the coefficient of recombination of gaseous ions produced by an x-ray flash decreases continuously as the ions are aged for times between 0.001 and two seconds. The effect was noted not only for ions formed in air, but for ions formed in argon, nitrogen, and other gases. Moreover, since the effect continues long after the ions have attained random distribution in the gas, it would seem that, after the very rapid "initial recombination", some other aging effect must be involved. This aging effect might consist of the formation of heavy ion clusters and a weeding out of the smaller, faster ions by selective recombination.

In view of these unexpected results obtained in measurements of the coefficient of recombination, it was thought worthwhile to measure the mobility of ions which had been aged over periods of time varying between 0.01 and 1 second. The recombination apparatus which has previously been described by L. C. Marshall,² and one of the authors¹ was slightly modified by the addition of an extra brush to the commutator system, thus permitting measurements of mobility by the simple Rutherford alternating current method.³ After the ions were formed by passing a flash of x-rays into the ionization chamber, they were allowed to age for various periods of time, and then drawn to the upper plate by an advancing potential applied through the commutator system. A bias of twenty percent or more was always maintained on the retarding potential to make sure that all the ions were removed before the conclusion of each cycle. In general, the aging periods, during

¹ O. Luhr, Phys. Rev. **35**, 1394 (1930); **36**, 24 (1930).

² L. C. Marshall, Phys. Rev. **34**, 618 (1929).

³ J. J. Thomson, Conduction of Electricity Through Gases, p. 102, 3rd Edition Cambridge, 1928.

which the volume of ionization was field-free, were long compared to the time required to sweep the ions out by the field. This would allow clustering and selective recombination to take place under the same conditions as in the recombination measurements.

It may be noted that, to the authors' knowledge, mobility measurements have never before been made with ions older than 0.1 second. Moreover, x-rays have seldom been employed in mobility measurements of any kind, especially in later years, and no specific effect has been noted.

RESULTS AND DISCUSSIONS

Figure 1 shows a typical series of curves for both positive and negative ions. The current in arbitrary units is plotted against the accelerating voltage and the straight part of the curves is extrapolated to the voltage axis.

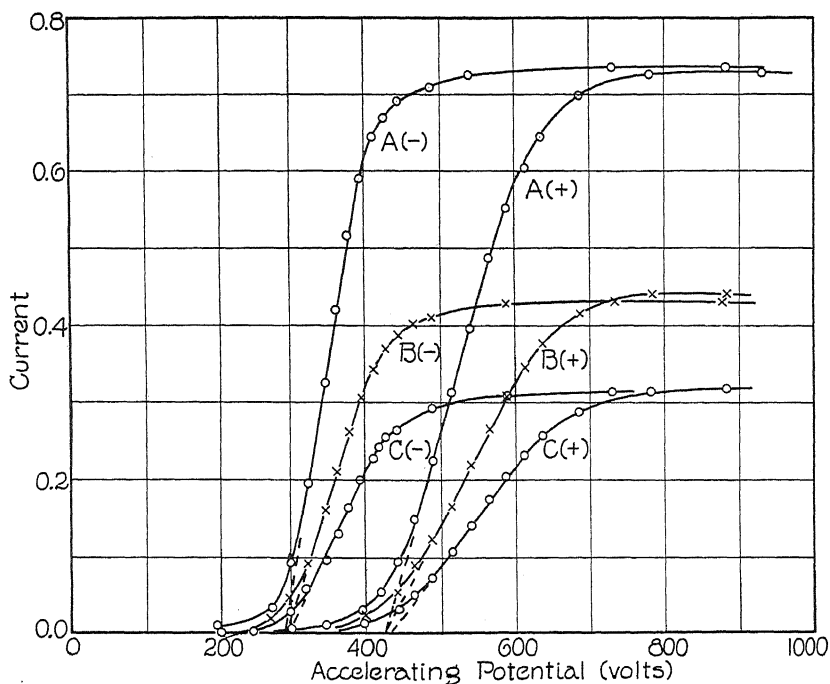


Fig. 1. Current plotted against voltage for negative and positive ions aged over periods of 0.06, 0.26, and 0.46 seconds for curves A, B, and C respectively. Extrapolation gives intercepts of 290 and 415 volts from which mobilities are calculated as 2.25 and 1.57 cm/sec per volt/cm for negative and positive ions.

The mobility is calculated from the relation $k = dD/VT$, where k is the mobility of the ions in cm/sec. per volt/cm, d is the distance from the volume of ionization to the collecting plate of the ionization chamber (5.9 cm), D is the distance between the plates (7.5 cm), V is the voltage at which the extrapolated line intercepts the axis, and T is the time the advancing voltage is applied.

The three series of curves, *A*, *B*, and *C* are for ions whose average ages were 0.06, 0.26, and 0.46 seconds respectively. These readings were all taken with the commutator revolving at the rate of one revolution per second, the setting being changed relative to the period of the x-ray flash to obtain the variation in age. The difference in saturation currents in the three cases shown represents the loss of ions by recombination during the time of aging. The mobilities obtained from the intercept points (415 volts and 290 volts) are: positive, 1.57; negative, 2.25. As can be seen from the figure, there is no evidence of the presence of more than one type of ion, or of any change in mobility with age which would result in different intercepts for the different curves.

The "asymptotic feet" obtained in every curve by this method throw a certain degree of uncertainty into the absolute value of the mobility. There is a sufficient straight portion in every case, however, to make the extrapolation quite certain, and better results can hardly be expected in a method of this kind where the volume of ionization is defined by the edges of an x-ray beam and where diffusion plays an important role.

The curves shown in Figure 1 are typical of a large number of runs, in which the age of the ions was varied between 0.01 and 1 second with commutator speeds of eight to one-half revolution per second. In no case was there any evidence of a decrease in mobility with age or of the presence of more than one type of ion. The weighted average of mobilities from some thirty runs was 1.64 for the positive ion and 2.25 for the negative. The results of each of the better runs fell within five percent of these values; so the absolute mobilities may be set at 2.25 ± 0.05 and 1.64 ± 0.05 . These values are in close agreement with those obtained by Loeb,⁴ Tyndall and Grindley, and other observers who have employed more accurate absolute methods.

In two cases values of the mobility markedly different from the average were obtained. The mobility was lowered to about 1.8 and 1.4 for negative and positive ions respectively when air from the room was substituted for the carefully purified air which had been passed through glass wool, sodium calcium hydrate, CaCl_2 , P_2O_5 , and liquid air traps. Such a result was to be expected as the effect of the presence of water vapor and other impurities in lowering the mobility is well known. The other case in which the value of the mobility differed considerably from the average was unexpected, and is probably worthy only of mention since the experimental conditions were very poor. If the driving field was low, and therefore the time of application long (i.e. slow commutator speed and long contact segment) the mobilities rose to values as high as three cm/sec for the negative ions and two cm/sec for the positive. In this case the driving field was of the order of ten volts/cm compared to fifty volts/cm when the best results were obtained. As conditions were the worst possible, with such factors as space charge, self-repulsion, and diffusion playing important roles, it is believed that the high values

⁴ L. B. Loeb, *International Critical Tables*, Vol. VI, p. 110, New York, 1929.

obtained are spurious. As in the other runs, there was no indication of a change in mobility with age.

It remains to discuss the question: What property of the ions can change with age so that the coefficient of recombination may become continually lower, while the mobility remains unchanged? A change of mass resulting from cluster formation would decrease the coefficient of recombination which, on the J. J. Thomson theory,⁵ is inversely proportional to the square root of the mass, but would not greatly affect the mobility which, according to the Langevin theory,⁶ varies for mass as $[(M+m)/m]^{1/2}$, a factor which at best could only decrease the mobility by a factor of the square root of two when the mass is increased from that of a single molecule to infinity. As it is probable that all ions have a mass considerably greater than that of a single molecule, it is very possible that an increase sufficient to reduce greatly the coefficient of recombination would not be detected in mobility measurements. However, such an increase in mass would very probably be accompanied by an increase of volume which must result in a shortening of the mean free path and a consequent decrease in the mobility proportional to that shortening. On the whole, the clustering and selective recombination hypotheses seem to be of doubtful tenability in the light of this experimental evidence. The solution to the problem may lie, then, in some change in the nature of the ion—possibly a redistribution of the electrical charge or a redistribution of the molecules in the cluster which makes the process of recombination more difficult, but does not change the mobility. Further speculation along this line is useless owing to a lack of definite knowledge concerning the nature of gaseous ions.

In conclusion, the authors wish to express their sincere appreciation to Professor Loeb for his guidance throughout the performance of these experiments.

⁵ L. B. Loeb and L. C. Marshall, *Jour. Frank. Inst.* 207, 371 (1929).

⁶ L. B. Loeb, *Kinetic Theory of Gases*, p. 468, New York, 1927

ON THE ENTROPY OF HYDROGEN*

BY D. MAC GILLAVRY

(Received August 9, 1930)

ABSTRACT

The entropy difference between ordinary hydrogen and hydrogen in perfect equilibrium, both in the solid phase at the absolute zero, has been calculated to be $(3/4)R \log 3 + R \log 4$. This value checks the result given by Giauque and Johnston. The method is the direct evaluation along a reversible path of $\int dQ/T$, under certain idealized assumptions, using partition functions. The thermodynamical and statistical aspects are examined.

IN a recent paper¹ I have indicated a theoretical way, by which the entropy difference between ordinary hydrogen and hydrogen in perfect equilibrium may be calculated. In this study I shall consider the details. With Fowler² I assume, that ordinary hydrogen is a mixture of para- and ortho-hydrogen in the fixed ratio 1:3, that thus transitions between para- and ortho-hydrogen do not occur in the ordinary mixture, and further, that para- and ortho-hydrogen and its different mixtures always have the same vapor pressure and the same heat of transition, so that the ratio 1:3 persists unchanged, when ordinary hydrogen is liquified or solidified. Recent experiments³ have shown that this last assumption is not exactly true. Calculations made on these assumptions must be regarded, therefore, only as first approximations.

All earlier investigations and measurements have shown that ordinary hydrogen, gaseous, liquid or solid, may behave like a substance in true equilibrium. We now must add, provided the experiments are not continued over too long a time. One may speak of reversible quasistatic changes of state, and thus, the entropy difference of ordinary hydrogen at higher and lower temperatures can be discussed.⁴ Going to rather high temperatures (above 500°C) the transition velocity becomes measurable, but at sufficiently high temperature we have again the proportion 1:3 anyway. It seems to me that there is no objection against idealizing the theory. Thus I suppose that the necessary experiments can be performed in such a short time, that the transition velocity may be regarded as negligibly small over the whole range of temperature. This concerns ordinary hydrogen.

* Contribution No. 635 from the Department of Chemistry, Columbia University, New York, N. Y.

¹ D. Mac Gillavry, *Rec. trav. chim.* **49**, 348 (1930).

² R. H. Fowler, *Proc. Roy. Soc. A* **118**, 52 (1928).

³ K. F. Bonhoeffer and P. Harteck, *Zeits. f. physik. Chem. Abt. B*, **4**, 113 (1929); *Naturwissenschaften* **17**, 182, 321 (1929). K. Clusius and K. Hiller, *Zeits. f. physik. Chem. Abt. B*, **4**, 158 (1929).

⁴ P. Ehrenfest and V. Trkal, *Verslag. Akad. Wetenschappen Amsterdam*, **28**, 906 (1920).

On the other hand one can discuss also the entropy of hydrogen in ideal perfect equilibrium. In this second case care should be taken that the experiments are extended over such a long time, that the transition velocity may be considered as extremely rapid. Or one can take advantage of suitable catalysts accelerating this transition velocity.⁵

Now, the difference between para- and ortho-hydrogen resides only in the different rotational states. But the masses of all the hydrogen molecules are equal and the distribution of translational velocities is exactly the same. Further the total entropy can always be written as the sum of the translational and the rotational entropy, disregarding at first the vibrational states. If we take gaseous ordinary and gaseous ideal hydrogen at the same temperature (and pressure), then the difference in entropy must be a difference in rotational entropy only. Also, according to the assumptions already made by Fowler (l.c.), the difference in entropy between solid ordinary and solid ideal hydrogen must be rotational entropy only; for either form the rotations in the solid phase can be described by the same partition function, which holds good for the corresponding gas phase. The rotational entropy, therefore, should be unaffected by a change in phase, if it were rigorously true, that the ratio of ortho- and para-hydrogen is not altered by a change of phase, in the case of ordinary, as well as in the case of ideal hydrogen.

In this paper I shall calculate the entropy difference at the absolute zero between the two solid forms of hydrogen (ordinary and ideal). The problem may be solved in this way. One calculates at first the rotational entropy difference between ordinary hydrogen at a very high temperature and at the absolute zero. One calculates in the same way the rotational entropy difference of ideal hydrogen at the same very high temperature and at the absolute zero. Finally one goes to the limit of infinitely high temperature. But at infinitely high temperature there is no difference between ordinary and ideal hydrogen. The distribution of energy over the rotational states becomes exactly the same at extremely high temperatures. *Therefore, the desired difference of entropy is obtained by simply subtracting the two indicated differences.* At the same time it is obvious, that one may disregard complications caused by vibrations and other mechanisms. In the neighborhood of absolute zero rotational states only are excited.

For the actual calculation we can best make use of the methods developed by Fowler. Although ordinary hydrogen is a mixture, we can omit at once the paradox term, for the ratio of the two constituents is assumed to remain exactly constant. The entropy η is related to the partition function F by the equation:⁶

⁵ K. F. Bonhoeffer and P. Harteck, reference 3. It is interesting to mention, that the catalysts, which catalyze the transitions between ortho- and para-hydrogen, also catalyze the combination of hydrogen and chlorine. Mellor in his *Comprehensive Treatise on Inorganic and Theoretical Chemistry* (Vol. II, page 159 top) says: "the mixed gases can be exploded by a piece of brick at 150°, while platinum black or charcoal may produce an explosion at ordinary temperature in the dark; in any case, they start the gases reacting—presumably by catalysis." Cf. *Rec. trav. chim.* 49, 348 (1930).

⁶ R. H. Fowler, *Phil. Mag.* 44, 823 (1922).

$$\eta_2 - \eta_1 = \left| \left(R + RT \frac{d}{dT} \right) \log F \right|_1^2. \quad (1)$$

The indices 1 and 2 indicate two states with temperature T_1 and T_2 ; the pressure does not influence the rotational properties of perfect gases. The partition function of ideal hydrogen is:

$$F_i = 1 + 5e^{-6\sigma} + 9e^{-20\sigma} + \dots + 3.3e^{-2\sigma} + 3.7e^{-12\sigma} + \dots = \phi_p + \phi_o, \quad (2.1)$$

and the partition function of ordinary hydrogen is:

$$F_c = (1 + 5e^{-6\sigma} + 9e^{-20\sigma} + \dots)^{1/4} \times (3.3e^{-2\sigma} + 3.7e^{-12\sigma} + \dots)^{3/4} = \phi_p^{1/4} \cdot \phi_o^{3/4}; \quad (2.2)$$

and where ϕ_p is the partition function for para-hydrogen:

$$\phi_p = 1 + 5e^{-6\sigma} + 9e^{-20\sigma} + \dots, \quad (3.1)$$

and ϕ_o is the partition function for ortho-hydrogen:

$$\phi_o = 3(3e^{-2\sigma} + 7e^{-12\sigma} + 11e^{-30\sigma} + \dots). \quad (3.2)$$

$$\sigma = h^2/8\pi^2IkT,$$

where h is the constant of Planck, k the constant of Boltzmann, I the moment of inertia. Thus, we have to form the expression:

$$\begin{aligned} \eta_c^* - \eta_i^* &= \{\eta_c(0) - \eta_c(\infty)\} + \{\eta_i(\infty) - \eta_i(0)\} \\ &= \lim_{T_2=\infty} \lim_{T_1=0} \left\{ - \left| R \left(1 + T \frac{d}{dT} \right) \log F_c \right|_1^2 + \left| R \left(1 + T \frac{d}{dT} \right) \log F_i \right|_1^2 \right\}. \quad (4) \end{aligned}$$

The indices c and i indicate ordinary and ideal hydrogen respectively.

That the substitution of F_i for ideal hydrogen and of F_c for ordinary hydrogen in formula (1) gives correct results, can be proved also with the general theorems given by Fowler in his monograph on "Statistical Mechanics." One finds on page 129 the theorem: that any particular species of free molecule contributes to the characteristic function of Planck:

$$k\bar{M} \left\{ \log \frac{F(T)}{\bar{M}} + 1 \right\}, \quad (5)$$

where \bar{M} is the average number present in the specified equilibrium state.⁷ One gets the entropy from Planck's characteristic function by applying the operator $(1 + T d/dT)$. Thus any entropy difference of ideal hydrogen, for instance, is given by:

$$\frac{\eta_{i2} - \eta_{i1}}{R} = \left| \left(1 + T \frac{d}{dT} \right) \left(\log \frac{F_i}{N} + 1 \right) \right|_1^2$$

⁷ Combination of the two theorems on page 128 and 129.

$$\begin{aligned}
&= \left| \left(1 + T \frac{d}{dT} \right) \log F_i \right|_1^2 + \left| \log \frac{1}{N} + 1 \right|_1^2 \\
&= \left| \left(1 + T \frac{d}{dT} \right) \log F_i \right|_1^2,
\end{aligned} \tag{1}$$

then \overline{M} here equals N , Avogadro's number, if we employ molar entropies.

It may be instructive to interpret ideal hydrogen also as a mixture of para- and ortho-hydrogen, between which two forms equilibrium has been established. One verifies easily that:⁸

$$\overline{M}_{pi} = \frac{\phi_p}{\phi_p + \phi_o} \times N \quad \text{and} \quad \overline{M}_{oi} = \frac{\phi_o}{\phi_p + \phi_o} \times N. \tag{6}$$

We first get:

$$\begin{aligned}
\frac{\eta_{i_2} - \eta_{i_1}}{R} = \\
\left| \left(1 + T \frac{d}{dT} \right) \left\{ \frac{\phi_p}{\phi_p + \phi_o} \left(\log \frac{\phi_p}{\overline{M}_{pi}} + 1 \right) + \frac{\phi_o}{\phi_p + \phi_o} \left(\log \frac{\phi_o}{\overline{M}_{oi}} + 1 \right) \right\} \right|_1^2,
\end{aligned}$$

which becomes:

$$\begin{aligned}
&\left| \left(1 + T \frac{d}{dT} \right) \left\{ \frac{\phi_p}{\phi_p + \phi_o} \log F_i + \frac{\phi_o}{\phi_p + \phi_o} \log F_i \right\} \right|_1^2 \\
&+ \left| \left(1 + T \frac{d}{dT} \right) \left\{ \frac{\phi_p}{\phi_p + \phi_o} \left(\log \frac{1}{N} + 1 \right) + \frac{\phi_o}{\phi_p + \phi_o} \left(\log \frac{1}{N} + 1 \right) \right\} \right|_1^2 \\
&= \left| \left(1 + T \frac{d}{dT} \right) \log F_i \right|_1^2.
\end{aligned} \tag{1}$$

The functions ϕ_p and ϕ_o depend on the temperature T .

I leave it to the reader to derive in an analogous way the formula for the entropy differences of ordinary hydrogen. I recall only that the concentrations of the para- and the ortho-forms now have the constant values:

$$(\overline{M}_p)_c = \lim_{T=\infty} (\overline{M}_p)_i = \lim_{T=\infty} \frac{\phi_p}{\phi_p + \phi_o} N = \frac{1}{4} N, \tag{7.1}$$

$$(\overline{M}_o)_c = \lim_{T=\infty} (\overline{M}_o)_i = \lim_{T=\infty} \frac{\phi_o}{\phi_p + \phi_o} N = \frac{3}{4} N. \tag{7.2}$$

The omission of the paradox terms from the two terms of equation (4) is legitimate, since they cancel if they are not omitted.

⁸ Cf. R. H. Fowler, *Statistical Mechanics*, p. 30 formula (51), or p. 106 formulae (310) and (311).

Equation (4) represents exactly

$$\int \frac{dQ}{T} = \int d\eta = \int \frac{c_r}{T} dT,$$

the integral taken along the reversible way examined in this study. It must be possible to check the theory experimentally step by step, measuring heat capacities, as is always done. From the thermodynamical arguments used thus far it is evident, that no further term has to be added to the two terms of equation (4).

Now, we regroup the terms of expression (4) in a more convenient way, omitting the indices 1 and 2:

$$\frac{\eta_c^* - \eta_i^*}{R} = \lim_{T=0} \left(1 + T \frac{d}{dT} \right) \log \frac{F_c}{F_i} - \lim_{T=\infty} \left(1 + T \frac{d}{dT} \right) \log \frac{F_c}{F_i}. \quad (4a)$$

We introduce two new functions, defined by the equations:

$$\begin{aligned} \phi_o &= e^{-2\sigma} \phi_o', \\ F_c &= (e^{-2\sigma})^{3/4} F_c' = e^{-3\sigma/2} F_c'; \end{aligned}$$

and we substitute F_c' in the first term of (4a), noticing that always:

$$\left(1 + T \frac{d}{dT} \right) \log e^{-a/T} = \left(1 + T \frac{d}{dT} \right) \left(-\frac{a}{T} \right) = -\frac{a}{T} + \frac{a}{T} = 0;$$

thus:

$$\frac{\eta_c^* - \eta_i^*}{R} = \lim_{T=0} \left(1 + T \frac{d}{dT} \right) \log \frac{F_c'}{F_i} - \lim_{T=\infty} \left(1 + T \frac{d}{dT} \right) \log \frac{F_c}{F_i}.$$

I will give the results at once:

$$\lim_{T=0} \log \frac{F_c'}{F_i} = \log 1^{1/4} \cdot 9^{3/4} = \log 9^{3/4}; \quad (8.1)$$

$$\lim_{T=0} T \frac{d}{dT} \log \frac{F_c'}{F_i} = 0; \quad (8.2)$$

$$\lim_{T=\infty} \log \frac{F_c}{F_i} = \log \left(\frac{1}{4} \right)^{1/4} \left(\frac{3}{4} \right)^{3/4}; \quad (8.3)$$

$$\lim_{T=\infty} T \frac{d}{dT} \log \frac{F_c}{F_i} = 0. \quad (8.4)$$

Thus:

$$\eta_c^* - \eta_i^* = R \log 9^{3/4} - R \log \left(\frac{1}{4} \right)^{1/4} \left(\frac{3}{4} \right)^{3/4} = \frac{3}{4} R \log 3 + R \log 4. \quad (9)$$

The mathematical material, necessary for the justification of equations (8), has already been furnished by Fowler.⁹

This analysis is sound from a thermodynamical standpoint. However, a statistician may ask, does expression (4) really represent the desired entropy difference? Should not a third term be added? At higher temperatures ordinary and ideal hydrogen have the same internal energy and the same specific heat of rotation. At one time it has been supposed that transitions were prohibited, and at a later time it has been supposed that transitions do occur. Does not this different viewpoint necessitate a third term? Let us now add a third term, representing the entropy difference arising from those two viewpoints:

$$\eta_c(\infty) - \eta_i(\infty),$$

using again the most general theorems; then the operator

$$\text{Lim}_{T=\infty} R(1 + T d/dT)$$

has to work on the expression:

$$\begin{aligned} & \frac{1}{4} \left(\log \frac{\phi_p}{N/4} + 1 \right) + \frac{3}{4} \left(\log \frac{\phi_o}{3N/4} + 1 \right) - \left(\log \frac{F_i}{N} + 1 \right) \\ &= \log \phi_p^{1/4} \phi_o^{3/4} - \log \left(\frac{1}{4} \right)^{1/4} \left(\frac{3}{4} \right)^{3/4} + \left(\log \frac{1}{N} + 1 \right) - \log F_i - \left(\log \frac{1}{N} + 1 \right) \\ &= \log \frac{F_c}{F_i} - \log \left(\frac{1}{4} \right)^{1/4} \left(\frac{3}{4} \right)^{3/4}. \end{aligned}$$

The application of the operator $\lim_{T=\infty} R(1 + T d/dT)$ yields zero,¹⁰ in accordance with the thermodynamical considerations.

We may consider hydrogen as a mixture, if the experiments do not take much time, and we may consider hydrogen as a single gas, if we always wait a sufficiently long time. The entropy of hydrogen in equilibrium at higher temperatures can not depend on the length of time we keep it in a vessel. The equality can only be obtained in statistics by inserting the appropriate paradox terms (logarithmic terms), and for hydrogen considered as a mixture, and for hydrogen considered as a single gas; then the term representing the difference vanishes. Here we have a case, that a mixed gas has the same entropy as a single gas (see below).

Let us now consider the analysis more carefully. From thermodynamical considerations two terms have arisen:

$$\eta_c(0) - \eta_c(\infty) \quad \text{and} \quad \eta_i(\infty) - \eta_i(0).$$

To complete the argument from a statistical standpoint a third term has been added:

⁹ One may refer concerning the limits (8.1) and (8.2) to Proc. Roy. Soc. A118, 52 (1928), and concerning the limits (8.3) and (8.4) to Statistical Mechanics p. 52, 53, and also Phil. Mag. 45, 11 (1923).

¹⁰ See equations (8.3) and (8.4).

$$\eta_c(\infty) - \eta_i(\infty).$$

In this way we have come to the equation:

$$\eta_c^* - \eta_i^* = \eta_c(0) - \eta_i(0) = \{\eta_c(0) - \eta_c(\infty)\} + \{\eta_c(\infty) - \eta_i(\infty)\} + \{\eta_i(\infty) - \eta_i(0)\},$$

which is trivial mathematically. It is obvious, that the mathematical calculation can at once be shortened in just this way, provided the general theorems are applied throughout. Therefore, we get:

$$\begin{aligned} & \frac{\eta_c(0) - \eta_i(0)}{R} \\ &= \lim_{T=0} \left(1 + T \frac{d}{dT} \right) \left\{ \frac{1}{4} \left(\log \frac{\phi_p}{N/4} + 1 \right) + \frac{3}{4} \left(\log \frac{\phi_o}{3N/4} + 1 \right) - \left(\log \frac{F_i}{N} + 1 \right) \right\} \\ &= \lim_{T=0} \log \frac{F_c'}{F_i} - \frac{1}{4} \log \frac{1}{4} - \frac{3}{4} \log \frac{3}{4}. \end{aligned} \quad (10)$$

Giauque and Johnston¹¹ give for this quantity

$$\eta_c^* - \eta_i^* = R \left(-\frac{1}{4} \log \frac{1}{4} - \frac{3}{4} \log \frac{1}{12} \right) = \frac{3}{4} R \log 3 + R \log 4, \quad (9a)$$

which is exactly our value. They consider ordinary hydrogen at the absolute zero as a mixture of para-hydrogen and of nine species of ortho-hydrogen, in accordance with the weight factor 3×3 of the lowest ortho-state. Although our final result is the same, Giauque and Johnston's interpretation of quantity (9a) as a paradox term does not seem *a priori* plausible. We do not compare ordinary hydrogen with the total of the separated constituents, but with 100% para-hydrogen. The conception of nine species of ortho-hydrogen is confined to the absolute zero, whereas our analysis, following Fowler, is generally applicable.

Fowler¹² gives the quantity $(3/4)R \log 9$, which value is not confirmed by the above given analysis. In fact, only the first term of expression (9) is given by Fowler. The second term, a paradox term, has resulted from our general *uniform* analysis. *This paradox term is intrinsic to entropy*. Its significance for diffusion problems constitutes only a special case.

In the monograph on Statistical Mechanics, page 163, one weight factor 3 is retained as an experiment, i.e., a correction $(3/4)R \log 3$ is used. The argument is, that nuclear weights must pursue hydrogen through all its combinations. If a nuclear spin accompanies hydrogen in all compounds, then I prefer to apply the full correction (9) to hydrogen and separate corrections to its combinations.

I am very much indebted to Dr. G. van Hasselt, Amsterdam, for many extensive discussions of the mathematical questions, and to Professor V. K. La Mer for the preparation of the manuscript.

¹¹ W. F. Giauque and H. L. Johnston, J. Am. Chem. Soc. 50, 3221 (1928).

¹² R. H. Fowler, Proc. Roy. Soc. A118, 52 (1928).

A NEW RELATIVITY THEORY OF THE
UNIFIED PHYSICAL FIELD

BY WILLIAM BAND

PHYSICS DEPARTMENT, YENCHING UNIVERSITY, PEPING, CHINA

(Received May 1, 1930)

ABSTRACT

This theory abandons the attempt to geometrize physics. Its aim is to give invariant differential equations of motion for mass-charge particles in regions where the indeterminacy of position and momentum is not significant.

Eddington's displacement rule is used to define an indeterminate vector field, and a simple generalization of it is used to define an indeterminate tensor field. The vector field gives the possible velocity of a mass-charge particle at any point, and vector lines in the field are necessarily the tracks of the particle. The tensor field defines an invariant element of arc by means of which the orbit equations are given in the familiar parametric form.

Physical or actual fields are necessarily determinate functions and are defined by the variations of the indeterminate fields round closed loops in the usual way; but an alternative definition is suggested which does not depend upon such abstract processes. The usual identifications of the gravitation and electric field tensors give the classical laws for small fields. In the pure gravitation field the vector lines become Einstein's "geodesics", and for negligible gravitation field they become the empirical equations of motion of a charge in regions remote from atomic nuclei.

The theory is purely a descriptive apparatus, and its usefulness is definitely limited by the principle of indeterminacy. This admitted limitation enables the theory to avoid the inconsistency between field and atomic theory, an inconsistency which appears as merely the result of ignoring the limitation.

INTRODUCTION

ALL unified field theories have hitherto been attempts to geometrize completely the theory of the physical field: and such is the loyalty to the geometrical ideal that quite unintelligible properties are introduced such as non-integrable length and generalized parallel displacement. Such geometrical analogies are entirely useless as aids to imaginative conception¹ and therefore, in the writer's opinion, a hindrance to sound mathematics and to further progress. In the present theory geometrical interpretation is dispensed with. Stated briefly the aim of the theory is to derive a spacetime description of the motion of a material particle in regions where the indeterminacy in the particle's position and momentum is not significant; the motion being given by differential equations of invariant form.

Apart from Whitehead's theory² which does not appear to have attracted much attention, and which was based on the reactionary principle of absolute

¹ For a statement of the opposite view see Eddington's "The Mathematical Theory of Relativity" Art. 83.

² Dr. A. N. Whitehead, "The Principle of Relativity" Chaps. IV, V.

acceleration, the theory of O. Klein³ appears to be the only theory which has succeeded in so deriving the equations of motion of charged particles in electric fields. Since the latter theory introduces an unknowable fifth dimension, it would seem less satisfactory than the present one which requires no such *ad hoc* hypothesis.

The writer has tried so to state the theory that it shall be obviously nothing more than a descriptive apparatus: not its validity, but only its usefulness as an apparatus depends upon the existence of the entities whose motions it proposes to describe. The limits to the usefulness of the method come out quite clearly when the fact of indeterminacy is taken into account. Thus the present theory will lead to the classical result that an accelerated electron must radiate energy, but it also contains the admission that such a result is meaningless when the acceleration is large and taking place in fields close to atomic nuclei. This seems to be a distinct advance on the classical theory, at least as usually stated; for no such admission is contained in the latter theory.

Thus the present theory suggests that the apparent inconsistency between the field theory and atomic theory is nothing more, in all probability, than a limitation in the usefulness of the field theory due to the fact of indeterminacy. Once the exact nature of this limited usefulness is defined the inconsistency evaporates.

I. THE VECTOR FIELD OF POSSIBLE VELOCITY

Begin with space time coordinates x_i , $i = 1, 2, 3, 4$, and the fundamental array Γ_{jk}^i , $i, j, k = 1, 2, 3, 4$. The latter is composed of sixty four independent continuous single-valued functions of the coordinates.

Select arbitrarily a 4-vector A^r at a definite point x_i and proceed by the rule

$$dA^r = -\Gamma_{si}^r A^s dx_i \quad (1)$$

to construct a vector field, by defining

$$A'^r = A^r + dA^r$$

at

$$x_i' = x_i + dx_i.$$

The field at any point will depend upon the track along which the rule (1) has been applied. We shall call this field the field of possible velocity, and use it to describe the motions of particles.

A vector line in this field will be a line, every element of which has coordinate components proportional to the components of the vector at the point; and so defined, will be the track of a particle with the corresponding initial conditions. The equations of a vector line follow immediately from Eq. (1) as

$$d^2x_i = -\Gamma_{jk}^i dx_j dx_k. \quad (2)$$

This is a set of four differential equations of the second order, their solutions containing eight arbitrary constants, the four components of initial velocity and the coordinates of the starting point.

³ O. Klein Zeits. f. Physik 46, 188 (1927).

II. THE FUNDAMENTAL TENSOR FIELD

Erect, again at any initial point, the (symmetrical tensor) components a_{ik} and just as in §1, define a tensor field by

$$\begin{aligned} da_{ik} &= (a_{rk}\Gamma_{is}^r + a_{ir}\Gamma_{ks}^r)dx_s \\ - da^{ik} &= (a^{rk}\Gamma_{rs}^i + a^{ir}\Gamma_{rs}^k)dx_s \end{aligned} \quad (3)$$

where a^{ik} is the usual normalised subdeterminant of a_{ik} .

An associated covariant vector

$$A_i = a_{ik}A^k$$

may be defined at any point, and combining Eqs. (1) and (3) shows

$$dA_i = \Gamma_{is}^k A_k dx_s. \quad (1')$$

Provided we remember that Eqs. (3) are not integrable, and that therefore the double partial differentiation of the a_{ik} 's is non-commutative, they can be expressed in the form

$$\partial a_{ik}/\partial x_s = a_{rk}\Gamma_{is}^r + a_{ir}\Gamma_{ks}^r \text{ etc.} \quad (3')$$

Insert these equations in the usual definition of the Christoffel three-index symbol of the second kind, we deduce that, if we put

$$\Delta_{jk}^i = \frac{1}{2}(\Gamma_{jk}^i + \Gamma_{ki}^j) \quad (4)$$

$$\nabla_{jk}^i = \frac{1}{2}(\Gamma_{jk}^i - \Gamma_{ki}^j) \quad (4')$$

then

$$\{ij, k\} = \Delta_{ij}^k + a_{ri}a^{ks}\nabla_{sj}^r + a_{rj}a^{ks}\nabla_{si}^r. \quad (5)$$

Using Eqs. (4), (4'), and (5), Eq. (2) becomes

$$d^2x_i + \{jk, i\}dx_jdx_k = 2a_{rj}a^{is}\nabla_{sk}^rdx_jdx_k. \quad (2')$$

III. FUNDAMENTAL INVARIANTS

If we define invariant

$$A^2 = A_s A^s$$

we can show by Eqs. (1) and (1') that the value of A is a constant independent of position, depending only on the initial values of A_s , A^s . Similarly if we define the invariant

$$ds^2 = a_{ij}dx_idx_j \quad (7)$$

and apply the rule of association

$$d \cdot dx_k = -\Gamma_{ij}^k dx_idx_j \quad (1'')$$

the value of ds will also be a constant depending only on the initial values of the displacement ds_i and the tensor a_{ij} . Comparison of Eqs. (1'') and (2)

shows that we may therefore use ds as an invariant differential to give the Eqs. (2) the form

$$d^2x_i/ds^2 + \Gamma_{jk}^i dx_j/ds dx_k/ds = 0. \quad (8)$$

Since ds is an invariant for coordinate transformations, we may use the variation equation

$$\delta \int ds = 0$$

to deduce⁴ the tensor character of the expression

$$d^2x_i + \{jk, i\} dx_j dx_k = t^i \quad (10)$$

and as usual also the tensor

$$D^{ij}_{,k} = \partial D^{ij} / \partial x_k + \{sk, i\} D^{sj} + \{sk, j\} D^{si}. \quad (11)$$

and the similar derivatives of tensors of different order.

Note that although (10) is a tensor at any point, it is not a determinate function of position; solutions of (9) are not fixed by the initial conditions, as are those of Eq. (2).

IV. ACTUAL PHYSICAL FIELDS

We have introduced the idea of a possible field, indeterminate at any point, but actual fields will be determinate at every point. Such fields may be obtained from the fundamental array in the usual way.

Thus the total change in the possible vector field on going round a closed space-time track is⁵

$$\Delta A^i = -\frac{1}{2} \iint *B^i_{jrs} A^j dS^{rs} \quad (12')$$

and similarly the change in the tensor field is⁶

$$\Delta a_{ij} = -\frac{1}{2} \iint (a_{kj} *B^k_{irs} + a_{ik} *B^k_{jrs}) dS^{rs} \quad (12'')$$

where

$$*B^r_{ijk} = -\partial \Gamma_{ij}^r / \partial x_k + \partial \Gamma_{ik}^r / \partial x_j + \Gamma_{ik}^s \Gamma_{sj}^r - \Gamma_{ij}^s \Gamma_{sk}^r \quad (12)$$

is a tensor determined by the array.

Define as usual

$$*R_{ij} = *B^r_{ijr} \quad (13)$$

$$*G_{ij} = \frac{1}{2}(*R_{ij} + *R_{ji}) \quad (13')$$

⁴ For an alternative deduction of the tensor character of (11) see the writer's "Mathematical Properties of a Continuum with Indeterminate Metric" shortly appearing in the P. R.S.

⁵ See Eddington, reference 1, Art. 92.

⁶ The proof of this is analogous to that of the preceding equation.

and

$${}^*F_{ij} = {}^*B_{rij} \quad (13'')$$

Then by Eq. (12) we can show that

$${}^*F_{ij} = \partial \Gamma_{si}^s / \partial x_j - \partial \Gamma_{sj}^s / \partial x_i \quad (14)$$

or that

$${}^*F_{ij} = {}^*K_{i,j} - {}^*K_{j,i} \quad (14')$$

where

$${}^*K_i = \Gamma_{si}^s + \partial f / \partial x_i \quad (14'')$$

in the original coordinates, but transforms as a vector; f being any function of position, invariant.

An alternative antisymmetrical tensor⁷ may also be defined by

$${}^*H_{ij} = {}^*K'_{i,j} - {}^*K'_{j,i} \quad (15)$$

where

$${}^*K'_i = \nabla_{is}^s. \quad (15')$$

In what follows no difference results from using ${}^*H_{ij}$ instead of ${}^*F_{ij}$.

(a). Pure gravitation field.

Let us limit our choice of the 64 array-components at any point by the twenty-four independent equations

$$\nabla_{jk}^i = 0. \quad (16)$$

Then Eqs. (4'), (4) and (5) show that Eq. (12) reduces to the classical Riemann-Christoffel tensor, both (15) and (13'') vanish, and (13') becomes Einstein's symmetrical field tensor. By virtue of (12'') the components a_{ij} become determinate functions of position, Eqs. (3) becoming mere identities. In this case therefore our theory is simply a restatement of Einstein's from a new point of view; the vector lines or particle orbits, becoming Einstein's so-called geodesics.

(b). Negligible gravitation field.

We wish to study the field of a small charged particle, in particular, of an electron. The gravitation field of an electron may be neglected⁸ to a first approximation, and if zero external gravitation field is taken then we may take the three index symbols as zero both in the orbit Eqs. (2') and in the derivatives (11).

Maxwell's first set of laws

$$\partial F_{ij} / \partial x_k + \partial F_{jk} / \partial x_i + \partial F_{ki} / \partial x_j = 0 \quad (17)$$

are identically satisfied if either (14) or (15) are used as the electric field tensor; and his second set

$$J^i = \partial F^{ij} / \partial x_j \quad (17')$$

⁷ For proof (of tensor nature) refer to the paper mentioned in reference (4) above.

⁸ See Eddington, reference 1, Arts. 78, 80.

are satisfied to the degree of approximation assumed, if we define

$$J^i = {}^*F^{ij}{}_{,j}. \quad (18)$$

Again we have approximately

$$\partial^2 D_i / \partial x_j \partial x_k = D_{i,jk} = D_{i,kj}$$

so that by (14') and (18)

$$J_{i,j} = a^{rs}({}^*K_{i,r} - {}^*K_{r,i})_{,js} = a^{rs}({}^*K_{i,jrs} - {}^*K_{r,sij})$$

or

$$J_{i,j} - J_{j,i} = a^{rs}({}^*K_{i,i} - {}^*K_{j,i})_{,rs}$$

giving

$$a^{rs}{}^*F_{ij,rs} = J_{i,i} - J_{j,i} \quad (19)$$

A solution of this⁹ is

$${}^*F_{ij} = (1/4\pi) \iiint (1/r)(J_{i,i} - J_{j,i}) dv \quad (20)$$

which gives the field at distance r from the volume dv containing the current density J_i . Suppose the current $J_i dv$ is due to a charge e moving with a velocity A_i , then $J_i dv = eA_i$, so that Eq. (20) becomes

$${}^*F_{ij} = (1/4\pi)(e/r)(A_{i,i} - A_{j,i})$$

or, by (1') and (4')

$${}^*F_{ij} = 2\nabla_{ij}{}^k A_k e / 4\pi r. \quad (21)$$

If the charge e is not considered a point singularity, it must be supposed to be such that each element has the same velocity, and Eq. (21) to have been integrated over the volume dv containing e .

Construct any sphere of radius a completely enclosing the charge e ; then it is easy to show that the average of the values of de/r at all points over the surface of the sphere is de/a , so that the average of e/r is also e/a , and the average of the field taken over the surface of the sphere will therefore be

$$F_{ij}' = \frac{e}{4\pi a} 2\nabla_{ij}{}^k A_k. \quad (21')$$

Suppose now that the external field varies only so slowly that its variation over the sphere of radius a can be neglected, then we may assume that it is possible to choose the sphere so that the external field F_{ij}'' is equal and opposite to the average F_{ij}' ; this sphere will be defined as the boundary of the charged particle, or even as the particle itself. Actually the sphere is only an approximation: a more accurate definition would be the surface, assumed to exist, over which the external field just balances the corpuscle's field at every point.

⁹ See Eddington, reference 1, Arts. 72, 74.

Granting this assumption,¹⁰ that the particle is bounded by a surface of zero field, the equations of motion of the charge e are given by putting in (2')

$$a_{rj}dx_j/ds = A_r, dx_k/ds = A^k,$$

and

$$2\nabla_{sk}{}^r A_r = (4\pi a/e)F_{sk}' = - (4\pi a/e)F_{sk}''$$

giving, of course with the approximation mentioned before,

$$m = e^2/4\pi a, m d^2 x_i/ds^2 = - e A^r F_{ri}'' \quad (22)$$

which, if m be interpreted as the mass of the particle, are the empirical equations of motion of charged particles, in regions where the field F_{ij}'' is not sensibly varied over the volume occupied by the charge.

V. THE PRINCIPLE OF INDETERMINACY

Heisenberg's principle of indeterminacy shows that the vector line method cannot give anything more than an approximate description of phenomena, for to do so it requires an exact knowledge of the initial conditions. The degree of approximation can be roughly estimated, however.

Let q, p be a typical pair of coordinates and momentum components actually measured as the initial conditions of the particle, and let the estimated uncertainties be $\Delta q, \Delta p$; definite values satisfying

$$\Delta q \cdot \Delta p = 0(\hbar). \quad (23)$$

Describe a sphere of diameter D and centre q , where

$$D > \Delta q, \text{ and } D - \Delta q = 0(\Delta q). \quad (24)$$

If this sphere is moved so that its centre follows the track found by putting the measured initial conditions in (22), then the particle will certainly remain within the sphere for a finite time T . The greater T or the smaller Δq and D , the more useful the vector line description, and vice versa. We must be careful not to assert that if exact initial conditions could be found, then Eqs. (22) would give an exact description of the motion; for such an assertion can never be experimentally verified. Essentially, therefore the time T must be determined experimentally in every case; it is not possible to deduce from the purely abstract descriptive apparatus any binding limits to its applicability; an appeal to experiment must be made.

Nevertheless the following argument which, for the above reasons, cannot claim to be rigorous, may not be without interest.

In zero external field, (that is zero after the initial measurements have been made) an electron obeying Eq. (22) will move with its initial velocity unchanged. Any initial discrepancy between its measured and its "actual"

¹⁰ Eddington's assumption (reference 1, Art. 80) that the two fields neutralise each other throughout the volume occupied by the charge could be used here just as well, but the one given in the text seems to be a useful alternative.

velocity will be transmitted as it were along its motion unchanged. Hence the time T in which the electron may drift out of the sphere of diameter D mentioned above will be

$$T = (D - \Delta q)/\Delta v$$

or by Eq. (23)

$$= (m/h)(D - \Delta q)(\Delta q) \quad (25)$$

For the electron $(m/h) = 0(1)$ so that by Eq. (24)

$$T = 0(\Delta q^2).$$

Suppose the initial velocity is measured as 10^8 cm/sec; and allow an uncertainty of no more than 10^3 cm/sec. Then by Eq. (23) the uncertainty in the initial position will be of the order of 10^{-3} cm. Thus T is of the order of 10^{-6} sec. and the length of track traversed in that time of the order of 100 cm.

When the field is not zero the initial discrepancy is not transmitted unchanged and the value of T becomes correspondingly uncertain, in general less. When the field varies so rapidly with position that it is sensibly different for different points within the sphere D , the various possible tracks starting from the points of Δq will in general diverge so rapidly that the sphere D will contain them only for a uselessly short time.

This non-rigorous argument thus leads us to suspect that in regions near atomic nuclei, where the space-variation of the field is great, the vector line method becomes useless; a result which is in full agreement with experimental data.

Independent of this argument is the further possibility that in the non-uniform fields near atomic nuclei, the boundary of the electron as defined in §4 can no longer exist. In this case the electron would cease to function as a particle and the process of deriving Eqs. (22) would no longer be possible.

LETTERS TO THE EDITOR

Prompt publication of brief reports of important discoveries in physics may be secured by addressing them to this department. Closing dates for this department are, for the first issue of the month, the twenty-eighth of the preceding month; for the second issue, the thirteenth of the month. The Board of Editors does not hold itself responsible for the opinions expressed by the correspondents.

Effect of Electric Field upon X-ray Diffraction Pattern of a Liquid

McFarlan's small positive effect (Phys. Rev. 35, 1469 (1930)) of an applied electric field on the x-ray diffraction halo of nitrobenzene is both interesting and important. He finds a definite increase of intensity at the maximum in the halo. He evidently favors the following suggestion: "The effect of the field is to bring about a more orderly arrangement of the molecular scattering centers with an increased regularity in the spatial distribution of these centers."

Attention should be called to the view that the nitrobenzene has a group structure without the electric field, and that the field, acting on the relatively large electric moment of each group, caused a change in the number of groups per unit volume oriented at any angle. The second is more acceptable for the following reasons:

(a) The existence of the semi-orderly, temporary groups (cybotaxis) accounts most readily for the numerous experiments in x-ray liquid diffraction in this laboratory and elsewhere.

(b) There is no reason to anticipate that the applied electric field would be powerful enough to alter the internal regularity of a group. McFarlan's computation on the effect on a single independent molecule shows that its orientation is negligible.

(c) Similarly there is not sufficient reason

to anticipate that the applied electric field would increase the size of the individual groups, and one could not be certain that such an increase would result in an increase in intensity, for the groups are imperfect and cannot be treated as small crystals.

(d) The effect of the electric field would be noticeable on these groups on account of the large value of the moment. Indeed, from McFarlan's experiments one can estimate the size of these groups, if one assumes either a permanent or an induced electric moment.

(e) The adoption of the group view explains both the original diffraction effect and the change caused by the field. As already said, it seems to the writer that the second view is much more plausible.

I may be permitted to emphasize McFarlan's suggestion that "the effect just described is not associated with the Kerr effect." An illustration may be given of the vast difference in similar optical and x-ray effects. Para-azoxyanisole in the liquid crystalline and, at higher temperatures, the transparent states, gives practically the same x-ray diffraction effect, though one is optically anisotropic and the other isotropic. The optical effects do not require crystallinity in the x-ray sense.

G. W. STEWART

University of Iowa

September 17, 1930

Interpretation of the Spectra of CaF and SrF

In the course of a search for isotope effects in the band spectra of the alkaline earth fluorides, we have obtained high dispersion spectrograms of the visible CaF and SrF bands in both emission and absorption. With CaF, the faint bands expected for Ca^{40}F could not be observed, as they would in all cases

be masked by the Ca^{40}F system. The SrF bands, however, are favorably placed for the detection of the lighter isotope, Sr^{86} , and we have identified several Sr^{86}F heads accompanying the main Sr^{88}F heads in the $(v+1, v)$ sequence of the yellow-green system. They lie to the violet of the main heads, the

average isotopic displacement of the first six members being 0.92 cm^{-1} . The mean deviation of observed from calculated displacements is only 0.03 cm^{-1} , and no trend is evident. By visual estimates the relative intensity of the Sr^{86}F to the Sr^{88}F bands is considerably below that predicted by the calculated abundance ratio, 1 to 5.5. Combined with a similar observation by Aston¹ with the mass-spectrograph, this indicates either an exceptionally large packing fraction for Sr, or an error in the accepted atomic weight.

By comparing these spectra in emission and absorption, we are able to draw conclusions about the rotational structure of the bands, direct measurement of which cannot be hoped for, even with a large grating. The green and red systems of CaF, and their analogues in SrF, have been ascribed by Johnson² to transitions ${}^2\Sigma \rightarrow {}^2\Sigma$ and ${}^2\Pi \rightarrow {}^2\Sigma$ respectively. Our results support these designations, but disagree with Johnson in several important respects. The near equality of rotational constants in the upper and lower states causes the heads to be formed at a very high value of J , at a considerable distance from the band origins. In this case data on the heads cannot give reliable values of the vibrational constants, since the distance from head to origin is not even approximately constant throughout the system. By assuming that the combination principle can be applied to measurements of the heads to find accurate values of the vibrational term-differences, Johnson has been led to wrong assignments of quantum numbers in the sequences ${}^2\Sigma(v+1) \rightarrow {}^2\Sigma(v)$ and ${}^2\Pi(v) \rightarrow {}^2\Sigma(v+1)$ in CaF. Furthermore, the value of J_{head} is so large in some cases that heads do not appear

at the temperature of the arc, a fact which explains Johnson's failure to observe certain sequences. The remarkable difference in the appearance of the ${}^2\Sigma \rightarrow {}^2\Sigma$ systems in emission and absorption³ can be readily interpreted as a temperature effect of the usual type if the double heads are ascribed not to R and Q branches, as suggested by Johnson, but to a doublet R branch, probably representing a very large p -type doubling.

Estimates of the molecular constants of CaF have been made from partial measurements of the fine structure, using formulas for the separation of the P and Q heads in the red system. The moment of inertia in the lower state is about $I_0'' = 86 \times 10^{-40}$, and is very nearly the same in the upper states. Johnson's interpretation of the heads in the ${}^2\Sigma \rightarrow {}^2\Sigma$ system, besides being incompatible with their appearance in absorption, leads to unreasonable values of the constants, since he places the origin (Q head) of the $(0, 0)$ band only 6.5 cm^{-1} from the R head. Using our approximate values of the rotational constants, the various unusual features of the band systems can be shown to be a necessary consequence of the type of structure postulated. Details of this work will be published elsewhere.

A. HARVEY,
F. A. JENKINS

Department of Physics
University of California
September 25, 1930

¹ F. W. Aston, *Nature* **113**, 856 (1924).

² R. C. Johnson, *Proc. Roy. Soc.* **122A**, 161 (1929).

³ O. H. Watters and S. Barratt, *Proc. Roy. Soc.* **118A**, 120 (1928).

Structure of K -radiation from C, B, and Be

In the "Physical Review" for the 15th of July Mr. L. Y. Faust has published the results of his research upon the structure of the softest K -radiation. He finds that the lines of carbon, boron and beryllium consist of a number of components, whose relative intensity varies with the angle of incidence and the tension. In order to confirm this statement I have microphotometered several lines of the carbon, boron and beryllium spectra, obtained with the special x-ray gratings ruled in this laboratory.¹ The results of this investigation will be published in the

"Zeitschrift für Physik." Though the dispersion is greater than that used by Mr. Faust and the resolving power of the microphotometer probably is larger, the blackening curve appears quite even in its course. Nothing corresponding to the components found by Mr. Faust was observed. Moreover the total blackening lies within a considerably smaller range of wave-length. By way of example Mr. Faust finds 9 components in the

¹ M. Siegbahn and T. Magnusson, *Zeits. f. Physik* **62**, 435 (1930).

carbon line, extending over the range from 43 to 48 Å, while the carbon lines on my plates are only about 1 Å wide. The cause of variance in the results obtained is probably due to inaccuracies in the gratings used by Mr. Faust. As has been pointed out by Dr. Fagerberg² even very small variations in

the grating constant can give rise to considerable errors in the structure of the lines.

MARTIN SODERMAN

Physical Laboratory,
University of Uppsala,
September 12, 1930

² S. Fagerberg, *Zeits. f. Physik* **62**, 457 (1930).

High Efficiencies of Emission from Oxide-Coated Filaments

Very high efficiencies of electron emission from oxide coated filaments have been observed. Inasmuch as these observations were made in connection with an entirely different problem, no complete investigation has been made as yet on this subject. The observations are here reported as being of interest in connection with emission phenomena.

The filaments were of nickel, coated with barium and strontium carbonates. They were given a conventional exhaust and activation.

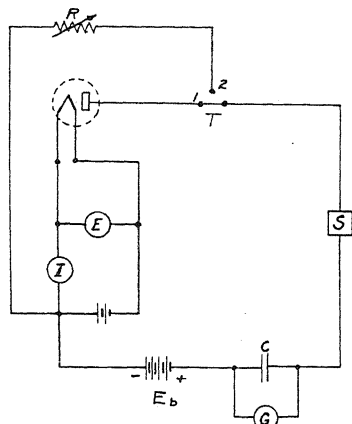


Fig. 1.

The method of measuring emission is illustrated in Fig. 1. The filament is heated to the proper temperature and the voltage E_b applied. With the switch T in position 1 the contactor S is operated. This contactor closes the circuit for a very short time (of the order of 10^{-3} second) during which time the emission current charges the condenser C . The deflection of the galvanometer G is read. Then the switch T is thrown to position 2 and the non-inductive resistance R adjusted until operating contactor S gives the same galvanometer deflection as before. The emission is then E_b/R . This method was adopted so that the full saturation emission could be

drawn without the filament temperature being changed appreciably.

At normal operating temperatures efficiencies of from one to four amperes per watt were obtained. These figures represent the range of a considerable number of filaments presumably operating at the same temperature. It should be pointed out that these observations were made on filaments representative of a large number, and that no special care was exercised to secure high activity in those tested. These results were checked by means of the standard power-emission chart. Readings were taken of emission in the usual way of applying a continuous potential to the anode at such low temperatures that the emission could not appreciably affect the filament temperature, and the curves extrapolated to determine the emission at normal temperature.

Fig. 2 shows the results obtained by the two methods. The agreement is as close as may be expected, since neither method gives exactly uniform results on the same filament at different times, due either to errors of measurement or to changes in the emission of the filament.

Fig. 3 shows the emission per square centimeter plotted against watts per square centimeter for representative filaments.

The temperatures of the filaments were determined by means of an optical pyrometer, and checked by computation from the watts per unit area and the probable thermal emissivity of the surface. From Dushman's equation¹

$$I = AT^2 e^{-b_0/T}$$

the values of b_0 and A were computed from the temperatures and emissions. On a representative filament, values of b_0 between 8,700 degrees and 10,500 degrees were computed. The value of A was about 0.3 ampere per

¹ S. Dushman, *Phys. Rev.*, Vol. 21 No. 6, p. 623, June, 1923.

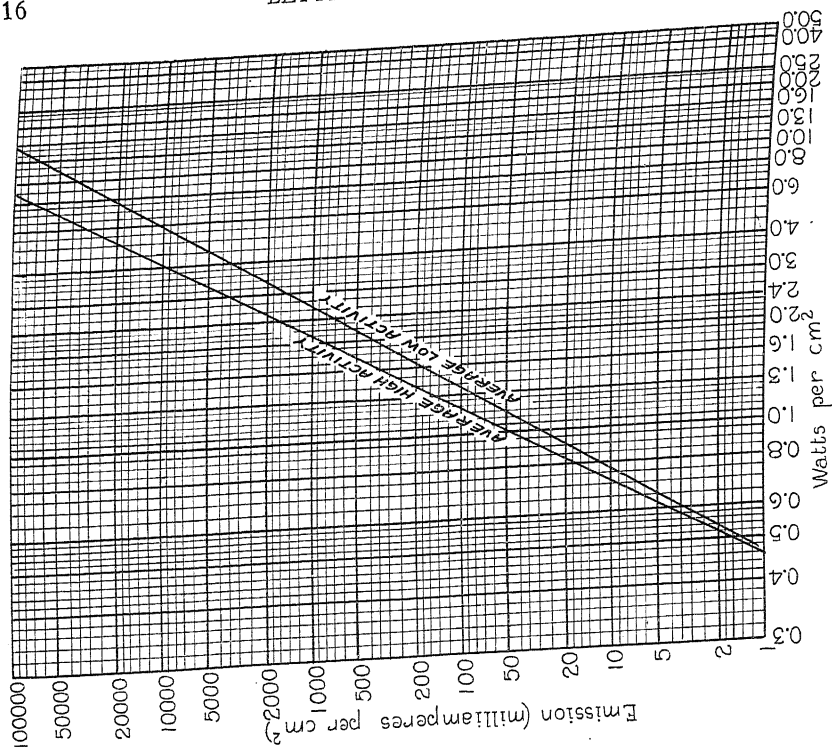


Fig. 3.

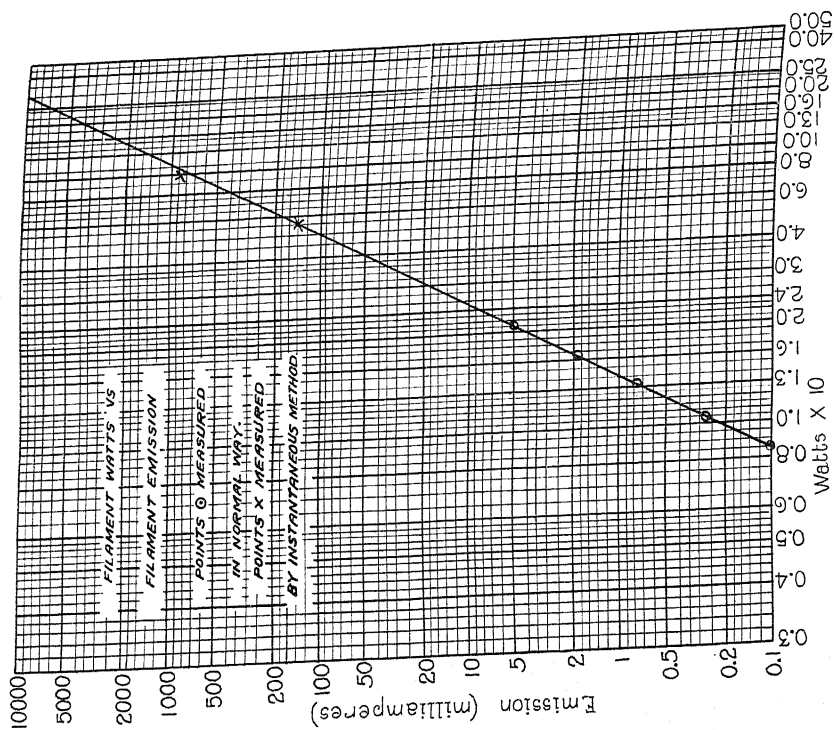


Fig. 2.

cm² degree². The values of work function ϕ_0 corresponding to the above values of b_0 are 0.75 volt and 0.905 volt.

A great deal of the work in connection with these measurements was performed by Mr. T. T. Eaton, and to him should go the

credit for first noticing the very high efficiencies here reported.

B. J. THOMSON

Vacuum Tube Engineering Department,
General Electric Co.,
September 24, 1930.

Negative Ions in Hydrogen and Water Vapor

In the course of the writer's¹ investigation of the positive ions produced in hydrogen by electron impact the presence of negative ions was observed. These were indicated by the appearance of two sharp peaks when the negative ion current was studied as a function of the electron velocity. They were suspected of being H⁻ ions and Bleakney upon re-examining hydrogen in his mass spectrograph² observed the ions and found them to have the e/m value of H⁻. The maxima of the peaks, corresponding to the maxima for the efficiency of their production occurred at electron velocities of 6.6 and 8.8 volts. These negative ions were found to possess kinetic energy, presumably acquired in the dissociation process which accompanies their formation. The velocity of the ions of the 6.6-volt group was about 1.5 volts while that of the 8.8-volt group could not be accurately determined because there were so few of them.

The negative ions were so few in number that it was thought they might be due to an impurity in the hydrogen—most probably water vapor. They persisted, however, after all reasonable precautions were taken to eliminate possible sources of the vapor. On the other hand when water vapor was admitted to the tube and the hydrogen removed the same H⁻ ions appeared in much greater abundance, and a determination of their velocities could be made.

A preliminary study of their kinetic energies showed that the velocity of the 6.6-volt group was about 1.5 volts while that of the 8.8-volt group was about 3.2 volts. This would mean that if they are formed by dissociation of H₂O⁻ the energy of the dissociated system is in the first case 5.1 volts above the normal H₂O state and in the second case 5.6 volts.

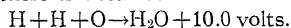
Bleakney has informed me that he has obtained H⁺ ions from H₂O at a minimum electron velocity of 19.2 volts. If we assume that these ions result from the dissociation of H₂O⁺ into H⁺+OH, we find, by adding an electron to the H⁺ that the energy of the system H+OH is 5.7 volts above the normal H₂O state.

Less than this by the electron affinity of the H atom would be the energy of the system H⁻+OH. Assuming that this is the system which results from the 6.6-volt electron impact we find the value 0.6 volts for the electron affinity of the hydrogen atom. It is interesting to note that Hylleraas³ gives 0.7 volts for this quantity.

The second group of H⁻ ions appearing at 8.8 volts may possibly result from the dissociation of H₂O⁻ into H⁻, excited, and OH. The energy of this system would be expected to lie above the energy of H⁻+OH by the amount of the excitation potential of H⁻ which would be in the neighborhood of 0.6 volts. (H⁻ would be expected to resemble He with an excitation potential near its ionization potential.) Actually its energy is 0.5 volts above the energy of the system resulting from the 6.6 volt impacts.

On the other hand if it be true that the H⁻ ions are formed by dissociation of H₂⁻ the energy of the system resulting from the 6.6-volt impacts would lie 3.6 volts above the normal state of the H₂ molecule and that resulting from the 8.8-volt impacts 2.4 volts above. The former might be regarded as the heat of dissociation of H₂ less the electron affinity which would give 0.8 volts for the affinity. There is no reasonable explanation of the energy of the state resulting from the 8.8-volt impacts.

Upon combining with thermochemical data the known heats of dissociation of H₂ and O₂ there is obtained



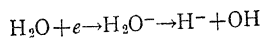
From the above consideration that H+OH lies 5.7 volts above the normal state of H₂O we see that the heat of dissociation of the OH molecule would be 4.3 volts. The writer has been unable to find any data concerning this.

¹ See paper in this issue.

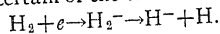
² W. Bleakney, Phys. Rev. **34**, 157 (1929); and Phys. Rev. **35**, 139 (1930).

³ E. A. Hylleraas, Zeits. f. Physik **63**, 291 (1930).

In conclusion I believe in the reality of the transition



but am not certain of the transition



It is hoped that more precise measurements in the future will throw additional light on the matter.

One interesting feature of the phenomena is the extremely narrow range of electron

velocities which are capable of producing these negative ions. The range is but little wider than the normal velocity distribution in the electron beam, as though the electrons, to produce a negative ion of a given type, were compelled to have a perfectly precise velocity.

W. WALLACE LOZIER

University of Minnesota

October 6, 1930

Wave Mechanics of Deflected Electrons

In a letter¹ appearing in the September 1 number of the Physical Review, Carl Eckart makes the assertion that the major conclusion of my paper² on the above subject is incorrect, and that the difference between $(e/m)_{\text{defl}}$ and $(e/m)_{\text{sp}}$ cannot be explained as a difference between wave and classical mechanics. He attributes the alleged error in my conclusion to the interpolation method of calculating the mean radius of curvature, admitting that the rest of the analysis is correct.

I had not neglected to verify the interpolation formula in question by direct calculation of the mean radius of curvature for the states $k=0$ and $k=1$. Shortly after seeing Dr. Eckart's letter, however, I noticed that the method of interpolation which I had employed is unnecessary, since the mean radius of curvature may be calculated rigorously from Eq. (43) of my paper. This equation does not lead to an infinite series even when p is fractional since k is a positive integer. For the mean radius of curvature it gives

$$\bar{\rho} = \frac{(\pi/2)^{1/2}}{s!} \left[\left(s - \frac{1}{2} \right)! \left(2s + \frac{1}{2} - k \right) + \frac{(s - 3/2)! k (2s - \frac{1}{2} - k)}{2^2 [1!]^2} + \frac{(s - 5/2)! k (k - 1) (10s - 3/2 - 9k)}{2^4 [2!]^2} + \dots \right].$$

For the first order correction we need only the first two terms. Using S and K as defined in my paper

¹ Carl Eckart, Phys. Rev. **36**, 1014 (1930).

² Leigh Page, Phys. Rev. **36**, 444 (1930).

$$\bar{\rho} = \left(\frac{\pi}{2} \right)^{1/2} \frac{(s - \frac{1}{2})!}{s!} S \left[1 - \frac{K + 1}{4S} \right],$$

and applying Stirling's formula

$$\bar{\rho} = S^{1/2} \left[1 - \frac{K - 1}{4S} \right],$$

which is (except for the negligible -1 in the numerator of the second term) the same formula as obtained by interpolation. Therefore it is clear that Dr. Eckart was mistaken in his assertion that I had been led to incorrect results by the method of interpolation used.

Dr. Eckart bases his criticism of my work on a supposed disagreement between my conclusions and those obtained by Kennard³ in an earlier paper. Working with the transformation theory of Dirac and Jordan, Kennard obtains the coordinates of the center of a wave packet moving in a magnetic field in terms of initial coordinates and momenta and notices that he is led to a formula identical with that given by classical electrodynamics. He does not, however, obtain the radius of curvature in terms of the energy, which is the significant relation from the experimental point of view. Therefore there does not seem to be any necessary conflict between Kennard's conclusions and mine.

LEIGH PAGE

Yale University
New Haven, Conn.
October 3, 1930

³ E. H. Kennard, Zeits. f. Physik **44**, 347 (1927).

BOOK REVIEWS

Astronomy, An Introduction. ROBERT H. BAKER. Pp. xii+521. D. Van Nostrand Company, Inc., New York: 1930. \$3.75.

A few years ago those who were teaching introductory courses in Astronomy in colleges felt the need of a new text. Young's "Manual of Astronomy" and Moulton's "Introduction to Astronomy" were extensively used and both of these books left much to be desired. The science had made such rapid progress since these texts were written that many new discoveries and theories were lacking altogether. With the introduction of "Astronomy" by Professor Baker there are at least five texts from which teachers of beginning courses in Astronomy may choose. The ranges of material presented and the matter of treatment is such that from one of the five texts a satisfactory selection can be made to suit the varying conditions found in different universities and colleges. Without exception the authors have avoided a mathematical presentation of the subject and have endeavored to set forth the fundamental facts and principles of the science with as few mathematical formulas as possible. They have kept in mind the fact that those who are reading the text have studied mathematics no further than trigonometry and have had, in high school or college, only an elementary course in physics. In many instances the authors have been a bit too cautious in the matter of avoiding mathematics. From the writer's own experience a mathematical formula now and then is a good thing even in a "non-mathematical" course. A few formulas sometimes bring a definiteness that satisfies the student and which, were the point in question explained in words, would have a vagueness, that is to say the least, undesirable. Most of the authors have had in mind a text that could be used in a three hour course extending through the college year and which by so doing will meet the requirements of most colleges and universities offering a course in Astronomy as one of the electives in the science group.

"Astronomy, An Introduction" by Doctor Robert H. Baker, Professor of Astronomy in the University of Illinois, is a text that will be found to be highly satisfactory from many points of view. To say that it is up-to-date in the presentation of new material is to cite only one of its merits. The text is printed with excellent type on good paper. It is well bound and illustrated in a manner worthy of the highest praise. Five hundred illustrations and drawings have been included which give added interest and which help in the explanation of the subject matter. The illustrative material is so designated that the chapter and paragraph with which each is associated is indicated. The decimal system has been used throughout. The number to the left of the decimal point indicating the number of the chapter, and the number to the right, the paragraph in the chapter. At the end of each division a list of references is given. These references have been carefully chosen and they form an admirable basis for an up-to-date astronomical library. Such a list of books, periodicals and charts should be available to every college student studying the subject.

The text begins with a chapter on "Aspects of the Sky." The student is introduced at this point to the coordinate systems and to many of the technical terms he will need in understanding the subject. A paragraph is included on "Learning the Constellations" and a few charts are given with directions as to how the constellations may be located in the sky. While this attempt is inadequate it is admittedly a difficult feature to include in a text. It is a mistake to place too much emphasis on the study of the constellations, but a knowledge of the principal configurations should be a part of the stock-in-trade of every student who studies astronomy, and this feature should not be omitted nor neglected. The problems of practical astronomy have been eliminated almost entirely and the relation of geology to astronomy is mentioned only in the briefest manner. More attention is given to a study of the earth's atmosphere and its astronomical effects than is usually found in most texts. The subject of celestial mechanics is dealt with in a concise but adequate manner. The author has succeeded in presenting this material in an interesting way even for one who does not have a special interest for this part of the subject. Of the twelve chapters one is devoted to the sun and five to the sidereal system.

This seems to be about a proper division of the material. The latter half of the text calls forth special commendation. In general controversial points are free from bias and new theories are put forth in a manner which in most cases will leave the student with the impression that these theories are only theories and not established facts. The last three chapters deal with The Constellation of the Stars, The Galactic System, and Exterior Galaxies. These chapters will be of interest to general readers who have not been able to keep abreast with recent astronomical literature. With these chapters a climax is reached. It is apparent that Astronomy is an old, yet new, science, that the frontiers offer thrilling adventure and that "What we know compared with what we do not know is immense."

On the whole the book is comparatively free from typographical errors and those, such as they are, will doubtless be eliminated in future printings. In places the mode of expression used by the author may startle the more conservative. Doubtless many will feel that this or that section could have been expanded to advantage. However it is an excellent text which will be welcomed by many who are teaching an introductory course in astronomy.

CLIFFORD C. CRUMP

Electron Physics. J. BARTON HOAG. Pp. 208. D. Van Nostrand Co., Inc., New York, 1930. Price \$3.00.

This book is more than a laboratory manual in that the larger part of it is devoted to the descriptions of the physical phenomena which are to be studied rather than to the description of the apparatus used in the experiments. Each chapter describes the fundamentals of a particular topic and concludes with directions for performing one or more experiments. These are designed to acquaint the student with the technique used in that field and to obtain an understanding of the subject such as is afforded by a good laboratory experiment. The discussion usually includes a number of different experiments which may be performed, but detailed procedures are given for only one or two of the possible experiments, selecting those which are best adapted to the use of simple apparatus and which will yield satisfactory results in the hands of the student. For example, in the chapter on "The Electron" the determination of $N.e$ by electrolysis, the determination of N from Brownian movements and from the recent measurements of x-ray wave-lengths by means of ruled gratings are given. Also the cloud expansion method, the balanced oil drop, and the shot effect methods of measuring e are described but detailed directions are given for the student to measure e by the oil drop method only.

There is given a number of experiments which may well displace some of those experiments which have become "classical" in the intermediate laboratory courses or which may be added to that group if time permits. For example, the test of Richardson's emission equation, the measurement of the thermionic work function, the characteristics of the photoelectric cell and of the three-electrode tube, measurement of ionization potentials and the absorption of x-rays are experiments well worth the attention of the student of modern physics. The book also gives a number of experiments in radioactivity.

Appendices on electrometers, electroscopes, pressure gauges, vacuum technique and the production of vacua, also a number of tables add to the value of the book. References at the end of each chapter and a group of numerical problems with answers are given.

J. W. BUCHTA

THE PHYSICAL REVIEW

IMPROVED TECHNIQUE FOR THE RAMAN EFFECT

By R. W. Wood

JOHNS HOPKINS UNIVERSITY, BALTIMORE

(Received September 15, 1930)

ABSTRACT

Mercury-arc excitation of Raman spectra. The unfiltered light from a mercury arc is not well suited for an analysis of Raman spectra. The confusion of interpretation which may result is illustrated in the case of benzene.

Filters for use with mercury arc.—The object of a filter is two-fold: the limitation of the excitation to light of a single wave-length (if possible) and the suppression of the continuous spectrum in the region in which the Raman spectrum appears. Raman spectra of benzene excited by the mercury arc through various filters are reproduced. Suggestions concerning the proper design and manipulation of arc, filter tubes and scattering tubes are given.

Helium-arc excitation of Raman spectra.—The use of the General Electric Company's hot cathode helium arc as a source for Raman spectra excitation is described. The Raman spectrum of benzene excited by this source through a nickel-oxide glass filter is reproduced.

THE ideal source of light for the study of the Raman effect should have a single very bright spectrum line, widely removed from other lines, and situated preferably in the region between 4000 and 4200A. The nearest approach to this is the hot-cathode helium arc, brought out by the research laboratory of the General Electric Company at Schenectady, with which I have been experimenting during the past winter. A number of photographs of Raman spectra made with a spiral helium discharge tube and a filter of nickel-oxide glass were published in the *Philosophical Magazine* for 1929,¹ and in this paper I stated that apparatus was in preparation for excitation by the helium arc.

The mercury arc which has been used exclusively heretofore, suffers from a number of disadvantages, but as it will doubtless continue to be used by the majority of investigators, it appeared to be worthwhile to improve the technique for this method of excitation.

MERCURY ARC EXCITATION

In the first place it is a great mistake to employ the total radiation of the arc without filters. Consider, for example, the region between the 4358 mercury line and wave-length 5100, shown in Fig. 1B which is the Raman spectrum of benzene excited by the mercury lines 4046-4077 and 4358-4348-

¹ R. W. Wood, *Phil. Mag.* 7, 744 (1929).

4339, the light being filtered through a concentrated solution of praseodymium which absorbs the continuous spectrum of the arc in the region of the Raman spectrum, and enables us to photograph fainter lines than would be recorded otherwise. It is obvious that more lines appear in this photograph than in any of the numerous ones of benzene that have been reproduced heretofore. This is due simply to the very perfect suppression of the continuous background, which ordinarily drowns out the fainter lines, a matter which will be taken up in detail presently.

As is now well-known the Raman spectrum of a large majority of organic compounds excited by Hg4358, consists of a group of lines in the region 4400–4700 and from one to three or more strong broad lines at about 5030 which, for brevity I shall call the 3.3μ band, the region between being free of lines. As I showed, however, in the paper on helium excitation,¹ the 3.3μ band is, in some cases accompanied on both sides by companion lines or doublets and the work of the past winter with the helium arc has shown, in the case of benzene at least, that the companions extend down nearly half way across the region usually regarded as free of lines. This is shown by Fig. 1F—the Raman spectrum of benzene excited by the helium arc filtered through a nickel-oxide glass tube. Excitation is by the 3888 line at the left, two other helium lines appear (indicated) but all of the others are Raman lines. The spectrum has been enlarged to such a scale as to coincide with Fig. 1B, the spectrum of benzene already referred to. The “coincidence” is for lines of the Raman spectrum and not for wave-lengths, of course. The complexity resulting from the circumstance that in case B the spectrum is excited by five mercury lines is at once apparent. Its analysis is shown by the diagram above and by the two spectra below, Fig. 1, C and D. The former excited by 4358–4348–4339 and the latter by 4046–4077.

The spectrum of the mercury arc, in the region near the 3.3μ band at 5030 is shown by Fig. 1A', No. 1 being the 4915 line. The short wave-length component of the 3.3μ band is in coincidence with mercury line No. 3, and its relative intensity is thus enhanced unless this spectral region is filtered out of the exciting radiation, since all radiations present in the exciting light are scattered with an intensity several hundred times that of the strongest Raman lines to which they give rise. We see from the diagram at the top of Fig. 1 that the main part of the Raman spectrum excited by the 4358 group is overlaid with the 3.3μ band and its companions, i.e., n and r are the 3.3μ bands excited by 4046 and 4077, and correspond to the 3.3μ band excited by 4358, near mercury line No. 3 of Fig. 1A'. If now there are numerous companions of the 3.3μ band, as is the case with benzene, the confusion resulting is obvious, and it is this circumstance that has been responsible for the numerous disputes over the assignment of the fainter lines of this substance.

We may take for example lines o , p , and q of Fig. 1B. Pringsheim and Rosen list only o and q giving incorrect assignments for both. This error was based on the assumption that r was excited by 4358 as well as by 4077, o and q being considered as excited by the companions of 4358, all of which is incorrect. Kohlrausch and Dadiou list o and q , give a wrong assignment

to *o*, deducing a frequency difference $\Delta\nu = 3160$ which is non-existent—and give no assignment for *q*. Bär claims that *o* does not exist, does not mention *p*, and gives a correct assignment for *q*. Söderquist omits *o*, and gives correct assignments for *p* and *q*, thus verifying the doublet companion on the long wave-length side of the 3.3μ band $\Delta\nu = 3046\text{--}3060$ which I found last year with helium excitation and which shows beautifully in Fig. 1, E and F, the former excited by the green mercury line and the latter by helium 3888.

The 3.3μ band has a strong companion on the short wave-length side $\Delta\nu = 2947$. In Fig. 1B this line, as excited by 4046 coincides with the line *m* excited by 4358 which gives $\Delta\nu = 1178$. Kohlrausch and Dadiou state in their paper that I "failed to find this line as can be seen by reference to their table of lines found by previous investigators." Though absent in *their* table it was present in *mine*, and showed as well as a strong line in the reproduction of the spectrogram, though they state that it was not present. We thus see that *m* and *o* are the short wave-length components *n* and *r*, (the 3.3μ bands excited by 4046 and 4077 respectively), while *p* and *q* constitute the long wave-length component (doublet) of *n*, the corresponding component of *r* being hidden by the strong doublet *st* excited by 4358. They appear as faint lines in Fig. 1D at the extreme right, in which case 4358 has been filtered out of the exciting light.

Uncertainties and errors such as those enumerated above are almost certain to occur with unfiltered mercury arc excitation, and can be avoided only by the use of suitable filters. Even with filters we have to contend with the difficulty that all strong Raman lines excited by 4358 are accompanied on the short wave-length side by two fainter companions excited by 4348 and 4339, while those excited by 4046 have a faint companion on the long wave-length side, due to 4047 excitation.

Lines in Fig. 1B not mentioned above are as follows:

a, the 3.3μ band excited by Hg 3906

bc, *hi*, *kl*, short wave-length companions of *d*, *j*, and *m* excited by 4358 (due to multiple excitation)

e, *f*, excited by 4046, $\Delta\nu 2542\text{--}2597$ (see following paper).

Filters for Hg-arc excitation:—We will now take up the subject of filters and how best to apply them. While the 4358 line is about four times as intense as 4046 it suffers from the disadvantage that the 3.3μ band (with its real companions) which it excites falls in a region of very low sensibility of most photographic plates and of only moderate dispersion of the prism spectrograph. The 4046 line, however, projects its entire Raman spectrum in the region of high and moderately uniform sensibility of the ordinary plate. The mercury lines 4077, 4108 and 4140 are superposed on the Raman spectrum and are liable to conceal important lines. Some substances, however, cannot be excited profitably by 4046 on account of strong fluorescence. The object of the filter is two-fold, the limitation of the excitation to the light of a single wave-length (if possible) and the suppression of the continuous spectrum of the mercury arc in the region in which the Raman spectrum appears.

The most convenient mercury arc that I have found for Raman spectra work is the new model brought out recently by the Hanovia Company of Newark, New Jersey. Both electrodes are of mercury, which obviates the tungsten blackening, and the burner is enclosed in a metal housing which can be rotated on trunnions, which in turn have an up and down adjustment of several inches. With the housing in the horizontal position the burner is just below and close to a narrow rectangular aperture in the top and the Raman tube can thus be brought very close to it, with interposed filters. At first I used shallow glass dishes of "Pyrex" (Petri dishes used by the biologists, superposing one above the other, when two solutions were used). The evaporation was rather rapid, however, even with air cooling by an electric fan.

A much better method is to enclose the filter solution in a glass tube 5 cm in diameter, which when mounted between the mercury arc and the Raman tube and as close to each as possible, acts as a cylindrical lens and filter combined. If two solutions are used, one of them is contained in an inner tube of smaller diameter, which is hermetically sealed. A concentrated solution of cuprammonium sulphate sealed up in a large tube looks very promising as a filter but I have not fully tried it out. An electric fan placed close to the lamp and blowing over the top is sufficient to keep the tubes cool. The Hanovia Company has obtained excellent results with a chimney attachment to the lamp, which I suggested they make up, and which causes a "down draught" through the slot in the top of the housing. With this attachment I hope to be able to dispense with the fan. (See Fig. 3.)

Raman spectra of benzene made with various combinations of filters are reproduced in Fig. 1. Spectrum B was obtained with a tube 3.5 cm in diameter filled with a saturated solution of the praseodymium double salt furnished by the Welsbach Light Company of Gloucester City, Pennsylvania. In this case the excitation is by 4046 and 4358, the filter absorbing the region between 4375 and 4800 where most of the Raman lines are found. Spectrum C was obtained with a combined filter of praseodymium and sulphate of quinine in dilute sulphuric acid, which absorbs 4046 and 4077, the excitation being by 4358. Spectrum D was made with a filter composed of a solution of cobalt sulphocyanate, made by adding a strong solution of ammonium sulphocyanate to one of cobalt chloride. This filter reduces the intensity of 4358 to the point at which it fails to yield Raman lines, though the group of three lines records itself in the spectrum. A strong solution of iodine in carbon tetrachloride is even better for removing 4358 and a spectrum made with this filter is reproduced (Spectrum H.) This spectrum, however, shows strong fluorescence to the right of the 4358 group, which is at the middle of the spectrum. This fluorescence is due to the 3650 group of mercury lines. A less concentrated solution of iodine transmits 4358 freely, and can be used for the suppression of the continuous background. Spectrum G was made with a double filter, the inner tube filled with a very dilute solution of potassium chromate and the outer with the iodine solution. Potassium chromate can be used only if diluted to the point at which it shows only a trace of

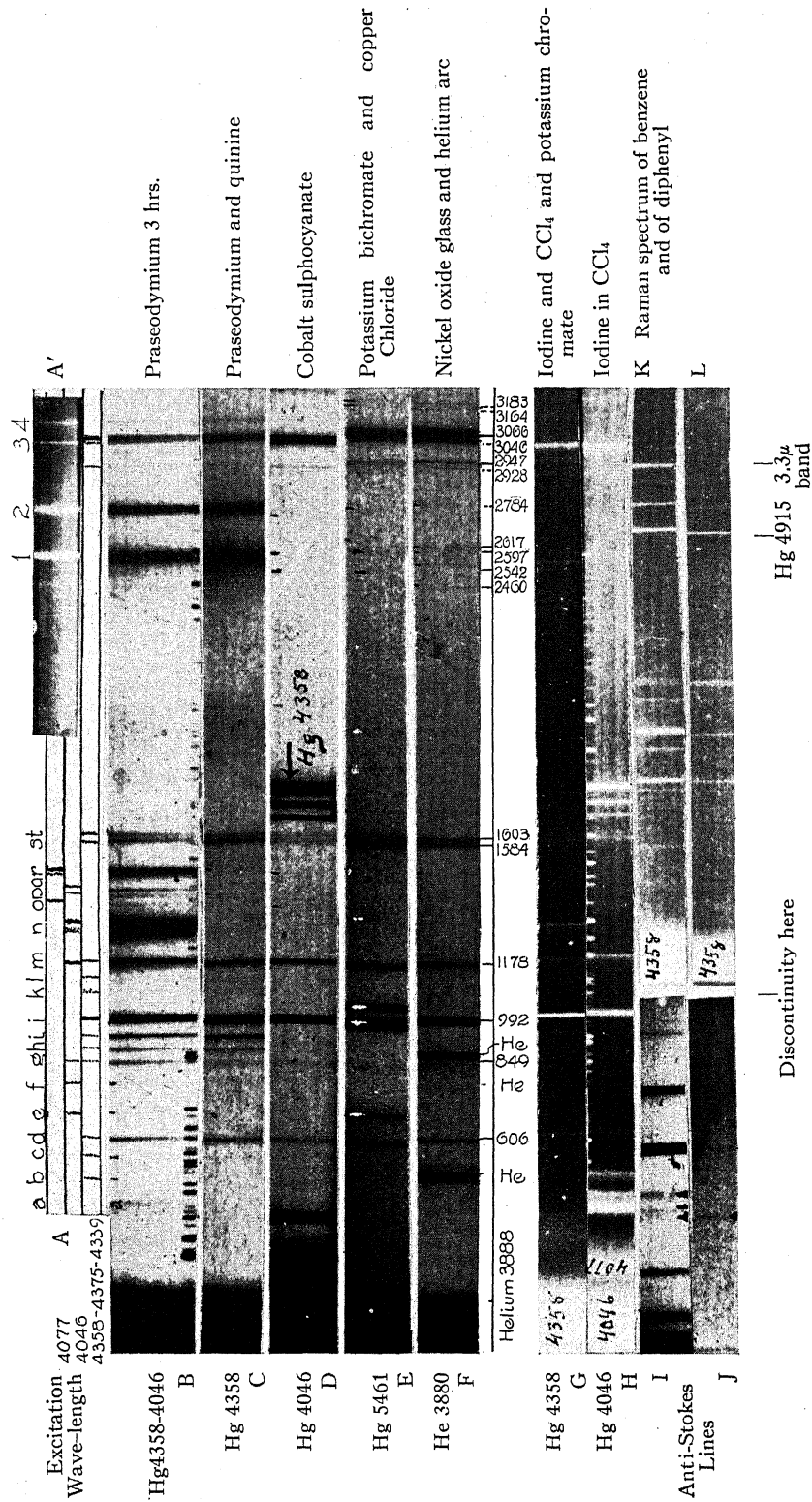


Fig. 1. Raman Spectra of benzene under various types of excitation.

yellow by daylight with the thickness employed, otherwise it absorbs 4358 too powerfully. In this concentration it only partially suppresses the 4046 group. Quinine sulphate in dilute sulphuric acid can be made sufficiently concentrated to completely suppress 4046 with practically no absorption of 4358 but it turns yellow rapidly and requires renewal every half hour.

The Zeiss Company makes a fluorescent glass (used in filter "C" in combination with cobalt glass) which appears to be similar to the Corning Noviol glass plates. I believe that a tube of this glass filled with a solution of iodine in carbon tetrachloride of moderate concentration, will prove the best filter for excitation 4358, and for 4046 excitation a strong solution of iodine contained in a tube of Corning "Noviol" 0, or "Nultra" of such thickness as to absorb 3660 and transmit freely 4046. If tubes of these glasses should not be available the iodine solution can be used in a tube of ordinary glass with a plate of the ultraviolet absorbing glass interposed between it and the Raman tube. I am informed by the Corning Company that their "Noviol A" is opaque to 4046 and transmits 50 percent of 4358, but I have not yet had the opportunity of comparing it with the Zeiss filter C. None of these glasses that I have tried however is much better than a solution of potassium chromate. By increasing the concentration of the solution 4046 can be practically abolished but only at the cost of increased time of exposure.

The absorbing power of a potassium chromate solution for 4046 and 4358 has been investigated by Mrs. M. Goeppert-Mayer in my laboratory. Her results are given in the following table, in which the two lines are regarded as having equal intensity with no filter. c = concentration in grams per liter, d = thickness of the filter in centimeters.

$c d$ concentration times thickness	I 4046	I 4358	Ratio
0	1	1	1
0.127	$\frac{1}{10}$	$\frac{1}{1.7}$	6
0.177	$\frac{1}{25}$	$\frac{1}{2.1}$	11
0.215	$\frac{1}{50}$	$\frac{1}{2.45}$	24
0.253	$\frac{1}{100}$	$\frac{1}{2.9}$	34
0.304	$\frac{1}{250}$	$\frac{1}{3.54}$	70
0.342	$\frac{1}{500}$	$\frac{1}{4.15}$	120
0.361	$\frac{1}{750}$	$\frac{1}{4.55}$	165
0.380	$\frac{1}{1000}$	$\frac{1}{4.87}$	205

This table shows very clearly just what can be accomplished: for example, 4046 is reduced to 1 percent with a reduction of 4358 to 34 percent almost exactly the same figures as given for the Zeiss C filter. If the mercury arc is of the type that operates only in the vertical position the filter tube can be mounted alongside of it, and the cooling accomplished by the convection currents in the fluid. The higher the tube, the more perfect the cooling. A tube 4 cm in diameter and 70 cm in height will be found sufficient to carry off the heat. If there is no objection to water cooling, a shorter tube can be used, the upper end wrapped with several layers of tin-foil on which is wound a close spiral of copper or lead tubing, as shown in Fig. 2.

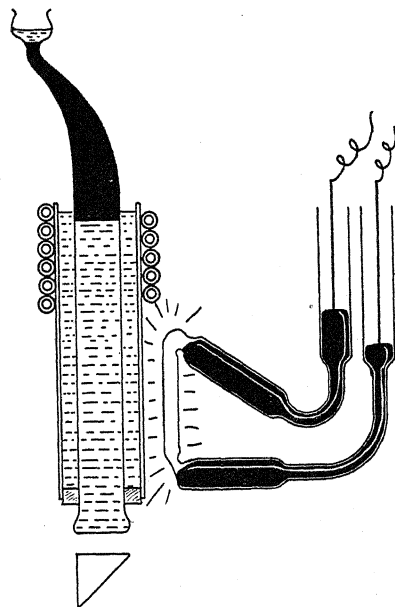


Fig. 2.

One of the most important points is to prevent any stray light from reaching the slit of the spectrograph. The entire optical path, from the window of the Raman tube to the slit should be enclosed by tubes of black paper, as diffused light, reflected from the window of the tube, or the lens used in forming the image on the slit, gives rise to a continuous background. The arc should be operated in a light-tight box, well ventilated, however, and placed as close as possible to the aperture in the wall.

If only very small quantities of material are available for study (10 cc or less) a form of tube which I described in a communication to the Faraday Society last year, may be used. It is shown one half natural size in Fig. 3. The Raman tube should be made of thin walled soft glass tubing (not Pyrex) about 13 mm in diameter, one end blown round and then flattened by holding it absolutely vertical above the tip of a very small bunsen flame which is burning quietly without flickering. If the tube is drawn off sharply at a right

angle preliminary to blowing the bulb the objectionable drop of glass at the center is avoided. Windows can be made in this way which give almost no distortion. A water-jacket tube about 23 mm internal diameter surrounds this tube, which is held in place by a rubber gasket at the bottom. These gaskets can be turned on a lathe from rubber stoppers with a sharp pen-knife as described in my first paper on the Raman effect² where more complete directions for making the flattened bulb are also given. After slipping the gasket over the tube the upper portion is drawn down as shown and painted with black "Duco." The upper portion of the large tube is wrapped in tin-foil wound with a copper tube 3 or 4 mm in diameter, the space between being filled with water or a filter solution. Cooling is effected by water circulating in the copper spiral. A concave 3/4 inch cylinder of polished

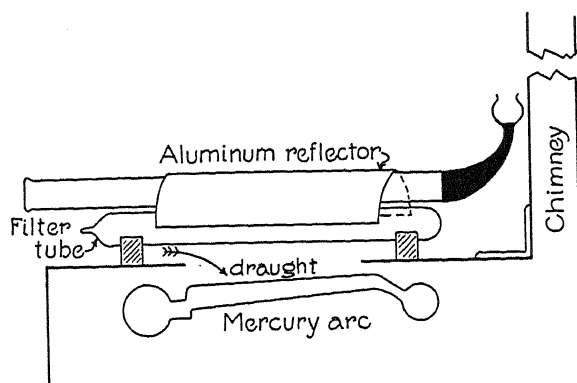


Fig. 3.

sheet aluminum is slipped around the inner tube on the side opposite the lamp, unless a filter solution which attacks aluminum is being used. The tube is illuminated with a capillary quartz mercury arc, almost in contact with the outer tube.

A few words regarding the best method of pointing the collimator of the spectrograph down the axis of the illuminated tube and forming the image on the slit may be found helpful.

In general, when the source of light is a long cylinder, seen end-on it is important to mount it at such a distance from the spectrograph that both ends of it can be fairly well focussed on the slit simultaneously. This means that the distance from the source to the lens should be much greater than the distance from the lens to the slit. If this condition is not fulfilled we are not utilizing all of the available light.

With the eye in such a position that it is looking exactly down the axis of the tube, bring the end of the match stick (mounted in a clamp stand) directly in front of the pupil. This marks the position of the spectrograph slit. The collimator is now pointed at the end of the tube, and the slit brought into coincidence with the end of the match.

² R. W. Wood, *Phil. Mag.* 6, 729 (1928).

Now look into the spectrograph from the position of the plate (i.e. from the focal plane of the camera) and if the aim has not been very bad, the end of the tube will appear as a small circle of light somewhere in the field of the camera lens. Next shift the spectrograph until the circle of light is in the center of the lens, keeping the slit position fixed.

To form an image of the end of the tube on the slit two methods are available. If a large spectrograph is being used, a small circle of paper should be mounted over the end of the tube and strongly illuminated with a lamp. This can then be focussed at once on the slit. With small spectrographs I have found the following method very convenient. The lens is first mounted practically in contact with the slit and the spot of light in the camera lens watched. As the lens is moved towards the tube and away from the slit the spot of light gradually enlarges, finally filling the entire field of the lens. The lens should be moved so as to keep the spot centrally placed in the field, and when the whole field is uniformly illuminated, the lens is in the correct position. This method enables us to utilize the brightest part of the source, if the illumination is not uniform, for, as the spot enlarges the attention can be focussed on the bright portion and this is then made to fill the field.

HELIUM ARC EXCITATION

Through the courtesy of Dr. Dushman of the Research Laboratory of the General Electric Company I was supplied with a hot cathode helium arc. This is more troublesome to operate than the mercury arc, as it requires a current of 9 amperes for heating the filament and 220 volts direct current for excitation. The filament current was supplied by a very inexpensive transformer, operated from the 110-volt A.C. mains, and the lamp started by spraying the tube with sparks from a small high-frequency apparatus (leak tester).

A tube of Pyrex glass with a window fused to one end was surrounded by a tube of nickel-oxide glass and mounted as close as possible to the helium arc, the whole being surrounded by a cylindrical tube of very thin and highly polished sheet aluminum, made by rolling up a rectangular piece of suitable size on a cylinder somewhat smaller than the size desired. The tube springs open to the desired diameter and can be still further opened and slipped over the other tubes. Sheet aluminum of this description is now obtainable commercially and is most useful for making reflectors of various shapes. There seems to be little point in going to the trouble of ellipsoidal reflectors as some investigators have done. Equally good illumination can be secured as described above, for the source is so large that only a small fraction of it is at the focus point, and the ellipsoid functions only for radiations originating at the focus. With the cylinder practically all of the light emitted by the arc gets into the Raman tube, with the exception of that lost by absorption. A large tube of Pyrex glass, silvered on the outside, similar to the reflector which I described many years ago in connection with the excitation of the resonance spectra of iodine, would give rather stronger illumination, but the aluminum is less troublesome and easier to fit over the tubes. The helium arc was sup-

ported in V-shaped notches lined with asbestos on two wooden upright supports, and the Raman tube, with its cover of nickel-oxide glass held in an iron clamp as shown. The end of the tube was drawn off obliquely and expanded into a bulb, to take care of expansion of the fluid. The tapering portion was painted with black "Duco" to secure a black background. Cooling was accomplished with the blast of an electric fan, directed into the aluminum cylinder by a paste-board cone. I have found nothing as good as this arrangement for investigating the region in the vicinity of $\Delta\nu = 3060$. The only objection is the presence in the Raman spectrum of the helium lines 3964 and 4026. The Raman spectrum of benzene excited in this way is reproduced in Fig. 1, Spectrum F, which will be more fully considered in the following paper.

RAMAN SPECTRA OF BENZENE AND DIPHENYL

By R. W. Wood

JOHNS HOPKINS UNIVERSITY, BALTIMORE

(Received September 15, 1930)

ABSTRACT

Raman spectrum of benzene.—By employing suitable filters with both mercury-arc and helium-arc excitation a number of new lines have been recorded. The complete spectrum given in frequency differences, $\Delta\nu$, is as follows: $\Delta\nu = 606, 849, 992, 1178, 1584, 1603, 2460, 2542, 2597, 2617, 2784, 2928, 2947, 3046, 3060, 3164$. *Anti-Stokes lines* corresponding to $\Delta\nu$ values 606, 849, 992 are verified.

Raman spectrum of diphenyl.—With mercury arc excitation and quinine sulphate filter fair spectra were obtained though the continuous background due to fluorescence was troublesome. The spectrum consisted of five faint diffuse lines and seven strong lines. Their $\Delta\nu$ values are: 416, 606, 731, 766, 810 (these are very faint) and 990, 1023, 1280, 1544, 1584, 1603, 3055, 3170. It will be noted that six of the lines are found in the spectrum of benzene.

THE Raman spectrum of benzene has been rather fully discussed in the previous paper, from the point of view of the assignment of the fainter lines, and it has been shown, that by employing suitable filters, and taking great precautions in the matter of excluding diffused and reflected light from the spectrograph, a number of new lines have been recorded in the region of the spectrum usually regarded as devoid of Raman radiations. This region lies between the main part of the Raman spectrum and the strong group corresponding to a frequency difference of about 3050, associated on the elementary theory with the absorption bands at 3.3μ . The complete spectrum of benzene, given in frequency differences, as I now believe it to be, is recorded in the following table.

TABLE I. Complete Raman spectrum of benzene. Frequency differences, $\Delta\nu$.

606	2460	2928
849	2542	2947
992	2597	3046)
1178	2617	3060} strong
1584	2784	3164
1603		3183

The anti-Stokes lines of frequency difference 990 and 605, the former being reported in my first paper confirming Raman's observation, have been obtained beyond any question with excitation by both the violet and green mercury lines.

THE ANTI-STOKES LINES

Raman, in his first paper, reported two anti-Stokes lines for benzene of frequency 23928 and 23541 with excitation by 4358, the former of which I verified in my earliest experiments. These observations have not been

confirmed by other observers, and Kohlrausch and Dadieu express doubt of their existence, claiming that with better conditions of illumination no trace of the lines was found. There seems, however, to be no doubt as to their existence as they appear distinctly on several of my plates. Their wavelengths are given in the following table, designated by the minus sign.

TABLE II. *Anti-Stokes lines of benzene.*

λ	Excit. λ	$\Delta\nu$	Filter
-4178	4358	990	praseodymium only
4181	4077	606	
4190	4046	849	
-4246.7	4358	605	praseodymium and quinine copper chloride neodymium and bichromate of potash.
-5180	5461	993	

Photographs showing the anti-Stokes lines are reproduced in Fig. 1 of the preceding paper (two small strips to the left marked I and J). The upper strip was printed from the same spectrogram as that reproduced in spectrum B, this portion lying between Hg 4046 and 4358 where the anti-Stokes lines excited by 4358 are found. The line -4178 (anti-Stokes) shows faintly on the negative while the lines 4181 and 4190 are strong. The three lines are indicated by ink marks at the bottom. The lower strip was made from a negative made with a quinine filter, lines 4181 and 4190 being absent while the anti-Stokes line -4178 comes out strong. The other line -4246.7 shows on the negative, but not on the print. The position of the two lines is indicated by dots below the spectrum. The 4246 line being nearly in coincidence with a strong line excited by 4046.

The first three lines were obtained with a praseodymium filter only, excitation being by the 4046 and 4358 groups. With praseodymium and quinine, lines 4178 and 4246 were obtained only, and with cobalt sulphocyanate 4181 and 4190 only. The proximity of the anti-Stokes line 4178 to the stronger line 4181 makes it seem possible the two may have been confused in the earlier investigations.

Line -5180 was obtained on the plate with excitation by the green line 5461. In the case of the excitation by helium 3888, Spectrum F (Fig. 1 of preceding paper), two faint lines appear between the doublet 1603-1584 and the 1178 line. The right hand one $\lambda 4127$ I have identified as $\Delta\nu 990$, excited by helium 3965, which is passed with some intensity by the filter. The other $\lambda 4114$ I cannot account for. If excited by 3888 it would give a $\Delta\nu$ of 1403, but no trace of such a line appears with any other type of excitation.

Spectrum E was taken with a filter of copper chloride, bichromate of potash and neodymium (a single solution). This transmits the green mercury line, with a trace only of the yellow lines. Mercury lines appearing in the Raman spectrum are marked with white dots, 577 and 579 being the most conspicuous. This photograph was made on an Ilford panchromatic plate, as the 3.3μ band lies in the red region.

New lines appear in the region to the right and left of the strong double band $\Delta\nu$ 3046-3060, most clearly recorded with helium excitation. There seems to be evidence of a variation in the position and number of these lines with the type of excitation, as can be seen by comparing Spectrum F with Spectra E and D, but this matter requires confirmation with more perfect filters and purer benzene. The subject is now under investigation. All other cases, in which a difference in the Raman spectra with different excitations has been suspected, have been shown to be spurious.

The Raman spectrum of diphenyl has never been reported, so far as I know. It should be of interest in connection with the benzene spectrum as diphenyl consists of two benzene rings linked together at one corner. Its spectrum was photographed with the apparatus described in the preceding paper for the investigation of substances available only in limited quantity. The water circulation in the coil was cut off, and the radiation of the quartz capillary arc was sufficient to keep the water in the outer tube above the fusion point of the diphenyl; and a minute pointed gas flame placed a few centimeters below the window of the tube kept the material fluid below the water level. The diphenyl was distilled in the high vacuum of an oil pump directly into the Raman tube, which was then hermetically sealed with a flame. I am under obligation to Mr. George B. Collins who gave much assistance in this part of the work.

The material was so powerfully fluorescent under the total radiation of the mercury arc that practically no trace of Raman lines appeared; but with sulphate of quinine in the water cell, very fair spectra were obtained; though the continuous background due to fluorescence was still very strong even in this case. Better results are hoped for by excitation with the green line or by the 4381 line of helium. The spectrum consisted of a group of five faint diffuse lines just barely visible on the continuous spectrum and seven strong lines, some of which coincided with benzene lines. They are given in the following table

TABLE III. *Raman spectrum of diphenyl.*

	λ	Diphenyl Int.	$\Delta\nu$	Benzene	
very faint	4439	(0)	416		
	4477	(0)	606	4476	
	4502	(0)	731		
	4509	(0)	766		
	4518	(0)	810		
	4557	(6)	990	4556	(50)
	4562	(2)	1023		
	4616	(4)	1280		
	4673	(1)	1544		
	4684.5	(6)	1584	4682	(8)
	4687.5	(8)	1603	4686	(6)
	5029		3055	5029	
	5048		3170	5048	

The first five lines form the diffuse group referred to above. Their wavelengths have not been very accurately determined as they were obtained

only with a spectrograph of small dispersion. One of them appears to coincide with a benzene line. The line 990, and the double line 1584-1603 of benzene appear, but 1178 is missing. The line 3170 is fairly strong with diphenyl but very weak with benzene, while 2947 is absent. Line 4557 of diphenyl has about the same intensity as the double line 4684-4687, while the same line of benzene is six or eight times as intense as the doublet.

Spectra of benzene and diphenyl are reproduced in coincidence in Fig. 1 of the previous paper (Spectra *K* and *L*). They were not enlarged to exactly the same scale, which accounts for the slight discrepancy in coincidence.

HEATS OF CONDENSATION OF ELECTRONS ON SEVERAL METALS IN SEVERAL IONIZED GASES

BY C. C. VAN VOORHIS, PRINCETON UNIVERSITY AND
K. T. COMPTON, MASSACHUSETTS INSTITUTE OF TECHNOLOGY

(Received September 17, 1930)

ABSTRACT

Heats of condensation ϕ_- of electrons on electrodes of Mo, Pt and W coated with K were measured in the ionized gases Ar, Ne, He, N₂ and H₂, by measuring the heat developed in Langmuir collectors of these metals when a known number of electrons of known energy were received by it. The values of ϕ_- varied as expected for the different metals, but also showed decided dependence on the surrounding ionized gas, even though this was a highly purified inert gas. The highest and lowest values recorded were 5.21 volts for Pt in N₂ and 0.93 for W+K in He. There is evidence that the specific effect of a purified gas is due to its ions rather than its neutral atoms. The accuracy of the experimental determinations is well within 1 percent.

IN A previous paper¹ a method for measuring the heat of condensation ϕ_- of electrons upon a metal collector in a gas discharge was described in detail. This method makes use of a small spherical Langmuir collector in which is imbedded a thermocouple. From the electron currents and the rates of heating at two different potentials (both somewhat negative to the space potential) and the application of some minor corrections, ϕ_- is obtained. Continuing with the same type of apparatus, additional measurements have been made on collectors of several metals in several gases. The inert gases used were all purified in the vacuum system by "misch metal" arcs, and the other gases were prepared and purified as previously described.

Corrections for the effect of contact potential difference between the collector and anode, hereafter called C.P.D., (corrections not applied in the previous paper) were found to be very necessary in order to get consistent results under some of the experimental conditions. This was due to variations in the C.P.D. following cleansing of the surface of the collector by positive ion bombardment, and was particularly evident when measurements were being made with a Pt collector. After the collector had been bombarded with positive ions accelerated by a field of a few hundred volts in order thoroughly to clean the surface and remove adsorbed gas layers, it was noticed that the electron current to the collector gradually increased while the potential of the collector, which was slightly negative to the space, was kept at the same value with respect to the anode, the general arc conditions remaining the same. The change in collector potential necessary to reduce the collector current to the value it had immediately after bombardment, is the change in C.P.D. Table I gives a typical set of results for platinum in argon extending over a period of about 1 hour after bombardment.

¹ K. T. Compton and C. C. Van Voorhis, Proc. Nat. Acad. Sci. 13, 336 (1927); C. C. Van Voorhis, Phys. Rev. 39, 318 (1927).

TABLE I. *Effect of contact potential difference change.*

Calculated from observations	Change in C.P.D.	ϕ_- Calculated for freshly bombarded collector
4.85 volts	0.05 volts	4.90 volts
4.78	.14	4.92
4.68	.22	4.90
4.65	.26	4.91
4.65	.27	4.92

When the previous paper was published there was considerable uncertainty as to the specific heat of molybdenum, the material of which the spherical collector had been made. Since then measurements of the specific heat of Mo have been made in two independent investigations^{2,3} the results agreeing within 1 percent in the range of temperature concerned in our measurements of ϕ_- . The present paper includes the revised results obtained by using these new specific heat values, as well as the results of some new measurements of ϕ_- for Mo in He, Ne and two gases previously used, A and N. The repeated measurements were made to take account of whatever C.P.D. change there might be. However, as will be seen from the result given in Table II, this effect was negligible in the measurements previously made in A and was small in N.

The results of these measurements are assembled in Table II.

TABLE II. *Values of ϕ_- and C.P.D. changes, Δ , in volts. Δ is the change in C.P.D. measured from the instant at which the positive ion bombardment (for cleansing the surface) was stopped.*

Collector Material	Argon		Neon		Helium		Nitrogen		H ₂ +inert gas	
	ϕ_-	Δ	ϕ_-	Δ	ϕ_-	Δ	ϕ_-	Δ	ϕ_-	Δ
Mo	4.14	0-0.2	3.69	0-0.1	3.53	0-0.1	4.47	0-0.1	—	—
Mo*	4.12	?	—	—	—	—	4.39	?	3.79	?
							(4.19)†	?	(3.47)	?
Pt	4.89	0-0.5	4.61	0-0.3	4.39	0-0.2	5.21	0-0.4	3.9±0.6	—
W+K†	1.11	0	1.05	0	0.93	0	—	—	—	—

* Old results¹ corrected by use of better specific heat values,^{2,3} but not for C.P.D. changes, which were not measured.

† W+K was a tungsten collector coated by distillation with potassium.

‡ () are doubtful, being perhaps due to a spurious C.P.D. change caused by some impurity. These lower values were not found with the new tube.

GENERAL DISCUSSION OF RESULTS

Results in the inert gases. When the previous paper¹ was published, we believed that the value of ϕ_- of a metal obtained in an inert gas discharge by this method would be the same as ϕ_- obtained by thermionic methods in a high vacuum, after correcting for the large difference in the temperatures involved in the two methods. The results show, however, that in gas discharges even in the inert gases the value of ϕ_- for a given metal depends upon the gas, for the values in A, Ne and He, respectively, differ from each other by amounts much larger than the experimental errors involved. We believe

² J. E. Stern, Phys. Rev. 32, 298 (1928).

³ D. Cooper and G. O. Langstroth, Phys. Rev. 33, 243 (1929).

that these differences are not due to differences in the amounts of active impurities in the respective inert gases, because the values of ϕ_- appear to be perfectly definite and reproducible, once the gas and apparatus are well cleansed, and are not modified by further strenuous purification.

Because of the following results obtained in mixtures of inert gases we suggest that these differences in the values of ϕ_- may be due to a layer of gas atoms or positive ions, probably the latter, on the collector. With a Pt collector in a 50%–50% Ne–A mixture, ϕ_- was 4.92 and 4.78 volts in 16 and 22 volt arcs respectively. In a 75%–25% He–A mixture ϕ_- was 4.80 and 4.68 volts in 18 and 30 volt arcs respectively and in a 50%–50% He–A mixture ϕ_- was 4.91 and 4.77 volts in 18 and 30 volts arcs respectively. Thus with an arc voltage lower than the ionizing potential of one of the gases in the mixture, the value of ϕ_- is near that characteristic of the gas with the lower ionizing potential, but with an arc of voltage high enough to ionize both gases, the value of ϕ_- is between the values of the two pure gases.

Also after the collector was bombarded with 200–300 volt positive ions in an inert gas mixture the C.P.D. *increased* for a short time immediately after bombardment when the arc voltage was high enough to ionize both gases, but when the arc voltage was high enough to ionize only one gas the C.P.D. decreased immediately after bombardment. This effect was rather small but was found in 50%–50% mixtures of any two of the inert gases used. Thus in the A–He mixture with a 30 volt arc the C.P.D. increased about 0.02 volt to a maximum in about 15 seconds, then decreased about 0.06 volt in the next minute; but with an 18 volt arc there was only the decrease of 0.06 volt starting immediately after bombardment. In the A–Ne mixture with a 25 volt arc the increase in C.P.D. was 0.015 in the first 30 seconds and then a decrease of 0.06 volt in the next two minutes, while with a 17 volt arc there was only the 0.06 volt decrease in C.P.D. during about 150 seconds after bombardment. In the He–Ne mixture with a 30 volt arc there was an increase in C.P.D. of 0.05 volt in 30 seconds and then a decrease of 0.09 volts in the next two minutes, whereas with a 21 volt arc there was only a decrease of about 0.06 volt in about 35 seconds starting immediately after bombardment.

These results, indicating that the specific influence of the inert gas on ϕ_- is due to its ions rather than to its atoms, further suggest that it arises from the halogen-like character and hence great chemical activity of the ions, which may lead to a prolonged period of attachment of the ion to the metal during the process of its neutralization. If each incoming positive ion were to remain in contact with the surface for 0.001 second the surface would be about 10 percent covered with ions.

General discussion. The new results for ϕ_- with a Mo collector in argon (see Table II) agree well with the corrected results from the former measurements while in nitrogen the new ϕ_- value differs from the old higher value by about the amount of C.P.D. corrections, but with the new tube there did not seem to be enough evidence of a lower value also, to warrant its inclusion in the table. The values of ϕ_- with a Pt collector have been calculated with

the use of the specific heat equation $C_T = 0.03165 + 0.0000060t$, based on the results of Magnus⁴ and White,⁵ and show the same order of variation as with Mo in the inert gases and nitrogen, but the values of ϕ_- with hydrogen present in the discharge were quite variable and not at all reproducible. It was not possible to maintain the discharge in pure hydrogen and though the hydrogen content of the gas mixtures was "cleaned up" rather rapidly, this is not the whole cause of the variableness of the results as the changes were not progressive but more or less random.

Similar variableness in results was found in the measurements of ϕ_- with a tungsten collector in argon, the values obtained ranging from 2.0 to 3.2 volts, in spite of prolonged attempts to get steady conditions. The fact that the tungsten used was ordinary thoriated "C" grade used in the lamp industry may account for these low values and the variableness of these results, but, because of this uncertainty, the values are not recorded in Table II. After a small amount of potassium had been vaporized into the discharge tube in the neighborhood of the W collector, the results were quite steady and reproducible, giving the values recorded in Table II. The specific heat equation used in calculating the W results was $C_T = 0.03194 + 0.00000613t$ from Zwikker⁶ which is in good agreement also with the more recent results of Magnus and Holzmann.⁷ With the potassium in the discharge tube no C.P.D. change was observed.

Accuracy of the results. The mean values given in Table II are the means of from 10 to 50 separate determinations of ϕ_- none of which differed from the mean by more than 0.10 volts, the rare values having a larger variation being discarded. Also each mean value is the result of averaging the results from at least three fillings of the gas used, in many cases other fillings of other gases being interspersed. In many cases under good experimental conditions the maximum variation in a series of 6 to 8 results would be less than 0.05 volts.

A small correction⁸ to take account of reflected electrons probably should be made. Any such correction should be *subtracted* from the values given for ϕ_- since the reflected electrons have delivered some of their energy to the collector. Just how large this correction should be is rather difficult to estimate since the average incident energy of the electrons is of the order of one volt and the measurements of Petry⁹ and others have shown that the reflection coefficient of slow electrons varies greatly with the surface conditions of the collector. However, since the reflection coefficient is small for slow electrons striking a collector covered by a gas layer we believe this correction to be less than 0.10 volt. In any case such a correction is too small and in the wrong direction to account for the difference in ϕ_- in the different inert gases.

⁴ A. Magnus, Ann. d. Physik 48, 997 (1915).

⁵ W. P. White, Phys. Rev. 12, 436 (1918).

⁶ C. Zwikker, Zeits. f. Physik 52, 668 (1928).

⁷ A. Magnus and H. Holzmann, Ann. d. Physik 3, 598 (1929).

⁸ The need for such a correction was called to our attention by H. M. Mott-Smith after the publication of the previous paper.¹

⁹ R. L. Petry, Phys. Rev. 26, 346 (1925) and Phys. Rev. 28, 362 (1926).

CONCLUSION

Our results show conclusively that ϕ_- in a gas discharge depends not only upon the material of the collector or cathode but also upon the gases in which the discharge takes place even though very pure inert gases are being used. Even a very slight impurity in the gas or collector material may lower the value of ϕ_- by a large amount. Consequently in evaluating the energy balance at the electrodes, fairly large errors may be made unless the value of ϕ_- for the existing experimental conditions is determined and used in the calculations.

In conclusion we wish to express our thanks to Mr. Donald C. Archibald who helped with the experimental work upon which this paper is based.

CORRELATION OF ATOMIC J VALUES AND MOLECULAR QUANTUM NUMBERS, WITH APPLICATIONS TO HALOGEN, ALKALINE EARTH HYDRIDE, AND ALKALI MOLECULES

BY ROBERT S. MULLIKEN*

RYERSON PHYSICAL LABORATORY, UNIVERSITY OF CHICAGO

(RECEIVED AUGUST 22, 1930)

ABSTRACT

Rules are given for determining the Ω values and symmetry properties of the molecular states obtainable from the union of two atoms with specified J values, assuming case c coupling in the molecule. These are used to determine the correlation of molecular Λ and S values with atomic J values, for cases where there is strong L , S coupling in one or both atoms. The correlation rules are applied to $I+I$, $Hg+H$, and $Cs+Cs$. Difficulties which exist when a similar correlation is attempted in cases where the L , S coupling is weak (e.g. $Mg+H$, or $Na+Na$) are discussed. Electron configurations and dissociation products are discussed in some detail in the case of the halogen molecules, and an interpretation is given, in terms of electron configurations, of the analogies and differences between the spectra of the members of homologous series of molecules such as F_2 , Cl_2 , Br_2 , I_2 , or Li_2 , Na_2 , K_2 ,

STATEMENT OF THE PROBLEM

WIGNER and Witmer¹ have given rules for completely determining, in terms of Λ and S values and symmetry properties, the possible molecular states which result from the union of two atoms with specified L and S values $L_1S_1L_2S_2$ and specified symmetry character (even or odd). Most of the results given by these rules can be obtained very simply² by assuming negligible L , S couplings in the atoms and determining the possible values of the projections M_{L_1} and M_{L_2} of L_1 and L_2 on the internuclear axis, and from these the possible Λ values ($\Lambda = |M_{L_1} + M_{L_2}|$). The resulting S values are $S_1 + S_2$, $S_1 + S_2 - 1$, . . . , $|S_1 - S_2|$, once for each M_{L_1} , M_{L_2} combination. In the case of two atoms of the same element^{2a}, in *unlike* states,³ each molecular state of given M_{L_1} , M_{L_2} , and S occurs twice, there being always one even (g) and one odd (u) state. For like^{2a} atoms in the *same* state,³ the number of molecular states is, however, not doubled. Here a consideration of the way

* Fellow of the John Simon Guggenheim Memorial Foundation.

¹ E. Wigner and E. E. Witmer, *Zeits. f. Physik*, **51**, 883 (1928).

² The method here indicated was first used by F. Hund. Wigner and Witmer later, by a more rigorous method, cleared up some doubtful points, and determined the symmetry properties of the molecular terms.

^{2a} The electron states of a molecule composed of two different isotopes of one element are not quite strictly, but are for all practical purposes, g and u . In respect to the rules given in this paper, different isotopes of an element may be regarded as identical.

³ "The same state" here means the same set of n 's and l 's and the same L and S , but not necessarily the same J 's or M 's. "Unlike states" means here states differing in some way other than in the J 's or M 's.

in which (in zeroth approximation) the atomic combine to give the molecular wave-functions is required to determine which molecular states are g and which are u . When $\Lambda=0$, it is necessary to distinguish Σ^+ and Σ^- states. When $\Lambda=0$ results from $M_{L_1} = -M_{L_2}$, there is always one Σ^+ and one Σ^- state, derived from a splitting up of the degenerate pair $+M_{L_1} - M_{L_2}$ and $-M_{L_1} + M_{L_2}$. When $\Lambda=0$ results from $M_{L_1} = M_{L_2} = 0$, however, a consideration of the forms of the atomic and molecular wave-functions is required to determine whether the resulting state is Σ^+ or Σ^- . The complete set of rules for all cases is given in convenient form in a recent paper by Hund.⁴ These rules are applicable to case a or b molecular states and hold regardless of whether or not the initial assumption of negligible L , S couplings in the atoms is true.

In cases where the actual L , S couplings are strong, so that atomic states with different J values differ considerably in energy, it is of interest to determine the molecular states capable of being formed from two atoms with specified L , S , and J values. For case a or b molecular states we should like to know to what J values (J_1 , J_2) each state of specified Λ and S (and Ω in case a) corresponds. The solution of this problem unfortunately cannot be given completely in terms of simple rules like those for the less detailed problem of the correlation of Λ and S with $L_1 S_1 L_2 S_2$. It can, however, be divided into two steps, for the first of which simple rules can be given. These steps are (1) determination of the possible Ω values, assuming case c coupling, for each pair of atomic J values ($J_1 J_2$), and (2) correlation of each such state of given Ω with one of the case a or b states whose Λ and S values are known from the Hund-Wigner-Witmer rules.

The results of the first step are of course directly applicable to case c molecular states, where Λ and S lack meaning, for example to certain excited states of the halogen molecules.⁵ It should also be noted that molecular states which for r near r_e have case a or b coupling tend normally to pass through case c when r is increased toward dissociation. Similarly, molecular states which have case c coupling for $r \sim r_e$ and $> r_e$ tend to go over to case a or b coupling when r is decreased.

RULES FOR CORRELATION OF Ω VALUES AND ATOMIC J VALUES

The problem of determining the Ω values of the molecular states derived from atoms with given J values is similar to that of the determination of Λ values when atomic L values are given. Most of the results can be obtained very simply, by considering the Ω values resulting from the possible projections M_1 and M_2 of J_1 and J_2 on the internuclear axis. For atoms of *different elements*, the Ω values are determined, if $\Omega > 0$, by $\Omega = |M_1 + M_2|$. When $\Omega = 0$,

⁴ F. Hund, Zeits. f. Physik, **63**, 723, 1930.

⁵ R. S. Mulliken, Phys. Rev., **36**, 699 (1930). This article unfortunately contains a number of minor errors, mainly typographical (e.g. use of small π for large Π).

⁶ Cf. Ref. 5, p. 702 and ref. 10, for definition and discussion of 0^+ and 0^- states, and nomenclature and selection rules for case c .

⁷ This is exactly analogous to the fact that when $\Lambda=0$ results from $M_{L_1} = -M_{L_2}$ (cf. text, above), there is always one Σ^+ and one Σ^- state.

we have to distinguish 0^+ and 0^- states.⁶ When $\Omega=0$ results from $M_1=-M_2$, there is always one 0^+ and one 0^- state, derived from the degenerate pair $+M_1-M_2$ and $-M_1+M_2$.⁷ When $\Omega=0$ results from $M_1=M_2=0$, a consideration of the atomic and molecular wave-functions is required to determine whether the resulting state is 0^+ or 0^- . In the case of two atoms of the *same element*^{8a} but in *unlike states*, each molecular state given by the above results is replaced by one even (*g*) and one odd (*u*) state.⁸ By "unlike states" are here meant atomic states which differ in respect to at least one quantum number, even if only in respect to *J* or *M*. (We are using the terms "like" and "unlike" states here in a different sense than in Ref. 3 and in a previous paragraph.) For *like atoms in the same state* (i.e. identical in all quantum numbers including *M*), the number of derived molecular states is the same as in the case of two unlike atoms. The symmetry (*g* or *u*) of such states can be determined by means of rules given by Wigner and Witmer.⁹ The complete set of rules for the determination of the possible Ω values derivable from two atoms having specified *J* values can be conveniently expressed as follows:¹⁰

A. *Unlike Atoms*

Let $J_1 \geq J_2$. The possible Ω values are as follows:

$$\begin{array}{c} J_1 + J_2, J_1 + J_2 - 1, \dots, \frac{1}{2} \text{ or } 0^+ \\ J_1 + J_2 - 1, \dots, \frac{1}{2} \text{ or } 0^- \\ \dots \\ \dots \\ J_1 - J_2, \dots, \frac{1}{2} \text{ or } 0^+ \text{ or } 0^- \end{array}$$

If J_1+J_2 is half-integral, the smallest Ω value is $\frac{1}{2}$. If J_1 and J_2 are both half-integral, the lowest Ω value is 0, and there are equally many 0^+ 's and 0^- 's. If J_1 and J_2 are both integral, there is an odd number of 0's and the *odd one* (which appears in the last line in the table of Ω values just given) is 0^+ or 0^- according as the sum $J_1+J_2+\Sigma l_1+\Sigma l_2$ (where l_1 and l_2 refer to the *l* values of the individual electrons in atoms 1 and 2), is even or odd.

B. *Like atoms in states differing in J or in some other quantum number, other than M*. The results are the same as under A, except that there is one odd (*u*) state and one even (*g*) state in place of each state given under A.

C. *Like Atoms in States Alike in all Quantum numbers with the possible*

⁸ Cf. Wigner and Witmer, *l. c.* p. 878-9, B and C.

⁹ Cf. Wigner and Witmer, *l. c.* p. 879, C. Wigner and Witmer's "positive" and "negative" eigenfunktionen are (in the case discussed in p. 879, C) respectively "even" and "odd" in the mode of description used here.

¹⁰ The relations given by these rules all follow directly from what has already been said together with what is said in Refs. 8-9, with the exception of (a) the rule under A for determining the symmetry character of the odd 0 in the case where J_1 and J_2 are both integral, and (b) the rule under C according to which for 0 states derived from like atoms in the same state, only 0^+_g and 0^-_u , but not 0^+_u or 0^-_g , are possible. These last rules follow indirectly from the results (*l. c.*, pp. 877-883) of Wigner and Witmer, or directly from a consideration of atomic and molecular wave functions.

exception of M . The results are the same as with $J_1 + J_2$ integral under A , except that approximately half the states are even, half odd according to the following schemes (here we write J in place of J_1 and J_2):

(1) J integral (numbers of electrons even in each atom)

$$\begin{aligned} (2J)_g, (2J-1)_g, (2J-2)_g, \dots, (0^+)_g \\ (2J-1)_u, (2J-2)_u, \dots, (0^-)_u \\ (2J-2)_g, \dots, (0^+)_g \\ \dots \\ \dots \\ (0^+)_g \end{aligned}$$

(2) J half-integral (number of electrons odd in each atom)

$$\begin{aligned} (2J)_u, (2J-1)_u, \dots, (0^-)_u \\ (2J-1)_g, \dots, (0^+)_g \\ \dots \\ \dots \\ (0^+)_g \end{aligned}$$

CORRELATION OF MOLECULAR Λ AND S VALUES WITH ATOMIC J VALUES. DISCUSSION OF I+I AS AN EXAMPLE

Let us now consider, as an example for the correlation of molecular quantum numbers with atomic J values, the union of two identical^{2a} halogen atoms, e.g. two I atoms, each in its 2P normal state ($L_1 = L_2 = 1, S_1 = S_2 = \frac{1}{2}, J_1 = \frac{1}{2}$ or $1\frac{1}{2}, J_2 = \frac{1}{2}$ or $1\frac{1}{2}$). First we must determine the Ω values. If both atoms have $J = 1\frac{1}{2}$, we have the following possibilities: (a) $M_1 = \pm 1\frac{1}{2}, M_2 = \pm 1\frac{1}{2}, \Omega = 3_u, 0_g^+, 0_u^-$; (b) $M_1 = \pm 1\frac{1}{2}$ or $\pm \frac{1}{2}, M_2 = \pm \frac{1}{2}$ or $\pm 1\frac{1}{2}, \Omega = 2_u, 2_g, 1_g, 1_u$; (c) $M_1 = \pm \frac{1}{2}, M_2 = \pm \frac{1}{2}, \Omega = 1_u, 0_g^+, 0_u^-$. If one atom has $J = 1\frac{1}{2}$, the other $J = \frac{1}{2}$, we get: (a) from $J_1 = 1\frac{1}{2}, M_1 = \pm 1\frac{1}{2}, J_2 = \frac{1}{2}, M_2 = \pm \frac{1}{2}$, and $J_2 = 1\frac{1}{2}, M_2 = \pm 1\frac{1}{2}, J_1 = \frac{1}{2}, M_1 = \pm \frac{1}{2}, \Omega = 2_g, 2_u, 1_g, 1_u$; (b) from $J_1 = 1\frac{1}{2}, M_1 = \pm \frac{1}{2}, J_2 = \frac{1}{2}, M_2 = \pm \frac{1}{2}$, and $J_1 = \frac{1}{2}, M_1 = \pm \frac{1}{2}, J_2 = 1\frac{1}{2}, M_2 = \pm \frac{1}{2}, \Omega = 1_g, 1_u, 0_g^+, 0_u^+, 0_g^-, 0_u^-$. If both have $J = \frac{1}{2}$, we have $M_1 = \pm \frac{1}{2}, M_2 = \pm \frac{1}{2}, \Omega = 1_u, 0_g^+, 0_u^-$. (The M 's have been written out in detail here in order to help make clear, through an example, the relations of the Ω values and symmetry properties to the M values.) Summarizing, ($1\frac{1}{2}, 1\frac{1}{2}$) gives one each of $3_u, 2_g, 2_u$, and 1_g , two each of $1_u, 0_g^+$, and 0_u^- ; ($1\frac{1}{2}, \frac{1}{2}$) gives one each of $2_g, 2_u, 0_g^+, 0_u^+$, 0_g^- , and 0_u^- , two each of 1_g and 1_u ; ($\frac{1}{2}, \frac{1}{2}$) gives one each of $1_u, 0_g^+, 0_u^-$.

For sufficiently small r values, we expect case a or b coupling. The correlation between large and small r values can be made (tentatively: cf. last section, on Qualifications and Difficulties) by means of the rules: the lowest 0_g^+ state for large r (case c) goes over into the lowest 0_g^+ state for small r (case a or b), the next lowest 0_g^+ state into the next lowest, and so on, with

corresponding rules for each other type of state ($2_u, 1_u, 0_u^-, 0_u^+, 1_g, 2_g, 0_g^-$). The energy of each individual state as a function of r , for stationary nuclei, may be called a $U(r)$ curve. The rules just given say that no two $U(r)$ curves which belong to the same Ω value and symmetry type can cross; it also implies that any two $U(r)$ curves differing in these respects *may* cross.¹¹

In order to apply the rule just given it is necessary to consider what such case c designations as 0_g^+ , 1_u , and so on, correspond to in cases a and b . We can best do this by going in the reverse direction. In case a states ($^1\Sigma^+$, $^1\Sigma^-$, $^1\Pi$, $^1\Delta$, \dots , $^2\Pi_{1/2}$, $^2\Pi_{3/2}$, $^2\Delta_{1/2}$, $^2\Delta_{3/2}$, \dots , $^3\Pi_0$, $^3\Pi_1$, $^3\Pi_2$, $^3\Delta_1$, $^3\Delta_2$, $^3\Delta_3$, \dots), Ω exists as in case c . Hence $^1\Sigma^+$ gives 0^+ , $^1\Sigma^-$ gives 0^- , $^1\Pi$ gives 1, $^1\Delta$ gives 2 of case c , and so on. $^3\Pi_0$ and all other states with $\Omega=0$ split in case c into 0^+ and 0^- .⁶ All other states go according to their Ω values. The symmetry property indicated by g or u is also maintained. Case b states with $\Lambda > 0$ can be correlated with case c states by first assuming the corresponding case a states. Case b states with $\Lambda=0$ go over as follows: $^2\Sigma^+$ or $^2\Sigma^-$ gives $\frac{1}{2}$ of case c ; $^3\Sigma^+$ gives 0^- and 1, $^3\Sigma^-$ gives 0^+ and 1 (cf. Fig. 1); $^4\Sigma^+$ or $^4\Sigma^-$ gives $\frac{1}{2}$ and $1\frac{1}{2}$; $^5\Sigma^+$ gives 0^+ , 1, and 2, $^5\Sigma^-$ gives 0^- , 1, and 2 (cf. Fig. 1); and so on.

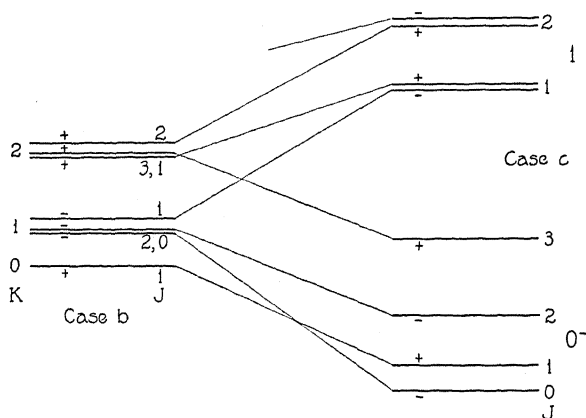


Fig. 1. Correlation of rotational levels of a typical case b $^3\Sigma^+$ state with those of the corresponding 0 and 1 states of case c . The positive (Wigner-Witmer nomenclature) or even (Kronig nomenclature) rotational levels are marked +, the negative or odd, $-$. If the case c 0 levels lay above instead of below the 1 levels, the correlations would be different, but the 0 state would still be 0^- , since the fact that the one level with $J=0$ in case b is a negative ($-$) level always brings it about that we have a 0^- state in case c . To obtain the relations for a case b $^3\Sigma^-$ state, which gives a 0^+ and a 1 state in case c , it is only necessary to reverse all the signs in Fig. 1. The relations for $^5\Sigma$ and other Σ states follow in a similar manner.

From the rules of Wigner and Witmer for Λ and S values, we know that the following case a and b states can be formed, using all the combinations $(J_1, J_2) = (1\frac{1}{2}, 1\frac{1}{2}), (1\frac{1}{2}, \frac{1}{2}), (\frac{1}{2}, \frac{1}{2})$, from two normal halogen atoms: $^1\Sigma_g^+$,

¹¹ For a general discussion of correlation problems in molecule formation, cf. W. Weizel, *Zeits. f. Physik*, 59, 320 (1930).

$^3\Pi_u$, $^1\Pi_u$, $^3\Sigma_g^-$, $^1\Delta_g$, $^1\Sigma_g^+$, $^3\Pi_g$, $^1\Pi_g$, $^3\Sigma_u^+$, $^3\Delta_u$, $^3\Sigma_u^-$, $^1\Sigma_u^-$. Let us assume that the order of these states, say for some single definite fairly small value of r , is as just given, i.e. with $^1\Sigma_g^+$ lowest, $^3\Pi_u$ next, and so on. Then according to the correlation rules given above, the lowest $^1\Sigma_g^+$ (small r) becomes 0_g^+ (large r) and gives $^2P_{1\frac{1}{2}} + ^2P_{1\frac{1}{2}}$ on dissociation. For brevity we shall write this $^1\Sigma_g^+$, $0_g^+(1\frac{1}{2}, 1\frac{1}{2})$. In a similar manner, we have $^3\Pi_{2u}$, $2_u(1\frac{1}{2}, 1\frac{1}{2})$; $^3\Pi_{1u}$, $1_u(1\frac{1}{2}, 1\frac{1}{2})$; $^3\Pi_{0u}$, $0_u^-(1\frac{1}{2}, 1\frac{1}{2})$ and $0_u^+(1\frac{1}{2}, \frac{1}{2})$; $^1\Pi_u$, $1_u(1\frac{1}{2}, 1\frac{1}{2})$; $^3\Sigma_g^-$, $1_g(1\frac{1}{2}, 1\frac{1}{2})$ and $0_g^+(1\frac{1}{2}, 1\frac{1}{2})$; $^1\Delta_g$, $2_g(1\frac{1}{2}, 1\frac{1}{2})$; $^1\Sigma_g^+$, $0_g^+(1\frac{1}{2}, \frac{1}{2})$; $^3\Pi_{2g}$, $2_g(1\frac{1}{2}, \frac{1}{2})$; $^3\Pi_{1g}$, $1_g(1\frac{1}{2}, \frac{1}{2})$; $^3\Pi_{0g}$, $0_g^-(1\frac{1}{2}, \frac{1}{2})$ and $0_g^+(\frac{1}{2}, \frac{1}{2})$; $^1\Pi_g$, $1_g(1\frac{1}{2}, \frac{1}{2})$; $^3\Sigma_u^+$, $0_u(1\frac{1}{2}, 1\frac{1}{2})$ and $1_u(1\frac{1}{2}, \frac{1}{2})$; $^3\Delta_{3u}$, $3_u(1\frac{1}{2}, 1\frac{1}{2})$; $^3\Delta_{2u}$, $2_u(1\frac{1}{2}, \frac{1}{2})$; $^3\Delta_{1u}$, $1_u(1\frac{1}{2}, \frac{1}{2})$; $^3\Sigma_u^+$, $0_u^-(1\frac{1}{2}, \frac{1}{2})$ and $1_u(\frac{1}{2}, \frac{1}{2})$; $^1\Sigma_u^-$, $0_u^-(\frac{1}{2}, \frac{1}{2})$.

A consideration of this example shows that if we assumed a sufficiently different order of molecular levels, the correlation with atomic J values would be more or less altered. For example, if we assumed the order of the molecular levels for small r to be $^1\Sigma_g^+$, $^3\Pi_u$, $^1\Pi_u$, $^1\Sigma_g^+$, $^3\Pi_g$, $^3\Sigma_g^-$, $^1\Delta_g$, etc., then we should have $^1\Sigma_g^+$, $^3\Pi_u$, and $^1\Pi_u$ with correlations just as before but then: $^1\Sigma_g^+$, $0_g^+(1\frac{1}{2}, 1\frac{1}{2})$ instead of $1\frac{1}{2}, \frac{1}{2}$ as before; $^3\Pi_{2g}$, $2_g(1\frac{1}{2}, 1\frac{1}{2})$ instead of $1\frac{1}{2}, \frac{1}{2}$; $^3\Pi_{1g}$, $1_g(1\frac{1}{2}, 1\frac{1}{2})$ instead of $1\frac{1}{2}, \frac{1}{2}$; $^3\Pi_{0g}$, $0_g^-(1\frac{1}{2}, \frac{1}{2})$ as before and $0_g^+(1\frac{1}{2}, \frac{1}{2})$ instead of $\frac{1}{2}, \frac{1}{2}$; $^3\Sigma_g^-$, $1_g(1\frac{1}{2}, \frac{1}{2})$ instead of $1\frac{1}{2}, 1\frac{1}{2}$ and $0_g^+(\frac{1}{2}, \frac{1}{2})$ instead of $1\frac{1}{2}, 1\frac{1}{2}$; $^1\Delta_g$, $2_g(1\frac{1}{2}, \frac{1}{2})$ instead of $1\frac{1}{2}, 1\frac{1}{2}$. A correct determination of the correlation of molecular Λ and S values with atomic J values therefore evidently depends in an essential manner on a knowledge of the energy order of the molecular levels. This order, however, cannot in general be predicted in advance. Nevertheless it can often be approximately predicted, or in simple cases exactly. Usually we know theoretically that many if not most of the molecular levels given by Wigner and Witmer's Λ and S rules have very high energies for small r values, and have very large r_e values and very small dissociation energies. Predictions of the kind just indicated, combined with an empirical knowledge of part of the levels in question, are often sufficient for practical purposes. Furthermore, there are always one or two "unique levels" for which the J correlation can be given without any knowledge of the energy order of the molecular levels. Unique levels are levels whose Ω and symmetry type occur only once in the list of states derivable from two atoms with given L and S values. In our example, the unique levels are 3_u of case c , which necessarily becomes $^3\Delta_{3u}$ of case a , 0_u^+ which necessarily becomes part of $^3\Pi_{0u}$, and 0_g^- which necessarily becomes part of $^3\Pi_{0g}$.

Fig. 2 illustrates how the foregoing considerations can be applied to the I_2 molecule. (Analogous relations doubtless hold for Br_2 , probably also for Cl_2). The normal state of I_2 is in all probability a $^1\Sigma_g^+$ state⁵ derived from two iodine atoms each in the 2P normal state. According to the rules given above it must be derived from two $^2P_{1\frac{1}{2}}$ atoms. The r_e value of the normal state of I_2 (let us call it r_N) is probably small enough so that we have approximately case $a-b$ coupling. As has been shown in a previous paper,⁵ the upper state of the visible I_2 absorption bands is in all probability a 0_u^+ state. The r_e value of this state is much larger than r_N and the coupling conditions, for $r \sim r_e$, probably approximate those of case c . If, however, we follow the $U(r)$

curve of this state to smaller r values, we may probably expect nearly case a coupling when $r \sim r_N$ or less. Now this 0_u^+ state is a "unique state" and we know that it must belong to a ${}^3\Pi_{0u}$ state in case a . But in case a we expect to find ${}^3\Pi_0$ accompanied by ${}^3\Pi_1$ and ${}^3\Pi_2$. In Fig. 2 we have assumed that these three levels form an inverted ${}^3\Pi$ whose width is of the same order of magnitude as that of the inverted 2P normal state of the atom. According to the rules given in preceding paragraphs, as well as empirically, the 0_u^+ component of ${}^3\Pi_{0u}$ is derived from ${}^2P_{1/2} + {}^2P_{1/2}$, while the ${}^3\Pi_2$ and ${}^3\Pi_1$ levels and the 0_u^- component of the ${}^3\Pi_0$ are according to our rules derived from two ${}^2P_{1/2}$ atoms. (A different correlation would be expected only if the states ${}^3\Sigma_u^+$ and ${}^3\Delta_u$ lie

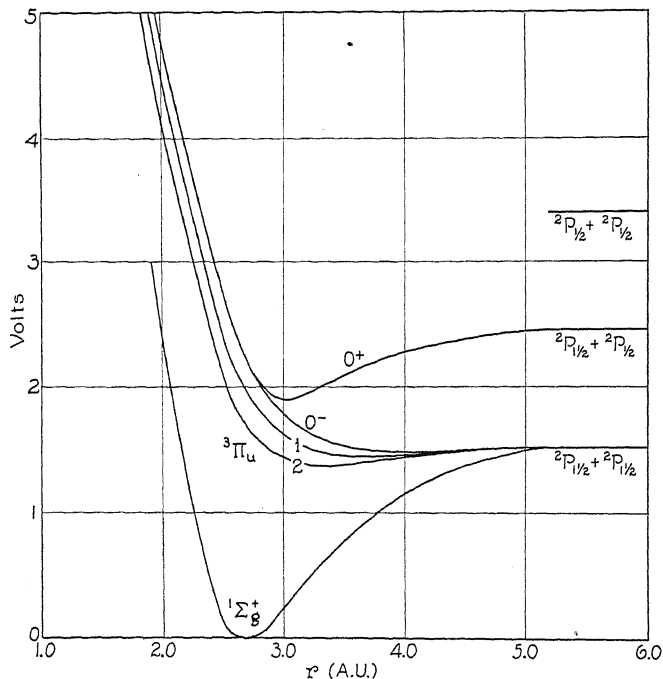


Fig. 2. $U(r)$ curves for ${}^1\Sigma_g^+$ and 0_u^+ states of I_2 drawn to scale according to Morse's function (P. M. Morse, Phys. Rev. 34, 57, 1929). $U(r)$ curves for the 0_u^- , 1_u , and 2_u components of ${}^3\Pi_u$ are sketched in a plausible way (cf. text). The numerous other $U(r)$ curves derivable from the normal (2P) atomic levels probably all correspond to unstable molecular states, and are omitted here. The family of $U(r)$ curves derived from normal atoms is probably crossed by one or more curves of large r_e but large D derived from $F^+ + F^-$ (cf. text).

below ${}^3\Pi_u$ for $r = r_N$, an arrangement which is seen to be very improbable when one considers possible electron configurations for the states last mentioned.) The assumption that the ${}^3\Pi$ state is an inverted ${}^3\Pi$ with large multiplet spacing is made probable by a consideration of electron configurations (see below). In Fig. 2, $U(r)$ curves are sketched for the normal state and the ${}^3\Pi_u$ state of I_2 , based on the facts and assumptions just discussed and on our experimental knowledge of the normal state and the 0_u^+ state. A study of possible electron configurations indicates that the numerous other molecular

states derivable from two normal halogen atoms (see above) probably all have larger r_e values and smaller D values than the 0_u^+ state. (To make Fig. 2 complete, the $U(r)$ curves of these states should be added.) To be sure, other states of I_2 are known in addition to $^1\Sigma_g^+$ and 0_u^+ , including one (state B of Pringsheim and Rosen) which for $r=r_e$ probably lies between $^1\Sigma_g^+$ and 0_u^+ . Although the data on this state are uncertain¹², they indicate that it has a small or rather small ω_e , hence a large or rather large r_e , but that it has at the same time a large D . These characteristics make it likely that it is derived from two ions ($I^+ + I^-$).

Before going farther with the theoretical discussion of the correlation of atomic and molecular states, we shall digress in order to consider some other interesting points about the halogen molecules which are brought out or suggested by Fig. 2. If Fig. 2 is correct, one would probably expect to find a strong continuous spectrum resulting from the transition $^3\Pi_{1u} \leftarrow ^1\Sigma_g^+$, and probably also weaker continua corresponding to $^3\Pi(0_u^-) \leftarrow ^1\Sigma_g^+$ and $^3\Pi_{2u} \leftarrow ^1\Sigma_g^+$. If the arrangement of the $U(r)$ curves for the $^3\Pi_u$ levels is correctly shown in Fig. 2, the continua just mentioned should in part overlies the discrete bands of the transition $0_u^+ \leftarrow ^1\Sigma_g^+$. So far as I know there is, however, no evidence of a strong continuum in this region.

ELECTRON CONFIGURATIONS AND $U(r)$ CURVES IN HALOGEN AND OTHER MOLECULES

By a consideration of electron configurations in connection with the above discussion, a qualitative explanation of the differences between the $0_u^+ \leftarrow ^1\Sigma_g^+$ bands of the four halogens can be given. These differences can be expressed as follows: for the upper level, D increases in the series F_2 to I_2 , for the lower level it decreases. The essential thing here is perhaps that the contrast between the two states decreases as the quantum numbers of the outer electrons increase.¹³ In terms of electron configurations this can be understood as follows. The normal, $^1\Sigma_g^+$, state of F_2 has an electron configuration (composed of closed shells) which for definiteness we shall write $1s^2 2p^2 2s^2 3p^2 3d^2 4s^2 4p^4$. (That the four least firmly bound electrons are π electrons is practically certain, although that they are $3d\pi$ is less certain.) The last ten electrons in $F_2(2p^4 3d^2 3d\pi^4)$ are very probably derived from the ten $2p$ electrons of the two normal F atoms. Of these ten, the $2p\pi$

¹² State B is observed in absorption, but only at high temperatures (P. Pringsheim and B. Rosen, *Zeits. f. Physik*, 50, 1, 1928), as the initial (lower) state of a band system not otherwise known. The upper state of these bands (state D) may be identical (Pringsheim and Rosen, *l.c.*) with the upper state of the ultraviolet absorption bands of I_2 , whose lower state is the normal $^1\Sigma_g^+$ state (state A). If this last is true, state D must be an odd state (u) and state B , like state A , an even (g) state, since g states combine spectroscopically only with u states. Pringsheim and Rosen's data indicate that state D , like B , has a large r_e and large D , and it seems likely that it also is derived from $I^+ + I^-$.

¹³ One should really compare the energies of the $^1\Sigma_g^+$ and $^3\Pi_u$ states at the same value of r , instead of at their respective r_e values. One might well, for instance, take $r=r_N$ and project upward from $U(r_e)$ of the $^1\Sigma_g^+$ state to the $U(r)$ curves of the $^3\Pi_u$ states. When this is done the contrast between F_2 and I_2 becomes very marked, as can be seen by comparing Fig 2. with a corresponding set of curves for F_2 .

are unpromoted and the $3d\pi$ are promoted, $2p\pi$ electrons of the atom, while $3d\sigma^2$ represents two promoted $2p\sigma$ atomic electrons. A further stage of promotion is also to be expected for the latter, in which they become probably $4f\sigma$ molecular electrons; these might be looked for in excited states of the molecule. The ${}^3\Pi_u$ state to which our case c 0_u^+ state belongs has very probably a configuration obtained by displacing one of the most loosely-bound electrons ($3d\pi$) to the first available σ orbit, very likely $4f\sigma$; the promoted orbit $3d\pi$ is thus replaced by a more strongly promoted orbit, and D is decreased. Analogous configurations presumably exist in the other halogen molecules; it would be difficult to explain in any other way their great chemical and spectroscopic analogy. For Cl_2 we may reasonably assume $\cdots 3s\sigma^2 4p\sigma^2 3p\pi^4 4d\sigma^2 4d\pi^4$ for the normal state and $\cdots 4d\pi^3 5f\sigma$ for the ${}^3\Pi_u$ state, and for Br_2 and I_2 configurations in which the quantum numbers of the outer electrons are increased by one and by two units respectively. In each case the $p\pi$ electrons are unpromoted atomic p electrons from the outermost shell, the $d\sigma$, $d\pi$, and $f\sigma$ electrons are promoted electrons from the same source. Now with increase in the principal quantum number of promoted and unpromoted electrons alike, the energy differences between promoted and unpromoted electrons and between different stages of promotion, should evidently decrease steadily. In particular, the energy difference between $nd\pi$ and $(n+1)f\sigma$, and with it the difference in D values between $\cdots nd\pi^4 {}^1\Sigma$ and $\cdots nd\pi^3(n+1)f\sigma {}^3\Pi$, should decrease steadily as n increases from 3 in F_2 to 6 in I_2 .¹³ This seems to explain satisfactorily the characteristics of the halogen levels discussed at the beginning of this paragraph.

Similar analogies and differences are known in other series of homologous molecules, e.g. O_2 , S_2 , Se_2 , Te_2 ; Li_2 , Na_2 , K_2 , Rb_2 , Cs_2 ; CN , SiN , $\cdots \text{BO}$, $\text{AlO} \cdots$. In all such cases, explanations analogous to that just given for the halogens are probably applicable.

FURTHER EXAMPLES

Fig. 3 shows the probable correlation of molecular states of HgH with J values of the Hg atom for the case of $\text{Hg}(\cdots 6s6p, {}^3P) + \text{H}(1s, {}^2S)$, using the rules above discussed. Similar correlations probably hold (but cf. Ref. 16) for CdH and ZnH .

As a further example we may consider the case of two alkali metal atoms with strong L, S coupling, say two Cs atoms, one in its normal (2S) state, the other in its lowest 2P state. For case $a-b$ we get the following states: ${}^3\Pi_u$, ${}^3\Sigma_g^+$, ${}^1\Sigma_u^+$, ${}^1\Sigma_g^+$, ${}^1\Pi_u$, ${}^3\Pi_g$, ${}^3\Sigma_u^+$, ${}^1\Pi_g$. For case c we get 1_g , 1_u , 0_g^+ , 0_u^+ , 0_g^- , 0_u^- , from ${}^2P_{1/2} + {}^2S$ and 2_g , 2_u , 1_g , 1_u , 1_g , 1_u , 0_g^+ , 0_u^+ , 0_g^- , 0_u^- from ${}^2P_{3/2} + {}^2S$. The unique states are 2_g and 2_u , which go over into ${}^3\Pi_{2g}$ and ${}^3\Pi_{2u}$. Experimentally, ${}^1\Sigma_u$ (lower) and ${}^1\Pi_u$ (higher) are known in the case of some of the alkali metal molecules. Assuming, as is probable from a consideration of possible electron configurations, that ${}^3\Pi_{0u}$ and ${}^3\Pi_{1u}$ come below ${}^1\Sigma_u$, we find (e.g. by drawing a diagram like Fig. 3) that ${}^1\Sigma_u$ and ${}^1\Pi_u$ must both be derived from ${}^2P_{1/2} + {}^2S$ (${}^3\Pi_{0u}$ and ${}^3\Pi_{1u}$ are then derived from ${}^2P_{3/2} + {}^2S$).

QUALIFICATIONS AND DIFFICULTIES

In the preceding discussion, we have been tacitly assuming that crossings of $U(r)$ curves occur only at r values where case c coupling holds. This assumption is implied in the use of the rule given above (p. 1443) for correlating

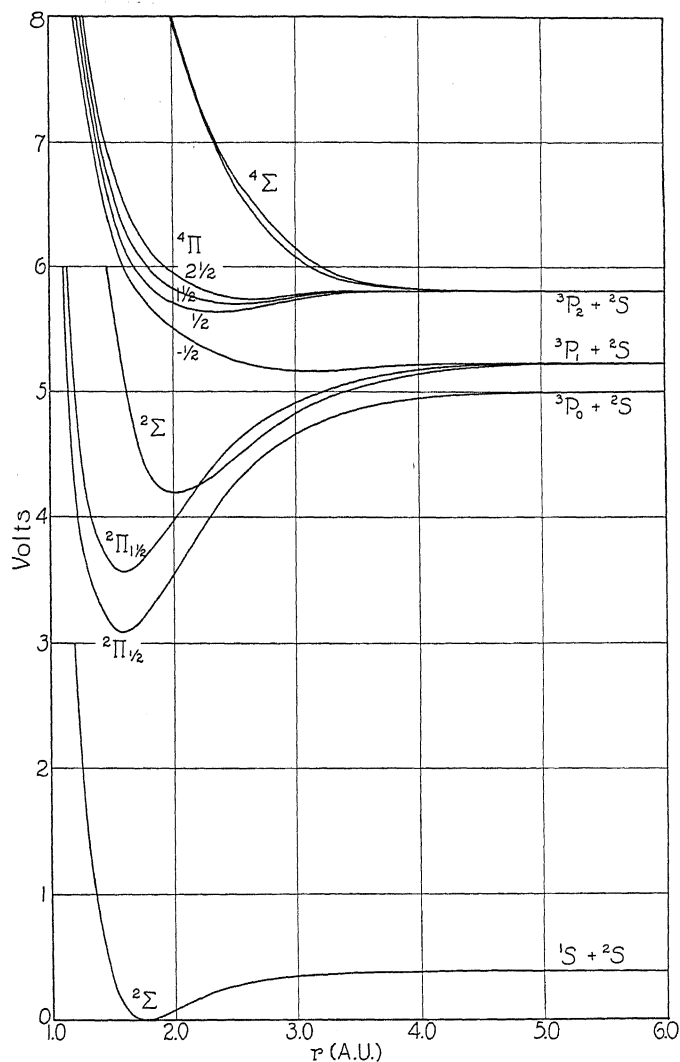


Fig. 3. Correlation of energy levels for separated atoms and molecular distances, for Hg ($\cdots 6s^2, {}^1S$) plus H ($1s, {}^2S$) and for Hg ($\cdots 6s 6p, {}^3P$) plus H ($1s, {}^2S$). The $U(r)$ curves for the ${}^2\Sigma$ and ${}^2\Pi$ states are drawn in accordance with Morse's formula, using experimental data on r_e and ν_e values, and using the experimental ω_e and D values of the lower ${}^2\Sigma$ state. The ${}^4\Sigma$ and ${}^4\Pi$ $U(r)$ curves are sketched in a plausible way.

case c with case $a-b$ states; according to this rule, crossings of $U(r)$ curves occur only for states differing in Ω or in symmetry properties (g or u , 0^+ or 0^-). But such an assumption is not general enough.¹¹ Crossings of $U(r)$

curves may occur or tend to occur at r values where there is case $a-b$ coupling. Here more crossings are possible than in case c , since in case $a-b$ $U(r)$ curves with the same Ω and symmetry properties may cross if they differ in Λ or S . Hence the correlation between atomic J values and molecular states (for $r=r_e$) may in many cases be somewhat different than it would be according to our previous rules. Actually, however, the number of $U(r)$ curves, other than those of "unique states," which tend to cross as r is decreased, hence the number of cases of doubtful correlation, is often small.

In the extreme case of very narrow atomic multiplets (very weak L , S couplings), case a or b molecular coupling exists practically all the way to dissociation, so that our correlation rules fail completely, except for the unique states. Fortunately, however, the correlation with atomic J values lacks importance, if not meaning, in such cases. In intermediate cases, where the atomic multiplets are of small to moderate width,¹⁴ the correlation problem is a complicated one. Considerable departures from our rules may often be expected, but our knowledge of the forces acting between atoms at large distances appears to be as yet insufficient to permit the setting up of better rules, except probably in the special case of the union of two ions, or of an atom and an ion, where the Stark effect probably determines to a first approximation the splitting up of the terms at large r values.¹⁵

The application of the preceding considerations to the examples discussed above indicates that with decreasing atomic weight of the atoms concerned, the correlations given above (except for "unique states") become less certain. Thus in $F+F$, the correlations may, for this reason and also perhaps because of a different order of some of the molecular levels, be in part different than in $I+I$, in $Mg+H$ different than in $Hg+H$, and in $Li+Li$ or $Na+Na$ different than in $Cs+Cs$.¹⁶

¹⁴ If the L , S couplings are weak in one atom, but strong in the other, we can determine the J correlation in the usual manner for the latter, but not for the former atom. In the special case that the latter atom is in an S state this does not matter (cf. e.g. $Hg+H$ in Fig. 3).

¹⁵ The Stark effect should quickly establish quantum numbers M_1 and M_2 (case c), or M_{L_1} and M_{L_2} (case a or b). The van der Waals forces (cf. R. Eisenschitz and F. London, *Zeits. f. Physik*, 60, 491, 1930, and subsequent paper by F. London) may cause some splitting up, but have little if any tendency to give axis-quantization (M_1 , M_2 , etc.).

¹⁶ Recent data of E. Svensson (*Zeit. f. Physik* 59, 349, 1930) suggest that even in CdH the correlations are different than in HgH , in that the upper $^2\Sigma$ state (cf. Fig. 3) may go to $^3P_0 + ^2S$ and the $^3\Pi_1$ state to $^3P_1 + ^2S$.

A NEW BAND IN THE ABSORPTION SPECTRUM OF METHANE GAS

BY DAVID M. DENNISON AND S. B. INGRAM*

UNIVERSITY OF MICHIGAN

(Received September 22, 1930)

ABSTRACT

The absorption spectrum of methane gas has been examined in the photographic infrared region from 6500Å to 9500Å in the hope of observing overtones of the known fundamental frequencies. A path length of 10 meters of gas at 70 cm pressure was used. The source of continuous radiation was a tungsten filament and the radiation was analysed with a grating spectrograph having a dispersion of 2.6Å per mm at 8000Å.

One band which may be attributed to methane was observed at about 8900Å and may be identified as the third overtone ($n=0 \rightarrow 4$) of the fundamental absorption band at 3.3μ . The fine structure appears to be very complex and irregular, consisting of more than a hundred lines of which about five are very intense.

In an attempt to reconcile the apparent irregularity of this structure with the simple and regular fine structure of the fundamental at 3.3μ , the theory of the overtones of a methane type molecule was examined. It is remarked that the higher energy states corresponding to this mode of vibration are in first approximation degenerate and have a weight $\frac{1}{2}(n+1)(n+2)$. A perturbation representing the anharmonic forces is now introduced and is postulated to have a tetrahedral symmetry. The secular determinant is then constructed and the resulting energy constant is given explicitly for the values $n=0,1,2,3,4$. It is found that for $n=4$ the 15 levels which originally coincided now group themselves into seven neighboring levels having the weights 3,3,3,2,2,1, and 1. These levels may all combine with the vibrationless state $n=0$ and thus it is to be expected that the overtone band under discussion will consist of seven nearly superimposed single bands. These considerations appear to explain the observed degree of complexity although it has not been possible as yet to make a detailed analysis of the positions of the individual lines.

THE infrared absorption spectrum of methane has been observed by Cooley¹ who found a number of bands in the region from 2μ to 8μ but particularly two strong ones at 3.3μ and 7.7μ which are without doubt due to two of the fundamental vibrations of the methane molecule. Higher harmonics of the fundamental at 3.3μ are to be expected in the region of wave-length less than 1μ where they are accessible to photographic investigation. It was therefore determined to search for such bands using a comparatively long light path in the gas (10 meters).

EXPERIMENTAL

The absorption tube was constructed of a piece of lap-welded steel pipe 15 cm in diameter and 5 meters long. Flat steel rings were set in the ends and soldered tightly to the pipe and against these two plate glass windows

* National Research Fellow.

¹ J. P. Cooley, *Astrophys. J.* 62, 73 (1925).

were sealed with picein wax. Side tubes and drying apparatus for admitting the gases, a water aspirator for rough evacuation of the chamber and a mercury manometer to indicate the pressure were attached.

A tungsten filament provided the source of continuous spectrum. The light passed from the lamp at one end of the tube to a concave mirror of seven meters radius of curvature placed at the other. This mirror reflected the light back through the tube, and focussed it directly on the slit of the spectrograph, a plane mirror being used to deflect the beam from the axis of the tube to the axis of the spectrograph. When observations were made in the region of wave-lengths greater than 8600A a large 45° glass prism was introduced in the convergent beam about one meter in front of the slit. This device produced a short spectrum on the spectrograph slit. Rotation of the prism selected particular regions of wave-length about 1000A in width and thus the scattered light of shorter wave-length which otherwise caused a general fogging on the plates during the long exposures necessary in this part of the spectrum could be easily disposed of. When this prism was not used a red glass filter served to cut out the blue light.

The spectrograph consisted of a concave Rowland grating of 7 meters radius in a Paschen mounting. This instrument gave a dispersion of 2.6A per mm at 8000A. Eastman Extreme Red and Infrared Sensitive plates were used and exposure times varied from 5 minutes to 24 hours, depending on the spectral region under investigation. Second order iron lines served as standards for the determination of wave-lengths.

Pressures in the absorption cell of about 70 cm were used. Even at this pressure the absorption lines seemed quite diffuse and broad so that no advantage was to be gained by pushing the large grating spectrograph to the limit of its resolving power. A similar observation has been made by Badger² in work on the absorption bands of ammonia.

The methane was taken from cylinders of compressed gas supplied by the Matheson Company. It was dried by passing over calcium chloride and through concentrated sulphuric acid but no further attempts were made to purify it. According to the makers this gas was 88% pure containing approximately 7% of ethane, 4% of propane, and 1% of butane. In order to be sure that none of these impurities was responsible for the observed absorption, photographs were taken successively through a 60 cm cell containing each of these gases. In no case could absorption be observed in the region containing the band under discussion. When the 60 cm cell was filled with methane three or four of the strongest absorption lines near 8870A could be detected on the plates, although the absorption was very faint with this relatively short path length.

RESULTS

A survey of the spectrum from 6500A to 9500A showed one band extending from 8800A to 9000A. In all over one hundred individual lines could be measured. Some of these were very strong and showed fairly complete

² R. M. Badger, *Phys. Rev.* 35, 1038 (1930).

absorption but the greater number were very weak and could be measured only with difficulty under the high magnification on the comparator. Table I gives the measured wave-lengths of the lines and eye estimates of the intensities. The last column gives the values of the wave-numbers reduced to

TABLE I. *Wave-lengths and intensities of the lines of a band in the absorption spectrum of methane.*

Int.	I.A.	ν	Int.	I.A.	ν	Int.	I.A.	ν	Int.	I.A.	ν
0*	8798.50	11362.46	0	8837.61	11312.18	1	8872.27	11267.99	0	8910.61	11219.50
0*	8806.15	11352.58	0*	8838.28	11311.32	1	8873.08	11266.96	0	8913.65	11215.68
0	8811.11	11346.19	0	8839.35	11309.95	3	8874.00	11265.79	0*	8916.16	11212.51
1	8812.17	11344.83	2	8842.03	11306.51	0*	8874.74	11264.85	0*	8917.13	11211.29
0	8813.11	11343.62	3	8843.36	11304.81	0	8875.67	11263.67	0*	8919.73	11208.02
1	8814.25	11342.16	0	8844.13	11303.83	0	8876.76	11262.29	1	8921.71	11205.54
1	8814.96	11341.24	0	8845.96	11301.49	1	8877.95	11260.78	0*	8923.53	11203.25
0*	8816.06	11339.82	0	8848.66	11298.04	0*	8879.16	11259.24	0*	8924.71	11201.77
0	8817.04	11338.56	0	8850.44	11295.77	1	8882.83	11254.58	1	8925.96	11200.20
0	8818.32	11336.92	0	8852.25	11293.46	0	8884.94	11251.91	0	8935.84	11187.82
0	8819.78	11335.04	2	8854.44	11290.67	0*	8886.99	11249.31	0*	8937.99	11185.13
0*	8821.02	11333.45	0	8856.35	11288.24	0*	8887.38	11248.82	0*	8940.35	11182.18
1	8822.60	11331.42	4	8859.21	11284.59	0	8888.38	11247.56	0*	8943.01	11178.85
0*	8823.79	11329.89	0*	8860.62	11282.80	0*	8890.36	11245.05	0*	8944.57	11176.90
0	8824.99	11328.35	0*	8861.42	11281.78	0*	8890.87	11244.41	0	8946.26	11174.79
0	8825.68	11327.46	0*	8862.45	11280.47	4	8892.60	11242.22	0	8947.33	11173.46
0	8827.04	11325.72	0	8863.78	11278.78	0*	8893.40	11241.21	0*	8948.78	11171.65
0	8828.15	11324.30	0*	8864.34	11278.06	0*	8896.72	11237.02	0*	8958.47	11159.56
0*	8829.77	11322.23	0*	8864.79	11277.49	0*	8898.20	11235.15	0*	8961.22	11156.13
0*	8830.18	11321.69	0*	8865.54	11276.54	0*	8900.18	11232.65	0	8963.13	11153.76
1	8831.19	11320.40	2	8866.30	11275.57	2	8901.20	11231.36	0*	8966.99	11148.95
1	8831.57	11319.91	2	8867.56	11273.97	0	8902.51	11229.71	0*	8982.97	11129.13
0*	8832.38	11318.87	0*	8868.13	11273.24	0*	8903.46	11228.51	0*	8984.84	11126.81
1	8832.87	11318.25	5	8868.77	11272.43	1	8904.18	11227.60	0*	8986.56	11124.68
2	8836.59	11313.48	0	8870.11	11270.73	0*	8905.69	11225.70	1*	8988.03	11122.86
0*	8837.07	11312.87	1	8871.36	11269.14	0*	8909.41	11221.01	0*	9001.89	11105.73
									0*	9010.14	11095.56

* Measured on one plate only.

vacuum. Independent determinations of the wave-lengths using two different plates indicate that the wave-lengths of the stronger lines are probably accurate to about 0.03Å. For the weaker lines, of course, the accuracy is considerably less and errors of 0.1Å may be present. Figure 1 gives a graph-

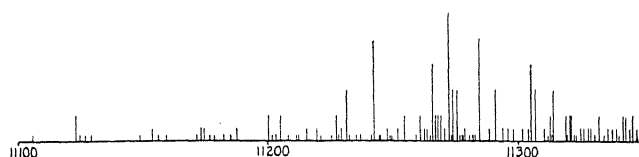


Fig. 1. Graphical picture of the absorption band in methane.

ical picture of the band. The absorption lines are plotted on a frequency scale, the vertical height of the lines representing their intensities.

It seems very probable that this absorption band is the third overtone ($n=0 \rightarrow 4$) of the fundamental ($n=0 \rightarrow 1$) band at 3.3μ . The first and second

overtone have been previously reported by Ellis³ as lying at 1.69μ and 1.15μ respectively. From the positions of these bands Ellis gives the following formula which is typical for series of this sort.

$$\nu = 3070n - 55n^2.$$

Substituting for $n=4$ we obtain $\nu = 11480 \text{ cm}^{-1}$ which we may compare with the most intense experimental lines at 11280 cm^{-1} . The agreement is satisfactory but could be improved by the formula

$$\nu = 3085n - 66n^2$$

which also represents Ellis' results within his experimental error.

The fine structure of the overtone reported in this paper appears to be very irregular and complex; a feature which seems surprising since the fundamental possesses a simple fine structure consisting of a regular positive, negative and zero branch as might be expected from a molecule whose three moments of inertia are equal. We shall however attempt to show that this overtone should consist of seven nearly superimposed simple bands of varying intensity. These considerations appear to account for the complexity of the observed fine structure even though we have not succeeded in analysing it in detail.

OVERTONES IN THE METHANE SPECTRUM

The normal vibrations of methane have been discussed by Dennison⁴ under the assumption that the molecule may be represented by a regular tetrahedron with the carbon atom at the center. The nine degrees of vibrational freedom give rise to only four independent frequencies ν_1 , ν_2 , ν_3 and ν_4 . Of these ν_1 single, and ν_2 double, are optically inactive. ν_3 and ν_4 are each triple frequencies and are optically active. They may be identified with the two strong bands of methane at 3.3μ and 7.7μ respectively. The band which is being reported in this paper is almost certainly the third overtone of ν_3 ($n=0 \rightarrow 4$) and we shall therefore confine ourselves to a discussion of this vibration. The considerations may be applied without change to overtones of ν_4 and might be extended to cover any general combination of the four fundamental frequencies. In the following work we have derived many important suggestions from two papers by F. Hund⁵ and by W. Elert⁶ on the symmetry properties of the methane type molecule, to which the reader interested in a further development of the subject is referred.

The normal mode of vibration ν_3 (or ν_4) involves the motion of all four of the hydrogen atoms together with the motion of the carbon atom. This system of the normal oscillator ν_3 (or ν_4) may be replaced by a simpler model which will possess all the properties of the ν_3 vibration and which will be found more convenient for discussion. Let a mass particle μ be elastically

³ J. W. Ellis, *Proc. Nat. Acad. Sci.* **13**, 202 (1927).

⁴ D. M. Dennison, *Astrophys. J.* **62**, 84 (1925).

⁵ F. Hund, *Zeits. f. Physik* **43**, 805 (1927).

⁶ W. Elert, *Zeits. f. Physik* **51**, 6 (1928).

bound to the origin of a rectangular set of axes x, y, z with a potential energy function whose leading term is, $V^0 = 2\pi^2\mu\nu^2(x^2 + y^2 + z^2)$. The remaining terms of the potential function V' may be considered as a perturbing potential and will have only one condition imposed upon them, namely that they must show a tetrahedral symmetry. This model may be visualized by thinking of the hydrogen atoms of methane as being rigidly fixed in space at the corners of a regular tetrahedron. The carbon atom is elastically bound to these four points and has as its equilibrium position the center of the tetrahedron. In first approximation the potential energy is V^0 and the frequency of vibration of the carbon atom is independent of the path of its motion.

When we discuss the model by means of the wave mechanics, we see that the wave equation is separable in the x, y, z coordinates and that in effect we have three independent linear harmonic oscillators each with the same frequency ν . The proper value for the system wave equation is the sum of the proper values for the individual linear oscillators and the wave function is the product of the individual wave functions. Since the theory of the harmonic oscillator and of separable wave equations is so well known, it will only be necessary to give the following results.

The energy of the system in first approximation is

$$W^0 = h\nu(n + 3/2) \quad n = 0, 1, 2, \dots$$

while the wave function ψ will be given in terms of three positive integer indices n_1, n_2, n_3 .

$$\psi = \psi_{(x)}^{n_1} \psi_{(y)}^{n_2} \psi_{(z)}^{n_3}.$$

In this expression $\psi_{(x)}^{n_1}$ is the n_1^{th} Hermitian orthogonal function having as its argument the variable $[4\pi^2\mu\nu/h]^{1/2}x$. The relation between the n , $n_1 + n_2 + n_3 = n$ shows that all the states for which n is not equal to zero are degenerate. For each value of n there will exist a number g_n of independent solutions to the wave equation. This number, which represents the weight of the n^{th} state may be easily found to be

$$g_n = (\frac{1}{2})(n + 1)(n + 2).$$

For simplicity we shall represent a wave function by the symbol $(n_1 n_2 n_3)$. Thus the lowest vibrational state has the single wave function (000) while the first state possesses three independent wave functions (100), (010) and (001), any linear combination of which will be a solution of the wave equation.

In first approximation as has been seen, for any value of n there will be g_n coincident energy levels. In higher order of approximation however when we take into account the anharmonic terms in the potential function, not all of these levels will exactly coincide and the purpose of the discussion is to determine the grouping of the levels. The method we shall employ is the familiar theory of perturbations of degenerate systems. For any particular value of n , the wave functions may be given the designation ψ_{nm} where m is an index running from 1 to $\frac{1}{2}(n+1)(n+2)$. Let the perturbing potential

energy be V' and the perturbed addition to the energy constant be W' . The so-called secular determinant is then constructed with the elements $|\int V' \psi_{nm} \psi_{nm}' dx dy dz - W' \delta_m^{m'}|$ where $\delta_m^{m'}$ is the Kroneker symbol. Setting the secular determinant to zero provides $\frac{1}{2}(n+1)(n+2)$ values for W' not all of which however need be distinct.

In our problem the secular determinant for small values of n becomes very simple since many of the elements vanish because of the tetrahedral symmetry of V' . Let the four corners of the tetrahedron be joined by six straight lines. Construct three axes each of which bisects one of the three opposite pairs of lines. These three axes which are mutually perpendicular, have an origin at the center of gravity of the system, and may be chosen as our x, y, z axes.

The potential function $V = V^0 + V'$ is a function of x, y and z and must have the symmetry of the tetrahedron. A little inspection discloses the following properties.

$$\begin{aligned} V(x, y, z) &= V(y, x, z) = V(z, y, x) \\ &= V(-x, -y, z) = V(-x, y, -z) = V(x, -y, -z). \end{aligned}$$

Thus the potential V or V' is unchanged by any permutation of the coordinate axes x, y, z . It is further unchanged if any two of the axes are reversed in direction. These properties describe the most general type of function having tetrahedral symmetry.

In constructing the elements of the secular determinant we may use the notation,

$$\alpha_{n_1 n_2 n_3}^{n_1' n_2' n_3'} = \int (n_1' n_2' n_3') V' (n_1 n_2 n_3) dx dy dz.$$

If we now remember that the Hermitian orthogonal function is an even or odd function of x depending upon whether n is an even or odd integer, it becomes evident that only those elements are non-vanishing for which $(n_1' + n_1)$, $(n_2' + n_2)$ and $(n_3' + n_3)$ are either all even integers or all odd integers. It is further clear from the symmetry properties of V' that,

$$\alpha_{n_1 n_2 n_3}^{n_1' n_2' n_3'} = \alpha_{n_2 n_1 n_3}^{n_2' n_1' n_3'} \text{ etc.}$$

The results of these considerations will now be tabulated for $n=0, 1, 2, 3, 4$. In every case values of the energy constant W' are given. The number in parenthesis immediately preceding W' indicates the number of levels having this value of the energy. This last degeneration (falling together of levels) can never be removed by introducing higher order perturbing terms provided they retain the symmetry of the tetrahedron.

$$\begin{array}{cc} n=0 & g_0=1 \\ (1)W' = \alpha_{000}^{000} & n=1 & g_1=3 \\ & (3)W' = \alpha_{100}^{100} \end{array}$$

$$n = 2 \quad g_2 = 6$$

$$(3)W' = \alpha_{110}^{110}$$

$$(2)W' = \alpha_{200}^{200} - \alpha_{020}^{200}$$

$$(1)W' = \alpha_{200}^{200} + 2\alpha_{020}^{200}$$

$$n = 3 \quad g_3 = 10$$

$$(1)W' = \alpha_{111}^{111}$$

$$(3)W' = \alpha_{210}^{210} - \alpha_{021}^{201}$$

$$(3)W' = \frac{1}{2}(\alpha_{300}^{300} + \alpha_{210}^{210} + \alpha_{021}^{201}) + \left[\frac{1}{4}(\alpha_{300}^{300} + \alpha_{210}^{210} + \alpha_{021}^{201})^2 - \alpha_{300}^{300}(\alpha_{210}^{210} + \alpha_{021}^{201}) + 2(\alpha_{120}^{300})^2 \right]^{1/2}$$

$$(3)W' = \frac{1}{2}(\alpha_{300}^{300} + \alpha_{210}^{210} + \alpha_{021}^{201}) - \left[\frac{1}{4}(\alpha_{300}^{300} + \alpha_{210}^{210} + \alpha_{021}^{201})^2 - \alpha_{300}^{300}(\alpha_{210}^{210} + \alpha_{021}^{201}) + 2(\alpha_{120}^{300})^2 \right]^{1/2}$$

$$n = 4 \quad g_4 = 15$$

$$(3)W' = \alpha_{310}^{310} - \alpha_{130}^{310}$$

$$(3)W' = \frac{1}{2}(\alpha_{310}^{310} + \alpha_{211}^{211} + \alpha_{130}^{310}) \pm \left[\frac{1}{4}(\alpha_{310}^{310} + \alpha_{211}^{211} + \alpha_{130}^{310})^2 - \alpha_{211}^{211}(\alpha_{310}^{310} + \alpha_{130}^{310}) + 2(\alpha_{112}^{310})^2 \right]^{1/2}$$

$$(2)W' = \frac{1}{2}(\alpha_{400}^{400} + \alpha_{220}^{220} - \alpha_{040}^{400} - \alpha_{202}^{220}) \pm \left[\frac{1}{4}(\alpha_{400}^{400} + \alpha_{220}^{220} - \alpha_{040}^{400} - \alpha_{202}^{220})^2 - (\alpha_{400}^{400} - \alpha_{040}^{400})(\alpha_{220}^{220} - \alpha_{202}^{220}) + (\alpha_{022}^{400} - \alpha_{220}^{400})^2 \right]^{1/2}$$

$$(1)W' = \frac{1}{2}(\alpha_{400}^{400} + \alpha_{220}^{220} + 2\alpha_{040}^{400} + 2\alpha_{202}^{220}) \pm \left[\frac{1}{4}(\alpha_{400}^{400} + \alpha_{220}^{220} + 2\alpha_{040}^{400} + 2\alpha_{202}^{220})^2 - (\alpha_{400}^{400} + 2\alpha_{040}^{400})(\alpha_{220}^{220} + 2\alpha_{202}^{220}) + (2\alpha_{220}^{400} + \alpha_{022}^{400})^2 \right]^{1/2}$$

A certain independent check on the above calculations may be made in the following manner. Suppose that V' possesses not only tetrahedral symmetry but spherical symmetry as well. This would mean that the α_s would be unchanged by a rotation of the x, y, z axes and this would lead to certain relations between them. Thus in the case $n=2$, it may be shown that if V' has spherical symmetry $\alpha_{200}^{200} - \alpha_{020}^{200} = \alpha_{100}^{110}$ and therefore instead of three groups of energy levels for the tetrahedron we obtain only two energy levels for the sphere (one with the weight 5 and the other with the weight 1). These results for a spherical potential may be obtained independently by introducing the spherical coordinates r, θ, ϕ in which case V' is a function of r alone. The results of applying these two methods were compared for the values of n under discussion and found to agree, thus furnishing at least one check on the numerical calculations. It may be of interest to state how the seven groups of levels for the tetrahedron for $n=4$ degenerate into three groups of levels (with the weights 9, 5, and 1) for the sphere. Let the perturbed energy W' be given an index running from 1 to 7 and corresponding

to the energies in the above table ($n=4$) respectively. When the tetrahedral symmetry degenerates into spherical symmetry we have the three levels, $W_1' = W_3' = W_5' = W_7'$, $W_2' = W_4'$ and W_6' .

We may now summarize the results which have been obtained. The first vibrational state $n=1$ is degenerate and is composed of three coincident levels which will not be separated by any perturbing potential having tetrahedral symmetry.⁷ The fundamental band ($n=0 \rightarrow 1$) is consequently a single band, a result which agrees with the simplicity of its observed fine structure.

The level $n=4$ is composed of seven neighboring levels having the weights 3, 3, 3, 2, 2, 1 and 1 respectively.⁸ All of these levels may combine with the lowest level $n=0$ and therefore the third overtone should consist of seven nearly superimposed bands. The intensity of any one of these bands will depend not only upon the weight of the upper state but also upon the exact nature of the perturbing function V' .

Each of these bands we suppose will have a fine structure consisting of a regular positive, negative and zero branch. By referring to the work of Elert⁶ on the symmetry properties of the wave functions, it may be seen that all the lines of the fine structure will be present with the possible exception of the first line of the zero branch. The intensity distribution will be somewhat irregular due to the spin of the hydrogen nucleus. It is not possible to predict whether the spacing of the lines in the positive and negative branches will be the same for each of the seven nearly superimposed bands since the mechanism of the coupling between rotation and vibration in the methane molecule is not yet understood. It will be remembered that the fine structure lines in the two fundamental bands ν_3 and ν_4 do not have the same spacing in frequency although this was to be expected on the basis of the simple theory involving no interaction between vibration and rotation.

Let us now return to a consideration of the observed structure of the overtone band $n=0 \rightarrow 4$. Although the lines are very irregularly spaced there seems to be a definite convergence on the short wave side of the band. This may be compared with the fact that Cooley¹ found a slight convergence of the fine structure lines of the fundamental band on the short wave side.

Among the hundred or so lines recorded on the plate some five or more lines stand out as being definitely much stronger than the rest and we should

⁷ For the sake of completeness we should remark that Hund⁵ and Elert⁶ have pointed out a further degeneracy arising from the fact that more than one equivalent space equilibrium configuration exists for the methane molecule. In fact each of the levels which we have treated as single is split into two separate levels having reciprocal symmetry character in the wave functions. The magnitude of the separation of these two levels is however very much smaller than the separations which we are considering here and will certainly be far too small to be observed experimentally. We have therefore omitted this type of degeneracy from the discussion.

⁸ It is obviously impossible to determine the W_s' when we do not know the exact form of V' . An estimate based on a potential function having spherical rather than tetrahedral symmetry indicates that the difference between two successive W_s' is smaller than any one of the W_s' but is yet not of an essentially smaller order of magnitude.

like to identify these as the zero branches of the seven single bands which have been predicted by the theory. A difficulty arises however which may make this interpretation untenable. The formula for the positions of the lines of the fundamental band as given by Cooley¹ is,

$$\nu = 3019.3 + 9.771m - 0.0351m^2, \quad m = \pm 1, \pm 2, \dots$$

If the mechanism of the coupling between vibration and rotation were similar to that for a diatomic molecule, the zero branch lines of any of the seven single bands comprising the third overtone would be given by,

$$\nu = A - 4(0.0351)m^2$$

where A is a constant of the order of 12000 cm.^{-1} . These zero branch lines would then not fall exactly together but starting from a head on the high frequency side would extend over several waves per cm. Actually the strongest lines on the plates appear to be much sharper than this and seem to have a half width no greater than one wave per cm. We should emphasize however that these considerations lie in the realm of speculation since each single band will probably have a different convergence factor whose magnitude can not be predicted without a more complete analysis of the interaction between vibration and rotation for this type of molecule.

Many difficulties lie in the way of a detailed ordering of the observed fainter lines into seven independent series of regularly spaced positive and negative branches. From the theoretical side we do not understand the nature of the coupling between the vibration and rotation and hence we can not be certain of the formulae giving the positions of the fine structure lines. From the experimental side we are not convinced that all the lines necessary for an analysis have been recorded and we believe that many of the lines may be enhanced due to the chance superposition of several faint lines. Our purpose has been rather to show that this overtone band may be expected to possess a complex structure composed of seven bands, each containing some thirty or more lines. The observed spectrum seems to possess about this same degree of complexity.

THE TRANSVERSE ZEEMAN EFFECT OF THE GREEN AURORAL LINE; AN EXPERIMENTAL PROOF OF THE EXISTENCE OF QUADRUPOLE RADIATION

BY RUDOLF FRERICHS* AND J. S. CAMPBELL

CALIFORNIA INSTITUTE OF TECHNOLOGY, PASADENA

(Received September 23, 1930)

ABSTRACT

The transverse Zeeman effect of the green auroral line was photographed. The pattern is of the type (1), 2/1, in complete agreement with the prediction made by Rubinowicz on the basis of the theory of quadrupole radiation.

THE problem of forbidden lines, long a complete mystery, has been to a great extent elucidated by two recent lines of investigation. I. S. Bowen¹ showed that the explanation of the nebular lines as forbidden transitions between the low metastable terms of the N II, O II, O III and S II ions requires us to regard these transitions as being conditioned by very small probability instead of being absolutely forbidden. He has further plausibly explained the occurrence of these lines in the nebulae as a consequence of the extremely low pressures prevailing there. Under these conditions there are very few collisions of the second kind between the ions, and because there are thus no radiationless transitions from these states the ion must after a long life-time emit the forbidden line.

The replacement of an absolute prohibition by a low transition-probability, however, still left unexplained the contradiction of the selection principle for dipole radiation, which remains rigorously valid in the new quantum theory. This apparent contradiction has been explained in recent theoretical papers² which show that while the dipole radiation is absent in the case of these forbidden lines, the contribution of the higher moments of the atom, principally of the quadrupole moment, may be present to an observable degree. Among those who have developed this view point, Rubinowicz³ has carried his calculations to the point of showing that an experimental difference between dipole and quadrupole radiation is to be found in the Zeeman pattern. The results of this calculation for the green auroral line, the forbidden combination $^1S_0 - ^1D_2$ in the O I spectrum, are given in Table I.

* International Education Board Fellow.

¹ I. S. Bowen, *Astrophys. J.* **67**, 1 (1928), see also the report of F. Becker and W. Gotrian, *Ergebnisse der exakten Naturwiss.* VII p. 8, 1928.

² I. Placinteanu *Zeits. f. Physik* **39**, 276 (1926); A. Rubinowicz, *Zeits. f. Physik* **53**, 267 (1929); J. Bartlett, *Phys. Rev.* **34**, 1245 (1929); A. F. Stevenson, *Proc. Roy. Soc. A* **128**, 591 (1930).

³ A. Rubinowicz, *Zeits. f. Physik* **61**, 338 (1930); L. Huff and W. V. Houston, *Phys. Rev.* **36**, 842 (1930).

TABLE I. Results of calculation for the Zeeman pattern of the green auroral line.

Δm	Polarization				
	transverse $\theta = 90^\circ$	$90^\circ > \theta > 45^\circ$	$\theta = 45^\circ$	$45^\circ > \theta > 0^\circ$	longitudinal $\theta = 0^\circ$
-2	σ	l. ell.	l. ell.	l. ell.	—
2	σ	r. ell.	r. ell.	r. ell.	—
-1	π	r. ell.	σ	l. ell.	l. circ.
1	π	l. ell.	σ	r. ell.	r. circ.
0	—	π	π	π	—

It can be seen from this table that for the case $\theta = 0$ the Zeeman pattern is indistinguishable from the normal Zeeman effect of dipole radiation. Therefore the existence of quadrupole radiation cannot be demonstrated on the basis of the older measurements⁴ of the *longitudinal* Zeeman effect of the auroral line. The table shows that a measurement of the *transverse* Zeeman effect of the auroral line offers a clear distinction between quadrupole and dipole radiation. In view of the extraordinary significance which an experimental test for quadrupole radiation has for the quantum theory, we have undertaken the investigation of this point.

Before the discussion of our measurements it is desirable to justify using for such an experiment the auroral line as produced in the laboratory. At first sight it seems irreconcilable with Bowen's hypothesis, that this line can be produced in the laboratory in discharges at relatively high pressures. It has therefore been often assumed that the appearance of this line in discharge tubes is due to electrical fields. Thus Bartlett⁵ states that the auroral line under laboratory conditions cannot be regarded as quadrupole radiation. However there seems to be no reason for regarding the production of the auroral line in the laboratory as fundamentally different from the production of the forbidden lines in the nebulae. It is true that in laboratory sources we have relatively high pressures and therefore numerous collisions, but Frayne⁶ has shown that in the case of the magnesium resonance line, which is also a line of low transition probability, the quenching effect of the surrounding atoms is almost negligible in comparison with that of the walls. It is in agreement with these results that the auroral line becomes stronger with increasing tube diameter. Moreover the intensity of the auroral line increases with increasing pressure, which indicates that the disturbing influence of pressure is small. Even though many more metastable oxygen atoms are destroyed by collisions in discharge tubes than would be under nebular conditions, this effect is compensated by the strong excitation of these states in the former source. Especially in the case of the oxygen-argon mixture, where the higher

⁴ Longitudinal measurements were first made visually by J. C. Mc Lennan, I. H. Mc Leod and W. C. Mc Quarrie Proc. Roy Soc, **114**, 15 (1927) giving the Zeeman effect as a doublet with normal separation. These measurements have been checked photographically by J. C. Mc Lennan, I. H. Mc Leod and R. Ruedy, Phil. Mag. **6**, 558 (1928) and independently by L. A. Sommer, Zeits. f. Physik **51**, 451 (1928).

⁵ J. Bartlett, reference 2.

⁶ J. G. Frayne, Phys. Rev. **34**, 590 (1929).

oxygen terms are not excited,⁷ the excitation of the metastable 1S_0 state is favored.

Since there seems to exist this parallelism between the excitation of the auroral line and that of the nebular lines, the investigation of the transverse Zeeman effect of the auroral line affords a quite general test of the theory of quadrupole radiation.

APPARATUS AND PROCEDURE

The magnetic field for the investigation was produced in a large solenoid already constructed and employed in a determination of e/m by the Zeeman effect which is being carried on by one of us (C). As a detailed description of its construction and calibration will be given in a later paper, only the principal data need be mentioned here. The winding consists of 2449 turns of No. 4 B&S (5.2 mm) square d.c.c. copper wire in 18 layers. The coil is 80 cm long, with an outer diameter of 39.7 cm and an inner diameter of 7.6 cm, and is enclosed in a brass shell. Cooling is accomplished by circulating kerosene between the layers, which are separated by narrow fiber spacers placed parallel to the axis. The dimensions of the solenoid were selected to give a field uniform to a tenth of a percent over an axial length of 6 cm at the center.

Calibrations of the solenoid for the measurement for which it was built gave its field as 36.82 gauss per ampere of exciting current. These calibrations were made by the following zero method, using a single layer standard solenoid. The dimensions of the standard solenoid were accurately measured on a comparator. From them the field for unit current in the standard was calculated. The standard solenoid was introduced in the 63.5 mm inner tube of the large solenoid. The currents in the two solenoids were regulated until their resultant field became zero. The point of balance was indicated by the absence of deflection of a sensitive ballistic galvanometer connected to a flip coil placed at the center. The disturbing effect of the earth's field was eliminated by reversing the current in both solenoids. The currents in the two solenoids were measured with separate shunts and separate potentiometers with a common standard cell. The ratio of the currents at the point of balance was used in connection with the calculated field of the standard solenoid to give the ratio of field to current in the large solenoid.

During an exposure, the exciting current was measured by means of a 0.001-ohm standard shunt and a Brooks type deflection potentiometer, and was held constant by controlling the field current of the generators used for supply. In this investigation the solenoid was used below its full current capacity. It is possible to maintain continuously a field of 7300 gauss, requiring 54 kilowatts, without exceeding a temperature of 50°C in the circulating kerosene.

It was necessary to use a light source emitting the green auroral line with considerable intensity from a small volume because the space available for

⁷ The narrow limitation of the excitation in argon-oxygen may be seen from Fig. 1. R. Frerichs, *Phys. Rev.* **36**, 398 (1930).

the transverse observation in the solenoid was much less than the diameter of the inner tube (63.5 mm).

Much work on the excitation of the green auroral line has been done by Mc Lennan and his collaborators. They have shown in numerous papers that the best conditions for producing the auroral line are heavy uncondensed discharges through mixtures of argon with slight traces of oxygen, in tubes of about 2 cm diameter. Because the specific intensity of such a source is small, end-on observation is necessary. Thus in their work on the longitudinal Zeeman effect, Mc Lennan and his collaborators used a positive column with an effective length of 25 cm; Sommer used a 50 cm positive column.

For our transverse observation it was necessary to use a light source of much greater specific intensity. The auroral line can be easily produced in narrow capillaries with a heavy D.C. discharge through commercial oxygen with sufficient intensity to be photographed with a 6.5 m grating.⁸ In order to observe the transverse Zeeman effect of such a source end-on, the discharge would be necessarily perpendicular to the magnetic field. It is well known that this arrangement is difficult to use; accordingly we placed the capillary parallel to the field and studied the transverse emission reflected by a 45° prism (see below). As the intensity of the auroral line so obtained was too weak to be photographed, other wider tubes were tried. The tube finally used, (Fig. 1), had a diameter of 28 mm and a total length of 1 m, so that the heavy aluminum electrodes were within the solenoid. The arrangement of the electrodes coaxially with the field had the advantage that the discharge did not strike and locally heat the glass wall. The light which left the central portion of the tube transversely was directed out of the solenoid by a 45° prism. Following a suggestion of Dr. Bowen, it proved to be very helpful to silver the tube on the outside of the 6 cm central portion and to observe the multiply reflected light through a small slit cut in the silvering. The intensity was greatly increased in this way, the transverse emission becoming nearly as strong as the emission end-on.

Photographs with this tube were first made with an argon-oxygen mixture. The oxygen was electrolytically generated and dried by passing through a liquid air trap. The commercially pure argon was purchased from the Air Reduction Co. It proved difficult, however, to maintain the best mixture, since the oxygen was rapidly absorbed by the electrodes in the heavy discharge of 600–700 m.a. direct current. As helium was available in larger quantities, we used for the final exposures a steady stream of a helium-oxygen mixture through the tube. (Fig. 1). The oxygen passed slowly from the liquid air trap where it was stored, liquefied at about 30 cm pressure, through a narrow capillary into the discharge tube, which was connected to an oil pump by a nearly closed stopcock. The rate of flow of the helium through another capillary was regulated by adjusting the pressure in a small intermediate bulb until the auroral line appeared with maximum intensity. With a few liters of helium it was possible to supply the discharge for many hours.

⁸ R. Frerichs, *Phys. Rev.* **34**, 1237 (1929).

For resolving the Zeeman pattern of the green auroral line we used a combination of Fabry Perot interferometer and prism spectrograph. The interferometer, a Hilger type instrument built in the Institute shop, was placed between the collimator and the Rutherford prism of the spectrograph. It

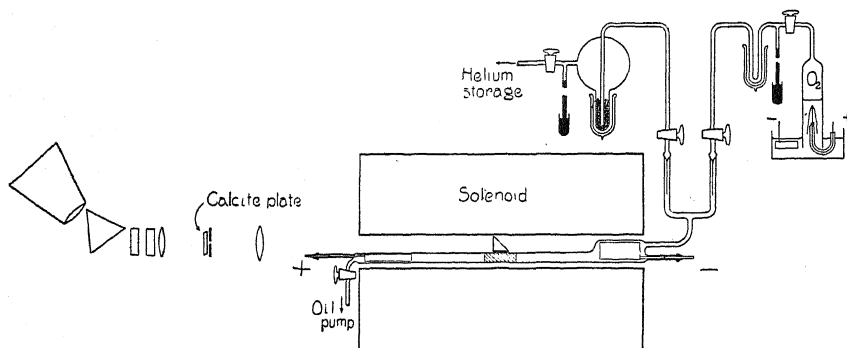


Fig. 1. Experimental arrangement; spectral apparatus, solenoid, discharge tube, and means of supplying a steady flow of helium-oxygen mixture.

was mounted in a tight wooden box, in which the temperature was observed with a Beckmann thermometer and regulated by electrical heating to within 0.05°C . The interferometer plates were 2.5 cm in diameter and had been silvered by sputtering.

In order to reduce the complexity of the interferometer pattern, and show clearly the states of polarization of the components observed, there was mounted immediately behind the slit a thin calcite plate, (Fig. 1) This plate was oriented to give close double images of the slit, the image lying toward the red end of the spectrum containing the light polarized perpendicular to the magnetic field (σ comp), the other image containing the light polarized parallel to the magnetic field (π comp.). The orientation of the calcite plate was made on a Nörrenberg polariscope, and was checked first visually with a Nicol prism, and second photographically on the Zeeman pattern of the argon line 7067A, occurring on some of our earlier plates.

For photographing the auroral line Eastman Slow Panchromatic plates proved to be superior to Ilford Extra Rapid Panchromatic plates and Eastman astronomical green sensitive plates after all three were hypersensitized with ammonia.

During the exposures, which required from 1 to 2 hours when the helium-oxygen mixture was employed, the discharge was frequently observed with a spectroscope of considerable dispersion. The mixture and pressure were adjusted to give maximum emission.

MEASUREMENT AND DISCUSSION

In many cases the appearance of forbidden lines has been ascribed to the disturbing influences of external electric or magnetic fields, which cause a breakdown of the selection principle. In order that the excitation of the auroral line should depend as little as possible upon such influences, we

worked with low magnetic fields. For a given Zeeman pattern the lower limit of the field required for its resolution is determined by the half-width of the line. Measurements by Babcock⁹ on the light of the night sky and by Mc Lennan and his collaborators¹⁰ on electrical discharges, gave 0.035A as the half-width of the auroral line. With the Zeeman pattern (1), 2/1 predicted by Rubinowicz, the smallest separation between the components of the same polarization is $2\Delta\nu$ norm. Thus we may expect that at any field over 2400 gauss the inner components are resolved.

The exposures were made with the interferometer plates separated by 7.1045 mm. This value was determined by measuring the fractional order of interference of five secondary standards of the neon spectrum and determining the whole order by systematic trial in the usual way.¹¹ With this interferometer distance and a field of 2578 gauss (corresponding to a solenoid current of 70.0 amp.) the Zeeman pattern predicted by Rubinowicz should appear with all four components clearly separated in each order, i.e. without overlapping. Fig. 2b is a reproduction of such an exposure, enlarged 6 times. In this pattern the π components are just separated; the σ components are already approaching the neighboring orders. In Fig. 2a the field has been increased to 3867 gauss at 105.0 amp. Here the π components are evenly spaced, but the σ components are just overlapping the adjacent orders. To permit measurements on the σ components plate 2c was taken with a field of 2025 gauss (55.0 amp.), to give them an even spacing. As expected the π components are not resolved, but are perceptibly broadened. For the sake of completeness Fig. 2d was taken without field. The increasing magnetic resolution with increasing magnetic field can be easily followed through the four exposures by means of the divergent lines, dotted lines for π components, full lines for σ components. Attention may be called to the absence of an undisplaced central component in Fig. 2a.

Table II contains the results of the measurements on plates 2a, 2b, and 2c.

TABLE II

Plate	Field	$\Delta\nu/\Delta\nu$ norm	
		σ comp.	π comp.
2a	3867	—	1.035
2b	2578	2.018	0.922
2c	2025	1.877	—
		Mean 1.948	0.979

The calculations were made in the following manner. From the ring diameters, D_n , as measured on a comparator, the fractional order of interference, δ , of each component at the center of the fringe system was found by the usual relation:

⁹ Babcock, *Astrophys. J.* **57**, 209 (1923).

¹⁰ J. C. Mc Lennan and J. H. McLeod, *Proc. Roy. Soc.* **A115**, 515 (1927).

¹¹ Lord Rayleigh, *Phil. Mag.* **9**, 685 (1906).

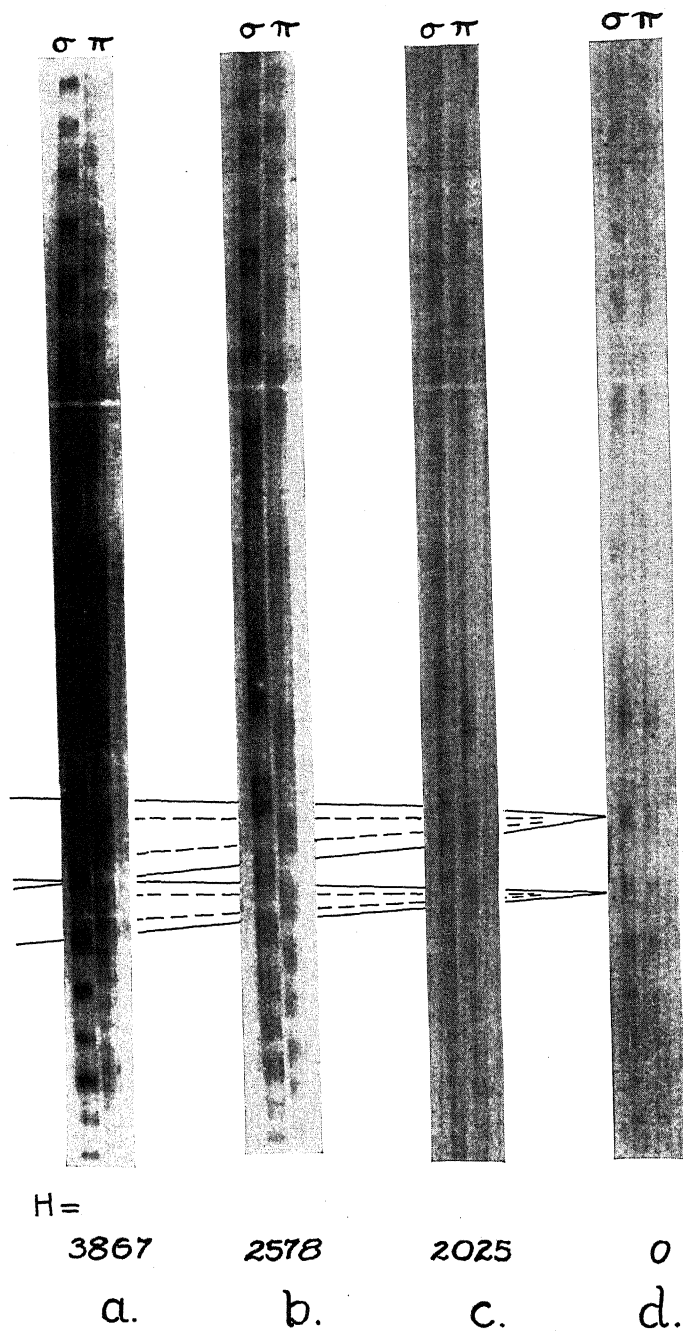


Fig. 2. Interferometer fringes of the auroral line at four values of the magnetic field. The full lines pass through σ -components, the dotted lines through π -components.

$$\delta = \frac{D_n^2}{D_n^2 - D_{n-1}^2} - n$$

D_n is the linear diameter of the n th fringe from the center. From the difference in order, $\delta - \delta'$ between the fringes corresponding to $+\Delta\nu$ and $-\Delta\nu$ in the Zeeman pattern, the separation in frequency is given by the expression

$$2\Delta\nu = \frac{\delta - \delta'}{2d},$$

where d is the interferometer plate distance. The values so obtained are divided by the normal Zeeman separation:

$\Delta\nu \text{ norm} = 4.674 \times 10^{-5} \times H$ derived from the value¹² $e/m = 1.761 \times 10^{-7}$.

The transverse Zeeman pattern predicted for the auroral line by Rubinowicz was (1), 2/1, with all components of the same intensity. The slight deviation of the positions of the components, 1.95 instead of 2 for the σ components, and 0.98 instead of 1 for the π components, lies within the experimental error. While the field was known and held constant to within 0.2 percent, the fringes could not be measured with as great accuracy, because surface irregularities in the calcite plate introduced local irregularities of intensity, as may be seen in the photographs. Thus we see no significance in the small deviation from the predicted values.

The two π components are of equal intensity, as are the two σ components. The slightly greater intensity of the σ components as compared with that of the π components is probably due to the polarizing influence of the various reflections encountered in the optical path, since all the other lines on the plates, with and without field, show darker σ components.

One of the authors (F.) is very much indebted to the Rockefeller Foundation for the grant of a fellowship and to Professor Millikan for the facilities extended to him in the Norman Bridge Laboratory.

¹² R. T. Birge, 'Probable Values of General Physical Constants,' Phys. Rev. Supplement 1, 1 (1929).

SPECTRAL DISTRIBUTION OF ENERGY RADIATED FROM A NEW TYPE OF TUNGSTEN MERCURY ARC

By B. T. BARNES

LAMP DEVELOPMENT LABORATORY, INCANDESCENT LAMP DEPARTMENT,
GENERAL ELECTRIC COMPANY

(Received September 24, 1930)

ABSTRACT

This paper describes measurements with a quartz monochromator and thermopile of the energy flux from the tungsten mercury arc which is the source of radiation in the General Electric Sunlamp. Data are given on the energy flux radiated in each of the principal mercury lines below 6000Å and a curve is given for the distribution of energy in the continuous spectrum between 2500 and 17000Å. The maximum in the continuous spectrum curve comes at about 10600Å where the energy flux in a 50Å band is 6.5 microwatts per cm² at one meter distance from the center of the arc in a direction normal to the plane of the leads when the arc is operated with 115 volts on the primary of the transformer. The energy maximum corresponds to that of tungsten at about 2500°K but the shape of the curve below 5000Å corresponds more closely to that of tungsten at 3250°K which is approximately the maximum temperature of the electrodes. For the radiation in a direction normal to the plane of the leads 1% of the total energy flux was found to lie between 2500 and 3200Å, 1% between 3200 and 4000Å, 10% between 4000 and 7600Å, 46% between 7600 and 17000Å, 29.6% between 17000Å and the cutoff (roughly 40,000Å) of a fused quartz plate 2.4 mm thick and the remaining 12.6% at longer wave-lengths.

IN RECENT years many new applications have been found for sources of radiation in the ultraviolet and infrared as well as the visible portion of the spectrum. With each new source put into use there has arisen the need for measurements of the spectral distribution of its radiant energy. This paper presents data of this sort for the tungsten mercury arc which is the source of radiation in the General Electric Sunlamp. An analysis of the spectrum of this source over the wave-length region from 2800 to 7400Å has been published by Benford.¹ An article by Coblentz² gives some data on the spectral distribution of the energy radiated from the complete Sunlamp unit. In the present article the average of energy flux values for a number of lamps are given for the principal mercury lines between 2500 and 6000Å and for the continuous spectrum up to 17000Å.

For making these measurements the quartz prism monochromator described in a recent paper³ was used. The lamp to be measured was mounted in front of the collimator slit without any intervening lens. It was turned so that the axis of the arc was perpendicular to the line from the center of

¹ F. Benford, *J. Motion Picture Eng.* **14**, 414 (Apr. 1930), N. T. Gordon, F. Benford, G. E. Rev. **33**, 290 (May 1930).

² W. W. Coblentz, *J.A.M.A.* **95**, 411-Aug. 9, 1930.

³ W. E. Forsythe and B. T. Barnes, *R.S.I.* (Oct. 1930).

the arc to the center of the slit. With this arrangement energy radiated from all parts of the arc and from the electrodes entered the monochromator. The slit height was 6.6 mm, the focal length of the collimator lens 12 cm, and the distance from the slit to the center of the lamp 15 cm. Thus, light from the region approximately 1 cm in diameter containing the electrodes and the arc would illuminate an area 20 mm high and 8 mm wide at the collimator lens. Since the latter is 30 mm in diameter there was practically no loss of light in the monochromator except by reflection. Correction was made for the latter by use of the transmission curve for this instrument shown in the article mentioned previously.³ For use in the red and infrared this curve was extended parallel to the calculated curve up to 17000Å. Such a long extrapolation, of course, introduces some uncertainty into the infrared values computed by use of the curve.

The energy passing through the rear slit of the monochromator fell on a thermopile. The sensitivity of the latter as determined by means of incandescent lamps calibrated by the Bureau of Standards is $2.3_1 \times 10^{-7}$ volts per microwatt when it is used behind a 0.70 mm slit. This thermopile could be connected to either a D'Arsonval high sensitivity or a Coblentz type moving magnet galvanometer. The latter was adjusted to a sensitivity about five times that of the D'Arsonval and used in the ultraviolet portion of the spectrum where the amount of energy to be measured was relatively small.

Below 6000Å readings were taken on the principal mercury lines and at suitable intervals between them. To get the radiation due to the lines alone it was necessary to subtract the deflection due to the continuous spectrum from the actual readings which included both line and continuous radiation. To accomplish this the readings at settings where line radiation was negligible were plotted and the deflection due to the continuous spectrum at each setting for a mercury line was obtained from the curves through these points. Below 4500Å the less important mercury lines which were necessarily included with the continuous radiation may have raised the curve appreciably since the continuous spectrum is relatively weak in the ultraviolet. On the other hand, in the red and infrared the mercury lines are too weak, compared with the continuous radiation from the tungsten electrodes, to be detected.

Having separated the line radiation from the continuous spectrum each may be reduced to absolute intensity. The energy flux in microwatts per cm^2 at one meter distance in the radiation comprising one of the lines of the mercury spectrum is:

$$E_L = Sd_Lx^2/tA$$

where S is the sensitivity of the galvanometer-thermopile combination in microwatts per cm deflection; d_L is the galvanometer deflection due to the line itself—that due to the continuous radiation having been deducted from the actual reading— x is the distance in meters from the center of the arc to the slit— t is the transmission of the spectrometer at the wave-length of the line in question, and A the area of the front slit. It is assumed that the rear

slit is at least as wide as the front slit. Actually the rear slit was set at 0.70 mm and the front slit at 0.50 mm so that for groups of neighboring lines such as at 3650 and 3130A all the radiation entering the front slit could pass through the rear slit and the above formula would still apply. In the case of the continuous spectrum it is desirable to introduce a dispersion factor to reduce the results to terms of a wave-length band of constant width. For the data given here this band was chosen as 50A. The energy flux in microwatts per cm² at one meter distance radiated in a band of continuous spectrum of this width is:

$$E_c = \frac{S d_c x^2}{t A} \cdot \frac{50}{w}$$

where d_c is the deflection produced by the continuous radiation and w is the width in Angstroms of the band passing through the rear slit (0.70 mm wide). For obtaining w the dispersion curve was computed from the formula for the refractive index of quartz given by Coode-Adams⁴ and the relation for minimum deviation—

$$\frac{ds}{d\lambda} \equiv f \cdot \frac{dD}{d\lambda} \equiv f \cdot \frac{dD}{dn} \cdot \frac{dn}{d\lambda} = \frac{4f}{(4 - n^2)^{1/2}} \cdot \frac{dn}{d\lambda}$$

where s represents distance along the spectrum, f is the focal length of the telescope lens (120.7 mm), D is the total deviation produced by both quartz prisms and n the refractive index.

No correction was made for impurity of the continuous spectrum due to finite slit-widths as it was found from computations on one set of data that the correction was not over 1% in any case. However, a correction for stray light in the ultraviolet portion of the spectrum was found necessary. Readings taken on a lamp with a purple Correx filter in front of the slit were divided by the transmission of the filter at each wave-length and the results subtracted from the corresponding readings without any filter. The difference—presumably due chiefly to light scattered from the more intense portions of the continuous spectrum—was subtracted from corresponding readings on all other lamps.

SPECTRAL DISTRIBUTION OF ENERGY FLUX BELOW 17000A

The averages of energy flux measurements made on twenty-six lamps, each operated with 115 volts on the primary of the transformer, are given by Figure 1. The curve shows the energy flux in microwatts per cm² at one meter distance in a direction perpendicular to the plane of the leads radiated in a band of the continuous spectrum 50A wide at any given wave-length. The energy radiated in the mercury lines is given by the length of the heavy lines drawn above the curve. These are plotted as if 50A wide so that the ratio of the area representing the line to the area under the curve for the continuous spectrum will be the ratio of the corresponding amounts of energy radiated from the lamp.

⁴ Coode-Adams Proc. Roy. Soc. A117, 209 (1927-8).

Several features of the curve for the continuous spectrum given in Fig. 1 are of interest. The peak of this curve comes at about 10600A which is quite close to the maximum in the curve for the energy radiated by tungsten at 2500°K. However, the shape of the energy flux curve below 5000A is approximately the same as that for tungsten at 3250°K which is the temperature of the hottest parts of the electrodes. Also the output of visible and ultraviolet radiation is much too high in comparison with the infrared energy for tungsten at 2500°K. These facts are easily explained if one takes into consideration the composite nature of the continuous radiation. The electrodes having temperatures above 3000°K radiate a relatively high proportion of energy in the visible and ultraviolet. The filament and the in-

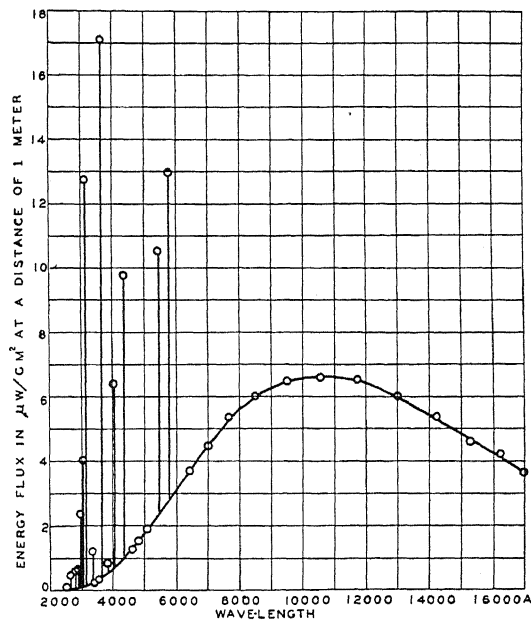


Fig. 1. Energy flux ($\mu\text{w}/\text{cm}^2$) 1 meter from center of arc in a direction normal to the plane of the leads. Lamp burning in the open (without reflector) with 115 volts on primary of transformer. Average lamp current and voltage 30.9_s amps. and 10.6 volts. Curve represents energy in 50A band of continuous spectrum. Heavy lines above curve give energy flux in lines or groups of lines in arc spectrum.

candescent portions of the leads which are at much lower temperatures, but which, taken together, have a larger area than that of the electrodes, contribute a considerable portion of the infrared radiation and shift the maximum in the continuous spectrum curve toward longer wave-lengths.

DISTRIBUTION OF TOTAL ENERGY FLUX FROM LAMP

Although the range of the monochromator limited the energy distribution measurements to the region below 17,000A the amount of radiation of longer wave-lengths was obtained by measuring the total energy flux and sub-

tracting from it the total flux of wave-lengths shorter than 17,000Å. Six of the lamps were mounted two meters in front of a calibrated thermopile and readings made on the total energy flux and that transmitted by a fused quartz plate 2.4 mm thick and by 2.5 cm of water in a Pyrex cell. Measurements with the water cell served as a check on the agreement between the energy flux measured after passing through the monochromator and that measured directly. The total energy flux transmitted by the cell was computed by multiplying the measured energy flux at each wave-length by the transmission of the cell and integrating. The value obtained by this method was 553 microwatts per cm^2 at one meter as compared with 560 measured directly. On a set of four lamps each located at one meter distance from the thermopile computations by the above method indicated that the average energy flux through the cell should be 588 microwatts per cm^2 at one meter distance. The measured value was 604. The agreement in both cases is within the limits of experimental error indicating that the extrapolation of the transmission curve of the monochromator was not seriously in error in the wave-length region between 5780 and 11,000Å.

The measured transmission of the water cell for the total energy flux from the lamp averaged 24.7 percent for the group of six lamps with the distance to the thermopile two meters and 23.5 percent for the group of four lamps located one meter from the thermopile. The difference may be due to increased absorption of the longer infrared rays by the water vapor in the air-making the proportion of the rays not transmissible by the water cell less at two meters than at one meter distance. The vapor pressure computed by psychrometric readings was 12.2 mm when the group of six lamps was measured and 11.3 mm when the group of four lamps was measured. The corresponding room temperatures were 25.3 and 24.0°C.

For these ten lamps the average cut-off of the water layer as defined by Stockbarger and Burns,⁵ *i.e.*, the wave-length for which the amount of radiation absorbed at shorter wave-lengths is equal to that transmitted for longer wave-lengths was 10500Å. The maximum transmission of the cell was 0.87—a slight deposit on the interior of the cell making the actual value somewhat less than the computed one. Then we find that of the total energy flux at one meter distance along a line perpendicular to the plane of the leads the fraction which is of wave-lengths shorter than 10500Å is approximately 0.24₂ divided by 0.87 or 0.27₈. This is an average of the two sets of data disregarding the increased absorption of the air path for the lamps tested at a distance of two meters.

Although the transmission curve for the fused quartz plate has not been determined, measurements with this filter give an upper limit to the amount of radiation beyond about 4 μ , the effective cut-off for a piece of crystalline quartz of the same thickness. Since the transmission of the fused quartz plate for the average total radiation for the ten lamps was 0.79₈ while the maximum transmission of quartz is 0.91₂ then 0.79₈ divided by 0.91₂ or 0.87₅ is the fraction of the radiation below the effective cut-off of the filter which

⁵ Stockbarger and Burns, Phys. Rev. 34, 1263 (1929).

is probably between 3.5 and 3.9μ . The bulb of the lamp having a temperature of about 300°C doubtless furnishes a large proportion of the energy of wave-lengths longer than 4μ .

By dividing the average value for the energy flux for each individual line by the average total energy flux one finds the fraction of the total radiation comprised in each line. Table I gives the results, representing the average of ten lamps, for the strongest lines and groups of lines in the mercury spectrum. The average total energy flux at one meter distance for these lamps was 2380 microwatts per cm^2 .² The average lamp current and voltage were 30.9_s amp. and 10.6 volts.

TABLE I. *Average energy flux for each of the principal mercury lines and corresponding percentages of average total energy flux.*

115 volts on primary of transformer.								
Wave-length	5780	5461	4358	4047	3905	3650	3342	3130
Microwatts/ cm^2 at 1 meter	9.7	8.2	9.0	5.8	0.4	17.4	1.1	13.8
Percent of total	0.4 ₁	0.3 ₄	0.3 ₈	0.2 ₅	0.01 ₇	0.7 ₃	0.04 ₆	0.5 ₇
Wave-length	3024	2967	2894	2804	2650	2537		
Microwatts/ cm^2 at 1 meter	4.4 ₀	2.5 ₄	0.7 ₁	0.6 ₉	0.6 ₆	0.1 ₂		
Percent of total	0.1 ₉	0.10 ₇	0.03 ₀	0.02 ₉	0.02 ₇	0.00 ₅		

These data apply only to the energy flux in a direction perpendicular to the plane of the leads. For the total radiation from the lamp in all directions the spectral distribution of energy would be somewhat different. The total energy flux in the direction specified averaged for the ten lamps was 2.38 milliwatts per cm^2 at one meter distance as compared with the calculated value of 2.61 if the entire input of the lamp were assumed to be radiated with a uniform distribution. The difference is due to absorption in the layer of air traversed, losses by conduction and convection and non-uniform distribution of the radiated energy.

A summary of the energy flux in certain wave-length regions is given by Table II. These results are the averages for the same ten lamps for which data are given in Table I and likewise refer to the energy flux along a line passing through the center of the arc normal to the plane of the leads.

TABLE II. *Average energy flux in microwatts per cm^2 at one meter distance. 115 volts on primary of transformer. Average lamp current and voltage 30.9_s amp. and 10.6 volts.*

Wave-length Region	2500-3200	3200-4000	4000-7600	7600-17000	>17000A	Total Radiation
Line spectrum	22.6	18.9	(32.7)*	—	—	—
Continuous spectrum	0.6	5.2	209	—	—	—
Continuous and lines	23.2	24.1	242	1090	1000	2380

* Red lines in Hg spectrum included with continuous spectrum.

The data of Table II show that the continuous spectrum furnishes less than 3% of the energy flux below 3200\AA but over 86% of the visible radiation. Since much of this continuous radiation is in the red end of the spectrum where the visibility is low the continuous spectrum furnishes only 76%

of the light radiated in a direction perpendicular to the plane of the leads. This result was obtained by multiplying the average data for twenty-six lamps plotted in Figure 1 by the relative visibility at each wave-length, integrating graphically for the continuous spectrum and summing for the mercury lines. Photometric measurements, on other lamps, made in this laboratory by Miss Easley indicated that for the direction perpendicular to the plane of the leads the continuous spectrum furnishes 75% of the total light. Benford¹ gives a corresponding figure of 76%, also obtained by a photometric method. There is very good agreement between the three sets of results. The energy of the weak red lines of mercury does not appreciably affect the computations of the total light radiated in all the mercury lines.

In the infrared the mercury spectrum could not be separated from the continuous radiation. Comparison with other mercury arcs indicates that between 1 and 2μ the radiation in the mercury lines is of the order of 1% of the total continuous radiation in this wavelength region.

The last line of Table II shows that for the energy flux at one meter distance in a direction perpendicular to the plane of the leads 1% of the total radiation is of wave-lengths shorter than 3200A, 1% is in the wave-length region between 3200 and 4000A, and 10% in the visible spectrum. Mercury arc radiation of wave-lengths shorter than 6000A comprises only 3% of the total energy flux in the direction specified.

Comparison of the data given in Table II and in the last two paragraphs with those published by Benford¹ indicates a fair agreement as to the amount of ultraviolet below 3200A. One would expect his values to be lower because the glass used for the bulbs which he tested had a somewhat lower transmission below 3200A than that used at the present time. Furthermore his lamps were operated at 30 amperes while ours were run with 115 volts on the primary of the transformer giving an average current of 30.9 $\frac{1}{2}$ amperes. One would not expect a close agreement.

The fact that Benford's data for the range from 3200 to 4000A is 41% higher than ours may be due to the circumstance that the line at 3650A which contributes the major part of this radiation varies considerably in intensity with varying mercury vapor pressure. Consequently different lamps may have a widely different output at this wave-length. Also the intensity of this line often increases over 50% during the first forty hours burning. Our data were taken on lamps which had been burned from three to five hours.

For the region from 4000 to 7000A our data gives the energy flux as 185 microwatts per cm² at one meter distance. Benford's value is 28% higher. This difference is hard to explain since most of the radiation in this region, being in the continuous spectrum, is little affected by mercury vapor pressure and therefore changes comparatively little in intensity during the first forty hours burning. For the group of twenty six lamps for which the distribution data is plotted in Figure 1 the average deviation of the values on individual lamps from the mean for the energy flux between 4000 to 7000A was

about one-fourth the difference between Benford's and our values and the maximum deviation only about one-half of this difference. It is possible, however, that the earlier lamps were less uniform than those being manufactured now with respect to the average temperature of the electrodes. The latter of course, determines the distribution and total amount of continuous radiation from the lamp.

A satisfactory comparison of the data given in this paper with those for the complete Sunlamp unit published by Coblenz² is not possible. There are not sufficient data on the amount and distribution of radiation in other directions than along the normal to the plane of the leads, or on the reflecting power and the concentration of the beam by the reflector. Furthermore data obtained in this laboratory by Miss Easley showed that for six lamps the average temperature of the mercury pool was 7° greater with the lamps in the reflector unit but without the screen in place than when they were operated in open air. Data previously published⁶ show that the intensity of the ultraviolet radiation below 3200Å would be 10 to 15% greater at the higher temperature. The intensity of the continuous spectrum would remain practically unchanged. In consideration of the above mentioned facts it should therefore be emphasized that the data in the present paper refer to the radiation from the lamp operated in the open and not to that received from the complete Sunlamp unit.

⁶ W. E. Forsythe, B. T. Barnes, M. A. Easley, G. E. Rev. 33, 364 (June 1930).

THE GENERAL ELECTRIC TYPE S-1 LAMP
AS A SPECTROSCOPIC SOURCE

BY DONALD DOOLEY

HIRAM COLLEGE, HIRAM, OHIO

(Received September 15, 1930)

ABSTRACT

The possibilities presented by the General Electric type S-1 lamp as a spectroscopic source have been investigated by employing lamps filled with argon, hydrogen, helium, neon and carbon dioxide. Nitrogen-filled lamps yielded the second positive bands of nitrogen greatly modified in form from that usually obtained from a Geissler tube discharge. The spectra of hydrogen-filled lamps which also contained mercury showed the mercury hydride bands while the spectra of carbon dioxide-filled lamps gave evidence only of the third positive bands of Deslandres. Further investigation of the more quantitative aspects of the problem will be studied.

THE extreme intensity of the radiation from the General Electric Type S-1 lamp has led to the suggestion that an investigation be made of its possibilities as a spectroscopic source when filled at various pressures, with other gases than argon which it normally contains. Descriptions of the stand-

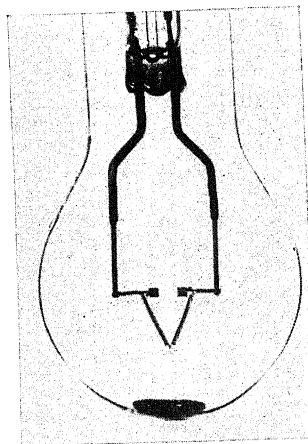


Fig. 1. Details of General Electric type S-1 lamp.

ard Type S-1 lamp will be found in the literature¹ and only a few general statements need be made here concerning it. The Type S-1 lamp is a 300-watt alternating current tungsten-mercury arc of the form pictured below. The salient features of its construction are the V-shaped coiled filament connecting the lead wires and the tungsten electrodes forming a spark gap between the ends of the filament (Fig. 1). It contains purified argon and a

¹ W. E. Forsythe, B. T. Barnes, M. A. Easley; *G. E. Review*, June, 1930, 358-365.
N. T. Gordon, F. Benford; *G. E. Review*, May 1930, 283-295.

small amount of mercury and operates off the secondary of a transformer which yields about 30 volts when the circuit is first closed. The filament carries in the neighborhood of 9.5 amperes at this voltage and attains a very high temperature which starts an arc across the tungsten electrodes. Immediately the current rises to nearly 30 amperes and the secondary voltage falls to about 10 volts at the lamp terminals due to the characteristics of the transformer. At this voltage the filament carries much less current than initially so that much the greater part of the total radiation originates in the intensely heated electrodes and the arc itself. Attention is called to the continuous radiation in the visible region observed on all spectrograms in spite of the fact that the image of the arc alone was projected upon the slit of the spectrograph. It is not certain whether this is scattered radiation from the tungsten electrodes or comes directly from the arc.

Examination of the spectrograms of radiation from the arc of a standard argon and mercury lamp (see Fig. 2) reveals the fact that, whereas for a few seconds when the lamp is first put in operation it emits a number of spectral

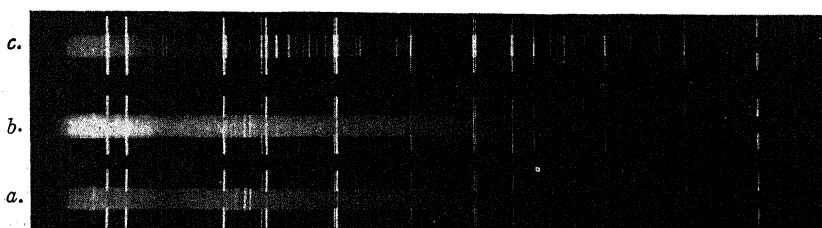


Fig. 2. Spectra of lamp containing argon and mercury. (a) Taken at start of lamp operation. (b) Taken after 10 sec. operation. (c) Taken after 60 sec. operation. Quartz mercury arc comparison.

lines attributable to argon, after a few minutes operation only mercury lines are emitted. The same characteristic is true of lamps containing helium, neon, nitrogen, and carbon dioxide together with mercury, an exception being observed in the case of hydrogen-filled lamps. The latter continue to radiate bands ascribed to mercury hydride² together with several other bands at shorter wave-lengths than the recognized mercury hydride bands (see Fig. 3).



Fig. 3. Spectrum of hydrogen filled lamp containing usual amount of mercury. Lower comparison is spectrum of standard type S-1 lamp. Upper comparison is quartz mercury arc.

Lamps containing gases alone without the mercury provide more interesting results in most cases. Notable in this class was the spectrum of nitro-

² A. Kratzer, *Ann. d. Physik* **71**, 102 (1923); R. S. Mulliken, *Nature* **113**, 489 (1924).

gen, which gas could be made to arc only with difficulty if the pressure was greater than a few millimeters. At a pressure of 5 millimeters the arc struck at normal operating voltage and the spectrograms showed the second positive bands of Deslandres greatly modified, the band subheads being entirely suppressed and the lines of each band being clearly visible at the head of the succeeding band (Fig. 4). This effect has been observed in other sources, Lewis³ associated it with the presence of an inductance coil in the secondary

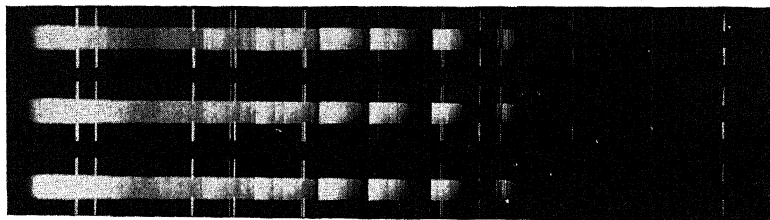


Fig. 4. Spectra of nitrogen filled lamp without mercury showing second positive bands of nitrogen. Quartz mercury arc comparison.

circuit of the transformer. However such a coil placed in the circuit failed to produce a visible effect in this case. Further investigation of this point will be undertaken soon.

With nitrogen at pressures of 25, 50 and 100 mm excitation of the gas could be initiated only by employing voltages high enough to melt the standard 30 volt filament, the arc starting at the break, quickly melted the filament back to the electrodes which in turn were melted if the applied voltage was not immediately reduced. Spectra of the lamps operating under these conditions with approximately 40 amperes across the arc and the electrodes frequently molten consist of a very great number of lines the emitter of which has not yet been determined (Fig. 5).

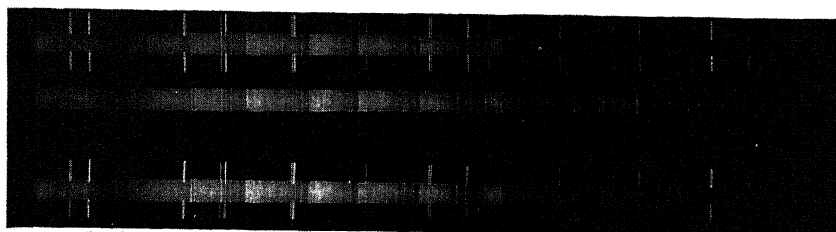


Fig. 5. Spectra of nitrogen filled lamp operated at unusually high current density. Quartz mercury arc comparison.

Similar rich line spectra were obtained with helium, neon and argon when lamps containing them were operated for a few minutes at the normal current of 30 amperes. However, as no attempt had been made to purify the samples of gases used, nitrogen could very well have been present in varying amounts. This was proved to be true in the case of the argon first used, spec-

³ E. P. Lewis, *Astrophys. Jour.* **40**, 148 (1914).

tograms of which showed the nitrogen bands when the arc carried moderate currents. In these rich line spectra many of the lines are common to the spectra from lamps containing nitrogen, neon, helium and argon. The wavelengths of the lines of several spectra have been measured but their identification has not been determined.

Carbon dioxide was especially interesting in that, at a pressure of less than a millimeter, both in lamps with mercury and in those without it the bands of the third positive group of Deslandres were present together with other bands in the visible, which are obscured by the background of continuous radiation.

All the spectra shown in this paper were obtained from lamps in the regular Corex bulb which does not have a very high transmission¹ for wave-lengths shorter than about 2700Å. Some spectra taken with the S-1 lamp in a quartz bulb⁴ show many lines as far down as the plates used were sensitive. This lamp in the regular Corex glass bulb makes a very good source for spectroscopic work and by using a quartz bulb the range can be considerably extended into the short ultraviolet. A continuation of the investigation is being undertaken in which more quantitative work will be done on the above mentioned gases and a number of others.

This work was performed in the Lamp Development Laboratory of the General Electric Company at Nela Park. The author wishes to acknowledge his appreciation of the privilege of working in the laboratory and also of the assistance and consideration afforded him by Dr. W. E. Forsythe and other members of the laboratory staff.

⁴ W. E. Forsythe, M. A. Easley, *Phys. Rev.* **36**, 150 (1930).

THE BEHAVIOR OF A MERCURY VAPOR ARC WITH A
JET OF LIQUID MERCURY AS CATHODE

BY AUSTIN M. CRAVATH*

PRINCETON UNIVERSITY

(Received September 22, 1930)

ABSTRACT

A mercury vapor arc in which the cathode was a jet of liquid mercury with a velocity up to 2400 cm per sec. was built to see if a stationary cathode spot with moving mercury could be obtained instead of the usual moving cathode spot and stationary mercury. Usually the arc refused to run to the exposed part of the jet. When a cathode spot did appear on the jet, it moved in the usual irregular manner, and increasing the jet speed tended to make the spot leave the jet.

THE motion of the cathode spot in the ordinary mercury vapor arc, with a pool of mercury acting as a cathode, interferes with the study of the conditions near the cathode (e. g. potential distribution, electron density and velocity). To avoid this difficulty, Compton and LaMar used a cathode consisting of a quartz tube, with a 2 mm hole at the top, kept filled with mer-

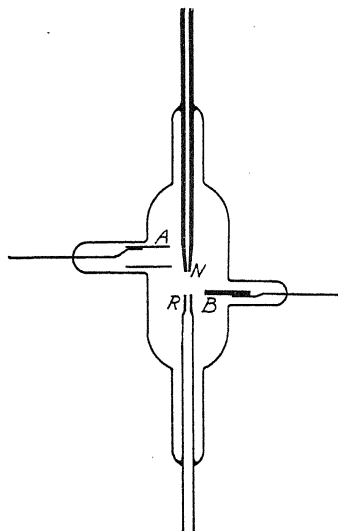


Fig. 1. The arc tube, showing the arrangement for the mercury jet cathode.

cury up to the level of the hole. This limited the range of motion, but did not stop it, and there was still that unsteadiness in the arc which results from the unsteadiness of the cathode spot.

While it is not to be expected that the relative motion of cathode spot and mercury surface can be prevented without radically changing the nature

* National Research Fellow.

of the spot (as is done by having a tungsten wire project up through the mercury surface), it occurred to the writer that it might be possible to obtain this relative motion by moving the mercury instead of the spot. An arc was therefore constructed, as shown in Fig. 1, in which the cathode was a jet of liquid mercury, 1 mm in diameter. Issuing from the nozzle *N* and passing into the receiver *R*. Two anodes, *A* and *B*, were provided.

OBSERVATIONS

The arc was run at various currents, from one ampere to ten amperes, and at various temperatures from room temperature up to probably 150°C. Both anodes, *A* and *B*, were tried. Various receivers were used, having openings from about 1.2 mm (so small that the jet had to be aimed by keeping one side of the tube heated while running) up to 5 mm. The arc was also turned on its side, and run with no receiver, but with the jet striking the end of the tube, the mercury being drained out at the bottom. Jet speed varied from 45 to 2400 cm per sec. The effect of a permanent magnet held near the arc in various positions was tried. In some cases an additional connection to the mercury was made in the receiver, and a current of 8 amperes was passed through the jet stream (superimposed on the arc current) from nozzle to receiver. This produces a magnetic field tending to drive the spot toward the nozzle.

At no time could a stationary cathode spot on the jet be obtained. With a receiver, the arc invariably ran into the receiver, forming a bright glow about the jet, but no regular concentrated cathode spot. The 8 ampere current passing through the jet stream from nozzle to receiver tended to drive the glow up toward the mouth of the receiver, and even to drive some diffuse glow out around the jet before it entered the receiver. A few times, with small diameter receiver, there was temporarily a regular concentrated cathode spot, running along the exposed part of the jet, in addition to the glow in the receiver, but this could not be reproduced. Increasing the jet speed increased the glow in the receiver, and thinned out the zigzag pattern traced by the spot on the jet. The distance to which the arc penetrated the receiver increased with increasing jet speed, and also depended on the receiver diameter, varying from as much as 20 cm sometimes, with a 5 mm receiver, to less than 1 mm with the smallest (about 1.2 mm) receiver.

With no receiver there was a regular cathode spot, running irregularly around the jet, at the point where it was breaking up. This was in the open at low speed, and against the wall at high speed.

The results may be summed up in the statement that in all cases the arc tended to run down stream, along the jet, and this tendency increased with increasing jet speed.

THE DIFFRACTION OF A CIRCULARLY SYMMETRICAL ELECTROMAGNETIC WAVE BY A CO-AXIAL CIRCULAR DISC OF INFINITE CONDUCTIVITY

BY JOHN BARDEEN

DEPARTMENT OF ELECTRICAL ENGINEERING, UNIVERSITY OF WISCONSIN

(Received August 22, 1930)

ABSTRACT

A disc of infinite conductivity, whose radius is a , and whose center is at the origin, lies in a plane which is perpendicular to the z -axis of cylindrical coordinates, r, z, ϕ . A circularly symmetrical electromagnetic wave of wave-length λ impinges on the disc, and the resultant field is required. The solution depends upon solving an integral equation of the first kind. When $2\pi a/\lambda < 1$, this equation reduces to an integral equation similar to Abel's which may be solved explicitly. As an illustration the solution is obtained for the diffraction of a wave due to an oscillating electric dipole whose axis is the axis of z . It is mentioned that these equations have been used in determining the powerflow into the earth below a vertical antenna which is grounded by a circular disc lying on the surface.

1. FORMULATION OF THE PROBLEM

CONSIDER a disc of radius a whose center is at the origin and whose plane is perpendicular to the Z -axis of cylindrical coordinates r, z, ϕ . A circularly symmetrical electromagnetic wave impinges on the disc, and the resultant field is required. Heretofore in such problems the disc has been treated as the limiting case of an oblate ellipsoid of revolution.¹ A solution in the form of a definite integral may, however, be directly obtained without making use of this limiting process.

The electric intensity E' and the magnetic intensity H' of the incident wave are assumed to be of such nature that:

$$H_r' = H_z' = E_\phi' = 0$$

and that H_ϕ' , E_r' , and E_z' are independent of ϕ . The dependence of this wave on time is to be of the form $e^{-i\omega t}$.

In diffraction problems, the field due to the disc is considered separately from the incident wave. This field alone will be considered here, the incident wave being taken into account only through the boundary conditions. The electric intensity E and the magnetic intensity H of the field due to the disc must satisfy Maxwell's equations for free space, which in this case reduce to:

$$H_r = H_z = E_\phi = 0 \tag{1}$$

¹ Hertzfeld, Wiener Berichte (1911) p. 1587; Möglich, Ann. der Physik 83, 609 (1927).

$$\left. \begin{aligned} i\omega\mu H_\phi &= \frac{\partial E_r}{\partial z} - \frac{\partial E_z}{\partial r} \\ -i\omega p E_r &= -\frac{\partial H_\phi}{\partial z} \\ -i\omega p E_z &= \frac{1}{r} \frac{\partial}{\partial r}(r H_\phi) \\ \frac{1}{r} \frac{\partial}{\partial r}(r E_r) + \frac{\partial E_z}{\partial z} &= 0 \end{aligned} \right\} \quad (2)$$

In these equations \mathbf{E} and \mathbf{H} are expressed in the rationalized practical system of units.²

The disc is assumed to be of infinite conductivity. Thus the radial component of the electric intensity of the total field must vanish on the surface of the disc. This requires that

$$(E_r)_{z=0} = f(r) \quad \text{for } r < a \quad (3)$$

where $f(r)$ is the negative of the radial component of the electric intensity of the incident wave at $z=0$. From symmetry considerations it is seen that

$$(E_z)_{z=0} = 0 \quad \text{for } r > a \quad (4)$$

and that

$$(H_\phi)_{z=0} = 0 \quad \text{for } r > a. \quad (5)$$

It is required further that \mathbf{E} and \mathbf{H} be continuous functions of (r, z) throughout space except at the disc, and that they vanish to proper orders at infinity.

2. SOLUTION OF THE PROBLEM

An appropriate solution of Eq. (2) is:

$$E_r = \int_0^\infty J_1(\lambda r) \phi(\lambda) (\lambda^2 - k^2)^{1/2} e^{\mp z(\lambda^2 - k^2)^{1/2}} d\lambda \quad (6)$$

$$E_z = \pm \int_0^\infty J_0(\lambda r) \phi(\lambda) \lambda e^{\mp z(\lambda^2 - k^2)^{1/2}} d\lambda \quad (7)$$

$$H_\phi = \mp i\omega p \int_0^\infty J_1(\lambda r) \phi(\lambda) e^{\mp z(\lambda^2 - k^2)^{1/2}} d\lambda^{1/2} \quad (8)$$

The upper signs are used for positive z , while $k = \omega/c$, where c is the velocity of light. The symbols J_0 and J_1 represent the ordinary Bessel's functions. The quantity $\phi(\lambda)$ is an arbitrary function of λ , independent of the coordinates.

² In this system: Magnetic intensity, H , is expressed in ampere-turns per cm. Magnetic flux density, B , is expressed in webers per sq. cm. ($=10^8$ maxwells per sq. cm.). Permeability, $\mu = B/H = 4\pi/10^{-9}$ for free space. Electric intensity, E , is expressed in volts per cm. Displacement, D , is expressed in coulombs per sq. cm. Permittivity, $p = D/E = 8.85/10^{-14}$ for free space.

It may be chosen in such a manner as to satisfy the boundary conditions (3), (4), and (5) and is, of course, subject to the restriction that it must produce proper convergence of the integrals.

The method of solution is somewhat analogous to Beltrami's theory of symmetrical potentials.³ Choose:

$$\phi(\lambda) = \int_0^a F(s) \cos [s(\lambda^2 - k^2)^{1/2}] ds \quad (9)$$

where $F(s)$ is arbitrary. From q. (7)

$$r(E_z)_{z=0} = \frac{\partial}{\partial r} r \int_0^\infty J_1(\lambda r) \phi(\lambda) d\lambda \quad (10)$$

Substituting the value of $\phi(\lambda)$ given by Eq. (9), and changing the order of integration, there results:

$$r(E_z)_{z=0} = \pm \frac{\partial}{\partial r} r \int_0^a F(s) ds \int_0^\infty J_1(\lambda r) \cos [s(\lambda^2 - k^2)^{1/2}] d\lambda \quad (11)$$

For $r > a$

$$r(E_z)_{z=0} = \pm \frac{\partial}{\partial r} r \int_0^a \frac{F(s) \cosh (ks) ds}{r} = 0. \quad (12)$$

Thus Eq. (4) is satisfied.

Next $F(a)$ will be chosen so that Eq. (5) is satisfied. From Eq. (8)

$$(H_\phi)_{z=0} = \mp i\omega p \int_0^\infty J_1(\lambda r) \phi(\lambda) d\lambda. \quad (13)$$

Now from Eq. (9)

$$\phi(\lambda) = F(a) \frac{\sin [a(\lambda^2 - k^2)^{1/2}]}{(\lambda^2 - k^2)^{1/2}} - \int_0^a F'(s) \frac{\sin [s(\lambda^2 - k^2)^{1/2}]}{(\lambda^2 - k^2)^{1/2}} ds. \quad (14)$$

Thus

$$(H_\phi)_{z=0} = \mp i\omega p \left[F(a) \int_0^\infty J_1(\lambda r) \frac{\sin [a(\lambda^2 - k^2)^{1/2}]}{(\lambda^2 - k^2)^{1/2}} d\lambda - \int_0^a F'(s) ds \int_0^\infty J_1(\lambda r) \frac{\sin [s(\lambda^2 - k^2)^{1/2}]}{(\lambda^2 - k^2)^{1/2}} d\lambda \right] \quad (15)$$

For $r > a$

$$(H_\phi)_{z=0} = \mp i\omega p \left[\frac{F(a) \sinh (ka)}{kr} - \int_0^a \frac{F'(s) \sinh (ks) ds}{kr} \right] = 0 \quad (16)$$

This equation gives $F(a)$ in terms of $F'(s)$:

$$F(a) = \int_0^a F'(s) \frac{\sinh (ks)}{\sinh (ka)} ds. \quad (17)$$

³ Webster: Partial Differential Equations of Mathematical Physics, p. 368 (1927).

Next $F'(s)$ is determined in such a manner that Eq. (3) is satisfied. Substituting Eq. (14) in Eq. (3):

$$(E_r)_{z=0} = \int_0^\infty J_1(\lambda r) \left[F(a) \sin [a(\lambda^2 - k^2)^{1/2}] - \int_0^a F'(s) \sin [s(\lambda^2 - k^2)^{1/2}] ds \right] d\lambda. \quad (18)$$

The value of $F(a)$ from Eq. (17) is now substituted in Eq. (18). Changing the order of integration:

$$(E_r)_{z=0} = \int_0^a F'(s) \frac{\sinh(ks)}{\sinh(ka)} ds \int_0^\infty J_1(\lambda r) \sin [a(\lambda^2 - k^2)^{1/2}] d\lambda - \int_0^a F'(s) ds \int_0^\infty J_1(\lambda r) \sin [s(\lambda^2 - k^2)^{1/2}] d\lambda. \quad (19)$$

For $r < a$

$$r(E_r)_{z=0} = f(r) = - \int_0^r s F'(s) \frac{\cos [k(r^2 - s^2)^{1/2}]}{(r^2 - s^2)^{1/2}} ds + i \int_0^a F'(s) \left[\frac{a \sinh [k(a^2 - r^2)^{1/2}] \sinh(ks)}{(a^2 - r^2)^{1/2} \sinh(ka)} - \frac{s \sinh [k(s^2 - r^2)^{1/2}]}{(s^2 - r^2)^{1/2}} \right] ds \quad (20)$$

This is an integral equation of the first kind for the determination of $F'(s)$. It probably possesses no solution of a simple form. If, however, the second integrand be expanded in a power series in ka , we find that the leading term is

$$\frac{iF'(s)ka}{\sinh(ka)} \left[\frac{4}{3} \frac{sr^2(a^2 - s^2)}{a^5} \frac{(ka)^5}{5!} + \text{higher order terms} \right]$$

Let us now assume that $ka < 1$, the final result being, of course, subject to this restriction. Remembering that r in Eq. (20) is less than a , it appears that the second integral of Eq. (20) will be much smaller than the first unless abnormally great values of $F'(s)$ occur between $s=r$ and $s=a$. We will therefore assume that the second integral of Eq. (20) is negligible as compared to the first. The validity of this assumption for any definite problem must be checked after $F'(s)$ is calculated, by direct test of the final result in the original conditions of the problem. In the special cases for which calculation has been completed, the error involved has been found to be less than one percent.

We thus have left an integral equation similar to Abel's equation,⁴ which may be solved in much the same manner. This equation is:

$$rf(r) = - \int_0^r \frac{F'(s)s \cos [k(r^2 - s^2)^{1/2}] ds}{(r^2 - s^2)^{1/2}}. \quad (21)$$

⁴ Bocher, An Introduction to the Study of Integral Equations, p. 8, (1914).

It is interesting to note that this equation for the determination of $F'(s)$ no longer contains the parameter a . Thus we will proceed formally as though the functions $f(r)$ were known⁵ for all values of r . In the final equations $F'(s)$ will involve a knowledge of $f(r)$ only from $r=0$ to $r=a$. Let

$$-F'(s) = \int_0^k \beta g[(k^2 - \beta^2)^{1/2}] I_0(\beta s) d\beta + \int_0^\infty \lambda g[(\lambda^2 + k^2)^{1/2}] J_0(\lambda s) d\lambda \quad (22)$$

where $g[\rho]$ is a function to be determined. Substituting this value for $F'(s)$ in Eq. (21) and changing the order of integration,

$$rf(r) = \int_0^k \beta g[(k^2 - \beta^2)^{1/2}] d\beta \int_0^r s I_0(\beta s) \frac{\cos[k(r^2 - s^2)^{1/2}]}{(r^2 - s^2)^{1/2}} ds \quad (23)$$

$$+ \int_0^\infty \lambda g[(\lambda^2 + k^2)^{1/2}] d\lambda \int_0^r s J_0(\lambda s) \frac{\cos[k(r^2 - s^2)^{1/2}]}{(r^2 - s^2)^{1/2}} ds$$

$$= \int_0^k \beta g[(k^2 - \beta^2)^{1/2}] \frac{\sin[r(k^2 - \beta^2)^{1/2}]}{(k^2 - \beta^2)^{1/2}} d\beta$$

$$+ \int_0^\infty \lambda g[(\lambda^2 + k^2)^{1/2}] \frac{\sin[r(\lambda^2 + k^2)^{1/2}]}{(\lambda^2 + k^2)^{1/2}} d\lambda \quad (24)$$

or, changing the variable of integration,

$$rf(r) = \int_0^\infty g(\rho) \sin(r\rho) d\rho. \quad (25)$$

This is a Fourier integral equation, the solution of which is

$$g(\rho) = \frac{2}{\pi} \int_0^\infty \alpha f(\alpha) \sin(\alpha\rho) d\alpha \quad (26)$$

$$= -2\alpha f(\alpha) \frac{\cos(\alpha\rho)}{\pi\rho} \Big|_0^\infty + \frac{2}{\pi} \int_0^\infty \frac{\partial}{\partial\alpha}(\alpha f(\alpha)) \frac{\cos(\alpha\rho)}{\rho} d\alpha. \quad (27)$$

Since $f(\alpha)$ vanishes to a higher order than $1/\alpha$ at $\alpha = \infty$, the first term vanishes. Substituting the remainder in Eq. (22)

$$-F'(s) = \frac{2}{\pi} \int_0^\infty \frac{\partial}{\partial\alpha}(\alpha f(\alpha)) d\alpha \int_0^k \beta I_0(\beta s) \frac{\cos[\alpha(k^2 - \beta^2)^{1/2}]}{(k^2 - \beta^2)^{1/2}} d\beta$$

$$+ \frac{2}{\pi} \int_0^\infty \frac{\partial}{\partial\alpha}(\alpha f(\alpha)) d\alpha \int_0^\infty \lambda J_0(\lambda s) \frac{\cos[\alpha(\lambda^2 + k^2)^{1/2}]}{(\lambda^2 + k^2)^{1/2}} d\lambda \quad (28)$$

$$F'(s) = -\frac{2}{\pi} \int_0^\infty \frac{1}{\alpha} \frac{\partial}{\partial\alpha}(\alpha f(\alpha)) \frac{\alpha \cosh[k(s^2 - \alpha^2)^{1/2}]}{(s^2 - \alpha^2)^{1/2}} d\alpha \quad (29)$$

The solution of the problem is now complete, since we may write from Eq. (14) and Eq. (17),

⁵ Since $f(r)$ is essentially a component of the incident field, it vanishes at infinity as $1/r^2$.

$$\phi(\lambda) = \int_0^a F'(s) \left[\frac{\sin [a(\lambda^2 - k^2)^{1/2}] \sinh(ks)}{(\lambda^2 - k^2)^{1/2} \sinh(ka)} - \frac{\sin [s(\lambda^2 - k^2)^{1/2}]}{(\lambda^2 - k^2)^{1/2}} \right] ds \quad (30)$$

and the components of the field are then obtained directly from Eq. (6), (7), and (8).

Thus

$$\begin{aligned} H_\phi &= \mp i\omega p \int_0^a F'(s) \frac{\sinh(ks)}{\sinh(ka)} ds \int_0^\infty J_1(\lambda r) e^{\mp z(\lambda^2 - k^2)^{1/2}} \frac{\sin [a(\lambda^2 - k^2)^{1/2}]}{(\lambda^2 - k^2)^{1/2}} d\lambda \\ &\quad \pm i\omega p \int_0^a F'(s) ds \int_0^\infty J_1(\lambda r) e^{\mp z(\lambda^2 - k^2)^{1/2}} \frac{\sin [s(\lambda^2 - k^2)^{1/2}]}{(\lambda^2 - k^2)^{1/2}} d\lambda \\ &= \pm \frac{i\omega p}{kr} \int_0^a F'(s) \left[\frac{e^{ikR_1} \sinh(kI_1) \sinh(ks)}{\sinh(ka)} - e^{ikR_2} \sinh(kI_2) \right] ds \end{aligned} \quad (31)$$

where

$$R_1 + iI_1 = [r^2 + (ia \pm z)^2]^{1/2}$$

and

$$R_2 + iI_2 = [r^2 + (is \pm z)^2]^{1/2}.$$

The upper signs are used for positive z and the lower for negative z . Derivatives of H_ϕ give E_r and E_z .

$$\left. \begin{aligned} E_r &= -\frac{i}{\omega p} \frac{\partial H_\phi}{\partial z} \\ E_z &= \frac{i}{\omega p r} \frac{\partial}{\partial r} (r H_\phi) \end{aligned} \right\} \quad (32)$$

In many important cases $f(\alpha)$ is given in the form of an integral.

$$f(\alpha) = \int_0^\infty h(\rho) J_1(\alpha \rho) d\rho. \quad (33)$$

Then

$$\frac{1}{\alpha} \frac{\partial}{\partial \alpha} (\alpha f(\alpha)) = \int_0^\infty \rho h(\rho) J_0(\alpha \rho) d\rho \quad (34)$$

and

$$\begin{aligned} F'(s) &= -\frac{2}{\pi} \int_0^\infty \rho h(\rho) d\rho \int_0^s \alpha J_0(\lambda \alpha) \frac{\cosh [k(s^2 - \alpha^2)^{1/2}]}{(s^2 - \alpha^2)^{1/2}} d\alpha \\ &= -\frac{2}{\pi} \int_0^\infty \rho h(\rho) \frac{\sin [s(\rho^2 - k^2)^{1/2}]}{(\rho^2 - k^2)^{1/2}} d\rho \end{aligned} \quad (35)$$

3. ILLUSTRATIVE EXAMPLE

As an example, $F'(s)$ will be calculated for the diffraction of a wave due to an oscillating electric dipole. The axis of the dipole is the Z -axis and it is located a distance H above the disc. Then

$$E_r' = - \int_0^\infty \rho^2 e^{-(H-z)(\rho^2-k^2)^{1/2}} J_1(\rho r) d\rho \quad (36)$$

so that

$$f(\alpha) = \int_0^\infty \rho^2 e^{-H(\rho^2-k^2)^{1/2}} J_1(\rho \alpha) d\rho \quad (37)$$

and

$$h(\rho) = \rho^2 e^{-H(\rho^2-k^2)^{1/2}}. \quad (38)$$

Thus from Eq. (35)

$$\begin{aligned} F'(s) &= -\frac{2}{\pi} \int_0^\infty \rho^2 e^{-H(\rho^2-k^2)^{1/2}} \frac{\sin [s(\rho^2-k^2)^{1/2}]}{(\rho^2-k^2)^{1/2}} d\rho \quad (39) \\ &= \frac{2}{\pi} \int e^{ikH} \left[\frac{k(H^2-s^2) \sinh(ks) + 2ikHs \cosh(ks)}{(H^2+s^2)^2} \right] \\ &\quad - e^{ikH} \left[\frac{(3H^2s-s^3) \cosh(ks) + i(3Hs^2-H^3) \sinh(ks)}{(H^2+s^2)^3} \right]. \quad (40) \end{aligned}$$

This value of $F'(s)$ is then substituted in Eq. (31) to obtain the components of the field. The resulting integrals are rather complicated, but may be numerically evaluated by mechanical means.

These equations have been used in determining the power flow into the earth below a vertical antenna which is grounded by a circular disc lying on the surface. (The disc is an idealized case. Actually a number of radial wires would be buried in the earth.) The results of this investigation will be published elsewhere.

worked with low magnetic fields. For a given Zeeman pattern the lower limit of the field required for its resolution is determined by the half-width of the line. Measurements by Babcock⁹ on the light of the night sky and by Mc Lennan and his collaborators¹⁰ on electrical discharges, gave 0.035A as the half-width of the auroral line. With the Zeeman pattern (1), 2/1 predicted by Rubinowicz, the smallest separation between the components of the same polarization is $2\Delta\nu$ norm. Thus we may expect that at any field over 2400 gauss the inner components are resolved.

The exposures were made with the interferometer plates separated by 7.1045 mm. This value was determined by measuring the fractional order of interference of five secondary standards of the neon spectrum and determining the whole order by systematic trial in the usual way.¹¹ With this interferometer distance and a field of 2578 gauss (corresponding to a solenoid current of 70.0 amp.) the Zeeman pattern predicted by Rubinowicz should appear with all four components clearly separated in each order, i.e. without overlapping. Fig. 2b is a reproduction of such an exposure, enlarged 6 times. In this pattern the π components are just separated; the σ components are already approaching the neighboring orders. In Fig. 2a the field has been increased to 3867 gauss at 105.0 amp. Here the π components are evenly spaced, but the σ components are just overlapping the adjacent orders. To permit measurements on the σ components plate 2c was taken with a field of 2025 gauss (55.0 amp.), to give them an even spacing. As expected the π components are not resolved, but are perceptibly broadened. For the sake of completeness Fig. 2d was taken without field. The increasing magnetic resolution with increasing magnetic field can be easily followed through the four exposures by means of the divergent lines, dotted lines for π components, full lines for σ components. Attention may be called to the absence of an undisplaced central component in Fig. 2a.

Table II contains the results of the measurements on plates 2a, 2b, and 2c.

TABLE II

Plate	Field	$\Delta\nu/\Delta\nu$ norm	
		σ comp.	π comp.
2a	3867	—	1.035
2b	2578	2.018	0.922
2c	2025	1.877	—
		Mean 1.948	0.979

The calculations were made in the following manner. From the ring diameters, D_n , as measured on a comparator, the fractional order of interference, δ , of each component at the center of the fringe system was found by the usual relation:

⁹ Babcock, *Astrophys. J.* **57**, 209 (1923).

¹⁰ J. C. Mc Lennan and J. H. Mc Leod, *Proc. Roy. Soc.* **A115**, 515 (1927).

¹¹ Lord Rayleigh, *Phil. Mag.* **9**, 685 (1906).

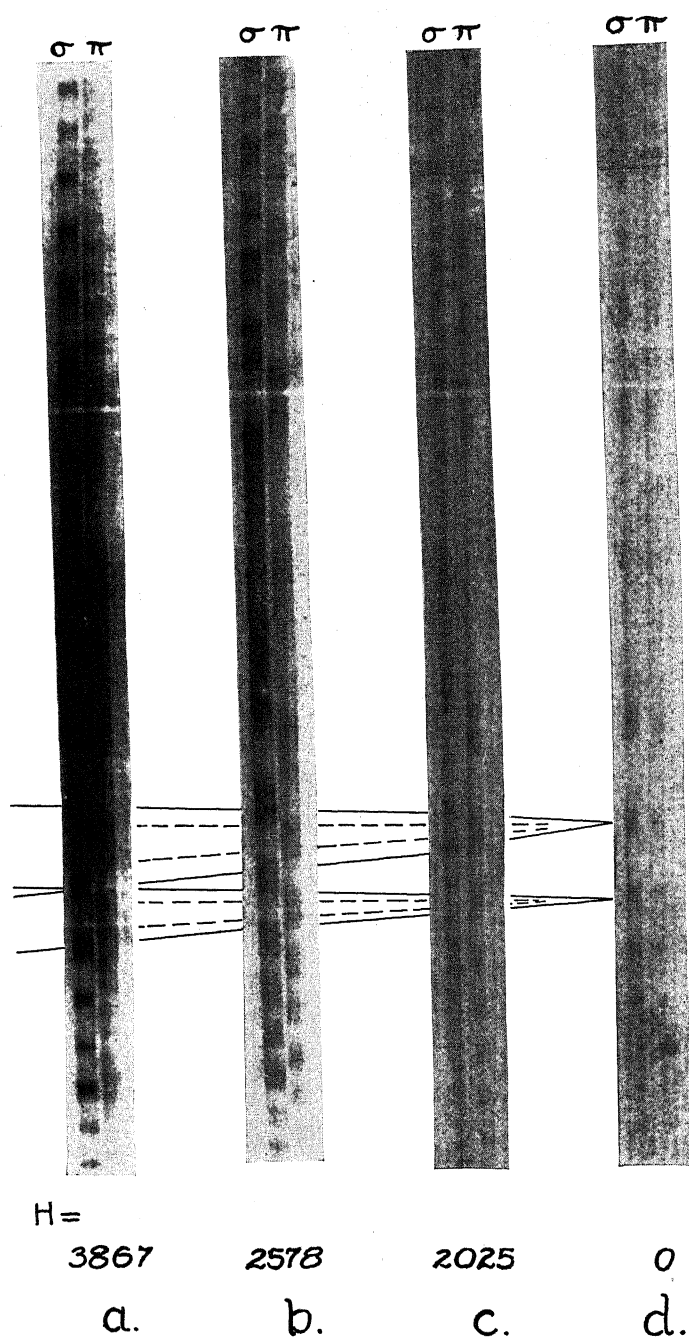


Fig. 2. Interferometer fringes of the auroral line at four values of the magnetic field. The full lines pass through σ -components, the dotted lines through π -components.

small tungsten filament. To overcome this effect a space-charge grid is placed between the filament and control grid which repels all ions since it is operated at a positive potential. This grid, of course, also increases the mutual conductance of the tube.

While photo-electrons are not emitted by pure nickel or molybdenum grids under action of light from the filament, there is invariably enough contamination to cause an appreciable current. This effect is greatly reduced by using thoriated filaments operated at a low temperature.

In order to determine the magnitude of the current emitted by soft x-rays from the anode several special tubes were constructed in which a nickel or molybdenum plate was so mounted that it received only soft x-rays produced by the impact of 4 to 10 volt electrons. With potentials above 6 volts the currents were in all cases greater than 10^{-15} ampere. Photoelectric emission due to such soft x-rays has been demonstrated by numerous investigators.^{7,8} By the use of very low anode voltages the currents due to this cause were reduced to an inappreciable value.

DESCRIPTION OF TUBE DEVELOPED

The tube as finally developed is, as mentioned, a space-charge grid tube. The control grid is brought out of the top of the bulb, while the other elements terminate in a standard UX base. The control grid is mounted on quartz beads shielded to prevent surface contamination. The filament is of thoriated tungsten and consists of two legs in parallel to keep the voltage low. The general structure is shown in the photograph. (Fig. 1).

The most desirable operating conditions and the characteristics at these conditions were found to be as follows:

Filament voltage	= 2.5 v.	Filament current	= 100 ma.
Plate voltage	= 6.0 v.	Plate current	= 40 μ a.
Control grid voltage	= -4.0 v.	Mutual conductance	= 25 μ a/v.
Space charge grid voltage	= 4.0 v.	Amplification factor	= 1.0
		Plate Resistance	= 40000 ohms.

Under these conditions representative tubes have a grid current of about 10^{-15} ampere while the input resistance is of the order of 10^{16} ohms. The input capacity is about 2.5×10^{-12} farad. Fig. 2 shows plate current and grid current plotted against grid voltage for such a tube.

The effects of filament temperature are shown in Fig. 3. The rapid increase in grid current above 2.5 volts on the filament is attributed to photoelectric emission from the grid due to the light from the filament. Fig. 4 shows the effects of plate-voltage variation. The considerable increase in grid current above 6 volts is due to photoelectric emission caused by soft x-rays, while the great increase above 8 volts is due to ionization.

⁷ O. W. Richardson, Proc. Roy. Soc. A110, 247 (1926).

⁸ C. H. Thomas, Phys. Rev. 25, 322 (1925).

METHODS OF MEASURING SMALL CURRENTS

The method used in measuring the grid current of the tubes consists in determining the rate of change of grid potential when the grid is free. The plate current of the tube serves as the indication of grid voltage. Of course, $i_c = C_g de_c/dt$. The input capacity C_g may be measured quite accurately, while the rate of change of grid voltage is readily determined with a stop watch. With this method there is practically no minimum limit on the mag-

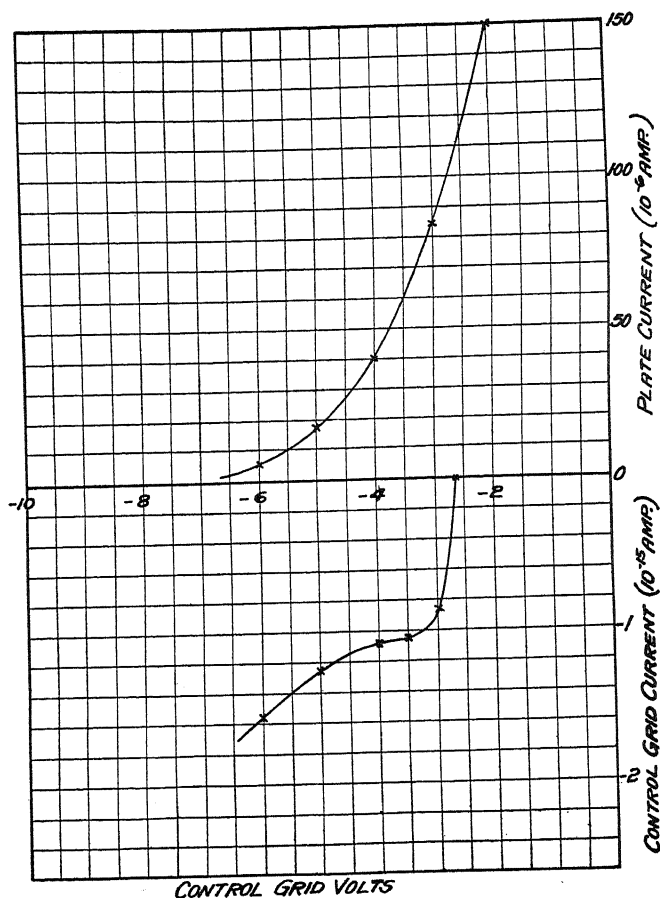


Fig. 2. Plate current and control grid current as a function of grid voltage.

nitude of the grid current which may be measured, except that imposed by the time required to obtain an appreciable deflection on the galvanometer used in the plate circuit.

This method may be applied to the measurement of any small current. If the current is of the order of 10^{-13} ampere or greater, the grid current may be neglected. For measuring smaller currents the grid current may be subtracted from the indicated value.

This tube may be used in any of the methods previously described^{1,2,3}

for indicating currents directly with better results than are obtained with ordinary tubes.

Neglecting for the moment variations in supply voltages, all currents of this tube are very steady, no drift in plate current being appreciable on a galvanometer having a sensitivity of 10^{-10} ampere per millimeter.

The variation in grid current should not produce an error of greater than 10^{-17} amperes in the measured current, so that the limiting value to be measured may be taken as of this order. If a direct indicating method is used the input resistance to give an appreciable deflection on a galvanometer of 10^{-10}

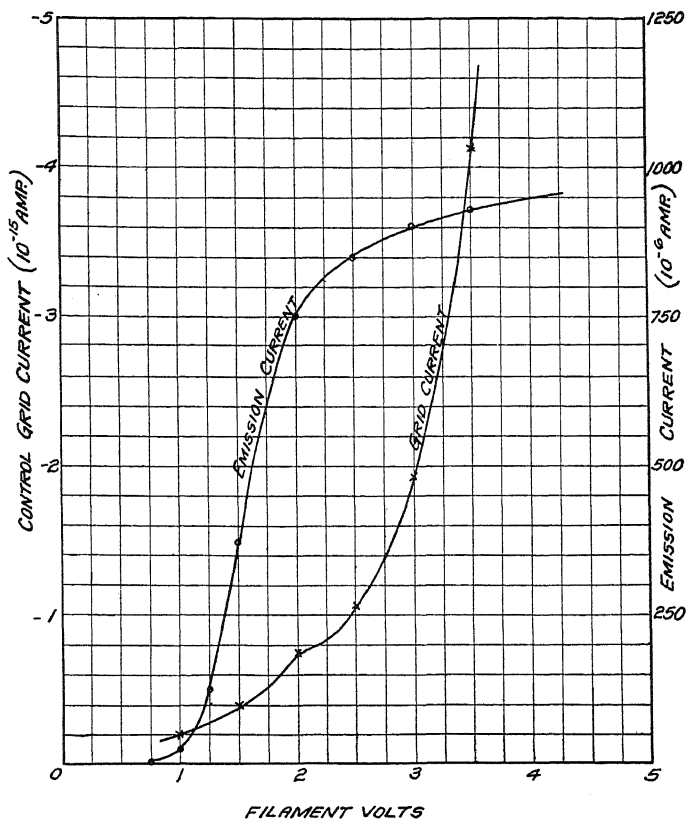


Fig. 3. Effect of filament temperature on grid current.

ampere sensitivity with a current of 10^{-17} ampere is 4×10^{11} ohms. Various means of obtaining such resistances have been described.^{3,9} With this galvanometer the sensitivity of the unit is 250,000 millimeters per volt. If amplification is added after the electrometer tube a smaller input resistance may be used, or a less sensitive galvanometer.

No leakage troubles are experienced with these tubes provided they are used in dry air. This has been accomplished by operating the tube in a relatively air-tight container with a dryer such as phosphoric pentoxide.

⁹ Mulder & Razek, J.O.S.A. & R.S.I. 18, 470 (1929).

Drift of supply potentials has been minimized by using storage batteries of ample capacity. Since the voltages and currents are very low this presented no problem.

It is felt that the tube as described will prove to be a very useful scientific

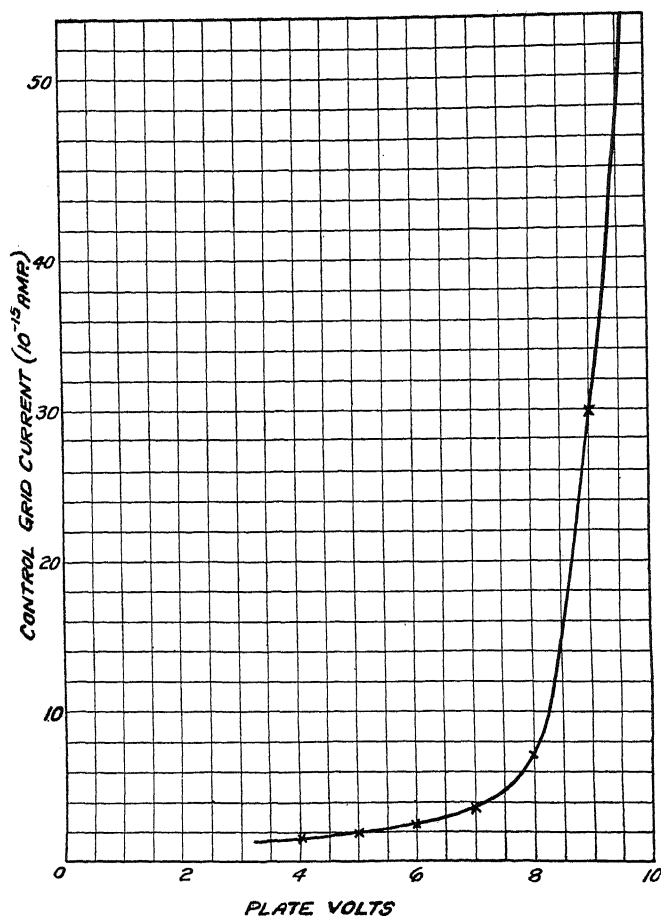


Fig. 4. Effect of plate-voltage variation on the grid current.

instrument, offering advantages in sensitivity and convenience over the common forms of electrometer.

The writers desire to acknowledge the helpful suggestions and the encouragement offered by Dr. A. W. Hull throughout this investigation, and the careful work of Mr. G. M. Rose in taking much of the data.

CATAPHORESIS IN ROTATING ELECTRIC FIELDS*

BY E. M. PUGH AND C. A. SWARTZ**

CALIFORNIA INSTITUTE OF TECHNOLOGY

(Received September 17, 1930)

ABSTRACT

A new method of making cataphoresis measurements on colloid particles has been developed and tested. The method makes use of a rotating electric field which causes the particles to move in circles. In this way it is easily possible to test the effect of variable speed of the particle on the distribution of the diffuse electric double layer surrounding it. The results obtained indicate that this effect is negligible. Furthermore, it has been discovered that the mobility of the small particles (below 10^{-4} cm in diameter) fluctuates widely and this is made very evident to the eye by the fluctuations in the circular paths of the particles. The fluctuations are quite violent with particles as small as 10^{-6} cm in diameter. Considerable study of these variations has been made as well as an attempt to explain them qualitatively.

INTRODUCTION

THE alternating field method of measuring cataphoresis of colloid particles in the ultramicroscope, first introduced by Cotton and Mouton,¹ has not come into general use for this purpose although it possesses the distinct advantage of measuring instantaneous mobilities of individual particles. This is undoubtedly due to the fact that the interpretations of such measurements have been open to question since the particles cannot have the uniform velocities, always assumed in cataphoretic theories, when in A.C. fields. They must have different velocities in different parts of their paths.

For example, Blüh² found that the apparent mobility of silver particles in water increased with the frequency—an unexplainable result.³ It was a question whether the diffuse double layer could be out of phase with the particle and thus noticeably influence the measurements.

The advantages of the A.C. method can be preserved and most of the objectionable features removed by using a rotating field⁴ produced by applying a two phase A.C. source to four electrodes placed at the corners of a square

* This paper contains results obtained in an investigation on "The Fundamentals of the Retention of Oil by Sand" listed as Project No. 36 of American Petroleum Institute Research. Financial assistance in this work has been received from a research fund of the American Petroleum Institute donated by Mr. John D. Rockefeller. This fund is being administered by the Institute with the cooperation of the Central Petroleum Committee of the National Research Council.

** American Petroleum Institute Research Fellows.

¹ Cotton and Mouton, *Compt. Rend.* **138**, 1584, 1692 (1904).

² Blüh, *Ann. d. Physik* **78**, 177 (1925).

³ Blüh, *Ann. d. Physik* **79**, 143 (1926); **80**, 181 (1926).

⁴ Cotton and Mouton, in *Compt. Rend.* **138**, 1584 (1904) suggested the possibility of using colloid particles in a rotating field as a kind of oscilloscope to analyze three-phase potentials.

in a cataphoretic cell. Over a small area in the center of the square, the field thus produced will be practically uniform, constant in magnitude, and rotating with a constant angular velocity. This rotating field will cause each particle in this small area to describe the circumference of a circle with each rotation of the field. The greater the mobility of the particle the larger will be the circle which it will be able to traverse, and its speed will be given simply by the product of the circumference of the orbit by the frequency applied. Particles with constant mobility thus will move at constant speed, and the double layer or ionic cloud generally assumed to surround all colloid particles will reach the same kind of dynamic equilibrium as it would if the particle were moving in a straight line.

In the cell here developed, the electrodes were spaced sufficiently far apart so that the entire field of view in the high power microscope was small enough to fulfill the requirement of being a small area. On looking into the microscope, one finds the entire field of view filled with small circles or toroids of light.

THEORY

In the small section of the cell under observation, the electrostatic field will be that due to the superposition of the two fields arising from the alternating potentials applied separately to the two opposite sets of electrodes, and its x and y components given as functions of time will be

$$X = F \cos \omega t$$

$$Y = F \sin \omega t.$$

Here F is the maximum value of the field strength, in the small region under consideration, due to the potential applied across one of the two sets of electrodes. The total resultant field is a uniform electric field of constant strength F rotating with the constant angular velocity ω .

In order to find the motion of a particle suspended in the liquid and acted upon by such a rotating field, some assumptions must be made from both the electrical and the hydrodynamic standpoints in order to make the problem soluble and yet represent the facts fairly accurately. It is, therefore, assumed that the force acting on the particle due to the electric field is directly proportional to the field strength and that the equations of motion of the particle are

$$\begin{aligned} A \frac{d^2 x}{dt^2} + B \frac{dx}{dt} &= kX = kF \cos \omega t \\ A \frac{d^2 y}{dt^2} + B \frac{dy}{dt} &= kY = kF \sin \omega t \end{aligned} \quad (1)$$

where A and B are constants. A represents the effect of the inertia of the particle and B represents the viscous drag of the liquid surrounding the particle. Solving these equations, neglecting the constant terms, and introducing the initial condition that the velocity is zero when $t=0$ we get

$$\begin{aligned} x &= R_0 \cos \delta \sin (\omega t - \delta) + R_0 \cos \delta \sin \delta e^{-\omega t / \tan \delta} \\ y &= -R_0 \cos \delta \cos (\omega t - \delta) - R_0 \sin^2 \delta e^{-\omega t / \tan \delta} \end{aligned} \quad (2)$$

where $R_0 = kF/B\omega$ and $\delta = \tan^{-1} \omega A/B$.

Omitting the last or transient term in each of these equations, the path of the particle is seen to be a circle of radius $R = R_0 \cos \delta$. The velocity of the particle is

$$R\omega = kF \cos \delta / B$$

whereas, in cataphoretic measurements in a straight line it would be $V = kF/B$ as seen from equations (1) and these two will agree within the limits of accuracy of our experiment if $\cos \delta$ is sufficiently near to unity. Now δ is the angle by which the velocity vector of the particle lags behind

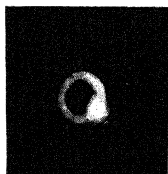


Fig. 1. Initial position and final path of oil particle. Diameter of particle 2×10^{-4} cm, field 225 volts/cm, frequency 21.5 r.p.s.

the electric field vector. One would expect it to be quite small because for colloid particles one would expect A to be very small compared to B . Fortunately, there is a simple experimental method of determining $\cos \delta$ with just

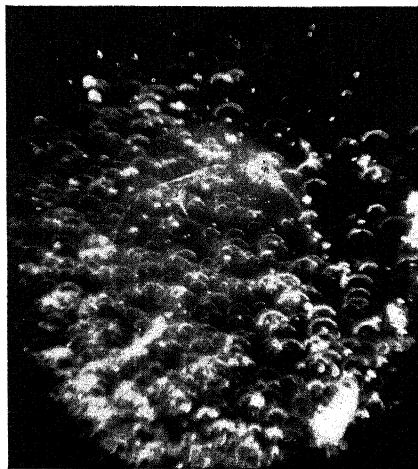


Fig. 2. Arcs of circular paths showing particles all of same sign but varying mobility.

the accuracy required, for on putting $t=0$ in equations (2), it is found that the initial position of the particle is at a distance R_0 from the center of the final circle of radius R . Long exposure microphotographs can then be taken in which the rotating field is not applied until the exposure is partly com-

pleted. The result is that the initial position and the final circle of the particle are recorded upon the plate from which R and R_0 can be measured, whence $\cos \delta = R/R_0$.

Fig. 1 is an example of such a photograph for a particle of mineral oil in water. It is seen that the initial position lies almost exactly in the path of the final circle. From this and several other such photographs, it can be concluded that $\cos \delta = 1$ within the limits of experimental error.

If particles of opposite sign should exist in the same sol, these could be detected by exposing the photograph for only a fraction of a period of revolution. Since particles of opposite sign must rotate in the same direction as the field but 180° apart in phase, they will produce arcs of circles curved in opposite directions. Fig. 2 is a photograph taken in this manner of a mineral oil emulsion with particles ranging in size from 10^{-6} to 10^{-5} cm.

APPARATUS

The apparatus consists essentially of three parts, the ultramicroscope and light source, the quartz cell (Fig. 3) containing the sol and electrodes, and the machine for producing the two phase A.C. potential (Fig. 4).

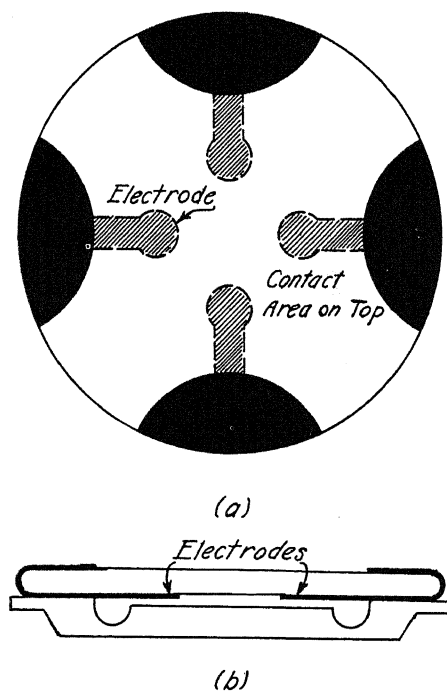


Fig. 3 a. Quartz cover glass with gold electrodes to produce rotating field.

Fig. 3 b. Cross-section of cataphoretic cell with cover glass.

The quartz cell, with its mounting and the high power oil-immersion objective are the special equipment made by Zeiss for colloidal work, and were adapted with slight modification for this purpose. The light source,

used in connection with a cardioid condenser, consists of a pointolite lamp for visual observation and a carbon arc passing from 15 to 75 amperes for photographic work.

The electrodes in the cell were formed by painting the proper design (Fig. 3a) on the under side of the cover glass with the gold paint used for decorating china and then heating in a furnace to 750°C . The cover glass with electrodes made in this way may be cleaned in hot cleaning solution without injury. Connection to the electrodes was made by strips of the gold paint which extend around the edge of the cover glass and connect to other painted areas on top. It was found necessary to grind the edges of the cover glass round and polish them in order to insure electrical connection. To these painted sections on top, connection is made directly by four spring clips which also serve to hold the cover glass firmly in place against the lower half of the cell.

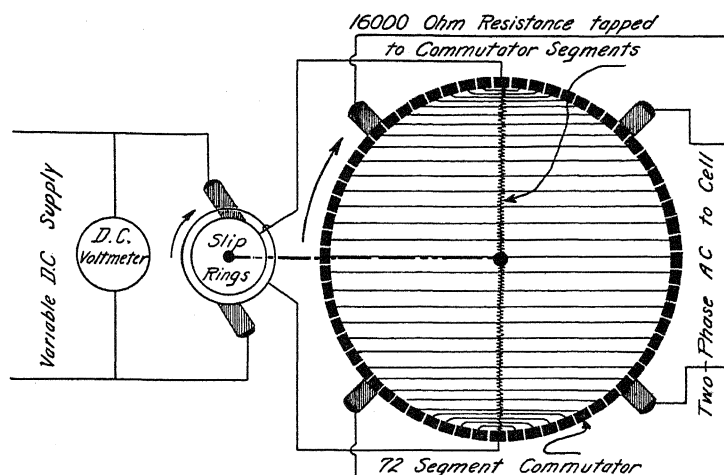


Fig. 4. Two-Phase A.C. potential generator allowing independent variation of voltage and frequency.

In this cell, it is found that the size of circles described by the colloids, and therefore the velocity of the particles, is not a function of the depth of the particle in the cell as is usually found in thin cells. This is due to the fact that the edges are free (Fig. 3b) and the endosmose can, therefore, move the entire layer of liquid in the center as a whole without causing pressures which will give rise to reverse currents. Blüh² made tests which seemed to show that endosmose could be entirely damped out by using a cell as thin as ours. Our results, however, indicate that the endosmose is only reduced and not entirely eliminated. In use, the cell thickness was about 10μ .

A specially constructed machine was used for producing the A.C. potential its principle being illustrated in Fig. 4. Thirty-six coils, each of proper resistance, were wound non-inductively on an old D.C. generator armature shaft from which the iron core and windings had been removed. The coils

were connected as shown to the seventy-two segments of the commutator so that, as one proceeds from segment to segment around the periphery, the resistance between the two diametrically opposite segments is a sine function of the angle. The coils were of No. 30 "advance" wire and in series they totaled 16000 ohms. When a D.C. potential supply is connected in series with them by means of slip rings and when the shaft is rotated at uniform speed, any number of sine function potentials may be obtained in any desired phase relation to each other by the use of sets of brushes properly spaced about the commutator. Two sets were placed 90° apart for the two phase. The advantage of this construction is that both the voltage and frequency of the A.C. potentials produced are variable over wide ranges and entirely independently of each other.

RESULTS AND DISCUSSION

If we calculate the mobility of particles as explained above, we get results in agreement with other observers. For instance, using a silver sol made by the Bredig method we find the mobility to vary between 2×10^{-4} and 4×10^{-4} cm²/volt · sec. which is practically the same range of mobility as given in Bancroft's "Applied Colloid Chemistry" for silver particles in water.⁵

In order to test the effect of a variable speed on the diffuse electric double layer assumed to surround the particle, several photographs of the same particle have been taken on the same plate, first with the rotating field, then with a straight alternating field obtained by disconnecting one of the phases composing the circular field. In the first case, the path is circular and the *speed* of the particle is constant; in the second case, the path is a straight line vibration and the *speed* varies over wide limits. All photographs thus taken show that the amplitude of the straight line vibration is just equal to the diameter of the corresponding circle. This indicates that the distorting effect of the variation in speed on the distribution of the diffuse double layer and the consequent variation of the effective force on the particle due to the field is very small if it exists at all. A sample of such a photograph is reproduced in Fig. 5. Furthermore, when several photographs are taken on the same plate of the same particle moving in circles with constant frequency but with different field strengths and consequently with different speeds, the diameters of the orbits are in the same ratio as the applied voltages, showing again that the variation in speed has no effect on the double layer, at least for the frequencies and voltages used.

According to the tests described in this paper, the rotating field method must give correct values for the mobilities of the colloid particles. The single phase A.C. method, should also give correct values, since it agrees with that of the rotating field. Why, then, did Blüh² using the A.C. method find an increase in his measured mobilities with increasing frequencies. Using the same sol,—Bredig silver in distilled water,—as he used, we repeated and checked his results. However, the test which he made to show that endos-

⁵ Bancroft, Applied Colloid Chemistry, p. 258.

mose was entirely eliminated did not seem conclusive. His peculiar results can be easily explained if we assume that there was some endosmose in his cell and that this motion was opposite in direction to the cataphoretic motion of his particles. Since the inertia of the liquid is relatively large, its oscillatory motion, due to endosmose which tends to reduce the motion of the silver particles, would become less and less noticeable as the frequency increased. Consequently, at low frequencies the measured mobility would be too low, but it would approach the true mobility as the frequency increased. Thus, the measured mobility would increase with frequency. If this explanation be correct, then similar experiments using a colloid of sign opposite to that of silver should give a decrease rather than an increase in measured mobility with increasing frequency. This was tried out with a sol of Bredig copper in distilled water, and the result was a definite decrease in mobility with increasing frequency as was expected. Thus Blüh's increase in mobility with frequency can be explained if the endosmose was not entirely eliminated from his cell as he assumed.



Fig. 5. Paths of an oil particle in the rotating field and in each of the component A.C. fields. (Four exposures)

Probably the most important result of this research is the observation that the mobility of individual particles as measured by the diameter of their orbits is not constant with time but fluctuates considerably. These fluctuations take place so rapidly that it is impossible to make quantitative visual measurements upon them. However, many hours of observation of the phenomena have yielded the following facts:

1. Each particle has one definite size of orbit or speed in which it is most frequently observed. This orbit will be called the preferred orbit. It is the same order of magnitude for all particles from the smallest to the largest found in a mechanically stirred oil emulsion, though it is slightly larger for the larger particles in agreement with Mooney's⁶ results.
2. Particles are very rarely found in orbits larger than their preferred orbits—almost all of the fluctuations take place between the preferred orbit and zero. The fluctuations are apparently quite random.
3. The amount and rapidity of these fluctuations depends upon the size

⁶ Mooney, *Phys. Rev.* **23**, 396 (1924).

of the particles in much the same way as the Brownian motion depends upon the size. They are hardly perceptible in particles larger than 10^{-4} cm diameter while the finest particles observable in the ultramicroscope fluctuate so violently that they seldom stay in any circle for one revolution.

4. The same type of fluctuation is found in all sols observed. Emulsions of mineral oil, olive oil and turpentine in distilled water; Bredig sols of copper and silver in distilled water; and Zigmondy's nuclear gold sol⁷ have been tried.

Why does the mobility fluctuate? Fluctuations in the charge on the particle seems the most reasonable explanation but how can a particle suddenly lose such a large charge. Calculations show that the change in charge necessary to produce some of the fluctuations observed must be at the very least several hundred electrons. It may be that the charge on all colloid particles is always fluctuating, or it may be that the strong electric field with the aid of an occasional heavy impact due to Brownian motion carries away some of the adsorbed layer of ions causing fluctuations in charge only while the colloid mobility is being observed. At present we cannot answer this question.

The authors wish to thank Dr. R. A. Millikan under whose direction it has been a pleasure to do this work and also the American Petroleum Institute for a grant which defrayed the expenses. During the latter part of the research one of the authors (E. M. P.) has been working as a National Research Fellow and wishes to express his gratitude to the National Research Council.

⁷ Rinde, Diss. Upsala, p. 25 (1928).

HALL EFFECT AND THE MAGNETIC PROPERTIES OF
SOME FERROMAGNETIC MATERIALS

BY EMERSON M. PUGH*

CALIFORNIA INSTITUTE OF TECHNOLOGY

(Received September 20, 1930)

ABSTRACT

The Hall effect and the magnetic properties have been measured simultaneously with considerable accuracy in K.S. magnet steel and in hardened high carbon steel. The Hall effect is found to be a single-valued straight-line function of the intensity of magnetization I , but is neither a single-valued nor a straight-line function of either the magnetic induction B or the magnetic field H . This is true on both the virgin curves and the broad hysteresis loops of these materials. The possibility of writing the Hall e.m.f. per unit current in a cm square as $\epsilon = R_0 H + R_1 I$ is considered. In the materials measured here R_0 is less than $0.005 R_1$. The formula may hold for non-ferromagnetic materials, but it could not be tested so simply.

INTRODUCTION

SHORTLY after the discovery of the Hall effect it was found that ferromagnetic materials behave differently than paramagnetic and diamagnetic substances. While the transverse Hall e.m.f.'s in the latter substances are directly proportional to the magnetic field for all fields obtainable, in the ferromagnetic materials the direct proportionality holds only up to the region of maximum permeability.¹ Above that point the rate of increase of the Hall e.m.f. with the field decreases.²

Many attempts have been made to explain this phenomenon. Many of the early authors thought that in ferromagnetic substances the effect was proportional to the intensity of magnetization I rather than to the induction B , which is the quantity that is always measured. In fact, Kundt³ in 1893 made experiments on iron, nickel, and cobalt which showed this to be the case. At low fields he could not possibly distinguish between B and I ; but at higher fields, near the saturation point of the material, his results are certainly good enough to show that the Hall e.m.f. is more nearly proportional to the magnetic intensity I than to either the magnetic induction B or the magnetic field H .

This might have been expected since both the direction and magnitude of the Hall coefficient depends upon the materials in which it is measured. This seems to indicate that the Hall effect is a phenomenon more dependent upon the characteristics of the material than upon the applied magnetic field. However, we find that since that time most of the theoretical work

* National Research Fellow.

¹ E. M. Pugh, Phys. Rev. 32, 824 (1928).² A. W. Smith, Phys. Rev. 30, 1 (1910).³ A. Kundt, Wied. Ann. 49, 257 (1893).

has been based upon the assumption that the effect is caused by the action of a uniform field on the electric current in the material.

Recently Smith and Sears⁴ have found it possible to separate the Hall e.m.f. in permalloy into two components; one of which they consider due to I and the other to H .

The usual expression for the Hall e.m.f. E is

$$E = RHI/t$$

and this may be written

$$Et/I = \epsilon = RH \quad (1)$$

where ϵ represents the Hall e.m.f. per unit current in 1 cm square of the test piece, R the Hall coefficient depending upon the material and H the field strength in gauss. This equation holds for nearly all non-ferromagnetic materials, although, as the author¹ has previously pointed out, the H should be replaced by B , where

$$B = H + 4\pi I \quad (2)$$

since it is the magnetic induction which is actually measured. While it might be legitimate to neglect the second member of (2) in non-ferromagnetic materials, where it is small compared to the first, it certainly is not legitimate in ferromagnetic materials.

From the work of Smith and Sears, equation (1) for ferromagnetic materials should be written

$$\epsilon = R_0H + R_1I \quad (3)$$

where R_0 is a constant which may be nearly independent of the material and R_1 is a constant which may have any value, either positive or negative, depending upon the material.

As far as our experimental knowledge goes on non-ferromagnetic materials, equation (3) might also be correct for them, for in them the quantities B , H and I are all proportional to each other. Therefore, the Hall e.m.f. is a straight line when plotted against any one of the three.

If we are to develop a workable theory of these galvanomagnetic and thermomagnetic effects, of which the Hall effect is only one, we should first settle the question as to what part of these effects is due to H and what part is due to I . With this in mind, the following experiment was started to correlate as accurately as possible the Hall effect with the magnetic properties of ferromagnetic materials.

Since H is so small compared to I in most materials, it was decided to use some materials which were not easily magnetized so that H would be a larger proportion of B . It was also decided to use materials with wide hysteresis loops to see if the effect followed the same law on the loops as on the virgin curve of the material. The K.S. Magnet Steel which was kindly furnished by Professor Honda of the Imperial University at Tokyo, Japan was admirably suited for this purpose.

⁴ Smith and Sears, Phys. Rev. 34, 1466 (1929).

METHOD

The same general method was used as was previously employed by the author,¹ though with many changes and refinements to obtain greater accuracy. This method measures the Hall effect in bars instead of sheets. It eliminates the uncertainties caused by the close proximity of the surfaces of the sheets to the interior where the effect is presumably taking place. This may be especially important with ferromagnetic substances which become polarized in the field, and thus have free poles on their surfaces. The method also makes it possible to measure the magnetic quantities in the material at the same time as the Hall effect is being measured. This is important because the behavior of magnetic materials depends so much upon their previous magnetic history that we must know the magnetic quantities at the particular time when the Hall e.m.f. is measured.

The experimental arrangement is illustrated in Fig. 1. A rectangular bar of the material to be tested was fitted into the pole pieces of an electro-

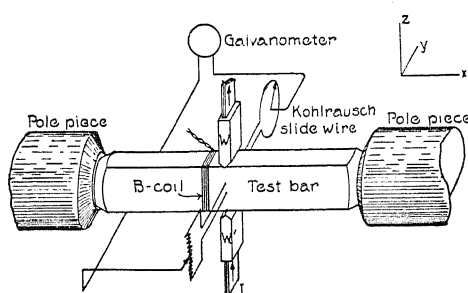


Fig. 1. Perspective diagram of experimental arrangement.

magnet, which made it possible to magnetize the bar longitudinally in the x -direction. A steady current of from 50 to 100 amps. from a large bank of storage batteries was passed through the bar in the z -direction by means of the heavy copper electrodes W and W' . The change in the Hall e.m.f. in the y -direction resulting from a change in the magnetization in the bar was measured by means of the Kohlrausch slide wire and high sensitivity galvanometer shown in Fig. 1.

Hall e.m.f. Any change in the magnetization in the bar causes a change in the Hall e.m.f., or a rotation of the equipotential surfaces in the bar about the lines of force, *i.e.* about the x -axis. Such a rotation changes the position of the contact on the Kohlrausch slide wire at which the galvanometer will not deflect. The change in position on the slide wire is then a measure of the change in the Hall e.m.f. The point on the slide wire representing zero Hall e.m.f. lies midway between the two points found by magnetically saturating the bar in opposite directions. Contact was made by two steel needles on each side of the bar. The needles were symmetrically spaced with respect to the center of the bar, 3 mm apart, and directly in line with the electrodes W and W' .

MAGNETIZATION

Both the virgin curves and the hysteresis loops were obtained by the step by step method using a ballistic galvanometer to measure the magnetic induction B . The Hall e.m.f. was measured between each of these steps. The search coil was wound on the bar as close to the center as the contacts would permit. The period of the ballistic galvanometer was made as large as possible, and the instrument was used greatly overdamped to avoid errors due to the fact that for each change in the e.m.f., a finite time is required for the magnetization to reach its final value. A number of tests were made to determine the extent of this error, and it was found to be entirely negligible with the hardened materials upon which the conclusions from this experiment are based. In soft annealed materials the errors were not negligible. For this reason, and because the low resistance of these materials made the method of measuring the Hall e.m.f. quite insensitive, little was done with such substances.

The electromagnet was wound with five coils which were connected in series. It was arranged that each of these coils could be reversed separately to obtain the necessary changes in e.m.f. In this way, two important errors were eliminated which would have been present had the steps been produced by changing the current in the coils. When the current is changed in a coil considerable time is required for it to reach its final value, for the temperature and resistance must change. This would cause grave errors in the step by step method of determining B . Also, in order to keep the temperature sufficiently constant, it was necessary that the heat loss in the coils be kept constant. The magnet and test bar were immersed in a constant temperature insulated oil bath.

The value of H can not be obtained directly. It was measured with a "saddle coil"⁵ connected to the ballistic galvanometer. The "saddle coil" was made to fit over the test bar at the center. This method was chosen because it has been shown to measure the average value of H over the small section which it covers. It therefore approximated very closely the value of H where the Hall e.m.f. was measured. As a further check upon the absolute value of H in the test bars and upon the calibration of the "saddle coil," the value of H was measured with an independently calibrated Chattock potentiometer.⁶

RESULTS

The results of this experiment on K.S. magnet steel are shown in Figs. 2, 3, 4, and 5. Fig. 2 shows the Hall e.m.f., E , plotted against H when the material was taken through a complete hysteresis loop. This E vs. H curve presents the same appearance as the usual B vs. H or I vs. H curves. In Fig. 3, the values of E plotted in Fig. 2 are replotted first against B and then against $(B-H)$. The E vs. B curve (points indicated by circles) is a very definite loop though quite narrow, while the E vs. $(B-H)$ (points indicated

⁵ Dictionary of Applied Physics, Vol. II Electricity, p. 464, 1922 edition.

⁶ Dictionary of Applied Physics, Vol. II Electricity, p. 467, 1922 edition.

by dots) curve is a straight line. It is seen from this that the Hall e.m.f. is not a single valued function of B , but it is a single valued function of $(B-H)$ which is proportional to the intensity of magnetization. This is quite significant because it shows that the same intensity of magnetization undoubtedly produces the same Hall e.m.f. whether it is a residual intensity or an intensity produced by the action of an external field. In Figs. 4 and 5 one of the many runs taken on the virgin curve of K.S. magnet steel has been plotted. In Fig. 4, E has been plotted first as a function of B (points indicated by dots) and second as a function of $(B-H)$ (points indicated by

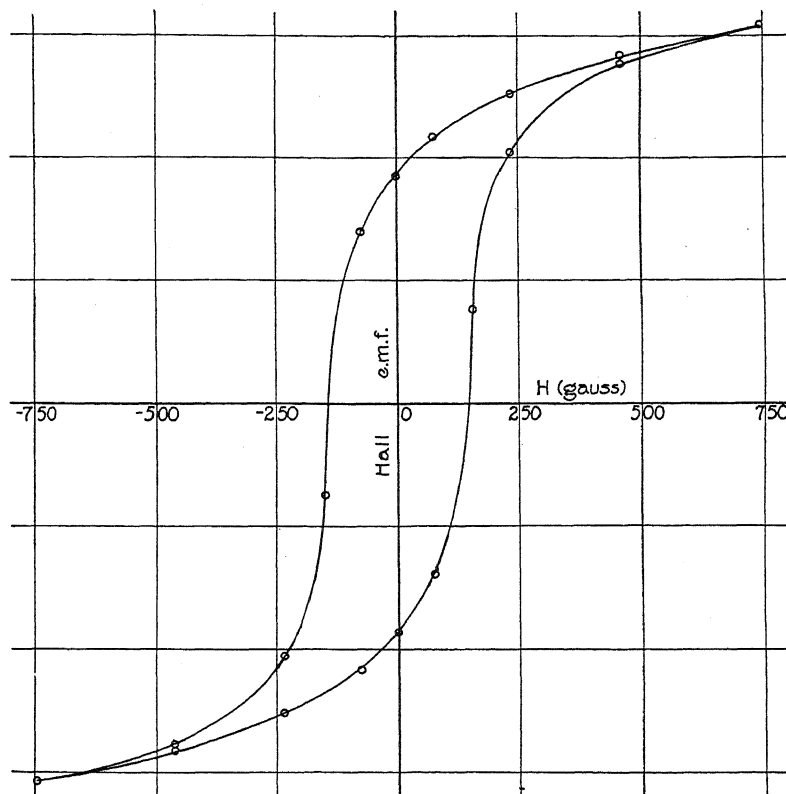


Fig. 2. Hall e.m.f. hysteresis loop for K.S. magnet steel.

circles) just as was done in Fig. 3. The accuracy of the experimental points could not be well shown in Figs. 3 and 4, so the deviations of the points in Fig. 4 from their respective straight lines have been shown in Fig. 5. The run plotted in Figs. 4 and 5 was chosen because it was taken under the most favorable conditions ever obtained. The slight deviation of the second point from the straight line in each of these figures is undoubtedly an error because it does not show up on other runs. Runs were also made on the first part of the virgin magnetization curve of K.S. magnet steel. Here H is small and consequently the difference between B and $(B-H)$ is very little,

yet even in this case, when the Hall e.m.f. is plotted against B , a slight curvature can be detected which straightens out when plotted against $(B-H)$.

These results show that within the limits of error of this experiment on K.S. magnet steel the Hall e.m.f. is a single valued, straight line function of I , while it is neither a single valued nor a straight line function of either B or H .

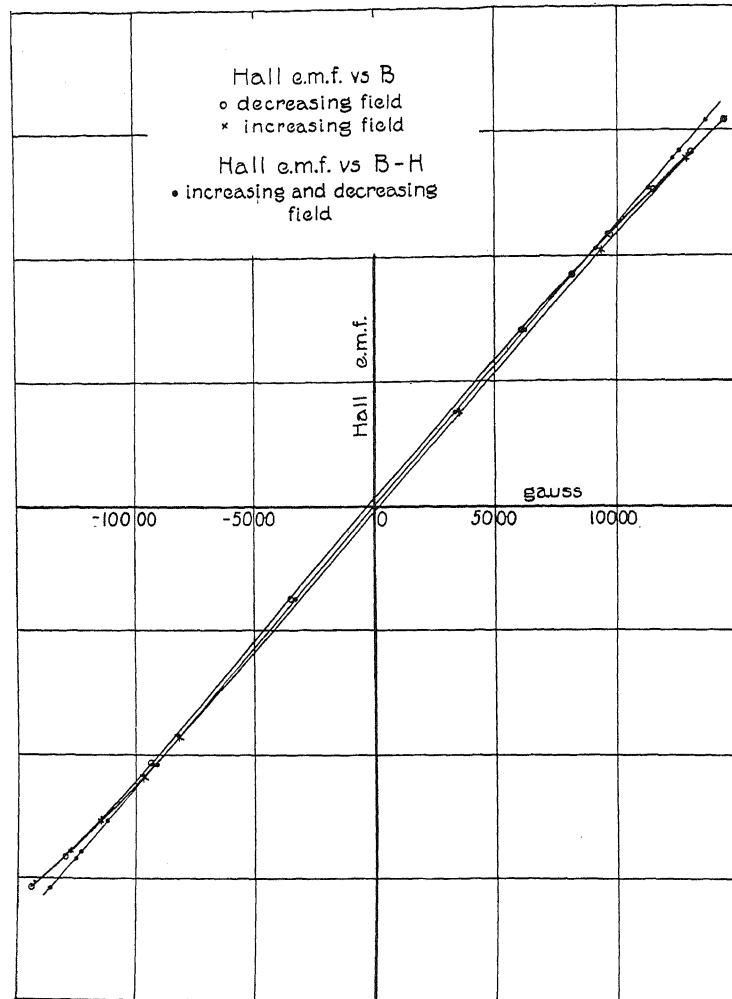


Fig. 3. Hall e.m.f. hysteresis loop for K.S. magnet steel plotted against B and $(B-H)$.

This is true whether the Hall e.m.f. is measured on the virgin curve or on a hysteresis loop.

The same tests were performed with a hardened high carbon steel (1.1 percent carbon) and the results were just the same as with the K.S. magnet steel.

Just recently Stierstadt⁷ has published an investigation of the change in

⁷ O. Stierstadt, Phys. Zeits. 31, 561 (1930).

electrical conductivity of ferromagnetic materials in longitudinal magnetic fields in which he also takes the materials around their magnetic hysteresis loops. He states that this change in resistance is a function of B and not of I , but the quantity which he measures and calls magnetic induction is actually intensity of magnetization. It seems that in ferromagnetic materials the change in resistance and the Hall effect are both functions of the intensity of magnetization rather than of the magnetic induction. One wonders

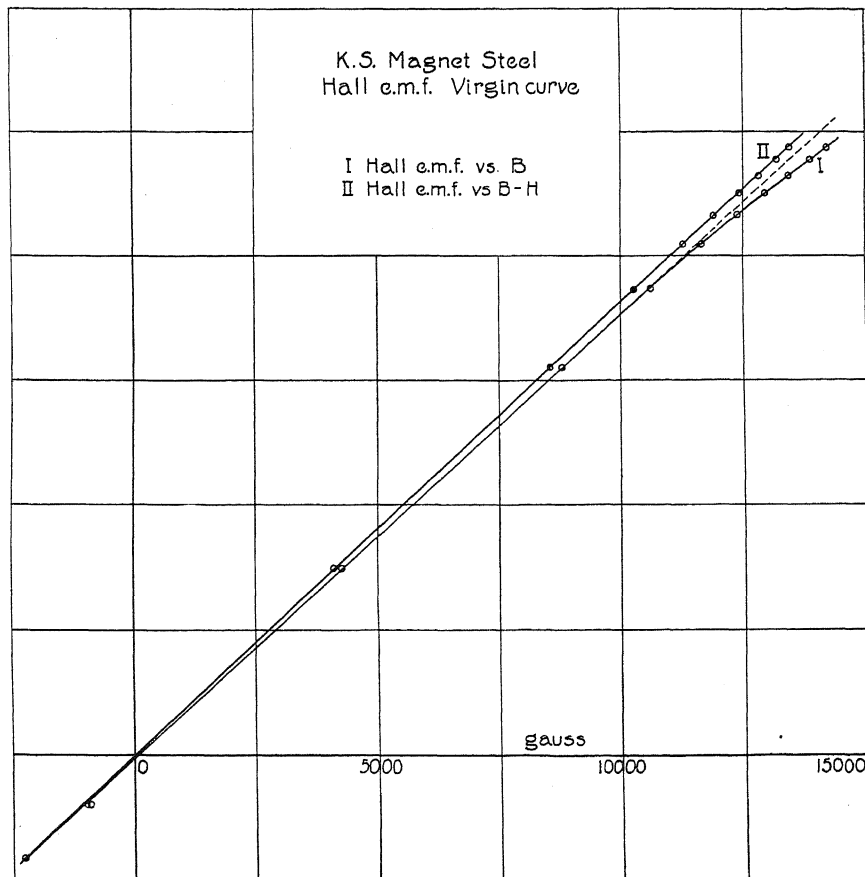


Fig. 4. Hall e.m.f. virgin curve for K.S. magnet steel plotted against B and $(B-H)$.

whether this might not be true of all the familiar galvanomagnetic and thermomagnetic effects in ferromagnetic substances.

Where the Hall effect is proportional to the intensity of magnetization it must mean that the part played by the uniform field is quite negligible. Is it not reasonable to suppose that if the uniform field plays a negligible part in the production of the Hall e.m.f. in some materials that it also plays a negligible part in others? Such an assumption would be difficult to test in paramagnetic and diamagnetic substances because in them the Hall e.m.f. gives a straight line whether it is plotted against B , H or I . It has been

possible to make the test in these ferromagnetic materials only because I and B are not proportional to each other.

The recent work of Smith and Sears⁴ in measuring the Hall effect on different permalloys differs from the results obtained here. They find that in all of their permalloys the Hall e.m.f. rises to a maximum and then decreases to negative values with increasing magnetic inductions. This may mean, as must be concluded from their explanation, that in equation (3) R_1 is positive while R_0 is negative and of the same order of magnitude as R_1 . It may also mean that the annealed permalloys were not homogeneous but had segregated into two magnetically different components, which have Hall coefficients R_1 and R_1' of opposite sign. In which case the component having the positive coefficient reached saturation long before the one having the negative coefficient.

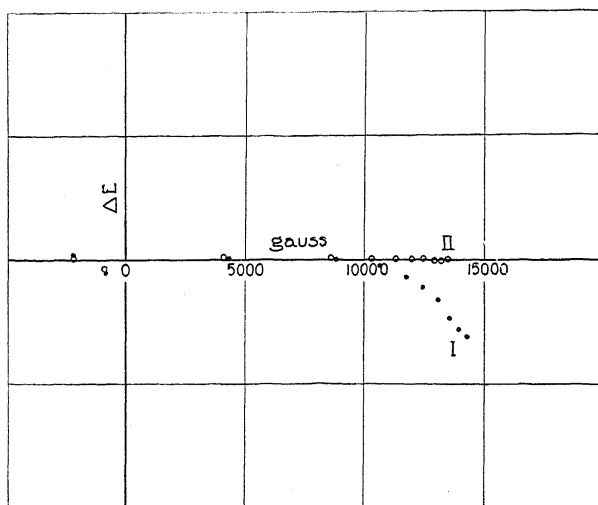


Fig. 5. Deviation from straight lines of the experimental points shown in Fig. 4.

Let us consider the first explanation. No experiment can prove that R_0 is zero. It can only be shown that R_0 is or is not negligible compared to R_1 . The best test in this experiment shows that R_0 is less than $0.004 R_1$. It is conceivable that while in some materials R_0 is negligible compared to R_1 this may not be true for others. However, if the absolute value of R_0 had been as large in the K.S. magnet steel as it was reported to be in the permalloy of Smith and Sears, it should have been possible to detect it here. Now let us consider the second explanation which assumes segregation of the permalloy into two components when it is annealed. Permalloy is an alloy of iron and nickel. Iron has a positive Hall coefficient and nickel has a negative one. If segregation occurs, we might expect the two components to have opposite signs for their Hall coefficients. Elman⁸ has found that certain alloys of iron, nickel, and cobalt, when annealed for a long time, have

⁸ G. W. Elman, Bell Tech. Journ. July 1929.

peculiar magnetic hysteresis loops which may be very nicely accounted for on the assumption that the alloy had segregated into two or more magnetic components which act individually. He could not detect the segregation in any other way. Since the permalloys of Smith and Sears were annealed they might have been segregated into two such components. If these components reached saturation at different times the reversal of the Hall e.m.f. with increasing induction would be perfectly possible. It should be stated that permalloys are very hard to investigate in this way on account of their extremely high initial permeability. Stray fields such as that of the earth or of the current flowing through the sheet itself may nearly saturate the permalloy when the applied field is apparently zero. This may help to account for the fact that the Hall e.m.f. vs. field curves of Smith and Sears depended so much upon the direction of the applied field.

The author wishes to thank Dr. A. Goetz for his assistance in planning and directing this research and Dr. W. V. Houston for his valuable suggestions.

LETTERS TO THE EDITOR

Prompt publication of brief reports of important discoveries in physics may be secured by addressing them to this department. Closing dates for this department are, for the first issue of the month, the twenty-eighth of the preceding month; for the second issue, the thirteenth of the month. The Board of Editors does not hold itself responsible for the opinions expressed by the correspondents.

The Molecular Field and Atomic Order in Ferromagnetic Crystals and in Hydrogenized Iron

The molecular field postulated by Weiss to explain ferromagnetism is regarded by Becker¹ as mechanical in origin, representing the control exerted by strain within any portion of a crystal upon the direction in which that portion may retain its magnetization in the absence of externally applied magnetic fields. More recently Becker and Kirsten² have discussed some interesting experiments upon the magnetization of nickel under tension. They arrive at the conclusion that at least for applied fields much larger than the coercive force—which becomes as small as one or two gauss under their extreme conditions—the magnetization may be predicted quantitatively from the maximal magnetostrictive shortening of well annealed metal and the saturation intensity of magnetization, both of which quantities are sufficiently well known from previous experiments by others. Their account of the effect of internal stresses over the cross-section of a wire specimen upon its magnetization is also very satisfactory. They point out, in the second foot-note to page 660, that the “extremely irreversible processes” observed in weak applied fields are not correctly represented by Becker’s theory, magnetic changes being observed at field values which are less than the theory predicts as necessary for their occurrence.³

Two other recent notes which present apparently contradictory opinions regarding the molecular field are by Frenkel and Dorfman⁴ and by Akulov.⁵ In the former the energies of magnetization and of the quasi-magnetic separation of a crystal into elementary regions magnetized in different directions are used in computing the minimum and average volumes of the magnetically saturated regions postulated by Weiss. In

the latter it is argued that such magnetic saturation of small regions is incompatible with the observed magnetic behavior of iron macro-crystals, and that therefore the internal energy of partially saturated states must be nearly the same as that of the saturated state.

A fourth position of interest in the present connection is that taken by Gerlach,⁶ who thinks that his own experiments and those of others are consistent only with the complete absence of magnetic hysteresis in perfect crystals of iron. Against this it may be urged that the hysteresis losses in the polycrystalline hydrogenized iron of Cioffi⁷ are at least as low as in any mono-crystalline iron yet described.

My recent studies on magneto- and elasto-

¹ R. Becker, *Zeits. f. Physik* **62**, 253–269 (1930).

² R. Becker, M. Kirsten, *Zeits. f. Physik* **64**, 660–681 (1930).

³ It may also be mentioned, though the facts are not pertinent to the present discussion, that the theory of the distorted dipole lattice, as the authors themselves state, predicts a magnetostriction of the wrong sign and amount, and that the similarity in the magnetic behavior of cold-worked and annealed specimens under great tension is not surprising in view of the fact that such tension is reported to have stretched the annealed specimen by as much as 10 percent.

⁴ J. Frenkel, J. Dorfman, *Nature* **126**, 274–275 (1930).

⁵ N. S. Akulov, *Zeits. f. Physik* **64**, 559–562 (1930).

⁶ W. Gerlach, *Zeits. f. Physik* **64**, 502–506 (1930).

⁷ P. P. Cioffi, *Nature* **126**, 200–201 (1930).

resistance⁸ have led me to suppose that the electrical resistance of a crystal in which the atomic magnets have been rendered parallel by magnetization or by mechanical strain is sensibly the same whether the magnetic axes of the elementary magnets all point in one direction—corresponding to magnetic saturation—or point indifferently in either direction—corresponding to magnetic neutrality. The two states have been distinguished in a paper before the American Physical Society⁹ as, respectively, “magnetic” and “mechanical” atomic order. This distinction affords a convenient starting point for a more precise treatment of ferromagnetism which may lessen the confusion of opinions noted in the papers first referred to herein.

In agreement with Becker, then, we may regard the molecular field of Weiss as wholly mechanical in origin.¹⁰ Since however the strain tensor does not fix the direction of the magnetic vector we will suppose that a given strain may in the absence of an applied magnetic field be associated with any degree of magnetization, of either sign, in the preferred direction. We must also suppose that the differences in internal energy between the various *magnetic* complexions associated with a given strain are small in comparison with the energy of the strain. This is the more likely because we know that the electrical resistance and the length in the direction of alignment are almost unaffected by changes in magnetization under these special conditions. This amounts to saying that the reversal of an atomic magnet involves little change in the internal energy of the crystal to which it belongs.

We differ from Akulov in supposing that an atomic magnet can pass from one strain-favored direction to the other without necessarily dissipating the energy required *per atom* in changing the common direction of all the atomic magnets from the initial direction to an intervening position for which the internal energy is greater. Akulov, for example, sets the minimum hysteresis loss per cycle for reversal of magnetization along a $\langle 100 \rangle$ direction at twice the energy difference for complete magnetization along $\langle 110 \rangle$ and $\langle 100 \rangle$ directions. This loss, as Akulov points out, is absurdly too great. We avoid his difficulty by denying that in the reversal of magnetization along a $\langle 100 \rangle$ direction the assembly of atomic magnets

ever has any other common direction. We are thus able to go through cycles of magnetization without working against the molecular field.

We cannot, however, go as far as Gerlach does in denying hysteresis losses altogether. The reversal method of changing magnetization must still involve some dissipation of energy because for one thing, there must be resultant eddy currents in the adjacent metal. This loss will not depend upon the frequency of traversing the cycle if, as seems safe to assume, the reversals are as quick as other atomic energy jumps. We will therefore regard the low values of coercive force which Gerlach and others have attained as closely approaching the limit to which perfect atomic order would permit us to go. The low values of coercive force reached by Becker and Kirsten by stretching nickel are still far higher than this limit, and indeed, the strains under even their extreme stresses must have been far from homogeneous on an atomic scale. The imperfections of real crystals may prevent our ever quite attaining the ideal case by purifying and annealing.

If these hypotheses are correct the calculations of Frenkel and Dorfman, which depend for their validity upon magnetic saturation of each elementary region, are no longer valid.

The effect observed by Cioffi is distinctly more puzzling. It is suggested as possible that hydrogen dispersed throughout the lattice of iron crystals—not at lattice points—

⁸ L. W. McKeehan, *Phys. Rev.* [2] **36**, 948–977 (1930).

⁹ L. W. McKeehan, O. E. Buckley, *Phys. Rev.* [2] **33**, 636 (1929).

¹⁰ This opinion has, of course, been held by others than Becker. My first explicit statement of the hypothesis was made in connection with the magnetostriction of permalloy—*Phys. Rev.* [2] **28**, 158–166 (1926)—where I said: “The more or less random stresses in ordinary metals would, in accordance with the views here expressed, do that for which this molecular field [of Weiss] was evoked, for they would in the case of all but favorably oriented atoms tend to maintain the established direction of magnetization against small disturbances, and thus confer upon magnetization that stability which the simple interaction of freely turning magnets cannot furnish.”

may act catalytically in the following way. Some of the iron atoms immediately adjacent to hydrogen atoms are thereby strained in a manner that favors increase in magnetization by their reversal along the direction of the applied field. We know nothing of the manner in which hydrogen atoms conduct themselves in iron at room temperature but it is at least possible that a single hydrogen atom may wander about sufficiently to strain in the favorable way a great many iron atoms in succession at each low value of the applied field. If this is the process involved the hydrogen atoms must repeatedly lose their energy of thermal agitation and therefore the iron must be cooled during the process and the energy must be supplied from outside by thermal conduction and by the magnetic field. If, as is the case, the reduction of area of the hysteresis loop is by more than 50 percent there will be a net cooling during each cycle, the hydrogenized iron being a refrigerating engine worked by cyclic magnetization. Experiments with alternating magnetic fields should be competent to fix not only the amount of cooling integrated over many cycles, but also the time interval required for the complete promotion of magnetization at each increment in magnetic field by the necessary random migration of hydrogen atoms. This explanation would be much more fanciful if we had not recently learned from the experiments of Ellwood¹¹ that cooling

may occur at certain stages in a hysteresis cycle and that the heat developed in the whole cycle may be less if the cycle is traversed in many steps so that there are periods of ageing under the important applied fields. In Ellwood's case, carbon, not hydrogen, is known to have been present, and carbon is also known to enter the lattice of iron not at lattice points but by crowding into interatomic spaces. Its diffusion rate in iron at room temperature would be expected to be much less than that of hydrogen.

On these views the possible ways in which magnetization may change are two (1) by reversals, without sensible magneto-resistance changes or magnetostriction, and with small but definite hysteresis losses probably closely conditioned by electrical conductivity and (2) by rotations through less than 180° , with magneto-resistance and magnetostriction, with hysteresis losses of important amount largely controlled by mechanical strains inherent or induced by applied stresses, and possibly subject to catalytic acceleration.

L. W. McKEEHAN

Sloane Physics Laboratory,
Yale University,
October 15, 1930.

¹¹ W. B. Ellwood, *Phys. Rev.* [2] **36**, 1066-1082 (1930).

The Wave Mechanics of Deflected Electrons

In a comment¹ on Leigh Page's paper² on the deflection of electrons by a magnetic field I made the statement that Kennard³ had proven that the mean radius of curvature of a cathode ray is given by the same formula as the curvature of the path of a classical electron. Several people have called my attention to the incorrectness of this statement: what was actually proven is that the path of the centroid of a wave-packet is given by the classical equations of motion of an electron. Page's calculation of ρ by interpolation is also justifiable, contrary to my statement.

While admitting these mistakes in my letter, I still wish to maintain that the difference between $(e/m)_{\text{defl}}$ and $(e/m)_{\text{sp}}$ cannot be explained as a difference between wave and classical mechanics. The heuristic argument supporting this proposition is

simple: the only cause which might produce such a discrepancy is diffraction, and since the de Broglie wave-length is so small compared to slit-widths, radii of curvature, inhomogeneities of field, etc., even this cause cannot be operative. Unfortunately there is no rigorous proof of the non-existence of other causes and therefore the following considerations may carry more weight.

Most deflection experiments consist in determining the centroid of a wave-packet of electrons. The correctness of Page's value for ρ is beside the point in these cases and Kennard's results are immediately appli-

¹ Carl Eckart, *Phys. Rev.* **36**, 1014 (1930).

² Leigh Page, *Phys. Rev.* **36**, 444 (1930).

³ E. H. Kennard, *Zeits. f. Physik.* **44**, 344 (1927).

cable.⁴ The method by which Wolf⁵ obtained the value of $(e/m)_{\text{defl}}$ which Birge considered most reliable belongs to this class. It involves the simultaneous deflection of a cathode ray by a rotating electric field and a stationary homogeneous magnetic field. The rotation of the electric field during the time the ray is under its influence is so small that it may be neglected; the physics of Wolf's method thus differs from the more usual one only in that the ray is defined by an opaque cross-hair rather than by a slit. Such a cross-hair produces a wave packet of "absence of electrons" which obeys the same laws as the more usual packet of "presence of electrons." This may be seen as follows: let ψ be the wave function on the cathode side of the cross-hair, ψ' on the other side. The function ψ may be analytically extended beyond the cross-hair as though the latter were not present; then $\psi'' = \psi - \psi'$ will satisfy the wave equation and represent a beam of electrons originating at the cross-hair. If this solution could be realized physically, it would produce

an image on the fluorescent screen which is the negative of that observed by Wolf. From Kennard's results it follows immediately that classical formulae may be used throughout.

CARL ECKART

Ryerson Physical Laboratory,
University of Chicago,
October 17, 1930.

⁴ It is surely a quibble to insist that Kennard's results apply only to wave packets which are small in all directions and not to the long rays which are actually used. Ray solutions of the wave equation can be built up by superposition of packet solutions, and the component packets will not disturb one another if the radius of curvature of the ray is large compared to the de Broglie wavelength. For exceedingly long and very narrow rays the "diffusion" of the packets would also play a role, but neither of these complications is to be feared under the usual conditions.

⁵ F. Wolf. Ann. d. Physik 83, 867 (1927).

The Non-Static Solution of Einstein's Law of Gravitation in a Spatially Symmetrical Field

In a spatially symmetrical field, I define the line element as,

$$ds^2 = h_1(r, t)dt^2 - \frac{1}{c^2} \{ h_2(r, t) dr^2 + h_3(t) r^2 d\theta^2 + h_4(t) r^2 \sin^2 \theta d\phi^2 \}$$

where the h 's are functions to be determined by the Einstein's Law of Gravitation $G_{\mu\nu} = 0$, where the c is the velocity of light, and where r, θ, ϕ, t are the ordinary spherical coordinates and time.

The solution is obtained *directly* from the differential equations $G_{\mu\nu} = 0$, and it is finally,

$$ds^2 = \left\{ 1 - \frac{m}{r(1-t/T)} \right\} \frac{dt^2}{(1-t/T)^2} - \frac{1}{c^2}$$

$$(1-t/T)^2 \left\{ \left[1 - \frac{m}{r(1-t/T)} \right]^{-1} dr^2 + r^2 d\theta^2 + r^2 \sin^2 \theta d\phi^2 \right\}$$

where T is a constant which, as will be seen from my paper, has been called the boundary of time or the disintegrating factor and m , nearly a constant, decreases slowly with the time. The manuscript is now in preparation and will be ready for publication within a month.

HSIN P. SOH
Massachusetts Institute of Technology,
Cambridge, Massachusetts,
October 11, 1930.

BOOK REVIEWS

The Physical Principle of the The Quantum Theory. W. HEISENBERG. Pp. 186, figs. 19. University of Chicago Press, 1930. Price \$2.00.

Die physikalischen Prinzipien der Quantum theorie. W. HEISENBERG. Pp. 117, figs. 22. Hirzel, Leipzig 1930. Price R.M. 8.50.

One might have known that Heisenberg would not write a conventional textbook; and he has not. In his Chicago lectures, now published in a small book both in English and in German, there is no intention of teaching the principles of quantum theory to one who does not know them. The lectures are rather addressed to one who has studied the mathematical side of the theory, who understands its conventional applications to problems, but who has never stopped to ask what it was all about, just what were the physical ideas behind it. There are too many such; and it is fortunate that one of the authority of Heisenberg, and one who has contributed so many of the ideas himself, should have taken the trouble to work out the theory of many elementary but illuminating problems.

The book is deceptive. It starts with descriptions of some single experiments, illustrating the parallel concepts of wave and particle. Its table of contents, its general arrangement, suggest a simple book: after the introduction, the chapters deal with critiques of the physical concepts of the corpuscular theory, and then of the wave theory; with the statistical interpretation of quantum mechanics; and with a discussion of important experiments. Following these is the mathematical appendix, more voluminous in the English than in the German, and suggesting that the main body of the book can be read without following the mathematics. But this is unfortunately not the case. Much of the mathematical theory has found its way into the elementary parts, so that one who was not familiar with the mathematical background would have constantly to refer to the appendix. There seems to be no intermediate way of reading the book between a rapid but superficial scanning, which, it is true, yields most of the interesting ideas, and a careful study. The latter is amply repaid, however, for Heisenberg has assembled and developed mathematical treatments of many of the advanced parts of quantum mechanics, greatly superior to those which have appeared before. As one would expect, the discussions of general matrix and transformation theory, and of electromagnetic fields, are particularly valuable. This mathematical material will probably prove for many readers to be almost as useful as the discussions of the physical meaning of quantum theory.

J. C. SLATER

Modern Physics. A General Survey of its Principles. THEODOR WULF, S. J. Translated from the second German Edition by C. J. Smith, Ph. D., M. Sc., A. R. C. S. 468 pages with 202 diagrams. E. P. Dutton and Company. \$10.80.

This book is written by an obviously good teacher; the translation is all that could be asked.

In his introduction Father Wulf states that his book has been written for readers who are not technical experts but desire to obtain an insight into the realm of physics. Particularly (he implies) is it written for those of philosophic bent. The result is a text book covering the entire field of physics and yet differing in its general scheme and on every page from the usual elementary text.

The book is divided into four parts: The Material World, The Atomic Structure of Matter, The Structure of the Atom, and the Physics of Aether. Under these headings the writer is able to present the fundamental principles of classical physics and yet to devote much of the book to more recent views. The viewpoint is quite unusual. Very clearly the fundamental laws of mechanics are presented, a chapter is given to the three laws of thermodynamics, and the nature of the electromagnetic wave is elucidated; though all of this is done with simple illustration, machines, locomotives and motors are not mentioned in the index. The book is not

mathematical and no numerical problems are solved; yet the author does not hesitate to use exponential and trigonometric functions when the subject demands. Concreteness of example and occasional ingenuity of presentation makes for clarity. The historical setting is continually presented. The book fairly bristles with names (in black type) of those who have carried on, from Democritus to Heisenberg. Too often in textbooks results are presented as *fait accompli* with little sympathy for their gradual development. Here we frequently see the matter through the eyes of the pioneering experimenter. Introducing radioactivity he says: "Owing to the newness of this type of phenomenon . . . all attempts to account for them were attended by considerable difficulties. . . . The following facts, however, played a very decisive role in the development of a theory which would explain radioactive phenomena." There is no dogmatism; a chapter usually ends with a question left for the future to settle.

The style is rather conversational. Exception can be taken to statements at times and *non sequiturs* occur. It is not evident to the reviewer that the second law of thermodynamics is far greater than the first nor that this second law would be of little importance if it only predicted in which way a reaction would proceed. Relativity is stressed throughout the book but always with the writer's eye upon the undiscoverable absolute. However the subject matter is in its nature debatable and the attitude of the author is non-dogmatic. The book has many diagrams but a few half tones would add to its attractiveness. The publishers believe that the book is suited to nontechnical readers among the general public. The reviewer feels that it has a place in second year college courses in Modern Physics, where something of the idealistic truth seeking attitude of the physicist should be seen through the intricate maze of his revolutionary discoveries.

Unfortunately the cost of the book is nearly prohibitive for elementary text book use but it would seem probable that the cost would be reduced if there were any considerable demand for the book.

JOHN A. ELDRIDGE

An Introduction to Mechanics. J. W. CAMPBELL. Pp. 384, figs. 154. Houghton Mifflin Company, Boston, 1929. Price \$3.50.

Teachers of mechanics courses for sophomore and junior engineers will find this text useful. It is, however, not purely an engineering text, stressing practical applications, but instead, we find emphasis on the fundamental concepts in mechanics. For example, the three laws of motion are treated as axioms and definitions, and care is taken that definitions will have meanings in terms of measurable quantities.

Calculus is used throughout the book, although in an elementary way in the first half of the book. The author suggests that a course in calculus may be started at the same time the work in this book is started. The student is taken by this text up to the point where he may profitably begin the study of the methods of Lagrange, Hamilton and Jacobi.

Numerous problems are given with an occasional numerical example worked out. Among the appendices on methods of calculation, mathematical theorems, etc., we note particularly one on the "Relative Character of the Center of Gravity."

J. W. BUCHTA

The General Properties of Matter. F. H. NEWMAN AND V. H. L. SEARLE. Pp. 388, figs. 113. Macmillan Company, New York, 1929. Price \$5.50.

The reviewer was particularly pleased with the opening sentence of the first paragraph Weight and Mass. "The mass of a body, usually described as the quantity of matter in it, is one of the fundamental entities which are more easily understood than adequately defined." Other points noted in the first chapter, which are seldom so explicitly stated, were that the first two laws of motion "may be regarded as definitions," that the third "contains a principle of great importance" that we separate physical quantities into scalar and vector quantities because of the different manner of adding them, that "it is possible to have angular acceleration at constant angular speed."

In the second chapter on The Acceleration of Gravity we find among the sixteen paragraphs the following three, which indicate the manner of treatment, Corrections applicable

to the Use of the Compound Pendulum; (a) Finite Arc of Swing, (b) Air Correction, (c) Curvature of Knife-Edges, (d) Yielding of the Support; Eötvös Balance, Acceleration of Gravity at Sea.

Chapters following are on Gravitation, Gyroscopic Motion and Elasticity, in each of which are found topics seldom treated in general texts. The book, however, is not limited to the chapter headings usually found in texts on mechanics. There is a chapter of fifty four-pages on Surface Tension, in which Gibbs' phase rule is developed and applied and the work of Hardy, Harkins, Langmuir and others on surface phenomena is discussed.

In the chapter on Viscosity are described various methods of measuring viscosities of liquids and gases. A discussion of lubrication is given. This is followed by chapters on the Kinetic Theory of Matter and Osmosis and Diffusion with a short one on Fourier's Theorem and Fourier's Series interposed.

The last part of the book deals with various types of differential equations as they are used in mechanics and hydro-dynamics, including vibrations, free, forced, and those with large amplitudes; also a chapter on Wave Motion in Liquids. The closing chapter is on Units and Dimensions.

The mathematical steps are generally given very completely. Vector methods are not used. A bibliography stressing the historical aspects is given at the end of each chapter. A good index is supplied. Some paragraphs would have been improved by small additions, for example, in discussing forced simple harmonic motions with damping, "maximum resonance" is defined as the condition giving maximum kinetic energy, that is, when the natural frequency without damping is equal to the frequency of the applied force. But the student is not warned that this condition does not give maximum amplitude, which it is often erroneously thought to do.

The book will probably fit exactly the requirements of very few courses given in American universities, since it covers a number of topics usually given in separate courses. But with the tendency to crowd out the courses on classical physics with those on modern physics, a course based on this book may be a way of getting the student in contact with these older subjects without the expenditure of too much time on the more detailed courses. In any case, the book appears to be ideal for general assigned reading for graduate students and for review in preparation for degree examinations.

J. W. BUCHTA

THE PHYSICAL REVIEW

SCATTERING OF HARD γ -RAYS

By C. Y. CHAO*

NORMAN BRIDGE LABORATORY OF PHYSICS, CALIFORNIA
INSTITUTE OF TECHNOLOGY

(Received October 13, 1930)

ABSTRACT

Measurements have been made on the scattering of γ -rays from Th C" by Al and Pb. For Al the scattering is, within experimental error, that predicted by the Klein Nishina formula. For Pb additional scattered rays were observed. The wavelength and space distribution of these are inconsistent with an extranuclear scatterer, and hence they must have their origin in the nuclei.

INTRODUCTION

IN A previous study of the absorption coefficient of hard γ -rays in various elements,¹ it was found that the absorption coefficient of light elements was predicted fairly well by the Klein-Nishina formula which assumes that the removal of the energy from the primary beam is entirely due to Compton scattering of the extranuclear electrons. For heavy elements, however, the experimental value was much larger than was to be expected from the Klein-Nishina formula or any other. Two causes can be suggested to explain this additional absorption. (a) It may be an extranuclear phenomenon due either to an ordinary photoelectric absorption or a breakdown of the Klein-Nishina formula for Compton scattering in these elements. (b) It may also be a nuclear phenomenon, such as the scattering by particles inside the nucleus or any other nuclear absorption (like the excitation or the photoelectric effect occurring there). In an attempt to obtain more information about these questions, a study of the scattered rays has been made.

EXPERIMENTAL RESULTS

In this experiment, γ -rays from Th C after being filtered through 2.7 cm of Pb were used as the primary beam. Al and Pb were chosen as the representatives of the light and the heavy elements. The scatterer was set about 50 cm from the source, which was contained in the same lead cylinder used in the previous experiment. The Al scatterer was $11 \times 8 \times 2.5$ cm in size, the Pb scatterer was approximately equivalent to this in total number of

* Research fellow of the China Foundation for the Promotion of Education and Culture.

¹ Chao, Proc. Nat. Acad. Sci. 16, 431 (1930).

electrons. The scattered rays were studied by means of an ionization chamber with 20 atmospheres pressure at a distance of about 20 cm from the scatterer. The work consisted of three parts.

(a) The comparison of the intensities scattered from Al and Pb is shown in Table I. Here $\lambda + \Delta\lambda$ gives the wave-length of the scattered rays according to Compton's formula, μ'_{Al} and μ'_{Pb} are their absorption coefficients in Al and Pb respectively. $S_{\text{K\&N}}$ gives the theoretical intensity distribution, expressed in terms of the number of the scattered quanta, according to the Klein-Nishina formula for $\lambda = 4.85$ x.u. (i.e. $\alpha = 5$), S_{D} gives that according to Dirac's old formula. S_{Al} is the observed distribution of quanta scattered by Al. Corrections are made for the absorption in the scatterer of both the primary and scattered rays and for the change of efficiency of ionization for different wave-lengths (the latter correction is made by assuming that the efficiency of ionization is proportional to the absorption coefficient in light elements). By comparing $S_{\text{K\&N}}$ and S_{Al} , we see that the agreement between the theory and the experiment is indeed fairly good.

Now, since we are mainly interested in the comparison of the scattered intensities from Al and Pb, a set of measurements was made which gives directly the ratio of the ionization currents due to the scattered rays from the two scatterers. If the scattered rays from Al and Pb are of the same hardness, the ionization current i should be proportional to the energy E of the scattered rays passing through the ionization chamber. In the table, $(E_{\text{Pb}}/E_{\text{Al}})_1$ is calculated by assuming that the scattered intensity at a definite angle is proportional to the number of the extranuclear electrons per cc, i.e. the value predicted by the Klein-Nishina formula. Here again correction is made for the absorption in the scatterer of both the primary and scattered rays, the variation of the ratio for different angles being due to this correction ($i_{\text{Pb}}/i_{\text{Al}}$) is the observed ratio of the ionization currents. It is to be noted here that in the forward direction ($i_{\text{Pb}}/i_{\text{Al}}$) is fairly close to $(E_{\text{Pb}}/E_{\text{Al}})_1$, but in the backward direction ($i_{\text{Pb}}/i_{\text{Al}}$) is much greater than $(E_{\text{Pb}}/E_{\text{Al}})_1$ and is even greater than $(E_{\text{Pb}}/E_{\text{Al}})_2$ which is calculated by assuming that the scattered intensity at a definite angle is proportional to the absorption coefficient at the scatterer. From this fact we can infer that in the case of Pb, beside the normal Compton scattering there is still a kind of anomalous scattering. This anomalous scattering, in fact, gives about three times as much ionization current as the normal scattering does at $\theta = 135^\circ$, as shown at the end of Table I.

TABLE I. Absorption coefficient of the primary rays, $\mu_{\text{Al}} = 0.109$, $\mu_{\text{Pb}} = 0.515$.
Mean wave-length, deduced from $\mu_{\text{Al}} = 5.2$ X.U.

Angle of Scattering	22.5°	35°	55°	90°	135°
$\lambda + \Delta\lambda$	7.0	9.6	15.5	29.4	47
μ'_{Al}	.129	.153	.193	.25	.29
μ'_{Pb}	.61	.74	1.02	2.0	4.8
$S_{\text{K\&N}}$		1	.493	.249	.180
S_{D}		1	.277	.061	.037
S_{Al}		1	.504	.254	.188
$(E_{\text{Pb}}/E_{\text{Al}})_1$.70	.72	.70	.57	.38
$(i_{\text{Pb}}/i_{\text{Al}})$.695	.75	.80	.96	1.44
$(E_{\text{Pb}}/E_{\text{Al}})_2$.965	.995	.97	.80	.53

(b) The hardness of the scattered rays is shown in Table II. Here i_0 is the ionization current due to the initial scattered rays, i' is that due to the scattered rays after passing through a Pb-absorber of 0.68 cm thickness. From Table II we see that the hardness of the scattered rays from Al agrees very well with that which is to be expected for ordinary Compton scattering, but the scattered rays from Pb are harder than is predicted by the simple theory for these angles. Later on, a separate investigation of the scattered rays from Pb was made with a thicker Pb-scatterer (1.36 cm) and less filtering (1.4 cm) of the primary rays in order to obtain greater intensity. The result of this investigation is shown in Table III. Here, the anomalous scattered rays seem to be almost monochromatic to the limit of accuracy of the present experiment.

TABLE II.

Angle of Scattering	90°		135°	
	Al	Pb	Al	Pb
$(\mu'_{\text{Pb}})_{\text{cnl.}}$	2.0		4.8	
i_0	310	297	75	108
i'	69	101	4	43
$(\mu'_{\text{Pb}})_{\text{obs.}}$	2.2	1.6	4.3	1.4

TABLE III.

Thickness of Absorber	0	.68	1.36	204 cm
90° $\left\{ \begin{array}{l} i \\ \mu'_{\text{Pb}} \end{array} \right.$	894	308	109	45
135° $\left\{ \begin{array}{l} i \\ \mu'_{\text{Pb}} \end{array} \right.$	448	151	55	19
		1.6	1.5	1.3
		1.6	1.5	1.6

(c) Assuming the absorption coefficient of the anomalous scattered rays to be 1.5 in Pb (It is probably too low owing to the fact that the absorbers were set at a distance of only 4 to 5 cm from the ionization chamber.), we can deduce the wave-length of these rays to be 22.5 X.U. From the result of Table I, we can now compute the intensity distribution of the anomalous scattered rays as given in Table IV. Since the absorption coefficient of the scattered rays plays a very important rôle in such calculations and the ratio of the anomalous scattered intensity to the normal scattered intensity is very small in the forward direction, these values can only give a rough idea.

TABLE IV. *Intensity distribution of the anomalous scattered rays.*

Angle	35°	55°	90°	135°
Intensity Distribution	.05	.06	.07	.08

DISCUSSION

In view of these results we shall consider the different possible causes as to the origin of the anomalous scattering.

(a) *Extranuclear hypothesis*: Under this heading we can include the following subdivisions. (1) The ordinary photoelectric effect. The anomalous scattering can not be explained in this way because, first, it should be very small theoretically, and, secondly, the scattered radiation is much harder than the K -radiation of Pb, which is the hardest that can be obtained from the change of the extra-nuclear electronic configuration. (2) The extra-nuclear Compton scattering. Since the intensity distribution of Al-scattering agrees fairly well with the Klein-Nishina formula and the intensity distribution of Pb-scattering is widely different, the anomalous scattering does not comply with this hypothesis. Still more important is the fact that the change of the wave-length is much smaller than is predicted for Compton scattering, this prediction is independent of any intensity formula. One might expect the scattering of the tightly bound electrons of inner shells to be different from the ordinary Compton scattering at first thought, but it does not seem adequate for the explanation in considering the fact that we have 2.7×10^6 volts photon against 7.5×10^4 volts for the binding energy of the K -electrons of Pb. Furthermore the change of wave-length found experimentally is not to be expected in the scattering of the tightly bound extra-nuclear electrons.

(b) *Nuclear hypothesis*: Under this heading we have again (1) the scattering process, the mechanism of which is not yet well known, (2) the re-emission after photoelectric absorption or nuclear excitation. Since inside the nucleus the separation of energy levels is greater, the change of wave-length can be accounted by either process. But in considering the fact that the intensity distribution of the anomalous rays is almost uniform in different directions, it seems more probable that it originates from the re-emission process.

Although the final solution of this problem is not yet reached, nevertheless from the present experiment it is fairly evident that the additional absorption as well as the anomalous scattering of hard γ -rays by heavy elements, at least Pb, originates in the nucleus.

The author wishes in this occasion to express his sincere thanks to Professor R. A. Millikan and especially Professor I. S. Bowen for their valuable suggestions and also to Professor W. V. Houston for his interest in this problem.

THE FINE STRUCTURE OF CERTAIN X-RAY EMISSION LINES

BY JOSEPH VALASEK

DEPARTMENT OF PHYSICS, UNIVERSITY OF MINNESOTA

(Received October 2, 1930)

ABSTRACT

The $K\alpha$ lines of Fe, Co, Ni, Cu, Mo, and Ag; and the $K\beta$ lines of Mo have been studied for possible fine structure with two different single crystal spectrometers especially constructed for the purpose. No structure was found. The widths of the various α_1 lines and the β_1 line of Mo were measured.

RECENTLY, Bergen Davis and his associates reported the discovery of satellites on the long wave sides of various emission lines in the K series of Ni, Cu, and Mo,¹ with a double crystal spectrometer.² Their results are collected in the following table.

TABLE I.

Element	Line	$\Delta\lambda$ X.U.	$\Delta\nu/R$	ΔV (volts)
Mo	$K\alpha_1$	0.085	0.155	2.09
	$K\alpha_2$	0.096	0.173	2.34
	$K\beta_1$	0.17	0.389	5.29
Cu	$K\alpha_1$	0.42	0.162	2.20
	$K\alpha_2$	0.35	0.134	1.80
Ni	$K\alpha_1$	0.45	0.150	2.03
	$K\alpha_2$	0.38	0.126	1.70

Attempts have been made to confirm these results with two different single crystal spectrometers of special construction. One of these was a new instrument recently built at Upsala in Professor Siegbahn's laboratory; the second was constructed at the University of Minnesota this year. In both cases the arrangement of crystal, Cr , slit, and plate P , was as shown in Fig. 1. With this arrangement, only a small part of the crystal surface is utilized for any one spectrum line. This has an advantage, for the use of large surfaces makes the effects of crystal imperfections more likely to appear. In both cases unpolished cleavage surfaces of calcite of excellent quality were used. At Upsala in particular, one of Siegbahn's "precision calcites" designated as P. K. 4 was used.

The resolving power of a spectrograph of the type employed depends on the width of the diffraction maxima given by the crystal, and on the width of the slit relative to the dispersion. The former depends on the quality of the crystal and has a definite minimum value for a perfect crystal. The second

¹ Davis and Purks, Proc. Nat. Acad. Sci. 14, 172 (1928); Purks, Phys. Rev. 31, 931 (1928).

² Schwarzschild, Phys. Rev. 32, 162 (1928).

factor depends on the slit width relative to the distance from the slit to the plate. To obtain the order of magnitude of the resolving power attainable, it will be assumed that the widths of the diffraction maxima are those given by the theory of Ewald, Darwin, and Waller.³ Calculations made by Allison and Williams⁴ lead to widths of 3.0 seconds of arc for $\text{MoK}\alpha$ in the first order

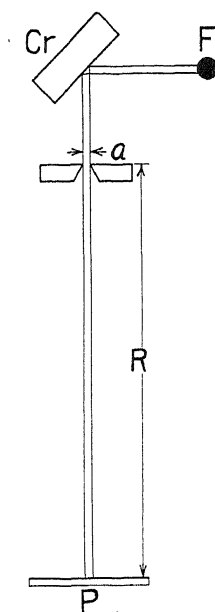


Fig. 1. Single crystal spectrometer. Arrangements of parts.

and 0.56 seconds in the second. For $\text{CuK}\alpha$ the corresponding values are 6.0 in the first order and 1.7 in the second. If a represents the width of the slit and R the distance to the plate, then the angular widths in seconds of arc of the intensity curves for a perfectly monochromatic radiation at $\text{MoK}\alpha$ would be:

$$\Delta\phi_1 = 3.0 + 2.07(a/R)10^5 \text{ in the first order,}$$

and

$$\Delta\phi_2 = 0.56 + 2.07(a/R)10^5 \text{ in the second order.}$$

At the wave-length of $\text{CuK}\alpha$ the following relations apply:

$$\Delta\phi_1 = 6.0 + 2.07(a/R)10^5$$

and

$$\Delta\phi_2 = 1.7 + 2.07(a/R)10^5.$$

³ Waller, Uppsala Universitets Arsskrift (1925).

⁴ Allison and Williams, Phys. Rev. 35, 149 (1930).

These formulae give the theoretical resolving powers for a single crystal spectrometer. A double crystal spectrometer would at best (neglecting the effect of slit height²) give angular resolutions obtained from the same formulae by multiplying the results for zero slit width by 1.414. Thus there is no great difference between the theoretical resolutions if the second term is made small enough by a suitable design and operation of the single crystal spectrometer. This can be done without making the intensity of the spectrum as low as is often assumed.

The values of the smallest resolvable wave-length differences may be obtained from the above angles by the use of Bragg's formula in the differential form. The result should give the narrowest doublet resolvable with an intensity minimum between the two lines. It might sometimes be possible to detect somewhat closer satellites by means of irregularities in the intensity curves. The wave-length resolutions for the data actually used in this work are given below.

TABLE II. *Theoretical resolving powers.*

<i>R</i> (cm)	<i>a</i> (mm)	order	Sec. at Cu K_{α}	Sec. at Mo K_{α}	X.U. at Cu K_{α}	X.U. at Mo K_{α}
296	0.03	1	8.1	5.1	0.28	0.15
114	0.015	2	4.4	3.3	0.13	0.10
114	0.01	2	3.5	2.4	0.10	0.07

FIRST ORDER SPECTRUM

The spectrometer used in the first order investigation had been recently designed by Professor Siegbahn and constructed in the instrument shops at the University of Upsala. Fig. 1 is a photograph of the instrument. The crystal is mounted at *Cr* in a holder that permits of accurate adjustment of the reflecting surface by the method of Siegbahn and Larsson.⁵ The precision scale *PS* enables one to obtain the position of the crystal to 2" by means of the microscopes *M*₁. The microscope *M*₂ is removed after adjusting the crystal. The slit is at *S* and the plate holder is at *P*. The latter can be clamped in four different positions along the three meter long *I*-beam. These are at 46, 96, 196, and 296 cm from the slit. The latter position was used in this work. The metal x-ray tube *T* is of the type described by Siegbahn and is mounted so that it can be rotated about the axis of the spectrometer by means of the cone at *C*. This cone serves to attach the tube to the Siegbahn molecular pump *MP* directly below the spectrograph. The settings of the tube are made with the aid of the circular scale at *Sc*.

Exposures were made of the K_{α} lines of Cu, Mo, and Ag, and the K_{β} lines of Mo. The current was usually 15 m.a. and the voltage was 45 k.v. The exposures required for the CuK_{α} lines were between 2 and 12 hours, the former being the time needed when an evacuated tube was placed between the slit and the plate holder. The MoK_{β} lines required an exposure of 20

⁵ Larsson, Phil. Mag. 3, 1136 (1927).

hours, and about half of this was enough for the $K\alpha$ lines. Enlargements of three of the plates obtained with this apparatus are shown in Fig. 2a, b, and c.

The microphotometer curves for the same plates are given in Fig. 3a, b, and d respectively. These were obtained with the Moll microphotometer at the University of Minnesota. It is well known that the Moll instrument gives such a short microphotometer spot that local variations in density such as those due to the granular structure of the photographic image produce irregular curves. In order to obtain an average of the blackening

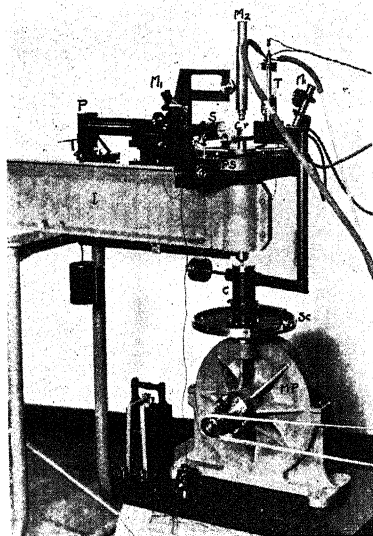


Fig. 2. Siegbahn's spectrometer for high resolving power.

along the spectrum lines, enlargements were made with the negative in regular slow motion in a direction parallel to the spectrum lines. This was found to give somewhat better results than a cylindrical lens in front of the objective. The magnification was only eight times. A reference mark on the projection screen was used to make sure that the motion was accurately parallel to the spectrum lines. It is thought that this adjustment can be made more easily by this method than if a cylindrical lens had been employed. Essentially the same adjustment is also required when a microphotometer with a long slit is used. Curves with an instrument of this type, a photoelectric microphotometer at Upsala, were also made with similar results.

The positions of the expected satellites are indicated in Figs. 2 and 3 by the vertical lines marked x . No conclusion can be drawn from the curve for $\text{Mo}K\alpha$. However, the satellites of $\text{Cu}K\alpha$ and $\text{Mo}K\beta$ must be very weak if present at all.

SECOND ORDER SPECTRUM

To take advantage of the greater resolving power attainable in the second order, a spectrograph was constructed having a camera 114 cm long with a carefully constructed slit with gold jaws at the crystal end. The general construction was along the lines of the instrument described by

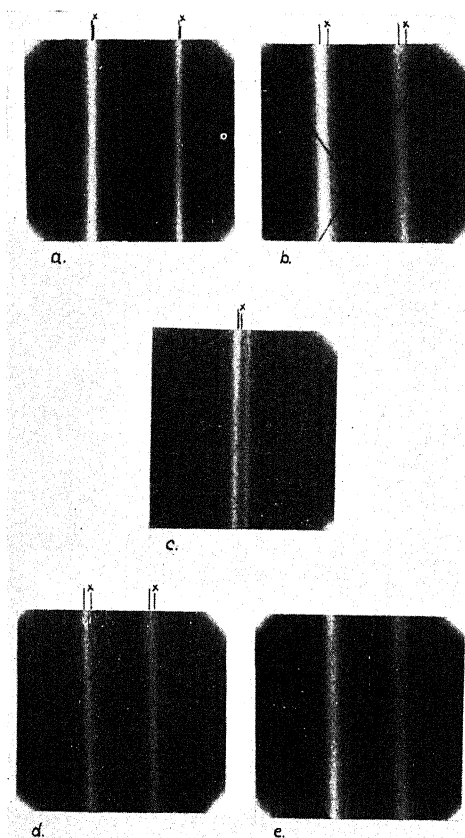


Fig. 3. Enlargements of plates taken in the first order with a 0.03 mm slit and 296 cm camera length; *x* marks the location of satellites reported by Davis and Purks: (a) $\text{MoK}\alpha_1$, (b) $\text{CuK}\alpha_1$ and α_2 , (c) $\text{MoK}\beta_1$ and β_3 .

Enlargements of plates taken in the second order with a 0.01 mm slit and 114 cm camera length: (d) $\text{NiK}\alpha_1$ and α_2 , (e) $\text{CoK}\alpha_1$ and α_2 .

Larsson⁵ except that many simplifications were made since the instrument was not intended for absolute measurement of diffraction angles. A narrower slit width could be used with this shorter camera length without unduly lengthening the time of exposure. The $K\alpha$ lines of Fe, Ni, Co, and Cu were exposed in the second order using about 26 k.v. and 6 to 15 m.a. depending on what the cooling would allow. The focal spot was about a millimeter in diameter so that a good specific intensity was obtained even with these rather low currents. The time of exposure was 10 to 15 hours in the second order with the camera partially evacuated.

Microphotometer curves of these plates are shown in Fig. 4. They likewise fail to show the structure sought for.⁶ That the resolving power was sufficient may be judged from the curves for $\text{MoK}\beta$, Fig. 3d and e, a doublet of 0.565 X.U. separation. The curve 3d is from a plate taken in the first order with Siegbahn's new spectrograph, while 3e is from a plate obtained in

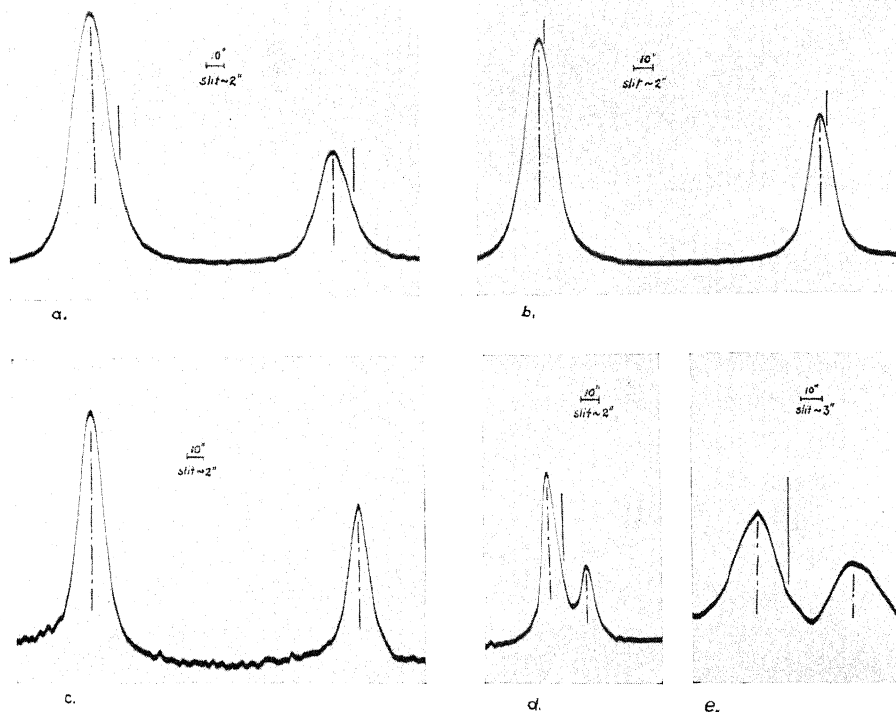


Fig. 4. Microphotometer curves from plates taken in the first order; solid vertical lines mark the location of satellites reported by Davis and Purks: (a) $\text{CuK}\alpha_1$ and α_2 , (b) $\text{MoK}\alpha_1$ and α_2 , (c) $\text{AgK}\alpha_1$ and α_2 , (d) $\text{MoK}\beta_1$ and β_2 , (e) $\text{MoK}\beta_1$ and β_3 in the second order with a 0.015 mm slit and 114 cm camera.

the second order at Minnesota. Comparison with the curves obtained by Davis and Purks,¹ and, more recently, by Allison and Williams⁴ with a double crystal spectrometer shows that the resolving power is comparable with theirs.

The natural width of spectrum lines makes resolution of doublets difficult or impossible if the two lines are too close together, e.g. $\text{MoK}\alpha$, Fig. 4b. However this difficulty cannot be removed merely by the choice of a

⁶ The curves show a lack of symmetry which is especially prominent in the $\text{FeK}\alpha_1$ and $\text{CoK}\alpha_1$ lines. Similar results have been obtained by Seljakow, Krasnikow, and Stelzsky, *Zeits. f. Physik* 45, 548 (1927), who used a spectrograph having a lower resolving power than that used in the present work. They associate the broadening toward the long wave side with the appearance of the $K\beta^1$ line.

spectrograph. An estimate may be made of the half-widths at half maximum of the various $K\alpha_1$ lines by measuring the half widths of the microphotometer curves at the levels of the peaks of the α_2 lines since these are known

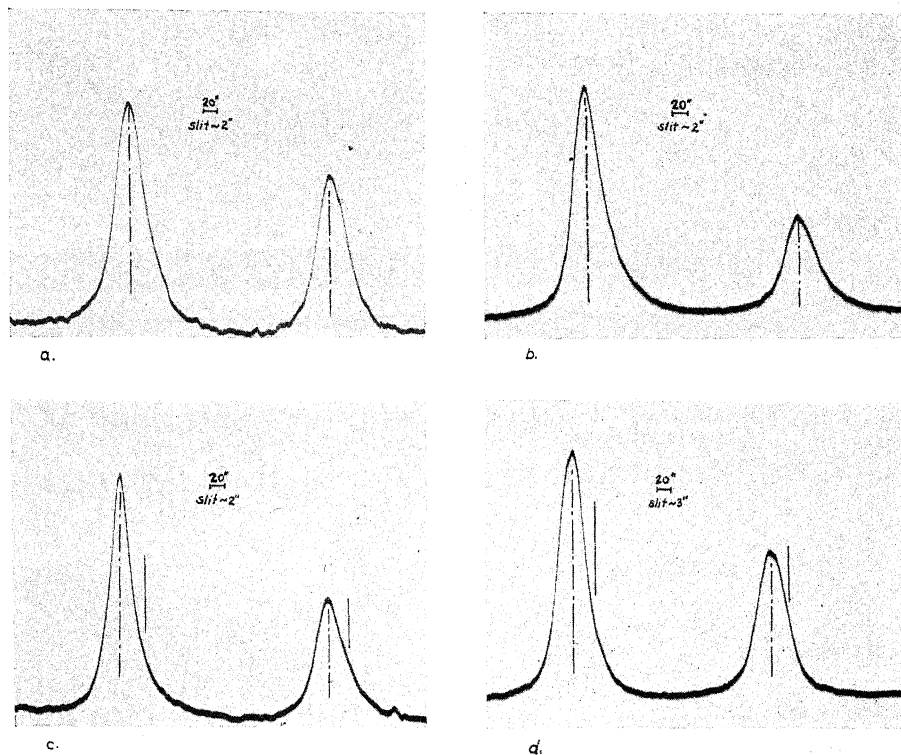


Fig. 5. Microphotometer curves from plates taken in the second order with a 0.01 mm slit and 114 cm camera length: (a) Fe $K\alpha_1$ and α_2 , (b) Co $K\alpha_1$ and α_2 , (c) Ni $K\alpha_1$ and α_2 , (d) Cu $K\alpha_1$ and α_2 (0.015 mm slit).

to be half as intense as the α_1 lines. The same holds good for the β_1 and the β_3 lines. The results of such measurements are given in Table III. The

TABLE III. Half-widths at half maximum of x-ray spectral lines.

Line	X.U. uncorrected	X.U. corrected	X.U. ⁷	X.U. ^{1b}	X.U. ⁴
Fe $K\alpha_1$	0.24	0.19			
Co $K\alpha_1$	0.34	0.29			
Ni $K\alpha_1$	0.23	0.18		0.33*	
Cu $K\alpha_1$	0.26	0.19	0.35	0.32	
Mo $K\alpha_1$	0.20	0.13	0.19	0.24	0.147
Mo $K\beta_1$	0.16	0.09	0.21	0.22	
Ag $K\alpha_1$	0.19	0.12	0.24	0.22	

* The measurements in the first order are given. In the second order the lines were apparently resolved into doublets with the components of Cu $K\alpha$, Cu $K\beta$, and Ni $K\alpha$ all 0.4 X.U. wide (half-width 0.2 X.U.).

⁷ Ehrenberg and Susich, *Zeits. f. Physik* **42**, 823 (1927).

direct measurements are given in the second column. These have been corrected for slit width and diffraction width by subtracting half of the values given in Table II. The corrected results are given in column three. Columns four, five, and six contain the results of other experimenters obtained with the use of double crystal spectrometers.

The agreement is not very good even among workers using the same type of apparatus. As has been noted before, there is a general tendency toward sharper lines with increase in atomic number. However, this effect is not as pronounced as many experimenters believe, because the decrease in diffraction width of the beam from the crystal as the wave-length diminishes is often overlooked. Ehrenberg and Susich have also studied the effects of voltage and current on the widths of x-ray lines and find no simple relation. Some of the difficulty may be experimental.

The first part of this work was carried out at the Physical Institute of the University of Upsala in Sweden. The writer takes this opportunity to thank Professor Siegbahn for suggesting this problem and providing the excellent equipment required. The work in the second order was carried out at the University of Minnesota with the aid of a grant from the Research Fund of the Graduate School.

CORRECTION AND EXTENSION OF THE SERIES OF THE SILVER ARC SPECTRUM, AG I.

BY H. A. BLAIR

PALMER PHYSICAL LABORATORY, PRINCETON, N. J.

(Received September 29, 1930)

ABSTRACT

Measurements, with a Schüller-tube source and helium standards, of the high series members of Ag I showed the older measurements to be rather poor. A few new lines have been added. No terms of the quartet system nor of the $d^9s^2\ ^2D$ were found from new arc measurements. The $d^{10}5s\ ^2S$ is at 61104.4, which gives an *ionizing potential* of 7.53 volts.

ALMOST no extension has been made to the classification of the silver arc spectrum as given in Fowler's Report.¹ McLennan and McLay² have since derived by analogy a probable $d^9s^2\ ^2D$ difference but were not able to establish the terms. The difficulty of classification is no doubt due to the fact that the lines of this spectrum are relatively few.

Recently in this laboratory both the silver and copper arc spectra, which should be similar in structure, have been photographed and measured. In each case the excitation was brought about in arcs in which the lower electrode, the positive, consisted of a piece of the metal laid on a plate of graphite. The cathode consisted of a rod of the metal. Enough current was used, about 3 amperes on a 350 volt line, to render the lower electrode molten. In the case of silver a small amount of copper was added which provided standards and also caused the arc to run more smoothly. The spectra from this type of source are almost entirely free of air bands, a circumstance which renders it possible to obtain measurements on the faint lines. By this method only about 200 lines were obtained in silver while about four times as many were obtained in copper in the region 2,000 to 7,000Å. No success attended an attempt to determine the quartet system using these silver lines. The lines belonging to this system, if present at all, must be much weaker than the corresponding ones in copper as there are few strong lines left unclassified.

While using the Schüller tube to excite the silver spark spectrum as previously described³ it was not noticed that the high series members of the arc spectrum were being brought out. After finding they were excited quite strongly in copper, a further search in silver showed that these members were present but the newly measured wave-numbers differed from the old by 10-15 units in many cases. As the new measures were obtained from photographs with the Hilger E. 1. spectrograph using helium standards they

¹ Report on Series in Line Spectra p. 112, 1922.

² McLennan and McLay, Trans. Roy. Soc. of Canada 22, 1 (1928).

³ Blair, Phys. Rev. 36, 173 (1930).

are probably no more in error than 0.5 cm^{-1} in any case. For this reason and on account of there being a few new lines it was thought worth while to give the complete series.

The Data. In the tables, the older measurements for the lower members of the series have usually been retained. For higher members, where the new measurements are used, the old have not been included as they can be eliminated from lists by referring to Fowler's Report. Both the arc intensities and the Schüller tube intensities are given as they supply some indication of the results of the two types of excitation. The wave-lengths were obtained by means of tables from the wave numbers which were calculated from the measurements.

TABLE I. *Diffuse series.*

λ	Auth.	I_1	I_2	ν	Designation	$nd^2D_{2\frac{1}{2}}1\frac{1}{2}$ observed	$nd^2D_{1\frac{1}{2}}$ calc.	R.D.
5471.52	E&H	50		18271.4	$5p^2P_{1\frac{1}{2}}^\circ - 5d^2D_{1\frac{1}{2}}$			
5465.47	E&H	200		18291.6	$5p^2P_{1\frac{1}{2}}^\circ - 5d^2D_{2\frac{1}{2}}$	12339.9		
5209.04	E&H	100		19192.1	$5p^2P_{\frac{3}{2}}^\circ - 5d^2D_{1\frac{1}{2}}$	12360.0	12360.0	2.9797
4212.68	B	35	100U	23731.2	$5p^2P_{1\frac{1}{2}}^\circ - 6d^2D_{1\frac{1}{2}}$			
4210.94	B	100	500U	23741.0	$5p^2P_{1\frac{1}{2}}^\circ - 6d^2D_{2\frac{1}{2}}$	6890.5		
4055.27	E&H	75	200R	24652.3	$5p^2P_{\frac{3}{2}}^\circ - 6d^2D_{1\frac{1}{2}}$	6899.8	6900.3	3.9880
3811.79*	B	5		26227.0	$5p^2P_{1\frac{1}{2}}^\circ - 7d^2D_{1\frac{1}{2}}$			
3810.93	B	40	5U	26232.9	$5p^2P_{1\frac{1}{2}}^\circ - 7d^2D_{2\frac{1}{2}}$	4398.6		
3682.47	B	30		27148.0	$5p^2P_{\frac{3}{2}}^\circ - 7d^2D_{1\frac{1}{2}}$	4404.1	4404.4	4.9918
3624.71	B	20		27580.6	$5p^2P_{1\frac{1}{2}}^\circ - 8d^2D_{2\frac{1}{2}}$	3050.9		
3508.08	B	20		28497.5	$5p^2P_{\frac{3}{2}}^\circ - 8d^2D_{1\frac{1}{2}}$	3054.6	3054.1	5.9937
3521.16	B	10		28391.6	$5p^2P_{1\frac{1}{2}}^\circ - 9d^2D_{2\frac{1}{2}}$	2239.9		
3410.78	B	8		29310.4	$5p^2P_{\frac{3}{2}}^\circ - 9d^2D_{1\frac{1}{2}}$	2241.7	2242.7	6.9963
3457.10	B	5		28917.7	$5p^2P_{1\frac{1}{2}}^\circ - 10d^2D_{2\frac{1}{2}}$	1713.8		
3350.56	B	3		29837.2	$5p^2P_{\frac{3}{2}}^\circ - 10d^2D_{1\frac{1}{2}}$	1714.9	1716.5	7.9995
3414.55	B	4		29278.1	$5p^2P_{1\frac{1}{2}}^\circ - 11d^2D_{2\frac{1}{2}}$	1353.4		
3310.51*	B	2		30198.2	$5p^2P_{\frac{3}{2}}^\circ - 11d^2D_{1\frac{1}{2}}$	1353.9	1356.0	9.0030
3282.53*	B	3		covered by 3382 He. 30455.6	$5p^2P_{\frac{3}{2}}^\circ - 12d^2D_{1\frac{1}{2}}$	1100.5	1098.1	9.9868

The Diffuse Series. The $^2P_{\frac{1}{2}} - ^2D_{1\frac{1}{2}}$ combinations were used to find a Ritz formula. After adjustment of the constants to give the best fit, the formula obtained was as follows:

$$(m+3)d^2D_{1\frac{1}{2}} = \frac{109737.1}{(m+0.9981-1.484 \times 10^{-6}D)^2}$$

The value of the lowest term $5s^2S$ is then obtained by adding to $5d^2D_{1\frac{1}{2}}$ the wave-numbers of the lines $5p^2P_{\frac{1}{2}}-5d^2D_{1\frac{1}{2}}$ and $5s^2S-5p^2P_{\frac{1}{2}}$. The value obtained is 61104.4, corresponding to an ionization potential of 7.53 volts.

The column of Table I headed " 2D , observed," gives the terms as obtained from the above limit and the observed lines. The calculated terms are those derived from the formula. The Rydberg denominators are calculated from the observed terms.

The Sharp Series. The limit got from the diffuse series was assumed for the limit of the sharp series. The terms then fit the following Ritz formula with reasonable accuracy.

$$(m+4)s^2S = \frac{109737.1}{(m+0.4685-1.957 \times 10^{-6}S)^2}.$$

The column headings of Table II have the same meanings as for the diffuse series.

TABLE II. *Sharp series.*

λ	Auth.	I_1	I_2	ν	Designation	ns^2S observed	ns^2S calc.	R.D.
8273.73	F			12083.1	$5p^2P_{1\frac{1}{2}}^\circ-6s^2S_{\frac{1}{2}}$	18548.4		
7688.12	F			13003.5	$5p^2P_{\frac{1}{2}}^\circ-6s^2S_{\frac{1}{2}}$	18548.6	18548.5	2.4323
4668.50	E&H	50	500u	21414.2	$5p^2P_{1\frac{1}{2}}^\circ-7s^2S_{\frac{1}{2}}$	9217.3		
4476.06	E&H	20	500u	22334.8	$5p^2P_{\frac{1}{2}}^\circ-7s^2S_{\frac{1}{2}}$	9217.3	9217.3	3.4505
3981.62	K	15	30u	25108.3	$5p^2P_{1\frac{1}{2}}^\circ-8s^2S_{\frac{1}{2}}$	5523.2		
3840.82	K	12	20u	26028.7	$5p^2P_{\frac{1}{2}}^\circ-8s^2S_{\frac{1}{2}}$	5523.4	5521.7	4.4574
3709.30	B	4	10U	26951.3	$5p^2P_{1\frac{1}{2}}^\circ-9s^2S_{\frac{1}{2}}$	3680.2		
3586.91	B	#	6U	27871.2	$5p^2P_{\frac{1}{2}}^\circ-9s^2S_{\frac{1}{2}}$	3680.9	3679.3	5.4604
3569.76	B	2		28005.1	$5p^2P_{1\frac{1}{2}}^\circ-10s^2S_{\frac{1}{2}}$	2626.4	2626.7	6.4638
3487.76	B	5		28663.5	$5p^2P_{1\frac{1}{2}}^\circ-11s^2S_{\frac{1}{2}}$	1968.0	1968.5	7.4674
3434.65	B	1	1	29106.7	$5p^2P_{1\frac{1}{2}}^\circ-12s^2S_{\frac{1}{2}}$	1524.8	1531.3	8.4836

The Principal Series. The $6p^2P$ difference, 203.4 cm^{-1} , derived from Shenstone's measurements with copper standards, is probably correct to 0.2 cm^{-1} . The $^2P-^2P$ combinations did not appear with the Schüller tube. The measurement of those lines in the arc can be expected to be relatively poor because of the extreme diffuseness of the lines in that source.

The $d^0 s^2 ^2D$. As pointed out by Shenstone⁴ this 2D may be expected to be nearly coincident with the $5p^2P$, thus its combinations with $6p^2P$ may be expected to lie about the middle of the visible spectrum. None of the lines obtained, however, appeared to represent these combinations. The conclusion to be drawn seems to be that the excited silver atom seldom emits energies allowing it to revert to this 2D state. If the state were metastable as

⁴ A. G. Shenstone, Phys., Rev. 31, 317 (1928).

in copper this would be unexpected. It thus appears probable that the 2D is not metastable, but lies closer to the limit than the $5p^2P$. The unusual relative strengths of the resonance lines would follow as readily from this circumstance as that supposed on the alternative explanation that the 2D

TABLE III. *Principal series.*

λ	Author	I_1	ν	Designation	$np^2P_{1\frac{1}{2}}$
3280.66	F	150	30472.9	$5s^2S_{\frac{1}{2}} - 5p^2P_{1\frac{1}{2}}^\circ$	30631.5
3382.86	F	150	29552.3	$5s^2S_{\frac{1}{2}} - 5p^2P_{\frac{3}{2}}^\circ$	31552.1
2061.21	S		48499.6	$5s^2S_{\frac{1}{2}} - 6p^2P_{1\frac{1}{2}}^\circ$	12604.8
2069.81	S		48296.2	$5s^2S_{\frac{1}{2}} - 6p^2P_{\frac{3}{2}}^\circ$	12808.2

and the $5p^2P$ are so close together that the collision processes in the arc raise the metastable atoms very quickly to the $5p^2P$ state.

If the 2D is higher than the $5p^2P$ its combinations with $6p^2P$ will be of greater wave-length than 5600. Only a very few weak lines were observed

TABLE IV. $5p^2P - 6p^2P$ combinations.

λ	Author	I_2	ν	Designation	Calculated
5608.95*	B	4U	17823.7	$5p^2P_{1\frac{1}{2}} - 6p^2P_{\frac{1}{2}}$	17823.3
5545.94	B	25U	18026.2	$5p^2P_{1\frac{1}{2}} - 6p^2P_{1\frac{1}{2}}$	18026.7
5333.73	B	7U	18743.4	$5p^2P_{\frac{3}{2}} - 6p^2P_{\frac{3}{2}}$	18743.9
5276.47	B	3U	18946.8	$5p^2P_{\frac{3}{2}} - 6p^2P_{1\frac{1}{2}}$	18947.3

F—taken from Fowler.
 E & H—Exner and Haschek.
 K—Kasper.
 S—Shenstone.
 B—author.
 I_1 —Schuler tube intensity.
 I_2 —Arc intensity.

u—diffuse.
 U—very diffuse.
 #—covered by He. 3587.
 *—new allocations.
 complete designations are $4d^{10}ns, np$, etc.

above 5600, the one of greatest wave-length being at 6450. If any of the combinations sought are represented by these lines they will probably only be the strongest.

The writer wishes to express his thanks to Professor A. G. Shenstone for much assistance, and to the Carnegie Institution for supplying the calculating machine used in obtaining the wave numbers from the measurements.

I. EFFECT OF GASES ON THE OPTICALLY EXCITED CADMIUM I SPECTRUM

BY PAUL BENDER

DEPARTMENT OF PHYSICS, UNIVERSITY OF IOWA

(Received October 6, 1930)

ABSTRACT

An apparatus producing intense optically excited cadmium radiation is used to study the effects of nitrogen, carbon monoxide, and hydrogen on the optically excited cadmium spectrum, which effects are compared to similar phenomena with mercury. Each gas produces a decrease in the intensity of each of the spectral lines; no increase occurs because of the lack of self-reversal in the lines of the exciting source. The quenching of the resonance line $\lambda 3261$ A.U. is less than that of the remainder of the spectrum. Nitrogen quenches very inefficiently, while carbon monoxide is considerably more efficient: about 35 mm and 3 mm, respectively, of gas pressure are necessary to reduce the intensity of the resonance line to half value. Both of these gases transfer the excited cadmium atom from the 2^3P_1 to the metastable 2^3P_0 state by kinetic energy collisions. Hydrogen quenches the cadmium radiation very effectively; a collision between the excited 2^3P_1 cadmium atom and a hydrogen molecule produces a normal cadmium hydride molecule and a hydrogen atom.

INTRODUCTION

AFTER Wood's¹ first discovery of the quenching of the resonance radiation of mercury by the addition of foreign gases, Wood and numerous other workers have studied the rather remarkable changes occurring in the radiation from optically excited mercury vapor produced by the addition of foreign gases under various conditions. The cadmium spectrum exactly parallels in structure that of mercury, but shows decidedly different energy relations within the atom, which facts gave promise of interesting comparisons in the effects of foreign gases on the optically excited spectra of the two metals. Also, the hydrogen-filled, high-voltage discharge tube available as a source of the cadmium spectrum, with its intense radiation without self-reversal, offered a very satisfactory source of excitation for the spectrum of cadmium. Accordingly the present investigation was undertaken, studying the effect on the optically excited cadmium radiation of the addition of nitrogen, carbon monoxide, and hydrogen. This paper discusses the effect of these gases on the cadmium I spectrum; the succeeding paper discusses the cadmium hydride bands appearing in the optically excited radiation with the presence of hydrogen, together with zinc hydride and mercury hydride bands appearing under parallel experimental conditions.

APPARATUS

The apparatus was constructed to produce intense optical excitation by the cadmium spectrum itself of cadmium vapor in the resonance tube *R*, as shown by the diagram in Fig. 1.

¹ Wood, Phys. Zeits. 13, 353 (1912).

The source of illumination was a long hydrogen-cadmium discharge tube *D*, of a type first described by Ellett² and successfully used for exciting resonance radiation of various metals. It was operated with a 10 K.V.A. transformer with a 1 to 60 ratio from a 110-volt source with from 30 to 50 amperes in the primary circuit controlled by a water rheostat. A spirally arranged quartz section of the discharge tube, making two complete turns around the resonance tube *R*, and a side tube, containing cadmium metal from which cadmium vapor was distilled into the discharge tube, were constructed. The resonance tube was made entirely of quartz, one end being drawn out obliquely to form a light trap, the other end having a plane quartz window through which the optically excited radiation passed to the spectrograph. The passage of light from the discharge tube to the spectrograph was avoided by painting with lampblack the entire resonance tube excepting the central portion of the window and the portion of the tube adjacent to the spiral of the discharge tube. The resonance tube and the adjacent portion of the

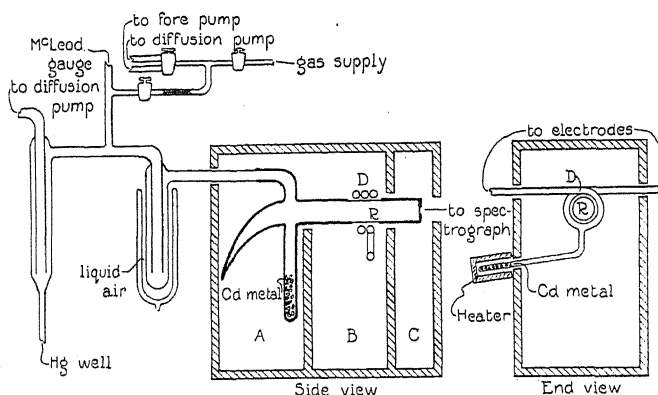


Fig. 1. Diagram of apparatus.

discharge tube were mounted in an asbestos box which was heated by electric heaters and the heat generated by the discharge tube. Cadmium metal in a side tube supplied to the resonance tube the necessary cadmium vapor, the pressure of which was maintained at about 0.008 mm of mercury (corresponding to about 260° C) and controlled by regulating the temperature in section *A* of the box containing the side tube. Sections *B* and *C* of the box were always maintained at a considerably higher temperature than *A* to avoid condensation of the metal in the main part of the tube. A mercury diffusion pump served to evacuate the tube, and a mercury seal made it possible to seal the pump from the resonance system. The usual liquid-air trap prevented diffusion of mercury vapor to the resonance tube.

This set-up permitted a very intense illumination of the cadmium vapor in the resonance tube, causing it to radiate, but producing no effect when the hydrogen discharge tube was operated without cadmium vapor. The

² Ellett, Jour. Opt. Soc. of Am. 10, 427 (1924).

optically excited radiation appeared as an intense bluish-green glow throughout the volume of the resonance tube with such strength that a ten-second exposure on a Hilger E1 quartz spectrograph sufficed to record all the strong lines in the cadmium spectrum.

The gases employed to modify the optically excited radiation were admitted into the resonance tube through a capillary tube and stop-cocks, as pictured in Fig. 1, which regulated the flow of gas, and which could be evacuated separately. The gas pressures up to 1 mm were measured on a McLeod gauge, and those above 1 mm were measured directly on the mercury seal.

To obtain pure gases for these experiments, the following methods of preparation were employed: Nitrogen was obtained from sodium azide, which was placed into a flask attached to the system and the entire system evacuated, after which the azide was gently heated to decompose it. Carbon monoxide was prepared from sodium formate and sulfuric acid: the formate was placed into a flask attached to the system, after evacuation the acid was admitted through a stop-cock, and the gas thus produced was passed through a liquid-air trap to freeze out any vapors. Hydrogen was prepared electrolytically and passed through a liquid-air trap.

To study the general effects of these gases on the optically excited radiation of cadmium, the radiation was photographed with a small quartz spectrograph having an average dispersion of about $\lambda 150$ A.U. per mm over the range from $\lambda \lambda 3000$ to 5000 A.U., and the intensity relations of the spectral lines compared by matching, visually, equal densities on the photographic film for different exposure times. No accurate quantitative measurements of intensity were attempted.

DISCUSSION

The gases used in the present investigation—nitrogen, carbon monoxide, and hydrogen—all produced a decrease in the intensity of the resonance radiation of cadmium, never an increase as observed by Wood³ for mercury. There are two reasons for this difference: First, the lines in the source are free from self-reversal, insuring maximum absorption from the central portion of the line. Second, the absorbing vapor is at a temperature approaching that of the source, giving a Doppler broadening to the absorption line practically the same as that of the absorbed line. Thus any additional broadening of the absorption line, due to collisions with the foreign gas molecules, will tend only to decrease the absorption; hence, even apart from the actual quenching collisions, the only influence of a foreign gas will be to decrease the resonance radiation.

In the optical excitation of the cadmium spectrum, cadmium atoms are first brought to the 2^3P_1 state by absorption of the resonance line $\lambda 3261$ A.U. ($2^3P_1 - 1^1S_0$), from which state they may either re-radiate the resonance line or absorb from the exciting light other frequencies corre-

³ Wood, Proc. Roy. Soc. A106, 679 (1924).

sponding to transitions ending on the 2^3P_1 state to bring them to still higher excited levels. These more highly excited atoms will then radiate what might be termed the secondary portion of the cadmium spectrum, that is, the portion other than the resonance line and depending on two or more successive absorptions by the same atom and, hence, also depending on the second or higher power of the intensity of the exciting light. This part of the spectrum will include principally those lines ending on the 2^3P levels, the transitions from the 2^3S_1 and the 3^3D levels being the most intense. (See energy-level diagram in Fig. 2.)

Now, in the process of quenching the optically excited radiation by gas collisions, this secondary portion of the spectrum will be quenched more effectively than the resonance line, depending upon the second or higher power of the gas pressure according as the particular excited state involved is reached by two or more successive steps, while the quenching of the resonance line will depend only upon the first power of the gas pressure.

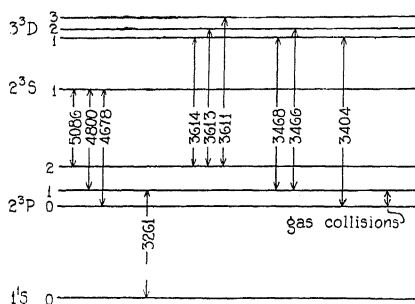


Fig. 2. Energy-level diagram for the cadmium atom.

This effect was observed in the cadmium spectrum with nitrogen and carbon monoxide, which produced a much greater decrease in the intensity of the secondary portion of the spectrum than of the resonance line. In the case of nitrogen, $\lambda 3261$ A.U. persisted with only slightly diminished intensity to rather high gas pressures, its intensity at a pressure of 35 mm of nitrogen being roughly half that with no gas present. The secondary portion of the spectrum could readily be detected at 35 mm nitrogen pressure, although it had only a small fraction of its original intensity. Carbon monoxide was more effective in quenching the resonance line, 5 mm of the gas decreasing the intensity slightly more than did 35 mm of nitrogen. This difference in the effects of the two gases is similar to that reported by Stuart⁴ in the case of mercury, although it seems to be considerably smaller. Stuart's method of excitation was such as to produce only the resonance line $\lambda 2537$ A.U. with measurable intensity, and under these conditions the pressures necessary to reduce the intensity of the resonance line to one-half value were, for nitrogen 30 mm, and for carbon monoxide 0.4 mm.

⁴ Stuart, *Zeits. f. Physik* **32**, 262 (1925).

Nitrogen and carbon monoxide also produced an increase in the relative intensity of the $\lambda 3404$ A.U. line ($3^3D_1-2^3P_0$) over the remainder of the secondary spectrum observed, including the 3^3D-2^3P lines in the ultraviolet and the 2^3S-2^3P lines in the visible. (The two 3^3D lines ending on 2^3P_1 and the three 3^3D lines ending on 2^3P_2 were not resolved by the spectrograph used). This effect was first noticeable with about 0.01 mm pressure of nitrogen and with a slightly lower pressure of carbon monoxide, reaching its maximum at about 0.1 mm gas pressure in both cases and persisting with a relative intensity ratio between the $\lambda 3404$ A.U. line and the remainder of the spectrum of about 2 to 1 throughout the whole range of pressures observed.

This phenomenon is apparently caused by an increased population of the metastable 2^3P_0 state of the cadmium atom, due to collisions of excited (2^3P_1) atoms with gas molecules. From the energy-level diagram (Fig. 2) it is evident that the 3^3D_1 level will be favored by an increase in the population of the metastable 2^3P_0 level, through absorption of $\lambda 3404$ A.U. from the exciting light. On the other hand, the 3^3D_2 and 3^3D_3 levels will be decreased in population by the transfer of cadmium atoms from the 2^3P_1 level to the metastable 2^3P_0 level. Thus, in re-emission by transfer from the D to the P levels, $\lambda 3404$ A.U. should show an increase in intensity as compared with the other two unresolved members of the D triplet.

A similar but much larger effect is observed in the case of mercury by Wood⁵ and Klumb and Pringsheim,⁶ nitrogen and carbon monoxide producing a very large increase in the population of the metastable 2^3P_0 state of the atom. Oldenberg⁷ has suggested that this is due to a resonance phenomenon between the excited mercury atom and the gas molecules, pointing out that the energy difference between the 2^3P_1 and 2^3P_0 levels of the mercury atom (0.218 volt) is nearly the same as the energy required to excite the normal gas molecule to its first vibration level (0.29 volt for N_2 and 0.265 volt for CO). In cadmium, however, the difference in energy between the two P levels is only 0.07 volt; consequently the same resonance phenomenon could not occur. But with so low an energy difference one would expect a large transfer of the excited cadmium atoms to the metastable state by collisions of the second kind with gas molecules, in which the excess atomic energy appears as kinetic energy of translation of the colliding molecules. Again, at the temperatures employed (about 350°C), at which the average kinetic energy of translation of the gas molecules is about 0.08 volt, collisions with a metastable cadmium atom will have a large probability of bringing it back to the 2^3P_1 state. Now, in the absence of a gas, the concentration of the metastable atoms is relatively low since they are destroyed by rapid diffusion to the walls of the tube and are formed only by emission of $\lambda\lambda 4678$ and 3404 A.U. from the 2^3S_1 and 3^3D_1 levels, respectively, which in turn are reached only by two or more successive absorptions. With the addition of

⁵ Wood, Phil. Mag. (7) 4, 466 (1927).

⁶ Klumb and Pringsheim, Zeits. f. Physik 52, 610 (1928)

⁷ Oldenberg, Zeits. f. Physik 49, 609 (1928).

a gas, two effects will tend to increase the population of the metastable state: first, the presence of the gas will decrease the rate of diffusion of the metastable atoms to the walls of the tube, thus increasing their effective life; and, second, the kinetic energy collisions of the gas molecules with the atoms in the 2^3P_1 and 2^3P_0 states will produce more metastable atoms than they will destroy. The final equilibrium with gas present, therefore, should have a larger population of the metastable state than does the condition without the gas. As pointed out above, this favors the population of the 3^3D_1 level by absorption of $\lambda 3404$ A.U. which in turn permits the observed increased re-emission of this same line.

Transfer of the 2^3P_1 cadmium atoms to the upper metastable state (2^3P_2) by collisions with gas molecules is highly improbable since the energy difference between the two levels (0.14 volt) is considerably in excess of the mean kinetic energy of the gas molecules (0.08 volt).

It is interesting to note here, also, in the cases of mercury and cadmium, a comparison of the pressures required to produce the first evidences of increased population of the metastable level by gas molecule collisions. For mercury the effect first appears at a gas pressure of about 0.1 mm, as stated by Pringsheim,⁸ while for cadmium it is evident at 0.01 mm pressure. This is to be expected from the difference in the mean lives of the two excited atoms (2^3P_1). The mean life for mercury is 0.98×10^{-7} sec.⁹ and for cadmium it is 2.30×10^{-6} sec.¹⁰, giving a ratio of the mean lives of the same order of magnitude as the ratio of the collision times required to produce the effects observed.

Hydrogen produced a quenching of the whole optically excited cadmium spectrum, with only a slightly greater efficiency for the secondary portion of the spectrum than for the resonance line $\lambda 3261$ A.U. The quenching was evident at pressures as low as 0.01 mm, and the resonance line was almost entirely extinguished at 4 mm gas pressure. Bates¹¹ and Hoffman¹² have observed this quenching effect of hydrogen. Bates attempted to produce the spectrum of cadmium by optical excitation of cadmium vapor in the presence of hydrogen, but found complete quenching. He failed to state the gas pressures employed, however. Hoffman studied the absorption of the $2^3S_1-2^3P$ lines ($\lambda\lambda 5086, 4800$ and 4678 A.U.) by electrically excited cadmium vapor in the presence of gases, and found varying degrees of absorption of these lines with nitrogen and the inert gases, but could detect no absorption in the presence of about 2 mm of hydrogen, which showed that the hydrogen very effectively destroyed the 2^3P atoms.

In the case of mercury, the excited atom has an energy (4.86 volts) only slightly greater than the dissociation energy of the hydrogen molecule

⁸ Pringsheim, *Fluorescenz und Phosphorescenz*, p. 117.

⁹ Olson, *Phys. Rev.* **32**, 443 (1928).

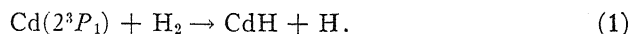
¹⁰ Ellett, *Phys. Rev.* **33**, 124 (1929).

¹¹ Bates, *Proc. Nat. Acad. Sci.* **14**, 849 (1928).

¹² Hoffman, *Zeits. f. Physik* **60**, 457 (1930).

(4.46 volts);¹³ the excited mercury atom is very effective, therefore, in dissociating the hydrogen molecule, losing, of course, its own energy of excitation in the process, as pointed out by Cario and Franck.¹⁴ Thus, only a small amount of hydrogen gas is necessary to quench the mercury resonance radiation. In cadmium, however, the energy of excitation of the first excited state (3.78 volts) is less than the dissociation energy of hydrogen, hence the same quenching process can not occur. Nevertheless, the quenching effect of hydrogen seems to be about as strong for cadmium as for mercury.

The present investigation, however, reveals the formation of the unexcited cadmium hydride molecule in the excited cadmium-hydrogen mixture (evidence for this is discussed in the succeeding paper), which leads directly to the explanation of the quenching of the cadmium radiation by hydrogen: an excited cadmium atom in the 2^3P_1 state collides with a hydrogen molecule, forming an unexcited cadmium hydride molecule and an atom of hydrogen,



Svensson,¹⁵ in his analysis of the cadmium hydride band system, gives for the dissociation energy of the normal CdH molecule the value 0.67 volt.¹⁶ In the collision represented by Eq. (1), therefore, the total energy available is the sum of the excitation energy of cadmium (3.78 volts) and the dissociation energy of the CdH molecule, which sum amounts to 4.45 volts. This is practically the same as the required dissociation energy of the hydrogen molecule (4.46 volts), which fact makes the process highly probable.

The present experiments gave evidence, also, of the formation of atomic hydrogen in the optically excited cadmium-hydrogen mixture, which is further verification of the process of molecule building represented by Eq. (1). With commercial (chemically pure) cadmium metal in the side tube of the resonance tube, optical excitation of the cadmium-hydrogen mixture in the resonance tube caused a large decrease in the hydrogen pressure, which decrease did not occur without optical excitation even when the mixture stood for a long period at the high temperature employed. The lost hydrogen was found as water frozen out by the liquid-air trap, which had been formed, presumably, through a reduction by atomic hydrogen of some oxide present in the cadmium supply. This was further verified by using in the resonance tube cadmium which had first been distilled in an atmosphere of hydrogen to reduce any oxide present; whereupon only a very small decrease in the hydrogen pressure occurred on operation of the tube.

¹³ Richardson and Davidson, *Proc. Roy. Soc. A* **123**, 54 (1929).

¹⁴ Cario and Franck, *Zeits. f. Physik* **11**, 161 (1922).

¹⁵ Svensson, *Zeits. f. Physik* **59**, 333 (1930).

¹⁶ The spacing between the vibration levels of the normal CdH molecule does not follow the empirical rule stated by Condon and Morse (*Quantum Mechanics* p. 159) as holding for many diatomic molecules. Applying this empirical rule to the three highest vibration levels recorded by Svensson yields the value given (0.67 volt) for the dissociation energy. Higher values are obtained when it is applied to other levels. This value must be considered, therefore, merely as a rough approximation.

In contrast with the effects of nitrogen and carbon monoxide, the spectrograms of the present investigation showed no evidence of an increased population of the metastable state with hydrogen present, which agrees with the observations of Klumb and Pringsheim⁶ for mercury. The reason in the present case of cadmium is obvious when we consider that a collision of the excited cadmium atom with a hydrogen molecule produces the CdH molecule, as described above, and hence will not transfer the cadmium atom to the metastable state.

In addition to the cadmium spectrum, cadmium hydride bands appear in the optically excited radiation from the cadmium-hydrogen mixture. This interesting phenomenon is discussed in the succeeding paper.

CONCLUSIONS

Nitrogen and carbon monoxide have a low quenching efficiency on the optically excited cadmium radiation, and are less effective in quenching the resonance line $\lambda 3261$ A.U. than the remainder of the spectrum.

Kinetic energy collisions of gas molecules with excited cadmium atoms transfer them from the 2^3P_1 to the metastable 2^3P_0 state.

Hydrogen is very effective in quenching the optically excited cadmium radiation, collisions with the 2^3P_1 cadmium atoms forming CdH molecules and atomic hydrogen.

To Professor A. Ellett, who suggested the present investigation and rendered valuable assistance in its execution, the writer wishes to express his appreciation.

II. OPTICAL EXCITATION OF CADMIUM HYDRIDE AND ZINC HYDRIDE BANDS

BY PAUL BENDER

DEPARTMENT OF PHYSICS, UNIVERSITY OF IOWA

(Received October 6, 1930)

ABSTRACT

Excitation of a cadmium-hydrogen gas mixture with light from a hydrogen-cadmium electric discharge produces with great intensity a portion of the band system of the CdH molecule, while excitation of the same mixture with light from a helium-cadmium discharge does not produce these bands. The process consists, first, of a collision between a 2^3P_1 cadmium atom and a H_2 molecule to form an unexcited CdH molecule, which molecule is then brought to the excited levels by absorption from the exciting light of the band frequencies themselves, whence it emits the band radiation in returning to the normal state. A weak excitation of the entire $^3\Pi-^2\Sigma$ band system also occurs independently of the optical excitation as a result of collisions of the second kind with excited cadmium atoms.

ZnH bands are also produced as a true optical resonance phenomenon under exactly parallel conditions. The formation of the ZnH molecule results in a selective quenching by hydrogen of the triplet zinc spectrum, while the singlet spectrum is unaffected.

The experiment of Gaviola and Wood, in which HgH bands are excited through collisions of the second kind, is repeated and discussed in the light of the above results.

CADMIUM HYDRIDE BANDS

WITH the apparatus described in the preceding paper, a cadmium-hydrogen mixture in the resonance tube was illuminated with the light from the hydrogen-cadmium electric discharge. This produced an optically excited radiation which contained a portion of the cadmium hydride

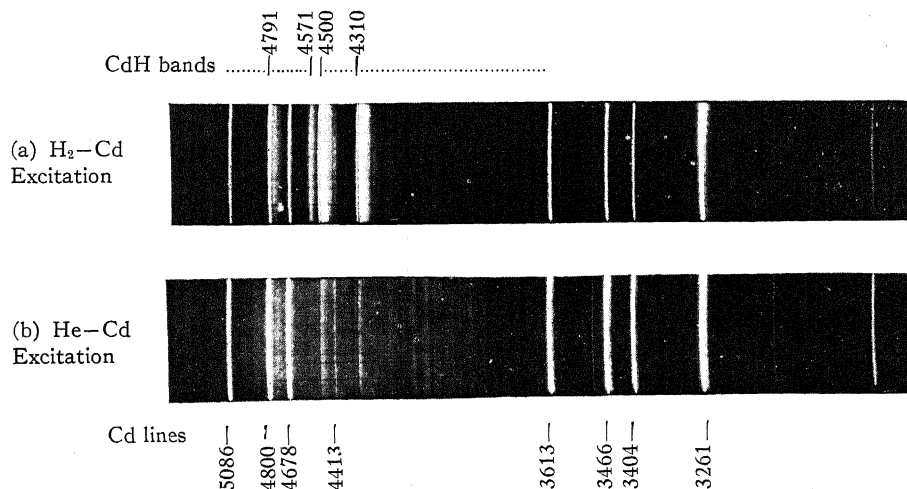


Fig. 1. Spectrograms of radiation from cadmium-hydrogen mixture optically excited by (a) hydrogen-cadmium and (b) helium-cadmium electric discharge.

band system. The bands with heads at $\lambda\lambda 4310$, 4500, 4571 and 4791 A.U. appeared very prominently, while, with somewhat longer exposures, those with heads at $\lambda\lambda 4835$, 4198, and 4026 A.U. were also faintly evident. The stronger of these bands appeared with fair intensity at hydrogen pressures in the cadmium resonance tube as low as 0.1 mm of mercury and reached a maximum intensity at about 0.5 mm pressure. At still higher pressures they became less intense, probably as a consequence of the quenching of the cadmium resonance radiation at such high pressures of hydrogen gas, as described in the previous paper. Under the optimum conditions for excitation of the bands, the two strongest bands, with heads at $\lambda\lambda 4310$ and 4500 A.U., had a gross intensity at least as great as that of the visible triplet of the cadmium spectrum; the bands at $\lambda\lambda 4571$ and 4791 A.U. had always a much lower intensity, however. These facts were shown by photographs of the optically excited radiation taken with a small quartz spectrograph having an average dispersion of about $\lambda 150$ A.U. per mm in the range $\lambda\lambda 3000$ to 5000 A.U. One of these spectrograms taken under the optimum conditions for band excitation is reproduced in Fig. 1a.

Fig. 2b is a large spectrogram of this same optically excited radiation taken with a four-hour exposure on a Hilger E1 quartz spectrograph. The original plate, of which this is a reproduction, showed definitely, in addition to the four prominent bands, the presence of the bands with heads at $\lambda\lambda 4835$, 4198, and 4026 A.U. (Those with heads at $\lambda\lambda 4835$ and 4198 A.U. may be seen faintly on the reproduction, but $\lambda 4026$ A.U. is beyond the range of the reproduction.) For the sake of comparison, a spectrogram of the radiation from the hydrogen-cadmium electric discharge tube used as an exciting light source is reproduced in Fig. 2a, and it is observed that this radiation contains the more complete CdH band system as compared to the relatively few bands appearing in the optically excited radiation. It is observed also that in the optically excited radiation the bands with heads at $\lambda\lambda 4310$, 4500, 4571, 4791, and 4835 A.U. have about the same relative intensities as they do in the radiation from the electric discharge. (Reference is made to this fact later in the paper.)

Since the CdH bands are present in the radiation from the hydrogen-cadmium discharge tube used as a source of illumination, it was thought possible that their excitation in the resonance tube was an optical resonance phenomenon. In order to determine whether this was the case, the discharge tube was operated with helium instead of hydrogen, thus eliminating the CdH band radiation from the source but giving as intense a cadmium spectrum as did the hydrogen discharge. When the cadmium-hydrogen mixture in the resonance tube was illuminated by this helium-cadmium source its radiation did not show the very strong CdH bands appearing before, but contained with very low intensity the entire ${}^2\Pi - {}^2\Sigma$ CdH band system. This weaker band radiation had not been observed earlier with the hydrogen source, but on returning to the hydrogen source, a very much longer exposure showed that with this method of excitation also the entire ${}^2\Pi - {}^2\Sigma$ system of bands was present. Most of the heads had about the same intensity under

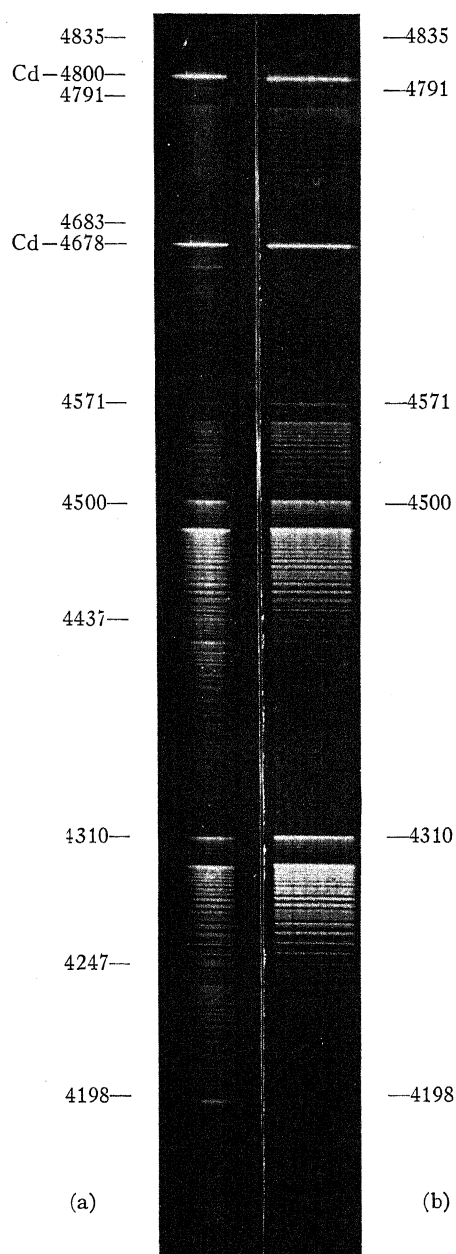


Fig. 2. (a) Spectrogram of the radiation from a hydrogen-cadmium electric discharge showing the most prominent portion of the CdH $^3\Pi-^2\Sigma$ band system. (b) Spectrogram of the optically excited CdH band radiation.

the two methods of excitation, but those mentioned above (with heads at $\lambda\lambda 4310, 4500, 4571$, and 4791 A.U.) came out with an intensity at least fifty times as great with the hydrogen cadmium excitation as with the helium-cadmium excitation. Fig. 1 is a reproduction of spectrograms of the Cd and CdH radiation as produced by the two methods of optical excitation. It will be observed that with the helium-cadmium excitation the bands are evident over nearly all of the range of wave-lengths between the cadmium lines $\lambda\lambda 5086$ and 3613 A.U., with the heads at $\lambda\lambda 4310$ and 4500 A.U. standing out slightly more prominently than the rest of the system. On the other hand, with the hydrogen-cadmium excitation the entire band system is present, but the heads at $\lambda\lambda 4310, 4500, 4571$, and 4791 A.U. have a very great intensity, much greater than that of the remainder of the system.

An additional experimental detail is of significance in this connection. For the helium discharge, a new discharge tube was built in order to avoid contamination of the helium with hydrogen evolved from the electrodes and metal deposited on the walls of the old discharge tube, which had been operated with hydrogen. The new tube, operated with helium, at first showed considerable hydrogen gas, which had been occluded by the aluminum electrodes. But after operating the tube at a high temperature and washing out the gases with successive charges of helium it was practically free from hydrogen. In the earlier spectrograms, taken with small quantities of hydrogen in the helium discharge tube, the prominent portion of the CdH spectrum (i.e., bands with heads at $\lambda\lambda 4310, 4500, 4571$, and 4791 A.U.) was considerably more intense, decreasing in intensity as the amount of hydrogen in the source was diminished. Under the final condition, with no hydrogen present, these prominent bands were reduced in intensity to a value comparable with that of the remainder of the band system, as shown by the spectrogram of Fig. 1b.

These results are direct evidence that we have here a true optical resonance of the CdH bands. An alternative possible method of excitation of the band radiation would be through collisions of the second kind with excited cadmium atoms, but under like conditions of excitation of the cadmium in the resonance tube containing cadmium and hydrogen the strong band radiation is excited only when the band frequencies themselves are present in the exciting light.

Additional indirect experimental evidence for the optical excitation of the CdH bands was obtained by filtering the exciting light from the hydrogen-cadmium discharge tube through Wood's nickel glass. This greatly reduced the intensity of the $\lambda 3261$ A.U. line but allowed it to pass with sufficient intensity to excite a relatively weak cadmium spectrum in the resonance tube. The 3^3D-2^3P Cd lines were passed without absorption, but the 2^3S-2^3P Cd lines and the $\lambda\lambda 4310$ and 4500 A.U. CdH bands were completely absorbed. Under these conditions the optically excited spectrum showed the 3^3D-2^3P lines, but the 2^3S-2^3P lines and the bands were absent. This absence of the bands is to be expected, obviously, from the theory that the bands are excited by absorption of the band frequencies themselves from the exciting radiation rather than by collisions with excited cadmium atoms.

In order that this resonance phenomenon can occur, CdH molecules must first be present in a state in which they are able to absorb the band frequencies. This state must be the lowest vibration level of the unexcited molecule, as is revealed by fitting the optically excited band system into the energy-level diagram of Svensson.¹ Thus the optical resonance of the band spectrum furnishes the evidence for the presence of the normal CdH molecule, the method of formation of which is discussed in the preceding paper.

The exact method of absorption and re-radiation of the bands by the CdH molecule is revealed by a study of the structure of the band system. Svensson¹ has analyzed the CdH band systems appearing in a hydrogen-cadmium electric discharge, such as was used in the present investigation for an exciting light source, and his analysis of the $2\Pi-2\Sigma$ system is represented in the energy-level diagram in Fig. 3a. A spectrogram of the most prominent portion of this system, taken by the writer on a Hilger El quartz

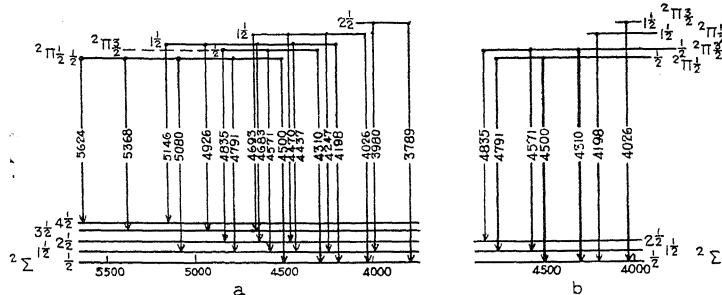


Fig. 3. Energy-level diagram of the CdH band system. (After Svensson)¹ (a) The entire system. (b) The portion of the system which is optically excited.

spectrograph, is reproduced in Fig. 2a. The energy-level diagram in Fig. 3b represents the portion of the band system which is optically excited, as shown by the spectrogram of Fig. 2b. The excitation and radiation proceed as follows: the CdH molecules in the normal $2\Sigma^{(1/2)}$ state absorb from the exciting light the frequencies of the bands with heads at $\lambda 4500$ A.U. ($2\Pi_{3/2}^{(1/2)} - 2\Sigma^{(1/2)}$) and at $\lambda 4310$ A.U. ($2\Pi_{1/2}^{(1/2)} - 2\Sigma^{(1/2)}$), bringing them to the excited $2\Pi_{3/2}^{(1/2)}$ and $2\Pi_{1/2}^{(1/2)}$ states, from which states they re-radiate the same band frequencies along with the other band frequencies which have these 2Π states as upper levels. This process yields the bands at $\lambda\lambda 4310, 4500, 4571, 4791$, and 4835 A.U. These radiated bands would be expected to have intensities proportional to their transition probabilities. This was observed, the transitions to the first, second, and third vibration levels of the normal (2Σ) CdH molecule having about the same intensity ratios as these same transitions in the hydrogen-cadmium electric discharge, as pointed out above. Again, a second process produces the bands at $\lambda 4198$ A.U. ($2\Pi_{3/2}^{(1/2)} - 2\Sigma^{(1/2)}$) and $\lambda 4026$ A.U. ($2\Pi_{1/2}^{(1/2)} - 2\Sigma^{(1/2)}$), which is also a true resonance phenomenon, these bands

¹ Svensson, Zeits. f. Physik **59**, 333 (1930).

² The superscript in parenthesis is the vibrational quantum number. This notation follows the suggestion of Mulliken, *Phys. Rev.* **36**, 611 (1930).

being absorbed directly from the exciting light to bring the molecules to the second vibration levels of the two ${}^2\Pi$ states, respectively, whence they are re-emitted by the absorbing molecules.

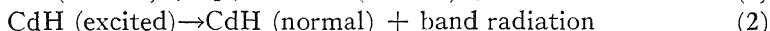
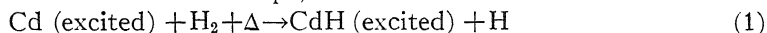
The much lower intensity in the resonance radiation of these latter bands, as compared with those arising from the ${}^2\Pi_{1/2}^{(1)}$ and ${}^2\Pi_{1/2}^{(3)}$ levels, is caused by the lower intensity of these same bands in the exciting light, the $\lambda\lambda 4198$ and 4026 A.U. bands being much weaker than the $\lambda\lambda 4310$ and 4500 A.U. bands. The absorption probability of a given resonance frequency is directly proportional to the second power of its intensity, hence the weaker resonance bands will be relatively less intense in the resonance radiation than in the exciting light, which is the case here.

One would expect absorption by the ${}^2\Sigma$ CdH molecule to occur also from vibration levels higher than the first if an appreciable number of molecules were found on these higher levels. Only a study of the absorption spectrum of the CdH molecule under the given conditions will give a direct answer to this question. All the phenomena observed in this investigation, however, are readily explained on the basis of absorption from the lowest level only. A consideration of the process of formation of the CdH molecule, described in the preceding paper, leads also to the conclusion that only this lowest level will be populated to any great extent. It was shown that the necessary 4.46 volts of energy required to dissociate the hydrogen molecule is almost exactly balanced by the sum of the excitation energy of the 2^3P_1 cadmium atom and the dissociation energy of the CdH molecule, totaling 4.45 volts, which energy would permit the molecule to find itself in the lowest vibration level of the ${}^2\Sigma$ state. Now, the energy difference between this lowest level and the second vibration level is 0.17 volt, a value too high to make very probable the possibility of finding the CdH molecule on the second level as a direct result of the process of molecule building or as a result of kinetic energy collisions of the CdH molecules with gas molecules, since the mean kinetic energy of translation at the temperatures employed is only 0.08 volt. Therefore, one would expect to find the population of the vibration levels higher than the first to be very small and absorption from these levels to be negligible.

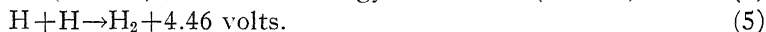
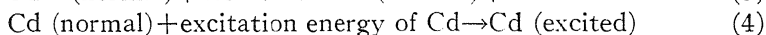
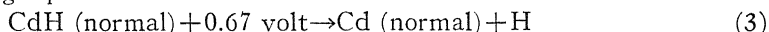
The excitation of the entire ${}^2\Pi - {}^2\Sigma$ band system with low intensity, when either the helium-cadmium or the hydrogen-cadmium discharge is used as a source of illumination, must be due to collisions of excited Cd atoms with either CdH molecules or H_2 molecules to form excited CdH molecules, which then radiate the band spectrum. A study of the energy relations involved in these collision processes is particularly instructive in determining the probability of their occurrence. In the CdH molecule the vibration levels of the ${}^2\Pi$ states have energy values above that of the lowest vibration level of the ${}^2\Sigma$ state ranging from 2.74 to 3.30 volts, so that, in order to excite it to the ${}^2\Pi$ levels, there must be given to the unexcited CdH molecule energy of an amount within this range corresponding to the particular ${}^2\Pi$ level that is to be excited. Now, if this energy results from a collision of the second kind with an excited cadmium atom, the atom will give up an amount of energy

corresponding to a transition from the particular excited state of the atom to a lower state. It will be observed, however, that the total energy of excitation of any of the excited states of the cadmium atom is considerably in excess of this range of CdH energies, the lowest value, that for the 2^3P_0 state, being 3.71 volts. Also, the 3^3D-2^3P transitions have energies (3.42 to 3.63 volts) somewhat above, while the 2^3S-2^3P transition energies (2.43 to 2.64 volts) lie somewhat below the range of CdH energies. This type of collision of the second kind seems, therefore, not to be very probable, although its probability is not entirely negligible.

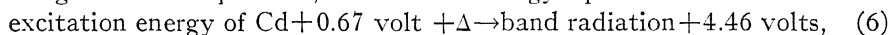
For the other type of collision excitation, involving an H_2 molecule the energy relations can be determined by representing the complete process of excitation and radiation in two steps, as follows:



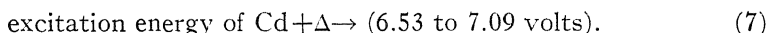
where Δ is an amount of energy, either positive or negative, to be supplied from kinetic energy. In order to balance the energies involved, one must add the following equations:



Adding these five equations, we have the energy equation



and putting in the limits of the band radiation energies, we obtain the equation



If, now, we supply the values of the excitation energies of cadmium in its various excited states (3.78 volts for 2^3P_1 , 6.35 volts for 2^3S_1 , 7.34 volts for 3^3D), we see that the 2^3P_1 level falls far short of having the required energy, and that the 2^3S_1 level will require at least 0.18 volt to be supplied from kinetic energy, while the 3^3D levels will have an excess of energy to appear as kinetic energy ranging from 0.25 to 0.81. volt. Thus, this process also will have a very low probability. The one or the other of the two collision excitation processes described above is responsible, no doubt, for the weak band spectrum observed without excitation by the band frequencies themselves; or it may be that these two processes together produce the phenomenon.

The $CdH^2\Pi-2\Sigma$ band system may then be excited in two ways under the conditions of the present experiments: first, by collisions of excited cadmium atoms with either CdH molecules or H_2 molecules, and, second, through absorption by the CdH molecules of the band frequencies themselves from the exciting light.

ZINC HYDRIDE BANDS

To study parallel phenomena, similar experiments were tried with zinc and mercury, whose hydride band spectra, as well as their atomic spectra, parallel those of cadmium. For zinc the same apparatus as was used for cadmium was employed, with the same technique, excepting that higher

temperatures were required. The resonance tube was maintained at a temperature of about 420°C and with a zinc vapor pressure corresponding to a temperature of about 380°C (0.036 mm of mercury). The discharge tube was operated first with hydrogen, then with helium, with small quantities of zinc vapor distilled from the side tube in each case. Illuminating a zinc-hydrogen mixture in the resonance tube with the hydrogen-zinc source produced in the optically excited radiation, in addition to the zinc spectrum, also some zinc hydride bands. A spectrogram of this radiation is reproduced in Fig. 4. When the discharge tube was operated with helium not entirely freed from hydrogen the optically excited band spectrum decreased in intensity as the amount of hydrogen in the source was diminished. This indicates an optical excitation of the ZnH bands similar to that in the case of the CdH bands.

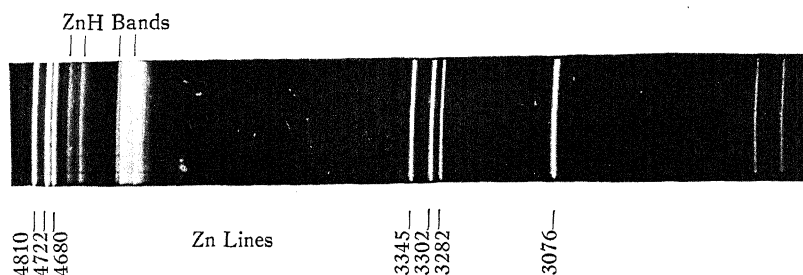
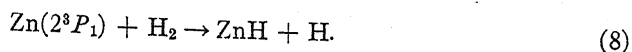


Fig. 4. Spectrogram of radiation from zinc-hydrogen mixture optically excited by hydrogen-zinc electric discharge.

The method of formation of the ZnH molecule is, apparently, also the same as in the case of cadmium. Illumination of the zinc vapor alone in the resonance tube produced an intense green glow of the optically excited zinc radiation; on the admission of hydrogen, however, at a pressure of about 0.02 mm the color of the glow changed to red. Now, the visible portion of the zinc spectrum contains most prominently the triplet blue-green lines $\lambda\lambda 4810, 4722, \text{ and } 4680 \text{ A.U.}$ ($2^3S_1 - 2^3P$) and the singlet red line $\lambda 6362 \text{ A. U.}$ ($3^1D_2 - 2^1P_1$). The green glow of the zinc radiation is due to the predominance of the three triplet blue-green lines, while the red glow on the admission of hydrogen results from the quenching of these triplet lines by the hydrogen gas, the singlet red line retaining its original intensity. The triplet lines are emitted after two successive absorptions, the first of which is the absorption of the resonance line $\lambda 3076 \text{ A.U.}$ bringing the atom to the 2^3P_1 state with an energy of 4.06 volts. Hulthén³ lists the dissociation energy of the normal ZnH molecule as about 0.9 volt, so that, if one considers a process analogous to that occurring in the case of cadmium, the total energy available (about 4.96 volts) will be such that a collision between the excited (2^3P_1) zinc atom and a hy-

³ Hulthén, Ark. f. Mat., Ast. och Fys. **21B**, No. 5 (1929). Although a dissociation energy for the ZnH molecule is listed in this article, a complete analysis of the ZnH band system has not been published, apparently.

drogen molecule can produce a zinc hydride molecule and an atom of hydrogen,



On the other hand, the first absorption necessary to produce the red singlet line, which also requires two successive absorptions, is the absorption of the second resonance line $\lambda 2139$ A.U. ($2^1P_1 - 1^1S_0$), bringing the atom to the first excited state in the singlet system. This state has an energy of 5.77 volts, which is far in excess of the 4.46 volts necessary to dissociate hydrogen, and hence collisions of zinc atoms in this state with hydrogen molecules do not effect a transfer of energy. The persistence of the red line demonstrates, in this manner, an interesting selective quenching effect due to hydrogen, in which only the states of the zinc atom (2^3P) which have an energy very nearly the same as that required to dissociate the hydrogen molecule lose their energy by the gas collisions. The rather remarkable results of this selective quenching, in which emission by the 2^3S_1 atoms is almost entirely wiped out, is possible in the case of zinc because of the absence of intercombination transitions between the singlet and triplet systems by which the 2^3S_1 level could be populated from the singlet levels.

It will be observed that the total energy available in the process of molecule building represented by Eq. (8) (about 4.96 volts) is considerably in excess of the required 4.46 volts, while the excitation energy of the zinc atom alone is not sufficient to dissociate hydrogen. Higher vibration levels that are yet below the dissociation level of the normal ZnH molecule may be, of course, the immediate end of this process, so that the total energy used will be more nearly the dissociation energy of hydrogen. It is evident, then, that the exact process of molecule building can be determined only after the ZnH band system has been analysed. Incidentally, this analysis should be aided materially by a study of the optically excited portion of the ZnH band system.

MERCURY HYDRIDE BANDS

For mercury the experiment of Gaviola and Wood⁴ was repeated, in which an ordinary water-cooled mercury arc was used as a source to illuminate mercury vapor in a resonance tube. A small amount of hydrogen and some nitrogen gas were admitted into the resonance tube, whereupon very weak HgH bands appeared in the optically excited radiation. Filtering the exciting light through bromine vapor produced no appreciable effect on the bands, although it greatly reduced the intensity of the $2^3S - 2^3P$ lines falling on the resonance tube, and hence also reduced their intensity in the optically excited radiation. This indicates that a population of the 2^3S_1 level of the mercury atom is not essential to the formation of the band spectrum.

Since there is no hydrogen in the mercury arc, the HgH radiation from the resonance tube could not be a resonance phenomenon, as in the cases of cadmium and zinc, but must be due entirely to collisions with excited mer-

⁴ Gaviola and Wood, *Phil. Mag.* (7) 6, 1191 (1928).

cury atoms. Also, the formation of the hydride molecule must be somewhat different in the case of mercury, since the excited 2^3P_1 mercury atom has more than sufficient energy (4.86 volts) to dissociate hydrogen. A collision between a 2^3P_1 mercury atom and a hydrogen molecule, therefore, should produce, apparently, two hydrogen atoms and a normal mercury atom, with considerable excess energy to appear as kinetic energy. Even the metastable 2^3P_0 mercury atom has energy (4.64 volts) in excess of the dissociation energy of hydrogen, so that collisions between the metastable atom and a hydrogen molecule should also produce complete dissociation. Perhaps the atomic hydrogen formed by these processes combines directly with a normal mercury atom to form the HgH molecule. It seems reasonable to suppose that the effect of nitrogen, which produces a large number of metastable 2^3P_0 atoms, in enhancing the HgH band spectrum is due to the indirect effect of increasing the concentration of atomic hydrogen. Collisions with nitrogen molecules will lengthen the effective life of the excited mercury atoms through transferring them to the metastable state, thus permitting more collisions of excited atoms with hydrogen molecules and increasing the concentration of atomic hydrogen. This will increase the probability of the collision of a normal mercury atom with an atom of hydrogen to form an HgH molecule. The subsequent excitation of the HgH bands would then be produced by collisions of the second kind of the HgH molecules with excited mercury atoms.

In this connection it should be particularly instructive to study the optical excitation of the HgH bands by a hydrogen-mercury electric discharge, which contains the HgH band radiation with great intensity, but lack of time prevented the execution of this project.

CONCLUSIONS

Optical excitation of CdH molecules by the band frequencies themselves produces a true resonance radiation of CdH bands.

CdH bands are produced also through excitation of CdH molecules by collisions of the second kind between excited cadmium atoms and either normal CdH molecules or H_2 molecules.

H_2 quenches the triplet portion of the optically excited Zn radiation, collisions with the 2^3P_1 zinc atoms forming ZnH molecules, but does not quench the singlet spectrum.

ZnH bands are optically excited as resonance radiation.

HgH bands are excited apparently by collisions of the second kind of HgH molecules with excited Hg atoms.

To Professor A. Ellett, who suggested the present investigation and rendered valuable assistance in its execution, the writer wishes to express his appreciation.

THE ISOTOPE EFFECT ON BAND SPECTRUM INTENSITIES

By J. L. DUNHAM*

RYERSON PHYSICAL LABORATORY, UNIVERSITY OF CHICAGO

(Received October 6, 1930)

ABSTRACT

Theory of the isotope effect on intensities.—It is shown that there is no change in the electronic part of the transition probability with nuclear mass, and that the vibrational part is the only part that does show an effect. This effect is calculated on the basis of Hutchisson's expressions for the vibrational transition probability. The effect of a change in nuclear mass on the population of the initial state is also found if this population is given by the simple Boltzmann distribution.

Application of the theory to specific cases.—The magnitude of the isotope effect is found for certain bands of O_2 , NO , and Cl_2 which have been used recently to measure the abundance of the isotopes of these substances by means of their band spectrum. The effect is small, being ordinarily less than ten percent, but it can not generally be neglected.

THE recent work of Babcock,¹ King and Birge,² and Naudé³ on the isotopes of oxygen, carbon and nitrogen has opened up the question of whether or not the transition probability of a given line is different for two isotopic molecules. The only method available at present for finding the relative abundance of the isotopes of these elements, a matter of great importance in the case of oxygen as it is used as the basis for the atomic weight scale, is to compare the intensities of corresponding lines from the different isotopic species. Giaque and Johnston⁴ have suggested that at least for symmetrical molecules like O_2 and C_2 it is possible that when the two component atoms are different isotopes the electric moment of the molecule would be greater than when both atoms are of the same weight, thus giving the lines of the unsymmetrical molecules a greater transition probability so that relative abundances estimated directly from intensities would be somewhat in error. This effect can be shown to be negligible, but obviously the whole matter needs discussion, and it is the purpose of the present paper to consider the possible effects of a difference in nuclear mass on the probabilities of transition between molecular states so as to make a more precise correlation between observed intensities and relative abundances possible. The isotope effect on the population of the initial state will also be considered for the cases where this population is given by the simple Boltzmann distribution. In the case of emission bands there are problems of differential excitation and possible effects of re-absorption, but as these can only be discussed in connection

* National Research Fellow.

¹ H. D. Babcock, *Proc. Nat. Acad. Sci.* **15**, 471 (1929); *Phys. Rev.* **34**, 540 (1929).

² A. S. King and R. T. Birge, *Astrophys. J.* July (1930).

³ S. M. Naudé, *Phys. Rev.* **36**, 333 (1930).

⁴ Giaque and Johnston, *Jour. Am. Chem. Soc.* **51**, 1436 (1929) and **51**, 3528 (1929) Cf. esp. p. 1439.

with the exact arrangements of a given experiment they will not be taken up here. To summarize the results it turns out that for bands with low quantum numbers and if the difference of equilibrium nuclear separation for the two states is small, there will be small effects; for large quantum numbers and large difference in r_e there will be large effects on the intensity. These general results will then be applied to various actual cases.

Since intensity measurements are most easily controlled when made on absorption lines we shall consider the effect of nuclear mass on absorption coefficients, though the results on transition probabilities can be applied directly to emission lines also. The effects we are looking for must be well over one percent to be appreciable as the accuracy of most intensity measurements is not under ten percent. However, as small corrections from different effects are likely to add up to give a large correction in the end, we shall consider all corrections which are greater than one percent.

The absorption coefficient, α_{ij} for the transition $i \rightarrow j$ (where i and j symbolize all the quantum numbers) is given by

$$\alpha_{ij} = \text{const. } b_i \nu_{ij} [P_{ij}]^2 \quad (1)$$

ν_{ij} is the frequency of the line, b_i is the Boltzmann factor giving the population of the initial state and $P_{ij} = \int P \psi_i \psi_j d\tau$, P being the electric moment of the molecule as a function of the coordinates of the electrons and nuclei and the ψ 's are the wave functions of the two states.

We are interested in the way in which α changes with the nuclear mass, so that all the factors which are independent of the nuclear mass have been put into the constant. ν_{ij} will vary slightly with mass, but ordinarily the isotopic frequency shift is very small compared to the whole frequency so that the effect of this can be neglected, and we can confine our attention to P_{ij} and b_i .⁵

Turning to P_{ij} we must find out first what the isotope effect on the ψ 's will be. The wave function of a molecular state can be approximated by the product of two wave functions, $\psi^e \psi^n$ of which ψ^e is the wave function for the motion of the electrons when the nuclei are held fast and ψ^n is the wave function for the motion of the nuclei assuming them to be bound by a force function equal to the total energy of the molecule for the fixed nucleus case. (This total energy is a function of the nuclear separation). Obviously ψ^e does not depend on the nuclear mass and so if this product is a sufficiently good approximation to the real wave function, we can confine our attention to ψ^n . Kronig,⁶ on the basis of some work of Slater⁷ has worked out the coefficient of the correction term which should be added to the product $\psi^e \psi^n$ to give a more accurate expression, and he finds that it will be very small

⁵ In the case of emission the intensity depends on the fourth power of ν_{ij} so that the effect would be greater and in extreme cases might be appreciable.

⁶ R. de L. Kronig, *Zeits. f. Physik.*, **50**, 347 (1928) esp. p. 353 ff. I am indebted to Prof. E. C. Kemble for pointing out the connection between separability and perturbations.

⁷ J. C. Slater, *Proc. Nat. Acad. Sci.* **13**, 423 (1927), also Born and Oppenheimer, *Ann. d. Physik.* **84**, 457 (1927).

(of the order of magnitude of the ratio of the electronic to the molecular mass) unless there is another state of a different electronic level which is very close to the state in question, and which can interact with it; in short, unless the level in question is perturbed.⁸ Consequently we may say that the wave function is separable to a high degree of approximation under ordinary circumstances and we can confine our attention to ψ^n . This means also that the effect suggested by Giauque and Johnston⁴ will be negligible ordinarily, as the electronic moment will not change appreciably between isotopic molecules even in cases like O_2 which are symmetrical.⁹

In discussing the isotope effect on ψ^n we can neglect the rotational part of the wave function because the rotational contribution to the transition probability is simply a function of the angular momentum quantum numbers and does not depend on the mass of the rotator so that the integrals involved in P_{ij} reduce to integrals of the two vibrational wave functions only, and are readily calculable.

Hutchisson¹⁰ has calculated these integrals using the wave functions of a simple harmonic oscillator. He considers them to be applicable only to symmetrical molecules, but they are of more general applicability than he states as the following argument shows. We are dealing with integrals of the type

$$\int P \psi_i^e \psi_i^n \psi_j^e \psi_j^n d\tau$$

where P and the ψ^e 's are functions of the coordinates of the electrons *and* the nuclei; the ψ^n 's depends on the nuclear coordinates only. If we integrate over the electronic coordinates there remains

$$\int P_{kk'}(r) \psi_i^n \psi_j^n d\tau$$

where k and k' are the electronic quantum numbers of the states i and j respectively and $P_{kk'}(r)$ is a sort of electronic electric moment and is a function of the nuclear coordinates, that is to say of r , as we are considering vibration only. $P_{kk'}(r)$ can be expanded in a Taylor's series about some convenient point and the integrals calculated for each term in the series. Since ordinarily $P_{kk'}(r)$ changes with r very slowly compared to the ψ^n 's and since it does not change very much in the region for which the ψ^n 's are appreciable it turns out that "for low quantum number" the constant term in the expansion of $P_{kk'}(r)$ gives the largest contribution to the integral and the others can be neglected.¹¹

⁸ Kronig's calculation can be greatly simplified if it is carried through in the original cartesian coordinates. The Euler's angles analysis is not necessary for this separability proof.

⁹ By the same reasoning we can see that the molecule $O^{16}O^{18}$, for instance, will have a very small permanent electric moment and hence the pure rotation and the vibration-rotation bands in the infrared will be exceedingly faint—too faint to be ordinarily detectable.

¹⁰ Elmer Hutchisson, *Phys. Rev.* **36**, 410 (1930).

¹¹ Cf. "Quantum Mechanics" Condon and Morse. McGraw-Hill 1929. p. 169 for a discussion of this subject. The fact that higher terms in the Taylor's expansion are negligible at least for low quantum numbers can be verified by direct calculation quite readily.

This reasoning is independent of whether or not the molecule is symmetrical, so that Hutchisson's formulas can be applied quite generally.

As the formulas for the integrals in the lower states are quite simple, we shall reproduce them here in a notation more suited to our problem. Using ω' and ω'' for the frequencies of vibration in the upper and lower states respectively, $\omega = \omega' + \omega''$, $B = \hbar^2/8\pi^2 I'' C$ (where I'' is the moment of inertia of the molecule in the lower state) and $\zeta = (r' - r'')/r''$ and $\beta = (\omega' \omega''/4B\omega)\zeta^2$, they are ^{12,13}

$$\begin{aligned} I_{00} &= \left(\frac{2(\omega' \omega'')^{1/2}}{\omega} \right)^{1/2} e^{-\beta} \\ I_{01} &= \frac{\omega''}{\omega} \left(\frac{\omega'}{B} \right)^{1/2} \zeta \left(\frac{2(\omega' \omega'')^{1/2}}{\omega} \right)^{1/2} e^{-\beta} \\ I_{02} &= \frac{1}{2^{1/2}} \frac{\omega'}{\omega} \left(\frac{2(\omega' \omega'')^{1/2}}{\omega} \right)^{1/2} e^{-\beta} \left(1 - \frac{\omega''}{\omega'} + \frac{\omega''^2 \zeta^2}{\omega B} \right) \\ I_{11} &= \frac{(\omega' \omega'')^{1/2}}{\omega} \left(\frac{2(\omega' \omega'')^{1/2}}{\omega} \right)^{1/2} e^{-\beta} \left(2 - \frac{\omega' \omega''}{\omega} \frac{\zeta^2}{B} \right). \end{aligned} \quad (2)$$

To find the isotope effect on the transition probabilities we need to find the effect of a change of nuclear mass on the expressions in Eq. (2). In calculating this we use the fact that the electronic part of the wave function is not affected by the nuclear mass, so that the "shape" of the nuclear binding potential will be the same in two isotopes. Hence ζ is unaffected by a change in nuclear mass, and the ω 's will vary inversely as the square root of μ , the reduced nuclear mass. B , of course, varies inversely as μ . It is therefore a simple matter to see how any of the expression's in Eq. (2) will vary with μ . In particular if ζ is large, so will be β , and the exponential will vary rapidly with μ . Also in this case the ruling term in the polynomial will be one in $(\omega/B)^{v'+v''/2}$ which will vary as $(\mu)^{v'+v''/4}$. However if ζ is small no definite statement can be made about which will be the ruling term and we can only say that the exponential will change slowly with μ . In general, therefore, we would expect large effects for transitions between states whose r_e 's differ considerably (i.e. large ζ) and for large vibrational quantum numbers, but this is not an exact rule and each case must be examined separately to see what the effect will be. It should be noted also that for very large vibrational quantum numbers, especially when ζ is large also, the higher terms in the expansion of the electric moment will no longer make a negligible contribution to the intensity and a more general calculation will be necessary.

¹² The constants ω' , ω'' , B and ζ are not necessarily $\omega_e B_e$ and ζ_e . We can go a long way toward taking account of the anharmonic character of the vibration by using ω_v , B_v and ζ_v instead.

¹³ Unfortunately Hutchisson has used the wrong normalization coefficients so that the quantity which he calls C_3 should be (using his notation) $C_3 = (2/\alpha(1+\alpha^2))^{1/2} e^{-\beta^2/2(1+\alpha^2)}$. This correction is of no importance in the calculations he makes as he is interested only in relative values, but where we are interested in dependence on mass it is necessary.

There is one other factor in the expression for α which depends on μ and that is the Boltzmann factor b . This factor is

$$b_i = \frac{e^{-E_i/kT}}{\sum_i e^{-E_i/kT}} \quad (3)$$

where E_i is the energy of the i th state, k is the ordinary gas constant and T the absolute temperature. For the rotational levels of a molecule $E_K = hcBK^2$ where K is the rotational quantum number (we do not need to bother about the refinement of using $K(K+1)$ in this case) and B has the same significance as in Eq. (2). Since hcB is small compared to kT , the denominator of Eq. (3) can be considered as the integral $\int e^{-hBK^2c/kT} dK$ and so we can readily evaluate the rate of change of b_K with μ , getting

$$\frac{1}{b_K} \frac{db_K}{d\mu} \Delta\mu = \left(K^2 \frac{B}{T} \frac{hc}{k} - \frac{1}{2} \right) \frac{\Delta\mu}{\mu} \quad (4)$$

For low rotational quantum numbers the first term in the parenthesis is small at ordinary temperatures so that the effect of μ on the population of the state will be one half the percentage change in μ . For lower temperatures or higher quantum numbers the effect will be smaller than this as shown by Eq. (4).

For the case of vibration the energy difference between successive levels is large and if the temperature is not too high, practically all of the molecules will be in the lowest state, in which case the summation in the denominator can be replaced by the first term of the sum only. In this case $E_v = h\omega_v(v + \frac{1}{2})$ so that we have

$$\frac{1}{b_v} \frac{db_v}{d\mu} \Delta\mu = v \frac{\omega_v}{T} \frac{hc}{k} \frac{\Delta\mu}{2\mu} \quad (5)$$

where v is the vibrational quantum number.

It is evident from this formula that there will be no isotope effect on the population of the lowest state ($v=0$), but there will be an effect on the population of higher states. It should be emphasized, however, that this formula can be applied only when the population of the excited states is absolutely negligible compared to that of the normal state. If this condition is not fulfilled the calculation is more elaborate.

Having discussed the possible sources of isotope effect on intensities we now turn to actual cases to apply our results.

In the case of oxygen, the measurements of abundance so far made are those of Babcock¹ on the atmospheric bands of O_2 and of Naudé³ on the γ bands of NO. Babcock measured a number of individual lines in the 0-0 band and found the intensity ratio to be one in 1250, but he does not give a probable error. However we may safely assume it to be over ten percent. For these bands the quantity ζ is very small indeed and a simple calculation using the first formula of Eq. (2) shows that the transition probability for the $O^{16}O^{18}$ molecule does not differ by more than 0.2 percent from that

for $(O^{16})_2$. As the bands were due to transitions from the lowest vibrational state there is no correction due to the vibrational Boltzmann factor, but the lines with low rotational quantum number will show an effect due to the rotational Boltzmann factor. This turns out to be about 2 percent for the lowest lines, but as Babcock used quite a number of lines for his measurement the average effect for all the lines will be less than this, so that, in view of the size of the experimental error, we can neglect the correction.¹⁴

Naudé's abundance estimate is based on the relative intensity of heads from the 1-0 band of the γ system of NO observed in absorption. The resolution was not sufficient to separate the lines so that they could be worked with separately, but the intensity of the heads as a whole was measured. A maximum error of about ten percent is given. In this case a calculation based on the second equation of Eqs. (2) shows that the transition probability for $N^{14}O^{18}$ is less than that for $N^{14}O^{16}$ by two percent.¹⁵ The rotational Boltzmann factor correction for the P_1 heads can be readily calculated from Eq. (4) using $\beta=1.70$ and $K=11$ for the quantum number of the lines at the head,¹⁶ and a correction of 2.7 percent is found in the opposite direction to that for the transition probability. As the two corrections cancel, it is evident that the intensity ratio gives the abundances directly.

The work of King and Birge² on carbon has not resulted in any numerical value of the abundance of the new isotope; in fact they report very anomalous behavior of the intensities which is as yet quite unexplained. There is therefore no point in calculating a numerical correction, but it can be said that the correction for the 0-1 band of the Swan system, which they have used so far, would be about one percent.

We now turn to the case of chlorine. Elliott¹⁷ has measured the intensity ratio of lines from the molecules $Cl^{35}Cl^{37}$ and $(Cl^{35})_2$ and has found a ratio different from that obtained from chemical data. The bands he has used are the 1-12, 2-12 and 2-6 bands in the visible absorption spectrum of Cl_2 , and his figure for the relative intensity is 1.40,¹⁸ whereas the chemical atomic weight in conjunction with the known weight of the two isotopes,¹⁷ shows that the relative abundance of the two types of molecules is 1.59 leaving a discrepancy of 14 percent. Now chlorine is a case where we would expect a large isotope effect because of the large difference in r_e for the two states, and a calculation based on Hutchisson's results for the 2-6 band shows that the transition probability is different by 19 percent in the two kinds of

¹⁴ In this case there is no question of the levels being perturbed by being near other levels. Babcock's analysis of the band shows that. C.f. also Dieke and Babcock, *Proc. Nat. Acad. Sci.* **13**, 670 (1927).

¹⁵ One might expect perturbations in this band because it lies on top of the 1-0 β band, but no perturbations have been found (Jenkins and Rosenthal, *Proc. Nat. Acad. Sci.* **15**, 382 (1929)) so that we can be pretty sure there will be no trouble about separability in this case.

¹⁶ C.f. R. Schmid, *Zeits. f. Physik.* **64**, 84 (1930).

¹⁷ A. Elliott, *Proc. Roy. Soc.* **A123**, 629 (1929) and **A127**, 638 (1930) also *Nature* **126**, 133 (1930).

¹⁸ Elliott corrects his measured ratio (1.35) to allow for the maximum possible effect of overlapping lines. 1.40 is obtained by using one half of that correction.

molecules. In applying Hutchisson's results to this transition a considerable simplification is possible because as ζ is fairly large, only one of the terms in the summation is appreciable. Further, this calculation was carried out using r_v and ω_v rather than r_e and ω_e . The 6th state of the upper level is markedly anharmonic and so it seemed of interest to carry out the calculation of the electric moment matrix using Morse's¹⁹ wave function for the upper state and the harmonic wave function for the lower state. The calculation in this fashion is fairly long-winded but the result is similar to that from the harmonic analysis, the isotope correction to the transition probability being 15 percent. No attempt was made to calculate the corrections for the 1-12 or the 2-12 transition, but they will probably be of the same general magnitude as that for the 2-6 transition. Since the bands were due to transitions from the 2nd level we should look to the vibrational Boltzmann factor for an effect, and a simple calculation shows that the heavier molecule will have 7 percent greater probability of being in the second state than the light one.²⁰ This is in the opposite direction from the 15 percent found for the difference of transition probabilities so the correction to Elliott's abundance ratio is 8 percent, making the corrected figure 1.29, which differs from the chemical value by 22 percent. It is not possible to say whether or not this discrepancy is within the experimental error of the measurements as Elliott does not give an estimate of his error, but it seems larger than one would expect.

In this connection it is interesting to note that Meyer and Levin²¹ measured the relative abundance of the chlorine isotopes from the infrared bands of HCl and obtained good agreement with the chemical value. The intensity ratio needs no correction in this case as the difference in μ between the two kinds of molecules is only a few tenths of one percent, and the probable experimental error is about twenty percent.

There are many other cases where bands due to two or more isotopic molecules have been observed, but, as in most of these cases the chief interest is in frequencies, the intensities are only estimated from the plates by eye and there is no point in applying the comparatively small isotope correction to these results.

¹⁹ P. M. Morse, *Phys. Rev.* **34**, 57 (1929).

²⁰ The rotational Boltzmann factor correction will be negligible in this case, because lines with relatively large rotational quantum numbers were used.

²¹ C. F. Meyer and A. A. Levin, *Phys. Rev.* **34**, 44 (1929).

THE ULTRAVIOLET LIGHT THEORY OF AURORAE
AND MAGNETIC STORMS. CONTINUED*

BY E. O. HULBURT

NAVAL RESEARCH LABORATORY

(Received September 29, 1930)

ABSTRACT

The ultraviolet light theory of aurorae and magnetic storms, *Phys. Rev.* **33**, 412 (1929), **34**, 344 (1929), did not agree with all the facts. Making use of the further development of the theory of the outer atmosphere, *Phys. Rev.* **34**, 1167 (1929), **35**, 240 (1930), the discrepancies in the ultraviolet theory are removed with no change in the original assumptions. The first phase of the average world-wide magnetic storm is attributed to the sudden increase in the eastward ion drift current which girdles the earth caused by an increase in the long free path ions produced by a solar ultraviolet flare. The second phase of the storm comes about from the heating of the high atmosphere by the flare. The atmosphere expands and the outward movement of the ionized regions across the earth's magnetic field gives rise to a westward current in the high atmosphere flowing around the earth. The movement also decreases the long free path ions and increases the short free path ions; this prolongs the westward current.

Assuming that the earth has no excess charge the high flying ions distilled from low latitudes fall into the top of the atmosphere of the auroral latitudes in maximum numbers at about 1 P.M. It takes them until about 6 P.M. to fall by diffusion and electrical drift down to the short free path levels at 100 km. They set up a system of electrical currents in the high atmosphere wheeling in a rather distorted course around a focus at about 6 P.M. in latitude 60° to 70° , one system in the arctic and one in the antarctic. The current systems give rise to the diurnal variations of the average world-wide magnetic storm. If the earth has a resultant charge in excess of about 50 coulombs the present theory would probably be untenable, or would require extensive modification.

The lower limits of the long and short free path ion banks of the polar atmosphere agree, respectively, with the observed lower boundaries of the streamers and the structureless luminosity of the aurora.

1. INTRODUCTION

THE ultraviolet light theory of aurorae and magnetic storms,¹ which was sketched out last year, was found to agree with the main features of the phenomena. However, the theory contained some unsettled points and did not agree with certain details of the observations. At the time it was difficult to know where the trouble lay. The further development of the theory of the high atmosphere^{2,3} has permitted a clearer insight into the actions which occur there and, as shown in the present paper, has removed some of the discrepancies which existed in the ultraviolet light storm theory. So that the theory without any changes in the original assumptions begins to assume a more finished appearance.

* Published with the permission of the Navy Department.

¹ Maris and Hulburt, *Phys. Rev.* **33**, 412 (1929).

² Hulburt, *Phys. Rev.* **34**, 1167 (1929).

³ Hulburt, *Phys. Rev.* **35**, 240 (1930).

2. THE WORLD-WIDE MAGNETIC STORM

During the average world-wide magnetic storm the horizontal component H_1 of the earth's magnetic field H increases quickly for a few minutes or a half-hour, the initial phase, and then in a few hours decreases to a value below normal returning gradually to normal in a day or so, the final phase. The vertical component H_2 experiences the opposite series of changes, first decreasing quickly then increasing to a value above normal and descending to its normal value slowly. (See the curves of Fig. 3, ref. 1.) The ultraviolet light theory attributed the initial phase of the storm to the eastward ion drift currents in the high atmosphere arising from a sudden increase in the ionization above 150 km levels caused by a sudden flare of ultraviolet light from the sun. The theory suggested that the final phase of the storm was due to the reaction of induced currents in the earth. Such a reaction would cause changes in agreement with those observed for H_1 but not for H_2 . It is now seen that all of the average storm variations of H_1 and H_2 are attributable to effects in the high atmosphere and that the earth currents are of secondary importance. Chapman⁴ in a recent criticism has dwelt upon the discrepancy which existed in the case of H_2 . The difficulty lay, however, in the fact that we used Chapman's⁵ value of the earth's conductivity to estimate the induced earth currents, and with his value the earth currents could not be neglected. It has turned out, see section 3, that his value is probably widely in error.

It was shown² that during solar quiescence there is a steady current of about 3×10^6 amperes flowing eastward around the earth in the high atmosphere which produces a northward magnetic field of about 400γ (γ is 10^{-5} gauss) at the equator in agreement with the observed value 450γ of the field of external origin. The current is due to the magnetic gravitational drift of the long free path ions. Over the daylight hemisphere the 3×10^6 ampere current is made up of an eastward current sheet of about 12×10^6 amperes in the long free path ion region, the D region, and a westward current sheet of 9×10^6 amperes in the underlying short free path ion region, the S region. The height z_0 above sea-level of the boundary between the D and S regions is at about 150 km at equinoctial noon at the equator. In the night hemisphere the current flows eastward in both the D and S regions and amounts to 3×10^6 amperes. The ultraviolet flare may be expected in general to increase the ionization in both the D and S regions, although different flares may increase the D and the S ions by different amounts. An increase in the D ions results in an increase in the eastward current in the daylight D region and hence in the 3×10^6 ampere current which girdles the earth. H_1 then increases and H_2 decreases as in the first phase of the storm. An increase in the daylight S ions causes an increase in the electrical conductivity of the daylight S region and hence an increase in the westward daylight S current. This reduces the eastward 3×10^6 ampere current and therefore amounts to a westward

⁴ Chapman, Monthly Notices Roy. Ast. Soc., Geophys. Sup. 2, 296 (1930).

⁵ Chapman, Phil. Trans. A218, 1 (1919).

storm current girdling the earth; H_1 is reduced and H_2 is increased, as in the second phase of the storm.

There is an additional effect which is common to all types of flares, namely a heating of the high atmosphere above the, say, 50 km level. The heating may be due to a direct absorption of the energy of certain wave-lengths in the spectrum of the flare or may come about directly. For example, the ionization produced at high levels descends to lower levels where recombination takes place and the energy of recombination heats the atmosphere. The heating causes an outward expansion of the upper atmosphere which has already been calculated for a particular case.¹ Evidence of the expansion is afforded by experiments with pulses of wireless signals which indicated that the ionized layers are lifted up during a magnetic storm.¹ The expansion of the atmosphere produces two reactions, a "dynamo" effect and an "engulfing" effect. The dynamo effect is the result of the movement of the S region across the earth's magnetic field, and is a maximum in tropical latitudes where H is approximately horizontal. An upward motion of the daytime S region gives rise to an induced westward electric field and therefore causes a westward current flowing around the earth; this reduces H_1 . An upward velocity of 25 km hr⁻¹ of the S region reduces H_1 by about 250γ at the equator, the case of an intense storm (ref. 2, section 30). The engulfing effect, also a maximum in tropical latitudes, depends on the fact that where H is approximately horizontal the D ions can only move a short distance across H between collisions and are therefore hindered from moving upward freely with the neutral particles of the expanding atmosphere. Thus, after the initiation of the storm, the D ions near the z_c level find themselves in a mounting tide of air molecules; their free paths are shortened and they become S ions. Since the D ions experience many collisions before being lost by recombination (ref. 2, section 29), the daylight S ions are increased at the expense of the D ions with a consequent effective westward storm current.

We may picture the sequence of events in the average world wide storm as follows: the solar flare by its ionizing energy first increases the D ions, increasing H_1 to a value above normal, as in the initial phase of the storm. In the second phase the heating effects of the flare make themselves felt, the high atmosphere expands, the ionized layers move upward and H_1 decreases for a few hours. When the layers cease their upward movement H_1 would increase to its previous value above normal were it not for the fact that in the meantime the engulfing effect has reduced the D ions, so that actually H_1 increases to some value below normal. Thereafter H_1 increases slowly to its normal value as the flare dies away, the storm ionization diminishes and the atmosphere settles down to its quiet day condition. Magnetic storms in which the initial phase is not pronounced, or is absent altogether, and which therefore consist only of the second phase, are fairly common. In these cases we may suppose that the flare emits mainly energy which heats the high atmosphere and produces S ionization without much D ionization. Storms made up only of the first phase are rare. Such a storm would be produced by a flare which gave rise to D ionization with little S ionization or heating; this

would seem to require a flare with unusual spectral characteristics. The fact that in general the most intense storms are of short duration is in keeping with the present theory because the more rapid the outward expansion of the atmosphere the greater is the induced westward current, due to dynamo action, in the second phase of the storm.

The intensity of the world-wide storm is a maximum at the equator, decreases with increasing latitude to a minimum at about 50° or 60° north or south, and then increases in the auroral zones around 70° . These facts find a simple explanation on the ultraviolet theory. The eastward storm current of the first phase of the storm has already been shown to be a maximum at the equator (ref. 1, section 13). With regard to the westward current during the second phase of the storm we note that the magnetic field H is horizontal at the equator and tilts up with increasing latitude; H is inclined 49° , 70° and 90° to the horizontal at magnetic latitudes 30° , 60° and 90° respectively. Therefore the dynamo effect in the S region and the engulfing of the D ions by the heated and expanding atmosphere are a maximum at the equator and fall off rapidly with increasing latitude. Hence the westward storm current is a maximum at the equator. The auroral latitudes receive a double contribution of ionization, that produced directly by the solar flare and that which distills in from the lower latitudes (see curve 2, Fig. 1). Therefore the storm effects will increase again at the high latitudes. It is hardly necessary to mention, what we have often stated before, that a complete theory would probable consider the winds which flow from the daylight to the night areas. In the high atmosphere the winds may be very rapid, especially during a magnetic storm and their effects may be important.

3. THE INDUCED CURRENTS IN THE EARTH

The electrical currents in the high atmosphere to which the present theory attributes the average world-wide storm variations in H will induce currents in the earth. From certain facts of the quiet day diurnal variations in H Chapman,⁵ following the method of Schuster, has calculated the resistivity ρ of the core of the earth to be 2.5×10^{12} e.m.u. the calculation was based on the assumption that ρ was constant throughout the earth, except of course for an outer crust of higher resistivity. The assumption was obviously faulty, and Gunn⁶ has recently shown that the method gives no exact information about ρ in the core of the earth. We can go a step farther and show that the value 2.5×10^{12} is untenable. The relaxation time τ for the current in a circuit of inductance L and total resistance R to fall to $1/e$ 'th of its value is

$$\tau = L/R. \quad (1)$$

The inductance of the earth⁷ is 7.8×10^8 e.m.u. and with $\rho = 2.5 \times 10^{12}$ R is about 10^4 e.m.u. From (2) $\tau = 22$ hours, which is roughly the duration of the westward atmospheric current during an average magnetic storm.

⁵ Gunn, Terr. Mag. and Atmos. Elec. 35, September (1930).

⁷ Lamb, Phil. Trans. 174, 519 (1883).

Therefore there would be a westward current induced in the earth after the westward atmospheric storm current dies away which would cause certain variations in H ; it would reverse the storm decrease in H_1 and maintain the storm increase in H_2 . Such variations are not observed and therefore ρ can not be 2.5×10^{12} in the earth's core. Because the core is hot it is reasonable to think that ρ is much less than 2.5×10^{12} . In such a case, taking into account "skin effect" calculated from the usual formula,⁸ the relaxation time will be much longer than 22 hours and the induced reactions in the core would be negligible for periods of the order of a day or less.

The effects of the induced reactions in the oceans are probably appreciable. The current will flow in large loops. With a loop about 30,000 km around, 10,000 km wide and 5 km thick, as might occur in the South Pacific Ocean, and with $\rho = 2 \times 10^{10}$ e.m.u. for sea water τ is about an hour, probably an over-estimate. Thus if the atmospheric currents undergo fluctuations of periods of an hour or so, as they often do, the ocean reactions may be pronounced. To work out the effects to be expected at any magnetic observatory due to the neighboring oceans promises to be complicated and we shall not go farther with the problem at this time. It may require a careful scrutiny of the data of magnetic observatories scattered over the earth. For earth girdling currents in the S region of the atmosphere τ is about 20 minutes.

4. DIURNAL MAGNETIC STORM VARIATIONS

The diurnal magnetic storm change in H varies with the local time of the observing station according to the curves of Fig. 4, ref. 1. By mistake curve 5 of the figure was drawn reversed; it should be similar to curve 4. The diurnal storm variation was ascribed to the influence of high flying ions distilled into the auroral regions from the lower latitudes. Neutral atoms and molecules were assumed to be sprayed out from the outer fringe of the atmosphere to distances as great as 50,000 km where they were ionized by the ultraviolet light of the sun. The ions in their descent back to the earth were guided by the magnetic field and accumulated in the auroral zones in the afternoon. By their diamagnetism they caused changes in the earth's magnetic field. The calculated changes agreed with most of the curves of Fig. 4, ref. 1, but not with all of them. Now that more is known about the conductivity of the upper atmosphere^{2,3} we see that the diamagnetism is not as important as the gravitational magnetic drift currents of the auroral ion concentration. As shown later, the magnetic effects of these currents agree with all of the facts as embodied in the curves of Fig. 4. In order, however, to calculate the magnetic effects we must examine in detail the course of the high flying ions in their descent into the atmosphere of the auroral regions.

The number of fast moving neutral particles sprayed away from the outer regions of the sunlit atmosphere in a direction θ was assumed to be proportional to $\cos \theta$, where θ is the angle with the line joining the earth and the

⁸ Jeans, *Electricity and Magnetism*, page 479 (1925).

sun.¹ Therefore, if the earth did not rotate on its axis and had no excess electrical charge, the ion concentration in the auroral latitudes from 60° to 70° magnetic produced by the high flying ions would be a maximum at noon. The earth does rotate, however, and we shall assume as was done throughout the earlier papers that the earth is uncharged as a whole. For this case Page⁹ has shown that ions beyond an earth's radius away from the outer atmosphere move along the lines of the earth's magnetic field without being influenced by the earth's rotation; that is, their paths are practically the same whether the earth rotates or not. Ions at nearer distances begin to partake of the earth's rotation until in the atmosphere they move with the full rotational velocity of the earth. (I pointed out¹⁰ that the effect of collisions between long free path ions and neutral molecules of the atmosphere might modify Page's calculation, but Page¹¹ showed that the effect could be included in those which he had already discussed⁹ on page 830). From Page's⁹ equation (16) it is seen that high flying ions formed on the noon meridian at heights around 30,000 to 50,000 km fall into the auroral zones at about 1 P.M.

Therefore q , the number of high flying ion pairs which descend per cm² per sec into the top of the atmosphere of the auroral zones is a maximum at about 1 P.M. and falls off roughly with the cosine of the longitude from the 1 P.M. meridian. q was estimated to be 3×10^7 ion pairs cm⁻² sec⁻¹ (ref. 1, page 421) during solar quiescence, probably a low estimate. During the magnetic storm q is greater than 3×10^7 and during the hours that the solar flare is most active we assume q to be 2×10^{11} . We take the daytime molecular densities in the high atmosphere of the auroral latitudes to be the same as those given by Maris¹² for a summer night in temperate latitudes. At any height z the molecular density n is given by¹³

$$n = n_0 e^{-pz}, \quad (2)$$

where $p = 1.41 \times 10^{-6}$. The 2×10^{11} ion pairs are probably positive ions and electrons. They fall freely along the lines of the earth's magnetic field into the atmosphere of the auroral zones and continue to descend through the atmosphere by temperature diffusion and electric-magnetic drift.² Calculating the temperature diffusion by the method of a former paper, ref. 13, page 1027, we find that the electrons form a bank with a maximum density at about 160 km. Below 160 km the electrons become attached rapidly to oxygen molecules to form negative oxygen molecular ions. The recombination of the electrons with positive ions is small compared to the attachment, and therefore the region above 160 km is a source of 2×10^{11} ion pairs. These form an ion bank as given by the y, z curve 1, Fig. 1. The maximum value of y is 2.35×10^9 at $z = 130$ km. 1.23×10^{11} ion pairs cm⁻² sec⁻¹ move downward across the 130 km level (calculated by equation (3), ref. 13) and therefore

⁹ Page, Phys. Rev. 33, 823 (1929), equation (16).

¹⁰ Hulburt, Phys. Rev. 35, 1587 (1930).

¹¹ Page, Phys. Rev. 36, 601 (1930).

¹² Maris, Terr. Mag. and Atmos. Elec. 33, 233 (1928); 34, 45 (1929).

¹³ Hulburt, Phys. Rev. 31, 1018 (1928).

their downward velocity is $1.23 \times 10^{11} \div 2.35 \times 10^9 = 52 \text{ cm sec}^{-1}$. Since the loss of ions by recombination is small above $z = 130 \text{ km}$ the downward diffusion velocity of the ions in these levels is proportional to $1/y$. In particular, the velocity is 250 cm sec^{-1} at $z = 140 \text{ km}$. The electric-magnetic drift velocity v , which is downward in the day hemisphere, has about this same value (section 27 and column 9 of Table 1, ref. 2) throughout the D ion region, i.e. above $z_c = 110 \text{ km}$. Therefore the y, z curve 1, Fig. 1, which has been calculated using gravity diffusion is approximately correct for z greater than about 135 km . Below this level the drift velocity v is more important than temperature diffusion, and hence from 135 km down to z_c we calculate the y, z curve by means of equation (16), ref. 2. This gives curve 2, Fig. 1. Below z_c temperature diffusion is important again, and the curve is found to fall to low values of y below $z = 100 \text{ km}$.

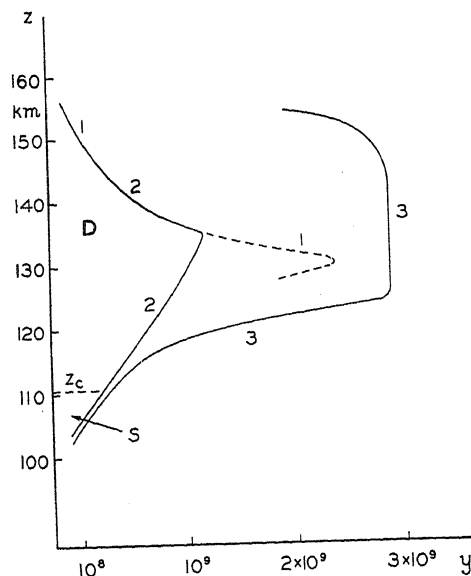


Fig. 1. Ion density y in auroral latitudes; curve 3 for noon on a quiet day, curve 2 the additional ions at about 6 P.M. during a magnetic storm.

Curve 2, Fig. 1, is approximately the ion bank which would be produced by $2 \times 10^{11} \text{ ions cm}^{-2} \text{ sec}^{-1}$ falling down into the atmosphere of the auroral zones and represents the increase in the ionization during a magnetic storm. However, the curve is not entirely correct, the values of y below $z = 125 \text{ km}$ being about twice as great as they should be, for two general approximations have entered into the calculations. In the first place we have determined the storm curve disregarding the ionization which was already present. The quiet day ionization at noon is given in curve 3, Fig. 2. This is the y, z curve of Fig. 2(c), ref. 2, with the ordinates lowered to accord with the n, z curve of equation (2). Since the rate of ionic recombination is proportional to y^2 (equations (7) and (9), ref. 13), it comes out that the storm ions produced

by $q = 2 \times 10^{11}$ which are added to the quiet day ions of curve 3, Fig. 1 are only about $\frac{1}{2}$ of the ions of curve 2, Fig. 1, in the region below 125 km. In the second place curve 2 is a steady state solution; it is the ion curve which would be formed if the rate of supply q persisted long enough. D , the total number of ion pairs in a 1 cm^2 column vertically upward through the ion bank of curve 2, is 2.6×10^{15} . With $q = 2 \times 10^{11}$ it would take 1.3×10^4 sec or 3.6 hours to build up the ion bank, if there were no losses; there are losses of course due to recombination. The solar flare may not persist at full intensity for this length of time. Or even if it did, q is not a constant, because of the rotation of the earth, and varies with the hour angle from 1 P.M. Thus a steady state may never be attained during the magnetic storm.

In spite of the numerous approximations we take curve 2, Fig. 1, as giving a rough idea of the storm ionization in auroral latitudes at 6 P.M. The total time for the ions to descend from the top of the atmosphere at about $z = 200$ km to the z_c level at 110 km is 4 or 5 hours. Since q is a maximum at 1 P.M. the ion density at z_c is a maximum at 5 or 6 P.M. The magnetic-gravitational

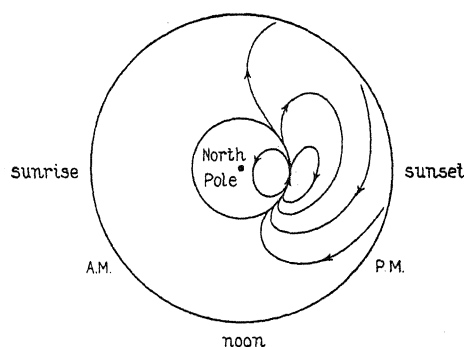


Fig. 2. Theoretical currents in the high atmosphere which cause the diurnal magnetic storm variations. View looking down on the North Pole. Aurorae and magnetic storms.

drift current^{1,2} of the D ions is eastward. The current is connected to the S ion region by the D ions which descend across z_c and the circuit is completed in the S region. Using the values of the electrical conductivity σ in the S region (Fig. 2, ref. 3), the lines of current flow are as sketched in Fig. 2; the figure is a view looking down on the North Pole of the earth. This current system causes changes in the earth's magnetic field in entire agreement with the observed diurnal magnetic storm variations in H . With $D = 2.6 \times 10^{15}$ the ion drift current density is 3.7×10^{-5} and 8.5×10^{-5} e.m.u. for atomic nitrogen and molecular oxygen ions, respectively (ref. 2, section 13), and the respective values of H_1 are 23 and 52γ . These values agree with the observed values which are around 40γ for an average storm.

5. THE AURORA

The ion storm curve 2, Fig. 1, leads to an explanation of some details of the aurora. It is the energy of these ions which gives rise to the strong auroral displays accompanying magnetic storms. These intense displays

occur usually in the evening hours in auroral latitudes.¹⁴ Vegard, Krogness, Störmer and others¹⁵ found that the lower limit of the auroral streamers was at about 100 km and of the clouds and diffuse arcs and draperies was at about 85 km. The z_c level of curve 2, Fig. 1, is at 110 km and if, instead of Maris' n, z curve for summer night which we have used to refer roughly to arctic day conditions, we use his n, z curve for winter night conditions, the ion curve 2 should be lowered about 10 km. This puts the night z_c level at 100 km. In the D region above z_c the free path of the ions is large compared to the radius of magnetic gyration. Therefore groups of D ions are guided by and outline the earth's magnetic field to form the auroral streamers. Below z_c the guidance of the magnetic field is lost, the streamers end at 100 km, and the luminosity in the S region is structureless. The S ionization falls to low values at about 10 km below z_c in accord with the observed lower boundary of the structureless luminosity at about 85 km. Altogether the agreement between the theory and the details of the aurora seems very striking.

6. THE BEARING OF THE ULTRAVIOLET LIGHT THEORY ON THE CHARGE ON THE EARTH

In general the theory of the ionization of the high atmosphere by solar ultraviolet light, and in particular those portions of the ultraviolet light theory of aurorae and magnetic storms which depend upon atmospheric ions flying at distances up to 70,000 km from the earth, and the recent theory of the zodiacal light¹⁶ would be disturbed by appreciable electric fields in the high atmosphere. Page⁹ showed that an excess charge on the earth of 72 coulombs would, if distributed in a certain way, give rise to an electric field which together with the earth's magnetic field would cause the high flying ions to swing around with the rotational velocity of the earth. They would then cause effects contrary to the experimental facts. We may conclude that if the total excess charge on the earth were greater than, say 50 coulombs, the ultraviolet light theories would be untenable, or would require considerable modification.

The earth, however, is observed to have a negative charge of about 10^5 coulombs; there is a positive electric gradient outward from the earth and an outflowing current of negative electricity in the air around us which, totalled over the earth, amounts to about 1400 amperes. The assumption of an earth electrically neutral as a whole was reconciled with these terrestrial electrical phenomena through the thunderstorm theory of C. T. R. Wilson.¹⁷ Wilson suggested, and obtained some experimental evidence in favor of his views, that the outflowing negative current is returned to the earth by thunder

¹⁴ Mawson, Australasian Antarctic Expedition 1911-14, Scientific Reports, Series B, Vol. 2, page 173 (1925).

¹⁵ Wien Harms, Handb. d. Exp. Phys. 25, 392 (1928).

¹⁶ Hulburt, Phys. Rev. 35, 1089 (1930).

¹⁷ Wilson, Trans. Roy. Soc. 221, 73 (1921); Proc. Phys. Soc. London, 37, 32D (1925); Nature 119, 502 (1927); Franklin Inst. Jr. 208, 1 (1929); etc.

clouds. Therefore we assumed (ref. 13, page 1022) that there was a positive charge in the atmosphere below, say 50 km equal to the negative charge on the earth, and approximately no excess charge and no electric field in the high atmosphere. W. Anderson's¹⁸ recent theory of the earth's negative charge assumed that positive electricity is continually annihilated in the earth thereby supplying the earth with the negative electricity necessary to maintain the observed negative charge and outflowing negative current. The theory apparently holds that the earth has an excess negative charge of something like 10^5 coulombs and that there is a strong electric field in the high atmosphere. It is seen that the ultraviolet light theory and Anderson's theory are based on conflicting assumptions and can not both be upheld at the same time.

¹⁸ Anderson, *Zeits. f. Physik* 42, 475 (1927); 44, 376 (1927).

THE DIELECTRIC CONSTANT OF AMMONIA AS A FUNCTION OF TEMPERATURE AND DENSITY

By FREDERICK G. KEYES AND JOHN G. KIRKWOOD*
RESEARCH LABORATORY OF PHYSICAL CHEMISTRY,
MASSACHUSETTS INSTITUTE OF TECHNOLOGY**

(Received October 13, 1930)

ABSTRACT

The dielectric constant of ammonia has been measured over a wide range of density at several temperatures. The Clausius-Mosotti function $(\epsilon-1)V/(\epsilon+2)$ was found to increase with increasing density. At the lower densities it was adequately represented by the following formula

$$\frac{\epsilon-1}{\epsilon+2} V = \frac{4\pi N p_0}{3} \frac{1}{1-\lambda\rho}$$

where p_0 is the molecular polarizability, ρ the density, and λ a constant expressible in terms of the equation of state constants, A and b , as

$$\frac{32\pi^2 p_0^2 N^2}{45b} \left(1 + \frac{1}{3} \frac{A}{bRT}\right).$$

Previous measurements of the dielectric constant of carbon dioxide are further discussed.

THE correlation of the molecular structure of a substance with its dielectric constant depends upon a knowledge of the average internal field effective in polarizing a molecule. A calculation of the internal field by the cavity method¹ leads to the Clausius-Mosotti equation

$$\frac{\epsilon-1}{\epsilon+2} V = \frac{4\pi N}{3} p_0 \quad (1)$$

where ϵ is the dielectric constant, V the molal volume, and N the Loschmidt number.

The molecular polarizability, p_0 , for weak fields and moderately high temperatures is given by

$$p_0 = \alpha + \frac{\mu^2}{3kT} \quad (2)$$

Here α is the sum of the electronic and atomic polarizabilities, μ the per-

* National Research Fellow.

** Contribution No. 252.

¹ Lorentz, *Theory of Electrons*, p. 305 (1923). In this method a spherical cavity is excised around a selected molecule in the dielectric. Under the assumption that the remainder of the dielectric is continuously polarized, the field acting at the center of the selected molecule is calculated as arising from an hypothetical surface charge on the interior of the cavity and on the outer boundary of the dielectric. Such an analysis appears highly artificial since in a region of molecular dimensions it is not justifiable to treat the dielectric outside the selected molecule as a continuum of polarized medium. Moreover, the influence of the fluctuations in the internal field, associated with the thermal motion of the surrounding molecules is completely ignored.

manent electric moment of the molecule, k Boltzmann's constant, and T the absolute temperature.

Although the Clausius-Mosotti relation has received adequate empirical confirmation in the case of gases at low pressures, its validity for more dense substances is open to some question. Recent measurements of the dielectric constant of carbon dioxide over a wide range of density² lead to the conclusion either that there exists a small deviation from the Clausius-Mosotti relation or that the molecular polarizability of carbon dioxide increases slowly with the density. The fact that the Clausius-Mosotti function shows itself independent of the temperature makes the existence of a dipole form of the carbon dioxide molecule in an appreciable proportion, extremely improbable. In the present article measurements of the dielectric constant of ammonia under similar conditions of temperature and density will be presented. The fact that the ammonia molecule is known to possess a permanent dipole makes these results of particular importance in supplementing the previous investigation on carbon dioxide.

EXPERIMENTAL RESULTS

The apparatus employed in the measurements has been previously described.² Except in a few minor details it was identical with that used in the measurement of the dielectric constant of carbon dioxide.

Ammonia from a commercial cylinder was purified by distillation and dried by allowing it to stand over metallic sodium for several months. It was afterwards slowly distilled into a steel reservoir in a pressure line of which the gas condenser was a part. Measurements were made at 100°, 125°, 150°, and 175°C. The results are listed in the accompanying tables.

The ammonia densities were obtained from the pressure-volume-temperature measurements of Beattie and Lawrence.³

The Clausius-Mosotti function, $(\epsilon - 1)V/(\epsilon + 2)$, has been plotted against density in Fig. 1. It will be observed that the curves for the different temperatures ascend slowly with decreasing slope as the density increases. The form of each of the curves is similar to that of the single curve obtained from the measurements on carbon dioxide at various temperatures, although the deviations from the lines

$$\frac{\epsilon - 1}{\epsilon + 2}V = f(T) \quad (2a)$$

are relatively much greater.

By extrapolation, the limiting values of the Clausius-Mosotti function at zero density were obtained. According to Eq. (1), undoubtedly valid in this limiting case.

$$\frac{\epsilon - 1}{\epsilon + 2}VT = \frac{4\pi}{3}N\alpha T + \frac{4\pi\mu^2}{9k} \quad (3)$$

² F. G. Keyes and J. G. Kirkwood, *Phys. Rev.* **36**, 754 (1930).

³ J. A. Beattie and C. K. Lawrence, *J.A.C.S.* **52**, 6 (1930).

TABLE I. *The dielectric constant of ammonia at 100°.*

Pressure (atm.)	$\epsilon - 1$	Molal volume (cc)	Density (mols/liter)	$\frac{\epsilon - 1}{\epsilon + 2} V$
20	0.0940	1385	0.72	42.07
25	.1230	1076	0.93	42.37
30	.1538	867	1.15	42.28
35	.1890	718	1.39	42.55
40	.2277	605	1.65	42.68
45	.2723	514	1.95	42.77
50	.3241	441	2.27	43.00
55	.3867	377	2.65	43.05

TABLE II. *The dielectric constant of ammonia at 125°.*

Pressure (atm.)	$\epsilon - 1$	Molal volume (cc)	Density (Mols/liter)	$\frac{\epsilon - 1}{\epsilon + 2} V$
20	0.0822	1512	0.66	40.32
30	.1318	966	1.04	40.65
40	.1892	689	1.45	40.88
50	.2568	521	1.92	41.08
60	.3381	406	2.40	41.12
70	.4396	322	3.11	41.15

TABLE III. *The dielectric constant of ammonia at 150°.*

Pressure (atm.)	$\epsilon - 1$	Molal volume (cc)	Density (mols/liter)	$\frac{\epsilon - 1}{\epsilon + 2} V$
20	0.0713	1636	0.61	37.98
30	.1125	1055	0.95	38.13
40	.1584	763	1.31	38.28
50	.2101	587	1.70	38.42
60	.2621	479	2.09	38.50
70	.3381	383	2.61	38.81
80	.4203	318	3.14	39.08
90	.5170	266	3.76	39.14
100	.6382	223	4.48	39.12

TABLE IV. *The dielectric constant of ammonia at 175°.*

Pressure (atm.)	$\epsilon - 1$	Molal volume (cc)	Density (mols/liter)	$\frac{\epsilon - 1}{\epsilon + 2} V$
20	0.0638	1753	0.57	36.49
30	.0998	1138	0.88	36.62
40	.1368	831	1.20	36.24
50	.1818	646	1.55	36.91
59	.2237	533	1.88	36.99
70	.2815	433	2.31	37.14
80	.3402	365	2.74	37.18
90	.4070	313	3.19	37.39
100	.4800	271	3.69	37.38

From the intercept of line obtained by plotting $(\epsilon - 1)VT/(\epsilon + 2)$ against T , the permanent electric moment of the ammonia molecule was calculated to be 1.44×10^{-18} e.s.u. This is in exact agreement with the value reported by Zahn⁴ from measurements of the dielectric constant of ammonia at low densities. The part of the molecular polarization independent of temperature, $4\pi N\alpha/3$, was calculated from the slope of the line to be 7.3 cc. The refractive index in the visible region, of ammonia at low densities yields a value of $(n^2 - 1)V/(n^2 + 2)$ of 5.9 cc. Due to infrared dispersion terms associated with the vibrational states of the molecule, it undoubtedly has a somewhat greater value at the frequency 1010 *k.c.*, of the present dielectric constant measurements.

DISCUSSION

In interpreting the experimental facts which have just been presented, two courses are open. We may assume either that the Clausius-Mosotti equation is valid and that the mean molecular polarizability increases with the density, or that the molecular polarizability, p_0 , remains constant and that the Clausius-Mosotti function $(\epsilon - 1)V/(\epsilon + 2)$ deviates from the molecular polarization, $(4\pi/3)Np_0$, as the density becomes great.

The first hypothesis may be justified by some very simple considerations. In a gas envisaged as an assembly of molecules in statistical equilibrium there exists a variety of possible molecular types as represented by the rotational and vibrational states of the molecule as well as by complex states arising from molecular association. The distribution among the various molecular states may be of importance in determining the mean molecular polarizability. Thus in the case of a fixed molecular dipole, the distribution among the rotational states of the molecule determines the form of the Debye term, $\mu^2/3kT$. It is possible that to the different vibrational and associational states of a molecule there correspond different atomic polarizabilities and different resultant electric moments.⁵ Moreover, if the transition energies of these states were of the order of magnitude of kT , a variation in temperature or density might be capable of producing changes in the distribution among them which would appreciably alter the mean molecular polarizability. It is therefore conceivable that an increase in density should produce an increase in the mean molecular polarizability of carbon dioxide or ammonia through the displacement of an equilibrium between molecular states of different polarizability. However, associated with this effect, a corresponding variation of polarizability with temperature would be expected, which in fact was not observed, at least for CO_2 . It is, of course to be remembered that the total observed variation of the Clausius-Mosotti function was small, and that the density range covered in the dielectric constant measurements was relatively much greater than the temperature range. It is accordingly possible that a small abnormal temperature effect associated with the observed density effect might well have escaped detection.

⁴ C. T. Zahn, *Phys. Rev.* **27**, 455 (1926).

⁵ C. T. Zahn, *Phys. Rev.* **35**, 1056 (1930); P. Debye, *Handbuch der Radiologie* p. 633 (1925).

The band spectra of both carbon dioxide and ammonia give evidence for the existence of frequencies associated with the molecular vibrational states for which $h\nu$ is of the order of magnitude of kT at $300^\circ\text{--}400^\circ\text{K}$.⁶ However, a quantitative discussion of the effect of the distribution among the various vibrational types on the mean molecular polarizability is impossible without independent information concerning the polarizabilities belonging to each type. Molecular association undoubtedly occurs in all gases to a greater or less extent and becomes increasingly important as the saturation region is approached. However, it is doubtful whether the loose coupling effective in such processes would be sufficient to influence the terms in the polarizability associated with the electrons and with the atoms. It might, however, affect the orientation of the permanent dipoles.

A deviation from the Clausius-Mosotti relation as suggested by the second hypothesis is indeed likely. Recently we have carried out a statistical calculation of the internal field which leads to the following relationship for gases up to moderately high densities

$$\frac{\epsilon - 1}{\epsilon + 2}V = \frac{4\pi}{3}Np_0 \frac{1}{1 - \lambda\rho} \quad (4)$$

where ρ is the density in mols per cubic centimeter. If for simplicity, the van der Waal's molecular model is employed, we find

$$\lambda = \frac{32N^2\pi^2p_0^2}{45b} \left(1 + \frac{1}{3} \frac{A}{bRT} \right) \quad (5)$$

where A and b are the constants of the van der Waal's type of equation of state. The constant λ has been computed and Eq. (4) has been plotted for ammonia at the various temperatures of the dielectric constant measurements. From Fig. 1 it may be seen that Eq. (4) conforms closely to the experimental curves until fairly high densities are reached. Thus at 175° , the deviation does not become appreciable until a pressure of 40 atm. is reached. The divergence of the two curves at higher densities is not surprising, for here the assumptions underlying the deduction of Eq. (4) undoubtedly begin to fail. Eq. (4) assumes that the molecules of the gas are continuously distributed in configuration, but when an appreciable fraction of the molecules are in quantized collision states arising in molecular association, this assumption loses its validity.

The application of Eq. (4) does not meet with similar success in the case of carbon dioxide. The observed deviation from the Clausius-Mosotti relation was found to be many times that predicted by Eq. (4). This may perhaps be explained in the light of the hypothesis which was first discussed. Eq. (4) assumes that the gas may be regarded as an assembly of molecules of identical polarizability. If carbon dioxide is to be regarded as a mixture of several vibrational types of different polarizability, this assumption is not justified. The abnormal behavior of the Clausius-Mosotti function may then be attributed to a variation of the mean molecular polarizability through

⁶ Dennison, *Phil. Mag.* 1, 195 (1926).

a displacement of an equilibrium between several molecular types. In this process only the infrared dispersion terms associated with the atomic oscillators would be affected. This is in accord with the fact that the refractive index of carbon dioxide in the visible region has been found to satisfy the Lorentz-Lorenz relation over a large part of the density range covered by our dielectric constant measurements.⁷

Both in the case of carbon dioxide and of ammonia, our dielectric constant measurements show a deviation from the Clausius-Mosotti relation. For ammonia, they are adequately represented up to moderately high densities by Eq. (4). For carbon dioxide Eq. (4) proves inadequate. In this case it seems necessary to assume the existence of several molecular types with different infrared dispersion terms.

⁷ P. Phillips, Proc. Roy. Soc. A47, 225 (1920).

NOTE ON THE PRODUCTION OF EXTREMELY HIGH VOLTAGES

By M. A. TUVE

DEPARTMENT OF TERRESTRIAL

MAGNETISM, CARNEGIE INSTITUTION OF WASHINGTON, WASHINGTON D. C.

(Received October 8, 1930)

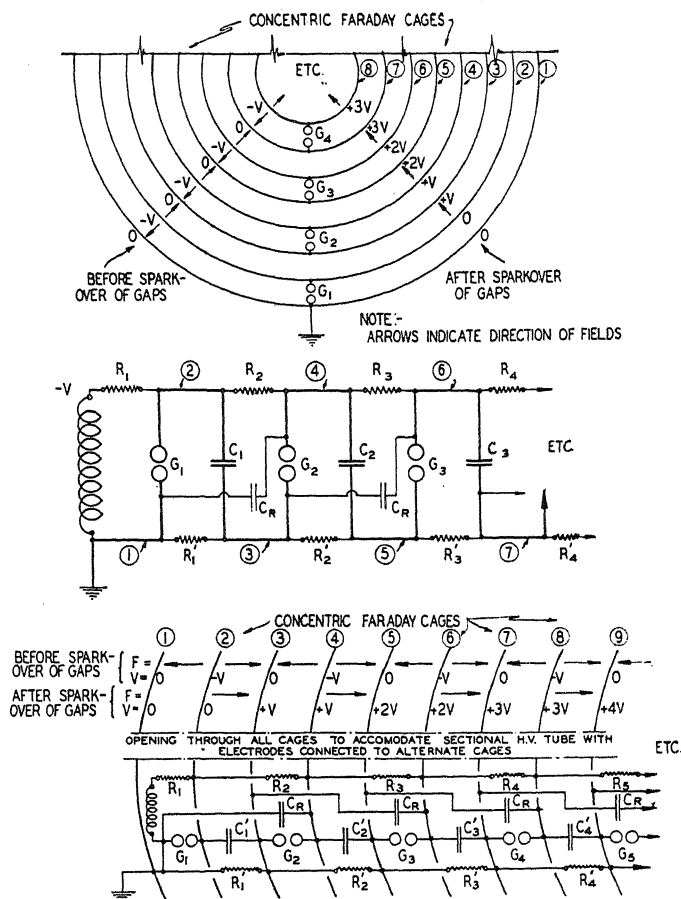
ABSTRACT

Ordinary methods for the production of high voltages for application to vacuum-tubes are satisfactory up to several million volts, but are subject to definite limitation due to corona or spark-over from the high-voltage terminal toward ground. A system of successive concentric Faraday cages, with the outermost cage grounded, is not so limited. An impulse-method for the production of extremely high voltages using such a system of Faraday cages is described. A system of $(2n+2)$ cages gives an impulse-voltage slightly less than nV on the innermost cage.

FOR many years it has become increasingly evident and recognized that a suitable artificial source of extremely high-energy particles and quanta must be developed as a tool before adequate studies of the atomic nucleus can be made. The most obvious approach to the development of such a tool has been the application of very high voltages to vacuum-tubes. Ordinary arrangements for this purpose are satisfactory for voltages up to several million volts, but it is clear that no matter what insulating medium is used a limitation is set by the corona or spark-over of the high-voltage terminal toward ground unless this point is completely surrounded by graded shields having intermediate voltages. Thus a system of successive Faraday cages, each inside of the next and charged to a higher voltage, is not subject to such a limitation. This fact of course has been long recognized. The inherent capacity between the Faraday cages, however, places very definite limitations on the type of voltage source which can be used to charge them. Using transformer-oil as an insulating medium, a voltage of even 1,000 k.v. would place unnecessarily high kilovolt-ampere requirements on the (cascaded) transformers to supply the wattless charging current. The use of kenotrons with such a system of cascaded transformers, however, charging the cages to successively higher and higher direct-current potentials, appears to be practical up to several million volts, but becomes complicated and very expensive. Voltage sources of the static-machine type for this purpose are not out of the question, but appear impractical at present for very high voltages. The familiar method of multiplication of voltage by charging condensers in parallel and discharging in series, however, has many advantages as source of intermittent high voltage. By reason of circuit time-constants, mechanical switching methods appear impractical for very high voltages,

but the impulse generator, as developed by Peek¹ and used by him for potentials up to 5 million volts is a method of obviously great possibilities. The impulse-generator used by Brasche and Lange² for high-voltage tube work is presumably of this type.

To eliminate the disadvantage of very great physical dimensions, however, and to remove the ultimate limitation on the attainable voltages



Figs. 1 to 3.—Method for the production of extremely high voltages—circuit-diagram for impulse-generator using successive Faraday cages.

with this device, it is necessary to use it in connection with successive Faraday cages. If successive units of the Peek impulse-generator are enclosed between successive Faraday cages several important difficulties are presented: The successive condensers must be connected through successive resistors to ground instead of directly, since a direct ground-lead cannot be insulated sufficiently to pass through all of the cages. This connection, how-

¹ F.W. Peek, Jr., Dielectric phenomena in high voltage engineering. 3rd ed., p.145 ff., 1929.

² Brasche and Lange, Naturwiss. 18, 16 and 765, 1930.

ever, does not cause the discharge of the first gap to throw over-voltages on the succeeding gaps, which in the Peek circuit causes the spark-overs which connect successive condensers in series. Even if provision is made to accomplish this, the capacity between cages in a few stages becomes comparable to the capacity of the condenser in each impulse-unit, and since the discharge of these condensers must elevate the successive cages in voltage with respect to each other, thus charging the inter-cage capacity, the effective multiplying power of the impulse-generator is lost after the first few stages.

In this connection, it occurred to the writer that a special type of impulse-generator could be devised which would be free from the above difficulties. The fundamental idea involved is indicated in Fig. 1. A series of "concentric" Faraday cages is charged alternately to two voltages, e.g., 0 and $-V$. The electric fields are then in opposite directions between alternate successive cages. If now a series of spark-gaps can be arranged to make sudden connections between alternate pairs of cages, all electric fields in one direction are wiped out and those in the opposite direction remain, raising the potential of each pair of cages by an amount V with respect to its predecessor, by the principle of the Faraday cage. If there are $2n+2$ cages and the outermost cage is grounded, the potential of the innermost cage will be raised to $n \cdot V$. The capacity between successive cages is thus no longer a disadvantage, being used as part of the essential capacity of the impulse-circuit.

An analysis of the original circuit devised for this purpose enabled its reduction to a form very similar to that of the Peek generator as indicated in Fig. 2, with *two* Faraday cages between successive units (eliminating the loss in "multiplying power" due to inter-cage capacity which occurs when only *one* is used), with the ground-connection made through successive resistors R_1' , R_2' , etc., instead of directly, and with the auxiliary condensers C_R added to throw an overvoltage on successive gaps when the gap G_1 first breaks. The complete circuit is shown inside of the Faraday cages in Fig. 3. The condensers C_1' , C_2' , etc., may be added between sections to make the effective capacities of all sections, including the inter-cage capacities, alike (C_1 , C_2 , etc., Fig. 2). The gaps should be sphere-gaps, to avoid time-lag and "impulse-ratio," and the condensers C_R should be no larger than is necessary to insure spark-over, e.g. 10 to 20 percent of C_1 , C_2 , etc. The addition of these condensers C_R reduces the theoretical voltage $n \cdot V$, by the amount used as overvoltage to cause the gaps to spark-over properly. It appears from consideration of time-constants that for effective charging R_1 should roughly approximate the sum of the other resistors R_2 , R_2' , R_3 , R_3' , etc. It seems most practical, perhaps, to use oil as the insulating medium between cages, with the gaps enclosed in vessels containing air. A further discussion of the practical features of the circuit and its possibilities and limitations is beyond the purpose of this note.

An opportunity has not been presented and may not arise for some time to make an adequate test of this circuit, but it has been thought worthy of calling to the attention of those interested. A test of the method has been made on a small scale, with satisfactory results.

A TWO DIMENSIONAL BOUNDARY VALUE PROBLEM FOR THE TRANSMISSION OF ALTERNATING CURRENTS THROUGH A SEMI-INFINITE HETEROGENEOUS CONDUCTING MEDIUM

BY HERBERT P. EVANS

DEPARTMENT OF MATHEMATICS, UNIVERSITY OF WISCONSIN

(Received October 13, 1930)

ABSTRACT

In this paper an infinitely long conductor parallel to the surface of a semi-infinite conducting medium is considered. The medium is supposed to consist of an upper stratum of uniform conductivity σ_1 , and having elsewhere a uniform conductivity σ_2 . The conductor is supposed to carry an alternating current for which the conducting medium forms the return path. The problem under consideration is that of determining the field vectors throughout space, subject to the condition that the frequency is sufficiently low that displacement currents may be neglected. This problem has been solved by Haberland by the case of a sufficiently thin stratum, this limitation arising through the use of approximate boundary conditions. A solution has also been given by Carson for the case of a homogeneous medium. The present treatment utilizes exact boundary conditions and permits the stratum to be of any thickness. The boundary conditions are formulated for a function ϕ which satisfied the wave equation throughout space. By means of the conditions which must hold at the surface of the conductor and at the two faces of the stratum, together with the conditions at infinity, the function ϕ may be expressed in terms of an infinite integral from which the field vectors are derivable. This integral is expanded into a convergent series of simpler integrals which are given physical interpretation.

STATEMENT OF THE PROBLEM

WE WILL consider an infinitely long overhead conductor parallel to the surface of the earth. This surface will be regarded as a plane and the earth will be regarded as a semi-infinite medium. The conductor is assumed to carry a harmonically varying current which will be taken as the real part of $Ie^{i\omega t}$, where I is a real constant. This excludes consideration of the case of displacement currents flowing in planes perpendicular to the conductor. The frequency will be supposed low enough so that axial displacement currents may also be neglected. In both the air and the earth the electric intensity vector will then be parallel to the conductor. The problem is that of determining the electric and magnetic intensities at any point of space. The solution of this problem will be an approximate solution for the case of a long overhead conductor of finite length, in the vicinity of the conductor and near its midpoint. Under these assumptions the field vectors will not vary in the z -direction, that is, in the direction of the conductor.

The foregoing problem has been solved for the case of a homogeneous earth by Carson,¹ and for the case of an earth covered by a thin conducting layer, of different conductivity from that of the earth, by Haberland.²

¹ Carson, Bell System Technical Journal, November, 1926. Carson also makes an important technical application considering attenuation due to radial displacement currents.

² Haberland, Zeits. f. Ange. Math. u. Mech. 6, (1926).

MATHEMATICAL FORMULATION OF THE PROBLEM

The Maxwell field equations are applicable to the problem in the form

$$\begin{cases} \text{curl } B = \frac{4\pi}{c}C \\ \text{curl } E = -\frac{i\omega}{c}B \\ C = \sigma E. \end{cases} \quad (1)$$

Written in this form the magnetic intensity B is expressed in c.g.s. electromagnetic units and all other quantities are in c.g.s. electrostatic units. The current density is designated by C , the conductivity by σ , the electric and magnetic intensities by E and B respectively, $(-1)^{\frac{1}{2}}$ by i , and the velocity of light by c . Let the origin of coordinates be taken at the surface of the layer and directly below the conductor. The x -axis will be taken in the surface of the layer perpendicular to a vertical plane containing the conductor, and the z -axis will be taken in the direction of the conductor. Since in our case

$$E_z = E_y = B_z = \frac{\partial}{\partial z} = 0$$

we may put $E_z = E$ and the system (1) takes the form

$$\frac{\partial B_y}{\partial x} - \frac{\partial B_x}{\partial y} = \frac{4\pi}{c}\sigma E \quad (2)$$

$$\begin{cases} \frac{\partial E}{\partial y} = -\frac{i\omega}{c}B_x \\ \frac{\partial E}{\partial x} = \frac{i\omega}{c}B_y. \end{cases} \quad (3)$$

From this point on we will consider only the electric field in our calculation, since with the aid of (3) it is clear that the magnetic field may be readily calculated therefrom. In Eq. (2) the conductivity σ is zero in the air and will be designated by σ_1 in the layer (region 1) and by σ_2 in the earth (region 2). Substitution of (3) in (2) gives

$$\nabla^2 E = \frac{4\pi\omega\sigma i}{c^2}E, \quad \text{where} \quad \nabla^2 = \frac{\partial^2}{\partial x^2} + \frac{\partial^2}{\partial y^2} \quad (4)$$

and σ , as in Eq. (2) depends upon the region of space under consideration. It should be noted that if E be determined from (4) the values of B_x and B_y are then obtainable at once from (3). Now Eq. (4) can be expressed in a simpler manner if we define

$$\gamma = \frac{c}{(4\pi\omega\sigma_1)^{1/2}}; \quad \xi\gamma = x; \quad \eta\gamma = y.$$

Then (4) becomes

$$\frac{\partial^2 E}{\partial \xi^2} + \frac{\partial^2 E}{\partial \eta^2} = i\kappa' E \quad (5)$$

where $\kappa' = 0$ in the air, $\kappa' = 1$ in the region 1 and $\kappa' = \sigma_2/\sigma_1$ in region 2.

The conductor is taken at a distance h above the surface of the layer, the thickness of which is d . Further, the distance from any variable reference point P to the conductor will be called r_0 and the distance from the same point P to the image of the conductor with respect to the surface of the layer will be called r_1 . In addition we put

$$h'\gamma = h, \quad d'\gamma = d, \quad \rho_0\gamma = r_0, \quad \rho_1\gamma = r_1.$$

The following figure then shows the system under consideration after all distances have been divided by the factor γ . In setting up the boundary conditions the radius of the conductor is assumed to be very small.

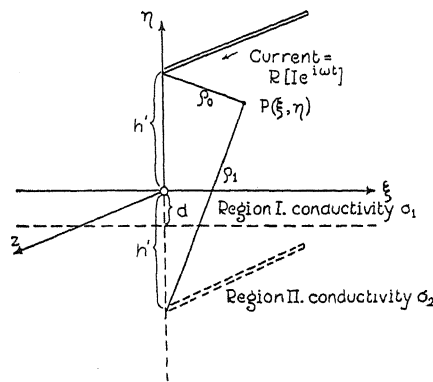


Fig. 1.

We will now formulate the boundary conditions for the system of differential Eqs. (5). At the surface of separation between the air and the layer, and at the surface of separation between the layer and the earth, the tangential components of E and B and the normal component of B must be continuous. It should be observed that the normal component of E , being everywhere zero, is of course continuous at these surfaces of separation. Now (3) may be written in the form

$$\frac{\partial E}{\partial \eta} = -\frac{\gamma i \omega}{c} B_x, \quad \frac{\partial E}{\partial \xi} = \frac{\gamma i \omega}{c} B_y$$

and therefore if $\partial E/\partial \xi$ is continuous, B_y will also be, and it is necessary only to require that $\partial E/\partial \eta$ be continuous in order to insure the continuity of B_x . The above requirements are therefore summarized by writing

$$E = E_1 \text{ and } \frac{\partial E}{\partial \eta} = \frac{\partial E_1}{\partial \eta} \text{ for } \eta = 0$$

$$E_1 = E_2 \text{ and } \frac{\partial E_1}{\partial \eta} = \frac{\partial E_2}{\partial \eta} \text{ for } \eta = -d'.$$

Two conditions remain. First, the field vectors must all be zero at infinity; that is,

$$E = 0; \eta = \infty \text{ and } E_2 = 0; \eta = -\infty$$

$$E = E_1 = E_2 = 0; \xi = \pm \infty.$$

Second, in the vicinity of the conductor the magnetic induction must approach the value.

$$|B^0| = \frac{2I}{r_0} \quad (6)$$

where B^0 denotes the primary field; i.e., the field due to the current in the wire alone. The direction of B^0 will then be normal to r_0 . By means of (3) the condition (6) may also be expressed in terms of electric intensity. For

$$B_x^0 = -\frac{2I}{r_0} \frac{y-h}{r_0} = -\frac{2I}{\gamma \rho_0^2} (\eta - h')$$

$$B_y^0 = \frac{2I}{\gamma \rho_0^2} \xi.$$

These values substituted in (3) give for the primary electric field

$$E^0 = \frac{2i\omega I}{c} \log \rho_0 + \text{constant}. \quad (7)$$

If we let E_0 denote the secondary air field; i.e., that due to earth currents, we have

$$E = E^0 + E_0$$

and since E must be zero at infinity it follows that the constant term in (7) must be zero. It will be convenient to replace the electric intensity E by a function ϕ defined by the equation

$$E = \frac{2\omega i}{c} \phi. \quad (8)$$

To summarize, then, the following boundary value problem³ is to be solved.

$$\frac{\partial^2 \phi}{\partial \xi^2} + \frac{\partial^2 \phi}{\partial \eta^2} = 0, \text{ in air} \quad (9)$$

$$\frac{\partial^2 \phi_1}{\partial \xi^2} + \frac{\partial^2 \phi_1}{\partial \eta^2} = i\phi_1, \text{ in region 1} \quad (10)$$

$$\frac{\partial^2 \phi_2}{\partial \xi^2} + \frac{\partial^2 \phi_2}{\partial \eta^2} = i\kappa \phi_2, \text{ in region 2} \quad (11)$$

³ The question of uniqueness of this boundary value problem has also been investigated and a complete uniqueness proof carried out for the case $\kappa=0$. This proof is omitted from the present paper as being chiefly of mathematical interest.

$$\phi = I \log \rho_0 + \phi_0 \quad (12)$$

$$\begin{cases} \phi = 0; \eta = \infty \text{ and } \phi_2 = 0; \eta = -\infty \\ \phi = \phi_1 = \phi_2 = 0; \quad \xi = \pm \infty \end{cases} \quad (13)$$

$$\phi = \phi_1 \text{ and } \frac{\partial \phi}{\partial \eta} = \frac{\partial \phi_1}{\partial \eta}; \eta = 0 \quad (14)$$

$$\phi_1 = \phi_2 \text{ and } \frac{\partial \phi_1}{\partial \eta} = \frac{\partial \phi_2}{\partial \eta}; \eta = -d'. \quad (15)$$

In these equations ϕ denotes the value of the ϕ -function in the air region, ϕ_1 the value in region 1, and ϕ_2 its value in region 2, while κ is used to denote the ratio of conductivities σ_2/σ_1 .

METHOD OF SOLUTION

A solution of (9) which satisfies both (12) and (13) and is symmetrical with respect to ξ is

$$\phi = I \log \frac{\rho_0}{\rho_1} + \int_0^\infty A_1(\beta) \cos \xi \beta e^{-\eta \beta} d\beta \quad (16)$$

where A_1 is an arbitrary function of β , subject to the condition that the integral exists and has second partial derivatives with respect to both ξ and η . A solution of (10) symmetrical with respect to ξ is

$$\phi_1 = \int_0^\infty A_2(\beta) e^{\alpha \eta} \cos \xi \beta d\beta + \int_0^\infty A_3(\beta) e^{-\alpha \eta} \cos \xi \beta d\beta; \quad -d' \leq \eta \leq 0 \quad (17)$$

where A_2 and A_3 are arbitrary functions of β and

$$\alpha = (\beta^2 + i)^{1/2}. \quad (18)$$

A solution of (11) which satisfies (13) and is symmetrical with respect to ξ is

$$\phi_2 = \int_0^\infty A_4(\beta) e^{\theta \eta} \cos \xi \beta d\beta; \quad \eta \leq -d' \quad (19)$$

where A_4 is an arbitrary function of β and

$$\theta = (\beta^2 + i\kappa)^{1/2}; \quad \kappa = \sigma_2/\sigma_1. \quad (20)$$

There remains to find functions A_1 , A_2 , A_3 , and A_4 which are consistent with the boundary conditions (14) and (15). In order to satisfy (14) the following equations must hold:

$$A_1 = A_2 + A_3 \quad (21)$$

$$- \int_0^\infty \beta A_1 \cos \xi \beta d\beta - 2I \frac{h'}{h'^2 + \xi^2} = \int_0^\infty \alpha (A_2 - A_3) \cos \xi \beta d\beta \quad (22)$$

In order for (15) to be satisfied we must have

$$A_2 e^{-\alpha d'} + A_3 e^{\alpha d'} = A_4 e^{-\theta d'} \quad (23)$$

$$\alpha(A_2 e^{-\alpha d'} - A_3 e^{\alpha d'}) = \theta A_4 e^{-\theta d'}. \quad (24)$$

These three algebraic equations and one integral equation are sufficient to determine the four unknown functions. We will first replace the integral Eq. (22) by an equivalent algebraic equation. Using Fourier's integral, we have

$$\frac{1}{h'^2 + \xi^2} = \frac{2}{\pi} \int_0^\infty d\beta \int_0^\infty \frac{\cos \xi \beta \cos \lambda \beta}{h'^2 + \lambda^2} \cdot d\lambda = \frac{1}{h'} \int_0^\infty e^{-\beta h'} \cos \xi \beta \cdot d\beta.$$

Substitution of this result in (22) gives

$$\beta A_1 + 2I e^{-\beta h'} = \alpha(A_3 - A_2). \quad (25)$$

If (21), (25), (23), and (24) are solved for A_1 , A_2 , A_3 , and A_4 the results are the following:⁴

$$A_1(\beta) = 2I e^{-\beta h'} \frac{e^{-\alpha d'}(\theta - \alpha) - e^{\alpha d'}(\theta + \alpha)}{e^{-\alpha d'}(\theta - \alpha)(\alpha - \beta) + e^{\alpha d'}(\theta + \alpha)(\alpha + \beta)} \quad (26)$$

$$A_2(\beta) = 2I e^{-\beta h'} \frac{e^{\alpha d'}(\alpha + \theta)}{e^{-\alpha d'}(\alpha - \theta)(\alpha - \beta) - e^{\alpha d'}(\alpha + \theta)(\alpha + \beta)} \quad (27)$$

$$A_3(\beta) = 2I e^{-\beta h'} \frac{e^{-\alpha d'}(\alpha - \theta)}{e^{-\alpha d'}(\alpha - \theta)(\alpha - \beta) - e^{\alpha d'}(\alpha + \theta)(\alpha + \beta)} \quad (28)$$

$$A_4(\beta) = 4I e^{-\beta h'} \frac{\alpha e^{\theta d'}}{e^{-\alpha d'}(\alpha - \theta)(\alpha - \beta) - e^{\alpha d'}(\alpha + \theta)(\alpha + \beta)} \quad (29)$$

Substitution of (26) in (16) gives,

$$\phi = I \log(\rho_0/\rho_1) + 2I \int_0^\infty \left[\frac{e^{-\alpha d'}(\theta - \alpha) - e^{\alpha d'}(\theta + \alpha)}{e^{-\alpha d'}(\theta - \alpha)(\alpha - \beta) + e^{\alpha d'}(\theta + \alpha)(\alpha + \beta)} \right] e^{-\beta(h' + \eta)} \cos \xi \beta d\beta. \quad (30)$$

In order to evaluate the integral in Eq. (30) a considerable advantage is gained, both from the standpoint of computation and of interpretation, if we put

$$\delta = \frac{\theta - \alpha}{\theta + \alpha} e^{-2\alpha d'}$$

and then expand the integrand in a series as follows:⁵

⁴ If these values of A_1 , A_2 , A_3 and A_4 are substituted in Eqs. (16), (17) and (19) it can be shown that the resulting integrals are convergent.

⁵ An independent study of Eq. (31) shows that it is legitimate to integrate this series term by term.

$$\begin{aligned}
\phi &= I \log \frac{\rho_0}{\rho_1} - 2I \int_0^\infty \frac{1-\delta}{\alpha+\beta} \frac{1}{1+\delta\left(\frac{\alpha-\beta}{\alpha+\beta}\right)} e^{-\beta(h'+\eta)} \cos \xi\beta d\beta \\
&= I \log \frac{\rho_0}{\rho_1} - 2I \int_0^\infty \left[\frac{1}{\alpha+\beta} \right. \\
&\quad \left. + \frac{2\alpha}{(\alpha+\beta)^2} \sum_{n=1}^\infty (-1)^n \delta^n \left(\frac{\alpha-\beta}{\alpha+\beta}\right)^{n-1} \right] e^{-\beta(h'+\eta)} \cos \xi\beta d\beta.
\end{aligned} \quad (31)$$

If only the first two terms of the series of integrals are taken, we have the approximate result

$$\begin{aligned}
\phi &= I \log \frac{\rho_0}{\rho_1} - 2I \int_0^\infty \frac{\cos \xi\beta}{\alpha+\beta} e^{-\beta(h'+\eta)} d\beta \\
&\quad - 4I \int_0^\infty \frac{\alpha(\alpha-\theta) \cos \xi\beta}{(\alpha+\beta)^2(\alpha+\theta)} e^{-(h'\beta+\eta\beta+2\alpha d')} d\beta.
\end{aligned} \quad (32)$$

In case the two conductivities σ_1 and σ_2 are equal, it is seen from (18) and (20) that $\alpha = \theta$, and the last term of (32) vanishes. The electric intensity then may be written in the form

$$E = \frac{2i\omega I}{c} \log \frac{\rho_0}{\rho_1} + \frac{4\omega I}{c} \int_0^\infty (\beta - (\beta^2 + i)^{1/2}) \cos \xi\beta e^{-\beta(h'+\eta)} d\beta.$$

This expression for the electric intensity agrees with that given by Carson for the homogeneous case.

Referring to Eq. (32), the first term only would be present if the conductivity of the earth were infinite; the second term arises due to its finite conductivity; and the third term arises on account of the difference in conductivities between the earth and the layer. The infinite series of integrals, which is necessary for the exact solution, converges very rapidly in case the layer is thick or in case the two conductivities are nearly equal.⁶

CALCULATION OF THE AIR FIELD FOR THE SPECIAL CASE WHEN $\kappa = 0$

It is of interest to compare the air field in the case of a homogeneous earth with the field obtained when only an upper stratum of the earth is conducting. Now Eq. (32) may be written

$$\begin{aligned}
\phi &= I \log \frac{\rho_0}{\rho_1} + 2Ii \int_0^\infty (\alpha - \beta) e^{-\beta p} \cos \xi\beta d\beta \\
&\quad - \frac{4Ii}{1-\kappa} \int_0^\infty [\alpha(\theta - \alpha)^2(\alpha - \beta)^2 e^{-\beta p - 2\alpha d'} \cos \xi\beta d\beta]
\end{aligned}$$

⁶ In fact, an upper bound for the error made if the three terms of (32) are used for computing ϕ is found to be

$$\frac{(\kappa-1)^2 e^{-2(\kappa)^{1/2} d'}}{(1+(\kappa)^{1/2})^2 \{ (1+(\kappa)^{1/2})^2 - |\kappa-1| e^{-2(\kappa)^{1/2} d'} \}} \left[\frac{1}{(h'+\eta)^2} + \frac{1}{h'+\eta} \right].$$

where

$$p = h' + \eta.$$

Now let

$$\begin{aligned} J_0 &= \int_0^\infty (\alpha - \beta) e^{-p\beta} \cos \xi \beta d\beta \\ J_1 &= \frac{1}{1 - \kappa} \int_0^\infty \alpha (\theta - \alpha)^2 (\alpha - \beta)^2 e^{-p\beta - 2\alpha d'} \cos \xi \beta d\beta. \end{aligned} \quad (33)$$

Then

$$\phi = I \log \frac{\rho_0}{\rho_1} + 2IiJ_0 - 4IiJ_1. \quad (34)$$

For the case in which only the layer is conducting, we have $\kappa=0$ and $\theta=\beta$, so there results in this case

$$J_1 = \int_0^\infty \alpha e^{-p\beta - 2\alpha d'} (\alpha - \beta)^4 \cos \xi \beta d\beta. \quad (35)$$

Now if we put

$$\alpha = r e^{i\lambda}$$

it may be shown that

$$r = (\beta^4 + 1)^{1/4}, \quad \lambda = \tan^{-1} \frac{((\beta^4 + 1)^{1/2} - \beta^2)^{1/2}}{((\beta^4 + 1)^{1/2} + \beta^2)^{1/2}}$$

and also that

$$\alpha - \beta = (\tau - (\tau^2 - 1)^{1/2})^{1/2} \cdot e^{i\chi}$$

where

$$\tau = \beta^2 + (\beta^4 + 1)^{1/2} \quad \text{and} \quad \chi = \tan^{-1} \frac{r \sin \lambda}{r \cos \lambda - \beta}.$$

It can also be shown that

$$e^{-2\alpha d'} = e^{-2r(\cos \lambda + i \sin \lambda) d'} \quad (36)$$

Now for brevity we put

$$P_1 = (\tau - (\tau^2 - 1)^{1/2})^{1/2}, \quad P_2 = ((\beta^4 + 1)^{1/2} - \beta^2)^{1/2}, \quad P_3 = ((\beta^4 + 1)^{1/2} + \beta^2)^{1/2}$$

With these substitutions we obtain

$$\begin{aligned} \sin \lambda &= \frac{P_2}{(2)^{1/2} r}, \quad \cos \lambda = \frac{P_3}{(2)^{1/2} r} \\ \alpha(\alpha - \beta)^4 &= r(\tau - (\tau^2 - 1)^{1/2})^2 e^{i(\lambda + 4\chi)}. \end{aligned}$$

Consequently, if this equation and Eq. (36) are substituted in (35), we obtain, after simplification,

$$J_1 = J_1^{(1)} + iJ_1^{(2)} \quad (37)$$

where $J_1^{(1)}$ and $J_1^{(2)}$ are both real and are defined by the equations

$$\begin{cases} J_1^{(1)} = \int_0^\infty r P_1^4 \cos(\lambda + 4\chi - 2rd' \sin \lambda) e^{-(p\beta + 2rd' \cos \lambda)} \cos \xi \beta d\beta \\ J_1^{(2)} = \int_0^\infty r P_1^4 \sin(\lambda + 4\chi - 2rd' \sin \lambda) e^{-(p\beta + 2rd' \cos \lambda)} \cos \xi \beta d\beta. \end{cases} \quad (38)$$

In like manner it may be shown that

$$J_0 = J_0^{(1)} + iJ_0^{(2)} \quad (39)$$

where $J_0^{(1)}$ and $J_0^{(2)}$ are both real and are defined by the equations

$$\begin{cases} J_0^{(1)} = \int_0^\infty P_1 \cos \chi e^{-p\beta} \cos \xi \beta d\beta \\ J_0^{(2)} = \int_0^\infty P_1 \sin \chi e^{-p\beta} \cos \xi \beta d\beta. \end{cases} \quad (40)$$

Substitution of (37) and (39) in (34) gives

$$\phi = I \left\{ \log \frac{\rho_0}{\rho_1} - 2J_0^{(2)} + 4J_1^{(2)} \right\} + 2iI \{ J_0^{(1)} - 2J_1^{(1)} \}$$

or, using Eq. (8), the electric intensity in the air is given by the equation

$$E = E^{(1)} + iE^{(2)} = (\{E^{(1)}\}^2 + \{E^{(2)}\}^2)^{1/2} \{ \cos \psi + i \sin \psi \}$$

where

$$\begin{aligned} E^{(1)} &= \frac{4\omega I}{c} \{ 2J_1^{(1)} - J_0^{(1)} \} \\ E^{(2)} &= \frac{2\omega I}{c} \left\{ \log \frac{\rho_0}{\rho_1} - 2J_0^{(2)} + 4J_1^{(2)} \right\} \\ \psi &= \tan^{-1} \frac{E^{(2)}}{E^{(1)}}. \end{aligned}$$

Finally, multiplying the electric intensity by the time factor $e^{i\omega t}$ and then taking the real part of the result, gives

$$R\{Ee^{i\omega t}\} = (\{E^{(1)}\}^2 + \{E^{(2)}\}^2)^{1/2} \cdot \cos(\omega t + \psi).$$

The determination of E^1 and E^2 depends upon the evaluation of the integrals of (38) and (40). These integrals are easily evaluated graphically with the aid of the following table in which those quantities appearing in the integrands which depend on β alone are tabulated.

In this table the substitutions

$$\Delta = \lambda + 4\chi - 2rd' \sin \lambda \text{ and } g = p\beta + 2rd' \cos \lambda$$

have been made.

TABLE I.

β	P_1	rP_1^4	x	Δ	g
0	1.00	1.00	45°	3.92-1.414 d'	1.414 d'
0.125	0.918	0.712	50° 6'	4.28-1.404 d'	0.125 p +1.424 d'
0.25	0.839	0.496	55° 6'	4.60-1.37 d'	0.25 p +1.456 d'
0.50	0.693	0.234	64°21'	5.15-1.25 d'	0.5 p +1.6 d'
1.00	0.463	0.055	77°39'	5.81-0.912 d'	p +2.2 d'
2.00	0.222	0.0049	86°34'	6.16-0.5 d'	2 p +4.03 d'

To take a definite example we will calculate the electric intensity at the surface of the earth directly below the conductor. The frequency will be taken as 1000 cycles per second, the conductivity of the layer as 9×10^8 electro-static units, the height of the conductor as 1000 cm, and the layer thicknesses d will be taken as 10, 500, 1000, 1500, and 2000 cm respectively. We have in this case

$$\omega = 2\pi f = 6.28 \times 10^3 \text{ rad./sec.}$$

$$p = h' + \eta = h' = \frac{h}{c}(4\pi\omega\sigma_1)^{1/2} = 0.281$$

$$d' = \frac{d}{c}(4\pi\omega\sigma_1)^{1/2} = 2.81 \times 10^4 d$$

$$\eta = 0, \xi = 0.$$

Using the above values for p and ξ , we find by graphical integration

$$J_0^{(1)} = 0.343 \text{ and } J_0^{(2)} = 0.980.$$

Similarly, corresponding to the various values of d , we find the following values:

TABLE II.

d	d'	$-J_1^{(1)}$	$-J_1^{(2)}$	$-E^{(1)}$	$-E^{(2)}$	$ E $
10	0.0028	0.0135	0.2785	0.370	1.537	1.58
500	0.14	0.0686	0.2089	0.480	1.398	1.48
1000	0.28	0.0822	0.1530	0.507	1.286	1.38
1500	0.42	0.0883	0.1148	0.520	1.210	1.31
2000	0.56	0.0891	0.0729	0.521	1.126	1.24
∞	∞	0	0	0.343	0.980	1.04

In this table the intensities were calculated aside from the constant factor $4\omega I/c$. This table shows that the electric intensity is approximately 50 percent greater at the surface of the conducting layer 10 cm thick than it is at the surface of the infinitely thick conductor having the same conductivity.

It will be observed from Table I that the evaluation of the integrals depends only on the parameters p , d' , and ξ instead of upon the six original parameters ω , h , η , ξ , σ_1 , and d' . This reduction in the number of parameters, together with the partial evaluation of the integrands in Table I, effects a considerable simplification in computation and makes possible the study of the behavior of the field as a function of one or more of its controlling factors.

LETTERS TO THE EDITOR

Prompt publication of brief reports of important discoveries in physics may be secured by addressing them to this department. Closing dates for this department are, for the first issue of the month, the twenty-eighth of the preceding month; for the second issue, the thirteenth of the month. The Board of Editors does not hold itself responsible for the opinions expressed by the correspondents.

Polarization of Mercury Lines in Stepwise Radiation

The polarization of several mercury lines appearing in fluorescence when a mixture of nitrogen and mercury vapor is radiated by light from a quartz mercury arc has been investigated. Wood and others have shown that when a mixture of mercury vapor and a few millimeters of nitrogen is radiated by a quartz mercury arc giving an unreversed resonance line (2^3P_1), mercury atoms in the normal (1^1S_0) state are raised by absorption of this line to the excited (2^3P_1) state where they collide with nitrogen molecules causing a large fraction of them to revert to the metastable (2^3P_0) state. These metastable mercury atoms, having a long mean life, may absorb other lines from the arc, thus carrying them to various higher states from which they may radiate a diversity of lines. We shall call this process "stepwise excitation."

In the present experiments a quartz tube containing mercury vapor at room temperature and 3 mm pressure of nitrogen was radiated by a water cooled and magnetically deflected quartz mercury arc. The fluorescence produced was observed at right angles to the exciting beam, and was tested for polarization by means of a Savart Plate, a Quartz Glans Prism and a small quartz spectrograph previously described.¹ By this method any line of the fluorescence showing more than a few percent polarization will appear on the spectra plate crossed by fringes perpendicular to the line, which will be more or less distinct depending on the degree of polarization of the line. The fluorescence tube was placed in a magnetic field parallel to the exciting beam. Mercury atoms reaching the 2^3S_1 state from the 2^3P_0 by absorption of the line 4047 from the arc, radiate 4047, 4358 and 5461 (not registered on plate used). The 3^3D_1 state is reached in the same manner by absorption

of 2967, from which 2967, 3131, and 3663 are radiated. A reproduction of a typical plate is seen below (Fig. 1). The lines 4047, 4358, 2967 and 3131 are all crossed by fringes, while the line at 3660 is not. The fringes on 4047 and 2967 are very distinct, indicating a large degree of polarization while those on 4358 and 3131 are indistinct showing only partial polarization. Moreover, the maxima

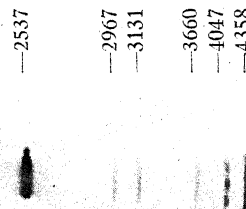


FIG. 1

of intensity of fringes on 3131 are at the same position as the minima on 2967, showing that they are polarized perpendicularly to each other. This is easily seen on the original plate but may not show distinctly on the reproduction. The line 4047 is strongly polarized corresponding to 2967, and 4358 is partially polarized perpendicularly to it, analogous to 3131.

These results can be explained by a consideration of the Zeeman levels for each line in question and their relation to the polarization of resonance radiation. The polarization of the lines 4047 ($2^3S_1 \rightarrow 2^3P_0$) and 4358

¹ A. C. G. Mitchell, Journ. Frankl. Institute 209, 747 (1930).

($2^3S_1 \rightarrow 2^3P_1$) have been explained by Hanle and Richter² who showed experimentally that with a magnetic field parallel to the exciting beam, 4047 was 100% polarized with its electric vector perpendicular to the magnetic field and 4358 33% polarized with its electric vector parallel to the field, in agreement with the theory. From the known Zeeman levels of 2967 ($3^3D_1 - 2^3P_0$) and 3131 ($3^3D_1 - 2^3P_1$), it is easy to show theoretically that 2967 should be 100% polarized corresponding to 4047 and 3131 33% corresponding to 4358. These experiments are in qualitative agreement with the theory.

It has further been shown, by using a large quartz spectrograph (Hilger E_1), that the line seen at 3131 on the small spectrograph is actually that line and not a composite of 3131 and 3125, the latter line being absent or at any rate very weak compared to 3131 in the fluorescence. The line at 3660 is a com-

posite of 3650, 3654 and 3663 and therefore shows no polarization.

The fact that the line 2967 is largely polarized (practically 100%) when 3 mm of nitrogen is present means that the 3^3D_1 state has a short mean life, for a calculation based on the time between collisions of mercury atoms and N_2 molecules shows that the mean life is probably 10^{-8} sec or less. The work is being continued with a view to measuring the mean life of this 3^3D_1 state by a magnetic depolarization experiment and will be reported in detail at a later time in this Journal.

ALLAN C. G. MITCHELL

Bartol Research Foundation
of the Franklin Institute.

October 24, 1930.

² W. Hanle and F. Richter, *Zeits. f. Physik* **54**, 811, (1929).

On the Attempt to Detect Collisions of Photons

A. L. Hughes and G. E. M. Jauncey (*Phys. Rev.* **36**, 772, (1930)) describe some experiments intended to detect the self-scattering of light bundles due to collisions of photons. Some years ago similar experiments were performed and published by me in Russian (*Jour. russ. phys. chem.* **60**, 555, 1928) with the same negative results. Light of condensed sparks was used, its momentum intensity being much greater than that of condensed sun light as used by the American authors. At the same time it was pointed out that experiments of this kind are unnecessary.

Phenomena in the neighborhood of the sun give us much more information about the subject. Very intense bundles meet and intercross near the sun's surface. In case collisions of photons exist—light in the neighborhood of the sun must be powerfully scattered. We know that near the sun some scattered light really exists—it is the solar corona.

From data about the intensity of the corona and from the law of distribution of its intensity as a function of the distance from the sun it is easy to calculate that the coefficient of the scattering near the sun is of the order 10^{-17} . Theories advanced about the corona explain this scattering as a scattering of sun light by atoms or electrons.

But even if we had some reasons to ascribe the corona to the hypothetical self-scattering of photons, its value (10^{-17}) must be so small that it is hopeless to detect it with terrestrial experiments. The effective radius of photons must be smaller than 10^{-20} cm.

The principle of superposition of the incoherent light bundles is also fulfilled with great accuracy.

S. VAVILOV

The States Electrotechnical Institut
U.S.S.R. Department of Physics.

October, 1930.

A Note on Zeeman Patterns

Many Zeeman patterns are quite unresolvable, even with powerful apparatus, and appear as spurious triplets or quartets, according as $\Delta J = \pm 1$ or 0. Shenstone and Blair,¹ assuming that in this case the measured position coincides with the theoretical center of intensity of the unresolved pattern, have derived formulae which are of great utility in

determining g -values from observations of complex spectra. The present note calls attention to the very simple values which the unresolved shifts assume when the g 's follow Landé's formula.

If B_σ , B_π are the mean displacements of

¹ *Phil. Mag.* **8**, 765-771 (1929).

the groups of σ or π components, J , $J+\Delta J$ the inner quantum numbers, and g_1 , g_2 the magnetic factors, their formulae may be written (after a little algebra)

$$\Delta J = -1 \quad 2B_\sigma = (J+1)g_1 - (J-1)g_2$$

$$B_\pi = 0$$

$$\Delta J = 0 \quad 2B_\sigma = g_1 + g_2$$

$$(4/3)B_\pi = \pm (g_1 - g_2) \frac{J(J+1)}{J + \frac{1}{2}} F.$$

When J is integral, $F=1$; when J is half-integral (even multiplicity) $J=1-(1/16)J^2$ ($J+1$)². This factor lies between 0.995 and 1, and may be neglected, except when $J=\frac{1}{2}$.

Substituting Landé's value, $g=3/2 + [S(S+1) - L(L+1)]/2J(J+1)$ and using J , L to denote always the *greater* of the two values involved in a transition, we find easily

	B_σ	B_π
Ordinary multiplets	$\frac{3}{2} - L/2J$	0
Diagonal lines		

	B_σ	B_π
First satellites	$\frac{1}{2}(g_1 + g_2)$	$3L/(2J+1)^*$
Second satellites	$\frac{3}{2} + L/2J$	0
Symmetrical multiplets		
Diagonal lines	g	0
Satellites	$\frac{3}{2}$	0

*When $J=\frac{1}{2}$, $B_\sigma=(4/3)L$

These formulae are remarkably simple. It is noteworthy that they do not involve S , except in the case of B_σ when $\Delta J=0$. It is only in this case that unresolved patterns can give any information about the multiplicity.

Even for resolved patterns, B_σ has a definite physical meaning; it is the weighted mean magnetic shift for all the radiation of a given state of polarization. It is noteworthy that these quantities come much nearer to satisfying Runge's rule of "simple denominators" than do the shifts for individual components.

HENRY NORRIS RUSSELL

Princeton University,
October 24, 1930.

Raman Effect of HBr and HI

With R. W. Wood's method (Phil. Mag. 7, 744 (1929)), a long mercury arc and a long tube containing gas at atmospheric pressure, we have measured modified lines scattered by HBr and HI, using a Hilger constant deviation spectrograph and iron arc standards. HBr lines were scattered from 4047 and 4358, HI from 4358 only, as all radiation of shorter wave-length had to be filtered out to decrease photochemical decomposition.

The shifts of the Raman lines, corresponding to (0, 1) vibrational transitions, are, according to these measurements: HBr 2556, HI 2233 vacuum wave-numbers. The value

of the center of the HBr vibration—rotation band is, according to Imes (Astrophys. J. 50, 251 (1919)), 2559. The center of the vibration—rotation band of HI has yet to be determined in absorption, though Czerny (Zeits. f. Physik 44, 235 (1927)) concluded that his measurements indicated it around 4.4μ (about 2270 wave numbers).

E. O. SALANT
A. SANDOW

Washington Square College,
New York University.
October 25, 1930.

Absorption and Collision Broadening of Resonance Radiation

In a recent paper in the Physical Review,¹ an expression was given for the optical absorption coefficient of a gas under conditions in which Doppler broadening of the absorption line was superimposed on collision broadening. The object of this letter is to mention that a similar expression was given by F. Reiche in a paper² with which I was not acquainted at the time. It can be readily shown

that the two expressions are mathematically identical.

M. W. ZEMANSKY

Kaiser Wilhelm Institut
für Physikalische Chemie,
Berlin-Dahlem, October 20, 1930.

¹ Zemansky, Phys. Rev. 36, 219 (1930).

² Reiche, Verh. d. D. Phys. Ges. 15, 3 (1913).

On the Incomplete Polarization of the Mercury Resonance Radiation

It has been shown by Ellett and McNair (Phys. Review 31, 180, 1928), that the incomplete polarization (80%) of the mercury resonance radiation in zero magnetic field is

due to the unpolarized radiations of the two outer components of the hyperfine structure of the 2537A mercury resonance line. According to these authors, the unpolarized part

of the resonance radiation is due to the absorption of the short wave-length component (-25.4 mA). This view was based on the fact, that the radiation is completely polarized in more intense magnetic fields, for which the short wave-length component is probably not absorbed, because it shifts in the direction of longer wave-lengths (parallel Zeeman component; observations in emission made by Mc Nair).

On the basis of this interpretation the author has hoped to obtain a totally unpolarized resonance radiation in zero magnetic field by irradiating the mercury vapor only with the short wave-length outer component of the resonance line of mercury. The study of Zeeman effect of the 2537 Å line in absorption made by the author last summer has shown, that this component in fact shifts for intense magnetic fields in the direction of longer wave-lengths and that we can in a very simple way let pass through the absorption cell only this single component (in magnetic fields parallel or perpendicular to the electric vector of the transmitted light) and let it irradiate a resonance vessel with mercury vapor. Observations made with resonance radiation excited monochromatically in this way at room tem-

perature and zero magnetic field (great care was taken to compensate the earth and stray magnetic fields) has shown, that the degree of polarization of this radiation is not smaller than for the resonance radiation excited with all five hyperfine structure components.

The measurements of the rotation of the polarization plane in weak magnetic fields lead to the same value 1.05×10^7 sec. for the mean life-time of the excited atoms when the fluorescence is excited by the outer component only, and when all five components are used for excitation.

The described experiments show, that these phenomena are more complicated than it has been supposed, and that it is necessary to extend the investigations to lower temperatures and to study the fine structure of the monochromatically excited resonance radiation. The author proposes to proceed with these investigations. A full report of the results already obtained will appear shortly in the Bulletin de l'Académie Polonaise (Cracovie).

S. MROZOWSKI

Physical Laboratory of the Society
of Sciences and Letters, Warsaw.

October, 17, 1930.

On the Entropy of Hydrogen

There has recently appeared a paper by D. MacGillavry "On the Entropy of Hydrogen" (Phys. Rev. 36, 1398 (1930)). The zero point (?) entropy of ordinary hydrogen with its 1:3 para, ortho mixture has been correctly calculated for certain assumed conditions by a lengthy but conventional method. Equilibrium hydrogen is carried from the absolute zero to some high temperature from which it is cooled as ordinary hydrogen with suspended equilibrium between the ortho and para forms. The resulting value was, as stated, in agreement with the value previously given by us (J. Am. Chem. Soc. 50, 3221 (1928)), namely 4.39 calories per degree per mole for the entropy of mixing of the two forms at low temperatures.

However MacGillavry states "They consider ordinary hydrogen at the absolute zero as a mixture of para-hydrogen and of nine species of ortho-hydrogen, in accordance with the weight factor 3×3 of the lowest ortho state. Although our final result is the same, Giaque and Johnston's interpretation of quantity (9a) as a paradox term does not

seem *a priori* plausible." Others have raised the same objection to the method used by us. For example—Rodebush (Proc. Nat. Acad. Sci. 15, 678 (1919)) has stated "Giaque and Johnston consider that there are ten varieties of molecules present at low temperatures and that the entropy should be increased by the entropy of mixing of these varieties. It seems doubtful if the entropy of a system of molecules which is not in statistical equilibrium can be calculated from *a priori* considerations."

The point involved in these identical criticisms is one that has wide application in the calculation of entropy and for this reason we consider further discussion desirable. Also the inference is that the results of calculations in which we expect to use the same method may be unreliable. We will not repeat the correct and simple numerical calculation given in our paper, but will call attention to an additional discussion of this subject by one of us which will soon appear in the Journal of the American Chemical Society (probably December). However we believe we can make

our point clear by means of a few brief remarks. Our point may be illustrated by considering any ideal system consisting, for example, of one or more chemical species of atoms or molecules distributed between rotational, vibrational, electronic or nuclear states. Whether these states are under complete equilibrium conditions or not we have an ideal solution of the various quantum species and *if the average number in each of the molecular states is known*, the entropy can be simply and rigorously calculated by means of the well-known formula for the entropy of mixing.

Let us consider a mixture consisting of one half mole each of hydrogen and helium gases. The absolute entropy is $R \ln 2$, the entropy of mixing, above that which these gases would have in their pure states at the same total pressure. However if our critics were consistent they would say that we could not plausibly determine the entropy in this way but must await the time when human ingenuity discovers an equilibrium path for the interconversion of hydrogen and helium. This would involve a knowledge of such excited states of our system as would be necessary for calculating the equilibrium path, for example excited states of the helium nucleus which may well exist as intermediate states. This is absurd. It is perfectly evident to us that the entropy of our system is determined by those quantum states which are present in appreciable concentrations according to any accuracy we require.

When the state of a system is known the entropy is known and unless we desire mathematical exercise we are not for our purpose necessarily concerned with the method by which a state arrived or could arrive at its condition. Changes that would take place if they could take place have nothing to do with the plausibility of an *a priori* calculation of the entropy of the particular state under consideration. If this were not so the calculation of entropy would indeed be in an unfortunate position since most of our known molecules and elements appear to be unstable with respect to others.

In our original paper we made it clear that while the usual extrapolation used in connection with the third law of thermodynamics would require the addition of 4.39 entropy

units, yet if the 1:3 mixture were to be cooled to the absolute zero under a limited equilibrium which would not permit interchange of ortho and para-hydrogen, that the system would nevertheless approach zero entropy. This would occur by relative instability of multiplets at very low temperatures, specific combination or separation into pure phases. This will happen in any solution if time is given for the attainment of that sort of equilibrium. That this precaution in our statement was well taken has been shown by the experimental results of Simon, Mendelssohn and Ruhemann (Naturwiss. 18, 34 (1930)) showing that in the liquid helium temperature range the heat capacity of mixtures of ortho and para-hydrogen increases with decreasing temperature. This is the beginning of the disposal of the 4.39 entropy units in the case of the ordinary mixture. However the combined attainment of sufficiently low temperatures, and high enough, rates of transformation to permit nearly complete experimental demonstration is very doubtful. See the interesting discussion of Pauling (Phys. Rev. 36, 430 (1930)).

We quote from the forthcoming paper mentioned above.

The absolute entropy of hydrogen is 33.98 E.U. at 298.1°K. The entropy calculated from statistics for the value which should be given by $\int_{0}^{298.1^{\circ}\text{K}} c_p d \ln T$ including a Debye extrapolation below 10°K is 33.98 - 4.39 = 29.59 E.U. The value calculated from experimental data is in excellent agreement, namely 29.7 ± 0.1 E.U.

Since the practical application of the third law of thermodynamics ignores the entropy effect due to nuclear spin in all known cases except that of hydrogen, it is suggested that the value 33.98 - $R \ln 4$ the (nuclear spin effect) = 31.23 E.U. be used in third law calculations.

We would like to thank Dr. MacGillavry for sending us the galley proof of his paper.

W. F. GIAUQUE
H. L. JOHNSTON

Chemical Laboratory of the University of California, Berkeley, California.

Chemical Laboratory of the Ohio State University, Columbus, Ohio.

October 28, 1930.

BOOK REVIEWS

A Manual of Experiments, to accompany A First Course in Physics for Colleges. MILLIKAN, GALE AND EDWARDS. Pp. 221, figs. 134. Ginn and Company, Boston, 1930. Price \$1.00.

In this manual are described fifty-five laboratory experiments, designed particularly to accompany a course based on the text by the same authors. The manual may, however, be easily used with another text as rather complete descriptions and discussions are given and the references given to the text could be changed by the instructor to another text.

The experiments are in general carefully selected and designed to give the student a definite conception of some physical principle. An exception is the experiment illustrating the second law of motion. In the first place, it seems to the reviewer as impossible logically to prove by experiment that $\text{force} = ma$ as to prove $\text{momentum} = mv$, that is, to prove a definition. However, for pedagogical purposes, an experiment on the second law perhaps should be included in a laboratory course, but the one in this text is none too clearly described. The essential part of the experiment is the measurement of the acceleration of a body down an inclined plane set at different angles. A weight (mg) is first attached to the body in such a manner that it must be raised as the body moves down the plane. This weight is adjusted so that the body moves without acceleration ($f = ma = 0$), then the weight is removed and the acceleration measured.

Suggested forms for the record of the experiment, preliminary questions and related exercises are given. The apparatus required is usually simple and inexpensive.

J. W. BUCHTA

Wave Mechanics. ARNOLD SOMMERFELD. Translated by Henry L. Brose. Pp. 304, figs. 33. E. P. Dutton and Company, New York, 1930.

This is the English translation of the "Wellenmechanische Ergänzungsband" of Sommerfeld's "Atombau und Spektrallinien" which was reviewed in this department last year (Phys. Rev. 33, 869 (1929)). The English edition is to some extent also a revision, several inaccuracies having been corrected and three notes added dealing with the photoelectric effect of atoms and the continuous spectrum of atomic hydrogen.

A very commendable feature is the index of German expressions commonly used in this field with their English equivalents.

It is of some interest to me (though perhaps to very few others) to note that Sommerfeld has allowed my remark on group velocity in the simple Zeeman effect to stand (p. 121) even though it was dismissed as "nicht stichhaltig" in Jordan's review of the German edition in *Die Naturwissenschaften*. The only possible quarrel with the remark that I can see is that the calculation appears to call for differentiation with regard to a quantum number, m , which since it is restricted to integer values, should not be treated as a continuous variable. But since the expression that is differentiated is linear in m the same result is obtained for a kind of group velocity that results from the superposition of waves whose quantum numbers are m and $m+1$, instead of the m and $m+\epsilon$ (with $\epsilon \rightarrow 0$) implied in the usual definition of group velocity.

E. U. CONDON

THE PHYSICAL REVIEW

ON THE QUESTION OF THE CONSTANCY OF THE COSMIC RADIATION AND THE RELATION OF THESE RAYS TO METEOROLOGY

BY ROBERT A. MILLIKAN

CALIFORNIA INSTITUTE OF TECHNOLOGY

(Received October 23, 1930)

ABSTRACT

Mean cosmic-ray intensities have been measured with much precision both at Pasadena, California (latitude 34) and at Churchill, Manitoba (latitude 59), the latter a distance of 730 miles from the North magnetic pole.

(1) The observed equality in these intensities indicates that these rays enter the earth's atmosphere as photons rather than as streams of electrons.

(2) Evidence is presented that the incoming rays are of a uniform intensity in all directions and in all latitudes, the small and apparently erratic fluctuations found by many observers at different stations arising simply from eruptions, waves, or ripples which change the thickness of the atmospheric blanket interposed between the source and the observer.

(3) The cosmic-ray electroscope thus acquires significance as a meteorological instrument.

(4) The influence of these rays in the maintenance of the earth's charge is considered.

I. LACK OF DEPENDENCE UPON LATITUDE

IN OUR trip to the Bolivian High Andes in 1926 Dr. Cameron and I, by taking continuous observations at sea from latitude 34 north to latitude 17 south, and also by observing at altitudes of about 15,000 feet both in California and in South America, proved to our own satisfaction that the cosmic-ray intensities are the same the world over at a given elevation above sea level, and also that they are independent of the positions of any celestial objects *within the limits of our experimental uncertainty*, which we estimated at about 3 percent but which in our report¹ we gave as 6 percent so as to have a sufficient margin of safety. This result has been questioned by other observers, and theories have been advanced which required a variation of cosmic-ray intensities both with latitude and with the positions of celestial objects, and I myself have thought it entirely possible that there might be small variations depending upon these elements. It was therefore very important for the theory of the origin of these rays to have much more exact measurements upon these points than we had yet made.

Having now an electroscope which by virtue of carrying a pressure of

¹ Millikan and Cameron, Phys. Rev. 31, 170 (1928).

450 pounds of air per square inch, and by virtue of other improvements in construction is fourteen times as sensitive as the one used in South America—it has not leaked a particle of air for more than two years—I have within the past fifteen months returned to the problem of studying variations with both latitude and sidereal time, since it is one of altogether fundamental importance for the understanding of the nature of these strange rays.

From the first we ourselves have thought the evidence satisfactory that these rays are ether waves of frequencies a thousand times and more those of the hardest x-rays, but others have thought that they might not be ether waves at all, but high-speed electrons instead.² If they were the latter, they would of necessity be influenced by the earth's magnetic field and should be stronger near the magnetic pole than at low latitudes, as is the case with other phenomena, such as the aurora, which depend upon the earth's magnetic field.

This summer I therefore went to the settlement which is much the nearest to the earth's north magnetic pole of any settlement on earth, namely, Churchill, 730 miles due south of the pole on the west side of Hudson's Bay—at present a construction camp where the Canadian Government is trying to make a three months summer harbor for the sake of bringing Manitoba and Alberta closer to Liverpool. It is estimated, for example, that eight cents a bushel can thus be saved on the transport of wheat from northwestern Canada to England. A construction train runs into Churchill once a week, crawling along at about 20 miles per hour over tracks laid partially on frozen swamps.

There, through the extreme courtesy of the Carter-Halls-Aldinger Engineering Co. Ltd., and also with transportation assistance for my 500 pounds of lead and other baggage from the Southern Pacific, the Canadian Pacific, and the Canadian National Railroads, I took observations continuously day and night for a week on the intensity of the cosmic rays, screening out the local rays with this shield of lead 7.6 cm (about 3 inches) thick. The aurora played brilliantly overhead on three of the six nights of observation, so that if cosmic rays and the aurora are phenomena that are in any way connected, the opportunity for bringing to light that connection could not have been better. The mean results, when compared with those similarly taken at Pasadena during the last week in July and the first in August show that *the cosmic rays have precisely the same intensity at Churchill, in latitude 59, as at Pasadena in latitude 34*, the mean results in the two places being 28.31 ions per cc per sec. and 28.30 ions per cc per sec., respectively, as measured in my particular electroscope. I think the error in these measurements cannot possibly be as much as 1 percent.

Table I gives the actual readings taken at six hour intervals, the rate of discharge in ions per cc per sec. during the six hours from midnight to 6 A.M. being labelled "night," that from 6 A.M. to noon being labelled "morning," that from noon to 6 P.M. being called "afternoon," and that from 6 P.M. to midnight "evening."

² Bothe and Kolhörster, *Zeits. f. Physik* 56, 751 (1929).

TABLE I. Comparison of cosmic ray intensities at Pasadena, California, latitude 34, and Churchill, Manitoba, Latitude 59.

Pasadena, July 26 to August 3, 1930							
Night		Morning		Afternoon		Evening	
Ions cc/sec	Barometer inches	Ions cc/sec	Barometer inches	Ions cc/sec	Barometer inches	Ions cc/sec	Barometer inches
29.77	29.13	29.19	29.14	29.96	29.10	30.08	29.09
29.10	29.08	29.42	29.16	29.98	29.15	29.65	29.16
29.27	29.19	29.49	29.18	29.70	29.15	29.33	29.12
29.37	29.14	29.46	29.14	30.23	29.10	29.58	29.11
29.56	29.16	29.22	29.16	29.52	29.13	30.24	29.13
29.68	29.12	28.93	21.12	30.00	29.08	30.16	29.06
29.42	29.09	29.52	29.10	29.56	29.09	29.94	29.11
29.35	29.14	29.21	29.18	29.07	29.18	29.28	29.17
Means	29.44	29.13	29.31	29.15	29.75	29.12	29.76
Mean Ions cc/sec=29.56 Mean barometer=29.13401 Corrected bar.=29.14							
Correction for local rays = $52.5 \times 2.4\% = 1.26$. Mean I cc/sec = $29.56 - 1.26 = 28.30$							
at mean barometer = 29.14.							
Churchill, August 25 to September 1							
Night		Morning		Afternoon		Evening	
Ions cc/sec	Barometer inches	Ions cc/sec	Barometer inches	Ions cc/sec	Barometer inches	Ions cc/sec	Barometer inches
28.33	29.54	28.40	29.42	28.72	29.41	28.30	29.44
28.24	29.49	27.88	29.58	28.46	29.66	28.53	29.77
28.69	29.79	28.12	29.79	28.38	29.72	28.80	29.59
27.82	29.47	29.10	29.35	29.17	29.27	29.25	29.26
28.83	29.30	28.18	29.35			28.89	29.41
28.57	29.45	27.63	29.51	28.06	29.61	28.39	29.63
28.60	29.52	28.13	29.57	28.81	29.46		
Means	28.44	29.51	28.21	29.51	28.60	29.52	28.69
Mean ions cc/sec = 28.48 Mean barometer = 29.51 - 0.07 Corrected bar. = 29.44							
Correction for local rays = $24. \times 2.4 = .58$. Mean I cc/sec = $28.48 - .58 = 27.90$							
Churchill ions cc/sec reduced to Pasadena barometer = $27.90 + 0.41 = 28.31$							
To compare with Pasadena observations 28.30							

It will be noticed that the rays producing the observed 29 ions per cc per sec. inside the lead are almost pure cosmic rays, since the local rays amount to but 4 percent of the total at Pasadena and to less than 2 percent of the total at Churchill. The exact amount of the local rays in each position was determined by taking a reading without the lead screen and subtracting from this reading the cosmic-ray intensity as read off for the given elevation from our depth-ionization curve taken in snow-fed lakes with this same electroscope. The percentage of these local rays getting through the lead screen was found by making preliminary direct measurements with standard samples of uranium and thorium. It thus found that 2.4 percent of the local rays appear inside the lead. The zero of this electroscope, i.e., the reading when entirely screened from all rays, was 1.2 ions cc/sec, so that at Pasadena, for example, it was found that 27.1 out of the observed 29.56 ions per cc/sec were due solely to the cosmic rays. The recorded barometer readings are the means of those directly observed on my "precision Paulin" aneroid at the beginning and end of each run, and the indicated corrections were furnished me by the weather bureau stations at both Los Angeles and Churchill as read on their standard mercury barometers.

Since the portion of the sky from which the rays come at Churchill is quite different from that at Pasadena, the indications of these experiments are, then, First, *that the cosmic rays enter the earth uniformly from all portions of the sky*; Second, *that they consist as they enter the earth's atmosphere of ether waves, not of electrons*.

II. LACK OF DEPENDENCE UPON THE POSITION OF ANDROMEDA OR THE MILKY WAY

But there are even more important conclusions than the foregoing that follow from the work thus far reported when it is taken in conjunction with the further experiments to be now considered.

When Dr. Cameron and I in 1925 proved³ that the difference in the intensities of the cosmic rays at two levels in the atmosphere could be computed from the thickness of the blanket of air interposed between the two levels it of course followed that the intensity of the rays at the earth's surface must vary with barometric pressures, since these simply reflect approximately the varying weights of the atmosphere above. So when we had completed, more than a year ago, the full curve showing the variation of intensity with depth beneath the surface of the atmosphere, and could thus, with the aid of this curve, reduce the readings taken over days, or weeks, or months, to a common barometer-reading, I expected that the variability in the measured cosmic-ray intensities would disappear under this procedure. But continuous readings taken every six hours with very delicate instruments a year ago last summer seemed to spoil this expectation. They still showed fluctuations after careful reduction to a common barometer-reading, and for a while I thought these fluctuations came at such a time of day as to indicate that the Milky Way exerted a small positive influence upon the intensities of the rays. Although I mentioned to some of my colleagues my apparent finding that the Milky Way might increase the intensity of the rays by perhaps a percent by its presence overhead, I made no publication of even such a small dependence of cosmic-ray intensity upon stellar-time, for I wished first to extend the observations to different times of the year when the Milky Way would be overhead at widely different times of day.

Such a prolonged and continuous following of the changes has now brought to light the fact that neither the Milky Way or the nearest of the spiral nebulae Andromeda, nor any other celestial object has anything to do with these changes, but rather that they are a diurnal affair occurring at the same time of day at widely different seasons of the year and having a connection with the diurnal barometric cycle. It is well known that this diurnal cycle carries the barometer—especially in warm regions free from summer storms—through a minimum late every afternoon and a maximum in the morning. The cosmic-ray intensities at Pasadena go through a *maximum every afternoon* and a *minimum every morning* even after corrections have been made to bring the readings to a common pressure. Table II exhibits these facts clearly, the readings from July 14–19 are entirely consistent with

³ Millikan and Cameron, Phys. Rev. 5, 851 (1926).

TABLE II. *Cosmic ray intensities.*

July 14 to 19, 1930									
Night			Morning		Afternoon		Evening		
12:08-8:52	29.81		9:11- 1:08	30.07	1:20-6:10	30.14	5:18-11:52	30.21	
12:07-7:47	29.69		8:00- 2:02	29.33	2:13-6:06	30.16	6:24-11:56	29.53	
12:30-8:12	29.62		8:22-12:25	29.77	12:33-4:22	31.15	6:20-12:15	29.87	
11:40-6:03	29.61		6:13-11:06	29.85	11:17-3:41	29.77	4:31-11:25	30.03	
10:26-1:44	29.94		9:31- 1:57	29.62	2:07-6:20	30.77	3:52-10:16	29.83	
1:53-9:22	29.63								
Means	29.71			29.73		30.39		29.89	
July 19 to 27, 1930									
Night			Morning		Afternoon		Evening		
12:38-6:39	29.78		6:40-12:20	29.72	12:32-6:02	30.01	6:30-12:24	29.53	
12:32-6:02	29.43		6:19-12:32	29.67	12:43-6:18	30.08	6:14-12:16	29.99	
12:40-6:45	29.85		7:08-12:38	29.72	12:48-6:26	29.82	6:28-12:26	30.09	
12:28-6:39	29.99		6:58- 1:22	30.12	1:53-6:32	30.69	6:36-12:06	30.04	
12:19-6:45	29.93		6:55-12:29	29.91	12:38-6:34	30.13	6:43-12:07	30.42	
12:33-6:41	29.42		6:57-12:32	29.75	12:42-6:33	30.35	6:46-12:22	30.35	
12:11-6:22	30.10		6:33-12:44	29.57	12:55-6:30	30.26	6:44-11:58	30.22	
12:03-5:57	29.43		6:09-11:55	29.78	12:05-6:05	30.35	6:44-11:50	30.35	
Means	29.74			29.78		30.21		30.12	
Milky Way overhead all this period			Milky Way overhead most of this time		Milky Way entirely out of sight		Milky Way partially overhead		
Oct. 6 to 12, 1929									
Night			Morning		Afternoon		Evening		
Date									
10/6/29	11:56-8:05	30.09	8:25- 2:14	30.01	2:22-6:49	30.77	6:54- 1:04	30.52	
10/7/29	1:11-10:24	30.30			10:33-6:22	30.53	6:30-11:40	30.65	
10/8/29	11:52-8:12	20.21	8:13- 1:47	30.08	1:57-7:07	30.54	7:16-12:21	30.34	
10/9/29	12:30-9:04	29.61	9:19- 2:15	29.90	2:26-6:50	30.63	6:59-11:69	30.20	
10/10/29	12:07-9:10	29.88	9:21- 3:30	30.37	3:40-7:00	30.54	7:10-11:51	30.30	
10/11/29	12:04-8:57	29.84	9:09- 2:04	29.73	2:15-6:20	30.80	6:29-11:57	30.24	
10/12/29	12:10-9:09	29.92	9:21- 2:22	30.32					
Means	29.98			30.07		30.63		30.37	
Milky Way overhead most of this time			Milky Way entirely out of sight		Milky Way partially overhead		Milky Way overhead all this period		

those taken from July 19-27, the "night" readings and the "morning" readings being in both cases lower than the "afternoon" and "evening" readings. Further, the night readings are the most consistent among themselves because the atmosphere is then in its most quiet condition. As indicated two-thirds of the way down the table the Milky Way was here entirely out of sight *when the cosmic ray intensities were at their afternoon maximum*. I at first thought that this must mean that the Milky Way, instead of exerting a positive influence as had been before suspected must instead act as an absorbing screen for the cosmic rays. But, as shown at the bottom of the table, in October 1929 I had taken a similar series of readings. The Milky Way had then moved forward about 6 hours, so that it was completely out of sight in the *morning* instead of the afternoon, *and yet the relation of the morning and afternoon readings had not been altered a particle by this fact*. That the readings are all a little higher in October, 1929, than in July, 1930, has no significance save that I was reducing to a different barometer reading at the former time. Table II yields quite exact and unambiguous proof, then, *that the Milky Way has no influence whatever, and therefore that the cosmic rays must originate "in the depths of space beyond the Milky Way."*

Table III shows again the same relations. The day was here divided into seven periods instead of into four, the time at the top of each column being merely the median clock-reading for the period. Here too, it is seen that the maximum is in the late afternoon and the minimum at night or in the early morning.

TABLE III. *Cosmic ray intensities.* (Observations August 1 to August 9, 1930).

12:40 P.M.		3:30 P.M.		6:15 P.M.		9:45 P.M.	
10:22-4:05	29.45	1:20-6:51	29.99	3:34-8:21	30.42	6:14-12:00	30.00
10:07-3:25	30.20	12:46-6:35	29.79	3:25-9:19	30.05	7:00-12:45	29.60
10:01-3:17	29.72	12:57-6:45	30.07	4:00-9:29	29.85	6:33-12:27	29.81
10:23-3:23	29.67	12:43-6:14	29.75	4:13-9:30	29.65	6:56-12:56	30.24
10:35-4:40	29.50	12:57-3:50	29.85	4:07-9:53	30.05	6:22-10:40	29.97
10:06-2:29	30.01			3:33-7:58	30.56	8:32-12:42	29.87
11:11-3:57	29.83			3:28-8:29	30.09	7:25-11:55	30.49
9:56-3:25	29.90			3:21-8:00	29.93	8:36-12:30	29.40
				2:47-7:53	29.57	8:11-12:22	29.80
Means	29.79		29.89		30.02		29.91
Milky Way a little in		Milky Way nearly out		Milky Way entirely out		Milky Way out	
3 A.M.		7:45 A.M.		9:45 A.M.			
12:11-6:28	29.69	5:53-11:03	29.95	6:33- 1:05	29.89		
12:55-6:43	29.66	5:34-10:16	29.52	6:50-12:48	29.73		
12:42-6:36	29.86	5:25-10:25	29.72	6:47-12:35	29.55		
11:50-5:47	29.91	5:10- 9:51	29.69	7:04-12:35	29.64		
1:03-6:53	29.52	5:59- 9:57	29.62	6:09-11:56	29.79		
10:51-5:12	29.65	4:32- 9:46	29.75				
9:43-3:36	29.62	4:10- 9:54	29.46				
12:53-6:45	29.50	3:47- 9:16	29.56				
7:45-3:53	29.51						
12:09-5:47	29.90						
12:41-6:55	29.89						
12:39-5:24	29.20						
12:32-5:13	29.98						
12:38-5:10	30.07						
Means	29.71		29.66		29.72		
Milky Way in		Milky Way in full		Milky Way mostly in			

The sort of consistency and precision in electroscope readings here attained is rather nicely shown by Tables II and III, which reveal that in three different sets of observations taken over three different groups of days the three "night" mean-readings were 29.71, 29.74, and 29.71, while the three morning mean readings were 29.73, 29.78, 29.72. The afternoon and evening readings fluctuate more because the atmosphere is then more disturbed.

III. EXPLANATION OF FLUCTUATIONS

The reason for the behavior shown in Tables II and III is now quite clear. As the sun rises and begins to heat the earth the barometer begins to rise, not at first because there is any larger weight of atmosphere above it, but solely because the temperature of the air, partially confined by its viscosity and inertia, is rising. Before night the column of air over the heated area has expanded upward, flowed over at the top, and left a miniature terrestrial "sun spot" or hole in the atmosphere through which the cosmic rays then reach the earth in greater intensity merely because the air-blanket has been partially removed locally by the heated spot.

In a word, the barometer is an instrument that responds both to the *temperature* and to the *weight* of the superincumbent air, i.e., to a mixture of static and kinetic conditions, while the cosmic-ray electroscope reflects only the *mass* of the superincumbent air, and is quite independent of temperature, or of kinetic effects of any kind. *The cosmic-ray electroscope is thus a simpler and a more fundamental instrument than the barometer.* I expect it to be an aid in bringing about advances in the as yet little developed science of meteorology, and ultimately to find a place in meteorological stations. The air is simply an absorbing blanket interposed between us and a constant

source of radiation coming into the earth uniformly from all directions. Every eruption, or wave, or ripple in that blanket is accurately reflected by the cosmic-ray electroscope of the type here used. The changes that it reveals are considerably larger than the changes revealed by the barometer, because it cares nothing about the temperature, but only about the mass of the interposed layer of air, while with the barometer a rise in temperature often masks the thinning of the air-blanket above. The two instruments between them furnish more information about the condition of the upper air than either one of them alone can do. The afternoon barometer minimum, corresponding to a mean drop of one-tenth inch of mercury, or one-third percent, may be accompanied by a cosmic ray rise of two percent, as Tables II and III show.

IV. CLEARING UP OF FORMER DISCREPANCIES

The fourth result to which I would call attention is that the proof that the cosmic rays that strike the atmosphere are all ether-waves, rather than a mixture of ether waves and high speed electrons, carries with it the conclusion that the rate of ionization within a vessel sent to the top of the atmosphere should not be a maximum at the top as we have heretofore assumed, but should pass through a maximum somewhere below the top. This removes the apparent contradiction between the early results of Hess and Kolhörster (1911-1914), who went up in manned balloons, and Bowen and myself (1922), who sent up recording electroscopes with pilot balloons to much higher altitudes. We obtained a very much smaller *mean* absorption coefficient than they did, and this is precisely what we should have done in view of this aforementioned maximum. This result also brings to light new evidence for the correctness of the interpretation made by Dr. Cameron and myself that the cosmic rays are due to the continuous formation "in the depths of space" of the common abundant elements helium, oxygen, silicon, and iron out of hydrogen; for, before these ether waves get into equilibrium with their train of secondary electrons they should show absorption coefficients of the same order of magnitude as, but *somewhat smaller than*, those computed for them by the Einstein equation, Aston curve, and the Klein-Nishina formula. This is exactly what they do show, and they show this departure least for the rays corresponding to the formation of helium, for which the difference is quite small, and most for those corresponding to the formation of iron. This, also, is exactly in accord with our observations, reported to the Academy at its fall meeting a year ago.

V. COSMIC RAYS AND ATMOSPHERIC ELECTRICITY

About forty percent of the ionization in the atmosphere at the earth's surface over the land is due to cosmic rays and sixty percent to the radioactive substances contained in the earth, but at the altitude of Pike's Peak (14100 feet) we have found the cosmic rays three times as intense as at sea level, and this checks roughly with Hess' and Kolhörster's observations made as early as 1911 to 1914. But at altitudes above say two thousand feet the influence of rays from the earth in producing atmospheric ionization has become negli-

gible, the cosmic rays alone being here effective, *so that practically the whole ionization of the atmosphere above its surface layer and below the great altitudes at which the Kennelly-Heaviside layer is found is due to the cosmic rays.* These rays must therefore exert a preponderating influence upon atmospheric electrical phenomena.

We have heretofore had considerable difficulty in finding a mechanism by which the earth can maintain its well-known negative charge,—a charge sufficient to produce a more or less constant potential gradient, near the surface, of some 100 volts per meter. The cosmic rays, by detaching negative electrons from the molecules of the atmosphere and hurling them with enormous energy into the earth, must contribute somewhat toward the maintenance of this gradient; but they are much too few in number, indeed, of an entirely wrong order of magnitude, to account for the observed effects. Indirectly, however, they assist greatly in maintaining the earth's charge, the mechanism being presumably somewhat as follows:

The ionization of the upper air by the ultraviolet light from the sun is undoubtedly very large, enormously larger than that due to cosmic rays, as is shown by the existence of the Kennelly-Heaviside layer. The result of this ionization, whatever its cause, ultraviolet light, cosmic rays, or what not, is to free, in the higher stretches of the atmosphere, the lightest possible gas, namely, an electron gas, about 1/50,000th the weight of nitrogen gas, and this, because of its extreme lightness and mobility, at once expands upward, *or tries to do so*, until stopped by the field that such expansion itself creates, the greater chance of attachment of the electrons that diffuse downward accentuating this process. This field is of course of such sign as to tend to drive all the negative ions formed within it, and especially the attached negatives which have no tendency to diffuse upward, in toward the earth, and to hold the positives in the air above them. In other words, the outermost layers of the atmosphere in view of this influence, should have an excess of negatives, the next lower layers an excess of positives, and below that there should be a layer in which negatives are again in excess.

Now, no one has gone far enough up to find the aforementioned outermost layer, but Wiegand⁴ and Idrac⁵ both report altitude observations in which the field drops from 100 volts per meter at the surface to nearly zero at 8 kilometers and then, in the region between 8 and 12 kilometers, rises in such a way as to indicate an excess of negatives, followed by an excess of positives between 12 and 19 kilometers, where the field has again dropped to zero.

Now water vapor is found up to 12 kilometers, and wherever below that it is rising, expanding and condensing on ions, it will condense, according to the C. T. R. Wilson effect, only on the negatives, although a droplet may afterward catch a positive by the diffusion process. Furthermore, atmospheric dust is usually found predominantly negatively charged. Negative capture seems, then, to be *strongly* favored by the C. T. R. Wilson effect, and to be somewhat facilitated by the excess of negatives between 8 and 12

⁴ Wiegand, Ann. d. Physik 66, 261 (1921).

⁵ Idrac, Comptes rendus 182, 1634 (1926).

kilometers, and also by the greater tendency of negatives, due to greater mobility, to collect on dust. After such capture gravity of course pulls this negatively charged dust and water vapor into the earth.

This gravitational effect on heavy, negatively charged carriers is, then, what creates a portion at least, of the negative gradient near the surface, a field that actually decreases rapidly with altitude, and if this theory is correct, should be reversed at high altitudes. A "gravity" theory of the maintenance of the earth's charge is not at all new, though there may be some elements of novelty in the foregoing elaboration of it. The purpose here is to point out the very important role that the cosmic rays play in it, since they must furnish practically all the atmospheric ions between the thin layer next the earth and the Kennelly-Heaviside layer.

VI. SUMMARY

In summary, then, we have presented convincing evidence

- (1) That the cosmic-ray intensities are independent of latitude.
- (2) That the cosmic-ray intensities are independent of sidereal time.
- (3) That the rays are constant all over the earth's surface, but that the fluctuations observed by many experimenters merely reflect changes in the thickness of the interposed atmospheric blanket.
- (4) That the cosmic-ray electroscope may be of use in meteorology.
- (5) That the cosmic rays enter the atmosphere as ether waves or photons, and hence produce their maximum ionization, not at the surface of the atmosphere, but somewhat farther down.
- (6) That the observed cosmic-ray effects are all in all good general agreement with the predictions of the Klein-Nishina formula, thus lending support to the view that the cosmic rays are due to atomic synthesis going on "in the depths of space."
- (7) That the cosmic rays are a very important factor in atmospheric electrical effects, especially in the maintenance of the earth's negative charge.

ON THE ELECTRICAL RESISTANCE OF CONTACTS BETWEEN SOLID CONDUCTORS

BY J. FRENKEL

DEPARTMENT OF PHYSICS, UNIVERSITY OF MINNESOTA

(Received October 30, 1930)

ABSTRACT

A contact between two solid conducting bodies is visualized as a small gap between them. This gap can be described as a potential-hill over which electrons, according to the wave-mechanical theory, can pass even with insufficient kinetic energy. The general expression of the resulting current intensity as function of the potential-difference is obtained and discussed for the case of two identical or different bodies in connection with the resistance of granular structures (thin metallic films) and the rectifying action of certain contacts.

INTRODUCTION

THE usual picture of an electrical contact between two solid conducting bodies is that their surfaces or part of their surfaces are at a distance of atomic dimensions from each other, so that the electrons can pass through the contact surface in the same way they pass through any surface within the same body.

Now such an intimate contact between two bodies along a large part of their surfaces is probably very rarely realized. Nor is it necessary for the conduction of electricity from one body to the other. Such conduction can also take place through those parts of their surfaces which lie rather far apart from each other, that is, at a distance many times larger than the usual atomic distance. In fact, according to a well-known principle of wave mechanics, which has been used already (and sometimes abused) for the explanation of a great many phenomena, an electron can jump over a "potential-hill" even if it does not have sufficient kinetic energy to do so according to the classical mechanics. Now the gap between two contiguous bodies may be considered as the top of such a hill, with practically vertical slopes at (or rather just beyond) the respective surfaces. There must be in general a steady flow of electrons across the gap in both directions, the difference between the two flows being the actually observed current intensity I . In the case of equilibrium the latter is of course equal to zero. If, however, an additional potential difference ϕ is maintained across the gap, I will be a certain function of ϕ , different from zero.

It will be our first object to determine the general character of this function $I(\phi)$. Before, however, proceeding further let us remark that this function can always be expanded in a power series and that for small values of ϕ one can simply put $I = \alpha_1 \phi$ in accordance with Ohm's law, α_1 , being the conductivity of the contact, that is the reciprocal of its electrical resistance. For larger values of ϕ one must get

$$I = \alpha_1\phi + \alpha_2\phi^2 + \alpha_3\phi^3 + \dots$$

The coefficients of the even powers of ϕ vanish in the case of a contact between two identical bodies. They must be however different from zero in the case of two bodies of different nature. One thus gets in this case, to the second approximation, $I = \alpha_1\phi + \alpha_2\phi^2$, which means that the current is changed in magnitude when the sign of ϕ is reversed. This means a rectification effect of the same type as that given by an electron valve on the curved part of the characteristic, and may be quite large for some particular contacts.

1. GENERAL THEORY

For the sake of simplicity we shall consider the contiguous surfaces of the two bodies (a, b) as two parallel infinite planes. Their distance apart will be denoted by δ . The potential energy curve will be represented by the full line $MNQRST$ (Fig. 1) $NQ = U_a$ and $SR = U_b$ denote the increase of potential energy of an electron crossing the surface of the respective body (from inside to the outside). The inclined line QR represents a homogeneous electrical field acting between the two bodies. The corresponding change of the poten-

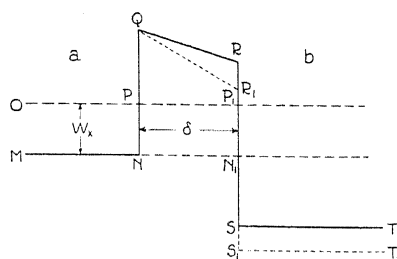


Fig. 1.

tial energy of an electron passing across the gap from a to b will be denoted by V and will be reckoned positive if this energy is diminished (as shown on the figure), that is, if the force F acting on the electron in the gap is directed from a to b ($F = V/\delta$). In the following it will be always supposed that the potential energy of an electron in a is *higher* than in b ; the difference represented by the line N_1S_1 will be denoted with U_{ab} . One has the obvious relation $U_b - U_{ab} + V = U_a$ or

$$U_{ab} = U_b - U_a + V \quad (1)$$

$NP = W_x$ represents the kinetic energy of an arbitrarily selected electron in a , or rather that part of its kinetic energy W , which corresponds to the x -component of the velocity, the x -axis being drawn in the direction ab . Every electron in a for which this component v_x is positive, will be able to pass through the gap, no matter how small W_x is, in comparison with the height of the potential wall NQ . On the other hand only those electrons of b will be able to jump over the gap to a for which the part of the kinetic energy corresponding to the x -component of the velocity (in the negative direction) is larger than $SN_1 = U_{ab}$.

The "transmission coefficient" for the a -electrons with the energy W_x will be denoted with $D(W_x)$. It is equal to the probability of any such electron passing from a to b (or the fraction of all the electrons succeeding in this enterprise). On the other side of the gap, that is in b , such an electron will have for the x -direction the kinetic energy $W_x + U_{ab}$. Reversing the direction of its motion we should get the same probability $D(W_x)$ for its getting back to a .¹ We thus see that $D(W_x)$ is the probability of a b -electron having for the negative x -direction the kinetic energy $W_x + U_{ab}$, to pass across the gap to a . The number of electrons per unit volume having velocity components in dv_x, dv_y, dv_z will be denoted by $f_a dv_x dv_y dv_z$ and $f_b dv_x dv_y dv_z$ for a and b respectively. So far as the *change in the velocity distribution of the electrons in each body*, due to the passage of the electrons to the other body or from the latter, can be neglected, f_a and f_b can be treated as functions of the resulting kinetic energy $W = W_x + W_y + W_z = \frac{1}{2}m(v_x^2 + v_y^2 + v_z^2)$. In case of two metals these are the well-known Fermi-Pauli-Sommerfeld functions.²

$$f_a = 2\left(\frac{m}{h}\right)^3 \frac{1}{e^{W/kT/A} + 1}, \quad f_b = 2\left(\frac{m}{h}\right)^3 \frac{1}{e^{W/kT/B} + 1}. \quad (2)$$

The number of electrons passing from a to b per unit surface per second is equal to

$$I_1 = \int_0^\infty dv_x \int_{-\infty}^{+\infty} \int_{-\infty}^{+\infty} dv_y dv_z D(W_x) f_a v_x.$$

For the corresponding number of electrons passing from b to a we get

$$I_2 = \int_{v_x^0}^\infty dv_x \int_{-\infty}^{+\infty} \int_{-\infty}^{+\infty} dv_y dv_z D(W_x - U_{ab}) f_b v_x.$$

Where v_x^0 is defined by the condition $\frac{1}{2}m(v_x^0)^2 = U$. These expressions may be simplified by introducing instead of v_x the variable $W_x = \frac{1}{2}mv_x^2$ and instead of v_y and v_z the variable $R = W_y + W_z = \frac{1}{2}m(v_y^2 + v_z^2)$ and the angle $\phi = \arctan(v_y/v_z)$. It will be remarked that $(2R/m)^{\frac{1}{2}}$ and ϕ are the polar coordinates replacing the rectangular coordinates v_y, v_z . We get then

$$I_1 = \frac{2\pi}{m^2} \int_0^\infty dW_x D(W_x) \int_0^\infty f_a(W_x + R) dR \quad (3)$$

and

$$I_2 = \frac{2\pi}{m^2} \int_{W_x^0}^\infty dW_x D(W_x - U_{ab}) \int_0^\infty f_b(W_x + R) dR$$

or replacing W_x by $W_x' = W_x - U_{ab}$,

$$I_2 = \frac{2\pi}{m^2} \int_0^\infty dW_x' D(W_x') \int_0^\infty f_b(W_x' + U_{ab} + R) dR. \quad (4)$$

¹ Cf. J. Frenkel, Einführung in die Wellenmechanik, p. 57.

² Cf. A. Sommerfeld, Zeits. f. Physik 47, 7 (1928).

The resulting flow of electrons from a to b is

$$I = I_1 - I_2 = \frac{2\pi}{m^2} \int_0^\infty dW_x D(W_x) \int_0^\infty [f_a(W_x + R) - f_b(W_x + U_{ab} + R)] dR. \quad (5)$$

We shall now suppose that $I=0$. This means that the two bodies are in a statistical equilibrium with respect to each other, as a result of the existence of a definite contact potential difference between them, corresponding to the drop of potential energy V in the gap.

This state of equilibrium must obviously be independent of the special shape of the function $D(W_x)$, which determines the velocity with which it is established or the time of relaxation. Therefore in the case of equilibrium the coefficient of $D(W_x)$, that is the integral over R in (5), must vanish for any value of W_x , whence it follows that the integrand must vanish. We get thus, as the condition of equilibrium

$$f_a(W) = f_b(W + U_{ab}) \quad (6)$$

This equation can be considered as the direct consequence of the principle of detailed balance.

Let us now assume that V is increased by the amount V_1 , corresponding to an additional (external) potential difference $\phi = V_1/e$ (e = charge of an electron). Instead of the initial potential energy curve Fig. 1, we shall get in this case the curve $MNQR_1S_1T_1$ (partially dotted line) if V_1 is positive (which it, of course, need not be). This will alter to some extent the transmission coefficient $D(W_x)$ replacing it by $D_1(W_x)$ say, and what is more important, change the potential energy difference U_{ab} replacing it by $U_{ab} + V_1$. As a result I_2 will now be smaller than I_1 (if $V_1 > 0$), and we shall have a current flowing through the gap in the direction of the applied electrical force. Taking account of the condition (6) we can determine this current by the formula

$$I = \frac{2\pi}{m^2} \int_0^\infty dW_x D_1(W_x) \int_0^\infty [f_b(W_x + U_{ab} + R) - f_b(W_x + U_{ab} + V_1 + R)] dR \quad (7)$$

For sufficiently small values of V_1 , we can put

$$f_b(W_x + U_{ab} + R) - f_b(W_x + U_{ab} + R + V_1) = -V_1 \frac{\partial f_b(W_x + U_{ab} + R)}{\partial R}.$$

This reduces the inner integral in (7), in view of $f_b(\infty) = 0$ to $V_1 f_b(W_x + U_{ab})$, so that neglecting the difference between D and D_1 , which is immaterial so far as second powers of V_1 are neglected, we get to a first approximation

$$\frac{I}{V_1} = \frac{2\pi}{m^2} \int_0^\infty dW_x D(W_x) f_b(W_x + U_{ab}) \equiv \alpha_1. \quad (8)$$

This expression, or rather its product with e^2 , may be defined as the reciprocal of the resistance of the contact (per unit surface). Putting $V_1 = eE\delta$ where E is the (additional) electrical field in the gap, we can define the quantity

$$\frac{eI}{E} = \frac{e^2 I \delta}{V_1} \equiv \sigma_g$$

that is

$$\sigma_g = \frac{2\pi e^2 \delta}{m^2} \int_0^\infty dW_x D(W_x) f_b(W_x + U_{ab}) \quad (9)$$

as the specific "conductivity" of the gap forming the contact.

Proceeding to the second approximation, we get

$$f_b(W_x + U_{ab} + R) - f_b(W_x + U_{ab} + R + V_1) = -V_1 \frac{\partial f_b}{\partial R} - \frac{V_1^2}{2} \frac{\partial^2 f_b}{\partial R^2}$$

$$D_1 = D + \frac{\partial D}{\partial V_1} V_1$$

(the arguments being in both cases those corresponding to $V_1 = 0$) whence

$$I = \alpha_1 V_1 + \alpha_2 V_1^2 \quad (10)$$

with the previous value of α_1 and

$$\alpha_2 = \frac{2\pi}{m^2} \int_0^\infty dW_x \left[\frac{1}{2} D(W_x) f_b'(W_x + U_{ab}) + \frac{\partial D}{\partial V_1} f_b(W_x + U_{ab}) \right] \quad (11)$$

f_b' denoting the first derivative of f_b .

It must be emphasized that the above results hold for the case only that $U_{ab} + V_1$ remains positive. If $U_{ab} + V_1 < 0$ the role of the bodies a and b will be exchanged.

2. APPLICATION TO THE CASE OF TWO IDENTICAL METALS AND TO GRANULAR STRUCTURES (THIN FILMS)

The last remark applies in particular to the case of a contact between two identical metals, which is characterized by U_{ab} (as well as V) being equal to zero. The second term in (10) will then vanish, and I will be an odd function of V_1 .

Introducing f for f_b in one of the expressions (2) we get in this case for the "specific conductivity" of the gap

$$\sigma_g = \frac{4\pi m e^2 \delta}{h^3} \int_0^\infty dW_x \frac{D(W_x)}{e^{W_x/kT/A} + 1} \quad (12)$$

It will be interesting to compare this expression with that of the usual specific conductivity of the corresponding metal σ as derived from Sommerfeld's theory. The latter expression can be put in the form

$$\sigma = \frac{e^2 l n}{m v_0} \quad (13)$$

where n denotes the number of electrons in unit volume, v_0 their maximum velocity for $T=0$, and l the mean free path of the electrons having this velocity.³ Putting

$$\begin{aligned} n &= 2 \left(\frac{m}{h} \right)^3 \int \int \int_{-\infty}^{+\infty} \frac{dv_x dv_y dv_z}{e^{W/kT/A} + 1} = 8\pi \left(\frac{m}{h} \right)^3 \int_0^{\infty} \frac{v^2 dv}{e^{W/kT/A} + 1} \\ &= \frac{8\pi m^2}{h^3} \int_0^{\infty} \frac{v dW}{e^{W/kT/A} + 1} \end{aligned}$$

we see that the integral

$$\frac{8\pi m^2}{h^3} \int_0^{\infty} \frac{v dW D(W)}{e^{W/kT/A} + 1} \quad (14)$$

can be considered as the mean value of $D(W)/v$ for all the electrons (irrespective of the direction of their velocity). We thus get, according to (12)

$$\sigma_g = \frac{1}{2} \frac{e^2 \delta n}{m} \left(\frac{\bar{D}}{v} \right) \quad (15)$$

or approximately—putting $(\bar{D}/v) = D/v_0$

$$\frac{\sigma_g}{\sigma} = \frac{1}{2} \frac{\delta \bar{D}}{l} \quad (15a)$$

This relation shows, that with respect to its conductivity the gap can be treated as a metal, where the free electrons have a mean free path of the order of magnitude of $\delta \bar{D}$. One can of course use it in the opposite way and treat a metal as a series of gaps. This interpretation roughly corresponds to the theories of Bloch and Peierls, where the electrons are considered as bound to the separate atoms, but still capable of jumping from one atom to the next one over the potential hill separating them.

The transmission coefficient D in the case of two identical metals $U_a = U_b = U$, that is for an energy-curve of the shape shown by the full line of Fig. 2, is given as a function of the energy $W_x = \frac{1}{2}mv_x^2$ so long as the

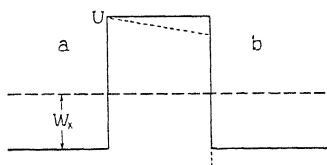


Fig. 2.

latter is smaller than U_0 , by the formula

$$D = \left[\cosh^2 \beta \delta + \frac{1}{4} \left(\frac{\beta^2}{\alpha^2} - \frac{\alpha^2}{\beta^2} \right) \sinh^2 \beta \delta \right]^{-1} \quad (16)$$

³ A. Sommerfeld, *Zeits. f. Physik* **47**, 1 (1928). Formulas (48c) and (42a).

where⁴

$$\alpha^2 = \frac{8\pi^2 m}{h^2} W_x, \quad \beta^2 = \frac{8\pi^2 m}{h^2} (U - W_x). \quad (16a)$$

For values of $\beta\delta$ which are large compared with 1, this reduces approximately to

$$D = 4e^{-2\beta\delta} \left[1 + \left(\frac{U}{2W_x} \frac{U - 2W_x}{U - W_x} \right)^2 \right]^{-1}. \quad (17)$$

It may be convenient to write β in the form $\beta = 2\pi/\lambda$ where λ can be defined as the wave-length of an electron moving with the positive kinetic energy $U_0 - W_x$. If expressed in volts this energy is equal to ϕ , then

$$\lambda = \frac{1.1 \times 10^{-7}}{\phi^{1/2}} \text{ cm} = \frac{11}{\phi^{1/2}} \text{ Angstrom units.}$$

For the electrons with velocity $v_x = v_0$, that is, the maximum velocity at zero-point of temperature, which approximately corresponds to the maximum of the Fermi distribution curve in the region of usual temperatures, the difference $U_0 - W_x$ is just equal to the work function of the metal (as measured directly in the Richardson effect).⁵ Putting $\phi \cong 4$ volts we get for these electrons (using Angstrom units for λ and for the distance δ):

$$\lambda \cong 5, \quad \beta \cong 1.2, \quad 2\beta\delta \cong 2.4\delta.$$

Since the expression in brackets in (17) is of the order of magnitude 1, we get as a rough estimate of the transmission coefficient D for $W_x = \frac{1}{2}mv_0^2$

$$D_0 \cong e^{-2.4\delta}.$$

If the mean value of D entering in (15a) could be identified with D_0 , we should have

$$\frac{\sigma_g}{\sigma} \cong \frac{\delta}{l} e^{-2.4\delta}$$

that is for $\delta = 10A$ with $l \cong 100$ (which roughly corresponds to the mean free path of the electrons at room temperature)

$$\sigma_g/\sigma \cong 10^{-10}.$$

To get absolute figures we note that for good conductors the specific resistance $1/\sigma$ is of the order of 10^{-5} ohms. The resistance of the contact $r = \delta/\sigma_g$ reckoned per unit surface (in cm^2 of course) thus turns out to be of the order of $10^{-7} \cdot 10^5 = 10^{-2}$ ohms. For a twice larger gap with $\delta = 20A = 2 \times 10^{-7}$ cm we should get in the same way a resistance about 10^{10} times larger than the previous one, that is, about 10^8 ohms. Further increase of δ

⁴ Cf. J. Frenkel, reference 1, p. 59.

⁵ A. Sommerfeld, reference 3, formula (53b).

would mean practically complete disappearance of current; for with $\delta = 20A$ it would require an electric field of 10 million volts per cm across the gap, corresponding to a potential difference of 2 volts, to obtain a current of the order of 10^{-8} amp/cm².

It must be remarked that for such high values of the field intensity—or rather of the potential difference—the current would no longer be proportional to the latter, but would increase much faster, gradually assuming the character of Millikan's "field-currents." It can be easily shown that this character, corresponding to a practically unidirectional flow of electrons (from a to b , that is in the direction of the applied force only), would be acquired for potential differences of the same order of magnitude as that corresponding to the potential jump at the surface of the metal (U_a/e).

We must now come back and test the validity of our assumption that the mean value of the transmission coefficient $\overline{D(W_x)}$ can be identified with its value D_0 for the electrons with the velocity $v_x = v_0 (=v_{\max}$ for $T=0$).

To do this we must find out the maximum of the function

$$F(W) = \frac{D(W)}{e^{W/kT}/A + 1}$$

which enters the integral (14) defining the mean value of $D(W)/v$. Leaving aside the case of extremely high temperatures we can put $A = e^{-W_0/kT}$ where $W_0 = \frac{1}{2}mv_0^2$. Neglecting the variations of the denominator of (17) when compared with that of the numerator we can further put, according to (16a),⁶

$$D(W) \cong e^{-[(U-W_0)/kT_1]^{1/2}} \quad (18)$$

the "effective temperature" T_1 , being defined by

$$1/kT_1 = 32\pi^2 m \delta^2 / h^2. \quad (18a)$$

This gives

$$F(W) = \frac{e^{-[(U-W)/kT_1]^{1/2}}}{e^{(W-W_0)/kT} + 1}$$

or with

$$\frac{W_0}{kT} = \xi_0, \quad \frac{W}{kT} = \xi, \quad \frac{U}{kT} = \xi_1, \quad \frac{U-W}{kT_1} = \gamma(\xi_1 - \xi), \quad \gamma = \frac{T}{T_1}$$

$$F(W) = \frac{e^{-[\gamma(\xi_1 - \xi)]^{1/2}}}{e^{\xi - \xi_0} + 1}. \quad (19)$$

The maximum of this function corresponds to the minimum of its reciprocal. Putting $\partial F^{-1}/\partial \xi = 0$ we get

$$1 + e^{-(\xi - \xi_0)} = 2[(\xi_1 - \xi)/\gamma]^{1/2}. \quad (19a)$$

It can be easily shown⁷ that this equation has either two solutions $\xi = \xi' < \xi_0$ and $\xi = \xi'' > \xi_0$, or none, depending upon the value of the parameter γ . The

⁶ This implies, of course the limitation to the case $W < U$, see below.

⁷ For instance, graphically, by tracing the exponential curve $Y = 1 + e^{\xi - \xi_0}$ and one branch of the parabola $Y = 2[(\xi_1 - \xi)/\gamma]^{1/2}$ (for $\xi < \xi_1$).

limiting value of this parameter is approximately equal to ξ_1 . When $\gamma \gg \xi_1$, the equation (19a) has no solution, which means that the function (19) steadily increases, as ξ increases from 0 to ξ_1 . In the opposite case $\gamma \ll \xi_1$, we get approximately

$$e^{\xi_0 - \xi'} \cong 2[(\xi_1 - \xi_0)/\gamma]^{1/2} \text{ and } 2[(\xi_1 - \xi'')/\gamma]^{1/2} \cong 1 \quad (20)$$

the first solution corresponding to a sharp maximum of $F(W)$ in the neighborhood of $W = W_0$, and the second to a faint minimum in the neighborhood of $W = W_1$. In order to see what case we have to deal with in practice, we must introduce numerical values.

If δ is measured in Angstroms, then it follows from (18a) $T_1 = 1.2 \times 10^4 / \delta^2$. Thus the "effective temperature" is high for $\delta = 1A$ which means an actual contact between the two metals, of the order of magnitude of the room temperature = 120°K for $\delta = 10A$ and becomes very small as δ increases beyond this value.

Assuming U_a to be equivalent to 14 volts and W_0 to 10 volts, and taking $T = 300^\circ\text{K}$, which corresponds with respect to the thermal energy kT to about 0.02 volts, we get $\xi_0 \cong 500$ and $\xi_1 \cong 700$.

We thus see, that in the above considered case of a gap $\delta = 10A$, the parameter γ is approximately equal to 2.5, that is, extremely small compared with its limiting value 700. For this case the first of the equations (20) gives approximately $\xi_0 - \xi' \cong 20$ and the second $\xi_1 - \xi'' \cong 2$. It can be easily verified that the maximum of $F(W)$ at $W = W' = kT\xi'$ is actually so sharp that $D(W)/v$ is practically equivalent to $D(W')/v'$ which is only very slightly different from the value $D(W_0)/v_0$ assumed above.

The condition $\gamma > \xi_1$ can be realized at $T = 300^\circ\text{K}$ for very broad gaps only with a width $\delta > 170A$. In this case the main part of the electric current—for sufficiently small values of the potential differences $\phi = V_1/e$, that is, for very small field intensities $E = \phi/\delta$ —should be due to electrons having a kinetic energy larger than U . For these electrons the transmission coefficient $D(W)$ is of the order 1, whereas their number for usual temperatures is extremely small. The electric current between a and b would have in this case the character of a thermionic current (and not of a field current) whose strength can be calculated by using the general expression (15a) for the effective conductivity of the gap with⁸

$$D \cong e^{-(\xi_1 - \xi_0)} = e^{-(U - W_0)/kT}. \quad (21)$$

Thus in this case the electrical resistance of the gap $r = \delta/\sigma_g$ should be independent of its width δ and should vary with the temperature as $e^{-(u - W_0)/kT}$. It would have an appreciable magnitude only for very high temperatures lying in the same range as the temperatures for which thermionic currents are observed. For usual temperatures, gaps of such width could no longer be treated as contacts, whereas in the case of shorter gaps with $\delta \cong 10A$ their resistance would be practically independent of the temperature and would vary exponentially with increase of δ .

⁸ This being (approximately) the relative number of electrons with a kinetic energy larger than U .

The above results may have interesting applications to the question about the electrical resistance of granular structures, such as metallic powders and probably also extremely thin metallic films obtained by means of cathode sputtering. As well known, the latter possess an abnormally high specific resistance, which for films with a thickness of about 10^{-6} cm and lower, may be 20 times larger than that of the same metal in block, and further abnormally small temperature coefficient of resistance, which in fact can become negative (decrease of resistance with increase of temperature). It has been often assumed⁹ that the high value of the specific resistance of very thin films is explained by the fact that their thickness may be smaller than the normal mean free path of the electrons (the latter being supposed to be scattered irregularly from both surfaces of the film). It would follow from this idea, that the "critical thickness" d for which the specific resistance should begin to increase, must be approximately equal to the mean free path l , and therefore must vary with the temperature in the same way as does the latter. According to the modern wave-mechanical theory of metallic conduction l varies inversely with T (or still faster in the region of very low temperatures), whereas as a matter of fact d remains practically independent of the temperature.

If on the other hand we adopt the equally often advocated granular theory of the constitution of thin films, and substitute for the usual conception of metallic contacts (which has been a serious obstacle for this theory) the conception developed in this paper, then the main properties of these films, distinguishing them from the metal in block, receive a satisfactory explanation. To say nothing of the abnormally high specific resistance, the smallness (or even the negative sign) of its temperature coefficient may be explained by the fact that the width of the gaps between adjacent grains is diminished, as a consequence of their thermal dilatation, with increase of temperature. Account should be taken of course of the thermal dilatation of the dielectric base upon which the film is deposited. But a comparison of the thermal dilation coefficients shows that they are as a rule larger in the case of the metals. This relation can be illustrated by the fact that the gaps between adjacent rails in a railway line decrease in the summer and increase in the winter time, and not vice versa. Denoting the length of a rail or grain with L and its effective dilation coefficient with α , we see that when the temperature is raised by ΔT the width of the gap is decreased by $\Delta\delta = -L\alpha\Delta T$. The relative decrease $\Delta\delta/\delta = -(L/\delta)\alpha\Delta T$ may be quite large even for a very small value of α ($\cong 10^{-5}$) if L is sufficiently large with respect to δ . And since the resistance of a gap varies exponentially with δ , this means a marked decrease of resistance, partially compensated by the normal increase of the resistance of the separate grains.

It is further well known that the resistance of thin films depends very largely upon the gas or gases present during their preparation. On our theory these gases must make thin monomolecular adsorbed layers on the surface of the separate grains of which the film is built up, thus changing

⁹ An assumption that has been worked out mathematically by J. J. Thomson long ago.

the potential energy U which determines the transmission coefficient according to (18) and consequently the resistance of the gaps between the grains. It may be remarked that this change of resistance must be quite parallel to the change of the thermionic emission of the corresponding metal owing to the presence of the adsorbed layer. In fact the difference $U - W_0$ in equation (18) may be identified with the "work function" $U - W_0$ which determines the thermionic emission in Sommerfeld's theory. It follows then from (15a) that the logarithm of the specific conductivity of a gap (contact) must vary with U , as the square root of the logarithm of the thermionic emission of the same metal for the "effective" temperature.

3. APPLICATION TO THE CASE OF TWO DIFFERENT CONDUCTORS AND TO THE PHENOMENON OF RECTIFICATION

Turning now to the consideration of a contact between two different conducting bodies (a, b) we shall first consider them as metals; the case of a non-metallic body (semi-conductor) may be obtained perhaps (see below) by taking the extreme form of the Fermi distribution law for a small concentration of free electrons which is nothing else but Maxwell's distribution law.

We have seen that when between two metals "in contact" that is at a small distance from each other, a potential difference V , determined by (1) and (6) is established, there will be no current flowing between them. Putting in (2) $A = e^{-W_a/kT}$ and $B = e^{-W_b/kT}$, we get, according to (6) $W - W_a = W - W_b + U_{ab}$ or according to (1).

$$V = (U_a - W_a) - (U_b - W_b). \quad (22)$$

This formula shows that the contact potential difference between two metals is equal to the difference of their respective work functions, as of course it should be.¹⁰

If a small additional potential difference V_1 is introduced, we must get a current determined by the "specific conductivity" (9). By the same argument as in the preceding paragraph we easily get

$$\sigma_g \cong \frac{1}{2} \frac{e^2 \delta n_b D(W_g)}{m v_g}$$

where $W_g + U_{ab} = W_b$, W_b being (practically) the maximum kinetic energy of the electrons in the body b at $T=0$. Since, according to the equilibrium condition $W_b - U_{ab} = W_a$, we get further, dividing σ_g by $\sigma_b = e^2 l_b n_b / m v_b$ the specific conductivity of the metal b ,

$$\frac{\sigma_g}{\sigma_b} \cong \frac{1}{2} \frac{\delta}{l_b} \frac{v_b}{v_a} D(W_a) \quad (23)$$

where $v_a = v_g$ is the largest velocity of the electrons in a at $T=0$. So far as v_a and v_b are of the same order of magnitude (which is the case for all metals)

¹⁰ Cf. C. Eckart, *Zeits. f. Physik* 38 (1928) and J. Frenkel, *Zeits. f. Physik* (1928).

we do not have to discuss this expression in detail, since it is practically the same as in the case of two identical metals.

A few words should be added with regard to the character of the function $D(W_x)$.

For the case of the energy curve $MNQRST$ of Fig. 1 with an inclined top, this function cannot be evaluated in a simple way. We can, however, simplify the problem by replacing the inclined top line QR by a horizontal line $Q'R'$ passing through its center. We shall thus get a practically equivalent energy curve $MNQ'R'ST$ (Fig. 3), for which the function D is given

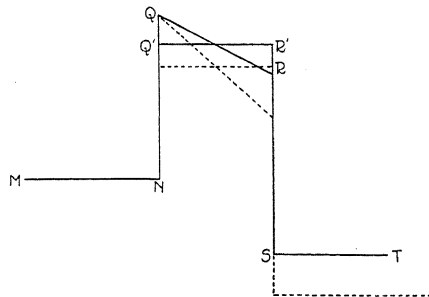


Fig. 3.

by the formula

$$D = \frac{4\alpha_a\alpha_b}{(\alpha_a + \alpha_b)^2 \cosh^2 \beta\delta + (\beta - \alpha_a\alpha_b/\beta)^2 \sinh^2 \beta\delta}$$

where

$$\alpha_a^2 = \frac{8\pi^2 m}{h^2} W_x, \quad \alpha_b^2 = \frac{8\pi^2 m}{h^2} (W_x + U'), \quad \beta^2 = \frac{8\pi^2 m}{h^2} (U_a' - W_x),$$

with $U_a' = NQ' = U_a - \frac{1}{2}V$, $U_b' = SR' = U_b + \frac{1}{2}V$, $U' = U_{ab}$. For sufficiently large values of $\beta\delta$, with which we are here concerned, the above expression reduces approximately to

$$D = \exp \left[- \left\{ (U_a - W_x - \frac{1}{2}V) / kT_1 \right\}^{1/2} \right] \quad (24)$$

with the previous definition of T_1 . In substituting this into (23) we must put $W_x = W_a$. We thus get the same expression for D as in the case of two identical metals, with the only difference that the "work function" $U_a - W_a$ is replaced by

$$U_a - W_a - \frac{1}{2}V = \frac{1}{2}[(U_a - W_a) + (U_b - W_b)] \quad (25)$$

that is by the arithmetic mean of the work functions of the two metals.

Now if V is increased by $V_1 \ll V$ the transmission coefficient is changed by the amount $(\partial D / \partial V) V_1$ where

$$\frac{\partial D}{\partial V} = \frac{D}{4[\frac{1}{2}kT_1(U_a - W_a + U_b - W_b)]}.$$

Introducing this expression and the expression (24) in (11) and putting for the sake of brevity

$$[2kT_1(U_a - W_a + U_b - W_b)]^{1/2} = \theta \quad (26)$$

we have

$$\alpha_2 = \frac{2\pi}{m^2} \frac{1}{2\theta} \int_0^\infty dW D(W) [f_b(W + U) + \theta f_b'(W + U)]$$

or so long as θ is small compared with $W + U$

$$\alpha_2 = \frac{\pi}{m^2 \theta} \int_0^\infty dW D(W) f_b(W + U + \theta). \quad (27)$$

Comparing this (8) we see that

$$\alpha_2 = \alpha_1' / 2\theta \quad (28)$$

where α_1' is the value taken by the coefficient α_1 , if U is increased by θ . It may be remarked that α_1 , is connected with the "specific conductivity" of the gap σ_g by the relation

$$\sigma_g = e^2 \delta \alpha_1.$$

Now α_1' , is but slightly different from α_1 , since θ is assumed to be small, so that we can finally put $\alpha_2 \cong \alpha_1 / 2\theta$. This relation could be of course obtained directly by neglecting the first term in the integral (11) which does not take account of the change of the transmission coefficient D caused by the introduction of the additional potential difference V_1 . It can be easily shown that the ratio of this term to the second term, which just characterized this change, is approximately equal to

$$\frac{\theta}{U_a - W_a + U_b - W_b} = \left(\frac{2kT_1}{U_a - W_a + U_b - W_b} \right)^{1/2}$$

that is, remains very small for values of T_1 corresponding to gaps of the width $\delta = 10A$ or even less than that.

The "characteristic curve" of our contact, considered as a rectifier, is thus the parabola

$$I = \alpha_1 V_1 (1 + V_1 / 2\theta)$$

This equation holds, of course, for sufficiently small values of V_1 only. It follows from it that the rectifying action of the contact becomes prominent for values of $|V_1|$ which are of the same order of magnitude as θ . Using the previous value of $T_1 = 120^\circ$ which corresponds to 0.01 volts and assuming for the mean work function of the two metals $\frac{1}{2}(U_a - W_a + U_b - W_b)$ a value corresponding to 4 volts, we get for θ about 0.4 volts.

This is a rather large figure, which explains the fact that metallic contacts cannot be used as detectors for radio-oscillations of small amplitude.

It seems possible, however, on our scheme to explain the detector action of contacts between metals and some semi-conducting "crystals" used for this purpose in simple radio receivers, by assuming that in these bodies we have to deal with a distribution of electrons different from that of Fermi.

The simplest assumption would be to replace the Fermi distribution by the usual Maxwellian one, corresponding to a relatively small number of free electrons per unit volume. This can be considered as a particular case of the preceding theory, since the Maxwell distribution is the limiting case

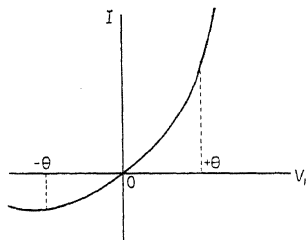


Fig. 4.

of the Fermi distribution which may be specified by putting the maximum kinetic energy of the electrons at $T=0$ equal to zero. It is clear that in this case the semi-conductor will play the role of the body a and the metal that of the body b , so that we shall have $W_a=0$, $V=U_a-(U_b-W_b)$, etc.¹¹

It seems at first sight that this will leave our formulas for α_1 , and α_2 unaltered since they depend upon the distribution function of the body b only and not on that of the body a . That this is not so, is clear, however, from equation (23), which with $W_a=0$ and $v_a=0$ would give $\sigma_a=\infty$. This shows that some of the approximations used in the evaluation of α_1 , and α_2 no longer hold in the limiting case we are now considering.

We shall not try to adjust our calculations to this case, for the implied picture of a semi-conductor as of a box enclosing a rarefied electron gas seems hardly adequate enough to deserve a quantitative treatment. It is, however, directly apparent without any calculations whatsoever, that the rectifying effect of a contact between two bodies, so far as it depends upon their dissimilarity with respect to the concentration and the velocities of the electrons, must increase for a given absolute value of V_1 as this dissimilarity becomes more pronounced.

A satisfactory extension of the above theory to the case of contacts between a metal and a semi-conductor, or between two semi-conductors will be possible only after an at least crude electron theory of such semi-conduc-

¹¹ We have designated with a that body for which the potential energy (inside) is higher than for the other when equilibrium is reached, that is, when the straight lines representing the kinetic energies W_a and W_b lie on the same level (that is, coalesce with each other).

tors shall have been developed. It will be further necessary to take account of the fact that in actual contacts the distance δ between contiguous surfaces does not remain constant, but varies in a more or less periodic manner, within a certain range, and that the adjacent (curved) surfaces of the two bodies need not be equipotential surfaces, as is the case if they are far apart.

X-RAY ABSORPTION IN GASES

BY W. W. COLVERT

RYERSON PHYSICAL LABORATORY, UNIVERSITY OF CHICAGO

(Received October 27, 1930)

ABSTRACT

X-ray spectral lines reflected from a platinum surfaced mirror and by a calcite crystal have been used for absorption measurements with neon, sulphur dioxide, chlorine and argon. The double reflection gives a more nearly homogeneous beam, since the mirror greatly reduces the higher orders of the shorter wave-lengths. The results are summarized in the following table.

MASS ABSORPTION COEFFICIENTS

	0.496A	0.561A	0.631A	0.710A	1.389A	1.539A	2.288A
Ne	0.84	1.20	1.69	2.50	16.0	23.4	75.5
Al	1.96	2.71	3.82	5.32	37.3	50.7	149.6
SO ₂	1.92	2.67	3.60	5.55	38.5	51.8	162.6
S (Calc)	3.40	4.64	6.89	9.96	66.4	88.4	284.0
Cl	4.14	5.76	8.18	11.52	76.9	102.7	315.0
A	5.06	6.89	9.80	13.0	85.7	114.0	339.4

INTRODUCTION

AN EXAMINATION of the tabulated values of x-ray absorption coefficients¹ reveals the scarcity of data for gases. In spite of the chances for contamination, gases are to be preferred to solids in some cases of absorption measurement. With the longer wave-lengths in particular, the thickness of solid absorbers is so small that the question of homogeneity presents serious difficulties. Such is not the case with gases.

In the present work neon, sulphur dioxide, chlorine and argon were studied. For comparison purposes, readings were also taken with aluminum. The K_{α} and K_{β} lines of silver, molybdenum and copper and the K_{α} line of chromium were used with each material.

APPARATUS

In order to secure significant absorption data, especial precautions were taken to obtain homogeneous x-rays of known wave-length, as well as to insure the purity of the absorbing materials. Homogeneity was obtained by totally reflecting the x-rays from a platinized mirror, and then selecting a strong spectral line by diffraction from a calcite crystal. The angle of the mirror can be so adjusted that the desired wave-length λ is totally reflected, whereas for wave-lengths $\lambda/2$, $\lambda/3$, etc. the glancing angle of incidence is greater than the critical angle and no appreciable reflection occurs. It is thus possible to apply relatively high potentials to the x-ray tube without danger

¹ International Critical Tables, Vol. VI, p. 12.

of introducing higher order reflections, an especially valuable feature for the longer wave-lengths.

The arrangement of the apparatus is shown in Fig. 1. The x-rays, after reflection from the platinized mirror *b*, traversed the absorption cell *c*, and were then reflected from the calcite crystal *d* into the ionization chamber. The figure is drawn approximately to scale.

For the source of x-rays, water cooled tubes of the Coolidge type were used. The Mo target tube was supplied by the Victor X-Ray Corporation; the silver, copper and chromium tubes were made by Siemens Reiniger Veifa. Lindemann glass windows in the latter two tubes avoided great absorption in the walls. As a source of high voltage a high tension transformer without

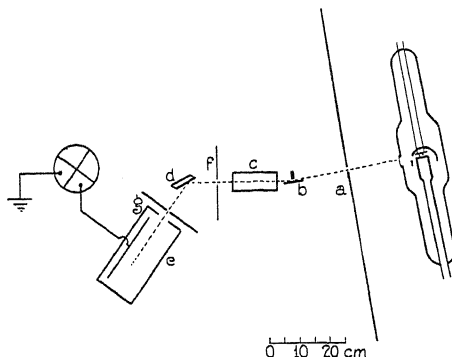


Fig. 1. Diagram of apparatus.

rectification was found satisfactory. An auto transformer and rheostat in the primary circuit served to control the voltage. The primary of the filament transformer was connected, through a variable resistance, across the primary of the high tension transformer. In spite of this precaution, however, it was not possible to eliminate completely the effect of fluctuations of the line voltage.

The spectrometer was of the double crystal type, designed by A. H. Compton, and constructed by the Societe Genevoise. The platinized mirror was placed in the position of the first crystal. A Compton electrometer was used for current measurements. The insulation was sulphur, and the ionization chamber was filled with argon.

THE ABSORPTION CELLS

Since one of the chief problems in working with gases is the obtaining of pure samples and the maintaining of that state during the observations, particular care was used in the selection of containers for the gases. Three types were used during the experiment. Fig. 2a represents the first type. These cells were made by fusing very thin glass windows to Pyrex tubing of the size indicated. Being curved, the windows could be made quite thin and yet stand atmospheric pressure during outgassing. This cell has the advantage that it may be thoroughly outgassed and that there is very little

chance of contamination after a cell is once filled and sealed off. The second type, Fig. 2b, was obtained by closing the ends of the Pyrex tubing with brass pieces which had narrow rectangular openings in the ends. These openings were covered with thin celluloid windows which were attached to the brass by means of "Duco Household Cement." The brass to glass connection was made by means of wax. The third type, Fig. 2c, was quite similar to the second. In this case, however, plane glass windows were fused to the tubing, rectangular slits cut in these windows and celluloid cemented over these openings. The third type was used only as a check on the second to see if any appreciable contamination might be detected by such a comparison.

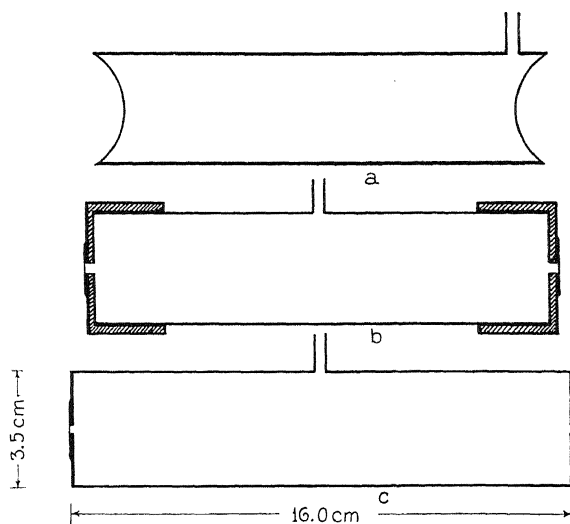


Fig. 2. Diagram of three types of cell used.

A cell of type *a* could be attached directly to the vacuum line, outgassed by baking for several hours, and filled with a purified gas without having the gas come in contact with anything except glass. For this reason seven such cells were used. The other cells were preferable however when the absorption in the glass windows became so great as to prevent accurate observations.

Purification of chlorine and sulphur dioxide was by a partial distillation method. The gas as furnished commercially was dried and solidified by cooling. Any unsolidified matter was removed by the vacuum system. On raising the temperature of the solidified material a few degrees above the boiling point of the particular gas the entire system was filled with the gas. The cell was then sealed off at an observed temperature and pressure. The neon was furnished in flasks, specially purified, by the Air Reduction Company. One cell was filled with argon furnished by the Air Reduction Company as pure. A second was filled with argon purified by means of a misch metal arc. A third cell was filled with argon containing known percents of impurities. As these three gave, on correction of the third, very nearly the same results,

gas of the last mentioned type was used throughout the latter part of the experiment.

THE DATA

A test of the homogeneity of the beam was made by means of Al foil. Three or more samples of aluminum were used in every case, and they were so selected as to give a total absorption of the same order of magnitude as with the gas-filled cells. If the values of the mass absorption coefficients with the various samples showed no decrease greater than the experimental error, it was assumed that the beam was sufficiently nearly homogeneous for the purposes of the experiment.

In order that the absorption of the gas be separable from that of the cell, readings were taken in each case with the cell evacuated and then filled to a measured pressure. Since, in several cases, the absorption by the gas was only a small part of the total measured quantity, it was very important that the cells be placed in the same position for all readings. Precautions were taken to insure that this be the case.

Corrections for the impurities in the argon were obtained by calculation from the Eq. (1)

$$m(\mu/\rho) = m_1(\mu/\rho)_1 + m_2(\mu/\rho)_2 + \text{etc.} \quad (1)$$

m being the mass and μ/ρ the mass absorption coefficient of the mixture; the terms on the other side of the equation representing the same quantities for the constituents. For the longer wave-lengths, values of μ/ρ for nitrogen and oxygen were obtained from table values by extrapolation. The data for sulphur were obtained from the sulphur dioxide values of the atomic absorption coefficients by subtracting the oxygen values in a similar manner.

In every case, the times for the rates of deflection over the same range were taken with the absorber alternately in and out of the path of the x-ray beam. These times were corrected for natural leak. From twenty-five to two hundred such pairs of readings constitute a single "set."

Data for four gases using a single cell and a single wave-length, K_α of Mo, are shown in Table I. Here i_1/i_0 represents the ratio of the transmitted to the incident intensity, μ/ρ is the mass absorption coefficient and μ_a the atomic absorption coefficient. The argon used in cell 5 contained 3% nitrogen and 0.4% oxygen. Corrected value = 85.6. The value of S from the SO_2 value = $(58.13 - 5.28) = 52.8$.

TABLE I. K_α of Mo. ($\lambda = 0.710$).

Cell	Absorber	Density (g/cc)	(Evac.)	i_1/i_0 (Filled)	μ/ρ	$\mu_a \cdot 10^{23}$
5	Ne	0.000512	$0.6093 \pm 1/7\%$	$0.6000 \pm 1/7\%$	2.42	8.07
5	SO ₂	.002045	.6093	.5280	5.50	58.13
5	Cl	.00166	.6093	.4780	11.44	66.92
5	A	.001589	.6093	.4700	12.78	84.1

In a similar way data were obtained for the other wave-lengths and using various absorption cells, giving the results summarized in Table II.

TABLE II. Mass absorption coefficients.*

Substance	AgK _β .496A	AgK _α .561A	MoK _β .631A	MoK _α .710A	CuK _β 1.389A	CuK _α 1.539A	CrK _α 2.288A
10 Ne	.84	1.20	1.69	2.50	16.0	23.3	75.5
13 Al	1.96	2.71	3.82	5.32	37.3	50.7	149.6
SO ₂	1.92	2.67	3.60	5.55	38.5	51.8	162.6
16 S (Calc)	3.40	4.64	6.89	9.96	66.4	88.4	284.0
17 Cl	4.14	5.76	8.18	11.52	76.9	102.7	315.0
18 A	5.06	6.89	9.80	12.98	85.7	114.0	339.4

Substance	0.496A	Atomic absorption coefficients × 10 ²³				1.539A	2.288A
		0.561A	0.631A	0.710A	1.389A		
10 Ne	2.8	4.0	5.63	8.33	53.3	77.6	252
13 Al	8.76	12.1	17.1	23.8	167	226	668
16 S	17.9	24.4	36.3	52.5	350	466	1497
17 Cl	24.2	33.7	47.8	67.4	450	601	1843
18 A	33.3	45.3	64.5	85.4	564	750	2233

Fig. 3 shows curves obtained by plotting $\log_e \lambda$ and $\log_e \mu/\rho$. Empirical

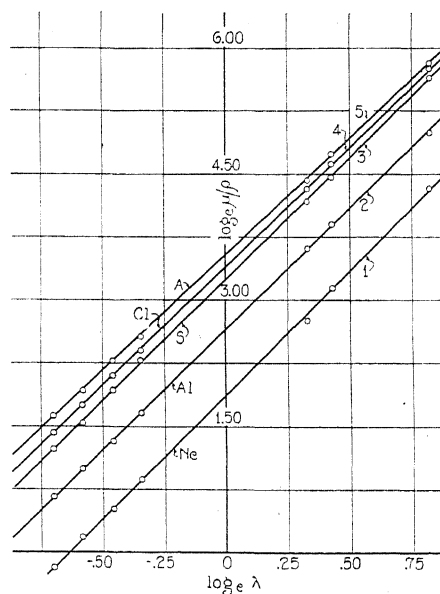


Fig. 3. Plot of $\log_e \lambda$ and $\log_e \mu/\rho$.

equations which represent these lines are as follows:

$$(\text{Ne}) \quad \log_e \mu/\rho = 2.92 \log_e \lambda + 1.87, \text{ or } \mu/\rho = 6.5 \lambda^{2.92} \quad (2)$$

$$(\text{Al}) \quad \log_e \mu/\rho = 2.88 \log_e \lambda + 2.67, \text{ or } \mu/\rho = 14.45 \lambda^{2.88} \quad (3)$$

$$(\text{S}) \quad \log_e \mu/\rho = 2.90 \log_e \lambda + 3.25, \text{ or } \mu/\rho = 25.8 \lambda^{2.90} \quad (4)$$

$$(\text{Cl}) \quad \log_e \mu/\rho = 2.84 \log_e \lambda + 3.40, \text{ or } \mu/\rho = 30.0 \lambda^{2.84} \quad (5)$$

$$(\text{A}) \quad \log_e \mu/\rho = 2.77 \log_e \lambda + 3.45, \text{ or } \mu/\rho = 34.5 \lambda^{2.77} \quad (6)$$

* An analysis of a sample of the aluminum used showed 0.45 percent iron. The values of the mass absorption coefficient for Al given in Table II are therefore too high for pure Al.

A comparison of experimental values with values calculated from these equations shows, in the majority of cases, discrepancies less than one per cent.

DISCUSSION OF RESULTS

From the equation

$$I_1 = I_0 e^{-\mu x} \quad (7)$$

it follows that

$$\mu/\rho = (-\log_e I_1/I_0)/\rho x \quad (8)$$

where I_1/I_0 is the ratio of the transmitted intensity to the incident intensity, μ is the linear absorption coefficient, x the thickness and ρ the density of the absorber. In order that the value I_1/I_0 be for the gas only it is necessary to use the ratio i_1/i_0 (filled) to i_1/i_0 (evacuated), i.e., for this calculation, $I_1/I_0 = (i_1/i_0)f/(i_1/i_0)_{ev}$. The uncertainty in the value of μ/ρ is therefore increased. The length x was known to about 1/3 percent, the value of the density to 1/5 percent and the value of i_1/i_0 to 1/7 percent. The value of I_1/I_0 is however by no means so accurate. A comparison of the data of Tables I and II shows that for neon in particular the uncertainty is rather large. This obviously results from the fact that the absorption by the gas was so small a part of the total measured quantity. In the case of gases of larger atomic number and even for neon at the longer wave-lengths this uncertainty is greatly diminished.

Other data for these gases, with which to compare the present results, are very meagre. Wingardth² has obtained some measurements on chlorine gas for $\lambda = 0.586, 0.631$ and 0.709\AA . For the latter wave-length he finds $\mu/\rho = 11.9$, which compares acceptably with the value 11.52 here obtained. Barkla and Collier³ also made some measurements many years ago on the absorption of fluorescent x-rays in sulphur dioxide. Because of the lack of true homogeneity, their data are of little significance for a precise comparison, though the agreement with the present results is as good as can be expected. Because of this lack of other existing absorption data, for these substances, the present data are perhaps of especial value.

In conclusion, I wish to express my appreciation to Professor A. H. Compton for his suggestions and interest both preceding and during the period of experimental work.

² Wingardth, Dissertation, Lund, 1923.

³ Barkla and Collier, Phil. Mag. **23**, 987 (1912).

DIFFRACTION OF X-RAYS IN LIQUIDS:
EFFECT OF TEMPERATURE

BY E. W. SKINNER

UNIVERSITY OF IOWA

(Received October 15, 1930)

ABSTRACT

The effect of temperature upon x-ray diffraction has been examined for the following liquids: mesitylene, 4-hydroxy-1,3-dimethylbenzene, 2-hydroxy-1,3-dimethylbenzene, phenol, naphthalene, benzene, cyclohexane, di-n-propyl carbinol, heptylic acid, tertiary butyl alcohol, lauryl alcohol, octane, 2,7-dimethyloctane and 2,4-trimethylpentane. (1) The peaks shift in the intensity-diffraction angle curve toward smaller angles with increase in temperature, which varies in amount in different planar spacings in the same liquid; (2), the peak intensity varies with temperature differently for the different spacings in a single liquid, the principal maxima showing a decrease in the intensity for some liquids (class I), and an increase in the intensity for other liquids (class II) with increase in temperature; (3) a greater diffuseness of the principal maxima was found at high temperatures, attaining a greater magnitude for class I liquids; (4) the percentage increase in peak width per degree change in temperature is greater for class II than for class I; (5) boiling had no effect on diffraction phenomena, (6), increased scattering at small angles was noted at high temperatures, the effect being greater for class II.

The foregoing results lead to the following conclusions. The evidence favors strongly the cybotactic space group condition of liquids and indicates that in some of the liquids space rearrangement within these groups takes place with changes in temperature. It may be said there is a change in molecular shape. Furthermore, within the groups of some liquids, expansion is apparently different in different directions, or internally anisotropic.

RESEARCHES carried on in this laboratory and elsewhere¹ on the diffraction of x-rays in liquids indicate that the molecular arrangement in a liquid consists of fairly orderly though temporary groups produced by molecular forces. These forces are most effective in producing such a regularity in unsymmetrical molecules. The groups evidently have neither perfect form nor sharp boundaries. Although numerous incidental suggestions as to the somewhat crystalline arrangement of molecules in a liquid antedate the work of this laboratory, yet it has been here that such a description, termed the "cybotactic condition," has been actively adopted and attempts have been made to establish its certainty by every systematic means of approach. Thus, the effect of increase in length of chain, and the differences in molecular arrangement of alcohol molecules with point of attachment of OH have been discovered. A determination of the influence of temperature is clearly of importance in such a study.

¹ See papers by Stewart and co-workers in *Phys. Rev.* 1927-1930; Stewart, *Rev. Mod. Phys.* 2, 116 (1930); Stewart, *Chem. Rev.* 6, 483 (1929); Drucker, *Phys. Zeits.* 29, 273 (1928).

APPARATUS AND METHOD

The x-ray spectrometer used, and the method of procuring diffraction curves were essentially the same as described by Stewart and Morrow.² The furnace for heating the liquid consisted of two coils of nichrome wire wound about two pieces of one inch iron pipe, each 2.5 inches long. The wire was insulated from the iron with asbestos. The heating coils were mounted vertically, one above the other, leaving room between their near ends for the passage of x-rays. The liquid was contained in a thin walled glass tube and placed so as to intercept the primary beam in this space. The thin walled

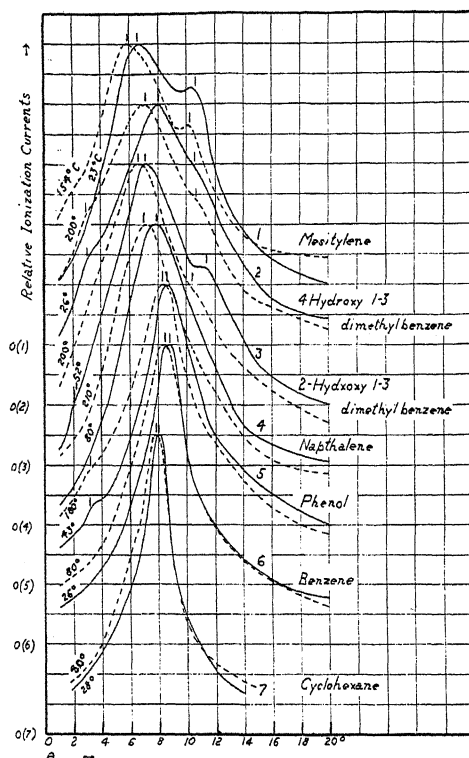


Fig. 1. Relative intensity liquid diffraction curves at two different temperatures.

glass tube was fused to a heavier tube leading to a Graham reflux condenser. The temperature was measured by means of a calibrated constantan-copper thermocouple, enclosed in a thin-walled capillary tube and inserted in the liquid.

The diameter of the tube containing the liquid was made definitely less than the optimum thickness of each particular liquid under observation, in order that there might be no effect from general radiation. The diffraction peaks obtained are produced by the Mo $K\alpha$ radiation. The voltage on the tube was such as to cause the maximum of the general radiation to fall at

² Stewart and Morrow, Phys. Rev. 30, 232 (1927).

about 6°. The curve for cyclohexane in Fig. 1 indicates the absence of any important effect of general radiation.

RESULTS

The diffraction curves are given in Figs. 1 and 2, the dotted curves giving the data for the higher temperatures. Both sets are plotted to the same scale, hence, in Figs. 1 and 2 intensity comparison can be made only for a single curve. In Table I, the values for percentage change in intensity were obtained from the original data, before reduction as shown in Figs. 1 and 2. The following facts are drawn from these curves and Table I.

TABLE I. *Effect of change in temperature on the planar dimensions.*

Liquid	Temperature	d_1 (A.U.)	d_2 (A.U.)	d_3 (A.U.)	Percentage change in intensity of peak corresponding to d_1 , d_2 , d_3 , respectively.
1. Mesitylene	23°C	—	6.00	3.86	—
Mesitylene	154°C	—	6.92	3.96	+18.0, -42.3
2. 4-Hydroxy	26°C	14.0	5.10	3.86	—
1.3 dimethyl benzene	200°C	13.6	5.75	3.82	+80.0, +5.1, -30.0
3. 2-Hydroxy	52°C	17.1	5.76	3.79	—
1.4 dimethyl benzene	200°C	—	6.17	3.92	+12.7, -37.8
4. Naphthalene	80°C	—	5.17	—	—
Naphthalene	210°C	—	5.76	—	+4.7
5. Phenol	43°C	12.7	4.73	—	—
Phenol	180°C	12.7	4.92	—	-38.0, +2.8
6. Benzene	26°C	—	4.64	—	—
Benzene	80°C	—	4.80	—	-1.1
7. Cyclohexane	28°C	—	5.08	—	—
Cyclohexane	80°C	—	5.24	—	-14.0
8. Di-n-Propyl Carbinol	24°C	10.2	4.87	4.35	—
Di-n-Propyl Carbinol	153°C	10.2	4.87	—	-6.7, +18.9
9. Heptylic Acid	28°C	17.7	4.64	—	—
Heptylic Acid	193°C	18.5	4.80	—	+18.5, -12.2
10. Tertiary Butyl Alcohol	27°C	8.51	4.80	—	—
Tertiary Butyl Alcohol	80°C	8.88	4.90	—	-37.7, +9.8
11. Lauryl Alcohol	27°C	22.7	4.54	—	—
Lauryl Alcohol	140°C	24.0	4.80	—	-2.4, -5.6
12. Octane	27°C	—	4.54	—	—
Octane	120°C	—	4.70	—	-7.3
13. 2,7-Dimethyloctane	27°C	—	4.75	—	—
2,7-Dimethyloctane	150°C	—	5.17	—	-10.3
14. 2,2,4 Trimethylpentane	27°C	—	5.67	—	—
2,2,4 Trimethylpentane	92°C	—	5.91	—	+0.5

Explanation: d_1 represents the planar distance given by the small maximum on the small angle side of the principal maximum; d_2 the distance given by the principal maximum; and d_3 the third dimension given by the remaining maximum when present.

(1) In general the maxima shifted toward the smaller angles of scattering with increase in temperature, the principal maxima being most consistent in this regard. The small peaks, denoting the largest spacing, showed no change in dimension except for tertiary butyl alcohol(10).

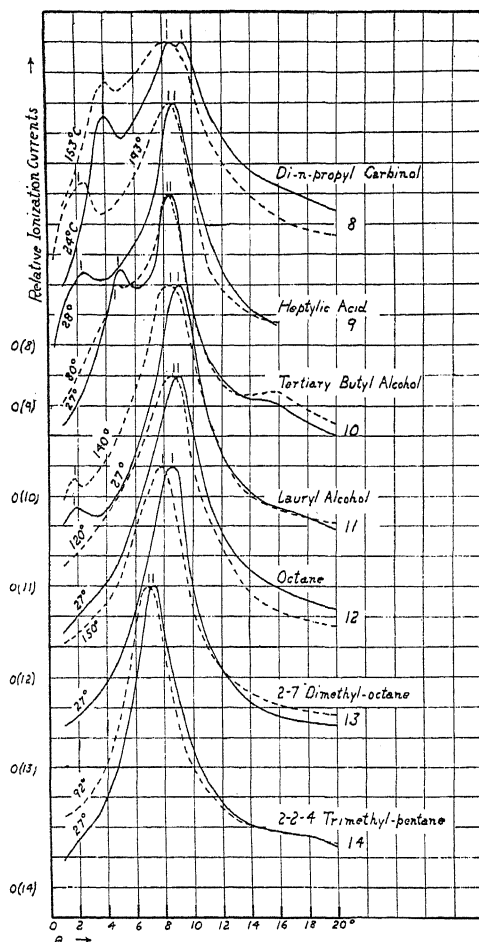


Fig. 2. Relative intensity liquid diffraction curves at two different temperatures.

(2) The effect of temperature upon the intensity is not uniform for all the liquids. In this respect, the liquids fall under two classifications:

Class I. Those liquids whose principal maxima show a decrease in intensity with increase in temperature, including nos. (6), (7), (9), (11), (12), and (13). (See Table I).

Class II. Those liquids whose principal maxima show an increase in intensity with increase in temperature, including nos. (1), (2), (3), (4), (5), (8), (10), and (14).

In general the smaller maxima in all liquids showed a decrease in intensity with increase in temperature.

(3) An increase in general scattering at small angles with increase in temperature was found in all cases, the increase being greater for liquids of class II.

(4) No observable difference in peak intensity was noted between that at the boiling point of tertiary butyl alcohol and a temperature a few degrees less.

(5) The percentage increase in peak width per degree change in temperature is five times as great for the liquids of class I, as for class II. As a matter of fact a graph showing the percentage change in peak width with difference in temperature is linear for both classes.

(6) A second order peak was noted in the case of tertiary butyl alcohol, but owing to the extreme diffuseness no conclusions regarding intensity change can be drawn.

These results may be compared with those obtained by Vaidyanathan³ who studied the influence of temperature on the haloes of camphene, mesitylene, acetic acid, butyric acid and ethyl alcohol, varying the temperature from 30° to 120° and 150°C. He observed a contraction of the haloes, an increase in their diffuseness and an increase in the scattering at small angles in all cases. In the case of liquids with two haloes, with rise of temperature, the separation between the inner and the outer halo tends to be effaced and the inner haloes become diffuse more quickly than the outer ones. As will be observed the results herein presented are in general agreement with those just cited, but not in detail.

DISCUSSION AND POSSIBLE INTERPRETATION OF RESULTS

(1) In general the effect of temperature upon liquid scattering is similar to the same effect in powdered crystals. This favors the conception of groups possessing space arrangement, simulating the effects of powdered crystals.

(2) The most obvious cause for the increase in planar dimension with increase in temperature is thermal expansion. A comparison of the expansion coefficients for d_2 , for example, as computed from the x-ray data, with corresponding values given in the International Critical Tables, shows no agreement. In fact, in some cases it showed as high as three times the true value. Furthermore, the expansion in molecular spacing in different directions in one liquid group is not the same. In consideration of these two facts, one is led to advance a new view of expansion in liquids which admits the possibility of anisotropic expansion within each group. Such a condition is common in crystals. The actual mechanism of expansion in the liquid might include an increase in warping of the molecules with increasing temperature. Such a warping might alone cause a decrease in separation of molecules in one direction and an increase in a direction perpendicular thereto. Such a condition of unequal expansion comparable to that of a crystal is not possible unless there exists, as is claimed, a temporary regularity of molecular arrangement in groups. This is designated as the cybotactic condition.

³ Vaidyanathan, Ind. J. Physics, III, III, 391, (1929).

(3) In the case of the liquids of class II, there is evidence of a group rearrangement, or a change in molecular shape causing such rearrangement. shown in (a) the increase in coherent scattering with increase in temperature. and (b), the small percentage increase in peak width per degree increase in temperature in comparison with class I liquids. This evidence, and that in the preceding paragraphs are not sufficient to assert that the rearrangement of groups actually occurs, but this interesting hypothesis seems a reasonable and straightforward explanation for the action of some liquids.

(4) In the case of the liquids in class I, the intensity decreases with an increase in temperature, and may be accounted for by two factors: (a) the decrease in density of the liquid due to the thermal expansion, (b) the disturbance of group regularity due to increased thermal agitation. That the first cause is not the only one, was proved by a special experiment. The relation between the intensity of the principal maximum and the mass intercepted by the primary beam was determined experimentally for cyclohexane. The actual change in mass intercepted over the given temperature change was computed, and the loss in intensity due to expansion determined. This was found to be 4 percent, whereas the actual loss was 14 percent.

In the view of the workers in this laboratory, the cybotactic condition is one in which at any instant small regions, occurring frequently throughout the liquid, have effective regularity of molecular spacing. A moment later a similar description applies, but with the regions of regularity altered in positions. Between these regions are to be expected less regularity of arrangement. But there are no sharp boundaries of regions of regularity of structure. Neither is there entire randomness anywhere. But with any failure to comply with perfect crystalline form, there would be a lack of coherent scattering and hence greater diffraction near the zero angle of diffraction. Class II, in which the group structure seems to be altered with increase in temperature, also shows a greater increase with temperature of the scattering near the zero angle than do the liquids of class I. These two phenomena are definitely correlated in the liquids here used. As could be anticipated from the view here stated, an increase in scattering near zero angle of diffraction would be caused by increase in temperature for all liquids. This expectation is verified.

The boiling point, in the very nature of the case, has no relation to the group arrangement of molecules. As should be expected, the approach to boiling point produced no marked alterations in the diffraction curves. As will be observed all of the results of these experiments are in accord with the conception that in the liquid state, the cybotactic condition is generally found.

The author wishes to take this opportunity to express his appreciation of the cooperation of the staff of the Physics Department and his thanks to Professor G. W. Stewart for his suggestions and inspiration in carrying on this research.

ON THE FLUORESCENCE OF QUARTZ UNDER THE INFLUENCE
OF CATHODE RAYS OF LOW VOLTAGE

BY HEINRICH PETERS, Rheydt

(Based upon experiments made in collaboration with Th. Schultes, Darmstadt)

(Received September 17, 1930)

ABSTRACT

Some experiments on the production of a red fluorescence in glass and quartz by cathode rays are described. It was found that the red glow could be produced in highly evacuated tubes and that the presence of oxygen or other gases was not essential. This is contrary to the conclusion of Wood. A spectroscopic study of the fluorescence showed a continuous spectrum with two maxima in the red, one in the green and one in the blue. No trace of any oxygen line was found. The observation that the red fluorescence disappears after about 70 hours of bombardment indicates that the SiO_2 group in the glass goes over into an allotropic modification.

LILIENTFELD¹ found that, under certain conditions, the discharge of electricity through rarefied gases was accompanied by a red (instead of the usual green) fluorescence. The red fluorescence appeared in tubes which had been flushed with oxygen and then evacuated to a pressure less than 0.01 mm Hg. Lilienfeld regarded the phenomenon as due to the bombardment by slow cathode rays of the glass walls on which a gas (probably oxygen) was occluded.

E. Goldstein² reported that he also noted the red fluorescence not only of glass but of other substances, such as rock crystal, fused quartz, etc., which contain SiO_2 . Since the fluorescence appeared not at all in tubes containing N_2 , H_2 , CH_4 , He or A, weakly with air and strongly with oxygen, he concluded also that oxygen was an essential factor in the production of the fluorescence.

On the other hand Konen³ pointed out that he could obtain the red fluorescence in tubes filled with helium. He suggested that CaO , present in minimal amounts, might constitute the fluorescent centers but admitted the difficulty of discriminating between this hypothesis and that of Lilienfeld and Goldstein.

Gehrke and Reichenheim⁴ examined the red fluorescence spectroscopically and found a continuous spectrum between 654–620 $\text{m}\mu$ with two maxima in intensity at 650 and 630 $\text{m}\mu$. Superposed on this was a continuous spectrum of all colors with a broad maximum in the blue.

Quite recently Wood⁵ has found the same red fluorescence accompanying the excitation of gases at very low pressures by high-frequency ($\lambda = 4\text{m}$), low-potential discharges. According to Wood the red glow appears only in

¹ I. E. Lilienfeld, Ber. d. deutsch. Phys. Ges. p. 631 (1906); Ann. d. Physik **32**, 673 (1910).

² E. Goldstein, Ber. d. deutsch. Phys. Ges. p. 598 (1907).

³ E. Konen, Ber. d. deutsch. Phys. Ges. p. 774 (1907).

⁴ Gehrke and Reichenheim, Ber. d. deutsch. Phys. Ges. p. 593 (1907).

⁵ R. W. Wood, Phys. Rev. **35**, 673 (1930).

very well cleansed tubes and goes over into a green fluorescence when the potential is increased. In this case a red fluorescent spot appears on the wall opposite the green fluorescence.

According to Wood the red fluorescence does not appear promptly after application of the potential but appears gradually in a few seconds or minutes, and is sometimes preceded by a green fluorescence. Further he remarks that if a bright discharge is produced at one end of the tube with a single ring electrode until the glass fluoresces with a red color and the ring is then moved to the other end, there will be no red fluorescence there. He concludes that some chemical alteration of the glass must be essential to the fluorescence. The red fluorescence could not be excited by the field of a 30m oscillator but after it had appeared in the field of a 2m oscillator it could be maintained by the 30m oscillations. Stroboscopic investigations showed that the excitation was by electron rays having a definite direction and that there was no special property of the high frequency discharge involved.

Spectroscopic examination established that, in addition to the continuous spectrum in the red, lines of the oxygen spectrum always appeared. For this reason Wood believed that the presence of oxygen was a necessary factor in the red fluorescence.

Independently, the author⁶ has also observed the red fluorescence under experimental conditions similar to those of Wood.⁵ Since the experimental results differ in some respects from those of Wood, it would seem appropriate briefly to mention them here.

Tubes of widely varying length were used. The electrodes were external and were excited by a vacuum tube oscillator. The oscillator in some of the experiments was of the push-pull type described by Eccles and Jordan.⁷ The wave-length was 6-7 meters and the output 150 watts. The potential was transmitted to the experimental tube by placing it at the loop position in an inductively coupled Lecher system (Figs. 1-3).

By varying length and diameter of the tubes it was found that the fluorescence was strongest in short, narrow tubes, i.e., in those in which the current density was greatest. In the wide tubes the glow did not appear unless the cathode rays were concentrated on individual spots by means of a magnetic field.

In other experiments a long-wave oscillator ($\lambda = 700\text{m}$) was used to determine whether or not a change of frequency materially affected the phenomenon. For these experiments a Hartley oscillator of about 80 watts capacity was used (Fig. 4). Oscillator and tube were connected by a Oudin resonator coil. In contrast to Wood's results it was found that all tubes showed the red fluorescence when excited by the long waves and that a preliminary excitation by short waves was not necessary. I believe that the difference which Wood observed between the long and short wave excitation was due to a difference in some discharge characteristic (probably potential) other than frequency.

⁶ Peters and Schultes, *Zeits. f. Elektrochemie*, im Erscheinen begriffen.

⁷ Eccles and Jordan, *Electrician* 83, 299 (1919).

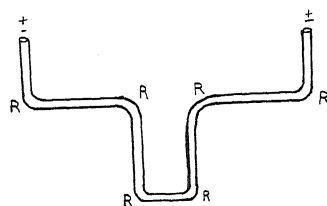


Fig. 1. Experimental tube of Lilienfeld for observation of the red phosphorescence at discharges with A.C. The points marked with *R* showed the red phosphorescence.

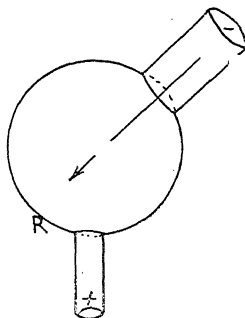


Fig. 2. Experimental tube of Lilienfeld for observations of the red phosphorescence at discharges with D.C. The point marked with *R* showed the phenomenon.

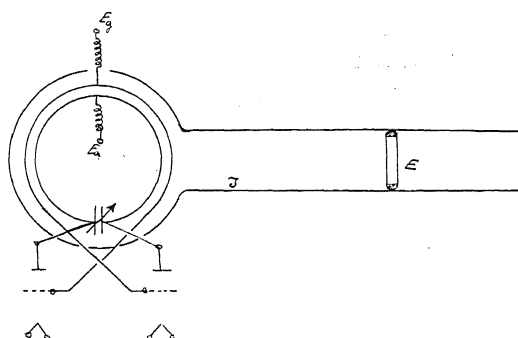


Fig. 3. Push-pull oscillator with inductively coupled Lecher system (*J*). *E* represents the experimental tube with exterior electrodes.

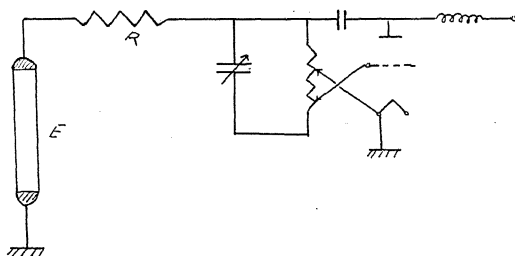


Fig. 4. Hartley oscillator, to which the experimental tube *E* is coupled by a resonator coil *R* of Oudin.

Experiments with internal electrodes also gave the red fluorescence at both high and low frequency alternating currents and with direct current.

When the high frequency current was led to the tubes through a suitable rectifier no new phenomena whatsoever appeared. It was observed that because of irregular field distribution the experimental tubes showed a detector action which makes the rise of cathode rays possible in one direction only. This observation corresponds with the stroboscopic experiments of Wood who found a periodic appearance of the fluorescence in rhythm with the alternating frequency. Experiments on the deflection of the cathode beam with a magnetic field showed that the red fluorescence was produced by electrons of lower velocity than those producing the green fluorescence. The "positive electron ray," thought by some authors to be the cause of the red fluorescence, appears to be a secondary electron ray moving in a direction contrary to the primary one.

Because the earlier spectroscopic observations⁴ were made with tubes having internal electrodes it seemed worthwhile to repeat them with tubes having external electrodes which could as a consequence be more thoroughly cleaned. The tubes were raised to a high temperature (just under the melting point) and evacuated with a steel Gaede pump. The results of the spectroscopic study of the red fluorescence are as follows:

Beginning of the red fluorescence	723.8m μ
First maximum	642.5m μ
Minimum	633.8m μ
Second maximum	628.5m μ
End of the red phosphorescence	589.5m μ
Maximum in the green part	560.0m μ
Maximum in the blue part	479.0m μ

The spectrum of the fluorescence consists of a continuum in the red with two maxima close together and a broad continuum in the green and the blue. The values agree well with those of Gehrke and Reichenheim.⁴

In none of the nearly 100 spectral tests made, with exposure times up to more than 50 hours, *did an oxygen line appear.*

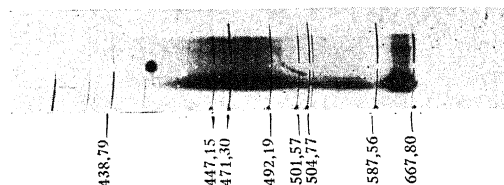


Fig. 5. Spectrographical test of the red phosphorescence. The lines are caused by a He-test, placed about in order to find the wave-length. The test shows that the red phosphorescence is a continuum and that no oxygen lines are present.

Fig. 5 gives a reproduction of one of the spectra. The double red as well as the green and blue maxima are to be seen distinctly. The lines visible in the figure are from helium and were added *subsequently* to serve as a wave-length guide. In order to make the two maxima in the red better visible, Fig. 6 shows a microphotometer curve of the spectrogram.

These spectroscopic results on heated, highly evacuated tubes proves that the red fluorescence will appear in the absence of any film of gas or water and that the presence of oxygen is not essential. This conclusion is at variance with that of Wood.

The red fluorescence was obtained with pure quartz also, which shows, in agreement with other publications,² that it is the SiO_2 group in the glass which is responsible for the fluorescence.

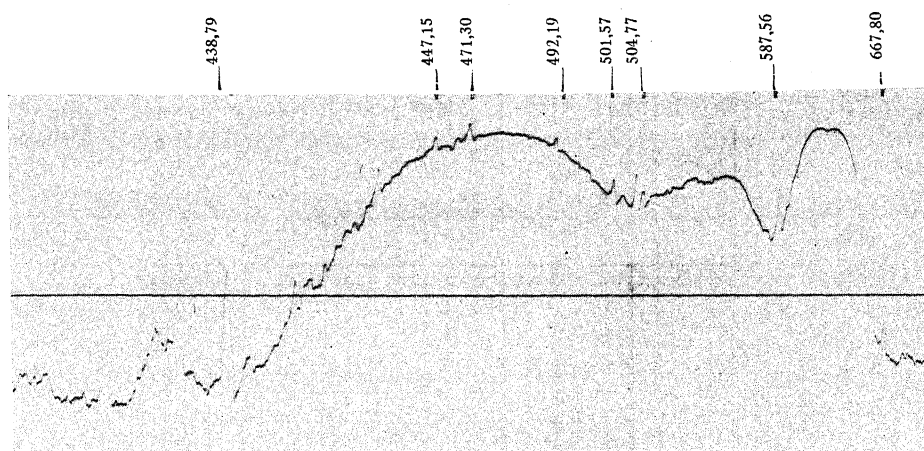


Fig. 6. Photometrical curve of the spectrographical test (Fig. 5). It shows distinctly the double maximum in the red part of the spectrum.

After continuously operating such tubes for nearly 70 hours it was found that the red fluorescence disappeared slowly. The points which had shown the red fluorescence now exhibited only the green fluorescence. Moreover, after having stood for weeks in an atmosphere of air, pure oxygen, hydrogen, steam, etc., the red glow did not appear again. The spectroscopic proof that the red glow is not due to oxygen is further strengthened by these results.

It has already been pointed out elsewhere⁶ that these observations make it probable that under the influence of slow cathode rays the SiO_2 group changes to another modification. For the normal modification, stable under ordinary conditions, I propose the name "erythrokeretic." Under the influence of slow cathode rays during the red fluorescence it changes to an allotropic form for which the proposed name is "lacinokeretic." This latter form has less energy and it is not possible to reduce it under simple conditions (heating, etc.) into the erythrokeretic form.

The existence of these two modifications is shown only by spectroscopic analysis and would probably be very difficult to demonstrate by more direct means. The only known method for transforming from one to the other is by bombardment by slow cathode rays and here the change takes place in a layer of minimal thickness. Nevertheless the possibility exists that the phenomena of poisoned quartz catalysers may find their explanation in this allotropy.

PRESSURE AND HIGH VELOCITY VAPOUR JETS AT CATHODES OF A MERCURY VACUUM ARC

BY E. KOBEL

PHYSICAL LABORATORY, BROWN, BOVERI AND COMPANY, LTD., BADEN, SWITZERLAND

(Received October 10, 1930)

ABSTRACT

The amount of vaporization of copper from the cathode of a copper arc measured by Tanberg as well as the velocity of this vapour calculated from the force of reaction on the cathode, agree closely with the values obtained by another method from the cathode of a mercury arc. With a mercury arc and fixed cathode spot the mercury vaporization is 0.017×10^{-3} gr/amp. sec. and the vapour velocity 16 to 43×10^5 cm/sec.

INTRODUCTION

DURING attempts to fix the rapidly moving cathode spot of the mercury arc in a conical tungsten insertion-piece, it was observed that when the entire surface of the mercury was covered by the cathode spot the force exerted on the mercury was considerable. The following experimental tests were carried out during the first six months of 1929 with the object of measuring this force. In the meantime, Mr. Tanberg¹ had published a description of a quantitative investigation of the force exerted on the cathode of a copper arc, and although the methods of measurement and the cathode materials are very different, the results agree very closely.

DESCRIPTION OF EXPERIMENTS

Fig. 1 shows diagrammatically the 3-anode rectifier with which the tests were carried out. *G* is a glass container of about 5.5 litres capacity, in the floor of which is the cathode *K*, and in the cover the three iron anodes *A*, equally spaced in the form of a triangle. The cathode is shown in section in Fig. 2. The conical and cylindrical-shaped tungsten insertion-piece *W* is extended in an upward direction by a quartz cone *Q*, so that the arc may be ignited in it by touching the mercury with the ignition anode *Z*. After ignition, the mercury is lowered into the cylindrical part of the tungsten insertion-piece by rotating the screw *S*. When increasing the cathode current, the mercury pressure must be adjusted at the same time by means of the screw *S*, so that the surface of the mercury, which is entirely covered by the cathode spot, neither rises nor sinks. The pressure can then be read on the slanting capillary glass tube *O*. In order to determine the amount of mercury vapour, the decrease in the mercury level in the tungsten insertion-piece and the corresponding ampère-seconds were determined at a constant temperature of the container and with the mercury feed pipe closed. It is well known that the vaporization of mercury at the cathode of a mercury arc with a free moving cathode spot has already often been established.² When the cathode spot

¹ R. Tanberg, Phys. Rev. 35, 1080 (1929).

² Zeits. f. Physik 2, 74-87 (1922); Phys. Zeits. 29, 857 (1928); Phys. Zeits. 30, 233 (1929).

is moving freely, the surface of the mercury is much larger than the area of the spot, and in this case the vaporization is greatly dependent upon the mean temperature of the surface of the mercury. When the cathode spot is fixed and covers the entire surface of the mercury, the amount of vaporization remains at a certain value which is no longer greatly dependent upon

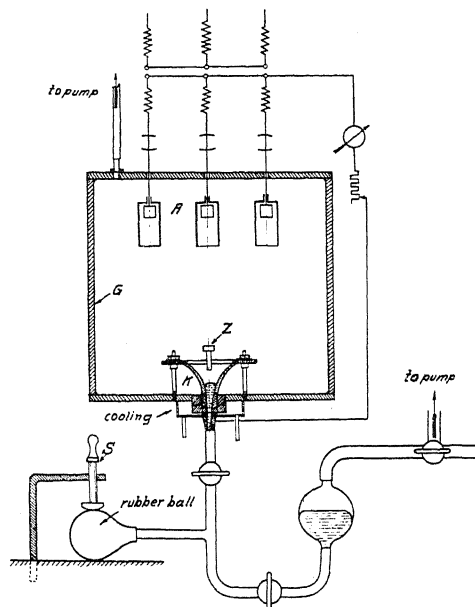


Fig. 1. Diagram of 3-anode rectifier.

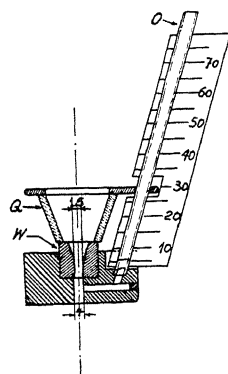


Fig. 2. Cross section of cathode.

the cooling of the cathode. This is also the case with a strongly-cooled copper-mercury cathode. The copper disk used as a cathode contained holes of about 2 mm diameter filled with mercury. A cooling liquid with a temperature of -10°C was circulated round a channel in the disk during the test. The arc only burned until all the holes covered by the cathode spot were used up. A subsequent examination of the copper disk showed that it had been scarcely burned by the arc, since an arc current of only 14 amp. was used.

RESULTS

The amount of mercury vapour at an average current of 35 amp. and with the cathode spot fixed in the tungsten insertion-piece was 0.017×10^{-3} gr/amp. sec.

The gas pressure in the container, arc current, force on the cathode spot and vapour velocity are given in Table I. The vapour velocity was calculated from formula (9) in Mr. Tanberg's article. No corrections for electrostatic and electrodynamic forces were made because they are of so little influence (less than 5 percent) that they do not effect the comparison of results which are already approximate.

TABLE I.

1	2	3	4	5	6
Arc current amp.	Current density in cathode spot amp./cm ²	Gas pressure mm Hg $\times 10^{-3}$	Height of mercury in glass tube cm	Force in dynes	(C ²) ^{1/2} vapour velocity in cm/sec.
30	1700	1	6.5	1470	42×10^5
37	2090	0.5	3.0	687	16
35	1980	1.5	6.5	1470	36
32	1810	0.5	7.0	1700	43

The figures in column 3 give only the gas pressure in the container, and not the mercury vapour pressure.

These values do not vary more than those of Mr. Tanberg. In the case of the above-described tests, the variation arises from the difficulty of adjusting the counter pressure of the cathode mercury. The close agreement of the results is of special interest considering the difference between the two methods of measurement. These results show that it is not possible to calculate the vapour velocity with a moving cathode spot; this velocity would be smaller but very variable. The well-known zig-zag movement of the cathode spot with mercury arcs is certainly due to the fact that the mercury transmits the pressure of the vapour to the sides of the vessel if the cathode spot is not held stationary.

Mr. Tanberg also calculates the absolute temperature of the cathode spot from the vapour velocity, and obtains a temperature of the order of 5 to 7×10^5 °K. Mr. Compton³ has since given us a new reason for the high vapour react. force, so that it is useless to calculate the temperatures from the velocities given here. On the other hand, the question arises why the amount of mercury vapour per amp. sec. in a mercury arc is the same as the amount of copper vapour in a copper arc. There appears to be some close relationship between the amount of cathode voltage drop and the thermal properties of the cathode material-specific heat, heat of fusion, heat of vaporization and heat-conductivity.

³ K. T. Compton, Phys. Rev. 36, 706 (1930).

PHOTOELECTRIC EMISSION FROM THIN FILMS OF CAESIUM

BY L. R. KOLLER

GENERAL ELECTRIC COMPANY, SCHENECTADY, NEW YORK

(Received October 22, 1930)

ABSTRACT

The photoelectric properties and the methods of preparing thin films of caesium are described. These are divided into two classes: (1) Those where a thin film of Cs is adsorbed on a thin layer of oxygen. (2) Those where a thin film of Cs is adsorbed on a layer of suboxides of Cs.

Surfaces of the latter type were prepared by coating a cathode with metallic caesium and then admitting oxygen in very small quantities. The photoelectric current was observed simultaneously. The measurements show that the most sensitive surfaces are obtained when the caesium has taken up sufficient oxygen to form a suboxide rather than the normal oxide Cs_2O . These films owe their properties to the arrangement of the molecules very near the surface.

RECENT workers^{1,2,3} have described some of the photoelectric properties of thin films of alkali metals. The following investigation was directed particularly at the physical structure and chemical composition of such surfaces.

The first precise measurements of the properties of thin films of atomic dimensions of the alkali metals as distinguished from the bulk metals were made by Ives,⁴ who also investigated the effect of the underlying material.

In this laboratory, Bainbridge and Charlton developed a method of obtaining thin very stable films of caesium giving high values of photoelectric emission. The method consisted in exhausting and silvering a photoelectric cell in the usual manner,⁵ then introducing a fairly large amount of caesium into the bulb and again baking out the cell while still on the exhaust system at a temperature of about 300°C. During this bake-out, the photo-sensitivity of the cell increases, passes through a flat maximum and if the bake-out is continued sufficiently long or the temperature is sufficiently high, falls to a very small value. The maximum probably coincides with the formation of an adsorbed monatomic film of caesium on the surface of the silver. The excess of caesium distills out through the top tube into the exhaust system.

It was later found possible to make more uniform surfaces and more sensitive surfaces by first adsorbing a thin layer of oxygen on the silver. This was done by heating the bulb (after silvering) to 360°C, admitting a

¹ N. R. Campbell, *Phil. Mag.* **6**, 633 (1928).

² Olpin, *Phys. Rev.* **36**, 251 (1930).

³ Zworykin and Wilson, Jr. *Opt. Soc.* **19**, 81 (1929).

⁴ Ives, *Astrophys. J.* **60**, 209 (1924).

⁵ Koller, *Trans. Soc. Motion Picture Eng.* **12**, 921 (1930).

few mm of oxygen and allowing the bulb to cool to room temperature before pumping out the gas. Caesium was then introduced and the cell treated as before. Surfaces formed in this way gave a spectral sensitivity curve as shown in Fig. 1. This type of cell will hereafter be referred to as Cs-O-Ag. The shape of the maximum at the edge of the ultraviolet is probably largely determined by the transmission of the glass. The curve, however, is radically

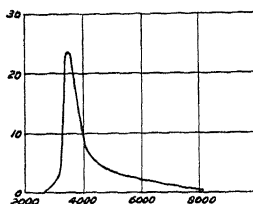


Fig. 1. Color sensitivity curve for Cs-O-Ag.

different from that determined for caesium in thick layers by Miss Seiler⁶ which shows a maximum at 5500 Å. These Cs-O-Ag surfaces are very stable and are not appreciably affected by temperatures below 100°C.

Similar results have been obtained with potassium on oxidized copper by N. R. Campbell.⁷

That these films are of atomic dimensions was shown for the case of potassium as follows. A long glass capillary was sealed to a photo-cell of the usual construction as shown in Fig. 2. At the end of this tube was a bulb containing some redistilled potassium. The bulb and capillary were immersed

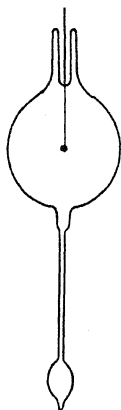


Fig. 2. Tube for determination of film thickness.

in an oil bath at a temperature of 155°C, while the photoelectric cell (still connected to the vacuum system) was maintained at room temperature. The quantity of potassium passing through the capillary per unit time was computed from Knudsen's formula

$$Q_2 = \frac{P_2 - P_1}{W_1(\rho_1)^{1/2}}$$

⁶ Seiler, *Astrophys. J.* 52, 1929 (1920).

⁷ Campbell, *Phil. Mag.* 6, 633 (1928).

where $P_2 - P_1$ is the difference in pressure between the ends of the tube; ρ_1 the density of gas at the temperature of the tube; $W_1 = 2.394l/D^3$ (l = length and D = diameter of tube); and Q_2 is the quantity of gas which flows through the tube per second.

The tube used was 10 cm long and 3 mm in diameter. The value for Q for these conditions was 3.62×10^{-8} gm/sec.

Since the area of the photo-cell was 170 cm², sufficient potassium to give a monatomic film would diffuse through the capillary in 2.5 minutes. Fig. 3 shows the change in sensitivity with time under these conditions. It passed through a maximum in 12.5 minutes. This was the time required for the deposition of a layer 5 atoms deep. As there is no reason for assuming the formation of a layer of uniform thickness over the entire bulb wall under these conditions the average thickness must have been of atomic dimensions.

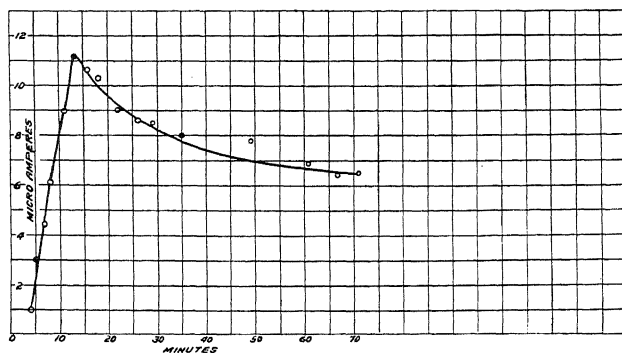


Fig. 3. Variation in photo current with time.

Cells were also made with a sheet of copper, plated electrolytically with silver as cathode. When treated as already described, this gave the same sensitivity as the evaporated metal deposit.

Throughout the discussion, unless otherwise specified, sensitivity will be taken to mean the response to the unresolved light of a tungsten filament lamp at 2400°K. Thus increasing sensitivity may be the result of an increase in the ordinates of any part of the spectral sensitivity curve or may be due to a lowering of the work function and consequent shift of the long wave limit toward the red.

When the oxidation of the silver cathode was carried out in such a manner as to give a layer of Ag₂O several hundred molecules deep, the results were radically different. If caesium was distilled into the tube and allowed to stand for a sufficiently long time, it gradually disappeared from the bulb walls and was completely absorbed by the silver oxide. It could be recovered again by very gentle warming of the plate. Such a surface shows only a very slight photo sensitivity. If the surface, however, is heated to temperatures in the neighborhood of 250°C, a reaction takes place and a compound is formed which is remarkably photo sensitive. Fig. 4 shows a spectral sensitivity curve for such a surface. Vacuum cells giving currents as high as 18

microamperes per lumen have been made in this way by Mr. H. E. Thomson who has done much of the development work in this field. This curve shows approximately the same maximum in the blue end of the spectrum as the Cs-O-Ag surfaces. Its high sensitivity is due to a pronounced maximum in the red and near infrared and a probable shift in the long wave limit toward the red.

These surfaces are very difficult to reproduce as their formation depends upon several factors which are not easily controlled. The silver oxide dissociates at 270°C . The amount of caesium condensed on the cathode depends upon the relative temperatures of the cathode and bulb wall, and consequently on the rate of heating and the masses of the various parts. In addition there is, of course, the problem of introducing definite small quantities of caesium. This type of surface owes its properties to the formation of a thick layer of oxides of Cs. The function of the silver is merely to provide an oxide which is readily reduced by caesium. This type of surface

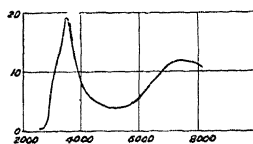


Fig. 4. Color sensitivity curve for Cs-CsO-Ag.

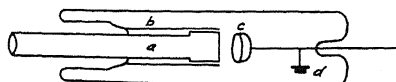
will be referred to as Cs-CsO-Ag. As will be shown later, the same results can be obtained with any base provided that the oxygen is introduced in the proper manner.

If the conditions during the exhaust of the cell were such that an excess of caesium remained in the bulb, the photosensitivity was invariably very low. On the other hand, if the heat treatment was continued so that the caesium was completely oxidized, the photo-sensitivity disappeared entirely. Apparently the optimum condition was a thin layer of caesium on top of a layer of caesium oxide. This condition could be arrived at, however, only when the oxide was formed by the reduction of Ag_2O by caesium. The normal oxide of caesium coated with a thin film of metallic caesium would not serve. Tubes were made up with a heavy deposit of caesium on the cathode, which was then completely oxidized, the oxygen was pumped out, and fresh caesium was distilled into the bulb. It was then sensitized in the usual way, but showed only the normal sensitivity for Cs-O-Ag.

Additional evidence in support of this view was obtained by making measurements of photo-sensitivity during the sensitizing bake-out. Since the photo-currents under these conditions are comparable with the thermionic currents⁸ and leakage currents, the light source was chopped up by a sector disc (three 60° openings rotated at 2200 r.p.m.) and the current observed on a simple a.c. amplifier. This indicated only the a.c. due to the photoelectric current. It was found that under these conditions the photo-sensitivity

⁸ Koller, Phys. Rev. 33, 1082 (1929).

never appeared until the exhaust oven was raised and the cell began to cool down, when it rose to its maximum value very rapidly. This may be interpreted as meaning that during the bake-out caesium atoms which reach the cathode surface are at once converted to a non-photosensitive caesium oxide. It is only as the cathode cools that a photo-sensitive layer of metallic caesium is formed there.



a HOLLOW COPPER CATHODE
b GLASS SLEEVE
c ANODE
d CAESIUM PELLET

Fig. 5. Tube with water-cooled cathode for observing effect of oxygen.

In an attempt to explain these phenomena, the problem was attacked in a slightly different manner. A tube was constructed, as shown in Fig. 5, with a hollow cathode which could be water cooled. This cathode was sealed

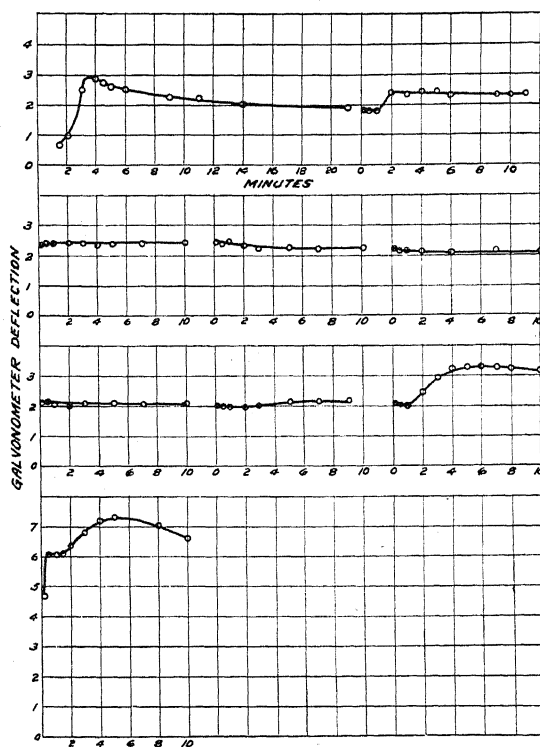


Fig. 6A. Effect on photo current of small "doses" of oxygen.

in by means of a chrome iron seal. A tight fitting glass sleeve covered the cathode so that only the end was exposed. The end of the cathode was a copper disk $3/4$ " in diameter. The anode was a nickel ring $7/8$ " in diameter spaced $1/2$ " from the cathode. In the upper part of the bulb were several Ni

pellets containing a mixture of $\text{Cs}_2\text{Cr}_2\text{O}_7$ and Si from which caesium could be liberated by heating with a high frequency induction furnace. The tube was well baked out while exhausting. A liquid air trap was used and all measurements were made with the tube on the exhaust system.

Fig. 6 shows a typical set of measurements. With no caesium in the tube, the photo-sensitivity of the cathode was 0. The caesium pellet was flashed

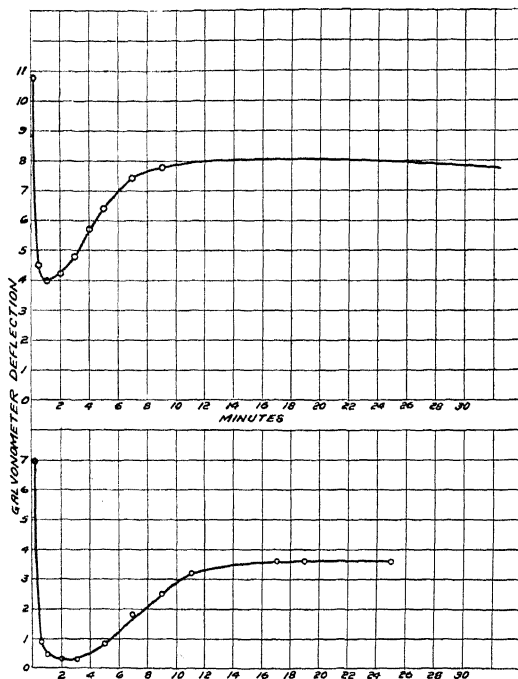


Fig. 6B.

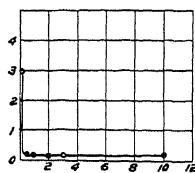


Fig. 6C.

and measurements of photo-sensitivity were made at frequent intervals. A stream of water was kept flowing through the cathode so that it was the coolest part of the bulb. The photo-sensitivity to unresolved light shows a fairly rapid increase with time, reached a maximum in about four minutes and eventually fell off to a constant value.

In about 20 minutes all of the caesium was condensed on the cathode. This was a thick visible deposit. Assuming 100 percent yield of caesium from the pellet, this was estimated to be 2×10^4 atoms thick. A small dose of

oxygen sufficient to fill the system to a pressure of 3.5μ was now admitted. As can be seen from the figure, this had no appreciable effect on the photo-sensitivity of the cathode. Measurements of pressure showed that the oxygen had been practically completely "cleaned up" by the caesium in the first three minutes. Successive doses of oxygen were admitted and photo-sensitivity and pressure observed. For the next six doses, the rate of clean up remained the same, and likewise the photo-sensitivity remained the same as for the clean caesium surface. The seventh dose, however, resulted in a 50 percent increase in sensitivity. The next dose also resulted in a large increase. The following dose, however, produced a strikingly different effect. The sensitivity passed through a maximum at least five times as large as the initial value within ten seconds of the admission of the oxygen, dropped to a low value and then gradually recovered. Additional doses of oxygen produced curves of similar shape but with a lower equilibrium value each time until finally all photo-sensitivity disappeared.

The maximum in the curve for pure caesium is of the right order of magnitude for the time required for sufficient caesium atoms to strike the surface to form a layer of atomic dimensions.

Once a thick layer of caesium is formed, small pressures of oxygen have no effect as the oxygen is absorbed as fast as it strikes the surface and the surface remains essentially a caesium surface. Finally a concentration of oxygen is reached, however, which corresponds very nearly to a suboxide of caesium. Under these conditions, the rate of absorption of oxygen is greatly reduced, the character of the final surface changes from a clean caesium surface to a composite surface consisting of atoms of caesium and oxygen. This is the condition represented by curves 7 and 8. Further doses of oxygen result in the formation of a layer containing the optimum amount of oxygen as represented by the peak in the curve, but this is rapidly destroyed by the excess of oxygen. The gradual recovery corresponds to a rearrangement of the surface as caesium diffuses out.

This experiment was repeated several times, always with the same results. In each case the amount of oxygen cleaned up corresponded to a suboxide of caesium. The oxygen could be measured to a high degree of accuracy, but there is always some uncertainty as to the yield from the pellet. The calculations were based on the assumption of 100 percent yield.

The experiment was now carried out under slightly different conditions. The same tube was used as before, but the oxygen, instead of being admitted in "doses," was allowed to flow into the tube continuously through a capillary leak. The rate of leak was made the same as the previously observed rate of clean up of oxygen, namely, 1μ per minute. After a thick film of caesium had been condensed on the cathode, the flow of oxygen was allowed to start through the capillary and measurements of pressure and photo sensitivity were made at frequent intervals.

The results are shown in Fig. 7. After the first minute the photo-sensitivity remained practically constant for twenty-six minutes when it began to increase, passed through a maximum and fell to zero. The amount of

O₂ which had been absorbed when the photo-sensitivity reached its maximum was 32μ , which is in good agreement with the amount determined by the discontinuous method. The pressure remained constant at 2.5μ throughout the experiment.

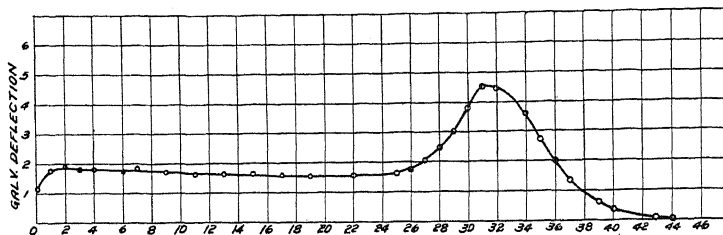


Fig. 7. Effect on photo current of small flow of oxygen.

$32/\mu$ corresponds to 82×10^{-6} gm of oxygen. Assuming that the yield of caesium was 9×10^{-3} gm, this gives a ratio of $\text{Cs/O} = 110$. The ratio for Cs_2O would be 33.

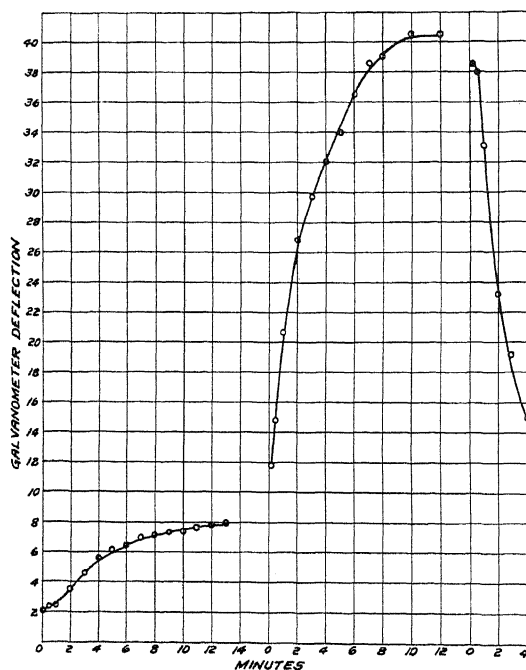


Fig. 8. Effect on photo current of small "doses" of oxygen at liquid air temperature.

The conclusion to be drawn from these experiments is that the highly photo-sensitive surface obtained by treating caesium with oxygen is due to a thin film of caesium upon a foundation of suboxides of caesium. If the caesium is present in large quantity, it must be entirely converted to suboxide before such a surface can be obtained. Until the entire amount of

caesium is oxidized, the process of diffusion maintains a practically clean caesium surface.

An experiment was undertaken to study such a surface in the absence of diffusion. The same tube was used as before, and after being thoroughly exhausted, the pellet was flashed. The cathode was then chilled with liquid air. Since the cathode was of heavy copper, the surface of caesium in contact with it was likewise at nearly liquid air temperatures. Fig. 8 shows the change in photo-sensitivity with time as the caesium condensed out upon it. This curve was very similar to the one obtained at room temperature. Oxygen was now admitted in very small doses, 0.6μ at a time. This quantity is sufficient to form a layer 6 atoms deep on the surface of the cathode. It is probable that some caesium remained on the bulb wall so that the first dose of oxygen may have been partly taken up elsewhere than at the surface of the cathode. The very first dose of oxygen now produced a four-fold increase in sensitivity, while the second dose raised the sensitivity to *twenty times* its initial value. This is in marked contrast with the effects at room temperature where fifty times this quantity of oxygen was required to produce an appreciable effect. The explanation lies in the fact that at the low temperature the oxygen cannot diffuse in, so that a very small amount can be effective in changing the surface structure. This experiment lends further support to the view that the chief function of the thick oxide layer in the Cs-CsO-Ag cells is to use up the free caesium so as to immobilize the surface layer.

THE MAGNETIC SUSCEPTIBILITY OF GASES II. TEMPERATURE DEPENDENCE

BY FRANCIS BITTER*

CALIFORNIA INSTITUTE OF TECHNOLOGY AND RESEARCH LABORATORIES,
WESTINGHOUSE ELECTRIC AND MANUFACTURING COMPANY

(Received October 20, 1930)

ABSTRACT

The susceptibilities of CO₂, N₂ and H₂ are measured at room temperature and at liquid air temperature using O₂ as a standard. The results are:

	298°K	88°K
CO ₂	-24.2	—
N ₂	-14.8	-14.2
H ₂	-5.8	-3.3

The relative values at room temperature are in fair agreement with most previous observations, but the absolute values are more diamagnetic than any previously recorded. The low temperature observation on N₂ can be interpreted as meaning that if a permanent moment is present, it is less than 1/25 of a Bohr magneton. The large change observed in H₂ is entirely unexpected, and the observations should be repeated.

IN A previous communication,¹ hereafter referred to as Part I, the proportionality between volume susceptibility of gases and pressure was established, thus clearing the way for an examination and interpretation of the temperature dependence. On the assumption that there is no diamagnetic orientation and that the molecular susceptibility of polyatomic gases is unaffected by temperature changes through such mechanisms as, for instance, slight differences in nuclear separations in various thermally excited states, the expression for the volume susceptibility may be written

$$K = \left(\frac{a}{T} + b \right) \frac{p}{T} \quad (1)$$

p and T stand for pressure and absolute temperature; a is a positive constant which measures the permanent moment of the molecule; b is a negative constant which measures the diamagnetism. The work described below is concerned chiefly with the gases O₂, H₂, and N₂. For O₂ b may be taken equal to zero, and in this form Eq. (1) has been tested² over a considerably range of temperatures and pressures and found to hold. For H₂ and N₂ it has heretofore been assumed that $a=0$, and it is the chief purpose of this paper to check this assumption, and to discuss the absolute values of the constant b .

* National Research Fellow.

¹ F. Bitter, Phys. Rev. 35, 1572 (1930).

² K. Onnes and E. Oosterhuis, Konink. Akad. Wetensch, Amsterdam, Proc. 15, 1404 (1913). Communication No. 134d from Phys. Lab. Leiden.

THE APPARATUS

The apparatus used in the following measurements is essentially the same as that described in Part I. A liquid air trap was introduced between the gasometer containing pump oil and the quartz furnace containing copper filings in order to prevent any vapors from reaching the furnace. Further, in order to reduce the volume of the purifying train, two of the three drying tubes were removed, leaving one tube containing P_2O_5 and the long spiral immersed in liquid air to accomplish the drying of the gases. The functioning of the train was checked spectroscopically as described in Part I.

Preliminary trials at low temperatures showed that the measuring apparatus described in Part I was not satisfactory. Even after the Dewar had been filled with liquid air and left standing for hours, the test body would not come to rest. This was due to slight convection currents, which were greatly reduced by enclosing the test body in a chamber of slightly different design as shown in Fig. 1. The resistance thermometer was eliminated

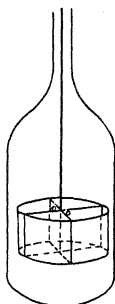


Fig. 1. Diagram of apparatus.

entirely. The container was immersed in liquid air up to the constricted portion. This was done by means of a Dewar flask which fitted between the pole-pieces of the magnet. In this way the test body was almost completely surrounded by walls at liquid air temperature, and heat was brought into the measuring chamber only along the long thin stem of the test-body. Further trials showed that this arrangement was satisfactory. The temperature was read on a pentane thermometer immersed in the liquid air bath. Its accuracy was first checked against the boiling point of pure O_2 .

THEORY OF MEASUREMENTS

Previous work had established the proportionality between, first, pressure and deflection of the test body; and second, pressure and volume susceptibility. From this, proportionality between deflection and susceptibility could be inferred for all measurements carried out at any given temperature. Thus if δO_2 and δH_2 represent the deflections produced by O_2 and H_2 at a pressure of say 1 cm, we may write

$$(K_{H_2})_{T,p} = \left(\frac{\delta H_2}{\delta O_2} \right)_T (K_{O_2})_{T,p} \quad (2)$$

In the following, oxygen was used as a standard, it being assumed³ that its volume susceptibility, K_{O_2} at 20°C and 76 cm pressure was 0.14×10^{-6} , and that its volume susceptibility at any other temperature T could be found by multiplying the above figure by $(293/T)^2$.

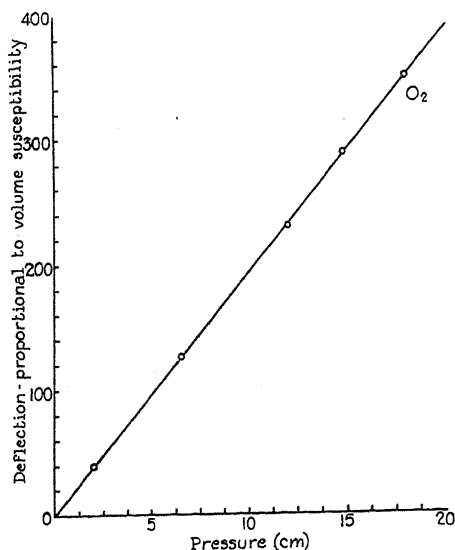


Fig. 2. Deflection, or volume susceptibility of O_2 in arbitrary units plotted as a function of the pressure, the observations being made at room temperature.

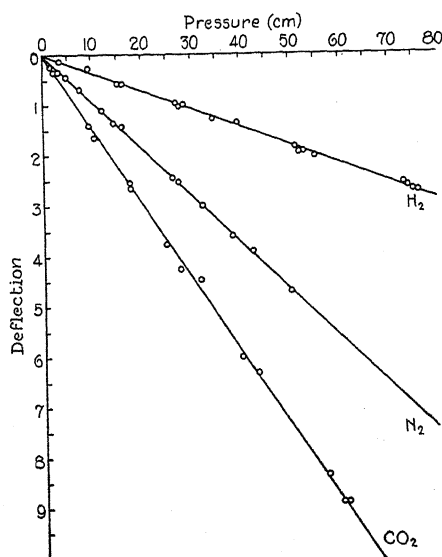


Fig. 3. Deflection or volume susceptibility of H_2 , N_2 , and CO_2 in the same units as those used in Fig. 2, plotted as a function of the pressure, the observations being made at room temperature.

³ J. H. Van Vleck, Phys. Rev. 31, 608 (1928).

In making a measurement the procedure was therefore the following: first plot the pressure vs. deflection curves, as in Figs. 2, 3, 4 and 5. From these obtain the quantities (δ_{H_2}), and by substituting the numbers thus

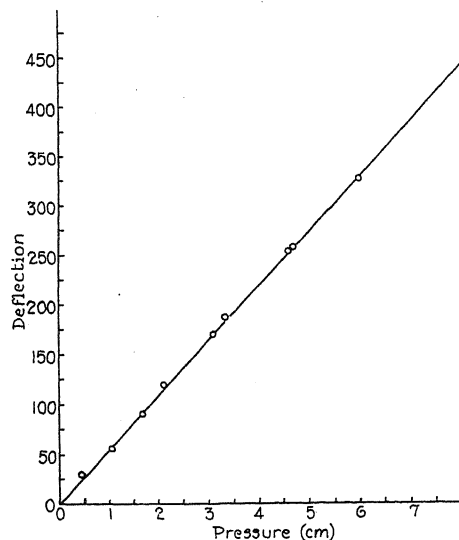


Fig. 4. Deflection, or volume susceptibility of O_2 in arbitrary units plotted as a function of the pressure, the observations being made at the temperature of liquid air.

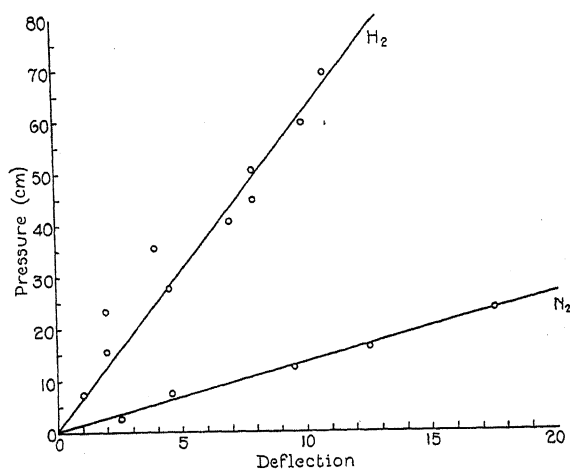


Fig. 5. Deflection, or volume susceptibility of H_2 and N_2 in the same units as those used in Fig. 4, plotted as a function of the pressure, the observations being made at the temperature of liquid air.

obtained into Eq. (2), the absolute values of the volume susceptibility at any temperature could be obtained.

RESULTS AT ROOM TEMPERATURE

As is evident from the above, these results may be divided into the following individual measurements: The ratio of the volume susceptibilities of a pair of gases; and the calibration, which involves the assumption of an absolute value for some standardizing substance. The division of the results into these two groups may conveniently be applied to the results of other observers, as most of their work has also been carried out in this fashion. Unless this is done, a faulty calibration would make all the measurements appear wrong, instead of showing up in the calibration as it ought. The results are shown in Table I.

TABLE I. Ratios and absolute values of the molecular susceptibilities of diamagnetic gases as found by various observers. (Vaidyanathan did not measure H_2 , but found an absolute value of -12.9×10^{-6} for N_2 , which multiplied by 0.39 gives (-5.0) which for the sake of comparison, is listed above. All the measurements were carried out at room temperature.)

	Hammar ⁴	Wills & Hector ⁵	Glaser ⁶	Lehrer ⁷	Vaidyanathan ⁸	Také Soné ⁹	Author
H_2/N_2	0.39	0.33	0.54	—	—	0.54	0.39
H_2/CO_2	.23	—	.22	.23	—	—	.24
N_2/CO_2	.59	—	.39	—	.63	—	.63
$H_2(\times 10^6)$		-3.94	—	-5.0	(-5.0)	-3.94	-5.8

In the first part of the table, the agreement for H_2/CO_2 is good, and the value may be taken with considerable confidence as 0.23 ± 0.01 . The next best is N_2/CO_2 where three of the four measurements point to 0.61 ± 0.02 as the correct value. The origin of the too low value for N_2 found by Glaser is not at all clear, and further work on this point should prove very interesting. Assuming that these two ratios are right, they give for H_2/N_2 $0.23/0.61 = 0.38$ in good agreement with the results of Hammar and myself (0.39). The agreement among the various absolute values for H_2 is very poor, and at present there seems to be no way of choosing the most nearly correct. I wish to add, however, that the use of the values for H_2 and N_2 found in this work would not invalidate the arguments advanced in an earlier paper¹⁰ on the susceptibility of organic gases, where the measurements of Wills and Hector on N_2 and H_2 were used as standards.

RESULTS AT LIQUID AIR TEMPERATURE

For N_2 the ratio of the molecular susceptibility at 298°K to that at 88°K was found to be 1.04, which means that, within the experimental error, the

⁴ G. W. Hammar. Thesis. California Institute of Technology. 1926.

⁵ A. P. Wills and L. G. Hector, Phys. Rev. **23**, 209 (1924). L. G. Hector, Phys. Rev. **24**, 418 (1924).

⁶ A. Glaser, Ann. d. Physik **75**, 459 (1924).

⁷ E. Lehrer, Ann. d. Physik **81**, 229 (1926).

⁸ V. I. Vaidyanathan, Phil. Mag. **5**, 380 (1928).

⁹ Také Soné, Phil. Mag. **39**, 305 (1920).

¹⁰ F. Bitter, Phys. Rev. **33**, 389 (1929).

susceptibility is expressible by an equation of the form $K = b\mu/T$. More accurately, it can be stated that if the N_2 molecule had a magnetic moment of $1/50$ of a Bohr magneton, this would just have sufficed to change the above ratio from 1.00 to 1.04, and that hence, if the N_2 molecule does actually have a permanent moment, this is surely less than, say $1/25$ of a Bohr magneton.

The result for H_2 is unexpected.

$$\frac{(\chi_{H_2})_{298^\circ K}}{(\chi_{H_2})_{83^\circ K}} = 1.82$$

This measurement involves considerable uncertainty, as is seen from the way the points are scattered about the line in Fig. 5. They represent data taken in two consecutive runs, and the difficulties in making accurate readings were due to unusually large random motions of the test body. It would have been highly advisable to repeat these observations, but this was impossible for lack of time. The above ratio is so large, however, that it is impossible to attribute it to any experimental error save that of O_2 contamination, which, in view of the precautions taken, seems out of the question. The result may therefore be stated by saying that at liquid air temperatures the molecular susceptibility of H_2 is only about half of its value at room temperature. Such an effect could be due to either an actual decrease in the size of the hydrogen molecule, or to an alignment of its axis parallel to the field in the ground state with no rotational energy. There seems to be no reason to expect either of these effects, even when the existence of a nuclear spin is taken into consideration. Future work on hydrogen should take into account possible differences between the para and ortho states.

THE MAGNETIC PROPERTIES OF CERTAIN
Pt-Co AND Pd-Co ALLOYS

BY F. WOODBRIDGE CONSTANT*

NORMAN BRIDGE LABORATORY, PASADENA, CALIFORNIA

(Received September 11, 1930)

ABSTRACT

If ferromagnetism is due to interaction between the electrons of neighboring ferromagnetic atoms, the effect on the magnetic properties of gradually separating these atoms is of interest. For this reason alloys of the Pt-Co and Pd-Co series were investigated. As the alloys were solid solutions, for small cobalt content the cobalt atoms could be regarded as partly isolated by the non-ferromagnetic atoms. The magnetic properties of these alloys showed a lowering of the Curie point and a decrease in the remanent magnetization and coercive force with decrease in the percentage of cobalt in accord with theory. An observed increase in the magnetization per cobalt atom is discussed along with recent theories of ferromagnetism.

I. INTRODUCTION

THE explanation of ferromagnetism has presented much greater difficulties than that of either diamagnetism or paramagnetism. X-ray experiments on ferromagnetic crystals have shown that the elementary magnet cannot be larger than the atom, and the most recent work of Barnett¹ on the gyromagnetic effect indicates that ferromagnetism can be attributed chiefly to the spinning electrons. But in spite of the supposed simple character of the elementary magnet experiments have shed little light on its behavior in ferromagnetic substances.

The point from which to attack the problem of magnetism most directly would seem to be the Gerlach and Stern² experiments, in which the magnetic moment and behavior of an individual atom is measured. The sodium and cobalt atoms have been found to possess magnetic moments of one and six Bohr magnetons respectively, but in the solid state sodium is only paramagnetic while the magnetic moment per cobalt atom, computed for saturation magnetization, is about 1.7 magnetons. However, in the gaseous state of an atomic beam neither element can be classed as ferromagnetic. The fundamental question is what special mechanism in the solid state makes cobalt ferromagnetic and sodium not. Ferromagnetism arises only when certain atoms, (notably Fe, Ni or Co), are brought into the close proximity which they find in the solid state. This was first explained by Weiss as due to a large internal magnetic field set up by these atoms in the solid state, and the most recent theories have attempted to account for the mechanism by which this field is created. Heisenberg³ deduces it from the resonance, (the "Austausch-

* National Research Fellow.

¹ S. J. Barnett, *Phys. Rev.* [2] 36, 789 (1930).² W. Gerlach and O. Stern, *Zeits. f. Physik* 9, 349 (1922), etc.³ W. Heisenberg, *Zeits. f. Physik* 49, 619 (1928).

phänomene"), between the spinning electrons of neighboring atoms, while Bloch⁴ believes the interaction takes place between the conduction electrons. It is therefore not surprising that ferromagnetism does not occur in liquids or gases where the separation of the atoms is greater. Further, as the orientations of the spinning electrons obeys a statistical energy distribution, the complicated nature of most ferromagnetic phenomena is accounted for, as well as the difficulty of using such measurements to work back to the mechanism of the individual atoms or electrons. Similar complications arise on the theoretical side, of a mathematical nature, and simplifying assumptions must be introduced, so that only predictions of a general character can be made.

In an attempt to simplify conditions it was thought interesting to observe the magnetic properties of ferromagnetic atoms in a state of isolation from one another intermediate between that of the pure solid metal and that of the Gerlach and Stern experiment. This suggested investigating alloys of a ferromagnetic with a non-ferromagnetic metal. By increasing the percentage of the latter the atoms of the former could be further and further isolated from each other and the corresponding effect on the magnetic properties noted. The present work is a continuation of that on the same subject previously reported by the author.⁵

2. EXPERIMENTAL METHOD

Several alloys of iron, nickel, or cobalt with other metals have been investigated. In nearly every case a small percentage of the non-magnetic element was sufficient to prevent ferromagnetism. For example, Lewkonja,⁶ has tested alloys of Co with Sn, Sb, Pb, Bi, Zn, Cd, Cr and Si and Tammann,⁷ those of Fe, Ni or Co with Sn, Sb, Pb, Bi, Zn, Si, Al and Mg. In many cases, such as the Ni-Cr series,⁸ the Curie point falls more and more rapidly to absolute zero as a few percent of, say, Cr is added. For Ni-Mn⁹ it decreases steadily to 0°C for 25 percent Mn. But in all these cases it is doubtful whether the two metals concerned form a continuous series of solid solutions, such as would be necessary for the purpose of this problem in order that the ferromagnetic atoms could be gradually further isolated. For the Ni-Cu series,¹⁰ however, the Curie point reaches -230°C for 65 percent Cu, and it is believed that these two metals are mutually soluble except for a small range around 50 percent Cu. But in the present work, alloys of cobalt have been selected in which the cobalt content can be made only a few percent without complete loss of ferromagnetism; these alloys belong to the Pt-Co and Pd-Co series. Although the diagram of thermal equilibrium has not been obtained for either of these series, Carter has investigated many high platinum alloys and believes platinum and cobalt to form an isomorphous series of solid solutions. As previous-

⁴ F. Bloch, *Zeits. f. Physik* **57**, 545 (1929).

⁵ F. W. Constant, *Phys. Rev.* [2] **34**, 1217 (1929).

⁶ K. Lewkonja, *Zeits. f. anorg. Chem.* **59**, 293 (1908).

⁷ G. Tammann, *Zeits. f. phys. Chem.* **65**, 73 (1909).

⁸ C. Sadron, *Comptes Rendus* **190**, 1339 (1930).

⁹ S. Kaya and A. Kussmann, *Naturwissenschaften* **17**, 995 (1929).

¹⁰ R. Gans and A. Fonseca, *Ann. d. Physik* [4] **61**, 742 (1920).

ly reported,¹¹ a microscopic investigation was made on each alloy used, confirming Carter's conclusions. Similar results were obtained for the Pd-Co alloys.

The first set of alloys investigated was the following, kindly supplied in the form of 30 mil wires by the Bell Telephone Laboratories:

10% Co-90% Pt

5% Co-95% Pt

10% Ni-90% Pt

5% Ni-95% Pt

The magnetic properties of these alloys have already been reported. The last two were not ferromagnetic, and the results obtained from the first two will be summarized below.

A second set of alloys was prepared, in the form of 10 mil wires whose compositions by weight were the following:

3% Co-97% Pt

1.5% Co-98.5% Pt

10% Co-90% Pd

5% Co-95% Pd

The first two alloys served as a continuation of the Pt-Co series, while in the last two palladium was substituted for platinum so that by comparison with the Pt-Co series the contribution to the magnetic behavior of the cobalt atoms alone might be more truly ascertained. The experimental method was the same as that used with the first set of alloys, the magnetic measurements being made by the ballistic method, with two identical rings connected differentially. Measurements were taken on (1) the variation of the magnetization, I , (magnetic moment per unit volume), with temperature, and the Curie point, (2) hysteresis loops between various maximum values of the applied magnetic force, H , and at different temperatures, and (3) the initial curve of magnetization for various fixed temperatures. For the higher temperatures, (50°C to 350°C), turpentine or paraffin baths were used, while for lower temperatures the specimens were placed in a Dewar flask containing liquid air or a bath of ether cooled by liquid air. Temperatures were measured by copper-constantan thermocouples.

The alloys were first tested in the hard-drawn state, when a microscopic examination showed the individual crystals greatly distorted and elongated; the wires were then annealed for three hours in a vacuum at about 1050°C, and afterwards allowed to cool gradually. The furnace was a small electric one, built by A. Goetz, consisting of two concentric cylindrical crucibles with between them the heating element, a slightly conical helix of tungsten wire which served as a thread in which the inner crucible could be tightly screwed. After annealing the wires appeared microscopically to be composed of much larger crystals forming a polygonal pattern, characteristic of solid solutions.

¹¹ F. W. Constant, Phys. Rev. [2] 35, 116 (1930).

3. RESULTS AND DISCUSSION

The results for all the alloys in both the hard-drawn and annealed states are summarized in Tables I, II, and III.

TABLE I. Curie Point.

Alloy	% Cobalt			Curie Point, ° Kelvin	
	by Wt.	by Vol.	Atomic	Hard-drawn	Annealed
90% Pt	10.0	21.4	26.9	578	522
95% Pt	5.0	11.4	14.9	322	322
97% Pt	3.0	7.1	9.3	193	179.5
98.5% Pt	1.5	3.7	4.8	—	87.5
90% Pd	10.0	13.4	16.8	511	462
95% Pd	5.0	6.8	8.7	359	301

In Table I are given the percentages of cobalt in each alloy by weight, by volume and from atomic considerations. The Curie points follow. For both series of alloys, in passing from 100 percent Co, with Curie point = 1388°K to 0

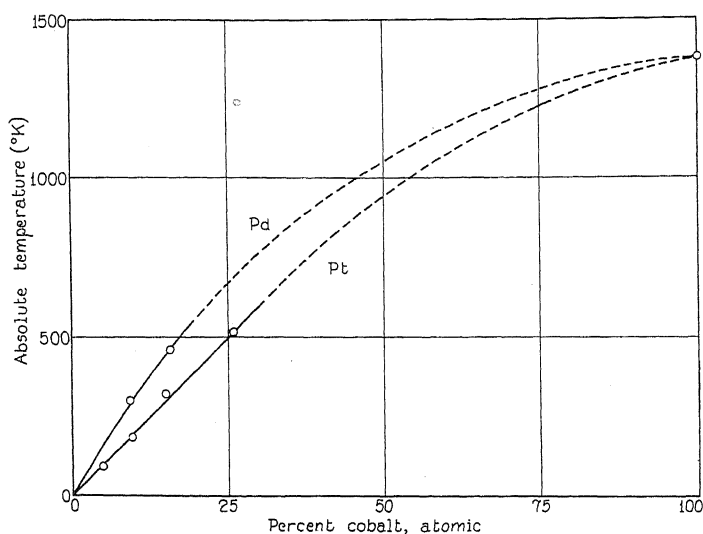


Fig. 1. Curie point as a function of the atomic percentage of cobalt.

percent Co, the Curie point decreases more slowly at first and then falls approximately linearly with the atomic percentage of cobalt, approaching absolute zero for 0 percent Co. This is shown in Fig. 1. In the magnetization-*vs.*-temperature curves the magnetization at first increased with rising temperature, later falling to zero at the Curie point. This initial rise was explained as due to lack of saturation for the values of H that could be applied.

Table II gives the characteristics of various hysteresis loops, the coercive force, H_c , and the remanent magnetization I_r , where H_{\max} is the limiting value of H for the loop.

TABLE II. *Coercive force and remanent magnetization.—190°C.*

Alloy	H_{\max}	H_c		I_r	
		Hard	Annealed	Hard	Annealed
90% Pt	260	—	30	—	189
95% Pt	260	90	18	200	107
97% Pt	260	80	14	73	53
98.5% Pt	260	30	0	1	0
90% Pd	260	120	110	—	142
90% Pd	650	420	115	210	167
95% Pd	260	50	88	—	83
95% Pd	650	410	110	145	108

The effect of annealing is seen to be to lower the Curie point and to decrease the magnetic hardness and hysteresis; the mechanical hardness was simultaneously decreased. This intimate connection between magnetic and mechanical hardness is in agreement with McKeehan's¹² theory of magnetostriction. O. v. Auwers and Sizoo¹³ have found that increasing the grain size by annealing produces just such results as these.

Decreasing the cobalt percentage always lowers the Curie point, and decreases H_c and I_r . As the hysteresis decreases the loops become less upright and more inclined, and for the 98.5 percent alloy, annealed, no hysteresis was observed. This is in complete accord with the recent resonance theories of ferromagnetism, for if residual magnetism and hysteresis are explained as due to interaction between neighboring spinning electrons this interaction must diminish and the Curie point fall as these electrons become less dense. Comparison between the platinum and the palladium alloys shows similar results for both series except that H_c is greater for the latter. The Pt or Pd atoms therefore seem to influence the hardness only and the ferromagnetism appears to be attributable to the cobalt atoms. It is of course possible that both Pt and Pd atoms contribute to the ferromagnetism in the same manner and degree but this seems less likely.

TABLE III. *Maximum values of I and the magnetic moment per cobalt atom.*

Alloy	Hard	I_{\max}		$I_{0,\infty}$ Annealed	$\sigma_a \times 10^{-20}$
		Hard	Annealed		
90% Pt	330		364	392	2.11
95% Pt	230		254	290	2.83
97% Pt	105		126	132	2.09
98.5% Pt	8		8	9	0.30
90% Pd	223		318	356	2.96
95% Pd	193		216	274	4.46

1 Bohr magneton = 0.92×10^{-20}

In Table III the second and third columns give the greatest values of I measured for each alloy. In most cases the greatest values of H which could be applied, namely, 600 to 1000 gauss, were not sufficient to produce saturation, but the approach toward saturation followed closely, especially in the case of the palladium alloys, the formula given by Weiss and Forrer,¹⁴

¹² L. W. McKeehan, Phys. Rev. [2] 26, 274 (1925).

¹³ O. v. Auwers and G. J. Sizoo, Zeits. f. Physik 60, 576 (1930).

¹⁴ P. Weiss and R. Forrer, Ann. d. Physique [10] 12, 279 (1929).

$$I_H = I_\infty \left(1 - \frac{a}{H} \right)$$

where I_H is the intensity of magnetization for a magnetic force H , I_∞ the magnetization at saturation, ($H = \infty$), and a a constant for a given alloy and temperature. Table IV shows how closely the values of I observed for the 10 percent Pd alloy fit those calculated from the formula

$$I_H = 356 \left(1 - \frac{131.4}{H} \right)$$

TABLE IV. Approach to saturation for 90% Pd—10% Co alloy.

H	I calc.	I obs.
270	182	190
361	226	225
450	252	252
564	273	272
700	289	289
767	295	295
903	304	304
∞	356	—

In this way values of I_∞ were computed at two different temperatures, that of liquid air and that of solid CO_2 and alcohol. They were very nearly the same; if not, the value of I_∞ at absolute zero, $I_{\infty,0}$ could be calculated by the Weiss¹⁴ formula for temperature dependence,

$$I_{\infty,T} = I_{\infty,0}(1 - AT^2)$$

where A is a constant and T the absolute temperature. Recently Bloch¹⁵ has obtained a closely similar formula from his theory of ferromagnetism; namely,

$$I_{\infty,T} = I_{\infty,0} \left[1 - \left(\frac{T}{\theta} \right)^{3/2} \right]$$

where $\theta \doteq T_c$, the Curie point. In agreement with this formula, $I_{\infty,T}$ showed greater dependence on T with those alloys whose Curie points were lowest. The fourth column of Table III gives the values computed for $I_{\infty,0}$ and the fifth these values divided by the number of cobalt atoms per cc, i.e. the magnetic moment per cobalt atom, σ_a , assuming the magnetization is entirely due to the cobalt. For pure cobalt σ_a is only about 1.6×10^{-20} so that as the cobalt content decreases to 5 percent σ_a increases, while for still further dilution it appears to decrease. This might be explained on Bloch's theory, according to which the spinning electrons between which resonance occurs are free conduction ones rather than associated with definite atoms. This electron gas can show ferromagnetism only if it is not completely degenerate so that its electrostatic energy may exceed its zero-point energy, (on the Sommerfeld theory). If decreasing the cobalt content in these alloys decreases the density of these free electrons the zero-point energy would decrease and this

¹⁵ F. Bloch, *Zeits. f. Physik* 61, 206 (1930).

might account for the increase in magnetic moment. At the same time, due to the lessening of the electrostatic energy a point would finally be reached where ferromagnetism would no longer be possible.

The theory of Bloch was prompted by the work of Dorfman, Jaanus and Kikoin¹⁶ on the change in atomic specific heat at the Curie point. Stoner¹⁷ has recently reported an important change in their results which alters the conclusion drawn from them that ferromagnetism is due to conduction electrons. But it is hard to distinguish between conduction and orbital electrons, and the peculiar electron arrangements in the Fe, Ni and Co atoms would seem to be the most likely source of the ferromagnetism of these metals. It is probable that greater values of σ_a would have been obtained with the 3 percent Co and 1.5 percent Co if the Curie points of these alloys had not been so low that measurements could only be taken a little below them.

In conclusion the following suggestions, along the lines of McKeehan's¹⁸ theory of ferromagnetism, are offered. Ferromagnetism occurs in certain metals only because in these metals the electrons are so arranged that resonance arises and the spins are oriented. Magnetic hardness arises because a change in the magnetization, or distribution of the spins, produces atomic magnetostriction, and hence gross magnetostriction unless the atomic magnetostriction of some of the atoms is of opposite sign so that compensation occurs. Such mechanical effects must be considered as partly influencing the degree of magnetization possible. As the percentage of non-magnetic or non-magnetostrictive atoms increases, the atomic magnetostriction per cobalt atom can increase for a given gross magnetostriction. Assuming the magnetostriction of these alloys to be the same as for cobalt this would mean a greater observable magnetic moment per cobalt atom, as each cobalt atom in the alloy would be more free, with increasing dilution, to take up its state of greatest possible magnetization, than in pure cobalt. However, too great dilution of the cobalt would prevent ferromagnetism from occurring.

The writer wishes to thank the National Research Council for its support, and Professor R. A. Millikan for his kind help and for the facilities of the Norman Bridge Laboratory.

¹⁶ J. Dorfman, R. Jaanus and I. Kikoin, *Zeits. f. Physik* **54**, 277, 289 (1929).

¹⁷ E. Stoner, *Nature* **125**, 973 (1930).

¹⁸ L. W. McKeehan, reference 12.

THE MAGNETIC ISOTROPY OF A PARAMAGNETIC ALUM

BY C. G. MONTGOMERY

SLOANE PHYSICS LABORATORY, YALE UNIVERSITY

(Received October 20, 1930)

ABSTRACT

It is shown that cubic crystals of potassium chromium alum are magnetically isotropic.

J. FORREST,¹ in 1926, was led from both theoretical and qualitative experimental grounds to the conclusion that a number of crystals had variations in the magnetic susceptibility with direction of the applied field which were not in strict accord with the Thomson-Voigt symmetry relations. In order to test this conclusion, measurements were made by the author on large single crystals of copper,² and it was found that there was no variation in the susceptibility greater than 1 percent. Copper is a diamagnetic material, and its magnetic properties are supposed to be mostly due to the Larmor precession of its closed shell of electron orbits. The theoretical basis on which Forrest was led to expect the anisotropies in question was derived from the use of a model consisting of elementary magnets fixed to points of a space lattice. It therefore seemed desirable further to test Forrest's conclusions using some paramagnetic substance, whose magnetic properties would be determined chiefly by incompletely filled shells of electrons, and would thus more closely approximate the theoretical model.

There are several paramagnetic alums with a cubic structure which can easily be obtained in large crystals suitable for this. Potassium chromium alum— $\text{K}_2\text{SO}_4 \cdot \text{Cr}_2(\text{SO}_4)_3 \cdot 24\text{H}_2\text{O}$ —was chosen for this purpose. Crystals were grown from saturated solutions of the pure salt by suspending small seed crystals in them. Two of these were ground into cylindrical shape for measurement, one having as the cylinder axis a $\langle 100 \rangle$ axis of the crystal, the other a $\langle 111 \rangle$ axis. The following were their dimensions.

Axis of cylinder	length	diameter
$\langle 111 \rangle$	0.610 cm	0.686 cm
$\langle 100 \rangle$	0.444	0.549

The structure of chrome alum has been determined by Vegard and Schjelderup,³ who place the chromium atoms on a face-centered cubic lattice. The magnetic susceptibility per unit mass is given in the International Critical Tables⁴ as 11.5×10^{-6} .

Measurements of the variation of the magnetic susceptibility were made with the apparatus previously described by the author.² Values of the susceptibility in arbitrary units were obtained for every 15° in the plane perpendic-

¹ J. Forrest, Trans. Roy. Soc. Edinburgh 54, 601-701 (1926).

² C. G. Montgomery, Phys. Rev. [2] 36, 498-505 (1930).

³ L. Vegard and H. Schjelderup, Ann. d. Physik [4] 54, 146-164 (1917).

⁴ International Critical Tables VI, p. 360.

ular to the axis of the cylinder. These relative values of the susceptibility were analyzed in a Fourier series in terms of the azimuth ϕ , the angle between the field and an arbitrary polar axis in the plane of the base of the crystal cylinder. This gave the following results:—

$$\begin{aligned} \chi_{\langle 100 \rangle} &= 85.85 + 2.32 \cos \phi - 0.34 \cos 2\phi - 1.36 \cos 3\phi + 0.12 \cos 4\phi \\ &\quad + 9.05 \sin \phi + 2.71 \sin 2\phi + 1.29 \sin 3\phi - 0.45 \sin 4\phi \\ \chi_{\langle 111 \rangle} &= 166.68 + 1.34 \cos \phi + 0.18 \cos 2\phi + 0.11 \cos 3\phi + 0.42 \cos 4\phi \\ &\quad + 3.81 \sin \phi + 0.27 \sin 2\phi + 0.72 \sin 3\phi - 0.38 \sin 4\phi \end{aligned}$$

These two runs were not made at the same sensitivity of the apparatus, and hence corresponding coefficients in the two series should not be compared. As in the previous work, the terms with the 360° period are to be ascribed to an instrumental error and should be ignored in the interpretation of the data. About a $\langle 100 \rangle$ axis, we should expect, if the crystal were other than isotropic, at least one large coefficient in the terms in 4ϕ . It is seen that the coefficients of these terms are much smaller than the coefficients of the 2ϕ and 3ϕ terms. These latter terms can have no physical significance, in view of the symmetry of the crystal. Hence we can assign none to the terms in 4ϕ . In a similar way, for the $\langle 111 \rangle$ axis, the 3ϕ term is small compared with the 2ϕ and 4ϕ terms. Thus we must conclude that chrome alum, as well as copper, forms magnetically isotropic crystals.

It remains to give an explanation, if possible, for the fact that Forrest obtained experimental evidence of some anisotropy in his crystals. Forrest gives a curve⁵ showing the dependence of the intensity of magnetization parallel to the field upon the direction of the field in the $\{100\}$ plane, for ammonium iron alum— $(\text{NH}_4)_2\text{SO}_4 \cdot \text{Fe}_2(\text{SO}_4)_3 \cdot 24\text{H}_2\text{O}$. The curve drawn shows a four-fold symmetry. This substance is identical in structure with chrome alum, and would be expected to behave magnetically in the same way. If we measure off in this figure the radius vectors of the experimental points, and subject them to a Fourier analysis, as above, we obtain the following result in centimeters:—

$$\begin{aligned} I_{11} &= 2.469 - 0.033 \cos \phi - 0.018 \cos 2\phi - 0.089 \cos 3\phi \\ &\quad + 0.072 \cos 4\phi + 0.000 \sin \phi - 0.048 \sin 2\phi + 0.041 \sin 3\phi \\ &\quad + 0.029 \sin 4\phi. \end{aligned}$$

We see that here the terms in 3ϕ have a larger amplitude than the terms in 4ϕ , and we conclude that to draw a curve through these points which shows a four-fold symmetry is not justifiable. The explanation of Forrest's curves for the transverse component of the intensity of magnetization is not evident. It should be pointed out, however, that if these curves represent real effects, there should be a dependence of the susceptibility of the material upon the strength of the field, an effect which has not been observed.

In conclusion, the author wishes to express his thanks to Professor L. W. McKeehan for much helpful discussion, and to the Sterling Fellowship Fund for financial support.

⁵ J. Forrest, reference 1, p. 615, outer curve, Fig. 1.

A METHOD FOR GROWING LARGE CRYSTALS
OF THE ALKALI HALIDES

BY JOHN STRONG

UNIVERSITY OF MICHIGAN

(Received August 13, 1930)

ABSTRACT

F. Stöber¹ has specified four conditions which must be fulfilled in order to grow large crystals from fused salts. Ramsperger and Melvin in applying Stöber's method encountered difficulty. They were able to grow large crystals which, however, broke upon cooling on account of unequal temperature contraction of the crystal and the melting pot as well as on account of strains caused by unequal temperature contraction throughout the crystal.

Two new supplementary conditions are specified which together with Stöber's conditions give a method for growing alkali halide crystals in cylindrical form 4.5 inches tall by 4.5 inches in diameter.

THE alkali halides are very transparent to infrared radiations. Rock salt (NaCl) is transparent to all infrared radiations from the red out to wave-lengths of 15μ , sylvine (KCl) is transparent out to wave-lengths of 22μ , and potassium bromide (KBr) to 30μ . No data are available for potassium iodide (KI) but one would expect it to be transparent even further than potassium bromide since its restrahlen lies deeper in the infrared.

Professor H. M. Randall, Director of the Physical Laboratory at the University of Michigan suggested to the author, the importance of these salts as possible materials from which to make windows and dispersing prisms for use in infrared spectroscopy and supported the undertaking to develop a method of making crystals sufficiently large for these purposes.

The method of growing crystals of the alkali halides as described in this paper is similar to a method described by P. W. Bridgman¹ where a mold containing the molten salt is slowly moved from the interior of a furnace maintained above the melting temperature to an external colder region. By the method described in this paper an iron pot is filled with the alkali halide and heated in a furnace in such a way that the temperature field moves instead of the pot. The molten salt is cooled in such a way that solidification starts at the bottom of the pot and proceeds upward.

This method of growing salt crystals has been made the subject of a paper by F. Stöber.² In this paper Stöber laid down several conditions which must be satisfied in order that the method yield large flawless crystals. These conditions may be summarized as follows:

1. The crystallization must start at a single point on the bottom of the container. If this condition is not satisfied more than one crystal may be formed in the pot.

¹ P. W. Bridgman, Proc. of the Amer. Acad. of Arts and Sciences 64, #2 December (1929).

² F. Stöber, Zeits. f. Kryst. 61, 299 (1925).

2. There must be a strong vertical temperature gradient in the molten salt. This helps to keep the crystal properly oriented and prevents twinning.

3. Isothermal surfaces within the pot must be nearly horizontal to prevent convection currents in the molten salt. The melting temperature isothermal surface must be raised up through the molten salt slowly and uniformly so that the crystal laid down below this surface will be sound and flawless.

Ramsperger and Melvin³ have applied the above principles with some measure of success but they were not able to make large crystals on account of the strains introduced by the heavy dishes used. They have attempted to get around this difficulty by using extremely thin walled crucibles made out of especially ductile platinum. In spite of this, however, they did not succeed in making sodium chloride crystals larger than one or two cm on an edge. They state, "All of these conditions are easily met and for all of the crystals which we prepared, we found that the entire contents of the dish became one large single crystal, but that in some cases this crystal broke along cleavage planes into several small crystals when the cooling was practically complete."

This experience of Ramsperger and Melvin has been found to agree with that of the author and as a consequence, two new conditions are added to those laid down by Stöber. When all five of these conditions are fulfilled, the preparation of large crystals is achieved without further difficulty.

A strong temperature gradient of 5.0 to 10.0°C per cm is maintained through the salt during the crystallization process. Thus, after the crystal is formed the top will be at a higher temperature than the bottom. When the crystal is slowly cooled to room temperature, the top is cooled through a greater temperature range than the bottom by about 100°C. This means that the contraction of the upper part of the crystal will be greater than that of the lower part—in other words, the crystal will be in a condition of strain.

It so happens that the alkali halides are quite plastic at high temperatures. If the equalization of temperature occurs when the crystal is plastic it will not break when cooled to room temperature. This is the basis for the first of the supplementary conditions to be fulfilled.

4. After the crystal has been formed and while it is still plastic, the bottom and top of the crystal must be brought to the same temperature in order that no strains will be introduced due to unequal contraction upon cooling to room temperature.

The last condition to be fulfilled is,

5. The crystal must be removed from the container before the cooling process begins in order to eliminate the strains introduced by the temperature contraction of the melting pot.

For the fulfillment of these conditions, an electric furnace was developed. The nickel resistor of the furnace was one arm of a self balancing Wheatstone bridge, and the furnace was heated by the bridge current. The resistor was wound around an alundum tube seven inches in diameter which is represented in Fig. 1. The resistor, as well as the melting pot, was protected from oxidation by an atmosphere of hydrogen within the furnace. Self-balancing was

³ Ramsperger and Melvin, J.O.S.A. 15, 359 (1927).

effected by changes in the bridge current resulting in changes of furnace temperature and consequently furnace resistance. The furnace in this manner, either held a temperature constant to $1/10^{\circ}\text{C}$ or changed its temperature at a uniform rate depending on whether the other resistances of the bridge were kept constant or gradually changed. During crystal growth the furnace temperature dropped about 10° per day.

The accompanying figures show in a diagrammatic way the conditions existing at three important stages of crystal growth. In Fig. 1, we have a representation of the conditions in the furnace during crystal formation. Heat flows from the hottest region of the furnace to the cooler regions by way of the molten salt and metal cooler. The dotted lines indicate how the isothermal surfaces in the molten salt are probably distributed. The rod attached to the bottom of the pot insures that this point in the pot is coolest and, therefore, it is at this point that crystallization will start. The thick metal cooler

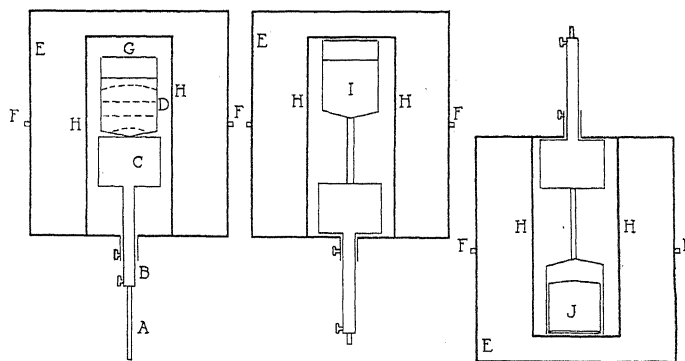


Fig. 1.

Fig. 2.

Fig. 3.

Diagrammatic representation of crystal growing furnace at three important stages of crystal growth.

A—Stem to raise or lower melting pot.

B—Sleeve to raise or lower metal cooler.

C—Metal cooler.

D—Dotted lines show probable isothermal surfaces. The melting temperature isothermal surface defines the boundary between crystal and molten salt.

E—Silocell heat insulation.

F—Axle for inverting furnace.

G—Lid to melting pot.

H—Alumina tube with nickel resistor.

I—Crystal at uniform temperature throughout.

J—Crystal free from melting pot.

immediately below the melting pot carries heat away from the bottom of the pot and insures the existence of a suitable temperature gradient. This metal cooler is movable from outside the furnace and may be adjusted to obtain the proper temperature gradient. As the furnace is gradually cooled the melting point isothermal surface moves up through the molten salt leaving a clear single crystal behind.

After the crystal has been formed the temperature gradient is removed by lowering the metal cooler and raising the pot until thermocouples at the top and bottom of the pot show equality of temperature throughout the crystal. At this time a slight plastic deformation occurs within the crystal but since this operation takes place at a temperature immediately below the melting point where the salt is quite plastic, no cracking occurs. This stage of crystal growth is illustrated by Fig. 2. In Fig. 3, we have a representation of the conditions existing just after the crystal has been melted out of the pot. When the temperature of the crystal has been equalized, the furnace is inverted and everything is then in readiness for the removal of the crystal from the pot. The furnace is strongly superheated for such a time as is necessary to melt the crystal away from the pot walls. A dull thud may be heard when the crystal drops onto the pot lid. This lid on to which the crystal drops is loose fitting so that the melted salt may run out of the pot. It is also corrugated so that it will catch and hold the crystal without causing it to suffer strains upon cooling due to unequal rates of contraction of the lid and crystal.

After this, it only remains to cool the crystal to room temperature which should not be so rapid as to cause cracking due to temperature contraction. For a single crystal weighing eight pounds, thirty hours time is sufficient for this cooling.

Large single crystals of cylindrical form have been prepared by this method ranging in size up to 4.5 inches tall by 4.5 inches in diameter. If the materials used are not pure a cloudiness will appear at the top of the crystal. Sometimes the top of the crystal is not clear because the temperature gradient at the top was insufficient. This cannot be conveniently avoided in the present form of the apparatus. Nevertheless, crystals have been made in the above size which are uniformly solid throughout.

Polished surfaces of potassium bromide and potassium chloride show less tendency to cloud than rock salt, when exposed to atmospheric moisture. A polished potassium bromide plate which has been exposed to room air for over two months shows no trace of reaction with the moisture in the air. Potassium iodide surfaces are less satisfactory in this respect yet they may be kept bright with sufficient care.

In conclusion the author wishes to acknowledge the skillful assistance of Mr. Paul Weyrich in making this undertaking a success.

LETTERS TO THE EDITOR

Prompt publication of brief reports of important discoveries in physics may be secured by addressing them to this department. Closing dates for this department are, for the first issue of the month, the twenty-eighth of the preceding month; for the second issue, the thirteenth of the month. The Board of Editors does not hold itself responsible for the opinions expressed by the correspondents.

Use of the Pierce Acoustic Interferometer

In the October 1 number (Phys. Rev. 30, 1262, 1930) appears a letter by Elias Klein and W. D. Hershberger in which the writers claim that they do not consider the determination of the absorption coefficient in gases for high frequency sound by the Pierce acoustic interferometer method justified. I wish to repeat the cautions in the use of this method which I stated in my articles on the subject. (Phys. Rev. 34, 1184, 1929 and Phys. Rev. 36, 1005, 1930). I published my interferometer data in connection with absorption because the reactance and decrement of the plate circuit apparently played but a small part at 1200 kilocycles; also because simultaneous absorption and velocity determinations are desirable. The values for A by the interferometer and by the pressure vane methods agree with each other better than do many other independently measured acoustic determinations. Correspondence with the

above writers revealed the fact that their letter was intended as a caution to others, particularly those contemplating the use of this method at lower frequencies.

In Phys. Rev. 35, 814, 1930, Charles D. Reid reports an unequal spacing of maxima and what might be termed an acoustic backlash of 0.48 mm, apparently at a frequency of 42 kilocycles per sec. The unequal spacing confirms my findings as published in Phys. Rev. 34, 1184, 1929 but I find the acoustic backlash, six wave-lengths from the crystal, to be less than 0.01 mm. ($\lambda = 0.0282$ cm; $\nu = 1219$ kc/sec.) The backlash or shift reported by Reid may be due to a persistence of resonance beyond the most favorable point in either direction.

W. H. PIELEMEIER

Pennsylvania State College
November, 1930

Wave Mechanics of Deflected Electrons

In the recent discussion¹ concerning the influence of quantum mechanics upon observations of e/m the actual method of experiment has not been analyzed very closely. In practice² an electron is caused to pass, first along a straight line through crossed electric and magnetic fields, then a further distance D through the same magnetic field alone. In the crossed fields we have, $eE = eHu$, whereas during the second part of its flight the electron is laterally displaced an amount (H and u being assumed small for simplicity) given by, $\delta = (eHu/m) (D^2/u^2)$; then $e/m = E\delta/H^2D^2$.

Now in the writer's paper³ cited by Dr. Eckart it is shown that the center of a wave-packet for a free electron in a uniform magnetic field revolves in a circle at the classical angular rate eH/m . The packet must therefore undergo the classical acceleration eHu/m where u is the speed of motion of the packet

along the circle. Similarly, in a uniform electric field the packet experiences the classical acceleration eE , superposed upon its quantum spreading. Accordingly the center of the packet should follow the classical path in the experiment upon e/m and the usual calculation of this quantity from the observations should be correct, as stated by Dr. Eckart. Apparently the only question that could arise would be as to a possible non-classical change in the packet speed u when it leaves the electric field. Since, however, the magnetic field is homogeneous throughout and the

¹ Cf. Page, Phys. Rev. 36, 1418 (1930).

² Cf. G. Neumann, Ann. d. Physik 45, 529 (1914).

³ E. H. Kennard, Zeits. f. Physik 44, 326 (1927).

electric field does not enter into the quantum-mechanical expression for packet speed, it seems safe to assert without detailed calculation that such a change cannot occur.

Professor Page interprets his results as referring to electrons having a certain energy. The "energy of an electron in a magnetic field," as distinguished from the total energy of electron and field, is, however, a complicated question even in classical theory and Page's results require, I think, further analysis before their significance can be properly appreciated.

Apparently no one has published a general formula for the motion of a wave-packet of any type in a general electromagnetic field. The writer has submitted for publication a paper in which this formula is obtained in a simple manner, the result being classical for uniform fields either in non-relativistic theory or for the relativistic electron of Dirac.

E. H. KENNARD

Cornell University,
Ithaca, N. Y.

November 5, 1930

Simple Isotopic Constitution of Caesium

By means of a mass-spectrograph similar to Dempster's, but of greater resolving power, caesium has been found to have but one isotope, within the limits of measurement. This result presents the possibility of a packing fraction of -14.3 compared to -5.3 ± 2 for Xe and I, or as an alternative, an error amounting to 0.077 percent in the accepted determination of the chemical atomic weight 132.81, assuming that the packing effect is similar to that for I and Xe. Aston¹ using photographic recording of the ion beam, likewise observed one isotope only, Cs¹³³. With electrical recording a lower limit may be placed on the relative abundance of any other isotope with respect to Cs¹³³.

If a packing fraction of -5.3 , (I and Xe -5.3 ± 2), is taken for Cs¹³³ on the $O^{16}=16.000$ scale then the following percentages of single isotopes would be required to give the chemically determined atomic weight 132.81. These amounts are expressed as percentage abundance relative to 132.93 taken as 100 percent.: 13.63 percent of isotope 131.93, 6.36 of 130.93, 4.16 of 129.93 or 3.1 of 128.93. If a lower limit of -7.3 is taken for the packing fraction of Cs¹³³ then relative to 132.903 the following percentages of any single isotope are 10.2 of 131.903, 4.87, of 130.903, 3.2 of 129.903 or 2.38 of 128.903. For oxygen = 16.000 on the chemical scale, the percentages of the other isotopes would lie between the above values on the basis of a packing fraction of -5.3 , equivalent to -6.55 on the $O^{16}=16.000$ scale. No indication has been obtained of any single one of

these possible isotopes being present to even one tenth of the above percentages. The resolving power, $M/\Delta M$, of the mass spectrograph was 200 to 230 for the five best runs with the peak value of the Cs¹³³ ion current ranging from 300 to 3600 mm (3×10^{-9} amperes), on the scale of a Compton electrometer with shunting resistances for current measurement. The caesium ions were obtained from a tantalum strip coated with pollucite from Newry, Maine.

Until the packing fraction of caesium is determined directly the source of the discrepancy between the simple isotopic constitution of caesium and the chemical atomic weight cannot be determined. It is, of course, quite possible that the chemical atomic weight is correct and that caesium has an abnormally low packing fraction. It is unfortunate that in the case of Aston's original measurement in 1921 no special accuracy of mass measurement² was sought with caesium, even though a packing fraction of -14.3 ($O^{16}=16.000$) was within the range of the mass spectrograph in use at that time.

This work is being extended to barium and strontium at the present time.

K. T. BAINBRIDGE

National Research Fellow

Bartol Research Foundation of the Franklin Institute,
Swarthmore, Pennsylvania
November, 1930

¹ F. W. Aston, *Phil. Mag.* **42**, 436 (1921).

² Reference 1, p. 440.

Problems in Acoustic Interferometry with Gases

In a recent communication to this journal Elias Klein and W. D. Hersberger (*Phys. Rev.* **36**, 1262, Oct. 1, 1930) point out that the

variation of plate current in the Pierce acoustic interferometer with increase in the length of the resonant column of gas is a function not

only of the absorption of the gas but of the circuit constants as well, and that accordingly the deductions of Pielemeier (Phys. Rev., 34, 1184-1203, Oct. 15, 1929) of ultrasonic absorption coefficients from plate current variations without taking circuit constants into account is probably not justified. Precisely this consideration together with the fact of the nonlinearity of the characteristics of vacuum tubes was the basis of experiments reported by me at the April meeting of the American Physical Society (Phys. Rev. 35, 1442, June 1, 1930). In these experiments the piezoelectric plate was part of a secondary circuit loosely coupled to a separate oscillator, and the very small (second order) cyclical changes of frequency caused by lengthening the gas column were compensated by adjusting a vernier condenser in the circuit. The quartz plate together with the column of gas was considered as a mechanical system of two degrees of freedom and its effect in the circuit was worked out in terms of circuit and mechanical constants, the frequency being constant. It is thus possible to express the absorption coefficient of the compressional waves in the gas in terms of the decrement of capacity compensation.

Since the time of presenting the above paper much improvement in procedure has been made. To secure data of significance on absorption the source of electrical oscillations must be safeguarded from reaction on it by the acoustic system. Methods have been devised of producing oscillations of constant frequency and of amplifying them so that a secondary system could be excited without disturbing the frequency or the amplitude of the exciting e.m.f. The circuit containing the piezoelectric plate and resonant air column is loosely coupled to the output of the amplifier and variation in current to the crystal electrodes as the gas column is lengthened is measured after the manner of W. G. Cady (Proc. I. R. E. 10, 83-114, 1922). The theory of this system is easily derived by extending the treatment given by Professor Cady so as to take account of the mechanical action of the gas. The results under these conditions are quite independent of vacuum tube characteristics. The greatest improvement in method has resulted from the use of two piezoelectric plates of nearly the same frequency, one of which is used in a piezoelectric oscil-

lator, the other of which is used in a simple circuit loosely coupled to the amplified output of the oscillator, and serves as a generator of compressional waves in the gas. Under these conditions frequency and amplitude of exciting e.m.f. are constant, considerations of the highest importance in the mathematical treatment.

One result of these measurements is the remarkable precision with which the resonance positions of the reflecting plate may be measured. Much difficulty has been encountered in securing screws of sufficiently small error and of sufficiently good design of mounting to hold their calibrations. Up to the present it is possible under best conditions to obtain values of velocity to one part in twenty thousand. For higher precision a screw system as good as that necessary for ruling an optical diffraction grating would be necessary. Incidentally, it may be remarked that the acoustic interferometer is a most convenient instrument for the calibration of screws. In the frequency limits in which I have so far worked (between 218 and 476 k.c.) I have not been able to detect any variation of velocity with path-length as reported by C. D. Reid (Phys. Rev. 35, 814-831, April 1, 1930) for lower frequencies. This may be due in part to the fact that the wave-length in gases being small compared with the dimensions of the face of the vibrating crystal, any part which may be played by diffraction is probably negligible. For the purpose of comparison of results with those of Reid, measurements are being made at lower frequencies.

As another result of these experiments I have at no time been able to detect any change of velocity with intensity as reported by W. H. Pielemeier (*loc. cit.*).

The experiments here outlined have been supported by a grant made in 1926 by the Rumford Committee of the American Academy of Arts and Sciences. This grant was renewed in 1928, but it was only during the spring of this year that active work could be undertaken. I am indebted to Mr. Alfred L. Loomis and to the Naval Research Laboratory for some of the crystals which I have used.

J. C. HUBBARD

Rowland Physical Laboratory
Johns Hopkins University
November 6, 1930

Magnetostriiction and Magnetic Hysteresis

In a recent paper on the nature of remanence and hysteresis losses in ferromagnetic materials¹ N. S. Akulov professes to prove that the magnetostriction of a single crystal, expressed as a function of its magnetization, is unaffected by the application of mechanical forces. Since my measurements on the magnetostrictions² and on the electrical resistance changes³ accompanying the magnetization of stretched and unstretched permalloy wires seem incompatible with Akulov's conclusion, I have been led to examine his argument in detail. His mistake lies in his separation of each of the strain components (ϵ_{ij}) into two parts, one of which (ϵ_{ij}) is said to depend *only* upon the mechanical forces, the other (λ_{ij}) *only* upon the magnetization. The assumption that such a separation is possible begs the question at issue.

My experiments, referred to above, and much other evidence of the same sort, make it abundantly clear that the "magnetic" strain components (λ_{ij}) can be set up either by magnetization or by suitable non-isotropic mechanical stresses. These strain components are not, of course, linear functions of the applied forces in either case, since they exhibit saturation phenomena. They are ordinarily ignored in elastic theory and experiment because their limiting values, of the order of 10^{-6} , are nearly negligible in comparison with permissible elastic strains in polycrystalline iron and nickel.

It should also be emphasized that experiment still discloses hysteresis losses and Barkhausen discontinuities in single crystals of iron and nickel, which Akulov regards as inherently free from both of these phenomena. Though the hysteresis losses are much smaller than in polycrystalline iron and nickel, they are, for equal ranges in magnetization, much greater than in polycrystalline permalloy that has never, since its preparation, been subjected to magnetic fields great enough to develop a "wasp-waisted" hysteresis loop. The explanation of permalloy offered by Akulov, which accounts only for the abnormal shape of extensive hysteresis loops, thus fails to account for the principal peculiarity of these materials. His conclusions as to the shapes of internal energy *versus* magnetization curves must, however, be essentially correct, and represent a real advance in the theory of ferromagnetism.

L. W. McKEEHAN

Sloane Physics Laboratory
Yale University

November 10, 1930

¹ N. S. Akulov, Zeits. f. Physik **64**, 817-829 (1930).

² L. W. McKeehan, P. P. Cioffi, Phys. Rev. [2] **28**, 146-157 (1925).

³ L. W. McKeehan, Phys. Rev. [2] **36**, 948-977 (1930).

Note on the Source of Dielectric Polarization

Dr. J. Hengstenberg has kindly called my attention to an error in my paper on the source of dielectric polarization (Phys. Rev. **36**, 65, 1930) Eq. (1), for the force on an ion in a cubic crystal lattice should read

$$f_e = \frac{K+2}{3} Ee \text{ dynes.}$$

This corrected formula gives, in the case of KCl, values for the fractional change in reflected intensity $\Delta I/I$ almost identical with those calculated by Hengstenberg (Zeits. f. Physik **58**, 345, 1929). My method consists of calculating first, the force on an ion within the lattice which is under electric stress, and then the restraining force constant for an ion from residual ray frequencies. The ratio of these quantities gives the displacement of the ions for any gradient E . Hengstenberg's

method consists in assigning one electronic charge to each ion and calculating the necessary displacement of these charges to account for the polarization. If the two theories lead to the same result, as is indicated by the numerical values in the case of KCl, then it should be possible to calculate the dielectric constant from the wave-length of the residual rays λ , the atomic mass m , the distance between adjacent oppositely charged ions r , and known constants. From Hengstenberg's paper

$$P = \frac{K-1}{4\pi} E = \frac{e}{2r^3} \delta r = \frac{e}{r^3} dx$$

whence

$$dx = \frac{(K-1)}{4\pi e} r^3 E$$

and my Eq. (3) as corrected

$$\delta = \frac{\lambda^2 e}{4\pi^2 c^2 m} \frac{K+2}{3} E$$

dx and δ are identical, whence

$$\frac{(K-1)}{4\pi e} r^3 E = \frac{\lambda^2 e (K+2)}{12\pi^2 c^2 m} E$$

and

$$\frac{K-1}{K+2} = \frac{\lambda^2 e^2}{3\pi c^2 m r^3}$$

If m is assumed to be the average mass of the ions of the lattice, then $m = M/2N$ where M is the molecular weight of the compound and N is Avogadro's number.

Then

$$\frac{K-1}{K+2} = \frac{2\lambda^2 e^2 N}{3\pi c^2 r^3 M} = a$$

Whence

$$K = \frac{2a+1}{1-a}$$

Taking the values $N = 6.06 \times 10^{23}$; $e = 4.77 \times 10^{-10}$; $c = 3 \times 10^{10}$

$$a = 3.25 \times 10^{-17} \frac{\lambda^2}{Mr^3}$$

The following table gives the values used in the calculation of K and the result together with observed values of dielectric constant for a number of crystals of the KCl type.

Compound	λ (in μ)	M	r (in A.U.)	a	K calc	K obs
KCl	63.4	74.6	3.14	0.56	4.8	5.0
NaCl	52.0	58.5	2.81	.68	7.4	6.1
AgCl	81.5	143.3	2.77	.71	8.4	11.2
KBr	82.6	119.0	3.30	.52	4.3	5.1
AgBr	112.7	187.8	2.90	.90	28.0	12.2
KI	94.1	166.0	3.53	.39	2.92	5.4
Diamond					1.00	16.5

The fact that these calculations lead to values for the dielectric constant in most cases of the same order of magnitude and in some cases almost identical with those observed, leads one to believe that ionic dis-

placement is an important factor in the polarization in a material of this sort. That this cannot be the only factor however is evident from the values for NaCl and AgBr where ion displacement alone predicts a greater dielectric constant than that actually observed. Further there are non-polar crystals of which diamond is an example, which on this basis should have a dielectric constant of unity instead of the observed value of 16.5. Hence the fraction β of the polarization due to ion displacement lies somewhere between 0 and 1, the value apparently varying from crystal to crystal. The resulting variation in intensity of reflected x-rays would then be for a given field strength, $(\Delta I/I) \propto \beta^2$.

Hengstenberg's experimental results indicate that β lies between 0.8 and 1.4 for his 1900 esu/cm observation and between 1 and 1.2 for his 3000 esu/cm observation. My results indicate that β is probably not more than 0.75 for a rough estimate over a comparatively large number of observations. My experimental values represent averages of ionization currents over long periods of time—a method of observing which tends to eliminate the effect of fluctuations; while those of Hengstenberg are direct readings of a quantity which is difficult to keep constant to 1/10%.

It seems worth while to call to mind in this connection the result of x-ray measurements on electron distribution in crystals of this sort. The results of such measurements indicate that the extra electron of the metal atom does not go over completely to the halogen atom. In other words the probable position of the extra electron is such that part of the time it is associated with the metal atom and part of the time with the halogen atom. This would lead to a value of β less than 1.

RALPH D. BENNETT

Ryerson Laboratory,
University of Chicago
November 5, 1930

A Diophantine Equation Connected with the Hydrogen Spectrum

The wave-length λ corresponding to a line in the hydrogen spectrum is given by Balmer's formula

$$\frac{1}{\lambda} = R \left(\frac{1}{m^2} - \frac{1}{n^2} \right),$$

where R is the Rydberg constant and the integers m and n are the principal quantum

numbers. The question then naturally arises whether two different pairs of quantum numbers (m, n) and (m_1, n_1) can correspond to the same wave-length, or in other words, whether the Diophantine equation

$$\frac{1}{m^2} - \frac{1}{n^2} = \frac{1}{m_1^2} - \frac{1}{n_1^2} \quad (1)$$

has any solutions.

It is readily verified that the formulas

$$\begin{aligned}\rho m &= v(u^2 - v^2 - w^2)(u^2 - v^2 + w^2), \\ \rho n &= u(u^2 - v^2 - w^2)(u^2 - v^2 + w^2), \\ \rho m_1 &= 2uvw(u^2 - v^2 - w^2), \\ \rho n_1 &= 2uvw(u^2 - v^2 + w^2),\end{aligned}\quad (2)$$

where u, v and w are integers and ρ a common divisor of all four numbers to the right, give a solution of (1). Conversely, when any solution of (1) is given, it is expressible in the form (2), since these equations give the following values of the ratios u/v and w/v : $u/v = n/m$, $w/v = n(n_1 - m_1)/m_1 n_1$.

From any solution of (1), an infinity of others are obtained by multiplying m, n, m_1 and n_1 by any integer; it is therefore of some interest to show that (1) has infinitely many solutions without a common divisor. Let v and w be relative primes, v odd and w even, and w not divisible by 3; making $u = 2v$ and $\rho = v$ in (2), we obtain

$$\begin{aligned}m &= (3v^2 - w^2)(3v^2 + w^2), \\ n &= 2(3v^2 - w^2)(3v^2 + w^2), \\ m_1 &= 4vw(3v^2 - w^2), \\ n_1 &= 4vw(3v^2 + w^2),\end{aligned}$$

and these four numbers have no common factor. In fact, m is not divisible by 2, nor has it any factor in common with v or w , so that a common factor of m, n, m_1 and n_1 must be a common divisor of $3v^2 - w^2$ and $3v^2 + w^2$ or, both these numbers being odd, a common divisor of $3v^2$ and w^2 , which is impossible.

We may obviously assume m to be the smallest of the four numbers; to obtain all the solutions of (1) corresponding to a given value of m , we note that since $n \geq m+1$, it follows from (1) that

$$\frac{1}{m^2} - \frac{1}{(m+1)^2} < \frac{1}{m_1^2},$$

which gives an upper bound for m_1 . Transposing n and m_1 in (1), it is seen that the same upper bound applies also to n , and the solution of (1) with m given is thus reduced to a finite number of trials. In this manner it is seen that there is no solution for $m = 1, 2, 3$ or 4, and that all solutions with $m \leq 10$ are those given in the following table, together with those obtained from it by transposing the two middle terms n and m_1 (in the cases where $n \neq m_1$).

m	n	m_1	n_1
5	6	9	90
5	7	7	35
6	8	9	72
7	8	14	56
10	11	22	55
10	11	24	1320
10	12	18	180
10	14	14	70

T. H. GRONWALL

Department of Physics,
Columbia University,
November 17, 1930.

BOOK REVIEWS

The Theory of Approximation. DUNHAM JACKSON. American Mathematical Society Colloquium Publications, Volume XI.

This book contains five short chapters, and constitutes, as the author states in his preface, "a brief essay in a field on which an encyclopedia might be written." In spite of this modest claim the author has assembled in compact yet lucid form a surprising number of fundamental theorems together with complete proofs. With the aid of this book a beginner in the field of approximations may become master of the essential concepts, methods, and results, without extensive reference to the original literature. To a large degree the material contained in the book is the fruit of the author's own extensive investigations in the subject of approximations.

In broad outline the problem which is dealt with throughout the book is the determination of the degree of accuracy by which a given function $f(x)$ can be represented by means of a polynomial of assigned degree or by a trigonometric sum of given order of the form

$$a_0 + a_1 \cos x + a_2 \cos 2x + \dots + a_n \cos nx \\ + b_1 \sin x + b_2 \sin 2x + \dots + b_n \sin nx$$

though brief reference is made to approximations using series of more general functions.

Chapter I, entitled "Continuous Functions," deals with the degree of approximation obtainable with a specified number of terms either of a polynomial or of a trigonometric sum for the case in which the given function has suitable properties of continuity. Chapter II, entitled "Discontinuous Functions; Limited Variation; Arithmetic Means;" treats the same problem for the case in which the given function or certain of its derivatives are discontinuous but are of limited variation. It also deals with the degree of convergence of the arithmetic means of a Fourier series. Chapter III treats the degree of approximation obtained by the method of least squares, in which the integral of the square of the error is a minimum, and by the method of least m th powers, in which the m th power of the absolute error is a minimum. The case of weighted approximation is also considered as well as the case of polynomial approximation over an infinite interval. Chapter IV considers the degree of approximation obtainable by means of a trigonometric sum which is determined by the method of trigonometric interpolation. Finally Chapter V, entitled "Introduction to the Geometry of Function Space," brings out interesting geometric interpretations of the formulas of multiple and partial correlation, a subject which is somewhat loosely related to the preceding work on approximation by the principle of Least Squares.

Since the approximate representation of functions plays such an important role in the technique of the mathematical physicist, and since a knowledge of the order of accuracy obtainable in each given case is equally important, this book should prove a valuable aid to physicists as well as to mathematicians.

W. E. MILNE

Allgemeine Physik der Röntgenstrahlen. FRITZ KIRSCHNER, Privatdozent an der Universität, München; comprising Volume 24, Part 1 of the Handbuch der Experimental Physik, edited by (the late) W. Wien and F. Harms. ix+548 pages. Akademische Verlagsgesellschaft m. b. H., Leipzig. Price bound, Rm 55.

Volume 24 of this well-known Handbuch is devoted to x-rays, Part II on X-Ray Spectroscopy having appeared somewhat earlier than the present Part I, which, as the title indicates, deals mainly with the fundamental principles of x-rays and their effects on matter.

The contents of the book can best be given by quoting the titles of its twelve chapters: The Production of X-Rays; High Voltage Sources; Current-Voltage Characteristics of X-Ray Tubes; The Intensity of the Radiation emitted by the X-Ray Tube; The Photoelectric Effect of X-Rays; Scattered (i.e. Compton recoil) Electrons; Characteristic X-Rays and Characteristic Electron emission; Secondary Effects of X-Rays Produced by Photo- and Scattered Electrons;

The Nature of Scattered Radiation; The Intensity of Scattered Radiation; Survey of the Theories of the Scattering of X-Rays; The Determination of X-Ray Wave-lengths by Diffraction and Interference.

With a thoroughness characteristic of the volumes in this series, the author has given a complete survey of each of the above-mentioned subjects. Not only are there copious references to the various articles, but numerous important articles are discussed in detail and very frequently data tables and graphs are reproduced. The discussion is seldom critical, however, and accordingly the reader must usually make his own evaluation of the importance of a given investigation.

Taken in combination with Part II, the present volume places before investigators and students a complete compendium of the more important experimental work which has been done in the field of x-rays. The volumes will be invaluable for both reference and study.

F. K. RICHTMYER

Les Statistiques Quantiques. LEON BRILLOUIN. Two volumes, pp. 404, figs. 26. Les Presses Universitaires de France, 1930. Price 125 francs.

A number of books on quantum mechanics have recently appeared in which the central theme is essentially spectroscopic. Although the development of this field has been most tremendously accelerated since Bohr's treatment of the hydrogen atom, the earliest work on black-body radiation, and some of the newest on the properties of solids, lie in other fields. Professor Brillouin has given a most delightful and stimulating resumé of many of the problems and accomplishments of the quantum theory along these lines. Although these volumes do not purport to be an exhaustive treatise on the subject, they do give a comprehensive treatment of quantum statistics with a wide variety of applications.

The rather classical treatment of black-body radiation is taken over, to a large extent, from the author's previous book and differs from the more common treatment by its emphasis upon the conditions in dispersive media. The discussion of phase, group, energy, and signal velocities is especially valuable at the present time. As is to be expected, the treatment of light quanta has been apparently much influenced by the ideas of deBroglie, with the result that a good deal of space is given to the equations of motion of the protons. A number of very interesting applications of these equations are made in this connection.

In the chapters on thermodynamics and statistics the connection between these two points of view is very nicely made. One could wish, however, that more emphasis had been laid upon the distinctions in point of view between the classical and the quantum theoretical methods of determining probabilities. In particular the work of Schroedinger lends a clarity of idea to the quantum method which is worthy of a good deal of attention. In connection with the discussion of the Fermi-Dirac statistics the applications made by Sommerfeld and Pauli to the electrons in metals are treated with a clear indication as to just what features are characteristic of the newer statistics.

In continuation of the subject of electrons in metals the first half of the second volume is devoted to the problem of the quantum mechanical evaluation of the mean free path. Professor Brillouin evidently does not consider the simpler methods as very significant, but he gives a thorough treatment of the more elaborate calculations of Bloch. He also gives an excellent presentation of the problem of an electron in a sinusoidal field of force. The remainder of the second volume is occupied by a discussion of the statistical treatment of the electron distribution in an atom, and of the distribution of atoms among various quantized states. There is also a very valuable and exhaustive bibliography.

To one who wishes an acquaintance with the wide applicability of quantum theory outside the field of spectroscopy, or to one who is interested in the possibilities of a satisfactory theory of solid bodies, these two volumes will be a most valuable aid.

W. V. HOUSTON

THE PHYSICAL REVIEW

POLARIZATION OF THE CONTINUOUS X-RAYS FROM SINGLE ELECTRON IMPACTS¹

BY BALEBAIL DASANNACHARYA
RYERSON PHYSICAL LABORATORY
UNIVERSITY OF CHICAGO

(Received November 8, 1930)

ABSTRACT

Experiments are described on the polarization of continuous x-rays from targets of aluminum sheets varying in the thickness from 6 to 250×10^{-5} cm. The velocities of the exciting electrons corresponded to voltages from 27 to 57 kilovolts. It was found that the polarization increased exponentially with decreasing thicknesses, suggesting perhaps a nearly complete polarization for a thickness of about 6×10^{-6} cm. The polarization diminished with an increase in the velocity of the exciting electrons.

The theory of the polarization of continuous x-rays developed by Sugiura seems to be in conformity with the experimental results obtained in the experiments described below.

THE old problem of the radiation due to the stoppage of electrons, attacked by Stokes and J. J. Thomson immediately after Röntgen's discovery of the x-rays, was extended by Sommerfeld² by the methods of the classical theory. Recently Sommerfeld³ extended his previous work by applying the mathematical methods of wave-mechanics to cases where the electrons were stopped in a single process (very thin anticathodes).

This new theory was well supported by the measurements of Kulenkampff⁴ on the angular distribution of the radiation produced in an aluminum target of thickness 6.5×10^{-5} cm. The intensity in the forward direction of motion of electrons was from these experiments extrapolated to be zero. Duane⁵ working with mercury vapour found that the intensities I_f in the forward direction and I_t at right angles were in the ratio of 1 to about 5.5. Defining the percent polarization as $(I_t - I_f / I_t + I_f) \times 100$, this might be interpreted as a polarization of 70 percent. Sommerfeld consequently made a generalized assumption according to which only those electron beams emerging from the target with zero velocity should give rise to complete polarization, i.e., the radiation corresponding to the short wave-length limit of the continuous spectrum should be completely polarized.

¹ A short account was given at the Chicago meeting of the American Physical Society, Nov. 27, 1929. Phys. Rev. 35, 129 (1930).

² A. Sommerfeld, Phys. Zeits. 10, 969 (1909).

³ A. Sommerfeld, Proc. Nat. Acad. Sci. 15, 393 (1929).

⁴ H. Kulenkampff Ann. d. Physik 87, 597 (1928).

⁵ W. Duane Proc. Nat. Acad. Sci. 14, 450 (1928).

P. Kirkpatrick⁶ calculated from his experiments with a thick tungsten anticathode a polarization of 11 percent for the short wave-length limit with a thick tungsten target. P. A. Ross⁷ using a method of balanced double filters obtained nearly complete polarization at the short wave-length limit with a thick tungsten target. Wagner and Ott⁸ reflected x-rays coming normal to the direction of the electron stream at the surface of a crystal and observed the intensity of the radiation thus reflected in directions along and at right angles to that of the electron beam. They found a maximum polarization of 47.5 for the short wave-length limit. Thus results so far recorded fail to show any general agreement.

It appeared therefore desirable to make some direct measurements on the polarization of continuous x-rays from thin targets, like aluminum foils of various thicknesses, with electrons accelerated by different potential drops.

APPARATUS

An electron stream (see Fig. 1) from a hot spiral cathode fitted with a focussing cup passes through two openings *A* and *B*, both of which form a single element and are earthed. The distance between *A* and *B* is 5 cm. The

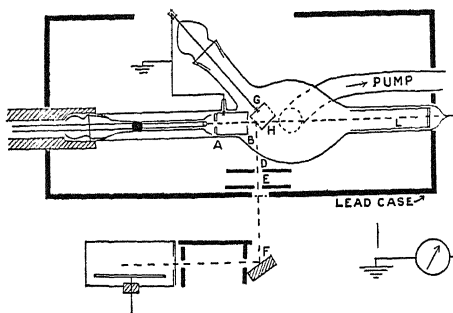


Fig. 1. Diagram of apparatus.

opening *A* is in the molybdenum disk facing the electron stream. *B* is in an iron sheet welded into the cylinder which carries the molybdenum. A centimeter behind *B* the electron beam meets the aluminum foils stretched across two rings *G* and *H*. The beam after passing through the aluminum passes without striking the sides of the lower ring *H* into a hollow cylinder *L* and through a millimeter to the earth. Circular openings *D* and *E* in lead sheets are so placed and are of such a size as to prevent x-rays formed at *B* from falling on the graphite block *F*. The effectiveness of the shielding was tested by observing the effect on the readings of the electrometer when the aluminum foils between *G* and *H* were rotated away from the path of the electron beam. Further, when an aluminum foil is in the path of the electron beam, it easily gets punctured at the place where the beam meets the foil. The size of this puncture, about 4 mm in diameter, and the place where it occurs, gives good indication of the path of the beam in the foil system *GH*.

⁶ P. Kirkpatrick, Phys. Rev. **22**, 226 (1923).

⁷ P. A. Ross, J. Opt. Soc. Am. **16**, 375 and 433; Phys. Rev. **28**, 425 (1926).

⁸ E. Wagner and P. Ott, Ann. d. Physik **85**, 425 (1928).

Pinhole photographs were also made for further confirmation. The openings in the diaphragms in front of the ionization chamber on a Bragg spectrograph were one square centimeter.

In order to avoid charge developing on the inside walls of the x-ray tube, and deflecting the electron beam, the inside surface from A to the end of the tube at L was platinized with platinum paint. Before the paint was heated it was nearly completely removed from that part of the wall through which the x-rays passed to the graphite F , in order to prevent any filtering action of the x-rays by the platinum layer.

The ionization current was measured in a Compton electrometer worked at a deflection of the reflected spot of about 30,000 mm per volt, with the scale at a distance of 2 meters from the mirror. The current from a transformer was rectified through a kenetron before being admitted into the x-ray tube.

EXPERIMENTAL RESULTS

The intensities I_i and I_r of the x-ray beam emerging from the graphite along the direction of the electron beam and at right angles to the same were

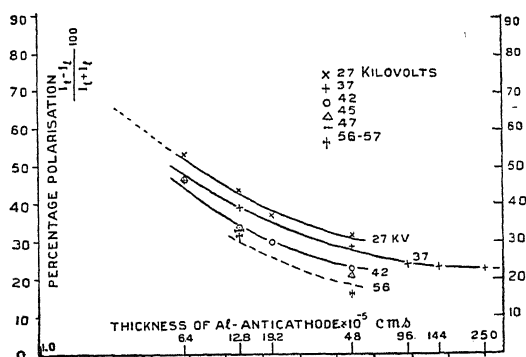


Fig. 2.

measured. Correction due to stray radiation when there was no aluminum foil in the path of the electron beam at C was found negligible. The thickness of the aluminum foils or plates varied from 6.4 to 250×10^{-5} cm. For the thinnest aluminum foil my obligations are due to Dr. Kulenkampff. These foils were stretched between the rings G and H , fastened with a paint made of fine aluminum powder and a little varnish dried over hot air.

The experiments of June 23rd (see Table I) showed that the polarization increased with the diminution of thickness as well as by a diminution of the accelerating voltage of the electrons. The value for 57 KV seems rather too low and that for 45 KV rather too high. The effect of voltage and thickness seems however to be unmistakable. The experiments of October 18 were carried out with one of the thinnest foils used previously, nearly 48.0×10^{-5} cm, and three others. The effects of voltage and thickness (see Fig. 2) are here more clearly marked.

A rough extrapolation for smaller thicknesses indicates that complete polarization may result for a thickness of about 6×10^{-6} cm. This thickness

TABLE I.

Date	Accelerating potential in kilovolts.	Thickness of the aluminum plates, in 10^{-5} cm	Percentage polarization $(I_t - I_i)/(I_t + I_i) \times 100$
June 23, 1929	37 ...	250 22.2
		144 22.3
		96 23.7
		48 28.5
	45 ...	48 26.3
	57 ...	48 16.3 (?)
Oct. 18, 1929	27 ...	48 31.5
		19.2 37.1
		12.8 43.5
		6.4 53.0
	37 ...	12.8 39.0
		6.4 46.2
	42 ...	48.0 22.5
		19.2 29.8
		12.8 33.8
		6.4 46.7
	56 ...	12.8 31.5
	47 ...	12.8 33.0

happens to be about the same as that (4×10^{-6} cm) for which the electron keeps its initial direction of motion, as calculated from theories of the diffusion of electrons through matter⁹ for an average accelerating potential of 34 KV. According to the diffusion theory, however, the length of path along which the electron keeps its initial direction should increase with increase in speed, which would mean greater polarization for greater electron speeds. Since this is contrary to the results of the present experiments, it would appear that the approximate agreement between the length of the undeviated path and the thickness for complete polarization is probably fortuitous.

According to Sugiura,¹⁰ who has recently developed a theory of the production of continuous x-rays somewhat on the lines followed by Sommerfeld, one should expect that the polarization at right angles to the direction of motion of the electron beam even for vanishing thickness of the target to be incomplete. The polarization should be greater for rays corresponding to electrons of smaller speed, a result which is in keeping with the findings of our present experiment.

It is interesting to note that Kulenkampff¹¹ has recorded a value of 45 per cent for the polarization with electron beams of 36 KV presumably for the thickness of aluminum the same as the least one in our present experiment.

⁹ Handb. d. Exptl. Physik, Kathodenstrahlen by Lenard and Becker pages 333, 379. Akad. Verl. Buchh., Leipzig, 1927.

¹⁰ Sugiura Sci. Papers I. P. C. R. 11, 251-290 (1929).

¹¹ H. Kulenkampff, Phys. Zeits. 30, 513 (1929).

Our value for the same is 47.5, within errors of experiment the same as the value obtained by Kulenkampff.

Duane¹² did not find any great difference between the polarizations with jets of mercury vapour as anticathode, the density of the vapour being varied from one to four. On an average the polarization decreased from 51.4 to 48.6, a result not contradicting our own findings, though Duane is inclined to believe that the difference perhaps is not very much greater than the experimental errors. Secondly, it may be that in Duane's experiment we are nearly at the maximum of polarization; or it may also be that in the case of mercury the change of polarization with thickness is small. Thirdly, a comparison of Duane's value (taking it to be nearly the maximum for mercury) with our own for Al extrapolated to smaller thicknesses than actually used, would lead us to suppose that an increase in the atomic number of the anticathode would result in a decrease in the polarization.

This last result as well as results of Duane just referred to would be hard to reconcile with the almost perfect polarization obtained by Ross¹³ with his double filter method, and using thick tungsten as anticathode. Perhaps the balancing of Ross's filters, which may have been perfect, or the error in the same inappreciable, when the differences are large, would cease to be so when the difference to be obtained is about of the order of the inaccuracy. As against Ross,⁷ Wagner and Ott⁸ using platinum as anticathode could get only 47.5 as the polarization for the short wave-length limit.

A ROUGH PICTURE OF THE PRODUCTION OF POLARIZATION IN CONTINUOUS X-RAYS

The polarization may depend on the following:

- (1). Initial direction of the impinging electron.
- (2). Its final direction, and probably also on,
- (3). The atomic number of the material of the anticathode, and
- (4). Electron configuration round the nucleus.

If the energy of the impinging electron is completely utilized in the production of the continuous x-ray, as would be the case for radiation at the short wave-length limit of the spectrum, and consequently (2) is negligible and if (3) and (4) should happen to be negligible too, the polarization may be complete. On the other hand, as we come to frequencies smaller than the limiting one, we may think of them as being produced by electrons leaving the atom with appreciable speeds in directions which however are arbitrary. Consequently (2) becomes increasingly appreciable so that the electric vector would deviate progressively from the initial direction. If we are to account for more complete polarization for smaller velocities, we have to assume that the probability is greater that an electron of a smaller speed would emerge from the atmosphere of an atom with comparatively greater loss of energy.

I wish to thank Professor A. H. Compton for suggesting the problem, for his continued encouragement and for his kindness in permitting me to work in his laboratory as a visiting foreign guest of the University.

¹² W. Duane, *Proc. Nat. Acad. Sci.* **15**, 805 (1929).

¹³ P. A. Ross, *J. Opt. Soc. Am.* **16**, 375 and 433. *Phys. Rev.* **28**, 425 (1926)

SPECTRUM OF THE RADIATION FROM A HIGH POTENTIAL
X-RAY TUBE

BY C. C. LAURITSEN

CALIFORNIA INSTITUTE OF TECHNOLOGY
PASADENA

(Received November 7, 1930)

ABSTRACT

A spectrograph of the Seemann type has been constructed for the purpose of investigating the radiation from the high potential x-ray tube at the California Institute. A typical spectrogram obtained with 600 kilovolts on the tube is presented. The photometer record shows a continuous spectrum with its maximum intensity at about 200 kilovolts and a short wave-length limit in the neighborhood of 600 kilovolts. The range covered is roughly from 100 to 20 x-units. It is proposed to use the apparatus for determining absorption coefficients by photographing the spectrum of radiation which has passed through an absorbing screen. No anomalies of any kind have been observed so far.

APPARATUS

THE high potential x-ray tube at the California Institute of Technology has recently been rebuilt and equipped with a hot cathode and a tungsten target. A description of the tube and its housing has been presented by Lauritsen and Cassen.¹ The tube in its present form operates satisfactorily at 600 kilovolts and it has been deemed advisable to investigate the available radiation before attempting to go to higher potentials.

In order to investigate the region of the x-ray spectrum from approximately 150 kilovolts and up, a crystal spectrograph was constructed following the principle described by Seemann,² Siegbahn³ and others. High precision cannot be expected with any reasonable time of exposure by this method since the whole of this region of the spectrum lies within an angle of less than one degree and thick slits are required because of the great penetrating power of the hard radiation. On the other hand, the method is convenient and sufficiently precise for the approximate determination of the short wave-length limit as well as of the general distribution of intensity in the spectrum. Also, if any prominent lines, bands or absorption edges or other unexpected irregularities exist in this region, they should be found most conveniently by this method.

The spectrograph consists essentially of a vertical slit 0.9 mm wide in a lead block 4 cm thick, in front of which a rock-salt crystal is placed. The crystal, slit and photographic plate are all rigidly mounted on a long arm which may be rotated through an angle of one degree on each side of the center, the rotation taking place about an axis through the vertical center line of the slit. Since the focal spot has the appearance of a thin horizontal

¹ C. C. Lauritsen and B. Cassen, *Phys. Rev.* **36**, 988 (1930).

² Seemann, *Phys. Zeits.* **18**, 242 (1917).

³ M. Siegbahn, *Phil. Mag.* **2**, 639 (1919).

disk approximately 5 mm in diameter, it is clear that radiation will reach the central planes of the crystal under all angles from zero to 50 minutes, provided that the distance from the focal spot to the crystal does not exceed 35 cm and that the spectrograph arm is set at an angle of 25 minutes on either side of the center line through the focal spot and the slit. Under these conditions the undeviated part of the light will produce an image of the focal spot as seen through the slit, the whole of the image being located on one side of and adjacent to the center line of the photographic plate. The reflected portion of the light will appear as a spectrum on the other side of the center line. The short wave-length limit is thus given by the distance from the center line to the edge of the continuous spectrum, and lines of equal wave-length are parallel to the center line. Since different wave-lengths originate from different lateral regions of the focal spot and since the intensity is not absolutely uniform throughout the whole of the area, it is not possible to obtain the intensity distribution in the spectrum directly with any degree of precision. Correction can, however, be made for this lack of uniformity

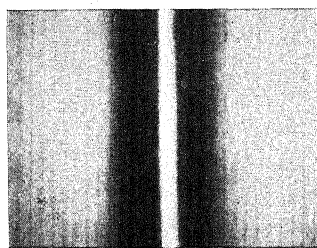


Fig. 1. Double spectrum 600 kv peak.

if the direct beam is reduced by means of a filter to an intensity comparable to the intensity of the spectrum. This is so because the direct beam is a true image of the focal spot and the spectrum is a specular image of the direct beam, except for the wave-length selectivity, and there appears to be no good reason why the radiation from different parts of the target should differ appreciably in hardness if the intensity is the same.

The photographic plate is placed 107.5 cm from the center of the slit. In spite of this comparatively great length, the resolution is not high on account of the wide slit, but it is sufficient for the present purpose.

In order to determine the exact zero on the photographic plate it is most convenient to photograph both right and left hand spectrum on the same plate. This is done by adjusting the spectrograph as described except that the direct image is blocked out completely by a heavy lead screen while one spectrum is being photographed. The spectrograph arm is then rotated into position on the opposite side of the center line and the direct image which now appears on the part of the plate which has been exposed is blocked off. The second exposure thus gives a spectrum on the part of the plate which was covered up during the first exposure. The result is two spectra which are symmetrical with respect to the center line or true zero. Fig. 1 is a positive reproduction of a double spectrum taken in this manner.

A dark line may be seen running diagonally through the spectrum in each of the spectra of Fig. 1. The origin of this line becomes apparent if we consider the geometry of the arrangement. The spectrum shown is due to reflection from vertical (100) planes of the rock-salt crystal, but if the crystal is adjusted so that the horizontal (100) planes are parallel to a horizontal plane through the focal spot and some part of the photographic plate, then it is clear that from each point of the target there will be a ray of a given wave-length which will make the same angle with the horizontal as with the vertical planes. The intensity of this ray will therefore be divided between the spectrum shown and a spectrum which falls above, below, or within the direct image.

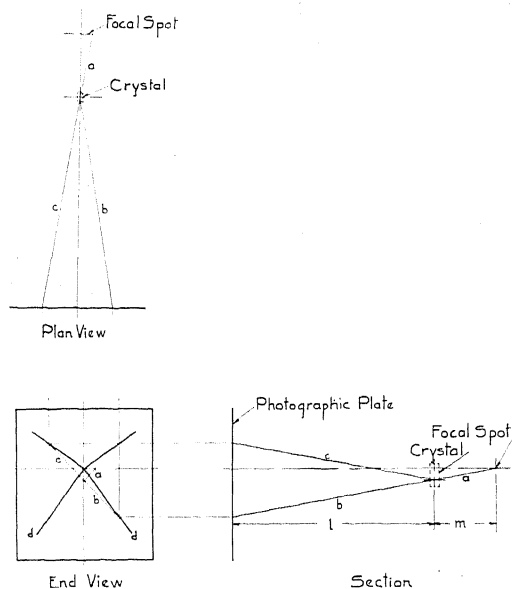


Fig. 2.

This second spectrum is of the type first obtained by Rutherford and Andrade and differs from the first in that the resolution is slightly less. The paths of a ray are shown by the lines a , b and c in Fig. 2, and the heavy lines d in the end view are the intersections with the photographic plate of all the rays which fulfill the foregoing condition. It is readily seen from the figure that the angle between the lines d and the vertical center line is given by

$$\tan \theta = \frac{b}{a + b}.$$

In the present case, this gives

$$\tan \theta = \frac{107.5}{142.5} = 0.755; \theta = 37.05^\circ$$

which agrees with the angles made by the dark lines in Fig. 1 with the center line.

The intensity distribution was obtained by means of a recording microphotometer. In Fig. 3 the galvanometer deflections obtained from the photometer records are plotted as ordinates against distance as abscissas. The tube was operated at 600 kilovolts peak and, as indicated in the graph, the short wave-length limit corresponds closely to this value. The maximum intensity occurs somewhat below one half of this potential, as might be expected since the tube is operated with alternating current and a "thick"

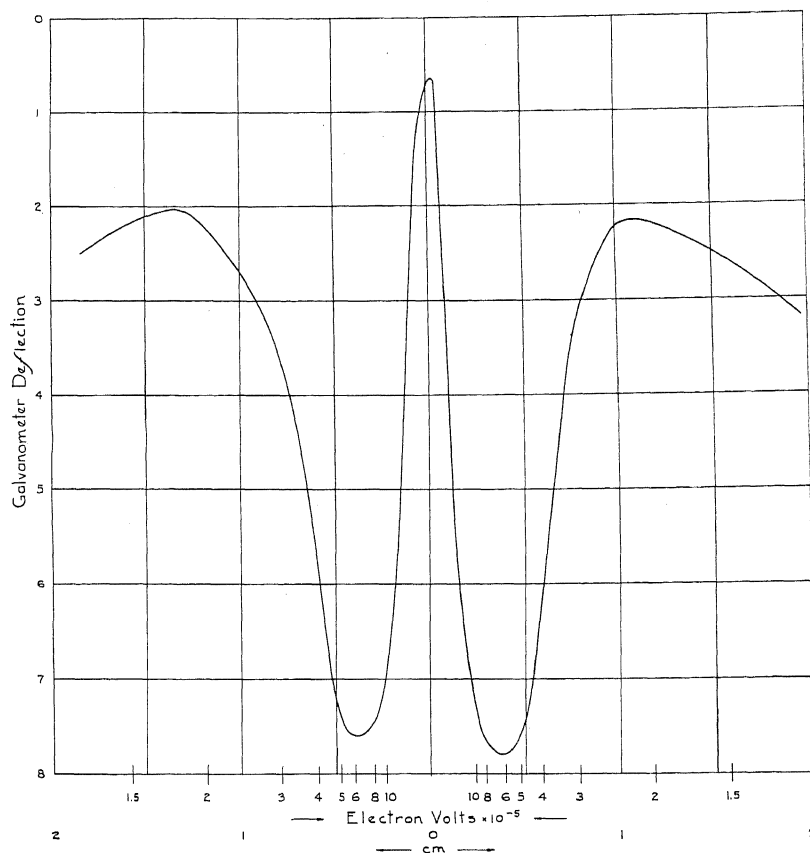


Fig. 3.

target is used. It should be noted, however, that the softer radiation is decreased somewhat in passing through both the 6 mm steel wall of the tube and the crystal. The lack of symmetry which is apparent in the graph is due partly to the aforementioned non-uniformity of the focal spot and partly to a slight difference in exposure.

RESULTS

From the photograph as well as from the photometer record we may conclude that, within the limits of the resolution used, there are no unexpected irregularities in the spectrum from tungsten in the region covered.

At the present time work is in progress to determine as accurately as possible how the spectrum is modified by different absorbers. The right half of Fig. 4 shows the spectrum after passing through lead screens. One screen, 0.28 in. thick, covers the whole image, and in addition the central portion is covered by a second screen 0.14 in. thick. The direct beam was decreased to a suitable intensity by a steel block 2 in. thick.

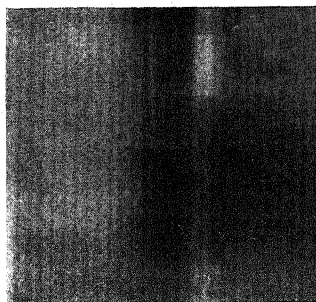


Fig. 4. Left, direct image. Right, spectrum.

The photometer records of spectra taken in this way show accurately how the spectrum is modified by any given absorber and it should therefore be possible to obtain from a single pair of records the absorption coefficient as a function of the wave-length.

If nuclear absorption levels or other unexpected irregularities exist in this region of the spectrum, they should be readily detected by this method. The spectra obtained so far and also the modifications due to absorbing screens of aluminum, iron, copper and lead are roughly what would be expected. There is no indication of any sudden changes in intensity with wave-length.

MULTIPLE SCATTERING IN THE COMPTON EFFECT

BY JESSE W. M. DUMOND

CALIFORNIA INSTITUTE OF TECHNOLOGY, PASADENA

(Received November 5, 1930)

ABSTRACT

In the experimental study of the spectral distribution of x-radiation scattered by light elements it has always, up to the present, been assumed that multiple scattering could be neglected. Recent improvements in experimental technique however make it possible to suppose that multiple (especially double) scattering may now be detectable from large scattering bodies. Multiple scattering may (1) affect the breadth of the modified line, (2) change the structure of the modified line, (3) distort the background in such a way as to render measurements of shift unreliable. It is therefore valuable to analyze the effect of multiple scattering in case some of the recent mutually discordant experimental results may be explained and harmonized in this way.

Assuming initially monochromatic radiation, scattering of any degree of multiplicity contributes a spectral band whose wave-length limits are here determined and discussed. The Breit, Compton, Jauncey formula taking polarization into account is adopted for the purposes of calculation of modified intensity. The results are thus fairly accurate for hard radiation scattered from very light elements. For softer radiation modified scattering at small scattering angles is greatly reduced below the values given by the Breit, Compton, Jauncey formula and unmodified scattering appears. The effect of this on the results of this paper is discussed in a qualitative way.

The case of double scattering from a spherical scatterer is computed in complete detail and a formula for the ratio of double to single scattering is derived. Curves of the spectral distributions due to double scattering are shown. The dependence of the total doubly scattered intensity on the primary scattering angle is plotted.

The natural width of the modified line is neglected throughout these calculations. Absorption in the scatterer is also neglected. The ratio of double to single scattering for a spherical scatterer observed under any given angle is proportional to the radius of the scatterer (neglecting absorption) and is given by

$$\frac{\text{Doubly scattered energy}}{\text{Singly scattered energy}} = \frac{9}{32} \sigma r R(\theta) \text{ where}$$

σ is the linear scattering coefficient for the material of the scattering sphere, r the radius of the sphere, θ the angle under which single scattering occurs. $R(\theta)$ never differs greatly from 2.5.

Triple scattering is negligible in comparison to single scattering.

Twice modified doubly scattered radiation may contribute a faint asymmetric line or edge at the shifted position

$$\Delta\lambda = 2(h/mc)(1 + \cos \frac{1}{2}\theta)$$

For hard radiation when the Thompson formula (with Breit correction) applies with fair accuracy to modified scattering alone twice modified doubly scattered radiation contributes a spectral band of breadth

$$4(h/mc) \cos \frac{1}{2}\theta$$

Once modified doubly scattered radiation may cause a slight broadening of the Compton line except in regions near $\theta=0$ and $\theta=180^\circ$.

INTRODUCTION

IN THE experimental study of scattered x-radiation it is impossible completely to eliminate multiple scattering. X-radiation whose direction is defined more or less closely within some solid angle $\delta\Omega_1$ is incident upon a scattering body. The apparatus (a spectrograph, ionization spectrometer or what not) is arranged so as to receive scattered radiation whose direction again is more or less closely defined within some solid angle $\delta\Omega_2$. The angle θ between the initial and final directions has thus assignable limits of inhomogeneity and is called the angle of primary scattering. A ray cannot be prevented, however, from suffering any number of scattering processes between its entry along the first direction and its exit along the last. It is the purpose of this paper to discuss theoretically the effect of such processes on the spectral distribution of the scattered radiation. The path of a multiply scattered ray is a broken line (in space) of $(M+1)$ straight segments, where M is the multiplicity of the scattering. The first and last segments have the fixed directions of the incident and scattered beams just mentioned. The other segments will be called *intermediate rays*. Their directions may be any whatever. In double scattering there is but one intermediate ray. The directions of the entry, exit and intermediate rays are to be plotted upon a sphere of unit radius by means of unit vectors originating at the center of the sphere and terminating on its surface. These vectors have the respective directions of propagation of the radiation along entry, exit and intermediate rays for their directions. The termini of these vectors thus locate $M+1$ points on the surface of the sphere and represent the $(M+1)$ directions taken by the M -tuple scattered ray. The first and last of these points are fixed upon the sphere and separated by the angle of primary scattering θ . The remaining $(M-1)$ points may have any position on the entire surface of the sphere. The problem of M -tuple scattering thus involves the $(2M-2)$ degrees of freedom of these points.

Each process of scattering splits an initially monochromatic ray into modified and unmodified components as regards wave-length. The modified ray suffers an increase of wave-length given by $\Delta\lambda = h/mc(1 - \cos \theta_i)$ where θ_i is the angle of scattering. There exist therefore $(M+1)$ cases in m -tuple scattering for the ray may be *scattered* M times but only *modified* 0, 1, 2, 3, etc. up to M times. Thus in double scattering the ray may be scattered twice without modifications, or modified at the first scattering but not at the second, or modified at the second scattering but not at the first, or modified twice successively. The two cases of singly modified doubly scattered radiation will be identical.

Unfortunately the law governing the partition of the scattered radiation between modified and unmodified rays is complicated and not very well known. For sufficiently hard radiation scattered by sufficiently light atoms however the unmodified radiation is negligible at nearly all scattering angles. In this paper only this limiting case will be discussed analytically in detail and therefore the total shift of the original wave-length will be the sum of all the separate shifts occurring at the successive scattering processes. The breadth of the shifted line will be neglected.

WAVE-LENGTH LIMITS OF MULTIPLY SCATTERED RADIATION

It is immediately possible to make the following obvious generalizations if M is both the number of scatterings and the number of shifts of a given ray:

1. When M is odd the maximum shift occurs for a primary scattering angle of $\theta = 180^\circ$.
2. When M is even the maximum shift occurs for $\theta = 0^\circ$.
3. Minimum shift for any multiplicity is always zero and always occurs at a primary scattering angle $\theta = 0$.
4. Maximum shift is always $2M(h/mc)$ where M is the multiplicity of scattering.

DOUBLE SCATTERING

Referring to Fig. 1, on the sphere, A is the direction of the entry ray, B the direction of the intermediate ray and C the direction of the scattered ray. The arc AC measures the fixed primary scattering angle θ and is bi-

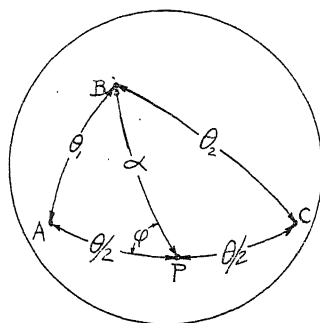


Fig. 1. Illustrating spherical coordinate system (α, ϕ) appropriate to the problem of double scattering.

sected at P . P is taken as the pole of a system of spherical polar coordinates (α, ϕ) which describe the location of the intermediate ray B whose two degrees of freedom are the independent variables of the problem.

That such a system of coordinates (α, ϕ) is appropriate to the problem will be seen from the following considerations:

The total shift

$$\Delta\lambda = \frac{h}{mc} \{ 2 - (\cos \theta_1 + \cos \theta_2) \} \quad (1)$$

If the letters A , B and C represent unit vectors, then

$$\begin{aligned} \Delta\lambda &= \frac{h}{mc} \{ 2 - (A \cdot B + B \cdot C) \} \\ &= \frac{h}{mc} \{ 2 - B \cdot (A + C) \} \\ &= \frac{2h}{mc} (1 - \cos \frac{1}{2}\theta \cos \alpha) \\ &\quad (\text{since } |A + C| = 2 \cos \frac{1}{2}\theta) \end{aligned} \quad (2)$$

Hence regions of constant total shift $\Delta\lambda$ correspond to directions of B lying in zones on the sphere described about P as a pole.

WAVE-LENGTH LIMITS OF DOUBLY SCATTERED DOUBLY SHIFTED RADIATION

Since $\cos \alpha$ may range from 1 to -1 , doubly scattered radiation may have a range of shifts defined by the inequalities

$$2h/mc(1 - \cos \frac{1}{2}\theta) < \Delta\lambda < 2h/mc(1 + \cos \frac{1}{2}\theta) \quad (3)$$

The limits of this range are evidently equidistant from the point $\Delta\lambda = 2h/mc$ and the total spectral width of the range is $4h/mc \cos \frac{1}{2}\theta$. Thus for a primary scattering angle of zero degrees double scattering contributes shifted radiation over a range of shifts from zero to $4h/mc$ while for a primary scattering angle of 180° double scattering contributes shifted radiation falling exactly at $2h/mc$ and extending over no range whatever. It is convenient to describe the spectral distributions caused by double scattering in terms of a variable x , which is defined as $x = (\Delta\lambda)/(2h/mc)$. This variable which is proportional to the shift in wave-lengths is a pure number.

THE LAW GOVERNING INTENSITY OF SCATTERING

In order to compute the distribution of intensity due to double scattering over the range determined for any particular primary scattering angle, some law must be adopted to express the scattered intensity as a function of the angle of scattering and of the polarization of the radiation. Kallman and Mark¹ have shown in a beautiful experiment that both shifted and unshifted radiations are completely polarized by scattering at 90° . In double scattering therefore the beam becomes partially polarized in the first scattering process and this fact is of importance in determining the intensity of scattering in the second scattering process.

We therefore assume in this computation that each scattering process gives modified radiation having the intensity and polarization dictated by the classical Thompson theory of scattering and then apply the Breit correction to this by multiplying by a factor $(1 + \alpha \text{ vers } \theta_1)^{-3} (1 + \alpha \text{ vers } \theta_2)^{-3}$ (c.f. Compton "X-Rays and Electrons" pp. 304-305). Fortunately $(1 + \alpha \text{ vers } \theta_1)^{-3} (1 + \alpha \text{ vers } \theta_2)^{-3}$ can be replaced by $(\lambda_0/\lambda_1)^3 (\lambda_1/\lambda_2)^3$ and hence by $(\lambda_0/\lambda_2)^3$ where λ_0 is the primary wave-length, λ_1 the wave-length after the first scattering, and λ_2 the wave-length after the second scattering. It is thus a very fortunate fact that the Breit correction factor depends only on the ratio of the initial and final wave-lengths in double scattering and not at all on the intermediate wave-length. Thus after the doubly scattered spectral distribution has been computed by the classical Thompson formula and the distribution is obtained as a function of $\Delta\lambda$ or x the Breit correction can be applied to the curves by simply multiplying each ordinate by the ratio $(\lambda_0/\lambda_2)^3$ applicable to its abscissa.

The above outlined method should give fairly accurate results for hard radiation and light scattering atoms where the presence of unmodified radiation and diminished modified radiation for small scattering angles can be neglected.

¹ Kallman and Mark, "Über einige Eigenschaften der Comptonstrahlung Zeits. f. Physik 36, 120-142 (1926).

Unfortunately the case of say $\text{MoK}\alpha$ radiation scattered by graphite is not such a one. The author has not succeeded in obtaining an analytic solution for double scattering rigorously applicable to this case taking account of the unmodified scattering and diminished modified scattering. Moreover the really great analytical difficulties incident to such a solution seem scarcely worth overcoming as a good qualitative idea of the spectral intensity distribution can be obtained by a rough examination of the effect of reduced modified scattering on the case which is here solved.

The shape of the scattering body also plays a part in determining the spectral distribution of doubly scattered radiation. It is of course practically impossible to take account of this factor and accordingly the solution here given can again only be applied to real cases qualitatively. In order to construct an ideal case in which the shape of the scatterer does not complicate the analysis we consider first only one electron at the center of a spherical scattering body. This electron receives primary radiation along the direction A and scatters in various directions B to all the other electrons in the scatterer which in turn scatter the radiation along the exit direction C . It is the spectral distribution of this radiation as affected by two wave-length modifications which we propose to investigate. Subsequently the reasoning is readily extended to initial scattering by *all* the electrons in the spherical scattering body.

COMPUTATION OF SPECTRAL DISTRIBUTIONS DUE TO DOUBLE SCATTERING

Referring to Fig. 2, let E_{n1} and E_{a1} be the primary component electric intensities E_{n1} being normal to the plane of the first angle of scattering θ_1

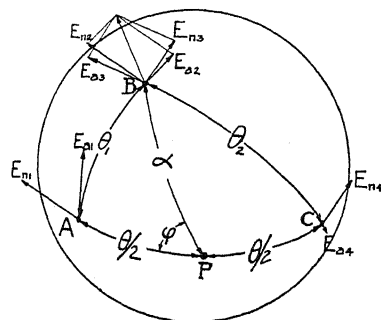


Fig. 2. Illustrating the components of the electric vector of the incident, intermediate and exit rays.

and E_{a1} parallel to that plane. At a distance r_1 from the first scattering electron along the intermediate direction B the scattered radiation will have electric components E_{n2} and E_{a2} again normal and parallel respectively to the plane of θ_1 given by the Thompson classical theory as:

$$E_{n2} = - \frac{E_{n1}e^2}{r_1mc^2} \quad (4)$$

$$E_{a2} = - \frac{E_{a1}e^2}{r_1mc^2} \cos \theta_1. \quad (5)$$

Let B represent the supplement of the angle B of the spherical triangle $A B C$. We now resolve the electric vector whose components are E_{n2} and E_{a2} along two new directions normal and parallel respectively to the plane of the second angle of scattering θ_2 and obtain E_{n3} and E_{a3}

$$E_{n3} = E_{n2} \cos B + E_{a2} \sin B \quad (6)$$

$$E_{a3} = E_{a2} \cos B - E_{n2} \sin B. \quad (7)$$

The scattered radiation having these components E_{n3} and E_{a3} is now scattered again by an electron at distance r_1 from the first, the new scattering angle being θ_2 . At distance r_2 from the second scattering electron along the direction C the doubly scattered radiation will have electric components E_{n4} and E_{a4}

$$E_{n4} = -\frac{E_{n3}e^2}{r_2mc^2} \quad (8)$$

$$E_{a4} = -\frac{E_{a3}e^2}{r_2mc^2} \cos \theta_2. \quad (9)$$

We now express E_{n4} and E_{a4} in terms of E_{n1} and E_{a1} and evaluate the square of the final electric intensity E_4^2

$$\begin{aligned} E_4^2 = E_{n4}^2 + E_{a4}^2 = & \frac{e^8}{r_1^2 r_2^2 m^4 c^8} [E_{n1}^2 \cos^2 B + E_{a1}^2 \cos^2 \theta_1 \sin^2 B \\ & + 2E_{n1}E_{a1} \cos B \sin B \cos \theta_1 + \cos^2 \theta_2 (E_{a1}^2 \cos^2 \theta_1 \cos^2 B \\ & + E_{n1}^2 \sin^2 B - 2E_{a1}E_{n1} \cos \theta_1 \cos B \sin B)] \end{aligned} \quad (10)$$

For unpolarized primary radiation we average over all possible orientations of E_1 about the primary beam giving all orientations equal weights. This means that $\{E_{n1}^2\} = \{E_{a1}^2\} = \frac{1}{2}E_1^2$ and $\{E_{n1}E_{a1}\} = 0$, the curly bracket here being used to indicate the average. The average doubly scattered intensity is then given by

$$\{E_4^2\} = \frac{1}{2}E_1^2 \frac{e^8}{r_1^2 r_2^2 m^4 c^8} [\cos^2 B + (\cos^2 \theta_1 + \cos^2 \theta_2) \sin^2 B + \cos^2 \theta_1 \cos^2 \theta_2 \cos^2 B] \quad (11)$$

Now from a well-known formula applying to spherical triangles we can express B in terms of θ_1 , θ_2 , and θ

$$\cos B = \frac{\cos \theta - \cos \theta_1 \cos \theta_2}{\sin \theta_1 \sin \theta_2}. \quad (12)$$

By appropriate substitutions employing this formula we obtain the doubly scattered intensity in terms of θ_1 , θ_2 and θ as

$$\begin{aligned} \{E_4^2\} = & \frac{1}{2}E_1^2 \frac{e^8}{r_1^2 r_2^2 m^4 c^8} [\cos^2 \theta_1 + \cos^2 \theta_2 \\ & + \cos^2 \theta - 2 \cos \theta \cos \theta_1 \cos \theta_2 + \cos^2 \theta_1 \cos^2 \theta_2]. \end{aligned} \quad (13)$$

We now transform this to an expression in α and ϕ the spherical coordinates of our problem by the use of the relations from spherical trigonometry

$$\cos \theta_1 = \cos \alpha \cos \frac{1}{2} \theta + \sin \alpha \sin \frac{1}{2} \theta \cos \phi \quad (14)$$

$$\cos \theta_2 = \cos \alpha \cos \frac{1}{2} \theta - \sin \alpha \sin \frac{1}{2} \theta \cos \phi. \quad (15)$$

This gives

$$\begin{aligned} \{E_4^2\} = & \frac{1}{2} E_1^2 \frac{e^8}{r_1^2 r_2^2 m^4 c^8} [2 \cos^2 \alpha \cos^2 \frac{1}{2} \theta + 2 \sin^2 \alpha \sin^2 \frac{1}{2} \theta \cos^2 \phi + \cos^2 \theta \\ & - 2 \cos \theta \cos^2 \alpha \cos^2 \frac{1}{2} \theta + 2 \cos \theta \sin^2 \alpha \sin^2 \frac{1}{2} \theta \cos^2 \phi \\ & + (\cos^2 \alpha \cos^2 \frac{1}{2} \theta - \sin^2 \alpha \sin^2 \frac{1}{2} \theta \cos^2 \phi)^2] \end{aligned} \quad (16)$$

or:

$$I_4 = \frac{1}{2} I_1 \frac{e^8}{r_1^2 r_2^2 m^4 c^8} [y(\alpha, \theta, \phi)]. \quad (17)$$

I_4 is the doubly scattered intensity. It is the energy per cm.² per second at a distance r_2 from the second scattering electron which in turn is at a distance r_1 from the first scattering electron.

The exit ray is confined to some solid angle $\Delta\Omega_3$ by the construction of the apparatus for studying the scattered radiation. If we multiply the last expression by the area $r_2^2 \Delta\Omega_3$ we obtain the energy scattered per second into the solid angle $\Delta\Omega_3$

$$I_4 r_2^2 \Delta\Omega_3 = \frac{1}{2} I_1 \frac{e^8 \Delta\Omega}{r_1^2 m^4 c^8} [y(\alpha, \theta, \phi)]. \quad (18)$$

Consider now a spherical shell of radius r_1 and thickness dr_1 described about the first scattering electron as a center. Let the volume density of electrons in the scatterer be ρ . In the solid angle between α and $\alpha+d\alpha$, ϕ and $\phi+d\phi$ there will be $\rho r_1^2 \sin \alpha dr_1 d\alpha d\phi$ electrons. The energy per second entering the solid angle $\Delta\Omega_3$ due to all the electrons just mentioned will be

$$I_4 r_2^2 \Delta\Omega_3 \rho r_1^2 \sin \alpha dr_1 d\alpha d\phi = \frac{1}{2} I_1 \frac{e^8 \Delta\Omega_3 \rho dr_1}{m^4 c^8} [y(\alpha, \phi, \theta) \sin \alpha d\alpha d\phi]. \quad (19)$$

Integrating this from $r=0$ to $r=r$, the distance from the first scattering electron to the furthestmost electron in the body in the direction (α, ϕ) , we have

$$\frac{1}{2} I_1 \frac{e^8 \Delta\Omega_3 \rho r_{\alpha\phi}}{m^4 c^8} [y(\alpha, \phi, \theta) \sin \alpha d\alpha d\phi]. \quad (20)$$

The total shift after two scatterings is independent of ϕ as has already been pointed out. We therefore obtain the total energy going into a zone between α and $\alpha+d\alpha$, all of which contributes to one and the same shifted position in the doubly scattered spectrum by integrating around the zone

from $\phi=0$ to $\phi=2\pi$. We thus obtain the energy per second passing out through the solid angle $\Delta\Omega_3$ after first scattering by one electron at the center of the *spherical* scattering body of radius, r , and then scattering by all other electrons in the body between the cones of half angle α and $\alpha+d\alpha$. It is

$$\begin{aligned} \frac{1}{2} I_1 \frac{e^8 \Delta\Omega_3 p r}{m^4 c^8} [y(\alpha, d\alpha, \theta)] &= \frac{1}{2} I_1 \frac{e^8 \Delta\Omega_3 p r}{m^4 c^8} \left[2\pi(2 - 2 \cos \theta) \cos^2 \alpha \cos^2 \frac{1}{2} \theta \right. \\ &+ \pi(2 + 2 \cos \theta) \sin^2 \alpha \sin^2 \frac{1}{2} \theta + 2\pi \cos^2 \theta + 2\pi (\cos^2 \alpha \cos^2 \frac{1}{2} \theta)^2 \\ &\left. - 2\pi \cos^2 \alpha \cos^2 \frac{1}{2} \theta \sin^2 \alpha \sin^2 \frac{1}{2} \theta + \frac{3}{4} \pi (\sin^2 \alpha \sin^2 \frac{1}{2} \theta)^2 \right] \sin \alpha d\alpha. \end{aligned} \quad (21)$$

We must now transform this expression to one in terms of x and dx the independant variable used to express the shift in the description of spectral distribution. $x = (\Delta\lambda)/(2h/mc)$. The shift is given by

$$\Delta\lambda = 2h/mc(1 - \cos \frac{1}{2} \theta \cos \alpha)$$

hence

$$x = (1 - \cos \frac{1}{2} \theta \cos \alpha) \quad (22)$$

$$dx = \cos \frac{1}{2} \theta \sin \alpha d\alpha \quad (23)$$

$$\sin \alpha d\alpha = dx / \cos \frac{1}{2} \theta \quad (24)$$

$$\cos^2 \alpha = \frac{(1-x)^2}{\cos^2 \frac{1}{2} \theta}; \quad \sin^2 \alpha \sin^2 \frac{1}{2} \theta = \sin^2 \frac{1}{2} \theta - (1-x)^2 \tan^2 \frac{1}{2} \theta.$$

Making these substitutions we obtain the total energy per second in the spectral region between x and $x+dx$; it is

$$\begin{aligned} I_4 dx &= \frac{1}{2} I_1 \frac{\pi e^8 \Delta\Omega_3 p r}{m^4 c^8} [y(x, \theta)] dx = \frac{1}{2} I_1 \frac{e^8 \Delta\Omega_3 p r \pi}{m^4 c^8} \left[\left(2 \cos^2 \theta \right. \right. \\ &+ \sin^2 \theta + \frac{3}{4} \sin^4 \frac{1}{2} \theta \left. \right) + \left(2 \sin^2 \frac{1}{2} \theta - \frac{3}{2} \sin^2 \frac{1}{2} \theta \tan^2 \frac{1}{2} \theta \right) (1-x)^2 \\ &\left. + \left(2 + 2 \tan^2 \frac{1}{2} \theta + \frac{3}{4} \tan^4 \frac{1}{2} \theta \right) (1-x)^4 \right] \frac{dx}{\cos \frac{1}{2} \theta}. \end{aligned} \quad (25)$$

This expression refers to one electron only at the center of the spherical scattering body as the first scattering agent. This same electron will by *single scattering* into the solid exit angle $\Delta\Omega_3$ scatter energy

$$I_2 = \frac{1}{2} I_1 \frac{e^4 \Delta\Omega_3}{m^2 c^4} (1 + \cos^2 \theta). \quad (26)$$

The ratio of double to single scattering is then

$$\frac{I_4}{I_2} dx = \pi \frac{e^4 p r}{m^2 c^4} \frac{[y(x, \theta)]}{1 + \cos^2 \theta} dx \quad (27)$$

but the "scattering coefficient" is;

$$\sigma = \frac{8}{3} \pi \frac{e^4 \rho}{m^2 c^4}$$

$$\frac{I_4}{I_2} dx = \frac{3}{8} \sigma r \frac{[y(x, \theta)]}{1 + \cos^2 \theta} dx. \quad (28)$$

The ratio of total doubly scattered energy to singly scattered energy is

$$\frac{\int_{1-\cos 1/2\theta}^{1+\cos 1/2\theta} I_4 dx}{I_2} = \frac{3}{8} \sigma r \frac{\int [y(x, \theta)] dx}{1 + \cos^2 \theta} = \frac{3}{8} \sigma r R. \quad (29)$$

Evaluating the integral in this expression we obtain the ratio of double to single scattering, it is

$$\frac{3}{8} \sigma r \frac{1}{1 + \cos^2 \theta} \left[2A + \frac{2}{3} B \cos^2 \frac{1}{2} \theta + \frac{2}{5} C \cos^4 \frac{1}{2} \theta \right] \quad (30)$$

where $A = (2 \cos^2 \theta + \sin^2 \theta + \frac{3}{4} \sin^4 \frac{1}{2} \theta)$

$B = (2 \sin^2 \frac{1}{2} \theta - \frac{3}{2} \sin^2 \frac{1}{2} \theta \tan^2 \frac{1}{2} \theta)$

$C = (2 + 2 \tan^2 \frac{1}{2} \theta + \frac{3}{4} \tan^4 \frac{1}{2} \theta)$

Both values of the bracket in the last expression and values of R are plotted in Fig. 3.

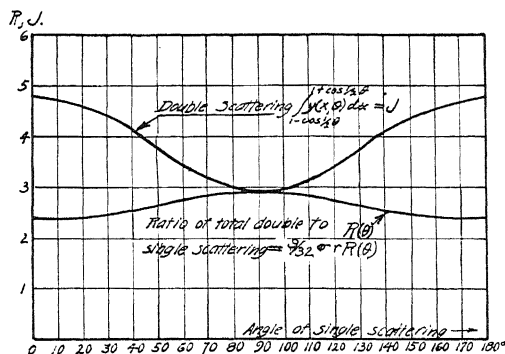


Fig. 3. Curves of the integral in Eq. (29) and also of the ratio R in that equation.

For scattering from the *central* electron in the spherical scatterer to all other electrons, the value of $r_{\alpha\phi}$ is the radius r of the spherical scatterer. For initial scattering from *all* electrons in the scatterer however an average² value of $\{r_{\alpha\phi}\} = \frac{3}{4}r$ must be taken. To obtain this we average the distance along any fixed arbitrary direction from each elementary volume in the spherical scatterer to the boundary of the sphere throughout the entire volume. Taking as volume elements of the sphere the space between two coaxial cylinders of radii r' and $r' + dr'$ with axis through the center of the

² The bracket $\{ \}$ is used to denote "average value."

sphere, the average distance in question is given by $1/(4/3)\pi r^3 \int_0^r (r^2 - r'^2) 4\pi r' dr' = \frac{3}{4}r$. Now $\sigma = 0.4$ per cm for Mo radiation scattered from graphite.

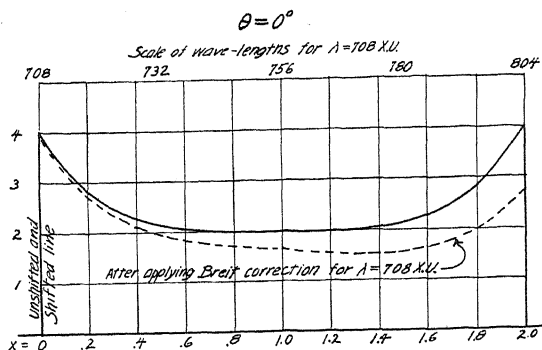


Fig. 4. Spectral distribution due to doubly modified double scattering for primary scattering angle of zero degrees.

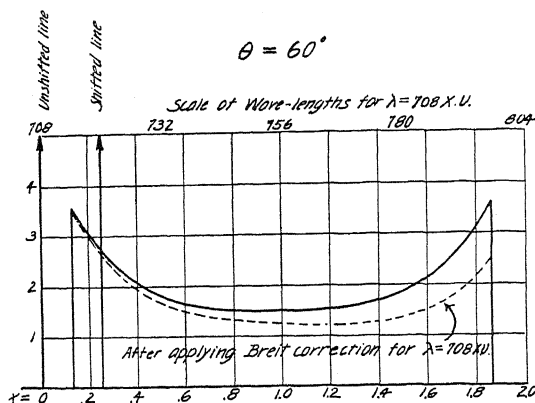


Fig. 5. Spectral distribution due to doubly modified double scattering for primary scattering angle of 60° .

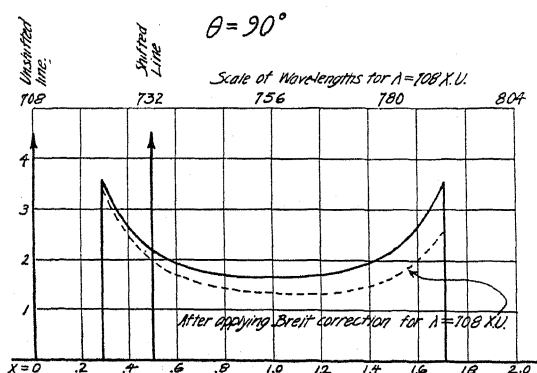


Fig. 6. Spectral distribution due to doubly modified double scattering for primary scattering angle of 90° .

It appears from Fig. 3 that R never differs very greatly from 2.5. The ratio then of total double scattering to single scattering for a spherical carbon

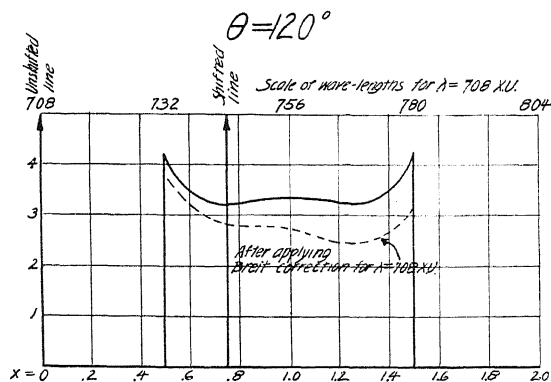


Fig. 7. Spectral distribution due to doubly modified double scattering for primary scattering angle of 120° .

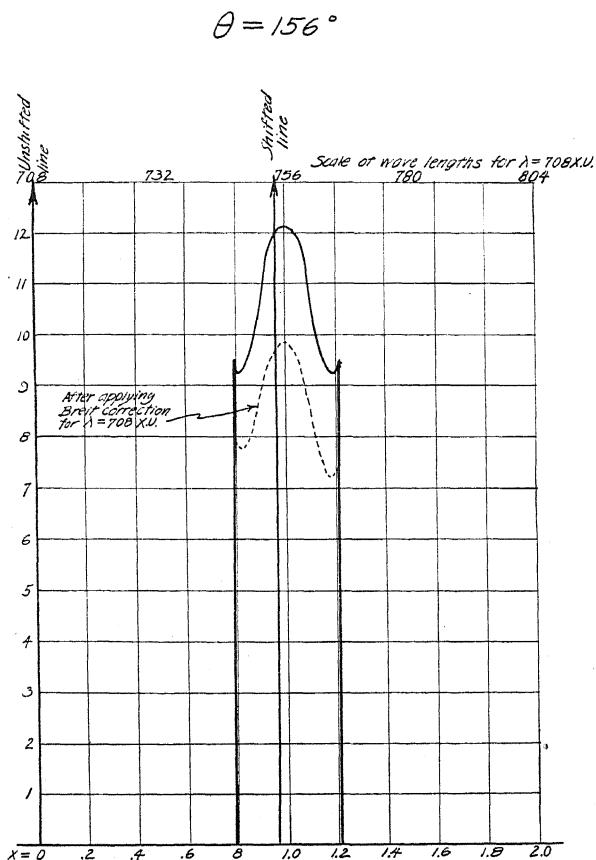


Fig. 8. Spectral distribution due to doubly modified double scattering for primary scattering angle of 156° .

scatterer 0.5 cm in radius scattering Mo radiation is about 0.140. This would increase in direct proportion to the radius of the spherical scatterer were it not for absorption. Except at $\theta=180^\circ$ however the doubly scattered energy is distributed over a considerable wave-length band.

The spectral distribution of double scattering is obtained from expression (25) for scattering angles θ between initial and final beams of 8° , 60° , 90° , 120° , 156° and 180° . These are exhibited in Figures 4 to 9. The curves both without and with the Breit correction computed for MoK radiation are shown. An interesting feature of these curves occurs when the angle of single scattering is 180° . At this angle the spectral distribution, due to doubly

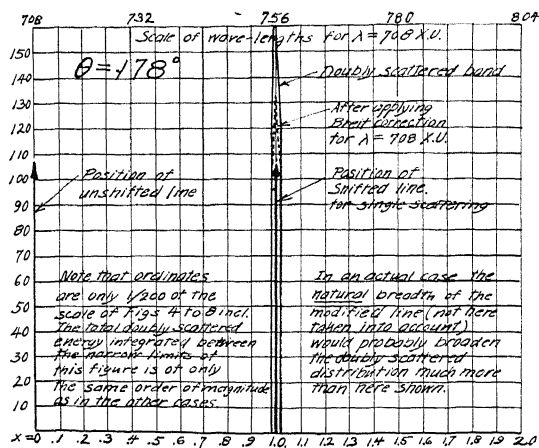


Fig. 9. Spectral distribution (with reduced ordinate scale) of doubly modified double scattering for primary scattering angle of 178° .

shifted scattering, narrows down to a sharp line (neglecting the natural breadth of the Compton shifted line itself). The presence of the term $(\cos \frac{1}{2}\theta)^{-1}$ in the expression (25) makes that expression indefinitely large for $\theta=180^\circ$. The energy associated with double scattering corresponding to the area under this infinitesimally narrow infinitely tall curve is of course finite.

QUALITATIVE DISCUSSION OF THE EFFECT OF UNMODIFIED AND DECREASED MODIFIED SCATTERING

Scattering of x-radiation of intermediate hardness (e.g. MoK radiation scattered by graphite) is of two well-known types; modified and unmodified. The total scattered energy follows the Thompson classical law with the Breit correction to a fair degree of approximation except at small scattering angles where the phenomenon of excess scattering occurs. Excess scattering is without doubt a phenomenon of interference of scattered x-radiation and applies therefore only to unmodified scattering (since modified scattering is incoherent). The total scattered energy is divided between the modified and unmodified types in proportions that depend on the scattering angle. Unfortunately the exact analytic form of this dependence is unknown. It is

doubtless very complex since it depends in an intimate way on the mechanics of the scattering atom. Jauncey has treated the problem theoretically for an approximate Bohr atom model. In Fig. 10 the work of Ross and Woo relative to MoK radiation scattered from graphite is collected in one curve showing the ratio of modified scattered radiation to unmodified scattered radiation as a function of scattering angle. Fig. 11 shows Hewlett's observations on total scattering. Applying the ratio of the previous curve to this we

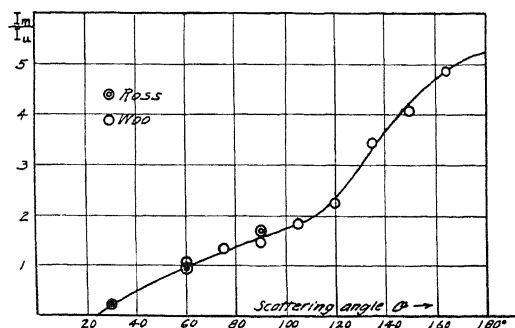


Fig. 10. Combined observations of P. A. Ross and Y. H. Woo of the ratio of modified to unmodified scattered intensity as a function of scattering angle.

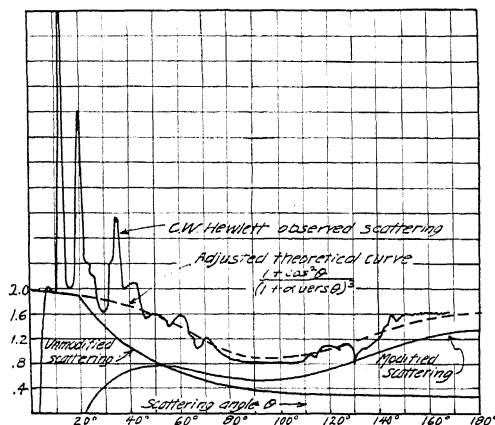


Fig. 11. Hewlett's observations of total scattering and the partition of this into modified and unmodified types in accord with Fig. 10.

obtain the two other curves which give the modified and unmodified scattered energies as a function of scattering angle. Note that below 90° modified scattering diminishes rapidly and disappears completely at about 20° . In this same region unmodified scattering becomes very strong.

To take account analytically of the effect of these phenomena on double scattering would doubtless be an extremely difficult task and one which would certainly not be warranted at present by the utility of its results. The main purpose of the present investigation is to obtain a qualitative idea

of the effect of double scattering regarded as an unavoidable impurity in the experimental study of single scattering. In this paper therefore we discuss only in a brief qualitative way the effect of excess unmodified scattering and diminished modified scattering on the results we have already obtained.

ONCE MODIFIED DOUBLE SCATTERING

Referring to Fig. 12 to which the same nomenclature of entry, exit and intermediate beams (respectively A , C , B) applies as before we obtain a rough approximation to the effect of once unmodified and once modified doubly scattered radiation by noting that the bulk of unmodified scattering will occur in the region of excess single scattering for θ_1 represented by the heavy shading around A . The zones of constant shift however are now no longer described around the bisector point P as before but around C the exit direction since the shift now occurs wholly in the second scattering process and depends only on θ_2 . From these considerations it is evident that

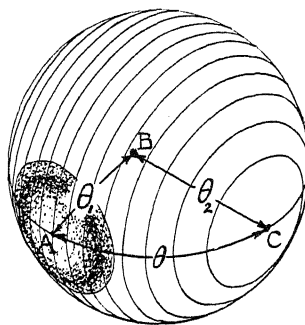


Fig. 12. Coordinate system for double scattering, unmodified at angle θ_1 but modified at angle θ_2 .

the only cases of importance are those where the intermediate ray point, B , lies in the shaded regions of excess unmodified scattering. The zones of constant shift have been so spaced in the drawing that they represent equal increments of shift. One can see immediately that the greatest intensity in the spectral distribution of once modified doubly scattered radiation occurs closely adjacent to and about symmetrically on either side of the position of the modified line for single scattering, and that there will also be a considerable contribution between these two positions. Since excess unmodified scattering has been observed to be many times as strong as ordinary unmodified scattering, there is just a chance that some of the observed excess breadth of the modified Compton line may be attributed to this effect. This argument however will not apply to explain the breadth of the Compton line for primary scattering angles of nearly 180° because here the entire shaded region is included in a very small range of shifts. Singly modified double scattering will be absent near $\theta = 0^\circ$ because in this case when B is in the shaded area θ will have values for which modified scattering is practically absent. If then the effect in question is the sole cause of the observed

excess breadth of the Compton line we should expect this excess breadth to be least for small and large angles of primary scattering, θ , and greatest for $\theta = 90^\circ$.

TWICE MODIFIED DOUBLE SCATTERING

The effect of decreased modified scattering at small angles on the already derived spectral distributions of twice modified doubly scattered radiation occurs principally in the left hand portions of the curves. We can approximate the facts roughly by imagining circles each about 45° in radius described about A and also C from which the point B is supposed to be excluded (see Fig. 13). For scattering angles, θ , up to 90° these excluded regions will lie entirely in the low shift hemisphere. We conclude then that the right hand halves of the curves, Figs. 4 to 6 inclusive, will remain practically unchanged and that the left hand halves will diminish monotonically as we pass to the left, vanishing almost completely at their left extremities.

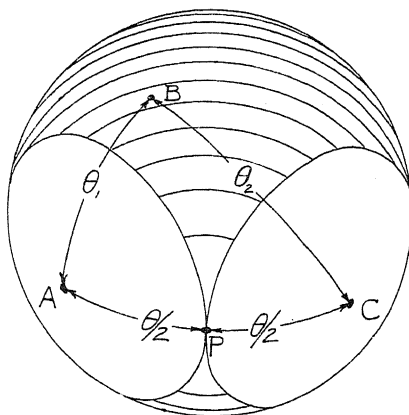


Fig. 13. Coordinate system for doubly modified double scattering taking into account the absence of modified scattering at small angles.

For scattering angles θ greater than 90° as the circles of exclusion move out of the low shift hemisphere into the high shift hemisphere, it is evident that energy will reappear in the left extremity of the spectral distributions and the suppressed portion of our curves will displace toward the right. The left hand regions or regions of low shift will however always be more depressed than the right hand regions of great shift. Fig. 14 shows the spectral distributions to be expected from the preceding discussion.

SUMMARY OF CONCLUSIONS

1. The ratio of double to single scattering for a spherical scatterer is proportional to the radius of the scatterer (neglecting absorption) and is given by the formula

$$\frac{\text{Doubly scattered energy}}{\text{Singly scattered energy}} = \frac{9}{32} \sigma r R(\theta)$$

in which the $R(\theta)$ is greatest for about $\theta=90^\circ$ and has minima at $\theta=0$ and $\theta=180^\circ$, the latter being the smaller (Fig. 3). R never differs greatly from 2.5.

2. For MoK radiation scattered by a sphere of graphite 1 cm in diameter double scattering is about 14% of single scattering (neglecting absorption).

3. From the last it seems probable that in most experiments the effect of triple and higher multiplicities of scattering can be completely neglected.

4. Once modified doubly scattered radiation may account for a slight broadening of the Compton line except in regions near $\theta=0$ and 180° .

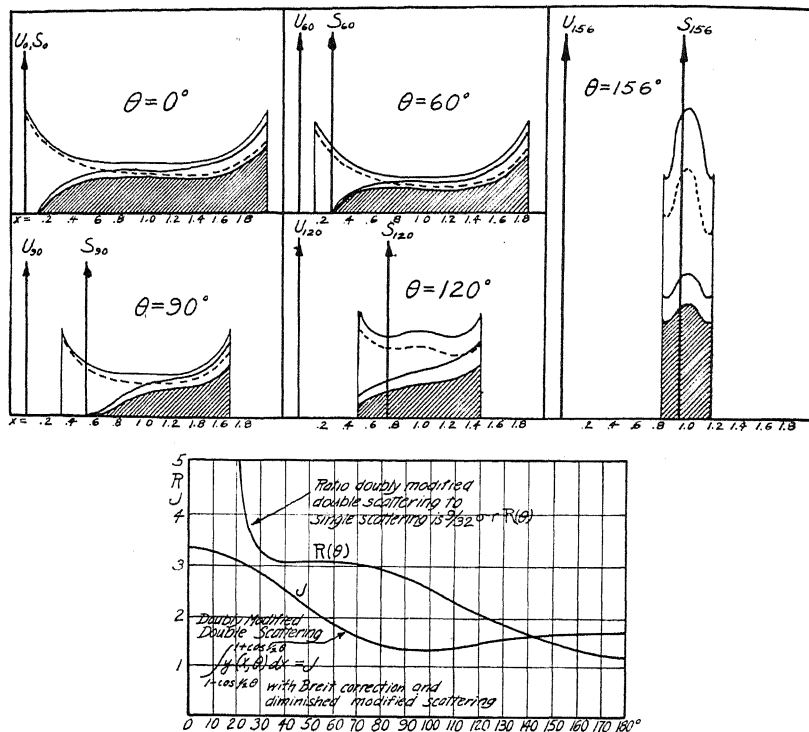


Fig. 14. Spectral distributions due to doubly modified double scattering corrected for diminished modified scattering at small angles (shaded curves). The two curves $R(\theta)$ and J are the same quantities as those shown in Fig. 3 after application of the Breit correction and correction for diminished modified scattering at small angles.

5. Twice modified doubly scattered radiation when corrected qualitatively for diminished modified scattering at small angles may contribute a faint asymmetric line or edge in the position

$$\Delta\lambda = 2\frac{h}{mc}(1 + \cos \frac{1}{2}\theta)$$

6. For hard radiation where the Thompson formula with the Breit correction applies with fair accuracy to modified scattering alone, twice modified doubly scattered radiation contributes a spectral band of breadth

$$4\frac{h}{mc}\cos \frac{1}{2}\theta$$

LIST OF SYMBOLS

- $\Delta\Omega, \delta\Omega$ —Solid angle measured in steradians.
 θ —The angle of single scattering.
 θ_1 —The first angle of double scattering.
 θ_2 —The second angle of double scattering.
 M —The multiplicity of scattering.
 λ_0 —The wave-length of the primary radiation.
 λ_1, λ_2 —The wave-lengths after first and second scatterings.
 h —Planck's constant.
 m —The mass of the electron.
 c —The velocity of light.
 A, B, C —Unit vectors representing the directions of the entry, intermediate, and exit rays in double scattering. (Fig. 2).
 α, ϕ —The colatitude and longitude angles of the spherical polar coordinates of reference in double scattering. (Fig. 2.)
 $x = (\Delta\lambda)/(2h/mc)$ —wave-length variable used for convenience in describing spectral distributions due to double scattering.
 $E_{n1}E_{a1}E_{n2}E_{a2}E_{n3}E_{a3}E_{n4}E_{a4}$ —components of the electric intensity in the radiation. The subscript, n , indicates the component normal to the plane of one scattering angle while the subscript, a , indicates the component parallel to that plane. The subscript 1 refers to the initial beam and the first scattering angle, subscript 2 refers to the intermediate beam and the first scattering angle, 3 to the intermediate beam and the second scattering angle, 4 to the final or exit beam and the second scattering angle. See Fig. 2.
 B —The dihedral angle between the planes of θ_1 and θ_2 . (Fig. 2.)
 r_1 —The distance from the point of first scattering to the point of second scattering.
 r_2 —The distance from the point of second scattering to the point of observation.
 r —The radius of the spherical scattering body.
 σ —The scattering coefficient for the material of the scatterer and the radiation used.

DESIGN AND TECHNIQUE OF OPERATION OF A
DOUBLE CRYSTAL SPECTROMETERBY JESSE W. M. DUMOND AND ARCHER HOYT
CALIFORNIA INSTITUTE OF TECHNOLOGY, PASADENA

(Received November 8, 1930)

ABSTRACT

The double crystal x-ray spectrometer is distinctly different in principle from the single crystal spectrometer and calls therefore for a completely new design rather than an adaptation of single spectrometer design. One such new design is described in this paper. Emphasis is laid on the fact that the wave-length selected by the process of two successive crystal reflections in any prescribed orders depends solely on the dihedral angle between the crystals. The advantages of rotating both crystals in equal and opposite directions with respect to a plane through their axes of rotation are pointed out and a spectrometer designed to accomplish this is described. In this spectrometer the turning of a single shaft drives the two crystals, the spectrometer as a whole and the x-ray tube, at the proper angular rates about the proper centers to insure that the x-ray beam will at all times remain centered on the crystal faces and the window of the stationary ion chamber. It is pointed out that spurious fluctuations may be introduced in spectral curves by the x-ray beam migrating across small steps in the cleavage surface reflecting the radiation. Description of design covers design of spectrometer and turning mechanisms, the tube housing, lead shields, the detecting system consisting of an ion chamber with internal grid of special design to minimize natural leak and a Hoffmann vacuum electrometer connected to it through a short evacuated shield. Description of operating technique covers optical method of accurately orienting the crystal faces, methods of aligning the tube, precautions to eliminate background.

THE Double crystal x-ray spectrometer first used in this country by A. H. Compton was developed by Bergen Davis¹ and his collaborators and has been very thoroughly investigated on the theoretical side by Schwarzschild² and on the experimental side by S. K. Allison³ and others.⁴ Its field of applicability seems to fall into two classes. First it may be used to study the properties of the crystals themselves (reflecting power, lattice perfections, etc.)⁵ Secondly it may be used as an x-ray spectrometer for exploring spectra (satellites, fine structure line breadths, Compton effect, etc.)⁶ In the development stage it was natural not to differentiate sharply in the design of double spectrometers for these different classes of work. It was also perfectly natural to adapt the general features of single crystal spectrometer design to the

¹ Bergen Davis, Phys. Rev. 17, 608 (1921), Phys. Rev. 27, 18 (1926), Phys. Rev. 32, 331 (1928).

² Schwarzschild, Phys. Rev. 32, 162 (1928).

³ Allison, Phys. Rev. 34, 176 (1929), 35, 1476 (1930).

⁴ Ehrenberg and Mark, Zeits. f. Physik 42, 807 (1927).

⁵ Davis & Purks, Phys. Rev. 34, 181 (1929).

⁶ DuMond & Hoyt, Phys. Rev. 36, 799 (1930), Bearden, Phys. Rev. 36, 791 (1930), Richtmyer & Taylor, Phys. Rev. 36, 1044, (1930).

double spectrometer. The authors feel however that now that so much is known about the possibilities and applications of this instrument the time has come to design it on its own merits in such a way as best to accomplish some particular function.

The double spectrometer here described was developed for the second of the above mentioned uses—the study of x-ray spectra. It is designed to be used entirely in the antiparallel positions (n, n) (Allison's notation)⁷ though slight modifications would permit "straddling two different orders."

The authors feel that much of the apparent complexity arising in connection with the double spectrometer comes from the introduction of such artificial frames of reference as the axis of rotation of the pivots supporting the crystals, or the axis of the slits which latter in the double spectrometer play an entirely different role from the slits of a single spectrometer.

THE IMPORTANT THING IS THE DIHEDRAL ANGLE BETWEEN THE CRYSTALS

It is of cardinal importance to note just what is measured in using the double spectrometer. A beam of x-rays reflected from a cleavage face of a

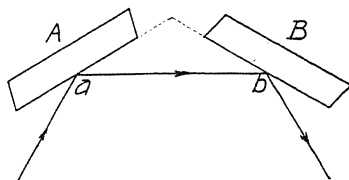


Fig. 1. Symmetrical ray selected by the bicrystalline reflection.

calcite crystal falls upon the face of a second calcite crystal and is again reflected into an ionization chamber. One or both of these crystals is turned slightly about an axis in the plane of the reflecting face and the ionization currents in the ion chamber are plotted as a function of the rocking angles of the crystal. For any given angle setting the two successive calcite reflections select out of the entire x-ray spectrum an exceedingly sharply defined narrow region of wave-lengths.

Precisely what angle determines the wave-length selected by the double x-ray reflection? Is it the angle through which one crystal rotates with respect to the slit system? Obviously not, since the horizontal slit width has nothing to do with the resolution of the double spectrometer. Neither do the pivots about which the crystals rotate constitute in any sense the system of reference with respect to which the rotation must be measured which determines the selected wave-length. The authors wish to emphasize most strongly that *the important thing is the dihedral angle formed by the two crystal faces themselves*. Let us consider for simplicity the case of first order reflection from two similar calcites in the anti-parallel position (1, 1). Fig. 1 represents the dihedral angle formed by the two crystals. Obviously the only rays which can be reflected twice selectively in the first order by both crystals are the

⁷ Allison & Williams, Phys. Rev. 35, 149 (1930).

symmetrical rays which make the same glancing angle at crystal *A* as at crystal *B*. A symmetrical ray, *ab*, is shown in Fig. 1 passing from crystal *A* to crystal *B*.

Define a plane *normal to the dihedral angle* formed by the crystal faces which for brevity and in accord with other writers we will call the "horizontal plane," (plane of the paper in Fig. 1). Now the ray, *a, b*, need not be parallel to the "horizontal plane" in order that it shall make equal glancing angles at each crystal and therefore be reflected. Such a ray oblique to the horizontal plane will in accord with Davis' terminology be said to have an angle of vertical divergence namely the angle α of obliquity with the horizontal plane. The projection of such an oblique ray will in Fig. 1 still be represented by the line, *a, b*, but the ray will in space actually suffer reflection at both crystals under a smaller glancing angle than rays which are not oblique. See Fig. 2.

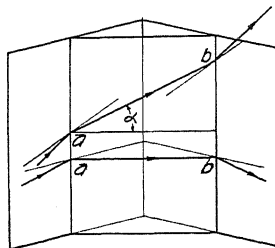


Fig. 2. Horizontal and oblique symmetrical rays.

We can assert then that the glancing angle (Bragg angle) selected by the process of the double selective reflection is half of the supplement of the dihedral angle between the crystal faces for horizontal rays and less than this for oblique rays. The band of wave-lengths selected then by the double reflection has a sharp limit on the long wave-length side determined only by the dihedral angle between the crystals. The band selected can be made as narrow as one pleases by limiting the vertical divergence.

Nothing in the above argument is made to depend on or refer to the pivots or axes of rotation of the crystals. It is of course obviously desirable that these axes of rotation should be parallel to the edge of the dihedral angle formed by the two crystal faces in order readily to permit the measurement of that dihedral angle and also to maintain the "horizontal ray" in a permanently fixed position with respect to the frame of the apparatus as the crystals rotate. The pivots, however, have nothing at all to do with the selective action of the double reflection and the dihedral angle between the crystals has everything to do with it. If this very fundamental fact is remembered all uncertainty as to the effect of various errors of alignment, etc., will vanish.

BAND PASS FILTER WIDTH

The theoretical spectral intensity curve of the wave-length band selected from a uniform or "flat" spectral energy distribution by the double crystal reflection in the (*n,n*) position with perfect crystals is shown in Fig. 3. It is

bounded on the long wave side by a vertical discontinuity and falls off on the short wave side more gradually, meeting the axis of abscissae so as to have a base breadth $\Delta\lambda$ related to the maximum vertical divergence permitted by the system of lead stops limiting the x-ray beam. Referring to Fig. 4 let θ_0

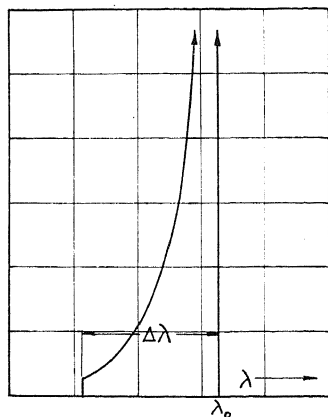


Fig. 3. Spectral intensity distribution selected by geometry of bicrystalline reflection *with crystals fixed*. This curve is not to be confused with the *shape of a spectral line* obtained by plotting reflected x-ray intensity against the dihedral angle between the crystals (or half of its supplement). Such line shapes are due to the overlapping of the "natural" line with the above curve as the latter is displaced spectrally with rotation of the crystals. The equation of the above curve is $y = k/[2(\lambda_0 - \lambda_\alpha)\lambda_0]^{1/2}$; $\lambda_0(1 - \frac{1}{2}\alpha^2) < \lambda_\alpha < \lambda_0$ calculated on the assumption that x-ray intensity is *uniformly distributed* over the permitted range of vertical divergences. The curve has a finite *area* in spite of the infinite *ordinate* at λ_0 . In a spectral exploration as such a curve progressively overlaps a spectral line the intensity will therefore always remain finite.

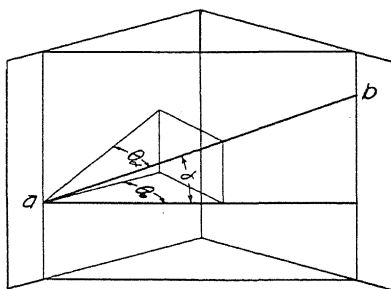


Fig. 4. Dependence of glancing angle on vertical divergence.

be the Bragg angle for a horizontally reflected ray, θ_α the Bragg angle for a ray of vertical divergence α . Then from the geometry of the case

$$\sin \theta_\alpha = \sin \theta_0 \cos \alpha$$

and since

$$n\lambda/2d = \sin \theta$$

we have

$$\lambda_\alpha = \lambda_0 \cos \alpha$$

$$\Delta\lambda = \lambda_0 - \lambda_\alpha = \lambda_0(1 - \cos \alpha)$$

and since in practice α is restricted to small values we have as a good approximation

$$\Delta\lambda = \frac{1}{2}\lambda_0\alpha^2.$$

DISTORTION OF LINES BY VERTICAL DIVERGENCES

The characteristic curve of Fig. 3 which may be regarded as the "frequency response curve" of the spectrograph for any given setting of the crystals displaces itself bodily toward longer wave-lengths as the dihedral angle between the crystal faces closes up. In this exploring process if a sharp line is encountered at some particular wave-length the ionization chamber will respond abruptly on the *short* wave side of the line and will diminish more gradually as the characteristic exploring curve moves to the *long* wave side of the lines. For this reason the distortion of spectral lines by the geometrical effect of vertical divergence alone is the *reverse* of Fig. 3, the discontinuous edge being on the *short* wave side. A good example of such distortions appears in Fig. 11 reproduced from a previous article⁸ published by the authors. It is an easy matter however to so limit the vertical divergence that its effect in broadening spectral lines is negligible in comparison to the effects of crystal imperfections and natural x-ray line breadths combined.

OBJECTIONS TO ROCKING ONLY ONE CRYSTAL

The fact that the rays selected by the mechanism of the double reflection are symmetrically orientated with respect to the dihedral angle between the crystal faces immediately suggests that in exploring the spectrum *both* crystals should be simultaneously rotated in equal and opposite directions with respect to a plane through their axes of rotation.

As a matter of fact however most double spectrometers are built so that only one crystal is rotated in exploring the spectrum. This necessitates rotating the other crystal from time to time and also changing the relative position of the two crystals to prevent the beam from falling partly or wholly off the reflecting faces. As one crystal alone is rotated the selected beam must of necessity progress across the faces of the two crystals in order that it shall continue to make equal glancing angles with both crystal faces. The objections to this procedure are:

1. The crystals may present different reflecting powers in different parts of their surfaces so that spurious intensity fluctuations would be introduced in a spectral exploration. In particular all calcite cleavage faces have multitudinous small "steps" where the fracture changes abruptly from one plane to another one parallel to it. At glancing angles such steps obviously cast shadows in the reflected ray which will diminish its intensity in different degrees according to whether the beam falls on a part of the surface with high steps or a part in which steps are nearly absent. If the beam is obliged to migrate across the crystal face these steps will surely introduce undesirable spurious fluctuations. Even though the beam remains centered at one point of the crystal surface the area of crystal surface employed in reflection will

⁸ DuMond and Hoyt, Phys. Rev. **36**, 799 (1930).

change with the glancing angle and some spurious fluctuations may thus be introduced by cleavage steps. These must however be regarded as an irreducible minimum.

2. If the source of radiation is not a point but has "horizontal" extension so as to permit reflection of one wave-length over a considerable area of the crystal a part of the beam which would otherwise be reflected may fall off one edge of the crystal introducing again spurious intensity fluctuations in a spectral exploration.

3. To avoid the above danger either very long crystals or a much reduced reflecting area must be used, both of which are rather serious difficulties.

4. The initial task of aligning the double spectrometer and locating a given spectral line is much harder in the instruments whose crystals do not rotate simultaneously.

As a corollary to what has just been said it is evidently desirable also to maintain the focal spot of the x-ray tube or other radiation source as well as the ionization chamber window always so situated with respect to the spectrometer that on one hand the selected beam from the tube will remain centered on the same reflecting region of the crystal faces for all glancing angles and on the other hand the selected radiation will always strike the ion chamber window at the same point. It is easy to see that large spurious fluctuations could be introduced by poor alignment of the beam entering a narrow ion chamber window and even with a broad window the transparency of the window might not be uniform over its area.

It seemed desirable to divorce the design of the double spectrometer completely from the single spectrometer and produce an instrument suited to the requirements of a large group of problems likely to be attacked without aspiring to achieve one so universal in its applicability that it would perform none of its functions well.

DESIGN OF THE SPECTROMETER

Fig. 5 is a general view of the spectrometer. Two circular tables *A* turning on conical pivots with accurately parallel axes support the crystals. The interpivotal distance is 5 inches. The pivot holes are bored in a single bed block of steel *B*, situated under the front end of the instrument. Two flat steel levers extending from the pivots to a similar steel bed block, *C*, under the rear end of the instrument can slide laterally, opening and closing like scissors, on top of this block so as to give equal and opposite rotations to the crystal tables. The levers are given their motion by a transverse shaft *D*, with right and left hand threads passing through nuts pivoted to the ends of the levers. The shaft is prevented from translating axially by a thrust bearing *E* half way between the levers. This bearing which has no axial play at all has sufficient lateral play to permit the screw shaft to translate in the direction of the crystal pivots as the levers spread apart. The action of the entire system is such that the crystal pivots and the driving nuts at the opposite ends of the two levers always stand at the four corners of a perfectly symmetrical isosceles trapezoid whose base is the screw shaft, whose sides are

the levers, and whose top is the line of centers of the crystal pivots. The top and sides are of constant length but the base and hence the altitude varies. It is for this reason that the thrust bearing on the screw provides for a slight lateral translation of the screw shaft. This same screw shaft carries a brass drum *F* on one projecting end on which the scale of glancing angles is engraved. The smallest divisions on this drum represent ten seconds of arc for the glancing x-ray reflection angles, and are separated by about three mm. A very important part of the design is a helical spring *G* running between two short posts on the under side of the two levers. The tension of this spring holds the levers together thus completely removing all backlash in the screw, nuts and pivots. The crystal tables are provided with angle scales engraved on their peripheries to facilitate setting. The levers can be clamped to and

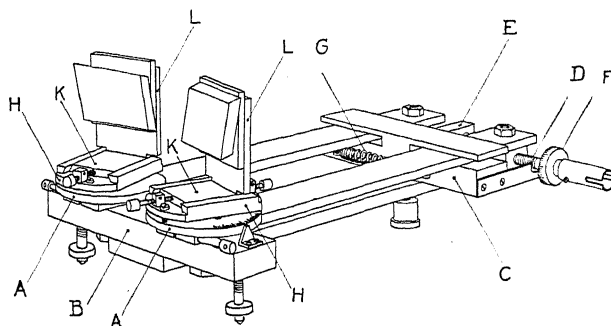


Fig. 5. Double spectrometer providing equal rotation of both crystals with respect to the line of pivot centers.

unclamped from the crystal tables in the same way as the tangent screws on a spectrometer or engineer's transit. The crystal tables are provided with removable false tops *H* which can rock about a horizontal axis. This is accomplished by two steel ball bearings lying between the crystal table disk and the false top in slight conical depressions provided for them and two opposing screws which clamp the false top to the crystal table with any desired slight inclination to the level. This adjustment is provided to permit of making the crystal faces accurately parallel to the axes of the pivots during the initial optical adjustment. A carriage *K* bearing the vertical crystal support slides in ways provided on each false top. This adjustment permits the crystal face to be brought in coincidence with the axis of rotation during the initial adjustment. The crystals are each fastened to a brass plate at three points with a very small quantity of beeswax. The brass plate can be fastened to the vertical crystal support *L* with two screws passing through holes large enough to permit of some adjustment in the position of the crystals. The vertical crystal support has a large hole bored through it at the point corresponding to the center of the crystal face. The reason for this hole is to permit sighting with a telescope and Gauss eyepiece at either side of a small interferometer plate which takes the place of the crystal during some of the initial adjustments. The entire spectrometer stands on leveling screws.

This instrument was very inexpensive to construct. The frame was built of pieces of cold rolled steel of rectangular section. No hand scraped surfaces were found necessary nor any precise circular divided scales. The one accurate requirement was that the pivot holes in the bed block *B* should have their axes as nearly parallel as possible. The spectrometer was built by one man in about five and one half days but in spite of its cheapness and simple construction a large amount of surprisingly precise work can be done with it.

THE SUBSIDIARY ROTATING MECHANISM

As before stated the quantities measured with the double spectrometer are: first, the angle between the crystals⁹ and second, the intensity of the twice reflected x-rays. The spectrometer just described measures the first quantity with high precision and reproducibility. It is however an important refinement to provide motion of the ionization chamber and x-ray source relative to the spectrometer in order to avoid the errors caused by shifting of the beam across the crystal faces and kindred objections already mentioned. It should be understood however that the requirement of precision in the motion of source and ion chamber is not as exacting as it is in the angular motion of one crystal relative to the other since the precise wave-length selected by the double reflection does not depend on the position of source or ion chamber so long as these are so situated that some radiation can suffer the double reflection. The wave-length selected by the double reflection depends wholly and solely on the angle between the crystals and it is this quantity which must be and is measured precisely and reproducibly on the drum of the spectrometer.

The motion of x-ray source and ion chamber relative to the spectrometer in the instrument here described is accomplished in such a way that the ion chamber remains stationary relative to the room. This means that relative to the room the spectrometer rotates about a center in line with the axis of rotation of the second crystal and at twice the rate of the second crystal. At the same time relative to the spectrometer the x-ray source rotates about a center in line with the axis of rotation of the first crystal at twice its rate of rotation. The scheme of holding the ion chamber stationary was adopted in order to permit the use of a short unarticulated vacuum sleeve surrounding a short lead wire of low and perfectly constant capacity connecting the ion collector to the electrometer. The ion chamber could probably be permitted to move relative to the room by using a vacuum tube amplifier such as has recently been developed for The General Electric Company in a shielded housing attached to the ion chamber to replace the electrometer. There is some question as to whether the enormous sensitivity, stability and reproducibility attainable with the Hoffmann type vacuum electrometer can be matched with the amplifier tube, and work is now being started to investigate the possibilities of this method in connection with a vacuum double crystal spectrometer now in process of design at this Institute.

⁹ The angles for which the drum is calculated are half the supplement of the dihedral angle between the crystals to facilitate their direct interpretation as glancing angles.

The above mentioned relative motions are obtained by means of two rotating false table tops of ply wood best shown in Figs. 6, 7. Ply wood was used instead of metal because the presence of the x-ray tube fed with high voltage made an insulating material convenient. The ply wood has proved to be quite free from warping and entirely satisfactory. The upper table top, *F*,

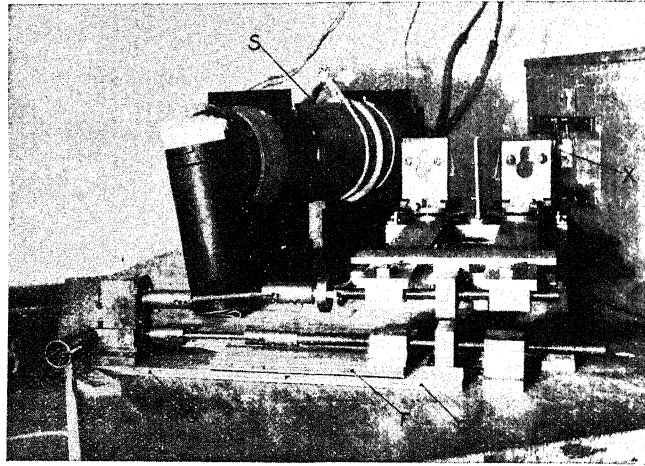


Fig. 6. General view of spectrometer, rotating table tops, rotating mechanism, and x-ray tube housing.

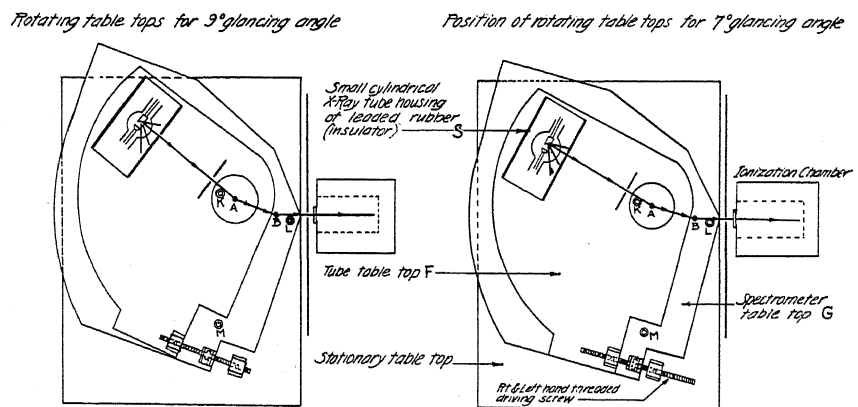


Fig. 7. Schematic diagram of table tops.

Figs. 6 and 7, carries the source of x-rays *S*. It rotates on a pivot centered at *A* consisting of a disk of ply wood 5 inches in diameter fixed to the second false table top *G*. This second table top in turn rotates on a stationary pivot centered at *B* and attached to the stationary table top. The centers *A* and *B* are separated by the same distance as the interpivotal distance on the spectrometer. The spectrometer rests entirely on the second table top *G*, the position of its three feet being at *K*, *L* and *M*. (The reason for the large diameter

pivot *A* is here obvious.) The pivots of the crystals are directly above and in line with the table top pivots *A* and *B*. The table tops are given the required angular rate of rotation by a second right and left hand screw with nuts and thrust bearing almost identical with the one on the spectrometer proper and having the same thread pitch. The two screws are connected through a simple type of universal joint transmission to gears having a ratio of two to one. The post supporting the gears is fastened to table top *G* and hence is stationary relative to the spectrometer. The entire mechanism is rotated by turning a shaft set at right angles to the screw shafts for accessibility the former driving the latter through bevel gears. This shaft terminates in a hollow brass tube *T* slotted axially on two diametrically opposite sides. A brass ball on the end of a long insulating handle can be inserted in this tube, and a rotary motion given to the tube by means of a diametral steel pin through the brass ball which engages in the slots of the tube. (The universal joints mentioned above are all of this simple ball and pin and slotted cylinder type and are very satisfactory.)

The kinematics of the table top drive is identical to that of the spectrometer. It is most easily grasped by taking as a reference, not the stationary table, but the false top *G* on which the spectrometer stands. The thrust bearing is attached to this top, and on turning the screw one nut causes the x-ray source on table *F* to rotate around the center *A*, relative to the spectrometer standing on *G*, at twice the rate of the crystal at *A*, while the other nut causes the table proper, and with it the room and the ion chamber, to rotate relative to the spectrometer standing on *G* around the center *B*, at twice the rate of the crystal at *B*. The same provision for lateral displacement of the shaft in the thrust bearing is provided for here as on the spectrometer. The whole device is of course open to the objection that it moves the source and ion chamber not accurately at twice the angular rate of the crystals, but rather at such a rate that the *sine* of one angle is twice the *sine* of the other angle. This however introduces far too small an error to cause trouble over the small rotations ordinarily required.

The lever arms of the spectrometer have each a range of motion of a little over one degree on each side of their position of mutual parallelism. The tables have each a range of two degrees on each side of their central position. A great deal of work can be done with even so small a range as this but slight modifications would suffice to increase the range. It is our practise to pick some definite angle setting near the midpoint of the range of glancing angles to be studied and then orient the crystals and other parts so that this angle corresponds to the zero position of the drum *F* (Fig. 5) with the levers in their central position. Details of this operation are described below.

MINOR SPECTROMETER DETAILS

The tube housing shown in Fig. 6 consists of a micarta tube large enough to contain the x-ray tube covered with a wrapping of two layers of the leaded rubber 1/16" thick such as is used by Röntgenologists for protective aprons. This material which can be obtained from surgical supply houses has the

advantage of being opaque to x-rays, flexible, and a good insulator. Its uses are manifest to anyone who has worked in x-rays. Since it is an insulator one can construct small and therefore light boxes of it to contain x-ray tubes.

Fig. 6 was taken with a copper target tube in the lead rubber housing provided with a projecting goose-neck tube with a charcoal trap dipping into a liquid air container. The latter is plainly visible standing on table *F*. An investigation over a period of two months¹⁰ was made with this copper target tube which had a mica window sealed on one side with DeKhotinsky cement. The liquid air and charcoal were found quite sufficient to maintain an excellent x-ray vacuum throughout the entire period.

The rotation required of the x-ray tube does not prevent the use of mercury pumps if necessary. These are installed under the table and are hung from table top *F* through holes bored in *G* and in the table top proper sufficiently large to permit the complete latitude of rotation. The pumps can be connected directly to the tube with an all-glass connection since no relative motion occurs between the two.

In order to insure smooth and easy operation of the table tops the bulk of the weight of the x-ray tube, housing, pumps and spectrometer is relieved by a simple system of lifting ropes going up to levers and counter weights hanging from the ceiling.

To give greater accessibility the entire table bearing all the parts so far described can be unclamped and moved away from the concrete wall shelf on which the detecting system consisting of electrometer and ion chamber stands.

DESIGN OF THE INTENSITY MEASURING SYSTEM

The essential requirements are that the x-ray intensity measuring system shall have high sensitivity coupled with great stability and reproducibility. It is also convenient to have as large an x-ray window in the ion chamber as possible to make the task of alignment less arduous. Fig. 8 shows a cross section of the entire ion chamber-electrometer system. The chamber is a large cylindrical brass can *A* nickel plated inside and out. A disk shaped cover *B* fastens on to the end of the can with six screws, but is electrically insulated from the can with a gasket and insulating washers under the screws. The cover is made gas tight by pressing a fillet of red universal laboratory wax into the groove *C* provided for it. The 1"×3" x-ray window in this cover is covered with a piece of paraffin impregnated Balsa wood—an extremely light yet stiff wood used in airplane model construction—with the grain running across the short dimension of the opening. The wood is attached to the cover with beeswax. The inner surface of the wood is coated with aluminum beryllium alloy 0.0002 inches thick making contact with the metal cover. The purpose of this coating is completely to define the potential all over the window so as to insure that the ions formed in this vicinity will not fail to be collected and also to prevent electrometer disturbances due to charges on the window inducing fluctuating charges on the collector.

¹⁰ Dumond and Hoyt, Phys. Rev. 36, 799–809 (1930).

A grid *D* of No. 36 nickel wire wound on and spot welded to a light nickel wire frame extends back from the window and surrounds the collector. This grid is supported on the brass cover *B* and by means of an external wire connected to the cover is brought to the potential of about 135 volts above ground, furnished by radio *B* batteries. The rest of the can which stands in contact with the electrometer housing is grounded.

The collector is led out of the can through a quartz insulator and as the can is itself grounded no guard ring is necessary. The collector of nickel wire can be fastened with a set screw into a brass cap on the top of the quartz

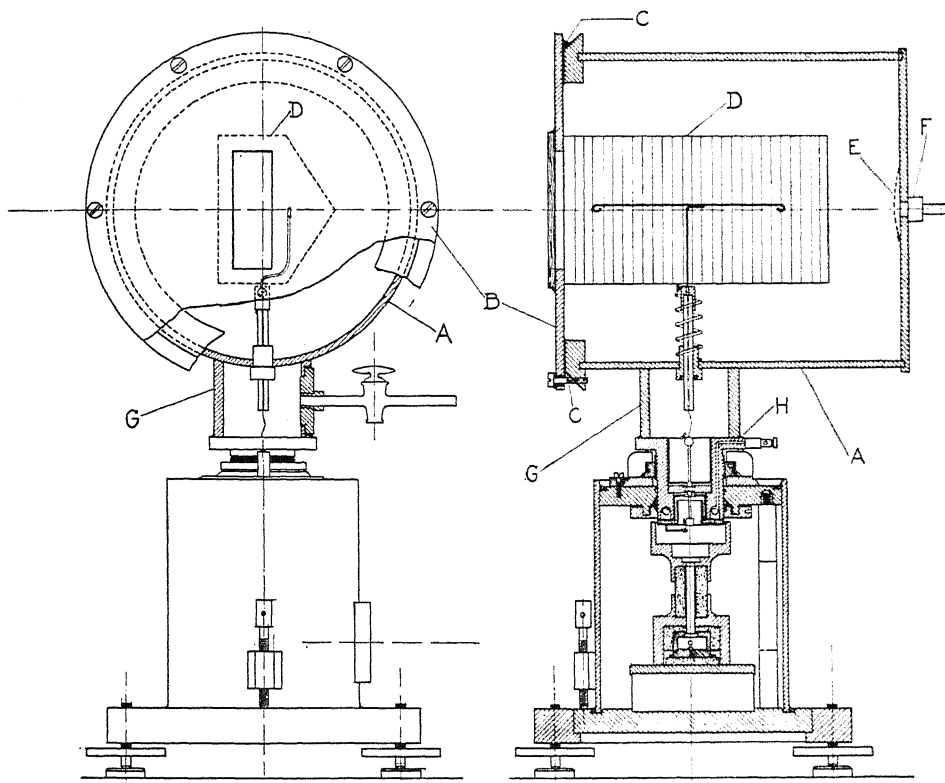


Fig. 8. Complete cross section of x-ray detecting system.

insulator. This collector is put in place through the x-ray tube window just before sealing on the Balsa wood cover. A small piece of fine mesh nickel screen *E* is welded over the inside opening of the gas connection *F*. This saves having to shield the glass tubes leading into the ion chamber by the usual method of covering them with tin foil.

The purpose of the internal grid is to minimize the fluctuations in the natural leak of the system caused by alpha-particles from the walls of the ion chamber. The space of about 5 cm from grid to chamber walls filled with about an atmosphere of methyl bromide accomplishes this very well.

The gas outlet from the ion chamber leads to a mercury manometer on

which any change in the methyl bromide pressure can be read. There is a glass cock for filling and a drying tube in constant connection with the chamber. It is important to keep the quartz insulator dry.

A fine No. 40 wire passing through the quartz insulator connects the collector to the highly insulated suspension of the Hoffman type electrometer. The connection is made through a short evacuated sleeve *G* which is made vacuum tight against the top flange of the electrometer with a fillet *H* of red universal wax.

Save for the flat flange just mentioned and for the use of universal wax instead of rubber gaskets to make the cylindrical case of the electrometer vacuum tight there are no changes in the design of the Hoffmann type vacuum electrometer. This remarkably satisfactory instrument has been completely described by its designer¹¹ and will not be given space in this article.

SENSITIVITIES AND REPRODUCIBILITIES OBTAINED

The spontaneous fluctuations in readings with this x-ray measuring system correspond to about 5×10^{-16} amperes. These fluctuations are the limiting feature at present on the smallest currents readable. They are only due in part to alpha-particles from the walls of the chamber. Their source is being studied and it is hoped that they can still be very greatly reduced. With these fluctuations at the present value currents of 6×10^{-14} amperes can be read with a reproducibility of one percent in a single reading of the order of a minute's duration. Currents of 10^{-15} amperes can be read with fair accuracy by taking several somewhat longer readings and averaging. We have succeeded in detecting the satellite $K\alpha_{34}$ of copper at only 1.75 KV above its critical excitation voltage with this outfit. This satellite had spectral ordinates protruding above the background *only one four hundred and fiftieth* as high as the maximum ordinate of $K\alpha_1$ its parent line six X.U. away.

The electrometer has a very stable zero that will remain constant within a few millimeters for months. The instrument as now used has a rather stiff suspension. Mr. Julius Pearson of this institute has succeeded recently in producing Wollaston wire suspensions for the Hoffmann electrometer with much longer period than the one now in use. The present rather low volt sensitivity could then be increased to about 10000 mm per volt. The capacity of the whole insulated system of electrometer and ion chamber is about 12 electrostatic units. We therefore do not believe the possibilities of the above described system are exhausted with the results here reported.

TECHNIQUE OF OPERATION

Method of orientating the crystals initially.

The procedure about to be described accomplishes in practice the fulfillment of the following required conditions. (These conditions are not all equally exacting.)

1. The crystal reflecting planes must be parallel to the axes of rotation of the crystal table pivots.

¹¹ G. Hoffmann, Ann. d. Physik 52, [7] 665-708 (1917).

2. The reflecting surfaces of each crystal must coincide with the axis of rotation of its pivot.

3. The two crystal reflecting planes must make equal angles with the plane through the axes of the pivots.

4. The dihedral angle between the two crystal planes must be set for some known value corresponding to the "zero" drum position of the screw and lever crystal turning mechanism to facilitate "finding" a spectral line.

The first condition is quite important since the accuracy with which the dihedral angle between the crystal faces can be determined and hence the accuracy to which the wave-length scale is known depends on this. Also if condition No. 1 is not fulfilled the so called "horizontal" plane i.e. the plane normal to the dihedral angle formed by the two crystals may be quite oblique to the pivot axes and the general line of the x-ray apertures causing an unsuspected vertical divergence of the rays from the "horizontal" plane. Requirement No. 1 evidently becomes more rigid due to both of these last named effects as the crystal planes approach parallelism.

The second condition cannot be fulfilled very rigidly since the plane of the face of the crystal is ill defined on account of the unavoidable cleavage steps. Its purpose is to minimize the gliding of the selected beam across the crystal face as the crystal rotates.

The third condition merely insures that the radiation from the first to the second crystal shall pass parallel to the line of centers of the two pivots thus facilitating the initial alignment of the apparatus. It need only be fulfilled to within a few minutes of arc.

The fourth condition is merely a convenience. We have however invariably succeeded by the technique about to be described in locating the crystals so closely that it was not necessary to *hunt* for a known spectral line over a range much greater than its own observed breadth.

A small optical spectrometer with collimator removed and with a Gauss eyepiece in the telescope is used. Calcite cleavage faces as Allison has noted are poor reflectors of visible light at normal incidence. It is however, possible to obtain a sufficiently intense image of the cross hairs for visibility if one employs a strong but small incandescent light, well shielded from directly striking the eye to illuminate the Gauss eyepiece. A small black disk of paper, say 0.5 mm in diameter, should be carefully attached with a little shellac to the intersection of the cross hairs. The period from a set of gummed letters such as are used to stick on drawings makes a good disk. This makes a spot large enough to see in the faint reflected image. Considerable patience is required in hunting for the faint image but the telescope and Gauss eyepiece furnish such an accurate method of alignment that it is worth while spending an hour or so, especially as it need not be done often.

A glancing angle θ_0 is first chosen as a setting for the crystals when the angle drum is set at zero and the levers and drum are then adjusted to that zero position. The optical spectrometer is then set on a bench in front of the x-ray spectrometer in such a position that in sighting the telescope alternately first at crystal one and then at crystal two the optical telescope must turn

through approximately the angle $2\theta_0$. The pivot axes of both spectrometers are then rendered accurately vertical with the leveling screws by taking reversed readings with a good level. A pair of light plumb lines of white silk thread are then adjusted so that they define a plane the perpendicular bisector of the plane through the two pivot axes. This can be done very precisely with a trammel which is engaged at one end in the conical center holes on which the crystal pivots were turned and is used as a "feeler" to strike four arcs in space centered each from a pivot and just making contact on either side with the plumb lines. The geometry is the simple Euclidian construction for a perpendicular bisector. The telescope is now adjusted to sight accurately down the line defined by the two plumb lines. The index of the divided circle on the optical spectrometer is then set on zero and clamped and the two spectrometers are rechecked for level and sealed to the bench with shellac or wax. The next step is to render the line of collimation of the telescope accurately normal to the pivot axes of the x-ray spectrometer. (Incidentally when this is done the line of collimation of the telescope will be horizontal.) A small plane parallel glass interferometer plate is stuck on with wax over the hole in the vertical brass crystal support and trial reflections are made from both sides of this plate turning the crystal table through 180° each time and correcting half the error at the plate and half in the level adjustment of the telescope (not the spectrometer of course) until the Gauss cross hairs coincide with their reflected image equally well with the plate facing either way. This condition must be fulfilled for both crystal pivots. The telescope collimation line is now accurately normal to both the x-ray and optical spectrometer pivot axes and its level must not be subsequently disturbed. The plane parallel glass plate is now removed and the calcites ready mounted on their brass plates are attached to the vertical crystal supports with screws. Care should be taken to locate them symmetrically over their axes of rotation at the same height above the turntables. At zero reading on the divided circle of the optical spectrometer the telescope is now normal to the plane through the axes of the x-ray spectrometer pivots. Turn the telescope through the angle θ_0 to right or left of this point as read on the divided circle of the optical spectrometer and sight at the crystal face. The crystal table is then unclamped and orientated and the false top tilted until the cross hair image normally reflected from the calcite coincides with the cross hairs. The crystal reflecting face is brought into coincidence with its pivot axis by screwing the crystal support carriage diametrically across until a tangential view of the face with the crystal rotated to either side the stationary line of sight shows no displacement. This should be done after rendering the crystals vertical but before finally clamping them to the levers at the correct horizontal orientation defined by the telescope.

The entire procedure requires three or four hours and need only be performed once for each pair of crystals used unless some accident disturbs them. The divided circles on the crystal turn tables should be carefully read and recorded.¹² This gives a fiducial reference from which the proper

¹² A scale capable of being read to within a few minutes of arc is sufficiently accurate.

settings for other glancing angles can be made without having further recourse to the Gauss eyepiece reflection method.

Alignment of other parts

It is necessary also to align the source of x-rays in the proper position with respect to the spectrometer. Furthermore the entire system of source and spectrometer must be aligned with respect to the ion chamber so that the rays will enter its window. We have found that this can all be done very conveniently after the crystals have been aligned by cutting a templet out of Bristol board such as is shown in Fig. (9). The edge segments *A*, *B*, of this templet are fitted against the crystals and the edges *C*, *D*, then point respectively in the direction of the source and the ion chamber window when their locations are correct. If the templet is carefully laid out with a precision vernier protractor and accurately cut with a razor blade held against a steel

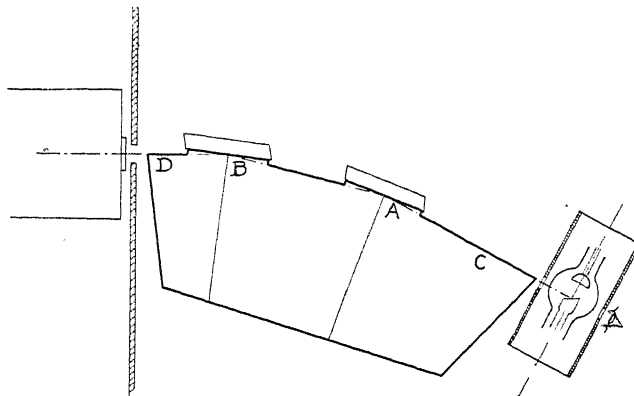


Fig. 9. Cardboard templet used in aligning table tops and x-ray tube.

straight edge the method is accurate to within a few minutes of arc. It is helpful to lay out the normals to the crystal faces on the cardboard. When the cardboard is properly orientated against the crystal faces the reflected image of these normals should line up straight with the normals themselves.

Needless to say the cardboard templet is laid out for the glancing angle θ_0 corresponding to the mid value of the spectral range chosen for the particular work to be done and the above described alignment procedure must be carried out with the spectrometer and the ply wood table tops set at the midpoint of their travel, i.e. at the point where the pivots of the nuts on the right and left hand screw shafts are separated by the same distance as the two crystal pivots.

ELIMINATION OF BACKGROUND

The detection and accuracy of measurement of faint lines is limited by the intensity of the x-ray background. Also the shapes and positions of lines are distorted by background structure. It is therefore essential to consider means of reducing background. The causes of background are:

1. Selective reflection of continuous or "white" radiation from the source.
2. Natural leak of ion chamber and electrometer system.
3. Amorphous or non-selective crystal scattering and fluorescent radiation excited in the crystals.
4. Leakage of x-rays without suffering double reflection in the prescribed orders.

It is not always desirable to eliminate all of the above factors. For example if one is interested in studying either the continuous "white" radiation or diffuse lines partaking of the nature of a continuous distribution No. 1 should obviously be retained. Methods of controlling the above sources of background are in the above order as follows.

1. The intensity of white radiation adjacent to a spectral line as measured by the ionization chamber relative to the intensity when the crystals are set for the peak of a line can be very widely controlled by controlling the cross-fire or vertical divergence of the x-ray beam. As long as the band of wavelengths selected by the bicrystal reflection is of larger order of magnitude than the natural line breadth, diminution of this band width reduces the background ordinates faster than the line ordinates. The vertical divergence angle is controlled by the height of defining lead openings and their distance apart. In the present instrument one such opening provided with adjustable jaws is arranged in the heavy lead wall dividing the spectrometer and x-ray source assembly from the electrometer and ion chamber.

2. Precautions for minimizing "natural leak" by means of the internal grid in the ion chamber have already been described as have also the use of quartz insulators kept dry with phosphorous pentoxide and the use of vacuum shields and a vacuum electrometer.

3. It is well known that scattering of x-rays is of two types namely modified and unmodified scattering. It is also well established that selective crystal reflection is solely of the unmodified type since this is the only type in which the incident and reflected beams are coherent. As regards modified scattering however the two calcite crystals might as well be two pieces of wood or graphite. All wave-lengths of radiation from the x-ray tube can be scattered into the ion chamber by the Compton modified scattering process independent of the angle setting of the crystals. The ratio of modified amorphous scattering to unmodified selective scattering increases with the hardness of the radiation. It is evident therefore that a great advantage in background reduction will be gained by filtering out all radiations from the source harder than those which are in the range being studied. This is especially true when the x-ray tube is being operated at voltages considerable higher than the critical voltage necessary to excite the radiation being studied. Thus in the study of the satellite $K\alpha_{34}$ of copper (parent, $K\alpha_1$) we have found that a filter made of a piece of nickel foil rolled out to 0.0005" thickness was extremely effective in reducing the ratio of background ordinates to line ordinates.

4. The same procedure evidently reduces the background due to char-

acteristic fluorescent radiations excited in the crystals themselves by the harder regions of the continuous spectrum from the x-ray tube.

4. Finally a judicious disposition of lead shields will be found to reduce the background very materially. A vertical lead knife edge should be placed

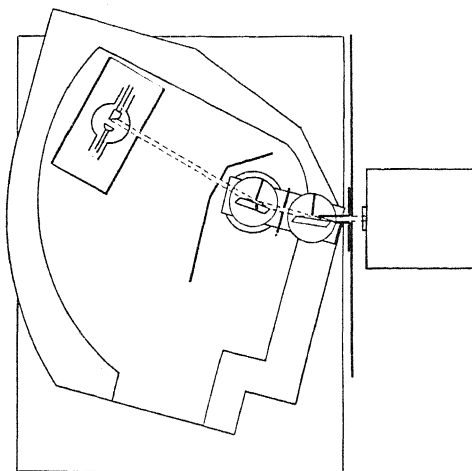


Fig. 10. Scheme of lead shielding.

normal to the reflecting face of each crystal, close enough to the face to prevent any radiation from reaching the ion chamber without suffering the double reflection. These knife edges if placed too close will cut down the

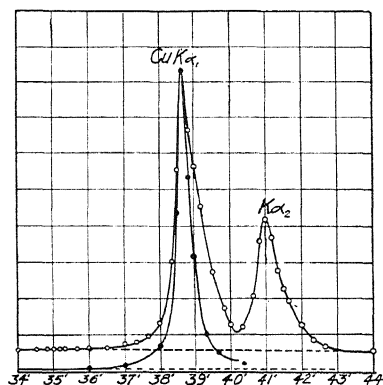


Fig. 11. Comparative curves of $\alpha_{1,2}$ before and after taking the precautions outlined in text for reducing relative background.

available intensity. A little experimentation is the best guide in this matter. A shield with a rectangular window of the proper dimensions placed symmetrically between both crystals is helpful as is also an extensive lead shield near the first crystal between it and the tube. Most effective of all is the use of a lead snout of rectangular cross section which hangs in front of the adjustable lead window in the lead partition between the spectrometer and

the detecting system and which projects forward to the second crystal. See X Fig. 6. The disposition of this snout if properly chosen will greatly reduce the solid angle from which stray radiation can enter the ionization chamber. Fig. 10 shows the system of lead shields.

The degree to which relative background can be reduced is shown in Fig. 11 by a comparison of the spectral curves of $K\alpha_1$ of copper before and

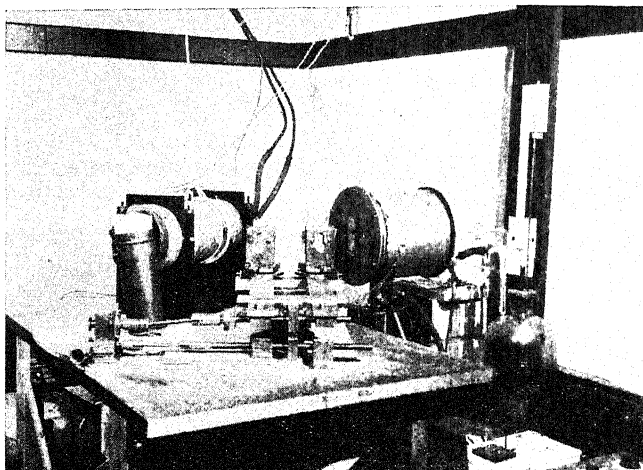


Fig. 12. General view of apparatus with lead shield between spectrometer and ionization chamber removed.

after taking the various precautions discussed above for reducing background. The ordinates of the curve with the low background have been plotted to a scale chosen so as to make both curves coincide at the maximum value of $K\alpha_1$. The relative reduction of background is very evident.

Fig. 12 is a general view of the apparatus with the lead shield removed from between ionization chamber and spectrometer.

THE VALUE OF e/m BY DEFLECTION EXPERIMENTS

BY G. E. UHLENBECK AND L. A. YOUNG

UNIVERSITY OF MICHIGAN

(Received November 10, 1930)

ABSTRACT

To clarify the discussion as to whether or not a quantum mechanical treatment of the motion of electrons in magnetic fields will lead to a formula for e/m , differing from that obtained by classical electro-dynamics the following problem was solved. A uniform magnetic field in the z -direction exists in the half-space $x > 0$. A plane monochromatic de Broglie wave, travelling in the positive x -direction representing electrons of arbitrary energy, impinges normally on the plane $x = 0$. Solutions of the wave equation were found fulfilling appropriate boundary conditions at the plane $x = 0$. Currents are calculated quantum mechanically and compared with the corresponding classical expressions. It was found that for electrons possessing energies of the order of magnitude used in deflection experiments, no *observable* deviations from classical results are predicted. Another quantum mechanical effect is diffraction at slits. Simple approximate calculations show that this effect can produce a fractional error in e/m of the order of the de Broglie wave-length divided by the slit width. These results are opposite to the conclusions reached by Page. We may remark that he solved a problem of "stationary states" which does not represent the actual experiments.

IN A recent issue of the Physical Review Professor Leigh Page¹ tried to explain the difference in the value of e/m obtained from deflection experiments and from spectroscopic evidence on the basis of quantum mechanics. This was later criticized by Eckart,² first, he doubted certain approximate calculations of Page which may, however, be shown to be correct;³ second, he referred to articles of Kennard⁴ and Darwin⁵ which prove quite conclusively that a wave packet representing an electron in a uniform magnetic field moves as in the classical theory. To this we may remark that in the deflection method the measurements are not made with a single particle but are statistical since we work with beams of electrons. However the work of Page does not seem conclusive because he considers the solutions of the wave equation corresponding to the completely quantized motion of isolated electrons in a magnetic field of infinite extension; whereas in the deflection experiments we have to deal with a problem of "streaming."

§2. In trying to decide the question as to whether or not quantum mechanics will lead to results appreciably different from those of the classical theory we have considered the following problem. A homogeneous magnetic field in the x -direction fills the half-space $x > 0$. Free electrons moving in the

¹ L. Page, Phys. Rev. 36, 444 (1930).

² C. Eckart, Phys. Rev. 36, 1014 (1930).

³ L. Page, Phys. Rev. 36, 1418 (1930).

⁴ E. H. Kennard, Zeits. f. Physik 44, 347 (1927).

⁵ C. G. Darwin, Proc. Royal Soc. A117, 258 (1927).

x -direction impinge on the plane $x=0$ and penetrate the magnetic field. Classically they will describe half-circles with centers on the plane $x=0$ and radii

$$r = \frac{cp}{eH} \quad (1)$$

where p represents the momentum of the particles. We find easily that in the magnetic field the components of the current density S are

$$S_x = 0 \quad S_y = \frac{2Ix}{(r^2 - x^2)^{1/2}} \quad (2)$$

and the total current $\int_0^r S_y dx = 2Ir$ where I is the current density of the incoming electrons. Quantum mechanically we have for $x > 0$ the wave equation

$$\left\{ \Delta_2 + \frac{2\pi i}{\lambda r} \left(x \frac{\partial}{\partial y} - y \frac{\partial}{\partial x} \right) - \left(\frac{\pi}{\lambda r} \right)^2 (x^2 + y^2) + \left(\frac{2\pi}{\lambda} \right)^2 \right\} \psi_1 = 0 \quad (3)$$

where Δ_2 is the Laplace operator for two dimensions and $\lambda = h/p$ is the de Broglie wave-length of the incident electrons. The incoming electrons are represented by a wave function $\psi_i = A \exp(2\pi i/\lambda x)$ and the outgoing electrons by $\psi_o = B \exp(-2\pi i/\lambda x)$ so that for $x < 0$ the total wave function $\psi_2 = \psi_i + \psi_o$. We must seek solutions of (3) which fulfill the boundary conditions at $x=0$:

$$\psi_1 = \psi_2 \quad (a)$$

$$(mv_x)_1 \psi_1 = (mv_x)_2 \psi_2 \quad (b)$$

$$(mv_y)_1 \psi_1 = (mv_y)_2 \psi_2 \quad (c) \quad (4)$$

$$\psi_1(\infty) = 0 \quad (d)$$

where

$$mv_x = \frac{h}{2\pi i} \frac{\partial}{\partial x} + \frac{e}{c} A_x$$

and

$$mv_y = \frac{h}{2\pi i} \frac{\partial}{\partial y} + \frac{e}{c} A_y.$$

In our case the components of the vector potential A_x and A_y are given by $A_x = -\frac{1}{2}Hy$ and $A_y = \frac{1}{2}Hx$. Making use of results given in a recent paper by Landau⁶ we find that

$$\psi_1 = \phi(x) e^{\pi i x y / \lambda r} \quad (5)$$

is a solution of (3) if $\phi(x)$ satisfies the equation

$$\phi''(x) + \left(\frac{2\pi}{\lambda} \right)^2 \left(1 - \frac{x^2}{r^2} \right) \phi(x) = 0. \quad (6)$$

⁶ L. Landau, Zeits. f. Physik 64, 629 (1930).

We may therefore write our boundary conditions (4) (conditions 4c is identically fulfilled)

$$\phi(0) = A + B \quad (a)$$

$$\phi'(0) = \frac{2\pi i}{\lambda}(A - B) \quad (b) \quad (7)$$

$$\phi(\infty) = 0 \quad (d)$$

It will be shown later that the condition $\phi(\infty)=0$ will, for a given λ determine $\phi'(0)/\phi(0)$ so that we may write for convenience

$$\frac{\lambda\phi'(0)}{2\pi\phi(0)} = q(\lambda) \quad (8)$$

where $q(\lambda)$ is a real quantity.

The first and second of the relations (7) then give

$$q(A + B) = i(A - B)$$

or

$$B = \frac{i - q}{i + q}A = Ae^{i\pi\tau}. \quad (9)$$

The phase of the outgoing electrons therefore differs from that of the incoming electrons by $\pi\tau$, where

$$\cos \pi\tau = \frac{1 - q^2}{1 + q^2}. \quad (10)$$

Thus

$$\phi(0) = A(1 + e^{i\pi\tau}). \quad (11)$$

§3. The current density is in general given by

$$S_x = \frac{e\hbar}{4\pi im} \left(\psi \frac{\partial \bar{\psi}}{\partial x} - \bar{\psi} \frac{\partial \psi}{\partial x} \right) - \frac{e^2}{mc} A_x \psi \bar{\psi}$$

with a similar expression for S_y . Substituting equation (5) and the vector potentials we find immediately

$$(S_x)_1 = 0 \quad (S_x)_2 = \frac{e}{m} \frac{\hbar}{\lambda} (B\bar{B} - A^2) = 0. \quad (12)$$

This latter expression is zero due to the fact that A and B are equal in absolute value from (9). The intensities of the incoming and outgoing waves are equal. Further

$$(S_y)_1 = -\frac{e}{m} \frac{\hbar}{\lambda\tau} x\phi\bar{\phi} \quad (S_y)_2 = 0. \quad (13)$$

At $x=0$ $(S_y)_1=(S_y)_2=0$. Continuity of the currents is therefore a consequence of the boundary conditions (4). Finally we can calculate the total current

$$\int_0^\infty (S_y)_1 dx = -\frac{eh}{\lambda r m} \int_0^\infty x \phi \bar{\phi} dx.$$

By integrating partially and using the differential equation (6) for ϕ and the fact that $\phi(\infty)=0$ it is found that

$$\int_0^\infty x \phi \bar{\phi} dx = \frac{1}{2} r^2 (1 + q^2) \phi(0) \bar{\phi}(0).$$

Substituting (11) and noting that $I = ehA^2/m\lambda$ we find that

$$\int_0^\infty (S_y)_1 dx = 2Ir$$

which is just the classical value.

§4. To get a clearer idea of $(S_y)_1$, a quantity which would be measured in a deflection experiment, we must study the solutions of (6) in more detail. Introducing $\xi = 2x(\pi/\lambda r)^{1/2}$, $\nu + \frac{1}{2} = \pi r/\lambda$ (6) becomes

$$\frac{d^2\phi}{d\xi^2} + \left(\nu + \frac{1}{2} - \frac{1}{4}\xi^2 \right) \phi = 0.$$

This equation is treated extensively in Chapter 16, page 341 of Whittaker and Watson "Modern Analysis." In their notation we obtain for a solution vanishing at $\xi = \infty$:

$$\phi(\xi) = a D_\nu(\xi) = a e^{-\xi^2/4} \xi^\nu \left\{ 1 - \frac{\nu(\nu-1)}{2\xi^2} + \frac{\nu(\nu-1)(\nu-2)(\nu-3)}{8\xi^4} - \dots \right\}$$

for large ξ (a is a constant to be determined from $\phi(0)$). If ν is an integer the series breaks off and we obtain the well-known harmonic oscillator eigenfunctions. This solution "connects" with the following solution for small ξ :

$$\phi(\xi) = a \left\{ \frac{\Gamma\left(\frac{1}{2}\right) 2^{\nu/2+1/4}}{\Gamma\left(\frac{1}{2} - \frac{\nu}{2}\right)} \xi^{-1/2} M_{\nu/2+1/4, -1/4}\left(\frac{\xi^2}{2}\right) + \frac{\Gamma\left(-\frac{1}{2}\right) 2^{\nu/2+1/4}}{\Gamma\left(-\frac{\nu}{2}\right)} \xi^{-1/2} M_{\nu/2+1/4, 1/4}\left(\frac{\xi^2}{2}\right) \right\}$$

where

$$M_{k,m}(\eta) = \eta^{1/2+m} e^{-\eta/2} \left\{ 1 + \frac{\frac{1}{2} + m - k}{1!(2m+1)} \eta + \frac{(\frac{1}{2} + m - k)(\frac{3}{2} + m - k)}{2!(2m+1)(2m+2)} \eta^2 + \dots \right\}$$

From this solution one can show easily that

$$q = 2(2\nu + 1)^{-1/2} \frac{\Gamma\left(\frac{\nu}{2} + 1\right)}{\Gamma\left(\frac{\nu}{2} + \frac{1}{2}\right)} \tan \frac{\nu\pi}{2} \quad (14)$$

$$\cong \tan \frac{\nu\pi}{2} \text{ for } \nu \gg 1$$

thus

$$\cos \pi\tau = \frac{1 - q^2}{1 + q^2} = \cos \nu\pi$$

or

$$\pi\tau = \pi\nu. \quad (15)$$

Thus the phase shift between the incoming and outgoing electrons is completely determined in terms of ν and therefore in terms of the energy of the incident electrons. It may be worth while to remark that ν is very simply related to the number N of de Broglie wave-lengths on the circumference of the classical half circle

$$\nu = N - \frac{1}{2} \text{ or } \pi\tau = (N - \frac{1}{2})\pi$$

or since λ is usually of the order of 10^{-8} cm, ν is of the order of magnitude 10^8 to 10^{10} . For quantum numbers of this order of magnitude one would hardly expect to find the differences between classical and quantum mechanical predictions to be measurable.

§5. To add weight to this belief we may consider the character of the function $\phi(x)$ in more detail. This is best done by considering the Wentzel-Brillouin-Kramers⁷ approximation. For $x > r$ $\phi(x)$ behaves as an increasing or decreasing exponential and to satisfy the condition $\phi(\infty) = 0$ we must choose the latter. We obtain

$$\phi(x) \cong \frac{a}{(x^2 - r^2)^{1/4}} \exp \left\{ -\frac{2\pi}{\lambda r} \int_r^x (x^2 - r^2)^{1/2} dx \right\}.$$

This "connects" according to Kramers with the oscillatory solution for $x < r$

$$\phi(x) \cong \frac{2a}{(r^2 - x^2)^{1/4}} \cos \left\{ \frac{2\pi}{\lambda r} \int_x^r (r^2 - x^2)^{1/2} dx - \frac{\pi}{4} \right\}.$$

We see immediately that this approximate solution determines $q(\lambda) = \lambda\phi'(0)/2\pi\phi(0)$ and we find for it again

⁷ G. Wentzel, *Zeits. f. Physik* **38**, 518 (1926); L. Brillouin, *C. R.*, Juli, 1926; H. A. Kramers, *Zeits. f. Physik* **39**, 828 (1926); A. Zwaan, *Utrecht Dissertation*, 1929; L. A. Young and G. E. Uhlenbeck, *Phys. Rev.* **36**, 1154 (1930).

$$q = \tan \frac{\nu\pi}{2}.$$

The constant a has to be determined from the value $\phi(0)$. We find from (11)

$$a = \frac{A(1 + e^{\pi i r})r^{1/2}}{\cos \frac{\pi\nu}{2}}.$$

Calculation of the current gives then for $x < r$

$$(S_y)_1 = \frac{4Ix}{(r^2 - x^2)^{1/2}} \cos^2 \left\{ \frac{2\pi}{\lambda r} \int_x^r (r^2 - x^2)^{1/2} dx - \frac{\pi}{4} \right\}. \quad (16)$$

The current, therefore, is "oscillatory" with an amplitude just twice the classical current. The distance between the maxima is, for small x , just $\lambda/2$ but increases as x approaches r . The distance Δ of the last maximum from $x=r$ is given by

$$\frac{2\pi}{\lambda r} \int_{r-\Delta}^r (r^2 - x^2)^{1/2} dx = \frac{\pi}{4}$$

or

$$\Delta = \frac{3^{2/3}}{8} \lambda^{2/3} r^{7/3}. \quad (17)$$

For $x > r$ the current is given by

$$(S_y)_1 = \frac{2Ix}{(x^2 - r^2)^{1/2}} \exp \left\{ -\frac{4\pi}{\lambda r} \int_r^x (x^2 - r^2)^{1/2} dx \right\}. \quad (18)$$

This current falls off very rapidly with increasing x , in fact in going a distance $n\Delta$ beyond $x=r$ the ratio of the current to the current at $x=r-\Delta$ is given by

$$\frac{1}{2(n)^{1/2}} \exp(-2n^{3/2}). \quad (19)$$

This ratio is equal to 0.001 for $n \cong 2.1$.

§6. These last results are perhaps doubtful since in the neighborhood of $x=r$ the approximation from which they were derived becomes invalid. We can, however, derive them more rigorously by observing that near $x=r$,

$$1 - \frac{x^2}{r^2} \cong 2 \left(1 - \frac{x}{r} \right).$$

Instead of (6) we have then

$$\phi''(x) + 2 \left(\frac{2\pi}{\lambda} \right)^2 \left(1 - \frac{x}{r} \right) \phi(x) = 0.$$

This equation has been thoroughly discussed by Kramers (reference 7) and the solution which "connects" properly with the exponential and oscillatory solutions of (6) is found immediately to be

$$\phi(x) = \omega \left\{ 2 \left(\frac{\pi r}{\lambda} \right)^{2/3} \left(1 - \frac{x}{r} \right) \right\} \quad (20)$$

$\omega(z)$ has been tabulated by van der Held (see Kramers, reference 7) and we find from his table

$$\Delta = \frac{1}{2} \pi^{-2/3} \lambda^{2/3} r^{1/3} \quad (17')$$

and in traveling a distance 2.5Δ the current drops to 0.001 of its maximum value.

§7. Returning now to the value of e/m we must distinguish between two quantum mechanical effects. The first is the one discussed above. If we observed the maximum current we would find it displaced a distance Δ from the classical position. If we calculated e/m from

$$\frac{e}{m} = \frac{cv}{H} \cdot \frac{1}{r}$$

we would obtain too *large* a value. This is in the right direction to explain the discrepancy between the deflection and spectroscopic values of e/m but quantitatively the relative error due to this is of the order $(\lambda/r)^{2/3}$ which is about 10^{-6} . The observed relative discrepancy is 4×10^{-3} .

A second quantum mechanical effect in an actual deflection experiment would be diffraction at the entrance slit. A rough calculation based on the uncertainty principle shows that this can give a relative error in e/m no larger than λ/d where d is the slit-width. For actual cases this is of the order 10^{-6} . We conclude therefore that the quantum mechanical analysis of the deflection experiments cannot explain the observed discrepancy. One might still think of relativistic or spin effects as a possible explanation of the e/m paradox, but we have a feeling that the resulting corrections will also be extremely small.

Note added in proof: We regret that, in preparing this manuscript we overlooked the article of Charlotte T. Perry and E. L. Chaffee (Phys. Rev. 36, 904; 1930) which seems to show quite conclusively that the discrepancy between the two values of e/m is due to an error in the experimental determination of the velocity of the electrons in the deflection experiments.

RELATIVISTIC WAVE MECHANICS OF ELECTRONS DEFLECTED BY A MAGNETIC FIELD

BY MILTON S. PLESSET*

SLOANE PHYSICS LABORATORY, YALE UNIVERSITY

(Received November 3, 1930)

ABSTRACT

It is shown that the relativistic wave equation for electrons in a uniform magnetic field leads to the same wave function as that already deduced by Page from the non-relativistic equation. As in the latter case the motion at right angles to the field is quantized.

An expression is found for the current density from the relativistic wave equation. The relativistic expression differs from the non-relativistic only by a constant factor which does not affect the calculation of the mean radii of curvature of the electron current.

Hence, for the relativistic case, as for the non-relativistic, the mean radius of curvature is less than that expected on the classical theory. It follows that the classical relativistic relation between ϵ/μ and the mean radius of curvature upon deflection gives a value of ϵ/μ which is too large.

THE non-relativistic Schrödinger wave equation which governs the motion of electrons in a uniform magnetic field has been solved by Page.¹ The solution which he obtains shows that the mean radius of curvature of the electron current is less than that given by the classical theory. An appreciable error is thus introduced in applying the classical relation to the determination of ϵ/μ from deflection experiments.

Since the energies of the electrons used in deflection experiments are so large, it was thought that a treatment of the problem by the relativistic wave mechanics would be of interest.

THE RELATIVISTIC WAVE EQUATION

The relativistic wave equation² for electrons in a magnetic field is

$$\nabla \cdot \nabla \psi - \frac{1}{c^2} \frac{\partial^2 \psi}{\partial t^2} - \frac{4\pi i e}{hc} \mathbf{A} \cdot \nabla \psi - \frac{4\pi^2}{h^2} \left(\mu^2 c^2 + \frac{\epsilon^2}{c^2} A^2 \right) \psi = 0 \quad (1)$$

where \mathbf{A} is the vector potential and μ is the rest mass of the electron. For a uniform field H in the X direction

$$\mathbf{A} = -j\frac{H}{2}z + k\frac{H}{2}y.$$

Eq. (1) then becomes in cylindrical coordinates r, θ, x ,

* Charles A. Coffin Fellow.

¹ Leigh Page, Phys. Rev. **36**, 444 (1930).

² L. Brillouin, J. de Phys. et Le Radium **8**, 74 (1927).

$$\frac{1}{r} \frac{\partial}{\partial r} \left(r \frac{\partial \psi}{\partial r} \right) + \frac{1}{r^2} \frac{\partial^2 \psi}{\partial \theta^2} + \frac{\partial^2 \psi}{\partial x^2} - \frac{1}{c^2} \frac{\partial^2 \psi}{\partial t^2} - \frac{2\pi i \epsilon H}{hc} \frac{\partial \psi}{\partial \theta} - \frac{4\pi^2}{h^2} \left(\mu^2 c^2 + \frac{\epsilon^2 H^2 r^2}{4c^2} \right) \psi = 0. \quad (2)$$

We put

$$\psi = R(r)X(x)e^{-im\theta}e^{-2\pi i(\epsilon/h)t} \quad (3)$$

where \mathcal{E} is the total energy, and m must be an integer for ψ to be single-valued. Eq. (2) then leads to the ordinary differential equations

$$\frac{d^2 X}{dx^2} + \alpha X = 0, \quad (4)$$

$$\frac{d^2 R}{dr^2} + \frac{1}{r} \frac{dR}{dr} + \left\{ \frac{4\pi^2 \mathcal{E}^2}{h^2 c^2} - \frac{4\pi^2 \mu^2 c^2}{h^2} - \frac{2\pi \epsilon H m}{hc} - \frac{\pi^2 \epsilon^2 H^2 r^2}{h^2 c^2} - \frac{m^2}{r^2} - \alpha \right\} R = 0, \quad (5)$$

in which α is the constant of separation. Eq. (4) states that the electrons moving parallel to the field act like free particles. If we introduce the quantity

$$W \equiv \frac{1}{2\mu c^2} (\mathcal{E}^2 - \mu^2 c^4) \quad (6)$$

into Eq. (5), the differential equation for R becomes identical in form with that deduced by Page from the non-relativistic wave equation. We have therefore, as in Page's development,

$$W = \left(s + \frac{1}{2} \right) h \left(\frac{\epsilon H}{2\pi \mu c} \right), \quad s = m + k = 0, 1, 2, \dots \quad (7)$$

The energy \mathcal{E} is thus completely quantized.³ We have also for the radius of curvature r of the deflected electrons⁴

$$r^2 = \frac{2\mu c^2 W}{\epsilon^2 H^2} \frac{x}{2s + 1} \quad (8)$$

in which $x \equiv (2\pi \epsilon H / hc) r^2$. Relativistic electrodynamics gives for the radius of curvature in terms of W as defined in Eq. (6)

$$r^2 = \frac{2\mu c^2 W}{\epsilon^2 H^2} \quad (9)$$

so that the same correction is introduced here by the wave mechanics treatment as in the non-relativistic case.

³ If the restriction of m to integral values is removed, the energy is no longer quantized. However, k remains integral in order that the series for R shall terminate, and the validity of subsequent calculations in both the non-relativistic and the relativistic case is not affected.

⁴ Page, Eq. (33).

THE CURRENT

It is necessary to deduce from Eq. (1) an expression for the current density. If the differential equation satisfied by $\bar{\psi}$ is multiplied by ψ and the result subtracted from the product of Eq. (1) and $\bar{\psi}$, we get

$$\bar{\psi} \nabla \cdot \nabla \psi - \psi \nabla \cdot \nabla \bar{\psi} - \frac{1}{c^2} \left(\bar{\psi} \frac{\partial^2 \psi}{\partial t^2} - \psi \frac{\partial^2 \bar{\psi}}{\partial t^2} \right) - \frac{4\pi i e}{hc} A \cdot (\bar{\psi} \nabla \psi + \psi \nabla \bar{\psi}) = 0. \quad (10)$$

Also

$$\bar{\psi} \nabla \cdot \nabla \psi - \psi \nabla \cdot \nabla \bar{\psi} = \nabla \cdot (\bar{\psi} \nabla \psi - \psi \nabla \bar{\psi}),$$

and

$$A \cdot (\bar{\psi} \nabla \psi + \psi \nabla \bar{\psi}) = \nabla \cdot (A \psi \bar{\psi}).$$

In addition we have

$$\begin{aligned} \bar{\psi} \frac{\partial^2 \psi}{\partial t^2} - \psi \frac{\partial^2 \bar{\psi}}{\partial t^2} &= \frac{\partial}{\partial t} \left\{ \bar{\psi} \frac{\partial}{\partial t} \left(\log \frac{\psi}{\bar{\psi}} \right) \right\} \\ &= -4\pi i \frac{\mathcal{E}}{h} \frac{\partial}{\partial t} (\psi \bar{\psi}) \end{aligned}$$

using Eq. (3). Eq. (10) may now be written

$$\frac{\epsilon h c^2}{4\pi i \mathcal{E}} \nabla \cdot (\bar{\psi} \nabla \psi - \psi \nabla \bar{\psi}) - \frac{4\pi i e}{hc} A \psi \bar{\psi} + \frac{\partial}{\partial t} (\epsilon \psi \bar{\psi}) = 0. \quad (11)$$

We identify Eq. (11) with the equation of continuity so that the current density is

$$j = \frac{\epsilon h c^2}{4\pi i \mathcal{E}} (\bar{\psi} \nabla \psi - \psi \nabla \bar{\psi}) - \frac{4\pi i e}{hc} A \psi \bar{\psi}. \quad (12)$$

This result is to be compared with the non-relativistic expression⁵

$$j = \frac{\epsilon h}{4\pi \mu i} (\bar{\psi} \nabla \psi - \psi \nabla \bar{\psi}) - \frac{4\pi i e}{hc} A \psi \bar{\psi}. \quad (13)$$

The factor $\epsilon h c^2 / 4\pi i \mathcal{E}$ appearing in Eq. (12) is, like that in Eq. (13), constant in the coordinates so that it does not affect the calculation of the mean radii of curvature averaged with respect to the current density. Hence the relativistic wave equation gives the same values for the mean radii of curvature as those calculated by Page.⁶

CONCLUSION

The relativistic wave equation leads to the same wave function for electrons in a uniform magnetic field as that determined from the Schrödinger equation.

⁵ Condon and Morse, *Quantum Mechanics*, p. 30.

⁶ Page, Eqs. (45) and (48).

The electron motion at right angles to the field is found to be completely quantized as before. The relativistic expression for the current density differs from the non-relativistic only in that \mathcal{E}/c^2 replaces μ ; this difference does not affect the calculation of the mean radii of curvature. We are led to a conclusion similar to that reached by the non-relativistic treatment: the classical relativistic relation between ϵ/μ and the mean radius of curvature upon deflection gives a value for ϵ/μ which is too large.

In conclusion the writer wishes to acknowledge his indebtedness to Professor Page for suggesting this problem and for his helpful criticism during its consideration.

THE HYPERFINE STRUCTURE OF S AND P TERMS OF
TWO ELECTRON ATOMS WITH SPECIAL
REFERENCE TO Li^+

BY G. BREIT AND F. W. DOERMANN

DEPARTMENT OF PHYSICS, NEW YORK UNIVERSITY

(Received October 28, 1930)

ABSTRACT

The proper form of the interaction energy between the nuclear magnetic moment and the electronic system of a many electron atom is discussed. The results of the Dirac equation for a single electron are taken as the guiding principle. A form for the interaction energy is set up as an expression involving Pauli's spin matrices. No convergence difficulties occur in the form here given.

The interaction Hamiltonian is applied to the 3S and 3P terms of two electron atoms for the case of Russell-Saunders coupling. An exact formula is derived for the resultant hyperfine structure of 3S terms and corrections to the Goudsmit Bacher formulas for 3P terms are given. It is shown that the Landé interval rule for 3S hyperfine structure levels is exact, and that therefore the ratio of intervals can be used to determine nuclear spin moments.

The formulas are applied to the Li^+ 5485Å line. Proper functions for S levels are worked out by the variational method and applied to the calculation of the magnetic moment of Li . With Schüler's wave-length data the nuclear g factor is 2.13 on the assumption that the nuclear spin is $3/2$.

The accuracy of the calculation is discussed. It is likely to be good to at least 2% in g . As a by-product of the calculation the lowest energy level of ortholithium has been computed as ≤ -1.1354 in units of the ionization potential of Li^{++} . The empirical value is -1.1358 .

INTRODUCTION

THE effect of nuclear spin on optical spectra has been treated mathematically by Casimir,¹ Fermi,² and Hargreaves.³ A somewhat more qualitative discussion has been given by Goudsmit and Bacher.⁴ In the first three of these discussions only one valence electron has been taken into account while in the last the more general problem of several valence electrons has been considered. Qualitatively the conclusions of Goudsmit and Bacher are doubtless correct. They do not pretend, however, to be exact quantitatively since the coupling between the nuclear spin and the electron system is supposed to be taking place only through one of the electrons—the most closely bound s electron. It is desirable to have a more exact quantitative theory taking into account the coupling of all electrons. This is particularly necessary if, say, two of them are s electrons. The desirability of having such a theory lies in its application to the absolute value of nuclear magnetic mo-

¹ See Goudsmit and Young, *Nature*, March 22, 1930.

² E. Fermi, *Zeits. f. Physik* **60**, 320 (1930).

³ J. Hargreaves, *Proc. Roy. Soc.* **124**, 568 (1929); **127**, 141 (1930); **127**, 407 (1930).

⁴ S. Goudsmit and R. F. Bacher, *Phys. Rev.* **34**, 1501 (1929).

ments. The observations of Schüler⁵ and of Granath⁶ show that the 3S level of Li^+ is split into three components under the action of the nuclear magnetic field and the separation between the two extreme components can be said to be 1.03 cm^{-1} . There seems to be no doubt that the three components in question are single. They are well and definitely resolved and so there is every reason to expect eventually a reliable determination of the nuclear magnetic moment from the determination of their frequency difference. The whole electron system consists in this case of only two electrons. The solution of the Schrodinger wave equation offers in this case a simpler problem than that of the heavy alkalis. An attempt at its approximate solution and its application to the calculation of the magnetic moment of the Li_7 nucleus is one of the objects of this paper. The other object is to formulate a theory for the interaction between the nucleus and the extranuclear electrons. A few words must be said as to why the formulation of such a theory is still subject to speculation.

For one electron an unambiguous result can be obtained by means of Dirac's equation. This has been done by Fermi and Casimir. The problem is not so clear when two or more electrons are discussed. There exists no satisfactory mathematical treatment of the relativistic two electron problem. It becomes necessary to use approximate equations. The simplest form for these is obtained through the introduction of Pauli's two row, two column spin matrices. It is known that interactions between electrons can be satisfactorily represented by means of these as long as the electronic velocities are not excessive. It might be expected that the interaction of nuclei and electrons can be reduced to the same basis. There is one important distinction between these two cases. The force between a nucleus and an electron is attractive while that between two electrons is repulsive. When an electron is close to the nucleus its velocity cannot be treated as small. For s electrons an important contribution to the interaction energy is due to the influence of the nucleus when the electron is very close to it. We have no reason to expect the interaction energy of the nucleus and the electron to be of the same form as that used for the approximate interaction energy of two electron spins. In fact it will be seen below that the two forms are different.

In order to derive the proper form of the interaction energy we consider first of all the one electron problem from the point of view of Dirac's equation, i.e. we write down the formulas found already in Fermi's paper. The two smaller Dirac wave-function components are then eliminated and an equation in the two large components is obtained. This equation involves Pauli's spin matrices and is equivalent to Dirac's for the discussion of the lighter nuclei. Having thus derived the proper interaction energy for one electron the result is generalized to the case of two or more. This forms the first section of the paper. In the second section the separations of spectral terms caused

⁵ H. Schüler, *Zeits. f. Physik* **42**, 487; (1927).

⁶ L. P. Granath, *Phys. Rev.* **36**, 1018, (1930), (letter). See also the forthcoming paper by P. Güttinger in the *Zeits. f. Physik* in which the feasibility of $i=3/2$ is explained and an approximate g value for the nucleus is derived.

by nuclear interactions are worked out. In the third the results of the second section are applied to Li^+

(I). THE INTERACTION ENERGY FOR ONE ELECTRON

We consider one electron of charge $-e$ under the influence of a single nucleus. The electrostatic potential due to the nucleus is A_0 . The electrostatic field due to the nucleus is central so that A_0 is a function only of r , the distance from the nucleus. The vector potential due to the nucleus is A . In special applications we take

$$A = \frac{[\mathbf{u} \times \mathbf{r}]}{r^3}. \quad (1)$$

With the abbreviations

$$\mathbf{p} = \mathbf{P} + (e/c)\mathbf{A}, \quad \mathbf{P} = (h/2\pi i)\nabla, \quad p_0 = E/c + (e/c)A_0 \quad (2)$$

Dirac's equation for a stationary state is

$$(\not{p}_0 + \alpha_1 \not{p}_1 + \alpha_2 \not{p}_2 + \alpha_3 \not{p}_3 + \alpha_4 mc)\psi = 0. \quad (3)$$

We suppose the α_s to be those given in Dirac's original paper. Equation (3) is, of course, a set of four equations in four ψ_s . It is convenient to eliminate ψ_1, ψ_2 as has been done by Darwin.⁷ The reader will verify that without approximations

$$\left\{ \not{p}_0 - mc - (\not{\mathbf{p}} \delta) \frac{1}{\not{p}_0 + mc} (\not{\mathbf{p}} \delta) \right\} \psi = 0 \quad (4)$$

where now the σ_k ($k=1, 2, 3$) are Pauli's matrices and the column matrix ψ contains only two rows: ψ_3, ψ_4 . Equation (4) must be satisfied for any solution of (3). It is not altogether equivalent to (3) if it is used for the determination of the eigenwerte E . In (3) it is required that $\psi_1^* \psi_1 + \psi_2^* \psi_2 + \psi_3^* \psi_3 + \psi_4^* \psi_4$ be integrable. Equation (4) is equivalent to (3) only if this last condition is added. If ordinary perturbation methods of quantum theory are applied to (4) it is more convenient to use the integrability of $\psi_3^* \psi_3 + \psi_4^* \psi_4$ as the restricting condition. As will be seen presently this circumstance is only of secondary importance. For the present we use (4) and derive its consequences as though $\psi_3^* \psi_3 + \psi_4^* \psi_4$ were integrable. Performing the operations indicated in the second term, using (2) and introducing the electric and magnetic fields by means of

$$\mathcal{E} = -\text{grad } A_0, \quad \mathcal{H} = \text{curl } A \quad (5)$$

we obtain

$$\begin{aligned} E = mc^2 - eA_0 + \frac{c^2}{E + mc^2 + eA_0} & \left[P^2 + \frac{e}{c}(PA + AP) + \frac{e^2}{c^2}A^2 + \frac{he}{2\pi c}(\mathcal{H}\delta) \right] \\ & + \frac{h}{2\pi i} \frac{c^2 e}{(E + mc^2 + eA_0)^2} \left[(\mathcal{E}P) + \frac{e}{c}(\mathcal{E}A) + i[\mathcal{E} \times P]\delta \right. \\ & \left. + i\frac{e}{c}[\mathcal{E} \times A]\delta \right] \end{aligned} \quad (6)$$

⁷ C. G. Darwin, Proc. Roy. Soc. 118, 654 (1928).

this is still an exact consequence of (2). At this point we make an approximation. The magnetic moment μ enters (6) only through A . It is sufficient to consider first order effects in μ and therefore in A . Quadratic terms in A are disregarded from here on. The perturbation energy may therefore be taken to be

$$H' = \frac{c^2}{E + mc^2 + eA_0} \left[\frac{e}{c} (PA + AP) + \frac{hc}{2\pi c} (\nabla \cdot \delta) \right] \\ + \frac{hc^2 e}{2\pi(E + mc^2 + eA_0)^2} \left[\frac{e}{c} [\mathcal{E} \times A] \cdot \delta - i \frac{e}{c} (\mathcal{E} A) \right]. \quad (7)$$

In this expression the first bracketed term corresponds to the ordinary interaction energy which is used in the ordinary discussions of two electrons. In the major portion of the configuration space eA_0 is negligible in comparison with $E + mc^2$ which itself is very nearly $2mc^2$. In this region the first bracketed term of (7) is on using (1)

$$H'' = \frac{e}{mc} \frac{M_{\mathbf{u}}}{r^3} + \frac{eh}{4\pi mc} \left\langle (\nabla \cdot \delta) (\nabla \cdot \mathbf{u}) \frac{1}{r} \right\rangle \quad (8)$$

where

$$M = [r \times P] \quad (8')$$

is the angular momentum operator and ∇ operates only on r^{-1} in the $\langle \rangle$. Only the expression (8) can be derived from the analogy of the electron and the nucleus to little magnets. For s terms the second term of (8) becomes indeterminate. A definite theory can be formulated by means of (8) if \mathbf{u} is defined as the limit of a spatial distribution of magnetic moment of very small extension in the limiting case of the extension approaching zero. It will be seen that the result of this limiting process is different from the application of the complete expression (7). For s electrons the result of (7) is (-2) times the result of (8). Hargreaves obtains zero for the perturbing effect of (8) in the case of s terms. He could have obtained any desired result since he has not defined the limiting process for the definition of the divergent integrals. Nevertheless his conclusion is correct. The exact effect of the first bracketed term of (7) is zero for s terms, the presence of eA_0 in the denominator making the radial integrals convergent. We see that the picture of the nucleus and electron as little magnets can be applied in this instance only with extreme caution.

If the field is central \mathcal{E} is perpendicular to A and the imaginary part of the second bracketed term of (7) disappears. Its real part containing $[\mathcal{E} \times A]$ is then combined advantageously with the second part of the first bracketed term containing $(\nabla \cdot \delta)$. The perturbation energy becomes

$$\begin{aligned}
H' = & \frac{(e/mc)(M\mathbf{y})}{1 + (E - mc^2 + eA_0)/2mc^2} \cdot \frac{1}{r^3} \\
& + \frac{hec/2\pi}{E + mc^2 + eA_0} \left\{ -\frac{(\mathbf{y}\delta)}{r^3} + \frac{3(\mathbf{r}\delta)(\mathbf{r}\mathbf{y})}{r^5} \right\} \\
& + \frac{(hec/2\pi)(e|\mathcal{E}|)}{(E + mc^2 + eA_0)^2} \left\{ \frac{(\mathbf{y}\delta)}{r^2} - \frac{(\mathbf{r}\delta)(\mathbf{r}\mathbf{y})}{r^4} \right\} \quad (9)
\end{aligned}$$

The perturbation energy (9) can now be applied to the calculation of the splitting of an s term. The first term of (9) can be disregarded because $M\psi=0$ for s terms and because the radial integration gives a finite result on account of eA_0 in the denominator. It is well known that the conservation of angular momentum makes it sufficient to calculate the average value of the coefficient of $\mu_z\sigma_z$ in the second line of (9). If this average be w and the nuclear spin k the s level is split into two components displaced by the amounts w , $(-1-k^{-1})w$ from the normal position.⁸ The first component is the one of higher fine quantum number $f=k+\frac{1}{2}$. The first term of the second line of (9) contributes nothing to the average, again on account of the presence of eA_0 in the denominator which makes the integration over r give a finite result. Using (5) we have on partial integration

$$w = - \int_0^\infty \frac{8\pi\mu}{3} \frac{hec}{2\pi} \frac{2\psi\psi'}{E + mc^2 + eA_0} dr \cong \frac{8\pi\mu}{3} \left(\frac{he}{4\pi mc} \right) \psi^2(0) \quad (10)$$

in agreement with Fermi.

The final result is not quite correct, but is very nearly so as long as the region in which $eA_0 < mc^2$ is negligible in comparison with the spatial extension of $\psi\psi'$ and as long as $E - mc^2 < mc^2$. Both of these conditions are satisfied by light nuclei. The difference between (10) and the correct result is of the order of the square of the fine structure constant.⁸ This example shows that the substitution of the integrability of $\psi_3^*\psi_3 + \psi_4^*\psi_4$ for the integrability of $\psi_1^*\psi_1 + \psi_2^*\psi_2 + \psi_3^*\psi_3 + \psi_4^*\psi_4$ is safe for the present purpose. We see also that the "empirical terms" used by Hargreaves are essentially the same as the terms derived above from Dirac's equation.

If instead of using Dirac's equation we were to use the perturbation energy (8) we should run into convergence difficulties. These may be avoided by endowing the magnetization of the nucleus with a finite spatial extension, say, by supposing that the magnetization is spread uniformly through the volume of a very small sphere. The first term then has no effect. The second gives rise to

$$w = \frac{\mu eh}{4\pi mc} \int \frac{\psi^2(P)}{3} \int f(P') \Delta_P \left(\frac{1}{r_{PP'}} \right) dV_P dV_P$$

⁸ See e.g. G. Breit, Phys. Rev. **35**, 1447 Equations (2), (3) (1930).

where P' refers to a point of the magnetization distribution, and $f(P')\mu dV_{P'}$ is the amount of magnetization in the element of volume $dV_{P'}$. The above double integral is easily evaluated if $I = \int f(P') (1/r_{PP'}) dV_{P'}$ is interpreted as the electrostatic potential at the point P due to a charge distribution of density $f(P')$. The total charge is $1 = \int f(P') dV_{P'}$. Outside the nucleus $\Delta_P I = 0$. Inside the nucleus Poisson's equation gives

$$\Delta_P I + 4\pi f(P) = 0,$$

and therefore

$$\int (\Delta_P I) dV_P = -4\pi.$$

In the limit of a very concentrated distribution $f(P')$ we may set therefore

$$\Delta_P \int f(P') \frac{1}{r_{PP'}} dV_{P'} = -4\pi \delta(P) \quad (11)$$

and we obtain then

$$w = -\frac{4\pi\mu}{3} \frac{ch}{4\pi mc} \psi^2(0). \quad (12)$$

This result must be multiplied by (-2) in order to give Fermi's result (10). The magnetic doublet model and Dirac's equation give in this case widely different results. The present evidence is that Dirac's equation is to be preferred so that (10) is the correct result.

The perturbation energy (9) must now be generalized to include the case of two or more electrons. As has been explained in the introduction we are unable to start with a relativistic treatment of two electrons and we must instead use (9) as an indication for the proper generalization. A number of possible generalizations could be made. Thus one could go back to (7) and use the field quantities \mathcal{E}, \mathcal{H} taking \mathcal{E}_1 to be the electric intensity at x_1, y_1, z_1 , due to the nucleus and also due to electron 2. Or else one may take $\mathcal{E}_1, \mathcal{H}_1$ to be due only to the nucleus. For the first choice we would have to prove that the imaginary term in (7) contributes nothing to the result. Also some generalization of A_0 would have to be made. Having no basis for forming such a generalization we make instead

$$H' = H_1' + H_2' \quad (13)$$

where H_1' is the result of using x_1, y_1, z_1, δ_1 , instead of x, y, z, δ in all of the terms of (9). The coupling between the nucleus and each electron is thus represented by a term in the Hamiltonian which depends only on the coordinates of that electron.

It may also be shown that for 3S terms the alternative generalization based on (7) leads to the same final result as (13) provided $\mathcal{E}_i = -\text{grad } A_{0i}$ ($i=1, 2$). The proof is not of sufficient interest to be quoted.

II. CALCULATION OF PERTURBATIONS IN TERMS OF SCHROEDINGER ψ IN CONFIGURATION SPACE

We use the method of sums.⁹ Consider first the 3S terms. It is convenient to define the following spin functions

$$S_1 = S_\alpha^1 S_\alpha^2, S_0 = 2^{-1/2}(S_\alpha^1 S_\beta^2 + S_\alpha^2 S_\beta^1), S_{-1} = S_\beta^1 S_\beta^2. \quad (14)$$

The upper indices refer to electrons 1 and 2. The functions S_α, S_β are as usual the column matrices $\begin{pmatrix} 1 \\ 0 \end{pmatrix}, \begin{pmatrix} 0 \\ 1 \end{pmatrix}$. The upper row corresponds to the spin being in the positive direction of the z axis. In the case of Russell-Saunders coupling there are three unperturbed functions for the 3S state. Each of these is the product of a coordinate function and of one of the three functions (14). The coordinate function ψ depends only on the shape and size of the electronic triangle and not on its orientation.¹⁰ The wave-function of the coupled system nucleus+electrons contains also the angular momentum specification of the nucleus. Denoting the angular momentum of the nucleus by k there are $2k+1$ nuclear functions

$$N_k = \begin{pmatrix} 1 \\ 0 \\ 0 \\ \vdots \\ 0 \end{pmatrix}, N_{k-1} = \begin{pmatrix} 0 \\ 1 \\ 0 \\ \vdots \\ 0 \end{pmatrix}, \dots N_{-k} = \begin{pmatrix} 0 \\ 0 \\ \vdots \\ 0 \\ 1 \end{pmatrix} \quad (15)$$

The vector matrix \mathbf{u} operates on these. The matrices for the components of \mathbf{u} we take to be the same as Fermi's. Among these the only matrix having diagonal elements is μ_z . It is a diagonal matrix with elements $\mu(1, k-1/k, \dots -1)$. The complete system of $3(2k+1)$ unperturbed eigenfunctions can be represented by means of

$$u_i^m = S_i N^m \psi \begin{pmatrix} i = 1, 0, -1 \\ m = k, k-1, \dots -k \end{pmatrix} \quad (16)$$

It is most conveniently arranged in a table:

Angular momentum:	$k+1$	k	$k-1$	-----	$-k+1$	$-k$	$-k-1$
	u_1^k	u_1^{k-1}	u_1^{k-2}	-----	u_{-1}^{-k}		
		u_0^k	u_0^{k-1}	-----	u_0^{-k+1}	u_0^{-k}	
			u_{-1}^k	-----	u_{-1}^{-k+2}	u_{-1}^{-k+1}	u_{-1}^{-k}

In Slater's method we are concerned only with diagonal elements of the perturbation energy matrix. The functions N^m are normal orthogonal and so are the S_i . We are therefore concerned only with coefficients of μ_z . This shows that the combined effect of the perturbations due to $\mathbf{M}_1\mathbf{u}$ and $\mathbf{M}_2\mathbf{u}$ is zero. In fact this perturbation is of the form $(\mathbf{B}_1 + \mathbf{B}_2)\mathbf{u}$. It, by itself, commutes with the total angular momentum. When it operates on u_1^k it gives $(B_{1z} + B_{2z})\mu u_1^k$ as well as other terms which do not count in the calculation

⁹ J. C. Slater, Phys. Rev. **34**, 1293 (1929).

¹⁰ E. Wigner, Zeits. f. Physik **43**, 624 (1927).

of the diagonal element $\int u_1^{*k} H' u_1^k$. The operation on u_{-1}^{-k} gives $-(B_{1z} + B_{2z})\mu u_{-1}^{-k}$. Thus $\int u_1^{*k} H' u_1^k = -\int u_1^{*k} H' u_1^k = 0$. The term of highest fine structure quantum number is therefore undisturbed. Considering the other functions in turn we see that there is no splitting due to terms not involving δ_1, δ_2 . This may also be verified by a short calculation of the average value of $A(r_1)\partial/\partial\phi_1 + A(r_2)\partial/\partial\phi_2$ in the six dimensional configuration space $x_1 \cdots z'_2$ for the case of $\psi = \psi(r_1, r_2, \cos\theta_{12})$. The terms in δ_1, δ_2 are easily treated if it is observed that, so far as the calculation of diagonal matrix elements is concerned, the symmetric operator $A_1\delta_1 + A_2\delta_2$ gives rise only to the following terms

$$(A_1\delta_1 + A_2\delta_2)(S_1, S_0, S_{-1}) \rightarrow (A_{1z} + A_{2z})(S_1, 0, -S_{-1}). \quad (17)$$

Letting now the energy perturbations of the three levels be w_1, w_2, w_3 , in the order of decreasing fine quantum numbers, we have from the first three columns of the table

$$\begin{aligned} w_1 &= \int \psi^*(A_{1z} + A_{2z})\psi, \quad w_1 + w_2 = \frac{k-1}{k}w_1, \quad w_1 + w_2 + w_3 \\ &= \left(-1 + \frac{k-2}{k}\right)w_1 \\ w &= w_1 \left(1, -\frac{1}{k}, -\frac{k+1}{k}\right). \end{aligned} \quad (18)$$

Here

$$A_{1z} = \frac{hec}{2\pi(2mc^2 + Ze^2/r_1)^2} \left\{ 2mc^2 \left(\frac{3z_1^2}{r_1^5} - \frac{1}{r_1^3} \right) + \frac{2Ze^2}{r_1^6} z_1^2 \right\}.$$

Performing one of the integrations over 1 for A_{1z} and over 2 for A_{2z} and then using the symmetry of ψ^2 in 1 and 2 we have

$$\begin{aligned} w_1 &= 16\pi/3 \mu\mu_0 \int \psi^2(0, 0, 0; x, y, z) dx dy dz \\ &(\mu_0 = eh/4\pi mc > 0). \end{aligned} \quad (19)$$

The only approximations made in deriving (19) are: (1) a definite case of Russell-Saunders coupling, (2) neglect of the square of the fine structure constant. The integral in (19) represents the probability of one electron being in a unit volume near the nucleus. The connection of this result with Goudsmit and Bacher is seen if one writes

$$\psi = (1/2^{1/2}) [\phi_n(q_1)\phi_m(q_2) - \phi_n(q_2)\phi_m(q_1)]. \quad (20)$$

If n refers to the inner electron state

$$\begin{aligned} \int \psi^2(0, q) dq &\cong \frac{1}{2} \phi_n^2(0), \text{ and} \\ w_1 &= (8\pi/3) \mu\mu_0 \phi_n^2(0). \end{aligned} \quad (21)$$

In this approximation (19) (18) are identical with the corresponding formulas of Goudsmit and Bacher. A discussion of the difference between (19) and (21) will be given in the third section.

If $k=1/2$ formula (18) remains correct if it is read from left to right and the last term is omitted. This is obvious from the order in which w_1, w_2, w_3 have been derived.

We may now consider 3P terms. There are three linearly independent coordinate eigenfunctions, each of these combining with the three spin functions (14) and thus forming a set of nine functions. The coordinate functions may be called $\psi_1, \psi_0, \psi_{-1}$ corresponding to components 1, 0, -1 of the orbital angular momentum in the z direction. The functions $\psi_i S_k$ do not themselves correspond to definite parts of the 3P term but certain linear combinations of them do. These linear combinations are

$$\begin{aligned} {}^3P_0 &: 3^{-1/2}(\psi_1 S_1 - \psi_0 S_0 + \psi_{-1} S_{-1}) \\ {}^3P_1 &: 2^{-1/2}(\psi_1 S_0 - \psi_0 S_1), 2^{-1/2}(\psi_1 S_{-1} - \psi_{-1} S_1), 2^{-1/2}(-\psi_{-1} S_0 + \psi_0 S_{-1}) \quad (22) \\ {}^3P_2 &: \psi_1 S_1, 2^{-1/2}(\psi_0 S_1 + \psi_1 S_0), 6^{-1/2}(\psi_1 S_{-1} + 2\psi_0 S_0 + \psi_{-1} S_1), \\ &2^{-1/2}(\psi_0 S_{-1} + \psi_{-1} S_0), \psi_{-1} S_{-1}. \end{aligned}$$

The functions $\psi_1, \psi_0, \psi_{-1}$ are supposed to be chosen so as to transform themselves under rotations as $2^{-1/2}(x+iy), -z, 2^{-1/2}(-x+iy)$. The set of functions (22) is convenient because each one of them corresponds to a definite value of the angular momentum in the direction of the z axis. There is no splitting for the 3P_0 and we consider first the 3P_1 term. The nucleus is brought in by means of the N_k just as in the case of 3S terms. The table which led to (18) is still correct, though now the functions u_l^m are different. Equation (18) still is valid although (19) is different. The validity of (18) is of course a consequence of the "cosine" law of interaction with the nucleus. It is very easy to prove this by writing $u_l^m = v_l N^m$. Denoting the coefficient of μ_z in the interaction energy by a_z we have on applying the diagonal sum theorem from both ends of the table $w_1 = I_1 = -I_{-1}$; $w_2 + w_1 = (k-1)/k I_1 + I_0 = -((k-1)/k) I_{-1} - I_0$ where $I_l = \mu \int v_l^* a_z v_l$. This shows that $I_0 = 0$ and (18) follows at once. It remains to determine w_1 . We may omit the correction in the denominator of the first term of (9). The second two terms are easily combined and we have

$$w_1 = (e\mu/mc) \int v_1^* (r_1^{-3} M_{1z} + r_2^{-3} M_{2z}) v_1 + \mu \int v_1^* (B_1 \delta_1 + B_2 \delta_2) v_1 \quad (23)$$

where

$$B_1 = \frac{hec}{2\pi \{2mc^2 + (Ze^2/r_1)\}^2} \left\{ 2mc^2 \left(3z_1 \frac{r_1}{r_1^5} - \frac{\zeta}{r_1^3} \right) + \frac{2Ze^2}{r_1^6} z_1 r_1 \right\}. \quad (24)$$

Here ζ is a unit vector along the z axis. B_2 is obtained from B_1 on substituting z_2, r_2 everywhere for z_1, r_1 . Performing the operations δ_1, δ_2 in (23) we have on letting

$$B = B_1 + B_2 \quad (25)$$

$$w_1 = \frac{e\mu}{2mc} \int \psi_1^* (r_1^{-3} M_{1z} + r_2^{-3} M_{2z}) \psi_1 + \frac{e\mu}{2mc} \int \psi_0^* (r_1^{-3} M_{1z} + r_2^{-3} M_{2z}) \psi_0 \\ + (\mu/2) \int \{ \psi_0^* B_z \psi_0 - \psi_1^* 2^{-1/2} (B_x + iB_y) \psi_0 - \psi_0^* 2^{-1/2} (B_x - iB_y) \psi_1 \} \quad (26)$$

This form for w_1 is correct quite regardless of any approximations which may be made as to the representation of the coordinate wave-functions $\psi_1, \psi_0, \psi_{-1}$. The most general forms of these functions are known and formula (26) is capable of giving exact results as long as the hypothesis of Russell-Saunders coupling applies.¹¹ In practical applications it appears to be unnecessary to use the general expressions for $\psi_1, \psi_0, \psi_{-1}$ and it will usually be sufficient to use the approximate representation of these coordinate functions as antisymmetric combinations of products of functions involving the coordinates of only one particle. We may then write

$$\begin{aligned} \psi_1 &= (3^{1/2}/4\pi) (F \sin \theta_1 e^{i\phi_1} - \tilde{F} \sin \theta_2 e^{i\phi_2}) \\ \psi_0 &= - (6^{1/2}/4\pi) (F \cos \theta_1 - \tilde{F} \cos \theta_2) \\ \psi_{-1} &= - (3^{1/2}/4\pi) (F \sin \theta_1 e^{-i\phi_1} - \tilde{F} \sin \theta_2 e^{-i\phi_2}) \end{aligned} \quad (27)$$

with

$$\begin{aligned} F &= f_1(r_1) f_2(r_2); \quad 4 \int F^2 r_1^2 r_2^2 dr_1 dr_2 = 1 \\ \tilde{F} &= f_1(r_2) f_2(r_1). \end{aligned} \quad (27')$$

The functions in (27) are chosen so as to give (22). The radial function f_1 is characteristic of the p state while f_2 describes the s state. If a single electron were in that s state it would be described by a normalized function ψ_s . Clearly

$$4\pi\psi_s(0)^2 = f_2(0)^2 / \left(\int f_2(r_2)^2 r_2^2 dr_2 \right). \quad (28)$$

It is now found on substitution of (27) (27')

$$(e/2mc) \int \psi_1^* (r_1^{-3} M_{1z} + r_2^{-3} M_{2z}) \psi_1 = (eh/4\pi mc) \overline{(r_1^{-3})} \quad (29)$$

where

$$\overline{(r_1^{-3})} = 4 \int F^2 r_1^{-3} r_1^2 r_2^2 dr_1 dr_2 \quad (29')$$

is the average of r^{-3} for a p electron described by a radial function f_1 . Also in

$$\frac{1}{2} \int \psi_0^* B_z \psi_0$$

¹¹ E. Wigner, reference 10; G. Breit, Phys. Rev. 35, 569 (1930).

we need

$$(3/16\pi^2) \int F^2 \cos^2 \theta_1 B_{1z} = (1/5)\mu_0 \overline{(r_1^{-3})} - (1/20)\mu_0 \overline{(r_1^{-4})} (Ze^2/mc^2).$$

A numerical estimate shows that the term in $\overline{r_1^{-4}}$ is much too small ordinarily to be worried about and this as well as similar terms will be neglected here. The most important contribution to (26) comes from terms of the type

$$(3/16\pi^2) \int F^2 \cos^2 \theta_1 B_{2z} = (2\pi/3)\mu_0 \psi_s(0)^2$$

using (28). The remaining contributions are from

$$-\frac{1}{2} \int \{\psi_1^* 2^{-1/2} (B_x + iB_y) \psi_0 + \psi_0^* 2^{-1/2} (B_x - iB_y) \psi_1\} = (3/5)\mu_0 \overline{(r_1^{-3})}.$$

It is thus found on substituting all the integrals into (26) that

$$w_1 = \mu\mu_0 \{ (4\pi/3) \psi_s(0)^2 + 2 \overline{(r^{-3})}_p \}. \quad (30)$$

This completes the calculation for the 3P_1 level.

For the 3P_2 term we have five electronic functions given by the last row of (22). These may be designated as v_l and the complete specification of the system is given by $u_l^m = v_l N^m$. Only now $l = (2, 1, 0, -1, -2)$ and the v_1, v_0, v_{-1} are, of course, now different from those just used for the 3P_1 term. In this case the table following equation (16) must be extended so as to have five rows. The method of sums does not suffice now to give all of the separation ratios. Denoting as before the coefficient of μ_z by a_z and letting $I_l = \mu \int v_l^* a_z v_l$ the method of sums shows directly that $I_2 = -I_{-2}$, $I_1 = -I_{-1}$, $I_0 = 0$ but it does not establish a relation between I_1 and I_2 . A calculation is easily made however for both I_1 and I_2 . We have:

$$I_2 = \frac{\mu e}{mc} \int \psi_1^* (r_1^{-3} M_{1z} + r_2^{-3} M_{2z}) \psi_1 + \mu \int \psi_1^* B_z \psi_1. \quad (31)$$

Substitution of the integrals used in deriving (30) gives

$$I_2 = \mu\mu_0 [(8\pi/3) \psi_s(0)^2 + (8/5) \overline{(r^{-3})}_p]. \quad (32)$$

Also

$$\begin{aligned} I_1 = & (\mu e/2mc) \int \psi_1^* (r_1^{-3} M_{1z} + r_2^{-3} M_{2z}) \psi_1 \\ & + (\mu/2) \int \{\psi_0^* B_z \psi_0 + \psi_1^* 2^{-1/2} (B_x + iB_y) \psi_0 + \psi_0^* 2^{-1/2} (B_x - iB_y) \psi_1\} \end{aligned} \quad (33)$$

so that I_1 can be obtained directly from (30) by subtracting $(6/5) \overline{(r^{-3})}_p$ inside the parenthesis. We have

$$I_1 = \mu\mu_0[(4\pi/3)\psi_s(0)^2 + (4/5)(\overline{r^{-3}})_p] = I_2/2. \quad (35)$$

Using the sum theorem we obtain for the first order energy perturbations

$${}^3P_2 = \mu\mu_0[(4\pi/3)\psi_s(0)^2 + (4/5)(\overline{r^{-3}})_p] \left(2, \frac{k-2}{k}, -\frac{3}{k}, -\frac{k+3}{k}, -2\frac{(k+1)}{k} \right) \quad (36)$$

which may be compared with

$${}^3P_1 = \mu\mu_0[(4\pi/3)\psi_s(0)^2 + 2(\overline{r^{-3}})_p] \left(1, -\frac{1}{k}, -\frac{k+1}{k} \right) \quad (36')$$

$${}^3S_1 = \mu\mu_0(8\pi/3)(1 + \epsilon)\psi_s(0)^2 \left(1, -\frac{1}{k}, -\frac{k+1}{k} \right). \quad (36'')$$

Here ϵ is a fractional correction due to the difference between (19) and (21).

III. APPLICATION TO THE SPECTRUM OF Li^+

The pattern of the ${}^3S-{}^3P$ line of Li^+ which has been observed by Schüler and Granath will now be considered using formulas (36) (36') (36''). The quantities $(\overline{r^{-3}})_p$ and ϵ are of the nature of correction terms and neglecting them these formulas become identical with those of Goudsmit and Young. The $\psi_s(0)^2$ for a hydrogenic s electron is related to the fine structure constant by

$$2\pi\psi_s(0)^2\mu_0^2 = R\alpha^2Z^3/n^3 \quad (37')$$

which is convenient for calculation. For $Z=3$ and $n=1$ we have in agreement with Goudsmit and Young $(8/3)R\alpha^2Z^3/1840n^3 = 0.228 \text{ cm}^{-1}$. Letting $(1840\mu/\mu_0) = g(k)$ we have therefore the approximate formulas:

$$\begin{aligned} {}^3P_2 &= 0.228(g(k)/4) \left(2, \frac{k-2}{k}, -\frac{3}{k}, -\frac{k+3}{k}, -2\frac{(k+1)}{k} \right) \\ {}^3P_1 &= 0.228(g(k)/4) \left(1, -\frac{1}{k}, -\frac{k+1}{k} \right) \\ {}^3S_1 &= 0.228(g(k)/2) \left(1, -\frac{1}{k}, -\frac{k+1}{k} \right) \end{aligned} \quad (37)$$

which are essentially the same as those of Goudsmit and Bacher. An application of (37) and the calculation of relative intensities of the different components of the pattern can be made for different values of k . As has been pointed out by Granath the experimental pattern seems to agree best with $k=3/2$. Most of the pattern appears to have a complicated structure which is due to unresolved components. Only the group of lines due to transitions from 3P_0 to 3S_1 is simple and consists of three fairly well resolved lines. It seems difficult at present to draw any definite conclusions from the other parts of the pattern on account of lack of resolution. We consider it more im-

portant therefore to have an accurate calculation of the correction factor $1 + \epsilon$ in (36'') than the exact evaluation of (36) (36'). There is, of course, no difficulty in evaluating $(\overline{r^{-3}})_p$. In the present instance the correction due to $(\overline{r^{-3}})_p$ amounts to about 1 percent change of scale for 3P_2 and 2 percent for 3P_1 .

In order to calculate the factor $1 + \epsilon$ in formula (36'') we must use the exact formula (19) which differs from (37) by the correction factor

$$1 + \epsilon = 2 \int \psi^2(0, q) dq / \psi_{1s}(0)^2. \quad (38)$$

The integral in the numerator is here the same as the integral in (19) the letter q having been written collectively for (x, y, z) . The denominator of (38) is the $\psi_{1s}(0)^2$ of (37') for $n=1, Z=3$.

We have tried a number of approximate forms for $\psi(q_1, q_2)$ using the variational method for the calculation of the term value of the 3S state and then, having adjusted the constants to satisfy the minimizing requirement, calculated by means of the minimized functions the corresponding value of $1 + \epsilon$. In all cases ϵ is a small quantity. Some of the functions give eigenwerte in good agreement with the spectroscopic term value while others give considerably too small absolute values of the eigenwert. It is of interest to see the results of the bad as well as the good functions. A very rough approximation to the solution can be obtained by tentatively expressing ψ as an antisymmetric combination of products of hydrogenic functions in the field of a certain nuclear charge. This charge is deliberately taken to be the same for both functions. The two functions entering are orthogonal and the calculation is very easy, only the common scale of the two functions being varied. In terms of the ionizing potential of Li^{++} the energy of the 2^3S state is known to be $\lambda = -1.1358$. In the same units the above function gives $\lambda = -1.1279$ and $1 + \epsilon = 0.96$. This is a deliberately poor function, possessing only one adjustable constant and giving a relatively poor agreement with the experimental λ . Hylleraas¹² has considered the 3S terms of two electron spectra particularly for He. In his paper functions are tried for the ortho state of He which may be called the one and the two term approximations. These give for He $\lambda = -1.0855$ and $\lambda = -1.0871$. The values of $1 + \epsilon$ for He would be 1.009 and 1.04 respectively. For Li^+ we have used only the one term function of Hylleraas giving $\lambda = -1.1337$, $1 + \epsilon = 1.02(6)$. From the analogy to He one would suppose that the two term function of Hylleraas would give an appreciably larger ϵ . The calculations with the two term function of Hylleraas are complicated, however, and we have found it more convenient to use another three constant function. It has also been possible to correct the first function of Hylleraas by a numerical method. In the latter case there is no definite way of using the eigenwert agreement as a check on the calculations and the procedure itself is somewhat arbitrary. Nevertheless it appears to be definite enough to show that $1 + \epsilon > 1.02$ and

¹² Hylleraas, Zeits. f. Physik 54, 347 (1929).

that $1 + \epsilon \approx 1.06$. The numerical method is based on the following consideration. In the units of length ($\hbar^2/8\pi^2mZe^2$) and energy ($RhcZ^2$) used by Hylleraas the differential equation to be satisfied by ψ is

$$\left[\frac{\partial^2}{\partial r_1^2} + \frac{2}{r_1} \frac{\partial}{\partial r_1} + \frac{\partial^2}{\partial r_2^2} + \frac{2}{r_2} \frac{\partial}{\partial r_2} + \left(\frac{1}{r_1^2} + \frac{1}{r_2^2} \right) \frac{1}{\sin \theta} \frac{\partial}{\partial \theta} \left(\sin \theta \frac{\partial}{\partial \theta} \right) + \frac{\lambda}{4} + \frac{1}{r_1} + \frac{1}{r_2} - \frac{1}{Zr_{12}} \right] \psi = 0. \quad (39)$$

The angle θ is the angle between the radii r_1, r_2 and r_{12} is the distance between electrons 1 and 2. A certain approximation to the exact solution can be obtained by supposing that ψ is a function only of r_1 and r_2 the angle θ being not very important for this particular state. The one term function of Hylleraas does not involve θ or r_{12} and is therefore an approximation of the above type. A systematic neglect of the dependence on θ leads of course to a definite eigenwert and to a definite eigenfunction if the variational method of solution is used. Substituting a general function $\psi(r_1, r_2)$ into the variational equation it is easy to obtain a differential equation for this ψ . This equation is

$$\left[\frac{\partial^2}{\partial r_1^2} + \frac{2}{r_1} \frac{\partial}{\partial r_1} + \frac{\partial^2}{\partial r_2^2} + \frac{2}{r_2} \frac{\partial}{\partial r_2} + \frac{\lambda}{4} + \frac{1}{r_1} + \frac{1}{r_2} - \frac{1}{Z\rho} \right] \psi = 0$$

$$\begin{aligned} \rho &= r_1 \text{ if } r_1 > r_2 \\ \rho &= r_2 \text{ if } r_1 < r_2. \end{aligned} \quad (39')$$

We assume for the present that the eigenvalue of λ and the function ψ of (39') is a sufficient approximation to λ and ψ of (39). For the 3S state ψ is antisymmetric in r_1, r_2 and vanishes therefore at $r_1 = r_2$. It may be represented in two dimensions. Along the axis of $r_2 = 0, \rho = r_1$. The last three terms behave as $1/r_2$. If ψ and its first and second derivatives are finite on this axis we must require in order to satisfy (39') that the term $2/r_2 \partial \psi / \partial r_2 + \psi / r_2$ should be finite i.e.

$$\left(\frac{\partial \log \psi}{\partial r_2} \right)_{r_2=0} = -\frac{1}{2}. \quad (40)$$

Any trial ψ can be checked qualitatively by means of (40) and it is important to require that (40) be satisfied in the region of large numerical values of ψ . This is especially advisable in the present instance because the result we wish to obtain is proportional to $\int \psi(r_1, 0)^2 r_1^2 dr_1$ and depends primarily on the relative values of ψ^2 at $r_2 = 0$ as compared with its value at other points of the r_1, r_2 plane.

The one term function of Hylleraas was tested by means of (40) and it was found that although the logarithmic derivative was fairly close to its correct value the differences were greater than could be desired. At a certain point of the r_1 axis (40) is satisfied exactly. This point lies at a higher value of $r_1 = r_{10}$ than that which corresponds to the maximum of $r_1^2 \psi^2$. At the maxi-

imum ψ does not decrease rapidly enough in absolute value with increasing r_2 . The dependence of ψ on r_2 has therefore been corrected by a numerical procedure so as to satisfy (40) in most of the important region. For values of $r_1 < r_{10}$ this was done by fitting the exponential curve $Ce^{-r_1/2}$ to the curve of ψ against r_2 . The fit was made quite accurate by calculating logarithmic derivatives $\partial \log \psi / \partial r_2$ of the Hylleraas function and choosing such an r_2 for every r_1 that $\partial \log \psi / \partial r_2 = -\frac{1}{2}$. This procedure is of course somewhat arbitrary because $e^{-r_1/2}$ is not an exact solution of the wave equation and because $\partial \log \psi / \partial r_2 = -\frac{1}{2}$ only at $r_2 = 0$. Nevertheless, as long as the correction applies only to a small region in the neighborhood of $r_2 = 0$ it is essentially correct. For values of $r_1 > r_{10}$ it is impossible to correct the function

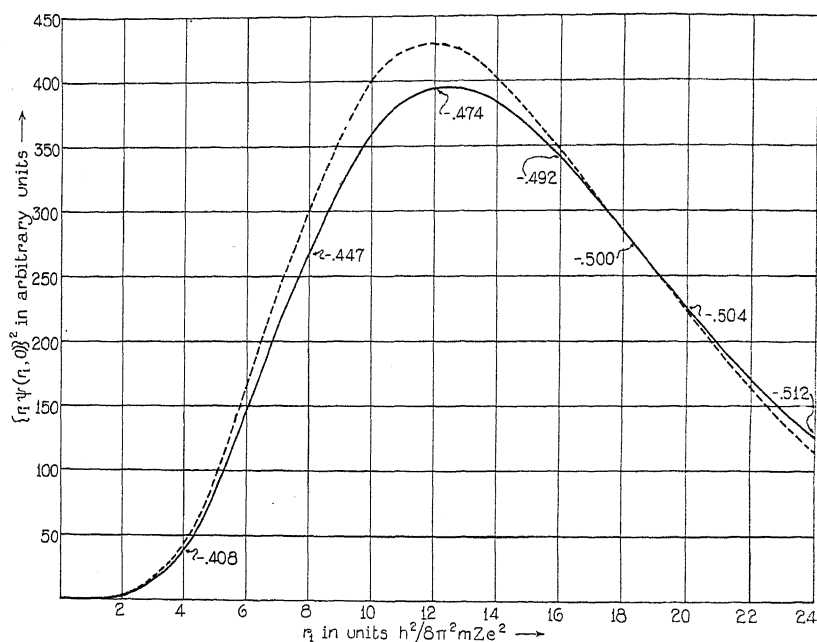


Fig. 1. The dotted curve is computed from the corrected, the full drawn curve from the uncorrected Hylleraas function. The values of $\partial \log \psi / \partial r_2$ are indicated along the curve.

by means of an exponential curve. The correction was made, therefore, by choosing for a given $r_1 = r_1'' > r_{10}$ a corresponding value of $r_1 = r_1' < r_{10}$ for which $\partial \log \psi / \partial r_2$ deviates from $-1/2$ by a numerically equal amount. The known corrections to ψ for $r_1 = r_1'$ and different values of r_2 were now applied to $r_1 = r_1''$ for the same values of r_2 . This means that the deviation of $\partial \log \psi / \partial r_2$ was taken as the criterion of the magnitude of the correction to ψ . The whole procedure has of course a meaning only as long as the corrections are small and can be applied therefore only in the region around the maximum of $r_1 \psi(r_1, 0)$. This maximum is at $r_1 = 12.5$ in the units of length used by Hylleraas. The correction becomes zero at $r_1 = 18.5$. The values of $(r_1 \psi(r_1, 0))^2$ at these points are 397.5 and 270 on an arbitrary scale. The relation of the corrected and the uncorrected $(r_1 \psi(r_1, 0))^2$ curves is shown in the Fig. 1.

Using these corrections the changes in $\int r_1^2 \psi^2(r_1, 0) dr_1$ and $\iint r_1^2 r_2^2 \psi^2(r_1, r_2) dr_1 dr_2$ were calculated. The corrections were taken into account only from $r_1=0$ to $r_1=24$. The resultant change in

$$\int r_1^2 \psi^2(r_1, 0) dr_1 \bigg/ \iint r_1^2 r_2^2 \psi^2(r_1, r_2) dr_1 dr_2$$

came out to be 4 per cent. The value of $1+\epsilon$ for the one term Hylleraas function is 1.02; the corrected value of $1+\epsilon$ is 1.06.

Our correction procedure may of course be criticized on account of its arbitrariness. It must be remarked however that the sign and the order of magnitude of the result depend primarily on the fact that an increase in the absolute value of ψ is required at the maximum by the logarithmic derivative condition. Thus even though mathematically the procedure lacks rigor we believe that for the present problem it is essentially correct.

Finally we have calculated the result by the variational method using the following trial function.

$$\psi = \phi(kr_1, kr_2); \phi = (r_1 - c)e^{-(a/2)r_1 - (b/2)r_2} - (r_2 - c)e^{-(a/2)r_2 - (b/2)r_1}.$$

This function is easily adapted to the variational procedure. It contains three constants a, b, c . The constants c and k can be treated algebraically in the variational procedure. Extensive arithmetic need be done only in connection with different values of a . The reason for this simplification is that the minimized value of k is always close to $k=1$ if $b=1$, the difference from 1 being usually of the order of 1 percent or less. The first step is to choose a value of a and to take $b=1$. Supposing that $k=1$ the minimizing is done for c analytically. Taking this value of c the result is minimized for k analytically. It is then usually unnecessary to minimize for c again because $k \approx 1$. The procedure is repeated for different values of a and the absolute minimum of λ is fixed by interpolation.¹³ We reproduce the final formulas for the minimizing procedure because they may be found useful in other connections. For $k=1$

$$\lambda/4 = (M - L_0 + L_1)/N \quad (41)$$

where

$$\begin{aligned} M = & 8a^{-3}b^{-3} + 24b^{-1}a^{-5} - 12a^{-1}b^{-1}\beta^{-7}(3\beta^{-1} - 2a^{-1}) \\ & - c[4a^{-2}b^{-3} + 12a^{-4}b^{-1} - 8ab\beta^{-6}(3\beta^{-1} - a^{-1})] \\ & + c^2[2a^{-1}b^{-3} + 2a^{-3}b^{-1} - 4ab\beta^{-6}]; \beta = (a+b)/2 \end{aligned} \quad (42)$$

$$\begin{aligned} L_0 = & 24a^{-4}b^{-3} + 48a^{-3}b^{-2} - 48\beta^{-7} - c[16a^{-3}b^{-3} + 24a^{-4}b^{-2} - 40\beta^{-6}] \\ & + c^2[4a^{-2}b^{-3} + 4a^{-3}b^{-2} - 8\beta^{-5}] \end{aligned} \quad (42')$$

¹³ The trick of minimizing for k is the same as that used by Hylleraas, ref. 12, and amounts physically to satisfying the requirement of having the kinetic energy $= -(1/2)$ times the potential energy in a system with Coulomb forces.

$$\begin{aligned}
ZL_1 = & 24[a^{-4}b^{-2}(a+b)^{-1} + a^{-3}b^{-2}(a+b)^{-2} + a^{-2}b^{-1}(a+b)^{-4} \\
& + 2a^{-1}b^{-1}(a+b)^{-5}] - (33/2)\beta^{-7} - c\{8[2a^{-3}b^{-2}(a+b)^{-1} \\
& + a^{-2}b^{-2}(a+b)^{-2} + a^{-2}b^{-1}(a+b)^{-3} + 3a^{-1}b^{-1}(a+b)^{-4}] \\
& - (25/2)\beta^{-6}\} + c^2\{4[a^{-2}b^{-2}(a+b)^{-1} + a^{-1}b^{-1}(a+b)^{-3}] - (5/2)\beta^{-7}\}.
\end{aligned}
\tag{42''}$$

Z = nuclear charge.

$$N/4 = 24a^{-5}b^{-3} - 18\beta^{-8} - 12c(a^{-4}b^{-3} - \beta^{-7}) + 2c^2(a^{-3}b^{-3} - \beta^{-6}) \tag{42'''}$$

With $L = L_0 - L_1$ the minimum for k comes at

$$k = L/2M, \quad \lambda/4 = L^2/(MN).$$

The correction factor $1 + \epsilon$ is obtained as

$$1 + \epsilon = k^3 I / (N/4) \tag{43}$$

where

$$I = 24a^{-5} - 12c(a^{-4} - \beta^{-4}) + 2c^2(a^{-3} + b^{-3} - 2\beta^{-3}). \tag{43'}$$

Using these formulas we obtain for $a=1/3$; the minimized values $c=1.446$, $k=1.0057$, $-\lambda/4=1.1344$; $1+\epsilon=1.082$. The minimized value of a is 0.380 giving $-\lambda/4=1.1354$; $1+\epsilon=1.063$. On the other side of the best value of a say at $a=0.395$, $1+\epsilon=1.055$ and $-\lambda/4=1.1353$. The calculations have been carried out to several more significant places and for several more values of a than given here. It is seen that $1+\epsilon$ varies slowly for the functions minimized for changes in c and k . We believe therefore that 1.063 is a fairly accurate result. It will be noted that this result is in agreement with that obtained by correcting Hylleraas' one term function, and that the agreement between the empirical value of $-\lambda/4=1.1358$ and the theoretical $-\lambda/4=1.1354$ indicates that the trial function used by us is good.

It is of course usually said that an eigenfunction may be quite inaccurate even if a good eigenwert is obtained. We must consider this in somewhat more detail. Eckart¹⁴ has already given a criterion for the accuracy of eigenfunctions. His reasoning may be extended so as to apply to the specific calculation of a given quantity.

With Eckart we let the solution obtained by the variational method with a given trial function be ϕ and the true eigenfunctions (in this case of the 3S system) we denote in order of decreasing term values by ψ_1, ψ_2, \dots ; the corresponding negatives of the energy we write as W_1, W_2, \dots . The functions ψ_1, ψ_2, \dots are supposed to be normalized and $\phi = a_1\psi_1 + a_2\psi_2 + \dots$ where $a_1^2 + a_2^2 + \dots = 1$. Eckart shows that if the trial function ϕ leads to

¹⁴ Carl Eckart, Phys. Rev. **36**, 878 (1930). In this very useful and interesting paper will be found also many other eigenfunctions. The one used for 3S states of two electron systems is very similar to ours. The eigenwert for Li^+ obtained by Eckart is almost as good as the one obtained by us. For our work we considered it important to minimize for c as well as the other constants because the result is fairly sensitive to c . See also D. S. Hughes and C. Eckart, Phys. Rev. **34**, 694 (1930) for the calculation of the isotope effect in the Li^+ spectrum.

an energy value of absolute amount W then $1 - a_1^2 < (W_1 - W)/(W_1 - W_2)$. We wish to calculate the average of some quantity $f(q)$ over the configuration space q . The function ϕ gives the approximate result $\bar{f}_0 = \int f(q) \phi^2(q) dq$ while the correct result is $\bar{f} = \int f(q) \psi_1^2(q) dq$. The error is

$$\bar{f}_0 - \bar{f} = (a_1^2 - 1)f_{11} + a_2^2 f_{22} + a_3^2 f_{33} + \cdots + 2a_1 a_2 f_{12} + \cdots$$

where $f_{ik} = \int \psi_i \psi_k f dq$. The terms in f_{ii} are of the order of $1 - a_1^2$ which in the present instance is of the order of 4×10^{-3} . The relative error due to these terms can be therefore neglected. The only important terms are those containing $f_{1i} (i \neq 1)$. Thus

$$\bar{f}_0 - \bar{f} \cong 2a_1 \sum_{i=2}^{\infty} a_i f_{1i} \cong 2 \sum_{i=2}^{\infty} a_i f_{1i}. \quad (44)$$

Any a_i^2 for $i > 1$ is $< 1 - a_1^2 < (W_1 - W)/(W_1 - W_2)$ and the general order of magnitude of (44) is that of $((W_1 - W)/(W_1 - W_2))^{1/2}$. The numbers f_{1i} are however also of influence. In order to estimate their order of magnitude we must use the special form of f . In our problem

$$f = \frac{1}{2}(\delta(0, q_2) + \delta(0, q_1))$$

q_1 and q_2 being the collective coordinates of electrons 1 and 2. We have then

$$f_{12} = \int \psi_1(0, q) \psi_2(0, q) dq. \quad (45)$$

Approximately

$$\begin{aligned} \psi_1 &\cong 2^{-1/2} [\phi_{1s}(q_1) \phi_{2s}(q_2) - \phi_{1s}(q_2) \phi_{2s}(q_1)] \\ \psi_2 &\cong 2^{-1/2} [\phi_{1s}(q_1) \phi_{3s}(q_2) - \phi_{1s}(q_2) \phi_{3s}(q_1)] \end{aligned}$$

where the ϕ_{1s} is a hydrogenic function in a central field of nuclear charge Z and ϕ_{2s}, ϕ_{3s} are hydrogenic functions in a central field of nuclear charge $Z - 1$. The hydrogenic functions ϕ_{2s}, ϕ_{3s} are orthogonal to each other. In this approximation $f_{12} \cong (1/2) \phi_{2s}(0) \phi_{3s}(0)$. It will now be remembered that $\phi_{ns}(0)^2$ in a field of charge Z is proportional to Z^3/n^3 . Thus $\phi_{2s}(0)^2/\phi_{1s}(0)^2 \cong (2/3)^3 (1/2)^3 = 1/27$ in the present instance. We may take $f_{12} < (1/30)f$. It is now seen that we are likely to over-estimate the error by setting $a_3 = a_4 = \cdots = 0$, and attributing all the error to a_2 . Doing this, $\bar{f}_0 - \bar{f} = 2a_2 f_{12} \cong (a_2/15)f$ and a_2 itself is of the order of $1/15$. Thus the accuracy is likely to be about $(1/2)$ percent.

This estimate of the probable error together with the agreement of this calculation with the numerically corrected Hylleraas one term function makes us think that the value 1.06 which we calculated by both methods is probably correct to 1 percent. We thus conclude

$$1 + \epsilon = 1.06. \quad (46)$$

Using this value in (36'') (37) and the separation between components (1) and (3) observed by Schüller we can derive the value of μ . According to Gran-

ath⁶ a slight correction must be applied to Schüler's value of ν_{vac} for component (3). Applying this correction and supposing that the nuclear spin is $k = 3/2$ we get

$$1840\mu/k = g = 2.13. \quad (46')$$

Thus Schüler's and Granath's present data and the present calculation indicate that the magnetic moment of the Li_7 nucleus is approximately equal to three times the theoretical magnetic moment of a proton. If the magnetic moment were exactly three times the theoretical protonic moment the g value in (46') would be $g = 2$. We have at present no explanation to offer for the result $g = 2.13$. It appears that the difference of 2 and 2.13 is a greater one than can be accounted for by experimental errors or by errors in our calculation. It must be remembered however that the measured position of component (1) may be slightly affected by the proximity of component (2) and that the whole separation between (1) and (3) is of the order of 1 cm^{-1} .

Note added in proof: If the coupling of the electronic orbits and spins is of the Russell-Saunders type and if the electronic interactions are not too large and yet considerably larger than the interactions with the nucleus it is possible to give general and simple formulas applying to the case of one electron being in an s state. The other electron is then supposed to be in an L state of azimuthal number l . We may write the energy perturbation as:

$$w = (\mu/k)(b/2)[f(f+1) - k(k+1) - j(j+1)] \quad (47)$$

where the perturbation Hamiltonian is taken to be $H' = (B\mathbf{u}) = (\mu/k)(B\mathbf{k})$ and \mathbf{k} denotes the angular momentum matrix vector of the nucleus in units $\hbar/2\pi$. If the electronic angular momentum \mathbf{J} is made diagonal in the sense of containing $\delta(j', j'')$ as a factor for every matrix element and if for a given j the matrix J_z is also diagonal then the diagonal elements of B_z for that j mb ; $m = (j, j-1, \dots, -j)$. The proof of this for B_z is exactly similar to the proof for σ_z in the usual derivation of Lande's g factor. The momentum J_z remains conserved under the perturbation B_z . We now imagine the coupling between the electron spins and between the two orbital momenta to be removed. The matrix elements may be referred to pairs of states such as $(^2S_{1/2})_{m_1}$ and $(^2L_{l+1/2})_{m_2}$. A canonical transformation does not change the sum of diagonal matrix elements belonging to a given $m = m_1 + m_2$. The values of b for 3L and 1L are thus related to the values for 2S , 2L by sum rule equations:

$$\begin{aligned} (l+1)b(^3L_{l+1}) &= (\tfrac{1}{2})b(^2S) + (l + \tfrac{1}{2})b(^2L_{l+1/2}) \\ l\{b(^3L_{l+1}) + b(^3L_l) + b(^1L_l)\} \\ &= (\tfrac{1}{2})b(^2S) + 2lb(^2L_{l+1/2}) + (l - \tfrac{1}{2})b(^2L_{l-1/2}) \text{ etc.} \end{aligned}$$

The values of b for the one electron terms are known:

$$b(^2L_l) = 2\mu_0 l(l+1)/j(j+1) \cdot \langle r^{-3} \rangle; \quad b(^2S) = (16\pi/3)\mu_0 \psi_S^2(0).$$

The value of $b(^1L_l)$ is easily computed directly and the remaining b are determined by the above relations. Thus:

$$\begin{aligned}
b(^3L_{l+1})/\mu_0 &= (8\pi/3)\psi_s^2(0)/(l+1) + 4l(\overline{r^{-3}})/(2l+3) \\
b(^3L_l)/\mu_0 &= (8\pi/3)\psi_s^2(0)/(l^2+l) + 2(\overline{r^{-3}}) \\
b(^3L_{l-1})/\mu_0 &= -(8\pi/3)\psi_s^2(0)/l + 4(l+1)(\overline{r^{-3}})/(2l-1) \quad (47') \\
b(^1L_l)/\mu_0 &= 2(\overline{r^{-3}}).
\end{aligned}$$

Formulas (36), (36') are special cases of (47), (47'). The fact that sum relations such as used here exist has already been mentioned on p. 210 of Pauling and Goudsmit, *Structure of Line Spectra*. According to an informal communication of Professor Goudsmit these sum rules have been used by him in the derivation of the general formula in *Phys. Rev.* **35**, 440 (1930). Formulas (47), (47') apply only to the case of Russell-Saunders coupling but have the advantage of simplicity.

THE THERMOANALYSIS OF METAL SINGLE CRYSTALS AND A NEW THERMOELECTRIC EFFECT OF BISMUTH CRYSTALS GROWN IN MAGNETIC FIELDS

BY ALEXANDER GOETZ AND MAURICE F. HASLER
CALIFORNIA INSTITUTE OF TECHNOLOGY, PASADENA

(Received September 29, 1930)

ABSTRACT

PART I. THE THERMOANALYSIS OF BI SINGLE CRYSTALS

Production of crystals.—Crystals of Bi of any desired orientation were grown by the method of Goetz, one half of each normally, the other half within a transversal magnetic field. The orientations, predetermined by a seed crystal, were not affected by this process. Two methods of growth—the continuous and the discontinuous—were used.

The thermoanalysis of a crystal.—A method and its experimental realization—the thermoanalyzer—were developed to measure and to localize any changes of the thermoelectric properties along the lengths of crystals without applying mechanical stresses to them, by progressive local heating of the specimens. Thus very small distortions and imperfections were detectable due to their thermoelectric asymmetry.

Types of thermoanalytic diagrams.—The types of diagrams to be expected in the cases of a perfect single crystal, a double-, and a triple-crystal are discussed and a method is developed to analyze simple diagrams by means of the theory of heat-conduction.

PART II. EXPERIMENTAL RESULTS OBTAINED FOR NORMAL AND MAGNETIC CRYSTALS WITH A DISCUSSION OF THE SAME

The thermoanalysis of normal crystals.—The application of the thermoanalysis to normal single crystals leads to the discovery of very small (0.1 mm^2) regions within a crystal which are distorted due to very slight variations of the cooling conditions during the growth of the crystal. It is however possible to avoid these faults and to produce comparatively perfect specimens. Hence it was possible to test the results of different methods of crystal production and thus to refine the method used as well as to measure quantitatively the influence of a magnetic field applied to the crystal during the time of its formation.

The thermoanalysis of "magnetic" crystals.—It was found that the normal half of a crystal has a thermoelectric e.m.f. against the "magnetic" half. The sign and size of this e.m.f. depend on many circumstances, though mainly on the orientation the growing crystal has with regard to the direction of the field lines.

The effect as a function of the orientation.—The effect is a maximum if the principal axis of the crystal grows normal to the lines of force and it is very small (probably zero) if the axis grows parallel. It depends furthermore on the orientation of the crystal with regard to the direction of the thermoelectric current, since the two orientations in which the principal axis is normal to the field show different effects: a small one if the axis is normal to the current, and a very large one if it is parallel. —The thermal e.m.f. obtained for the latter case is 4.3 microvolts/degree which would correspond to a change in orientation of ca. 21° though no actual change could be observed.

The effect as a function of the method of growth.—The thermal e.m.f. depends largely upon the method of growth, i.e., whether the crystal is grown by the continuous or the discontinuous method.

The effect as a function of impurities.—The thermal e.m.f. for one and the same method of growth depends also on the amount of chemical impurities. Four kinds of purest Bi of different provenience were used in which the total amount of other substances was less than 0.2%. The metals were spectroscopically examined and it appeared that the purest (electrolytic) metal showed the smallest effect. It was *ca.* 40 times smaller than the effect of another metal. Traces of Ag and Pb seem to affect the "magnetic" sensibility of Bi most whereas Sb is rather ineffectual.

The effect as function of the field strength.—The effect is influenced by the strength of the applied field through this problem is not yet settled quantitatively. The influence of a small field (10^2 Gauss) is comparatively large, whereas fields of more than 13000 Gauss seem to decrease the effect. The maximum seems to depend largely on the kind of the impurity.

The effect as a function of temperature.—The Peltier-effect (extrapolated from the $E-f(\theta)$ curve) shows a sharp discontinuity between 75° and 90°C , indicating a different relation with regard to the transformation of Bi in this region. No indication could be found that annealing above this point (16 hours) and aging (1 month) destroys the difference between the normal and the "magnetic" half of a crystal.

Discussion.—The results obtained are brought into relation with the diamagnetic anisotropy of Bi. They are discussed with regard to the investigations of other authors and it appears possible to describe the effect as due to a change in the secondary (mosaic) lattice of the Bi crystal.

PART I. THE THERMOANALYSIS OF BI SINGLE CRYSTALS

INTRODUCTION

IN A previous paper,¹ one of the authors (G) described a method of producing Bi-single crystals which permits the application of strong, transverse, magnetic fields at the zone of crystallization. The influence of the field with regard to the orientation of the growing crystal was studied. It was stated that the orientation frequently obtained was such that the trigonal axis of the growing crystal was parallel to the lines of force, in case the crystal formed its first center of crystallization within the field. This result was partly to be expected if one considers the anisotropic nature of the diamagnetic susceptibility in Bi-crystals. Since this susceptibility is at a minimum along the trigonal axis and at a maximum in a direction normal to it, the crystal assumes an orientation which corresponds to a minimum of free energy. This result is in agreement with the early observations of Plücker² and Leduc.³ It was, however, unexpected that the orienting forces of the strongest magnetic fields (*ca.* 22000 Gauss) did not show any effect as soon as the orientation of the growing crystal was already predetermined before entering the field. Yet for several reasons, it seemed to be interesting to investigate whether or not a crystal, one half of which was grown without, the other half within a strong transverse magnetic field showed any differences at all between portions, despite the fact that the orientation remained unchanged.

Such differences were to be expected when, for instance, one considers

¹ A. Goetz, *Phys. Rev.* **35**, 193 (1930).

² S. Plücker, *Pogg. Ann.* **76**, 583 (1849).

³ M. A. Leduc, *C. R.* **140**, 1022 (1905).

such observations as those by Tieri⁴ concerning the Hall-coefficient of Bi specimens crystallized within a strong magnetic field. A large difference of the Hall-e.m.f. was found with regard to different directions of the field lines crossing the solidifying specimen, but no interpretation was possible as these experiments were only of a qualitative kind and made on polycrystals.

Production of crystals. Since the method of producing bismuth single crystals introducing a minimum of mechanical stresses has already been described^{1,5} as well as the way the magnetic field was applied to the growing crystal only a few additional details need be mentioned.

The orientation of the crystal was as usual predetermined by a seed. Three main orientations were grown, which represent the possible primary relations between trigonal axis, the (111) plane, and the lines of force (see below). Two methods of growth were employed which differ principally both in the forces applied to the growing crystal at the moment when the field was energized and in the results obtained.

The first, entitled the *discontinuous method*, consisted of two distinct processes. A crystal was first grown completely without any magnetic field present (the residual field of the magnet was eliminated by removing the pole pieces). It was then removed from the growing trough, etched, and carefully examined with regard to irregularities. In case none could be detected, the crystal was put back into the trough, which in turn was put back into the furnace so far that only one half of the crystal melted again, the temperature of the furnace being regulated so as to bring the border between solid and liquid-crystal exactly in the middle of the pole-pieces of the magnet. This process had to be done very carefully in order to avoid irregularities along the molten part of the crystal. As soon as thermal equilibrium was reached, which condition could easily be recognized since the progress of the molten region into the space between the pole-pieces stopped as soon as the heat distribution along the crystal became stable, then the magnetic field was excited and the driving mechanism of the crystal apparatus started, thus the second half of the crystal recrystallized within a magnetic field.

The second, entitled the *continuous method*, allowed the growth of the unmagnetic and magnetic portion of the crystal in one operation. This was done by growing the crystals in the usual manner but with the pole-pieces in position, a precaution that was essential as pole-piece moving with its attendant jarring was prohibitive during crystal growth. This method had the advantage over the other process in that the growing forces remained undisturbed when the magnetic field was applied. In the early work, however, it had the disadvantage in that the residual field of the magnet (200–300 gauss) was present while the first portion of the crystal, the so-called “unmagnetic” half, was growing. Later this was eliminated by providing a magnetic by-pass of soft iron across the pole-pieces and above the trough, which was removed just before the magnet was energized. All these crystals

⁴ L. Tieri and E. Persico, Linc. Rend. 30, 464 (1921).

⁵ A. Goetz and M. F. Hasler, Proc. Nat. Acad. 15, 646 (1929).

were grown in an atmosphere of CO_2 to prevent oxidation so that in this respect they also differ from those grown by the discontinuous method.

The first observation which was made on crystals produced by the discontinuous method with fairly high fields was the difference in reflectivity of light between the two halves. This was most noticeable in the P_1 orientation, i.e. where (111) plane is parallel to the lines of force. It seems improbable that this difference was due entirely to the second recrystallisation, as etching off a layer one mm or more thick does not destroy the phenomenon. This effect must indicate a change of the structure of the crystal-faces within the magnitude of the wave-length of visible light and it thus seems possible that it concerns the mosaic lattice as described by Zwicky⁷ and Goetz⁸. This possibility will be treated at length in another paper.

The thermoanalysis of a crystal. Concerning a sensitive and effective method for determining possible differences between these two halves of one and the same crystal, it seemed that the measurement of the thermoelectric effect fulfilled the requirements the most easily. Nevertheless, it was experimentally rather difficult to perform, since it was not only necessary to measure the thermal e.m.f., but also, to localize it as exactly as possible. Several methods had to be tried until it was possible to obtain reliable results and since such methods, allowing one to measure as well as to localize a thermal e.m.f. within a metal rod, are excellent indicators of inhomogeneities undetectable by other means, their applicability is not limited to this special problem. Thus it seems worth while to give a more detailed description of them. (A similar idea has been put into realization independently by Terada and his collaborators.^{9,10,11} Their experiments had been started for testing the reality of the Benedix effect and the method used was fundamentally the same as ours, though quite different in its experimental procedure. It is excellent for the detection of the "residual" thermal e.m.f.'s. but its sensitivity and reproducibility does not meet the requirements of the thermoanalysis of single crystals).

A simple method first tried was as follows: The crystal was first protected by a coat of Duco paint. Leads from the ends were connected to a galvanometer, the contacts with the crystal being kept at constant temperature. The crystal held horizontally, had a small portion heated locally by the touch of a mercury meniscus which topped a column of that metal heated by an electric furnace. If the meniscus was moved slowly along the crystal and the deflections of the galvanometer were observed with relation to the position of the heated point on the crystal, then a thermoelectric analysis of each increment of length could be made. As soon as the heated region came near the border between the "magnetic" and the normal part of the crystal, an

⁶ A. B. Focke, *Phys. Rev.* **36**, 319 (1930).

⁷ F. Zwicky, *Proc. Nat. Acad.* **15**, 253, 816 (1929); **16**, 211 (1930).

⁸ A. Goetz, *Proc. Nat. Acad.* **16**, 99 (1930).

⁹ T. Terada and T. Tsutsui, *Proc. Imp. Acad. Tokio*, **5**, 132 (1929).

¹⁰ T. Terada, T. Tsutsui and M. Tamano, *Sc. Pap. Inst. Res. Tokio*, **7**, 201 (1927).

¹¹ T. Terada, T. Tsutsui and M. Tamano, *Proc. Imp. Acad. Tokoi*, **3**, 507 (1927).

e.m.f. was indicated, but its size could not be measured accurately enough inasmuch as it depended on the contact conditions of the meniscus which could not be made reproducible. This method was therefore soon abandoned.

The next method that was tried was to heat the crystal locally by focusing radiation of a powerful incandescent lamp upon it. This method had the advantage over the previous one in that it was not necessary to protect the surface of the crystal against amalgamation, with a covering that was necessarily a poor heat conductor. A large number of observations were made with this apparatus, but due to certain inherent difficulties of the method, it was abandoned. These difficulties were, for instance, providing air cooling

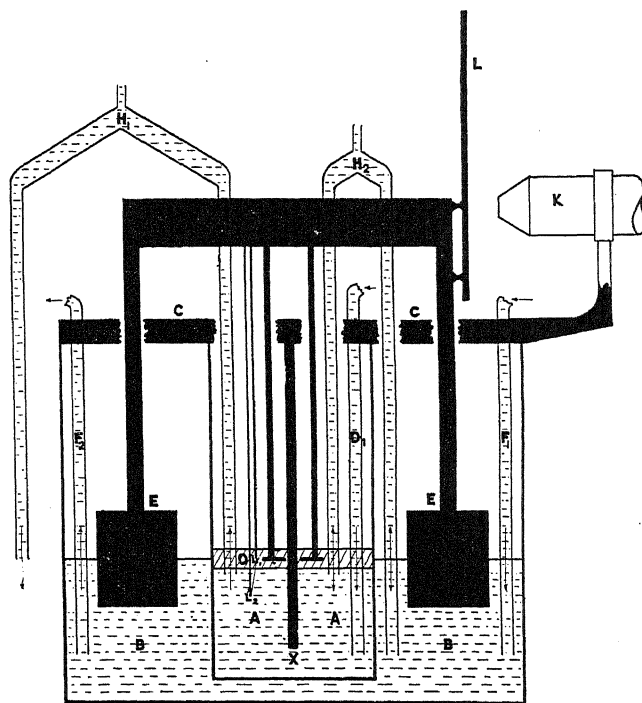


Fig. 1. Diagram of the thermoanalyzer.

of the crystal as a whole while preventing local convection currents at the point of heating, measuring the temperature at the heated point, and preventing surface irregularities of the crystal from nullifying results.

The final arrangement which avoided the above difficulties and made possible quantitative measurements is sketched in principle in Fig. 1. A cylindrical glass-container *A*, 18 cm long and 9 cm wide is held in the center of a large glass-container *B*, 24 cm wide, 22 cm long, by means of the bridge *C*. The glass tube *D*₁ is fixed in *A* and brings water at a definite temperature and under constant pressure into *A*. The vessel *B* is also filled partially with water, the level of which determines the position of a ring-shaped float *E*. Two tubes *F*₁ and *F*₂ fixed in *B* permit the raising or lowering

of the water level of B , which in turn changes the position of the float E . Fixed to this float E is a frame arrangement which carried several devices among which are the syphons H_1 and H_2 and the scale L . The latter serves to measure the position of the float (incl. oil-layer, furnace, etc). with regard to the crystal by means of the reading microscope K attached to the frame C . The syphons H_1 and H_2 have one end in A just underneath the water level, the other end of H_1 going outside of B , the corresponding end of H_2 ending beneath the water level in B . The horizontal part of both syphons is shaped to separate air bubbles from the flowing water, while adjustments for bringing the tubes into correct positions with regard to the water levels are provided. Beside the syphons, the float carries an electric heater consisting of a horseshoe-shaped thin mica sheet around which chromel wire is coiled. Other mica sheets above and below insulate this heater from two thin copper plates which bind the whole, making for equal heat-distribution and rigidity. This whole heater is only 1 mm thick. Its position with regard to the frame is so adjusted that it is slightly above the water level in A when the ends of H_1 and H_2 are just beneath that level. On top of the water in A , an oil layer of 5–10 mm thickness is put in order to surround the heater completely.

The arrangement works as follows: A constant flow of water is sent into A filling it up to a certain point, any surplus being syphoned off. The water level in A is therefore determined by the position of the syphons H_1 and H_2 or what amounts to the same thing, by the position of the float E in B . Thus a permanent circulation of the water underneath the heated oil layer results and consequently a constant temperature. If a certain amount of water is added through F_1 , the water in B rises and with it the float E holding the syphons and the heater. The oil layer in turn maintains its relative position with regard to the heater since its supporting water column rises as the syphons rise. It follows that the water has to be added into B at a rate sufficiently slow to permit hydrostatic equilibrium in A . Therefore, the cross sections of H_1 and H_2 are large compared with the cross-sections of F_1 , F_2 and D_1 . As an indicator of this equilibrium, a differential thermocouple is also attached to the frame of E . It consists of two copper wires L_1 and L_2 the ends of which, ending one in the middle of the oil-layer, the other within the water flow, are connected by a very thin constantan wire. This arrangement is extremely sensitive because the smallest displacement of the heater with respect to the oil and water level changes the temperature of the L_1 -junction and thus produces a change in the thermal e.m.f.

The reason the syphon H_2 is used in addition to H_1 is first, to tie the water systems of B and A together so that no appreciable differences in levels can result, though when everything is properly adjusted this link is largely static, and second to minimize the irregularities of the flow in H_1 caused by small differences in the surface tension of the water at the outside opening of H_1 , since H_2 allows the large volume of B to be used as a "shock-absorber."

Thus an arrangement is obtained which permits the production of a constant gradient of temperature which can progress regularly along a crystal X hung perpendicularly in the vessel A as indicated in Fig. 1. To com-

plete the ensemble, it is only necessary to mount the crystal in a holder which keeps it in a fixed position with regard to *A*, to provide connections at both ends with a galvanometer, and to keep the upper contact at a constant temperature, a temperature as nearly as possible equal to that of the water in *A*. All this was conveniently done with the so-called "crystal holder."

The bakelite tube *J* in Fig. 2 carries at one end the adjustable fork *K*, while close to the other, the clamp *L*. Through *J* sealed in, runs a copper wire, the upper end of which is connected directly with the galvanometer. The other end, bent, has a silver wire (0.1 mm) soldered to it. Furthermore, *J* carries an adjustable clamping device *M* which permits one, with the aid of a similar one on the bridge *C* (Fig. 1), to fix the holder into any position desired with respect to *A*. To cool the upper end of the crystal, a copper cylinder *N* is used, provided with two small side-tubings *N*₁ and *N*₂, *N*₁ being

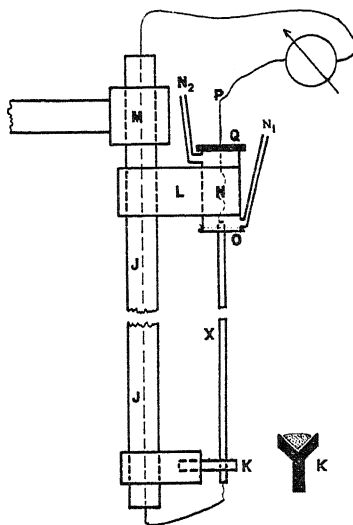


Fig. 2. Diagram of the crystal-holder of the thermoanalyzer.

connected with a water reservoir of constant temperature and hydrostatic pressure. In this way, a water flow is sent into *N*₁ and leaves by *N*₂. To fix the upper end of the crystal *X* in a position within the water flow without applying any fatal strain to it, a thin rubber membrane *O* (toy balloon), with a small central hole burned into it is stretched over one end of *N*. After a silver wire similar to the one previously mentioned is spark-welded to the crystal, the hole in *O* is momentarily widened, the crystal is introduced and the membrane released, thus forming a tight sleeve around *X* able to withstand the water pressure in *N*. The silver wire protruding now from the other side of *N* is soldered onto the copper wire *P* which is fixed in the bakelite plate *Q*. After a contact is thus made between *P* and *X* the plate *Q* is sealed tight onto *N*, thereby closing the water chamber. *N* and *X* are fixed into the clamps *L* and *K* respectively and the silver wire at the lower end is also spark-welded onto *X*. The whole arrangement is then put

vertically into *A* in such a way as to bring *X* exactly through the central opening of the heater. The wire *P* is connected through a resistance box to the galvanometer, thus completing the circuit. Fig. 3 shows a photograph of the apparatus for thermoelectric analysis and Fig. 4 a picture of a crystal in its holder. It is necessary to mention that the task of mounting crystals without distortion is a very difficult one and requires a special apparatus which avoids critical stresses by facilitating manipulation.

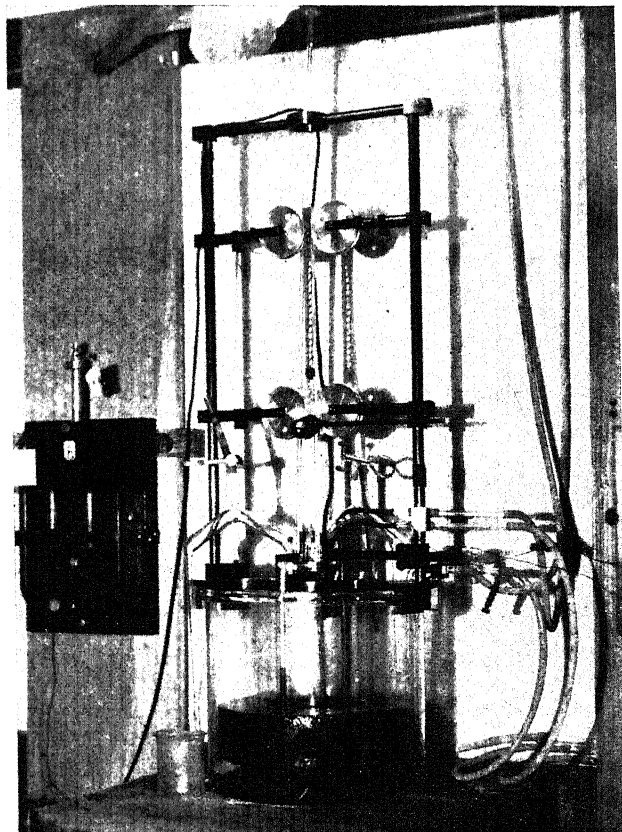


Fig. 3. Photographic view of the thermoanalyzer.

After the crystal, mounted in its holder, is fixed in the vessel *A*, the different water flows are started and the furnace-plate is heated, in general to a temperature 18° above the temperature of the running water. After thermal equilibrium is reached measurements are taken, i.e. the deflections of the galvanometer are measured as a function of the position of the oil-layer relative to the crystal. Simultaneously the e.m.f. of the differential-thermocouple is measured to assure the maintenance of thermal equilibrium. Schematically, this is shown in Fig. 5 where *X* is the crystal, *W*₁ is the water cooling the lower end of the crystal and *W*₂ that cooling the upper end, *G*₁ is the galvanometer measuring the thermal e.m.f. of the crystal, and *G*₂ one

measuring the difference of temperature between the heated oil layer O and the water W_1 .

Types of thermoanalytic diagrams. First it will be considered what type of curve one would expect to obtain with this kind of an arrangement. The obvious way of plotting the diagrams is to represent the thermal e.m.f. indicated by G_1 (Fig. 5) as ordinates and the position X of the heated oil layer with respect to the crystal as abscissas. If one considers first, the diagram that would be obtained by the thermoanalysis of a perfectly homogeneous crystal, one realizes immediately that it should not show any thermo-

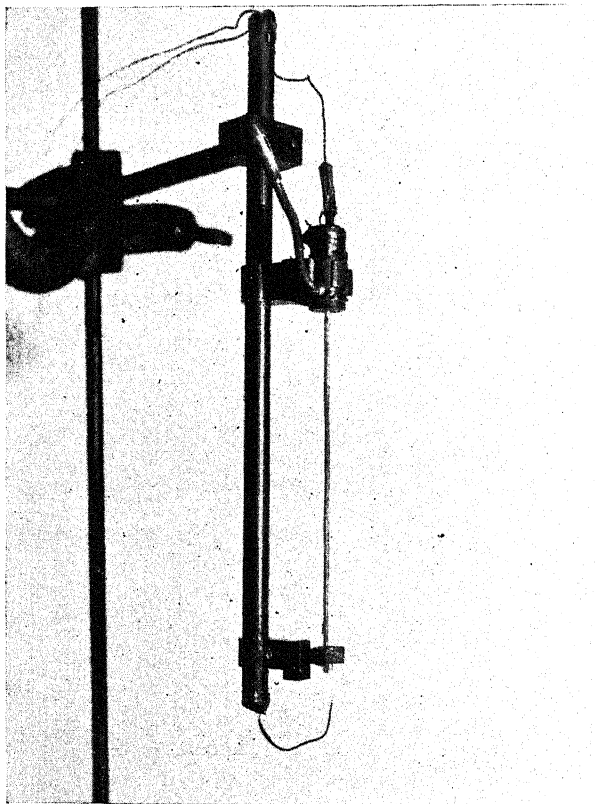


Fig. 4. Photographic view of the crystal-holder.

electric potential (Magnus' Law). However, certain deviations from this purely theoretical concept would be expected as a result of imperfect cooling conditions and the heat-conductivity of the crystal. Hence, a curve of the type (Fig. 6a) should be expected where the dotted line would represent a constant thermal e.m.f. (τ) due to a slight difference of temperature between the two different end cooling systems; while the curve drawn in full with its deviations from linearity would be obtained under normal conditions, where the cooling of the ends of the crystal is not sufficient to prevent a slight heating by conductivity through the metal. To make this "end-effect" as small as possible, the crystal used has to have a small cross-section.

The second case to be considered is shown in Fig. 6b, which represents an unhomogeneous crystal consisting of two halves (I and II) which have a thermal e.m.f. against each other. In this case, a curve as shown would be obtained, where a maximum would permit the exact localization of the junction

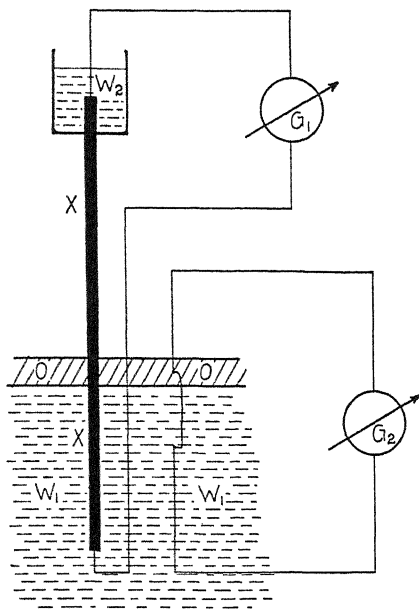


Fig. 5. The electrical connections of the thermoanalyzer.

tion of the two halves. Superimposed upon this would be the effects previously mentioned (Fig. 6a) though the constant thermal e.m.f. due to unequal end cooling would have a different value since the thermoelectric

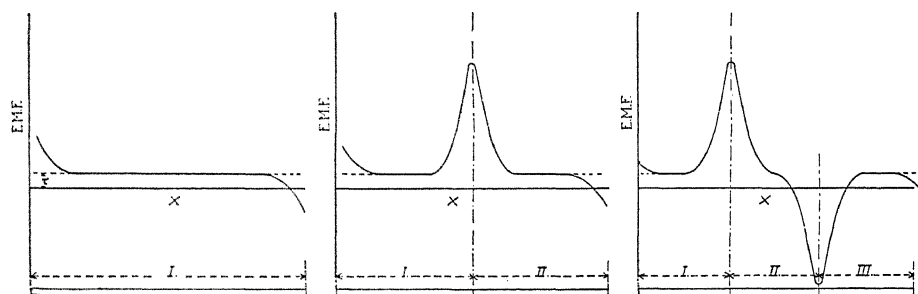


Fig. 6. a. b. c. Ideal thermoanalytic diagrams of a perfect single-crystal (a), a perfect double-crystal (b), and a perfect triple-crystal (c).

power of the two halves against the contact metal would be different from that in the case of a single crystal. Also, the end effects due to heat conduction would be slightly asymmetrical since the two different halves are involved. The sharpness of the maximum would depend on the gradient of

temperature along the crystal and the extension of the heated zone, thus the former should be as large while the latter as small as possible.

The third case in which the crystal consists of three sections, the second of which has the same thermal e.m.f. against the first and third (I: III, Fig. 6c) would result in a curve which is more complicated. With the heated oil layer at the junction of part I and II, there would be a maximum similar to that of Fig. 6b. Furthermore, on reaching the transition from II to III, the same thing would happen but in the opposite direction. Of course, the shape of the whole curve would depend very much on the relative sizes of the three sections. For a given thermoelectric difference of II against III, and a given difference of temperature in the analyzing apparatus, the maximum and minimum would not change their size as long as II is large enough to contain the whole drop of temperature given by the analyser. If II is smaller, the maxima would decrease and finally there is a size below which no effect whatsoever would be observed. This threshold determines the resolving power of the arrangement and depends on the construction of the analyser and the cross-section, thermal conductivity, etc., of the crystal as follows: The thermal conditions along the crystal within the thermo-analyser are easily treated by the general equation of the temporal and local distribution of temperature in a linear conductor:¹²

$$\frac{\partial \theta}{\partial t} = \frac{\sigma}{\rho c} \frac{\partial^2 \theta}{\partial x^2} - \frac{h}{\rho c} \frac{U}{S} \theta \quad (1)$$

where: θ is the temperature for (x) and (t) ; r the radius of the crystal; U the circumference of a cross-section of the crystal; S the cross-section of the crystal; x the length-coordinate of the crystal; h , the thermal emissivity of the crystal surface; c the specific heat; ρ the density; and σ the specific heat-conductivity.

Since the movement of the oil-layer along the crystal within the thermo-analyser is very slow we assume stationary condition, i.e. $\partial \theta / \partial t = 0$. Thus Eq. (1) becomes:

$$\frac{\partial^2 \theta}{\partial x^2} = \frac{U}{S} \frac{h}{\sigma} \theta = \frac{2}{r} \frac{h}{\sigma} \theta \quad (2)$$

and:

$$\theta = A \exp [-(2h/r\sigma)^{1/2}x] + B \exp [(2h/r\sigma)^{1/2}x]. \quad (3)$$

For the assumption of $x = \infty$, i.e. in case the crystal cools down so fast that the gradient is zero before the end of the crystal (which fact is indicated by the absence of the end-effects mentioned above), B and therewith the second term of Eq. (3) equals zero; hence we obtain:

$$\theta = A \exp [-(2h/r\sigma)^{1/2}x] \quad (4)$$

where A equals θ_{\max} , the temperature of the oil layer, if one assumes the absence of any gradient across the crystal as was already done for the entire crystal implicitly in Eq. (1).

¹² Enzyklopädie d. Math. Wiss. 5, I, 181.

The graphical interpretation of the records of the thermoanalyzer is more convenient if Eq. (4) is transformed into a logarithmic system:

$$\ln \theta = \ln A - (\alpha h)^{1/2} x \quad (5)$$

where $\alpha = 2/r\sigma$. If $\ln \theta$ is chosen as ordinate and $(h^{1/2}x)^{-1}$ as abscissa, the cooling curve becomes a straight line as shown in Fig. 7a, its inclination ($\text{tg } \phi$)

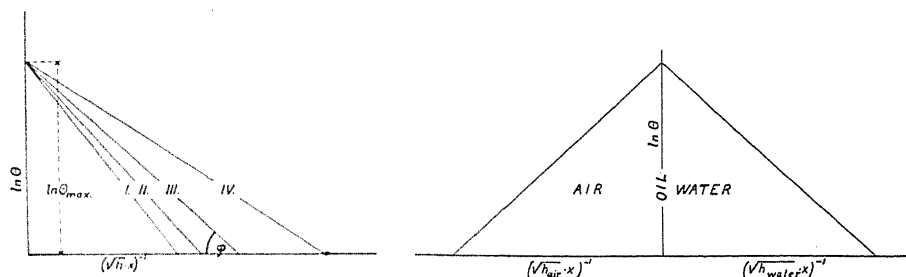


Fig. 7. a. b. Ideal logarithmical diagrams of a perfect double-crystal. The difference between the thermal "emissivity" for water (h_{water}) and air (h_{air}) of the crystal surface is compensated to obtain a symmetrical diagram. (Read +1 for -1 as abscissa-exponent!)

is for the same crystal directly proportional to $\ln \theta_{\text{max}}$ and $h^{-1/2}$, since r as well as σ is constant for a perfect single crystal over its whole length. However h differs with the surrounding medium, for instance is $h_{\text{air}} < h_{\text{water}}$. Hence the diagram is simplified if the abscissa indicates $\xi = (h^{1/2}x)$ instead of x , since in this case $\text{tg } \phi$ is the same for the cooling curve above and below the oil layer (Fig. 7b).

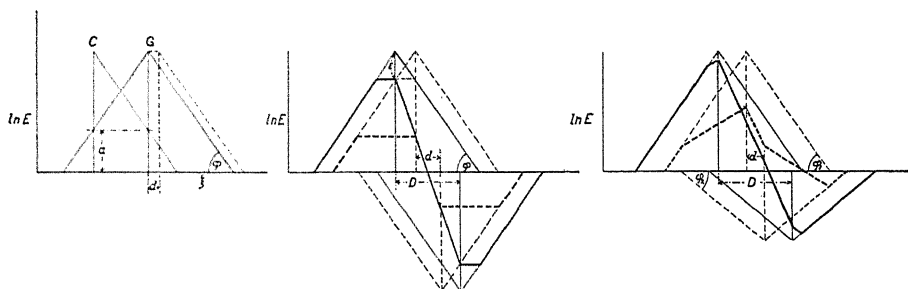


Fig. 8. a. b. c. The geometric construction of an ideal thermoanalytic diagram of a double crystal (a), a symmetrical triple-crystal (b), and an asymmetrical triple-crystal (c). 8b and 8c show each two different cases, the diagram of a large intersection (D ; full-drawn lines) and of a narrow one (d ; dotted lines).

If the rather valid assumption be made that E , the thermoelectric force is directly proportional to the (small) difference of temperature between oil and water (resp. air), then equation (5) may be written:

$$\ln E + \ln E_{\text{max}} - \alpha^{1/2} \xi \quad (6)$$

where E_{max} represents the value of E for $\theta = \theta_{\text{max}}$.

The e.m.f. produced at the ends of a double crystal (Fig. 6b) in a certain position (G) of the oil layer (C) (Fig. 8a) is given by the intersection with

the $\ln E$ - ξ line (a). Hence it is evident that the thermoanalytic curve $E = f(x)$ will follow that line in the coordination used if one moves the intersection gradually through the oil layer; i.e. the diagram (Fig. 8a) thus obtained is identical with the measured curve to be expected from an ideal double crystal if one considers (according to the medium surrounding the intersection) the two different values of h which are easy to find empirically.

It goes without saying that the assumption of a two-dimensional oil layer is not justified by the actual conditions, since the oil layer is of considerable thickness (d), its temperature is not uniform, and $d\theta/dx$ has a definite value as well as being a function of x_{oil} .

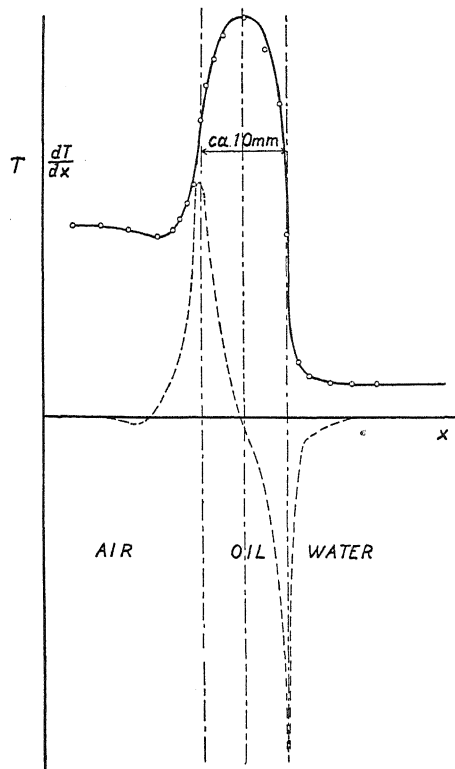


Fig. 9. The temperature diagram of the thermoanalyzer. The full drawn curve shows $T=f(x)$, the dotted lines show $dT/dx=f(x)$.

However the real curves are not fundamentally different from the constructed ones as soon as the oil layer is comparatively thin and the thermal conductivity of the crystal is large. If those conditions are fulfilled one can account for the oil layer by moving the starting point of the second half of the diagram the distance d (dotted in Fig. 8a). This also is only a first approximation on account of the neglect of $\partial^2\theta/\partial x^2 \neq \text{const.}$

Fig. 9 shows the measured temperature-curve within the thermoanalyzer (full line). The latter can be found readily by putting a very thin thermocouple into the thermoanalyzer instead of the crystal. The dotted line in Fig. 9.

indicates the temperature gradient obtained by graphical differentiation of the first curve. It shows that very large gradients could be obtained at the boundary layer of oil and water and furthermore that the theoretical assumptions are not very far from the facts.

In the case of a triple-crystal (Fig. 6c) the construction of the curve is more complicated though fundamentally the same. Here it is necessary to subtract the intersections of the $\ln E$ - ξ lines crossing one transition from those crossing the other. The diagram obtained thus has ordinates $(\ln E_1 - \ln E_2)$, while what is actually desired is $\ln (E_1 - E_2)$. Since the latter, however, give curves it was considered advisable from the view-point of a convenient graphical synthesis of the analytic curves to plot the former, which give the correct position of the maxima though not the correct amplitudes. The ordinates of the two elementary curves have to be plotted into the opposite direction since the sign of the e.m.f. is negative in one case. Fig. 8b. shows the diagrams of two different triple-crystals, one with a large II-section (full lines) (distance D) the other with a small section (dotted lines) (distance d). The thermal e.m.f. between I and II, and II and III is the same in both cases.

It is apparent that the size of the maxima depends on the length of the heterogeneous section II as soon as $d < x_0$; (x_0 means the distance from the heated intersection to where θ is so small that the thermal e.m.f. cannot be measured anymore).

The decrease of E_{\max} is then simply given by:

$$\ln \epsilon = (\xi_0 - d) \operatorname{tg} \phi \text{ for } d < (h^{1/2} \cdot x_0) = \xi_0. \quad (7)$$

Moreover it is evident that the width of the maxima increases with the decrease of their sharpness.

Fig. 8c. shows another case of a triple crystal, for different lengths of section II. Hence where all three sections are thermoelectrically different, one obtains asymmetrical curves as well as an asymmetrical decrease of the maxima with the length of section II.

The dependence of the size of the maxima indicated by the thermo-analyzer on the length of the straight section II determines the resolving power of the analyzer in each case since it is related to the indicated e.m.f. in the limit by the relation:

$$de = - E_{\max} \left(\frac{2h}{r \sigma} \right)^{1/2} \exp [- (2h/r\sigma)^{1/2} x] dx \quad (8)$$

which, if the oil layer is at section II reduces to:

$$de = - E_{\max} \left(\frac{2h}{r \sigma} \right)^{1/2} dx. \quad (8a)$$

The resolving limit of the analyzer is then given by a value dx which cannot produce a measurable de .

The above considerations show that the analyzer, since it does not necessitate the slightest stress to the specimen, is a very useful instrument

for the detection of all kinds of invisible imperfections and inhomogenities in a metal rod, especially in a delicate single crystal. The size of the smallest imperfection still resolved distinctively was *ca.* 0.1 mm. It is evident that thin rods (2 mm diameter in the present case) give better results than those of large diameter since the method integrates necessarily over the whole cross-section.

PART II. EXPERIMENTAL RESULTS OBTAINED FOR NORMAL AND MAGNETIC CRYSTALS WITH A DISCUSSION OF THE SAME

The Thermo-analysis of normal crystals. It is obvious that the described method of thermoanalysis can serve the purpose of detecting and locating imperfections within a crystal only when the size of these imperfections is above the resolving power of the analyzer. Furthermore, it is only possible to detect imperfections which cause a thermoelectric force, though it seems

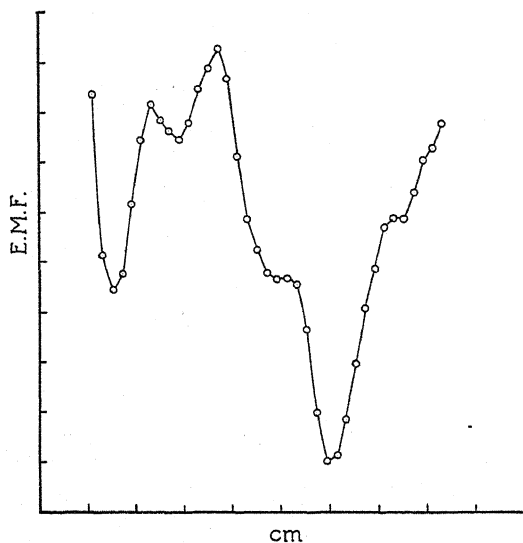


Fig. 10. The thermoanalytic curve of a Bi crystal grown in a glass tube.

very probable that any imperfection due to a distortion or change in the orientation within the crystal causes one, the detection of which depends only on the sensitivity of the galvanometer used. Thus this method is an excellent one to detect and locate heterogeneous inclosures and local plastic deformations. The latter became particularly evident in the case of bismuth since they result in the production of twin lamellae, a phenomenon treated at length in other papers.^{1,8}

Because of the effectiveness of this method, the different means used for the production of single-crystals were examined as to their results, and the development of a method of crystal growth—a method to be used in the final experiments—was guided step by step by this kind of an analysis. First crystals grown in glass tubes by the ordinary method (Tammann, Bridgman) were analysed. The deviations of the thermoanalysis curves from

linearity were to be expected especially as the taking off of the glass cover caused many twin lamellae. Fig. 10 shows a diagram of such a crystal.

The lower curve in Fig. 11 shows a crystal with one maximum (M) due to a magnetic effect (see later). After the analysis had been taken, the crystal was plastically deformed just enough to produce two small sets of twin lamellae visible under the magnifying glass. The diagram taken afterwards

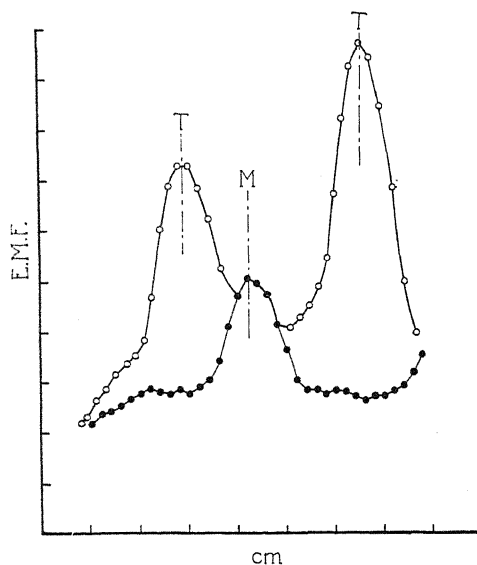


Fig. 11. The thermodynamic curve of a crystal before (black points) and after artificial deformations at the points $T-T$ (white points). M is the starting point of the magnetic field.

is shown as the upper curve where now two new maxima (T, T) occur, the position of which coincided exactly with the location of the twin-sets.

Fig. 12 shows the diagram of a crystal of the same orientation (P_3) as Fig. 11 as homogenous as it could be produced by means of the graphite

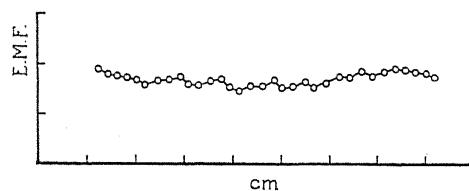


Fig. 12. Thermodynamic diagram of a "perfect" Bi crystal grown after the method of Goetz. Orientation: P_3 ; Kind "B."

trough, protecting atmosphere, etc., as previously described.¹ Since the scale of this diagram is the same as that of the previous ones it is quite evident that the method used for the production of the crystals gave quite uniform results.

Among the large number of diagrams which have been taken, it occurred very often that an apparently perfect crystal (as far as its examination after

etching was concerned) showed one or more distinct maxima. If the crystal then was cleaved at the point where a maximum had occurred, a microscopic investigation led always to the detection of the inclusion of a crystal of different orientation, which orientation was usually that of a twin. Fig. 13 is a microphotograph of an inclosure of that kind which shows distinctly a twinned region within a normal (111) plane, characterized by an alternating penetration of $(11\bar{1})$ planes through the original (111) plane bordered by (110) planes. The cause of these imperfections was, in general, a disturbance

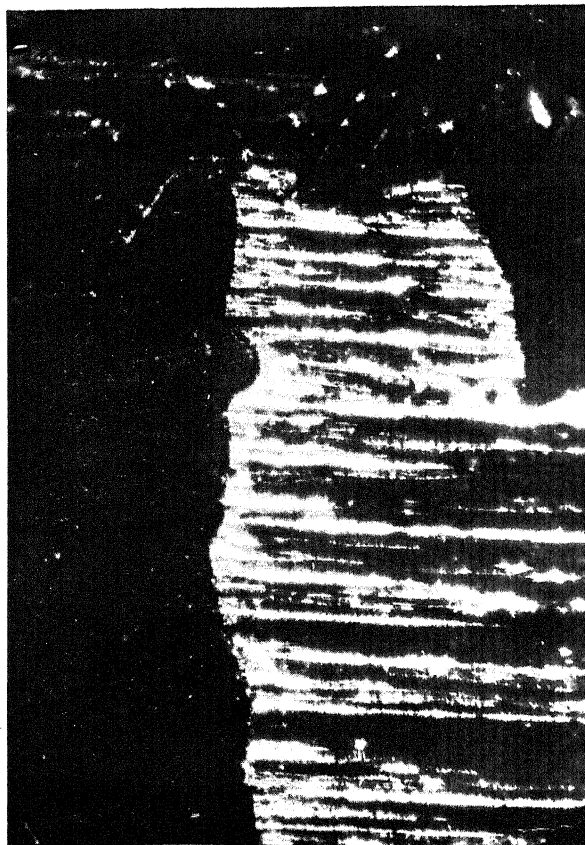


Fig. 13. Microphotograph of an etched (111) plane (ca. $120\times$), illuminated by polarized light, showing the inclosure of a region of periodical twinning.

(vibration, shock, etc.) happening at the time when this section of the crystal was forming.

The Thermoanalysis of "magnetic" crystals. The described method of thermoanalysis was applied to crystals, one half of which was grown without, the other half within a magnetic field. *It was found that the border between the magnetic and the normal half of the same crystal was the origin of a thermoelectric force.* Furthermore, the thermoanalysis gave evidence that *the origin of this force is exactly at the point where the magnetic field was applied.*

Nevertheless, it proved to be very difficult to measure this force quantita-

tively and not even the sign of the force could at first be reproduced although each curve showed a maximum if it was not fogged by other maxima due to distortions of the kind mentioned in the previous chapter.

To obtain a higher degree of reproducibility, certain definite conditions were imposed, both on the growth and on the analysis of the crystals. In the case of the former, four factors were considered in detail; orientation, method of growth, impurities in the metal, and field strength. For the latter, two were considered: temperature of the analyser, and annealing.

The actual results obtained indicate that at least for the first group of factors the thermoelectric effect is a very complicated function. Despite this complexity, however, duplication of results, for any given set of conditions, with less than ten percent deviation was always possible which indicates that all the principal variants were being controlled.

In presenting the results, the effect of each of the factors on the thermoelectric e.m.f. will be considered separately, the stationary values of the

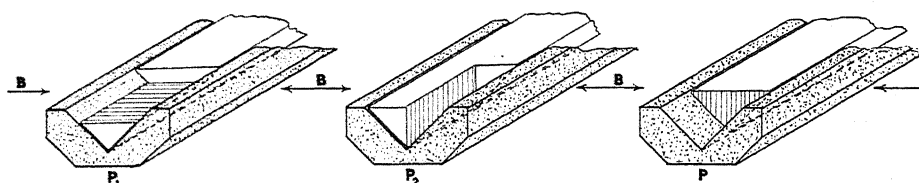


Fig. 14. Scheme of the three principal orientations used. The hatched plane indicates (111), the arrow shows the direction of the field lines.

other factors being given in each case. Up to date, no attempt has been made systematically to evaluate the effect for a large number of values of each of the factors involved, thus the results given can be considered as merely illustrating the type of variation to be expected.

For all the curves to be presented unless specifically stated, the temperature difference in the analyzer was 18°C measured above tap water temperature of 19° to 21°C .

TABLE I. *The three orientations of the crystal.* The third column entitled "vector" shows the direction of the heat flow and the electric current during the thermoanalysis.

Name	Trigonal axis to field			(111) plane to field		
	rod		vector	rod		vector
P_1	\perp	\perp	\perp	\parallel	\parallel	\parallel
P_2	\perp	\parallel	\perp	\perp	\perp	\perp
P_3	\parallel	\perp	\parallel	\perp	\parallel	\perp

The ordinate scale for the curves unless designated otherwise is 7.8×10^{-6} volts per division. It indicates positive volts for increasing values. The units of the abscissa (length of the crystal) are centimeters.

The solid line, mid-way along the abscissa scale on the curves, indicates the position of the furnace at the intersection between magnetic and normal

portions of the crystal.* The dotted lines indicate the extent of the oil layer to each side of the furnace.

The Effect as a function of the orientation. As stated already in a previous paper,¹ there are three different orientations the crystal can have with regard to the rod, or to the direction of the lines of force, which are essentially different from each other.** Fig. 14 shows the trough *G* dotted, and the crystal white, the latter cut parallel to its main cleavage plane. These three orientations are given in Table I.

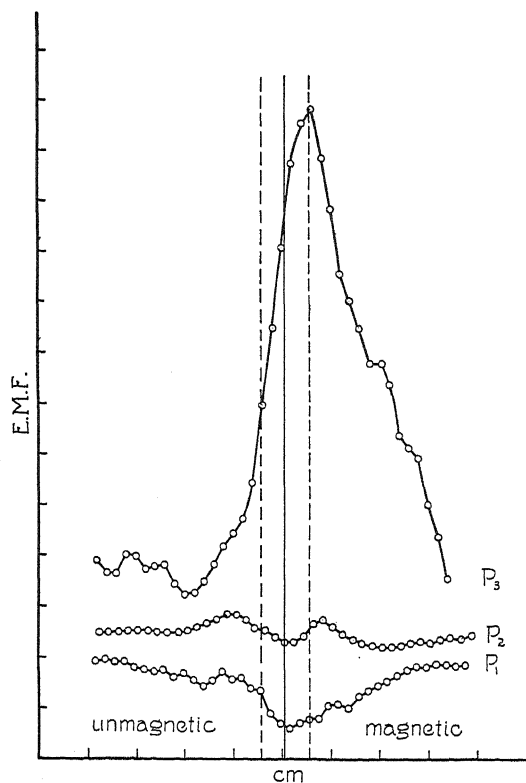


Fig. 15. The thermoanalytic curves of three principal orientations of crystals (kind "B") grown discontinuously. Field: 21,000 Gauss.

Fig. 15 shows analysis curves typical for crystals of these three orientations. The method of growth employed was the discontinuous (see Part I), the metal of purity "B" (see later), and the field strength 21,000 Gauss.

* The thickness of the center line is misleading in so far as the furnace plate was 1 mm thick and since it was impossible to measure exactly its location within the oil layer.

** The possibilities of azimuthal variation were neglected in these experiments. There are:

- two for P_1 with regard to field and vector;
- two for P_2 with regard to vector;
- two for P_3 with regard to field;

which differ essentially from each other.

The diagram shows that the thermal e.m.f. depends very much on the orientation of the principal axis of the crystal to the field lines. The effect is very large for P_3 and very small for P_2 ; it is even very probable that the latter effect does not exist at all, and that the deviations of the P_2 -diagram are due to inaccuracies in orientation.

The thermal e.m.f. is positive for P_3 and negative for P_1 .*** Furthermore it is apparent from Fig. 15 that the thermal e.m.f. is different from what should be expected, (see Part I) since the maximum of the P_3 -curve is not at the intersection with the center line, i.e. within the region where θ is largest (see Fig. 9), but at the border between oil and water, where $d\theta/dx$ is a maximum, a fact which seems to be of fundamental importance.

The size of the thermal e.m.f. of the P_3 curve seems remarkable (7.8×10^{-5} volt or 4.33×10^{-6} volt. degree $^{-1}$), if one calculates the change in orientation of the crystal necessary to produce this e.m.f. due to the thermoelectric anisotropy of the Bi crystal. Taking the data from Bridgman's last paper¹³ one finds that change would have to be 21° **** though it is certain that there is no larger change of orientation at the intersection than 0.5° , which fact makes it quite impossible that the thermal e.m.f. is just caused by a change of orientation at the intersection.

The Effect as a Function of the method of growth. The methods of growth employed have been described in detail in Part I of this paper. They were the so-called continuous and discontinuous methods. Fig. 16 shows curves obtained from crystals of P_3 orientation produced in these different ways. "1" represents the former, "3" the latter; in both these cases, no appreciable residual field was present over the so-called unmagnetic portion of the crystal. "2" on the other hand, represents a crystal of continuous growth with the residual field present during the growth of the first portion of the crystal.

It was entirely unexpected to find that the thermal e.m.f. depended on the method of growth to such an extent as shown in Fig. 16. The fundamental difference between "3" and "1" is that there exists only one maximum in the former (the small second maximum at "b" has a different cause and will be discussed later) and a maximum and a minimum in the latter. The sign of these maxima is opposite in "1" and "3" but their positions coincide again with the extreme values of $d\theta/dx$ in the thermoanalyzer, for "1" the thermo-analytic curve is even an exact repetition of the $d\theta/dx$ curve in Fig. 9. The case of "2" shows the large effect of a small field strength which seems to suppress entirely the first maximum.

*** The thermal e.m.f. is called positive, if the end of the "magnetic" part of the crystal had a potential positive with regard to the end of the normal half, if the temperature of the intersection was higher than the temperature of the ends.

**** This diagram (Fig. 16, page 384) shows the thermal e.m.f. as a function of $\cos^2 \phi$ (angle of orientation). The units of the ordinate are 3.10×10^{-4} volt for a difference of temperature of 68° . Since the curve is no straight line it is necessary to measure at an orientation corresponding to P_3 , i.e., starting from $\cos^2 \phi = 1.0$. Since the e.m.f. unit in that diagram equals $3.10 \times 10^{-4} / 68^\circ = 4.56 \times 10^{-6}$ volt. degree $^{-1}$ our e.m.f. corresponds to $4.33 / 4.56 = .95$ units. For the P_3 -orientation ($\cos \phi = 1$) .95 ordinate-units correspond to 1.3 units of the abscissa, i.e. $\cos \phi = (0.87)^{1/2}$, $\phi = 21^\circ$.

The effect as a function of the impurities. It became evident that the magnitude of the effect depended on the purity of metal used to a very large extent. The crystals were therefore prepared from four kinds of Bi, obtained

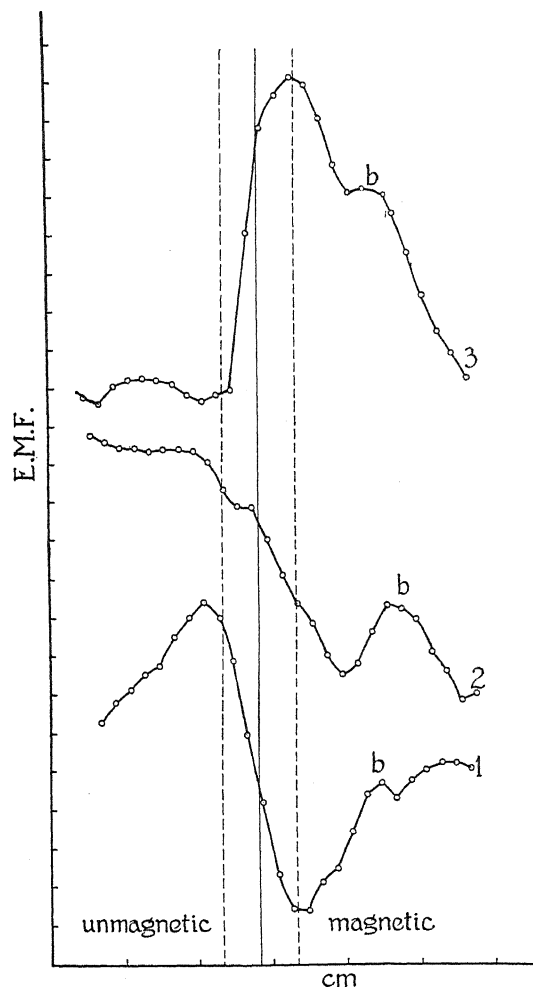


Fig. 16. The thermoanalytic curves of three different types of growth:

1. represents the continuous method without residual field. Field: 13,800 Gauss; kind "B₁;" orientation: P_3 .
2. represents the continuous method with residual field.
3. represents the discontinuous method.

from different sources which were designated as "A", "B", "C", and "D" as shown in the following table:

TABLE III. Sources of the bismuth used.

Designation	Characterization	Source
"A"	Bismuth C. P.	Brown Corp., Philadelphia, Pa.
"B"	Bismuth purissimum	Hartmann & Braun, Frankfurt a. M.
"C"	Electrolytic bismuth	"
"D"	Bismuth "Kahlbaum"	Kahlbaum A. G., Adlershof.

Fig. 17 shows curves of the P_3 orientation made from these four different kinds of Bi by the discontinuous method, whereas Fig. 18 represents the corresponding crystals of continuous growth.

Since from this work as well from papers of Bridgman¹³ and Kapitza¹⁴ it was well-known how large the influence of small impurities on the electric effects of Bi can be, an accurate chemical analysis of the different kinds of bismuth was made. The results obtained showed that a very small trace of

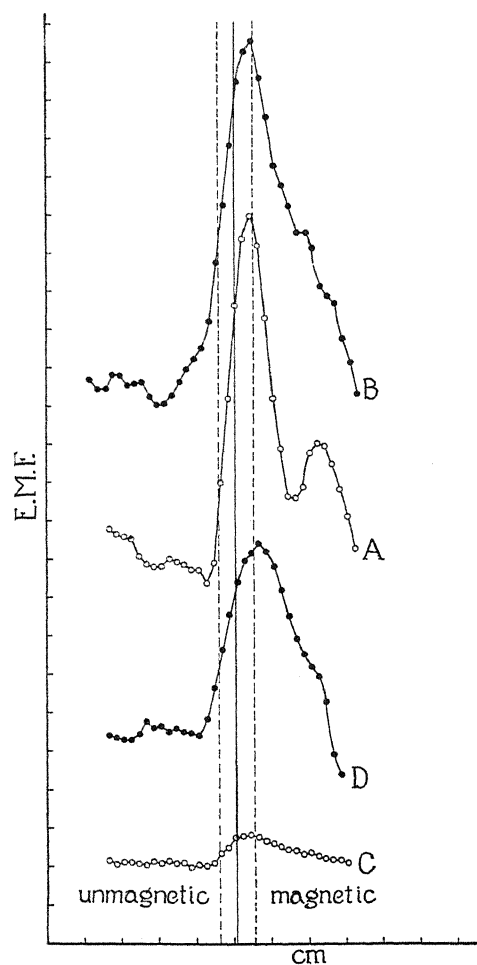


Fig. 17. The thermoanalytic curves for P_3 crystals of four different degrees of chemical purity, grown discontinuously; field: 21,000 Gauss.

silver was present in "A" and "B" though the amount was too small to measure accurately. Since this indicated that the impurities involved were only present in extremely small amounts, a spectral analysis seemed necessary. Dr. R. M. Badger was kind enough to perform this type of analysis

¹³ P. W. Bridgman, Proc. Am. Acad. 63, 351 (1929).

¹⁴ P. Kapitza, Proc. Roy. Soc. A119, 358 (1929).

on our different metals. The amount of any impurity was measured by comparing the intensities of its different lines as observed for the specimen, with the intensity of the lines obtained from these metals by themselves in a spark. The bismuth electrodes were prepared by putting the metal into Pryex tubes after it had been ascertained that the glass did not contain any of the metals

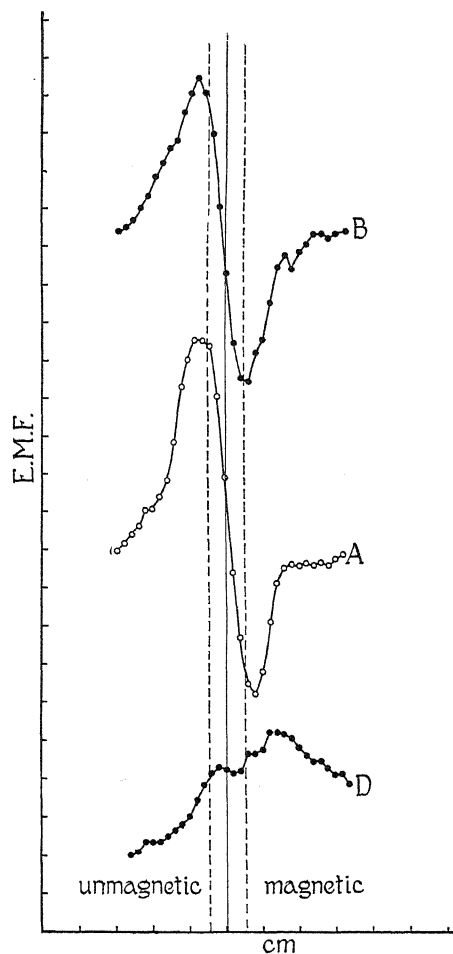


Fig. 18. The thermoanalytic curves for P_3 crystals of three different degrees chemical purity, grown continuously; field: 13,800 Gauss.

involved in the analysis. The results are given in the following table, where the numbers give the approximate relative intensities of the indicated lines of the different impurities.

In general, it can be said that the amount of impurity is probably on the whole, smaller than 0.2 percent in the worst case which is "B". It is smaller for "A" which contains less Pb. "D" differs from "B" in its smaller content of Pb, though in its Ag content, it compares badly whereas "C" is by far the purest metal.

TABLE IV. Spectroscopic analysis of Bi samples.

Sample	Ag		Cu		Sn	Pb					Zn			Sb					
	3281	3383	3247	3274	3262	2863	4058	3683	3639	3275	2802	2613	4810	4722	3345	3267	3232	2598	2528.5
A	4	1	1		?		5	1			?								?
B ₁	5	2	1		?		10	4	3										
B ₂	5	2	1		?		10	4	2										
C ₁	1		5	3	?		1						?						?
C ₂	1		5	3			1	?					?						?
D ₁	7	3	1-0		1		6	1											
D ₂	7	4			1		5												?

Thus it is apparent from the diagrams that the purest metal shows the smallest effect and also that the shape of the curve is but little affected. However the secondary maximum ("b" in Fig. 16) depends apparently on certain impurities, since it is very large for "A" (Fig. 17) and extremely small for "C". The method of continuous growth shows very little difference between "A" and "B" and a large one for "D". It is however doubtful whether the latter measurement is a correct one, since it is based only on a few crystals.

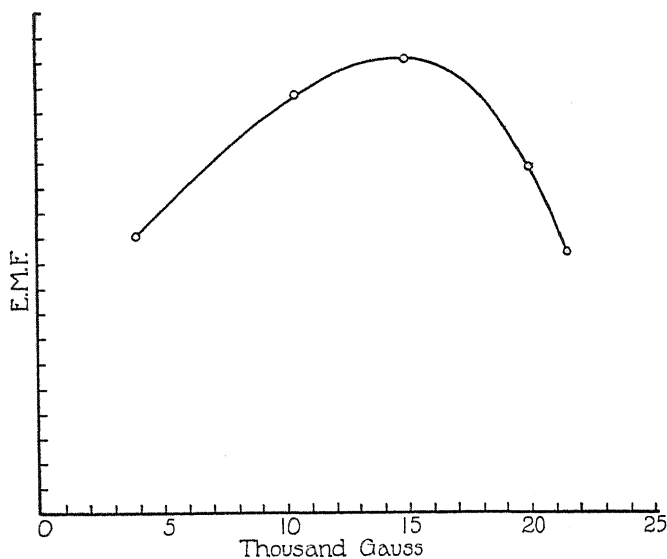


Fig. 19. The size of the maximum thermal e.m.f. as a function of the field strength for P_3 crystals, kind "B," grown discontinuously.

The effect as function of the field strength. Although it is very important to investigate what influence the strength of the applied field has upon the thermoelectric effect, it appeared very difficult to obtain reliable results, since the effect does not depend merely on the orientation of the crystal but also on the method of growth, the degree of impurity, etc. Thus

it has not yet been possible to obtain results of sufficient generality in spite of a great number of experiments. It seems however quite safe to state that there exists a large influence of the field strength upon the effect for crystals of the P_3 -orientation. (Other orientations have not yet been investigated.) The influence of weak fields is very large whereas strong fields (20,000 Gauss) decrease the effect considerably in the case of the discontinuous method of growth.

Fig. 19 shows the variation with field strength obtained for crystals grown with the P_3 orientation, composed from a series of curves of the type of Fig. 15.

The field which produces the maximum thermoelectric effect seems to depend on the degree of impurity.

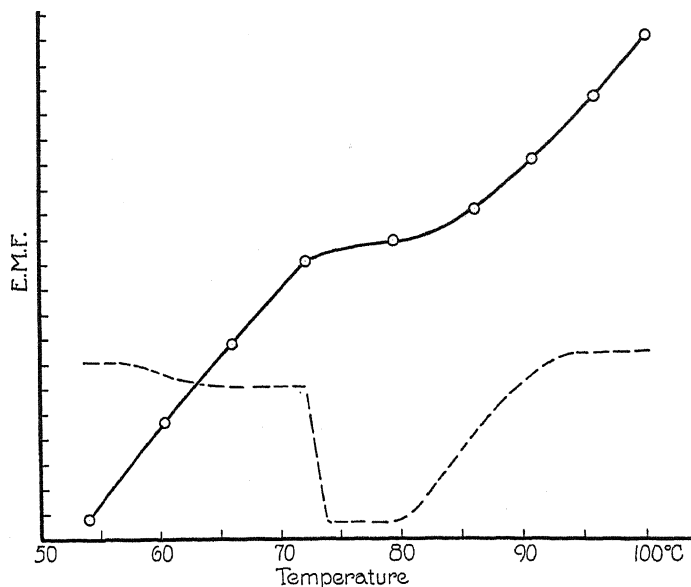


Fig. 20. The size of the maximum thermal e.m.f. as a function of the temperature (The hypothetical transformation of α into β -bismuth.) P_3 -crystal, grown discontinuously, kind "B," field: 21,000 Gauss. The dotted curve gives $dE/dT=f(T)$.

The effect as a function of the temperature. Fig. 20 shows the thermoelectric effect between the magnetic and the normal half of a crystal as a function of the temperature of the analyzer and its differential curve (dotted). The curve was taken by first finding the exact position of the maximum e.m.f. with regard to the crystal (crystal of the type shown in Fig. 15) and then keeping the oil layer in this position while its temperature was gradually increased.

This experiment performed on many crystals of different types showed that the temperature function is independent of the impurity as far as the general shape of the curve is concerned. It seems quite interesting that the differential curve $dE/d\theta$ shows a large discontinuity between 75° and 90°C.

Since it is well known that this type of curve is obtained in case of an allotropic transformation (as for instance typically represented by the thermoelectric effects of pure iron¹⁵) the shape of the curve obtained indicates that the discontinuity in that region of temperature affects the magnetic half of the crystal in a different way than the normal.*

In order to decide whether or not the magnetic state is just a more or less unstable allotropic state caused by strains, such as magnetostriction for instance, specimens showing large effects were reinvestigated after being annealed. The temperature of annealing was chosen sufficiently high, above 90°C, to see whether the transition into the normal state would occur at all. Since this annealing temperature lies above the point of the mentioned "allotropic" transformation, it is probable that the instability of the magnetic state should increase, or the transformation speed into the normal state should be larger.

Hence a crystal (P_3 of "B") was analyzed the day it had been grown, it was then annealed for 16 hours at 100°C and analyzed again a month later. No change of any kind could be detected which indicates that the magnetic state is either perfectly stable or that it has an extremely slow speed of transformation. It is certainly not affected by passing the critical temperature of normal Bi. (75°–90°C)

This experiment shows also that the effect of "aging" Bi crystals does not occur in specimens of good crystallographic perfection, either for normal or for magnetic crystals.

* The question of the existence of an allotropic state of Bi is still unsettled; Cohen¹⁶ and Cohen and Moesveld¹⁷ concluded from their pyknometric and dilatometric measurements the existence of an α and a β modification, of which the α -state is stable below 75°C having a larger density than the β -state. However those authors found other transformations at 81° and 90° where the volume of the metal changed suddenly according to its thermal history. Würschmidt¹⁸ found also the transformation point at 75° indicated by a large contraction, whereas the temperature coefficient of the conductivity of Bi as investigated by Bridgman¹⁹ and Holborn²⁰ does not indicate such transformation at all.—Furthermore the thermoelectric effects as a function of temperature of Bi single crystals were investigated by Boydston;²¹ his $E=f(\theta)$ curves show a slight indication of an irregularity in this region of temperature which becomes much more evident in the case of the Peltier effect curve: $\Pi = T \, dE/d\theta = f(\theta)$. A recent investigation of the Peltier and Thomson effect by Fagan and Collins²² would have cleared this question, if the authors had extended their measurements into this region of temperature. The exact coincidence of the critical temperatures in our measurements with the transformation-point of Cohen, Moesveld, and Würschmidt seem to render the existence more probable. It may be however another example of "pseudo-allotropy" due to traces of impurities as shown recently in the case of extremely pure Zn by Guertler and Anastasiadis.²³

¹⁵ A. Goetz, *Phys. Zeits.* **25**, 562 (1924); **26**, 260 (1925).

¹⁶ E. Cohen, *Akad. Amsterdam Verls.* **23**, 1224 (1914/15).

¹⁷ E. Cohen and A. L. Th. Moesveld, *Zeits. f. Phys. Chem.* **85**, 420 (1913).

¹⁸ J. Würschmidt, *Verh. d. Dt. Phys. Ges.* **16**, 799 (1914).

¹⁹ P. W. Bridgman, *Proc. Am. Acad.* **52**, 636 (1916/17).

²⁰ L. Holborn, *Ann. d. Physik* (4) **59**, 152 (1919).

²¹ R. W. Boydston, *Phys. Rev.* **30**, 911 (1927).

²² H. D. Fagan and T. R. D. Collins, *Phys. Rev.* **35**, 421 (1930).

²³ W. Guertler and L. Anastasiadis, *Zeits. f. Metallkd.* **21**, 338 (1929).

DISCUSSION

Generally speaking the above results are far from sufficient to start an explanation of the effect on a theoretical basis. However the results seem to us complete enough to describe the phenomenology of the new effect approximately.

In the first place, it becomes quite apparent that the forces acting at the moment of crystallization affect the physical properties of the final crystal, though neither orientation nor any other macroscopic quality of the crystal is changed.

The effect as a function of the orientation of the crystal with regard to the field seems the most obvious of all the different variations of the experimental conditions. Here we obtain the largest thermal e.m.f. if the principal axis is normal to the field lines and parallel to the heat flow, i.e. the direction of the thermoelectric current (P_3); whereas the effect is extremely small if the axis is parallel to the lines of force and normal to the flow (P_2).

If one considers the anisotropy of the diamagnetic susceptibility of Bi crystals as measured recently by Focke⁶ a relation between the two effects is quite evident, since in case of P_3 the crystal is in a position where the direction of the largest diamagnetism is parallel to the lines of force, and in the case of P_2 the most "paramagnetic" direction is parallel to the field. Hence there is a difference between the content of free energy in these cases, for the stability of the latter orientation is larger than of the former. If thus a crystal is grown first under normal conditions and then in a field the stability does not change in case of P_2 but is does considerably in case of P_3 . One knows from other observations that a crystal prefers the P_2 orientation when forming its first center of crystallization in a transverse field and also that the field does not even change the opposite orientation if the latter is enforced on it by inoculation with a seed crystal. The fact that the point where the field (i.e. the instability) started is indicated by a thermal e.m.f. shows that the crystal undergoes a change in spite of the constancy of the orientation. Thus the question about the nature of this change becomes quite interesting.

Regarding the shape of the thermoanalytic curves it seems as if the curves of discontinuous growth (Fig. 15) were due to a double-crystal, and the curves of continuous growth (Fig. 18) represent a triple crystal, as has been discussed in Part I of this paper. The interpretation however of the latter diagram as being produced by a triple-crystal seems to be inadequate in view of the fact that the length of sandwiched section (d in Fig. 8b and 8c) would have to coincide with the thickness of the oil layer to produce the maxima and minima at the borders of the layer, which coincidence would seem highly improbable; i.e. the maxima and minima of the diagrams are too close together to be sufficiently resolved if caused by a section smaller than the thickness of the oil layer. Furthermore those points are not situated at the hottest part of the oil layer of the thermoanalyzer (Fig. 9), which means that the e.m.f. does not reach its maximum if the intersection of the crystal passes θ_{\max} . This concerns also the simpler curves of discontinuously grown crystals.

It is very remarkable that the maximum of the thermoanalytic curves of P_3 crystals of that kind does not coincide with the position of the maximum of temperature, it does however with the maximum of the $d\theta/dx$ curve (Fig. 9), i.e. at the border of water and oil. *The only simple interpretation is thus that the thermal e.m.f. must depend on the temperature gradient or the density of the heat flow crossing the intersection between the normal and the magnetic half of the crystal.*

It is apparent that such effect cannot be caused simply by a double or a triple crystal, since the normal thermoelectric effect between two different metals or orientations of a crystal depends on the difference of the temperature and is quite independent of the gradient.

Although the assumption of such a type of a thermoelectric effect seems to be quite uncertain in view of the fact that the passing of the opposite gradient (air-oil, see Fig. 9) is much less expressed by the thermoanalytic curves of discontinuously grown crystals, such interpretation gains some probability in the case of continuously grown crystals (Fig. 18). Here we have curves which are the exact duplicates of the $d\theta/dx$ -curve in Fig. 9. The sign of the effect is opposite in these two cases as follows: If the heat flow passes the intersection *from* the magnetic *to* the unmagnetic half of the crystal, the magnetic half is *positive* for *continuous* growth and *negative* for *discontinuous* growth, it is opposite if the heat flows the other way. In case of the discontinuous kind of growth the flow in the latter direction seems to be quite ineffective.

It is apparent that the influence of the impurities makes the effect very complex since the amount as well as the kind of impurity affects the thermal e.m.f. considerably as is to be expected from a consideration of the dependence of the anisotropy of the electric qualities of the crystal on the impurities present. Hence the mentioned instability of a growing crystal for certain orientations to the field should increase with an increasing anisotropy due to impurities and one should expect a kind of proportionality of the thermal e.m.f. with the impurity. This however is misleading, since it seems highly probable from the behavior of the metal "C" that an ideally pure Bi would not show any effect at all though the electric anisotropy still exists. Thus one is forced to assume that the whole effect is due to disturbances of the odd atoms in the Bi lattice, which disturbance is the more distinct the better the crystal is grown. The disturbance for a given amount and kind of odd atoms depends apparently on their arrangement and is easily affected by external influences during the act of crystallization.

Very little can be said as yet about the actual nature of the disturbance though the fact that an extremely small amount of impurities has such a large influence seems to indicate a surface effect, i.e. an effect due to a formation of mono- or bimolecular layers of odd atoms sandwiched between perfect sections of the crystal. Such arrangement similar to the "II-planes" of the mosaic structure of Zwicky^{7,24} would require an extremely small amount of impurity to affect the electronic relations inside the lattice. In case of such an interpretation one has to assume that the arrangement of the odd atoms is changed under the influence of the magnetic field. It is quite plausible that such a

change differs with different crystallographic planes as well as that its effect works differently upon an electric current, which might explain the difference between the thermoanalytic curves of P_1 and P_3 . (As has been mentioned already, these two orientations do not differ with regard to the field though they do with regard to the direction of the thermoelectric current and the heat flow.)

The arrangement of the odd atoms within the crystal must depend furthermore on the growth of the crystal, since any disturbance during the formation will affect the structure of the impurity layers to a certain extent and therewith the final influence of the magnetic field. This would explain the difference between the thermoanalytic curves of continuous and discontinuous growth. The highly metastable state of the configuration of the odd atoms within the Π -planes during the formation of the mosaic structure is probably the cause of the extreme experimental difficulties in obtaining reproducible results.

Before closing, some comparisons with Kapitza's work¹⁴ may be made. Concerning his observations of the change of the resistance of Bi crystals in a strong magnetic field, it is to be expected from the above hypothesis that the Bi which produced an extremely small effect (K.'s crystal "B" in his Fig. 13, p. 407, l.c.) would produce in our case one of medium magnitude, since his metal corresponds to our "D" whereas his crystal "A" which produced large effects was of metal of the same source as our "C" giving—for our work—the smallest values. Since the influence of an external field upon the change of the resistance depends on the size of the disturbances within the lattice, our experience with "D" and "C" compares very well with Kapitza's result, his effect being fogged by impurities and ours depending apparently wholly on their presence.

With regard to the orientation effects, a few comparisons can also be made. Being limited to only one direction of both the field to the rod, and the thermoelectric current to the rod, only one kind of Kapitza's experiments can be considered for comparison, i.e. where the field is normal to the current. Neglecting the azimuthal effects which seem in our case small, at best, comparison shows that the largest values obtained of the ratio R/R_0 is for our so-called P_3 orientation, while the value obtained for P_1 was only a fractional part of that for P_3 , both facts being analogous to our results. In the case of P_2 however, a larger value of R/R_0 than the P_1 case was obtained which might be interpreted as suggested above, because our effect shows no appreciable influence of the odd atoms upon this orientation.

CONCLUSION

Although these experiments were begun several years ago during which time a very large number of measurements have been taken, it is not yet possible to give more than a rather vague hypothetical explanation as outlined above. Since the experimental difficulties proved to be very large the

¹⁴ F. Zwicky, *Helv. Phys. Acta* **3**, 269 (1930).

actual progress has been slow and the present paper cannot be more than a first report about the new effect.

Systematic measurements concerning the electrical conductivity, the specific gravity, and the magnetic susceptibility were performed and are still going on, as well as a detailed x-ray analysis of the "magnetic" crystals. Papers concerning these subjects will be published in near future.

In conclusion, the authors wish to express their great obligation to Dr. R. A. Millikan for the interest he has taken in the work, to Dr. R. M. Badger to whom they owe the spectroscopical analysis of the bismuths, to Mr. J. Pearson for his helpful technical advice and to Mr. A. Focke for his general assistance.

THE SECOND VIRIAL COEFFICIENT FOR GASES: A
CRITICAL COMPARISON BETWEEN THEORETICAL
AND EXPERIMENTAL RESULTS

BY HENRY MARGENAU

SLOANE PHYSICS LABORATORY, YALE UNIVERSITY

(Received November 5, 1930)

ABSTRACT

On the basis of a recent theory developed by London the second virial coefficient of the following gases is computed: He, Ne, A, H₂, N₂, O₂, CO₂, NH₃, H₂O. For the latter two, which have a dipole moment, the contribution of the dipole interaction is also calculated. The results are compared graphically with experimental values. Except in the case of He and H₂, where the disagreement can be accounted for by the presence of zero point energy, the accordance is as good as is compatible with the inaccuracies involved in the calculation.

IN CLASSICAL mechanics it was necessary to attribute the attractive forces between molecules, demanded by the empirical equation of state, to the action of permanent or induced electric poles. Quadrupoles of considerable moment had to be assigned to molecules such as H₂ and the rare gases, which were known to carry no permanent dipoles. On the basis of the old atomic models the required assumption of quadrupoles was entirely reasonable, but it is inconsistent with the more uniform distribution of molecular charges calculated by wave mechanics. Moreover, molecular quadrupoles are not yet accessible to measurement, so that a theory based on their presence is unsatisfactory for its lack of verification. This difficulty was very successfully removed when Eisenschitz and London¹ recognized the significance of attractive forces appearing in the second order perturbation in the interaction problem of two H atoms. They showed that Van der Waals' constant a derived from these forces had the correct order of magnitude. In a recent paper London² made a more comprehensive study of these forces (arising from what he terms the "dispersion effect") and discussed in particular their relation to two other types of attractive forces existing between molecules having electric moments (resulting from Keesom's effect of "alignment" and Debye's induction effect).³ He also calculates the contribution to the molecular interaction energy of the dispersion effect and finds that this is for many gases the dominant constituent of the interaction, resulting in a van der Waals' a which is in good agreement with the value for a computed from critical data. This is indeed a most interesting and significant observation which goes far in confirming the validity of the theory. Now it is well known that van der Waals' equation with a independent of the

¹ R. Eisenschitz and F. London, *Zeits. f. Physik* **60**, 491 (1930).

² F. London, *Zeits. f. Physik* **63**, 245 (1930).

³ Cf.² for literature.

temperature does not represent the empirical equation of state, nor does the a value computed from critical data coincide of necessity with the factor of $1/T$ in the equation of state. It is the purpose of this communication to make a closer comparison between the predictions of London's theory and experimental data, and also to include in this comparison the results of a recent paper⁴ dealing with forces between dipole molecules. We shall express the second virial coefficient, B , as a function of the temperature and examine its correspondence to the empirically known values of B for various temperatures. The results can best be shown by graphs.

It will appear that the calculation of B is of necessity very crude because idealized assumptions and lack of accurate knowledge of certain quantities involved; hence one is justified to look for qualitative agreement only. The method used is essentially the same as that employed by London to compute a and is subject to the same errors.

NON-POLAR GASES

It may be recalled that B is the coefficient of $1/V$ in an expansion of pV/RT as a power series in $1/V$. It measures the deviation from Boyle's law for small concentrations (large V) and is given analytically by:

$$B = 2\pi N \int_0^{\infty} (e^{-\epsilon/kT} - 1)r^2 dr, \quad (1)$$

where ϵ is the interaction energy of two molecules expressed as a function of r , the distance between the molecules. If N is Avogadro's number, B is in cc per mole. The result of London's⁵ investigation concerning the dispersion effect is:

$$\frac{3}{4} \frac{\alpha^2 V_a}{r^6} \leq -\epsilon \leq \frac{3}{4} \frac{\alpha^2 V_i}{r^6} \quad (2)$$

where α is the polarizability, V_a the excitation potential, and V_i the ionization potential of the substance. An accurate theoretical expression for ϵ involves the energy values and matrix elements of the molecules and is, therefore, in general difficult to evaluate. At $r < d$ the interaction energy ceases to be given by (2), ϵ merges into the rapidly rising exponential curve characteristic of the valence forces.⁶ Here the assumption will be made that

$$\epsilon = +\infty \text{ for } r < d \quad (3)$$

corresponding essentially to the supposition that the molecules have a diameter d and are impenetrable. Refinements, such as introducing a dependence of d on T , as would be necessary to take account of the finite slope of the exponential curve at $r = d$ are possible but can be omitted in view of the general lack of precision of the premises on which we are compelled to make

⁴ H. Margenau, *Zeits. f. Physik* **64**, 584 (1930).

⁵ Reference 2, p. 256.

⁶ See Fig. 1 in the paper by Eisenschitz and London.

the calculation. We shall therefore assume an empirical value for d , independent of T . Moreover we shall put

$$\epsilon = -\frac{3}{4} \frac{\alpha^2 V_i}{r^6} \quad (4)$$

introducing thereby a considerable error. (There is reason to suppose that in general ϵ is nearer the upper limit in (2).)⁷ Expanding the exponential in (1) and performing the integration using (3) and (4) we obtain

$$B = \frac{2\pi N d^3}{3} \left\{ 1 - 0.75 \frac{\theta_1}{T} - 9.4 \times 10^{-2} \left(\frac{\theta_1}{T} \right)^2 - 1.4 \times 10^{-2} \left(\frac{\theta_1}{T} \right)^3 \right. \\ \left. - 1.9 \times 10^{-3} \left(\frac{\theta_1}{T} \right)^4 - 2.2 \times 10^{-4} \left(\frac{\theta_1}{T} \right)^5 \right. \\ \left. - 2.2 \times 10^{-5} \left(\frac{\theta_1}{T} \right)^6 - \dots \right\}, \quad (5)$$

where

$$\theta_1 = \frac{\alpha^2}{d^6} \frac{V_i}{k}.$$

If we put

$$\frac{2\pi N d^3}{3} = B_0$$

we have

$$\theta_1 = \frac{4\pi^2 N^2}{9k} \frac{\alpha^2 V_i}{B_0^2}.$$

B_0 can be determined from the empirical B curve and is essentially the same as van der Waals' b . The values of B_0 used in the computation of B are taken from Beattie and Bridgeman's⁸ work, except for O_2 and CO_2 . For these two gases the experimental and the theoretical B obtained from the data listed by the latter authors proved to be peculiarly discrepant, more so than could be explained by the crudeness of the calculation. It may be observed, however, that while for all other gases listed here Beattie and Bridgeman's B_0 is in the neighborhood of the usual b -values (as computed from critical data), it is considerably higher for O_2 and CO_2 (46 and 105). Also, in the case of He, Ne, A, N_2 their constants are derived from isothermals up to $400^\circ C$, whereas for the two gases in question only temperatures up to $100^\circ C$ were used. If now it is remembered that B_0 is the limit of B for high temperatures one could be led to suppose that though Beattie-Bridgeman's B_0 , together with their other constants, describe the behavior of O_2 and CO_2 very well over the range of lower temperatures, it may not actually be the limit which is here required.⁹

⁷ See reference (1), action of the continuous spectrum.

⁸ Cf. for instance *Zeits. f. Physik* **62**, 95 (1930).

⁹ At 258° Beattie and Bridgeman's constants for CO_2 give a value of B which is, compared to Amagat's measurements, about 50 percent too small.

If this supposition is erroneous the discrepancy spoken of would have to be admitted as unexplained. We have in the following assumed B_0 values for O_2 and CO_2 equal to the b -values from critical data, which are in agreement with our knowledge about the size of molecules derived from other sources (viscosity). If they are chosen the experimental and the theoretical B -curves agree quite well.

Table I contains the experimental data on the basis of which the computation of B was made. The ionization potentials of some of the gases may be in considerable doubt, but in view of the other uncertainty concerning the

TABLE I.

	$\alpha \times 10^{24}$	B_0	V_i (volts)	θ_1
He	0.20	14	24.5	92
Ne	0.39	20	21.5	150
A	1.63	39	15.4	500
H_2	0.81	21	16.4	440
N_2	1.74	50	17	385
O_2	1.57	32 (46)	13	580 (280)
CO_2	2.9	42 (105)	10	880 (180)

value of V to be used (Eq. (2)) this need not disturb us particularly. It is interesting to observe the magnitude of θ_1 . The calculation of van der Waals' a^{10} neglects higher powers of θ_1/T than the first, which seems unsatisfactory, even if due consideration is given to the large errors in our assumptions. CO_2 , though having a small dipole moment ($\mu = 0.06 \times 10^{-18}$) is included in the list of non-polar gases.

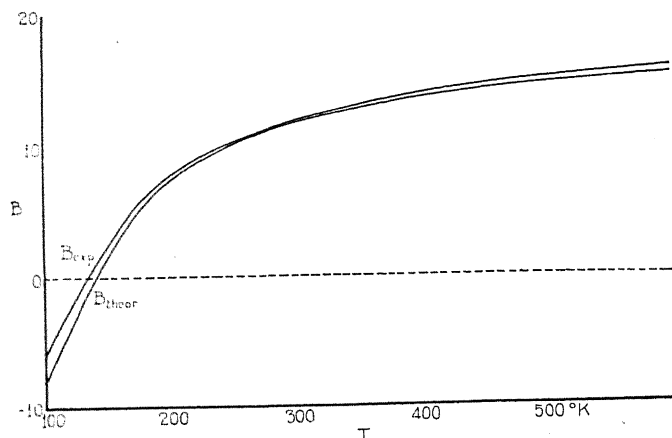


Fig. 1. Neon.

The curves in Figs. 1-7 show the results, the ordinates being in cc per mole, the abscissae in absolute degrees. Except for CO_2 (where the experimental B -values were taken from Amagat's diagram) the experimental points were computed from Beattie and Bridgeman's constants. The broken curves

¹⁰ F. London, reference 2.

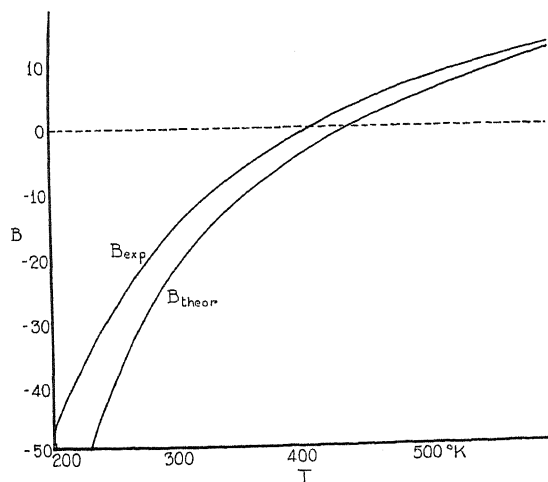


Fig. 2. Argon.

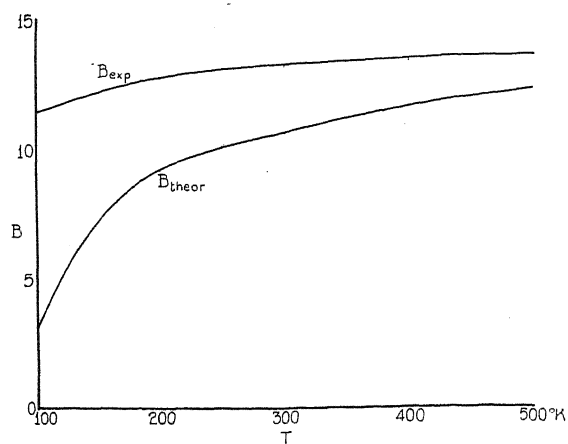


Fig. 3. Helium.

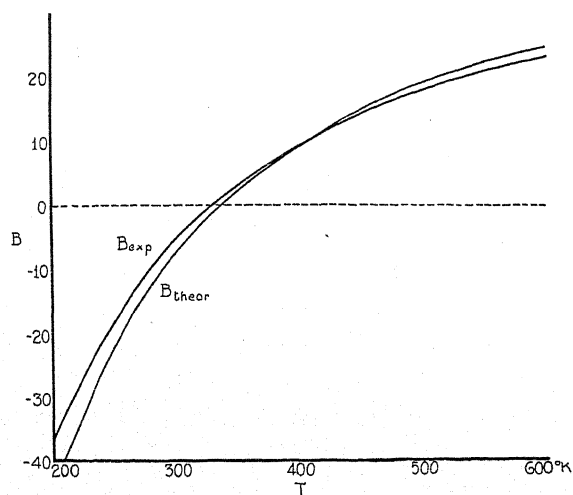


Fig. 4. Nitrogen.

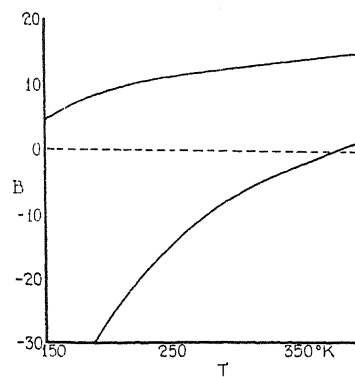
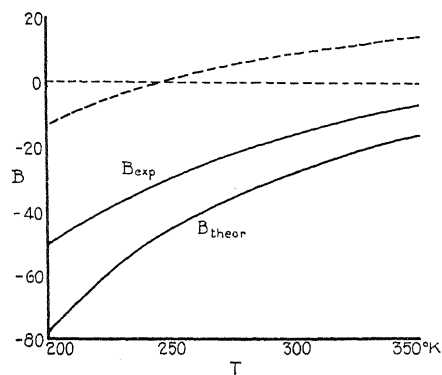
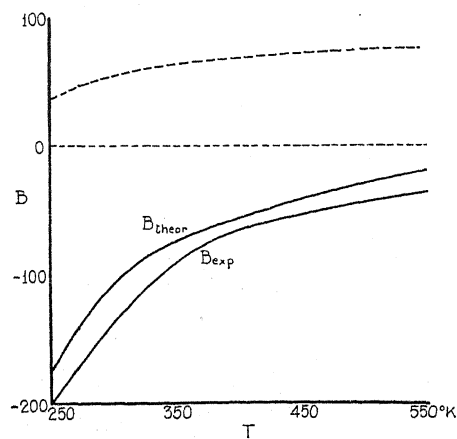


Fig. 5. Hydrogen.

Fig. 6. Oxygen. The broken curve was computed on the assumption $B_0 = 46$.Fig. 7. Carbon dioxide. The broken curve was computed on the assumption $B = 105$.

in Figs. 6 and 7 represent the values obtained by using $B_0 = 46$ and 105 respectively. The agreement is seen to be good for all substances with the exception of He and H_2 , where the large deviation can be accounted for qualitatively by the zero point energy of the interacting molecules. As London has pointed out, this is negligible for molecules of larger mass, but would, in the case of He and H_2 , cause the theoretical curves to be displaced toward the experimental ones.

POLAR GASES

It has been shown¹¹ that for sufficiently high temperatures ($kT \gg h^2/8\pi^2 A$) the virial coefficient of polar molecules is given by

$$B = \frac{N^2}{8\pi} \int_{\Omega} \int_0^{\infty} (e^{-V/kT} - 1) r^2 dr d\Omega \quad (6)$$

where the first integration is extended over all orientations of the two molecules and V is their classical potential energy in terms of r and the angles. For dipole molecules capable of polarization we find, if μ is the dipole moment,

$$V = \frac{\mu^2}{r^3} [-2 \cos \theta_1 \cos \theta_2 + \sin \theta_1 \sin \theta_2 \cos (\phi_1 - \phi_2)] \\ - \frac{\mu^2 \alpha}{2r^6} (3 \cos^2 \theta_1 + 3 \cos^2 \theta_2 + 2) \text{ neglecting small terms.} \quad (7)$$

The B computed from (6) will have to be added to the B resulting from the dispersion effect, but in doing so it must be remembered that the integration over r from 0 to d has already been counted, and the relevant part of (6) results from \int_d^{∞} . Expression (6) has been calculated by Falkenhagen.¹² He finds for several dipole gases, among them NH_3 and H_2O , good agreement between experimental data and the results of (6). This is very surprising from our present point of view, for it would seem to indicate that, if the dispersion effect also were taken into consideration the total B would be much too large. This difficulty, we feel, resolves itself on closer examination. It is impossible to check Falkenhagen's calculations in detail because the numerical values used in them are not all stated. (If we use the values of d derived from the B_0 of Table II, the agreement found by him is considerably disturbed.) We also note that his potential energy expression contains a polarization term (the second term in the brackets of (7)) twice as large as ours, which circumstance we are inclined to attribute to a numerical error in his G_2 . This tends to enlarge the contribution of (6) to B .

¹¹ H. Margenau, *Zeits. f. Physik* **64**, 584 (1930). In Eq. (1) of this paper a bar was omitted. It should read, of course,

$$B = 2\pi N^2 \int_0^{\infty} (\overline{e^{-V(R, \omega)/kT}} - 1) R^2 dR.$$

¹² H. Falkenhagen, *Phys. Zeits.* **23**, 87 (1922).

In evaluating (6) we remember that

$$\int_{d\Omega} = \int \int \int \int \sin \theta_1 d\theta_1 \sin \theta_2 d\theta_2 d\phi_1 d\phi_2,$$

and obtain, after expanding the exponential, for the dipole contribution to the total B ,

$$\begin{aligned} B' = & -\frac{2\pi Nd^3}{3} \left\{ 2z \frac{\theta_2}{T} + [0.33 + 0.73z^2] \left(\frac{\theta_2}{T} \right)^2 + [0.27z + 0.35z^3] \left(\frac{\theta_2}{T} \right)^3 \right. \\ & + [1.3 \times 10^{-2} + 0.21z^2] \left(\frac{\theta_2}{T} \right)^4 + 2.3 \times 10^{-2} z \left(\frac{\theta_2}{T} \right)^5 \\ & \left. + 5.2 \times 10^{-4} \left(\frac{\theta_2}{T} \right)^6 \right\}. \end{aligned} \quad (8)$$

Here

$$\begin{aligned} \theta_2 &= \frac{\mu^2}{kd^3} = \frac{2\pi N}{3k} \cdot \frac{\mu^2}{B_0} \\ z &= \frac{\alpha}{d^3} = \frac{2\pi N}{3B_0} \alpha. \end{aligned}$$

There is but little sense in using more terms since (1) would probably lose its validity for temperatures in which these terms become significant. The only dipole gases for which a comparison can be made at present are NH_3 and H_2O on account of the lack of experimental data for others. Table II shows the data from which the B values of these two gases were computed.

TABLE II.

	$\alpha \times 10^{24}$	B_0	V_i	$\mu \times 10^{18}$	θ_1	θ_2	z
NH_3	2.21	34	11	1.50	880	610	0.085
H_2O	1.48	34	13	1.84	470	920	0.055

B_0 for NH_3 was taken from Beattie and Bridgeman's work and the experimental B computed from their constants, while for H_2O it was necessary to take the critical data b , using for comparison experimental data by M. Jacob¹³ from which Falkenhagen¹⁴ has calculated the second virial coefficient.

In Figs. 8 and 9 the experimental curves are plotted together with values obtained from (a) (5), (b) (5) + (8). It is seen in both cases that the dipole effect is a very essential part of the interaction causing B . For NH_3 the agreement between B_{exp} and $B_{\text{disp+dipole}}$ is quite good, showing that the two effects here considered suffice to explain the molecular interaction. For H_2O , however, it is evident that they do not suffice, and that we must look, for quad-

¹³ M. Jacob, Zeits. f. Ing. 1912, p. 1980.

¹⁴ Reference 12.

rupole interaction to fill the space between the two lower curves of Fig. 9. It is plausible to assume that water molecules have a quadrupole moment, and one can without difficulty compute it from the last figure, for Keesom's

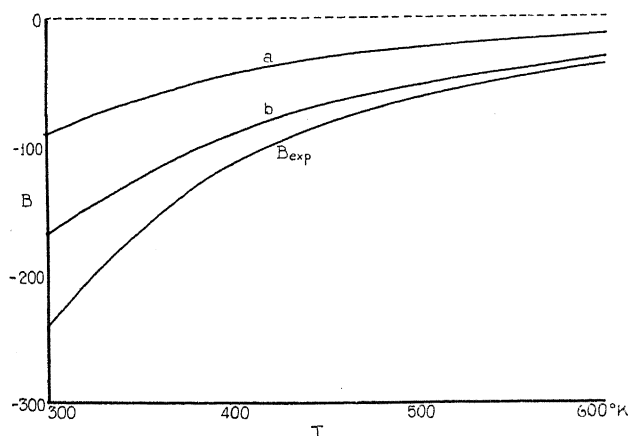


Fig. 8. Ammonia. Curve *a* represents values of *B* due to the dispersion effect, curve *b* those due to dispersion plus dipole effect.

theory, and the formulae he developed,¹⁵ have been shown to be applicable from the point of view of wave mechanics provided that the temperatures

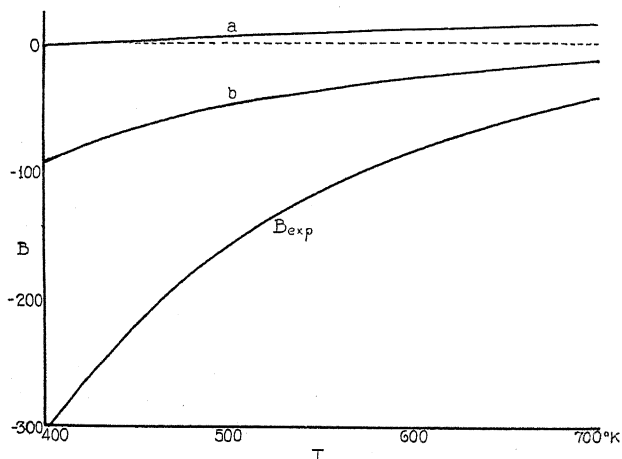


Fig. 9. H_2O . Curve *a* represents values of *B* due to the dispersion effect, curve *b* those due to dispersion plus dipole effect.

are sufficiently high.¹⁶ The result is about 5×10^{-26} for the quadrupole moment. But there appears to be no way at present of checking this value by independent experiments.

¹⁵ W. H. Keesom, Phys. Zeits. 22, 129 (1921).

¹⁶ H. Margenau, reference 11.

TEMPERATURE EQUILIBRIUM IN A STATIC GRAVITATIONAL FIELD

BY RICHARD C. TOLMAN AND PAUL EHRENFEST

NORMAN BRIDGE LABORATORY OF PHYSICS, PASADENA, CALIFORNIA

(Received October 27, 1930)

ABSTRACT

In the case of a gravitating mass of perfect fluid which has come to thermodynamic equilibrium, it has previously been shown that the proper temperature T_0 as measured by a local observer would depend in a definite manner on the gravitational potential at the point where the measurement is made. In the present article the conditions of thermal equilibrium are investigated in the case of a general static gravitational field which could correspond to a system containing solid as well as fluid parts. Writing the line element for the general static field in the form

$$ds^2 = g_{ij}dx_i dx_j + g_{44}dt^2 \quad i, j = 1, 2, 3,$$

where the g_{ij} and g_{44} are independent of the time t , it is shown that the dependence of proper temperature on position at thermal equilibrium is such as to make the quantity $T_0\sqrt{g_{44}}$ a constant throughout the system.

§ I. INTRODUCTION

IN SEVERAL previous articles the principles of relativistic thermodynamics have been discussed¹ and then applied² to determine the conditions for thermodynamic equilibrium in the presence of gravitational fields. In the case of a gravitating mass of perfect fluid which has come to thermodynamic equilibrium, it was shown in the course of the work³ that the proper temperature as measured by a local observer would depend in a definite manner on the gravitational potential at the point where the measurement is made. Thus if we write the line element, for a spherical mass of fluid which has come to equilibrium, in the form

$$ds^2 = -e^\mu(dr^2 + r^2d\theta^2 + r^2\sin^2\theta d\phi^2) + e^\nu dt^2 \quad (1)$$

where μ and ν are functions of the coordinate r , the dependence of the proper temperature T_0 on position was found to be given by the equation

$$\frac{d \log T_0}{dr} = -\frac{1}{2} \frac{d\nu}{dr}. \quad (2)$$

This result is a very interesting one since uniform temperature throughout a system which has come to thermodynamic equilibrium has hitherto been regarded as an inescapable part of thermodynamic theory. In accordance with this equation, however, the proper temperature is found to

¹ Tolman, Proc. Nat. Acad. 14, 268 (1928); *ibid.* 14, 701 (1928); Phys. Rev. 35, 875 (1930); *ibid.* 35, 896 (1930).

² Tolman, Proc. Nat. Acad. 14, 348 (1928); *ibid.* 14, 353 (1928); Phys. Rev. 35, 904 (1930).

³ See reference 2, last article.

increase as we move inwards towards the center of the sphere, and this can be qualitatively interpreted by ascribing to heat the property of weight and regarding the increase in temperature as we move inwards as necessary in order to prevent the flow of heat from higher to lower gravitational levels.

Integrating equation (2) we obtain the result

$$\log T_0 + \frac{\nu}{2} = \text{const.}$$

or

$$T_0 e^{\nu/2} = T_0 \sqrt{g_{44}} = \text{const.} \quad (3)$$

and have thus obtained a quantity which has a constant value throughout the fluid even though the proper temperature itself does not. This result, however has so far only been proved for the equilibrium condition of a perfect fluid, and the question naturally arises whether the quantity $T_0 \sqrt{g_{44}}$ would also have a constant value in the case of a more complicated system containing solid parts. In the present article we shall investigate temperature equilibrium in the case of a general static gravitational field by considering that the parts of the system whose temperatures are to be compared are in thermal contact with a small connecting tube containing radiation. Such a tube may be called a *radiation thermometer*, and by calculating the change in pressure as we go from one portion of the tube to another it will be easy to show that the radiation has the same value of $T_0 \sqrt{g_{44}}$ throughout the thermometer.

§ 2. THE ENERGY-MOMENTUM TENSOR FOR BLACK-BODY RADIATION

In order to solve our problem by the method suggested, we shall need an expression for the energy-momentum tensor for black-body radiation and shall take this as given by the equation

$$T^{\mu\nu} = (\rho_{00} + p_0) \frac{dx_\mu}{ds} \frac{dx_\nu}{ds} - g^{\mu\nu} p_0 \quad (4)$$

with

$$\rho_{00} = 3p_0 \quad (5)$$

where ρ_{00} is the proper macroscopic density of the radiation at the point of interest, p_0 its proper pressure, and the velocities dx_μ/ds correspond to the macroscopic motion of the radiation; i.e., to the motion, in the coordinate system which is being used, of an observer who finds on the average no net flow of energy in the radiation field.

Equation (4) is well known in general relativity as being an expression for the energy-momentum tensor of a perfect fluid,⁴ and the primary justification for adopting it as applying to black body radiation resides in its

⁴ See for example Eddington, "The Mathematical Theory of Relativity," Cambridge 1923, equations (54.81) and (54.82).

general applicability in studying the relativistic mechanics of any system whose local properties can be specified by the two scalars, proper density ρ_{00} and pressure p_0 . And such is evidently the case for black-body radiation, with the additional simplification $\rho_{00} = 3p_0$.

In addition to this primary justification, however, it will also be of interest to start with the usual relativistic generalization of the Maxwell-Lorentz electromagnetic equations and derive the above expression for the energy-momentum tensor by treating black-body radiation as an electromagnetic phenomenon.

In accordance with this relativistic generalization, the electromagnetic field at any point can be specified by a certain antisymmetric tensor $F_{\mu\nu}$ whose components are directly related in Galilean coordinates to the classical components of electric field strength X, Y, Z and magnetic field strength α, β, γ . And the energy-momentum tensor is given in terms of the $F_{\mu\nu}$ by the equation⁵

$$T^{\mu\nu} = -g^{\mu\gamma}F^{\nu\alpha}F_{\gamma\alpha} + \frac{1}{4}g^{\mu\nu}F^{\alpha\beta}F_{\alpha\beta}. \quad (6)$$

Using Galilean coordinates at the point of interest and substituting for the components of $F_{\mu\nu}$ the values which they then have, it is found that the components of $T^{\mu\nu}$ assume the values indicated by the following typical examples⁶

$$\begin{aligned} T^{11} &= -\frac{1}{2}(X^2 - Y^2 - Z^2) - \frac{1}{2}(\alpha^2 - \beta^2 - \gamma^2) \\ T^{12} &= -\alpha\beta - XY \\ T^{14} &= -\beta Z + \gamma Y \\ T^{44} &= \frac{1}{2}(X^2 + Y^2 + Z^2) + \frac{1}{2}(\alpha^2 + \beta^2 + \gamma^2) \end{aligned} \quad (7)$$

Thus in Galilean coordinates T^{11} , T^{22} , T^{33} , T^{12} , T^{13} , and T^{23} become the classical components of the stress in the field, T^{14} , T^{24} , and T^{34} become the classical components of the Poynting vector, and T^{44} becomes the classical density of energy.

If now we consider that the electromagnetic field in question corresponds to black-body radiation, and take a proper system of Galilean coordinates in which the radiation as a whole is at rest, it is evident that we shall have *on the average*

$$X^2 = Y^2 = Z^2 \quad \text{and} \quad \alpha^2 = \beta^2 = \gamma^2 \quad (8)$$

since the average field strength will be independent of direction,

$$XY = YZ = ZX = 0 \quad \text{and} \quad \alpha\beta = \beta\gamma = \gamma\alpha = 0 \quad (9)$$

since the lack of phase relations between waves will make it equally probable that the instantaneous values of these products will have positive or negative magnitude, and

⁵ See Eddington, reference 4, equation (77.2).

⁶ See Eddington, reference 4, equations (77.41-2-3-4).

$$-\beta Z + \gamma Y = -\gamma X + \alpha Z = -\alpha Y + \beta X = 0 \quad (10)$$

since there will be no net flow of energy in the proper system of coordinates that we are now using. Hence, introducing these results into equations 7, it is evident that in proper coordinates the averaged energy-momentum tensor for black-body radiation will have as its only surviving components

$$T^{11} = T^{22} = T^{33} = p_0 \quad \text{and} \quad T^{44} = \rho_{00} \quad (11)$$

with

$$\rho_{00} = 3p_0 \quad (12)$$

where ρ_{00} is the proper macroscopic density at the point of interest and the three surviving components of the stress are each equal to the pressure p_0 .

This expression for the energy-momentum tensor of black-body radiation holds, however, only for a set of proper coordinates x, y, z, t , in which there is no net flow of energy, and to pass to a general set of coordinates x'_1, x'_2, x'_3, x'_4 we shall have to substitute the above values into the general transformation equation

$$T'^{\mu\nu} = \frac{\partial x'_\mu}{\partial x_\alpha} \frac{\partial x'_\nu}{\partial x_\beta} T^{\alpha\beta}.$$

Doing so we at once obtain

$$T'^{\mu\nu} = (\rho_{00} + p_0) \frac{\partial x'_\mu}{\partial t} \frac{\partial x'_\nu}{\partial t} + p_0 \left(\frac{\partial x'_\mu}{\partial x} \frac{\partial x'_\nu}{\partial x} + \frac{\partial x'_\mu}{\partial y} \frac{\partial x'_\nu}{\partial y} + \frac{\partial x'_\mu}{\partial z} \frac{\partial x'_\nu}{\partial z} - \frac{\partial x'_\mu}{\partial t} \frac{\partial x'_\nu}{\partial t} \right) \quad (13)$$

For the macroscopic velocity of the radiation in our new set of coordinates, however, we can evidently write

$$\frac{dx'_\mu}{ds} = \frac{\partial x'_\mu}{\partial x} \frac{dx}{ds} + \frac{\partial x'_\mu}{\partial y} \frac{dy}{ds} + \frac{\partial x'_\mu}{\partial z} \frac{dz}{ds} + \frac{\partial x'_\mu}{\partial t} \frac{dt}{ds} = \frac{\partial x'_\mu}{\partial t} \quad (14)$$

owing to the null value for the components $dx/ds, dy/ds$ and dz/ds and the equality of dt and ds in proper coordinates. And from the transformation equation

$$g'^{\mu\nu} = \frac{\partial x'_\mu}{\partial x_\alpha} \frac{\partial x'_\nu}{\partial x_\beta} g^{\alpha\beta}$$

we obtain

$$g'^{\mu\nu} = -\frac{\partial x'_\mu}{\partial x} \frac{\partial x'_\nu}{\partial x} - \frac{\partial x'_\mu}{\partial y} \frac{\partial x'_\nu}{\partial y} - \frac{\partial x'_\mu}{\partial z} \frac{\partial x'_\nu}{\partial z} + \frac{\partial x'_\mu}{\partial t} \frac{\partial x'_\nu}{\partial t}. \quad (15)$$

Hence, substituting (14) and (15) into (13) and dropping primes we at once obtain the result which was to be proved

$$T^{\mu\nu} = (\rho_{00} + p_0) \frac{dx_\mu}{ds} \frac{dx_\nu}{ds} - g^{\mu\nu} p_0$$

with

$$\rho_{00} = 3p_0.$$

The second justification which we have thus presented for our expression for the energy-momentum tensor for black-body radiation suffers from the fact that it makes our final expression, which contains none but macroscopically measurable quantities, a consequence of the relativistic generalization of the Maxwell-Lorentz equations, which assume possibilities of microscopic measurement in conflict with the modern ideas of quantum mechanics. Nevertheless, in view of the primary justification which we presented, it is evident that our expression for the energy-momentum tensor for black-body radiation may be used with reasonable confidence at the present time, and may actually be regarded as more certain than the basis of the second justification. At some future time, the expression might have to be modified in the light of a successful unified field theory if that should ever be achieved.

§ 3. THE LINE ELEMENT

Having justified the expression which we shall use for the energy-momentum tensor of radiation, we are now ready to proceed to our problem of determining the distribution of radiation in a static gravitational field.

For the case of a general static system which may contain solid parts we can not assume spherical symmetry as a necessary accompaniment of equilibrium, and must take the line element in the *general static* form

$$ds^2 = g_{ij}dx_i dx_j + g_{44}dt^2 \quad i, j = 1, 2, 3 \quad (16)$$

where $g_{ij}dx_i dx_j$ is a negative quadratic form.

We adopt the convention of using Latin indices i, j , etc. to correspond with the spatial coordinates x_1, x_2 and x_3 , and shall reserve Greek indices α, β etc. to correspond with all four coordinates x_1, x_2, x_3 and t . In accordance with the usual definition of a static system we take the potentials g_{14}, g_{24} and g_{34} equal to zero, and take the other potentials g_{ij} and g_{44} as independent of the time t , although depending in any arbitrary way desired on the spatial coordinates x_1, x_2 and x_3 .

For the potential g_{44} , we note from the form of the line element that we have the simple relation

$$g^{44} = \frac{1}{g_{44}}. \quad (17)$$

§ 4. ENERGY-MOMENTUM TENSOR FOR BLACK-BODY RADIATION IN A STATIC FIELD

We must now consider the form taken by the energy-momentum tensor for black-body radiation in the field defined by the above line element. Returning to our general Eq. (4) for the energy-momentum tensor

$$T^{\mu\nu} = (\rho_{00} + p_0) \frac{dx_\mu}{ds} \frac{dx_\nu}{ds} - g^{\mu\nu} p_0 \quad (18)$$

we note that in a static system the macroscopic velocities dx_μ/ds will evidently be zero for $\mu = 1, 2, 3$

$$\frac{dx_i}{ds} = 0 \quad (19)$$

and taking account of Eq. (17) will reduce for the case $\mu = 4$ to

$$\frac{dx_4}{ds} = \frac{dt}{ds} = \frac{1}{\sqrt{g_{44}}} = \sqrt{g^{44}}. \quad (20)$$

Substituting in (18), the energy-momentum tensor degenerates into

$$\begin{aligned} T^{ij} &= -g^{ij}p_0 \\ T^{44} &= g^{44}\rho_{00} \end{aligned} \quad (21)$$

And on lowering suffixes we have

$$\begin{aligned} T_i^i &= g_{i\alpha}T^{i\alpha} = -g_{i\alpha}g^{i\alpha}p_0 = -g_i^i p_0 \\ T_4^4 &= g_{44}g^{44}\rho_{00} = \rho_{00} \end{aligned}$$

so that the only surviving components become

$$T_1^1 = T_2^2 = T_3^3 = -p_0 \quad T_4^4 = \rho_{00}. \quad (22)$$

§ 5. APPLICATION OF THE PRINCIPLES OF MECHANICS

We can now investigate the pressure of radiation in our thermometer by applying the principles of relativistic mechanics in the form of the well-known equation

$$\frac{\partial \mathfrak{T}_\mu^\nu}{\partial x_\nu} - \frac{1}{2} \mathfrak{T}^{\alpha\beta} \frac{\partial g_{\alpha\beta}}{\partial x_\mu} = 0. \quad (23)$$

Taking the case $\mu = 1$ and substituting Eqs. (21) and (22), we obtain

$$\frac{\partial}{\partial x_1} (-p_0 \sqrt{-g}) - \frac{1}{2} (-g^{ij} p_0 \sqrt{-g}) \frac{\partial g_{ij}}{\partial x_1} - \frac{1}{2} (g^{44} \rho_{00} \sqrt{-g}) \frac{\partial g_{44}}{\partial x_1} = 0$$

which can evidently be rewritten in the form

$$\begin{aligned} \sqrt{-g} \frac{\partial p_0}{\partial x_1} + p_0 \frac{\partial \sqrt{-g}}{\partial x_1} - \frac{1}{2} p_0 \sqrt{-g} \left(g^{ij} \frac{\partial g_{ij}}{\partial x_1} + g^{44} \frac{\partial g_{44}}{\partial x_1} \right) \\ + \frac{1}{2} (\rho_{00} + p_0) \sqrt{-g} g^{44} \frac{\partial g_{44}}{\partial x_1} = 0 \end{aligned} \quad (24)$$

This equation can easily be simplified, however, since we are permitted to write in accordance with a well-known result of tensor analysis

$$g^{ij} \frac{\partial g_{ij}}{\partial x_1} + g^{44} \frac{\partial g_{44}}{\partial x_1} = g^{\alpha\beta} \frac{\partial g_{\alpha\beta}}{\partial x_1} = \frac{1}{g} \frac{\partial g}{\partial x_1} \quad (25)$$

and if this is substituted in Eq. (24), it is found that the second and third terms will cancel. Making other obvious simplifications, we then obtain for the dependence of pressure on position the simple expression

$$\frac{\partial p_0}{\partial x_1} + \frac{\rho_{00} + p_0}{2} \frac{\partial \log g_{44}}{\partial x_1} = 0 \quad (26)$$

and similar relations will hold with respect to the other spatial coordinates x_1 and x_2 .

For the case of radiation, moreover, we have the additional simplification

$$\rho_{00} = 3p_0$$

so that equation (26) further reduces to

$$\frac{\partial \log p_0}{\partial x_1} + 2 \frac{\partial \log g_{44}}{\partial x_1} = 0 \quad (27)$$

and since similar relations hold for the other spatial coordinates, we can express the dependence of radiation pressure on position in our gravitational field by the remarkably simple equation

$$p_0(g_{44})^2 = \text{const.} \quad (28)$$

§ 6. DEPENDENCE OF TEMPERATURE ON POSITION

Finally, however, in the case of radiation we can connect proper pressure and proper temperature by the well-known result of Boltzmann

$$p_0 = \frac{a}{3} T_0^4 \quad (29)$$

where a is the Stefan Boltzmann constant, and substituting this into Eq. (28) we at once obtain the desired conclusion for the dependence of proper temperature on position in the case of a general static gravitational field

$$T_0 \sqrt{g_{44}} = \text{const.} \quad (30)$$

§ 7. DISCUSSION

In conclusion several remarks may be made with respect to the above result which will be of interest.

In the first place it should be noted from the method of derivation that the constancy of $T_0 \sqrt{g_{44}}$ has been proven in the first instance solely for points inside the radiation thermometer. Nevertheless since we shall expect T_0 and g_{44} to be continuous functions of position, we shall feel justified in concluding that $T_0 \sqrt{g_{44}}$ is also constant in the system itself where it comes in thermal contact with the thermometer.

In the second place it should be noted that the derivation was carried out on the assumption that the system had already been provided with a radiation thermometer connecting the parts whose temperatures were to be compared. Hence in the case of a given system of interest the question arises

whether a thermometer can be inserted to connect the desired points without thereby seriously altering the system itself. Thus if we had a gravitating system containing solid parts it would be necessary to make a hole into the solid and insert a radiation thermometer if we wished to obtain information as to the temperature of the interior by the method that we have suggested. This procedure, however, would certainly affect the gravitational potentials $g_{\mu\nu}$ which are themselves completely determined by the distribution of the matter and energy in the system. Nevertheless since the equation of connection

$$-8\pi\rho_0 \frac{dx_\mu}{ds} \frac{dx_\nu}{ds} = -8\pi T^{\mu\nu} = G^{\mu\nu} - \frac{1}{2}Gg^{\mu\nu} + \Lambda g^{\mu\nu} \quad (31)$$

is a differential one giving the distribution of matter and energy in terms of the $g_{\mu\nu}$ and their first and second differential coefficients, it seems correct to assume that the insertion of a thermometer of small dimensions can be made without appreciably affecting the values of the $g_{\mu\nu}$ themselves. This question might bear further investigation, however, since singular cases of interest might be found.

Finally, it might be emphasized that although the proper temperature itself, T_0 , varies from point to point in a gravitational system which has come to equilibrium, nevertheless the constancy of the combined quantity $T_0\sqrt{g_{44}}$ provides many of the advantages of the older principle of constant temperature throughout as necessary for equilibrium. Indeed it would be possible to label $T_0\sqrt{g_{44}}$ as *the* temperature of a system, except for the undesirability of multiplying the different things that are signified by that word. In this connection it is also interesting to recall that Einstein himself was led in his early speculations on the nature of gravitation⁷ to distinguish between a quantity, called "wahre Temperatur," which would be constant throughout a system in thermal equilibrium and a second quantity, called at the suggestion of Ehrenfest "Taschentemperatur," which would vary with gravitational potential. The considerations were of only a limited applicability since this was at a time before Einstein's complete development of the general theory of relativity; the quantities in question, however, were quite analogous to our present $T_0\sqrt{g_{44}}$ and T_0 .

⁷ Einstein, Ann. d. Physik 38, 443 (1912).

LETTERS TO THE EDITOR

Prompt publication of brief reports of important discoveries in physics may be secured by addressing them to this department. Closing dates for this department are, for the first issue of the month, the twenty-eighth of the preceding month; for the second issue, the thirteenth of the month. The Board of Editors does not hold itself responsible for the opinions expressed by the correspondents.

The Inner Potential of a Copper Crystal

From electron diffraction experiments Rupp (Ann. d. Physik 5, 453, 1930) obtains values for the inner potentials of several metals. His value of the inner potential for any one metal is approximately constant and independent of the electron wave-length. In some results for a copper crystal obtained by the writer (Phys. Rev. 34, 679, 1929) it appears that the inner potential decreases with increase of wave-length or decrease of voltage. It is to be noted that, in his calculation for copper, Rupp uses the distance between adjacent (100) planes as 3.59Å. This is the value for the edge-length of an elementary cube, but since the copper crystal is a face-centered cube, the distance between adjacent (100)

planes is one-half the above value. With a gas-free Cu crystal Rupp obtains maxima at 54 and 134 volts for which he chooses the values 3 and 4, respectively, for n . If the distance 1.8Å between adjacent planes is used, the above values of n must be divided by two to give the same values for the inner potential. This, however, requires the use of a half-integer. If only whole integers are used then equal values for the inner potential from the observed two maxima are not obtained.

H. E. FARNSWORTH

Brown University

Providence, R. I.

November 15, 1930

Differences in the Absorption Spectrum of Benzene in the Liquid and Vapor State

The absorption spectra of benzene, liquid and vapor, in the 1.1μ and 1.6μ regions have been recorded with an effective slit width of 6Å. Four meters of saturated vapor and two millimeters of liquid were used, both at room temperature and pressure. Several interesting differences between the liquid and vapor absorptions appear when this resolution is attained. The vapor spectrum is shifted towards higher frequencies. The 1.1μ band is shifted 28 cm^{-1} . Two shifts appear in the 1.6μ region, 18 cm^{-1} and 28 cm^{-1} , due to the fact that the 1.6μ absorption is a combination of overtones of two fundamentals. The absorption in the 1.6μ region is similar in intensity for the two phases while the vapor absorbs only 4-6 percent as much as the liquid in the 1.1μ region.

These preliminary results yield information

as to the distribution of energy in the vibrational states of the molecule in the two phases, and show the effect of the proximity of the molecules in the liquid state. The two shifts in the 1.6μ region are about equally divided between the twenty lines observed. This enables a separation of the overtones of the two fundamentals that overlap in this region. An extensive investigation of this general problem is now under way and a comprehensive report will be published in the near future.

E. D. McALISTER

H. J. UNGER

Division of Radiation & Organisms

Smithsonian Institution

Physics Department.

University of Oregon

November 25, 1930.

Relative Intensities in Hyperfine Structure Multiplets

The extension of the Landé interval rule to hyperfine structure energy levels was first made by Bach and Goudsmit¹ from observations of hyperfine patterns in bismuth. Since the observed intervals followed very closely the interval rule, the nuclear spin, I , was calculated to be $(9/2)(h/2\pi)$. This was later verified by them² in the Zeeman splitting up of each line into ten components, in a paper which is now considered a classic.

The interval rule has since been shown by the author to hold for over a hundred hyperfine patterns in praseodymium. With the partially resolved patterns of three lines in manganese, the patterns or graphs of many lines were predicted for Mn I by making the assumption that the intensity rules as well as the interval rule were, in general, valid. These predictions fit the observed patterns so beautifully that the interval rule was used in computing all of the hyperfine levels.³ The interval rule, as pointed out in a short note by Goudsmit and Fisher,⁴ should hold in general and is therefore a powerful tool that may be used in analysing hyperfine-structure patterns.

Since each tiny hyperfine multiplet in Mn I has not been completely resolved the intensities of several lines were qualitatively given by the authors³ in diagrams or graphs. With intensity rules⁵ similar to those for ordinary

multiplets, relative intensities have been calculated for quite a number of the hyperfine multiplets already published. The qualitative agreement with the observed patterns is so remarkable for all patterns studied that accurate measurements are now contemplated. A comparison of the two figures, here shown, with the graphs and microphotometer curves of the same lines³ strongly confirms their interpretation. It is now clear why the *off-diagonal* or faint components are rarely observed.

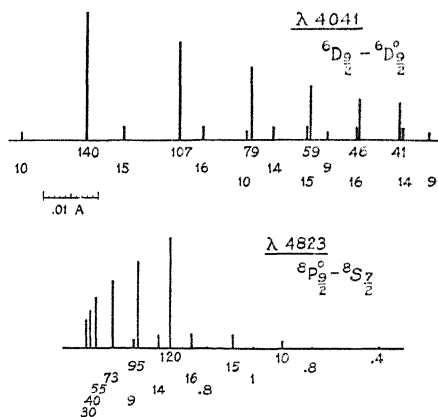


Fig. 1.

While very few accurate intensity measurements are known for hyperfine lines, qualitative measures indicate that in general the intensity rules hold as well as the interval rule. This should be true even though the ordinary multiplet to which the hyperfine pattern belongs does not follow *LS* coupling or the intensity rules.

H. E. WHITE

University of California,
Berkeley, California
November 22, 1930.

¹ Bach and Goudsmit, Zeits. f. Physik **43**, 321 (1927).

² Bach and Goudsmit, Zeits. f. Physik **47**, 174 (1928).

³ White and Ritschl, Phys. Rev. **35**, 1146 (1930).

⁴ Goudsmit and Fisher, Paper presented at the Amer. Phys. Soc. November 29, 1930.

⁵ For hyperfine intensity rules see Hill, Nat. Acad. Sci. **15**, 779 (1929).

The Vibrational and Rotational Analysis of the S_2 Bands.

The absorption and emission spectrum of S_2 has been photographed from $\lambda 5300$ to $\lambda 2400$ with greater dispersion than that used by other investigators. The absorption spectrum was obtained by means of a quartz cell which contained pure sulphur and could be heated electrically up to about 700°C . A hydrogen continuous source was used. The absorption photographs were taken with an E_1 Hilger quartz

spectrograph, and also in the first order of a 21-foot Rowland grating. For the rotational analysis we have used emission plates taken in the third order of the Rowland grating.

Our work confirms essentially the vibrational analysis as given by Rosen (Zeits. f. Physik **43**, 69, 1927). However, the assignment of quantum numbers to some of the bands has been changed and several other

band heads have been measured. Numerous perturbations have been found mainly among the levels of the upper electronic state. $v' = 10$ is the first level showing diffuseness due to predissociation (c.f. V. Henri, *Structures des Molecules*, Paris, 1925). This is shown definitely in both our emission and absorption plates. In absorption all bands with $v' = 10$ are diffuse, while in emission no bands are obtained with $v' = 10$. The 9-0 band does not appear in our emission plates. This can be attributed to the small probability in the Franck-Condon parabola rather than to predissociation. From $v' = 10$ to $v' = 15$ the diffuseness decreases and for $v' = 16$ it increases greatly. Our interpretation of the predissociation differs somewhat from that of Herzberg (*Zeits. f. Physik* **61**, 604, 1930).

We have used for the fine structure analysis the bands 9-1, 7-0, 8-1, 9-2, and 7-1. These were photographed in emission in the third order of a 21-foot Rowland grating with a dispersion of 0.8Å per mm. The overlapping is such that even with this dispersion a considerable number of lines are not clearly separated. The lines can be arranged in two *P* and two *R* branches, one series of each kind being considerably stronger than the other. Each of the stronger branches, however, split into two series of equal intensity for high quantum numbers. This structure (three *P* and three *R* branches of approximately equal intensity) is that of a $^3\Sigma^- \rightarrow ^3\Sigma^-$ transition, and the bands are presumably analogous to the Schumann-Runge bands of O_2 ($^3\Sigma_g^- \rightarrow ^3\Sigma_u^-$). The rotational constants B_e' (extrapolated) and B_e'' are 0.319 and 0.414 cm^{-1} . These give $r_e' = 0.573$ and $r_e'' = 0.503\text{Å}$. The upper rotational states belonging to $v' = 9$ are irregular in that their spacing corresponds to a larger value of *B* than that for the lower rotational states. This is thought to be due to perturbations in the rotational states, since these levels are close to the predissociation limit. Just as in the case of O_2 , alternate rotational levels, hence

alternate band lines, are missing in each series, showing that the sulphur atom S^{32} has zero nuclear spin. In the lower $^3\Sigma$ state, the levels with even *K* values are missing, in the upper state the odd *K* values, as in the Schumann-Runge bands of O_2 .

Our analysis does not agree with that given recently by Rompe (*Zeits. f. Physik* **65**, 404, 1930), according to which the bands are due to a $^1\Pi \rightarrow ^1\Sigma$ transition. Rompe's analysis was based on fluorescence spectra of sulphur excited by various lines of the mercury arc and were photographed with relatively low dispersion. He did not use single line excitation, and although fluorescence spectra in general facilitates the analysis of complex bands, the use of several exciting lines simultaneously, the proximity of the sulphur levels as well as the dispersion used makes it difficult to interpret the results.

The analysis is complete except for a number of weak satellite heads found mainly in absorption which are probably due to a different electronic transition.

Gilles (*C.R.* **188**, 1607, 1929) and Van Iddekinge (*Nature* **51**, 858, 1930) have reported a new system due to S_2 in the ultra-violet. These bands, however, are due to CS and not to S_2 , and the vibrational analysis of this system has been given by Jevons (*Proc. Roy. Soc. A* **117**, 351, 1927-1928). They are very intense and a small impurity of carbon in the discharge tube is sufficient to bring them out prominently.

A detailed discussion of both the rotational and vibrational analyses will appear shortly. The authors wish to express their appreciation to Professor Mulliken for his interest and assistance.

S. MEIRING NAUDÉ
ANDREW CHRISTY

Ryerson Physical Laboratory,
University of Chicago,
December 12, 1930.

Erratum

I note in my letter concerning efficiency of emission of oxide-coated filaments published in the October 15th issue of the *Physical Review* that the value of *A* has been printed as 0.3 ampere per cm^2 degree². This is a typo-

graphical error and should be 0.03 ampere per cm^2 degree².

B. J. THOMPSON
Vacuum Tube Engineering Department
General Electric Company,
November 5, 1930.

AUTHOR INDEX TO VOLUME 36

References marked (A) are to abstracts of papers presented at meetings of the Physical Society, those marked with (L) refer to Letters to the Editor.

- Adams, E. Q. Penetration of radiation—1020(L)
 Adams, J. M. Polar properties of single crystals of ice—788(A)
 Albright, C. L. Hyperfine structures of some cadmium lines and the hypothesis of nuclear spin—847
 Allison F. and E. J. Murphy. Probable number of isotopes of eight metals as determined by a new method—1097(L)
 Anderson, W. A remark on the paper of R. C. Tolman: "Mechanical treatment of temperature distribution in the case of radiation"—365(L)
 Andrews, D. H. (see Kettering, C. F.)—531
 ——— Relation between the Raman spectra and the structure of organic molecules—544
 Arnott, E. G. F. (see Smyth, H. D.)—1023
 Atanasoff, J. V. Dielectric constant of helium—1232
 Babcock, H. D. Classification of iron lines—784(A)
 Bainbridge, K. T. Simple isotopic constitution of Cs—1668(L)
 Baker, E. B. Application of the Fermi-Thomas statistical model to the calculation of potential distribution in positive ions—630
 Band, W. A new relativity theory of the unified physical field—1405
 Bardeen, J. Diffraction of a circularly symmetrical electromagnetic wave by a co-axial circular disc of infinite conductivity—1482
 Barnes, R. B. Infrared absorption of some organic liquids under high resolution—296
 Barnes, B. T. Spectral distribution of energy radiated from a new type of tungsten mercury arc—1468
 Barnes, S. W. (see Richtmyer, F. K.)—1017(L)
 Barnett, S. J. Discovery and rough measurement of a new electron inertia effect—786(A)
 ——— Further work on the rotation of soft iron and permalloy by magnetization and the gyromagnetic anomaly—789(A)
 Bartlett, J. H., Jr. Orbital valency—1096(L)
 Beams, J. W. Propagation of luminosity in discharge tubes—997
 Bearden, J. A. A double crystal study of scattered x-rays—791
 Beattie, J. A. A rational basis for the thermodynamic treatment of real gases and mixtures of real gases—132
 ——— (see Gillespie, L. J.)—743, 1008
 Bedell, F. and J. Kuhn. Linear correction for cathode ray oscillograph—993
 Beese, N. C. Thermionic emission of oxide coated cathodes containing a Ni-Ba alloy core—1309
 Bender, P. I. Effect of gases on the optically excited cadmium I spectrum—1535
 ——— II. Optical excitation of cadmium hydride and zinc hydride bands—1543
 Bennett, R. D. A search for the source of dielectric polarization—65, 1670 (L)
 Bergstein, M., J. F. Rinke, and C. M. Gutheil. Studies in contact rectification. II. Cupric sulfide-magnesium junction—587; errata—1022
 Bingham, E. C. and H. J. Fornwalt. Chemical constitution and association—381(A)
 Bitter, F. On the magnetic properties of metals—978
 ——— Magnetic susceptibility of gases. II. Temperature dependence—1648
 Blair, H. A. Spark spectra of silver and palladium (Ag II and Pd II)—an extension—173
 ——— Correction and extension of the series of the silver arc spectrum Ag I—1531
 Bleakney, W. Ionization potentials and probabilities for the formation of multiply charged ions in helium, neon and argon—1303
 Bouma, T. (see Ornstein, L. S.)—679
 Bowen, I. S. Presence of neutral oxygen in the gaseous nebulae—600(L)
 Boyce, J. C. (see MacInnes, J. M.)—368(L)
 Boynton, W. P. Equations of state and thermodynamic functions for a substance with variable specific heat—787(A)
 Bradbury, N. E. (see Luhr, O.)—1394
 Braun, M. L. Current, pressure, and frequency relationships for the initiation and maintenance of the electrodeless glow discharge—1195
 Breit, G. Fine structure of He as a test of the spin interactions of two electrons—383
 ——— and F. W. Doermann. Magnetic moment of the Li_7 nucleus—1262(L)
 ——— and F. W. Doermann. Hyperfine structure of *S* and *P* terms of two electron atoms with special reference to Li^+ —1732

- Breit, G. and E. O. Salant. Note on frequency shifts in dispersing media—871
- Bridgman, P. W. Book review—155, 781
- Browne, T. E., Jr. and F. C. Todd. Extinction of short a.c. arcs between brass electrodes—726
— (see Todd, F. C.)—732
- Bryan, A. B. (see Heaps, C. W.)—326
- Buchta, J. W. Book reviews—1420, 1517, 1594
- Busang, P. F. (see Smith, W. O.)—524
- Campbell, J. S. (see Frerichs, R.)—151(L), 1460
- Cassen, B. (see Lauritsen, C. C.)—988
- Caswell, A. E. A note on the quantization of the solar system—787(A)
- Chaffee, E. L. (see Perry, C. T.)—904
- Chaffee, M. A. (see Lawrence, E. O.)—1099(L)
- Chao, C. Y. Scattering of hard γ rays—1519
- Chapman, S. Wind mixing and diffusion in the upper atmosphere—1014(L)
- Chase, C. T. Scattering of fast electrons by metals. I. Sensitivity of the Geiger point-discharge counter—984
— Scattering of fast electrons by metals. II. Polarization by double scattering at right angles—1060
- Christy, A. (see Crane, W. O.)—421
— (see Naudé, S. M.) 1801 (L)
- Clark, J. C. (see Ross, P. A.)—378(A)
- Coade, E. N. X-ray scattering coefficient as a function of wave-length and atomic number—778(L), 1109
- Cohn, B. E. (see Nyswander, R. E.)—1257
- Collins, J. R. Effect of high pressure on the near infrared absorption spectrum of certain liquids—305
- Colvert, W. W. X-ray absorption in gases—1619
- Compton, K. T. An interpretation of pressure and high velocity vapor jets at cathodes of vacuum arcs—706
— (see Van Voorhis, C. C.)—1435
- Condon, E. U. Theory of complex spectra—1121.
— Book reviews—156, 369, 1594
- Constant, F. W. Magnetic properties of dilute cobalt alloys—786(A)
— Magnetic properties of certain Pt-Co and Pd-Co alloys—1654
- Cook, R. V. Formation of striae in a Kundt's tube—1098(L)
- Cook, S. R. On an electromagnetic theory of sight and color vision—790(A)
- Cooksey, C. D. (see Cooksey, D.)—80
— and D. Cooksey. Precision measurements of the glancing-angle of reflection from calcite for silver ($K\alpha_1$) x-rays by the "method of displacement"—85
- Cooksey, D. and C. D. Cooksey. Unreliability of photographic emulsions on glass for recording distances and a method of minimizing this defect—80
- Cooksey, D. (see Cooksey, C. D.)—85
- Copeland, L. C. Heat of formation of molecular oxygen—1221
- Cork, J. M. False lines in x-ray grating spectra—665
- Cotton, J. C. (see Knauss, H. P.)—1099(L)
- Crane, W. O. and A. Christy. Vibrational quantum analysis of the potassium infrared absorption bands—421
- Cravath, A. M. Rate at which ions lose energy in elastic collisions—248
— Behavior of a mercury vapor arc with a jet of liquid mercury as cathode—1480
- Crump, C. C. Book review—1419
- Dahl, O. (see Tuve, M. A.)—1261(L)
- Dasannacharya, B. Polarization of the continuous x-rays from single electron impacts—1675
- Davisson, C. J. Book review—782
- Dennison, D. M. Book review—608
— and S. B. Ingram. A new band in the absorption spectrum of methane gas—1451
- Dershchem, E. and M. Schein. Apparatus for measuring absorption coefficients of soft x-rays in gases and the absorption in air of the $K\alpha$ line of carbon—378(A)
- Doermann, F. W. (see Breit, G.)—1262(L), 1732
- Donal, J. S., Jr. Abnormal shot effect of ions of tungstous and tungstic oxide—1172
- Dooley, D. General Electric type S-1 lamp as a spectroscopic source—1476
- Dumond, J. W. M. Breadth of Compton modified line—146(L)
— Evidence for the Richtmyer double jump hypothesis of x-ray satellites—1015(L)
— Multiple scattering in the Compton effect—1685
— and A. Hoyt. Energy of $K\alpha_3$ of copper as a function of applied voltage with the double crystal spectrometer—799
— and A. Hoyt. Design and technique of operation of a double crystal spectrometer—1702
- Dunham, J. L. Isotope effect on band spectrum intensities—1553
- Easley, M. A. (see Forsythe, W. E.)—150(L)
- Eckart, C. Calculation of energy values—149(L)
— Theory and calculation of screening constants—878
— Wave mechanics of deflected electrons—1014(L), 1514(L)
— (see Hughes, D. S.)—694
- Ehrenfest, P. (see Tolman, R. C.)—1791
- Eldridge, J. A. Book review—1516
- Ellis, J. W. (see Kinsey, E. L.)—603(L)
- Ellwood, W. B. An experimental determination of the change in temperature accompanying change in magnetization of iron—1066

- Evans, H. P. A two dimensional boundary value problem for the transmission of alternating currents through a semi-infinite heterogeneous conducting medium—1579
- Ewing, M. An x-ray study of the structure of electrets—378(A)
- Farnsworth, H. E. and V. H. Goerke. Distinction between contact-potential effects and true reflection coefficients for low-velocity electrons—1190
 ——— Inner potential of a copper crystal—1799(L)
- Faust, L. Y. Fine structure of the *K*-radiation of the lighter elements—161
- Ffolliott, C. F. Raman spectra of geometric isomers—367(L)
- Findlay, J. H. Spark spectrum of cobalt, Co II—5
- Focke, A. B. Principal magnetic susceptibilities of bismuth single crystals—319
- Foot, P. D. (see Smith, W. O.)—524
- Fornwalt, H. J. (see Bingham, E. C.)—381(A)
- Forsythe, W. E. and M. A. Easley. Some peculiarities of the spectrum of the tungsten mercury arc—150(L)
- Found, C. G. (see Langmuir, I.)—604(L)
- Franklin, D. and E. R. Laird. Raman effect in trimethylethylene—147(L)
- Freed, S. and C. Kasper. A simple accurate method for measuring the diamagnetic susceptibility of dissolved substances—1002
- Frenkel, J. On the electrical resistance of contacts between solid conductors—1604
- Frerichs, R. and J. S. Campbell. Experimental evidence for the existence of quadrupole radiation—151(L), 1460
 ——— Singlet system of the oxygen arc spectrum and the origin of the green auroral line—398
- Froman, D. K. A photographic method of determining atomic structure factors—1330
 ——— A note on the extrapolation of atomic structure factor curves—1339
- Geer, W. (see Utterback, C. L.)—785(A)
- Gessner, G. S. Luminescence of zinc sulphide under the action of alpha, beta and gamma-rays—207
- Giauque, W. F. and H. L. Johnston. On the entropy of hydrogen—1592(L)
- Gillespie, L. J. Gibbs-Dalton law of partial pressures—121
 ——— and J. A. Beattie. Thermodynamic treatment of chemical equilibria in systems composed of real gases. I. An approximate equation for the mass action function applied to the existing data on the Haber equilibrium—743
 ——— and J. A. Beattie. Thermodynamic treatment of chemical equilibria in systems composed of real gases. II. A relation for the heat of reaction applied to the ammonia synthesis reaction. Energy and entropy constants for ammonia—1008
- Gingrich, N. S. Double crystal analysis of scattered x-rays—364(L)
 ——— An analysis of scattered x-rays with the double crystal spectrometer—1050
- Goerke, V. H. (see Farnsworth, H. E.)—1190
- Goetz, A. and M. F. Hasler. Thermoanalysis of metal single crystals and a new thermoelectric effect of bismuth crystals grown in magnetic fields—1752
- Goucher, F. S. Contact resistance and microphonic action—375(A)
- Granath, L. P. Angular momentum of the Li₇ nucleus—1018(L)
- Gray, F. Contact resistance and microphonic action—375(A)
- Green, J. B. Incomplete Paschen-Back effect—157; 379(A)
- Green, M. C. Effect of small angle scattering on the electron absorption coefficient—239
 ——— Scattering of electrons in small angles by gas molecules and its effect on the electron absorption coefficient—786(A)
- Gronwall, T. H. A diaphantine equation connected with the hydrogen spectrum—1671(L)
- Gunn, R. Origin of the variations in the sun's rotational velocity—1251
- Gutheil, C. M. (see Bergstein, M.)—587; 1022
- Hafstad, L. R. (see Tuve, M. A.)—1261(L)
- Ham, W. R. (see LeGalley, D. P.)—379(A)
- Hartig, H. E. Book review—156
- Hasler, M. F. (see Goetz, A.)—1752
- Harrington, M. C. (see Uytterhoeven, W.)—709
- Harrison, G. R. and P. A. Leighton. Fluorescent dry plates for photographic photometry—779(L)
- Harvey, A. and F. A. Jenkins. Interpretation of the spectra of CaF and SrF—1413(L)
- Heaps, C. W. and A. B. Bryan. Discontinuous changes in length accompanying the Barkhausen effect in nickel—326
- Henderson, G. H. and J. L. Nickerson. Range of the α -particles from thorium—1344
- Henderson, J. E. and E. B. Jordan. Reflection of x-rays from thin metallic films—785(A)
- Hershberger, W. D. (see Klein, E.)—1262(L)
- Hicks, V. Experiments on the relative intensities of x-ray lines in the *L*-spectrum of tantalum—785(A), 1273
- Hidnert, P. and W. T. Sweeney. Thermal expansion of M-M-M alloy—787(A)
- Hilberry, N. (see Smith, H.)—374(A)
- Hoffmann, B. (see Veblen, O.)—810
- Holzer, R. E. Absorption of slow hydrogen positive rays in hydrogen—788(A), 1204
- Hopfield, J. J. Continuous spectrum in the region 500-1100A—784(A)
 ——— New oxygenspectra in the ultraviolet—789(A)

- Hopfield, J. J. New spectra in nitrogen—789(A)
- Hoxton L. G. Note on the pressure variation of specific heats of gases derived from compressibility data—1091
- Houston, W. V. Book review—1674
 — (see Huff, L. D.)—842
- Hoyt, A. (see Dumond, J. W. M.)—799, 1702
- Hoyt, F. C. Structure of emission lines—380(A), 860
- Hubbard, J. C. Problems in acoustic interferometry in gases—1668(L)
- Huff, L. D. and W. V. Houston. Appearance of "forbidden lines" in spectra—842
- Hughes, A. L. and G. E. M. Jauncey. An attempt to detect collisions of photons—773
 — and C. M. Van Atta. A second ionization potential in potassium vapor—214
- Hughes, D. S. and C. Eckart. Effect of the motion of the nucleus on the spectra of Li I and Li II—694
- Hulburt, E. O. Spectra of gases lighted with strong electrical discharges—13
 — Wind mixing and diffusion in the upper atmosphere—1264(L)
 — Ultraviolet light theory of aurorae and magnetic storms (continued)—1560
- Hull, A. W. Book review—369
- Humphreys, C. J. Interference measurements in the first spectra of krypton and xenon—380(A)
- Hutchisson, E. Band spectra intensities for symmetrical diatomic molecules—410
- Huxford, W. S. (see Stowell, E. Z.)—1348
- Hyatt, J. M. (see Wold, P. I.)—375(A)
- Hyman, H. H. Resonance (*B-A*) band system of the hydrogen molecule—187
- Ingram, S. B. (see Dennison, D. M.)—1451
- Jauncey, G. E. M. (see Hughes, A. L.)—773
- Jenkins, F. A. (see Harvey, A.)—1413(L)
- Johnson, T. H. Diffraction of hydrogen atoms—381(A)
- Johnston, H. L. (see Giauque, W. F.)—1592(L)
- Jordan, E. B. (see Henderson, J. E.)—785(A)
- Kabakjian, D. H. Luminescence due to radioactivity—379(A)
- Kaplan, J. Band intensities—778(L)
 — Some properties of the third positive carbon and associated bands—784(A)
 — Quenching of mercury resonance radiation by nitrogen and carbon monoxide—788(A)
- Kasper, C. (see Freed, S.)—1002
- Kemble, E. C. and F. F. Rieke. Interaction between excited and unexcited hydrogen atoms at large distances—153(L)
- Kennard, E. H. Wave mechanics of deflected electrons—1667(L)
- Kettering, C. F., L. W. Shutts and D. H. Andrews. A representation of the dynamic properties of molecules by mechanical models—531
- Keyes, F. G. and J. G. Kirkwood. Dielectric constant of carbon dioxide as a function of temperature and density—754
 — and J. G. Kirkwood. Dielectric constant of ammonia as a function of temperature and density—1570
- Kievit, B. and G. A. Lindsay. Fine structure in the x-ray absorption spectra of the *K* series of the elements calcium to gallium—648
- Kimball, W. S. Entropy, elastic strain and the second law of thermodynamics, the principles of least work and of maximum probability—377(A)
- Kinsey, E. L. and J. W. Ellis. Electrolytic dissociation of nitric acid as revealed by its infrared absorption spectrum—603(L)
- Kirkwood, J. G. (see Keyes, F.)—754, 1570
- Klein, E. and W. D. Hershberger. Use of the Pierce acoustic interferometer for the determination of absorption in gases for high frequency sound waves—1262(L)
- Knauss, H. P. and J. C. Cotton. Intensity changes of Cameron bands in the electrodeless discharge—1099(L)
- Kobel, E. Pressure and high velocity vapour jets at cathodes of a mercury vacuum arc—1636
- Koller, L. R. Photoelectric emission from thin films of caesium—1639
- Kozanowski, H. N. and N. H. Williams. Shot effect of the emission from oxide cathodes—1314
- Kruger, P. G. New lines in the arc and spark spectrum of helium—855
- Kuhn, J. (see Bedell, F.)—993
- Kurth, E. H. On the recombination of electrons with caesium ions—374(A)
- Laird, E. R. (see Franklin, D.)—147(L)
 — (see Sterling, V.)—148(L)
- Langmuir, I. and C. G. Found. Metastable atoms and electrons produced by resonance radiation in neon—604(L)
- Lauritsen, C. C. and B. Cassen. High potential x-ray tube—988
 — Spectrum of the radiation from a high potential x-ray tube—1680
- Lawrence, E. O. and L. B. Linford. Effect of intense electric fields on the photoelectric properties of metals—482
 — and M. A. Chaffee. On the direction of emission of photoelectrons from potassium vapor by ultraviolet light—1099(L)
- LeGalley, D. P., W. R. Ham, and M. W. White. Some measurements of currents through the walls of x-ray tubes—379(A)
- Lewis, A. B. Coupled vibrations with applications to the specific heat and infrared spectra of crystals—568

- Lewis, G. N. Principle of identity and the exclusion of quantum states—1144
- Leighton, P. A. (see Harrison, G. R.)—779(L)
- Lille, H. R. Margules method of measuring viscosities modified to give absolute values—347
- Linder, E. G. Organic reactions in gaseous electrical discharge. I. Normal paraffin hydrocarbons—374(A), 1375
- Lindsay, G. A. (see Kievit, B.)—648
- Linford, L. B. (see Lawrence, E. O.)—482
- Electrostatic surface fields near thoriated tungsten filaments by a photoelectric method—1100(L)
- Livingood, J. J. (see Shenstone, A. G.)—380(A)
- Loeb, L. B. Mobility of Na^+ ions in H_2 —152(L) 790(A)
- Lozier, W. W. A study of the velocities of H^+ ions formed in hydrogen by dissociation following electron impact—1285
- Negative ions in hydrogen and water vapor—1417(L)
- Lucy, A. A method offered as a means of computing Planck's constant without involving the charge on the electron—367(L)
- Luhr, O. Recombination of ions in argon, nitrogen and hydrogen—24, 788(A)
- Recombination of ions in air and oxygen in relation to the nature of gaseous ions—787(A)
- and N. E. Bradbury. Mobility of aged ions in air—1394
- Lynch, W. A. (see Smith, H.)—374(A)
- MacDougall, F. H. Book review—371
- MacGillavry, D. On the entropy of hydrogen—1398
- MacInnes, J. M. and J. C. Boyce. Gas discharge wave-length list in extreme ultraviolet—368(L)
- McAlister, E. D. High resolution in the near infrared—784(A)
- and H. J. Unger. Differences in the absorption spectrum of benzene in the liquid and vapor state—1799(L)
- McKeehan, L. W. Book review—608
- Electrical resistance of nickel and permalloy wires as affected by longitudinal magnetization and tension—948
- Magnetostriction in nickel—1014(L)
- Molecular field and atomic order in ferromagnetic crystals and in hydrogenized iron—1512(L)
- Magnetostriction and magnetic hysteresis—1670(L)
- McMillen, J. H. Angle and energy distribution of electrons scattered by helium, argon and hydrogen—1034
- Mack, J. Book review—609
- Manning, K. V. (see Richtmyer, F. K.)—1017(L)
- Margenau, H. Second virial coefficient for gases: a critical comparison between theoretical and experimental results—1782
- Maxwell, L. R. Average life for ionized helium—379(A)
- Mazumder, K. C. Absorption of x-rays by lithium—457
- Merritt, E. and D. R. Morey. Polarized fluorescence of solutions of rhodamine-B and uranine—1386
- Metcalf, G. F. and B. J. Thompson. A low grid current vacuum tube—1489
- Michels, W. C. Optical excitation function of helium—604(L), 1362
- Millikan, R. A. On the question of the constancy of the cosmic radiation and the relation of these rays to meteorology—1595
- Milne, W. E. Book review—1673
- Mitchell, A. C. G. Behavior of positive ions in hydrogen—381(A)
- Polarization of mercury lines in stepwise radiation—1589(L)
- Montgomery, C. G. Magnetic isotropy of copper crystals—498
- Magnetic isotropy of a paramagnetic alum—1661
- Morey, D. R. (see Merritt, E.)—1386
- Morse, P. M. (see Stueckelberg, E. C. G.)—16
- (see Robertson, H. P.)—375(A)
- Mrozowski, S. On the origin of the bands in the spectrum of mercury vapor—1168
- On the incomplete polarization of the mercury resonance radiation—1591(L)
- Mulliken, R. S. Interpretation of the visible halogen bands—364(L)
- Report on notation for spectra of diatomic molecules—611
- Electronic states in the visible halogen bands—699
- Correlation of atomic J values and molecular quantum numbers with applications to halogen, alkaline earth hydride, and alkali molecules—1440
- Murnaghan, F. D. Book review—609
- Murphy, E. J. (see Allison, F.)—1097(L)
- Muskat, M. Dispersion formula and Raman effect for the symmetrical top, an erratum—363
- Muzzey, D. S. Jr. Some measurements of the longitudinal elastic frequencies of cylinders using a magnetostriction oscillator—935
- Nadai, A. Some applications of the theory of plastic deformations of ductile metals—762
- and A. Christy. Vibrational and rotational analysis of the S_2 bands—1801(L)
- Naudé, S. M. Isotopes of nitrogen, mass 15, and oxygen, mass 18 and 17, and their abundances—333

- Nickerson, J. L. (see Henderson, G. H.)—1344
- Nottingham, W. B. Work functions and thermionic constant "A" determined for toriated tungsten—376(A)
- Nutting, F. L. Position and structure of the modified line of the spectrum of scattered x-rays—1267
- Nyswander, R. E. and B. E. Cohn. Tribothermoluminescence—1257
- O'Brien, B. Energy distribution in the ultraviolet spectrum of skylight—381(A)
- Olpin, A. R. Method of enhancing the sensitiveness of alkali metal photoelectric cells—251
—— Inhibition of photoelectric emission by near infrared light—376(A)
- Ornstein, L. S. and T. Bouma. Intensity measurements in the spectrum of nickel and cobalt—679
—— (see Uhlenbeck, G. E.)—823
- Osgood, T. H. Book reviews—781, 782
- Page, L. Deflection of electrons by a magnetic field on the wave mechanics—444
—— Effect of the earth's electric and magnetic fields on ions in the atmosphere—601(L)
—— Wave mechanics of deflected electrons—1418(L)
—— Book reviews—369, 610
- Pauling, L. Rotational motion of molecules in crystals—430
- Perry, C. T. and E. L. Chaffee. A determination of e/m for an electron by direct measurement of the velocity of cathode rays—904
- Peters, H. On the fluorescence of quartz under the influence of cathode rays of low voltage—1631
- Pfund, A. H. Infrared filters of controllable transmission—71
- Pielemeier, W. H. Ultrasonic velocity and absorption in oxygen—1005
—— Use of the Pierce acoustic interferometer—1667(L)
- Plesset, M. S. (see Weigle, J. J.)—373(A)
—— Relativistic wave mechanics of electrons deflected by a magnetic field—1728
- Pugh, E. M. Hall effect and the magnetic properties of some ferromagnetic materials—1503
—— and C. A. Swartz. Cataphoresis in rotating electric fields—787(A), 1495
- Rashevsky, N. On chain reactions caused by physical structure—376(A)
- Reich, H. J. A new type of glow-discharge tube—373(A)
- Richtmyer, F. K., S. W. Barnes, and K. V. Manning. Hyperfine structure of x-ray lines—1017(L)
—— and L. S. Taylor. Intensity of x-ray satellites—1044
—— Book review—1673
- Rieke, F. F. (see Kemble, E. C.)—153(L)
- Rinke, J. F. (see Bergstein, M.)—587; 1022
- Robertson, H. P. and P. M. Morse. Effect of collisions on potential distribution in positive ion sheaths—375(A)
- Roller, D. Photoelectric behavior of solid and liquid mercury—738
- Rolnick, H. Tension coefficient of resistance of metals—506
- Rosen, N. and M. S. Vallarta. Spherically symmetrical field in the unified theory—110
- Ross, P. A. and J. C. Clark. Modified line in scattered x-rays—378(A)
- Rossi, B. On the magnetic deflection of cosmic rays—606(L)
- Ruark, A. E. Book review—155
- Russell, H. N. A note on Zeeman patterns—1590(L)
- Salant, E. O. (see Breit, G.)—871
—— and A. Sandow. Raman effect of HBr and HI—1591(L)
- Sandow, A. (see Salant, E. O.)—1591(L)
- Sawyer, R. A. Excitation processes in the hollow cathode discharge—44
- Schein, M. (see Dershem, E.)—378(A)
- Shenstone, A. G. and J. J. Livingood. Spark spectrum of rhodium—380(A)
—— Note on wave-lengths in the vacuum copper arc—603(L)
—— Arc spectrum of palladium—669
—— Book review—607
- Shereshefsky, J. L. Corresponding state of maximum surface tension of saturated vapors—377(A)
- Shutts, L. W. (see Kettering, C. F.)—531
- Silverman, S. Adsorption of methyl alcohol films on rock-salt—311
- Skinner, E. W. Diffraction of x-rays in liquids: effect of temperature—1625
- Slater, J. C. Atomic shielding constants—57
—— Book review—1516
- Smith, H., W. A. Lynch and N. Hilberry. Electrodeless discharge in mercury vapor—374(A)
- Smith, P. T. Ionization of helium, neon, and argon by electron impact—1293
- Smith, S. A note on the spectra of doubly and trebly ionized lead—1
- Smith, W. O., P. D. Foote and P. F. Busang. Capillary retention of liquids in assemblages of homogeneous spheres—524
- Smyth, H. D. and E. C. G. Stueckelberg. Ionization of carbon dioxide by electron impact—472
—— and E. G. F. Arnott. Canal ray and electron excitation of the band spectrum of nitrogen—1023
—— (see Stueckelberg, E. C. G.)—478
- Soderman, M. Structure of K-radiation from C, B, and Be—1414(L)
- Soh, H. P. Non-static solution of Einstein's law

- of gravitation in a spatially symmetrical field—1515(L)
- Soller, T. Velocity distribution of secondary electrons from molybdenum—1212
- Stauffer, L. H. Electro-optical modification of light waves—1352
- Stauss, H. E. Use of the refraction of x-rays for the determination of the specific charge of the electron—1101
- Steadman, L. T. Wave-length measurements of gamma-rays from radium and its products—460
- Sterling, V. and E. R. Laird. Raman effect in solutions of sodium nitrate of varying concentration—148(L)
- Stewart, G. W. Effect of electric field upon x-ray diffraction pattern of a liquid—1413(L)
- Book review—1265
- Stewart, J. Q. Fundamental correspondences between geometry and thermodynamics—377(A)
- Stibitz, G. R. Vibrations of a non-planar membrane—513
- Stowell, E. Z. and W. S. Huxford. Possibilities of the oscillating arc in spectrochemical analysis—1348
- Strong, J. A method for growing large crystals of the alkali halides—1663
- Stueckelberg, E. C. G. and P. M. Morse. Computation of the effective cross section for the recombination of electrons with hydrogen ions—16
- and H. D. Smyth. Ionization of nitrous oxide and nitrogen dioxide by electron impact—478
- (see Smyth, H. D.)—472
- Swann, W. F. G. Book review—1265
- Swartz, C. A. (see Pugh, E. M.)—787(A), 1495
- Sweeney, W. T. (see Hidnert, P.)—787(A)
- Taylor, L. S. (see Richtmyer, F. K.)—1044
- Terenin, A. Photoionization of salt vapors—147(L)
- Thomas, C. H. Potential drop-current relations of a Geissler discharge from a hollow cathode—374(A)
- Thompson, B. J. High efficiencies of emission from oxide-coated filaments—1415(L); erratum—1802
- (see Metcalf, G. F.)—1489
- Thompson, G. E. Velocity of ultrasonic waves in water vapor—77
- Tiedeman, J. A. Relation between the number of electrons ejected photoelectrically from the cathode and the time lag of the spark—376(A)
- Todd, F. C. (see Browne, T. E. Jr.)—726
- and T. E. Browne, Jr. Restriking of short a.c. arcs—732
- Tolman, R. C. A remark on the letter of W. Anderson—365(L)
- Book review—370
- and P. Ehrenfest. Temperature equilibrium in a static gravitational field—1791
- Tuve, M. A., L. R. Hafstad, and O. Dahl. High-voltage tubes—1261(L)
- Note on the production of extremely high voltages—1576
- Uhlenbeck, G. E. and L. S. Ornstein. On the theory of the Brownian motion—823
- (see Young, L. A.)—1154
- and L. A. Young. The value of e/m by deflection experiments—1721
- Unger, H. J. Near infrared spectrum of Hg—784(A)
- (see McAlister, E. D.)—1799(L)
- Utterback, C. L. and W. Geer. Electronic emission from a metal target bombarded with positive ions—785(A)
- Uyterhoeven, W. and M. C. Harrington. Secondary emission from metals by impact of metastable atoms and positive ions—709
- Valasek, J. Fine structure of certain x-ray emission lines—1523
- Vallarta, M. S. (see Rosen, N.)—110
- Van Atta, C. M. (see Hughes, A. L.)—214
- Van Voorhis, C. C. and K. T. Compton. Heats of condensation of electrons on several metals in several ionized gases—1435
- Vavilov, S. On the attempt to detect collisions of photons—1590(L)
- Veblen, O. and B. Hoffmann. Projective relativity—810
- Wall, C. N. Potential and potential energy of space lattices—1243
- Watson, W. W. Evidence for Be isotope of mass 8 in the BeH band spectrum—1019(L)
- Zeeman effect in the ZnH and CdH bands—1134
- Weigle, J. J. and M. S. Plesset. Preliminary measurements of the mean free path of potassium atoms in nitrogen—373(A)
- Werth, M. Relative efficiency of the Hg-arc lines in exciting the Raman spectrum of benzol—1096(L)
- White, H. E. Relative intensities in hyperfine structure multiplets—1800(L)
- White, M. W. (see LeGalley, D. P.)—397(A)
- Williams, N. H. (see Kozanowski, H. N.)—1314
- Winans, J. G. New bands in the absorption spectrum of mercury—1020(L)
- Winch, R. P. Photoelectric outgassing—601(L)
- Wold, P. I. and J. M. Hyatt. Hall effect in tellurium amalgams—375(A)
- Wood, R. W. Improved technique for the Raman effect—1421
- Raman spectra of benzene and diphenyl—1431
- Workman, E. J. A new method of measuring the variation of the specific heats (c_p) of gases with pressure—1083

- Wyckoff, R. W. G. Atomic scattering powers of nickel, copper and iron for various wave-lengths—1116
- Yates, R. C. Elastic character of the homopolar chemical bond—555
—— Study of the small vibrations of six particles in a system analogous to the benzene ring—563
- Young, L. A. and G. E. Uhlenbeck. On the Wentzel-Brillouin-Kramers approximate solution of the wave equation—1154
—— (see Uhlenbeck, G. E.)—1721
- Zahl, H. A. Reflection of cadmium and zinc atoms from sodium chloride crystals—893
- Zeleny, J. Mobilities of ions in dry and moist air—35
—— Book review—156
- Zemansky, M. W. Absorption and collision broadening of the mercury resonance line—219, 380(A)
—— New experimental determination of effective cross-sections for the quenching of mercury resonance radiation—919
—— Absorption and collision broadening of resonance radiation—1591(L)
- Zener, C. Analytic atomic wave functions—51
- Zwicky, F. Energy changes related to the secondary structure of crystals—378(A)

ANALYTIC SUBJECT INDEX TO VOLUME 36

References marked (A) are to abstracts of papers presented at meetings of the American Physical Society, those marked with (L) refer to letters to the Editor.

Absorption of light (see also **X-Rays, absorption**)

Hg 2537 in Hg vapor, broadening, M. W. Zeman-sky—219, 380(A), 1591(L)

Liquids, infrared, effect of pressure, J. R. Collins—305

Organic liquids in infrared, high resolution, R. B. Barnes—296

Acoustics

Absorption of high frequency sound, E. Klein, W. D. Hersberger—1262(L)

Kundt's tube, striae, R. V. Cook—1098(L)

Ultrasonic velocity and absorption in oxygen, W. H. Pielemeier—1005, 1667(L); J. C. Hubbard—1668(L)

Ultrasonic waves, velocity in water vapor, G. E. Thompson—77

Adsorption

Methyl alcohol on rock salt, S. Silverman—311

Alloys

Electrical resistance, magnetization and tension of Ni and permalloy, L. W. McKeehan—948

Gyromagnetic anomaly and rotation by magnetization of permalloy, S. J. Barnett—789(A)

Magnetic properties of Pt-Co and Pd-Co, F. W. Constant—786(A), 1654

Thermal expansion of M-M-M, P. Hidnert, W. T. Sweeney—787(A)

Thermionic emission from oxide-coated Ni-Ba alloy, N. C. Beese—1309

Alpha particles

Range from Th, G. H. Henderson, J. L. Nickerson—1344

Arcs (see also **Discharge of electricity in gases, Sparks**)

Extinction of short a.c. arcs between brass electrodes, T. E. Browne, Jr., F. C. Todd—726

General Electric type S-1 lamp, spectrum, D. Dooley—1476

Hg arc, moving jet cathode, A. M. Cravath—1480

Oscillating arc in spectrochemical analysis, E. Z. Stowell, W. S. Huxford—1348

Pressure and vapor jets at cathode, K. T. Comp-ton—706; E. Kobel—1636

Restriking of short a.c. arcs, F. C. Todd, T. E. Browne, Jr.—732

Tungsten mercury arc, spectral energy, B. T. Barnes—1468

Tungsten mercury, peculiarities in spectrum, W. E. Forsythe, M. A. Easley—150(L)

Astrophysics

Quantization of solar system, A. E. Caswell—787(A)

Variations in the sun's rotational velocity, R. Gunn—1251

Atmospheric electricity

Aurorae and magnetic storms, theory of, E. O. Hulburt—1560

Ionization of cosmic rays, R. A. Millikan—1595

Ions in upper atmosphere, motion of, L. Page—601(L)

Atomic beams

Cs⁺ in H₂, pressure changes, A. C. G. Mitchell—381(A)

Diffraction of H atoms, T. H. Johnson—381(A)

Hydrogen ions in H₂, absorption of, R. E. Holzer—788(A), 1204

Potassium atoms in nitrogen, mean free path, J. J. Weigle, M. S. Plesset—373(A)

Reflection of Cd and Zn atoms from NaCl crystals, H. A. Zahl—893

Atomic radii (see also **Collision diameter**)

Absorption of H ions in H₂, R. E. Holzer—788(A), 1204

Atomic and molecular radii (see **Collision diameter**)**Atomic structure factors**

Electron distribution in atoms of KCl and MgO, D. K. Froman—1330, extrapolation of factors, D. K. Froman—1339

Atoms

Wave functions, approximate, for any atom, J. C. Slater—57

Wave functions for Be, B, C, N, O, F, Ne, C. Zener—51

Aurora

Green line, Zeeman effect, R. Frerichs, J. S. Campbell—151(L)

Origin of auroral green line, R. Frerichs—398

Transverse Zeeman effect of green auroral line, quadrupole radiation, R. Frerichs, J. S. Campbell—1460

Barkhausen effect

Discontinuous changes in length of Ni, C. W. Heaps, A. B. Bryan—326

Book reviews

- Baker, Robert H., *Astronomy, An Introduction*—1419
- Brillouin, Leon, *Les Statistiques Quantiques*—1674
- deBroglie, L., *Einführung in die Wellenmechanik*—369
- Campbell, J. W., *An Introduction to Mechanics*—1517
- Castelfranchi, Gaetano. *Physique Moderne*—155
- Emeléus, K. G. *The conduction of Electricity through Gases*—156
- Grube, Georg., *Grundzuge der Theoretischen und Angewandten Elektrochemie*—371
- Haas, A., *Einführung in die Theoretische Physik*—610
- Halpern, O. and H. Thirring. *Die Grundgedanken der neueren Quantentheorie*—156
- Heisenberg, W., *The Physical Principle of the Quantum Theory*—1516
- Hoag, J. Barton., *Electron Physics*—1420
- Jackson, D., *The Theory of Approximation*—1673
- Jäger, Gustav. *Theoretische Physik*—610
- Jahrbuch des Forschungs, Instituts der Allgemeinen Elektrizitäts-Gesellschaft, Erster Band, 1928-1929*—782
- Handbuch der Experimentalphysik, Volume 24, 1 Teil, Kirchner, F. Allgemeine Physik der Röntgenstrahlen—1673; 2 Teil, Lindh, Axel, Röntgenspek troskopie*—609
- Kiebitz, F. *Radio Technic. VI. Die electrishen Wellen*—156
- Lichtenstein, L., *Grundlagen der Hydromechanik*—609
- Longinescu, I.-N. *Essai sur les Principes de la Thermodynamique*—155
- Millikan, Gale and Edwards. *A Manual of Experiments, to accompany A First Course in Physics for Colleges*—1594
- Moulton, F. R., *Differential Equations*—1265
- Newman, F. H. and V. H. L. Searle. *The General Properties of Matter*—1517
- Pauling and Goudsmit. *Structure of Line Spectra*—607
- Peek, F. W. Jr., *Dielectric Phenomena in High Voltage Engineering*—369
- Planck, Max, *Einführung in die Theorie der Wärme, Volume V*—781
- Pohl, R. W., *Einführung in die Mechanik und Akustik*—1265
- Schaefer, Cl. and F. Matossi, *Das Ultrarote Spektrum*—608
- Silberstein, Ludwig, *The Size of the Universe*—370
- Sommerfeld, Arnold, *Wave Mechanics*—1594
- Thibaud, J., *Les Rayons X*—781
- Worsnop, B. L., *X-Rays*—782
- Wulf, Theodor, *Modern Physics*—1516
- Wyckoff, Ralph W. G., *The Analytical Expression of the Results of the Theory of Space Groups*—608
- Zeleny, Anthony, *Elements of Electricity*—369
- Brownian motion**
Theory of, G. E. Uhlenbeck, L. S. Ornstein—823.
- Canal rays**
Spectra in N₂ excited by, H. D. Smyth, E. G. F. Arnott—1023
- Capillary action** (see **Surface tension**)
- Cataphoresis**
In rotating electric fields, E. M. Pugh, C. A. Swartz—787(A), 1495
- Cathode rays** (see **Electrons, Electrons in gases**)
- Chemical bonds**
Elastic character of the homopolar, R. C. Yates—555
Vibration of system analogous to benzene ring, R. C. Yates—563
- Chemical constitution**
And association of homologous compounds, E. C. Bingham, H. J. Fornwalt—381(A)
- Chemical reaction**
Chain reactions caused by physical structure, N. Rashevsky—376(A)
Organic reactions in gaseous electrical discharge, E. G. Linder—374(A), 1375
Thermodynamic treatment of chemical equilibria in systems composed of real gases, ammonia synthesis, I. Mass action function, L. J. Gillespie, J. A. Beattie—743; Heat of reaction, entropy, L. J. Gillespie, J. A. Beattie—1008
- Collision diameter** (see also **Electrons in gases, Electron scattering**)
Calculated values, Fermi-Thomas statistics, E. B. Baker—630
From scattering of electrons, M. C. Green—239, 786(A)
- Colloids**
Cataphoresis in rotating electric fields, E. M. Pugh, C. A. Swartz—787(A), 1495
- Compton effect** (see **X-Rays, diffraction, scattering**)
- Constants, physical**
Planck's constant, h , method of computing, A. Lucy—367(L)
- Contact potential**
Effect on reflection coefficients, H. E. Farnsworth, V. H. Goerke—1190
- Contact resistance**
Microphonic action, F. Gray—375(A); F. S. Goucher—375(A)
Wave mechanical theory, J. Frenkel—1604
- Cosmic rays**

- Constancy and relation to meteorology, R. A. Millikan—1595
- Magnetic deflection, B. Rossi—606(L)
- Crystals and crystal structure**
- Calcite, glancing angle for Ag $K\alpha_1$ rays, C. D. Cooksey, D. Cooksey—85
- Cu, magnetic susceptibility, C. G. Montgomery—498
- Growing large crystals of the alkali halides, J. Strong—1663
- Ice, polar properties of single crystals, J. M. Adams—788(A)
- Inner potential of a copper crystal, H. E. Farnsworth—1799(L)
- Potential and potential energy of space lattices, C. N. Wall—1243
- Properties of metal crystals grown in magnetic fields, A. Goetz, M. F. Hasler—1752
- Rotational motion of molecules in crystals, L. Pauling—430
- Secondary structure, energy changes, F. Zwicky—378(A)
- Cybotactic state**
- Organic liquids, temperature effect, E. W. Skinner—1625
- Dielectric constant**
- CO₂, temperature and density variations, F. G. Keyes, J. G. Kirkwood—754
- H₂, calculated, J. V. Atanasoff—1232
- NH₃, temperature and density variations, F. G. Keyes, J. G. Kirkwood—1570
- Dielectric properties**
- Polarization, search for source, R. D. Bennett—65, 1670(L)
- Diffraction of atoms (see Atomic beams)**
- Diffraction of electrons (see Electrons, diffraction)**
- Diffraction of corpuscles**
- H atoms, T. H. Johnson—381(A)
- Diffraction of radiation (see X-Rays, diffraction)**
- Discharge of electricity in gases (see also Arc, spark)**
- A.c. arcs, extinction of, T. E. Browne, Jr., F. C. Todd—726
- A.c. arcs, restriking of, F. C. Todd, T. E. Browne, Jr.—732
- Electrodeless discharge, current, pressure, and frequency relations—M. L. Braun—1195
- Electrodeless, Hg vapor, characteristics, H. Smith, W. A. Lynch, N. Hilberry—374(A)
- Geissler, hollow cathode, characteristics, C. H. Thomas—374(A)
- Heats of condensation of electrons on Mo, Pt and W-K, C. C. Van Voorhis, K. T. Compton—1435
- Hollow cathode, excitation processes, spectra, R. A. Sawyer—44
- Luminosity, propagation of, J. W. Beams—997
- Ne arc, metastable atom and resonance radiation, I. Langmuir, C. G. Found—604(L)
- New type of glow-discharge tube, H. J. Reich—373(A)
- Organic reactions in gaseous electrical discharge, E. G. Linder—374(A), 1375
- Positive ion sheaths, effect of collisions on potential distribution, H. P. Robertson, P. M. Morse—375(A)
- Secondary electrons produced by metastable atom and positive ions, W. Uytterhoeven, M. C. Harrington—709
- Spectra, variation with discharge, characteristics, E. O. Hulburt—13
- Vapor jets in Hg arc, E. Kobel—1636
- Dissociation**
- Nitric acid from absorption spectra, E. L. Kinsey, J. W. Ellis—603(L)
- H₂ velocities of H⁺ ions formed, W. W. Lozier—1285
- H₂O and formation of negative ions in H₂ and H₂O, W. W. Lozier—1417(L)
- Dissociation, heat of (see also Molecular structure and constants)
- O₂, heat of formation, L. C. Copeland—1221
- Elasticity**
- Longitudinal vibration of rods, D. S. Muzzey, Jr.—935
- Plastic deformations of ductile metals, A. Nadai—762
- Electrets**
- X-ray study of structure, M. Ewing—378(A)
- Electrical conductivity and resistance**
- Contact between carbon spheres, microphonic action, F. Gray—375(A); F. S. Goucher—375(A)
- Contact resistance, wave-mechanical theory, J. Frenkel—1604
- Electrical discharge in gases (see Discharge of electricity in gases)**
- Electromagnetic theory**
- Diffraction of a circularly symmetrical electromagnetic wave by a co-axial circular disc, J. Bardeen—1482
- Transmission of alternating currents through a semi-infinite heterogeneous conducting medium, H. P. Evans—1579
- Unified theory, spherically symmetrical field, N. Rosen, M. S. Vallarta—110
- Electrons**
- Deflection in magnetic field on wave mechanics and value of e/m , L. Page—444; criticism, C. Eckart—1014(L), 1514(L); reply, L. Page—1418(L); G. E. Uhlenbeck, L. A. Young—1721; M. S. Plesset—1728; E. H. Kennard—1667(L)
- e , by x-ray refraction, H. E. Stauss—1101

- e/m* from velocity measurements, C. T. Perry, E. L. Chaffee—904
- e/m* measurements from inertia effects, S. J. Barnett—786(A)
- Heat of condensation of electrons on Mo, Pt and W-K, C. C. Van Voorhis, K. T. Compton—1435
- Polarization by double scattering, C. T. Chase—1060
- Recombination with Cs^+ , E. H. Kurth—374(A)
- Recombination with protons, theory, E. C. G. Stueckelberg, P. M. Morse—16
- Reflection coefficients and contact potentials, H. E. Farnsworth, V. H. Goerke—1190
- Scattering by gas molecules, M. C. Green—239, 786(A)
- Scattering and operation of Geiger counter, C. T. Chase—984
- Electrons, diffraction**
- Inner potential of a copper crystal, H. E. Farnsworth—1799(L)
- Electrons in gases**
- Formation of, W. Bleakney—1303
- Ionization of helium, neon, and argon by electron impact, efficiency, P. T. Smith—1293
- Scattering in He, A and H_2 , angular and energy distribution, J. H. McMillen—1034
- Electrons, photoelectric (see Photoelectric effect)**
- Electrons, scattering (see also Electrons in gases)**
- Effect of small angle scattering on absorption coefficient, M. C. Green—239, 786(A)
- Electrons, secondary**
- From metals bombarded by positive ions, C. L. Utterback, W. Geer—785(A)
- Metastable atoms and positive ions, produced by, W. Uyterhoeven, M. C. Harrington—709
- Velocity distribution of secondary electrons from molybdenum, T. Soller—1212
- Electron tubes**
- Cathode ray oscillograph, F. Bedell, J. Kuhn—993
- High potential x-ray tube, C. C. Lauritsen, B. Cassen—988
- Energy states of atoms**
- Average life of ionized helium, L. R. Maxwell—379(A)
- Method of calculation, C. Eckart—149(L)
- Energy states of molecules**
- As effected by interaction, E. C. Kemble, F. F. Rieke—153(L)
- Excitation function**
- He, spectra, W. C. Michels—604(L), 1362
- Filters, light**
- Infrared, controllable transmission, A. H. Pfund—71
- Fine structure (see also Hyperfine structure)**
- He 2^3P level, test of spin interaction, G. Breit—383
- K radiation of lighter elements, L. Y. Faust—161; M. Soderman—1414(L)
- K series, Ca to Ga, B. Kievit, G. A. Lindsay—648
- $K\alpha$ of Fe, Co, Ni, Cu, Mo and Ag, $K\beta$ of Mo, J. Valasek—1523
- $\text{MoK}\alpha$ lines, double crystal spectrometer, N. S. Gingrich—1050
- Unmodified scattered x-rays, J. A. Bearden—791
- Fluorescence**
- Polarized, of rhodamine-B and uranine, E. Meritt, D. R. Morey—1386
- Quartz, under low voltage cathode rays, H. Peters—1631
- ZnS, under α , β , γ rays, decay characteristics, G. S. Gessner—207
- Gamma rays**
- Wave-length in spectrum of Ra, RaB, RaC, and RaD, including intensity measurements of line and continuous spectra, L. T. Steadman—460
- Geiger-counters**
- Sensitivity, C. T. Chase—984
- Geophysics**
- Wind mixing and diffusion in the upper atmosphere, S. Chapman—1014(L); reply, E. O. Hulburt—1264(L)
- Hall effect**
- Te amalgams, P. I. Wold, J. M. Hyatt—375(A)
- Heat of dissociation (see Dissociation)**
- High voltages**
- Production, M. A. Tuve—1576; M. A. Tuve, L. R. Hafstad and O. Dahl—1261(L)
- Hyperfine structure**
- Cd lines and nuclear spin, C. L. Albright—847
- Hyperfine structure and interval rule, H. E. White—1800(L)
- S and P terms of Li^+ , G. Breit, F. W. Doermann—1732
- $\text{WK}\alpha$, F. K. Richtmyer, S. W. Barnes, K. V. Manning—1017(L)
- Infrared spectra :see also Spectra, molecular;**
- Hg, arc, H. J. Unger—784(A)
- High resolution in near infrared, E. D. McAlister—784(A)
- Instruments (see Methods and instruments)**
- Intensities in spectra**
- Bands of diatomic molecules, theory, E. Hutchison—410
- Cameron bands, intensity changes, H. P. Knauss, J. C. Cotton—1099(L)
- Ni I, Ni II, Co I multiplets, L. S. Ornstein, T. Bouma—679
- X-ray lines in the tantalum L-spectrum, V. Hicks—785(A), 1273

- X-ray satellites, intensity ratios, F. K. Richtmyer, L. S. Taylor—1044
- Ionization by impact**
- CO₂ by electrons, H. D. Smyth, E. C. G. Stueckelberg—472
- He, Ne, and A, efficiency by electrons 0-4500 volts, P. T. Smith—1293
- K and Hg vapors, extra ionization potentials, A. L. Hughes, C. M. Van Atta—214
- Multiply charged ions, He, Ne and A, W. Bleakney—1303
- NO₂ and N₂O, by electrons, E. C. G. Stueckelberg, H. D. Smyth—478
- Velocities of H⁺ ions formed, W. W. Lozier—1285
- Ions**
- Cs⁺ in H₂, pressure changes, A. C. G. Mitchell—381(A)
- Negative ions in hydrogen and water vapor, W. W. Lozier—1417(L)
- Recombination of H⁺ with electron, theory, E. C. G. Stueckelberg, P. M. Morse—16
- Ions in gases**
- Energy losses at elastic collisions, A. M. Cravath—248
- Recombination in A, N₂ and H₂, O. Luhr—24, 788(A); in air and O₂—787(A)
- Ions, mobility**
- Aged ions in air, O. Luhr, N. E. Bradbury—1394
- In dry and moist air, J. Zeleny—35
- Na⁺ in H₂, L. B. Loeb—152(L), 790(A)
- Isotopes**
- Be⁹, band spectrum of BeH, W. W. Watson—1019(L)
- Cs, K. T. Bainbridge—1668(L)
- Effect on band spectrum intensities, J. L. Dunham—1553
- N₁₅, O₁₈, O₁₇, abundances, from band spectra, S. M. Naudé—333
- Number of isotopes of eight metals, F. Allison, E. J. Murphy—1097(L)
- Kinetic theory of gases**
- Second virial coefficient, experimental and theoretical, H. Margenau—1782
- Light waves**
- Electro-optical modification of, electric oscillations on Kerr cell, L. H. Stauffer—1352
- Frequency shifts in dispersing media, G. Breit, E. O. Salant—871
- Luminescence**
- Due to α , β , γ rays, mechanism, D. H. Kabakjian—379(A)
- ZnS under α , β , γ rays, decay characteristics, G. S. Gessner—207
- Magnetic properties**
- Barkhausen effect in Ni, discontinuous changes in length, C. W. Heaps, A. B. Bryan—326, criticism, L. W. McKeehan—1014(L)
- Cu and Ag, susceptibilities of and structure sensitivity, F. Bitter—978
- Electrical resistance, tension and magnetization of Ni and permalloy, bibliography included, L. W. McKeehan—948
- Gyromagnetic anomaly and rotation by magnetization, S. J. Barnett—789(A)
- Hall effect in ferromagnetic materials, E. M. Pugh—1503
- Hall effect of Te amalgams, P. I. Wold, J. M. Hyatt—375(A)
- Isotropy of a paramagnetic alum, C. G. Montgomery—1661
- Li₇ nucleus, momentum of, L. P. Granath—1018(L); see also G. Breit, F. W. Doermann—1262(L)
- Molecular field and atomic order in ferromagnetic crystals, L. W. McKeehan—1512(L), 1670(L)
- Pt-Co and Pd-Co alloys, F. W. Constant—786(A), 1654
- Susceptibility measurements, S. Freed, C. Kasper—1002
- Susceptibilities of Bi single crystal, A. B. Focke—319
- Susceptibility of Cu crystals, C. G. Montgomery—498
- Susceptibility of gases, temperature dependence, F. Bitter—1648
- Temperature change on magnetization, W. B. Ellwood—1066
- Magnetostriction oscillator**
- For elastic studies, D. S. Muzzey, Jr.—935
- Mechanics**
- Coupled systems of linear oscillators, A. B. Lewis—568
- Solar system, quantization and inverse square law A. E. Caswell—787(A)
- Vibrations of mechanical systems representing organic molecules, R. C. Yates—555
- Vibrations of non-planar membrane, G. R. Stibitz—513
- Vibration of system representing benzene ring, R. C. Yates—563
- Mechanics, quantum**
- Complex spectra, theory, E. U. Condon—1121
- Calculation of energy values, C. Eckart—149(L)
- Deflection of electrons in magnetic field and value of e/m , L. Page—444; criticism, C. Eckart—1014(L); 1514(L); reply, L. Page—1418(L); G. E. Uhlenbeck, L. A. Young—1721; M. S. Plesset—1728; E. H. Kennard—1667(L)
- Dielectric constant H₂, J. V. Atanasoff—1232

- Electrical resistance of contacts, J. Frenkel—1604
Energy states of molecules as affected by interaction, E. C. Kemble, F. F. Rieke—153(L)
Extrapolation of atomic structure factor curves, D. K. Froman—1339
Frequency shifts in dispersing media, G. Breit, E. O. Salant—871
Intensities in band spectra, E. Hutchisson—410
Isotope effect on intensities, J. L. Dunham—1553
Magnetic moment of Li_7 nucleus, G. Breit, F. W. Doermann—1262(L)
Motion of nucleus, effect on spectra, D. S. Hughes, C. Eckart—694
Orbital valency, J. H. Bartlett, Jr.—1096(L)
Paschen-Back effect, incomplete, J. B. Green—157, 379(A)
Principle of identity and the exclusion of quantum states, G. N. Lewis—1144
Recombination of electron and H^+ , E. C. G. Stueckelberg, P. M. Morse—16
Relativity, unified field, W. Band—1405
Rotational motion of molecules in crystals, L. Pauling—430
Screening constants, calculation of, C. Eckart—878
Spin interactions as tested by fine structure of He, G. Breit—383
Structure of emission line, theory, F. C. Hoyt—380(A), 860
Symmetrical top, dispersion formula, Raman effect—an erratum, M. Muskat—363
Wave equation, solution, L. A. Young, G. E. Uhlenbeck—1154
Wave functions, approximate, for any atom, J. C. Slater—57
Wave functions for Be, B, C, N, O, F, Ne, C. Zener—51
- Mechanics, statistical**
Brownian motion, theory of, G. E. Uhlenbeck, L. S. Ornstein—823
Entropy of H_2 , D. MacGillavry—1398, W. F. Giaque, H. L. Johnston—1592(L)
Fermi-Thomas method applied to positive ions, E. B. Baker—630
- Metastable atoms**
Ne, in arc by resonance radiation, I. Langmuir, C. G. Found—604(L)
- Meteorology (see also Atmospheric electricity)**
Cosmic rays and meteorology, R. A. Millikan—1595
- Methods and instruments**
Calorimeter to measure small heat changes, W. B. Ellwood—1066
Cathode ray oscillograph, correction, F. Bedell, J. Kuhn—993
Diamagnetic susceptibility measurements, S. Freed, C. Kasper—1002
False x-ray lines, J. M. Cork—665
Filters, infrared, controllable transmission, A. H. Pfund—71
Fluorescent dry plates for photographic photography, G. R. Harrison, P. A. Leighton—779(L)
Geiger counter, voltage effects, C. T. Chase—984
Glow discharge tube—new type, H. J. Reich—373(A)
High potential x-ray tubes, C. C. Lauritsen, B. Cassen—988
High voltage tubes, M. A. Tuve, L. R. Hafstad and O. Dahl—1261(L)
Infrared, high resolution in, E. D. McAlister—784(A)
Low grid-current vacuum tube for current measurements, G. F. Metcalf, B. J. Thompson—1489
Mass spectrograph, H. D. Smyth, E. C. G. Stueckelberg—472
Mechanical models to represent dynamic properties of molecules, C. F. Kettering, L. W. Shutts, D. H. Andrews—531
Minimizing errors in reading distance on photographic plates, D. Cooksey, C. D. Cooksey—80
Optically excited radiation, P. Bender—1535
Photoelectric cells, methods of enhancing sensitivity, O. R. Olpin—251
Photographic method of determining atomic structure factors, D. K. Froman—1330
Pierce acoustic interferometer, high frequencies, E. Klein, W. D. Hersherberger—1262(L)
Rectifier, cupric sulfide-magnesium junction, M. Bergstein, J. F. Rinke, C. M. Gutheil—587; 1022
Refraction of x-rays, H. E. Stauss—1101
Shot-circuit impedance measurements, H. N. Kozanowski, N. H. Williams—1314
Specific heat variation with pressure, E. J. Workman—1083
Velocity Measurement of electrons, C. T. Perry, E. L. Chaffee—904
Viscosimeter, Margules method for absolute values, H. R. Lille—347
X-ray spectrometer, double crystal, J. W. M. Dumond, A. Hoyt—1702
- Microphone**
Microphonic action of contact resistance, F. Gray—375(A); F. S. Goucher—375(A)
- Mobility of ions (see Ions, mobility)**
- Molecular structure and constants (see also Spectra, molecular)**
Atomic J values and molecular quantum numbers, R. S. Mulliken—1440
Benzene ring model and Raman spectra, R. C. Yates—563

- Homopolar chemical bond and Raman spectra, R. C. Yates—555
- K₂, heat of dissociation, vibrational constants, W. O. Crane, A. Christy—421
- Mechanical models to represent dynamic properties, C. F. Kettering, L. W. Shutts, D. H. Andrews—531
- Methane gas, new absorption band, D. M. Denison, S. B. Ingram—1451
- O₂, heat of formation, L. C. Copeland—1221
- Orbital valency, J. H. Bartlett, Jr.—1096(L)
- Multiplets**
- Intensity ratios Ni I, Ni II, Co I, L. S. Ornstein, T. Bouma—679
- Packing effect**
- Cs, K. T. Bainbridge—1668(L)
- Paschen-Back effect**
- For intermediate fields, theory, J. B. Green—157, 379(A)
- Photoelectric cells**
- Methods of enhancing sensitiveness, O. R. Olpin—251
- Photoelectric effect**
- Cs thin films on O, L. R. Koller—1639
- Direction of emission of photoelectrons, E. O. Lawrence, M. A. Chaffee—1099(L)
- Effect of intense electric fields, E. O. Lawrence, L. B. Linford—482; see also L. B. Linford—1100(L)
- Inhibition by infrared light, A. R. Olpin—376(A)
- Outgassing, action of photoelectrons, R. P. Winch—601(L)
- Photoionization of salt vapors, A. Terenin—147(L)
- Threshold and current variation with temperature (Hg), D. Roller—738
- Photography**
- Fluorescent dry plates for photographic photometry, G. R. Harrison, P. A. Leighton—779(L)
- Unreliability of photographic emulsions for recording distances, improvements, D. Cooksey, C. D. Cooksey—80
- Photons**
- Collisions of, A. L. Hughes, G. E. M. Jauncey—773; S. Vavilov—1590(L)
- Planck's constant, h**
- Method of computing not involving e , A. Lucy—367(L)
- Polarization, electrical** (see Dielectric properties)
- Potentials, critical** (see also Spectra)
- Ag I, ionization, spectra, H. A. Blair—1531
- CO₂, ionization by electrons, H. D. Smyth, E. C. G. Stueckelberg—472
- CO II, ionization, spectra, J. H. Findlay—5
- Ionization potentials, successive, calculated, E. B. Baker—630
- Ionization of He, Ne and Ar, W. Bleakney—1303
- K and Hg vapor, extra ionization potentials, A. L. Hughes, C. M. Van Atta—214
- NO₂ and N₂O, ionization by electrons, E. C. G. Stueckelberg, H. D. Smyth—478
- Proceedings of the American Physical Society**
- Ithaca Meeting, June 19 to 21, 1930—372
- Eugene Meeting, June 19 to 21, 1930—783
- Quadrupole radiation**
- Experimental evidence, R. Frerichs, J. S. Campbell—151(L); 1460
- Quantum mechanics** (see Mechanics, quantum)
- Radiation**
- Penetration, therapeutic use, E. Q. Adams—1020(L)
- Quenching of resonance radiation (Hg), M. W. Zemansky—919
- Radio**
- Diffraction of a circularly symmetrical electromagnetic wave by a co-axial circular disc, J. Bardeen—1482
- Radioactivity**
- Range of α particles from Th, G. H. Henderson, J. L. Nickerson—1344
- γ -ray scattering, ThC, C. Y. Chao—1519
- Wave-length measurements of gamma rays for Ra, RaB, RaC, and RaD, L. T. Steadman—460
- Raman effect**
- Benzene and diphenyl, anti-Stokes lines, R. W. Wood—1431
- Excitation efficiency, relative, of Hg lines, M. Werth—1096(L)
- Geometric isomers, C. F. Ffolliott—367(L)
- HBr and NI, E. O. Salant, A. Sandow—1591(L)
- Hg and He arc excitation, filters and improved technique, R. W. Wood—1421
- Solutions of NaNO₃, V. Sterling, E. R. Laird—148(L)
- Structure of organic molecules, D. H. Andrews—544
- Trimethylethylene, D. Franklin, E. R. Laird—147(L)
- Recombination**
- Electron and H⁺, theory, E. C. G. Stueckelberg, P. M. Morse—16
- Of ions in Ar, N₂ and H₂, O. Luhr—24, 788(A)
- Electrons with Cs⁺, E. H. Kurth—374(A)
- Rectifiers**
- Cupric sulfide-magnesium junction, M. Bergstein, J. F. Rinke, C. M. Gutheil—587; errata—1022
- Relativity**
- Mechanical treatment of temperature distribution in case of radiation W. Anderson—365(L); reply, R. C. Tolman—365(L)
- Non-statical solution of Einstein's law of gravitation, H. P. Soh—1515(L)

- Projective relativity, O. Veblen, B. Hoffmann—810
 Relativistic wave mechanics, of deflected electrons, M. S. Plesset—1728
 Temperature equilibrium in a static gravitational field, R. C. Tolman, P. Ehrenfest—1791
 Unified physical field, W. Band—1405
 Unified theory, spherically symmetrical field, N. Rosen, M. S. Vallarta—110
Resistance of metals (see **Electrical conductivity and resistance**)
 Tension coefficient of, H. Rolnick—506
Resonance radiation
 Width of line as function of geometry of tube and vapor density, M. W. Zemansky—219, 380(A), 1591(L)
Screening constants
 Theory and calculation of, C. Eckart—878
Shielding constants
 For any atom, approximate, J. C. Slater—57
Shot effect
 Abnormal effect of ions, J. S. Donal, Jr.—1172
 Oxide coated filaments, H. N. Kozanowski, N. H. Williams—1314
Skylight
 Energy distribution in ultraviolet, B. O'Brien—381(A)
Spark
 Time lag, relation to photoelectrons from cathode, J. A. Tiedeman—376(A)
Specific heats
 Gases, variation with pressure, calculated values, L. G. Hoxton—1091
 Gases, variation with pressure, experimental values, E. J. Workman—1083
 Organic crystals, calculated from mechanical models, A. B. Lewis—568
Spectra, absorption
 Benzene in the liquid and vapor state, E. D. McAlister, H. J. Unger—1799(L)
 Nitric acid dissociation, by absorption spectra, E. L. Kinsey, J. W. Ellis—603(L)
Spectra, atomic
 Ag II and Pd II, extension, H. A. Blair—173
 Ag I, classification and new lines, H. A. Blair—1531
 Atomic *J* values and molecular quantum numbers, R. S. Mulliken—1440
 Auroral green line, Zeeman effect, quadrupole radiation, R. Frerichs, J. S. Campbell—151(L), 1460
 Co II, classification, J. H. Findlay—5
 Cu arc, correction to published list, A. G. Shenstone—603(L)
 Diaphantine equation, hydrogen spectrum, T. H. Gronwall—1671(L)
 Energy states, calculation, C. Eckart—149(L)
 Excitation function of helium, W. C. Michels—604(L); 1362
 Excited in hollow cathode discharge, R. A. Sawyer—44
 Fe lines, classification, H. D. Babcock—784(A)
 Forbidden lines and quadrupole terms, L. D. Huff, W. V. Houston—842
 He, new lines in arc and spark, P. G. Kruger—855
 Hg lines, fluorescence, polarization of, A. C. G. Mitchell—1589(L)
 Hg 2537, ratio of emission to absorption line width, M. W. Zemansky—219, 380(A), 1591(L)
 Hyperfine structure Cd lines, C. L. Albright—847
 Hyperfine structure of *S* and *P* terms of two electron atoms, G. Breit, F. W. Doermann—1732
 Kr and Xe, wave-lengths, C. J. Humphreys—380(A)
 Li I and Li II, calculated effect of motion of nucleus, D. S. Hughes, C. Eckart—694
 Nitrogen atomic, resonance series, J. J. Hopfield—789(A)
 Ni I, Ni II, Co I, intensity measurements, multiplet intensity ratios, L. S. Ornstein, T. Bouma—679
 O, singlet system, origin of auroral line, R. Frerichs—398
 Oxygen, atomic, resonance series, J. J. Hopfield—789(A)
 Pb III and Pb IV, classification, S. Smith—1
 Pd I analysis, A. G. Shenstone—669
 Polarization of Hg resonance line, S. Mrozowski—1591(L)
 Quenching of Cd lines by gases, P. Bender—1535
 Rh, term values, A. G. Shenstone, J. J. Livingood—380(A)
 Structure of emission line, theory, F. C. Hoyt—380(A), 860
 Theory of complex spectra, E. U. Condon—1121
 Wave equation, application to hydrogenic atoms, L. A. Young, G. E. Uhlenbeck—1154
 Wave-length list for extreme ultraviolet, J. M. MacInnes, J. C. Boyce—368(L)
Spectra, continuous
 From gases lighted by strong discharge, E. O. Hulburt—13
Spectra, general
 Excitation function of helium, W. C. Michels—604(4); 1362
 Fluorescence of quartz, H. Peters—1631
 Fluorescence, polarization of, E. Merritt, D. R. Morey—1386
 From gases lighted by strong discharge, E. O. Hulburt—13
 General Electric type S-1, spectrum, D. Dooley—1476

- He, continuous spectrum in condensed discharge 500-1100A, J. J. Hopfield—784(A)
- Hg vapor absorption bands, origin of, S. Mrozowski—1168
- Optical excitation, P. Bender—1543
- Oscillating arc in spectrochemical analysis, E. Z. Stowell, W. S. Huxford—1348
- Oxygen, auroral and nebular lines, I. S. Bowen—600(L)
- Quenching of mercury resonance radiation by nitrogen and carbon monoxide, J. Kaplan—788(A)
- Radiation from a high potential x-ray tube, C. C. Lauritsen—1680
- Tungsten mercury arc, peculiarities, W. E. Forsythe, M. A. Easley—150(L)
- Tungsten mercury arc, spectral energy, B. T. Barnes—1468
- Spectra, molecular**
- Absorption bands of K_2 , W. O. Crane, A. Christy—421
- Atomic J values and molecular quantum numbers, R. S. Mulliken—1440
- Band in Be^8H spectra, W. W. Watson—1019(L)
- Bands in the absorption spectrum of mercury, J. G. Winans—1020(L)
- CaF and SrF , interpretation of, A. Harvey, F. A. Jenkins—1413(L)
- Cameron bands in CO , intensities, H. P. Knauss, J. C. Cotton—1099(L)
- CO third positive group, J. Kaplan—784(A)
- Electronic states in halogen bands, R. S. Mulliken—699
- Energy states, effect of interaction, E. C. Kemble, F. F. Rieke—153(L)
- Halogen bands, interpretation, R. S. Mulliken—364(L)
- H_2 , $B-A$ resonance bands, quantum assignments, H. H. Hyman—187
- Intensities in bands, J. Kaplan—778(L)
- Isotope effect on intensities, J. L. Dunham—1553
- Liquids, absorption in infrared, effect of pressure, J. R. Collins—305
- Methane gas, new absorption band, theory of overtones, D. M. Dennison, S. B. Ingram—1451
- N_2 , absorption bands, J. J. Hopfield—789(A)
- N_2 and O_2 , abundances of N_{18} , O_{18} and O_{17} , S. M. Naudé—333
- N_2 band spectra, by canal ray excitation, H. D. Smyth, E. G. F. Arnott—1023
- Notation, report on, R. S. Mulliken—611
- O_2 bands, new, J. J. Hopfield—789(A)
- Optical excitation of CdH and ZnH bands, P. Bender—1543
- Organic liquids, absorption in infrared, high resolution, R. B. Barnes—296
- S_2 , vibrational and rotational analysis—S. M. Naudé, A. Christy—1801(L)
- Symmetrical diatomic molecules, intensities, theory, E. Hutchisson—410
- ZnH and CdH bands, Zeeman effect, W. W. Watson—1134
- Spectrograph, spectrometer**
- X-ray, double crystal, J. W. M. Dumond, A. Hoyt—1702
- Spectroscopic technique**
- Unreliability of photographic emulsions for recording distances, improvements, D. Cooksey, C. D. Cooksey—80
- Sun (see Astrophysics)**
- Surface tension**
- Of saturated vapors, maximum, J. L. Shereshefsky—377(A)
- Retention of liquids between homogeneous spheres, W. O. Smith, P. D. Foote, P. F. Busang—524
- Susceptibility, magnetic (see Magnetic properties)**
- Thermal expansion**
- M-M-M alloy, P. Hidnert, W. T. Sweeney—787(A)
- Thermionic emission of electrons**
- Efficiency of emission from oxide coated filaments, B. J. Thompson—1415(L); erratum—1802(L)
- Oxide coated filaments, shot effect, H. N. Kozanowski, N. H. Williams—1314
- Oxide coated Ni-Ba alloy, N. C. Beese—1309
- Shot effect, abnormal, of ions, J. S. Donal Jr.—1172
- Work function and constant A for thoriated tungsten, W. B. Nottingham—376(A)
- Thermodynamics**
- c_p variation, calculated from p-v-t data, L. G. Hoxton—1091
- Entropy, elastic strain, W. S. Kimball—377(A)
- Entropy of crystalline hydrogen, L. Pauling—430
- Entropy of H_2 , D. MacGillavry—1398; W. F. Giauque, H. L. Johnston—1592(L)
- Equations of state and thermodynamic functions for a substance with variable specific heat, W. P. Boynton—787(A)
- Equilibrium, ammonia synthesis reaction. I. Mass action function, L. J. Gillespie, J. A. Beattie—743. II. Heat of reaction entropy, L. J. Gillespie, J. A. Beattie—1008
- Fundamental correspondence to geometry, J. Q. Stewart—377(A)
- Gibbs-Dalton law of partial pressures, L. J. Gillespie—121
- Mechanical treatment of temperature distribution of radiation, W. Anderson—365(L); reply, R. C. Tolman—365(L)
- Real gases and mixtures, J. A. Beattie—132

- Surface tension of saturated vapors, J. L. Shershensky—377(A)
- Temperature equilibrium in a static gravitational field, R. C. Tolman, P. Ehrenfest—1791
- Thermoelectric effect**
In crystals grown in magnetic fields, A. Goetz, M. F. Hasler—1752
- Triboluminescence**
In crystals, glass and frits, R. E. Nyswander, B. E. Cohn—1257
- Ultrasonic waves**
Velocity and absorption in O_2 , W. H. Pielemeier—1005, 1667(L); J. C. Hubbard—1668(L)
Velocity in water vapor, G. E. Thompson—77
- Vacuum tubes**
High voltage, M. A. Tuve, L. R. Hafstad, O. Dahl—1261(L)
Low grid-current tube, type F. P.-54, G. F. Metcalf, B. J. Thompson—1489
- Viscosity**
Margules method, absolute values, H. R. Lille—347
- Vision theory of**
Electromagnetic theory of sight and color vision, S. R. Cook—790(A)
- Wave functions**
For any atoms, approximate, J. C. Slater—57
For Be, B, C, N, O, F, Ne, C. Zener—51
- Work function** (see Thermionic emission)
- X-rays, absorption**
By Li, K. C. Mazumder—457
Elements Ca to Ga, fine structure, B. Kievit, G. A. Lindsay—648
In gases, W. W. Colvert—1619
Penetration, therapeutic use, E. Q. Adams—1020(L)
Soft rays in gases, C $K\alpha$ in air, E. Dershem, M. Schein—378(A)
- X-rays, diffraction, reflection and scattering**
Compton effect, position and structure of modified line, F. L. Nutting—1267
Compton shift, accurate measure, N. S. Gingrich—364(L)
Electric fields and diffraction pattern of a liquid, G. W. Stewart—1413(L)
Fine structure lines, with double crystal spectrometer, N. S. Gingrich—1050
Fine structure of unmodified line, J. A. Bearden—791
Liquids, effect of temperature, E. W. Skinner—1625
Multiple scattering in the Compton effect, J. W. M. Dumond—1685
- Scattering coefficient as a function of wave-length and atomic number, E. N. Coad—778(L), 1109
Scattering power of Ni, Cu, Fe, for various wave-lengths, R. W. G. Wyckoff—1116
Thin metallic films, reflection from, J. E. Henderson, E. B. Jordan—785(A)
Width and structure of modified $K\alpha_1$, $K\alpha_2$, P. A. Ross, J. C. Clark—378(A)
- X-rays, emission**
Fine structure, $K\alpha$ of Fe, Co, Ni, Cu, Mo and Ag, $K\beta$ of Mo, J. Valasek—1523
Hyperfine structure W $K\alpha$, F. K. Richtmyer, S. W. Barnes, K. V. Manning—1017(L)
 $K\alpha_2$ of Cu, origin of, and Richtmyer double group hypothesis, J. W. M. Dumond, A. Hoyt—799; J. W. Dumond—1015(L)
Ta, L -spectrum relative intensities of lines, V. Hicks—785(A), 1273
- X-rays, polarization**
Continuous x-rays from single electron impacts, B. Dasannacharya—1675
- X-rays, reflection and refraction**
Glancing angle of calcite for Ag $K\alpha_1$ C. D. Cooksey, D. Cooksey—85
- X-rays, scattering**
Breadth of modified line, J. W. M. Dumond—146(L)
- X-rays, spectra**
Fine structure in K -radiation of lighter elements, L. Y. Faust—161; M. Soderman—1414(L)
- X-rays, spectra and spectroscopy**
False lines in x-ray grating spectra, J. M. Cork—665
Intensity ratios of satellites, F. K. Richtmyer, L. S. Taylor—1044
Radiation from a high potential x-ray tube, C. C. Lauritsen—1680
- X-rays, tubes**
Currents through walls, D. P. LeGalley, W. R. Ham, M. W. White—379(A)
- Zeeman effect**
Auroral green line, R. Frerichs, J. S. Campbell—1460
Incomplete Paschen-Back effect, calculation, J. B. Green—157, 379(A)
In Co II spectrum, J. H. Findlay—5
In quadrupole radiation, R. Frerichs, J. S. Campbell—151(L)
Misplacements and g values, H. N. Russell—1590(L)
ZnH and CdH bands, W. W. Watson—1134